2023 Annual Meeting of the American Society for Bone and Mineral Research

October 13-16, 2023

The *Journal of Bone and Mineral Research* (ISSN: 0884-0431 [print]; 1523-4681 [online]) provides a forum for papers of thehighest quality pertaining to bone, muscle, and mineral metabolism. Manuscripts are published on the biology and physiology of bone and muscle, relevant systems biology topics (e.g., osteoimmunology), and the pathophysiology and treatment of sarcopenia,and disorders of bone and mineral metabolism. All authored papers and editorial news and comments, opinions, findings, conclusions or recommendations in the *Journal* are those of the author(s) and do not necessarily reflect the views of the *Journal* and its publisher, nor does their publication imply any endorsement.

The JOURNAL OF BONE AND MINERAL RESEARCH (ISSN: 0884-0431), is published monthly on behalf of the American Society for Bone and Mineral Research by Wiley Subscription Services, Inc., a Wiley Company, 111 River St., Hoboken, NJ 07030-5774. Periodical Postage Paid at Hoboken, NJ and additional offices.

Postmaster: Send all address changes to JOURNAL OF BONE AND MINERAL RESEARCH, John Wiley & Sons Inc., C/O The Sheridan Press, PO Box 465, Hanover, PA 17331. **Information for subscribers:** The *Journal of Bone and Mineral Research* ispublished in 12 issues per year. Institutional subscription prices for 2023 are: Print &Online: US$1481 (US), US$1481 (Rest of World),€1064 (Europe),£908 (UK). Prices are exclusive of tax. Asia-Pacific GST, Canadian GST and European VAT will be applied at the appropriate rates. For more information on current tax rates, please go to www.wileyonlinelibrary.com/tax-vat. The price includes online access to the current and all online back files to January 1st 2012, where available. For other pricing options, including access information and terms and conditions, please visit www.wileyonlinelibrary.com/access. **Commercial Reprints:** Beth Ann Rocheleau, Reprints and Eprints Manager, Rockwater, Inc., PO Box 2211, Lexington, SC 29072, USA; Tel: +00 (1)803-359-4578; Fax: +00 (1)803-753-9430; E-mail: asbmr@rockwaterinc.com. For submission instructions, subscription and all other information, visit: www.jbmr.org

The *Journal of Bone and Mineral Research* is the official journal of the American Society for Bone and Mineral Research, 2001 K Street, NW, 3rd Floor North, Washington, D.C. 20006, USA. **Advertising:** Address advertising inquiries to Joseph Tomaszewski, Advertising Sales Executive, Wiley, 111 River St., Hoboken, NJ 07030, (201) 748-8895 (Tel); jtomaszews@wiley.com (email). Advertisements are subject to editorial approval and must adhere to ASBMR's advertising policy as specified here: https://onlinelibrary.wiley.com/page/journal/15234681/homepage/Advertise.html. Publication of the advertisements in JBMR® is not an endorsement of the advertiser's product or service or the claims made for the product in such advertising. **Disclaimer:** No responsibility is assumed, and responsibility is hereby disclaimed, by the American Society for Bone and Mineral Research, the *Journal of Bone and Mineral Research*, and the Publisher for any injury and/or damage to persons or property as a matter of products liability, negligence or otherwise, or from any use or operation of methods, products, instructions or ideas presented in the *Journal*. Independent verification of diagnosis and drug dosages should be made. Discussions, views and recommendations as to medical procedures, choice of drugs and drug dosages are the responsibility of the authors. Advertisers are responsible for compliance with requirements concerning statements of efficacy, approval, licensure, and availability. The *Journal of Bone and Mineral Research* is a **Journal Club™** selection. The Journal is indexed by *Index Medicus, Current Contents/Life Science, CABS (Current Awareness in Biological Sciences), Excerpta Medica, Cambridge Scientific Abstracts, Chemical Abstracts, Reference Update, Science Citation Index*, and Nuclear Medicine Literature Updating and IndexingService.

GUIDELINES FOR ABSTRACT READERS

The JBMR® Supplement 1 Abstracts serves as a compiled version of the Abstracts. Authors submit their own abstracts and are charged a fee to do so. Each abstract must be sponsored by a current ASBMR member. Authors are responsible for the accuracy of the content that they post. Authors are responsible for ensuring compliance with applicable human subject and animal subject procedures. When an abstract is submitted, one person is identified as the Presenting Author, the person who is expected to present the abstract at the ASBMR Annual Meeting.

The ASBMR depends upon the honesty of the authors and presenters and relies on their assertions that they have had sufficient full access to the data to be and are convinced of its reliability. The ASBMR expects that authors and presenters:

- Will disclose any conflicts of interest, real or perceived.
- Should disclose any relationship that may bias one's presentation or which, if known, could give the perception of bias.
- Will affirm, for any study funded by an organization with a proprietary or financial interest, that they had full access to all the data in the study.
- Are responsible for the content of abstracts, presentations, slides, and reference materials.
- Keep the planning, content and execution of abstracts, speaker presentations, slides, abstracts and reference materials free from corporate influence, bias or control.
- Should give a balanced view of therapeutic options by providing several treatment options, whenever possible, and by always citing the best available evidence.
- Should disclose when any commercial product is not labeled for the use under discussion or that the product is still investigational.

The ASBMR:

- Will note those speakers who have disclosed relationships, including the nature of the relationship and the associated commercial entity.
- Will peer-review the abstracts according to categories, but only to determine which will be selected for oral presentation, for poster presentations or for any awards. Abstracts are not otherwise subject to any quality or content review by ASBMR or JBMR®.
- Expects the audience for the Abstracts to be researchers, physicians and other health and allied health professionals.
- Protects the Abstracts by copyright, and prohibits the reproduction, distribution or transmission of the abstracts without the express written permission of ASBMR.
- Embargoes the Abstracts for public release in written, oral or electronic communications – until the start time of the session in which the presentation is being made at the ASBMR Annual Meeting

Disclaimer. All authored abstracts, findings, conclusions, recommendations or oral presentations are those of the author(s) and/or speaker(s) and do not reflect the views of the American Society for Bone and Mineral Research or imply any endorsement. No responsibility is assumed, and responsibility is hereby disclaimed, by the American Society for Bone and Mineral Research for any injury and/or damage to persons or property as a matter of products' liability, negligence or otherwise, or from any use or operation of methods, products, instructions or ideas presented in the abstracts or at the ASBMR Annual Meeting. Independent verification of diagnosis and drug dosages should be made. Discussions, views and recommendations regarding medical procedures, choice of drugs and drug dosages are the responsibility of the authors and presenters.

TABLE OF CONTENTS

JBMR® Journal of Bone and Mineral Research

Official Journal of the American Society for Bone and Mineral Research

wileyonlinelibrary.com/journal/jbmr

OFFICERS

Mary Bouxsein, Ph.D., President
Laura Calvi, M.D., President-Elect
Peter Ebeling, AO, M.D, FRACP, Past-President
René St-Arnaud, Ph.D., Secretary-Treasurer

COUNCILORS

Carolyn Crandall, M.D., MS
Tamara Alliston, Ph.D.
Joseph Stains Ph.D.
Christopher J. Hernandez, Ph.D.
Joy Wu, M.D., Ph.D.
Melissa Kacena, Ph.D.
Nina Ma, M.D.
Nicola Napoli, M.D., Ph.D.
Megan Weivoda, Ph.D.
Rajesh Thakker, FRS FMedSci FRCPath FRCPE FRCP, *Ex-Officio*
Deborah Veis, M.D., Ph.D., *Ex-Officio*

ASBMR STAFF

Angela Belusik, *Associate Executive Director*
Taylor Collison, *Marketing Manager*
Michele Cook, *Program Coordinator*
John Curle, *Senior Accounting Manager*
Erin Dalder-Alpher, Program Manager
Melissa Dewey, *Event Director*
Katie Duffy, *Senior Director of Publications*
Douglas Fesler, *Executive Director*
Emily Flint, *Conference Manager*
Jennifer Jasas, *Exhibits and Sponsorship Fulfillment Manager*
Deborah Kroll, *Director of Development*
Greg Maciog, *Senior Membership Manager*
Alana Stewart, *Membership & Operations Coordinator*
Isabella Rosanova, *Tradeshow Support*
Rachel Schneider, *Convention Support*
Kat Seiffert, *Marketing Director*
Amy Truong, *Staff Accountant*

ASBMR BUSINESS OFFICE

2001 K Street, NW
Third Floor North
Washington, DC 20006
USA
Tel: +1 (202) 367-1161
Fax: +1 (202) 367-2161
E-mail: asbmr@asbmr.org
Internet: http://www.asbmr.org

2023 PROGRAM COMMITTEE

President: Mary Bouxsein, Ph.D.
Program Chair: Larry Suva, Ph.D.
Basic Co-Chair: Hannah Taipaleenmaki, Ph.D.
Translational Co-Chair: Joy Wu, M.D., Ph.D.
Clinical Co-Chair: Sabashini Ramchand, FRACP, MBBS

2023 PROGRAM ADVISORY COMMITTEE

Natasha Appelman-Diskstra, M.D., Ph.D.
Belinda Beck, Ph.D.
Andrea Bonetto, Ph.D.
Aline Bozec, Ph.D.
Andrea Burden, Ph.D.
Manju Chandran, M.D.
Angela Cheung, M.D., Ph.D.
Roberto Civitelli, M.D.
Patricia Clark, Ph.D.
Adi Cohen, M.D.
Martine Cohen-Solal, M.D., Ph.D.
Lindsay Dawson, Ph.D.
Jesus Delgado-Calle, Ph.D.
Mathew Drake, M.D., Ph.D.
Emma Duncan, M.D.
Gustavo Duque, M.D.
Claire Edwards, Ph.D.
Roberta Faccio, Ph.D.
Mathieu Ferron, Ph.D.
Antonella Forlino, Ph.D.
Lora Giangregorio, Ph.D.
Matthew Greenblatt, M.D., Ph.D.
Agi Grigoriadis, Ph.D.
Diego Grinman, Ph.D.
Ed Guo, Ph.D.
Nicholas Harvey, MB Bchir, Ph.D., FRCP
Nan Hatch, D.M.D., Ph.D.
Chris Hernandez, Ph.D.
Eric Hesse,
Eason Hildreth, DVM
Lorenz Hofbauer, M.D.
Yuuki Imai, Ph.D.
Rachelle Johnson, Ph.D.
Patricia Juarez Camacho, Ph.D.
John Kemp, Ph.D.
Sundeep Khosla, M.D.
Stavroula Kousteni, Ph.D.
Ron Kwon, Ph.D.
Alex Lambi, M.D., Ph.D.
Bente Langdahl, M.D., Ph.D.
Ben Leder, M.D.
Joshua Lewis, Ph.D.
Karl Lewis, Ph.D.
Jason Lim, Ph.D.
William Lu, Ph.D.
Christa Maes, Ph.D.
Michelle McDonald, Ph.D.
Nicola Napoli, M.D.
Noriaki Ono, Ph.D.
Nathan Pavlos, Ph.D.
Sun Peck, Ph.D.
Daniel Perrien, Ph.D.
Allison Pettit, Ph.D.
Lilian Plotkin, Ph.D.
Martina Rauner, Ph.D.
Yumie Rhee, M.D.
Brent Richards, M.D.
Fernando Rivadeneira, M.D., Ph.D.
Eric Rush, M.D.
Erica Scheller, D.D.S., Ph.D.
Claudia Sedlinsky, M.D.
Steven Stegen, Ph.D.
Emily Stein, M.D.
Sakae Tanaka, M.D., Ph.D.
Anna Teti, Ph.D.
Rodrigo Valderrabano, M.D.
Bram van der Eerden, Ph.D.
Shirley Wang, Ph.D.
Leanne Ward, M.D.
Kate Ward, Ph.D.
Natalie Wee, Ph.D.
Nicole Wright, Ph.D.
Shirley (Jialiang) Yang, Ph.D.
Elaine Yu, M.D.
Maria Zanchetta, M.D.
Ayse Zengin, Ph.D.

2023 ABSTRACT REVIEWERS

Cheryl Ackert-Bicknell, Ph.D.
Robert Adler, M.D.
Kylie Alexander, Ph.D.
Maria Almeida, Ph.D.
Thomas Levin Andersen, Ph.D.
Natasha Appelman-Dijkstra, M.D.
Ugur Ayturk, Ph.D.
Laura Bachrach, M.D.
Yangjin Bae, Ph.D.
Kristen Beavers, Ph.D., M.P.H.
Belinda Beck, M.S., Ph.D., FACSM
Zhanna Belaya, M.S.
Teresita Bellido, Ph.D.
Laura Bilek, Ph.D.
Edith Bsonnelye, Ph.D.
Nicolas Bonnet, Ph.D.
Elizabeth Bradley, Ph.D.
Giacomina Brunetti, Ph.D.
Angela Bruzzaniti, Ph.D.
Andrea Burden, Ph.D.
Andrew Burghardt, B.S.
Frederic Cailotto , Ph.D.
Ernesto Canalis, M.D.
Diana Carlone, Ph.D.
Geert Carmeliet, M.D.., Ph.D.
Jane Cauley, Dr.P.H.
Peggy Cawthon, Ph.D.
Andrei Chagin, Ph.D.
Abhishek Chandra, Ph.D.
Abhishek Chandra, Ph.D.
Manju Chandran, M.D., FACP, FACE, FAMS., CCD
Julia Charles, M.D., Ph.D.
Patricia Clark, M.D., Ph.D.
Gregory Clines, M.D., Ph.D.
Michael Collins, M.D.
Celine Colnot, Ph.D.
Cyrille Confavreux, M.D., Ph.D.
Felicia Cosman, M.D.
Robin Daly, Ph.D.
Rachel Davey, Ph.D.
Lindsay Dawson, Ph.D.
Jesus Delgado-Calle, Ph.D.
Ruban Dhaliwal, M.D., M.P.H.
Hans Peter Dimai, M.D.
Neha Dole, M.D.
Madison Doolittle, Ph.D.
Patricia Ducy, Ph.D.
Amel Dudakovic, Ph.D.
Emma Duncan, M.D., Ph.D.
Gustavo Duque, M.D., Ph.D.
Grahame Elder, M.B.B.S., Ph.D.
Florent Elefteriou, Ph.D.
Klaus Engelke, Ph.D.
Kristine Ensrud, Ph.D.
Reinhold Erben, D.V.M., M.D.
Roberta Faccio, Ph.D.
Astrid Fahrleitner-Pammer, M.D.
Mathieu Ferron, Ph.D.
David Findlay, Ph.D.
Melissa Formosa, Ph.D.
Pierrick Fournier, Ph.D.
Renny Franceschi, Ph.D.
Michael Friedman, Ph.D.
Benjamin Frisch, Ph.D.
Fernanda Gazoni, Ph.D.
Anne Gingery, Ph.D.
Natalie Glass, Ph.D.
Francesca Gori, Ph.D.
Struan Grant, Ph.D.
Marc Grynpas, Ph.D.
Rosaria Guzzo, Ph.D.
Melanie Haffner-Luntzer, Ph.D.
Shawn Hallett, B.S.
Stephen E Harris, Ph.D.
Nicholas Harvey, M.D., Ph.D.
Mohamed Hassan, D.D.S., M.S., Ph.D.
Quamarul Hassan, Ph.D.

Federico Hawkins Carrabza, Ph.D.
Eric Hesse, M.D., Ph.D.
Evelyn Hsieh, M.D., Ph.D.
Marja Hurley, M.D.
Yuuki Imai, M.D., Ph.D.
Erik Imel, M.D.
Steven Ing, M.D.
Daisuke Inoue, M.D., Ph.D.
Suzanne Jan de Beur, M.D.
Muhammad Kassim Javaid, M.D., Ph.D.
Elise Jeffery, Ph.D.
Karl Jepsen, Ph.D.
Smita Jha, M.D.
Fjola Johannesdottir, Ph.D.
Patricia Juarez Camacho, Ph.D.
Melissa Kacena, Ph.D.
Ivo Kalajzic, M.D., Ph.D.
Lamya Karim, Ph.D.
Courtney Karner, Ph.D.
Deepak Kumar Khajuria, Ph.D.
Sang Wan Kim, M.D., Ph.D.
Ha-Neui Kim , Ph.D.
Joseph Kindler, Ph.D.
Ben Kirk, Ph.D.
Gordon Klein, M.D.
Frank Ko, Ph.D.
Tatsuya Kobayashi, M.D., Ph.D.
Sung Hye Kong, M.D.
Ken Kozloff, Ph.D.
Richard Kremer, M.D., Ph.D.
Anjali Kusumbe , Ph.D.
Marie-Helene Lafage-Proust, Ph.D.
Alex Lambi, M.D., Ph.D.
Nancy Lane, M.D.
Bente Langdahl, M.D., Ph.D.
Lisa Langsetmo, Ph.D.
Beate Lanske, Ph.D.
Michaël Laurent, M.D., Ph.D.
Ben Leder, Ph.D.
Richard Lee, M.D.
Bill Leslie, M.D., M.S.
Itamar Levinger, Ph.D.
Chuanju Liu, M.D.
Gabriela Loots, Ph.D.
Maureen Lynch, Ph.D.
Naim Maalouf, M.D.
Christa Maes, Ph.D.
Michael Mannstadt, M.D.
Sarah Manske, Ph.D.
David Maridas, Ph.D.
Aline Martin, Ph.D.
Brya Matthews, Ph.D.
Michael McClung, M.D.
Michelle McDonald, Ph.D.
Meenal Mehrotra, Ph.D.
Mark Meyer, Ph.D.
Laetitia Michou, M.D., Ph.D.
Jose Luis Millan, Ph.D.
Salvatore Minisola, M.D.
Elise Morgan, Ph.D.
Suzanne Morin, M.D., M.Sc.
Sofia Movérare-Skrtic, Ph.D.
Dobrawa Napierala, Ph.D.
Tuan Nguyen, Ph.D.
Toru Ogasawara, D.D.S., Ph.D.
Olufemi Ogundipe, Ph.D.
Shinsuke Ohba, D.D.S., Ph.D.
Wanida Ono, D.D.S., Ph.D.
Noriaki Ono, D.D.S., Ph.D.
Susan Ott, M.D.
Keiichi Ozono, M.D., Ph.D.
Julien Paccou, M.D., Ph.D.
Gabriel Pagnotti, Ph.D.
Andrea Palermo, M.D., Ph.D.
Feng Pan, M.D., Ph.D.
Rodis Paparodis, M.D.
Dongsu Park, Ph.D.
Serkin Park, D.D.S., Ph.D.
Elefterios Pascalis, Ph.D.
Nathan Pavlos, Ph.D.
Lilian Plotkin, Ph.D.
Kristin Popp, Ph.D.
Richard Prince, MBCHb, B.Sc., M.D.(Mel)
Sylvain Provot, Ph.D.
Chamith Rajapakse, Ph.D.
Saravana Ramasamy, Ph.D.
Madhumati Rao, M.D., Ph.D.
Martina Rauner, Ph.D.
Michaela Reagan, Ph.D.
Thomas Register, Ph.D.
Perla Reyes Fernandez, Ph.D.
Ryan Riddle, Ph.D.
Pamela Robey, Ph.D.
Manuela Rocha-Braz, M.D., Ph.D.
Alexander Rodriguez, M.D., Ph.D.
Ryan Ross, Ph.D.
Kenneth Saag, M.D.
Fayez Safadi, Ph.D.
Shivani Sahni, Ph.D.
Hitoshi Saito, Ph.D.
Cheryl Sanchez-Kazi, M.D.
Amy Sato, Ph.D.
Throsten Schinke, Ph.D.
Ernestina Schipani , M.D., Ph.D.
John Schousboe, M.D., Ph.D.
Deborah Sellmeyer, M.D.
Alana Serota, M.D.
Jad Sfeir, M.D.
Viral Shah, M.D.
Charles Sharp, M.D.
Eileen Shore, Ph.D.
Matthew Silva, Ph.D.
Despina Sitara, Ph.D.
Brenda Smith, Ph.D.
Kent Soe, Ph.D.
Joe Stains, Ph.D.
Steven Stegen, Ph.D.
Elsa Strotmeyer, Ph.D.
Maya Styner, M.D.
Lauren Surface, Ph.D.
Michaela Tencerova, Ph.D.
Cyril Thouverey, Ph.D.
Robert Tower, Ph.D.
Trupti Trivedi, Ph.D.
Elena Tsourdi, M.D.
Jan Tuckermann, Ph.D.
Serra Ucer Ozgurel, Ph.D.
Rodrigo Valderrabano, M.D., M.S.
Bram van der Eerden, Ph.D.
Nick van Gastel, Ph.D.
Andre van Wijnen, Ph.D.
Deepak Vashishth, Ph.D.
Reina Villareal, M.D.
Yongmei Wang, Ph.D.
Shirley Wang, Ph.D.
Stuart Warden, Ph.D.
David Weber, M.D.
Natalie Wee, Ph.D.
Marc Wein, M.D., Ph.D.
Megan Weivoda, Ph.D.
Deborah Wenkert, M.D.
Ken White, Ph.D.
Elizabeth Winter, M.D., Ph.D.
Christian Wright, Ph.D.
Nicole Wright, Ph.D.
Colleen Wu, Ph.D.
Yingzi Yang, Ph.D.
Elaine Yu, M.D.
Maria Zanchetta, M.D.
Ayse Zengin, Ph.D.
Carola Zillikens, M.D., Ph.D.

ASBMR COMMITTEE MEMBERS AND REPRESENTATIVES

ADVOCACY/SCIENCE POLICY COMMITTEE

Michael Hadjiargyrou, Ph.D., *Chairperson*
Blake Eason Hildreth, D.V.M., Ph.D.
Jenna Leser
Megan McGee-Lawrence, Ph.D.
Katherine Motyl, Ph.D.
Sabrina Noel, Ph.D.
Orhan Oz, M.D., Ph.D.
Ryan Ross, Ph.D.
Kristi Tough Desapri, M.D.
Rodrigo Valderrábano, M.D.
Tamara Alliston, Ph.D., *Council Liaison*
Douglas Fesler*, Staff Liaison*

DEVELOPMENT COMMITTEE

Andrea Alford, Ph.D., *Chairperson*
Kristina Astleford-Hopper
Elizabeth Bradley, Ph.D.
Beth Bragdon, Ph.D.
Julia Charles, M.D., Ph.D.
Francesca Gori, Ph.D.
Lamya Karim, Ph.D.
Joseph Kindler, Ph.D.
Joseph Kindler, Ph.D., CTR
Maureen Lynch, Ph.D.
Orhan Oz, M.D., Ph.D.
Nicola Napoli, M.D., Ph.D., *Council Liaison*
Deborah Kroll, *Staff Liaison*

DIVERSITY, EQUITY, AND INCLUSION COMMITTEE

Nilsson Holguin, Ph.D, *Chairperson*
Alison Boyce, M.D.
Michael Econs, M.D.
Pouneh Fazeli, M.D., M.P.H.
Ronald Kwon, Ph.D.
Seungyong Lee, Ph.D.
Fei Liu, Ph.D., D.D.S.
Gabriela Loots, Ph.D.
Dolores Shoback, M.D.
Earnest Taylor, Ph.D.
Yingzi Yang, Ph.D.
Sylvia Christakos, Ph.D., *Non-Voting Advisor*
Kristy M. Nicks, Ph.D. *Non-Voting Advisor*
Joy Wu, M.D., Ph.D., *Council Liaison*
Greg Maciog, *Staff Liaison*
Alana Stewart, *Staff Liaison*

EARLY STAGE INVESTIGATOR SUBCOMMITTEE

Rachelle Johnson, Ph.D., *Co-Chairperson*
Benjamin Frisch, Ph.D., *Co-Chairperson*
Tania Amorim, Ph.D.
Erin Bumann, D.D.S., Ph.D.
Joseph Collins
Serra Ucer Ozgurel, Ph.D.
Shawn Hallett, D.D.S., Ph.D.
Katharine Hubert
Karl Lewis, Ph.D.
Melanie Mendez, Ph.D.
Chad Novince, DDS, Ph.D.
Renee Ormsby, Ph.D.
Garyfallia "Fay" Papaioannou, M.D., Ph.D.
Jessica Pierce, Ph.D.
Cassandra Smith, Ph.D.
Lauren Surface, Ph.D.
Christian Wright, MS, Ph.D.
Fayez Safadi, Ph.D., *MEC Liaison*
Greg Maciog, *Staff Liaison*
Alana Stewart, *Staff Liaison*

EDUCATION ADVISORY COMMITTEE

Jesus Delgado-Calle, Ph.D., *Co-Chairperson*
Anne Schafer, M.D., *Co-Chairperson*
Elena Ambrogini, M.D., Ph.D.
Natasha Appelman-Dijkstra, M.D., Ph.D.
Pamela Cabahug-Zuckerman, Ph.D.
Joshua Farr, Ph.D.
Jean Jiang, Ph.D.
Deborah Mitchell, M.D.
Elizabeth Zimmerman, Ph.D.
Megan Weivoda, Ph.D., *Council Liaison*
Angela Belusik, *Staff Liaison*

ETHICS ADVISORY COMMITTEE

Eileen Shore, Ph.D., *Chairperson*
Eve Donnelly, Ph.D.
Elisabeth Eekhoff, M.D., Ph.D.
Roman Eliseev, M.D., Ph.D.
Kristine Ensrud, M.D., MPH
Nan Hatch, DMD, Ph.D.
Beata Lecka-Czernik, Ph.D.
Emily Stein, M.D.
Peter Ebeling, AO, M.D., FRACP, *Ex-Officio*
Doug Fesler, *Staff Liaison*

FINANCE COMMITTEE

Rene St-Arnaud, Ph.D., *Chairperson*
Maria Luisa Brandi, M.D., Ph.D.
Patricia Juarez Camacho, Ph.D.
Michaela Reagan, Ph.D.
Eileen Shore, Ph.D.
Michael Wacker, Ph.D.
Elaine Yu, M.D.
Mary Bouxsein, Ph.D., *Ex Officio*
Melissa Kacena, Ph.D., *Council Liaison*
Doug Fesler, *Staff Liaison*
Angela Belusik, *Staff Liaison*
John Curle, *Staff Liaison*

INNOVATION COMMITTEE

Michael Mannstadt, M.D., *Chairperson*
Fjola Johannesdottir, Ph.D.
Rachelle Johnson, Ph.D.
Dobrawa Napierala, Ph.D.
Ryan Riddle, Ph.D.
Natalie Sims, Ph.D.
Hannah Taipaleenmaki, Ph.D.
Rachana Vaidya, Ph.D.
Christopher Hernandez Ph.D., *Council Liaison*
Angela Belusik, *Staff Liaison*

MEMBERSHIP ENGAGEMENT COMMITTEE

Fayez Safadi, Ph.D., *Chairperson*
Claire Clarkin, Ph.D.
Rosa Guzzo, Ph.D.
Yi-Hsiang Hsu, M.D., ScD
Smita Jha, M.D.
Richard Lee, M.D., M.P.H.
Radhika Narla, M.D.
Julia Paik, M.D.
Dongsu Park, Ph.D.
Sun Peck, Ph.D.
David Scott, Ph.D.
Yusuke Shiozawa, M.D., Ph.D., *Ad-Hoc Member*
Jennifer Kelly, D.O., FACE, CCD, *Non-Voting Advisor*
Joseph Stains, Ph.D., *Council Liaison*
Benjamin Frisch, Ph.D., *Early Stage Investigator Subcommittee Co-Chair*
Rachelle Johnson, Ph.D., *Early Stage Investigator SubCommittee Co-Chair*
Greg Maciog, *Staff Liaison*
Alana Stewart, *Staff Liaison*

PROFESSIONAL PRACTICE COMMITTEE

Matthew Drake, M.D., Ph.D., *Chairperson*
Erik Imel, M.D.
Bente Langdahl, M.D., Ph.D., DMSc
Suzanne Morin, M.D., Msc
Kendall Moseley, M.D.
Joy Tsai, M.D.
Elena Tsourdi, M.D.
David Weber, M.D., MSCE
Carola Zilikens, M.D., Ph.D.
Carolyn Crandall, M.D., MS, *Council Liaison*
Douglas Fesler, *Staff Liaison*
Alana Stewart, *Staff Liaison*

PUBLICATIONS COMMITTEE

Cheryl Ackert-Bicknell, Ph.D., *Chairperson*
Joel Boerckel, Ph.D.
Julie Hughes, Ph.D.
Christine Lary, Ph.D.
Saravana Ramasamy, Ph.D.
Ernestina Schipani, M.D., Ph.D.
Maya Styner, M.D.
Ken White, Ph.D.
Deborah Veis, M.D., Ph.D., *JBMR® Plus EIC & Council Liaison*
John P. Bilezikian, M.D., *Primer EIC*
Rajesh Thakker, M.D., *JBMR® EIC & Council Liaison*
Katie Duffy, *Staff Liaison*

ASBMR PRIMER EDITORIAL BOARD - 10th Edition

John Bilezikian, M.D., Ph.D.(hon)
Editor-in-Chief
Senior Associate Editors
Teresita Bellido, Ph.D.
Lorenz Hofbauer, M.D.
Marcella Walker, M.D.
Associate Editors
Susan Bukata, M.D.
Manju Chandran, M.D.
Michael Collins, M.D.
Matthew Drake, M.D., Ph.D.
Erin Ealba Bumann, DDS, MS, Ph.D.
Richard Eastell, M.D.
Peter Ebeling, FRACP, MBBS, M.D.
Ghada El-Hajj Fuleihan, M.D., MPH
Klaus Engelke, Ph.D.
David Goltzman, M.D.
Evan Keller, DVM, Ph.D.
Stavroula Kousteni, Ph.D.
Bente Langdahl, M.D., Ph.D.
E. Michael Lewiecki, M.D.
Jian-Min Liu, M.D., Ph.D.
Karen Lyons, Ph.D.
Christa Maes, Ph.D.
Claudio Marcocci, M.D.
Laurie McCauley, DDS
Michael McClung, M.D.
Martina Rauner, Ph.D.
Fernando Rivadenieira, M.D., Ph.D.
Cliff Rosen, M.D.
Ego Seeman, M.D.
Barbara Silva, M.D., Ph.D.
Rajesh Thakker, M.D.
Laura Tosi, M.D.
Michael Whyte, M.D.
John Wysolmerski, M.D.
Maria Belen Zanchetta, M.D.
Murray J. Favus, M.D., *Founding Editor*

SOCIAL MEDIA COMMITTEE

Michaël Laurent, M.D., Ph.D., *Co-Chairperson*
Sun Peck, Ph.D., *Co-Chairperson*
Ahmed Al Saedi, Ph.D.
Lena Batoon, Ph.D.
Madhura Nijsure, MS
Noriaki Ono, DDS, Ph.D.
Garyfallia "Fay" Papaioannou, M.D., Ph.D.
Rachel Pessah Pollack, M.D., FACE
Emily Quarato, M.S.
Parinya Samakkarnthai, M.D.
Cristina Sanchez de Diego, Ph.D.
David Scott, Ph.D.
Mustafa Unal, Ph.D.
Danielle Whittier, Ph.D.
Taylor Collison, *Staff Liaison*
Greg Maciog, *Staff Liaison*
Alana Stewart, *Staff Liaison*

WOMEN IN BONE AND MINERAL RESEARCH COMMITTEE

Michelle McDonald, Ph.D., Co-*Chairperson*
Lilian Plotkin, Ph.D., Co-*Chairperson*
Edith Bonnelye, Ph.D.
Aline Bozec, Ph.D.
Manju Chandran, M.D.
Erica Clinkenbeard, Ph.D.
Rachel Davey, Ph.D.
Deborah Galson, Ph.D.
Amna Khan, M.D.
Kelsey Mangano, Ph.D.
Amy Sato, Ph.D.
Natalie Wee, Ph.D.
Michaela Tencerova, Ph.D.
Nicole Wright, Ph.D.
Nina Ma, M.D. *Council Liaison*
Greg Maciog, *Staff Liaison*
Alana Stewart, *Staff Liaison*

ASBMR REPRESENTATIVES TO FASEB

Brendan Boyce, M.B., Ch.B.
Member, Board of Directors

Thomas L. Clemens, Ph.D.
Finance Committee

Frank Ko, Ph.D.
Science Policy Committee (SPC)

Stavroula Kousteni, Ph.D.
Excellence in Science Award Committee

Ronald Kwon, Ph.D.
Diversity, Equity, and Inclusion Committee

Yousef Abu-Amer, Ph.D.
Animals in Research and Education

Rafio Agoro, Ph.D.
Animals in Research and Education Subcommittee, SPC

Zhengqiang Yao, Ph.D.
Research Conferences Advisory Committee

Courtney Karner, Ph.D.
Publications and Communications Committee

Thomas Lang, Ph.D.
FASEB Editorial Board

Yousef Abu-Amer, Ph.D.
FASEB Open Access Journal Editorial Board

Katie Duffy, Senior Director of Publications
FASEB Publications Staff Liaison

ASBMR REPRESENTATIVES TO OTHER GROUPS

Jonathan Lowery, Ph.D.
U.S. Bone and Joint Initiative

Roland Baron, D.D.S., Ph.D.
International Federation of Musculoskeletal Research Societies (IRMRS), Co-Chair

Nicola Napoli, M.D.
IFMRS ASBMR Board Representative

Meghan McGee-Lawrence, Ph.D.
IFMRS Future Global Leaders Committee

Lynda Bonewald, Ph.D.
IFMRS Big Data Working Group, Co-Chair

David Karasik, Ph.D.
IFMRS Big Data Working Group

Douglas Kiel, M.D.
IFMRS Big Data Working Group

Jane Lian, Ph.D.
IFMRS Big Data Working Group

Douglas Kiel, M.D.
IFMRS Musculoskeletal Knowledge Portal Chair

Lynda Bonewald, Ph.D.
IFMRS Musculoskeletal Knowledge Portal

David Karasik, Ph.D.
IFMRS Musculoskeletal Knowledge Portal

Natasha Appelman-Dijkstra, M.D., Ph.D
International Education Core Group

Douglas Kiel, M.D.
Society on the Global Leadership in Sarcopenia (GLIS) Steering Committee, Co-Chair

ASBMR AMBASSADORS

Asia/Australia
Janine Danks, Ph.D.
Hiroshi Kawaguchi, M.D.
Ambrish Mithal, M.D.
Yumie Rhee, M.D., Ph.D.
Tingting Tang, Ph.D.

Europe/Middle East
Zhanna Belaya, M.D., Ph.D.
Pascale M. Chavassieux, M.D.
Emma Duncan, FRACP, MBBS, M.D., Ph.D.
Ghada El-Hajj Fuleihan, M.D.
Bente Langdahl, M.D., Ph.D.
Christian Meier, M.D.
Nicola Napoli, M.D., Ph.D.
Martina Rauner, Ph.D.
Annegreet Velhuis-Vlug, M.D., Ph.D.
Kate Ward, Ph.D.

North America
Jacques P. Brown, M.D.
Patricia Juarez Camacho, Ph.D.
Aliya Khan, M.D., FRCP, FACP, FACE
Jonathan Lowery, Ph.D.
Joy Y. Wu, M.D., Ph.D.

South America
Lucas Brun, M.D., Ph.D.
Charles Heldan De Moura Castro, M.D., Ph.D.
Gabriela Picotto, Ph.D.
Claudia Sedlinsky, M.D.
Maria Belen Zanchetta, M.D.

AWARDS

WILLIAM F. NEUMAN AWARD
Richard Eastell, M.D.

FULLER ALBRIGHT AWARD
Marc Wein, M.D., Ph.D.

FREDERIC C. BARTTER AWARD
Bente Langdahl, M.D., Ph.D.

LOUIS V. AVIOLI FOUNDERS AWARD
Fanxin Long, Ph.D.

LAWRENCE G. RAISZ AWARD
Peter Croucher, Ph.D.

PAULA STERN ACHIEVEMENT AWARD
Lilian Plotkin, Ph.D.

SHIRLEY HOHL SERVICE AWARD
Rhonda Prisby, Ph.D.

STEPHEN M. KRANE AWARD
Melissa Kacena, Ph.D.

GIDEON A. RODAN EXCELLENCE IN MENTORSHIP AWARD
Roberto Civitelli, M.D.

ADELE L. BOSKEY AWARD
Dobrawa Napierala, Ph.D.

EARLY CAREER CLINICAL INVESTIGATOR AWARD
HONORING ROBERT MARCUS, M.D.
Elaine Yu, M.D.

2023 ASBMR RAISZ-DREZNER AWARD
Madison L. Doolittle, Ph.D.

2023 ASBMR MOST OUTSTANDING BASIC ABSTRACT AWARD
Sarah L. Dallas Ph.D.

2023 ASBMR MOST OUTSTANDING CLINICAL ABSTRACT AWARD
Rachel I. Gafni, M.D.

2023 ASBMR MOST OUTSTANDING TRANSLATIONAL ABSTRACT AWARD
Japneet Kaur, Ph.D.

2023 ASBMR PRESIDENT'S AWARD
Han Jiao, MBBS

2023 ASBMR FELIX BRONNER YOUNG INVESTIGATOR AWARD
Lisbeth Koch Thomsen, Cand.scient.san

2023 ASBMR FUND FOR RESEARCH AND EDUCATION YOUNG INVESTIGAOR AWARDS
Sanchita Agarwal, M.S.
Eren Bora Yilmaz

2023 ASBMR FUND FOR RESEARCH AND EDUCATION DIVERSITY YOUNG INVESTIGATOR AWARD

Daniel Dapaah

GIDEON A. RODAN EXCELLENCE IN MENTORSHIP AWARD

Maisa Monseff R. da Silva, M.D.

2023 ASBMR YOUNG INVESTIGATOR AWARDS

Supported by donations from:
Korean Society for Bone and Mineral Research (KSBMR)
Kyowa Kirin
Texas A & M University School of Veterinary Medicine and Biomedical Sciences
UAMS Musculoskeletal Hub, University of Arkansas for Medical Sciences
University of California San Francisco Musculoskeletal Center
University of Pennsylvania Perelman Medical School
Washington University in St. Louis Musculoskeletal Research Center

Lama Alabdulaaly, BDS DMSc
Dima A. Alajlouni, MScMed
Kristina Astleford-Hopper
Seoyeon Bok, Ph.D.
Stephanie Chinwo
Amy Creecy, Ph.D.
Emily Crowe
Judith Everts-Graber, M.D.
Jinxiao Fan, Ph.D. Candidate
Giulia Furesi, Ph.D.
Qinghe Geng, Ph.D.
Nicole R. Gould, Ph.D.
Zubeyir Hasan Gun, M.D.
Guoli Hu, Ph.D.
Rui Hua, Ph.D.
Sabrina E. Kosnik
Elis J. Lira dos Santos, Ph.D.
Shauni Loopmans
Marta Martinez Calle, Ph.D.
Jillian L. McCool
Steven J. Meas
Jacob A. Moore
Joeri Nicolaes, MSc
Tian Nie
Omar Al Rifai, Ph.D.
Tânia Amorim, Ph.D.
Diana Athonvarangkul
Ogulcan Caliskan
Adriana Carvalho, Ph.D.
Ahyoun Choi
Andrea Cowan
Hamid Y. Dar, Ph.D.
Caroline de Carvalho Picoli
Rachel E. Elam, M.D.
Emily Maria Eul, B.S.
Donghao Gan, M.D.
Judit Gimenez Roig
Sofya Gronskaia, M.D.
Ngoc B Huynh
Zhiming He
Koji Ishikawa, M.D., Ph.D.
Min Kim, Ph.D.
Rachel E. Klassen
Joe Kodama
Eileen H. Koh, M.D.
Alex G. Lambi, M.D., Ph.D.
Seunghyun Lee
Aleda M. Leis, Ph.D.
Qiwen Li, DMD, Ph.D.
Xing Li, MBBS
Linyi Liu
Hanghang Liu, Ph.D., D.D.S.
Jiawei Lu
Eugenie Macfarlane, Ph.D.
Antonio Maurizi, Ph.D.
Nicole Migotsky, Ph.D.
Genna E. Monahan
Ananya Nandy, Ph.D.
Gia Huy Nguyen, B.E. (Hons)
Shion Orikasa, D.D.S., Ph.D.
Yongli Qin
Sowmya Ramesh, Ph.D.
Hayley M. Sabol, M.S.
Merle Schene, M.D.
Seung Shin Park, M.D.
Ernesto Solorzano
Silvia Storoni, M.D.
Eri Takematsu, Ph.D.
Nicha Tokavanich, D.D.S.
Haydee M. Torres, Ph.D.
David Villani, Ph.D.
Jiekang Wang
Haichao Zhang, M.D.
Michail Zoulakis, M.D.

2023 Class of ASBMR fellows

Cheryl Ackert-Bicknell Ph.D.
Catherine Anastasopoulou M.D., Ph.D.
Belinda Beck Ph.D.
Marco Brotto B.S.N., MPharm., Ph.D.
Andrei Chagin Ph.D.
Sarah Dallas Ph.D.
Hong-Wen Deng Ph.D.
Pawel Szulc M.D., Ph.D.
Nicole Wright Ph.D., M.P.H.
Kate Ward, Ph.D.

2023 SUPPORTERS

The ASBMR gratefully acknowledges the following companies for their support as of as of September 13, 2023:

SILVER LEVEL

Alexion, AstraZeneca Rare Disease
Amgen, Inc.
Ipsen Biopharmaceuticals, Inc.
Kyowa Kirin
Sandoz, a Novartis Division

BRONZE LEVEL

Ascendis Pharma A/S
Inozyme Pharma
UCB

FRIEND LEVEL SUPPORTERS

Amolyt
Calcilytix Therapeutics, Inc., (a BridgeBio company)
Hologic, Inc.
Radius Health
Regeneron Pharmaceuticals, Inc.
Takeda
Ultragenyx Pharmaceutical Inc.

2023 Corporate Advisory Board

The ASBMR gratefully acknowledges the following companies for their membership:

Alexion AstraZeneca Rare Diseases
Amgen, Inc.
Ascendis Pharma A/S
Ipsen Biopharmaceuticals, Inc.
Kyowa Kirin
Radius Health
Regeneron Pharmaceuticals, Inc.
Sandoz, a Novartis Division
Takeda
UCB
Ultragenyx Pharmaceutical Inc.

GENERAL MEETING INFORMATION

ASBMR 2023 Annual Meeting Location

All ASBMR sessions will take place in the Vancouver Convention Centre, Vancouver, BC, Canada, West Building, unless otherwise stated. The Vancouver Convention Center is located at 1055 Canada Place, Vancouver, BC, V6C 0C3, Canada.

Annual Meeting Evaluation

The ASBMR 2023 Annual Meeting Evaluation will be accessible online starting Thursday, October 19. An email will be sent to all meeting attendees who provided their email addresses at the time of registration. The email will provide a hyperlink to the online evaluation site. It will also to be accessible via the ASBMR website at https://www.asbmr.org/annual-meeting. We strongly encourage and welcome all attendees to provide us with feedback on the meeting. Your input is very important to us.

Registration Hours

Registration desks will be open for new registrants and material pick-up in the Vancouver Convention Center in the Ballroom Lobby during the following hours:

Thursday, October 12 ..... 7:00 am – 6:00 pm
Friday, October 13 ..... 7:00 am – 6:00 pm
Saturday, October 14 ..... 7:00 am – 6:30 pm
Sunday, October 15 ..... 7:30 am – 6:00 pm
Monday, October 16 ..... 7:30 am – 12:00 pm

Discovery Hall Hours

Exhibits are located in the ASBMR Discovery Hall on the Exhibition Level, Exhibit Halls A and B of the Vancouver Convention Center. Please note that children aged 16 and under are not permitted in Discovery Hall at any time.

Friday, October 13 ..... 6:00 pm – 7:30 pm
Saturday, October 14 ..... 9:30 am – 4:30 pm
Sunday, October 15 ..... 9:30 am – 4:30 pm

Future ASBMR Annual Meeting Dates

ASBMR 2024 Annual Meeting
Metro Toronto Convention Centre, Toronto, ON, Canada
September 27-30, 2024

ASBMR 2025 Annual Meeting
Washington State Convention Center, Seattle, WA, USA
September 4 - 8, 2025

DISCLOSURE POLICY

The ASBMR is committed to ensuring the balance, independence, objectivity and scientific rigor of all its individually sponsored or industry-supported educational activities. Accordingly, the ASBMR adheres to the requirement set by ACCME that audiences at jointly-sponsored educational programs be informed of a presenter's (speaker, faculty, author, or planner) academic and professional affiliations, and the disclosure of the existence of any significant financial interest or other relationship a presenter or their spouse has with any proprietary entity over the past 12 months producing, marketing, re-selling or distributing health care goods or services, consumed by, or used on patients, with the exemption of non-profit or government organizations and non-health care related companies. When an unlabeled use of a commercial product, or an investigational use not yet approved for any purpose, is discussed during the presentation, it is required that presenters disclose that the product is not labeled for the use under discussion or that the product is still investigational. This policy allows the listener/attendee to be fully knowledgeable in evaluating the information being presented. The On-Site Program book will note those speakers who have disclosed relationships, including the nature of the relationship and the associated commercial entity.

Disclosure should include any affiliation that may bias one's presentation or which, if known, could give the perception of bias. This includes relevant financial affiliations of a spouse or partner. If an affiliation exists that could represent or be perceived to represent a conflict of interest, this must be reported in the abstract submission program by listing the name of the commercial entity and selecting the potential conflict(s) by clicking in the box next to the relationship type. Disclosures will be printed in the program materials. These situations may include, but are not limited to: 13. Grant/Research Support; 14. Consultant; 15. Speakers' Bureau; 16. Major Stock Shareholder; 17. Other Financial or Material Support.

ABSTRACT PRESENTATION KEY

1001 - Fri-577	Friday Oral Presentations
1021 - LB Sat-660	Saturday Oral Presentations
1041 - LB Sun-660	Sunday Oral Presentation
1081 - 1140	Monday Oral Presentations

1001

Metastatic Breast Cancer Cells Induce Osteocyte Senescence Contributing to Osteolytic Bone Destruction *Japneet Kaur[1], Manish Adhikari[1], Hayley Sabol[1], Aric Anloague[1], Sharmin Khan[1], Lowry Barnes[1], Jeffrey Stambough[1], Michela Palmieri[1], Olivia Reyes-Castro[1], Elena Ambrogini[2], Maria Jose Almeida[2], Charles O'Brien[3], Intawat Nookaew[1], Jesus Delgado-Calle[1]. [1]University of Arkansas for Medical Sciences, United States. [2]Central Arkansas VA Healthcare System, Univ of Arkansas for Medical Sciences, United States. [3]Univ of Arkansas for Medical Sciences, United States

Breast cancer (BCa) bone metastases cause extensive bone destruction and are typically incurable. We studied the impact of BCa bone metastasis on osteocytes (Ots) - recently identified as key cells of the tumor niche - using single-cell RNA sequencing (scRNAseq). First, we injected murine E0771 BCa cells or PBS into 8-wk female NuTRAP reporter mice crossed with Dmp1-8kb-Cre mice and, after 2 wks, sorted Dmp1-8kb-GFP+ cells to study Ots. Bioinformatic analyses showed that Ots from BCa bone metastases had upregulation of genes enriched in GO terms linked to senescence, senescence-associated secretory phenotype (SASP), and inflammatory response, and had an increased senescence/SASP score compared to naïve mice. Histology revealed 4 times more p16+ (RNAscope) and senescence-associated distension of satellites (SADS)+ (centromere-FISH; 2 vs 14%) Ots, hallmarks of cellular senescence, in the cortical bone of BCa-bearing mice. Conditioned media (CM) from E0771 or human MDA-MB-231 BCa cells increased senescence-associated ?-galactosidase activity and upregulated senescence-related genes p16, p21, Mmp13, and Il6 in cultured Ocy-454 cells. Remarkably, MDA-MB-231 BCa cells led to similar gene expression changes in ex vivo organ cultures of human bone. Collectively, these results support the idea that signals from metastatic BCa cells cause Ot senescence. Next, we treated 8-wk female mice with intratibial E0771 BCa tumors with a cocktail of the senolytics (D+Q) Dasatinib (5 mg/kg) and Quercetin (50mg/kg) once a wk, starting two days after tumor inoculation. D+Q, known to eliminate senescent cells, prevented the histological increases in p16+ and SADS+ Ots induced by BCa cells. D+Q did not affect tumor burden but decreased lytic lesions and preserved cancellous bone mass (30% higher vs untreated BCa-mice). scRNAseq showed Ots from BCa-bones had elevated Rankl, Mmp13, Il6, Lgals3, Serpine2, Cd9, and Vegfa, and reduced Cthrc1 expression, suggesting increased osteoclastogenic potential. Consistent with this, D+Q restored the elevated p21, p16, and Mmp13 mRNA levels and reduced by 40% the increase in CTX in bones-bearing BCa cells cultured ex vivo. D+Q did not affect P1NP levels, which remained decreased in bones with BCa cells, suggesting senolytics preserved bone by inhibiting resorption. Our data demonstrate that metastatic BCa cells change the bone microenvironment and cause Ot senescence, which in turn induces osteoclastogenesis and osteolytic disease.

***Disclosures: Japneet Kaur**, None*

1002

Local and Systemic Effects of Dickkopf-1 During Breast Cancer Progression by Limiting NK Cell-Mediated Killing *Seunghyun Lee[2], Biancamaria Ricci[2], David Clever[2], Roberta Faccio[3]. [2]Washington University in St.Louis, . [2]Washington University in St.Louis, United States. [3]Washington University in St Louis School of Medicine, United States

Elevated levels of the Wnt inhibitor dickkopf-1 (Dkk1) are detected in breast cancer patients and correlate with the progression of bone metastases. We found that breast cancer patients with progressive metastatic bone disease unresponsive to standard-of-care therapies have higher Dkk1 levels than patients with stable disease. Intriguingly, serum Dkk1 levels do not always correlate with Dkk1 expression in cancer cells. Thus, it is important to understand the source and role of Dkk1 in breast cancer to better identify patients that could benefit from Dkk1-targeted therapies.In this study, we used mice orthotopically injected with PyMT, EO771, and 4T1 breast cancer lines. Although Dkk1 was not expressed in these cells, Dkk1 serum levels were upregulated in all models. Strikingly, Dkk1 neutralizing antibody (?-Dkk1) significantly reduced tumor growth in the primary site and in the bone compared to IgG, in all models.To understand the source of Dkk1 in the tumor-bearing mice, we examined Dkk1 transcripts in the bone and tumor stroma. Dkk1 was highly expressed by the osteoblasts (OBs) in the bone and to a less extent by the cancer-associated fibroblasts (CAFs) in the tumor stroma. To address the role of bone- versus CAF-derived Dkk1, we generated mice with specific deletion of Dkk1 in the OBs (OsxCre;Dkk1fl/fl), or CAFs (Fsp1Cre;Dkk1fl/fl and aSMACreERT2;Dkk1fl/fl). To our surprise, all models showed a significant reduction in primary tumor growth. Furthermore, WT mice co-injected with PyMT and Dkk1 KO CAFs showed reduced tumor growth compared to mice co-injected with Dkk1 WT CAFs. These results suggest systemic and local effects of Dkk1.To understand how Dkk1 supports tumor growth, we performed bulk RNAseq on tumor cells isolated from IgG and ?-Dkk1 treated mice. Intriguingly, immune response-related pathways were upregulated in the ?-Dkk1 treated tumors. Supporting the involvement of immune cells, ?-Dkk1 did not reduce tumor growth in the NSG immune-compromised mice. Next, we treated tumor-bearing mice with ?-Dkk1 and depleting antibodies against T or NK cells. Surprisingly, only NK cell depletion abrogated ?-Dkk1 anti-tumor effects. Further confirming that Dkk1 directly affects NK cells, we found that the NK cell killing efficiency against PyMT tumor cells in vitro was significantly reduced by recombinant Dkk1.In sum, our data show that Dkk1 exerts local and systemic effects to promote tumor progression by modulating the killing efficiency of NK cells.

***Disclosures: Seunghyun Lee**, None*

1003

PD-1 blockade disrupts bone microarchitecture and compromises bone strength in breast cancer bone metastasis *GWENYTH JOSEPH[1], Lawrence A. Vecchi III[2], David Kell[3], Sasidhar Uppuganti[2], Margaret Durdan[4], Wei Chen[2], David Harrison[2], Jeffry Nyman[2], Megan Weivoda[5], Rachelle Johnson[2]. [1], United States. [2]Vanderbilt University Medical Center, United States. [3]Vanderbilt University, United States. [4]University of Michigan, United States. [5]Mayo Clinic, United States

Immune checkpoint blockade (ICB) enables anti-tumor immunity by blocking immunoregulatory receptor-ligand interactions [e.g., programmed cell death protein 1 (PD-1) and its ligand (PD-L1)]. ICB has revolutionized cancer treatment but has lower efficacy in patients with bone metastases, and bone loss and increased fracture risk are reported in patients receiving treatment. To study mechanisms of ICB-induced bone loss, we inoculated 8-week-old WT female C57Bl/6 mice with E0771 mouse mammary carcinoma cells by intracardiac injection and treated with IgG or ?-PD-1 for 2 weeks (n=6-10), at which point the mice were euthanized due to paralysis. Tumor naïve mice were included to assess the baseline skeletal phenotype following 2 or 4 weeks of ?-PD-1 treatment (n=10). In tumor naïve mice, 2 weeks of ?-PD-1 treatment reduced BMD by DXA compared to IgG treatment (4%, p=0.04); after 4 weeks, BV/TV by ?CT was lower in ?-PD-1-treated mice compared to IgG controls (17%, p=0.04), consistent with reports of bone loss in patients receiving ICB therapy. We observed a similar reduction in BV/TV in young, adult, and aged PD-1 KO female mice compared to WT controls (n=5, 32-81%, p<0.01). We also assessed bone strength in tumor naïve mice by 3 point bending and saw no effect from ?-PD-1. As with tumor naïve mice, E0771-inoculated mice had reduced BMD (8%, p=0.04); in contrast, ultimate strength was lower in E0771-inoculated ?-PD-1 treated mice and 8-week-old PD-1 KO mice (n=7) compared to controls (12-16%, p<0.005). Thus, PD-1 blockade only weakens the bone if tumor cells are present. Importantly, flow cytometric analysis of the bone marrow revealed a similar number of tumor cells in ?-PD-1-treated mice compared to IgG controls, suggesting the impact of PD-1 blockade on bone strength is not due to changes in tumor burden. Serum CTX-1 was also elevated in E0771-inoculated PD-1 KO mice vs WT controls (1.8-fold, p=0.04), suggesting elevated bone resorption. CD8+ effector memory T cells, capable of promoting IFN?-mediated osteoclastogenesis in chronic inflammation, were also enriched in the bone marrow in tumor naïve and tumor bearing ?-PD-1 treated mice (1.4-1.8-fold, p<0.03), as was Ifng (5.8-8.2-fold, p<0.002). These data suggest that PD-1 blockade compromises bone microarchitecture by promoting infiltration of T cells that enhance bone resorption, and the presence of bone metastases reduces bone strength and increases fracture risk in the setting of immune checkpoint blockade.

***Disclosures: GWENYTH JOSEPH**, None*

1004

Bimodal Bone-Targeted Therapy Repairs Damage Bone and Overcomes Drug Resistance in Multiple Myeloma *Hayley Sabol[1], Manish Adhikari[1], Cody Ashby[1], Aric Anloague[1], Japneet Kaur[1], Sharmin Khan[1], Michela Palmieri[1], Lawry Barnes[1], Elena Ambrogini[1], Venkatesan Srinivasan[2], Alison Frontier[2], Frank H. Ebetino[2], Jesus Delgado-Calle[1]. [1]University of Arkansas for Medical Sciences, United States. [2]University of Rochester, United States

Multiple myeloma (MM) remains incurable due to drug-resistant cells and disease relapse. Further, MM induces high bone resorption, increasing fracture risk, and osteoblast suppression, which impedes the restoration of damaged bone. Thus, drug resistance and bone repair remain major challenges in MM. Because Notch signals promote MM growth and bone destruction, and Wnt inhibition suppresses osteoblasts, we postulated that a bimodal therapy inhibiting Notch (bone-targeted ?-secretase (GS) inhibitor; BT-GSI) and activating Wnt signaling (anti-Sclerostin; Scl-Ab) should decrease tumor burden and repair bone. To test this idea, we injected OPM2 human MM cells, which have the high-risk t(4;14) translocation linked to poor prognosis/survival, in the tail vein of NSG mice. After 1wk, mice had tumor engraftment and decreased bone mass (20%). We then randomized mice to groups receiving BT-GSI (2.5mg/Kg, 3x/wk), Scl-Ab (100mg/Kg, 1x/wk), or a combination of both. After 3wks, all untreated mice bearing MM tumors died. Scl-Ab did not improve tumor burden or survival. In contrast, BT-GSI, alone or with Scl-Ab, decreased tumor burden by 75% and improved survival (9/11 alive). Untreated mice had a 40% decrease in bone mass, 53% CTX increase, and 40% P1NP reduction. BT-GSI reduced CTX by 58% but did not improve bone mass. However, Scl-Ab, alone or with BT-GSI, increased bone mass (70%) and restored P1NP to naïve controls. Remarkably, the bimodal therapy also reduced tumor growth (85%) and CTX (75%) and elevated P1NP (55%) in human bones bearing OPM2 cells cultured ex vivo. Because Notch signals also promote chemoresistance, we next assessed if the expression of genes of the Notch activator GS complex (PSEN1, PSENEN, APH1, or NCSTN) correlates with therapeutic responses in MM in patients using the CoMMpass database (n=750). Newly diagnosed MM patients with high vs. low expression of these genes had worse responses to Bortezomib (BOR)-based therapies. We then studied if inhibiting GS with BT-GSI improves responses to Bortezomib (BOR) in an ex vivo bone

organ culture established with BOR-resistant MM cells. BT-GSI reduced MM growth by 30% and doubled BOR's anti-MM efficacy (35% vs 70%, BOR alone vs BOR+BT-GSI, respectively). Our data demonstrates that a bimodal bone-targeted therapy based on Notch inhibition and Wnt activation is a safe and clinically relevant approach to control tumor growth, repair damaged bone, and improve therapeutic responses to chemotherapy in MM.

***Disclosures: Hayley Sabol**, None*

1005

Targeting tumor innervating neurons via chemical and genetic approaches to improve osteosarcoma disease progression *Sowmya Ramesh[1], QIZHI QIN[3], Lingke Zhong[3], Ankit Uniyal[4], Masnsen Cherief[1], Mary Archer[1], Leslie Chang[3], Yun Guan[4], Edward F. McCarthy[5], Thomas Clemens[6], Aaron James[3]. [1]Department of Pathology, Johns Hopkins University, United States. [3]Johns Hopkins University, . [3]Johns Hopkins University, United States. [4]Department of Anesthesiology and Critical Care Medicine, Johns Hopkins University, United States. [5]Department of Orthopedics, Johns Hopkins University, United States. [6]University of Maryland, Baltimore, United States

Osteosarcoma (OS) is a bone malignancy affecting young adults. Bone pain is a common symptom in OS patients, however the importance of abnormal sensory innervation in OS progression remains unclear. Here, we perturbed nerve signaling using a combination of transgenic-mice and FDA-approved local analgesic to mitigate pain and OS growth. TrkAF592A mice carry a point mutation in Ntrk1 gene, resulting in inactive signaling upon small-molecule treatment. Human 143B OS cells (1x106) were injected into the tibia and assayed for OS growth for 4wks using caliper measurements. Innervation was assessed using pan-neuronal marker Beta III Tubulin (TUBB3) immunostaining and vascularity was assessed using Endomucin (EMCN). Molecular changes were studied using single cell-RNA sequencing (scRNA-seq) of the OS xenograft tissue. Bupivacaine liposomes (B-LNP) was used as a neurotoxic agent. Along with OS cells, Scid mice received tibial injection of 10mg/kg B-LNP while the sham received saline (PBS). Behavioral test of mechanical sensitivity was conducted using von Frey filament (0.4 g).TUBB3+ axons were found adjacent to human and mice OS implants and upon TrkA disruption nerve density reduced by 88%. Overall, OS size (51%), Ki67 proliferative index (80%), vasculature (47%), and incidence of lung metastasis were significantly reduced upon denervation. Consistent with these phenotypic changes, scRNA-seq of denervated OS tumors suggested a decrease in Notch signaling and reduced oxidative-phosphorylation. Ligand-receptor interactome between mouse dorsal root ganglia (DRG) neurons and OS-associated endothelial cells identified putative growth factors that may play a role in neural regulation of OS growth and angiogenesis. In a translational effort, intratumoral injection of B-LNP demonstrated a 60% decrease in OS size with concomitant decreases in Ki67 proliferative index (25%), TUBB3+ axons (16.4%) and EMCN+ vessels (31%). Besides, von Frey test showed a 30% decrease in paw-withdrawal rate in B-LNP-treated mice, suggesting an alleviation of mechanical pain hypersensitivity. TrkA-expressing primary sensory neurons promoted OS progression. Importantly, neural inhibition attenuated OS-associated pathological nerve sprouting, secondarily leading to reduced OS-associated vasculature, disease progression, metastasis and overall survival. The FDA-approved B-LNP may have a dual therapeutic use in patients with OS, both as a local analgesic and a negative regulator of OS growth.

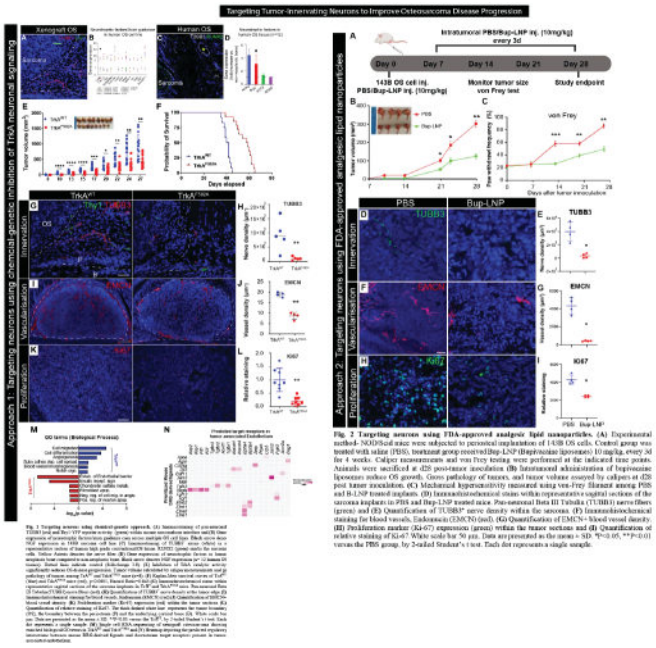

***Disclosures: Sowmya Ramesh**, None*

1006

Comparative Effectiveness of Denosumab versus Zoledronic Acid among Postmenopausal Women with Osteoporosis in the U.S. Medicare Program *Jeffrey Curtis[1], Tarun Arora[2], Ye Liu[3], Tzu-Chieh Lin[6], Leslie Spangler[6], Vanessa Brunetti[6], Robert Stad[6], MICHELE MCDERMOTT[7], Brian Bradbury[6], Min Kim[8]. [1]University of Alabama at Birmingham, United States. [2]Foundation for Advancing Science, Technology, Education and Research, United States. [3]Univesity of Alabama at Birmingham, United States. [6]Amgen Inc., United States. [6]Amgen Inc., United Kingdom. [6]Amgen Inc., Switzerland. [7]Amgen, United States. [8], United States

ObjectivesAlthough clinical trials have shown that denosumab (Dmab) significantly increases bone mineral density at key skeletal sites more than zoledronic acid (ZA), evidence from randomized trials evaluating fracture outcomes is lacking. This retrospective cohort study evaluated the comparative effectiveness of Dmab versus ZA in reducing fracture risk among women with postmenopausal osteoporosis (PMO) in the U.S.MethodsFemale Medicare fee-for-service beneficiaries >= 66 years of age who newly initiated Dmab (n=89,990) or ZA (n=36,861) between Jan 1, 2012 to Dec 31, 2018 with no prior history of osteoporosis treatment were followed from treatment initiation (index date) until the first instance of a given fracture outcome, treatment discontinuation (defined as the end of exposure according to usual dosing intervals + 60-day gap) or switch, Medicare disenrollment, death, end of available data (Dec 31, 2019), or 5 years post-index date. A doubly robust inverse-probability of treatment (weights estimated from multivariate logistic regression models) and censoring (weights estimated from multivariate Cox Proportional Hazards regression models) weighted function was used to estimate the relative risk (RR) associated with the use of Dmab compared with ZA for major osteoporotic (MOP; nonvertebral and hospitalized vertebral), hip, nonvertebral (NV; includes hip, humerus, pelvis, radius/ulna, other femur), non-hip, nonvertebral (NHNV), and hospitalized vertebral (HV) fractures for the overall study period and by year of follow-up.ResultsOver a maximum of 5 years of follow-up, Dmab reduced the risk of MOP by 26% (RR=0.74; 95% CI: 0.59-0.89), hip by 34% (0.66; 0.43-0.90), NV by 33% (0.67; 0.52-0.82), and NHNV by 31% (0.69; 0.50-0.88), and HV fractures by 10% (0.90; 0.56-1.24) compared with ZA (Figure). Over time, Dmab reduced the risk of MOP fractures by 9% (0.91; 0.83-0.99) at year 1, 12% (0.88; 0.80-0.96) at year 2, and 12% (0.88; 0.78-0.98) at year 3. An increase in the magnitude of fracture risk reduction with increasing duration of exposure was also observed for other NV outcomes. ConclusionIn a cohort of over 125,000 treatment-naive women with PMO, we observed robust, clinically meaningful reductions in the risk of MOP, hip, NV, and NHNV fractures for patients on Dmab compared to ZA, with greater reductions in fracture risk with longer duration of exposure.

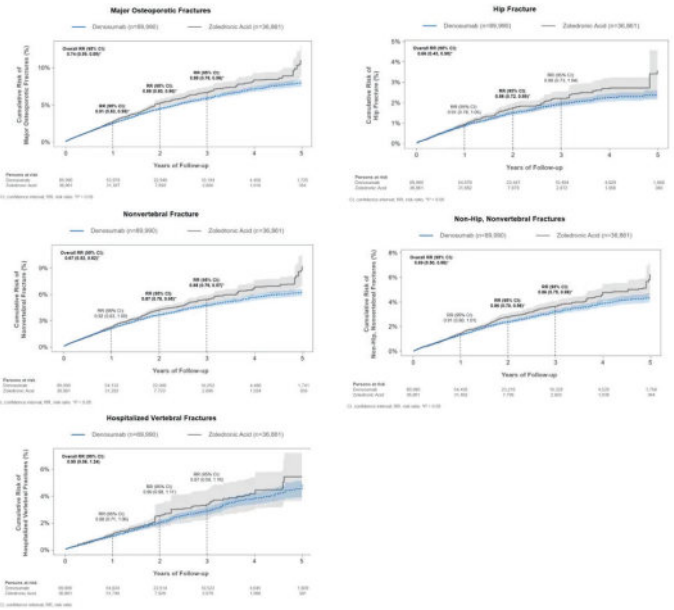

***Disclosures: Jeffrey Curtis**, Amgen Inc., Consultant, Amgen Inc., Grant/Research Support*

1007

Different effects of daily teriparatide and weekly high-dose teriparatide on cortical and trabecular BMD of vertebra and proximal femur: Sub-analysis by QCT from the TERABIT study *Ko Chiba[1], Ryosuke Takahashi[1], Makoto Osaki[1]. [1]Nagasaki University Graduate School of Biomedical Sciences, Japan

Purpose:The effects of daily teriparatide (D-PTH) (20 μg) or weekly high-dose teriparatide (W-PTH) (56.5 μg) on the vertebra and proximal femur were investigated in post-

menopausal women with osteoporosis using quantitative computed tomography (QCT). Methods:A total of 131 postmenopausal osteoporosis patients with a history of fragility fractures were randomized to receive D-PTH, W-PTH, or a bisphosphonate (BP) (oral alendronate or risedronate). The efficacy of these drugs was investigated by comparing bone turnover markers (BTMs), dual-energy X-ray absorptiometry (DXA), and QCT at baseline and after 18 months of treatment.Results:BTMs showed that, in the D-PTH group, P1NP increased (+52.9%), whereas TRACP-5b remained high; in the W-PTH group, P1NP was maintained at the baseline level, whereas TRACP-5b decreased (-26.7%); and in the BP group, both TRACP-5b (-54.1%) and P1NP (-69.8%) decreased.In terms of DXA, D-PTH, W-PTH, and BP all increased lumbar spine areal bone mineral density (aBMD) (median +11.1%, +7.9%, +6.7%, respectively) and total hip aBMD (+2.6%, +2.1%, +3.0%) after 18 months.QCT of the vertebral bodies (T12 and L1) showed that D-PTH, W-PTH, and BP increased total volumetric BMD (Tot.vBMD) (+34.8%, +18.2%, +11.1%), trabecular volumetric BMD (Tb.vBMD) (+50.8%, +20.8%, +12.2%), and cortical volumetric BMD (Ct.vBMD) (+20.0%, +14.0%, +11.5%). The increases in Tb.vBMD was greater in the D-PTH group than in the W-PTH and BP groups.QCT of the proximal femur showed that D-PTH, W-PTH, and BP all increased Tot.vBMD (+2.8%, +3.6%, +3.2%) and Tb.vBMD (+7.7%, +5.1%, +3.4%). Although there was no significant increase in Ct.vBMD in the D-PTH group (-0.1%, +1.5%, +1.6%), cortical bone volume increased in all three treatment groups (+2.1%, +3.6%, +3.1%). The increase in Ct.vBMD was greater in the W-PTH and BP groups than in the D-PTH group.Conclusions:D-PTH had a strong effect on trabecular bone of vertebra. Although D-PTH did not increase cortical BMD of proximal femur, it increased trabecular BMD and cortical bone volume. W-PTH had a moderate effect on trabecular bone of vertebra, while improving both cortical and trabecular BMD of proximal femur.

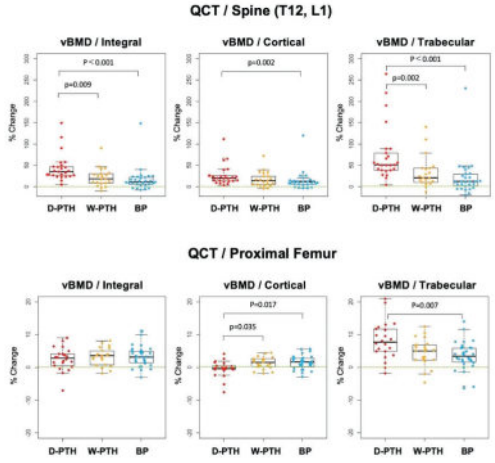

***Disclosures: Ko Chiba**, Asahi Kasei Pharma Corporation, Grant/Research Support, Eli Lilly Japan K.K., Grant/Research Support*

1008

Assessment of Romosozumab Treatment on Spine Bone Strength Using Biomechanical Computed Tomography Virtual Stress Tests *Tony Keaveny[1], Mary Oates[2], Donald Betah[2], Yifei Shi[2], Jen Timoshanko[3], Corinna Zygourakis[4], Mohamad Bydon[5], Kelly Krohn[6], Koji Ishikawa[7]. [1]University of California, Berkeley, United States. [2]Amgen Inc., United States. [3], United Kingdom. [4]Stanford University School Medicine, United States. [5]Mayo Clinic, United States. [6]U of AZ College of Medicine Phoenix, United States. [7]Showa University School of Medicine, Japan

BackgroundOsteoporosis (OP) is characterized by decreased bone density and strength, which increase the risk of fractures. OP is common in older patients undergoing spinal fusion and is a significant risk factor for post-surgical complications. Romosozumab (Romo), a sclerostin inhibitor, has been shown to increase bone mineral density (BMD) and vertebral strength and reduce fracture risk. Using a novel Finite Element Analysis we studied the pedicle screw-bone connection in pullout test and physiological spinal loads with different OP treatments, including Romo.MethodsThis retrospective secondary analysis used lumbar spine computed tomography (CT) data from postmenopausal women with low BMD or OP in the imaging substudies of the Phase 2 (NCT00896532) and Phase 3 ARCH (NCT01631214) trials. For the Phase 2 study, treatment groups were: Romo 210 mg QM, placebo [Pbo], or teriparatide [Tptd] for 12 months. In ARCH, treatment groups were: Romo or alendronate [Aln] for 12 months, then Aln for all for a second 12 months. For each patient, CT scans at baseline (BL) and follow-up (6, 12, and/or 24 months), were used to create a finite element model at each timepoint for the patient's L1 vertebra, virtually implanted with a pedicle screw, in a "shear pullout" configuration. Percent changes from BL in shear bone strength (N), volume of failed tissue (cm3) associated with shear bone loading related to weak bone, and periprosthetic BMD (mg/cm3) were compared by analysis of covariance models adjusting for baseline covariates.ResultsData were analyzed for 79 patients from each study (Phase 2: Romo, 24; Pbo, 27; Tptd, 28; ARCH: Romo/Aln, 44; Aln/Aln, 35). BL characteristics were similar across treatment groups within each study. In the Phase 2 study, at M12 compared to BL, Romo significantly increased shear bone strength, decreased volume of failed tissue, and increased periprosthetic BMD, compared to both Pbo and Tptd (Table 1A). In ARCH, at M6 and M12 compared to BL, Romo significantly increased shear bone strength, decreased volume of failed tissue, and increased periprosthetic BMD compared to Aln, and these changes were maintained at M24 after switching from Romo to Aln (Table 1B).ConclusionFor both studies, compared to its respective comparators, Romo significantly increased shear bone strength by finite element analysis and periprosthetic BMD and lowered the amount of failed tissue. These data demonstrate Romo's efficacy vs Tptd or Aln for improving lumbar spine bone density and strength associated with pedicle screw fixation.

Table 1

1A. Phase 2 study (NCT00896532)

	Placebo (N=27)	Teriparatide 20 µg SC QD (N=28)	Romo 210 mg SC QM (N=24)
Percentage change from baseline in Shear Bone Strength (N) at Month 12			
LS mean (95% CI)	−2.2 (−5.8, 1.5)	14.8 (11.3, 18.4)	24.7 (20.8, 28.6)
Romosozumab difference from Placebo			
LS mean (95% CI)			26.9 (21.6, 32.2)***
Romosozumab difference from Teriparatide			
LS mean (95% CI)			9.9 (4.5, 15.2)***
Percentage change from baseline in Volume of Failed Tissue (cm^3) at Month 12			
LS mean (95% CI)	8.2 (−0.4, 16.8)	−29.3 (−37.6, −21.1)	−44.0 (−53.3, −34.8)
Romosozumab difference from Placebo			
LS mean (95% CI)			−52.2 (−65.0, −39.5)***
Romosozumab difference from Teriparatide			
LS mean (95% CI)			−14.7 (−27.0, −2.4)*
Percentage change from baseline in Periprosthetic BMD (mg/cm^3) at Month 12			
LS mean (95% CI)	−2.5 (−5.2, 0.2)	10.5 (7.9, 13.1)	19.1 (16.3, 22.0)
Romosozumab difference from Placebo			
LS mean (95% CI)			21.6 (17.8, 25.5)***
Romosozumab difference from Teriparatide			
LS mean (95% CI)			8.6 (4.8, 12.5)***

CI, confidence interval; BMD, bone mineral density; LS, least squares; N, number of subjects with evaluable data at Month 12; QD, once every day; QM, once every month; Romo, Romosozumab; SC, subcutaneous. Percentage changes from baseline were assessed by analysis of covariance model adjusting for treatment, geographic region, and baseline value of the measure. ***p<0.001, **p<0.01, *p<0.05.

1B. Phase 3 ARCH study (NCT01631214)

	Aln 70 mg QW/ Aln 70 mg QW (N=35)	Romo 210 mg QM/ Aln 70 mg QW (N=44)	Difference from Aln 70 mg QW/ Aln 70 mg QW
Percentage change from baseline in Shear Bone Strength (N) by visit			
Month 6			
n	32	42	–
LS mean (95% CI)	6.1 (4.2, 8.1)	21.6 (17.8, 25.4)	15.5 (11.2, 19.7)***
Month 12			
n	34	44	–
LS mean (95% CI)	7.3 (5.0, 9.6)	26.3 (22.1, 30.6)	19.0 (14.1, 23.9)***
Month 24			
n	20	25	–
LS mean (95% CI)	5.7 (3.2, 8.2)	25.2 (19.9, 30.5)	19.5 (13.6, 25.3)***
Percentage change from baseline in Volume of Failed Tissue (cm^3) by visit			
Month 6			
n	32	42	–
LS mean (95% CI)	−0.7 (−4.2, 2.7)	−15.4 (−22.4, −8.4)	−14.7 (−22.5, −6.9)***
Month 12			
n	34	44	–
LS mean (95% CI)	−4.5 (−8.9,−0.2)	−19.9 (−28.3, −11.6)	−15.4 (−24.9, −6.0)**
Month 24			
N	20	25	–
LS mean (95% CI)	−1.4 (−4.1, 1.3)	−23.0 (−34.0, −11.9)	−21.6 (−33.0, −10.1)***
Percentage change from baseline in Periprosthetic BMD (mg/cm^3) by visit			
Month 6			
n	32	42	–
LS mean (95% CI)	4.9 (3.2, 6.6)	16.6 (13.9, 19.3)	11.7 (8.5, 14.9)***
Month 12			
n	34	44	–
LS mean (95% CI)	5.4 (3.4, 7.5)	20.7 (17.7, 23.7)	15.3 (11.7, 18.9)***
Month 24			
n	20	25	–
LS mean (95% CI)	4.8 (3.2, 6.3)	20.7 (16.8, 24.7)	16.0 (11.7, 20.2)***

Aln, alendronate; CI, confidence interval; BMD, bone mineral density; LS, least squares; N, Number of subjects with values at baseline and at-least one post-baseline visit; n, Number of subjects with evaluable data at the time point of interest; Romo, romosozumab; QM, once every month; QW, once every week. Percentage changes from baseline were assessed by analysis of covariance model adjusting for treatment, presence of severe vertebral fractur at baseline, and baseline value of the measure. Missing values were imputed by carrying forward the last non-missi post-baseline value prior to the missing value and within the treatment period. ***p<0.001, **p<0.01, *p<0.05.

***Disclosures: Tony Keaveny**, O.N. Diagnostics, Major Stock Shareholder*

1009

Can We Treat Osteoporosis, Obesity And Neurodegeneration With A Single FSH-blocking Drug? *Judit Gimenez Roig[1], Anusha Rani Pallapati[1], Satish Rojekar[1], Funda Korkmaz[1], Damini Sant[2], Orly Barak[1], Farhath Sultana[1], Ofer Moldavski[1], Anisa Azatovna Gumerova[1], Hasni Kannangara[1], Uliana Cheliadinova[1], Clifford J. Rosen[3], John N. Caminis[4], Marcia Meseck[1], Victoria Elise DeMambro[3], Darya Vasilyeva[1], Steven Sims[1], Sakshi Gera[1], Ronit Witztum[1], Sari Miyashita[1], Vitaly Ryu[1], Mansi Saxena[1], Tal Frolinger[1], Anne Macdonald[1], Se-Min Kim[1], Georgii Pevnev[1], Daria Lizneva[1], Tony Yuen[1], Mone Zaidi[1]. [1]Icahn School of Medicine at Mount Sinai, United States, [2]Max Planck Institute for Biology of Ageing, Germany, [3]Maine Medical Center Research Institute, United States, [4]Shire, United States

Pharmacological and genetic studies suggest that FSH is an actionable target for diseases affecting millions, notably osteoporosis, obesity and Alzheimer's disease (AD). Blocking FSH action prevents bone loss (1, 2), fat accrual (3) and AD-like features in mice (4). We recently developed a first-in-class, humanized, epitope-specific FSH blocking antibody that binds to a 13-amino-acid-long sequence of FSH?-MS-Hu6-with a KD of 7.52 nM (5). We showed that MS-Hu6 binds specifically to FSH?, without binding to LH and TSH. For efficacy studies, we have blocked FSH action using either MS-Hu6 or the parent murine antibody, Hf2, targeted to the same epitope. Using our Good Laboratory Practice platform (Code of Federal Regulations, Title 21, Part 58), we report that FSH blockade prevents obesity, osteoporosis and AD in mice. We injected 20-week-old C57BL/6 male mice on a high-fat diet with a range of doses of Hf2 or vehicle s.c. five-days-a-week for 8 weeks. Hf2 (100 µg/mouse/day) reduced the increase in fat mass by 33% starting week 3, with a 7% reduction in body weight. In separate studies, MS-Hu6 not only caused beiging of white adipose tissue in UCP1-reporter ThermoMice (IVIS imaging), but also improved bone density and microstructure (micro-CT) by elevating bone formation (dynamic histomorphometry). The increase in bone mass and improved microstructure were replicated in Cliff Rosen's lab using C57BL6 mice 24 weeks post-ovariectomy. Novel Object Recognition testing of AD-prone, ovariectomized 3xTg mice showed a deficit in recognition memory, which was reversed after 8 weeks of Hf2 (100 µg/mouse/day for 5-days-a-week) exposure. Biodistribution studies using 89Zr-labelled, biotinylated or unconjugated MS-Hu6 in mice and monkeys showed localization to bone, bone marrow, fat depots and brain tissue. MS-Hu6 displayed a ? phase t½ of 7.8 days in humanized Tg32 mice. In monkeys, an acute single injection of MS-Hu6 did not affect vitals, and biochemical parameters remained within the normative range. We tested 215 variations of excipients using a range of physicochemical techniques, including protein thermal shift, size exclusion chromatography, dynamic light scattering, Fourier-transform infrared spectroscopy, circular dichroism spectroscopy, and differential scanning calorimetry, to yield a formulation with thermal, colloidal, monomeric and structural stability at an ultra-high concentration (100 mg/mL) with acceptable viscosity, clarity and turbidity parameters. MS-Hu6 showed the same "humanness" as human IgG1 in silico and was non-immunogenic in ELISPOT assays for IL-2 and IFN? in human PBMC cultures. In conclusion, MS-Hu6 is efficacious, durable and manufacturable, and is therefore poised for human testing as a multipurpose therapeutic for obesity, osteoporosis, and perhaps for AD. 1Cell, 2006; 2PNAS, 2018,; 3Nature, 2017; 4Nature, 2022; 5. PNAS, 2020, eLife, 2022.

***Disclosures: Judit Gimenez Roig**, None*

1010

Bisphosphonates Maintain BMD after Sequential Teriparatide and Denosumab in Premenopausal Women with Idiopathic Osteoporosis (PremenIOP) *Mafo Kamanda-Kosseh[1], Stephanie Shiau[2], Sanchita Agarwal[1], Ananya Kondapalli[1], Ivelisse Colon[1], Nayoung Kil[1], Mariana Bucovsky[1], Robert Recker[3], Joan Lappe[3], Julie Stubby[3], Elizabeth Shane[4], Adi Cohen[5]. [1]Columbia University Irving Medical Center, United States, [2]Rutgers University School of Public Health, United States, [3]Creighton University, United States, [4]Columbia University College of Physicians and Surgeons, , [5]Columbia University Medical Center, United States

We previously reported that teriparatide (TPTD) for 2 yrs followed by denosumab (Dmab) for 2-3 yrs leads to substantial increases in spine (LS) and hip BMD in PremenIOP. After completing sequential TPTD-Dmab, 24 PremenIOP (aged 43+/-8 yrs) enrolled in an open label Bisphosphonate Extension Study in which either (patient-centered choice) alendronate (ALN) 70mg po weekly or zoledronic acid (ZOL) 5mg IV was initiated 7M after the last Dmab dose. All were severely affected with low trauma adult fractures (range 0-12; 9 with vertebral fractures) and/or very low BMD. BMD by DXA and serum C-telopeptide (CTX) were measured every 6M; vertebral fracture assessment (VFA) was performed annually.On sequential TPTD-Dmab, the participants had large increases in BMD: 25+/-9% at LS, 11+/-6% at the total hip (TH), and 14+/-7% at the femoral neck (FN). Pretreatment baseline LS BMD Z score was -2.0+/-0.9, increasing to -0.1+/-1.0 after completing TPTD-Dmab. Mean CTX was 342+/-166 pg/mL at baseline and 173+/-203 pg/mL at end of Dmab.During the Bisphosphonate Extension Study, mean BMD and CTX changes in the entire group were small and not statistically significant at 6 or 12M (Figure). The 6 women who selected ZOL and the 18 who chose ALN did not differ at baseline by age, BMI, fractures, BMD, calciotropic hormones or CTX. In the ZOL group, there were small declines in BMD and increases in CTX, particularly between 6M and 12M, while greater stability was observed in the ALN group. The ZOL group had significantly greater increases in CTX and decreases in TH BMD than the ALN group (Fig B & D).Changes in BMD and CTX did not differ by duration of Dmab (36M vs <36M) and did not differ between 20 women who remained premenopausal and 4 who transitioned into menopause. Pre-TPTD CTX, likely reflecting baseline remodeling status, was inversely related to 12M BMD %change on bisphosphonate at the LS (r=-0.6; p=0.005) and FN (r=-0.5; p=0.04). No new vertebral (clinical or VFA-based) or non-vertebral fractures occurred.In summary, the large increases in BMD achieved after sequential TPTD-Dmab therapy in PremenIOP were maintained during a bisphosphonate transition year. Our data also suggest that weekly ALN may provide greater suppression of CTX and more stable BMD than ZOL, particularly at the hip and between 6 and 12M. Higher baseline CTX predicted more bone loss after Dmab cessation. We conclude that bisphosphonate therapy prevents significant bone loss after sequential TPTD-Dmab in PremenIOP.

Figure: Change in BMD and CTX on 12M of Bisphosphonate after Denosumab Withdrawal
*p<0.05 for Alendronate vs Zoledronic Acid; #p<0.05 for within group change vs baseline

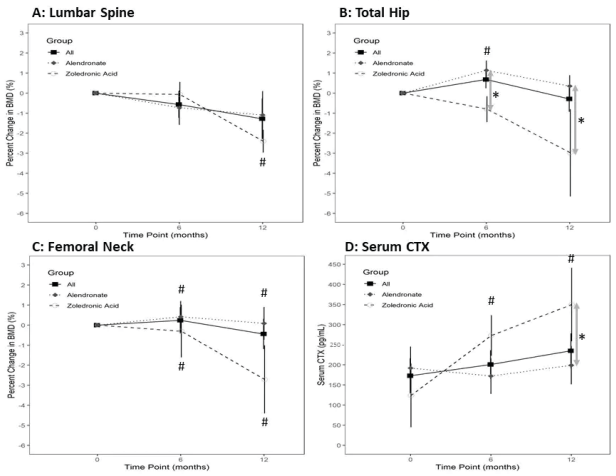

***Disclosures: Mafo Kamanda-Kosseh**, None*

1011

Phlpp2 Limits the Protective Effects of Estrogen on Cortical Bone *ISMAEL KARKACHE[3], Elizabeth Vu[2], David Molstad[3], Kim Mansky[3], Elizabeth Bradley[4]. [3]University of Minnesota, , [2]University of Minnesota Twin Cities, United States, [3]University of Minnesota, United States, [4]University of Minnesota , United States

Pleckstrin Homology Domain and Leucine Rich Repeat Protein Phosphatases (Phlpp) are metal-dependent protein phosphatases solely comprised of isozymes Phlpp1/2 that dampen anabolic kinase activity. In women, age and estrogen status modulate Phlpp1 levels. Prior research demonstrated that osteoclast-directed deletion of Phlpp1 enhanced trabecular bone in females, but that Phlpp1 ablation did not protect against ovariectomy (Ovx) induced bone loss. Estradiol (E2) reduces osteoclast number by decreasing osteoclast progenitor (OCP) cellular respiration and enhancing apoptosis. These data suggest that Phlpp isoforms facilitate E2 actions on the skeleton, but the role of Phlpp2 is not known. We generated Phlpp2 deficient mice via conditional deletion in LysM-Cre expressing cells (Phlpp2 cKO). We first confirmed deletion of Phlpp2 within osteoclasts in vivo via IHC and within in vitro generated osteoclasts. In contrast to Phlpp1, 12-week-old Phlpp2 cKO female mice exhibited an 11% greater femoral midshaft cortical thickness than controls as revealed by micro-CT, but no changes in trabecular bone (n=8-10/group). Importantly, no differences were observed of Phlpp2 ablated males. We next performed Ovx or sham surgeries on 12-week-old female Phlpp2 ablated mice and their control littermates (n=7 per group). We confirmed enhanced endosteal midshaft femoral cortical thickness of Sham Phlpp2 cKO females. Ovariectomy reduced cortical thickness of littermate controls by 10% and Phlpp2 deficiency did not protect against this loss (Fig.1A). To discern the mechanisms for these effects, we next surveyed expression of estrogen receptor gene expression, Esr1/2, within Phlpp1/2 ablated osteoclasts. qPCR analysis revealed that Phlpp2 ablation enhanced Esr1 expression, whereas Esr2 expression increased with Phlpp1 deletion (Fig. 1B). These data mirror the compartment-specific localization of Esr2/1 and the effects of Phlpp1/2 ablation to trabecular and cortical bone, respectively. We further show that Phlpp2 ablation increases OCP responses to E2 via enhanced TUNEL-positive OCPs (Fig 1C, D), leading to decreased osteoclast numbers. Our data asserts that an intact estrogen status facilitates the effects of Phlpp2 to maintain cortical bone and that Phlpp2 ablated OCPs have increased sensitivity to estradiol, driving apoptosis. Overall, our findings demonstrate that Phlpp1/2 distinctly orchestrate maintenance of trabecular and cortical bone in an estrogen dependent-fashion.

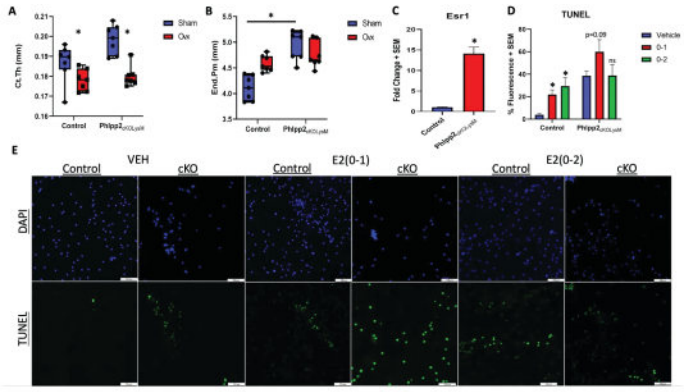

Figure 1: Enhanced Estrogen Sensitivity in Phlpp2 Ablated Osteoclast Progenitors Following, Despite Ovariectomy. Asterisks indicate statistical significance (*p <0.05). A-B) Female Phlpp2 cKO_{LysM} mice and their control littermates (n=7) were aged to 12-weeks at which ovariectomy or sham surgeries were performed. Micro-CT was performed at 8 weeks post-surgery and mid-shaft cortical thickness and endosteal/periosteal perimeter was measured. C-E) BMMs were harvested from 6-8-week-old female Phlpp2 cKO_{LysM} mice and their control littermates and cultured in osteoclastogenic conditions (50ng/ml MCSF, 90ng/ml RANKL) for three days. C) RNA was isolated from day 3 pre-osteoclast cultures and qPCR was performed to assess differential expression of Esr1. D-E) Cultures were treated with E2 in a time window from days 0-1, 0-2, or in vehicle for days 0-2. On day 3, cultures were fixed and TUNEL/DAPI stained. Images taken under a fluorescent microscope (10x) were merged and percentage TUNEL-positive/DAPI-positive cells were quantified. Scale bar is 100 microns.

***Disclosures: ISMAEL KARKACHE**, None*

1012

GIRK3 deletion increases bone mass but does not prevent ovariectomy-induced bone loss *SAMANTHA WEAVER[2,] Jennifer Westendorf[2,] [2]Mayo Clinic, United States[,] [2]Mayo Clinic,

GIRK3 is one of four subunits of GIRK channels. GIRK channels are activated when GPCR ligands stimulate pertussis toxin-sensitive Gi/o-G proteins and the liberated G?? subunit binds to GIRK channels and increases gating, resulting in K+ efflux. Deletion of Girk3 increased femoral bone mineral density (BMD), bone volume fraction, and trabecular number in six-month-old male and female mice. In female mice, cortical bone thickness and tissue mineral density were also increased. Three-point bend tests of the femurs of female Girk3-/- mice revealed increased energy to failure and maximum load. No changes in cortical microarchitecture or strength were detected in males. Static histomorphometry revealed moderately reduced osteoclast activity (osteoclast surface / bone surface), mineral apposition rate, and bone formation rate in Girk3-/- mice, suggesting that osteoblast and osteoclast activity was coupled, but suppressed. Calvarial osteoblasts from Girk3-/- mice differentiated faster in vitro and expressed reduced levels of Wnt pathway inhibitors Sost and Sfrp4, and increased expression of pro-osteogenic Sfrp3 on day 14 of culture. Dkk1 prevented increased mineralization in Girk3-/- osteoblasts. These data demonstrate that Girk3 deletion increases in vitro mineralization in part through a WNT-dependent mechanism. To determine whether Girk3 deletion in osteoblasts was sufficient to recapitulate the high bone mass phenotype in Girk3-/- mice, we generated mice with a deletion of Girk3 in osteoblasts using the 2.3kb-Col1a1 promoter (Girk3-CKO). Male Girk3-CKO had increased trabecular and cortical bone mass, as well as increased energy to failure and maximum load, compared to Cre- controls. There was no phenotype in females. These data suggest that deletion of Girk3 in osteoblasts is sufficient to induce high bone mass in a sexually dimorphic manner. Finally, ovariectomy (OVX) was performed to determine if Girk3 deletion was sufficient to prevent bone loss caused by sex hormone withdrawal. Both sham-operated and OVX Girk3-/- mice had increased bone mass compared to WT mice at 24-weeks-old. WT-OVX mice had 16% lower BMD than WT-SHAM mice, while Girk3-/--OVX mice had 13% lower BMD than Girk3-/--SHAM mice. Girk3 deletion was therefore unable to completely prevent OVX-induced bone loss. Taken together, these data indicate that Girk3 deletion increases bone mass in adult mice through an osteoblastic, partially WNT-dependent mechanism.

***Disclosures: SAMANTHA WEAVER**, None*

1013

Hdac1 and Hdac2 positively regulate N1ICD pathogenic signaling in committed osteoblasts *Haydee Torres[1,] Leetoria Hinojosa[2,] Ashley VanCleave[2,] Tania Rodezno[2,] Danielle May[3,] Kyle Roux[3,] Jennifer J. Westendorf[4,] Jianning Tao[5,] [1]Cancer Biology & Immunotherapies Group at Sanford Research; Department of Chemistry and Biochemistry, South Dakota State University; Department of Orthopedic Surgery, Mayo Clinic , United States[,] [2]Cancer Biology & Immunotherapies Group at Sanford Research, United States[,] [3]The Biochemistry Core at Sanford Research, United States[,] [4]Department of Orthopedic Surgery, Mayo Clinic; Department of Biochemistry & Molecular Biology, Mayo Clinic, United States[,] [5]Cancer Biology & Immunotherapies Group at Sanford Research; Department of Chemistry and Biochemistry, South Dakota State University; Department of Biomedical Engineering, University of South Dakota , United States

Notch receptors belong to a core evolutionarily conserved short-range cell communication signaling pathway that determine cell fate in developmental processes. Regulated successive intramembranous proteolytic-cleavages of the Notch receptor leads to nuclear translocation of the Notch intracellular domain (NICD), where it forms a Notch transcription complex with DNA-binding factors and co-regulators to induce target genes. We utilized a proximity-dependent biotin identification (BioID) method that revealed core Notch circuitry and identified N1ICD associating with chromatin co-regulators, including the NuRD complex (the nucleosome remodeling and deacetylase), SWI/SNF complex (SWItch/Sucrose Non-Fermentable), methyltransferases, and SUMO proteins (Small Ubiquitin-like Modifiers). Our protein-protein interaction network analysis predicted Histone deacetylase 1 (HDAC1) to be the top critical node in an activated Notch state. While an HDAC1-NICD interaction has been studied in vitro and in Drosophila melanogaster wing development, its role in vertebrate skeletal development and homeostasis is unclear. Here, we tested our hypothesis that HDAC1 plays a critical role in the pathogenesis of N1ICD-induced osteosclerosis. Conditional knockout of Hdac1 and Hdac2 in osteoblasts expressing N1ICD mutations had sexually dysmorphic effects on osteosclerosis. Male N1ICD mutant mice with homozygous deletions of Hdac1/2 (Col2.3kb-Cre;TGRosaN1ICD/+;Hdac1f/f;Hdac2f/f) had a 40% decrease in BV/TV and a 22% decrease in trabecular thickness at 4 weeks old when compared to mice with heterozygous deletions of Hdac1/2 (Col2.3kb-Cre;TGRosaN-1ICD/+;Hdac1f/+;Hdac2f/+). Female N1ICD mutant mice with a homozygous deletions of Hdac1/2 exhibited a 38% decrease in BV/TV, 15% decrease in trabecular thickness, and a 25% decrease in trabecular number when compared to mice with heterozygous deletions of Hdac1 (Col2.3kb-Cre;TGRosaN1ICD/+;Hdac1f/+;Hdac2f/f), implicating that HDAC1 deficiency mitigates N1ICD-induced osteosclerosis. Moreover, we found that mice with only deletion of Hdac1/2 and normal NICD (Col2.3kb-Cre;Hdac1f/f;Hdac2f/f) did not exhibit significant changes in skeletal microarchitecture at 4 weeks old. Ongoing studies of transcriptome changes in these mutant bones of mice may provide the molecular basis for these phenotypes. Thus, our studies may provide an insight how HDAC1 may positively regulate N1ICD pathogenic signaling in vivo.

***Disclosures: Haydee Torres**, None*

1014

Cellular and molecular mechanisms underlying regulation of bone homeostasis by the zinc receptor GPR39 *Noam Levaot[1,] Biplab Chaterjee[1,] Gal Gozlan[1,] Chen Abramovitch-Dahan[1,] Katharina Jähn-Rickert[2,] Björn Busse[2,] [1]Department of Physiology and Cell Biology, Ben-Gurion University of the Negev, Israel[,] [2]Department of Osteology and Biomechanics, University Medical Center Hamburg- Eppendorf, Hamburg, Germany., Germany

Zinc is a trace element that is crucial for cellular function and is regulated by various transporters and metallothioneins. G Coupled protein receptor 39 (GPR39) is a specialized zinc receptor which signals through Gq and Gs pathways. We previously showed that GPR39 is important for bone homeostasis and bone collagen content in male mice. In this study, we investigated the role of GPR39 in regulating bone homeostasis in females and found that GPR39 deficiency has a more severe impact on bone health in females than males. Structural and histological analyses revealed lower bone mass and abnormal mineralization in GPR39-deficient mice, with abnormal osteoclast distribution contributing to the reduction in bone volume in females. GPR39-deficient females also exhibited higher osteoporotic bone loss compared to normal female mice when challenged with ovariectomy. We also investigated the cellular basis for the impact of GPR39 deficiency on the skeleton using mice with a conditional deletion in the osteoblast lineage. Our results showed that osteoblast-specific deletion of GPR39 recapitulates the bone phenotype of mice with the germline deletion, indicating that the impact of GPR39 deficiency on the skeleton likely derives from its activity in the osteoblast lineage.Finally, we demonstrated that zinc signaling through GPR39 regulates the expression of collagen alpha 2 chain, providing a possible explanation for the abnormal collagen levels observed after GPR39 deletion in vivo and in vitro. Additionally, we found that GPR39 activity is essential for the regulation of collagen expression by TGF?, a central factor known to regulate collagen expression in normal and clinical conditions.In conclusion, this study provides insights into the cellular and molecular

mechanisms involved in sex-specific bone health and highlights the potential of GPR39 as a therapeutic target for bone-related disorders.

***Disclosures: Noam Levaot**, None*

1015

A Novel Role of TRAPPC9 in Bone Remodeling and Osteoclast Differentiation
*Gabrielle Robinson[2], Alexander Powell[2], Hope Ball[2], Fayez Safadi[2]. [2]Northeast Ohio Medical University, United States. [2]Northeast Ohio Medical University,

Intellectual disability (ID) affects about 4.92 million Americans, which accounts for approximately 17% of the American population. Skeletal abnormalities have been described in patients with ID. X-linked forms of ID have been investigated, while the autosomal-recessive forms of ID have yet to be studied. Specifically Non-syndromic autosomal-recessive intellectual disability (NSARID) develops as a result of mutations in the trafficking protein particle complex subunit 9 (TRAPPC9) gene. Patients possessing this mutation exhibit obesity, develop microcephaly, and skeletal abnormalities inclusive of an increase in bone mass, resulting in a denser cranium, limb deformities, and the loss of teeth. The direct linkage by which TRAPPC9 mutations contribute to skeletogenic homeostasis has yet to be characterized and explained. To definitively understand the impact of TRAPPC9 on skeletogenesis, we investigated the physiological role of TRAPPC9 in bone homeostasis. We characterized the skeletal phenotype of TRAPPC9 global knockout (KO) mice. When analyzing the bone weight across both the TRAPPC9 WT and KO mice, at ages 8 weeks and 8 months. At 8 weeks of age, TRAPPC9 KO mice showed no significant differences from the WT mice, while at 8 months the KO mice had an increased body weight by 1.3-fold when compared to WT animals. We then performed dual X-ray absorptiometry (DEXA) to analyze the bone mineral density (BMD). DEXA analysis showed TRAPPC9 KOs increased in BMD as they aged, while WT's BMD decreased with age. Suggesting that TRAPPC9 deficiency protects against age-related bone loss. Next, we analyzed the serum biomarker of CTX and found that the TRAPPC9 KOs exhibited significantly lower serum CTX levels at 8 months compared to 8 weeks of age. As expected, TRAPPC9 WT's exhibited increased serum levels of CTX at 8 months than at 8 weeks. qPCR analysis performed on calvaria, and humeri of 8-week-old mice showed that the TRAPPC9 KO mice exhibited lower expression levels of osteoclast markers (Cathepsin-K, TRAP). Taken together, these data show that TRAPPC9 deficiency contributes to skeletogenic homeostasis via the dysregulation of osteoclast differentiation and function, resulting in increased bone mass. These findings correlate with findings observed in TRAPPC9 mutation in patients. The data generated in this study is the first to characterize the skeletal phenotype of this TRAPPC9 null mice, aiding in the development of therapeutic approaches for NSARID.

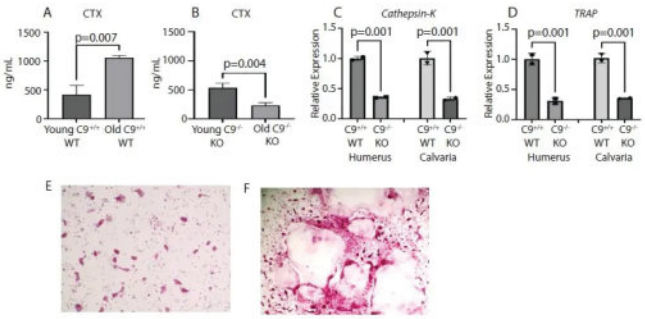

A. The CTX Serum levels in young and old TRAPPC9 WT mice, the old WT mice had increased serum levels of CTX. **B. The CTX Serum levels** in young and old TRAPPC9 KO mice, the young WT mice had increased serum levels of CTX. **C. Cathepsin-K** mRNA expression levels in the calvaria and humeri were decreased in TRAPPC9 KO mice compared to TRAPPC9 WT. **D. TRAP** mRNA expression levels in the calvaria and humeri were decreased in TRAPPC9 KO mice than the TRAPPC9 WT. **E &F.** Osteoclast differentiation derived from the TRAPPC9 WT **(E)** and TRAPPC9 KO mice **(F)**, stained for TRAP and imaged at 10x magnification. TRAPPC9 Kos have increased osteoclast differentiation compared to WT mice.

***Disclosures: Gabrielle Robinson**, None*

1016

The HIF-1?/PLOD2 axis regulates collagen cross-linking and mesenchymal progenitor cell fate responsible for traumatic heterotopic ossification
*Heeseog Kang[1], Amy L. Strong[2], Yuxiao Sun[1], Alec C. Bancroft[1], Ji Hye Choi[1], Conan Juan[1], Lei Guo[3], Juhoon Lee[4], Robert N Kent III[5], David Hudson[6], Brendon M. Baker[5], Kevin Dalby[4], Lin Xu[3], Benjamin Levi[1]. [1]Center for Organogenesis and Trauma, Department of Surgery, University of Texas Southwestern, United States. [2]Section of Plastic Surgery, Department of Surgery, University of Michigan, United States. [3]Quantitative Biomedical Research Center, Department of Population and Data Sciences, University of Texas Southwestern, United States. [4]Division of Chemical Biology and Medicinal Chemistry, College of Pharmacy, University of Texas at Austin, United States. [5]Biomedical Engineering, University of Michigan, United States. [6]Department of Orthopaedics and Sports Medicine, University of Washington, United States

Heterotopic ossification (HO) is a debilitating condition, where ectopic bone formation occurs within extra-skeletal soft tissues. The inflammatory response to tissue damage activates hypoxic signaling that modulates cell proliferation, survival, metabolism, and aberrant differentiation leading to HO and progression. Previously, we reported that activation of hypoxia-inducible factor 1? (HIF-1?) promoted ectopic bone formation in traumatic HO, however, the underlying mechanisms by which hypoxia and the HIF-1? pathway contribute to the aberrant bone formation have yet to be elucidated. Using a well-established burn/tenotomy (BT) HO mouse model, we performed scRNA-seq, immunofluorescent histology, and primary cultures of HO-forming mesenchymal progenitor cells (MPCs) to better define the role of HIF-1? in traumatic HO. Zeugopod-specific mesenchymal cell deletion of Hif1a (Hoxa11-CreERT2;Hif1afl/fl) significantly mitigated HO volume in the BT injury mouse model. ScRNA-seq analysis revealed that Hoxa11(+) lineage specific KO of Hif1a significantly decreased expression of genes associated with glycolysis and collagen cross-linking associated enzymes, many of which were upregulated during HO formation. Consistently, in vitro studies using cultured MPCs isolated from the HO site of Hoxa11-CreERT2;Hif1afl/fl mice demonstrated decreased lactate production and down-regulated expression of collagen cross-linking associated enzymes, including lysyl oxidases (LOX) and procollagen-lysine,2-oxoglutarate 5-dioxygenase 2 (PLOD2). Immunofluorescent staining and second harmonic generation imaging of Hoxa11-CreERT2;Hif1afl/fl demonstrated decreased expression of the collagen cross-linking associated enzymes and impaired collagen cross-linking at the injury site. Treatment of mice post-BT with ?-aminopropionitrile (BAPN), a LOX inhibitor, dramatically and significantly diminished HO volume even with a brief treatment period. Furthermore, in vitro studies using MPCs treated with newly screened PLOD2 inhibitor compounds revealed that inhibition of PLOD2 activity significantly decreased collagen cross-linking, alignment of collagen fibers, MPCs migration and osteogenic differentiation, supporting the central role of the HIF-1?/PLOD2 axis in MPCs metabolic reprogramming, collagen cross-linking, and MPC fate. These results suggest targeting the molecular components in the HIF-1?/PLOD2 pathway to be a promising therapeutic strategy to mitigate HO formation and progression.

***Disclosures: Heeseog Kang**, None*

1017

Loss of TFAM in PRX1 lineage cells causes an Osteogenesis Imperfecta-like phenotype and increased HIF1a activity prevents it
*Mohd Parvez Khan[1], Giulia Lanzolla[1], Elena Sabini[1], Brittany M Laslow[1], Dian Wang[1], Fanxin Long[2], Ernestina Schipani[1]. [1]University of Pennsylvania, United States. [2]CHOP, Philadelphia, Pennsylvania, United States

Once thought to be a consequence of the state of the cell, glycolytic metabolism is now known to control cell differentiation. Both glycolysis and oxidative phosphorylation (OXPhos) are required for osteoblastogenesis. To gain insights into the role of OXPhos in bone mass accrual, we generated a mutant mouse lacking Mitochondrial Transcription Factor A (TFAM) in mesenchymal progenitors of the limb bud and their descendants by using the PRX1-Cre driver (TFAM mice). TFAM regulates transcription of the mitochondrial genes that encode thirteen subunits of the electron transport chain and thus controls OXPhos. TFAM mice display a significant shortening of the long bones, which is already detectable at birth, worsens postnatally, and is associated with growth plate abnormalities and deformities. More importantly, spontaneous mid-shaft fractures are present in mutant long bones by three weeks of age. MicroCT and histomorphometry analysis showed a severe thinning of cortical bone in mutants compared to controls. This was secondary to a dramatic impairment of osteoid accumulation and bone formation rates in the diaphyseal periosteum. Osteoclast number was also significantly increased at that site, implying that augmented resorption may contribute to the phenotype. The long bone phenotype of TFAM mutants, namely shortening, increased fragility, and spontaneous fractures, is reminiscent of Osteogenesis Imperfecta (OI). Single-cell RNA sequencing of periosteal cells revealed that the pool of osteoblastic cells was reduced in mutants, whereas the number of mesenchymal progenitors identified by concomitant expression of markers such as Sca1, PRX1, PDGFRa, and CD90 was increased. Moreover, expression of genes encoding collagens, enzymes involved in posttranslational modifications of collagens, and endoplasmic reticulum chaperons, including serpinH, was downregulated in mutant osteoblastic cells. Levels of osteocalcin mRNA were also significantly lower in the same cells. Conversely, mRNAs encoding downstream targets of TgFbeta signaling such as p21 and serpine1, were upregulated. To establish wheth-

er this phenotype could be corrected by augmenting glycolysis, we bred TFAM mice with mice expressing a mutant Hypoxia Inducible Factor 1alpha (HIF1a), which is constitutively active independently of oxygen levels (HIF1dPA) in PRX1 lineage cells (TFAM/HIF1dPA mice). TFAM/HIF1dPA mice did not develop spontaneous fractures; moreover, thickness of cortical bone and the ability of periosteal cells to accumulate osteoid were fully restored in double mutant mice. HIF1a promotes glycolysis and posttranslational modifications of collagens; we are now investigating whether both events contribute to "rescuing" the bone phenotype of TFAM mice. In conclusion, loss of TFAM in PRX1 lineage cells causes an OI-like phenotype that is prevented by increased HIF1a activity in the same cells.

***Disclosures: Mohd Parvez Khan**, None*

1018

Glucocorticoid-induced Reduction in Osteogenesis and Angiogenesis is Coupled through Altered Skeletal Stem Cell Lineage Dynamics *Thomas Ambrosi[1], Yuting Wang[2], Matthew Murphy[2], Charles Chan[2], Nancy Lane[3]. [1]UC Davis, United States, [2]Stanford University, United States, [3]University of California, Davis Medical Center, United States

Glucocorticoids (GCs) are potent anti-inflammatory compounds, however, continued exposure results in bone loss and osteonecrosis. Skeletal stem cells (SSCs) are crucial for osteogenesis; it is tempting to speculate that GCs might affect their function. Detrimental changes to angiogenesis have been implicated in GC-induced bone loss. The mechanism by which GCs alter vascularity remains unknown. Our study aimed to evaluate GC-effects on both osteogenesis and angiogenesis, as well as if treatment with PTH modifies the effects in a mouse model of GC bone loss. BALB/cj male mice, age 9wks were randomized to placebo (PLB) for 28 or 56 days (d) or GC (MP pellets of 2.5mg) for 28d, then recovery (29-56d) or 56d, or GC for 28d followed by hPTH (29-56d). Outcome measures included bone mass, histology, flow cytometry for SSCs and multipotent progenitors (BCSPs), vascular progenitors (CD31, Tie2), in vitro SSC cultures for osteogenesis, chondrogenesis, and single cell RNA sequencing (scRNAseq). Flow cytometry-purified SSCs were lentivirally barcoded and transplanted into the renal capsule for 28d during GC and hPTH treatments to investigate clonal lineage dynamics and signaling using scRNAseq. GC exposure led to trabecular, but not cortical, bone loss and reduced mechanical strength in 28- and 56d exposure regimens. Similarly, we observed reduced surface-based bone formation rate and increased osteoclast activity by TRAP staining and BM cultures. SSCs and BCSPs of GC mice were reduced in frequency and showed impaired osteogenic and chondrogenic differentiation capacity in vitro compared to controls. In contrast, CD31+ endothelial cells were increased but displayed distorted phenotypical features in immunohistological staining. Interestingly, removal of GC pellets after 28d did not improve any of these parameters with or without PTH treatment. However, GCs + hPTH treatment reversed all GC-induced changes back to control levels. Bone tissue scRNAseq confirmed these findings, as GC reduced osteochondrogenic and increased CAR and Smooth muscle cells. This was accompanied by increased pro-endothelial and pro-inflammatory signaling. Altered clonal SSC differentiation dynamics in vivo perpetuated the reduction in bone formation driving altered endothelial morphogenesis that could only be reversed by PTH treatment with concurrent GC exposure. These findings help to explain the cellular basis of how PTH treatment can mitigate GC induced bone loss and possibly osteonecrosis.

***Disclosures: Thomas Ambrosi**, None*

1019

CAR/LepR+ Cells Express BMP Inhibitors Negatively Regulating Bone Formation in Vivo *Wei Zou[1], Nidhi Rohatgi[1], Aersilan Alimasi[1], Steven Teitelbaum[1]. [1]Washington University in St. Louis School of Medicine, United States

C-X-C motif chemokine 12 (CXCL12)-abundant reticular (CAR) cells, which are LepR+, are marrow residing stromal cells believed to be osteoblast progenitors. The mechanism by which CAR/LepR+ cells differentiate into osteoblast is not well known. Our lab has generated an inducible fat deletion mouse model by mating mice expressing an inducible DTR to those bearing adiponectin (ADQ)-Cre. Within 4 days of DTR activation, the systemic bone mass of DTRADQ mice begins to increase due to stimulated osteogenesis, with a 1,000% enhancement by 10-14 days. This adipocyte ablation-mediated enhancement of skeletal mass reflects bone morphogenetic protein (BMP) receptor activation following the elimination of its inhibitors, Gremlin1 and Chrdl1 by depletion of marrow residing adiponectin-expressing cells. In our recent work, we found virtually all CAR/LepR+ cells are derived from adiponectin positive lineage cells and DTR activation completely depletes marrow of CAR cells. By sorting CAR cells from Cxcl12-GFP reporter mice, we found they are the principal source of the BMP inhibitors. To further explore the effect of CAR/LepR+ cells on bone, we mated floxed DTR mice with LepR Cre (DTRLepR). Depletion of CAR/LepR+ cells by DTR activation decreases BMPR inhibitors expression in marrow, and induces 5-6 fold increase of bone mass in diaphysis of DTRLepR mice in 10 days compared with WT control, while marrow adipose cells were not significantly affected in DTRLepR mice. Similar to DTRADQ mice, administration of BMP inhibitors completely blocks the bone mass enhancement, indicating that BMPR activation mediates new bone formation in DTRLepR. BMP targeted cells in DTRADQ mice are early committed osteoblast lineage cells driven by the 3.6Col1a1 promoter likely differentiating into mature osteoblasts characterized by activated 2.3Col1a1 promoter. Taken together, our data show CAR/LepR+ cells are not only osteoblast progenitors differentiating into osteoblasts, but are also the principal source of BMP inhibitors in marrow negatively regulating bone formation in vivo. Thus, unexpectedly, elimination of CAR/LepR+ cells, which are osteoblast progenitors, rapidly increases bone mass due to BMP activation of more committed osteoblast lineage cells.

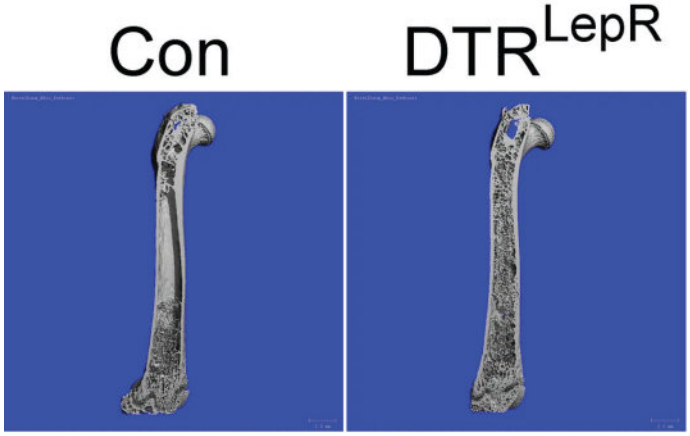

***Disclosures: Wei Zou**, None*

1020

ERK Suppresses the Plasticity of Periosteal Skeletal Stem Cells *Alisha Yallowitz[1], Shawon Debnath[2], Hwanhee Ho[3], Michelle Cung[3], Yeon-Suk Yang[4], Jae Hyuck Shim[4], Matthew Greenblatt[5]. [1]Weill Cornell Medicine, United States, [2]Weill Cornell Medicine, Cornell University, , [3]Department of Pathology and Laboratory Medicine, Weill Cornell Medicine, United States, [4]UMASS Medical School, United States, [5]Weill Cornell Medical College, United States

We previously reported a periosteal stem cell (CTSK+ skeletal stem cells, CTSK+ SSCs) that mediates intramembranous ossification under baseline conditions (Debnath et al. Nature 2018). However, these cells undergo a plasticity event after skeletal fracture whereby they acquire the gene expression profile and endochondral bone formation capacity of endosteal stem cells. The molecular pathways by which these normally intramembranous-specialized CTSK+SSCs interconvert into cells with the properties of endosteal stem cells and mediate endochondral fracture repair is unknown. Here, we have identified that the ERK signaling pathway acts as a molecular regulator of fracture induced plasticity in CTSK+SSCs. The ERK pathway is constitutively active in CTSK+SSCs and suppresses their plasticity under basal conditions. When the ERK pathway is disrupted in CTSK+SSCs, as in Mek1flox/flox; Mek2-/- CTSK-cre mice (Mek1CTSKMek2-/-), CTSK+SSCs expand and display a cell intrinsic gain in the capacity to mediate endochondral ossification. In contrast, enforced activation of the ERK pathway in CTSK+SSCs via a conditional constitutively active Mek1 allele (Mek1DDCTSK mice) prevents CTSK+SSC plasticity and inhibits the formation of the cartilaginous callus during fracture healing, resulting in nonunion. Thus, ERK-regulated CTSK+SSC plasticity is critical for fracture repair. Additionally, Mek1CTSKMek2-/- mice develop spontaneous osteochondroma formation in the periosteum, a phenotype that is similar to human multiple exostoses/osteochondroma. Thus, osteochondromas represent induction of the fracture induced CTSK+SSC plasticity pathway in the absence of fracture. Altogether, these findings confer a surprising link between osteochondroma formation and fracture repair and identifies the first molecular regulator of plasticity among SSC types.

***Disclosures: Alisha Yallowitz**, None*

FRI-055

Examining the Role of Zinc Fingers and Homeoboxes 2 (Zhx2) in Chronic Kidney Disease-related Bone & Cardiovascular Health *Jordan Matz[1], Corinne Metzger[3], Huda Mahmood[3], Christopher Miller[3], Arelis Quintana-Martinez[3], Gagandeep Sooch[4], Matthew Allen[3], Erica Clinkenbeard[3]. [1]IU School of Medicine, , [3]Indiana University School of Medicine, , [3]Indiana University School of Medicine, United States, [4]Marian University College of Osteopathic Medicine, United States

Chronic Kidney Disease (CKD) is estimated to affect more than 1 in 7 US adults. CKD-mineral and bone disorder (CKD-MBD), a common sequela, independently leads to vascular calcification, increased fracture risk, and mortality. Mice placed on CKD-inducing 0.2% adenine diet (AD) for 8 weeks show increased cortical bone porosity, osteoclast activity, and marrow adiposity, mirroring human patients. The differentiation skewing between osteoblast and adipocyte in CKD however remains unclear. Zinc finger and homeobox 2 (Zxh2), a transcriptional repressor, was previously shown to be critical for odontoblast differentiation. Further, lack of Zhx2 promotes hepatic steatosis with high fat diet. We hypothesize Zhx2 potentiates osteoblast commitment by inhibiting adipocyte gene expression. We utilized BALB/cJ (/cJ) mice which harbor a hypomorphic mutation in the Zhx2 locus,

drastically decreasing Zhx2 mRNA compared to normal BALB/c (/c) mice. AD feeding in both sexes significantly increased serum Blood Urea Nitrogen vs casein control consistent with CKD; however, /cJ mice had significantly lower values than /c mice. On casein, /cJ females exhibited lower trabecular bone volume (Tb.BV/TV; p<0.01), reduced Bglap mRNA (p<0.01), and increased adipogenic Lpl mRNA (p<0.05) vs /c. AD-fed /c females lost Tb.BV/TV and reduced Bglap mRNA comparable to /cJ levels which correlated with reduced bone Zhx2 mRNA vs /c casein. Male /cJ mice exhibited reductions in Bglap (5-fold, p<0.01), Alpl (2.5-fold; p<0.01), and Dmp1 (2.5-fold, p<0.01) mRNA compared to /c on casein, with no differences in Lpl mRNA or trabecular bone parameters. In contrast to females, AD-fed /c males had modestly increased Tb.BV/TV whereas Tb.BV/TV decreased in AD-fed /cJ males. Consistent with CKD, AD-fed /cJ mice exhibited modestly elevated serum phosphate and fibroblast growth factor 23 (FGF23) vs /c mice. Thus, we assessed tissues for downstream calcifications via X-ray. Analysis of isolated hearts showed AD-fed /c mice incurred heart calcifications (2/7 females; 4/6 males), whereas BALB/cJ mice appeared protected (0/8 male and female). In conclusion, Zhx2 is a transcription factor that exhibits influence on outcomes related to CKD and mineral metabolism. Most notably, /cJ mice lacking Zhx2 were protected from cardiac calcification incidence. These results have important implications for patients with CKD-MBD and downstream outcomes related to disrupted mineral metabolism.

***Disclosures: Jordan Matz**, None*

FRI-074

Bariatric Surgery is Associated with Increased Fracture Risk Among Veterans *Eileen H. Koh[1], Tiffany Y. Kim[2], Hui Shen[2], Mary A. Whooley[2], Matthew L. Maciejewski[3], Theodore S. Z. Berkowitz[4], Valerie Smith[3], Lygia Stewart[2], Anne L. Schafer[2]. [1]University of California, San Francisco, United States. [2]University of California, San Francisco and San Francisco Veterans Affairs Health Care System, United States. [3]Durham Veterans Affairs Health Services Research and Development and Duke University, United States. [4]Durham Veterans Affairs Health Services Research and Development, United States

Despite its metabolic and mortality benefits, bariatric surgery has negative skeletal effects. The Roux-en-Y gastric bypass (RYGB) procedure is associated with increased fracture risk in the general bariatric surgery population, who are predominantly premenopausal women. It is unclear whether postoperative fracture risk is increased in men, and whether patients with obesity who undergo sleeve gastrectomy (SG), now the most commonly performed procedure, are more likely to fracture than nonsurgical patients. We compared fracture risk among US Veterans who underwent bariatric surgery from 2000-2020 at a Veterans Affairs (VA) facility or paid for by VA and matched Veterans with obesity who did not have surgery. Surgical patients were matched 1:3 to nonsurgical patients by age, sex, year, and pre-op BMI. We used ICD codes to capture incident fracture from VA electronic health records, VA purchased care claims, and Medicare claims. Cox proportional hazards models were used to determine the relationship between bariatric surgery and subsequent fracture risk. Our surgical cohort, comprised of 8357 patients [3182 RYGB, 4168 SG, 291 adjustable gastric banding (AGB)], was 70% men with mean age 52+/-10 years and BMI 45+/-7 kg/m2. Compared to 25,057 matched Veterans who did not have surgery, surgical patients had higher baseline rates of obesity-related comorbidities including diabetes (48% vs 36%). During an average 7 years follow-up, surgical patients had higher rates of incident fracture (25.1 vs 13.9 per 1000 person-years). Bariatric surgery was associated with a 67% increased risk of incident fracture (HR 1.67, 95% CI 1.56-1.79, p<0.001) after adjustment for race/ethnicity, geographic location, and comorbidities. Bariatric surgery was also associated with incident hip fracture (HR 2.42, 95% CI 1.97-2.96, p <0.001), spine fracture (HR 1.81, 95% CI 1.60-2.05, p<0.001), and radius fracture (HR 2.36, 95% CI 2.03-2.75, p< 0.001). Compared to matched controls, RYGB was associated with increased risk of fracture (HR 1.91, 95% CI 1.73-2.11, p<0.001), as was SG (HR 1.48, 95% CI 1.31-1.67, p<0.001), but there was no difference in fracture rates between RYGB and SG (p=0.18). There was no evidence for an association between AGB and fracture risk (HR 0.97, 95% CI 0.68-1.40, p=0.88). Our findings show that RYGB and SG are associated with increased risk of fracture in this Veteran population of predominantly older men, including at major osteoporotic fracture sites.

***Disclosures: Eileen H. Koh**, None*

FRI-127

Osteocytes Induce Drug Resistance via the NOTCH3-CXCL12 Signaling Axis in Multiple Myeloma *Hayley Sabol[1], Cody Ashby[1], Manish Adhikari[1], Japneet Kaur[1], Aric Anloague[1], Sharmin Khan[1], Samrat Roy Chodhury[1], Michela Palmieri[1], Lawry Barnes[1], Elena Ambrogini[1], Carolina Schinke[1], Intawat Nookaew[1], Jesus Delgado-Calle[1]. [1]University of Arkansas for Medical Sciences, United States

Multiple myeloma (MM) remains incurable due to disease relapse and drug resistance. Notch signals between MM cells and cells of the tumor niche (TME) confer drug resistance, but the cellular/molecular mechanisms are not entirely known. Using in silico analysis of clinical and transcriptomic public and internal databases, we found that 1) NOTCH3 is upregulated in MM cells from newly diagnosed MM patients (NDMM) vs. healthy donors, 2) increases in relapsed/refractory MM (RRMM) vs. NDMM patients, and 3) NDMM patients with high NOTCH3 expression have worse responses to Bortezomib (BOR)-based therapies. Because NOTCH3 mRNA levels did not correlate with somatic mutations in NOTCH3, we tested if NOTCH3 is regulated by TME cells and its role in responses to chemotherapy. Osteocytes (Ots), recently defined as key cells in the TME, increased NOTCH3 in MM cells and protected them from apoptosis induced by BOR or VRd (BOR+Lenalidomide+Dexamethasone) in vitro. This protection was lost by NOTCH3 knockdown (NOTCH3KD) and enhanced by NOTCH3 activation (NOTCH3OE) in MM cells. Next, we compared BOR (0.1 mg/kg, 5x/wk) responses in control (C) vs NOTCH3OE MM cells in vivo. All untreated mice bearing C or NOTCH3OE cells died at 4 wks. In mice injected with C MM cells, BOR reduced tumors by 65%, improved survival (7/10 alive), and had 38% more bone mass, 25% more P1NP, and 29% less CTX than untreated mice. In contrast, in NOTCH3OE-bearing mice, BOR only reduced tumors by 23% and did not improve survival (1/10 alive), bone mass, or serum markers, supporting NOTCH3 confers BOR resistance. We then compared the MM cell transcriptome of NDMM patients with high vs. low NOTCH3 expression to find the mechanism for BOR resistance. We found that high NOTCH3 NDMM and RRMM patients had enrichment in chemokine and cell adhesion pathways and CXCL12 upregulation. Ots upregulated CXCL12 and activated the CXCR4/ERK pathway in MM cells in vitro. These effects were blunted in NOTCH3KD and enhanced in NOTCH3OE MM cells. Genetic inhibition of CXCL12 in NOTCH3OE cells prevented Ot's protection and restored BOR/VRd sensitivity, supporting CXCL12 works in an autocrine fashion. Lastly, Plerixafor, a CXCR4/CXCL12 inhibitor, restored NOTCH3OE MM cells sensitivity to BOR/VRd in vitro and in human bones bearing NOTCH3OE tumors cultured ex vivo. Our clinical and experimental data show Ots transmit drug resistance signals and unravel a novel targetable NOTCH3-CXCL12 pro-survival signaling axis in the MM TME.

***Disclosures: Hayley Sabol**, None*

FRI-131

Osteoblasts are a source of bone metastases-associated fibroblasts (BMAFs) *Jennifer Zarrer[1], Marie-Therese Haider[2], Nicole Ridlmaier[2], Rafael Preuer[2], Daniel J. Smit[3], Hiroaki Saito[1], Eric Hesse[1], Hanna Taipaleenmäki[1]. [1]Institute of Musculoskeletal Medicine, University Hospital, LMU Munich, Munich, Germany, Germany. [2]Molecular Skeletal Biology Laboratory, Department of Trauma, Hand and Reconstructive Surgery, University Medical Center Hamburg-Eppendorf, Hamburg, Germany, Germany. [3]Institute of Biochemistry and Signal Transduction, University Medical Center Hamburg-Eppendorf, Hamburg, Germany, Germany

In breast cancer bone metastases the abundance of adjacent osteoblasts (OBs) is diminished. To determine the fate of OBs, we combined a lineage-tracing model (Osx-cre-ERt+;Ai9) with intracardiac injection of 4T1 breast cancer cells and performed single cell RNA sequencing (scRNAseq) of tdTomato-positive (tdTom+) OBs in metastases-bearing and healthy control animals. Bioinformatic analysis revealed a distinct cluster of tdTom+ OBs in metastases-bearing mice that express genes related to tumor microenvironment, fibrosis and cancer-associated fibroblast (CAF) proliferation (e.g. Cxcl12, Tnc, Mmps, Pdgfr-?, Pdgfr-?). CAFs reside inside tumors providing a micro-milieu that supports tumor growth. However, little is known about metastasis-associated fibroblasts (MAFs), in particular in bone metastases. Based on our findings, we hypothesized that OBs might abandon the bone surface and become MAFs. Supporting our hypothesis, histological analysis demonstrated elongated tdTom+ OBs within metastases, which we termed bone metastases-associated fibroblasts (BMAFs), while only a few OBs were present on nearby bone surfaces. Consistently, MC3T3-E1- and primary OBs acquired a spindle shape morphology upon stimulation with medium conditioned by 4T1 or MDA-MB-231 breast cancer cells (CCM), which also increased OB migration and OB-induced collagen remodeling. Furthermore, in an ex vivo co-culture model, OBs in the vicinity of cancer cells became elongated and migrated in-between tumor cells. Immunoblot, qRT-PCR, scRNAseq and histological analyses revealed a reduction of OB markers (Runx2, Osx) and an increase of BMAF-associated genes (e.g. Pdgfr-?, Pdgfr-?) in CCM-stimulated OBs and cancer-associated tdTom+ OBs. To elucidate the mechanisms transitioning OBs to BMAFs, we performed RNA sequencing and identified an activated IL-17A signaling pathway in CCM-stimulated OBs compared to controls, which was confirmed by immunoblot and qRT-PCR analyses of downstream targets (C/ebp, Ccl2). Furthermore, recombinant IL-17A promoted OB migration and acquisition of a BMAF phenotype while inhibition of IL-17A signaling using an anti-IL-17 antibody restored the CCM-induced morphological changes and OB migration. In vivo, anti-IL-17A reduced the number and growth of bone metastases determined by bioluminescence imaging and histology. Together, these results demonstrate that OBs give rise to BMAFs at least in part through IL-17A, which might contribute to metastatic growth.

***Disclosures: Jennifer Zarrer**, None*

FRI-163

Bone fracture causes long-term impairment of the bone marrow niche for hematopoietic stem cells *Elise Jeffery[1], Sean Ahler[1], Bethany Davis[1], Sean Morrison[1]. [1]UT Southwestern Medical Center, United States

Bone fracture is estimated to occur in 2.3% of people every year (GBD Fracture Collaborators, The Lancet, 2021). In addition to damaging bone, fracture also significantly damages the bone marrow (BM), which is the primary site of hematopoiesis in healthy adults. Hematopoietic stem cells (HSCs) in the BM reside adjacent to sinusoidal blood vessels and

perivascular stromal cells, which secrete chemokines essential for HSC maintenance and survival (Crane et al, Nat Rev Immun, 2017). During fracture repair, the BM stroma is regenerated in part by periosteal cells that contribute to the formation of the fracture callus (Jeffery et al, Cell Stem Cell, 2022). However, it's unclear to what extent the regenerated BM stroma supports hematopoiesis. To investigate this, we analyzed the frequency of HSCs, restricted progenitors, and mature lineages in mice five weeks after tibial fracture, a time point when the bone cortex has fully re-formed and the marrow has regenerated (Jeffery et al, Cell Stem Cell, 2022). We found a striking three-fold reduction in the frequency of HSCs in post-fracture BM compared to that of the contralateral uninjured tibia. In contrast, there was no difference in the frequencies of lineage restricted progenitors or of mature hematopoietic populations. These data suggest that post-fracture BM is specifically toxic to HSCs. The degree of fracture stabilization did not affect the phenotype, as we observed a similar reduction in HSC frequency after non-stabilized fracture and pin-stabilized fracture. Surprisingly, the reduction in HSC frequency was maintained for at least six months post-fracture, suggesting that fracture has a long-term effect on the hematopoietic microenvironment. We hypothesized that this reduction in HSC frequency was due to impaired niche cell function in the regenerated BM. However, we found no significant changes in stromal cell number, morphology, or niche factor expression in stromal cells from regenerated BM compared to stromal cells from normal BM. In contrast, when we analyzed the morphology of endothelial cells following fracture, we found a significant increase in the number of arterioles, as well as irregular organization of sinusoids with high variability in sinusoid width. These data suggest that the sinusoidal niche for HSCs may be compromised in regenerated BM, and that the regrowth and remodeling of blood vessels in the BM is a limiting factor for the proper resumption of hematopoiesis following fracture.

***Disclosures: Elise Jeffery**, None*

FRI-183

PTH Stimulates Osteoblast Secretion of Slit3 to Repel Aberrant Vertebral Innervation and Relieve Low Back Pain Associated with Spinal Degeneration
*Weixin Zhang[1], Arryn Otte[2], Sisir Kumar Barik[3], Mei Wan[2], Xu Cao[2], Janet Crane[2]. [1]Johns Hopkins university, , [2]Johns Hopkins University, United States, [3],

Low back pain (LBP) is the leading cause of disability globally, affecting one out of every four people. Nonspecific LBP is associated with spinal degeneration, particularly with vertebral endplate bone expansion and sclerosis. We have analyzed two mouse models with spinal degeneration, aging mice and lumbar spine instability (LSI) and found that parathyroid hormone (PTH) treatment reduced vertebral endplate sclerosis and improved pain behaviors. Most notably, porosity of the vertebral endplate significantly decreased while the tolerance of mechanical pressure significantly increased in PTH treated (40 μg/kg/day) groups relative to the vehicle groups in both aging mice and wild type (WT) LSI mice. Aberrant innervation noted in the vertebral body and endplate during spinal degeneration was reduced with PTH treatment as quantified by PGP9.5+ nerve fibers. Beta-3tubulin+ and CGRP+ neurons also significantly decreased in dorsal root ganglion within PTH treatment relative to vehicle control in both mice models. To explore the mechanism of PTH-reduction of innervation, we screened multiple axon guidance cues. The neuronal repulsion factor Slit3 significantly increased in the endplate after PTH treatment in WT LSI model. E47 and Foxa2, two transcription factors of Slit3, were significantly increased after PTH treatment (100 nmol for 3 days) in MC3T3 cells with osteoblast differentiation inducible culture medium. CHIP assay further indicated that the expression of Slit3 was significantly increased by Foxa2 with PTH stimulation in vitro. In vivo models deleting PTH type 1 receptor (PPR) in osteoblasts (OsteocalcinCrePPRf/f LSI mice) prevented PTH-reduction of endplate porosity and improvement in pressure tests, whereas PPR deletion in chondrocytes (Col2aCreERt2P-PRf/f LSI mice) continued to improve to PTH in regard to porosity and pressure tests. Furthermore, deletion of Slit3 in osteoblasts (OsteocalcinCreSlit3f/f LSI mice) did not differ between PTH and vehicle treatment in regard to total endplate porosity nor pressure test. Altogether, PTH stimulates Slit3 to repel sensory nerve innervation and provides symptomatic relief of LBP associated with spinal degeneration.

***Disclosures: Weixin Zhang**, None*

FRI-312

In vivo stimulation of Tfeb, a master regulator of autophagy and lysosomal biogenesis, via in vivo CRISPR activation increases bone mass and strength
*Alicen James[2], James Hendrixson[2], Ilham Kadhim[2], Jacob Laster[2], AMY SATO[3], Stuart Berryhill[2], Julie Crawford[2], Melda Onal[2]. [2]University of Arkansas for Medical Sciences, , [2]University of Arkansas for Medical Sciences, United States, [3]UAMS, United States

Autophagy is a recycling pathway in which cellular components, including damaged or dysfunctional proteins, protein aggregates, and organelles are delivered to lysosomes for degradation. Reduction or insufficiency of autophagy is thought to contribute to a number of skeletal diseases such as skeletal aging. Accordingly, elimination of autophagy from the entire osteoblast lineage or only from osteocytes reduces osteoblast number, decreases bone formation, and causes low bone mass. However, whether increasing autophagy in osteoblast lineage cells is beneficial for bone health under physiological or pathological conditions is unknown. To address this, we generated a novel model to increase endogenous Tfeb expression in the osteoblast lineage. Transcription factor EB (Tfeb) is a master transcriptional regulator of autophagy and lysosomal biogenesis. Consistent with this, Tfeb overexpression (OE) induces autophagy in cultured osteoblasts. We stimulated expression of the endogenous Tfeb gene in osteoblast lineage cells of mice via in vivo CRISPR activation. Specifically, we expressed a sgRNA targeting the Tfeb transcription start site from the Rosa26 locus and activated a dCas9::SPH transgene using the Osx1-Cre transgene. This maneuver increased Tfeb expression 2.5-fold in RNA isolated from whole bones. At 8 weeks of age, the skeletal phenotype of mice overexpressing Tfeb was similar to littermate controls. However, at 4 months of age, Tfeb overexpressing male mice displayed increased femoral and vertebral cortical thickness. Histological analysis revealed that the increase in femoral cortical thickness was due to increased bone formation. Tfeb OE was also anabolic for femoral and vertebral cancellous bone. Analysis of osteoblast and osteoclast marker gene expression in lumbar vertebrae revealed that the anabolic impact of Tfeb OE was associated with high bone turnover. Moreover, the anabolic actions of Tfeb OE were sufficient to elevate bone strength as determined by femoral three-point bending analysis. Similar to males, serial BMD measurements of female mice showed that Tfeb OE in the osteoblast lineage also increases bone mass of female mice. Moreover, the high bone mass of female mice became more pronounced between 3 to 8 months of age. In conclusion, Tfeb overexpression in osteoblast lineage cells is anabolic and results in mechanically stronger bones and may represent an effective approach to combat age-associated bone loss.

***Disclosures: Alicen James**, None*

FRI-341

Osteoclast-specific Deletion of ?2-Adrenergic Receptor Limits Trabecular Bone Acquisition in Male, but not Female Mice
*Rebecca Peters[3], Ryan Neilson[2], Hannah Feliciano[3], Katherine Motyl[4]. [3]MaineHealth Institute for Research, , [2]MMCRI, United States, [3]MaineHealth Institute for Research, United States, [4]MaineHealth, United States

The sympathetic nervous system (SNS) is important for maintenance of bone homeostasis through ?-adrenergic signaling. Our lab and others found that osteoclasts are direct targets of the SNS, and that ?-blockers limit osteoclast differentiation. Osteoclasts express both ?1- and ?2-adrenergic receptor (?2AR), but ?2AR is more highly expressed. To directly examine the effects of ?2AR on osteoclasts, we developed an osteoclast-specific ?2AR knockout mouse model. Adrb2fl/fl mice were crossed with the myeloid lineage specific Lyz2Cre/Cre (a.k.a. LysM-Cre) mice. We tested the efficiency of deletion with Adrb2fl/fl-Lyz2Cre/+ (Cre/+) and Adrb2fl/flLyz2Cre/Cre (Cre/Cre) mice and found deletion of Adrb2 was comparable in both using gene expression and in situ hybridization in the distal femur. Using μCT, we measured the bone microarchitecture of wildtype (+/+) and Cre/+ male and female mice at 8 and 26 weeks of age (N=7-10). In male mice with the deletion, L5 vertebrae trabecular bone parameters (BV/TV, BMD, Tb.Th) were significantly lower. Distal femur trabecular BMD was reduced by 10% and SMI was elevated by 35% in Cre/+ compared to +/+ ($p<0.05$). Cortical bone (Ct.Ar/Tt.Ar, Ct.TMD) tended to be lower in Cre/+ mice ($p<0.09$). Both osteoclast and osteoblast marker genes were reduced in tibia, including Acp5, Alpl, Col1a1 and Tnfsf11 (Rankl). Although no changes in serum CTX-1 or P1NP were observed in untreated mice, ?2AR deletion in osteoclasts attenuated the elevated CTX-1 caused by the ?2AR agonist salbutamol (N=3, $p=0.031$). The low bone mass phenotype subsided by 26 weeks, suggesting age-related bone loss is unaffected by Adrb2 deletion in osteoclasts in male mice. Female mice had no significant changes in bone microarchitecture or serum bone remodeling markers at 8 or 26 weeks of age. Although global deletion of Adrb2 has been reported to cause a high bone mass phenotype, our work indicates that ?2AR function in bone is sex, age, cell-type, and stress dependent. We have also found that ?2AR deletion in osteoclasts may have indirect effects on osteoblast function, indicated by lower osteoblast marker gene expression. Future studies will examine this using osteoblast culture and co-culture studies with osteoclasts. These studies will aid in our understanding of mechanisms through which stress and ?-blockers influence bone density, which may inform osteoporosis prevention and treatment strategies.

***Disclosures: Rebecca Peters**, None*

FRI-350

Interventional and integrative subcellular sequencing (i2scseq) clarifies the multi differentiation stages embedded inside mature osteoclast *Hiroyuki Okada[1], Yuta Terui[2], Yasunori Omata[3], Masahide Seki[4], Shoichiro Tani[5], Junya Miyahara[6], Kenta Makabe[6], Asuka Terashima[7], Sanshiro Kanazawa[8], Masahiro Hosonuma[9], Shoko Onodera[10], Fumiko Yano[11], Hiroyuki Kajiya[12], Taku Saito[6], Yutaka Suzuki[4], Koji Okabe[12], Roland Baron[13], Sakae Tanaka[6], Ung-il Chung[14], Hironori Hojo[14]. [1]Center for Disease Biology and Integrative Medicine, Graduate school of Medicine, the University of Tokyo; Department of Orthopaedic Surgery, the University of Tokyo; Department of Oral Medicine, Infection, and Immunity, Harvard School of Dental Medicine, Japan. [2]Department of Single Cell Solution, Product Strategy Department, Marketing Center, Life Business HQ, Yokogawa Electric Corporation, Japan. [3]Department of Orthopaedic Surgery, the University of Tokyo; Bone and Cartilage Regenerative Medicine, the University of Tokyo Hospital, Japan. [4]Department of Computational Biology and Medical Sciences, Graduate School of Frontier Sciences, the University of Tokyo, Japan. [5]Center for Disease Biology and Integrative Medicine, Graduate school of Medicine, the University of Tokyo, Japan. [6]Department of Orthopaedic Surgery, the University of Tokyo, Japan. [7]Bone and Cartilage Regenerative Medicine, the University of Tokyo Hospital, Japan. [8]Department of Oral and Maxillofacial Surgery, Graduate School of Medicine, the University of Tokyo, Japan. [9]Department of Clinical Immuno Oncology, Clinical Research Institute for Clinical Pharmacology and Therapeutics, Showa University; Showa University Pharmacological Research Center, Japan. [10]Department of Biochemistry, Tokyo Dental College, Japan. [11]Department of Biochemistry, Showa University School of Dentistry, Japan. [12]Department of Physiological Science and Molecular Biology, Fukuoka Dental College, Japan. [13]Department of Oral Medicine, Infection, and Immunity, Harvard School of Dental Medicine, United States. [14]Center for Disease Biology and Integrative Medicine, Graduate school of Medicine, the University of Tokyo; Department of Bioengineering, Graduate School of Engineering, the University of Tokyo, Japan

The transcriptome at single-cell resolution clarifies the diversity of cell populations. Single-cell RNA-seq (scRNA-seq) has already been adopted for giant cells such as osteoclasts (OCs) (Omata, Okada, JBMR plus 2022). Although large OCs could not pass through a fluid-based cell dissociation device because of their diameter, acid-producing mature OCs were captured using conventional scRNA-seq.At ASBMR 2022, we presented intra-single cell sequencing (iSCseq) (Okada, bioRxiv 2022). iSCseq is a combinatorial method of high-resolution confocal imaging, picking of intracellular components, including a single nucleus, using the Single CellomeTM System SS2000 (Yokogawa, Japan), and next-generation sequencing at high resolution for mRNA. Our previous results showed that individual nuclei within the same cell are heterogeneous in terms of gene expression.The next version of iSCseq called i2scseq (interventional and integrative subcellular sequencing) can also collect cytoplasm in a small ordinary cell with a 3um probe and capture the living subcellular transcriptome. The average number of genes per cell detected by a 10um probe is much higher, and one by a 3um is equivalent to traditional fluid-based sequencing.i2scseq was used for the in vitro lineage of cells differentiating into OCs. i2scseq clarified that some small cells, which were not morphologically regarded as OCs, were classified into the final cluster of lineages, and vice versa, that giant OC contain immature nuclei in terms of gene expression. With integrative analysis of i2scseq and fluid-based sequencing datasets using a deep machine learning method, large OCs have embedded components at many stages of differentiation.i2scseq clarified the subcellular heterogeneity of mature OCs at a higher resolution than previous iSCseq. We partially solved the question of why conventional scRNA-seq has captured so-called mature OCs. i2scseq is expected to be a core method in cell biology.

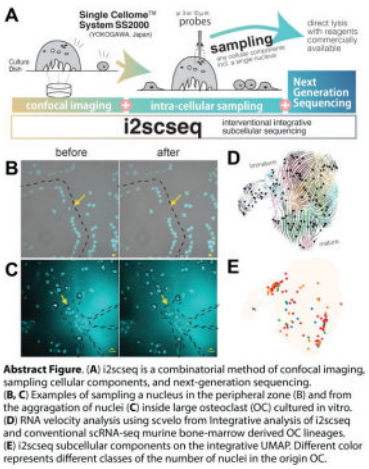

Abstract Figure. (**A**) i2scseq is a combinatorial method of confocal imaging, sampling cellular components, and next-generation sequencing. (**B, C**) Examples of sampling a nucleus in the peripheral zone (**B**) and from the aggregation of nuclei (**C**) inside large osteoclast (OC) cultured in vitro. (**D**) RNA velocity analysis using scvelo from Integrative analysis of i2scseq and conventional scRNA-seq murine bone-marrow derived OC lineages. (**E**) i2scseq subcellular components on the integrative UMAP. Different color represents different classes of the number of nuclei in the origin OC.

***Disclosures: Hiroyuki Okada**, None*

FRI-402

Estimating 'Skeletal Age' by Bone Loss in Elderly Men and Women *Ngoc Huynh[1], Krisel De Dios[1], Thach Tran[1], Tuan Nguyen[2]. [1]University of Technology Sydney, Australia. [2]University of Technology Sydney , Australia

Background and Aim: Skeletal Age is defined as the age of the skeleton as a result of a fracture or exposure to risk factors that elevate the risk of fracture. Higher rates of bone loss are associated with an elevated risk of both fracture and mortality. In this study, we aimed to assess the impact of bone loss on bone fragility by estimating skeletal age using bone loss in elderly men and women. Methods: We analyzed the data from the Study of Osteoporosis Fracture (SOF) and Osteoporotic Fractures in Men (MrOS) that included 9704 women and 5994 men aged 64 years and above. Bone mineral density (BMD) at the femoral neck was measured at baseline and subsequent visits. Mortality was ascertained from death certificates and hospital records. We limited the analysis to those with at least 3 BMD measurements (3848 women and 2925 men). The linear regression model was used to estimate the rate of change in BMD for each individual. The multivariable Cox's proportional hazard model was used to quantify the contribution of the rate of BMD change to mortality, adjusted for age, body mass index, smoking status, alcohol consumption, dietary calcium intake, estrogen and bisphosphonate treatment. The magnitude of the association between bone loss and mortality was then transformed into the number of years of life lost using Gompertz's law of mortality and the US life table. Skeletal age is then determined by the sum of chronological age and years of life lost. Results: In women, the average rate of change in femoral neck bone mineral density (BMD) was found to be -0.61 +/- 1.2% [mean+/-SD] per year, while in men, it was -0.16 +/- 0.9% per year. Throughout the study, 1942 women and 1949 men died. For women, each standard deviation [SD] increase in femoral neck BMD loss was linked to a 1.2-fold (95%CI, 1.1-1.3) increase in total mortality, while for men, the increase was 1.4-fold (95%CI, 1.35-1.5) after adjusting for age, baseline FNBMD, BMI, smoking and drinking status. Additionally, each SD increase in bone loss was associated with a loss of 1.9 years and 3.5 years of life in women and men, respectively. For the same rate of bone loss, men experienced a more substantial loss of years of life than women. Moreover, a 60-year-old woman with a femoral neck BMD loss of more than 2% is estimated to have a skeletal age of 63.5 years. Conclusion: In elderly men and women, excess bone loss is associated with an increased loss of years of life and accelerated bone fragility.

***Disclosures: Ngoc Huynh**, None*

FRI-455

Influence of age on the efficacy of pharmacologic treatments on fracture risk reduction and increases in BMD: Results from the FNIH-ASBMR SABRE Project *Marian Schini[2], Tatiane Vilaca[2], Eric Vittinghoff[3], Lui Li-Yung[4], Susan Ewing[3], Douglas Bauer[5], Dennis Black[6], Mary Bouxsein[7], Richard Eastell[2]. [2]University of Sheffield, . [2]University of Sheffield, United Kingdom. [3]Department of Epidemiology & Biostatistics, University of California, San Francisco, San Francisco, CA, USA, United States. [4]Research Institute, California Pacific Medical Center, San Francisco, CA, USA , United States. [5]University of California, San Francisco, United States. [6]UC San Francisco, . [7]Beth Israel Deaconess Medical Center, Harvard Medical School, United States

PurposeAntiosteoporosis medications are given to individuals of various ages, but we do not know whether the effect is similar in different age groups. The aim of this study was to use data from key trials of antiosteoporosis medications to determine whether the anti-fracture efficacy or BMD changes associated with treatment differ in people above and below 70 years. The threshold was set at this age as it gave similar numbers of subjects in the studies with vertebral fracture as the endpoint.MethodsWe used individual patient data from 23 randomised placebo-controlled clinical trials of antiosteoporosis medications. Data were stratified by age (<70 and >=70 years old), and the treatment-related fracture risk reduction was estimated in each subgroup, using logistic regression for morphometric vertebral fractures and Cox regression for all clinical, non-vertebral, hip and "all" (combination of non-vertebral and clinical or morphometric vertebral fractures) fractures. The treatment effect on 24-month change in BMD was estimated in each subgroup using linear regression. We performed analyses on all trials, and again separately on trials of bisphosphonates only. We tested the interaction between age subgroup and treatment in all analyses.ResultsThese analyses included 123,164 participants; 57% 0.05) (Figure). The use of antiosteoporotic drugs in people aged 70 and older resulted in significantly greater absolute and percent increases in BMD at 24 months at the total hip (3.8% [3.7, 3.9] vs. 3.1% [3.0, 3.2]), femoral neck (3.4% [3.3, 3.5] vs. 3.0% [2.9, 3.1]) and lumbar spine ((4.4% [4.2, 4.5] vs. 3.9% [3.8, 4.0]) (all p<0.0001).ConclusionsIn summary, antiosteoporotic medications reduced the risk of fractures similarly among those above and below 70 years of age but were more effective at increasing BMD among those at least 70 years.

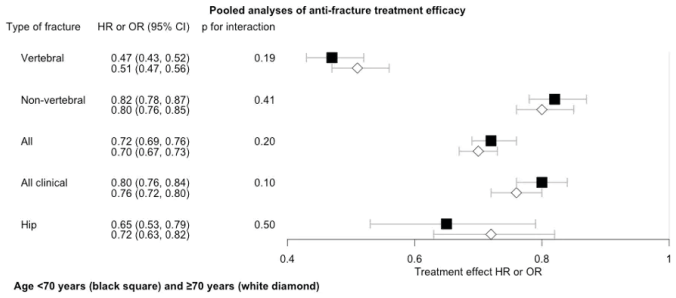

***Disclosures: Marian Schini**, None*

FRI-577

Type 2 Diabetes is Associated with Better Bone Microarchitecture, higher BMD, but Impaired Physical Function and Increased Risk of Incident Fracture in Older Swedish Women from the SUPERB study. *Lisa Johansson[1], Kristian Axelsson[2], Mattias Lorentzon[3], Henrik Litsne[4], Michail Zoulakis[5]. [1]Institute of medicine, , [2]Institute of Medicine, Sahlgrenska Academy, Gothenburg University, , [3]Sahlgrenska Academy, University of Gothenburg, Sweden, [4]Sahlgrenska Osteoporosis Centre,University of Gothenburg, , Sweden, [5]Sahlgrenska Osteoporosis Centre, Institute of Medicine,University of Gothenburg, Sweden

Several studies have shown that type 2 diabetes mellitus (T2DM) is associated with incident fracture, but it is not clear if the risk increase is due to impaired bone microarchitecture, low bone material strength index (BMSi) or poor physical function. The aim of this study was to determine if T2DM is associated with bone microarchitecture, BMSi, physical function, and risk of incident fracture in older Swedish women.In total, 3028 Swedish women, 75-80 years old were included in the prospective SUPERB study. At baseline, information on clinical risk factors (CRFs) was collected using questionnaires. Bone mineral density (BMD) was measured with dual-energy X-ray absorptiometry, bone microarchitecture with HR-pQCT (XtremeCT), and BMSi obtained using the Osteoprobe device (n=630). Physical function was assessed using timed up and go (TUG), one leg standing (OLS), grip strength, chair stand test and by measurements of gait speed. Data on incident fractures were retrieved from a regional x-ray archive.At baseline, the 294 women with T2DM were compared to women (n=2714) without diabetes. Women with T2DM had higher BMD at all sites (total hip 4.7%, femoral neck (FN) 3.9% and lumbar spine L1-L4 5.4%, all p<0.01) than women without. At the ultradistal tibia, T2DM women had a greater cortical area (7.3%, p<0.01) and density (1.2%, p=0.03), as well as higher trabecular bone volume fraction (8.6%, p<0.01). There was no difference in BMSi between groups (n=630; T2DM 77.8+/-8.1 vs. controls 78.1+/-7.3, p=0.81). Women with T2DM performed significantly worse on all physical function tests than their non-diabetic controls. For example, grips strength was 10.1% lower, gait speed 10.2% slower, and TUG time 13.1% (p<0.001 for all comparisons) slower in women with T2DM than in those without.During 7.3 (4.4, 8,4) years (median (IQR) of follow-up there were 1071 incident any fractures, 797 major osteoporotic fractures (MOF), and 232 hip fractures. In adjusted (for age, BMI, FRAX CRFs and FN BMD) Cox regression models T2DM was associated with an increased risk of any fracture (HR 95% CI 1.26 [1.04-1.53], but the associations with MOF (HR 1.16 [0.92-1.46]) or hip fracture (HR 1.31 [0.85-2.00]) did not reach statistical significance.In conclusion, older women with T2DM have considerably better bone microarchitecture, and no different BMSi, but substantially poorer physical function than nondiabetic women, which could be the principal reason for the increased fracture risk observed in T2DM women.

***Disclosures: Lisa Johansson**, None*

FRI-001

Automated immunohistochemistry for TRAcP facilitates osteoclast detection and counting for bone histomorphometry: A validation study *Marie-Josée Bégin[1], Natalie Dion[2], Louis-Georges Ste-Marie[1]. [1]Division of Endocrinology, Department of Medicine, Centre hospitalier de l'Université de Montréal, Université de Montréal, Canada, [2]Department of Pathology, Centre hospitalier de l'Université de Montréal, Université de Montréal, Canada

Histomorphometric analysis of undecalcified bone specimens is the gold standard for diagnosis of complex bone disorders. This analysis requires the measurement of many variables, including osteoclasts (Oc) count per bone perimeter (N.Oc/B.Pm). Oc are identified by their morphology and multinuclearity on Goldner's trichrome stained (GTS) sections. To facilitate Oc count, histological sections are stained by an enzymatic histochemical reaction (EHR) of Tartrate Resistant Acid Phosphatase (TRAcP), an Oc biomarker. This technique has certain limitations including the possible alteration of enzymatic activity by bone tissue preparation with ethanol fixation and methyl methacrylate embedding (EFMMAE). In pathology laboratories, biomarkers such as TRAcP are routinely detected by automated immunohistochemistry technique (AIHC) performed on sections of formalin-fixed and paraffin-embedded (FFPE) of decalcified bone biopsies. We aim to validate the use TRAcP detection by AIHC on sections of undecalcified bone tissue EFMMAE in order to improve Oc identification and counting. To this end, transiliac bone biopsies from 20 adult patients (68.7 +/- 8.7 yo) affected by various metabolic bone diseases were studied. AIHC was performed with a Ventana BenchMark ULTRA system (Roche-Diagnosis) using mouse monoclonal antibody for TRAcP (clone 9C5) on deplastified sections with a protocol usually used for FFPE tissue. Osteoclastic detection by AIHC was confirmed by GTS on consecutive sections (Figure 1), as well as with EHR TRAcP and with AIHC Cathepsin K. The AIHC TRAcP showed a strong positive correlation with N.Oc/B.Pm measurements on GTS (r=0.90), as well as with bone formation rate per bone surface (BFR/BS) (r=0.84). Interestingly, there was a significantly greater detection of Oc with AIHC than with GTS (p<0.001). Furthermore, the difference in Oc counts between the two methods was significantly higher in high turnover states compared to low turnover (p=0.021). Taken together, this study validates the use of AIHC TRAcP on undecalcified bone tissue EFMMAE as an effective technique for Oc detection and outperformed Oc count by standard GTS method, especially in the high turnover states. AIHC should be considered as an alternative and easier method to EHR TRAcP. To our knowledge, this is the first time that AIHC has been successfully performed on undecalcified bone tissue EFMMAE, paving the way for the detection of other cellular biomarkers for clinical purposes.

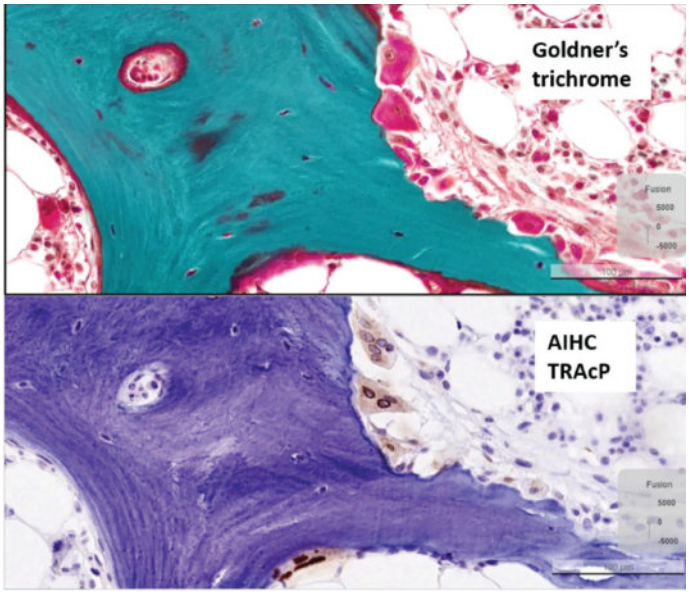

***Disclosures: Marie-Josée Bégin**, None*

FRI-005

Effectiveness of Asfotase Alfa for Treatment of Adults With Hypophosphatasia: Results from a Global Registry *Priya S. Kishnani[1], Gabriel Ángel Martos-Moreno[2], Agnès Linglart[3], Anna Petryk[4], Andrew Messali[4], Shona Fang[4], Cheryl Rockman-Greenberg[5], Keiichi Ozono[6], Wolfgang Högler[7], Lothar Seefried[8], Kathryn M. Dahir[9]. [1]Duke University Medical Center, United States, [2]Hospital Infantil Universitario Niño Jesús, IIS La Princesa, Universidad Autónoma de Madrid, CIBERobn, ISCIII, Spain, [3]Paris-Saclay University, AP-HP and INSERM, France, [4]Alexion, AstraZeneca Rare Disease, United States, [5]University of Manitoba, Canada, [6]Osaka University, Japan, [7]Johannes Kepler University Linz, Austria, [8]University of Würzburg, Germany, [9]Vanderbilt University Medical Center, United States

Objectives: To assess asfotase alfa's effectiveness on mobility, functional status, quality of life (QOL), and pain in adults with hypophosphatasia (HPP).Methods: Patients enrolled in the Global HPP Registry (NCT02306720; EUPAS13514) who had an alkaline phosphatase below the LLN for age and sex and/or a documented ALPL gene variant, initiated asfotase alfa at age >=18 years, and been treated for >=6 months at last follow-up were included. Outcomes were evaluated as mean change from mean baseline (BL) value through 36 months; assessments were not performed at all timepoints for all patients.Results: Among included patients (N=190), median age at treatment start was 45.5 years; 91.1% were characterized as having pediatric-onset HPP. 6MWT distance walked was 404 m (n=31) at BL and improved over time vs BL (change: 93 m at 12 months [95%CI: 47, 138; n=18], 62 m at 24 months [95%CI: 0, 124; n=15], and 45 m at 36 months [95%CI: ?83, 172; n=7]). The SF36v2 Physical Component Summary score was 35.7 (n=48) at BL and improved over time (change: 4.68 at 6 months [95%CI: 0.16, 9.21; n=34], 4.61 at 12 months [95%CI: 1.02, 8.19; n=28], 4.94 at 24 months [95%CI: ?2.23, 12.11; n=22], and 5.13 at 36 months [95%CI: ?0.96, 11.21; n=21]). SF36v2 Mental Component Summary score improvements were not statistically significant at all timepoints. Health Assessment Questionnaire-Disability Index

scores were generally unchanged over time. Self-reported Brief Pain Inventory Short Form scores improved at all timepoints from a BL of 4.86 (change: ?0.72 at 6 months [95%CI: ?1.23, ?0.21; n=38], ?1.07 at 12 months [95%CI: ?1.62, ?0.52; n=31], ?1.13 at 24 months [95%CI: ?1.76, ?0.51; n=26], and ?0.97 at 36 months [95%CI: ?1.70, ?0.24; n=23]). The most common AEs were injection site reactions and injection-associated reactions, occurring in 29 (13.4%) and 13 (6.0%) patients, respectively. Eleven serious AEs related to asfotase alfa were reported in 7 patients.Conclusion: Adults with HPP who received asfotase alfa for >=6 months experienced improvements in mobility, physical function, QOL, and pain, which were maintained over 3 years of follow-up.

***Disclosures: Priya S. Kishnani**, Alexion, AstraZeneca Rare Disease, Grant/Research Support, Alexion, AstraZeneca Rare Disease, Consultant, Alexion, AstraZeneca Rare Disease, Other Financial or Material Support*

FRI-006

Mobility and Health-related Quality of Life in Adults with Pediatric-onset Hypophosphatasia Treated With Asfotase Alfa: Interim Analysis From the UK Managed Access Agreement *Katie E. Moss[1,] Richard Keen[2,] Shona Fang[4,] Alexandros Zygouras[4,] Muhammad Javaid[5,] Tarekegn Geberhiwot[6,] Kenneth Poole[7,] Peter Selby[8,] Jennifer S. Walsh[9,] Judith S. Bubbear[2,] [1]St. George's University Hospitals, United Kingdom, [2]Royal National Orthopaedic Hospital, United Kingdom, [4]Alexion, AstraZeneca Rare Disease, United States, [4]Alexion, AstraZeneca Rare Disease, United Kingdom, [5]Oxford University, United Kingdom, [6]Queen Elizabeth Hospital, United Kingdom, [7]Cambridge NIHR Biomedical Research Centre, Addenbrooke's Hospital; University of Cambridge, United Kingdom, [8]Manchester Royal Infirmary, United Kingdom, [9]University of Sheffield, United Kingdom

Background: Asfotase alfa is a tissue-nonspecific alkaline phosphatase enzyme replacement therapy used to treat hypophosphatasia (HPP). Data describing effects of asfotase alfa on mobility, pain, and health-related quality of life (HRQoL) in adults with HPP are limited. Methods: This analysis used data from the UK Managed Access Agreement to assess mobility and HRQoL in adults with pediatric-onset HPP treated with asfotase alfa. Data were collected at enrollment, 3 and 6 months after enrollment, and every 6 months thereafter. All adults initiated asfotase alfa treatment after enrollment. Interim results are presented as median (min, max; n); change from baseline to Month 24 is reported as median (95% confidence interval).Results: Of 25 adults enrolled, 17 with >6 months of exposure were included in the study population (12 women, 5 men); 21 who received >=1 dose of asfotase alfa were evaluated for safety. Age at enrollment was 44.0 (22.0, 60.0) years. Treatment duration was 1.5 (0.5, 3.2) years. Bleck score improved from a baseline of 6.0 (2.0, 9.0; n=17) by 2.0 (1.3, 2.7; n=8). The 6-Minute Walk Test distance walked improved from a baseline of 130.0 (28.0, 360.0; n=10) by 160.0 (2.5, 290.9; n=5) meters. Pain severity score improved from a baseline of 8.0 (4.3, 10.0; n=16) by ?3.2 (?5.6, 0.9; n=7). EQ-5D-3L utility score improved from a baseline of 0.1 (?0.3, 0.5; n=17) by 0.3 (0.1, 0.5; n=8). Of 13 adults prescribed opioids, 2 stopped and 5 reduced use after starting asfotase alfa. One vertebral (1 patient) and 2 metatarsal (1 patient) fractures occurred 1 week and 13.5 months, respectively, after initiating asfotase alfa. Serious adverse events were infrequent (n=3, 4 events), with 2 events related to asfotase alfa (injection site reaction, dysesthesia; Figure). No patients discontinued asfotase alfa.Conclusion: asfotase alfa improved mobility, pain, and HRQoL in adults with pediatric-onset HPP, with a favourable benefit/risk profile.

	Any		Related to AA Treatment		Not Related to AA Treatment	
	Patients, n (%)	Total Events	Patients, n (%)	Total Events	Patients, n (%)	Total Events
Adverse events of special interest	12 (57.1)	30	12 (57.1)	28	1 (0.05)	2
Injection-associated reaction	3 (14.3)	4	2 (9.5)	2	1 (4.8)	2
Injection-site reaction	12 (57.1)	25	12 (57.1)	25	0 (0)	0
Medication error	1 (4.8)	1	1 (4.8)	1	0 (0)	0
Serious adverse events	3 (14.3)	4	2 (9.5)	2	2 (9.5)	2
Femur fracture (right)	1 (4.8)	1	0 (0)	0	1 (4.8)	1
Dysesthesia	1 (4.8)	1	1 (4.8)	1	0 (0)	0
Flank pain	1 (4.8)	1	0 (0)	0	1 (4.8)	1
Injection-site reaction	1 (4.8)	1	1 (4.8)	1	0 (0)	0

***Disclosures: Katie E. Moss**, Alexion, AstraZeneca, Other Financial or Material Support*

FRI-009

Abdominal aorta calcification detected on vertebral fracture assessment DXA scans and all-cause and cardiovascular mortality in adults. *Carlos Orces[1,] [1]Laredo Medical Center,

Objective: Abdominal aorta calcification (AAC) is a well known risk factor of cardiovascular events and mortality. Whether AAC detected on vertebral fracture assessment DXA scans is associated with all-cause and cardiovascular mortality has not been extensively studied. Methods: The present study was based on data from participants aged 50 years and older in the National Health and Nutrition Examination Survey cycle 2013-2014. Vertebral fracture assessment on lateral spine scans was conducted using Hologic Discovery model A densitometers (Hologic, Inc., Marlborough, Massachusetts), which also provided AAC measurement for L1-L4. The AAC8 score was used to estimate the total length of calcification of the anterior and posterior aortic walls in front of the spine L1-L4. The AAC8 scores were grouped into "0" if no calcification was seen; "1" if the calcification was equal to the height of one vertebra or less; "2" if the length of calcification was more than one but less than or equal to the height of two vertebrae; >= 3 if calcification occurred in more than two vertebrae. Mortality was examined using the NHANES 2019 public-use linked mortality files. Time to death was calculated in months. Results: A total of 2,243 participants with a mean age of 63.0 (SE 0.2) years comprised the study sample. During a median follow up of 71 months, a total of 256 (9.3%) participants died. Of those, 84 (32.8%) deaths occurred from cardiovascular diseases. As shown in Figure 1, the proportion of subjects with AAC8 >= 3 score had significantly lower survival than their counterparts with minor AAC8 scores. Moreover, survival across AAC8 scores diverged about 40 months into the study. Adjusted Cox proportional hazards regression demonstrated that participants with AAC8 >= 3 score had 1.8 times higher risk of all-cause mortality than those with AAC8 = 0 (HR 1.82; 95% CI, 1.15 to 2.89; p < .05). Similarly, the risk of cardiovascular mortality was 1.5-fold higher in participants with AAC8 score >= 3 thant those without calcification. However, this association did not reach statistical significance (HR 1.57; 95% CI, 0.80 to 3.10; p = .018).Conclusions: AAC severity detected on vertebral fracture assessment DXA scans was associated with increased risk of all-cause mortality in a nationally representative sample of U.S. adults.

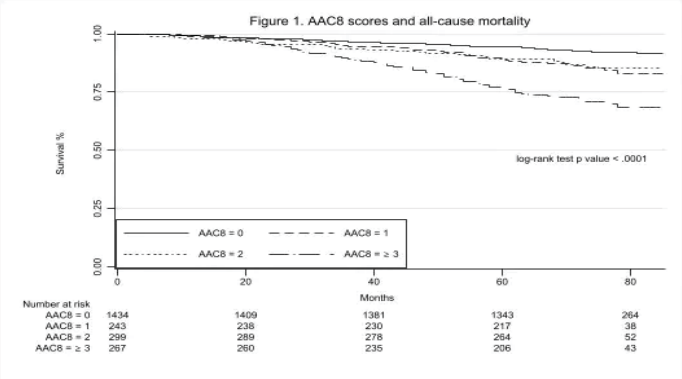

***Disclosures: Carlos Orces**, None*

FRI-011

A single infusion of Zoledronic acid suppressed bone turnover markers for up to seven years: Results from the Zoledronate in the Prevention of Paget's disease (ZiPP) study. *Jonathan Tang[1,] William Fraser[1,] Jonathan Phillips[2,] Isabelle Piec[1,] Rachel Dunn[1,] Catriona Keerie[2,] Steff Lewis[2,] Stuart Ralston[2,] ZiPP inverstigators[2,] [1]University of East Anglia, United Kingdom, [2]University of Edinburgh, United Kingdom

Background: Zoledronate in the Prevention of Paget's disease (ZiPP) trial (ClinicalTrials.gov ID: NCT03859895) is a multi-centre, double-blind, placebo-controlled, randomised trial of intravenous Zoledronic acid (ZA) in sequestosome 1 (SQSTM1) mutation carriers. SQSTM1 mutation has high penetrance and is associated with the early onset of Paget's disease of bone. Methods: Participants with the SQSTM1 genotype were randomised to receive either a single dose of 5mg zoledronic acid (Aclasta, Novartis); intervention group (n=111), age mean (range) 49.8 (32-74)yrs, or a placebo (n=111), 50.5 (32-75)yrs, by intravenous infusion. Serum samples collected were rapidly centrifuged and stored frozen for bone markers CTX (resorption), PINP (formation) and BSALP (osteoblasts activity) every 12 months from baseline for five years and at end-of-study (EoS) 2-yr follow-up. Urine bone resorption marker uNTX and radionuclide bone scans were performed at baseline/EoS).Results: In the Intervention group, CTX and PINP showed respective decreases in serum concentrations of average -44.8% and -29.2% across all time points; the greatest reductions were observed at 12 mths (CTX -57.6%, PINP -46.7%), and remained below baseline concentrations to EoS (CTX -15.2%, PINP -20%). Serum BSALP showed a -20.9% decrease at 12 mths, then returned to baseline concentration at 36 mths. uNTX showed a -36% decrease at EoS. Treatment effect (zoledronate vs placebo) was highly significant for CTX and PINP (ANCOVA p<0.0001) and significant for BSALP (p=0.0005). Bone scans revealed ZA treatment effect was associated with lower risks of developing new bone lesions (odds ratio, 95% CI: 0.406,

0.0-3.425, p=0.246) and further activities of existing lesions in patients (0.083, 0.0-0.424, p=0.003).Conclusion: Our findings showed in SQSTM1 mutation carriers, a single treatment of 5mg ZA can achieve long-term suppression of bone resorption and formation markers for up to 7 years. ZA treatment is beneficial against the formation of bone lesions and improves outcome in patients with existing lesions. The different rates of decrease in bone markers offer insights into the bone remodelling process post ZA administration.

***Disclosures: Jonathan Tang**, None*

FRI-012

Assessment of Pain, Stiffness, and Physical Functioning Pre and During Burosumab Among Adults With X-linked Hypophosphatemia: Results from a Multinational, Long-term, Prospective Outcomes Disease Monitoring Program *Erru Yang[1], Zunqiu Chen[1], Joel Hetzer[1], Alison Skrinar[1]. [1]Ultragenyx Pharmaceutical Inc., United States

Purpose: Loss-of-function mutations in PHEX gene lead to excess FGF23 that in turn results in hypophosphatemia, leading to chronic debilitating musculoskeletal impairments in patients with X-linked hypophosphatemia (XLH). Treatments include burosumab, a fully-human monoclonal antibody to FGF23, or the combination of oral phosphate and active vitamin D (Pi/D). XLH symptoms in adults include bone/joint pain, stiffness, and fatigue. Previous research validated the Western Ontario and McMaster Universities Osteoarthritis Index (WOMAC) in adults with XLH. This study assesses burosumab impact on WOMAC among adults from an XLH Disease Monitoring Program (XLH-DMP; NCT03651505). Methods: The DMP is a 10-year study to collect real-world data on the safety and effectiveness of supportive care and burosumab for the treatment of XLH in adults and children. WOMAC has 24 items divided into three subscales: Pain (5 items), stiffness (2 items), and physical function (PF, 17 items). WOMAC scores collected from adults at enrollment were compared to scores obtained one year later for three cohorts: 1, burosumab-naïve at enrollment with burosumab dosed within 90 days post-enrollment; 2, burosumab-naïve at enrollment with burosumab dosed between 91-180 days post-enrollment; 3, no-burosumab at/before enrollment and during one year post enrollment.Results: As of February 2023, 30 and 14 burosumab-naïve and 55 no-burosumab patients from North America were selected into cohort 1, 2 and 3, respectively. Average WOMAC scores were 38, 52.1, 34 for pain, stiffness, and PF for cohort 1, and 40.7, 51.8, 37 for cohort 2, and 26.4, 36.6, 21.1 for cohort 3 at enrollment. At year 1, reduction of 11.8, 11.7 and 8 scores were observed in pain, stiffness, and PF for cohort 1; and reduction of 15.3, 13.4, and 9.1 were observed for cohort 2. No-burosumab cohort had minimal reduction of scores in pain (2.1) and PF (0.9), with 5-score reduction in stiffness.Conclusion: Adult patients with XLH who initiated burosumab within 180 days of DMP enrollment had worse pre-burosumab quality of life in terms of WOMAC scores in pain, stiffness and PF compared with patients without burosumab. Clinically meaningful improvement in pain (>9.7) and stiffness (>10) with burosumab were observed one year after DMP enrollment among adults with XLH and were consistent with results from a randomized, double-blind placebo-controlled registration study.

***Disclosures: Erru Yang**, Ultragenyx, Other Financial or Material Support*

FRI-026

Experimental and Computational Mechanics of Bone Fragility in Type-2 Diabetes: A Longitudinal Investigation using Zucker Diabetic Fatty (ZDF) Rats *Genna Monahan[1], Marissa Britton[1], Jessica Schiavi-Tritz[2], Ted Vaughan[1]. [1]Biomechanics Research Centre (BioMEC), School of Engineering, University of Galway, Ireland. [2]Université de Lorraine, CNRS UMR 7274, Nancy, France, France

While Type-2 Diabetes (T2D) is associated with an increased bone fracture risk, the pathophysiological factors that contribute to impaired bone biomechanics remain poorly understood. The objective of this study was to investigate biological, biophysical and biomechanical factors that contribute to bone fragility in T2D using a Zucker Diabetic Fatty (ZDF) rat.Femora and blood serum were collected from male [ZDF: fa/fa (T2D) and Lean: fa/+ (Control)] rats, euthanized at 12-, 26- and 46-wk of age (n = 7-9, per age, per condition). Serum markers such as HbA1c/ HbA1 and interlukin-6 (IL-6) and bone turnover markers such as sclerostin (Sost) and C-telopeptide of collagen alpha-I (CTX-I) were measured using ELISA kits. Fluorometric assays and high performance liquid chromatography were used to measure bulk AGEs and adducts carboxylmethyl-lysine (CML), respectively. Cortical and trabecular regions of bone were scanned using micro-computed tomography (micro-CT). Pre- and post-fracture scans of the right proximal femurs were imaged, while a region of cortical and trabecular bone from the distal metaphysis were imaged. Biomechanical analysis was carried out on the femora using a fracture toughness test and sideways fall configuration using a custom-built rig. Finally, image-based finite element models were generated to simulate the sideways fall test and prediction tissue-level stress/strain.Firstly, serum markers showed that the diabetic state disrupted normal bone homeostasis in 46-wk diabetic rats versus controls (HbA1c/ HbA1, 2-fold ?, IL-6, 2.3-fold ?), with possibly impaired osteoblast activity (Sost, 3.7-fold ?). Along with altered cellular activity, changes to the organic component of the bone matrix were shown to be affected, whereby CML, a non-fluorescent AGE trended towards an increase in the 46-wk diabetic rats than controls ($p = 0.07$). Micro-computed tomography (micro-CT) showed that diabetic rats had higher cortical porosity than controls ($p < 0.001$). Biomechanical fracture toughness testing revealed that the sub-tissue alterations lead to significant reductions in tissue-level cracking toughness (Tcr, 45.5% ?) and work-to-fracture (Wf, 31.6% ?) in 46-wk diabetic rats versus controls, highlighting that diabetic tissue has significantly reduced energy dissipation capacity. Overall, this study provides a novel insight into the pathophysiological mechanisms and sequence of events that lead to bone fragility in severe T2D in this ZDF rat model.

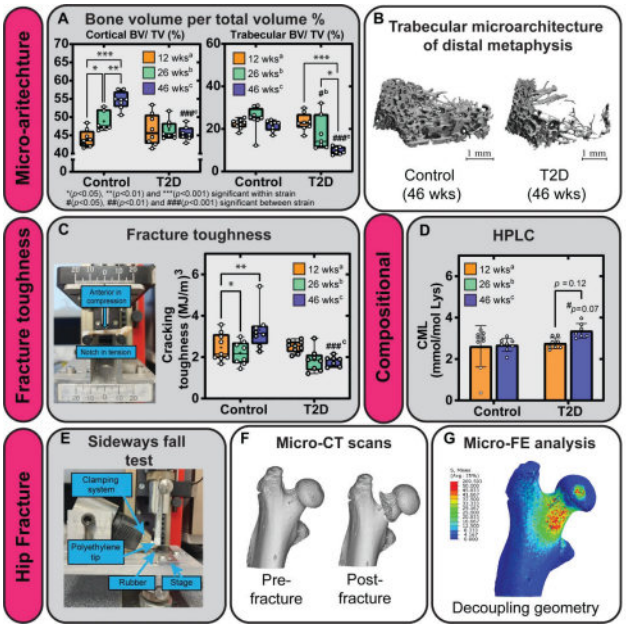

***Disclosures: Genna Monahan**, None*

FRI-030

Chromosomal sex (XX vs XY) contributes to bone and muscle mass independently of the gonadal sex (ovaries vs testis) in the 4 core genotype mouse model. *Lilian Plotkin[1], Matthew Arnett[2], Dyann Segvich[3], Padmini Deosthale[1], Chiebuka Okpara[4], JULIAN BALANTA-MELO[5], FABRIZIO PIN[6], Joseph Wallace[7]. [1]Indiana University School of Medicine, United States. [2]I, United States. [3]Indiana University-Purdue University Indianapolis, United States. [4]Lehigh University, United States. [5]Universidad del Valle, Colombia. [6], United States. [7]Indiana University Purdue University Indianapolis (IUPUI), United States

Vertebrate sexual dimorphism is ascribed to the presence of testis or ovaries, and, hence, to gonad-specific hormone production. Sex differences also stem from the presence of sex chromosomes (XX or XY). To tease out the contribution of chromosome (CS) from gonad (GS) sex, the Sry gene that dictates testis formation was either deleted in XY mice, resulting in XYF mice with ovaries or overexpressed in XX mice, resulting in XXM mice with testis. These mice, together with XY males (M) and XX females (F) form the 4core genotype (FCG) model. It has been shown that levels of estrogen in XXF/XYF and androgen in XXM/XYM are similar. We now show that the musculoskeletal phenotype of 2 and 4 month (m) FCG mice depends on both GS and CS. Mice were scanned for DXA, blood/tissues were collected, and bones were tested by µCT and 3-point bending. GS/CS effects were assessed by 2-way ANOVA (Tukey post-hoc test). GS influenced body weight (BW), and total/femur/spine BMD at 2m, and BW and total/femur BMD at 4m, all lower in gonadal females (Table1). A GS-CS interaction was found in 2m mouse spine BMD, which was lower in XYF than XYM, but similar in XXF and XXM mice. At 4m, XY mice show lower BW and BMD at the 3 sites than XX mice, whereas % lean mass was higher in XYM and XYF than the respective XX mice, and % fat mass was lower in XYM vs XXM, indicating CS effects (Table2). Skeletal muscle weights were lower in gonadal females (XXF/XYF) than in males (XXM/XYM) at 2m (Table3) whereas soleus muscle weight was higher in XYM than in XXM mice and no different in females. Fewer differences were found at 4m, with a CS-dependent effect in QC weight (higher in XXM than in XYM). µCT showed GS and CS contribution to structural parameters and TMD in femur mid-diaphysis -lower in XYF vs XXF, no different in males- whereas only GS affected marrow cavity and total tissue area and MOI at 4m (Table4). Bone mechanical properties were overall lower in gonadal females (Table5). CS only affected ultimate force - lower in XYF vs XXF, no different in males. GS affected all distal femur trabecular structural parameters, which were lower in gonadal females, but only partially L5 vertebrae (Table4). L5 tissue mineral density TMD depended on CS and was higher only in XXF vs XYF. Finally, GS and CS also affected serum chemokine levels, which might explain changes in bone and muscle cell function (Table6). Thus, while GS has a major role, CS is a so far unrecognized contributor to bone/muscle mass and bone strength.

Musculoskeletal phenotype of FCG mice at 2 and 4 months of age. Values indicate mean±sd, only parameters that are significantly different at least for one comparison are shown by 2-way ANOVA: @= gonadal sex effect; £= chromosome sex effect; &=G5xC5 interaction. Tukey post-hoc test: * p<0.05 vs corresponding gonadal sex, # p< 0.05 vs corresponding chromosome sex. Underlined bold corresponds to p<0.05 for gonadal female XX vs gonadal male XY.

		2months				4months				
	measurement	XXM	XXF	XYM	XYF	measurement	XXM	XXF	XYM	XYF
Table1. body weight (g) / bone mineral density (mg/cm³)	body weight @	25.1±2.9	**20.6±1.9***	**24.8±1.6**	19.3±1.5*	body weight (g) @£	32.7±3.5	**24.8±2.4***	**29.0±1.7 ***	23.3±1.8*
	total @	49.8±4.0	**46.8±1.9***	**50.0±2.7**	45.3±1.4*	total @ £	52.5±3.5	52.0±1.6*	52.4±2.3	49.5±1.6**
	femur @	69.4±7.2	**59.2±2.6***	**67.5±5.6**	56.2±3.1*	femur @ £	77.1±6.5	70.0±2.9*	73.8±5.1	63.4±3.3**
	spine @	53.9±5.1	54.2±2.8	56.1±3.2	51.4±3.2*	spine £	58.9±5.6	58.0±3.5	54.6±3.4	56.7±3.3
Table2. body composition (% body weight)	lean body mass	No significant differences				lean body mass £	76.6±5.0	**76.3±3.5**	**81.1±2.3#**	79.7±2.6#
	fat mass					fat mass £	21.9±5.2	**21.3±3.8**	**17.3±2.4#**	18.6±2.6#
Table3. skeletal muscle mass (muscles for both limbs combined, g)	EDL @	.02±.00	**.01±.00***	**.02±.00**	.01±.00*	EDL	No significant differences			
	TA @	.08±.00	**.06±.01***	**.08±.01**	.06±.01*	TA @	.11±.04	.08±.01*	.09±.01	.09±.03
	GC @	.24±.02	**.17±.03***	**.26±.03**	.15±.02*	GC @	.34±.06	**.29±.04***	**.34±.03**	.26±.04*#
	SL @	.01±.00	**.01±.00**	**.02±.00**	.01±.00*	SL	No significant differences			
	QC @	.30±.04	**.20±.03***	**.30±.05**	.20±.04*	QC @ £	.45±.04	**.34±.05**	**.38±.05**	.31±.04
Table4. µCT - femur mid-diaphysis	BA/TA (%)	Not measured				BA/TA (%) @ £ &	49.6±2.8	**53.3±2.4***	**47.6±3.6**	48.2±2.4#
	CtTh (mm)					CtTh (mm) @ £	.25±.02	.24±.01	.24±.02	.21±.01*#
	tissue area (mm²)					tissue area (mm²) @	2.32±0.29	**1.83±0.08***	**2.28±0.21**	1.85±0.14*
	marrow area (mm²)					marrow area (mm²) @	1.18±0.19	**0.86±0.05***	**1.20±0.16**	0.86±0.05*
	Imax (mm⁴)					Imax (mm⁴) @ £	0.47±0.1	**0.31±0.04***	**0.43±0.07**	0.27±0.04*
	TMD (mg HA/cm³)					TMD (mg HA/cm³) @ £	1.18±0.03	**1.22±0.02***	**1.16±0.04**	1.17±0.03#
Table4. µCT - distal femur	BV/TV (%)					BV/TV (%) @	23.7±7.0	**5.71±1.6***	**22.07±4.7**	5.7±2.7*
	Tb.N (/mm)					Tb.N (/mm) @	2.95±0.60	**0.94±0.24***	**2.97±0.55**	0.91±0.39*
	Tb.Th (mm)					Tb.Th (mm) @	.08±.01	**.06±.00***	**.08±.01**	.06±.01*
	Tb.Sp (mm)					Tb.Sp (mm) @	0.19±0.02	**0.28±0.02***	**0.20±0.02**	0.30±0.04*
	TMD (mg HA/cm³)					TMD (mg HA/cm³) @	.71±.03	**.67±.02***	**.70±.02**	.65±.03*
Table4. µCT - L5	BV/TV (%)					BV/TV (%) @	32.6±6.3	**22.2±4.6***	**31.14±5.71**	21.10±4.82*
	Tb.N (/mm)					Tb.N (/mm) @	4.07±0.68	**2.88±0.18***	**4.06±0.52**	2.78±0.53*
	Tb.Sp (mm)					Tb.Sp (mm) @	.16±0.2	**.23±.03***	**.16±.02**	.24±.04*
	TMD (mg HA/cm³)					TMD (mg HA/cm³) £	.71±.03	.72±.01	.71±.03	.69±.02#
Table5. biomechanical properties (3-point bending)	Ultimate force (N)					Ultimate force (N) @ £	20.58±4.94	17.31±1.72*	19.20±2.62	14.25±1.37**
	Yield Force (N)					Yield Force (N) @	12.86±3.00	12.07±1.14	13.08±14.7	10.96±1.81*
	Stiffness (N/mm)					Stiffness (N/mm) @	114.8±23.0	110.4±9.3	118.1±17.8	99.7±16.3*
	Modulus (GPa)					Modulus (GPa) @	4.59±1.25	**6.35±0.64***	**4.96±0.86**	5.94±1.57
	Yield Stress (MPa)					Yield Stress (MPa) @	76.6±19.9	94.7±6.9*	81.8±13.5	89.6±20.8
Table6. circulating chemokines	IL-13 (ng/ml)					IL-13 (ng/ml) £ &	33.6±5.9	24.5±8.5	18.4±5.3#	24.0±5.5
	CXCL10 (ng/ml)					CXCL10(ng/ml) @ &	162.6±34.0	263.6±61.2*	205.4±33.7	178.0±17.6#
	RANTES (ng/ml)					RANTES (ng/ml) @ £ &	7.74±4.9	13.4±5.0	18.3±8.8	230.9±179.8**
	CCL11 (µg/ml)					CCL11 (µg/ml) @ £ &	1.32±0.3	**0.95±0.1***	**1.56±0.2#**	1.13±0.1#
	LIX/Cxcl5 (µg/ml)					LIX/Cxcl5 (µg/ml) @	5.06±0.23	4.88±1.07	5.05±0.53	3.91±0.42*

a: p=0.08 vs XXF; b: p=0.08 vs XXF; c: p=0.06 vs XXM; d: p=0.08 vs XXM; e: p=0.09 vs XXM. EDL: extensor digitorum longus; TA: tibialis anterior (TA); GC: gastrocnemius; SL: soleus; QC: quadriceps

***Disclosures: Lilian Plotkin**, None*

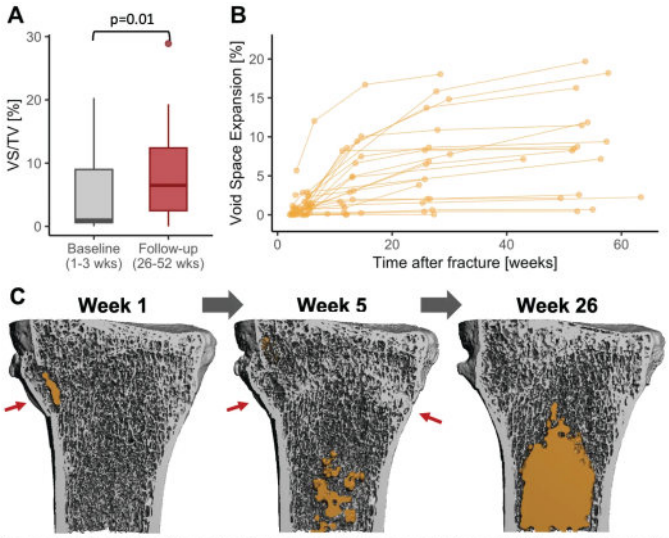

Figure: A) VSTV at the first and last timepoint. B) Void space expansion of individual patients during fracture healing, relative to baseline bone volume. C) Representative HR-pQCT scan from a 29-year-old woman during fracture healing. Red arrows indicate the fracture line and yellow region is the void space.

***Disclosures: Danielle Whittier**, None*

FRI-040

Fracture Healing Leads to Localized Structural Bone Loss Quantified using Void Space Analysis *Danielle Whittier[1], Matthias Walle[2], Charles Ledoux[3], Penny Atkins[1], Caitlyn Collins[4], Julia Holtmann[5], Matthias Zumstein[6], Patrik Christen[7], Kurt Lippuner[8], Ralph Müller[3]. [1]Institute for Biomechanics, ETH Zurich; Department of Osteoporosis, University Hospital of Bern, Switzerland. [2]ETH Zurich, . [3]Institute for Biomechanics, ETH Zurich, Switzerland. [4]Virginia Tech, United States. [5]Department of Orthopaedic Surgery and Traumatology, University Hospital of Bern, Switzerland. [6]Department of Orthopaedic Surgery and Traumatology, University Hospital of Bern; Sonnenhof Orthopaedics, Bern, Switzerland, Switzerland. [7]Institute for Information Systems, FHNW, Switzerland. [8]Department of Osteoporosis, University Hospital of Bern, Switzerland

High-resolution peripheral quantitative computed tomography (HR-pQCT) has shown rapid changes in bone mineral density (BMD), morphology, and biomechanical properties at the distal radius during fracture healing. However, patient outcomes in terms of BMD are highly variable, suggesting that changes in bone microarchitecture may also play a role in patient-specific recovery and long-term bone strength. This study uses void space analysis to identify regions of adverse localized structural bone loss during fracture healing.Twenty-six patients (21 female, 5 male; aged 18-79 years) with conservatively-treated distal radius fractures were scanned using HR-pQCT (XtremeCT II, 61 µm) at 6 timepoints post-fracture (weeks 1, 3, 5, 12, 26, and 52). The common scan region across timepoints was determine using 3D rigid registration, and total BMD (TtBMD), bone volume fraction (BVTV), and void space volume faction (VSTV) were quantified at the first and last available timepoint for each participant. The cumulative formation of VSTV across sequential timepoints (termed void space expansion) was also quantified to capture structural voids that developed during fracture healing as opposed to those that arose due the fracture incident. Changes in BMD, BVTV, and VSTV between the first and last visit were compared using paired t-tests or Wilcoxon test, depending on data distribution.The median time of the first and last post-fracture visits were 1.1 weeks (IQR = 0.9-1.1) and 52.3 weeks (42.9-54.1), respectively. During this interval, VSTV increased five-fold in size from 1.0% (0.6-9.0%) to 5.5% (2.5-12.4%) (Figure 1A, p=0.01). Void space expansion occurred more rapidly in the first 26 weeks of fracture healing (Figure 1B) and did not necessarily occur in the immediate fracture region, but rather the surrounding area (Figure 1C). In contrast, TtBMD and BVTV did not significantly differ between the first and last study visits, where TtBMD was 283 +/- 55 mg HA/cm3 and 269 +/- 62 mg HA/cm3 (p=0.16) at the first and last visit, and BVTV was 42 +/- 2% and 41 +/- 2% (p=0.48) at the first and last visit, respectively.This study suggests that there may be adverse changes in bone microarchitecture during fracture healing, despite the potential preservation of overall TtBMD and BVTV in the fracture and surrounding region. The formation of void spaces may have long-term implications on patient bone strength and could provide insight into who is at risk of re-fracture.

FRI-043

Bone Microarchitecture and Bone Strength at the Distal Radius Related to the Pubertal Growth Spurt in Adolescence *Imanma Tiffany Egeonu[1], James Johnston[1], Saija Kontulainen[1]. [1]University of Saskatchewan, Canada

Increase incidence of forearm fractures at the time of the adolescent growth spurt is well documented but it is unclear if bone structure is weaker during this rapid period of growth. The purpose of this research was to compare bone strength and micro-architectural outcomes of the distal radius across the pubertal growth spurt. We categorized 143 typically developing children (60 females) into 3 groups, based on their estimated somatic maturity (years from the age at peak height velocity, APHV): Pre -0.5y prior to APHV; Peri +/-0.5y within APHV, and Post >0.5y post to APHV. We analyzed distal radius HR-pQCT images to obtain trabecular and cortical bone microstructure and finite element (FE) derived strength outcomes. We created an FE model with mechanical properties scaled in relation to image bone mineral density to estimate: stiffness, off-axis fracture load, and related factor-of-risk. We compared bone strength and microarchitecture across the groups using MANCOVA (age, height, and body mass as covariates), followed by pairwise comparisons. Age and body size adjusted distal radius strength and micro-architecture differed across the groups (Wilks' Lambda, p<0.05). Peri group had 20% lower bone stiffness than Pre (p=0.01), and 39% higher factor-of-risk than Post (p=0.01) groups. Peri had 12-19% lower trabecular thickness, bone volume, trabecular bone density and total bone density than Pre group. Peri group also had 5-19% lower cortical thickness, cortical bone mineral density and tissue mineral density, cortical total and bone volume, and cortical area than Post group (p<0.05). Findings indicate lower bone strength and maturity-specific deficits in trabecular and cortical bone micro-architecture and density at the distal radius around the age at peak height velocity. Prospective monitoring of bone strength development over the pubertal growth spurt is warranted. These findings support the hypothesis of transient weakness in bone development during the peak growth spurt in adolescence.

***Disclosures: Imanma Tiffany Egeonu**, None*

FRI-050

Splenectomy Specifically Ameliorated Osteosclerosis in Lumbar Vertebra of Female Mpig6b null (Mpig6b?/?) Mice *Sirion Aksornthong[1], Kerstin Tiedemann[2], Svetlana V. Komarova[2]. [1]Department of Experimental Surgery, McGill University; Shriners Hospital for Children, Canada, Canada. [2]Faculty of Dental Medicine and Oral Health Sciences, McGill University; Shriners Hospital for Children, Canada, Canada

Myeloproliferative neoplasms are a group of blood cancers, in which abnormalities in bone marrow are associated with abnormal bone gain and osteosclerosis. Bone marrow megakaryocytes (MKs) strongly implicated in osteosclerosis (OS), are maintained in a resting state with the help of the inhibitory receptor G6b-B. Null and loss-of-function mutations in the gene coding G6b-B, Mpig6b in mice and MPIG6B in humans lead to myelofibrosis associated with macrothrombocytopenia, splenomegaly and osteosclerosis. MKs can affect bone cells through cell-cell contact or soluble factors. In female Mpig6b?/? mice, megakaryopoiesis was shifting to the spleen, however, OS progression continued. The goal of this project was to assess the role of circulating factors in mediating osteosclerosis in Mpig6b?/?

mice using a clinically relevant procedure of splenectomy. At the age of 31-37 weeks, when long bone OS is established, but other skeletal sites are not yet affected, female Mpig6b?/? and littermate control (LC) mice were subjected to splenectomy or sham surgery, and 20 weeks later, the hematopoietic parameters, and bone structure by μCT at the femur and lumbar vertebra were analyzed. Macrothrombocytopenia with decreased counts ($p < 0.01$) of larger ($p < 0.05$) platelets persisted in splenectomized and sham-operated Mpig6b?/? mice. The analysis of the femur indicated increased BV/TV ($p < 0.01$) and trabecular thickness ($p < 0.05$) and the decreased medullary area ($p < 0.01$) in 52-week-old splenectomized and sham-operated Mpig6b?/? mice compared to LC, no change in microarchitectures and mechanical properties of the femur was found between splenectomized Mpig6b?/? mice and sham group. In contrast, in vertebra of sham-operated Mpig6b?/? mice, osteosclerosis continued to develop, while splenectomy led the decreased BV/TV ($p < 0.05$) and a tendency to decrease trabecular number with increased trabecular separation in lumbar vertebrae of Mpig6b?/? mice compared to both the sham-operated Mpig6b?/? and splenectomized LC. Using the quantitative plasma proteomics, we identified three proteins, the coagulation factor V, Ig kappa chain C region and intercellular adhesion molecule 2, which were significantly affected in Mpig6b?/? mice compared to LC, and reversed to normal levels after splenectomy. This study contributes to determining molecular interactions between bone and bone marrow in myelofibrosis and will enable the development of novel treatments for patients with this disorder.

***Disclosures: Sirion Aksornthong**, None*

FRI-051

Osteoblast-specific ablation of FGF23 attenuates obesity-induced bone loss in male mice *Napatsorn Imerb[1], MIN YOUNG PARK[2], Despina Sitara[3]. [1]Chiang Mai University, , [2], United States, [3]New York University College of Dentistry, United States

FGF23 is a phosphotropic hormone, mainly produced by osteoblasts/osteocytes, which regulates mineral homeostasis. Recent studies demonstrated that FGF23 is linked to chronic metabolic conditions, including cardiovascular disease, type II diabetes, obesity, and osteoporosis. High circulating levels of FGF23 are positively correlated with greater fat accumulation in obesity and low bone mass in menopausal women, implying a role of FGF23 in energy metabolism and the crosstalk between bone and fat. However, the action of FGF23 in osteoblasts and its role in bone metabolism in obesity have not been demonstrated. We generated osteoblast-specific Fgf23 null mice using Cre recombinase under the control of the mouse collagen type 2.3 (Col2.3) promoter. Male control (Fgf23flox/flox) and knockout (KO, Col2.3CreFgf23flox/flox) mice were fed high fat diet (HFD) (60 %kcal fat) for 24 weeks starting at 8 weeks of age. Body weight and body fat measurements were taken weekly during the 24 weeks of HFD intervention. Serum, femur, and tibiae were collected upon sacrifice. Micro-computed tomography was used to evaluate bone microarchitecture in left femur. Expression of bone- and adipocyte-specific genes in bone and bone marrow were assessed by qRT-PCR. Our data show that bone Fgf23 expression was almost completely abolished (85-90% reduction) in the KO mice. After 24 weeks of HFD, control and KO mice had comparable gain in body weight and percentage of body fat. However, KO mice fed HFD exhibited a higher BV/TV fraction and reduced trabecular separation compared to control mice, and these were associated with a significant decrease in bone and bone marrow mRNA levels of osteoclastic genes such as RANKL and TRAP5. Moreover, osteoblast-specific genes such as Runx2 and osteocalcin were also decreased in the bone and bone marrow of KO mice compared to control mice. Interestingly, expression of PPAR, and TNF-? in bone and bone marrow were significantly decreased in KO mice compared to controls. Together, our data suggest that osteoblastic Fgf23 modulates bone marrow adiposity, inflammation, and bone resorption. In summary, our findings demonstrate for the first time that osteoblast-specific ablation of Fgf23 improves bone mass and alleviates obesity-induced bone loss by regulating bone marrow adiposity and attenuating bone resorption in male mice. Targeting osteoblastic Fgf23 may be a potential strategy for treating metabolic bone disease in obesity.

***Disclosures: Napatsorn Imerb**, None*

FRI-053

miR122 regulates FGF23 cleavage in iron deficiency *Jane Joy Thomas[1], JOHN VON DRASEK[2], GUILLAUME COURBON[3], JADAEH SPINDLER[2], Aline Martin[2], Valentin David[1]. [1]Northwestern University, Feinberg School of Medicine, United States, [2]Northwestern University, United States, [3]Center for Translational Metabolism and Health, France

Proteolytic cleavage of intact fibroblast growth factor 23 (iFGF23) yields C-terminal FGF23 peptides (Cter-FGF23) that play a protective role in iron metabolism during acute inflammation. Increased circulating Cter-FGF23 levels are also observed in iron deficiency anemia (IDA) due to simultaneous increase in production and cleavage of intact iFGF23. O-glycosylation of iFGF23 176-RXXR-179 cleavage site by GALNT3 protects iFGF23 from cleavage, but the regulation of GALNT3 in IDA is unknown.We found that IDA increases the expression of miR-122-5p (miR122), which is a predicted inhibitor of Galnt3 expression. We hypothesized that inhibition of GALNT3 by miR122 results in increased iFGF23 cleavage in IDA.Since miR122 is mainly produced by the liver, we generated mice harboring a conditional deletion of miR122 in hepatocytes (miR122cKO) by crossing miR122 floxed mice with mice expressing a Cre recombinase driven by the Albumin promoter. We induced IDA by feeding 3-week-old wild-type (WT) and miR122cKO mice either a control diet (Ctr) or a low iron diet (IDA) for 3 weeks. At 6 weeks of age, we analyzed serum biochemical and hematological parameters as well as bone Galnt3 expression in all mice.Compared to WT-Ctr, miR122cKO-Ctr mice exhibited reduced miR-122 levels, increased bone Galnt3 expression and iFGF23 levels, despite normal total cFGF23. These mice also showed reduced iron levels and transferrin saturation, but normal hemoglobin levels and red blood cells counts. As expected, WT-IDA mice were anemic and showed higher levels of miR122, reduced Galnt3 expression along with a 3.6-fold increase in total cFGF23 compared to WT-Ctr, and a slight but significant increase in iFGF23. Compared to WT-IDA, miR122cKO-IDA mice showed increased Galnt3 expression, total cFGF23 levels and higher iFGF23, resulting in an increased i/cFGF23 ratio, a surrogate marker of FGF23 cleavage. miR122cKO-IDA mice also exhibited further reduced levels of iron and transferrin saturation, but this did not aggravate the severity of anemia in these mice.Our results demonstrate that iron deficiency increases miR122, which inhibits Galnt3 osseous expression and results in increased FGF23 cleavage, elevated Cter-FGF23 but reduced iFGF23. miR122 could be a potential therapeutic target to reduce iFGF23 and thus improve adverse outcomes in diseases associated with iFGF23 excess.

***Disclosures: Jane Joy Thomas**, None*

FRI-055

Examining the Role of Zinc Fingers and Homeoboxes 2 (Zhx2) in Chronic Kidney Disease-related Bone & Cardiovascular Health *Jordan Matz[1], Corinne Metzger[3], Huda Mahmood[3], Christopher Miller[3], Arelis Quintana-Martinez[3], Gagandeep Sooch[4], Matthew Allen[3], Erica Clinkenbeard[3]. [1]IU School of Medicine, , [3]Indiana University School of Medicine, , [3]Indiana University School of Medicine, United States, [4]Marian University College of Osteopathic Medicine, United States

Chronic Kidney Disease (CKD) is estimated to affect more than 1 in 7 US adults. CKD-mineral and bone disorder (CKD-MBD), a common sequela, independently leads to vascular calcification, increased fracture risk, and mortality. Mice placed on CKD-inducing 0.2% adenine diet (AD) for 8 weeks show increased cortical bone porosity, osteoclast activity, and marrow adiposity, mirroring human patients. The differentiation skewing between osteoblast and adipocyte in CKD however remains unclear. Zinc finger and homeobox 2 (Zxh2), a transcriptional repressor, was previously shown to be critical for odontoblast differentiation. Further, lack of Zhx2 promotes hepatic steatosis with high fat diet. We hypothesize Zhx2 potentiates osteoblast commitment by inhibiting adipocyte gene expression. We utilized BALB/cJ (/cJ) mice which harbor a hypomorphic mutation in the Zhx2 locus, drastically decreasing Zhx2 mRNA compared to normal BALB/c (/c) mice. AD feeding in both sexes significantly increased serum Blood Urea Nitrogen vs casein control consistent with CKD; however, /cJ mice had significantly lower values than /c mice. On casein, /cJ females exhibited lower trabecular bone volume (Tb.BV/TV; $p<0.01$), reduced Bglap mRNA ($p<0.01$), and increased adipogenic Lpl mRNA ($p<0.05$) vs /c. AD-fed /c females lost Tb.BV/TV and reduced Bglap mRNA comparable to /cJ levels which correlated with reduced bone Zhx2 mRNA vs /c casein. Male /cJ mice exhibited reductions in Bglap (5-fold, $p<0.01$), Alpl (2.5-fold; $p<0.01$), and Dmp1 (2.5-fold, $p<0.01$) mRNA compared to /c on casein, with no differences in Lpl mRNA or trabecular bone parameters. In contrast to females, AD-fed /c males had modestly increased Tb.BV/TV whereas Tb.BV/TV decreased in AD-fed /cJ males. Consistent with CKD, AD-fed /cJ mice exhibited modestly elevated serum phosphate and fibroblast growth factor 23 (FGF23) vs /c mice. Thus, we assessed tissues for downstream calcifications via X-ray. Analysis of isolated hearts showed AD-fed /c mice incurred heart calcifications (2/7 females; 4/6 males), whereas BALB/cJ mice appeared protected (0/8 male and female). In conclusion, Zhx2 is a transcription factor that exhibits influence on outcomes related to CKD and mineral metabolism. Most notably, /cJ mice lacking Zhx2 were protected from cardiac calcification incidence. These results have important implications for patients with CKD-MBD and downstream outcomes related to disrupted mineral metabolism.

***Disclosures: Jordan Matz**, None*

FRI-057

Membrane Estrogen Receptor-? Signaling in POMC Neurons is Crucial for Normal Bone Metabolism in Female Mice *Yiwen Jiang[1], Karin Horkeby[1], Jianyao Wu[1], Karin Nilsson[2], PETRA HENNING[3], Sofia Movérare-Skrtic[4], Claes Ohlsson[5], Marie Lagerquist[4]. [1]Sahlgrenska Osteoporosis Centre, Centre for Bone and Arthritis Research at Institute of Medicine, Sahlgrenska Academy at University of Gothenburg, Sweden, Sweden, [2], Sweden, [3]UNIVERSITY OF GOTHENBURG, Sweden, [4]Medicine, Sweden, [5]Center for Bone and Arthritis Research at the Sahlgrenska Academy, Sweden

Estrogen receptor-? (ER?) signaling in the central nervous system is involved in the regulation of bone metabolism1,2. We have previously shown that deletion of ER?, specifically in proopiomelanocortin (POMC) neurons, increases bone mass and mechanical strength3. We and others have also revealed that membrane-initiated estrogen receptor-? (mER?) signaling plays an important role in regulating estrogenic effects in bone. However, it remains unknown whether mER? signaling in POMC neurons is involved in mediating estrogenic effects in bone.For this purpose, we have generated a novel ER?-C451Aflox/flox mouse

model (C451Af/f) in which the C451A mutation disables the membrane localization of ER?. C451Af/f mice were mated with POMC-Cre mice to breed POMC-C451A mice, lacking mER? signaling in POMC-expressing neurons, and homozygous C451Af/f littermate controls.Phenotyping at 16 weeks of age showed multiple changes between POMC-C451A mice (n=8) and C451Af/f littermate controls (n=9). Areal bone mineral density (BMD), measured by DEXA, was significantly increased in POMC-C451A mice (total body, +5%, p<0.001; lumbar spine, +16%, p<0.001). Cortical thickness and trabecular BMD, measured by pQCT, were increased in long bones (cortical thickness: femur, +13%, p<0.001, tibia, +13%, p<0.001; trabecular BMD: femur, +32%, p<0.05, tibia, +29%, p<0.001). In addition, cortical bone in vertebrae L5 and bone volume fraction (BV/TV), measured by ?CT, were also increased in POMC-C451A mice compared with controls (BV/TV: +37%, p<0.001; cortical thickness: +18%, p<0.01). Uterus weight was unaffected in POMC-C451A mice, suggesting normal sex steroid feedback regulation.In conclusion, our study emphasizes the inhibitory effect of neuronal ER? signaling on bone mass, in contrast to the stimulatory bone effects by peripheral ER? signaling. This demonstrates that mER? signaling in POMC neurons plays an important role in this negative regulation of bone mass.Reference1. Herber CB, et al. Nat Commun, 2019.2. Ohlsson C, et al. Proc Natl Acad Sci U S A, 2012.3. Farman HH, et al. Endocrinology, 2016.

***Disclosures: Yiwen Jiang**, None*

FRI-058

L- ?-aminoisobutyric Acid (L-BAIBA) Treatment Enhances Musculoskeletal Properties in Combination with Voluntary Wheel Running Exercise in Male Mice *Julian Vallejo[1], Yukiko Kitase[2], Thiagarajan Ganesh[3], Mark Dallas[4], Yixia Xie[4], Mark Johnson[5], Lynda Bonewald[6], Michael Wacker[7]. [1]University of Missouri-Kansas City, School of Medicine, United States. [2]Indiana University, School of Medicine, United States. [3]University of Missouri-Kansas City, School of Science and Engineering, United States. [4]University of Missouri-Kansas City, School of Dentistry, United States. [5]University of Missouri, Kansas City Dental School, United States. [6]Indiana University School of Medicine, United States. [7]University of Missouri-Kansas City School of Medicine, United States

L-BAIBA is a metabolite secreted from contracting skeletal muscle. Exercise is commonly known to produce system-wide benefits and L-BAIBA appears to play a role in this process. In addition to metabolic homeostasis, recent studies suggest that L-BAIBA may also promote cardiac health and maintenance of bone. We have shown that L-BAIBA treatment in mice prevents musculoskeletal decline during chronic disuse. However, the effects of L-BAIBA on musculoskeletal and cardiac tissue in exercising mice are unknown. Therefore, we hypothesized that the combination of exercise with L-BAIBA treatment would promote greater benefits than exercise alone. Male 12 month old C57BL6 mice performed voluntary wheel running (VWR) with L-BAIBA treatment (VWR+L-BAIBA; n=7), VWR only (n=9), L-BAIBA only (n=8), or none (control; n=8) for three months. L-BAIBA was supplied in the drinking water (100 mg/kg/day). At the end of the study, hearts had no significant differences in conscious electrocardiogram parameters or size between groups. In bone, VWR had no significant effect alone, however VWR+L-BAIBA maintained higher trabecular thickness (VWR+L-BAIBA: 0.043+/-0.01 vs Control: 0.035+/-0.00mm, p<0.05) and connectivity (VWR+L-BAIBA: -3.7+/-1.4 vs Control: -1.3+/-1.5mm-1, p<0.05). Although VWR+L-BAIBA showed smaller bone diameter (VWR+L-BAIBA: 2.2+/-0.1 vs VWR: 2.5+/-0.2mm, p<0.05) thereby lower Moment of Inertia (VWR+L-BAIBA: 0.20+/-0.02 vs VWR: 0.24+/-0.02mm4, p<0.05), tibia mechanical testing revealed higher Modulus of Elasticity (VWR+L-BAIBA: 4.77+/-0.36 and L-BAIBA: 4.78+/-0.36 vs VWR: 4.13+/-0.43GPa, p<0.05), suggesting L-BAIBA retains better bone material properties. Therefore, the VWR+L-BAIBA required less compensatory periosteal expansion, which resulted in no differences in biomechanical properties of Elastic Stiffness among groups. VWR+L-BAIBA showed lower femoral bone marrow adipose compared to control (VWR+L-BAIBA: 0.03+/-0.03 vs Control: 0.08+/-0.03mm2, p<0.05). Soleus skeletal muscles from VWR+L-BAIBA mice were significantly larger (VWR+L-BAIBA: 10.4+/-1.0 vs Control: 12.3+/-0.7mg, p<0.05) and contracted with more force (VWR+L-BAIBA: 301.2+/-37.6 vs Control: 263.6+/-19.1mN, p<0.05). In EDL muscle VWR improved fatigue resistance and recovery from fatigue (p<0.01) while VWR+L-BAIBA did not. These findings suggest a physiological interaction between exercise and L-BAIBA to enhance bone structural and material qualities, prevent an increase in bone marrow adipose, and improve muscle mass and strength.

***Disclosures: Julian Vallejo**, None*

FRI-060

Fluid Flow Shear Stress Bone Conditioned Media Increases Intracellular Cardiomyocyte Calcium *Anuhya Dayal[1], Julian Vallejo[2], Nuria Lara-Castillo[3], Mark Johnson[3], Michael Wacker[2]. [1]University of Missouri - Kansas City, School of Medicine , United States. [2]University of Missouri - Kansas City, School of Medicine , United States. [3]University of Missouri - Kansas City, School of Dentistry, United States

Bone is a dynamic organ, serving countless endocrine functions in the body. As fluid flows through bone, via the lacunar-canalicular system and interstitially, it generates fluid flow shear stress (FFSS). FFSS variably stresses osteocytes, impacting the subsequent cytokines and endocrine factors released.We previously demonstrated that administration of FFSS osteocyte conditioned media (CM) to murine whole hearts increased both peak force and area under contractile waveforms by approximately 25% (p<0.01, n=6-7). Here, we aim to elucidate the cellular signaling for this response. Cardiomyocyte calcium (Ca2+) release is widely established as one of the primary mechanisms for increasing cardiac contractility. Thus, we hypothesized that FFSS CM administration to cardiomyocytes will increase intracellular Ca2+ levels. Cultured H9C2 cardiomyocytes were differentiated for 7 days at 37oC then stained with fluo-8 AM (Ca2+ indicator dye). Blank (control) and FFSS conditioned media obtained from osteocyte-like MLOY4 cultured cells were perfused over the H9C2 cells both with and without electrical pacing (1 Hz). Intracellular fluorescence was monitored for 20 min, with perfusion in this order: 5 min Ringer's solution (baseline), 7 min 7.5% FFSS media or 7.5% blank media, 7 min 2.5 mM KCl (positive control). For analysis, fluorescence was reported as a percentage of KCl response.We observed an increase in intracellular Ca2+ with FFSS CM perfusion of cardiomyocytes compared to control; average cell Ca2+ levels after FFSS CM were 72 +/-21% of its max response (KCl) and blank was 28 +/- 11% (p=0.01; n=4 series; 20-30 cells/series). Not only did the magnitude of intracellular Ca2+ increase with FFSS osteocyte CM, but the number of cells demonstrating elevated Ca2+ also increased 1.4-fold (p<0.0001). Interestingly, these increases were absent in experiments without pacing (p=0.001, n=16 series, 20-30 cells/series).Our findings strongly indicate a connection between osteocyte FFSS CM increasing cardiomyocyte Ca2+ as a mechanism to increase cardiac contractility. These effects were only observed with electrical pacing; thus, it is likely that bone factors in FFSS CM sensitize or activate targets such as voltage-gated Ca2+ channels. These conclusions further elucidate bone-heart crosstalk and provide significant, exciting data supporting our hypothesis that bone release factors that impact the heart, indicating implications for cardiovascular health in exercise and aging.

***Disclosures: Anuhya Dayal**, None*

FRI-061

Deletion of Fra1 in osteoblasts by Runx2-Cre causes a reduced adipose tissue mass *Julia Luther[1], Mona Neven[1], Olga Winter[1], Lana Rosenthal[1], Michael Amling[1], Jean-Pierre David[1], Thorsten Schinke[1]. [1]Institute for Osteology and Biomechanics (IOBM), University Medical Center Hamburg-Eppendorf, Hamburg, Germany, Germany

The activator protein-1 (AP-1) transcription factor family member Fra1 has been described to cause increased bone mass and decreased adipose tissue mass when ubiquitously overexpressed in mice. Epiblast-specific deletion of Fra1 by More-Cre, conversely, caused osteopenia due to a decreased bone formation rate. In vitro experiments with primary calvarial osteoblasts showed a reduced mineralizing activity. Osteoclast number and activity was not affected in vivo, however, osteoclasts showed a differentiation defect in vitro.To analyse the cell autonomous phenotype in vivo, we generated mice with an osteoclast- or an osteoblast-specific deletion of Fra1 (Fosl1) using LysM-Cre and Runx2-Cre, respectively. Deletion of Fra1 specifically in osteoclasts did not lead to a change in trabecular bone mass in 12-week- or in 1-year-old LysM-Cre;Fra1fl/fl mice compared to control animals (14.23+/-3.49% (control) versus 12.85+/-2.733% (LysM-Cre;Fra1fl/fl) at the age of 1 year). In addition, osteoclast number per bone perimeter was not affected in young mice (N.Oc/B.Pm: 4,307+/-1,86mm-1 (control) versus 4,928+/-1,42mm-1 (LysM-Cre;Fra1fl/fl)), confirming that Fra1 is not necessary for osteoclast differentiation in vivo. When deleting Fra1 in osteoblasts no significant change in bone mass was observed in 12-week as well as 1-year-old Runx2-Cre;Fra1fl/fl compared to control mice (15.53+/-2.243% (control) versus 13.36+/-0.7766% (Runx2-Cre;Fra1fl/fl) at the age of 1 year). Furthermore, the number of osteoblasts was unchanged in 12-week-old mice (N.Ob/B.Pm: 32,24+/-6,54mm-1 (control) versus 39,38+/-9,66mm-1 (Runx2-Cre;Fra1fl/fl)). However, we could observe a significantly reduced adipose tissue mass accrual in mice with an osteoblast-specific deletion of Fra1, accompanied by a lack of increase in adipocyte cell diameter in 1-year-old Runx2-Cre;Fra1fl/fl mice. Thus, Fra1 expression in Runx2-Cre positive pre-osteoblasts regulates adipose tissue metabolism. In contrast, the bone-anabolic function might be driven by Fra1 expression in early mesenchymal osteoblast progenitors rather than in committed pre-osteoblasts.

***Disclosures: Julia Luther**, None*

FRI-062

Spatial histomorphometry reveals that local peripheral nerves modulate but are not required for skeletal adaptation to applied load *ALEC BEEVE[1], Anna Li[2], MOHAMED HASSAN[1], Matthew Silva[3], Erica Scheller[2]. [1], . [2]Washington University, United States. [3]Washington University in St. Louis School of Medicine, United States

Mechanical loading is required for bone health and results in skeletal adaptation to optimize strength. Local nerve axons, particularly within the periosteum, may respond to load-induced biomechanical and biochemical cues. However, their role in the bone anabolic response remains controversial. We hypothesized that spatial alignment of periosteal nerves with sites of load-induced bone formation in both intact and denervated conditions would clarify this relationship. To achieve this, we developed RadialQuant, a new custom tool for spatial histomorphometry. Tibiae of control and neurectomized (sciatic/femoral nerve cut) pan-neuronal Baf53b-tdTomato reporter mice were loaded with a 5-day regimen to induce lamellar bone formation prior to analysis after 6-days. Mineralizing surface (MS), mineral apposition rate (MAR), bone formation rate (BFR), bone area, cortical thickness, and periosteal nerve axon density were quantified simultaneously in non-decalcified sections of the

mid-diaphysis using RadialQuant. In control animals, anabolic loading induced maximal periosteal bone formation at the site of peak compression, as has been reported previously. Loading did not significantly change overall periosteal nerve density. However, a trending 28% increase in periosteal axons in loaded limbs was noted at the site of peak compression, possibly indicating subtle, local nerve sprouting after applied load. Neurectomy depleted 88% of all periosteal axons, with near-total depletion on load-responsive surfaces. Neurectomy alone also caused de novo bone formation on the lateral aspect of the mid-diaphysis. However, neurectomy did not inhibit load-induced increases in periosteal bone area, MS/BS, MAR, or BFR. Rather, neurectomy spatially redistributed load-induced bone formation towards the lateral tibial surface. This spatial shift resulted from reduction in periosteal bone formation indices at the site of peak compression (-38-63%) and enhancement of indices of skeletal adaptation at the lateral surface (+70-1300%), altogether contributing to comparable load-induced changes in total bone area (+5.5% with load in control mice; +8.9% with load in neurectomized animals). Our results show that local skeletal innervation modulates but is not required for skeletal adaptation to applied load. This supports the continued use of loading and weight-bearing exercise as an effective strategy to increase bone mass, even in patients with peripheral nerve damage or dysfunction.

***Disclosures: ALEC BEEVE**, None*

FRI-067

IL-34 mediated osteolysis exacerbates pathogenic features of Alzheimer's disease *Anny Ho[4], CHIAKI YAMADA[2], Bidii Ngala[3], Amilia Nusbaum[3], Carolina Duarte[4], Juliet Akkaoui[5], Christopher Michael Garcia[6], William Kochen[4], Alexandru Movila[3]. [4]Nova Southeastern University, United States. [2], . [3]Indiana University School of Dentistry, United States. [4]Nova Southeastern University, . [5]Florida International University, United States. [6]Indiana University School of Medicine, United States

Alzheimer's disease (AD) is characterized by progressive neurodegeneration and a gradual decline in memory and cognitive functions. The hallmark features of AD are associated with elevated accumulation of aggravated amyloid beta (A?) peptides, hyperphosphorylated Tau (p-Tau), and neuroinflammation. Emerging evidence indicated that inflammatory osteolysis exacerbates AD neurodegeneration and neuroinflammation via unknown molecular mechanisms. Signaling through the colony-stimulating factor-1 receptor (CSF-1r) is critical for maintaining the physiological and pathological signaling of blood myeloid cells and microglia. CSF-1r is activated by macrophage colony-stimulating factor-1 (M-CSF) and interleukin-34 (IL-34). While the impact of M-CSF in bone physiology and pathology is well addressed, it remains controversial whether IL-34-mediated bone osteolysis promotes AD neuroinflammation and neurodegeneration. Surprisingly, we observed that IL-34 plays a critical role in inflammatory osteolysis in wild-type mice. To evaluate the effects of IL-34 on AD cognitive behavioral phenotype and neuroinflammation, female and male triple transgenic 3x-Tg AD mice and corresponding control were randomly divided into two experimental groups (10 mice/sex/group). Mice were subcutaneously injected with 100 µl of mouse recombinant IL-34 protein solution in PBS or PBS alone over the calvaria bone every other day for 42 days. In addition, we compared the effects of IL-34 and M-CSF on macrophages, microglia, and RANKL-mediated osteoclastogensis in relation to AD pathology. This study demonstrated that local calvaria injection of recombinant IL-34 protein dramatically elevated AD-like memory loss, pathogenic amyloidogenesis, p-Tau, and neuroinflammation-associated RAGE expression in female 3x-Tg mice. Furthermore, IL-34 promoted calvaria inflammatory osteolysis compared to the sham control injected group of female and male mice. Our data also indicated that IL-34-microglia and bone-marrow-derived macrophages isolated from 3x-Tg mice released significantly higher amounts of pro-inflammatory cytokines, TNF-?, IL-1?, and IL-6, compared to M-CSF-proliferated cells in vitro. In addition, IL-34 elevates RANKL-primed osteoclastogenesis in the presence of key AD-associated A?40 and A?42 peptides. Therefore, our data indicated that a novel therapeutic regimen targeting IL-34 could suppress neuroinflammation, neurodegeneration, and elevated bone loss observed in patients with AD.

***Disclosures: Anny Ho**, None*

FRI-070

Crohn's and Bones: Examining Bone Quality using HR-pQCT *Rachel E. Klassen[1], Aysha J. Macci[2], Cathy Lu[3], Lauren A. Burt[1], Steven K. Boyd[1]. [1]McCaig Institute for Bone and Joint Health , Canada. [2]Division of Gastroenterology and Heptaology, Canada. [3]Division of Gastroenterology and Hepatology, Canada

Introduction: Crohn's Disease (CD) negatively affects bone density through factors including diet and physical activity changes, steroid use, bowel resections, and disease mediated inflammatory pathways. Two problems prevent the optimization of skeletal health in individuals with CD: 1) inadequate knowledge of the mechanisms underpinning skeletal fragility associated with CD, and 2) the failure to identify individuals with CD who are at risk for low bone mineral density (BMD). Using high resolution peripheral quantitative computed tomography (HR-pQCT) and dual X-ray absorptiometry (DXA), the aims of this study were to determine differences in bone quality, quantity, and strength between controls and individuals with CD, and within the CD group between inflammatory and fibrostenotic CD phenotypes. Methods: Male and female participants aged 55 years and over were recruited. HR-pQCT scans at the radius and tibia were obtained in addition to standard DXA analysis of the hip and spine. Controls were age, sex, and body mass index matched at a 1:1 ratio. Blood work, health history questionaires, and medical chart review captured various health history and disease severity data. An estimate of strength was determined using finite element analysis. A measure of the void spaces from HR-pQCT was conducted and statistical analyses compared group differences. Results: A total of 45 CD and 45 controls were recruited. Significant differences in density, microarchitecture, and geometry parameters were found between controls and the CD group. A sub-analysis found additional differences between inflammatory versus fibrostenotic CD phenotypes. Overall, the CD and fibrostenotic groups had weaker, less dense, and poorer bone microarchitecture than the control and inflammatory groups. Void spaces were more prevalent, appearing 48% of the time at the radius and 39% of the time at the tibia in the CD group (Figure 1). Conclusions: Pathological endosteal resorption may explain the bone microarchitecture observed in the CD group; this is enhanced in the fibrostenotic group. Our future work will examine lifestyle factors, disease severity, CD treatment type, and time since diagnosis. Earlier identification and diagnostic evaluation from HR-pQCT data combined with known risk factors for low BMD may allow for more timely preventative medical therapy.

Figure 1. Left: the radius of a healthy control. Centre and right: radius and tibia from the CD group showing poor bone quality and void spaces.

***Disclosures: Rachel E. Klassen**, None*

FRI-074

Bariatric Surgery is Associated with Increased Fracture Risk Among Veterans *Eileen H. Koh[1], Tiffany Y. Kim[2], Hui Shen[2], Mary A. Whooley[2], Matthew L. Maciejewski[3], Theodore S. Z. Berkowitz[4], Valerie Smith[3], Lygia Stewart[2], Anne L. Schafer[2]. [1]University of California, San Francisco, United States. [2]University of California, San Francisco and San Francisco Veterans Affairs Health Care System, United States. [3]Durham Veterans Affairs Health Services Research and Development and Duke University, United States. [4]Durham Veterans Affairs Health Services Research and Development, United States

Despite its metabolic and mortality benefits, bariatric surgery has negative skeletal effects. The Roux-en-Y gastric bypass (RYGB) procedure is associated with increased fracture risk in the general bariatric surgery population, who are predominantly premenopausal women. It is unclear whether postoperative fracture risk is increased in men, and whether patients with obesity who undergo sleeve gastrectomy (SG), now the most commonly performed procedure, are more likely to fracture than nonsurgical patients. We compared fracture risk among US Veterans who underwent bariatric surgery from 2000-2020 at a Veterans Affairs (VA) facility or paid for by VA and matched Veterans with obesity who did not have surgery. Surgical patients were matched 1:3 to nonsurgical patients by age, sex, year, and pre-op BMI. We used ICD codes to capture incident fracture from VA electronic health records, VA purchased care claims, and Medicare claims. Cox proportional hazards models were used to determine the relationship between bariatric surgery and subsequent fracture risk. Our surgical cohort, comprised of 8357 patients [3182 RYGB, 4168 SG, 291 adjustable gastric banding (AGB)], was 70% men with mean age 52+/-10 years and BMI 45+/-7 kg/m2. Compared to 25,057 matched Veterans who did not have surgery, surgical patients had higher baseline rates of obesity-related comorbidities including diabetes (48% vs 36%). During an average 7 years follow-up, surgical patients had higher rates of incident fracture (25.1 vs 13.9 per 1000 person-years). Bariatric surgery was associated with a 67% increased risk of incident fracture (HR 1.67, 95% CI 1.56-1.79, p<0.001) after adjustment for race/ethnicity, geographic location, and comorbidities. Bariatric surgery was also associated with incident hip fracture (HR 2.42, 95% CI 1.97-2.96, p <0.001), spine fracture (HR 1.81, 95% CI 1.60-2.05, p<0.001), and radius fracture (HR 2.36, 95% CI 2.03-2.75, p< 0.001). Compared to matched controls, RYGB was associated with increased risk of fracture (HR 1.91, 95% CI 1.73-2.11, p<0.001), as was SG (HR 1.48, 95% CI 1.31-1.67, p<0.001), but there was no difference in fracture rates between RYGB and SG (p=0.18). There was no evidence for an association between AGB and fracture risk (HR 0.97, 95% CI 0.68-1.40, p=0.88). Our findings show that RYGB and SG are associated with increased risk of fracture in this Veteran population of predominantly older men, including at major osteoporotic fracture sites.

***Disclosures: Eileen H. Koh**, None*

FRI-075

Impact of Osteoporosis Pharmacotherapy on Functional Outcomes after Ischemic Stroke *So Young Park[1], Sang-Hwa Lee[2]. [1]Division of Endocrinology and Metabolism Department of Internal Medicine, Kyung Hee University College of Medicine, , Republic of Korea. [2]Department of Neurology, Chuncheon Sacred Heart Hospital, Hallym University College of Medicine, Republic of Korea

Purpose: This study evaluated whether osteoporosis pharmacotherapy (OPT) affects functional outcome in acute ischemic stroke patients with osteoporosis.Methods: Using a single-center registry database, we consecutively registered acute ischemic stroke patients between May 2016 and December 2020. All patients older than 55 years underwent routine bone densitometry within 7 days of stroke onset. OPT prescription was confirmed by reviewing medical records. We classified the patients into OPT and no OPT groups. We performed propensity score matching (PSM) to overcome the imbalance in multiple covariates between the two groups. We investigated whether OPT affects 1-year functional outcomes by multivariate analysis using PSM cohort.Results: Among 1,307 consecutively registered acute ischemic stroke patients, 381 patients were enrolled in this study, of whom 134 (35.2%) were prescribed OPT at discharge, which was maintained for 1 year. In multivariate analysis using PSM cohort. the OPT group had a lower risk of dependency (odds ratio [OR], 0.52; 95% confidence interval [CI], 0.27-0.996) and poor functional outcome at 1 year (OR, 0.24; 95% CI, 0.10-0.57). The OPT group also had increased chance of late functional improvement (OR, 6.16; 95% CI, 1.12-33.79).Conclusion: This study showed that OPT could reduce dependency and poor functional outcome and increase the chance of improving functional outcome at 3 months and 1 year after ischemic stroke onset, and these findings could be helpful for improving functional outcomes and bone health after ischemic stroke.?

***Disclosures: So Young Park**, None*

FRI-077

Fractures and JAK-inhibitors: Evidence of a Safety Signal from the WHO Global Pharmacovigilance VigiBase Data *Andreas Clausen[1], Adrian Martinez-De la Torre[1], Andrea Burden[2], Stefan Weiler[1]. [1]Swiss Federal Institute of Technology (ETH) Zurich, Institute of Pharmaceutical Sciences, Switzerland. [2]Swiss Federal Institute of Technology (ETH) Zurich, Switzerland

Background: The Janus Kinase (JAK) inhibitors are promising new treatments for inflammatory rheumatic diseases. However, numerous safety concerns have been raised. Most recently, the European Medicines Agency (EMA) updated the warning to include an elevated risk of fractures for tofacitinib, but not upadacitinib or baricitinib.Objective: We conducted a global pharmacovigilance analysis of tofacitinib, upadacitinib, and baricitinib to describe and evaluate the safety signal for fractures.Methods: Individual case safety reports (ICSRs) for tofacitinib, upadacitinib, and baricitinib were identified from the World Health Organization (WHO) global pharmacovigilance database, VigiBase on March 14 2023. The primary outcome of interest was a bone fracture (excluding tooth and avulsion fractures). ICSR demographics were summarized overall and among those with a fracture. A disproportionality analysis using reporting odds ratios (RORs) and 95% confidence intervals (CIs) evaluated the reporting of a bone fracture with one of the JAK-inhibitors compared to all other drugs in the VigiBase, during the same period.Results: We identified 122,037 ICSRs for tofacitinib, 27,786 ICSRs for upadacitinib, and 14,616 ICSRs for baricitinib between 2011 and 2023. Among the ICSRs, we identified 2,202 (1.8%), 634 (2.3%), and 144 (1.0%) reports where a bone fracture was reported for tofacitinib, upadacitinib, and baricitinib, respectively. ICSR characteristics are provided in Table 1. Those with a bone fracture, were more often female, older, and had a higher number of co-reported medications (Table 1). ICSRs with a fracture had a higher reported prevalence of glucocorticoids, opioids, and bisphosphonates. All JAK-inhibitors were associated with increased reporting for fracture (Table 1): tofacitinib (ROR 3.39, 95% CI 3.25 - 3.53), upadacitinib (ROR 4.28, 95% CI 3.95 - 4.63), baricitinib (ROR 1.82, 95% CI 1.54 - 2.14).Conclusion: While a warning for fractures is only included for tofacitinib, the results from this global pharmacovigilance analysis identified elevated reporting of fractures with tofacitinib, upadacitinib, and baricitinib. However, ICSRs with fractures were older and more likely to have other drugs that may indicate a baseline fracture risk reported. Therefore, further causality assessment is required.

Table 1. Characteristics of Individual Case Safety Reports and Disproportionality Analysis for Tofacitinib, Upadacitinib, and Baricitinib

	Tofacitinib		Upadacitinib		Baricitinib	
	All cases (n=122,037)	Fracture cases (n=2202)	All cases (n=27,786)	Fracture cases (n=634)	All cases (n=14,616)	Fracture cases (n=144)
ICSR Characteristics*						
Female	77.4	88.6	72.7	84.9	74.1	88.2
Unknown sex	3.2	0.8	5.3	1.6	3.6	1.4
Mean age (sd)	59.4 (13.8)	66.6 (10.9)	57.2 (14.2)	64.7 (10.6)	59.7 (14.2)	66.8 (10.4)
Unknown age	12.3	5.2	49.1	43.4	34.1	30.6
Number of medications						
0-4	86.7	75.7	89.2	79.8	87.1	79.9
5-9	8.2	11.9	6.7	10.6	9.7	13.9
≧10	5.1	12.4	4.1	9.6	3.2	6.2
Co-reported medications						
Glucocorticoids	7.2	14.1	5.1	8.2	9.4	10.4
Opioids	2.8	6.1	2.3	5.5	2.7	4.9
Bisphosphonates	0.9	3.8	0.6	1.6	1.0	4.2
NSAIDs	8.3	15.4	5.6	9.0	7.7	10.4
Disproportionality analysis†						
	Tofacitinib		Upadacitinib		Baricitinib	
	ROR	95% CI	ROR	95% CI	ROR	95% CI
	3.39	3.25 – 3.53	4.28	3.95 – 4.63	1.82	1.54 – 2.14

Abbreviations: ICSR=individual case safety report; sd=standard deviation; NSAIDs=non-steroidal anti-inflammatory drugs; ROR=Reporting odds ratio; CI=confidence interval

*All characteristics are reported as the column percentage, unless otherwise stated

† reporting odds ratios (RORs) calculated as the number of fractures reported with the drug of interest, compared to the number of fractures reported for all other drugs in the database during the same time period.

***Disclosures: Andreas Clausen**, None*

FRI-080

Comparative effects of antihypertensive medications on fracture risk in elderly patients with hypertension *Seung Shin Park[3], Hanna Jang[2], Sung Hye Kong[3], Hyunmook Jeong[3], Siyeon Yi[3], Seung Hun Lee[4], Jeonghoon Ha[5], Kwangsoo Kim[3], Jung Hee Kim[3], SANG WAN KIM[6], Chan Soo Shin[7]. [3]Seoul National University Hospital, Korea, Democratic People's Republic of. [2]Seoul National University Bundang Hospital, Korea, Democratic People's Republic of. [3]Seoul National University Hospital, Republic of Korea. [4]Asan Medical Center, Korea, Democratic People's Republic of. [5], Republic of Korea. [6]Seoul National University College of Medicine, Boramae Medical Center, Republic of Korea. [7]Seoul National University College of Medicine, Republic of Korea

Background:Hypertension and osteoporosis commonly coexist in the elderly, and some antihypertensive medications have been reported to potentially lower the risk of fractures. However, there is limited data comparing the effects of different antihypertensive agents and their combinations on fracture risk. We aimed to investigate the individual and combined effects of antihypertensive drugs on fracture risk in this study.Methods:A total of 28,247 patients who received antihypertensive medications for at least one year between 2008 and 2012 at Seoul National University Hospital were retrospectively reviewed using common data model. Patients were categorized into groups based on their antihypertensive medication use: antiotensin receptor blocker (ARB), calcium channel blocker (CCB), beta blocker (BB), ARB with CCB, ARB with BB, ARB with thiazide, CCB with BB, and ARB with BB and thiazide, for the purpose of analysis. Fracture risks, defined as major osteoporotic fractures (MOFs), vertebral fractures (VFs), and hip fractures (HFs), were analyzed using the Cox proportional hazard model with adjustments made for age, sex, body mass index, previous history of fractures, secondary osteoporosis-related conditions, diabetes mellitus, drug use, and the use of osteoporosis medications.Results:The number of patients using ARB, CCB, BB, ARB with CCB, ARB with BB, ARB with thiazide, CCB with BB, and ARB with BB and thiazide were 5,515, 7,514, 4,940, 5,022, 1,055, 1,965, 1,874, and 362, respectively. Among the total patient population, females accounted for 50.6%, and the average age and BMI were 65.8 years and 24.5 kg/m2, respectively. Compared to the CCB group, the BB group showed a significantly increased risk of osteoporotic fractures (MOFs) and vertebral fractures (VFs) (Hazard ratio (HR) 1.24, 95% confidence interval (CI) [1.01, 1.52] for MOFs; HR 1.40, 95% CI [1.08, 1.91] for VFs). In contrast to the BB group, the ARB with BB group and ARB with BB and thiazide groups demonstrated decreased HRs for VFs of 0.51 and 0.29, respectively (95% CI [0.28, 0.94] and [0.09, 0.93]). No significant differences in fracture risk were observed between the ARB monotherapy group and the ARB with BB, ARB with CCB, or ARB with thiazide groups (HR 1.07, 1.03, and 0.87 respectively). Conclusion:In hypertensive patients with concomitant osteoporosis, prioritizing the use of ARB and thiazide over BB when selecting medications may help reduce the risk of fractures.

***Disclosures: Seung Shin Park**, None*

FRI-083

Associations Between the Changes in Gut Microbiota and Bone and Muscle Outcomes After Sleeve Gastrectomy *Angela Yang[1], Julie-Catherine Coll[2], Thibault Varin[3], Serge Simard[3], Suzanne Morin[4], Fabrice Mac-Way[5], André Tchernof[6], Bettina Willie[4], Stéfane Lebel[7], André Marette[3], Claudia Gagnon[8]. [1]Universite Laval, , [2]CHU de Québec Research Centre, Quebec Heart and Lung Institute Research Centre, Canada. [3]Quebec Heart and Lung Institute Research Centre, Canada. [4]McGill University, Canada. [5]CHU de Québec Research Centre, Department of Medicine, Laval University, Canada. [6]Quebec Heart and Lung Institute Research Centre, Department of Medicine, Laval University, Canada. [7]Quebec Heart and Lung Institute Research Centre, Department of Surgery, Laval University, Canada. [8]CHU de Quebec, Universite Laval, Canada

The mechanisms leading to bone and muscle loss after sleeve gastrectomy (SG) remain unclear. We aimed to determine whether changes in the gut microbiota following SG are associated with this bone and muscle loss.This is an exploratory analysis of a multicentre prospective cohort study, in which 70 participants with severe obesity had the following parameters measured before and one year after SG: lumbar spine, total hip, and femoral neck areal bone mineral density (aBMD) and whole-body lean mass by dual-energy X-ray absorptiometry; lumbar spine, total hip, femoral neck, tibia, and radius volumetric BMD (vBMD), bone strength (maximum cross-sectional moment of inertia [CSMI] and maximum section modulus [Z]), and mid-femur muscle cross-sectional area by quantitative computed tomography; serum bone turnover markers (C-terminal crossed-linked telopeptide of type 1 collagen [CTX], procollagen type 1 N-terminal propeptide [P1NP], osteocalcin); lower limb absolute and relative muscle strength by isometric dynamometry. Gut microbiota from stool samples was analyzed by 16S rRNA gene sequencing at baseline and one year after SG. Results are presented as percentage or mean+/-SD. Linear regression analyses adjusted for age and sex were used to assess the associations between microbial, bone, and muscle parameters.A preliminary sample of 19 participants (79.0% women [26.7% postmenopausal], 57.9% with type 2 diabetes, mean age 45.3+/-9.5 years, mean BMI 40.1+/-0.6 kg/m2 at baseline) was analyzed. One year after SG, weight (-26.3+/-6.1%), aBMD (-6.4 to -8.5% depending on skeletal sites), vBMD (-1.0 to -7.4% depending on skeletal sites), whole-body lean mass and mid-femur muscle cross-sectional area as well as lower limb absolute muscle strength all decreased significantly (Table). Bone strength parameters did not change. All serum bone turnover markers increased significantly. Alpha diversity, represented by Shannon (p=0.04) and Simpson (p=0.02) indices, increased significantly while beta microbial diversity did not change (p=0.60).In this preliminary sample, significant associations were identified between bacteria genera and some bone parameters, but not between microbial and muscle parameters. Further analysis of the additional participants is ongoing to confirm that associations observed between gut microbiota composition and bone outcomes after SG persist in the larger cohort.

	Percent change (%)	p-value[a]
Bone mass outcomes		
Areal BMD (g/cm^2)		
Lumbar spine	-1.9 ± 6.8	0.1426
Total hip	-8.5 ± 3.5	**0.0002**
Femoral neck	-6.4 ± 4.1	**0.0002**
Volumetric BMD (g/cm^3)		
Lumbar spine (L2-L3)	-1.0 ± 1.3	**0.0016**
Total hip	-7.4 ± 3.1	**< 0.0001**
Femoral neck	-4.3 ± 2.7	**< 0.0001**
Distal tibia	-1.5 ± 4.5	0.2065
Distal third radius	-5.1 ± 3.6	**< 0.0001**
Bone strength outcomes		
Max CSMI femoral neck (cm^4)	0.1 ± 13.0	0.4037
Max CSMI tibia (cm^4)	-3.5 ± 8.0	0.1336
Max CSMI radius (cm^4)	-2.6 ± 13.4	0.6435
Max Z femoral neck (cm^3)	-3.1 ± 7.4	0.1628
Max Z tibia (cm^3)	-1.4 ± 6.1	0.2288
Max Z radius (cm^3)	-1.7 ± 9.8	0.5293
Serum bone turnover markers		
CTX (ng/ml)	134.2 ± 95.4	**< 0.0001**
Osteocalcin (ng/ml)	90.8 ± 59.9	**< 0.0001**
P1NP (ng/ml)	64.8 ± 65.4	**0.0006**
Muscle mass outcomes		
Whole-body lean mass (g)	-13.4 ± 7.3	**0.0001**
Mid-femur muscle cross-sectional area (cm^2)	-19.1 ± 5.7	**0.0002**
Muscle strength outcomes		
Lower limb absolute strength (kg)	-29.0 ± 20.0	**< 0.0001**
Lower limb relative strength (kg/kg body weight)	-3.9 ± 26.5	0.6397

Data are expressed as mean ± SD.
[a]Wilcoxon signed-rank tests were used to compare paired outcome values between the baseline and one-year study visits.

***Disclosures: Angela Yang**, None*

FRI-085

Treatment With Monthly Romosozumab Injections Increases Areal Bone Mineral Density at the Lumbar Spine and Hip in Women With Chronic Spinal Cord Injury *W. Brent Edwards[1], Laura E. Crack[1], Tudor Muresan[1], Narina Simonian[2], Thomas J. Schnitzer[2]. [1]University of Calgary, Canada. [2]Northwestern University Feinberg School of Medicine, United States

Sublesional bone loss is a known complication of spinal cord injury (SCI) with low bone mineral density (BMD) and increased fracture risk persisting into the chronic phase of injury. While existing literature focuses on pharmaceutical treatment options to prevent bone loss in acute SCI, limited investigations have examined potential therapies to increase BMD in chronic SCI. Romosozumab, a monoclonal antibody that inhibits sclerostin, has illustrated significant bone growth in pre-clinical models and among able-bodied post-menopausal clinical populations. The purpose of this study was to examine the efficacy of romosozumab to increase BMD in women with chronic SCI and an inability to ambulate. Twelve women with a mean (SD) age of 45.4 (9.1) years and injury duration of 15.1 (11.2) years, were administered monthly subcutaneous injections of romosozumab (210 mg) for one year. Areal BMD of the lumbar spine and hip (total hip and femoral neck) were measured at baseline and after 6 and 12 months using dual energy x-ray absorptiometry (DXA). The study is on-going and currently nine of the 12 participants have completed all aforementioned data collection. A preliminary analysis was conducted using longitudinal mixed-effects models to examine the effect of one year of romosozumab treatment on DXA-derived areal BMD measures. Areal BMD at the lumbar spine significantly increased ($p<0.001$) by an average of 6.1 (3.6)% and 9.3 (3.1)% after 6- and 12-months, respectively (Fig. 1). DXA-derived BMD at the total hip increased ($p<0.001$) with average gains of 2.2 (2.6)% and 4.1 (3.1)% after 6- and 12-months, respectively. Results were similar when isolating the femoral neck ($p=0.014$), which increased by an average of 1.8 (6.9)% at 6-months and 4.6 (4.9)% at 12-months. These results are comparable to the treatment efficacy of romosozumab for post-menopausal osteoporosis, which induced an annual increase in areal BMD of approximately 17% at the lumbar spine and 5% at the hip1. These preliminary findings demonstrate that treatment with romosozumab in women with chronic SCI increases areal BMD at the lumbar spine and hip, similar to effects in post-menopausal osteoporosis in able-bodied women. On-going data collection in this clinical trial will lead to further analysis with a larger sample size, and evaluation of bone mineral at the knee and hip using computed tomography.[1] Ishibashi H et al. (2017). Bone. 103:209-215

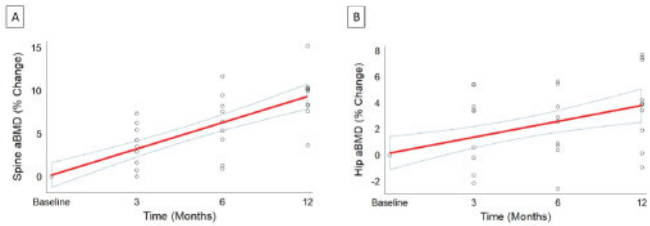

Figure 1. Individual (n=9) and average (95% CI) percentage change in lumbar spine (A) and total hip (B) areal bone mineral density (aBMD) throughout 12 months of treatment with subcutaneous injections of romosozumab (210 mg)

***Disclosures: W. Brent Edwards**, Amgen, Grant/Research Support*

FRI-086

IL-4 Protects the Male Mouse from Age-Associated Trabecular Bone Decline, While IL-4 Deficiency May Contribute to Bone Loss and Fracture in People Living With HIV. *Sadaf Dabeer[1], Daiana Weiss[1], Tatyana Vikulina[1], Ashish Tripathi[1], Ajay Chawla[2], Ighovwerha Ofotokun[3], M. Neale Weitzmann[4]. [1]Emory University, United States. [2]University of California, United States. [3]The Grady Healthcare System, United States. [4]Emory University School of Medicine, United States

HIV infection leads to bone loss in People living with HIV (PLH). This is aggravated by antiretroviral therapy (ART), resulting in high rates of fractures in PLH. The mechanisms driving HIV-induced bone loss prior to ART are multifactorial, and incompletely delineated. IL-4, a potent inhibitor of osteoclastogenesis and bone resorption, is secreted by CD4+ Th2 cells. As CD4 T cells are depleted in HIV infection, we hypothesized that an ensuing decline in IL-4 levels in PLH, may contribute to bone loss. We thus quantified IL-4 in PLH prior to ART and in uninfected controls and found a significant decline in serum levels of IL-4. Furthermore, serum levels of IL-4 were significantly, inversely associated with serum CTX, a marker of bone resorption. To further investigate the effect of IL-4 deficiency on bone, we used prospective in vivo μCT to phenotype the skeletons of male and female WT control and IL-4 knockout (KO) mice, from 2 to 20 months of age. The data revealed a significant decrease in BV/TV and bone structure indices, in both male and female IL-4 KO mice at 10 months of age. Between 6 and 20 months of age, female WT and IL-4 KO mice underwent age associated bone loss that was exacerbated in female mice between 6 and 10 months but resolved at later timepoints. By contrast, BV/TV was stable in WT male mice between 6 and 20 months, while IL-4 KO male mice underwent significant progressive bone loss. The data highlight an important sex difference and suggest that IL-4 may protect the male skeleton from age-related declines in trabecular bone. To further explore the mechanisms of

IL-4 action in vivo, mice with a conditional deletion of the IL-4 receptor alpha (IL-4R?) in the monocyte/osteoclast lineage, were generated by crossing IL-4R? floxed mice with LysM-Cre mice. The conditional deletion of IL-4 signaling in the monocyte/osteoclast lineage resulted in a significant decline in BV/TV and in structural indices in both male and female mice at 10 months of age, implicating the monocyte/osteoclast-cell lineage as major target cells of IL-4 in vivo. Overall, the data suggest that IL-4 may play a crucial role in protecting the male skeleton from age-related trabecular bone loss. The data further support the hypothesis that a decline in IL-4 due to HIV infection, may contribute to increased bone loss and fracture risk in PLH. Therefore, IL-4 could be a novel potential biomarker and therapeutic target for reversing HIV and age-related bone loss.

***Disclosures: Sadaf Dabeer**, None*

FRI-090

Mechanisms of the Anti-Anabolic Action of Progranulin from Transcriptional Profiling *Robert Nissenson[1.] [1]VA Medical Center and University of California, San Francisco, United States

Deficient bone formation is a prominent feature of bone loss associated with inflammation and aging. Progranulin (PGRN) is a protein that is implicated in the immune response in disorders that affect bone health such as rheumatoid arthritis. We have shown that global deletion of the Grn gene that encodes PGRN results in protection of female mice from bone loss that occurs between 3 and 12 months of age. Similar protection was seen with targeted deletion of Grn in Cx3cr1-cre positive myeloid cells. These results suggest that the negative effect of PGRN on bone formation results from an interaction between bone marrow macrophages (BMMs) and osteoblasts (OBs). To gain insight into the mechanism behind this, we have compared the BMM populations in WT vs Grn KO female mice. FACS analysis identified a discrete population of BMMs in WT mice that displayed low level expression of the marker Mac2 (galectin-3). This Mac2 Lo population was almost completely absent in Grn KO mice. Transcriptome analysis demonstrated that Mac2 Lo BMMs were enriched (> 5-fold) in the expression of several genes involved in inflammatory responses (Nlrp3, Il1b, Ptgs2, Ccr1, Cxcl2, Selplg, Clec7a, Trem1, Csf1, Il17ra, Tlr6, Ccl3). To explore how expression of PGRN by BMMs influences osteogenesis, we carried out transcriptomic studies of WT vs. Grn KO bone marrow stromal cells (BMSCs). BMSCs were isolated from adult female WT and Grn KO mice and were induced to undergo osteogenesis. At cell culture day 21, genome wide transcriptome analysis was carried out by RNAseq. 160 genes were up-regulated >2-fold in Grn KO cultures in three paired data sets. Bioinformatic analysis of these genes identified “mitosis” and “cell cycle regulation” as highly enriched pathways. 77 genes were down-regulated > 2-fold in Grn KO cultures in these three paired data sets. Bioinformatic analysis of these genes identified “signaling by G protein-coupled receptors” and “Gi signaling events” as the most enriched pathways. These findings indicate that PGRN expression maintains a distinct pro-inflammatory population of BMMs in adult female mice. PGRN may act to suppress proliferation while promoting Gi signaling in OBs. Our previous results demonstrate that blockade of Gi signaling in OBs in vivo has effects on bone that phenocopy the effects seen in Grn KO mice. Taken together, these findings suggest that BMM-derived PGRN may function upstream of OB Gi signaling to suppress bone formation in adult female mice.

***Disclosures: Robert Nissenson**, None*

FRI-092

Inflammasome activation is an important mechanism in chemotherapy-induced bone loss *Chun Wang[1.] Gabriel Mbalaviele[2.] [1]Division of Bone and Mineral Diseases, Washington University School of Medicine, United States. [2]Washington University in St. Louis School of Medicine, United States

Doxorubicin is a widely used chemotherapy drug for the treatment of a variety of tumors including breast cancer. Despite its success in improving survival rates of cancer patients, it causes deleterious side effects, including bone marrow toxicity, neutropenia, irreversible heart muscle damage, osteoporosis, and fracture risk, but the underlying mechanisms remain unknown. We hypothesized that doxorubicin causes DNA damage, which leaks to the cytoplasm, and cell death, which releases DNA to the extracellular environment. We further hypothesized that mislocalized DNA is sensed by inflammasomes, intracellular protein complexes that propagate inflammation through various mechanisms, including the maturation and secretion of IL-1?. To test these ideas, we used a non-tumor-bearing mouse model, which allowed the assessment of direct tissue off-target effects of this drug in the absence of tumor confounding outcomes. A single injection of 5 mg/kg doxorubicin to wild-type (WT) mice caused NETosis, a form of neutrophil cell death that follows the release to the extracellular space of genomic DNA and granular contents known as neutrophil extracellular traps (NETs). Specifically, doxorubicin administration increased serum levels of NETosis markers such as citrullinated histone 3 and myeloperoxidase. This response correlated with cytopenia, elevated IL-1? serum levels, increased osteoclast number (N.Oc/BS: vehicle = 4.84+/-0.43; doxorubicin = 12.53+/-1.56), and bone loss (BV/TV: vehicle = 29.21+/-3.93%; doxorubicin = 12.29+/-1.82%). Since damaged or mislocalized DNA is mainly detected by inflammasomes assembled by AIM2 or NLRP3 sensors, we determined their role in doxorubicin actions. Consistent with our hypothesis, doxorubicin osteopenic effects were attenuated in animals lacking AIM2 inflammasome or NLRP3 inflammasome, to some extent (BV/TV: WT = 12.29+/-1.82%; Aim2-/- = 23.33+/-4.05%; Nlrp3-/- = 16.68+/-2.05%). Thus, off-target actions of doxorubicin cause inflammasome activation, a response that ultimately, leads to bone loss.

***Disclosures: Chun Wang**, None*

FRI-093

Hematopoietic and stromal Dmp1-Cre labeled cells form a unique niche in the bone marrow *Sierra Root[1.] Brya Matthews[2.] Elena Torreggiani[1.] IVO KALAJZIC[3.] [1]Center for Regenerative Medicine and Skeletal Development, UConn Health, United States. [2]University of Auckland, New Zealand. [3]University of Connecticut Health Center, United States

Skeletogenesis and hematopoiesis are interdependent. Niches are formed between cells of both lineages and support specific lineage commitment. Because of the complex topography of the bone marrow (BM) space, the identity and function of cells within specialized niches has not been fully elucidated. DMP1-Cre animals have been utilized in bone biology studies as mature osteoblasts and osteocytes highly express DMP1. However, DMP1 has been identified in nonmineralized tissue including CXCL12+ BM cells and an undefined CD45+ hematopoietic population. We aimed to investigate the role of this unconsidered BM population. We crossed DMP1-Cre with Ai9 reporter mice and analyzed the tdTomato+ (tdT+) population and niche. By flow cytometry and Image Stream, 1% of cells are CD45+tdT+ and express myeloid markers including CD11b. By histology, tdT+CXCL12+ stromal cells are in direct contact with F4/80+ macrophages. CD45+tdT+ cells are established early in ontogeny by E15.5. CD45+tdT+ cells phagocytose latex beads, respond to LPS, and are radioresistant. Furthermore, depletion of macrophages with clodronate liposomes and 5-FU treatment caused a significant decrease in the tdT+CD11b+ gated F4/80+Ly6G+ population. Characterization of resident macrophage populations identified CD45+tdT+ cells to be erythroid island macrophages (EIM). Flow cytometric analysis of intact erythroid blood islands (EBI) demonstrated enrichment of tdT+ cells that were Ly6G+CD51+VCAM1+CD169+ER-HR3+. Upon treatment with GCSF, CD45+tdT+ EBIs and EIM significantly decrease. By histology, endogenous DMP1 protein was evaluated with tdT reporter. Extracellular DMP1 protein was located next to or on the processes of tdT+ stromal cells and in direct contact with tdT+ macrophages expressing cytoplasmic and nuclear DMP1. Using tamoxifen inducible DMP1-CreER, a myeloid CD45+tdT+ population expands in adult mice. By histology tdT+ stromal cells express RANKL, stromal processes are seen in direct contact with B cells and tdT+ sorted cells express a key niche factor for B cells, IL7. Secondary hematopoietic organs were also analyzed and a similar tdT+ population that express RANKL found to reside in thymus. In conclusion, DMP1-Cre labels a unique macrophage/stromal niche expressing key microenvironmental factors RANKL and IL7.In memory of Dr. Hector Leonardo Aguila †

***Disclosures: Sierra Root**, None*

FRI-094

Quantitative Lightsheet microscopy of human bones reveals a highly vascularized but degenerated sinusoidal environment for skeletal stem cells with aging *tszlong chu[1.] EMIL KRIUKOV[1.] DANA TROMPET[1.] Misty Shuo Zhang[2.] Ostap Dregval[3.] Björn Barenius[4.] Lars Sa?vendahl[5.] Andrei Chagin[3.] [1], . [2]First Affliated Zhejiang Univeristy Hospital, China. [3]Gothenburg University, Sweden. [4]Södersjukhuset, Karolinska Institutet, Sweden. [5]Karolinska Institutet and Karolinska University Hospital, Sweden

The current understanding of human bone and its marrow spatial organization is largely limited to 2D analysis of tissue sections. Here we developed a tissue-clearing approach coupled with multiplexed detection of mRNAs and proteins, which allows 3D visualization, reconstruction, and quantification of various structures and markers in large samples of aged human bone. As a proof-of-principle, quantitative automated 3D profiling of 380,000 osteocytes embedded within the bone matrix revealed a drastic loss of SOST-expressing (mRNA) osteocytes, i.e., Romosozumab targeted cells, the relocation of the remaining SOST+ cells toward the bone surface, and increased spatial dispersion with age. Multiplex RNA probing of DMP1+FGF23+SOST+ cells revealed that the lineage continuum of osteocytes was relatively sustained thereby indicating the reduction of SOST+ cells with age was not primarily caused by upstream reduction of immature osteocyte supply. By combining 3D mRNA and protein detection, we further characterized CXCL12-expressing stromal cells (CAR cells) in the human bone marrow in relation to arteriolar and sinusoidal vasculature, adipocytes, and bone matrix. The density of CAR cells did not change significantly with age, but their surrounding did. In young bones, CAR cells were found in close proximity to both the bone surface and sinusoids (Endoglin+ vessels), whereas with age these cells were found mostly near arteriolar bed with about 25% of cells trapped within adipocytes. Quantification of CD271+ and CD146+ subsets of CXCL12+ stroma revealed that these two populations of skeletal stem and progenitor cells occupy distinct trabecular and arteriolar niches while sharing a sinusoidal environment that degenerates with age. Therefore our work provides the first comprehensive spatial characterization of changing bone microenvironment in relation to human aging.

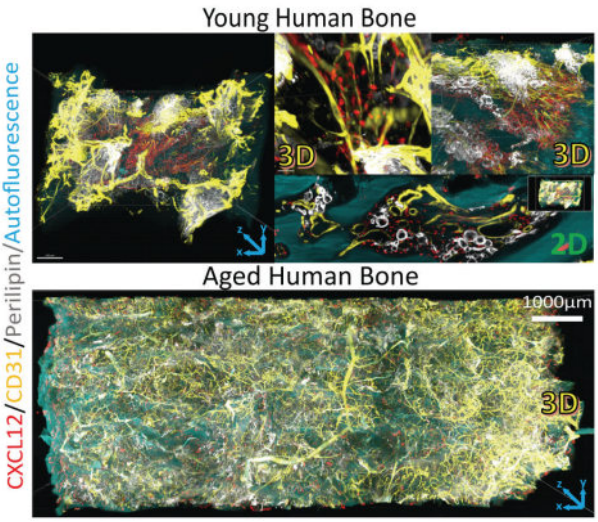

***Disclosures: tszlong chu**, None*

FRI-101

Osteoblast-triggered downregulation of Nucleoporins transforms myelodysplastic cells to induce development of acute myeloid leukemia *Alvaro Cuesta-Dominguez[1], Ioanna Mosialou[1], Brygida Bisikirska[1], Marta Galan-Diez[1], Abdullah Ali[2], Diana Kotini[3], Malgorzata Olszewska[3], Manon Jaud[3], Stephanie Braunstein[4], Aaron Viny[4], Junfei Zhao[5], Raul Rabadan[5], Eirini Papapetrou[3], Azra Raza[2], Stavroula Kousteni[1]. [1]Department of Physiology and Cellular Biophysics, Columbia University Irving Medical Center, United States. [2]Center for Myelodysplastic syndromes, Columbia University Irving Medical Center, United States. [3]Department of Oncological Sciences, Icahn School of Medicine at Mount Sinai, United States. [4]Department of Genetics and Development, Columbia University Irving Medical Center, United States. [5]Department of Systems Biology, Columbia University Irving Medical Center, United States

Acute myeloid leukemia (AML) often transforms from pre-AML states such as myelodysplastic syndromes (MDS). To gain mechanistic insight into the transformation of MDS to AML we compared the transcriptional profile of hematopoietic stem and progenitor cells (HSPCs) from mouse models of osteoblast-induced MDS and AML mice as well as of bone marrow mononuclear cells from patients at their MDS and AML transformed stages. We found a decrease in the expression of Nucleoporin (NUP) family members with transformation to AML that was confirmed in two additional MDS to AML mouse models and following analysis of publicly available human data. Notably, low NUPs expression associates with poor prognosis in AML. shRNA knockdown of NUPs in HSPCs from MDS mice and transplantation to wild type recipients led to fully penetrant AML with blast infiltration in blood, bone marrow and spleen. To examine the relevance of NUPs in human disease we downregulated NUPs expression in a model of induced Pluripotent Stem Cell (iPSC)-derived HSPCs harboring the MDS-relevant SRSF2P95L and ASXL1646fs*12 mutations (SA). shNUPS-SA overcame exhaustion and loss of CD34 expression that is typical of MDS cells. Surviving cells maintained growth for as long as 10 months, acquired phenotypic characteristics of AML blasts and presented a 2.5-fold upregulation of the leukemic biomarker CD123. Unlike MDS cells, shNUPS-SA HSPCs engrafted in NSG mice, establishing the transformative potential of NUP downregulation in a humanized in vivo model. Transcriptional changes caused by NUPs downregulation in MDS-SA HSPCs captured transformation by comparison to gene expression datasets of iPSC-HSPC models of MDS and AML. GSEA analysis revealed upregulation of a signature that is highly expressed in pediatric AML and encompasses genes involved in mitochondrial biogenesis and neutrophil activation. Chromatin accessibility analysis by ATACseq in the human MDS-L cell line showed increased accessibility in genes involved in proliferation (MAPK10, RAB36, RAB7A), apoptosis (PIM3), cell cycle (CDK7) and ribosomal biogenesis (RPS12, RPL19, RPL18A, RPS19). Thus, low NUPs expression drives transformation of MDS to AML by activating a multi-pronged network of AML-favoring biological outcomes that involve rescuing MDS cells from apoptosis and promoting their entry to cell cycle and proliferation, while at the same time enhancing their metabolic activity to fuel blast expansion and activation of the immature myeloid lineage.

***Disclosures: Alvaro Cuesta-Dominguez**, None*

FRI-105

An IAP antagonist combined with a novel adoptive dendritic cell targeting delivery of TNF to treat breast cancer *Rong Duan[1], Philip Milton[1], Jun Wu[1], Md. Mahmudul Hasan Akash[1], Xin Liu[1], Brendan Boyce[1], Zhenqiang Yao[2]. [1]University of Rochester Medical Center, United States. [2]University of Rochester, United States

Inhibitor of apoptosis proteins (IAPs) restrain caspase-mediated apoptosis. The IAP antagonist, SM-164, which efficiently degrades IAPs, does not kill cancer cells, but we found that it enabled TNF? to strongly induce breast cancer (BC) cell apoptosis in vitro, and combined with TNF? it significantly reduced the % of leg bones with metastases from heart-injected MDA-MB-231 BC cells in a mouse model (40% vs 88% in vehicle, p<0.01). SM-164 alone or a standard chemotherapy (SCT) regimen reduced tumor burden in bone, but not the % of bones with metastases. However, SM-164+TNF? more effectively reduced tumor burden in bone than SM-164 or SCT. Treatment of mice inoculated with MDA-MB-231 cells with a TNF antibody or with clodronate, which depletes macrophages, reduced the inhibitory effect of SM-164 on tumor growth in bone, and clodronate inhibited osteolysis. These findings suggest that TNF?+SM-164 could be an effective therapy to reduce BC bone metastasis. However, systemically administrated TNF? can have serious side effects and is not a practical therapy. Thus, we examined the effects of targeted delivery of TNF?+SM-164 on BC. Overexpression of Mucin1, a surface glycoprotein on epithelial cells, is associated with tumorigenesis and metastases. We induced and expanded dendritic cells (DCs) from human peripheral blood using M-CSF and GM-CSF and engineered them to express TNF? and chimeric CD66b-Mucin1 scFv, which was constructed by linking Mucin1 monoclonal Ab scFv to the extracellular domain of a truncated portion of myeloid cell receptor, CD66b, to target BC. We called these novel engineered DCs Mucin1-directed DCs producing TNF? (M-DCsTNF). Conditioned medium from M-DCsTNF (contains 300 pg/ml TNF?) strongly induced MDA-MB-231 cell death in the presence of SM-164 in vitro; this was blocked by a TNF Ab. Specific binding of M-DCsTNF to MDA-MB-231 cells was confirmed in bones in NSG mice. Importantly, SM-164 given with a one-time injection of M-DCsTNF significantly reduced the growth of human BC from orthotopically-injected Her2+ BT474 BC cells (median tumor weight 6.25 vs. 98.4 mg in vehicle, p<0.01) and patient-derived xenograft (PDX) of triple-negative BC (tumor wt. 0.78+/-0.42 vs. 1.56+/-0.82 g in vehicle, p<0.05) in NSG mice. In contrast, SM164 alone did not inhibit BC growth in the PDX model. Our findings suggest that an adoptive cell targeted delivery of TNF? to BC deposits combined with SM-164 may be a novel effective approach to treat breast cancer.

***Disclosures: Rong Duan**, None*

FRI-106

Prostate Cancer Bone Metastasis Alters Gut Microbiota Composition by Enhancing Gut Leakiness *Kelly Contino[1], Jenna Ollodart[1], Yang Yu[1], Sidharth Mishra[2], Laiton Steele[1], Katherine Cook[3], Hariom Yadav[2], Yusuke Shiozawa[1]. [1]Department of Cancer Biology, Wake Forest University Health Sciences, United States. [2]University of South Florida Morsani College of Medicine, United States. [3]Department of Hypertension, Wake Forest University Health Sciences, United States

In a state of dysbiosis, the physical, biochemical, and immune barriers separtating gut bacteria from systemic circulation become compromised. This loss of gut barrier integrity, referred to as “leaky gut”, has been implicated in the pathogenesis of numerous diseases including cancer. The translocation of the gut derivatives as a result of leaky gut has been shown to drive tumorigenesis and cancer progression, including prostate cancer (PCa). Despite this link to tumor formation/progression, the relationship between leaky gut and metastasis, specifically to the bone, remains unexplored. To begin understanding the complex mechanisms between the gut and bone metastasis, the leading cause of death in PCa patients, we intrafemorally inoculated murine PCa cell line RM-1 cells into C57BL/6 mice. Bulk RNA sequencing of intestinal tissue from these mice revealed that markers of intestinal tight junctions (physical barrier) and gut mucosal membranes (biochemical barrier) were downregulated in the intestinal tissue of PCa-bearing mice. This data suggests that bone metastasis alone is capable of inducing leaky gut. To validate these findings, serum ELISAs for LPS binding protein (LBP) and sCD14, well-established markers of leaky gut, were performed. Significantly higher levels of LBP and sCD14 were observed in the serum of PCa-bearing mice, compared to that of sham mice, further supporting the notion that leaky gut occurs as a result of bone metastasis. Then, to examine whether bone metastasis induces changes in gut microbial composition,16s rRNA sequencing of the mouse stool was conducted. Interestingly, elevated levels of Dorea formicigenerans and Ruminococcus gnavus, mucin degrading bacteria known to enhance leaky gut, were found in the stool of PCa-bearing mice. Several butyrate generating bacteria were found to be upregulated in the stool of PCa-bearing mice. Butyrate is a short chain fatty acid known to contribute to bone formation. Clostridum scindens, known to convert glucocorticoids into androgen, was also elevated in the stool of PCa-bearing mice. Conversely, Faecalibaculum rodentium, known to be protective against intestinal tumor growth, was significantly enhanced in the stool of sham mice. Collectively, these results suggest that bone metastasis alters the gut microbiota composition by enhancing gut leakiness. Future studies are clearly warranted to further reveal the mystery of gut-bone metastasis axis.

***Disclosures: Kelly Contino**, None*

FRI-108

Effect of Autologous Dendritic Cell Vaccine and Anti-MDSC Treatment Against 4T1 Breast Cancer Cells in Mice *Pierrick Fournier[1], Paloma Almeida Luna[2], Danna Arrellano[2], Samanta Jimenez[3], Patricia Juarez[4]. [1]Centro de Investigacion Cientifica y de Educacion Superior de Ensenada (CICESE), Mexico. [2]Posgrado en Ciencias de la Vida, CICESE, Mexico. [3]Centro de Investigación Cientifica y de Educacion Superior de Ensenada (CICESE), Mexico. [4]Center for Scientific Research and Higher Education, Mexico

Immunotherapies can cause long-term response in cancer patients. Autologous dendritic cell (DC) vaccines (DC-Vax) can induce T and B cell-mediated anti-tumor response. However, its efficacy still seems limited in breast cancer and has not been assessed for bone metastases. We sought here to test the effect of an autologous DC-Vax in the 4T1 breast cancer syngeneic model, and whether its efficacy could be improved by increasing DC maturation with natural PAMP or combining with 5-Fluorouracil (5FU) to decrease the immunosuppressive myeloid-derived suppressor cells (MDSC).Bone marrow cells from Balb/C mice were differentiated to DC cells ex vivo (>80%). Loading DC with antigens (Ag) from 4T1 mammary fat pad (mfp) tumors did not induce their maturation, assessed by MHC-II, CD80 and CD86 expression by flow cytometry. However, combined treatment with LPS or Ag from a vaccine against rabies increased MHC-II and CD86 expression. In mice, 2 doses of LPS-treated DC increased the levels of anti-4T1 antibodies without increasing T cell infiltration, resulting in a modest decrease of 4T1 mfp tumor volume (-16%). The combined treatment LPS/rabies Ag of the DC did not improve their anti-tumor efficiency.5FU was reported to decrease MDSC levels in other cancer models, so we tested its efficacy against MDSC in 4T1 mfp tumors. 5FU at 25mg/kg decreased polymorphonuclear (PMN-) MDSC, but not monocytic (M-) MDSC in 4T1 tumors and increased infiltrating CD4+ T cells. While 50mg/kg 5FU decreased both PMN- and M-MDSC, it decreased the levels of T cells infiltrating the tumors. However, both doses decreased the volume of 4T1 mfp tumors (-18% and -33%, respectively). In 4T1 bone metastases, 5FU had similar effects on MDSC and T cells in bone.Consequently, we tested the effect the autologous DC-Vax combined with 5FU at 25mg/kg. However, although the combined treatment decreased of the amount of circulating MDSC and increased circulating levels of CD4+ and CD8+ T cells as wells as the levels of anti-4T1 antibodies in plasma, it did not decrease the volume of 4T1 mfp tumors.Based on these results, we conclude that while autologous DC vaccines are a promising personalized treatment option for patients with breast cancer, its efficacy remains limited at the pre-clinical level. Further research is needed to improve the preparation and maturation of the DC and combined treatment to increase the immune response is needed in order to support patients suffering from breast cancer.

***Disclosures: Pierrick Fournier**, None*

FRI-110

Bone-derived Dickkopf-Related Protein 1 promotes primary breast cancer tumor growth and supports hematopoietic stem and progenitor cells *Emily Eul[1], Biancamaria Ricci[1], Seunghyun Lee[1], Giulia Furesi[1], Roberta Faccio[1]. [1]Washington University in St. Louis , United States

Dickkopf-related protein 1 (Dkk1), a Wnt/?-catenin signaling inhibitor, is produced in the bone, and is best known for suppressing bone formation and increasing bone resorption. Interestingly, Dkk1 is upregulated in cancer patients and correlates with poor prognosis. Recent work has shown that Dkk1 can exert immune suppressive effects by altering the frequency and function of immune cell subsets in various cancer models. However, the role of Dkk1 in breast cancer progression and the mechanisms by which Dkk1 can affect so many immune cell types remain unclear.We found that mice bearing luminal B, ER+ PyMT-B6 tumors exhibit increased Dkk1 expression in the bone and higher systemic serum levels compared to no tumor bearing controls. To assess the role of Dkk1 during breast cancer tumor progression, female C57BL/6 mice were orthotopically injected with PyMT-B6 cells and treated with Dkk1 neutralizing antibody (?Dkk1) or IgG control antibody (10mg/kg every 48 hrs). We observe a striking reduction in tumor growth of ?Dkk1 treated mice, and systemic alterations to immune cell population frequencies. We also find similar results in mice bearing the metastatic basal-like ER- EO771-LMB breast tumors. To study the effects of bone-dervied Dkk1 we utilized osteoblast lineage specific Dkk1 overexpressing mice (2.3kbCol1?1Dkk1Tg) injected with PyMT-B6 cells and observed increases in tumor growth and changes in the immune landscape.To uncover how Dkk1 can modulate a variety of immune cell populations, we investigated the impact of tumor progression and Dkk1 on hematopoietic stem and progenitor cells (HSPCs) in the bone marrow of tumor bearing mice. Based on previous reports indicating that Dkk1 can influence HSPC regeneration and exhaustion, we performed noncompetitive bone marrow transplantation (BMT) assays using Dkk1 overexpressing mice and osteolineage conditional ckO mice, tTA-TetOFFOsx-Cre; Dkk1fl/fl and saw an increase in the engraftment of HSPC populations from over expressing mice. Additionally, we treated mice with PyMT-B6 or EO771-LMB with ?Dkk1 or IgG and discovered that Dkk1 strickingly reduced HSPC frequencies only in the EO771-LMB model, suggesting that Dkk1 may regulate hematopoiesis in a breast cancer subtype dependant manner.Together this data demonstrates that Dkk1 expression is upregulated in the bones and supports breast cancer tumor growth and hematopoiesis, overall, highlighting the existence of a bone-tumor crosstalk to promote tumor progression.

***Disclosures: Emily Eul**, None*

FRI-112

Bone-derived Osx+ Cells Infiltrate Mammary Tumors and Contribute to Extracellular Matrix Reorganization and Tumor Progression *GIULIA FURESI[1], Roberta Faccio[2]. [1]Washington University in St. Louis, School of Medicine, United States. [2]Washington University in St Louis School of Medicine, United States

Osterix (Osx) is a crucial transcription factor for osteoblast differentiation and bone mineralization. Interestingly, we detected expression of Osx in the stroma of various breast tumors (PyMT, E0771, 4T1) in adult mice, as well as in patients with advanced breast carcinomas. Using lineage tracing TdT-Osx+ mice, we demonstrated that tumor-infiltrating Osx+ cells support tumor growth when co-injected with cancer cells. To determine if ectopic Osx+ cells at the tumor site are derived from the bone marrow (BM), we lethally irradiated CD45.1 WT recipient mice and transplanted BM from CD45.2 TdTOsx+ mice to generate TdTOsx+>WT chimeric mice. After tumor inoculation, TdTOsx+ cells were detected both in circulation and at the primary tumor site, thus confirming a bone origin. Next, we wanted to assess the tumor-promoting abilities of bone resident Osx+ cells. In contrast to the tumor-infiltrating Osx+ cells, TdT-Osx+ populations isolated from the BM did not increase tumor growth when co-injected with PyMT cells. To further elucidate the identity of tumor-infiltrating Osx+ cells, we orthotopically injected PyMT cells into TdTOsx+ mice and performed Immunofluorescence and FACS analysis. Tumor sections showed the presence of TdTOsx+ stromal cells with elongated morphology, a common feature of cancer-associated fibroblasts (CAFs). RNA-seq and flow cytometry analyses of these cells confirmed the expression of CAF markers, such as alpha-SMA, Fsp1, PDGFR?, PDGFR?, Ly6C, and CD146, as well as genes associated with ECM reorganization and skeletal development. Next, to determine whether Osx directly drives the pro-tumorigenic effects of tumor-infiltrating Osx+ cells or merely marks BM mesenchymal populations at the tumor site, we ectopically expressed Osx or empty vector in murine mammary fibroblasts (MMF+Osx or MMFctr) and co-injected them with PyMT cells into WT mice. MMF+Osx significantly increased PyMT growth ($p>0.001$) compared to MMFctr or tumor cells alone. Interestingly, expression of Osx in mammary fibroblasts resulted in the upregulation of matrix-related genes. In line with these observations, second-harmonic generation imaging revealed higher collagen deposition ($p>0.05$) in the tumors co-injected with MMF+Osx compared to MMFctr. In conclusion, our findings demonstrate the existence of BM-derived osteolineage Osx+ cells in extra-skeletal tumors, which possess tumor-promoting effects and may represent a novel subset of matrix-producing CAFs.

***Disclosures: GIULIA FURESI**, None*

FRI-114

Breast cancer bone metastasis is mediated by the PTHrP NLS and C-terminal domain in a TGF-?/SNAI2/ZEB1 cascade *DEJA GRANT[1], Julia Ahn[2], Courtney Edwards[3], Jasmine Johnson[4], T. John Martin[5], Rachelle Johnson[4]. [1], United States. [2]Vanderbilt University, United States. [3]Vanderbilt University , . [4]Vanderbilt University Medical Center, United States. [5]St. Vincent s Institute of Medical Research, Australia

Breast cancer cells frequently metastasize to bone, where they may proliferate or enter a dormant state. Parathyroid hormone-related protein (PTHrP) expressed by breast cancer cells promotes tumor outgrowth in bone by increasing bone resorption and stimulating tumor cell exit from dormancy. PTHrP has multiple biological domains that determine its autocrine, paracrine, and intracrine functions, but the role of the PTHrP nuclear localization signal (NLS) and C-terminus is not well understood. To assess the role of PTHrP biological domains in breast cancer bone colonization, we stably expressed full-length secreted PTHrP, PTHrP with deletion of the NLS, or PTHrP with deletion of the NLS and C-terminus in human MCF7 breast cancer cells, which normally lay dormant in bone. MCF7 cells expressing these proteins were termed FLSEC, DNLS, and DNLS+CTERM mutant cell lines, respectively, and inoculated into athymic nude mice by intracardiac injection to facilitate bone colonization (n=8-10/group). Osteolytic lesion area and number, assessed by radiography, and tumor burden in the bone marrow quantified by flow cytometry, were significantly higher in mice inoculated with DNLS (5.9-fold, $p<0.05$) and DNLS+CTERM (4.19-fold, p77% decrease, $p<0.0023$), while ZEB1 was significantly upregulated in DNLS+CTERM cells (2.19-fold, $p<0.05$), compared to MSCV controls. Crosstalk within the TGF-?/Slug/ZEB-1 pathway is exceedingly complex, with bi-directional regulation, depending on the cell type and context. It is also well established that TGF-? positively regulates PTHrP; however, our data suggest that downregulation of Slug may be important for breast tumor progression in bone downstream of PTHrP, and this pathway may or may not converge on ZEB1. Taken together, our data indicate that PTHrP-mediated breast cancer-induced osteolysis involves the NLS and C-terminal domains signaling through EMT-associated pathways.

***Disclosures: DEJA GRANT**, None*

FRI-115

Non-bone metastatic Head and Neck Cancer promote osteocyte changes in patients and mice bearing the MLM3 HNC cells *Alexander J. Jones[1], Anika Shimonty[2], Joshua Huot[3], Daniel Marks[4], ANDREA BONETTO[5], Lynda Bonewald[6], Michael Moore[1], FABRIZIO PIN[7]. [1]Department of Otolaryngology - Head & Neck Surgery, Indiana University School of Medicine, Indianapolis, United States, [2]Indiana Center for Musculoskeletal Health, Indiana University School of Medicine, Indianapolis, United States, [3]Department of Anatomy, Cell Biology and Physiology, Indiana University School of Medicine, Indianapolis, United States, [4]Oregon Health & Science University, Portland, Oregon, United States, [5]University of Colorado Anschutz, United States, [6]Indiana University School of Medicine, United States, [7], United States

It is estimated that 54,000 people in the US will be diagnosed with Head and Neck Cancer (HNC) in 2023 ADDIN EN.CITESiegel202346[1]464617Siegel,R. L.Miller, K.D.Wagle, N. S.Jemal,A.Surveillanceand Health Equity Science, American Cancer Society, Atlanta, Georgia,USA.Cancer statistics,2023CA Cancer JClinCACancer JClin17-48731MaleHumansFemaleUnitedStates/epidemiologyMiddleAgedAged*Neoplasms/epidemiologyRegistriesIncidenceRacialGroups*Lung Neoplasms/epidemiology*Melanoma*MultipleEndocrine Neoplasia Type 1cancercasescancerstatisticsdeath rates-mortality2023Jan1542-4863(Electronic) 0007-9235(Linking)36633525https://www.ncbi.nlm.nih.gov/pubmed/3663352510.3322/caac.21763MedlineNLM[1]. HNC patients are at high risk of developing debilitant musculoskeletal alterations during the course of the disease ADDINEN.CITE ADDINEN.CITE.DATA 3C456E644E6F74653E3C436974653E3C-
417574686F723E4A6F6E65733C2F417574686F723E3C596561723E-
323032323C2F596561723E3C5265634E756D3E34373C2F5265634E756D3E3C-
446973706C6179546578743E5B322C20335D3C2F446973706C6179546578743E-
3C7265636F72643E3C7265632D6E756D6265723E34373C2F7265632D6E-
756D6265723E3C666F726569676E2D6B6579733E3C6B6579206170703D22454E22206
4622D69643D2272736673747864643064726674696530783573357872663676657761613
9783270303264222074696D657374616D703D2231363833323231363433223E3437
3C2F6B65793E3C2F666F726569676E2D6B6579733E3C7265662D74797065206E616D-
653D224A6F75726E616C2041727469636C65223E31373C2F7265662D747970653E3C6
36F6E7472696275746F72733E3C617574686F72733E3C617574686F723E4A6F6E-
65732C20412E204A2E3C2F617574686F723E3C617574686F723E44617669732C-
204B2E20502E3C2F617574686F723E3C617574686F723E4E6F76696E6765722C-
204C2E204A2E3C2F617574686F723E3C617574686F723E426F6E6574746F2C20412E-
3C2F617574686F723E3C617574686F723E4D616E-
747261766164692C20412E20562E3C2F617574686F723E3C617574686F723E53696D-
2C204D2E20572E3C2F617574686F723E3C617574686F723E596573656E736B-
792C204A2E20412E3C2F617574686F723E3C617574686F723E4D6F6F72652C-
204D2E20472E3C2F617574686F723E3C2F617574686F72733E3C2F636F
6E7472696275746F72733E3C617574682D616464726573733E4465706172746D656E742
06F66204F746F6C6172796E676F6C6F6779202D204865616420616E64204E65636B-
20537572676572792C20496E6469616E6120556E6976657273697479205363686F6F-
6C206F66204D65646963696E652C20496E6469616E61706F6C69732C20496E6469616E
612C205553412E262378443B4465706172746D656E74206F6620537572676572792C204
96E6469616E6120556E6976657273697479205363686F6F6C206F-
66204D65646963696E652C20496E6469616E61706F6C-
69732C20496E6469616E612C205553412E3C2F617574682D616464726573733E3C-
7469746C65733E3C7469746C653E506F73746F706572617469766520636F6E736571756
56E636573206F662063616E6365722063616368657869612061667465722068656164206
16E64206E65636B206672656520666C6170207265636F6E737472756374696F6E3C2F-
7469746C653E3C7365636F6E646172792D7469746C653E48656164204E65636B-
3C2F7365636F6E646172792D7469746C653E3C2F7469746C65733E3C706572696F-
646963616C3E3C66756C6C2D7469746C653E48656164204E65636B3C2F66756C-
6C2D7469746C653E3C2F706572696F646963616C3E3C70616765733E313636352D-
313637373C2F70616765733E3C766F6C756D653E34343C2F766F6C756D653E3C6E-
756D6265723E373C2F6E756D6265723E3C-
65646974696F6E3E32303232303432393C2F65646974696F6E3E3C6B-
6579776F7264733E3C6B6579776F72643E4164756C743C2F6B6579776F72643E3C6B-
6579776F72643E43616368657869612F6574696F6C6F67793C2F6B-
6579776F72643E3C6B6579776F72643E46656D616C653C2F6B6579776F72643E3C6B-
6579776F72643E2A467265652054697373756520466C6170732F-
6164766572736520656666656374733C2F6B6579776F72643E3C6B6579776F72643E-
2A4865616420616E64204E65636B204E656F706C61736D732F636F6D-
706C69636174696F6E732F737572676572793C2F6B6579776F72643E3C6B-
6579776F72643E48756D616E733C2F6B6579776F72643E3C6B6579776F72643E4D-
616C653C2F6B6579776F72643E3C6B6579776F72643E506F7374
6F706572617469766520436F6D706C69636174696F6E732F65706964656D696F-
6C6F67792F6574696F6C6F67792F737572676572793C2F6B6579776F72643E3C6B-
6579776F72643E2A506C617374696320537572676572792050726F636564757265732F-
6164766572736520656666656374733C2F6B6579776F72643E3C6B-
6579776F72643E526574726F737065637469766520537475646965733C2F6B-
6579776F72643E3C6B6579776F72643E4E737169703C2F6B6579776F72643E3C6B-
6579776F72643E63616368657869613C2F6B6579776F72643E3C6B-
6579776F72643E6672656520666C61703C2F6B6579776F72643E3C6B-
6579776F72643E6865616420616E64206E65636B2063616E6365723C2F6B-
6579776F72643E3C6B6579776F72643E706F73746F7065726174697665206F7574636F-
6D65733C2F6B6579776F72643E3C2F6B6579776F7264733E3C64617465733E-
3C796561723E323032323C2F796561723E3C7075622D64617465733E3C646174653E-
4A756C3C2F646174653E3C2F7075622D64617465733E3C2F64617465733E-
3C6973626E3E313039372D303334372028456C656374726F6E696329262378443B-
3130343332D3330373420284C696E6B696E67293C-
2F6973626E3E3C616363657373696F6E2D6E756D3E33353438383436393C2F61636365
7373696F6E2D6E756D3E3C75726C733E3C72656C617465642D75726C733E3C-
75726C3E68747470733A2F2F7777772E6E6362692E6E6C-
6D2E6E69682E676F762F7075626D65642F33353438383436393C2F75726C3E3C2F-
72656C617465642D75726C733E3C2F75726C733E3C-
656C656374726F6E69632D7265736F757263652D6E756D3E31302E313030322F686564
2E32373037323C2F656C656374726F6E69632D7265736F757263652D6E756D-
3E3C72656D6F74652D64617461626173652D6E616D653E4D65646C696E-
653C2F72656D6F74652D64617461626173652D6E616D653E3C72656D6F74652D64617
461626173652D70726F76696465723E4E4C4D3C2F72656D6F74652D646174616261736
52D70726F76696465723E3C2F7265636F72643E3C2F436974653E3C436974653E-
3C417574686F723E536F6C69732D4D617274696E657A3C2F417574686F723E-
3C596561723E323032323C2F596561723E3C5265634E756D3E34383C2F5265634E-
756D3E3C7265636F72643E3C7265632D6E756D6265723E34383C2F7265632D6E-
756D6265723E3C666F726569676E2D6B6579733E3C6B6579206170703D22454E22206
4622D69643D2272736673747864643064726674696530783573357872663676657761613
9783270303264222074696D657374616D703D2231363833323231373239223E3438
3C2F6B65793E3C2F666F726569676E2D6B6579733E3C7265662D74797065206E616D-
653D224A6F75726E616C2041727469636C65223E31373C2F7265662D747970653E3C6
36F6E7472696275746F72733E3C617574686F72733E3C617574686F723E536F-
6C69732D4D617274696E657A2C204F2E3C2F617574686F723E3C617574686F723E416
C766172657A2D416C74616D6972616E6F2C204B2E3C2F617574686F723E3C-
617574686F723E43617264656E61732C20442E3C2F617574686F723E3C-
617574686F723E5472756A696C6C6F2D436162726572612C20592E3C2F-
617574686F723E3C617574686F723E46756368732D5461726C6F76736B792C20562E-
3C2F617574686F723E3C2F617574686F72733E3C2F636F6E7472696275746F-
[illegible]
5723E3C2F7265636F72643E3C2F436974653E3C2F456E644E6F74653E00[2, 3]
[illegible]

756D6265723E34373C2F7265632D6E756D6265723E3C666F726569676E2D-
6B6579733E3C6B6579206170703D22454E222064622D69643D22727366737478646430
647266746965307835733578726636766577616139783270303264222074696D65737461
6D703D2231363833323231363433223E34373C2F6B65793E3C2F666F726569676E2D-
6B6579733E3C7265662D74797065206E616D653D224A6F75726E616C-
2041727469636C65223E31373C2F7265662D747970653E3C636F6E7472696275746F72
733E3C617574686F72733E3C617574686F723E4A6F6E65732C20412E204A2E3C2F-
617574686F723E3C617574686F723E44617669732C204B2E20502E3C2F-
617574686F723E3C617574686F723E4E6F76696E6765722C204C2E204A2E3C2F-
617574686F723E3C617574686F723E426F6E6574746F2C20412E3C2F-
617574686F723E3C617574686F723E4D616E747261766164692C20412E20562E3C2F-
617574686F723E3C617574686F723E53696D2C204D2E20572E3C2F-
617574686F723E3C617574686F723E596573736E736B792C204A2E20412E3C2F-
617574686F723E3C617574686F723E4D6F6F72652C204D2E20472E3C2F-
617574686F723E3C2F617574686F72733E3C2F636F6E7472696275746F72733E3C-
617574682D616464726573733E4465706172746D656E74206F66204F746F-
6C6172796E676F6C6F6779202D204865616420616E64204E65636B-
20537572676572792C20496E6469616E6120556E6976657273697479205363686F6F-
6C206F66204D65646963696E652C20496E6469616E61706F6C69732C20496E6469616E
612C205553412E262378443B4465706172746D656E74206F6620537572676572792C204
96E6469616E6120556E6976657273697479205363686F6F6C206F-
66204D65646963696E652C20496E6469616E61706F6C-
69732C20496E6469616E612C205553412E3C2F617574682D616464726573733E3C-
7469746C65733E3C7469746C653E506F73746F706572617469766520636F6E736571756
56E636573206F662063616E6365722063616368657869612061667465722068656164206
16E64206E65636B206672656520666C6170207265636F6E737472756374696F6E3C2F-
7469746C653E3C7365636F6E646172792D7469746C653E48656164204E65636B-
3C2F7365636F6E646172792D7469746C653E3C2F7469746C65733E3C706572696F-
646963616C3E3C66756C6C2D7469746C653E48656164204E65636B3C2F66756C-
6C2D7469746C653E3C2F706572696F646963616C3E3C70616765733E313636352D-
313637373C2F70616765733E3C766F6C756D653E34343C2F766F6C756D653E3C6E-
756D6265723E373C2F6E756D6265723E3C-
65646974696F6E3E32303232303432393C2F65646974696F6E3E3C6B-
6579776F7264733E3C6B6579776F72643E4164756C743C2F6B6579776F72643E3C6B-
6579776F72643E43616368657869612F6574696F6C6F67793C2F6B-
6579776F72643E3C6B6579776F72643E46656D616C653C2F6B6579776F72643E3C6B-
6579776F72643E2A467265652054697373756520466C6170732F-
6164766572736520656666656374733C2F6B6579776F72643E3C6B6579776F72643E-
2A48656164206E64204E65636B204E656F706C61736D732F636F6D-
706C69636174696F6E732F737572676572793C2F6B6579776F72643E3C6B-
6579776F72643E48756D616E733C2F6B6579776F72643E3C6B6579776F72643E4D-
616C653C2F6B6579776F72643E3C6B6579776F72643E506F7374
6F706572617469766520436F6D706C69636174696F6E732F65706964656D696F-
6C6F67792F6574696F6C6F67792F737572676572793C2F6B6579776F72643E3C6B-
6579776F72643E2A506C617374696320537572676572792050726F636564757265732F-
6164766572736520656666656374733C2F6B6579776F72643E3C6B-
6579776F72643E526574726F737065637469766520537475646965733C2F6B-
6579776F72643E3C6B6579776F72643E4E737169703C2F6B6579776F72643E3C6B-
6579776F72643E63616368657869613C2F6B6579776F72643E3C6B-
6579776F72643E6672656520666C61703C2F6B6579776F72643E3C6B-
6579776F72643E6865616420616E64206E65636B2063616E6365723C2F6B-
6579776F72643E3C6B6579776F72643E706F73746F7065726174697665206F7574636F-
6D65733C2F6B6579776F72643E3C2F6B6579776F7264733E3C646174657333E-
3C796561723E323032323C2F796561723E3C7075622D64617465733E3C646174653E-
4A756C3C2F646174653E3C2F7075622D64617465733E3C2F64617465733E-
3C6973626E3E313039372D303334372028456C656374726F6E696329262378443B-
313034332D333330373420284C696E6B696E67293C-
2F6973626E3E3C616363657373696F6E2D6E756D3E33353438383436393C2F61636365
7373696F6E2D6E756D3E3C75726C733E3C72656C617465642D75726C733E3C-
75726C3E68747470733A2F2F7777772E6E6362692E6E6C-
6D2E6E69682E676F762F7075626D65642F33353438383436393C2F75726C3E3C2F-
72656C617465642D75726C733E3C2F75726C733E3C-
656C656374726F6E69632D7265736F757263652D6E756D3E31302E313030322F686564
2E32373037323C2F656C656374726F6E69632D7265736F757263652D6E756D-
3E3C72656D6F74652D64617461626173652D6E616D653E4D65646C696EE-
653C2F72656D6F74652D64617461626173652D6E616D653E3C72656D6F74652D64617
461626173652D70726F76696465723E4E4C4D3C2F72656D6F74652D646174616261736
52D70726F76696465723E3C2F7265636F72643E3C2F436974653E3C436974653E-
3C417574686F723E536F6C69732D4D617274696E657A3C2F417574686F723E-
3C596561723E323032323C2F596561723E3C5265634E756D3E34383C2F5265634E-
756D3E3C7265636F72643E3C7265632D6E756D6265723E34383C2F7265632D6E-
756D6265723E3C666F726569676E2D6B6579733E3C6B6579206170703D22454E22206
4622D69643D2272736673747864643064726674696530783573357872663676657761613
9783270303264222074696D657374616D703D2231363833323231373239223E3438
3C2F6B65793E3C2F666F726569676E2D6B6579733E3C7265662D74797065206E616D-
653D224A6F75726E616C2041727469636C65223E31373C2F7265662D747970653E3C6
36F6E7472696275746F72733E3C617574686F72733E3C617574686F723E536F-
6C69732D4D617274696E657A2C204F2E3C2F617574686F723E3C617574686F723E416
C766172657A2D416C74616D6972616E6F2C204B2E3C2F617574686F723E3C-
617574686F723E43617264656E61732C20442E3C2F617574686F723E3C-
617574686F723E5472756A696C6C6F2D436162726572612C20592E3C2F-
617574686F723E3C617574686F723E46756368732D5461726C6F76736B792C20562E-
3C2F617574686F723E3C2F617574686F72733E3C2F636F6E7472696275746F72733E3C2F-
72733E3C617574682D616464726573733E556E697665727369646164205465636E6F-
6C6F67696361206465204D657869636F2C20436975646164206465204D657869636F-
2C204D657869636F2E262378443B436C696E6963616C204E-
7574726974696F6E20556E69742C20486F73706974616C2047656E-
6572616C206465204D657869636F202671756F743B44722E204564756172646F-
204C6963656167612671756F743B2C204D657869636F2E262378443B-
466163756C7479206F66204D65646963696E652C20496E7374697475746F206465204E7
574726963696F6E2C2047656E65746963612079204D657461626F6C69736D6F-
2C20556E6976657273696461642064656C20426F737175652C20426F676F-
74612C20436F6C6F6D6269612E262378443B556E697665727369646164204175746F6E
6F6D61206465204D657869636F2C20436975646164206465204D657869636F2C204D-
657869636F2E3C2F617574682D616464726573733E3C7469746C65733E3C-
7469746C653E43616E63657220436163686578696120416666656374732050617469656E
74732077697468204865616420616E64204E65636B2043616E63657220696E20416C-
6C20537461676573206F6620446973656173653A20412050726F73706563746976652043
726F73732D53656374696F6E616C2053747564793C2F7469746C653E-
3C7365636F6E646172792D7469746C653E4E75747269656E74733C2F7365636F6E646F
6E646172792D7469746C653E3C2F7469746C65733E3C706572696F646963616C3E3C-
66756C6C2D7469746C653E4E75747269656E74733C2F66756C6C2D-
7469746C653E3C2F706572696F646963616C3E3C70616765733E38322D-
38393C2F70616765733E3C766F6C756D653E37343C2F766F6C756D653E3C6E-
756D6265723E313C2F6E756D6265723E3C-
65646974696F6E3E32303231303131363C2F65646974696F6E3E3C6B-
6579776F7264733E3C6B6579776F72643E2A43616368657869612F-
646961676E6F7369732F65706964656D696F6C6F67792F6574696F6C6F67793C2F6B-
6579776F72643E3C6B6579776F72643E43726F73732D53656374696F6E616C-
20537475646965733C2F6B6579776F72643E3C6B6579776F72643E-
2A4865616420616E64204E65636B204E656F706C61736D732F636F6D-
706C69636174696F6E733C2F6B6579776F72643E3C6B6579776F72643E48756D-
616E733C2F6B6579776F72643E3C6B6579776F72643E50726F73706563746976652053
7475646965733C2F6B6579776F72643E3C6B6579776F72643E536B-
6579776F72643E537175616D6F75732043656C6C2043617263696E6F6D-
61206F66204865616420616E64204E65636B3C2F6B6579776F72643E3C2F6B-
6579776F7264733E3C646174657333E3C796561723E-
323032323C2F796561723E3C2F64617465733E3C6973626E3E313533322D-
373931342028456C656374726F6E696329262378443B303136332D-
3535383120284C696E6B696E67293C2F6973626E3E3C616363657373696F6E2D6E-
756D3E33333435353436343C2F616363657373696F6E2D6E756D3E3C75726C733E3C-
72656C617465642D75726C733E3C75726C3E68747470733A2F-
2F7777772E6E6362692E6E6C6D2E6E69682E676F762F7075626D65642F-
33333435353436343C2F75726C3E3C2F72656C617465642D75726C733E3C2F-
75726C733E3C656C656374726F6E69632D7265736F757263652D6E756D3E31302E313
038302F30313633353538312E323032302E313836393739323C2F-
656C656374726F6E69632D7265736F757263652D6E756D3E3C72656D6F74652D-
64617461626173652D6E616D653E4D65646C696E653C2F72656D6F74652D-
64617461626173652D6E616D653E3C72656D6F74652D64617461626173652D7072
6F76696465723E4E4C4D3C2F72656D6F74652D64617461626173652D70726F7669646
5723E3C2F7265636F72643E3C2F436974653E3C2F456E644E6F74653E00. These alterations reduce the response to chemotherapy, and lead to reduced quality of life and survival due to muscle loss and weakness ADDINEN.CITE vonHaehling201450[4]505017vonHaehling, S.Anker, S.D.Instituteof Innovative Clinical Trials, Department of Cardiology and Pneumology,University of Gottingen Medical School, Robert-Koch-Strasse 40, 37075,Gottingen, Germany, stephan.von.haehling@web.de.Prevalence,incidence and clinical impact of cachexia: facts and numbers-update2014J Cachexia SarcopeniaMuscleJCachexia SarcopeniaMuscle261-3542014Dec2190-5991(Print) 2190-6009 (Electronic) 2190-5991(Linking)25384990https://www.ncbi.nlm.nih.gov/pubmed/25384990PMC424841110.1007/s13539-014-0164-8PubMed-not-MEDLINENLM[4]. Unfortunately, little is known regarding the consequences of non-bone metastatic HNC on bone homeostasis. For this reason, this study is aimed to elucidate the bone alterations associated with a non-bone metastatic model of HNC.C57BL/6J male mice (8-week-old) were intrascapularly and subcutaneously injected with 3 × 106 MLM3 HNC cells. The MLM3 tumor growth caused body and skeletal muscle wasting as previously described [5]. In addition, tumor hosts displayed severe loss of trabecular and cortical bone as suggested by the reduction of the Tb.BV/TV, Tb.Th, Tb.N. and Ct.BV/TV and Ct.Th. The assessment of mechanical properties of the femur reveled that HNC bearers have weaker bones as suggested by the reduced ultimate force, stiffness, and energy to failure. Since osteocytes are key regulator of bone resorption, we analyzed the mRNA expression of important pro-resorptive genes such as Tnfsf11, Tnf-? and IL-6 and found them increased in the osteocyte enriched samples from MLM3 bearers. To determine if these changes also characterized human HNC, mRNA was isolated from bone derived from patients who underwent HNC ablation followed by osseous free tissue reconstruction. As a control tissue, we used bone samples derived from patients who underwent trauma surgery. These data showed increased mRNA expression of Tnfsf11 (RANKL) whereas Tnfrsf11b (OPG) was unchanged, resulting in an increased Rankl/Opg ratio. Interestingly, also the mRNA expression of IL-6 was increased in the bone of the HNC patients.Our study clearly shows that HNC, even in the absence of direct metastases to the bone, has severe detrimental effects on the musculoskeletal system. For the first time, we are showing that osteocytes acquire a pro-inflammatory phenotype that could directly drive bone and muscle loss in HNC patients. Consideration of co-treatments that maintain musculoskeletal health as well as assessment of the presence of osteoporosis should be taken in non-bone metastatic HNC patients.

1. Siegel RL, Miller KD, Wagle NS, Jemal A. Cancer statistics, 2023. CA Cancer J Clin. 2023;73(1):17-48. doi: 10.3322/caac.21763.
2. Jones AJ, Davis KP, Novinger LJ, Bonetto A, Mantravadi AV, Sim MW, et al. Postoperative consequences of cancer cachexia after head and neck free flap reconstruction. Head Neck. 2022;44(7):1665-77. doi: 10.1002/hed.27072.
3. Solis-Martinez O, Alvarez-Altamirano K, Cardenas D, Trujillo-Cabrera Y, Fuchs-Tarlovsky V. Cancer Cachexia Affects Patients with Head and Neck Cancer in All Stages of Disease: A Prospective Cross-Sectional Study. Nutr Cancer. 2022;74(1):82-9. doi: 10.1080/01635581.2020.1869792.
4. von Haehling S, Anker SD. Prevalence, incidence and clinical impact of cachexia: facts and numbers-update 2014. J Cachexia Sarcopenia Muscle. 2014;5(4):261-3. doi: 10.1007/s13539-014-0164-8.
5. Olson B, Norgard MA, Levasseur PR, Zhu X, Marks DL. Physiologic and molecular characterization of a novel murine model of metastatic head and neck cancer cachexia. J Cachexia Sarcopenia Muscle. 2021;12(5):1312-32. doi: 10.1002/jcsm.12745.

***Disclosures: Alexander J. Jones**, None*

FRI-119

Elevated Lactate in Acute Myeloid Leukemia (AML) Contributes to Bone Marrow Microenvironment Dysfunction through GPR81-Mediated Macrophage Polarization and Leukemia Cell Growth *Benjamin Frisch[1], Maggie Lesch[2], Joshua Munger[2], Celia Soto[2]. [1]University of Rochester School of Medicine and Dentistry, United States. [2]University of Rochester, United States

Acute myeloid leukemia (AML) has a survival rate of ~30% at five years due to bone marrow dysfunction and relapse following treatment. Metabolomics revealed higher metabolite levels in the bone marrow of AML patients at diagnosis compared to healthy controls, including lactate (mmol/L = 3.62 vs 1.31, $p < 0.05$, n = 5). We hypothesized that excess lactate advances leukemia progression by polarizing macrophages to an immunosuppressive (M2-like) phenotype and promoting cancer aggressiveness. Further, as bone marrow is a unique tumor microenvironment, research is needed on the contribution of lactate to altered hematopoiesis. This study used: (i) a murine AML model of blast crisis chronic myelogenous leukemia (bcCML) that recapitulated the metabolomic analysis of human AML, and (ii) C57BL/6J wild type mice or a transgenic knockout of the extracellular lactate receptor GPR81 (GPR81-/-). Leukemia-associated macrophages (LAMs) were found to overexpress the mannose receptor CD206, an M2-like marker. LAMs in GPR81-/- bcCML mice had a reduced expression of CD206 (fold-change MFI compared to non-leukemic = 4.98 vs 2.06, $p < 0.05$, n = 11). RNA sequencing of LAMs detected multiple upregulated T cell pathways. Expression of arginase-1 RNA, a functional M2-like protein, was observed in lactate-polarized bone marrow-derived macrophages (BMDMs) in vitro and was substantially lower in GPR81-/- BMDMs. Next, leukemia progressed more slowly when bcCML was initiated using GPR81-/- leukemia cells compared to wild type (% leukemic bone marrow cells at day 13 = 11.75 vs 45.54, p 7 passages, n = 2). These results suggest that GPR81 is critical for LAM polarization, leukemia cell growth, and repopulation. Lastly, bone marrow support for hematopoiesis was assayed by coculturing murine hematopoietic stem and progenitor cells (HSPCs) over a stromal monolayer of macrophages and mesenchymal stem cells, a key cell type of the hematopoietic stem cell niche; exposure to physiologically-relevant elevated lactate levels (10 mmol/L) reduced HSPC colony-forming ability when plated in methylcellulose-containing media (fold-change colonies = 0.41, $p < 0.001$, n = 14). This research identifies lactate as a critical driver of AML progression, highlighting GPR81 as an exciting and novel therapeutic target for both AML cells and LAMs.

***Disclosures: Benjamin Frisch**, None*

FRI-120

Targeting S1PR1 and p62-mediated signaling as a therapeutic approach to multiple myeloma bone disease *Daniela N. Petrusca[1], Silvia Marino[2], Attaya Suvannasankha[1], Judith Anderson[1], Evgeny Berdyshev[3], Kelvin P. Lee[1], G. David Roodman[1], Deborah L. Galson[4]. [1]Department of Medicine, Hematology/Oncology Division, Indiana University School of Medicine, United States. [2]Department of Physiology and Cell Biology, University of Arkansas for Medical Sciences, United States. [3]Department of Medicine, National Jewish Health, United States. [4]Department of Medicine, Division of Hematology/Oncology, UPMC Hillman Cancer Center, McGowan Institute for Regenerative Medicine, University of Pittsburgh, United States

Multiple myeloma (MM) is an incurable plasma cell malignancy that causes osteolytic bone lesions in most patients. Thus, novel treatments which effectively target both the MM cells and the bone microenvironment are needed. We previously reported that MM-induced upregulation of GFI1 in bone marrow stromal cells (BMSC) causes prolonged suppression of osteoblast (OB) differentiation. In addition, we described the pivotal role of GFI1 in MM proliferation via intracellular S1P-dependent increased c-Myc stability and enhanced extracellular release of S1P for a pro-survival autocrine and paracrine feedback loop through S1PR1. We employed XRK3F2, a p62-ZZ domain competitive inhibitor that can decrease GFI1 expression in both MM cells and in MM-educated BMSC in vitro, in combination with Ozanimod (Oza), a selective S1PR1 functional antagonist. We found S1P levels significantly elevated in the BM plasma of MM patients when compared to healthy donors. Also, S1PR1 and p62 are highly expressed in MM primary cells when compared with healthy donors and negatively correlate with overall survival of MM patients. Microenvironmental soluble factors (IL6, S1P, TNF?, hypoxia) and the direct co-culture of MM cells with BMSC cells, significantly increase S1PR1 transcription as well as GFI1 (mRNA and protein expression) levels in both cell types. We found that XRK3F2 significantly downregulated both p62 and GFI1 levels in MM cells even in the presence of IL-6, and Oza significantly decreased S1PR1 levels even in the MM cells overexpressing GFI1. Each drug alone significantly reduced viability in MM cells and their combination further enhanced the pro-death effect. Either drug alone significantly decreased GFI1 and P-cMyc protein levels in MM cells as well as c-Myc chromatin bound levels. These effects were further accentuated by the drugs in combination. We found that XRK3F2 and OZA, alone and in combination, improve differentiation of pre-OB. Moreover, either drug alone significantly rescued TNF? suppression of OB differentiation, and their combination completely restored it as measured by Col1a1 levels. Oza treatment of MM downregulated IL6 and RANKL levels even in MM cells overexpressing GFI1. IL6 and RANKL increase MM viability and osteoclast recruitment and activation, respectively. These data support the idea that p62 and S1PR1 might be effective targets in MM treatment and the potential of using the Oza-XRK3F2 combination as a novel therapeutic approach for treating MMBD.

***Disclosures: Daniela N. Petrusca**, None*

FRI-122

Stimulation of Osteoclasts by Extracellular Vesicles without RANKL Released from Adult T-Cell Leukemia *Nitin Pokhrel[1], Amanda Panfil[2], Haniya Habib[1], Sham Seeniraj[1], Ancy Joseph[3], Daniel Rauch[3], Robert Sprung[4], Petra Gilmore[4], Qiang Zhang[4], Reid Townsend[4], Yu Lianbo[5], Ayse Selen Yimaz[6], Rajeev Aurora[7], William Park[7], Lee Ratner[3], Katherine Weilbaecher[8], Deborah Veis[9]. [1]Division of Bone & Mineral Diseases, Musculoskeletal Research Center, Washington University School of Medicine, United States. [2]Veterinary Biosciences, The Ohio State University, United States. [3]Division Molecular Oncology, Washington University School of Medicine, United States. [4]Division of Endocrinology, Washington University School of Medicine, United States. [5]College of Public Health, The Ohio State University, Columbus, Ohio, USA; [6]Department of Biomedical Informatics, Bioinformatics Shared Resource, Comprehensive Cancer Center, The Ohio State University, United States. [6]Department of Biomedical Informatics, Bioinformatics Shared Resource, Comprehensive Cancer Center, The Ohio State University, United States. [7]Department of Molecular Microbiology and Immunology, School Of Medicine, Saint Louis University, United States. [8]Washington University School of Medicine, United States. [9]Washington University in St. Louis School of Medicine, United States

Adult T cell Leukemia (ATL), caused by chronic infection of human CD4+ T cells with HTLV-1, is associated with hypercalcemia and osteolytic lesions. To study the direct effect of HTLV-1-infected T cells (HTLV/T) on osteoclasts (OC), we generated a panel of clonal HTLV/T (n=9 from 2 donors) and ATL patient cell lines (ATL/P) (n=3). Supernatants (sup) from HTLV/T and ATL/P were added to murine and human OC precursors cultured in suboptimal osteoclastogenic conditions. HTLV/T sup variably stimulated OC differentiation (4 high, 1 medium, 4 low), but showed identical effects on murine and human cultures. ATL/P sup all stimulated OC generation. Expression of RANKL and OPG mRNAs by HTLV/T and ATL/P was variable, but we found no correlation between OC effects and either RANKL levels or RANKL/OPG ratio, suggesting an alternative mechanism. Concordantly, we previously showed that osteolysis in a humanized mouse model of HTLV-1 infection was only partially blocked by anti-RANKL antibodies. HTLV/T and ATL/P produce small extracellular vesicles (sEV), known to facilitate HTLV-1 infection. We hypothesized that these sEV also mediate bone loss by targeting OC. We isolated sEV from both HTLV/T and ATL/P, and found they carried most of the activity of sup. In contrast, sEV from uninfected activated T cells had little effect. Pre-treatment of HTLV/T by exosome inhibitor GW4869 blunted the OC stimulatory activity of sup. We further characterized the sEV, finding no viral particles using transmission EM. LC-MS/MS of HTLV/T sEV (n=7) showed no RANKL, but ~18% of sEV proteins correlated with strength of osteoclastogenic effect; gene ontogeny analysis of this group showed increased representation of proteins involved in bone resorption such as cytoskeletal proteins and GTPases. MicroRNA profiling of HTLV/T sEV with high osteoclastogenic activity revealed top microRNAs (mir 21, mir 155, mir 92a1) with previously noted effects on OC. To determine if in vitro findings correlate with true osteolysis, HTLV/T lines (2 high and one low effect) were injected into tibias of immunodeficient NCG mice, and trabecular bone mass was followed by vivaCT. HTLV/T with high in vitro activity caused profound bone loss by 4-8 weeks regardless of RANKL expression ($p<0.01$), while bone injected with the low effect line was not significantly different from uninjected controls. Our study suggests that sEV, which lack RANKL, directly stimulate OC, likely mediated by multiple components of their cargo.

***Disclosures: Nitin Pokhrel**, None*

FRI-123

Blocking PTH1R inhibits prostate cancer metastases *Yawei Zhao[1], Xiaohong Li[1]. [1]The University of Toledo, United States

The causative effects of parathyroid hormone-related protein (PTHrP) in bone metastases have been demonstrated. However, clinical trials on blocking PTHrP have not yet been successful. On the other hand, parathyroid hormone receptor 1 (PTH1R) is the only receptor that PTHrP binds to. PTH1R belongs to the G protein-coupled receptor (GPCR) family. In general, GPCRs comprise 35% of the current clinical drug targets. Therefore, we explore

the effects of blocking PTH1R in prostate cancer metastases using both genetic and pharmacological approaches.Physiologically, PTH1R is expressed in the mesenchymal lineage of cells. To determine the paracrine effect of PTH1R in advanced prostate cancer metastases, we crossed the floxed Pth1r (Pth1rFloxE2) mouse with the Col1?2 CreERT mouse. This mouse line was further bred into immunodeficient NSG background. We then xenografted the human castration-resistant prostate cells, PC3 (labeled with luciferase), intracardially into the Pth1rFloxE2 and Pth1rColCreERT KO littermates. Note that we did not observe phenotypic changes in the Pth1rColCreERT KO mice, compared to the Pth1rFloxE2 littermates or wild-type controls. Luminescent signals and bone lesions were monitored weekly. We found metastases in multiple organs, including bone and liver. The overall and organ-specific metastases, such as bone metastases, were significantly inhibited in the Pth1rColCreERT KO, compared to the Pth1rFloxE2 littermates. These data showed that blocking the paracrine effects of PTH1R inhibits prostate cancer metastases. Furthermore, prostate cancer cells also express PTH1R. To determine the autonomous effect of PTH1R inhibition, we treated the prostate cancer cells with either a small molecule inhibitor, XC039, or the peptide antagonist, (Asn10,Leu11,D-Trp12)-PTHrP(7-34) amide [PTHrP(7-34) amide]. We found that XC039 significantly inhibited prostate cancer cell growth but not PTHrP(7-34) amide, although both PTHrP(7-34) amide and XC039 can significantly suppress the ligands (PTH or PTHrP) induced downstream cAMP signaling. Furthermore, our preliminary study in mice also showed a trend of bone metastasis inhibition of C4-2B-induced bone lesion development by PTHrP(7-34) amide. Taken together, these studies prove the concept and demonstrate potential efficacy in blocking PTH1R for prostate cancer metastases.

***Disclosures: Yawei Zhao**, None*

FRI-127

Osteocytes Induce Drug Resistance via the NOTCH3-CXCL12 Signaling Axis in Multiple Myeloma *Hayley Sabol[1,] Cody Ashby[1,] Manish Adhikari[1,] Japneet Kaur[1,] Aric Anloague[1,] Sharmin Khan[1,] Samrat Roy Chodhury[1,] Michela Palmieri[1,] Lawry Barnes[1,] Elena Ambrogini[1,] Carolina Schinke[1,] Intawat Nookaew[1,] Jesus Delgado-Calle[1,] [1]University of Arkansas for Medical Sciences, United States

Multiple myeloma (MM) remains incurable due to disease relapse and drug resistance. Notch signals between MM cells and cells of the tumor niche (TME) confer drug resistance, but the cellular/molecular mechanisms are not entirely known. Using in silico analysis of clinical and transcriptomic public and internal databases, we found that 1) NOTCH3 is upregulated in MM cells from newly diagnosed MM patients (NDMM) vs. healthy donors, 2) increases in relapsed/refractory MM (RRMM) vs. NDMM patients, and 3) NDMM patients with high NOTCH3 expression have worse responses to Bortezomib (BOR)-based therapies. Because NOTCH3 mRNA levels did not correlate with somatic mutations in NOTCH3, we tested if NOTCH3 is regulated by TME cells and its role in responses to chemotherapy. Osteocytes (Ots), recently defined as key cells in the TME, increased NOTCH3 in MM cells and protected them from apoptosis induced by BOR or VRd (BOR+Lenalidomide+Dexamethasone) in vitro. This protection was lost by NOTCH3 knockdown (NOTCH3KD) and enhanced by NOTCH3 activation (NOTCH3OE) in MM cells. Next, we compared BOR (0.1 mg/kg, 5x/wk) responses in control (C) vs NOTCH3OE MM cells in vivo. All untreated mice bearing C or NOTCH3OE cells died at 4 wks. In mice injected with C MM cells, BOR reduced tumors by 65%, improved survival (7/10 alive), and had 38% more bone mass, 25% more P1NP, and 29% less CTX than untreated mice. In contrast, in NOTCH3OE-bearing mice, BOR only reduced tumors by 23% and did not improve survival (1/10 alive), bone mass, or serum markers, supporting NOTCH3 confers BOR resistance. We then compared the MM cell transcriptome of NDMM patients with high vs. low NOTCH3 expression to find the mechanism for BOR resistance. We found that high NOTCH3 NDMM and RRMM patients had enrichment in chemokine and cell adhesion pathways and CXCL12 upregulation. Ots upregulated CXCL12 and activated the CXCR4/ERK pathway in MM cells in vitro. These effects were blunted in NOTCH3KD and enhanced in NOTCH3OE MM cells. Genetic inhibition of CXCL12 in NOTCH3OE cells prevented Ot's protection and restored BOR/VRd sensitivity, supporting CXCL12 works in an autocrine fashion. Lastly, Plerixafor, a CXCR4/CXCL12 inhibitor, restored NOTCH3OE MM cells sensitivity to BOR/VRd in vitro and in human bones bearing NOTCH3OE tumors cultured ex vivo. Our clinical and experimental data show Ots transmit drug resistance signals and unravel a novel targetable NOTCH3-CXCL12 pro-survival signaling axis in the MM TME.

***Disclosures: Hayley Sabol**, None*

FRI-131

Osteoblasts are a source of bone metastases-associated fibroblasts (BMAFs) *Jennifer Zarrer[1,] Marie-Therese Haider[2,] Nicole Ridlmaier[2,] Rafael Preuer[2,] Daniel J. Smit[3,] Hiroaki Saito[1,] Eric Hesse[1,] Hanna Taipaleenmäki[1,] [1]Institute of Musculoskeletal Medicine, University Hospital, LMU Munich, Munich, Germany, Germany, [2]Molecular Skeletal Biology Laboratory, Department of Trauma, Hand and Reconstructive Surgery, University Medical Center Hamburg-Eppendorf, Hamburg, Germany, Germany, [3]Institute of Biochemistry and Signal Transduction, University Medical Center Hamburg-Eppendorf, Hamburg, Germany, Germany

In breast cancer bone metastases the abundance of adjacent osteoblasts (OBs) is diminished. To determine the fate of OBs, we combined a lineage-tracing model (Osx-creERt+;Ai9) with intracardiac injection of 4T1 breast cancer cells and performed single cell RNA sequencing (scRNAseq) of tdTomato-positive (tdTom+) OBs in metastases-bearing and healthy control animals. Bioinformatic analysis revealed a distinct cluster of tdTom+ OBs in metastases-bearing mice that express genes related to tumor microenvironment, fibrosis and cancer-associated fibroblast (CAF) proliferation (e.g. Cxcl12, Tnc, Mmps, Pdgfr-?, Pdgfr-?). CAFs reside inside tumors providing a micro-milieu that supports tumor growth. However, little is known about metastasis-associated fibroblasts (MAFs), in particular in bone metastases. Based on our findings, we hypothesized that OBs might abandon the bone surface and become MAFs. Supporting our hypothesis, histological analysis demonstrated elongated tdTom+ OBs within metastases, which we termed bone metastases-associated fibroblasts (BMAFs), while only a few OBs were present on nearby bone surfaces. Consistently, MC3T3-E1- and primary OBs acquired a spindle shape morphology upon stimulation with medium conditioned by 4T1 or MDA-MB-231 breast cancer cells (CCM), which also increased OB migration and OB-induced collagen remodeling. Furthermore, in an ex vivo co-culture model, OBs in the vicinity of cancer cells became elongated and migrated in-between tumor cells. Immunoblot, qRT-PCR, scRNAseq and histological analyses revealed a reduction of OB markers (Runx2, Osx) and an increase of BMAF-associated genes (e.g. Pdgfr-?, Pdgfr-?) in CCM-stimulated OBs and cancer-associated tdTom+ OBs. To elucidate the mechanisms transitioning OBs to BMAFs, we performed RNA sequencing and identified an activated IL-17A signaling pathway in CCM-stimulated OBs compared to controls, which was confirmed by immunoblot and qRT-PCR analyses of downstream targets (C/ebp, Ccl2). Furthermore, recombinant IL-17A promoted OB migration and acquisition of a BMAF phenotype while inhibition of IL-17A signaling using an anti-IL-17 antibody restored the CCM-induced morphological changes and OB migration. In vivo, anti-IL-17A reduced the number and growth of bone metastases determined by bioluminescence imaging and histology. Together, these results demonstrate that OBs give rise to BMAFs at least in part through IL-17A, which might contribute to metastatic growth.

***Disclosures: Jennifer Zarrer**, None*

FRI-133

DDRGK1 regulates proteostasis by modulating the ribosomal protein RPL26 during chondrocyte differentiation in spondyloepimetaphyseal dysplasia *Yangjin Bae[2,] Monika Weisz-Hubshman[2,] Carolina Leynes[2,] Sung Yun Jung[2,] Brendan Lee[2,] [2]Baylor College of Medicine, United States, [2]Baylor College of Medicine,

DDRGK1 is a substrate of the ufmylation process, a post-translational modification mediated UFM1.It is required for subsequent ufmylation of other substrates by forming complex with ULF1 (E3 ligase). The physiological importance of DDRGK1 was elucidated by the finding of mutations in Shohat-type Spondyloepimetaphyseal dysplasia (SEMD). Moreover, other genes in this pathway have since been associated with this spectrum of skeletal dysplasias. We previously showed that osteochondroprogenitor-specific (Prx1-Cre; Ddrgk1f/f) and mature chondrocyte- specific (Agn1-CreERT2; Ddrgk1f/f) knockout mouse models recapitulated the SEMD phenotype. In brief, Prx1-Cre; Ddrgk1f/f mice showed severe chondrodysplasia including progressive shortening of the limbs with an abnormal growth plate and a delayed epiphyseal ossification. In Agn1-CreERT2; Ddrgk1f/f mice, we consistently found disorganized growth plate and reduced level of proteoglycan in growth plate and articular cartilage. These in vivo results highlight the essential role of UFM1 modification in cartilage development and homeostasis. Hence, to uncover the potential cartilage-specific complexes and novel substrates of the ufmylation, we have generated ATDC5 (murine chondrocyte cell line) stably expressing the components of the ufmylation machinery, i.e., UFC1-FLAG; UFL1-MYC; HA-HIS-UFM1 via doxcyclin induction and performed IP-MS assay. Based on GO analysis, we found proteins enriched in protein ufmylation (as internal control), ER stress, protein translation pathways and ribosome. Among these, ribosomal protein RPL26 was previously reported as the substrate of UFM1 modification and also the cause of with a human ribosomopathy. Similar to the function of Ddrgk1 in proteostasis, we found that total protein synthesis was reduced by SUnSET assay (Surface Sensing of Translation) when Rpl26 was knockdown in ATDC5, with associated impairment of ATDC5 chondrocyte differentiation. We also found that Sox9 protein level was decreased similarly when Ddrgk1 was knockdown in ATDC5. These data suggest that ufmylation may be a critical post-translational modification for cartilage homeostasis by modulating the protein stability/function of subset of ribosomal proteins such as RPL26. Furthermore, this

mechanism underscore the evidence of tissue-specific ribosomal function as a pathological cause of human chondrodysplasia.

***Disclosures: Yangjin Bae**, None*

FRI-134

Loss of function variant in histone reader SPIN4 causes a new X-linked overgrowth syndrome *Julian Lui[1], Jacob Wagner[1], Elaine Zhou[1], Kevin Barnes[1], Lijin Dong[2], Youn Hee Jee[1], Jeffrey Baron[1]. [1]Section on Growth and Development, NICHD, United States. [2]National Eye Institute (NEI), United States

Overgrowth syndromes can be caused by pathogenic genetic variants in epigenetic writers, such as DNA and histone methyltransferases. However, no overgrowth disorder has previously been ascribed to variants in a gene that acts primarily as an epigenetic reader. Here, we studied a male individual with generalized overgrowth of prenatal onset. Exome sequencing identified a hemizygous frameshift variant in Spindlin 4 (SPIN4), with X-linked inheritance. We found evidence that SPIN4 binds specific histone modifications, promotes canonical WNT signaling, and inhibits cell proliferation in vitro and that the identified frameshift variant had lost all of these functions. Ablation of Spin4 in mice recapitulated the human phenotype with generalized overgrowth, including increased longitudinal bone growth. Growth plate analysis revealed increased cell proliferation in the proliferative zone and an increased number of progenitor chondrocytes in the resting zone. We also found evidence that loss of Spin4 in mice led to decreased canonical Wnt signaling in growth plate chondrocytes, potentially contributing to increased pool of progenitor cells in the resting zone.Taken together, our findings provide strong evidence that SPIN4 is an epigenetic reader that negatively regulates mammalian body growth, and that loss of SPIN4 causes an overgrowth syndrome in humans, expanding our knowledge of the epigenetic regulation of human growth.

***Disclosures: Julian Lui**, None*

FRI-135

DNA methylation determines bone length through growth plate mineralization by regulating chondrocyte energy metabolism *Yuta Yanagihara[1], Masatomo Takahashi[2], Yoshihiro Izumi[2], Takeshi Bamba[2], Yuuki Imai[1]. [1]Division of Integrative Pathophysiology, Proteo-Science Center, Ehime University, Japan. [2]Division of Metabolomics/Mass Spectrometry Center, Medical Research Center for High Depth Omics, Medical Institute of Bioregulation, Kyushu University, Japan

Chondrocytes differentiated from mesenchymal stem cells play a role in determining skeletal patterns by ossification. However, it is still unclear how the maintenance DNA methylation regulates chondrocyte differentiation and skeletal formation. Dnmt1 is recruited to hemi-methylated DNA sites by Uhrf1 and is essential for maintenance DNA methylation. In Musculoskeletal Knowledge Portal from IFMRS, common variant gene-level of Dnmt1 was significantly associated with “Height” (p=4.22e-35). Therefore, we analyzed the function of Dnmt1 in chondrocytes using limbs specific Dnmt1 deficient (cKO) mice. cKO mice exhibited remarkably short long bones about 45-60% of control (Ctrl) mice. Histological analyses revealed that cKO showed thinner proliferative zone, wider and more calcified hypertrophic zone than Ctrl littermates at 1 week old. Surprisingly, growth plate of cKO mice was disappeared at 6 weeks old. These results suggested that Dnmt1 regulate skeletal formation via controlling chondrocyte differentiation. Then, to identify factors that are directly regulated by Dnmt1 and influence chondrocyte differentiation, candidate genes were identified by integrated analysis of RNA-Seq and MBD-Seq. Among candidate genes, ossification related genes were significantly enriched. Consistent to this result, mineralization of cKO primary cultured chondrocyte was remarkably facilitated. In addition, the top 4 genes increased by reduction of DNA methylation were related to energy metabolism. cKO chondrocytes showed enhanced mitochondrial respiratory function compared to Ctrl chondrocytes by flux analyzer. Furthermore, metabolomic analysis revealed that almost all metabolites in TCA cycle and glycolytic process, including ATP, were increased in cKO chondrocytes. ATP is well known important metabolite for mineralization. Moreover, Ctrl chondrocytes completely failed to mineralize in culture media without glucose and glutamine, however, cKO chondrocytes could successfully mineralize under same condition. These results indicate that Dnmt1 mediated maintenance DNA methylation governs chondrocyte mineralization by regulating energy metabolism through both gene expression and metabolite supply. Finally, the expression of Dnmt1 was decreased and TETs expression was increased along with chondrocyte differentiation. These data totally suggested that appropriate DNA methylation status in chondrocytes can organize growth plate mineralization, followed by determine bone length.

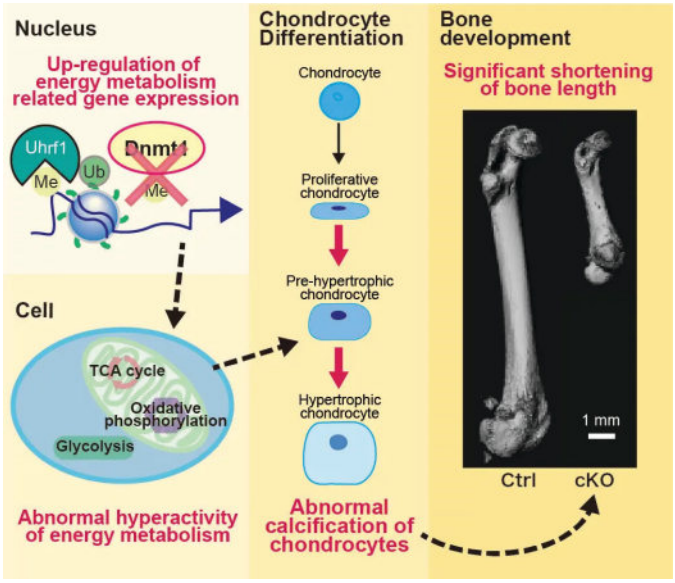

***Disclosures: Yuta Yanagihara**, None*

FRI-136

Piezo1 activation accelerates endochondral osteogenesis-mediated fracture healing and the targeted intervention effect of resveratrol *Donghao Gan[1], Wenjing Zhang[2], Qingyun Jia[3], Guozhi Xiao[1]. [1]Southern University of Science and Technology of China, China. [2]Shenzhen Institute of Advanced Technology, China. [3]Linyi People’s Hospital, China

Background Fracture is one of the most common injuries in humans, and despite advances in surgical treatment, approximately 5-10% of patients will progress to delayed union or nonunion. Therefore, it is urgent to explore therpeutic targets for promoting fracture healing and shorten the healing time.Objectives To investigate the effects of Piezo1 activation on bone fracture healing and to explore Piezo1-targeting fracture healing treatment.Methods The expression levels of Piezo1 were determined in human and mice fresh callus tissue. Mice with genetic Piezo1 deletion in chondrocytes or local injection of the Piezo1 activator Yoda1 were utilized to determine the effects on fracture healing. In an effort to define Piezo1-targeting drugs for potential fracture treatment, via virtual docking technology in the constructed compound library, we found that Resveratrol (RSV) may be a PIEZO1-targeting drug. Then, we developed an injectable RSV loaded hydrogel platform as a high payload and sustainable release for fracture treatment.Results Piezo1 expression was elevated in callus tissue chondrocytes in human and bone fracture mouse model. Piezo1 deletion in chondrocytes largely delays fracture healing and callus mineralization. In contrast, local injection of Yoda1 markedly accelerated fracture healing in bone fracture mice. PIEZO1 activation increases, while PIEZO1 siRNA knockdown decreases, expression of osteogenic markers such as RUNX2, Col1a1 and Osterix in primary human articular chondrocytes (HACs) induced by osteogenesis and fluid shear stress stimuli. Interestingly, we found that Yoda1 reduced, while Piezo1 deletion increased, the expression of Runx2-degraded E3 ligase smurf1 in HACs, inhibits ubiquitin-proteasome degradation of Runx2, and promotes Runx2 transcription and osteogenic phenotype. virtual docking simulation revealed Piezo1 molecule with strong binding ability to RSV. Results from primary HACs showed that RSV activates the PIEZO1-mediated calcium flux. Results from in vitro experiments confirmed that RSV decreased the Runx2 degradation and reversed by Piezo1 deletion in HACs. Hydrogel conjugated with RSV were stable and nontoxic, with long time slow release, high cartilage uptake, and penetration capabilities, and is used for in vivo research. When compared with control mice, the RSV-treated mice displayed marked accelerated fracture healing, and upregulated osteogenic genes. Importantly, RSV-induced increases in the bone trabeculae formation, callus mineralization and fracture gap union were dramatically delayed or completely abolished by Piezo1 deletion.Conclusions We establish a critical role of Piezo1 in promoting bone fracture healing and define RSV, Piezo1-targeted compound, as a potential bone fracture treatment.

***Disclosures: Donghao Gan**, None*

FRI-138

SDHA inhibition is involved in Lin28a osteoarthritic chondrocyte reprogramming *ZOHRA BOUCHEMLA[1], Inès Slitine[2], Valentin Duong[2], Fawaz Alzaid[3], Lucie Orliaguet[3], Augustin Latourte[4], Pascal Richette[4], Hang-Korng EA[4], MARTINE COHEN-SOLAL[5], Eric Hay[6]. [1], France. [2]U1132 Inserm, France. [3]Cordeliers Research Center, INSERM, France. [4]U1132 Inserm and Lariboisière APHP hospital, France. [5]Inserm U1132 Bioscar and université Paris-Cité, France. [6]INSERM u1132, France

We have previously shown that Lin28a induces cartilage regeneration during osteoarthritis by inhibiting Let7. Loss of hypoxia is associated with OA progression, inducing energetical metabolism dysfunction. We focused here on the effect of Lin28a on this process and how energetical metabolism is involved in cartilage reprogramming.We performed RNAseq, RT-qPCR, WB, and immunofluorescent staining on murine primary chondrocytes overexpressing or not Lin28a in control or osteoarthritic (Wnt3a) conditions. For ex vivo analysis we used mouse femoral heads and human cartilage explants. Osteoarthritis was induced in WT or TgLin28aflox/flox/Col2CreERt2 by meniscectomy or aging. Knee joints were used for qPCR and histological analysis.In vitro RNAseq analysis showed that Wnt3a induces an increase in oxidative stress associated genes and mitochondrial impairment. Seahorse assay demonstrated a dramatic decrease of the spare respiratory capacity, indicating mitochondrial failure induced by Wnt3a treatment. On the other hand, reduced mitochondrial respiration and increased glycolysis were found with Lin28a overexpression (RNAseq and Seahorse). RNAseq indicates that the mitochondrial enzyme SDHA is oppositely regulated by Wnt3a and Lin28a. In vitro, Wnt3a increases SDHA gene and protein expression whereas Lin28a reduces it. This result was confirmed ex vivo on mouse femoral head explants. In OA mice (meniscectomized or aged), we observe an increase of SDHA expression whereas it is dramatically decreased in TgLin28a mice. This result was confirmed in human OA cartilage samples. To investigate the role of SDHA in chondrocyte protective effect, we used Aptenin5, an SDHA inhibitor. Aptenin5 inhibits the increased expression of mmp13 and adamts5 induced by Wnt3a. This effect was also found in human explants cultured with Wnt3a and Aptenin5. Because SDHA is involved in the conversion of succinate to fumarate, we hypothesized that the accumulation of succinate is responsible for the protective effect on chondrocytes. To demonstrate this, we treated murine chondrocytes and explants with Wnt3a with and without succinate. We found that succinate blocks the pro-catabolic and anti-anabolic effects of Wnt3a.Alltogether, these data indicate that energetic metabolism reprogrammed by Lin28a overexpression participates in cartilage protection during OA through SDHA inhibition. These results suggest that chondrocyte energy metabolism could be a new insight on OA therapeutics.

***Disclosures: ZOHRA BOUCHEMLA**, None*

FRI-139

Apolipoprotein E Is a Novel Marker for Chondroprogenitor Cells in The Murine Growth Plate *JOE KODAMA[3], Kevin Wilkinson[2], Takeshi Oichi[3], Masahiro Iwamoto[4], Motomi Enomoto-Iwamoto[5], Satoru Otsuru[2]. [3]University of Maryland, Baltimore, United States. [2]University of Maryland, United States. [3]University of Maryland, Baltimore, . [4]University of Maryland School of Medicine, United States. [5], United States

Recent studies suggest that the progenitor cells are located in the resting zone of the murine growth plate and consist of heterogeneous cell populations such as Pthlh+ cells and Foxa2+ cells. However, neither the spatial distribution nor the temporal hierarchy of these different cell populations is fully understood. We newly identified that Apolipoprotein E (encoded by Apoe) specifically and ubiquitously marks the progenitor cells in the resting zone of the murine growth plate after the formation of the secondary ossification center. We generated Apoe-mCherry reporter mice and confirmed the specific expression of mCherry in the resting chondrocytes (Fig.A). Sorted mCherry-positive chondrocytes have demonstrated the potential to differentiate into the trilineage in vitro culture. Single-cell RNA sequencing (scRNAseq) analysis and flow cytometry analysis of Apoehigh growth plate chondrocytes revealed at least two distinct progenitor populations (cluster 0 and cluster 1 in Fig.B). Cluster 0 had the highest Apoe and Clu expressions, whereas Cluster 1 had lower Clu expressions (Fig.C). Trajectory analysis suggested that the Cluhigh population gave rise to the other Apoehigh cells (Fig.B). RNA in situ hybridization of the growth plate of Apoe-mCherry mice identified that the Cluhigh population was located in the upper layer of the mCherry-positive resting zone (Fig.A). Pulse-chase experiments with daily injection of EdU for 8 days during the growth spurt demonstrated that mCherry+ progenitors were slow cycling compared to the columnar chondrocytes. Interestingly, mCherry+Cluhigh progenitors were barely incorporated with EdU, suggesting that they are more quiescent than mCherry+Clulow progenitors. These findings are also supported by our scRNAseq analysis showing that Cluhigh cells (Cluster 0) express the lowest Ccnd1, a cell cycle marker, further indicating that they are quiescent cells. These results suggest that mCherry+Cluhigh progenitors are upstream of the mCherry+Clulow progenitors in the hierarchy. Future characterization of these two populations may lead to a better understanding of the dynamic role of chondroprogenitors in the resting zone during longitudinal bone growth.

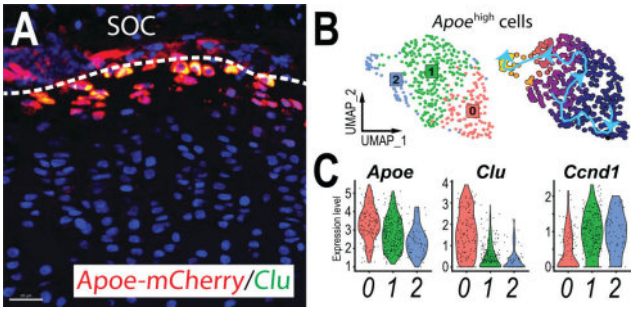

***Disclosures: JOE KODAMA**, None*

FRI-143

Hedgehog activation promotes osteogenic cell fates of growth plate resting zone chondrocytes *Shion Orikasa[1], Noriaki Ono[1]. [1]University of Texas Health Science Center at Houston School of Dentistry, United States

The resting zone of the postnatal growth plate is organized by slow-cycling chondrocytes expressing parathyroid hormone-related protein (PTHrP), which include a subgroup of skeletal stem cells that contribute to the formation of columnar chondrocytes. The PTHrP-Indian hedgehog (Ihh) feedback regulation is essential for sustaining growth plate activities; however, molecular mechanisms regulating cell fates of PTHrP+ resting chondrocytes and their eventual transformation into osteoblasts remain largely undefined. In this study, we hypothesized that Hedgehog signaling facilitates osteogenic cell fates of PTHrP+ resting chondrocytes through multiple mechanisms. We utilized a tamoxifen-inducible PTHrP-creER line that can exclusively mark PTHrP+ chondrocytes in the resting zone of the postnatal growth plate without marking any other cell types in long bones. To specifically activate Hedgehog signaling in PTHrP+ resting chondrocytes and visualize the fate of their descendants within growth plate and bone marrow, we also used Patched-1 (Ptch1 encodes a Hedgehog receptor which inhibits its downstream Smoothened signaling) floxed and R26R-tdTomato reporter alleles. All mice received a single dose of tamoxifen at postnatal day (P) 6 and were chased for up to 3 months. Histological and three-dimensional micro-computed tomography (3D micro-CT) analyses were performed at P14, 21, 28, 36, 42, 56, 70, 96. Hedgehog-activated PTHrP+ chondrocytes formed large concentric clonally expanded cell populations within the resting zone (‘patched roses’) at P21 and generated significantly wider columns of chondrocytes, resulting in hyperplasia of the growth plate at P36. Interestingly, Hedgehog-activated PTHrP+ cell descendants migrated away from the growth plate and eventually transformed into trabecular osteoblasts in the diaphyseal marrow space, leading to increased trabecular bone mass in the diaphysis at P96. Therefore, Hedgehog activation drives resting zone chondrocytes into transit-amplifying states as proliferating chondrocytes and eventually converts these cells into osteoblasts, unraveling a novel Hedgehog-mediated mechanism that facilitates osteogenic cell fates of PTHrP+ skeletal stem cells. These findings provide a solid foundation to understand how therapeutic intervention to the Hedgehog signaling pathway may impact a group of stem cell populations residing in the resting zone of the growth plate of growing individuals and subsequently affect bone formation.

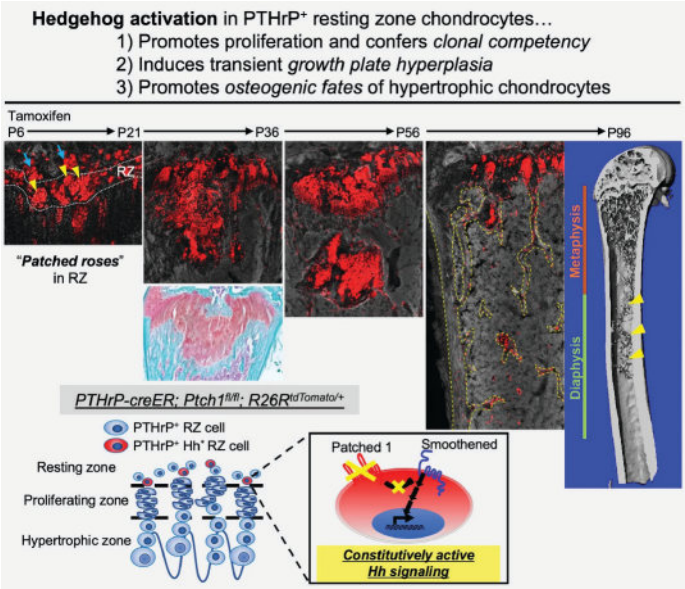

***Disclosures: Shion Orikasa**, None*

FRI-147

Identification of Novel Somatic Pathogenic Menin 1 Mutations without Germline Origin in an Atypical Parathyroid Tumor *An Nguyen[1], Dolores Shoback[2], Roubin Wu[3], Quan-Yang Duh[4], Janet Chiang[1]. [1]UCSF Endocrinology, United States. [2]UCSF Endocrinology, SFVA Medical Center, United States. [3]UCSF Pathology, United States. [4]UCSF Endocrine Surgery, SFVA Medical Center, United States

Atypical parathyroid tumors (APTs) are rare lesions and can have worrisome features even without invasion or metastases like PT cancer. The loss of parafibromin staining in these tumors suggests a germline or somatic mutation that produces either hyperparathyroidism (HPT)-jaw tumor or familial HPT syndromes. However, parafibromin expression does not exclude a possible mutation.A 69-year-old woman with end-stage renal disease received a living donor kidney transplant after being on peritoneal dialysis for 16 months. While on dialysis and cinacalcet 120mg daily, serum Ca was ~9.0 mg/dL (normal, 8.6-10.4), and PTH values were 1100-1500 pg/mL (normal, 16 -77). One-month post-transplant, PTH remained elevated to 600 pg/mL, serum Ca to 11.8 mg/dL. Neck ultrasound identified a 1.9 x 1.8 x 2.2 cm left posterior hypoechoic candidate lesion with heterogeneity and irregular borders which was co-localizied on Sestamibi scan. PTH level in the washings of the fine needle aspiration of this lesion was >2500 ng/L. At left neck exploration, a large superior parathyroid gland was found to be embedded in the thyroid, requiring lobectomy with parathyroidectomy. Histology revealed a markedlyn enlarged glandtumor with 95% cellularity, without significant mitotic activity, necrosis or infiltration into surrounding tissue. There was retention of nuclear parafibromin staining, consistent with APT. Postoperatively, PTH decreased to 140 pg/mL (serum Ca 9.7 mg/dL) off cinacalcet. The patient denied any family history of MEN. Molecular testing of the tumor revealed pathogenic missense Menin 1 mutation MEN1 p.P320L (40% allele frequency) and pathogenic frameshift MEN1 p.V80W (38% allele frequency) - the latter being a novel mutation. Germline genetic testing was negative for both variants.For molecular testing for somatic mutations, the general cutoff of at least 50% allele frequency strongly supports a germline origin. The MEN1 p.P320L missense mutation is known to result in reduced protein stability leading to rapid degradation and is a germline mutation in hereditary MEN1 and a somatic mutation in sporadic endocrine tumors. The p.V80W mutation in MEN1 is novel and predicted to be pathogenic, given its truncating effect potentially early in protein translation. Overall, this case unites several concepts of recognition, diagnosis, and treatment, as well as application of molecular and genetic testing to identify somatic and germline mutations in APT and in endocrine tumors.

***Disclosures: An Nguyen**, None*

FRI-150

Bone microarchitecture and disorganized bone tissue in a young woman with pycnodysostosis and an atypical femur fracture: A case report *Cat Shore-Lorenti[4], Heshan Witanachchi[4], Colin Chen[4], Simon Zhang[4], Hanh Nguyen[2], Christian Girgis[3], Roger Zebaze[4], Peter Ebeling[5]. [4]Monash University, Australia. [2], Australia. [3]Westmead Hospital , . [4]Monash University, . [5]School of Clinical Sciences, Monash University, Australia

Abstract: Pycnodystosis (PYCD) is a rare autosomal recessive lysosomal storage disorder, involving a loss of function mutation of the gene encoding cathepsin K (CTSK). The loss of function of this osteoclastic lysosomal protease reduces bone resorption, increases bone mineral density (BMD), but impairs the structure and material properties of bone. This case report demonstrates that bone fragility in a young woman with PYCD, presenting with an atypical femur fracture (AFF), was not explained by changes in bone density but by microarchitectural defects, disorganized bone and microcracks.Clinical Case: A 24-year-old woman with PYCD presented with an AFF in 2020 following a long history of prior minimal trauma fractures (MTF). PYCD was diagnosed in childhood and as an adult this patient displayed several signs and symptoms, including, but not limited to: short stature; dystrophic nails; short fingers; prominent forehead; prognathism, and; a significant history of 10 peripheral MTFs. Her first MTF occurred at 6-years-of-age. No other medical conditions or significant family history were identified. Her parents were consanguineous.At the time of the AFF, the patient was treatment naïve. Three years prior she gave birth via Caesarean-section and was able to breastfeed her baby for 12 months. Following the AFF, her vitamin D was slightly reduced (45 nmol/L), while P1NP and CTX were high, at 124 ug/L and 518 ng/L, respectively. Other pathology results were unremarkable.In the year following the AFF, BMD was high at the spine (T-score = +3.3), total hip (+5.4); and femoral neck (+6.7). High-resolution peripheral quantitative computed tomography (HR-pQCT) of the distal tibia detected unexpected cortical lucencies and sclerotic lesions in the trabecular compartment of the distal tibia (Fig1). Both total and trabecular volumetric BMD (vBMD) were high and trabecular numbers were increased in both the distal radius and tibia. Disorganization analysis using a novel software showed chaotically disorganized femoral shaft with spike shape masses at locations corresponding to a pseudofracture and sclerotic lesions.Clinical Conclusion: These imaging techniques detected disorganized bone and microarchitectural defects in a treatment naïve patient with PYCD and an AFF. The suppression of bone resorption in PYCD allows the accumulation of microdamage and disorganized bone that produces bone fragility. Antiresorptive therapy should be avoided.

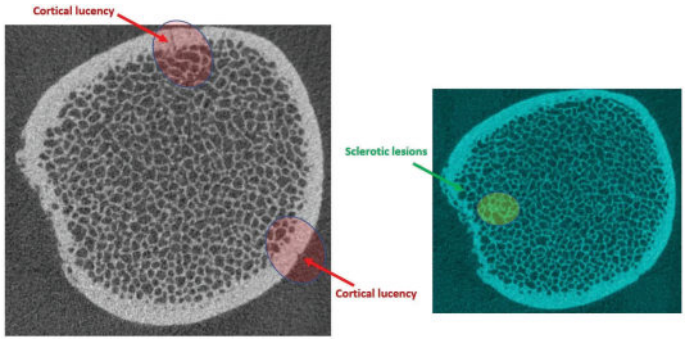

***Disclosures: Cat Shore-Lorenti**, None*

FRI-152

Evidence of Reduced Dentin Sialophophoprotein Expression and Impaired Cell Process Formation in Odontoblasts in Patients with Hypophosphatasia *Akira Nozoe[1], Kazuaki Miyagawa[1], Chiho Nakano[1], Shinji Takeyari[2], Makoto Fujiwara[4], Yasuhisa Ohata[4], Keiichi Ozono[2], Takuo Kubota[2], Susumu Tanaka[1]. [1]First Department of Oral and Maxillofacial Surgery, Osaka University Graduate School of Dentistry, Japan. [2]Osaka University Graduate School of Medicine, Japan. [4]Osaka University, . [4]Osaka University, Japan

Background: Hypophosphatasia (HPP) is a genetic disorder characterized by the premature loss of deciduous teeth due to defects in cementum formation. In addition, insufficient calcification of mantle dentin, which is essential for cementum formation, is also observed. But the underlying pathology remains unclear. Our objective of this study is to elucidate the underlying pathogenesis of dental defect in patients with HPP.Methods: We utilized induced pluripotent stem cells (iPSCs) from healthy individuals to generate odontoblast-like cells (ODs) via neural crest cells and mesenchymal stem cells (MSCs). We then examined various parameters, including odontoblastic differentiation markers and protein expressions, morphology, and calcification function using RT-qPCR, western blotting, immunostaining, and alizarin red staining. As a control group, we also induced osteoblast-like cells (OBs) from the same healthy MSCs. In addition, we created an HPP-iPSC from a patient with perinatal severe-type HPP (c.1559delT/c.1559delT: Perinatal), genetically rescued Perinatal-iPSCs by repairing both alleles using the CRISPR-Cas9 system (WT/WT: resHPP), and an odonto-type HPP model (WT/c.550C>T: odonto) from the resHPP-iPSCs using prime editing.

We then assessed their isogenic odontogenesis.Results: In WT-ODs, we observed significant increase in DSPP and NES protein expressions, compared to MSCs. The expression of RUNX2 protein increased in the early differentiation stages and then decreased in the late differentiation stages. Additionally, calcification and ALP activity increased over time. We also noted significant increase in MAPT and NEFL gene expressions, in WT-ODs compared to WT-OBs. Moreover, WT-ODs displayed a polarized nucleus and elongated cell process in one direction, Compared to Perinatal-ODs and Odonto-ODs, resHPP-ODs showed significant increase in ALP activity, DSPP protein expression, and mineralization during odontogenesis. Notably, RUNX2 protein expression was sustained until the late differentiation stage in Perinatal-ODs. The length of cell processes in Perinatal-ODs and Odonto-ODs were shorter than that in resHPP-ODs.Conclusion: We successfully established ODs differentiated from iPSCs. Our findings suggested that reduced DSPP expression, decreased ability to form cell process and lower calcification ability may be involved in the underlying pathogenesis of dental defect in HPP.

***Disclosures: Akira Nozoe**, None*

FRI-153

Comparison of Cd11b+ cells of the mandibular and femoral bone marrow at single-cell resolution *Rachel Phillips[1], Elizabeth Bradley[1], Kim Mansky[2], Amy Tasca[1]. [1]University of Minnesota , United States. [2]University of Minnesota, United States

Osteoclast activity within craniofacial bones orchestrates critical processes such as tooth eruption and skull modeling. Recent lineage tracing experiments in mice demonstrate that proper tooth eruption and skull generation requires embryonic but not adult myeloid cells. These data suggest that cellular ontogeny imparts fundamental differences between adult bone marrow-derived as compared to embryonic-derived tissue resident osteoclast progenitor cell populations; however, we lack essential knowledge about the osteoclast progenitors found in the marrow of craniofacial bones. Moreover, we completely lack transcriptomic data describing craniofacial-derived osteoclast progenitors. This knowledge gap impairs our understanding and treatment of pathological conditions including osteonecrosis of the jaw, primary or metastasized facial bone malignancies and osteomyelitis. Our lab has demonstrated that mandible-derived osteoclast precursors proliferate less, have increased osteoclast size and upregulation of osteoclast genes including Nfatc1, Dc-stamp, Ctsk, and Rank compared to osteoclasts derived from the femur bone marrow. To develop a better understanding of the transcriptome differences between mandible- and femur-derived osteoclast precursors, we performed scRNA sequencing of CD11b+ cells from mandible and femur bone marrow. CD11b+ cells were isolated from the femur and mandible derived bone marrow of 2-month-old male C57Bl/6 mice using Cd11b+ isolation microbeads. Six samples (3 femoral and 3 mandibular) were submitted for single-cell RNA sequencing. Six single cell captures targeting 10,000 cells each were performed by ST G chip for 3' gene expression. Using two-dimensional t-SNE representations of the expression levels of each of the samples, unique cell populations and differentially expressed genes were identified. Femur gene expression levels were used as the baseline for analysis. Differentially expressed genes pathways included up-regulation of TNF-?, AGE-RAGE and FOXO signaling pathways. While genes involved in cell adhesion, Fc gamma R mediated phagocytosis and autophagy pathways were down regulated in mandible derived cells. Currently expression of genes within these pathways are being verified by qRT-PCR. Together this data suggests that mandible derived osteoclast precursors have a unique gene signature compared to femur derived osteoclast precursors.

***Disclosures: Rachel Phillips**, None*

FRI-155

Conditional Knockout of Neural Sarm1 Improves Body Mass and Metabolic Health with High Fat Diet *Lila Dabill[3], IVANA SHEN[2], XIAO ZHANG[2], Aaron DiAntonio[3], Erica Scheller[4]. [3]Washington University in St. Louis, , [2], , [3]Washington University in St. Louis, United States. [4]Washington University, United States

Sterile alpha and TIR motif containing 1 (Sarm1) is a toll-like receptor, highly expressed in the nervous system, that is activated with injury, inflammation, and oxidative stress to promote axon degeneration and dysfunction. Previous findings with global knockout of Sarm1 showed evidence of metabolic improvements in high-fat diet (HFD) induced type 2 diabetes (T2D) as well as reduced peripheral axon degeneration. We hypothesize that this is due to the actions of Sarm1 in the nervous system. To test this hypothesis, we used Baf53b-Cre to knock out Sarm1 in all neurons throughout the body (Sarm1-cKO). Both control and Sarm1-cKO mice were fed HFD for 24 weeks, starting at 4-6 weeks of age. Quantitative PCR (qPCR) analysis confirmed high Sarm1 expression in the dorsal root ganglia (DRG) with a significant decrease in Sarm1-cKO mice; no significant difference in Sarm1 expression was observed in bone, testis, liver, or iWAT tissue between control and Sarm1-cKO mice. Over the 24-week study period, Sarm1-cKO mice fed HFD gained 20% less body mass than controls (20.8g mass gain on average in cKO vs 26g mass gain in control mice). Furthermore, subcutaneous inguinal fat, but not visceral gonadal fat, was preferentially reduced by 26% in Sarm1-cKO mice. Sarm1-cKO mice on HFD also showed evidence of metabolic rescue with smaller livers and less steatosis. Lastly, insulin tolerance testing (ITT) results show that Sarm1-cKO mice on HFD were more sensitive to insulin than controls. Micro-computed tomography and biomechanical testing are pending to determine if Sarm1-cKO mice have improved bone microarchitecture or strength with HFD feeding, respectively. Sarm1 inhibitors are currently under clinical development for the treatment of neurodegenerative disease. These results show that inhibition of Sarm1-dependent neurometabolic regulatory pathways also has the potential to support metabolic health in settings of obesity and T2D.

***Disclosures: Lila Dabill**, None*

FRI-158

The NAD salvage pathway in osteoblast lineage cells is indispensable for skeletal homeostasis *Olivia Reyes-Castro[1], Aaron Warren[1], Ha-Neui Kim[2], Maria Jose Almeida[3]. [1]University of Arkansas for Medical Sciences, United States. [2]Univ. Arkansas for Medical Sciences, Central Arkansas VA Healthcare System, United States. [3]Central Arkansas VA Healthcare System, Univ of Arkansas for Medical Sciences, United States

Nicotinamide adenine dinucleotide (NAD+) - a critical cofactor for cellular energy metabolism and numerous cellular processes, including cell division, DNA damage repair, and mitochondrial function - can be synthesized via several pathways. NAD+ levels and the expression of nicotinamide phosphoribosyltranferase (Nampt), the rate limit enzyme of the NAD+ salvage pathway, are lower in osteoblastic cells from old when compared to young mice. Moreover, administration of NAD+ precursors to aging mice attenuates the loss of bone mass and the involution of many other tissues. To examine the role of Nampt in osteoblastic cells and whether a decline in Nampt could contribute to skeletal aging, we initially generated mice lacking Nampt in Prx1-cre targeted cells. However these mice exhibited severe developmental phenotypes due to effects in chondrocytes, which precluded the examination of effect of Nampt on bone formation. In the work reported herein, we crossed Nampt-flox and Osx1-Cre mice to generate Nampt?Osx1 and Osx1-cre control mice. Nampt?Osx1 mice were born at the expected Mendelian ratio and were grossly undistinguishable from Osx1-Cre control littermates at birth. Evaluations of body weight, as well as spine and femur DXA BMD at 4 weeks of age revealed no differences between Nampt?Osx1 female or male mice when compared to the respective littermate controls. In contrast, femoral BMD in male and female Nampt?Osx1 mice was decreased at 12 weeks of age compared with Osx1-cre mice. Cultures of bone marrow derived osteoblastic cells from Nampt?Osx1 mice had lower NAD+ levels and exhibited decreased mineralization, as determined by Alizarin Red staining. Micro-CT analysis of femur from male and female Nampt?Osx1 revealed a decrease in cortical thickness due to a decrease in periosteal circumference. No changes were detected at the endosteal circumference. Trabecular bone volume at the distal femur and vertebrae (L5) was also lower in male Nampt?Osx1. These changes were due to a decrease in both trabecular number and thickness. No differences in trabecular bone were found in female. These results indicate that in osteoblast lineage cells Nampt contributes to bone homeostasis. Together with the earlier findings in Nampt?Prx1 mice, these results highlight that the dependency of osteoblast on Nampt is of much lower magnitude than that of chondrocytes.

***Disclosures: Olivia Reyes-Castro**, None*

FRI-159

Effects of Carboxylated and Uncarboxylated Osteocalcin on Glucose Sensitivity in Severe Osteoporotic Non-Diabetic Patients and In Vitro on Human ?-cells and Primary Adipocytes *Veronica Sansoni[1], Laura Gerosa[1], Chiara Verdelli[1], Marta Gomarasca[1], Martina Faraldi[1], Giovanni Mennuni[2], Riccardo Pasquali[3], Giuseppe Banfi[1], Sabrina Corbetta[4], Giovanni Lombardi[1]. [1]Laboratory of Experimental Biochemistry, IRCCS Istituto Ortopedico Galeazzi, Italy. [2]Laboratory Medicine Service, IRCCS Istituto Ortopedico Galeazzi, Italy. [3]Endocrinology and Diabetology Service, IRCCS Istituto Ortopedico Galeazzi, Italy. [4]Bone Metabolism and Diabetes Unit, IRCCS Istituto Auxologico Italiano, Italy

Extra-skeletal roles of carboxylated (GlaOC) and uncarboxylated (GluOC) forms of osteocalcin (OC) have been described in heterologous in vitro models and in vivo in rodents, where GluOC has been reported to affect glucose metabolism by stimulating pancreatic ?-cells proliferation, insulin expression and secretion and by improving insulin sensitivity and glucose uptake by skeletal muscle and adipose tissue. However, data in humans and human cells are limited and contrasting.This study aims at investigating: i) the relationship between GlaOC, GluOC and the indexes of glucose metabolism and insulin resistance in severe osteoporotic non-diabetic women randomized to either teriparatide (TPT) treatment or TPT associated with vitamin K (TPT+MK7) supplementation; ii) the effects of GlaOC and GluOC on human ?-cell function, and iii) on adipogenic differentiation of human subcutaneous adipose-derived stromal cells (ASCs).At present, 65 patients out of 82, aged >=65 years, have been enrolled. Six TPT and 6 TPT+MK7 patients completed the 18-month follow-up. At baseline, circulating GlaOC and GluOC do not associate with the indexes of glucose metabolism, while GlaOC positively correlates with waist circumference. GlaOC increases and GluOC/GlaOC decreases, both consistently although not significantly, in TPT+MK7 patients. Oral glucose insulin sensitivity (OGIS) significantly increases and fasting glycaemia decreases after TPT treatment, together a higher GluOC/GlaOC.The putative receptor for OC, GPRC6A, is expressed in immortalized human EndoC-?H1 ?-cell; 72h treatment with either GlaOC or GluOC (5, 20, 40 ng/mL) do not affect the glucose-stimulated insulin secretion (glucose: 0, 2.8, 5.6, 11, 20 mM). Further, 6h treatment with OC forms do not affect the expression of key genes in ?-cell function and sensitivity to glucose.GPRC6A is also ex-

pressed in ASCs. OC forms do not affect the adipogenic differentiation potential of ASCs; indeed, GluOC 40ng/mL induces a significantly increased expression of UCP1 gene, marker of brown adipocyte, without affecting LPL gene expression, marker of white adipocytes. UCP1 induction is independent from PGC1? expression, while associates with Cited1 induction, marker of the beige intermediate phenotype.In conclusion, human in vivo and in vitro data suggest no direct effects of OC on insulin secretion while supporting mild positive effects on peripheral insulin sensitivity and potential stimulation of a brown-like adipocytic phenotype.

***Disclosures: Veronica Sansoni**, None*

FRI-163

Bone fracture causes long-term impairment of the bone marrow niche for hematopoietic stem cells *Elise Jeffery[1,] Sean Ahler[1,] Bethany Davis[1,] Sean Morrison[1.] [1]UT Southwestern Medical Center, United States

Bone fracture is estimated to occur in 2.3% of people every year (GBD Fracture Collaborators, The Lancet, 2021). In addition to damaging bone, fracture also significantly damages the bone marrow (BM), which is the primary site of hematopoiesis in healthy adults. Hematopoietic stem cells (HSCs) in the BM reside adjacent to sinusoidal blood vessels and perivascular stromal cells, which secrete chemokines essential for HSC maintenance and survival (Crane et al, Nat Rev Immun, 2017). During fracture repair, the BM stroma is regenerated in part by periosteal cells that contribute to the formation of the fracture callus (Jeffery et al, Cell Stem Cell, 2022). However, it's unclear to what extent the regenerated BM stroma supports hematopoiesis. To investigate this, we analyzed the frequency of HSCs, restricted progenitors, and mature lineages in mice five weeks after tibial fracture, a time point when the bone cortex has fully re-formed and the marrow has regenerated (Jeffery et al, Cell Stem Cell, 2022). We found a striking three-fold reduction in the frequency of HSCs in post-fracture BM compared to that of the contralateral uninjured tibia. In contrast, there was no difference in the frequencies of lineage restricted progenitors or of mature hematopoietic populations. These data suggest that post-fracture BM is specifically toxic to HSCs. The degree of fracture stabilization did not affect the phenotype, as we observed a similar reduction in HSC frequency after non-stabilized fracture and pin-stabilized fracture. Surprisingly, the reduction in HSC frequency was maintained for at least six months post-fracture, suggesting that fracture has a long-term effect on the hematopoietic microenvironment. We hypothesized that this reduction in HSC frequency was due to impaired niche cell function in the regenerated BM. However, we found no significant changes in stromal cell number, morphology, or niche factor expression in stromal cells from regenerated BM compared to stromal cells from normal BM. In contrast, when we analyzed the morphology of endothelial cells following fracture, we found a significant increase in the number of arterioles, as well as irregular organization of sinusoids with high variability in sinusoid width. These data suggest that the sinusoidal niche for HSCs may be compromised in regenerated BM, and that the regrowth and remodeling of blood vessels in the BM is a limiting factor for the proper resumption of hematopoiesis following fracture.

***Disclosures: Elise Jeffery**, None*

FRI-167

Rhythmic Circulating Glucocorticoid Levels Play a Critical Role in Bone Loss Driven by Chronic Disruption of Circadian Rhythms *Eugenie Macfarlane[1,] Lauryn Cavanagh[1,] Colette Fong-Yee[1,] Markus Seibel[1,] Hong Zhou[1.] [1]Bone Research Program, ANZAC Research Institute, University of Sydney, Sydney, Australia, Australia

Chronic disruption of circadian rhythms (CR) from shiftwork or sleep disorders is associated with bone loss and low bone mineral density. However, the mechanisms that drive these detrimental effects on bone are unknown. Adrenal glucocorticoid (GC) secretion follows a diurnal rhythm and is a potent regulator of CR by synchronizing the cellular clocks throughout the body. We therefore asked whether GC signaling in osteoblasts/osteocytes mediates bone loss induced by chronic CR disruption using conditional glucocorticoid receptor (GR) knockout mice. Col2.3Cre/GRf/f (obGRKO) mice and their wild-type (WT) littermates were exposed to an established model of chronic CR disruption for 22-weeks. Mice were maintained on either a normal 12:12hr light-dark cycle (non-shifted) or exposed to weekly 12hr phase-shifts, equivalent to spending alternate weeks in Sydney and London (shifted; Fig.1A). Chronic disruption of CR abolished the diurnal rhythmicity of circulating corticosterone, characterised by a loss in the normal daily peak of serum corticosterone (prior to wakening at 6pm) in all shifted mice (regardless of genotype, $p<0.0001$). Consequently, rhythmic expression of the major clock gene Bmal was absent in tibiae of shifted WT mice ($p=0.0004$) but maintained in shifted obGRKO mice (Fig.1B-C, $p=0.0409$). This indicates that blocking arrhythmic osteoblastic GC signaling allows a self-sustaining rhythm in Bmal1 expression to persist in these bone cells. Micro-CT analysis revealed that chronic CR disruption caused pronounced trabecular bone loss ($p=0.005$) and reduced volumetric bone mineral density (vBMD, $p<0.0001$) in shifted compared to non-shifted WT mice. While non-shifted obGRKO mice had lower trabecular BV/TV than non-shifted WT mice ($p<0.0001$), chronic disruption of CR increased trabecular BV/TV in obGRKO mice ($p<0.0001$), with vBMD maintained (Fig. 1D-E). Notably, shifted WT mice displayed significantly greater numbers of empty osteocyte lacunae compared to non-shifted WT mice ($p=0.0464$), suggestive of cellular apoptosis. In contrast, no such changes in osteocyte lacunae were observed in shifted compared to non-shifted obGRKO mice (Fig. 1F-G). In conclusion, chronic circadian rhythm disruption abolishes glucocorticoid rhythmicity which thereby disturbs skeletal circadian gene expression and induces bone loss. These novel findings provide valuable insight into how chronic disruption of circadian rhythm drives detrimental effects on skeletal health in shift workers.

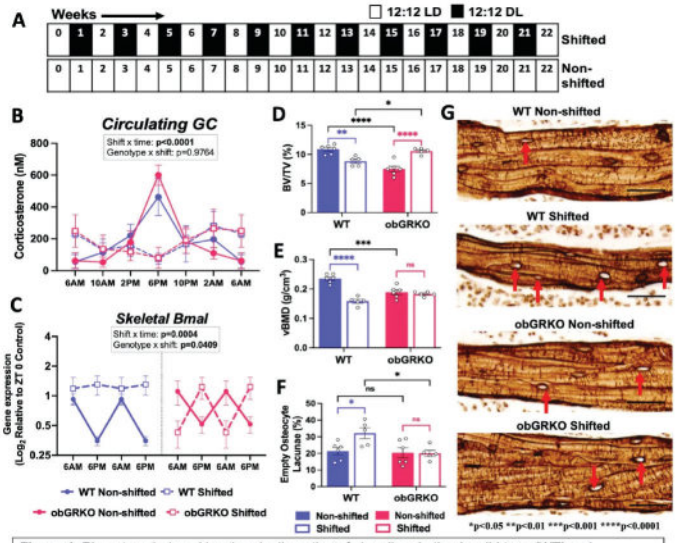

Figure 1. Phenotype induced by chronic disruption of circadian rhythm in wild-type (WT) and osteoblast/osteocyte glucocorticoid receptor knockout (obGRKO) mice. GC, glucocorticoid; Bmal, brain and muscle ARNT-Like protein; LD, Light:Dark. Analysed by two- or three-way ANOVA, n=5-6/group.

***Disclosures: Eugenie Macfarlane**, None*

FRI-168

Two-Pronged Mediation of Adrenal Steroidogenesis by Oxytocin *Uliana Cheliadinova[2,] Georgii Pevnev[2,] Vitaly Ryu[2,] Tal Frolinger[2,] Steven Sims[2,] Ofer Moldavski[2,] Funda Korkmaz[2,] Orly Barak[2,] Judit Gimenez Roig[2,] Farhath Sultana[2,] Natan Kramskiy[2,] Soleil Wizman[2,] Michelle Orloff[2,] Tony Yuen[2,] Daria Lizneva[2,] Mone Zaidi[3,] Anisa Gumerova[2.] [2]Icahn School of Medicine at Mount Sinai, United States [2]Icahn School of Medicine at Mount Sinai, [3]Mount Sinai Medical Center, United States

Stress-stimulated glucocorticoid release affects diverse biological processes, including pregnancy and childbirth. The controversy surrounding effects of OXT on stress prompted us to investigate its actions on adrenal cortical function in mice. RNAscope and immunohistochemistry provided unequivocal evidence for abundant OXT receptor (OXTR) expression in the adrenal cortex, predominantly in zona fasciculata and zona reticularis. Female mice displayed higher adrenal cortical Oxtr expression, more than a range of other tissues under study. Oxtr expression was also detected in the adenohypophysis solely in female mice, while both male and female mice expressed Oxtr in the pars intermedia of the hypophysis. Aging impressively attenuated Oxtr expression in female mice in both the adrenal gland and adenohypophysis. For loss-of-function studies, we generated tissue-specific Star-CreERT2/Oxtrfl/fl mice in which the Oxtr was deleted from steroidogenic tissues, namely adrenals and ovaries. Deletion was confirmed by RNAscope and immunohistochemistry. We found no difference in serum corticosterone between tamoxifen-induced and uninduced mice; however, the elevation of serum corticosterone upon ACTH stimulation or after four weeks of stress was attenuated in tamoxifen-induced mice. Bulk RNAseq of adrenals from tamoxifen-induced mice revealed the downregulation of key steroidogenic genes, namely Cyp17a1, Hsd3b3, Hsd17b2, Cyp3a41b, and Serpina6 (a corticosteroid-binding globulin). In gain-of-function studies, a single OXT injection led to a rise of serum ACTH in tamoxifen-induced mice, which was greater in magnitude than uninduced controls. However, after five days of OXT injections, corticosterone levels became elevated, whereas ACTH levels declined to baseline. This suggests that OXT acts directly on OXTRs on corticotropes to initiate a stress-like response, with a negative feedback loop that inhibits further ACTH secretion. Of note is that male mice did not display any difference between tamoxifen-induced and uninduced groups, consistent with their low hypophyseal Oxtr expression. In all, we describe a novel gender-specific two-pronged circuit through which OXT may precisely regulates the production of corticosterone from the adrenal cortex. In the first arm, OXT directly stimulates ACTH secretion through adenohypophysis OXTRs. In the second arm, OXT prevents excessive stress-induced adrenal stimulation by downregulating steroidogenic genes. Our discovery lays the foundation for the emergence of new physiology that may relate to a fundamental role for oxytocin in the stress response during procreation, notably, when levels are elevated during pregnancy and lactation.

***Disclosures: Uliana Cheliadinova**, None*

FRI-170

Dio3-Dio3os regulatory function in thyroid hormone linked bone formation
*Quamarul Hassan[1], Yuechuan Chen[2]. [1]University of Alabama, United States. [2]Univerisity of Alabama At Birmingham,

Consumptive hypothyroidism, a skeletal consequence due to aberrant deiodinase 3 (Dio3) expression, delays adolescent bone development, inhibits adult bone turnover due to defective thyroid hormone (TH) signaling. The long non-coding (lncRNA) Dio3os and coding Dio3 genes overlap and transcribe in opposite directions; however, we lack the knowledge of how Dio3os activates neighboring gene Dio3 (in cis) and silences osteoblast (OB)-specific genes at a distance (in trans) to inactivate TH signaling in osteoblast cells. The proposed research investigates the osteoblast-specific functions by which Dio3os controls cis and trans transcriptional activities in maintaining thyroid hormone (TH) signaling and bone formation in vivo. Recently, we found that the Dio3os is a critical regulator for osteogenesis, and CRISPR-mediated Dio3os transcriptional repression or exon deletion significantly decreased local Dio3 expression and increased non-local OB-specific gene expression. Preliminary RNA and chromatin accessibility (ATAC) sequencing analysis from Dio3os-deleted OBs further revealed that Dio3os directly controls the chromatin accessibility and modifications of TH-controlled bone-forming genes through a trans-regulatory mechanism by recruiting nucleosomal remodeling deacetylase (NuRD) complex. Furthermore, RNA immunoprecipitation with Dio3os followed by mass spectrometry analysis identified a group of nucleosome remodelers associated with deacetylase activity and belonging to the NuRD complex. Our central hypothesis is that Dio3os functions as a critical regulator of TH signaling during bone synthesis and maintenance by activating Dio3 locally and by repressing transcription of distant OB-specific genes.

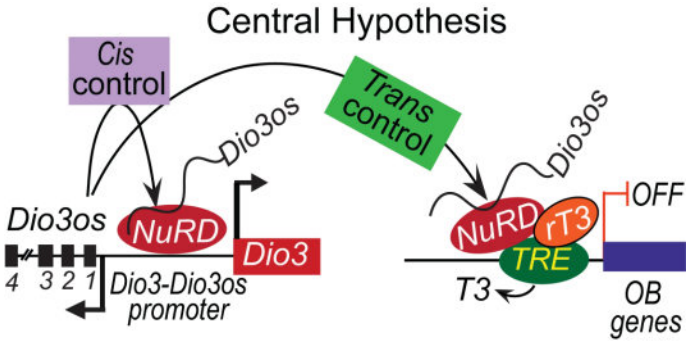

***Disclosures: Quamarul Hassan**, None*

FRI-172

Comparative Analysis of PTH (1-34), PTHrP (1-36), and Abaloparatide Effects on Murine Osteoblast Transcriptome
*ZHIMING HE[4], Michael Mosca[2], Florante Ricarte[3], CAROLE LE HENAFF[4], Nicola Partridge[5]. [4]New York University, . [2]NYU Langone Medical Center, . [3]Department of Molecular Pathobilogy, New York University college of Dentistry, United States. [4]New York University, United States. [5]New York University College of Dentistry, United States

Teriparatide (PTH (1-34)) and its analogs, PTHrP (1-36) and abaloparatide (ABL) have been used for the treatment of osteoporosis, but their efficacy over long-term use is significantly limited. Our laboratory has shown that PTH (1-34), PTHrP (1-36), and ABL exert time and dose-dependent differential responses in osteoblasts, leading us to hypothesize that they may also differentially modulate the osteoblast transcriptome. Here, we treated mouse calvarial osteoblasts with 1 nM of the 3 peptides for 4 h and analyzed the resulting RNA-Seq data. Gene-set enrichment analysis revealed that PTH (1-34) regulated 367 genes, including 194 unique genes; PTHrP (1-36) regulated 117 genes, including 15 unique genes; and ABL regulated 179 genes, including 20 unique genes. There were 74 genes shared exclusively between PTH (1-34) and ABL, 16 genes shared exclusively between PTH (1-34) and PTHrP (1-36), and 83 genes shared among all 3 peptides. The significant differences in the expression of various genes from the 3 peptides indicate gene ontology specific differences, including differences in Wnt signaling, cAMP-mediated signaling, bone mineralization, morphogenesis of a branching structure in biological processes; cytokine receptor/binding activity, ligand-activated transcription factor activity, cAMP phosphodiesterase activity in molecular functions. The 3 peptides increased Vdr, Cited1 and Pde10a mRNAs in a differential fashion similar to Rankl expression. These findings were confirmed via qRT-PCR with additional cultured samples. mRNA abundance of other genes of interest based on gene/pathway analyses, including Wnt4, Wnt7, Wnt11, Pde10a, Sfrp4, Dkk1, Kcnk10, Hdac4, Epha3, Tcf7, Crem, Fzd5, Pp2r2a, and Dvl3 were also examined; some genes were stimulated similarly by all 3 peptides; others were not. Finally, experiments with siRNA knockdowns of SIK1/2/3 and CRTC1/2/3 in PTH (1-34) treated cells showed that some of these genes are regulated by SIKs and CRTCs (Vdr, Wnt4), while others are not. Although many studies have examined PTH signaling in the osteoblast/osteocyte, ours is the first to examine the global effects of these peptides on the osteoblast transcriptome. Further delineation of which signaling events are attributable to PTH (1-34), PTHrP (1-36) and ABL exclusively and which are shared among all 3 will help improve our understanding of the effects these peptides have on the osteoblast and lead to the refinement of PTH-derived treatments for osteoporosis.

***Disclosures: ZHIMING HE**, None*

FRI-174

Calorie Restriction Profoundly Suppresses Bone Remodeling and Causes Cortical but not Trabecular Bone Loss in Mice
*Linyi Liu[1], Phuong T. Le[1], Roland Baron[2], Victoria DeMambro[1], Samantha Costa[1], Ziru Li[1], Clifford J. Rosen[1]. [1]MaineHealth Institute for Research, United States. [2]Harvard School of Dental Medicine, United States

Weight loss, by most means, causes bone loss, although the mechanism for that loss is unclear. Some studies have shown increased bone resorption, such as in anorexia nervosa while others have demonstrated uncoupled remodeling with reduced bone formation and enhanced bone marrow adiposity. Several lines of evidence from our previous studies suggested there was differential loss of cortical but not trabecular bone mass. To characterize the mechanisms inherent in weight loss-induced bone loss, we performed 30% calorie restriction (CR) for 8 weeks in both male and female 8-week-old C57BL/6J mice compared to a control diet. We examined areal BMD, micro-architecture, histomorphometric parameters, in vitro trajectories of osteoblast and adipocyte differentiation, and stromal cell bioenergetics using Seahorse technology. After 8 weeks, both CR male and female mice lost weight and exhibited femoral and whole body loss of BMD vs. controls ($p<0.05$). By uCT, CR males and females both had lower cortical bone volume fraction vs. control diet mice ($p<0.05$) (Figure 1), but trabecular parameters increased by diet in female mice vs. controls. Histomorphometric analysis revealed that CR male and female mice had a profound suppression in trabecular MAR, BFR/BV, and MS/BS ($p<0.001$ vs control), and very reduced EC and PS MAR, BFR/BV and MS/BS in cortical bone vs. control ($p<0.001$ for all parameters). These features were due to reduced osteoblast and osteoclast numbers on the endosteal, endocortical and periosteal surfaces. Importantly, there was a 6-fold increase in bone marrow adipocytes; Cfd (adipsin) was one of the top up-regulated bone marrow genes by qRT-PCR vs. control marrow. In vitro, the pace of adipogenesis in BMSCs was greatly accelerated with more oil red O staining, whereas osteogenic differentiation was reduced. CR BMSCs had a bioenergetic profile that revealed marked suppression in both oxidative phosphorylation and glycolysis (Figure 2) vs. controls ($p<0.001$). Taken together, these lines of evidence support the tenet that calorie restriction causes cortical bone loss due to a profound suppression in bone turnover, almost certainly related to a reduced supply of energy substrates. The increase in marrow adipocytes is related to both progenitor recruitment and lipid storage in the face of widespread nutrient insufficiency. Long term dietary restrictions may lead to a greater risk of cortical bone fractures.

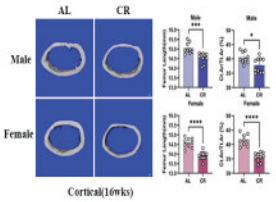

Fig1. Caloric restriction decreased cortical bone area fraction in both male and female mice

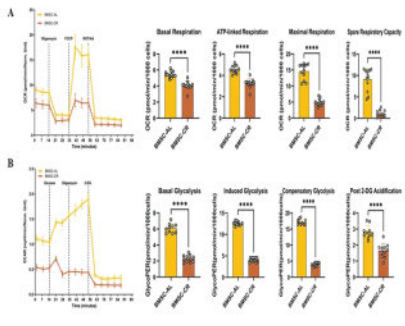

Fig2. Caloric restriction suppressed both oxidative phosphorylation and glycolysis in female mice

***Disclosures: Linyi Liu**, None*

FRI-176

EXT608 for the Treatment of Hypoparathyroidism: Phase 1 Trial Design and Results *Laura Hales PhD[1], Kate Didio MBA[1], Leon Shi PhD[2], Daniel Hall PhD[1], Poul Strange MD PhD[2], Daniel Dickerson MD PhD FAAFP[3], Tarik Soliman PhD[1]. [1]Extend Biosciences, United States; [2]IMD, United States; [3]ICON plc, United States

Extend Biosciences is developing EXT608, a long-acting parathyroid hormone (PTH 1-34)-based therapy designed to replace the physiological effects of PTH with significantly less frequent dosing and improved bioavailability. EXT608 was developed using the company's D-VITylation® platform, which harnesses the biology of vitamin D and the reversible binding properties of the serum-circulating vitamin D binding protein. By utilizing this natural pathway, D-VITylation prevents a vitamin D-conjugated therapeutic from renal clearance, thereby significantly extending its half-life. Bioactivity is not compromised and as such, EXT608 is fully active as-is at the PTH receptor.A double-blind, randomized, placebo-controlled Phase 1 trial involving 24 healthy participants (3:1 active:placebo) across 6 cohorts was conducted with EXT608. The primary endpoint was to characterize the safety and tolerability profile of escalating dose levels of EXT608 when administered to healthy adult subjects as a single injection by 1) observing the incidence, nature, and severity of adverse events (AEs) and withdrawals due to treatment emergent AEs, 2) noting the frequency and severity of post-dose change from baseline in hematology, serum chemistries, urinalysis, electrocardiogram, vital signs, and physical examination findings, and 3) determining the percentage of subjects with injection or infusion site reactions. Secondary endpoints included 1) determining plasma pharmacokinetic parameters, and 2) assessing the pharmacodynamic profile by measuring post-dose change from baseline in serum chemistries and urinalysis. The results show that EXT608 was safe and well tolerated, with no serious adverse events reported. It also shows a dose dependent increase in serum calcium. A prolonged suppression of endogenous parathyroid hormone was also observed, as anticipated. The pharmacokinetic analysis suggests that EXT608 can be effective when dosed once-weekly. The data provide a strong rationale to proceed to the next stage of clinical development and also offer valuable guidance for selecting a starting dose in the Phase 2 trial.

***Disclosures: Laura Hales PhD**, Extend Biosciences, Major Stock Shareholder*

FRI-181

Targeting Synovial Connexin Hemichannels Ameliorates Osteoarthritis Progression *Rui Hua[1], Yi Tian[1], Manuel A. Riquelme[1], Xuewei Wang[1], Liang Ma[1], Sumin Gu[1], Jean X. Jiang[1]. [1]UT Health San Antonio, United States

Osteoarthritis (OA) is a degenerative joint disease characterized by progressive articular cartilage deterioration, subchondral bone sclerosis, and synovial inflammation. The gap junction protein connexin 43 (Cx43), a key regulator of musculoskeletal homeostasis, is overexpressed in cartilage and synovium of OA patients. However, the contributions of Cx43 to OA pathogenesis remains largely elusive. Cx43 forms hemichannels (HCs) and mediate the release of small molecules (< 1.2 KDa), such as ATP and PGE2, into the extracellular environment. To determine whether deletion of Cx43 in joint tissue could ameliorate OA symptoms, we adopted adeno-associated virus (AAV) mediated Cre expression in Cx43 fl/fl mice using a destabilization of the medial meniscus (DMM) surgery induced OA model. Intra-articular injection of AAV-Cre decreased Cx43 level, with a higher efficiency in the synovium (p=0.001) than in the cartilage (p=0.065). MicroCT analysis showed reductions in subchondral BV/TV, Tb.Th, and BMD with AAV-Cre mediated Cx43 deletion. Moreover, reduced Cx43 expression mitigated OA-related pain behaviors evaluated by von Frey and open-field tests. To further investigate the role of Cx43 HCs in OA progression, a monoclonal Cx43(M1) antibody that specifically blocks Cx43 HCs was developed. In vivo Evens blue dye uptake assay showed that DMM increased HCs opening by 2 folds, which was inhibited by the antibody. Impeded Cx43 HCs by the antibody improved cartilage structure as quantified by OARSI score, decreased degree of synovitis, along with reduction of MMP13 and Collagen X levels. Subchondral sclerosis and OA pain symptoms were also alleviated in the Cx43 antibody treated group. Remarkably, in vivo distribution of this antibody is predominantly in synovium, including macrophages and fibroblasts, with sustained presence for over 2 weeks. In addition, OA induced increase of M1 macrophages, as indicated by the iNOS/CD68 double positive cells, was attenuated after antibody treatment. In vitro study using mouse macrophages or human synovial fibroblasts demonstrated the inhibition of LPS or IL1?-induced HCs opening and inflammatory genes expression (COX2, ADAMTS 4/5, and MMP3/13) by Cx43 HC-blocking antibody. In summary, our results highlight the crucial role of Cx43 and HCs in regulating pro-inflammatory mediators under OA conditions. Targeting synovial Cx43 HCs, thus, is a potential therapeutic strategy to mitigate the inflammatory environment during OA progression.

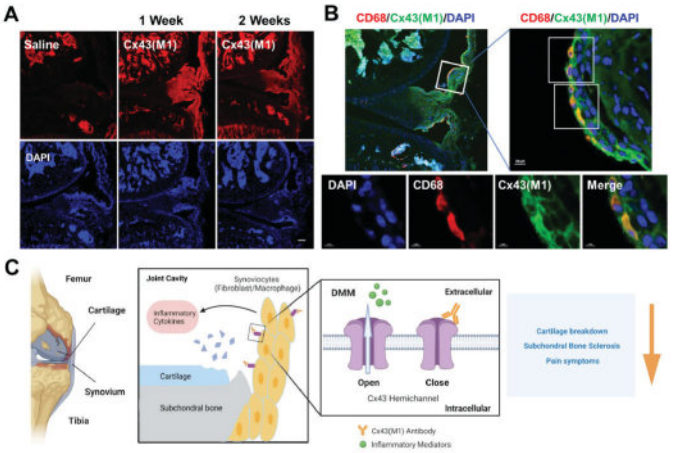

Targeting synovial connexin 43 hemichannel as a potential therapeutic target of OA

(A) *In vivo* distribution of Cx43(M1) antibody shows accumulation primarily in the synovium with sustained presence for over 2 weeks. **(B)** Colocalization of Cx43(M1) antibody with macrophage marker CD68. **(C)** Schematic illustration showing the administration of Cx43(M1) antibody blocks hemichannel opening and release of inflammatory cytokines, thus improving joint structure, subchondral bone sclerosis and pain symptoms.

***Disclosures: Rui Hua**, None*

FRI-183

PTH Stimulates Osteoblast Secretion of Slit3 to Repel Aberrant Vertebral Innervation and Relieve Low Back Pain Associated with Spinal Degeneration *Weixin Zhang[1], Arryn Otte[2], Sisir Kumar Barik[3], Mei Wan[2], Xu Cao[2], Janet Crane[2]. [1]Johns Hopkins university, , [2]Johns Hopkins University, United States; [3],

Low back pain (LBP) is the leading cause of disability globally, affecting one out of every four people. Nonspecific LBP is associated with spinal degeneration, particularly with vertebral endplate bone expansion and sclerosis. We have analyzed two mouse models with spinal degeneration, aging mice and lumbar spine instability (LSI) and found that parathyroid hormone (PTH) treatment reduced vertebral endplate sclerosis and improved pain behaviors. Most notably, porosity of the vertebral endplate significantly decreased while the tolerance of mechanical pressure significantly increased in PTH treated (40 µg/kg/day) groups relative to the vehicle groups in both aging mice and wild type (WT) LSI mice. Aberrant innervation noted in the vertebral body and endplate during spinal degeneration was reduced with PTH treatment as quantified by PGP9.5+ nerve fibers. Beta-3tubulin+ and CGRP+ neurons also significantly decreased in dorsal root ganglion within PTH treatment relative to vehicle control in both mice models. To explore the mechanism of PTH-reduction of innervation, we screened multiple axon guidance cues. The neuronal repulsion factor Slit3 significantly increased in the endplate after PTH treatment in WT LSI model. E47 and Foxa2, two transcription factors of Slit3, were significantly increased after PTH treatment (100 nmol for 3 days) in MC3T3 cells with osteoblast differentiation inducible culture medium. CHIP assay further indicated that the expression of Slit3 was significantly increased by Foxa2 with PTH stimulation in vitro. In vivo models deleting PTH type 1 receptor (PPR) in osteoblasts (OsteocalcinCrePPRf/f LSI mice) prevented PTH-reduction of endplate porosity and improvement in pressure tests, whereas PPR deletion in chondrocytes (Col2aCreERt2P-PRf/f LSI mice) continued to improve to PTH in regard to porosity and pressure tests. Furthermore, deletion of Slit3 in osteoblasts (OsteocalcinCreSlit3f/f LSI mice) did not differ between PTH and vehicle treatment in regard to total endplate porosity nor pressure test. Altogether, PTH stimulates Slit3 to repel sensory nerve innervation and provides symptomatic relief of LBP associated with spinal degeneration.

***Disclosures: Weixin Zhang**, None*

FRI-187

Differential osseous gene expression in swim-trained anosteocytic and osteocytic teleost fish *JOSEPHINE T. TAUER[1], Tobias Thiele[2], Catherine Julien[3], Lior Ofer[4], Paul Zaslansky[5], Ron Shahar[4], Bettina Willie[6]. [1]Shriners Hospital, Canada; [2]Julius Wolff Institute, Charité - Universitätsmedizin Berlin, Germany; [3]Shriners Hospital for Children-Canada, Montreal; Faculty of Dental Medicine and Oral Health Sciences, McGill University, Canada; [4]Koret School of Veterinary Medicine, The Robert H. Smith Faculty of Agriculture, Food and Environmental Sciences, The Hebrew University of Jerusalem, Israel; [5]Department of Operative and Preventive Dentistry, Charité - Universitätsmedizin Berlin, Germany; [6]McGill University, Canada

Introduction: Osteocytes are considered mechanosensory bone cells that regulate bone (re)modeling in response to mechanical stimuli. Surprisingly, evolutionarily advanced fish

lack osteocytes but still exhibit bone formation in response to loading. While there is knowledge of the molecular mechanisms controlling mammalian mechanoadaptation, fish data is lacking. Thus, we aimed to identify molecular mechanisms in anosteocytic bones (ricefish; RF) and osteocytic bones (zebrafish; ZF) after loading.Methods: Fish were trained by swimming for 5 minutes against a current and sacrificed after 1-, 8-, or 24 hours (h). Vertebrae were analyzed using RNA sequencing and compared to non-trained controls (n=6 fish/genotype).Results: At each time point, 26,099 and 21,129 gene reads for ZF and RF have been identified, respectively. After filtering non-skeletal genes (Ayturk et al. JBMR, 2013:28), 14, 54, and 977 differentially expressed genes (DEGs) have been identified in ZF, and 353, 284, and 763 DEGs in RF at 1h, 8h, and 24h, respectively. Enrichment analysis showed in ZF that upregulated DEGs were related to protein translation at 1h, and to DNA transcription and cell cycle processes at 24h, while downregulated DEGs were linked to muscle function, circadian rhythm, and metabolic processes at 24h. In RF, upregulated DEGs were associated with ion channel activity related to metabolic processes in muscle at 8 and 24h, while downregulated DEGs were related to cytoskeletal organization at 8h. Osteoblast differentiation associated enriched DEGs were identified in ZF at 8 and 24 h, but not in RF. Applying a customized 'osseous analysis panel' identified 87 'osseous DEGs' (oDEGs) in ZF and 71 in RF, primarily upregulated in ZF and downregulated in RF. Only one upregulated oDEG was identified in RF, myocilin, a regulator of osteoblast differentiation, at 1h and 24h post-training.Conclusion: Zebrafish benefited from numerous osteocytes for bone formation in response to mechanical stimuli, while ricefish exhibited delayed skeletal modeling after swim training. It's speculated that in anosteocytic bone, non-osteocytic cells, such as bone lining osteoblasts, chondrocytes, and chordoblasts, sense and respond to mechanical load differently over time (Ofer et al. PLoS Biol, 2019:17). Our findings challenge the current paradigm of osteocytes as the exclusive regulators of bone remodeling and suggest the existence of multivariate feedback networks involved in bone remodeling.

***Disclosures: JOSEPHINE T. TAUER**, None*

FRI-188

Osteocyte-Specific Endocannabinoid Receptor 1 (CB1) Deficiency Influences Cancellous Bone Mass, But Does Not Affect Bone Response To Disuse *Rachel DeNapoli[1], Evan Buettmann[2], Aron Lichtman[2], Henry Donahue[2], [1], United States, [2]Virginia Commonwealth University, United States

Disuse-induced bone loss during prolonged bedrest, injury, or paralysis, is a major health and financial concern for the general population. Endocannabinoid receptor 1 (CB1) influences bone in an age, sex, and strain dependent manner. In particular, our lab found skeletally mature male C57BL/6J mice with a global CB1 deletion (KO) are more sensitive to disuse-induced bone loss than male wildtype, while disuse-induced bone loss was mitigated in female KO mice during single limb immobilization [1]. To further determine CB1's role in bone, we hypothesized that mice with a conditional knockout of CB1 in osteocytes, the predominate mechanoregulatory cell in bone, would be more sensitive to bone loss than wildtype during hindlimb suspension (HLS).All animal procedures were conducted with approval of the VCU IACUC. We generated novel homozygous DMP1-Cre(+); CB1flox/flox mice (cKO) and DMP1-Cre(-); CB1flox/flox mice (WT) for this experiment. 20-week-old male and female mice (n=7-9/group) were assigned to either HLS or control group for three weeks. Skeletal phenotype was assessed using in vivo micro-CT scans following 21 days of HLS. Cancellous bone at epiphyseal and metaphyseal regions were analyzed. Data were analyzed using repeated measures 3-way ANOVA with Sidak post-hoc test ($p<0.05$).MicroCT analysis at D21 demonstrated that loss of CB1 in DMP1 expressing cells led to lower metaphyseal and epiphyseal BV/TV versus WT. HLS resulted in all groups experiencing bone loss from baseline in the femoral metaphyseal and epiphyseal region. However, genotype had no influence on disuse-induced bone loss. Interestingly, in the epiphyseal region, there was an interaction of HLS and sex, with male mice having greater disuse-induced decreases in BV/TV from baseline than female mice.These results suggest for the first time that CB1 expression in DMP1 lineage cells plays an important role in bone mass within the epiphyseal and metaphyseal regions, but not in the response to disuse. These results, when compared to our previous studies, suggest CB1 receptor in osteocytes controls bone mass under basal conditions, while deficiency in earlier osteoblastic cells may control response to disuse.[1] DeNapoli, R. C. et al. Journal of Biomechanics (2023)

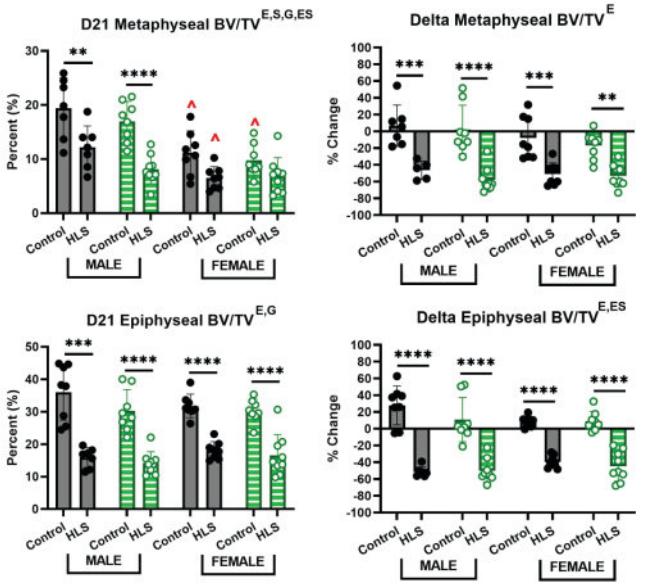

Figure 1: Femoral metaphyseal and epiphyseal trabecular bone BV/TV for male and female WT (filled, black) and cKO (striped, green) at day 21 of HLS and change from baseline. Data depict mean ± standard deviation. Significant main effects on HLS (E), Sex (S), Genotype (G), and interaction between HLS and Sex (ES). ^p<0.05 vs same limb of opposite sex, *p<0.05, **p<0.01, ***p<0.001, p<0.0001

***Disclosures: Rachel DeNapoli**, None*

FRI-193

Osteocytic Connexin 43 Deficiency Attenuates HLS-Induced Epiphyseal Bone Loss in Female, but not Male, C57Bl/6J Mice *Gabriel Hoppock[1], Evan Buettmann[2], Jolene Windle[2], Henry Donahue[2], [1], [2]Virginia Commonwealth University, United States

Preceding research has shown that gap junction communication and mechanical stimulation, or lack thereof, influence bone development and remodeling, however, the mechanisms by which this occurs remain unclear. Our lab and others have shown deficiency of connexin 43 (Cx43), bone's predominant gap junction protein, in early osteoblasts/osteocytes protects against unloading-induced bone loss in mice.1,2 It is unclear, however, if this protection is due to Cx43 deficiency in osteoblasts or osteocytes, the latter being the most abundant and primary mechanosensory bone cell. To address this, we used a Cx43-deficient mouse targeting later osteoblasts/osteocytes to test the hypothesis that osteocyte-specific Cx43 deficiency protects against hindlimb suspension (HLS)-induced bone loss.All animal procedures were approved by the VCU IACUC. At 6 months of age, male and female osteocyte-specific Cx43 deficient mice (Cx43?OCY) and their wildtype littermates (WT) with C57Bl/6J backgrounds underwent HLS or normal ambulation (control) for 21 days (n=8-11 per group). MicroCT scans were taken on days 1 and 22 and images the left femur was analyzed. Separate 2-way ANOVAs with Bonferroni's post-hoc tests were used to assess female and male mice for significant effects of genotype and HLS ($p<0.05$).At baseline Cx-43?OCY mice had decreased diaphyseal cortical bone compared to WT (Figure 1A). In the epiphysis and metaphysis, male mice showed an increase in bone volume due to Cx43 deficiency, but female mice did not. The basal differences between WT and Cx43?OCY mice show osteocytic Cx43 plays a sexually dimorphic role in postnatal bone volume. After 21 days of HLS, significant effects of HLS were found in all female and male epiphyseal and metaphyseal changes as well as in Ct.Ar/T.Ar (Figure 1B). Interestingly, osteocyte-specific Cx43 deficiency protected against HLS-induced decreases in epiphyseal BV/TV in female but not male mice. Cx43 deficiency did not affect HLS-induced decreases in metaphyseal or cortical bone in either male or female mice. These results suggest osteocytic Cx43 deficiency causes increased trabecular and decreased cortical bone basally. The data also show osteocytic Cx43 deficiency protects against HLS-induced epiphyseal bone loss in female mice whereas early osteoblast Cx43 deficiency likely also protects against metaphyseal bone loss, as shown previously by our lab.21. Grimston et al. J Bone Miner Res. 2011. 2. Lloyd et al. J Bone Miner Res 2012.

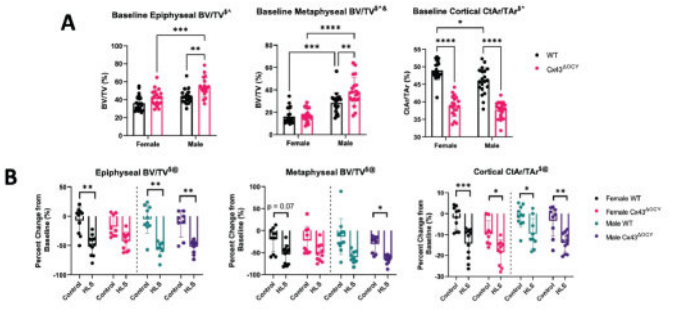

Figure 1. A. Osteocyte specific Cx43 deficiency led to increased trabecular bone but decreased cortical bone fraction. Baseline microCT data for WT and Cx43$^{\Delta OCY}$ female and male mice analyzed by 2-way ANOVA for effects of sex and genotype. $ Significant main effect of sex. ^ Significant main effect of genotype. & Significant main interaction of sex and genotype. **B. Cx43 deficiency protects against HLS-induced epiphyseal bone loss in female, but not male, mice.** Percent change from baseline after 21 days of HLS. Females and males analyzed by separate 2-way ANOVAs for effects of HLS and genotype. $ Significant main effect of HLS in females. @ Significant main effect of HLS in males. * p < 0.05; * p < 0.005; * p < 0.0005; **** p < 0.0001 by Bonferroni post-hoc.

***Disclosures: Gabriel Hoppock**, None*

FRI-200

Gene expression profiles in fibroblast growth factor 23 (FGF23)-producing tumors provide new insights on diagnostics and therapeutic intervention. *Sofya Gronskaia[1], Ruslan Devitiarov[2], Sergey Popov[1], Svetlana Rodionova[3], Yuriy Buklemishev[3], Liudmila Rozhinskaya[1], Oleg Gusev[2], Zhanna Belaya[1]. [1]Endocrinology Research Centre, Russian Federation. [2]Regulatory Genomics Research Center, Kazan Federal University, Russian Federation. [3]National Medical Research Center of Traumatology and Orthopedics named after. N.N. Priorov, Russian Federation

Background: Fibroblast growth factor 23 (FGF23)-producing tumors are histologically known as phosphaturic mesenchymal tumors (PMT). A PMT causes an oncogenic osteomalacia (OOM), which is associated with multiple fractures, severe pain, and muscle weakness.Aim: To analyze gene expression profiles of PMT versus control tissue.Methods: PMT and surrounding control tissue samples were obtained during tumor resection in 5 patients (Age 62 [45; 65], iFGF23 (ELISA Kit Biomedica BI-20700 -113 [50; 203] pg/ml (ref. range 14.8 [3.8;25.0]pg/ml), serum phosphorus 0.51 [0.4; 0.53]mM/L (ref. range 0.74-1.52 mM/l)). Based on histological verification we obtained 4 PMT samples (2 -mandibular bones, 1 - femur bone, 1 - metatarsal bone) and performed bulk RNA sequencing. We used Gene Ontology (GO) and the Kyoto Encyclopaedia of Genes and Genomes (KEGG). Results: A total of 976 genes were differently expressed between PMT and control samples. The four PMT samples were homogeneous according to their gene expression profiles. The genes most up-regulated (n=10) in PMT were LOC105377323/FGF1/MB/SPRY2/LOC105378029/DMP1/FGF23/BMP7/PHEX/LOC124903699. The genes most negatively regulated in PMT were LOC102724638/LOC124901874/LOC124901875/IGLL5/IGKC/IGLC1/LOC105377460/LOC105376032/IGK/IGHG1 (FDR < 0.05). We found that PMT overexpressed genes that are typical for osteoblast activity and differentiation including the most known OPG, RANKL (KEGG: p-value 0.03). We also found increased expression of the Wnt signaling antagonists SOST, DKK1 (KEGG: p-value 0.02). In PMT we found upregulated genes that are typical for secretory active osteocytes surrounded by high phosphate(FGF23/DMP1/ENPP1/PHEX/GALNT3/FAM20C/AKNA/DSPP/MEPE/EN1). Genes and pathways related to mineral ion transport were also up-regulated: Phospholipase D signaling pathway (KEGG p-value 0.003); signaling receptor binding (GO p-value < 0.001); solute: sodium symporter activity (GO p-value 0.004); calcium ion binding (GO < 0.001) and PiT1 (SLC20A1), which encodes the inorganic phosphate transporter. We found that PMT highly expressed osteopontin, CENPK and genes involved in PI3K/AKT (KEGG: p-value 0.006); ERK1/2 pathways (KEGG p-value 0.02) that are associated with castrate-resistant prostate cancer. The most up-regulated pathways in PMT were ECM-receptor interaction and gastric cancer related genes. We identified human membrane protein genes that were highly expressed in the PMT compared to control tissue PHEX/SYT12/PCDH7/RAMP1/CD44/NRG3/ILDR2/ECEL1/CHST3/ LRFN4/PCDH9, FGFR1/EVA1A/AREG/PTGIS/VSIG2/ENPP1/NRCAM/WSCD2.Conclusion: PMT expresses gene that are typical for secretory active osteoblast cells, including RANKL/OPG, phosphaturic genes, and wnt signaling antagonists. Newly identified gene expression profiles may expand our knowledge on diagnostics and therapeutic intervention in PMT.

***Disclosures: Sofya Gronskaia**, None*

FRI-201

Phosphate Signaling Is Mediated via Parathyroid Hormone Receptor 1-PLC-PKC Pathway in Committed Osteogenic Cells *Nadine Robert[1], Sandeep Chaudhary[2], Mairobys Socorro[1], Sana Khalid[1], Catherine Roberts[1], Juan Taboas[1], Dobrawa Napierala[1]. [1]University of Pittsburgh, United States. [2]Institute of Oral Health Research, University of Alabama at Birmingham, United States

Phosphate (Pi) is a main component of hydroxyapatite crystals that form the skeletal tissues. Pi also acts as a signaling molecule to regulate mineralization. Previous studies demonstrated the involvement of Na+/Pi cotransporters, FGFR1 and Erk1/2 kinase in Pi signaling. However, the molecular mechanisms of Pi sensing and cellular mediators of Erk1/2 activation in response to Pi have not been elucidated. Our goal is to decipher Pi signaling in cells producing bone (osteoblasts) and dentin (odontoblasts). Hence, we selected two committed osteogenic cell lines, the 17IIA11 odontoblast and MLO-A5 osteoblast/pre-osteocytes, which rapidly undergo mineralization in standard osteogenic conditions. From two independent lines of experiments, we observed the 17IIA11 cells failed to respond to Pi, as evaluated by Erk1/2 activation, when the parathyroid hormone receptor 1 (Pth1r) expression is downregulated. Therefore, we hypothesized that Pth1r is required for Pi signaling in committed osteogenic cells. To test this hypothesis, we used shRNA technologies to generate Pth1r-deficient 17IIA11 and MLOA5 stable cell lines. Unlike WT and shScr controls, Pth1r-deficient cells failed to activate Erk1/2 in response to stimulation with Pi nor mineralized under osteogenic conditions. As Pth1r can modulate various signaling cascades, including protein kinase A (PKA)-cAMP and phospholipase C (PLC)-protein kinase C (PKC), we analyzed which signaling axis downstream of Pth1r transmits the response to Pi in the presence and absence of specific pharmacological inhibitors. PKA inhibition with H-89 did not prevent Erk1/2 phosphorylation (pErk1/2) whereas inhibition of phospholipase C (PLC) with D609 attenuated that response. In addition, we observed a dose-dependent decrease of pErk1/2 levels in comparison to untreated controls when PKCs were inhibited by pan-classical PKC inhibitor Bisindolylmaleimide I (GF109203X). To identify which PKC isoform is involved in Pi signaling, we utilized two selective PKC inhibitors Sotrastaurin (inhibits classical PKCs- PKC? and PKC?, but not PKC?) and Staurosporine (inhibits PKC? and PKC?, but not PKC?). We observed a dose-dependent decrease in Erk1/2 activity only with Staurosporin, while Sotrastaurin had no effect on pErk1/2. Our in vitro studies in committed osteogenic cells propose the Pth1r as a candidate receptor/sensor of Pi, that mediates Pi signaling through PLC-PKC? axis.

***Disclosures: Nadine Robert**, None*

FRI-204

Genome-wide Analyses Reveal TGF? Signaling as a Regulator of Osteogenic Phosphate Sensing *Dylan Kuennen[1], Long Tran[2], Michael Mannstadt[3], Lauren Surface[2]. [1]University of Michigan, United States. [2]University of Michigan School of Dentistry, United States. [3]Massachusetts General Hospital Harvard Medical School, United States

Organismal phosphate (Pi) is an essential regulator of many cellular processes necessary for healthy tissue and organismal function. The skeleton is a key regulatory site in the control of organismal Pi homeostasis. However, the mechanisms of the Pi-sensing circuitry in osteogenic cells are poorly understood. Using in vitro approaches, our goal is to elucidate how the factors responsible for serum Pi sensing in osteogenic cells enable the endocrine Pi response to inform future therapeutics.To understand the transcriptional response in osteogenic cells during exposure to Pi, we performed an RNA-seq time course on MC3T3-E1, a pre-osteoblast cell line, and OCY454, an osteocytic cell line. We observed differential expression of gene categories related to bone mineralization as well as TGF?, MAPK, and EGF signaling. Based on these findings, we developed two flow cytometry-based readouts of the response to increased extracellular Pi; a Dmp1-2A-mCherry fluorescent reporter and a cell surface antigen stained with an antibody (SEMA7A). Using flow cytometry, we confirmed that inhibiting FGFR1 and ERK signaling blocks these responses to Pi. To identify factors that mediate Pi sensing, we combined our reporters with genome-wide CRISPRi screens and identified ~38 hits common to screens in both reporters. To prioritize physiologically relevant pathways, we intersected these hits with loci associated with circulating Pi and FGF23 levels by GWAS, and identified TGFB2 as a hit that is also top genetic polymorphism associated circulating FGF23 levels, supporting a potential physiological role for TGF? signaling in controlling the endocrine Pi response.We find that TGF-?2 co-treated with Pi enhances the response of osteogenic cells both increasing early Erk phosphorylation and the response of our reporters after 24 hours. We observe that TGF? signaling affects calcium (Ca2+) flux, leading to an increase in extracellular Ca2+, and that an inhibitor of store-operated calcium entry (SOCE) blocks the effect of TGF-?2 suggesting that SOCE mediates this response. Ca2+ may boost the response of osteogenic cells to Pi, likely through calciprotein particle (CPP) formation. We hypothesize that TGF-?2 increases the available extracellular Ca2+ to form CPP with Pi, thereby boosting the Pi response. These results may provide critical insights into Pi homeostasis, particularly in the setting of chronic kidney disease in which both circulating TGF? and FGF23 levels are increased.

***Disclosures: Dylan Kuennen**, None*

FRI-206

A novel approach combining in vitro and in vivo RNAseq/ATACseq identified key FGF23 target genes dysregulated with loss of Klotho in kidney single-cell subpopulations *Emmanuel Solis[1], Kayleigh Jennings[1], Yamil Marambio[1], RAFIOU AGORO[1], Megan Noonan[2], Sheng Liu[1], Jun Wan[1], Kenneth White[1]. [1]Indiana University School of Medicine, United States. [2]Indiana University , United States

Background: The osteocyte-produced hormone FGF23 controls phosphate and vitamin D synthesis in the kidney via its co-receptor ?Klotho (KL), however, the cellular responses to FGF23 during normal and disease states are not fully understood. We hypothesize that

FGF23 induces unique and generalized changes in transcription and genomic accessibility within specific nephron cell populations.Methods: An HEK293 cell line stably expressing membrane Klotho (HEK-mKL cells) was treated with FGF23 (50 ng/mL) for 4 and 16 hours, then processed for ATACseq and RNAseq libraries. Differentially expressed genes were validated by qPCR as well as in an independent single-cell 10X Multiomics dataset from KL-KO mice. Dimensionality reduction via Uniform Manifold Approximation and Projection (UMAP) was used to identify distinct nephron cell types.Results: HEK-mKL cell groups treated with FGF23 displayed clear segregation for both RNAseq and ATACseq following principal component analysis (PCA), with 9 and 7-fold increases in MAPK target genes EGR1 and FOS. Both vitamin D 24-hydroxylase CYP24A1 (2-fold) and VDR (1.5-fold) were increased at 4 and 16h, supporting this model. ATACseq showed FGF23 rapidly influenced genomic regions to control MAPK signaling as demonstrated by opening chromatin accessibility of an EGR1 distal enhancer by 4h. In confirmation, HOMER motif discovery predicted enrichment in transcription factor binding for MAPK targets FOS, JUN, AP1, and EGR1 (P<0.01) across the genome. At both 4 and 16h, FGF23 bioactivity was associated with novel induction of ETV transcription factor family mRNAs (ETV1 (3.7 fold), ETV4 (8-fold), and ETV5 (7.5 fold)), known to serve important roles in kidney development, mitochondrial biogenesis, and acute kidney injury repair. Furthermore, FGF23 bioactivity increased the expression of ETV1/4/5 target genes MMP1(7.3-7.7 fold), PTGS2 (3.5-4.2 fold), and VEGF (1.3-1.4 fold). Conversely, in vivo, 10X Multiome analysis of KL-KO mouse kidney proximal tubule-S1/S2 cells showed a 27% decrease in Etv5 mRNA. Further, Etv1 expression and chromatin accessibility decreased by 70% and 92%, respectively, contrary to the increase of these key factors with FGF23 treatment.Conclusion: A unique combination of unbiased in vitro ATACseq/RNAseq pinpointed novel FGF23-induced transcriptional and genomic reprogramming. Translation to in vivo kidney cell subpopulations demonstrated these changes may influence cell-specific outcomes in FGF23-related diseases.

***Disclosures: Emmanuel Solis**, None*

FRI-213

Bone alterations in ALS mice appear earlier than muscle atrophy and correlate with reduced expression of complement factors and interferon signaling in osteocytes *Melanie Haffner-Luntzer[1], Stefano Antonucci[2], Baiba Vilne[3], Jan-Moritz Ramge[4], Anita Ignatius[4], Francesco Roselli[4]. [1]University Medical Center Ulm, Germany; [2]Ulm Unversity, Germany; [3]Riga University, Latvia; [4]Ulm University, Germany

Amyotrophic lateral sclerosis (ALS) is a neurodegenerative disease characterized by progressive muscle atrophy. It is well known that muscle loss and thereby reduced mechanostimulation of the skeleton leads to bone loss. Therefore, it was proposed that mice suffering from ALS display severe osteoporosis after the onset of muscular symptoms, while presymptomatic mice do not show bone alterations. However, it was recently investigated that human SOD1 mutation carriers already display metabolic alterations before the onset of muscular symptoms. Therefore, we aimed to analyze the bone phenotype in a mouse model of ALS-associated SOD1 mutation in more detail before and after the onset of muscular symptoms in order to understand pathogenic mechanisms. Femurs of SOD1(G93A)-mutated male mice and respective wildtype controls were analyzed at p45 and p110 of age (pre- and post-symptomatic) using bending test, µCT, histomorphometry and RNA sequencing. We found that force to failure was significantly reduced in pre- and postsymptomatic ALS mice. Furthermore, both cortical and trabecular bone parameters were significantly diminished in pre- and postsymptomatic ALS mice, with the effect being more pronounced in older mice (cortical thickness WT p45: 0.183+/-0.007mm vs. SOD1 p45: 0.172+/-0.009mm; WT p110: 0.227+/-0.014mm vs. SOD1 p110: 0.184+/-0.009mm; trabecular BV/TV WT p45: 25.5+/-1.8% vs. SOD1 p45 20.1+/-1.9%; WT p110: 26.5+/-4.9% vs. SOD1 p110: 17.3+/-3.7%). Cellular analysis revealed reduced osteoblast numbers in pre- and postsymptomatic ALS mice, while osteoclast numbers were only increased in postsymptomatic mice. RNA sequencing and GO term analysis of flushed femurs (mainly containing osteocytes) revealed that genes related to the complement system and interferon signaling were significantly downregulated in pre- and postsymptomatic ALS mice (e.g. C3, C6, Ifit1). Immunohistochemical staining confirmed osteocytic expression of complement markers. Our data shows that in contrast to previous reports, SOD1-mutated mice do already display bone alterations before the onset of muscular symptoms. Reduced bone mass correlated with reduced expression of complement and interferon-associated factors. Because it has already been shown that the complement system plays an important role in bone cells, this might be an interesting target to further explore treatment options for human mutation carriers. It remains to be studied which role interferon-related signaling plays in this context.

***Disclosures: Melanie Haffner-Luntzer**, None*

FRI-217

Age-related decline of TNF receptor-associated factor 3 expression in skeletal muscle causes sarcopenia and remotely stimulates bone loss *Xing Li[1], Yaning Xing[1], Brendan Boyce[2], Hailin Zhang[1], Jinbo Li[1]. [1]Hebei Medical University, China; [2]University of Rochester Medical Center, United States

Skeletal muscles supply contraction forces and stem cells to bone to help maintain bone homeostasis and regeneration; however, how the aging process in skeletal muscle itself affects age-related bone loss remains poorly understood. To study this, we first performed bulk RNASeq and found that inflammatory cytokine/receptor interaction, involved in TNF receptor and interleukin receptor super families were significantly upregulated in gastrocnemius muscles from aged (20-mon-old) than young (4-mon-old) mice (KEGG; p=0.0006). Protein levels of TNF receptor-associated factor 3 (TRAF3), an adaptor protein of these receptors, was decreased during aging in mouse and human skeletal muscles, and in mouse skeletal muscle stem cells (MuSCs; Integrin ?7+CD45-CD31-CD11b-Sca1-) and myocytes (CD45-CD31-CD11b-Sca1-). To examine the function of TRAF3 in MuSCs and myocytes, we generated MCKCreTRAF3fl/fl (M-cKO) and Pax7CreERTRAF3fl/fl (P7-cKO) mice with Traf3 deletion in myocytes and MuSCs, respectively. Both cKO mice developed obvious sarcopenia by 3-mon-old, with shrinkage of MyHC IIA+ myofibers in particular, loss of myocytes per fiber, and impaired myotube formation capacity in-vitro. This sarcopenic phenotype in M-cKO mice was more marked than in age-matched P7-cKO mice and does not appear to be mediated by non-canonical NF-?B signaling because RelB and p100/p52 double knockout mice have normal muscle mass. Surprisingly, the M-cKO mice also developed early onset osteoporosis with significantly lower tibial trabecular bone mass (BV/TV: (10.8+/-3.0)% vs. (17.4+/-5.5)% in WT; p=0.010) and cortical bone thickness (143+/-7 vs. 204+/-9 ?m in WT; p2; p<0.05) elevated in both naturally aged C57 mice and young M-cKO mice; mRNA and protein levels of musclin (also known as osteocrin), a novel exercise-responsive myokine, were significantly higher in gastrocnemius from aged and M-cKO mice than in controls. In addition, osteoclast precursors treated with musclin formed more osteoclasts (11.2+/-2.6 vs. 6.3+/-2.5/mm2 in vehicle; p=0.002). These findings implicate TRAF3 reduction causes age-related sarcopenia and osteoporosis via an NF-?B-independent mechanism and suggest that increased musclin expression by aging muscles may enhance osteoclastic bone resorption to promote age-related bone loss.

***Disclosures: Xing Li**, None*

FRI-221

Progranulin inhibits C5a/C5aR1 signaling via direct binding to C5a and its deficiency exaggerates osteoarthritis due to hyper-activation of the complement system *Wenyu Fu[1], Guiwu Huang[1], Chuan-ju Liu[1]. [1]New York University Grossman School of Medicine, United States

The prevalence of osteoarthritis (OA) is increasing globally, with significant economic impacts and negative effects on quality of life. Accumulating evidence demonstrates that complement activation is involved in the pathogenesis of OA, although the molecular events involved remain to be elusive. While previous research has shown that C5 deficiency can attenuate arthritis in mouse OA model, the mechanisms of C5/C5a in OA have not been understood. Our lab has long-standing interest in investigating the role of progranulin (PGRN), a growth factor like molecule, in the pathogenesis of OA. The findings that PGRN bind to cysteine-rich domains (CRDs) of various proteins, together with the fact that complement proteins contain CRDs, suggesting that PGRN may interact with and affect the complement system. We thus conducted solid-phase binding assays to screen the interactions between PGRN and central complement components, including C1-C9, C5a and C3a. Our results showed that PGRN strongly binds to C5 and dose-dependently binds and saturates C5a. Additionally, PGRN/C5a complex formation in mouse sera was confirmed by Co-IP, and PGRN binds to C5a with a high affinity of KD 7.18+/-0.07nM measured by Analytical Surface Plasmon Resonance. Further functional assays demonstrated that PGRN inhibits C5a binding to C5aR1 and effectively blocks C5a binding to cell surfaces, indicating that PGRN acts as a natural antagonist of C5a signaling. PGRN was also found to antagonize C5a's effect on macrophage polarization.ELISA analysis showed a significant increase in C5a levels in the synovial fluid of OA patients than healthy controls, indicating hyperactivation of the complement cascade in OA synovial fluid. PGRN levels were also significantly higher in the synovial fluid of OA patients compared to healthy controls. Furthermore, a positive correlation was found between the levels of PGRN and C5a in OA patients ($r = 0.5475$, $P < 0.0001$). The interaction and interplay of PGRN/C5a were also investigated in vivo using various genetically deficient mice with surgically induced DMM model. The results showed that deletion of C5aR1 partially reversed the exaggerated OA phenotype, including severe cartilage loss and increased OA-associated pain observed in PGRN-/- OA mice. These findings suggest that PGRN interacts with C5a/C5aR1 signaling to regulate macrophage function, and PGRN mitigates OA by suppressing proinflammatory activities of C5a through interrupting C5a/C5aR1 signaling (Fig.1).

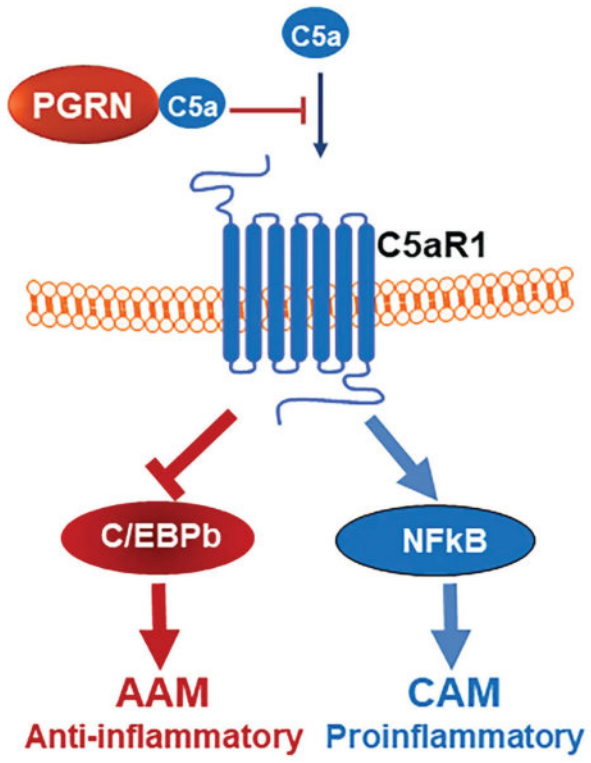

Fig1. A proposed model illustrating the interplays between PGRN and C5a/C5aR1 signaling in regulating macrophage polarization. PGRN directly binds to C5a and inhibits C5a/C5aR1 signaling, and resultant macrophage polarization regulation and OA progression.

***Disclosures: Wenyu Fu**, None*

FRI-224

Blocking CCN2 Reduces Established Palmar Muscle Fibrosis and Entheseal Damage following Repetitive Overuse Injury *Alex Lambi[1], Robert DeSante[2], Steven Popoff[3], Mary Barbe[4]. [1]University of New Mexico, [2]Center for Translational Medicine, Lewis Katz School of Medicine of Temple University, United States. [3]Lewis Katz School of Medicine at Temple University, United States. [4]Temple University School of Medicine, United States

Upper extremity overuse injuries are a leading cause of long-term pain and disability. Underlying tendinopathies, muscle fibrosis, and joint disorders occur. We have shown that the matricellular protein connective tissue growth factor (CTGF/CCN2) is critical to early progression of chronic forelimb muscle fibrosis and grip strength declines in a rat model of overuse injury. Here we tested whether an anti-CCN2 antibody reduces established forepaw and entheseal changes corresponding to improved grip strength. All experiments were approved by the Institutional Animal Care and Use Committee. Adult female rats (3 mo at onset) performed a high repetition high force (HRHF) task for 18 wks, consisting of 4 reaches/min, at 1.22N, 2hr/d, 3d/wk. One subset was euthanized after 18 wks of task performance (HRHF-Untreated, n=9). Two subsets were provided 6 wks of rest post-task, with concurrent treatment with anti-CCN2 monoclonal antibody FG-3019 (HRHF-Rest/anti-CCN2, n=8) or an IgG as a vehicle control (HRHF-Rest/IgG, n=9). Results were compared with age-matched controls (Control-IgG, n=11). We analyzed histologic data from forepaw muscles (thenar, hypothenar, and deep intrinsic) and wrist/forepaw entheses. Muscle fibrosis (% muscle area with collagen) in combined forepaw muscles was significantly increased in HRHF-Untreated and HRHF-Rest/IgG rats, but not HRHF-Rest/anti-CCN2, compared to Controls ($p<0.01$). Forepaw and carpal entheses were graded on six domains: tidemark, fissuring, void space, vascular invasion, attachment site holes, and underlying bone remodeling. Each domain was graded binarily (1 indicating present). The overall enthesis score of damage was significantly increased in HRHF-Untreated rats compared to Controls and HRHF-Rest/anti-CCN2 ($p<0.05$), with tidemark changes showing the greatest change ($p<0.05$). We found an inverse correlation between muscle fibrosis and grip strength ($r=-0.33$, $p=0.01$). Analyzed for percent grip strength change by group, we found a significant decrease in HRHF-Untreated compared to Controls ($p=0.02$), and significant increases in HRHF rest groups, more so in HRHF-Rest/anti-CCN2 ($p<0.05$). These studies demonstrate for the first time that anti-CCN2 treatment reduces established forepaw muscle fibrosis and entheseal damage following overuse injury. As these findings alone do not account for the percent change in grip strength, ongoing work seeks to determine what other factors contribute to functional changes in these forepaws.

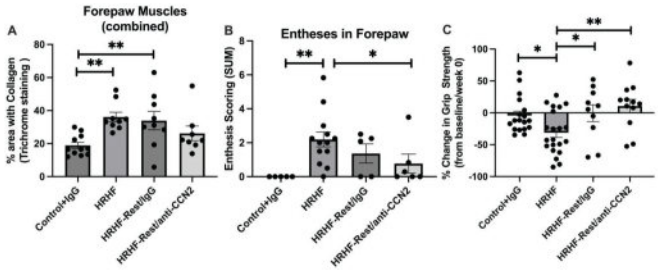

***Disclosures: Alex Lambi**, None*

FRI-230

Foxc1 and Foxc2 Function in Osteochondral Progenitors for the Progression Through Chondrocyte Hypertrophy and Mineralization of the Primary Ossification Center *Fred Berry[1], Asra Almubarak[1]. [1]University of Alberta, Canada

The forkhead box transcription factor genes Foxc1 and Foxc2 are expressed in the condensing mesenchyme of the developing skeleton prior to the onset of chondrocyte differentiation. To determine the roles of these transcription factors in limb development we deleted both Foxc1 and Foxc2 in lateral plate mesoderm using the Prx1-cre mouse line. Resulting compound homozygous mice died shortly after birth with exencephaly, and malformations to this sternum and limb skeleton. Notably distal limb structures were preferentially affected, with the autopods displaying reduced or absent mineralization. The radius and tibia bowed and the ulna and fibula were reduced to an unmineralized rudimentary structure. Molecular analysis revealed reduced expression of Ihh leading to reduced proliferation and delayed chondrocyte hypertrophy at E14.5. At later ages, Prx1-cre;Foxc1?/ ?;Foxc2 ? / ? embryos exhibited restored Ihh expression and an expanded COLX-positive hypertrophic chondrocyte region, indicating a delayed exit and impaired remodeling of the hypertrophic chondrocytes. Osteoblast differentiation and mineralization were disrupted at the osteochondral junction and in the primary ossification center (POC). Levels of OSTEOPONTIN were elevated in the POC of compound homozygous mutants, while expression of Phex was reduced, indicating that impaired OPN processing by PHEX may underlie the mineralization defect we observe. Together our findings suggest that Foxc1 and Foxc2 act at different stages of endochondral ossification. Initially these genes act during the onset of chondrogenesis leading to the formation of hypertrophic chondrocytes. At later stages Foxc1 and Foxc2 are required for remodeling of HC and for Phex expression required for mineralization of the POC

***Disclosures: Fred Berry**, None*

FRI-234

Elevated PDGFR? Signaling Causes Knee Joint Fusion by Disrupting Synovial Progenitor Differentiation *John Woods[1], Lorin Olson[1]. [1]Oklahoma Medical Research Foundation, United States

Mouse knee joint development begins at E11.5-E13.5 when a cartilage template is divided in two by the formation of an interzone, an anlage that gives rise to all the structures of a mature joint. Before interzone formation, the cartilage template expresses cartilage genes Sox9 and Col2a1. These genes are downregulated upon interzone formation and replaced by Gdf5, a member of the bone morphogenic protein family. Platelet-derived growth factor receptor-? (PDGFR?) is not expressed in the cartilage template of the limb, but it is expressed in the perichondral mesenchyme and Gdf5+ interzone cells. Based on this expression pattern, we hypothesized that tight regulation of PDGFR? signaling may be crucial for joint development. To investigate this role of PDGFR?, we used gain-of-function (?GOF) and loss-of-function approaches with Prx1-Cre, which is active in the early limb bud mesenchyme. Loss-of-function did not affect joint formation. However, ?GOF mice were born with knee joints fused by ectopic cartilage and lacking ligaments and menisci. Interzone specification occurred normally in ?GOF mutants up to E13.5, but Gdf5 expression was decreased. Further, there was expansion of Sox9 protein expression into domains that are normally Sox9-negative. These results suggest that elevated PDGFR? signaling interferes with joint progenitor differentiation by redirecting Gdf5+ interzone cells from a synovial connective tissue fate to a Sox9+ chondrogenic fate. Thus, PDGFR? signaling has pro-chondrogenic properties that must be tightly regulated to allow differentiation of ligaments, menisci, and

other connective tissue cell types. This property of PDGFR? signaling may be important in other contexts such as de novo cartilage formation in fracture healing.

***Disclosures: John Woods**, None*

FRI-235

Racial disparities in osteoporosis screening and treatment among older adults in a centralized, secondary prevention Fracture Liaison Service

*Richard Lee[1], Cathleen Colon-Emeric[2]. [1]Duke University, United States. [2]Duke University Medical Center, United States

Background: Published studies have shown significant racial disparities in osteoporosis screening and treatment. We evaluated whether our well-established Fracture Liaison Service (FLS) may mitigate these disparities.Method: This is a retrospective analysis of patients in the VISN6 Bone Health Service (BHS), a centralized FLS, located at the Durham VA Medical Center, serving 4 medical centers within the VA Integrated Service Network 6. The BHS identifies adults > age 50 years, who have sustained a recent low-trauma fracture and reviews their medical record for risk factors of osteoporosis. Recommendations are provided the electronic health record to the patient's primary care provider and implemented by a dedicated BHS Nurse. Recommendations may include DXA screening, initiation of calcium/vitamin D supplementation, initiation of bisphosphonate therapy, and/or referral to a metabolic bone specialty clinic. Data were obtained from the BHS clinical database from Oct 2012 to Mar 2022, regarding osteoporosis recommendations. Statistical analysis for differences was performed by chi square by race.Results: 2552 patients with incident low-trauma fracture were identified during the study period, among whom 72.9% were White, 21.2% were Black, and 5.9% were other racial groups. 12.2% of Black adults sustained a hip fracture, compared to 11.1% White and 17.2% other groups; however, only 6.5% of Black adults had vertebral fracture, compared to 16.2% White and 11.9% other groups ($P < 0.01$). After controlling for fracture location, Black adults were more likely to be recommended for DXA screening (82.3%, vs. 72.9% White and 72.8% other groups), but less likely to be recommended for initiation of calcium/vitamin D (18.9%, vs. 31.1% White and 25.2% other groups) and of bisphosphonates (15.7%, vs. 26.0% White and 25.2% other groups) [$P < 0.01$ for all comparisons]. There were no significant differences in referral to Metabolic Bone Clinic ($P = 0.50$). Additionally, there were no differences among racial groups regarding implementation of BHS recommendations, with 85.5% among White, 85.2% among Black, and 88.7% among other racial groups ($P = 0.53$).Conclusion: The BHS program improved osteoporosis screening among older adults with recent low-trauma fracture, with no significant differences in implementation of recommendations among racial groups. Similar FLS programs may help reduce racial disparities and improve guideline-based treatment in osteoporosis care.

***Disclosures: Richard Lee**, None*

FRI-247

Role of Discoidin Domain Receptor 2 in Tooth Socket Healing

*RENNY FRANCESCHI[1], Rajay Kamath[1]. [1]University of Michigan, United States

Discoidin Domain Receptor 2 (DDR2) is a collagen-activated tyrosine kinase required for skeletal development and regeneration of the calvaria and long bones, however, possible functions in alveloar bone have not been examined. The present study used lineage tracing, as well as global and conditional knockout approaches, to examine functions of Ddr2 in alveolar bone regeneration during tooth socket healing. The following mouse lines were used: DDR2LacZ (where the bacterial LacZ gene is inserted into the Ddr2 locus creating an effective null allele), Ddr2CreERT2; Rosa26GtTdtomato and Gli1CreERT2 Rosa26GtTdtomato for lineage tracing, and the Gli1CreERT2; DDR2fl/fl mice for the selective knockout of Ddr2 in GLI1+ skeletal progenitors. For lineage tracing, 4w old Ddr2CreERT2; Rosa26GtTdtomato and Gli1CreERT2 Rosa26GtTdtomato mice were induced with one dose of tamoxifen and the 1st molars were extracted after 2 or 7 days. In both cases, TdTomato+ cells migrated into the sockets where they co-localized with OSX, a preosteoblast marker. Thus, both DDR2 and GLI1+ cells contribute to socket healing. The considerable overlap observed between DDR2+ and GLI1+ cells suggested that DDR2 largely functioned in GLI1+ cells, which are known to have skeletal progenitor properties. Consistent with localization data, both global Ddr2 (Ddr2LacZ/LacZ) or conditional knockout (Gli1CreERT2; Ddr2fl/fl) mice exhibited reductions in socket healing 1-week post extraction as measured by µCT, but not after 2 or 4 weeks. However, analysis of collagen fibril orientation by picrosirius red staining revealed that collagen fibril orientation was disrupted in tooth sockets at all times examined, suggesting that even though loss of DDR2 only had a transient effect on socket bone fill, it has long-term effects on ECM structure and, potentially, mechanical properties. In summary, this work demonstrates a role for DDR2 in alveolar bone regeneration, a finding that may have therapeutic implications for the treatment of alveolar bone loss assciated with periodontal disease and other disorders.

***Disclosures: RENNY FRANCESCHI**, None*

FRI-250

Spatial Transcriptomics and Bulk-RNA Sequencing show distinct spatial and time-dependent effect of Abaloparatide at the sites of Fracture Repair

*ASHUTOSH PARAJULI[1], Andre van Wijnen[2], Daniel Bikle[3]. [1], [2]University of Vermont, United States. [3]Endocrine Research Unit, Division of Endocrinology UCSF and VAMC, United States

Fracture repair involves multiple cell types from periosteum, bone cortex, and bone marrow. Our study (Wang 2020, JBMR) identified three distinct repair sites (Site 1, 2 & 3; Fig. 1), but the underlying interaction mechanism between progenitors at these sites remains unclear. Abaloparatide (Abl), a PTHrP analog for osteoporosis treatment, enhances bone formation at these sites (Parajuli, ASBMR 2021; Fig. 1) by activating specific osteoblast and chondrocyte genes (Parajuli, ASBMR 2022). In this study, we investigated the effect of Abaloparatide (Abl) on the gene expression patterns at the specific sites (Spatial transcriptomics) as well as the whole callus (Bulk RNA-Seq) at day 10, 15 and 28 post Fx. Closed-unstabilized fracture model (12-wk C57BL/6J mice, 3-pt. bending) was used to create the fracture (midshaft of tibia). Mice received subcutaneous Abl (40ug/kg/day) or vehicle for 28 days. We performed RNA-Seq on the whole callus at day 10, 15, and 28 post Fx. Spatial transcriptomics was performed on paraffin sections using 10x Genomics Visium kit at the same time points. PCA and heatmap analysis (Fig. 2) revealed significant Abl-induced changes in gene expression within the healing callus at all time points. Differential gene expression analysis (Fig. 3) showed increasing Abl effects over time (8 DGEs at day 10, 305 at day 15, and 5351 at day 28). Spatial transcriptomics confirmed Abl's distinct effects at Site 1, 2, and 3 (Fig. 4). Heatmap analysis of selected osteogenic and chondrogenic markers (Fig. 5) showed site and time-specific responses to Abl. At day 10, Abl increased osteogenic activity at Site 1, while chondrogenic activity remained stable. At Site 2 and 3, Abl upregulated cartilage markers and downregulated osteogenic markers. At day 15, osteogenic markers increased, while chondrogenic markers decreased across all sites (compared to Day 10), with minimal Abl impact. By day 28, osteogenic marker expression decreased compared to day 15, but all three sites showed slightly higher osteogenic activity and decreased chondrogenic activity with Abl. These findings indicate distinct effects of Abl on all three sites during Fx repair. Further investigation aims to elucidate the molecular pathways involved at these sites and understand how Abl selectively promotes Fx repair.

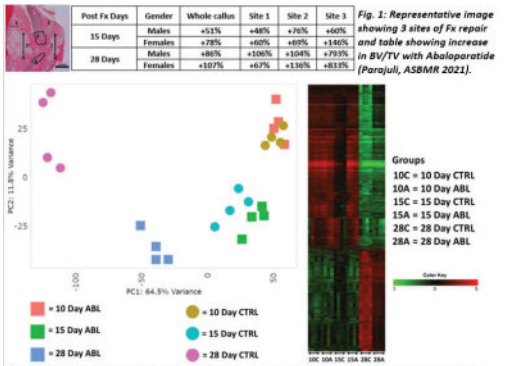

Fig. 1: Representative image showing 3 sites of Fx repair and table showing increase in BV/TV with Abaloparatide (Parajuli, ASBMR 2021).

Fig.2: (Left) PCA and (Right) Heatmap of top 1000 genes' expression profile in each of the samples. Heatmap columns left to right : 10D CTRLS, 10 D ABL, 15D CTRL, 15D ABL, 28D CTRL, 28D ABL (4 samples each).

10 Days (ABL - CTRL)	Down-Regulated	4
	Up-regulated	4
15 Days (ABL - CTRL)	Down-Regulated	283
	Up-regulated	22
28 Days (ABL - CTRL)	Down-Regulated	2129
	Up-regulated	3222

Fig. 3: Number of differentially expressed genes at Day 10, 15 and 28 with Abl treatment.

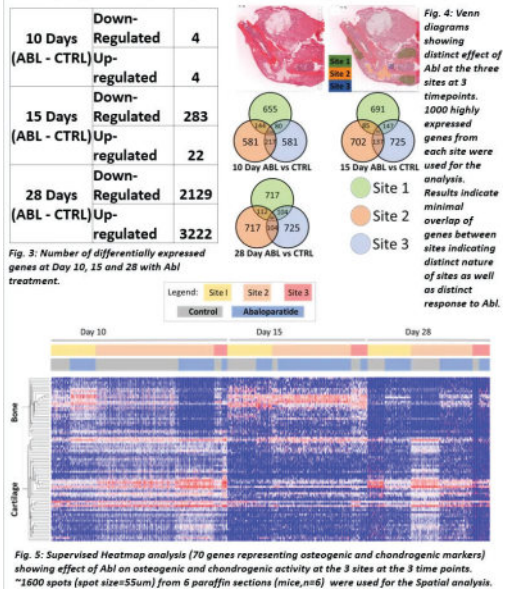

Fig. 4: Venn diagrams showing distinct effect of Abl at the three sites at 3 timepoints. 1000 highly expressed genes from each site were used for the analysis. Results indicate minimal overlap of genes between sites indicating distinct nature of sites as well as distinct response to Abl.

Fig. 5: Supervised Heatmap analysis (70 genes representing osteogenic and chondrogenic markers) showing effect of Abl on osteogenic and chondrogenic activity at the 3 sites at the 3 time points. ~1600 spots (spot size=55um) from 6 paraffin sections (mice,n=6) were used for the Spatial analysis.

***Disclosures: ASHUTOSH PARAJULI**, None*

FRI-252

Schwann cells and skeletal stem/progenitor cells in periosteum drive fibrosis and congenital pseudarthrosis of the tibia in NF1 *Simon Perrin[1], Sanela Protic[1], Ingrid Laurendeau[2], Oriane Duchamp de Lageneste[1], Nicolas Panara[2], Cécile-Aurore Wotawa[1], Odile Ruckebusch[3], Marine Luka[4], Cécile Masson[5], Théodora Maillard[6], Stéphanie Pannier[7], Philippe Wicart[7], Smail Hadj-Rabia[8], Katarzyna Radomska[1], Mickael Ménager[4], Dominique Vidaud[6], Piotr Topilko[1], Béatrice Parfait[2], Céline Colnot[1]. [1]Univ Paris Est Creteil, INSERM, IMRB, Creteil, France, France. [2]INSERM UMR S1016, Institut Cochin, Université de Paris, Paris, France, France. [3]Univ Paris Est Creteil, INSERM, IMRB, Plateforme de Cytométrie en flux, Creteil, France., France. [4]Paris Cité University, Imagine Institute, Laboratory of Inflammatory Responses and Transcriptomic Networks in Diseases, Atip-Avenir Team, INSERM UMR 1163, Paris, France., France. [5]Bioinformatics Core Facility, Institut Imagine-Structure Fe?de?rative de Recherche Necker, INSERM U1163 , France. [6]Service de Médecine Génomique des Maladies de Système et d'Organe, Hôpital Cochin, DMU BioPhyGen, Assistance Publique-Hôpitaux de Paris, AP-HP, Centre-Université Paris Cité, F-75014 Paris, France, France. [7]Department of Pediatric Orthopedic Surgery and Traumatology, Necker-Enfants Malades Hospital, AP-HP, Paris Cité University, Paris, France, France. [8]Department of Dermatology, Reference Center for Rare Skin Diseases (MAGEC), Imagine Institute, Necker-Enfants Malades Hospital, AP-HP, Paris Cité University, Paris, France. , France

The periosteum, the outer layer of bones, is a crucial source of skeletal stem/progenitor cells (SSPCs) for bone healing. The role of periosteum in bone repair disorders is poorly understood but suspected in congenital pseudarthrosis of the tibia (CPT). CPT is a severe pathology marked by tibial bowing leading to spontaneous fractures and fibrous non-union. Half of CPT cases are linked to Neurofibromatosis type 1 (NF1), a genetic disorder caused by mutations in the NF1 gene, encoding the RAS negative regulator neurofibromin. NF1 is characterized by a wide range of symptoms, such as tumors (neurofibromas, NFBs), skin hyperpigmentation and skeletal manifestations, including CPT. While NF1 neurodermatological manifestations are known to arise from NF1 biallelic inactivation in Schwann cells and melanocytes, the cellular origin of CPT remains unknown. Recently, analysis of the Prss56-Nf1 KO mice, revealed that boundary-cap cells, a transient population of neural-crest derivatives, is the population responsible for both neurofibromas and skin hyperpigmentation (Radomska et al.). These results raised the question of a possible common cellular origin of NF1 neurodermatological and skeletal symptoms.In this study, we unraveled the cellular origin and pathogenic mechanisms of CPT through analyses of bone samples from 17 CPT patients and Prss56-Nf1 KO mice. We showed that CPT is associated with NF1 biallelic inactivation in human periosteum. SSPCs in pathological periosteum exhibit NF1 biallelic inactivation and a pro-fibrotic phenotype. We identified an increased proportion of pERK+ Schwann cells (SCs) in pathological periosteum. Overall, analyses of CPT patients revealed SSPCs and SCs as affected cell types in CPT. In parallel, we described the pseudarthrosis phenotype of Prss56-Nf1 KO mice, due to Nf1 loss in boundary cap-derived SSPCs and SCs in periosteum. Single nuclei analyses of the periosteum showed that Nf1 KO SSPCs fail to undergo chondrogenic differentiation leading to fibrogenic differentiation. More strikingly, we identify Nf1 KO SCs as the main driver of fibrotic accumulation in CPT as they acquire a pro-fibrotic function and promote fibrotic fate of wild-type SSPCs via TGF?. We demonstrate that TGF? inhibition prevents pseudarthrosis in Prss56-Nf1 KO mice. These results establish the pro-fibrotic role of boundary cap-derived SCs and SSPCs causing CPT in NF1. This study suggests new therapeutic strategies targeting SC-derived pro-fibrotic factors, including TGF?, for CPT.

***Disclosures: Simon Perrin**, None*

FRI-255

Evidence of Bisphosphonate-Conjugated Fluoroquinolone Analog Eradication of Established Methicillin-Resistant S. aureus Infection with Osseointegration in Murine Models of Implant-Associated Osteomyelitis *F Hal Ebetino[1], Shuting Sun[1], Youliang Ren[2], Jason Weeks[2], Thomas Xue[3], Joshua Rainbolt[3], Karen de Mesy Bentley[3], Ye Shu[3], Yuting Liu[3], Elysia Masters[3], Philip Cherian[4], Charles E McKenna[5], Jeffrey Neighbors[6], Edward M Schwarz[2], Chao Xie[2]. [1]BioVinc, United States. [2]University of Rochester Medical Center, United States. [3]University of Rochester Medical School, United States. [4]BioVinc LLC, United States. [5]University of Southern California, United States. [6]Pennsylvania State University, United States

Eradication of methicillin-resistant Staphylococcus aureus (MRSA) infection of bone requires elimination of distinct biofilms including bacteria within osteocyte-lacuno-canalicular networks (OLCN) and Staphylococcus abscess communities (SAC) in the bone marrow. To overcome the limited efficacy of standard of care (SOC) vancomycin(vn) therapy, we developed bisphosphonate(BP)-conjugated sitafloxacin analogs (BCS, BV600072 and HBCS, BV63072), to achieve "target-and-release" drug delivery proximal to the bone infection. We evaluated their efficacy in a murine 1-stage exchange femoral plate model with bioluminescent MRSA (USA300LAC::lux). Chronic osteomyelitis was confirmed by CFU on the explants and bioluminescent imaging (BLI) after implant exchange surgery on day 7, and mice were randomized into 7 groups: 1) Baseline (day 7, no trtmt); 2) HPBP (BCS BP control) + vn; 3) HPHBP (HBCS BP control) + vn; 4) vn; 5) sitafloxacin; 6) BCS + vn; and 7) HBCS + vn. BLI prior to euthanasia on day 21 (day 14 post-revision) confirmed that MRSA infection persisted in all groups except for mice treated with BCS or HBCS + vn. X-ray and micro-CT analyses revealed catastrophic femur fractures in all groups except for mice treated with BCS or HBCS + vn which also displayed significant decreases in peri-implant bone loss, osteoclast numbers, and biofilm as assessed by histomorphometry ($p<0.05$ via 1-way ANOVA). (Figure 1.) TEM images of the bacteria within SACs or canaliculi of the infected bone are shown at low power (×5,000) (Fig 2A,C,E,G,I) and with high-power images (×25,000) (Fig 2B,D,F,H,J). Regions of interest (Fig 2A,C,E,G,I) illustrate the morphology of the bacteria on day 14 post 1-stage revision. TEM demonstrated strong evidence of HBCS- and BCS- induced bacterial cytotoxicity (cell swelling with large numbers of vacuoles). We also assessed the efficacy of vancomycin, sitafloxacin, and HBCS monotherapy in a transtibial implant model of chronic MRSA osteomyelitis. X-ray, histology, and transmission electron microscopy analyses confirmed that all mice treated with vancomycin remained infected, while all mice treated with HBCS had evidence of infection control including SAC's, and some had evidence of osseous integrated septic implants, suggesting biofilm eradication. This is the first evidence that biofilms within SACs and the OLCN can be eradicated in chronic models and demonstrates the potential of HBCS to eradicate MRSA osteomyelitis as an adjuvant to SOC therapy.

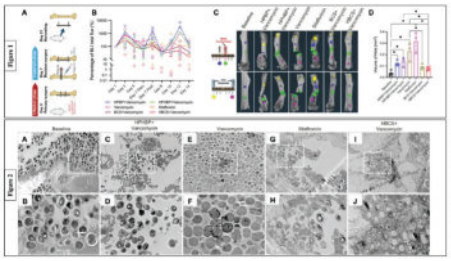

Figure 1. *In vivo* BLI and quantifiable Micro-CT and histological evaluation show a promising antimicrobial efficacy of BCS and HBCS in a 1-stage revision murine model. (A) Schematic illustration of the surgical procedure (Fig 1A). Longitudinal BLI (B) and micro-CT (C,D) images and data are presented for each animal with mean +/-SD (*p<0.05).

Figure 2. TEM evidence of BCS and HBCS killing of MRSA within SACs and biofilm within the bone marrow space. Histological section from the infected femurs were processed for subsequent TEM. Representative TEM images of the bacteria within bone marrow space of the infected bone are shown at low power (A, C, E, G, I), and high-power images of the dashed boxed region of interest (B, D, F, H, J) are shown to illustrate the morphology of the bacteria within SACs on day 21 post-infection.

***Disclosures: F Hal Ebetino**, BioVinc, Major Stock Shareholder*

FRI-261

Lumbar instability initiates endplate remodeling via Hippo signaling activation *Hao Chen[1], Hanwen Li[2]. [1]Yangzhou University, China. [2]The First Affiliated Hospital of Soochow University, China

Introduction: Protic endplates with sensory innervation contribute to low back pain. However, the origin and developing mechanism of the porotic endplate remain unclear.Objectives: This study aims to explore the regulatory mechanism of cartilage endplate (CEP) remodeling caused by abnormal stress.Methods: In vivo, we constructed lumbar spine instability (LSI) model in mice. We then analyzed the forces on the CEP using finite element analysis (FEA). In vitro, we used a mechanical tensile machine to simulate the abnormal stress conditions of the endplate cartilage cells (ECs). WB, RT-qPCR, and immunofluorescence staining were used to analyze the cell status. We use high-throughput sequencing to find out the key signaling regulating this process. Then, we created cartilaginous YAP elimination mice (Col2a1-CreER::YAPfl/fl). After that, we used YAP agonists both in vivo and in vitro to rescue CEP remodeling. Finally, we conducted therapeutic experiments by using AAV5-carrying Yap1 plasmids.Results: Here in this report, we discovered lumber instability-induced cartilage endplate remodeling is responsible for making the cheese-endplate and subsequent lumber disc degeneration by employing the lumbar spine instability (LSI) model in vivo and the mechanical tensile model in vitro. We confirmed that lumbar instability-induced abnormal stress and initiated cartilage endplate remodeling. Transcriptome analysis revealed Hippo signaling was enriched in this process. Activation of Hippo signaling or knock out of YAP in the cartilage endplate impressively severed the endplate and disc degeneration after LSI surgery, while blocking the Hippo signaling reversed this process. Meanwhile, we observed osteoclast differentiating factors were also enriched in the endplate chondrocytes under lumbar instability-induced abnormal stress stimulation, in which the release of CCL3 helped to form osteoclasts and proceed for cartilage remodeling. Finally, we successfully rescued LSI-induced lumbar degeneration by local injection of AAV5-Yap1 over-expression plasmid.Conclusions: Our study sought to demonstrate that YAP is like the guard for the endplate cartilage, which can maintain CEP homeostasis. We also confirmed that this may be related to the CCL3-regulation of osteoclast activation, which is induced by YAP. These findings suggest that the Hippo signaling activation in the cartilage endplate by lumbar instability is a potential new target for the management of lumbar degeneration and low back pain.

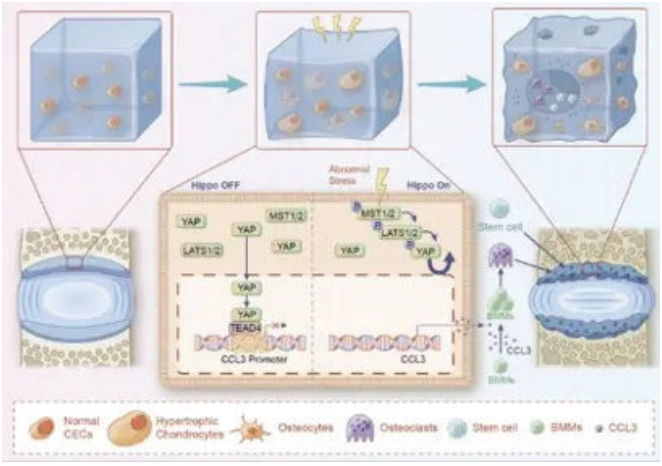

***Disclosures: Hao Chen**, None*

FRI-262

Epigenetic modification to prevent heterotopic ossification *Tao Yue[1], ji Hae Choi[1], Alec Bancroft[1], yuxiao sun[1], Conan Juan[1], Robert Tower[2], Pranathi Dasari[1], Sowmya Ramesh[3], Aaron W James[3], Katherine A Gallagher[4], Benjamin Levi[1]. [1]University of Texas Southwestern, United States, [2]University of Texas Southwestern Medical Center, , [3]Johns Hopkins University, United States, [4]University of Michigan, United States

Heterotopic ossification (HO) is defined by the abnormal formation of bone tissue outside of the skeleton, accompanied by chronically progressive pain and limited mobility. However, identifying evolutionally conserved epigenetic modifiers that regulate the formation of HO is challenging due to our limited understanding of the molecular and cellular mechanisms implicated in HO. Here, a proven burn-tenotomy (BT) mouse model was used to investigate the role of epigenetic modification in traumatic HO formation. Our single-cell RNA sequencing (scRNA-seq) analysis of 150 human-conserved epigenetic modifiers from the injury site of this mouse model revealed that the histone demethylase Kdm6b had the most dramatic upregulation in HO-driving macrophages (Fig.1 A-B), with expression peaking by day 7 and maintained at the highest levels until day 42 (Fig.1 C). We also found KDM6B protein highly expressed in myeloid cells in human HO tissues (Fig.1 D). Mechanistically, we first uncovered that Kdm6b expression is upregulated by the activation of toll-like receptor signaling in injury-site macrophages. Single-nucleus Assay for Transposase-Accessible Chromatin (sn-ATAC) and Chromatin immunoprecipitation-qPCR (Chip-qPCR) further demonstrated that increased Kdm6b levels in macrophages led to demethylation of the repressive trimethylated lysine 27 on histone H3 (H3K27me3) at genomic loci of its target genes (Il1b, Tnfa, Tgfb1, and Pdgfa), and enhanced chromatin accessibility for elevated transcription of these proinflammatory and HO-promoting genes. Of note, KDM6B, also expressed in injury-site mesenchymal progenitor cells (MPCs), remodels the epigenetic landscape of MPCs in response to inflammatory stimuli after injury, thereby promoting their osteochondral differentiation during traumatic HO formation (Fig.1 E). Targeted inhibition of KDM6B in vivo with myeloid-specific genetic inactivation (Kdm6bf/f; Lyz2Cre+) or pharmacological inhibition with GSK-J4 in the mouse model of HO, significantly reduced inflammation, and markedly attenuated HO formation (Fig.1 F). Thus, our findings show that KDM6B acts as a critical HO-promoting epigenetic factor in both macrophages and MPCs, and targeting KDM6B could be an effective therapeutic intervention to limit HO development and progression.

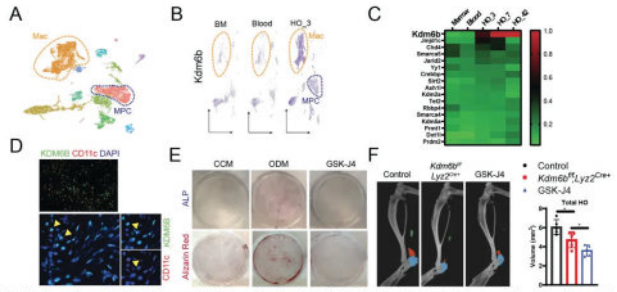

Fig.1 Epigenetic modification to prevent HO formation. (A and B) UMAP showing *Kdm6B* highly expressed in macrophages and MPCs. (C) Heatmap showing *Kdm6B* highly expressed in infiltrating macrophages at different time points after the traumatic injury. (D) Immunostaining showing that KDM6B is expressed in macrophages of human HO tissue samples. (E) ALP and Alizarin Red staining showing that GSK-J4 treatment inhibits osteogenic differentiation of MPCs in vitro. (F) Myeloid-specific genetic inactivation or pharmacological inhibition of JMJD3 in the mouse model mitigates HO formation.

***Disclosures: Tao Yue**, None*

FRI-268

The Role of Clec3b+ Muscle Cells in Fracture Healing and Heterotopic Ossification *JACOB MOORE[1], EZGI AYDIN[2], Ugur Ayturk[2, 1], [2]Hospital for Special Surgery, United States

Loss of Clec3b expression results in impaired healing of bone, connective tissue and skin injuries. We previously generated a Clec3b.creERT2 knock-in allele and found that Clec3b+ cells are located in muscle, outer periosteum and connective tissues, and are completely absent in the marrow, endosteum or growth plate. Further, Clec3b+ cells are osteogenically inactive during skeletal development and remodeling, but can contribute to the healing of drill hole injury or BMP2-driven heterotopic ossification (HO).Our goal with the current study was to determine the specific cell types Clec3b+ cells can convert to in trauma situations, and whether these changes are physiologically significant. We induced stabilized long bone fractures in Clec3b.creERT2; Ai14.R26.tdTomato; Bglap.eGFP mice. Using scRNA-seq, flow cytometry and fluorescent histology, we confirmed that Clec3b-lineage cells become fibroblasts, chondrocytes, osteoblasts, osteocytes, and bone marrow stromal cells in the fracture callus. To determine whether these Clec3b-lineage cells arise from the muscle or periosteum, we performed periosteum removal and bone graft transplantation experiments. All results indicated that muscle-resident Clec3b+ cells are the predominant contributors to bone healing. To test the significance of these contributions, we ablated Clec3b+ cells in Clec3b.creERT2; R26.DTA mice during fracture healing. MicroCT analysis showed that Clec3b+ cell-depleted fracture calluses had less bone volume (BV) than same-sex, littermate controls ($p < 0.05$).To determine whether Clec3b+ cells also play a significant role in HO, we activated the Acvr1.Q207D mutation in Clec3b+ cells (which results in BMP-gain-of-function) and confirmed muscle mineralization with microCT. To test loss of function, we depleted Clec3b+ cells with the DTA allele after inducing HO by intramuscular BMP2-injection. Surprisingly, Clec3b+ cell depletion (confirmed by histology) did not reduce but instead increase ectopic bone volume (both TV and BV, $p < 0.05$). These data suggest that Clec3b+ cell apoptosis during HO stimulates bone formation by cells that do not undergo Cre-recombination, either due to inefficient Cre-activation or lack of Clec3b-expression.Overall, our data show that Clec3b+ interstitial muscle cells play significant roles in regenerative and pathologic bone formation processes. Studying the mechanisms regulating Clec3b+ cells can lead to new strategies to promote fracture healing and prevent HO.

***Disclosures: JACOB MOORE**, None*

FRI-271

Fgfr3-expressing endosteal stromal cells form osteosarcoma-like lesions through unregulated self-renewal upon loss of p53 tumor suppressor *Yuki Matsushita[1], Noriaki Ono[2]. [1]Nagasaki University, Japan, [2]University of Texas Health Science Center at Houston School of Dentistry, United States

Skeletal stem cells (SSCs) are found in various bone marrow stromal compartments and provide an important source bone-forming osteoblasts. We recently described that bone marrow stromal cells expressing fibroblast growth factor receptor 3 (Fgfr3) reside in the endosteal space and actively participate in bone formation under homeostatic and regenerative conditions. However, how Fgfr3+ endosteal stromal cells participate in aberrant bone formation under pathological conditions remains unclear. First, we conditionally deleted p53 tumor suppressor in Fgfr3+ cells using Trp53-floxed allele. We pulsed cohorts of Fgfr3-creER; Trp53fl/+; R26RtdTomato (Control) and Fgfr3-creER; Trp53fl/fl; R26RtdTomato (Fgfr3-p53 cKO) mice at postnatal day (P) 21 and analyzed these mice at 9 months of age. Strikingly, a substantial fraction of Fgfr3-p53 cKO mice (5/17 mice) developed highly-trabecularized bone tumors radiating from the marrow space, which destroyed the pre-existing cortical bones. In all Fgfr3-p53 cKO bones examined (17/17 mice), the marrow space was dominated by unorganized trabecular bone-like structures entirely composed of Fgfr3CE-P21?p53 tdTomato+ cells. In contrast, conditional deletion of p53 by Osx-creER (pulsed at P21) or Lepr-cre did not induce apparent bone tumor-like lesions at 9 months, indicating that Fgfr3+ endosteal stromal cells, but not Osx+ or LepR+ cells, can transform into bone tumor cells upon p53 loss. Subsequently, we investigated mechanisms underlying tumorigenic potential of Fgfr3+ cells by colony forming unit-fibroblast (CFU-F) assays. Fgfr3CE-?p53 tdTomato+ clones exhibited substantially faster cell growth and higher passage-ability compared to wild-type tdTomato+ clones, associated with significant upregulation of osteoblast markers and cell proliferation genes as identified by RNA-seq, indicating that p53 loss introduces stem cell-like properties and an osteogenic bias in Fgfr3+ CFU-Fs. Further, transplantation of Fgfr3CE-?p53 tdTomato+ clones into the femoral marrow cavity of NSG mice resulted in the formation of highly trabecularized structures throughout the marrow space, which were reminiscent of early-stage osteosarcoma-like lesions. Therefore, Fgfr3+ endosteal stromal cells develop aggressive osteosarcoma-like lesions upon loss of p53 tumor suppressors through unregulated self-renewal and aberrant osteogenic fates.

***Disclosures: Yuki Matsushita**, None*

FRI-273

Periosteal CD51+ progenitor cells contribute to local healing *YE CAO[1], IVO KALAJZIC[2], Brya Matthews[3, 1], New Zealand, [2]University of Connecticut Health Center, United States, [3]University of Auckland, New Zealand

The periosteum is a major source of cells that contributes to fracture healing. However, complexity of the fracture model includes response of bone marrow derived skeletal stem/progenitor cells (SSPCs). In this study, we evaluated the response of periosteum and defined populations of periosteal injury-responsive SSPCs using a periosteum-specific scratch injury.Following injury, periosteal progenitors expanded by day 3 and formed fibrocartilage by day 7. Fibrocartilage was gradually replaced by new bone formation with marrow infiltration from day 14 to day 21. Bone and periosteum were remodeled, and healing was complete by day 28.We used multicolor spectral flow cytometry combined with ?SMACreER/tdTom/Col2.3GFP, a lineage tracing model of skeletal progenitors (?SMA+) and osteoblasts (Col2.3+). Within total periosteal CD45- cells, enrichment of ?SMA and CD90 cells was detected on day 3 (10.4% and 27.9%) and day 7 (28.0% and 36.0%) after injury compared with uninjured (3.4% and 17.9%). Markers of progenitors Sca1+CD51+, Sca1-CD51+ were expanded by 7 days after injury.Histologically, most periosteal Sca1 cells were located on the outer periosteum layer. They showed minimal expansion with injury. CD51 and CD90 cells were more abundant in the inner layer and expanded immediately with injury. In contrast with flow result, Sca1+CD51+ cells were rare in the periosteum in situ. Some CD51+ cells were Col2.3+ on day 14 following injury, indicating the contribution of CD51+ cells to osteoblasts.Periosteal Sca1+CD51+ cells were multipotent, and Sca1-CD51+ cells were committed osteoprogenitors in vitro. We further examined the in vivo lineage potential of Sca1-CD51+ and, Sca1+CD51+ cells by subcutaneous transplant. In contrast to the in vitro results, Sca1-CD51+ cells exhibited greater engraftment and more osteoblast formation than the other populations tested.Stimulation of Notch signalling enhances bone healing. Using ?SMACreNICD mice, which have increased Notch signalling in ?SMA+ cells, we found the frequency of CD51+ was tripled in NICD+ mice compared to controls, indicating that CD51+ cells may improve healing at early stages.In conclusion, periosteal Sca1-CD51+ and CD90+ cells are multipotent progenitors that respond rapidly to local injury in vivo. Enhanced bone healing is correlated with the rapid expansion of CD51+ osteoprogenitors.

***Disclosures: YE CAO**, None*

FRI-275

Refining the identity of mesenchymal cell types associated with murine bone *Intawat Nookaew[1], Jinhu Xiong[1], Melda Onal[1], Cecile Bustamante-Gomez[1], Visanu Wanchai[1], Qiang Fu[1], Ha-Neui Kim[1], Maria Almeida[1], Charles O'Brien[1], [1]University of Arkansas for Medical Sciences, United States

Single cell RNA sequencing (scRNA-seq) quantifies mRNAs in individual cells. The transcriptomic profile can be used to cluster cells with similar profiles. Combining this information with known gene expression patterns can be used to define clusters of cells as specific cell types. Several recent studies have used scRNA-seq to define mesenchymal cells associated with murine bone. However, these studies do not agree on the number of different cell types. To address this inconsistency in cell type designation, we created an atlas of murine bone-associated cells by harmonizing published datasets with in-house data from cells targeted by Osx1-Cre and Dmp1-Cre driver strains. Over 100,000 mesenchymal cells were mapped to reveal 11 major clusters designated fibro-1, fibro-2, chondrocytes, articular chondrocytes, tenocytes, adipo-CAR, osteo-CAR, pre-osteoblasts, osteoblasts, osteocytes, and osteo-X, the latter defined in part by Postn expression. In situ hybridization revealed that osteo-X, osteo-CAR, and pre-osteoblasts were closely associated with osteoblasts on trabecular bone, suggesting a continuum of cells spanning from osteoblast progenitors to mature osteoblasts. To determine if any of these cell populations are dependent on ongoing bone remodeling, we suppressed osteoclast formation using denosumab and examined the impact by scRNA-seq. To ensure our analysis produced cluster annotations consistent with the harmonized atlas, we constructed a reference-based mapping model using the Azimuth pipeline. Denosumab dramatically reduced osteoblast number, consistent with the suppression of bone remodeling. The abundance of pre-osteoblasts was also slightly reduced as was expression of the pre-osteoblast marker Spp1. In contrast, the abundance of osteo-CAR and adipo-CAR cells was not altered. Consistent with these results, in situ hybridization revealed an almost complete loss of Bglap-positive osteoblasts on trabecular bone in denosumab-treated mice. Pre-osteoblasts, as defined by Spp1 expression, showed robust staining on trabecular bone in vehicle-treated mice, which was reduced but not abolished after denosumab. In contrast, the osteo-CAR marker Limch1 and the osteo-X marker Postn displayed little change after denosumab administration. Thus osteoblasts, and to some extent pre-osteoblasts, are highly dependent on bone resorption and coupling factors for their existence but osteo-CAR and osteo-X cells, and their close association with the bone surface, are not.

***Disclosures: Intawat Nookaew**, None*

FRI-276

SHP2 Regulation of the Plasticity of OSTERIX+ Bone Marrow Stroma and Hematopoietic Niches *Lijun Wang[1], Huiliang Yang[1], Nathalie Oulhen[2], Jiahui Huang[1], Gary M. Wessel[2], Vicki Rosen[3], Shaomeng Wang[4], Hicham Drissi[5], Douglas C. Moore[1], Wentian Yang[1], [1]Brown University, Department of Orthopaedic Surgery, United States, [2]Brown University, Departments of Molecular Biology, Cell Biology, and Biochemistry, United States, [3]Harvard School of Dental Medicine, United States, [4]University of Michigan, Departments of Internal Medicine, Pharmacology, and Medicinal Chemistry, United States, [5]Emory University, United States

Objective: Live-cell fate mapping has identified a pivotal population of bone marrow (BM) Osterix (Sp7)-positive mesenchymal stem and progenitor cells (O+MSPC). These O+MSPC also express variable levels of Nestin, Cxcl12, LepR and Pdgfr?/Sca-1, their functions in skeletal development and BM homeostasis remain elusive. SHP2 (encoded by PTPN11) is a widely expressed tyrosine phosphatase and has been implicated in MSPC maintenance. This study aims to understand how the self-renewal and lineage commitment of O+MSPC are regulated by SHP2, and how SHP2 in O+MSPC modulates osteogenesis and hematopoietic niche formation.Materials and Methods: Mice lacking SHP2 in O+MSPC were generated by crossing the Ptpn11 floxed allele to Tg(Sp7-cre) mice. Tg(Rosa26ZSG) was bred in as a lineage reporter in some studies. Control and SHP2 mutants were sacrificed at the indicated time points and examined via X-Ray, μ-CT, histological, biochemical, scRNA-seq, and biological analyses. All mice were maintained on the C57BL/6 background and studied in accordance with the IACUC-approved protocols.Results and Discussion: Phenotypic characterization of the SHP2 mutants and their cellular derivatives reveals that SHP2 is a critical regulator of O+BMPC. SHP2 ablation in O+BMSC substantially reduced bone mass. OB abundance and function were markedly reduced in affected mutants. These mice also exhibited delayed closure of the cranial sutures and fontanelles, phenotypically mimicking the features of human Cleidocranial Dysplasia in which RUNX2 loss-of-function mutations have been described1-3. SHP2 mutants also have increased BM adipocyte accumulation and altered BM vasculature, likely by impairing pericyte development. Importantly, SHP2 ablation in O+BMSC skewed hematopoiesis, significantly reducing common lymphoid progenitors (CLPs) and B cells in BM, although the number of HSC is comparable between control and SHP2 mutants. Mechanistically, SHP2 regulated the lineage commitment of O+BMSC by modulating the RUNX2 and OSTERIX expression, and CLP and B cell survival by promoting IL7 secretion. BM hematopoietic niches are 3D stromal complexes that contain MSPCs, their progeny, and cells of vascular origin. These cells are known to provide key signals that support HSC survival, proliferation, and differentiation. Our data and published literature4 together emphasize a crucial role for SHP2 in the formation and functional regulation of hematopoietic niches and osteogenesis.

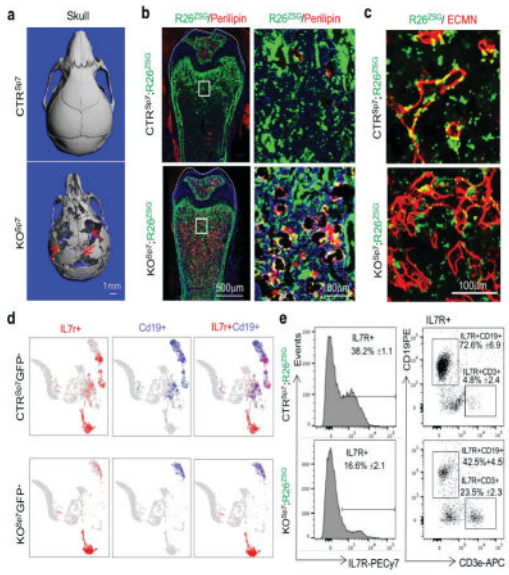

Fig.1 **a.** μCT images demonstrate the gross skull morphology of 4-week-old SHP2CTR^{Sp7} and SHP2KO^{Sp7} mice. Note that SHP2 deletion impairs frontal and parental bone mineralization (red arrows). **b-c.** Immunostained distal femoral sections show the massive accumulation of Perilipin+ adipocytes and altered BM vasculature (ECMN+) in SHP2KO^{Sp7};R26^{ZSG} mice, compared to SHP2CTR^{Sp7};R26^{ZSG} controls. **d.** scRNA-seq analysis and UMAP plots show the diminish of IL7r+Cd19+ pro- and pre-B cell clusters in FACS-enriched R26^{ZSG}- BM populations in SHP2KO^{Sp7};R26^{ZSG} mice, compared to age and sex matched SHP2CTR^{Sp7};R26^{ZSG} controls. **e.** Representative FACS data show a marked reduction of BM IL7R+CD19+ subpopulation in SHP2KO^{Sp7};R26^{ZSG} mice, compared to SHP2CTR^{Sp7};R26^{ZSG} controls.

***Disclosures: Lijun Wang**, None*

FRI-277

AdipoQ lineage bone marrow progenitors are the major cellular source of M-CSF for bone marrow macrophage development, osteoclastogenesis and bone metabolism *Yongli Qin[1], Kazuki Inoue[1], Yuhan Xia[1], Jie Han[2], Ruoxi Yuan[3], Jun Sun[4], Ren Xu[2], Jean X. Jiang[5], Matthew B. Greenblatt[1], Baohong Zhao[1]. [1]Weill Cornell Medical College and Hospital for special surgery, United States. [2]The first Affiliated Hospital of Xiamen University, China. [3]Hospital for special surgery, United States. [4]Weill Cornell Medical College , United States. [5]University of Texas Health Science Center, United States

M-CSF, encoded by Csf1, is a critical growth factor for myeloid lineage cells, including monocytes, macrophages, and osteoclasts. Tissue-resident macrophages in most organs rely on local M-CSF. However, it is unclear what specific cells in the bone marrow produce M-CSF to maintain myeloid homeostasis. We performed an integrative scRNAseq analysis based on five published bone marrow scRNAseq datasets and human bone marrow scRNA-seq datasets. Although the current paradigm indicates osteoblasts as the main cellular source of M-CSF in bone marrow, we surprisingly found that the osteoblasts do not express Csf1 in vivo. In contrast, we identified that Adipoq-lineage (Adipoq+) bone marrow progenitor cells possess the predominant and highest Csf1 expression level in bone marrow. The Adipoq-lineage progenitors with high CSF1 expression also exist in human bone marrow. We further generated Csf1 conditional knock out (cKO) mice, in which Csf1 is specifically deleted in Adipoq+ cells by crossing Csf1flox/flox mice with Adipoq-cre mice (hereafter referred to as Csf1?Adipoq). Csf1 deficiency in Adipoq+ cells lead to a drastic decrease in bone marrow macrophages and a severe osteopetrotic phenotype in mice with significantly reduced osteoclast numbers and enhanced bone mass. Without exogenous M-CSF, RANKL is able to induce osteoclastogenesis in bone marrow harvested from the control mice, but not from Csf1?Adipoq bone marrow. These results further support an essential role for M-CSF secreted from Adipoq+ bone marrow cells in osteoclastogenesis in vivo. Interestingly, Csf1 is undetectable in other Adipoq highly expressed cells, including peripheral mature adipocytes or mature bone marrow adipocytes. Tissue macrophages in other organs appear normal in Csf1?Adipoq mice. Furthermore, the lack of the Adipoq+ cell-produced M-CSF prevented the estrogen-deficiency induced excessive osteoclast formation and osteoporosis, indicating a potential novel therapeutic strategy for postmenopausal bone loss by targeting M-CSF produced by Adipoq+ cells. Collectively, our data reveal a specifically high Csf1 expression feature of the Adipoq+ bone marrow progenitor cells. These cells constitute approximately only 0.05% of bone marrow cells, but are the major cellular source of M-CSF in bone marrow. These findings challenge the current paradigm and have profound implications for our understanding of bone marrow macrophage development, osteoclastogenesis, bone homeostasis, and pathological bone loss.

***Disclosures: Yongli Qin**, None*

FRI-279

In Vivo Tracking of Human Fetal Skeletal Stem Cell Lineage Dynamics at the Single Cell Level *Thomas Ambrosi[1], Rahul Sinha[2], Charles Chan[2]. [1]UC Davis, United States. [2]Stanford University, United States

With the increasing socioeconomic impact of skeletal disorders and the absence of reliable treatments, innovative approaches are required to prevent bone loss and restore skeletal tissues. Skeletal stem cells (SSCs) show great potential as a new therapeutic option; however, progress has been hindered by a lack of understanding regarding the identity and function of these cells in humans. Here, we utilized a combination of prospective flow cytometric isolation and SmartSeq2 single cell RNA-sequencing (scRNAseq) to interrogate the diversity of over 4,000 human SSCs from ten distinct skeletal sites at 20 weeks gestational age. In vivo tracing of lentivirally barcoded fetal human SSCs was combined with scRNA-seq readouts to assess unique clonal dynamics of human growth plate and periosteal SSCs. RNAscope was employed to map SSC subsets in situ. A xenograft model of fetal skeletal elements together with scRNAseq was used to further deconstruct the human SSC lineage tree in fetal long bones. Transcriptomic analysis of single fetal SSCs from distinct skeletal sites revealed diversity of SSCs tied to specialized features correlating with anatomical localization. Intriguingly, gene expression in specific types of SSCs residing in different bone regions was linked to skeletal phenotypes caused by genetic mutations. For example, XYLT1, a gene that if mutated leads to dwarfism, was highly expressed in growth plate SSCs but not cranial, periosteal, pelvic or vertebra SSCs, while SEC24D, a gene associated with craniosynostosis, was highly expressed in suture SSCs. Overall, we identified two major types of SSCs - an osteochondral SSC and a stromal SSC. We also found that growth plate and periosteal SSCs of long bones, representing examples of the two specialized SSC subtypes, presented with distinct clonal dynamics thereby differentially contributing to skeletal development. Functional and bioinformatic approaches highlighted that neither of the two SSC types were dispensable and that they tightly interacted to facilitate proper bone growth and maintenance. Lastly, index-sort analysis of prospectively isolated SSC lineage subsets was able to reconstruct stem cell dynamics and identify additional new subsets of specified, more committed skeletal lineage cell populations. In summary, our research provides novel insights into human skeletal stem cell biology and offers experimental vantage points to study skeletal development and disease at an unprecedented resolution.

***Disclosures: Thomas Ambrosi**, None*

FRI-282

Mitochondrial Metabolism Determines Mesenchymal Stem Cell Fate *CHEN YU[3], RUBENS SAUTCHUK JR[2], Roman Eliseev[3]. [3]University of Rochester, , [2], , [3]University of Rochester, United States

Aging-related changes in bone marrow stromal (a.k.a. mesenchymal stem) cells (BMSCs) shift cell fate away from osteogenesis and towards adipogenesis. The mechanism(s) underlying such changes are not completely understood. Mitochondria are important cell organelles that not only produce energy but also determine cell behavior by regulating metabolism, signaling, calcium homeostasis, apoptosis, and other cellular processes. We have previously shown that mitochondrial activation is important during osteogenesis of BMSCs. In aged bone tissue, we observed pathological opening of the mitochondrial permeability transition pore (mPTP) which leads to mitochondrial dysfunction, oxidative phosphorylation uncoupling, and cell death. Cyclophilin D (CypD) is a mitochondrial protein that facilitates opening of the mPTP. We found that CypD is downregulated during osteogenesis of BMSCs leading to lower mPTP activity and, thus, protecting mitochondria from dysfunction. On the other hand, we observed that during adipogenesis, BMSC alternative fate, cells significantly upregulate glycolysis and increase CypD expression and mPTP activity. Confocal imaging shows that mitochondrial morphology remains rounded and fragmented during this process (Figure). CypD gene, Ppif, promoter analysis reveals multiple binding sites for adipogenic C/EBP and inflammatory NF-?B transcription factors. Luciferase assay and ChIP-PCR analysis confirm C/EBP? as a transcriptional activator of CypD. NF-?B p65 translocates to the nucleus during adipogenesis and shows synergistic effect with C/EBP? in inducing Ppif expression, suggesting a potential link between ‘inflammaging’ and altered BMSC fate. In vitro CypD overexpression enhances, whereas CypD knockdown impairs adipogenesis. Pharmacological inhibition of CypD by NIM811 also impairs adipogenesis in vitro. Prx-1Cre-mediated deletion of CypD in Ppiff/f mice decreases bone marrow fat in 13-month-old mice. Currently we are pursuing the effect of Prx1Cre-mediated CypD overexpression in mice. In summary, BMSCs maintain or upregulate CypD expression during adipogenesis leading to increased mPTP activity, activated glycolysis and low mitochondrial function, thus establishing a metabolic profile that appears to be favorable for adipogenic lineage. The overall goal of this study is to define the potential role of CypD/mPTP during BMSC adipogenesis, facilitating the understanding of stem cell fate determination and molecular mechanism of age-related bone loss.

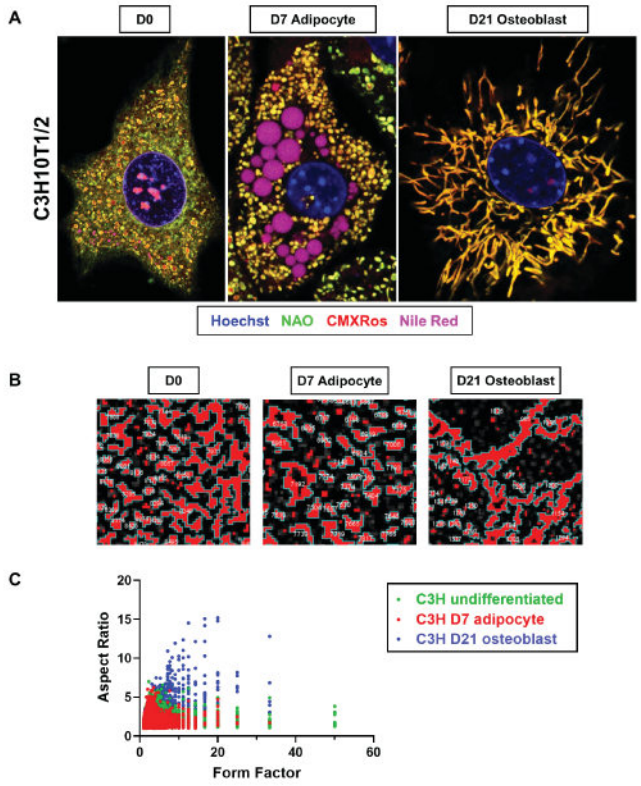

Figure. Mitochondrial network during osteogenesis and adipogenesis in C3H10T1/2.
A) Representative images of mitochondrial morphology in C3H/10T1/2 cells. Cells were cultured in adipogenic media for 7 days or osteogenic media for 21 days. After staining, images were taken by confocal microscopy at 63x magnification. B) Representative images of mitochondrial morphology analysis in C3H10T1/2. Analysis was performed with CMXRos staining using ImageJ. C) Quantification of mitochondrial morphology. For each group, three cells were randomly selected for analysis.

***Disclosures: CHEN YU**, None*

FRI-287

Effect of Protein Supplementation during Weight Loss on Trabecular and Cortical Bone Mineral Density of the Hip in Older Adults with Obesity: a Randomized Controlled Trial *Ashley Weaver[1], Katelyn Greene[2], Joshua Stapleton[3], Xiaoyan Leng[4], Leon Lenchik[4], Mary Lyles[4], Barbara Nicklas[4], Sue Shapses[5], Denise Houston[4]. [1]Wake Forest University, United States; [2]Wake Forest School of Medicine, , [3], , [4]Wake Forest University School of Medicine, United States; [5]Rutgers University/ Rutgers RWJ Medical School, United States

Weight loss (WL) to treat obesity is controversial in older age as it can exacerbate bone loss. We conducted a double-blind, randomized controlled trial in 187 low-functioning older adults with obesity (mean+/-SD: 71.0+/-4.3 yrs; BMI 34.2+/-4.1 kg/m2; 34% men) to assess the effect of protein supplementation during WL on hip volumetric bone mineral density (vBMD). Participants were enrolled in a 6-month WL intervention (caloric restriction and moderate-intensity treadmill walking 3d/wk) followed by 12 months of follow-up and randomized to one of 3 groups: 50 g/d of supplemental protein (PRO; n=62) or carbohydrate (CHO; n=62) for the 6-month WL period, or 50 g/d of supplemental PRO for the 18-month WL plus follow-up period (n=63). Computed tomography (CT) scans at baseline and 18 months were analyzed to assess trabecular and cortical vBMD of the total hip, femoral neck, and intertrochanter and differences in change were examined using analysis of covariance adjusted for age, sex, race, baseline weight, and baseline bone measure. Spearman's correlations of WL vs bone changes adjusted for age, race, and sex were also examined. Protein intake at 18 months was higher in the 18-m PRO group compared to the 6-m PRO and 6-m CHO groups (mean+/-SD: 1.0+/-0.4 vs 0.8+/-0.3 and 0.8+/-0.3 g/kg/d, respectively; p<0.01). 18-month WL did not differ by group (-5.2+/-5.6, -4.9+/-5.4, -4.3+/-5.3 kg for 18-m PRO, 6-m PRO and 6-m CHO, respectively). Total hip cortical vBMD improved over 18 months (Fig A) but did not differ by group (adjusted mean+/-SE: 12.8+/-4.3, 13.4+/-4.2, 11.6+/-3.9 mg/cm3 for 18-m PRO, 6-m PRO and 6-m CHO, respectively; all p<0.05). Similar trends were observed in cortical vBMD changes of the femoral neck and intertrochanter. Trabecular vBMD losses (mg/cm3) did not differ by group (Fig B), but there was more preservation in the 18-m PRO group at the total hip (0.0+/-1.4 vs -1.7+/-1.4 and -1.0+/-1.4 for 6-m PRO and 6-m CHO, respectively), femoral neck (0.9+/-2.2 vs -1.8+/-2.1 and -0.7+/-2.1) and intertrochanter (-0.7+/-1.8 vs -2.4+/-1.7 and -2.3+/-1.7). Greater weight loss was associated with more trabecular vBMD loss at the total hip (?=0.22, p=0.03) and intertrochanter (?=0.29, p<0.01). In low-functioning older adults with obesity in a weight loss trial, hip cortical vBMD increased (possibly due to more physical activity) and trabecular vBMD declined; trends suggest protein supplementation for 18 months better preserved trabecular bone compared to protein or carbohydrate supplementation for 6 months.

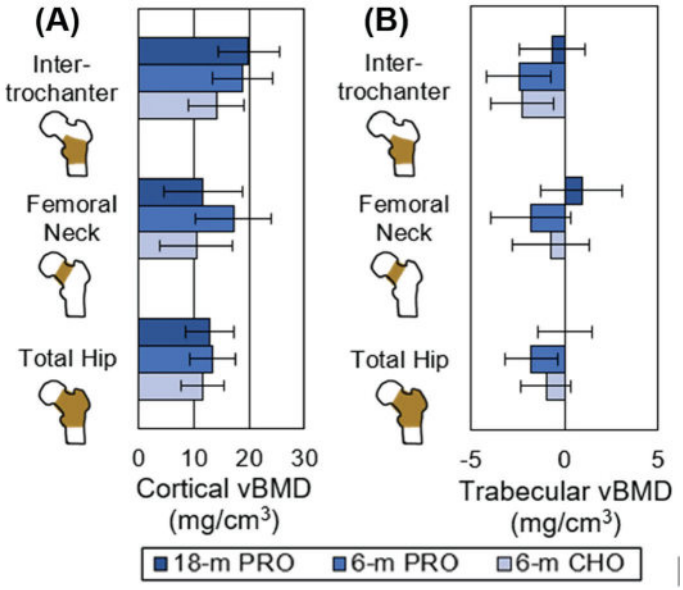

***Disclosures: Ashley Weaver**, None*

FRI-291

Exploring a Network of Pathways and Proteins: A Proteomic Analysis of ENPP1 Deficiency *Juancarlos Torres[1], Shira Ziegler[2], Carlos Ferreira[3]. [1]NHGRI, NIH, United States; [2]Johns Hopkins University School of Medicine, United States; [3]National Institutes of Health,

Ectonucleotide pyrophosphatase/phosphodiesterase 1 (ENPP1) deficiency leads to a slew of symptoms, including arterial calcification, hypophosphatemic rickets, cervical vertebral fusions, retinal involvement and auditory impairment. The molecular mechanisms leading to these protean manifestations remain largely unknown. To try to better understand the pathogenesis of this rare disease, we performed proteomic analysis from patients' plasma and calvarial osteoblasts from mutant mice. Specifically, we compared protein levels from 18 ENPP1-deficient patients v. 22 controls, and cell lysates from calvarial osteoblasts obtained from 5 Enpp1asj/asj mice v. 5 littermate controls. Proteomic analysis was performed by the SomaScan® Assay, which uses Slow Off-Rate Modified Aptamers to quantify 7,322 different proteins. Proteomics data visualization and analysis were performed with ProViz, and the results filtered based on Fold Change and adjusted p-value. These results were uploaded to QIAGEN Ingenuity Pathway Analysis (IPA), which uses a built-in library to group the proteins into pathways to find overrepresentation of biological functions. The enriched pathways were sorted by adjusted p-value and Z-score into eight groups: Cardiac, FGF Signaling, Insulin, MAPK, mTOR/PTEN, Rho (including RHOGDI), G-proteins, P2Y Purinergic Receptor Signaling, and Miscellaneous Signaling Pathways. All pathways in these groups, except for RHOGDI and PTEN Signaling, were upregulated in patients and mutant mice. The proteins identified by ProViz were further analyzed, and four (SRC, SMAD5, PAK6, and RAC1) were selected based on their fold changes and p-values (PAK6 was prominent in plasma results, RAC1 was prominent in lysate results, while SRC and SMAD5 were prominent in both), for independent confirmation of results via ELISA assays, which are currently underway. Finally, upstream analysis performed through IPA predicted that the activation of regulators including TGFB1 and FGFR1 heavily influenced the change in expression of the target proteins. In summary, we performed proteomic analysis in patients' plasma and calvarial osteoblasts obtained from a mouse model of ENPP1 deficiency and found overrepresentation of several proteins and pathways that are shared between ENPP1-deficient patients and mutant mice. Our work increases understanding of the pathomechanisms of ENPP1 deficiency and opens new avenues for research into this rare disease.

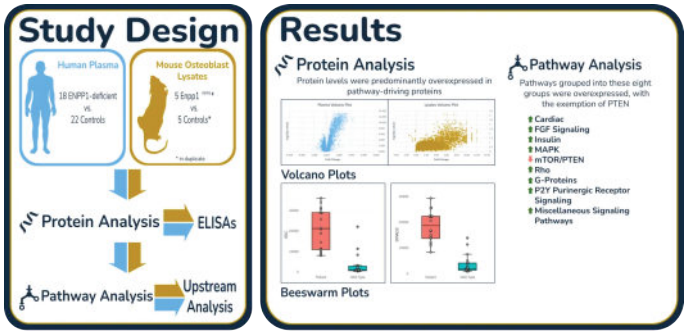

***Disclosures: Juancarlos Torres**, Inozyme Inc, Grant/Research Support*

FRI-293

Protein-Based Risk Scores Improve Hip Fracture Prediction More than Available Genetic Risk Scores *Thomas Austin[1], Howard Fink[2], Anna Törnqvist[3], Diana Jalal[4], Petra Buzkova[5], Joshua Barzilay[6], Tianyuan Lu[7], Laura Carbone[8], Maiken Gabrielsen[9], LOUISE GRAHNEMO[10], Kristian Hveem[11], Christian Jonasson[9], Jorge Kizer[12], Arnulf Langhammer[13], Kenneth Mukamal[14], Robert Gerszten[14], Maria Nethander[3], Bruce Psaty[15], John Robbins[16], Yan Sun[17], Anne Heidi Skogholt[9], Bjørn Olav Åsvold[18], Rodrigo Valderrabano[19], Brent Richards[20], Jie Zheng[21], Eivind Coward[9], Claes Ohlsson[22]. [1]Cardiovascular Health Research Unit, University of Washington, Seattle, WA, United States. [2]Minneapolis VA Medical Center, United States. [3]Department of Internal Medicine and Clinical Nutrition, Institute of Medicine, Sahlgrenska Osteoporosis Centre, Centre for Bone and Arthritis Research at the Sahlgrenska Academy, University of Gothenburg, Gothenburg, Sweden, Sweden. [4]Division of Nephrology, Department of Internal Medicine, Carver College of Medicine AND Iowa City VA Medical Center, Iowa City, IA, United States. [5]Department of Biostatistics, University of Washington, Seattle, WA, United States. [6]Division of Endocrinology, Kaiser Permanente of Georgia, Atlanta, GA, United States. [7], [8]Augusta University, United States. [9]K.G. Jebsen Center for Genetic Epidemiology, Department of Public Health and Nursing, Norwegian University of Science and Technology, Trondheim, Norway, Norway. [10]University of Gothenburg, Sweden. [11]K.G. Jebsen Center for Genetic Epidemiology, Department of Public Health and Nursing, Norwegian University of Science and Technology, Trondheim AND HUNT Research Centre, NTNU, Levanger, Norway, Norway. [12]Cardiology Section, San Francisco VA Health Care System AND Department of Medicine, Epidemiology and Biostatistics, University of California San Francisco, San Francisco, CA, United States. [13]HUNT Research Centre, NTNU AND Levanger Hospital, Nord-Trøndelag Hospital Trust, Levanger, Norway, Norway. [14]Department of Medicine, Beth Israel Deaconess Medical Center, Brookline, MA, United States. [15]Iowa City VA Medical Center, Iowa City, IA AND Departments of Medicine, Epidemiology, and Health Systems and Population Health, University of Washington, Seattle, WA, United States. [16]Department of Medicine, University of California, Davis, CA, United States. [17]Department of Epidemiology, Rollins School of Public Health, Emory University, Atlanta, GA, United States. [18]K.G. Jebsen Center for Genetic Epidemiology, Department of Public Health and Nursing, Norwegian University of Science and Technology AND Department of Endocrinology, Clinic of Medicine, St. Olavs Hospital, Trondheim University Hospital, Trondheim, Norway, Norway. [19], United States. [20]McGill University, Canada. [21]MRC Integrative Epidemiology Unit (IEU), Bristol Medical School, University of Bristol, Oakfield House, Oakfield Grove, Bristol, BS8 2BN, United Kingdom, United Kingdom. [22]Center for Bone and Arthritis Research at the Sahlgrenska Academy, Sweden

Hip fractures are associated with significant disability and mortality. Early identification of patients at high risk of hip fracture is important to inform efficient intervention strategies. Published genetic risk scores (GRS) improve hip fracture prediction modestly. The present study aimed to develop and validate a protein-based risk score (PrRS) for hip fracture prediction.In the Cardiovascular Health Study (CHS) and the HUNT study, we performed a comprehensive circulating protein association study on incident hip fractures using the aptamer-based 5K SomaScan assay, including 4,979 aptamers. A PrRS was developed in CHS (3,171 subjects, mean 74.4 yrs, 39% men, 456 hip fractures) using two different strategies. In the first strategy, univariate associations between protein levels and hip fractures were calculated using age and sex-adjusted Cox regression models. A weighted PrRS (W-PrRS) was developed, including the 18 proteins passing the significance level after adjustment for multiple testing. In the second strategy, using machine learning (ML), LASSO with repeated splits of training (70%) and testing data sets (30%) was carried out to develop a PrRS including 6 proteins (ML-PrRS) with optimal improvement of c-index.The performances of the two PrRSs to predict incident hip fractures were determined in the independent HUNT validation cohort (3,259 subjects, mean 64.5 yrs, 61% men, 187 hip fractures). Age and sex-adjusted Cox regression models revealed that both the W-PrRS (Hazard ratio (HR) 1.51, 95% confidence interval 1.25-1.81 per standard deviation increase in risk score) and the ML-PrRS (HR 1.42, 1.19-1.69) improved fracture prediction more than GRSs previously developed using 47 genome-wide significant markers for femoral-neck BMD (FN-BMD-GRS; HR 1.14, 0.98-1.32) or using ML (21,716 genetic markers) of ultrasound-derived speed of sound in the heel (gSOS-GRS; HR 1.09, 0.94-1.26). Hip fracture prediction for the two PrRSs were only marginally attenuated after adjustment for clinical risk factor based FRAX score (W-PrRS, HR 1.45, 1.19-1.75; ML-PrRS, HR 1.37, 1.14-1.64). Discriminative analyses revealed that both the W-PrRS and the ML-PrRS ($p<0.05$), but not the FN-BMD-GRS or the gSOS-GRS, improved the c-index for hip fractures compared with an age and sex-adjusted base model.In conclusion, our developed PrRSs improve hip fracture prediction more than available GRS and may add clinically useful information for hip fracture prediction.

***Disclosures: Thomas Austin**, None*

FRI-294

Rare Coding Variant in SERT is Associated with Improved Bone Mass in Mice and Humans *Emily Larson[1], Hillary Larson[1], Eric Orwoll[2], Robert Klein[1]. [1]Veterans Affairs Portland Health Care System, United States. [2]Oregon Health & Science University, United States

Common susceptibility loci thus far identified by genome-wide association studies (GWAS) account for a small proportion of the estimated genetic heritability of bone mineral density (BMD). One explanation for the missing heritability is the existence of less common variants with larger biological effects that are poorly detected by GWAS. We hypothesized that genes contributing to biological pathways that regulate BMD could be identified by studying subjects at the phenotypic extremes for BMD. Subjects from the Osteoporotic Fractures in Men Study (MrOS) with the lowest total hip BMD (N =?98) and highest BMD (N =?110) were selected for exome sequencing. We observed an amino-terminal-localized Gly56Ala substitution (rs6355) in the serotonin transporter (SERT or SLC6A4) with a minor allele frequency 4-fold higher in the high BMD pool (4.1%) compared to the low BMD pool (1%). In the entire MrOS European-American population (n=5,008) associations between rs6355 and total hip BMD (maf 1.8%; ? = 0.31; p = 5x10-5) and femoral neck BMD (maf 1.8%, ?= 0.29; p = 1x10-4) were again confirmed. Inspection of the GEFOS Femoral Neck BMD 2012 Data Release provided concordant support for this variant (maf 2.4%; ? = 0.06; p = 0.014). To further explore this novel association, we examined SERT Ala56 mouse knock-in mice (provided by R. Blakely, Florida Atlantic University). Compared to wild-type Gly56Gly littermates, male SERT Ala56Ala knock-in mice demonstrated increased whole body (3.3%; $p < 0.01$) and femoral (3.3%; $p < 0.01$) BMD and greater resistance to 3-point bending (12%; $p < 0.001$). In contrast, no genotype-dependent effect on any skeletal parameter was observed in female SERT Ala56Ala knock-in mice. The rs6355 variant has been demonstrated to exhibit tonic elevation of serotonin (5-HT) transport activity in transfected cells and human lymphoblasts in vitro and when examined in a SERT Ala56 knock-in mouse model leads to an increased 5-HT clearance rate in vivo, along with altered sensitivity to SERT regulatory signaling pathways. The mechanisms whereby this variant results in the acquisition and/or maintenance of increased bone mass are unclear, but our results in both mice and humans suggest that serotonin signaling is involved in skeletal physiology and manipulating this pathway is a potential target for the treatment of osteoporosis.

***Disclosures: Emily Larson**, None*

FRI-295

A comprehensive single cell transcriptomic atlas of adult human bone marrow *Michael Duffy[3], Shovik Bandyopadhyay[2], Kyung Jin Ahn[2], Kai Tan[2], Ling Qin[3]. [3]University of Pennsylvania, . [2]Children's Hospital of Philadelphia, United States. [3]University of Pennsylvania, United States

Bone marrow (BM) is primarily made of mesenchymal and hematopoietic lineage cells to provide mechanical support and produce blood. While mouse BM has been characterized at the single cell level, the rareness of mesenchymal cells in human BM aspirate has led to a lack of heterogeneity in scRNA-seq datasets and hindered human studies. Here, we developed a robust protocol to enzymatically isolate cells from fresh femoral head BM acquired after total hip arthroplasty. We separately enriched non-hematopoietic (CD45 depletion) and hematopoietic progenitor (CD34 selection) cells and then mixed them with RBC-depleted BM cells at 10:3:3 ratio for scRNA-seq using 10x genomics. From 12 samples (age 52-74, median 65+/-8), we profiled 53,417 hematopoietic and 29,325 non-hematopoietic cells at 3117 genes/cell and identified 35 cell clusters (Fig 1) of hematopoietic (25), mesenchymal (7), endothelial (2), and smooth muscle cells (1). Further analyzing 6 groups of mesenchymal cells, Fibro-mesenchymal stromal cells (MSCs), Osteofibro-MSCs, Osteo-MSCs, Osteoblasts, Adipo-MSCs, and THY1+ MSCs, with distinct markers, only Fibro-MSCs, marked by HAS1, DPT, and PDPN, expressed canonical mesenchymal stem markers and were identified as the most primitive population by CytoTRACE. Contributing a variable proportion of mesenchymal cells (52% +/- 31%, mean +/- SD), THY1+ and Adipo-MSCs highly expressed adipogenic markers. However, THY1+ MSCs had a unique expression profile including THY1 and LBP, and a high CytoTRACE score. We designed a flow panel to sort Fibro-, Thy1+-, Osteo-, and Adipo-MSCs. Fibro-MSCs showed the highest CFU-F forming ability and maintained the highest proliferative status over the long term culture, followed by THY1-MSCs, while Osteo- and Adipo-MSCs grew poorly. Fibro-MSCs also differentiated into osteogenic and adiopogenic cells efficiently in culture, confirming their stem and progenitor properties. CellChat analysis revealed that Adipo- and Thy1+-MSCs produce the highest amount of CXCL12 and KITL to regulate HSPCs and specifically express IL7 to regluate lymphopoiesis. Csf1, a major melopoiesis cytokine, was expressed in Adipo-MSCs, and Notch ligands, which are also important for lymphopoiesis, were mainly produced by arteriol endothelial cells. Together, our work presents a first comphrehensive cellular atlas of adult human bone marrow, identifies a new primitive MSC population, and reveals the importance of adipoprecursors in supporting hematopoeitic function.

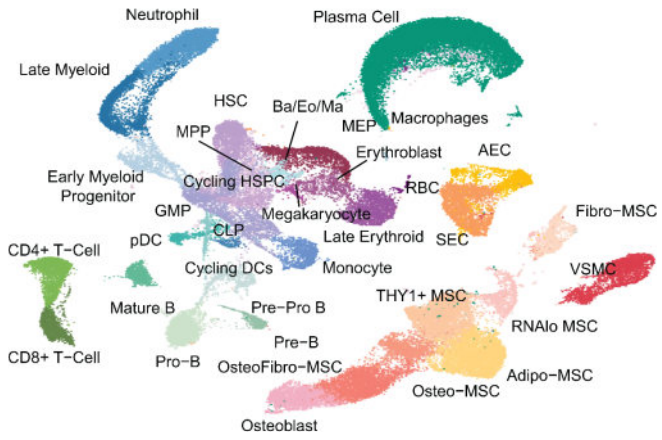

***Disclosures: Michael Duffy**, None*

FRI-296

Spatial Proteomics via Mass Spectrometry Imaging of Human Tibial Plateaus Reveals Alterations to Subchondral Bone Precede Cartilage Loss in Medial Osteoarthritis *Charles Schurman[6], Jonathan Woo[2], Nannan Tao[3], Tamara Alliston[4], Peggi Angel[5], Birgit Schilling[6]. [6]Buck Institute for Research on Aging, , [2]University of California - San Francisco, United States, [3]Bruker Scientific, United States, [4]University of California, San Francisco, United States, [5]Medical University of South Carolina, United States, [6]Buck Institute for Research on Aging, United States

Osteoarthritis (OA) of the knee is a degenerative condition of the skeletal extracellular matrix (ECM) marked by the loss of articular cartilage and changes in the underlying bone. OA commonly displays spatial discrimination preferring either the lateral or medial joint, while evidence of early degenerative changes may be found across the entire joint and even in 'healthy' joints of aged individuals. Matrix-assisted laser desorption/ionization (MALDI) mass spectrometry imaging (MSI) offers the ability to spatially investigate the proteomic landscape of OA progression in bone and cartilage to elucidate mechanisms of joint degeneration.Human tibial plateaus from BMI matched male donors aged 60-75 with and without diagnosed medial OA (N=5 patients each) were formalin fixed and decalcified to prepare for paraffin embedding and sectioning. Mounted tissue sections were prepared for MSI with a collagenase treatment to target ECM components and imaged utilizing the Bruker timsTOF fleX mass spectrometer. Untargeted and guided statistical comparisons of collected MS1 mass spectra were processed using the Bruker SCiLS Lab software package.We demonstrate the first simultaneous collection of spatial ECM proteomic spectra from human bone and cartilage from tibial plateaus of healthy and OA patients. Visualization of detected ions revealed striking separation in the abundance of features assignable to human cartilage and bone via principal component analysis (PCA). Unsupervised spatial clustering of the top 500 MS1 precursor ions from diseased joint tissue revealed progressive subchondral bone sclerosis from the medial joint where cartilage loss was the greatest into the lateral joint despite a thick identifiable cartilage layer. Statistical comparison via SCiLS found 35 ions specific to the most severe OA regions that were confirmed as derived from bone and cartilage collagen chains ?-1(I) and ?-1(II) while new unannotated peptides were identified by MS/MS as belonging to other 10 other collagen sub-types and 37 additional ECM proteins including aggrecan, biglycan, and others. Some of these signature markers were identified at lower abundance in the transitional region between cartilage and bone in aged-control joint samples, offering possible novel markers of early OA with age. The spatial up-regulation of certain collagens and ECM-derived peptides in OA and their unexpected appearance in aged-healthy joints reveal new molecular details about the development of OA.

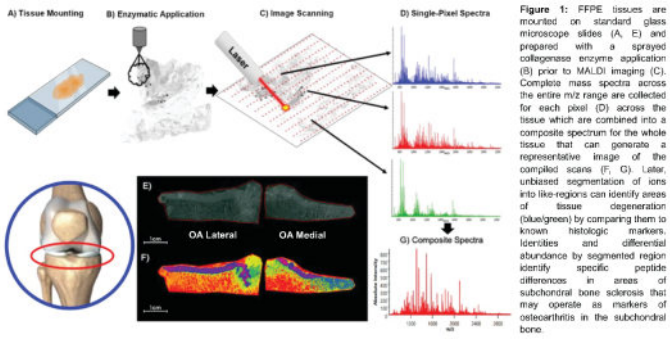

Figure 1: FFPE tissues are mounted on standard glass microscope slides (A, E) and prepared with a sprayed collagenase enzyme application (B) prior to MALDI imaging (C). Complete mass spectra across the entire m/z range are collected for each pixel (D) across the tissue which are combined into a composite spectrum for the whole tissue that can generate a representative image of the compiled scans (F, G). Later, unbiased segmentation of ions into like-regions can identify areas of tissue degeneration (blue/green) by comparing them to known histologic markers. Identities and differential abundance by segmented region identify specific peptide differences in areas of subchondral bone sclerosis that may operate as markers of osteoarthritis in the subchondral bone.

***Disclosures: Charles Schurman**, None*

FRI-298

Large-Scale Integration of Human Bone Proteomics, Circulating Proteomics and Genetics to Discover Molecular Pathways and Risk Factors of Osteoporotic Fractures *Yi-Hsiang Hsu[1], Sjur Reppe[2], Fangtang Yu[3], Xue Zeng[4], Ming-Ju Tsai[3], Ronald Kwon[5], Kaare Gautvik[2]. [1]HSL Institute for Aging Research, Harvard Medical School, United States, [2]Oslo Univ. Hosp., Oslo, Norway, Norway, [3]HSL Marcus Institute for Aging Research , United States, [4]Amgen, United States, [5]University of Washington, United States

Despite significant progress being made in mapping the basic blueprints (DNA variants) of human diseases, we have yet to comprehensively decipher the myriad end products (proteins) contributing towards these diseases. Thus, proteomics is an emerging tool and a deeper view of proteome alterations in bone tissues from fractures will advance our understanding of molecular pathways and enhance new drug target discovery. In addition, identifying circulating protein biomarkers allows us to identify high risk subjects of fractures. Two proteomics studies were conducted. (1) Bone proteomics was measured by mass spectrometry on human hip bone biopsies from 180 hospitalized adults due to hip replacement surgeries. The whole genome seq was done and DXA FNBMD was measured at non-fracture hip. (2) Serum (circulating) proteomics was measured by OLINK immunoassays in 48,000 UK Biobank subjects. Incident osteoporotic fractures were assessed via eHR. Among them, 237 had osteoporotic fractures and 5,217 had DXA BMD. In both studies, differential protein expression analyses were performed w/wo adjusting for BMD to identify proteins contributing to fractures independently from BMD. Mendelian randomization (MR) analyses were performed to inference causally relations. We observed 6,154 proteins from hip bone biopsies. 198 (88 higher and 110 lower expressed) proteins significantly differentially expressed ($p < 1.7x10-5$) in fracture subjects comparing to controls. These proteins are enriched in terpenoids biosynthesis, ECM-receptors, cytokine-ligand-receptor interactions and TGF-beta, NFKB, PPAR signaling pathways. For example, SOST, VKDPs and EFEMP1 are associated with increased fracture risks. COL6A1, osteoadherin and osteopontin are associated with decreased risks. MR analyses adjusted for BMD identified proteins (e.g. CA2, EIF3I, EFEMP1) associated with fractures independently from BMD. For circulating proteomics, 2,941 proteins were measured. 81 (69 higher and 12 lower expressed) proteins significantly associated with incident osteoporotic fracture (e.g. SOST, GDF15, IL6). In conclusion, we identified novel proteins causally associated with osteoporotic fracture from hip bone biopsies. Not all the fracture-associated proteins observed in bone biopsies could be observed in circulating (plasma); thus, our finding provided tissue-specific molecular insights underlying osteoporotic fractures. We also identified novel circulating proteins predicating risks of incident fractures.

***Disclosures: Yi-Hsiang Hsu**, None*

FRI-300

Pharmacogenetic and microRNA mechanisms of beta blocker treatment response in bone *Christine Lary[2], Griffin Scott[2], Hongyu Chen[2], Archana Nagarajan[3], Elizabeth Atkinson[4], David Monroe[5], Aaron Brown[6], Katherine Motyl[7], Sundeep Khosla[8]. [2]Northeastern University, , [2]Northeastern University, United States, [3]Tufts University School of Biomedical Sciences, , [4]Mayo Clinic, United States, [5]Mayo Foundation, United States, [6]MaineHealth Institute for Research, United States, [7]MaineHealth, United States, [8]Mayo Clinic College of Medicine, United States

Atenolol, a beta-1 selective beta blocker (BB), is being evaluated to prevent postmenopausal bone loss in the randomized clinical trial, "Atenolol for the Prevention of Osteoporosis". Atenolol inhibits norepinephrine binding of the beta-1 and beta-2 adrenergic receptors (b1-AR and b2-AR) on osteoblasts and osteoclasts (Figure A). Previous pharmacogenetic effects have been found in b1-AR (ADRB1) and in HDAC4, a histone deacetylase that stabilizes ATF4-mediated upregulation of TNFSF11 (RANK Ligand) in osteoblasts. We have also shown that miR-19a-3p, which is associated with BB treatment response for hypertension, and which targets both b1-AR and HDAC4, is positively associated with BB use, bone mineral density (BMD), and reduced fracture risk. However, these associations have not been studied longitudinally with BB treatment. We analyzed pharmacogenetic data using variants from ADRB1, ADRB2, and HDAC4 in a pilot clinical trial performed at the Mayo Clinic in 155 postmenopausal women randomized to placebo, propranolol (40 mg or 80 mg), atenolol (50 mg), or nebivolol (5 mg) daily for 20 weeks. We also collected miRNA-seq data at baseline and endpoint from 24 participants, 9 each from the atenolol group with high response (HR) or low response (LR) based on changes in C-terminal telopeptide (CTX), and 6 from the placebo group. We modeled the change in BMD at the femoral neck (FN), lumbar spine (LS), or ultradistal radius (UDR) or in serum CTX as a function of baseline values, SNP dosage, treatment group, and their interaction. Longitudinal miRNA-seq data was analyzed using negative binomial regression with generalized linear mixed models. An increase in UDR BMD for the propranolol 80 mg group was found compared to placebo for each additional copy of the ADRB1 rs1801252 G allele (Figure B), and an increase in LS BMD and decrease in CTX was found for the atenolol group for each additional copy of the HDAC4 rs11124190 G allele (LS BMD in Figure C). miR-19a-3p was associated with a significant increase in the low responder group over time compared with placebo (OR = 2.8, p= 0.028) and with a trend towards significance in the combined atenolol groups (OR = 2.2, p=0.06, Figure D). Taken together these results are consistent with a mechanism in which genetic variation or miR-19a-3p-induced suppression of b1-AR and HDAC4 is associated

with improved treatment response. These results will be validated in an ongoing ancillary study for the APO clinical trial.

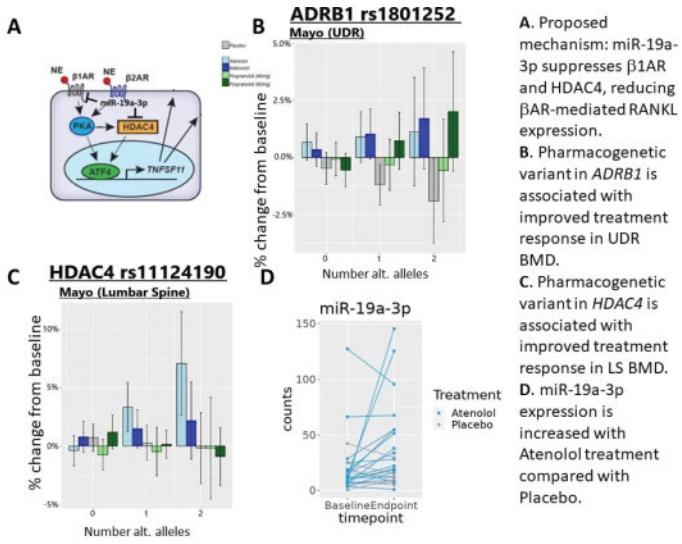

A. Proposed mechanism: miR-19a-3p suppresses β1AR and HDAC4, reducing βAR-mediated RANKL expression.
B. Pharmacogenetic variant in *ADRB1* is associated with improved treatment response in UDR BMD.
C. Pharmacogenetic variant in *HDAC4* is associated with improved treatment response in LS BMD.
D. miR-19a-3p expression is increased with Atenolol treatment compared with Placebo.

***Disclosures: Christine Lary**, None*

FRI-302

Augmentation of BMP signaling leads to ectopic cartilages through changes in chromatin structures *YUJI MISHINA[1,] Hiroki Ueharu[1.] [1]University of Michigan,

Dysregulation of proliferation, migration, and differentiation of cranial neural crest cells (NCCs) develop craniofacial anomalies. We have reported that enhanced BMP signaling in NCCs (caAcvr1; P0-Cre mice, mutant mice hereafter) developed ectopic cartilages in the midfacial region at embryonic day 14.5 (E14.5). Pharmacologic rescue experiments using an inhibitor for BMP signaling revealed that a time window for suppression of ectopic cartilage formation is at E11.5, which is a stage before the initiation of the ectopic cartilage formation. We hypothesize that augmentation of BMP signaling directs the multipotency of cranial NCCs towards chondrogenesis. This study aims to reveal the mechanism for cell fate specification of cranial NCCs by BMP signaling. We compared gene expression profiles in cranial NCCs between control and mutant mice at E10.5 by single cell RNA sequence. In the mutant embryos, cranial NCCs formed the ectopic cartilages, but trunk NCCs did not, thus we speculated that genes changed only in cranial NCCs of mutant mice but not in trunk NCCs involve in the formation of ectopic cartilage. Through these 2 way comparisons, we identified 11 genes of which expressions are specifically changed in mutant cranial NCCs. Among these genes, we found that Xist, a main player for X chromosome inactivation, is significantly increased in cranial NCCs of mutant mice. We further observed that cranial NCCs in mutant female embryos have ectopic X chromosome inactivation: one cell has two inactive X chromosomes that are entirely coated with Xist RNA. Surprisingly, ectopic X chromosome inactivation was also found in cranial NCCs of mutant male mice, which should not have X chromosome inactivation. This finding may explain the fact that both male and female mutant mice develop ectopic cartilage in a comparable manner. We demonstrated that silencing of Xist in cranial NCCs decreases chondrogenic differentiation capacity in vitro, and genetic reduction of Xist in mutant mice by deletion of Kdm5C, a known factor positively regulates Xist expression, significantly reduced formation of ectopic cartilages. These results suggested that enhanced BMP signaling develops the ectopic cartilages through induction of ectopic X chromosome inactivation. This is for the first time to demonstrate BMP-Xist axis contributes cell fate specification of cranial NCCs in both sexes.

***Disclosures: YUJI MISHINA**, None*

FRI-306

Differential transcriptional responses to intracellular infection by S. aureus in osteoclasts and their precursors. *Luke O'Connor[1,] Deborah Veis[2.] [1], [2]Washington University in St. Louis School of Medicine, United States

S. aureus is an opportunistic pathogen that causes 30-50% of all osteomyelitis (OM) cases. During OM, S. aureus survive in colonies, as well as within osteocytes, osteoblasts, and osteoclasts (OCs). We have recently shown that OCs, unlike their bone marrow macrophage (BMM) precursors, allow bacteria to replicate intracellularly and the magnitude of growth increases with OC differentiation . We hypothesized that OC differentiation alters host-pathogen interactions by changing nutrient availability and host defense pathways to favor intracellular S. aureus growth. To test this, we conducted dual RNA-seq to analyze host and S. aureus gene expression at 4 critical infection timepoints: prior to infection, after bacterial internalization (2h), during bacterial metabolic transition (6h), and after bacterial expansion in OCs or killing in BMMs (21h). Bone marrow was cultured from 6-7 week-old male B6/alb mice, and BMMs (MCSF only) or OCs (3 days RANKL) generated prior to infection with USA300 MRSA strain TI3. To ensure data robustness we sequenced 3 batches of pooled samples per cell type, with each pool representing 3 mice and 3 separate infections (total: 18 mice, 10 infections). S. aureus transcripts were aligned to S. aureus USA300_FPR3757 and DESeq2 used to analyze genes differentially expressed by cell type (BMM vs OC) over the time course. In parallel, we used PyModulon to analyze modules of co-regulated genes in bacteria. These analyses show that bacteria in OCs have lower expression of Fur regulated iron scavenging genes as well as genes related to CodY, PerR, PurR, and CymR, which regulate amino acid metabolism. Thus, S. aureus in OCs may be less stressed for iron and amino acids than bacteria in BMMs. Murine host transcripts were aligned to Mm39 and analyzed in DESeq2, followed by supplemental analysis with Gene Ontology (GO) enrichment and using weighted coregulated gene network analysis (WGCNA). GO analysis highlights that OC and BMM responses largely differ in host defense and bacterial response pathways. WGCA of all differentially expressed genes and a subset of genes from the top 10 GO identify Pi3kr1, Id2, and ZO-2 as genes highly interconnected with differential host response and indicate a potential roles for PI3K, TGF-?, and Hippo signaling pathways. Collectively these results suggest OCs have an altered response to infection and provide greater access to nutrients than their BMM precursors, allowing S. aureus expansion in OCs but not BMMs.

***Disclosures: Luke O'Connor**, None*

FRI-312

In vivo stimulation of Tfeb, a master regulator of autophagy and lysosomal biogenesis, via in vivo CRISPR activation increases bone mass and strength *Alicen James[2,] James Hendrixson[2.] Ilham Kadhim[2.] Jacob Laster[2.] AMY SATO[3,] Stuart Berryhill[2.] Julie Crawford[2.] Melda Onal[2.] [2]University of Arkansas for Medical Sciences, [2]University of Arkansas for Medical Sciences, United States, [3]UAMS, United States

Autophagy is a recycling pathway in which cellular components, including damaged or dysfunctional proteins, protein aggregates, and organelles are delivered to lysosomes for degradation. Reduction or insufficiency of autophagy is thought to contribute to a number of skeletal diseases such as skeletal aging. Accordingly, elimination of autophagy from the entire osteoblast lineage or only from osteocytes reduces osteoblast number, decreases bone formation, and causes low bone mass. However, whether increasing autophagy in osteoblast lineage cells is beneficial for bone health under physiological or pathological conditions is unknown. To address this, we generated a novel model to increase endogenous Tfeb expression in the osteoblast lineage. Transcription factor EB (Tfeb) is a master transcriptional regulator of autophagy and lysosomal biogenesis. Consistent with this, Tfeb overexpression (OE) induces autophagy in cultured osteoblasts. We stimulated expression of the endogenous Tfeb gene in osteoblast lineage cells of mice via in vivo CRISPR activation. Specifically, we expressed a sgRNA targeting the Tfeb transcription start site from the Rosa26 locus and activated a dCas9::SPH transgene using the Osx1-Cre transgene. This maneuver increased Tfeb expression 2.5-fold in RNA isolated from whole bones. At 8 weeks of age, the skeletal phenotype of mice overexpressing Tfeb was similar to littermate controls. However, at 4 months of age, Tfeb overexpressing male mice displayed increased femoral and vertebral cortical thickness. Histological analysis revealed that the increase in femoral cortical thickness was due to increased bone formation. Tfeb OE was also anabolic for femoral and vertebral cancellous bone. Analysis of osteoblast and osteoclast marker gene expression in lumbar vertebrae revealed that the anabolic impact of Tfeb OE was associated with high bone turnover. Moreover, the anabolic actions of Tfeb OE were sufficient to elevate bone strength as determined by femoral three-point bending analysis. Similar to males, serial BMD measurements of female mice showed that Tfeb OE in the osteoblast lineage also increases bone mass of female mice. Moreover, the high bone mass of female mice became more pronounced between 3 to 8 months of age. In conclusion, Tfeb overexpression in osteoblast lineage cells is anabolic and results in mechanically stronger bones and may represent an effective approach to combat age-associated bone loss.

***Disclosures: Alicen James**, None*

FRI-316

Wnt10b is required for the bone anabolic effect of a natural antibody that blocks oxidized phospholipids. *Michela Palmieri[1,] Intawat Nookaev[2,] Maria Jose Almeida[3,] Ha-Neui Kim[4,] Teenamol E Joseph[1,] Stavros Manolagas[3,] Charles O'Brien[5,] Elena Ambrogini[3.] [1]Division of Endocrinology and Metabolism, Center for Musculoskeletal Disease Research, University of Arkansas for Medical Sciences and the Central Arkansas Veterans Healthcare System, United States, [2]2Department of Biomedical Informatics, University of Arkansas for Medical Sciences, United States, [3]Central Arkansas VA Healthcare System, Univ of Arkansas for Medical Sciences, United States, [4]Univ. Arkansas for Medical Sciences, Central Arkansas VA Healthcare System, United States, [5]Univ of Arkansas for Medical Sciences, United States

Oxidized phospholipids containing phosphatidylcholine (PC-OxPLs), present on oxidized low-density lipoproteins (OxLDL) and apoptotic cells, are pathogenic in many dis-

eases, including osteoporosis, atherosclerosis, and non-alcoholic steatohepatitis. OxPLs decrease Wnt and BMP2 signaling, induce ferroptosis and stimulate pro-inflammatory cytokine production. The natural antibody IgM E06 binds PC-OxPLs and blocks their deleterious effects. Transgenic expression of the antigen-binding domain of E06 (E06-scFv) increases bone mass in 6-month-old mice and attenuates high fat diet- and age-induced bone loss by increasing osteoblast number and function. It was shown earlier that E06-scFv upregulates the expression of Wnt10b and Wnt signaling in vivo, but not other Wnt ligands. We investigated the mechanism(s) mediating the anabolic effect of E06-scFv. Single cell RNA-sequencing (scRNA-seq) of mesenchymal cells, isolated from long bones of 7-month-old female mice, revealed a 3-fold increase in Wnt10b expression (adj-P=3.04E-11) in pre-osteoblasts and osteoblasts obtained from E06-scFv transgenic mice compared to cells from WT mice. Wnt target genes were also upregulated. An integrated analysis of 9 published scRNA-seq datasets from bone resident mesenchymal and hematopoietic cell types revealed that the bulk of Wnt10b in the bone microenvironment originates from cells of the osteoblast lineage. Consistent with this evidence, OxLDL decreased Wnt10b and Wnt target genes in calvaria- and bone marrow-derived osteoblastic cell cultures but had no impact on ferroptosis of osteoblastic cells. Moreover, gene expression markers of ferroptosis, as well as BMP2 signaling pathways, were similar in the mesenchymal cells from E06-scFv and WT mice as determined by scRNA-seq. Expression of inflammatory cytokine genes was also similar in vertebral bone by bulk-RNA-seq, and in myeloid cells by scRNA-seq, of WT and E06-scFv mice. To examine the requirement of Wnt10b in the anabolic activity of E06-scFv, we next determined the effect of Wnt10b deletion on the bone phenotype in WT vs E06-scFv transgenic male mice at 6 months of age. We found that both the increase in BMD by DXA and BV/TV of vertebral and femoral cancellous bone by micro-CT were prevented in E06-scFv transgenic mice lacking Wnt10b. Collectively, these findings indicate that the bone anabolic effect of E06-scFv is due to increased Wnt10b expression that results from removal of the suppressive effects of PC-OxPL.

***Disclosures: Michela Palmieri**, None*

FRI-317

Inactivation of the Polycomb Repressive Complex 2 in Osteoblasts Increases Trabecular Bone Mass and Results in Mechanically Stronger Bones *Amel Dudakovic[1,] Sofia Jerez[1,] Christopher Paradise[1,] M. Lizeth Galvan[1,] Oksana Pichurin[1,] Padmini Deosthale[2,] Roman Thaler[1,] Lilian Plotkin[2,] Andre van Wijnen[3,] [1]Mayo Clinic, United States, [2]Indiana University School of Medicine, United States, [3]University of Vermont, United States

Epigenetics, including post-translational modifications of histones, control osteoblast activity and bone formation. The Polycomb Repressive Complex 2 (PRC2) methylates H3 at lysine 27 (H3K27me3), a heterochromatin mark that suppresses gene expression. PRC2 is made of two main structural proteins, Eed and Suz12, and one of two methyltransferases, Ezh1 or Ezh2. We and others showed that Ezh2 inhibition stimulates osteoblast differentiation in vitro and bone formation in vivo. However, Ezh2 loss in osteoblasts (Osx-Cre) is not bone stimulatory in vivo. Thus, the mechanistic understanding of the divergency between Ezh2 inhibition and Ezh2 loss on bone formation remains elusive. These studies build on our findings that Ezh2 is expressed in progenitors while Ezh1 is expressed in committed osteoblasts. We reasoned that loss of the entire PRC2 function will stimulate bone formation. We generated mice in which Ezh1 is depleted globally and Ezh2 is lost in osteoblasts (control = Osx-Cre; Ezh1 KO = Ezh1-/-: Osx-Cre; Ezh2 cKO = Ezh2f/f: Osx-Cre; dKO = Ezh1-/-: Ezh2f/f: Osx-Cre). Ezh1 and Ezh2 dKOs male and female mice exhibited significantly increased trabecular bone (μCT) and bone strength (3-point bending) when compared to controls, Ezh1 KOs, and Ezh2 cKOs (8 weeks). While doxycycline (Cre suppression) prevented this phenotype in dKOs (8 weeks), its removal (8 weeks) to inactivate Ezh2 in osteoblasts (on a Ezh1 null background) lead to a significantly higher trabecular bone mass (14 weeks). We next assessed the effects of targeting PRC2 scaffolding proteins. Eed inhibitors A395 and EED226 enhanced osteogenic differentiation of MC3T3 pre-osteoblasts as assessed by RNA expression (e.g., Bglap and Ibsp) and alizarin red staining (mineral deposition). Similarly, siRNA mediated Eed or Suz12 loss stimulated MC3T3 differentiation. Because Eed can be targeted by small molecules, our initial in vivo studies focused on Eed over Suz12. μCT analysis revealed a significant enhancement of trabecular bone and bio-mechanical bone properties in male and female Eed cKOs (8 weeks). Together, these studies reveal that loss of PRC2 functionality in osteoblasts, through dual Ezh1 and Ezh2 or Eed inactivation, results in high bone mass and mechanically stronger bones. Our findings may enhance the development of novel therapeutic strategies focused on the inactivation of PRC2 to stimulate short-term or sustained bone formation.

***Disclosures: Amel Dudakovic**, None*

FRI-319

WNT16 Regulates Mitochondrial Function and Smooth Muscle Cell Phenotype Via Yap /Taz Signals To Restrain Vascular Remodeling and Mitigate Cardiovascular Risk *Abraham Behrmann[1,] Dalian Zhong[1,] Li Li[1,] Shangkui Xie[1,] Megan Mead[1,] Parastoo Sabaeifard[1,] Mohammad Goodarzi[1,] Andrew Lemoff[1,] Julia Kozlitina[1,] Dwight Towler[1,] [1]UT Southwestern Medical Center, United States

Deterioration in bone and vascular health are frequent concomitants with aging, highlighted by the surgeon-pathologist Jean Lobstein who first coined the terms “osteoporosis” and “arteriosclerosis” as he described this relationship. Wnt16 is selectively expressed in bone and arterial vascular smooth muscle (VSM), and hypomorphic WNT16 alleles convey fracture risk. We show that these same WNT16 cSNPs also convey risk for composite cardiovascular (CV) events in the Dallas Heart Study (OR = 1.25, p = 0.02; adjusted for age, systolic blood pressure / SBP, body mass index, sex & ancestry)/ To better understand Wnt16’s role in vascular medicine, we generated Wnt16-deficency in LDLR-/- mice, a validated background for studying CV disease. SBP & vessel stiffness were reduced in Wnt16-/-;LDLR-/- mice vs. LDLR-/- controls. Ascending aorta (AscAo) aneurysm following angiotensin-II (AngII) infusion was worsened with Wnt16 deficiency. VSM contractile markers such as Acta2 - known to convey AscAo aneurysm risk & reduce SBP with genetic deficiency - were down-regulated in Wnt16-/- VSM, with reduction in TGFbeta-induced contraction. Mitochondrial spare respiratory capacity was significantly impaired with Wnt16 deficiency and restored by exogenous Wnt16 treatment. LC-MS/MS revealed Acta2 protein was reduced in Wnt16-/-;LDLR-/- VSM as was aortic Ankrd1- a target of Yap and Taz(Wwtr1) activation via nuclear TEAD-directed transcription. Wnt16-/- VSM exhibited reduced nuclear Yap+Taz protein. RNAi targeting either Wnt16 or Taz phenocopied Wnt16 deficiency, inhibited Wnt16 up-regulation of the mature contractile VSM phenotype & reversed C3 (dedifferentiation biomarker) suppression. By contrast,Yap1 mediated cytokine suppression. RNAi targeting Yap/Taz inhibitory kinases Lats1/2 or Ccm2 -- but not Ccm3 or Stk3/Stk4 -- elicited responses reciprocal to Wnt16 deficiency. Biotin proximity labeling following Taz-BioID2 expression identified TEAD1, IQGAP3, & GPR180 as functionally important Wnt16 signaling mediators. TEAD cognates in the Acta2 promoter conveyed transcriptional responses to Wnt16 and Taz+Tead1, and Wnt16 treatment increased Taz association with the Acta2 promoter in aortic VSM. Thus, in addition to known roles in bone, Wnt16 also promotes the VSM contractile phenotype and mitochondrial function in the vasculature ro regulate arterial remodeling. Strategies that augment Wnt16 signaling relays may help preserve both cardiovascular and skeletal health with aging.

***Disclosures: Abraham Behrmann**, None*

FRI-320

C-Jun N-terminal Kinase (JNK) Isoform 2 Augments Human Osteoblast Differentiation by Integrating Bone Morphogenetic Protein Signaling and Canonical Notch Signaling *Yadav Wagley[1,] Benjamin Graham[2,] Kurt Hankenson[2,1], [2]University of Michigan, United States

The c-Jun N-terminal kinases (JNK) are evolutionary conserved regulators of proliferation, differentiation, and cell death responses. In vivo studies have shown that Jnk1-/- and Jnk2-/- mice display varying degrees of osteopenia due to impaired bone formation. However, JNK1 and JNK2 isoform specific contribution to human osteoblast differentiation is lesser known. Here, we used small interfering RNA-mediated knockdown of JNK1 and JNK2 in bone-marrow derived human mesenchymal stem cells (hMSC) to evaluate their role in BMP-mediated osteoblast differentiation. Histochemical staining for alkaline phosphatase (ALP) expression and extracellular matrix mineralization using Alizarin red S showed that JNK2 activity is essential for hMSC osteoblastic differentiation, whereas JNK1 activity was dispensable. Gene expression analysis revealed a minimal effect on BMP-dependent RUNX2 and SP7 expression after JNK2 knock-down, but their levels were enhanced in JNK1 silenced cells. Since, BMP signaling requires canonical Notch signaling to promote human osteoblastogenesis, we evaluated JNK-isoform specific effects on Notch signaling components. The expression of Notch ligand JAG1 and downstream Notch target genes HES1 and NOTCH3 was reduced in response to BMP stimulation of JNK2 silenced cells, while the effects were modest after JNK1 knock-down. Consequently, the absolute requirement of JAG1 for BMP-mediated hMSC osteoblastogenesis was established as JAG1 silenced hMSC failed to enhance ALP expression and extracellular matrix mineralization. Finally, we generated JNK2-deficient immortalized hMSC using CRISPR-Cas9 genome editing and subjected these cells to BMP2 stimulation. Corresponding to the results with siRNA, JNK2 knock-out cells failed to produce extracellular matrix mineralization in response to BMP2. Collectively, these results establish a regulatory role of JNK2 in human osteoblast differentiation and suggest that it functions by integrating canonical BMP/SMAD signaling and Notch signaling in human cells.

***Disclosures: Yadav Wagley**, None*

FRI-322

ClC-3 and ClC-5 are essential to drive normal bone mineralization. *Quitterie Larrouture[2], Irina Tourkova[2], Deborah Nelson[3], Paul Schlesinger[4], Harry Blair[2]. [2]University of Pittsburgh, , [2]University of Pittsburgh, United States, [3]University of Chicago, United States, [4]Washington University , United States

Osteoblasts form an epithelial-like layer that separates the extracellular fluid (ECF) that contains the essential components to bone formation from the bone matrix. The production of hydroxyapatite in bone matrix produces a massive number of protons and their removal is essential to avoid stopping the mineralization process. Previously we established that Na/H exchangers 1 and 6 are highly expressed at secretory osteoblast basolateral surfaces and neutralize massive acid loads. We hypothesized that high-capacity proton transport from matrix into osteoblast cytosol must exist to support acid transcytosis for mineral deposition. Gene screening of cultured mineralizing osteoblasts showed dramatic expression of chloride-proton antiporters ClC3 and ClC5. Localization of ClC3 and ClC5 proteins at the apical secretory surface facing the bone matrix was confirmed by antibody labeling, at the EM level, of plasma membrane ClC3, and ClC5, in ClC3 knockout mice (Figure). To study the importance of ClC3 and ClC5 in bone mineralization in vivo and in vitro we used ClC-5 KO mice as well as ClC-3 KO mice. The whole exome sequencing confirmed the deletion of the whole exon 7 in ClC-3 KO mice and the deletion of part of the exon 6 in ClC-5 KO mice. No additional deletions were detected. The ClC-3 KO mice sowed a mildly disordered mineralization (microCT) and serum level of ALP and TRAP compared to WT. Surprisingly, at 3-5 months, body weights of ClC-5 KO females were significantly higher than control mice and 3D morphometry of the lumbar vertebrae showed a significant increase in bone surface/volume ratio in CLC-5 KO mice compared to control. Mass spectrometry-based proteomics confirmed that both KO mice have the presence of modified dysfunctional protein not seen in WT mice). In CLC-3 KO mice the normal CLC-5 protein was increased confirming what we showed previously that cultured ClC-3 KO osteoblasts have an increase in ClC-5 protein expression. After isolation from the bone marrow, CLC-3 KO and CLC-5 KO stromal stem cells were differentiated on PET membrane showing a lower alkaline phosphatase activity, a weak staining with Von Kossa as well as a decrease in collagen production, suggesting a decreased bone turnover. We conclude that regulated acid export, mediated by chloride-proton exchange, is essential to drive normal bone mineralization, and that CLC transporters also regulate fine patterning of bone.Figure: Transmission electron microscopy of mouse vertebrae showing the presence of CLC-5 (immunogold labeling, 12nm) at the apical secretory surface (red arrows) of an osteoblast facing the bone matrix (blue stars).

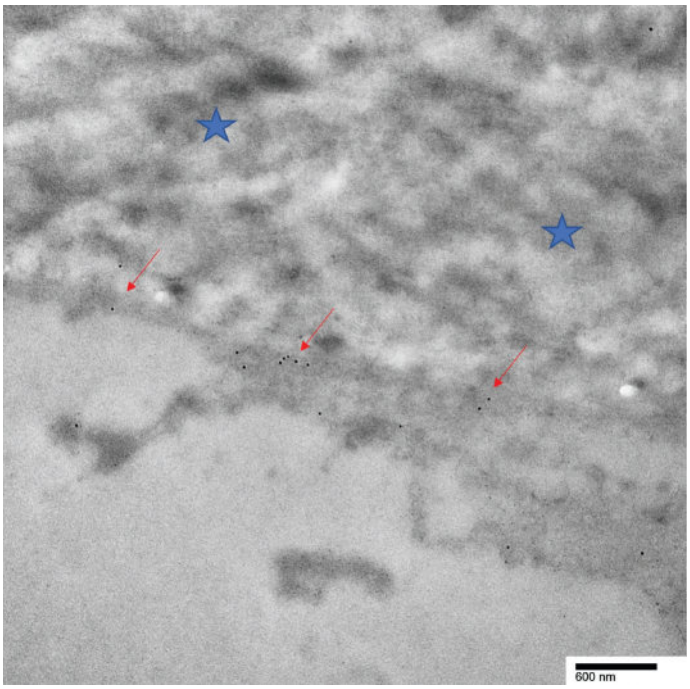

***Disclosures: Quitterie Larrouture**, None*

FRI-324

Nuclear factor I A (NFIA) regulates osteoblast differentiation of skeletal progenitor cells in bone growth and fracture healing in mice *Hiroaki Manabe[1], Noriaki Ono[2]. [1]The University of Texas Health Science Center at Houston, United States, [2]University of Texas Health Science Center at Houston School of Dentistry, United States

NFIA is a transcription factor belonging to the nuclear factor I family and has key roles in the development of multiple organs. NFIA is known to interact with other transcription factors such as SOX9 during glial cell differentiation; however, the function of NFIA in skeletal development remains unknown. We evaluated the skeletal phenotype of mice in which NFIA was conditionally deleted in a cell type-specific manner. For this purpose, Nfia-floxed mice were crossed with Col2a1-cre (chondrocytes), Osx-creER (osteoblasts, pulsed at postnatal day (P) 3) or Prrx1-cre (skeletal progenitor cells) drivers. Deletion of NFIA in chondrocytes or osteoblasts did not cause any apparent bone phenotype. In contrast, NFIA deletion in skeletal progenitor cells using Prrx1-cre (Prrx1-NFIA cKO) resulted in a significant decrease in trabecular bone mass at P21 and 8 weeks of age (W), associated with an increased cortical thickness at 8W. Bone histomorphometry revealed a reduction in osteoblast numbers and an unchanged osteoclast number per bone perimeter in Prrx1-NFIA cKO mice, associated with decreased trabecular but increased cortical bone formation rates as determined by calcein double labeling, accompanied by the significant reduction of the serum bone formation marker PINP level. In contrast, the growth plate of Prrx1-NFIA cKO mice showed only modest structural changes, associated with no overt change in the expression level of chondrocyte marker genes as determined by qPCR. In addition, upon the complete fracture of the mid-shaft, Prrx1-NFIA cKO femurs showed normal callus formation but delayed calcification of the healing site. In primary cell culture, bone marrow stromal cells (BMSCs) isolated from Prrx1-NFIA cKO mice showed reduced alkaline phosphatase and alizarin red staining, indicating impaired osteogenic potential of skeletal progenitor cells. Bulk RNA-seq analyses of NFIA-deficient BMSCs identified 53 differentially expressed genes including downregulation of Ibsp (encoding bone sialoprotein, BSP), Igfbp2, and Camk4, which are known to play important roles in osteoblast differentiation. Interestingly, inspection of the genome-wide association study (GWAS) catalog database revealed 6 SNPs statistically significantly associated with heel bone mineral density, implicating a role of NFIA in human bone metabolism. Our study demonstrates that NFIA plays an important role in osteoblast differentiation of skeletal progenitor cells in bone growth and fracture healing.

***Disclosures: Hiroaki Manabe**, None*

FRI-326

Mitochondrial dysfunction and integrated stress response in G610C mouse osteoblasts *Elena Makareeva[1], Megan Sousa[1], Laura Gorrell[1], Shakib Omari[1], Satoru Otsuru[2], Sergey Leikin[1]. [1]National Institutes of Health, United States, [2]University of Maryland, United States

Osteoblast cell stress caused by the misfolding of procollagen has been shown to be an important factor in bone pathology resulting from Gly substitutions in osteogenesis imperfecta (OI). Our previously published studies of G610C mice with a Gly610Cys substitution in the triple helical region of the ?2(I) chain of type I collagen revealed increased EIF2? phosphorylation and ensuing integrated stress response (ISR) in osteoblasts without upstream unfolded protein response (UPR). Instead, upregulated expression of Hspa9 and Atf5 encoding mitochondrial paralogues of BIP and ATF4 suggested mitochondrial involvement in the ISR activation, probably via disruption of ER-mitochondria contacts. In the present study, we tested this hypothesis in primary osteoblast cultures by investigating which of the four EIF2? kinases activate the ISR and by imaging mitochondrial dynamics, ATP, and reactive oxygen species (ROS). We observed altered mitochondrial fission, increased ROS production in differentiating osteoblasts, reduced ATP synthesis in mature cells, and EIF2? phosphorylation by GCN2 rather than PERK in response to the G610C mutation. Taken together with our published studies of G610C procollagen trafficking in osteoblasts, these observations suggest the following ISR activation mechanism. Like all secretory proteins, the procollagen precursor of collagen is folded in the ER and exported through ER exit sites (ERESs). Its triple helix misfolding, however, is detected at ERESs rather than in the ER lumen. Blockage and depletion of functional ERESs due to the retention of misfolded procollagen by ERESs disrupts the exit of all secretory proteins and causes their accumulation in the ER. The resulting ER dilation disrupts ER-mitochondria contacts, leading to mitochondrial dysfunction and activation of the mitochondrial, not ER, arm of the ISR, in which EIF2? is phosphorylated by GCN2 rather than PERK. This novel pathway of ISR activation by secretory protein misfolding in the ER may present new opportunities for therapeutic targeting of osteoblast malfunction in classical OI.

***Disclosures: Elena Makareeva**, None*

FRI-328

Extrachromosomal circular DNA is produced by bone cells and may regulate physiological and pathological bone remodeling in mice and humans *Alongkorn Kurilung[1], Pratomporn Krangvichian[1], Manish Adhikari[2], Michela Palmieri[3], Lowry CL Barnes[4], Simon C Mears[4], Jeffrey B Stambough[4], Benjamin Stronach[4], Elena Ambrogini[3], Jesus Delgado-Calle[2], Intawat Nookaew[1]. [1]Department of Biomedical Informatics, University of Arkansas for Medical Sciences, United States. [2]Department of Physiology and Cell Biology, University of Arkansas for Medical Sciences, United States. [3]Division of Endocrinology, University of Arkansas for Medical Sciences, United States. [4]Department of Orthopaedic Surgery, University of Arkansas for Medical Sciences, United States

Extrachromosomal circular DNAs (eccDNAs) are nuclear, closed-circular DNAs derived from chromosomes. eccDNAs have been implicated in oncogene amplification and gene expression regulation in cancer cells. A population of eccDNAs encodes full-length transcripts, leading to high-copy number and transcription levels. eccDNAs also carry enhancers and genes encoding for miRNAs, which regulate chromatin accessibility and gene expression. Recent breakthroughs in eccDNA detection and functional analysis revealed that these molecules play important roles in cancer progression. However, current knowledge about eccDNA production and function in normal bone cells or destructed bone by cancers is limited. We have, therefore, searched for eccDNA circulomes in bone cell lines and tissue specimens from mice and humans, using a novel eccDNA enrichment method and our high-accuracy bioinformatic tool, CReSIL. Using third-generation sequencing, we detected eccDNA molecules (per 5?g of genomic DNA) in murine osteocyte-like MLOY4 cells (~12,000), primary murine osteoblasts (~20,000). eccDNAs were also detected in murine cortical bone (~4,000) and human trabecular bone obtained from femoral heads resected during hip replacement surgery (~4,000). Approximately 10% of the eccDNAs harbored full/truncated genes and miRNAs, including genes directly involved in bone homeostasis, in both MLO-Y4 (Apod, Adm2, Ecm1, Ilk, Mat2a, Sosc1, miR-200a, miR-429) and primary Obs (Bglap2, Elf3, miR-101, miR-137). Wee next performed functional GO term analysis of the genes carried by the identified eccDNAs from whole murine cortical bone. We found enrichment in terms associated with RNA transcription, Wnt signaling, mesenchymal differentiation and bone growth. It has been shown earlier that apoptosis and the consequent DNA fragmentation stimulate eccDNA formation and its production. Consistent with this evidence,we detected a 3-fold increase in eccDNA molecules in the cortical bone of mice bearing human multiple myeloma tumors, in which osteoblast and osteocytes undergo premature apoptosis, compared to naïve mice. This observation suggests that apoptotic osteoblastic cells are a source of regulatory eccDNA molecules in the multiple myeloma tumor niche. Taken all together, these findings provide compelling evidence for the existence of eccDNAs in bone and suggesta role in the regulation of cellular and molecular events influencing physiological and pathological bone remodeling.

***Disclosures: Alongkorn Kurilung**, None*

FRI-330

Targeted Expression of Claudin (Cldn)-11 in Osteoblasts Increases Trabecular Bone Mass by Stimulating Bone Formation and Reducing Marrow Adiposity in Mice *Weirong Xing[1], Sheila Pourteymoor[2], William Tambunan[2], Subburaman Mohan[3]. [1]Musculoskeletal Disease Center, Jerry L. Pettis Memorial Veteran s Admin., United States. [2]VA Loma Linda Healthcare System, United States. [3]Jerry L. Pettis Memorial VA Medical Center, United States

The claudin (CLDN) family comprises 24 members of 20-34 kDa tetraspan transmembrane proteins of tight junctions. In addition to their established canonical role as barriers controlling the flow of molecules in the intercellular space between cells, a distinct non-canonical role for CLDNs is now emerging in which they serve as mediators of cell signaling. In previous studies, we showed that mice with global deletion of Cldn-11 gene exhibited reduced trabecular bone mass. However, the impact of Cldn11 expression osteoblast lineage cells in vivo remains undefined. Here, we generated osteoblast-specific transgenic lines expressing Cldn11 transgene driven by the ColCAT2.3 promoter and characterized their skeletal phenotype. Micro-CT analysis of distal femoral metaphysis showed that trabecular bone mass was increased by 50% and 38% (both $P<0.01$, n=8-10 per gender), respectively, in the transgenic male and female mice compared to littermate control mice that was caused by a significant increase in trabecular number and reduction in trabecular separation. Trabecular bone mass was also increased by 43% ($P<0.01$) in the proximal tibial metaphysis of transgenic mice of both genders. Histology and serum biomarker studies revealed that increased bone formation, and not reduced bone resorption, is the cause for increased trabecular bone mass in the Cldn11 Tg mice. Accordingly, expression levels of bone formation (Alp, Bsp) but not bone resorption (Ctsk) markers were increased in the bones of Cldn11 transgenic mice. Since bone marrow stromal cells are common precursors for osteoblasts and adipocytes and marrow adipose tissue (MAT) is known to correlate with trabecular bone mass inversely, we measured MAT by micro-CT of osmium tetroxide labeled bones. MAT was reduced by 86% ($P<0.05$) in the proximal tibia of transgenic male mice compared to control mice. Accordingly, the expression levels of the adipogenic markers (adiponectin and Asc1) and regulators of MAT (adipsin and leptin), were significantly reduced by 45-53% ($P<0.05$) in the bones of transgenic male mice. Our data are consistent with the possibility that CLDN11 exerts anabolic effects in osteoblasts by promoting the differentiation of mesenchymal stem cells towards osteoblasts at the expense of adipocytes.

***Disclosures: Weirong Xing**, None*

FRI-332

Phospholipase C beta 4 regulates RNAKL-mediated osteoclastogenesis via its interaction with MKK3 and p38 *Dong-Kyo Lee[1], Xian Jin[1], Xiangguo Che[1], Poo-Reum Choi[1], Ying Cui[1], Sihoon Lee[2], Hyun-Ju Kim[1], Je-Yong Choi[1]. [1]School of Medicine, Kyungpook National University, Republic of Korea. [2]Gachon University College of Medicine, Republic of Korea

Phospholipase C beta (PLC?) exerts diverse biological functions including inflammatory response, tumorigenesis and neurogenesis, but its role in bone cell function is largely unknown. Among the PLC? isoforms (?1-?4), we found that PLC?4 was highly upregulated during osteoclastogenesis. Here, using global and osteoclast lineage-specific PLC?4 conditional knockout mice (LysM;PLC?4fl/fl), we show that PLC?4 is a key regulator of osteoclast differentiation induced by RANKL. Both global and osteoclast lineage-specific deletion of PLC?4 in mice led to a significant reduction in osteoclast formation in vitro and decreased osteoclast marker gene expression. Importantly, compared to WT littermates, LysM;PLC?4fl/fl male mice had higher bone mass and lower osteoclast numbers in vivo without altering osteoblast histomorphometric indices. Mechanistically, PLC?4 formed a complex with mitogen-activated protein kinase kinase (MKK) 3 and p38 MAPK and modulated p38 activation after RANKL stimulation. Subsequently, RANKL-induced phosphorylation of p65, a downstream target of p38, was blocked in LysM;PLC?4fl/fl cells. Overall, our findings reveal that PLC?4 controls osteoclastogenesis via RANKL-dependent MKK3-p38-p65 pathway, and that PLC?4 may be a potential therapeutic candidate for bone diseases such as osteoporosis.

***Disclosures: Dong-Kyo Lee**, None*

FRI-333

Short-term RAGE inhibition enhances osteoclast activity in a mouse model of type 2 diabetes *KAITLYN BROZ[1], Remy Walk[2], Simon Tang[3, 1]. [2]Washington University in St. Louis, . [3]Washington University in St Louis, United States

Patients with type 2 diabetes experience more fractures in spite of increased bone mineral density. One likely contributor is the accumulation of advanced glycation endproducts (AGEs) and activation of the receptor of AGEs (RAGE). We previously showed that the systemic genetic ablation of RAGE from 6-8 month-old type 2 diabetic mice protected against the decline of osteocyte density and increased AGEs in the vertebrae. To translate these findings, we sought to determine the effects of short-term RAGE inhibition on the vertebrae of db/db mice.Female leptin receptor deficient (db/db) mice and littermates at 5 months-old were injected daily with 1mg/kg/ml of FPS-ZM1, a small molecular inhibitor of RAGE, in 0.05% DMSO or with vehicle (n=4-5/group) for 60 days. Body weight was monitored biweekly. L4 vertebra were scanned by microCT (Scanco vivaCT 40, 10um, 70 keV, 170uA, 300ms integration) before treatment and then again immediately prior to sacrifice. The L3 vertebra were stained with TRAP / H&E to measure osteoclast activity (osteoclast surface per bone surface, Oc.S/BS) and osteocyte density. Mice were injected with calcine 2 days prior to sacrifice to measure osteoblast activity (mineralizing surface per bone surface, MS/BS). L5 vertebra were scanned by microCT and tested in compression and an AGE fluorometric assay was performed.Body weight for all groups was unchanged throughout. BV/TV was unchanged in wt mice with and without treatment, and BV/TV was increased in the untreated db/db mice. The changes in BV/TV were concomitant with an increase in Oc.S/BS in the db/db treatment group, with a trending effect of treatment on MS/BS. Diabetes reduced osteocyte density, increased vertebral AGEs, and impaired mechanical properties, and these were unaffected by RAGE inhibition.Inhibiting RAGE for 60 days in db/db mice enhances osteoclast action and prevents the bone accumulation. RAGE inhibition did not affect bone matrix AGEs, osteocyte lacunae density, though osteoblast mineral apposition was modestly increased. Our previous study revealed that systemic, constitutive RAGE ablation in 6-8 month-old db/db mice rescued osteocyte lacunar density, enhanced bone mineralizing surface, but not osteoclast function. Taken together, short-term RAGE inhibition may stimulate the actions of osteoclasts to stimulate bone removal, but prolonged treatment may be required to stimulate the sustained actions of the osteoblast and the osteocyte to restore bone matrix quality.

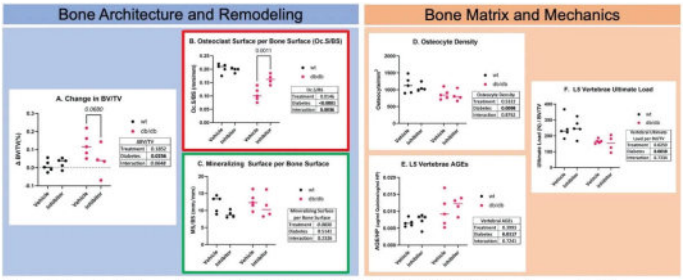

Figure 1. Bone Architecture and Remodeling: [A] The administration of a RAGE inhibitor nearly prevented the accumulation of bone in the db/db (p = 0.068). [B] The inhibition of RAGE also restored the Oc. S/BS in the db/db animals, suggesting that the osteoclast function is enhanced. [C] Inhibiting RAGE did not appear to affect osteoblast function. Bone matrix and mechanics: [D] Osteocyte density is reduced in db/db animals and not affected by RAGE inhibition. [E] AGEs also accumulated in vertebrae of db/db animals with no effect of treatment. [F] Finally, the fragility observed in the db/db animals was not affected by the treatment.

***Disclosures: KAITLYN BROZ**, None*

FRI-335

Docosahexaenoic acid inhibits TNF-?-induced osteoclast formation and bone resorption through GPR120 *Jinghan Ma[2,] Hideki Kitaura[2,] Fumitoshi Ohori[3,] Takahiro Noguchi[2,] Aseel Marahleh[2,] Ria Kinjo[4,] Kayoko Kanou[4,] Itaru Mizoguchi[2,] [2]Tohoku University, , [2]Tohoku University, Japan, [3]Tohoku University Graduate School of Dentistry, Japan, [4]Tohoku University Tohoku University Graduate School of Dentistry, Japan

Objectives: Docosahexaenoic acid (DHA), an omega-3 fatty acid which exerts its function via G protein-coupled receptor 120 (GPR120). DHA possesses anti-inflammatory effects and inhibits osteoclastogenesis. Orthodontic force induces the expression of tumor necrosis factor-? (TNF-?) which supports osteoclastogenesis by increasing RANKL expression. In our studies, we investigated the effect of DHA on TNF-?-induced osteoclastogenesis in vivo and in vitro. We also observed the effect of DHA on TNF-?-induced NF-?B pathway activation through GPR120. Furthermore, we also aim at the inhibitory effect of DHA on osteoclast formation and bone resorption in bone marrow chimeric mouse by using WT and GPR120 deficient mouse.Materials and methods: WT and GPR120-KO mice were administered supracalvarial injections with either PBS; TNF-?; DHA and TNF-?; or DHA. Calvaria were analyzed for bone resorption and osteoclastogenesis. We also analyzed RANKL mRNA expression in both kinds of mice osteoblasts treated as above. Then measured osteoclastogenesis in co-cultures of GPR120-KO osteoclast precursors and osteoblasts from WT or GPR120-KO mice. To observe how DHA influence proinflammatory signaling pathway, we stimulated osteoblast of both kinds of mice by TNF-? then analyzed by immunofluorescence. Finaly, we generated chimeric mice by transplanting the bone marrow cells from donor into the irradiated recipient mice, which resulting chimeric mice have stromal cells derived from the recipient and macrophages derived from the donor. Then, these mice were also received DHA and TNF-? injection and were used for histological examination. Results and Discussion: Calvaria of WT but not GPR120-KO mice injected with DHA and TNF-? had less bone resorption and osteoclastogenesis than mice injected with TNF-? alone. TNF-?-induced RANKL mRNA expression was reduced in WT mice but not GPR120-KO osteoblasts treated with DHA. DHA also inhibited TNF-?-enhanced osteoclast formation in co-culture of osteoblasts obtained from WT mice but not GPR 120-KO mice. Moreover, DHA exerted inhibitory effects on the NF-?B pathway activated by TNF-? in osteoblasts of WT mice but not GPR120-KO mice. Osteoclast number and bone resorption were increased in the chimeric mice which have GPR120-KO stromal cells compared to those owns WT stromal cells.Conclusion: DHA suppresses osteoclast formation and bone resorption induced by TNF-? in vivo and in vitro, and inhibits osteoclastogenesis and bone resorption via GPR120. Moreover, stromal cells contribute more to osteoclast formation than macrophages during this process. Additionally, DHA directly inhibits RANKL expression in osteoblasts in vitro via GPR120.

***Disclosures: Jinghan Ma**, None*

FRI-336

Identification of glutamine metabolism as a metabolic vulnerability in osteoclasts *GUOLI HU[1,] Yilin Yu[3,] Robert Tower[3,] Guo-fang Zhang[4,] Courtney Karner[3,] [1]UT Southwestern Medical Center, , [3]University of Texas Southwestern Medical Center, United States, [3]University of Texas Southwestern Medical Center, , [4]Duke University, United States

Osteoclasts are bone resorbing cells that are essential to maintain skeletal integrity and function. Excessive osteoclast activity causes both age-related and pathological bone loss associated with several diseases including osteoporosis. While many of the growth factors and molecular signals that govern osteoclastogenesis are well studied, a large gap in our knowledge exists about the role and regulation of cellular metabolism during osteoclastogenesis. Advances in our understanding of differentiation associated metabolic changes will aid in identifying metabolic vulnerabilities that can be exploited therapeutically to reduce bone resorption and pathological bone loss. Here, we used a multifaceted approach to define the metabolomic signature of osteoclasts. When compared to bone marrow monocyte and macrophage cultures, mature osteoclasts (mOC) have significantly increased abundance of amino acids and purine and pyrimidine nucleotides. Osteoclasts must increase the consumption and metabolism of glutamine which provides carbon and nitrogen for amino acid and nucleotide biosynthesis. Importantly, inhibiting glutamine metabolism in mOC resulted in a complete loss of the metabolomic signature and prevented osteoclast differentiation in vitro. Deletion of a floxed Gls allele (Glsfl) in myeloid progenitor cells using LysmCre resulted in significantly higher bone mass at 4- and 6-months of age in male and female mice. The LysmCre;Glsfl/fl bone phenotypes were attributed to a reduction in osteoclast numbers and bone resorption with no change osteoblast parameters. Conversely, expressing a doxycycline inducible Gls allele (tetoGls) using LysmCre (LysmCre;R26rtTA;tetoGls) increased osteoclastogenesis, enhanced bone resorption and rapidly reduced bone mass. Highlighting the therapeutic implications of these findings, genetically inhibiting glutamine metabolism prevented ovariectomy induced bone loss in mice. Collectively, our data provide genetic evidence that glutamine metabolism is essential to regulate osteoclast metabolism, osteoclastogenesis and bone resorption in mice. Moreover, our study demonstrates osteoclasts are reliant on glutamine metabolism like cancer cells. Targeting glutamine dependency using Telaglenastat is being developed as a potential cancer treatment. Our findings indicate it may be possible to repurpose this strategy to prevent excessive bone resorption.

***Disclosures: GUOLI HU**, None*

FRI-338

A Novel Fluorogenic Probe for Intravital Microscopic Imaging of Enzymatically Active Cathepsin K in Functional Osteoclasts *Eun Jung Lee[1,] Seyoung Koo[2,] Da Hyeon Yoon[1,] Jong Seung Kim[2,] SERK IN PARK[1,] [1]Korea University College of Medicine, Republic of Korea, [2]Department of Chemistry, Korea University, Republic of Korea

Cathepsin K (CTSK) is a lysosomal cysteine protease that is essential to the osteolytic activity of functional osteoclasts. Several fluorescence-based probes for CTSK have been developed for preclinical studies on osteoclast inhibitors but the sensitivity and signal intensity are insufficient for real-time live imaging in mice. To overcome this limitation, we synthesized a novel fluorescence resonance energy transfer (FRET)-based fluorogenic CTSK probe and tested its efficacy in vitro using a confocal microscope and in vivo using an intravital microscope. A peptide substrate specific to CTSK was conjugated with a TAMRA fluorophore and a BHQ-2 quencher. Upon addition of a nano-molar range of recombinant CTSK, the TAMRA fluorophore was cleaved from the quencher, resulting in a strong fluorescence signal, which was fully suppressed by odanacatib, a CTSK inhibitor. Notably, our probe exhibited over 60-fold higher sensitivity than previously reported probes. For in vitro imaging, osteoclasts were formed by treating murine bone marrow monocytes with RANKL and M-CSF on collagen-coated plates or dentin discs, followed by fixation, permeabilization and staining with the probe, phalloidin and DAPI. Confocal microscopy demonstrated the subcellular localization of CTSK in osteoclasts (Figure Panel A). A strong fluorescence signal was localized in the ruffled border, indicating that the probe is sensitive and specific to functional CTSK in bone-resorbing osteoclasts. For intravital imaging, we used three different mouse models: an ovariectomy-induced osteoporosis model, a RANKL injection bone loss model, and a bone metastasis model using intra-tibial injection of breast tumor cells. The CTSK probe was administered by tail-vein injection (50?mol), and live real-time images were captured in the proximal tibia with a small skin incision under anesthesia. No significant toxicities were noted in multiple injection groups of mice. Two-photon intravital microscopy showed clear real-time images of osteoclasts on the endosteal surface or trabecular bone of live animals (Figure Panel B). The fluorescence signal was not detectable in negative control mice, and the signal was significantly reduced in mice treated with zoledronic acid or odanacatib. In conclusion, we developed a novel probe for sensitive and specific visualization of functional CTSK in real-time live mice that can be useful in bone biology research and in the development of therapeutics for CTSK or osteoclasts.

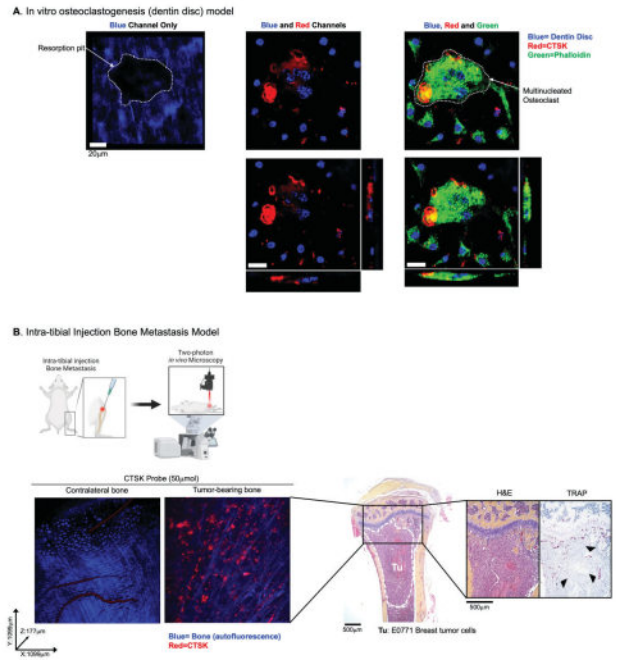

***Disclosures: Eun Jung Lee**, None*

FRI-339

Interactome of Galectin-8 Isoforms to Dissect their Impact on Human Osteoclasts *Leopold Mbous Nguimbus[1], Michèle Roy[1], Marie A. Brunet[2], Sophie Roux[1]. [1]Rheumatology, Department of Medicine, Sherbrooke University, Canada. [2]Department of Biochemistry and Functional Genomics, Sherbrooke university, Canada

Using a screening strategy, we previously showed an alternative splicing (AS) event in LGALS8 encoding galectin-8 (gal-8) in overactive pagetic osteoclasts (OCs), with a decrease in long spliced isoform while total gal-8 was upregulated compared to controls (Klinck et al. 2014). LGALS8 AS leads to the formation of distinct splice variants that only differ in their linker region whose length and structure could influence its biological functions. The best-characterized functions of gal-8 are performed extra-cellularly, where it binds glycans to modulate cell-matrix interactions. The functions of intracellular gal-8 are less well known, but cytosolic gal-8 has been shown to act as a danger recognition receptor. Our objective was to evaluate the impact of gal-8 isoforms on OC phenotype, and to identify interacting partners for each isoform to better understand their role in OCs. We used fetal monocytes to generate OCs, adding isoform-specific knockdown (siRNA) at the end of long-term cultures. Inhibiting gal-8 expression decreased OC nuclearity and bone resorption, mainly attributable to the short isoform as its targeting significantly decreased the number of multinucleated cells and the resorbed surface area compared to control siRNA. Targeting gal-8 long isoform did not induce any phenotypic changes. The two isoforms may interact with distinct proteins and pathways, which led us to analyze the interactome of gal-8 isoforms by liquid chromatography mass spectrometry in HEK293T cells transfected with either isoform. Results were scored using SAINTexpress which identified 31 gal8-interacting proteins, including 22 proteins shared by both isoforms, as well as 9 specific to the short isoform. Proteins specific to the short isoform of gal-8 included proteins involved in cell adhesion (ITGA4, ITGA5, TPBG), lysosomal proteins (LAMP1, SCL17A5, GLMP) or membrane receptors (M6PR, PTGFRN). The tertiary structure of each isoform was generated with AlphaFold2 and could also suggest spatial interference of the long isoform with some binding sites. GO enrichment analyses confirmed specificity in some cell adhesion or lysosomal pathways for the short isoform. Finally, 3 protein-protein interactions with gal-8 were confirmed by double immunofluorescence staining in resorbing OCs. Our proteomics approach of the interaction partners allowed to identify some molecules or pathways associated with the short isoform that drive gal-8 pro-OC activity in humans.

***Disclosures: Leopold Mbous Nguimbus**, None*

FRI-341

Osteoclast-specific Deletion of ?2-Adrenergic Receptor Limits Trabecular Bone Acquisition in Male, but not Female Mice *Rebecca Peters[3], Ryan Neilson[2], Hannah Feliciano[3], Katherine Motyl[4]. [3]MaineHealth Institute for Research, . [2]MMCRI, United States. [3]MaineHealth Institute for Research, United States. [4]MaineHealth, United States

The sympathetic nervous system (SNS) is important for maintenance of bone homeostasis through ?-adrenergic signaling. Our lab and others found that osteoclasts are direct targets of the SNS, and that ?-blockers limit osteoclast differentiation. Osteoclasts express both ?1- and ?2-adrenergic receptor (?2AR), but ?2AR is more highly expressed. To directly examine the effects of ?2AR on osteoclasts, we developed an osteoclast-specific ?2AR knockout mouse model. Adrb2fl/fl mice were crossed with the myeloid lineage specific Lyz2Cre/Cre (a.k.a. LysM-Cre) mice. We tested the efficiency of deletion with Adrb2fl/fl-Lyz2Cre/+ (Cre/+) and Adrb2fl/flLyz2Cre/Cre (Cre/Cre) mice and found deletion of Adrb2 was comparable in both using gene expression and in situ hybridization in the distal femur. Using µCT, we measured the bone microarchitecture of wildtype (+/+) and Cre/+ male and female mice at 8 and 26 weeks of age (N=7-10). In male mice with the deletion, L5 vertebrae trabecular bone parameters (BV/TV, BMD, Tb.Th) were significantly lower. Distal femur trabecular BMD was reduced by 10% and SMI was elevated by 35% in Cre/+ compared to +/+ ($p<0.05$). Cortical bone (Ct.Ar/Tt.Ar, Ct.TMD) tended to be lower in Cre/+ mice ($p<0.09$). Both osteoclast and osteoblast marker genes were reduced in tibia, including Acp5, Alpl, Col1a1 and Tnfsf11 (Rankl). Although no changes in serum CTX-1 or P1NP were observed in untreated mice, ?2AR deletion in osteoclasts attenuated the elevated CTX-1 caused by the ?2AR agonist salbutamol (N=3, $p=0.031$). The low bone mass phenotype subsided by 26 weeks, suggesting age-related bone loss is unaffected by Adrb2 deletion in osteoclasts in male mice. Female mice had no significant changes in bone microarchitecture or serum bone remodeling markers at 8 or 26 weeks of age. Although global deletion of Adrb2 has been reported to cause a high bone mass phenotype, our work indicates that ?2AR function in bone is sex, age, cell-type, and stress dependent. We have also found that ?2AR deletion in osteoclasts may have indirect effects on osteoblast function, indicated by lower osteoblast marker gene expression. Future studies will examine this using osteoblast culture and co-culture studies with osteoclasts. These studies will aid in our understanding of mechanisms through which stress and ?-blockers influence bone density, which may inform osteoporosis prevention and treatment strategies.

***Disclosures: Rebecca Peters**, None*

FRI-342

Pim1 contributes to maintenance of bone homeostasis via regulation of osteoclast function *Soo Young Lee[1], Ryeojin Ko[1], Jeongin Seo[1]. [1]Ewha Womans University, Republic of Korea

ObjectiveThe proviral integration site for Moloney murine leukemia virus 1 (Pim1) protein is a highly conserved serine/threonine kinase that is involved in a variety of cellular processes including cell survival, proliferation, and apoptosis. In addition, Pim1 has been shown to regulate the differentiation of osteoclasts. Mature osteoclasts absorb bone matrix by forming an actin ring between themselves and the bone surface. However, the role of Pim1 in the bone-resorbing function of osteoclasts is largely unknown.MethodsIn this study, we generated Pim1-/- mice to investigate the role of Pim1 in the regulation of bone metabolism. We conducted immunofluorescence staining of actin and acetylated tubulin in osteoclast on dentin slices and coverslips in wild-type and Pim1-/- mice. To identify whether Pim1 deletion affects bone growth in vivo, we examined the microstructure of the distal femur from 8 weeks old male mice wild-type and Pim1-/- mice using micro-computed tomography (micro-CT) analysis.ResultsWe demonstrated that Pim1 deletion does not affect the differentiation of osteoclasts. However, a significant reduction in resorption area was observed in Pim1-/- mice. In addition, Pim1-deficient osteoclasts were unable to form normal actin rings, and the acetylation pattern of microtubules was abnormal. Furthermore, an increase in distal femoral bone mass was observed in Pim1-/- mice compared to wild-type mice.Conclusions-These results indicate that Pim1 plays an important role in the bone-resorbing function of osteoclasts. Therefore, the control of osteoclast activity via targeting Pim-1 will provide a novel therapeutic option for the treatment of bone diseases.

***Disclosures: Soo Young Lee**, None*

FRI-344

Transcriptional Reprograming during Human Osteoclastogenesis Identifies Targets for Predicting and Modulating Osteoclast Differentiation and Activity *Morten S. Hansen[1], Kaja Madsen[2], Maria Price[3], Kent Søe[1], Caroline M. Gorvin[3], Morten Frost[1], Alexander Rauch[2]. [1]Odense University Hospital, Denmark. [2]University of Southern Denmark, Denmark. [3]University of Birmingham, United Kingdom

Background: Increased osteoclastogenesis and osteoclast activity are important causes of postmenopausal osteoporosis. Understanding the transcriptional reprogramming during osteoclastogenesis has the power to identify targets for novel anti-osteoporotic drugs.Purpose: Define gene expression dynamics during human osteoclast differentiation for the alignment with bone mineral density related expression and GWAS data, the construction of

transcriptional networks and the identification of G-protein-coupled receptors and surface molecules that allow interference with osteoclast activity and the prediction of subject-specific resorptive potential.Methods: Human osteoclasts were differentiated (t=10 days) in vitro from CD14+-monocytes from eight female donors aged 18-49 years. RNA-sequencing was performed at four time points (day 0 prior to and 2-, 5-, and 9-days post-differentiation). GPCRs were targeted with agonist and/or antagonists and FACS based surface molecule expression was determined in relation to bone resorbing activity.Results: We identified 8446 differentially expressed genes with high reproducibility across donors that were grouped into eight temporal patterns which based on network analysis are linked by mutual and temporal dependencies. These patterns were enriched for distinct molecular functions, metabolic pathways, and genes that are flanked by bone mineral density associated SNPs. Compared to normal, osteoporotic bones exemplified gene signatures of mature osteoclasts and absence of precursor related genes. Using pharmacological interference with differentially expressed GPCRs, we found activation of somatostatin receptor 2 (SSTR2) to decrease osteoclast resorption, activation of free fatty acid receptor 4 (FFAR4/GPR120) to decrease both osteoclast numbers and activity, and activation of complement C5a receptor 1 (C5AR1) to increase osteoclast numbers. FACS analysis affirms expression of oxidised LDL receptor 1 (LOX1) and activated CDC42 kinase 1 (ACK1) on precursors to be correlating with activity of the mature cells. Conclusions: We provide a consecutive map of the transcriptional reprogramming during human osteoclastogenesis that highlights the strong implication of osteoclast genes in the aetiology and genetics of human bone loss. Targeting stage specifically expressed GPCRs as well as the quantifying resorption-associated surface molecules highlights the identification of targets and monitors for anti-resorptive treatment options.

***Disclosures: Morten S. Hansen**, None*

FRI-346

The endosomal RANKL-LGR4 signaling during osteoclast differentiation *Wonbong Lim[1], Beomchang Kim[1], Young Jong Ko[1], Yuria Jang[1]. [1]Department of Premedical Science, College of Medicine, Chosun University, Republic of Korea

LGR4 (Leucine-rich repeat-containing G-protein coupled receptor 4, also known as GPR48) is a membrane receptor and known as a negative regulator of RANK signaling cascade during osteoclast differentiation. Although cell signaling and endocytic membrane trafficking from membrane receptor have traditionally been viewed as distinct processes, it is now recognized that these processes are intimately and bidirectionally linked. In this study, we investigated the difference between membrane-bound LGR4 signaling and internalized LGR4, and whether the LGR4 signaling cascade gives RANKL signal in internalized endosomes as an potential regulator during RANKL-induced osteoclastogenesis. Herein, we showed that LGR4 is endocytosed to endosome after binding to RANKL in osteoclast precursor cells RAW 264.7s. The internalized LGR4 activates LGR4-RANKL signaling in the early endosome. When RANKL is bound to LGR4, it is endocytosed and located in the Rab5 positive ealry endosome. In LGR4-down regulated RAW 264.7 cells, it was analyzed that the early endosome signal increased and the inhibitory phosphorylation of GSK-3beta decreased. Raw 264.7 cells treated with Dynasore (Dynamin inhibitor) confirmed the same reduction in inhibitory P-GSK3B as LGR4 CKO(Conditional Knock-out) cells. With similar results, it was confirmed that the reduced inhibitory P-GSK3B was recovered when DRG2 KO mice were treated with Dynasore, which is similar to the results of DRG2 WT mice. As a result of confirming NFATC1 nuclear translocation by RANKL treatment in LGR4 CKO Raw 264.7 cells and DRG2 KO mouse, nuclear translocation of NFATC1 increased in both groups. In addition, decreased bone density and increaesd TRAP activity in DRG2 KO mice which is known to be increased the early endosome duration were investigated. Taken together, our result showed that the internalized LGR4 could be a potential regulator for the modulation of osteoclast differentiation via RANKL-LGR4 signaling in endosomes.

***Disclosures: Wonbong Lim**, None*

FRI-347

Proteomics Analyses Unveil Leucine Repeat Rich Kinase 1 (LRRK1) Signaling Targets Proteins Critical for Endosome/Lysosome Sorting and Trafficking in Osteoclasts *Subburaman Mohan[1], Weirong Xing[2]. [1]Jerry L. Pettis Memorial VA Medical Center, United States. [2]Musculoskeletal Disease Center, Jerry L. Pettis Memorial Veteran s Admin., United States

LRRK1 plays a pivotal role in regulating osteoclast activity and bone resorption. Global knockout (KO) of Lrrk1 gene in mice caused severe osteopetrosis due to failure of osteoclast to resorb bone. The molecular mechanism of LRRK1 regulation of osteoclast function is not fully understood. Since LRRK1 is a serine/threonine kinase and most aspects of cellular biology and protein function are regulated by protein phosphorylation, we performed a 2D DIGE phosphor-proteomics analysis to identify potential LRRK1 target proteins in osteoclasts. Osteoclasts derived from Lrrk1 KO, and control WT mice were differentiated for 5 days, starved in M-CSF and RANKL-free media for 1 hour, followed by 1 hour M-CSF and RANKL stimulation. The cells were then lysed, and total cellular proteins were extracted. For phosphoprotein profiling, same amounts of lysate from Lrrk1 KO and WT osteoclasts were labeled with Cy3-dye and run on 2D SDS PAGE. The gels were then stained using Pro-Q® Diamond Phosphoprotein Gel Stain. For the protein profiling, lysates from Lrrk1 KO and control WT cells were labelled with Cy3- and Cy5-dye, respectively. Labelled proteins were mixed and analyzed on the same 2D SDS PAGE. The fluorescent intensities of overlapped spots on the gels were scanned using Typhoon TRIO and analyses using DeCyder software. Phosphor-ratio of two samples (WT/KO) were calculated by adjusting phosphor-ratios with protein ratios in LRRK1 deficient vs. control WT cells. Differentially phosphorylated spots between the two types of cells were picked up by Ettan Spot Picker, digested with modified porcine trypsin in the gel, and identified by MALDI-TOF MS and TOF/TOF tandem MS/MS. Twenty-four phosphoproteins were identified, six of which involved in endosome/lysosome sorting, vacuolar protection, and trafficking SNX2, VPS35, VTA1, CFL1, and CTSA proteins were significantly hypo-phosphorylated while SNX3 was hyper-phosphorylated in LRRK1-deficient osteoclasts. Phosphorylated VPS35 was reduced by 80% while phosphorylated SNX3 was elevated by 4-fold in LRRK1 deficient osteoclasts. Since both VPS35 and SNX3 are critical retromer complex components responsible for membrane trafficking, and the phosphorylation of SNX3 at serine 72 is known to block its phosphoinositide binding to control release of endosomal SNX3 to the cytosol, our results suggest that LRRK1 signaling target proteins critical for endosome/lysosome sorting and trafficking in osteoclasts.

***Disclosures: Subburaman Mohan**, None*

FRI-350

Interventional and integrative subcellular sequencing (i2scseq) clarifies the multi differentiation stages embedded inside mature osteoclast *Hiroyuki Okada[1], Yuta Terui[2], Yasunori Omata[3], Masahide Seki[4], Shoichiro Tani[5], Junya Miyahara[6], Kenta Makabe[6], Asuka Terashima[7], Sanshiro Kanazawa[8], Masahiro Hosonuma[9], Shoko Onodera[10], Fumiko Yano[11], Hiroyuki Kajiya[12], Taku Saito[6], Yutaka Suzuki[4], Koji Okabe[12], Roland Baron[13], Sakae Tanaka[6], Ung-il Chung[14], Hironori Hojo[14]. [1]Center for Disease Biology and Integrative Medicine, Graduate school of Medicine, the University of Tokyo; Department of Orthopaedic Surgery, the University of Tokyo; Department of Oral Medicine, Infection, and Immunity, Harvard School of Dental Medicine, Japan. [2]Department of Single Cell Solution, Product Strategy Department, Marketing Center, Life Business HQ, Yokogawa Electric Corporation, Japan. [3]Department of Orthopaedic Surgery, the University of Tokyo; Bone and Cartilage Regenerative Medicine, the University of Tokyo Hospital, Japan. [4]Department of Computational Biology and Medical Sciences, Graduate School of Frontier Sciences, the University of Tokyo, Japan. [5]Center for Disease Biology and Integrative Medicine, Graduate school of Medicine, the University of Tokyo, Japan. [6]Department of Orthopaedic Surgery, the University of Tokyo, Japan. [7]Bone and Cartilage Regenerative Medicine, the University of Tokyo Hospital, Japan. [8]Department of Oral and Maxillofacial Surgery, Graduate School of Medicine, the University of Tokyo, Japan. [9]Department of Clinical Immuno Oncology, Clinical Research Institute for Clinical Pharmacology and Therapeutics, Showa University; Showa University Pharmacological Research Center, Japan. [10]Department of Biochemistry, Tokyo Dental College, Japan. [11]Department of Biochemistry, Showa University School of Dentistry, Japan. [12]Department of Physiological Science and Molecular Biology, Fukuoka Dental College, Japan. [13]Department of Oral Medicine, Infection, and Immunity, Harvard School of Dental Medicine, United States. [14]Center for Disease Biology and Integrative Medicine, Graduate school of Medicine, the University of Tokyo; Department of Bioengineering, Graduate School of Engineering, the University of Tokyo, Japan

The transcriptome at single-cell resolution clarifies the diversity of cell populations. Single-cell RNA-seq (scRNA-seq) has already been adopted for giant cells such as osteoclasts (OCs) (Omata, Okada, JBMR plus 2022). Although large OCs could not pass through a fluid-based cell dissociation device because of their diameter, acid-producing mature OCs were captured using conventional scRNA-seq.At ASBMR 2022, we presented intra-single cell sequencing (iSCseq) (Okada, bioRxiv 2022). iSCseq is a combinatorial method of high-resolution confocal imaging, picking of intracellular components, including a single nucleus, using the Single CellomeTM System SS2000 (Yokogawa, Japan), and next-generation sequencing at high resolution for mRNA. Our previous results showed that individual nuclei within the same cell are heterogeneous in terms of gene expression.The next version of iSCseq called i2scseq (interventional and integrative subcellular sequencing) can also collect cytoplasm in a small ordinary cell with a 3um probe and capture the living subcellular transcriptome. The average number of genes per cell detected by a 10um probe is much higher, and one by a 3um is equivalent to traditional fluid-based sequencing.i2scseq was used for the in vitro lineage of cells differentiating into OCs. i2scseq clarified that some small cells, which were not morphologically regarded as OCs, were classified into the final cluster of lineages, and vice versa, that giant OC contain immature nuclei in terms of gene expression. With integrative analysis of i2scseq and fluid-based sequencing datasets using a deep machine learning method, large OCs have embedded components at many stages of differentiation.i2scseq clarified the subcellular heterogeneity of mature OCs at a higher resolution than previous iSCseq. We partially solved the question of why conventional scRNA-seq has captured so-called mature OCs. i2scseq is expected to be a core method in cell biology.

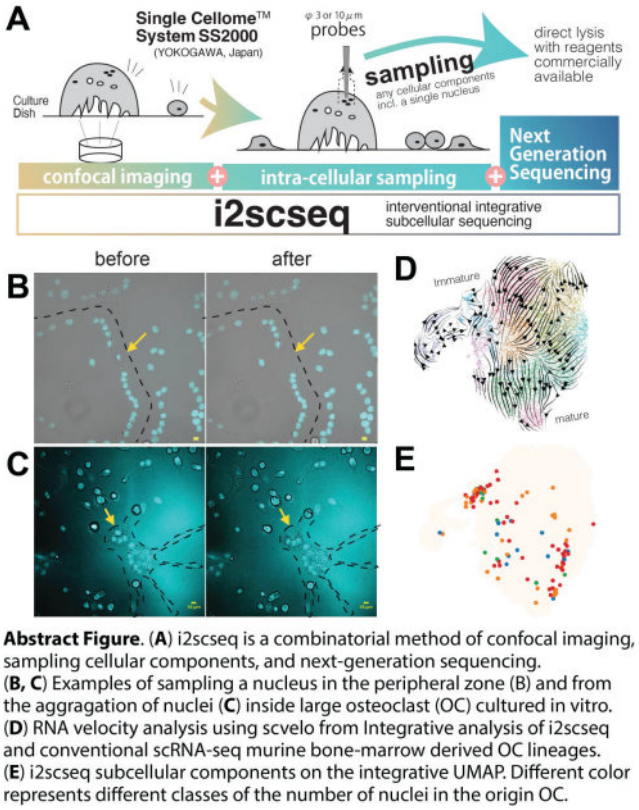

Abstract Figure. (**A**) i2scseq is a combinatorial method of confocal imaging, sampling cellular components, and next-generation sequencing. (**B, C**) Examples of sampling a nucleus in the peripheral zone (B) and from the aggragation of nuclei (**C**) inside large osteoclast (OC) cultured in vitro. (**D**) RNA velocity analysis using scvelo from Integrative analysis of i2scseq and conventional scRNA-seq murine bone-marrow derived OC lineages. (**E**) i2scseq subcellular components on the integrative UMAP. Different color represents different classes of the number of nuclei in the origin OC.

***Disclosures: Hiroyuki Okada**, None*

FRI-352

La, a repurposed RNA-binding protein, regulates osteoclast multinucleation and function. *Jarred M. Whitlock[1], Evgenia Leikina[1], Kamran Melikov[1], Luis Fernandez De Castro Diaz[2], Sandy Mattijssen[1], Richard Maraia[1], Michael Collins[2], Leonid Chernomordik[1]. [1]NICHD, United States. [2]NIDCR, United States

Multinucleated osteoclasts, essential for skeletal remodeling in health and disease, are formed by the fusion of osteoclast precursors, where each fusion event raises their bone-resorbing activity. Here we show that the nuclear RNA chaperone, La protein has an additional function as an osteoclast fusion regulator. Monocyte-to-osteoclast differentiation starts with a drastic decrease in La levels. As fusion begins, La reappears as a low molecular weight species at the osteoclast surface, where it promotes fusion. La's role in promoting osteoclast fusion is independent of canonical La-RNA interactions and involves direct interactions between La and Annexin A5, which anchors La to transiently exposed phosphatidylserine at the surface of fusing osteoclasts. Disappearance of cell-surface La, and the return of full length La to the nuclei of mature, multinucleated osteoclasts, acts as an off switch of their fusion activity. Targeting surface La in a novel explant model of fibrous dysplasia inhibits excessive osteoclast formation characteristic of this disease, highlighting La's potential as a therapeutic target.

***Disclosures: Jarred M. Whitlock**, None*

FRI-353

The PDE4 inhibitors Roflumilast and Rolipram Rescue ADO2 Osteoclast Resorption Dysfunction *Jung Hong[1], Angela Bruzzaniti[1], Rita O'Riley[2], Dena Acton[2], Imranul Alam[2], Michael Econs[2]. [1]Indiana University School of Dentistry, United States. [2]Indiana University School of Medicine, United States

Autosomal Dominant Osteopetrosis type II (ADO2) is a rare bone disease of impaired osteoclastic bone resorption caused by heterozygous missense mutations in the chloride channel 7 (CLCN7). Previous reports have shown that ADO2 knock-in mouse models containing the CLCN7 mutation exhibit elevated bone mass. A CLCN7 mutation is thought to affect not only Clcn7 chloride exchange activity but also affect endosomal-lysosomal trafficking which is critical for formation of the resorption lacunae of active osteoclasts. It is well known that adenylate cyclase is critical for lysosomal acidification in osteoclasts and other cells. Adenylate cyclase catalyze the formation of cyclic adenosine monophosphate (cAMP), an important small second messenger that activates key cellular target proteins. Intracellular cAMP concentration is tightly regulated at the level of its synthesis by adenylate cyclase and hydrolysis by specific phosphodiesterase (PDEs). We investigated the cellular mechanism involved in ADO2 OC dysfunction and found that both immature and mature ADO2 osteoclasts exhibit reduced cAMP levels, compared to wild-type OCs, implicating the signaling pathways that regulate cAMP synthesis or hydrolysis. QPCR analysis revealed higher expression levels of the three PDE4 subtypes (4a, 4b, 4d) in ADO2 osteoclasts compared in WT. Next, we examined the effects of two cAMP specific PDE4 inhibitors, roflumilast and rolipram, on ADO2 osteoclast formation and resorption activity in vitro. Non adherent bone marrow macrophages from ADO2 and WT mice were cultured with RANKL and MCSF in the presence of roflumilast or rolipram (0-250 nM). Roflumilast and rolipram increased osteoclast formation in a dose-dependent manner in both ADO2 and WT osteoclasts. Importantly, the PDE4 inhibitors also displayed a concentration-dependent increase in osteoclast resorption activity which was greater in ADO2 osteoclasts than WT osteoclasts. The key findings from our studies demonstrate that ADO2 mice exhibit reduced cAMP levels and that PDE4 inhibition by rolipram and roflumilast rescue ADO2 osteoclast activity dysfunction in vitro. Further understanding of this mechanism will potentially lead to the development of new approaches for the treatment of clinically affected ADO2 patients.

***Disclosures: Jung Hong**, None*

FRI-354

Proton-Activated Chloride Channel Enhances Endplate Porous Osteoclast Resorption to Induce Spinal Pain *Weixin Zhang[1], Peng Xue[2], Shenyu Wang[2], Jiachen Chu[2], Janet Crane[2], Mei Wan[2], Zhaozhu Qiu[2], Xu Cao[2]. [1]Johns Hopkins university, . [2]Johns Hopkins University, United States

Proton-activated chloride (PAC) channel is responsive to pathological acidic pH in ischemic brain injury in mice and acid-induced neuronal cell death as a completely new ion channel family. Our PAC structure study revealed that the protein exists in two states: namely, a high-pH resting closed state and a low-pH proton-bound non-conducting state. PAC channel undergoes striking conformational changes when the pH drops from 8 to 4, leading to an opening of the channel and the conduction of anions across cellular membranes, thereby inducing diseases associated with tissue acidosis (acid-induced cell death). Skeletal pain in bone disorders is often associated with aberrant osteoclast-mediated resorption due to very low pH environments. But the role of PAC in pathological osteoclast resorption and spinal pain is still unexplored. Chronic low back pain (LBP) can severely affect daily physical activity and is one of the leading risk factors for the development of immobility and frailty. Aberrant osteoclast-mediated resorption during spinal degeneration leads to the development of a porous endplate that in turn allows for the sensory innervation of the spinal unit, leading to LBP. But the mechanism by which aberrant osteoclast activity occurs during spinal degeneration is unclear. Here, we report that the expression of proton-activated chloride channel (PAC) is induced specifically in the apical membrane of osteoclasts in the porous endplates via a RANKL-NFATc1 signaling pathway. Extracellular acidosis evokes the ICl, H current in the cell membrane of osteoclasts by activating the PAC-encoded Cl? channel. Thus, a combination of an acidic environment of porous endplates and elevated PAC expression results in enhanced osteoclast fusion and resorption that, in turn, provokes LBP. Further, we find that genetic knockout of PAC significantly reduces endplate porosity and spinal pain in a mouse model of spine degeneration, but it does not affect bone development or homeostasis of bone mass in adult mice. Aberrant osteoclast-mediated resorption is found in most skeletal disorders, including osteoarthritis, ankylosing spondylitis, rheumatoid arthritis, heterotopic ossification, enthesopathy, and Paget disease, in addition to spine degeneration. Thus, elevated PAC expression and PAC activity could be a common mechanism for various bone pathologies and thus a potential therapeutic target.

***Disclosures: Weixin Zhang**, None*

FRI-357

The Effect of Osteocyte-Derived RANKL on Bone Graft Remodeling *Balazs Feher[1], Carina Kampleitner[2], Patrick Heimel[2], Stefan Tangl[2], Jill Helms[3], Ulrike Kuchler[2], Reinhard Gruber[2]. [1]Harvard School of Dental Medicine, United States. [2]Medical University of Vienna, Austria. [3]Stanford University School of Medicine, United States

Autologous bone is considered the gold standard for grafting, yet it suffers from a tendency to undergo resorption over time. While the exact mechanisms of this resorption remain elusive, osteocytes have been shown to play an important role in stimulating osteoclastic activity through their expression of receptor activator of NF-?B (RANK) ligand (RANKL). During physiological remodeling, this activity is also necessary for bone formation. We hypothesized that osteocyte-derived RANKL plays an important role in the remodeling of bone grafts by suppressing resorption and thus potentially preventing new bone formation.In 8-week-old Tnfsf11fl/fl;Dmp1-Cre osteocyte-specific RANKL knockout and Dmp1-Cre control mice, we harvested a 2.6 mm bone disk from the left parietal bone and transplanted it either into a subcutaneous pouch above or as a subperiosteal onlay graft onto the right parietal bone, creating 4 groups in total. We performed histology and micro-computed tomography of the grafts as well as the donor regions 28 days after grafting.Histology revealed marked resorption of subcutaneous control Dmp1-Cre grafts (Fig. 1A) and new bone formation around subperiosteal Dmp1-Cre grafts (Fig. 1C). In contrast, Tnfsf11fl/fl;Dmp1-Cre grafts showed effectively no signs of either bone resorption or formation (Fig. 1B, D). Quantitative micro-computed tomography of the bone disks (Fig. 1E-H) revealed a significant difference in residual graft area between subcutaneous and subperiosteal Dmp1-

Cre grafts ($p < 0.01$, Fig. 1I). This difference was not observed between subcutaneous and subperiosteal Tnfsf11fl/fl;Dmp1-Cre grafts ($p = 0.17$). Residual graft volume ($p = 0.08$, Fig. 1J) and thickness ($p = 0.13$, Fig. 1K) did not differ significantly among the groups. Regeneration of the donor areas was comparable between Tnfsf11fl/fl;Dmp1-Cre and Dmp1-Cre mice and restricted to the defect margins.Without osteocyte-derived RANKL, bone grafts remained virtually unreactive, showing neglectable signs of either resorption or new bone formation. Bone grafts with undisturbed osteocytic expression of RANKL showed substantial resorption when placed subcutaneously, and resorption as well as visible new bone formation when placed subperiosteally. Within the limitations of our study, the results suggest an active function of osteocyte-derived RANKL within the bone graft remodeling cascade.

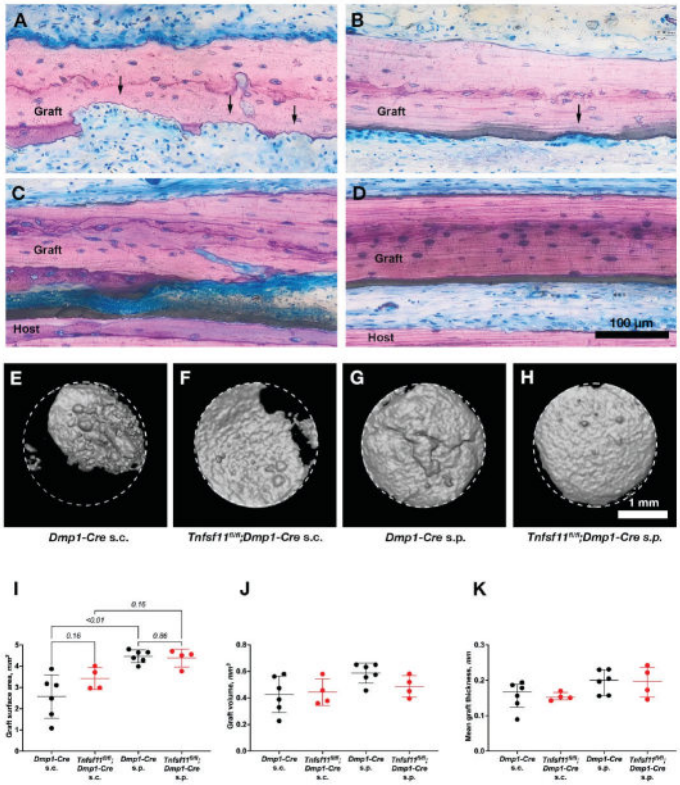

***Disclosures: Balazs Feher**, None*

FRI-359

Live Cell, Confocal and Tissue Clearing/3D Imaging in Mice Expressing a Membrane-GFP targeted to Osteocytes, Odontoblasts and Cementocytes
*Yixia Xie[1], David Moore[1], Eleanor Ray[1], Lisa Le[1], Sarah Dallas[1]. [1]University of Missouri - Kansas City, United States

High resolution 3D imaging of cells in hard tissues is challenging due to the light scattering properties of mineralized matrix. Resolving fine detail of osteocyte, cementocyte & odontoblast dendritic processes requires cell-specific staining methods targeting the membrane or specific substructures in the dendrites. Using transgenic mice expressing a membrane-bound GFP driven by the 10kb Dmp1 promoter (Dmp1-mGFP mice) or mice co-expressing Dmp1-mGFP & a LysM-Cre/tdTomato reporter to target osteoclasts, we have used 3D confocal imaging & tissue clearing/3D imaging to define tissue localization of the mGFP reporter and fine cellular detail of osteocytes, odontoblasts & cementocytes in the lower jaw. Samples were counterstained with alexa555-phalloidin to visualize F-actin and DAPI to label nuclei. Dmp1-mGFP mice were also used for confocal live cell imaging to examine osteocyte embedding dynamics. 3D confocal imaging on 50?m cryosections in 7d mandibles showed Dmp1-mGFP expression in osteocytes, odontoblasts, pulpal cells adjacent to odontoblasts and a subset of mature osteoblasts. Membrane-targeting of GFP enabled resolution of branching & fine detail of odontoblast processes (Fig.1) and osteocyte dendrites. Dmp1-mGFP was also expressed in cementocytes in 2mo mice. Dmp1-mGFP also labeled 80-500nm extracellular vesicle-like particles, at the dentin-enamel junction adjacent to odontoblast processes (Fig 1, arrows) and throughout the mineralized bone & cementum matrix, which likely represent matrix vesicles that initiate mineralization. PEGASOS clearing enabled deep tissue imaging and lightsheet imaging enabled 3D reconstruction of Dmp1-mGFP & LysM-Cre/td tomato expression in the intact mandible and virtual sectioning in any plane. This also revealed Dmp1-GFP expression in a subset of cells in blood vessels supplying the cervical loop region of the incisor. Long term live cell imaging of osteocyte embedding in calvarial explant cultures revealed Dmp1-mGFP first switching on in post mitotic polygonal cells that extended and retracted dendrites during embedding/positioning. Live imaging of osteoclasts & osteocytes revealed that the majority (95%) of osteocytes die during the process of bone resorption. We conclude that the Dmp1-mGFP mouse is a valuable tool for studying differentiation of mineralizing cell types and imaging their fine structure and is compatible with high resolution confocal imaging, tissue clearing/3D lightsheet imaging & live cell imaging.

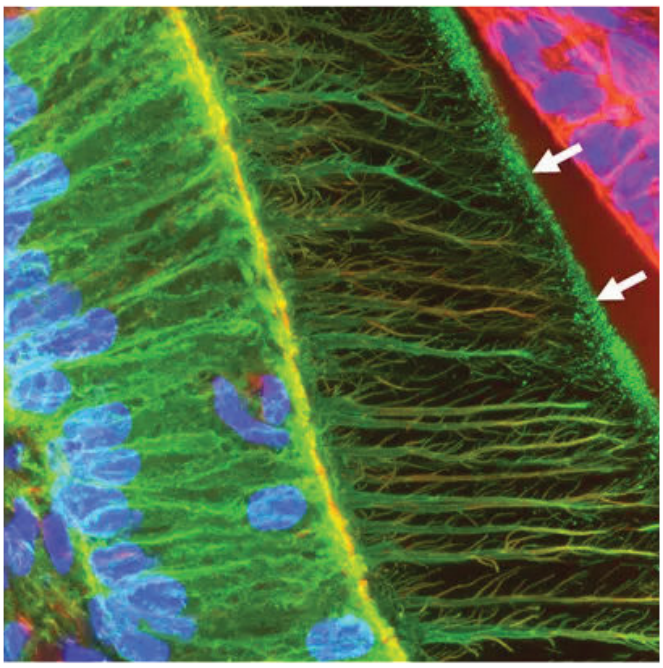

Fig. 1: Dmp1-mGFP expression in odontoblasts showing fine detail of odontoblast processes and GFP positive vesicles close to the dentin- enamel junction (arrows). (green – Dmp1-mGFP, blue = nuclei; red = F-actin)

***Disclosures: Yixia Xie**, None*

FRI-360

The role of NFATc1 in 1,25 dihydroxyvitamin D mediated regulation of osteocyte lacuno-canalicular remodeling *Supriya Jagga[1], Niusha Manoochehri Arash[2], Melissa Sorsby[2], Eva Liu[1]. [1]1 Division of Endocrinology, Diabetes, and Hypertension, Brigham and Women's Hospital, Boston, Massachusetts 02115 2 Harvard Medical School, Boston, Massachusetts 02115, United States. [2]Division of Endocrinology, Diabetes, and Hypertension, Brigham and Women's Hospital, Boston, Massachusetts 02115, United States

Osteocytes are multifunctional bone cells that act as modulators of mineralized matrix resorption. They reside in small cavities of bone called lacunae and form an extensive canalicular network of dendrites (lacuno-canalicular network, LCN) for cell-cell interaction. Bones from mice with X-linked hypophosphatemia (Hyp), which have impaired production of 1,25 dihydroxyvitamin D (1,25D), demonstrate abnormal LCN organization, with enlarged lacunae, impaired canalicular structure, and enhanced osteocyte expression of bone resorption genes compared to WT. Administration of 1,25D or an anti-FGF23 targeting antibody to Hyp mice improves LCN organization, supporting a role for 1,25D in regulating LCN remodeling. In support of this, bones from mice lacking the vitamin D receptor (VDR) in osteocytes (VDRf/f;DMP1Cre+) have impaired LCN organization compared to control, demonstrating that osteocyte-specific actions of 1,25D regulate LCN remodeling. In osteoclasts, the transcription factor nuclear factor of activated T cells cytoplasmic 1 (NFATc1) induces the expression of matrix resorption genes to acidify the extracellular environment and enhance bone resorption. Since osteocytes also acidify their microenvironment and resorb matrix, we hypothesize that NFATc1 plays a role in 1,25D-mediated LCN remodeling. Consistent with this hypothesis, 1,25D suppresses Nfatc1 mRNA expression in IDG-SW3 osteocytes, and knockdown of Nfatc1 expression by lentivirus carrying anti-Nfatc1 shRNA in IDG-SW3 cells attenuates the 1,25D-mediated suppression of matrix resorption gene expression and blocks the 1,25D-mediated suppression of RANKL-induced acidification of the osteocyte microenvironment. These data show that NFATc1 is required for 1,25D-mediated regulation of perilacunar remodeling in vitro. Corresponding with the in vitro data, VDRf/f;DMP1Cre+ osteocytes have enhanced Nfatc1 and matrix resorption gene

expression. To determine the role of NFATc1 in 1,25D mediated LCN remodeling, histomorphometric analyses of tibiae from mice lacking osteocyte-specific NFATc1 (NFATc1f/f;-VDRf/f;DMP1Cre+) were performed, demonstrating that bones from these mice have decreased lacunar size, decreased immunoreactivity for matrix resorption marker cathepsin K, and improved canalicular structure compared to VDRf/f;DMP1Cre+ control. Taken together, the current study demonstrates that NFATc1 is necessary for 1,25D-mediated regulation of osteocyte LCN remodeling.

***Disclosures: Supriya Jagga**, None*

FRI-362

Bone formation by osteoid-osteocytes and osteocytes in C57Bl/6 mice *Sarah Ford[1], Svetlana Komarova[2], Katharina Jähn-Rickert[3], Kerstin Tiedemann[2], Elizabeth Zimmermann[2, 1], [2]McGill University, Canada, [3]University Medical Center Hamburg-Eppendorf, Germany

Purpose: Bone formation is described as occurring on bone surfaces by osteoblasts. However, as bone forming osteoblasts become entrapped in the bone matrix, these so-called osteoid-osteocytes may continue to produce bone matrix while differentiating into osteocytes [1]. Mature osteocytes deeply embedded in the bone have also been observed to remodel their surrounding bone matrix in lactation and hibernation: a process termed perilacunar remodeling [2]. The contribution of osteocyte-driven bone remodeling in the regulation of healthy bone tissue is currently unknown.Methods: Skeletally mature female C57Bl/6 mice received two calcein injections. MMA-embedded undecalcified L3-L5 vertebrae sections were prepared. A region of interest (ROI) of trabecular bone was identified and the bone area of the ROI was measured on brightfield images. Osteocyte lacunae with calcein labels were identified on z-stacks imaged with confocal microscopy. Lacunae were classified (Fig. 1) as osteoid-osteocytes (in or adjacent to the line of osteoblast bone formation) or mature osteocytes (> 3 µm from osteoblast bone formation labels). Bone formation rate (BFR) due to osteoblast activity on bone surfaces followed ASBMR guidelines. BFR of mature osteocytes was measured as follows:BFRosteocyte=(L.Th)/(Ir.L.t) ((sLSocy)/(Ocy.S)) L.Th is label thickness, Ir.L.t is time between calcein injections, and sLSocy is lacunar label length. Ocy.S is total osteocyte surface calculated as the product of lacunar density, bone area and average lacunar perimeter.Results: Active bone formation was observed in 206 +/- 64 lacunae/mm2. Around 80-90% of labeled lacunae were associated with bone forming osteoid-osteocytes (173 +/- 50 lacunae/mm2) and 16% mature osteocytes (33 +/- 6 lacunae/mm2). The osteoblast BFR was 3.17 µm/day and the osteocyte BFR was 0.078 nm/day (not including osteoid osteocytes).Conclusion: Here, we observed that a majority of bone formation at lacunae occurs at osteoid-osteocytes, which should be distinguished from mature osteocytes. BFR due to osteocyte activity may seem small, but perilacunar remodeling is an emerging phenomenon for which the implications on bone quality and bone fragility are not fully understood.References:1. C Palumbo, et al. Cells Tissues Organs. 137:350-358, 1990.2. KJähn-Rickert & EA Zimmermann, Curr. Osteoporos. Rep. 19:391-402, 2021.

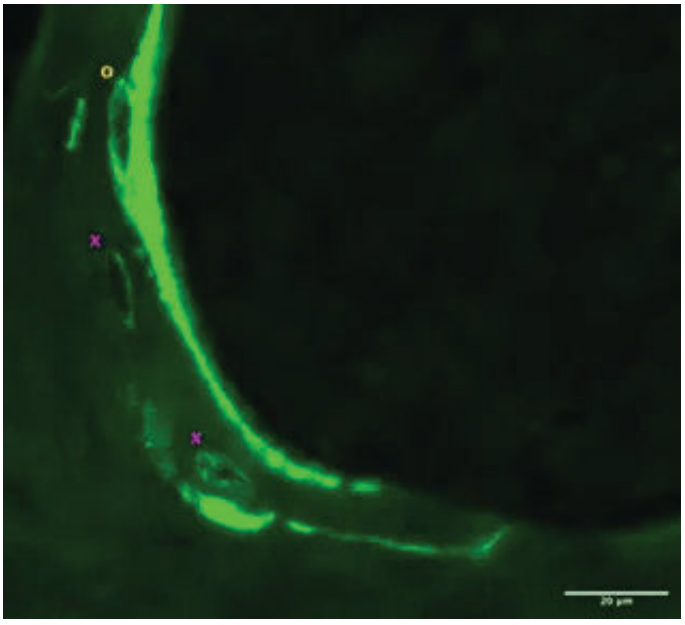

***Disclosures: Sarah Ford**, None*

FRI-363

Hypoxia Inducible Factor-2? Predominantly Contributes to Cortical Microarchitecture of Vhl cKO mice *Sarah Mendoza[5], Benjamin Osipov[2], Deepa Murugesh[3], Blaine Christiansen[4], Gabriela Loots[5], Damian Genetos[6], Clare Yelllowley[5, 5]University of California, Davis, , [2]UC Davis Health, , [3]Lawrence Lvermore National Lab, United States, [4]University of California Davis Health, United States, [5]University of California, Davis, United States, [6]University of California, Room 1020 VM3B, United States

Osteoporosis causes more than 8.9 million bone fractures every year, predominantly affecting the increasingly aging population. Current osteoporotic therapies are undeniably suboptimal due to their adverse side effects and attenuated efficacy. Thus, identification of novel therapeutic targets that provide lifelong improvements in bone mass and quality are necessary. Hypoxia inducible factor (HIF) signaling is required for skeletal health and maintenance. HIFs are transcription factors composed of an oxygen-dependent HIF-? subunit (transcriptionally active isoforms: HIF-1?, HIF-2?) and a constitutively stable nuclear HIF-? subunit. Under normoxic conditions, HIF-? subunits are hydroxylated and targeted for degradation by an E3 ligase complex Von Hippel-Lindau (VHL). Under hypoxic conditions, HIF-? subunits escape VHL-mediated degradation, complex with HIF-?, and induce osteoanabolic gene expression. We've shown that deletion of osteocytic (OCY) Vhl generates a strikingly high bone mass (HBM) phenotype, and deletion of OCY Hif1a or Hif2a showed no effect on skeletal microarchitecture. However, expressing a degradation-resistant OCY HIF-2?, not HIF-1?, generated a HBM phenotype. To determine the requirement of HIF-2? in generating the Vhl cKO HBM phenotype, we utilized 16-week-old mice with dual OCY Vhl and Hif1a (Vhl;Hif1a cKO) or Hif2a (Vhl;Hif2a cKO) deletion. Micro-computed tomography revealed that deletion of Vhl with Hif1a (n=5) or Hif2a (n=3) partially mitigated the trabecular phenotype, whereas dual deletion of Hif2a and Vhl fully mitigated the cortical phenotype. To determine effects on biomechanical integrity, we conducted three-point bending tests on contralateral femora from Vhl;Hif1a cKO (n=2), Vhl;Hif2a cKO (n=2), Vhl cKO (n=3) and cre-negative control (n=3) mice. We found that dual deletion of Vhl and Hif1a or Hif2a fully mitigated cortical stiffness, postyield displacement (PYD), and ultimate force to cre-negative levels, while the Vhl cKO showed increased stiffness and ultimate force with decreased PYD. Although HIF-2? appears to predominantly determine cortical microarchitecture in the Vhl cKO, HIF-? isoform-specific contributions to biomechanical integrity are less clear. Future studies will evaluate HIF-? isoform-specific effects on tissue mechanical properties and collagen orientation that contribute to the mitigated biomechanical phenotype we observe. DKM and GGL conducted work under the auspices of the USDOE by LLNL (DE-AC52-07NA27344).

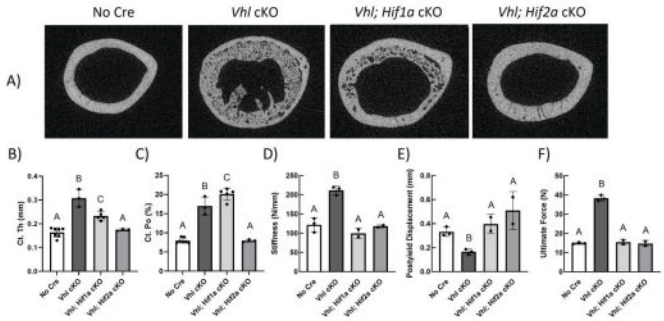

Hypoxia inducible factor-2α predominantly contributes to cortical microarchitecture of *Vhl* cKO mice. Representative microCT mid-sagittal images of left femora from (A) *cre*-negative, *Vhl* cKO, *Hif1a*; *Vhl* cKO, and *Hif2a*; *Vhl* cKO mice. Quantification of cortical thickness (B), cortical porosity (C), cortical stiffness (D), post yield displacement (E), and ultimate force (F) of the femoral mid-diaphysis from *cre*-negative (n=3), *Vhl* cKO (n=3), *Hif1a*; *Vhl* cKO (n=2), and *Hif2a*; *Vhl* cKO (n=2) mice. Bars represent mean ± SD; groups with different letters are statistically different from each other.

***Disclosures: Sarah Mendoza**, None*

FRI-365

Investigating Osteocyte Morphology in Crtap -/- Mouse Model of Recessive Osteogenesis Imperfecta *Carolina Leynes[1], Ellen Busschers[1], Mary Adeyeye[1], Iwen Song[1], Yangjin Bae[1], Brendan Lee[1, 1]Baylor College of Medicine, United States

Osteogenesis Imperfecta (OI) is characterized by short stature and brittle bones. OI type VII has been associated with the loss of CRTAP (Cartilage-associated protein) which is responsible for post-translational modifications of type I collagen via 3-hydroxylation of Pro986 of chain alpha1(I) and Pro707 of chain alpha2(I). Currently, Crtap-/- mice are used as a model for recessive OI as mice present with a decrease in body size, osteo-chondrodysplasia, kyphosis, and severe osteopenia. Furthermore, our lab and others have shown Crtap-/- mice have upregulated transforming growth factor-? (TGF-?) resulting in decreased bone volume to total bone volume (BV/TV), maximum load, and ultimate strength. In addition, an increase in osteoclast, osteoblast, and osteocyte was observed in Crtap-/- mice. Previous studies in children with OI type I and V have also shown an increase in osteocyte number in cortical and trabecular bone compared to age match controls. Given osteocytes' mechanosensory and bone regulatory role via sclerostin and RANKL secretion, we studied

morphological changes in osteocytes of Crtap-/- mice. In this study, we collected femurs from Crtap-/- and WT mice of 4 months of age (n=6) and performed phalloidin staining on 30 ?m sections. Using Imaris analysis software, we processed the images and analyzed osteocyte dendrite length, branch depth, branch level, and area. Our analysis showed an increase osteocyte number, consistent with our and others' previous report, and a decrease in dendrite branch length, depth, level, and area in Crtap-/- mice compared to WT control mice. Our data suggest Crtap-/- mice have decrease osteocyte branching complexity which might be correlated to the decrease in bone mass, maximum load, and ultimate strength previously published by our group. Future studies will further determine the changes in dendrite network after 1D11, an anti-TGF-? treatment, in Crtap-/- mice and investigate the underlying molecular changes in osteocytes of OI models such as Crtap-/- mice and additional OI mouse models.

***Disclosures: Carolina Leynes**, None*

FRI-367

Poloxamer-188 treatment rescues osteocytes with an impaired ability to repair plasma membrane disruptions caused by mechanical loading *Anik Tuladhar[2], Joseph Shaver[2], Wesley McGee[2], KANGLUN YU[3], Wendy B. Bollag[2], Mark W. Hamrick[2], Meghan McGee-Lawrence[4]. [2]Augusta University, , [2]Augusta University, United States. [3], , [4]Medical College of Georgia, Augusta University, United States

We and others have seen that osteocytes sense high-impact osteogenic mechanical loading via transient plasma membrane disruptions (PMDs) which initiate downstream mechanotransduction. However, a PMD must be repaired for the cell to survive this wounding event. The protein Prkd1 (PKC-?) was suggested to play a crucial role in PMD repair via vesicular exocytosis, and our previous studies implicated it as an important mediator of bone adaptation to mechanical loading, where inhibition or deletion of Prkd1 in osteocytes delayed PMD repair rate, decreased cell viability, and blunted the bone's response to in vivo mechanical loading. To determine if impaired osteocyte PMD repair rate can be rescued, the current study investigated whether the FDA-approved synthetic copolymer Poloxamer 188 (P188) can mediate membrane repair and stability in Prkd1-targeted osteocytes. We generated an osteocyte-targeted Prkd1 conditional knockout (CKO) mouse from which primary osteocytes were isolated, and used MLO-Y4 cells and Prkd1 inhibitors to test the effects of P188 on PMD repair rate. MLO-Y4 cells were treated with P188 (2%) for 24hrs followed by Prkd1 inhibitors (kbNB 142-70, 10 ?M; staurosporine, 100 nM) or vehicle for 30 minutes and subjected to laser wounding using a 2-photon microscope (Zeiss) in the presence of membrane impermeant FM1-43 fluorescent dye. Prkd1 inhibitors significantly delayed PMD repair rate (p=0.017), and this effect was rescued by P100 treatment (p=0.001). Similar beneficial effects of P188 treatment on PMD repair rate were seen in Prkd1 CKO primary osteocytes (p=0.010). MLO- Y4 cells were seeded into flow chamber slides, treated with P188 followed by Prkd1 inhibitors as described above, and exposed to fluid flow shear stress (50 dynes/cm^2; 5 minutes; Harvard Apparatus). Viability was assessed 10 minutes after flow exposure ceased via PI staining. Prkd1 inhibition impaired post-wounding cell survival in osteocytes (p=0.0005) subjected to flow, but treatment with P188 significantly (p=0.00006) improved post-wounding viability. To test the efficacy of P188 treatment in vivo, we injected the Prkd1 CKO mice with P188 (460mg/kg) 30mins before osteogenic tibial loading bouts (alternating days for 2 weeks) and saw a significant improvement in the bone mineral density in the loaded tibia (p=0.0006) as compared to the controls. Our findings suggest a potential therapeutic application of P188 in improving osteocyte membrane repair and promoting bone health.

***Disclosures: Anik Tuladhar**, None*

FRI-368

Irisin modulates murine osteocytic osteolysis in a sex and age-specific manner *Anika Shimonty[1], Fabrizio Pin[1], Matt Prideaux[1], Gang Peng[1], Lynda Bonewald[1]. [1]Indiana University School of Medicine, United States

Irisin, a hormone generated by the proteolytic cleavage of Fibronectin type III Domain Containing protein 5 (FNDC5) has been described to have beneficial effects on the brain and fat, but effects on bone are contradictory [1], as some studies have found positive effects but our studies have shown that irisin deletion protects against bone loss due to ovariectomy [3]. Recently we have shown that irisin deletion also protects against bone loss with lactation and a low calcium (Ca) diet in females but exacerbates male mice bone loss due to a low Ca diet. To determine if irisin plays a role in bone loss with aging, 5 and 20-month (mo)-old mice were compared. No differences were observed between WT and FNDC5 global KO female mice (BV/TV; 57.5% WT:58.5% KO), however, male KO mice, 5 and 20 mo, had higher BV/TV (60.8% KO:57.6% WT) but less biomechanical strength compared to WT males (ultimate force; 18.5N KO:22.1N WT, stiffness;78.6Nmm KO:94.3Nmm WT). With a low Ca diet, both 5 and 18 mo female KO were partially protected against bone loss and weakness: (BV/TV;43.2% KO:40.4% WT), ultimate force (17.8N KO:15.7N WT) and stiffness (59.8Nmm KO:43.4 Nmm WT). In contrast, both 5 and 18-mo male KO mice lost more bone and had lower bone volume (BV/TV; 48.6% KO:55.4% WT) on a low Ca diet and lower ultimate force (14.9N KO:18.4N WT). To begin to identify responsible molecular mechanisms, RNAseq was performed on osteocyte-enriched bone from 5 mo old animals as two major functions of the osteocyte are to remove their perilacunar matrix to provide calcium and to produce RANKL to activate osteoclasts. Sex differences showed that the female WT osteocyte transcriptome had higher expression of genes responsible for osteocytic osteolysis including Acp5, Ocstamp, Dcstamp, Ctsk, Tnfsf11, and Mmp13 compared to WT males. This difference was not evident in KO females compared to KO males. On a low Ca diet, KO females had lower expression of osteocytic osteolysis genes such as Tnsfs11 and Ocstamp compared to WT females. Analysis of the osteocyte transcriptome is ongoing. In summary, in young females irisin aids or primes the osteocyte to release Ca under Ca-demanding conditions to possibly aid in offspring survival, however in the aging female, this effect of irisin on osteocyte function becomes detrimental with sex hormone and/or Ca deficiency. In contrast, irisin appears beneficial for males at any age, but especially with aging.1.Maak et al, Endocr Rev, 20212. Kim et al, Cell, 2018

***Disclosures: Anika Shimonty**, None*

FRI-370

Deletion of Osteocyte-Intrinsic MMP13 is Protective from Temporal Mandibular Joint Osteoarthritis *Cristal Yee[1], Marianne Demirdji[1], Karsyn Bailey[1], Alena Larios[1], Christoforos Meliadis[1], Clarissa Aguirre Luna[1], Sunil Kapila[2], Tamara Alliston[1]. [1]University of California, San Francisco, United States. [2]University of California, Los Angeles, United States

Osteocytes support the crosstalk between cartilage and subchondal bone that maintains joint homeostasis. In human knee osteoarthritis (OA), osteocyte perilacunar-canalicular remodeling (PLR) and MMP13 expression are suppressed. Using mice with an osteocyte-intrinsic deficiency in MMP13 (MMP13ocy-/-), we showed that suppression of MMP13-dependent PLR is sufficient to cause early OA in the knee. However, whether these mechanisms are conserved in the fibrocartilaginous temporomandibular joint (TMJ), which differs from the knee in its anatomy, cell types, and OA progression, remains unclear. We aim to determine the cellular and molecular mechanisms that distinguish progression of knee and TMJ osteoarthritis (TMJOA) and if osteocytic MMP13 plays a causal role in the TMJ degeneration as it does in the knee. Given the importance of osteocytic MMP13 in knee joint homeostasis, we hypothesize that osteocytic-ablation of MMP13 will compromise PLR and exacerbate degeneration of the TMJ.Male MMP13ocy-/- mice and littermate controls (Ctrl, n=6 mice/group) at 12 weeks of age, were injected with saline or 0.10 mg of monosodium iodoacetate (MIA) in the intra-articular joint of the TMJ, a model of TMJOA. After 28 days post injection, TMJs were assessed for cartilage degeneration and lacunar canalicular network (LCN) integrity. Unlike the knee, genotype-dependent differences in the TMJ cartilage were not apparent in a modified Mankin score among the uninjured controls or saline-treated Ctrl and MMP13ocy-/- mice. As expected, MIA significantly increased the TMJ Mankin score in Ctrl mice, with excessive Safranin-O staining of the chondrocyte pericellular matrix, disorganization of TMJ chondrocytes, and changes in the histological boundary between cartilage and bone. However, MMP13ocy-/- mice were protected from MIA-induced TMJOA. MIA-injected MMP13ocy-/- TMJs showed no change in Mankin scores compared to the MMP13ocy-/- saline-injected group. Further, silver nitrate staining of the LCN showed an MIA-dependent increase in subchondral bone osteocyte number in the Ctrl mice that was absent in the MMP13ocy-/- TMJ. Therefore, we find that ablation of MMP13 in TMJ osteocytes plays a protective role in the TMJ, preventing MIA-induced OA and osteocytic deregulation. Thus, osteocyte-intrinsic MMP13 plays a distinct role in knee and TM joint homeostasis, providing new insight into the differential susceptibility of these joints to OA.

***Disclosures: Cristal Yee**, None*

FRI-372

Sex Differences in in vivo Osteocyte Ca2+ Signaling and Gap Junction Inhibition *JAMES BOORMAN-PADGETT[1], Randy Valcourt[2], Bridget Saw[3], Jelena Basta-Pljakic[2], Mia Thi[4], David Spray[3], Mitchell Schaffler[5]. [1], United States. [2]City College of New York, United States. [3]Albert Einstein College of Medicine, United States. [4]ALBERT EINSTEIN COLLEGE OF MEDICINE, United States. [5]The City College of New York, United States

INTRODUCTION: Osteocytes (Ot) in vivo exhibit a highly coordinated Ca2+ signaling response to mechanical loading, in which number of responding Ot increases in proportion to increasing applied strain [1,2]. Earlier studies established this signaling pattern in female mice. Whether Ot in males respond similarly to loading is unknown. Here, we compared Ot Ca2+ signaling responses to loading in male vs female mice and further tested whether signaling in both sexes responded similarly to gap junction inhibition.METHODS: Osteocyte Ca2+ signaling responses to mechanical loading were examined in tamoxifen inducible GCaMP6f Ca2+ indicator mice (4 mo, n=22F/30M). Studies used urethane anesthesia, which unlike isoflurane does not interfere with gap junctions [3]. This allowed us to test gap junction function using the inhibitor carbenoxolone (CBX). 3rd metatarsals (MT3s) were cyclically loaded to test strains of 250-3000 ??; 2-photon microscopy was used to image Ca2+ fluorescence in diaphyseal Ot during loading [1,2]. CBX was given after the first (baseline) loading bout and 20 minutes were allowed for diffusion into the bone; loading and imaging studies were then repeated. Cumulative in vivo fluorescent signal intensity as a function of time was calculated for each osteocyte in the region of interest (>1000 cells/group). Ot Cx43 gene and protein expression were determined.RESULTS: Ot in male mice showed ~40% greater cumulative fluorescent signal intensity with loading than Ot in female mice [Fig 1A] and occurred at all strain levels. Blocking gap junctions slightly reduced cumulative signal

intensity in males. In contrast, blocking gap junctions in females dramatically attenuated Ca2+ signal intensity. Cx43 mRNA and protein levels were significantly higher in male than female Ot [Fig 1B, 1C - mRNA: 1.4-fold; Protein: ~2.5-fold].DISCUSSION: Our studies reveal unexpected differences in loading-induced osteocyte Ca2+ signaling in male and female mice. The reasons underlying this sex difference in Ot response to loading remain obscure, but may include sex hormones effects and/or intrinsic biological differences between males and female cells [4,5]. Indeed, the more profound Ot response to gap junction inhibition in female mice may reflect such a biological difference, as female Ot express comparatively less Cx43 at both gene and protein levels.REFERENCES:1)Lewis+ PNAS 2017 2)Lewis+ JoVE 2023 3)Burt+ Cir Res 1989 4)Lewis+ Bone 2021 5)McNamara+ Curr Ost Rep 2021

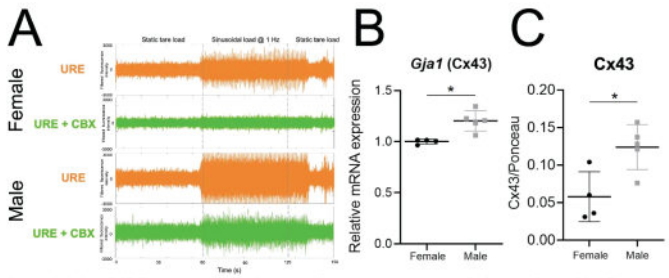

Figure: (A) Overlaid fluorescence intensity traces from ~1000 osteocytes during mechanical loading protocol at 2000 με. (B) Gene expression of *Gja1* in bones of female and male mice (C) Protein expression of Cx43 in bones of female and male mice

***Disclosures: JAMES BOORMAN-PADGETT**, None*

FRI-373

Disparate impact of osteocyte oxygen-sensing mechanisms on bone quality *Kristina Wells[1], Sarah Mendoza[4], Alice Wong[1], Deepa Murugesh[3], Gabriela Loots[4], Clare Yellowley[5], Damian Genetos[6]. [1]UC Davis, United States. [4]University of California, Davis, . [3]Lawrence Lvermore National Lab, United States. [4]University of California, Davis, United States. [5]University of California School of Veterinary Medicine, United States. [6]University of California Davis, United States

Bone strength involves bone quantity and quality, with bone quantity receiving greater engagement and investigation than bone quality. Ideal osteoanabolic therapies will involve both the quantity and the quality of bone matrix. We have recently demonstrated that constitutive osteocytic oxygen sensing (degradation resistant HIF2a, HIF2cDR) or a regulatory protein upstream of oxygen sensing (Vhl cKO) produce unique high bone mass phenotypes. While both disruptions increase cortical and trabecular bone, HIF2cDR does not phenocopy Vhl KO either in quantity of bone produced or apparent bone organization. Understanding overlapping and unique contributions to bone quality in Vhl cKO vs. HIF2cDR will identify ideal targets for osteoanabolic therapies. We developed mice with osteocyte-enriched (10kb-Dmp1-cre) deletion of Vhl, Hif1a, or Hif2a or degradation-resistant HIF1A or HIF2A and established distinct impact of these deletions on bone strength, which was increased in Vhl cKO and reduced in HIF2cDR mice compared to wild-type controls. We next used ?CT to evaluate total mineral density distribution of knockout and transgenic femora. Both Vhl cKO and HIF2cDR mice had reduced mid-cortical peak mineral and mean mineral density, indicating impaired tissue material properties despite distinct impact on bone strength. Collagen alignment, analyzed by second-harmonic generation, was altered in each genotype relative to wild-type controls. Finally, we sought a potential mechanism for the differences in bone quality. SPARC - a matrix mineralization protein involved in collagen fibrillogenesis- is regulated by both hypoxia and Vhl in myriad cell types; absence of SPARC causes osteopenia and impairs both the organic and mineral content of bone. IHC staining revealed higher Sparc levels in both HIF2acDR and Vhl cKO compared to wild-type bones, with greater staining in Vhl cKO compared to Hif2cDR. In summary, manipulating oxygen-sensing pathways in osteocytes elicits high bone mass phenotypes with diverse outcomes on bone quality.DKM and GGL conducted work under the auspices of the USDOE by LLNL (DE-AC52-07NA27344)

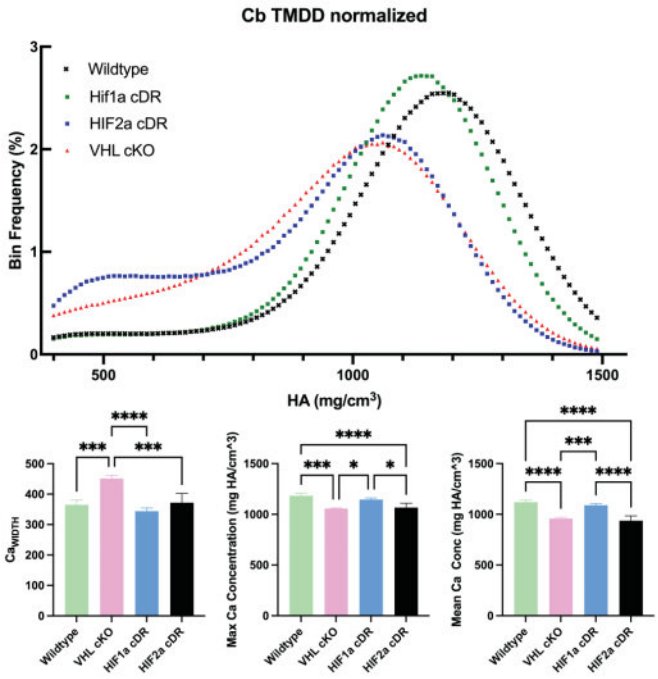

***Disclosures: Kristina Wells**, None*

FRI-387

Previous Fracture and Subsequent Fracture Risk: A Meta-analysis to Update FRAX *Eugene McCloskey[5], Helena Johansson[2], Nicholas Harvey[3], Enwu Liu[4], Marian Schini[5], Liesbeth Vandenput[4], Mattias Lorentzon[6], William Leslie[7], John Kanis[4], and the FRAX Meta-analysis Cohort Group. [8]. [5]University of Sheffield, United Kingdom. [2]University of Gothenburg, Sweden. [3]University of Southampton, . [4]Australian Catholic University, Australia. [5]University of Sheffield, . [6]Sahlgrenska Academy, University of Gothenburg, Sweden. [7]University of Manitoba, Canada. [8]Sheffield, United Kingdom

The aim of this study was to quantify the fracture risk associated with a prior fracture on an international basis and to explore the relationship of this risk with age, sex, time since baseline and bone mineral density (BMD).We studied 665,971 men and 1,438,535 women from 64 cohorts in 32 countries followed for a total of 19.5 million person-years. The effect of a prior history of fracture on the risk of any clinical fracture, any osteoporotic fracture, major osteoporotic fracture and hip fracture alone was examined using an extended Poisson model in each cohort. Covariates examined were age, sex, BMD and duration of follow up. The results of the different studies were merged by using the weighted ?-coefficients.A previous fracture history, compared with individuals without a prior fracture, was associated with a significantly increased risk of any fracture (Hazard ratio, HR = 1.88; 95% CI = 1.72-2.07). The risk ratio was similar for the outcome of osteoporotic fracture (HR = 1.87; 95% CI = 1.69-2.07), major osteoporotic fracture (HR = 1.83; 95% CI = 1.63-2.06) or for hip fracture (HR = 1.82; 95% CI = 1.62-2.06). There was no significant difference in risk ratio between men and women. Subsequent fracture risk was marginally downward adjusted when account was taken of BMD. Low BMD explained a minority of the risk for any fracture (14%), osteoporotic fracture (17%), and for hip fracture (33%). The risk ratio for all fracture outcomes related to prior fracture decreased significantly with adjustment for age and time since baseline examination.A previous history of fracture confers an increased risk of fracture of substantial importance beyond that explained by BMD. Its quantitation on an international basis permits the more accurate use of this risk factor in case finding strategies.

***Disclosures: Eugene McCloskey**, Osteoporosis Research Ltd, Other Financial or Material Support*

FRI-390

Development of Artificial Intelligence System for Predicting Areal Bone Mineral Density from Plain Radiographs *Huy Nguyen[1], Dinh Tan Nguyen[2], Thach Tran[3], Lan Ho-Pham[4], Tuan Nguyen[5]. [1]The University of Technology Sydney, . [2]University of Technology Sydney, . [3]Garvan Institute of Medical Research, Australia. [4]Saigon Precision Medicine Research Center, Viet Nam. [5]University of Technology Sydney , Australia

Background and Aim: Currently, dual-energy X-ray absorptiometry (DXA) is the gold standard for measuring bone mineral density (BMD) and diagnosing osteoporosis, but DXA is not widely available in low-resource settings. In this study, we developed an Artificial Intelligence (AI) system to estimate BMD from plain radiographs for osteoporosis screening. Methods: The development of AI algorithms was based on 5134 plain X-rays, and the testing was based on 1926 plain X-rays from the Vietnam Osteoporosis Study. Anteroposterior and oblige digital X-ray hip and spine were taken by FCR Capsula XLII (Fujifilm Corp., Tokyo, Japan). We used seven backbone models, including VGG16, VGG19, ResNet34, ResNet50, ViTB16, ConvNextB, and RegNetY16F, to extract 1000 features from each radiograph. From the features, we developed models to estimate areal BMD at the lumbar spine, total hip, and femoral neck. We termed the estimated BMD as 'xBMD'. We then compared xBMD with DXA-based areal BMD (aBMD) measured at the lumbar spine, total hip, and femoral neck (Hologic Horizon, Hologic Corp., Bedford, MA, USA). The concordance between xBMD and aBMD was assessed by the coefficient of correlation and the Bland-Altman approach. Results: The correlation between xBMD and aBMD was 0.87, 0.91, and 0.90 for the lumbar spine, total hip, and femoral neck, respectively. The correlation was greater in women than men, but the difference was not statistically significant (p-overall = 0.568). When aBMD was used to classify into osteoporosis vs non-osteoporosis, the discrimination of xBMD was high, with area under the ROC curve (AUC) being 0.92 for lumbar spine, 0.95 for total hip and 0.94 for femoral neck.Conclusion: These results suggest that it is possible to accurately predict areal BMD from plain radiographs, and that the AI system developed here can be used as an effective tool for opportunistic screening osteoporosis in high-volume settings.

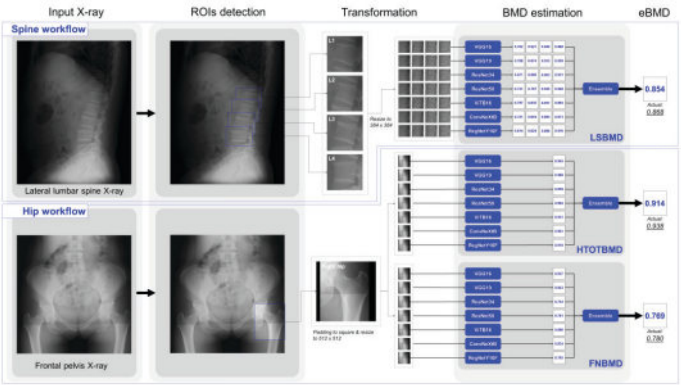

***Disclosures: Huy Nguyen**, None*

FRI-395

Automated Deep Learning-based CT-Scout View Assessment of Prevalent Vertebral Fractures *Eren Bora Yilmaz[1], Till Yannik Fricke[2], Claus-C Glueer[3], Carsten Meyer[2]. [1]Christian-Albrechts-Universität Kiel , . [2]Ostfalia University of Applied Sciences, Germany. [3]Christian Albrechts Universitaet zu Kiel, Germany

Automated detection and grading of vertebral fracture status on computed tomography (CT) scout scans using artificial intelligence (AI) may be useful for both diagnosis and opportunistic prognostic evaluation of fracture risk (no added radiation dose). 2D localizer images (scout scans) taken as part of a CT protocol to select the scan range usually cover a larger area of the spine than the final 3D CT volume and thus may provide more comprehensive information on prevalent vertebral fractures, a key risk factor for future fracture. Aim: To develop and test an AI tool for classification and grading of fractures on CT scout scans. Method: "fNet" is a deep CNN that was previously applied to 3D CT volumes (Yilmaz et al., 2023) and was modified to work with 2D scout scans. It was used to classify the fracture status of individual vertebrae based on 2D image patches centered on vertebral bodies (47 × 47 mm at 1 mm/px) that were extracted using ground truth vertebral body center coordinates. The model was trained on scout scans from the Diagnostik Bilanz dataset (147 scout scans from 7 centers, 1798 vertebrae, 127 fractured, 101 with fracture grade>=2, 32 with grade 3). Ground truth (vertebral body center coordinates and per-vertebra fracture status) for T4-L4 was previously annotated by a trained radiologist using slices of 3D CT volumes. Experiments were conducted in a 4-fold cross-validation setting also used to compute mean confidence intervals (noted +/- in the following). Results: For classifying osteoporotic fractures (positive class; Genant SQ grades 1 - 3) versus normal vertebrae (negative class; Genant SQ grade 0 and deformities), the model achieved 90.6%+/-1.5% ROC-AUC. At a classification threshold of ?=0.05 the sensitivity was 81%+/-4%, the specificity 86%+/-1.3%. When regarding Genant SQ grades 2 and 3 as positive class, ROC-AUC, sensitivity and specificity (?=0.05) were 91.5%+/-0.8%, 85%+/-2% and 85%+/-1.0%, respectively. Finally, with only SQ grade 3 as positive class, we obtained 95.9% 0.8%, 87%+/-7% and 90.6%+/-0.8%, respectively. Discussion: In previous experiments on 3D CT volumes instead of scout scans we reported AUC=98.4%+/-0.4%for the classification of "0-1 vs 2-3". 2D vs 3D differences and image quality of the scout scans could be reasons for lower AUC. Conclusion: To our knowledge this is the first automatic vertebral fracture assessment method on CT scout scans. We demonstrated robust classification performance across three fracture classification tasks.

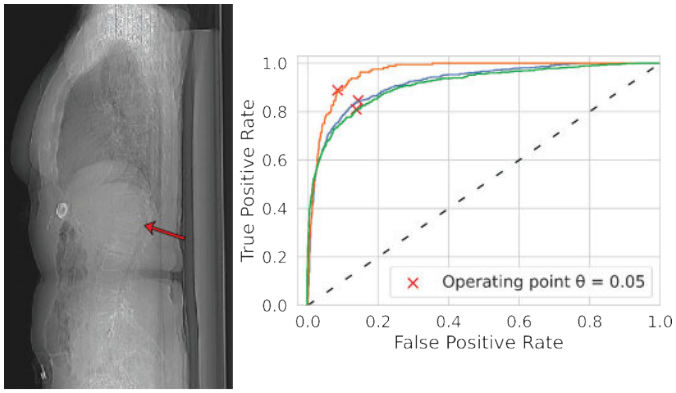

Figure: Vertebral fracture detection on CT scout scans. Left: Arrow indicates indicates Genant SQ grade 3 fracture fracture that was correctly detected by the model. Right: ROC-Curves for binary classifications of fracture grades "0 vs 1-3" (green line), "0-1 vs 2-3" (blue line), and "0-2 vs 3" (orange).

***Disclosures: Eren Bora Yilmaz**, None*

FRI-399

Joint Prediction Incident Fractures by Prevalent Vertebral Fracture & Abdominal Aortic Calcification Ascertained by Automated Algorithms in Clinical Practice *John Schousboe[1], Joshua Lewis[5], Barret Monchka[3], Siobhan Reid[3], Michael Davidson[3], Doug Kimelman[3], Mohamed Jafari Jozani[3], Cassandra Smith[4], Marc Sim[5], Zulqarnain Gilani[5], David Suter[5], William Leslie[3]. [1]Park Nicollet Clinic HealthPartners Institute University of Minnesota, . [5]Edith Cowan University, Australia. [3]University of Manitoba, Canada. [4]Victoria University, . [5]Edith Cowan University,

Background: Prevalent vertebral fracture (PVFx) and abdominal aortic calcification (AAC) jointly are associated with incident fractures. The need for trained interpreters of lateral spine bone mineral density (BMD) images remains a barrier to widespread ascertainment of PVFx and AAC in older adults. Our aim was to estimate the joint associations of PVFx and AAC ascertained by automated algorithms in clinical practice with incident major osteoporotic (MOF), hip, and any clinical fracture.Methods: Separate convolutional neural networks (CNNs) were used to develop automated algorithms to identify fractured thoracolumbar vertebrae and score AAC using the Framingham scale on lateral spine bone density images obtained in the province of Manitoba at the time of bone densitometry between 2010 and 2017. In a separate test set of 6,371 individuals (mean [SD] age 75.8 [6.9], 93% female), automated vertebral fracture status was determined and AAC scored and categorized as low (score 0-1), moderate (2-5) or high (6-24). Cox models were used to estimate associations of PVFx and AAC with incident fractures, adjusted for other covariates and each other. Cumulative incidence of fractures over 5 years in subsets defined by AAC level and PVFx status were calculated accounting for competing mortality. The importance of predictor variables relative to each other for prediction of all three fracture types was compared using Wald chi-square statistic of the full model with each single predictor variable left out vs included.Results: 15% had PVFx, 41% had low AAC, 33% had moderate AAC, and 27% had high AAC. PVFx had higher importance than any other predictor for MOF, second most important for any clinical fracture prediction after age (Figure), and third most important for hip fracture prediction after age and BMD. AAC was of moderate importance for predicting all fracture types. Compared to low AAC, those with high AAC had a fully-adjusted HR 1.32 (95% CI 1.05-1.66) for MOF and HR 1.42 (95% C.I. 0.95-2.11) for hip fracture. The 5-year cumulative incidence of MOF was 7.1% in those with low AAC and no PVFx, 10.1% in those with high AAC and no PVFx, 12.9% in those with low AAC & PVFx, and 16.7% in those with high AAC and PVFx.Conclusions: Ascertainment of both PVFx and AAC on lateral spine bone density images using automated algorithms can aid fracture risk assessment and stratification amongst older individuals undergoing bone densitometry in clinical practice.

Figure: Variable Importance* for Prediction of Incident Fractures

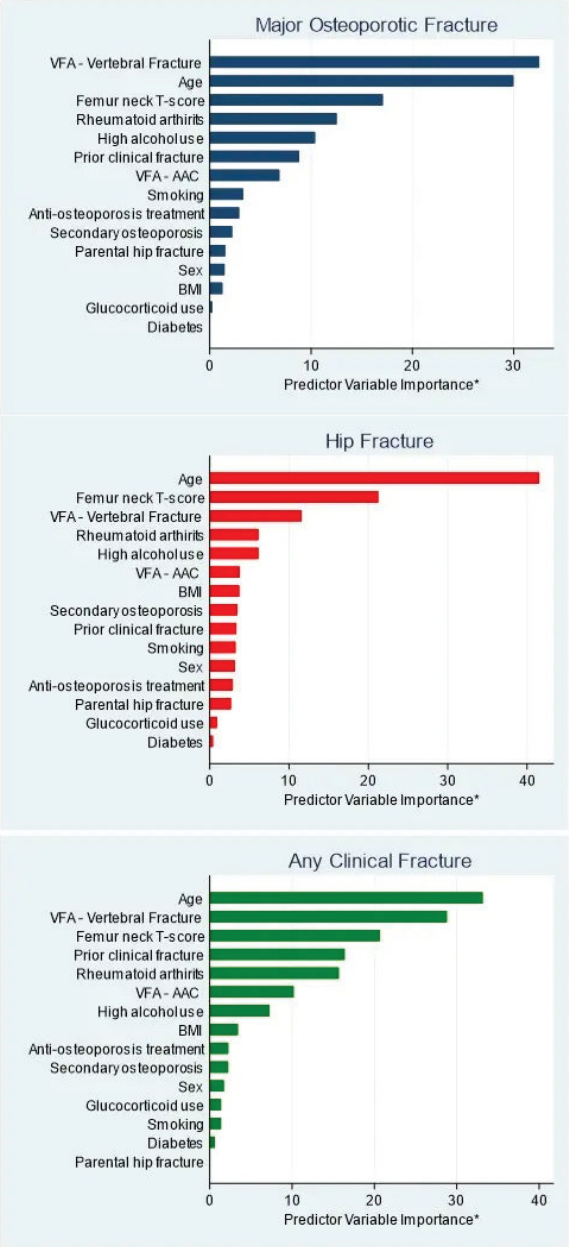

*measured with Wald chi-square statistic

***Disclosures: John Schousboe**, None*

FRI-402

Estimating 'Skeletal Age' by Bone Loss in Elderly Men and Women *Ngoc Huynh[1], Krisel De Dios[1], Thach Tran[1], Tuan Nguyen[2]. [1]University of Technology Sydney, Australia. [2]University of Technology Sydney , Australia

Background and Aim: Skeletal Age is defined as the age of the skeleton as a result of a fracture or exposure to risk factors that elevate the risk of fracture. Higher rates of bone loss are associated with an elevated risk of both fracture and mortality. In this study, we aimed to assess the impact of bone loss on bone fragility by estimating skeletal age using bone loss in elderly men and women. Methods: We analyzed the data from the Study of Osteoporosis Fracture (SOF) and Osteoporotic Fractures in Men (MrOS) that included 9704 women and 5994 men aged 64 years and above. Bone mineral density (BMD) at the femoral neck was measured at baseline and subsequent visits. Mortality was ascertained from death certificates and hospital records. We limited the analysis to those with at least 3 BMD measurements (3848 women and 2925 men). The linear regression model was used to estimate the rate of change in BMD for each individual. The multivariable Cox's proportional hazard model was used to quantify the contribution of the rate of BMD change to mortality, adjusted for age, body mass index, smoking status, alcohol consumption, dietary calcium intake, estrogen and bisphosphonate treatment. The magnitude of the association between bone loss and mortality was then transformed into the number of years of life lost using Gompertz's law of mortality and the US life table. Skeletal age is then determined by the sum of chronological age and years of life lost. Results: In women, the average rate of change in femoral neck bone mineral density (BMD) was found to be -0.61 +/- 1.2% [mean+/-SD] per year, while in men, it was -0.16 +/- 0.9% per year. Throughout the study, 1942 women and 1949 men died. For women, each standard deviation [SD] increase in femoral neck BMD loss was linked to a 1.2-fold (95%CI, 1.1-1.3) increase in total mortality, while for men, the increase was 1.4-fold (95%CI, 1.35-1.5) after adjusting for age, baseline FNBMD, BMI, smoking and drinking status. Additionally, each SD increase in bone loss was associated with a loss of 1.9 years and 3.5 years of life in women and men, respectively. For the same rate of bone loss, men experienced a more substantial loss of years of life than women. Moreover, a 60-year-old woman with a femoral neck BMD loss of more than 2% is estimated to have a skeletal age of 63.5 years. Conclusion: In elderly men and women, excess bone loss is associated with an increased loss of years of life and accelerated bone fragility.

***Disclosures: Ngoc Huynh**, None*

FRI-404

Effect of Race/Ethnicity on United States FRAX Calculations and Treatment Qualification: A Registry-Based Study *William Leslie[1]. [1]University of Manitoba, Canada

Since 2008 the United States has had four race/ethnic FRAX® calculators: White ("Caucasian"), Black, Asian, and Hispanic. The ASBMR Task Force on "Clinical Algorithms for Fracture Risk" has been examining the implications of retaining race/ethnicity in the US FRAX calculators.AIM: To compare treatment qualification based upon existing US FRAX race/ethnicity calculators and a hypothetical US population-based FRAX calculator. METHODS: The study sample consisted of all DXA assessments in Manitoba women aged 50 years or older from 1996-2018, with at least one year of prior coverage to assess FRAX inputs. Race/ethnicity was self-identified (119,243 White, 485 Black, 2,816 Asian, insufficient Hispanic for analysis). We computed FRAX scores according to each US calculator and the proportion exceeding intervention cutoffs (>20% for major osteoporotic fracture, MOF; >3% hip for fracture, and combined with prior fracture and T-score criteria as per the Bone Health and Osteoporosis Foundation, BHOF). We then estimated these measures for a hypothetical population-based FRAX calculator derived as the weighted mean for the US population based upon current US Census Bureau statistics.RESULTS: With identical inputs, the highest FRAX measurements were seen with the White FRAX calculator, lowest measurements with the Black calculator, with intermediate measurements for the Asian and Hispanic calculators. The percentage of women with FRAX scores exceeding the hip fracture treatment threshold was 32.0% for White, 1.9% for Black and 19.7% for Asian women; the MOF treatment threshold was exceeded for 14.9% of White, 0.0% of Black, and 3.5% of Asian women. Disparities in treatment qualification were reduced when additional BHOF criteria including DXA T-score were considered. When fracture risk was recalculated for non-White women using the White FRAX calculator, mean values for Asian women slightly exceeded those for White women but for Black women remained substantially below those for White women. When using a single population-based FRAX calculator for non-White women the mean probability of fracture and treatment qualification increased across the age range, and for Asian women slightly exceeded that for White women.CONCLUSION: Use of a single population-based FRAX calculator, rather than existing US race/ethnic FRAX calculators, will reduce differences in treatment qualification and may ultimately enhance equity and access to osteoporosis treatment.

Proportion of women with high fracture risk according to self-reported race/ethnicity using race/ethnicity-concordant FRAX calculator and population-based FRAX calculator.

WHITE WOMEN	WHITE FRAX MOF ≥ 20%	WHITE FRAX HIP ≥ 3%	WHITE FRAX BHOF GUIDELINES	POP-BASED FRAX MOF ≥ 20%	POP-BASED FRAX HIP ≥ 3%	POP-BASED FRAX BHOF GUIDELINES
50-59 years	2.8%	5.2%	20.3%	1.4%	3.6%	19.5%
60-69 years	9.2%	16.9%	33.0%	5.4%	13.1%	31.0%
70-79 years	23.1%	55.4%	61.4%	16.5%	49.4%	57.2%
80+ years	41.7%	87.1%	87.5%	29.1%	81.7%	83.1%
All ages	14.9%	32.0%	43.4%	10.0%	28.0%	40.9%
BLACK WOMEN	BLACK FRAX MOF ≥ 20%	BLACK FRAX HIP ≥ 3%	BLACK FRAX BHOF GUIDELINES	POP-BASED FRAX MOF ≥ 20%	POP-BASED FRAX HIP ≥ 3%	POP-BASED FRAX BHOF GUIDELINES
50-59 years	0.0%	0.0%	13.1%	0.8%	0.8%	13.1%
60-69 years	0.0%	0.0%	19.3%	1.0%	4.0%	21.8%
70-79 years	0.0%	3.0%	15.0%	1.5%	15.8%	21.1%
80+ years	0.0%	17.9%	50.0%	7.1%	71.4%	75.0%
All ages	0.0%	1.9%	18.4%	1.4%	10.3%	22.5%
ASIAN WOMEN	ASIAN FRAX MOF ≥ 20%	ASIAN FRAX HIP ≥ 3%	ASIAN FRAX BHOF GUIDELINES	POP-BASED FRAX MOF ≥ 20%	POP-BASED FRAX HIP ≥ 3%	POP-BASED FRAX BHOF GUIDELINES
50-59 years	0.8%	2.5%	26.3%	1.5%	5.1%	26.3%
60-69 years	1.3%	10.9%	42.1%	6.4%	21.8%	43.7%
70-79 years	7.4%	42.4%	58.3%	19.0%	59.8%	68.5%
80+ years	18.2%	82.5%	84.4%	39.6%	94.8%	94.8%
All ages	3.5%	19.7%	43.6%	9.7%	29.8%	47.2%

MOF, Major osteoporotic fracture. BHOF, Bone Health and Osteoporosis Foundation.

***Disclosures: William Leslie**, None*

FRI-406

Postmenopausal women with normal BMD who have fracture have deteriorated microarchitecture by HRpQCT: a prospective analysis from The OFELY Study *Elisabeth Sornay-Rendu[1], Roland Chapurlat[2], francois duboeuf[2]. [1]INSERM UMR1033, Universit? de Lyon, France. [2]INSERM UMR 1033, France

Alterations of bone microarchitecture (MA) contribute with low areal BMD to skeletal fragility but the contribution of cortical and trabecular (Tb) architecture to the risk of fracture (Fx) has rarely been evaluated prospectively in women with normal areal BMD. The aim of this study was to prospectively investigate the prediction of fragility Fx by bone MA assessed by HR-pQCT in postmenopausal women without low BMD.We measured at the 14th annual follow-up of the OFELY study, bone MA at the distal radius and tibia with HR-pQCT (XTreme CT, Scanco Medical AG, Bassersdorf, Switzerland) in addition to areal BMD with DXA, in 589 postmenopausal women. Among them, 169 (29%) women, mean (SD) age 65 (9) yr, had normal BMD defined as a T score>=-1 at the lumbar spine, femoral neck and total hip. During a median [IQR] 14 [12-15] yr of follow-up, 46 of those women sustained incident fragility Fx, including 19 women with a major osteoporotic Fx (hip, clinical spine, shoulder or wrist). Women who sustained Fx did not differ for age, BMI, tobacco use, prior Fx, FRAX, aBMD and TBS compared with women without incident Fx. In contrast, they had significant impairment of volumetric densities (vBMD) (-0.4 to -0.6 SD), cortical area (Ct.Ar) and cortical thickness (Ct.Th) (-0.7 SD) at the radius, and alterations of stiffness (K) and estimated failure load (FL) (-0.4 to -0.6 SD) at both sites, compared with women without incident Fx .At the radius, each SD decrease of several baseline values of bone MA was significantly associated with an increased MOF risk with hazard ratios [HR(95%CI)] of 2.69 (1.45-4.97) for Tt.vBMD, 2.10 (1.15-3.82) for Tb.vBMD, 1.73 (1.05-2.84) for Ct.vBMD, 1.75 (1.05-2.94) for Ct.Ar, 2.20 (1.30-3.72) for Ct.Th, 2.01 (1.13-3.59) for K and 1.97 (1.10-3.51) for FL. At the tibia, each SD decrease of Tt.vBMD, Ct.Ar, K and FL were also significantly associated with an increased MOF risk (HR from 2.10 to 2.26).We conclude that fragility fractures are associated with deterioration of bone MA even in women with normal areal BMD,that may justify a therapeutic intervention.

***Disclosures: Elisabeth Sornay-Rendu**, None*

FRI-407

Trajectories of Areal Bone Mineral Density Significantly Differ by Patterning of Femoral Neck Area and Bone Mineral Content Across the Menopausal Transition *Aleda Leis[1], Karl Jepsen[1], Kerry Richards-McCullough[2], Tom Richards[2], ERIN BIGELOW[3], Robert Goulet[4], Carrie Karvonen-Gutierrez[5]. [1]University of Michigan, United States. [2]University of Michigan , United States. [3]UNIVERSITY OF MICHIGAN, United States. [4]Michigan Medicine, University of Michigan, United States. [5], United States

Clinical use of areal bone mineral density (aBMD) to identify individuals at risk of fracturing assumes that aBMD change reflects bone mineral content (BMC) change. However, differences in the rate and magnitude of BMC and bone area changes over time may affect the reliability of aBMD. Understanding how different trajectories of BMC and area affect aBMD is thus central to improving our use of DXA measures to monitor bone health. This study examined the differential impact of BMC and area trajectories across the menopausal transition (MT) on aBMD. The Michigan Bone Health and Metabolism Study (MBHMS) is a longitudinal study of women; participants aged 24-50 were recruited in 1992 and followed near-annually through 2010. Femoral neck bone data were assessed using DXA. The sample included 138 women with an observed non-surgical final menstrual period (FMP); a DXA scan 10 years prior to FMP; and at least one post-FMP DXA. Group-based growth trajectory modeling was used to determine trajectory groups of area and BMC. Smoothed loess curves were constructed to examine trajectories of aBMD within each area (lowest, middle, highest) and BMC (slowest decline, moderate decline, and fastest decline) trajectory combination. Cross-tabulations of area and BMC trajectory group showed very few individuals in both the BMC fastest decline trajectory group and the area lowest trajectory group, and in the BMC slowest decline trajectory group and area highest trajectory group. The most common combinations were lowest area/slowest decline BMC (23.2%) and middle area/moderate decline BMC (21.0%). Those in the highest area/fastest decline BMC trajectory groups had the largest decline in aBMD from first to last study visit (mean 13.3% decrease, SD 8.7%; Fig. 1), while those in the highest area trajectory and the slowest BMC decline trajectory had the least decline in aBMD (mean 2.2% decrease, SD 5.9%). Understanding bone health with aging using trajectories of BMC and area change represents a novel approach to examining the significant heterogeneity across the MT, a critical life stage for musculoskeletal health. Notably, our analysis showed women who started at higher aBMD with significant BMC loss may not have been identified earlier as high risk though they show the greatest loss pattern. This information may be highly informative in identifying women at greatest risk for low aBMD and future risk for fracture.

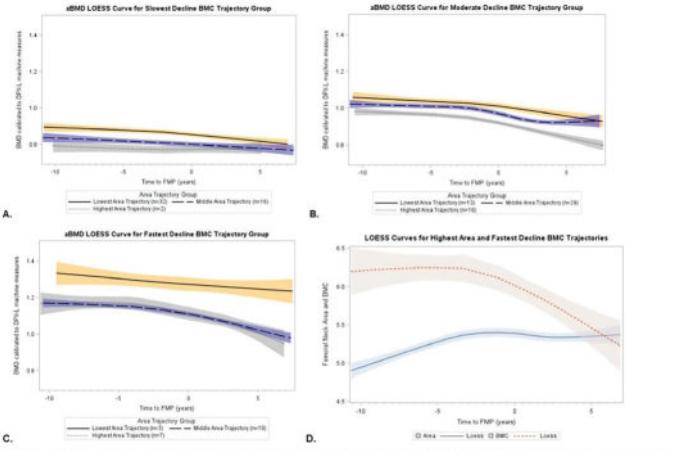

Figure 1. Loess curves for (A) aBMD by area trajectory group for those in the slowest decline BMC trajectory group, (B) aBMD by area trajectory group for those in the moderate decline BMC trajectory group, (C) aBMD by area trajectory group for those in the fastest decline BMC trajectory group, and (D) femoral neck area and BMC for those in the highest area and fastest decline BMC cross-tab trajectory group.

***Disclosures: Aleda Leis**, None*

FRI-410

Associations of Cardiorespiratory Fitness with HR-pQCT Bone Parameters in Older Adults: The Study of Muscle, Mobility and Aging (SOMMA) *Nina Heilmann[2], Kerri Freeland[2], Reagan Moffit[2], Nancy Glynn[2], Lauren S. Roe[3], Tong Yu[2], Nicole Sekel[2], Kristen Koltun[2], Katelyn Guerriere[4], Julie Hughes[4], Bradley Nindl[2], Ashley Weaver[5], Paolo Caserotti[6], Peggy Cawthon[7], Anne Newman[2], Jane A. Cauley[8], Elsa Strotmeyer[2]. [2]University of Pittsburgh, . [2]University of Pittsburgh, United States. [3], . [4]US Army Research Institute of Environmental Medicine, United States. [5]Wake Forest University, United States. [6]Department of Sports Science and Clinical Biomechanics and the Center for Active and Healthy Ageing, Denmark. [7]San Francisco Coordinating Center, United States. [8]UNIVERSITY OF PITTSBURGH, United States

Cardiorespiratory fitness and bone mass and strength decline with age, yet few studies have assessed the relationship of cardiorespiratory fitness with bone health in older adults. Physical activity (PA) is related to cardiorespiratory fitness and is recommended for preventing bone loss and osteoporosis. Whether cardiorespiratory fitness is associated with bone health independent of PA is unknown. The Study of Muscle, Mobility and Aging (SOMMA) included baseline assessments of VO2peak from treadmill cardiopulmonary exercise testing using the modified Balke protocol. We investigated associations of absolute VO2peak (mL/min) with bone mineral density (BMD) from dual-energy X-ray absorptiometry (DXA) and bone microarchitecture and strength from high-resolution peripheral quantitative computed tomography (HR-pQCT) collected in the SOMMA Bone Ancillary Study at the year 1 visit. In 124 men (age 76.2+/-4.3 years, 93% White) and 189 women (age 76.2+/-4.2 years, 87% White), relative VO2peak (mL/kg/min) was higher in men (23.8+/-5.5) vs. women (19.6+/-4.6; p<0.001). Bone outcomes differed between men and women (p<0.001) so analyses were stratified with sex-specific z-scores used in linear regression. Models (Table 1) were adjusted for age (years), race (White/non-White), weight (kg), >=1 alcoholic drink/week (y/n), total activity counts from valid wrist-worn accelerometry (>=3 days with >=10 h wear), comorbidity count (0-7), and limb length. In men, higher VO2peak was associated with higher tibial (standardized[std] ?=0.26, p<0.05) and radial (std ?=0.30, p<0.05) failure load, but not with DXA or other HR-pQCT parameters. Higher VO2peak was associated with higher radial trabecular (Tb) BMD (std ?=0.26, p<0.05) and cortical (Ct) area (std ?=0.25, p0.05) after adjusting for total activity. Associations were consistent when adjusting for moderate-to-vigorous PA instead of total activity counts. No significant associations were found between VO2peak and bone outcomes in women. Positive associations of VO2peak with failure load found in older men suggest cardiorespiratory fitness is associated with bone outcomes in a sex-specific manner. Future studies need to explore reasons for sex differences of VO2peak and bone outcomes.

Table 1. Adjusted linear regression std β coefficients of VO_2peak associations with DXA and HR-pQCT outcomes

	VO_2peak (mL/min)	
	Women mean 1350±257	**Men** mean 1966±429
Distal tibial HR-pQCT	*n=170*	*n=111*
Est. Failure load, N	0.05	**0.26***
Ct.BMD, mg/cm^3	0.12	0.11
Tb.BMD, mg/cm^3	-0.05	0.14
Ct.Ar, mm^2	0.08	0.14
Tb.Ar, mm^2	0.10	0.09
Distal radial HR-pQCT	*n=153*	*n=105*
Est. Failure load, N	0.07	**0.30***
Ct.BMD, mg/cm^3	0.13	0.18
Tb.BMD, mg/cm^3	-0.03	0.15
Ct.Ar, mm^2	0.08	0.22
Tb.Ar, mm^2	0.001	0.07
DXA parameters	*n=163*	*n=112*
Total hip BMD, mg/cm^2	-0.02	0.09
FN BMD, mg/cm^2	-0.08	0.04

***P<0.05**; Models adjusted for age (years), race (White/non-White), weight (kg), ≥1 drink/week (y/n), total activity counts (ActiGraph), comorbidity count (0-7), and tibia/ulna length. Abbreviations: cortical BMD (Ct.BMD), Ct. area (Ct.Ar), FN (femoral neck), trabecular BMD (Tb.BMD), Tb. area (Tb.Ar)

***Disclosures: Nina Heilmann**, None*

FRI-411

Associations of Muscle Strength and Functional Power to Longitudinal Change in HR-pQCT Bone Parameters: the Osteoporotic Fractures in Men (MrOS) Study *Nina Heilmann[2], Kerri Freeland[2], Tong Yu[2], Paolo Caserotti[3], Andrew Burghardt[4], Mary Winger[5], Nancy Lane[6], Jane A. Cauley[7], Elsa Strotmeyer[2]. [2]University of Pittsburgh, , [2]University of Pittsburgh, United States, [3]University of Southern Denmark, Denmark, [4]University of California, San Francisco, United States, [5]UPMC Insurance Services Division, United States, [6]University of California, Davis Medical Center, United States, [7]UNIVERSITY OF PITTSBURGH, United States

Both bone and muscle function decline with age and are anatomically and functionally related. However, whether and to what extent muscle function (i.e., strength and power) may predict longitudinal changes in bone microarchitecture and strength is unclear. The Osteoporotic Fractures in Men Study (MrOS) included assessments of peak jump muscle power (W) from force plate and grip strength (kg) from dynamometer tests, both normalized to body weight at Visit 4 (2014-2016). We investigated associations of power and grip strength with annual % change in tibial and radial bone parameters of geometry, structure and estimated failure load from high-resolution peripheral quantitative computed tomography (HR-pQCT) between Visit 4 and Visit 5 (2020-2022; 6.2+/-0.6 years follow-up; N=224; age 82.8+/-3.0 years; 88% White). Mean power was 22.9+/-5.6 W/kg and grip strength was 0.49+/-0.1 kg/kg. The largest declines were observed for tibial (-1.0+/-1.3%/year) and radial (-1.1+/-1.8%/year) failure load. Partial correlations of power and grip strength with % change in HR-pQCT outcomes adjusted for age, race, study site, height, and limb length were weak (all r<0.30), though significant associations were largely maintained in multivariable linear regression (Table 1), additionally adjusting for respective HR-pQCT initial values, % absolute weight change, and history of myocardial infarction and congestive heart failure. Higher power was associated with greater %/year increase in tibial Tb.Ar, though greater %/year decrease in tibial Ct.Ar and Ct.Th (all p<0.05). Higher grip strength was significantly associated with greater %/year increase in tibial Tb.Ar (p<0.05) and marginally associated with %/year decrease in tibial Ct.Th (p=0.05). Power and grip strength were not associated with change in failure load or Tb.Th at either site, or with radial Ct.Ar, Tb.Ar, and Ct.Th. Most associations of higher jump power and grip strength in older men were with tibial components of bone geometry and structure. Future analyses will examine changes in tibial and radial BMD. For the tibial site, both power and grip strength predicted changes in Tb.Ar, Ct.Ar, and Ct.Th, suggesting potential mechanisms for bone loss and targets for musculoskeletal interventions.

Table 1. Adjusted linear regression standardized β coefficients of power & grip strength with change in HR-pQCT outcomes

	%/year Change in HR-pQCT parameters				
	Est. failure load, N	Ct.Ar, mm^2	Tb.Ar, mm^2	Ct.Th, mm	Tb.Th, mm
	Distal tibia (N=218)				
Mean % change	*-1.04 ±1.3*	*-0.11 ±2.5*	*0.06 ±0.5*	*0.22 ±2.1*	*-0.07 ±0.6*
Power (W/kg)	0.05	**-0.14***	**0.15***	**-0.17***	0.14
Grip strength (kg/kg)	-0.04	-0.10	**0.12***	**-0.12***	0.07
	Distal radius (N=202)				
Mean % change	*-1.06 ±1.8*	*-0.65 ±1.8*	*0.17 ±0.4*	*-0.29 ±2.0*	*0.23 ±0.7*
Power (W/kg)	0.12	-0.05	0.04	-0.09	0.06
Grip strength (kg/kg)	0.06	-0.02	0.05	-0.03	0.07

***P≤0.05**; Models adjusted for age, race, study site, height, respective HR-pQCT initial value, % absolute weight change, history of myocardial infarction and congestive heart failure, and for tibia or ulna length respectively. Abbreviations: cortical area (Ct.Ar), Ct. thickness (Ct.Th), trabecular area (Tb.Ar), Tb. thickness (Tb.Th)

***Disclosures: Nina Heilmann**, None*

FRI-413

Degree of Trauma in Clinical Fractures with Advancing Age in Older Men *Kristine Ensrud[1], Sheena Patel[2], Lisa Langsetmo[3], Peggy Cawthon[4], Howard Fink[3], John Schousboe[5], Douglas Bauer[6], Jane A. Cauley[7], Eric Orwoll[8]. [1]University of Minnesota and Minneapolis VA Health Care System, United States, [2], , [3]Minneapolis VA Medical Center, United States, [4]San Francisco Coordinating Center, United States, [5]Park Nicollet Clinic HealthPartners Institute University of Minnesota, , [6]University of California, San Francisco, United States, [7]UNIVERSITY OF PITTSBURGH, United States, [8]Oregon Health & Science University, United States

Among community-dwelling older adults, the proportion of fractures (fxs) due to severe trauma is higher in men vs. women. However, the extent to which the degree of trauma in fxs in older men varies with advancing age is unknown.We used data from 1424 MrOS men aged >=65 yrs at baseline who experienced 2351 clinical fxs during a mean (SD) follow-up of 9.9 (5.7) yrs. Participants were contacted every 4 mos until death, termination from study or Feb 2023 to ascertain incident fxs confirmed by radiographic reports. When a fx was reported, staff interviewed the participant about circumstances. Fxs were classified as fall or nonfall related and coded according to degree of trauma. Degree of trauma was considered minimal (fall from <= standing height), moderate (fall on stairs, steps or curb), or severe (fall from > standing height) for fall related fxs, and minimal (coughing), moderate (collisions with objects during normal activity without falling), or severe (motor vehicle accident) for nonfall related fxs.Of the 2351 fxs, 298 (12.7%) occurred in men <75 yrs, 370 (15.7%) in men 75-79 yrs, 613 (26.1%) in men 80-84 yrs and 1070 (45.5%) in men >=85 yrs. 1891 (80.4%) of all fxs were the result of a fall; this proportion was greater with older age at the time of the fx, ranging from 65.8% in men <75 yrs up to 84.7% in men >=85 yrs (p<0.001 across age groups). Six of every 10 (61.5%) of the 1891 fall related fxs were due to minimal trauma, while over half (53.5%) of the 460 nonfall related fxs were due to severe trauma. The proportion of fxs due to severe trauma was lower in a graded manner with advancing age, irrespective of whether the fx was due to a fall or not (Figure). The proportion of fxs due to a fall with severe trauma was 18.5% in men <75 yrs declining to 3.8% in men >=85 yrs (p<0.001 across age groups); the proportion of fxs due to severe trauma without a fall was 19.5% in men <75 yrs declining to 8.4% in men >=85 yrs (p<0.001 across age groups). In contrast, the proportion of fxs due to a fall with minimal trauma was higher in a graded manner with increasing age (p0.98).Among community-dwelling older men, proportions of both fall and nonfall related fxs due to severe trauma decrease with advancing age. Fall-related fxs due to minimal trauma are increasingly common with advancing age and comprise an increasing proportion of all fx events.

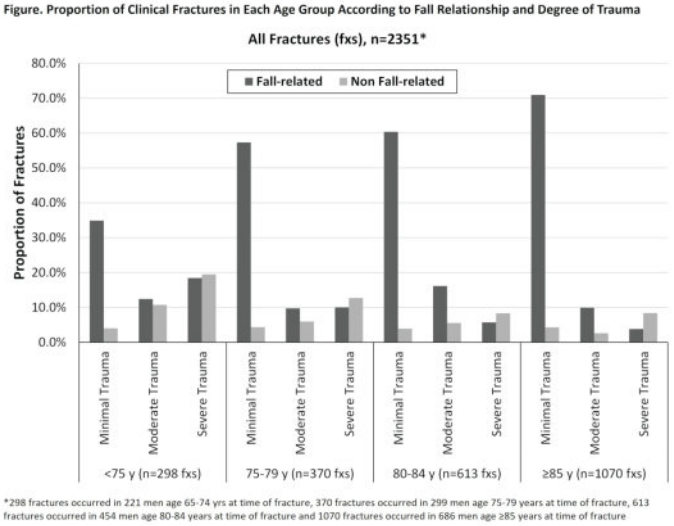

***Disclosures: Kristine Ensrud**, None*

FRI-419

Current trends in the risk of subsequent fracture after initial fracture, and post-fracture treatment among commercially insured postmenopausal women in the United States *Min Kim[1], Vanessa Brunetti[9], Felicia Cosman[3], Jeffrey Curtis[4], Mike Lewiecki[5], Matthew Phelan[6], Peter Samai[7], MICHELE MCDERMOTT[8], Tzu-Chieh Lin[9], M Alan Brookhart[10], Kathleen Hurwitz[6, 1], United States. [9]Amgen Inc., United Kingdom. [3]Columbia University College of Physicians and Surgeons, United States. [4]University of Alabama at Birmingham, United States. [5]New Mexico Clinical Research & Osteoporosis Center, United States. [6]Target RWE, Inc, United States. [7]University of North Carolina at Chapel Hill, United States. [8]Amgen, United States. [9]Amgen Inc., United States. [10]Duke University, United States

BackgroundRecent studies suggest that post-fracture pharmacologic management has been declining in the U.S. despite an increase in the burden of osteoporosis (OP). In light of this treatment gap, few studies have reported on the incidence of subsequent fracture risk among commercially insured postmenopausal women with a history of fracture.MethodsWe assembled a retrospective cohort of women aged >=50 years from 2012-2021 using an administrative claims database of privately insured or employer-sponsored Medicare Advantage coverage. Osteoporotic fractures were identified by >=1 insurance claims with a relevant diagnosis and/or procedure code for an open or closed fracture. Treatments for osteoporosis were identified by prescription fills or medical procedure claims. The cumulative incidence of a new, subsequent fracture at the same or a different anatomic site was estimated for any (clinical vertebral, hip, femur, pelvis, tibia, fibula, radius/ulna/distal forearm, humerus, clavicle, rib, sternum), major (any fracture excluding extremities, clavicle, rib, sternum), hip, and clinical vertebral fractures occurring >=90 days of initial index fracture to up to 2 years. Women were followed from the index fracture for up to 2 years to estimate the cumulative incidence of any treatment uptake. All analyses used inverse probability weighting to adjust for differential censoring due to differences in demographics and clinical risk factors. ResultsAmong the 483,564 women with any initial fracture (mean age 74.8), the 1-year cumulative incidence of a subsequent fracture at any site was 11.6%, which increased to 19.1% at 2 years (Figure). The same-site subsequent fracture risk was highest for women with an initial clinical vertebral fracture: 10.1% experienced a subsequent vertebral fracture at year 1 and 15.9% at year 2. Among women with an initial hip fracture, 12.2% and 19.6% experienced a subsequent fracture at any site after 1 and 2 years, respectively, while 8.0% and 12.2% experienced a subsequent hip fracture at 1 year and 2 years, respectively. Most patients did not receive pharmacological treatment one year (91.7%) and two years (89.4%) after their initial fracture.ConclusionAlthough clinical guidelines specify that OP is a lifelong, chronic disease requiring ongoing management, recent data over a 10-year period show that recurrent fracture rates within 2 years are high, while pharmacological treatment remains underutilized in this high-risk population.

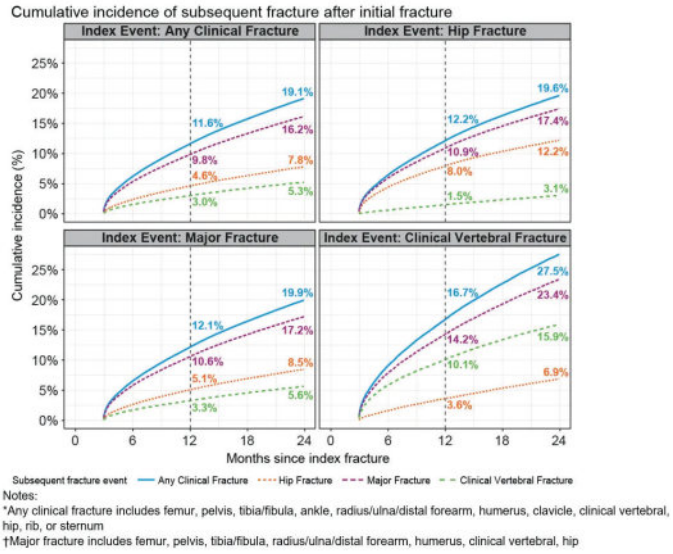

***Disclosures: Min Kim**, Amgen Inc., Other Financial or Material Support*

FRI-421

Associations of Metabolic Syndrome (MetS) with Fall Rates and Fall Injuries: Results from the Objective Physical Activity and Cardiovascular Health in Older Women (OPACH) *Chen Hu[1], Kerri Freeland[1], Michael LaMonte[2], Marcia Stefanick[3], Kristine Ensrud[4], Jane Cauley[1], Andrea LaCroix[5], Elsa Strotmeyer[1]. [1]University of Pittsburgh, United States. [2]University of Buffalo, United States. [3]Stanford University, United States. [4]University of Minnesota Twin Cities, United States. [5]University of California San Diego, United States

MetS is an increasingly prevalent disorder that consists of a cluster of metabolic conditions. Previous studies found individual MetS components were associated with falls and fall injuries in older adults, though the association of MetS, as a constellation, with these outcomes is unknown. We aimed to evaluate whether MetS was associated with higher fall rates and fall injury risk among older women in a community-based cohort in the OPACH, an ancillary study of the Women's Health Initiative (WHI). Participants were 5,548 women (mean 79.0+/-6.7 years; 63.4% White; 30.8% obese) who had a blood draw and physical measurements during 2012-2013, and >1 month of fall calendars over a 13-month follow-up. MetS (Y/N) was defined as having?>=3 of 5 criteria per NCP/ATP-III guidelines: waist circumference?>88 cm, fasting glucose >=100 mg/dL or hypoglycemic medication use, systolic BP?>=130 or diastolic BP?>=85 mmHg, high-density cholesterol?<50 mg/dL, and triglycerides >=150 mg/dL. Falls and fall injuries were ascertained by monthly fall calendars and telephone interviews. Poisson regression examined MetS associations with fall rates. Weighted logistic regression was used for MetS associations with fall injuries (Y/N), while accounting for sampling strategies for interviews. MetS (N=1,125) was present in 20.3% the cohort and 43.6% (N=2,417) reported >=1 fall. Fall injuries were reported in 35.6% (508/1,428) over mean 11.9+/-2.3 mo. of follow-up. In unadjusted models, MetS was associated with 17% higher fall rates (RR=1.17, 95%CI=1.10-1.24) and 17% higher odds of fall injuries (OR=1.17, 95% CI=1.02-1.34). After adjusting for age, race (White/Black/other), ethnicity (Hispanic/non) and obesity (BMI>=30) the association persisted between MetS and fall rates (RR=1.12, 95%CI=1.04-1.20), but the association between MetS and fall injuries was attenuated to null (OR=1.08, 95%CI=0.93-1.24). In addition to MetS, obesity was an independent risk factor of higher fall rates (RR=1.16, 95%CI=1.08-1.25). Age-stratified adjusted analyses found MetS associated with higher fall injuries (OR=1.18, 95%CI=1.00-1.39) in women aged 65-85 years (N=1,159), but a non-significant inverse association (OR=0.83, 95%CI=0.57-1.10) in women aged >85 years (N=269). MetS was associated with higher fall rates in women >=65 years and injurious falls in women <85 years. Further studies should evaluate potential mechanisms of individual MetS components and how comorbidities may contribute to these associations.

***Disclosures: Chen Hu**, None*

FRI-423

Evaluating Fractures by Race and Ethnicity in a Diverse Sample of Postmenopausal Women - Results from the Women's Health Initiative

*Nicole Wright[1], Steven Ing[2], Joseph Larson[3], Carolyn Crandall[4], Shawna Follis[5], Marcia Stefanick[5], Jane A. Cauley[6]. [1]University of Alabama at Birmingham, United States. [2]The Ohio State University Wexner Medical Center, United States. [3]Fred Hutchinson Cancer Center, United States. [4]University of California, Los Angeles, United States. [5]Stanford Prevention Research Center, Department of Medicine, Stanford University, United States. [6]UNIVERSITY OF PITTSBURGH, United States

Background: The Women's Health Initiative (WHI) recently released more comprehensive race and ethnicity to provide much needed longitudinal fracture data in multiple race and ethnic groups.Methods: The WHI recruited 161,808 postmenopausal women. Women identified as one of the following racial categories: White, Black/African American, American Indian/Alaskan Native, Asian Indian, Chinese, Filipino, Japanese, Korean, Vietnamese, Other Asian, Native Hawaiian, Samoan, Guamanian or Chamorro, or Other Pacific Islander; and one of the following Hispanic ethnic categories: Not Spanish/Hispanic, Cuban, Mexican, Puerto Rican, Other Spanish. Fractures of interest included any clinical fracture, hip, and major osteoporotic fracture (MOF). We computed crude fracture incidence rates per 10,000 woman-years and used Cox proportional hazards model to estimate fracture risk compared to non-Hispanic White women after adjusting for age. For Asian and Hispanic women, we estimated within group fracture risk using the most prevalent subgroup as the reference.Results: Our final analytic sample included 154,948. Over 17.2 years of follow-up 67,213 (43.4%) women experienced any clinical fracture, including 8,677 (5.6%) and 34,545 (22.3%) hip and MOFs, respectively. Women sustaining a fracture were significantly older, White, not Hispanic, highly educated, more physically active, and reported more falls in the past year. Compared to White women, Black, Asian, and Native Hawaiian/Pacific Islander women had significantly lower risk of any clinical fracture and MOF (Table). Black and Asian women had significantly 71% and 52% lower risk of hip fracture compared to White women, respectively (Table). Within Asian women, Filipino women had 23% [0.77 (0.61, 0.99)] lower risk of fracture compared to Japanese women (Table). Hispanic women had 8%, 44%, and 10% lower risk of any clinical, hip, and MOF compared to non-Hispanic women, respectively (Table). Within Hispanic women, Cuban women had 95% [1.95 (1.05, 3.63)] higher risk of hip fracture compared to Mexican women (Table).Discussion: Our study showed significant differences in fracture rates and fracture risk by race, Hispanic ethnicity, and within Asian and Hispanic groups. These data can be used to provide current and more granular information on fractures in communities of color for future research and updates to fracture risk prediction tools that incorporate race and ethnicity.

Table: Fractures in the WHI by Race and Ethnicity

	Total Fracture		Hip		MOF	
	Crude IR[1] (95% CI)	Adj HR[2] (95% CI)	Crude IR[1] (95% CI)	Adj HR[2] (95% CI)	Crude IR[1] (95% CI)	Adj HR[2] (95% CI)
Race						
White	352 (349, 354)	1.00 (ref)	36 (35, 37)	1.00 (ref)	154 (153, 156)	1.00 (ref)
Black	186 (180, 192)	**0.58 (0.56, 0.60)**	7 (6, 8)	**0.29 (0.25, 0.34)**	52 (49, 55)	**0.40 (0.37, 0.42)**
American Indian/Alaskan Native	337 (286, 397)	1.03 (0.88, 1.22)	14 (7, 29)	0.55 (0.28, 1.10)	107 (83, 139)	0.81 (0.62, 1.05)
Asian	236 (223, 251)	**0.68 (0.64, 0.72)**	16 (13, 20)	**0.48 (0.39, 0.59)**	94 (86, 103)	**0.63 (0.58, 0.70)**
Native Hawaiian/Pacific Islander	216 (157, 297)	**0.69 (0.50, 0.95)**	9 (2, 38)	0.41 (0.10, 1.65)	54 (30, 97)	**0.43 (0.24, 0.78)**
Asian Subgroup						
Japanese	247 (229, 267)	1.00 (ref)	18 (14, 23)	1.00 (ref)	99 (88, 111)	1.00 (ref)
Asian Indian	295 (205, 425)	1.42 (0.98, 2.07)	0	-	111 (65, 192)	1.56 (0.89, 2.73)
Chinese	229 (202, 260)	0.95 (0.82, 1.10)	12 (7, 20)	0.69 (0.39, 1.20)	86 (71, 104)	0.91 (0.73, 1.13)
Filipino	177 (141, 222)	**0.77 (0.61, 0.99)**	14 (7, 30)	0.99 (0.45, 2.19)	74 (53, 104)	0.87 (0.61, 1.24)
Korean	237 (161, 348)	1.01 (0.68, 1.49)	16 (4, 62)	1.02 (0.25, 4.18)	126 (76, 209)	1.43 (0.85, 2.41)
Vietnamese	149 (37, 596)	0.76 (0.19, 3.04)	0	-	149 (37, 596)	2.51 (0.62, 10.15)
Other	242 (162, 361)	1.03 (0.68, 1.55)	26 (8, 81)	2.01 (0.63, 6.47)	80 (42, 154)	0.92 (0.47, 1.79)
Hispanic Ethnicity						
Not Hispanic	336 (334, 339)	1.00 (ref)	34 (33, 34)	1.00 (ref)	145 (144, 147)	1.00 (ref)
Hispanic	273 (260, 286)	**0.92 (0.87, 0.96)**	13 (11, 16)	**0.56 (0.46, 0.69)**	107 (99, 115)	**0.90 (0.84, 0.97)**
Hispanic Subgroup						
Mexican	257 (238, 276)	1.00 (ref)	11 (8, 15)	1.00 (ref)	103 (92, 114)	1.00 (ref)
Puerto Rican	270 (238, 308)	1.01 (0.87, 1.17)	13 (8, 22)	0.97 (0.52, 1.82)	106 (88, 128)	0.94 (0.76, 1.18)
Cuban	313 (265, 369)	1.17 (0.98, 1.41)	24 (14, 41)	**1.95 (1.05, 3.63)**	119 (93, 152)	1.05 (0.80, 1.37)
Other	288 (264, 313)	1.04 (0.93, 1.17)	14 (10, 19)	0.87 (0.53, 1.44)	109 (96, 124)	0.92 (0.78, 1.10)

WHI = Women's Health Initiative; MOF = Major Osteoporotic Fracture; IR = Incidence Rate; CI = Confidence Interval; HR = Hazards Ratio
[1]IR per 10,000 woman-years
[2]Model adjusted for age

***Disclosures: Nicole Wright**, None*

FRI-429

Medications, Fracture Risk and Oral Bisphosphonate Efficacy - Evidence from a Well-Characterized Prospective Clinical Trial in Older Women

*Andre Tan[1], Eugene McCloskey[7], Zhangan Zheng[3], Nicholas Harvey[4], Mattias Lorentzon[5], John Kanis[6], Marian Schini[7]. [1]National University Health System, Singapore. [7]University of Sheffield, United Kingdom. [3]The Second People's Hospital of Wuhu, China. [4]University of Southampton, . [5]Sahlgrenska Academy, University of Gothenburg, Sweden. [6]Australian Catholic University, Australia. [7]University of Sheffield,

Epidemiological studies have reported several medication classes to be associated with effects on bone mineral density and fracture risk but have largely been unable to adjust for potential confounders. Having observed an interaction between NSAID use and oral bisphosphonate efficacy, we explored the relationship between other baseline medication use and fracture risk in the same cohort.This was a post-hoc analysis of a well-documented, randomized, placebo-controlled study of the oral bisphosphonate, clodronate, in 5212 community dwelling women aged 75 years or more followed for 3-5 years. At baseline, medication classes used by at least 250 women (approximately 5% of the cohort) were identified. Cox regression analysis was used to investigate the hazard ratio (HR) between medication class and osteoporotic fracture risk in univariate and adjusted models. Potential covariates included age, BMI, BMD, other FRAX risk factors excluding alcohol exposure, bone turnover markers, muscle strength and recent falls.In the placebo arm, no association with fracture risk was observed for beta-blockers, angiotensin-converting enzyme inhibitors, loop diuretics, thiazide diuretics, nitrates, digoxin, proton pump inhibitors (PPIs), H2 receptor antagonists, antacids, tricyclic antidepressants, or first-generation antipsychotics. However, compared to non-users of the drug class, the incidence of osteoporotic fractures was higher in users of calcium channel blockers (CCB, n=843, HR 1.49, 1.11-2.01, p = 0.008) and benzodiazepines (BNZ, n=690, HR 1.59, 95% CI 1.15-2.18, p = 0.004) in unadjusted models. When adjusted for significant differences from non-users in risk factors, CCB but not BNZ remained associated with osteoporotic fractures (HR 1.59, 1.13-2.23, p = 0.007). In the clodronate arm, neither BNZ nor CCB were associated with fracture risk. However, PPI use was significantly associated with increased osteoporotic fracture risk in clodronate treated women (HR 1.63, 1.23-2.16, p < 0.001) but not placebo treated women. This association persisted following adjustment for risk factors (HR 1.93, 1.26-2.97, p=0.003).The association of BNZ with fracture risk appears to be largely mediated through co-existing risk factors. The increased risk of osteoporotic fractures with CCB appears independent of measured risk factors but is prevented by bisphosphonate therapy. Concomitant PPI use negated the effect of clodronate in reducing fracture risk.

***Disclosures: Andre Tan**, None*

FRI-431

Impact of Bisphosphonate Use Following Hip Fracture: A Decade-Long Follow-Up of a Cohort Within a Private Healthcare System

*Betiana Perez[1], Maria Eugenia Vera[1], Luisa Carmen Plantalech[1], Maria Diehl[1]. [1]Hospital Italiano de Buenos Aires, Argentina

Bisphosphonate use after hip fracture is useful for secondary prevention and may reduce post-fracture morbidity and mortality. Aims To evaluate the long-term impact of bisphosphonate use after hip fracture in mortality and morbidity. Methods Retrospective cohort study of patients >=50 years from a closed health system hospitalized for a fragility hip fracture between July 2005 and December 2010. Deaths and readmissions were analyzed. Kaplan Meier survival analysis and Cox regressions were performed. Sensitivity analysis with propensity score matching (PSM), considering age, sex, previous fracture and comorbidities was employed to adjust for prescription bias. Results We included 965 patients. The median age was 82.4 years (IQR 77.8-86.6), and 80.7% were female. Secondary prevention with bisphosphonates was administered to 39% of cases within the year after hip fracture. Mortality in the first year was 14.9% and at 10 years 73.2%. Median survival was 5.6 years. The median survival of patients with hip fracture treated with bisphosphonates was 8.33 years, and for those not treated it was 4.06 years (p<0.0001), and remained significantly different after PSM (p= 0.022). Median survival free of readmissions was 2.93 years; 4.02 years for treated with bisphosphonates, and 2.09 years for not treated (p<0.0001), and also remained different after PSM (p= 0.045). Multivariate Cox regression showed that secondary prevention with bisphosphonates remains an independent predictor of survival and survival free of readmissions, even after adjusting for significant covariates (table 1). Conclusions Bisphosphonates positively impacted survival and readmissions in our study after adjusting by demographic variables, comorbidities. However, we could not assess other relevant covariates such as educational level and social support.

	Mortality	Readmissions
Age (each year)	1.08(1.07-1.09) [a]	1.04 (1.03-1.05) [a]
Male sex	1.22(1.01-1.48) [b]	1.12 (0.92-1.37)
Intracapsular fracture	1.46(1.22-1.74) [a]	1.32 (1.10-1.59) [c]
Charlson Index (each point)	1.14(1.08-1.20) [a]	1.17 (1.11-1.23) [a]
Dementia	1.74(1.46-2.07) [a]	1.23 (1.03-1.48) [d]
Congestive heart failure	1.68(1.30-2.17) [a]	1.99 (1.50-2.65) [a]
Secondary prevention with bisphoshonate	0.68 (0.58-0.80) [a]	0.72 (0.61-0.86) [a]

a. p<0.0001 b. p=0.043 c. p=0.003 d. p=0.026

***Disclosures: Betiana Perez**, None*

FRI-434

Comparative Effectiveness of Denosumab versus Bisphosphonates among Treatment-Experienced Postmenopausal Women with Osteoporosis in the U.S. Medicare Program *Jeffrey Curtis[1], Tarun Arora[2], Ye Liu[1], Tzu-Chieh Lin[4], Leslie Spangler[4], Vanessa Brunetti[4], Robert Stad[4], MICHELE MCDERMOTT[5], Brian Bradbury[4], Min Kim[4]. [1]University of Alabama at Birmingham, United States. [2]Foundation for Advancing Science, Technology, Education and Research, United States. [4]Amgen Inc., United States. [4]Amgen Inc., Switzerland. [5]Amgen, United States

ObjectivesAlthough clinical trials have shown that transitioning from bisphosphonates (BP) to denosumab (Dmab) increases bone mineral density at key skeletal sites more than remaining on BP, evidence from head-to-head studies evaluating fracture outcomes is lacking. This retrospective observational study compared the effectiveness of Dmab versus BP in reducing fracture risk among treatment-experienced women with postmenopausal osteoporosis (PMO) in the U.S.MethodsFemale Medicare fee-for-service beneficiaries >= 66 years of age with prior history of treatment with an oral BP, who newly initiated Dmab (n~108,000), a different oral BP (alendronate, ibandronate, or risedronate; n=100,649), alendronate (Aln; n=53,165), or zoledronic acid (ZA; n=35,100) between Jan 1, 2012 to Dec 31, 2018 were followed from treatment initiation (index date) until the first instance of a fracture, treatment discontinuation (defined as the end of exposure + 60-day gap) or switch, Medicare disenrollment, death, end of available data (Dec 31, 2019), or 5 years post-index date. A doubly robust inverse-probability of treatment (weights estimated from multivariate logistic regression models) and censoring (weights estimated from multivariate Cox Proportional Hazards regression models) weighted function was used to estimate the relative risk (RR) associated with the use of Dmab compared with oral BP, Aln, and ZA for hip, nonvertebral (NV; includes hip, humerus, pelvis, radius/ulna, other femur), non-hip, nonvertebral (NHNV), hospitalized vertebral (HV), and major osteoporotic (MOP; nonvertebral and hospitalized vertebral) fractures for the overall study period and by year of follow-up. ResultsOver a maximum of 5 years of follow-up, Dmab reduced the risk of hip fracture by 45% (RR=0.55; 95% CI: 0.42-0.68), 37% (0.63; 0.51-0.75), and 38% (0.62; 0.32-0.91), and reduced the risk of MOP fracture by 31% (0.69; 0.61-0.76), 25% (0.75; 0.67-0.82), and 31% (0.69; 0.57-0.82) compared with oral BP, Aln, and ZA respectively (Figure). Similar results were observed for NV, NHNV, and HV fractures, with an increase in the magnitude of fracture risk reduction with increasing duration of exposure across all fracture outcomes. ConclusionIn a large cohort of treatment-experienced women with PMO, we observed robust, clinically meaningful reductions in the risk of hip, NV, NHNV, HV, and MOP fractures for patients on Dmab compared to oral BP, Aln, and ZA; greater reductions in fracture risk were observed with longer duration of exposure.

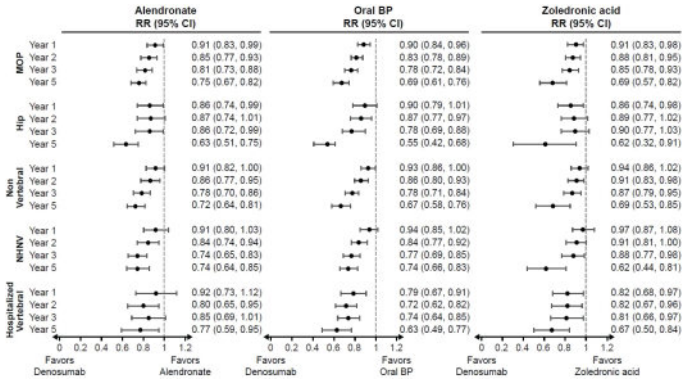

***Disclosures: Jeffrey Curtis**, Amgen Inc., Grant/Research Support, Amgen Inc., Consultant*

FRI-437

Romosozumab Increases Modeling-based Bone Formation and Creates a Positive Bone Balance in Remodeling Units at 2 and 12 Months *Erik Eriksen[1], Rogely Boyce[2], Yifei Shi[2], Jacques Brown[3], Donald Betah[2], Cesar Libanati[4], Mary Oates[2], Roland Chapurlat[5], Pascale Chavassieux[5]. [1]Faculty of Odontology, Oslo University, Norway. [2]Amgen Inc., United States. [3]CHU de Québec Research Centre and Laval University, Canada. [4]UCB Pharma, Belgium. [5]INSERM UMR 1033, Université de Lyon, Hospices Civils de Lyon, France

Romosozumab (Romo), a monoclonal antibody against sclerostin, causes an early increase in bone formation that attenuates with treatment and a sustained decrease in bone resorption. Histomorphometric analyses revealed the primary bone-forming effect of Romo is transient early stimulation of modeling-based bone formation (MBBF) on cancellous (Cn) and endocortical (Ec) surfaces. Preclinical studies have demonstrated that Romo may effect changes in the remodeling unit resulting in positive bone balance. Here we compared remodeling bone balance in women treated with Romo vs placebo (Pbo).We analysed bone biopsies from the FRAME clinical trial (NCT01575834) using remodeling site reconstruction to quantify and characterize the changes in bone balance within bone multicellular units (BMU) on Cn/Ec surfaces that may contribute to the progressive improvement in bone mass/structure and reduced fracture risk in women with osteoporosis at high fracture risk. At month (M) 2, the median percentage of MBBF referent to the total bone surface was significantly increased with Romo vs Pbo on Cn (18.0% vs 3.8%; P=0.005) and Ec (36.7% vs 3.0%; P=0.001), but not periosteal (5.0% vs 2.0%; P=0.37) surfaces, with no significant difference in the surface extent of remodeling-based bone formation (RBBF) on all three bone surfaces. Final erosion depth (E.De) at M2 was decreased significantly on the Ec (42.7µm vs 50.7µm; P=0.021) and non-significantly on the Cn surface (38.5µm vs 44.6µm; P=0.11) with Romo vs Pbo. Sector analysis of early Ec formative sites revealed in sector 2 significant increases in osteoid thickness (29.9µm vs 19.2µm; P=0.005) and mineralized wall thickness (W.Th; 18.3µm vs 11.9µm; P=0.004) with Romo vs Pbo. These evolving BMUs may reflect early stimulation of bone formation contributing to the increase in completed W.Th at M12. At M12, there were significant increases in bone balance with Romo vs Pbo on Cn (+6.1µm vs +1.5µm; P=0.012) and Ec (+5.2µm vs ?1.7µm; P=0.02) surfaces; the increase in bone balance was due to a significant decrease in final E.De (40.7µm vs 43.7µm; P=0.05) on Cn surfaces and increased completed W.Th (50.8µm vs 47.5µm; P=0.037) on Ec surfaces.These data suggest that Romo induces a positive bone balance due to effects on bone resorption and formation at the level of the remodeling unit, contributing to the positive effects on bone mass, structure, and fracture risk. This positive balance is further enhanced by significant activation of MBBF.

***Disclosures: Erik Eriksen**, Lilly, Merck, Mylan, Takeda, Speakers' Bureau, Amgen, Takeda, Grant/Research Support, Ascendis, Amgen, Lilly, Merck, Takeda, Consultant*

FRI-440

Antiresorptive Therapy to Reduce Fracture Risk and Effects on Dental Implant Outcomes in Patients with Osteoporosis: A Systematic Review and Consensus Statement *Aliya A. Khan[1], Dalal S. Ali[1], Reza Mirza[2], Archibald Morrison[3], Salvatore Ruggiero[4], Gordon Guyatt[2], Sotirios Tetradis[5]. [1]Division of Endocrinology and Metabolism, McMaster University, Canada. [2]Department of Health Research Methods, Evidence, and Impact at McMaster University, Canada. [3]Citadel Oral and Maxillofacial Surgery, Canada. [4]NYCOMS, United States. [5]University of California, Los Angeles, United States

Background: Placement of a dental implant in a patient on antiresorptive therapy has been hypothesized to increase the risk of Medication-Related Osteonecrosis of the Jaw (MRONJ) and/or impact implant survival. In patients with osteoporosis, the risk of MRONJ with antiresorptive therapy is only marginally higher than observed in the general population1. Due to the invasive nature of implant placement and the increased risk of MRONJ seen in patients undergoing an oral procedure or event2, the International ONJ Taskforce further evaluated this issue.Methods: A systematic review of the literature was conducted and evaluated the outcomes of implant placement in individuals with osteoporosis or osteopenia receiving antiresorptive therapy. The risk of implant failure was evaluated in comparison to age matched individuals not on antiresorptive therapy.Results: Seven studies reported comparative risk estimates of dental implant failure with and without antiresorptive therapy for osteoporosis or osteopenia. A random-effects meta-analysis revealed a non-significant increased risk with antiresorptive agents with wide confidence intervals (RR 1.56, 0.43 - 5.70). The data were reviewed by the International Taskforce, and consensus was achieved on the graded recommendation3,4.Conclusion: In patients with osteoporosis on antiresorptive therapy, the Taskforce suggests that antiresorptive therapy does not need to be stopped prior to proceeding with dental implant (weak recommendation, very low-quality evidence). Current evidence does not suggest an association between antiresorptive therapy and implant failure. There is no evidence that cessation of bisphosphonate or denosumab therapy improves implant survival or reduces the development of MRONJ. Cessation of denosumab is not advised as it has been associated with rebound bone loss and an increased risk of multiple vertebral fractures. This presentation will provide the recommendations of the International Taskforce and also provide details regarding possible pathogenesis and differences in healing following dental extraction in comparison to implant placementReferences: 1.Khan, et al., Diagnosis and Management of ONJ: A Systematic Review and International Consensus. JBMR, 2015. 30(1): p. 3-23. 2.Watts, et al., Invasive Oral Procedures and Events in Postmenopausal Women With Osteoporosis Treated With Denosumab for Up to 10 Years. JCEM, 2019. 104(6): p. 2443-2452. 3.Mirza et al OI (submitted) 4. Tetradis et al OI (submitted)

***Disclosures: Aliya A. Khan**, Alexion, Amgen, Ascendis, Chugai, Radius, Takeda, Grant/Research Support*

FRI-442

Perioperative Bisphosphonates Did not Impact Healing Following Osteoporotic Fracture Surgery: A Systemic Review and Meta-analysis *Guolin Meng[1], Yuhong Zeng[2], Yuan Yang[3], Jue Wang[3]. [1]Department of Orthopaedics, Xijing Hospital, Fourth Military Medical University, China. [2]Department of Osteoporosis, Red Society Hospital, Xi'an Jiaotong University, China. [3]MA & OR, Organon Research and Development, Organon China, China

Background: Treatment guidelines recommend early bisphosphonates (BPs) following fragility fracture surgery to prevent more fractures. However, the clinical practice needs evidence to guide the timing to initiate BPs. We performed a systematic review and meta-analysis to investigate the effect of perioperative initiation of BPs versus non-perioperative BP

use on healing following fragility fracture repair.Method: The study included randomized controlled trials (RCTs) and cohort studies on adults with fragility fractures at different anatomical sites for surgical procedures (including reduction or fixation). Healing rates and time to healing at the follow-up were primary outcomes and compared between perioperative BP initiation versus non-perioperative BP use [before surgery (prior use) and >=1 month postoperative (delayed use)]. The search was performed in PubMed, Web of Science, the Cochrane Library, and Embase. The analysis presented risk ratio (RR) and mean difference (MD) for binary and continuous outcomes with 95%CI. I2 statistic assessed heterogeneity.Results: The primary analysis pooled 7 studies (5 RCTs; 2 cohort studies, n=912) on patients with alendronate, risedronate, and zoledronic acid and fragility fracture repair. Fracture sites were the spine, the femoral neck, the hip, and the intertrochanteric area. Healing rates at the follow-up for fracture repair did not differ between patients with perioperative and non-perioperative BP initiation (prior or delayed BP use) (RR: 1.00, 95%CI: 0.98, 1.02, I2: 16%). Analysis of pooled RCTs suggested similar results (RR: 1.01, 95%CI: 0.96, 1.06; I2: 58%). Perioperative BP initiation did not significantly shorten the time to healing at the follow-up (MD vs. control: -0.57 week, 95% CI: -2.12, 0.97, I2: 41%). These findings were independent of fracture site or BP treatment. Perioperative BP initiation reduced screw-loosening risk (RR: 0.39, 95% CI: 0.03, 4.56, p=NS). Secondary analysis showed perioperative BP initiation resulted in significantly more reductions in VAS at month 6 (MD: -0.46, 95%CI: -0.81, -0.12) and 12 (MD: -0.75, 95%CI: -1.10, -0.41) following fracture repair than no BP initiation postoperatively.Conclusion: Perioperative BP initiation was not associated with a clinical impact on healing but remarkably improved the long-term pain following fracture repair. Findings may support perioperative BP initiation as an option for osteoporotic patients with fragility fracture surgery.

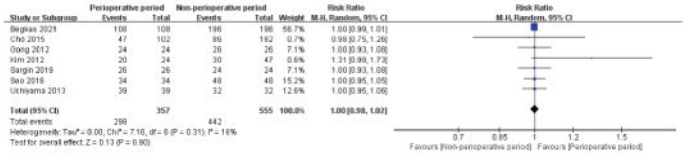

***Disclosures: Guolin Meng**, None*

FRI-445

Effectiveness of zoledronic acid treatment within 14 days of hip fracture surgery. *Betiana Perez[1], Ariela Kitaigrodsky[1], Natalia Aliquo Maciel[1], Ullman Tamara[1], Lucia Coli[1], Rodrigo Greco[1], Ivan Huespe[1], Mirena Buttazzoni[1], Maria Diehl[1]. [1]Hospital Italiano de Buenos Aires, Argentina

Treatment with zoledronic acid (ZA) within 90 days after surgical repair of a hip fracture reduces the occurrence of clinical fractures and mortality. However, there is limited available data regarding the effectiveness of using ZA within the first two weeks. As lockdown limited follow-up during Covid-19 pandemic, ZA began to be indicated during hospitalization with calcium and vitamin D supplementation in our institution. AimTo evaluate the effectiveness of administering ZA within 14 days after surgical resolution of a hip fracture.MethodsRetrospective cohort study of patients >=65 years from a closed health system hospitalized in a tertiary care hospital for a fragility hip fracture between 04/2018 and 04/2022, comparing patients who received ZA within 14 days after surgery (Early-ZA) with those treated between days 15 and 90 after surgery (Later-ZA). The main outcome was the combined event of death or refracture. Analysis was made with chi2 or Fisher for qualitative variables and Wilcoxon for quantitative variables. We performed Kaplan-Meier survival analysis and Cox regressions. We adjusted the regression analysis considering age, Charlson Index and length of the initial hospital stay as potential confounders.ResultsOut of 848 patients, 220 received ZA within 90 days: 163 (74%) within 14 days following hip fracture surgery (Early-ZA) and 57 (26%) between days 15 and 90 (Later-ZA). Median age Early-ZA 88 (IQR 81-92) and Later-ZA 85 (IQR 80-88) p=0.054; 14% male without differences between groups (15.3% vs 10.5%, p=0.36). Median Charlson Comorbidity Index was significantly higher in patients receiving Early-ZA (median 5 IQR 4-5; vs Later-ZA 0 IQR 0-1; p<0.0001). Median hospitalization for hip fracture was 7 days (IQR 5-9) for both groups (p=0.76). During a median follow-up of 502 days, 38 patients died (17.3%); 27 had new fractures (12.3%). Regarding the combined outcome (death or refracture) we did not observe significant differences (Figure), with a crude HR of 1.314 (95%CI 0.74-2.35), and an adjusted HR of 1.011 (95%CI 0.46-2.22). ConclusionsZA administration during in-hospital stay enhances access to secondary fracture prevention. We did not observe differences in the combined outcome of refracture or mortality between Early-ZA and Later-ZA after hip fracture in this preliminary study. After adjusting for confounding variables, HR changed substantially, suggesting a higher burden of comorbidities in patients treated in the first two weeks.

***Disclosures: Betiana Perez**, None*

FRI-448

A Single Dose of Zoledronic Acid after Stopping Denosumab in Early Hormone-receptor-positive Breast Cancer Patients: a Randomized Controlled Trial *Georg Pfeiler[1], Christian F. Singer[1], Dominik Hlauschek[2], Diether Manfreda[3], Ferdinand Haslbauer[4], Paul Sevelda[5], Kristin Koeck[6], Karl Tamussino[7], Arno C. Reichenauer[8], Florian Fitzal[9], Dietmar Heck[10], Richard Greil[11], Anita Jallitsch-Halper[2], Christian Fesl[2], Michael Gnant[12]. [1]Department of Gynecology and Gynecological Oncology and Comprehensive Cancer Center, Medical University of Vienna, Vienna, Austria, Austria. [2]ABCSG, Austrian Breast and Colorectal Cancer Study Group, Vienna, Austria, Austria. [3]Doctor's office Manfreda, Klagenfurt, Austria, Austria. [4]Department of Internal Medicine, Salzkammergutklinikum Hospital Vöcklabruck, Vöcklabruck, Austria, Austria. [5]Department of Gynecology, Karl Landsteiner Institute for Gynecologic Oncology and Senology, Hospital Hietzing, Vienna, Austria, Austria. [6]Department of Gynecology and Obstetrics, Hospital Klagenfurt, Klagenfurt, Austria, Austria. [7]Department of Gynecology and Obstetrics, Medical University of Graz, Graz, Austria, Austria. [8]Department of Surgery, Hospital BHB St. Veit, St. Veit/Glan, Austria, Austria. [9]Department of General Surgery and Breast Health Center of the Comprehensive Cancer Center, Medical University of Vienna, Austria, Austria. [10]Department of Hematology and Oncology, Ordensklinikum Linz - Barmherzige Schwestern, Linz, Austria, Austria. [11]Department of Internal Medicine III with Haematology, Medical Oncology, Haemostaseology, Infectiology and Rheumatology, Oncologic Center, Paracelsus Medical University Salzburg, Salzburg, Austria, Austria. [12]Medical University of Vienna, Comprehensive Cancer Center, Vienna, Austria; ABCSG, Austrian Breast and Colorectal Cancer Study Group, Vienna, Austria, Austria

Background: The placebo controlled randomized phase III ABCSG-18 trial demonstrated that denosumab significantly reduced clinical fractures in postmenopausal patients with breast cancer. Concern exists about a potential rebound effect after treatment discontinuation with denosumab. In line with this, an earlier analysis of ABCSG-18 showed an increased risk for vertebral and multiple vertebral fractures after stopping denosumab. We have therefore conducted a randomized sub-study investigating the use of a single dose of zoledronic acid (ZA) at the end of denosumab therapy. Here we present the first data on bone turnover markers (BTM).Patients And Methods: Patients of the ABCSG-18 trial who had completed denosumab treatment were randomized to a single dose of ZA 5mg i.v. versus nil(=SOC). ZA was administered 8 months+/-4 weeks after the last dose of denosumab (day 1 of this sub-study). DXA scans, lateral spine X-rays and BTM (CTX and osteocalcin) were assessed at baseline and at 6, 12 and 18 months thereafter. New fractures were assessed throughout. The percent change from baseline was derived and compared between arms with stratified Wilcoxon rank sum tests.Results: 50 patients with a median age of 71 years were randomized into this prospective sub-study. 24 received ZA, and 26 did not. Patient groups were well balanced with respect to baseline bone health factors. All patients of the ZA arm and 25 of the SOC arm received 7 doses of denosumab in the ABCSG-18 trial. At baseline, mean CTX was 0.57 ng/ml in both arms, mean osteocalcin was 19.5 ng/ml in the ZA arm and 18.8.ng/ml in the SoC arm. Percentage change of CTX differed significantly between the two arms with a median decrease of CTX after 6 months (-50.0%) and 12 months (-49.5%) in the ZA arm, and a median decrease after 6 months (-7.0%) and after 12 months (-6.5%) in the SOC arm. Accordingly, osteocalcin decreased by a median 17.0% after 6 months and 13.9% after 12months in the ZA arm, but increased by 110.8% after 6 months and by 29.4% after 12 months in the SOC arm. No significant difference of the BTM could be seen after 18 months.

Importantly, the observed increase of BTM in the SOC arm was driven by a few patients with major changes - up to 778.6% for CTX and up to 679.6% for osteocalcin.Conclusion: These first data of the randomized sub-study of the ABCSG-18 trial demonstrate that a single dose of ZA prevents a high bone turnover state that occurs in some patients of the SOC arm after stopping denosumab.

***Disclosures: Georg Pfeiler**, Pfizer, Roche, AstraZeneca, Seagen, MSD, Gilead, Accord Healthcare, Daiichi, Novartis, Lilly, Speakers' Bureau, Pfizer, Roche, Seagen, Novartis, AstraZeneca, Daiichi, MSD, Lilly, Gilead, Consultant, Pfizer, Accord Healthcare, Roche, AstraZeneca, MSD, Grant/Research Support*

FRI-451

The efficacy of sequential therapy with romosozumab followed by denosumab compared to denosumab alone in hemodialysis patients *Yuichiro Tamagawa[1], Hitoshi Tanigawa[2]. [1]Japan Community Health care Organization Shiga hospital, Japan. [2]Center for Regenerative Medicine and Skeletal Development, Uconn Health, United States

Hemodialysis patients have a high rate of osteoporosis and are a high-risk group for fractures. However, some osteoporosis drugs are contraindicated to severe renal failure patients, and treatment strategies for patients with severe osteoporosis aren't well established. Romosozumab is a monoclonal anti-sclerostin antibody that has the dual effect of increasing bone formation and suppressing bone resorption, reducing the risk of fracture within 12 months. This study aimed to compare the effects of one year of romosozumab followed by one year of denosumab (group R) to two years of denosumab (group D) on bone mineral density (BMD) and bone metabolism markers in hemodialysis patients with severe osteoporosis. This study was a single-center, retrospective study. 19 patients were in group R and 23 in group D, they are all hemodialysis patients. All patients were given these treatments as their first treatment for osteoporosis. Both groups showed significant increase in BMD(T-score) at the lumbar spine and femoral neck after 6 months treatment (group D: +0.32; group R: +0.70), with group R showing a significant increase compared to group D in BMD at the lumbar spine (p=0.0024). The bone metabolism marker P1NP increased significantly in group R at 6 months (+57.4%, p=0.002 vs baseline), and decreased significantly at 12 months (-17.4%, p=0.001 vs baseline). Adverse events were few and none were fatal, including cardiovascular events. P1NP level of group D showed a consistent decrease from baseline. The bone resorption marker TRACP-5b also showed a significant decrease compared to baseline after 6 months in both groups (group D: -42.9%; group R: -17.4%), with group D showing a consistently greater decrease in all the periods. No obvious fractures were not observed. These results suggest that romosozumab treatment followed by denosumab may be a potentially good strategy for hemodialysis patients with severe osteoporosis.

***Disclosures: Yuichiro Tamagawa**, None*

FRI-455

Influence of age on the efficacy of pharmacologic treatments on fracture risk reduction and increases in BMD: Results from the FNIH-ASBMR SABRE Project *Marian Schini[2], Tatiane Vilaca[2], Eric Vittinghoff[3], Lui Li-Yung[4], Susan Ewing[3], Douglas Bauer[5], Dennis Black[6], Mary Bouxsein[7], Richard Eastell[2]. [2]University of Sheffield, . [2]University of Sheffield, United Kingdom. [3]Department of Epidemiology & Biostatistics, University of California, San Francisco, San Francisco, CA, USA, United States. [4]Research Institute, California Pacific Medical Center, San Francisco, CA, USA , United States. [5]University of California, San Francisco, United States. [6]UC San Francisco, . [7]Beth Israel Deaconess Medical Center, Harvard Medical School, United States

PurposeAntiosteoporosis medications are given to individuals of various ages, but we do not know whether the effect is similar in different age groups. The aim of this study was to use data from key trials of antiosteoporosis medications to determine whether the anti-fracture efficacy or BMD changes associated with treatment differ in people above and below 70 years. The threshold was set at this age as it gave similar numbers of subjects in the studies with vertebral fracture as the endpoint.MethodsWe used individual patient data from 23 randomised placebo-controlled clinical trials of antiosteoporosis medications. Data were stratified by age (<70 and >=70 years old), and the treatment-related fracture risk reduction was estimated in each subgroup, using logistic regression for morphometric vertebral fractures and Cox regression for all clinical, non-vertebral, hip and "all" (combination of non-vertebral and clinical or morphometric vertebral fractures) fractures. The treatment effect on 24-month change in BMD was estimated in each subgroup using linear regression. We performed analyses on all trials, and again separately on trials of bisphosphonates only. We tested the interaction between age subgroup and treatment in all analyses.ResultsThese analyses included 123,164 participants; 57% 0.05) (Figure). The use of antiosteoporotic drugs in people aged 70 and older resulted in significantly greater absolute and percent increases in BMD at 24 months at the total hip (3.8% [3.7, 3.9] vs. 3.1% [3.0, 3.2]), femoral neck (3.4% [3.3, 3.5] vs. 3.0% [2.9, 3.1]) and lumbar spine ((4.4% [4.2, 4.5] vs. 3.9% [3.8, 4.0]) (all p<0.0001).ConclusionsIn summary, antiosteoporotic medications reduced the risk of fractures similarly among those above and below 70 years of age but were more effective at increasing BMD among those at least 70 years.

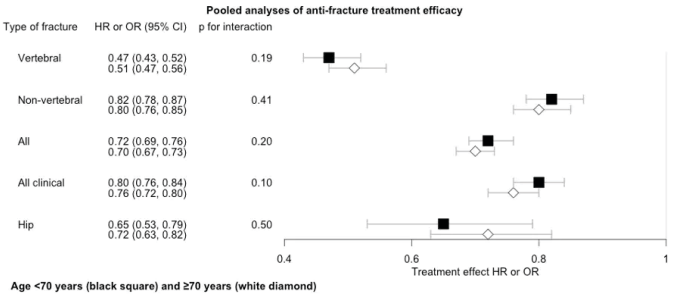

***Disclosures: Marian Schini**, None*

FRI-464

From bench to bedside: Transcriptome profiling in a medaka fish osteoporosis model identifies CXCL9 as a blood marker that predicts the risk for osteoporotic hip fractures in men *Christoph Winkler[1], Quang Tien Phan[1], Kevin Yiqiang Chua[1], Aizhen Yin[1], Woon-Puay Koh[1]. [1]National University of Singapore, Singapore

Bone homeostasis requires reciprocal communication between bone-forming osteoblasts and bone resorbing osteoclasts to maintain bone health. Communication failures result in bone diseases, such as osteoporosis, where uncontrolled osteoclast activity results in excessive bone resorption and bone fractures. To identify novel signalling factors implicated in osteoblast-osteoclast communication, our lab had earlier conducted transcriptome profiling of bone cells in a medaka fish osteoporosis model, which allows high-resolution live imaging of dynamic bone cell behaviour in intact specimen. In this model, transgenic induction of the osteoclast inducer Rankl resulted in excessive osteoclast formation and osteoporotic bone lesions. We showed that under Rankl+ conditions, osteoblasts strongly upregulated expression of the chemokine Cxcl9l. This chemokine in turn led to osteoclast recruitment and differentiation at bone matrix and excessive bone resorption. Mutations in cxcl9l and its cognate receptor cxcr3.2, or treatment with chemical Cxcr3.2 antagonists prevented excessive osteoclast formation and protected medaka bone form osteoporotic lesions. To validate a possible association of the CXCL9 ortholog and osteoporosis or fracture risk in humans, we conducted a matched case-control study nested in the prospective, population-based Singapore Chinese Health Study. This study included 55 men and 119 women who had experienced a hip fracture with an average of 6.3 years after their blood was collected. Participants were matched individually to controls who did not develop hip fractures. We found significantly higher levels of CXCL9 in pre-fracture blood samples of men with subsequent hip fractures compared with their non-fracture controls. Surprisingly, no such differences were seen in women. This suggests that elevated CXCL9 levels affect older men and women differently, possibly due to changes in sex hormone levels during aging. These findings open the possibility that early interventions targeting CXCL9-CXCR3 signalling could be beneficial in preventing hip fractures in older men. This work is funded by a grant from the Singapore Ministry of Education (MOE-T2EP30221-0008).

***Disclosures: Christoph Winkler**, None*

FRI-465

Endothelin Receptor Blockade Restores SARS-CoV-2-induced Bone Loss in Hamsters *Junguo NI[1], Man Ting Au[1], Kaiming Tang[2], Marianne Lauwers[1], Cuiting Luo[2], Shuofeng Yuan[2], Chunyi WEN[3]. [1]Department of Biomedical Engineering, The Hong Kong Polytechnic University, Hong Kong. [2]State Key Laboratory of Emerging Infectious Diseases, Department of Microbiology, School of Clinical Medicine, Li Ka Shing Faculty of Medicine, The University of Hong Kong, Hong Kong. [3]Hong Kong Polytechnic University, Hong Kong

Purpose: SARS-CoV-2-induced persistent bone loss has been documented in humans and animals. Yet there is no cure for such post-COVID skeletal complications till now. Endothelin signaling, known as a key player in bone homeostasis and disease, was recently shown to upregulate in hospitalized COVID patients. Hereby, we aim to investigate the efficacy of FDA-approved endothelin receptor antagonist, Macitentan, in treating bone loss in hamsters after SARS-CoV-2 infection.Methods: A total of 10 female golden Syrian hamsters at the age of 10-16 weeks were infected intranasally at day 0 with 1×105 PFU SARS-CoV-2. They were randomly allocated to the placebo (PBS) or treatment (0.3 mg/kg Macitentan) groups, that is five hamsters per group. The treatment was initiated during the sub-acute infection phase, i.e. at 16 days post SARS-CoV-2 infection (dpi) and continued for two weeks, which was delivered intraperitoneally with the same volume of PBS as placebo. Five additional hamsters were used as control and received mock infection at the same age as the infected groups. All hamsters were sacrificed at 30 dpi and hind limbs were harvested for ?CT, histopathological and immunohistochemical analysis.Results: At 30dpi, a significant decrease in growth plat thickness, chondrocyte number, and BMD and BV/TV in primary spongiosa was observed compared to mock infection. It was accompanied by a reduction in the number of TRAP+ osteoclasts and SP7+ osteoblasts per bone perimeter. SARS-CoV-2

nucleocapsid and spike proteins were detected in bone marrow cavity in the vicinity of blood vessels. Noteworthily, the number of caspase 3-positive apoptotic growth plate chondrocytes remarkably increased with upregulated expression of endothelin type A and B receptors. Surprisedly, 2-week Macitentan treatment in the sub-acute phase of viral infection could mitigate growth plate chondrocyte apoptosis, increase the number of chondrocytes and SP7+ osteoblasts, fully restore the thickness of growth plate and bone mass.Conclusion: SARS-CoV-2 infection triggers growth plate chondrocyte dropout and causes bone loss. Endothelin receptor blockade via Macitentan is a promising therapeutic strategy to rescue growth plate injury and persistent bone loss after SARS-CoV-2 infection. This treatment remains effective even when not initiated during the acute phase of viral infection.Note: JGN, MTA, and KMT are equal contributions. CYW and SFY are the corresponding authors.

***Disclosures: Junguo NI**, None*

FRI-468

Sclerostin Loop3-LRP4 Interaction Required by Sclerostin for Antagonizing Wnt Signaling and Osteogenic Potential in Osteoblasts *Luyao Wang[1], Xiaohui Tao[1], Hewen Jiang[2], Ning Zhang[2], Dijie Li[1], Jin Liu[1], Yuanyuan Yu[1], Yihao Zhang[1], Aiping Lyu[1], Baoting Zhang[2], Ge Zhang[1]. [1]Law Sau Fai Institute for Advancing Translational Medicine in Bone and Joint Diseases (TMBJ), School of Chinese Medicine, Hong Kong Baptist University, Hong Kong. [2]The Chinese University of Hong Kong, Hong Kong

Sclerostin becomes a novel bone anabolic target. Sclerostin loop2 was reported to bind to YWTD repeats within LRP5/6 of osteoblasts, thereby antagonizing bone anabolic Wnt/?-catenin signaling pathway. Humanized sclerostin antibody which targeted sclerostin loop2 promoted bone formation, whereas imposed sever cardiovascular events in clinical trials. In our published work, sclerostin loop3 was notably found to contribute to the antagonistic effect of sclerostin on bone formation, while the cardiovascular protective effect of sclerostin was independent of loop3. Targeting sclerostin loop3 by our screened sclerostin loop3-specific aptamer promoted bone formation in SOSTki mice, ovariectomized osteoporotic rats and Col1a2+/G610C mice, without increasing cardiovascular risk. The sclerostin loop3 aptamer for osteogenesis imperfecta was granted Orphan Drug Designation by US-FDA (DRU-2019-6966). However, how sclerostin loop3 participates in the antagonistic effect of sclerostin on bone formation remains unclear. In our pull-down and biolayer interferometry (BLI) studies, sclerostin loop3 was found to bind to LRP4 in osteoblasts (Fig.1a-b). It was reported that osteoblastic LRP4 could facilitate the binding of sclerostin to LRP6 for antagonizing bone formation. After identification of the interaction residues, LRP4m (LRP4-Y200A, G201A, L214A, D215A, I216A, Y217A, H218A, C219A) was designed to genetically block sclerostin loop3-LRP4 interaction in vitro. The antagonistic effect of sclerostin on Wnt signaling and osteogenic potential in osteoblasts were inhibited upon LRP4m, while no changes in Wnt signaling and osteogenic potential were found in the absence of sclerostin before and after expression of LRP4m (Fig.1c-d). Based on the interaction, a peptide tool LRP4-Pep was designed to pharmacologically block sclerostin loop3-LRP4 interaction. The antagonistic effects of sclerostin on Wnt signaling and osteogenic potential in osteoblasts were inhibited after pretreatment of the exogenous LRP4-Pep (Fig.1e-f). Sclerostin loop3-LRP4 interaction was required by sclerostin for antagonizing Wnt signaling pathway and osteogenic potential in osteoblasts in vitro.

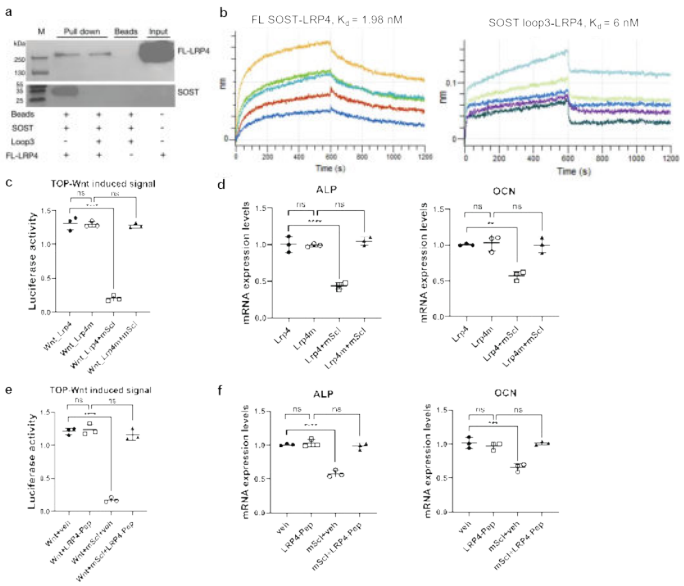

***Disclosures: Luyao Wang**, None*

FRI-474

High Physical Activity Is Associated with Greater Cortical Bone Size, Better Physical Function, and Lower Risk of Incident Fracture Independently of Clinical Risk Factors and BMD in Older Women *Lisa Johansson[1], Kristian Axelsson[2], Henrik Litsne[3], Mattias Lorentzon[4]. [1]Institute of medicine, . [2]Institute of Medicine, Sahlgrenska Academy, Gothenburg University, . [3]Sahlgrenska Osteoporosis Centre, University of Gothenburg, Sweden. [4]Sahlgrenska Academy, University of Gothenburg, Sweden

The Physical Activity Scale for the Elderly (PASE) is a validated test to assess physical activity in older persons. It has not been investigated if physical activity level, according to PASE, can improve fracture risk prediction beyond the commonly used clinical risk factors (CRFs) in the FRAX algorithm. The purpose of this study was to evaluate if PASE score is associated with bone characteristics, physical function, and predicts incident fracture in older women, independently of CRFs in FRAX with femoral neck (FN) bone mineral density (BMD).SUPERB is a population-based study of 3,028 older Swedish women. Included women were 75-80 years, answered questionnaires regarding CRFs in FRAX, and underwent physical function tests, detailed bone phenotyping with DXA (Hologic) of the FN, and bone geometry, volumetric BMD, and microstructure at the ultradistal tibia with HRpQCT (XtremeCT). Incident fractures were x-ray verified. Cox regression models were used to assess the association between PASE score and incident fractures, with adjustments for CRFs and FN BMD.In total, 3014 women completed the PASE assessment and were divided into quartiles (PASE score median (range) Q1 52.1 (0.0-65.0), Q2 78.6 (65.1-96.1), Q3 113.9 (96.3-134.2), Q4 164.8 (134.2-385.3)). At baseline, women in Q4 had greater cortical volumetric BMD (vBMD) and cortical area than women in Q1, with quartile differences corresponding to 1.56% for cortical vBMD (p=0.007), and 4.03% for cortical area (p=0.022). Similarly, women in Q4 had shorter timed up and go test compared to women in Q1 (7.7+/-1.9 vs 10.6+/-4.7 seconds, p<0.001). During 8 years (median, range 0.20-9.9) of follow-up, 1077 women had any incident fracture, 806 had a major osteoporotic fracture (MOF; spine, hip, forearm, humerus), and 236 had a hip fracture. Women in Q4 had a 30% lower risk of any fracture, 23% lower risk of MOF, and 54% lower risk of hip fracture, compared to women in Q1. These associations remained after adjustment for CRFs in FRAX and FN BMD (Table).In conclusion, high physical activity was associated with a lower risk of any fracture, MOF, and hip fracture, independently of risk factors used in FRAX with FN BMD. Better physical function and greater cortical bone size may explain the lower fracture risk observed in those with high physical activity. These results suggest that fracture risk assessments in older women may be improved if the physical activity level is considered.

Table. Quartiles of Physical Activity According to PASE and Risk of Fracture in Older Women.

	Quartile 1 n=754	Quartile 2 n=753	Quartile 3 n=753	Quartile 4 n=754
Any fracture				
No. (%)	305 (40.5)	277 (36.8)	251 (33.3)	244 (32.4)
Per 1000 person-years	69.4	58.2	50.6	48.6
CRFs in FRAX + FN BMD	1 [Ref]	0.85 [0.72-1.00]	0.75 [0.63-0.89]	0.73 [0.62-0.87]
MOF				
No. (%)	229 (30.4)	206 (27.4)	196 (26.0)	175 (23.2)
Per 1000 person-years	48.6	40.6	37.7	33.2
CRFs in FRAX + FN BMD	1 [Ref]	0.86 [0.71-1.04]	0.81 [0.67-0.99]	0.74 [0.60-0.90]
Hip				
No. (%)	80 (10.6)	57 (7.6)	53 (7.0)	46 (6.1)
Per 1000 person-years	14.9	10.0	9.2	7.9
CRFs in FRAX + FN BMD	1 [Ref]	0.65 [0.46-0.92]	0.62 [0.44-0.89]	0.54 [0.37-0.78]

CRFs=Clinical Risk Factors. FN BMD = Femoral Neck Bone Mineral Density. MOF=Major Osteoporotic Fracture. Hazard Ratios with 95% confidence intervals are shown.

***Disclosures: Lisa Johansson**, None*

FRI-483

Functional Characterization of Novel Lunatic Fringe Variants in Spondylocostal Dysostosis Type-III with Scoliosis *Parker Wengryn[1], Karina Da Costa Silveira[1], Connor Oborn[1], Carrie-Lynn Soltys[1], Alex Beke[1], Inara Chacon-Fonseca[2], Nadirah Damseh[3], Marco Quesada Rodriguez[4], Ramsés Badilla Porras[4], Peter Kannu[1]. [1]University of Alberta, Canada. [2]Lakeridge Health Oshawa, Canada. [3]University of Toronto, Canada. [4]Hospital Nacional de Niños, Costa Rica

Purpose: Rare Mendelian diseases provide a unique opportunity to investigate genetic pathways contributing to normal spinal development and variability in phenotypic presentation. Spondylocostal Dysostosis Type-III (SCD3) is a rare, autosomal recessive disorder characterized by rib fusions, vertebral abnormalities, and varying degrees of scoliosis. SCD3 is caused by variants in the Lunatic Fringe (LFNG) gene encoding a ?-1-3-N-acetylglucosaminyltransferase. This enzyme transfers N-acetylglucosamine to NOTCH1 during somitogenesis to promote normal vertebral formation. We have identified compound heterozygous LFNG variants-of-uncertain-significance (VUS; the genetic variant has an unknown effect on health) in a proband with a SCD phenotype. However, the proband is taller (Height: 10th-25th%), has a longer trunk (Arm span-to-height ratio: 1.07), and more vertebrae (>20) than the six previously reported SCD3 cases. The purpose of our study is to determine whether the c.766G>A (p.G256S) and c.521G>A (p.R174H) LFNG variants lead to diminished N-acetylglucosaminyltransferase activity, protein mis-localization, and/or dysregulated

pre-pro-processing. We hope that this will inform the relationship between genotype and phenotype.Methods: HEK293T cells were transiently transfected with 3XFLAG-hLFNG. Fusion protein was immunoprecipitated and assessed with a quantitative glycosyltransferase luciferase assay. NIH3T3 cells were transiently transfected with LFNG-HA, incubated with anti-HA and anti-GM130 antibodies, then assessed for signal colocalization through confocal microscopy. Finally, NIH3T3 cells were transfected with LFNG-HA and whole cell lysate was processed for protein, western blotted, and semi-quantitatively analyzed. Results: The p.G256S and p.R174H variants displayed significantly less enzymatic activity than wildtype. The p.G256S substituion was comparable to negative control whereas p.R174H was significantly more active than p.G256S. Both variants were correctly localized to the Golgi and normally pre-pro-processed.Conclusions: We have discovered the first hypomorphic (p.R174H) and report the fourth functionally null (p.G256S) LFNG variants associated with SCD3. This is the first clinically identified combination of partially active and completely inactive LFNG. This data may suggest that the hypomorphic variant partially rescued the probands height, trunk length, and vertebral number, but not segmentation defects nor scoliosis.

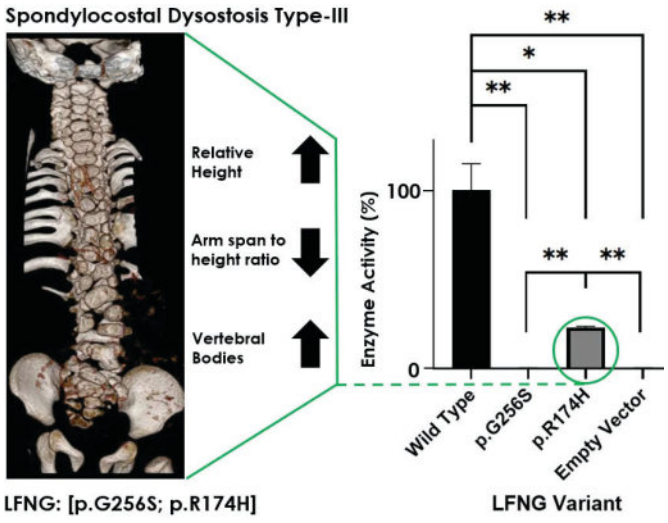

***Disclosures: Parker Wengryn**, None*

FRI-484

Women with Pregnancy and Lactation associated Osteoporosis (PLO) Have Substantial Volumetric BMD Deficits at the Spine by Central QCT *Sanchita Agarwal[1], Thomas Lang[2], Mafo Kamanda-Kosseh[1], Dany El-Najjar[1], Mariana Bucovsky[1], Ivelisse Colon[1], Ananya Kondapalli[1], Nayoung Kil[1], Joan M. Lappe[3], Julie Stubby[3], Robert R. Recker[3], Adi Cohen[1]. [1]Columbia University Irving Medical Center, United States, [2]School of Dentistry, University of California San Francisco, United States, [3]Creighton University Medical Center, United States

PLO is a rare, severe, early form of osteoporosis, most commonly presenting with multiple vertebral fractures (Fx) associated with pregnancy/lactation. Most women with PLO have no known secondary cause; mechanisms and etiologies are largely unknown. Herein we report central QCT (cQCT) findings at the lumbar spine (LS; L1-L2) in the largest structurally characterized cohort of PLO women to date in comparison to both (1) healthy nonosteoporotic premenopausal controls and (2) premenopausal women with idiopathic osteoporotic Fx not associated with pregnancy/lactation (nonPLO IOP).Clinical and skeletal characteristics were compared between 3 treatment naïve premenopausal cohorts: 34 controls, 49 nonPLO IOP and 48 PLO. Among PLO, 19 were studied <=12M (Recent PLO), while 29 were studied >12M postpartum (Distant PLO). NonPLO IOP and controls were studied >12M postpartum. cQCT parameters: cQCT-derived AP and lateral (LAT) 2D LS aBMD, total density (with posterior elements; Tot_vBMD), Tb density (Tb_vBMD), vertebral integral density (excludes posterior/transverse elements; Int_vBMD), and mid vertebral integral density (Mid_vBMD) and strength index (SI; =density2*area, approximating compressive strength) both computed from a 10mm vertebral body mid-section. Student's t-tests were used for between groups comparisons.Clinical presentation was more severe in PLO than nonPLO IOP: more Fx, childhood Fx, multiple Fx, and vertebral Fx (Table). Skeletal structure was also most severely affected in PLO. Compared to controls, PLO had substantial deficits in all LS aBMD and vBMD parameters (all p<0.001). Compared to nonPLO IOP, PLO also had significantly lower aBMD and vBMD, but SI did not differ.To study natural history of PLO, we compared patients at different postpartum stages. Compared to Distant PLO, Recent PLO had lower LS aBMD by DXA, and Tot_vBMD and Mid_vBMD by cQCT (all p<0.05; data not shown). These results support our hypothesis that Recent PLO, studied soon after they fractured and prior to full recovery of pregnancy/lactation related bone loss, would have the most profound structural deficits.In summary, PLO women have substantial aBMD and vBMD deficits at the LS compared to both controls and nonPLO IOP. The Recent PLO group had the most profoundly affected bone structure, particularly in the vertebral mid-section. This structural investigation increases mechanistic understanding of the spine predominant bone fragility presentation that characterizes PLO.

Table: Clinical and skeletal characteristics by DXA and cQCT in healthy premenopausal controls, nonPLO IOP and PLO (mean ± SD or %).

	Clinical characteristics				
	Controls (N=34)	NonPLO IOP (N=49)	PLO (N=48)	p-value (PLO vs Controls)	p-value (PLO vs IOP)
Age (years)	36.8 ± 8.5	37.1 ± 8.1	34.3 ± 5.6	0.11	0.05
Height (cm)	165.4 ± 7.2	164 ± 7.1	164 ± 7.3	0.4	0.99
Weight (kg)	70 ± 15.6	62.5 ± 14.8	64.2 ± 12.2	0.06	0.53
BMI (kg/m^2)	25.5 ± 4.7	23.2 ± 5.1	23.9 ± 4.6	0.13	0.47
Age at Menarche (years)	12.8 ± 1	12.8 ± 1.1	13.2 ± 1.5	0.19	0.13
Age at 1st Pregnancy (years)	25.8 ± 5.8	26.2 ± 6.1	29.1 ± 5.4	**0.02**	**0.03**
Parity (n)	1.4 ± 1.3	1.3 ± 1.2	2 ± 2	0.12	**0.03**
Parous (%)	64.7	59.2	100	**<0.001**	**<0.001**
History of Childhood Fx (%)	17.6	42.9	47.9	**0.01**	0.77
Number of Adult Fx	NA	2.4 ± 1.7	4.9 ± 3.0	NA	**<0.001**
Multiple Adult Fx (%)	NA	65.3	89.6	NA	**0.01**
Vertebral Fx (%)	NA	12.2	79.2	NA	**<0.001**
	DXA and cQCT of the Lumbar Spine				
DXA LS aBMD (L1-L4) (g/cm^2)	1.09 ± 0.10	0.87 ± 0.14	0.77 ± 0.11	**<0.001**	**<0.001**
Simulated AP LS aBMD (L1-L2) (g/cm^2)	1.19 ± 0.11	0.94 ± 0.16	0.83 ± 0.14	**<0.001**	**<0.01**
Simulated LAT LS aBMD (L1-L2) (g/cm^2)	0.74 ± 0.08	0.59 ± 0.09	0.50 ± 0.13	**<0.001**	**<0.001**
Total vBMD (g/cm^3)	0.27 ± 0.02	0.23 ± 0.03	0.20 ± 0.03	**<0.001**	**<0.001**
Trabecular vBMD (g/cm^3)	0.18 ± 0.03	0.14 ± 0.03	0.12 ± 0.05	**<0.001**	0.07
Vertebral Integral vBMD (g/cm^3)	0.21 ± 0.02	0.17 ± 0.02	0.15 ± 0.03	**<0.001**	**<0.001**
Mid Vertebral Integral vBMD (g/cm^3)	0.19 ± 0.02	0.15 ± 0.02	0.13 ± 0.03	**<0.001**	**<0.01**
Strength Index (g^2/cm^4)	0.33 ± 0.07	0.20 ± 0.07	0.16 ± 0.14	**<0.001**	0.13

***Disclosures: Sanchita Agarwal**, None*

FRI-485

Bone microarchitecture and strength in Osteogenesis Imperfecta using HR-pQCT: comparison with normative data taking into account limb length and deviating axial scan angles *MELISSA BEVERS[1], Bert Rietbergen[2], Arjan Harsevoort[3], Koert Gooijer[3], Hans Feenstra[3], Guus Janus[3], Caroline Wyers[4], Joop Van Den Bergh[5]. [1]VieCuri Medical Center, , [2]Eindhoven University of Technology, Netherlands, [3]Expert Center for adults with Osteogenesis Imperfecta Isala Hospital, Netherlands, [4]VieCuri Medical Centre, Netherlands, [5]VieCuri MC Noord-Limburg and Maastricht UMC,

Purpose: Patients with osteogenesis imperfecta (OI) have increased bone fragility and fracture risk. High-resolution peripheral quantitative CT (HR-pQCT) has been used to study bone microarchitecture in OI as compared to non-OI groups, but short stature and bone deformities in OI may cause deviations in scanned region and limit comparison. The aim of this study was to assess bone microarchitecture and strength in adults with OI as compared to normative data using HR-pQCT with a limb-length dependent scan protocol and by taking into account deviating scanned regions. Methods: Limb-length dependent HR-pQCT scans of the distal radius and tibia were obtained from 118 adults with OI (41.8 [IQR: 25.1] year old). To evaluate potential deviations in the scanned region, the axial scan angle was computed using a new algorithm that quantifies the angle between the areal center of the bone on the first and last slice of a scan. The angle was compared to that of limb-length dependent HR-pQCT scans of 13 healthy young women. It was considered to be deviated when being outside the fence of 1.5xIQR from Q1 and Q3 in those women. Bone microarchitecture and strength were quantified and compared to normative data from literature (Warden et al. Osteoporos Int 2021). Results: 102 radius and 105 tibia scans could be analyzed, of which the axial scan angle was found to be deviating in 11 (radius; 10.8%) and 14 (tibia; 13.3%). In the radius scans without deviating angle, total BMD was low (Z-score: -1.0+/-1.8) as were trabecular BMD (Z-score: -1.6+/-1.3) and number (Z-score: -2.5+/-1.4) and total bone stiffness (Z-score: -1.4+/-1.5). Trabecular separation was high (Z-score: -2.7 [2.7]). Trabecular thickness and cortical BMD and microarchitecture were normal. Larger deviations were seen at the tibia. In the scans with a deviating axial angle, deviations from the normative data were smaller or similar (cortical bone) but more often larger (total and trabecular bone) than in the scans without deviating angle, most pronounced at the tibia (Fig.1). Conclusion: Bone microarchitecture and strength in OI are impaired, in particular at the trabecular compartment. It likely contributes to the increased fracture risk in OI and may provide valuable insights to improve treatments of reduced bone quality. Scans with a deviating scanned region, likely due to bone deformities and scan positioning limitations in OI, should be excluded in HR-pQCT studies on OI, especially when comparing study groups.

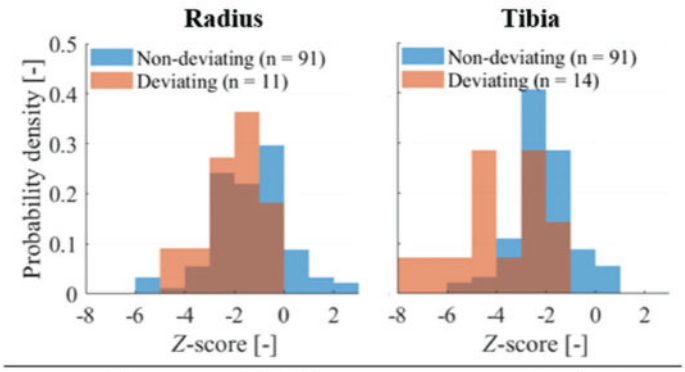

	Non-deviating	Deviating	Non-deviating	Deviating
Z<-1	51 (56%)	9 (82%)	78 (86%)	14 (100%)
Z<-4	4 (4%)	1 (9%)	5 (5%)	7 (50%)

Fig.1: Z-scores for bone stiffness at the distal radius (left) and tibia (right) from scans with and without deviating axial angle.

***Disclosures: MELISSA BEVERS**, None*

FRI-487

A Prospective Study to Evaluate Patient-Reported Quality of Life Before and After Asfotase Alfa Treatment in Adults with Pediatric-Onset Hypophosphatasia *Kathryn Dahir[1], Steven Ing[2], Chad Deal[3], Andrew Messali[4], Toby Bates[4], Eric T. Rush[5]. [1]Vanderbilt University Medical Center, United States, [2]The Ohio State University Wexner Medical Center, United States, [3]Cleveland Clinic Foundation, United States, [4]Alexion, AstraZeneca Rare Disease, United States, [5]Children's Mercy Kansas City; University of Missouri - Kansas City School of Medicine, United States

Purpose: To evaluate the impact of asfotase alfa on patient-reported outcomes (PROs) in adults with pediatric onset hypophosphatasia (HPP).Methods: A longitudinal telephone-based survey was administered to adults with pediatric-onset HPP at baseline (prior to asfotase alfa initiation) and follow-up (3 [3M], 6 [6M], and 12 months [12M] post-initiation). Demographics and PROs (Patient Health Questionnaire-9 [PHQ-9], Patient-Reported Outcomes Measurement Information System [PROMIS-29], Routine Assessment of Patient Index Data 3 [RAPID3], and Work Productivity and Activity Impairment-Specific Health Problem [WPAI-SHP]) were assessed (Figure). McNemar's or Cochran-Mantel-Haenszel tests or paired t-tests were performed, as appropriate.Results: Among 50 enrolled patients, 29 were evaluable at 12M. Mean age at baseline was 46 (+/-15.4) years; 80% were female and 94% were White. At 12M, a statistically significant improvements from baseline were observed for PHQ-9 total score (10.6 baseline vs 4.2 12M, P<0.0001), PROMIS-29 domain scores (physical functioning: 38.0 vs 46.5, P<0.0001; anxiety: 57.5 vs 47.9, P<0.0001; depression: 52.6 vs 47.4, P=0.003; fatigue: 63.3 vs 51.3, P<0.0001; sleep disturbance: 58.8 vs 51.6, P=0.0008; social roles and activities: 42.6 vs 50.7, P=0.0001; pain interference: 63.8 vs 54.9, P<0.0001), and RAPID3 domain scores (functional status: 2.7 vs 1.1, P<0.0001; pain tolerance: 6.0 vs 3.2, P<0.0001; global health estimate: 5.1 vs 2.7, P<0.0001). WPAI-SHP domains showed significant improvement at 12M in presenteeism (39.6% vs 14.0%, P<0.0001), activity impairment (64% vs 30.0%, P<0.0001), and work productivity loss (41.9% vs 20.0%, P=0.012); however, the significant improvement seen at 6M in absenteeism (4.7% vs 0%, P=0.025) was not maintained at 12M (vs 8.0%, P=0.65). By 12M, the use of analgesic medications decreased from baseline (20%, n=10 vs 10.3%, n=3).Conclusion: Treatment with asfotase alfa improved anxiety, depression, physical functioning, fatigue, sleep, pain, and improved work and social relationships. These results illustrate the potential utility of adapting existing PRO instruments validated in diseases phenotypically similar to HPP.

Overview of Patient-reported Outcomes Questionnaires Collected in the Study

Information	Patient Health Questionnaire-9 (PHQ-9)	Patient-Reported Outcomes Measurement Information System (PROMIS-29)	Rourtine Assessment of Patient Index Data 3 (RAPID 3)	Work Productivity and Activity Impairment - Specific Health Problem (WPAI-SHP)
Concept of interest	• Depression	• Health-related quality of life	• Disease activity	• Work-related productivity and activity impairment
Recall period	• Past 2 weeks	• Past 7 days • Except Physical Functioning, which does not have a specified timeframe	• Over the last week for Physical Function and Pain • At this time for Patient Global Estimate	• Past 7 days
Domains covered	• Unidimensional	• Physical Function (4 items) • Anxiety (4 items) • Depression (4 items) • Fatigue (4 items) • Sleep Disturbance (4 items) • Ability to participate in Social Roles and Activities (4 items) • Pain Interference (4 items) • Pain Intensity (1 item)	• Physical Function (13 items) • Pain (1 item) • Patient Global Estimate (1 item)	• Work Productivity (5 items) • Daily Activities (1 item)
Response scale & score range	• Range: 0–27 • PHQ severity categories: minimal (0-4), mild (5-9), moderate (10-14), moderately severe (15-19), severe (20-27)	• Standardized T-score with a mean of 50 and a standard deviation of 10	• Range: 0–10 • RAPID3 qualitative description Categories: near remission (0–1.0), low severity (1.3–2.0), moderate (2.3–4.0), high (4.3–10.0)	• Scores are multiplied by 100 to be expressed as impairment percentages
Directionality	Higher = More severe depressive symptoms	Higher = Better for positively worded concepts Higher = Worse for negatively worded concepts	Higher = More active disease	Higher = Greater impairment & less productivity

Note: All PROs were measured at baseline (prior to initiation of asfotase alfa) and follow-up (3 months and 6 months post-initiation)>

***Disclosures: Kathryn Dahir**, Alexion, AstraZeneca Rare Disease, Consultant, Alexion, AstraZeneca Rare Disease, Grant/Research Support*

FRI-489

A Multicenter Study Evaluating Hypertension in Children with X-Linked Hypophosphatemia *Irene Chen[5], Anna Ryabets-Lienhard[2], Sreya Molakalapalli[3], Jennifer Ringrose[5], Leanne Ward[4], Robert T Alexander[5], Chelsey Grimbly[5]. [5]University of Alberta, Canada, [2]Children's Hospital Los Angeles , , [3]Children's Hospital of Los Angeles, United States, [4]Children s Hospital of Eastern Ontario, Canada, [5]University of Alberta,

X-linked Hypophosphatemia (XLH) is associated with elevated fibroblast growth factor 23 (FGF23) resulting in renal phosphate wasting and decreased 1,25 dihydroxyvitamin D. It is a multi-system disease with significant co-morbidities. Current treatment options include conventional therapy (phosphate and 1,25 dihydroxy vitamin D) or burosumab (anti-FGF23 therapy). High rates of hypertension (HTN) have been reported in adults, but it is unclear if HTN develops in childhood. We present data on HTN in pediatric XLH.Methods: We evaluated medical records of children (<18 years of age) with XLH followed at two tertiary care centers, the Stollery Children's Hospital (Edmonton, Canada), and the Children's Hospital of Los Angeles (Los Angeles, United States) from 2014-2022. Patients were included if they had three or more blood pressure (BP) recordings. Clinical data was collected including laboratory and treatment data and renal ultrasound results. HTN was defined as systolic or diastolic BP (SBP, DBP) greater than the 95th percentile for age, sex and height on three or more occasions, as per the Fourth Report on the Diagnosis, Evaluation, and Treatment of High Blood Pressure in Children and Adolescents. Descriptive analyses were performed. Results: Our cohort included 56 children (35 female, 63%) with XLH. HTN was found in 19 children (34% of the cohort, n=10 female), diagnosed at a mean age of 7.9 years (SD 4.2). SBP was higher than DBP with a SBP percentile average of 76 and DBP percentile average of 58 (p<0.01). 14 children had isolated systolic HTN, 4 had a combination of diastolic and systolic HTN, and 1 child had isolated diastolic HTN. HTN was not associated with body mass index, serum parathyroid hormone levels, nephrocalcinosis, or average weight-based phosphate or 1,25 dihydroxyvitamin D treatment over the study period. Furthermore, BP percentiles did not change with initiation of Burosumab therapy.Conclusion: Children with XLH demonstrate a high prevalence of hypertension as a third of our cohort met criteria for HTN. It is unclear why children with XLH develop HTN. FGF23 has been associated with vascular morbidity and elevated FGF23 drives the pathology in XLH. We did not see that anti-FGF23 treatment (Burosumab) lowered BP percentiles, but this could be confounded by a small sample size and the limited duration of follow up. HTN is an important comorbidity in XLH, and further studies are needed to identify risk factors.

***Disclosures: Irene Chen**, None*

FRI-491

Flare-Ups in Patients with Fibrodysplasia Ossificans Progressiva Reduced by Garetosmab Treatment: LUMINA-1 Data *KATHRYN DAHIR[1], Jennifer McGinniss[2], Eduardo Forle-Neto[2], Scott Mellis[2], Robert Sanchez[2], Maja Di Rocco[3], Richard Keen[4], Philippe Orcel[5], Christian Roux[6], Jacek Tabarkiewicz[7], Javier Bachiller-Corral[8], Angela Cheung[9], Mona Al Mukaddam[10], Kusha Mohammadi[2], Dushyanth Srinivasan[2], Andrew Rankin[2], Aris Economides[2], Dinko Gonzalez Trotter[2], Frederick Kaplan[11], Elisabeth Eekhoff[12], Robert Pignolo[13]. [1]Vanderbilt University Medical Center, . [2]Regeneron Pharmaceuticals, Inc., United States. [3]Department of Pediatrics, Unit of Rare Diseases, IRCCS Istituto Giannina Gaslini, Italy. [4]Royal National Orthopaedic Hospital, United Kingdom. [5]Service de Rhumatologie - DMU Locomotion, AP-HP. Nord - Université de Paris, France. [6]Department of Rheumatology, Cochin Hospital, Assistance Publique - Hôpitaux de Paris, France. [7]Rzeszów University, Rzeszów, Poland. [8]Hospital Universitario Ramón y Cajal, Spain. [9]University Health Network, University of Toronto, Canada. [10]Departments of Orthopaedics, Medicine and the Center for Research in FOP & Related Disorders, University of Pennsylvania Perelman School of Medicine, United States. [11]University of Pennsylvania, United States. [12]Amsterdam UMC, location VU University Medical Center, Amsterdam, The Netherlands, Netherlands. [13]Mayo Clinic, United States

Purpose: Fibrodysplasia ossificans progressiva (FOP) is a rare disorder, characterized by progressive heterotopic ossification (HO) and soft tissue inflammatory events known as flare-ups. Garetosmab, an investigational, fully human monoclonal antibody against activin-A, prevents formation of new HO lesions. Here we describe the impact of garetosmab on flare-up events in the LUMINA-1 study (NCT03188666).Methods: This was an analysis of garetosmab data from LUMINA-1, a phase 2, randomized, double-blind, placebo-controlled study that evaluated the safety and efficacy of garetosmab 10 mg/kg every 4 weeks intravenous in adult patients with FOP over 28 weeks (Period 1), followed by a 28-week open-label treatment (Period 2) and open-label extension (Period 3). Patient-reported flare-ups were collected via a patient diary and symptom severity was reported as mild, moderate, or severe.Results: In Period 1, the proportion of patients reporting flare-ups (35% vs 71%, p=0.032) was significantly reduced with garetosmab (n=20) vs placebo (n=24), respectively. The overall number of patient-reported flare-ups (13 vs 34) and median days experiencing new flare-ups (15.0 days vs 48.0 days) were also reduced with garetosmab vs placebo, respectively. Most flare-ups occurred in the back in garetosmab-treated patients, and the lower extremities and back for those on placebo. Pain was the most frequent symptom in both cohorts. Severity of flare-up associated symptoms were reduced in the garetosmab-treated cohort. No patients reported severe swelling or severe decrease in movement. One patient treated with garetosmab reported severe pain and joint stiffness. In Period 2, the proportion of patients experiencing flare-ups (68% vs 14%, p=0.0005) and number of patient-reported flares (31 vs 11) was significantly reduced in patients who crossed over from placebo to garetosmab (n=22). Patients who continued on garetosmab (n=18) maintained a reduction in number of flare-ups (12 vs 6) and the proportion of patients experiencing flare-ups (33% vs 22%). Reductions were maintained through Period 3.Conclusions: Patients treated with garetosmab experienced significant and sustained reductions in the frequency, duration, and severity of flare-ups. Therefore, garetosmab may provide a meaningful therapeutic option for patients with FOP.

***Disclosures: KATHRYN DAHIR**, Alexion, Consultant, Ultragenyx, Grant/Research Support, Regeneron Pharmaceuticals, Inc., Grant/Research Support, Inozyme, Consultant, AM Pharma, Consultant, Alexion-Astra Zeneca, Grant/Research Support, Ultragenyx, Consultant*

FRI-492

A Phase 1, Open-label, Dose-escalating Study to Evaluate the Safety, Tolerability, Pharmacokinetics, and Pharmacodynamics of ALXN1850 in Adults With Hypophosphatasia *KATHRYN DAHIR[1], Derek Dunn[2], Jawad Hasan[2], Amy Shannon[2], Wei-Jian Pan[2]. [1]Vanderbilt University Medical Center, . [2]Alexion, AstraZeneca Rare Disease, United States

Hypophosphatasia (HPP) is a rare, inherited disorder associated with recurrent fractures/pseudofractures, orthopedic/dental burden, pain, mobility impairments, and diminished quality of life. ALXN1850 is an investigational enzyme replacement therapy being developed for the treatment of HPP.1-3 The primary objective of this study was to assess the safety and tolerability of ALXN1850 administered by IV weekly as 1 dose and SC for 3 weeks. Secondary objectives included pharmacokinetics (PK) of 1 IV and 3 SC doses, absolute bioavailability of SC, pharmacodynamic (PD) effects of 1 IV and 3 SC doses, and immunogenicity potential of ALXN1850. Of the 23 adult patients with HPP who signed informed consent, 15 were dosed, and each cohort of 5 received ALXN1850 (15, 45, or 90 mg) as 1 IV dose weekly and SC for 3 weeks; 3 patients missed doses due to COVID-19 but did not discontinue the study. Following IV and SC doses, peak and total exposure of ALXN1850 increased dose dependently (15-90 mg). Effective t1/2 was estimated at 3-6 days depending on dose. Mean bioavailability of SC doses was ~43% (range: 6%-75%). ALXN1850 achieved maximal lowering (nadir) of plasma inorganic pyrophosphate (PPi) in 7 days; ~40% post-dose PPi concentrations were below the limit of quantification (0.75µM). Mean PPi concentration was reduced for 3-4 weeks post-dose. There was no apparent impact of immunogenicity on ALXN1850 PK/PD. ALXN1850 has acceptable safety, tolerability, and PK profiles, demonstrating a sustained reduction in PPi concentrations in patients with HPP. These results will inform the selection of an appropriate therapeutic dose in future studies.References:1. Baumgartner-Sigl S et al. Bone. 2007;40(6):1655-1661.2. Whyte MP et al. J Clin Invest. 1985;76(2):752-756.3. Whyte MP. Academic Press. 2012:771-794.Acknowledgments: The authors would like to thank the patients, their families, and the investigators of the trial (NCT04980248), and Loredana Cuccia (Medical Lead/Medical Monitor, Alexion, AstraZeneca Rare Disease) for their commitment to this research. Medical writing and editorial support were provided by Danielle Dalechek, MSc, of Oxford PharmaGenesis Inc., Newtown, PA, USA, and were funded by Alexion, AstraZeneca Rare Disease, Boston, MA, USA.

Safety Overview Table

Safety finding, n (%)	Description (N = 15) of 4 weeks treatment with ALXN1850
Any TEAE	12 (80.0%); 46 events
Related TEAE	10 (66.7%); 29 events
Injection site reactions (ISRs)	8 (53.3%); 10 out of 41 (24.4%) SC injections led to an ISR event* • Four patients with 1 ISR (erythema) • One patient with 1 ISR (soreness, swelling, and redness) • One patient with 1 ISR (erythema and bruising) • One patient with 3 ISRs, 1 per each SC administration (erythema and pruritus; erythema and ecchymosis; erythema) • One patient with 1 ISR (bruise) Four patients had 1 ISR each of erythema, not reported as TEAEs but included in this ISR total. One patient experienced induration following the IV dose, which is not included in this ISR total
Injection associated reactions • **Systemic reactions**	1 (6.7%) Headache (grade 1), considered related to study drug,*** occurred following the start of the IV dose and resolved the same day following medical intervention.
TESAE	1 (6.7%) Atrial fibrillation (grade 3) considered not drug related***
TEAE/TESAE leading to study drug withdrawal	0
Immunogenicity (ADA+)**	4 (26.7%) Only 1 (6.7%) was treatment emergent; ADAs persisted to the end of the study. Per protocol, patient was offered follow-up via the HPP registry. No patients tested NAb+

*Most cases of erythema resolved in less than 2 hours following the SC dose. There was no pattern observed in the timing of SC administration (ie, first, second, or third dose) and the occurrence of erythema.
**Assays for measuring anti-ALXN1850 antibodies and neutralizing antibodies (NAbs) were fully validated for precision, specificity, selectivity, sensitivity, robustness, and drug tolerance following the current 2019 FDA guidance on ADA method validation.
***By the investigator.
ADA, antidrug antibody; AE, adverse event; HPP, hypophosphatasia; IV, intravenous; NAb, neutralizing antibody; SC, subcutaneous; TEAE, treatment-emergent adverse event; TESAE, treatment-emergent serious adverse event.

***Disclosures: KATHRYN DAHIR**, Alexion, AstraZeneca Rare Disease, Consultant*

FRI-494

Prevalence of ENPP1 variants among patients with ossification of the posterior longitudinal ligament *Hajime Kato[1], Shivani Srivastava[2], Paul Stabach[3], Soichiro Kimura[4], Takashi Sunouchi[4], Yoshitomo Hoshino[4], Naoko Hidaka[4], Minae Koga[4], DEMETRIOS BRADDOCK[5], Nobuaki Ito[6]. [1], . [2]Department of Pathology, Yale University, United States. [3]Department of Pathology, Yale Universty, United States. [4]Division of Nephrology and Endocrinology, The University of Tokyo Hospital, Japan. [5]YALE UNIVERSITY, United States. [6]The University of Tokyo Hospital, Japan

Background: Ossification of the posterior longitudinal ligament (OPLL) is a multifactorial disease that is caused by genetic and environmental factors. On the other hand, some hereditary FGF23-related hypophosphatemic rickets/osteomalacia (heterozygous PHEX mutation, homozygous ENPP1 mutation, homozygous DMP1 mutation) are known to develop OPLL. We, therefore, hypothesized that mild or undiagnosed cases of these diseases are included in the patients diagnosed with OPLL.Methods: We prospectively evaluated the frequency of cases with low-frequency variants (allele frequency in gnomAD: <0.5%) in the exonic regions of PHEX, ENPP1, and DMP1 genes in patients who underwent surgery for OPLL at our hospital. Clinical and biochemical data (i.e. calcium, phosphate, FGF23) of were collected. Plasma inorganic pyrophosphate (PPi) levels, which ENPP1 produces by hydrolyzing ATP, were also measured to evaluate the effect of the detected variants on ENPP1 catalytic activity.Results: The total of 50 patients with OPLL were included in this study (median age, 68 years [range, 37-86 years]; 14 women [28%]). All OPLL patients underwent genetic testing, and four types of heterozygous rare ENPP1 variants (c.802T>C [p.Y268H], c.1352A>C [p.Y451C], c.2089G>A [p.V697M], c.2335A>C [p.T779P]) were found in seven patients (14%). Clinical and biochemical data analysis showed that FGF23 levels of the OPLL patients with ENPP1 variants (median: 46 pg/mL [range: 36-102 pg/mL]) were higher than those of OPLL patients without ENPP1 variants (median: 36 pg/mL [range: 14-86 pg/mL]) (p=0.01). All of seven OPLL patients with heterozygous ENPP1 variants presented low plasma PPi levels (median: 1.8µM [range: 1.0-1.9 ?M], reference value 2-5 ?M). In vitro kinetic assays showed p.Y268H, p.Y451C, p.V697M and p.T779P variants possessed a catalytic velocity of 5%, 30%, 30%, and 1%, respectively, compared with that of wild-type ENPP1.Conclusion: This study revealed that patients with heterozygous ENPP1 variants were included in patients with OPLL and the prevalence of ENPP1 variant in this

cohort was 14%. The establishment of the appropriate diagnostic criteria to select cases with pathogenic ENPP1 variants would be warranted.

***Disclosures: Hajime Kato**, None*

FRI-495

The Relationship of Flare-Ups and Heterotopic Ossification in Patients with Fibrodysplasia Ossificans Progressiva: LUMINA-1 Data *Richard Keen[1], Jennifer McGinniss[2], Eduardo Forleo-Neto[2], Scott Mellis[2], KATHRYN DAHIR[3], Maja Di Rocco[4], Ma?gorzata Szczepanek[5], Javier Bachiller-Corral[6], Angela Cheung[7], Mona Al Mukaddam[8], Jing Gu[2], Aris Economides[2], Dushyanth Srinivasan[2], Dinko Gonzalez Trotter[2], Frederick Kaplan[9], Elisabeth Eekhoff[10], Robert Pignolo[11]. [1]Centre for Metabolic Bone Disease Royal National Orthopaedic Hospital NHS Trust, United Kingdom. [2]Regeneron Pharmaceuticals, Inc., United States. [3]Vanderbilt University Medical Center, . [4]Department of Pediatrics, Unit of Rare Diseases, IRCCS Istituto Giannina, Italy. [5]Rzeszów University, Rzeszów, Poland. [6]Hospital Universitario Ramón y Cajal, Spain. [7]University Health Network, University of Toronto, Canada. [8]Departments of Orthopaedics, Medicine and the Center for Research in FOP & Related Disorders, University of Pennsylvania Perelman School of Medicine, United States. [9]University of Pennsylvania, United States. [10]Amsterdam UMC, location VU University Medical Center, Amsterdam, The Netherlands, Netherlands. [11]Mayo Clinic, United States*

Purpose: Fibrodysplasia ossificans progressiva (FOP) is an ultra-rare autosomal dominant disorder, characterized by progressive heterotopic ossification (HO) and painful soft tissue inflammatory events known as flare-ups. Flare-ups can precede HO formation, but prospective data are limited. Here, we describe the relationship between flare-ups and HO from the placebo cohort of the LUMINA-1 study (NCT03188666).Methods: This was a post hoc analysis of the placebo cohort from a phase 2, randomized double-blind placebo-controlled study that evaluated the safety and efficacy of intravenous garetosmab 10 mg/kg every 4 weeks vs placebo in adult patients with FOP over 28 weeks. Patient-reported flare-ups were collected via a patient diary. This analysis focused on new HO lesions as assessed by 18F-NaF positron emission tomography and computed tomography (CT) at week 8, and week 28. Total volume of HO was determined by CT.Results: Of the 44 individuals enrolled in the study, 24 received placebo. Seventeen of these placebo patients reported new flare-ups, 10 of which also developed HO. Furthermore, of the 29 reported new HO lesions, which developed in 11 placebo patients, 12 (41.4%) occurred in the same limb or region as a previous flare-up, and 17 (58.6%) did not. Patients with new flare-ups had a higher volume of HO lesions at week 28, with mean (SD) total volume of new lesions of 14.2 (21.6) cm3 vs 0.5 (1.2) cm3 in patients without flare-ups, resulting in a mean (SD) change from baseline of 19.0 (33.9) cm3 vs 10.9 (21.5) cm3, respectively. In patients with new HO lesions, those with flare-ups (n=10) had a higher volume of newly formed heterotopic bone at week 28, mean (SD) of 24.2 (23.7) cm3 vs 3.2 cm3 in one patient with new HO but no flare-ups.Conclusions: Most placebo patients who reported a flare-up developed new HO lesions and had a higher volume of HO lesions; however, newly developed HO did not occur at the flare-up site in most instances. These results suggest that flare-ups within a year may reflect disease activity and be a prognostic indicator of higher volumetric growth of HO lesions.

***Disclosures: Richard Keen**, Regeneron Pharmaceuticals Inc., Grant/Research Support, Clementia/Ipsen, Grant/Research Support*

FRI-497

Evidence Based Guidelines On Diagnosis, Management and Monitoring of X-Linked Hypophosphatemia (XLH) in The Pediatric and Adult Population 2023 *Aliya A. Khan[1], Dalal Ali[2], MARIA LUISA BRANDI[3], Eric Rush[4], Gordon Guyatt[1], Natasha Appelman-Dijkstra[5], Catherine Chaussain[6], Suzanne Jan De Beur[7], Thomas Carpenter[8]. [1]McMaster University, Canada. [2], . [3]FONDAZIONE FIRMO, Italy. [4]Children's Mercy Kansas City, United States. [5]Leiden Center for Bone Quality, Netherlands. [6]Université Paris Cité and APHP, France. [7]Johns Hopkins University, United States. [8]Yale University School of Medicine, United States*

Background: Over the past 5 years, there have been rapid advances in our understanding of the multisystem manifestations of XLH and the development of new treatment paradigms. To offer guidance to clinicians and to promote evidence-based care, an International Working Group (IWG) of 52 experts in guideline development methodology and XLH in the pediatric and adult population has convened to develop new evidence-based guidelines on the evaluation, management, and monitoring of XLH.Methods: Four systematic reviews and meta-analyses were completed using the GRADE methodology addressing the management of XLH in relation to patient important outcomes and surrogate outcomes. In addition to the systematic reviews, expert clinical practices were captured with a comprehensive, 280 item questionnaire developed by the panel and administered to 44 experts treating patients with XLH. Data derived from the questionnaire were captured in expert-opinion based narrative reviews that address: 1) diagnosis of XLH including the role of genetic testing, 2) dental complications, 3) indications for treatment, 3) selection of treatment, 4) disease and treatment monitoring, 5) pregnancy and lactation in XLH, 5) agenda for future research.The new international guidelines on XLH will be reviewed by stakeholders including professional medical societies and patient advocacy organizations interested in endorsing these guidelines.Conclusions: These new guidelines will be presented for the first time internationally at the upcoming meeting of the ASBMR in October 2023.International Working Group Members:Aliya A. Khan (Chair), Dalal S. Ali, Maria L. Brandi, Eric Rush, Hajar Abualarob, Hatim Alalwani, Abdulrahman Alamri, Rana Aldabbagh, R.Todd Alexander, Farah Alsarraf, Natasha Appelman-Dijkstra, Signe Sparre Beck-Nielsen, Martin Biosse Duplan,Tom Carpenter, Catherine Chaussain, Martine Cohen-Solal, Rachel K. Crowley, Karel Dandurand, Guido Filler, Lisa Friedlander, Seiji Fukumoto, Claudia Gagnon, Paul Goodyer, Corinne Grassmann, Chelsey Grimbly, Gordon Guyatt, Dieter Haffner, Erik A. Imel, Suzanne M. Jan de Beur, Kassim Javaid, Sarah Khan, Aneal Khan, Anna Lehman, Willem F. Lems, E. Michael Lewiecki, Agnès Linglart, Outimaija Makitie, Karen McAssey, Ciara McDonnell, Reza D. Mirza, Emmett Morgante, Archibald Morrison, Anthony Portale, Frank Rauch, Lars Rejnmark, Yumie Rhee, Salvatore Ruggiero, Heide Siggelkow, Sotirios Tetradis, Laura Tosi, Pablo Florenzano Valdes, Leanne M. Ward

***Disclosures: Aliya A. Khan**, Amgen, Amolyt and Takeda, Consultant, Alexion, Amgen, Ascendis, Chugai, Radius, Takeda, Grant/Research Support*

FRI-501

Efficacy of growth hormone therapy on height in children with achondroplasia *Takuo Kubota[1], Hirofumi Nakayama[2], Takeshi Ishimi[3], Chieko Yamada[3], Yukako Nakano[3], Ikumi Ueda[3], Tatsuya Nakamichi[3], Hiroyuki Saitou[3], Kenichi Yamamoto[4], Makoto Fujiwara[6], Yasuhisa Ohata[6], Taichi Kitaoka[1], Keiichi Ozono[1]. [1]Osaka University Graduate School of Medicine, Japan. [2]Department of Pediatrics, Graduate School of Medicine, The first Department of Oral and Maxillofacial Surgery, Graduate School of Dentistry, Osaka University , Japan. [3]Department of Pediatrics, Osaka University Graduate School of Medicine, Japan. [4]Department of Pediatrics, Division of Health Sciences, Osaka University Graduate School of Medicine, Japan. [6]Osaka University, . [6]Osaka University, Japan*

Background: Achondroplasia (ACH) is a skeletal disorder with marked short stature and short limbs. The mean adult height has been reported to be 130.4 cm in males and 124.0 cm in females, respectively, in Japan, resulting in difficulties of daily life. Growth hormone (GH) therapy is available in children with ACH in Japan, although evidence on the efficacy of GH therapy on height growth is limited. Aim: To elucidate the efficacy of GH therapy on height growth in children with ACH. Methods: Children with ACH who visited our department from January 2011 to December 2022 and received GH therapy were included in this study. Height data between a year before and 5 years after the initiation of GH therapy were collected annually. Height SD values for healthy and ACH children and annual growth velocity (AGV) were evaluated. No further data were included after discontinuation of the therapy. A height increase due to lower limb lengthening was subtracted from the height measured. Results: Forty?one children (25 males) with ACH were included in the study. The median age was 4.00 years (range: 3.04 to 8.50) at the beginning of GH therapy. Height SD at that time was ?4.95 +/- 0.75 (mean +/- SD) for healthy children and ?0.24 +/- 0.71 for children with ACH. AGV was 4.45 +/- 1.62 cm. Regarding the efficacy of the therapy, the mean height SD of ?4.28, ?4.01, ?3.69, ?3.83, and ?3.84 for healthy children significantly increased 1 to 5 years after GH therapy, respectively, compared to that at the therapy initiation. In addition, the mean height SD of 0.25, 0.51, 0.95, 1.03 and 1.18 for children with ACH significantly increased in 1 to 5 years after GH therapy, respectively. AGV was 7.40, 5.76, 5.66, 4.84 and 4.77 cm 1 to 5 years after GH therapy, respectively, and significantly higher 1 to 3 years after GH therapy compared to that at the therapy initiation. Four and one patients underwent adenotonsillectomy and lower limb lengthening, respectively, after GH therapy initiation. GH therapy in 3 patients was changed to C-type natriuretic peptide analogue treatment. Except for the medical treatment change, no discontinuation of GH therapy occurred. Discussion: Height SD for both healthy and ACH children, and annual growth velocity were improved at least 1 to 3 years during GH therapy in this study, which shows the efficacy of GH therapy on height in children with ACH. Adult height needs to be evaluated in many patients with ACH after GH therapy.

***Disclosures: Takuo Kubota**, BioMarin Pharmaceutical Japana, Speakers' Bureau, Eli Lilly Japan, Grant/Research Support, Novo Nordisk Pharma, Speakers' Bureau*

FRI-502

Bone matrix properties in adults with osteogenesis imperfecta are not adversely affected by Setrusumab - A sclerotin neutralizing antibody *Maximilian Rummler[1], Victoria Schemenz[1], Samantha McCluskey[2], Anton Davydok[3], Frank Rauch[4], Francis Glorieux[5], Matthew Harrington[6], Wolfgang Wagermeier[1], Bettina Willie[6], Elizabeth Zimmermann[6]. [1]Max Planck Inst Colloids and Interfaces, Germany. [2]Shriners Hospital for Children-Canada, Canada. [3]Deutsches Elektronen-Synchrotron , Germany. [4]Shriners Hospital for Children, Montreal, Canada. [5]Shriners Hospital for Children and McGill University, Canada. [6]McGill University, Canada*

Osteogenesis imperfecta (OI) is a skeletal dysplasia characterized by low bone mass and frequent fractures. Children with OI are commonly treated with bisphosphonates to

reduce fracture rate, but treatment options for adults are limited. In the Phase 2b ASTEROID trial, setrusumab (a sclerostin neutralizing antibody, SclAb) improved bone density and strength in adults with type I, III and IV OI. Here, we investigate bone matrix material properties in tetracycline-labeled trans-iliac biopsies from three groups: i) control: individuals with no metabolic bone disease (n = 7), ii) OI: individuals with OI (n = 4), iii) SclAb-OI: individuals with OI after six months of setrusumab treatment as part of the ASTEROID trial (n = 5). In addition to bone histomorphometry, bone mineral and matrix properties were evaluated with nanoindentation, Raman spectroscopy, second harmonic generation imaging, quantitative backscatter electron imaging, and small-angle x-ray scattering. Spatial locations of fluorochrome labels were identified to differentiate inter-label bone of the same tissue age and intra-cortical bone. No difference in collagen orientation was found between the groups. The bone mineral density distribution (Fig. 1) and analysis of Raman spectra indicate that OI and SclAb-OI groups have greater mean mineralization, greater relative mineral content and lower crystallinity than the control group, which was not altered by SclAb treatment. Finally, a lower modulus and hardness were measured in the inter-label bone of the OI-SclAb group compared to the OI group. Previous studies suggest that even though bone from OI has a higher mineral content, the extracellular matrix has comparable mechanical properties. Therefore, fragility in OI may stem from contributions from other yet unexplored aspects of bone organization at higher length scales. We conclude that SclAb treatment leads to increased bone mass while not adversely affecting bone matrix properties in individuals with OI.

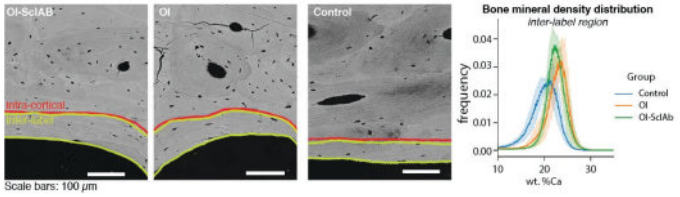

***Disclosures: Maximilian Rummler**, None*

FRI-504

A Phase 1/2, Open-Label, Multiple Ascending Dose Clinical Study to Evaluate the Safety, Tolerability, Pharmacokinetics, and Pharmacodynamics of INZ-701 in Adults with ENPP1 Deficiency *Yves Sabbagh[1], Robert Wermers[2], Rainard Fuhr[3], Dirk Schnabel[4], Terra Arnason[5], Alix Besancon[6], Borut Cizman[1], Deborah Wenkert[7], Kurt Gunter[1]. [1]Inozyme Pharma, United States. [2]Mayo Clinic, United States. [3]Parexel International GmbH, Early Phase Clinical Unit Berlin, Germany. [4]Charitè, Universitätsmedizin Center for Chronic Sick Children, Pediatric Endocrinology, Germany. [5]University of Saskatchewan, Division of Endocrinology, Canada. [6]Hôpital Universitaire Necker Enfants Malades, Endocrino-diabetologie pediatrique , France. [7]Wenkert and Young, LLC, United States

Background: ENPP1 Deficiency is a rare disorder due to inactivating mutations in the ENPP1 gene. It is characterized by low levels of inorganic pyrophosphate (PPi), a critical regulator of mineralization; subsequent pathologic soft tissue calcification results in ~50% infant mortality and life-long musculoskeletal and cardiovascular morbidities. No targeted therapy exists for this disease. INZ-701 is a recombinant ENPP1-Fc investigational product which has demonstrated efficacy in preclinical models of ENPP1 Deficiency.Purpose: To determine the safety, tolerability, immunogenicity, pharmacokinetics and pharmacodynamics of INZ-701 following subcutaneous administration in adults with ENPP1 Deficiency. Methods: Phase 1/2, multicenter, open-label, multiple ascending dose study including three cohorts of three adults each, with genetic confirmation and PPi <1300 nM (NCT04686175). Participants were dosed at Day 1, then twice weekly from Day 8 to the end of the study. Results: In all 3 dosing cohorts as of January 10, 2023, INZ-701 was well-tolerated with no related serious or severe adverse events. Low titers of non-neutralizing anti-drug antibodies (<160) were observed in 7/9 patients. Rapid increase in mean PPi from baseline of 426+/-407 nM of was noted in all patients, reaching the healthy volunteer range within 6 hours of the first dose. Mean PPi across the 0.2, 0.6, and 1.8 mg/kg dosing groups from day 32 through last data cut was 1299+/-490 nM, 1472+/-516 nM, and 1462+/-233 nM, respectively. Six of eight evaluable participants showed improvements in overall health on the Global Impression of Change (GIC) scale, as reported by both participants and clinicians. Long half-life of approximately 126 hours and drug accumulation as shown by a greater than dose proportional exposure suggests the potential for once weekly dosing. All participants enrolled in the phase 2 portion of the study.Conclusions: INZ-701 demonstrated a rapid and sustained increase in PPi levels in all participants, was well tolerated, and exhibited a favorable safety profile with a potential for once weekly dosing. Improvements in GIC score were observed in 6/8 patients and this ongoing study will elucidate the impact of INZ-701 on additional clinical and functional endpoints.

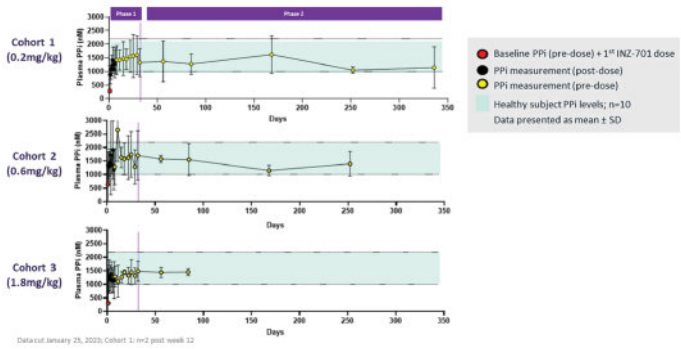

***Disclosures: Yves Sabbagh**, Inozyme Pharma, Other Financial or Material Support*

FRI-505

A Phase 1/2, Open-Label, Multiple Ascending Dose Study to Evaluate the Safety, Tolerability, Pharmacokinetics, and Pharmacodynamics of INZ-701 Followed by an Open-Label Long-Term Extension Period in Adults with ABCC6 Deficiency Manifesting as Pseudoxanthoma Elasticum (PXE): An Interim Analysis *Yves Sabbagh[1], Magdy Shenouda[2], Jorg Taubel[3], Mark Lebwohl[4], Kurt Gunter[1]. [1]Inozyme Pharma, United States. [2]Clinilabs Drug Development Corporation, United States. [3]Richmond Research Institute, St George's University of London, United Kingdom. [4]Department of Dermatology, Icahn School of Medicine, United States

Background: Pseudoxanthoma elasticum (PXE) is a rare mineralization disorder caused by mutations in the ABCC6 gene. The ABCC6 protein transports nucleotides, including ATP, into the extracellular space where it is metabolized by the ENPP1 enzyme to AMP and inorganic pyrophosphate (PPi), a critical inhibitor of mineralization. PXE therefore is associated with reduced levels of PPi and ectopic calcification. Adults with PXE experience progressive dermatologic, ophthalmologic, and cardiovascular morbidities, and there are no therapies that target the underlying disease process. INZ-701 is a recombinant ENPP1-Fc investigational product which has demonstrated efficacy in preclinical models of ABCC6 Deficiency. Purpose: To determine the safety, tolerability, immunogenicity, pharmacokinetics and pharmacodynamics of INZ-701, an ENPP1-Fc fusion protein, following subcutaneous administration in adults with ABCC6 Deficiency manifesting as PXE. Methods: Phase 1/2, multicenter, open-label, multiple ascending dose study including 3 cohorts of 3 adults in each with confirmed clinical diagnosis of PXE and biallelic ABCC6 mutations, and PPi <1300 nM (NCT05030831). Participants received 0.2, 0.6 or 1.8 mg/kg INZ-701 SC on day 1, then twice weekly from day 8 to the end of the study. Results: In all 3 dosing cohorts as of January 16, 2023, INZ-701 was generally well-tolerated with no serious or severe adverse events. Mild injection site reactions occurred in 4/9 patients. One patient was withdrawn from the study due to moderate erythema and urticaria. A rapid (within 24 hours) increase in PPi was noted in 8 patients after a single dose of INZ-701, from a mean of 947+/-193 nM at screening. From day 11-32, mean PPi across the 0.2, 0.6 and 1.8 mg/kg dosing groups was 1023 +/- 454 nM, 1119 +/- 216 nM and 1415 +/- 509 nM respectively, suggestive of a dose response relationship. A dose dependent exposure of INZ-701 in a greater than dose proportional manner was observed. The half-life of INZ-701 (~126 hrs) suggests the potential for once-weekly dosing. Eight of 9 participants transitioned to the phase 2 portion of the study and continue on INZ-701. Conclusions: At all 3 doses evaluated, INZ-701 rapidly increased PPi levels into the normal range. A PPi dose response was observed, and at the highest dose (1.8 mg/kg) mean PPi remained in the normal range through last data cut. INZ-701 was generally well tolerated and exhibited a favorable safety profile with potential for once weekly dosing.

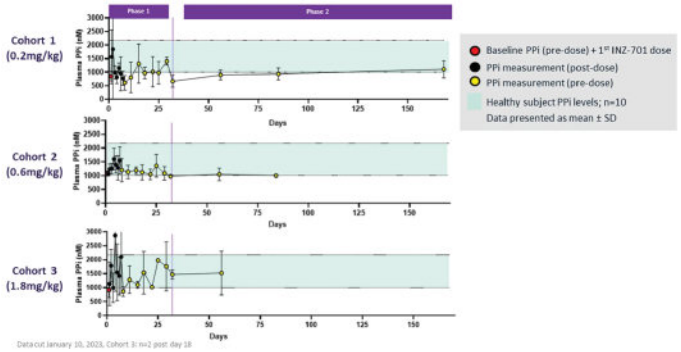

***Disclosures: Yves Sabbagh**, Inozyme Pharma, Other Financial or Material Support*

FRI-507

Development of an 18F-NaF PET/CT-Based Tool for Quantification and Characterization of Soft Tissue Calcification in Hyperphosphatemic Familial Tumoral Calcinosis (HFTC) *Aaron Sheppard[1], Faraz Farhadi[2], IRIS HARTLEY[3], Rachel Gafni[7], Michael Collins[5], Babak Saboury[6], Kelly Roszko[7]. [1]NIH, United States. [2]Geisel School of Medicine, Dartmouth, United States. [3]NIDCR/NIH, . [7]National Institutes of Health, United States. [5]NIDCR, NIH, United States. [6]Clinical Center, Department of Radiology and Imaging Sciences, NIH, United States. [7]National Institutes of Health,

Hyperphosphatemic familial tumoral calcinosis (HFTC) is a rare disorder which results from a deficiency of FGF23 signaling. Biochemical abnormalities include hyperphosphatemia and an elevated calcium x phosphate product, which likely drives the development of disabling soft tissue calcification. The study of HFTC and its response to treatment suffers from the lack of a quantitative technique to measure disease burden and activity. To address this, we developed 18F-NaF PET/CT and CT only imaging and analysis techniques to characterize and quantify calcifications in the NIH HFTC cohort. 11 patients with HFTC underwent either CT or 18F-NaF PET/CT imaging and the PET and CT voxel-level data were exported to and analyzed with MIM and MATLAB software. Analyses included CT-based bone data - volume and density (Hounsfield Units, HU), and PET-based mineral metabolic activity (Standardized Uptake Value, SUV).82% of patients had ectopic calcifications. The most frequently occurring and largest lesions were at the hips (n=9) and shoulders (n=5), 546.5 +/- 573.5 cm3 and 388.8 +/- 535.1 cm3 respectively. Large variations in total lesion volume and individual lesion volume over the cohort illustrated the great degree of heterogeneity in HFTC. Calcifications were also identified in the sclera of the eye, the colonic mucosa, the brain parenchyma and meninges/dura, and the para-vertebral region of the neck. In one patient who had four CT scans, we found that surgical intervention or repeated trauma increased the rate of growth of the lesions. Another patient had two 18F-NaF PET/CT scans, and voxel-by-voxel analysis found that the lesion increased in volume and density while decreasing in metabolic activity. These data demonstrate the utility of 18F-NaF PET/CT in identifying and quantifying the presence and mineral metabolic activity of calcific lesions and illustrate that CT and PET data provide complementary information that may inform the underlying pathomechanisms of calcification in HFTC. This technique will be useful in quantifying response to treatment in HFTC and likely applicable to other diseases of ectopic calcification.

***Disclosures: Aaron Sheppard**, Ultragenyx, Grant/Research Support*

FRI-508

Altered Collagen I And Premature Pulmonary Embryonic Differentiation In Patients With OI type II *SILVIA STORONI[1], Luca Celli[2], Marjolein Breur[2], Dimitra Micha[2], SARA VERDONK[1], Alessandra Maugeri[2], Joost g. Van den Aardweg[2], Mara Riminucci[3], Elisabeth Eekhoff[4], Marianna Bugiani[2]. [1], Netherlands. [2]Amsterdam UMC, Netherlands. [3]University La Sapienza, Italy. [4]Amsterdam UMC, location VU University Medical Center, Amsterdam, The Netherlands, Netherlands

AbstractIntroduction Pulmonary hypoplasia and respiratory failure are primary causes of death in patients with Osteogenesis Imperfecta (OI) type II. OI is a genetic skeletal disorder caused by pathogenic variants in genes encoding collagen type I. It is still unknown if the collagen defect also affects lung development and structure, causing lung hypoplasia in OI type II.Objective The aim of this study was to investigate the intrinsic characteristics of OI embryonic lung parenchyma and to determine whether altered collagen type I may compromise airway development and lung structure.Methods Lung tissue from nine fetuses with OI type II and six control fetuses, matched by gestational age, was analyzed for TTF-1 and collagen type I expression by immunohistochemistry, to evaluate the state of lung development and amount of collagen.Results The differentiation of epithelium into type 2 pneumocytes during embryonic development was premature in OI type II fetuses compared to controls ($p<0.05$). Collagen type I showed no significant differences between the two groups. However, the amount of alpha2(I) chains was higher in fetuses with OI and the ratio of alpha1(I) to alpha2(I) lower in OI compared to controls.Conclusion Cell differentiation during lung embryonic development in patients with OI type II is premature and impaired. This may be the underlying cause of pulmonary hypoplasia. Altered cell differentiation can be secondary to mechanical chest factors or a consequence of disrupted type I collagen synthesis. Our findings suggest that collagen type I is a biochemical regulator of pulmonary cell differentiation, influencing lung development.

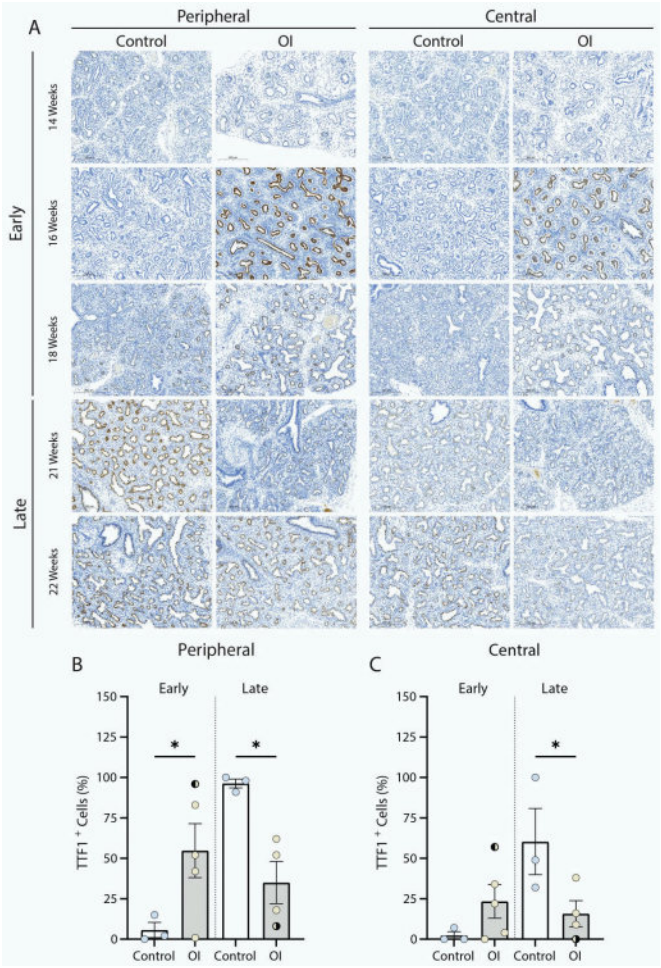

***Disclosures: SILVIA STORONI**, None*

FRI-510

18F-NaF PET/CT is a Sensitive Tool for Detection of Prevalence and Activity of Enthesopathies in X-linked Hypophosphatemia *Aaron Sheppard[1], Babak Saboury[2], Juan Carlos Quintana[3], Oscar Contreras[3], Macarena Jimenez[4], Danisa Ivanovic-Zuvic[5], Annette Madison[5], Michael Collins[1], Pablo Florenzano[5]. [1]National Institutes of Health, National Institutes of Dental and Craniofacial Research, United States. [2]National Institutes of Health, Department of Radiology and Imaging Sciences, United States. [3]Pontificia Universidad Catolica de Chile, Radiology Department, Chile. [4]Pontificia Universidad Catolica de Chile, Endocrinology Department, Chile. [5]Pontificia Universidad Catolica de Chile, Endocrinology D, Chile

X-linked hypophosphatemia (XLH) is a rare metabolic bone disorder characterized by increased FGF23 production, which leads to chronic hypophosphatemia. Clinically, it presents with impaired skeletal mineralization and abnormal soft-tissue calcifications, including enthesopathies (Ens), leading to pain and diminished quality of life (QoL). To date, the natural history of Ens in XLH has been ill defined, due to the lack of a sensitive quantitative tool for its characterization and follow-up. Adult patients with genetically confirmed XLH were included. Clinical evaluations included severity surveys to assess QoL (SF23V), pain (BPI) and functionality (WOMAC/6MWT). 18F-NaF PET/CT scans, which can detect both the presence and metabolic activity of Ens, were acquired for all patient, and a comprehensive review of each patient's scan was performed. A subset of 14 common tendon/ligament insertion sites were chosen for further analysis, characterizing each site as CT-positive only (CT+) (macro-En) or PET-positive/CT-negative (PET+/CT-) (micro-En). Associations of macro- and micro-Ens with relevant clinical variables were performed, including linear regressions and Pearson's correlations. 20 patients were included, 70% women. Mean age at study was 35 years (21-62), with a mean age at diagnosis of 10 years (0.3-32). 18F-NaF PET was able to detect developing Ens in many locations before detection by CT (14.6% of all Ens). Notably, the number of PET+/CT- Ens was negatively correlated with age ($r=-0.634$, $p=0.0027$). The number of CT+ Ens had an insignificant positive correlation with age ($r=+0.29$, $p=0.200$). In addition, 18F-NaF PET offered synergistic information to CT,

allowing the differentiation between metabolically active (PET+) vs stable (CT+/PET-) Ens. To illustrate, only 25% of macro-Ens at the ischial tuberosity were 18F-NaF avid, while 95.7% at the Achilles tendon were 18F-NaF avid. This, the first study to describe the use of 18F-NaF PET in characterizing Ens in XLH, demonstrated the ability of this modality to detect early En development at many sites. The fact that the number of detectable micro-Ens (PET+/CT-) was negatively correlated with age, suggests a progression pattern from a metabolically active early-lesion to a more structurally detectable, inactive lesion. 18F-NaF PET/CT is a promising tool that opens a window to better understand the natural history of the disease and may be used to assess the response of early Ens to therapeutic interventions.

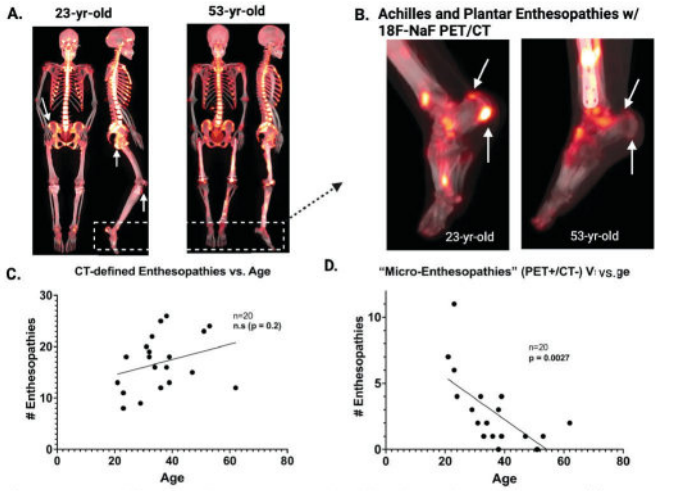

[18]F-NaF PET/CT differentiates between active and stable enthesopathies (Ens) in XLH. *(A) maximum intensity projection (MIP) of [18]F-NaF PET scan overlayed on CT MIP for a 23-yr-old patient and a 53-yr-old. (B) A focused look at the heel of the same 23- and 53-yr-old patients. Increased [18]F-NaF PET signal is greatest at the Achilles and plantar ligament in the younger patient, illustrating how this modality may detect the actively forming Ens earlier in life. (C) The number of CT+ Ens was insignificantly positively correlated with age, whereas (D) the number of PET+/CT- Ens was negatively correlated with age*

Disclosures: Aaron Sheppard*, Ultragenyx, Grant/Research Support*

FRI-511

Osteopathia striata with cranial stenosis can be caused by a somatic missense variant in the CTNNB1 gene encoding ?-catenin *YENTL HUYBRECHTS[1], Natasha Appelman-Dijkstra[2], Ellen Steenackers[3], Wouter Van Beylen[3], Geert Mortier[4], Gretl Hendrickx[4], Wim Van Hul[3, 1], Belgium, [2]Leiden Center for Bone Quality, Netherlands, [3]University of Antwerp, Belgium, [4]University of Leuven, Belgium

Osteopathia striata with cranial sclerosis (OSCS) is a rare bone disorder with X-linked dominant inheritance, characterized by a generalized high bone mass in the skull and long bones and typical metaphyseal striations in the long bones. So far, loss-of-function variants in AMER1 (also known as WTX or FAM123B), encoding the APC membrane recruitment protein 1 (AMER1), have been described as the only molecular cause for OSCS. AMER1 promotes the degradation of ?-catenin via AXIN stabilization, acting as a negative regulator of the WNT/?-catenin signaling pathway, a central pathway in bone formation. A Dutch adult woman was seen with an OSCS phenotype, i.e. generalized high bone mass and characteristic metaphyseal striations, but without a genetic variant affecting AMER1. Whole exome sequencing led to the identification of a mosaic missense variant (c.876A>C; p.Lys292Asn) in CTNNB1, coding for ?-catenin. The variant substitutes an amino acid known to be involved in the interaction with AXIN, a key factor in the ?-catenin destruction complex. Western blotting experiments demonstrate that the p.Lys292Asn variant does not significantly affect the ?-catenin phosphorylation status, and hence stability in the cytoplasm. Additionally, luciferase reporter assays were performed to investigate the effect of p.Lys292Asn ?-catenin on canonical WNT signaling. These studies indicate an average 70-fold increase in canonical WNT signaling activity by p.Lys292Asn ?-catenin. In conclusion, this study indicates that somatic variants in the CTNNB1 gene could explain the pathogenesis of unsolved cases of osteopathia striata with cranial sclerosis.

Disclosures: YENTL HUYBRECHTS*, None*

FRI-513

Assessment of Serum Alkaline Phosphatase, Serum Phosphate, Rickets Severity Score, Spinal Stenosis, Nephrocalcinosis, and Renal Function with Burosumab or Conventional Therapy Among Patients with X-linked Hypophosphatemia (XLH): Results from a Multinational, Long-term, Prospective Outcomes Disease Monitoring Program (DMP) *Leanne Ward[1], KATHRYN DAHIR[7], Hamilton Cassinelli[3], Pablo Florenzano[4], Erik Imel[5], Aliya Khan[6], Jill Simmons[7], Suzanne Jan De Beur[8], Carolina Moreira[9], Anna Ryabets-Lienhard[10], Zhiyi Li[11], Zunqiu Chen[12], ANTONIO NINO[13], Thomas Carpenter[14], [1]Children s Hospital of Eastern Ontario, Canada, [7]Vanderbilt University Medical Center, , [3]CEDIE, Centro de Investigaciones Endocrinologicas Dr Cesar Bergada, Division de Endocrinologia, Hospital de Niños Ricardo Gutierrez, Argentina, [4]Pontificia Universidad Catolica de Chile, Chile, [5]Indiana University School of Medicine, United States, [6]McMaster University, Canada, [7]Vanderbilt University Medical Center, United States, [8]Johns Hopkins University, United States, [9]Endocrine Division (SEMPR), Department of Internal Medicine, Federal University of Parana, Brazil, [10]Children's Hospital Los Angeles , , [11]Kyowa Kirin, Inc., United States, [12]Ultragenyx Pharmaceutical Inc., United States, [13]Ultragenyx, United States, [14]Yale University School of Medicine, United States

Purpose: To provide an update from the XLH DMP, which is an ongoing, non-interventional, prospective study with a 10-year planned duration, that characterizes disease progression and long-term effectiveness and safety of burosumab and other treatments (NCT03651505).Methods: Children (peds; <18 years) and adults (>=18 years) at DMP enrollment (Month 0; M0) were grouped according to burosumab treatment: Group 1 (Gr1) began burosumab in a prior clinical trial and have the longest exposure among the study population; Group 2 (Gr2) began commercial burosumab prior to/during the DMP; Group 3 (Gr3) had no burosumab exposure, but most received conventional therapy (CT; eg, oral phosphate and active vitamin D). Results from patients (pts) who completed Year 3 (Y3) at data cutoff are reported.Results: As of February 2023, 347 peds and 461 adults were enrolled in the DMP; mean (SD) age at M0 was 9.0 (4.8) years and 39.0 (14.7) years, respectively. Mean duration of burosumab exposure was similar between peds (133.1 [65.5] weeks) and adults (135.0 [72.0] weeks). At Y3, mean serum alkaline phosphatase was lower in peds receiving burosumab vs CT (Gr1: 287.3 [151.6] U/L; Gr2: 277.0 [142.4] U/L; Gr3: 474.5 [170.2] U/L). Additionally, mean serum phosphate levels were higher in peds receiving burosumab vs CT (Fig 1A). Mean serum phosphate levels were also higher in Gr1 and Gr2 adults vs Gr 3 adults (Fig 1B). Rickets severity scores (RSS) in Gr1 peds remained low at Y3 (-0.1 change from M0) and improved in Gr2 peds (-0.7 change from M0); no Gr3 pts had completed RSS at Y3. At M0, 75 (16%) adults across all 3 groups reported an existing diagnosis of spinal stenosis (SS) or spinal cord (SC) compression, including 36 pts (37%) in Gr1, 28 pts (14%) in Gr2, and 11 pts (7%) in Gr3. The majority of pts who had a previous diagnosis of SS or SC compression did not report worsening of their condition and did not undergo a related surgery at Y3. Comparing M0 to Y3, 4 pts (2 each from Gr2 and Gr3) had renal ultrasound score increases of >=2 and 1 pt from Gr2 showed improvement with score decreases of >=2; no Gr1 pts had score increases >=2. Burosumab was not associated with declines in renal function (as assessed by eGFR), urinary protein/creatinine ratio, or any new safety concerns in peds or adults.Conclusions: Long-term exposure to burosumab for up to 3 years in the DMP was consistent with its previously reported benefits vs CT and positively affected markers of disease activity.

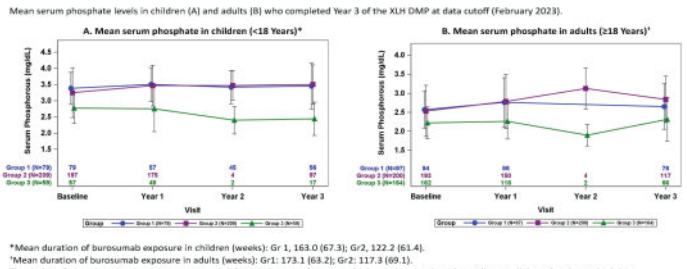

Disclosures: Leanne Ward*, Ultragenyx Pharmaceutical Inc., Grant/Research Support, Ultragenyx Pharmaceutical Inc. , Consultant*

FRI-514

Genotype-Phenotype Correlations in Osteogenesis Imperfecta: A Retrospective Study in 294 Patients *Jay Byrd[1], Andrew White[1], Makayla Schissel[1], Matthew VanOrmer[1], Danita Velasco[1], Maegen Wallace[1], [1]University of Nebraska Medical Center, United States

BACKGROUND: Osteogenesis imperfecta (OI) is an inherited disorder characterized by bone fragility with extraskeletal manifestations. Mutations in COL1A1 and COL1A2 account for most OI, yet non-COL1A1/2 mutations are responsible for many cases. There are 16 widely accepted genes causing OI; however, literature on genotype-phenotype correlation

and incidence of non-skeletal clinical features are limited. This study aims to identify genotype-phenotype correlations in patients with OI, allowing clinicians to better inform families of prognosis, optimize patient care, and facilitate evidence-based clinical decision-making. METHODS: A retrospective review of 294 patients with OI was performed to collect demographic data, clinical characteristics, and genotypic information. Patients were stratified by COL1A1/2 vs. non-COL1A1/2 mutations to evaluate differences in phenotype. Data were summarized with descriptive statistics, followed by Chi-square or Fisher's Exact tests for categorical variables and independent samples T-tests or Wilcoxon Rank sum tests for continuous variables. A p-value of <0.05 was considered statistically significant.RESULTS: The majority of OI was due to mutations in COL1A1/2 (91%), with the remaining 9% due to non-COL1A1/2 mutations. 147 (50.0%) are male and 147 (50.0%) are female. Most patients in the COL1A1/2 group were White compared to the non-COL1A1/2 group (78% vs. 50%; p=0.004). COL1A/2 patients had higher incidence of blue sclerae (83% vs. 50%, p=0.002), dentinogenesis imperfecta (49% vs. 15%, p<0.001), and family history of OI (34% vs. 12%, p=0.03). Those in the non-COL1A1/2 group have higher rates of scoliosis compared to those in the COL1A1/2 group (62% vs. 40%, p=0.04), as well as higher rates of expressive language disorder/delay (15% vs. 0.4% in non-COL1A1/2 and COL1A1/2 patients, respectively; p<0.001).CONCLUSIONS: Identifying the underlying molecular etiology early is imperative for optimal clinical care, allowing for appropriate risk counseling, identification of affected relatives, and improved anticipatory care and management. This data supports that rare subtypes of OI occur more frequently in non-White individuals and demonstrated genetic associations with incidence of blue sclera, dentinogenesis imperfecta, scoliosis, and expressive language disorders.

***Disclosures: Jay Byrd**, None*

FRI-521

OCL-IGF1-induced OCy senescence promotes RANKL production and induces pagetic bone lesions in Paget's disease *Hirofumi Tenshin[1], Jolene J. Windle[2], Mark A. Subler[2], John M Chirgwin[3], Brendan F. Boyce[4], G. David Roodman[1], Noriyoshi Kurihara[1]. [1]Division of Hematology and Oncology, Department of Medicine, Indiana University, United States; [2]Department of Human and Molecular Genetics, Virginia Commonwealth University, United States; [3]Research Service, Roudebush Veterans Administration Medical Center, United States; [4]Pathology & Laboratory Medicine, University of Rochester School of Medicine & Dentistry, United States

Paget's disease (PD) is characterized by persistent focal bone lesions, typified by increased bone resorption by abnormal osteoclasts (OCLs) that is followed by rapid formation of increased woven bone. Measles virus nucleocapsid protein (MVNP) expression in OCLs of PD patients increases OCL IGF1 production (OCL-IGF1), which in turn stimulates osteoblast differentiation. Conditional deletion of Igf1 in OCLs of TRAP-MVNP (T-MVNP) transgenic mice blocked the development of pagetic bone lesions (PDLs). These results suggest that OCL-IGF1 is sufficient to induce PDL formation in PD. To determine the role of OCL-IGF1 in PD, we generated TRAP-Igf1 (T-Igf1) transgenic mice, whose OCLs expressed similar levels of IGF1 as T-MVNP mice and developed the same PD phenotype as T-MVNP mice. PDLs were detected in vertebrae, femora, and tibiae of 50% of 16-month-old T-Igf1 mice by μ-CT and histological analysis. Thus, increased IGF1 expression in the absence of MVNP in OCLs is sufficient to induce PDLs. The results support IGF1 as a major PD-OCL product driving PDL formation in T-MVNP mice. Senescence increases RANKL expression by osteocytes (OCys), and OCy-derived RANKL is required for cortical bone loss that occurs with age (Kim HN et al, JCI-Insight 2020). We hypothesized that MVNP-expressing OCLs drive the accumulation of senescent OCys and increased RANKL expression in OCys in PD. However, we do not know if IGF1 secreted by OCLs in PD directly affects senescence to regulate RANKL production by OCys, bone resorption and development of PDLs. We determined the expression of telomere dysfunction-induced foci expression as a marker of senescence. 10% of OCys were senescent in 16-month-old WT mice, and 20% of OCys in T-Igf1 and T-MVNP mice. We used in situ hybridization to determine if mRNAs for p16INK4A and Rankl are upregulated in OCys in vivo. Rankl-expressing OCys were detected within 50 μm of OCLs, and almost all p16INK4A-positive OCys in T-MVNP mice expressed Rankl, while OCys in WT mice did not. There was no relationship between the expression of p16INK4A and IL-6 or sclerostin. OCys in MVNP-expressing PD patients showed similar levels of senescence and RANKL expression as T-MVNP mice. These results suggest that increased senescence in OCys is induced by OCL-IGF1, and accompanied by increased OCy RANKL, promoting the formation of PDLs. These findings support a model where senescent OCys expressing RANKL may initiate PDL formation in PD.

***Disclosures: Hirofumi Tenshin**, None*

FRI-522

Genetic Modulation of Hedgehog Signaling Influences Exostoses Elongation, Orientation, and Proliferation in a Mouse Model of Hereditary Multiple Exostoses (HME) *Sarah Catheline[1], Christina Mundy[2], Maurizio Pacifici[3]. [1]University of Rochester, United States; [2]Children's Hospital of Philadelphia, United States; [3]The Children's Hospital of Philadelphia, United States

Hereditary Multiple Exostoses (HME) is a congenital pediatric disorder in which cartilaginous tumors called osteochondromas or exostoses develop perpendicular to growth plates of skeletal elements. Most HME patients have a mutation in?EXT1?or?EXT2 causing heparan sulfate (HS) deficiency. Normally, HS-rich proteoglycans (HSPGs) restrict growth factor availability, and the HS deficiency in HME growth plates could result in freely available growth factors, inducing exostosis formation. However, it is unknown why the exostoses grow orthogonally to the growth plate main axis. The Indian hedgehog (IHH)/PTHrP signaling axis is critical for growth plate zonal organization, and hedgehog proteins bind HSPGs. Thus, HS deficiency in HME could allow the proteins to escape the growth plate and trigger a neo IHH-PTHrP axis within perichondrium, causing orthogonal exostosis formation. To test this novel thesis, we used AggrecanCreERT2? mice to drive?Ext1?deletion in chondrocytes and perichondrium in 5 week-old mice. To ask whether hedgehog signaling is necessary and sufficient for exostosis formation, we combined this model with: (a) conditional deletion of hedgehog receptor?Smo?resulting in Hedgehog loss of function (LOF); or (b) conditional deletion of?Ptch1, a negative regulator of signaling, resulting in gain of function (GOF). Acan-Cre+/-ERT2; Ext1f/f;?Smof/f?mice displayed delayed exostosis formation 10 days after tamoxifen relative to Acan-Cre+/-ERT2; Ext1f/f?(Ext1 mutant) mice, significantly decreasing exostosis number and size 4 weeks post tamoxifen. In contrast,?Acan-Cre+/-ERT2; Ext1f/f; Ptch1f/+?mice showed greater number of exostoses at 10 days relative to Ext1?mutant mice, resulting in significantly longer, wider and more numerous exostoses by 4 weeks. Notably, Ext1 mutants showed enriched cell proliferation marked by Ki67 in perichondrium at the site of new exostoses, while LOF mice lacked proliferating perichondrial cells and GOF mice showed the greatest number of Ki67-positive cells, suggestive that hedgehog helps initiate perichondrial proliferation. ?-catenin expression throughout the exostoses, and Pthrp-LacZ specifically present at their leading edge, both increased in Ext1 mutant mice and were further increased in GOF mice, suggesting that crosstalk between these pathways is important in exostosis formation. Our current data implicate IHH/PTHrP signaling as a critical regulator of osteochondroma formation and orthogonal growth.

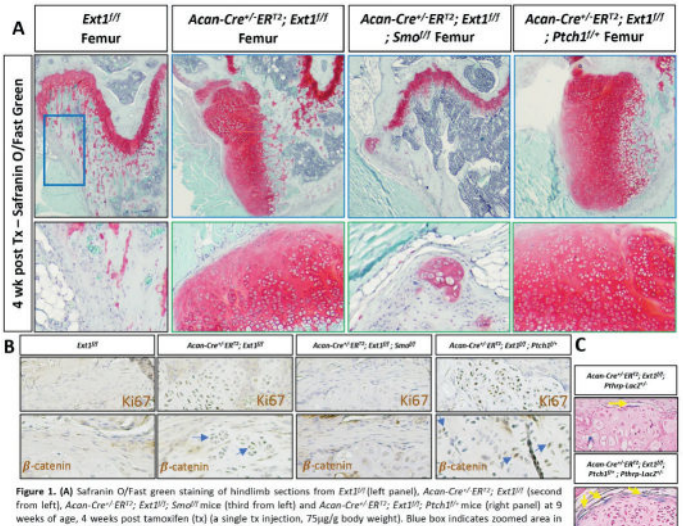

Figure 1. (A) Safranin O/Fast green staining of hindlimb sections from *Ext1$^{f/f}$* (left panel), *Acan-Cre$^{+/-}$ER^{T2}; Ext1$^{f/f}$* (second from left), *Acan-Cre$^{+/-}$ER^{T2}; Ext1$^{f/f}$; Smo$^{f/f}$* mice (third from left) and *Acan-Cre$^{+/-}$ER^{T2}; Ext1$^{f/f}$; Ptch1$^{f/+}$* mice (right panel) at 9 weeks of age, 4 weeks post tamoxifen (tx) (a single tx injection, 75μg/g body weight). Blue box indicates zoomed area in bottom panels. **(B)** Ki67 IHC (top panels) and β-catenin IHC (bottom panels) from the same genotypes as in **(A)** at 6.5 weeks of age, 10 days post tx induction; blue arrows indicate β-catenin+ cells. **(C)** β-gal/Nuclear fast red staining of hindlimb sections from *Acan-Cre$^{+/-}$ER^{T2}; Ext1$^{f/f}$; Pthrp-LacZ$^{+/-}$* or *Acan-Cre$^{+/-}$ER^{T2}; Ext1$^{f/f}$; Ptch1$^{f/+}$; Pthrp-LacZ$^{+/-}$* mice 2 weeks post tx. Yellow arrows indicate *Pthrp+* cells.

***Disclosures: Sarah Catheline**, None*

FRI-523

A novel mouse model for osteogenesis imperfecta type I shows altered TGF? signaling *Ellen Busschers[1], Yuqing Chen-Everson[1], I-Wen Song[1], Brian Dawson[1], Brendan Lee[1]. [1]Baylor College of Medicine, United States

Osteogenesis imperfecta (OI) is a genetic skeletal disorder that is characterized by low bone mass, frequent fractures, and bone deformities as well as multiple extra-skeletal manifestations. The vast majority of OI is caused by either quantitative defects of type I collagen or qualitative defects of type I collagen characterized by post-translational over-modification. Type I OI is caused by haploinsufficiency of collagen type 1 (COL1A1 or COL1A2). On the mild end of the disease spectrum, it accounts for more than 50% of OI cases. The previously reported Mov13 mouse model with a retroviral insertion into Col1a1 was originally reported as a putative type I OI model; however, the mice develop lymphoma which makes molecular and long-term study difficult. Therefore, we set out to generate a new mouse model of OI type 1.We generated a novel Col1a1 haploinsufficient type I OI mouse model by crossing mice with a Col1a1 floxed allele to CMV-Cre mice to create a full body heterozygous deletion of Col1a1. Micro-CT analysis showed that these mice have a decrease in both trabecular bone volume as well as a decrease in cortical thickness of the femur. Currently, there are no FDA-approved treatments for OI. Clinically, bisphosphonates have become the standard of care medication to treat bone fragility in mild OI; however, the benefit of long-term use is inconclusive. Increased TGF? signaling has been shown to be a major pathogenic driver in multiple models of moderate and severe OI characterized by collagen over modification. Here, inhibition of TGF? was shown to increase bone volume and strength. Therefore, we also measured the level of TGF? signaling in OI mice that have reduced

quantity, but otherwise normal collagen modification. We show that phospho-SMAD2 protein expression is increased by western blot and immunohistochemistry. We further saw an increase in mRNA expression of TGF? target genes by qPCR. Overall, these data suggested that TGF? signaling was also increased in these mice. To determine if inhibition of TGF? has a beneficial effect, we treated these mice for 8 weeks with the TGF? neutralizing antibody 1D11. Our preliminary results suggest this results in an increase in bone volume in these mice. Here, we describe a novel mouse model for OI type I that shows a mild OI phenotype and increased TGF? signaling in bone. These studies support extending the clinical study of anti-TGF? approach to OI type I patients as is currently in progress (NCT05231668).

***Disclosures: Ellen Busschers**, None*

FRI-525

Deciphering phenotypic and mechanistic variability in Bruck syndrome and Osteogenesis imperfecta, through a zebrafish model with loss of fkbp10

*Tamara Jarayseh[1], Hanna De Saffel[1], Toon Rosseel[1], Mauro Milazzo[1], Sophie Debaenst[1], Paul Eckhard Witten[2], Andy Willaert[1], Paul Coucke[1]. [1]Center for Medical Genetics, Department of Biomolecular Medicine, Ghent University, Ghent, Belgium, Belgium. [2]Department of Biology, Ghent University, Ghent, Belgium. , Belgium

Bruck syndrome (BS) is a disorder characterized by bone fragility and congenital contractures that has a clinical overlap with Osteogenesis imperfecta (OI) disease. BS is caused by recessive biallelic mutations in either the FKBP10 or PLOD2 gene. The FKBP65 protein, encoded by FKBP10, acts in the folding of collagens and is involved, together with the LH2 enzyme (PLOD2), in the hydroxylation of collagen telopeptide lysine residues, which is important for collagen crosslinking in the extracellular matrix. A pronounced phenotypic variability ranging from fractures without contractures, to fractures and contractures and even only contractures, in the presence of an identical causal genetic variant is frequently observed in Bruck syndrome patients. This suggests that modifier genes contribute to the phenotypic severity through a network of interactions with the causative gene.To further investigate the mechanistic role of FKBP10 in BS/OI pathogenesis, and to unravel the cause of this phenotypic variability, we created a zebrafish model carrying an fkbp10a frameshift mutation by using CRISPR-Cas9 technology. Deep skeletal phenotyping of the vertebral column using X-ray imaging, Alizarin red mineral staining, micro-CT scanning and bone histology for fkbp10a mutant siblings, revealed a wide phenotypic variability, similar to what is observed in human patients, with variable mineralization, fracture incidence, shortened body axis and skeletal deformations. To identify potential modifiers, we conducted whole exome sequencing of the 7 most mildly and 7 most severely affected mutant siblings, followed by SNP-based linkage analysis. This revealed a linked region (LOD score= 4.4) on chromosome 13, ~15Mb in size and contains 268 protein coding genes, which segregates with the phenotypic severity.In conclusion, FKBP10 mutant zebrafish show molecular and tissue abnormalities in the skeletal system and our findings suggest that the linked region in chromosome 13 could contain the potential modifier gene that explains the phenotypic variability, thus could lead to a novel therapeutic avenues in this syndrome.

***Disclosures: Tamara Jarayseh**, None*

FRI-527

Osteopathy in Gorham-Stout Disease Animal Model

*ERNESTO SOLORZANO[1], Gabrielle Robinson[5], Hope Ball[5], Adam Sanchez[3], Alexander Powell[3], Michael Kelly[4], Fayez Safadi[5]. [1], United States. [5]Northeast Ohio Medical University, . [3]NEOMED, United States. [4]Cleveland Clinic Foundation, United States. [5]Northeast Ohio Medical University, United States

Gorham-Stout Disease (GSD) is a rare condition associated with aggressive lymphatic invasion into bone leading to massive bone loss. To date, the mechanism of bone loss identified in GSD remains to be elucidated. Most recently, a lymphatic-specific KRAS somatic activating mutation was identified in GSD patients. A mouse model recapitulating this mutation in Prox1 expressing lymphatic cells showed detrimental lymphatic valve formation. To better understand the abnormal bone loss present in GSD patients, we generated a tamoxifen-induced lymphatic endothelial cell KRAS somatic activating mutation in mice and characterized the skeletal phenotype. These mutant animals exhibited decreased body weight compared to wild-type littermates. In addition, we observed extensive lymphatic fluid accumulation in the thoracic cavity in comparison to wild-type littermates. Soft tissue immunohistochemical analysis of LYVE-1 (lymphatic endothelial cell marker) revealed lymphatic vessel invasion into the kidneys. Subsequently, bone mineral density, content, and area were all found to be decreased in KRAS mutants compared to wild-type mice. These results were also observed in KRAS mutant spine, femur, and tibia compared to wild-type controls. In addition, a decrease in total fat and lean muscle mass was also observed. Further, we next assessed bone mRNA expression and found a decrease in Runx2 and Collagen type I in mutant mice. However, the expression of osteoclast-related markers (TRAP, DC-Stamp, and Cathepsin-K) was increased in mutants compared to wild-type animals. When assessing bone marrow-derived macrophages, we found a decrease in cell proliferation associated with decreased total osteoclast count in mutant compared to wild-type. Interestingly, TRAP activity per osteoclast was increased in mutant compared to wild-type. Our findings show how a lymphatic-specific KRAS mutation leads to a decrease in bone mass in vivo and induces cell-autonomous changes in osteoclast differentiation ex vivo. For this reason, we predict mutant lymphatic tissue actively secretes bone-regulating factors capable of modulating bone homeostasis. In conclusion, our studies are the first to describe abnormal bone phenotypes found in KRAS mutant mice. Future studies aimed to identify lymphatic secreted factors responsible for bone loss and changes in osteoclast homeostasis observed in the GSD mouse model.

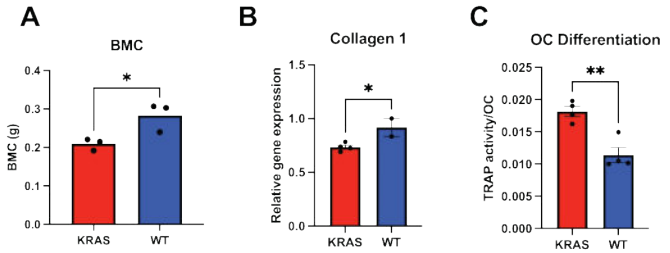

Figure 1. Osteopathic changes found in GSD animal model. Lymphatic specific KRAS activating mutation led to a decrease in bone mineral content (BMC) on mutant animals (KRAS) when compared to wild-type (WT) (**A**). Bone mRNA expression of collagen 1 was decreased in KRAS when compared to WT (**B**). Osteoclast (OC) TRAP activity per cell was higher in KRAS animals when compared to WT (**C**).

***Disclosures: ERNESTO SOLORZANO**, None*

FRI-529

Distinct molecular mechanisms of bone and lung pathologies in a G610C Mouse Model of OI

*ELENA MAKAREEVA[1], Megan Sousa[1], Muthulakshmi Sellamani[1], Edward L. Mertz[1], Satoru Otsuru[2], Sergey Leikin[3]. [1]NIH, United States. [2]University of Maryland, United States. [3]National Institutes of Health, United States

Lung function in osteogenesis imperfecta (OI) is affected by both chest deformities and intrinsic lung tissue pathology. Alveolar disruption has been reported in mouse models and bronchial wall thickening in humans. The present study aims to provide mechanistic insights into the causes of the lung-intrinsic pathology in a G610C mouse model of moderate OI, which carries the same mutation in type I collagen alpha2(I) chain as in Old Order Amish patients. We previously demonstrated that bone pathology in G610C mice is largely caused by osteoblast and hypertrophic chondrocyte malfunction because of misfolded procollagen accumulation in the ER and consecutive cellular stress, specifically integrated stress response (ISR). Surprisingly, we found that lung pathology in G610C mice is more severe than bone pathology, homozygous (Hom) G610C neonates die at birth from lung failure caused by poorly developed saccular structures and massive parenchymal bleeding. In Hom E18.5 embryos, bone pathology was comparable to severely affected yet surviving Het animals while the lung pathology was more dramatic. In lung fibroblasts, unlike osteoblasts, we observed no ER disruption in electron microscopy (EM) and no ISR marker gene upregulation in single cell (scRNASeq) or spatially resolved (srRNASeq) RNASeq. Instead, EM, histology, immunofluorescence, scRNASeq, srRNASeq, and in situ mRNA hybridization revealed deficient extracellular matrix (ECM) deposition, myofibroblast deficiency, and disorganization of lung epithelial cells, which filled the developing lung saccules instead of lining them. Altered gene expression by myofibroblasts and epithelial cells suggested abnormal cell interactions with the deficient ECM. In Het embryos, the lung pathology was less severe, but in 3- and 5-week-old Het mice we observed alveolar disruption, reduced alveolar surface/volume ratio, and increased respiratory frequency and volume/minute at rest (potentially compensating for the alveolar surface loss). In addition, many 3- and 5-week-old Het mice had lesions with inflammatory cell infiltration and various degrees of fibrosis, probably resulting from weak ECM being prone to injury. In 10-week-old Het mice, the alveolar disruption, lesions, and respiratory abnormalities were less pronounced, likely because of continuous lung remodeling in mice. These observations suggest that disruption of rapidly forming ECM and cell-ECM interactions by secreted mutant collagen molecules in embryos and young animals is the primary cause of the lung-intrinsic pathology in G610C mice, which is distinct from bone pathology.

***Disclosures: ELENA MAKAREEVA**, None*

FRI-532

Osteogenic impairment in novel pre-clinical mouse model of osteofibrous dysplasia

*Jonathan Rios[1], Nandina Paria[2], Carol Wise[3], Kristin Denton[4], Aysha Khalid[4]. [1]Scottish Rite for Children, United States. [2]Texas Scottish Rite Hospital for Children, United States. [3]Texas Scottish Rite Hospital, United States. [4]Scottish Rite Hospital for Children, United States

Osteofibrous dysplasia (OFD) is a skeletal disorder affecting the periosteal surface of bone. We previously identified inherited and somatic mutations in the gene encoding the MET tyrosine kinase receptor in patients with OFD. MET gene mutations alteres the juxtamemrane domain (JMD), thereby reducing ubiquitin-mediated receptor degradation and resulting in a ligand-dependent gain-of-function mechanism. We developed the first pre-clinical mouse model of OFD by engineering mice lacking the Met JMD (Met?JMD) and com-

pared our results to mice conditionally lacking Met in the bone periosteum (Postn-cre;Met-flox/flox; herein MetPostn). We compared matched bone periosteal explant cells (PECs) to bone marrow stromal cells (BMSCs) from control mice, Met and Hgf expression was significantly higher in PECs compared to BMSCs, consistent with human OFD. Consistent with the ligand-dependent gain-of-function mechanism, Met activation following stimulation with HGF was prolonged with delayed return to baseline in BMSCs from Met+/?JMD mice compared to control . Moreover, downstream Erk activation was significantly higher in PECs from Met+/?JMD mice compared to control, which was attributed to growth factors present within the cell culture media. Osteogenic differentiation of BMSCs and PECs from Met+/?JMD mice was significantly impaired compared to control. However, µCT analysis demonstrated no significant differences in trabecular and cortical parameters between control and Met+/?JMD mice. To test the impact that inhibition of Met has on osteogenic differentiation and skeletal development, we repeated ostogenic differentiation experiments using PECs from MetPostn mice. In contrast to results from Met+/?JMD mice, osteogenic differentiation of PECs from MetPostn mice was enhanced compared to control mice. Our results identify Met as a bidirectional key regulator of osteogenic differentiation and implicate impaired osteogenic differentiation in the pathogenesis of OFD. Results from this study suggest further research into the use of MET inhibitors to treat MET?JMD -associated OFD.

***Disclosures: Jonathan Rios**, None*

FRI-535

Global Wnt Inhibition with the Porcupine Inhibitor LGK974 Decreases Trabecular Bone in a Murine Model with Fibrous Dysplasia-Like Bone *Hsuan Lung[1], KELLY WENTWORTH[2], Tania Moody[3], Ariane Zamarioli[3], Apsara Ram[3], Gauri Ganesh[3], Misun Kang[4], Sunita Ho[4], Edward Hsiao[5]. [1]Kaohsiung Chang Gung Memorial Hospital and Chang Gung University College of Medicine, University of California, San Francisco, Taiwan, Province of China. [2]University of California-San Francisco, Zuckerberg San Francisco General Hospital, United States. [3]Division of Endocrinology and Metabolism, the Institute for Human Genetics, and the Eli and Edythe Broad Institute for Regeneration Medicine, Department of Medicine, University of California, San Francisco, CA 94143, United States. [4]Oral and Craniofacial Sciences Graduate Program, School of Dentistry, University of California, San Francisco, CA 94143, United States. [5]University of California, San Francisco, United States

G protein-coupled receptors (GPCRs) mediate many physiological functions, including skeletal development, remodeling, and repair. Fibrous dysplasia (FD) of the bone is characterized by fibrotic, expansile bone lesions caused by activating mutations in GNAS. Col1(2.3)+/Rs1+ mice with hyper-activation of Gs-GPCR signaling in osteoblastic cells develop FD-like bone lesions that can be reversed by normalizing Gs-GPCR signaling, suggesting that targeting Gs-GPCR or downstream signaling is a potential therapeutic strategy for FD. While Wnt signaling is implicated in FD pathogenesis, the specific Wnts and which cells produce them remain largely unknown. Single cell RNA sequencing on long-bone stromal cells of 9-wk-old male Col1(2.3)+/Rs1+ mice and littermate controls showed numeric and proportional stromal cell expansion in Col1(2.3)+/Rs1+ mice (6.37% (391 cells/5632 Col1(2.3)+/Rs1+ cells) v. WT 0.99% (57 cells/5767 WT cells). Pathway analysis of this cluster showed activation of Wnt/?-catenin signaling, likely driven by a predominance of Col1(2.3)+/Rs1+ cells. Subclustering found individual Wnt ligands were variably expressed by multiple fibroblastic subclusters. Wnt9a and Wnt11 were significantly upregulated in all of the fibroblastic stromal cell sub-clusters (c8.0, 8.1, 8.2, 8.5) compared to non-stromal cell lineages. Col1(2.3)+/Rs1+ mice treated with the porcupine inhibitor LGK974, which blocks Wnt signaling broadly, showed a significantly lower femoral BV/TV (0.34 vs. 0.46, $p<0.006$) and trabecular thickness (16.53 vs. 20.58 mm, $p<0.0055$) compared to vehicle-treated Col1(2.3)+/Rs1+ mice, but only qualitative changes in the craniofacial skeleton. Bone fibrosis remained evident after treatment, suggesting a dissociation between the fibrotic and trabecularization phenotypes in FD. Notably, LGK974 caused significant bone loss in control mice indicating that broad Wnt blockade is detrimental to the normal skeleton. Our scRNAseq results revealed that Col1(2.3)+/Rs1+ mice with FD-like bone lesions have a significant expansion of a fibroblastic cell population. A surprisingly broad number of cell types express Wnt ligands. Also, broadly inhibiting Wnt signaling using a porcupine inhibitor reversed established FD-like bone trabecularization in Col1(2.3)+/Rs1+ mice, but the fibrotic cell infiltrate remained unchanged. These findings will guide future studies testing how individual Wnt ligands contribute to FD pathogenesis.

***Disclosures: Hsuan Lung**, None*

FRI-538

Phenotype of the first mouse model of Cole Carpenter Syndrome. *Antonio Maurizi[1], Piergiorgio Patrizii[1], Katie Desmond[1], Oriana Newman[1], Elisa Pucci[1], Antonella Stoppacciaro[2], Paolo Mené[2], Anna Teti[1]. [1]University of L'Aquila - Department of Biotechnological and Applied Clinical Sciences, Italy. [2]University Sapienza, Department of Clinical and Molecular Medicine, , Italy

The Cole Carpenter Syndrome (CCS) is a rare genetic disease displaying an autosomal dominant inheritance with a prevalence 0.05). However, the bone phenotype, assessed by µCT in 1, 3, 6 and 12 months old male and female CCS mice showed marked osteopenia compared to the WT counterpart ($p<0.05$). In addition, the Indentation Distance and the Total Indentation Distance were dramatically increased (+1.7fold;$p=0.03$) in CSS femurs compared to WT, indicating a poor bone quality. Interestingly, the metabolic analysis revealed a significant reduction of postprandial blood glucose levels in 1 and 6 months old CCS male mice compared to WT (-28 and -14%, respectively, $p<0.05$), along with an unchanged glucose and insulin tolerance. This finding could be linked to renal defects found in CSS mice consisting of an extensive tubular vacuolization, along with intracellular protein deposits, intraluminal protein cylinders and glomerular shrinkage, which can lead to an excessive glucose leakage in the urines. At the subcellular level, Western blot analysis conducted in primary CCS mouse osteoblasts showed a significant reduction of type 1 collagen production (-25%;$p=0.05$) associated with an increased pro-collagen 1 expression (+2.9;$p=0.03$) compared to WT cells. In line with this, in vivo serum PINP1 levels, a marker of type I collagen turnover in the bone matrix, were lower in CCS mice as well (-60%;$p<0.01$). Overall, our data indicate the presence of a severe bone phenotype in CCS mice, consistent with the skeletal features of the human disease, and the pathogenic involvement of organs beyond the bone, such as kidneys. Moreover, we demonstrated the presence of a defective type 1 collagen biosynthesis.

***Disclosures: Antonio Maurizi**, None*

FRI-540

Bone-targeted ENPP1-Fc suppresses spinal hyperostosis and prevents hearing loss and spinal osteoporosis in murine ENPP1 deficiency. *Shivani Srivastava[1], Paul Stabach[1], Keith Weise[1], Simon Von Kroge[2], Ralf Oheim[2], Thomas Carpenter[3], Steven Tommasini[4], Demetrios Braddock[1]. [1]Department of Pathology, Yale University School of Medicine, United States. [2]University Medical Center Hamburg-Eppendorf, Germany. [3]Department of Pediatrics, Yale University School of Medicine, United States. [4]Department of Orthopædics and Rehabilitation, Yale University School of Medicine, United States

Background: Biallelic ENPP1 deficiency is associated with GACI and ARHR2, and monoallelic ENPP1 deficiency with Diffuse idiopathic skeletal hyperostosis (DISH), Ossification of the Posterior Longitudinal Ligament (OPLL), and early onset osteoporosis. DISH and OPLL are characterized by entheses in the paraspinal tendons and ligaments, similar to the spinal phenotype in ARHR2. Moreover, increased FGF23 and decreased plasma Pi is associated with rapidly progressing OPLL, as in ARHR2. Experimental Plan: To determine the effects of soluble (1118) or bone targeted (2000) ENPP1 on the skeletal phenotype, hearing acuity, and plasma analytes in 17-week-old Enpp1 deficient (Enpp1asj) mice treated between weeks 3-17 with 1118 and weeks 5-17 with 2000. Results: We found that 2000 normalized the increased FGF23 levels in Enpp1asj mice in at 1 mg/Kg per week, which 1118 did not suppress at any level. Moreover, the elevated levels of alkaline phosphatase and PTH in Enpp1asj mice were suppressed more potently by 2000 than 1118, which required doses 2-4 times greater. The dramatic spinal hyperostosis present in Enpp1asj mice was suppressed 16% with 1 mg/Kg per week of 2000, but not with 1118 at any dose. Hearing acuity, measured by auditory brainstem response, was impaired by 193% at 8 MHz in Enpp1asj mice and was normalized with 2 mg/Kg per week of 1118 and 0.5 mg/Kg per week of 2000. Femoral maximum load until fracture was reduced 23% in Enpp1asj mice and was normalized to WT levels at 1 mg/Kg of 1118 and 2000, while post yield deflection in the femurs increased 105% and was only normalized with 2000 at doses of 0.5 mg/Kg. Finally, biomechanics in the spines of 17-week-old Enpp1asj mice revealed that spinal stiffness and maximum load until fracture was decreased by 51% and 37% respectively and was restored to WT levels at doses of 0.5 and 2 mg/Kg per week, respectively with 2000.Conclusions: Both soluble and bone targeted ENPP1 improved biomechanics and hearing loss, but only bone targeted ENPP1 suppressed paraspinal enthesopathies, normalized plasma FGF23, and corrected post-yield deflection in long bones. Moreover, bone targeted ENPP1 demonstrated increased potency correcting plasma analytes and bone microarchitecture than soluble ENPP1. Our findings have important implications for the treatment of spinal enthesopathies in OPLL, DISH, and spinal hyperostosis in Ankylosing Spondylitis.

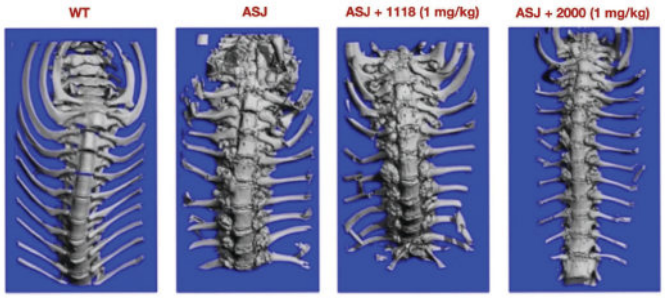

***Disclosures: Shivani Srivastava**, None*

FRI-544

Frailty is associated with greater long-term risk for fall- and fracture-related hospitalizations and mortality in community-dwelling older Australian women *Marc Sim[1], Elsa Dent[2], Jack DallaVia[1], Trent Bozanich[1], Emiel Hoogendijk[3], Abadi Gebre[1], Cassandra Smith[1], Richard Prince[4], Joshua Lewis[1]. [1]Edith Cowan University, Australia. [2]Torrens University Australia, Australia. [3]VU University, Netherlands. [4]University of Western Australia,

Frailty is a complex condition associated with declines in multiple systems with detrimental effects on capacity and quality of life. An underlying assumption being the frailer an individual is, the more likely they are to fall and fracture. We examined whether grades of frailty are related to long-term risk of hospitalized falls and fractures as well as all-cause mortality in community-dwelling older women. 1261 women (mean +/- SD 75.1 +/- 2.7 years) were followed over 14.5 years. Frailty was operationalized using a frailty index (FI) of cumulative deficits from 33 variables (as developed by Rockwood) across multiple health domains (physical, psychosocial, comorbidities) at baseline. Participants were graded as either fit (FI <=0.12), mildly frail (FI >0.12-0.24), moderately frail (FI >0.24-0.36) or severely frail (FI >0.36) based on established criteria. Fall- (n=498), any fracture (n=347) and hip fracture-related hospitalizations (n=137) and deaths (n=482) were obtained from linked health records. Associations between FI grades and each of the clinical outcomes were analyzed using multivariable-adjusted Cox-proportional hazard models including risk factors such as age, treatment (calcium/placebo), body mass index, smoking history, socioeconomic status, plasma 25-hydroxyvitamin D status plus season obtained, physical activity, self-reported prevalent falls and fractures. At baseline, women were classified as fit (n=713, 56.5%), mildly- (n=350, 27.8%), moderately- (n=163, 12.9%) and severely-frail (n=35, 2.8%). In the multivariable-adjusted analysis, compared to fit women, those with mild, moderate and severe frailty had significantly higher hazards for a fall- (46%, 104%, 168%), any fracture- (88%, 193%), hip fracture-related hospitalization (93%, 127%, 129%) and all-cause mortality (47%, 126%, 242%) (Figure). When DXA-derived hip BMD was included as an additional covariate to the multivariable-adjusted model (subset of women with available data, n=865), the results remained unchanged. For community-dwelling older women, our study supports the use of the FI to identify women at risk for falls and fractures requiring hospitalization, as well as all-cause mortality. Accordingly, the FI may be incorporated into falls assessment and fracture prevention strategies to identify older women with poorer clinical prognosis who will benefit from tailored primary prevention programs.

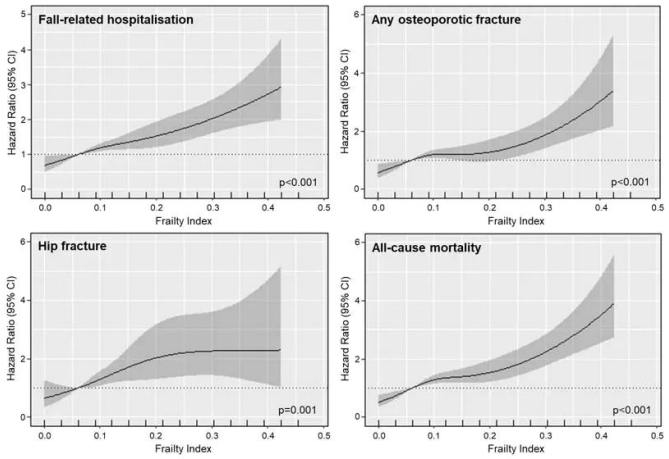

Figure. Multivariable-adjusted relationship between frailty index, fall-, any fracture- and hip fracture-related hospitalizations and all-cause mortality. Hazard ratios are obtained in comparison to the median frailty index score for mildly frail (0.16), frail (0.28) and severely frail (0.41) women, compared to fit women (0.06).

***Disclosures: Marc Sim**, None*

FRI-545

Antihyperglycemic Medications and Fall Related Injuries in a High Risk Population of Older Adults *Sarah Berry[1], Melissa Riester[2], Richa Joshi[2], Kathleen Hayes[2], Lori Daiello[2], Andrew Zullo[2], Douglas Kiel[3]. [1]Hebrew SeniorLife/Beth Israel Deaconess Medical Center, United States. [2]Brown University, United States. [3]Hinda and Arthur Marcus Institute for Aging Research Hebrew SeniorLife, United States

In the past decades, new antihyperglycemics have been approved for type-2 diabetes (T2D) including dipeptidyl peptidase-4 inhibitors (DPP-4i), glucagon-like peptide-1 receptor agonists (GLP-1-RA), and sodium-glucose cotransporter-2 inhibitors (SGLT2-i). Antihyperglycemics can increase fracture risk through long-term effects on bone and more immediately on falls risk through polyuria. Our objective was to compare the incidence of hip fracture and fall related injuries (FRI) among older adults with T2D and DPP-4i, GLP-1-RA, and SGLT2-i use. We hypothesized that SGLT2-i use would increase FRI.Our sample was comprised of Medicare beneficiaries aged ?66 years with a dispensing of a diabetes medication (2013-2019). MedPAR and Part B and D claims were linked with clinical assessments (i.e., Minimum Data Set). We restricted to patients with a T2D diagnosis and a dispensing of DPP-4i, GLP-1-RA, or SGLT2-i while receiving care in a nursing home. We excluded patients with a dispensing in the prior180 days and dialysis patients. Hip fractures and FRI were identified using hospitalization claims. Patients were followed from the date of the new antihyperglycemic dispensing until the first occurrence of fracture/FRI, death, Medicare disenrollment, or 1-year. Cause-specific Cox proportional hazards regression models that accounted for mortality were used to compare outcomes among DDP-4-I, GLP-1-RA, and SGLT2-i adjusting for 30 covariates including measures of function, comorbidities, concomitant medications, and facility-level characteristics.55,149 patients initiated DPP-4i, 6,629 GLP-1-RA, and 2,343 SGLT2-i. The mean (SD) age was 80.8 yrs (+/-8.2) and 66.1% were female. Most patients had multiple comorbidities, including dementia (67.2%). During a mean follow-up of 282 (+/-123) days, 2,993 (4.7%) experienced a FRI, and 17,598 (27.4%) died. Unadjusted rates of hip fracture were 2.19/100 person-yrs (PY) for DPP-4i, 1.32/100 PY for GLP-1-RA, and 1.78/100 PY for SGLT2-i. (Table). Adjusted models found that compared with adults using DPP-4i, the one-year rate of hip fracture and FRI was similar for GLP-1-RA and SGLT2-i users.In a large sample of older adults with T2D receiving care in a nursing home, we found no difference in the rates of hip fracture or injurious falls among persons initiating DPP-4i, GLP-1-RA, or SGLT2-i. Given the potential therapeutic advantages, these results do not suggest that any of the new antihyperglycemics increase FRI risk in a high risk population

	Incidence Rate of Injurious Falls /100 person yrs (95% CL)	Cause specific: Unadjusted Hazards ratio (95% CL)	Cause specific: Adjusted Hazards ratio (95% CL)
Hip Fractures			
DPP-4i	2.19 (2.05, 2.33)	REF	REF
GLP1-RA	1.32 (1.05, 1.60)	0.61 (0.48, 0.78)	0.94 (0.73, 1.20)
SGLT2-i	1.78 (1.20, 2.36)	0.82 (0.58, 1.16)	1.07 (0.75, 1.51)
Fall Related Injuries			
DPP-4i	6.41 (6.17, 6.65)	REF	REF
GLP1-RA	4.53 (3.95, 5.10)	0.72 (0.63, 0.82)	0.92 (0.81, 1.06)
SGLT2-i	4.92 (3.99, 5.86)	0.78 (0.63, 0.96)	0.93 (0.75, 1.14)

***Disclosures: Sarah Berry**, Wolters-Klewer, Other Financial or Material Support*

FRI-557

Higher PEN and CML Levels are Independently Associated with Increased Fracture Risk in Type 2 Diabetes with Suboptimal Glycemic Control *Ruban Dhaliwal[1], Susan Ewing[2], Bowen Wang[3], SAMUEL STEPHEN[4], Deepak Vashishth[3], Ann Schwartz[5]. [1]State University of New York Upstate Medical University, . [2]University of California San Francisco, United States. [3]Rensselaer Polytechnic Institute, United States. [4], . [5]University of California, San Francisco, United States

Advanced glycation end-product (AGE) accumulation occurs with aging and diabetes diminishing the mechanical properties of bone. We have previously shown in two separate analyses that Pentosidine (PEN), a crosslinking AGE and Carboxymethyl-lysine (CML), a

non-crosslinking AGE are risk factors for fracture in type 2 diabetes (T2D), independent of bone mineral density, glycemia and other factors. However, whether PEN and CML have independent relationships with fractures in T2D is unknown. We assessed whether PEN and CML are associated with incident clinical fractures in T2D, independent of each other, in a well characterized cohort of men and women ages 70-79 years from the Health, Aging, and Body Composition study. In addition, we examined the effect of glycemic control on these associations. Determinants of T2D were use of hypoglycemic medication or elevated fasting glucose (>=126 mg/dl). Cox proportional hazards models were used to analyze the associations between log-transformed baseline AGE and risk of clinical fractures. At baseline, mean age of T2D participants (n=501) was 73.6 +/- 2.9 years. Incident clinical fractures occurred in 97 participants over mean follow-up of 9.4 years. In multivariate models, the risk of incident clinical fractures significantly increased 32% per SD increase in log CML and 46% per SD increase in log PEN (Table 1); these estimates were not statistically different (p=0.84). In a model including CML and PEN, only PEN was independently associated with fracture risk (HR=1.37; 95% CI: 1.07, 1.77). Associations with PEN were stronger in those with suboptimal glycemia (HbA1c>7.5%) compared with optimal glycemia (all interaction p<0.10); the pattern for CML was similar but differences by glycemia status were not statistically significant. In those with suboptimal control, CML (HR=1.43; 95% CI: 1.01, 2.02) and PEN (HR=1.51; 95% CI: 1.06, 2.16) were both independently associated with fracture risk. In a sensitivity analysis, adjusting for diabetes duration did not substantially alter these results. In conclusion, crosslinking and non-crosslinking AGEs play independent roles in the pathophysiology of bone fragility in diabetes, possibly through different mechanisms on collagen and bone matrix.

Table 1. Risk of incident clinical fracture per SD increase in log CML versus log PEN in T2D and by glycemic control

	Overall HR (95% CI) (n = 501)	A1c ≤7.5% HR (95% CI) (n = 215)	A1c >7.5% HR (95% CI) (n = 286)	P-value for interaction*
N with fracture	n = 97	n = 46	n = 51	
Serum CML				
Multivariate adjusted model[a]	**1.32 (1.05, 1.66)**	1.24 (0.86, 1.77)	**1.61 (1.16, 2.25)**	0.32
Multivariate adjusted model + PEN	1.18 (0.92, 1.52)	1.17 (0.80, 1.71)	**1.43 (1.01, 2.02)**	0.24
Urine PEN				
Multivariate adjusted model[a]	**1.46 (1.16, 1.85)**	1.34 (0.91, 1.96)	**1.71 (1.22, 2.41)**	0.06
Multivariate adjusted model + CML	**1.37 (1.07, 1.77)**	1.28 (0.86, 1.90)	**1.51 (1.06, 2.16)**	**0.047**

[a]Adjusted for age, race, sex, clinic, BMI, total hip BMD, current smoking status, weight loss of 5+ pounds in year before baseline, cystatin-C, A1c (in overall model only), and medication use (vitamin D supplements, calcium supplements, oral steroids, osteoporosis drugs, thiazide diuretics, statins, oral estrogen, use of insulin and thiazolidinediones).
Bolded HRs signify p < 0.05.
Bolded p values for interaction signify p < 0.10.
*P for interaction: between continuous A1c and AGE

***Disclosures: Ruban Dhaliwal**, None*

FRI-563

Type 2 diabetes mellitus and incident fracture risk in UK Biobank: Impact of disease duration and diabetes medications *Elizabeth Curtis[1], Rebecca Moon[1], Stefania D'Angelo[1], Zahra Raisi-Estabragh[2], Cyrus Cooper[1], Nicholas Harvey[1]. [1]MRC Lifecourse Epidemiology Centre, University of Southampton, United Kingdom; [2]William Harvey Research Institute, NIHR Barts Biomedical Research Centre, Queen Mary University of London, United Kingdom

Type 2 diabetes (DM2) has been associated with increased fracture risk, but the impact of disease duration and related medications has not been well characterised in a large uniformly-assessed, prospective population. We therefore investigated these relationships in the UK Biobank cohort.DM2 diagnosis at baseline was defined using self-report, nurse interview and ICD code data. We used Poisson regression with robust standard errors to calculate incidence rate ratios (IRRs) for osteoporotic fracture during prospective follow-up in patients with DM2 versus non-diabetic controls. IRRs below and above follow-up times were compared in cumulative one-year increments. Secondly, within the cohort of DM2 patients, we examined associations between diabetic medications and incident osteoporotic fracture risk. Associations were adjusted for traditional clinical risk factors (age, sex, smoking, alcohol use, deprivation, physical activity, co-morbidities).There were 498,949 participants, 20,551 of whom had a diagnosis of DM2. The presence of DM2 was associated with an increased risk of OP fracture, independent of traditional risk factors [IRR: 1.14 95% CI (1.04,1.26)]. Associations were similar by sex. The fracture association for DM2 increased with greater duration of disease [1.01 (1.00, 1.02)], with a statistically significant effect emerging at eight years follow-up [IRR for <8 years duration: 1.12 (1.00,1.25)]. Within the DM2 cohort (users of specific medication versus all other DM2 patients), the use of insulin (n=546) and sulfonylureas (n=5,387) were associated with a trend towards increased OP fracture risk [IRR 1.64 (0.98, 2.73) and 1.19 (0.99, 1.42) respectively] and thiazolidinediones (n=2,036) were significantly associated with increased risk [IRR 1.31 (1.02, 1.67)]. Metformin use (n=11,839) was not associated with increased risk (all after adjustment for clinical risk factors).In UK Biobank, DM2 is associated with increased risk of fracture, with the association increasing in magnitude with greater duration of disease. The risk interaction with follow-up time and associations with insulin, sulfonylureas and thiazolidinediones treatment inform risk assessment in clinical practice. This work was undertaken using the UK Biobank resource under approved application 3593.

***Disclosures: Elizabeth Curtis**, None*

FRI-566

Chronic kidney disease is associated with lower cortical measures at proximal femur as assessed by 3D-DXA *M. Kužma[1], Z. Kužmová[1], L. Humbert[2], M. Lopez Picazo[2], J. Falat[1], J. Smaha[0], P. Jackuliak[1], Z. Killinger[0], J. Payer[1]. [1]5th department of Internal Medicine, Comenius University Faculty of Medicine, University Hospital , Bratislava, Slovakia, Slovakia; [2]3D-Shaper Medical, Barcelona, Spain, Spain; [0]5th department of Internal Medicine, Comenius University Faculty of Medicine, University Hospital , Bratislava, Slovakia, Slovakia

Introduction: Patients with chronic kidney disease (CKD) has 2-14 fold increase in fracture risk, especially in later stages of the CKD. The gold standard for the diagnosis of osteoporosis represents DXA, but its use is limited due to lack of possibility to measure trabecular and cortical characteristics and interference of aortic calcifications with BMD. Specific information about bone microstructure and turnover could be obtained by bone biopsy, but this is limited due to invasiveness.Aim: To compare several non-invasive DXA-derived methods used for assessment trabecular and cortical parameters, such a s trabecular bone score (TBS), 3D-Shaper and hip structure analysis (HSA) in subjects across all CKD stages.Patients and methods: In total, 89 CKD (38 females / 51 males; mean age 69,5 years) subjects were included in the analysis. According to glomerular filtration rate (GFR) there were 12; 23; 10; 14; 14 and 16 subjects in stage G1, G2, G3a, G3b, G4 and G5, respectively. BMD at lumbar spine (LS) and proximal femur (hip and neck) was analyzed by Hologic Horizon device. LS TBS was analyzed by TBS Insight software. Proximal femur parameters such as cortical and trabecular volumetric (v) BMD, cortical thickness (CTh) and surface (s) BMD and HSA parameters such as buckling ratio (BR), cross-sectional area (CSA) and section modulus (Z) were analyzed by 3D-Shaper-research v. 2.12.1. In all subjects bone turnover markers such as CTx, P1NP and Osteocalcin was measured.Results: Cross-sectional comparison between each CKD stage showed gradually decreasing LS BMD, cortical vBMD (neck and TH), TH Cth and neck BR starting from G3b, G4 and G5 stages; but not in earlier stages of CKD (G1-G3a). Comparison of means between earlier stages (G1-G3a) versus later stages (G3b-G5) of CKD showed significant differences in CTx (386 vs. 1053 ng/l); TH aBMD (0,991 vs 0,859 g/cm2), cortical vBMD at TH (831 vs 795 mg/cm3) and neck (837 vs.788 mg/cm3), TH cortical sBMD (170 mg/cm2) and TH Cth (2,03 vs 1,92 mm) (all p<0.05). Among all subjects, strong positive associations between GFR and cortical parameters (neck/TH vBMD and TH Cth) were observed (p<0.01).Conclusion: This study showed that later stages of CKD (G3b - G5) CKD have lower cortical bone parameters, such as vBMD, sBMD and CTh, as assessed by 3D Shaper. In addition, most of the cortical parameters are associated with GFR, showing direct relationship of kidney function and bone. These results agree with the previous findings provided by bone histomorphometry. As such, it is likely that 3D Shaper as non-invasive DXA derived method can be of use in assessment of fracture risk in CKD subjects especially in later stages of the disease. However, further prospective studies with greater amount of subjects and fracture data are needed.

***Disclosures: M. Kužma**, None*

FRI-568

Longitudinal changes of QCT-derived bone parameters by indices of beta cell function and insulin resistance in non-diabetic community-dwelling adults *Namki Hong[1], Graham Treece[2], Hyeon Chang Kim[3], Yumie Rhee[4]. [1]Division of Endocrinology, Republic of Korea; [2]University of Cambridge, United Kingdom; [3]Department of Preventive Medicine, Yonsei University College of Medicine, Republic of Korea; [4]Department of Internal Medicine, Endocrine Research Institute, Yonsei University College of Medicine, Republic of Korea

Beta cell dysfunction and insulin resistance, two culprit pathophysiology of type 2 diabetes mellitus, may have distinctive impact on cortical and trabecular bone parameters. We aimed to investigate longitudinal changes of QCT-derived bone parameters according to beta cell function and insulin resistance in non-diabetic community-dwelling adults. From a community-based cohort, longitudinal changes in bone parameters of individuals without diabetes mellitus aged 50 or older were analyzed using baseline and 5-year follow-up QCT scans. Homeostasis Model Assessment for beta cell function (HOMA-b) and for Insulin resistance (HOMA-IR) were calculated using fasting glucose and insulin level. Cortical bone mapping technique were applied to analyze cortical and trabecular bone parameters of hip. Mean age of participants (n=377) was 56.6 years and 68% were women. Compared to highest HOMA-b quartile (Q4, reference), individuals in lowest quartile (Q1) had lower body mass index (BMI, 24.4 vs. 23.1 kg/m2), higher fasting glucose, lower insulin and lower disposition index (HOMA-b/HOMA-IR). Individuals in HOMA-b Q1 had highest risk of new-onset T2DM (8.5%) compared to other quartiles (1.1 to 2.1%, p=0.020). Compared to HOMA-b Q4, HOMA-b Q1 had greater decrease in lumbar spine volumetric BMD (-12.0% vs. -8.6%) and total hip trabecular density (-7.5% vs. -4.8%, p<0.05 for all) at 5-year follow-up, which remained robust after adjustment for age, sex, BMI, baseline BMD, and HOMA-IR (adjusted beta -4.0, p=0.007 [Q1 vs. Q4] for lumbar spine BMD changes; adjusted beta -2.4, p=0.008 [Q1 vs. Q4] for total hip trabecular density changes). Changes in bone parameters did not differ between HOMA-IR quartiles. Spatial heterogeneity of hip bone trabecular density loss was observed, with greater loss at femoral neck and greater trochanteric regions in lower HOMA-b quartiles. In summary, beta cell dysfunction was associated with greater loss of trabecular bone density at lumbar spine and hip in non-diabetic community-dwelling adults.

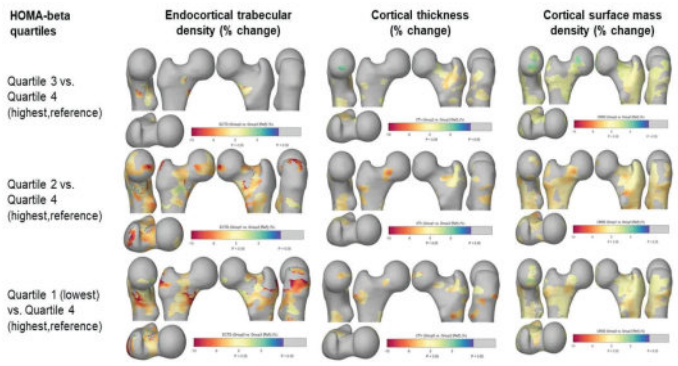

***Disclosures: Namki Hong**, None*

FRI-570

Association of Sodium-Glucose Cotransporter 2 Inhibitor Use With Risk of Osteoporotic Fracture Among Older Women: A Nationwide, Population-Based Cohort Study *Seunghyun Lee[1], Min Heui Yu[2], Namki Hong[3], KYOUNG JIN KIM[4], Hae Kyung Kim[5], Yumie Rhee[6], Minyoung Lee[5], Kyoung Min Kim[7]. [1]Wonju Severance Christian Hospital, Yonsei University Wonju College of Medicine, Wonju, Korea, . [2]SENTINEL team, Division of Endocrinology, Department of Internal Medicine, Yonsei University College of Medicine, Seoul, Korea, Republic of Korea. [3]Division of Endocrinology, Republic of Korea. [4]Korea University College of Medicine, Republic of Korea. [5]Institute of Endocrine Research, Department of Internal Medicine, Yonsei University College of Medicine, Seoul, Korea, Republic of Korea. [6]Yonsei University College of Medicine, Republic of Korea. [7]Yongin Severance Hospital, Yonsei University College of Medicine, Republic of Korea

Sodium-glucose cotransporter-2 inhibitor (SGLT2i) is a widely recommended anti-diabetic medication (ADM) due to its cardioprotective and renoprotective benefits. However, the effects of SGLT2i on fracture risk have been debated. The Canagliflozin Cardiovascular Assessment Study showed that SGLT2i increased hip fracture risk during the mean 6-year follow-up period. However, in most other large randomized controlled trials of SGLT2i, SGLT2i use was not associated with increased fracture risk. Although the fracture risk associated with SGTL2i use is controversial, there are concerns regarding fracture risk due to the increased risk of falls caused by volume depletion or disturbance of calcium phosphate balance. Therefore, in the present study, the association between SGLT2i use and fracture risk in elderly women (>= 65 years of age) who were newly prescribed ADMs was investigated using a national cohort database.?We used the data for this population-based cohort study obtained from the National Health Insurance Service of Korea between January 1, 2013, and December 31, 2020. Women older than 65 years old diagnosed with type 2 diabetes mellitus who were newly prescribed ADMs other than glucagon-like peptide-1 receptor agonists and thiazolidinedione and who had available comprehensive health check-up data were included.A total of 1,333 SGLT2i users was analyzed and compared with covariate (e.g., body mass index (BMI), age-matched non-SGLT2i users at a 1:2 ratio (n = 2,626). After propensity score matching, mean age (70.3 years vs. 70.3 years, p = 0.830), BMI (27.4 kg/m2 vs. 27.4 kg/m2, p = 0.924), number of oral ADMs (1.4 vs. 1.3, p = 0.092), and other covariates were well-balanced between SGLT2i users and non-SGLT2i users. During the follow-up period, SGLT2i use was associated with a significantly increased risk of vertebral fracture compared with non-SGLT2i use (incidence rate 19.2 vs. 13.8 per 1,000 person-years; hazard ratio 1.40, 95% confidence interval 1.00-1.96, p = 0.049). Regarding the risk of other types of fracture, any fractures, hip fractures, and non-hip or non-vertebral fractures, significant differences were not observed between SGLT2i users and non-SGLT2i users.In conclusion, SGLT2i use showed a 40% higher risk of vertebral fracture than non-SGLT2i use in elderly women. Although further validation is required, SGLT2i should be cautiously prescribed in older women due to the potential association with fracture risk in this vulnerable population.

***Disclosures: Seunghyun Lee**, None*

FRI-572

The Association between Intrahepatic Lipid Content and Bone Microarchitecture and Strength (Assessed by HR-pQCT): The Maastricht Study. *VEERLE VAN HULTEN[1], Johanna Driessen[2], Marleen van Greevenbroek[3], Carla van der Kallen[3], Annemarie Koster[4], Martijn Brouwers[3], Eline Kooi[5], Pieter Dagnelie[6], Coen Stehouwer[3], Joop Van Den Bergh[7]. [1]Maastricht University, . [2], Netherlands. [3]Department of Internal Medicine, MUMC+, Netherlands. [4]Department of Social Medicine, Maastricht University, Netherlands. [5]Department of Radiology, MUMC+, Netherlands. [6]School for Cardiovascular Diseases, Maastricht Universiity, Netherlands. [7]VieCuri MC Noord-Limburg and Maastricht UMC,

Background: It is known that type 2 diabetes (T2D) is associated with a number of comorbidities, such as an increased fracture risk, possibly due to impaired bone quality. T2D has also been associated with non-alcoholic fatty liver disease (NAFLD) characterized by a high intrahepatic lipid (IHL) content. In turn, NAFLD has been shown to be a risk factor for osteoporotic fractures.Purpose: To determine the association of IHL content with parameters of bone microarchitecture and strength assessed by high-resolution peripheral quantitative computed tomography (HR-pQCT).Methods: This study includes cross-sectional data from 2104 participants of the Maastricht Study who underwent a HR-pQCT scan (first generation) at the distal radius. MRI was performed to determine IHL content, expressed as the percentage of hepatic triglyceride content in the total liver volume. Multiple linear regression models were used to investigate the association of IHL content with HR-pQCT parameters of bone microarchitecture and strength. Analyses were stratified by sex due to inherent differences in bone metabolism, and were adjusted for glucose metabolism status, age, comorbidities, medication and lifestyle factors.Preliminary Results: We included 1057 men and 1047 women. Male participants were on average 60 (+/-8.7) years old, and female participants were on average 58 (+/-8.8) years old. After adjustment, IHL content was positively associated with total bone mineral density (BMD) and cortical BMD in the distal radius in men and women, and with trabecular BMD, cortical area, stiffness, and failure load in women (Table 1). When BMI was added to the linear regression model, all significant associations between IHL content and HR-pQCT parameters were strongly attenuated and not statistically significant.Conclusion: These findings suggest that bone quality may not be impaired in individuals with an increased IHL content, and that bone strength may even be greater in women with NAFLD. However, it is possible that this finding is at least partially due to the association of BMI with IHL content and with bone density, stiffness and failure load, since no statistically significant associations between IHL content and HR-pQCT parameters remained when BMI was added to the linear regression model.

Table 1: The association between IHL content and bone architecture and bone strength in the distal radius (assessed by HRpQCT)

	IHL content	
	Men (ß (95% CI)) †	**Women** (ß (95% CI)) †
Tt.BMD (mg HA/cm³)	0.76 (0.13; 1.39) * ↑	0.90 (0.23; 1.57) * ↑
Ct.BMD (mg HA/cm³)	0.70 (0.05; 1.35) * ↑	1.05 (0.29; 1.81) * ↑
Tb.BMD (mg HA/cm³)	0.17 (-0.2; 0.55)	0.52 (0.12; 0.91) * ↑
Tt.Ar (mm²)	-0.58 (-1.30; 0.14)	0.08 (-0.42; 0.59)
Ct.Ar (mm²)	0.18 (0.00; 0.36)	0.20 (0.08; 0.32) * ↑
Tb.Ar (mm²)	-0.70 (-1.42; 0.03)	-0.06 (-0.57; 0.45)
Ct.Th (mm)	0.00 (0.00; 0.01)	0.00 (0.00; 0.01)
Tb.N (mm⁻¹)	0.00 (0.00; 0.01)	0.00 (0.00; 0.01)
Tb.Sp (mm)	0.00 (0.00; 0.00)	0.00 (0.00; 0.00)
Log Ct.Po (%)	0.00 (-0.01; 0.00)	0.00 (-0.01; 0.00)
Stiffness (kN/mm)	-0.10 (-0.15; 0.34)	0.28 (0.12; 0.43) * ↑
Failure load (kN)	4.94 (-6.45; 16.33)	12.51 (5.19; 19.83) * ↑

** Denotes statistically significant finding*
† Adjusted for age, educational level, time gap (time in months between baseline visit and HR-pQCT scan), alcohol use, smoking behavior, medication affecting bone metabolism, estimated glomerular filtration rate, moderate-to-vigorous physical activity and history of cardiovascular disease.
CI, confidence interval; Ct.Ar, cortical area; Ct.BMD, cortical density; Ct.Po, cortical porosity; Ct.Th, cortical thickness; HbA1c, glycated hemoglobin; IHL, intrahepatic lipid; NGM, normal glucose metabolism; Tb.Ar, trabecular area; Tb.BMD, trabecular density; Tb.N, trabecular number; Tb.Sp, trabecular separation; Tt.Ar, total area; Tt.BMD, total density.

***Disclosures: VEERLE VAN HULTEN**, None*

FRI-574

Relation between switching from noninsulin antidiabetic drugs to insulin and hip fracture risk in Japan: a nationwide study *JUNKO TAMAKI[1], Kenji Fujimori[2], Shigeyuki Ishii[3], Sumito Ogawa[4], Shinichi Nakatoh[5], Nobukazu Okimoto[6], Masayuki Iki[7]. [1]Osaka Medical and Pharmaceutical University, Japan. [2]Tohoku University School of Medicine, Japan. [3]Tokyo University of Pharmacy and Life Sciences, Japan. [4]The University of Tokyo, Japan. [5]Asahi General Hospital, Japan. [6]Okimoto Clinic, Japan. [7]Kindai University Faculty of Medicine, Japan

Aims We aimed to identify hip fracture risks in patients who switched to or were prescribed noninsulin antidiabetic drugs in addition to insulin using a nationwide health insurance claims database in Japan.Methods This study included the information of 7,54,767 patients aged >=50 years who were started on noninsulin antidiabetic drugs at the outpatient department between 2012 and 2019 fiscal years from the National Database of Health Insurance Claims and Specific Health Check-ups of Japan (NDBJ). Of the 7,54,767 patients, 2,22,311 were selected using propensity score to predict the prescriptions of insulin agents

as second antidiabetic drugs and optimal variable rate matching revealed that 63,516 patients switched to insulin and 1,58,795 switched to noninsulin antidiabetic drugs.Results The hip fracture incidences (per 10,000 person-year) of the patients who switched to or were additionally prescribed insulin and noninsulin antidiabetic drugs were 89.1 and 35.4, respectively, during the first 2 months after the switch. The patients who switched to or were additionally prescribed insulin exhibited increased hip fracture risk compared with patients prescribed noninsulin drugs during the 2 months [log-rank test; p < 0.001, sex- and age-adjusted hazard ratio (HR) (95% CI), 2.20 (1.54, 3.16)]. The sex- and age-adjusted HR during the first half of the month after the switch was 3.09 (1.81, 5.27) with a p-value of <0.001 in the log-rank test. The sex- and age-adjusted HRs during the first 2 months among patients whose age at switching drugs were <80 and >=80 years were 3.76 (1.90, 7.44) and 1.88 (1.23, 2.89), respectively, with a p-value of <0.001 in the log-rank test for both.Conclusions Patients whose second diabetic drugs was insulin demonstrated increased risk of hip fractures compared with those prescribed with noninsulin antidiabetic drugs, especially immediately after switching to insulin. Increased fracture risk was observed in older and middle-aged patients with diabetes.

***Disclosures: JUNKO TAMAKI**, None*

FRI-576

Relationship of Biomarkers of Cellular Senescence with Skeletal Parameters in Type 2 Diabetes Mellitus *Caroline Hoong[2], Joshua Farr[2], Thomas White[2], Elizabeth Atkinson[2], Amanda Tweed[2], Stephanie Vos[2], Matthew Drake[3], Nathan LeBrasseur[2], Sundeep Khosla[4], Jad Sfeir[2]. [2]Mayo Clinic, , [2]Mayo Clinic, United States, [3]College of Medicine, Mayo Clinic, United States, [4]Mayo Clinic College of Medicine, United States

Patients with type 2 diabetes (T2D) have increased risk of fractures and impaired bone microarchitecture, despite a preserved or increased areal BMD. We have previously demonstrated premature accumulation of senescent osteocytes in the bone microenvironment of T2D mice (JCI Insight 2020; 5:e135236). Here, we report on the biomarkers of cellular senescence in patients with obesity with and without T2D, and their relationship with skeletal phenotypes. We compared 27 postmenopausal women with obesity and T2D [median age 66.7 yrs (IQR 62.8-71.4); BMI 36.3 (34.0-38.7); A1c >6.5%] to 29 age-matched controls with obesity but no T2D [median age 64.7 yrs (IQR 59.7-73.7); BMI 34.7 (32.0-39.9); A1c <5.9%] and 37 age-matched lean controls [median age 70.1 yrs (IQR 63.0-72.2); BMI 22.7 (21.6-23.7); A1c <5.9%]. We measured circulating senescence-associated secretory phenotype (SASP) proteins that have been identified as biologically relevant in vitro (via commercially available multiplex magnetic beads immunoassays) and mRNA gene expression in peripheral T-lymphocytes of cyclin-dependent kinase inhibitors (p16 and p21, via rt-qPCR). Skeletal parameters included bone microarchitecture parameters using HRpQCT at the radius and tibia. Expression of p16 and p21 mRNA was significantly increased the obese group and further increased in patients with T2D. Similarly, a cluster of the SASP proteins (TNF?, IL-8, IL-6, GDF-15, TNFR1, TNFR2, Fas, Activin-A) showed increases that were most pronounced in patients with obesity and T2D (Table). Interestingly, p16 expression was associated with age in lean and obese patients but not in T2D, where it remained elevated in all age groups. There was a significant correlation between p16 and the SASP protein cluster with cortical parameters on HRpQCT in patients with T2D: p16 was negatively correlated with cortical thickness at both the radius and tibia; Fas negatively correlated with cortical thickness at the radius and cortical vBMD at the tibia; GDF-15 negatively correlated with cortical vBMD at the tibia; IL-8 negatively associated with stiffness and failure load at the radius. These findings demonstrate an increase in cellular senescence burden in patients with obesity, and further increases with T2D. Collectively, these results indicate a central role for cellular senescence in mediating skeletal fragility in patients with T2D.

Senescence markers, median (IQR)	T2D (n=27)	BMI>30 (n=29)	BMI<25 (n=37)	p value
p16* ($x10^{-3}$)	1.4 (1.19-1.83)	1.11 (0.91-1.30)	1.05 (0.87-1.22)	<0.001
p21* ($x10^{-4}$)	2.2 (1.7-2.5)	1.6 (1.3-2.0)	1.5 (1.2-1.7)	<0.001
TNFα^	14.2 (12.8-16.4)	12.1 (10.2-15.0)	11.4 (10.0-12.7)	0.001
IL-8^	16.6 (14.3-22.7)	12.5 (10.7-18.2)	12.1 (10.5-15.5)	0.002
IL-6^	3.85 (2.85-4.56)	2.98 (2.51-4.02)	1.71 (1.32-2.16)	<0.001
GDF-15	1244.1 (847.4-1671.1)	612.4 (553.4-195.9)	583.3 (478.0-192.9)	<0.001
TNFR1	1557.8 (1216.1-2005.2)	1382.5 (1226.3-1681.8)	1148.1 (923.4-1283.3)	<0.001
TNFR2	3419.2 (2358.0-4691.3)	2967.2 (2582.9-3743.1)	2518.9 (1888.8-3052.7)	0.009
Fas	9409.3 (8263.2-10974.5)	8858.1 (7946.8-10304.1)	7655.4 (6198.6-8950.2)	0.001
Activin-A	346.2 (272.6-438.7)	339.4 (268.9-365.9)	273.0 (239.7-308.5)	0.005

* rt-qPCR, expressed in normalized expression
^ measured by automated ELISA immunoassay

***Disclosures: Caroline Hoong**, None*

FRI-577

Type 2 Diabetes is Associated with Better Bone Microarchitecture, higher BMD, but Impaired Physical Function and Increased Risk of Incident Fracture in Older Swedish Women from the SUPERB study. *Lisa Johansson[1], Kristian Axelsson[2], Mattias Lorentzon[3], Henrik Litsne[4], Michail Zoulakis[5]. [1]Institute of medicine, , [2]Institute of Medicine, Sahlgrenska Academy, Gothenburg University, , [3]Sahlgrenska Academy, University of Gothenburg, Sweden, [4]Sahlgrenska Osteoporosis Centre,University of Gothenburg, , Sweden, [5]Sahlgrenska Osteoporosis Centre, Institute of Medicine,University of Gothenburg, Sweden

Several studies have shown that type 2 diabetes mellitus (T2DM) is associated with incident fracture, but it is not clear if the risk increase is due to impaired bone microarchitecture, low bone material strength index (BMSi) or poor physical function. The aim of this study was to determine if T2DM is associated with bone microarchitecture, BMSi, physical function, and risk of incident fracture in older Swedish women.In total, 3028 Swedish women, 75-80 years old were included in the prospective SUPERB study. At baseline, information on clinical risk factors (CRFs) was collected using questionnaires. Bone mineral density (BMD) was measured with dual-energy X-ray absorptiometry, bone microarchitecture with HR-pQCT (XtremeCT), and BMSi obtained using the Osteoprobe device (n=630). Physical function was assessed using timed up and go (TUG), one leg standing (OLS), grip strength, chair stand test and by measurements of gait speed. Data on incident fractures were retrieved from a regional x-ray archive.At baseline, the 294 women with T2DM were compared to women (n=2714) without diabetes. Women with T2DM had higher BMD at all sites (total hip 4.7%, femoral neck (FN) 3.9% and lumbar spine L1-L4 5.4%, all p<0.01) than women without. At the ultradistal tibia, T2DM women had a greater cortical area (7.3%, p<0.01) and density (1.2%, p=0.03), as well as higher trabecular bone volume fraction (8.6%, p<0.01). There was no difference in BMSi between groups (n=630; T2DM 77.8+/-8.1 vs. controls 78.1+/-7.3, p=0.81). Women with T2DM performed significantly worse on all physical function tests than their non-diabetic controls. For example, grips strength was 10.1% lower, gait speed 10.2% slower, and TUG time 13.1% (p<0.001 for all comparisons) slower in women with T2DM than in those without.During 7.3 (4.4, 8,4) years (median (IQR) of follow-up there were 1071 incident any fractures, 797 major osteoporotic fractures (MOF), and 232 hip fractures. In adjusted (for age, BMI, FRAX CRFs and FN BMD) Cox regression models T2DM was associated with an increased risk of any fracture (HR 95% CI 1.26 [1.04-1.53], but the associations with MOF (HR 1.16 [0.92-1.46]) or hip fracture (HR 1.31 [0.85-2.00]) did not reach statistical significance.In conclusion, older women with T2DM have considerably better bone microarchitecture, and no different BMSi, but substantially poorer physical function than nondiabetic women, which could be the principal reason for the increased fracture risk observed in T2DM women.

***Disclosures: Lisa Johansson**, None*

1021

Results from the PROPEL 2 dose-finding study: oral infigratinib leads to significant increases in height velocity with good tolerability in children with achondroplasia *Ravi Savarirayan[1], Josep Maria De Bergua[2], Paul Arundel[3], Jean Pierre Salles[4], Vrinda Saraff[5], Borja Delgado[6], Antonio Leiva-Gea[7], Helen McDevitt[8], Marc Nicolino[9], Massimiliano Rossi[10], Maria Salcedo[11], Valerie Cormier-Daire[12], Mars Skae[13], Peter Kannu[14], Michael B. Bober[15], John Phillips III[16], Howard Saal[17], Paul Harmatz[18], Christine Burren[19], Toby Candler[19], Terry Cho[20], Elena Muslimova[20], Richard Weng[20], Supriya Raj[21], Julie Hoover-Fong[22], Melita Irving[23], Daniela Rogoff[20]. [1]Murdoch Children's Research Institute, Australia. [2]Hospital Vithas San José, Spain. [3]Sheffield Children's NHS Foundation Trust, United Kingdom. [4]Children Hospital, Toulouse University Hospital, France. [5]Birmingham Women's and Children's NHS Foundation Trust, United Kingdom. [6]Campus de Teatinos sin número, Hospital Universitario Virgen de la Victoria, Spain. [7]Instituto de Investigación Biomédica de Málaga - IBIMA, and Hospital Universitario Virgen de la Victoria, Spain. [8]NHS Greater Glasgow and Clyde, United Kingdom. [9]Hôpital Femme Mère Enfant, Hospices Civils de Lyon, France. [10]Lyon University Hospital, Bron, France. [11]Hospital Universitario La Paz, Spain. [12]Imagine Institute, Hôpital Necker-Enfants Malades, University of Paris, France. [13]Manchester University NHS Foundation Trust, University of Manchester, United Kingdom. [14]Department of Medical Genetics, University of Alberta, Canada. [15]Nemours Children's Hospital, United States. [16]Vanderbilt University Medical Center, United States. [17]Cincinnati Children's Hospital Medical Center, United States. [18]UCSF Benioff Children's Hospital Oakland, United States. [19]University Hospitals Bristol and Weston NHS Foundation Trust, United Kingdom. [20]QED Therapeutics, United States. [21]Murdoch Children's Research Institute, Australia. [22]Johns Hopkins University, United States. [23]Guy's and St Thomas' NHS Trust, United Kingdom

Background: Achondroplasia (ACH), the most common short-limbed skeletal dysplasia, is characterized by impaired endochondral ossification resulting from gain-of-function pathogenic variants in the fibroblast growth factor receptor 3 (FGFR3) gene, a negative regulator of endochondral bone growth. People with ACH are at risk for several significant co-morbidities, including brainstem compression due to foramen magnum stenosis, sleep-disordered breathing, chronic otitis media with conductive hearing loss, and symptomatic spinal stenosis. Infigratinib is an oral, selective FGFR1-3 tyrosine kinase inhibitor being investigated for treating children with ACH.Methods: PROPEL 2 (NCT04265651) is a phase 2 dose-finding, open-label study of infigratinib in children 3?11y with ACH who participated for >=6m in PROPEL (NCT04035811), a non-interventional clinical assessment study. The PROPEL 2 dose-escalation (DE) phase includes 5 ascending dose cohorts from 0.016 to 0.25mg/kg/d. Primary endpoints: safety; change from baseline in annualized height velocity (AHV); infigratinib pharmacokinetics.Results: Children enrolled in PROPEL 2 DE completed >=6m of treatment at the assigned dose. Cohorts 1-3 (n=37; 0.016, 0.032, 0.064mg/kg/d) did not show a significant increase in AHV and these doses were assessed as non-efficacious. Treatment at the cohort 4 dose (0.128mg/kg/d) resulted in an increase in AHV from baseline of 1.52cm/y in children >=5y old (n=11; p=0.02). Infigratinib at the cohort 5 dose (0.25mg/kg/d, n=10, m6) resulted in a significant mean increase from baseline of 3.03cm/y (p=0.0022). In cohort 5, collagen X marker, a biomarker of endochondral ossification, showed a median increase of 28% from baseline at m6 (n=6). Infigratinib was well tolerated with no serious AEs or AEs leading to study discontinuation, with most AEs mild/moderate in severity. At the cohort 5 dose, no grade 3 AEs or treatment-related AEs were reported.Conclusion: Oral infigratinib in children with ACH was well tolerated and showed dose-dependent increases in AHV, with a significant mean change from baseline of +3.03cm/y at the cohort 5 dose (0.25mg/kg/d). The safety and efficacy of this oral, once-daily dose of infigratinib will be further explored in a phase 3 randomized controlled study. If these phase 2 data are confirmed, infigratinib could potentially offer children with ACH the first safe and effective oral therapy to improve growth, enhance functionality and decrease medical complications.

***Disclosures: Ravi Savarirayan**, BioMarin, Consultant, Ascendis Pharma, BioMarin, QED Therapeutics, Sanofi, Other Financial or Material Support, Ascendis Pharma, BioMarin, QED Therapeutics, Theracon, Grant/Research Support*

1022

Sodium Fluoride-18 PET/CT Visualizes Disease Activity and New Bone Formation in Adult Chronic Nonbacterial Osteomyelitis/Synovitis, Acne, Pustulosis, Hyperostosis, Osteitis-Syndrome (CNO/SAPHO) *Anne Leerling[1], Frits Smit[2], Zita Sp?th[1], Ana Navas Cañete[3], Lioe-Fee De Geus-Oei[2], Alina Van der Burgt[4], Olaf Dekkers[5], Wouter Van der Bruggen[6], Natasha Appelman-Dijkstra[1], Dennis Vriens[2], Elizabeth Winter[1]. [1]Department of Internal Medicine, Division of Endocrinology, Center for Bone Quality, Leiden University Medical Center, Netherlands. [2]Department of Radiology, Division of Nuclear Medicine, Center for Bone Quality, Leiden University Medical Center, Netherlands. [3]Department of Radiology, Center for Bone Quality, Leiden University Medical Center, Netherlands. [4]Department of Nuclear Medicine, Alrijne Hospital, Netherlands. [5]Department of Clinical Epidemiology, Leiden University Medical Center, Netherlands. [6]Department of Nuclear Medicine, Slingeland Ziekenhuis, Netherlands

Background: Chronic nonbacterial osteomyelitis/synovitis, acne, pustulosis, hyperostosis, osteitis syndrome (CNO/SAPHO) is a rare disease characterized by inflammatory bone lesions with increased bone turnover. CNO/SAPHO lacks biochemical and radiological biomarkers that are sensitive for disease activity. Sodium fluoride positron emission tomography ([18F]NaF-PET/CT) produces quantitative data on bone turnover that correlate with disease activity in other metabolic bone disorders. We quantitate 18F-uptake in CNO/SAPHO for the first time, to evaluate its capacities as a diagnostic and disease activity biomarker.Methods: Cohort study among CNO/SAPHO patients (n=43) and mimicking controls (n=16) presenting at our expert clinic with [18F]NaF-PET/CT performed. Images were qualitatively compared between patients and controls and maximal standardized uptake values (SUVmax (g/ml)) were calculated for bone lesions and soft tissue/joint lesions plus thoracic vertebra 5 as reference bone. SUVmax was correlated with clinical disease activity. Results: Qualitative analysis of [18F]NaF-PET/CT revealed manubrial and costal sclerosis/hyperostosis, and calcification of the costoclavicular ligament as core radiologic features associated with CNO/SAPHO. SUVmax of bone lesions was higher compared to reference bone in patients (mean paired difference 11.4, 95%CI 9.4-13.5, p<0.001) and compared to controls (mean difference 12.4, 95%CI 9.1-15.8, p<0.001). Highest SUVmax was found in soft tissue/joint lesions like the costoclavicular ligament and the manubriosternal joint, and also correlated with erythrocyte sedimentation rate (r=0.546, p<0.002). Receiver operator characteristic analysis demonstrated excellent discriminatory value of SUVmax of bone and soft tissue/joint lesions (area under curve 0.95 95%CI 0.88-1.00 and 0.98 95%CI 0.96-1.00 respectively).Conclusion: Adult CNO/SAPHO patients display distinctive imaging features that are well-captured on [18F]NaF-PET/CT, and show higher SUVmax in bone and soft tissue/joint lesions compared to reference bone and controls, the latter correlating with inflammatory disease activity. SUVmax therefore qualifies as a first diagnostic and disease activity biomarker in CNO/SAPHO. Highest SUVmax was seen in soft tissue/joint areas, which are known locations of new bone formation in CNO/SAPHO. [18F]NaF-PET/CT visualizes this pathogenic process, and can invaluably steer therapeutic decision-making.

***Disclosures: Anne Leerling**, None*

1023

Encaleret?(CLTX-305) Normalizes Mineral Homeostasis Parameters in Patients with Autosomal Dominant Hypocalcemia Type 1 over 18 months in a Phase 2 Study (NCT04581629) *Rachel Gafni[2], Iris Hartley[2], Kelly Roszko[2], Edward Nemeth[3], Karen Pozo[2], Arun Mathew[4], Mary Scott Roberts[4], Scott Adler[4], Michael Collins[2]. [2]National Institutes of Health, United States. [2]National Institutes of Health, . [3]MetisMedica, Canada. [4]Calcilytix Therapeutics, United States

Autosomal dominant hypocalcemia type 1 (ADH1), caused by gain-of-function variants in the calcium-sensing receptor (CaSR) gene, is characterized by low parathyroid hormone (PTH), hypocalcemia, hypercalciuria, hyperphosphatemia, and hypomagnesemia. Calcium (Ca) and active vitamin D treatment worsens hypercalciuria and can lead to renal morbidity. Calcilytics (negative allosteric CaSR modulators) decrease the sensitivity of hyperactive receptors to extracellular Ca and normalize blood and urine abnormalities in ADH1 rodent models.This Phase 2b open-label study of the oral investigational calcilytic encaleret included 3 periods followed by a long-term extension (LTE). Periods 1&2 were inpatient dose-finding and safety evaluations. Period 3 (P3) assessed safety/efficacy over 24 outpatient weeks; participants then continued in the outpatient LTE.Thirteen adults with ADH1 were treated with encaleret, titrated to normalize albumin-corrected Ca (cCa). Encaleret was well-tolerated with no serious adverse events reported. There were no treatment discontinuations or withdrawals prior to the LTE; one participant withdrew in the LTE. The mean+/-SD encaleret sulfate dose was 86+/-70mg BID at P3 Week 24 (P3W24) and 75+/-66mg BID at LTE Month 12 (LTEM12). Mean mineral indices normalized over 18 months of encaleret (Figure). Analyses comparing P3W24 and LTEM12, respectively, to baseline (BL), were as follows: PTH rose from 6.3+/-7.8 pg/mL (nl 10-65) to 35.3+/-10.2 and 36.9+/-15.2 (p<0.01). Hypocalcemia (cCa=7.1+/-0.4 mg/dL [nl 8.4-10.2]) corrected and remained normal at 9.2+/-0.5 and 9.2+/-0.4 (p<0.01). BL urinary calcium of 395+/-216 mg/d (nl<250-300) decreased to 202+/-83 and 177+/-94 (p<0.05). Blood phosphate (4.5+/-1.1 mg/dL [nl 2.3-4.7]) decreased to 3.4+/-0.4 and 3.4+/-0.5 (p<0.01). Blood magnesium increased from 1.7+/-0.2 mg/dL [nl 1.6-2.6]) to 2.0+/-0.2 and 2.1+/-0.2 (p<0.01). Bone turnover markers increased from BL (n=7, CTX=253+/-111 pg/mL; P1NP=34+/-10

mcg/L) to P3W24 (n=13, CTX=744+/-565; P1NP=104+/-87) and LTEM12 (CTX=988+/-652; P1NP=83+/-49) p<0.01. Except for Total hip, DXA BMD Z-scores (n=11) did not change from BL?LTEM12: AP spine Z=2.6+/-1.5?2.5+/-1.7; Total hip Z=2.2+/-1.4?2.0+/-1.3 (p<0.05); 1/3 radius Z=0.2+/-0.9?0.5+/-0.5.This study represents a molecularly targeted, precision medicine approach to treatment of ADH1. The consistent, sustained results over 18 months of encaleret treatment support Phase 3 evaluation of encaleret efficacy/safety as the first potential treatment indicated for ADH1.

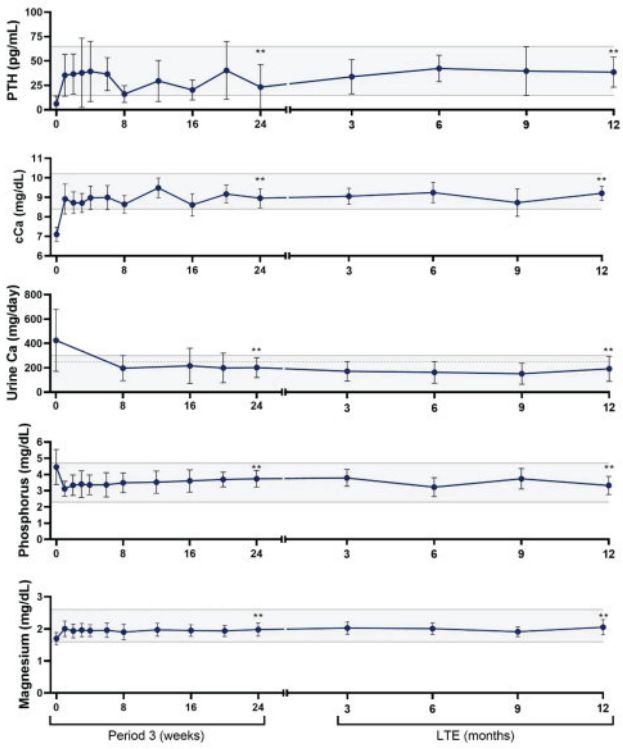

Data reported as mean±SD. Gray shading = normal range. Solid line for urine calcium = upper limit for men, dashed line = upper limit for women. Values below limit of assay quantitation recorded as "0". The measures shown for weeks 0, 8, 16, and 24 are pre-encaleret. ** p-value < 0.01 Period 3 Week 24 or LTE Month 12 compared to Baseline.

***Disclosures: Rachel Gafni**, Hypoparathyroidism Association, Consultant, Calcilytix Therapeutics, Grant/Research Support, Ascendis Pharmaceuticalss, Consultant*

1024

Intermittent Parathyroid Hormone Treatment Activates Osteoclast-Mediated, but not Modeling-Based, Bone Formation: A Randomized Clinical Trial in Patients with Hypoparathyroidism *Lisbeth Koch Thomsen[1], Galina Pronina[1], Tanja Sikjaer[2], Jesper Skovhus Thomsen[3], Christina M Andreasen[4], Lars Rejnmark[2], Thomas Levin Andersen[5]. [1]Molecular Bone Histology Lab, Research Unit of Pathology, Department of Clinical Research, University of Southern Denmark & Department of Pathology, Odense University Hospital, Odense, Denmark, Denmark. [2]Department of Endocrinology and Internal Medicine, Aarhus University Hospital, Aarhus, Denmark, Denmark. [3]Department of Biomedicine, Aarhus University, Aarhus, Denmark, Denmark. [4]Molecular Bone Histology Lab, Research Unit of Pathology, Department of Clinical Research, University of Southern Denmark & Department of Pathology, Odense University Hospital, Odense, Denmark, Denmark. [5]Molecular Bone Histology Lab, Research Unit of Pathology, Department of Clinical Research, University of Southern Denmark & Department of Forensic Medicine, Aarhus University, Aarhus, Denmark, Denmark

Treatment with intermittent parathyroid hormone (iPTH) has been reported to increase the proportion of osteoclast-independent modeling-based bone formation (MBF) in patients with osteoporosis. However, to our knowledge a similar investigation of osteoclast-mediated bone formation in patients with hypoparathyroidism treated with iPTH has not been made thus far.We have developed a new histological method to distinguish osteoclast-mediated formation (Remodeling Based Formation (RBF) and overflow Remodeling Based Formation (oRBF)) from MBF, utilizing the osteopontin-rich cement lines and the lamellar structure of the underlying bone in the entire bone structural unit (BSU). We applied this method to 68 iliac crest biopsies collected from patients with chronic hypoparathyroidism. As add-on to conventional therapy participants were randomized to 6 months of treatment with i) placebo (PLB6; n=25) or ii) 100 µg s.c./daily rhPTH(1-84)(PTH6; n=25) followed by 24 months open-labeled of iii) conventional treatment (CON; n=5), iv) 100 µg s.c./daily rhPTH(1-84)(PTH30; n=5), or v) rhPTH withdrawal (PTHw; n=8) (figure). Tetracycline was administered twice 8 days apart ending 2 days prior to biopsy collection. Using the tetracycline labels, bone formation at the cancellous and endocortical envelopes was identified and measured. Subsequently, the bone formation was categorized as either RBF, oRBF, or MBF based on adjacent osteopontin immunostained sections.At the cancellous envelope, PTH6 group had a 33-fold higher proportion of mineralizing surfaces (p<0.0001) relative to PLB6 and mineralizing surfaces correlated with increased P1NP-levels (p<0.05), but not with mineral apposition rate at 6 months. At month 30, PTHw had significantly reduced mineralizing surfaces (p<0.01) relative to PTH6 (median 0 versus 21%). Moreover, compared to PTH6 the PTH30 group also had significant lower mineralizing surfaces (p<0.05). RBF, oRBF, and MBF were all significantly increased in the PTH6 compared to PLB6 group, but osteoclast-mediated bone formation (RBF median 16.7% p<0.0001; oRBF median 9.0%, p<0.001), and not MBF (median 0.00% p <0.01), was by far the main type of bone formation. Interestingly, oRBF exhibited a significantly increased mineral apposition rate (3-fold, p<0.05). All data were reproduced at the endocortical envelope.Collectively, this study demonstrates that the rhPTH-induced bone formation in hypoparathyroidism is osteoclast-mediated RBF and oRBF, and not MBF.

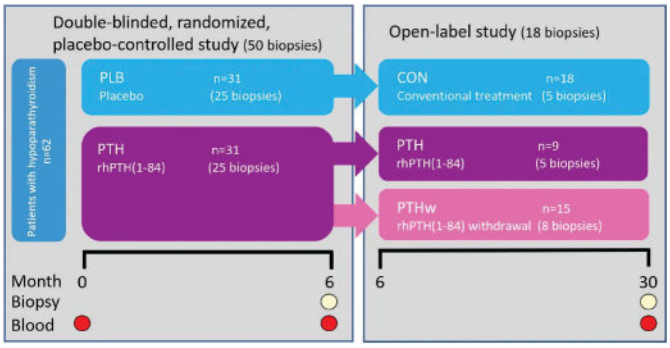

***Disclosures: Lisbeth Koch Thomsen**, None*

1025

Genetic testing and targeted intervention to prevent development and progression of Paget's disease of bone *Jonathan Phillips[1], Deepak Subedi[1], Catriona Keerie[1], Steff Lewis[1], Owen Cronin[1], Mary Porteous[1], Rosemary Cetnarsky[2], Lakshminarayan Ranganath[3], Peter Selby[4], Tolga Turgut[4], Geeta Hampson[5], Rama Chandra[6], Shu Ho[7], Jonathan H Tobias[8], Stephen Young-MIn[9], Malachi McKenna[10], Rachel Crowley[10], William Fraser[11], Jonathan Tang[11], Luigi Gennari[12], Rannuccio Nuti[12], Maria Luisa Brandi[13], Javier del Pino-Montes[14], Jean-Pierre Devogelaer[15], Anne Durnez[15], Giovanni Isaia[16], Marco Di Stefano[17], Nuria Guanabens[18], Josep Blanch[19], Markus Seibel[20], John Walsh[21], Sarah Rea[22], Mark Kotowicz[23], Geoff Nicholson[24], Gabor Major[25], Emma Duncan[24], Anne Horne[26], Nigel Gilchrist[27], Stuart Ralston[1]. [1]University of Edinburgh, United Kingdom. [2]University of Dundee, United Kingdom. [3]University of Liverpool, United Kingdom. [4]Manchester Royal Infirmary, United Kingdom. [5]St. Thomas' Hospital, United Kingdom. [6]King's College Hospital, United Kingdom. [7]10 The Robert Jones and Agnes Hunt Orthopaedic and District Hospital, United Kingdom. [8]University of Bristol, United Kingdom. [9]Queen Alexandra Hospital, United Kingdom. [10]University College Dublin, Ireland. [11]University of East Anglia, United Kingdom. [12]University of Sienna, Italy. [13]University Hospital of Careggi, Italy. [14]University Hospital of Salamanca, Spain. [15]Clinique Universitaires Saint-Luc, Belgium. [16]University of Torino, Italy. [17]L'Ospedale S. Giovanni Battista Antica Sede, Italy. [18]Hospital Clinic, CIBERehd, Spain. [19]Hopital del Mar, Spain. [20]Concord Repatriation General Hospital, Australia. [21]Sir Charles Gairdner Hospital, Australia. [22]Murdoch University, Australia. [23]University Hospital Geelong, Australia. [24]University of Queensland, Australia. [25]32 Rheumatology, Bone and Joint Institute, Royal Newcastle Center, Australia. [26]University of Auckland, New Zealand. [27]The Princess Margaret Hospital, New Zealand

BackgroundPaget's disease of bone (PDB) often presents with irreversible skeletal damage. Early detection of PDB coupled with prophylactic bisphosphonate therapy may help prevent progression of the disease to an advanced stage.MethodsWe conducted a randomised trial of a single infusion of 5mg zoledronic acid (ZA) versus placebo in 222 individuals who were genetically at increased risk of PDB because of pathogenic mutations in SQSTM1. The primary outcome was emergence of new bone lesions assessed by radionuclide bone scan. Secondary outcomes included change in existing lesions, biochemical markers of bone turnover and skeletal events related to PDB. Participants were followed up for a median of 84 months (range 0-127) and 180 (81%) completed the study.ResultsAt baseline, PDB lesions were present in 9 (8.1%) of the ZA group and 12 (10.8%) of the pla-

cebo group. Two participants in the placebo group developed new lesions during the study versus none in the ZA group (OR 0.41, 95% CI 0.00 to 3.43, p=0.25). Eight participants in the placebo group had a poor outcome (lesions which were new, unchanged, or progressing) compared with none in the ZA group (OR =0.08, 95% CI 0.00-0.42, p=0.003). By the end of study, there were 2 lesions in the ZA group compared with 26 in the placebo group (p<0.0001). Biochemical markers of bone turnover were significantly reduced in the ZA group throughout the study. One participant allocated to placebo required rescue therapy with ZA because of symptomatic disease. The number, severity and type of adverse events did not differ between the groups.ConclusionsGenetic testing for SQSTM1 mutations coupled with intervention with ZA is well-tolerated and has favourable effects on progression of early PDB. (ISRCTN 11616770)

***Disclosures: Jonathan Phillips**, None*

1026

Association of Clinical Factors and Incident Fracture in Overweight and Obese Middle-aged and Older Persons with Type 2 Diabetes Mellitus *Rachel Elam[1], Hongyan Xu[1], Laura Carbone[1], Carlos Isales[1], Yanbin Dong[1], Karen Johnson[2]. [1]Augusta University, United States. [2]University of Tennessee Health Science Center, United States

Purpose: Persons with type 2 diabetes mellitus (T2DM) have increased bone fragility despite preserved bone mineral density. We aimed to identify clinical factors associated with incident fracture in overweight and obese persons with T2DM.Methods: A retrospective cohort study of overweight and obese adults with T2DM enrolled in the multicenter Look AHEAD (Action for Health in Diabetes) Randomized Clinical Trial was conducted. Ethnically diverse men and women 45-75 years old were recruited to Look AHEAD from 2001-2004 and randomized to an intensive lifestyle intervention versus diabetes support and education. Incident fractures were ascertained every 6 months by self-report and confirmed with central adjudication of medical records. Clinical factors ascertained at baseline included: treatment arm; age; gender; race/ethnicity; height; weight; body mass index; smoking; alcohol use; prevalent cardiovascular disease, rheumatoid arthritis, and peripheral neuropathy; age at menopause (in women); duration of T2DM; hemoglobin A1C (HbA1C); estimated glomerular filtration rate; urinary albumin-to-creatinine ratio; and medication use thought to affect bone health, including diabetes drugs. Potential covariates were screened with Least Absolute Shrinkage and Selection Operator (LASSO) Cox regression, censoring on first incident fracture, death, loss to follow-up, or study year 18, whichever was first. The final multivariate Cox model was selected with optimal LASSO penalty to maximize the Harrell C-index.Results: Over a median follow-up of 16.6 years, 649 incident fractures occurred in 4,703 persons. In the final multivariate model (C-index: 0.63), modifiable clinical factors associated with incident fracture were tricyclic antidepressant use [hazard ratio (HR):2.24, 95% confidence interval (CI):1.14-4.43], insulin use (any form) [HR:1.26, 95% CI:1.02-1.57], and higher HbA1C [HR:1.12 per 1% increase in HbA1C, 95% CI:1.04-1.20]. Other significant covariates in the final model included age [HR:1.02, 95% CI:1.01-1.04], female gender [HR:2.20, 95% CI:1.83-2.66], race/ethnicity, and estrogen use [HR:0.65, 95% CI:0.44-0.98] (Figure 1).Conclusions: Tricyclic antidepressants should be used judiciously in adults with T2DM as their use confers the highest hazard of incident fracture in our study, independent of prevalent peripheral neuropathy. Improving glycemic control, without insulin use if possible, may prevent fractures in overweight and obese adults with T2DM.

Figure 1: Hazard ratios (95% confidence intervals) for covariates in the final multivariate Cox model for incident fracture

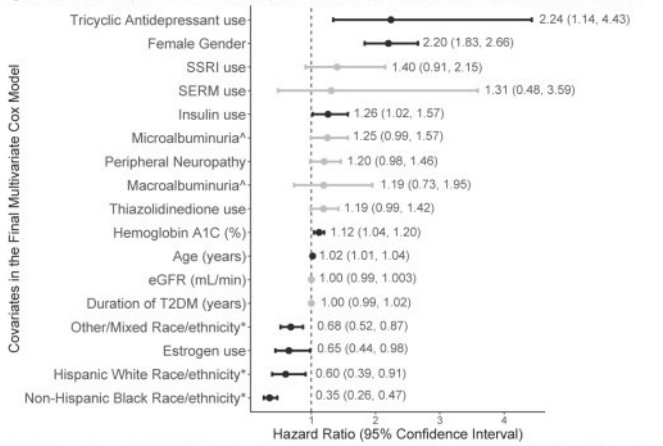

SSRI: Selective serotonin reuptake inhibitor; SERM: Selective estrogen receptor modulator; eGFR: estimated glomerular filtration rate; T2DM: Type 2 diabetes mellitus
^Comparator group is No albuminuria (urinary albumin-to-creatinine ratio < 30 mg/g)
*Comparator group is Non-Hispanic White Race/ethnicity

***Disclosures: Rachel Elam**, None*

1027

The Association of SGLT2-Is Versus DPP4-Is as Add-on to Metformin and Fracture Risk in Patients With Type 2 Diabetes Mellitus *Veerle van Hulten[1], Johanna Driessen[2], Jakob Starup-Linde[3], Zheer Al-Mashhadi[4], Rikke Viggers[5], Olaf Klungel[6], Patrick Souverein[6], Peter Vestergaard[5], Coen Stehouwer[7], Joop Van Den Bergh[8]. [1]1Department of Clinical Pharmacy and Toxicology, Maastricht University Medical Centre+ (MUMC+), Netherlands. [2], Netherlands. [3]Department of Endocrinology and Internal Medicine, Aarhus University Hospital, Denmark. [4]Steno Diabetes Center Aarhus, Aarhus University Hospital, Denmark. [5]Steno Diabetes Center North Denmark, Denmark. [6]Division of Pharmacoepidemiology & Clinical Pharmacology, Utrecht Institute for Pharmaceutical Sciences, Utrecht University, Netherlands. [7]Department of Internal Medicine, Cardiovascular Research Institute Maastricht, Maastricht University Medical Centre+ (MUMC+), Netherlands. [8]VieCuri MC Noord-Limburg and Maastricht UMC,

Background: T2D is a major burden to public health and healthcare costs. It is known that T2D is associated with an increased fracture risk. Additionally, the use of SGLT2-Is, a relatively new class of glucose lowering drugs, has recently been linked with an increased risk of fractures.Purpose: To study if SGLT2-I use as compared to DPP4-I use as add-on to Metformin is associated with the risk of any fracture or major osteoporotic fractures (MOFs).Methods: A cohort study using the Clinical Practice Research Datalink (CPRD) Aurum database was conducted. The CPRD contains medical records of primary care practices in the United Kingdom. All patients aged 18 years and older with a first ever prescription of a DPP4-I or a SGLT2-I as add-on to Metformin between 1-1-2013 and 30-6-2020 were selected. Patients starting with SGLT2-I were matched (up to 1:3) on propensity scores to patients starting with DPP4-Is. Propensity scores were calculated based on sex, age, BMI, comorbidities, comedication and lifestyle factors. Cox proportional hazard models were used to estimate the risk of any fracture with SGLT2-I use as compared to DPP4-I use. As the secondary analysis the risk of major osteoporotic fracture (MOF) was estimated. Results: A total of 13,807 SGLT2-I users (55.4+/-10.6 y/o, 36.7% female) were included in this study, matched with 28,524 DPP4-I users (55.4+/-8.0 y/o, 36.4% female). The risk of any fracture with current SGLT2-I use was similar compared with current DPP4-I use (adjusted hazard ratio (aHR) 1.09; 95% CI: 0.91-1.31), as was the risk of MOFs (aHR 0.89; 95% CI: 0.64-1.22) and the risk of fractures at any of the individual MOF sites. Additionally, no association was found with the duration of SGLT2-I use (longest duration >811 days), with any of the individual SGLT2-I agents, or after stratification by sex and age. All analyses were repeated in CPRD GOLD and yielded similar results.Conclusion: SGLT2-I use was not associated with the risk of any fracture, MOFs or fracture at the individual MOF sites when compared to DPP4-I use.

***Disclosures: Veerle van Hulten**, None*

1028

Maternal Diabetes Is Associated with Higher Risk of Fractures in Offspring: A Population-Based Analysis *Viral Shah[1], William Leslie[2], Maria-Elena Lautatzis[3], Kun Liu[4], Heather Prior[4], Brandy Wicklow[3]. [1]University of Colorado Denver, United States. [2]University of Manitoba, Canada. [3]Department of Pediatrics and Child Health, University of Manitoba, Canada. [4]Manitoba Centre for Health Policy, Canada

Purpose: Fracture risk is 1.2-1.5 fold higher in people with type 2 diabetes and 2-to 6-fold higher in people with type 1 diabetes. The intra-uterine environment is known to affect offspring risk for type 2 diabetes and cardiovascular disease. We studied the effect of in-utero exposure to maternal diabetes (type 2 diabetes and gestational diabetes) on offspring fracture risk.Methods: Administrative data was accessed between 1980-2020 from the Manitoba Population Research Data Repository to identify a cohort of offspring born to women with and diabetes. The primary outcome was any fracture (defined using ICD-9 CM/ICD-10-CA diagnosis codes) by maternal diabetes status adjusting for potential confounders.Results: Of 585,176 total deliveries, 26,397 offspring were born to women with diabetes (mean maternal age 30.7+/-5.9) and 558,779 were born to women without diabetes (age 27.9+/-5.6). A higher percentage of offspring born to women with diabetes were large for gestational age (27.7% vs 12.0%) and had a diabetes diagnosis (2.4% vs 1.2%). After adjusting for potential confounders, risk for any fracture [HR 1.070 (95% 1.027-1.115), p=0.0012; Figure 1] was 7.0% higher and risk for non-traumatic fracture was 6.7% higher [1.067 (1.023-1.113), p=0.0026] among offspring born to women with diabetes compared to offspring of women without diabetes). There was significant increase in risk for long bone upper extremity [1.065 (1.005-1.129, p=0.033)]; however, long bone lower extremity [1.027 (0.932-1.130), p=0.59] and vertebral fractures [1.195 (0.769-1.859), p=0.42] were not significantly higher in offspring born to mother with diabetes.Conclusion: To our knowledge, this is the first study identifying increased fracture risk among offspring of women with diabetes during pregnancy. This study highlights the potentially detrimental role that intra-uterine glucose exposure may have on skeletal health of offspring. Further studies are needed to evaluate the effect of intrauterine hyperglycemia on offspring bone morphology and bone mass accrual.

Figure 1: Survival curve of cumulative incidence of any fracture in offspring by maternal diabetes status

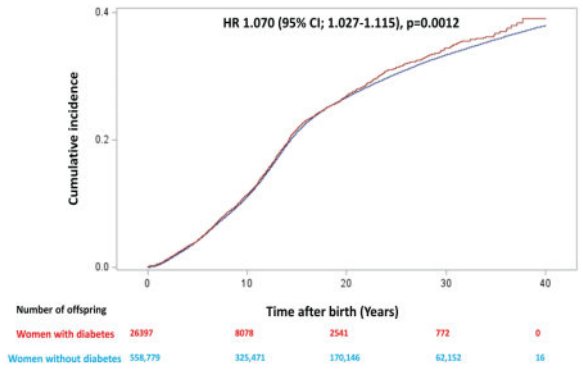

***Disclosures: Viral Shah**, None*

1029

High Glucose and Type 2 Diabetes Mellitus Condition Stimulate Osteocyte-Mediated Sclerostin Production by Inhibiting Autophagy *Cyril Thouverey[1], Sara Delon[1], Nicolas Bonnet[2], Serge Ferrari[3]. [1]University Hospital of Geneva, Switzerland. [2]Nestlé research, Switzerland. [3]Geneva University Hospital and Faculty of Medicine, Switzerland

Serum levels of sclerostin are elevated in patients with type 2 diabetes mellitus (T2DM), inversely related to serum levels of bone formation marker, and associated with increased fracture risk. Moreover, sclerostin is highly expressed by osteocyte-like cell lines treated with high glucose in vitro, and by osteocytes in a diabetic rat model. Since high glucose can potentially alter autophagy in osteoblast lineage cells in vitro, we hypothesized that T2DM condition and high glucose could increase sclerostin expression by affecting autophagy in osteocytes. To test this hypothesis, we cultured KUSA-A1 cells for 16 days in osteogenic medium until complete mineralization and expression of osteocyte markers, including sclerostin (Sost gene), then treated those cells with vehicle solution (Veh), 25 mM mannitol or 25 mM glucose for 6 days, and monitored autophagic flux and sclerostin expression/secretion. In addition, mice treated with a high fat diet for 3 months and receiving a single low dose of streptozotocin (HFD + STZ) were injected with Veh or 0.5 mg/kg rapamycin (to stimulate autophagy) 3 times a week for the last 2 months. Fully mineralized KUSA-A1 cells cultured under high glucose condition displayed high Sost mRNA expression (5-fold versus Veh- and mannitol-treated cells) and sclerostin protein secretion (5-fold), but unchanged expressions of osteocyte markers Gp38 and Mepe. Furthermore, mineralized KUSA-A1 cells treated with high glucose exhibited reduced autophagic flux (lower LC3II/LC3I ratio than in Veh- and mannitol-treated cells) and diminished expressions of autophagy effectors Beclin, Atg5 and Atg7. High glucose stimulated phosphorylation/activation of mammalian target of rapamycin (mTOR), while it decreased that of UNC-51-like kinase 1 (a positive regulator of autophagy whose activation is inhibited by mTOR). Inhibition of mTOR by 25 nM Torin2 restored autophagic flux and normal sclerostin secretion in high glucose-treated mineralized KUSA-A1 cells. Finally, our murine model of T2DM (HFD + STZ) showed reduced cortical bone thickness at femoral midshaft (-11% versus mice receiving a control diet, p=0.002), decreased bone tissue expressions of Beclin, Atg5 and Atg7, and elevated Sost expression (8-fold). In this context, rapamycin treatment could restore normal Sost expression and cortical thickness. In conclusion, our findings show that high glucose and T2DM condition stimulate osteocyte-mediated sclerostin production by inhibiting autophagy.

***Disclosures: Cyril Thouverey**, None*

1030

Effect of Romosozumab on Tissue Thickness-Adjusted Trabecular Bone Score in Postmenopausal Women with Osteoporosis and Diabetes: Results From the ARCH Study *Serge Ferrari[1], Donald Betah[2], Robert Feldman[3], Bente Langdahl[4], Mary Oates[2], Jen Timoshanko[5], Zhenxun Wang[2], Ruban Dhaliwal[6]. [1]Geneva University Hospital , Switzerland. [2]Amgen Inc, United States. [3]MemorialCare Saddleback Medical Center, United States. [4]Aarhus University Hospital, Denmark. [5]UCB Pharma, United Kingdom. [6]Massachusetts General Hospital, United States

Diabetes mellitus is associated with reduced bone strength and increased fracture risk (Walle 2022, Curr Osteoporos Rep). Trabecular bone score (TBS), a gray-level texture index derived from lumbar spine (LS) DXA scans, has been reported to be decreased in patients with diabetes and is associated with an increased fracture risk, independent of bone mineral density (BMD). In the ARCH trial (Saag 2017, NEJM), romosozumab (Romo), an osteoanabolic with the dual effect of increasing bone formation and decreasing bone resorption, significantly improved bone mass and bone strength leading to superior fracture risk reduction vs alendronate (Aln) alone. Here, we examined the effect of Romo-to-Aln vs Aln-to-Aln on LS BMD and TBS in ARCH patients with diabetes.In ARCH, postmenopausal women with osteoporosis and prior fracture were randomized 1:1 to Romo 210mg SC monthly or Aln 70mg PO weekly for 12 months (M), followed by Aln 70mg PO weekly for 24 M in both groups. This post hoc analysis included a subgroup of women from ARCH who had diabetes mellitus at baseline (BL) and had LS DXA scan measurements at BL and >=1 post-BL visits (Romo-to-Aln, n=195; Aln-to-Aln, n=165). BMD and TBS (determined by an updated tissue thickness-adjusted TBS algorithm [TBSTT]; TBS iNsightTM v4.0 [Medimaps]; Shevroja 2019, JBMR) were assessed on LS DXA scans at BL, M12, M24, and M36.BL LS BMD was -2.63 for Romo and -2.89 for Aln; BL LS TBSTT was 1.006 and 1.010, respectively. Romo led to significantly greater gains in LS BMD and TBSTT at M12 vs Aln, and greater gains with Romo were maintained after transition to Aln and persisted significantly at M24 and M36 vs Aln alone (Figure). In the Romo-to-Aln group, the percentage of women with "normal" TBS values (TBSTT>1.074; Hans 2022, Osteoporos Int) increased from 23.6% at BL to 50.0% at M36 and those with "degraded" TBS values (TBSTT<=1.027) decreased from 55.8% to 33.9% (P<0.001). A similar trend, albeit with smaller improvement, was observed in the Aln-to-Aln group. TBSTT percentage changes were unrelated to LS BMD percent changes from BL to M36 (Romo-to-Aln, r2=0.1493; Aln-to-Aln, r2=0.0429).In conclusion, in postmenopausal women with osteoporosis and diabetes, 12 M of Romo followed by 24 M of Aln significantly improved LS BMD and TBS as measured by TBSTT (independently of BMD) to a greater extent when compared with 36 M of Aln alone. These changes may reflect a greater improvement of bone strength by Romo vs Aln in patients with diabetes.

Figure: Percentage change from baseline by visit and treatment group for LS BMD and TBS_{TT}

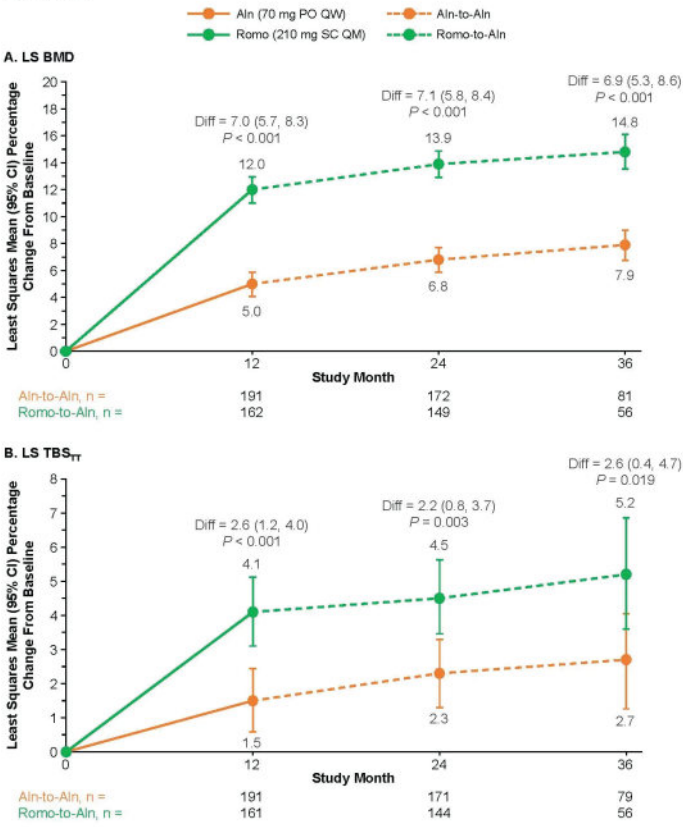

LS BMD and TBS_{TT} data were analyzed based on repeated measures model adjusting for treatment, presence of severe vertebral fracture at baseline, visit, treatment-by-visit interaction, baseline BMD or TBS value as fixed effects, with machine type and baseline BMD or TBS value-by-machine type interaction as covariates, using either a compound symmetry variance covariance structure for BMD or an unstructured variance covariance structure for TBS.

Aln = alendronate; BMD = bone mineral density; CI = confidence Interval; Diff = percentage change from baseline for Romo treatment group minus percentage change from baseline for Aln treatment group; LS = lumbar spine; PO = orally; QM = monthly; QW = weekly; Romo = romosozumab; SC = subcutaneous; TBS = trabecular bone score; TBS_{TT} = tissue thickness–adjusted trabecular bone score.

***Disclosures: Serge Ferrari**, Amgen, UCB, Agnovos, Grant/Research Support, Amgen, UCB, Agnovos, Radius, Myovant, Flowbone, Amolyt, Ascendis, Fresenius, Parexel, Consultant*

1031

I?B? Is a Central Modulator of Rheumatoid Arthritis Pathology *Gaurav Swarnkar[1], Krishna Bhan Singh[1], Dorothy Kate Mims[1], Syeda Kanwal Naqvi[1], Musarrat Naaz[1], Yousef Abu-Amer[1]. [1]Washington University School of Medicine, United States

Rheumatoid Arthritis (RA) is a chronic inflammatory autoimmune disease considered as one of the leading causes of disability worldwide. IL-1?, TNF?, IL-17, IL-6, and other highly abundant cytokines and catabolic enzymes such as MMPs from a variety of synovial

cells in RA, perpetuate a vicious inflammatory cycle in the joint tissue, leading to the demise of articular cartilage and subchondral bone. As such, current therapies targeting inflammatory cytokines show limited efficacy owing to cytokine redundancies and many adverse side effects on normal physiology. NF-?B signaling plays a crucial role in the production and function of these inflammatory cytokines. However, given the essential role of NF-?B in physiologic processes, a more effective approach is needed to target pathway downstream of NF-?B, which regulates expression of inflammatory cytokines in RA. Using transcriptomics, we have identified I?B? (gene: Nfkbiz) as a unique inflammatory signature of NF-?B that controls transcription of inflammatory cytokines only under pathologic conditions. Our qPCR, western blot, ELISA and RNAseq results show that deletion of Nfkbiz attenuates production of these inflammatory cytokines and catabolic enzymes such as MMPs in various cell types involved in RA pathology. Further, RNA-Seq of CD11b+ cell from joints of WT and LysMcre: Nfkbiz-/- knockout mice, subjected to serum-induced arthritis (STIA), showed decreased expression of IL-6, IL-17, IL-1?, TNF? and other inflammatory signals in KO mice. To determine if genetic global deletion of Nfkbiz attenuates experimental mouse arthritis, we subjected Ubc-ERT2-Cre+/-: Nfkbiz-/-, CAGG-ERT2-Cre+/-: Nfkbiz-/- and littermate wildtype (WT) control animals to STIA. Paw measurements, microCT and bulk RNAseq analysis showed significant inhibition in joint swelling, joint erosion, and decrease expression of inflammatory cytokines. Finally, we identified Dimethyl Itaconate (DI) and 8-Hydroxyquinoline (8HQ) as selective pharmacological inhibitors of I?B? activity without affecting NF-?B activity. We show that systemic administration of DI and/or 8HQ significantly inhibit joint swelling and joint erosion. In summary, our study holds promise to establish I?B? as an inflammation-specific target for therapeutic intervention in RA while sparing the broad beneficial effects of NF-?B

***Disclosures: Gaurav Swarnkar**, None*

1032

Conditional Deletion of MCP1 in the Colonic Epithelium is Protective in the OA of Obesity *David Villani[1], Honey Hendesi[1], Celia Mbazoa[1], Samantha Landgrave[2], Toru Ishii[1], Ann Gill[3], Lacey Favazzo[1], Karin Payne[1], Steven Gill[3], Michael Zuscik[4]. [1]CU Anschutz, United States. [2]University of Colorado Anschutz Medical Campus, United States. [3]University of Rochester, United States. [4]University of Colorado, United States

One of the leading risk factors for the development of osteoarthritis (OA) is obesity. In addition to causing joint overloading, obesity is associated with a gut microbiome dysbiosis that initiates colonic, systemic, and joint inflammation that ultimately accelerates joint degeneration in OA. It follows that obesity-associated gut microbiome dysbiosis leads to an infiltration of pro-inflammatory macrophages into the colon, which triggers colonic inflammation during obesity. This phenotype is driven by an increase in monocyte chemoattractant protein one (MCP1), a chemokine encoded by the Ccl2 gene. MCP1 is responsible for recruiting pro-inflammatory macrophage populations to the colon, an initiating factor that may drive both systemic and joint inflammation, ultimately accelerating OA progression. Here, we sought to test if knocking out Ccl2, the gene that encodes MCP1, in the intestinal epithelium, can blunt colonic inflammation and, as a result, protect against obesity-related OA. To test this idea, tamoxifen-inducible Vil1-CreERT2;Ccl2fl/fl mice (Vil-Ccl2cKO) were placed on a lean or high-fat diet. Tamoxifen was administered to conditionally delete Ccl2 from the intestinal epithelium, and OA was initiated via surgical destabilization of the medial meniscus. Three months post-injury, colon, joints, and serum were collected for molecular analysis. Flow cytometry indicated that there was a reduction in the number of macrophages and NK1.1+ NK cells within the colon of obese Vil-Ccl2cKO animals, consistent with parallel immunohistochemistry detection of reduced MCP1 levels in the colonic epithelium (Figure 1A). Serum cytokine analysis revealed decreases in circulating MCP1 and IL-1? in obese Vil-Ccl2cKO animals (Figure 1B). Finally, in DMM-injured joints, histomorphometry indicated that obese Vil-Ccl2cKO mice are protected from the accelerated OA phenotype (Figure 1C). Specifically, obese Vil-Ccl2cKO animals had an increase in both calcified and total femur cartilage area compared to diet-matched control mice (Figure 1D). In summary, using Vil-Ccl2cKO mice, we show that inhibition of colonic inflammation during the OA of obesity via deletion of Ccl2 in the intestinal epithelium, can protect against obesity associated OA. These findings suggest that approaches to reduce obesity-associated colonic inflammation may represent a novel strategy for addressing systemic and joint inflammation that leads to accelerated OA in the context of obesity.

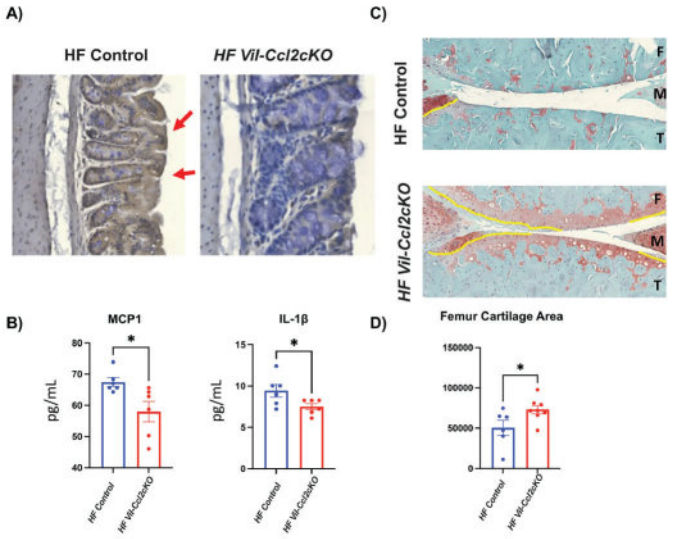

***Disclosures: David Villani**, None*

1033

Altered glucose and glutamine metabolism drives chondrocyte dysfunction in osteoarthritis *Steve Stegen[1], Frederique Cornelis[2], Ingrid Stockmans[1], Karen Moermans[1], Silvia Monteagudo[2], Rik Lories[2], Geert Carmeliet[1]. [1]Clinical and Experimental Endocrinology, KU Leuven, Belgium. [2]Skeletal Biology and Engineering Research Center, KU Leuven, Belgium

Osteoarthritis (OA) is the most common degenerative joint disease for which there is no curative treatment. OA etiology is multifactorial, but dysfunctional behavior of the articular chondrocytes is considered as a major contributor to disease onset and progression. Increasing evidence suggests that during OA the metabolic profile of articular chondrocytes is altered, but whether disturbed metabolism causes cellular dysfunction is still unknown. To investigate the metabolic changes in OA chondrocytes, we employed a combinatory approach of (i) single-cell RNA sequencing using the medial meniscus destabilization (DMM) mouse model and (ii) mass spectrometry-based metabolomics on OA patient-derived articular chondrocytes or cytokine-treated mouse chondrocytes. We found that OA chondrocytes displayed increased glycolysis and enhanced activity of the pentose phosphate pathway (PPP) and hexosamine biosynthesis pathway (HBP), whereas oxidative phosphorylation and glutathione synthesis were decreased. These metabolic alterations affected chondrocyte function at multiple levels. First, the typical hypertrophic and catabolic gene signature of OA chondrocytes was caused by stimulation of the HBP. More precisely, increased PPP-mediated glucose flux and glutamine metabolism into the HBP caused enhanced protein O-glycosylation, which resulted in the induction of genes involved in chondrocyte hypertrophy (Col10a1) and matrix degradation (Mmp13). Second, OA chondrocytes undergo ferroptosis, a type of cell death caused by oxidation of cell membrane lipids by reactive oxygen species (ROS). As a mechanism, more ROS was produced by NADPH-oxidases, mediated by increased PPP-driven NADPH generation, whereas less ROS was scavenged due to decreased glutamine-dependent glutathione synthesis. To causally link metabolic maladaptation to cellular dysfunction, we inhibited key enzymes in the PPP (by G6PDi) and glutamine metabolism (by EGCG), which fully normalized the oxidative stress phenotype and hypertrophic/catabolic gene expression, and prevented cartilage loss in the DMM model in mice.Together, our data show that dysbalanced glucose and glutamine metabolism in OA chondrocytes results in oxidative stress and protein O-glycosylation, leading to cell death and increased catabolic gene expression (Fig 1). Pharmacological inhibition of altered metabolic enzymes prevented cartilage loss in mice, suggesting that targeting chondrocyte metabolism is an appealing strategy to treat OA.

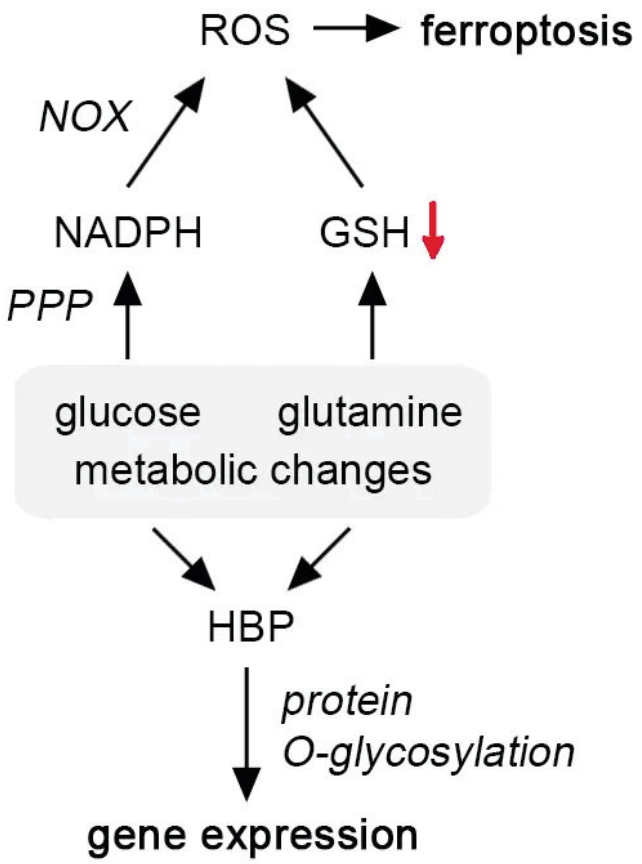

***Disclosures: Steve Stegen**, None*

1034

Functional Studies of Transcription Factor Dlx5 During Mouse Chondrogenesis and Osteoarthritis Progression *Jinnan Chen[1], Fangzhou Chen[2], Dongmei Liu[3], Tiaotiao Han[1], Huiqin Bian[1], Chen Chen[1], Xuan Wu[1], Qian Wang[1], Yaojuan Lu[3], Qiping Zheng[1]. [1]Department of Hematology and Hematological Laboratory Science, Jiangsu Key Laboratory of Medical Science and Laboratory Medicine, School of Medicine, Jiangsu University Zhenjiang, Jiangsu 212013, China, China. [2]Department of Pathology, the Affiliated People's Hospital of Jiangsu University, Zhenjiang, Jiangsu 212002, China, China. [3]Shenzhen Walgenron Bio-Pharm Co., Ltd. Shenzhen 518118, Guangdong, China, China

The transcription factor DLX5 (Distal-Less Homeobox 5) has been implicated roles in chondrocyte hypertrophy during osteoarthritis (OA) progression. We have recently reported DLX5 transactivation of the hypertrophic chondrocytes-specific Col10a1 gene expression in a mouse model of OA. Herein, we further performed the expression profiling of DLX5 in OA patients and in induced OA like cell model. The effect of DLX5 regulation of chondrocyte maturation and matrix mineralization in vitro was evaluated by Alizarin Red S, Alcian Blue, and ALP staining after ITS induction of ATDC5 cells. To gain insights about its role during endochondral ossification and OA progression, we have established a chondrocyte-specific Dlx5 knock out mouse model using the CRISPR-Cas9 and Cre-LoxP technology. Our results showed that DLX5 and COL10A1 were both significantly elevated in the damaged zone of OA patients as well as in OA-like chondrocytes after TNF-? and LPS induction. Forced expression of Dlx5 facilitated chondrocyte hypertrophy and matrix mineralization, while knock down of Dlx5 attenuated hypertrophic phenotype of ATDC5 cells. In vivo results revealed that mice with conditionally knock-out (CKO) Dlx5 in chondrocytes [Dlx5f/fCol2Cre(F/F/?)] leads to smaller body size and shortened hypertrophic zone of the ribs compared with the littermate controls Dlx5f/f (F/F). Delayed mineralization of the distal phalanges and metatarsals of the Dlx5 CKO mice was also observed after whole skeletal alcian blue-alizarin red S staining. Meanwhile, histologic analysis revealed shortened hypertrophic zones in growth plate of Dlx5 CKO mice with reduced number of trabecula bone and the inhibition of osteogenic mineralization. The DMM-induced OA mouse model was also established in Dlx5 CKO mice and their littermate controls. Relatively intact microstructure of the trabeculae with high number and connectivity of subchondral was detected in Dlx5 CKO mice with Micro-CT and Safranin O- Fast Green staining, indicating its less destruction of the knee joint. Together, our results suggest that DLX5 is an essential transcription factor for chondrocyte hypertrophy during endochondral ossification and OA progression, and may serve as a biological marker for OA diagnosis and therapeutics.

***Disclosures: Jinnan Chen**, None*

1035

Synovium and infrapatellar fat pad share common mesenchymal progenitors and undergo coordinated changes in osteoarthritis *Jun Li[1], Tao Gui[1], Lutian Yao[1], Hanli Guo[1], Yu-Lieh Lin[1], Jiawei Lu[1], Jiankang Fang[1], Michael Duffy[1], Miltiadis Zgonis[1], Robert Mauck[1], Nathaniel Dyment[1], Yejia Zhang[2], Carla Scanzello[3], Patrick Seale[4], Ling Qin[1]. [1]Department of Orthopaedic Surgery, Perelman School of Medicine, University of Pennsylvania, United States. [2]Translational Musculoskeletal Research Center, Corp. Michael J Crescenz, VA Medical Center, United States. [3]4Translational Musculoskeletal Research Center, Corp. Michael J Crescenz, VA Medical Center, United States. [4]Department of Cell and Developmental Biology, Perelman School of Medicine, University of Pennsylvania, United States

Osteoarthritis (OA) affects multiple tissues in the knee joint. Past OA research focused on articular cartilage and bone, but often overlooked surrounding soft tissues, such as synovium (Syn) and infrapatellar fat pad (IFP). In knees, IFP attaches to Syn in a seamless fashion and both tissues undergo drastic morphologic changes in OA progression. To investigate tissue heterogeneity, we performed scRNA-seq on Syn/IFP from control (n=20 mice) and DMM-treated adult mice (1 week, n=8 mice; 2 months, n=12 mice). Unsupervised clustering of 29,763 cells revealed 9 clusters, including fibroblasts, endothelial cells, mural cells, and immune cells. Further analysis on 17,097 fibroblasts identified 5 subtypes: mesenchymal progenitor cells (MPCs), synovial lining fibroblasts (SLFs), myofibroblasts (MFs), preadipocytes 1 and 2 (preAD1 and 2). MPCs, preAD1s and 2s were largely overlapped with Dpp4+, Icam1+, and F3+ progenitors previously identified in subcutaneous white adipose tissue (sWAT). Computational analysis predicted MPCs as common progenitors for SLFs and adipocytes and for a rapid induction of MFs after DMM. Immunofluorescence imaging of Dpp4-CreER Td and Prg4-CreER Td knees, in which Td labels MPCs and SLFs, respectively, revealed that Dpp4+ MPCs reside in the synovial sublining layer and give rise to Prg4+ SLFs and adipocytes during joint development and DMM or loading-induced OA. While Syn/IFP contained much more Prg4+ cells (22.0%) than Dpp4+ cells (1.7%), CFU-F colonies formed by Syn/IFP cells were mainly derived from Dpp4+ cells but not from Prg4+ cells. Sorted Dpp4+ cells proliferated much faster than Dpp4- cells in culture and had multi-lineage differentiation ability. On the contrary, Prg4+ SLFs did not contribute to adipocytes and sorted Prg4+ cells barely grew in vitro. Lineage tracing showed that both MPCs and SLFs become highly proliferative MFs (labeled by ?SMA staining or Scx-GFP expression) after DMM. Those MFs gained myofibroblast features and remained in the thickened synovium in late OA, thus contributing to synovial and fat pad fibrosis. Importantly, Dpp4+ cells were present at a similar location in human Syn/IFP. Based on the trajectory analysis of scRNA-seq and snRNA-seq datasets from healthy and OA patients, Dpp4+ cells also gave rise to Prg4+ SLFs and adipocytes in the Syn/IFP. Taken together, we demonstrate that Syn/IFP is indeed one functional tissue sharing common mesenchymal progenitors and undergoing coordinated changes in OA.

***Disclosures: Jun Li**, None*

1036

MMP13 Regulation of Perilacunar Remodeling is Cathepsin K-Dependent and Required for Lactation-Induced Osteocytic Osteolysis and Trabecular Bone Loss *MAISA MONSEFF SILVA[1], JIAMING ZHANG[2], YINBO NIU[3], SHUANG LIANG[4], Daniel Brooks[5], Mary Bouxsein[6], Francisco Jose De Paula[7], Francesca Gori[8], Roland Baron[9, 1], [2]Harvard University, [3]Key Laboratory for Space Bioscience & Biotechnology, School of Life Sciences, Northwestern Polytechnical University, China. [4]Harvard University , United States. [5]BIDMC/MGH, [6]Beth Israel Deaconess Medical Center, Harvard Medical School, United States. [7]Ribeirao Preto Medical School- USP, Brazil. [8]Harvard School of Dental Medicine, United States. [9]Harvard Medical School and School of Dental Medicine, United States

During lactation, bone resorption supplies calcium in milk via osteoclastic bone resorption and osteocytic osteolysis during perilacunar remodeling (PLR). Osteocytes (Ocy) modulate their micro-environment and respond to hormonal and mechanical cues, engaging in matrix resorption and/or deposition, altering their lacunar space. The molecular mechanisms underlying Ocy PLR regulation during lactation and the interaction between Ocy and their microenvironment are yet to be fully elucidated. We performed bulk RNA seq of highly enriched Ocy preparations from lactating and virgin mice. As anticipated, a significant upregulation of resorption-related genes was observed. Among the key genes were cathepsin K (Ctsk) and matrix metalloproteinase 13 (Mmp13). To explore the role of these two secreted enzymes in PLR, we first generated Mmp13ocy mice using the 10 kb-Dmp1-cre. BSEM revealed that cortical Ocy lacunar area (LcA) was significantly larger (p=<0.01) in Mmp13ocy mice vs control. Thus, Mmp13 maintains a positive PLR balance at steady state. In contrast, Mmp13 deletion prevented lactation-induced LcA enlargement, suggesting that in lactating mice, MMP13 enhances the osteolytic aspect of PLR. Furthermore, virgin Mmp13ocy mice

exhibited a higher trabecular (Tb) bone volume (BV/TV) than control virgin mice and did not lose bone during lactation: ?CT analysis showed that lactating Mmp13ocy mice had significantly higher BV/TV (+86.16%, p<0.001), Tb number (Tb.N) (+60,7%, p<0.001), and Tb connectivity (Conn.D) (+188,1%, p<0.001) vs control lactating mice. Because MMP13 deletion increases Ctsk expression in Ocy, we then asked whether the increase in LcA in Mmp13ocy mice was due to increased Ctsk expression. Ocy-targeted deletion of Ctsk in Mmp13ocy (DKO) prevented LcA enlargement in virgin mice, confirming a role for Ctsk in the Mmp13ocy LcA enlargement. Furthermore, DKO not only prevented the expected increase in LcA during lactation, lactation-induced Tb bone loss but also further increased BV/TV over Mmp13ocy at both steady state and in lactation. In conclusion, counter-intuitively, Mmp13 deletion triggers Ocy osteolysis and lacunar expansion and this is prevented by the deletion of Ctsk. Thus, at steady state, Mmp13 favors a positive balance in PLR, whereas during lactation its favors Ctsk-dependent Ocy osteolysis and bone loss. These results highlight the crucial contribution of Ocy-derived Mmp13 and Ctsk in PLR and skeletal homeostasis.

***Disclosures: MAISA MONSEFF SILVA**, None*

1037

Coupling of osteocytic osteolysis to functional osteoclasts during lactation *Roland Baron[1], Diana Athonvarangkul[2], John Wysolmerski[3], Zainah Salloot[4]. [1]Harvard Medical School and School of Dental Medicine, United States. [2]Yale University, United States. [3]Yale School of Mediicne, United States. [4]Harvard School of Dental Medicine, United States

Osteocytic osteolysis may contribute to bone loss in lactation. The connection between osteocytes and osteoclasts to regulate lactational bone resorption is not understood. In this study, we provide novel evidence that bone resorption in lactation is coordinated between osteocytes and osteoclasts. In particular, loss of functional osteoclasts prevents osteocytic osteolysis during lactation.We initially hypothesized that inhibition of osteoclast activity would lead to a compensatory increase in osteocytic osteolysis during lactation. We treated 10 week-old lactating CD1 mice with recombinant osteoprotegerin (OPG, 10mg/kg) to block RANKL signaling, zoledronic acid (ZA,100 ug/kg) to inhibit osteoclasts or vehicle, from delivery through mid-lactation (day 12). Eliminating osteoclast function with either OPG or ZA prevented lactational trabecular BMD loss measured by microCT. The average osteocyte lacunar area, measured by backscatter electron microscopy, did not significantly differ among the groups. However, OPG and ZA tended to prevent the shift to large osteocyte lacunae (30-60 uM) that was observed in the lactation group, reflecting loss of osteocytic osteolysis and the presence of osteocyte heterogeneity. Lactational increases in gene expression of the key resorptive enzymes tartrate-resistant acid phosphatase, cathepsin K, and matrix metallopeptidase 13 were not observed in osteocyte-enriched RNA samples from OPG and ZA groups, suggesting that loss of active osteoclasts interferes with the phenotypic switch in osteocytes.Since the above results suggested that osteocytic osteolysis depends on RANKL signaling, we asked whether osteocytes might express RANK during lactation. We crossed the mT/mG reporter mouse with the RANK-Cre mouse to identify cells expressing RANK by their switch from red to green fluorescence. All osteocytes remained red, which indicated that RANK is not expressed on osteocytes. Therefore, the inhibition of osteocytic osteolysis by OPG must be mediated indirectly by osteoclasts or another RANK-expressing cell.Here we showed that osteoclastic resorption is coordinated with osteocytic osteolysis in lactation. Our working theory is osteocytes are stimulated by RANKL-dependent coupling factor(s) from active osteoclasts to induce a bone resorption gene program. Identifying clastokines that couple the activity of osteoclasts and osteocytes could be important for pathophysiology outside of lactation and may lead to therapeutic targets for pathologic bone turnover.

***Disclosures: Roland Baron**, None*

1038

Osteoclast-Independent Osteocyte Morphology Defects in Mice Bearing an Osteogenesis Imperfecta-Causing SP7 R316C Mutation *Jialiang S. Wang[1], Katelyn Strauss[1], Michael Bruce[1], Daniel J. Brooks[2], Tatsuya Kobayashi[1], Mary L. Bouxsein[2], Marc N. Wein[1]. [1]Massachusetts General Hospital, Harvard Medical School, United States. [2]Massachusetts General Hospital, Beth Israel Deaconess Medical Center, Harvard Medical School, United States

BackgroundSP7 is a transcription factor with a well-known role in osteoblast differentiation. Recent studies suggest a novel role of SP7 in osteocyte development. Rare SP7 mutations have been reported to cause recessive and dominant osteogenesis imperfecta. Homozygous SP7 R316C patients were characterized by short stature, recurrent fractures and high cortical porosity. In this abstract, mice with the osteogenesis imperfecta-causing SP7 R316C mutation show osteocyte dendrite defects and increased intracortical bone resorption. However, at present we do not understand the relationship between osteocyte morphology defects and intracortical osteoclast activity in this model. Methods/ResultsWe generated SP7R316C knock-in mice using CRISPR-Cas9 gene editing. First, skeletal analyses were performed in 8-week-old mice to recapitulate the bone development from childhood to adulthood. Compared to littermate controls, male and female mutant SP7R316C/R316C mice demonstrated significantly increased cortical porosity and reduced cortical bone mineral density. This is consistent with the phenotypes observed in R316C patients. Homozygous SP7R316C mice had osteocyte dendrite defects, increased osteocyte apoptosis, elevated Rankl expression, and increased osteoclast activity (Fig. 1A). Next, we assessed if the dendrite defect seen in SP7R316C mice is dependent on osteoclast activity by treating mice with OPG-Fc. Female mutant SP7R316C/R316C mice and their control littermates were injected once weekly with OPG-Fc or vehicle starting at 6 weeks old (four injections total). OPG-Fc treatment showed expected effects, including reduced serum CTX-1, increased trabecular bone mass, and reduced cortical porosity in both wild type and SP7R316C/R316C mice (Fig. 1B). In contrast, osteocyte dendrite defects in SP7R316C/R316C mice were not rescued by OPG-Fc treatment (Fig. 1C). Taken together, these results demonstrate that the SP7 R316C mutation leads to cortical bone loss by disrupting the osteocyte dendrite connectivity. Increased bone resorption does not cause osteocyte morphology defects in the SP7 R316C mutant mice. ConclusionsHere we report a novel mouse model of osteocyte defects due to the SP7 R316C mutation. The osteocyte defects observed in this SP7 mutant mouse model are independent of increased osteoclast activity. This model provides a valuable resource to test novel therapeutic approaches to treat osteocyte defects in addition to bone loss.

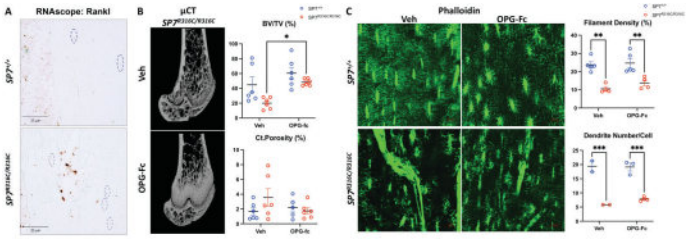

Figure 1. Osteocyte dendrite defects in $SP7^{R316C/R316C}$ mice were not rescued by OPG-Fc treatment. A. Rankl level is increased in $SP7^{R316C/R316C}$ mice compared to wild-type littermates by *in situ* hybridization (RNAscope). **B.** µCT analysis from the femur reveals increased bone mass and reduced cortical porosity in $SP7^{R316C/R316C}$ mice with OPG-Fc treatment. **C.** 10-week-old control and $SP7^{R316C/R316C}$ tibia were stained with phalloidin to visualize actin filaments within dendrites. Dendrite defects could not be rescued by OPG-Fc treatment in $SP7^{R316C/R316C}$ mice.

***Disclosures: Jialiang S. Wang**, None*

1039

Prematurely Aging PolgA Mice Exhibit Sex-specific Hallmarks of Musculoskeletal Aging *Dilara Yilmaz[1], Thurgadevi Parajasingam[1], Lorena Gregorio[1], Christian Gehre[1], Francisco Correia Marques[1], Neashan Mathavan[1], Xiao-Hua Qin[1], Esther Wehrle[1], Gisela Anna Kuhn[1], Ralph Mueller[1]. [1]ETH Zurich, Switzerland

Age-related frailty is highly associated with senile osteoporosis and has been shown to be sex specific. Emerging evidence suggests that osteocytes serve as a promising therapeutic target for mitigating age-related bone loss. The PolgD257A/D257A (PolgA) mouse model displays premature aging and develops clinically relevant hallmarks of musculoskeletal aging. However, the relevance of this model in investigating age-related osteoporosis and the underlying mechanism responsible for age-associated changes in the osteocyte network remains unclear. In this study, we used male and female PolgA mice exhibiting hallmarks of premature aging to investigate age- and sex-related changes in frailty, bone structure, and osteocyte network.Frailty scoring was performed in young (12 weeks) and adult (34 weeks) male and female PolgA mice and their age-matched wild-type littermates (WT) (n=10-16 mice/group). Bone morphometric parameters were evaluated from the right femurs of PolgA mice (n=9-16 mice/group) and WT by micro-CT (voxel size: 10 µm). Phalloidin-Hoechst-stained osteocytes from the cortical bone of young (20 weeks) and old adults (40 weeks) PolgA and WT mice were imaged with 3D confocal microscopy and quantified with IMARIS (n=2-4 mice/group). Multiple t-test with Sidak-Bonferroni correction was used for statistical analysis.PolgA mice showed a higher frailty index (FI) with aging compared to young and age-matched WT mice at 34 weeks (males:+51%, females:+36%) (Figure 1B), followed by reduced cortical bone volume fraction (BV/TV) at 40 weeks (males:-10%, females:-9%)(Figure 1C). 3D visualization of osteocytes and dendrites demonstrated osteocyte sex-specific network disruption in PolgA mice with aging (Figure 1A). Osteocyte analysis revealed a significant reduction in dendrite length (males:-46% and females:-52%) and osteocyte area (males:-41%, females:-46%) in 40-week-old PolgA mice compared to WT and young PolgA mice (males:-45%, females:-44%; males:-61%, females:-63%) respectively(Figure 1D-E).We showed PolgA mice exhibited sex-specific hallmarks of musculoskeletal aging with increased frailty, reduced cortical BV/TV, and a disrupted osteocyte network, which was more pronounced in females than males. Since a similar age-related degeneration of the osteocyte network has been observed in humans, our results suggest that the PolgA mouse could be a valuable model to investigate the molecular mechanism responsible for age-related bone loss and senile osteoporosis.

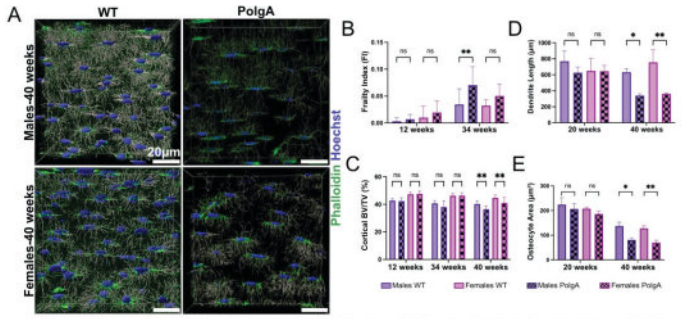

Figure 1: Age- and sex-related changes in PolgA mice: A) 3D visualization of osteocytes and their dendrites using automated filament tracing in iMARIS B) frailty index, C) cortical BV/TV, D) dendrite length, E) osteocyte area

***Disclosures: Dilara Yilmaz**, None*

1040

Conditional deletion of PTH1R in osteocytes abolishes lactation-induced alterations in canalicular pericellular space and increases bone microstructure deterioration *Xiaoyu Xu[1], Yilu Zhou[1], Rosa M Guerra[2], Yuanhang Li[1], Wonsae Lee[1], Tala Azar[1], Kira Lu[1], Liyun Wang[3], Xiaowei Liu[4]. [1]McKay Orthopaedic Research Laboratory, University of Pennsylvania, United States. [2]Center for Biomechanical Engineering Research, University of Delaware, United States. [3]University of Delaware, United States. [4]University of Pennsylvania, United States

During lactation, the female skeleton undergoes substantial loss of bone mineral by both osteoclast resorption and osteocyte (Ocy) perilacunar/canalicular remodeling (PLR). Our previous study suggested that PLR-induced alterations in the Ocy pericellular environment would amplify the mechanical and biochemical signal transduction to Ocys, in turn enhancing mechanical adaptation of maternal bone to maintain its load-bearing function (Fig A). Therefore, we hypothesized that abolishing Ocy PLR would result in greater bone loss and microstructure deterioration during lactation. In order to abolish lactation-induced PLR, we deleted PTH/PTHrP Receptor 1 in osteocytes (cKO: 10kb-Dmp1-Cre; PPRfl/fl) of C57BL6 mice and compared them with their wildtype (WT) littermates (n=4-6 in Virgin, Lactation, and Post-Weaning groups of both WT and cKO mice). Histology by Ploton silver nitrate staining indicated that 12-day lactation in WT mice resulted in 20% and 9% greater lacunar area and perimeter, respectively, which returned to baseline levels as in WT Virgin mice 14 days after weaning. In contrast, these lactation-induced changes were not found in the cKO mice (Fig B-D). Furthermore, transmission electron microscopy (TEM) images showed a 48% enlargement of the pericellular area surrounding the Ocy dendrite processes, leading to a 30% increase in canalicular area in WT Lactation vs. Virgin mice, whereas relevant increases were not found in cKO mice (Fig E-G). Unlike the recovered pericellular area in WT Post-Weaning mice, pericellular and total canalicular areas in cKO mice remained elevated after weaning. Interestingly, μCT results indicated greater lactation-induced bone loss and microstructure deterioration in cKO vs. WT mice (Figure H-K; cKO: 48% and 26% lower BV/TV and Tb. Th, and 48% higher SMI in Lactation vs. Virgin mice; WT: 30% lower Tb. Th in Lactation vs. Virgin mice). This is the first study that quantified the lactation-induced alterations in the ultrastructure of canaliculi and demonstrated active remodeling of the pericellular matrix surrounding Ocy dendrites during lactation and post-weaning. Inhibiting lactation-induced PLR may prevent the amplification of mechano-signal transduction in the Ocy network, leading to accelerated bone loss in lactating cKO mice (Fig A). Future studies will continue to elucidate critical roles of Ocy PLR in regulating the balance between mineral resorption and mechanical integrity of the maternal skeleton.

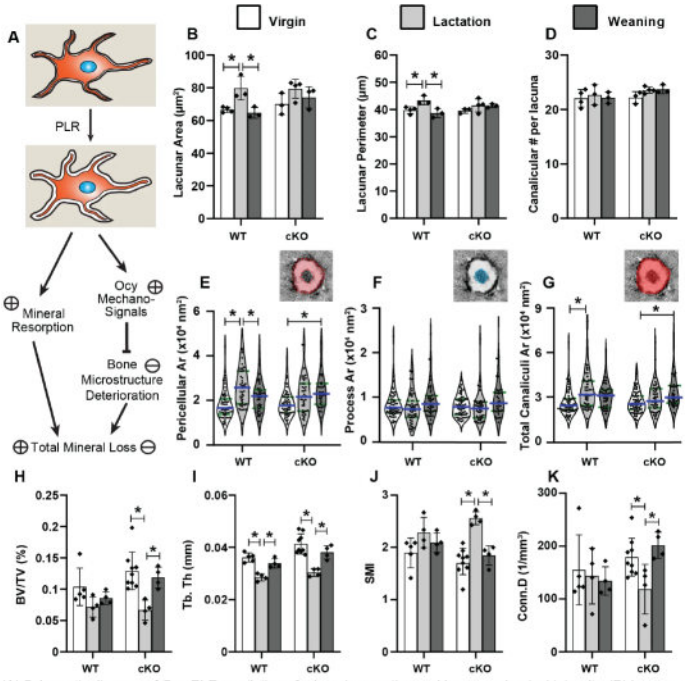

(A) Schematic diagram of Ocy-PLR regulation of mineral resorption and bone mechanical integrity. (B) Lacunar area, (C) lacunar perimeter , and (D) canaliculi number per lacuna derived from Ploton silver nitrate staining images of cKO and WT mice with different reproductive statuses. (E) Pericellular area of Ocy dendrite processes (area between the two red dashed lines), (F) process area (central area highlighted in blue), and (G) total canaliculi area (the area highlighted in red) derived from TEM images of tibial cortical bone of cKO and WT mice with different reproductive statuses. (H-K) L4 trabecular bone morphometry by μCT (7.5 μm) in cKO and WT Virgin, Lactation, and Post-weaning mice. Asterisk (*) indicates a significant difference between reproductive statuses (Virgin, Lactation, and Post-weaning) of cKO or WT mice by one-way ANOVA ($p<0.05$).

***Disclosures: Xiaoyu Xu**, None*

Disclosures:

SAT-002

Low Cortical Volumetric BMD Predicts Complications in Men Undergoing Spine Fusion Surgery *Emma Billings[1], Joe Raphael[1], Alex Dash[1], Han Jo Kim[1], Matthew Cunningham[1], Darren Lebl[1], Donald McMahon[2], Jeri Nieves[3], Emily Stein[1]. [1]Hospital for Special Surgery , United States. [2]Columbia University College of Physicians and Surgeons, . [3]Columbia University and Hospital for Special Surgery,

Spine fusion surgery is one of the most common orthopedic procedures, with nearly 500,000 performed annually in the United States alone. Complications occur in up to one third of cases, increasing morbidity and health care costs. Many complications relate to poor bone quality, however; identification of high-risk patients remains a challenge. Men are infrequently referred for pre-operative skeletal evaluation, and no studies have focused on bone health in men having fusion. The FUSED SPINE (FUsion and Skeletal Evaluation in patients unDergoing SPINE surgery) ongoing prospective cohort study investigates relationships between pre-operative bone health and post-operative outcomes. This substudy focused on bone health and rates of skeletal complications in men. We hypothesized that men with microarchitectural abnormalities would have higher rates of complications. Pre-operative skeletal imaging included areal BMD by DXA, volumetric BMD (vBMD) and microarchitecture of the distal radius and tibia by high resolution peripheral QCT (HRpQCT, Xtreme CT2). Cox hazard models were used to identify the best predictors of post-operative complications among clinical indices (age, alcohol, smoking, BMI, # of vertebrae involved in surgery) and imaging measurements. Of 54 men enrolled mean age was 61 (range 25-82 yrs), and BMI 29 kg/m2. Mean Z-Scores by DXA were within or above normal at the spine (1.9), total hip (0.1), femoral neck (0.1), and 1/3 radius (0.1). Six men (11%) reported a history of atraumatic fracture. None reported use of medications for osteoporosis. Median post-operative follow-up was 12 months. Twenty-one men (39%) sustained skeletal complications. Cortical vBMD at the tibia predicted time to skeletal complication (HR 0.72, 95% CI 0.53-0.98; Figure). No other HRpQCT feature independently predicted risk of complications, nor did aBMD by DXA at any site. Our data suggests that despite normal appearing DXA, older men undergoing spinal fusion surgery have high rates of complications, and cortical deficits are associated with complication risk. As cortical bone is the site of insertion of surgical hardware, men with low cortical vBMD may lack adequate bone to provide early stability to hardware necessary for de novo bone formation and successful fusion to occur. Additional studies are needed to better elucidate the specific risk factors for complications and therapeutic strategies to improve bone quality in men.

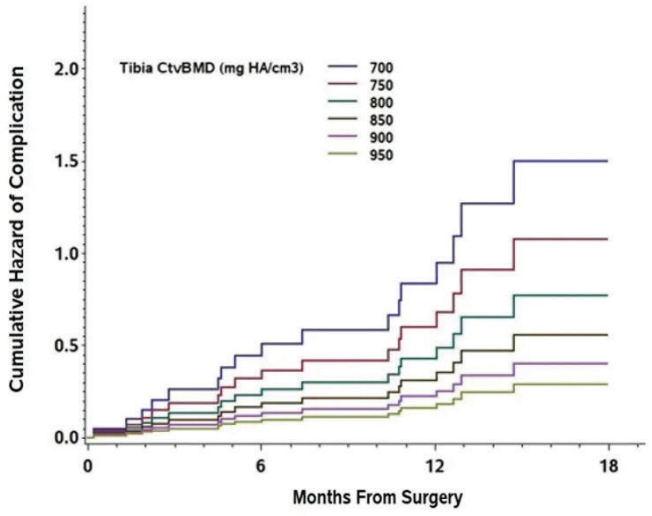

***Disclosures: Emma Billings**, None*

SAT-003

Changes of intact and C-terminal FGF23 levels in patients with primary hemochromatosis following iron depletive treatment: a pilot study *Luciano Colangelo[1], Sergio Terracina[2], Chiara Sonato[3], Viviana De Martino[4], Giancarlo Ferrazza[5], Enrico Panzini[5], Luciano Nieddu[6], Cristiana Cipriani[4], Stefania Trasarti[7], Jessica Pepe[4], Salvatore Minisola[5]. [1]Department of Clinical, Internal, Anesthesiologic and Cardiovascular Sciences, "Sapienza" University of Rome, Italy. [2]"Sapienza" University of Rome, Italy. [3]"Sapienza" University of Rome, Italy. [4]Department of Clinical, Internal, Anesthesiologic and Cardiovascular Sciences, "Sapienza" University of Rome, Italy. [5]Department of Immunohaematology and Transfusion Medicine, Sapienza University of Rome, Policlinico Umberto I, Italy. [6]Faculty of Economics, UNINT University, Italy. [7]Department of Translational and Precision Medicine, "Sapienza" University of Rome, Italy

Background: Fibroblast growth factor 23 (FGF23) has a crucial role in phosphate homeostasis. However, other factors play a role in the regulation of this hormone (e.g. anemia, inflammation, and iron status), even though the underlying mechanisms are not completely understood.Aim: To determine the behavior of FGF23 levels in a clinical condition of iron overload, i.e., hereditary hemochromatosis, following iron depletive treatment.Methods: We enrolled 26 consecutive patients with genetically confirmed hereditary hemochromatosis (HE), without organ damage (mean years +/-SD: 43.80+/-10.40) on maintenance therapy with phlebotomy every five months. They were evaluated at baseline and seven days after iron depletive treatment. Nineteen blood donors (mean age: 42.40+/-12.80) were also recruited as a control group (C). FGF23 was evaluated by both intact (DiaSorin, Stillwater, MN, USA) and C-terminal (Biomedica GmbH kit) assays.Results: We found no differences in mean values of intact FGF23 levels between the two groups neither at baseline (HE0: iFGF23 54.3+/-14.4 pg/mL vs C0: iFGF23 52.8+/-17.6 pg/mL) nor 7 days after phlebotomy (HE7: iFGF23 54.7+/-15.5 pg/mL vs C7: iFGF23 53.2+/-15.9 pg/mL). Mean basal C-terminal values were 7.4+/-3.0 pg/mL in HE vs 9.5+/-6.7 pg/mL in C. After 7 days, mean values were: HE 9.0+/-6.7 pg/mL NS vs basal values; C: 13.8+/-8.4 pg/mL, ($p < 0.014$ vs basal values). The ratio of Intact/C-terminal FGF23 was significantly reduced at 7 days in C (8.2+/-5.8 vs 5.3+/-3.7, $p < 0.017$) but unchanged in HE (8.7+/-5.3 vs 8.7+/-4.8) There we no changes in mean values of serum phosphate at 7 days in respect to basal values.Conclusion: Our data suggest that in normal subjects preservation of phosphate homeostasis is maintained by increased cleavage of intact FGF23. Other mechanisms seem to be responsible in patients with primary HE on long-term iron depletive treatment. Alternatively, an earlier peak of C-terminal FGF23 was not captured at 7 days post-phlebectomy.

***Disclosures: Luciano Colangelo**, None*

SAT-004

The Use of Adjusted Calcium in Alberta: A Population-Based Study *Noémie Desgagnés[1], James A. King[2], Gregory A. Kline[3], Isolde Seiden-Long[4], Alexander A. Leung[5, 1] Department of Medicine, University of Calgary, Calgary, Alberta, Canada. , Canada. [2]Data and Research Services , Alberta Strategy for Patient Oriented Research Provincial Research Data Services, Alberta Health Services, Canada. [3]Division of Endocrinology and Metabolism, Department of Medicine, University of Calgary, Calgary, Alberta, Canada. , Canada. [4]Alberta Precision Laboratories and Department of Pathology and Laboratory Medicine, University of Calgary Foothills Medical Centre, Calgary, Alberta Canada, Canada. [5]Division of Endocrinology and Metabolism, Department of Medicine, University of Calgary, Calgary, Alberta, Canada. ,Department of Community Health Sciences, University of Calgary, Calgary, AB, Canada. , Canada

Background: Adjustment of total calcium is commonly performed in clinical settings in order to account for states of altered protein-binding. However, studies have shown that albumin-adjusted calcium correlates poorly with ionized calcium, and yet remains a common practice. Therefore, we aimed to describe the epidemiology of calcium measurements in the province of Alberta by evaluating the correlation between adjusted calcium and total calcium against contemporaneously measured ionized calcium as a reference standard.Methods: We assembled a population-based cohort of all adults who were tested for serum total calcium and ionized calcium within a 24-hour interval in Alberta between January 1, 2013, to October 31, 2019. When available, we extracted data for serum albumin, serum creatinine, and pH, as these variables may be incorporated into calcium adjustment formulas. We then analyzed the correlation between total calcium and adjusted calcium using the Payne (total calcium (mg/100mL) - albumin (g/100mL) + 4), Payne simplified (total calcium (mmol/L) + 0.02 [40 - albumin (g/L)]), and six other formulas against ionized calcium. Overall agreement for each pair of comparisons was assessed with correlation coefficients and linear regression methods. Furthermore, we determined the frequency of serum total calcium, ionized calcium, and albumin that were measured within 24 hours to estimate ordering pattern of serum calcium. Results: A total of 74 971 patients had total calcium and ionized calcium sampled within 24 hours, among whom 52 469 individuals also had a coinciding serum albumin measurement. Unadjusted total calcium correlated modestly with ionized calcium ($R2=51.1\%$) as well as all correction formulas ($R2=40.2$-$66.\%$). The simplified Payne formula, which is the most used method in clinical practice, performed similarly to total calcium ($R2=50.9\%$), while the original Payne formula had a weaker correlation ($R2=44.8\%$) (see Table). In the same study period, we identified 7,356,939 tests for total calcium amongst which the majority (56.5 %, N=4,156,248) also had an albumin result within 24-hour interval.Conclusion: Most total calcium tests were ordered within 24-hours of a serum albumin suggesting that albumin-adjusted calcium is still commonly used in clinical practice, however, our preliminary data showed that total calcium correlates similarly to most adjustment formulas with ionized calcium, including the commonly used simplified Payne formula.

Table. Correlation between ionized calcium and other adjusted calcium formulas

Comparison	Formulas	First per patient	
		N	R^2 (95% CI)
Total calcium		74 971	51.1% (50.6, 51.5)*
Payne	total calcium (mg/100mL)[a] – albumin (g/100mL)[b] + 4	52 469	44.8% (44.2, 45.3)*
Simplified	total calcium (mmol/L) + 0.02 [40 – albumin (g/L)]	52 469	50.9% (50.3, 51.4)*
Orrell	total calcium (mmol/L) +0.0177 [34 – albumin (g/L)]	52 469	53.0% (52.5, 53.5)*
Berry	total calcium (mmol/L) +0.0225 [46 – albumin (g/L)]	52 469	48.0% (47.5, 48.5)*
Thode	total calcium (mmol/L) x [2.7 / (1.7 + (albumin (g/L) / 42 (g/L)]	52 469	48.5% (47.9, 49.0)*
James	total Ca (mmol/L) +0.012 [39.9 – albumin (g/L)]	52 469	56.1% (55.6, 56.6)*
Antonio (A)	0.815 x total calcium$^{0.5}$ (mmol/L)	74 971	49.0% (48.6, 49.5)*
Antonio (B)	0.826 x total calcium$^{0.5}$ (mmol/L) – 0.023 x renal function (RF) where RF is: • normal function (eGFR > 60 ml/min/1.73m^2) = 0 • moderate dysfunction (eGFR 30-59ml/min/1.73m^2) = 1 • severe dysfunction (eGFR<30 ml/min/1.73m^2) = 2	8768	66.4% (65.4, 67.3)*
Antonio (C)	0.813 x total calcium$^{0.5}$(mmol/L) – 0.006 x Alb$^{0.75}$ (g/L) + 0.079	52 469	54.0% (53.5, 54.5)*
Pekar	adjusted calcium (mmol/L) = 2.567 – 2.045e -3[albumin (g/L)] – 5.601e - 4 [creatinine (mg/L)] +0.4493[total calcium (mmol/L)] – 0.307[pH]	46 824	40.2% (39.6, 40.8)*

*p<0.001; [a]mg/100mg x 0.25 = mmol/L; [b]g/100 ml x 10 = g/L

***Disclosures: Noémie Desgagnés**, None*

SAT-006

See Friday Plenary Number FRI-006

SAT-007

Automated Segmentation Scheme to Evaluate CKD Patient Bone HR-pQCT images using a Trained Deep Learning Model *YoungJun Lee[1], Minwoo Park[2], Sangjun Park[3], Stuart Warden[4], RACHEL SUROWIEC[5]. [1]Purdue University, [2]Department of Laboratory Medicine, St. Vincen'ts Hospital, The Catholic University of Korea, Republic of Korea, [3]Department of Radiation Therapy, Samsung Medical Center, The Sungkyunkwan University of Korea, Republic of Korea, [4]Indiana University School of Health & Human Sciences, United States, [5]Indiana University Purdue University,

Chronic kidney disease (CKD) predominately affects cortical bone resulting in trabecularization of the endocortical surface and cortical porosity development. High-resolution peripheral quantitative computed tomography (HR-pQCT) is a noninvasive imaging modality that can assess bone microarchitecture, making it particularly attractive in CKD. However, CKD's hallmark bone phenotype complicates available segmentation methods required for accurate and reproducible separation of trabecular and cortical bone. Thus, we present a deep-learning model trained with normal volunteers to evaluate skeletal abnormalities associated with CKD via HR-pQCT. HR-pQCT (XtremeCT II, SCANCO) volumes of distal and diaphyseal cortices (radius and tibia) from 3 healthy volunteers (F, 52 +/- 0.70 yrs) and one CKD patient (F, 39 yrs) were used for training and testing, respectively. Ground truth masks were segmented and produced using 3D slicer and computed using Google-Colab. The model was trained by U-Net architecture and tested for CKD patients. For evaluation metrics, we utilized the dice similarity coefficient and dice loss to compare and assess the bone density of healthy volunteers vs. CKD. The training sets for the four deep learning models -distal and diaphyseal radial and tibial cortices - had dice loss values of 0.0689, 0.0254, 0.0738, and 0.0426, respectively; thus, all models were used for the binary cross-entropy loss function, of which it took 5 to 20 minutes to train with 504 HR-pQCT images for 50 and 200 cycles, and the model inference for 169 test set images took an average of 3 and 5 seconds, respectively. Test set (CKD) model performance was excellent for dice similarity coefficients- 0.8419, 0.9652, 0.8701, and 0.9630, respectively and had low dice loss values- 0.1290, 0.0726, 0.0840, and 0.0652. Overall, the diaphyseal cortical models (radius, tibia) required lower iterations and outperformed distal cortical models. Finally, several results from the trained models visually outperformed the ground truth masks and did not overestimate the manually segmented masks.Findings indicate automated segmentation of CKD patient bone using the presented deep learning approach could improve the precision and reproducibility of HR-pQCT outcomes and could be particularly valuable for application in diseases marked by severe microarchitectural changes to the cortices and trabecularization of endosteal surfaces. Ongoing work will improve distal cortices models through varying hyperparameters and apply the model to scans from CKD patients across stages (1-5).

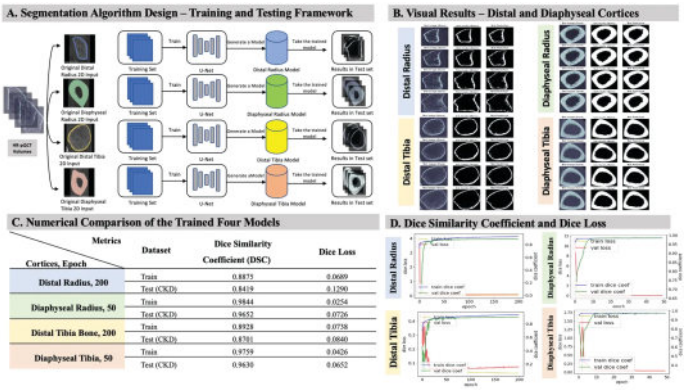

Cortices, Epoch	Dataset	Dice Similarity Coefficient (DSC)	Dice Loss
Distal Radius, 200	Train	0.8875	0.0689
	Test (CKD)	0.8419	0.1290
Diaphyseal Radius, 50	Train	0.9844	0.0254
	Test (CKD)	0.9652	0.0726
Distal Tibia Bone, 200	Train	0.8928	0.0738
	Test (CKD)	0.8701	0.0840
Diaphyseal Tibia, 50	Train	0.9759	0.0426
	Test (CKD)	0.9630	0.0652

A. Each cortical bones' deep learning model – distal and diaphyseal radius & tibia – was trained based on U-Net architecture 50 and 200 iterations with 3 normal volunteers and then tested with 1 CKD patient, respectively. All ground-truth masks in the training sets were manually segmented by a specialized medical researcher. Each result produced by each model was compared with evaluation metrics. B. Representative results – orderly and evenly extracted from the upper to the lower - of CKD patient tested by using the trained deep learning. The first column is the HR-pQCT image from the CKD patient, the middle column is the ground truth mask using the 3D slicer segmentation tool, and the third column is the predicted mask generated by our trained deep learning model. C. Dice similarity coefficient and dice loss values from our four models and (D) corresponding plots. All reported low values of the dice loss result from the Binary CrossEntropy loss function. Values of dice similarity vary depending on hyperparameters such as epoch, optimizer, batch size, etc. Although data is presented on a small sample, the diagnostic performance of this algorithm was high. Overall, the diaphyseal cortices models (radius and tibia) perform very well, with model inference scores of 0.9652 and 0.9630, respectively, and required a low epoch (50).

***Disclosures: YoungJun Lee**, None*

SAT-008

Difference of fat compositions in lumbar vertebral bone marrow according to age and relation to bone mineral density *Yuji Kasukawa[1], Michio Hongo[1], Koji Nozaka[1], Hiroyuki Tsuchie[1], Daisuke Kudo[1], Hayato Kinoshita[1], Ryota Kimura[1], Yuichi Ono[1], Kento Okamoto[1], Naohisa Miyakoshi[1]. [1]Akita University Graduate School of Medicine, Japan

Purpose: The proton density fat fraction (PDFF) by the Iterative Decomposition of water and fat with Echo Asymmetry and Least-squares estimation-iron quantification (IDEAL-IQ) method of magnetic resonance imaging (MRI) can quantitatively measure the amount of fat in the vertebral body. Although intravertebral fatty change may be a risk factor for fracture, it has not been investigated whether the PDFF in lumbar vertebrae varies with age or is related to bone mineral density (BMD). In this study, we investigated the relationship between (1) age-related differences in PDFF in lumbar vertebrae and (2) BMD and bone metabolic markers.Methods: (1) Age difference in PDFF: Thirty patients (18 males and 12 females), aged 14 to 87 years (median 63 years), whose PDFF was measured in the lumbar spine by the sagittal images of IDEAL-IQ method of MRI were included in this study. We compared PDFF in the trabecular bone region of the L4 vertebral body between 62 years of age or younger and 64 years of age or older, divided by a median age of 63 years. (2) Association of PDFF with BMD and bone metabolic markers: Forty-six women aged 60 years or older with PDFF measured on lumbar spine with MRI sagittal images, and measured BMD as well as bone metabolic markers within six months before and after MRI imaging were included. Intra-vertebral PDFF was evaluated by the mean value of intra-vertebral PDFF at L1 or L3 to L5 (LS PDFF or L3-5 PDFF). BMD of lumbar spine and femur were measured by dual energy x-ray absorptiometry, and bone metabolism markers were measured by serum propeptide of type I procollagen (P1NP) and tartrate-resistant acid phosphatase-5b (TRACP-5b). The association with PDFF and BMD or bone metabolic markers were evaluated by Pearson correlation coefficient.Results: (1) Intra-vertebral L4 PDFF (%) was significantly higher in patients aged 64 years or older at 62.1 than in those aged 62 years or younger at 53.6 ($p < 0.05$). Both LS PDFF and L3-5 PDFF were not significantly correlated with BMD of lumbar spine and femur, nor were serum P1NP and TRACP-5b.Conclusion: Fat mass measured with PDFF in the vertebral body of L4 increased significantly with increasing age, but there was no significant association between PDFF of lumbar spine and BMD of lumbar spine or femur in women over 60 years of age, nor with bone metabolism markers.

***Disclosures: Yuji Kasukawa**, None*

SAT-009

See Friday Plenary Number FRI-009

SAT-010

Comparative effectiveness of therapeutic interventions for pregnancy and lactation-associated osteoporosis: a systematic review and meta-analysis *PANAGIOTIS ANAGNOSTIS[1], KALLIOPI Lampropoulou-Adamidou[2], JULIA BOSDOU[1], GEORGE TROVAS[2], EFSTATHIOS CHRONOPOULOS[2], DIMITRIOS GOULIS[1], SYMEON TOURNIS[2]. [1]Unit of Reproductive Endocrinology, 1st Department of Obstetrics and Gynecology, Medical School, Aristotle University of Thessaloniki, Greece, [2]Laboratory for the Research of Musculoskeletal System "Th. Garofalidis", School of Medicine, National and Kapodistrian University of Athens, KAT General Hospital, Athens, , Greece

Objective: Pregnancy and lactation-associated osteoporosis (PLO) is a rare disease, which significantly affects quality of life. However, the optimal management of this entity has not yet been designated. The aim of this study was to systematically investigate and meta-analyze the best available evidence regarding the effect of different therapeutic interventions on bone mineral density (BMD) in these patients.Methods: A comprehensive search was conducted in PubMed and Scopus databases up to December 20th, 2022. Data were expressed as weighted mean difference (WMD) with 95% confidence intervals (CI). The I2 index was employed for heterogeneity.Results: Initial search provided 5503 results after excluding duplicates, 65 of which were included in the qualitative analysis (40 case-reports, 17 case-series and eight cohort studies), yielding a total of number of 454 women with PLO (follow-up time range: 6-264 months; age range: 19-42 years). The vast majority of fractures (89.2%) occurred during lactation and involved the thoracolumbar spine (number range: 1-12). Non-vertebral fractures were reported in 17 patients (3%).Calcium plus vitamin D (CaD) increased lumbar spine (LS) BMD by 2-7.5%, 9.6%, 11-12.2% and 41.8% at 12, 18, 24 and 36 months, respectively (FN BMD increase: 6.1% at 18 m). Bisphosphonates increased LS BMD by 5-36.3%, 10.2-171.9% and 20-38.9% at 12, 24 and 36 months, respectively, and FN BMD by 3.4-71.6%, 0.7-18% and 3.3% at 12, 24 and 36 months, respectively. Teriparatide increased LS BMD by 8-24.4%, 7.4-36%, 24.1-32.9% and 23.4-30.3% at 12, 18, 24 and 36 months, respectively, and FN BMD by 3.9-12.6%, 3.7-13.8%, 8.4-18.6% and 10-16.3% at 12, 18, 24 and 36 months, respectively. Denosumab increased LS BMD by 14-21.2% and 32%, and FN BMD by 0-5.6% and 13%, at 12 and 18 months, respectively New fractures occurred in 66 (14.5%) patients (six in subsequent pregnancies).Meta-analysis was performed only for two retrospective studies with teriparatide, which also included a control group. Teriparatide induced a greater increase in both LS and FN BMD, compared with CaD [11.45% (95% CI 4.89-18.01%, p=0.001; I2 50.9%) and 5.43% (95% CI 1.24-9.62%, p=0.011; I2 8.1%), respectively].Conclusions: Despite the high heterogeneity among studies, pharmaceutical intervention, mainly with teriparatide, exerts a more beneficial effect on BMD than CaD in women with PLO.

***Disclosures: PANAGIOTIS ANAGNOSTIS**, None*

SAT-011

See Friday Plenary Number FRI-011

SAT-012

See Friday Plenary Number FRI-012

SAT-013

Mitigation of proximal junctional kyphosis with post to preoperative vertebral loading comparison using biomechanical analysis *Fatemeh Alavi[1], Chistopher Nielsen[1], Stephen Lewis[1], Raja Rampersaud[1], Angela Cheung[2]. [1]University Health Network (UHN), Canada. [2]University Health Network-University of Toronto, Canada

Proximal junctional kyphosis (PJK) remains one of the most common mechanical complications of adult spinal deformity (ASD) surgery. Interventions proposed to limit the rate of PJK include tethering, cementing upper instrumented vertebra (UIV) and/or UIV +1, as well as changing sagittal alignment parameters, which are still debated in ASD. We hypothesized that excessive post- to preoperative vertebral loading at proximal junction is associated with PJK development. In this retrospective study, eighteen consecutive patients (7 PJK and 11 non-PJK) with scoliosis who underwent fusion surgery from T10 to the sacrum were included. Individualized musculoskeletal models were created from pre and immediate post-operative EOS images. Then, vertebral loading including shear and compressive forces were calculated. Finally, pre and postoperative vertebral loading at UIV and UIV+1 were compared. To consider the influence of bone mineral density on PJK development, finite element (FE) analysis under the postoperative loading was performed to identify fracture location for PJK patients. In this study, we define shear difference as the difference between shear forces on the bottom and top surfaces of UIV or UIV+1. The difference in bone mass index and the average of post to preoperative compressive loading ratio between PJK and non-PJK groups were not significant. However, 85% of PJK patients experience more postoperative anterior-posterior shear loading at UIV+1 or UIV compared to their preoperative alignments (|ratio_(Post-Pre) |>1) and the ratios for 63% of non-PJK patients are less than 1. While, on average postoperative shear difference at UIV or UIV+1 for PJK group is 96 N more than preoperative shear difference, this difference for non-PJK patients with (|ratio|>1) is 31.3 N and for non-PJK patients with (|ratio|<1) is -92.9 N. The results illustrate the effect of excessive postoperative shear loading on PJK development. As shown in figure 1, we found a good agreement between FE-based predicted and actual postoperative fracture locations. Post to preoperative comparison of vertebral loading at UIV and/or UIV+1 is introduced as an effective measure to identify the risk of PJK development. Utilizing a developed framework to calculate vertebral loading based on pre and postoperative EOS images, provides the opportunity to select individualized postoperative targets to design an alignment with vertebral loading less than preoperative one and elucidates the way to mitigate PJK.

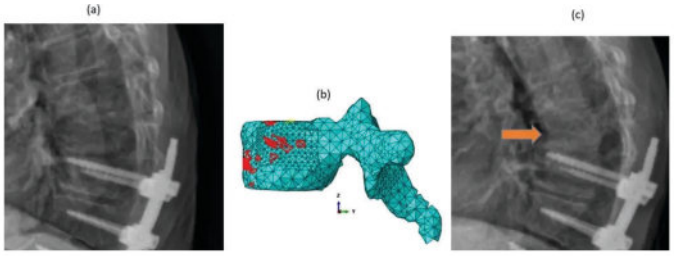

***Disclosures: Fatemeh Alavi**, None*

SAT-014

Differential Effects of Diabetes and Sodium-Glucose Co-Transporter 2 Inhibitors on Skeletal Microstructure *Sanchita Agarwal[1], Keity Okazaki[2], Ananya Kondapalli[1], Carmen Germosen[1], Ivelisse Colon[1], Nayoung Kil[1], Isabella Rosillo[1], Mariana Bucovsky[1], Marcella Walker[1]. [1]Division of Endocrinology, Department of Medicine, Columbia University, United States. [2]Department of Medicine, Columbia University Irving Medical Center, New York Presbyterian, United States

Type 2 diabetes (T2DM) is characterized by a 3-fold increased risk of fracture. The pathophysiology of skeletal fragility is unclear. Areal bone mineral density (aBMD) by DXA is normal or elevated in T2DM. Sodium-glucose co-transporter 2 (SGLT2) inhibitors may further increase fracture risk. We studied bone health in adults >= age 65 from a multi-ethnic population-based study in New York City using DXA, High Resolution peripheral Quantitative Computed Tomography (HRpQCT), and Trabecular Bone Score (TBS) in 565 women (mean age 77+/-6 yrs; 31% Black, 26% White, 42% mixed race; 55% Hispanic). Compared to non-diabetics, women with T2DM (n=175) were more likely to be mixed race, Hispanic, immigrants, and have lower education and income. Compared to non-diabetics, women with T2DM had lower alcohol use, menopause age and physical activity, had higher BMI, and were less likely to use proton pump inhibitors. All models were adjusted for covariates. T-scores by DXA were higher at all sites (all p<0.05) in T2DM, while TBS did not differ. Using HRpQCT, T2DM had higher trabecular (Tb) density and microstructure with 6% higher failure load (FL; all p<0.05) at the radius. At the distal tibia, cortical (Ct) density was 2% lower and porosity was 10% higher in T2DM, but more favorable Tb indices led to 5% higher FL. Using individual trabecula segmentation (ITS), T2DM had 6% more Tb plates and 7% more rods at the radius only. Higher glycosylated hemoglobin (9%) was not associated with worse microstructure. Among T2DM, aBMD at the hip, femoral neck, and 1/3-radius was 7%, 6% and 5% lower respectively in those with (n=72) versus those without fractures (all p<0.05). TBS was 4% lower (p=0.04) in the fracture group. By HRpQCT, T2DM with fractures had 8% lower total and 4% lower Ct density, 8% lower Ct thickness, and 13% lower FL at the radius. Similar differences were seen at the tibia with lower plate, but higher rod volume (all p<0.01). SGLT2 inhibitor use (n=19) was associated with 18-34% higher Tb heterogeneity at the radius and tibia respectively and 3% lower radial rod tissue mineral density (all p<0.05). In summary, T2DM negatively affects the bone cortex. Those with T2DM and fractures have more severe cortical deficits than those without fractures. In contrast, SGLT2 inhibitors use is associated with trabecular deficits, including poor trabecular connectivity and mineralization. Further work is needed to understand the pathophysiology by which SGLT2 inhibitors may affect bone metabolism.

Table: Differences in demographics, DXA, TBS, and HR-pQCT in type 2 diabetes (T2DM) vs controls. Data is presented as Mean ± SD. Statistical significance tested by student's t-test or chi-square test.

Diabetes	Controls (N=390)	T2DM (N=175)	p-value	Adj p-value
Age (years)	77.0 ± 6.1	76.3 ± 6.2	0.27	
Ethnicity (% Hispanic)	49.7	66.9	**<0.001**	
Race (%)			**<0.001**	
Black or African American	30	32		
White	31.8	12.6		
Mixed	36.7	54.9		
Other	1.5	0.6		
Education (%)			**<0.001**	
Grammar school	29.5	48.6		
High school	32.3	30.3		
College or advanced degree	38.2	21.1		
Household Income (%)			**<0.001**	
<$50k	78.1	94		
$50-$200k	21.1	5.4		
>$200k	0.8	0.6		
Born in USA (%)	45.9	32	**<0.01**	
Height (inches)	61.8 ± 3.1	61.4 ± 2.7	0.17	
Weight (pounds)	156.3 ± 35.3	166.3 ± 35.0	**<0.01**	
BMI (kg/m2)	28.8 ± 6.1	31.0 ± 5.8	**<0.001**	
Alcohol Intake	1.415 ± 3.399	0.618 ± 2.314	**<0.01**	
Physical Activity Score	85.5 ± 45.7	70.3 ± 46.4	**<0.001**	
Current PPI Use (%)	23.8	32	**0.03**	
DXA				
LS Total T-score	-0.9 ± 1.6	-0.2 ± 1.6	**<0.001**	**<0.001**
Femoral Neck T-score	-1.6 ± 1.1	-1.1 ± 1.1	**<0.001**	**<0.001**
Total Hip T-score	-1.3 ± 1.1	-0.8 ± 1.0	**<0.001**	**0.01**
Radius 1/3 T-score	-1.5 ± 1.4	-1.0 ± 1.4	**<0.001**	**<0.001**
TBS	1.219 ± 0.119	1.183 ± 0.124	**<0.01**	0.24
HRpQCT Radius (4% offset)				
Tot.vBMD (mgHA/ccm)	229 ± 60	245 ± 57	**<0.01**	0.05
Tb.vBMD (mgHA/ccm)	123 ± 40	132 ± 36	**0.01**	**0.02**
Tb.N (1/mm)	1.22 ± 0.25	1.29 ± 0.23	**<0.01**	**<0.01**
Tb.Th (mm)	0.226 ± 0.016	0.230 ± 0.026	0.05	0.23
Tb.Sp (mm)	0.832 ± 0.251	0.770 ± 0.174	**<0.01**	**<0.01**
Tb.1/N.SD (mm)	0.374 ± 0.232	0.324 ± 0.141	**<0.01**	**0.03**
Ct.vBMD (mgHA/ccm)	792 ± 74	803 ± 74	0.11	0.72
Ct.Po (%)	1.13 ± 0.77	1.09 ± 0.62	0.62	0.87
Ct.Th (mm)	0.76 ± 0.18	0.82 ± 0.18	**<0.001**	0.05
Failure Load (N)	2360 ± 815	2595 ± 744	**<0.01**	**0.03**
Tb plate number	7486 ± 2503	8091 ± 2354	**<0.01**	**0.02**
Tb rod number	9687 ± 2790	10340 ± 2790	**0.01**	**<0.01**
HRpQCT Tibia (7.3% offset)				
Tot.vBMD (mgHA/ccm)	230 ± 55	241 ± 51	**0.02**	0.13
Tb.vBMD (mgHA/ccm)	140 ± 41	145 ± 38	0.15	0.05
Tb.N (1/mm)	1.18 ± 0.25	1.20 ± 0.25	0.28	**0.04**
Tb.Th (mm)	0.251 ± 0.019	0.253 ± 0.021	0.19	0.75
Tb.Sp (mm)	0.87 ± 0.272	0.848 ± 0.276	0.38	0.12
Tb.1/N.SD (mm)	0.411 ± 0.31	0.383 ± 0.349	0.34	0.34
Ct.vBMD (mgHA/ccm)	779 ± 84	779 ± 91	0.97	**0.03**
Ct.Po (%)	4.06 ± 1.72	4.24 ± 1.81	0.28	**0.02**
Ct.Th (mm)	1.15 ± 0.29	1.25 ± 0.29	**<0.001**	**0.03**
Failure Load (N)	7580 ± 2185	8166 ± 1795	**<0.01**	0.05

***Disclosures: Sanchita Agarwal**, None*

SAT-015

The Role of AGEs in Bone Fragility Associated with Type 2 Diabetes and Chronic Kidney Disease *Daniel Dapaah[1], Shoutaro Arakawa[2], Mitsuru Saito[2], Thomas Willett[1]. [1]University of Waterloo, Canada. [2]Jikei University School of Medicine, Japan

Type-2 diabetes (T2D) patients often present with normal to high BMD [1]. Elevated advanced glycation end products (AGEs) in T2D and chronic kidney disease (CKD) has been proposed as an alternate reason for increased fracture risk [1,2]. AGEs are widely thought to inhibit collagen network ductility [3]. However, beyond pentosidine measured ex vivo, there have been limited comprehensive measurements of AGE accumulation in human cortical bone. Hence, in this study, a variety of AGEs (adducts and crosslinks) and the lysyl oxidase (LOX) catalyzed crosslinks were measured in human cortical bone from donors with and without a history of T2D and/or CKD. Relationships with the state of the collagen and the cortical bone fracture toughness were explored.Single edge notched bend (SENB) specimens were prepared from 57 cadaveric human femora. Twenty-two of the donors had T2D and/or CKD. Each specimen underwent a 3-point bend fracture test from which fracture toughness measures (JIc, J-int) were determined. After fracture, de-mineralized (EDTA) por-

tions were used in mass spectrometry [4] to measure AGEs (carboxy-methyl-lysine (CML), carboxy-ethyl-lysine (CEL), 5-hydro-5-methyl-4-imidazolon-2-yl-ornithine 1 (MG-H1) and pentosidine (PEN)), as well as mature and immature LOX crosslinks. The state of the collagen was measured using differential scanning calorimetry. Differences between the donor groups (+/-T2D/CKD) were tested using Student's t-test. Pearson's correlations were generated between AGEs, LOX crosslinks, collagen network properties and fracture toughness measures.AGE contents were 30 to 80% higher in the T2D/CKD group. There were negative correlations between HLNL, an immature LOX crosslink, and all AGEs as well as between collagen's enthalpy of denaturation and all AGEs (Table 1). No significant relationships were detected between the AGE contents and the fracture toughness measures. However, HLNL and enthalpy of denaturation correlated positively with J-int, a measure of the J-integral fracture toughness at the point of crack instability. These results suggest an indirect pathway by which AGEs may negatively affect fracture resistance in cortical bone through disruption of the collagen network by obstructing immature crosslinking, specifically HLNL, and reducing the energetic cost of collagen denaturation. In turn, this may lead to reduced fracture resistance because collagen molecules mechanically denature during bone fracture [5].

Table 1: Pearson's correlations between AGEs, LOX immature crosslink HLNL, enthalpy of denaturation of the collagen, and two cortical bone fracture toughness measures (ns stands for not significant).

Pearson's correlation	J_{IC}	J-int	HLNL	Enthalpy of denaturation
CML	ns	ns	r= -0.61, p<0.001	r= -0.33, p=0.011
CEL	ns	ns	r= -0.70, p<0.001	r= -0.37, p<0.01
MG-H1	ns	ns	r= -0.59, p<0.001	r= -0.34, p<0.01
Pentosidine	ns	ns	r= -0.52, p<0.001	r= -0.38, p<0.01
HLNL	ns	r= 0.31, p=0.018	-	r= 0.26, p=0.048
Enthalpy of denaturation	r= 0.38, p<0.01	r= 0.43, p<0.001	r= 0.26, p=0.048	-

***Disclosures: Daniel Dapaah**, None*

SAT-016

Alendronate Treatment in Fatigue-Damaged Bone Exacerbates Deleterious Effects of Microdamage on Bone Material Properties *Niovi Dollas[1] Lukasz Witek[2] Abigail Coffman[1] Mitchell Schaffler[1] [1]The City College of New York, United States [2]New York University, United States

PURPOSE: Bone microcracks (?Crks) and bisphosphonates are implicated in atypical femoral fractures, though the nature of their interaction is not well understood[1]. Previous canine studies found altered material properties after long-term alendronate (ALN) use[2]. However, canine cortical bone remodels extensively, so separating biomechanical effects of inhibiting remodeling (which increases material stiffness) from deleterious effects of ?Crks has proven challenging. To address this, we examined bone material property changes that occur in fatigue-damaged bone with ALN treatment in a model that has no baseline intracortical remodeling[3].METHODS: Diaphyseal sections were obtained from a previous study of osteocyte changes and ?Crks after long-term ALN in fatigued rat ulnar cortex[4]. Briefly, ?Crks were induced by fatigue loading of ulnar diaphyses of young-adult female Sprague Dawley rats (n=16). Material property changes were assessed in sections from fatigued-Baseline ulnae (FAT-B, no survival), fatigued-Survival rats treated with ALN for 4 months (FAT-S+ALN), and non-loaded control (NoFAT) ulnae. Nanoindentation was used to measure elastic modulus at varying distances around microcracks and equivalent regions in control tissues. Tissue modulus (ET) was calculated as mean for all indents/bone. Individual indent moduli (Ei) were also examined as a function of distance from a ?Crk.RESULTS: ET in FAT-B was reduced moderately (~20%) vs NoFAT-B bone (Fig 1). In FAT-B bone, modulus loss was localized around ?Crks (~5 ?m), beyond which Ei were similar to control (Fig 2). ET of FAT-S+ALN bone was further reduced, >40% vs controls, but this trend was not significant (p<0.1) due to limited number of available samples. Furthermore, modulus loss around ?Crks was greater in magnitude and extended further into the tissue than was observed for baseline ?Crks (Fig 2).DISCUSSION: The current studies suggest that ALN use in fatigue-damaged bone has a marked, negative effect on local tissue material properties-greater than acute fatigue ?Crks alone. How ALN exacerbated loss of material properties remains obscure. Potential mechanisms include additional matrix damage that occurs when the initial ?Crks cannot be remodeled, and osteocyte effects such as localized osteocyte death and regulatory changes in the remaining osteocytes near ?Crks that affect matrix integrity[5].REFERENCES: 1)Starr+ 2018; 2)Allen+ 2006; 3)Bentolila+ 1998; 4) Coffman+ 2021; 5)Kaya+ 2017

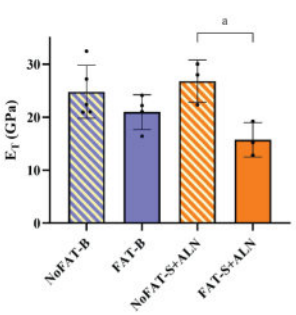

Figure 1: Tissue average moduli for experimental groups. Mean ± SD. a) p = 0.1

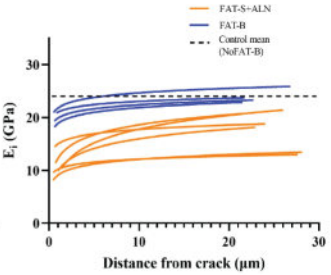

Figure 2: Log-fitted regression curves of individual indent moduli vs. distance from a µCrk. Correlation coefficients (R) for regression lines: FAT-B R: 0.5-0.6; FAT-S+ALN R: 0.5-0.8

***Disclosures: Niovi Dollas**, None*

SAT-017

A Systematic Review and Meta-Analysis of the Effect of Tea, Tea Polyphenols and Tea Extracts on Bone Outcomes in Rodent Models *Rebekah S. Feld[1] Michael D. McAlpine[1] Jenalyn L. Yumol[1] Russell J. de Souza[2] Wendy E. Ward[1] [1]Brock University, Canada [2]McMaster University, Canada

Tea and its polyphenols are potential modulators of bone metabolism through anti-inflammatory or antioxidant activity. The objective of this systematic review was to determine the effect of Camellia sinensis provided as whole tea or an extract on measures of bone health in rodent models. A systematic search of Medline and 4 other databases from inception through July 8, 2021, identified 2548 studies. Of the 37 studies that met the inclusion criteria, 73% investigated green tea or extract (27/37), 16% investigated black tea or extract (6/37), and the remaining 11% included other teas or extract including white and pu-erh. The quality of each study was analyzed using both the Systematic Review Center for Laboratory Animal Experimentation (SYRCLE) risk of bias tool and the Animal Research: Reporting of In Vivo Experiments (ARRIVE) Essential 10 and Recommended Set. A random-effects meta-analysis was conducted for intervention studies in intact rats consuming a green tea extract. Pooled standardized mean differences (SMD) and corresponding 95% confidence intervals (CI) were used for areal bone mineral density (aBMD), bone volume fraction (BV/TV) and cortical thickness (Ct.Th). Analysis was performed separately at each bone site investigated (femur, tibia) and heterogeneity ($I2 > 50$) was explored for sex-specific effects. Compared to the control group, rats consuming green tea extract demonstrated greater aBMD at the femur (n = 80 rats [60 F, 20 M], SMD = 1.00, 95% CI [0.53, 1.48], $I2 = 0\%$, $P < 0.0001$). Overall, BV/TV was greater for green tea extract compared to the control intervention (overall: n = 114 rats [80 F, 34 M], SMD = 0.64, 95% CI [0.16, 1.11], $I2 = 34\%$, $P = 0.009$; femur: n = 54 rats, SMD = 0.50, 95% CI [-0.27, 1.28], $I2 = 48\%$, $P = 0.20$; tibia: n = 60 rats, SMD = 0.76, 95% CI [0.06, 1.46], $I2 = 41\%$, $P = 0.03$) but not Ct.Th (femur: n = 34 rats [20 F, 14 M], SMD = 0.61, 95% CI [-0.81, 2.03], $I2 = 74\%$, $P = 0.40$). Only the effect of tea on Ct.Th differed by sex ($P = 0.048$). One study in males (14 M) reported no significant effect, whereas the study in females (20 F) reported a positive effect. Findings from this study suggest green tea extract may support bone mineral metabolism and bone quality.

***Disclosures: Rebekah S. Feld**, None*

SAT-018

A Comparison of Bone Surface Speckle Pattern Preparation on Digital Image Correlation Efficacy *Beatriz Garcia[2] Kevin Hoffseth[2] [2]Louisiana State University, [2]Louisiana State University, United States

Purpose: This study investigates use of bone's natural microstructure in conjunction with traditional methods of speckle pattern application for digital image correlation (DIC) to determine if it can be used to improve deformation measurement during mechanical loading. Bone has a natural random and nonuniform pattern due to its microstructures[1]. Current research using DIC as a method of determining strain in cortical bones during load relies on traditional speckling methods such as paint[2]. However, overlaying a speckle pattern on a specimen results in a loss of visualization of fracture and the influence of microstructure as it propagates through the material.Methods: DIC is commonly used to measure displacements and strain of materials under mechanical loading, with growing biomedical application. Here we implement DIC with DICe software with a random nonuniform speckle pattern applied on the surface of beams under 3-point loading while recording deformation using an Edgertronic SC2+ camera at 200 FPS to provide full-field[3] values of strain and displacement of the tested specimen(s) in the speckled zone. Beams were sectioned out of bovine cortical bone and polished at a high grit to flatten the surface and minimize surface roughness. The surface of the bone specimens was prepared using traditional speckling methods as well as histological dyes, to enhance microstructure of bone.Results: Preliminary results from testing may be seen in Figure 1, which shows a comparison between traditional speckle preparation (Fig 1 A-B) and toluidine blue dyed bone (Fig 1 C-D). The microstructure of the bone is

visible in the dyed samples, but the DIC software is unable to detect as many subsets due to low contrast between the dyed and undyed areas of the bone. This problem may be remedied by manipulating the image to enhance contrast and improve visibility of microstructural features of the bone (Fig 1 E-F).Conclusions: Dyeing of bone shows promises in DIC analysis by enhancing the natural features of bone as a speckle-like pattern. More research is needed during fundamental loading configurations, for example 3-point bending conditions, to compare the accuracy of DIC results with different speckling methods.References: [1] Rho, J.; et al., Med Eng Phys 1997, 20. [2] Grassi, L.; et al., J Biomech Eng 2014, 136 (11). DOI 10.1115/1.4028415. [3] Vaananen, S. P.; et al., J Biomech 2013, 46 (11), 1928-32. DOI 10.1016/j.jbiomech.2013.05.021.

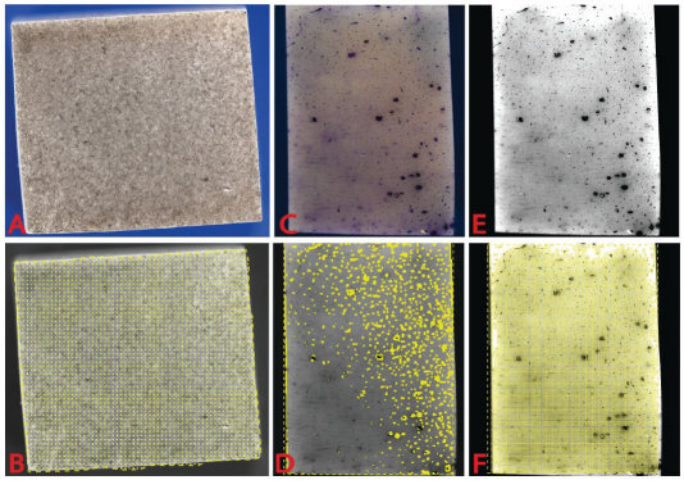

***Disclosures: Beatriz Garcia**, None*

SAT-019

Distal Radius Fracture Healing: A 12-month Follow-up Using HR-pQCT and Finite Element Analysis *Ifaz Haider[1], Phillip Spanswick[1], Erin Davison[1], Robert Korley[1], Paul Duffy[1], Ryan Martin[1], Andrew Dodd[1], Steven Boyd[1], Prism Schneider[1]. [1]University of Calgary, Canada

Introduction: Distal radius fractures (DRFs) are commonly treated non-operatively with closed reduction and cast immobilization. Insufficient or overly long immobilization durations are associated with poor outcomes, but no guidelines exist for optimal immobilization duration. Finite element (FE) modeling based on high-resolution peripheral computed tomography (HR-pQCT) may help study healing after DRF. We previously documented stiffness recovery up to six months after injury and now aim to investigate changes in FE-predicted bone stiffness over 12 months in patients with DRF.Method: This is a prospective cohort of consecutive adult patients with DRF amenable to treatment with cast immobilization. HR-pQCT scans of bilateral distal radii were taken at baseline, and the injured limb was scanned 2-,4-,6-,8-,12-,26-, and 52-weeks post-fracture (68 kVP, 1.47 mA, 61 µm nominal isotropic voxel size). An FE model of 8-noded hexahedral elements was generated via voxel conversion, with bone tissue modelled as a homogeneous solid (Modulus = 8748 MPa). To characterize stiffness, the distal surface was fully constrained while both compressive or rotational displacement was applied to the proximal end. Using the baseline uninjured distal radius as reference, we computed percent difference in stiffness of the injured limb at each timepoint; one-sided t-tests were used to determine if a non-zero percent difference in stiffness was detected.Results: A total of 57 patients (50.5 yrs +/- 16.0 yrs, 46 females) are being followed. Preliminary results from the first 20 patients (51.2 yrs +/- 16.0 yrs) to complete their 52-week scan are presented here. Compared to the uninjured limb, we observed lower compressive (-12.5%, 95%CI: -20.1 to -5.0%; p = 0.002) and torsional (-14.7%, 95%CI: -22.5 to -6.8%; p = 0.0006) stiffness at week two. Stiffness increased progressively over the 52-week follow-up period up to +16.1% for compression (95%CI: 4.9 to 27.4%; p = 0.007) and +14.2% for torsion (95%CI: 4.1 to 24.4%; p = 0.008) (Figure 1).Discussion: Fractured distal radius stiffness was low at baseline and increased progressively. At 52 weeks, the injured limb demonstrated greater stiffness than the uninjured limb. Stiffness was typically restored between 12 and 28 weeks, but substantial variability between individuals was observed; follow-up to understand the source of variability is ongoing. Assessment via HR-pQCT-based FE shows promise to personalize cast removal timing decisions.

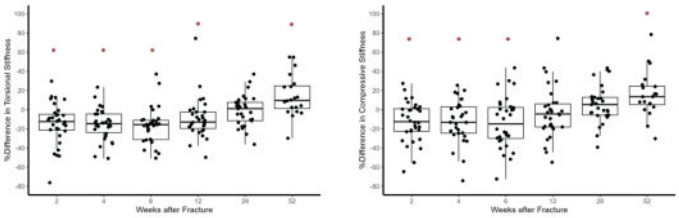

***Disclosures: Ifaz Haider**, None*

SAT-020

Region-specific Equivalent Densities for Phantomless Internal Reference Calibration *Zac Haverfield[3], Amanda Agnew[2], Lauren Hayden[3], RANDEE HUNTER[4]. [3]The Ohio State University, . [2]The Ohio State University, United States. [3]The Ohio State University, United States. [4]SKELETAL BIOLOGY RESEARCH LABORATORY, United States

Assessments of volumetric BMD (vBMD) are often quantified using phantom based (PB) or phantomless (PL) Hounsfield Unit (HU) calibration methods. While PB calibration methods are standard, phantom rods may not be available in opportunistic screening scenarios. Retrospective PL quantification of vBMD can be conducted using internal reference tissues (e.g., fat and muscle) and air for HU calibration. However, the equivalent densities (EqDen) of these media are inconsistently reported and may vary across skeletal sites. Therefore, the purpose of this study is to identify differences in EqDen of air, fat, and muscle between skeletal sites that may influence PL calibration methods.Whole-body clinical CT scans of n=100 male post-mortem human subjects (PMHS) (24-102 years of age) were analyzed. Consistent acquisition parameters of 120 or 140kVp and a reference 250mA were used for each scan that included INTableTM phantom rods. For each PMHS, skeletal site-specific volumes of interests (VOI) for air, fat, and muscle were created to obtain HU from slices associated with the left humerus, radius, femur, tibia, and calcaneus and the 2-4th lumbar vertebra regions. Using site-specific PB calibration, the EqDen of each air, fat, and muscle VOI was calculated. Kruskal-Wallis multiple comparisons tests demonstrated significant site-specific differences in air, fat, and muscle HU ($p<0.001$) and EqDen ($p<0.001$). Differences in air EqDen and HU were largely found between sites from the trunk of the body compared to the extremities. This may result from differential x-ray attenuation at denser body regions that influences calculations. Variation in fat and muscle EqDen and HU were observed across skeletal regions with the largest difference between the humerus (Hum-50) and the distal tibia (Tib-4). In addition to x-ray attenuation, these differences are also likely associated with local physiologic and mechanical loading environments.The use of PL calibration methods to quantify vBMD may provide a unique retrospective approach towards clinical assessments of bone quality. However, results from this study indicate that PL methods that use air, fat, and muscle are subject to the influence of x-ray attenuation and heterogenous fat and muscle densities. As these variations may influence resulting vBMD values, using site-specific PL calibration methods is recommended to provide more accurate assessments of bone quality and fracture risk.

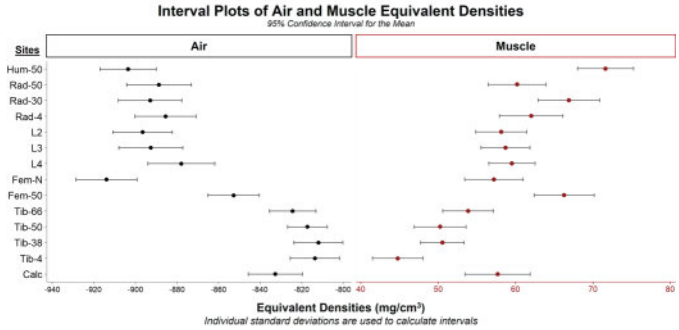

***Disclosures: Zac Haverfield**, None*

SAT-021

Effects of An In Vitro Oxidative Damage Model on the Tensile Mechanical Properties of Cortical Bone *Faezeh Iranmanesh[1], Jindra Tupy[2], John Montesano[2], THOMAS WILLETT[3]. [1]University of waterloo, . [2]University of Waterloo, Canada. [3],

Bone is a complex tissue composed of mineral and organic components [1][2]. Collagen, the major bone protein, contributes to bone yield and post-yield mechanical properties [3]-[7]. Aging and disease can affect bone collagen structure and function [6]. Oxidative stress results from excessive reactive oxygen species produced by the body [8], and is a

major contributor to numerous diseases and age-related disorders [9]. It can damage collagen and compromise bone health [10][11]. Little is known about the effects of physiological levels of oxidative damage on bone mechanical properties. In this study, we are testing the hypothesis that in vitro oxidative damage deteriorates the tensile mechanical properties of cortical bone.Oxidative damage was induced in bovine cortical bone in vitro to assess its effects on bone tensile mechanical properties. Longitudinally-oriented tensile test specimens were cut from three bovine tibiae using a mini-CNC mill. The specimens were oxidized using neutral hypocholorous acid (HClO) solution (5% Acetic acid (HOAc), 5% Sodium Hypochlorite (NaClO). HClO is a strong and stable oxidant produced by osteoclasts and other cells in bone biology and inflammation. Two groups (n=3) were incubated for 48 and 96 hours at 37°C. Two control groups (n=3) were also prepared (submerged in PBS at 37 °C or at room temperature). Uniaxial tensile tests were conducted (?TS, Psylotech, IL, USA) while strain was measured using digital image correlation. One-way ANOVA was used to detect statistically significant differences in group means.Representative stress-strain curves for the four groups are shown in the figure below. These graphs show that the yield and post-yield tensile properties of cortical bone in the longitudinal direction decrease with increasing exposure to the oxidant solution. Yield and ultimate strengths, and ultimate strain, were all strongly and negatively related to incubation time (R^2>0.8,p<0.005). As expected, because damage of the bone mineral is not expected, correlation between the elastic modulus and oxidation time was not significant (p=0.146). One-way ANOVA detected differences among group means (p<0.008). These findings a) support our hypothesis that in vitro oxidative damage deteriorates bone mechanical properties, due to bone collagen damage, and b) suggest a new model for understanding degradation of bone quality in aging and chronic diseases.

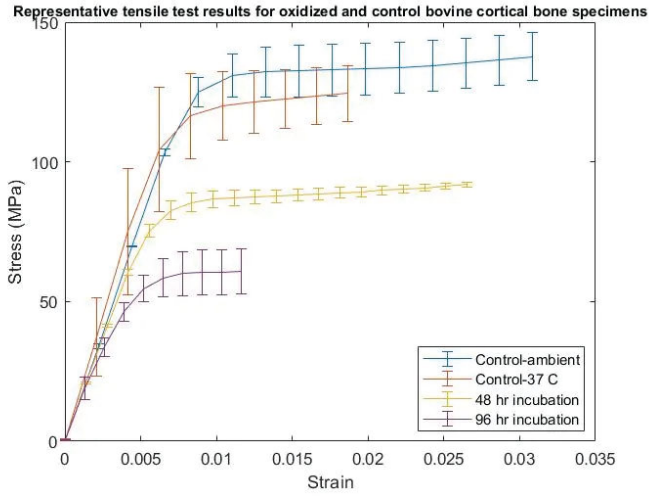

***Disclosures: Faezeh Iranmanesh**, None*

SAT-022

Tailoring the Mechanical Microenvironment to Enhance Osteogenesis in Bone Tissue Engineering Scaffolds *Timothy Josephson[2,] ELISE MORGAN[2,] [2]Boston University, , [2]Boston University, United States

Skeletal cells are influenced by a variety of stimuli in their microenvironments. Two of these stimuli, surface curvature and strain, have been identified as particularly influential, for example in migration and osteogenic differentiation of marrow stromal cells (MSCs) [1-3]. Methods of delivering optimal levels of these stimuli in 3D physiological environments, such as bone injuries, are lacking. Biomaterial scaffolds are candidates for treating these injuries; further, by tuning the internal architecture of the scaffold, one can control the types and magnitudes of the stimuli delivered to the cells. Prior work on optimizing scaffold architecture has been limited by both the types of stimuli considered and the size of the design space. To overcome these limitations, we used a topology optimization approach that seeks to maximize the amount of osteogenically favorable microenvironments within the scaffold architecture.Scoring functions were developed based on published data on the influence of local cues-specifically curvature [1,3,4] and shear strain [2]-on osteogenesis. The individual scoring functions were combined multiplicatively to create a composite local score for each region within the scaffold, and the fitness of the entire scaffold was evaluated by taking an area-weighted sum of local scores. Mixed-topology scaffolds were then generated by taking weighted sums of the mathematical definitions of a set of triply periodic minimal surfaces (TPMS) architectures: primitive, gyroid, and diamond. A gradient-free optimization method was used to identify optimal scaffold designs. Different optimization cases targeted different stimuli (curvature, strain, and both), with and without constraints on the macroscale stiffness of the scaffold.Each optimization case yielded a design that improved the scaffold fitness relative to the baseline design, which was an even mix of the three TPMSs. The final design obtained by jointly optimizing for curvature and strain had a nearly 5-fold increase in fitness score over the baseline design and also outperformed all of the original three TMPS structures. These results demonstrate the potential of mixed-topology TPMS designs to achieve optimal architectures with both micro- and macroscale considerations.[1] Werner et al., Adv. Sci. 2017.[2] Prendergast et al., J Biomech. 1997.[3] Callens et al., Nat. Commun. 2023.[4] Swanson et al., Int. J. Mol. Sci. 2022.

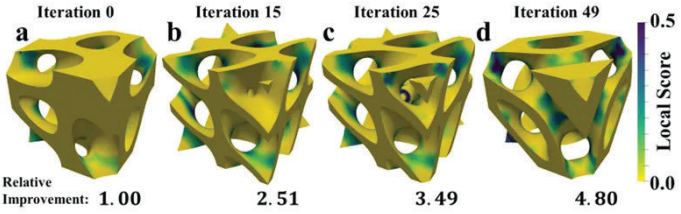

***Disclosures: Timothy Josephson**, GE HealthCare, Grant/Research Support*

SAT-023

Methodology to Analyze Stress Distribution in Long Bones using Computer-Aided Design *Kyung Kang[1, 1]Marian University, United States

Mechanical stress is an important factor to affect mechanosensing, bone-regulating osteocytes, especially in load-bearing long bones. Since signals released from osteycytes control neighboring bone-forming and bone-resorbing activities, region-specific mechanical stress is considered a key contributor to local bone remodeling. Traditional mechanical tests, such as a three-point bending, compression, and torsion, are common methods to measure macro mechanical properties, however, such tests do not provide spatial stress distribution in bones. Computer simulation has been utilized to predict the stress, while many of such research articles did not sufficiently demonstrate region-specific data with various loading cases. Therefore, we propose to use widely-used Computer-Aided Design (CAD) engineering software to estimate spatial stress distribution in long bones under various loading conditions. This research summarizes how CAD software (Fusion 360, AutoDesk) can visualize stress distribution inside a long bone under various loadings. First, a series of micro-CT DICOM scans of a mouse tibia was converted into a single STL file using 3D Slicer (open-source software). Then, the STL file was imported into Fusion 360 and converted into a meshed (solid) model. We ran static stress analysis on this solid tibia model under axial compression, torsion, and bending forces. For the static stress analysis, users can define materials property, constraints (where to fix) and loading conditions, such as types, directions, and magnitudes of loadings. The computation results demonstrate that Fusion 360 provides not only the estimated stress, but also the displacement (deformation) as well as safety factors in the entire tibia model. The stress can be visualized on any desired cross-section that is defined by users in a three-dimensional axis. These quantified results are difficult to directly compare with the macro mechanical properties from the traditional testing methods, due to the assumptions used in the computation. However, this technique provides sufficient information on relative spatial changes in stress under a given loading condition. Therefore, this will be a useful tool to identify the regional stress distribution inside bones under different loadings and/or genetic conditions, which will potentially give us an insight into stress region-specific behavior of osteocytes.

***Disclosures: Kyung Kang**, None*

SAT-024

Determinants of juvenile trabecular bone quality *MARIANA KERSH[1,] Annette McCoy[1,] Sara Moshage[1, 1]University of Illinois at Urbana-Champaign, United States

Adult bone quality is influenced by mechanical loading during ontogeny and can also be negatively impacted by juvenile bone disorders or injury. Understanding the determinants of mechanical properties will help to provide bone quality targets for both the diagnosis of impaired bone strength and interventions designed to improve bone quality in young individuals. Bone samples were harvested from foals (age: 4 - 48 weeks) euthanized for reasons unrelated to this study. Longitudinal trabecular cores from the third metacarpal (MC3, n=85) and proximal phalanx (P1, n=49) were imaged with micro-computed tomography (µCT) at 144µm prior to compression testing. The µCT data was used to measure bone mineral density, bone volume fraction (BVTV), trabecular thickness (Tb.Th), trabecular spacing, degree of anisotropy (DA), and connectivity density. Mechanical properties quantified included elastic modulus, yield stress and strain, and ultimate stress and strain.P1 mineral density was 14% higher and connectivity density was 51% higher than the MC3 (Fig F,K). In contrast, DA was 15% higher in the MC3 (Fig J). There was no difference in the elastic moduli; however, yield and ultimate stress were 26% and 24% higher in the P1 (Fig B,C), ultimate strain was 6% higher. Mineral density was the strongest predictor of mechanical properties - in particular in the P1 (r2 = 0.81, Fig L) compared to the MC3 (r2 = 0.62, Fig M). Mineral density tended to increase with age but with more variability in the MC3. In general, the distal segments (e.g. P1) mature first in foals - likely because they are ambulatory from birth. However, the growth plates of the P1 and MC3 close at the same time suggesting that modeling occurs over a similar amount of time. Our data suggests that the rates of mineralization may be different. Curiously, Tb.Th was more strongly correlated to mechanical properties in the P1 (r2 = 0.55) compared to the MC3 (r2=0.31) despite the fact that there were no statistical differences in Tb.Th though may be explained by the moderate

increase in range of Tb.Th values in the P1. While both the P1 and MC3 are considered long bones, the mechanical environment that influences bone formation are likely different due to overall shape differences and mechanisms of load transfer during equine locomotion. Our data shed light into the interplay between compositional and microstructural determinants of bone strength.

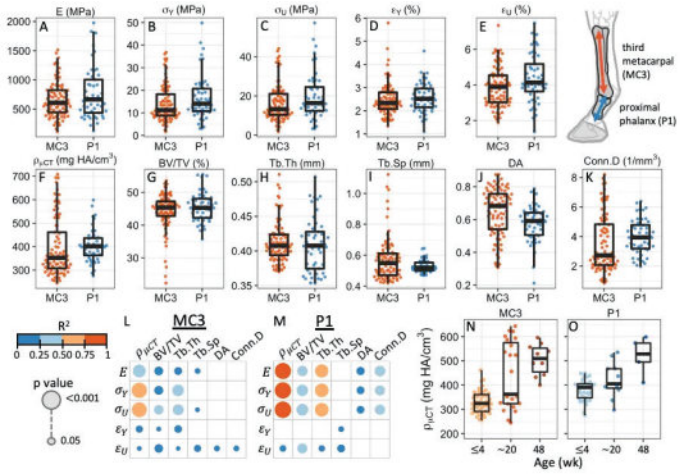

***Disclosures: MARIANA KERSH**, None*

SAT-025

A preliminary study on the effect of intramedullary pressure on bone resorption: Effects of hypertension on osteoporosis *Taekyeong Lee[1], Jaemin Kim[2], Soonmoon Jung[2], Youngho Lee[2], Hyeyeong Song[2], Yeeun Kang[2], Junghwa Hong[2]. [1]BNR R&D Center, Republic of Korea. [2]Korea University, Republic of Korea

Recently, it has been found that hypertension, one of the representative chronic diseases, greatly increases the risk of not only cardiovascular diseases but also osteoporosis(L Do Carmo et al, 2020). In addition, it has been found that bone loss in young mice with hypertension is associated with increased inflammation(EM Hennen et al, 2022), and increased inflammation affects bone density and strength(UA Gurkan, O Akkus, 2008).In other words, the hypothesis that an increase of intramedullary pressure in bone tissue interferes with bone metabolism for stable nutrient supply and waste discharge in bone tissue, resulting in a decrease in bone mass due to the expression of inflammatory proteins is accepted. However, these studies are only the results of statistical analysis or that the results of antihypertensive drugs administration affect bone loss, and there is no research result that direct pressure increase has an effect on bone loss(N Yarema et al, 2020; H Nakagami, RMorishita, 2013; K llic et al, 2013; X Hu et al, 2019; Z Hu et al, 2021).In this study, the intramedullary pressure of the bone fluid flow in the bone marrow space was increased and the cytokine were analyzed.After inserting the specimen(fabricated and processing a 5-10 mm specimen from the left/right femur of NZW Rabbit) into a tightly fitting chamber using the bone on a chip device manufactured in the previous study, a controlled medium was injected for 2 weeks. For the injection fluid pressure, 3.3 kPa was used as the control group, and 6.6 kPa, which is twice the pressure, as the experiment group, referring to the intramedullary pressure of rabbit femur through literature review, and experiments were conducted three times each(UA Gurkan, O Akkus, 2008). Bone formation/resorption analysis(ELISA) were performed though cytokine analyses of output medium.As a result of the experiment, the Rankl/Opg ratio of the experimental group to which 2 times the pressure was applied was about 1.8 times higher than that of the control group. BMP-2 and OCN were expressed relatively low in the experimental group, and CTX and COX-2 were expressed relatively high in the experimental group compared to the control group, confirming that they were affected by bone resorption, not bone formation. These results show that excessive intramedullary pressure greatly affects bone loss, suggesting that high blood pressure may increase the incidence of bone loss and osteoporosis.

***Disclosures: Taekyeong Lee**, None*

SAT-026

See Friday Plenary Number FRI-026

SAT-027

Are Enzymatic Collagen Cross-links the Real Culprit in Fracture Occurence in Type 1 Diabetes Patients? *Eleftherios Paschalis[1], Laura Graeff-Armas[2], Sonja Gamsjaeger[3], Sue Bare[4], Robert Recker[5], Mohammed Akhter[6]. [1]Ludwig Boltzmann Institute for Osteology, Austria. [2]University of Nebraska Medical Center , United States. [3]Ludwig Boltzmann Institute of Osteology, Austria. [4]Osteoporosis Research Center, Creighton University, United States. [5]Creighton University, United States. [6]Creighton University Osteoporosis Research Center, United States

Increased fracture risk in type 1 diabetes (T1D) patients is not fully captured by bone mineral density outcomes, leading to the hypothesis that alterations in bone quality (material & structural properties) are responsible. Advanced glycation endproducts (AGEs) have been implicated in the increased fracture risk in T1D, yet recent publications [1, 2] question whether this is associative or causative.To test the hypothesis that enzymatic collagen cross-links rather than AGEs correlate with fracture incidence in T1D, we analyzed iliac crest biopsies from sex-matched, 5 fracturing T1D patients (T1D Fx; median age, BMI, and HbA1c values: 38, 27.1, 8.1, respectively), 6 nonfracturing T1D patients (T1D NoFx; median age, BMI, and HbA1c values:38, 24.4, 7.1, respectively), and 6 healthy subjects (HC; median age, BMI, and HbA1c values: 37, 24.2, 5.2, respectively), by Raman microspectroscopy as a function of tissue age (based on double fluorescent labels), in trabecular bone. Both T1D groups had significantly higher ($p<0.05$) HbA1c values compared to HC.The pyridinoline (Pyd; enzymatic collagen cross-link), as well as the content of two AGEs, namely CML (?-N-Carboxymethyl-L-lysine) and PEN (Pentosidine) were calculated. Data were compared by 2-way ANOVA against HC.Results are shown in Figure below. Mean and SEM are plotted as a function of tissue age (TA1 = mid-distance between the second fluorescent label and the mineralizing front; TA2 = mid-distance between the two labels; TA3 = 2 µm behind the first label), whereas the included table summarizes the mean and SD values for the three groups when all tissue ages are averaged. There were no differences between the 3 groups in either CML or PEN content. Pyd content was elevated in the T1D Fx group compared to either HC or T1D NoFx ($p<0.001$ and $p<0.001$, respectively) ones, while no differences were evident between HC and T1D NoFx.Collagen fibers with high Pyd content are more brittle. Thus, a plausible suggestion is that it is the enzymatic collagen cross-links that either by themselves or in combination with the adverse effects of increased AGEs accumulation, that result in fragility fracture in T1D.[1] M. Unal, et al, Effect of ribose incubation on physical, chemical, and mechanical properties of human cortical bone, J Mech Behav Biomed Mater 140 (2023) 105731.[2] T.L. Willett, et al, Causative or associative: A critical review of the role of advanced glycation end-products in bone fragility, Bone 163 (2022) 116485.

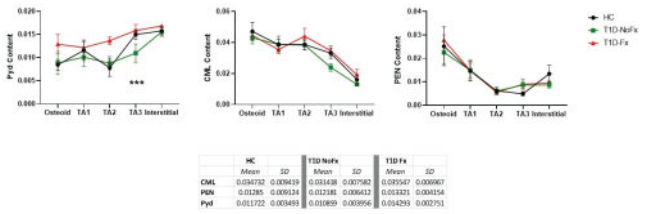

	HC		T1D NoFx		T1D Fx	
	Mean	SD	Mean	SD	Mean	SD
CML	0.034732	0.009419	0.031438	0.007582	0.035547	0.006967
PEN	0.01285	0.009124	0.012181	0.006612	0.013321	0.008154
Pyd	0.011722	0.003493	0.010859	0.003956	0.014293	0.002751

***Disclosures: Eleftherios Paschalis**, None*

SAT-028

Sex- and Site-Specific Reference Data for Size-Invariant Bone Properties using Multi-Stack HR-pQCT *Simone Poncioni[1], Dominique Lüscher[1], Daniela Frauchiger[2], Michael Indermaur[1], Christian Meier[3], Philippe Zysset[1], Kurt Lippuner[2]. [1]ARTORG Centre for Biomedical Engineering Research, University of Bern, Switzerland. [2]Department of Osteoporosis, Bern University Hospital, University of Bern, Switzerland. [3]Div. of Endocrinology, Diabetes and Metabolism, University Hospital Basel, Switzerland

Reference data for bone architecture in adults were recently reported for ~10 mm distal bone sections scanned by second generation HR-pQCT [1]. To overcome the limitations of this small section size for follow-up, a multi-stack scan protocol followed by a non-linear, homogenised finite element (hFE) analysis to compute bone strength was developed and validated in our lab [2]. Here, we aimed to collect reference data with this new protocol and identify key size-independent structural and strength parameters to optimise the continuous assessment of bone health in radius and tibia. Data from 4 clinical studies conducted at the Policlinic for Osteoporosis of the University Hospital in Bern were combined. 276 healthy participants (157 M & 119 F, age 20-92) underwent double- and triple-stack scans at the distal radius and tibia, respectively, using HR-pQCT (XtremeCT II, SCANCO Medical) as described in [2]. Following standard structural evaluation, hFE was performed according to [3]. Exploratory statistical analysis stratified for sex and anatomical site was conducted. Six key size-independent variables were selected: total and cortical volumetric bone density (Tot.vBMD, Ct.vBMD), relative cortical thickness (Rel Ct.Th), cortical to trabecular area ratio (Ct./Tb.Ar), trabecular bone volume over total volume (Tb.BV/TV), and apparent ultimate stress (Ult.S). Baseline values and corresponding coefficients of variation (CV) were calculated for participants aged 37 years. T-scores were plotted in equally distributed age

groups (50, 63, 76, 89 years, Fig. 1). A minimal CV of 2% was found for Ct.vBMD. For the radius, Ult.S decreased by 1.13% and 0.88% per year in females and males respectively. For the tibia, these changes were 0.80% and 0.82%. All T-scores decreased in both females and males, with the highest change in females' Ct.vBMD: -0.16 SD and -0.08 SD per year at the tibia and radius, respectively. Ct.vBMD of the weight-bearing tibia, which includes cortical porosities at all scales, is the most sensitive variable with age. To conclude, the proposed set of size-independent variables provides a synthetic overview of distal bone health for practical follow-up in a clinical setting.References: [1] Whittier et al. J Bone Miner Res, 2020. [2] Schenk et al. J Mech Behav Biomed Mater, 2022. [3] Arias-Moreno et al. Osteoporos Int, 2019.

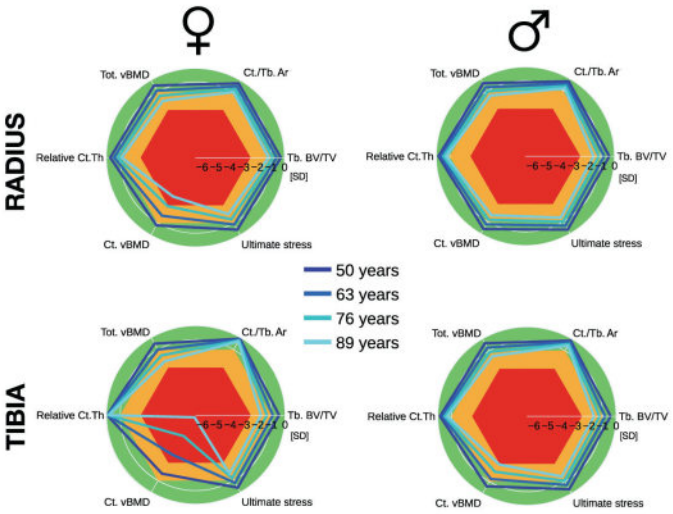

***Disclosures: Simone Poncioni**, None*

SAT-029

In Vitro Vitamin B Treatment Reduces Formation of the Non-Enzymatic Crosslink Pentosidine in Human Cortical Bone *Christian L. Ray[1], Ramina Behzad[1], Zackery J. Silva[1], Lamya Karim[1]. [1]University of Massachusetts Dartmouth, United States

Diabetic patients are at an elevated risk of bone fractures, which may be due to having poor bone quality. Accumulation of non-enzymatic crosslinks known as advanced glycation end-products (AGEs) in bone has been suggested as one source of poor bone quality. It has been shown that Vitamin B6 (VitB) may prevent AGE formation in other tissues by inhibiting glycation reactions [1]. Our goal was to test its effects in human bone in vitro, and we hypothesized that VitB treatment will decrease fluorescent AGEs (fAGE) and the specific fAGE pentosidine (PEN), with a consequent improvement in bone mechanical properties.Sixty cortical beams (2x2x30 mm) were acquired from the midshaft of female human cadaveric tibias (young/old, diabetic/non-diabetic). Tissue mineral density (Ct.TMD) and porosity (Ct.Po) was assessed by microCT, and then beams were randomly distributed into 5 groups: Control, Ribose (R), R + 50 mM VitB, R + 75 mM VitB, and R + 100 mM VitB. They were incubated for 14 days at 37°C in solutions [2], with Ribose and VitB groups containing 0.6 M ribose and respective concentrations of VitB. 6 mm segments of the beams were mechanically tested by cyclic Reference Point Indentation (cRPI), and then hydrolyzed to extracted bone collagen. Extracts were assessed for fAGEs by a fluorometric assay and PEN by high-performance liquid chromatography (HPLC).There was no difference in Ct.TMD, Ct.Po, or cRPI properties between groups. Total fAGEs were higher in ribose vs vehicle specimens (+99%, p<=0.05), but no differences were detected between ribose and VitB groups. PEN was greater in ribose (+53%, p <=0.001) and R + 50 mM VitB (+47%, p <= 0.01) groups vs vehicles, and lower in R + VitB 100 mM group vs ribose group (-25%, p<=0.05) (Figure).There was increased glycation in the ribose group than in vehicles, indicating a successful induction of in vitro AGEs. fAGE measurement is a broad indicator of glycation that does not consider individual crosslinks. Our measurement of PEN, a single fAGE, showed that treatment of cortical bone with the highest dose of vitB reduced glycation. However, there was no change in cRPI measures, suggesting the decrease in glycation may not directly impact tissue-level mechanical properties. Other mechanical properties such as fracture toughness need to be assessed to further evaluate the impact of vitB on bone mechanical behavior.References: [1] Mascolo and Verni, Int J Mol Sci, 2020; [2] Merlo, et al., J Orthop Res, 2020

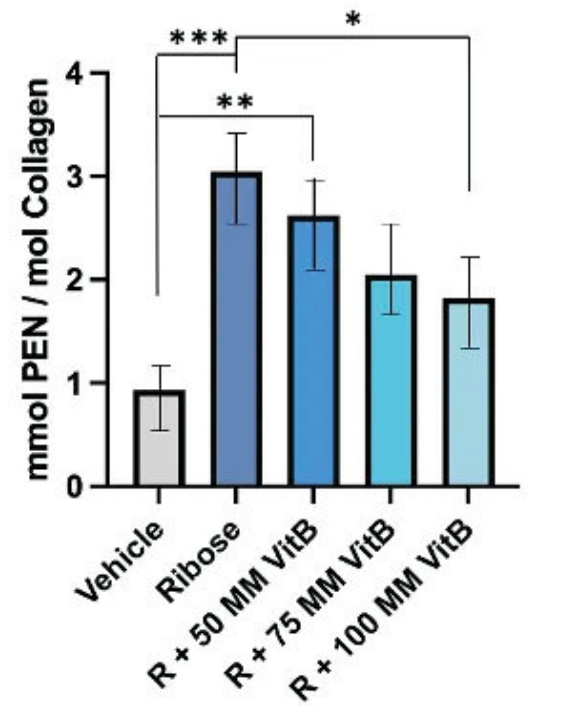

Figure. Pentosidine measurements by HPLC in ratio of mmol PEN / mol collagen. (* $P \leq 0.05$, ** $P \leq 0.01$, *** $P \leq 0.001$)

***Disclosures: Christian L. Ray**, None*

SAT-031

The Relationship between Bone Strain Index (BSI), Bone Mass, Microarchitecture and Mechanical Behavior in Human Vertebrae: an Ex Vivo Study *Jean-Paul Roux[1], Francois Duboeuf[1], Elisabeth Sornay-Rendu[1], Luca Rinaudo[2], Fabio Massimo Ulivieri[3], Julien Wegrzyn[4], Roland Chapurlat[1]. [1]INSERM UMR 1033, University of Lyon, Lyon, France., France. [2]Tecnologie Avanzate Srl, Torino, Italy., Italy [3]Casa di Cura la Madonnina, Milano, Italy., Italy [4]Department of Orthopedic Surgery, Lausanne University Hospital and University of Lausanne, Switzerland., Switzerland

The measurement of areal bone mineral density (aBMD) does not completely identify future fracture because there is an overlap of BMD in patients with or without fractures. DXA-based bone indexes were developed to improve the predictive role of BMD in clinical practice. The first was the trabecular bone score (TBS), a texture parameter evaluating local variations in gray level from DXA image of the lumbar spine to estimate bone microarchitecture. Bone Strain Index (BSI) is a new DXA-based bone index which represents the finite element analysis of the bone deformation under load. The current study aimed to assess whether the BSI is associated with 3D microarchitecture and the mechanical behavior of human lumbar vertebrae.Lumbar vertebrae (L3) were harvested fresh from 31 human donors (16 men, and 15 women, age: 76 +/- 10 yrs for men and 75 +/- 10 yrs for women). The anteroposterior BMC (g) and aBMD (g/cm2) of the vertebral body were measured using DXA (Delphi W, Hologic) and then the BSI was automatically derived with a dedicated external software from the same area. The trabecular bone volume (Tb.BV/TV), trabecular thickness (Tb.Th), degree of anisotropy (DA), and structure model index (SMI) were measured using µCT with a 35-µm isotropic voxel size (Skyscan 1076). Quasi-static uniaxial compressive testing was performed on L3 vertebral bodies under displacement control (0.5mm/min) to assess failure load (N) and stiffness (N/mm). TBS was extracted in a subset of 16 vertebrae. The BSI was significantly correlated (Pearson correlation) with failure load and stiffness (r=-0.60, -0.59; p<0.0001), aBMD and BMC (r=-0.93, -0.86; p<0.0001); Tb.BV/TV and SMI (r=-0.58, 0.51; p=0.001 and 0.004 respectively). No significant correlation was found between BSI and TBS. After adjustment for aBMD, the association between BSI and stiffness, BSI and SMI remained significant (r=-0.51; p=0.004 and r=-0.39; p=0.03 respectively, partial correlations) and the relation between BSI and failure load was close to significance (r=-0.35; p=0.06).In conclusion, the BSI was significantly correlated with microarchitecture

and mechanical behavior of L3 vertebrae and these associations remained statistically significant regardless of aBMD.

***Disclosures: Jean-Paul Roux**, None*

SAT-032

Establishment Of Normative Curves of Specific Microarchitecture and Bone Resistance Per Age Group and Sex Obtained By Second Generation of High-Resolution Peripheral Quantitative Computed Tomography (HR-pQCT II) In Healthy Brazilians *RODRIGO SANTOS[1], Isabela Silva[2], Edson Campos[2], Gabriela Vieira[2], Leonardo Bandeira[3], MONIQUE OHE[4], Sergio Maeda[2], MARISE LAZARETTI-CASTRO[5]. [1]Federal University of Sao Paulo, , [2]Federal University of São Paulo, Brazil. [3]Department of Endocrinology, Federal University of São Paulo, UNIFESP, Brazil, Brazil. [4]UNIFESP-EPM, Brazil. [5]Escola Paulista de Medicina, Brazil

HR-pQCT provides quantitative 3D parameters of microarchitecture and volumetric density (vBMD) from cortical (Ct.) and trabecular bone (Tb.). An upgrade of this device brought greater accuracy to the measurements but requires the definition of specific normal curves. The existence of a high degree of miscegenation, particular lifestyles, and climate make the Brazilian population unique, which further increases the need for specific normative curves for all parameters obtained from HRpQCT II. Purpose: To develop reference curves for Brazilian healthy adults grouped by age and sex of different parameters, such as microarchitecture, vBMD, and bone strength, of distal radius and tibia. Methods: 500 healthy individuals without osteoporosis from the community aged from 20 to 80 years old will be included. Non-dominant radius and tibia are scanned using HR-pQCT (XTremeCT II; Scanco, Switzerland). The standard segmentation methods are used to verify the bone parameters. Virtual bone stiffness (St) is evaluated by finite element analysis (St). Participants undergo densitometry by DXA to obtain areal BMD and total body composition. A questionary is applied to verify health history and self-reported race. The data will be described as median and quartile. Regression models will be developed according to age, biometrics variables, and lifestyles. Some parameters of interest will be associated with the Person correlations coefficient. Results: Currently, 215 volunteers have been evaluated (145 females; 70 males). An initial analysis showed that Total vBMD peaked at close to 30 years of age. Radius'Ct.Po increased by 100% in females from the third to sixth decades ($p<0.0001$). An inverse correlation was observed in the female group between age and Ct.vBMD (Fig. E) and positively with Ct. Po (Fig. C). Age correlated with Ct.Po diameter and Tb.inhomogeneity ($p=0.0006$) in males. When all individuals were analyzed in the same group, age had a significant inverse correlation with Tt.vBMD and St in both limbs (Figure). Conclusion: In healthy Brazilians, volumetric bone density peaks during the 3rd decade of life. Aging is associated with the deterioration of structural parameters and bone stiffness. Among the measures, cortical porosity increased significantly in the age group above 60. Establishing normative curves using the HR-pQCT II will be an essential database for future Brazilian studies, clinical applications, and comparative studies between different populations.

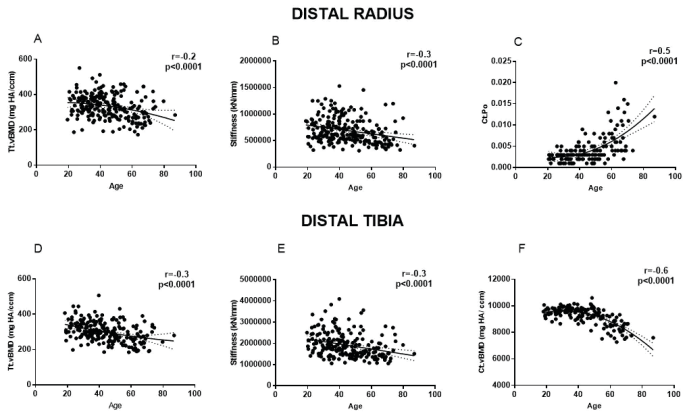

Figure 1. Abbreviations: mg HA/ccm: milligrams of hydroxyapatite per cubic centimeter; Volumetric bone mineral density, vBMD; Stiffness: Whole bone stiffness; kN/mm: Kilonewton millimeter. A) Person' correlations and Reference curves, according to age, of the parameters of vBMD, Stiffiness, and cortical porosity being (A,D) total volumetric density (Tt.vBMD) and (B, E) Stiffness of all volunteers; (C) Cortical Porosity (Ct.Po) and (F) cortical volumetric density (Ct.vBMD) of females, obtained by HR-pQCT II in the non-dominant distal radius and tibia in healthy subjects. The solid line represents the mean from the regression model, and the dashed lines represent the 95% confidence interval.

***Disclosures: RODRIGO SANTOS**, None*

SAT-033

Collagen Denaturation Correlates With Human Cortical Bone Fracture Resistance *Corin Seelemann[1], Daniel Dapaah[1], THOMAS WILLETT[2]. [1]University of Waterloo, , [2],

Bone tissue, primarily composed of hydroxyapatite, collagen, and water, has a multi-scale structure which provides toughening mechanisms to resist fracture. Recent research has examined the relationship between collagen state and fracture resistance of cortical bone [1]. The underlying mechanisms could be vital to understanding bone fragility. Previously, we have shown in bovine cortical bone that collagen denatures during fracture. The extent of denaturation on the fracture surfaces correlated with the work to fracture [2] Here we test the hypothesis that collagen denatures because of fracture in human cortical bone, and the extent of denaturation positively correlated with the work to fracture.Five single edge notched beams from human femurs, each from a different donor (aged 19-61), were fractured under 3-point bending. The beams (2.5 mm x 5 mm x 50 mm) were fractured with the crack propagating circumferentially on the transverse plane. The R curve, a measure of fracture toughness, was calculated for each specimen, then integrated to compute the work needed to grow the crack by approximately 250 µm. This excludes large deflections, which complicate the analysis. The fracture surfaces and a negative control were cut from each specimen using a metallurgical saw. These were surface decalcified (EDTA), stained with fluorescently labelled collagen hybridizing peptides (F-CHP) and imaged using laser scanning confocal microscopy. Each negative control was polished to remove damage from preparation and was used to establish a threshold level for intrinsic denaturation. The threshold was set to exclude 99.95% of the stained pixels in the control and was applied to the fracture surface images to visualize denaturation. The percentage of pixels above that threshold within the first 250 µm of crack growth was used to measure the extent of collagen denaturation.Human bone collagen consistently denatured because of fracture. Every specimen demonstrated increased staining in the region analyzed. Collagen denaturation correlated to work done (R2 = 0.87), as shown in figure. This corroborates with our past work in bovine cortical bone [2]. One limitation of this study is that the collagen denaturation could not be analyzed over a larger range of crack growth due to large crack defections.[1]T. L. Willett, D. Y. Dapaah, S. Uppuganti, M. Granke, J. S. Nyman, Bone 2019, 120, 187.[2]C. A. Seelemann, T. L. Willett, J Mech Behav Biomed Mater 2022, 131, 105220.

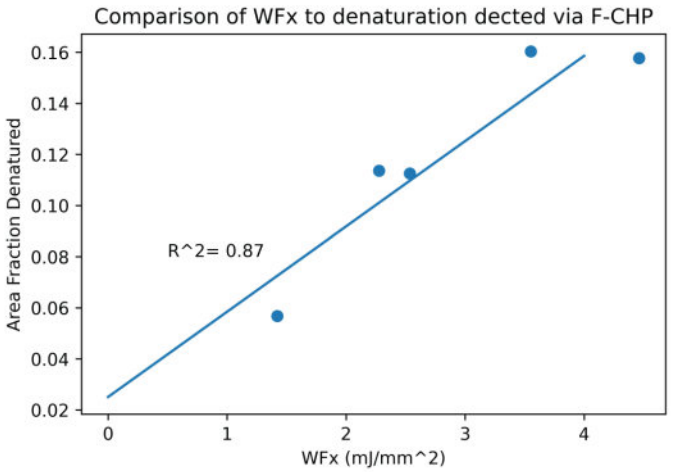

***Disclosures: Corin Seelemann**, None*

SAT-034

Automated Detection of Bone Marrow Lesions in Acute ACL Tears using MRI *Callie Stirling[3], Nathan Neeteson[3], Richard Walker[2], Steven Boyd[3]. [3]University of Calgary, , [2]Department of Radiology, Cumming School of Medicine, University of Calgary, Canada. [3]University of Calgary, Canada

Bone marrow lesions (BMLs) represent tissue damage and bleeding within the inner bone structure following a traumatic anterior cruciate ligament (ACL) injury. BMLs are typically caused by a collision of the tibia and the femur and are indicative of significant joint damage, associated with an elevated risk of developing post-traumatic osteoarthritis (PTOA) [1]. Magnetic resonance imaging (MRI) is useful for detecting BMLs qualitatively, but quantitative assessment may be helpful to determine risk factors for PTOA. Quantitative assessment includes measuring the volume and distribution of BMLs over time. However, manual segmentation of BMLs can be time-consuming. Deep learning methods have been shown to accurately segment regions of interest, giving clinicians crucial data for diagnosis, prognosis, and treatment [2-5].This study aims to develop a model that accurately locates, segments, and measures BMLs in patients with ACL injuries using knee MRI scans performed within 6 weeks of injury. To enhance the generalization ability of the model, pre-processing steps such as intensity normalization, bias field correction, and data augmentation techniques were employed on fat-suppressed fast spin echo T2-weighted MRI images. The model was initially trained on a labelled dataset. Any discrepancies in the resulting segmentation were corrected, and the newly labelled data was integrated into the training set. The re-segmented images were then used to retrain the model. The iterative training approach allowed the model to learn from its mistakes and improve its accuracy.To assess the performance of the final segmentation model, a four-fold cross-validation method was used, and the Dice similarity coefficient (DSC) was calculated between the ground truth and predicted segmentations. The initial iteration of the model yielded a DSC of 0.78, indicating good agreement between the manual and predicted segmentations. Continued iterative training aims at achieving a DSC greater than 0.85. By identifying and quantifying BMLs through

automated detection and segmentation, clinicians and researchers can more accurately estimate the severity of ACL injuries and track bone changes over time. BMLs are also a potential imaging biomarker to identify patients at elevated risk of PTOA.1 Keil, Experimental Orthopaedics, 20222 Dang, BRO Neuroscience Reports, 20223 Paing, Entropy, 20224 Ronneberger, Springer International, 20155 Mauer, Int J Legal Med, 2021

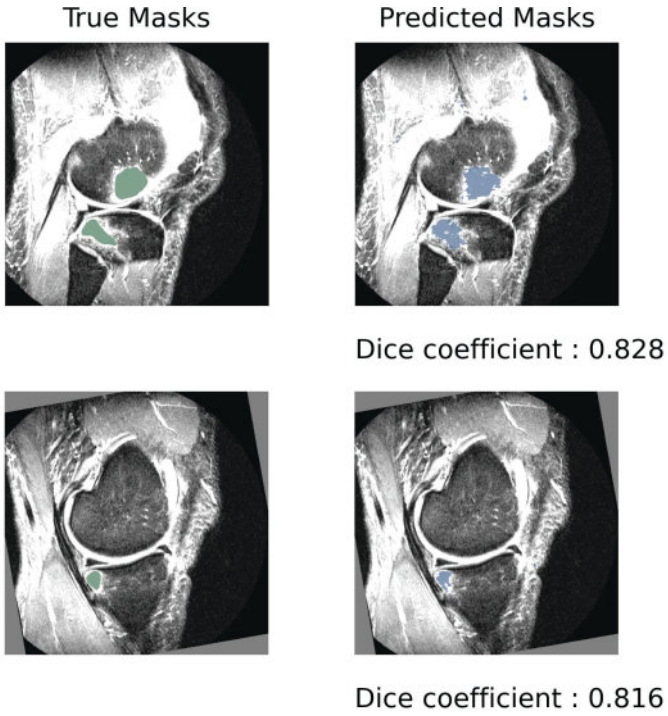

***Disclosures: Callie Stirling**, None*

SAT-035

The Effect of Chemically Induced Diabetes on Bone Architecture Changes Across Bone Length *Carlos Urrego[1], Morgan Bolger[1], David Kohn[2]. [1]University of Michigan, Ann Arbor Dept. of Biomedical Engineering, United States. [2]University of Michigan, United States

Type 1 diabetes (T1D) decreases bone quality and increases fracture risk. Conventional fracture risk assessment tools underdiagnose diabetic subjects due to the lack of understanding of the effects of T1D on bone quality. Moreover, bone quality changes spatially in healthy bone, but the spatial effects of T1D are unknown. The purpose of this study is to evaluate how T1D affects bone architecture along the length and within the cross-section of the femur using a mouse model of chemically induced diabetes, to determine the spatial effect of T1D on bone architecture. Femoral proximal metaphysis, diaphysis, and distal metaphysis of 22 weeks-old Streptozotocin-induced diabetic male mice (n=12) were evaluated. Micro-Computed Tomography was used to evaluate bone mineral density (BMD), bone volume (BV), bone fraction (BV/TV), cross-sectional moments of inertia and rotation of the principal axis (?). No significant effect of diabetes was found in trabecular bone, whereas cortical bone exhibited changes in all regions evaluated. Diabetic femoral distal metaphysis BV was significantly lower compared to age and weight-matched nondiabetic controls (p=0.0427). Diabetic diaphyseal BMD and BV/TV were significantly lower compared to control (p=0.0082 and p=0.0108 respectively). At the proximal metaphysis, BV, BMD, and BV/TV were significantly lower in diabetic samples compared to controls (p= 0.0198, p=0.0159 and p=0.002 respectively). While no changes were found in cross-sectional moments across bone length, ? increased significantly at the proximal metaphysis in the diabetic group compared to control (p=0.0328). T1D femora displayed increased distance from the centroid to the anterior surface at the proximal metaphysis (p=0.0341), decreased distance to the anterior surface at the distal metaphysis (p=0.0257) and decreased distance to the medial surface at the proximal metaphysis (p=0.0013) compared to control. The effect of diabetes on bone architecture increases from the distal end towards the proximal metaphysis, affecting only cortical tissue. The significant increase in the rotation of the principal axis may be a compensatory response to reduce the effect of architecture changes on bone strength. The strong location-dependent effect of T1D on bone suggests that standard femoral neck BMD may not represent the spatial effect of T1D on bone, and that additional properties and areas of interest should be considered.

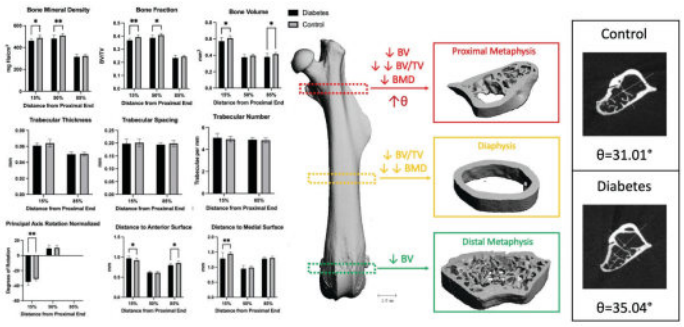

***Disclosures: Carlos Urrego**, None*

SAT-036

Molecular-Level Porosity Differences in Osteogenesis Imperfecta Bone Revealed by Positron Annihilation Lifetime Spectroscopy (PALS) Imaging *Richard Vallery[1], David Gidley[2], Taeyong Ahn[3], Mark Banaszak-Holl[4], Kenneth Kozloff[2]. [1]Grand Valley State University, United States. [2]University of Michigan, United States. [3]Indiana University School of Medicine, United States. [4]University of Alabama, United States

Bone is a complex hierarchical material composed primarily of collagen, mineral, and water. How bone quality, and thus fragility, is regulated at the level of the collagen fibril and mineral interface remains incompletely described. Positron annihilation lifetime spectroscopy (PALS) is a metrology that correlates the positron annihilation lifetime and intensity with nanoscale pore size and relative volume fraction respectively. We demonstrated that PALS is an effective probe of the nanoscale porosity in bone in multiple species, which all showed four distinct pore populations with sizes less than 10 nm. Here we have extended the technique to evaluate nanoscale porosity changes in models of altered collagen structure resulting in varying skeletal fragility.Femora from four 10 wk female heterozygous mouse models of osteogenesis imperfecta (OI) (n=3/genotype plus n=3 WT) were prepared. Brtl/+ and G610C/+ arise from Gly->Cys substitution in col1a1 and col1a2 respectively, resulting in moderate fragility. Jrt/+ arises from a premature splice site mutation in col1a1 (severe) while Mov13/+ is haploinsufficient for col1a1 (mild). Femora were harvested, lightly pulverized, and subject to PALS measurements in dehydrated conditions. Differences in OI mouse spectra were compared to corresponding WT (Figure).The average intra-collagen lifetime/pore size was conserved vs. WT among all mice, while the density of these voids was substantially reduced, suggesting reductions in collagen content. In the three larger pores, the lifetimes/ pore sizes indicate minor differences with WT but all present significantly higher density of pores, consistent with reduced collagen content. Moreover, three of the genotypes presented smaller voids at the collagen-mineral interface suggesting the mineral plate spacing is reduced- consistent with higher mineralization with OI. We have confirmed this reduced plate spacing for deproteinated male Brtl/+ samples. Finally we note that Jrt/+, which exhibits the greatest collagen molecular structural change and the most severe OI symptoms, also presented the most extreme differences in PALS lifetimes and intensities.By probing bone at the nanoscale level, we reveal novel measures of bone quality differences arising from collagen deficiency and structural mutation. Jrt/+ showed the greatest dysregulation of terminal collagen spacing and collagen-mineral interface, suggesting the importance of these features in contributing to bone fragility.

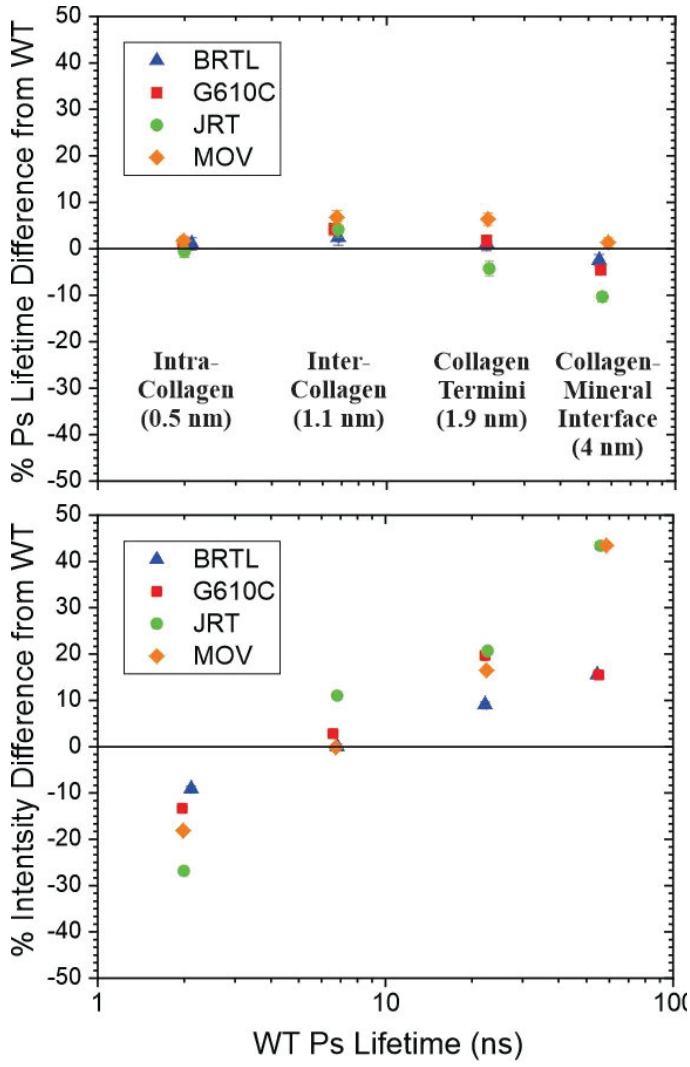

***Disclosures: Richard Vallery**, None*

SAT-037

Accuracy of BMD measurement in weight bearing, cone-beam CT *Tadiwa Waungana[3,] Keven Qiu[2,] Justin Tse[3,] Donald Anderson[4,] Sarah Manske[3,] [3]University of Calgary, [,2]University of Waterloo, Canada[,3]University of Calgary, Canada[,4]University of Iowa, United States

PurposeKnee osteoarthritis (KOA) is a common, painful, and disabling joint disorder. Changes in BMD at the knee are associated with worsening clinical and radiographic outcomes, such as pain and structural progression of KOA. Weight-bearing, cone-beam CT (WBCT) allows cross-sectional, functional imaging of the knee for assessment of bone and joint structures but is challenged by artefacts that may compromise the accuracy and precision of BMD measures. Therefore, we compared BMD measurement accuracy between WBCT and multi-slice CT (MSCT) using a BMD calibration phantom. In addition, we sought to determine the dependence of BMD measurement on the presence of a participant to determine whether synchronous BMD calibration is feasible.MethodsWe scanned a BMD calibration phantom (QRM, Möhrendorf, Germany) including three hydroxyapatite cylindrical inserts of 100, 400 and 800 mgHA/cm3 with WBCT (HiRise, CurveBeam) and MSCT (Revolution GSI, GE). Two image acquisitions were completed with each scanner: 1) a phantom image (asynchronous calibration) and 2) a phantom + participant image (synchronous calibration). Within each BMD insert, we selected four regions of interest to facilitate BMD calibration and uniformity analysis. We used one sample t-tests and relative error measurements to compare measured BMD to true BMD, whilst paired t-test, regression and Bland-Altman analysis were used to compare measured BMD between scanners and calibration techniques.ResultsFor all CT scans, measured BMD values were significantly different from the true BMD value ($p < 0.001$; Fig. 1). Relative errors from true BMD were larger for WBCT (-16% to 8%) than for MSCT (-1.3% to 3%). Although the mean BMD measurements for synchronous WBCT images were closer to the true BMD, the standard deviations were 2.0% - 10.3% higher (w.r.t. true BMD) compared to asynchronous images. In contrast, MSCT scans were unaffected by the presence of a participant. Whilst regression analysis showed a high association between WBCT and MSCT measures (R2>0.99), Bland-Altman analysis suggested that WBCT and MSCT showed better agreement when BMD was measured asynchronously.ConclusionOur results suggest that WBCT BMD measures are more variable than MSCT measures. Furthermore, WBCT measures are more accurate when measured with a participant in the scan and may need to be calibrated at the height where BMD will be measured. Together, our data support the use of synchronous calibration for BMD measurement using WBCT.

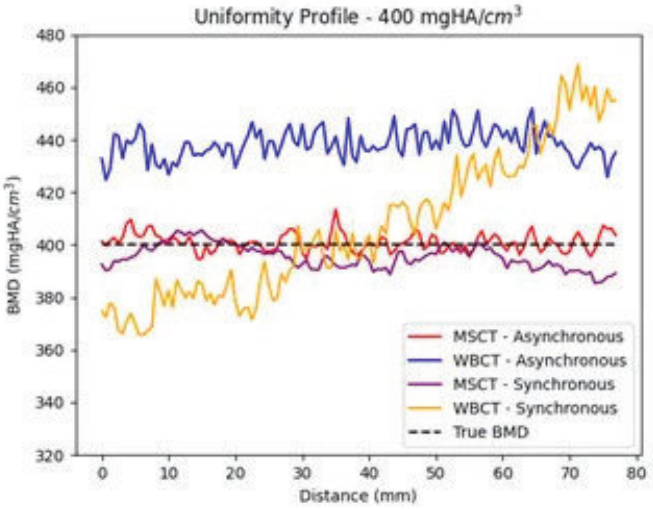

***Disclosures: Tadiwa Waungana**, None*

SAT-038

A Systematic Review and Meta-Analysis of the Effect of Probiotics on Bone Outcomes in Rodent Models *Jenalyn L. Yumol[1,] William Gittings[1,] Russell J. de Souza[2,] Wendy E. Ward[1,] [1]Brock University, Canada[,2]McMaster University, Canada

Probiotics are live bacteria intended to produce a health benefit, one of which may include supporting a strong, healthy skeleton. The purpose of this systematic review was to determine if probiotic supplementation, compared to no supplementation, improves bone mineral density (BMD) and bone structure outcomes in rodent models. A systematic search of the literature using MEDLINE and Embase via OVID and CINAHL Complete was performed on August 27, 2021. Intervention studies (N = 51) examining the effect of oral consumption of any probiotic strain on BMD or bone structure in rodents were included. Risk of bias and quality assessment were performed using the Systematic Review Center for Laboratory Animal Experimentation risk of bias tool and the Animal Research: Reporting of In Vivo Experiments Guidelines, respectively. Meta-analyses were conducted separately by study model (ovariectomized, intact) and bone site (femur, tibia, spine) to determine the pooled standardized mean difference (SMD) between treatment and control groups for volumetric BMD (vBMD), bone volume fraction (BV/TV) and cortical thickness (Ct.Th) following supplementation. Heterogeneity was explored (probiotic genus, sex, mice versus rats). Using an ovariectomized model, probiotic supplementation resulted in greater vBMD at the femur (SMD = 1.35, 95% CI [0.92, 1.78], I2 = 25%, $P < 0.05$) and tibia (SMD = 1.88, 95% CI [0.89, 2.86], I2 = 59%, $P < 0.05$) but not at the spine (SMD = 1.29, 95% CI [-0.08, 2.66], I2 = 83%, P = 0.06) when compared to the control. At these sites, there was higher BV/TV (femur: SMD = 1.03, 95% CI [0.56, 1.50], I2 = 52%, $P < 0.05$; tibia: SMD = 2.66; 95% CI [0.93, 4.40], I2 = 86%, $P < 0.05$; spine: SMD = 1.92, 95% CI [0.77, 3.08], I2 = 82%, $P < 0.05$) and Ct.Th (femur: SMD = 0.57, 95% CI [0.17, 0.96], I2 = 0%, $P < 0.05$; tibia: SMD = 2.16; 95% CI [0.15, 4.18], I2 = 87%, $P < 0.05$) with the probiotic compared to the control. The effects were not modified by probiotic genera or rodent species. In intact rodents, probiotic supplementation increased vBMD at the femur (SMD = 0.61, 95% CI [0.20, 1.02], I2 = 12%, $P < 0.05$) without changes in bone structure (BV/TV: SMD = 0.33, 95% CI [-0.03, 0.68], I2 = 31%, P = 0.07; Ct.Th: SMD = 0.19, 95% CI [-0.20, 0.57], I2 = 9%, P = 0.32). In conclusion, probiotic use may be a beneficial strategy for improving bone outcomes in rodent models. However, high-quality studies are needed to define intervention dose and duration.

***Disclosures: Jenalyn L. Yumol**, Lallemand Health Solutions, Other Financial or Material Support*

SAT-039

Correlation between lattice element (LE) and finite element (FE) methods in prediction of trabecular bone apparent elastic modulus *Mahsa Zojaji[1], Keyvan Ferasat[1], Roshni Rainbow[1], Heidi-Lynn Ploeg[1], Laurent Karim Béland[1]. [1]Dept. of Mechanical and Materials Engineering, Queen's University, Kingston, ON, Canada, Canada

Prediction of bone mechanical properties including apparent elastic modulus is commonly used in pre-clinical diagnosis of bone disorders such as osteoporosis and bone cancer. The objective of this study is to utilize lattice element method (LEM) implemented in an open-source package as an alternative method to finite element analysis (FEA). The LEM builds a discretized continuum solid using particles and springs. The spring constants are calculated by equalizing the total elastic energy from LEM and continuum mechanics. We proposed a new scheme for LEM-firm and floppy boundary method (FFLEM)-that is more cost- and time-efficient than the FEA. Fifteen trabecular bone cores were ?-CT scanned (20x20 microns), segmented, and surface mesh refinement were completed in 3-Matic (Materialise, version 16.0) before exporting to Abaqus/CAE (version 2017, Simulia, Johnston, RI, USA) for further mesh generation (quadratic tetrahedral with a max edge length size of 2.00 microns). FFLEM is a capable and reliable alternative to FEA to study elastic response of trabecular bones.

***Disclosures: Mahsa Zojaji**, None*

SAT-041

A Multimodal Analysis of Cement Lines in Human Osteonal Bone *Astrid Cantamessa[1], Stéphane Blouin[5], Shahrouz Amini[3], Maximilian Rummler[3], Andrea Berzlanovich[4], Richard Weinkamer[3], Markus A. Hartmann[5], Davide Ruffoni[6]. [1]University of Liège, , [5]Ludwig Boltzmann Institute of Osteology, Austria. [3]Max Planck Institute of Colloids and Interfaces, Germany. [4]Center of Forensics Medicine, Austria. [5]Ludwig Boltzmann Institute of Osteology, Germany. [6]University of Liege, Belgium

Cement lines (CLs) are thin layers separating secondary osteons from each other or from interstitial bone. Previous evidence suggests that CLs protect osteons by deflecting microcracks. However, their composition and structure still remain uncertain. In the present study, we characterize CLs mineral content and mechanical properties at the micrometer scale using cortical bone samples from 2 human femurs. We perform backscattered electron imaging, both quantitative (qBEI) and at higher resolution (hrBEI), to obtain 2D maps of mineral content and nanostructural features of 74 osteons. We manually segment CLs from their corresponding osteon, also considering concentric layers of bone (~1.1 ?m in width) adjacent to the CLs. We compare the mineral content of CLs to the mineral content of the inside and outside neighboring layers of their corresponding osteon. We also measure the reduced modulus (Er) and hardness across the CLs using nanoindentation (nIND) in 25 selected regions to correlate them with mineral content. At the micrometer scale, CLs appear 10 +/- 3.5% more mineralized than their corresponding osteon. The CL mineral content is quite heterogeneous but has a stronger spatial correlation with the mineral content of the layers outside rather than inside the osteon ($p < 0.01$). This may suggest an interplay between the CLs mineralization and the mineral content of the surrounding bone, which is locally recycled to build the new osteon [Roschger, Acta Bio 2020]. As illustrated with a specific region in Fig. 1, we exploit indentation maps to compute the average Er inside each CL, as well as within stiffer and more compliant lamellae (here 26.45 +/- 1.31 GPa, 22.98 +/- 2.71 GPa and 20.69 +/- 2.05 GPa, respectively) by analyzing the corresponding post-nIND hrBEI image. Overall, we highlight a periodic alternation of stiffer and softer regions ($p < 0.01$) corresponding to lamellae of different fibers orientations. Additionally, CLs are stiffer and harder ($p < 0.01$) than their corresponding osteon. This mechanical contrast between CLs and lamellar regions may be one additional factor for hampering cracks entering the osteons. Recent findings that CLs have reduced nanoscale porosity in comparison to adjacent lamellar bone could explain the measured higher mineral content and stiffness [Tang, JBMR 2023]. Ongoing work focuses on the mineral properties of CLs measured with X-ray scattering as well as on the interplay between CLs and the osteocyte lacuno-canalicular network.

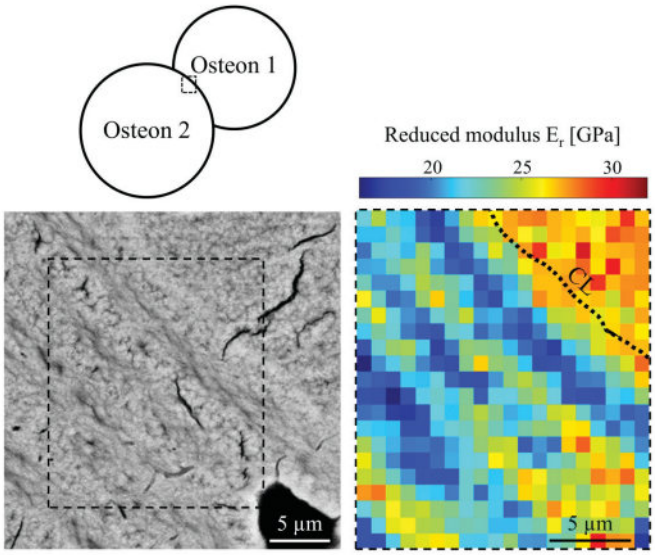

***Disclosures: Astrid Cantamessa**, None*

SAT-042

Longitudinal Evaluation of Female Distal Radius Bone Properties Viewed through 3 Maturational Lenses: Implications for Adolescent Fracture Risk and Site-specific Peak Bone Mass *Jodi Dowthwaite[1], Stephanie Kliethermes[2], Tim Cole[3], Tamara Scerpella[4]. [1]SUNY Upstate Medical University; Binghamton University, United States. [2]University of Wisconsin - Madison, United States. [3]University College London, United Kingdom. [4]University of Wisconsin, United States

Purpose: Distal radius fracture risk is high in adolescence and senescence, and peak young adult bone values set baseline adult fracture risk. Adolescent fracture risk is high at peak height velocity (PHV), while menarche represents increased estrogen exposure, which modulates epiphyseal fusion and bone structure. To assess forearm bone accrual patterns in these contexts, we used 3 age clocks: standard chronological age, age relative to PHV, and age relative to menarche, to evaluate timing of peak growth velocities and peak young adult values for radius bone mass, geometry, and density, in US females with diverse organized physical activity and forearm mechanical loading exposures.Methods: We collected longitudinal data (1997-2023) via annual DXA scans for 1/3 and ultradistal (UD) radius bone mass (BMC, g), projected area (AREA, cm2), and areal bone mineral density (BMD, g/cm2), contemporaneous with height (cm) & body mass (Wt, kg). We used SuperImposition by Translation And Rotation (SITAR package, R) to model growth curves using 3 age clocks (years, y), centered at birth (chronological age, CAGE), individual age at PHV (PHVAGE), and individual age at menarche (gynecological age, GYNAGE). For each DXA outcome and age clock, we report ages at peak velocity (AGEPkV; PkV), ages at peak value (AGEPEAK), and model R2.Results: We included data for 124 white non-Hispanic females, median 11 annual observations [IQR 7-13, range 3-23; CAGE 8y to 36y; GYNAGE -8y to +24y; PHVAGE -5y to +25y; CAGE<10y n=45; CAGE>18y n=96]. Grand means by CAGE were: AGE@PHV=12.4y; AGE@MENARCHE=13.2y; AGE@WtPkV=13.4y. Radius AGEPkVs ranged from: CAGE 12y to 14y; PHVAGE -1y to +3y; GYNAGE -0.5y to +1y (Table 1). All Radius AGEPkVs and AGE@WtPkV lagged after PHV, except 1/3AREA, for which AGEPkV preceded PHV by 1 year. All 1/3 AGEPkVs & AGE@WtPkV were well-centered around menarche, but UD AGEPkVs lagged. All model R2 exceeded 90%.Conclusion: Ultradistal AGEPkVs lag relative to PHV, weight PkV, and 1/3 diaphysis PkVs, suggesting an extended period of metaphysis fracture risk. Ultradistal lags may be due to growth plate proximity and trabecular sensitivity to loading/unloading, estrogen, and metabolic factors. Failure to detect 1/3 BMC & BMD AGEPEAKs suggests diaphysis bone accrual/remodeling may extend into adulthood. Future work will detail nutrient intakes, physical activity, and mechanical loading as time-varying factors for tissue-specific bone mass, geometry, and density growth.

TABLE 1

Clock	Variable	Site	df	AGE_{PkV} [95% CI] (y)	AGE_{PEAK} (y)	R^2
C_{AGE} (y)	AREA (cm^2)	UD	5	12.3 [11.9, 12.6]	15.8	93.0
		1/3	5	13.2 [12.8, 13.6]	14.4	95.4
	BMC (g)	UD	4	13.9 [13.6, 14.3]	21.8	95.1
		1/3	5	13.0 [12.9, 13.2]	NO PEAK	97.6
	BMD (g/cm^2)	UD	4	14.1 [13.1, 15.1]	19.5	91.0
		1/3	5	13.0 [12.5, 13.6]	NO PEAK	93.1
PHV_{AGE} (y)	AREA (cm^2)	UD	4	1.2 [0.8, 1.6]	3.9	92.9
		1/3	4	-1.0 [-1.4, 4.6]	5.8	94.9
	BMC (g)	UD	4	2.6 [2.1, 3.0]	10.6	94.8
		1/3	5	1.6 [1.4, 1.8]	NO PEAK	97.4
	BMD (g/cm^2)	UD	4	2.9 [2.3, 3.6]	8.8	90.2
		1/3	4	1.5 [1.3, 1.8]	NO PEAK	92.5
GYN_{AGE} (y)	AREA (cm^2)	UD	4	-0.5 [-1.2, -0.3]	1.9	93.1
		1/3	5	-0.0 [-2.0, 1.9]	1.6	95.4
	BMC (g)	UD	4	0.8 [0.2, 1.4]	8.5	95.2
		1/3	4	-0.3 [-0.4, -0.1]	NO PEAK	97.6
	BMD (g/cm^2)	UD	4	1.0 [0.3, 1.6]	6.4	90.9
		1/3	4	-0.1 [-0.4, 0.1]	NO PEAK	93.5

***Disclosures: Jodi Dowthwaite**, None*

SAT-043

See Friday Plenary Number FRI-043

SAT-044

Wide Range of Calcium-Sensing Receptor Response to Small Pediatric Burns *Gordon Klein[1] [1]University of Texas Medical Branch, United States

Severe burns in children up-regulate the parathyroid calcium-sensing receptor (CaSR) but the CaSR response to small burns remains unclear. The aim of the study was to review data on smaller pediatric burns and compare circulating ionized calcium (iCa) and parathyroid hormone (iPTH) to those seen in previously published pediatric patients with severe burns (Klein et al J Pediatr 1997). We examined previously published data from 37 anonymized pediatric patients, ages 1-15 yr, with total body surface area burns <20% with known age and length of stay as an index of severity of burn. Admission intact PTH and iCa data were available and correlated with age and length of stay. Findings: No correlation was found between length of stay and iCa, r2=0.22, p- 0.38, or between length of stay and iPTH, r2=0.07, p=0.016. Similarly, no correlation was observed between patient age and admission iCa (r2=0.094, p=0.065) or iPTH (r2=0.04, p=0.21) . Of interest, circulating iCa was low in 34 of 37 of the patients (95%), similar to the published findings in severely burned patients (J Pediatr 1997), However, the distribution of iPTH values, in contrast to values previously published in severely burned pediatric patients, 19 of the 37 patients (51%), were in the normal range (10-65 pg/ml), 10 of the 37 patients (27%) had iPTH in the low range, and 8 of the 37 patients (22%) had iPTH levels above normal despite low circulating iCa. The variability of the iPTH response to small burns compared to large burns (>40% total body surface area) in the presence of low circulating iCa suggests that CaSR gene expression may be affected by severity of burn and the attendant inflammatory and stress responses.

***Disclosures: Gordon Klein**, None*

SAT-045

Self-Reported Sleep Duration and Timing and Bone Mineral Density in Adolescents *Jessica Decker[1] Kimberly Yolton[2] Joseph Braun[3] Heidi Kalkwarf[4] Jessie Buckley[5] Bruce Lanphear[6] Aimin Chen[7] Kim M. Cecil[2] Babette Zemel[8] Jonathan Mitchell[9] [1]CHOP, United States [2]CCHMC, United States [3]Brown University, United States [4]Cincinnati Children's Hospital Medical Center, United States [5]Johns Hopkins, United States [6]Simon Fraser University, Canada [7]UPenn , United States [8]Children s Hospital of Philadelphia, United States [9]Children's Hospital of Philadelphia, United States

Background: Bone accretion can be optimized to maximize peak bone mass during childhood to prevent or delay the onset of osteoporosis in adulthood. Emerging evidence indicates that impaired sleep may be associated with lower bone mineral density. We aimed to determine if an association exists between sleep duration and timing with bone mineral density in adolescents.Methods: We analyzed cross-sectional data from the Health Outcomes and Measures of the Environment (HOME) Study collected in early adolescence. Dual-energy X-ray absorptiometry (DXA) scans yielded the following bone mineral density content (BMC) or areal bone mineral density (aBMD) traits as outcome variables: total body less head (TBLH) BMC, spine aBMD, total hip aBMD, femoral neck aBMD, and distal radius aBMD. All BMC and aBMD variables were converted to age and sex specific Z-scores and adjusted for height-for-age Z-score. Sleep duration (hours) and sleep onset times (hours from 00:00) on week and weekend nights were self-reported. Linear regression models were constructed to examine the association between sleep variables and bone Z-scores, adjusted for sex, race, household income, calcium intake, physical activity, and Tanner stage.Results: The study participants were 229 adolescents, aged 11-14 years; 56% were female and 57.2% non-Hispanic White. Average sleep onset time was 21:30 on weeknights and 00:42 on weekend nights and average sleep duration was 9.1 [standard deviation (SD): 1.1] hours on weeknights and 10.1 (SD: 1.8) hours on weekend nights. We observed no associations between sleep duration on weeknights or weekend nights and the bone outcomes. Similarly, we observed no associations between the timing of going to bed on weeknights or weekend nights and bone outcomes, with one exception. Later time in bed on weekend nights was associated with higher femoral neck aBMD (1 SD later time in bed on weekend nights: b=0.18; 95% CI: 0.02, 0.34; P=0.030). No sex or Tanner stage differences were detected with respect to the association between sleep exposures and the bone Z-score outcomes. Conclusion: Self-reported sleep duration and timing were not associated with TBLH-BMC or aBMD in this study. Future studies using actigraphy to assess sleep patterns are needed to advance this area of research.

***Disclosures: Jessica Decker**, None*

SAT-046

Circulating preosteoclasts and mesenchymal stem cells are decreased in adolescents with Duchenne muscular dystrophy on chronic glucocorticoids whom have a significant fracture history *Angela Sadlowski[1] Julia See[1] Weixin Zhang[2] Arryn Otte[1] Emely Loscalzo[1] Sisir Barik[1] Janet Crane[3] [1]Johns Hopkins University, Department of Pediatrics, Division of Endocrinology, United States [2]Johns Hopkins University, Department of Orthopedic Surgery, Center for Musculoskeletal Research, United States [3]Johns Hopkins University, Department of Pediatrics, Division of Endocrinology and Department of Orthopedic Surgery, Center for Musculoskeletal Research, United States

By adolescence, 80% of people with Duchenne muscular dystrophy (DMD) on chronic glucocorticoids (GCs) have sustained a vertebral compression fracture. We have previously shown in a young GC-induced osteoporosis (GIO) mouse model that GCs decrease preosteoclast platelet-derived growth factor type BB (PDGF-BB), ultimately impairing bone angiogenesis and osteogenesis. As PDGF-BB stimulates the migration of endothelial precursor cells (EPCs) and mesenchymal stem cells (MSCs) to support angiogenesis and osteogenesis, we conducted a case-control study to determine if there is an association between serum PDGF-BB concentrations or peripheral blood mononuclear cell (PBMC) subpopulations representative of circulating bone precursor cells with DMD-GIO. Cases included 8-20-year-old DMD patients with GIO as defined by a significant fracture history (DMD-GIO, n=14); two control groups included disease controls, defined as DMD patients on chronic GCs without a significant fracture history (DMD-control, n=10) and healthy controls (n=9) whom were age- and sex-matched people not on any prescription medications and without a significant fracture history. The mean GC duration was 12.8 years for the DMD-GIO group and 9.0 years for the DMD-control group (P=0.06), partially explained by the DMD-GIO group being slightly older (16.5 years vs 14.4 years, P=0.3). Preliminarily, mean serum PDGF-BB concentration in DMD-control (n=6) was significantly lower relative to DMD-GIO (n=9) and healthy controls (n=9) ($P < 0.05$). PBMC percentage of preosteoclasts (CD14+, Stro-1-, CD105-) was significantly decreased in both DMD groups (DMD-GIO, n=11; DMD-control, n=4) relative to healthy controls (n=8). The percent of EPCs (CD34+, CD14-, Stro-1-, CD105-) was similar between DMD-GIO and healthy controls but increased significantly in DMD controls. The percent of MSCs (Stro-1+, CD105+, CD14-, CD45-) was lowest in DMD-GIO, intermediate in DMD controls, and highest in healthy controls. (P=0.05). In prospective follow-up, 8 of the DMD controls have sustained at least one vertebral compression fracture, such that additional analyses are underway to determine if a specific biomarker correlates with the probability of future fracture. Overall, a low circulating percent of preosteoclasts and MSCs was observed in patients with DMD-GIO,

whereas DMD-controls had low concentrations of PDGF-BB, low circulating preosteoclasts and MSCs, but high EPCs relative to age- and sex-matched healthy controls

***Disclosures: Angela Sadlowski**, None*

SAT-047

Saphenous Nerve Transection Results in Sensory and Sympathetic Denervation of the Mouse Tibia *Talia Lizotte[1,] Gesele Henderson[1,] Jacob Hickey[1,] Peter Caradonna[1,] Victoria Eaton[1,] Gabriel DeOliveira[1,] Derek Molliver[1,] TAMARA KING[1,] Kathleen Becker[1,] [1]University of New England, United States

The saphenous nerve is a sensory nerve that is commonly injured during ACL repair, varicose vein surgery, and other procedures, resulting in numbness or pain. Retrograde labeling studies have suggested that the tibia is innervated by the saphenous nerve, but this has not been confirmed with nerve transection. While sensory and sympathetic input to bone impacts bone metabolism, little is known about the specific consequences of saphenous nerve injury on tibial innervation and bone mineral density (BMD). We hypothesize that saphenous nerve transection will result in a decrease in sensory nerve fibers in the tibia. A greater understanding of elements regulating tibial innervation will help identify risk factors influencing tibial BMD.To demonstrate that the saphenous nerve innervates the tibia, fast blue dye was injected into the proximal tibia of saphenous nerve transected or sham 8-week-old female C57BL/6J mice. The L2-L5 dorsal root ganglia (DRG) were isolated one week post-injection and fast blue positive cells were quantified in the DRG. The highest level of retrograde labeling was observed in the L2 and L3 DRG of sham surgery mice. To determine if transection of the saphenous nerve resulted in tibial denervation, the saphenous nerve was unilaterally transected in 8-week-old female C57BL/6J mice and the ipsilateral and contralateral control tibiae were isolated 2 weeks post-nerve transection. Retrograde labeling from the tibia to the L2 DRG was reduced by 75% in mice with saphenous nerve transection, consistent with the paradigm that the saphenous nerve is the primary source of tibial innervation. Immunohistochemical analysis of sensory and sympathetic innervation was performed using immunofluorescent staining for calcitonin gene-related peptide (CGRP, sensory fiber), tyrosine hydroxylase (TH, sympathetic fiber) and ?III-tubulin (?3T, pan-neuron). CGRP, TH, and ?3T positive fibers were reduced by 40-60% in the proximal, lateral-most periosteum of the tibia ipsilateral to the saphenous nerve transection. Longitudinal analysis of saphenous nerve transected animals indicated no long-term hindlimb unloading. These data show that saphenous nerve denervation reduces sensory and sympathetic innervation of the tibia. Our findings demonstrate that the saphenous nerve is a critical source of tibial innervation making transection of the saphenous nerve a versatile model to study the impact of innervation on bone.

***Disclosures: Talia Lizotte**, None*

SAT-048

Chronic kidney injury induced bone loss through downregulation of the runt-related transcription factor 2-alkaline phosphatase signaling pathway *Yu-Pin Chen[1,] Tso-Hsiao Chen[1,] Ruei-Ming Chen[2,] [1]Wan Fang Hospital, Taiwan, Province of China, [2]Taipei Medical University, Taiwan, Province of China

In Taiwan, the population density of kidney dialysis is the highest in the world. Unfortunately, the patients suffering from end-stage renal disease (ESRD) usually also raise the risk of bone disorders. This study was aimed to investigate the effects of chronic kidney injury (CKI) on loss of bone mass and the possible mechanisms. Administration of male ICR mice with 0.2% adenine for 4 weeks significantly elevated levels of serum creatinine, blood urea nitrogen, and urea, finally resulting in server insults to the kidneys. In parallel, our results by micro-computed tomography (?CT) displayed that administration of mice with CKI significantly decreased trabecular bone numbers, bone volumes, and trabecular thickness, but caused an elevation in trabecular separation. As to the mechanisms, exposure of female ICR mice to 0.2% adenine for 4 weeks diminished levels of runt-related transcription factor 2 (Runx2), a critical transcription factor of osteogenesis, in the femur. Alkaline phosphatase (ALP) is a typical biomarker of osteoblasts. A bioinformatics search revealed that there are 3 Runx2-specific DNA-binding elements existing in the 5'-promoter of the alp gene. Treatment of mice with CKI meaningfully inhibited ALP mRNA and protein expressions. Furthermore, our in vitro analysis also confirmed that exposure of MC3T3-E1 cells to indoxyl sulfate, a uremic toxin, significantly inhibited runx2 and alp gene expressions and consequently suppressed cell mineralization. Therefore, this study has shown that CKI could induce loss of bone bass through downregulating the Runx2-ALP signaling events.

***Disclosures: Yu-Pin Chen**, None*

SAT-049

The Time Course of Bone Resorption Following Muscle Paralysis is Sex-Dependent *Leah Worton[3,] Phillipe Huber[3,] Brandon Ausk[3,] Steven Bain[3,] Adrian Piliponsky[2,] Edith M. Gardiner[3,] Ted Gross[3,] [3]University of Washington, United States, [2]Seattle Children's Research Institute, United States, [3]University of Washington,

Transient calf paralysis in female mice rapidly initiates osteoclast mediated trabecular bone resorption in the ipsilateral proximal tibia metaphysis. In this study, we explored whether: 1) transient muscle paralysis induces acute bone resorption in male mice as it does in female mice, and 2) if elevated Substance P (SP), a neuropeptide precursor to neurogenic inflammation, precedes the initiation of trabecular bone resorption in female and male mice. First, 8 female and 8 male C57BL/6 mice underwent right calf paralysis and serial microCT imaging of the proximal tibia and tibia midshaft (d-1, d6, d13, and d21). Standard trabecular and cortical bone morphology outcome measures were determined as a percentage of d-1. Second, 41 female and 25 male C57BL/6 mice were randomly assigned to a naïve group (F:11; M:5) or right calf paralysis (F:30; M:20). Right tibia bone marrow was removed on d1, d3, d7, and d14 post-paralysis and SP was quantified via ELISA (F: > n=6/timepoint, 3 independent experiments; M: n=5/timepoint, 1 experiment). For each experiment, data were expressed as a percentage of mean naïve group SP. Consistent with the literature, female mice demonstrated significant proximal tibia trabecular bone loss by d6 vs baseline (BV/TV, mean +/- SE: -45.0 +/- 5.9%, $p<0.01$) that progressed through d13 (-73.1 +/- 2.0%, $p<0.001$) and then plateaued (d21: -77.1 +/- 2.6%, $p<0.001$). In contrast, trabecular bone loss was not observed in male mice at d6 vs d-1 (BV/TV: 1.3 +/- 9.9%, $p=0.33$), but it was evident by d13 (-50.6 +/- 7.5%, $p=0.002$) and was similar in magnitude to female mice by d21 (-72.8 +/- 3.6%, $p<0.001$). Midshaft endocortical expansion (a surrogate for osteoclastic resorption) demonstrated the same pattern of delayed initiation but a similar endpoint (F v M: d6 3.9 +/- 1.6 % vs -0.4 +/- 0.5%, $p=0.02$; d21: 10.4 +/- 2.0% vs 8.1 +/- 2.0%, $p=0.43$). SP expression in female mice was rapidly elevated vs naïve (d1: 48.0 +/- 10.9%, $p<0.01$) and returned to normal levels by d14 (-17.1 +/- 19.0%). SP expression in male mice was not elevated at any time point vs naïve mice. In summary, trabecular and cortical bone loss induced by transient muscle paralysis was delayed in male vs female mice. Further, acute upregulation of SP in female mice, but not male mice, suggests sex-based differences in neurogenic signaling following transient muscle paralysis. As a result, successful interventions to mitigate paralysis induced bone loss may require sex-specific targeting.

***Disclosures: Leah Worton**, None*

SAT-050

See Friday Plenary Number FRI-050

SAT-051

See Friday Plenary Number FRI-051

SAT-052

Morphine-induced Bone Loss is Associated with Altered Bone miRNA Expression in Male C57BL/6J Mice *Audrie Langlais[1,] Claire Morrow[1,] Katherine Motyl[1,] [1]MaineHealth Institute for Research, United States

Opioids pose a serious risk to bone health by reducing bone mineral density and increasing fracture risk. Previously, we identified morphine-induced bone loss was due to reduced bone formation in male but not female mice. This was associated with differentially expressed circulating micro RNAs (miRNA) in serum and altered target gene expression in bone. However, miRNA changes in bone have not yet been assessed. We delivered morphine (17 mg/kg) or vehicle (0.9% saline) subcutaneously via osmotic minipumps to 8-week-old C57BL/6J male mice (N = 12/group) for four weeks. Femur and vertebrae were isolated for micro-computed tomography and mRNA/miRNA was extracted from tibia for qPCR. Consistent with our previous study, trabecular bone volume fraction was reduced by 10% in the L5 vertebrae ($p<0.05$) and cortical area fraction was reduced by 5% in the femur midshaft. We confirmed that the top differentially expressed miRNAs from serum were also expressed in tibia bone marrow and cortical bone. miR-223-3p was significantly elevated in serum but downregulated in bone marrow and not altered in cortical bone. Interestingly, miR-223-3p has been previously associated with opioid use in humans and shown to regulate osteogenesis through its targets, including Foxo3 and Igf1r. Alternately, miR-28a-3p was downregulated in serum and cortical bone. Although the function of this miRNA has not been previously investigated within bone, several predicted and validated targets (e.g., Tgif1, Sox2) suggest an influence on osteoblast function. Furthermore, within bone marrow, expression of all six miRNAs examined were significantly lower, which is consistent with morphine causing a negative skew in miRNA expression in serum in our previous study. Due to the robust suppression of miRNA levels in marrow, we assessed expression of miRNA biogenesis genes (Dicer1, Drosha, Ago2 and Xpo5), but none were altered by morphine. Future studies will test whether the nervous system, the major target of morphine, is the source of suppressed miRNA levels in marrow and serum. Furthermore, we will test how opioids and miRNA gene targets collectively impact osteoblast function to cause bone loss. This

work will critically expand our understanding of how opioids impair bone and may influence future clinical treatment and prevention strategies.

***Disclosures: Audrie Langlais**, None*

SAT-053

See Friday Plenary Number FRI-053

SAT-054

Osteoclast and neuronal crosstalk as a mechanism for chest wall pain in lung cancer patients receiving thoracic radiosurgery *Sun Park[1], Joseph Moore[1], Kaitlyn Reno[1], Michael Farris[1], Christopher Peters[2], Jeffery Willey[1]. [1]Department of Radiation Oncology, Wake Forest University School of Medicine, United States. [2]Department of Anesthesiology, Wake Forest University School of Medicine , United States

Purpose: Thoracic stereotactic body radiation therapy (SBRT) for the treatment of lung tumors near the chest wall unavoidably delivers high doses of radiation to the surrounding normal tissues. This predisposes patients to debilitating radiation-induced chest wall pain (CWP). CWP may present and resolve acutely or may develop and persist chronically over years with or without bone fractures. The underlying mechanisms of CWP are unclear, but could involve damage to intercostal peripheral nerves, and or RT induced osteoclast mediated bone degradation. While RT induced nerve damage has typically been thought of as a separate process from RT induced bone damage, we describe here evidence of potential crosstalk between factors released from irradiated osteoclasts and nerves.Methods: We utilized an in vitro culture system involving a pre-osteoclast mouse cell line (Raw264.7) and primary mouse thoracic dorsal root ganglion (DRG) neuron cultures. Mature osteoclast cells were plated on Osteoassay plates to measure resorption of a bone proxy surface. Osteoclasts were irradiated with a single fraction of 10Gy using Cs137 ?-rays, and conditioned media (CM) from these cells was collected at 24h and applied to non-irradiated neurons. Changes in neurite growth was assessed with immunohistochemistry and alterations in gene expression of pain-associated molecular markers, including substance P (SP), calcitonin gene-related peptide (CGRP),and nerve growth factor (NGF) were measured using quantitative real time PCR. Unpaired t-tests were used for statistical analyses (?=0.05).Results: Radiation induced osteoclast activity at 24h as measured with Osteoassay disks. Non-irradiated neurons treated with CM, demonstrated no change in total nerve length. However, neurons exposed to CM expressed a higher level of CGRP (+38.5%), substance P (+29.5%), and NGF (+14.5%) compared to control media.Conclusions: RT induced damage to intercostal nerves may be influenced by the release of factors from nearby resident osteoclasts within ribs or vertebrae, triggering expression and release of pain related neuropeptides. This osteoclast mediated elevation in neuropeptides could contribute to debilitating radiation related CWP. Understanding the crosstalk between osteoclasts and peripheral nerves may identify potential targets for preventating CWP, and provide clinicians an opportunity to achieve higher tumor dosing with reduced toxicity.

***Disclosures: Sun Park**, None*

SAT-055

See Friday Plenary Number FRI-055

SAT-056

3D Genomic features across >50 diverse cell types reveal insights into the differing genomic architectures of BMD determination and osteoporotic fracture pathogenesis *Khanh B. Trang[1], Matthew C. Pahl[1], James A. Pippin[1], Alessandra Chesi[2], Yadav Wagley[3], Babette Zemel[4], Kurt Hankenson[5], Andrew D. Wells[6], Struan Grant[6]. [1]Children's Hospital of Philadelphia, United States. [2]University of Pennsylvania, United States. [3], , [4]Children s Hospital of Philadelphia, United States. [5]University of Michigan, United States. [6]Children s Hospital of Philadelphia / University of Pennsylvania, United States

The incomplete correlation between bone mineral density (BMD) determination and the pathogenesis of osteoporotic fracture suggests a degree of difference in underlying biological processes. Genome-wide association studies (GWAS) have identified numerous genetic variants associated with either BMD or osteoporotic fracture, where indeed the genetic overlap is also only partial. There is much that remains to be characterized for such loci, including cellular context, underlying causal variants and corresponding effector genes. Leveraging our existing 3D genomic datasets across >50 diverse human cell types consisting of high-resolution promoter-focused Capture-C/Hi-C, ATAC-seq and RNA-seq, enables us to contrast both the causal variants and the corresponding effector genes for these two orthogonal traits. These cell types include those closely relevant to bone biology, such as human mesenchymal stem cell (hMSC)-derived osteoblasts, plus those spanning more broadly across metabolic, neuronal and immune cell types. Using stratified LD regression, we calculated the proportion of genome-wide SNP heritability attributable to our derived cell type specific features via the integration of the most recent adult BMD and osteoporosis fracture GWAS summary statistics. These analyses revealed a statistically significant enrichment ($P<0.05$) for osteoporotic fracture across multiple immune cell types (plasmacytoid and classical CD1c+ dendritic cells, along with several classes of T-cells), pancreatic ?-cells and adipocytes; while in contrast, the features related to BMD were more enriched for bone-related cell types (hMCS-derived osteoblasts, the human fetal osteoblasts hFOB cell line), as well as several derived neuron and neural progenitor cell lines. Subsequent application of our chromatin contact-based 'variant-to-gene' mapping of these loci identified key "hub" genes, functional pathways, and biological processes, including regulation of extracellular matrix remodeling and immune response. These observations further reinforce the prevailing hypothesis that GWAS-implicated variants confer their effects via complex polygenetic regulatory mechanisms involving key signaling pathways. In conclusion, our comprehensive appraisal of 3D genomic datasets in a myriad of different cell types drives greater genomic understanding of both the similarities and the differences across BMD determination and osteoporotic fracture pathogenesis.

***Disclosures: Khanh B. Trang**, None*

SAT-058

See Friday Plenary Number FRI-058

SAT-059

Secoisolariciresinol exerted bone protective effects via inhibiting intestinal tryptophan hydroxylase 1 (Tph-1) and altering circulating serotonin *Yu-Xin Zhu[1], Hong-Yu Peng[1], Man Sau Wong[2], Hui-Hui Xiao[1]. [1]The Hong Kong Polytechnic University Shenzhen Research Institute, China. [2] The Hong Kong Polytechnic University, Hong Kong

We previously demonstrated that the lignan-rich fraction from Sambucus williamsii Hance could exert bone protective effects indirectly by suppressing serotonin synthesis via inhibiting the intestinal tryptophan hydroxylase 1 (TPH-1) protein, a rate-limiting enzyme of serotonin synthesis, and modulating gut microbiota composition. However, there was no direct evidence for the modulating actions of lignans on TPH-1 protein. This study aims to verify the direct actions of a major lignan Secoisolariciresinol (SECO) from S. williamsii on TPH-1 protein, and its mechanism on bone protection via modulating circulating serotonin. The molecular docking, surface plasmon resonance (SPR), TPH-1 protein activity, TPH-1 protein expression, mRNA expression as well as mice serum serotonin level and bone properties upon SECO treatment were determined. Molecular docking study and SPR analysis revealed that SECO exhibited high binding affinities to Tph-1 protein. SECO significantly inhibited the TPH-1 activity and protein expressions in RBL 2H3 cells. It also decreased the serotonin level, inhibited intestinal TPH-1 protein expressions, and improved bone properties in OVX mice. Our results indicated that SECO is a new TPH-1 inhibitor and it induced decreased circulating serotonin level may account for its bone protective effects.

***Disclosures: Yu-Xin Zhu**, None*

SAT-060

See Friday Plenary Number FRI-060

SAT-062

See Friday Plenary Number FRI-062

SAT-063

The Impact of Zoledronic Acid on Bone health and Fracture Risk in Intestinal Transplant Patients *Ayat ElSherif[1], LEILA KHAN[2], Krupa Doshi[3], James Bena[4], Kareem Abu-Elmagd[1]. [1]Center of Gut Rehabilitation and Transplantation, Cleveland Clinic Foundation, OH, USA, United States. [2]CLEVELAND CLINIC FOUNDATION, United States. [3]Mayo Clinic Arizona, , [4]Department of Quantitative Health Sciences, Cleveland Clinic Foundation, OH, USA, United States

BACKGROUND: Intestinal transplant is the standard of care for patients with gut failure (GF) who can no longer be maintained on total parenteral nutrition (TPN). The intestinal transplant recipients are at increased risk of osteoporosis and deleterious metabolic effects of TPN than their solid organ counterparts. However, existing literature about bone health in intestinal transplant recipients is sparse. The use of alendronate in solid organ and intestinal transplantation was shown to be associated with a reduction in bone loss. However, the use of oral bisphosphonates (only 1-4% of which are absorbed from the gut) may not be the ideal answer for intestinal transplant recipients. This is the first study to examine pre-surgical use of one or more doses of zoledronic acid in intestinal transplant recipients and to evaluate its impact on the fracture risk post-transplantation.METHODS: An institutional review board-approved prospective database was reviewed of patients with total parenteral nutrition-dependent catastrophic and chronic GF who were referred for surgical

intervention particularly transplantation from 2013-2019 and had received at least one dose of zoledronic acid. Patient demographics, status of digestive health, total parenteral nutrition details, type of allograft received and mineral data were collected. Date of zoledronic acid, number of doses received and incidence of fragility fractures post- transplant were analyzed. RESULTS: A total of 28 patients were identified. Fifty-seven percent of the patients (n=16) were females. Median age was 47 years (IQR 33, 55) and median BMI was 24.7 (IQR 21.7, 27.9). The incidence of post-transplant fragility fracture in the cohort was 14% (n=4). The time between first pre-transplant zoledronic acid injection and surgery was the only significant risk factor for fragility fracture (p=0.024). Age, sex, BMI, duration of gut disease, and TPN duration were not associated with increased fracture risk. A significant increase in vitamin D levels was noted from pre-transplant to post-transplant (Median 25 [IQR 20, 30] vs 54 [37, 61], p=0.009).CONCLUSION: Pre-transplant zoledronic acid has a protective effect against fragility fracture in patient undergoing transplant patients.

Table. Predictors of Fracture

Characteristic	N	Overall, N = 28[1]	No Fracture, N = 24	Fracture, N = 4	p-value[2]
Years of Reclast, Median [IQR]	28	1 [1, 2]	2 [1, 2]	1 [1, 2]	0.64
Years from Reclast to Surgery, Median [IQR]	28	0.31 [0.04, 0.59]	0.39 [0.12, 0.69]	-0.50 [-1.19, 0.07]	**0.024**
TPN duration (years), Median [IQR]	28	3.8 [2.0, 5.4]	3.3 [1.6, 5.4]	4.2 [3.5, 5.1]	0.77
Age, Median [IQR]	28	47 [33, 55]	47 [33, 55]	44 [37, 51]	0.97
Sex, n (%)	28				>0.99
F		16 (57)	14 (58)	2 (50)	
M		12 (43)	10 (42)	2 (50)	
BMI, Median [IQR]	28	24.7 [21.7, 27.9]	24.7 [21.9, 28.1]	23.6 [19.9, 27.3]	0.45
Illness Duration (years), Median [IQR]	26	8 [4, 13]	10 [4, 19]	6 [5, 8]	0.64
Ileocecal valve, n (%)	27	1 (3.7)	1 (4.3)	0 (0)	>0.99
End stoma, n (%)	18	8 (44)	7 (50)	1 (25)	0.59

[1]Median [IQR]; n (%)
[2]Wilcoxon rank sum test; Fisher's exact test

***Disclosures: Ayat ElSherif**, None*

SAT-064

Association between bone mineral density and body composition among Mongolian adult women *Narantsetseg Jargalsaikhan[1], Giimel Ajnai[1], Sarnai Gunsenkhorloo[1]. [1]Research and Development Office, Fourth Hospital, Mongolia

Background: Maintaining bone health is an important public health issue and challenge (concern) in women for preventing a determinant of the risk of developing osteoporosis later in life. The aim of the present study is to investigate the relationship between bone mineral density (BMD) analysis, and body composition in a female population in Mongolia. Methods: A sample of 309 women aged between 20 and 39 underwent scans between January and December 2022 by dual x-ray absorptiometry (DXA) in Fourth Hospital, Ulaanbaatar City. The correlation between bone mineral density analysis and total fat mass, lean mass, and bone mass was analyzed by Pearson correlation and multiple linear regression analysis. Results: According to the DXA results, 76.4% of women had normal bone mineral density, and 20.1% and 3.6% were diagnosed with osteopenia and osteoporosis, respectively. Multiple linear regression analysis indicated BMD was positively associated with total fat mass (?: 0.042, p<0.001), total lean mass (?: 0.083, p<0.001), and bone mass (?: 0.857, p<0.001). The positive correlation of BMD and lean and bone mass was significant in younger women aged <30 years, whereas women over 30 were positively associated with lean mass and fat mass. There were no significant relationships between BMD and body weight, percentage of body fat, and android/gynoid ratio parameters. Conclusions: Our results indicate that women younger than 30 were associated with BMD, lean, and bone mass. Emphasizing lean mass and bone mass in young Mongolian women may be valuable for improving bone health.

***Disclosures: Narantsetseg Jargalsaikhan**, None*

SAT-065

Injectable Levonorgestrel Butanoate Does Not Result in a Decline in Z-Scores in Reproductive-Age Women *Jeffrey Kroopnick[1], Min Lee[1], David Archer[2], Mitchell Creinin[3], Jeffrey Jensen[4], Aaron Lazorwitz[5], Lori Gawron[6], Carolyn Westhoff[7], Katharine White[8], Diana Blithe[1]. [1]Contraceptive Development Program, Eunice Kennedy Shriver National Institute of Child Health and Human Development, NIH, United States. [2]Clinical Research Center, Department of Obstetrics and Gynecology, Eastern Virginia Medical School, United States. [3]Department of Obstetrics and Gynecology, University of California, Davis, United States. [4]Department of Obstetrics and Gynecology, Oregon Health & Science University, United States. [5]Department of Obstetrics and Gynecology, University of Colorado Anschutz Medical Campus, United States. [6]Department of Obstetrics and Gynecology, University of Utah, United States. [7]Department of Obstetrics and Gynecology, Columbia University, United States. [8]Department of Obstetrics and Gynecology, Boston University, United States

Purpose: The NICHD Contraceptive Development Program has developed levonorgestrel butanoate (LB) as an injectable contraceptive that will inhibit ovulation for 3 or more months, with the goal of reducing side effects, such as weight gain and mood issues, compared to depot medroxyprogesterone acetate (DMPA), the only marketed injectable progestin available in the U.S. The FDA has issued a warning to DMPA users of significant decreases in bone mineral density (BMD) and possible increased fracture risk with long-term use. Levonorgestrel has a well-established history of clinical use in a variety of contraceptives, including pills, intrauterine devices, and implants. Its efficacy and safety are well-recognized, particularly for obese women or women with other risk factors for which estrogen is contraindicated. Here, we report the change in Z-scores pre- and post- treatment in subjects receiving escalating LB doses.Methods: Participants received one dose of LB intramuscularly or subcutaneously and were followed until return to ovulation occurred. Subjects received LB 40 mg (20 mg/mL) intramuscularly (Group A) or subcutaneously (Group B). Group B2 received LB 40 mg (70 mg/mL) subcutaneously. Baseline and post-treatment Dual Energy X-ray Absorptiometry (DXA) scans were obtained. Two subjects were excluded from analysis due to a baseline Z-score of <= -2.0. We compared pre- and post-treatment Z-scores at the lumbar spine (LS) and total hip (TH) using a two-tailed t-test for two independent means and considered a post-treatment Z-score <= -2.0 as clinically significant.Results: We enrolled 86 participants into Groups A (n=24), B (n=31), and B2 (n=31) with median duration from baseline to post-treatment DXA scans of 129, 185, and 205 days. In Group A, mean pre- and post-treatment Z-scores at the LS were 0.04 and 0.00, respectively (p=0.58) and at the TH were 0.00 and -0.05, respectively (p=0.90). In Group B, LS scores were 0.28 and 0.25, respectively (p=0.91) and TH scores were 0.24 and 0.18, respectively (p=0.84). In Group B2, LS scores were 0.47 and 0.29, respectively (p=0.57) at TH scores were 0.36 and 0.45, respectively (p=0.76). No subject had a post-treatment Z-score <= -2.0.Conclusion: We found no clinically significant decline in Z-scores among participants receiving injectable LB over the treatment period in our study. Once a treatment dose is identified, larger, long-term studies are needed to assess bone density with prolonged use.

***Disclosures: Jeffrey Kroopnick**, None*

SAT-066

Prevalence of Low Vitamin D Level among Older US Asian and Pacific Islander Women *Joan Lo[1], Malini Chandra[1], Jennifer Park-Sigal[1], Jeanne Darbinian[1], Catherine Lee[1], Wendy Yang[1]. [1]Kaiser Permanente Northern California, United States

Asian women are at higher risk for low Vitamin D level compared to non-Hispanic White (NHW) women, but differences may exist among subgroups. Large population studies among US Asian subgroups remain lacking. PURPOSE: We compared the prevalence of low vitamin D among Asian and Pacific Islander (PI) and NHW women aged 50-89y. METHODS: Data from Asian/PI and NHW women in a Northern California health plan who had body mass index (BMI) assessed at a clinical encounter in 2010-2019 and measurement of 25-hydroxy-vitamin D (25OHD) within 1 year of the visit were examined. The earliest BMI and 25OHD level in the specified time frame was ascertained. Prevalence of low vitamin D (25OHD <20 ng/mL) was examined by race and ethnicity, reported with 95% confidence intervals [CI]. Modified Poisson regression was used to calculate prevalence ratios (PRs), adjusting for age and BMI. RESULTS: Among 50,728 Asian/PI women (average age 60.0+/-9.8y; 13,865 Chinese, 12,629 Filipina, 3902 South Asian, 3238 Japanese, 2170 Vietnamese, 1320 Korean, 1212 Native Hawaiian/Pacific Islander (NHPI), 807 other Southeast Asian, and 11,585 unspecified or other Asian/PI) and 181,862 NHW women (average age 63.2+/-10.8y), prevalence of low 25OHD was 19.4% [19.0-19.7%] for Asian/PI women and 14.8% [14.7-15.0%] for NHW women. Among Asian/PI women, prevalence ranged from 15.7% [14.4-16.9%] for Japanese, 17.4% [16.7-18.1%] for Filipina, 19.2% [18.6-19.9%] for Chinese, 20.4% [18.2-22.6%] for Korean, 23.6% [21.9-25.4%] for Vietnamese, 22.7% [19.8-25.6%] for other Southeast Asian, 23.9% [22.5-25.2%] for South Asian, and 30.9% [28.3-33.5%] for NHPI women. Adjusted PRs for low 25OHD (NHW as reference) were 1.29 [1.19-1.40] for Japanese, 1.33 [1.28-1.39] for Filipina, 1.65 [1.59-1.71] for Chinese, 1.74 [1.56-1.93] for Korean, 1.75 [1.65-1.85] for South Asian, 1.96 [1.80-2.13] for NHPI, 2.06 [1.91-2.22] for Vietnamese, and 1.79 [1.58-2.04] for other Southeast Asian women. CONCLUSION: In a community-based population of older Asian/PI women receiving healthcare, low Vitamin D prevalence was higher than NHW women but varied widely by Asian/PI ethnicity, ranging from 30% higher for Japanese and Filipina women, to 65-75% higher for Chinese, Korean, and South Asian women, and twofold higher for NHPI and Vietnamese women, accounting for age and BMI. While these findings are limited by lack of data on Vitamin D intake or treatment, they emphasize the much higher risk of low vitamin D among selected Asian/PI subgroups.

***Disclosures: Joan Lo**, None*

SAT-068

Low bone density screening rate in patients treated with long term glucocorticoid therapy *Tasma Harindhanavudhi[1], Rebecca Freese[2], Nolawit Tesfaye[1], Susanne Trost[1]. [1]Division of Endocrinology, Diabetes and Metabolism, Department of Medicine, University of Minnesota, United States. [2]Clinical and Translational Science Institute, University of Minnesota, United States

Glucocorticoid is the most common cause of secondary osteoporosis. Approximately 10% of patients who receive long-term glucocorticoid treatment sustain a fracture. Previous data derived from U.S. health maintenance organizations in 2000-2001 found only 9.8% of the total population received a bone density measurement. However, no recent data are available. Our aim is to understand the clinical practice pattern of bone density screening (DXA) in patients who are prescribed long-term glucocorticoid therapy (for 3 months or longer).

This retrospective cohort study (n=8924) used the electronic medical record's databases to identify patients who were dispensed 2.5 mg of prednisone or equivalent per day for at least 3 months between 2017 to 2022. Approximately half of the patients (51%) were women and the majority of participants were Caucasian (88.6%). Overall, 15% of the patients (n=1378) had at least one DXA measurement within 2 years prior and 1 year after the index glucocorticoid prescription. Among patients who received bone density screening, 17% had more than one DXA measurement. Among DXA measurements performed, 62.4% (n=1041) were performed within 2 years before the glucocorticoid initiation, while 21.9% (n=366) and 15.7% (n=262) were performed within 6 months and between 6 months to 1 year after glucocorticoid initiation, respectively. Our study found suboptimal bone density screening in patients receiving long-term glucocorticoid therapy as recommended in the clinical practice guideline. Future efforts should focus on quality improvement to understand the barriers and improve the frequency of bone density screening to facilitate osteoporosis management.

***Disclosures: Tasma Harindhanavudhi**, None*

SAT-069

The association of muscle (amount and function) with bone mass in women diagnosed with anorexia nervosa followed up by a multidisciplinary team
*Iana Mizumukai de Araujo[1], Carlos Ernesto Garrido Salmon[2], Francisco Jose De Paula[3]. [1]Ribeirão Preto Medical School - University of São Paulo, Brazil, [2]University of São Paulo, Brazil, [3]Ribeirao Preto Medical School- USP, Brazil

Introduction: Anorexia nervosa (AN) is a psychiatric disorder in which the individual presents extreme aversion to weight gain, leading to self-imposed fasting. The catabolism in muscle and adipose tissues is accompanied by bone loss and marrow adipose tissue (MAT) expansion. The present study was designed to evaluate the association of muscle mass and metabolism with bone properties and MAT composition in AN patients.Methods: The study comprised 13 women with AN and 25 healthy women (C). A multidisciplinary team is treating the AN group. BMD was measured by DXA in several regions, while MAT composition (saturated/unsaturated/total) were assessed by 1H-MR Spectroscopy in proximal tibia. Phosphocreatine (PCr) and inorganic phosphorus (Pi) were measured by 31P-MR Spectroscopy in rest in the soleus muscle. Trabecular bone score (TBS) was assessed via the software TBS iNsight v.3.0. Lean mass index (LMI) was calculated as appendicular skeletal muscle mass adjusted by height squared and Fat mass index (FMI) calculated as body fat mass dividing by height squared. p-value<0,05 was considered as statistical threshold.Results: We present the medians of the results. The groups were matched by age (Median: C=24, A=21y) and height (C:1.63; AN=1.60m). The BMI was higher in C than in AN (C=21.1; AN=19.1). AN showed lower BMD and Z-score in lumbar spine, total hip, and femoral neck than C. TBS was also lower in AN than in C (C=1.462, AN=1.302). The total (C=93.4, AN=94.85%), saturated (C=39.49, AN=36.3%), and unsaturated (C=7.69, AN=7.98%) MAT were similar between the groups. Lean mass index was similar between the groups (C=6.1, AN=5,4 kg/m²). FMI was lower in AN than in C group (C=7.3, AN=5.5 kg/m²). OC, albumin, PTH, and 25-hydroxyvitamin D were similar between the groups. Rest PCr and Pi were similar between the groups. There was a positive correlation between FMI and TBS (r=0.58). LMI was positively associated with L1-L4, TH, and FN BMD (respectively r=0.45, 0.44, 0.38). Conclusion: Our data reaffirms that bone loss is a long-lasting complication for women with AN. In addition, our results contribute to this line of investigation by showing that muscle mass is positively associated with bone mass. People with AN have bone mass and quality loss. In addition, the AN group showed lower adipose tissue but similar LMI in comparison to controls. An adequate nutritional approach can mitigate muscle mass loss and limit the expansion of MAT in anorexia nervosa.

***Disclosures: Iana Mizumukai de Araujo**, None*

SAT-070

See Friday Plenary Number FRI-070

SAT-071

Bone Mineral Density and Body Composition in Postmenopausal Primary Hypothyroid Females on Replacement Dose of Levothyroxin and its Correlation with TSH and Duration of Hypothyroidism
*Eram Nahid[1], Parth Jethwani[2], Kamla Kant Shukla[3], Madhukar Mittal[4], M K Garg[5], Ravindra Shukla[4]. [1]Resident, Department of Endocrinology and Metabolism, All India Institute of Medical Sciences(AIIMS),Jodhpur, India. [2]Resident, Department of Endocrinology and Metabolism, All India Institute of Medical Sciences, Jodhpur, India. [3]Associate professor, Department of Biochemistry, All India Institute of Medical Sciences(AIIMS), Jodhpur, India. [4]Additional Professor, Department of Endocrinology and Metabolism, All India Institute of Medical Sciences, Jodhpur, India. [5]Professor, Department of Endocrinology and Metabolism, All India Institute of Medical Sciences, Jodhpur, India

Background:Long term use of Levothyroxin (LT4) is known to increase the risk of fracture,but there is limited knowledge on Bone mineral density (BMD) and body composition in postmenopausal primary hypothyroid female patients. Body composition measures such as Visceral adipose tissue (VAT) and Total body fat (TBF%) are important determinants of cardiometabolic diseases.Aim/Purpose:To assess BMD and body composition in postmenopausal primary hypothyroid female patients on replacement dose of LT4 by Horizon-A DXA scanner and to explore association of BMD with dose of LT4,duration of hypothyroidism & level of serum TSH.Methodology:This is single-centre cross-sectional study conducted among 104 postmenopausal primary hypothyroid females on replacement dose of LT4. The outcome included BMD of femur neck, total hip, lumbar spine, distal forearm and whole body, along with body composition. Furthermore, effect on BMD was analysed with respect to age, duration of the disease and treatment, physical activity, and thyroid status. The analyses were performed using Spearman's correlation.ResultA total of 104 postmenopausal women who were taking LT4 for mean duration of 5.83 years were analysed. 50(48.8%) patients were found to have osteopenia and 36 (34.62%) were found to have osteoporosis. A comparison of BMD showed that neither TSH nor LT4 dose and duration of hypothyroidism was correlated with BMD at various sites. The number of years post-menopause, as well as age were inversely correlated with BMC at all the sites (p-value<0.05). Physical activity (METs/week) was strongly correlated with BMC at all the sites (P value<0.001). On subgroup analysis patients who has suppressed TSH (5IU/L.63 females (60.57%) were obese based on Southeast Asia specific BMI cut offs. However 102 females (98%) were having TBF > 30%. Critical VAT (VAT area > 100 cm2) present in 73 (70.1%) and VAT area >160cm2 was present in 24 (23%) patients. Metabolically obese normal weight (MONW) defined as a VAT area >100 cm2 with a normal BMI (<25kg/m2) constituted a total of 19.2% (n=20). 49 females (47%) had appendicular lean mass index (ALM/height2) <6 kg/m2.ConclusionThis study found no significant correlation between BMD and serum TSH, duration of hypothyroidism or LT4 dose.98% patients were obese according to TBF% and 70% had significantly high VAT suggesting high cardiometabolic risks.

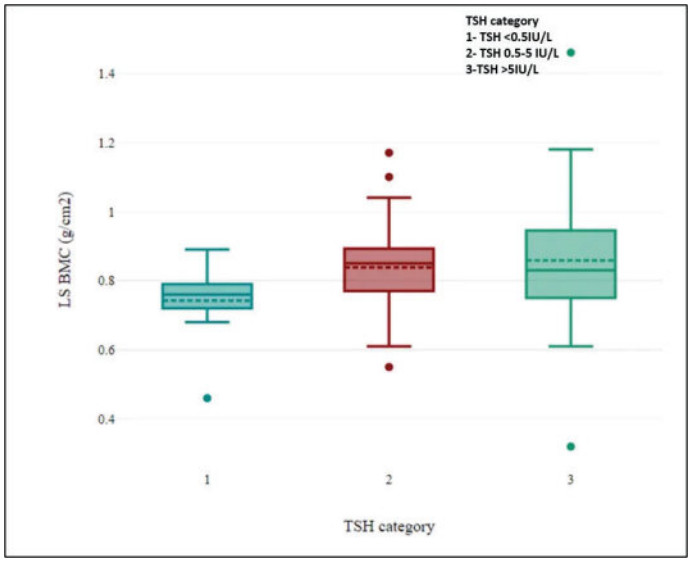

***Disclosures: Eram Nahid**, None*

SAT-072

Artificial Neural Network (ANN) model employing Immunometabolic factors is better than FRAX for predicting fragility fractures (FF) in postmenopausal women with autoimmune hypothyroidism
*ravindra shukla[1], eram nahid[1], Ayan Roy[2], kamalakant shukla[1], MK Garg[1], divyangi mishra[3]. [1]AIIMS Jodhpur, India. [2]AIIMS Kalyani, India. [3]SNMC Jodhpur, India

Introduction: Various observational studies have shown conflicting evidence between primary hypothyroidism and fragility fracture risk in postmenopausal women. Unlike autoimmune diseases like SLE, RA (which have FF risk) , systemic manifestations of autoimmune hypothyroidism have been poorly understood. In this study we explore veritability immunometabolic factors Versus traditional FRAX score in predicting fragility fractures in autoimmune hypothyroidism Methods: In this single center cross-sectional study , consecutive subjects of post menopausal women with primary hypothyroidism on stable levothyroxine and positive anti TPO antibody were evaluated for symptoms, metabolic (HbA1C,lipid, visceral adipose tissue,hypertension,thyroid hormones),inflammatory(vit D,IL6,hsCRP, DHEAS, antiTPO Ab, N/L ratio) and Bone (BMD indices,TBS,Ca,Phosphorus,parathormone) profile.Those with rheumatological disease,diabetes mellitus or any other endocrine disorder, recent (<2 months) viral illness or hospitalization were excluded.Of 243 screened 104 were included in the study. The subjects were divided into two groups: those who had fragility fractures & those who did not. FRAX for major osteoporotic fracture (MOF)calculated online. Discriminant analysis was done to find out factors associated with metabolic inflammation. Levothyroxine dose (?g/kg/day) , dose-duration exposure (?g.months), neutrophil to lymphocyte(NL) ratio, 25 (OH)Vit D,Parathormone, anti TPO Ab, Free T4, freeT3, DHEAS , LDL,Triglycerides,IL-6, HbA1c ,Visceral Adipose tissue index, hypothyroidism duration(in yrs), Presence or absence of Hypertension or any musculoskeletal symptoms was used to construct Multilayer perceptron (MLP) using artificial neural networking

(ANN). ROC analysis of FRAX MOF & MLP in predicting FF was done and Area Under Curve (AUC) compared. SPSS ver21 used Results: Comparison of FRAX based risk (Fig1a) versus MLP based immunometabolism model (Figure 1b) in predicting Fragility fracture in primary hypothyroidism showed MLP to be better than FRAX (AUC 0.67 Vs 0.754). ANN with 18 immunometabolic parameters shown in fig2 Conclusion: ANN algorithm employing immunometabolic factors is more effective than traditional FRAX MOF scores in predicting fragility fracture. Future studies defining fracture risk in primary autoimmune hypothyroidism should focus on disease specific immunometabolic factors.

Figure 1a

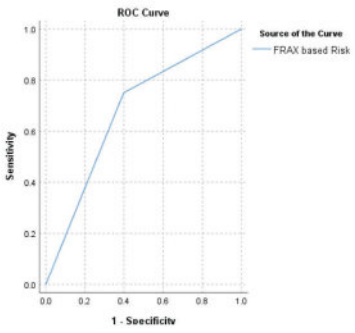

Figure 1b

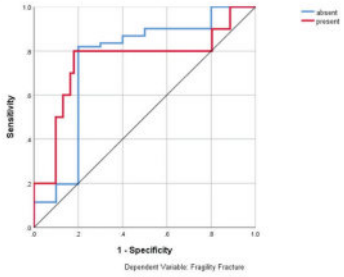

Figure 2

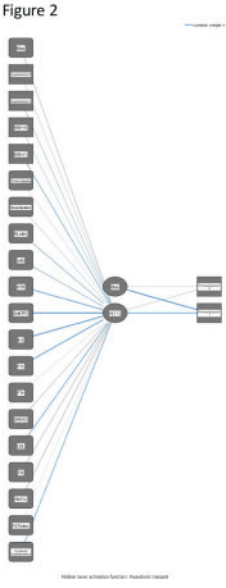

***Disclosures: ravindra shukla**, None*

SAT-073

Bone Deficits in Ambulatory Children and Adults with Cerebral Palsy Are Not Severe or Progressive *Tishya Wren[1], Adriana Liang[1], Veronica Beltran[1], Robert Kay[1]. [1]Children's Hospital Los Angeles, United States

Children with severe cerebral palsy (CP) are known to have low bone mass, with dual-energy x-ray absorptiometry (DXA) areal bone mineral density (BMD) Z-scores several standard deviations below normal. Less is known, however, about bone mass in adults and more functional persons with CP. The purpose of this study was to measure DXA Z-scores in ambulatory children and adults with CP to determine the effects of age and severity level. We hypothesized that Z-scores would be lower in less functional subjects and would decrease with age. 83 subjects (52 male) with CP ages 6-46 years (mean 19.0, SD 9.4) underwent DXA imaging (Hologic Horizon A) of the spine and bilateral hips following standard clinical procedures. CP severity was classified using the Gross Motor Function Classification System (GMFCS). All subjects were ambulatory (using assistive devices if needed) with 28 (34%) in GMFCS I, 36 (43%) in GMFCS II, and 19 (23%) in GMFCS III. The relationship of DXA BMD Z-scores from the lumbar spine, right femoral neck, and right total hip to age and GMFCS level was examined using univariate, followed by multivariate, linear regression. Surprisingly, DXA Z-scores showed no relationship to GMFCS level or age in univariate and multivariate analysis ($p>0.45$). Z-scores were slightly below normal, averaging -0.67 (SE 0.15) for the lumbar spine ($p<0.0001$), -0.83 (SE 0.14) for the femoral neck ($p<0.0001$), and -0.58 (SE 0.14) for the total hip ($p=0.0001$). In contrast to more severely involved children with CP in GMFCS levels IV and V, who are non-ambulatory or minimally ambulatory and have very large deficits in BMD, ambulatory children and adults with CP appear to have much smaller bone deficits through middle age with average Z-scores between -0.5 and -0.9. In addition, bone deficits did not worsen with age or disease severity, contrary to expectations. These results suggest that most ambulatory persons with CP generate enough mechanical loading to build and maintain bone mass close to peers of the same age. While modest bone deficits are present and age-related bone loss is still a concern, osteopenia and osteoporosis may not be as severe a problem as feared for more functional and ambulatory persons with CP.

***Disclosures: Tishya Wren**, None*

SAT-075

See Friday Plenary Number FRI-075

SAT-076

Significant bone loss in bone marrow transplant patients over 3884 person-years of follow up *Joanna Gong[1], Cherie Chiang[2], John Wark[3], David Ritchie[4], Yvonne Panek-Hudson[5], Minh Le[1], Lydia Limbri[6], Nicolo Fabila[6], Spiros Fourlanos[7], Christopher Yates[8]. [1]The Royal Melbourne Hospital, Australia. [2]Head of Chemical Pathology, The Royal Melbourne Hospital, and The Peter MacCallum Cancer Centre, Australia. [3]Previous Head of Bone & Mineral Medicine, The Royal Melbourne Hospital, and Professor of Medicine, The University of Melbourne, Australia. [4]Head of Allogeneic Stem Cell Transplantation, The Royal Melbourne Hospital & The Peter MacCallum Cancer Centre, Australia. [5]The Peter MacCallum Cancer Centre, Australia. [6]The University of Melbourne, Australia. [7]Director of the Department of Diabetes & Endocrinology, The Royal Melbourne Hospital, Australia. [8]Head of Bone & Mineral Medicine and Head of the Bone Densitometry Unit, The Royal Melbourne Hospital, and Co-director of Research, Department of Endocrinology & Diabetes, Western Health, Australia

As outcomes from allogeneic bone marrow transplantation (BMT) continue to improve, monitoring for longer-term complications becomes increasingly important. Decline in bone health post BMT is well-established, although the pathophysiology is multifactorial and unique. Currently available fracture risk calculators do not adequately predict fracture risk in these patients.We aimed to evaluate the fracture risk and decline in areal bone mineral density (aBMD) and trabecular bone score (TBS) post BMT.Patients who attended Royal Melbourne Hospital BMT clinic from 2005-2018 and responded to a patient questionnaire, and those who underwent BMT and had a DXA scan with TBS between 2019-2021, were included. Patient characteristics and DXA values were collected from the electronic medical record and questionnaires. TBS iNsight was used to calculate TBS and FRAX® was used to calculate probability of fracture.337 patients were eligible for inclusion. Patients were primarily male (60%) and mean age was 45.6+/-13.4 years. Baseline DXA T-scores for aBMD were relatively preserved: median (IQR) T-score -0.56 (-1.40?0.48) at the lumbar spine, -1.00 (-1.79?0.02) at the femoral neck, and -0.59 (-1.39?0.39) at the total hip. The annualised decline in aBMD was greater at the femoral neck (4.6%; 3.2g/cm2 (0.18?8.2)) and total hip (4.7%; 4.6g/cm2 (0.64?9.5)), compared to the spine (3.2%; 2.4g/cm2 (-0.16?7.6)). BMD loss occurred most rapidly in the first year post BMT, after which the rate of decline slowed. Post BMT, 18 patients (5.3%) had 19 fractures over 3884 person-years of follow-up (median 11 years (8.2?15)). This corresponds to a 4.9% fracture prevalence over 10 years, significantly higher than FRAX estimates. For the 50 patients with TBS data, the FRAX risk of major osteoporotic fracture was 2.7%. There was no association between fracture post BMT and graft-versus-host disease, total body irradiation or annualised decline in aBMD at any site. Twenty-one (6.2%) patients received antiresorptive therapy; among fracture patients, only 8 (44%) received treatment. In the subgroup of 50 patients with TBS and sequential DXA data, TBS declined independently of aBMD T-scores at all sites.There is significant bone loss post BMT, with a higher fracture rate than predicted by FRAX®. Novel tools such as TBS may help to assess bone fragility in this group. Adjustments to existing fracture risk calculators may be required to guide the use of antiresorptive therapy.

***Disclosures: Joanna Gong**, None*

SAT-077

See Friday Plenary Number FRI-077

SAT-078

Western Diet Alters Gut-bone Axis in IL-10 KO Mice in a Sex Dependent Manner *Pelumi A. Adedigba[1], Sanmi E. Alake[2], Bethany H. Hatter[2], Islam Proapa[2], Leo Perez[2], John A. Ice[2], Trina A. Knotts[3], Edralin A. Lucas[2], Brenda J. Smith[4]. [1]Indiana Center for Musculoskeletal Health, Indiana University-Purdue University Indianapolis, United States. [2]Department of Nutritional Sciences, Oklahoma State University., United States. [3]Department of Surgery, Center for Alimentary Metabolic Sciences, UC Davis Health, United States. [4]Department of Obstetrics and Gynecology and Indiana Center for Musculoskeletal Health, Indiana University-Purdue University Indianapolis, United States

Loss of interleukin (IL)-10, an anti-inflammatory cytokine, has been associated with gut inflammation and bone loss in animal models and patients with inflammatory bowel diseases. A high fat, high sugar western diet (WD) contributes to gut dysbiosis and bone loss. This study aimed to determine if the absence of IL-10 exacerbates the impact of a WD on the gut-bone axis in male and female mice. 8-wk-old B6.129P2-Il10tm1Cgn/J (KO) and C57BL/6 (WT) were assigned to 4 groups in 2x2 factorial with diet (Control [CO] or WD) and strain (WT or KO). After 3 mo, bone mineral density (BMD) and trabecular and cortical bone microarchitecture, serum biomarkers, gene expression, and the gut microbiota profile were assessed. Data were analyzed using 2-way ANOVA. Both the female and male KO mice exhibited reduced (P<0.001) whole body BMD and trabecular bone volume (BV/TV) in the femur compared to WT mice. In WT mice on WD, BMD was unaltered in either sex, but BV/TV was decreased in the females. Only the female KO mice on WD exhibited an unexpected increase (P<0.001) in BMD and BV/TV compared to KO-CO. WD increased (P<0.05) femoral cortical thickness and cortical area in both strains and sexes. In females, the expression of bone morphogenetic protein 2 (BMP2), osteocalcin (BGALP-2), and collagen, type 1, (COL1A1), genes involved in osteoblast differentiation and activity, as well as genes expressed by osteocytes (i.e., dentin matrix acidic phosphoprotein 1 (DMP1), SOST, phosphate-regulating endopeptidase homolog X-linked (PHEX)) were increased (P<0.05) in KO-WD vs. KO-CO, but not in WT mice. However, there were no changes in gene expression in male mice. In females, WT-WD increased (p<0.05) serum intact FGF-23 (iFGF-23) compared to WT-CO. In contrast, WD normalized the KO-induced increase in iFGF-23. In male mice, WD reduced (P<0.01) iFGF-23, irrespective of strain. Intestinal activity of ?-glucuronidase (bGUS), which deconjugates estrogens, was reduced (P<0.01) in the male and female KO mice, and WD increased (P<0.01) bGUS in both strains and sexes. The microbiota analysis revealed the relative abundance of lactobacillus and bifidobacterium was suppressed (P=0.05) by WD. Our findings indicate that WD does not exacerbate the bone phenotype in IL-10 KO mice. However, in the absence of IL-10, WD consumption restored bone in female but not male mice, a response potentially mediated through gut-derived estrogens and Fgf23 signaling.

***Disclosures: Pelumi A. Adedigba**, None*

SAT-079

LSD1 is Important for Physiological, but not Inflammatory Induced Osteoclast Differentiation *Kristina Astleford-Hopper[1], Jennifer Auger[2], Bryce Binstadt[2], Elizabeth Bradley[3], Kim Mansky[4]. [1]University of Minnesota School of Dentistry, United States. [2]University of Minnesota Medical School, United States. [3]University of Minnesota , United States. [4]University of Minnesota, United States

Receptor activator of NF-kB ligand (RANKL) is the only known physiological inducer of osteoclast differentiation; however, we understand much less about the mechanisms driving osteoclast differentiation during inflammatory conditions. Therapies that block TNF-? successfully inhibit bone erosion in RA; however, we still do not understand why inflammatory cytokines such as TNF-? do not induce osteoclastogensis independent of RANKL. A recent study demonstrated that TGF-? reprograms TNF-? stimulation of macrophages towards inflammatory osteoclast differentiation by downregulating interferon regulated genes. Lysine-specific demethylase 1 (LSD1, KDM1A) functions as a transcriptional co-repressor/co-activator and histone demethylase catalyzing the removal of mono- and di-methyl groups from histone 3 lysine 4 (H3K4) and histone 3 lysine 9 (H3K9). To determine the role LSD1 plays in regulating cells of the myeloid lineage including osteoclasts, we bred Lsd1fl/fl mice with mice expressing LysM-driven Cre. Our previous data demonstrated that conditional deletion of LSD1 (Lsd1cKO) reduced osteoclast differentiation leading to osteopenia in female mice. Additionally, increased expression of IFN-? stimulated genes resulted in decreased osteoclast differentiation of Lsd1cKO mice. To better understand the role of LSD1 in osteoclasts under inflammatory conditions, we sequentially primed Lsd1WT and Lsd1cKO bone marrow macrophages (BMMs) with TGF-? for two days before stimulating with TNF-? in the absence of RANKL. Additionally, we used a rheumatoid arthritis model (K/BxN serum transfer) to determine if loss of LSD1 mitigates bone loss in inflammatory diseases. We found that treating Lsd1cKO BMMs with TGF-? followed by TNF-? did not impact the size and number of TRAP+ multinuclear cells as compared to Lsd1WT. These results contrast with our previous data where Lsd1cKO monocytes were stimulated with RANKL and M-CSF. Additionally, we found that Lsd1WT and Lsd1cKO mice given K/BxN serum have statistically similar clinical scores and ankle thickness, supporting that under inflammatory conditions, the loss of LSD1 does not significantly affect osteoclast differentiation. These data demonstrate that ablation of LSD1 reduces bone loss mediated by physiological osteoclast activity, but other LSD1-independent pathways promoting inflammatory-induced osteoclastogenesis.

***Disclosures: Kristina Astleford-Hopper**, None*

SAT-081

Impact of FasL deficiency on osteoblastic cells with focus on intramembranous bones *Adela Kratochvilova[1], Martina Zapletalova[1], Janka Gregorkova[1], Reinhard Gruber[2], Eva Matalova[1]. [1]Institute of Animal Physiology and Genetics CAS, Czech Republic. [2]University Clinic of Dentistry, Medical University of Vienna, Austria

FasL is a key molecule in the immune system participating in regulation of cell number via apoptosis, however the spectrum of its functions appears much broader. This applies also for the bone. Recently, FasL was demonstrated to impact expression of sclerostin (Sost), the major osteocytic marker, and also to be required for osseous healing in extraction sockets. The latter finding was shown in gld (FasL deficient) mice.To further follow these observations, the transcriptomic profile (based on RNA Sequencing) of primary gld osteoblastic cells with potential to differentiate into osteocytes (Sost-positive cells) was compared with corresponding wild type samples (intramembranous bone origin). To this type of bones belongs also the alveolar bone being a component of the periodontal apparatus necessary for functional dentition.The majority of affected genes have been involved in formation and mineralization of the extracellular matrix (ECM). The alterations were morphologically visible also in the cell cultures and based on activity of alkaline phosphatase. Along with these core groups of genes, those known from regulation of vasculature development (angiogenesis), cell migration and morphogenesis were identified. Notably, some genes associated with tooth mineralization were also impacted. In more details, Tgfb ligands were investigated to follow possible interactions within cytokine networks and metalloproteinases (Mmps) as the key proteases within the ECM. While Tgfb ligands were upregulated, the majority of Mmps was downregulated in the gld cells. The reactome analysis pointed to several additional groups of genes being recently investigated to provide a more complex evaluation of the data.In general, there was obtained a robust dataset which can be used for further analyses of non-apoptotic functions of FasL in tooth and bone related cells, including tooth-bone interface.

***Disclosures: Adela Kratochvilova**, None*

SAT-082

Deletion of Vhl in Dmp1-expressing cells induces splenic stress erythropoiesis *Janna Emery[1], Betsabel Chicana[1], Hanna Taglinao[1], Citlaly Ponce[1], Cristine Donham[1], Aimy Sebastian[2], Scott Trasti[3], Jennifer Manilay[1]. [1]University of California, Merced, United States. [2]Lawrence Livermore National Laboratory, United States. [3]Texas Tech University Health Sciences Center, United States

In recent years, several hypoxia-inducible factor (HIF)-prolyl hydroxylase (PHD) enzyme inhibitors have been developed for the treatment of anemia of renal disease and more recently, for osteoporosis. However, it remains a challenge to target the HIF signaling pathway without dysregulating the skeletal and hematopoietic system and causing off target metabolic, hormonal, and renal effects. Previous work in Dmp1-Cre; Vhl conditional knockout (VhlcKO) mice, where Vhl is deleted in subsets of mesenchymal stem cells, late osteoblasts, and osteocytes, indicated drastic defects in B lymphocyte development in the bone marrow (BM), which could be a potential side effect in HIF-PHD inhibitor-treated patients. Here, we examined the effects of Vhl deletion in bone by performing longitudinal analyses of VhlcKO mice at 3, 6, 10, and 24 weeks of age, where at 10 and 24 weeks of age, high bone mass and splenomegaly are present. Using flow cytometry, we observed increased frequency (%) of CD71-TER119+ orthochromatophilic erythroblasts in 10- and 24-week-old VhlcKO BM, which correlated with the elevated erythropoietin (EPO) levels in the BM, and our complete blood count analysis, where we found increased number of red blood cells (RBC) in circulation. The absolute numbers of myeloerythroid progenitors (MEPs) in the BM were significantly reduced. Bulk RNA-Seq of the MEPs showed upregulation of Hif1a and Hif2a in VhlcKO MEPs, consistent with a response to hypoxia, and genes involved in erythrocyte development, actin filament organization, and response to glucose. Vhl expression was similar in control and VhlcKO MEPs, ruling out aberrant activity of Dmp1-Cre in MEPs. WT?VhlcKO chimeras confirmed a cell-extrinsic effect on erythroblast development. We also observed a polycythemic phenotype and marked hypoglycemia in VhlcKO mice, which may reflect increased glucose uptake in both RBC and bone. Additionally, histological analysis of VhlcKO spleens revealed red pulp hyperplasia and the presence of megakaryocytes, both of which are features of extramedullary hematopoiesis (EMH). EMH in the spleen was correlated with the presence of mature stress erythroid progenitors, suggesting that stress erythropoiesis is occurring to compensate for the BM microenvironmental irregularities. Our studies implicate HIF-driven alterations in skeletal homeostasis with BM microenvironmental changes that accelerate erythropoiesis.

***Disclosures: Janna Emery**, None*

SAT-084

Effects of Systemic PPAR? Inhibition on Bone and Immune Cells in Aged Female Mice *Xingming Shi[1], Kehong Ding[1], Raysa Rosario[1], Ashwin Ajith[1], Yun Su[1], Sean Shaw[1], Meghan McGee-Lawrence[2], Xin-Yun Lu[1], Anatolij Horuzsko[1], Carlos Isales[1]. [1]Augusta University, United States. [2]Medical College of Georgia, Augusta University, United States

This study investigates the effects of peroxisome proliferator-activated receptor gamma (PPAR?) inhibition on bone and immune cell profile in aged female mice, as well as in vitro MSC osteogenic differentiation and inflammation gene expression. The hypothesis was that inhibition of PPAR? would increase bone mass and alter immune and other cellular functions. Our results showed that treatment with PPAR? antagonist GW9662 for six weeks reduced bone volume and trabecular number and increased trabecular spacing. However, inhibition of PPAR? had no significant effect on marrow and spleen immune cell composition in aged female mice. In vitro experiments indicated that GW9662 treatment increased the expression of osteogenic genes but did not affect adipogenic genes. Additionally, GW9662 treatment decreased the expression of several inflammation related genes. Overall, these findings suggest that PPAR? inhibition may have adverse effects on bone in aged female mice.

***Disclosures: Xingming Shi**, None*

SAT-086

See Friday Plenary Number FRI-086

SAT-087

C. acnes Related Bone Prothesis Infection: How Osteoblasts May Rule the Innate Immune Response *Léa Thoraval[1], Min Tang-Fichaux[1], Jennifer Varin-Simon[1], Christine Guillaume[1], Sophie C. Gangloff[1], Céline Mongaret[1], Fany Reffuveille[1], Frédéric Velard[1]. [1]URCA, EA 4691 BIOS, France

Purpose: Cutibacterium acnes is a commensal skin bacterium, involved in bone prosthesis infections (BPI) [Boisrenoult, 2018]. C. acnes infections mainly present low-grade clinical symptoms that delay the diagnosis [Portillo, 2013]. This led us to hypothesize that C. acnes could escape immune system in bone site. This work aims to study the ability of osteoblasts (OB) infected with clinical and non-clinical strains of C. acnes to trigger innate immune cells response.Methods: Human primary OB (n=4), cultured on titanium alloy, were infected with two C. acnes strains (a reference and a BPI-related strain) for 3h (MOI 20:1 and 200:1). After 24h, human primary neutrophils (PMN) (n=16) were put into contact with infected OB for 4h. Pro-inflammatory mediators' production (IL-8, TNF-?, MCP-1, IL-6, MIP-1?) by OB, infected or not with C. acnes, and then by the PMN/OB/C. acnes trio or PMN challenged with infected OB conditioned supernatants, was determined by ELISA. Confocal fluorescence microscopy and scanning electron microscopy allowed to visualize these complex interactions.Results: We demonstrated a C. acnes-induced increased secretion of IL-8, IL-6 and MCP-1 by OB ($p<0.05$ vs uninfected OB) only at MOI 200:1. Conditioned supernatants from infected OB did not trigger PMN response, whereas PMN/infected OB contact elicited a MOI-dependent production of IL-8, TNF-? and MIP-1? ($p<0.05$ vs uninfected OB/PMN interaction) by PMN. OB-mediated IL-6 and MCP-1 production was also noticed but only in the triple interaction thanks to cell/cell contact with PMN. Previous data evidenced a more sustained inflammatory response with BPI strain in direct contact with PMN or in mice air pouch model in vivo, conversely, no differences were found here between both strains. Fluorescence microscopy showed the presence of C. acnes in both OB and PMN, while scanning electron microscopy highlighted an absence of bacteria at the cell surface, indicating an effective clearance by PMN, and a real ability of OB to hide C. acnes from PMN.Conclusion: This work suggests that C. acnes could escape immune system by at least partial internalization within the OB. The immune response elicited in this model appeared to be reduced for the clinical strain compared to that observed without OB in our previous work. Even if precise mechanisms remain to be elucidated, these results show for the first time that OB may temper the immune response to C. acnes despite production of inflammatory mediators.

***Disclosures: Léa Thoraval**, None*

SAT-088

Compromised Bone Microarchitecture and Fragility in Ovariectomized Mice is Reversed by a Novel Immunotherapy *Di Wu[2], Anna Cline-Smith[2], Deborah Veis[3], Rajeev Aurora[2]. [2]Saint Louis University School of Medicine, . [2]Saint Louis University School of Medicine, United States. [3]Washington University in St. Louis School of Medicine, United States

Patients with low bone mineral density (BMD) are at high risk of fragility fractures. However, accumulating clinical data demonstrates that ~ 15% of people with normal BMD experience fragility fractures, indicating that bone mass and bone quality are independent parameters. The osteolineage, which includes osteoblasts and the osteocytes, plays a key role in maintaining the microarchitecture. Bone quality is reflected by the microarchitecture, and its contribution to fracture resistance is less well understood than bone mass. Over the past three decades, studies revealed that T-cell produced cytokines, particularly TNF? and IL-17A, play a role in the pathogenesis of postmenopausal osteoporosis (PMOP) by stimulating osteoclasts to favor bone resorption. Our lab has described a pathway in which TNF? and IL-17A produced by memory T cells in the bone marrow is necessary for bone erosion in ovariectomized (OVX) mice. We hypothesize that inflammation post estrogen loss targets the osteolineage to degrade bone quality. In this study, we evaluated bone quality by four parameters: collagen organization by picrosirius red staining and CT-FIRE analysis; lacunar-canalicular network (LCN) integrity by rhodamine staining; osteocyte network connectivity by phalloidin staining; and biomechanical strength normalized to bone mass. We show that OVX of 12-week-old C57BL/6 (n = 5 in each group) leads to diminished fracture resistance, disorganized collagen matrix, disrupted LCN and decreased osteocyte connectivity. To determine whether these alterations are dependent on T-cell produced TNF? and IL-17A, we are comparing C57BL/6, TCR?KO, and IL-15RA?TKO mice. We expect this comparison to illuminate the different contributions of estrogen loss, T cells and cytokines. In addition, our lab has also shown that pulsed low dose RANKL (pRL) induces CD8+ FoxP3+ regulatory T cells (TcREG). TcREG induction in OVX mice is anti-resorptive, bone anabolic, and limits production of TNF? and IL-17A. Here, we show that pRL treatment improves the biomechanical properties of the bone post OVX in WT mice. We also show that the anabolic effects of pRL is IL-10 dependent, as treatment in IL-10KO mice post OVX had no effect on bone quality. Taken together, our data demonstrates that the compromised microarchitecture observed in PMOP can be modeled using OVX in mice and that pRL is a promising immunotherapy that improves bone quality in addition to bone mass.

***Disclosures: Di Wu**, None*

SAT-090

See Friday Plenary Number FRI-090

SAT-091

In vitro effects of Tanshinone and Ligustrazine promoting the differentiation of primary endothelial cells into type H vascular endothelial cells *Xiaohui Hu[1], Kanghui Sun[1], Liqiang Guo[1], Ziyu Huang[1], Jing Wang[2], Yongjian Zhao[1], Dongfeng Zhao[1], Yongjun Wang[1], Bing Shu[2]. [1]Longhua Hospital, Shanghai University of TCM, China. [2]Shanghai University of TCM, China

Background: type H blood vessels play an important role in the process of osteogenesis, and Tanshinone and Ligustrazine can protect vascular endothelial cells and promote angiogenesis. Objective: to observe the effects of Tanshinone and Ligustrazine on primary endothelial cells differentiation into type H vascular endothelial cells. Methods: primary endothelial cells were obtained from bone tissue of mice, and were treated with different concentrations of Tanshinone or Ligustrazine solutions respectively for 7 days. The cell survival rate was assessed using the CCK-8 kit, and the generation of CD31+ EMCN+ type H vascular endothelial cells and their proportion in the total cells were detected by immunofluorescence staining and flow cytometry, respectively. Results: no significant effects on cell survival of different concentrations of Tanshinone and Ligustrazine were observed. Tanshinone and Ligustrazine dose-dependently promoted the differentiation of primary endothelial cells into type H vascular endothelial cells. Ligustrazine solution of 100 ?M could increase the percentage of type H vascular endothelial cells in primary endothelial cells to nearly 20%. Conclusion: Both Lanshinone and Ligustrazine can promote the differentiation of primary endothelial cells into type H vascular endothelial cells, which may contributed inthe process of bone repair.

***Disclosures: Xiaohui Hu**, None*

SAT-093

See Friday Plenary Number FRI-093

SAT-094

See Friday Plenary Number FRI-094

SAT-095

Real Life Use of Bone-Targeting Agents for Bone Metastases in France: the OPTIMOS Study *Cyrille Confavreux[1], Béatrice Bouvard[2], Nicolas Girard[3], Pauline Bosco-Levy[4], Clarisse Marchal[5], Manon Walter[5], Eric Lehmann[6], Gaelle Desamericq[6], Manon Belhassen[5]. [1]INSERM UMR1033-University of Lyon-Hospices Civils de Lyon, France. [2]CHU d'Angers-Univ Angers, Nantes Université, Oniris, UMR 1229 RMeS, France. [3]Institut Curie - Paris Saclay, UVSQ, France. [4]Bordeaux PharmacoEpi-INSERM CIC-P 1401-Université de Bordeaux, France. [5]Pharmaco-Epidémiologie Lyon (PELyon), France. [6]Amgen, France, France

Purpose. Progress in oncology improved survival of bone metastatic (BM) patients highlighting bone health issue. We aimed to describe recent use of bone-targeting agents (BTA) in BM patients in France.Methods. We accessed EGB, a French National Health Insurance database corresponding to 1/97 of the whole population. The algorithm identified adult BM patients either through BM ICD-10 hospitalization code or through the onset of a skeletal-related event (SRE): pathologic fracture, cimentoplasty, spondyloplasty, spinal cord compression, palliative radiotherapy, orthopaedic surgery and malignant hypercalcemia. Inclusion period covered the years 2009-2018. Patients not affiliated to the general health system and patients with primary sarcoma or with prevalent BM during the 3 years preceding inclusion date, have been excluded. Dispensations of clodronate, IV bisphosphonates (zoledronate, pamidronate- IVBP) and denosumab (Dmab), the BTA marketed in France, were recorded. Discontinuation was defined as absence of dispensation of more than 30 days after the end of coverage period.Results. We identified 6663 new BM patients. Mean (SD) age was 69.7 yrs (13.2). Charlson comorbidity index was >= 5 in 5532 (83.0%) of cases. Major primary cancer sites were breast (15.8%), prostate (13.4%), lung (12.6%) and digestive (10.6%). Among BM patients, 4300 (64.5%) had SRE at inclusion. The median [Q1-Q3] follow-up was 1.3 yrs [0.3-3.4] mainly interrupted by death (63.5%) or end of study (35.6%).After inclusion, only 621 (9.3%) patients initiated BTA (327 received Dmab). Median initiation delay was 99 days [37-241] similar in Dmab and IVBP. Patients initiating BTA decreased by two-fold overtime. Proportion of BM patients who discontinued was lower with Dmab than IVBP (43% vs 56%). Treatment persistence lasted longer with Dmab than IVBP (302 days [152-616] vs 180 [90-427]). Among patients included with SRE, the ones with early (<100 days) BTA initiation (N=118 vs 125) had a reduced incidence rate of 2nd SRE (12.9% pers-yrs [8.4-18.9] vs 20.7% [15.7-26.7]) corresponding to a cumulative incidence at 12 months of 13.6% [8.1-20.4] vs 21.6% [14.8-29.2]. Conclusion. Proportion of BM patients treated with BTA in France is low even in secondary prevention. Early BTA treatment is efficient to reduce second SRE. This highlights the need for optimizing BM management in France in accordance to the ESMO guidelines.

***Disclosures: Cyrille Confavreux**, Amgen, Grant/Research Support*

SAT-096

Osteosarcoma growth in Fos-transgenic mice is limited by Rsk2 and Lrp5 deficiency via different mechanisms *Armelle Carreau[1], Christina Baldauf[1], Mona Neven[2], Olga Winter[1], Julia Luther[1], Michael Amling[1], Jean-Pierre David[1], Thosten Schinke[1]. [1]Department of Osteology and Biomechanics University Medical Center Hamburg-Eppendorf, Germany. [2] Department of osteology and Biomechanics University Medical Center Hamburg-Eppendorf, Germany

Since specific treatment options for osteosarcoma are still limited, it is required to better understand the molecular mechanisms that control proliferation and/or differentiation of the transformed bone-forming osteoblasts. Using a Fos-transgenic mouse model spontaneously developing osteosarcomas, we have previously shown that inactivation of the ribosomal S6 kinase 2 (Rsk2) strongly impairs osteosarcoma growth.Using cell lines derived from FosTg;Rsk2-/- tumors we observed that Rsk2 deficiency impaired the growth advantage of FosTg cells, which was explained by aberrant nuclei number due to impaired cytokinesis suggesting the induction of "mitotic catastrophe". A similar influence was observed by treatment of FosTg cells with a pharmacological Rsk inhibitor (BI-D1870). Moreover, since BI-D1870 administration to FosTg cell lines reduced expression of aurora kinase B, the influence of a pharmacological aurora kinase B inhibitor (Hesperadin) was also tested. Similar to BI-D1870, Hesperadin caused impaired cytokinesis, resulting in the accumulation of polynuclear cells, an effect that was not only observed in FosTg cell lines, but also in the human osteosarcoma cell line U2OS.We next focused on targeting a more osteoblast-specific pathway involving the transmembrane protein Lrp5, which acts as a co-receptor of Wnt ligands. To analyze the role of Lrp5 in osteosarcoma growth, FosTg mice were crossed with Lrp5-deficient mice or with mice carrying a high bone mass mutation of Lrp5 (Lrp5A213V/+). It was found that Lrp5 deficiency drastically reduced the osteosarcoma volume in FosTg mice, which was explained by a decreased number of active osteoblasts at the tumor surfaces associated with the appearance of large unmineralized areas. Cell lines were established from the three FosTg mouse models with different Lrp5 genotypes, however growth curve and mineralization analyses did not reveal significant differences, thereby suggesting a non-cell-autonomous mechanism.Taken together, this study identified the relevance of both, the Rsk2 and the Lrp5 pathway, for osteosarcoma formation, yet the impairment of osteosarcoma growth by Rsk2 or Lrp5 deficiency are explained by different mechanisms.

***Disclosures: Armelle Carreau**, None*

SAT-097

Population Dynamics-Based Model to Predict Tumor Cell Interactions with Bone Resident Cells *Natalie Bennett[1], Alexandra Gutierrez Vega[2], Leonard Harris[2], Julie Rhoades[1]. [1]Vanderbilt University, United States. [2]University of Arkansas, United States

Tumor-induced bone disease (TIBD) is the result of signaling between tumor cells and bone resident cells, such as osteoclasts and osteoblasts, that ultimately results in osteolysis. This leads to severe clinical manifestations such as pain and pathologic fractures. Standard-of-care cancer therapies such as chemotherapy and immunotherapy are not curative for bone metastases, and the unique physical and cellular characteristics of the bone microenvironment can lead to drug resistance and immune exclusion. Computational models are a valuable tool to better understand how cell-cell interactions can lead to disease progression. There are several published mathematical models that demonstrate the process of homeostatic bone remodeling via interactions between osteoclasts and osteoblasts, including some that incorporate key signaling components such as the receptor activator of nuclear factor kappa-B (RANK) - RANK ligand axis. While some models of the bone microenvironment include malignant cells, there are none to our knowledge that specifically model the interactions between bone resident cells and metastatic breast cancer cells. We aim to develop a population dynamics-based mathematical model that can demonstrate how signaling between breast cancer cells, osteoclasts, and osteoblasts drives bone destruction. While many other models are based on theoretical data, our analyses will be based on tumor growth and bone destruction measurements in experimental murine models of TIBD. Our preliminary model is able to recreate experimental data of tumor growth and resultant bone loss. Furthermore, our model will incorporate tumor-secreted parathyroid hormone-related protein (PTHrP), a downstream target of the transcription factor Gli2, which is an essential driver of bone metastases. The outputs of this model can then be verified with in vitro co-culture experiments and in vivo tumor models with modified Gli2 and PTHrP activity. Overall, capturing the critical cell-cell interactions in TIBD via this novel computational model will enhance our understanding of the bone metastatic microenvironment and can eventually be expanded by incorporating additional cell populations. Computational modeling is a robust technique to evaluate the potential clinical impacts of targeting pathways that drive disease, which is an essential step toward overcoming drug resistance in TIBD.

***Disclosures: Natalie Bennett**, None*

SAT-098

The role of SWAP-70 in bone formation and osteosarcoma progression *Laura Di Giuseppe[1], Jacopo Di Gregorio[2], Sara Terreri[2], Madalina Maftei[2], Giulia Battafarano[2], Salvatore Minisola[1], Andrea Del Fattore[2], Michela Rossi[2]. [1]Department of Clinical, Internal, Anaesthesiology and Cardiovascular Sciences, Policlinico Umberto I, "Sapienza" University of Rome, Rome, Italy, Italy. [2]Bone Physiopathology Unit, Genetics and Rare Diseases Research Area, Bambino Gesù Children's Hospital, IRCCS, Rome, Italy, Italy

Introduction: Osteosarcoma is the most common primary bone tumour, particularly prominent among adolescents and young adults. The therapeutic strategies for osteosarcoma involve both surgery and chemotherapy, but the identification of new therapeutic targets is needed in patients with chemo-resistance, recurrence and metastases. Our study aims to investigate the mechanisms by which the phosphatodylinotsitol trisphophate (PIP3) binding protein SWAP-70 controls osteosarcoma progression. SWAP-70 is involved in actin rearrangement, phagocytosis and cell migration. It also plays an important role in the oncogenesis of many malignant tumors. However, the role of SWAP-70 in osteosarcoma has not been previously investigated.Methods: Gene and protein expression, proliferation, cell migration, invasion, apoptosis, ALP activity and mineralization were evaluated by in vitro assays.Results: To understand the role of SWAP-70 in tumour progression, we analysed its expression in mesenchymal stem cells (MSC), osteoblasts and Saos-2 osteosarcoma cells. Our data evidenced that SWAP-70 increases during osteoblast differentiation from MSC to osteoblasts and its expression is not detected in Saos-2. To further study the role of SWAP-70 in osteosarcoma, we transfected Saos-2 cells with vector overexpressing SWAP-70 (pSWAP-70) or empty plasmid (pEmpty). The overexpression of SWAP-70 in Saos-2 increased the expression of RUNX2, SP7, ALP, DMP1 and MEPE. SWAP-70 overexpressing Saos-2 cells showed reduced proliferation rate [Proliferative rate; pEmpty: 1.000+/-0.007, pSWAP-70: 0.815+/-0.119. **p<0.01], decreased migration [Wound closure (%); pEmpty: 100.000+/-1.000, pSWAP-70: 52.110+/-20.760. *p<0.05] and invasion abilities [Absorbance (%); pEmpty: 100.000+/-1.000, pSWAP-70: 62.540+/-11.260. **p<0.01] compared to empty vector transfected cells. No substantial changes between pEmpty- and pSWAP-70-transfected cells were detected in the apoptosis induced by H2O2 treatment. Moreover, increased ALP [ALP intensity; pEmpty: 1.000+/-0.008, pSWAP-70: 1.386+/-0.157. **p<0.01] and 2-fold higher ability to form mineralized nodules were revealed in SWAP-70 overexpressing cells.Conclusion: Our results showed that the overexpression of SWAP-70 in Saos-2 induced osteoblast differentiation of osteosarcoma cells, suggesting that SWAP-70 could act as an onco-suppressor and represent a novel therapeutic target for this rare paediatric tumour.

***Disclosures: Laura Di Giuseppe**, None*

SAT-099

High dose melphalan induces senescence features in multiple myeloma cells

*ANGELO GUILATCO[1], GABRIEL ALVARES BORGES[1], Tamar Tchkonia[2], James L Kirkland[2], Taxiarchis Kourelis[3], Matthew Drake[4], Megan Weivoda[5]
[1], , [2]Robert and Arlene Kogod Center on Aging, Mayo Clinic, United States, [3]Division of Hematology, Mayo Clinic, United States, [4]College of Medicine, Mayo Clinic, United States, [5]Mayo Clinic, United States

Multiple myeloma (MM) is a clonal plasma cell malignancy. MM cells can persist after treatment, where they exhibit growth arrest and chemotherapy resistance: features consistent with tumor dormancy. These cells may regain proliferative capacity to drive relapse. Thus, understanding these cells is key to achieving durable response in MM. Cytotoxic chemotherapies, including those used in MM (e.g., high dose melphalan, HDM), drive senescence in many tissues. Senescence shares many features with dormancy, including growth arrest and apoptosis resistance. Therefore, we hypothesize that MM cells persisting after HDM exhibit therapy-induced senescence.5TGM1 mouse MM cells were treated with vehicle (Veh) or HDM (10uM, IC90) for 6 hours. Cells were washed and plated in the presence/absence of wildtype C57BL/6 bone marrow stromal cells (BMSCs) in normal media for 2 weeks. Cells were counted during media changes to track proliferation. HDM-5TGM1 cells exhibited substantial cell death following treatment; HDM-5TGM1 cultured alone did not survive past 48 hours. Co-culture with BMSCs maintained survival of a portion of HDM-5TGM1 cells. This was not reproduced with BMSC conditioned media, suggesting that direct cell interactions are required. HDM-5TGM1 with BMSCs exhibited a significant growth arrest and increased size compared to Veh-5TGM1 for at least 10 days. To validate senescence features, Day 10 HDM-5TGM1 cells were stained for telomere-associated DNA damage foci (TAFs) and assessed for gene expression. HDM-5TGM1 had significantly more TAFs than Veh-5TGM1, reflecting persistent DNA damage signaling in senescence. HDM-5TGM1 demonstrated upregulation of myeloid/dormancy markers (Axl, Fcer1g, Csf1r, Mpeg1) as well as significantly increased senescence markers (Cdkn1a, Cdkn1c, Glb1), anti-apoptosis (Bcl2l1), and senescence associated secretory phenotype genes (Ccl5, Icam1, Mmp13). Further, HDM-5TGM1 were more sensitive to navitoclax senolysis. After 14 days, clusters of HDM-5TGM1 that regained proliferative capacity were detectable, suggesting escape from senescence-like growth arrest.Our findings demonstrate that direct interactions with BMSCs facilitate survival of HDM MM cells, which go on to develop features of therapy-induced senescence. However, this is a temporary response. These data suggest that targeting senescence anti-apoptosis pathways following HDM may be a viable therapeutic strategy to eliminate surviving MM cells and prevent disease relapse.

***Disclosures: ANGELO GUILATCO**, None*

SAT-100

Abnormal Structures in Prostate Cancer Metastatic Bone Lesions as a Fracture Risk Factor

*Naomi Jung[1], Qiong Wang[2], Felipe Eltit Guersetti[1], Danmei Liu[3], Samuel Xu[1], Sheryl Munshan[1], Eva Corey[4], Colm Morrissey[4], Lawrence True[5], Rizhi Wang[6], Michael Cox[1], [1]Department of Urologic Sciences, University of British Columbia; Vancouver Prostate Centre, Canada, [2]Department of Materials Engineering, University of British Columbia, Canada, [3]Centre for Aging SMART at VCH, Canada, [4]Department of Urology, University of Washington, United States, [5]Department of Pathology and Laboratory Medicine, University of Washington, United States, [6]Department of Materials Engineering, University of British Columbia; School of Biomedical Engineering, University of British Columbia , Canada

Prostate cancer (PC) is the most frequently diagnosed male cancer. Improved treatments have dramatically improved survival rates, but 20% of patients will develop metastatic disease, ~70% of whom will suffer from PC bone metastases (PCBM). PCBM reduces quality of life due to intractable pain and high risk of fracture. PCBM lesions are defined as being predominantly osteoblastic/sclerotic. We hypothesize that pain and fracture risk are caused by aberrant matrix deposition in the sclerotic lesions. This study aims to characterize the structure of PCBM-involved bone and the connection between structural changes and increased risk of fracture.We evaluated the bone macrostructure and trabecular properties of 13 PCBM, and 12 control, cadaveric vertebral specimens using micro computed tomography (microCT, Scanco µCT35) at 10 µm voxel size. We performed quantitative backscattered electron scanning electron microscopy (QBSE-SEM) to observe microstructural details. A custom MATLAB script was used to identify lacunae density and properties in osteoblastic bone and control trabeculae.We observed 3 qualitative phenotypes by microCT imaging: mixed-osteolytic with thinned trabeculae and patches of sclerosis (n=4), osteosclerotic with residual trabeculae where new bone deposits on the surface of trabeculae and medullar spaces (n=7), and osteosclerotic with minimal residual trabeculae (n=2). PCBM samples had significantly higher trabecular number, bone volume/total volume, and connectivity density, and significantly lower trabecular separation and tissue mineral density compared to controls. PC sclerotic bone had a greater lacunae density and lacunae area/bone area compared to residual trabeculae by QBSE-SEM. Lacunae in PC sclerotic bone have significantly increased area, circularity, and minor axis length, and decreased major-to-minor axis ratio and eccentricity. Lacunae in sclerotic lesions exhibited a significant loss of anisotropy relative to their strongly aligned organization in trabecular bone.PCBM lesions have altered trabecular bone architecture with a predominantly osteoblastic presentation, and abnormal lacunae density and lacunar characteristics. This macrostructural analysis demonstrates distinct qualitative and quantitative differences between control vertebrae and PCBM lesions. These multiple pathologic structural details indicate that PCBM lesions are subjected to irregular loading of the bone that can elevate fracture risk.

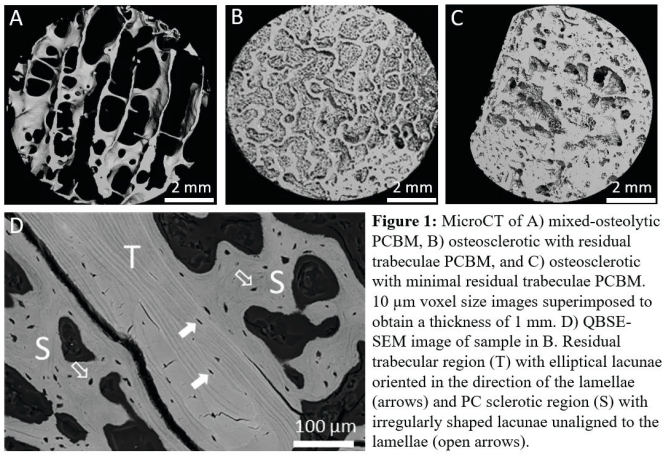

Figure 1: MicroCT of A) mixed-osteolytic PCBM, B) osteosclerotic with residual trabeculae PCBM, and C) osteosclerotic with minimal residual trabeculae PCBM. 10 µm voxel size images superimposed to obtain a thickness of 1 mm. D) QBSE-SEM image of sample in B. Residual trabecular region (T) with elliptical lacunae oriented in the direction of the lamellae (arrows) and PC sclerotic region (S) with irregularly shaped lacunae unaligned to the lamellae (open arrows).

***Disclosures: Naomi Jung**, None*

SAT-101

See Friday Plenary Number FRI-101

SAT-102

Role of Advanced Glycation End Product in Malignancy on Chondrosarcoma via the Activation of Cancer Stemness

*Rong-Sen Yang[1], Shing-Hwa Liu[2], Ting-Yu Chang[2], [1]National Taiwan University Hospital, Taiwan, Province of China, [2]National Taiwan University, Taiwan, Province of China

Despite epidemiologic evidence suggests that diabetes mellitus is a risk factor for cancer, the link between diabetes mellitus and primary bone cancer is rarely discussed. Chondrosarcomas are primary malignant cartilage tumors with poor prognosis and high metastatic potential. N?-(1-Carboxymethyl)-L-lysine (CML), an advanced glycation end product (AGE), is the major AGE immunological epitope detected in the tissue proteins of diabetes patients. It remains unclear whether AGE affects the stemness and malignancy of chondrosarcoma cells. This study aimed to clarify the role of CML/AGE in the stemness and malignancy of chondrosarcoma. A commercial human chondrosarcoma tissue microarray was used to test the expression of CML and receptor for AGE (RAGE). Human chondrosarcoma cell lines JJ012 and SW1353 cells were cultured. The concentrations at 5-100 ?M of CML were used for in vitro experiments. Male non-obese diabetic (NOD)/severe combined immunodeficiency (SCID) mice with or without streptozotocin (STZ)-induced diabetes with high AGE levels were used for in vivo tumor xenograft experiments (n=10/group) (IACUC approval has been obtained). CML and RAGE were highly expressed in patients' chondrosarcoma tissues with advanced grade (Fig. 1A: representative images; total samples: 80, $p<0.0001$). CML at the concentrations of 25 and 50 ?M enhanced tumor sphere formation (a) and cancer stem cell marker expression (b) (Figure 1B) in both JJ012 and SW1353 cells ($n >= 3$, $p<0.05$). The epithelial-mesenchymal transition (EMT) process and the migration and invasion (Figure 1C) abilities were also induced with CML treatment in both JJ012 and SW1353 cells ($n>=3$, $p<0.05$). Moreover, CML increased the expression levels of RAGE and phosphorylated NF?B-p65 protein in both JJ012 and SW1353 cells (Figure 1D; $n>=3$, $p<0.05$). We also found that diabetic hyperglycemia decreased the body weights (a), facilitated the tumor metastasis (increased lung tissue weights and nodules) (b), and increased blood CML levels (c) in a STZ-treated NOD/SCID mouse model (Figure 1E; $n=10$, $p<0.05$). Our findings revealed the role of CML in chondrosarcoma stemness and metastasis, leading to tumorigenesis and malignancy. CML induced cancer stemness properties, cell migration/invasion, and EMT process in chondrosarcoma cells. These results figure out the importance of CML in chondrosarcoma progression, and may provide a potential prognostic strategy for chondrosarcoma patients, especially in diabetic conditions.

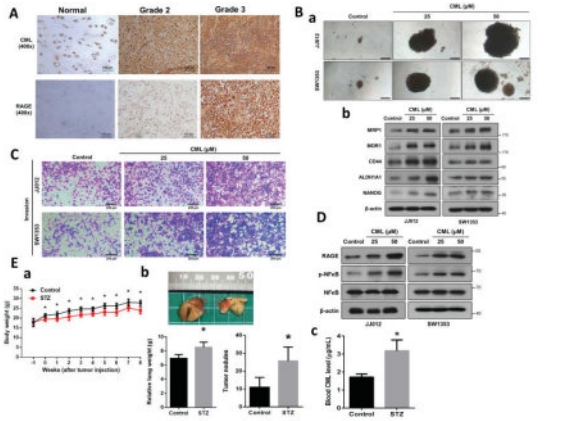

Figure 1. Role of CML in malignancy on chondrosarcoma via the activation of cancer stemness. (A) The CML and RAGE stains in patients' tumor tissues were shown. (B-D) The in vitro sphere formation (B-a) and cancer stem cell marker expression (B-b), transwell invasion (C), and RAGE/NFκB expression (D) were shown. (E) The in vivo xenograft mouse model for body weight (a), tumor lung metastasis (b), and blood CML level (c) were shown. In vitro: results are shown as mean±SD of three independent experiments. In vivo: Tumor nodules were counted in lung tissue. Results are shown as mean±SD (n=10 mice/group). *, $p < 0.05$, compared to the control.

***Disclosures: Rong-Sen Yang**, None*

SAT-103

CD36-Sphingosine 1-Phosphate Axis in Non-Malignant Osteoblasts Contributes to Osteosarcoma Progression *InHong kang[1], Uday Baliga[2], Zachariah Hedley[2], Besim Ogretmen[2], Meenal Mehrotra[2]. [1]Medical university of South Carolina, United States. [2]Medical University of South Carolina, United States

Osteosarcoma (OS) is a primary malignant bone sarcoma and main cause of cancer-related mortality in adolescents/young adults, characterized by abnormal osteoid formation. Despite wide-margin surgery and intensification of chemotherapy, overall survival rates have plateaued at 60%. Novel treatment modalities are therefore needed, but mechanisms underlying its spread/metastasis are still largely unclear. Role of tumor microenvironment in tumor progression has recently gained attention. OS develops in a complex/dynamic milieu made up of calcified extracellular matrix as well as bone, stromal, vascular, and immune cells. Although the contribution of other cells has been characterized, very little is known about the contribution of bone cells, particularly osteoblasts. Our findings show that non-malignant osteoblasts (nmObs) significantly increase OS cell invasion in vitro and their metastatic potential in vivo, suggesting a role for nmObs itself in OS progression. RNA sequencing of nmObs showed enhanced accumulation of components of the sphingolipid signaling pathway ($p<0.003$). Increased sphingosine-kinase (SphK1) levels were observed in nmObs in presence of OS cells which co-related with increased Sphingosine-1-phosphate (S1P) levels in the microenvironment in nmObs. S1P significantly increased OS invasion. No increase in OS invasion was seen in the presence of SphK1-/- nmObs, which was restored when S1P was added. Importantly, nmObs-mediated OS cell invasion was prevented by the functional S1P antagonist FTY720. Also, presence of OS cells greatly elevated expression of the fatty acid transporter, CD36, in nmObs. Moreover, CD36-/- nmObs as well as blocking CD36 expression in wild type nmObs by the specific inhibitor SSO or with shRNA, significantly decreased SphK1 expression, S1P secretion into the microenvironment and OS cell invasion. Additionally, OS invasion was significantly increased when S1P was added to CD36-/- nmObs. Furthermore, simultaneous inhibition of CD36 and SphK1 has an additive effect on the decrease in OS progression in vitro and in vivo. We, thus, hypothesize that SphK1 activity is elevated by CD36 mediated lipid intake and increases S1P which in turn is exported to the tumor microenvironment, where it promotes OS development and metastasis. Thus, inhibiting this interaction between CD36-SphK1-S1P and in turn between nmObs and OS cells in the tumor microenvironment, will aid in the development of novel therapeutics to halt OS progression.

***Disclosures: InHong kang**, None*

SAT-104

Vertebral Osteosclerotic Bone Metastasis Lesions of Prostate Cancer Acquire Altered Extracellular Matrix Characteristics *Bita Mojtahedzadeh[1], Dennis Xie[1], Hans Adomat[1], Felipe Eltit[2], Raphaële Charest-Morin[3], Colm Morrissey[4], Eva Corey[4], Lawrence True[4], Michael Cox[2]. [1]Vancouver Prostate Centre, Canada. [2]Department of Urologic Sciences, University of British Columbia, Canada. [3]Department of Orthopedics, University of British Columbia, Canada. [4]Department of Urology, University of Washington, Seattle, United States

Prostate cancer (PC) bone metastases (BM) is a debilitating disease morbidity that primarily affects the axial skeleton. PCBMs are mixed blastic/lytic with increased, irregular, bone density and deposition, loss of collagen alignment and increased porosity. Under pathological conditions or repair, bone matrix composition is altered and can include cartilage-associated proteins. We hypothesize that PCBMs induce dysregulated repair-like bone remodeling activity resulting in differential deposition and organization of extracellular matrix (ECM) factors relative to residual trabecular bone.We analyzed lumbar vertebrae specimens from 13 cadaveric PCBMs, 6 biopsies from patients undergoing decompression surgery, and 4 age-matched cancer-free donors. We used mass spectrometry (MS) to compare the protein content of sclerotic and lytic vertebral PCBMs vs. cancer-free controls. We performed Goldner's trichrome staining to compare bone matrix organization among specimens. We performed immunohistochemistry (IHC) using antibodies against collagens (COL-I, -II, -III), osteocalcin (OSC), osteopontin (OSP), aggrecan, bone morphogenic protein 2 (BMP2), and alkaline phosphatase (ALP) to evaluate the composition of irregular and residual trabecular PC-associated bone matrix. MS analysis differentially segregated sclerotic and lytic PCBMs from control specimens (Fig. 1A). Differential Goldner's staining of irregular PC-associated bone and lamellar bone under brightfield, and loss of collagen alignment under polarized light in the PCBM specimens confirmed irregular bone interspersed with lamellar (residual trabeculae) bone (Fig. 1B,C). Stronger COL-III (Fig. 1D), OSC and OSP (Fig 1F), and ALP and BMP2 staining in sclerotic regions of PCBMs validated noted MS findings from the sclerotic PCBM specimens. Aggrecan and COL-I levels were indistinguishable between specimen groups, and COL-II was not detected in sclerotic, PC-associated bone. We did not observe evidence of a collagenous matrix switch based on the absence of COL-II and aggrecan. High COL-III content suggests that a process akin to bone repair occurs in the PCBM, while elevated levels of polyanionic proteins, such as OSP, suggest an accelerated process of mineralization. Our observations demonstrate structural and biochemical alterations in irregular PC-associated bone consistent with a hyperblastic dysregulation of matrix deposition that results in a disorganized sclerotic matrix distinct from healing physiology.

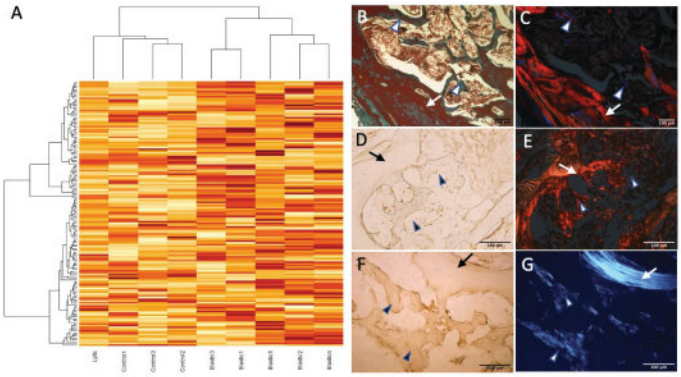

Figure 1. Bone matrix composition and collagen alignment differences between irregular PC-associated bone and lamellar bone. **A)** Differential expression of proteins in sclerotic bone (label: blastic1-5) compared to lytic bone (label: lytic) and cancer-free control bone (label: control1-3) seen via Mass Spectrometry. Protein expression shows higher similarity within groups. **B)** Goldner's trichrome stain shows lamellar bone stained red (arrow) while irregular PC-associated bone stains green (arrowhead). **C,E,G)** Polarized light imaging shows collagen alignment in lamellar bone and non-organized alignment in the irregular PC-associated bone. **D)** Increased staining of collagen-III in irregular PC-associated bone (arrowhead) compared to lamellar bone (arrow). **E)** Increased staining of osteopontin in irregular PC-associated bone (arrowhead), compared to lamellar bone (arrow). Scale Bar = 100 μm.

***Disclosures: Bita Mojtahedzadeh**, None*

SAT-105

See Friday Plenary Number FRI-105

SAT-107

Recombinant Adeno-associated Viruses Designed to Target Pediatric Osteosarcoma and Bone Stromal Cells *Patrick Mulcrone[1], Anh K. Lam[1], Erika A. Dobrota[1], Dylan A. Frabutt[1], Pankita H. Pandya[1], Karen E. Pollok[1], Weidong Xiao[1]. [1]Indiana University School of Medicine, United States

As new first-line therapies for primary bone cancers have not been developed for decades, the need for effective, genomically-guided treatments for these tumors is warranted. The viral-based gene therapy, recombinant adeno-associated virus (rAAV), is a powerful biological tool making a positive clinical impact on various diseases, yet it is an underexplored treatment strategy for cancers, including pediatric osteosarcoma (OS). The AAV3 serotype is known to transduce various tumor cells, and AAV9 is being researching for various bone pathologies. In this exploratory project, we hypothesize that rAAV3 and 9 serotype construct designs can be assembled to transduce human OS cells for therapeutic means. We prioritized the p16INK4a cell cycle regulator as aggressive OS typically harbors loss of the CDKN2A gene encoding p16. As high levels of p16 may be a favorable prognostic factor in OS progression, AAV gene therapy could restore proper function of this tumor suppressor. We observed in vitro transduction of the OS cell lines U2OS and Saos2, and the patient-derived xenoline TT2, developed at IUSM, with AAV serotypes 2, 3, and 9. Transduction with rAAV2 or rAAV9 driving expression of the tumor suppressor p16INK4a resulted in elevated levels of p16 protein and significant decreases in proliferation and cell number in vitro. In 3D cultures, a decrease in U2OS tumor spheroid volume transduced with rAAV2-p16INK4a compared to the control rAAV2-eGFP was evident. Additionally, chemical modification of rAAV9 protein capsid with the organic compound N-ethylmaleimide (NEM) led to a greater increase in transduction in U2OS and Saos2 cell lines via luciferase activity. To determine if

this NEM modification also altered rAAV9 transduction of non-transformed bone cells, we transduced murine bone marrow stromal cells, or their derivative osteoblasts and adipocytes with the NEM-modified rAAV9 or the WT rAAV9. Only primary osteoblasts were effectively transduced by rAAV9-NEM, suggesting that NEM alters AAV's trafficking and/or interaction of surface membranes or receptors on bone and OS cells. Overall, our data demonstrates that rAAVs efficiently transduce bone and OS cells, and that specific designs and modification can be used to dictate their tropism in vitro. More research, including in vivo OS cancer models, is underway to characterize the translational efficacy of our rAAV designs.

***Disclosures: Patrick Mulcrone**, None*

SAT-108

See Friday Plenary Number FRI-108

SAT-109

Evaluating Changes in Estrogen Receptor Signaling in Breast Cancer at Stiffnesses Related to the Bone Marrow *LOGAN NORTHCUTT[1], Marjan Rafat[2], Julie Rhoades (Sterling)[3]. [1], . [2]Vanderbilt University, United States. [3]Vanderbilt University Medical Center, United States

Estrogen receptor (ER) status is a primary marker used to predict breast cancer (BC) outcomes and metastatic disease. Clinical studies have indicated that ER+ patients often have bone-only metastatic disease. However, previous studies have indicated that ER+ cells lack factors for osteoclast-mediated bone destruction. It is well-established that tumors are heterogenous in ER expression and studies in primary tumor sites suggest that changes in stiffness can alter ER signaling. However, it remains unclear how ER may change through the stiffnesses of the bone microenvironment, which can be 20 times stiffer than the breast. We reasoned that the stiffness of the bone and bone marrow may drive changes in ER signaling that alters epithelial-to-mesenchymal transition (EMT). Understanding how the bone environment may alter ER signaling leading to changes in EMT and osteolytic factors may lead to a better understanding of how ER+ BC may be able to induce osteoclast-mediated bone destruction.We hypothesize that higher stiffnesses of the bone marrow and bone decrease estrogen receptor sensitivity of ER+ BC cells which increases the expression of genes that can drive osteoclast-mediated bone destruction. To evaluate this, we seeded ER+ (MCF7s) and ER- (MDAs) cells on CytoSoft® Rigidity Plates that mimicked the stiffness of the bone marrow (0.5 - 32 kPa). After 2 days in culture, RNA and protein were extracted to analyze factors associated with osteolysis (ITGB3, TGFB-RII, Gli2, and PTHLH). Additionally, we probed the expression of ER and phosphorylated ER (pS118ERa) to evaluate estrogen activity. Preliminary results show that gene expression of osteolytic factors PTHLH and Gli2 were changed at various stiffnesses. We predict that increased other osteolytic factors will be altered at these stiffnesses.Overall, this work gives insight into how estrogen signaling is changed in the bone marrow compared to the primary site. For our next steps, we plan to re-evaluate the expression of osteolytic genes when given aromatase inhibitors at varying stiffnesses and perform RNA-sequencing to gain an understanding of what other signaling pathways change in ER+/ER- bone metastatic tumors. These studies may lead to more targeted therapies in ER+ breast cancer patients that no longer respond to hormone-targeted therapies, which may help reduce the negative effects of therapies and better predict which patients may develop bone metastatic disease.

***Disclosures: LOGAN NORTHCUTT**, None*

SAT-111

Investigating the Role of EphA2 in Breast Cancer-Mediated Osteoclast Expansion and Function *Dominique Parker[2], Verra Nwga[2], Jin Chen[2], Julie Rhoades (Sterling)[3]. [2]Vanderbilt University, . [2]Vanderbilt University, United States. [3]Vanderbilt University Medical Center, United States

Bone metastases are present in over 70% of metastatic breast cancer patients and are complicated by the development of tumor-induced bone disease (TIBD). Frequently, TIBD is characterized by an increase in osteoclast proliferation and bone-resorbing activity, and patients often experience pain and increased fractures. Additionally, bone metastatic patients are often resistant to first- and second-line therapies highlighting an importance for research in this area. Moreover, the receptor tyrosine kinase, Ephrin-type-A 2 receptor (EphA2), is highly expressed in bone metastases, and previous evidence suggests its involvement in TIBD and anti-tumor immunity. EphA2 participates in both forward and reverse signaling during receptor/ligand engagement and is known for its role in inflammation and bone homoeostasis. Previous data shows a reduction in osteoclast number and bone lesions following EphA2 knockout. However, the mechanism by which EphA2 mediates the expansion of osteoclasts is not well understood. We therefore hypothesize that increased expression of EphA2 in breast cancer cells at the site of bone metastasis promotes osteoclast expansion, leading to TIBD. In agreement with previous work, our data shows that EphA2 deletion in murine breast cancer (BC) cell line, 4T1, reduces bone lesion area and number and reduces the presence of bone metastasis-associated macrophages, which are important in tumor establishment and expansion in the bone. To assess the effects of EphA2 deletion on the behavior of 4T1 cells, we conducted a wound healing assay. We observed a reduction in wound healing capacity in 4T1 cells following EphA2 deletion. This suggests that EphA2 expression in BC cells may increase their metastatic potential. Our future studies will investigate EphA2 signaling and reverse signaling in BC cell lines, myeloid progenitor cells, osteoclasts, and bone metastasis-associated macrophages. We will utilize murine and human BC cell lines to elucidate the effects of EphA2 deletion on immune cell populations, bone metastasis, and tumor progression. Additionally, we will investigate how EphA2 reverse signaling impacts osteoclasts' ability to modulate immune cells. We aim to reduce TIBD and tumor burden by reducing the expansion of osteoclasts and shifting the immune cells to an anti-tumorigenic phenotype. Our studies will provide additional insight into the underlying mechanisms of TIBD which will offer new treatment strategies for osteolytic breast cancer.

***Disclosures: Dominique Parker**, None*

SAT-112

See Friday Plenary Number FRI-112

SAT-113

68Ga-PSMA-11 (Gozetotide) PET Radiomic Features of Prostate Gland Related to Osseous Metastatic Disease. *Orhan Oz[1], Jin Qi[2]. [1]University of Texas Southwestern Medical Center, Dallas, United States. [2]Parkland Heath System & UTSW Medical Center, United States

Purpose:To test the hypothesis whole prostate 68Ga-PSMA-11 (Gozetotide) PET radiomic features can be identified that are predictive of/portend a higher probability for osseous metastasis.Materials & Methods:One hundred three subjects with available preoperative PET imaging were included in this IRB-approved retrospective study. Two radiologists, with 30 years (OKÖ) and 15 years (JQ) experience, jointly interpreted the PET/CT scans and agreed on the presence of metastatic disease. The study cohorts were established based on the location of the metastases on the scans: Bone only ("osseous metastases" (OM)), nodes only ("nodal metastases", (NM)), both bone and nodal metastases, (OM+NM), and "non-osseous metastases (NOM)", or "both nodal and osseous metastases" designation for each scan. Whole prostate semi-automated segmentation and feature extraction were performed on axial PET/CT images using public domain 3D slicer software (V5.2.1). The Pyradiomic features were compared between "osseous metastases" (OM), "non-metastases (NOM)" via Mann Whitney U test. Features with P values < 0.05 were considered to build the multivariable model. Logistic regression analysis was performed to discriminate two groups using GraphPad Prism 9.Results:To explore the radiomic features that only related to osseous metastasis in this initial study, 44 of the 103 pre-operative subjects were excluded- 12 subjects with both nodal and osseous metastases, and 32 subjects with only nodal metastases were excluded. The study cohort consisted of 59 subjects with pre-operative Gozetotide PET/CT and intact prostate glands. Scans of 37 subjects constituted the NOM cohort, 22 the OM cohort. Among 108 features, the most statistically predictive features differentiating OM from NOM on PET images were: the Maximum2DDiameterRow (p= 0.0275), JointEnergy (p=0.0001), JointEntropy entropy (p=0.0001), SmallAreaLowGrayLevelEmphasis (p=0.0001), DependenceNonUniformityphase (p= 0.0464), Coarseness (p=0.0420), wavelet-LHH_ Coarseness (p= 0.0109) (Table 1). Multivariable analysis of radiomics achieved an AUC (95%CI) of osseous metastatic predictive power of 0.85 Figure 1.Conclusions:To our knowledge, this is the first study to determine that there are radiomic features of the primary prostate that have predictive power for osseous metastases. 68Ga-PSMA-11 PET radiomic features of the whole prostate were identified that could play a role in improving predictive capability in diagnosing osseous metastasis in prostate cancer. This information could inform follow-up periods after initial scanning. Future larger studies may help determine the clinical significance of our findings. Features will be tested for the ability to predict nodal metastases and the feature sets will be expanded to include the other 1000 or more other features available to test.

Table 1: Selected Radiomics features differentiated osseous metastases from non- osseous metastases

Feature Group	Description	Features Name	P value
Shape Features 2D	Maximum diameter	Maximum2DDiameterRow	0.0275
Gray Level Cooccurrence Matrix (GLCM)	Spatial Relationship	JointEnergy	<0.0001
Gray Level Cooccurrence Matrix (GLCM)	Spatial Relationship	JointEntropy	<0.0001
Gray Level Cooccurrence Matrix (GLCM)	Intensity	SmallAreaLowGrayLevelEmphasis	<0.0001
Gray Level Dependence Matrix (GLDM)	Uniformity	DependenceNonUniformity	0.0464
Neighboring Gray Tone Difference Matrix (NGTDM)	Complexity	Coarseness	0.042
Gray Level Small Affinity Matrix (GLSAM)	Uniformity	SmallAreaLowGrayLevelEmphasis	<0.0001
wavelet-LHH	Complexity	Coarseness	0.0109

GLCM: gray-level co-occurrence matrix; GLSZM: gray level S zone; GLDM: gray level dependence matrix; NGTDM: neighboring gray tone difference Matrix.

Figure 1: Multivariable Model Analysis of Prostate Radiomic Features to Predict Osseous Metastases

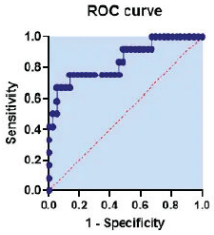

***Disclosures: Orhan Oz**, None*

SAT-115

See Friday Plenary Number FRI-115

SAT-116

Aging of the bone marrow niche awakens dormant breast cancer cells and promotes overt bone metastasis *Alexander Scaeffer[1], Ioanna Tsoukala[1], Mohammed Mosa[1], Devona Soetopo[2], Maresa Weitmann[3], Wadim Kisel[4], Sophia Thevissen[5], Jennifer Beavarlet[6], bernhard drotleff[7], theodore alexandrov[7], Lisa Sevenich[3], Thomas Broggini[8], Marcus Czabanka[8], Halvard Boenig[9], Katharina goetze[6], Aline Bozec[10], Klaus Pantel[11], Lorenz Hofbauer[12], Martina Rauner[13], Hind Medyouf[1]. [1]Georg-Speyer-Haus, Germany, [2]Georg-Speyer-Haus-haus, Germany, [3]Georg-speyer-haus, Germany, [4]TU Dresden, Germany, [5]Georg-Speyer-haus, Germany, [6]TUM, Germany, [7]Embl, Germany, [8]Goethe University Frankfurt, Germany, [9]German Red Cross, Germany, [10]UK Erlangen, Germany, [11]UKE Hamburg-Eppendorf, Germany, [12]TU Dresden University Medical Center, Germany, [13]Medical Faculty of the TU Dresden, Germany

Background: Despite substantial advances in the treatment of primary tumors, metastases are associated with poor outcome and remain the major source of cancer-related deaths. In breast cancer (BCa), bone is one of the major sites of metastasis, with autopsy studies showing occurrence in up to 70% of BCa patients. In patients with hormone receptor positive BCa, bone metastatic manifestations frequently follow an indolent disease course, where disseminated tumor cells (DTCs) remain initially dormant for years up to a decade before overt outgrowth and symptomatic disease manifestation. Notably, besides the hormone receptor status, advanced age is the second most significant predictor of overt bone metastasis occurrence in BCa. However, the molecular mechanisms that underpin this association, remain largely unknown. Methods and Results: Here, we used a newly generated immunocompromised model that recapitulates bona-fide features reminiscent of physiological aging, to demonstrate that age-related alterations in the bone marrow niche, dictate growth dynamics of human breast cancer DTCs in the bone. More specifically, our data point to a prominent tumor-extrinsic control of dormancy that is linked to aging of specific structural niche cell types. To confirm this in a fully human setting and dissect the cellular origin of the observed phenotype, we used bone metastatic cell lines and patient-derived circulating tumor cells (CTCs) in a newly established 3D human organotypic marrow environment (3D-HOME). We demonstrate that age-related alterations in the cell-fate decision of mesenchymal niche cells towards adipocytes, generates an adipo-rich local microenvironment that drives the awakening of quiescent DTCs. Metabolomic analysis revealed specific dependencies, targeting of which, effectively reverted the outgrowth phenotype. Current work is additionally exploring whether these new metabolic dependencies could be exploited to sensitize the DTCs to a specific form of programmed cells death, to enable disease eradication. Conclusion: This work shows that DTC-niche dependencies dynamically evolve with age. The findings will enhance our ability to propose disease-stage and age-adapted therapeutic interventions and inform the rational design of new treatment strategies for patients with bone metastasis.

***Disclosures: Alexander Scaeffer**, None*

SAT-117

Mechano-activation of Osteocytic Connexin Hemichannels Prime Microenvironment in Suppressing Breast Cancer Bone Metastasis *Xuewei Wang[1], Rui Hua[2], Manuel Riquelme[2], Jingruo Zhang[2], Francisca Acosta[2], Jean Jiang[2]. [1]University of Texas Health Science Center at SAn Antonio; University of Texas at San Antonio, , [2]University of Texas Health Science Center at San Antonio, United States

Previous studies have shown that moderate mechanical stress prevents the growth of metastatic breast cancer (BC) and bone destruction by transducing mechanical stimulation into downstream cellular signals. Connexin 43 (Cx43) is abundantly expressed on the plasma membrane of osteocytes and forms both gap junctions (GJs) and hemichannels (HCs, unpaired GJs), which enable communication between neighboring cells or intra-extracellular microenvironment, respectively. Our recent study demonstrated that Cx43 HCs activation in osteocytes, induced by mechanical stress, inhibited the migration of triple-negative BC cells and HC-released factors such as ATP and PGE2 were involved in this process. To investigate if activation of osteocytic Cx43 HCs cultivates bone microenvironment that is BC suppressive, we examined the ER+ BC cells that have a greater potential to metastasize to the bone. We adopted a 3D tumor spheroid model for human ER+ BT-474 cells that closely mimics tumor growth in situ and cultured cells with conditioned medium (CM) collected from osteocytes after treated with fluid shear stress (FSS). The results showed that the FSS-CM significantly reduced BC cell growth and increased numbers of apoptotic cells; however, this inhibitory effect was attenuated with the CM collected from osteocytes treated with a specific HC-blocking antibody (Panel A). To further investigate the impact of activation of osteocytic Cx43 HCs by mechanical stress on bone microenvironment and BC metastasis in vivo, we applied mechanical loading to the left tibia for two weeks (5 minutes/day, 5days/week, peak strain: 1000 ??). After loading, murine Py8119 BC cells were implanted in both loaded and unloaded tibiae of wild type (WT) and two osteocyte-specific transgenic mice expressing dominant negative mutants: R76W (impaired GJs) and ?130-136 (impaired both HCs and GJs). The unloaded right tibia had greater cancer cell proliferation, tumor growth, and bone damage than pre-loaded left tibia in WT and R76W mice with functional HCs. However, no significant differences were observed in ?130-136 mice with impaired HCs (Panel B). ATP and PGE2 released by Cx43 HCs were elevated in loaded tibiae of WT and R76W mice but not ?130-136 mice. This study suggests that activation of Cx43 HCs by mechanical stress associated with the release of the factors changes the bone from tumor-supportive to suppressive microenvironment that inhibits BC metastasis (Panel C).

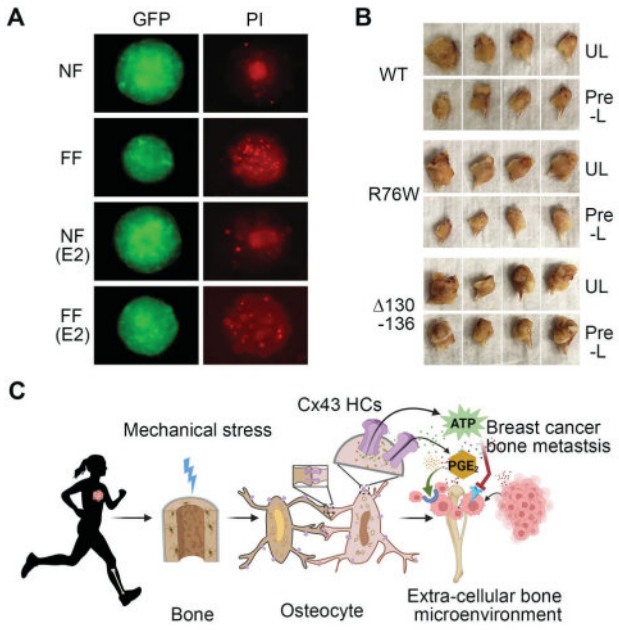

***Disclosures: Xuewei Wang**, None*

SAT-118

Prostate Cancer Engages Osteoblasts and Osteocytes via Soluble Signals *Kristina Wells[1,] Stephen Wilson[2,] Aimy Sebastian[2,] Gabriela Loots[1,] Damian Genetos[3,] [1]University of California, Davis, United States, [2]Lawrence Livermore National Laboratory, United States, [3]University of California, Room 1020 VM3B, United States

Prostate cancer (PCa) is the fifth leading cause of death worldwide. PCa's preferential metastasis to bone bodes terribly for survival, where 5-year survival rates plummet from 56% to <1%. Thus, mitigating bone metastasis is critical for improving the health- and lifespan of PCa patients. How PCa metastasizes to bone or engages bone cells to promote its survival are incompletely understood. Previous research established that PCa engages bone-building osteoblasts (OB) and bone-resorbing osteoclasts to promote PCa growth and survival; less is known about PCa interactions with osteocytes (OCY), the long-living cells in bone that orchestrate remodeling. We sought how PCa indirectly engaged OBs and OCYs as well as common and distinct transcriptional responses.We created PCa conditioned media (CM) by culturing C4-2B PCa cells to 80% confluence, adding fresh RPMI1640, then growing cells for 24 hours. We treated MC3T3-E1 pre-OBs or OCY-like OCY454 cells with PCa CM or naïve media for 24 hours. PCa CM dose-dependently increased MC3T3-E1 apoptosis without affecting OCY454. Bulk RNA sequencing was performed to establish PCa impact on transcription vs. naïve media. PCa CM impacted OBs more than OCYs, affecting 1536 MC3T3-E1 transcripts vs 423 OCY454 transcripts. Only 38 differentially expressed genes (DEGs) affected in both cell types when treated with PCa CM. Gene ontology analysis revealed changes in expected and novel pathways. In MC3T3-E1 cells, 'cholesterol biosynthetic process,' 'regulation of endothelial cell differentiation,' and 'regulation of nitric oxide biosynthetic process' were among enriched processes. In OCY454 cells, 'regulation of nitric oxide synthase biosynthetic process' and 'regulation of wnt signaling pathway' were enriched. In both MC3T3-E1 and OCY454 cells, 'epithelial to mesenchymal transition' and 'cell junction assembly' were enriched by PCa CM. Overall, MC3T3-E1 cells were more strongly impacted by treatment with PCa CM compared to OCY454 cells, in terms of apoptosis, total DEGs, and gene ontology analysis. Few genes or pathways were differentially expressed in response to PCa CM in both MC3T3-E1 and OCY454 cells. Thus, MC3T3-E1 cells, a pre-OB cell line, appear to be more strongly impacted by the presence of PCa than the OCY-like cell line OCY454. This suggests that PCa may more effectively engage OBs than OCYs, despite their common origin.AS and GGL conducted work under the auspices of the USDOE by LLNL (DE-AC52-07NA27344).

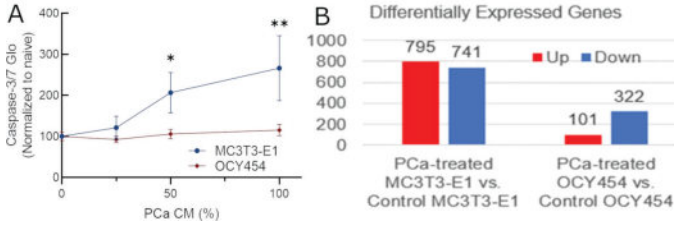

***Disclosures: Kristina Wells**, None*

SAT-119

See Friday Plenary Number FRI-119

SAT-121

Assessing Effects Of Immune Checkpoint Inhibitors On Bone Using Opportunistic Computerized Tomography Bone Densitometry: A Translational Pilot Study In Oncology *Carrie Ye[1,] Jacob Jaremko[1,] John Walker[1,] Jasmine Gill[1,] Bryn Matheson[2,] Cassandra Gallant[1,] William Leslie[3,] Michael Kolinsky[1,] Steven Boyd[2,] [1]University of Alberta, Canada, [2]University of Calgary, Canada, [3]University of Manitoba, Canada

Many therapies in oncology are associated with decline in bone mineral density (BMD) and increased risk of fragility fractures. The newest class of cancer drugs, immune checkpoint inhibitors (ICIs), have become standard of care for treatment of several types of cancer. ICIs work by activating T-cells to attack cancer cells, but T-cell activation is known to activate osteoclast maturation, leading to increased bone resorption. Increased fracture rate has been reported after ICI initiation, but the direct effects of ICI on BMD have never been studied.AIM: To investigate the effects of ICI on BMD using clinical computed tomography scans (CT).METHODS: We performed a retrospective cohort study of patients treated at the Cross Cancer Institute or Kaye Edmonton Clinic in Edmonton, Canada. The study cohort included individuals with stage III melanoma, treated with at least 6 months of ICI and the control cohort included individuals with stage II melanoma, not treated with ICIs. Inclusion criteria required that each individual have a baseline and 12-month follow-up CT that included the lumbar spine. Using an automated segmentation algorithm and internal calibration, lumbar spine BMD obtained from CT images will be compared between baseline and follow-up using a mixed-effects regression model. Glucocorticoid exposure between the baseline and follow-up CT was ascertained and stratified analysis will be completed for those exposed to long-term glucocorticoids.PRELIMINARY RESULTS: 42 study patients and 49 control patients have been identified with available baseline and follow-up CT images. All CT images have been collected and are undergoing analysis including automated segmentation of lumbar spine vertebrae and BMD measurement. Preliminary results demonstrated approximately 7% decline in lumbar spine (L1-5) BMD 12-months after ICI initiation (Figure).CONCLUSION: It is feasible to obtain BMD from clinical CT using machine learning and internal calibration. Full longitudinal BMD results for all study participants is ongoing.

Bone	Baseline BMD (mg/cc)	Follow-up BMD (mg/cc)	Percent Difference
L5	349.3	322.9	-8.2
L4	348.6	316	-10.3
L3	330.5	312	-5.9
L2	323.3	304.7	-6.1
L1	299.6	284.6	-5.3
		Mean Percent Difference	-7.2

***Disclosures: Carrie Ye**, None*

SAT-123

See Friday Plenary Number FRI-123

SAT-124

Persistent DNA Damage in Chondrocytes May Contribute to Osteoarthritis Onset *Mark James[2], Eduardo Peralta-Herrera[2], Danielle Benoit[3], Jennifer Jonason[4]. [2]University of Rochester, . [2]University of Rochester, United States. [3]Phil and Penny Knight Campus to Accelerate Scientific Impact, University of Oregon, United States. [4]UNIVERSITY OF ROCHESTER, United States

Background: Osteoarthritis (OA) is the most common form of arthritis and is characterized by progressive loss of articular cartilage which can cause pain and loss of mobility. Aging is a significant risk factor for OA and while DNA damage is associated with aging, the role of DNA damage in chondrocyte aging and OA remains unclear. It was recently shown that aged and OA human knee chondrocytes contain more damaged DNA relative to young healthy chondrocytes. In response to DNA double-strand breaks (DSBs), stimulator of interferon gene (STING) activates the nuclear factor ?B (NF-?B) pathway. We previously showed increased NF-?B activity in aged chondrocytes and chondrocyte-specific induction of NF-?B activity promotes early OA onset in mice. We hypothesize that accumulating DNA damage leads to chronic proinflammatory signaling in aging chondrocytes, ultimately resulting in OA onset.Design: To investigate the role of DNA damage in chondrocytes and OA, we induced DNA DSBs in cultured chondrocyte-like cells using etoposide and modulated STING activity using siRNA or a small molecule STING agonist before collecting protein and RNA for respective immunoblot and RT-qPCR analyses. We also induced DNA damage using targeted X-rays in the knee joints of young and aged adult mice and assessed DNA damage, proinflammatory signaling, and cell senescence by histology at 2 hours, 2 days, and 1 week after irradiation. We also included a separate cohort of mice to assess histology, pain and mobility 6 months after irradiation.Results: We found that inducing DNA DSBs in cultured, chondrocyte-like cells led to proinflammatory signaling, as evidenced by increased NF-?B activity. We also showed that knockdown of STING by siRNA partially reduced this proinflammatory response while STING agonist treatment elevated NF-?B target gene expression. In vivo, we found that chondrocytes contained more persistent DNA damage a week after irradiation compared to synoviocytes. Histology and behavioral studies on mice 6 months after irradiation are currently in progress.Conclusions: We learned that chondrocytes contained more persistent DNA damage compared to synoviocytes after irradiation. Our future work will determine whether radiation-induced DNA damage may cause OA using histological and behavioral techniques. Understanding how DNA damage impacts articular cartilage could inform future clinical radiation therapies as well as provide new pathways to inhibit inflammation and prevent OA.

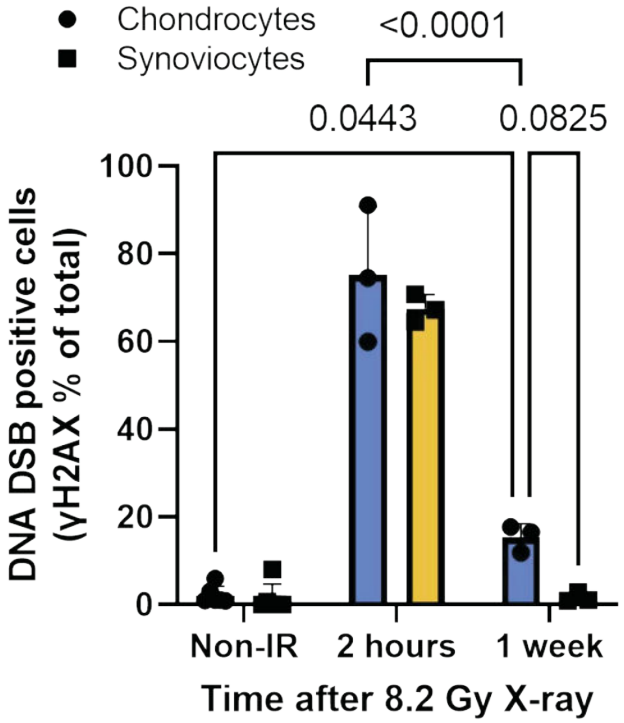

Quantification of tibial articular cartilage (blue) and synovium (yellow) of γH2AX IHC which marks DNA DSBs in non-irradiated (non-IR) and at time-points after 8.2 Gy X-irradiation.

***Disclosures: Mark James**, None*

SAT-125

Single-cell Transcriptomic Analysis supports GP stem cell hierarchy and reveals FoxA2+ long-term skeletal stem cells (LTSSC) and PTHrP+ short-term stem cells (STSSC) clusters are independent of each other. *Yiwei Kong[1], Yu Zhou[2], Shreya Kumar[1], Shanmugam Muruganandan[1], Shobana Sekar[1], Rachel Pierce[1], Hannah Alberico[1], Dori Woods[1], Andreia Ionescu[3]. [1]NORTHEASTERN UNIVERSITY, United States. [2]Boston Children's Hospital Harvard Medical School, United States. [3]Northeastern University,

We recently discovered a FoxA2+LTSSCs population at the top of growth plate (GP) resting zone (RZ), with higher clonogenicity and longevity than the previously identified PTHrP+STSSCs. To validate the newly discovered GP stem cell hierarchy, we performed 10x genomics single-cell RNA sequencing on GP cells isolated from P18 C57B6 mice (Fig.1A). We separated clusters positive for chondrocyte markers (Acan, col2a1) from erythroid cells, B cells, neutrophils, osteoblasts, macrophages, endothelial cells, NK cells and monocytes. We performed Seurat-based specific sub-clustering of the chondrocytes, yielding 1444 cells separated in 9 independent clusters (0-8). High expression level of Col2a1 was observed in all clusters (A1). Cluster 6 was enriched for proliferation markers Mki67 and Cdk1 (A2-3). Clusters 2, 3, 6 showed enrichment for columnar chondrocytes marker Gdf10 and hypoxia-associated gene Cox4i2 (A4-5). Cluster 4 has high levels of hypertrophic chondrocytes markers Col10a1 and Ihh (A6-7). Cluster 5 was enriched for S100a7a (A8) and Cdkn1c (p57), expressed in pre/hypertrophic chondrocytes. Cluster 1 expressed markers of late hypertrophic chondrocytes Mmp13 and Bmp7 (A10-11). The remaining clusters (0, 8, 7) were annotated as RZ cells positive for skeletal stem cell markers Pdpn, Xrcc2 and Srpx2 (A12-14). In line our previous studies, FoxA2 marks two distinct populations, the FoxA2+col.10-LTSSC group in the RZ (cluster 8), and the FoxA2+col.10+ HZ chondrocytes (cluster 4) (A16). Consistent with GP geography, hypoxia-induced gene, Mif was highly expressed in all clusters except for Cluster 8 (RZ FoxA2+ layer - at the top of the GP) and Cluster 1 (late hypertrophic chondrocytes - at the bottom of the GP) (A15). Lastly, PTHrP expression is mapped to RZ cluster 0, consistent with specific localization of PTHrP+ cells at the bottom of the RZ. Future investigations need to determine whether RZ cluster 7 are progenitor cells. These results confirm a distinct separation of FoxA2+LTSSC and PTHrP+STSSC in the GP RZ. To further validate cluster hierarchy, we performed Monocle 3 pseudotime cell trajectory analysis, assigning cluster 8 (FoxA2+LTSSC) as a starting point. This analysis showed a continuous trajectory linking RZ chondrocytes (clusters 8, 0, 7), going through columnar chondrocytes (clusters 2, 3, 6), to terminal differentiated hypertrophic chondrocytes (clusters 5, 4, 1) (Fig.1B) supporting previously identified GP stem cell hierarchy.

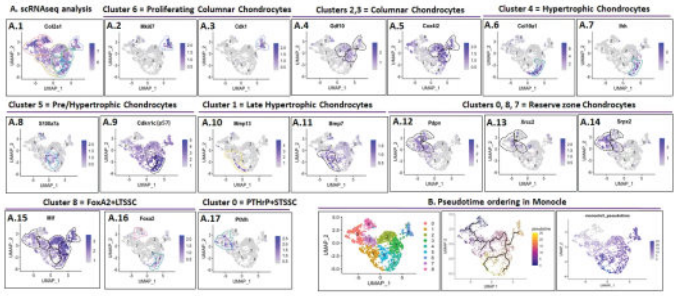

***Disclosures: Yiwei Kong**, None*

SAT-126

Nutrition-dependent stunted growth in neonatal mice is associated with decreased chondrocyte proliferation but not the activity of skeletal stem cells within the growth plate. *Daniela Schnyder[1], Anna Usanova[1], Baoyi Zhou[1], Jussi Heinonen[1], Jose M Lopez-Pedrosa[2], Ricardo Rueda[2], Andrei S Chagin[1]. [1]Department of Physiology and Pharmacology, Karolinska Institutet, Stockholm, Sweden, Sweden. [2]Abbott Nutrition R&D, Granada, Spain, Spain

Introduction: One of the leading causes of stunted and/or retarded longitudinal growth in children and adolescents is nutrient depletion. In the year 2020, 149.2 million children under the age of five were affected by stunted growth worldwide. Recently, it was shown that catch-up growth after nutrition-dependent growth retardation is associated with the regulation of skeletal stem and progenitor cells (SSPCs) in the growth plate1. However, the effect of stunted growth retardation on SSPCs is unknown.Method: Extensive nutrition deprivation was induced by litter size expansion to 15-16 pups per dam at postnatal day 7 (P7). Restriction lasted until pups were starting to eat by themselves between P17 and P21. SSPCs were assessed by employing the PTHrP-mCherry mouse strain and their ability to form progeny by PTHrP-CreERT2:tdTomato mice as described2.Results: Body weight was significantly reduced in nutrition-deprived mice as early as P14 and was not restored until the end of the study period, 2 months of age. At the same time, decreased tibia and femur length were restored to control values at day P35. Systemically, the malnourishment caused a dramatic reduction of serum levels of insulin and IGF1 and while insulin levels were restored to control at P21, levels of IGF1 remained low at P21. Locally, a profound decrease in proliferation (28.8% of control, normal-fed pups) was observed throughout the growth

plate including PTHrP-mCherry SSPCs (33.3% of control). However, the number of SSPCs normalized to the length of the growth plate was not significantly changed by malnourishment. The formation of committed progeny was not affected by malnourishment as assessed in PTHrP-CreERT2:tdTomato mice pulsed with tamoxifen one day prior to the initiation of malnourishment. We also noticed a mild reduction in the number of hypertrophic chondrocytes during malnourishment (86% of control), which was restored to normal at P21, but not their size.Conclusion: We concluded that malnourishment-caused growth retardation in neonatal and early postnatal periods is not associated with SSPCs behavior in the growth plate, but instead all chondrocytes respond by dramatic reduction of their proliferation. The effect is probably regulated by insulin/IGF1 serum levels.References:1. Oichi T, et al. Nutrient-regulated dynamics of chondroprogenitors in the postnatal murine growth plate. Bone Res. 2023 Apr 21;11(1):20. doi: 10.1038/s41413-023-00258-9. PMID: 37080994; PMCID: PMC10119120.2. Mizuhashi, K. et al. Resting zone of the growth plate houses a unique class of skeletal stem cells. Nature 563, 254-258 (2018).

***Disclosures: Daniela Schnyder**, None*

SAT-128

Runx2 activity in hypertrophic chondrocytes regulates postnatal cartilage and bone turnover *Caris Smith[1], Harunur Rashid[2], Vashti Convers[3], Katelynn Clark[3], Amjad Javed[4]. [1]The University of Alabama at Birmingham, United States, [2]University of Alabama Birmingham, United States, [3]The University of Alabama at Birmingham School of Dentistry, United States, [4]University of Alabama at Birmingham, United States

Resting chondrocyte specific deletion of Runx2 gene blocks chondrocyte differentiation and endochondral ossification resulting in perinatal lethality. Importantly, expression of Runx2 increases progressively from resting to hypertrophic chondrocytes (HCs). HCs regulate endochondral ossification by secreting matrix resorbing enzymes and angiogenic factors. However, HCs specific role of Runx2 during postnatal chondrogenesis remains unknown. We deleted Runx2 gene specifically in HCs using the type-X collagen-Cre mice. Endochondral ossification was assessed from birth to adulthood using molecular, biochemical, and histological approaches. Homozygous (Runx2HC/HC) mice survive but show limb dwarfism and enlarged growth plates. A significant decrease in apoptosis of Runx2-defecient HCs resulted in doubling of the HC zone in the growth plate. Consistent with this observation, expression of HC marker type-X collagen was increased in Runx2HC/HC littermates. Evaluation of 10-weeks-old mice revealed a significant increase in the articular and growth plate cartilage. Interestingly, the expression of collagen type 2 and major proteoglycans was unchanged. In sharp contrast, expression of collagenases and aggrecanases was markedly decreased during both embryonic and postnatal chondrogenesis. Cartilage islands were extended into the mid-diaphysis of the Runx2HC/HC mice indicating impaired resorption of the cartilage matrix. Histomorphometry and ?CT analyses revealed a significant increase in trabecular BV/TV, trabecular number, thickness, and a concomitant decrease in trabecular space in Runx2HC/HC mice. Osteoblast number and the expression of early and late osteoblast markers were comparable among the littermates. Furthermore, dynamic bone synthesis showed no differences in mineral apposition or bone formation rates. Despite an increased trabecular bone mass 3-point-bending test revealed bone fragility in Runx2HC/HC mice. TRAP staining showed a significant decrease in number and surface of osteoclasts in Runx2HC/HC mice. Runx2 deficient HCs showed a significant decrease in the expression of Rankl and IL-17. Bone marrow culture from Runx2HC/HC mice showed few, smaller osteoclasts. Impaired osteoclast differentiation was evident by a marked decrease in expression levels of mature osteoclast markers. Thus, Runx2 controls endochondral ossification by regulating the expression of cartilage resorbing enzymes and osteoclast differentiation factors in hypertrophic chondrocytes.

***Disclosures: Caris Smith**, None*

SAT-129

Observer-independent Identification of the Cellular Zone and Rates of Mineral Deposition in the Mouse Growth Plate Using Image Analysis Algorithms *Seung-Hyun Hong[1], Li Chen[2], Xiaonan Xin[2], Zhihua Wu[2], David Rowe[2]. [1]University of Connecticut, United States, [2]University of Connecticut Health, United States

Previously we have demonstrated the use of multimodal fluorescent and chromogenic imaging of single cryosectioned mouse growth plate section of a 4 week old mouse that was injected with EdU and alizarine complexone (AC) one day prior to sacrifice. Captured in the imaging process is the deposited mineral, the surfaces of active mineral deposition, TRAP positive cells (osteoclasts and columnar chondrocytes), EdU positive columnar chondrocytes and marrow cells, and AP positive osteoblasts and chondrocytes, all of which are aligned to an aqueous DAPI and Safranin O/ Fast Green image taken in color and Cy5 autofluorescence. In this abstract we describe how the individual image files from each round of scanning (11 files) are vertically aligned utilizing registration beads and how specific layer combinations are used to assign a line that separates specific zones. The imaging algorithms were designed to replicate the cellular and structural features that the human observers use as criteria of distinguishing each zone. In most cases, more than one criteria for a border line was generated from the multiple images from which the computer averaged the subtle differences into a final dividing line. Distinguishing features of the germinal, proliferative, prehypertrophic and hypertrophic zones of the growth plate and the metaphyseal and diaphyseal zone of the invading bone allowed the calculation of the width/area (absolute and relative) of each zone. Comparison of the zonal level of the accumulated mineral, deposited AC and expressed AP allow the calculation of the 1 day mineralization rate of cartilage and bone component of the growth plate. Other features of the columnar zone that can be computed is the proliferation index and the relative alignment of the columnar stacks. The images also capture the activity of the zone of Ranvier which is EdU and AP positive with a mineralizing front. We believe that this imaging and analysis workflow will be useful for high throughput screening of knockout mouse lines for cartilage abnormalities and a baseline for histological spatial localization of specific cell types identified by either CODEX or MERFISH technologies.

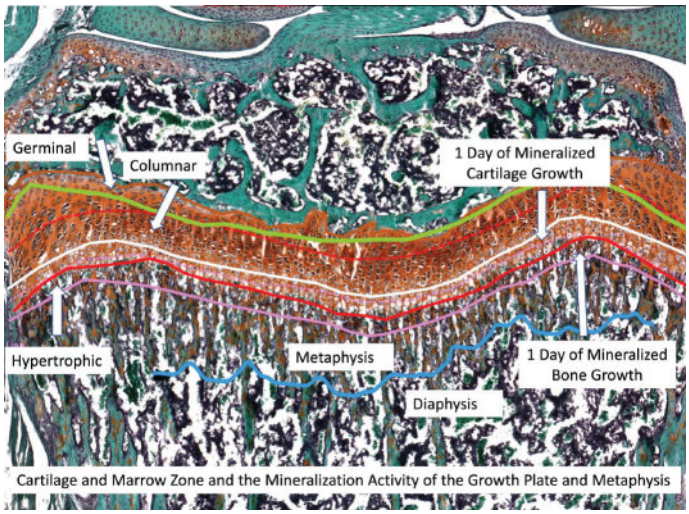

***Disclosures: Seung-Hyun Hong**, None*

SAT-130

Modified Periodic Acid-Schiff (PAS) is an alternative to Safranin O for discriminating bone-cartilage interfaces *Maria A Serrat[1], Kelsey M Kjosness[2], Philip L Reno[2]. [1]Marshall University School of Medicine, United States, [2]Philadelphia College of Osteopathic Medicine, United States

Safranin O is a cationic dye that binds to proteoglycans in cartilage and is routinely used to assess growth plate dynamics and/or fracture repair at bone-cartilage interfaces. When used with a counterstain such as fast green, Safranin O can offer exquisite differentiation of cartilage from surrounding bone. However, various decalcification and processing methods can deplete proteoglycans, rendering inconsistent, weak, or absent Safranin O staining with indiscriminate bone-cartilage boundaries. We sought to develop an alternative staining method that preserves the contrast of bone and cartilage in cases of proteoglycan depletion. Periodic acid-Schiff (PAS) is a carbohydrate-specific stain used to demonstrate glycogen and other polysaccharides, such as the mucopolysaccharides in cartilage. This two-step reaction involves exposure to periodic acid, which oxidizes glycol groups to aldehydes, followed by Schiff's reagent, which turns the aldehydes a rose-violet color. PAS preferentially targets glycol groups with a neutral charge, making this reaction more sensitive than Safranin O for staining cartilage matrix. We developed a simple and novel modification of a standard PAS protocol using Weigert's iron hematoxylin and light green stains that produces a contrast between bone (blue-green) and cartilage (purple).Juvenile mouse fore- and hindlimb bones (N=87) were fixed in formalin, decalcified in 10% EDTA and processed for routine paraffin histology. Modified PAS staining was performed using a commercially available kit (Sigma-Aldrich) with several modifications to the manufacturer's protocol: sections were exposed to periodic acid for 5 minutes, rinsed, immersed in Schiff's reagent for 10 minutes, rinsed and counterstained with Weigert's iron hematoxylin, after which they were "blued" in PBS, rinsed, and stained with 1% light green.In all samples tested, this modified PAS method consistently rendered purple staining in cartilage and blue-green staining in bone. Importantly, our technique provided a clear distinction of the bone-cartilage interface even when Safranin O staining did not (Figure 1). This modified PAS protocol provides a practical solution for differentiating bone and cartilage when Safranin O staining is not detected following decalcification and paraffin processing. This method can be a useful alternative for studies in which identification of the bone-cartilage interface is essential but may not be preserved with standard staining approaches.

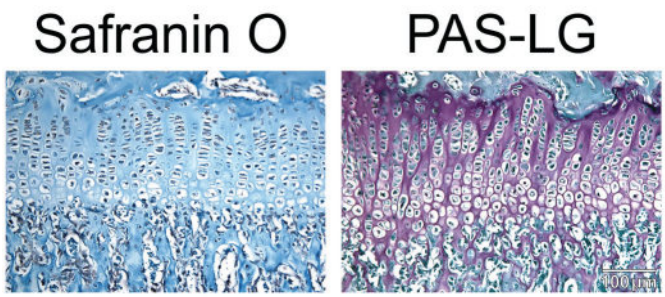

***Disclosures: Maria A Serrat**, None*

SAT-132

A Crucial Role For microRNA-433-3p in Endochondral Ossification: suppressing miR-433-3p in the osteochondral lineage alters growth plate morphology and bone growth *Prachi Thakore[1], Sangita Karki[2], Anne Delany[2]. [1]University of Connecticut Health Center, United States. [2]UConn Health, United States

Spatiotemporal regulation of gene expression is critical for establishing the cartilaginous scaffold needed for endochondral ossification, and there is little understanding of how small non-coding microRNAs (miRNAs) regulate growth plate biology. Mutation of a miR-433 binding site in human HDAC6 leads to X-linked chondrodysplasia, suggesting its clinical relevance. In vitro, miR-433 was induced >10 fold during chondrogenic differentiation of primary mouse mesenchymal cells. Decreasing miR-433 activity increased the expression of chondrogenic marker genes Sox9, Col2a1, and ColXa1, suggesting that miR-433 restrains chondrogenesis.To study the function of miR-433 in vivo, a miR-433 tough decoy (TuD) inhibitor was knocked into the Rosa26 locus; its expression is activated in cre expressing cells and their progeny. To suppress miR-433 activity in the osteochondral lineage RosamiR-433TuD/+ mice were crossed with Prrx1-cre, targeting limb bud mesenchyme. Femurs of both male and female miR-433 decoy (Prx-RosamiR433TuD/+) were shorter than littermate controls at 3, 6 and 12 weeks of age, with males more severely affected. Histology of tibias from 6 week males showed that miR-433 decoy mice exhibited disordered chondrocyte columns and reduced column length, indicating a critical role for miR-433 in growth plate organization.microCT analysis revealed that femurs from 6 week miR-433 decoy mice were narrower, with a 35% decrease in total cortical area. miR-433 decoy mice also had a 40% decrease in trabecular bone volume fraction, driven by decreased trabecular thickness. While trabecular bone volume increased from 6 to 12 weeks of age for both control and miR-433 decoy mice, the percent change in bone volume in this interval was 5 fold higher in decoy mice compared with controls. Thus, by 12 weeks, trabecular parameters in miR-433 decoy mice were similar to controls, supporting the concept that miR-433 dampens osteoblast function. In contrast, 12 week miR-433 decoy bones remained narrower and shorter, highlighting the impact of miR-433 on growth.Some validated miR-433 targets include Runx2 and Hdac6, which are known to regulate chondrocyte proliferation and maturation; we are currently examining how genes associated with chondrogenesis are affected by miR-433. Our study demonstrates that suppressing miR-433 in the osteochondral lineage significantly impacts growth plate morphology and bone accrual, indicating a crucial role of miR-433 in endochondral bone formation.

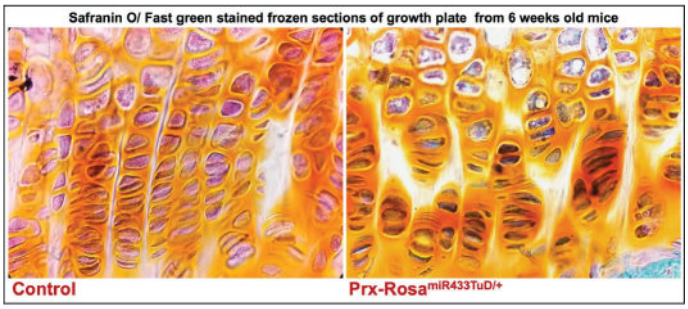

***Disclosures: Prachi Thakore**, None*

SAT-135

See Friday Plenary Number FRI-135

SAT-137

Piezo1 activation accelerates osteoarthritis progression and the targeted intervention effect of artemisinin *Donghao Gan[1], Guozhi Xiao[2], Qinnan Yan[1], Xiaowan Jin[1], Chu Tao[1], Yiming Zhong[1], Qingyun Jia[3]. [1]Southern University of Science and Technology of China, China. [2]Southern University of Science and Technology, China. [3]Linyi People's Hospital, China

Purpose: Osteoarthritis (OA) is a devastating whole-joint disease affecting a large population worldwide with no cure, its mechanism remains poorly defined. Abnormal mechanical stress is the main pathological factor of OA. Here we investigate the effects of Piezo1 activation on osteoarthritis (OA) development and progression and to explore Piezo1-targeting OA treatment.Methods:The expression levels of Piezo1 were determined in human OA cartilage and experimental OA mice. Mice with genetic Piezo1 deletion in chondrocytes or intra-articular injection of the Piezo1 activator Yoda1 were utilized to determine the effects on DMM-induced OA progression. In an effort to define PIEZO1-targeting drugs for potential OA treatment, via virtual docking technology in the constructed small molecule compound library, we found that artemisinin (ART), a potent antimalarial drug, may be a PIEZO1-targeting drug. Effects of ART, on Piezo1 activation, chondrocyte metabolism and OA lesions were determined.Results: Piezo1 expression is up-regulated in articular chondrocytes in human OA and destabilization of medial meniscus (DMM)-induced mouse OA cartilage. Inducible deletion of Piezo1 in articular chondrocytes in adult mice largely attenuates DMM-induced OA lesions. In contrast, intra-articular injection of Yoda1, a selective activator of Piezo1, aggravates the knee joint OA lesions induced by DMM in adult mice, while Yoda1 treatment did not cause marked OA lesions in sham mice. PIEZO1 activation increases, while PIEZO1 siRNA knockdown decreases, expression levels of RUNX2 and catabolic enzymes MMP13 and ADAMTS5 in primary OA-human articular chondrocytes (HACs) in a PI3K-AKT dependent manner. Similar results were observed in DMM mice articular cartilage. Of potential translational significance, we find that ART may have strong binding ability with several amino acid residues near the ion channel pore of Piezo1 molecule through computer protein-ligand docking simulation. We have provided strong evidence supporting that ART is a novel and potent inhibitor of Piezo1 activation in primary OA-HACs and all cell lines examined, including human endothelial HUVEC cells, ATDC5 chondrocyte-like cells and MLO-Y4 osteocytes-like cells. Results from in vitro experiments confirmed that ART decreases the Yoda1-induced increases in the levels of OA-related genes and p-PI3K and p-AKT proteins in OA-HACs and alleviates DMM-induced OA lesions in mice.Conclusions: We establish a critical role of Piezo1 in promoting OA development and progression and define ART as a potential OA treatment.

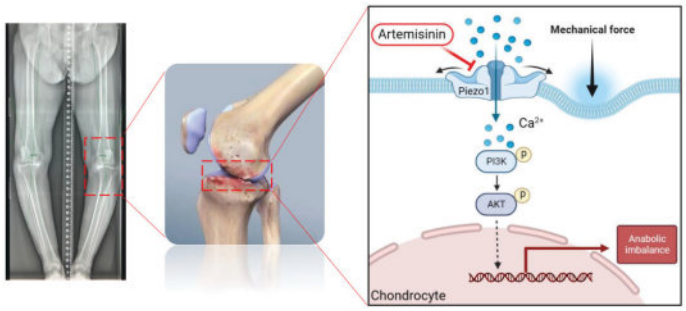

***Disclosures: Donghao Gan**, None*

SAT-139

See Friday Plenary Number FRI-139

SAT-140

Falsely Elevated Lumbar Spine BMD Due to Overlying Calcified Fibroid *Jovan Milosavljevic[1], Vafa Tabatabaie[2], Priyanka Mathias[1], Jenna Le[3]. [1]Division of Endocrinology, Department of Medicine, Montefiore Medical Center, Albert Einstein College of Medicine, United States. [2]Division of Endocrinology, Department of Medicine, and Department of Orthopedic Surgery, Montefiore Medical Center, Albert Einstein College of Medicine, United States. [3]Department of Radiology, Montefiore Medical Center, Albert Einstein College of Medicine, United States

Introduction: Dual-energy X-ray absorptiometry (DXA) is widely recognized as the gold standard for evaluating bone mineral density (BMD). However, approximately one-third of patients have artifactual findings on lumbar spine (LS) DXA imaging, resulting in the exclusion of at least one vertebral level. Identifying the presence of artifacts is crucial, as they can substantially influence BMD measurements. We present a case of falsely elevated LS BMD due to overlapping calcified uterine fibroma.Clinical Case: A 51-year-old woman was referred to endocrinology for evaluation of primary hyperparathyroidism (PHPT). Laboratory tests showed a serum calcium level of 10.6 mg/dL (normal 8.5 - 10.5 mg/dL) and an

inappropriately elevated serum PTH level of 163 pg/mL (normal 20.0 - 80.0 pg/mL) establishing diagnosis of PHPT. She denied history of prior fragility fractures. Bone densitometry was performed using a Hologic DXA scan and showed a total lumbar BMD of 1.701 g/cm2 and a T-score of 5.9. Individual lumbar T-scores were as follows: L1 = 1, L2 = 3.7, L3 = 8.3, and L4 = 8.7. The total hip BMD was 1.225 g/cm2 with a T-score of 2.3, femoral neck BMD was 1.159 g/cm2 with a T-score of 2.8, and the distal third of the left forearm BMD was 0.787 g/cm2 with a T-score of 1.8. An artifact overlying L2-L4 levels of the spine was identified, corresponding to a calcified uterine fibroid, measuring 18.3 x 14.9 x 14.2 cm, previously observed on a CT scan of the pelvis. Taking into account the measurements hip, and forearm, it was determined that the patient had normal bone mineral density. Due to the artifact obscuring 3 vertebral bodies, spine was excluded from the analysis.Conclusion: This case report emphasizes the significant influence of artifacts, in this case presence of a calcified uterine fibroma, on the evaluation of lumbar spine BMD. Providers interpreting DXA scans should routinely examine the images and be aware of various artifacts that can falsely alter interpretation of BMD values.

***Disclosures: Jovan Milosavljevic**, None*

SAT-141

Regional citrate anticoagulation with continuous renal replacement therapy: a rare cause of hypercalcemia *Leor Needleman[1,] Michael S. Hughes[1,] Ralph Mohammed Mohty[2,] Pedram Fatehi[2,] Deborah Sellmeyer[3.] [1]Division of Endocrinology, Stanford University School of Medicine, United States. [2]Division of Nephrology, Stanford University School of Medicine, United States. [3]Stanford University, School of Medicine, United States

Introduction: Regional citrate anticoagulation is used to prevent clotting in continuous renal replacement therapy (CRRT) circuits by chelating ionized calcium. On CRRT, patients with impaired citrate clearance can develop hypercalcemia due to citrate toxicity manifest as an elevated total calcium and low ionized calcium (a high "calcium ratio") and high anion gap metabolic acidosis. A calcium ratio (tCa:iCa) above 10 is considered high. We present three cases of citrate toxicity that resulted in significant total hypercalcemia. Clinical Case 1: A 61-year-old female with cirrhosis was admitted 11 months after liver transplantation with septic shock and renal failure. Serum calcium on admission was 9.6 mg/dL (8.4-10.5 mg/dL), albumin 2.4 g/dL (3.5-5.2 g/dL). She was placed on CRRT and underwent combined liver and kidney transplantation. Serum calcium increased to 13.1 mg/dL with ionized calcium 0.70 mmol/L (1.12-1.32 mmol/L) and calcium ratio 18.7. CRRT was discontinued and total and ionized calcium levels normalized. Case 2: An 80-year-old female was admitted with heart failure from carcinoid heart disease and AKI due to cardiorenal syndrome. Calcium on admission was 8.0 mg/dL, albumin 2.7 g/dL. Three days after starting CRRT serum calcium rose to 11.9 mg/dL with ionized calcium 0.91 mmol/L (calcium ratio 13.1). Rate of citrate infusion was reduced and within two days the serum calcium panel normalized. Case 3: A 41-year-old female with cirrhosis was admitted with AKI due to hepatorenal syndrome; admission calcium was 9.4 mg/dL. Within two days of starting CRRT, serum calcium increased to 11.9 mg/dL with ionized calcium 0.96 mmol/L (calcium ratio 12.4). She was transitioned to hemodialysis and the serum calcium levels normalized within two days. Conclusion: Because the clearance of exogenous citrate relies heavily on hepatocyte mitochondrial metabolism, citrate accumulation correlates inversely with residual hepatic function. This case series illustrates the importance of recognizing citrate toxicity as a cause of total hypercalcemia in patients on CRRT. An important diagnostic clue is an elevated total to ionized calcium ratio. Citrate toxicity is associated with high mortality although occurs in a critically ill patient population with a high underlying mortality. Endocrinologists should be aware of citrate accumulation and toxicity as causes of hypercalcemia and work closely with nephrologists to minimize the risk of hypercalcemia in patients on CRRT.

***Disclosures: Leor Needleman**, None*

SAT-142

The Use of Ketoconazole for Hypercalcemia Resulting from Lymphoma *Katlyn Sawyer[1,] Monique Maher[1,] Micol Rothman[2,] Lisa Kosmiski[1.] [1]University of Colorado, United States. [2]University of Colorado- Denver, United States

Introduction: 1,25- dihydroxyvitamin D mediated hypercalcemia is associated with lymphoma, granulomatous infections, or autoimmune disease. This is a case of severe hypercalcemia from 1,25-dihydroxyvitamin D excess treated with ketoconazole. Case presentation: A 79-year-old male with history of elevated prostate-specific antigen (PSA) and monoclonal gammopathy of undetermined significance (MGUS) was brought in by family for altered mental status. On admission, corrected calcium was 19.1 mg/dL (ref range: 8.1-10.5 mg/dL). Subsequent labs revealed a low parathyroid hormone (PTH) of 8.1 pg/mL (ref range: 9.0-55.0 pg/mL), mildly elevated parathyroid hormone-related protein (PTHrP) of 4.4 pmol/L (ref range: 0.0-2.3 pmol/L), phosphorus of 3.5 mg/dL (ref range: 2.7-4.8 mg/dL), eGFR of 24 mL/min/1.73m2, elevated PSA of 27.19 ng/mL (ref range: 20 ng/mL for years and a nuclear medicine whole body bone scan without evidence of osseous metastatic disease. He was treated with aggressive intravenous fluids, one dose of pamidronate 60 mg, and four doses of calcitonin at 4 U/kg. Corrected calcium improved to 16.1 mg/dL along with mild improvement in mental status. The presence of diffuse lymphadenopathy raised suspicion for lymphoma or granulomatous disease, prompting lymph node biopsy. Steroid therapy was not initiated to ensure accurate pathological diagnosis. Hypercalcemia persisted and he received a 3.3 mg dose of zoledronic acid with only a mild calcium reduction. Another 48 hour treatment of calcitonin was given simultaneously with ketoconazole 200 mg PO three times daily. Corrected calcium level went from 12.2 mg/dL to 10.5 mg/dL after four days of ketoconazole treatment. The calcium nadir on ketoconazole therapy was 9.9 mg/dL. Ultimately, lymph node pathology confirmed large B-cell lymphoma. Clinical Conclusions: Ketoconazole can be used for 1,25-dihydroxyvitamin D mediated hypercalcemia when steroids are contraindicated or ineffective. 1 alpha-hydroxylase can become autonomously active in the macrophages of granulomas and in malignant lymphocytes, increasing conversion of 25-hydroxyvitamin D to 1,25-dihydroxyvitamin D. Both glucocorticoids and ketoconazole inhibit 1-alpha hydroxylase.

***Disclosures: Katlyn Sawyer**, None*

SAT-144

Successful management of sarcoid-mediated hypercalcemia with anti-TNF-alpha antibody adalimumab. *Aidar Gosmanov[1.] [1]Stratton VAMC,

Background: Glucocorticosteroids is therapy of choice in the management of sarcoid-mediated hypercalcemia. Rarely, some patients may require high doses of steroids which result in spectrum of side effects. It is unknown if alternative approaches may be offered to these patients to control hypercalcemia in attempt to mitigate burden of adverse effects from high-dose steroid therapy. Clinical Case: A 54-year old Caucasian male with a history of type 2 diabetes treated with oral hypoglycemia agents, psoriatic arthritis (PA) and recent diagnosis of biopsy-proven pulmonary and hepatic sarcoidosis was admitted to hospital in March 2020 with newly-diagnosed hypercalcemia. On admission his serum albumin-adjusted calcium was 14.0mg/dL (8.3-10.4), 25-OH vitamin D level 14.8ng/mL (20-50), phosphorus 3.0mg/dL (2.5-4.5) and undetectable parathyroid hormone (PTH) level (14-72pg/mL). His 1,25-dyhydorxy vitamin D was inappropriately high-normal at 59pg/mL (18-72) and ACE level was elevated at 177U/L (9-67). Based on clinical and biochemical evaluation, sarcoid-induced hypercalcemia diagnosis was made and prednisone 10mg daily initiated. During follow up, his hypercalcemia persisted and prednisone regimen was gradually intensified to 40mg daily. This however led to marked deterioration of glycemic control resulting in initiation and then intensification of insulin therapy reaching regimen of 1.5 units/kg/day. As part of PA care, his rheumatologist in December 2021 has initiated weekly injections of 40mg adalimumab, an anti-tumor necrosis factor (TNF)-alpha antibody. One month after adalimumab commencement, routine biochemical evaluation incidentally showed marked improvement of calcium levels allowing to gradually reduce and then stop prednisone over 2-month period while maintaining eucalcemia. Nine months after stopping prednisone, he remains eucalcemic and PTH level is now normal associated with marked reduction in insulin requirement. Discussion: This case report for the first time demonstrated robust hypocalcemic effect of adalimumab in a patient with sarcoid-induced hypercalcemia who was failing intensive prednisone regimen. TNF-alpha inhibition in patients with extra-pulmonary manifestations of sarcoidosis is poorly studied and considered to be a third-line therapy for these patients. Our case report illustrates that TNF-alpha blockade can prove to be a rescue agent in cases of sarcoid-induced hypercalcemia that are difficult to control with glucocorticosteroids.

***Disclosures: Aidar Gosmanov**, None*

SAT-145

Acute decompensated heart failure from hypocalcaemia induced cardiomyopathy due to osteoblastic bone metastases only reversed after correction of hypocalcaemia *Ariel Woo[1,] Donovan Tay[2.] [1]Department of Endocrinology, Sengkang General Hospital, Singhealth, Singapore. [2]Sengkang General Hospital, United States

Calcium is essential for physiologic excitation-contraction coupling in cardiac myocyte and severe hypocalcaemia leads to reduced cardiac contractility and dilated cardiomyopathy. Failure of response to standard heart failure therapy has been reported unless calcium has been sufficiently repleted. Loop diuretics increase urinary calcium excretion and further worsen hypocalcemia. We share our experience in treating a patient with acute decompensated heart failure from hypocalcaemic induced cardiomyopathy due to disseminated osteoblastic bone metastases from prostatic malignancy with resolution of heart failure following the correction of serum calcium.An elderly Chinese man with no history of cardiac disease presents after a fall complicated by right humeral and left pubic ramus fracture with dyspnea and pedal edema. He did not complain of muscle cramp, perioral numbness, and peripheral paraesthesia.Clinical examination revealed elevated jugular venous pressure, bilateral crepitations and left sided reduced breath sounds with stony dull percussion. There were no audible cardiac murmurs.Investigations showed high pro-BNP (23681 pg/mL; NR<99). Serial cardiac enzymes were normal. ECG showed sinus rhythm, T-wave inversion in the anterior leads and prolonged QTc (470ms). CXR showed left pleural effusion, cardiomegaly, and pulmonary edema. Echocardiogram showed low ejection fraction of 34%.Hypocalcaemia was noted on Day 4 (Ca 1.86 mmol/L; NR 2.1-2.6), normal PO4 (1.05 mmol/L; NR 0.8-1.5), secondary hyperparathyroidism (PTH 31.7 pmol/L; NR 1.6-6.9), low 25OHD (7 ug/L), high ALP (1762 U/L; NR 40-129) and renal impairment (Cr 156umol/L; NR 59-104). CTAP showed diffuse patchy sclerosis in the skeleton and an unenlarged prostate. Bone scan showed a "super scan" appearance from extensive osteoblastic bone metastases. TRUS prostate biopsy confirmed prostatic acinar adenocarcinoma.He was treated with oxygen, fluid restriction and IV frusemide but pulmonary edema persisted. A calcium gluconate infusion was started with oral calcium and vitamin D supplementation and titrated till an eventual

dose of CaCO3 1.25g qds, calcitriol 0.25mcg bd, and cholecalciferol 1000IU/day. There was a clear positive response to diuretics once his serum hypocalcaemia was corrected. He was started on androgen-deprivation therapy, Bicalutamide.Severe hypocalcaemia can induce heart failure that may be resistant to diuretic treatment but responds only when normocalcemia is achieved.

***Disclosures: Ariel Woo**, None*

SAT-146

Marked phenotype of the Dentin-Enamel Junction in murine model of Dentinogenesis Imperfecta Type 1 *Kai Clarke[1], Sobhan Katebifar[2], Roland Kröger[3], Alix Deymier[2]. [1]Department of Biomedical Science, UConn Health Center, United States. [2]Department of Biomedical Engineering, UConn Health Center, United States. [3]School of Physics, Engineering and Technology, United Kingdom

Dentinogenesis Imperfecta (DGI) is an inherited autosomal dominant disorder characterized by abnormal dentin mineralization that affects 1 in 6,000-8,000 people worldwide. DGI type I is caused by mutations in the collagen 1 gene, which are also associated with Osteogenesis Imperfecta (OI), resulting in dentin hypertrophy and enamel attrition. The loss of enamel predominantly occurs near the Dentin-Enamel Junction (DEJ), the interfacial tissue that connects these two mechanically dissimilar materials, suggesting that DGI may negatively affect the DEJ. However, due to its small hierarchical organization the structural and mechanical changes of the DEJ caused by DGI remain unknown. It has been shown that compositional and structural gradients cross the DEJ provide it with mechanical robustness in healthy dentition; therefore, we hypothesize that DGI type I affects the graded structure of the DEJ causing increased fracture risk.Incisors (n=6) were collected from 12-week-old DGI type 1 mice (Col1a2oim) and their wildtype littermate controls (WT) according to UConn Health Institutional Animal Care and Use Committee. Incisors were embedded in EpoKwick FC, polished, and data was collected using a WiTec Alpha 300 Raman Spectrometer. Spectra were collected across DEJ to obtain compositional information in the dentin and enamel. The 960 cm-1 phosphate peak was fit to obtain peak intensity, peak position, and full width half max (FWHM) as a function of location. Gradients width of these values were calculated.The position of the phosphate peak in the dentin trended (p=0.086) towards higher wavenumbers compared to WT. This was not seen in the enamel. Peak FWHM, which is inversely correlated to atomic order, was unchanged between DGI and WT for both dentin and enamel near the DEJ. The ratio of peak intensities between the tissues was unchanged for DGI vs. WT. Gradients in peak intensity, position, and fwhm were present for all samples but their width did not vary between DGI and WT.These results suggest that DGI does not affect mineral content or atomic order of the dentin near the DEJ; however, it does cause the mineral to be more hydroxyapatite-like. This may point to a reduction in substitutions in the DGI mineral which affects mineral stiffness. An increase in mineral modulus near the DEJ could cause stiffening of the interface and changes to the DEJ mechanics. This may explain in part the increase in fracture risk with DGI.

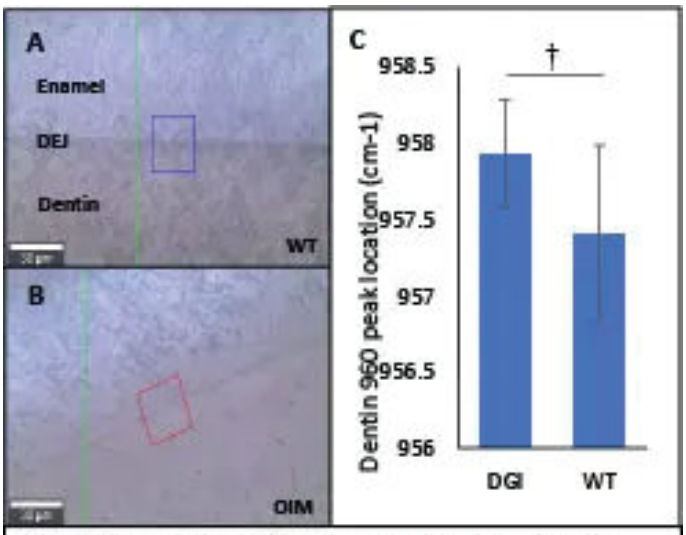

Figure 1: The effect of DGI on the phosphate peak position in dentin. (A-B) Image of the DEJ for WT and OIM incisor showing area of interest (C) Plot of the 960 peak location for the Dentin. † indicates p<0.1.

***Disclosures: Kai Clarke**, None*

SAT-148

Impact of Dental Cement on Peri-implant Disease Development: A Preclinical Study in Lewis Rats *Bhuvana Lakkasetter Chandrashekar[1], Claudia Biguetti[2], Alexandra Arteaga[1], Andres Miramontes[1], Danieli Rodrigues[1]. [1]The University of Texas at Dallas, United States. [2]University of Texas Rio Grande Valley, United States

Cement mediated peri-implantitis accounts for about 1.9-75% of dental implant failures associated with peri-implant diseases, of which most are associated with residual cements. However, there is a lack of preclinical studies that evaluate dental cements as a primary cause of peri-implant disease development. Understanding these failures will further help initiate better treatment methods and prognosis. Thus, in this study, we investigated the impact of residual dental cement on osseointegrated implants using a rat model. A total of 25 rats (12 weeks old) were distributed into 5 groups: negative controls soft (S) diet and (H) diet; positive controls S and H diet (n=3); Implant+Cement (BC) S and H diet (n=4). Commercially pure titanium screws (0.76x1mm) were placed on either sides of the maxillae and were treated with standard H diet for 14 days. At day 14 post-implantation, both sides of experimental groups were subjected to re-entry surgery for implant head exposure to simulate a clinical cementation procedure. The right side was loaded with 0.61mg of permanent bioceramic cement, while the left side was used as sham. Standard chow moistened with water was introduced in S diet groups. Bone samples containing the implants were harvested for microtomographic (MicroCT), and histological analysis (H&E and Goldner's Trichrome stains) for evaluation of distance between the implant head and the alveolar bone crest, tissue healing/inflammatory infiltrate and Bone to Implant contact (BIC) percentage respectively. Quantitative data was analyzed by one way ANOVA and Tukey tests ($p<0.05$). MicroCT results indicated circumferential bone resorption around BC implants in comparison to NC group. H&E stains revealed remaining cements particles surrounded by foreign body giant cells adjacent to the implant thread area accompanied by biofilm resembling structures in the soft tissue for S groups. Both cemented and sham sides of BC indicated intense bone loss and resorption around the threads accompanied by signs of osteolysis and biofilm infiltration when compared to NC rats (Fig1). Additionally, cemented groups depicted significantly lower BIC than NC. Altogether, these findings point to the negative biological effect of cement extravasation on healed peri-implant tissues depicting that excess of dental cements affect peri-implant health leading to adverse foreign body reaction. Thus, careful consideration must be given to the use of dental cements with implant prostheses.

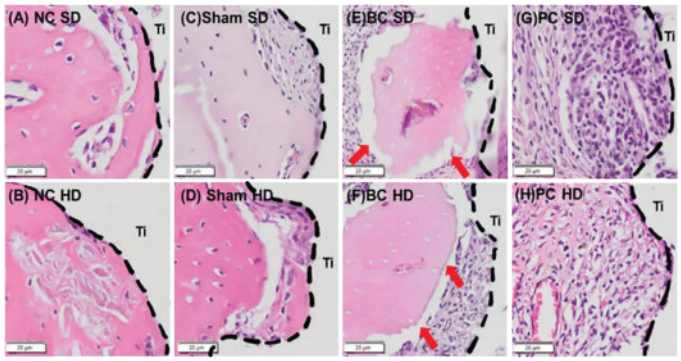

***Disclosures: Bhuvana Lakkasetter Chandrashekar**, None*

SAT-149

Selcopintide Assists the Elongation of PDL Fibroblasts by Altering Microtubules with TAU *Eunhoo Park[1], Joo-cheol Park[1]. [1]Dental Research Institute and School of Dentistry, Seoul National University, Republic of Korea

Ligaments are dense fibrous tissue that connects bones and essential in order that the musculoskeletal system functions properly. In a similar context, the periodontal ligament(P-DL) that connects the root of the tooth and the alveolar bone is indispensable for the correct function of teeth. Although a gomphosis constituted by teeth and alveolar bones doesn't show dynamic movement unlike general synovial joints, PDLs should also tolerate various mechanical forces such as tensile, compressive, and shear forces caused by mastication. Just as general ligaments are formed by tenocytes, PDLs are formed by PDL fibroblasts, which have different properties from those of tenocytes. Not only do they secrete collagen, but they also elongate themselves and are directly involved in the formation of PDLs. Thus, the elongation of PDL fibroblasts are important phenomenon.To ensure that Selcopintide assists the elongation of PDL fibroblasts by altering microtubules with TAU, a series of in vitro study was conducted with siTAU-transfected human PDL fibroblasts. Live cell imaging and laser scanning microscopy were used to investigate their morphologic transition and cytoskeletal structure. Subsequently, immunoblotting is done for evaluating post-translational modification of Tubulin and its associated proteins.Selcopintide promoted the elongation of PDL fibroblasts, it couldn't take its effect on siTAU-transfected cells. Active lamellipodia were observed in TAU-transfected cells, however they withdrew soon showing short-periodic reciprocating manner and couldn't grow into long and thin celluar process. Also, Selcopintide disentangled condensed microtubules of lamellipodial region both in normal

and siTAU-transfected cell. However, their direction corresponds with that of microfilament only in normal cell, not in siTAU-transfected cell. Total amount of ?-Tubulin wasn't altered by siTAU nor Selcopintide, however acetylation of ?-Tubulin was decreased by siTAU and recovered by Selcopintide.Therefore, this study indicates that Selcopintide makes microtubules follows actin filaments and promoting ?-Tubulin acetylation. It also implies that TAU is involved in the effect of Selcopintide that cause the elongation of PDL fibroblasts.

***Disclosures: Eunhoo Park**, None*

SAT-151

Comparative Effects of Metformin and Melatonin on Alveolar Bone Remodeling in Doxorubicin-treated Rats *Bhumrapee Srivichit[1], Chanisa Thonusin[2], Ratchaneevan Aeimlapa[3], Narattaphol Charoenphandhu[3], Nipon Chattipakorn[2], Siriporn Chattipakorn[4]. [1]Department of Oral and Maxillofacial Surgery, Faculty of Dentistry, Chiang Mai University, Thailand. [2]Department of Physiology, Faculty of Medicine, Chiang Mai University, Thailand. [3]Department of Physiology, Faculty of Science, Mahidol University, Thailand. [4]Department of Oral Biology and Diagnostic Sciences, Faculty of Dentistry, Chiang Mai University, Thailand

Doxorubicin (Dox) is a widely used chemotherapeutic agent for several types of cancers. However, previous studies reported that Dox increased the risk of alveolar bone loss, leading to periodontitis, delayed wound healing, and dental implant failure. Melatonin and metformin have been shown to increase alveolar bone mass in certain types of oral surgery and dental implantation, but their potential benefits in alleviating Dox-induced alveolar bone impairment have never been investigated. Herein, 24 male Wistar rats were randomly divided into 4 groups (n = 6/group) to receive either (i) 1 mL of normal saline solution on days 0, 4, 8, 15, 22, and 29 (Control), (ii) 3 mg/kg/day of Dox i.p. on day 0, 4, 8, 15, 22, and 29 (Dox), (iii) 3 mg/kg/day of Dox i.p. on day 0, 4, 8, 15, 22, and 29 plus 10 mg/kg/day of melatonin orally on day 0-29 (Dox + Mel), or (iv) 3 mg/kg/day of Dox intraperitoneally on days 0, 4, 8, 15, 22, and 29 plus 250 mg/kg/day of metformin orally on day 0-29 (Dox + Met). The rats were euthanized on day 30. Blood and left maxillary alveolar bone were collected to evaluate oxidative stress using malondialdehyde (MDA) measurement. The right maxillary alveolar bone was used to assess the microarchitecture and periodontal status by using an ultra-high-resolution E-Class VecTor6CT system in 5 µm voxel size. The results showed that Dox-treated rats exhibited increases in serum and bone MDA levels, decreased trabecular bone volume fraction (BV/TV), decreased trabecular thickness (Tb.Th), decreased mineral density, and increased periodontal ligament (PDL) space, as compared to the control group (Fig. 1A-1F). Melatonin and metformin equally decreased serum MDA levels in Dox-treated rats to become comparable with that of the control (Fig. 1A). Interestingly, melatonin was superior to metformin in terms of reducing bone MDA levels and restoring bone microarchitecture, but both drugs were equally effective in improving periodontal status in Dox-treated rats (Fig. 1B-1F). In conclusion, our findings suggested that melatonin is more effective than metformin in attenuating Dox-induced alveolar bone impairment.

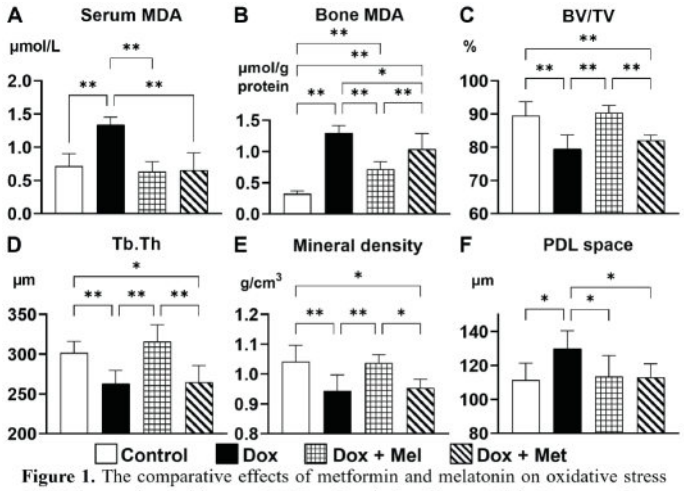

Figure 1. The comparative effects of metformin and melatonin on oxidative stress (A, B), bone microarchitecture (C-E), and periodontal status (F) in Dox-treated rats. Data are expressed as mean ± SD. Statistical analysis was performed using one-way ANOVA with Tukey's post-hoc test. * $p < 0.05$; ** $p < 0.01$ compared between the indicated groups.

***Disclosures: Bhumrapee Srivichit**, None*

SAT-154

Elevated Pedf contributes to increased bone mineralization in diabetes *Maude Gerbaix[1], Badoud Isabelle[1], Delphine Farlay[2], Ryan Tomlinson[3], Marie Helene Lafage-Proust[4], Frederic Dutheil[5], Serge Ferrari[6]. [1]Division of Bone Diseases, Geneva University Hospitals and Faculty of Medicine, Geneva, Switzerland, Switzerland. [2]INSERM, UMR1033; Universite De Lyon, France. [3]Thomas Jefferson University, United States. [4]SAINBIOSE, INSERM U1059, Jean Monnet University, SAINT-ETIENNE, France, France. [5]Université Clermont Auvergne, CHU Clermont-Ferrand,University Hospital of Clermont-Ferrand Preventive and Occupational Medicine, Clermont Ferrand, France, France. [6]Geneva University Hospital and Faculty of Medicine, Switzerland

Diabetic bone is characterized by low bone turnover and a higher degree of mineralization. Pigment Epithelium derived factor (Pedf) is expressed by bone-forming cells and activates bone mineralization by attracting mineralizing factors at osteoid surfaces. We previously observed increased Pedf bone gene expression in mice fed with high fat diet (HFD) and decreased expression in response to caloric restriction (CR) and exercise. Here we investigate circulating Pedf levels in relation to bone turnover in type 2 diabetic subjects (T2D) and the role of Pedf on bone properties in a diabetic mouse model.Pedf serum levels, Hb1Ac and bone turnover markers (BTMs: OCN, P1NP and CTx) were assessed in 29 obese T2D and 50 control (Ctr) subjects from the ReSoLVE trial (Dutheil et al. 2013) before and 6-month after CR plus exercise. Pedf -/- and Pedf +/+ adult male mice were fed with Chow or HFD during 8wks and assessed for metabolic markers, bone microarchitecture (µ-CT), formation and mineralization (histology), gene expression (Nanostring) and material properties (nano-indentation).T2D subjects had higher Pedf levels (+20%; $p<0.05$) and lower BTMs (-40% to -56%; $p<0.001$) vs. Ctr. CR + Exercise significantly decreased Hb1ac and Pedf serum levels, respectively improved BTMs in T2D. Pedf correlated positively with Hb1Ac (r =0.468; $p<0.001$) and negatively with CTX, OCN and P1NP (range r =-0.414 to -0.331; $p<0.001$).As compared to WT, Pedf -/- mice exhibited lower Tb. BV/TV (-50%), higher Tb. osteoid surfaces (+326%), and lower mineralization gene expression levels (Mepe, Alpl, BSP, OPN and osteonectin, range -67 to -34%; $p<0.05$), confirming the role of pedf on bone mineralization.HFD induced higher body weight, insulin levels and insulin resistance (AUCglucose) in both genoptypes (Pedf +/+HF : +30%, +210%, +28% vs Pedf +/+chow; Pedf -/-HF: +37%; +308%,+23% vs Pedf -/- chow; pHF< 0.001; pgenoNS). HFD increased Tb. MS/BS, Tb. BFR and Pedf, Mepe and Alpl bone genes expression in Pedf +/+ mice (+34%, +80%, +29%, +62%, +29%; pHF<0.05), but not Pedf -/- (pgeno<0.05). In turn HFD increased endosteal tissue hardness in Pedf +/+ but not in Pedf -/- mice (Pedf +/+HF : +58%; pHF<0.05; pgeno<0.01).Overall, these data suggest that Pedf is involved in bone mineralization and material properties alterations induced by insulin resistance. The degree of bone mineralization in these diabetic mice is currently being analyzed by micro-radiography. Elevated serum Pedf levels could potentially reveal pathological increases in bone mineralization in T2D.

***Disclosures: Maude Gerbaix**, None*

SAT-155

See Friday Plenary Number FRI-155

SAT-156

Effect of endogenous melatonin depletion on metabolic markers in bone, fat and muscle in AA-NAT KO transgenic mice *Afsana Jahan[1], Afsin Malik[1], Yong Myoung[1], Diane Carlisle[2], Robert Friedlander[2], Paula Witt-Enderby[3]. [1]Duquesne University School of Pharmacy Div Pharm Sci, United States. [2]University of Pittsburgh School of Medicine Dept Neurological Surgery, United States. [3]Duquesne University,School of Pharmacy, United States

Background: Therapeutic doses of melatonin (~6mg nightly dose or 50nM in vitro) have been shown in in vitro, pre-clinical and clinical studies to produce strong effects on osteoblastogenesis to increase bone density, bone formation, and normalize bone marker turnover. In MSCs, melatonin induces osteoblastogenesis through MT2s and MEK1/2 and MEK5 pathways. In MSCs and mouse bone, melatonin, via MT2/MEK1/2- and MEK5-mediated pathways, inhibit PPAR?, the metabolic switch driving MSCs down an osteoblastic lineage, and away from an adipogenic lineage. Although much is known about the role of pharmacogical doses/concentrations of melatonin on bone and MSCs, little to no information is known about the role of physiological levels of melatonin on bone and the proteins that govern its physiology. This is important because conditions that suppress nocturnal melatonin levels (i.e., shift work, light at night) in people demonstrate decreases in bone mineral density and increases in fracture risk.Objective: To determine the role of endogenous melatonin on PPAR? and metabolic proteins governing this switch point (i.e., UCP-1, C/EBP, ACRP30, DIO2) in bone and metabolic tissues (white fat, WAT, brown fat, BAT and muscle) in an AA-NAT (melatonin-depleted) knockout model and compared to wild-type (WT; CBA) mice. The AA-NAT KO mice were made on CBA background known to have robust melatonin synthesis and circadian rhythms similar to WT mice.Methods: Tissue lysates were prepared from bone, muscle, WAT and BAT taken from AA-NAT KO mice. Protein levels were measured by western blot analysis and quantified using Odyssey and LiCor Imaging systems. Protein bands were normalized by total protein levels detected

using Revert 700.Results: The results of this study demonstrate that in AA-NAT knockout mice and when compared to WT mice, PPAR?, UCP-1, C/EBP, ACRP30 and DIO2 levels decreased in BAT; no changes in protein levels were observed in the other tissues except for ACRP30, which demonstrated trends (p= 0.0655) towards increases in muscle.Conclusion: These data demonstrate that melatonin produces distinct effects on metabolic proteins in bone and metabolically active tissues dependent upon dose suggesting that to achieve beneficial effects of melatonin on bone, pharmacological doses may be required. Further studies on bone biomechanics and density are required.

***Disclosures: Afsana Jahan**, None*

SAT-157

Osteoblast RNA Sequencing in T1D Mice Reveals Genetic Signature of Maladaptation to Hypoxia and Compromised Collagen Synthesis *Se-Min Kim[5], Juhyeon hong[2], Farhath Sultana[3], Eleanor Shelly[4], Funda Korkmaz[4], Judit Gimenez[4], Tony Yuen[5], Ilse Daehn[6], Jungmin Choi[7], Mone Zaidi[8]. [5]Icahn School of Medicine at Mount Sinai, , [2]Department of Biomedical Sciences, Korea University College of Medicine, Seoul, Republic of Korea , Republic of Korea. [3]1Center for Translational Medicine and Pharmacology, Icahn School of Medicine at Mount Sinai, New York, NY, United States. [4]Center for Translational Medicine and Pharmacology, Icahn School of Medicine at Mount Sinai, United States. [5]Icahn School of Medicine at Mount Sinai, United States. [6]Department of Medicine, Division of Nephrology, Icahn School of Medicine at Mount Sinai, United States. [7]Department of Biomedical Sciences, Korea University College of Medicine, Republic of Korea. [8]Mount Sinai Medical Center, United States

The main feature of skeletal abnormality in type 1 diabetes (T1D) is low bone turnover with decreased osteoblastic bone formation [1, 2]. However, the mechanism of osteoblast dysfunction remains unclear. We generated T1D mice using low dose streptozotocin (STZ). T1D mice showed lower bone mass (g/cm2) at the femur (0.07 vs. 0.09*) and trends at lumbar spine (0.05 vs. 0.06, p=0.08) compared with control group at 8 weeks after inducing T1D. Osteoblasts were differentiated using bone marrow mesenchymal stem cells, and RNAseq was performed to analyze the transcriptome of osteoblasts. In gene set enrichment analysis, several pathways including immune, hypoxia, and glycolytic pathway were enriched. The osteogenic genes panel showed decreased Bglap and Col1a1 expression, together with lower expression of Bmp2 and Wnt5a, suggesting decreased bone formation might be related to the suppression of BMP and WNT signaling. Particularly, P4ha2, encoding prolyl 4-hydroxylase subunit alpha-2, which are responsible for posttranslational modification of collagen were downregulated in T1D osteoblasts (log2FC = - 1.7**). Among genes in hypoxia pathway, Egln3 encoding prolyl hydroxylase domain-containing protein 2 and Vhl encoding von Hippel-Lindau tumor suppressor, both of which stabilize HIF-? were downregulated (log2FC = - 2.8** and - 0.31*, respectively) likely for promoting HIF-? dependent gene expression in hypoxia. However, genes of the growth signaling pathway, namely Pgf, Vegfa, and Igf1r, which were normally upregulated in hypoxic condition, were downregulated (log2FC = - 3.1**, - 0.4* and - 0.5**, respectively). Altogether, our findings suggest that maladaptation to hypoxic condition in T1D with compromised growth signaling pathway and impaired collagen synthesis might be related to osteoblasts dysfunction in T1D bone. (* $p < 0.05$ and ** $p < 0.001$)

***Disclosures: Se-Min Kim**, None*

SAT-159

See Friday Plenary Number FRI-159

SAT-160

High-fat Diet Induced Skeletal Muscle Metabolic Memory and Its Implication in Hyperglycemia and Associated Muscle Atrophy *Wei Ting Hsiao[1], Yuk-wai Lee[2], Chien-Wei Lee[3]. [1]Department of Orthopaedics & Traumatology, Faculty of Medicine, The Chinese University of Hong Kong, Hong Kong SAR, China, Hong Kong. [2]Li Ka Shing Institute of Health Sciences, The Chinese University of Hong Kong, Prince of Wales Hospital, Hong Kong SAR, China, Hong Kong. [3]Center for Translational Genomics & Regenerative Medicine Research, China Medical University Hospital, China Medical University, Taichung 40402, Taiwan, Taiwan, Province of China

Metabolic memory is a description of the lasting effects of pre-exposed stimulations, which can be manifested in a variety of aspects, including transcription, translation, post-translational modification, epigenetic modification, etc. In diabetes, long-term clinical trial follow-up studies showed that metabolic memory leads to a higher risk of diabetic complications and mortality. However, the role of metabolic memory in the early stage of hyperglycemia is unclear. Since skeletal muscle insulin resistance is an early response to hyperglycemia development and disease progression, we hypothesized that short-term repeated high-fat diet (HFD) feeding causes metabolic memory in skeletal muscle and influences the development of hyperglycemia.This study aimed to investigate the effects of repeated HFD on muscle structure and function in 12-week-old male C57BL/6J mice. The continuous control diet (CTL) and the repeated HFD feeding regimens shown in Figure 1 were used to investigate metabolic memory phenomenon. Six mice were sacrificed at each designated timepoints, then extensor digitorum longus (EDL) and gastrocnemius (GA) muscles were collected for analysis. Bulk RNA Sequencing was performed to identify DEGs during the treatment. In vitro functional experiments were employed to verify the in vivo findings. Two-way ANOVA statistical analysis was used in this study.According to the definition of metabolic memory which proposed by Poonam in 2020, persistent alteration metabolic memory patterns, including ECM remodeling, muscle stiffening, contraction relaxation deterioration, and force reduction, as well as increased sensitivity metabolic memory patterns, including the extent of hyperglycemia and weight gain, were identified in HFD group when compared with the CTL group (Figure 2.) Furthermore, the RNA Sequencing analysis revealed two clusters of DEGs exhibiting metabolic memory-like patterns, which are enriched with ECM remodeling and AGE-RAGE signaling pathways. In vitro experiments with myoblast cell line showed a causal relationship between substrate stiffness and the preservation of high-glucose-induced insulin resistance.Our findings revealed that muscle structural and functional alteration occurred at least 2 weeks before the fasting glucose was upregulation; thus, altering aberrant ECM remodeling in muscle through more in-depth investigation could provide a new avenue to develop new approaches to ameliorate the disease onset/progression.

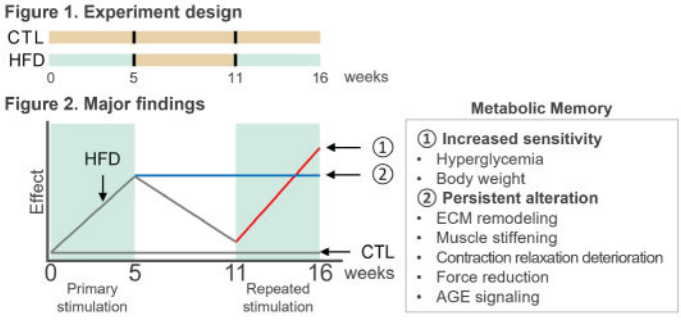

***Disclosures: Wei Ting Hsiao**, None*

SAT-161

Placental tissue derived allograft enhances bone healing and reduces pain behaviors in a surgically induced murine fracture model. *UPASANA GANGULY[1], Sonali J Karnik[2], Amy Creecy[3], Aamir Tucker[2], Murad Nazzal[2], Marko V Dragisic[2], Saveda Majety[2], Sarah L Mostardo[2], Rachel J Blosser[2], Fletcher A White[4], Jill C Fehrenbacher[5], Melissa Kacena[6, 1], , [2]Department of Orthopaedic Surgery, Indiana University School of Medicine, Indianapolis, IN, United States, United States. [3], United States. [4]Department of Anesthesia, Indiana University School of Medicine, IN, USA, United States. [5]Department of Pharmacology and Toxicology, Indiana University School of Medicine Indianapolis, IN USA, United States. [6]Indiana University School of Medicine, United States

Connective Tissue Matrix (CTM) allografts are structural implants intended to supplement or replace damaged or inadequate tissues. Generated from human amnion, chorion, and umbilical elements, these allografts contain structural proteins as well as tissue-specific and -agnostic growth factors. In damaged dermal and mucosal tissues, application of CTM allografts is associated with lower levels of pro-inflammatory cytokines in vivo. In these studies, we examined the efficacy of CTM allografts to improve bone healing and whether CTM alters injury-associated pain behaviors in a pre-clinical animal model. Forty-five, 12-week-old, male C57BL/6J mice were divided into four groups: Saline Control, Membrane, Paste, and Membrane+Paste. All mice underwent a surgically induced femur fracture and treatments were administered intraoperatively. Baseline and weekly post-surgery complete blood counts were conducted, and no significant change in the blood cell numbers were noted. Additionally, upon euthanasia no gross abnormalities with any organs were noted, suggesting no obvious cross-species immune reaction. X-rays were performed twice weekly post-surgery. Surgical and contralateral femurs were collected and processed for µCT and histological analysis. µCT analysis demonstrated that the Membrane+Paste group showed a significant 13% increase in the trabecular number and 98% increase in the mineralized callus area when compared to the saline controls ($p<0.05$ and $p<0.0001$, respectively). Histological analysis indicated the Membrane+Paste group exhibited a 90% increase in the percentage of bone within the callus when compared to the saline controls ($p<0.01$). Open field assessments demonstrated no significant differences in the activity of mice among groups. Weightbearing testing demonstrated that the Membrane+Paste group was able to bear more weight on their fractured limb 4 days post-surgery ($p<0.05$) and a stimulus-evoked nociception assay using Von Frey probes suggested that the same group displayed significantly less “pain-like” behavior ($p<0.01$). In the studies described here, allograft application at the fracture site is associated with increased bone formation in the callus and reduced pain-like behavior. The latter may allow earlier weightbearing and accelerated bone healing. Taken together, these findings suggest that CTM allografts may promote fracture repair and support a randomized control trial in humans for fracture repair in weightbearing bones.

***Disclosures: UPASANA GANGULY**, None*

SAT-162

Quantifying Tibial Stress Fractures Using Computed Tomography Finite Element Analysis *Rashad Madi[1], Makayla Clark[1], Rasleen Grewal[1], Julio Ojea Quintana[1], Christiana Cottrel[1], Scott Epsley[2], Gregory Chang[3], Chamith S. Rajapakse[4]. [1]University of Pennsylvania, United States. [2]Independent Researcher, United States. [3]New York University, United States. [4]Univeristy of Pennsylvania, United States

Introduction: Recent advancements in computed tomography (CT) scans have facilitated high-resolution imaging of tibial stress fractures in clinical settings. This has led to the application of finite element analysis (FEA) for studying the biomechanical properties of diseased bone (1). In our study, we employed FEA modeling to test the hypothesis that stiffness in stress fractures (measured in kN/mm) is lower than the stiffness in normal bone for the same individual in the same bone.Methods: We examined 10 tibial CT scans from 9 patients diagnosed with anterior/posteromedial tibial stress fractures (Figure 1A), including one patient with bilateral stress fractures. The study population comprised 6 males and 4 females with a mean age of 34 +/- 18. Each CT scan was individually analyzed using Sectra MSK (Version 24.2.6.5829, Linkoping, Sweden). In-house software was used to segment fracture regions. To simulate "pre-fracture" bone, we modified the 3D models by virtually filling the fracture region with normal cortical bone HU values derived from neighboring regions without fractures. We then employed FEA to model the tibia and simulate compression along the bone's axial direction, as described by Rajapakse et al. (2).Results: Our findings revealed a 2.8% [1.58% - 6.68%] decrease in bone stiffness in stress fracture patients compared to the pre-fracture baseline (Table 1B). HU analysis demonstrated that stress fractures have significantly lower HU values than normal bone, with a mean difference of 300 HU and a P-value of < 0.001 (Figure 1C). As the bone of a stress fracture heals and returns to its normal state, both HU and stiffness increase until they reach values indicative of normal bone.Discussion: By utilizing FEA modeling, we calculated the stiffness of bone in both pre- and post-stress fractures. These measurements can aid in determining when an athlete is ready to return to competition without risking further complications. Moreover, they provide valuable insights into an individual's bone health and progress toward full bone strength recovery.

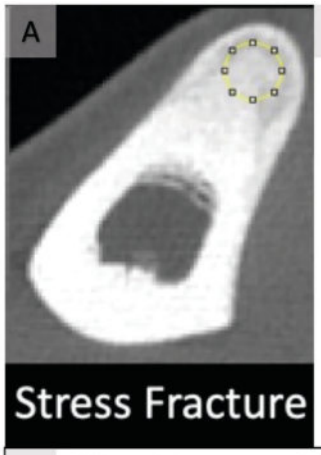

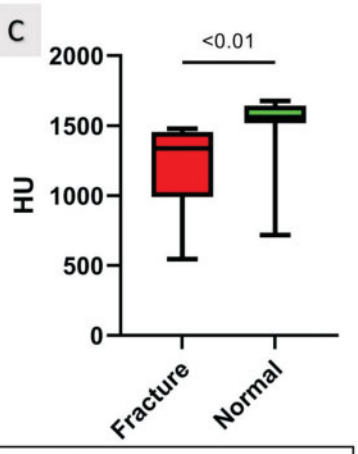

B

Stiffness with Fracture (kN/mm)	Stiffness Before Fracture (kN/mm)	% Change
15.2687	15.7282	5.5
9.98245	10.8762	15.4
1.06443	1.11781	9.0
2.91142	2.946	2.2
2.09041	2.10309	1.1
2.95535	2.97432	1.2
2.9238	3.01813	5.9
2.44075	2.46282	1.7

***Disclosures: Rashad Madi**, None*

SAT-163

See Friday Plenary Number FRI-163

SAT-164

Automated quantification of lipid storage and cellular dysfunction induced by glucocorticoid signaling in BMSC-derived osteoblasts *Colby Gross[1], HUSAM BENSRETI[2], Meghan McGee-Lawrence[3]. [1]Department of Cellular Biology and Anatomy, Medical College of Georgia at Augusta University, , United States. [2], United States. [3]Medical College of Georgia, Augusta University, United States

Glucocorticoids (GCs) are released in a circadian manner and during stress to regulate tissue metabolic activity. GCs can bind either glucocorticoid receptors (GR) or mineralocorticoid receptors (MR), which then act as transcription factors to mediate downstream effects. We previously showed that GC-induced signaling promoted lipid storage and dysfunction in BMSC-derived osteoblasts, but the relative contributions of the GR and MR were unclear. Here we report the effects of two experimental GR/MR inhibitors on the in vitro behavior of BMSCs using a novel automated method for quantifying intracellular lipid storage. Bone marrow stromal cells (BMSC) from 12-wk old female CD-1 mice were cultured for 14 days in osteogenic media with or without the GC dexamethasone (Dex). Cells were fixed and stained with Oil Red O (ORO) to detect lipids and Hoechst to highlight the nucleus (for easier counting of total cell number). Automated imaging and quantification were performed using a Cytation 5 plate reader and Gen5 software (Agilent BioTek). Manual quantification of ORO+ cells was used for verification. To test this new methodology in a previously established mouse model, BMSC from 6 mo old Osx-Cre: GR conditional knockout (GR- CKO) and WT littermates were cultured in osteogenic media in the presence of Dex and either the GR-specific inhibitor Relacorilant (RELA) or the GR/MR targeting drug Miricorilant (MIRI) for 14 or 21 days. Comparison between manual and automated quantification of ORO-containing osteoblasts showed no difference (p=0.806) between the approaches; both methods demonstrated that Dex significantly increased osteoblastic lipid storage compared to osteogenic media alone (p=0.0003, p=0.0115, respectively). Applying this methodology in our GR-CKO model, the GR-CKO cultures showed 30% more ORO-containing osteoblasts than WT cells, comparable to our previous reports. RELA increased lipid storage in WT cells by nearly 25%, while MIRI treatment rescued lipid storage in the GR-CKO cultures back to WT levels. These effects on lipid storage impacted mineralized matrix production, as the blunted matrix production seen in GR-CKO cultures (-6% vs. WT) was rescued to above WT levels by MIRI. Together, these data support a role for GC-mediated signaling via GR and MR in osteoblast lipid storage and dysfunction and established an unbiased, automated methodology for quantifying this phenomenon.

***Disclosures: Colby Gross**, None*

SAT-165

Evocalcet suppresses cyclin D1 oncogene-derived parathyroid cell proliferation in a murine model for primary hyperparathyroidism *Yasuo Imanishi[1], Tomoe Hirakawa[2], Waka Haruyama[3], Keigo Tsushida[3], Mariko Sakai[3], Tetsuya Kitayama[3], Takehisa Kawata[4], Ikue Kobayashi[1], Andrew Arnold[5], Masanori Emoto[1]. [1]Department of Metabolism, Endocrinology, and Molecular Medicine, Osaka Metropolitan University Graduate School of Medicine, Japan. [2]Department of Metabolism, Endocrinology and Molecular Medicine, Osaka Metropolitan University Graduate School of Medicine, Japan. [3]Biomedical Science Research Laboratories 1, Research Unit, R&D division, Kyowa Kirin Co. Ltd., Japan. [4]Medical Affairs Department, Kyowa Kirin Co., Ltd., Japan. [5]Center for Molecular Oncology and Division of Endocrinology & Metabolism, University of Connecticut School of Medicine, United States

Background: Evocalcet, a calcimimetic compound, suppresses parathyroid (PTH) hormone secretion from parathyroid glands in both primary hyperparathyroidism (PHPT) and secondary hyperparathyroidism (SHPT) similar to cinacalcet's activity. We previously reported the suppressive effect of cinacalcet on parathyroid cell growth in vivo in a PHPT model mouse, in which parathyroid-targeted overexpression of the cyclin D1 oncogene caused chronic biochemical hyperparathyroidism and parathyroid cell hyperplasia. In this study, the effect of evocalcet on parathyroid cell proliferation was analyzed in the PHPT mice.Methods: Evocalcet (0.25 mg/g chow) or cinacalcet (1 mg/g chow) was mixed into the rodent diet and orally administrated to 59-71 week-old PHPT mice for 10 days before sacrifice. 5-bromo-2'-deoxyuridine (BrdU) (240 µg/day) was infused by an osmotic pump for five days before sacrifice, followed by immunostaining of the thyroid-parathyroid complex using an anti-BrdU antibody to estimate parathyroid cell proliferation.Results: Compared to untreated PHPT mice, evocalcet or cinacalcet significantly suppressed both serum calcium and PTH and increased serum phosphate. The proportion of BrdU-positive cells to the total cell number in the parathyroid glands increased considerably in untreated PHPT mice (5.23 +/- 4.64%, mean +/- SD) compared to wild-type mice (1.15 +/- 0.82%), and was significantly suppressed by evocalcet (1.87 +/- 2.34%) or cinacalcet (1.38 +/- 0.95%). These compounds did not affect the expression of calcium-sensing receptor or vitamin D receptor in the parathyroid cells of the PHPT mice.Conclusions: These data suggest that evocalcet suppressed both serum PTH levels and parathyroid cell proliferation as effectively as cinacalcet in vivo in PHPT.

***Disclosures: Yasuo Imanishi**, Kyowa Kirin Co. Ltd., Grant/Research Support*

SAT-166

Loss of 24-Hydroxylase in Murine Fetuses Causes Hypercalcemia and Hypophosphatemia *David Bennin[1], Sarah A. Hartery[1], Alexandre S. Maekawa[1], Beth J. Kirby[1], René St-Arnaud[2], Christopher S. Kovacs[1]. [1]Memorial University of Newfoundland, Canada; [2]McGill University and Shriners Hospital for Children-Canada, Canada

Calcitriol circulates at low levels in normal human and rodent fetuses due to increased 24-hydroxylation of calcitriol and 25-hydroxyvitamin D. Prior human and animal studies have shown that absence of vitamin D, calcitriol, or vitamin D receptor do not disturb fetal mineral homeostasis or skeletal development. However, whether high concentrations of calcitriol affect fetal bone and mineral metabolism has not been assessed. Inactivating mutations of CYP24A1 cause high postnatal levels of calcitriol and the human condition of infantile hypercalcemia type 1, but whether the fetus is disturbed by this is unknown.We hypothesized that loss of Cyp24a1 in fetal mice will cause high calcitriol, hypercalcemia, and increased placental calcium transport.Cyp24a1+/- mice were mated to create pregnancies with WT, Cyp24a1+/- (HET) and Cyp24a1-/- (null) fetuses. On embryonic day (ED) 18.5, maternal and fetal blood, placentas, and intact fetuses were collected. On ED 17.5, amniotic fluid was collected; placental calcium and phosphate transport were assayed after intracardiac injections of 45Ca and 32P to the mother. Intact fetuses were either reduced to ash with ash mineral content assayed by atomic absorption spectroscopy, or were rendered transparent and stained with Alcian blue and alizarin red S to visualize the intact skeletons. Placental and kidney gene expression were examined by qPCR.Null fetuses were markedly hypercalcemic (3.37+/-0.81[SD] vs 2.15+/-0.80 mmol/L in WT, p<0.001) and hypophosphatemic (1.44+/-0.46 vs 1.97+/-0.68 mmol/L in HET, p<0.02). They also showed increased calcitriol (358+/-124 vs 190+/-42 pmol/L in WT, p<<0.001) and FGF23 (706+/-50 vs 204+/-47 pg/mL in WT, p<<0.001) while PTH was unchanged. qPCR confirmed absence of Cyp24a1 and 2-fold increases in S100g, Ncx1 and Casr in null placentas but not fetal kidneys; these changes predicted an increase in placental calcium transport. However, placental 45Ca and 32P transport were unchanged in nulls. Fetal ash weight and mineral content, placental weight, crown-rump-length, and skeletal morphology did not differ among the genotypes. Overall, loss of Cyp24a1 in fetal mice caused increased calcitriol, hypercalcemia, hypophosphatemia, increased FGF23, but no disturbance in placental mineral transport or skeletal development and mineralization. These results indicate that the human condition of infantile hypercalcemia type 1 likely begins with hypercalcemia in utero.

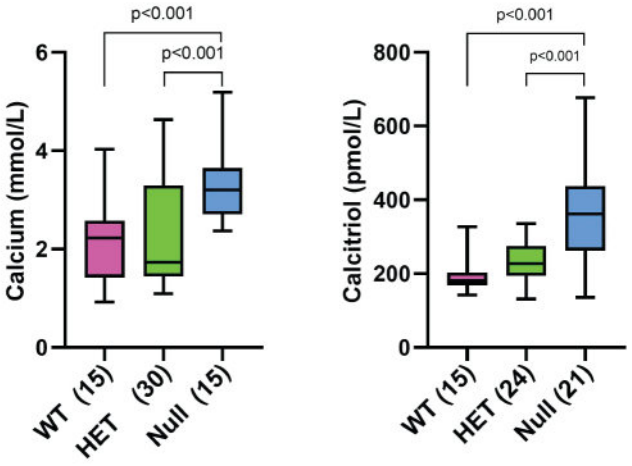

***Disclosures: David Bennin**, None*

SAT-167

See Friday Plenary Number FRI-167

SAT-169

Cyp24a1 Ablation in Mice Causes Increased Intestinal Calcium Absorption, Hypercalcemia in Pregnancy, and Reduced Lactational Bone Loss *Alexandre S. Maekawa[1], David Bennin[1], Sarah A. Hartery[1], Beth J. Kirby[1], René St-Arnaud[2], Christopher S. Kovacs[1]. [1]Memorial University of Newfoundland, Canada; [2]McGill University and Shriners Hospital for Children-Canada, Canada

Homozygous inactivating mutations of 24-hydroxylase (CYP24A1) cause mild hypercalcemia in humans, which can become severe and life-threatening during pregnancy (gestational hypercalcemia). The mechanisms are unclear and effects on lactation and post-weaning have not been studied.We studied the effects of Cyp24a1 ablation in mice on maternal calcium and bone metabolism during pregnancy, lactation, and post-weaning. We hypothesized that a normal 2-3 fold rise in calcitriol during pregnancy would be greater due to loss of its catabolism. In turn this would cause a marked increase in intestinal calcium absorption (IntCaAbs) during pregnancy; if sustained during lactation, less bone resorption would result.WT and Cyp24a1 null sisters were mated to Cyp24a1+/- males. Main timepoints included before mating (BL), late pregnancy (LP), mid-lactation (ML), late lactation (LL), and weekly to 28 days post-weaning (R1-4). Bone mineral content (BMC by PIXImus DXA), serum, and urine were collected at all time points. IntCaAbs was assayed after oral gavage of 45Ca. Serum and urine minerals, calcitriol, FGF23, and PTH were measured.At LP, whole body BMC increased equally ~12% in null and WT. Calcitriol was 2.5 fold higher in nulls vs WT (189+/-68 vs 76+/-20 pmol/L, p<0.001), accompanied by higher IntCaAbs (3.6+/-0.5 vs 1.2+/-0.2%, p<0.002), hypercalcemia (3.2+/-0.5 vs 2.7+/-0.4 mmol/L, p<0.05), hypercalciuria (9.4+/-9.6 vs 1.0+/-1.5 mmol/L, p<0.001), and higher FGF23 (1716+/-803 vs 260+/-151 pg/mL, p<0.001). PTH was suppressed in both. 20% of null dams died during delivery but their serum calcium at LP was the same as null survivors.At ML, calcitriol, IntCaAbs, and FGF23 had declined in both genotypes but remained higher in nulls over BL (91+/-49 vs 20+/-5 pmol/L, 2.2+/-0.9 vs 0.5+/-0.3%, and 736+/-752 vs 203+/-75 pg/mL, respectively). By LL, nulls were still hypercalcemic vs WT (2.61+/-0.48 vs 2.07+/-0.38, p<0.05), and had lost less mean whole body BMC (11% vs. 21%) to reach 0.572+/-0.056 vs 0.519+/-0.035 g, p<0.02. Lactational losses in BMC were restored by R4 in both.In summary, ablation of Cyp24a1 caused increased IntCaAbs during pregnancy and lactation, hypercalcemia at both time points, reduced lactational bone loss, and late gestational mortality in some nulls. Treating women with gestational hypercalcemia from CYP24A1 mutations should focus on methods to reduce IntCaAbs or lower calcitriol, since increased bone resorption is not the mechanism for hypercalcemia in this condition.

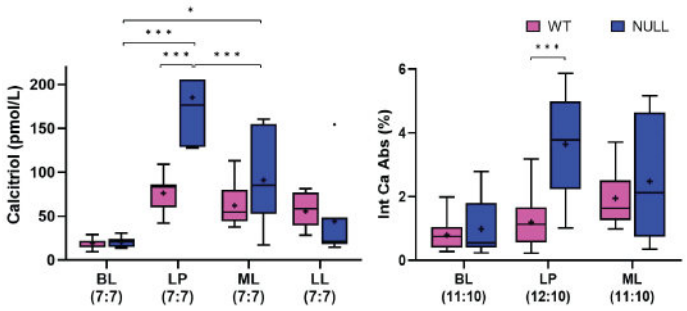

***Disclosures: Alexandre S. Maekawa**, None*

SAT-170

See Friday Plenary Number FRI-170

SAT-171

Gender Affirming Hormone Therapy does not impair skeletal maturation in young mice and regulates Bone via the Gut Microbiome *Subhashis Pal[1], Hamid Dar[1], Andreea Stoica[2], Yijuan Hu[3], Rheinallt M. Jones[3], Neale Weitzmann[4], Roberto Pacifici[4]. [1]Post Doctoral Researcher, Emory University, United States; [2]Research Specialist, Emory University, United States; [3]Associate Professor, Emory University, United States; [4]Professor, Emory University, United States

Gender affirming hormone therapy (GAHT) is used by ~80 % of transgenders to alleviate gender dysphoria and to align physical characteristics with the affirmed gender. GAHT is often started during adolescence, potentially impacting skeletal maturation. In this study, we evaluate the effects of GAHT on postnatal skeletal development and the involvement of gut microbiome in the skeletal effects of GAHT. We modeled GAHT used by transwomen by performing orchidectomy (orx) in 6-weeks-old male mice and treating orx mice with estrogen (E2) for 10 weeks. GAHT used by transmen was modeled by treating intact female mice with testosterone from 6 to 16 weeks of age. Neither E2 treatment of orx male mice, nor testosterone treatment of eugonadic female mice impaired skeletal maturation, bone structure, or turnover, in 6-16 weeks old animals. In fact, GAHT in male mice, resulted in better bone microarchitecture and higher serum osteocalcin, a marker of bone formation. Measurement of gut permeability through serum lipopolysaccharide and sCD14 quantification revealed that GAHT didn't alter gut permeability in male or female mice. Intriguingly, GAHT did result in sex-specific changes in the composition of the gut microbiome, and induced modifications to bacterial metabolic pathways within the microbiome that were associated with changes in bone structure. Confirming the causal role of the microbiome change, fecal material transfer studies revealed that GAHT-shaped gut microbiome was a communicable regulator of gut permeability, bone structure, and turnover in mice. Mediation analysis identified three strains of Bacteroides (Bacteroides acidifaciens JCM 10556, Bacteroides caecimuri, and Bacteroides caecimuris) as responsible, in part, for the skeletal effects of GAHT in male mice. Bacteroides promote the expansion of intestinal regulatory T cells (Tregs), a sex steroid-regulated T cell population known to affect bone formation and resorption. Accordingly, GAHT was found to regulate the frequency of intestinal and bone marrow Tregs, indicating that a higher number of Tregs could account for the improved bone microarchitecture of GAHT-treated male mice. In summary, GAHT treatment mice did not

impair skeletal maturation in young male and female animals, and improved bone structure in male mice. GAHT acted, in part, by regulating microbiome composition and function. Mechanistically, GAHT-induced microbiome changes may regulate bone maturation affecting Treg differentiation.

***Disclosures: Subhashis Pal**, None*

SAT-173

A Diurnal Trough in Glucocorticoid Signaling is Essential for Bone Health *Annelies Smit[1], Jan Kroon[1], Sander Kooijman[1], Maaike Schilperoort[2], Salwa Afkir[1], Bram van der Eerden[3], Marijke Koedam[3], Patrick Rensen[1], Onno Meijer[1], Elizabeth Winter[4]. [1]Department of Medicine, Division of Endocrinology, Leiden University Medical Center, Leiden, the Netherlands, Netherlands. [2]Department of Medicine, Columbia University Irving Medical Center, New York, USA, United States. [3]Department of Internal Medicine, Erasmus MC, Rotterdam, Netherlands, Netherlands. [4]Department of Medicine & Center for Bone Quality, Division of Endocrinology, Leiden University Medical Center, Leiden, the Netherlands, Netherlands

PurposeWe recently have shown that a flattened glucocorticoid (GC) circadian rhythm in itself induces an osteoporotic phenotype in mice. Here, we investigated whether the diurnal trough in GC signaling is essential to preserve bone mass and structure.MethodsFemale C57Bl/6J mice were implanted with slow-release 7.5 mg corticosterone (CORT) or vehicle pellets for 7 weeks to flatten GC circadian rhythm without increasing total exposure. Additionally, mice received daily subcutaneous injections with vehicle or non-specific GC receptor antagonist RU-486 to reintroduce a diurnal trough in GC signaling. To investigate a timing effect, mice were injected either at the time of the endogenous GC trough, i.e. zeitgeber time (ZT) 1, or GC peak (ZT11). Bone remodeling was assessed by serum turnover markers, osteoblast and osteoclast surface area was determined via osteocalcin and tartrate-resistant acid phosphatase (TRAP) staining respectively, and bone microarchitecture was evaluated by micro-CT (n=12/group).ResultsThe various interventions did not affect serum bone resorption marker TRAP levels. The timing of peak bone formation marker procollagen type I N-terminal propeptide (P1NP) levels was notably synchronized to the timing of RU-486 injection, resulting in a reversed P1NP pattern in mice injected at ZT11, as compared to vehicle. Osteoclast and osteoblast surface area were unchanged across groups. CORT pellets induced a loss of lean mass compared to vehicle (-6.5%, $p<0.01$), which was rescued by RU-486 injection at both ZT1 and ZT11, suggesting prevention of bone wasting. Indeed, CORT pellets significantly reduced cortical thickness (-13.0%, $p<0.001$), cortical bone area (-10.0%, $p<0.01$) and trabecular bone volume (-31.8%, $p<0.05$), as compared to vehicle. RU-486 injection at either timepoint significantly improved cortical thickness (ZT1 +10.5%, $p<0.01$; ZT11 +9.2%, $p<0.01$) and cortical bone area (ZT1 +8.7% $p<0.05$; ZT11 +9.5% $p<0.01$), as compared to CORT mice. Notably, RU-486 injection at ZT1 prevented trabecular bone volume loss, while RU-486 injection at ZT11 did not (-30.6%, $p<0.05$, as compared to vehicle).ConclusionReinstating a diurnal trough in GC signaling under the condition of flattened GC levels is sufficient to rescue bone mass and structure. The fact that these effects were more pronounced when the GC receptor antagonist was injected at the time of the endogenous GC trough suggests that the circadian context of bone tissue is also important.

***Disclosures: Annelies Smit**, None*

SAT-174

See Friday Plenary Number FRI-174

SAT-175

Paradoxical effects of abaloparatide on 1,25-dihydroxyvitamin D formation and blood calcium level change *Yanmei Yang[1], Wei-Ju Tseng[1], Bin Wang[1]. [1]The Center for Translational Medicine, Departments of Medicine, Sidney Kimmel Medical College, Thomas Jefferson University, Philadelphia, Pennsylvania 19107, United States

Paradoxical effects of abaloparatide on 1,25-dihydroxyvitamin D formation and blood calcium level changeYanmei Yang, Wei-Ju Tseng, and Bin WangThe parathyroid hormone (PTH)-related peptide(1-34) analog, abaloparatide (ABL) is the second anabolic agent for the treatment of osteoporosis. Previous research demonstrated that ABL had a potent anabolic effect but caused hypercalcemia at a significantly lower rate. 1,25-dihydroxyvitamin D [1,25(OH)2D] plays an important role in intestinal calcium absorption and renal calcium reabsorption. However, it is unknown whether ABL affects 1,25(OH)2D synthesis and its downstream signaling. Osteocalcin (Ocn) is synthesized by osteoblasts and is the most abundant non-collagenous protein in bone. The carboxylated Ocn (Gla-Ocn) is released into the circulation and exhibits high affinity to bind ionized calcium (Figure 1), which in turn induces Gla-Ocn conformational change and then increases Gla-Ocn binding to hydroxyapatite to form new bone matrix. During the bone remodeling, Gla-Ocn in bone matrix can be converted into a form with a lower grade of carboxylation and uncarboxylated Ocn (Glu-Ocn), and then be released into the bloodstream when osteoclasts are activated to form acidic pH. Although ABL was reported to increase total Ocn formation in the circulation, the effects of ABL on both Gla-Ocn and Glu-Ocn levels and their ratio in bloodstream and bone are unknown. Our in vivo data showed that ABL significantly increased rat 1,25(OH)2D formation, however, without raising the blood calcium values. ABL also significantly augmented the levels of Gla-Ocn and Glu-Ocn, as well as the ratio of Gla-Ocn to Glu-Ocn in blood and bone. The in vitro data showed that 1,25(OH)2D concentration-dependently induced Gla-Ocn formation in rat osteoblastic cells, confirming that Ocn is the downstream signaling of 1,25(OH)2D. ABL had little direct effects on 1,25(OH)2D synthesis and Ocn formation in non-renal cells (rat osteoblastic cells). However, ABL significantly promoted both 1,25(OH)2D and Gla-Ocn formation when 25-hydroxyvitamin D, the substrate of 1alpha-hydroxylase, was added to the cells. Our data also showed that the increased Gla-Ocn levels are vitamin K-dependent in osteoblasts. Thus, the increased 1,25(OH)2D levels in rats treated by ABL result in high level of Gla-Ocn and transient calcium increase in the circulation. The ionized calcium then binds to Gla-Ocn that increases Gla-Ocn to bind to hydroxyapatite to form new bone matrix. We conclude that Gla-Ocn at least, in part, eliminates the paradoxical effects of abaloparatide on 1,25(OH)2D formation and blood calcium level change, which may help understand the mechanism of ABL for osteoporosis therapy.

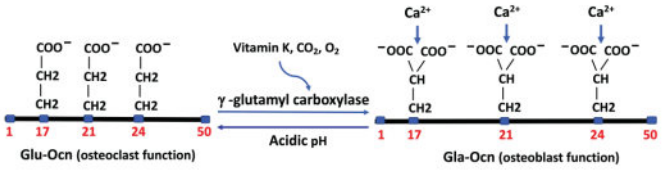

Figure 1. Schematics of osteocalcin (Ocn) post-translational modification. Post-translational carboxylation at three glutamic acid residues at positions 17, 21 and 24 in rat occurs by γ-glutamyl carboxylase that uses vitamin K, CO_2, and O_2 as cofactors, which results in the formation of three Ca^{2+}-binding γ-carboxyglutamates (Gla) in osteoblasts. The carboxylated form of OCa (Gla-Ocn) can be converted into a form with a lower grade of carboxylation (Glu-Ocn) when osteoclasts are activated to form acidic pH. In contrast to Gla-Ocn, Glu-Ocn has no affinity to ionized calcium.

***Disclosures: Yanmei Yang**, None*

SAT-177

PTH-dependent stabilization of RANKL mRNA is associated with a selective increase in binding of phosphorylated KSRP, an AU-rich element binding-protein, to RANKL transcripts. *Gang-Qing Yao[1], Meiling Zhu[2], Karl Insogna[1]. [1]Yale University School of Medicine, United States. [2]Yale University, United States

PTH1R agonists promote bone formation but also increase osteoclastogenesis in part by increasing RANKL expression. Consistent with previous reports, we observed a significant 10+/-1.2-fold increase in RANKL mRNA expression in UAMS cells treated with PTH for 6 hours. However, despite pretreating these cells with triptolide, a powerful inhibitor of transcription, PTH still increased RANKL transcript levels by 7.4+/-2.4-fold. RANKL mRNA stability is regulated by AU-Rich Element binding proteins (ABPs), which bind to AREs (AU-Rich Elements) in the 3' UTR of RANKL transcripts. PTH did not change transcript expression levels of four ABPs: KSRP, AuF1, HuR, and TTP. ABPs are phosphorylated by protein kinases and dephosphorylated by Pin1. Phosphorylating Pin1 blocks Pin1's enzymatic activity. PTH increases the phosphorylation of KSRP and Pin1 in opossum kidney cells1, suggesting that PTH-dependent phosphorylation of KSRP reflects inhibition of Pin1. Whether these pathways are operative in bone is not currently known.Levels of phosphorylated KSRP in UAMS cells pretreated with triptolide and subsequently treated with PTH, were significantly increased compared to those treated with vehicle (0.225+/-0.012 µg/ per 106 cells vs. 0.083+/-0.009 µg/ per 106 cells, $p<0.001$). Phosphorylation of AuF1, HuR, and TTP proteins either remained unchanged or were slightly reduced in response to PTH treatment. KSRP was subsequently immunoprecipitated from PTH-treated cells and the RANKL mRNA content of the immunoprecipitated quantified by RT-PCR. The immunoprecipitates from PTH-treated cells contained considerably more RANKL mRNA than did vehicle treated cells. In an initial experiment the amount of RANKL mRNA in immunoprecipitates of AuF1, HuR, and TTP did not change significantly with PTH treatment. There were no changes in the cellular content of phospho-Pin1 protein with PTH treatment. We speculate that PTH selectively increases binding of phosphorylated KSRP (which is not active) to RANKL mRNA and either displaces, or competes for binding of non-phosphorylated KSRP to the mRNA, thereby stabilizing the transcript.We conclude that, 1) PTH induces KSRP phosphorylation by a mechanism that does not involve changing the activity of Pin 1. 2) PTH appears to selectively increase binding of phosphorylated KSPR to RANKL transcripts, which may play an important role in PTH-independent RANK mRNA stabilization.

1. Murray R. Merchant M. Hardin E. Clark B. Khundmiri S. Lederer E. Identification of an RNA-binding protein that is phosphorylated by PTH and potentially mediates PTH-induced destabilization of Npt2a mRNA. American journal of physiology. Cell physiology 310:C205-C215, 2016

***Disclosures: Gang-Qing Yao**, None*

SAT-178

Dual anti-resorptive and anti-inflammatory activity of tanshinone IIA-sulfonate attenuates rheumatoid arthritis in mice *Preety Panwar[1], Pierre M Andrault[2], Dieter Bromme[2]. [1]University of British Columbia, Canada. [2]The University of British Columbia, Canada

Rheumatoid arthritis (RA) is an autoimmune disease characterized by joint inflammation and tissue destruction. An effective treatment for RA needs to combine both anti-inflammatory and anti-resorptive properties. Here, we demonstrate the potent dual activity of tanshinone IIA sulfonate (T06) effectively reducing inflammation as well as cartilage/bone loss in a mouse arthritis model. T06 effectively suppresses the percentage of synovial fibroblast, various immune cells and osteoclasts which was corroborated by the decreased production of inflammatory cytokines (tumor necrosis factor (TNF)-?, interleukin-1? (IL-1?), IL-17, IL-6, IFN?, and RANKL. Interestingly, a significant reduction in T helper (Th17) cells that activate osteoclasts by inducing synovial fibroblasts via IL-17 is caused by T06 resulting in less osteoclasts and bone resorption. The anti-inflammatory activity of T06 is based on the interference of the NF-kB pathway by preventing the phosphorylation of I?B?/NF-?B signaling in immune cells, and thus its nuclear translocation resulting in the reduced expression of inflammatory cytokines. We also demonstrated that the activation, nuclear location, and DNA binding of NF-kB is decreased by T06-treatment. The anti-resorptive activity of T06 is based upon its interference with the formation of collagenolytically active CatK oligomers resulting in a selective inhibition of its bone and cartilage-destroying collagenase activity. In contrast, the selective active-site-directed CatK inhibitor, odanacatib, reduced bone and cartilage resorption but did not alleviate inflammation. Our study illuminates the immune regulatory and antiresorptive effect of T06 in arthritis.

***Disclosures: Preety Panwar**, None*

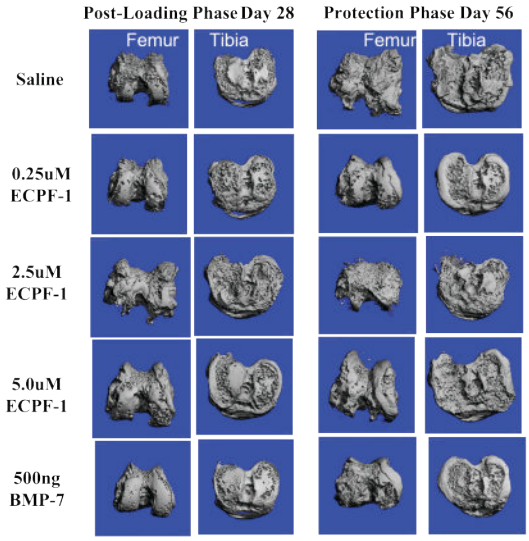

µCT comparison of femoral condyles and tbial plateau Post-Loading (day 28) and Protection (day 56) Phases. Smooth areas represent intact cartilage, while pitted areas represent cartilage erosion and subchondral bone. **Saline**(negative control) displays considerable cartilage degradation and exposure of subchondral bone **0.25 µM, 2.5 µM and 5.0 µM ECPF-1** display improved appearance compared to saline control at 56 days. **5.0 µM ECPF-1** appearance is improved from saline control and comparable with BMP-7 (positive therapeutic control) treatment. **500 ng BMP-7**: Served as positive therapeutic control. **Outcome**: ECPF-1, specifically at 5.0 µM, and BMP-7 treatment indicate long-term chondroprotection in post-traumatic OA.

Saturday Orals

***Disclosures: Marina D'Angelo**, ProteaPex Therapeutics, LLC, Major Stock Shareholder*

SAT-179

Extracellular Matrix Protection Factor 1, a Novel Therapeutic, Demonstrates Chondroprotective Properties in a Rat Model of Post-Traumatic Osteoarthritis *Marina D'Angelo[1], Amy Bhatt[1], Brian Heist[1], Lyudamila Lukashova[2], Patrisia Mattioli[1], Victoria Datillo[1], Ellen Cho[1], Sarah Chmielewski[1], Tiffany Holmes[1], Abdulhafez Selim[1]. [1]Philadelphia College of Osteopathic Medicine, United States. [2]University of Pittsburgh, United States

Osteoarthritis (OA) is a common degenerative joint disease causing pain and disability in more than 654 million, or 23% of adults worldwide. Post-traumatic osteoarthritis (PTOA) occurs after articular or meniscal injury to the joint and accounts for 12% of symptomatic OA cases. PTOA offers an opportunity to explore novel therapeutic treatments because the starting point is clear. Current pharmacological treatment targets inflammation and pain management through non-steroidal anti-inflammatory drugs and intraarticular corticosteroids. Extracellular Matrix Protection Factor 1 (ECPF-1) is a novel therapeutic that inhibits specific matrix metalloproteinases that are involved in degradation of the cartilage extracellular matrix (ECM) during PTOA. In this study, an experimental rat model of PTOA was replicated by an injection of mono-iodoacetate (MIA) infrapatellar to the ligament of 150g male, Wistar rats. This model is characterized by osteophyte formation at the edges of the joint, fibrillation and erosion of the cartilage within 30 days of the injections. One week following MIA, animals were injected weekly for 4 weeks with various doses of ECPF-1(0.25uM - 5uM), saline (negative control), or BMP-7 (500 ng, positive control) and sacrificed between 28 and 56 days. Total mineralization in the femur and tibial cartilages and 3D reconstructions were scanned through µCT of 15um voxel size, 55KVp, 0.36 degrees rotation step (180 degrees angular range) and a 600ms exposure per view from joints immersed in phosphate buffered saline solution (Scanco µCT software and HP, DEC windows Motif 1.6). Volumes were segmented using a global threshold of 0.4g/c for bone and 0.25g/c for soft tissue. Following µCT scanning, specimens were decalcified, embedded in paraffin, sectioned and stained with Safranin-O to detect proteoglycans or Periodic-acid Schiff for general cartilage architecture. The µCT images showed that at both the 28-day post-loading (4 weekly injections) and 56-day protection phase (4 weeks beyond the final injection), ECPF-1 decreased ECM degradation compared to untreated controls. Improved articular cartilage histological staining of the ECPF-1 treated joints supported the µCT image data for the femur and tibia. We are currently compiling the µCT mineralization data. These preliminary results suggest a chondroprotective property to ECPF-1 and its potential as a therapeutic that may slow the progression of PTOA.

SAT-180

Characterisation of Spatial Variations of Epiphyseal Growth Plate Bridging In Loaded Post-traumatic Murine Model of Osteoarthritis *Hasmik Jasmine Samvelyan[1], Kamel Madi[1], Livia Rocha Dos Santos[1]. [1]Dr, United Kingdom

Our recent studies indicated uncharacteristic growth plate (GP) changes may contribute to osteoarthritis (OA) in mouse models. However, the precise relationship between spatial variation in GP bridging and cartilage mechanics has yet to be determined, and how this may increase OA vulnerability.We investigated GP dynamics in non-invasive mechanically loaded murine model of OA, to understand associations between abnormalities in these dynamics and biomechanical material properties of calcified cartilage, found beneath the hyaline cartilage, underpinning post-traumatic OA development.The right knee joints of 19-week-old wild type C57BL/6 male mice (n=7) were subjected to dynamic axial mechanical loading for 7 min/day, 3 alternate days a week for 2 weeks to induce OA-like changes in vivo. Left knee joints were non-loaded controls in each animal. Subchondral bone (SCB) and trabecular bone (Tb.) parameters were measured using microCT in tibiae of these mice (n=14) and correlated to GP bridging using novel 3D quantification method. All procedures were approved by University Ethics Committee.3D quantification revealed enriched GP bridging (540+35 vs 750+19; p<0.001) and higher bridge densities (16+1 vs 21+0.5; p<0.001) in medial compared to lateral tibiae in loaded knee joints. Anatomical variations were observed in all samples, with focal high-density clusters forming in anterior region of medial loaded tibiae compared with those more central and posterior of non-loaded tibiae. GP dynamics were associated with increased SCB and epiphyseal Tb. volume fraction (BV/TV) in medial compared to lateral tibiae of loaded knee joints.Results confirm AC chondrocyte transiency and characteristic thickening of medial tibiae SCB and Tb. in loaded model of post-traumatic OA. We reveal spatial variation of GP bridging in this model and how these may contribute to anatomical variation in vulnerability of OA development. Ongoing experiments will further determine these associations, establish biomechanical and morphological properties across calcified cartilage underpinning post-traumatic OA development and examine relevance to human OA.

***Disclosures: Hasmik Jasmine Samvelyan**, None*

SAT-182

Implant loosening in bone can be detected by bone biomarkers in rodents *Andreas A. Kurth[1], Björn Habermann[2], Konstantinos Kafchitsas[3]. [1]Marienhaus Klinikum Mainz, Germany. [2]Dep. Orthopedic Surgery, University Medicine Mainz, Germany. [3]Spine Center Oberpfalz, Orthopaedic Hospital Lindenlohe, Germany

Aseptic loosening of implants is the leading cause of implant failure. Currently, this can only be diagnosed with a combination of medical history, clinical symptoms and imaging. Detection of aseptic implant loosening at an early stage would improve surgical outcome, and future pharmacologic intervention may prevent further bone destruction. Since aseptic implant loosening is caused by increased periprosthetic bone resorption, parameters of periprosthetic bone metabolism may offer an option for early detection.Material and methods:60 female OVX Wistar rats were randomized into experimental group (n=50) and control group (n=10). All animals in the experimental group were implanted with a tibial hemiarthroplasty, and polyethylene particles were continuously infused into the operated joint via a diffusion pump to induce implant loosening. All animals in the control group underwent sham surgery.

Blood was taken preoperatively every 42 days, once on the day of surgery and postoperatively every 7 days. In the serum, osteocalcin (OC) and PINP were determined as parameters of bone formation, and C-terminal type I collagen telopeptide (CTX) and tartrate-resistant acid phosphatase 5b (TRAP 5b) as parameters of bone resorption.Results:_ OC showed an identical course in both groups. PINP showed significantly increased concentrations postoperatively in the experimental group ($p<0.05$). CTX showed significantly higher postoperative concentrations in the experimental group only on day 14 and 21 ($p<0.05$). TRAP 5b showed significantly higher activity postoperatively in the experimental group ($p<0.05$). Conclusion:Implant loosening was expected from day 28 in the model used. CTX showed increased concentrations prior to the expected changes, but is not very sensitive enough to bone resorption, and has a pronounced circadian rhythm. TRAP 5b activity was significantly increased temporally before and during the first histological changes and could therefore be considered as a predictor of aseptic implant loosening. PINP was elevated due to ineffective bone formation in the context of aseptic prosthesis loosening and may contribute to the early diagnosis of aseptic prosthesis loosening in combination with TRAP 5b serum activity. Due to the low influence of metabolism, food intake and circadian rhythmicity, TRAP 5b has many merits for clinical application and should be investigated further for its clinical use in identifying the initial stage of aseptic implant loosening.

***Disclosures: Andreas A. Kurth**, None*

SAT-183

See Friday Plenary Number FRI-183

SAT-184

Static Strain, but Not Dynamic, Inhibits the Hippo Pathway to Activate YAP in MSC *Zhihui Xie[1], Buer Sen[1], Sean Howard[2], Cody McGrath[1], Maya Styner[1], Gunes Uzer[2], Janet Rubin[1]. [1]UNC@Chapel Hill, United States; [2]Boise State, United States

Skeletal progenitors require mechanical input to direct appropriate formation of the skeleton. In-vitro application of dynamic mechanical force to mesenchymal stem cells (MSC) promotes stemness and constrains adipogenesis (1). Nuclear transport of YAP (Yes-associated protein) is involved in force signaling: YAP nuclear entry due plating of MSC stiff substrate has been ascribed primarily to stretching of nuclear pores via F-actin/LINC connections (2). We previously showed in primary murine marrow MSC that application of static stretch promoted YAP translocation, but that dynamic strain did not (3). As both strain applications generate indistinguishable accretion of phalloidin stained F-actin cables in the cytoplasm and crossing the nucleus, we asked what distinguishes static strain, which allows YAP entry, from dynamic strain, which does not. We examined the Hippo pathway, which when activated, induces phosphorylation of YAP and prevents its transport to the nucleus (pMST? pLATS? pYAP? nuclear exclusion of YAP). Hippo protein phosphorylation and immunofluorescence microscopy were performed 3 hours after application of 2% strain using murine MSC: a) static = x 1/hold and b) dynamic = x 200 cycles @ 0.2 Hz with release. We found dynamic strain increased phosphorylation of MST (180%) and YAP (113%), and that nuclear YAP did not increase (micrography assessment of nuclear YAP). In contrast, static strain induced de-phosphorylation of MST, LATS and YAP on western blots (50%, 57% and 38% respectively). To investigate the mechanism whereby static strain caused dephosphorylation of Hippo pathway members, we pulled down MST and found that association of the STRIPAK phosphatase catalytic subunit PP2AC was increased. Inhibiting PP2A with okadaic acid prevented static strain YAP nuclear entry. To ascertain a potential contribution of F-actin/LINC forces on the nucleus to YAP transfer, we utilized MSC transfected with a lentiviral DOX-inducible dominant-negative KASH expression: preventing F-actin association with LINC member KASH disrupts mechanical force on the nucleus. Treatment with DOX induced expression of DN KASH labelled with cherry red. In DOX treated cells, DN-KASH expression did not impair static strain induced nuclear YAP entry. Our results indicate that the predominant effect of static strain, rather than altering nuclear membrane mechanics, is to promote PP2AC association with MST, thus preventing activation of the Hippo pathway to phosphorylate YAP. Dynamic strain, in contrast, activates the Hippo pathway, preventing the nuclear transport of YAP through promoting its phosphorylation.1. Sen JBMR 2020 2. Elosegui-Artola Cell 2017 3. Sen, Stem Cells 2022.

***Disclosures: Zhihui Xie**, None*

SAT-185

Adaptive Response to Loading is Impaired in a Mouse Model of Osteogenesis Imperfecta *David Bertrand[1], JOSEPHINE T. TAUER[2], Joan Marini[3], Frank Rauch[4], Bettina Willie[1]. [1]McGill University, Canada; [2]Shriners Hospital, Canada; [3]National Institute of Child Health and Human Development, United States; [4]Shriners Hospital for Children, Montreal, Canada

IntroductionOsteogenesis imperfecta (OI) is a connective tissue disorder characterized by increased bone fragility with frequent fractures. The cross-sectional area of long bones, as measured by periosteal circumference, is consistently low in individuals with OI This appears to be due to reduced periosteal bone apposition and may be related to a reduced adaptive loading response. Thus, we aimed 1) to determine strains engendered in tibias during locomotion and assess strain-load relationship, and 2) to examine the bone remodeling response in OI mice following a 2-week in vivo tibial loading.MethodsStrain gauges were attached to the antero-medial surface of the tibias of ten-week-old female Brtl+/- mice and wild type (WT) littermates (n=7/genotype). Strains engendered during walking and cyclic tibial compressive loading (3N to 12N) were then measured. Based on these results, the bone adaptive response to two weeks of in vivo tibial loading (5 days/week) at 10N was assessed in both Brtl+/- and WT mice (n=10/genotype; left tibia loaded, right tibia nonloaded control). The change in bone mass and microstructure was assessed via in vivo ?CT (? =day 15-day 0). ?CT-based timelapse morphometry was performed to assess endocortical (Ec) and periosteal (Ps) mineralized and eroded volumes and surface areas over the 15-day interval. Activity analysis, dynamic fluorochrome-based histomorphometry, assessment of bone formation markers (P1NP, TRAP5b), and characterization of the osteocyte lacunocanalicular network (LCN) are ongoing.ResultsAt day 0, as expected, Brtl+/- mice showed significantly reduced cortical area (CtAr), total area (TtAr), marrow area (MaAr), second moment of area (Imax, Imin) and cortical thickness (CtTh) compared to WT. Following two weeks of loading, ?CtAr, ?CtTh, Ec. MV/BV, Ec. MS/BS were significantly increased in loaded compared to non-loaded limbs for both genotypes. Strikingly, ?TtAr, Ps.MV/BV and Ps. MS/BS were significantly increased in the loaded vs non-loaded limb of WT mice, but not in Brtl+/- mice. In terms of resorption, both Ec and Ps EV/BV and ES/BS were reduced in the loaded compared to control limb of both genotypes.ConclusionOur results suggest that Brtl+/- mice have a diminished loading-bone formation response on the periosteal surface, which is believed to be a contributing factor to their low bone mass phenotype. Ongoing research aims to investigate the mechanisms responsible for this reduced mechano-adaptive response.

***Disclosures: David Bertrand**, None*

SAT-186

Detrimental Effects of Microgravity on Osteoblast and Osteoclast Activity *Isaiah Taylor[2], Sardar Uddin[2], David Komatsu[3]. [2]Stony Brook University, ; [2]Stony Brook University, United States; [3]Stony Brook University, Dept. of Orthopaedics and Rehabilitation, United States

Mars 2030 is rapidly approaching, and despite recent breakthroughs in space biology, sending the first humans to Mars remains a significant challenge. During space flight, astronauts lose 1-1.5% of their bone mass per month. Because of our inadequate understanding of the mechanisms causing microgravity-induced bone loss, as well as the difficulties in developing effective remedies, NASA has designated microgravity-induced bone loss as a high-priority knowledge gap.Osteoblast-osteoclast coupling is a dynamic process regulating bone remodeling. This study uses osteoblast-osteoclast co-cultures to identify the direct and indirect cell communication pathways disrupted by microgravity (MG). Simulated MG is hypothesized to disrupt osteoblasts-osteoclasts communication, resulting in increased resorption and decreased bone formation.Primary human osteoblasts and osteoclasts (25,000 cells/chip) were seeded on tricortical human decellularized blocks and subjected to either microgravity or gravity using a rotary cell culture system (Synthecon®) for 28 days. The mechanical integrity of tricortical blocks was assessed using unconstrained uniaxial compression. Briefly, a monotonic load to failure was applied at 5mm/min, and data were analyzed for stiffness, energy to failure, yield force, ultimate force, and failure force.The biomechanical strength was significantly reduced in MG-exposed samples compared to samples experiencing normal gravity. Specifically, stiffness was 140% lower, energy to failure was 419% lower, yield force was 274% lower, ultimate force was 269% lower, and failure force was 269% lower in microgravity conditions compared to gravity. The biomechanical results for osteoclasts are in progress.Future experimental work includes RNAseq, ELISA, histomorphometry, and biomechanical analysis. The functional analyses will show the effects of osteoblast-osteoclast decoupling on bone structure and mechanical integrity. The utilization of primary human cells in the physiological environment significantly enhances the data's translational value in providing potential therapeutic targets for reducing microgravity-induced bone loss and further recognizing potential clinical targets for treating osteoporosis and osteopenia. In addition, the data from these studies will enhance our understanding of the effects of microgravity on the osteoblast-osteoclast coupling and identify biomolecular targets to regulate bone remodeling and regeneration.

***Disclosures: Isaiah Taylor**, None*

SAT-188

See Friday Plenary Number FRI-188

SAT-189

Effects of zoledronic acid on skeletal phenotype in female C57BL/6 mice undergoing chemical or surgical estrogen deficiency *Claudia Biguetti[1], Nataira Momesso[2], Ana Carolina Bacelar[2], Juliana Meira[2], Antonio Hernandes[2], Edilson Ervolino[2], Mariza Matsumoto[2]. [1]Research Laboratory of Regenerative Medicine, School of Podiatric Medicine, University of Texas Rio Grande Valley, United States; [2]School of Dentistry, São Paulo State University (UNESP), Brazil

Animal models are crucial for studying osteoporosis, but diverse induction methods may impact investigations on antiresorptive drugs and bone health. The purpose of this study was to evaluate the differences in chemical or surgical models of induced ovarian failure with or without treatment with zoledronate (ZL) in analyzing the skeletal microar-

chitecture of female C57Bl/6 mice. Twenty-two female C57Bl/6 mice, weighing around 28 grams and 4-6 months old, were divided into five groups: CT (negative control), OVX (ovariectomized), VCD (treated with 160 mg/Kg/day of diepoxyd 4-vinylcyclohexene), CT+ZL (treated with 500µg/Kg of ZL, once a week), OVX+ZL (ovariectomyzed treated with ZL), and VCD+ZL (treated with VCD and ZL). ZL treatment was administered throughout 7 consecutive weeks, initiating 10 days before confirming permanent diestrus of the animals that underwent induced ovarian failure and matched time with the animals of CT+ZL group. After the experiment, femurs and L5 vertebrae were microCT scanned to quantify cancellous bone (BV mm³, BV/TV%, Tb.N, 1/mm, Tb.Th, mm, Tb.Sp, mm, and SMI for L5 vertebra). Data was analyzed using Shapiro-Wilk and Two-way ANOVA followed by Tukey test ($p<0.05$). While femurs did not present significant differences induced by ovarian failure models (OVX and VCD), vertebrae of OVX and VCD mice presented significantly reduced values of BV/TV, BV, and Tb/Th in comparison with CT. However, femurs of the CT+ZL group presented significantly increased values of BV/TV and BV in comparison with CT and significantly reduced values of Tb.Sp in relation to CT. ZL treatment was also effective in vertebrae of OVX and VCD groups, with significantly increased values of BV/TV, BV, Tb.Th, and Tb.N when compared with the non-treated mice. SMI values were also significantly higher in OVX and VCD groups in comparison with their matched ZL-treated groups. Both models of induced ovarian failure, OVX and VCD, induced osteoporosis in the present animal model. ZL treatment improved trabecular quality in the mice vertebrae; however, it was not observed in the distal metaphysis of the femur. In conclusion, the study showed that both chemical and surgical methods of inducing ovarian failure in female C57BL/6 mice resulted in osteoporosis. Furthermore, treatment with ZL improved the trabecular quality of vertebrae in both mice models with induced ovarian failure but did not have the same effect on the distal metaphysis of the femur.

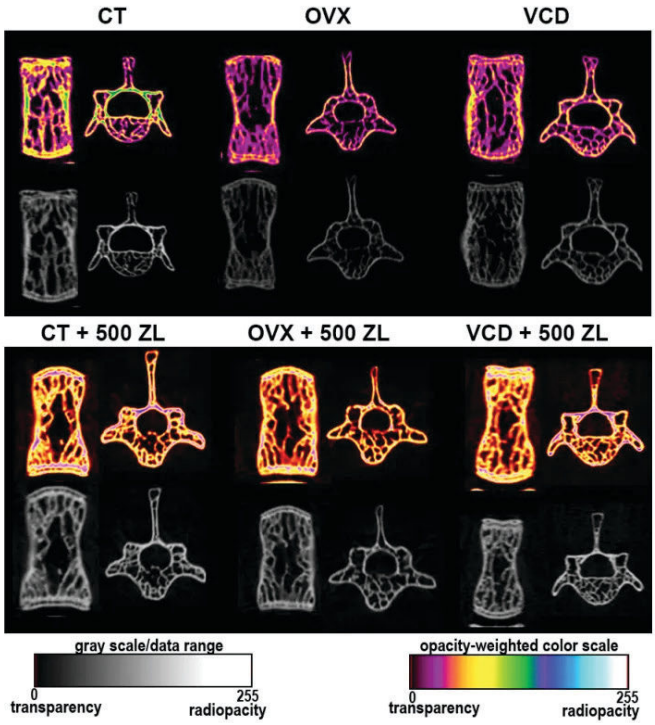

***Disclosures: Claudia Biguetti**, None*

SAT-190

Dose Dependent Response of the Murine Musculoskeletal System to Artificial Gravity Induced by Centrifugation on the International Space Station (MHU-8): A NASA-JAXA Collaboration *Jennifer Coulombe[1], Anna Wadhwa[2], Marie Mortreux[3], Shannon Emerzian[4], Jason Ciola[5], Jarred Chow[2], Daniel Brooks[6], Jeffrey Willey[7], Charles Fuller[8], Satoru Takahashi[9], Martha Hotz-Vitaterna[10], Mary Bouxsein[11]. [1]Center for Advanced Orthopedic Studies, Department of Orthopedic Surgery, Beth Israel Deaconess Medical Center, Harvard Medical School, United States. [2]Center for Advanced Orthopedic Studies, Beth Israel Deaconess Medical Center and Department of Orthopedic Surgery, Harvard Medical School, United States. [3]Department of Nutrition and Food Sciences, University of Rhode Island, United States. [4]Beth Israel Deaconess Medical Center, United States. [5]Ann Romney Center for Neurologic Diseases, Department of Neurology, Brigham and Women's Hospital and Harvard Medical School, United States. [6]BIDMC/MGH, . [7]Department of Radiation Oncology, Wake Forest School of Medicine, Bowman Gray Center, United States. [8]Department of Neurobiology, Physiology and Behavior, University of California, United States. [9]Department of Anatomy and Embryology, Faculty of Medicine, University of Tsukuba, Japan; , Japan. [10]Department of Neurobiology, Northwestern University, United States. [11]Beth Israel Deaconess Medical Center, Harvard Medical School, United States

Artificial gravity (AG) by centrifugation is a potential countermeasure to mitigate deleterious musculoskeletal changes associated with microgravity (µG). Yet, the responses of the musculoskeletal system to varied magnitudes of AG are not known.Adult (12 weeks) male C57Bl/6 mice were exposed to either 0G, 0.33G, 0.67G, or 1G (n=5-6/group) via centrifugation using the JAXA Multiple Artificial-gravity Research System (MARS), during a 30-day mission on the International Space Station. Ground controls were housed in an identical environment (HGC, n=12). Groups were assigned based on pre-flight body mass, no significant differences between mean body mass was detected between groups. Mice underwent pre- and postflight testing of grip strength, body composition and BMD via DXA (lnAlyzer, Medikors). Following euthanasia, the hindlimb muscles were harvested and weighed. Bone microarchitecture of the femur was assessed via microcomputed tomography (Scanco Medical). Group differences were evaluated using a one-way ANOVA with Tukey's Post Hoc Test in R.Pre-flight body mass was similar among the groups. HGC animals gained significantly more mass than 0.66G mice (+4.0% vs -1.9%, $p<0.05$). Gastrocnemius wet mass was lowest in 0G (-18.2% less than HGC), and inversely related to level of AG (Fig. 1A). Soleus wet mass showed a similar pattern. Front paw grip strength declined ~ 50% in 0G and 0.33G, but was unchanged in the 0.67, 1G and HGC groups. Rear paw grip strength did not differ among groups. At the distal femur, trabecular (Tb) BV/TV (-31.0%, $p<0.0001$), Tb thickness (-10.6%, $p<0.01$), Tb.BMD (-20.6%, $p<0.0001$, Fig. 1C), cortical (Ct) thickness (-9.6%, $p<0.0001$, Fig. 1B), and Ct area (-12.8%, $p<0.05$) were lower in the 0G compared to HGC and 1G. AG had varied effects on bone microstructure, but AG groups tended to show similar intermediate values as compared to those observed in 0G and 1G.Mice exposed to different levels of artificial gravity via centrifugation during one month of spaceflight dose-dependently mitigated atrophy of the gastrocnemius and soleus, and front paw grip strength. Declines in bone density and microarchitecture due to microgravity were partially mitigated by artificial gravity. Ongoing work will further explore the mechanisms underlying the musculoskeletal response to AG.

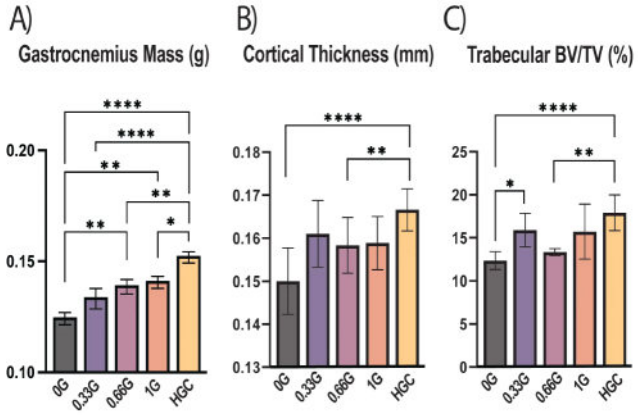

Figure 1: Muscle mass and bone microarchitectural changes associated with micro- and artifical gravity. **A)** Gastrocnemius wet mass, **B)** Cortical Thickness, and C) Trabecular Bone Volume Fraction (BV/TV). Data are presented as mean and standard deviation. Statistical significance of Tukey's post hoc test: * - $p<0.05$, ** - $p<0.01$, *** - $p<0.001$, **** - $p<0.0001$.

***Disclosures: Jennifer Coulombe**, None*

SAT-191

Targeted next generation sequencing of germline and somatic mutations in primary hyperparathyroidism Indian patients and evaluation of their gene expression *Sheenam Garg[1], Poonam Kumari[2], Ashutosh Kumar Arya[3], Rimesh Pal[4], Naresh Sachdeva[5], Ritambhara Nada[6], Divya Dahiya[7], Sanjay Kumar Bhadada[8], Sudhaker Rao[9]. [1]Research Associate I, Department of Endocrinology, PGIMER, India. [2]Ph.D Scholar, Department of Endocrinology, PGIMER, India. [3]Assistant Professor, Endocrinology & Metabolism, AIIMS, India. [4]Assistant Professor, Department of Endocrinology, PGIMER, India. [5]Professor, Department of Endocrinology, PGIMER, , India. [6]Professor, Department of Histopathology, PGIMER, , India. [7]Professor, Department of General Surgery, PGIMER, , India. [8]PGIMER, chandigarh, India, India. [9]Henry Ford Hospital, United States

Background: Primary hyperparathyroidism (PHPT) is characterized by hypercalcemia with elevated parathyroid hormone (PTH). In India, the known genetic causes of familial forms of PHPT such as multiple endocrine neoplasia 1 (MEN1), MEN2A, MEN4, hyperparathyroidism-jaw tumour syndrome and familial isolated hyperparathyroidism has been published in the form of few case reports, however, there is no comprehensive study of genetic analysis of sporadic and familial PHPT cases till now.Aim: To establish an Indian database of both germline and somatic variants in 18 genes panel of parathyroid tumour and its validation through PCR array.Methods: 20 PHPT patients and 5 normal were recruited. Post operatively, histopathological characteristics were checked for parathyroid tumours by H & E staining of the respective patients followed by their demographic, clinical and biochemical profile. Further, the blood and tissue samples were analysed for germline and somatic variants respectively through targeted next generation sequencing. Also, real-time PCR array of the respective genes was performed keeping 18S as housekeeping gene.Results: The mean age of the patients recruited was 43.50 +/- 12.6 years with sporadic: familial ratio of 15:5. Clinical manifestations were bone pain, renal stone disease, fractures and osteoporosis. Biochemically, the corrected serum calcium (11.3 +/- 1.4 mg/dL), vitamin D (27.7 +/- 16.3 ng/ml), serum PTH (1058 +/- 1029 pg/ml), and phosphorus (3.8 +/- 4.4 mg/dL) levels were fluctuated in comparison to control. For genetic analysis, libraries for both germline and somatic samples were prepared in two different pools generating ~20 GB and ~60 GB respectively. Using in-silico approaches, two germline frameshift and non-synonymous pathogenic mutations were observed in MEN1 gene. A total of 7 somatic mutations have been observed out of which 2 were non-synonymous likely pathogenic and 1 stop gain mutations in EZH2 gene; 2 non-synonymous likely pathogenic mutations in GNA11 gene; 1 stop gain pathogenic mutation both in MEN1 and CASR genes respectively. Finally, the gene expression of MEN1, EZH2 and GNA11 genes was upregulated and CASR was downregulated in parathyroid tumours.Conclusion: It is the first comprehensive study of identification of somatic and germline variants in parathyroid tumours in Indian patients which might lead to design a DNA based targeted gene panel to be used as clinical diagnostic method for sporadic or familial PHPT.

ABSTRACT

Title: Targeted next generation sequencing of germline and somatic mutations in primary hyperparathyroidism Indian patients and evaluation of their gene expression

Authors: **Sheenam Garg**, Poonam Kumari, Ashutosh Kumar Arya, Rimesh Pal, Naresh Sachdeva, Ritambhara Nada, Divya Dahiya, Sanjay Kumar Bhadada, Sudhaker D. Rao

Corresponding Author: *Sanjay Kumar Bhadada, Professor and Head, Department of Endocrinology, PGIMER, Chandigarh - 160012

Background: Primary hyperparathyroidism (PHPT) is characterized by hypercalcemia with elevated parathyroid hormone (PTH). In India, the known genetic causes of familial forms of PHPT such as multiple endocrine neoplasia 1 (MEN1), MEN2A, MEN4, hyperparathyroidism-jaw tumour syndrome and familial isolated hyperparathyroidism has been published in the form of few case reports, however, there is no comprehensive study of genetic analysis of sporadic and familial PHPT cases till now.

Aim: To establish an Indian database of both germline and somatic variants in 18 genes panel of parathyroid tumour and its validation through PCR array.

Methods: 20 PHPT patients and 5 normal were recruited. Post operatively, histopathological characteristics were checked for parathyroid tumours by H & E staining of the respective patients followed by their demographic, clinical and biochemical profile. Further, the blood and tissue samples were analysed for germline and somatic variants respectively through targeted next generation sequencing. Also, real-time PCR array of the respective genes was performed keeping 18S as housekeeping gene.

Results: The mean age of the patients recruited was 43.50 ± 12.6 years with sporadic: familial ratio of 15:5. Clinical manifestations were bone pain, renal stone disease, fractures and osteoporosis. Biochemically, the corrected serum calcium (11.3 ± 1.4 mg/dL), vitamin D (27.7 ± 16.3 ng/ml), serum PTH (1058 ± 1029 pg/ml), and phosphorus (3.8 ± 4.4 mg/dL) levels were fluctuated in comparison to control. For genetic analysis, libraries for both germline and somatic samples were prepared in two different pools generating ~20 GB and ~60 GB respectively. Using *in-silico* approaches, two germline frameshift and non-synonymous pathogenic mutations were observed in MEN1 gene. A total of 7 somatic mutations have been observed out of which 2 were non-synonymous likely pathogenic and 1 stop gain mutations in EZH2 gene; 2 non-synonymous likely pathogenic mutations in GNA11 gene; 1 stop gain pathogenic mutation both in MEN1 and CASR genes respectively. Finally, the gene expression of MEN1, EZH2 and GNA11 genes was upregulated and CASR was downregulated in parathyroid tumours.

Conclusion: It is the first comprehensive study of identification of somatic and germline variants in parathyroid tumours in Indian patients which might lead to design a DNA based targeted gene panel to be used as clinical diagnostic method for sporadic or familial PHPT.

***Disclosures: Sheenam Garg**, None*

SAT-192

Sea Snails Conotoxins As Bone Remodeling Therapeutic Agents *Brenda Iduarte-Frias[1], Pavel Galindo-Torres[1], Claudia Ventura-Lopez[1], Johanna Bernaldez-Sarabia[1], Alexei Licea-Navarro[1], Pierrick Fournier[2], Patricia Juarez[3]. [1]Centro de Investigación Científica y de Educación Superior de Ensenada (CICESE), Mexico. [2]Centro de Investigacion Cientifica y de Educacion Superior de Ensenada (CICESE), Mexico. [3]Center for Scientific Research and Higher Education, Mexico

Disruption of the normal cycle of bone renewal causes an excess of bone producing high bone mass and bone fragility diseases, including osteosarcoma and bone metastases. New molecules that modulate bone remodeling are needed. Conotoxins, small peptides from the venom sea snails, exhibit high affinity and selectivity for ion channels, and transporters are also present in bone cells. Thus, we characterize the effects of two synthetic conotoxins on bone cells and their microenvironment.Transcriptomic analysis of osteoblast treated with conotoxin revealed a significant down-regulation of multiple genes associated with Gene Ontology categories such as “ossification”, “bone development”, “bone mineralization”, and “osteoblast differentiation”. In vitro, conotoxins decreased the mineralization of mice osteoblasts and increased the differentiation of mouse bone marrow cells into osteoclasts by RANKL and M-CSF. In contrast, osteoclast resorption activity was significantly increased (p=0.0003). Cultures without RANKL demonstrated that this pro-osteoclastic effect was RANKL-dependent.RT-qPCR revealed that conotoxins modulated the expression of nAChR on bone cells and downregulated the expression of osteoblastic genes like Runx2, Alpl, and Col1a1. In contrast, osteoclastic genes such as Nfatc1 and Rank were upregulated. Conotoxins treatment in osteocyte-enriched bone significantly increased gene expression of Dmp1, Mepe, Rankl, Sost, and nAChR.Lastly, We tested the effect of conotoxins on an ex vivo calvaria culture model. Histological analysis of calvaria treated with conotoxins indicated a significant decrease in the bone area (p=0.0053) and an increase in the number of osteoclasts associated with a reduction in the expression of Runx2, and increased Rankl/Opg ratio, Ctsk, and Sost expression levels.Our results indicate that the evaluated conotoxins can disrupt bone remodeling, affecting bone cell differentiation and activity in vitro and ex vivo. These results support the potential use of conotoxins as a therapeutic strategy for bone-related diseases, particularly those characterized by excessive bone formation.

***Disclosures: Brenda Iduarte-Frias**, None*

SAT-194

Aberrant Expression Of Polycomb Repressive Complex 2 Key Components EZH2/EED/SUZ12 And Its Clinical Correlation In Patients With Sporadic Primary Hyperparathyroidism. *Poonam Kumari[1], Sheenam Garg[2], Ashutosh Kumar Arya[3], Naresh Sachdeva[4], Divya Dahiya[5], Uma Nahar Saikia[6], Sanjay Kumar Bhadada[7], Sudhaker Rao[8]. [1]Ph.D Student, Department of Endocrinology, PGIMER, India. [2]Research Associate I, Department of Endocrinology, PGIMER, India. [3]Assistant Professor, Endocrinology & Metabolism, AIIMS, India. [4]Professor, Department of Endocrinology,PGIMER, , India. [5]Professor, Department of General Surgery, PGIMER, , India. [6]Professor, Department of Histopathology, PGIMER, , India. [7]PGIMER, chandigarh, India, India. [8]Henry Ford Hospital, United States

Introduction Primary hyperparathyroidism, a common endocrine disorder characterized by hypercalcemia and elevated parathyroid hormone. Recently, an epigenetic modification was found to play a pivotal role in gene silencing in PHPT patients. Among these factors, the polycomb group (PcG) proteins encompassing enhancer of zeste 2 (EZH2), embryonic ectoderm development (EED), and suppressor of zeste 12 homolog (SUZ12) was found to regulate gene activity at the chromatin level through histone modifications having a crucial role in tumor development. The lacunae exist in the expression and mechanisms by which PRC2 repress target genes in PHPT. Therefore, this study has been designed to investigate the clinical and prognostic significances of EZH2, EED and SUZ12 in PHPT patients. ObjectiveTo analyse the gene and protein expression of PRC2 complex key components (EZH2, EED, SUZ12) and its clinico-pathological correlation in patients with sporadic parathyroid tumorsMethodologyA total of 40 parathyroid tumors (25 non-aggressive and 15 aggressive and 5 normal parathyroid tissues samples) were collected in this study. mRNA and protein expression analysis of PRC2 components (EZH2, EED, SUZ12) was evaluated by quantitative real-time PCR and immunohistochemistry respectively.ResultsWe found that overall mRNA expression of EZH2 with mean fold change [Mean+/-S.E; (9.1+/-1.6 vs 1.2 +/-0.3, p=0.005), EED; (6.1+/-1.0 vs 1.5+/-0.5,p=0.01) and SUZ12; (4.9+/-0.9 vs 0.95+/-0.2,p=0.02)] was significantly increased in aggressive PHPT and non -significantly in non-aggressive [EZH2; (4.2+/-2.7 vs 1.2 +/-0.3, p=0.4), EED (2.1+/-1.9 vs 1.5+/-0.5,p=0.9), SUZ12 (2.6+/-1.6 vs 1.2 +/-0.3,p=0.5)] in comparison to normal parathyroid tissues. This increase in EZH2 expression is statistically correlated with serum calcium (p=0.0002), PTH levels (p=0.006) and tumor weight (p=0.005). Moreover, EED (p=0.03) and SUZ12 mRNA expression (p=0.05) was also directly associated with elevated PTH levels in aggressive parathyroid tumors. Furthermore, the protein expression is also consistent with the gene expression having 90% nuclear positive of EZH2 , 80% nuclear positive of EED and SUZ12 (50% cytoplasmic and membranous positivity) in aggressive parathyroid tumors in comparison to normal parathyroid gland (negative staining).ConclusionsThis was the first expression study that elucidated the high expression of EZH2, EED and SUZ12 components that might contribute to the parathyroid tumorigenesis.

Title: Aberrant Expression of Polycomb Repressive Complex 2 Key Components EZH2/EED/SUZ12 And Its Clinical Correlation In Patients With Sporadic Primary Hyperparathyroidism.

Authors: **Poonam Kumari**, Sheenam Garg, Ashutosh Kumar Arya, Naresh Sachdeva, Divya Dahiya, Uma Nahar Saikia, Sanjay Kumar Bhadada, Sudhaker D. Rao
Corresponding Author: *Sanjay Kumar Bhadada, Professor& Head, Department of Endocrinology, PGIMER, Chandigarh-160012

Introduction
Primary hyperparathyroidism, a common endocrine disorder characterized by hypercalcemia and elevated parathyroid hormone. Recently, an epigenetic modification was found to play a pivotal role in gene silencing in PHPT patients. Among these factors, the polycomb group (PcG) proteins encompassing enhancer of zeste 2 (EZH2), embryonic ectoderm development (EED), and suppressor of zeste 12 homolog (SUZ12) was found to regulate gene activity at the chromatin level through histone modifications having a crucial role in tumor development. The lacunae exist in the expression and mechanisms by which PRC2 repress target genes in PHPT. Therefore, this study has been designed to investigate the clinical and prognostic significances of EZH2, EED and SUZ12 in PHPT patients.

Objective
To analyse the gene and protein expression of PRC2 complex key components (EZH2, EED, SUZ12) and its clinico-pathological correlation in patients with sporadic parathyroid tumors

Methodology
A total of 40 parathyroid tumors (25 non-aggressive and 15 aggressive and 5 normal parathyroid tissues samples) were collected in this study. mRNA and protein expression analysis of PRC2 components (EZH2, EED, SUZ12) was evaluated by quantitative real-time PCR and immunohistochemistry respectively.

Results
We found that overall mRNA expression of EZH2 with mean fold change [Mean±S.E; (9.1±1.6 vs 1.2 ±0.3, p=0.005), EED; (6.1±1.0 vs 1.5±0.5,p=0.01) and SUZ12; (4.9±0.9 vs 0.95±0.2,p=0.02)] was significantly increased in aggressive PHPT and non -significantly in non-aggressive [EZH2; (4.2±2.7 vs 1.2 ±0.3, p=0.4), EED (2.1±1.9 vs 1.5±0.5,p=0.9), SUZ12 (2.6±1.6 vs 1.2 ±0.3,p=0.5)] in comparison to normal parathyroid tissues. This increase in EZH2 expression is statistically correlated with serum calcium (p=0.0002), PTH levels (p=0.006) and tumor weight (p=0.005). Moreover, EED (p=0.03) and SUZ12 mRNA expression (p=0.05) was also directly associated with elevated PTH levels in aggressive parathyroid tumors. Furthermore, the protein expression is also consistent with the gene expression having 90% nuclear positive of EZH2 , 80% nuclear positive of EED and SUZ12 (50% cytoplasmic and membranous positivity) in aggressive parathyroid tumors in comparison to normal parathyroid gland (negative staining).

Conclusions
This was the first expression study that elucidated the high expression of EZH2, EED and SUZ12 components that might contribute to the parathyroid tumorigenesis.

***Disclosures: Poonam Kumari**, None*

SAT-195

Effect of the Bone-Targeted Prostaglandin E2 Receptor 4 Agonist Mes-1022 on a Rat Model of Duchenne Muscular Dystrophy *Juliana Marulanda[1], Ashok Narasimhan[2], Lin Yi[2], Katie Day[2], Keitaro Yamanouchi[3], Fabio MV Rossi[2], Frank Rauch[1]. [1]Shriners Hospital for Children, McGill Univeristy, Canada. [2]School of Biomedical Engineering, University of British Columbia, Canada. [3]Department of Veterinary Physiology, Graduate School of Agricultural and Life Sciences, The University of Tokyo, Japan

Background: Duchenne muscular dystrophy (DMD) is a devastating muscle disorder that also leads to bone loss and fractures. In this study, we characterized bone mass in a rat model of DMD and performed treatment studies with a novel bone anabolic drug, Mes-1022, a bone-targeting prostaglandin E2 receptor EP4 agonist.Methods: The bone phenotype of CRISPR/CAS9-generated male DMD rats (Nakamura et al. Sci Rep. 2014;4:5635) was analyzed by microCT at various ages. Vehicle or Mes-1022 (3mg per kg body mass) was administered subcutaneously once a week for 8 weeks, starting at 30 weeks of age.Results: We found that, compared to wild type littermates, DMD rats had consistently lower trabecular bone mass at the distal femur at 1, 3, 6 and 9 months of age, becoming significant at 6-9 months. No differences were detected in the midshaft femur periosteal and endosteal diameter at any timepoint, but cortical thickness was slightly higher in 9-month-old DMD rats than in controls. Treatment with Mes-1022 was associated with significantly increased amounts of trabecular bone, both at the distal and the midshaft femur. At the distal femur, trabecular bone volume was markedly increased in the treated group, due to a higher trabecular number, whereas trabecular thickness was similar between groups. At the midshaft femur, cortical geometry (periosteal diameter, endosteal parameter and cortical thickness) was similar in Mes-1022 and vehicle-treated rats, but cortical porosity and trabecular bone volume were higher in rats that had received Mes-1022.Conclusion: The DMD rat appears to be a suitable model for bone-targeting treatment studies. Treatment with Mes-1022 was associated with a markedly higher trabecular bone mass at the femur. Mes-1022 warrants further study for the treatment of DMD-associated bone disease.

***Disclosures: Juliana Marulanda**, None*

SAT-196

Differences Between the Effects of Anti-Catabolic and Anabolic Treatments on Bone in Adult Ovariectomized Rats *Jukka Morko[1], Jukka Vaaraniemi[1], Katja M. Fagerlund[1], Mari I. Suominen[1], Jukka P. Rissanen[1]. [1]Pharmatest Services Ltd, Finland

Human osteoporosis is a systemic skeletal disease characterized by low bone mass, deterioration of bone microarchitecture, and increased risk for fractures. Effective osteoporosis therapies are available including various anti-catabolic and anabolic agents. These treatments have been associated with adverse effects on the skeleton, including atypical fractures and osteosarcoma. Therefore, new therapies are needed with improved efficacy/safety ratio. In nonclinical efficacy studies, ovariectomized (OVX) rats suffering from osteopenia are used as the major small animal model of human postmenopausal osteoporosis. In this study, we compared the effects of anti-catabolic and anabolic treatments on bone in more detail in adult OVX rats. Nitrogen-containing bisphosphonate zoledronate (ZOL) was used as the anti-catabolic agent and recombinant human parathyroid hormone (PTH) analog (1-34) as the anabolic agent. Female Sprague-Dawley rats were ovariectomized or Sham-operated at 6 months of age. OVX rats were treated subcutaneously with ZOL at 20 ?g/kg, PTH(1-34) at 40 ?g/kg/d or vehicle, and Sham-operated rats with vehicle for 2 months. Treatment effects were evaluated by peripheral quantitative computed tomography, bone histomorphometry, bone ash weight determination, biomechanical testing, and the measurements of bone turnover biomarkers. Surgical OVX operation decreased the amount of metaphyseal trabecular bone, and enhanced osteoclastogenesis, bone resorption, and bone formation on the trabecular surface and bone formation on the periosteal surface. Both ZOL and PTH(1-34) prevented the OVX-induced reduction in the amount of metaphyseal trabecular bone and the OVX-induced enhancement of osteoclastogenesis on the trabecular surface as well as increased ash weight in the femur and tibia. ZOL prevented and PTH(1-34) enhanced the OVX-induced increase in bone formation on the trabecular surface. PTH(1-34) enhanced the OVX-induced increase in bone formation on the periosteal surface, increased the amount of diaphyseal cortical bone and bone formation on the endocortical surface, and improved bone strength in the femoral neck and tibial shaft. This study demonstrated significant differences between the effects of anti-catabolic ZOL and anabolic PTH(1-34) treatments on bone in adult OVX rats. The anabolic PTH(1-34) treatment was more potent, also increasing the amount of diaphyseal cortical bone and improving bone strength in the femoral neck and long bone diaphysis.

***Disclosures: Jukka Morko**, None*

SAT-197

Sclerostin-neutralizing antibody reverses alveolar bone loss and promotes periodontium repair in type 2 diabetes *Xue Yuan[1], Hakan Turkkahraman[2], Shannan Flanagan[1], Tianli Zhu[2], Nisreen Akel[3], Silvia Marino[4], Dayane Ortega-Gonzalez[1], Teresita Bellido[5]. [1]Indiana University School of Medicine, United States. [2]Indiana University School of Dentistry, United States. [3]University of Arkansas for Medical Sciences, United States. [4]University of Arkansas, United States. [5]University of Arkansas for Medical Sciences , United States

Type 2 diabetes (T2D) is on the rise worldwide and is associated with several complications of the oral cavity. Developing an appropriate model of adult-onset T2D is essential to identifying novel approaches for treating diabetes-induced oral diseases. We recently established a T2D mouse model in the setting of high-fat diet (HFD) feeding and streptozotocin (STZ) injection, allowing for both environmental as well as temporal control of T2D onset. Utilizing this adult-onset diabetes model, we characterized the periodontal alterations in mice eight weeks after T2D was established. T2D mice had inflamed gingiva with increased immune cells, disintegrated periodontal ligaments (PDL) with reduced cell numbers and osteogenic potential, and overwhelming alveolar bone loss with unbalanced bone formation and resorption. Further, the Wnt signaling inhibitor sclerostin was elevated in the T2D mice. Thus, we investigated whether a sclerostin-neutralizing antibody (Scl-Ab) could rescue the periodontium in T2D mice. Four weeks after T2D was established, Scl-Ab was administered subcutaneously once a week for four weeks. Scl-Ab significantly increased bone mass by inhibiting osteoclasts and promoting osteoblasts in both control and T2D mice, completely rescuing the bone loss under the T2D condition. Scl-Ab treatment also stimulated PDL cell proliferation, partially rescued the PDL fibers, and suppressed the inflammation in the periodontium. Additionally, the Scl-Ab treatment slightly enlarged the edentulous bone and mandible but displayed a minimal effect on the premaxillary suture. In conclusion, our results describe a novel T2D-induced periodontitis model in mice characterized by inflammation and tissue degeneration. Systemic administration of Scl-Ab effectively reverses the detrimental effects of T2D on the periodontium while displaying minor effects on other craniofacial hard tissues.

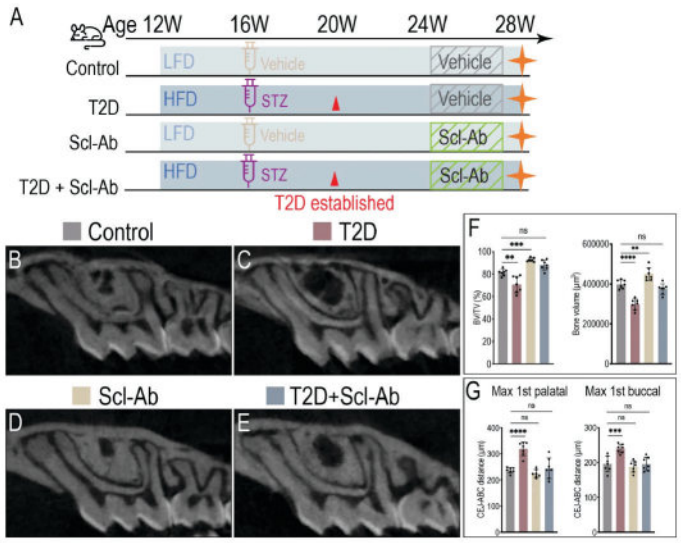

Figure 1

***Disclosures: Xue Yuan**, None*

SAT-198

Deficiency of Trps1 in Osteoblasts and Cementoblasts-compromises Formation of Alveolar Bone and Cementum *Kaoru Fujikawa[1] Mairobys Socorro[1] Priyanka Hoskere[1] Catherine Roberts[1] Lyudmila Lukashova[1] Konstantinos Verdelis[1] Dobrawa Napierala[1] [1]University of Pittsburgh, United States

Objectives: Trichorhinophalangeal syndrome (TRPS) is caused by heterozygous mutations in the TRPS1 gene, which encodes a GATA-type transcription factor. TRPS is characterized by abnormal skeletal, craniofacial, and dental development, including delayed development of endochondral bones and small mandible. TRPS1 has been also associated with bone mineral density and periodontal disease risk by genome-wide association studies. Periodontium comprises two mineralized tissues - alveolar bone and cementum, ligament that connects them, and the gingiva. Proper function of the periodontium depends on its structural integrity. However, the role of Trps1 in the development and homeostasis of the periodontium is unknown. Since Trps1 is expressed is osteoblasts and cementoblasts, we hypothesized that Trps1 supports formation of bone and cementum by regulating expression of genes critical for the formation of these tissues.Methods: We compared alveolar bone and tooth roots of 1st mandibular molars of 4wk old WT and Trps1col1a1 cKO mice (N=5/genotype/sex) by micro-Computed Tomography (µCT), histology, and immunohistochemistry.Results: µCT analyses revealed significantly lower alveolar bone volume, and shorter and thinner tooth roots in Trps1Col1a1 cKO compared with WT mice. Semi-quantitative histological analyses detected reduced the cellular cementum area and unevenly distributed cementoblasts (?III Tubulin-positive cells) in Trps1Col1a1 cKO mice compared to WT mice. There were fewer Osterix-positive cells on the surface of the alveolar bone and cementum in Trps1Col1a1 cKO mice. Moreover, we detected decreased levels of tissue-nonspecific alkaline phosphatase (TNAP) in alveolar bone, cementum, and periodontal ligament in Trps1Col1a1cKO mice. Bone sialoprotein (Bsp) was unevenly distributed and accumulated in the margin of the alveolar bone matrix in Trps1Col1a1 cKO mice, while there was no difference in the Bsp distribution in the cementum. Picrosirius staining revealed impaired organization of collagen fibers in periodontal ligaments in Trps1Col1a1 cKO mice.Conclusions: Trps1 transcription factor supports expression of key proteins required for proper formation of the alveolar bone, cementum, and the structure of the periodontium, hence highlight the importance of Trps1 for the function of osteoblasts and cementoblasts. Our data suggest that the compromised periodontal structure in Trps1 deficiency is the contributing factor to predisposition to periodontal disease.

***Disclosures: Kaoru Fujikawa**, None*

SAT-199

Spatial transcriptomics identified in vivo FGF23 and CKD-mediated transcriptional reprogramming within distinct kidney nephron segments *Lainey Hibbard[1] Sheng Liu[1] RAFIOU AGORO[1] Yamil Marambio[1] Kayleigh Jennings[1] Steven Welc[1] Jun Wan[1] Kenneth White[1] [1]Indiana University School of Medicine, United States

Background: Osteocyte-secreted FGF23 acts in the kidney via Klotho (KL) to control phosphate metabolism. However, in CKD, KL is lost and FGF23 is pathologically increased, disrupting mineral homeostasis. KL is expressed in multiple nephron segments, thus localization of FGF23 actions on intra-nephron regions remain unclear. Herein, we tested for novel FGF23 bioactivity localized with KL, as well as hypothesized that CKD alters FGF23/KL signaling and causes spatially unique transcriptional reprogramming.Methods: Visium spatial transcriptomics (ST) was performed on kidney sections from normal mice injected with FGF23 (250 ng/kg) for 1 or 4 h, and male mice with adenine diet induced CKD (0.2% for 4 weeks).Results: The FGF23-injected and CKD kidney sections had >6900 genes/sequencing spot and formed 12 and 10 UMAP cell clusters, respectively. Mapping nephron segment-specific markers showed clear demarcation of cortical and medullary gene expression. Proximal tubule S1/S2 marker Slc5a2 was highly expressed in the cortex, and S3 marker Eci3 localized to the outer stripe of the medulla (OSOM). FGF23 increased MAPK-dependent transcription factor Egr1 more at 1 h (2.3 log2-fold) compared to 4 h (1.2 log2-fold). The vitamin D metabolic enzymes Cyp24a1 and Cyp27b1 mRNAs were increased (2.3 log2-fold) or decreased (22%), respectively, at 4 h and overlapped with KL. The ST data were validated by qPCR as well as in independent kidney scRNAseq data from FGF23-injected mice. We also identified novel changes in response to FGF23, including increased Cyp4b1 in the cortex at 4 h, which decreases in CKD. Mice with CKD had a 55% reduction in KL mRNA and increased Cyp27b1. Consistent with CKD fibrosis, Col1a1, -1a2, -3a1, and -4a1 were ubiquitously increased, although Col3a1 was more focused to the inner stripe of the medulla (ISOM). Further, pro-fibrotic Tgfb1 broadly increased, whereas its target Mmp7 was elevated in the ISOM. In contrast, the damage and injury markers C3 and Havcr1 were restricted to the cortex and OSOM, respectively. Finally, evidence of wider immune infiltration was present in CKD with increased neutrophil marker Lcn2, and macrophage markers Cd68 and Ptprc.Conclusion: Using ST, we identified unbiased, spatially identifiable effects of FGF23 bioactivity in kidney, including potentially new FGF23 targets. This approach also localized pathologic KL-dependent and -independent CKD gene alterations that differentially occur within distinct cell populations.

***Disclosures: Lainey Hibbard**, None*

SAT-202

The Effects of Nfi-C Epithelium-Specific Deletion on Ameloblast Differentiation *Joo-Cheol Park[1] Hyun-Sook Bae[2] Si Hyoung Ki[1] [1]Department of Oral Histology-Developmental Biology, School of Dentistry and Dental Research Institute, Seoul National University, Republic of Korea [2]Department of Oral Hygiene, Namseoul University, Cheonan, Republic of Korea, Republic of Korea

Rodent incisors continuously grow throughout their whole life. This growth is made by the complicated interactions between epithelium and ectomesenchyme during tooth formation. The Nuclear factor I (NFI) family consists of four genes (NFI-A, NFI-B, NFI-C, and NFI-X). In our previous research, we found that conventional Nfic Knock-Out (KO) mice exhibited defective phenotypes in molar roots and incisor. Furthermore, Nfic is necessary for maintaining the stem cell population in several mineralized tissues by controlling Sox2 expression. continuously The purpose of this study is to compare phenotypes of Nficfl/fl, K14-Cre;Nficfl/-(Hemi), and K14-Cre;Nficfl/fl (Homo) to clarify the mechanism of Nfic-mediated tooth formation.To investigate the phenotypic changes in epithelium-specific Nfic KO mice, K14-Cre;Nficfl/-, and K14-Cre;Nficfl/fl mice were generated using the Cre-loxP system. Histological analysis was performed using microscope.1-month-old K14-Cre;Nficfl/-, and K14-Cre;Nficfl/fl mice did not exhibit any morphogenetic changes in their teeth, including dentin. However, In the 6-months-old K14-Cre;Nficfl/- and K14-Cre;Nficfl/fl mice, incisor pulp space was narrowed compared to Nficfl/fl mice, respectively. Compared to Nficfl/fl mice mature ameloblasts of K14-Cre;Nficfl/- mice exhibited lost their polarity, and mature ameloblasts of K14-Cre;Nficfl/fl showed flatten shape.Our findings suggest that Nfic deficiency in dental epithelium could alter late-stage ameloblast differentiation.

***Disclosures: Joo-Cheol Park**, None*

SAT-203

The Vitamin D Receptor (VDR) in Osteoblastic Cells but Not Parathyroid Hormone (PTH) Secretion Is Critical for Soft Tissue Calcification Induced by the Proresorptive Activity of 1,25(OH)2D3 *Yuko Nakamichi[1] Ziyang Liu[2] Tomoki Mori[2] Zhifeng He[3] Hisataka Yasuda[4] Naoyuki Takahashi[3] Nobuyuki Udagawa[5] [1]Matsumoto Dental University, Japan [2]Graduate School of Oral Medicine, Matsumoto Dental University, Japan [3]Institute for Oral Science, Matsumoto Dental University, Japan [4]Oriental Yeast Co., Ltd., Japan [5]Department of Biochemistry, Matsumoto Dental University, Japan

VDR is expressed most abundantly in osteoblasts and osteocytes (osteoblastic cells) in bone, and regulates bone resorption and calcium (Ca) and phosphate (P) homeostasis in concert with PTH. We reported that near-physiological doses of vitamin D analogs suppressed bone resorption through VDR in osteoblastic cells (JBMR 2017). We also reported that supra-physiological doses of 1?,25-dihydroxyvitamin D3 [1,25(OH)2D3] increased bone resorption, serum Ca and FGF23 levels, and decreased the body weight via VDR in osteoblastic cells. Serum P levels tended to increase but did not significantly elevate (Endocrinology 2020). The present study demonstrated that the latter, a proresorptive dose of 1,25(OH)2D3, induced soft tissue calcification through VDR in osteoblastic cells. Excess amounts of vitamin D affect various organs and induce ectopic calcification, with increases in bone resorp-

tion, serum Ca and FGF23 levels, and decreases in body weight. Such a wide range of symptoms is called as hypervitaminosis D, which is caused by not only too much intake of vitamin D but also malfunctions of vitamin D metabolism and diseases that produce 1,25(OH)2D3 ectopically. To clarify a biological process hierarchy in hypervitaminosis D, a proresorptive dose of 1,25(OH)2D3 was administered to wild-type mice whose bone resorption was suppressed with neutralizing anti-RANKL antibody. Proresorptive doses of 1,25(OH)2D3 increased the serum Ca x P product, induced calcification of the aortas, lungs, and kidneys, and decreased serum PTH levels in the control-IgG pretreated wild-type mice. Pretreatment of wild-type mice with anti-RANKL antibody did not affect the down-regulation of PTH levels by 1,25(OH)2D3, but inhibited the increase in the serum Ca x P product and soft tissue calcification induced by 1,25(OH)2D3. Consistent with the effects of anti-RANKL antibody, VDR ablation in osteoblastic cells also did not affect the down-regulation of PTH levels by 1,25(OH)2D3, but inhibited 1,25(OH)2D3-induced increase of the serum Ca x P product and calcification of soft tissues. These data suggest that bone resorption induced by VDR signaling in osteoblastic cells is crucial for the pathogenesis of hypervitaminosis D, but PTH is not relevant to it. These findings indicate that the use of bone resorption inhibitors is a treatment option not only for patients with hypervitaminosis D but also for patients with other diseases having complications of hypercalcemia and ectopic calcification.

***Disclosures: Yuko Nakamichi**, None*

SAT-205

Multi-Trait Analysis of Mineral Metabolism Markers Identifies Novel Genetic Associations for PTH *Nicholas Vartanian[1], Cassianne Robinson-Cohen[1], Elvis Akwo[1]. [1]Vanderbilt University Medical Center, United States

Introduction: Genome-wide association studies (GWAS) have identified numerous genetic loci associated with mineral metabolism markers but have exclusively focused on single-trait analysis. In this study, we performed a multi-trait analysis of GWAS data of mineral metabolism markers, exploring overlapping genetic architecture between the traits, to identify novel genetic associations for parathyroid hormone.Methods: We applied multi-trait analysis of GWAS (MTAG) to genetic variants common to GWAS of 5 genetically correlated mineral metabolism markers (phosphorus, fibroblast growth factor-23, calcium, 25-hydroxyvitamin D and PTH) in European-ancestry subjects. We integrated information from the UKBioBank GWAS for phosphate and calcium (n=366,484), and two GWAS from the CHARGE consortium for PTH (n=29,155) and FGF23 (n=16,624).Results: MTAG increased the effective sample size for all mineral metabolism markers, to over 50,000 for PTH. After clumping, MTAG identified independent genome-wide significant SNPs for all traits, including 47 loci for PTH. Many of these loci have not been previously reported in single-trait analyses, including loci involved in inflammation, lipid metabolism, glucose metabolism, and bone health.Conclusions: MTAG boosted the number of genome-wide significant loci PTH. Our findings highlight the importance of performing multi-trait analysis in GWAS studies of mineral metabolism markers to identify novel genetic associations. These genetic loci may provide insight into the biological mechanisms underlying mineral metabolism and may have implications for the development of therapies for mineral-related disorders.

***Disclosures: Nicholas Vartanian**, None*

SAT-206

See Friday Plenary Number FRI-206

SAT-207

Local activation of endogenous glucocorticoids by 11?-hydroxysteroid dehydrogenase type 1 in bone contributes to musculoskeletal decline during aging *HUSAM BENSRETI[2], DIMA ALHAMAD[2], KANGLUN YU[2], Wendy B. Bollag[3], Mark W. Hamrick[4], Carlos Isales[5], Meghan McGee-Lawrence[6, 2], United States[, 2], , [3]Department of Physiology Medical College of Georgia at Augusta University , United States[, 4]Department of Cellular Biology and Anatomy, Medical College of Georgia at Augusta University, , United States[, 5]Augusta University, United States[, 6]Medical College of Georgia, Augusta University, United States

Glucocorticoids (GCs) have been implicated in the fate of BMSCs differentiating into osteogenic vs. adipogenic lineages. Unlike most signaling mechanisms, GC signaling has an additional layer of regulation in the form of enzymes 11?-hydroxysteroid dehydrogenase type 1 and 2 (Hsd11b1/2) that control local GC activation and downstream signaling. The current study explored the role of Hsd11b1 in the aging skeleton. Hsd11b1 expression was measured by qPCR in cortical bone from wildtype (WT) mice at 12 and 23 mo of age. BMSC and sorted MSCs (Sca1+ / CD29+ / CD44+) from 22 mo old mice were treated with an Hsd11b1 inhibitor (385581) for 21 days in osteogenic media and mineralization was evaluated with Alizarin red. Hsd11b1 floxed mice were crossed with Osx-Cre to generate Hsd11b1-WT and osteoprogenitor-targeted Hsd11b1 conditional knockout (Hsd11b1-CKO) mice. Mice were raised on doxycycline until 3 mo of age to negate the developmental impact of Osx Cre. Musculoskeletal phenotype data were collected at 21 mo of age. Muscle endurance was measured via hang time and muscle strength and fatigue via grip strength meter (Bioseb). Body composition and BMD were measured via DXA. Groups were compared by t-tests or two-way ANOVA as appropriate. Hsd11b1 was significantly up-regulated in bone from aged mice, with a 20-fold increase over adult animals (p=0.04), and osteoblasts from aged mice exhibited enhanced mineralization with pharmacological Hsd11b1 inhibition. Osx-Cre-mediated recombination of Hsd11b1 was seen in bone but not off-target tissues such as skeletal muscle, liver, kidney, spleen, or white or brown fat depots. Whole-body BMD was 12% higher in aged CKO as compared to WT littermate mice, suggesting a beneficial impact from the loss of Hsd11b1 activity on the skeleton. While DXA revealed no effect of Osx-Cre-mediated Hsd11b1 knockdown on whole body composition, brown fat pads tended to be smaller in the CKO mice, and aged CKO mice had higher muscle endurance and lower muscle fatigue score as measured by forelimb muscle grip testing (p=0.002). While we previously saw no difference in fasting blood glucose levels between WT and CKO mice at 6 mo old, aged Hsd11b1 CKO mice exhibited elevated fasting blood glucose levels (p=0.02). These results suggest a crucial role of local GC activation by Hsd11b1 in bone homeostasis during aging and support the importance of local endogenous glucocorticoid signaling in mechanisms of skeletal crosstalk with other organ systems.

***Disclosures: HUSAM BENSRETI**, None*

SAT-208

Alterations in Soft Tissue Quality and Quantity in People Living with HIV *Zehra Akkaya[1], Katie Kenny[2], Jannis Bodden[3], Bo Fan[1], Isra Saeed[1], Phyllis Tien[4], Gabby Joseph[1], Thomas Link[1], Roland Krug[1], Galateia Kazakia[1]. [1]University of California, San Francisco, Department of Radiology and Biomedical Imaging, San Francisco, CA, United States[. 2]University of California Berkeley, Department of Biomedical Engineering, Berkeley, CA, United States[. 3]Technical University of Munich Diagnostic and Interventional Neuroradiology Clinic, Munich, Germany, Germany[. 4]University of California, San Francisco, Department of Medicine and Department of Veterans Affairs Medical Center, San Francisco, CA, United States

People living with HIV (PLWH) experience systemic and metabolic alterations particularly involving adipose tissues. Chronic HIV infection and earlier anti-retroviral therapy (ART) regimens were known to cause subcutaneous adipose tissue (SAT) loss. With contemporary ART, lipoatrophy is of less concern, while visceral adipose tissue (VAT) has become a growing concern. In addition to differences in quantity, density of adipose tissue, measured by quantitative computed tomography (QCT), was shown to be positively associated with inflammatory biomarkers in PLWH. Sarcopenia is characterized by deteriorated skeletal muscle quantity and function and is also associated with chronic inflammation. There are contradictory reports on HIV-associated sarcopenia.The aim of this study was to investigate the impact of HIV on 1) adipose tissue quality and quantity in the thigh and trunk, and 2) skeletal muscle quality and quantity in the thigh.This cross-sectional study included 109 participants (mean age=58.8+/- 4.93 years) comprised of 54 PLWH (40 M / 14 F; on stable long-term antiretroviral therapy) and 55 age-matched seronegative control subjects (SNC; 22 M / 33 F). QCT measurements of cross-sectional areas and densities of abdominal VAT and SAT and non-dominant thigh SAT and thigh muscles (total, quadriceps, and hamstrings) were obtained using in-house developed software built on the MIPAV platform. The impact of HIV serostatus on QCT measurements were investigated by linear regression models, adjusted for a) age, sex and race and b) age, sex, race, and BMI.VAT area and thigh SAT density were statistically significantly higher in PLWH in demographically adjusted models as well as models also adjusted for BMI (Table 1). Intramuscular quadriceps fat density was higher in PLWH but reached significance only in models additionally adjusted for BMI (p=0.038). Quadriceps total and lean areas were lower in both models in PLWH. Total thigh area and thigh muscle bundle area were lower in PLWH but reached significance only in models after BMI adjustment (p=0.012 and p=0.020, respectively).In conclusion, PLWH have higher adipose tissue density at the thigh, both subcutaneously and in the intramuscular quadriceps fat depots when compared to those without HIV. These may reflect increased inflammatory burden as a consequence of chronic HIV infection and ART. Being HIV seropositive is associated with lower total and lean muscle areas in the quadriceps which supports that chronic HIV infection may be associated with sarcopenia.

Table 1. The beta coefficient (β) represents the difference in the outcome measure of interest (i.e., total thigh area) between PLWH and SNC (reference group). Models are adjusted for age, sex, and race (a), and age, sex, race, and BMI (b). Bold indicates statistically significant results ($p < 0.05$).

	β (95% CI)	p-value a	β (95% CI)	p-value b
Total thigh area (cm^2)	-13.3 (-31.0, 4.4)	0.140	**-9.3 (-17.1, -1.5)**	**0.012**
Thigh SAT area (cm^2)	-5.3 (-18.8, 8.2)	0.439	-6.1 (-17.0, 4.7)	0.263
Thigh SAT density (HU)	**4.9 (2.1, 7.9)**	**0.001**	**5.1 (2.2,7.9)**	**0.001**
Thigh muscle bundle area (cm^2)	-8.7 (-18.1, 0.6)	0.067	**-9.3 (-1.7, -0.1)**	**0.020**
Thigh muscle bundle intramuscular fat area (cm^2)	-1.03 (-4.1, 2.0)	0.508	-1.2 (-3.7, 1.2)	0.329
Thigh muscle bundle intramuscular fat density (HU)	2.3 (-2.0, 6.7)	0.290	2.5 (-1.6, 6.6)	0.232
Thigh muscle bundle lean area (cm^2)	-7.7 (-16.5, 1.04)	0.084	-8.1 (-16.2, 0.05)	0.051
Thigh muscle bundle fat area (cm^2)	-0.84 (-3.12, 1.44)	0.467	-0.96 (-2.90, 0.98)	0.326
Thigh muscle bundle lean density (HU)	1.01 (-.66, 2.68)	0.235	1.06 (-0.54, 2.66)	0.190
Thigh muscle bundle fat density (HU)	1.75 (-1.69, 5.18)	0.315	1.88 (-1.30, 5.07)	0.243
Quadriceps total area (cm^2)	**-6.60 (-11.08, -2.12)**	**0.004**	**-6.62 (-10.76, -2.48)**	**0.002**
Quadriceps lean area (cm^2)	**-6.41 (-10.86, -1.97)**	**0.005**	**-6.43 (-10.68, -2.17)**	**0.003**
Quadriceps fat area (cm^2)	-0.08 (-0.46, 0.29)	0.625	-0.08 (-0.40, 0.23)	0.602
Quadriceps lean density (HU)	1.31 (-0.28, 2.90)	0.106	1.31 (-0.20, 2.83)	0.088
Quadriceps fat density (HU)	3.38 (-0.11, 6.88)	0.058	**3.46 (0.20, 6.73)**	**0.038**
Hamstring total area (cm^2)	0.75 (-1.67, 3.17)	0.539	0.65 (-1.58, 2.88)	0.564
Hamstring lean area (cm^2)	1.23 (-1.07, 3.53)	0.290	1.18 (-1.07, 3.43)	0.301
Hamstring fat area (cm^2)	-0.46 (-1.21, 0.30)	0.235	-0.49 (-1.20, 0.23)	0.179
Hamstring lean density (HU)	1.54 (-0.95, 4.02)	0.135	1.60 (-0.83, 4.03)	0.194
Hamstring fat density (HU)	4.31 (-0.88, 9.50)	0.103	4.57 (-0.35, 9.50)	0.068
Visceral adipose tissue area (cm^2)	**46.80 (18.52, 75.08)**	**0.001**	**45.03 (22.42, 67.64)**	**<0.001**
Abdominal SAT area (cm^2)	2.10 (-45.69, 49.89)	0.931	-1.85 (-30.77, 27.07)	0.899
Visceral adipose tissue density (HU)	-0.96 (-4.53, 2.62)	0.597	-0.74 (-3.68, 2.19)	0.617
Abdominal SAT density (HU)	1.52 (-1.29, 4.33)	0.287	1.64 (-0.91, 4.20)	0.204

HU: Hounsfield units, SAT: Subcutaneous adipose tissue

***Disclosures: Zehra Akkaya**, Zehra Akkaya received consulting fees from Calico Life Sciences LLC unrelated to the subject matter of this research, Consultant*

SAT-209

The impact of neutrophil efferocytosis by MSCs on MSC mitochondrial function and inflammatory signaling *Sandra Castillo Aguirre[1], Matthew McArthur[1], Emily Quarato[4], Laura Calvi[3], Roman Eliseev[4]. [1]University of Rochester , United States, [4]University of Rochester, , [3]University of Rochester School of Medicine, United States, [4]University of Rochester, United States

Bone marrow stromal, a.k.a. mesenchymal stem, cells (MSCs) senescence plays a critical role in age-related musculoskeletal diseases and bone loss. Despite their role in bone homeostasis and repair, the mechanism of age-dependent MSC dysfunction remains incompletely understood. Studies have shown that MSCs can perform efferocytosis, i.e., phagocytosis and clearing of apoptotic cells. Efferocytosis of end-stage neutrophils by MSCs increases with age, as aged marrow macrophages exhibit impaired efferocytotic capacity. This upregulation is accompanied by oxidative stress and mitochondrial fission and dysfunction, which in non-professional phagocytes such as MSCs may lead to inflammation, senescence, and decreased osteoblastic differentiation. The significance of efferocytosis in MSC function and osteoimmunology is unknown.Therefore, our objective is to understand the mechanism of efferocytic neutrophil attraction, MSC mitochondrial dysfunction, and inflammation. We have observed that after neutrophil efferocytosis, mitochondria in MSCs become less functional, more ROS-producing, and fragmented. To investigate the effect of high efferocytic loads on inflammatory signaling in a mice bone marrow MSC cell line (ST2), we seeded cells on a chamber slide. We treated them with end-stage neutrophils using ratios of 0, 1:1, 3:1, and 10:1 (neutrophils: MSC). After 24 hours, p65 nuclear translocation was visualized using a confocal microscope. We observed an increase in the percent of positive cells for nuclear translocation from 7.4% for the 0 ratios to 39.75% for the 10:1 ratio, indicating a trend for higher inflammation with increased efferocytic load. To study the paracrine crosstalk between MSCs, and neutrophils, we will use a microdevice as an in vitro platform to mimic the interactions in the bone marrow. Preliminary observations confirm the transendothelial migration of neutrophils to the MSC monolayer. Ongoing studies are focused on manipulating oxidative stress using primary bone marrow MSCs isolated from the following mouse models: a) expression of mitochondrial catalase (mCatTG) to combat oxidative stress, mitochondrial fission (Drp1ff and Mfn1ff), and inflammation (Relaff). Cells will be infected with GFP or Cre adenovirus to induce recombination in vitro and treated with different efferocytic loads, then analyze with flow cytometry after 3- and 24-hours post-neutrophil addition and updated data will be presented on these findings.

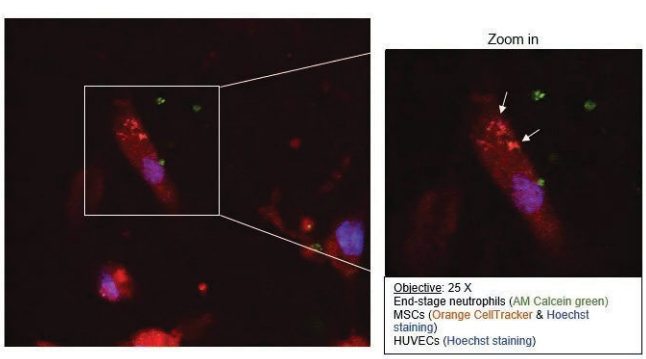

Figure 1. Efferocytosis of end-stage neutrophils by hMSCs. A) Two-photon microscopy image depicts efferocytosis of neutrophils by MSCs (white arrows) in a microdevice with a dual scale ultrathin (<100 nm) silicon-based membrane (μSiM device), containing nanopores and micropores. It shows the transendothelial migration of neutrophils (green) across the membrane containing a human umbilical vein endothelial cells (HUVECs) barrier to the MSC monolayer.

***Disclosures: Sandra Castillo Aguirre**, None*

SAT-210

Early Clearance of p21+ Senescent Cells Suppresses the Radiation -Induced Pro-Inflammatory Secretome from Cd11b+ Myeloid Cells and Mitigates Chronic Bone Loss *Abhishek Chandra[4], MADISON DOOLITTLE[2], Sundeep Khosla[3], Robert Pignolo[4]. [4]Mayo Clinic, , [2]University of Rochester, United States, [3]Mayo Clinic College of Medicine, United States, [4]Mayo Clinic, United States

We recently demonstrated that injury to bone by focal radiation treatment (RTx) is a p21-dependent process. Using p21-ATTAC mice, we showed that bi-weekly clearance of p21-positive senescent cells over a 42-day period resulted in significant mitigation of bone damage generated by 24Gy of RTx. To identify the RTx-induced p21-expressing cell types and their senescent-associated secretory phenotype (SASP), we performed single-cell mass Cytometry by Time of Flight (CyTOF) and identified several cell clusters based on their cell surface or intracellular protein expression profile. Interestingly, we identified unique clusters for p21+ and p16+ expressing cells. On day 4 post-RTx, Cd11b+ myeloid cells had the highest p21 expression, accompanied by elevated SASP factors, such as pNf?b, Cxcl1, Il6, Pai-1, and Il1?. To confirm the source of these factors, magnetic-sorted Cd11b+ cells were isolated from non-radiated (NR) and radiated (R)-bones before and after clearance of p21+SEN cells. As expected, Cd11b+SEN cells showed elevated levels of Ccl2 (~150-fold), Ccl3 (~20-fold), Ccl5 (~3-fold), Ccl7 (~200-fold), Cxcl1 (~50 fold), Cxcl12 (~2.5-fold), Il6 (~15-fold) and Mmp12 (~12 fold) in R-bones, suggesting that Cd11b+ myeloid cells were the major contributors to the SASP in RTx-induced bone loss. Upon clearance of p21+SEN cells in the p21-ATTAC mice, the SASP of magnetically sorted Cd11b+ myeloid cells were significantly reduced in the R-bones [AP20187(AP)-group], as compared to the R-bones (vehicle) group, and approaching the levels found in NR bones. To further understand the dynamics of the early events post-RTx, we performed a targeted clearance of p21+SEN cells limited to first week post-RTx, with no subsequent treatment before ?CT analysis at 6-weeks. Bone parameters assessed by ?CT on day 42 post-RTx showed improved BV/TV (11.2% in AP vs -46.5% in veh, p=0.01), improved Tb.N. (-10.8% in AP vs -25.6% in veh, p=0.011), reduced Tb.Sp. (12.9% in AP vs 39.2% in veh, p= 0.015), and increased Tb.Th. (20.9% in AP vs -4.3% in veh, p=0.013). In summary, early clearance of p21+SEN cells abrogated bone loss caused by RTx. Thus, our data strongly indicate that acute generation of Cd11b+SEN cells following RTx are predominately responsible for the deleterious SASP and identifies an early therapeutic window within which targeting these senescent cells or their SASP may be effective to prevent RTx-induced bone deterioration.

***Disclosures: Abhishek Chandra**, None*

SAT-211

Bisphosphonates Protect Against Oxidative Stress Induced Apoptosis via an FPPS-independent pathway *Helen Knowles[3], Jinsen Lu[3], Srinivasa Rao Rao[3], Haoqun Zhan[3], Anne Horne[2], Ian Reid[2], R Graham Russell[3], James Edwards[3]. [3]University of Oxford, United Kingdom, [2]University of Auckland, New Zealand, [3]University of Oxford,

Bisphosphonates (BP) are the leading medicines targeting disorders of excessive bone loss (eg. osteoporosis, cancer-induced bone disease). BPs inhibit farnesyl pyrophosphate synthase (FPPS) within the mevalonate pathway, impairing protein prenylation. Two placebo-controlled trials have shown Zoledronate reduces mortality whilst several observational studies indicate BPs confer beneficial effects in diverse age-related disorders (cardiovascular disease, cancers, respiratory infections). Increased accumulation of reactive oxygen species in tissues of older individuals is a key ‘hallmark of aging’ and contributing factor

to age-related disease. To test whether BPs alter the cellular response to increased oxidative stress seen in aging organs, we challenged monocytes (THP1), T cells (Jurkat), fibroblast (MRC-5), kidney (HEK) and cardiomyocyte (HL-1) cell lines in an oxidative stress environment (H2O2) +/- pre-treatment with a panel of BPs, and assessed cellular responses by live cell imaging and involvement of new and established mechanisms of action. Levels of antioxidant proteins following BP treatment in osteopenic patients was also assessed. High dose BP treatment (>10uM, up to 7d) led to consistent cell death ($p<0.0001$), which was blocked by a key downstream metabolite in the mevalonate pathway, geranylgeraniol (GGOH, 10mM, 3d, $p<0.01$), confirming the role of FPPS-inhibition. Low dose BP treatment (0.1nM-100nM) protected against basal cell death and prolonged lifespan/proliferation in monocytes, fibroblasts, T cells (up to 67% in 0.1nM ZOL-treated fibroblasts, $p<0.05$). A correlation between basal level of cell death and BP protection was observed ($R2=0.7679$) where cells with lower levels of basal apoptosis have this reduced even further by 0.1nM BP. Treatment with GGOH did not alter this effect suggesting a FPPS-independent effect. Oxidative stress-induced apoptosis (50-300uM H2O2, 24h) was reduced by pre-treatment with BPs (48h) in monocytes, cardiomyoblasts (0.1nM-1uM, $p<0.001$), with up to 99% protection by 100nM ALN in monocytes ($p<0.001$). Addition of GGOH showed no effect. Osteopenic women treated with ZOL showed significantly increased levels of the plasma antioxidant catalase known to accelerate the decomposition of H2O2 ($log2FC=0.67$, $p<0.001$), and reduced levels of pro-oxidants ROCK2, STAT3 and MAPK14. These data suggest treatment with BPs protect against oxidative stress through mechanisms independent of mevalonate pathway inhibition.

***Disclosures: Helen Knowles**, None*

SAT-212

Anti-inflammatory effects of Selcopintide by recovering mitochondrial function in periodontitis *Howon Jang[1], Dong-Seol Lee[2], Ji-Huyn Lee[2], Joo-Cheol Park[1]. [1]Seoul National University, Republic of Korea. [2]HysensBio, Republic of Korea

Periodontitis is a chronic inflammatory disease caused by bacterial plaque accumulation around the tooth-supporting tissues. Long-term uncontrolled inflammation of the gums can lead to loss of periodontal tissue, and treatment or preventive solutions for periodontitis are lacking. Mitochondria are cell organelles that produce energy and regulate cellular metabolism, apoptosis, and calcium signaling. Mitochondrial dysfunction has been linked to various human diseases, and recent studies have suggested a potential association between mitochondrial dysfunction and periodontitis. Studies have reported that mitochondria in patients with periodontitis show decreased function, increased oxidative stress, and inflammatory responses. These functional changes in mitochondria may be related to the progression of periodontitis. Previously, our results reported that Selcopintide (SCPT), a CPNE7-derived peptide, repairs the periodontal ligament by TAU-mediated cytoskeleton reorganization and regulation of cementum attachment protein to enhance the attachment activity of periodontal ligament cells (PDLCs). However, the anti-inflammatory effects of SCPT in periodontal diseases are unknown. In this study, we examined the potential anti-inflammatory effect of SCPT in the periodontal ligament and its possible association with mitochondrial function. To investigate the effects of SCPT, we induced an inflammatory response in PDLCs and ligature-induced periodontitis animal models. Inflammatory responses of PDLCs were stimulated by LPS. Mice were used and divided into three groups (no ligature, ligature only, ligature and SCPT treatment), and periodontal tissue damage and alveolar bone loss were confirmed by histological analysis. The gene expression levels of pro-inflammatory cytokines were significantly reduced after treatments with SCPT with or without LPS-stimulated PDLCs. Furthermore, the expression of fusion and fission protein were upregulated after SCPT treatments. These findings suggest that the SCPT-mediated regulation of mitochondria function may contribute to the alleviation of oxidative stress in PDLCs with inflammation. In vivo micro-CT analysis showed that bone loss occurred in the ligature group. However, the SCPT treated group was protected from periodontal damage and attenuated periodontitis compared to the control (ligature-only) group. These results indicated that Selcopintide might be a potential preventive and therapeutic agent for periodontal diseases.

***Disclosures: Howon Jang**, None*

SAT-213

See Friday Plenary Number FRI-213

SAT-214

Long-term Voluntary Wheel Running Generates Skeletal Muscle-derived Anti-inflammatory Oxylipins correlating with Osteocyte-derived Anti-inflammatory Cytokines in Aging Female Mice *Yukiko Kitase[1], Zhiying Wang[2], Chenglin Mo[3], Julian A. Vallejo[4], Michael Wacker[5], MARCO BROTTO[6], Lynda Bonewald[7]. [1]Indiana University, School of Medicine, United States. [2]Bristol Myers Squibb Princeton, United States. [3]The University of Texas at Arlington, United States. [4]University of Missouri-Kansas City, United States. [5]University of Missouri-Kansas City School of Medicine, United States. [6]University of Texas-Arlington (UTA), United States. [7]Indiana University School of Medicine, United States

Low-grade, systemic, chronic inflammation is a key contributor to tissue dysfunction leading to aging-related disease. Exercise reduces chronic inflammation and prevents the loss of skeletal muscle and bone. We have previously shown that long-term exercise initiated in middle age has positive effects against aging-induced skeletal muscle and bone deterioration in female mice. To identify potential mechanisms, muscle was analyzed for oxylipins, bioactive lipid mediators known to regulate inflammation, and RNA-seq was performed on bones from female mice that were allowed access to wheels from 12 mo to 18 mo of age. The animals were divided into high body weight (HBW) and low body weight (LBW) based on median body weight for analysis. There were no differences in run distance between these two groups. Oxylipins in skeletal muscle were quantitated by LC-MS/MS, and Spearman correlation analyses were performed to determine if VWR plays a role in muscle-bone crosstalk through muscle oxylipins and bone inflammatory cytokines.The anti-inflammatory oxylipin 13-KODE, known to reduce LPS-induced inflammation, was elevated in muscle from the VWR mice ($p<0.05$). However, the anti-inflammatory oxylipin, 15-HETE, known to inhibit the formation of leukotriene, a pro-inflammatory oxylipin, was only elevated in muscle from HBW ($p<0.05$) but not LBW mice. 13-KODE showed positive correlations with soleus muscle functions, such as maximal force with calcium depletion, fatigue, and recovery. GO analysis of bone RNA-seq identified the immune system as the topmost significantly impacted biological process with elevated anti-inflammatory genes and decreased pro-inflammatory genes. 13-KODE negatively correlated with inflammatory genes in bone, including Tnfsf11 mRNA (?=-0.94, p=0.017), coding for RANKL, but positively correlated with Il-27 mRNA (?=0.89, p=0.033), an interleukin known to antagonize RANKL-induced osteoclastogenesis. Il-27 showed a positive correlation with soleus muscle mass and maximal force with calcium depletion and with EDL relaxation rate. In contrast, Tnfsf11, shown to have a negative effect on muscle function and myogenesis, was negatively correlated with muscle function. In summary, VWR elevated anti-inflammatory oxylipins in skeletal muscle from HBW mice and reduced pro-inflammatory cytokines in bone. Correlation analyses suggest that the beneficial effects of VWR on the aging musculoskeletal system are due to reciprocal crosstalk between muscle and bone.

***Disclosures: Yukiko Kitase**, None*

SAT-215

Inhibition of Schnurri-3 protects from systemic and articular bone loss in murine serum transfer arthritis *Priyanka Kushwaha[1], Ellen M. Gravallese[1], Jae-Hyuck Shim[2], Catherine A. Manning[1], Tadatoshi Sato[2], Yeon-Suk Yang[2]. [1]Brigham and Women's Hospital, United States. [2]University of Massachusetts Chan Medical School, United States

Rheumatoid arthritis (RA) is a chronic inflammatory disease that activates osteoclasts (OCs) to resorb bone while simultaneously suppressing the ability of osteoblasts (OBs) to build bone. Current therapeutic agents are inadequate to fully prevent inflammation-induced systemic and articular bone loss. Our previous studies identified Schnurri-3 (SHN3) as a potent suppressor of bone formation and inhibition of SHN3 protects from systemic trabecular bone loss and articular joint bone erosion in RA models. These data suggest that inhibition of SHN3 could be a promising approach to limit bone loss and promote bone repair in RA1. To test SHN3's role in bone erosion healing at articular sites, we used the K/BxN serum transfer arthritis model. We administered arthritogenic serum generated in K/BxN mice to induce inflammation in wildtype mice, then allowed inflammation to completely resolve within 28-30 days. To test whether Shn3 knockdown could promote healing of articular erosions once established, we administered a bone-targeting recombinant adeno-associated virus (rAAV) vector carrying an artificial miRNA that silences expression of Shn3 (amiR-Shn3) or control (amiR-Ctrl) at day 7, three days prior to peak inflammation. Expression of SHN3 was reduced in bone (by ~17%) in amiR-Shn3 mice. Furthermore, microcomputed tomography analysis suggests that knockdown of SHN3 promotes bone formation at the articular erosion site as inflammation resolved. Clinical inflammation scores and joint inflammation scores are comparable in both amiR-Ctrl and amiR-Shn3 groups, demonstrating that knockdown of SHN3 does not affect inflammation. Importantly, AAV treated mice didn't lose body weight and have normal activity, supporting safety of this approach. These results suggest that bone-targeting AAV-mediated silencing of SHN3 may be a promising and safe therapeutic strategy to treat bone loss in rheumatoid arthritis and may promote erosion healing. Reference: 1: Stavre Z, Kim J-M, Yang Y-S, Nündel K, Chaugule S, Sato T, Park KH, Gao G, Gravallese EM, Shim JH et al. Schnurri-3 inhibition suppresses bone and joint damage in models of rheumatoid arthritis. Proc Natl Acad Sci U S A. 2023;120: e2218019120.

Inhibition of Schnurri-3 protects from systemic and articular bone loss in murine serum transfer arthritis

*Priyanka Kushwaha[1], Catherine A. Manning[1], Tadatoshi Sato[2,3,4], Yeon-Suk Yang[2,3], Jae-Hyuck Shim[2,3] and Ellen M. Gravallese[1].

[1]Department of Medicine/Division of Rheumatology, Inflammation and Immunity, Brigham and Women's Hospital; Boston, MA 02115, USA. [2]Department of Medicine/Division of Rheumatology, University of Massachusetts Chan Medical School; Worcester, MA 01605, USA. [3]Horae Gene Therapy Center, University of Massachusetts Chan Medical School; Worcester, MA 01605. USA.[4]Massachusetts General Hospital, Endocrine unit/Harvard Medical School, Boston MA, 02114.

Rheumatoid arthritis (RA) is a chronic inflammatory disease that activates osteoclasts (OCs) to resorb bone while simultaneously suppressing the ability of osteoblasts (OBs) to build bone. Current therapeutic agents are inadequate to fully prevent inflammation-induced systemic and articular bone loss. Our previous studies identified Schnurri-3 (SHN3) as a potent suppressor of bone formation and inhibition of SHN3 protects from systemic trabecular bone loss and articular joint bone erosion in RA models. These data suggest that inhibition of SHN3 could be a promising approach to limit bone loss and promote bone repair in RA[1]. To test SHN3's role in bone erosion healing at articular sites, we used the K/BxN serum transfer arthritis model. We administered arthritogenic serum generated in K/BxN mice to induce inflammation in wildtype mice, then allowed inflammation to completely resolve within 28-30 days. To test whether Shn3 knockdown could promote healing of articular erosions once established, we administered a bone-targeting recombinant adeno-associated virus (rAAV) vector carrying an artificial miRNA that silences expression of *Shn3* (*amiR-Shn3*) or control (*amiR-Ctrl*) at day 7, three days prior to peak inflammation. Expression of SHN3 was reduced in bone (by ~17%) in *amiR-Shn3* mice. Furthermore, microcomputed tomography analysis suggests that knockdown of SHN3 promotes bone formation at the articular erosion site as inflammation resolved. Clinical inflammation scores and joint inflammation scores are comparable in both *amiR-Ctrl* and *amiR-Shn3* groups, demonstrating that knockdown of SHN3 does not affect inflammation. Importantly, AAV treated mice didn't lose body weight and have normal activity, supporting safety of this approach. These results suggest that bone-targeting AAV-mediated silencing of SHN3 may be a promising and safe therapeutic strategy to treat bone loss in rheumatoid arthritis and may promote erosion healing.

Reference:
1: *Stavre Z, Kim J-M, Yang Y-S, Nündel K, Chaugule S, Sato T, Park KH, Gao G, Gravallese EM, Shim JH et al. Schnurri-3 inhibition suppresses bone and joint damage in models of rheumatoid arthritis. Proc Natl Acad Sci U S A. 2023;120: e2218019120.*

*Presenting Author

***Disclosures: Priyanka Kushwaha**, None*

SAT-216

Hindlimb Unloading Induces Microarchitectural and Transcriptomic Changes in the Femur and Tibia in an Age- and Sex-Dependent Manner *STEVEN MEAS[1], Gabriella Daire[1], Michael Friedman[1], Henry Donahue[1]. [1]Virginia Commonwealth University, United States

Age and disuse-related bone loss both result in decreases in BMD, cortical thickness, and trabecular thickness and connectivity. An emerging concept is that disuse induces physiological changes in bone similar to those seen with aging. Animal studies used 4, 6, and 22-month-old C57BL/6J male and female mice that were hind-limb unloaded (HLU) for 3 weeks. Ingenuity Pathway Analyses (IPA) included a publicly available dataset (GLDS647) from 3-month female C57BL/6 mice unloaded for 7 days.In females, three weeks of HLU induced an intermediary bone phenotype in femurs between 6-month-old and 22-month-old mice. Specifically, CTAr/TAr significantly decreased in young HLU mice (n=7) and further in aged control mice (n=13) compared to young ground control mice (n = 7; young control: 55%, young HLU: 48.86%, aged control: 43.25%; $p < 0.0001$). In males, CTAr/TAr remained similar between young control mice (n=8, 42.63%) and young HLU mice (n=8, 42.25%) but there was a decrease in CTAr/TAr with aged control (n=11, 38.91%) and aged HLU mice (n=3, 34.00%). Metaphyseal trabecular bone indices were unchanged. Epiphyseal trabecular bone volume (BV/TV) in female mice was lower in young HLU mice (22.0%) compared to young control (29.7%, $p < 0.05$) and aged control (28.7%, $p < 0.05$) mice. Male mice demonstrated similar trends, with a decrease in BV/TV due to HLU ($p < 0.05$).RNA extracted from whole-bone marrow-flushed tibias was sequenced and analyzed. Gene ontology analysis demonstrated that mitochondrial function was downregulated after HLU whereas cell-cycle transition was downregulated with aging. These ontologies suggest that HLU leads to dysfunctional mitochondria that can perhaps lead to cellular errors in transcription and translation, whereas in aging there is primarily a downregulation of cell cycle processes. IPA was used to identify the leading canonical pathways and upstream regulators in each HLU age group. IPA identified "Senescence Pathway" as the fourth leading canonical pathway enriched in mice exposed to HLU. HLU induced activation of the senescence pathway in 3 month ($p < 0.05$, $z = 3.464$) and 4 month ($p < 0.001$, $z = 0.6$) old mice, inhibited it in 6 month ($p < 0.01$, $z = -3.153$) old mice and did not change it in 22 month ($p = 0.1$, $z = -1$) old mice.In conclusion, we demonstrate that hind-limb unloading initiates changes in bone microarchitecture and gene expression similar to aging, but with distinct differences.

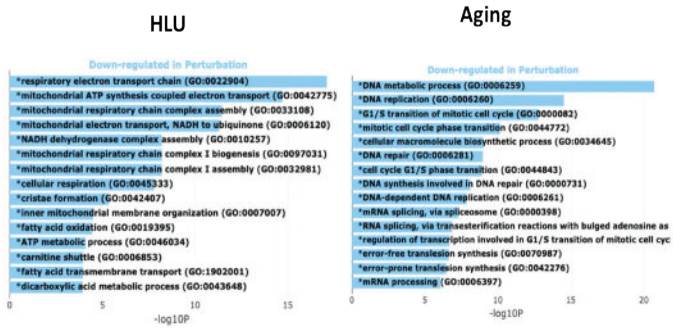

***Disclosures: STEVEN MEAS**, None*

SAT-217

See Friday Plenary Number FRI-217

SAT-218

High levels of efferocytosis by mesenchymal stromal cells increases their senescence and decreases bone *Emily Quarato[2], Noah Salama[2], Yuko Kawano[2], Allison Li[3], Roman Eliseev[2], Laura Calvi[4]. [2]University of Rochester, . [2]University of Rochester, United States. [3]Yale University, United States. [4]University of Rochester School of Medicine, United States

Age-dependent bone loss is a manifestation of skeletal aging. Hallmarks of skeletal aging include mesenchymal stromal/stem cell (MSC) dysfunction and cellular senescence. However, the mechanisms inducing MSC senescence remain unclear. We found that MSCs contribute to the clearance of apoptotic cells in the bone marrow (efferocytosis). While rates of efferocytosis are low at homeostasis, in aging, MSCs increase their efferocytic activity. Thus we hypothesized that excess efferocytosis may contribute to MSC dysfunction and senescence, and represent a previously unknown mechanism of bone loss. In vitro, excess efferocytosis induced MSC dysfunction through increased mitochondrial fission and metabolic disruption. Additionally, MSCs with high efferocytic burden had transcriptional evidence of increased senescence, which we confirmed functionally. In a mouse model of enhanced efferocytosis by MSCs (Bai1xPrxCre), we confirmed increased efferocytosis by MSCs (70% to 85%), and found that efferocytic MSCs had increased rates of senescence compared to controls (40% vs 20%). Consistent with a negative effect of excessive efferocytosis on bone homeostasis, Bai1xPrxCre mice at 3 months had decreased cortical thickness, which significantly declined with age (12m) compared to controls. In this model, MSC dysfunction was also decreased by CFU-F/OB. We next profiled the efferocytic machinery in MSCs, and identified Axl as the primary efferocytic receptor on MSCs. In mice with global loss of Axl, MSCs had decreased efferocytic efficiency, and increased bone mineral density/content and cortical thickness, in both young (3m) and aged (24m) mice. To determine the translation potential of this finding, we tested small molecule inhibitors of the TAM receptors (Tyro3, Axl, MerTK) on MSC in vitro and found that combined Axl and Tyro3 inhibition blocks MSC efferocytosis. Collectively, our data support the idea that excess efferocytosis is a novel mechanism of bone loss. MSC efferocytosis is activated by defects in professional phagocytic cells, such as macrophages. Therefore, senescence induced by excessive MSC efferocytosis may be an underappreciated mechanism of bone loss in settings of defective macrophages, as in aging, obesity, and diabetes-induced bone loss. Given the unique reliance of MSC efferocytosis on Axl, this novel mechanism may be pharmacologically targetable for the treatment of bone loss in aging and in other diseases caused, in part, by MSC efferocytic excess.

***Disclosures: Emily Quarato**, None*

SAT-219

Dementia Is More Associated With Osteosarcopenia Than With Other Musculoskeletal Phenotypes. Results From the Sarcos Study *Lorena Sallovitz[1], Angela Paes[1], ALBERTO FRISOLI JUNIOR[2]. [1]FICSAE, Brazil. [2]UNIVERSIDADE FEDERAL SAO PAULO,

Dementia has been associated with low physical activity and inflammatory process. These conditions are associated with sarcopenia and osteoporosis. However the association between dementia and the musculoskeletal phenotypes remain unclear.Aim: To evaluate the association between dementia and osteosarcopenia, sarcopenia and osteoporosis phenotypes using two different diagnosing methods of sarcopenia, in older adults.Methods: SARCOS is a prospective cohort study on the association between sarcopenia and osteoporosis and difficult outcomes in older adults with cardiovascular disease. Population: subjects aged > 60 years from the cardiovascular disease outpatient clinic. All patients underwent DXA analysis for appendicular muscle mass, bone mineral density, in addition, handgrip strength and walking speed were measured. Sarcopenia was diagnosed following the EWGSOP II (EW)

and SDOC recommendations. Osteoporosis was diagnosed according to the WHO guidelines. Osteosarcopenia was categorized into four phenotypes (osteosarcopenia-OPSAR, sarcopenia-only-SAR, osteoporosis-only-OP, and robust-ROB) for each sarcopenia diagnosis. Dementia was defined by recommended score on the Mini Mental State Examination (MMSE). Regression analyses were adjusted for significant variables for osteosarcopenia SDOC and EWGSOP II (Age>80, depression, chronic obstructive pulmonary disease and years of schooling).Results: In this study, 408 patients were evaluated. The mean age was 77.87(7.6) years, female gender 57.5%(235). Dementia occurred in 68,4%(279); osteosarcopenia phenotypes: OPSAR-SDOC: 17.9% (73), SAR-SDOC: 26.7% (109), OP-SDOC: 11.5% (47); p<0.013; and OPSAR-EW: 9.6% (39); SAR-EW: 7.8%(32); OP-EW: 19.9% (81); p=0.197. In patients with dementia, 21.5% had OPSAR-SDOC, 11.5% OPSAR-EW; 27.6% SAR-SDOC, 6.8% SAR-EW; 9.7% OP-SDOC and 19.7% OP-EW. In regression analyses, dementia showed odds ratio for OPSAR-SDOC: 2.36 (1.16-4.81; 0.018), SAR-SDOC: 1.25 (0.73-2.14; 0.405); OP-SDOC 0.72 (0.37-1.41; 0.344), while for phenotypes with EW, the OR for OPSAR-EW: 1.87 (0.77-4.55; 0.165); SAR-EW: 0.64 (0.3-1.38; 0.258); OP-EW: 0.994 (0.58-1.72; 0.983).Conclusions: In our study dementia showed greater association only with the osteosarcopenia phenotype by SDOC recommendation. Implications: These results highlight the importance of differentiating osteosarcopenia phenotypes in clinical practice.

***Disclosures: Lorena Sallovitz**, None*

SAT-220

Diet Stimulated Marrow Adiposity Fails to Worsen Early, Age-Related Bone Loss *Cody McGrath[1], Sarah E. Little-Letsinger[1], Gabriel M. Pagnotti[2], Buer Sen[1], Zhihui Xie[1], Gunes Uzer[1], Guniz B. Uzer[1], Xiaopeng Zong[3], Brandie M. Ehrmann[4], Diane Wallace[4], Martin A. Styner[5], Janet Rubin[1], Maya Styner[1]. [1]University of North Carolina, Chapel Hill, School of Medicine, United States. [2]Department of Endocrine, Neoplasia, and Hormonal Disorders, MD Anderson Cancer Center, United States. [3]3Radiology and Biomedical Research Imaging Center, University of North Carolina , United States. [4]Department of Chemistry, University of North Carolina, United States. [5]5Departments of Computer Science and Psychiatry, University of North Carolina, United States

Introduction: Longitudinal effect of diet-induced obesity on bone is uncertain. Prior work showed both no effect versus a decrement in bone density or quality when obesity begins prior to skeletal maturity. We aimed to quantify long-term effects of obesity on bone and bone marrow adipose tissue (BMAT) in adulthood. Methods: Skeletally mature, female C57BL/6 mice (n=70) aged 12-weeks were randomly allocated to low-fat (LFD; 10%kcal fat; n=30) or high-fat (HFD; 60%kcal fat; n=30) diet, with analyses at 12,15,18 and 24-weeks (n=10/group). Tibial microarchitecture was analyzed by µCT, and volumetric BMAT was quantified via 9.4T MRI/advanced-image-analysis. Histomorphometry of adipocytes and osteoclasts, qPCR, and bone metabolomic subset analyses were performed. Results: Body weight and visceral white adipose tissue accumulated in response to HFD started in adulthood. Trabecular bone parameters declined with advancing experimental age. BV/TV declined 22% in LFD (p=0.0001) and 17% in HFD (p=0.0022) by 24-weeks. HFD failed to appreciably alter BV/TV and had negligible impact on other microarchitecture parameters. Both dietary intervention and age accounted for variance in BMAT, with regional differences: distal femoral BMAT was more responsive to diet, while proximal femoral BMAT was more attenuated by age. BMAT increased 60% in the distal metaphysis in HFD at 18 and 24 weeks (p=0.0011). BMAT in the proximal femoral diaphysis, unchanged by diet, decreased 45% due to age (p=0.0002). Marrow adipocyte size via histomorphometry supported MRI quantification. Osteoclast number did not differ between groups. Tibial qPCR showed attenuation of some adipose, metabolism, and bone genes. A regulator of fatty-acid ?-oxidation, Cytochrome C (CYCS), was 500% more abundant in HFD-bone (p<0.0001; diet effect). CYCS also increased due to age, but to a lesser extent. HFD mildly increased OCN, TRAP, and SOST. Metabolomic subset analysis (24-week HFD vs LFD; n=3/group) showed enrichment in some fatty acid and amino acid pathways in bone. Conclusions: Long-term high fat feeding after skeletal maturity, despite upregulation of visceral adiposity, body weight, BMAT, and attenuation of local energy metabolism, failed to worsen bone microarchitecture. In adulthood, we found aging to be a more potent regulator of microarchitecture than diet-induced obesity.

***Disclosures: Cody McGrath**, None*

SAT-222

Follistatin-compound hFST?HBS-FC improves bone, muscle mass and body weight during immobilization and ageing and adds to bone effect of bisphosphonates *Bram van der Eerden[1], Andreas Lodberg[2], Mikkel Bo Brent[2], Marijke Koedam[3], Renate Brandt[4], Jeroen Essers[4], Jesper Skovkus Thomsen[2], Ingrid van der Pluijm[5], Annemarie Brüel[6], Johannes Van Leeuwen[7]. [1]Erasmus MC, Netherlands. [2]Department of Biomedicine, Health, Aarhus University, Denmark. [3]Dept. Internal Medicine, Erasmus MC, Netherlands. [4]Department of Molecular Genetics, Erasmus MC, Netherlands. [5]Department of Vascular Surgery, Erasmus MC, Netherlands. [6]Department of Biomedicine, Health, Aarhus University, , Denmark. [7]Erasmus University Medical Center, Netherlands

Background: Sarcopenia, loss of muscle mass and strength, and osteoporosis, loss of bone mass and strength, are natural consequences of aging and often related. Sarcopenia is associated with increased fracture risk, while immobilization leads to loss of muscle and bone mass. We developed a follistatin (FST)-based compound (hFST?HBS-FC) that can bind activin A and myostatin and prevents OVX-induced bone loss (Lodberg et al, FASEB J. 33:6001; 2019)Aim: In this study we examined the impact of hFST?HBS-FC on bone and muscle mass in a premature aging mouse model (Ercc1 ?/-) and a botox-induced immobilization mouse model. We also examined the combined treatment of hFST?HBS-FC and zoledronate (ZOL).Methods: For both models, female mice (Botox model 16 weeks old; Ercc1 ?/- model, 8 weeks old) were treated with either vehicle, 10 mg/kg hFST?HBS-FC twice a week intraperitoneally, a single subcutaneous injection of 100 ?g/kg zoledronate once, or a combination of both treatments. After 3 weeks, animals were sacrificed, and tissues were harvested.Results: Botox-treatment led to a decrease in both bone mass (BV/TV(%): 11.1>6.7%) and muscle mass (quadriceps: -17%). hFST?HBS-FC and ZOL both increased BV/TV (6,7>8,6% and 6.7>16.9, respectively), which was further elevated by the combination treatment of hFST?HBS-FC with ZOL (6.7>20.3%). Similar effects were observed for other bone parameters like Tb.N and Tb.Sp. hFST?HBS-FC prevented weight loss and the loss of muscle mass caused by systemic stress of immobilization. ZOL did not affect muscle mass. Bone and muscle mass were both reduced in the premature aging model compared to wild type mice (Vermeij et al. Nature 537:427; 2016). ZOL prevented the decrease in bone mass which was strongly further enhanced by co-treatment with hFST?HBS-FC (see Table). hFST?HBS-FC also increased muscle mass (+20%) as well as total body weight (+7%) in prematurely aging mice, which was not observed for ZOL.Conclusion: hFST?HBS-FC not only improves bone mass and bone structure but also increases muscle mass and prevents weight loss in conditions reflecting immobilization and aging. hFST?HBS-FC adds to the positive treatment effect of bone loss by zoledronate. These results hold promise for a hFST?HBS-FC combination therapy with bisphosphonates against bone loss with the additional benefit of a muscle anabolic effect.

Ercc1 $^{\Delta/-}$ mice	Control	hFST$_{\Delta HBS}$-FC	ZOL	hFST$_{\Delta HBS}$-FC + ZOL
BV/TV (%)	4.7+/- 0.57	7.1+/-0.82	16.6+/-1.0	24.73+/-3.6
Tb.N (mm^{-1})	1.1+/-0.1	1.6+/-0.15	3.3+/-0.15	4.2+/-0.71
Tb.Sp (µm)	375.2+/-38	250.4+/-21	113.2+/-5.4	84.4+/-13.7
TB.Pf (mm^{-1})	43.7+/-2.5	37.33+/-2.7	21.5+/-0.92	19.5+/-2.6
Tb.Th (µm)	44.4+/-1.5	43.5+/-1.5	50.43+/-1.2	52.6+/-1.5
SMI	2.6+/-0.05	2.33+/-0.07	1.78+/-0.07	1.30+/-0.24

+/- SEM, n=8 or 9 mice

***Disclosures: Bram van der Eerden**, None*

SAT-223

Captopril Alleviates Chondrocyte Senescence and Cartilage Loss In Spontaneous Hypertensive Rats *Yuqi Zhang[1], Chunyi WEN[2]. [1]Department of Biomedical Engineering, The Hong Kong Polytechnic University, Hung Hom, Kowloon, Hong Kong, China, Hong Kong. [2]Hong Kong Polytechnic University, Hong Kong

Background: Mounting epidemiological evidence suggests a close association between hypertension and osteoarthritis (OA). Their causal relationship remains not established yet. Hereby, we aimed to examine knee joint structural integrity in spontaneously hypertensive rats (SHR) compared to normotensive Wistar Kyoto (WKY) rat with or without surgical induction, and investigate the efficacy of FDA-approved anti-hypertensive medication, captopril, on joint structure in SHR.Method: First, we used 6 male SHR and 6 male WKY at the age of 4 months for comparison. They were randomly allocated to sham or anterior cruciate ligament transection (ACLT) groups with n=3 for each group. Then we further tested the efficacy of captopril on SHR. SHR were divided into the placebo and captopril treatment groups (n=3 for each group). In addition to blood pressure, carotid arterial stiffness and knee joint vascularity were measured non-invasively via ultrasonic and photoacoustic imaging at baseline, 1 and 2 months after surgery. Bone mass and microstructure of knee joint was evaluated via in-vivo micro-CT. The animals were sacrificed at postoperative 2 months and knee joints and aorta were harvested for routine histology and immunostaining for detection of p16INK4a+ senescent cells and MMP13 expression.Results: Hypertension induced p16IN-

K4a+ senescent cells accumulation not only in the aorta but also knee joint, increased expression of MMP13 in knee joint, and ultimately contributed to cartilage degradation in SHR compared to WKY. Captopril not only lowers blood pressure but also removes p16INK4a+ senescent cells from aorta and knee joint, reduced the level of MMP13 in joint cartilage, and preserved the thickness of articular cartilage in SHR. SHR showed bone loss, but captopril did not rescue bone loss. After ACLT induction, WKY and SHR have almost the same degree of cartilage senescence and damage in joints.Conclusion: Hypertension contributes to senescent cells accumulation and cartilage degeneration. Anti-hypertensive medicine such as captopril emerges as a promising senolytic approach for rescue of degenerative joint disorder. However, for joints already suffering from OA, hypertension did not further aggravate OA, or the aggravation effect was very weak.

***Disclosures: Yuqi Zhang**, None*

SAT-224

See Friday Plenary Number FRI-224

SAT-225

Laminopathy-like pathology due to Runx2-dependent downregulation of LINC protein expression underlies the pathogenesis of Cleido cranial dysplasia *Akiko Saito[1], Shoko Onodera[1], Natsuko Aida[1], Hiroyuki Okada[2], Hironori Hojo[2], Shigeaki Kato[3], Toshifumi Azuma[4]. [1]Tokyo Dental College, Japan. [2]Tokyo University, Japan. [3]Iryososei Unicersity, Japan. [4]Tokyo Dental Collge, Japan

Severe laminopathies (such as Hutchinson-Gliford progeria syndrome) caused by mutations in the LINC protein genes, including the lamin A/C genes, exhibit bone lesions such as clavicle and cranial suture. RUNX2 heterozygous deficiency, cleido cranial dysplasia (CCD), are known to exhibit bone lesions in areas similar to laminopathy. Hoewever, it is not known whether RUNX2 and LaminA/C share any common roles in the development of bone lesions. In this study, we used human RUNX2-deficient iPS cells to elucidate the mechanisms of chromosome dynamics regulation and epigenetic control mechanisms mediated by nuclear lamina and nuclear conformation by the RUNX2-LaminA/C-nesprin 1 axis. LINC protien(Nesprin 1) and LaminA/C were substantially downregulated in RUNX2-deficient iPS cell-induced osteoblast, and abnormal laminopathy-like nuclear morphology, such as abnormal deep nuclear groovesm was observed in RUNX2 hetero-and homo- deficient cells. Observation of cellular and nuclear propeties by atomic force microscopy and cytoskeletal distribution by fluorescence microscopy revealed prominent nuclear deformation and greatly reduced physical rigidity in RUXN2 -/- cells with loss of perinuclear action cap structure and actin stress fibers and significantly reduced intracellular tension. In RUNX2 -/- cellls with forced expression of Nesprin1, nuclear deformations, nuclear membrane stiffness, nuclear actin cap structure, actin stress fibers and intracellular tensions were recovered to normal. LaminA/C CUT & RUN assay showed that LaminA/C was enriched in the TSS region both RUNX2+/+ cells and RUNX2-/- with forced expression of Nesprin1 cells, while LaminA/C was sparse in the TSS region in RUNX2-/- cells. Single cell RNAseq analysis showed that RUNX2 mRNA was detected even in the Runx2-/- cells, but the RUNX2-positive cells were detected at about half the the frequency of RUNX2+/+ cells, whereas RUNX2-/- with Nesprin 1 cells had the same frequency as RUNX2 +/+ cells. These results indicate that marked downregulation of LaminA/C and Nesprin1 similar to laminopathy by RUNX2 deletion underlies CCD pathogenesis due to nuclear membrane abnormalty, loss of perinuclear actin cap, reduced intracellular tensions, althered chromosome dynamics and dysregulation of LINC protein epigenetic control mechanisms. Therefore we propose that RUNX2-LINC protein axis is a newly discovered osteogenic checkpoint

***Disclosures: Akiko Saito**, None*

SAT-226

Mice Lacking COX2 Cyclooxygenase Activity Display Sexual Dimorphism and Respond to Osteogenic Mechanical Loading *Alexandra Ciuciu[1], Ryan Tomlinson[2]. [1]Thomas Jefferson University , . [2]Thomas Jefferson University, United States

Non-steroidal anti-inflammatory drugs (NSAIDs) relieve pain and inflammation by inhibiting prostaglandin synthesis by the cyclooxygenase (COX) enzymes COX1 and COX2. Regular NSAID use is associated with increased stress fracture incidence, but it is unknown if the inhibition of COX2 signaling causes this effect. To investigate COX2-dependent and COX2-independent effects of NSAIDs, we used Ptgs2-Y385F mice, which harbor a point mutation that inhibits the cyclooxygenase activity of COX2 but maintains its peroxidase activity (similar to a COX2-selective NSAID). In adult mice (15-18 weeks old), microCT revealed that female Ptgs2-Y385F mice had significantly increased trabecular BMD (+35%, p=0.05). Surprisingly, male Ptgs2-Y385F mice have significantly reduced relative endosteal BFR/BS (-48%, p=0.042). There were no other significant differences in histomorphometric parameters. Potential compensation by COX2 in the Ptgs2-Y385F mice is being investigated at the mRNA and protein levels. Nonetheless, these data indicate that Ptgs2-Y385F mice are a valuable tool for examining COX2-independent effects of NSAIDs in bone and underscore the need to consider sex as a biological variable when analyzing the effects of NSAIDs in bone.

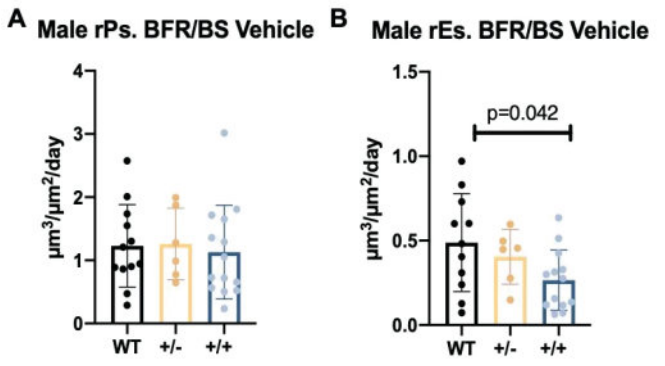

Figure 1: A) Relative periosteal bone formation rate per bone surface of vehicle treated male wild-type (WT), heterozygous (+/-), and Ptgs2-Y385F mice (+/+). B) Relative endosteal bone formation rate per bone surface of vehicle treated male WT, heterozygous, and Ptgs2-Y385F mice. (n=6-13 per genotype)

***Disclosures: Alexandra Ciuciu**, None*

SAT-227

Chronic treatment with the ?2-adrenoceptor agonist clonidine affects the morphophysiology of epiphysel groth plates but does not modify the longitudinal bone growth of mice. *Vitor Torres[1], Cecilia Gouveia[2]. [1]University of Sao Paulo, Brazil. [2]University of Sao Paulo, Institute of Biomedical Sciences, Brazil

We have demonstrated that ?2-adrenoceptors (?2-AR) are expressed in the epiphyseal growth plates (EGP) of mice, and that mice with isolated gene inactivation of ?2A-AR and ?2C-AR have lower body length and EGP dysgenesis. We showed that tibias isolated from these knockout animals and kept in organ cultures present lower rate of longitudinal bone growth (LBG). We also showed that treatment of wild-type tibias (in organ cultures) with UK, an ?2-AR agonist, decreases the number of hypertrophic chondrocytes (HC) in the EGP, suggesting that ?2-ARs mediate local and negative actions of the sympathetic nervous system (SNS) in the EGP. Considering that ?2-AR agonists are used in clinical practice for various purposes, the present study aimed to investigate whether the chronic use of clonidine (CLO), an ?2-AR agonist, affects the EGP morphology and LBG. C57BL/6J mice (21 day-old) were treated daily with subcutaneous injections of 35 ?g/kg CLO or saline (CLO and control groups, respectively; n=10/group) for 30 days. We showed that CLO treatment did not affect body weight, body growth, and the longitudinal growth of the femur and tibia. However, CLO reduced the thickness and area of the EGP and hypertrophic zone (HZ), while increased the number of proliferative chondrocytes (PC) and decreased the ration between the hypertrophic and proliferative zones (HZ/PZ) of the EGP, which suggests a negative effect of CLO on the differentiation of HC and a positive effect on chondrocyte proliferation. Treatment with CLO did not alter EGP gene expression of IGF-1, Runx-2 and Wnt4, but increased the expression of type II collagen. These findings demonstrate that chronic treatment with CLO does not affect the LBG, but promotes changes in the EGP. Considering that CLO stimulates pituitary secretion of growth hormone (GH), it is possible that CLO acts indirectly and positively in the EGP, via GH actions (chondrocyte proliferation), which probably compensates its direct and negative effects (inhibition of terminal differentiation of chondrocytes), resulting in normal LBG.

***Disclosures: Vitor Torres**, None*

SAT-228

Hypertrophic Chondrocyte-Autonomous Roles of YAP/TAZ Signaling in Embryonic Bone Development *Christopher Panebianco[1], Joel Boerckel[1]. [1]University of Pennsylvania, United States

The appendicular skeleton forms through endochondral ossification, in which chondrocytes proliferate, undergo hypertrophy, and then are remodeled at the chondro-osseous junction to form bone. Previously, we found that deleting the transcriptional regulators YAP and TAZ from Osterix (Osx) -expressing cells caused bone fragility, perinatal lethality, hypertrophic zone (HZ) elongation, and a cone shaped chondro-osseous junction.1 Since Osx is expressed in hypertrophic chondrocytes (HCs) and osteoblast-lineage cells, it remains unknown whether the HZ phenotype is caused by HC-autonomous defects or by disrupted chondro-osseous junction remodeling.To answer this question, we generated mice featuring allele dosage-dependent deletion of YAP/TAZ in ColX-expressing cells (i.e., HCs). Wild-type (WT) and ColX-conditional knockout (cKO) mice were evaluated by whole mount imaging and μCT at birth (P0), and by histology at E17.5. In contrast to Osx-cKO mice, ColX-cKO mice were viable, fertile, and had no perinatal bone fractures (Fig 1A). Nonetheless, ColX-cKO mice were smaller, had reduced body mass, and had reduced bone volume

compared to WT littermates (Fig 1B). To explore the cellular basis of this phenotype, we analyzed the growth plate of the E17.5 proximal tibia. ColX-cKO mice had an elongated HZ compared to WT littermates, though both groups exhibited a normal, flat profile at the chondro-osseous junction (Fig. 1C).Our results indicate an HC-autonomous contribution of YAP/TAZ signaling to endochondral ossification. Our previous work with Osx-cKO mice found that deleting YAP/TAZ in HCs and osteoblast-lineage cells impaired growth plate remodeling through HC-autonomous and non-autonomous mechanisms.1 The elongated HZ phenotype present in ColX-cKO mice demonstrates the importance of YAP/TAZ signaling in HC-autonomous matrix remodeling. However, since chondro-osseous junction shape was normal, we verify that non-autonomous mechanisms of matrix remodeling are independent of HC YAP/TAZ signaling. These results are similar to Col2-cKO mice, which displayed HZ elongation and a flat chondro-osseous junction.2 Future studies will study potential mechanisms by which HC-autonomous YAP/TAZ signaling affects endochondral ossification (e.g., HC differentiation, HC matrix degradation), but our data shows that HC-autonomous YAP/TAZ signaling is necessary for proper endochondral ossification.Refs: [1] Collins+ BioRxiv 2023; [2] Vanyai+ Development 2020

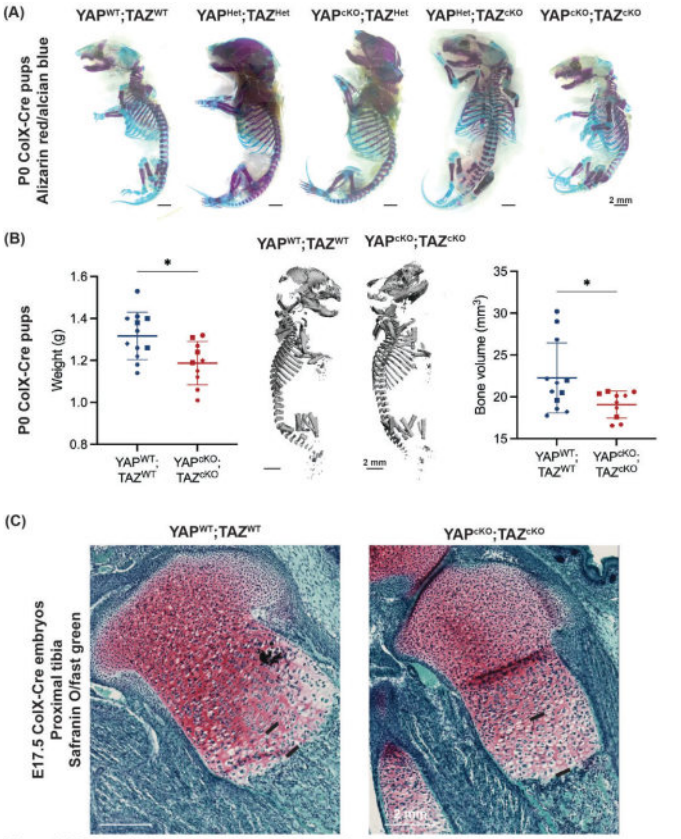

Figure 1. HC-specific YAP/TAZ deletion inhibits endochondral ossification through HC-autonomous mechanisms. ***(A)*** *Whole mount images of P0 skeletons stained with alizarin red/alcian blue. WT = wildtype, Het = heterozygous, cKO = conditional knockout. Bar = 2 mm.* ***(B)*** *Weight and bone volume quantifications for P0 pups. Bar = 2 mm. * = p<0.05.* ***(C)*** *Safranin O/fast green staining of E17.5 proximal tibia. Black lines indicate HZ. Bar = 2 mm.*

Disclosures: Christopher Panebianco*, None*

SAT-229

Elucidating the Consequences of Wnt16 Cysteine Deletion on Bone *Emily G. Ramirez[1], Maria F. Rojas[1], Jyoti Rai[1], Claire J. Watson[1], Ronald Young Kwon[1]. [1]Department of Orthopaedics and Sports Medicine, University of Washington School of Medicine , United States

Osteoporosis, a polygenic disease characterized by low bone mineral density (BMD) and increased fracture risk, afflicts over 200 million people worldwide [1]. WNT16 is a member of the WNT protein family that has been specifically linked to genetic influence on BMD and fracture risk. The majority of WNT proteins contain 24 conserved cysteines (c1-c24), and mutations for almost half of these cysteines are associated with human diseases or disrupted development in animal models [2]. However, the impact of cysteine 10 (c10) alteration remains unknown. Previous analyses suggest that c10 may form a disulfide linkage with cysteine 11 that contributes to the structure of the thumb-like domain recognized by Frizzled receptors [2]. Previously, our lab showed that wnt16-/- mutant zebrafish exhibit impaired spine development and morphology [3]. We hypothesized that c10 is necessary for WNT16 structure and function, and that loss of c10 in zebrafish will phenocopy wnt16-/- mutants. To test this, we used CRISPR-based gene editing to generate zebrafish harboring mutations at the wnt16 locus at the c10 position, and isolated wnt16w1012 mutants. Sanger sequencing revealed a three amino acid deletion at Cys214, corresponding to c10 (p.Cys214_Gly216del). Calcein staining of wnt16w1012 mutant fish at 14 days post fertilization (dpf) revealed altered mineralization in vertebrae compared to age-matched controls (n=10/group). Analysis of microcomputed tomography scans at 90 dpf revealed significantly reduced centrum length ($p<0.0001$), along with a significant increase in neural arch angle ($p=0.0002$) in wnt16w1012 mutants (n=10/group). Moreover, wnt16w1012 mutants exhibited significantly reduced centrum volume ($p=0.0088$) and significantly increased centrum ($p=0.0404$), haemal arch ($p=0.0264$), and neural arch ($p=0.0166$) tissue mineral density compared to controls. No significant differences were observed between wnt16w1012 and wnt16-/- mutants, indicating that wnt16w1012 mutants phenocopy wnt16-/- mutants. Computational modeling of the encoded protein for wnt16w1012 revealed conformational changes predicted to affect recognition by Frizzled receptors. These studies indicate that c10 is essential for WNT16 function. Our findings suggest that mutations affecting c10 in WNT16 could influence BMD and fracture risk.1. Sözen et al., 2017, Eur. J. Rheumatol.2. MacDonald et al., 2014, J. Biol. Chem.3. Watson et al., 2022, PLoS Genet.

Disclosures: Emily G. Ramirez*, None*

SAT-230

See Friday Plenary Number FRI-230

SAT-231

Effects of Tetrahydrocannabinol on Prenatal Skeletal Development *Faisal Sadar[1], Nihamul Ehan[1], Samantha Penman[2], Gabriela Miletsky[2], Rania Ahmed[2], Michael Hadjiargyrou[3], Panayotis Thanos[2], David Komatsu[4]. [1]Department of Orthopaedics and Rehabilitation, Stony Brook University, United States, [2]Behavioral Neuropharmacology and Neuroimaging Laboratory on Addictions, Clinical Research Institute on Addictions, Department of Pharmacology and Toxicology, Jacobs School of Medicine and Biosciences, State University of New York at Buffalo, United States, [3]Department of Biological and Chemical Sciences, New York Institute of Technology, United States, [4]Stony Brook University, Dept. of Orthopaedics and Rehabilitation, United States

The rapid expansion of legalized marijuana has been accompanied by an increase in the number of people using this drug. Clinical studies have reported that users of marijuana have an increased incidence of skeletal fractures and decreased bone mineral density. Other studies have shown that 2-5% of woman use marijuana regularly during their pregnancies. Tetrahydrocannabinol (THC) is the primary psychoactive component in marijuana and can cross the placental barrier and potentially affect fetal development. Currently, nothing is known about the effects of prenatal THC exposure on skeletal development. Therefore, we conducted a study in which rats were prenatally exposed to THC. Rat dams were exposed to THC (0.8mg/kg) via inhalation or normal air daily from 3 days prior to pairing for breeding until they gave birth. This dose results in peak THC blood plasma levels of 71.6 +/- 10.9 ng/mL which is similar to the clinical levels detectable after smoking marijuana. The pups were then euthanized on postnatal day 60, corresponding to the end of adolescence in humans. Digital caliper measurements were taken to ascertain tibial and femoral length and mid-diaphyseal diameter on the anterior-posterior (AP) and medial lateral axes (ML). Biomechanical analyses were performed by subjecting femora to 3-point bending tests to determine energy to failure, stiffness, ultimate force, failure force, and yield force. Results were compared between THC and normal air (control) within the male and female cohorts. Sample sizes were 8 for each group. For the caliper measurements, significant differences were found between the control group and the group exposed to THC for tibial ML diameter in both males and females. Specifically, tibial ML diameter was 57% wider in male controls compared to THC exposed and 29% wider in the female controls compared to THC. We also found that femoral length in females was 4% longer in controls compared to THC. Biomechanically, only male femoral yield force differed significantly, with THC exposure resulting in a 28% increase compared to control. Ongoing analyses include safranin O/fast green staining to assess tibial growth plates and tibial microCT to measure bone density and microstructure. The current data suggest that the effects of prenatal exposure to THC on skeletal development are relatively minor. The completion of these studies will provide us with a better understanding of the effects of prenatal THC exposure on skeletal development.

Disclosures: Faisal Sadar*, None*

SAT-232

Key Characteristics of Clinicians with Competence in Bone Health Management *Lesley Jackson[1], Sindhu Johnson[2], KEN SAAG[3], Maria Danila[4]. [1]The University of Alabama at Birmingham, United States, [2]University of Toronto, Canada, [3]THE UNIVERSITY OF ALABAMA AT BIRMINGHAM, , [4]University of Alabama at Birmingham, United States

Background: Osteoporosis is managed by clinicians across many specialties. No specific certification in bone health/osteoporosis management exists and the key competencies of clinicians delivering these services have not been systematically established. We aimed to develop a decision rule to define the threshold of adequate bone health competence for a

clinician serving as a referral source for osteoporosis/post-fracture care.Methods: In part 1 using a modified Delphi method, we invited clinicians with expertise in treating osteoporosis and patient advocacy group representatives to create a list of desirable characteristics of a clinician with bone health competence. Characteristics were coded into "attributes" with "levels" within each attribute. Participants prioritized levels by perceived importance. We included levels receiving the highest median scores in the final list of criteria. In part 2, to identify the cutoff for defining adequate competence, participants ranked 20 hypothetical clinicians defined by various levels of attributes from highest to lowest likelihood of having bone health competence. In part 3, we conducted a discrete choice experiment (DCE) to generate a weighted score for each attribute/level such that the sum of weights across the highest level for each attribute would equal 100%. The threshold for competence was a priori determined as the total weighted score at which >=70% of participants agreed a clinician had bone health competence.Results: 13 participants completed Part 1, and 30 participants completed both Parts 2 and 3. The Delphi exercise generated a list of N=108 characteristics, which were coded and grouped into common attributes. Through an iterative process, the attribute categories were reduced to 8 categories. The maximum possible score in the final criteria was 25. Category weights are shown in the Table. A summed threshold score of >12 points classified a clinician as having adequate competence in bone health. For lack of continuing medical education, 1.2 points (~5% of maximum total score) were subtracted from the clinician's score.Conclusions: We developed a numeric additive decision rule to classify clinicians across multiple specialties as having adequate competence in managing bone health/osteoporosis. Our data provides the critical definition of a clinician with competence in bone health and can be used to quantitate the skills of clinicians participating in bone health research and clinical care.

Table. Relative weights of criteria and levels defining a clinician with competence in bone health.

Criteria	Subcriteria	Weighted Score*
Provides bone health care	Performs osteoporosis workup and treatment monitoring, but does not have a dedicated Bone Health Clinic	3.9
	Performs osteoporosis workup and prescription monitoring, has ≥1/2 day per week Bone Health Clinic time	5.7
Prescribing practices	Prescribes only bisphosphonates and denosumab	2.1
	Prescribes all osteoporosis drugs (i.e., anabolic drugs)	4.8
Attends bone health continuing medication education (CME)	None	-1.2**
	Every 2-5 years	1.9
	Once or more per year	3.3
Dual-energy x-ray absorptiometry (DXA) competence	Interprets < 100 DXA scans/year	1.9
	Interprets ≥100 DXA scans/year	2.8
Fracture liaison service (FLS) participation	Leads or participates	2.7
Vertebral Fracture Assessment (VFA) competence	Orders and interprets	2.0
Subspecialty board (Endocrinology, Rheumatology) certification	Currently certified and practicing	1.9
International Society for Clinical Densitometry (ISCD) certified	Certified	1.8

*Summed across all categories, a minimum score of >12 points classifies a clinician as having competence in bone health management.
**If the clinician does not attend CME, subtract 1.2 points from total score.

***Disclosures: Lesley Jackson**, None*

SAT-233

The POWER Program: Personalized Osteoporosis Care with Early Recognition, Incorporating Virtual Tools Into an Outpatient Fracture Liaison Service *Leah Kennedy[1], Stephanie Yee[1], Melissa Kallas-Koeman[1], Emma Billington[1], Prism Schneider[1]. [1]University of Calgary, Canada

Background: Individuals experiencing a fragility fracture (FF) are 2- to 4-times more likely to have another FF in the future. The COVID-19 pandemic increased existing osteoporosis (OP) care gaps, likely due to reduced assessments, screening, and testing. Provincial treatment initiation declined for oral (43%) and intravenous (26%) bisphosphonates and denosumab (35%) from March to June 2020. Without early identification, investigation, and intervention (3i model), FF incidence will continue to increase globally. Our study evaluated the feasibility, effectiveness, and patient satisfaction regarding a multidisciplinary outpatient fracture liaison service (OFLS), utilizing virtual case conferences and follow-ups and a smartphone application (app).Methods: In August 2020, a 3i OFLS was implemented at our Level 1 trauma centre. Active case finding identified patients >50 years with a new wrist, shoulder, or pelvis FF. The nurse completed a bone health history for each patient, followed by case discussion with the lead physician. We provided education, ordered tests, and initiated pharmacotherapy as needed. Virtual multidisciplinary case conferences were held monthly to review complex patients. Individualized care plans were initiated within three months of enrollment. Participants were followed for 1-year prior to transfer of care to the primary care physician with a bone health care plan. Patient satisfaction surveys were completed serially. Descriptive statistics are presented.Results: Within 12 months, 128 patients were enrolled (mean age=65 [SD +/- 9.9]; 87.5% female), with mainly distal radius (62%) and proximal humerus (21%) fractures. Fifty-four patients were reviewed in multidisciplinary case conferences, with only six requiring referrals for in-person specialist assessment. The virtual conferences required <10 hours of specialist time and avoided over 48 in-person consultations for a minimum estimated direct cost-savings of $12,720 annually. An estimated 270 FFs could be prevented annually at a provincial level. Thirty-nine (30.5%) patients were started on new OP medication. All patient respondents (100%) felt that the OFLS was "good" or "excellent."Conclusions: Our study utilized virtual tools to improve OP education, evaluation, and treatment, and demonstrated promising patient satisfaction, cost-savings, and feasibility. Future directions include provincial implementation of a virtual OFLS to quantify economic impact and fracture prevention.

***Disclosures: Leah Kennedy**, None*

SAT-235

See Friday Plenary Number FRI-235

SAT-236

Emerging Roles of Prostaglandin E2 In Skeletal Muscle Repair and Regeneration *Kamal Awad[1], Jian Huang[2], Leticia Brotto[3], Lynda Bonewald[4], MARCO BROTTO[5]. [1]The University of Texas at Arlington , United States. [2]Rush University Medical Center, United States. [3]Bone-Muscle Research Center, The University of Texas at Arlington, United States. [4]Indiana University School of Medicine, United States. [5]University of Texas-Arlington (UTA), United States

Introduction: Prostaglandin E2 (PGE2) is a signaling molecule protecting skeletal muscle and enhancing regeneration1. was demonstrated that in vivo PGE2 treatment inhibits apoptosis of Hematopoietic stem and progenitor cells2, however this mechanism has not been validated in muscle. Previous studies indicated that Barium Chloride (BaCl2) can induce cell-death in various cell types including muscle cells3. We hypothesized that establishing an in-vitro muscle injury model using BaCl2 to study underlying molecular mechanisms and screen potential therapeutics for muscle regeneration. We tested the role of PGE2 on muscle repair and regeneration after damage by BaCl2.Methods: In-vitro muscle damage using BaCl2 model was developed. Studies using C2C12 and primary muscle cells were performed. Live/dead assay was used to monitor cell's death. Fusion index (FI) calculation was used to quantify the differentiation and muscle damage. Live dynamic imaging used to quantify cell's migration and muscle regeneration. Pathway finder q-PCR array was used to uncover the activated pathways. Ex-vivo FDB myofibers were damaged with BaCl2 and treated with PGE2 while monitored the Ca transient. All experiments were tested with n=4 and in triplicates. T-Test and ANOVA were performed.Results: BaCl2 induces myoblast cell death as indicated by significant increase in number of dead cells after 6 hrs. BaCl2 induced muscle damage via breakdown of myotubes as indicated by significant decrease in FI (p=0.001); while PGE2 attenuated this effect. PCR results indicated that BaCl2 treatment upregulates the BCl-2 gene, involved in programmed cell death "apoptosis". Treatment with PGE2 significantly upregulated the anti-apoptotic gene, Birc-3 (~7.5-fold) vs control. Ex-vivo data from FDB muscle confirmed the same rescuing mechanism with 50 nM PGE2 treatment.Conclusion: BaCl2 induced muscle damage and dysregulated the regeneration through the upregulation of BCl-2 gene, while PGE2 normalizes muscle regeneration after BaCl2 through the upregulation of Birc-3. This study establishes a new in vitro model of BaCl2 damage in muscle cells. The data suggests that BaCl2 induces damage via cell apoptosis, while PGE2 exerts anti-apoptotic effects and rescuing mechanism during muscle damage.1- Mo, C., et. al., (2012). Recent patents on biotechnology, 6(3), 223-229.2- Porter L., et al., (2011). Blood, Volume 118, Issue 21.3- Morton, A. B., et. al. (2019). Skeletal muscle, 9(1), 27.

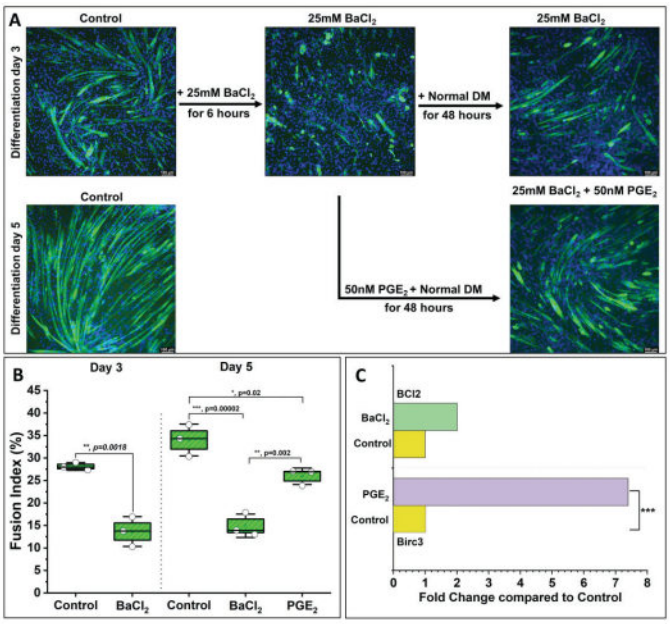

Figure1: $BaCl_2$ significantly damage skeletal muscle while PGE_2 attenuates the damage and significantly enhances the regeneration (A&B) via the upregulation of anti-apoptotic Birc3 gene (C).

***Disclosures: Kamal Awad**, None*

SAT-237

Osteoimmunity-regulating nanosilicate-reinforced hydrogel for enhancing osseointegration *Juny Chen[1], Yuanyuan Li[1], Qianbing Wan[1]. [1]West China Hospital of Stomotology, Sichuan University, China

As osteoimmunomodulation was identified as a new and important strategy to enhance material osseointegration, designing an appropriate immune response after biomaterial implantation become a major challenge for efficient bone repair. In this study, a nanosilicate-reinforced sodium alginate (SA) hydrogel is fabricated by introducing montmorillonite (MMT) nanoparticles, meanwhile immunoregulator,harmine (HM) is loaded and released to induce macrophages to differentiate into M2 type. The release of HM and MMT can directly induce bone formation, meanwhile, the release of HM can stimulate the macrophages towards M2 phenotype and secrete osteoblast-related cytokines to indirectly promote bone formation, designed to maximize the material's osteoblastic induction potential (Scheme 1). The fabricated SA/MMT/HM(SMH) hydrogel exhibited improved mechanical stiffness and stability. The hydrogel loaded with HM efficiently promoted macrophage anti-inflammatory M2 phenotype polarization, enhanced the secretion of pro-tissue healing cytokines to induce a favorable immunomodulatory microenvironment for osteogenic differentiation of BMSCs. Further rat air-pouch model and the critical-size bone defect model results showed that SMH hydrogel induced macrophage infiltration into the surrounding tissues and increased the proportion of M2 macrophage, markedly reduces local inflammation while enhancing desirable new bone formation. Transcriptomic analysis revealed that SMH induced acceleration of the M1-to-M2 transition of macrophages by inhibited relevant inflammatory signaling pathways and activation of PI3K-AKT1 signaling pathway. The results above demonstrate that this immunomodulation high-intensity hydrogel might be a promising biomaterial for bone regeneration, which also provides a valuable base and positive enlightenment for massive bone defect repair.

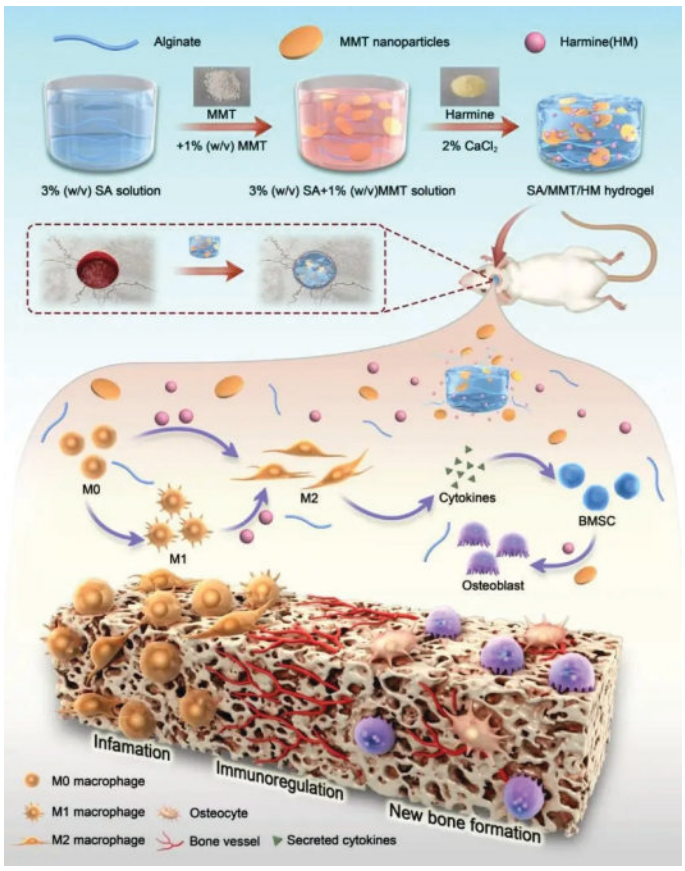

***Disclosures: Juny Chen**, None*

SAT-238

The Collagen Receptor, Discoidin Domain Receptor 2 (DDR2), is Required for BMP-induced Osteogenesis *RENNY FRANCESCHI[1], Fashuai Wu[2], Chunxi Ge[3]. [1]University of Michigan, United States. [2]University of Michigan School of Dentistry, United States. [3]Univ of Michigan School of Dentistry, United States

Objectives: DDR2 is required for normal bone development where it functions in GLI1+ skeletal progenitor cells (SPCs). However, it is not known if it can regulate BMP-dependent bone formation.Methods: Mouse lines used: Ddr2slie/slie (global Ddr2-deficient), Ddr2Mer-icre-Mer;R26RtdTomato; Gli1CreERT;R26RtdTomato and Gli1CreERT;Ddr2loxp/loxp and Ddr2loxp/loxp. Bone formation was measured by subcutaneously implanting BMP2-containing GelfoamTM sponges in mice followed by analysis using microCT, histology, and immunofluorescence (IF). Osteoblast differentiation was measured in BMSCs isolated from Ddr2loxp/loxp mice. BMP signaling was measured by Western blot. RNA-seq was conducted by the University of Michigan Sequencing Core.Results: Comparison of BMP2-induced bone formation in wildtype and Ddr2-deficient (Ddr2slie/slie) mice revealed a strong requirement for DDR2. Similarly, implanted BMSCs from Ddr2-deficient mice are unable to form bone. Lineage tracing in tamoxifen-treated Ddr2Mer-icre-Mer;R26RtdTomato and Gli1CreERT;R26RtdTomato mice showed Ddr2 and Gli1 are expressed in connective tissue cells that rapidly migrate into Gelfoam implants with or without BMP2. In addition, IF analysis showed extensive cellular colocalization (approx. 85%) for DDR2 and GLI1. In the presence of BMP2, DDR2/GLI1-positive cells form bone via an endochondral process. Conditional knockout of Ddr2 in GLI1+ cells using tamoxifen-treated Gli1CreERT;Ddr2loxp/loxp mice strongly inhibited BMP-induced bone formation.The basis for DDR2 actions was explored using BMSCs isolated from Ddr2loxp/loxp mice treated with control or Cre adenovirus. Ddr2 inactivation strongly inhibited osteoblast differentiation. However, it had only a minor effect on rapid BMP2 responses (SMAD1/5/8 phosphorylation/nuclear translocation, AKT and ERK1/2 phosphorylation). In contrast, Ddr2 deficiency was associated with reduction in BMP-induced gene expression as measured by RNAseq and reduction of nuclear/cytoplasmic YAP/TAZ distribution, changes that may explain the loss of osteoblast differentiation.Conclusions: DDR2 is necessary for BMP2-induced bone formation where it functions in GLI1+ SPCs that migrate into implants from adjacent connective tissue. DDR2 is also necessary for BMP2-induced osteoblast differentiation, a response that may be mediated by Hippo signaling.

***Disclosures: RENNY FRANCESCHI**, None*

SAT-239

Central Nervous System Injury Dysregulates Muscle MiRNAs Signaling to Promote Heterotopic Ossifications *Dorothée Girard[1], Jules Gueguen[2], Bastien Rival[1], Juliette Fernandez[1], Marie-Emmanuelle Goriot[1], Sébastien Banzet[1]. [1]IRBA / INSERM UMRS-MD 1197, France. [2]Institut de Recherche Biomédicale des Armées, France

Neurogenic heterotopic ossifications (NHOs) are intra-muscular ectopic bone formations that develop following central nervous system (CNS) damage. NHOs occur in the vicinity of major joints and induce ankylosis, pain, nervous and vascular compressions, ultimately impairing patient recovery. The role of the CNS lesion in the onset of NHO is still poorly understood while therapeutic solutions, apart from surgical resection, remain unsatisfying. At the cellular level, pro-inflammatory macrophages are known to be involved in the pathogenesis by promoting aberrant osteogenic commitment of muscle fibro-adipogenic progenitors (FAPs). In this study, we investigated miRNAs signaling dysregulation in the muscle tissue from a clinically relevant NHO mouse model and in FAPs from NHO patients. NHO was induced in C57Bl/6J mice by combining spinal cord injury (SCI) and cardiotoxin injection (CDTX) in the gastrocnemius muscle. Muscles were harvested at day 2, 4 and 7 for miRNA profiling and FAPs were isolated to study osteo-chondrogenic mRNA and miRNAs expression. Human FAPs were isolated from muscle surrounding NHO and cultured in osteogenic conditions with pro-inflammatory conditioned medium from LPS stimulated macrophages (CM+). Osteo-chondrogenic mRNAs and miRNAs expression were assessed after 1, 3, 7 and 10 days. Human FAPs were also transfected with either miRNAs inhibitors or mimics for functional analysis.We observed the overexpression of osteo-chondrogenic Runx2 and Sox9 mRNAs along with the overexpression of osteo-suppressive miRNAs in CDTX muscle. When combining CDTX with SCI injury, intramuscular mineralization nodules developed and osteo-suppressive miR-199a-3p and miR-214-3p response was hindered. In FAPs isolated from CDTX muscle, SCI induced a global downregulation of osteo-suppressive miRNAs while osteo-chondrogenic Alpl, Runx2 and Sox9 mRNAs were overexpressed. In osteogenic condition, pro-inflammatory CM+ exarcerbated human FAPs in vitro mineralization activity and stimulated ALPL, RUNX2 mRNAs and osteo-suppressive miRNAs expression. Functional analysis of miRNAs candidates confirmed that miR-20a-5p, miR-199a-5p, miR-146a-5p and miR-214-3p were able to inhibit human FAPs mineralization capacities by downregulating osteo-chondrogenic mRNAs expression.This study provides insight into an osteo-suppressive mechanism regulated by miRNAs in response to muscle injury that is ablated by CNS damage in the early stages of NHO pathophysiology.

***Disclosures: Dorothée Girard**, None*

SAT-240

mRNA profiling of human fracture callus and nonunion tissues *Rishika Thayavally[1], Peter Kloen[2], Leonidas Salichos[1], Michael Hadjiargyrou[1]. [1]New York Institute of Technology, United States. [2]Academic University Medical Centre, Netherlands

Fracture repair is a complex regenerative biological process that ultimately restores the bone's biomechanical, biochemical, physiological and functional properties. In the United States alone, 16 million people each year fracture a bone and most heal within 6-12 weeks with full recovery of function. Unfortunately, for some patients, the fracture does not heal, and it becomes a non-union, needing (revision) surgery. At the molecular level, not much is known about the mechanisms that lead to a nonunion and thus it is imperative that we explore this. In an effort to identify the expression of known mRNAs during human fracture repair, we analyzed RNAseq data from normal fracture callus (FC, Control) and nonunion tissue (Hypertrophic and Oligotrophic; HNU and ONU; experimental) from patient samples. RNA from each condition, FC (n=6), NHU (n=8) and ONU (n=9) was analyzed in order to identify differentially expressed genes between these tissues. Following analysis of RNAseq data and comparison/normalization to the FC sample, 67 and 81 mRNAs were differentially expressed in the HNU and ONU, respectively. From these differentially expressed genes, 20 were common between the two non-union samples. Moreover, out of the 20 common genes, 8 were upregulated and 12 were downregulated. To explore the biological significance of these differentially expressed genes, we analyzed gene ontology and pathway enrichment analyses using the Database for Annotation, Visualization and Integrated Discovery (DAVID) Bioinformatics Resources and identified several relevant and common biological processes (i.e. positive/negative regulation of transcription; positive/negative regulation of inflammatory response; actin filament organization; circadian regulation of gene expression; etc). Taken together, these data provide a comprehensive examination of mRNA expression in fracture callus and nonunion tissues and hopefully they will enable us to decipher some of the molecular mechanisms responsible for normal physiological repair and nonunions.

***Disclosures: Rishika Thayavally**, None*

SAT-241

Biocompatibility and Osteogenic Properties of a new type of Absorbable Magnesium-Based Amorphous Alloy *Talante Juma[1], Yongping Cao[1]. [1]Peking university first hospital, China

Purpose: The treatment of bone defects has always been a difficult problem in orthopedic clinical practice, emerging development of amorphous alloys has been a new hope due to their unique characteristics. In this study, the biological safety and osteogenic property of a new, absorbable magnesium-based amorphous alloy (Mg66Zn30Ca3Sr1) were investigated through animal experiments.Method: 30 SD rats were randomly divided into a blank group, a control group, and an experimental group. Bone defects with the size of 4.5*4.5*5mm were made in the lateral condyle of the left hind leg of all rats. The blank group closed the wound after establishing the bone defect model. The control group was implanted with zinc-magnesium powder and chondroitin sulfate gel in the bone defect, while Mg66Zn30Ca3Sr1 amorphous alloy particles and chondroitin sulfate gels were implanted in the experimental group. Blood samples were collected for detection of serum osteogenic protein levels (BMP-2, OPG, OPN, and RUNX2), serum magnesium ion concentration (Mg2+), zinc ion concentration (Zn2+), blood panel test (white blood cell, hemoglobin, platelet), blood biochemical test (alanine aminotransferase, aspartate transferase, creatinine, urea nitrogen) at 4 weeks, 8 weeks and 12 weeks after the operation. After all the rats were sacrificed 12 weeks postoperatively, X-ray and micro-CT of left knee joints were conducted, as well as the HE and Masson's staining of the knee joint sections.Result: The postoperative conditions of all rats were normal, as well as the blood panel test and blood biochemical test results of all rats at every checkpoint. The ELISA results showed that Mg66Zn30Ca3Sr1 amorphous alloy could promote all of the tested osteogenic protein levels compared to a blank group while the zinc-magnesium powder only promoted the levels of OPG and BMP-2 ($P<0.05$). Compared with the zinc-magnesium powder group, all the tested osteogenic protein levels of the Mg66Zn30Ca3Sr1 amorphous alloy group were significantly increased at every checkpoint ($P<0.05$). Micro CT analysis showed that the volume fraction of new bone and the number of trabeculae both in the Mg66Zn30Ca3Sr1 amorphous alloy group and zinc-magnesium powder group were significantly higher than the blank group at 12 weeks after the operation ($P<0.05$). The volume fraction of new bone and the number of trabeculae in the Mg66Zn-30Ca3Sr1 amorphous alloy group were significantly higher than in the zinc-magnesium powder group ($P<0.05$). HE staining and Masson's staining showed there were more new bone formation and less metal degradation in Mg66Zn30Ca3Sr1 amorphous alloy group than in the zinc-magnesium powder group.Conclusion: Mg66Zn30Ca3Sr1 amorphous alloy is a new kind of degradable material with good biocompatibility and osteogenic ability, which could provide a new sight in the treatment of bone defects.KEYWORDS: Amorphous alloy, Magnesium based, Biocompatibility, Osteogenic ability.

***Disclosures: Talante Juma**, None*

SAT-242

Lipoxin A4 accelerates osseous wound healing in two independent models of bone repair *AMY KOH[1], Ann Decker[2], Conor Locke[2], Kenneth Kozloff[2], Laurie McCauley[3], Hernan Roca[2]. [1]U OF MICHIGAN, United States. [2]University of Michigan, United States. [3]University of Michigan School of Dentistry, United States

Injured bone navigates the healing process via phases including cell apoptosis, inflammation, resolution and remodeling. Lipoxin A4 (LXA4), an eicosanoid lipid mediator derivative of arachidonic acid, is one of the most abundant lipoxin specialized pro-resolving mediators. LXA4 promotes inflammation resolution and has positive osseous effects in conditions that induce bone loss such as periodontitis and ovariectomy, in part due to its inhibitory actions on osteoclasts. In this study, the effects of LXA4 on bone healing were investigated in two models: tooth extraction socket and ulnar stress fracture (sFx). In the socket model, C57Bl/6 male mice (12wk) were anesthetized, and the first maxillary molar extracted. LXA4 (10ng/g; IP) or vehicle (Veh) was administered daily for 14d starting immediately after extraction. µCT analyses revealed a significant increase in bone volume/total volume ($p<0.05$) within the socket with LXA4 treatment. There was a significant decrease in trabecular (Tb) number and a significant increase in Tb thickness and BMD ($p<0.05$). There was no systemic impact of LXA4 as seen via µCT of the tibia, serum TRAcP5b (indicator of OC number), or serum P1NP (indicator of bone formation). Nor were there any differences on TRAP+OC or F4/80+ (macrophage) cell numbers within the socket. In the second wound healing model, C57Bl/6 female mice (16wk) underwent cyclical uniaxial compressive loading to create a sFx in the right ulna. LXA4 (50ng/g; IP) or Veh was administered daily for 5, 7 or 12 days starting immediately after sFx. µCT analyses of sFx sites at d7 showed LXA4 treatment significantly decreased callus bone volume ($p<0.05$), as well as callus ($p<0.01$) and fracture longitudinal length ($p<0.05$), while BMD was unchanged. Serum markers of resorption (TRAcP5b) and formation (P1NP) were also unchanged. At d5, collagen2a1 staining was decreased in the callus ($p<0.05$) in the LXA4 group correlating with the subsequent decrease seen in bone volume at d7. At d12, callus bone volume was no longer different between groups, however mechanical 4-pt bending analyses revealed that LXA4 increased stiffness in the loaded ulna compared to Veh ($p<0.05$). Altogether, these data reveal that the pro-resolving mediator, LXA4 accelerates osseous wound healing in two independent wound regeneration models. Our analysis showed no effect on osteoclasts in these models, highlighting that further studies into the mechanism of LXA4 mediating bone healing are needed.

***Disclosures: AMY KOH**, None*

SAT-243

The role of wnt16 in satellite cell activation *Sumaya Addish[1], W. Joyce Tang[2], Ronald Kwon[2]. [1]University of Washington, United States. [2]University of Washington School of Medicine, United States

The recapitulation of WNT signaling pathways that dually influence bone and muscle during embryonic morphogenesis is a promising approach for developing novel regenerative therapeutics that target both tissues. WNT16 plays a critical role in mediating genetic influence on bone mineral density and fracture risk and is actively being pursued as a target for osteoporosis therapies. Recent work from our lab has demonstrated wnt16 to have dual roles in zebrafish spine and muscle morphogenesis [1]. In embryos, wnt16 was coexpressed with pax7 in the dermomyotome, which contributes myogenic precursors to developing muscle. Prior studies have shown that pax7 promotes muscle differentiation and is a marker of satellite cells that support skeletal muscle regeneration. These findings indicate that wnt16 is necessary for muscle morphogenesis, however, its specific function remains unclear. We hypothesized that wnt16 contributes to skeletal muscle regeneration by regulating pax7 in satellite cells. To test this, we performed a skeletal muscle injury in 3 days post fertilization (dpf) zebrafish. To visualize pax7 and wnt16 expression, we performed HCR RNA FISH at 1 day post injury (dpi) and imaged animals using a confocal microscope. Consistent with previous studies [2], we found that pax7 was upregulated at the injury site and in adjacent tissue. No noticeable changes in wnt16 expression in injured muscle was observed. We previously showed that wnt16 mutants did not exhibit clear differents in pax7 expression during embryonic development [1]. Our studies indicate that wnt16 expression is dispensable for pax7 activation during development and following injury, suggesting that the influence of wnt16 on muscle morphogenesis occurs independently of pax7 regulation. Further investigation into underlying mechanisms is needed to better understand the potential to target WNT16 to treat musculoskeletal disorders and injuries. References:1. Watson et al., 2022, PLoS Genet; 2. Pipalia et al., 2016, DMM

***Disclosures: Sumaya Addish**, None*

SAT-244

Association between musculoskeletal disorders and physical activity in COPD mice *Takayuki Nabeshima[1], Manabu Tsukamoto[1], Yosuke Mano[1], Daisuke Arakawa[1], Takafumi Tajima[1], Yoshiaki Yamanaka[1], Eiichiro Nakamura[1], Ke-Yong Wang[2], Kagaku Azuma[3], Akinori Sakai[1]. [1]Department of Orthopaedic Surgery, School of Medicine, University of Occupational and Environmental Health, Japan. [2]Shared-Use Research Center, School of Medicine, University of Occupational and Environmental Health, Japan. [3]Department of Anatomy, School of Medicine, University of Occupational and Environmental Health, Japan

Introduction: The pathogenesis of musculoskeletal disorders associated with Chronic Obstructive Pulmonary Disease (COPD) is unclear. Since COPD patients have multi factors that contribute to the development of those disorders, basic research using animal models will be needed. We demonstrated that intratracheally administered elastase (PPE) induces emphysema in a mice model (COPD mice), which exhibits trabecular bone loss, fiber type shift from type I to type II muscle fibers and muscle atrophy, however we did not investigate considering physical activity. Our study aimed to investigate whether the musculoskeletal disorders in COPD mice were due to reduced physical activity. Methods: Twelve-week-old male C57BL/6J mice were intratracheally administered saline (Saline group) or PPE (PPE group), and every 4 weeks, food intake, water intake, urine volume, fecal volume and spontaneous activity were measured using a metabolic gauge and the EthoVision XT (Noldus, Wageningen, Netherlands), respectively. At 24 weeks after intratracheal administration, the animals were sacrificed and weighed for leg muscles. Lungs, femurs, and tibiae were harvested, and lungs were measured for mean inter-alveolar distance (Lm) in tissue specimens. The bone microstructure and histomorphometry were analyzed using micro-CT images and tissue specimens. In addition, bone marrow cells were harvested and CAGE-seq was performed. Results: No significant differences in food intake, water intake, urine volume, feces volume, and spontaneous activity were found between the two groups at each time point. At 24 weeks after intratracheal administration, the PPE group had significantly larger Lm values than the Saline group and showed pulmonary emphysema. The value of soleus muscle weight was significantly smaller in the PPE group. In bone histomorphometry of the leg bones, the values of BV/TV, vBMD, Tb.Th, Tb.N, Ob.S/BS and Ob.N/BS were significantly lower in the PPE group. CAGE-seq showed that the expression of musculoskeletal-related genes was decreased in the PPE group. Discussion: In COPD mice, disease-nonspecific factors (age, weight, nutritional status, smoking, and steroids) for muscle and bone were eliminated as much as possible, and physical activity was no exception. Further investigation is needed to take disease-specific pathophysiology into account. Conclusions: COPD mice did not show decreased spontaneous activity, and musculoskeletal disorders occurred regardless of physical activity.

***Disclosures: Takayuki Nabeshima**, None*

SAT-245

Recovering Bone Tissue Strength Through Fecal Microbiota Transplantation in Adult Mice *CHONGSHAN LIU[2], Erika Cyphert[2], Angie Morales[2], Jacob Nixon[2], Christopher Hernandez[3]. [2]Cornell University, . [2]Cornell University, United States. [3]University of California, San Francisco, United States

Alterations to the gut microbiome can cause reductions in bone strength that are not explained by bone density or geometry. However, it is unclear if microbiome-induced changes in bone tissue mechanical properties can be reversed. Here we ask if repairing the gut microbiota using fecal microbiota transplant (FMT) could improve bone tissue strength. Male and female mice were randomly divided into 5 groups: untreated, initial dosing reconstituted, initial dosing unrecovered, delayed dosing and continuous (134 animals, n=12-17/group/sex). The gut microbiome was altered with antibiotics in drinking water (1g/L ampicillin and 0.5g/L neomycin). Initial dosing groups were treated from 1 to 4 months of age then either received FMT (reconstituted) or no further treatment (unrecovered). The other groups were dosed from 4 to 6 months (delayed) or 1 to 6 months (continuous). At 6 months of age animals were euthanized and the femurs collected. In males, whole bone strength was significantly reduced in the unrecovered ($p = 0.040$), delayed ($p = 0.005$), and continuous ($p = 0.001$) groups as compared to the untreated, indicating impaired bone tissue strength. The whole bone strength in the reconstituted group was comparable to the untreated group (Fig. 1a). Similar trends among groups were seen in females, although differences were not statistically significant ($p = 0.13$, Fig. 1b). The composition of the fecal microbiota mirrored the differences in bone tissue strength, with the continuous, unrecovered, and delayed groups showing a composition similar to one another and distinct from the other groups (which clustered together, Fig. 1c and 1d). Only a small amount of bone tissue is resorbed/formed in the cortex between 4-6 months of age, that changes in the gut microbiome over this period alter bone tissue strength suggests that changes in bone tissue strength do not require matrix turnover, indicating the existence of a yet-to be described mechanism that changes the mechanical properties of existing bone matrix. While future studies are required to characterize this mechanism, our findings provide the first evidence that microbiome-induced alterations to bone tissue strength are recoverable in adults.

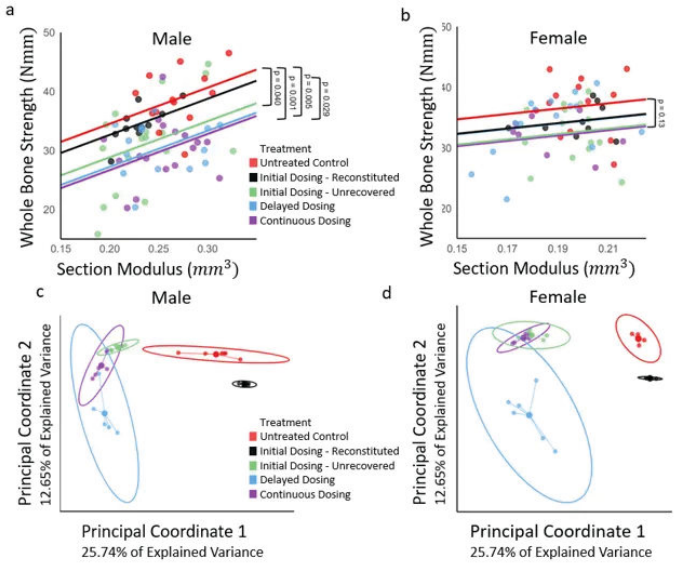

Fig 1. (a, b) Differences in the relationship between section modulus and whole bone strength indicate alterations in bone tissue strength. (c, d) The composition of the fecal microbiota is shown (beta diversity). Clusters closer to one another are more similar to each other.

***Disclosures: CHONGSHAN LIU**, None*

SAT-246

Yolk-sac Erythromyeloid Progenitors in Fracture Healing and Regeneration *Choiselle Marius[1], Koji Ishikawa[1], Puvi Nadesan[1], Vijitha Puviindran[1], Tomasa Barrientos De Renshaw[1], Tuyet Nguyen[1], Savanna Ma[1], Benjamin Alman[1]. [1]Duke University, United States

Bone fractures are common injuries. However, delayed, and incorrect fracture healing can be a major health issue, particularly in the context of aging. Therefore, strategies to improve the pace of repair and prevent non-union (the body's inability to heal a fracture) will substantially improve patient outcomes as well as lower health care costs. As fracture healing is a dynamic process, many cell types from various lineages are required to restore a broken bone. Macrophages are known to play a critical role in bone healing, and these cells have several embryonic origins enabling unique functions. Yolk-sac derived macrophages are one research candidate, as previous work from our lab identified a reservoir of yolk-sac derived macrophages that reside in the spleen and are capable of not only migrating to a

fracture site, but also differentiating into osteoclasts to contribute to repair. Osteoclasts are essential players in bone repair, serving to resorb unnecessary bone to initiate osteogenesis. Additionally, previous work has shown that when osteoclasts are compromised or macrophages are depleted, fracture healing slows immensely, and the quality of repair suffers. However, while we know that these yolk-sac derived macrophages/osteoclasts can hone to fracture sites, their specific functions are not understood. Yolk-sac derived macrophages also precede the development of hematopoietic stem cells, populate organs, and maintain their populations through self-renewal in peripheral organs, serving as a novel extramedullary source of progenitors. This proposal will further characterize the functions of these yolk-sac derived cells and could potentially also identify targets for future osteogenic therapeutics.

***Disclosures: Choiselle Marius**, None*

SAT-248

Transcriptional changes in periosteum of an early callus *Sanja Novak[1], Vijender Singh[2], Kurt Hankenson[3], IVO KALAJZIC[4]. [1]UConn Health, , [2]UConn, Institute for Systems Genomics, Computational Biology Core, United States, [3]University of Michigan, United States, [4]University of Connecticut Health Center, United States

Bone has great regenerative capacity that depends on a pool of skeletal stem/progenitor cells (SSPC) and intercellular signaling between mesenchymal and hematopoietic populations. Following fracture there is a dramatic expansion of SSPC within a very short time followed by their commitment to chondrogenic and osteogenic lineages. It is critical to understand the early events regulating fracture healing. Our data showed improved healing ability when Notch1 signaling was overexpressed in ?SMA osteoprogenitors. The aim of this study was to determine molecular changes in SSPC and in hematopoietic lineages and to determine mechanisms involved in improved healing process with Notch1 activation.We have completed single cell RNA-seq from intact and fractured periosteal cells (3 days after the fracture) in ?SMACre+/NICD1 and Cre-/NICD1 mice. Live, mesenchymal (CD45-) and hematopoietic (CD45+) cells were sorted and single cell RNA-seq performed (10x Genomics). Rstudio and Seurat package were used for data analysis. Principal component (PC) analysis was performed, and clusters were identified using 40 PCs at the resolution of 0.25 for CD45- cells and 0.4 for CD45+ cells.We identified endothelial, satellite and muscle cell clusters and trajectories from SSPCs into chondrocytes, osteoblasts. We identified a quiescent cluster termed MSC1 with characteristics of stem cells (inhibition of cell cycle genes and mitosis) that initiates proliferation after fracture and transition into highly proliferating MSCs (cluster 2, 3 and 4).NICD1 (Cre+) injured periosteum had significantly increased expression of Alpl and Ibsp compared to injured Cre-. Unexpectedly, overexpression of NICD1 lead to increases in interferon signaling genes (Ifit1, Ifit3, Iigp1, Ifi203, Ifi27l2a) in mesenchymal and endothelial clusters. We show increased Isg15 and Ifit1 mRNA in isolated periosteal cells upon Jag1 treatment, confirming the scRNA-seq data. In hematopoietic population NICD1 overexpression in the ?SMA expressing cells resulted in decreased pro-inflammatory signals (Tnf and Il6) after bone injury.Induced Notch1 activation in SSPCs led to increased expression of osteogenic genes within CD45- and decreased pro-inflammatory genes within CD45+ populations. We confirmed the importance of Notch signaling in osteoprogenitors leading to distinct transcriptional changes affecting not only osteoprogenitors and their lineage, but also hematopoietic cells during the healing process.

***Disclosures: Sanja Novak**, None*

SAT-249

A Refined Murine Growth Plate Injury Model Using Tri-lineage Collagen Reporter Technology *Sierra Root[1], Natasha Patel[2], Sarah Feltz[2], Olivia Ferrigno[2], IVO KALAJZIC[3], Christy Lottinger[4], Liisa Kuhn[2]. [1]UConn Health, School of Dental Medicine, , [2]Department of Biomedical Engineering, UConn Health, United States, [3]University of Connecticut Health Center, United States, [4]Department of Oral Maxillofacial Surgery, UConn Health, United States

The cartilage growth plate (GP) is the most fragile area of growing bones in children making it highly susceptible to injuries. Approximately 30% of GP related injuries will develop an undesirable partial bony closure of the GP from the epiphysis to the metaphysis at the site of injury. Bony bridge formation can hinder normal growth resulting in orthopedic problems such as limb length discrepancy and bone angulation deformity. Small rodent models to study GP injuries are lacking due to the small and difficult to see GP in young mice that developmentally mimic young children. The few models published often involve damage to other areas of the bone including articular cartilage. We aimed to develop a reproducible GP injury model in mice to test future regenerative approaches. Triple transgenic mice fluorescing cyan for Collagen 2a1 expressing chondrocytes, mCherry for Collagen 10a1 expressing hypertrophic chondrocytes and Topaz for Col1a1(3.6 kb) expressing preosteoblasts and osteoblasts were generated. Using tri-lineage fluorescent reporters for collagen types I, II and X, the GP and adjacent bone were visualized under a fluorescent dissecting microscope and enabled the creation of precise injuries with a dental bur. GP injury with a 0.5 mm and 1.4 mm bur were analyzed for limb length discrepancies, bony bridge formation by micro-CT and histology using fluorescent tri-lineage collagen reporters to assess cell types within injured GP. A unicortical defect created with a 1.4 mm bur over the anteromedial aspect of the tibia GP reproducibly caused GP fusion with bony bridge formation starting as early as 1-week post-injury. Light sheet fluorescent microscopy (LSFM) was used to evaluate positive Collagen I Topaz reporter expression in the GP. LSFM allowed us to gain valuable 3D information with respect to cell infiltration that could not be observed in micro-CT or by histology. In conclusion, the use of tri-lineage collagen reporter mice allowed for a consistent GP injury model that mimics limb discrepancies and stunting found in severe GP injuries. Tri-lineage collagen reporter technology also provides a simple histological readout of the location and differentiation status after healing and can be used to test therapeutic strategies to prevent GP fusion.

***Disclosures: Sierra Root**, None*

SAT-250

See Friday Plenary Number FRI-250

SAT-251

Mitochondrial function regulates ROS-mediated patterning following injury *Mimi Sammarco[1], Anyonya Guntur[2], Robert Tower[3]. [1]Tulane University, United States, [2]Maine medical center research institute, United States, [3]University of Texas Southwestern Medical Center,

Regeneration of bone and soft tissue after injury has two key requirements: energetic demand and spatial patterning to create a regenerative map. Evidence has emerged that the mitochondria serve a dual function as a hub for reactive oxygen species (ROS) signaling and ATP generation, linking growth signaling and cell metabolism to a single organelle. While ROS signaling is critical, excessive ROS is detrimental. As a result, ROS and the mitochondria that generate them, are tightly regulated through elimination of dysfunctional mitochondria (mitophagy). We unexpectedly found that two mitophagy proteins previously known to function only in mitochondrial or cell homeostasis play key roles in regeneration - BNIP3 (BCL2 interacting protein 3) and NIX (BCL2 interacting protein 3-like) - both separately impeding regeneration. BNIP3 functions to eliminate dysfunctional mitochondria (mitophagy) and modulates cell metabolism to meet the carbon and ATP needs of the cell(1). NIX also regulates mitophagy(2), however, unlike BNIP3, NIX functions to also remodel mitochondrial networks resulting in more efficient mitochondria for cell functions such as differentiation(3, 4). Very little is known about their impact during injury and regeneration. Our preliminary data has led us to hypothesize that BNIP3 and NIX function in a spatially distinct relationship where NIX supports differentiation in the blastema in response to adjacent signaling gradients generated by BNIP3 in the wound epithelium.

***Disclosures: Mimi Sammarco**, None*

SAT-253

The Regulatory Role of Osteoblast-derived Matrix Vesicles *ANNE SKELTON[1], David Cohen[2], Zvi Schwartz[2], BARBARA BOYAN[2]. [1], , [2]Virginia Commonwealth University, United States

Matrix vesicles (MVs) are nano-sized extracellular vesicles that are produced by bone and cartilage cells and become anchored in the extracellular matrix (ECM). They are historically involved in mineralization during endochondral bone formation, but further research has revealed that they are heterogeneous and are enriched with proteins and microRNA, suggesting a role in cell regulation and intercellular communication. The role and mechanism of action of MVs, particularly in bone, remains to be elucidated. In the present study we examined the regulation of osteoblasts by osteoblast-derived MVs and explored the role of caveolae as the endocytic pathway used in their uptake.MVs were isolated from confluent cultures of human MG-63 osteoblast-like cells grown in growth medium (GM) by centrifuging trypsin digests of the ECM at 100,000xg. Additional MVs were isolated in the same manner from MG-63 cells grown in osteogenic differentiation medium (OM) for 10 days. MG-63 cells in GM were treated with either MV(GM) or MV(OM) for 24 and 48 hours followed by assessment of osteoblastic differentiation and production of inflammatory markers. MG-63 cells were also pre-treated with methyl-?-cyclodextrin (?-CD) prior to MV treatment for 48 hours and evaluated for MV uptake to assess the use of caveolae-mediated endocytosis.Treatment with MV(GM) reduced alkaline phosphatase specific activity and interleukin-6 (IL-6) production at 24 and 48 hours and osteocalcin and vascular endothelial growth factor (VEGF) production at 48 hours with no changes in DNA content. MV(OM) caused a similar reduction in alkaline phosphatase at 48 hours and osteocalcin and IL-6 at 24 and 48 hours. In addition, treatment with MV(OM) caused a significant increase in IL-10 production at 48 hours. Pre-treatment with ?-CD prevented the incorporation of MV(GM)s into the cells and prevented the decrease in alkaline phosphatase specific activity, suggesting inhibition of the MV effect when caveolae are disrupted.In conclusion, our results indicate that MVs have a direct regulatory effect on osteoblasts after their incorporation into these target cells through the caveolae system. They suggest that MV composition is sensitive to the culture conditions, resulting in different cellular responses. Osteoblast-derived MVs may contribute to bone formation and remodeling in a more nuanced manner modulating the rate of osteoblast differentiation to ensure formation occurs at the correct location.

***Disclosures: ANNE SKELTON**, None*

SAT-255

See Friday Plenary Number FRI-255

SAT-256

DLL4 deletion in endothelial cells affects fracture healing *Hitoshi Tanigawa[1], Sanja Novak[1], Sierra Root[1], Kurt Hankenson[2], Ivo Kalajzic[1]. [1]Uconn Health, Center for Regenerative Medicine and Skeletal Development, United States. [2]Department of Orthopaedic Surgery, University of Michigan Medical School, United States

Fracture healing involves interactions of different cell types and signaling cascades. Both in homeostasis and healing angiogenesis is coupled with osteochondrogenesis. Notch signaling has been known as an important regulator of skeletal cell proliferation and differentiation. Our previous study showed that activation of Notch signaling promotes fracture healing. Aim of this study was to determine the effects of Notch ligand Dll4 (Delta-Like-ligand 4) deletion in endothelial cells on the fracture healing process.We performed single cell RNA-seq from cells isolated from intact and periosteum, day 3 after fracture (DPF) in ?SMACre+/NICD1 and Cre-/NICD1 mice. Live, mesenchymal CD45- cells were sorted and single cell RNA-seq performed (10x Genomics). Our analysis identified endothelial cells (EC), satellite and muscle cell clusters and trajectories from skeletal progenitors into chondrocytes, and osteoblasts.Expression of Notch ligands Dll4 and Jag2 was restricted to EC while Jag1 was expressed in mesenchymal cells. We did not detect significant expression of Dll1 and 3 in periosteum. Notch1 has strong expression in EC, and in committed mesenchymal progenitors and preosteoblasts, satellite and muscle cells while low level of Notch2 is present in all CD45- cells within the callus.Based on gene expression analysis, we decided to use conditional knockout of Dll4 (Dll4?) in EC, using Cdh5/CreERT2. Fracture healing was assessed in 8-10-week-old male mice. Cre activity was induced by intraperitoneal injection of tamoxifen (75mg/kg) on 0, 2 and 4 DPF and healing evaluated by performing real time qPCR, histology and ?CT.Dll4 deletion in EC confirmed by real time qPCR, led to decreased expression of Hey1, Hes1 and OCN compared to Cre- mice. Cre+ mice have smaller callus with less cartilage 1 week post fracture (WPF). At this point, proportion of EdU+ cells within the smaller Cre- callus was higher than in Cre+ mice, displaying phenotype of delayed healing. However, there was no significant difference in bone volume at 3 WPF analyzed by ?CT, as Jag1 ligand could have potential to compensate for Dll4.We showed a negative effect on the early fracture healing process when Dll4 is deleted in EC. This data suggests that early Notch signaling through endothelial Dll4 expression is important for healing initiation (bigger callus with more cartilage) and potentially osteoprogenitor differentiation (increased OCN) in fracture healing process.

***Disclosures: Hitoshi Tanigawa**, None*

SAT-257

Investigating Correlated Changes to Bone Repair Physiology in Mice Selectively Bred for Accelerated Bone Growth *Colton Unger[2], Sarah Manske[2], Campbell Rolian[2]. [2]University of Calgary, . [2]University of Calgary, Canada

Bone fracture repair is a rare form of true tissue regeneration in mammals, and recapitulates many aspects of endochondral ossification seen in developing long bones. During both processes, multipotent progenitors undergo cell migration, differentiate into both chondrogenic and osteogenic lineages, induce vascularization, and subsequently produce, remodel, and mineralize cartilaginous scaffolds into bone. Transgenic studies in mice have shown that many genes involved in endochondral ossification also play important roles in bone repair. However, the full extent to which these processes overlap is poorly understood. To better understand the nature of endochondral ossification in bone repair, we employed the Longshanks mouse. Longshanks mice produce 15-20% longer tibiae than random bred Controls in the same developmental timeframe, a phenomenon driven in part by enhanced endochondral ossification. We hypothesized that if bone repair and development are largely overlapping at the gene regulatory and cellular levels, then there would be correlated changes in the bone repair dynamics of Longshanks adults. In other words, we predict that bone growth and repair are so fundamentally similar, that selection to alter one process will tend to indirectly alter the other. To test this, we induced experimental tibial fractures in sex-balanced and age-matched Longshanks and Control mice and monitored their recovery over six weeks using longitudinal live-µCT imaging during key milestones in fracture repair. In parallel, we analyzed callus tissue composition through histological analysis of a cross-sectional cohort of Longshanks fractures throughout the repair process. We show that mice with enhanced endochondral ossification rates in development also produce larger, more robust fracture calluses during the endochondral ossification phase of fracture callus repair compared to Controls. Moreover, we show that differences in fracture mineralization correlate with differences in the cellular properties of Longshanks calluses, which mimic observed trends in their developing long bone growth plates. These findings demonstrate that bones that grow faster, also heal faster, and highlights a deep conservation of endochondral ossification in both repair and development that may be leveraged to help heal fractures better in clinical settings.

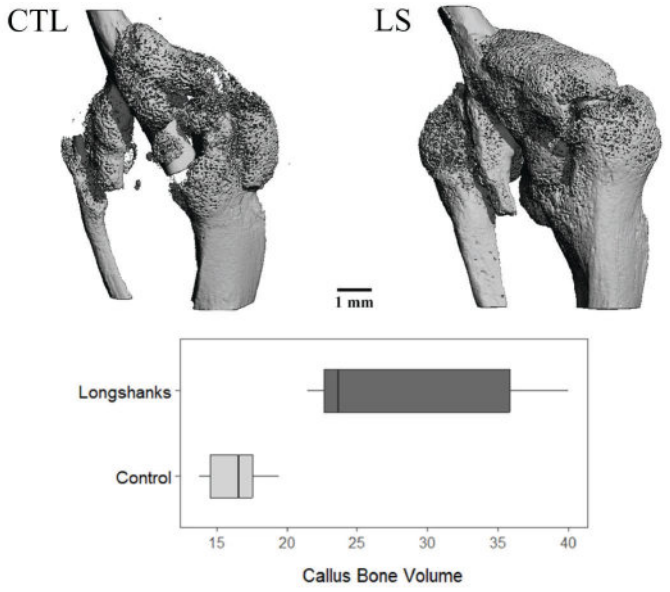

***Disclosures: Colton Unger**, None*

SAT-259

Kidney-tonifying traditional Chinese medicine (TCM) formula Er Zhi Wan (EZW) promotes myogenesis in myoblasts of aging osteosarcopenic animal model *CHRISTINA POON[1], Chun Au-Yeung[2], Yan Zhang[3], Man-Sau Wong[4]. [1]THE HONG KONG POLYTECHNIC UNIVERSITY, Hong Kong. [2]The Hong Kong Polytechnic University, Hong Kong. [3]Longhua Hospital, affiliated to Shanghai University of Traditional Chinese Medicine, China. [4]Hong Kong Polytechnic University, Hong Kong

The co-existence of osteoporosis and sarcopenia (also known as osteosarcopenia) in the older adults contributes to their higher risk for falls and fragility fractures due to reduced support from skeletal muscles. However, pharmaceutical remedies for treatment of osteosarcopenia are currently unavailable. Traditional Chinese medicine (TCM) has long been used for strengthening tendon and bone. Er Zhi Wan (EZW) is a TCM formula which contains two herbs, Fructus Ligustri Lucidi (FLL) and Ecliptae Herba (EH) at a ratio of 1:1 (w/w). Both herbs were recognized for their actions in tonifying "kidney yin" to exert potent bone protective activity. The role of muscle-bone crosstalk contributes to the pathogenesis of osteosarcopenia, however, the regulation of intracellular events of primary myoblasts, muscle satellite cells (MuSCs), and vitamin D metabolism still remains elusive. Thus, the present study aimed to determine if EZW could exert in vivo protective effects against age-related muscle loss by promoting myogenesis in MuSCs isolated from osteosarcopenic animal model. Vitamin D diet group will be included as the positive control to determine if the effects of EZW on myogenesis are comparable to the current available recommended vitamin D supplementation. Aging (10-month-old) male senescence-accelerated mouse prone 8 (SAMP8) and the control mice senescence accelerated mouse resistant 1 (SAMR1) without sarcopenia were randomly arranged and treated with EZW (14 g/kg/day), vitamin D supplementation diet (5.7 IU/g) or vehicle (saline) for 8 weeks. The primary MuSCs from hindlimbs of those mice were isolated by enzymatic dissociation and cultured into primary myoblasts. We have demonstrated that EZW could exert stimulatory effects on myogenesis in MuSCs by promoting myogenic differentiation, in which they significantly increased both number and area of myotubes ($p<0.05$). EZW was found to significantly upregulate the expressions of the myogenic markers (MHC, MyoD, Myogenin and Pax7) in differentiated myoblasts ($p<0.05$), which are essential for muscle regeneration and repairing. This study provides the evidence for supporting the use of EZW for management of age-related osteosarcopenia. Further study will determine the mechanisms that involved in mediating the multi-targets actions of EZW on muscle-bone crosstalk.Acknowledgements:This work was supported by the Health and Medical Research Fund of Hong Kong Health Bureau (19200411) and PolyU Dean's Reserve internal fund (1-ZVXG). We also thank the University Research Facility in Life Sciences at The Hong Kong Polytechnic University for the technical support.

***Disclosures: CHRISTINA POON**, None*

Saturday Orals

SAT-260

The Sodium Alginate Effect: Improving Tissue Printing from a Cellular Point of View *Ahmed Yacoub[1], Kamal Awad[2], MARCO BROTTO[3], Venu Varanasi[2]. [1]Bone Muscle Research Center, United States. [2]The University of Texas at Arlington , United States. [3]University of Texas-Arlington (UTA), United States

Introduction: Volumetric muscle loss requires external support to facilitate the healing. Biomaterials can mimic the mechanical behavior of muscles and be used as muscle grafts. They can provide improved functionality, compatibility, and regeneration, making them promising solutions for muscle regeneration. Gelatin methacrylate (GelMA) is a hydrogel material used in tissue engineering, but it has some limitations such printability, shape fidelity, and degradation. One promising strategy is to incorporate sodium alginate into GelMA hydrogels to overcome its limitations. This study investigates the advantages of this approach, including improved stability and mechanical properties, which could ultimately make GelMA hydrogels more suitable for a lot of tissue engineering applications.Methods: The methodology employed for this investigation includes rheology, 3D printing, and cell cultures. The rheological testing utilized a frequency sweep test, which provided information on the storage and loss modulus of the materials and their behavior under shear stress1. GelMA-alginate blends were extruded using a BioX 3D printer and crosslinked using UV light2. Cell viability was assessed using a LIVE/DEAD assay3. All experiments were tested with n=3 and in triplicates.Results: Firstly, we evaluated the rheological characteristics of muscle to determine the optimal properties of hydrogels that closely resemble the extracellular matrix of skeletal muscle. All formulations showed shear thinning behavior. GELMA + 1%, 2%, and 4% Alg exhibited an increase in the storage modulus. Storage modulus of the tested hydrogel attained a value of 950 +/- 56.5 Pa, which is consistent with the storage modulus of skeletal muscle. All GelMA alginate bio-inks exhibit superior printability when compared to GelMA alone. Live/dead assay demonstrated superior cell viability for GelMA+1%-alginate, compared to other tested formulations.Conclusion: The study showed that incorporating sodium alginate into GelMA hydrogels improves mechanical properties and stability for tissue engineering, specifically for muscle and neuronal cells. These findings are a significant advancement in the field of regenerative medicine, as they offer new possibilities for creating more effective and durable tissue constructs for transplantation and drug delivery.1- Zhang, J., et. Al., 2018. ACS Biomater. Sci. Eng. 4, 3036-3046.2- Gao, T., et. Al., 2018. Biofabrication.3- Siller, I.G., et. Al., 2019. Materials.

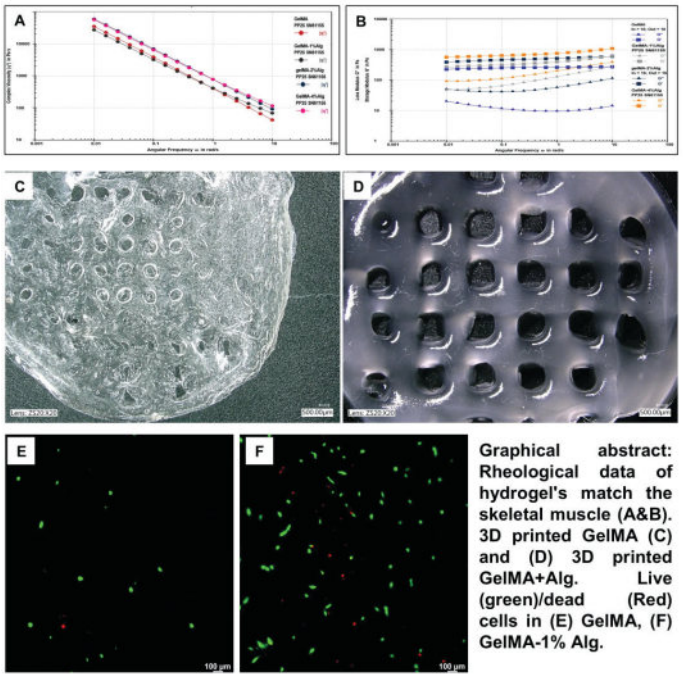

Graphical abstract: Rheological data of hydrogel's match the skeletal muscle (A&B). 3D printed GelMA (C) and (D) 3D printed GelMA+Alg. Live (green)/dead (Red) cells in (E) GelMA, (F) GelMA-1% Alg.

***Disclosures: Ahmed Yacoub**, None*

SAT-261

See Friday Plenary Number FRI-261

SAT-262

See Friday Plenary Number FRI-262

SAT-263

Molecular Phenotyping of Bone Forming Cells *Atenisa Caci[1], Nicholas Ditzel[2], Moustapha Kassem[1], Alexander Rauch[1]. [1]Molecular Endocrinology & Stem Cell Research Unit (KMEB), Department of Endocrinology and Metabolism, Odense University Hospital, Odense, Denmark and Department of Clinical Research, University of Southern Denmark, Odense, Denmark., Denmark. [2]Faculty of Health Science, Biomedical laboratory, University of Southern Denmark, Odense, Denmark, Denmark

Background: Bone Marrow stromal cells (BMSCs), are capable of multilineage differentiation. However, hBMSCs are heterogenous, not only in vivo due to the local niche, but also under standard culture conditions as clonal cell lines differ greatly in their potential to form bone.Purpose: Characterize the transcriptional heterogeneity of clonal MSC lines with distinct bone forming potential in vivo to define gene signatures that favor bone forming potential and to test the secretory capacity to transfer bone-forming potential from high to low-bone forming clones.Methods: Determine the cellular heterogeneity of clonal cell lines (high/low bone forming) using scRNA-seq analysis and quantify both in vitro and in vivo osteogenic potential of high, low, or mixtures of high and low bone-forming clones.Results: Cells with low bone-forming potential show higher osteogenic differentiation in vitro, which sought us to hypothesize that these cells either lack a positive signal required for or have a negative signal that prevents bone formation in vivo (A). At the single cell level, clones with similar bone forming potential show an alike cellular heterogeneity that is distinct between high and low bone forming clones and distinct to the parental hBM-MSC-TERT4 cells (B, bar plots). Bone-forming potential is characterized by the presence of cells with high regulation of cytoplasmic ribosomal proteins and PI3K-AKT mTOR signaling and the absence of HIPPO and VEGFA-VWGFR2 signaling. Bone formation assays in immunodeficient mice show that the presence of HBF cells in mixed cultures has a positive effect on bone formation in vivo beyond the linear relationship of cell numbers between high and low bone-forming clones (C).Conclusion: PI3K-AKT mTOR pathway activity seems to be beneficial for high bone-forming potential which can transferred on non-bone forming clones via secretory or cell-to-cell adherence mechanisms.

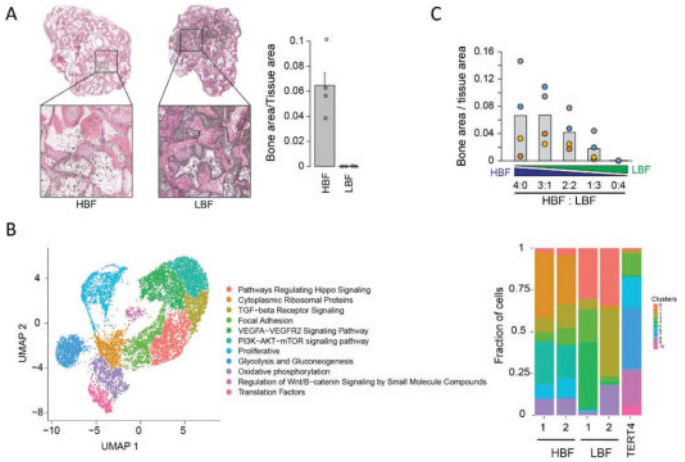

***Disclosures: Atenisa Caci**, None*

SAT-264

Identification and characterization of novel skeletal stem cell populations in mice and humans *Daniel Coutu[1], Stephanie Farhat[2], Bahaeddine Tilouche[3], Spencer Short[3]. [1]Ottawa Hospital Research Institute, Canada. [2]Univeristy of Ottawa, Canada. [3]University of Ottawa, Canada

Skeletal tissues possess an amazing capacity to regenerate. However, this regenerative capacity decreases with age and comorbidities. In older individuals, skeletal tissues heal slowly and imperfectly despite advances in orthopedic surgery and rehabilitation. Current experimental approaches involve tissue engineering and stem cell-based regenerative therapies. Indeed, stem cells are responsible for growth, maintenance, and repair of skeletal tissues. However, they remain poorly characterized at the cellular and molecular levels which is a clear limitation for their clinical use. Our aim was to identify and characterize novel skeletal stem cell populations in murine and human tissues. To achieve this, we used genetic lineage tracing, spectral 3D confocal imaging, computational image analysis, single cell transcriptomics and in vitro assays on mouse and human tissues. We show that the adult mouse skeleton contains self-renewing, multipotent skeletal stem cells (SSCs) with osteogenic, chondrogenic and adipogenic potential. These bona fide SSCs express Sox9 and are located in the resting zone of the growth plates and in periosteum. We further show that they persist after epiphyseal fusion in mature and old animals. Transcriptome analysis revealed that these cells express other putative SSCs markers, as well as genes involved in skeletal development, stem cell self-renewal, and fate decision. This data provides testable

drug targets to pharmacologically manipulate SSCs fate decisions in situ. We showed that human tissues contain SSCs akin to murine tissues. This is the first experimental proof of self-renewal in postnatal SSCs in vivo. These findings provide actionable insights for the use of culture-expanded stem cell product for regenerative medicine product or pharmacological targeting of these stem cells in situ.

***Disclosures: Daniel Coutu**, None*

SAT-265

The Decreased Expression of Sestrin 2 Contributes to a Decline in Osteogenesis and an Increase in Adipogenesis of Bone Marrow Mesenchymal Stromal Cells in Aged Individuals *Jeong-Hwa Baek[1], Hyun-Jung Park[2], Do Yeun Kim[2]. [1]Seoul National University, School of Dentistry, Republic of Korea. [2]Seoul National University School of Dentistry, Republic of Korea

Sestrin 2 belongs to the sestrin family of stress-induced proteins, which exert antioxidant activity by regulating AMPK and mTOR signaling. Although previous reports have shown that sestrin 2 is associated with the aging process, its role in the differentiation of osteoblasts and adipocytes remains unclear. Therefore, in this study, we investigated whether aging regulates the expression levels of sestrin 2 in bone marrow-derived mesenchymal stromal cells (BMSCs) and whether sestrin 2 has a regulatory effect on the differentiation of osteoblasts and adipocytes from BMSCs. Human BMSCs obtained from old donors (between 70 and 82 years old) showed cellular senescence characteristics such as higher levels of ?-galactosidase staining and expression of p16, p21, and ?H2AX proteins compared to the BMSCs from young donors (18 and 22 years old). RNA-seq analysis showed that the expression of SESN2 in old BMSCs was significantly lower than that in young BMSCs. Quantitative RT-PCR and western blot analysis confirmed the decreased expression level of sestrin 2 in old BMSCs. To examine the effect of decreased sestrin 2 expression on osteogenic and adipogenic differentiation, we induced sestrin 2 knockdown in mouse BMSCs using siRNAs. Knockdown of sestrin 2 suppressed the mRNA expression of osteogenic marker genes (Alpl, Ibsp, and Bglap), alkaline phosphatase activity, and matrix mineralization. Furthermore, sestrin 2 knockdown enhanced the mRNA expression of adipogenic marker genes (Cebpa, Pparg, Adipoq, and Plin1) and oil red O staining. These results suggest that the aging-associated down-regulation of sestrin 2 expression contributes to the enhanced adipogenic potential but reduced osteogenic potential of BMSCs.

***Disclosures: Jeong-Hwa Baek**, None*

SAT-266

Transcriptional Plasticity of Human Bone Marrow Stromal Cells for the Osteogenic and Adipogenic Lineage in vitro *Ali Jamil[1], Moustapha Kassem[2], Alexander Rauch[1]. [1]University of Southern Denmark, Denmark. [2]Odense University Hospital, Denmark

Both aging related and idiopathic osteoporosis show a strong inverse association between bone mass and bone marrow adiposity. Human bone marrow-derived (mesenchymal) stromal cells (hBM-MSCs) are progenitors capable of differentiating into bone forming osteoblasts and fat storing adipocytes. A preferential lineage speciation of hBM-MSCs into adipocytes on the cost of osteoblasts has been suggested as an underlying cause of osteoporotic bone fragility. However, whether activating the transcriptional networks of the osteogenic or adipogenic lineage modulates the multi-lineage potential of the cell, i.e. the capacity to change cell fates, has not been studied in detail. The aim of this study was to quantify the cellular and transcriptional plasticity of hBM-MSCs.Immortalized and primary hBM-MSCs were either subjected to osteogenic or adipogenic differentiation or exposed to single or multiple rounds of switching between osteogenic and adipogenic differentiation cocktails. Gene expression was quantified at the bulk and single cell level and by real time PCR for selected markers. Cellular differentiation was quantified by histochemical staining at the population and fluorescent staining at the single cell level.Immortalized hBM-MSCs show strong plasticity at the bulk and single cell expression level upon cross-differentiation, and fully differentiated cells either direct- or cross-differentiated towards the same lineage are almost indistinguishable (fig. 1A-B). Trajectory analysis in scRNA-seq data suggest that cells committing to one lineage remain capable to activate gene signatures of the other lineage confirmed by the generation of adipocytes with osteogenic characteristics upon osteogenic stimulation. Surprisingly, activation of a lineage selective gene program in hBM-MSCs does not reduce but rather enhance their differentiation capacity to the opposing lineage. In line, cross-differentiating primary hBM-MSCs that are refractory to osteogenic stimulation allowed the cells to mineralize (fig. 1C). Finally, multiple consecutive turns (8 x 4 days) of osteogenic and adipogenic stimulation leads to hybrid cells capable of mineralization and lipid droplet formation with high ALP activity.This study highlights a strong molecular plasticity between the transcriptional networks of osteoblast and adipocyte differentiation and that initiation of lineage speciation is associated with an increase rather than decrease in the multilineage potential of hBM-MSCs.

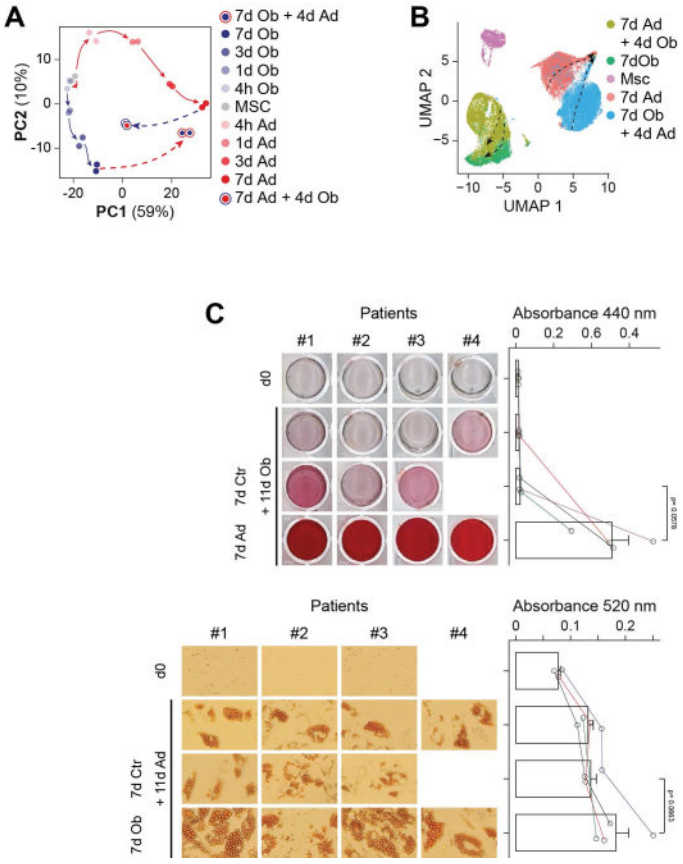

***Disclosures: Ali Jamil**, None*

SAT-267

Lgr6 regulates multiple pathways during osteoblastogenesis *Justin King[1], Archana Sanjay[2], Kurt Hankenson[3], IVO KALAJZIC[4], Matthew Wan[4]. [1]University of Connecticut School of Medicine, . [2]UCHC, United States. [3]University of Michigan, United States. [4]University of Connecticut Health Center, United States

The periosteum is crucial for proper bone healing and harbors skeletal stem and progenitor cells (SSPCs). We recently reported that leucine-rich repeat-containing G protein-coupled receptor 6 (Lgr6) is upregulated in the periosteum following fracture and is essential for promoting a robust periosteal response for proper fracture healing. To further understand Lgr6's involvement in fracture healing, we examined published single-cell RNA sequencing (scRNA-seq) data of periosteal cells from intact and three-day-old fractured tibiae. We found robust Lgr6 expression in SSPC clusters, exclusively in the injured samples. Lgr5 expression was not detected, and Lgr4 had minimal expression in uninjured and injured samples. Interestingly, Rspo2 and Rspo3, well-known ligands of Lgr6, displayed minimal expression in all clusters. Among growth factors essential for fracture healing, Bmp2 expression paralleled the Lgr6 expression pattern. We also investigated published scRNA-seq datasets of Cxcl12+ and LepR+ stromal cells isolated from intact and injured whole bones, uncovering minimal or no expression of Lgr6 and Bmp2 in all datasets. We conducted bulk RNA-sequencing on Lgr6-null and wild-type (WT) BMSC osteogenic cultures. KEGG analysis showed significant downregulation of the TGF-? signaling pathway gene set ($p<0.001$), which encompasses BMP signaling. In agreement, RT-qPCR indicated reduced expression of Bmp2 and BMP target genes. In subsequent mechanistic studies, Lgr6-null cells exhibited a diminished response to Bmp2 treatment, characterized by weakened SMAD1,3,5 phosphorylation and decreased expression of Id1 and Noggin in Lgr6-null cultures. However, the canonical Wnt (cWNT) signaling response was unimpaired in Lgr-null cultures. The addition of recombinant Bmp2, Wnt3a, or Rspo2, individually or combined, failed to restore impaired osteogenesis in Lgr6-null cultures. The spatiotemporal interplay between the Wnt and BMP pathways in regulating osteogenesis is important; studies suggest that Bmp2 operates downstream of cWnt, facilitating cells in passing the Sp7+/Col1a1+ "checkpoint." In light of our findings, Lgr6, a known Wnt pathway modulator, also regulates Bmp2 signaling during osteogenesis, demonstrating Lgr6's necessity for proper fracture healing and offering mechanistic insights into the signaling pathways controlling osteogenesis. Our findings contribute foundational knowledge to developing anabolic therapies for orthopedic applications.

***Disclosures: Justin King**, None*

SAT-270

iPSC-derived Osteoblasts for Musculoskeletal Regenerative Medicine

*Feini Qu[1], Omolabake Oyebamiji[1], Farshid Guilak[1]. [1]Washington University in St. Louis, United States

Humans have limited regenerative potential of musculoskeletal tissues following limb loss. To this end, successful attempts to regrow missing limbs could significantly improve the prognosis for amputees. The murine digit has been used to study mammalian limb regeneration, where stem/progenitor cells regrow the digit tip after distal amputation, but the mechanisms controlling skeletal elongation and patterning remain unclear. We hypothesize that the expression of a limb-like developmental program in osteoprogenitors is required for proper bone morphogenesis after digit amputation. To address this question in vitro, we sought to develop a procedure to derive osteoblasts from murine induced pluripotent stem cells (iPSCs). To this end, we differentiated murine iPSCs toward a mesenchymal state using a high-density micromass to produce pre-differentiated iPSCs (PDiPSCs; Fig. 1A). PDiPSCs (passage 3) in monolayer were exposed to the following media conditions: growth (Control; DMEM-HG base with basic fibroblast growth factor), osteogenic (Osteo; ?-MEM base with l-ascorbic acid, dexamethasone, ?-glycerophosphate), or osteogenic with supplements (Osteo+; Osteo with insulin, transferrin, and sodium selenite, nonessential amino acids, 2-mercaptoethanol). As a positive control, MC3T3 murine pre-osteoblasts (passage 7) were cultured in growth (Control; ?-MEM base) and Osteo media. At 0, 14, 21, and 28 days after osteogenic culture, cells were fixed and stained with Alizarin Red and Oil Red O to assess calcium deposition and lipid accumulation, respectively. We found that both PDiPSCs and MC3T3s produced mineralized cultures when exposed to standard osteogenic media (Osteo), which increased over time as measured by Alizarin Red staining (Fig. 1). While additional supplements to the Osteo media (Osteo+) significantly enhanced PDiPSC osteogenesis, Alizarin Red staining remained lower than MC3T3s in Osteo media at 21 and 28 days (Fig. 1C). Osteo+ media also increased adipogenesis, as evident by Oil Red O staining (Fig. 1B). In contrast, there was no mineral detected in PDiPSCs and MC3T3s cultured in their respective Control media over time. However, PDiPSCs exposed to Control media readily accumulated lipid, a feature that was absent in MC3T3s. These data indicate that PDiPSCs may be driven toward osteogenesis and/or adipogenesis depending on the soluble cues present, representing a novel in vitro platform to probe the mechanisms of osteogenic differentiation.

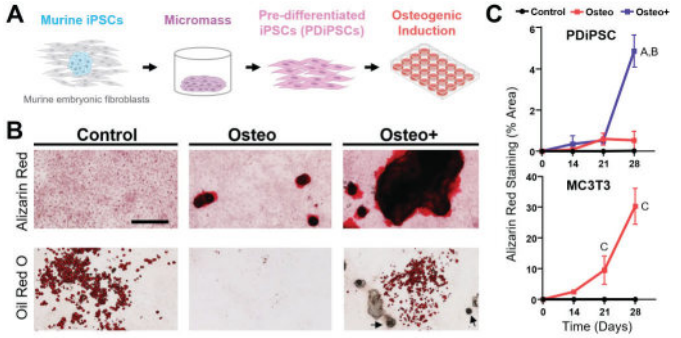

Fig. 1. (**A**) Schematic of iPSC differentiation. (**B**) PDiPSCs stained with Alizarin Red and Oil Red O after 28 days of culture. Arrows show mineralized nodules. Scale: 0.5 mm. (**C**) Alizarin Red staining (% area) over time (n=3-4/group, mean ± SD). A=p<0.05 vs. Control. B=p<0.05 vs. Osteo. C=p<0.05 vs. all other groups.

***Disclosures: Feini Qu**, None*

SAT-271

See Friday Plenary Number FRI-271

SAT-272

Differential Regulation of Calvarial vs Long Bone Skeletal Stem Cells in Bone Homeostasis and Osteogenesis Imperfecta

*JEA GIEZL SOLIDUM[3], YOUNGJAE JEONG[4], Francisco Heralde III[3], Dongsu Park[4]. [3]Department of Biochemistry and Molecular Biology, College of Medicine, University of the Philippines Manila, United States; [4]Baylor College of Medicine, ; [3]Department of Biochemistry and Molecular Biology, College of Medicine, University of the Philippines Manila, Philippines; [4]Baylor College of Medicine, United States

Reconstruction of craniomaxillofacial (CMF) defects is important but clinically challenging in patients with Osteogenesis Imperfecta (OI) or CMF deformities. Recently, calvarial suture skeletal stem cells (SuSSCs), including PRX1+ SuSSCs, were identified as a main stem cell popultaion for adult CMF bone regeneration. While much is known about skeletal stem cells in long bones, how the molecular and regulatory mechanisms of SuSSCs are different from long bone SSCs during skeletal development and injury healing have not yet been well elucidated. Further, their differences in normal and OI conditions are essentially unknown. Given that PRX1 is a common marker for calvarial and long bone SSCs, we compared PRX1+ SuSSCs with PRX1+ long bone SSCs to identify the differential function and molecular signatures during postnatal skeletal development and OI bone regeneration. By using inducible Prx1-CreER-EGFP+/-; Rosa26-tdTomato (WT) and G610c (a moderate OI) mouse models, we performed in-vivo imaging, immunofluorescence (IF) analysis, and single-cell (sc)RNA sequencing analysis. We found that PRX1+ SuSSCs and long bone SSCs differentially contribute to bone healing in both WT and OI mice. Further, in-vivo imaging of calvaria injury showed delayed migration of SuSSCs and delayed healing in OI mice. IF staining also showed less proportion of osteoblast progenies in the tibia injury site in OI mice. Single cell analysis revealed that calvarial and long bones have unique progenitor clusters with PRX1 and skeletal stem/progenitor cell (SSPC) marker expression. Consistent with development, long bone specific clusters express chondrogenic markers. Interestingly, calvaria specific clusters have higher expression of TGF?, FGFR, Twist1, and WNT-inhibitory pathways compared to long bones, suggesting potential targets for calvarial bone regeneration and repair. Overall, PRX1+ SSPCs contribute to injury repair in both WT and OI mice, with delay in OI bone healing. Further study of the molecular profiles and underlying mechanisms of PRX1+ SSPCs in WT and OI mice is warranted to provide valuable insghts to develop effective therapeutic options for CMF and long bone regeneration in healthy and OI conditions.

***Disclosures: JEA GIEZL SOLIDUM**, None*

SAT-274

Enrichment of osteogenic lineage cells from pluripotent stem cells and integration with dynamic stress-relaxing hydrogels for bone tissue regeneration

*Hongqiang Yu[1], Eileen Gentleman[1], Karen J Liu[1], Agamemnon E Grigoriadis[1]. [1]King's College London, United Kingdom

The ability to regenerate bone efficiently for tissue engineering purposes is dependent on robust bone grafting systems that are composed of productive cells and instructive biomaterials. Through formation and enrichment of mesodermal populations by precise temporal control of exposure to specific growth factors, we have identified a novel osteochondral progenitor population from mouse embryonic stem cells (mESCs) which gives rise to both chondrocytes and osteoblasts. Interestingly, exposure to BMP4 in a defined window during mesoderm enrichment completely abolished chondrogenic lineage commitment and enriched the population towards committed osteoprogenitors. Flow cytometry, western blot and qPCR analysis confirmed that BMP4 treatment converted Sox9/Runx2 double-positive cells to a population of Runx2 single-positive cells that expressed lateral plate mesodermal markers that are destined to contribute to the appendicular skeleton.To investigate the translatable potential of this BMP-induced osteogenic population, we encapsulated cells into stress-relaxing alginate hydrogels. Viscoelasticity is the natural property of many tissues and stress-relaxing hydrogels have been shown to enhance MSC osteogenic differentiation. We compared single cell and spheroid encapsulation of BMP-induced ESC-derived osteogenic cells in both RGD and non-RGD peptide functionalized hydrogels. Spheroids encapsulated in stress-relaxing hydrogels showed significantly enhanced ostoegenic differentiation compared to spheroids generated in liquid culture, demonstrating that self-assembled spheroids provide the best structure to maximize the osteogenic potential when encapsulated in dynamic hydrogels. We investigated the potential mechanosensing mechanisms underlying this enhanced differentiation and observed increased F-actin bundle and decreased N-cadherin expression in encapsulated spheroids, concomitantly with elevate levels of YAP expression. As YAP is a major mechanotransducer and is thought to directly regulate Runx2 expression, we further demonstrated increased Runx2 nuclear localization in encapsulated spheroids. Taken together, we've successfully established efficient differentiation of a pluripotent stem cell-derived osteogenic population in a dynamic hydrogel, which provides a robust system that serves as a powerful tool for not only bone regeneration but for understanding the essential parameters in directing stem cell fate and exploring cell-biomaterial interactions.

***Disclosures: Hongqiang Yu**, None*

SAT-275

See Friday Plenary Number FRI-275

SAT-276

See Friday Plenary Number FRI-276

SAT-278

The Effect of Protein Supplementation on Markers of Bone Metabolism following Repeated Whole-Body Resistance Exercise in Men and Women: A Randomised Controlled Trial *Julie Greeves[1], Joanne Mallinson[2], Sophie Wardle[1], Philip Atherton[2], Paul Greenhaff[2], Dan Wilkinson[2], Jonathan Tang[3], William Fraser[3], Thomas O'Leary[1]. [1]UK Ministry of Defence, United Kingdom, [2]University of Nottingham, United Kingdom, [3]University of East Anglia, United Kingdom

This study examined acute, dose-dependent effects of protein supplementation on markers of bone metabolism in young healthy adults following two repeated same-day bouts of whole-body resistance exercise in a randomised controlled trial. Resistance-trained men (n = 24) and women (n = 24) aged 18 to 35 y performed two within-day whole-body resistance sessions in the morning (Ex 1) and afternoon (Ex 2), separated by 4 h. Exercises comprised 3 × 8 repetitions at 75% 1 rep max (2 min rest between sets) involving latissimus dorsi pull down, single-leg press, and chest press. Participants (8 men and 8 women per group) were randomly assigned to drink either 15 g, 30 g or 60 g whey protein immediately after each exercise session. Resting venous blood samples were drawn after an overnight fast at 0 h (before Ex 1), 4 h (before Ex 2), 8 h and 24 h. Samples were analysed for ?CTX, P1NP, BALP, OC, RANKL, OPG, Sclerostin (SOST), PTH, adjusted-calcium. The dose-dependent effects of protein supplementation were analysed using Linear Mixed Effects Models. p values were adjusted using the Holm-Bonferroni method and significance was accepted at $p < 0.05$. ?CTX decreased between 0 h and 4 h, and 0 h and 8 h ($p < 0.001$); P1NP decreased between 0 h and 24 h ($p = 0.008$); OC decreased between 0 h and 4 h, and 0 h and 8 h ($p < 0.001$); and sRANKL decreased between 0 h and 4 h, 0 h and 8 h, and 0 h and 24 h ($p < 0.001$). OPG decreased between 0 h and 8 h ($p = 0.008$). PTH decreased between 0 h and 8 h ($p=0.003$) (mean (+/-SD) in Table 1). No significant changes were observed for BALP or SOST. Protein supplementation ingested immediately after two repeated same-day resistance exercise sessions did not increase markers of bone formation at any dose. A decrease in markers of bone resorption, molecular signalling makers of bone metabolism, and PTH are likely due to responses in circadian variation.

Table 1. Bone metabolic markers over time for each protein dose. Data are mean ± SD.

	15 g				30 g				60 g			
	0 h	4 h	8 h	24 h	0 h	4 h	8 h	24 h	0 h	4 h	8 h	24 h
CTX	0.66 ± 0.28	0.46 ± 0.15	0.49 ± 0.14	0.70 ± 0.27	0.56 ± 0.36	0.37 ± 0.26	0.40 ± 0.25	0.58 ± 0.30	0.62 ± 0.32	0.32 ± 0.13	0.36 ± 0.13	0.62 ± 0.30
P1NP	92 ± 36	93 ± 38	97 ± 41	88 ± 34	90 ± 70	91 ± 61	92 ± 65	87 ± 67	86 ± 36	84 ± 32	84 ± 32	81 ± 33
OC	30 ± 9	27 ± 8	29 ± 8	30 ± 9	30 ± 14	27 ± 14	28 ± 16	30 ± 16	32 ± 12	26 ± 9	27 ± 10	30 ± 11
sRANKL	0.25 ± 0.19	0.16 ± 0.13	0.18 ± 0.11	0.21 ± 0.16	0.21 ± 0.10	0.15 ± 0.05	0.15 ± 0.06	0.21 ± 0.11	0.21 ± 0.12	0.14 ± 0.08	0.13 ± 0.07	0.16 ± 0.09
OPG	2.38 ± 0.78	2.68 ± 0.97	2.32 ± 0.68	2.43 ± 0.87	2.76 ± 1.46	2.90 ± 1.59	2.51 ± 1.24	2.94 ± 1.66	3.05 ± 0.85	2.91 ± 0.86	2.69 ± 0.81	3.32 ± 1.06
PTH	4.20 ± 0.99	3.41 ± 0.79	3.39 ± 0.78	4.47 ± 1.22	4.38 ± 1.58	3.96 ± 0.97	4.03 ± 1.14	4.59 ± 1.11	4.33 ± 1.61	4.16 ± 1.39	4.04 ± 1.31	4.46 ± 1.82

***Disclosures: Julie Greeves**, None*

SAT-280

Effects of glucose-dependent insulinotropic polypeptide on bone metabolism: a systematic review and meta-analysis of randomized controlled trials *Wang Shin Lei[1], XianYan Chen[1], Andrea Kelly[2], Carlos Isales[3], Joseph Kindler[4]. [1]University of Georgia, United States, [2]The Children's Hospital of Philadelphia, United States, [3]Medical College of Georgia at Augusta University, United States, [4]The University of Georgia, United States

Glucose-dependent insulinotropic polypeptide (GIP) and glucagon-like peptide 1 (GLP-1) are gut-derived hormones that not only augment post-prandial insulin production for glucose control, but also regulate bone metabolism. Bone-resorbing osteoclasts possess receptors for incretins, and clinical trials have tested the effects of acute incretin administration on bone metabolism. These studies support an anti-resorptive effect of incretins, but results from these trials have not been systematically evaluated and summarized. We performed a systematic review and meta-analysis summarizing randomized controlled crossover trials testing the effect of GIP/GLP-1 administration on bone resorption in adults. A systematic search of PubMed was performed for studies published between January 2000-2023 that reported baseline carboxy-terminal collagen crosslinks (CTX) and percent change in CTX relative to baseline following placebo and incretin administration. Among the 168 records that were originally identified, 24 underwent full-text review, and 9 met criteria for inclusion in this analysis. Two studies performed GLP-1 administration (n=27) and seven trials performed GIP administration (n=77, 100% male), so a meta-analysis was only performed for GIP. Among the GIP studies, most included healthy subjects, with the exception of two that included 22 people with diabetes. Five studies performed intravenous infusion (n=59) and two performed subcutaneous injection (n=18). For each study, baseline CTX and percent change in CTX following GIP and placebo administration were extracted, and a mean difference (MD) between the two treatments was computed. A random-effects meta-analysis of MDs was performed using the 'R package meta' in R. GIP administration was associated with a greater decrease in CTX compared to placebo ($P<0.01$, Fig. 1), but there was relatively high heterogeneity ($I2=87.2\%$, $P<0.01$). Comparing the MD between studies of people with diabetes (MD: 0.12, 95% CI: 0.08-0.16) vs. without diabetes (MD: 0.19, 95% CI: 0.15-0.23), the decrease in CTX following GIP administration was greater in those without diabetes ($P=0.03$). Route of GIP administration (infusion vs. injection) was not associated with the effect estimate. Egger's test revealed an absence of publication bias ($P=0.014$). In summary, GIP has a bone anti-resorptive effect, which may be modified in people with diabetes. Involvement of GIP in diabetes-related bone pathology requires further attention.

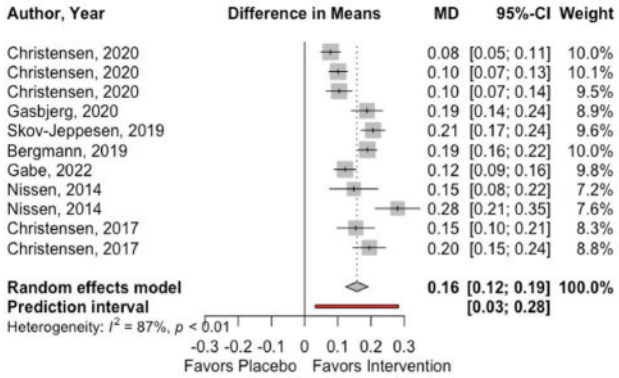

Fig. 1. Forest plot of total MD. Data represents overall study-level MD. Grey squares and horizontal lines represent the MD of each study and their 95% confidence interval. The sizes of the grey squares are proportionate to the study-level weights. Dashed line represents the overall pooled estimate. MD, mean difference, 95%-CI, 95% confidence interval.

***Disclosures: Wang Shin Lei**, None*

SAT-281

Prevention of bone loss in mice by suppression of adipocyte-like cell differentiation by phenolic acids *Perry Caviness[1], Oxana Lazarenko[2], Michael Blackburn[2], Christopher Randolph[3], Jovanny Zabaleta[4], Jin-Ran Chen[5]. [1], [2]Arkansas Children's Nutrition Center, United States, [3]Arkansas Children's Research Institute, United States, [4]Louisiana State University Health Sciences Center, United States, [5]Arkansas Children s Nutrition Center / UAMS, United States

Phenolic acids, such as hippuric acid (HA) and 3-(3-hydroxyphenyl) propionic acid (3-3-PPA), are present in the human body throughout life from microbiome digestion of polyphenols and may be involved in facilitating bone development and protection from degeneration. Currently the mechanisms by which these chemicals prevent bone deterioration are unknown. In this report, we show that HA and 3-3-PPA suppression of bone resorption is slightly less effective than zoledronic acid (ZA) in an ovariectomy (OVX) induced osteoporotic mouse model but is still able to recover µCT parameters back to sham levels (BV/TV% for tibia trabecular bone; Sham: 3.11 +/- 0.60, OVX-PBS: 2.33 +/- 0.44, OVX-HA: 3.17 +/- 0.51, OVX-3-3-PPA: 3.17 +/- 0.24, OVX-ZA: 4.06 +/- 0.60). ZA treatment, unlike HA or 3-3-PPA treatment, was shown to fuse the tibial growth plate in mice. We hypothesize that HA and 3-3-PPA inhibit bone resorption through suppression of adipose tissue formation in bone marrow. HA and 3-3-PPA treatments were shown to significantly decrease bone marrow adipocyte-like cell formation in OVX bone tissue (Average # of adipocyte-like cells at 20X magnification; Sham: 49.63 +/- 14.93, OVX-PBS: 82.75 +/- 19.30, OVX-HA: 44 +/- 9.17, OVX-3-3-PPA: 43.38 +/- 15.01, OVX-ZA: 21.86 +/- 9.66). Decreased number of adipocyte-like cells is likely through decreased expression of lipoprotein lipase (Lpl) as determined by RNA-seq analysis. Gene expression of the key adipogenesis regulator, peroxisome proliferator activated receptor gamma (PPAR?), was shown to be upregulated in OVX mice and downregulated after HA or 3-3-PPA treatments. In addition, ChIP experiments show that the association between PPAR? and Lpl promoter region in pre-adipocyte-like cells (ST2 and mouse Calvaria) was significantly suppressed following HA, 3-3-PPA or ZA treatment (ST2 fold enrichment; DMEM: 0.53 +/- 0.13, Adipogenic media (AM): 1.62 +/- 0.15, AM + HA: 0.84 +/- 0.11, AM + 3-3-PPA: 0.53 +/- 0.22, AM + ZA: 0.61 +/- 0.37) (Mouse calvaria fold enrichment; DMEM: 0.46 +/- 0.07, AM: 1.04 +/- 0.29, AM + HA: 0.43 +/- 0.12, AM + 3-3-PPA: 0.45 +/- 0.27, AM + ZA: 0.49 +/- 0.12) Contrasting HA and 3-3-PPA, ZA significantly increased the number of TRAPase positive cells and suppressed bone cell proliferation, likely through increased apoptotic pathways. These findings suggest HA

or 3-3-PPA may be alternative options for protecting against bone deterioration without the potential negative side effects induced by ZA.

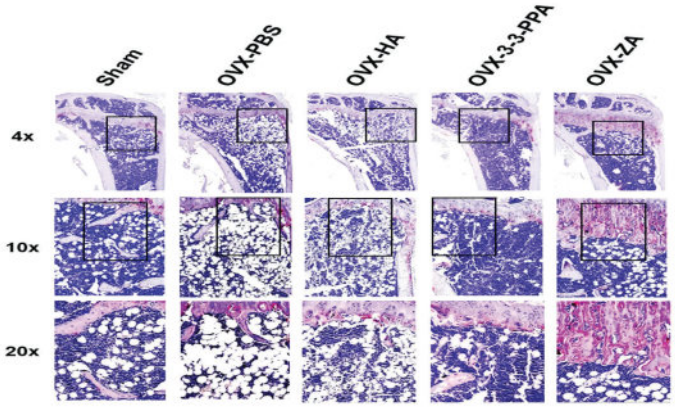

***Disclosures: Perry Caviness**, None*

SAT-283

Optimizing Nutrition Education at an Osteoporosis Centre: The Bites for Bones Randomized Controlled Pilot Trial *Julia MacLaren[1,] Heidi Piovoso[2,] Adrienne Feasel[3,] Charlie Hasselaar[6,] Sarah Rose[6,] April Matsuno[3,] Tanis R. Fenton[6,] Catherine B. Chan[5,] Gregory Kline[6,] Emma Billington[6, 1], Canada. [2]Albert Health Services, Canada. [3]Alberta Health Services, Canada. [6]University of Calgary, Canada. [5]University of Alberta, Canada. [6]University of Calgary,

Nutrition recommendations for bone health frequently target single nutrients in isolation and often do not address strategies to obtain these nutrients as part of a balanced diet. The emerging field of Culinary Medicine (CM) offers a pragmatic approach to improve dietary quality and health outcomes, but CM interventions are untested for bone health. The purpose of this pilot trial was to assess the feasibility of implementing and evaluating a dietitian-led virtual CM intervention for bone health as an adjunct to usual care at our specialty osteoporosis centre. This study received ethics approval. A total of 40 adults age >=45 years, referred to our centre for assessment of fracture risk, were randomized to receive either usual care (didactic nutrition education from a dietitian) or usual care plus a CM program. The CM program consisted of a 1.5-hour virtual (Zoom) group session, co-facilitated by two dietitians. Participants were provided a recipe package and had the option of cooking along or viewing the session as a demonstration. Six weeks after the CM session the CM group were offered an optional virtual follow-up with a dietitian where they could ask further questions regarding home cooking and nutrition. The usual care group was invited to attend the CM program after study completion (i.e. wait-list control). At baseline and 3 months, participants completed surveys asking about home cooking patterns and confidence in eating well for bone health and were asked to complete 2 dietary recalls. The CM group also completed a program acceptability survey immediately following the CM session. Primary feasibility outcomes were: recruitment (target : 100% of participants recruited in 6 months), adherence (target: >85% of participants received allocated intervention), and retention (target: >85% of participants provided follow-up data). Feasibility data are shown in the Table . We achieved our target recruitment of 40 participants (95% female, median age 68 years) in 2 months. Targets were also met for adherence and retention (shown in bold); sub parameters reflect difficulties participants experienced in completing the dietary recalls, with only 5 participants (12.5%) completing all 4 recalls. Our findings indicate that evaluation of a CM program as an adjunct to usual care at our specialty osteoporosis centre is feasible, although, to achieve adequate retention, future studies will require data collection processes that are less onerous for participants.

Table. Feasibility of delivering and evaluating a dietitian-led virtual Culinary Medicine (CM) program for bone health

Feasibility Outcomes	Target, n	Achieved, n (%)	Target achieved (Yes/No)
Recruitment			
Recruited in 6 months	**40**	**40 (100%)**	**Yes**
Adherence			
All participants	**40**	**38/40 (95%)**	**Yes**
CM group			
Attended CM session	20	18 (90%)	Yes
Attended optional follow-up session	-	12 (60%)	-
Usual care group			
Did not attend any CM programming during study	20	20 (100%)	Yes
Retention			
Completed all surveys	**40**	**32 (80%)**	Yes
Completed baseline survey	40	35 (87.5%)	Yes
Completed 3 month survey	40	32 (80%)	Yes
Completed post-CM session survey (CM group only)	20	17 (85%	Yes
Completed baseline dietary recall x2	40	11 (27.5%)	No
Completed 3 month dietary recall x2	40	5 (12.5%)	No
Completed all dietary recalls	40	5 (12.5%)	No

Primary feasibility outcomes are bolded.

***Disclosures: Julia MacLaren**, None*

SAT-284

The Role of Vitamin D Sulfates in Breastmilk *Carmen Reynolds[1,] Roy Dyer[1,] Sara Oberhelman-Eaton[1,] Brianna Konwinski[1,] Ravinder Singh[1,] Thomas Thacher[1. 1]Mayo Clinic, United States

Vitamin D is essential to infants for normal calcium metabolism and bone development, but the concentration of vitamin D3 (VitD3) in breastmilk is low or undetectable unless mothers receive high-dose vitamin D supplement. However, infant serum 25-hydroxyvitamin D3 (25OHD3) correlates with maternal serum 25OHD3, suggesting that alternative vitamin D metabolites may contribute to the infant's nutrition. Serum 25OHD3 is also observed conjugated to a polar sulfate group that increases metabolite solubility. In milk, such sulfate-conjugated vitamin D metabolites (D-Sulfates) could disperse into the aqueous phase for advantages such as enhanced stability or alternate digestion. We hypothesized that D-sulfates, vitamin D3-sulfate (VitD3-S) and 25-hydroxyvitamin D3-sulfate (25OHD3-S), are present in breastmilk and that these metabolites increase with high-dose VitD3 supplementation. We measured D-sulfates in breastmilk from 10 healthy lactating women >=2 weeks after delivery, before and after high-dose VitD3 supplementation. Those with premature birth (<37 weeks gestation), history of sarcoidosis or renal disease, or consuming VitD >=600 IU/day for 30 days prior were excluded. Breastmilk and serum were collected at baseline and after 28 days (d28) of supplementation with VitD3 5000 IU/day. VitD3-S and 25OHD3-S were measured by a newly developed LC-MS/MS method optimized for milk assessments. Subjects were enrolled in the fall and early winter (Oct-Dec). All women had baseline 25OHD3 values >=25 ng/ml and mean +/- SD serum 25OHD3 increased from 32.0 +/- 5.5 ng/mL at baseline to 42.7 +/- 4.5 ng/mL (d28; P <0.001). The D-sulfates in serum were 35.4 +/- 6.0 ng/mL 25OHD3-S and 2.3 +/- 0.2 ng/mL VitD3-S and did not increase from the supplement. In milk, baseline VitD3-S was 12.6 +/- 7.1 ng/mL and 16.3 +/- 9.4 ng/mL on d28 (P=0.3). Baseline 25OHD3-S was 3.5 +/- 2.2 ng/mL and 4.3 +/- 2.5 ng/mL on d28 (P = 0.4). Milk VitD3-S was positively correlated with milk 25OHD3-S (r=0.87, P<0.0001), but neither correlated with serum analytes (25OHD3, VitD3-S, or 25OHD3-S). In conclusion, VitD3-S and 25OHD3-S are present in milk from mothers who are not deficient in serum 25OHD3. These D-sulfates do not correspond to serum analytes or supplementation, thereby suggesting that a regulatory mechanism may exist within mammary glands.

***Disclosures: Carmen Reynolds**, None*

SAT-285

Vitamin C deficiency deteriorates bone microarchitecture and mineralization in a sex-specific manner in adult mice *Stephane Blouin[1,] Farzaneh Khani[2,] Phaedra Messmer[1,] Paul Roschger[1,] Markus Hartmann[1,] Andre van Wijnen[3,] Roman Thaler[4,] Barbara Misof[1. 1]Ludwig Boltzmann Institute of Osteology at Hanusch Hospital of OEGK and AUVA Trauma Centre Meidling, 1st Med. Dept. Hanusch Hospital, Austria. [2]Department of Orthopedic Surgery, Mayo Clinic, United States. [3]University of Vermont, United States. [4]Mayo Clinic, United States

Vitamin C is essential for bone health and low vitamin C serum levels associate with an increased risk for skeletal fractures. However, if and how vitamin C affects bone mineralization is still unknown. Using micro-computed tomography (μCT), histologic staining as well as quantitative backscattered electron imaging (qBEI) we assessed the effects of

vitamin C on femoral structure and microarchitecture, bone formation and bone mineralization density distribution (BMDD) in the vitamin C incompetent Gulo-/- mouse model. For this purpose, 20 week old, vitamin C supplemented mice were compared to age-matched counterparts where dietary vitamin C intake was abrogated from week 15. We found that the cortical thickness of the diaphyseal shaft as well as bone volume around the growth plate are severely decreased in vitamin C depleted Gulo-/- mice (e.g., BV/TV of primary spongiosa -43%, p<0.001). Concurrently, the amount of newly formed bone tissue is clearly reduced as visualized by histology and by calcein labeling of the active mineralization front. Furthermore, the BMDD analysis reveals a shift to higher calcium concentrations, including higher average and peak calcium concentrations in the epiphyseal and metaphyseal spongiosa (e.g. average calcium concentration increases by 10%, p<0.001, in female Vitamin C depleted versus Vitamin C supplemented mice) suggesting increased bone tissue age. Importantly, many of the observed effects are significantly more pronounced in female mice indicating a higher sensitivity of their skeleton to vitamin C deficiency. In summary, our results unveil that vitamin C plays a key role in bone formation, propose low vitamin C levels as a contributing factor for the higher prevalence of bone degenerative diseases in females and suggest leveraging this vitamin against these conditions.

***Disclosures: Stephane Blouin**, None*

SAT-286

Prevalence for urinary calcium level among people in 9 provinces of China: a multi-center cross-section study *Li Shen[1], Zhenlin Zhang[2]. [1]Shanghai Sixth People's Hospital, China. [2]Shanghai Sixth People's Hospital, China

Objective: Population-based data of urinary calcium level in Chinese population is lacking. We aimed to investigate the urinary calcium level and obtain the profile of urinary calcium level according to gender and age.Methods: This is a multi-center, cross-section study, involving the method of multi-stage stratified sampling. Eligible participants (>=18 years) of Chinese ethnicity were enrolled from 9 provinces in China (9 centers). Dietary information was collected through questionnaire survey. 24-hours urine collection (24HUC) were collected and analyzedResults: A total of 1081 subjects with mean ages of (46.89+/-18.27) years (age range: 19-91 years) were included in the final analysis, of whom 434 (40.1%) were men and 674 (59.9%) were women. The median 24-hour urinary calcium excretion were 2.10mmol/24h(Q1-Q3: 1.29-3.37mmol/24h), there was no statistically significant difference in urinary calcium excretion between men and women. The total number of subjects with low urinary calcium excretion(<=2.5 mmol/24h) in this study was 641(59.5%), of which 234(54.0%) were men and 407(63.1%) were women. The total number of subjects with high urinary calcium excretion(>7.5 mmol/24h) in this study was 46(4.3%), of which 28(6.5%) were men and 18(2.8%) were women. The prevalence of 24-hour urinary calcium excretion in different provinces are shown in Figure 1, and the level difference in different provinces were statistically significant (P<0.001). The profile according to age showed that urinary calcium excretion were the highest at the age of 31-45 years in men[3.64mmol/24h(95%CI=2.92-4.35mmol/24h)] and over 46 years. However,it quickly decreased. In women, the highest urinary calcium excretion level was age of 46-60 years [2.99mmol/24h(95%CI=2.49-3.49 mmol/24h)], and over 60 years, it decreased with age. Conclusion: Low urinary calcium excretion was found to be high in China, which requires addressing as a public health priority. Further study is needed to understand the epidemiology of urinary calcium level and Influencing factors in more details to tailor intervention programs.Keywords: 24-hour urinary calcium level, calcium level, epidemiology, cross-sectional studyAcknowledgement: We thank the Chugai Pharma China Co., Ltd for funding this study

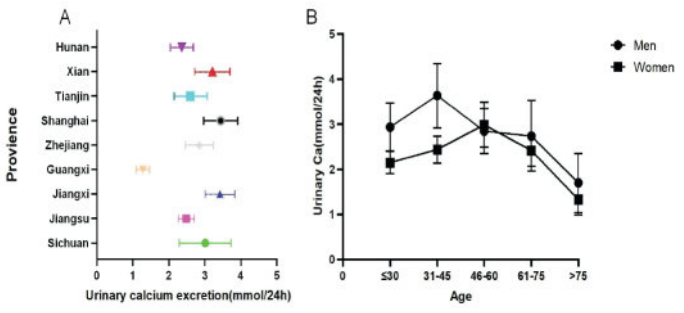

***Disclosures: Li Shen**, None*

SAT-287

See Friday Plenary Number FRI-287

SAT-288

The landscape of osteoblast dysregulation in osteoporosis revealed by single cell 'omics *Ryan Chai[2], Marcelo Sergio[2], Torsten Gross[3], Juliana Cudini[3], Lorenzo Ramos-Mucci[3], Amaia Vilas Zornoza[3], Jake Taylor-King[3], Edith Hessel[3], Sarthak Chopra[4], Nathaniel Bradford[5], Horng Lii Oh[6], Peter Croucher[2], Rebecca McIntyre[3]. [2]Garvan Institute of Medical Research, . [2]Garvan Institute of Medical Research, Australia. [3]Relation Therapeutics, United Kingdom. [4]St. Vincent's Hospital, Australia. [5]St Vincent's hospital, Australia. [6]St Vincent's Hospital, Australia

Osteoporosis is a common skeletal disease of older age that is thought to affect ~200 million people worldwide. Despite the large healthcare burden of fracture surgery and the significantly increased post-surgery mortality (~20% lower than expected for up to 10 years post-fracture), only a small fraction of osteoporotic individuals are therapeutically treated. With the global population aging, there is an urgent need to identify novel therapeutic targets and early disease biomarkers.Here, we present a comprehensive single cell atlas of human femoral head and neck from both osteoporotic patients and non-osteoporotic controls. We established a pipeline to process bone cores for single cell RNA-seq (scRNA-seq), ATAC-seq (scATAC-seq), DEXA, microCT and histopathology. For scRNA-seq, we removed the majority of CD45-positive immune cells and CD235a-positive cells by cell sorting to improve resolution of the bone-lineage cells. We performed unsupervised clustering to identify 27 clusters of cells, inferred cell-cell communication and performed trajectory analysis to identify the multiple stages of osteoblast differentiation from mesenchymal stromal cells (MSCs) through to mature osteoblasts and early osteocytes. We cross-referenced expression profiles against genes known to regulate bone mineral density and found that the vast majority of the genes involved in the monogenic form of osteoporosis, osteogenesis imperfecta, were expressed highly in osteoblasts at a specific stage of differentiation. We characterized these cells further using flow cytometry and histopathology. These findings represent the first data describing the cellular landscape of patients with osteoporosis and identified osteoblast populations that may be associated with disease pathogenesis/abnormal bone mass. Our results to date provide a vast resource and enable prioritization of genes and disease-relevant pathways in key disease effector cell types, greatly facilitating the development of novel therapeutics and disease biomarkers.

***Disclosures: Ryan Chai**, None*

SAT-289

The Impact of Genomic Structural Variations on Osteoporosis Risk: Insights from Whole-Genome Sequencing *Kuan-Jui Su[1], Yong Liu[1], Anqi Liu[2], Jonathan Greenbaum[1], XIAO ZHANG[2], Zhe Luo[1], Qing Tian[1], Li Wu[1], CHUAN QIU[3], Hui Shen[4], Hong-Wen Deng[4]. [1]Tulane Center for Biomedical Informatics and Genomics, United States. [2], . [3], United States. [4]Tulane University, United States

Genomic structural variations (SVs) are large-scale differences in the genome that can lead to genetic diversity. While small-scale copy number variations are known to affect osteoporosis, a heritable metabolic bone disorder characterized by low BMD, the role of large-scale SVs in osteoporosis susceptibility is not well understood. This study aims to investigate the diverse patterns of SVs and their potential association with osteoporosis in the human genome. Whole-genome sequencing was performed on 4982 subjects from the Louisiana Osteoporosis Study, including 50% males, 23% Black, and 57% White participants, to analyze genomic deletions, duplications, insertions, and inversions using an ensemble-SV method. A gene-based burden test was applied to determine the association between the presence of SVs within a gene and hip, femoral neck (FNK), and lumbar spine (SPN) BMD. We used a false discovery rate procedure for multiple tests correction. We also performed post-analytic interrogation using webTWAS, GWAS Catalog, ROADMAP epigenome, and enrichment analysis. Additionally, we explored the sex- and race-specific effects of SVs on bone traits through stratification. We identified a total of 31,304 high-confidence SVs, comprising four SV types. Among the pooled samples, we found 243 unique BMD-related SVs. Over than 50% of these SVs were simultaneously associated with two skeletal sites in combined and sex/race-specific analyses, but none of the SVs were found to be simultaneously associated with all three bone traits. Furthermore, we noted a higher number of FNK-related SVs compared to HIP and SPN-BMD SV associations. We found that many BMD-related SVs were located near centromeres/telomeres, which have been suggested as relevant to human diseases as sources of genomic instability or repositories of haplotypes containing causative mutations. Additionally, we discovered 55 GWAS bone signals that co-occurred with BMD-related SVs. Our analysis also identified 157 GO terms and 32 KEGG pathways and annotated with several enhancers and promoters in osteoblasts, myoblasts, CD14+monocytes, and other cell types (Fig 1). Overall, our study highlights how different sets of SVs can influence BMD at different skeletal sites as well as common enriched biological functions that could provide new insights into the pathophysiology of osteoporosis.

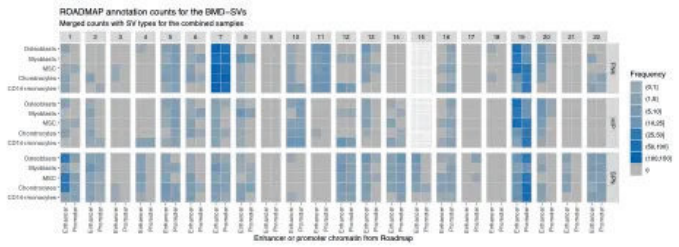

***Disclosures: Kuan-Jui Su**, None*

SAT-290

Metabolomics signatures associated with fracture prediction; cox proportional hazard model and random forest survival analysis *Sohyun Jeong[1], Paul Okoro[1], Sarah Berry[2], Douglas Kiel[3], Yi-Hsiang Hsu[4]. [1]Marcus Institute for Aging research and Hebrew seniorlife, United States. [2]Hebrew SeniorLife/Beth Israel Deaconess Medical Center, United States. [3]Hinda and Arthur Marcus Institute for Aging Research Hebrew SeniorLife, United States. [4]HSL Institute for Aging Research, Harvard Medical School, United States

Measurement of multiple metabolites has shown some success in understanding bone metabolic processes that contribute to skeletal health. We aimed to identify metabolomics signatures that are associated with the risk of fracture. We leveraged large-scale UK Biobank data which has high-throughput NMR-based measures of 249 metabolites spanning 14 lipoprotein subclasses, fatty acids, low-molecular weight amino acids, ketone bodies, and glycolysis metabolites. A total of 121,733 individuals with metabolomics profiling were selected. Missing metabolite values (0.1%) were imputed by assigning half of the minimum positive values. We had a 2-step approach; 1) Cross-sectional study between individuals with fracture events within 6 months before/after blood sampling and those with no fracture history (case;295, control;115,862); significantly different metabolomics (Log2FC, pval <.05) were determined using Limma, 2) Cohort study in individuals with no fracture history before blood sampling (n=119,081); metabolomics selected in the first step were considered as predictors of 6-month and 1-year fracture outcomes; cox proportional hazard model adjusting for age at sampling, sex, BMI, genetic European ancestry, hypertensive disease, diabetes (Type1/Type2), lipid disorder and chronic kidney disease and random forest survival analysis (randomForestSRC R package) were conducted. Mean age was 57.14 (+/-8.13) and 54% were female. Among 249 metabolomics screened, 20 were selected in the first step. Next in the cohort study, none of the metabolomics were significantly associated with 6-month fracture outcome. However, at 1-year follow-up,"Phospholipids to Total Lipids in Small HDL percentage" (HR:3.99, pval<.001), "Cholesterol to Total Lipids in Small HDL percentage" (HR:4.84, pval:0.005), and "Monounsaturated Fatty Acids to Total Fatty Acids percentage" (HR:1.44, pval: 0.008) were significantly associated with increased fracture whereas "Monounsaturated Fatty Acids" (HR: 0.067, pval:0.019) was associated with decreased fracture risk. Additionally, we put 4 significant metabolomics with all covariates in random forest survival analysis. The model fitted well to predict 1-year fracture risk with OOB CRPS (Continuous Ranked Probability Score), 0.0014 and OOB performance error, 0.460. We demonstrated 4 lipoprotein and fatty acid related metabolomics were associated with fracture risk at 1 year of follow up and previous studies support the association.

***Disclosures: Sohyun Jeong**, None*

SAT-291

See Friday Plenary Number FRI-291

SAT-292

Identification of a Novel, MSC-Induced Macrophage Subtype via Single-Cell Sequencing: Implications for IVDD Therapy *JINSHA KOROTH[1], CASEY CHITWOOD[1], RAMYA KUMAR[1], WEI-HAN LIN[1], THERESA REINIKE[1], ARIN ELLINGSON[1], CASEY JOHNSON[1], LAURA STONE[1], BRENDA OGLE[1], ELIZABETH BRADLEY[1]. [1]University of Minnesota, United States

Intervertebral disc (IVD) degeneration is a common pathological condition associated with lower back pain. Recent evidence suggests that mesenchymal signaling cells (MSCs) promote IVD regeneration, but the mechanisms are poorly defined. MSCs encounter drastic oxygen tension declines when injected into the avascular IVD. IVD degeneration likewise associates with altered oxygen tension via vasculature invasion, and macrophage infiltration; thus, understanding how different oxygen tensions affect interactions between MSCs and macrophages may offer clues as to how MSCs act therapeutically. To gain insight, we investigated how conditioned medium (CM) derived from MSCs cultured in hypoxia altered macrophage subsets. We cultured human, bone marrow-derived Stro3+ MSCs in hypoxia (2% O2) or normoxia and collected CM. We then cultured human bone marrow-derived macrophages (e.g., Cd11b+/Cd14+ cells) with IFN-y for 24 hours, followed by either hypoxic or normoxic Stro3+ MSC CM. We also cultured macrophages in hypoxic MSC CM in the presence of IL-4. After 24 hours in CM, we collected cells for scRNA-seq analyses. Bioinformatic analyses confirmed multiple subpopulations of macrophages within human bone marrow. To gain insight into how MSCs exposed to different oxygen tensions affected macrophage subsets, we first performed comparison analyses between macrophages cultured in hypoxic and normoxic MSC CM. Integration of these two data sets showed large overlap between most macrophage subsets; however, we identified a unique macrophage cluster induced by hypoxic MSC CM. This cluster represented approximately 2-3% of macrophages (Fig 1A, B). Gene Ontogeny (GO) analyses revealed enrichment in several Reactome Pathways, including IL-10, Ccl5/Ccr5, G alpha (i) Signaling and Rho GTPases within this unique cluster (Fig 1C, D). To determine if factors from MSC CM simulated IL-4, we integrated the data from macrophages cultured in hypoxic MSC CM with and without IL-4 addition. Integration of these two data sets showed considerable overlap, demonstrating that hypoxic MSC CM simulates the effects of IL-4. Interestingly, macrophages cultured in normoxic MSC CM did not significantly show the unique cluster within our comparison analyses; thus, normoxic conditions did not approximate the effects of IL-4. Our study identifies a unique macrophage subset induced by MSCs within hypoxic conditions, and offers clues towards mechanisms by which MSCs promote IVD regeneration.

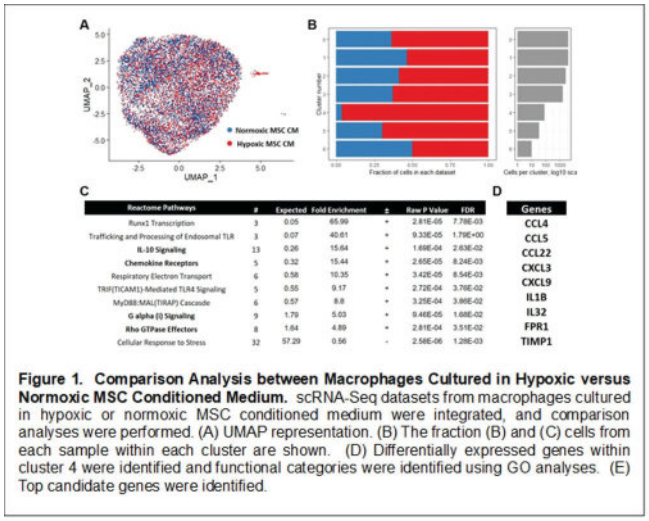

Figure 1. Comparison Analysis between Macrophages Cultured in Hypoxic versus Normoxic MSC Conditioned Medium. scRNA-Seq datasets from macrophages cultured in hypoxic or normoxic MSC conditioned medium were integrated, and comparison analyses were performed. (A) UMAP representation. (B) The fraction (B) and (C) cells from each sample within each cluster are shown. (D) Differentially expressed genes within cluster 4 were identified and functional categories were identified using GO analyses. (E) Top candidate genes were identified.

***Disclosures: JINSHA KOROTH**, None*

SAT-293

See Friday Plenary Number FRI-293

SAT-296

See Friday Plenary Number FRI-296

SAT-297

Identification of Osteoporosis Biomarkers and Biological Interactions Using Multi-omics Data Integration *Anqi Liu[2], Lindong Jiang[2], Kuan-Jui Su[2], XIAO ZHANG[2], YUN GONG[2], CHUAN QIU[3], Zhe Luo[2], Qing Tian[2], Zhengming Ding[2], Hui Shen[2], Hong-Wen Deng[2]. [2]Tulane University, . [2]Tulane University, United States. [3], United States

Osteoporosis is a medical condition characterized by a decrease in bone density and a deterioration of bone microarchitecture, which increases the risk of fractures. The development of high-throughput technologies and integrative strategies has created new possibilities to explore the underlying pathophysiological mechanisms associated with osteoporosis. Currently, omics-based technologies have been put forward to enhance our comprehension of the biological mechanisms contributing to decreased bone mineral density (BMD). While each omics technology can capture a portion of biological information, integrating multiple types of omics data can provide a more holistic picture of the underlying biological processes. In this study, we produced multi-omics data from our own Trans-omics Integration of Multi-omics Studies for Male Osteoporosis Study (including single nucleotide variations, copy number variations, mRNA gene expression, miRNA, DNA methylation, metabolomics, lipidomics and clinical data) from 181 subjects with high (n=57) and low (n=124) BMDs. We employed a multi-omics integrative method using multi-view graph convolutional networks for high BMD and low BMD classification. This method jointly explored omics-specific learning with graph convolutional networks and cross-omics correlation learning with view correlation discovery network (VCDN) for effective multi-omics data classification. In conclusion, we identified 105 important biomarkers associated with

low BMDs from various omics. We revealed functional interactions among the 36 annotated genes from 105 biomarkers and pinpointed osteoporosis-related pathways related with other biomarkers. The identification of osteoporosis biomarkers and the understanding of their biological interactions would be transformed into consistent benefits for the effective prevention, intervention, and treatment for osteoporosis.

***Disclosures: Anqi Liu**, None*

SAT-299

Multi-Omics Data Integration Revealed Osteoporosis-Associated DNA Methylation and Transcription Variations in Human Peripheral Blood Monocytes *XIAO ZHANG[2], YUN GONG[2], Kuan-Jui Su[3], Anqi Liu[2], CHUAN QIU[4], Zhe Luo[3], Qing Tian[3], Melanie Ehrlich[3], Hong-Wen Deng[3], Hui Shen[3, 2], , [2], United States, [3]Tulane University, United States, [4], United States

Osteoporosis (OP) is a common bone disorder characterized by low bone mineral density (BMD) and increased risk of fractures in both women and men. About one third of worldwide fractures occur in men and OP in men has received little attention. Despite extensive research efforts, the underlying molecular mechanisms driving OP remain poorly understood. Multi-omics integration has emerged as a promising approach to address this issue by integrating data from various molecular layers, such as epigenomics (DNA methylation) and transcriptomics (RNA-seq and miRNA-seq). In this study, we integrated a set of 519 independent male (both Caucasians and African Americans) subjects' multi-omics data derived from peripheral blood (classical) monocytes using Multi-Omics Factor Analysis (MOFA) to study osteoporosis risk in men. We determined nine factors and identified known and novel putative genes and BMD-associated features associated with OP, with the model explains > 10% of the variation in the DNA methylation annotated in CpG islands, active enhancer- and promoter-chromatin region in monocytes. One of the identified factors prioritized a CpG site (chr19:4,053,428/hg19) which annotated to active enhancer-chromatin in monocytes and located in intron 2 of ZBTB7A. The encoded protein, ZBTB7A, is known to play a role in osteoclast differentiation. Through the integration analysis, we identified significant and novel OP-associated coding and non-coding genes whose expression is epigenetically dysregulated.

***Disclosures: XIAO ZHANG**, None*

SAT-301

Trabecular bone texture is sensitive to Strontium Ranelate treatment and improves the prediction of knee osteoarthritis progression: Data from the SEKOIA Trial *Ahmad Almhdie-Imjabbar[1], Hechmi Toumi[1], Eric Lespessailles[2], [1]Translational Medicine Research Platform, PRIMMO, University hospital center of Orleans, France, France, [2]Centre Hospitalier Universitaire d'Orleans, France

Trabecular bone texture (TBT) analysis of subchondral bone on conventional knee X-ray has been shown to be a promising method to identify patients at risk for knee osteoarthritis (KOA) progression.The aim of this study was to investigate an approach combining the use of TBT, with a set of radiological severity scores and clinical covariates, to predict radiological progression (joint space narrowing (JSN) >= 0.5 mm over 3 years) and radioclinical progression (JSN >= 0.5 mm and lack of improvement in WOMAC pain <= 20% over 3 years) in the Strontium-ranelate (SR) Efficacy in Knee Osteoarthritis trIAl (SEKOIA). The study also examined the longitudinal effects of the SR treatment on TBT variations.This study included 905 patients from the SEKOIA dataset. Radiographs were automatically segmented to determine 16 regions of interest (ROIs). Several statistical models were developed using logistic regression to evaluate the performance gain in including not only clinical covariates (age, gender and BMI), WOMAC pain scores and radiological KL grades and minimum joint space width, named hereafter TBT-excluded models, but also TBT descriptors, named hereafter TBT-included models.The TBT-included models were predictive of radiological progression and the AUC was 0.64 (95% CI: 0.57-0.70), significantly outperformed TBT-excluded models (AUC=0.52, 95% CI: 0.46-0.59, p-value=0.002). The performance of TBT-included models in prediction of radioclinical progression (AUC=0.62, 95% CI: 0.52-0.73) also outperformed, but not statistically significantly, those of TBT-excluded models (AUC=0.58, 95% CI: 0.49-0.68).The highest increase in TBT was 3% in specific ROIs, in both the placebo and treated group (Strontium Ranelate). The highest variations were observed in the horizontal direction, in the extreme medial and lateral ROIs, see Figure 1.The proposed combined model provides a good performance in the prediction of radiological and radioclinical progression over 3 years, in the setting of a multicenter international trial. The current study confirms the ability of the TBT-included models to predict KOA progression in different databases. TBT provides a responsive outcome measure for subchondral tibial bone microarchitecture in longitudinal KOA trial.

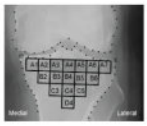

Medial		ROIs				Lateral
A1	A2	A3	A4	A5	A6	A7
	B2	B3	B4	B5	B6	
		C3	C4	C5		
			D4			

Placebo (non-progressors)						
2	0	0	0	0	0	3
	1	0	0	0	0	
		0	0	0		
			0			

Placebo (progressors)						
3	1	0	0	0	0	3
	1	0	0	0	0	
		0	0	0		
			0			

SR treated (non-progressors)						
2	0	0	0	0	0	2
	1	0	0	0	0	
		0	0	0		
			0			

SR treated (progressors)						
3	0	0	0	0	0	2
	1	0	0	0	0	
		0	0	0		
			0			

SR refers to Strontium-Ranelate
A1:A7, B2:B6, C3:C5 and D4 refer to the selected 16 regions of interest

***Disclosures: Ahmad Almhdie-Imjabbar**, None*

SAT-303

Evaluation of a Novel Computed Tomography Application to Monitor Knee Osteoarthritis *REECE BLAY[2], Grace Roskam[2], Yvonnne Golightly[2], Laura Bilek[3], [2]University of Nebraska Medical Center, , [2]University of Nebraska Medical Center, United States, [3]UNIVERSITY OF NEBRASKA MEDICAL CENTER, United States

PurposeKnee osteoarthritis (KOA) affects nearly 1 in 5 adults over the age of 45 in the United States. Its prevalence is rapidly increasing in recent decades, partly due to the obesity epidemic. Identifying the pathologic mechanism of KOA development requires the detection of early changes in bone. No validated tool exists to examine the role of bone in the initiation of KOA in those at risk for the disease. X-ray is not sensitive enough to detect changes, and advanced imaging techniques such as CT and MRI are not routinely used in practice, as they require a significant amount of time to capture images. There is a need for a quick, accessible, and low-radiation tool to accurately assess bone at the knee in people at risk of KOA development. This methodological study evaluates the effectiveness of a peripheral quantitative computed tomography (pQCT) scan to assess bone density of the proximal tibia and distal femur.MethodsParticipants include adults over the age of 23 who can transfer independently into and out of the pQCT. Pregnant women and those who had prior surgery on their right knee were excluded. Participants underwent two trials during a single visit, with images of their right knee captured using a Stratcom XCT3000 pQCT. The knee angle was kept neutral with straps and padding to stabilize the patient's position. A radiographic technician identified the image reference lines of the femur and tibia (densest area of the medial subchondral endplate) using a scout image. The femur was scanned at a distance 2 mm proximal to the femoral reference line, and the tibia was scanned 12 mm distal to the tibial reference line. These sites represent subcortical and trabecular bone, respectively. Between trials, participants exited the pQCT. The process was repeated to capture a second image. Each trial took approximately 12 minutes. Endpoints include total, trabecular, and cortical density of the medial and lateral condyles of the femur and total, medial, and lateral hemispheres of the tibia. Bland Altman analysis assessed bias (95% CI) between pQCT scans.ResultsThe study sample included 52 participants (mean age 50 years, 81 % female, BMI 27.98 kg/m2). Bland Altman Bias (95% CI) between pQCT scan trials is reported in Table 1.ConclusionpQCT is a reliable modality to assess tibial and medial femoral bone at the knee. Since KOA changes occur primarily in the tibia, the reliability of pQCT to monitor bone changes in this area is significant.

Table 1: Bland Altman Bias (95% CI) between pQCT scan trials, N=52

Scan Location	Density Measure	Bland Altman Bias (95% CI)
Medial Femoral Condyle (2mm)	Total	0.77 (0.66 to 0.88)
	Trabecular	0.67 (0.57 to 0.77)
	Cortical	-0.4 (-0.44 to -0.36)
Lateral Femoral Condyle (2mm)	Total	3.92 (3.29 to 4.55)
	Trabecular	4.49 (4.09 to 4.89)
	Cortical	1.96 (1.64 to 2.29)
Total Tibia (12mm)	Total	0.58 (0.54 to 0.62)
	Trabecular	0.59 (0.56 to 0.62)
	Cortical	1.99 (1.81 to 2.18)
Medial Tibial Hemisphere (12mm)	Total	-0.31 (-0.36 to -0.26)
	Trabecular	-0.47 (-0.51 to -0.42)
	Cortical	0.22 (0.13 to 0.30)
Lateral Tibial Hemisphere (12mm)	Total	-0.35 (-0.40 to -0.31)
	Trabecular	-0.17 (-0.22 to -0.13)
	Cortical	0.42 (0.31 to 0.54)

***Disclosures: REECE BLAY**, None*

SAT-304

Bone Mineral Density and Structure in the Human Femoral Head - A Synchrotron CT Study *Doris Liang[1], Qiong Wang[2], Ning Zhu[3], Danmei Liu[4], David Cooper[5], Pierre Guy[6], Marc Grynpas[7], Rizhi Wang[8]. [1]School of Biomedical Engineering, Centre for Aging SMART, University of British Columbia, Canada. [2]Department of Materials Engineering, University of British Columbia, Canada. [3]Canadian Light Source, Canada. [4]Centre for Aging SMART, University of British Columbia, Canada. [5]Department of Anatomy Physiology and Pharmacology, University of Saskatchewan, Canada. [6]Department of Orthopaedics, Centre for Aging SMART, University of British Columbia, Canada. [7]Samuel Luenfeld Research Institute, Mount Sinai Hospital, Department of Laboratory Medicine and pathobiology, Institute of Biomedical Engineering, University of Toronto, Canada. [8]Department of Materials Engineering, School of Biomedical engineering, Centre for Aging SMART, University of British Columbia, Canada

Osteoarthritis is a joint degenerative disease, the alteration in cartilage and underlying bone could concurrently change the microstructure and mechanical performance of osteoarthritic femoral heads due to the dynamic nature of human bones. Bone adaptation occurs in the direction of loading as stated by Wolff's law. Although some evidences suggest bone structure heterogeneity in regions under different degrees of loading [1], little is known about mineral deposition in response to load alteration at microscopic level across femoral head. Synchrotron Radiation Computed Tomography (SRCT) offers the advantage of three-dimensional visualization, precise mineralization quantification and mineral distribution of the whole femoral head. This study uses SRCT technique to compare the bone mineral density (BMD) between regions subjected to different degrees of loading, with a specific focus on the stressline observed along principal compressive trabeculae [Figure 1].Osteoarthritic femoral heads collected from patients of 42, 59, 69, 89 years old were scanned with SRCT at beamline 05ID-2 at the Canadian Light Source. Images at different bit depth were used for microstructural and density analysis. Bone cores of 10 mm in diameter were then drilled from the superior, medial and inferior region of femoral heads with descending order of loading magnitude. Cores were cut, ground, polished and scanned under scanning electron microscope (SEM) for quantitative backscattered electrons (qBSE) analysis. qBSE offers two dimensional quantitative calcium content analysis from grayscale values, which was compared and correlated with the grayscale values of the matched SRCT slice in an attempt to confirm the observed stressline spanning down the main loading direction.SRCT data from patients at age 59 and 89 demonstrated that the superior region exhibits the highest mean volumetric BMD (1.74 g/cm^3) whereas the inferior region showing the lowest (1.50 g/cm^3). Regions with pronounced color intensity on the heatmap showed higher BMD. Preliminary analyses also suggested a correlation between qBSE and SRCT, indicating higher degree of mineralization along the principal compressive trabeculae.Reference: [1] G. Li, L. Chen, Q. Zheng, Y. Ma, C. Zhang, and M. H. Zheng, "Subchondral bone deterioration in femoral heads in patients with osteoarthritis secondary to hip dysplasia: A case-control study," J. Orthop. Transl., vol. 24, pp. 190-197, Sep. 2020, doi: 10.1016/j.jot.2019.10.014.

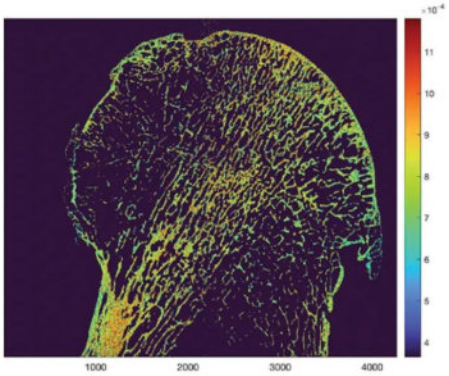

Figure 1.Heatmap of femoral head slice with pronounced stress line in the direction of loading. Grayscale values outside of the range of 2 standard deviations from the mean are excluded. X-axis shows the pixel scale with a pixel size of 13.07um. The grayscale of SRCT is represented by color intensity,where red represents high grayscale an d blue represents low grayscale.

***Disclosures: Doris Liang**, None*

SAT-305

Single-Cell Transcriptomic Analysis Reveals Molecular Complexity and Key Genes Involved in Osteoarthritis *Zhengwu Xiao[1], Chong Cao[2], Yan Chen[2], Junxiao Yang[1], YUN GONG[3], Xiao Zhang[3], Kaizhi Wen[1], Hui Shen[3], Lijun Tan[2], Hong-Wen Deng[3], Hongmei Xiao[1]. [1]Central South University, China. [2]Hunan Normal University, China. [3]Tulane University, United States

Osteoarthritis (OA) is the most common multifaceted degenerative joint disease which is characterized by degeneration and loss of cartilage and bone. These alterations are mediated by various bone-related cells, such as osteoblasts (OBs) in bone, and potential cell subtypes (cellular heterogeneity). Despite extensive research efforts, the underlying molecular mechanisms driving OA remain poorly understood, especially at single cellular level. In this study, we performed comparative single-cell transcriptomics (scRNA-seq) analysis on freshly isolated OBs obtained from femur head of three OA individuals and three controls with femoral neck fractures. We obtained a total of 42,855 cells and revealed three distinct OB subtypes (pre-, metaphase, and mature OBs) through gene expression profiling, which each with unique functional roles. The pre-OBs exhibit to participate in angiogenesis and adipocyte differentiation; the metaphase OBs may regulate neutrophil-related immune responses; and, the mature OBs display ossification properties. Differential gene expression analysis revealed three upregulated genes (APOE, PTGDS, and CFD) in OA. Using weighted gene co-expression network analysis (WGCNA), we identified a critical gene co-expression network associated with OA, which featuring CFD as the central hub gene. Our findings shed light on the molecular intricacies of OA in OBs and its subtypes, uncovering potential biological processes and essential genes that may guide future diagnostic and therapeutic research.

***Disclosures: Zhengwu Xiao**, None*

SAT-307

Higher CAROC Fracture Risk is Associated with Progressive Knee Symptoms in Postmenopausal Women: the AMBERS Cohort Study *Andy Kin On Wong[1], Shannon Reitsma[2], Ali Naraghi[3], Rakesh Mohankumar[3], Alexandra Papaioannou[4], Jonathan Adachi[5]. [1]University Health Network, Canada. [2]Division of Rheumatology, Medicine, McMaster University, Canada. [3]Joint Department of Medical Imaging, University Health Network, Canada. [4]McMaster University , Canada. [5]St. Joseph s Hospital/McMaster University, Canada

Purpose: To examine fracture risk's impact on knee osteoarthritis (OA) symptom progression in postmenopausal women.Methods: The Appendicular Muscle and Bone Extension Research Study (AMBERS) recruited women 60-85 years old at baseline through primary care in Hamilton, Canada. Participants completed a total hip DXA and a single slice peripheral QCT scan at the 66% site (0.500x0.500x2.3mm, 38 kVp energy, 0.3 mA current) at baseline. Muscle was separated from subcutaneous fat and bone using fixed thresholds (40 mg/cm3) on pQCT scans after filtration (F03F05F05). Muscle density (MD) was computed as mass/volume. At year 5 and 6 of follow-up, the Knee OA Outcomes Scores (KOOS) and Gender Role Expectations in Pain (GREP) questionnaires were completed. Information on use of corticosteroids, pain medications for the knee, and history of diabetes were collected annually. The Canadian Association of Radiologists and Osteoporosis Canada (CAROC) Fracture Risk category (low, moderate, high) was determined using DXA femoral neck

T-score, sex, and age.Statistical analyses: KOOS subcategory change from year 5 to 6 was dichotomized according to whether the decrease (more symptoms) exceeded the respective minimum detectable change (MDC) (1) or not (0), and used as the outcome in logistic regression. The primary exposure was CAROC fracture risk category. All models adjusted for MD as a secondary exposure, covariates: age, BMI, use of corticosteroids, knee pain medication, and history of diabetes. GREP score was reversed and normalized to its maximum value and used as a weight to mitigate gender bias in willingness to report pain, pain endurance, and sensitivity.Results: Among 284 women with complete data (age: 75.0+/-6.0 yrs, BMI: 29.56+/-5.69kg/m2, Total Hip T-score: -0.89+/-1.80), KOOS subcategory decreases beyond MDC ranged from 18.0% (symptoms) to 35.6% (quality of life). Overall, 8.8% of women were at high and 54.2% at moderate CAROC fracture risk. Odds for worsening knee symptoms beyond MDC was higher for every unit greater CAROC category, ranging from 1.51 (symptoms) to 2.33 (quality of life)-fold (Table 1). Each standard deviation lower MD was also predictive of worse KOOS scores (Odds ratios: 1.13 to 1.85). These effects remained significant with minimal effect size differences after accounting for use of antiresorptives. Conclusions: Having a higher fracture risk is associated with greater likelihood of experiencing worse knee symptoms in postmenopausal women.

		CAROC Fracture Risk Category			Muscle Density		
KOOS Subcategory	N	OR	Lower	Upper	OR	Lower	Upper
Knee Pain	284	1.69	1.20	2.38	1.57	1.12	2.19
Symptoms	284	1.51	0.96	2.38	1.13	0.72	1.78
Activities of Daily Living	284	1.56	1.09	2.23	1.82	1.29	2.58
Quality of Life	284	1.28	0.80	2.08	5.14	2.36	11.24

***Disclosures: Andy Kin On Wong**, None*

SAT-308

**Computed Tomography (CT) Parameters Used for the Assessment of Subchondral Bone in Osteoarthritis (OA) - A Systematic Review ***Jemima E Schadow[1], David Maxey[2], Toby O Smith[3], Mikko A J Finnilä[4], Sarah Manske[5], Neil Segal[6], Andy Kin On Wong[7], Rachel Davey[8], Tom Turmezei[9], Kathryn Stok[1]. [1]Department of Biomedical Engineering, The University of Melbourne, Australia. [2]epartment of Radiology, Norfolk and Norwich University Hospitals NHS Foundation Trust, United Kingdom. [3]Warwick Medical School, University of Warwick, United Kingdom. [4]4Research Unit of Health Science and Technology, Faculty of Medicine, University of Oulu, Finland. [5]University of Calgary, Canada. [6]Department of Rehabilitation Medicine, The University of Kansas Medical Center, United States. [7]University Health Network, Canada. [8]University of Melbourne, Australia. [9]Norwich Medical School, University of East Anglia, United Kingdom

IntroductionBone plays a major role in the pathology of OA, a common musculoskeletal disease [1]. For the assessment of OA, radiography and magnetic resonance imaging are the main imaging modalities considered. However, CT has advantages over those imaging modalities for bone imaging. Particularly, its capability of producing high resolution three-dimensional image reconstructions that enable standardised bone structure analysis. Therefore, we aimed to systematically review CT parameters for osteoarthritic subchondral bone assessment and gain an overview of current practices and standards in the realm of OA imaging with CT.MethodsMedline, Embase and Cochrane Library databases were searched from 2010 to January 2023 with bespoke search strategies. Two independent reviewers screened the search results against inclusion/exclusion criteria; studies utilising CT for subchondral bone assessment in vivo/ex vivo of human adults (>18 years) with OA were deemed eligible. Data was extracted and combined in a qualitative summary and formal narrative synthesis.ResultsIn the 202 included studies, imaging of subchondral bone in OA was performed with four CT groups (Fig. 1a) across nine anatomical locations (Fig. 1b). The reported subchondral bone parameters measuring related OA features were classified in six categories: (i) microstructure, (ii) bone adaptation, (iii) gross morphology, (iv) mineralisation, (v) joint space, and (vi) mechanical properties (Fig. 1c).Figure 1 | Reporting frequency overview of a) CT groups, b) anatomical locations, and c) parameter categories. ConclusionsCT is gaining increasing popularity for the assessment of OA. CT parameters with clinical relevance for osteoarthritic subchondral bone assessment were identified, as well as measurements with the potential to become clinically meaningful. To ensure the sensibility and reproducibility of these parameters, quantification is imperative. Additionally, reporting consistency and standardised measurement protocols are required to improve their value in future OA research and clinical practice.References1. Altman, R., et al., Arthritis & Rheumatism. 29(8):1039-1049, 1986.

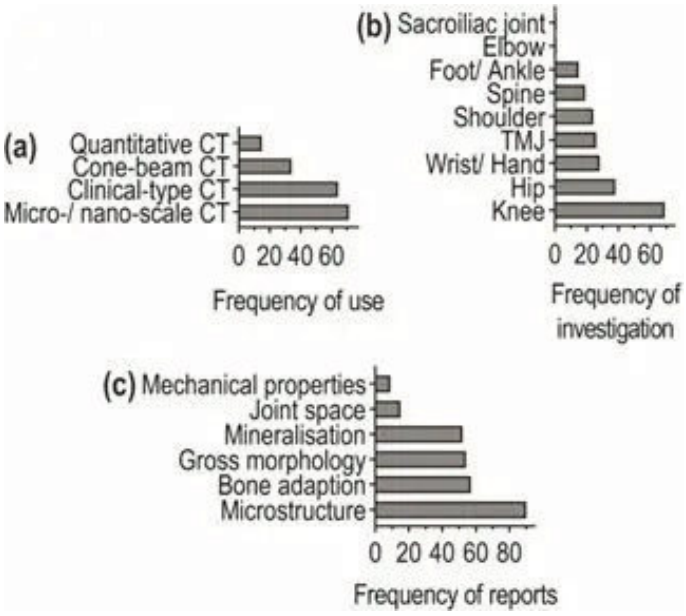

***Disclosures: Jemima E Schadow**, None*

SAT-309

**Comparison between UK Biobank and Shanghai Changfeng suggests distinct hip morphology may contribute to ethnic differences in the prevalence of hip osteoarthritis ***Jiayi Zheng[1], Monika Frysz[2], Benjamin Faber[2], Huandong Lin[3], Raja Ebsim[4], Jieyu Ge[1], Yanling Yong[5], Fiona Saunders[6], Jennifer Gregory[6], Richard Aspden[6], Nicholas Harvey[7], Bing-Hua Jiang[5], Timothy Cootes[4], Claudia Lindner[4], Xin Gao[3], Sijia Wang[1], Jonathan Tobias[2]. [1]Chinese Academy of Sciences, China. [2]University of Bristol, United Kingdom. [3]Fudan University, China. [4]The University of Manchester, United Kingdom. [5]Zhengzhou University, China. [6]University of Aberdeen, United Kingdom. [7]University of Southampton,

Background: Joint morphology is a key risk factor for the development of hip osteoarthritis (HOA) and could explain established ethnic differences in HOA prevalence. Therefore, we aimed to compare hip morphology and prevalence of radiographic HOA (rHOA) in the predominantly White UK Biobank (UKB) and exclusively Chinese Shanghai Changfeng (SC) cohorts.Methods: Left hip iDXA scans (GE Lunar) were used to quantify rHOA, from a combination of osteophytes and joint space narrowing, and hip morphology. Using an 85-point Statistical Shape Model (SSM) we evaluated cam/pincer morphology and acetabular dysplasia based on alpha angle (AA) and lateral center-edge angle (LCEA), respectively. Composite hip shape was derived from the first ten SSM modes, which explain 86.3% of hip shape variance. Measures of hip geometry were also obtained (femoral neck width (FNW), hip axis length (HAL) and femoral head diameter (DFH)). Results were adjusted for differences in age, height and weight.Results: Complete data were available for 5,924 SC and 39,020 White UKB participants. rHOA prevalence was considerably lower in female (2.3% versus 13.1%) and male (12.0% and 25.1%) SC versus UKB participants. Cam morphology, rarely seen in females, was less common in SC compared with UKB males (6.3% versus 16.5%). Inspection of composite SSM modes, scaled to the same overall size, revealed SC participants to have a wider femoral head compared to UKB participants. FNW and HAL were smaller in SC compared to UKB, whereas DFH was similar, and DFH/FNW ratio was higher in SC.Conclusions: The prevalence of rHOA was lower in SC compared with UKB participants. Several differences in hip shape were observed, including the frequency of cam morphology, FNW and DFH/FNW ratio. These characteristics have previously been identified as risk factors for HOA, and may contribute to observed differences in HOA prevalence.

Table 1 | Demographic characteristics, hip geometry and prevalence of rHOA in UKB and SC cohorts

	Female					Male				
	Shanghai Changfeng (n=3,417)	UK Biobank				Shanghai Changfeng (n=2,507)	UK Biobank			
		White (n=20,374)	Asian (n=171)	Black (n=134)	Chinese (n=65)		White (n=18,646)	Asian (n=266)	Black (n=119)	Chinese (n=51)
			mean±SD					mean±SD		
Age (years)	62.6±9.4*	63.1±7.4	60.2±7.9*	58.9±7.0*	58.8±7.3*	64.5±9.7	64.5±7.6	60.3±8.5*	58.3±7.3*	61.0±6.5*
Height (cm)	156.8±6.0*	163.7±6.4	158.4±6.8*	163.9±7.8	158.9±5.1*	168.1±6.2*	177.3±6.6	172.2±6.2*	176.6±6.5	169.9±5.8*
Weight (kg)	59.3±9.1*	69.2±12.8	63.8±11.0*	74.9±15.0*	56.9±8.2*	70.0±9.9*	83.3±13.4	76.4±12.1*	86.0±14.2*	69.1±9.9
FNW (mm)	28.5±2.1*	29.0±2.0	27.9±2.1*	28.4±2.3*	27.9±2.1*	33.5±2.3*	34.6±2.4	33.1±2.5*	32.9±2.6*	33.6±2.1*
HAL (mm)	87.8±4.3*	90.9±4.8	88.5±5.2*	88.5±5.1*	87.4±4.5*	99.5±4.8*	103.2±5.4	100.4±5.9*	100.5±5.2*	99.6±5.1*
DFH (mm)	43.1±2.3	43.1±2.2	41.9±2.5*	42.2±2.5*	42.7±2.3	49.0±2.5	49.1±2.6	47.8±2.6*	47.9±2.7*	48.7±2.2
DFH/FNW ratio	1.51±0.08*	1.49±0.07	1.50±0.07	1.49±0.08	1.53±0.09*	1.46±0.07*	1.42±0.07	1.44±0.08*	1.46±0.08*	1.45±0.08*
rHOA			N (%)					N (%)		
Minimal	70 (2.0)	1,768 (8.7)	17 (9.9)	7 (5.2)	1 (1.5)	267 (10.7)	2,641 (14.2)	38 (14.3)	20 (16.8)	4 (7.8)
Mild	7 (0.2)	712 (3.5)	7 (4.1)	12 (9.0)	0 (0.0)	33 (1.3)	1,526 (8.2)	20 (7.5)	9 (7.6)	2 (3.9)
Moderate	1 (0.03)	146 (0.7)	0 (0.0)	0 (0.0)	0 (0.0)	0 (0.0)	393 (2.1)	2 (0.8)	0 (0.0)	0 (0.0)
Severe	0 (0.0)	44 (0.2)	0 (0.0)	0 (0.0)	0 (0.0)	0 (0.0)	113 (0.6)	0 (0.0)	0 (0.0)	0 (0.0)
Total rHOA	78 (2.3)	2,670 (13.1)	24 (14.0)	19 (14.2)	1 (1.5)	300 (12.0)	4,675 (25.1)	60 (22.6)	29 (24.4)	6 (11.8)
hip morphology			N (%)					N (%)		
Cam (AA≥60)	30 (0.9)	302 (1.5)	2 (1.2)	0 (0.0)	0 (0.0)	159 (6.3)	3,068 (16.5)	27 (10.2)	13 (10.9)	1 (2.0)
Pincer (LCEA≥45)	267 (7.8)	1,820 (8.9)	18 (10.5)	7 (5.2)	2 (3.1)	234 (9.3)	1,802 (9.7)	35 (13.2)	14 (11.8)	2 (3.9)
AD (LCEA<25)	259 (7.6)	1,235 (6.1)	8 (4.7)	12 (9.0)	9 (13.9)	146 (5.8)	1,040 (5.6)	13 (4.9)	6 (5.0)	3 (5.9)

* P value <0.05 *-test versus UK Biobank White participants. FNW, HAL, DFH were adjusted for age, height and weight.
Abbreviations: FNW = femoral neck width; HAL = hip axis length; DFH = diameter of femoral head; rHOA = radiographic hip osteoarthritis; AA = alpha angle; LCEA = lateral center-edge angle; AD = acetabular dysplasia.
rHOA Category (grade 0-4) : minimal= grade 1 only; mild = grade 2 only; moderate = grade 3 only; severe = grade 4 only; total rHOA = grade > 0. Cam morphology was defined as AA≥60 degrees. Pincer morphology was defined as LCEA≥45 degrees. Acetabular dysplasia was defined as LCEA<25 degrees.

***Disclosures: Jiayi Zheng**, None*

SAT-310

Comparison of bone structure between weight-bearing and non-weight-bearing bones in patients with rheumatoid arthritis: A study using HR-pQCT and 3D-SHAPER on DXA *Ikuko Tanaka[1], Shigenori Tamaki[2], Yusuke Suzuki[2], Takashi Kato[3], Hisaji Oshima[4]. [1]NAGOYA Rheumatology Clinic, Japan, [2]Nagoya Rheumatology Clinic, Japan, [3]National Center for Geriatrics and Gerontology, Japan, [4]Tokyo Medical Center, Japan

Background and purposeIn rheumatoid arthritis (RA), anti-CCP antibodies (ACPA) and inflammatory cytokines activate osteoclasts, resulting in increased systemic bone resorption. Recently, the introduction of an analysis software, 3D-SHAPER (3DS) on DXA systems has made it possible to simulate quantitative CT-like three-dimensional bone structural analysis of the proximal femur. The purpose of this study was to investigate the bone structure in RA patients by analyzing the bone structure of non-weight bearing bones (the distal radius) by HR-pQCT and weight-bearing bone (the proximal femur) by 3DS.MethodsSubjects were 80 patients with ACPA-positive RA (RA group, 61+/-12 years old, male/female=3/77) and 147 patients with ACPA-negative non-RA diseases (control group, 63+/-12 years old, male/female=5/142). They underwent DXA scans (Horizon A, HOLOGIC) of the lumbar spine and the proximal femur and HR-pQCT scans (XtremeCT II, Scanco Medical) of the distal radius. Three-dimensional bone structure analysis was performed on the DXA data of the proximal femur using 3DS to obtain the structural measurements of the cortical and trabecular bones. HR-pQCT images were used to obtain structural parameters of the cortical and trabecular bones of the distal radius on the side where no synovitis was observed in the wrist joint on previous ultrasound examinations. The bone measurements were compared between the RA group and the control group.ResultsThere were no significant differences in bone mineral density at the lumbar spine or proximal femur, but it was -2.5% lower on average in the RA group than in the control group. 3DS showed a decrease in cortical volumetric bone mineral density (mean -2.0%, p<0.05) and cortical surface bone mineral density (mean -3.7%, p=0.06) in the RA group compared to the control group. HR-pQCT showed a decreasing tendency in cortical bone porosity (mean -14.3% p=0.15) and cortical bone thickness (mean -1.8%) in the RA group. In the trabecular bone, there was no apparent difference in any of the measurements by 3DS and HR-pQCT between RA and the control group.ConclusionThe bone structural measurements were more reduced in the distal radius than in the proximal femur in the RA group compared to the control group. The results indicate that in the RA group, structural strength loss may be more likely to occur in the weight-bearing bones than in the non-weight bearing bone.

***Disclosures: Ikuko Tanaka**, None*

SAT-311

Caveolin-1 microdomains modulate parathyroid hormone receptor type 1 signaling and osteogenic actions in bone cells *Sara Heredero-Jimenez[1], Eduardo Martin-Guerrero[1], Joan Pizarro-Gómez[1], Irene Tirado-Cabrera[1], Arancha R. Gortázar[1], Juan A. Ardura[1]. [1]Department of Basic Medical Sciences, Bone Physiopathology Laboratory, Universidad San Pablo?CEU, CEU Universities, Alcorcón, Madrid, Spain

Caveolin-1, a key component of caveolae, regulates the trafficking and signaling of some cell surface receptors. Parathyroid hormone (PTH) receptor type 1 (PTH1R) modulates osteoblast and osteocyte actions during bone remodeling and formation after activation by ligands such as the PTH-related protein (PTHrP). Activated PTH1R may lead to different biological actions depending on its association with different membrane or intracelular molecules. Since PTH1R presents a potential caveolin-1 binding domain we hypothesize that PTH1R trafficking, signaling and gene expression responses are regulated by interactions with caveolin-1 in cells of the osteoblastic lineage. Mouse osteoblastic MC3T3-E1 and osteocytic MLO-Y4 cells were transfected with GFP-PTH1R, mCherry-Caveolin-1 or specific caveolin siRNAs and stimulated or not with PTHrP (1-37). Using confocal microscopy we performed live-cell time-lapse imaging and fluorescence recovery after photobleaching analysis to evaluate PTH1R and caveolin-1 trafficking and receptor-caveolin-1 interactions, respectively. Intracellular calcium accumulation was evaluated by Fluo-4AM microscopy and cAMP levels were analyzed with an ELISA kit. ERK1/2 was assassed by western blotting. Caveolin-1, runx2, osteocalcin, bone alkaline phosphatase, OPG and RANKL mRNA expression were studied in osteoblastic cells and in femora of C57BL/6 mice ranging from 2-18 months of age by qPCR.Caveolin-1 interacts with PTH1R at membrane-bound vesicles in osteoblastic cells. This interaction causes PTH1R temporarily retention at caveolin-1 microdomains upon receptor activation by PTHrP, delaying receptor internalization. Moreover, caveolin-1 overexpression modified PTHrP-dependent signaling and actions in osteoblastic cells by decreasing intracellular calcium accumulation, increasing cAMP levels and inducing runx2, osteocalcin, bone alkaline phosphatase and OPG gene overexpression. In contrast, caveolin-1 silencing caused over-phosphorylation of ERK1/2 kinase, over-production of calcium, reduced expression of runx2, osteocalcin and alkaline phosphatase and increased the percentage of dead cells. Analysis of bone-related genes in femora of mouse of different groups of age revealed that the gene expression of caveolin-1 positively correlated with that of runx2, osteocalcin and OPG.Our observations suggest that PTH1R signaling and osteogenic actions are regulated by caveolin-1 in cells of the osteoblastic lineage.

***Disclosures: Sara Heredero-Jimenez**, None*

SAT-312

See Friday Plenary Number FRI-312

SAT-313

Omega-6 and Omega-9 Fatty Acids Negatively Impact Osteoblast Function Before and After Mineralization *Beatriz Bermudez[1], Veronica Butler[2], Michael David[2], David Karasik[3], Cheryl Ackert-Bicknell[4]. [1]University of Colorado Denver, United States, [2]University of Colorado Anschutz Medical Campus, United States, [3]Azrieli Faculty of Medicine, Bar-Ilan University, Israel, [4]University of Colorado, United States

Western diets are increasing in prevalence around the world and contain significant amounts of omega-3 (?-3) and omega-6 (?-6) fatty acids (FA). Therefore, these FAs and omega-9 FAs are commonly consumed, and current studies show mixed effects on bone health and fracture risk. Osteoblast function relies on energy generated through oxidative phosphorylation and therefore changes in cell metabolism due to the availability of various FA could impact osteoblast function. This study aimed to examine how specific ?-3, ?-6, and ?-9 FAs influence osteoblast mineralization, metabolism, and differentiation using the MC3T3-E1 pre-osteoblast cell line. Before differentiation, we quantified the effect of FAs on proliferation and cellular energetics, and then after differentiation, we looked at mineralization and cellular energetics. Cells were treated for 48 hours with vehicle (VEH) (?-3 VEH: ethanol, ?-6, ?-9 VEH: cell culture media) or with linoleic acid (?-3, 40 uM), alpha-linolenic acid (?-6, 250 uM), and oleic acid (?-9, 100 uM), respectively. Proliferation was assessed by quantifying a fluorescent ki67 marker. Immunofluorescent images were taken to count the percent of ki67 positive cells using QuPath software. A Mito Stress Test assay was conducted using a Seahorse XFe96 Analyzer to measure oxygen consumption and extracellular acidification rates after FA treatment. Mineralization was quantified over ten days using the IRDye 800CW BoneTag. Data are presented as the mean +/- SEM with significance set at p<0.05. Proliferation was reduced in MC3T3-E1 cells by 58% with ?-3 FA, 11% with ?-6 FA, and 32% with ?-9 FA. Maximal respiration before differentiation was reduced in cells treated with all FAs when compared to VEH-treated cells (Figure 1A-C) and ATP production (5.46+/-0.14 vs. 4.55+/-0.12 pmol/min) before differentiation was reduced in cells treated with ?-6 FA compared to VEH-treated cells. Proton leak after mineralization was reduced in cells treated with ?-6 FA (1.43+/-0.06 vs. 1.23+/-0.06 pmol/min) compared to VEH-treated cells. Mineralization was decreased at all time points in cells treated with ?-6 and ?-9 FAs (Figure 1D-F). Our results suggest that reducing the intake of ?-6 and ?-9 FAs has the potential to improve bone health since we found that acute treatment of FAs has a detrimental effect on osteoblast function before differentiation. In addition, ?-6 and ?-9 FAs negatively influence the osteoblasts after mineralization.

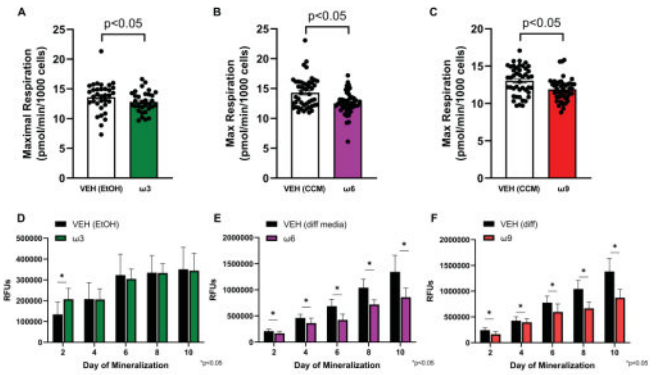

Figure 1: MC3T3-E1 cells after 48 hour treatment of alpha-linolenic acid (ω-3), linoleic acid (ω-6), and oleic acid (ω-9). Maximal Resipration before differentiation in cells treated with (A) ethanol vehicle or ω-3 fatty acid, (B) media vehicle or ω-6 fatty acid, and (C) media vehicle or ω-9. Mineralization after differentiation in cells treated with (D) ethanol vehicle or ω-3 fatty acid, (E) media vehicle or ω-6 fattyacid, and (F) media vehicle or ω-9 fatty acid.

***Disclosures: Beatriz Bermudez**, None*

SAT-314

Thrombospondin Status Affects Gene Expression in MSC-Osteoblasts from Adult Mice *Andrea Alford[1], Meredyth Bowman[1]. [1]University of Michigan, United States

The matricellular extracellular matrix (ECM) proteins thrombospondin (TSP) 1 and 2 affect bone mass and quality in growing mice. Our preliminary data suggest that TSP2 expression increases with age. In MSC-osteoblast cultures, conditioned medium TSP2 protein per cell layer DNA content increased between 5-9 months and 12 months of age (322.70+/-84.5 vs. 67.84+/-11.4 p<0.0001; N=5-6 female mice/age). However, contributions of TSP1 and 2 to osteoblast and osteocyte physiology in the adult and aging skeleton are not known. Marrow derived mesenchymal stem cells (MSC) from 10-month-old male TSP1-/- (N=6), TSP2-/- (N=3) TSP1/TSP2 double knockout (DKO, N=6), and wildtype (WT, N=3) mice were used to study effects of TSP status on osteoblast phenotype. RNA interference was employed to determine impacts of acute TSP2 knockdown in MSC from 2-year-old male mice (N=3). DMP1, OPG, RANKL, col1a1, col1a2, alkaline phosphatase, runx2 and PHEX expression were determined by rtPCR. Beta-actin was the house keeping gene. Significance (p<0.05) was determined using students t-test or ANOVA and Tukey test. Data are mean and SD.Mineralization was qualitatively reduced in TSP2-/- and DKO cultures, but not in TSP1-/- cultures (Figure 1). DMP1 expression was reduced in DKO, but it trended up in TSP2-/- MSC (p=0.11. Figure 1). TSP2-shRNA also led to elevated DMP1 expression compared to LacZ-shRNA in MSC from 2-year-old male WT mice (3.21+/-1.0 vs. 1.0+/-0.7 (n.s) at day 3 post-transduction and 6.88+/-3.0 vs. 0.87+/- 0.05 (p<0.01) at day 14 post-transduction. PHEX gene expression was reduced in DKO MSC, but not TSP1-/-, TSP2-/-MSC or in MSC transduced with TSP2-shRNA. OPG and RANKL were elevated ~2-fold over WT in TSP1 (p<0.0001 for both) but not TSP2-/- or in TSP2-shRNA treated MSC. OPG and RANKL were also elevated in DKO MSC (p<0.01), but the magnitude of the increases were reduced compared to TSP1-/- (~40% over WT for both).Our data suggest that TSP1 and 2 make unique and cooperative contributions to osteoblast and osteocyte gene expression in the adult and aging skeleton. The data also suggest overlap between the consequences of global TSP2 deficiency and acute reduction of TSP2 gene expression.

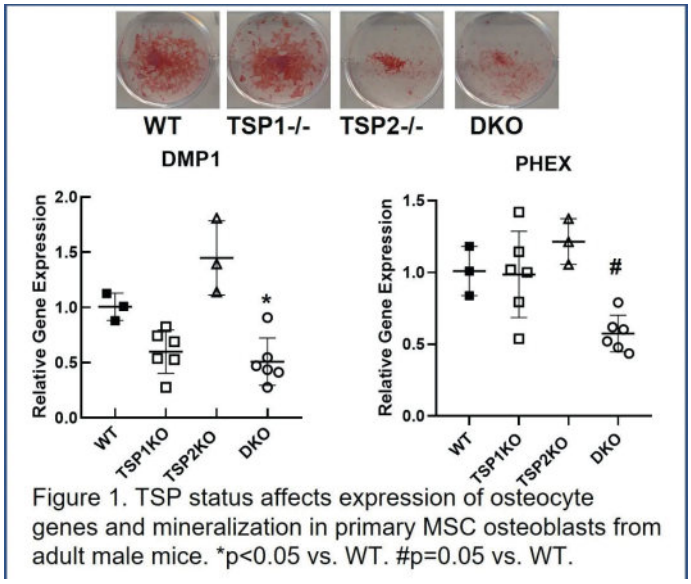

Figure 1. TSP status affects expression of osteocyte genes and mineralization in primary MSC osteoblasts from adult male mice. *p<0.05 vs. WT. #p=0.05 vs. WT.

***Disclosures: Andrea Alford**, None*

SAT-315

Mapping the local protein interactome of PHEX in osteoblasts by proximity biotinylation *Chirada Dusadeemeelap[1], Takuma Matsubara[1], Shoichiro Kokabu[1], William Addison[1]. [1]Kyushu Dental University, Japan

Inactivating mutations in PHEX cause impaired matrix mineralization and hypophosphatemia in X-linked dominant hypophosphatemic rickets (XLH). PHEX is a Type II membrane protein with an extracellular endopeptidase catalytic domain. To better understand the molecular mechanisms and protein-protein interactions which dictate PHEX's critical functions and underly XLH, we used proximity-dependent biotin identification (BioID) combined with mass spectrometry (MS) to define the PHEX interactome in osteoblast cells. BioID utilizes the fusion of a mutant form of BirA biotin ligase to a bait protein thereby permitting the specific labeling of proximal proteins in live cells within a delimited time period. Unlike classical affinity-purification proteomic approaches, BioID is well suited for the identification of insoluble matrix proteins, transient or weak associations and the membrane-anchored topology of PHEX.Protein fractionation, immunofluorescent imaging, PNGaseF analysis and PHEX activity assays confirmed that fusion of the biotin ligase to the C-terminal extracellular domain of PHEX (PHEX-BIOID) did not adversely affect PHEX subcellular localization, transmembrane orientation, glycosylation or endopeptidase activity in MC3T3-E1 osteoblast cells. MC3T3-E1 cells stably expressing PHEX-BIOID were differentiated for 12 days, treated with biotin for 24 hours and candidate factors identified by biotin-affinity capture and MS analysis. We discovered a PHEX proximity interaction network consisting of 21 proteins. Notably, several candidates with documented roles in endochondral bone morphogenesis, extracellular structure organization and collagen fibril organization were identified. Gene ontology analysis also revealed factors with underappreciated roles in integrin activation and cell adhesion molecule binding. Coimmunoprecipitation validated direct interaction of PHEX with selected candidate factors.In summary, our study provides a comprehensive map of the local PHEX interactome and provides a resource for unraveling the molecular mechanisms underlying PHEX-related functions and XLH disease. We show that the BioID approach is a powerful tool to explore membrane-matrix relationships in osteoblasts.

***Disclosures: Chirada Dusadeemeelap**, None*

SAT-318

The Effects of Hypochlorous Acid Antiseptic Solution on Cultured Osteoblast Proliferation *Madison Gregory[1], Ryan Moon[1], Patrick Brooks[1], Joshua Smith[1], Amanda Brodeur[1]. [1]Missouri State University, United States

Stabilized hypochlorous acid (HOCl) solutions have broad microbicidal activity at very low concentrations. With low toxicity to human tissues, these solutions are increasingly used as antiseptics in wound treatments. Contaminated orthopedic injuries such as compound fractures have a high rate of chronic infection despite operative irrigation and use of parenteral antibiotics. HOCl may be useful as an operative irrigant in this setting, yet the effects of hypochlorous acid on bony tissue and osteoblasts are unknown.Investigating the potential role of HOCl irrigation for contaminated orthopedic wounds, cultured osteoblasts were incubated with varying concentrations of a commercially available stabilized HOCl solution (Pure&Clean, Nixa, MO). Osteoblast survivability and proliferation was assessed. The LD50 of HOCl solution was assessed for Staphylococcus aureus, the most common pathogen in post-traumatic osteomyelitis, as well as for other common bacterial contaminants

of compound fractures. Bacterial cultures were exposed to hypochlorous acid at various concentrations and remaining colony forming units were calculated.Osteoblast cells were incubated in differing concentrations of HOCl and counted at varying durations following exposure. This work suggests that osteoblasts exposed to various concentrations of HOCl solution maintain proliferation in the short term. At the highest concentrations tested of up to 100 ppm, osteoblast survivability is not negatively impacted by HOCl, and survivability may be enhanced by its presence. Through culturing techniques and experimentation, osteoblast survivability appears more dependent on buffering conditions of incubation solutions. This work suggests that osteoblast growth media promotes greater survivability than HEPES and PBS. Finally, the potent bactericidal effects of hypochlorous acid were confirmed by reaching the LD50 against Staphylococcus aureus, Escherichia coli, and Pseudomonas aeruginosa at solution concentrations of less than 10 ppm.HOCl has bactericidal effects at extremely low concentrations yet does not show toxicity to osteoblasts in culture at concentrations used in some commercially available HOCl antiseptics. Overall, this study contributes to the growing body of research that HOCl may be safe as an irrigation solution for living cells, and potentially osteoblasts. Further investigation into the feasibility of HOCl irrigation of contaminated orthopedic tissues is warranted.

***Disclosures: Madison Gregory**, None*

SAT-319

See Friday Plenary Number FRI-319

SAT-321

Discovery of a novel tubulin isotype switch in microtubule cytoskeleton during osteoblast differentiation. *Shreya Patel[1], Marcus Winogradzki[1], Waddell Holmes[1], Niyati Patel[1], Ahmad Othman[1], Ryan Ross[1], Jitesh Pratap[1]. [1]Rush University Medical Center, United States

Differentiation of osteoblasts (OB) involves remarkable changes in gene expression, cytoskeletal proteins, and secretory activity. A network of microtubules (MT) supports intracellular vesicular trafficking and secretion. However, specific changes in the MT structure and function during differentiation are currently unknown. We show that disruption of MT structure inhibits differentiation. MTs are composed of heterodimers of ?- and ?-tubulins. The ?- and ?-tubulin isotypes and their post-translational modifications control the properties and functions of the MTs, a concept known as the 'tubulin code'. The objective of our study was to understand the changes in tubulin code during OB differentiation. First, we examined the expression levels of the 7 tubulin isotypes in primary mouse calvarial OB, fetal human OB, and mouse IDG-SW3 differentiation models via qRT-PCR and western blots. We found a robust increase in the mRNA and protein levels of TUB ?2, while a decrease of TUB ?3, indicating a novel tubulin isotype switch during differentiation. We validated these findings in vivo using mouse femurs revealing differential staining of OB in the endosteum and periosteum regions, suggesting a spatiotemporal function of TUB ?2 and TUB ?3 isotypes. The expression levels and integration of the isotypes into the MT polymer control its stability and regulate the interaction of MT-associated proteins. We then examined the post-translational modifications of tubulins and found a significant increase in the acetylation levels of Lys-40 of the ?-tubulin during differentiation. Acetylation prevents MT breakage and makes them more stable. Our immunofluorescence studies showed a differential subcellular distribution of TUB ?2 and TUB ?3 and their colocalization with acetylated MTs. These changes in the tubulin code indicate specific modifications in MTs to promote subcellular vesicular trafficking and secretion of matrix proteins. To understand the regulation of the code, we analyzed ChIP-Seq data from differentiating OB. We found increased recruitment of Runx2 on the TUB ?2 gene locus, revealing a novel role of Runx2 in controlling the isotype switch. Taken together, we discovered a tubulin isotype switch reflecting increased MT stability during differentiation. Our findings show a novel regulation of OB differentiation via tubulin code. Understanding the control mechanism of the tubulin code may lead to the development of targeted therapies for osteoporosis and osteopenia.

***Disclosures: Shreya Patel**, None*

SAT-323

Osteoblasts and Bone Nodules in vitro enhance understanding of how osteoblasts produce bone matrix: mechanism of bone labeling by calcium binding fluors *Quitterie Larrouture[2], Irina Tourkova[2], Deborah Nelson[3], Paul Schlesinger[4], Harry Blair[2]. [2]University of Pittsburgh, . [2]University of Pittsburgh, United States. [3]University of Chicago, United States. [4]Washington University , United States

Osteoblasts in vivo form an epithelial-like layer with tight junctions between cells. Bone formation involves mineral transport into the matrix and acid transport to balance pH in the bone with extracellular fluid. To study how osteoblasts mineralize in vitro, we cultured stromal stem cells (SSCs) on perforated polyethylene terephthalate membranes. SSCs prepared from murine bone marrow were used to investigate alternative conditions whereby osteoblast differentiation would better emulate in vivo bone development. SSCs were characterized by flow cytometry with CD44, Sca-1 and CD105 positive labeling and CD45 negative. Initially the SSC produced a monolayer; at 2.5 weeks we noted resistance of 100+/-10% ohms.cm2 across the cell layer. Calcein is commonly used as a marker for identification of bone growth in vivo, however, the mechanism is not well understood. Osteoblasts accumulate the fluorescent calcium binding protein (calcein), possibly via ATCC1, the only MDR transporter in avian osteoblasts greenscreen. In culture, the osteoblasts accumulate calcein, on their apical surface where mineral formation is observed which is the opposite site of the PET membrane. We incubated plates with 5 μM calcein and with 10 μM of the non-fluorescent inhibitors of multidrug resistance protein transport vinblastine or diltiazem. This showed calcein transport in the initial layer of osteoblasts that behaves as a tight epithelium is inhibited by two known inhibitors of the MDR mechanism. Mineralization was validated with paracellular alkaline phosphatase activity and mineral deposition. Cross-section of bone nodule formed by mineralizing osteoblasts revealed its structure with osteocyte-like cells within the nodule, surrounded by a dense collagenous matrix. The surface of the bone nodule is covered by cuboidal osteoblast-like cells. Membrane attached osteoblasts in vitro had abundant mitochondria consistent with active transport that is mediated in vivo by surface osteoblasts. These findings suggest that osteoblasts produce bone matrix on their apical side, transport protons from the apical side to the basolateral side and release the protons in the ECF. This in vitro model is a major advancement in modeling bone in vivo for understanding of osteoblast bone matrix production.Figure 1: Mineralizing osteoblasts cultured with calcein fluorescence and non-fluorescent MDR inhibitors. Bone nodule at 2 weeks of differentiation on PET membrane, 20x.

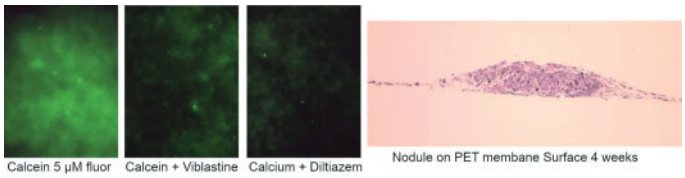

***Disclosures: Quitterie Larrouture**, None*

SAT-324

See Friday Plenary Number FRI-324

SAT-325

Analysis of the molecular influence of Wnt1 using osteogenic cell lines *Wenbo Zhao[1], Michael Amling[1], Timur Alexander Yorgan[1], Thorsten Schinke[1]. [1]University Medical Center Hamburg-Eppendorf, Germany

Mutations of WNT1 have been identified to cause either early-onset osteoporosis or osteogenesis imperfecta type XV, and the key role of Wnt1 for skeletal integrity was further confirmed by the analysis of corresponding mouse models. Moreover, although we observed a remarkable osteoanabolic influence of Wnt1 in transgenic mice with inducible Wnt1 expression in osteoblasts, the underlying mechanisms still remain to be established.To identify putative receptors of Wnt1 in osteoblasts and transcriptional targets mediating this response, we treated mesenchymal ST2 cells, MC3T3-E1 cells or primary murine osteoblasts with a recombinant Wnt1/Sfrp1 complex. Long-term treatment (15 days) with reWnt1/Sfrp1 during osteogenic differentiation significantly promoted osteogenesis of mesenchymal ST2 cells but not of MC3T3-E1 or primary osteoblasts. Based on these findings we analyzed the expression of all known Fzd genes encoding putative components of a Wnt1 receptor complex. We observed remarkably higher expression of Fzd2 and Fzd4 in Wnt1-responsive ST2 cells, when compared to MC3T3-E1 or primary osteoblasts. We additionally investigated the expression of all Fzd genes during osteogenic differentiation in primary osteoblasts, where we observed a general pattern of higher expression in early stages, especially for Fzd1, Fzd2 and Fzd9.In order to explore down-stream effects of Wnt1, we performed genome-wide expression analysis of short-term (6h) reWnt1/Sfrp1 treated ST2 cells. Here we observed significantly higher expression of known Wnt target genes (such as Apcdd1), but also of Osteomodulin (Omd) and Periostin (Postn). Importantly, the two latter genes were also identified to be strongly induced in another genome-wide expression analysis, where we analyzed ST2 cells 3 days after the transfection of a Wnt1 expression plasmid.Our data not only demonstrate that two established osteogenic cell lines display different responsiveness to Wnt1 administration, but also suggest that Wnt1 primarily acts on osteoblast progenitors. Based on our molecular findings, it now remains to be verified, if Omd and Postn are relevant downstream mediators of Wnt1 to promote bone formation, and if one of the Fzd genes with relatively higher expression in ST2 cells encodes a physiologically relevant Wnt1 receptor.

***Disclosures: Wenbo Zhao**, None*

SAT-327

?-catenin phosphorylation by ?2-adrenergic activation: New insights into sympathetic inhibition of osteoblasts *Leah Worton[3], Anna Curtin[2], Edith Gardiner[3]. [3]University of Washington, United States. [2]The University of Washington, United States. [3]University of Washington,

The sympathetic nervous system modulates bone mass by increasing bone resorption and inhibiting bone formation through osteoblastic ?2-adrenergic receptor (?2AR). ?-adrenergic activation in osteoblasts stimulates cAMP/PKA signaling upstream of the tran-

scriptional inhibition of proliferation/differentiation and support of osteoclastogenesis. The present study expands the signaling/mechanism by which this activation regulates osteoblast function. All data were generated from at least 3 independent culture studies and are presented as percentage change from the mean. Treatment of differentiating MC3T3 pre-osteoblastic cells with the ?-adrenergic agonist isoproterenol (ISO) resulted in decreased mineralization (-36%, p<0.001); this was mirrored in primary BMSCs from WT but not ?2AR KO mice. Further, ?-adrenergic stimulation in MC3T3 cells with ISO increased cell attachment (+165%, p<0.001) and reduced transwell migration (-45%, p<0.05). This decrease in migration was confirmed in osteoblastic outgrowth cells from WT mice (-48%, p<0.001) but negated in ?2AR KO cultures. Activation of ?-adrenergic signaling in MC3T3 cells also resulted in a higher cytoskeletal G/F-actin ratio, with F-actin decreased by ISO treatment (-85%, p<0.001). Investigating this inhibition of osteogenic signaling we found increased phosphorylation of ?-catenin at serine residues 552 and 675 downstream of ?2AR activation with ISO (p<0.05). These phosphorylation events were inhibited by pre-treatment with the ?-adrenergic antagonist propranolol or PKA inhibitor H89, suggesting that ?-catenin phosphorylation downstream of ?2AR is via G-protein coupled signaling. These phosphorylation events were also dependent on activation of PAK4 kinase. ISO did not affect GSK3? phosphorylation, activation of ?-catenin at S33/S37/T41, or canonical Wnt target gene expression. Co-immunoprecipitation suggested enhanced interaction of pS552/675 ?-catenin with Cadherin 11/?E-catenin after ISO treatment. This ?2-adrenergic response in osteoblasts may divert ?-catenin from its canonical Wnt pathway transcriptional role, instead promoting cadherin interaction at the cell membrane, reducing actin polymerization and cell migration and enhancing cell attachment, thereby modulating osteoblast function. These data reveal ?-catenin as a novel downstream effector of ?2-adrenergic signaling, which has not previously been reported in osteoblasts or any other cell type.

***Disclosures: Leah Worton**, None*

SAT-328

See Friday Plenary Number FRI-328

SAT-329

Effects of PTH on Osteoblast Bioenergetics in Response to Glucose *VICTORIA DEMAMBRO[1], Li Tian[2], Dr. Clifford ROsen[3], Anyonya Guntur[1]. [1]MaineHealth Institute for Research, United States. [2]West China Hospital, Sichuan University, China. [3]Maine Medical Center, United States

Parathyroid hormone acts through its receptor, PTHR1, expressed on osteoblasts, to control bone remodeling. Metabolic flexibility for energy generation has been demonstrated in several cell types coupled to substrate availability. Recent studies have identified a critical role for PTH in regulating glucose, fatty acid and amino acid metabolism thus stimulating both glycolysis and oxidative phosphorylation. Therefore, we postulated that PTH stimulates increased energetic output by osteoblasts either by increasing glycolysis or oxidative phosphorylation depending on substrate availability. To test this hypothesis, undifferentiated and differentiated MC3T3E1C4 calvarial pre-osteoblasts were treated with PTH to study osteoblast bioenergetics in the presence of exogenous glucose. Significant increases in glycolysis with acute ~ 1hr PTH treatment with minimal effects on oxidative phosphorylation in undifferentiated MC3T3E1C4 in the presence of exogenous glucose were observed. In differentiated cells, the increased glycolysis observed with acute PTH was completely blocked by pretreatment with a GLUT1 inhibitor (BAY-876) resulting in a compensatory increase in oxidative phosphorylation. We then tested the effect of PTH on the function of complexes I and II of the mitochondrial electron transport chain in the absence of glycolysis. Utilizing a novel cell plasma membrane permeability mitochondrial (PMP) assay, in combination with complex I and II specific substrates, slight but significant increases in basal and maximal oxygen consumption rates with 24hr PTH treatment in undifferentiated MC3T3E1C4 cells were noted. Taken together, our data demonstrate for the first time that PTH stimulates both increases in glycolysis and the function of the electron transport chain, particularly complexes I and II, during high energy demands in osteoblasts.

***Disclosures: VICTORIA DEMAMBRO**, None*

SAT-331

Irisin Enhances Mitochondrial Function in Differentiating Osteoclast Progenitors *Eben Estell[1], Tsunagu Ichikawa[2], Cliff Rosen[1]. [1]MaineHealth Institute for Research, United States. [2]University of New England College of Medicine, United States

Irisin is a signaling factor released from muscle during exercise1 known to modulate bone remodelling2,3. We have shown that irisin influences the resorptive processes of remodelling by stimulating osteoclastogenesis. The ability of brief initial irisin exposure to yield increased osteoclast numbers later in culture points to a rapid action on the progenitor4. Osteoclasts and their progenitors support the high energy demands of differentiation and resorption with increased mitochondrial glucose metabolism compared to other cells5. We have previously demonstrated via mitochondrial stress testing that irisin enhances mitochondrial respiration in the osteoclast progenitor, elevating basal oxygen consumption rate and significantly increasing maximal and spare energy capacity. The present study further investigates this mechanism with the hypothesis that enhanced respiration is due to an overall increase mitochondrial biogenesis in the osteoclast progenitor. Primary murine osteoclasts were differentiated in vitro from bone marrow progenitors as previously described5 for 48 hours with or without 10 ng/mL irisin prior to visualization of cellular content of mitochondria and reactive oxygen species via fluorescence microscopy. Irisin treatment resulted in a significant increase in mitochondrial content as quantified by relative fluorescence intensity of the MitoTracker Red CMXRos dye, averaged for the body of individual cells (Figure 1a-c). Similarly, irisin treatment resulted in a significant increase in intercellular levels of reactive oxygen species, as quantified by cellular fluorescence of the CellROX Green dye (Figure 1d-f). Together these data support previous mitochondrial stress test results by showing that irisin enhances mitochondrial content and production of reactive oxygen species, an output of mitochondrial respiration that plays a vital signaling function during osteoclastogenesis6. This enhancement of mitochondrial function may thus be a driving mechanism in the stimulation of osteoclastogenesis by irisin, providing both an energy source and key intercellular signaling factors to differentiating progenitors. Ongoing work weeks to elucidate the utilization of different metabolic processes during osteoclastogenesis, and the influence of irisin thereupon. References: 1) Bostrom et al. Nature 2012. 2) Kim et al. Cell 2018 3) Colaiannia et al PNAS 2015. 4) Estell et al. eLife 2020. 5) Kim et al. Cell Physiol Biochem 2007. 6) Lee et al. Blood 2005.

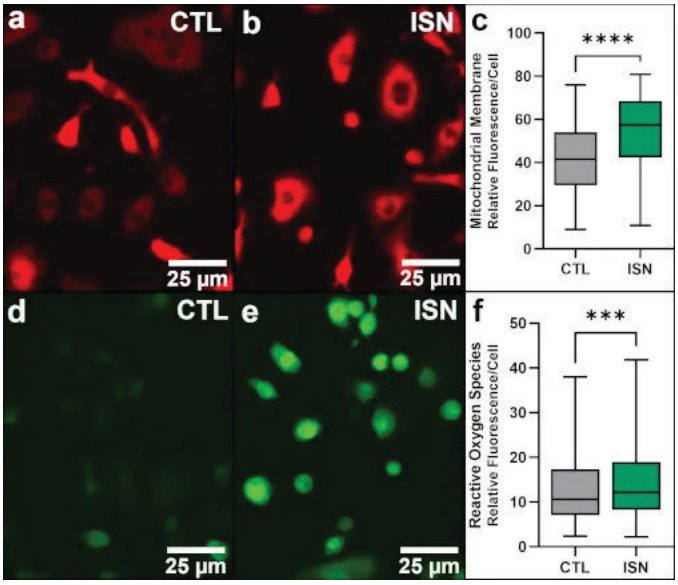

***Disclosures: Eben Estell**, None*

SAT-332

See Friday Plenary Number FRI-332

SAT-333

See Friday Plenary Number FRI-333

SAT-334

Expression of Ubiquitin-Specific Peptidase 4 (USP4) and its Impact on Bone Resorption in Human Osteoclasts *Victor Goguen-Couture[1], Papa Yaya Badiane[1], Michèle Roy[1], Jean-Philippe Brosseau[2], Sophie Roux[1]. [1]Rheumatology, Department of Medicine, Sherbrooke University, Canada. [2]Department of Biochemistry and Functional Genomics, Sherbrooke University, Canada

Alternative splicing (AS) plays a central role in protein diversity and may regulate OC activity. Using a PCR-based screening strategy, we previously identified an alternative splicing event in USP4 (encoding ubiquitin-specific protease 4) significantly associated with the overactive phenotype of osteoclasts in Paget's disease of bone (Klinck et al, 2014). USP4 is a de-ubiquitinase that exhibits specificity for both degradative (Lys48) and regulatory (Lys63) ubiquitin chains. In other systems, some USP4 targets involve signaling components, such as TAK1, TRAF6 or PDK1, all components known to be critical in osteoclasts. In mice and humans, two isoforms of USP4 are produced by AS, differing by 47 residues (exon7), which may regulate substrate selectivity as their relative abundance varies between tissues and also alters the subcellular distribution of USP4. In addition, most of the phosphorylation sites of USP4 are located in exon 7, suggesting a different regulation for the isoforms of the protein. Since USP4 had never been studied in osteoclasts, our first objective was to investigate the localization and the roles of USP4 in human osteoclasts. We used cord blood monocytes as osteoclast precursors in in vitro long-term cultures (N=5). We first confirmed USP4 protein

expression by western blot, as well as its subcellular localization by immunofluorescence in bone resorbing osteoclasts. The impact of USP4 on osteoclast activity was studied by comparing osteoclast transfected at D17 of three-week cultures with USP4-specific DsiRNAs or a negative control, or left untransfected, allowing an average 60% decrease in USP4 expression in presence of USP4-specific vs control DsiRNA. Inhibiting USP4 induced a significant 2/3 decrease in bone resorption compared with negative controls, with an associated decrease in the number of multinucleated cells. The impact of isoforms on nuclearity and resorption is being evaluated. Thus, USP4 may have a potential role in the regulation of osteoclast bone resorption in human osteoclasts, although the exact mechanism and the osteoclast targets remain to be elucidated, as does the impact of spliced isoforms.

***Disclosures: Victor Goguen-Couture**, None*

SAT-335

See Friday Plenary Number FRI-335

SAT-337

Vitamin A Enhances Periosteal Osteoclastogenesis by Stimulating Macrophage/Osteoclast Progenitor Cell Proliferation *Petra Henning[1], Anna Westerlund[1], Karin Horkeby[1], Vikte Lionikaite[1], Sofia Movérare-Skrtic[1], H. Herschel Conaway[1], Ulf H. Lerner[1]. [1]Sahlgrenska Academy at University of Gothenburg, Sweden

A deleterious effect of elevated levels of vitamin A on bone health has been reported in numerous clinical studies. Mechanistic studies in rodents have shown that numbers of periosteal osteoclasts are increased, while endocortical osteoclasts are simultaneously decreased by vitamin A treatment. These observations indicate that osteoclastogenesis on the endocortical and periosteal surface of bone is differentially controlled by vitamin A. The present study investigated the in vitro effect of all-trans retinoic acid (ATRA), the active metabolite of vitamin A, on osteoclast differentiation using periosteal osteoclast progenitors. Mouse calvarial bone cells were cultured in media containing ATRA, with or without the osteoclastogenic cytokine RANKL, on plastic dishes or bone discs. Whereas ATRA did not stimulate osteoclast formation alone, the compound robustly potentiated the formation of RANKL-induced bone resorbing osteoclasts. This effect was due to stimulation by ATRA (EC50 ~3nM) on the numbers of macrophages/osteoclast progenitors in the bone cell cultures, as assessed by mRNA and protein expression of several macrophage and osteoclast progenitor cell markers, such as M-CSF receptor, RANK, F4/80 and CD11b, as well as by FACS-analysis of CD11b+/F480+/Gr1- cells. The stimulation of macrophage numbers was independent of increased M-CSF and IL-34. These observations demonstrate a novel mechanism by which vitamin A enhances osteoclast formation specifically on periosteal surfaces.

***Disclosures: Petra Henning**, None*

SAT-339

See Friday Plenary Number FRI-339

SAT-340

Downregulation of receptor activator NF-kB (RANK) expression by CpG methylation of its gene promoter in aging model. *Riko Kitazawa[1], Ryuma Haraguchi[2], Sohei Kitazawa[3]. [1]Ehime University, Graduate School of Medicine, Japan. [2]Ehime University Graduate School of Medicine, Japan. [3]Ehime University, Japan

The precise mechanism of senile osteoporosis, which occurs in the elderly regardless of gender, remains largely unknown. We investigated the regulation of the receptor RANK gene expression by methylation using a high-passaged mouse osteoclast progenitor cell line, RAW264.7, as an in vitro model of aging. A comprehensive DNA methylation analysis was implemented with the use of low- and high-passaged RAW264.7 and bone marrow stromal cell line, ST2. CpG-island located in a regulatory region of RANK gene was maintained in a hypomethylated state in RAW264.7 cells, but accumulated in ST2 cells, suggesting that hypermethylation of CpG-island in RANK gene promoter is involved in its cell type-specific expression. In the RAW264.7 cells after prolonged passaging, receptor RANK expression was downregulated, resulting in decreased sRANKL-induced osteoclastogenesis and expression of TRACP and CTSK. Epigenome study of high-passaged RAW264.7 cells revealed that genes important in osteoclastogenesis, such as NFATc1, MITF, AP-1, and PU.1, did not change methylation status. On the other hand, methylation-specific PCR and bisulfite mapping confirmed hypermethylation of a small fraction of CpG-island (methylation at 22 out of 25 sites) in high-passaged cells. ICON probe-mediated in situ demonstration of methylated-cytosine at this CpG site revealed that the percentage of cells with methylation in the RANK gene increased in a passage-dependent manner in RAW264.7 cells. Conversely, upon treatment with demethylating agent 5-azacytidine, high-passaged RAW264.7 cells showed restoration of RANK expression, osteoclastogenesis, TRACP and CTSK expression. Ex vivo cultures of splenic macrophages from young (10.5W) and aged (12M) mice also showed that CpG methylation was predominant and RANK expression and osteoclastogenesis were reduced in the aged animals. In macrophage lineage cells, including osteoclast progenitors, overall DNA methylation was not significantly affected by passage loading, but for the RANK gene, its downregulation by methylation was observed in some aging osteoclast progenitor cells in both cell line RAW264.7 and mouse individuals. Reduced RANK expression by age-related accumulation of DNA methylation (type A methylation), albeit seen in some population of osteoclast precursor cells, may be involved in low-turnover bone in aged populations.

***Disclosures: Riko Kitazawa**, None*

SAT-341

See Friday Plenary Number FRI-341

SAT-343

AhR ligands regulate subchondral bone remodeling via osteoclast differentiation *Yuri Yoshikawa[1], Takashi Izawa[2], Yusaku Hamada[1], Yuuki Namba[1], Gohji Kozaki[1], Hiroshi Kamioka[3]. [1]Department of Orthodontics, Graduate School of Medicine, Dentistry and Pharmaceutical Sciences, Okayama University, Japan. [2]Okayama University Grad Sch, Japan. [3]Okayama University Graduate School of Medicine, Dentistry, and Pharmaceutical Sc, Japan

Bone loss due to smoking represents a major risk factor for fractures and bone osteoporosis. Signaling through the aryl hydrocarbon receptor (AhR) and its ligands contributes to both bone homeostasis and inflammatory diseases. The aim of this study was to investigate possible mechanisms which mediate bone loss in the TMJ due to smoking. In particular, whether benzo[a]pyrene (B[a]P), a carcinogen of tobacco smoke, induces expression of the AhR target gene, Cyp1a1, in mandibular condyles. Possible functions of an endogenous ligand of FICZ, were also investigated in a TMJ-osteoarthritis (OA) mouse model. B[a]P was administered orally to wild-type and AhR?/? mice and bone metabolism was subsequently examined. Therapeutic functions of FICZ were detected with ?CT and histology. Exposure to B[a]P accelerated bone loss in the mandibular subchondral bone. This bone loss manifested with osteoclastic bone resorption and upregulated expression of Cyp1a1 in an AhR-dependent manner. In a mouse model of TMJ-OA, FICZ exhibited a dose-dependent rescue of mandibular subchondral bone loss by repressing osteoclast activity. Meanwhile, in vitro, pre-treatment with FICZ reduced RANKL-mediated osteoclastogenesis. B[a]P regulates mandibular subchondral bone metabolism via the Cyp1a1. The AhR ligand, FICZ, can prevent TMJ-OA by regulating osteoclast differentiation.

***Disclosures: Yuri Yoshikawa**, None*

SAT-345

A novel biomaterial for functional and analytical recapitulation of osteoclastogenesis in vitro *Yongkuk Park[1], Jungwoo Lee[2]. [1]University of Massachusetts Amherst, . [2]University of Massachusetts-Amherst, United States

Osteoclasts, the multinucleated bone-resorption cells that exclusively develop on the bone surface during bone remodeling, is a primary target for osteoporosis drug development as their relatively increased activity leads to bone loss. Accurate in vitro recapitulation of osteoclast biology is essential for screening potential toxicity and predicting pharmacological responses. Recent animal studies have revealed the critical roles of osteoblasts in regulating osteoclast function and the longer lifespan of osteoclasts than previously thought, partly through fission and recycling. However, existing osteo-culture and assay platforms are limited in reproducing these newly identified processes. Here, we introduce a novel in vitro osteoclast differentiation and functional assay platform utilizing osteoid-inspired demineralized bone paper (DBP), a thin slice of demineralized compact bone matrix. DBP supports rapid, structural mineral deposition by osteoblasts while retaining optical transparency for imaging. Osteoblasts and bone marrow monocytes coculture on DBP under biochemical stimulation recapitulated in vivo-relevant osteoclastogenesis. Longitudinal fluorescent monitoring substantiated osteoclast fusion, mineral resorption, and fission. Finally, a simulated clinical scenario of bisphosphonate treatment demonstrated with significantly reduced the number and lifespan of osteoclasts due to mineral-bound bisphosphonate. The DBP-based bone model can significantly facilitate the development of osteoclast-targeting drugs and understanding various aspects of bone remodeling biology with high fidelity and analytical power.

***Disclosures: Yongkuk Park**, None*

SAT-347

See Friday Plenary Number FRI-347

SAT-348

Osteoclast Deletion of Kalirin, a Dual GTP Exchange Factor Protein, Decreases Bone?Mass *Katie Chester[1], Daniel Godfrey[1], Jung Min Hong[1], Mauro Tudares[2], Angela Bruzzaniti[3]. [1]Indiana University School of Dentistry, United States. [2]Indiana Unversity School of Dentistry, United States. [3]Indiana University School of Dentistry , United States

Kalirin is a multi-faceted protein with dual GTP/GDP activity which has previously been characterized in neurons, but its skeletal role remains unclear. Our group reported that Kalirin global knock-out mice exhibit profound decrease in bone mass, with females demonstrating more bone loss than males, compared to sex- and age-matched wild-type littermates. To investigate the contributing cellular mechanisms, we examined Kalirin deletion in osteoclasts (OCs) by crossing Kalirin flox/flox (Kal) mice with Cathepsin K (CatK) and TRAP Cre-recombinase mice. Male and female Kal-CatK-Cre and Kal-TRAP-Cre and Cre- littermates underwent in-vivo Lunar Piximus Densitometer analysis at 8-, 14- and 26-weeks (n=7-10). Changes in femoral bone mineral content (BMC), bone area and bone mineral density (BMD) were determined. Female Kal-CatK-Cre mice showed a significant decrease in BMC (-7.0%), bone area (-3.3%) and BMD (-4.0 %) at 14-weeks, with no statistical changes observed at 8- and 26-weeks. No significant changes were observed in male Kal-CatK-Cre mice at the ages examined. To assess OC formation in vitro, non-adherent bone marrow cells were differentiated with RANKL and MCSF, resulting in increased OC formation in Kal-CatK-Cre, compared to Cre- mice. Consistent with the Kal-CatK-Cre data, Kal-TRAP-Cre females showed a significant decrease in BMC (-6.3%) and bone area (-7.5%) ($p<0.05$) at 14-weeks. These results indicate that Kalirin regulates OCs and bone mass in female mice. In addition, other bone cell types or alternative physiological mechanisms contribute to the regulation of total bone mass by Kalirin. Expanded longitudinal assessment of mice with cell-targeted deletion of Kalirin will elucidate the individual or combinatory mechanisms regulating Kalirin's effects on overall bone mass.

***Disclosures: Katie Chester**, None*

SAT-351

Human Osteoclast Assays for Identifying Antiresorptive Treatments with Different Mechanisms of Action *Katja Fagerlund[1], Mervi Ristola[1], Jenni Mäki-Jouppila[1], Jukka Rissanen[1]. [1]Pharmatest Services Ltd, Finland

Several agents are approved for the treatment of osteoporosis, of which antiresorptive treatments primarily target osteoclasts by reducing their lifespan or activity. Zoledronic acid, a third generation nitrogen containing bisphosphonate, accumulates in bones where it binds to hydroxyapatite crystals. For years, zoledronic acid has been used to prevent or treat osteoporosis and regarded as the standard of care for patients with advanced cancer and bone metastasis to prevent skeletal complications. As an alternative therapeutic option, denosumab has also been found to be potent antiresorptive for treatment of osteoporosis and effective in delaying skeletal-related events in advanced cancer. Denosumab, a human monoclonal antibody against receptor activator of nuclear factor kappa-B ligand (RANKL), blocks the RANKL/RANK signalling pathway. In this study, effects of zoledronic acid and denosumab on osteoclast differentiation and bone resorption activity were studied using human osteoclast precursor cells that were cultured on bovine bone slices in 96-well plates for 7 days in the presence of RANKL and M-CSF, allowing them to differentiate into mature osteoclasts. In the osteoclast differentiation assay, zoledronic acid (0.001 - 500 µM) and denosumab (0.01 - 10 µg/ml) were added into the culture medium at day 0. Tartrate-resistant acid phosphatase 5b (TRACP 5b) activity was measured in the culture medium at day 7 as an index of osteoclast differentiation. In the osteoclast activity assay, the test compounds were added into the culture medium at day 7, and the formed osteoclasts were allowed to resorb bone for 3 days. C-terminal crosslinked telopeptides of type I collagen (CTX-I) was measured in the culture medium at day 10 as an index of bone resorption. Denosumab and zoledronic acid showed strong concentration dependent inhibition of osteoclast differentiation and resorption activity. We conclude that this osteoclast culture system can be used for identifying new potential compounds affecting osteoclasts with different mechanisms of action.

***Disclosures: Katja Fagerlund**, None*

SAT-355

Development of a Semi-Automated Digital Imaging Pipeline for Evaluation of Osteoclast Phenotypes in vitro *Anders Narum[3], MARGARET DURDAN[2], ANGELO GUILATCO[2], Christine Hachfeld[3], GABRIEL ALVARES BORGES[3], Megan Weivoda[3]. [3]Mayo Clinic, . [2]Mayo Clinic/University of Michigan, . [3]Mayo Clinic, United States

Osteoclasts (OCs) are myeloid-derived, bone-resorbing cells and are essential for healthy bone remodeling. In traditional in vitro osteoclastogenesis assays, OCs are quantified manually as multinucleated (>=3 nuclei) cells positive for Tartrate Resistant Acid Phosphatase (TRAP) activity. However, this method is time consuming and doesn't capture important characteristics of OC size, number of nuclei, and nuclear distribution that may be informative about OC functions and in vivo bone phenotypes. The goal of this study was to develop digital imaging analysis pipelines to automate the quantification of OC, including morphologic characteristics. Further, resorptive activity on bovine bone chipsOCs were generated from young (4 months) and old (32 months) male C57BL/6 mouse bone marrow macrophages using recombinant M-CSF and RANKL (n=3 per group). OC cultures were fixed after five days of differentiation; cells were TRAP stained and counterstained with Hoechst to assess nucleation. Whole wells were imaged using an EVOS automated fluorescent microscope. Images were run through a custom CellProfiler pipeline, identifying TRAP+ primary objects. Nuclei were detected as secondary objects and quantified per primary object (TRAP+ cell). Primary object morphometric data, including secondary object (nuclei) quantification was exported for analysis. Using this pipeline to compare young and old mouse derived OCs, we identified significant increases in the number of small (3-5 nuclei) and medium OCs (6-10 nuclei, p10 nuclei) was not significantly different; however, the area of large osteoclasts derived from old mice was trending larger than those from young mice. The overall morphometric parameters allow for principal component analysis and clustering of single OCs. These data are currently being tested for correlation with OC resorptive behavior on bovine bone chips in vitro as well as in vivo bone phenotype (micro computed tomography, histomorphometry, serum markers of bone remodeling). This semi-automated pipeline will facilitate the analysis of heterogeneity in OC and functional behavior and how these in vitro measures inform in vivo bone phenotypes.

***Disclosures: Anders Narum**, None*

SAT-356

Sclerostin and Wnt Signaling in Idiopathic Juvenile Osteoporosis *Renata Pereira[1], Isidro Salusky[2], Barbara Gales[2], Kathleen Noche[2], Lauren Albrecht[3]. [1]UCLA, United States. [2]University of California Los Angeles , United States. [3]University of California Irvine , United States

Idiopathic juvenile osteoporosis (IJO) is a condition characterized by low bone mass that can increase the risk of fractures in children. The molecular mechanisms underlying the initiation and progression of disease is incompletely understood, especially compared to adult osteoporosis, because it is uncommon. A key driver of osteoporosis in adults is sclerostin given its inhibitory roles on osteoblast activity and Wnt signaling. To evaluate the role of sclerostin in IJO, high-resolution confocal microscopy analyses were performed on bone biopsies collected from 13 pediatric patients. We report for the first time that sclerostin is increased in bone of IJO patients. Bone biopsies stained with sclerostin antibodies showed elevated expression across osteocytes and increased sclerostin-positive osteocytes. Skeletal sclerostin was associated with static and dynamic histomorphometric parameters. Further, colocalization analyses showed that bone sclerostin colocalized with phosphorylated ?-catenin, a hallmark of Wnt signaling that indicates Wnt inhibition. In contrast, sclerostin-positive osteocytes were not colocalized with "active" unphosphorylated form of ?-catenin. These results provide evidence that Wnt signaling plays a role in this disease and suggest that future studies of sclerostin in IJO could help in the development of biomarkers or therapies.

***Disclosures: Renata Pereira**, None*

SAT-357

See Friday Plenary Number FRI-357

SAT-358

Nitric Oxide Contributes to Sclerostin Protein Degradation Following Mechanical Load *HEATHER BUCK[3], Joseph Stains[2], Olivia Torre[2], Jenna Leser[2], NICOLE GOULD[3], Christopher Ward[2, 3], United States. [2]University of Maryland School of Medicine, United States. [3],

Following sufficient fluid-shear stress (FSS), osteocytes produce NOX2-derived reactive oxygen species, inducing calcium influx via TRPV4 channels. Increased intracellular calcium results in calcium-calmodulin dependent protein kinase II (CaMKII) activation, which regulates the lysosomal degradation of sclerostin. Here, we extend our discoveries identifying nitric oxide (NO) as a regulator of sclerostin degradation downstream of mechano-activated Ca2+ influx.Pharmacological inhibition of nitric oxide synthase (NOS) activity in Ocy454 osteocyte-like cells prevents FSS-induced sclerostin degradation. Conversely, short-term treatment with a NO donor in Ocy454 cells (10µM, 5min) or isolated murine long bones (15min) is sufficient to induce the rapid lysosomal degradation of sclerostin. Together these data show that NO is necessary and sufficient for sclerostin protein control.To interrogate the hierarchy of NO production within the mechano-transduction cascade that controls sclerostin protein abundance, we subjected Ocy454 cells to FSS in the presence of NOX2 or TRPV4 antagonists. Blocking NOX2 and TRPV4 prevents FSS-induced NO production, supporting that NO production is downstream of these signal transducers. Consistent with this hierarchy, NO donation was insufficient to induce Ca2+ influx in Ocy454s. Inhibition of lysosomal acidification did not alter NO production in mechanically-stimulated Ocy454s. NOS3 was identified as the predominant NOS gene expressed in Ocy454s via qPCR. Preliminary data show that siRNA knockdown of NOS2 or NOS3 abrogates FSS-induced sclerostin degradation.Emerging data show that NO donation (1min) appears sufficient to drive CaMKII activation, while NOS2/3 knockdown may also alter CaMKII activation in response to FSS. Conversely, loss of sclerostin protein expression in isolated long bones following treatment with a NO donor is abrogated in CaMKII?? dKO mice relative to WT.In conclusion, it seems that NOS3- and NOS2-dependent NO plays an essential role in the post-translational

degradation of sclerostin protein, suggesting a link between mechano-activated NO production and physiological responses initiating de novo bone formation.

***Disclosures: HEATHER BUCK**, None*

SAT-360

See Friday Plenary Number FRI-360

SAT-361

Sympathetic autonomic signaling promotes osteocyte-driven bone resorption

*Galen Goldscheitter[1], Alexandra Hooks[2], Evan Buettmann[3], Henry Donahue[3, 1], [1]United States, [2]Virginia Commonwealth University Department of Biomedical Engineering, United States, [3]Virginia Commonwealth University, United States

The sympathetic autonomic nervous system, which mediates the fight-or-flight response, has a complex role in skeletal health. Its primary effector, norepinephrine, acts on adrenergic receptors in bone. Of these, most evidence supports the role of ?1 and ?2 receptors in bone metabolism. Previous work demonstrated a catabolic effect of ?2 agonism. Further, studies suggest treatment with ?-adrenergic antagonists enhance the anabolic effect of loading via an unknown mechanism. Here, we show ?1/?2 agonism by isoproterenol (ISO) promotes a resorptive secretory phenotype in osteocyte-like cells, the primary mechanoresponsive bone cell, while ?1/?2 antagonism by propranolol (PRO) ablates this effect.OCY-454 cells were cultured at 33.5 °C to confluence in ?-MEM containing 10% FBS and 1% Penicillin/Streptomycin and exposed to vehicle (HBSS), PRO (10 ?M), and/or ISO (10 ?M) for 48 hours at 37 °C. Gene expression was measured via RT-qPCR.Treatment with the ?-receptor agonist ISO increased expression of Tnfsf11 (encodes RANKL) relative to Tnfrsf11B (encodes OPG). Treatment with PRO, alone, resulted in no change in expression. The effect of ISO was reversed when cells were co-treated with PRO. Treatment with ISO also reduced expression of ?2 adrenergic receptor (Adrb2), but not ?1 adrenergic receptor (Adrb1). No effect was seen on Phex expression, a component of the DMP1-FGF23 pathway and a marker of osteocyte differentiation.RANKL is an activator of osteoclast differentiation, and thus, a driver of bone resorption. It is inhibited by OPG which inhibits its binding on osteoclast precursors. Treatment with ISO increases relative expression of Tnfsf11 to Tnfrsf11B in osteocyte-like cells, key regulatory cells of bone metabolism. Suppression of this effect by PRO suggests this effect is driven by a primary ?1/?2-mediated mechanism. OCY-454 cells express both Adrb1 and Adrb2, and treatment with ISO decreases expression of Adrb2, but not Adrb1. Decreased receptor expression is a signal desensitization mechanism, thus suggesting ?2 is the primary mediator of this effect. Finally, ISO and PRO do not change Phex expression, suggesting this effect is not mediated by cellular differentiation state. These data introduce a novel mechanism of bone catabolism in response to sympathetic outflow; in which osteocytes secrete RANKL secondary to ?2 receptor agonism. This supports work done by other authors and suggests ?2 antagonism enhances osteogenic stimuli.

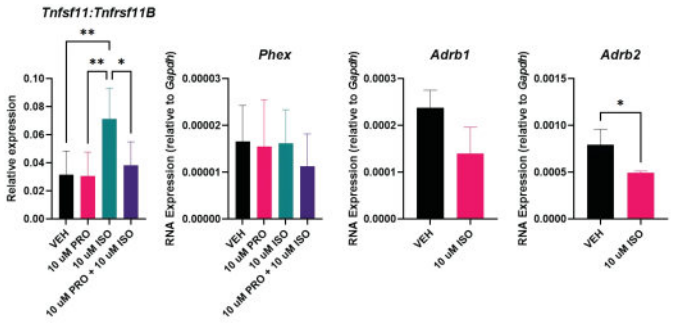

RT-qPCR of cell lysates from OCY-454 cells. Cells were treated with isoproterenol (ISO, 10 uM), propranolol (PRO, 10 uM) or vehicle (VEH) for 48 hours after reaching confluence. Statistical comparisons were made via one-way ANOVA and Tukey's post-hoc test (Tnsfs11:Tnfrsf11B, Phex) or student's t-test (Adrb1, Adrb2). * p < 0.05, ** p < 0.01

***Disclosures: Galen Goldscheitter**, None*

SAT-363

See Friday Plenary Number FRI-363

SAT-364

Hyperglycemia Induces Extensive Alternative Splicing Changes In Osteocyte-Enriched Cultures With Minimal Transcriptional Alterations

*Aseel Marahleh[1], Sherif Rashad[2], Hideki Kitaura[3], Jiayi Ren[3], Fumitoshi Ohori[4], Takahiro Noguchi[3], Itaru Mizoguchi[3]. [1]Tohoku University, Frontier Research Institute for Interdisciplinary Sciences, Japan. [2]Tohoku University, Graduate School of Biomedical Engineering, Japan. [3]Tohoku University, Graduate School of Dentistry, Japan. [4]Tohoku University Graduate School of Dentistry, Japan

Hyperglycemia is a hallmark of type II diabetes mellitus (T2D), and it is associated with reduced bone remodeling due to decreased bone resorption and bone formation. This state of reduced bone turnover leads to skeletal fragility and increased risk of fractures. Osteoblasts and osteocytes are the cells responsible for orchestrating the events necessary for bone remodeling to take place. Since bone cell gene expression was shown to be permanently impacted by high glucose, we reasoned that hyperglycemia would lead to extensive differential gene expression in osteocyte-enriched populations. First, we used Dmp1-Topaz neonatal calvaria, which express the topaz variant of GFP under the influence of the 8-kb Dmp1 promoter, to obtain osteocyte-enriched cultures through enzymatic digestion and cell sorting. Isolated cells were cultured under euglycemic (5.5 mM) and hyperglycemic conditions (25 mM) over 72 hours, where cell viability was comparable in both conditions as revealed by ethidium homodimer 1 staining. Second, RNA-seq data analysis revealed that high glucose diversifies the transcriptome by regulating RNA transcripts' splicing program rather than impacting gene transcription. Third, gene set enrichment analysis (GSEA) displayed a cellular environment of decreased adaptive response to oxidative stress and inflammation and increased susceptibility to apoptosis. Also, GSEA revealed a state of inhibited regulation of extracellular matrix (ECM) remodeling, including downregulation of biological processes involved in collagen catabolism and upregulation of the Hippo signaling pathway leading to YAP suppression which is implicated in poor bone accrual and poor mechanotransduction. Finally, computational analyses were performed for all five types of alternative splicing (AS) patterns and identified 2536 differential AS events between the two groups involving 719 genes, the most common of which were alternative spliced transcripts of Col1a1 and Col11a2. Additionally, we identified potential regulators of AS based on motif search analysis and found a significant enrichment in binding motifs of LIN28A/B, SRSF1 and HNRNP family and a significant depletion of KHDRBS1 and RBM41 motifs. In conclusion, we reveal that high glucose impacts AS events mostly without significant changes to gene expression, resulting in reduced cell adaptive response and an inhibited role in ECM remodeling.

***Disclosures: Aseel Marahleh**, None*

SAT-366

RNA Sequencing Analysis of Osteoclast Related Genes in Osteocyte-like Cell Line Cultured in Hypoxic Environment.

*Kohei Narita[1], Hideki Kitaura[1], Fumitoshi Ohori[2], Takahiro Noguchi[1], Aseel Marahleh[1], Jinghan Ma[1], Kayoko Kanou[1], Mariko Miura[1], Jiayi Ren[1], Itaru Mizoguchi[1]. [1]Tohoku University, Japan. [2]Tohoku University Graduate School of Dentistry, Japan

Purpose: In orthodontic tooth movement (OTM), bone resorption occurs on the compression side by osteoclasts. In compression side, orthodontic force compresses the periodontal ligament, which affects blood vessels, causes hypoxia due to lack of blood flow. It is considered that osteocytes in the alveolar bone on the compression side are also in a hypoxia environment. Recently, it has been found that osteocytes play an important role in osteoclastogenesis. In fact, it has been reported that hypoxia increases the expression of RANKL in osteocytes and promotes osteoclastogenesis. However, it is unclear that the mechanism of hypoxia environment promotes osteoclastogenesis through osteocytes. The purpose of this study is to elucidate the effect of osteocytes in hypoxia environment on osteoclastogenesis by using RNA sequencing analysis. Materials and Methods: Osteocyte-like cells (MLO-Y4 cell) were seeded in a 10 cm dish and cultured for 24 hours. Then, they were cultured for another 24 hours under hypoxia conditions (2% O2) using a hypoxia culture kit as the hypoxic culture group. The normal oxygen group were also cultured for another 24 hours (20% O2). After culturing, total RNA was extracted from all samples and analyzed for purification of RNA by RIN (RNA Integrity Number). RNA sequencing was performed using NovaSeq6000 for gene expression analysis. In addition, gene expression was mapped to the mouse genome using DRAGEN and calculated TMP values. Statistical analysis was then performed between the hypoxic culture group and the normal oxygen culture group. Results and Discussion: RIN analysis confirmed that all samples from osteocyte-like cells had a high-quality RNA. The most upregulated gene in osteocyte-like cells cultured under hypoxia conditions was Ndor1, while the most downregulated gene was Ifnb1. Additionally, it was observed that increased expression of several osteoclast related genes, such as Tnfsf11. The results suggested that hypoxic cultured osteocytes increase various osteoclastogenic factors including RANKL. Conclusion: The expression of osteoclast related gene in osteocytes by hypoxic cultured was found. It has been suggested that osteocytes in hypoxic condition promote osteoclastogenesis.

***Disclosures: Kohei Narita**, None*

SAT-367

See Friday Plenary Number FRI-367

SAT-369

Lack of osteoblast lineage autophagy does not alter the response to mechanical load *James Hendrixson[3], Robert Shaver[2], Alicen James[3], Jacob Laster[3], Julie Crawford[3], Jinhu Xiong[4], Melda Onal[3]. [3]University of Arkansas for Medical Sciences, United States. [2]University of Arkansas Fayetville, United States. [3]University of Arkansas for Medical Sciences, . [4]Univ of Arkansas for Medical Sciences, United States

Autophagy is a catabolic process by which cells recycle cytoplasmic content. Autophagy can play various cellular functions ranging from cellular stress response to cell differentiation. Previous studies have shown that mice lacking Atg7, an essential component of the autophagy pathway, from the entire osteoblast lineage exhibit very low cancellous and cortical bone mass associated with a 50% fracture rate. This phenotype was associated with a significant reduction in osteoblast number and bone formation. However, the underlying mechanisms are still unclear. Osteocytes are thought to serve as mechanosensing cells in bone and a reduction of the osteocyte network is thought to contribute to reduced mechanosensitivity. Notably, the deletion of Atg7 from the osteoblast lineage also caused a reduction in the osteocyte lacunocanalicular network. Additionally, mechanical strain has been shown to stimulate osteocyte autophagy in culture. Based on this, we hypothesized that autophagy contributes to mechanosensitivity by maintaining an intact osteocyte lacunocanalicular network. In support of this, Atg7floxed;Osx1-Cre (cKO) mice exhibited a low periosteal perimeter relative to control mice, a finding common to murine models with reduced mechanical response. To test our hypothesis, we isolated calvaria from cKO and Osx1-Cre (control) mice, and treated these ex vivo organ cultures with 10?M Yoda or vehicle for 24 hours. Yoda is a Piezo1 agonist, used to mimic mechanical strain in culture. Yoda treatment increased the expression of mechanosensitive genes such as Ptgs2 and Tnfsf11 independent of autophagy levels. However, transcriptional changes after a short-term mechanical stimulation in culture may not be representative of the long-term anabolic response to loading in vivo. Therefore, we tested if lack of autophagy altered the response to loading in vivo by performing tibial axial loading in 4-month-old cKO and control mice. The tibia of each mouse was loaded with equal compressive strain for 9 days within a 2-week period. MicroCT analysis revealed that mechanical loading increased cortical thickness similarly in both cKO and control mice. These results indicate that mice that lack autophagy respond normally to mechanical loading. Therefore, reduced mechanosensitivity is not responsible for the low bone formation levels and reduced periosteal perimeter of cKO mice.

***Disclosures: James Hendrixson**, None*

SAT-370

See Friday Plenary Number FRI-370

SAT-371

Sex dimorphic response to osteocyte miR21 deletion in calvaria bone as determined by RNAseq analysis. *Gang Peng[1], Padmini Deosthale[1], Hannah M. Messersmith[1], Lilian Plotkin[1]. [1]Indiana University School of Medicine, United States

Low microRNA (miR) 21 levels may explain the increase in osteocyte (Ot) apoptosis with Cx43 deletion and aging in female mice. Yet, further studies showed that miR21 exerts a sex-divergent role in osteocytes, regulating bone mass and architecture through non-cell autonomous effects on osteoblasts and osteoclasts, through sex-specific regulation of Ot cytokine production. Yet, miR21 deficiency improves bone strength in males and females, to a higher extent in male miR21-deficient mice. To understand the molecular basis for the sex-dependent or independent effects of miR21 deletion, mRNA was isolated from calvaria bones of males and females expressing miR21fl/fl (controls) or in which miR21 was deleted by 8kbDMP1-Cre (miR21?Ot mice). miR21 was 50% lower in mir21?Ot whole bone, compared to miR21fl/fl mice. 4 samples/sex and genotype were submitted for RNAseq. RNAseq reads were aligned to GRCm38 using HISAT and read counts for each gene were extracted with featureCounts. Following principal component analysis, Sample 173 (female miR21?Ot) was removed from the analysis. There were 152 genes with 1 absolute log2 fold change in the analysis of male data. Most of these genes were higher expression in miR21fl/fl group. With the 152 significant genes, the 8 male samples could be hierarchically clustered into miR21fl/fl and miR21?Ot groups. 2 of the genes, Actn3 and Myh4, had a false discovery rate <0.1. Gene enrichment analysis of significant genes on both KEGG pathways and GO gene sets shows the significant genes were enriched in muscle contraction. Some muscle related genes like Actn3 were included in multiple significant pathways. For females, only 65 genes had 1 absolute log2 fold change. The remaining 7 female samples can be clustered into miR21fl/fl and miR21?Ot groups by the 65 genes. Yet, no significant KEGG or GO pathways including >=5 significant genes were seen. Interestingly, we did not find any overlap of significant genes between male and female data. We conclude that deletion of miR21 has a stronger effect on male transcriptome, consistent with a positive effect on bone mass and remodeling, and a higher increase in bone strength compared to miR21fl/fl mice. Further, although there are some genes significantly changing in females, they are not enriched in any pathways. Either there are not difference between two groups in female or the effect size is small, and we need a larger sample size data to find differences.

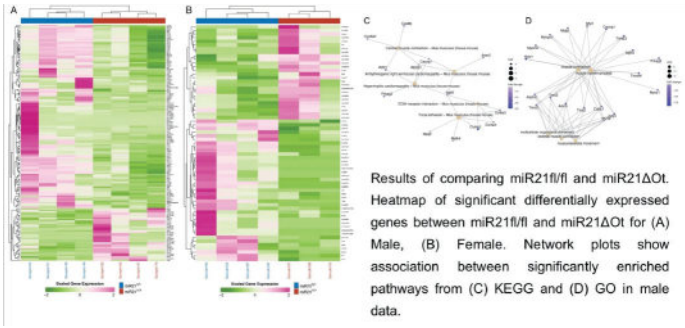

Results of comparing miR21fl/fl and miR21ΔOt. Heatmap of significant differentially expressed genes between miR21fl/fl and miR21ΔOt for (A) Male, (B) Female. Network plots show association between significantly enriched pathways from (C) KEGG and (D) GO in male data.

***Disclosures: Gang Peng**, None*

SAT-374

Differences in the architecture of the osteocyte lacunocanalicular network between mouse strains *Maximilian Rummler[1], Victoria Schemenz[1], Wolfgang Wagermaier[1], Markus A. Hartmann[2], Stéphane Blouin[2], Bettina M. Willie[3], Richard Weinkamer[1]. [1]Max Planck Institute for Colloids and Interfaces, Department of Biomaterials, Potsdam, Germany, Germany. [2]Ludwig Boltzmann Institute of Osteology at the Hanusch Hospital of OEGK and AUVA Trauma Centre Meidling, 1st Medical Department Hanusch Hospital, Vienna, Austria, Austria. [3]McGill University, Shriners Hospital for Children, 1003 Decarie Blvd, Montreal H4A 0A9, QC, Canada, Canada

Osteocytes reside in the mineralized bone matrix organized as a cell network. Their cell bodies are accommodated within pores called lacunae and their cell processes in channels called canaliculi. Lacunae and canaliculi together form the lacunocanalicular network (LCN). Besides facilitating transport, an important function of the LCN is to enable mechanosensation by osteocytes due to load-induced fluid flow through the LCN [1]. We follow the research strategy to detect differences in the LCN architecture and try to relate them to the network's function. In this study our aim is (i) to relate spatial heterogeneities of the LCN and material properties in whole mouse tibial cross-sections and (ii) to analyze differences in the LCN between different mouse strains.Our analysis included both tibiae of five BALB/c and four C57BL/6 mice (female, 12-week-old). After rhodamine staining the LCN in the whole tibial cross-section was imaged using confocal laser scanning microscopy (CLSM) and network properties were determined using a self-developed software. Quantitative backscattered electron imaging (qBEI) was employed to measure spatial differences in the calcium content in the same samples.In the tibial cross-sections of both mouse strains contiguous regions of high/low network density and high/low calcium content were identified, but these regions do not coincide. We asked the question whether differences in the network density are due to a different number of branching points in the network or due to a different number of branches emerging from a branching point. We found that spatial heterogeneities of the LCN were more strongly related to differences in the number of branching points. The LCN in C57BL/6 mice is denser compared to BALB/c and the difference can be explained by a network with more branching points.Spatial differences in network and material properties give important clues about the development of the bone. Since fluid flow through the LCN is influenced by its architecture, differences in the mechanoresponse between the two mouse strains have to be related to variations in their LCN.[1] van Tol et al., PNAS (2020).

***Disclosures: Maximilian Rummler**, None*

SAT-375

High-glucose environment reduces the response to mechanical stimulation by affecting its communication with other cells in the bone marrow. *Arancha Gortazar[1], JUAN ANTONIO ARDURA[2], Joan Pizarro-Gomez[3], Irene Tirado-Cabrera[3], Sara Heredero-Jimenez[3]. [1]IMMA- School of Medicine, San Pablo CEU University, Madrid Spain, Spain. [2]MADRID, Spain. [3]IMMA- School of Medicine San Pablo CEU University, Spain

Osteocytes can detect mechanical stimuli and translate it in a biochemical signal. The response of osteocytes to mechanical stimuli has important effects on bone microenvironment. Diabetes mellitus (DM) is a highly prevalent disease with negative impact on the skeleton, which markedly increases fracture risk. Both in vivo and in vitro studies have indicated that Diabetes mellitus and high glucose concentration media reduce some of the beneficial effects of mechanical stimulation, such as bone formation or osteocyte survival. Osteocyte responses to mechanotransduction also influence other cells present in the bone marrow. Based on this, we hypothesize that hyperglycemia may modify the communication of osteocytes with bone marrow cells, including macrophages, lymphocytes, or mesenchymal cells.MLO-Y4 osteocytes were mechanically stimulated by fluid flow (FF) or not (static conditions, SC) at normal (5mM D-Glucose; NG) or high glucose (25 mM D-glucose; HG) concentration. Conditioned media (CM) and RNA were collected 18h after treatments. RAW 264.7 murine macrophage cells were stimulated with lipopolysaccharide (LPS) or IL-4 for 24h to induce M1 or M2 macrophage polarization, respectively. In these conditions we eval-

uated the effect of CM from osteocytes on macrophage polarization by qPCR analysis of M1 or M2 specific markers in normal or high glucose media. Migration studies were carried out using CM from osteocytes on C3H/10T1 mesenchymal cells and JURKAT lymphocytes . qPCRs were performed with SYBR green and specific primers for GAPDH, TNF-?, INOS and CD206.CM from osteocytes stimulated by FF or not (SC) did not modify LPS-induced M1 polarization in macrophages cultured in normal or HG conditions. In contrast, SC-CM potentiated while FF-CM inhibited M2 polarization induced by IL-4. Interestingly, CM from osteocytes treated in HG conditions completely reversed these effects. Moreover, HG significantly reduce M1 or M2 polarization induced by LPS or IL-4, respectively. In addition, FF-CM stimulated both mesenchymal C3H/10T1 and lymphocyte JURKAT cell lines migration in NG but not in HG conditions.Our results suggest that a high glucose environment weakens osteocyte communication with bone marrow cell populations, buffering osteocyte actions on mesenchymal and lymphocyte migration and macrophage polarization in response to mechanical stimulation.

***Disclosures: Arancha Gortazar**, None*

SAT-376

A Comparison of Fixed versus Relative Offset Positioning for HR-pQCT *Annabel Bugbird[2], Rachel Klassen[2], Olivia Bruce[2], Lauren Burt[2], William Edwards[2], Steven Boyd[2]. [2]University of Calgary, , [2]University of Calgary, Canada

IntroductionIn HR-pQCT imaging, there are then two main approaches to define this scan position: (1) the fixed offset positioning, and (2) the relative offset positioning (relative to bone length). Differences between the use of these two methods may be problematic for comparison between studies and participants. It is thought that when using the fixed offset positioning, a shorter individual may result in an image captured more proximally, and in taller individuals an image captured more distally. The concern raised about a relative offset positioning method is that it assumes that the underlying bone structure scales linearly with bone length, which to the best of our knowledge has not been verified.The objectives of this study were (1) to determine how anatomical landmarks scale with whole bone length, and (2) to evaluate both a fixed and relative offset positioning for providing a consistent anatomical location for scan acquisition.MethodsUsing clinical computed tomography (CT) images of the radius (N = 25) and tibia (N = 42), 10 anatomical landmarks were selected along the bone's length. The location of these landmarks was then converted to a percent length along the bone, and the variation in the location of the landmarks was evaluated across all bones in the dataset. In addition, the absolute location of the HR-pQCT scan position using both offset methods were identified for all bones and converted to a percent length position. ResultsThere was a lack of allometric scaling in the landmarks across the dataset, with a range of 3.6% at the radius sites (Figure 1A), and 4.5% and the tibia sites. The range in the position of the scan at the radius was 0.6% and 0.3% (Figure 1B), and at the tibia 2.4% and 0.5%, for the fixed and relative offset, respectively.ConclusionIn summary, we demonstrate there is considerable normal variation in anatomical landmark positions in relation to bone length and that it is greater than the difference in scan position when comparing the fixed and relative offset positioning methods. This suggests that the difference between using the fixed or relative offset method is inconsequential as there is inherent variability in the scan location regardless of the offset method used. Therefore, there is no clear benefit of either offset method, and the intrinsic variation in the underlying architecture suggests that it is reasonable to compare studies and participants using different positioning methods.

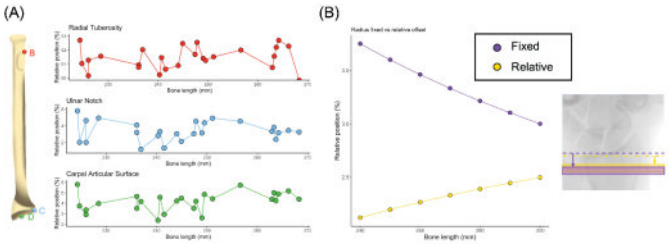

***Disclosures: Annabel Bugbird**, None*

SAT-377

Gaussian Process Regression Modeling for Real-Time Fracture Risk Prediction from 2D-DXA scans *Heesun Choi[1], Luca Quagliato[1], YOON-SOK (MARTIN) CHUNG[2], Taeyong Lee[1]. [1]Ewha Womans University, Republic of Korea. [2]Ajou University School of Medicine, Republic of Korea

Bone fracture risk assessment for osteopenia and osteoporotic patients is essential for the adoption of early countermeasures and avoid discomfort and hospitalization. Currently employed methodologies, such as FRAX®, provide calculation over a five to ten years period without showing the main variables influencing the prediction nor how they can be targeted in the short term. Thus, a lesser black-box approach where the fracture risk can be assessed in real time from a commonly employed analysis, such as dual-energy X-ray absorptiometry (2D-DXA), would help clinicians and patients alike. Accordingly, this study presents a real-time fracture risk assessment model, coupled with a feature augmentation algorithm, based on the results of a 2D-DXA scan.In this study, a ~10,000 adult Korean cohort, 70% female and 30% male ranging from 50 to 90 years of age where ~30% of the database is relevant of subjects who experienced an osteoporosis-related skeletal fracture. The 2D-DXA analyses performed on each patient allowed collecting 23 parameters, including the patients' age, BMI, gender, and fracture history, for a total of 25 scalar and one binary variable. To enhance the prediction accuracy, a feature augmentation algorithm (FAA) was developed and employed to allow for a better refinement of the parameters influence on the target function.The defined database was used to training of a Gaussian Process Regression (GPR) machine learning (ML) model, coupled with a Radial Basis Function (RBF) kernel, and validated through a 5-foldalidation and by considering various training-validation redistributed datasets. Unlike other ML models that predict exact values, the GPR algorithm, which is grounded on a Bayesian approach, presents a standard deviation of the predicted value.The GPR prediction, connected with the standard deviation, allows defining a 0-to-1 range with the associated standard deviation, allowing for the definition of the osteoporotic risk assessment, where a value close to zero represents no fracture risk whereas a value close to one a high risk. The GPR-RBF model already showed good accuracy in predicting fracture likelihood with an 89%, afterward improved to 96% thanks to the application of the FAA technique. In addition, the progressive integration of more augmented data in the training process allowed defining the limit beyond which the application of the FAA becomes counterproductive and leads to overfitting issues.

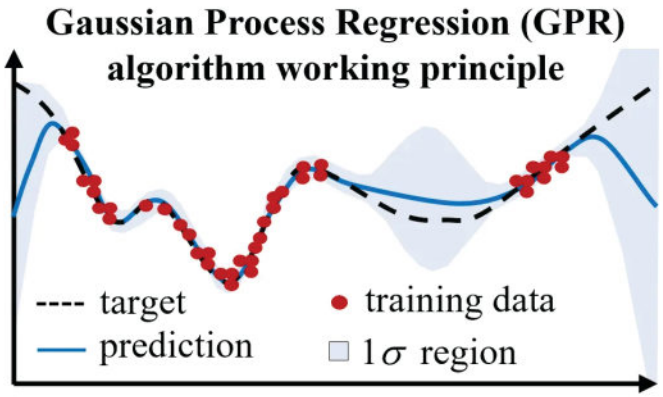

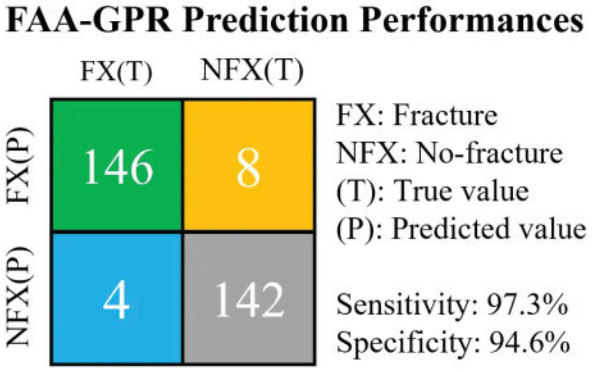

***Disclosures: Heesun Choi**, None*

SAT-378

Soft Bone During Spine Surgery and Its Significance: Relationships Between Subjective Intra-operative Assessment of Bone Quality, Bone Mineral Density and Biomechanical Properties of Bone *Alexander Dash[1], Fernando Quevedo Gonzalez[2], Ryan Breighner[3], Emma Billings[4], Han Jo Kim[2], Matthew Cunningham[2], Darren Lebl[2], Emily Stein[2]. [1]Icahn School of Medicine at Mount Sinai, , [2]Hospital for Special Surgery, United States. [3]Hospital for Special Surgery/Weill Cornell Medicine, United States. [4]Hospital for Special Surgery ,

Spinal fusion surgery is one of the most common and complex orthopedic procedures. Complications occur in up to one-third of cases. While poor bone quality increases risk of post-operative complications, many patients are not evaluated for skeletal deficits pre-operatively. Further, artifact from spinal pathology may mask osteoporosis on spine DXA. As a result, patients with poor bone quality are often only identified when surgeons encounter "soft" bone while placing orthopedic hardware. Few studies have investigated whether this subjective assessment of intra-operative bone quality (SBQ) relates to objective measurements of skeletal integrity. The FUSED SPINE (The FUsion and Skeletal Evaluation in patients unDergoing SPINE surgery) is an ongoing prospective cohort study investigating relationships between pre-operative bone health, intra-operative measures and post-operative outcomes. This sub-study related bone mineral density (BMD) and biomechanical

properties to SBQ. We hypothesized that patients with lower BMD and stiffness by would have lower SBQ. Pre-operative assessments included areal BMD (spine, hip, forearm) by DXA, phantom calibrated spine vBMD by QCT and whole bone stiffness by finite element analysis. Intra-operatively, surgeons blind to QCT and FEA rated bone on a 3-point scale (poor, fair, good) based upon resistance to the insertion of pedicle screws. Analysis of variance compared imaging parameters to the surgeon's assessment. This cohort included 59 patients who underwent lumbar spine fusion. Mean age was 61 years (range 25-81), 51% were women, 80% non-Hispanic White. Mean Z-scores by DXA were within the normal range at all sites. Mean vBMD (L1-L2) was 164 mg/cm3. Intra-operative SBQ was rated as poor in 7 patients (12%), fair in 23 (39%), and good in 29 (49%). Patients rated as having poor SBQ were older than those with good bone (70 vs 57 yrs; p<0.05). Spine aBMD was not related to SBQ. Compared to patients with good SBQ, those with poor SBQ had lower aBMD at the hip, femoral neck and 1/3 radius (-29 to -37% lower, p<0.05 for all). Further, those with poor SBQ had lower vBMD (-34%, p<0.01) and whole bone stiffness (-63%, p<0.01) at L1 (figure). In summary, there were direct relationships between BMD, stiffness and SBQ in patients undergoing spine fusion surgery. Our findings suggest that these subjective determinations may have clinical importance as a means of identifying patients with compromised bone.

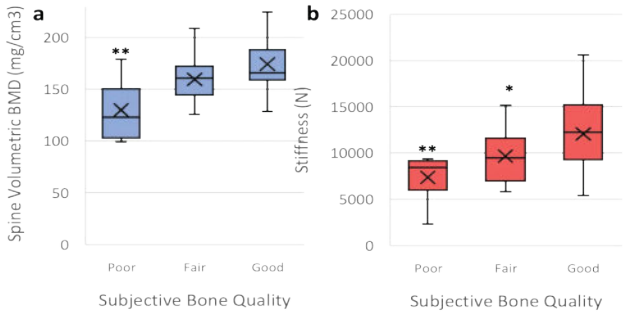

Figure: Volumetric BMD (a) and stiffness (b) at L1 according to subjective intra-operative bone quality assessment. Center line denotes median and X denotes mean values. Box encompasses 25th through 75th percentiles of dataset. *p <0.05 and **p<0.01 compared to good SBQ.

***Disclosures: Alexander Dash**, None*

SAT-379

The utility of clavicle cortex index as a screening tool for low bone mineral density among spine and hip surgery patients *Yusuke Dodo[1], Ichiro Okano[1], Koki Tsuchiya[1], Soji Tani[1], Chikara Hayakawa[1], Ryo Yamamura[1], Hiroshi Maruyama[1], Yoshifumi Kudo[1]. [1]Showa University, Japan

Background: Low bone mineral density (BMD) has been considered as a risk factor for mechanical complications after spine and hip surgeries. Currently, the Dual-energy X-ray absorptiometry (DXA) is the gold standard for the evaluation of bone mineral density. However, DXA scan is not always readily available for spine surgery patients. In this study, we focused on clavicle cortical bone thickness that can be easily assessed on routine chest radiograph to predict low bone mineral density among spine surgery patients. Purpose: To investigate the associations between clavicle cortical thickness index and DXA-BMDs in various anatomical locations. Methods: The records of patients who underwent elective spine and hip surgery were retrospectively reviewed. The bilateral clavicles shown on the chest radiograph was divided equally into four equal portions (A: distal, B: middle-distal, C: middle-proximal, D: proximal) and the thickness of each cortical and trabecular bone was measured at each point. The clavicle index was defined as the following formula: (cortical + trabecular) / trabecular bone. Pearson's correlation coefficients were calculated to compare the clavicle cortical index at each point, unilateral and bilateral average values, and BMDs in the proximal femur, lumbar spine, and distal radius. The receiver operating characteristic (ROC) curve analysis was also performed to assess the predictive value of the index for diagnosing osteoporosis defined as BMD <70% of young adult mean value. Results: A total of 219 patients (61.2% female) with mean age of 68.03 years were included in the final analysis. Mild but significant correlations were found between the middle-distal clavicle cortex index (MCDI) and BMDs in the radius (r=0.409) but weak correlations in the femur (r=0.313) and spine (r=0.209). Female was a factor for stronger correlations between MCDI and BMD in the radius (r=0.63). In spine surgery patient, mild correlations were observed between MCDI and BMDs in the femur (r=0.42) and radius (r=0.432) but weak correlations in lumbar BMD (r=0.223). In hip surgery patient, mild correlations were observed between the MDCI and BMDs in lumbar BMD (r = 0.223) and radius (r=0.446) but weak correlations in femur BMD (r=0.186). The ROC analyses demonstrated that the areas under the curve (95%CI) of MCDI for osteoporosis diagnosis were moderately accurate: 0.69 (0.55-0.83) with femur BMD, 0.716 (0.57-0.861) with lumbar BMD, and 0.834 (0.737-0.931) with radius BMD. Conclusions: Our results indicated that the middle-distal clavicle cortex index was significantly correlated with BMDs especially in the radius among spine and hip surgery patients. The clavicle cortex index is calculated easily using a routine chest radiograph, hence, the index can be utilized as an osteoporosis screening tool for spine and hip surgery patients.

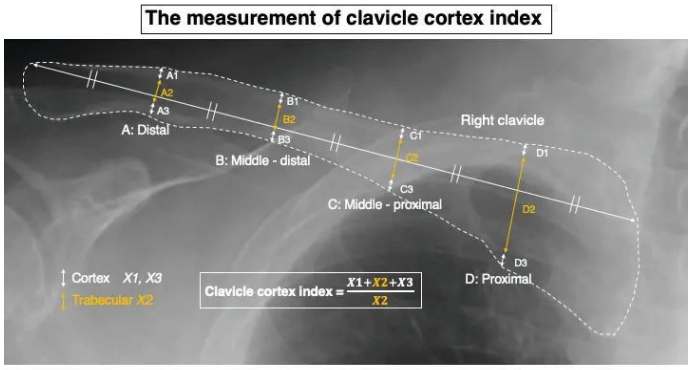

***Disclosures: Yusuke Dodo**, None*

SAT-380

The Influence of Contrast on Opportunistic Computed Tomography Bone Mineral Density Analysis *KIRSTEN BOTT[2], Ainsley Smith[2], Richard Walker[2], Steven Boyd[2], Sarah Manske[2]. [2]University of Calgary, , [2]University of Calgary, Canada

Opportunistic computed tomography (CT) analysis leverages CT images acquired for clinical diagnosis for secondary analysis of bone, without the need for a phantom within the field of view. Recent developments implement phantomless internal density calibration, using tissues captured in the scan field of view (e.g., blood, adipose, muscle, bone) and air as density referents for bone mineral density (BMD) analysis. However, many routine clinical scans often use contrast enhancement which may interfere with the internal calibration process. Therefore, the aim of this project was to investigate the effect of contrast enhancement on opportunistic BMD analysis, with the goal of quantifying error and determining whether corrective measures may be applied. The influence of contrast enhancement was addressed using retrospective CT scans from hematuria patients (n = 225). Hematuria patients are typically healthy and undergo a protocol that includes multiphasic CT imaging, a) without contrast b) during the nephrographic phase and c) 10-minute delayed post-contrast imaging). The vertebra from a subset (n = 39) of the abdominopelvic CT scans were automatically segmented and identified using the freely available Anduin web tool (https://anduin.bonescreen.de). The internal referents were manually selected for air, adipose, muscle, and bone; blood was not included due to the contrast enhancement. CT images were calibrated based on the mass attenuation coefficients of the internal referents. The results indicated that BMD was lower in the nephrographic phase (149.7 +/- 35.4 mg/cm3; p < 0.001) and delayed phased (141.8 +/- 36.1 mg/cm3; p < 0.001) contrast CT scans compared to the nonenhanced CT scan (170.1 +/- 39.5 mg/cm3), with a less significant difference between the two post-contrast phase scans (p < 0.05). The BMD from nonenhanced CT scans was linearly correlated with BMD in both the nephrographic (r2 = 0.70) and delayed (r2 = 0.67) phase contrast CT scans. The strong relationship between the multiphasic CT imaging with and without contrast suggests a linear equation may be able to correct differences in BMD results with contrast. Similarly, previous research using asynchronous BMD calibration also reported a strong correlation. Development of a robust opportunistic CT protocol will allow for greater applicability to analyze available clinical data, including corrections for contrast enhanced CT scans to comprehensively analyze changes in bone.

***Disclosures: KIRSTEN BOTT**, None*

SAT-381

Improving DXA Lumbar Spine BMD Outcomes with a new AI-Based Spine Segmentation Application *Guillaume Gatineau[1], El Hassen Ahmed Lebrahim[2], Karen Hind[2], Olivier Lamy[1], Elena Gonzalez Rodriguez[1], Lionel Beaugé[2], Didier Hans[3]. [1]Center of Bone Diseases, Rheumatology Unit, Bone and Joint Department, Lausane University Hospital, & University of Lausanne, Switzerland. [2]Medimaps group SA, Switzerland. [3]Center of Bone Diseases, Rheumatology Unit, Bone and Joint Department, Lausane University Hospital, & University of Lausanne, Switzerland, Switzerland

Introduction: Dual-energy X-ray absorptiometry (DXA) is commonly used to diagnose osteoporosis by measuring bone mineral density (BMD). However, DXA's accuracy in assessing lumbar spine BMD can be limited due to factors like degenerative changes, osteophytes, and artifacts. These limitations may lead to inaccurately high BMD values, resulting in misdiagnosis and undertreatment of osteoporosis. To overcome these challenges, a new AI-based spine segmentation (SpS) application has been developed by Medimaps Group, Switzerland, aiming to enhance the accuracy and efficiency of DXA-based spine BMD analysis. This study aimed to assess the effectiveness of this AI SpS application in improving DXA lumbar spine BMD outcomes. Methods: The study included 1,052 postmenopausal women (mean age=70.3+/-7.4 y, BMI=26.0+/-4.4 kg/m²) from the OsteoLaus cohort who

had a LS (L1-L4) DXA scan during the third visit (GE Lunar iDXA). Among these women, 568 had vertebral anomalies based on the ISCD criteria, which involves a +1 SD T-score difference between adjacent vertebrae. For this subgroup, LS BMD and T-score were analyzed using three SpS approaches: the default DXA manufacturer, an AI application, and the criterion set by a clinical expert. Statistical analysis involved Student's t-tests to compare outcomes. The impact of each SpS method on BMD classification (osteoporosis, osteopenic, or normal) was examined. Contingency tables were used to compare and analyze sensitivity and specificity for the Default and AI classifications. Kappa index was used to calculate the agreement levels of the default and AI SpS with the Expert's classification. Results: LS BMD outcomes differed significantly between Expert and Default SpS (p=0.005**, Table 1). No significant differences were found between Expert and AI SpS for LS BMD (p=0.098, Table 1). The prevalence of LS osteoporosis was 16.4% for Expert SpS, 9.3% for Default SpS, and 13.7% for AI SpS (Tables 2, 3). Osteoporosis classification sensitivity was 0.57 for Default SpS and 0.84 for AI SpS (Table 4). AI showed higher agreement with Expert (Kappa=0.892) compared to Default (Kappa=0.755) classifications.Conclusion: The AI SpS demonstrated improved LS BMD measurements and greater agreement of densitometric osteoporosis classifications with the extert compared with the default. These results suggest that AI SpS may be a valuable tool to improve the accuracy of LS BMD analysis and individual level diagnosis.

Table 1: Differences in LS BMD outcomes between the default, AI and expert (criterion) spine segmentation methods

		Mean (SD)		Mean (SD)	p-value
LS BMD	Expert	1.058 (0.186)	AI	1.077 (0.191)	0.096
LS BMD	Expert	1.058 (0.186)	Default	1.088 (0.174)	0.005 * *

Table 2: Lumbar spine BMD T-score classification using AI spine segmentation

		BMD T-score classification -Expert SpS		
		Normal	*Osteopenia*	*Osteoporosis*
BMD T-score classification - AI SpS	*Normal*	255	21	0
	Osteopenia	0	179	15
	Osteoporosis	0	0	78

Table 3: Lumbar spine BMD T-score classification using the manufacturer default spine segmentation

		BMD T-score classification - Expert SpS		
		Normal	*Osteopenia*	*Osteoporosis*
BMD T-score classification - Default SpS	*Normal*	248	38	0
	Osteopenia	2	162	40
	Osteoporosis	0	0	53

Table 4: Sensitivity and specificity outcomes for BMD T-score classification using default vs. AI SpS methods

		BMD T-score classification - Expert SpS		
		Normal	*Osteopenia*	*Osteoporosis*
AI SpS Kappa : 0.892	Sensitivity	1.00	0.89	0.84
	Specificity	0.93	0.96	1.00
Default SpS Kappa : 0.755	Sensitivity	0.99	0.81	0.57
	Specificity	0.87	0.80	1.00

***Disclosures: Guillaume Gatineau**, None*

SAT-382

Substantially Improved Identification of Patients At High Risk of Osteoporotic Fracture Through a Revised Risk Assessment Strategy: The Manitoba BMD Registry *Claus-C Glueer[1], Klaus Engelke[2], Friederike Thomasius[3], William Leslie[4]. [1]Christian Albrechts Universitaet zu Kiel, Germany. [2]University Hospital Erlangen, Germany. [3]Frankfurt Bone Health Center, Germany. [4]University of Manitoba, Canada

Purpose. Current strategies for case finding do not exploit the full potential for identification of patients at high(est) risk of fracture. A revised strategy is proposed emphasizing (i) hip fracture (HF) and vertebral fracture (VF) over other non-hip/non-vertebral osteoporotic fractures (oOF), (ii) a wider range of clinical risk factors (cRFs), (iii) spine aBMD and TBS in addition to total hip aBMD (iv) and prediction times of 3 and 1 years.Aim. To test whether this strategy leads to clinically relevant and statistically significant incremental improvement in fracture prediction.Methods. An expanded set of risk factors for HF or VF risk was selected based on systematic literature review (2267 publications, Oxford evidence criteria) and availability in the Manitoba BMD registry. Cox models to predict 3-yr HF, VF and oOF were built in 7 steps requiring significant improvement and clinically relevant increases in AUC>0.005 for each step : (0) base of 8 primary risk factors from FRAX (without secondary osteoporosis or DXA) (1) disaggregating FRAX prior fracture into subgroups of individual fractures ? (2) cRFs from FRAX secondary osteoporosis plus other bone disorders ? (3) cRFs from neurological disorders ? (4) adding total hip aBMD ? (5) adding lumbar spine aBMD ? (6) adding TBS; (7) comparison of the final 3-year fracture risk model with the same model for 1- and 10-yr fracture risk.Results. The sample included 56,129 women; over 3 years 292 HF, 260 clinical VF and 1556 oOF were recorded. Table shows improvement in AUC with each step adding significantly and at least AUC increase>0.005. Overall 3yr AUCs improved by +0.054 (from 0.830 to 0.884) for incident HF and by +0.068 from (0.727 to 0.795) for incident VF. Compared to 3yr risk models, imminent 1yr AUCs further increased to by +0.023 (to 0.907) for HF and by +0.055 (to 0.850) for VF. In contrast, the 10yr AUC was substantially lower at 0.825 (-0.059 vs 3yr AUC) for HF and at 0.771 (-0.024) for VF. For non-hip/non-vertebral oOFs, AUCs at all steps were consistently lower than for HF and VF.Conclusion. Four strategic changes, i.e. (i) focus on risk of hip and VF; (ii) novel clinical risk factors; (iii) including spine aBMD and TBS (for VF); (iv) assessing risk over 3-yr (and 1-yr imminent risk) instead of 10-yr all substantially improved risk profiling. The large improvement in AUC observed mandates consideration of a change in clinical approach to the identification of high-risk individuals.

Step	Change type	AUC HF	Increase AUC HF	AUC VF	Increase AUC VF	AUC oOF	Increase AUC oOF
0	**Basic 3-yr model w/o DXA**	**0.830**		**0.727**		**0.624**	
1	disaggregating FRAX prior fx	n.b.	n.b.	**0.748**[1]	0.021	n.b.	n.b.
2	expanded secondary osteop.	**0.837**[2]	0.007	n.b.	n.b.	**0.630**[3]	0.006
3	neuro cRFs	**0.848**[4]	0.011	**0.766**[5]	0.018	n.b.	n.b.
Step 3 vs 0	**Best 3-yr model w/o DXA**	**0.848**	0.018	**0.766**	0.039	**0.630**	0.006
4	& aBMD hiptot	**0.884**	0.036	**0.783**	0.017	**0.659**	0.029
5	& aBMD lumbar spine	n.b.	n.b.	**0.790**	0.007	n.b.	n.b.
6	& TBS lumbar spine	n.b.	n.b.	**0.795**	0.005	**0.664**	0.005
Step 6 vs 3	**Best 3-yr model with DXA**	**0.884**	0.036	**0.795**	0.029	**0.664**	0.034
Step 6 vs 0	**Total improvement 3-yr model**		**0.054**		**0.068**		**0.040**
7	1-yr vs 3-yr model with DXA	**0.907**	0.023	**0.850**	0.055	**0.679**	0.015
Step 7 vs 0	**Total improvement 1-yr model**		**0.077**		**0.123**		**0.055**

[1] predictors: prior VF, prior non-VF
[2] predictors: insulin dep diabetes, not insulin dep diabetes, hypogonadism, sec. liver disease
[3] predictors: insulin dep diabetes, celiac disease
[4] predictors: Parkinson, multiple sclerosis, dementia, seizure
[5] predictors: Parkinson, muscular dystrophy, stroke, seizure
AUC: area under receiver operating characteristic (ROC) curve; n.b.: no added clinical benefit

***Disclosures: Claus-C Glueer**, None*

SAT-383

The Association Between Body Mass Index and Fracture is Dependent on Femoral Neck BMD: An International Meta-Analysis *Nicholas Harvey[1], Helena Johansson[2], Eugene McCloskey[3], Enwu Liu[2], Marian Schini[4], Liesbeth Vandenput[2], Mattias Lorentzon[2], William Leslie[5], John Kanis[3], FRAX Meta-analysis Cohort Group[3]. [1]MRC Lifecourse Epidemiology Centre, University of Southampton, United Kingdom. [2]Mary McKillop Institute for Health Research, Australian Catholic University, Australia. [3]Centre for Metabolic Bone Diseases, University of Sheffield, United Kingdom. [4]Department of Oncology & Metabolism, University of Sheffield, United Kingdom. [5]Department of Medicine, University of Manitoba, Canada

We undertook an international meta-analysis to quantify the predictive value of body mass index (BMI) for incident fracture and to explore the relationship of this risk with age, sex, time since baseline and femoral neck bone mineral density (BMD). The analysis dataset comprised 1,824,804 men and women from 62 cohorts in 32 countries followed for a total of 17.6 million person-years. We investigated the relationship between BMI (kg/m2) and risk of any clinical fracture, any osteoporotic fracture, major osteoporotic fracture (MOF) and hip fracture alone using an extended Poisson model in each cohort. Covariates examined were age, sex, BMD and duration of follow up. The results of the different studies were merged by using the ?-coefficients (weighted by sample size). After adjustment for age and time since baseline, greater BMI was associated with lower risk of incident fracture in both men and women. For example, hazard ratio [HR (95% CI)] for MOF per kg/m2 greater BMI was 0.98 (0.97, 0.98) in women and 0.98 (0.97, 0.99) in men. Associations appeared similar by fracture outcome category and in the subset of cohorts in which BMD was measured. Here, after further adjustment for BMD, the relationships inverted such that greater BMI was associated with greater fracture risk. For example, for women HR (95%CI): 1.01 (1.00, 1.02) and for men 1.02 (1.02, 1.03). Dependent on sex and fracture category, the magnitude of associations varied by age and/or follow-up time. In the largest ever meta-analysis undertaken to date, greater BMI was protective for incident fracture without adjustment for femoral neck BMD, but a risk factor after accounting for BMD. Ongoing analyses will elucidate relationships by individual fracture site, BMI category and in non-linear models to inform the second version of the FRAX tool.

***Disclosures: Nicholas Harvey**, None*

SAT-384

Use of 3D-DXA as a new tool to evaluate bone loss after bariatric surgery *C. Gómez-Vaquero[1], M. López Picazo[2], L. Humbert[2], M. Perez-Prieto[3], L. Hernandez-Montoliu[6], O. Jermakova[4], L. Huanuco[0], F. Guerrero-Perez[4], J. Osorio[6], L. Sobrino[0], N. Vilarrasa[4]. [1]Rheumatology. Hospital Universitari de Bellvitge, L'Hospitalet, Spain, Spain. [2]3D-Shaper Medical, Barcelona, Spain, Spain. [3]Endocrinology and Nutrition. Hospital Universitari de Bellvitge, L'Hospitalet, Barcelona, Spain. [6]Endocrinology and Nutrition. Hospital Universitari de Bellvitge, L'Hospitalet, Spain, Spain. [4]Endocrinology and Nutrition. Hospital Universitari de Bellvitge, L'Hospitalet, Spain, Spain. [0]Endocrinology and Nutrition. Hospital Universitari de Bellvitge, L'Hospitalet, Spain. [6]General and Gastrointestinal Surgery, L'Hospitalet, Spain, Spain. [0]General and Gastrointestinal Surgery, L'Hospitalet, Spain, Spain

Objective: To analyze changes in bone structure using 3D-DXA in patients with severe obese after different types of bariatric surgery (BS).Methods: Prospective, single center and non-blinded study in patients with obesity undergoing BS. BMD at lumbar spine (LS, L1-L4), femoral neck (FN) and total hip (TH) was measured by DXA (Horizon Wi; Hologic Inc., Waltham, MA, USA) prior and 12 months after surgery. Proximal femur 3D-DXA parameters including cortical and trabecular volumetric(v) BMD, cortical thickness (CTh) and surface(s) BMD at TH, FN, trochanter and shaft were analyzed using 3D-Shaper software v.2.12.1 (3D-Shaper Medical, Barcelona, Spain).Results: 153 patients, 81% female, aged 50+/-9 years and BMI 38+/-9 kg/m2 were evaluated. In 54.3% of them underwent Sleeve gastrectomy (SG), 29.4% Duodenal Switch/SADIS and 16.3% Roux-en-Y Gastric bypass (RYGB). Baseline characteristics were comparable between groups, except BMI that was lower in RYGB. Weight loss was greater after DS/SADIS compared to SG and RYGB (-34+/-12 vs 27+/-9 vs 27+/-11, p< 0.001). After surgery DMO losses were significantly greater at all sites in DS/SADIS and RYGB (p<0.001) compared to SG. In the whole cohort, significant changes from baseline were found in 3D-DXA measurements at the TH. Cortical sBMD decreased by -4.4+/-4.8%; Cortical vBMD by -1.4+/-2.8%; CTh by -3.1+/-3.9%; and Trabecular vBMD by -8.0+/-6.6 (p<0.05). Similar results were found at all hip regions except the neck where a 2.1+/-7.3% increase in CTh was found (increase from baseline statistically significant (p<0,05) only after SG). Cortical and trabecular BMD losses were greater in DS/SADIS and RYGB (p<0.01). Final Z-scores for Cortical sBMD and Trabecular vBMD were 0.96 (IC 95%: 0.73 to 1.19) and -0.17 (IC 95%: -0.32 to -0.02).Conclusion: Patients undergoing BS showed a significant decrease in LS and hip BMD assessed by DXA. 3D-DXA analysis showed greater decreases in trabecular vBMD, compared to cortical sBMD. More hypoabsortive techniques induced a greater bone loss. After one year, bone density remains within or above mean reference values from the general population.

***Disclosures: C. Gómez-Vaquero**, None*

SAT-385

An MRI-based Approach for Characterizing Bone Mineral Density and Cortical Porosity: Comparing Ultrashort Echo Time MRI with HR-pQCT *Andrea Jacobson[1], Christopher Newman[2], Thomas Siegmund[3], Joseph Wallace[4], Matthew Allen[5], RACHEL SUROWIEC[6]. [1]Department of Biomedical Engineering, Indiana University Purdue University Indianapolis, United States. [2]Department of Radiology and Imaging Sciences, Indiana University School of Medicine, United States. [3]School of Mechanical Engineering, Purdue University, United States. [4]Indiana University Purdue University Indianapolis (IUPUI), United States. [5]Anatomy, Cell Biology and Physiology, Indiana University School of Medicine, United States. [6]Indiana University Purdue University,

Current imaging modalities used to quantify cortical bone density and microarchitecture rely on X-ray radiation to image the mineral phase. However, recent work suggests ultra-short echo-time MRI (UTE-MRI) can innocuously characterize cortical porosity and potentially bone mineral density (BMD) based on MRI's signal intensity. Additionally, UTE-MRI can provide insight into bone water and matrix organization, making a comprehensive bone evaluation with a singular imaging modality feasible. Toward this goal, we sought to establish UTE-MRI's ability to characterize mineral density and microarchitecture at clinical field strength and compare this to high-resolution peripheral quantitative computed tomography (HR-pQCT).Femoral bone from ten fresh cadaveric specimens (83.5 +/- 10.1 yrs) underwent 3D radial UTE MRI using a short (0.04 ms) and long (2.8 ms) echo time (3.0 T, Siemens, 0.45 mm resolution), and HR-pQCT (XtremeCT II, SCANCO, 0.06 mm resolution) imaging (Fig1A-B). For UTE-MRI, specimens were imaged with the following phantoms: H2O, hydroxyapatite (CHA), and a series of D2O-doped water. Multi-modal images were registered, and a 4.5 mm region of interest was created from the HR-pQCT image and used across two multi-modal images per specimen (MATLAB) (Fig1C). Statistical relationships between the following outcomes were determined using Pearson Correlations: porosity index [1] (UTE-MRI), a novel signal-intensity (SI)-based MRI surrogate for BMD [2] (UTE-MRI), and cortical porosity (%), pore volume, and BMD (HR-pQCT). Both % porosity and pore volume significantly and positively correlated with porosity index (Fig1D-E). For BMD, two HR-pQCT scans are pending analysis. Still, the abbreviated dataset showed SI BMD has a moderate, albeit insignificant, positive relationship with BMD (Fig1F). SI MRI BMD significantly and negatively correlated to porosity index indicating the more porous the bone, the lower the SI MRI BMD (Fig1G). Finally, SI BMD, but not porosity index, significantly and negatively correlated with specimen age (Fig1H).UTE-MRI correlated with HR-pQCT for cortical porosity measures and captured changes in BMD due to age and increasing porosity. Work is underway to extract bone water content and organic matrix organization from the UTE-MRI, where the sum of these efforts will describe a comprehensive set of bone imaging biomarkers to characterize bone health using a single innocuous clinical imaging modality.

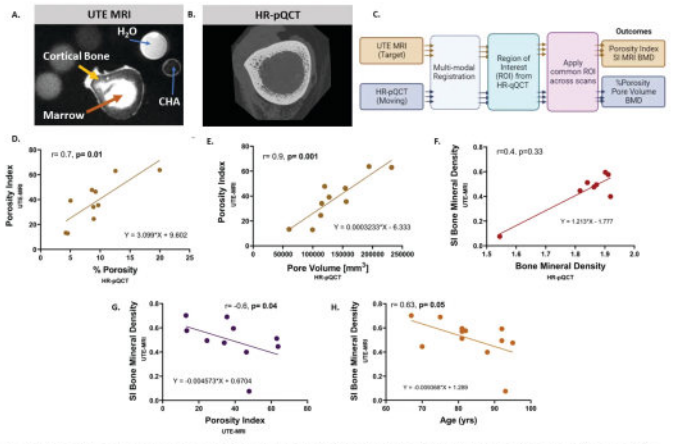

Figure 1. Ten 5cm long cadaveric femoral bone specimens from the proximal femoral shaft underwent (A) UTE-MRI with the bone fully submerged in a fluoroinert solution to reduce susceptibility and maintain hydration (flip angle: 12°, FOV: 160 mm3, 2 averages, 50K radial spokes, readout BW: 250 kHz, 0.45 mm isotropic resolution, TA: 20min 2s). (B) HR-pQCT imaging was acquired with the specimen wrapped in phosphate buffered saline-soaked gauze. (C) Images were registered, and a 4.5 mm proximal region of interest (ROI) was delineated using a structure-based mask in HR-pQCT images and applied to the UTE-MRI creating a common ROI for analysis. Porosity index and a signal intensity (SI) MRI based BMD was calculated from UTE-MRI and %porosity, pore volume, and BMD from HR-pQCT. Pearson correlation coefficients revealed that porosity index significantly and positively correlated with HR-pQCT measures of %porosity (D) and pore volume (E). SI MRI BMD was not significantly correlated to BMD perhaps due to ongoing troubleshooting with several HR-pQCT scans which could not be included in analysis. (G) SI MRI based BMD significantly and negatively correlated with porosity index; the more porous the bone the lower the BMD. While porosity did not correlate with specimen age, we observed a significant negative relationship between specimen age and SI MRI base BMD (H). The older the specimen, the lower the BMD.

***Disclosures: Andrea Jacobson**, None*

SAT-386

Utilization, Diagnoses, Medications, and Laboratory values in the Electronic Health Record can Predict Fractures Independently of FRAX *Rajesh Jain[1], Eric Polley[1], Mark Weiner[2], Amy Iwamaye[3], Elbert Huang[1], Tamara Vokes[1]. [1]University of Chicago, United States. [2]Weill Cornell Medicine, United States. [3]Lewis Katz School of Medicine at Temple University, United States

Introduction: FRAX is the fracture prediction tool most commonly used in the United States. We recently demonstrated that FRAX probabilities derived using information from electronic health records (EHRs) were generally as accurate as studies where patients were directly asked. FRAX includes 11 risk factors; however, it is not known if variables available in the EHR would add predictive value independently of FRAX. Thus, our study sought to assess the ability of routinely available EHR variables to predict fracture.Methods: We used data from the EHR in years 2010-2019 obtained at an academic medical center in Philadelphia, PA. All patients over 50 years of age who had received routine care were included. FRAX 10-year major osteoporotic fracture (MOF) predictions were based on at least 1 year of data in the EHR, and subsequent incident MOFs were captured by diagnosis codes. Additional variables besides those in FRAX were examined based on their known or suspected association with fracture, or because of high frequency in the data. These included categories such as utilization, vital signs, diagnoses, medications, and laboratory values. Missing values in vital signs or labs were imputed using a random forest imputation algorithm in RStudio 02.03. All other analyses were done in Stata 17.Analyses were done using Cox regression. First, each variable was analyzed while controlling for FRAX 10-year probability and the risk factors within FRAX. Then, we created a model that included all the statistically significant variables (p<0.05), as well as FRAX variables, and removed variables using a backwards stepwise approach. We allowed variables to remain in the model if p-value <0.2. We compared Harrell's C-statistic of our final model versus that of FRAX 10-year estimates. Results: There were 24,189 patients included with mean age 62.8 +/- 9.7 and 3.8 +/- 1.8 years of follow up. Overall, the MOF rates were 4.3 and 6.0 MOFs per 1,000 person-years in men and women, respectively. There were 26 risk factors significantly associated with MOF independently of FRAX, of which 14 met criteria for the final model. Table 1 shows the risk factors in the final model. The final model demonstrated a C-statistic of 0.69 versus FRAX alone of 0.63 (p<0.001).Conclusion: Information from the EHR can predict fractures independently of FRAX and may allow for automated fracture prediction at the point of care, reducing the clinician burden of ascertaining risk factors verbally.

Table 1: Risk factors in an Electronic Health Record-derived Final Model (in addition to FRAX variables) to predict major osteoporotic fracture

Risk Factor	Individual Model HR[1]	95% CI, p-value	Final Model HR[2]	95% CI, p-value
Pulse SD (per 5 BPM)	1.18	1.07-1.18, p=0.002	1.11	1.00-1.24, p=0.06
Visits with PCP (per 1 visit)	1.03	1.02-1.04, p<0.001	1.05	1.01-1.08, p=0.02
GABA use	1.60	1.20-2.14, p=0.001	1.27	0.94-1.71, p=0.12
PPI use	1.39	1.14-1.69, p=0.001	1.23	1.01-1.51, p=0.04
Anticonvulsant use	2.14	1.47-3.11, p<0.001	1.73	1.18-2.53, p=0.005
TZD use	1.87	1.19-2.95, p=0.007	1.80	1.14-2.84, p=0.01
Loop diuretic use	1.81	1.38-2.39, p<0.001	1.39	1.05-1.85, p=0.02
Sodium level (per 1 mmol/L)	0.94	0.90-0.98, p=0.001	0.97	0.93-1.01, p=0.11
CKD Stage 3b or worse	1.91	1.37-2.67, p<0.001	1.48	1.05-2.09, p=0.02
Alkaline phosphatase (per 25 U/L)	1.09	1.05-1.14, p<0.001	1.07	1.02-1.12, p=0.003
Albumin (per 1 g/dL)	0.56	0.46-0.69, p<0.001	0.72	0.58-0.91, p=0.006
RDW (per 1%)	1.09	1.03-1.15, p=0.001	1.04	0.98-1.11, p=0.17
Psychoses	3.07	1.72-5.50, p<0.001	2.65	1.48-4.75, p=0.001
Musculoskeletal Pain	1.35	1.10-1.65, p=0.003	1.24	1.01-1.52, p=0.04

[1] Controlled for FRAX 10-year probability and individual risk factors within FRAX
[2] Controlled for individual risk factors within FRAX and all other variables listed
HR, Hazard Ratio; SD, Standard Deviation; BPM, Beats per Minute; PCP, Primary Care Provider; GABA, Gabapentinoid use (such as gabapentin or pregabalin); PPI, Proton pump inhibitor; TZD, thiazolidinone (such as pioglitazone); CKD, Chronic Kidney Disease; RDW, Red Cell Distribution Width

***Disclosures: Rajesh Jain**, Amgen Foundation, Grant/Research Support*

SAT-387

See Friday Plenary Number FRI-387

SAT-388

Subject-Specific Fall Probability Improves Hip Fracture Prediction Beyond Bone Mineral Density: AGES-Reykjavik Study *Fjola Johannesdottir[1], Thor Aspelund[2], Sigurdur Sigurdsson[3], Vilmundur Gudnason[2], Mary Bouxsein[4]. [1]Beth Israel Deaconess Medical Center & Harvard Medical School , , [2]Icelandic Heart Association Research Institute and University of Iceland, Iceland, [3]Icelandic Heart Association Research Institute, Iceland, [4]Beth Israel Deaconess Medical Center, Harvard Medical School, United States

Current assessment of fracture risk does not directly include the probability of falling despite the fact that nearly all hip fractures are due to a fall. It remains unknown whether incorporation of subject-specific probability of falling improves assessment of hip fracture risk. Thus, we aimed to develop a subject-specific fall risk tool to evaluate probability of falling and test whether combining probability of falling and hip BMD would improve hip fracture risk assessment beyond BMD alone among older men and women from the AGES-Reykjavik study.We used baseline data from 3242 individuals (58% women) to predict repeated falling >=2 in the past 12 mos at follow-up (~5yrs later) by finding the best predictive logistic regression model using stepwise variable selection procedure (data were partitioned into training set 65% and test set 35%) considering age, sex, fall history, neuromuscular function, dynamic balance and medications as predictors. Further, in a prospective case-cohort study design of 698 hip fracture cases and 1348 controls from AGES cohort with median follow-up of 10yrs (6.1-13.9), we used Cox proportional hazards models to predict hip fracture. We tested whether fall probability combined with CT-derived femoral neck (FN) aBMD predicts hip fracture better than FN aBMD alone by comparing the time-dependent area under the receiving operating characteristic curve (AUC).295 individuals had >= 2 falls in the past 12 mos prior to follow-up visit. The best model to predict future falls at follow-up included fall history, timed up-and-go test and grip strength (AUC for predicting falls in test set = 0.67 (0.61-0.72)). The probability of falling predicted incident hip fracture independently of FN aBMD in both sexes. Individuals in the highest two quantiles of fall risk were 2.03-2.56 fold more likely to sustain a hip fracture than the ones in the lowest quantile, after adjusting for age, sex height, weight and FN aBMD. (Table). AUC for the model predicting 5 and 10 yrs hip fracture risk was greater when fall probability was combined with FNaBMD compared to FNaBMD alone (p<=0.001), as it was 76% (72-79, 95%CI) vs 73% (70-77, 95%CI) for 5-yrs and 80% (77-82, 95%CI) vs 78% (76-81, 95%CI) for 10yrs. In a population-based study of older adults, the probability of falling predicted incident hip fracture and improved hip fracture prediction beyond FNaBMD. Thus, subject-specific fall risk may provide added value in clinical assessment of hip fracture risk.

Table: Hazard ratios for incident hip fracture (95%, CIs) according to fall probability (Model 1: Fall probability, Model 2: Fall probability adjusted for FNaBMD)

Outcome predictor	Model 1#	Model 2#
Fall probability		
Q2vsQ1	1.60 (1.16-2.20)	1.40 (1.01-1.95)
Q3vsQ1	1.71 (1.24-2.35)	1.59 (1.14-2.21)
Q4vsQ1	2.33 (1.69-3.23)	2.03 (1.45-2.83)
Q5vsQ1	2.93 (2.08-4.13)	2.56 (1.80-3.66)
Femoral neck aBMD*	-	1.78 (1.58-2.00)

#All models adjusted for age, sex, weight and height
*per SD decrease

***Disclosures: Fjola Johannesdottir**, None*

SAT-389

Discordance in secular trends of bone mineral density measurements in different ages of postmenopausal women *Kwang Yoon Kim[1], Bom Taeck Kim[2]. [1]Myungju hospital / Ajou university hospital, Republic of Korea, [2]Ajou university hospital / School of medicine of Ajou university, Republic of Korea

Background: Age-adjusted bone mineral density (BMD) in postmenopausal women decreases in developed countries whereas incidence of osteoporotic fracture decreases or remains stable. We investigated secular trends of bone density from 2008 to 2017 among different age groups of postmenopausal women.Methods: We analyzed BMD data obtained from health check-up of 4905 postmenopausal women during three survey cycles from 2008 to 2017. We divided them into 3 groups by age (50-59 years, 60-69 years, and 70 years or more) and observed the transition of lumbar and femoral BMD in each group, before and after adjusting for variables that may affect BMD.Results: Age-adjusted BMD, bone mineral content (BMC), and T-score demonstrated a declining trend over the survey period at lumbar spine (-2.8%), femur neck (-3.5%) and total femur (-4.3%), respectively. In the analysis for the age groups, the BMD, BMC, and T-score presented linear declining trend (-6.1%) in younger postmenopausal women while women aged over 70 or more showed linear increasing trends (+6.3%) at lumbar spine during the survey period. Femoral neck and total femur BMD demonstrated a declining linear trend only in the 50-59 and 60-69 years groups (-5.5%, -5.2%, respectively), but not in the above 70 group.Conclusion: BMD in younger postmenopausal women has decreased considerably but has increased or plateaued in elderly women. This discordance of BMD trends among different age groups may contribute to decreased incidence of osteoporotic fracture despite a recent declining BMD trend in postmenopausal women.

***Disclosures: Kwang Yoon Kim**, None*

SAT-390

See Friday Plenary Number FRI-390

SAT-391

Automated Deep Learning-based Bone Mineral Density Assessment of Vertebral Bodies in CT Scans *Nicolai Krekiehn[1], Eric Orwoll[2], Eren Bora Yilmaz[3], Claus-C Glueer[4]. [1]Christian-Albrechts-Universität zu Kiel, Germany, [2]Oregon Health & Science University, United States, [3]Christian-Albrechts-Universität Kiel , , [4]Christian Albrechts Universitaet zu Kiel, Germany

Automated measurement of volumetric vertebral trabecular bone mineral density (vBMDvt) on computed tomography (CT) scans using artificial intelligence (AI) methods may be useful for both diagnosis of osteoporosis and opportunistic fracture risk prediction (no added radiation dose).Aim: To develop and test an AI tool for automated assessment of vBMDvt on lumbar CT scans.Methods: A convolutional neural network (U-Net) architecture for segmenting individual vertebrae was trained on Verse data (236 CT scans, 1793 vertebrae). Subsequently the individual vertebral masks (VM) are automatically reduced to the trabecular region of the vertebral body (VB), where vBMDvt value is measured. This pipeline has already been tested on an external dataset, a subset of Diagnostik Bilanz study. We tested the method on the MrOS CT sub cohort. vBMDvt results (central 70% of the VB) previously generated by classical quantitative CT (QCT) image processing were used as reference. Since QCT segmentation masks were not available the segmentation step had to be tested without re-training of the AI model. For selection of the vBMDvt region a fully automated multistep peeling procedure was applied: we first reduce the VM of the cortex to the center core region of the VB. Subsequently, the VM is enlarged again to cover as much trabecular volume as possible. Third, 0 to 4 peeling steps are applied to shrink the VM to its final shape. If two VBs were available per subject, the vBMDvt results were averaged, cases with missing data were excluded. In order to test whether AI-based BMD results are likely to be good predictors for future fracture risk we ran logistic regression to test whether they discriminated between men with and without prevalent vertebral fractures.Results: The pipeline produced segmentation masks in 1300 of 1331 men (97.7%) included. QCT

based and AI based vBMDvt results were highly correlated (r=0.94). In 1151 of 1300 cases (88.5%) the subsequent peeling process could be finished fully automatically. vBMDvt significantly discriminated between men with and without vertebral fracture (Genant SQ grade >=2). AI based age adjusted standardized odds ratios (sOR) ranged up to sOR=4.1(2.8-6.1), AUC 0.76 after 3 or 4 peeling steps (see figure) versus sOR=3.2(2.2-4.6), AUC 0.74 for QCT.Conclusions: Compared to QCT on same data our AI based vBMD assessment method performed at least as well in discriminating vertebral fracture and will next be tested as predictor of future fracture.

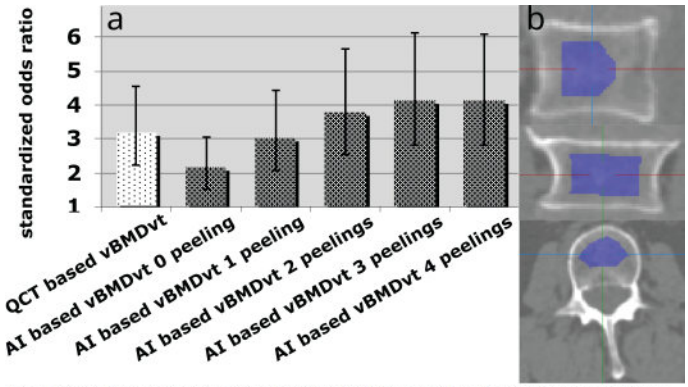

Figure: **a)** Age-adjusted standardized odds ratio for discrimination of men with and without prevalent vertebral fractures based on QCT based vBMDvt versus AI based vBMDvt with different amounts of peelings. **b)** AI based mask after four peeling steps

***Disclosures: Nicolai Krekiehn**, None*

SAT-392

FRAX® Adjustment Using Renormalized Trabecular Bone Score (TBS) from L1 Alone is Optimal for Fracture Prediction: The Manitoba BMD Registry *William Leslie[1], Heenam Goel[2], Neil Binkley[3], Eugene McCloskey[4], Didier Hans[5]. [1]University of Manitoba, Canada. [2]CentraCare, St. Cloud, United States. [3]University of Wisconsin, Madison, United States. [4]University of Sheffield, United Kingdom. [5]Lausanne University Hospital & University of Lausanne, Switzerland

Lumbar spine trabecular bone score (TBS) used in conjunction with FRAX® improves 10-year fracture prediction. The derived FRAX adjustment is based upon TBS measured from L1-L4, designated TBSL1-L4-FRAX. Previous studies show that TBS measurements that include L1 and exclude L4 give better fracture stratification than L1-L4. However, TBS limited to upper lumbar vertebral levels is lower than L1-L4 and direct entry into the FRAX adjustment will overestimate fracture risk.AIM: To compare fracture risk stratification from TBS-adjusted FRAX using TBS derived from different combinations of upper lumbar vertebral levels renormalized for level-specific differences.METHODS: We included individuals from the Manitoba Bone Density Program aged >40 years with baseline assessment of TBS and FRAX. TBS measurements for L1-L3, L1-L2 and L1 alone were calculated after renormalization for mean level-specific differences. Corresponding TBS-adjusted FRAX scores designated TBSL1-L3-FRAX, TBSL1-L2-FRAX and TBSL1-FRAX were compared with TBSL1-L4-FRAX for fracture risk stratification. Incident major osteoporotic fractures (MOF) and hip fractures were assessed through linkage to population-based data sources. The primary outcome was incremental change in area under the curve (?AUC) compared using the Hanley-MacNeil method.RESULTS: The study population included 71,209 individuals (mean age 64 years, 89.8% female). Mean TBS for L1-3, L1-L2 and L1 was significantly lower and TBS-adjusted FRAX significantly higher than from using TBSL1-L4. These differences were largely eliminated when TBS was renormalized for level-specific differences. During mean follow-up of 8.7 years 6745 individuals sustained incident MOF and 2039 sustained incident hip fractures. Compared with TBSL1-L4-FRAX, use of FRAX without TBS was associated with lower stratification (?AUC = -0.009, p<0.001). There was progressive improvement in MOF stratification using TBSL1-L3-FRAX (?AUC = +0.001, p<0.001), TBSL1-L2-FRAX (?AUC = +0.004, p<0.001) and TBSL1-FRAX (?AUC = +0.005, p<0.001). TBSL1-FRAX was significantly better than all other combinations for MOF prediction (p<0.001). Incremental improvement in AUC for hip fracture prediction showed a similar but smaller trend.CONCLUSION: This single large cohort study found that TBS-adjusted FRAX performance for fracture prediction was improved when limited to the upper lumbar vertebral levels, and was greatest for L1 alone. Validation is required in other cohorts.

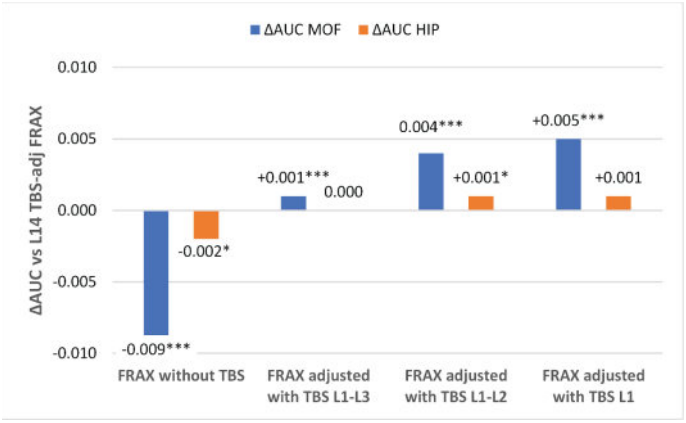

***Disclosures: William Leslie**, None*

SAT-393

Establishing error bounds for internal calibration on quantitative computed tomography (QCT) *Bryn Matheson[2], Nathan Neeteson[2], Steven Boyd[2]. [2]University of Calgary, . [2]University of Calgary, Canada

The current gold standard for osteoporosis screening uses dual X-ray absorptiometry (DXA) to calculate bone mineral density (BMD) at the hip and spine. However, DXA has limitations, such as low population screening rates and the lack of 3D bone geometry. To address this, computed tomography (CT) scans that include the osteoporotic bones of interest can be repurposed to assess fracture risk. However, most clinical CT scans do not contain calibration phantoms within the field of view (FOV), and it remains a challenge to perform accurate and precise phantomless, or internal, calibration of CT images. The current study aims to develop error bounds for the measurement of BMD using internally calibrated CT. Clinical CT scans containing the lumbar vertebrae and proximal femur were obtained at the University of Calgary's Centre for Mobility and Joint Heath. These scans follow the standard CT imaging protocol for the kidneys, urinary tract, and bladder and included a Mindways Model 3 CT calibration phantom in the FOV. Five tissue regions of interest (for internal calibration) and the bones of interest were extracted by segmentation from the scans. The error bounds of our previously established internal calibration1 method were estimated using Monte Carlo simulation and standard error propagation. For gold-standard phantom calibration, the calibration rods were extracted and a linear relationship was used to convert the scan to its equivalent K2HPO4 values. Integral BMD was calculated using both density calibration techniques. The agreement between internal and gold-standard phantom calibration results was evaluated by determining whether the internal calibration error bounds contained the reference mean BMD, calculated using phantom-calibrated densities, for the fourth lumbar vertebra (L4) and both femurs. With a dataset of 25 scans, we found the 95% confidence interval for the internal calibration estimations of BMD consistently captured the reference phantom BMD for both femurs and L4 vertebrae (Figure 1). The mean difference is 8.2 mg/cc [~2.5% error bound]. The estimated error bounds for internally calibrated CT measurements of BMD account for error sources related to variation across scanners and imaging artifacts. With our new method for estimating the accuracy of internal calibration, future work using this tool can focus on modifying the calibration procedure to narrow the error bounds.1. Michalski A, et al. Clin Med (Lond). 2020; 32(8):364-376

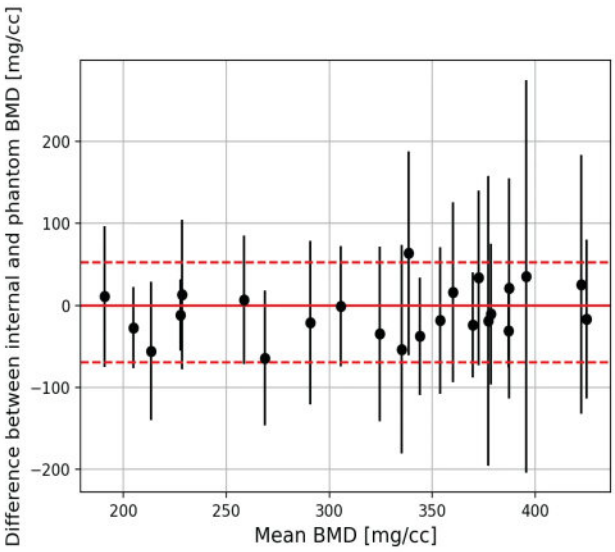

***Disclosures: Bryn Matheson**, None*

SAT-394

Establishing Japanese Osteoporosis Equivalent Femoral Strength Using Biomechanical CT (E-JOS Femoral Study) *Taro Mawatari[1], Shoji Baba[1], David Lee[2], Satoshi Hagio[1], Koichiro Kawano[1], Reima Sueda[1], Satoru Harada[1], Junta Mawatari[1], Yasuharu Nakashima[3], Tony Keaveny[2]. [1]KKR Hamanomachi Hospital, Japan. [2]O.N. Diagnostics, LLC, United States. [3]Kyushu University, Japan

Purpose: This study aimed to establish population-specific reference values for osteoporosis equivalent femoral strength using nonlinear finite element analysis (biomechanical CT) in a Japanese cohort, while taking into account the substantial difference in physique between Japanese and Americans. This would allow for more accurate assessment and treatment of osteoporosis in Japanese individuals. Methods: This study included a total of 717 patients (327 male and 390 female) aged 45-90 years who visited a general hospital for a CT scan including the hip joint and had a bone density test within 3 months before and after the scan. Up to 63 patients in each 5-year age group who met certain inclusion criteria were randomly selected. Femoral strength was calculated by phantom-less calibration from existing CT data. Osteoporosis and osteopenia equivalent femoral strength values were calculated based on femoral neck bone mineral density by DXA in Japanese subjects. Results and Discussion: The results showed that the osteoporosis equivalent femoral strength and osteopenia equivalent femoral strength in Japanese men were 3,000N and 4,000N, respectively, while those in Japanese women were 2,500N and 3,500N, respectively. These values were approximately 500N lower than the reported values for Americans. However, external factors, such as height, weight, BMI, and skeletal structure, also differ between the two populations. Conclusions: The study highlights the importance of using population-specific reference values for accurate assessment and treatment of osteoporosis. The estimated Japanese male and female osteoporosis equivalent femoral strength were found to be lower than reported values for Americans, emphasizing the need for region-specific reference values. Incorporating these population-specific reference values in the assessment of osteoporosis could help improve the accuracy of diagnosis and treatment.

***Disclosures: Taro Mawatari**, Teijin Pharma Limited, Grant/Research Support*

SAT-396

Differences in Cortical Bound and Pore Water Concentrations between Osteoporotic and Non-Fracture Cases *Jeffry Nyman[1], Thammathida Ketsiri[2], Elizabeth Louie[1], Kevin Harkins[1], Mary Kate Manhard[3], Donald Lee[1], Bobo Tanner[1], Mark Does[2]. [1]Vanderbilt University Medical Center, United States. [2]Vanderbilt University, United States. [3]Cincinatti Children's, United States

Many fragility fractures occur in adults with T-scores of the hip and spine above -2.5. Moreover, the current clinical assessment of fracture risk lacks diagnostic information about the inherent quality of a person's bone tissue. Using MRI to quantify both tissue hydration and porosity in cortical bone, we hypothesized that concentrations of bound water (Cbw) and pore water (Cpw) are lower and higher, respectively, in adults with a fragility fracture (Fx) than in sex-matched adults without osteoporosis (Non-Fx). We enrolled patients who experienced a fragility fracture of the distal radius and matched them to volunteers with no history of Fx. Adiabatic inversion recovery (AIR) and dual adiabatic full-passage (DAFP) sequences were used to acquire pore and bound water maps (Fig. A) of the distal-third radius (non-fracture side). For quantification of Cbw and Cpw, we assumed fixed relaxation rates of bound water (T1=290 ms and T*2=0.35 ms) and pore water (T1 =450 ms and T*2=2.6 ms) and used signal from a phantom (20%H2O/80%D2O/20-24 mM CuSO4) to convert intensity signals into moles of 1H per liter of bone. After acquiring DXA scans, 3 patients (F 59 yo, M 28 yo, and M 58 yo) in the Fx group were not eligible for MRI, leaving an age disparity between Fx and non-Fx groups for MRI measurements (Fx subjects were on average 21% older; Welch's p=0.030). Among the remaining 20 Fx and 20 Non-Fx subjects, there were no significant differences in BMI (Mann-Whitney, M-W, p=0.794) and in 10-year probability of major osteoporotic fracture (FRAX) between the 2 groups (M-W p=0.794). The 10-year probability of hip fracture (FRAX) was significantly higher (M-W p=0.027) in Fx [0.75% (0.10%, 2.45%)] than in Non-Fx group [0.20% (0.00%, 0.70%)]. Cbw was significantly lower (t-test p=0.003) in Fx (22.3+/-8.7 mol 1H/L) than in Non-Fx (30.8+/-7.9 mol 1H/L), while Cpw was higher (Welch's p=0.001) in Fx (26.7+/-7.8 mol1H/L) than in Non-Fx (19.2+/-4.1 mol 1H/L). The 2 groups tend to cluster in Cbw vs. Cpw plots (Fig. B). In logistic regressions of all imaging measurements, age, and BMI, the combination of Cpw, Cbw, and hip BMD best predicted the 2 cases (Fig C). Without MRI, hip BMD had the highest area under the receiver operating characteristic curve (AUC=0.73). Without DXA, the Cpw plus Cbw (AUC=0.88) was best (adding age didn't improve prediction). MRI offers new quantitative markers of fracture risk that are specific to the hydration state of collagen and pore space within cortical bone.

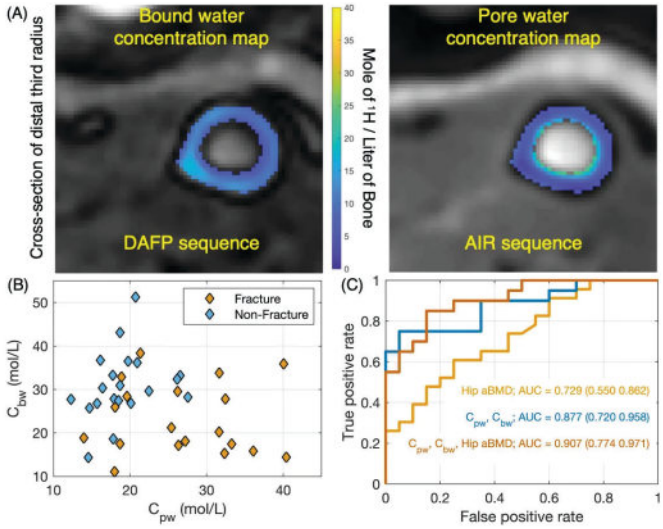

***Disclosures: Jeffry Nyman**, None*

SAT-397

Cystatin C-derived renal function parameters and Volumetric Bone Density and estimated Failure Load Among Older Men for the Osteoporotic Fractures in Men Study (MrOS) Research Group *Eugenie Koumakis[1], Alison Potok[2], Kristine Ensrud[3], Andrew Burghardt[4], Nancy Lane[5], Kerri Freeland[1], Charles Ginsberg[6], Jane A. Cauley[7]. [1]University of Pittsburgh, United States. [2]Division of Nephrology-Hypertension, University of California San Diego, San Diego, CA., United States. [3]University of Minnesota and Minneapolis VA Health Care System, United States. [4]University of California, San Francisco, United States. [5]University of California, Davis Medical Center, United States. [6]UCSD, . [7]UNIVERSITY OF PITTSBURGH, United States

Serum cystatin (Cys) C has been proposed to be superior to creatinine(Cr)-based measures of kidney function in detecting mild to moderate decreases in kidney function in older adults, in part because it is less dependent on muscle mass. Higher Cys C is associated with an increased risk of hip fracture independent of traditional risk factors including hip bone mineral density (BMD). Recently, eGFRdiff, the difference between eGFRCys and eGFRCr has been found to be associated with frailty in older adults. To date, the association between Cys C, eGFRCys and eGFRdiff, and bone microarchitecture assessed by High-resolution peripheral quantitative computed (HR-pQCT) has not been investigated.We used data from 555 community-dwelling men in MrOS with measurements of Cys C, creatinine and HR-pQCT parameters at the Year 14 exam. eGFRdiff (eGFRCys-eGFRCr) was calculated using 2021 CKD-EPI equations. We used linear regression to examine the association of Cys C, eGFRCys, and eGFRdiff with estimated failure load, total volumetric BMD (Tt.BMD), trabecular and cortical BMD (Tb.BMD, Ct.BMD) at the distal radius and tibia.Among the 555 men assessed, mean age was 84 years (SD 4); 181(32.6%) had an eGFRCr<=60 ml/min/1.73m2. Median eGFRCys was 51 ml/min/1.73m2, and median eGFRdiff was -16mL/min/1.73m2. In the unadjusted model, higher Cys C, lower eGFRCys and lower eGFRdiff were each associated with lower Ct.BMD at the tibia and radius, whereas eGFRCr was not related to Ct.BMD. These associations remained at the tibia after accounting for age, race, BMI, clinical center, CKD category by eGFRCr, smoking status, diabetes, hypertension, cal-

culated D3Cr muscle mass, serum albumin, self-reported physical activity, and femoral neck aBMD. Lower eGFRCys and lower eGFRdiff were also each associated with lower total tibia and radius BMD in unadjusted and multivariate models. Although lower eGFRdiff was associated with lower estimated failure load and Tb.BMD at the radius in the unadjusted model, these associations did not remain after adjustment.Older community-dwelling men with higher Cys C, and lower eGFRCys and eGFRdiff have lower total and cortical BMD which may contribute to the higher risk of fracture in this population. Creatinine-based eGFR was not associated with these HR-pQCT indices. Future studies should evaluate whether addition of Cys C-based eGFR measurements to traditional models improves identification of people at the highest risk of fracture.

Table. Linear regression model of Association of Cystatin C, $eGFR_{Cys}$, $eGFR_{diff}$, and $eGFR_{Cr}$ with Distal Tibia and Radius volumetric BMD and failure Load.

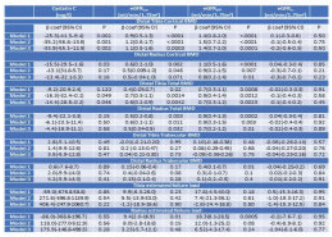

β coefficient represents the change in volumetric BMD for every 1-unit increase in Cystatin C, $eGFR_{Cys}$, $eGFR_{diff}$, and $eGFR_{Cr}$.
Model 1: unadjusted model.
Model 2: adjusted for age, race, body mass index (BMI), clinical center, chronic kidney disease (CKD) category by $eGFR_{Cr}$ (≥ 60 or < 60 ml/min/1.73m²), smoking status, diabetes, hypertension, muscle mass, and serum albumin.
Model 3: further adjusted for self-reported physical activity, and femoral neck aBMD.
$eGFR_{Cr}$ not adjusted for CKD in model 2 and 3.

***Disclosures: Eugenie Koumakis**, None*

SAT-398

Quiescent bone surface is not so "quiescent": An important but overlooked index for the estimation of bone remodeling *Shijing Qiu[1], Sudhaker Rao[2]. [1]Henry Ford Health, United States. [2]Henry Ford Hospital, United States

Bone surface (BS) is composed of: 1) quiescent surface (QS), where the bone remodeling begins; 2) eroded surface (ES) caused by osteoclastic bone resorption and 3) osteoid surface (OS) produced by osteoblastic bone formation (Fig 1). Currently, bone remodeling is assessed by tetracycline-based histomorphometry of bone tissue. In this study, we tested the hypothesis that QS decreases with increasing bone remodeling.Trans-iliac bone biopsies were obtained after double tetracycline labeling in 144 bone healthy women (43 blacks aged 24-70y and 109 whites aged 20-74y). Histomorphometric measurements were performed in cancellous, intracortical and endocortical bone envelopes. The relationship of static quiescent bone surface (QS/BS) with tetracycline-based bone remodeling variables, including mineralizing bone surface (MS/BS), surface-based bone formation rate (BFR/BS), and activation frequency (Ac.f) were analyzed in each bone envelop for black, white and all women using Spearman method.The results showed that QS/BS was strongly negatively correlated with bone remodeling related variables in all 3 bone envelops in black, white, and all women. R values ranged from 0.53 to 0.87 (all p values <0.0001; Table). However, there were no significant differences in QS/BS and other bone remodeling variables in all bone envelops between black and white women (data not shown).QS/BS is a static variable that does not contain tetracycline-based variables. Therefore, it is appropriate to perform correlation analyses between QS/BS and bone remodeling variables. Based on the strong correlations between QS/BS and the tetracycline-based bone remodeling variables in all bone envelops, we propose that QS/BS as a valid indicator to estimate bone remodeling in the absence of tetracycline labeling. Since bone remodeling always takes place on quiescent bone surface, QS/BS would decrease with increasing bone remodeling. Accordingly, the change in QS/BS can be used to estimate bone remodeling status in bone samples without tetracycline labeling such as from surgery, biopsy, or autopsy. Understanding of bone remodeling in these often discarded but readily available bone samples may provide valuable information in the research of osteoporosis, metabolic bone diseases and efficacy of pharmaceutical agents.

Fig 1. Types of bone surface

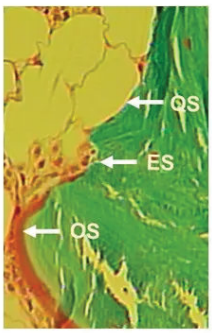

Table 1.Correlation of QS/BS with bone remodeling variables

	MS/BS	BFR/BS	Ac.f
Whole group (n=144)	**r values (all p < 0.0001)**		
Cancellous QS/BS	-0.627	-0.600	-0.615
Intracortical QS/BS	-0.634	-0.614	-0.605
Endocortical QS/BS	-0.719	-0.657	-0.675
Black women (n=35)			
Cancellous QS/BS	-0.873	-0.830	-0.843
Intracortical QS/BS	-0.750	-0.699	-0.625
Endocortical QS/BS	-0.776	-0.735	-0.735
White women (n=109)			
Cancellous QS/BS	-0.548	-0.527	-0.535
Intracortical QS/BS	-0.597	-0.590	-0.599
Endocortical QS/BS	-0.698	-0.632	-0.660

***Disclosures: Shijing Qiu**, None*

SAT-399

See Friday Plenary Number FRI-399

SAT-400

Communicating Fracture Risk: Results from the RICO Study *Mitali Sharma[1], Charlotte Beaudart[2], Mickael Hiligsmann[2], Stuart Silverman[3]. [1]The OMC Research Center, United States. [2]Department of Health Sciences Research, Maastricht University, Netherlands. [3]Cedars-Sinai/UCLA, United States

Objective: The Improving Risk Communication in Osteoporosis (RICO) study aims to identify and improve the apparent communication gap between patients and physicians when discussing fracture risk. RICO was a global initiative to understand patient preferences for fracture risk communication as well as the impact of age, fracture history, and education on the patient's willingness to initiate osteoporosis medication.Materials & Methods: Across eleven sites in nine different countries, 332 women with osteoporosis or at high risk of fracture were given a structured survey, in which they voiced their preferences for fracture risk communication as well as their attitudes towards initiating a prescription osteoporosis medication. Willingness to start a medication was measured in terms of fracture risk decision point (FRDP) or the lowest hypothetical fracture risk-in terms of FRAX score-at which the participant would initiate an osteoporosis medication with minimal, transient side effects. Results: 85.7% of participants indicated that it was important to receive information about their fracture risk with a mean rating of 6.22+/-1.40 on a Likert scale from 1-7. However, only 55.7% reported that they had been told about their fracture risk by a healthcare provider, and only 47% of patients could remember whether their risk was low, moderate, or high. Additionally, participants across all age groups indicated a significant preference for visual presentation of FRAX score-rather than numeric- ($p<0.001$) and reported interest in a two-year FRAX presentation in addition to the existing ten-year timeframe ($p=0.022$). In terms of willingness to initiate medication, participants with higher education expressed a significantly higher FRDP of 10% fracture risk when compared to those with high school education or less-who had a FRDP of 5% fracture risk ($p<0.001$). However, FRDP did not vary significantly based on participants' age ($p=0.082$) or fracture history ($p=0.175$).Discussion: These results confirm a communication gap with regards to how osteoporosis patients receive information regarding fracture risk. Furthermore, understanding the impact of demographic and clinical risk factors on attitudes toward medication initiation may assist both patient and physician in shared clinical decision-making.

***Disclosures: Mitali Sharma**, None*

SAT-401

Assessing osteoporosis in postmenopausal women: Preliminary results using a novel lumbar spine phantom-based MRI scoring method *Rahman Ud Din[1], Haisheng Yang[1]. [1]Beijing University of Technology, China

PurposeDual-energy X-ray absorptiometry (DXA) may have limitations in distinguishing between patients with osteoporosis and associated fractures. Hence, a new method for detecting osteoporosis has been proposed, which is based on novel magnetic resonance imaging (MRI) lumbar phantom scoring and utilizes fundamental MRI principles.MethodsA study was conducted after obtaining approval from the ethical board, which included testing of four different oils with varying T1 relaxation times, as well as 62 consenting females aged 55 years and above. Participants with bone issues were excluded. Both MRI (with novel phantom) and DXA scans were performed on the participants (November 2022 and March 2023). Two experienced readers evaluated the signal intensities (SI) on T1- and T2-weighted parametric images of 146 vertebrae. Median L1-L5 SI divided by T1 and T2 control SI was used to calculate F- and W-scores, respectively. The diagnostic performance of the new scores in detecting osteoporosis and vertebral fractures was assessed using ROC analysis. Nonparametric Mann-Whitney, regression analysis, box-whisker plots, and descriptive statistics were also used for the analysis.ResultsThirty eligible participants (mean age, 62.56 years +/-6.15; BMI, 28.78+/-6.15) were enrolled out of 62. Coconut oil and deionized water were used as reference controls in the MRI phantom. Higher mean F- and W-scores were reported in individuals with osteoporosis (3.81 and 2.28, respectively) compared to those without (3.05 and 1.78, respectively), with correlation coefficient (ICC) of 0.92 for F-score and 1.00 for W-score. Similar findings were observed in individuals with osteoporotic (3.82 and 2.47, respectively) and non-osteoporotic groups (3.13 and 1.69). The F- and W-scores achieved higher AUC values in individuals with osteoporosis (0.86 and 0.75, respectively) compared to vertebral bone quality (VBQ) (0.71) and signal-to-noise ratio (0.68) with p-values <.05 and p=.093, respectively. The new scores AUC (F-score, 0.80 and W-score, 0.86) better-differentiated participants with osteoporotic vertebral fractures (13/30 or 43.3%) compared to DXA (aBMD, 0.27) with p<.01 and p=.03, respectively.ConclusionA novel MRI lumbar spine phantom was developed and real-time safely tested. The newly defined F- and W-scores exhibited a capability to distinguish osteoporosis from non-osteoporosis, and further demonstrated improved detection ability of osteoporotic vertebral fractures when compared to DXA.

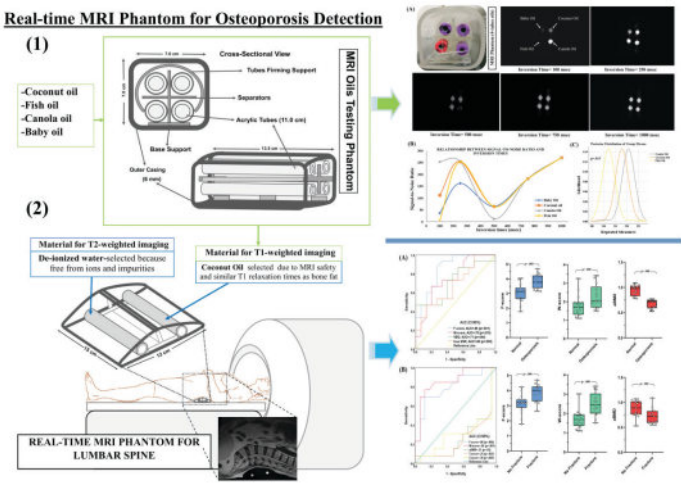

***Disclosures: Rahman Ud Din**, None*

SAT-403

Osteoporosis and Its Role in Periprosthetic Fractures of Total Hip Arthroplasty Patients *Mark Wishman[1], Katherine Haseltine[3], Joseph Lane[3]. [1]Weill Cornell Medical College, United States. [3]Hospital for Special Surgery, . [3]Hospital for Special Surgery, United States

Purpose:Patient undergoing total hip arthroplasty (THA) are routinely under screened for metabolic bone disease at the time of surgery leaving these patients at risk for poor outcomes including periprosthetic fractures (PPFx). As the number of THA procedures increases over the next few decades, the number of patients at risk will also increase. Therefore, there is a need to identify patients at highest risk for PPFx following THA so they can undergo appropriate screening and treatment for osteoporosis if necessary.Methods:We identified fifty-four periprosthetic fracture patients following primary THA. These patients were matched 2:1 to unfractured control THA patients by age and sex. Retrospective chart review was used to collecte demographic variables and past medical history. We then compared Fracture RIsk Assessment Tool (FRAX) scores and associated risk factors as well as treatment with vitamin D/calcium and osteoporosis medications. All data was gathered at the time of fracture PPFx group. In the control patients, an office visit that occurred at the same age as their fracture counterpart's hospitalization occurred was used for data collection. Statistical analysis was done using student t-tests for continuous variables and chi-square analysis for categorical variables. An alpha value of .05 was used to determine significance. Results:When comoparing PPFx patients to unfractured controls there was no difference in age (78.5 +/- 10.87 years vs 78.19 +/- 10.02, p=.79) or sex (?2(1) = 0, p=1). PPFx patients had increased 10-year risk of major osteoporotic fracture (21.86 +/- 10.7 vs 15.86 +/- 9.85, p=.0005) and hip fracture (10.81 +/- 8.48 vs 7.09 +/- 6.59, p.002) by FRAX analysis. PPFx patients had lower BMI (24.85 +/- 5.16 vs 27.92 +/- 6.03, p=.0023) and were more likely to have a history of fragility fracture (?2(1) = 30.65, p=<.00001), be current smokers (?2=(1) = 6.57, p=.0103), and have secondary risk factors for osteoporosis (cirrhosis, diabetes mellitus, etc.)(?2(1) = 16.73, p=.0004) compared to control patients. There was no difference in Vit D/Ca (?2(1) = 1.63, p=.201) or osteoporosis medication usage (?2(1) = 0.12, p=.729) in these groups.Conclusion:These findings suggest that despite PPFx patients having identifiabile risk factors for osteoporosis including increased FRAX scores, lower BMI, and history of fragility fractures, tobacco use, and secondary osteoporosis there is no difference in osteoporosis treatment in these groups.

***Disclosures: Mark Wishman**, None*

SAT-405

Retrospective study on the effectiveness and the clinical usefulness of bone turnover marker in patients with osteoporosis: A multicenter study in Korea *Jun-Il Yoo[1], Deog-Yoon Kim[2], Yong-Chan Ha[3], Seong Hee Ahn[4]. [1]Inha University Hospital, Republic of Korea. [2]Kyung Hee University Hospital, Republic of Korea. [3]Seoul Bumin Hospital, Republic of Korea. [4]Inha University Hospital, Inha University School of Medicine, Republic of Korea

Background: The purpose of this study is to investigate real-world data of CTX, P1NP, and Osteocalcin through present multicenter clinical study, and retrospectively analyze the usefulness of bone turnover markers (BTM) in Koreans. The observed data values would provide information that can be used as reference values for the diagnosis and treatment of osteoporosis in patients.Methods: The study focused on pre- and post-menopausal patients diagnosed with osteoporosis and excluded patients without certain test results or with test intervals of more than 1 year. The collected data included age, gender, menopause, fracture history, drug history, osteoporosis treatment history, and three bone turnover markers (CTX, P1NP, and Osteocalcin). The patients were classified by demographic characteristics and the concentrations of the bone turnover markers were analyzed by group.Results: In women who had no history of fractures, the levels of P1NP (n = 2100) were 43.544 +/- 36.902, CTX (n = 1855) were 0.373 +/- 0.927, and osteocalcin (n = 219) were 10.81 +/- 20.631. For men who had no history of fractures, the levels of P1NP (n = 221) were 48.498 +/- 52.892, CTX (n = 201) were 0.370 +/- 0.351, and osteocalcin (n = 15) were 7.868 +/- 10.674. Treatment with teriparatide led to an increase in P1NP levels after three months in both men and women, with a 50% increase observed in women. Similarly, treatment with Denosumab led to a decrease in CTX levels after three months in both men and women, with a reduction of 60% observed in women.Conclusions: The results of this study can contribute to appropriately evaluating the bone replacement status in Koreans. We also provide the PINP level in the Korean population for future comparative studies with other populations.

***Disclosures: Jun-Il Yoo**, None*

SAT-406

See Friday Plenary Number FRI-406

SAT-408

Skeletal Muscle Energetics and HR-pQCT Bone Parameters: The Study of Muscle, Mobility and Aging (SOMMA) *Jane A. Cauley[1], Tong Yu[4], Lauren S. Roe[3], Nina Heilmann[4], Kerri Freeland[4], Nicole Sekel[4], Kristen Koltun[4], Katelyn I. Guerriere[5], Julie Hughes[5], Bradley Nindl[4], Ashley Weaver[6], Nancy Glynn[4], Philip Kramer[6], Peggy Cawthon[7], Theresa Mau[8], Anne Newman[4], Paul Coen[9], Elsa Strotmeyer[4]. [1]UNIVERSITY OF PITTSBURGH, United States. [4]University of Pittsburgh, . [3], . [4]University of Pittsburgh, United States. [5]US Army Research Institute of Environmental Medicine, United States. [6]Wake Forest University, United States. [7]California Pacific Medical Center, United States. [8]University of California, San Francisco , United States. [9]Adventhealth, Translational Research Institute, United States

Mitochondria are important in aging muscle as they generate the energy needed for contraction. The SOMMA Bone study was designed to improve our understanding of the bone-muscle crosstalk. Here, we examined associations between muscle mitochondrial energetics and high resolution peripheral quantitative tomography (HR-pQCT) parameters. Bone microarchitecture, volumetric bone mineral density (BMD) and bone strength (failure load) were assessed by HR-pQCT. Muscle oxidative capacity was determined by 31 P-Magnetic Resonance Spectroscopy (ATPmax) and state-3 respiration (Max OXPHOS) was assessed in muscle biopsies. A total of 117 community dwelling older men and 178 women participated; mean age, 76.1+/-4.5 years; 86% White. HR-pQCT scans were obtained at the distal radius (DR) and tibia (DT). Failure load, total (Tt) BMD, and cortical (Ct) and trabecular (Tb) BMD, bone area (Ar), thickness (Th) and number (N) were measured. Linear regression models were used to examine the association between ATPmax and Max OXPHOS with sex-specific standardized HR-pQCT parameters. In minimally adjusted models (age, race, limb length), higher DR failure load, Tb.BMD and Ct.Ar were associated with higher ATPmax in men while there was no association in women, Table 1. At the DT, Tt.Ar was associated with higher ATPmax in women and Tb.N in men. There was no association with Max OXPHOS in women or men at the DR. At the DT, Max OXPHOS was positively related to the Tb.N in men and Tb.Ar in women. In the fully adjusted models (age, race, limb length, smoking, alcohol and comorbidities), the association between ATPmax and failure load at the DR (?=0.269*), and Tb.N at the DT (?=0.264*) in men retained significance. The association between ATP max and Tb.BMD at the DT in men became significant (?=0.228*). The fully adjusted association between Max OXPHOS and Tb.N at the DT in men also became significant (?=0.238*). There were no associations between muscle energetics and Ct.Th or Ct.Po at either the DR or DT. In conclusion, these preliminary results suggest that there may be an association between skeletal muscle energetics, specifically ATP max and failure load, Tb.BMD and Ct.Ar in men at the DR. The associations were generally not significant in women and may suggest gender differences in bone-muscle crosstalk. There was little association with Max OXPHOS. Further analyses will explore other markers of skeletal muscle energetics with bone.

Table 1: Associations of skeletal muscle energetics with HR-pQCT parameters at the distal radius and distal tibia in SOMMA older men and women. Standardized β are shown from linear regression models.

	Distal Radius				Distal Tibia			
	ATPmax		Max OXPHOS		ATPmax		Max OXPHOS	
	Women	Men	Women	Men	Women	Men	Women	Men
Failure load	-0.087	0.284*	0.025	0.015	0.021	0.154	0.092	0.005
Tt.BMD	-0.076	0.161	0.038	-0.071	-0.066	0.136	0.061	0.063
Tb.BMD	-0.015	0.210*	0.085	0.105	-0.002	0.180	0.088	0.146
Ct.BMD	-0.019	0.096	-0.006	-0.093	-0.001	-0.013	0.086	-0.017
Ct. Ar	-0.152	0.195*	-0.012	-0.124	-0.014	0.125	0.042	-0.073
Tt.Ar	-0.005	0.115	0.077	0.107	0.170*	0.101	0.034	-0.045
Tb.Th	0.022	0.137	0.025	0.059	-0.033	0.034	-0.123	0.105
Tb.N	-0.040	0.182	0.090	0.087	0.060	0.264*	0.109	0.154
Tb.Ar	0.093	0.045	0.047	0.087	0.171*	0.010	0.018	-0.049

*denotes p<0.05 for minimally adjusted models (age, race/ethnicity, limb length) .
Abbreviations: *ATPmax*, adenosine triphosphate maximal production; *Max OXPHOS*, maximal oxidative phosphorylation; *Tt.BMD*, Total bone mineral density; *Tb.BMD*, Trabecular bone mineral density; *Ct.BMD*, cortical bone mineral density; *Ct.Ar*, cortical area; *Tt.Ar*, total area; *TB.Th*, trabecular thickness; *Tb.N*, trabecular number; *Tb.Ar*, trabecular area.

***Disclosures: Jane A. Cauley**, None*

SAT-409

Background incidence rates for 1-year all-cause mortality, myocardial infarction, and stroke in U.S. male and female osteoporosis population in the year 2020 *Hsu-Chih Chien[1], Mary Oates[1], MICHELE MCDERMOTT[1], Tzu-Chieh Lin[1]. [1]Amgen, United States

BackgroundPublished literature on all-cause mortality and incidence of myocardial infarction (MI) and stroke has been limited in osteoporosis (OP) to women receiving OP medication or is based on older data. For OP-treated women, the literature reports 1-year MI incidence and stroke of 3 to 13, and 16-38 per 1,000 person-years respectively. In this epidemiology study, we aimed to update clinical knowledge with more recent data that includes both men and women with OP in the U.S.MethodsMen and women with OP >=50 years of age defined by either having a diagnosis of OP, fracture, or a prescription for OP medication among all available history prior to 1 January 2020 were included from Optum's de-identified Clinformatics® Data Mart Databases (Optum CDM). Individuals with a history of Paget's disease and metastatic cancer were excluded. Eligible patients were followed from 1 January 2020 for 1 year to identify study outcomes including all-cause mortality, MI, and stroke (ischemic, hemorrhagic, and uncertain type) using validated claims-based ICD algorithms. Kaplan-Meier (KM) method was applied to estimate the incidence rate and 95% CI for each study outcome. Event rates within each age subgroups (50-64, 65-74, 75-84, and 85 years and older) were also reported.Results1,078,263 OP patients met inclusion criteria in Optum data in 2020. Of these, 17.3% (186,761) of patients were men and 82.7% (891,502) were women; 79.6% of men and 89.4% of women were >=65 years of age. Fracture was experienced in 72.9% (136,210) of male OP patients and 37.0% (329,801) of female OP patients. Treatment was received by 23.8% (44,375) of male patients and 57.2% (510,092) of female patients.Overall, event rates per 1,000 patient-years were higher than women across all study outcomes (all-cause mortality, men: 95.7 [95% CI: 94.3, 97.1]; women: 55.9 [95% CI: 55.4, 56.4]; MI, men: 13.6 [95% CI: 13.1, 14.2]; women: 7.6 [95% CI:7.5, 7.8] ; stroke, men: 19.6 [95% CI: 19.0, 20.3]; women: 13.9 [95% CI: 13.7, 14.2]). The event rates increased with age and individuals >= 85 years old had the highest rates. Higher rates were also observed in men and women who experienced fracture across all age groups. (Figure 1)ConclusionWe updated the background rates of all-cause mortality, MI and stroke in men and women with OP in U.S. in 2020. The overall rates were within the range from published literature, and we observed a higher rate in men (vs women), older age and those with fracture history.

Figure 1. 1-year Incidence Rates of Myocardial Infarction, Stroke and All-cause Mortality in US Osteoporosis Population in 2020

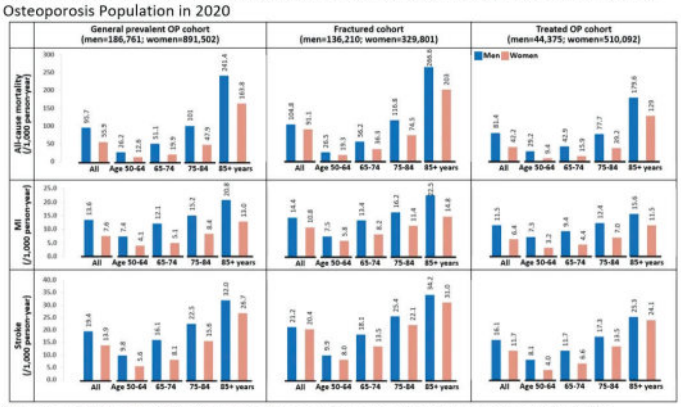

MI: myocardial infarction, OP: osteoporosis. Osteoporosis treatment included anabolic agents (including romosozumab and PTH analogues [teriparatide and abaloparatide]), denosumab, oral bisphosphonates (alendronate, risedronate and ibandronate) and intravenous zoledronic acid

***Disclosures: Hsu-Chih Chien**, Amgen, Other Financial or Material Support*

SAT-411

See Friday Plenary Number FRI-411

SAT-412

Race/ethnicity and Fracture Prediction in Younger Postmenopausal Women: Results from the Women's Health Initiative Study *Carolyn Crandall[1], Joseph Larson[2], John Schousboe[3], JoAnn Manson[4], Nelson Watts[5], John Robbins[6], Peter Schnatz[7], Rami Nassir[8], Aladdin Shadyab[9], Karen Johnson[10], Jane A. Cauley[11], Kristine Ensrud[12]. [1]University of California, Los Angeles, United States. [2]Fred Hutchinson Research Center, United States. [3]Park Nicollet Clinic HealthPartners Institute University of Minnesota, . [4]Harvard Medical School, United States. [5]Mercy Health Osteoporosis and Bone Health Services, . [6]University of California Davis Medical Center, United States. [7]Reading Hospital/Tower Health and Drexel University, United States. [8]University of California, Davis, United States. [9]University of California, San Diego, United States. [10]University of Tennessee Health Science Center, United States. [11]UNIVERSITY OF PITTSBURGH, United States. [12]University of Minnesota and Minneapolis VA Health Care System, United States

Importance: The best approach to identify younger postmenopausal women for osteoporosis screening in uncertain. The Fracture Risk Axsessment Tool (FRAX), which includes self-identified race/ethnicity information, and the Osteoporosis Self-Assessment Tool (OST), which does not, are risk assessment tools recommended by United States Preventive Services Task Force Guidelines to identify candidates for bone mineral density (BMD) testing in this age group.Objective: To compare the ability of FRAX vs. OST to discriminate between younger older postmenopausal women who do and do not experience incident fracture during 10-year follow-up in the four racial/ethnic groups specified by FRAX.Design: This observational study of Women's Health Initiative Study participants included 67,169 women aged 50-64 years at baseline with 10 years of follow-up for major osteoporotic fracture (MOF). at 40 U.S. clinical centers. Incident MOF and BMD (in a subset of 4,606 women) were assessed. The area under the receiver operating characteristic curve (AUC) for FRAX (without BMD information) and OST were calculated within each racial/ethnic category. Results: Mean (SD) participant age at baseline was 57.8 (4.1 years); 1,486 self-identified as Asian, 5,927 as Black, 2,545 as Hispanic, and 57,211 as White. During follow-up, 5,594 women experienced MOF. For discimination of MOF, AUC values (95% confidence interval) for FRAX were 0.65 (0.51-0.78) for Asian, 0.55 (0.49-0.61) for Black, 0.60 (0.52-0.68) for Hispanic, and 0.55 (0.53-0.57) for White women. AUC Values for OST were 0.67 (0.54-0.79) for Asian, 0.55 (0.48-0.61) for Black, 0.50 (0.52-0.68) for Hispanic, and 0.56 (0.54-0.58) for White women. See Figure 1. For discrimination of femoral neck osteoporosis, AUC values were excellent for OST (range 0.79-0.85), higher for OST than FRAX (FRAX AUC range 0.72-0.74), and similar in each of the four racial/ethnic groups. Conclusions: Within each racial/ethnic category, the U.S. FRAX tool and OST have suboptimal performance in discimination of MOF in younger postmenopausal women. In contrast, for identifying osteoporosis, OST was excellent. The U.S. version of FRAX should not be routinely used to make screening decisions in younger postmenopausal women.

Figure 2. Receiver Operating Characteristic (ROC) Curves by Race/Ethnicity for Major Osteoporotic Fracture during 10 years of Follow-up among Women aged Between 50 and 64 years at Baseline, by Race/Ethnicity[1]

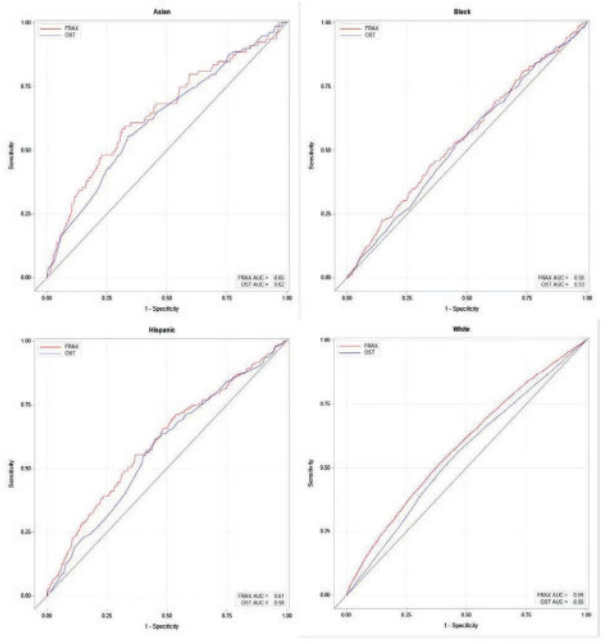

[1] FRAX vs. OST: All Participants, p<0.001; Asian, p=0.59; Black, p=0.50; Hispanic, p=0.35; White, p<0.001; p-values from a Chi-square statistic on 1 degree of freedom testing the difference between each paired group

***Disclosures: Carolyn Crandall**, None*

SAT-414

Vitamin D Status in Patients with Non-Vertebral Fragility Fractures *Satoshi Hagio[1], Taro Mawatari[2], Reima Sueda[3], Satoru Harada[3], Koichiro Kawano[3], Shoji Baba[3]. [1]HAMANOMACHI HOSPITAL, Japan. [2]Hamanomachi Hospital, Japan. [3]KKR Hamanomachi Hospital, Japan

Introduction:Vitamin D insufficiency or deficiency is a global health issue, and studies have reported that half of osteoporosis patients in Japan have vitamin D deficiency. This study aimed to investigate the vitamin D status in patients with non-vertebral fragility fractures, including distal radius (DRF), proximal humerus (PHF), femoral neck (FNF), and femoral trochanteric (FTF) fractures, who visited a hospital in Japan.Patients and Methods:A retrospective analysis was conducted on the serum 25(OH)D levels of 436 patients (107 males, 329 females, mean age 73 years) who visited a regional public general hospital in Japan for surgical treatment of non-vertebral fractures. Available information on other blood chemistry data and bone mineral density measured by dual-energy X-ray absorptiometry was also collected. The institutional review board approved this study.Results:Serum 25(OH)D levels were measured in patients with non-vertebral fragility fractures, including DRF (n=99), PHF (n=54), FNF (n=164), and FTF (n=119). The mean serum 25(OH)D levels were 15.7 ng/ml for DRF (mean age 65.3 years), 13.7 ng/ml for PHF (mean age 69.8 years), 11.9 ng/ml for FNF (mean age 77.9 years), and 11.3 ng/ml for FTF (mean age 83.6 years). Significant differences in serum 25(OH)D concentrations were observed between patients with DRF and those with FNF, as well as between those with DRF and FTF ($p<0.05$).No correlation was found between age and serum 25(OH)D ($R=0.03$), but significant differences were found in all groups except for PHF and DRF ($p<0.05$). The incidence of vitamin D deficiency, defined as serum 25(OH)D levels <20 ng/ml, was 76% for DRF, 81% for PHF, 89% for FNF, and 94% for FTF. The rates of severe deficiency, defined as serum 25(OH)D levels <10 ng/ml, were 18%, 31%, 48%, and 51%, respectively.Discussion and Conclusion:This study found that vitamin D insufficiency or deficiency is prevalent in patients with non-vertebral fragility fractures, especially in older patients with FNF and FTF. The incidence of vitamin D deficiency in this patient population is higher than the general population in Japan, highlighting the importance of monitoring and addressing vitamin D status in these patients. Fracture site differences in serum 25(OH)D levels suggest a potential relationship between the degree of vitamin D deficiency or insufficiency and the location of the fracture.

***Disclosures: Satoshi Hagio**, None*

SAT-415

Self-reported physical function is associated with increased fracture and mortality risk *Dana Bliuc[1], Thach Tran[1], Dunia Alarkawi[1], Weiwen Chen[2], Robert Blank[3], Jacqueline Center[1]. [1]Garvan Institute of Medical Research, Australia. [2]Garvan Institute, Australia. [3]Medical College of Wisconsin, Division of Endocrinology,

Poor muscle strength and physical performance, as measured by common tests, increase the risk of falling and fracture, particularly for men. However, those unable to perform these tests have the highest fracture risk, suggesting that simpler qualitative measures might be useful. This study investigated the association between self-reported physical function (PF) and fracture risk in women and men.45 and Up is a prospective population-based cohort of 116,001 (from 267,357) people with complete baseline questionnaire data linked to hospital, emergency, and mortality datasets. Four self-reported measures of PF (walking, lifting, climbing stairs and bending) were analysed. Fractures were identified from hospital admission and emergency care administrative data, and mortality from vital statistics data over the first 5 years of follow-up.The association of PF measures and fracture and mortality risk were determined using cause-specific Cox models, a competing risk approach which produces simultaneous estimates of fracture and mortality risk. The models were further adjusted for age, weight, prior fracture and falls. Given a significant interaction with self-reported PF, Cox models were stratified by age (< 75, >= 75).Approximately 20% of participants reported limitation in at least one PF domain. Interestingly, most participants reported limitation in all PF domains (Figure). During the first 5 years of follow-up, there were 7190 fractures and 4958 deaths in women and 4267 fractures and 7845 deaths in men. All PF domains were associated with an increased risk of fracture and mortality in both age groups and genders. Those who reported a limitation in all 4 PFs had the highest risk. In those < 75, the hazard ratio was 1.73 (95% CI, 1.58 - 1.89) for fracture and 1.21 (95% CI, 1.12 - 1.32) for death in women and 1.64 (1.45 - 1.86) and 1.28 (1.19 - 1.37) in men. In those >= 75, the respective hazard ratios for fracture and death were 2.16 (95% CI, 1.88 - 2.47) and 1.46 (95% CI, 1.34 - 1.60) in women and 2.44 (2.09 - 2.84) and 1.50 (1.40 - 1.58) in men. Approximately 8% of fractures and 5% of deaths were attributable to PF impairment in those aged 75.PF limitation is common and is associated with increased fracture and mortality risk. Our findings suggest that simple self-assessment may be a useful clinical tool for selecting candidates for further investigation and intervention.

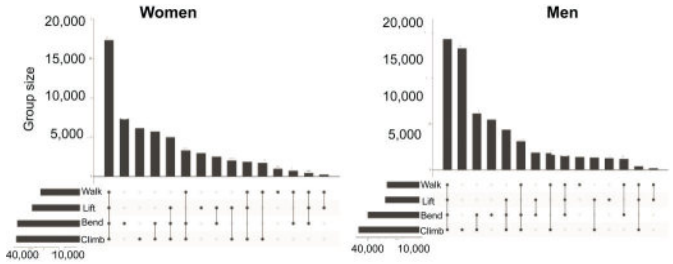

***Disclosures: Dana Bliuc**, None*

SAT-416

The Relationship between Sarcopenia and Bone Mineral Density in Community-Dwelling Subjects Aged 50 Years or Older in Men and Postmenopausal Women in Korea *Dong Jin Chung[1], Bitz-Na Kim[2], Jin Ook Chung[1], Dong Hyeok Cho[2], Jeong-Ran Cho[3]. [1]Chonnam National University Medical School, Republic of Korea. [2]Chonnam National University Hospital, Republic of Korea. [3]Kwangju Women's University, Republic of Korea

Sarcopenia is a progressive and generalized skeletal muscle disorder associated with poor health outcomes such as falls, fractures, cardiovascular, metabolic disease, lower quality of life, disability, and mortality. In this study, we used nation-wide data from 2008 to 2011 Korea National Health and Nutrition Examination Survey (KNHANES) to analyze the association between bone mineral density (BMD) and sarcopenia in community-dwelling men and women. Subjects with history of medication for osteoporosis or with illness or malignancy affecting bone metabolism were excluded. Data of anthropometric measurements and demographic characteristics were collected by trained examiner. Serum was separated from peripheral venous blood samples obtained after 8 hours of fasting. BMD was measured at the lumbar spine, femur neck and total femur using dual-energy X-ray absorptiometry (DXA). Sarcopenia was defined using the revised Asian Working Group for Sarcopenia (AWGS) classification with SMI (skeletal muscle index; <7.0 kg/m2 for men and <5.4 kg/m2 for women). We included 2,133 subjects aged 50 years or older in men (N=1,246, 887 without sarcopenia, 359 with sarcopenia) and postmenopausal women (N=887, 692 without sarcopenia, 195 with sarcopenia). All data analyses were performed using a weighted complex sample design. Prevalence of sarcopenia was significantly higher in men (28.8%) than women (22.0%). Compared with subjects without sarcopenia, men with sarcopenia had lower BMD at the lumbar spine, femur neck and total femur, whereas, women with sarcopenia had lower BMD at the femur neck and total femur. In multiple regression analysis, sarcopenia was significantly associated with low bone mass at the lumbar spine, femur neck and total femur BMD after adjusting age, obesity, hyperlipidemia, hypertension, smoking

status, alcohol consumption, monthly house income, physical activity, daily calcium intake and vitamin D concentration in men. However, there was no association between sarcopenia and bone mass in women in same analysis. In conclusion, sarcopenia is significantly related to low bone mass, especially in men aged >=50 years in Korea.

***Disclosures: Dong Jin Chung**, None*

SAT-417

Association of Sex Steroid Hormone Changes and Femoral Neck Area and Bone Mineral Content Across the Menopausal Transition: Findings from the Michigan Bone Health and Metabolism Study *Carrie Karvonen-Gutierrez[1], Irena Chen[2], Aleda Leis[3], Kerry Richards-McCullough[1], Tom Richards[1], ERIN BIGELOW[4], Robert Goulet[5], Karl Jepsen[3]. [1]Department of Epidemiology, University of Michigan, United States. [2]Department of Biostatistics, University of Michigan, United States. [3]University of Michigan, United States. [4]UNIVERSITY OF MICHIGAN, United States. [5]Michigan Medicine, University of Michigan, United States

Bone mineral density (BMD) declines rapidly during the menopausal transition (MT); nearly 50% of lifetime BMD loss in women occurs during the MT. It also a period of rapid endocrinologic change, with accelerated rises in follicle-stimulating hormone (FSH), beginning five years before the final menstrual period (FMP) and accelerated declines in estradiol (E2), beginning 2 years before the FMP. Given the co-occurrence of these two processes - endocrinologic and bone changes - sex hormones are hypothesized to have a major role in the regulation of bone metabolism, but the evidence is mixed. The majority of research has focused solely on BMD, a summary measure of bone change, which can obscure unique impacts on bone area and bone mineral content (BMC). In this analysis, we evaluate the relationship between E2 and FSH levels across the MT and patterns of change in bone area and BMC. Data are from 211 women (1929 observations) in the Michigan Bone Health and Metabolism Study, initiated in 1988 with 15 follow-ups through 2009. At each visit, participants received a DXA scan of the femoral neck and a blood sample was obtained in days 3-5 of the follicular phase of the menstrual cycle. E2 and FSH were assayed in duplicate and log-transformed for analysis. Models were adjusted for baseline BMC and area and included random intercepts to account for within-woman correlation. Time to FMP was fit with a linear spline, with knots at -2 and +2 years for E2 models and -2 and +1 years for FSH models. Analyses were conducted in R Studio. Latent class analysis was used to estimate trajectory groups representing patterns of change in BMC and area across the MT. In models relating BMC trajectory group to sex hormones, there were no statistically significant associations with E2 or FSH. However, a one unit higher baseline BMC was associated with an 11% lower FSH. In models relating area trajectory groups to sex hormones, women in the group with the highest but slightly declining area had 22% lower FSH as compared to women in the group with low but slightly increasing area. Further, a one unit higher baseline bone area was associated with a 19% higher FSH value. There were no statistically significant associations between bone area and E2. These findings suggest that increases in bone area are associated with higher FSH values. More research is needed to elucidate the relationship between sex hormone changes and changes in bone morphology across the MT.

***Disclosures: Carrie Karvonen-Gutierrez**, None*

SAT-418

Epidemiology of fractures in different ethnic groups across the lifespan in New Zealand *Brya Matthews[1], Subhajit Konar[1], Zhenqiang Wu[1], David Musson[1], Sarah-Jane Paine[1], Roger Harris[2]. [1]University of Auckland, New Zealand. [2]Australia and New Zealand Fragility Fracture Registry, New Zealand

Fractures lead to increased morbidity and mortality in the elderly, but they are a musculoskeletal issue that occurs at all ages. Fracture rates are often estimated based on hospitalisation data, which only gives a complete picture for certain fracture types. In New Zealand, injuries are covered by a no-fault national insurance system known as ACC. Most fractures that require clinical attention are recorded as ACC claims. The aim of this study was to determine the frequency of fractures in New Zealand overall and at key sites in different genders and ethnic groups across the lifespan.Individualised fracture claim data were obtained from ACC for 2010-2018. 851,544 fracture claims were included in the analysis. Prioritised ethnicity was reported (order of priority is Maori, Pacific peoples, Asian, Other, European) for 98% of claims. Census data was used to calculate fracture incidence. A setting where the injury occurred was reported in 91% of claims.Males accounted for 52.8% of fractures in the entire dataset, however over the age of 50, fracture incidence is 67% higher in women (Table). All ethnicities showed peaks in fracture incidence in adolescence and the elderly. We noted aging-related increases in fracture incidence at all anatomical sites except hands and feet, including sites like lower leg, ribs and skull and face that are not typically considered sites of fragility fracture. Europeans had the highest fracture incidence overall, and Maori and Pacific people have lower incidence of fractures than Europeans in all age groups in women and all but 20-39 years of age in men. Asians had the lowest fracture incidence overall, particularly in males. Hip fractures mainly occur in the elderly and show higher incidence in Europeans than other ethnicities (Table). Almost half of all fractures occurred at home, rising to over 80% in the elderly. 30% of fractures in people aged 10-39 occurred in a place of recreation or sports. Males consistently had more fractures outside the home than females.Age, gender and ethnicity all affect fracture incidence, with peaks in adolescents, young men, and the elderly. Non-Europeans in New Zealand generally have lower fracture rates than Europeans. Our data suggest that most types of fractures in older people could be indicators of skeletal fragility.

Table: Total fracture incidence in New Zealand 2010-2018 (per 10,000 people/year)

	Female					Male				
Age	European /Other	Maori	Pacific Peoples	Asian	All	European /Other	Maori	Pacific Peoples	Asian	All
0 -9	258	141	152	107	199	251	148	165	120	200
10-19	370	185	159	104	278	570	360	383	200	464
20-29	164	107	79	38	125	310	299	294	80	266
30-39	140	104	76	40	113	207	215	191	73	185
40-49	143	96	63	49	122	176	156	118	64	160
50-59	195	117	84	90	172	148	129	92	63	138
60-69	230	116	110	130	212	127	106	76	59	122
70-79	267	143	130	163	256	138	110	93	84	136
80+	527	260	317	348	530	286	179	206	157	289
All	233	131	112	75	192	242	219	215	96	222
50+	267	127	112	124	243	154	121	91	69	146
Hip fractures										
50+	27.7	7.6	9.2	8.3	25.1	13.2	5.3	4.9	3.9	12.3
80+	140.2	67.0	96.0	91.0	144.5	78.5	42.5	59.1	36.6	81.1

***Disclosures: Brya Matthews**, None*

SAT-419

See Friday Plenary Number FRI-419

SAT-420

Osteoporosis Risk Prediction by Machine Learning Approach Using Clinical and Metabolomic Data *Chuan Qiu[2], XIAO ZHANG[2], Anqi Liu[2], Luo Zhe[2], Qing Tian[2], Hui Shen[2], Hong-Wen Deng[2], Kuan-Jui Su[3], YUN GONG[2]. [2]Tulane University, United States. [2]Tulane University, , [3]Tulane.edu, United States

Osteoporosis, characterized by low bone mineral density (BMD), is an increasingly serious public health issue. So far, several traditional machine learning (ML) algorithms have been proposed for predicting osteoporosis risk. However, these models have shown relatively low accuracy in clinical implementation. Recently proposed deep learning (DL) approaches, such as deep neural network (DNN), which can discover knowledge from complex hidden interactions, offer a new opportunity to improve predictive performance. In addition, recent multi-omics studies showed that metabolomics has a great potential to identify predictive biomarkers for complex human diseases. Therefore, DL-based disease prediction methods, integrating multi-omics data such as metabolites, as well as conventional clinical factors, could be a promising approach for disease prediction and prevention. In this study, we aimed to assess whether DNN can achieve a better performance in osteoporosis risk prediction, especially by adding metabolomics data into the prediction model. By utilizing hip BMD and extensive demographic and routine clinical data of 2,376 subjects from the Louisiana Osteoporosis Study (LOS), we constructed a DNN framework for predicting osteoporosis risk and compared its performance in osteoporosis risk prediction with four conventional ML models, namely random forest (RF), artificial neural network (ANN), k-nearest neighbor (KNN), and support vector machine (SVM), as well as a traditional regression model termed osteoporosis self-assessment tool (OST). Model performance was assessed by area under the 'receiver operating curve' (AUC) and accuracy. By using 16 discriminative variables, we observed that the DNN approach achieved the best predictive performance (AUC = 0.793) in classifying potential osteoporosis (hip BMD T-score <= -1.0) and non-osteoporosis risk (hip BMD T-score > -1.0) subjects, compared to the other approaches. Feature importance analysis showed that the top 5 most important variables identified by the DNN model were weight, height, age, gender, and grip strength. Furthermore, we assessed the effects of metabolomics data on the predictive performance of these tested models. Notably, the predictive performance was further improved (AUC = 0.815) by integrating the metabolomics data into the DNN model. In conclusion, DNN was an effective algorithm for the early diagnosis and intervention of osteoporosis.

***Disclosures: Chuan Qiu**, None*

SAT-422

Higher Muscle Power and Strength are Associated with HR-pQCT Volumetric Bone Density, Microarchitecture and Strength: the Study of Muscle, Mobility and Aging *Elsa Strotmeyer[2], Nina Heilmann[2], Kerri Freeland[2], Tong Yu[2], Lauren S. Roe[3], Nicole Sekel[2], Kristen Koltun[2], Katelyn Guerriere[4], Julie Hughes[5], Bradley Nindl[2], Ashley Weaver[6], Paolo Caserotti[7], Peggy Cawthon[8], Anne Newman[2], Jane A. Cauley[9]. [2]University of Pittsburgh, United States. [2]University of Pittsburgh, , [3], , [4]Military Performance Division, United States Army Research Institute of Environmental Medicine, United States. [5]US Army Research Institute of Environmental Medicine, United States. [6]Wake Forest University, United States. [7]University of Southern Denmark, Denmark. [8]San Francisco Coordinating Center, United States. [9]UNIVERSITY OF PITTSBURGH, United States

Muscle and bone may be connected via mechanostat loading or by muscle-bone signaling. We hypothesized that higher muscle function in the Study of Muscle, Mobility and Aging (SOMMA) was associated with better high-resolution peripheral quantitative computed tomography (HR-pQCT) distal tibia (DT) and radius (DR) bone density (BMD), microarchitecture and strength, in the SOMMA Bone Study at year 1 (Pittsburgh, PA site, N=297; 59.0% women; 87.9% White; 77.2+/-4.6 years). Muscle function tests included best stair climb ascend power (Watts=W) of 3 stair climb laps, single leg press peak power (W; 40-70% 1-RM) and strength (1-RM, kg), and grip strength (kg). Muscle function was higher in men vs. women (all p<0.001). Partial correlations of muscle function and DT and DR outcomes adjusted for sex, age, race, limb length, height and weight were weak (all r<=0.2); though positive and significant for DT (failure load: all but grip strength, Ct.BMD: leg power and strength, Tt.Ar: leg power and strength, Ct.Ar: all, Tb.Ar: leg strength, and Ct.Th: leg power), and DR (failure load: all, Tt.Ar: leg/grip strength, Ct.Ar: stair climb power, Tb.Th: leg power, and Tb.Ar: leg/grip strength), which were mostly consistent for men and women. In multivariable linear regression, muscle function was associated with sex-specific z-score outcomes (except total BMD), and results varied by sex, tests, and DT/DR site (Table 1). For DT, more findings in women (N=152) were for leg power and leg/grip strength and only leg strength with Tt.Ar in men (N=109). For DR, more findings in women (N=137) were for stair climb power and in men (N=103) for grip strength. Higher muscle function was associated with higher DT Tt.Ar (women: grip strength; women and men: leg strength), DR Tt.Ar (men: leg power and strength) and DR failure load (women: stair climb power; men: grip strength). In women, higher muscle function was associated with higher Ct. outcomes (DT Ct.BMD: leg power and strength; DT Ct.Ar: all; DT Ct.Th: leg power, grip strength; DR Ct.BMD, Ct.Ar and Ct.Th: stair climb; DR Ct.Ar: grip strength), but higher DR Tb outcomes in men (Tb.Ar: leg strength; DR Tb.BMD and Tb.Th: grip strength). Higher muscle function in older women (power and strength) and men (mostly strength) was associated with varied tests and DT/DR outcomes, notably DR failure load which predicts fracture. Muscle-bone differences by sex for Ct vs. Tb bone and upper vs. lower extremity sites may also impact fracture risk.

Table 1. Multivariable linear regression of muscle function predictors (standardized β of stair climb power, leg power, leg strength and grip strength) and HR-pQCT sex-specific z-score outcomes in women and men

	Power				Strength			
	Stair climb power		Leg power		Leg strength		Grip strength	
	Women	Men	Women	Men	Women	Men	Women	Men
Outcomes	151±36	186±41	143±42	241±72	143±39	205±54	22±5 kg	34±8 kg
Distal tibial (DT)	W	W	W	W	kg	kg		
Est. Failure load, N	0.18†	0.10	0.13	0.16	0.09	0.18†	0.10	-0.02
Ct.BMD, mg/cm^3	0.16	0.10	***0.16****	0.13	***0.16****	0.10	0.08	-0.03
Tb.BMD, mg/cm^3	-0.07	0.01	-0.13	0.12	-0.14†	0.02	-0.10	-0.09
Tt.Ar, mm^2	0.08	-0.01	0.10	0.09	***0.13****	***0.19****	***0.13****	0.04
Ct.Ar, mm^2	***0.25****	0.08	***0.30****	0.11	***0.18****	0.14	***0.27****	0.05
Tb.Ar, mm^2	0.04	-0.01	0.03	-0.06	0.08	0.09	0.08	0.04
Ct.Th., mm	0.17†	0.06	***0.23****	0.08	0.11	0.03	***0.18****	0.04
Tb.Th., mm	-0.004	0.07	0.06	0.11	-0.07	0.02	0.02	0.04
Distal radial (DR)								
Est. Failure load, N	***0.22****	0.08	0.09	0.10†	0.05	0.14	0.15†	***0.20****
Ct.BMD, mg/cm^3	***0.23****	-0.15	0.11	-0.12	0.04	-0.14	0.11	-0.18†
Tb.BMD, mg/cm^3	-0.05	0.21†	-0.07	0.12	-0.01	0.08	-0.04	***0.21****
Tt.Ar, mm^2	-0.04	0.22†	-0.03	***0.22****	0.07	***0.29****	0.16†	0.18†
Ct.Ar, mm^2	***0.38****	-0.03	0.10	-0.03	0.04	0.02	***0.19****	0.04
Tb.Ar, mm^2	-0.09	0.17	-0.02	0.16	0.07	***0.25****	0.13†	***0.18****
Ct.Th., mm	***0.28****	-0.11	0.09	-0.07	-0.01	-0.13	0.09	-0.03
Tb.Th., mm	-0.02	0.08	0.06	0.17	0.02	0.03	-0.06	***0.22****

†p<0.10 and >0.05; ***p≤0.05; ****p<0.01;* Models adjusted for age (years), race (White/non-White), height (m), weight (kg), total activity counts (Actigraph), drinker (y/n), smoking (y/n), and comorbidity count (0-7), with tibial and radial outcomes respectively adjusted for tibia length and ulna length. Abbreviations: cortical BMD (Ct.BMD), trabecular BMD (Tb.BMD), total area (Tt.Ar), Ct. area (Ct.Ar), Tb. area (Tb.Ar), Ct. thickness (Ct.Th), Tb. thickness (Tb.Th).

***Disclosures: Elsa Strotmeyer**, None*

SAT-423

See Friday Plenary Number FRI-423

SAT-424

Comparison of Risk Factors for Initial Fragility Fractures vs. Recurrent Fractures *Lucas Steele[2], Amina Anwar[2], Aamir Kadri[2], Madhumathi Rao[2]. [2]University of Kentucky, United States. [2]University of Kentucky,

Fragility fractures refer to low trauma fractures and are often the first indication of underlying osteoporosis. The occurrence of a fracture sharply increases the risk of a second fracture by 2- to 3-fold, but other risk factors may also contribute to the occurrence of recurrent fractures. In this study, we aimed to characterize the differences between patients presenting with an initial fragility fracture and those presenting with a recurrent fracture, as this has yet to be performed in such a population.A retrospective chart review was performed to collect data pertaining to variables such as age, sex, race, BMI, comorbidity, osteoporosis risk factors, and types of fractures. Admission lab values were obtained for all patients, including metabolic, hematologic, inflammatory, and bone turnover markers. Categorical data were analyzed with Chi-squared analysis; means were compared using independent sample T-tests and sex, age, and BMI-adjusted means were compared using regression analysis with significance set at p=0.05.In total, we had 196 patients, mean age 78.1 +/- 9.6 years, 76.5% female; 92 patients presented with an initial fracture and 104 with a recurrent fracture. There were no significant differences in sex, BMI, or race, prior osteoporosis treatment history or osteoporosis risk factors such as cancer, steroid history, and tobacco exposure. Notably there was no difference in age (78.6 +/- 9.3 vs 77.7 +/- 10.0) between patients who presented with an index fracture compared to those with recurrent fractures. Patients presenting with an index fracture had higher baseline serum creatinine (1.12 vs 1.01, SE = 0.095, p = 0.001 after adjusting for sex and BMI). Patients with a prior fracture history also had a significantly higher prevalence of microvascular comorbidities (92.3% vs 81.5%, p = 0.024). Lastly, 63.3% of index fractures were femur fractures, compared to 53.8% in the recurrent group (p = 0.05).Our results suggest that patients presenting with recurrent fractures may be those who begin fracturing at a younger age and have more microvascular disease (hypertension and diabetes). Patients that presented with an index fracture appeared to have a higher overall baseline creatinine and were more likely to present with a femur fracture. Improved characterization of these differences would help with better risk stratification for preventive strategies.

***Disclosures: Lucas Steele**, None*

SAT-425

Clinical outcomes of COVID-19 infection in patients with osteoporosis: A nationwide cohort study in Korea *Seong Hee Ahn[1], Sung-Hyo Seo[2], Chai Young Jung[3], Dong Han Yu[4], Youngjoon Kim[1], Yongin Cho[1], Da Hea Seo[1], So Hun Kim[1], Jun-Il Yoo[5], Seongbin Hong[1]. [1]Department of Endocrinology and Metabolism, Inha University Hospital, Inha University School of Medicine, Republic of Korea. [2]Department of Research Planning, Gyeongsang National University Hospital, Republic of Korea. [3]Biomedical Research Institute, Inha University Hospital, Republic of Korea. [4]Big Data Department, Health Insurance Review and Assessment Service, Republic of Korea. [5]5Department of Orthopedic Surgery, Inha University Hospital, Inha University School of Medicine, Republic of Korea

Background: The association between comorbidities and severe COVID-19 outcomes has been extensively researched, but little is known about the clinical outcomes of COVID-19 patients with osteoporosis. To address this gap, we conducted a nationwide cohort study in Korea to investigate the clinical outcomes of COVID-19 patients with a history of osteoporosis before their infection.Methods: We conducted a retrospective cohort study using data from Health Insurance Review and Assessment Services encoded in the Observational Medical Outcomes Partnership Common Data Model. We included patients >=50 years old diagnosed with COVID-19 infection between 1 January 2020 and 30 April 2022 and stratified them into two groups according to a history of osteoporosis before COVID-19 infection. Clinical outcomes within 30 days after COVID-19 infection were analyzed using propensity score stratification and logistic regression analysis.Results: Of the 597,011 COVID-19 patients included in the study, 105,172 had a history of osteoporosis. COVID-19 patients with osteoporosis had a lower risk of mortality than those without osteoporosis (OR 0.82, P <0.002). However, among COVID-19 patients with osteoporosis, those who also had a history of fracture had a higher risk of mortality, pneumonia, hospitalization, major adverse cardiovascular events (MACE), and venous thromboembolism than COVID-19 patients without osteoporosis (OR 1.32-1.58, P<0.001 to P=0.001). In male COVID-19 patients, those with osteoporosis had an increased risk of pneumonia, hospitalization, and MACE compared to those without osteoporosis (OR 1.11-1.18, P<0.001 to P=0.026), and the risk of mortality was not significantly different between the two groups. In female COVID-19 patients, the risk of mortality was lower in those with osteoporosis than those without osteoporosis (OR 0.84, P<0.001).Conclusion: Our study suggests that patients with severe osteoporosis who have experienced fractures have an elevated risk of mortality and other severe complications with COVID-19. However, patients with osteoporosis who have not experienced fractures and have sought medical attention have demonstrated a lower risk of

mortality. Effective management of osteoporosis may result in better clinical outcomes in the context of COVID-19, despite the potential impact of deteriorating bone health itself on the severity of COVID-19 complications.*This study used OMOP-CDM data made by Health Insurance Review & Assessment Service.

***Disclosures: Seong Hee Ahn**, None*

SAT-426

PPI use is not associated with bone microarchitecture and bone strength in a 3-year follow-up study of FLS patients *MERLE SCHENE[1], MELISSA BEVERS[2], Wim Van Der Vijgh[3], Johanna Driessen[4], Lisanne Vranken[5], Robert van der Velde[6], HANNA C. WILLEMS[7], Joop Van Den Bergh[8], Caroline Wyers[9]. [1]Viecuri Medisch Centrum , , [2]VieCuri Medical Center, , [3]VU University Medical Center, , [4], Netherlands. [5]Department of Internal Medicine, VieCuri Medical Center; 2 NUTRIM School of Nutrition and Translational Research in Metabolism, Maastricht University, Netherlands. [6]Department of Internal Medicine, VieCuri Medical Center, Netherlands. [7]Amsterdam UMC, Netherlands. [8]VieCuri MC Noord-Limburg and Maastricht UMC, , [9]VieCuri Medical Centre, Netherlands

The use of proton pump inhibitors (PPI) has been associated with an increased fracture risk in observational studies. Proposed biological mechanisms include a decreased calcium absorption, hypergastrinemia and increased bone resorption. However, the association between PPI use and bone mineral density (BMD), bone microarchitecture and strength is inconsistent. The aim of this study was to assess the association between PPI use and bone microarchitecture and strength using high resolution peripheral quantitative CT (HR-pQCT). This three-year prospective cohort study included 323 patients aged >=50 years with a recent fracture (median age 62 [IQR 56-69], 68.7% women) who attended the Fracture Liaison Service (FLS) and had no treatment indication with anti-osteoporosis medication. At the FLS visit (T0), 63 (19.5%) patients used PPI. At baseline, female PPI users had a significantly higher BMI and more often probable sarcopenia (EWGSOP2) compared to non-users. Male PPI users had more often a hip/major fracture than non-users. In both men and women, PPI users had more cardiovascular co-morbidities than non-users. HR-pQCT scans of the distal radius and tibia were acquired at T0 and at three-year follow-up (T3). Scans of sufficient quality at T0 and T3 were available for assessment of bone microarchitecture and strength in 166 women at the distal radius (33 PPI-users and 133 in non-users) and 190 at the distal tibia (34 and 156, respectively) and for 76 men at the distal radius (14 and 62) and 90 men at the distal tibia (19 and 71). Sex-stratified linear regression analyses were used to investigate the association between PPI use and bone microarchitecture and strength parameters at T3. Covariates included age, HR-pQCT parameter at T0, vitamin-D deficiency (<30 nmol/L), prednisone use, and cardiovascular co-morbidity in the models for men and women. In men, fracture type (major/hip vs. all others) and in women probable sarcopenia were additional covariates. In both men and women, when compared to non-use, PPI use was not associated with bone microarchitecture and strength at T3 at the distal radius and tibia, except for a marginally decreased trabecular thickness at the distal radius in men (B= -0.003, p=0.048). To conclude, PPI-use was not associated with bone microarchitecture and strength in FLS patients at 3 years of follow-up. This indicates that bone quality might not be related to fracture risk of PPI users found in observational studies.

***Disclosures: MERLE SCHENE**, None*

SAT-427

Cardiovascular events and bone fragility in a large population: a study based on the CARTaGENE cohort *Clément Vachey[1], Aurélie Dufour[2], Laetitia Michou[2], Claudia Gagnon[1], Mohsen Agharazii[1], Fabrice Mac-Way[3]. [1]CHU de Quebec, Universite Laval, Canada. [2]Universite Laval, Canada. [3]L Hotel-Dieu de Quebec, Canada

Purpose: An association between bone fragility and cardiovascular health has been previously reported. Our study aimed to evaluate the impact of osteoporosis on cardiovascular events (CVE) risk in the Quebec (Canada) population.Methods: From the large population-based cohort CARTaGENE, which represents 1% of the Quebec population aged from 40 to 70 years old, recruited between 2009 and 2010, we studied the impact of osteoporosis on CVE risk in subjects without any prior CVE. We then evaluated the impact of fragility fractures, occurring after 40, on CVE risk. A semi-parametric Cox model was used with adjustment for age, cardiovascular risk factors and medications. We also investigated whether sex was an effect modifier.Results: We included 18 644 subjects (mean age 54.2+/-7.9, women 52.9%, osteoporosis 4.4%, prior fragility fracture 7.8%). We observed a total of 342 CVE after a median follow-up time of 5.8 years. In multivariable analyses adjusted for cardiovascular risk factors, a diagnosis of osteoporosis was associated with a significant increased risk of CVE (Hazard Ratio (HR) =1.60, 95% confidence interval (95%CI): 1.02-2.50). We did not observe any effect modification by sex on this association. The occurrence of a fragility fracture after 40 was not marginally associated with a significant increased risk of CVE (HR=1.14, 95%CI: 0.78-1.66). However, there was a substantial increased risk in women (HR=1.89, 95%CI: 1.08-3.30) versus men (HR=0.82, 95%CI: 0.49-1.39). After adjustment for potential confounding medications, osteoporosis was still associated with CVE risk (HR=1.55, 95%CI: 0.99-2.44) while fragility fractures was associated with CVE risk only in women (HR=1.85, 95%CI: 1.06-3.24).Conclusion: In a relatively young and low cardiovascular risk population, osteoporosis is associated with CVE while the occurrence of a fragility fracture after 40 is associated with cardiovascular morbidity only in women.

***Disclosures: Clément Vachey**, None*

SAT-428

Force Plate Leg Power and Velocity Was Associated With the Risk of Major Osteoporotic Fractures (MOF): the Osteoporotic Fractures in Men Study (MrOS) *Tong Yu[1], Elsa Strotmeyer[1], Nina Heilmann[1], Deborah Kado[2], Kristine Ensrud[3], Mary Winger[4], Paolo Caserotti[5], Peggy Cawthon[6], Jane Cauley[1]. [1]University of Pittsburgh, United States. [2]Stanford University, United States. [3]University of Minnesota, Minneapolis VA Health care system, United States. [4]UPMC Insurance Services Division, United States. [5]University of Southern Denmark, United States. [6]University of California San Francisco, California Pacific Medical Center, Research Institute, United States

MOFs are clinical fractures at the vertebrae, hip, wrist and humerus, which may negatively impact physical function and quality of life. Previous studies found that lower extremity muscle function is associated with risk of falls and fractures, however, most studies have examined strength (force), but not power (force*velocity). A novel jump test on a force plate measures weight-bearing leg power and allows the dissection of peak power into its components, force and velocity. We investigated the association between jump test leg power measures and MOF risk in men from the MrOS study.The study included 1841 older men (median age 84 years, range 77-101 years) who completed the Year 14 visit (2017). Peak jump power (Watt/kg body weight), force (Newton/kg body weight) at peak power, and velocity (m/s) at peak power were measured by jump tests on a force plate at Year 14 visit. Follow-up times were truncated at 5 years to avoid extrapolating the effect of leg power on fractures. Fractures were identified by triannual questionnaires, with all self-reported fractures confirmed by medical record. Cox proportional hazards models were used to estimate hazard ratios (HR) and 95% Confidence Intervals (CIs) of MOFs by continuous (per one SD increment) and quartiles of jump test measurements. Participants that did not do jump tests mainly due to low physical function were classified into the "lowest" power group (referent).Incident clinical fractures occurred in 265/1841 (14%) within 5 years, of which 136 (51%) were MOFs. In the fully adjusted model, one SD increment of peak power/kg body weight was associated with 29% lower risk of MOF (HR 0.71, 95% CI 0.54-0.92). Similarly, one SD increment of velocity at peak power was associated with 24% lower risk of MOF (HR 0.76, 95%CI:0.59-0.98). Further adjustment of femoral neck (FN) bone mineral density (BMD) and fall history did not attenuate the association. Compared to the referent group, the fourth (highest) quartile of power and velocity were also significantly associated with decreased risk of MOF, P=0.003 and P=0.025 for trend, respectively. For force at peak power, only the highest quartile was significantly associated with lower risk of MOF, but not after adjusting for FN BMD.Peak leg power and velocity, but not force, during a force plate jump test predicted MOF risk independent of FN BMD. Power, which incorporates velocity, may play a more important role than force in reducing the risk of a fracture.

Table 1. Hazard ratio estimates from Cox regression models for associations between jump test measures and major osteoporotic fracture risk.

Variable	Fully[1] adjusted (n=83/1230) cont[2] (n=136/1819) quar[3]		Fully adjusted + FN BMD (n=80/1209) cont (n=130/1768) quar		Fully adjusted + fall history (n=83/1230) cont (n=136/1819) quar	
	HR	95% CI	HR	95% CI	HR	95% CI
Peak power (Watts/kg)						
Per 1 SD increment	**0.71**	**0.54 - 0.92**	**0.69**	**0.53 - 0.92**	**0.73**	**0.56 - 0.95**
4th quartile (highest)	**0.35**	**0.17 - 0.74**	**0.31**	**0.14 - 0.68**	**0.39**	**0.18 - 0.82**
3rd quartile	0.62	0.35 - 1.07	0.63	0.36 - 1.12	0.65	0.37 - 1.14
2nd quartile	1.10	0.69 - 1.75	1.06	0.66 - 1.73	1.18	0.74 - 1.89
1st quartile	0.93	0.57 - 1.52	1.00	0.61 - 1.66	0.97	0.59 - 1.59
Unable (lowest, referent)	1.0 (ref)		1.0 (ref)		1.0 (ref)	
P trend	**0.003**		**0.002**		**0.007**	
Velocity at peak power (m/s)						
Per 1 SD increment	**0.76**	**0.59 - 0.98**	**0.73**	**0.56 - 0.95**	0.78	0.61 - 1.01
4th quartile (highest)	**0.48**	**0.25 - 0.93**	**0.42**	**0.22 - 0.83**	0.53	0.27 - 1.01
3rd quartile	0.81	0.48 - 1.36	0.84	0.49 - 1.44	0.88	0.52 - 1.48
2nd quartile	0.77	0.46 - 1.31	0.76	0.44 - 1.29	0.83	0.49 - 1.41
1st quartile	1.00	0.61 - 1.64	1.10	0.67 - 1.82	1.04	0.63 - 1.69
Unable (lowest, referent)	1.0 (ref)		1.0 (ref)		1.0 (ref)	
P trend	**0.025**		**0.010**		0.052	
Peak force (N/kg)						
Per 1 SD increment	0.85	0.66 - 1.08	0.90	0.69 - 1.16	0.86	0.67 - 1.10
4th quartile (highest)	**0.51**	**0.26 - 0.99**	0.50	0.25 - 1.01	0.54	0.28 - 1.05
3rd quartile	0.87	0.52 - 1.45	0.96	0.57 - 1.61	0.95	0.57 - 1.58
2nd quartile	0.61	0.35 - 1.07	0.58	0.33 - 1.03	0.65	0.37 - 1.15
1st quartile	1.05	0.66 - 1.67	1.04	0.65 - 1.68	1.10	0.69 - 1.76
Unable (lowest, referent)	1.0 (ref)		1.0 (ref)		1.0 (ref)	
P trend	**0.038**		0.061		0.062	

[1] Full adjustment includes age, race/ethnicity and clinical sites, smoke, alcohol use, height, number of comorbidities.
[2] MOF events / Number at risk in model with continuous jump test measures.
[3] MOF events / Number at risk in model with quartiles of jump test measures.
[4] Significant HRs in bold font.

***Disclosures: Tong Yu**, None*

Saturday Orals

SAT-429

See Friday Plenary Number FRI-429

SAT-430

OsteoboostTM Is Effective in Preserving Bone Strength and Density of the Spine in Women with Low Bone Mass *Laura Bilek[2], LAURA FLORES[2], Nancy Waltman[3], Lynn Mack[3], Derek Hillstrom[4], Laura Yecies[4], Kara Smith[5], Meghan Griffin[4], Michael Jaasma[4]. [2]UNIVERSITY OF NEBRASKA MEDICAL CENTER, United States. [2]UNIVERSITY OF NEBRASKA MEDICAL CENTER, , [3]University of Nebraska Medical Center, United States. [4]Bone Health Technologies, United States. [5]Universithy of Nebraska Medical Center, United States

Introduction: Fragility fractures result in significant morbidity and mortality, which is of particular concern in postmenopausal women who are at high risk of fractures due to loss of estrogen. Pharmaceutical interventions are effective but have low uptake and adherence and are generally not indicated for patients with osteopenia. Vibration has the potential to prevent bone loss and holds promise as an effective, yet minimal risk, treatment. The OsteoboostTM, a novel wearable device delivering targeted vibration to the lumbar spine and hips, is designed to improve bone strength and bone density. Thus, this study aims to evaluate the efficacy of a 12-month intervention with the Osteoboost on preserving strength of the first lumbar vertebrae in postmenopausal women with low bone mass.Methods: This double-blinded, randomized controlled trial enrolled postmenopausal women with low bone mass who were not taking bone-active medications. Women had a bone density DXA and assessment of thyroid function to screen for eligibility Those who qualified were randomized to receive Osteoboost treatment 5x/week for 12 months with the belt in either the active or sham setting. The sham device created a sound but did not deliver vibration. Compressive strength (N) and volumetric density of the 1st lumbar vertebra (L1) was analyzed using Finite Element Analysis (FEA) of computed tomography (CT) scans of lumbar spine by ON Diagnostics.Results: 126 women (64 Active, 62 Sham) with low bone mass participated in the study, with an average age of 62.1 years (SD +/- 5.8) and 60.6 years (+/- 5.3) in the Active and Sham groups, respectively. Most participants were of White race (98%) and non-Hispanic (96%). There were no significant differences in baseline demographics between the sham and active groups.Intent to treat analysis revealed no significant difference in percent change in vertebral bone strength between the Active and Sham groups over time (baseline to 12 months). When stratified by age category, significant differences in percent change in vertebral bone strength were present in the 50-60 year old category; the Sham group lost 3.4% of their vertebral bone strength compared to a 0.5% loss in the Active group (p=0.018). While bone was preserved in the active group relative to the sham in the women over 60, it was not significant (p=0.20). With analysis of those who met the compliance criterion of 3x/week, the Sham group lost 2.84% compared to 0.48% in the Active group (p=0.014); representing a 5 times greater loss in the Sham group. Additionally, the Osteoboost treatment preserved volumetric bone density of L1, with the Active treatment group losing 0.29% BMD relative to a 1.97% loss in the Sham group; representing a 6.8 times greater loss in the Sham group (p=0.008).Conclusion: Osteoboost holds promise as a therapeutic intervention for women with low bone mass to prevent decline to osteoporosis and reduce fracture risk.

***Disclosures: Laura Bilek**, Bone Health Technologies, Grant/Research Support, Bone Health Technologies, Consultant*

SAT-432

Does femoral bowing expedite bisphosphonate-related atypical femoral fracture? *Dong Won Byun[1], Young-Kyun Lee[2], Hyoung-Moo Park[3], Deog-Yoon Kim[4], Yong-Chan Ha[5]. [1]Soonchunhyang University Hospital, Republic of Korea. [2]Seoul National University Bundang Hospital, Republic of Korea. [3]Grace Women Hospital, , Republic of Korea. [4]Kyung Hee University Medical Center, Republic of Korea. [5]BUMIN Hospital, Republic of Korea

Background ; Long-term use of bisphosphonate is a risk factor for atypical femoral fractures (AFFs). Femoral bowing is known to be associated with diaphyseal AFFs. However, whether the femoral bowing quickens the occurrence of AFF is unknown. We hypothesized severe anterolateral femoral bowing expedites the occurrence of AFF.Purpose ; The purpose of this study was to determine whether AFF occurs earlier in patients with severe femoral bowing than in those without severe bowing.Methods; One hundred and sixty-six AFF patients (179 AFFs), who were diagnosed from January 2006 to December 2018, were eligible for this study. Among them, we excluded 41 patients (42 AFFs), who had bony metastasis or metabolic bone disease, in whom the duration of bisphosphonate use was uncertain, or in whom the femoral bowing could not be measured. The remaining 125 patients (137 AFFs) were subjects of this study. According to severity of the femoral bowing, patients were divided into two groups; (1) severe bowing group (the line between the tip of the greater trochanter and the center of the intercondylar notch passes medial to the medial cortex of the femoral shaft, 20 patients) and (2) non-severe bowing group (105 patients). We compared the time of AFF occurrence after bisphosphonate therapy using cumulative percentage between the two groups.Results; Age and gender were similar between the two groups, while body mass index was lower in the severe bowing group. The duration of bisphosphonate use was shorter in the severe bowing group (3.2+/-3.6 years) than in the non-severe bowing group (4.7+/-4.2 years). However, the difference was not statistically significant (p=0.114). Cumulative percentage plot of AFFs in the severe bowing group was left-shifted compared to the non-severe bowing group.Conclusion; Severe femoral bowing expedites AFF development. In osteoporosis patients with severe femoral bowing, the duration of bisphosphonate use should be shortened.

***Disclosures: Dong Won Byun**, None*

SAT-433

Drug utilization patterns of anabolic agents - romosozumab and parathyroid hormone analogues - among postmenopausal women in the U.S., 2019-2021 *Hsu-Chih Chien[1], Ye Liu[2], Tzu-Chieh Lin[1], Tarun Arora[3], Mary Oates[1], MICHELE MCDERMOTT[1], Jeffrey Curtis[2]. [1]Amgen, United States. [2]University of Alabama at Birmingham, United States. [3]Foundation for Advancing Science Technology Education and Research, United States

BackgroundRomosozumab (Romo) and parathyroid hormone analogues (PTHA) are anabolic agents for postmenopausal women with osteoporosis (OP) at high risk of fracture. This study aims to describe the real-world utilization patterns of Romo and PTHA in the early period following Romo's U.S. approval.MethodsWomen >=66 years old who newly initiated Romo or PTHA (teriparatide or abaloparatide) were identified in Medicare Fee-For-Service Claims data (Medicare FFS) during April 1, 2019-October 1, 2021. The 12-month adherence (the proportion of days covered [PDC] by medication) and interruption (defined as a patient who did not refill a medication within 30 days after exhaustion of the days' supply of the previous dispensing, or usual dosing interval) were calculated for both Romo and PTHA groups. Kaplan-Meier method was applied to estimate the interruption rate and 95% confidence interval [CI], with censoring points of completing 12 doses, death, disenrollment, and the end of the follow up or the end of data (September 30, 2021). In a subgroup of Romo users with >=15 months available follow-up time, completion rates of 12-doses and follow-up treatment sequences (where individuals were required to have at least 1 additional month of coverage) were described.ResultsWe identified 8,408 new Romo and 7,428 PTHA users in Medicare FFS data. Romo users were slightly older (76.1+/-6.8 vs 75.5+/-6.8 years) and with less recent fracture history (33.4% vs. 38.3%) and higher previous OP treatment history (59.4% vs. 45.7%). Higher 12-month adherence was found among Romo users (PDC, Romo: 73.8+/-28.3%; PTHA: 57.3+/-33.8%. p<0.01). Lower 12-month interruption rate was observed among Romo users (Romo: 52.8%, 95% confidence interval [CI]: 50.6-54.9%; PTHA: 62.7%, 95% CI: 60.6-64.9%). Among individuals with >=15 months data available, 57.9% Romo users completed 12 doses. 21.8% of completers did not receive any OP treatment following the completion. Among those switching to another OP therapy following Romo treatment completion, denosumab was the most often used (83.2%) OP medication (Table 1).ConclusionWe observed higher adherence and fewer interruptions among Romo users versus PTHA users in the Medicare population. While more than half of Romo users completed the 12-doses within 15 months, a meaningful fraction (>20%) did not receive subsequent treatment, despite treatment guideline recommendations advising following Romo with antiresorptive therapy to prevent bone density decline.

Table 1: Selected baseline characteristics and utilization patterns in new romosozumab and PTH analogue users in Medicare FFS

	Romosozumab*,[a] users (N= 8,408)	PTHA users* (N= 7,428)
Age (mean [SD])	76.1 (6.8)	75.5 (6.8)
Osteoporosis related health information (n, %)[b]		
Fracture history (any sites)	3660 (43.5)	3388 (45.6)
Recent fracture history (any sites)[c]	2805 (33.4)	2846 (38.3)
History of OP medication use	4997 (59.4)	3391 (45.7)
Utilization pattern		
Adherence (PDC, %)		
By the end of the 6th month		
Mean (SD)	80.6 (24.7)	67.4 (30.7)
>=80%	71.3	50.7
By the end of the 12th month		
Mean (SD)	73.8 (28.3)	57.3 (33.8)
>=80%	62.4	39.4
Interruption (KM estimates [95% CI], %)		
By the end of the 6th month	33.3 (31.6, 35.1)	45.4 (43.4, 47.4)
By the end of the 12th month	52.8 (50.6, 54.9)	62.7 (60.6, 64.9)
Treatment completion in Romo users with >=15 months follow up time		
	N=4,858	
Completion rate (n, %)	2,811 (57.9)	
Next OP medication in Romo completers with >=1 month of follow up time		
	N=2,770	
No next OP medication	603* (21.8)	
Next OP medication	N=2,167*	
Denosumab	1,804 (83.2)	
Oral BP[d]	39 (1.8)	
IV zoledronic acid	313 (14.4)	
PTHA[c]	<11 (<0.5)	

BP: bisphosphonate, IV: intravenous, OP: osteoporosis, PTHA: parathyroid hormone analogues, Romo: romosozumab, PDC: proportion of days covered by medication, KM: Kaplan-Meier, CI: confidence interval
*Romosozumab and PTH analogues users were both identified with specific codes of National Drug Code and Healthcare Common Procedure Coding System (HCPCS codes). [a]Validated algorithm was implemented to identify romosozumab records in Medicare data before the issue of specific HCPCS codes for romosozumab in October 2019. [b]Defined with all available historical data except for those specified. [c]Fracture occurred within a year before the index date [d]The use of oral BP and PTHA after Romo completion might be under captured given incomplete part D coverage during the follow up time.

***Disclosures: Hsu-Chih Chien**, Amgen, Other Financial or Material Support*

SAT-434

See Friday Plenary Number FRI-434

SAT-435

Daily Administration of An Oral Robotic Pill (RT-102) Safely and Reliably Delivers Teriparatide with High Bioavailability in Women Volunteers: A Phase I Study *Joshua Myers, MS[1], Anvesh Dasari, PhD[1], Archana Battiwala, MS[1], Nidhi Patel, MS[1], April Toledo Vo, MS[1], Alyson Yamaguchi, DVM[1], Kyle Horlen, DVM[1], Leonard Fung, MS[1], Baber Syed, MS[1], Son Nguyen, PhD[1], Jacques Van Dam, MD, PhD[1], Mir Imran, BS[1], Mir Hashim, PhD[1], Arvinder Dhalla, PhD[1]
[1]Rani Therapeutics, United States

Purpose: Teriparatide, an effective osteoanabolic agent, requires chronic daily subcutaneous (SC) injections which can impact patient compliance and quality of life. We have developed an oral robotic pill (RP) designed to deliver biotherapeutic agents with bioavailability rivaling that of parenteral injections. Here we present data from a Phase I study on the safety and tolerability of repeat administrations of an oral RP containing teriparatide (RT-102), 20µg, in healthy and post-menopausal women volunteers. Methods: Every day for 7 consecutive days, overnight-fasted participants (N=17) orally ingested a single RT-102 capsule followed by a meal 3 hours later. Fluoroscopic images were taken daily to track the transit and deployment status of the RP in the GI tract. During Days 1-6, drug delivery success was determined by the detection of drug in at least one of 3 blood samples taken at 3-hour intervals every day following the oral dose. On Day 7, a full PK profile of RT-102 was generated from serially collected serum samples in which teriparatide was quantified using an ELISA. Results: Safety: A total of 104 RT-102 capsules were swallowed by study participants with no observed serious adverse events (SAEs). Seven participants were excluded per protocol with 10 completing the full study. Mild and transient adverse events (AEs) observed in 4 participants were attributed to either the drug (2) or the device (3). No participants were excluded due to any RT-102-related AEs. In all participants, capsule remnants were excreted without sequelae within 1.9 +/- 0.9 days. Reliability: Based on detectable drug levels in the 10 participants who completed the study, the overall success rate of drug delivery was 91% (63/69 capsules). Bioavailability: With a Cmax of 296 +/-243 pg/mL and a Tmax of 57 +/- 35 minutes, RT-102 delivered teriparatide with higher estimated bioavailability compared to that of historical Forteo® SC data. Effect of Food: During Days 1-6, similar rates of successful deployments of RT-102 occurred before (35) and after food was consumed (37), suggesting that the presence of food did not impact RP performance. Conclusions: This study provides the first clinical evidence of safe and successful repeat delivery of oral teriparatide administered daily to human participants via the RP with high reliability and bioavailability. These data suggest that RT-102 can potentially offer an oral osteoanabolic treatment option to osteoporosis patients.

***Disclosures: Joshua Myers, MS**, Rani Therapeutics, Other Financial or Material Support*

SAT-436

Safety and Immunogenicity of Proposed Denosumab Biosimilar GP2411 Compared with Reference Denosumab in Postmenopausal Women with Osteoporosis at 78 Weeks: The Randomized, Double-Blind, ROSALIA Study *S?awomir Jeka[1], Eva Dokoupilová[2], Alan Kivitz[3], Susmit Sekhar[4], Samik Banerjee[4], Natalia Krivtsova[4], Johann Poetzl[4], Arnd Schwebig[4], Jean-Jacques Body[5], Richard Eastell[6]. [1]Clinic and Department of Rheumatology and Connective Tissue Disease, University Hospital No.2. Bydgoszcz, Collegium Medicum in Bydgoszcz, UMK, Poland. [2]Masaryk University, Faculty of Pharmacy, Department of Pharmaceutical Technology, Czech Republic. [3]Altoona Center for Clinical Research, United States. [4]Hexal AG, Germany. [5]Department of Medicine, University Hospital Brugmann, Belgium. [6]Department of Oncology and Metabolism, University of Sheffield, United Kingdom

BackgroundDenosumab is a human monoclonal antibody to RANK ligand for osteoporosis in postmenopausal women with high fracture risk. Similarity of GP2411, a proposed denosumab biosimilar, with reference denosumab (ref deno) has been demonstrated at 52 weeks; here we report cumulative 78-week data, including a treatment switch.MethodsROSALIA (NCT03974100) was an international, double-blind, parallel group, Phase III study postmenopausal women with osteoporosis aged 55-80 years, with a bone mineral density (BMD) T-score <=-2.5 and >=-4.0 at the lumbar spine (LS-BMD). Patients were randomized (1:1) to 60 mg s.c. of GP2411 or EU-authorized ref deno on Day 1 and Week 26. Prior to the third dose at Week 52, patients in the ref deno group were re-randomized (1:1) to ref deno or GP2411 (switch period). Safety and immunogenicity (binding anti-drug antibodies [ADAs] and neutralizing antibodies [NAbs]) were assessed in the switch period. Efficacy was analyzed descriptively with percentage change from baseline (%CfB) in LS-BMD, femoral neck BMD (FN-BMD), and total hip BMD (TH-BMD). Outcomes were evaluated up to Week 78.ResultsIn subjects who reached Week 52 and received a third dose (502 of 527 randomized), the cumulative (78 week) incidence rate of all-grade treatment-emergent adverse events (TEAEs) was similar between groups. Most TEAEs were Grade 1 or 2 and not treatment related (Table 1); none led to study or treatment discontinuation. The most common TEAEs were hypocalcemia, COVID-19 infection, and nasopharyngitis; there were no fatal or serious treatment-related TEAEs. The vast majority of observed ADAs had very low, non-reportable titers (<20 ng/mL), were non-neutralizing, and transient (Table 2). There were no clinically meaningful differences between groups in the rate of new vertebral fractures (GP2411/GP2411: 9.9%; ref deno/ref deno: 13.6%; ref deno/GP2411: 13.7%) or in %CfB of LS-BMD, FN-BMD, or TH-BMD. Switching from ref deno to GP2411 did not affect the incidence and severity of TEAEs, and immunogenicity profiles were similar between groups. ADAs were not associated with hypersensitivity reactions.ConclusionsROSALIA demonstrated comparable safety, immunogenicity, and efficacy up to 78 Weeks between proposed denosumab biosimilar GP2411 and ref deno in postmenopausal women with osteoporosis, with switching to GP2411 having no impact.

Table 1. Summary of 78 weeks cumulative safety data in patients who received a third treatment dose at Week 52.

Category	GP2411/GP2411 N=253 n (%)		Ref deno/ref deno N=125 n (%)		Ref deno/GP2411 N=124 n (%)	
	All grades	Grades 3–4	All grades	Grades 3–4	All grades	Grades 3–4
TEAEs	161 (63.6)	14 (5.5)	95 (76.0)	6 (4.8)	95 (76.6)	4 (3.2)
Treatment-related	38 (15.0)	0	27 (21.6)	0	25 (20.2)	0
Serious TEAEs[a]	13 (5.1)	10 (4.0)	5 (4.0)	3 (2.4)	2 (1.6)	0
Fatal serious TEAEs[b]	0	0	0	0	0	0

Deno, denosumab; ref, reference; TEAEs, treatment-emergent adverse events.
Column headings indicate the treatment used prior to/after the switch. A patient with multiple severity grades for an adverse event is only counted under the maximum grade. MedDRA version 25.0, CTCAE version 5.0.
[a]No serious TEAEs were treatment related.
[b]In the period prior to administration of the third dose, there was one fatal serious TEAE in the GP2411 group that was considered not related to study drug.

Table 2. Summary of 78 weeks cumulative ADA status in patients who received a third treatment dose at Week 52.

	GP2411/GP2411 N=253 n (%)	Ref deno/ref deno N=125 n (%)	Ref deno/GP2411 N=124 n (%)
ADA positive	113 (44.7)	58 (46.4)	60 (48.4)
ADA titer positive[a]	2 (0.8)	2 (1.6)	0
NAb positive	2 (0.8)	1 (0.8)	1 (0.8)
Transient[b]	108 (42.7)	53 (42.4)	57 (46.0)
Persistent[b]	5 (2.0)	5 (4.0)	3 (2.4)

Deno, denosumab; ref, reference.
Column headings indicate the treatment used prior to/after the switch.
[a]'ADA titer positive' indicates a patient with a positive ADA result and a reportable titer value. Remaining patients experiencing a positive ADA result outside this category had non-quantifiable titers (<20 ng/mL).
[b]'Persistent' indicates a patient experiencing a positive ADA result at the final visit and with at least 2 consecutive positive ADA results. 'Transient' indicates a patient experiencing a positive ADA result but not qualifying as 'Persistent'.

***Disclosures: S?awomir Jeka**, None*

SAT-437

See Friday Plenary Number FRI-437

SAT-438

12 months experience with romosozumab: A real-life descriptive study *Mariana Gonzalez Pernas[1], Jesica Pingel[1], Natalia Lopacsek[1], Vanesa Longobardi[1], Paula Garibaldi[1], Lorena Conejos[1], Patricia Slavinsky[1], Soledad Sosa[1], Marcelo Sarli[1], Mariela Sesta[1], Maria Belen Zanchetta[1]. [1]IDIM, Argentina

Introduction: Recent guidelines recommend romosozumab (ROMO) as initial therapy for women with a very high risk of fracture, including those with a very low T-score (< -3.0), high fracture probability by FRAX, or multiple vertebral fractures. ROMO can also be used to reduce vertebral, hip, and nonvertebral fractures in cases of previous osteoporosis therapy failure. ROMO became available in Argentina in August 2021. This study aims to describe the baseline characteristics and 12-month outcomes of the first 10 postmenopausal women who completed ROMO treatment.Methods: A prospective study to assess clinical and densitometric features (spine, hip, and radius), muscle health (performance, hand grip (HG), IMME by DXA), spine RX, fatigue (FACIT), bone microarchitecture by HR-pQCT and bone biomarkers. This partial cross-sectional analysis includes clinical, BMD, muscle quality, vertebral fracture assessment of the first 10 postmenopausal women who completed 12 months of ROMO treatment until April 2023.Results: The study population had a median age of 76 (54-82) yo and all had a history of fractures: wrist (1), hip (1), and vertebral (9 (17 VTFx)). Half of them had two or more vertebral fractures, and all of them with imminent fracture risk. 30% of the patients were treatment-naïve, while the rest had received one or more drugs: 70% bisphosphonates, 20% sequential treatment (teriparatide-denosumab); mean treatment duration was 11.2 years. Baseline densitometric values (T-Score) reflected osteoporosis: LS -3, FN -2.2, and TH -2.3. After 12 months of ROMO treatment, there were significant increases in BMD at all measured sites: 12.9% LS, 3.6% FN, and 3.4% TH. Mean final T-score was -2.3 in LS, -2.1 FN, and -2 TH (p=0.03, p=0.02). No new fractures were reported in these patients. Mean baseline HG, sit-stand, and IMME values were: 14+/-2kg, 12+/-2s, and 6.1+/-0.9kg/m2. A significant improvement in muscle strength tests was observed with 12 months of treatment: HG 16,6+/-3kg (+18,5%), SS 9.8+/-3s (-18%) (p=0.04). Discussion: Beyond the limitations of the use of new osteoactive treatment in real life, in this study we show that the results are similar to those reported in pivotal studies. Treatment with ROMO can effectively improve BMD in postmenopausal women with very high-risk osteoporosis. It also seems to have a positive effect on muscle mass, however more studies are needed to confirm these data.

***Disclosures: Mariana Gonzalez Pernas**, None*

SAT-439

Effects of denosumab or zoledronic acid on bone density and muscle mass in drug-naive patients with postmenopausal osteoporosis : multicenter 3-year observational study *Jeonghoon Ha[1], Jinyoung Kim[1], Chaiho Jeong[1], Jeongmin Lee[1], Yejee Lim[2], Ki-Hyun Baek[1]. [1]The Catholic University of Korea, Republic of Korea. [2]Seoul National University Bundang Hospital, Republic of Korea

Objectives: Denosumab and zoledronic acid are potent anti-resorptive agents used to treat osteoporosis in postmenopausal women. However, limited research exists on their direct comparison in drug-naïve patients. This study aimed to compare the effects of denosumab and zoledronic acid in drug-naïve Korean postmenopausal women with osteoporosis. Methods: This prospective, observational, nonrandomized study included 120 patients, with 60 receiving denosumab and another 60 receiving zoledronic acid. Throughout the 3-year treatment period, patients were monitored for bone density and biochemical parameters, and changes in skeletal mass were evaluated using bioelectric impedance analysis.Results: Baseline characteristics, including age, BMI, and prevalent fracture, were similar between the two groups. Serum 25(OH), Ca, and P levels, as well as baseline bone mineral density (BMD), were also comparable between the groups before treatment. After the 3-year treatment period, both groups demonstrated significant increases in BMD from baseline. The denosumab group exhibited a BMD increase of 9.7% at the lumbar spine and 5.1% at the total hip, while the zoledronic acid group showed a BMD increase of 7.1% at the lumbar spine and 4.4% at the total hip. However, only the denosumab group displayed a significant increase in skeletal muscle mass at 1 year, with a notable increase in those with a baseline T score of -3.0 or lower.Conclusions: In conclusion, both denosumab and zoledronic acid are effective anti-resorptive agents with significant increases in BMD observed over the 3-year treatment period in drug-naïve patients. Nonetheless, denosumab may be a more suitable initial treatment option for patients with combined osteosarcopenia due to its significant increase in skeletal muscle mass.

***Disclosures: Jeonghoon Ha**, None*

SAT-441

Zoledronic acid dosing frequency among older adults in the community *Kaleen Hayes[1], Natalia Konstantelos[2], Angela Cheung[3], Suzanne Cadarette[2]. [1]Brown University, . [2]University of Toronto, Canada. [3]University Health Network-University of Toronto, Canada

Background: Zoledronic acid (ZOL, 5mg/100mL) is typically administered annually in outpatient infusion clinics to treat osteoporosis. A post-hoc analysis identified similar fracture protection when ZOL was dosed every 18 months compared to annual dosing. Evidence on ZOL dosing frequency in real-world practice is limited.Objectives: To describe ZOL dosing frequency overall and by prior osteoporosis medication history among older community-dwelling adults.Methods: We identified community-dwelling residents aged >=66 years initiating ZOL between 01/2006-10/2021 using Ontario healthcare administrative data. We excluded those who had a malignant cancer diagnosis captured through the Ontario Cancer Registry, a history of bone-related health conditions (e.g., Paget's disease), or a second dose administered within 31 to 334 days after the initial dose (to identify potential off-label dosing for cancer). We looked forward until October 31, 2022 to identify subsequent dispensings of ZOL after initiation. We described each patient's history of other osteoporosis medication use (oral bisphosphonates [alendronate/risedronate], denosumab, other [calcitonin, etidronate, raloxifene, teriparatide]) within 5 years prior to ZOL initiation. For patients with more than one administration of ZOL, we described the median length of time between each dose and described the number and timing of ZOL doses by other osteoporosis medication history.Results: We identified 4,337 eligible patients starting ZOL (average age 76 [SD 6.9] years, 82% female). Fifty-eight percent had a history of osteoporosis pharmacotherapy: 45% alendronate or risedronate, 10% denosumab, and 3% another osteoporosis medication (primarily raloxifene or etidronate). Among all ZOL initiators, 64% received only 1 dose during follow-up, 18% received 2 doses, and 18% received 3 or more doses. Among those with at least two administrations of ZOL, the median time between the first and second dose of therapy was 391 (IQR 366-456) days. For those with >=3 ZOL administrations, the median time between the second and third dose was 379 (IQR 364-422) days. Time between doses did not meaningfully differ by osteoporosis medication history.Conclusions: Among ZOL initiators, around two-thirds received a single dose. Many have a history of oral bisphosphonate use. Among those with more than one dose of ZOL, dosing largely aligns with labeling recommendations (annually).

***Disclosures: Kaleen Hayes**, None*

SAT-442

See Friday Plenary Number FRI-442

SAT-443

Under-treatment of Osteoporosis in "Very Elderly" Elective Orthopedic Surgical Patients *Aamir Kadri[1], Amina Anwar[2], Lucas Steele[2], Madhumathi Rao[1]. [1]University of Kentucky, . [2]University of Kentucky College of Medicine, United States

Introduction: Osteoporosis is associated with adverse orthopedic surgical outcomes. Post-operative use of anabolic or anti-resorptive therapies minimize osteoporosis related complications. However, the benefits of these medications are not well studied in the "very elderly" patient age >=80. We hypothesized that "very elderly" fracture patients received post-operative anti-osteoporosis medications less often than patients aged 50-79 (elderly) after surgical fixation of low energy fractures despite meeting clinical indications for treatment.Methods: Between June 2021-December 2022, 98 patients age >=80 were compared with 97 patients aged 50-79 who were referred to a single institution's bone health clinic after surgical fixation. Fracture Risk Assessment (FRAX) scores without BMD were calculated. Osteoporosis was defined by a history of hip or spine fracture, FRAX MOF risk >=20% or hip risk >=3%, or T-score < -2.5.Results: In the "very elderly" compared to the elderly, mean age was 87.6 vs 71.1 (p=0.001), BMI 26.1 vs 29.5 (p=0.002), and 72% vs 75% were female. The fracture requiring surgical fixation occurred at the hip/spine in 43% of "very elderly" vs 39% of elderly patients. Prior fracture after age 50 was present in 25% vs 54% (p=0.002). Current tobacco use was present in 36% vs 52% (p=0.01). Indications for treatment were met in 100% of "very elderly" and 92% of elderly patients. In the "very elderly," excluding non-ambulatory patients, those with active co-morbidities precluding therapy, and those who died prior to initiating therapy, 82% were candidates for treatment, which was prescribed in 2% of "very elderly" vs 12% of elderly patients (p=0.002).Conclusion: "Very elderly" patients received anti-osteoporosis therapies less often than the elderly despite most meeting indications for treatment. This finding suggests that, despite sustaining fractures diagnostic for osteoporosis, "very elderly" patients may be undertreated due to limited data on the efficacy of osteoporosis therapies in this age group. Further research evaluating the safety and efficacy of pharmacologic treatment in this age group is warranted. Recognizing simple risk factors, such as prior fracture or current tobacco use, may help identify patients at risk for surgical complications related to bone disease who may benefit from pharmacologic treatment, representing an opportunity to improve secondary fracture care and reduce mortality risk associated with fracture in this age group.

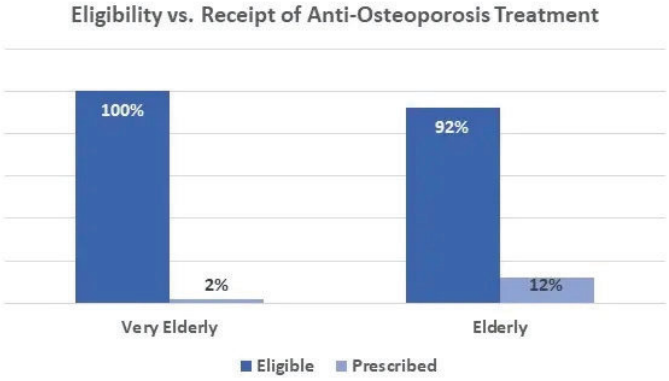

***Disclosures: Aamir Kadri**, None*

SAT-444

Reduction in the Non-adherence Rate to Denosumab Therapy with Clinical Pharmacy Collaboration: A Quality Improvement Project in an Osteoporosis Clinic *Amna Khan[1], Jaliyah Johnson, RN[2], Alexandria Tsikouras PharmD[3], Anna Zuschnitt, PharmD[3]. [1]University of Pennsylvania and Philadelphia VA medical center, United States. [2]Division of Endocrinology, Diabetes and Metabolism, University of Pennsylvania , United States. [3]University of Pennsylvania , United States

BACKGROUNDInterrupting or delaying Denosumab (DMab) beyond 7 months (210 days) from the last injection leads to transient increase in bone turnover known as rebound phenomenon, resulting in rapid loss of bone density and increased vertebral fracture. Risk of missing or delaying DMab therapy increased especially during the COVID-19 national emergency.Numerous studies suggest that clinical pharmacist participation in chronic disease state management leads to positive clinical outcomes and increase in medication adherence. Very few studies have evaluated pharmacist-physician collaboration for osteoporosis management and reduction in care gap and no study has evaluated the impact of this collaboration on preventing interruptions or delays in DMab therapy.METHODSThe Plan Do Study Act (PDSA) method of quality improvement was used for this project. Baseline review of charts revealed a non-adherence rate of about 21% amongst patients receiving this therapy for osteoporosis. Root cause analysis was performed.The aim of this study was to reduce the non-adherence rate to less than 5% by April 2023.INTERVENTIONSIn July 2021, 2 clinical pharmacists joined the Osteoporosis Clinic and hence the pharmacist-physician collabora-

tion was initiated.The first intervention began in October 2021. The pharmacists provided education to all patients starting DMab.The second intervention was implemented in March 2022. The pharmacists created an active reminder list of all patients receiving DMab in the electronic medical record system. They reviewed the list weekly. Lab reminders were sent to patients 1 month prior to their injection due date electronically and/or telephonically. Physician was alerted to review the labs for injection scheduling. Reminder closed 2 weeks post injection administration.RESULTSResults were analyzed using Statistical Process Control (SPC) G chart method (see attached). With these interventions, number of correct administrations between incorrect ones (delayed beyond 210 days) improved from an average of 4.8 to 13.5. These effects became visible about 10 weeks post intervention resulting in a reduction of non-adherence rate from 21% to 6.8% by April 2023.CONCLUSIONS-Pharmacist-Physician collaboration can reduce the non-adherence rate for drugs such as Denosumab, interruption of which can result in serious consequences. This can also relieve the overburdened nurses and physicians resulting in reduced burnout of healthcare teams.

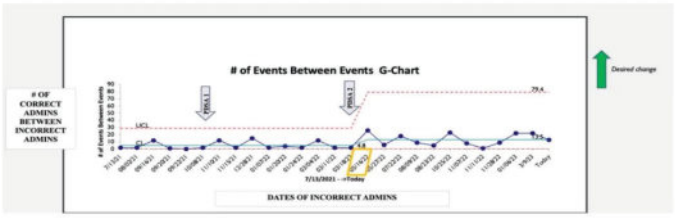

Statistical Process Control (SPC) G chart method

***Disclosures: Amna Khan**, None*

SAT-446

Bone mineral density change over three years before, during and after switching to Romosozumab followed by Denosumab *Yoichi Kishikawa[1.] [1]Kishikawa Orthopedics, Japan

BackgroundThese days, in considering life time management of severe osteoporosis, when and how to switch anabolic agents to anti-resorptive agents, and vice versa, is the key in keeping strong healthy bones. When switching from Denosumab (DSMb) to Romosozumab (RZMb), bone formation is activated, but bone resorption is activated as well. This change of bone metabolism is quite different from naïve or switching from Bisphosphonates (BPs) case, and the difference make a great influence on bone mineral density (BMD). The follower after RZMb is also important because the bone metabolism change still continues at the 12th administration of RZMb. I usually chose DSMb for severe osteoporosis patients as a follower to follow RZMb.PreviouslyI reported at the ASBMR annual meeting 2020 and 2021 as follows. Bone metabolism markers OC, ucOC, ucOC/ OC increased significantly in both groups after 4 months after switching from Bisphosphonate (BPs) or Denosumab (DSMb) to Romosozumab (RZMb), and TRACP5b increased when switching from DSMb however it decreased when switching from BPs. I reported neither Femoral total nor neck BMD change significantly in either group, however Lumbar spine BMD significantly increased in BPs group after 1year from switching.Subjects and methodThis time I followed 20 cases in the DSMb group and 19 cases in the BPs group of RZMb followed by DSMb in both groups. Subjects were retrospectively observed and statistically demonstrated from the point of BMD (Lumbar, Femoral neck and total) before switching from Bisphosphonate or Denosumab to RZMb, during RZMb for one year, and after switching from RZMb to Denosumab one year later.ResultsBone metabolism markers change were just the same results I reported before. TRACP5b increased when switching from DSMb however it decreased when switching from BPs.1.DSMB groupBone mineral density (BMD) change in DSMb group, BMD increased in lumbar and decreased in femoral total and neck during RZMb, then BMD increased in each site after Denosumab following RZMb. The changing rate of each BMD significantly increased in each site when comparing before and after RZMb for one year.2. BPs groupBMD in BPs group increased in each site administrating RZMb, then BMD increased in each site after Denosumab following RZMb. The changing rate of each BMD significantly increased in lumbar and femoral total while not significantly increased in femoral neck when comparing before and after RZMb for one year.

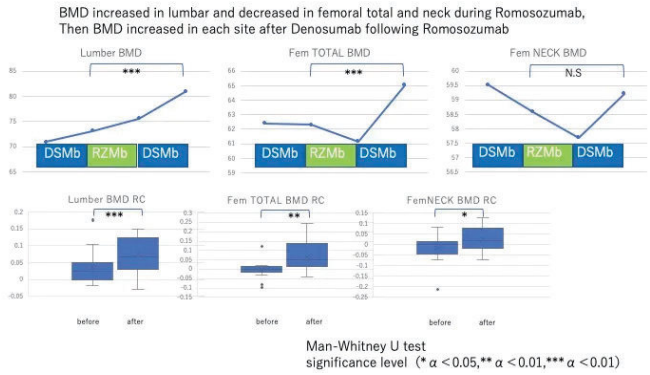

***Disclosures: Yoichi Kishikawa**, None*

SAT-447

A Phase I, Randomized, Double-blind, Single-dose Study to Evaluate the Biosimilarity of SB16 (Proposed Denosumab Biosimilar) with Reference Denosumab in Healthy Male Subjects *Hyuna Lee[1.] Sujung Kim[1.] Hyoryeong Seo[1.] Soyeon Kim[1.] [1]Samsung Bioepis, Republic of Korea

Background: SB16 has been developed as a biosimilar of the reference denosumab (DEN). Denosumab is a human monoclonal antibody, which inhibits the osteoclast formation and osteoclast-mediated bone resorption. It is currently indicated for postmenopausal osteoporosis, osteoporosis in men, breast cancer treatment-induced bone loss, prostate cancer treatment-induced bone loss, and glucocorticoid-induced osteoporosis. Objective: The primary objective of this phase I study was to demonstrate the pharmacokinetic (PK) equivalence between SB16, EU sourced DEN (EU-DEN), and US sourced DEN (US-DEN). Pharmacodynamic (PD), safety, tolerability, and immunogenicity were also evaluated as secondary objectives.Methods: In this double-blind, three-arm, multi-center, parallel group and single-dose study, healthy male subjects between 28-55 years of age were randomized in a ratio of 1:1:1 to receive a single 60 mg dose of either SB16, EU-DEN, or US-DEN subcutaneously. PK, PD, safety, tolerability, and immunogenicity were evaluated for 197 days. The primary PK endpoints were area under the concentration-time curve (AUC) from time zero to infinity, AUC from time zero to the last quantifiable concentration, and maximum serum concentration. Equivalence was determined if 90% confidence intervals (CIs) for the ratio of geometric least squares means (LSMeans) of the treatment groups compared were within the equivalence margin of 0.80 to 1.25. Results: A total of 168 subjects (56 per groups) were randomized. All of the corresponding 90% CI of geometric LSMean ratio of primary PK parameters for comparison of SB16 and EU-DEN, SB16 and US-DEN, and EU-DEN and US-DEN were within the pre-defined equivalence margin. The mean area under the effect curve from time zero to Day 197 for C-telopeptide of type I collagen (CTX) percent inhibition was comparable for SB16, EU-DEN, and US-DEN. The incidence of treatment-emergent adverse events (TEAEs) was comparable between the treatment groups. The majority of TEAEs were mild to moderate in severity. Three serious adverse events (SAEs) were reported in SB16 only but all the events were considered not related to investigational product. The overall incidence of subjects with post-dose anti-drug antibodies positive to denosumab was also comparable.Conclusion: This study demonstrated PK bioequivalence between SB16, EU-DEN, and US-DEN in healthy male subjects. PD, safety, and immunogenicity profiles were comparable.

***Disclosures: Hyuna Lee**, None*

SAT-449

Short-Term Effects of Sclerostin Inhibition on Calcium Homeostasis *Savannah Ryan[1.] Mackenzie Jordan[1.] Sabashini Ramchand[1.] Joy Tsai[1.] Benjamin Leder[1.] Sherri-Ann Burnett-Bowie[1.] [1]Massachusetts General Hospital, United States

Background: Romosozumab is a monoclonal antibody that inhibits osteocyte-derived sclerostin and thus stimulates bone formation and inhibits resorption. While the effects of romosozumab on bone mineral density (BMD), serum markers of bone remodeling, and blood calcium are known, romosozumab's effects on other measures of mineral metabolism and their potential consequences are less well defined. Thus, we explored the effects of romosozumab on mineral metabolism in postmenopausal women receiving adequate calcium and vitamin D intake.Methods: As part of a clinical trial, 31 postmenopausal women at high fracture risk (mean age 69) received monthly romosozumab 210-mg SC for 3 months. Subjects consumed approximately 1200-mg elemental calcium and a minimum of 400IU vitamin D daily from diet/supplements. Fasting serum calcium, albumin, 25hydroxyvitamin D (25OHD), parathyroid hormone (PTH), phosphate (PO4), and alkaline phosphatase (ALP) were compared at baseline and 3 months (paired t-test).Results: As shown in the Table, after 3-months of romosozumab, albumin-corrected calcium decreased by 3.1% (P<0.0001), PTH

increased by 57% (P<0.0001) and ALP increased by 20% (P<0.0001). There was no significant change in PO4 (P=0.9) or 25OHD (P=0.06). At month 3, of the 31 patients treated with romosozumab, three subjects (10%) developed asymptomatic hypocalcemia (calcium 77 pg/mL). While changes in serum PTH and ALP were not correlated, there was a significant negative correlation between the changes in serum PTH and calcium (R= -0.38, P=0.03). Conclusions: In postmenopausal osteoporotic women receiving calcium and vitamin D supplementation, 3 months of romosozumab treatment decreased serum calcium, resulting in significant increases in PTH and secondary hyperparathyroidism that impacted 1/3 of subjects. Despite the increase in PTH, serum PO4 was unchanged, which raises the question of possible compensatory changes in other mineral metabolism factors (such as FGF-23). Providers should be aware that secondary hyperparathyroidism may occur and persist in patients treated with romosozumab despite optimal 25OHD levels and calcium intake. Further larger studies are needed to determine whether these metabolic changes influence the clinical response to romosozumab and limit or mediate the observed gains in BMD.

	Week 0	Week 12	Delta	P value
Calcium (8.6-10.4 mg/dL)	9.2 (0.3); 8.6-9.9	8.9 (0.3); 8.4-9.6	-0.3 (0.3); -3.1 (3.4)	< 0.0001
PO_4 (2.1-4.3 mg/dL)	3.5 (0.4); 2.8-4.2	3.5 (0.4); 2.6-4.5	0.01 (0.3); 0.4 (8.7)	0.9
PTH (16-77 pg/mL)	45 (13); 22-69	68 (23); 37-137	23 (20); 57 (48)	< 0.0001
25OHD (30-100 ng/mL)	40 (12); 25-74	43 (11); 25-68	3 (9); 11 (25)	0.06
ALP (37-153 U/L)	64 (15); 42-102	76 (15); 54-115	12 (10); 20 (18)	< 0.0001

***Disclosures: Savannah Ryan**, None*

SAT-450

HIgh Frequency of Acute-Phase Response After Zoledronate: Who Has More Risk? *VANESA LONGOBARDI[1], Fernando Jerkovich[1], María Fernanda Carballo[1], Marcela Esparza Ramirez[1], MARIANA GONZALEZ PERNAS[1], ruben abdala[2], Rodolfo Gorris[1], Walter Sandoval[1], Nancy Sire[1], MARIA ZANCHETTA[3]. [1]IDIM, Argentina. [2]Instituto de Diagnóstico e Investigaciones Metabólicas, Argentina. [3]idim, universidad del salvador, Argentina

Introduction: Zoledronate (ZOL) is an effective treatment for several metabolic bone diseases. The reported frequency of acute-phase reactions (APRs) is widely variable.Aim: To describe the frequency of APRs after ZOL infusion and to identify associated factors. Methods: A prospective and observational study was designed. Patients who received 5 mg infusion of ZOL at our institution were invited to participate. After consent, they received 2 electronic questionnaires at 3 and 7days after infusion. APRs were divided into fever, musculoskeletal (ME) (myalgia, arthralgia, bone pain), general (malaise, fatigue, headache, dizziness, chills), gastrointestinal (GI) (abdominal pain, nausea, vomiting), and ocular (pain, red eye) symptoms (outcomes). Intensity for each symptom was classified on a scale of 1 to 10. Intensity >= 8, interference with daily activities, body T >= 37.8° or if the patient responded that would not receive ZOL again was considered a "severe symptom". The following variables were assessed: age >= 66 yo., sex, number of infusions, smoking, prior use of oral bisphosphonates (BP) and preventive NSAIDs. A uni- and multivariate analysis was performed.Results: Out of 653 patients invited to participate, 252 signed informed consent and completed at least one questionnaire. The mean age was 66.3 +/- 9 yo., 95% women. ZOL was administered for the first time in 138 (55%) patients, 58 of whom had received previous treatment (30 denosumab, 23 oral BP, 5 anabolic therapy). The frequency of APRs were: at least one symptom 207 (82%), general 173 (69%), ME 156 (62%), GI 70 (46%), fever 66 (43%), oculars 30 (20%), and severe 101 (40%). Significant associations between factors and APR symptoms were detailed in Table 1. First infusion of ZOL was significantly associated with a higher chance of having general, ME, GI, ocular and severe symptoms. It was also associated with higher frequency of fever although non-significant (p=0.063). Older age (>=66 yo.) was associated with a less chance of developing severe symptoms. 229 (91%) responded that if needed they will receive ZOL again.Conclusion: We observed a high frequency of APRs probably due to immediate and exhaustive. First ZOL infusion was the most important factor associated with practically all APRs symptoms and severity. Precise knowledge about the potential APRs after ZOL and effectively communicating this information with patients, will surely improve our clinical practice.

Table. Significant associations between variables and APRs after ZOL infusion
Only positive results are shown

Univariate Analysis
[a]Student's t-test; [b]Chi-squared test; [c]Fisher's exact test; [d]Mann-Whitney U Test

Variable	Outcome	p	OR (95% CI)
• **Age ≥ 66 ys**	Fever	0.007[b]	0.44 (0.25-0.80)
• **Prior oral BP**	Fever	0.016[b]	0.19 (0.04-0.83)
• **Prior oral BP**	ME symptoms	0.017[b]	0.34 (0.13-0.84)

Multivariate Analysis
(Binary logistic regression)

Variable	Outcome	p	OR (95% CI)
• **First Infusion**	General symptoms	0.003	2.42 (1.34-4.38)
	ME symptoms	0.030	1.88 (1.06-3.40)
	GI symptoms	0.008	2.59 (1.31-5.38)
	Ocular symptoms	0.004	6.21 (1.76-21.8)
	Severe Symptoms	<0.001	3.42 (1.83-6.38)
• **Age ≥ 66ys**	Severe Symptoms	0.005	0.95 (0.91-0.98)

***Disclosures: VANESA LONGOBARDI**, None*

SAT-452

Effect of gender on the evolution of pain and quality of life after treatment of symptomatic vertebral fragility fracture. *Pilar Peris Bernal[1], Jordi Blasco[2], Ana Monegal[1], Helena Florez[1], Nuria Guañabens[1], Josep Lluis Carrasco[3]. [1]Rheumatology Departament, Hospital Clinic, Spain. [2]Neurointerventional Departament, Spain. [3]Basic Clinical Practice, University of Barcelona , Spain

In a previous randomized clinical study comparing the effect of vertebroplasty (VP) vs. conservative therapy (CT) on pain evolution and quality of life (QoL) of patients with symptomatic vertebral fractures (VF), we observed the development of chronic back pain in 23% of subjects, independently of the therapy received. This study analyses the effect of gender on the evolution of pain and QoL in these subjects.Methods: 118/125 randomized patients (27 males/91 females) with recent symptomatic VF were evaluated. All received standardized analgesic and antiosteoporotic treatment. Pain and QoL were evaluated by VAS and Qualeffo-41, respectively, at baseline, at 2 weeks and 2 and 6 months. We compared pain evolution and QoL after treatment (CT vs. VP) according to gender, and analysed factors including age, time of evolution, treatment received, baseline VAS, previous VF (total and recent), incidental VF, lumbar and femoral T-scores, analgesic and antiosteoporotic treatment.Results: At baseline, there were no differences in age (males 74.8+/-11.2 vs. females:73.2+/-8.7 years), time of pain evolution, number of VF (males:3.8+/-2.4 vs. females: 3.1+/-2.4), treatment received (VP, males: 59%, females: 45%), lumbar or femoral T-scores, baseline VAS (males:6.8+/-2.1 vs. females: 6.8+/-2.2) or Qualeffo score (males:52.2+/-24.4 vs. females:59.7+/-20.6). Pain and QoL evolution differed according to gender, being better in males (figure 1). These differences were significant after two months and were independent of the treatment and the development of incidental VF during follow-up (males: 18.5 vs. females 12.1%).Conclusion: Pain and QoL evolution after a symptomatic VF differs according to gender, with a worse evolution in women independently of the treatment received.

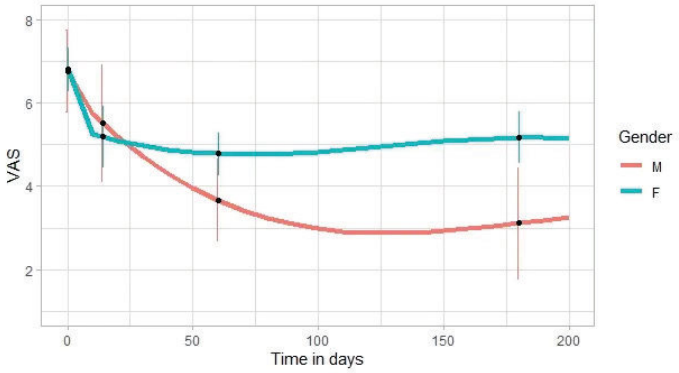

***Disclosures: Pilar Peris Bernal**, None*

SAT-453

Coronary artery calcification is associated with smaller increases in femoral neck bone mineral density in patients on anti-resorptive therapy *Rachael Hii[1], Nitesh Nerlekar[1], Peter Ebeling[2], Alexander Rodriguez[3]. [1]Monash Heart, Australia. [2]School of Clinical Sciences, Monash University, Australia. [3]Monash University, Australia

IntroductionAnti-resorptive medications are first-line treatments for osteoporosis. Additionally, patients with osteoporosis are at high cardiovascular risk, partly due to vascular calcification, such as in the coronary vessels. It is uncertain if the presence of coronary artery calcification (CAC) effects bone mineral density (BMD) response to anti-resorptive treatment. We therefore assessed changes in BMD following initiation of anti-resorptive treatment for osteoporosis in patients with and without evidence of CAC.MethodsIndividuals dispensed at least one prescription for an anti-resorptive medication (bisphosphonates or denosumab) at Monash Health between 2009-2022 were identified. Unique record numbers for these individuals were then cross-matched against the cardiac CT imaging service at Monash Heart (HREC#73603). CAC was detected by CT coronary angiogram (CTCA) using a Aquilion Vision (Canon Medical Systems Corporation, Otawara, Japan). We included only those patients having a baseline BMD measurement within two years of CTCA. The annualised percentage change in femoral neck BMD was calculated and adjusted for age, sex, height, weight, and number of years on anti-resorptive treatment.Results106 individuals were identified of which 85 (women=70 [85%], median age=73 years [interquartile range 64-79 years]) had a follow-up BMD measurement including 19 with, and 66 without, evidence of CAC. Those with CAC were older (76 years versus 64 years, p<0.001). There were 70 bisphosphonate users and 15 denosumab users. Individuals with evidence of CAC experienced, on average, a 1.2% lower increase [(0.345% (0.343 to 0.348) versus -0.881% (-0.883 to -0.879), mean difference -1.226% (-1.493 to -0.959; p<0.05)] in annualized femoral neck BMD with anti-resorptive therapy after adjusting for important clinical risk factors. InterpretationThese preliminary data suggest that CTCA-determined CAC may negatively impact femoral neck BMD increases with anti-resorptive therapy. Analysis of the full cohort is presently underway.

Coronary calcification	n	Annualised change in femoral neck BMD (%)^
Absent	19	0.345 (0.343 to 0.348)
Present	66	-0.881 (-0.883 to -0.879)
Mean difference		-1.226 (-1.493 to -0.959)

^Adjusted for age, sex, height, weight, number of years on anti-resorptive

***Disclosures: Rachael Hii**, None*

SAT-454

KER-012, A Modified ActRIIB Ligand Trap, Increased Bone Density in Healthy, Post-menopausal Women *Harveen Natarajan[1], Sylvain Bedard[1], Richard Friend[2], Ying Jiang[1], Jennifer Lachey[1], Jasbir Seehra[1], Simon Cooper[1]. [1]Keros Therapeutics, United States. [2]Nucleus Network, Australia

Background: TGF-? superfamily ligands are known to play a fundamental role in bone homeostasis. More specifically, activins A and B negatively regulate bone remodeling and suppress bone growth1. KER-012 is an investigational modified ActRIIB ligand trap designed to bind and inhibit activins to increase bone mass. A research form of KER-012 (RKER-012) not only prevented but reversed bone loss in multiple preclinical models of bone loss2. Further, in healthy post-menopausal women, KER-012 elicited rapid and robust increases in bone formation biomarkers3. The data presented here further support the potential effects of KER-012 on bone remodeling.Methods: A two-part Phase 1 study has been conducted with KER-012 in healthy post-menopausal women. Participants received either placebo or a single dose of KER-012 ranging between 0.75 and 5.0 mg/kg in Part 1 or multiple doses between 0.75 and 4.5 mg/kg in Part 2, subcutaneously once every 4 weeks over a 12-week period. Safety, PK, and biomarkers of activin target engagement were assessed. Additionally, bone mineral density was assessed temporally by DXA in Part 2 of the study. Informed consent was obtained from all subjects prior to enrollment in the study.Results: KER-012 was generally well tolerated at dose levels up to 5 mg/kg as a single dose and at dose levels up to 4.5 mg/kg administered Q4W for a total of 3 doses3. As previously reported at ASBMR 20223, biomarkers of bone formation were elevated post-KER-012 administration in both Part 1 and Part 2. Trends towards increases in whole-body bone mineral density were observed at all dose levels in Part 2 with a mean increase of 1.48% (median 2.8%, range -1.8 to 3.6%) at day 113 after three doses of KER-012 in the highest dose group vs an increase of 0.02% (median -0.40, range -1.9 to 2.7%) in the placebo group.Conclusions: KER-012 was generally well tolerated in this Phase 1 study in healthy post-menopausal women and elicited rapid and robust increases in bone formation biomarkers along with trends towards increasing whole-body bone mineral density. The observed safety profile along with the observed change in bone mineral density is supportive of further development of KER-012 in patients with disorders with diminished bone mass.References:1. Zou et al Front Mol Biosci. 2021 May 5;8:593310. 2. Materna C et al Am Society Bone Mineral Res 2021 Annual Meeting. Sept 9-12, 20213. Natarajan H et al 2022 J Bone Miner Res 38 (Suppl 1)

***Disclosures: Harveen Natarajan**, Keros Therapeutics, Other Financial or Material Support*

SAT-455

See Friday Plenary Number FRI-455

SAT-456

Pharmacokinetic (PK) Profile of EBP05/EB613 Oral Teriparatide Tablets in Women of Post Menopausal Age Versus Young Adult Men *Arthur C. Santora[2], Gregory Burshtein[2], Constantin Itin[2], Hillel Galitzer[2], Anke Hoppe[2], Miranda Toledano[2], Chana Sternberg[3], Auryan Szalat[4], Yoseph Caraco[4]. [2]Entera Bio, United States. [2]Entera Bio, Israel. [3]CSC Ltd, Israel. [4]Hadassah Medical Center, Israel

Background: EBP05/EB613 is an oral, daily tablet formulation of teriparatide [hPTH(1-34)] being developed by Entera Bio for the treatment of osteoporosis. A 161 patient, placebo-controlled, six-month Phase 2, dose-ranging study of EBP05/EB613 in postmenopausal women met biomarker and Bone Mineral Density endpoints (NCT04003467; ASBMR 2021: LB-1116). The 2.5 mg daily dose was selected for evaluation in a registrational Phase 3 study. An earlier Phase 1 study in young male volunteers (NCT02202603) and a Phase 2 study in female and male patients with hypoparathyroidism (NCT03516773; ASBMR 2019: LB SUN-972) evaluated the PK profile of EBP05/EB613 at a top dose of 2.25 mg. The current retrospective analysis compares PK data of EBP05/EB613 in the two different populations (young adult men vs. women of menopausal age), obtained from these studies. Methods: Evaluable PK profiles were obtained from nine young men (mean age of 23, range 21-26), and six women of menopausal age (mean age of 60, range 49-63) after administration of 2.25 mg EBP05/EB613 tablets in the morning, following an overnight fast. Subjects received up to 3 administrations of the treatment. For the current analysis, each administration is regarded as an independent event, resulting in a total number of 11 evaluable PK profiles obtained from this group.Results: Following the administration of a 2.25 mg dose of EBP05/EB613, the PK profiles obtained in young men and in women of menopausal age were found to be similar (Fig 1). Median Cmax was 425 (range 131-1772) vs 521 (172-2610) pg/mL and median AUClast was 157 (range 45.6-547) vs 158 (33.1-1078) pg*hour/mL in young men and women of menopausal age, respectively.Discussion: This retrospective comparison evaluating a 2.25mg dose of EBP05/EB613 in healthy males versus the target postmenopausal female population showed a consistent PK profile and bioavailability. A phase 3 study in postmenopausal women with osteoporosis is being planned.

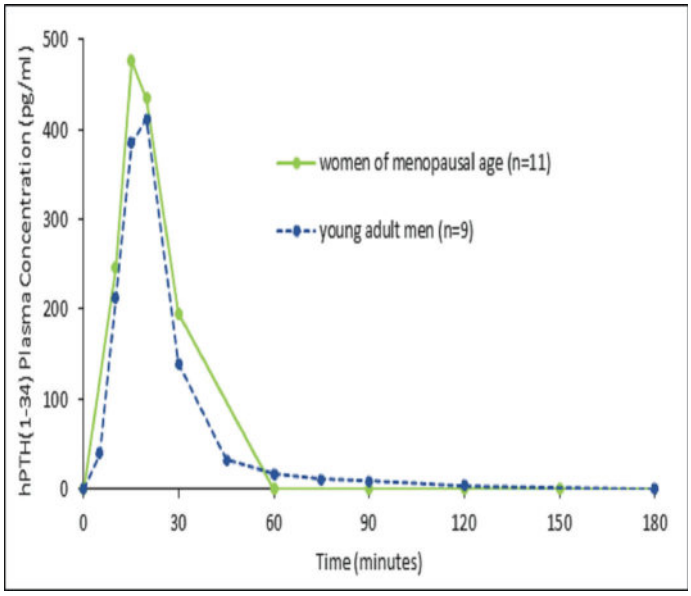

***Disclosures: Arthur C. Santora**, Entera Bio, Other Financial or Material Support*

Saturday Orals

SAT-457

Cost-Effectiveness of Sequential Abaloparatide/Alendronate for US Women and Men at Very High Risk of Fracture: an Economic Evaluation Based on Network Meta-Analysis *Mickael Hiligsmann[1], Stuart Silverman[2], Andrea Singer[3], LENY PEARMAN[6], Yamei Wang[5], John Caminis[6], Jean-Yves Reginster[7]. [1]Maastricht University, Netherlands. [2]Cedars-Sinai/UCLA, United States. [3]MedStar Georgetown University Hospital, United States. [6]Radius Health, . [5]Radius Health, Inc., United States. [6]Radius Health, United States. [7]University of Liège, Belgium

Current clinical evidence supports the use of a sequential treatment with an anabolic agent first followed by an antiresorptive in patients at very high fracture risk. In addition to clinical evidence, cost-effectiveness analyses are needed to assess the economic value of this strategy due to the higher cost of anabolic agents. Few economic analyses have been conducted so far, and to our knowledge, none have used efficacy data derived from network meta-analyses. In this study, a network meta-analysis-based economic evaluation was conducted to assess the cost-effectiveness of sequential treatment with abaloparatide (ABL) followed by alendronate (ALN) compared to alternative treatments in US men and women at very high risk of fracture. A previously validated economic model assessed lifetime healthcare costs (expressed in 2022 dollars) and outcomes (measured in quality-adjusted life years [QALYs]) of sequential ABL/ALN compared to a similar sequence with unbranded teriparatide (TPTD/ALN), to monotherapy with ALN and to no treatment. Efficacy data were derived from a recent network meta-analysis (Willems et al. Clin Ther 2022;44[1]:81-97). Populations included men and women aged 50-90 years with a recent fracture and densitometric osteoporosis (bone mineral density T-score <=?2.5). The results of the analyses were expressed in incremental cost-effectiveness ratios (ICERs) defined as the difference in costs between sequential ABL/ALN and alternative strategy, divided by their differences in QALYs. In all simulations, sequential ABL/ALN was associated with more QALYs for lower costs compared to sequential unbranded TPTD/ALN, being therefore dominant. In men, sequential ABL/ALN was also shown to be cost-effective at the US cost-effectiveness threshold (ie, $150,000 per QALY gained) compared to no treatment and to monotherapy with ALN over the full age range. In women, sequential ABL/ALN was cost-effective compared to no treatment in those aged >=60 years and compared to monotherapy with ALN in those aged >=65 years. In conclusion, this network meta-analysis-based cost-effectiveness analysis suggests that sequential ABL/ALN incurs less costs for more QALYs than sequential unbranded TPTD/ALN in both men and women aged 50-90 years, and is also cost-effective compared to monotherapy with ALN in men aged >=50 years and women >=65 years.

***Disclosures: Mickael Hiligsmann**, UCB, Consultant, ViiV, Grant/Research Support, Radius Health, Inc., Grant/Research Support, Amgen, Grant/Research Support, Mylan Pharmaceuticals, Other Financial or Material Support*

SAT-458

The Preference of the Treatment of Glucocorticoid-induced Osteoporosis in Korean Patients with Autoimmune Diseases *Chang-Hee Suh[1], Ji-Won Kim[1]. [1]Ajou University School of Medicine, Republic of Korea

PurposeGlucocorticoid-induced osteoporosis (GIOP) is common in patients with autoimmune disease who were prescribed with long-term glucocorticoids. The most commonly used drugs for GIOP is bisphosphonate. Zoledronate is a convenient treatment option that allows compliance to be advantageous over other bisphosphonates. Our aim is to evaluate the efficacy compared to other bisphosphonates as well as the preference and patient satisfaction of zoledronate.MethodsFifty patients with autoimmune diseases were recruited with new fractures or osteoporosis found in follow-up bone densitometry after taking oral bisphosphonates for at least 1 year for the treatment of GIOP. After 1 year of treatment with zoledronate, patients completed the survey to rate their preference and satisfaction. The treatment efficacy was analyzed by comparing the changes in bone density and fractures with patients maintaining oral bisphosphonates as controls.ResultsMean age of zoledronate group and oral bisphosphonates group was 64.1 vs 63.1 years, 96% vs 98% were female, and the mean duration of GIOP was 5.5 vs 4.2 years, respectively. There was no difference in the cumulative glucocorticoid doses of the two groups. Thirty-nine patients (78%) preferred and were more satisfied with intravenous zoledronate over oral bisphosphonates, and satisfaction was strongly affected by the administration interval and convenient regimen. The infusion-related adverse events of zoledronate were only 2 patients (4%). In addition, there were no significant differences in annualized percentage change in bone density in the lumbar spine (1.9 +/- 3.91 g/cm2 vs. 1 +/- 5.3 g/cm2, p = 0.355), femur neck (-0.91 +/- 6.31 g/cm2 vs. 0.41 +/- 5.07 g/cm2, p = 0.264), and hip (0.29 +/- 2.91 g/cm2 vs. 0.41 +/- 5.07 g/cm2, p = 0.888) between patients who received zoledronate and those who took oral bisphosphonates. The occurrence of new fractures was two in each of the two groups, showing no difference. ConclusionsZoledronate was preferred and more satisfactory by patients with autoimmune disease, and the treatment efficacy for osteoporosis was similar to oral bisphosphonates. Therefore, zoledronate is recommended as an appropriate treatment for GIOP.

***Disclosures: Chang-Hee Suh**, None*

SAT-459

Bisphosphonates preserve bone mineral density and suppress bone turnover markers in early menopausal women: A systematic review and meta-analysis of randomized trials *Aria Ahadzadeh Ardebili[4], Fariba Aghajafari[2], Timothy Fu[2], Nicole Dunnewold[3], Emma Billington[4]. [4]University of Calgary, . [2]Cumming School of Medicine, Canada. [3]Health Sciences Library, Canada. [4]University of Calgary, Canada

Women can lose up to 30% of their bone mass within the first 5 years following menopause. As such, 50% of postmenopausal women will experience a fracture within their lifetime. However, most women are ineligible for pharmacologic osteoporosis treatment until they have irreversible bone loss or have sustained a fracture. These outcomes may be preventable by short or intermittent bisphosphonate therapy courses initiated around the time of menopause. As such, the goal of this systematic review and meta-analysis was to determine the effects of nitrogen-containing bisphosphonate therapy on fracture incidence, bone mineral density (BMD) and bone turnover markers in early menopausal women.MEDLINE, EMBASE, CENTRAL, and CINAHL were systematically searched from their inception to July 2022. Randomized controlled trials (RCTs) over >=12 months examining the effects of nitrogen-containing bisphosphonates on fracture incidence, BMD, and bone turnover markers in early menopausal women (perimenopausal or <5 years postmenopausal) were included. Risk of bias was evaluated using the Cochrane Risk of Bias 2 tool and random effect meta-analysis was undertaken using RevMan v5.3.Fourteen articles (12 trials) were included (N = 1722 women). Four studies were assessed as having low risk of bias and 8 studies raised some concerns. Three studies reported on the incidence of fracture, all being infrequent. Bisphosphonate therapy improved BMD over 12 months versus placebo (mean percentage difference [95% CI]) at the lumbar spine (4.32[3.10-5.54]%, P<0.0001, N=8 studies), femoral neck (2.56[1.85-3.27]%, P=0.001, N=6 studies), and total hip (1.22[0.16-2.28]%, P=0.002, N=4 studies). Long-term (24-72 months) bisphosphonate therapy improved BMD at the lumbar spine (5.81[4.71-6.91]%, P<0.0001, N=8 studies), femoral neck (3.89[2.73-5.05]%, P=0.0001, N=5 studies) and total hip (4.09[2.81-5.37]% P<0.0001, N=4 studies). Bisphosphonate therapy reduced urinary N-telopeptide (-52.2[-60.3,-44.2]%, P<0.00001, N=3 studies) and bone-specific alkaline phosphatase (-34.2[-42.6,-25.8]%, P<0.00001, N=4 studies) over 12 months of treatment versus placebo.We conclude that nitrogen-containing bisphosphonate therapy improves BMD in early menopause. These BMD improvements are comparable to those in high fracture risk women following bisphosphonate therapy. These results warrant further investigations on bisphosphonate therapy for osteoporosis prevention in early menopausal women.

***Disclosures: Aria Ahadzadeh Ardebili**, None*

SAT-460

Assessing the robustness of evidence for the efficacy of anti-fracture medications *Nick Tran[1], Thach Tran[2], Tuan Nguyen[3]. [1]Macquarie University, Australia. [2]Garvan Institute of Medical Research, Australia. [3]University of Technology Sydney , Australia

Background: The evidence of the efficacy of anti-fracture medications is conventionally derived from randomized controlled clinical trials (RCTs) with P-values < 0.05 being the gold standard. However, the robustness of the evidence at this P-value threshold has never been examined. This study sought to quantify the fragility of the RCT evidence for ant-fracture medications.Methods: We searched for RCTs published in high-impact medical journals that reported a statistically significant result (P< 0.05) for at least one fracture site as either a dichotomous or time-to-event outcome. We included parallel trials that allocated participants in a 1:1 ratio to treatment and control groups. The fragility of the evidence was assessed by the 'Fragility Index' (FI) which is defined as the minimum number of patients whose condition would need to change from non-fracture to fracture to invalidate a statistically significant outcome.Results: This analysis included 22 RCTs which generated 110 positive results (P < 0.05); of these 37 (~34%) used fracture as the primary endpoint. The median FI of these analyses was 9 (interquartile range [IQR]: 3, 11), indicating that adding as few as 9 fracture patients (~0.4% of the study size) to the intervention group would eliminate the previously documented evidence of fracture prevention efficacy. Notably, in 65% of these analyses, the number of participants lost to follow-up exceeded the corresponding FI. Among the 34 results with P < 0.001, the median FI was 25 (IQR: 17 to 47) which was lower than the number of participants lost to follow-up in 25 results. Specifically, the anti-fracture efficacy of denosumab and calcium/vitamin D supplementation would be statistically lost if only an additional 4 (IQR: 3 to 17) and 6 (IQR: 2 to 16) patients respectively, sustained a fracture during the follow-up period (see Figure). Even when fracture was the primary outcome measure, the evidence for anti-fracture efficacy remained fragile, with a median FI being 15 (IQR: 8 to 25). In 86% of the positive results (P<0.05), the number of participants lost to follow-up was higher than that required to render the results statistically non-significant.Conclusions: These data indicate that the existing RCT evidence of anti-fracture efficacy is relatively fragile. In order to increase the robustness of the anti-fracture evidence, the P-value threshold should be lower than 0.001.

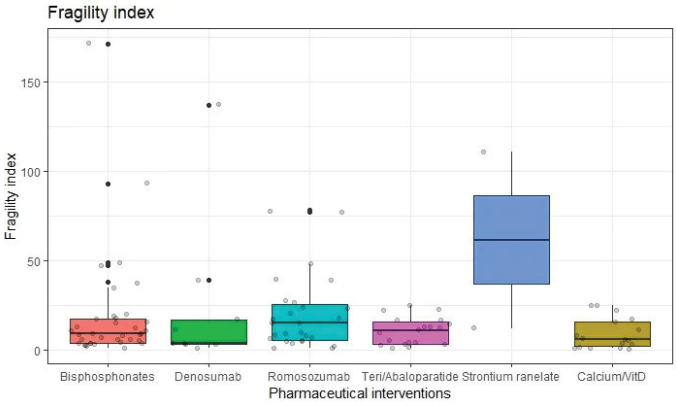

***Disclosures: Nick Tran**, None*

SAT-461

One versus 2 years of Alendronate Following Denosumab: The CARD Extension *Joy Tsai[1], Mackenzie Jordan[2], Savannah Ryan[2], Sabashini Ramchand[3], Hang Lee[4], Benjamin Leder[5]. [1]MASSACHUSETTS GENERAL HOSPITAL, United States. [2]Massachusetts General Hospital, United States. [3]Melbourne University, . [4]Biostatistics Center, Massachusetts General Hospital, United States. [5]Massachusetts General Hospital Harvard Medical School, United States

Background: When denosumab (DMAB) is discontinued, antiresorptive therapy is critical to attenuate high-turnover bone loss. The ideal choice and duration of antiresorptive therapy is not yet defined, however. In the CARD study, we demonstrated that 12-months of alendronate (ALN) was better able to maintain the BMD gains achieved with 12-months of DMAB versus 12-months of raloxifene (RAL). In this extension, we wished to determine if 12-months of ALN would be sufficient in maintaining these DMAB-induced BMD gains. Methods: In the CARD study, postmenopausal osteoporotic women aged 60-79 at high fracture risk received 12 months of DMAB 60-mg SC every 6 months followed by 12 months of either ALN 70-mg weekly (N=26) or RAL (N=25). All subjects in the ALN arm were then offered participation in a 1-year extension in which they were randomized to continue ALN for an additional 12 months (N=10) or to receive calcium and vitamin D (Ca/Vit D) alone (N=8). The primary outcome was change in PA spine BMD between months 24 and 36. Exploratory endpoints included changes in aBMD at other anatomic sites as well as changes in serum bone turnover markers.Results: The results of the CARD study, which demonstrated the effectiveness of 12-months ALN in preserving DMAB-induced BMD gains were presented previously and are currently in press. As shown in the Figure, in the extension, aBMD was maintained at the PA spine, TH and FN in both those randomized to an additional year of ALN and those randomized to Ca/Vit D alone. We did, however, observe a transient comparative decrease between months 24-30 in the Ca/Vit D group at the TH (P=0.008) and FN (P=0.040). At the end of 24 months of the CARD study, CTX and PINP were suppressed in both groups and then increased more between months 24-36 in the Ca/Vit D group than the ALN group (P=0.051 for CTX, P=0.030 for P1NP). Both CTX and PINP remained below the month 0 baseline in both groups (P<0.05 for all comparisons).Conclusions: With the limitations of our small sample size, these data suggest that both 1 and 2 years of ALN effectively maintain BMD gains achieved with one year of DMAB and prevented any rebound in bone turnover marker levels above pre-DMAB baseline. This is the first randomized trial to assess minimum duration of bisphosphonate after short term DMAB and may be helpful to guide clinical care. Similar studies performed after longer durations of DMAB would be helpful to further define optimal management.

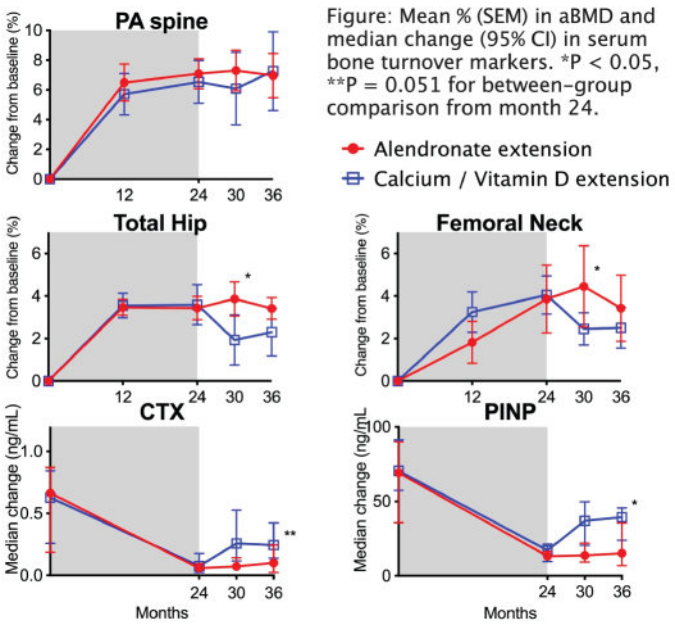

***Disclosures: Joy Tsai**, Amgen, Other Financial or Material Support*

SAT-462

Targeted coaching to improve osteoporosis therapy adherence: a single arm variation of the C-STOP study *Carrie Ye[1], Finlay McAlister[1], Debbie Bellerose[1], Meng Lin[2]. [1]University of Alberta, Canada. [2]Alberta Health Services, Canada

Despite having medications that are efficacious at preventing bone loss and fractures, suboptimal treatment rates are further attenuated by poor medication adherence and persistence. In our original C-STOP Trial, we found that a Nurse Case Manager (CM) could significantly increase testing for osteoporosis and starting treatment and that 12-month adherence rates were high (79%) in both the active control group and the CM group in the C-STOP Trial.AIM: In this pre-planned variation of the C-STOP Trial, we evaluate if adherence-specific coaching by the case manager (CM) can further improve adherence and persistence rates compared to those seen in the original C-STOP Trial.METHODS: We conducted a prospective observational cohort study of community-dwelling adults 50 years or older who suffered an upper extremity fracture, not previously treated with osteoporosis medications, to assess whether a well-trained CM can partner with patients to improve adherence and persistence to oral bisphosphonates. The primary outcome was adherence (taking >?80% of prescribed doses) to oral bisphosphonate at 12 months after study enrollment. Secondary outcomes included primary adherence and 12-month persistence to oral bisphosphonate, and calcium and vitamin D supplement intake at 12 months.RESULTS: The study cohort consisted of 84 participants, 84.5% women, mean age 64.9 years, with mean total hip BMD T-score of -1.4. 30 were prescribed an oral bisphosphonate (Figure). Twenty-two (73.3%) started treatment within 3 months. The adherence rate at 12-months was 77.3%. The persistence rate at 12-months was 95.5%. 62.8% of those not prescribed oral bisphosphonate were taking supplemental calcium and 93.0% were taking supplemental vitamin D at 12-months. Depression was a significant predictor of 12-month non-adherence (adjusted OR 9.8, 95% CI 1.2-81.5).CONCLUSION: Adherence-specific coaching by a CM did not further improve the medication adherence achieved in the original C-STOP study. Importantly, these negative results can inform future adherence intervention studies.

Figure. Flow and outcomes of study participants

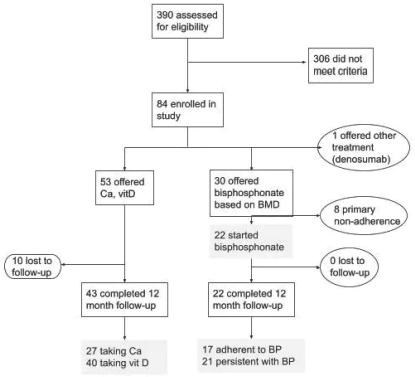

BP, bisphosphonate. Ca, calcium supplement. Vit D, vitamin D supplement. BMD, bone mineral density.

***Disclosures: Carrie Ye**, None*

SAT-463

A randomized controlled trial of the effect of raloxifene plus cholecalciferol versus cholecalciferol alone on bone mineral density in postmenopausal women with osteopenia *Sungjae Shin[1], Namki Hong[2], Yumie Rhee[3]. [1]Division of Endocrinology, Department of Internal Medicine, Endocrine Reasearch Institute, National Health Insurance Service Ilsan Hospital, Goyang, Korea, Republic of Korea. [2]Division of Endocrinology, Republic of Korea. [3]Yonsei University College of Medicine, Republic of Korea

Raloxifene increases lumbar spine bone mineral density (BMD) and lowers vertebral fracture risk in patients with osteoporosis. However, few prospective clinical trials have studied its efficacy in postmenopausal women with osteopenia. This study investigated the efficacy of raloxifene in postmenopausal women with osteopenia. A single-center, randomized, prospective controlled trial was performed in 112 postmenopausal women with osteopenia. Participants were randomly assigned to receive raloxifene 60 mg/day plus cholecalciferol 800 IU/day (RalD group) or cholecalciferol 800 IU/day (VitD group) for 48 weeks. Osteopenia was defined based on the lowest BMD T-score in the lumbar spine, femoral neck, or total hip. A favorable response was defined as an improvement of BMD at the lumbar spine above 95% least significant change (>=2.76%). The trial was registered with ClinicalTrials.gov (NCT05386784). Compared with the VitD group, the RalD group had a greater increase in lumbar spine BMD (RalD vs. VitD; 2.6% vs. ?0.6%, p=0.005) and less bone loss in total hip BMD (?0.3% vs. ?2.9%, p=0.003). The differences remained significant after adjustment for age, body mass index, baseline BMD, and other covariates. The proportion of favorable responders was higher in the RalD group than the VitD group (54% vs. 25%, p=0.003). During the study period, one wrist fracture and four adverse events (two leg cramps, one hot flushes, and one dry mouth) occurred in the RalD group. In conclusion, RalD significantly improved lumbar spine BMD and attenuated total hip BMD loss compared with VitD alone in postmenopausal women with osteopenia.

***Disclosures: Sungjae Shin**, None*

SAT-465

See Friday Plenary Number FRI-465

SAT-466

Comparative Study of the Effects of Bisphosphonates and Recombinant Human Parathyroid Hormone on Osteogenic Gene Expression and Mineralization in Human Osteogenic Sarcoma Cells. *takdeer kaur[1], Vandana Dhiman[2], Sanjay Kumar Bhadada[3], Naresh Sachdeva[4], Sudhaker D Rao[5], Ravi Pratap Barnwal[6]. [1]Senior Research fellow, India. [2]Senior Demonstrator, Department of Endocrinology Post Graduate Institute of Medical Education and Research, , India. [3]PGIMER, chandigarh, India, India. [4]professor Department of Endocrinology, India. [5]Henry Ford Hospital, United States. [6]Assistant Professor, Pu Chandigarh, India

Title: Comparative Study of the Effects of Bisphosphonates and Recombinant Human Parathyroid Hormone on Osteogenic Gene Expression and Mineralization in Human Osteogenic Sarcoma Cells.Takdeer Kaur, Vandana Dhiman, Sanjay Kumar Bhadada, ,Naresh Sachdeva, Ravi Pratap Barnwal, Sudhaker Dhanwada RaoAbstract: Despite more than two decades of clinical experience, molecular mechanisms of anti-fracture drugs, are not completely understood. Recent studies suggest fundamentally different mechanism of action of key anti-fracture drugs, bisphosphonates and recombinant human parathyroid hormone (rhPTH) at the tissue level, however their molecular basis of action has not explored completely. Accordingly, we studied the effects of varying cncentrations of zoledronic acid (ZOL; 1µM and 5µM) and rhPTH (5 µg and 10 µg) on Human Osteogenic sarcoma cells (U2OS cells). Cellular viability, mineralization, and osteogenic gene expressions were assessed to elucidate the effects of these two prototypic drugs with diametrically different mechanisms of action. Cellular viability was not affected either by ZOL or rhPTH alone or in tandem treatments. Osteoblastic activity (alkaline phosphatase activity and mineralization) increased significantly with rhPTH followed by ZOL. Further, alkaline phosphatase activity increased significantly with in tandem treatment of rhPTH followed by ZOL both at the mRNA (p<0.001) and protein levels (p<0.04). Moreover, osteoblastic genes (COL1A1 and osteocalcin) were significantly modulated by sequential treatment with rhPTH followed by ZOL. We conclude that rhPTH (5µg) treatment followed by ZOL (1µM) showed the best anabolic effects. Our results warrant further research in assessing similar combinations of anti-fracture drugs which augment osteogenesis to maximize their anabolic effects in preventing osteoporosis in susceptible individuals.

Title: Comparative Study of the Effects of Bisphosphonates and Recombinant Human Parathyroid Hormone on Osteogenic Gene Expression and Mineralization in Human Osteogenic Sarcoma Cells.

Takdeer Kaur, Vandana Dhiman, Sanjay Kumar Bhadada, ,Naresh Sachdeva, Ravi Pratap Barnwal, Sudhaker Dhanwada Rao

Abstract: Despite more than two decades of clinical experience, molecular mechanisms of anti-fracture drugs, are not completely understood. Recent studies suggest fundamentally different mechanism of action of key anti-fracture drugs, bisphosphonates and recombinant human parathyroid hormone (rhPTH) at the tissue level, however their molecular basis of action has not explored completely. Accordingly, we studied the effects of varying cncentrations of zoledronic acid (ZOL; 1µM and 5µM) and rhPTH (5 µg and 10 µg) on Human Osteogenic sarcoma cells (U2OS cells). Cellular viability, mineralization, and osteogenic gene expressions were assessed to elucidate the effects of these two prototypic drugs with diametrically different mechanisms of action. Cellular viability was not affected either by ZOL or rhPTH alone or in tandem treatments. Osteoblastic activity (alkaline phosphatase activity and mineralization) increased significantly with rhPTH followed by ZOL. Further, alkaline phosphatase activity increased significantly with in tandem treatment of rhPTH followed by ZOL both at the mRNA (p<0.001) and protein levels (p<0.04). Moreover, osteoblastic genes (COL1A1 and osteocalcin) were significantly modulated by sequential treatment with rhPTH followed by ZOL. We conclude that rhPTH (5µg) treatment followed by ZOL (1µM) showed the best anabolic effects. Our results warrant further research in assessing similar combinations of anti-fracture drugs which augment osteogenesis to maximize their anabolic effects in preventing osteoporosis in susceptible individuals.

***Disclosures: takdeer kaur**, None*

SAT-467

Lithocholic Acid Induced Bone and Renal 25-hydroxyvitamin D-1alpha hydroxylase (CYP27B1) Expression and Activities in vitro and in vivo *Chung Yan Lam[1], Wen Xuan Yu[3], Yayi Shen[3], Man-Sau Wong[4]. [1]The Hong Kong Polytechnic University , Hong Kong. [3]The Hong Kong Polytechnic University, China. [3]The Hong Kong Polytechnic University, Hong Kong. [4]Hong Kong Polytechnic University, Hong Kong

Lithocholic acid (LCA), a gut-derived bile acid, is believed to play a regulatory role in bone health. We hypothesize that LCA regulates bone metabolism via the activation of renal and extra-renal CYP27B1 expression and activities. The present study aimed to study the effects of LCA on CYP27B1 expression and activities in kidney and bone tissues in vitro and in vivo. CYP27B1 protein expression and activities in vitro were studied in human osteoblastic-like MG-63 cells and renal proximal convoluted tubule HKC-8 cells treated with either different concentrations of LCA (10-12 to 10-6 M), PTH (10-7M), or its vehicle for 4 hours. The in vivo time-dependent effects (1, 3, 5, 8, 12 and 24 hours) of LCA (25mg/kg) on serum 1,25(OH)2D3 levels and renal and extra-renal CYP27B1 and CYP24A1 (25-hydroxyvitamin D 24-hydroxylase) protein expression were studied using mature (4-month-old) male C57BL/6 mice.LCA was shown to significantly induce CYP27B1 protein expression at 10-12 to 10-8M in MG-63 cells (P<0.01) and at 10-12 to 10-6M in HKC-8 cells (P<0.05). In addition, LCA significantly induced CYP27B1 activity in MG-63 cells at 10-10M (P<0.05) and in HKC-8 cells at 10-6M (P<0.01). LCA at 25mg/kg significantly induced circulating 1,25(OH)2D3 levels at 3 hours in male C57BL/6 mice (P<0.05) and the level showed a trend returning back to basal level from 5 hours to 24 hours. Renal CYP27B1 expression was found to be significantly increased in male mice upon treatment with LCA for 1 hour (P<0.01). Renal CYP24A1 expression significantly decreased in male mice in response to treatment with LCA for 3 hours (P<0.05) and increased back to basal level. Extra-renal CYP27B1 expression in iliac crest slightly increased by LCA at 1 hour and decreased significantly at 3 and 12 hours (P<0.01 and P<0.001). CYP24A1 expression in iliac crest significantly increased by LCA at 5 hours (P<0.001). Renal CYP27B1 was more responsive than extra-renal CYP27B1 in mice to the treatment of LCA. Renal CYP27B1 and CYP24A1 appeared to exert a negative feedback mechanism to tightly control the level of serum 1,25(OH)2D3 level.In summary, both in vitro and in vivo results showed that LCA is able to regulate renal and extra-renal CYP27B1 expression, which in turn might account for its stimulatory effects on circulating 1,25(OH)2D3 levels. Our study indicated

that LCA might play an important role in bone health via its role in the regulation of vitamin D metabolism.

***Disclosures: Chung Yan Lam**, None*

SAT-469

Protein Kinase A activity modulates osteoclastogenesis *CAROLE LE HENAFF[1], YONGLI QIN[2], Henry Kronenberg[3], Lawrence S Kirschner[4], Baohong Zhao[5], Nicola Partridge[6]. [1]New York University, United States, [2], United States, [3]Massachusetts General Hospital, United States, [4]Departments of Cancer Biology and Genetics and the Division of Endocrinology, Diabetes, and Metabolism, Department of Internal Medicine, The Ohio State University Wexner Medical Center, United States, [5]Hospital for Special Surgery, United States, [6]New York University College of Dentistry, United States

Protein Kinase A action in osteoclasts has not been clearly investigated. Previous studies were mainly done in vitro without clear results yielding controversies in PKA activity in osteoclastogenesis or osteoclast activity. A few studies, such as with calcitonin, associated PKA activation to an inhibition of osteoclastogenesis or osteoclast activity whereas other studies, such as with dopamine showed the opposite. To elucidate the role of PKA activity during osteoclastogenesis and in osteoclast activity, we constitutively modulated this enzyme activity in osteoclastic lineages (from monocytes to mature osteoclasts) using LysM-Cre in mice: first, we deleted the PKA regulatory subunit 1A (Prkar1a) to increase PKA activity (PKAhighOC) and secondly, we hypoactivated PKA using a dominant negative mouse model (PKAlowOC) which results in a mutation in the cAMP binding site of the regulatory subunit and blocks the release of the active catalytic subunit. At 2 months of age, in our mouse models, hyperactive osteoclastic PKA caused a decrease in trabecular bone volume (-23% in males and -33% in female mice), thickness (-12%) and number (-15% to -24%) and an increase in trabecular separation (14%). Conversely, hypoactive osteoclastic PKA increased trabecular bone volume (18%) with increased trabecular thickness (9% to 12%) and separation (23% to 45%). The cortical thickness was decreased in hyperactive mice in the metaphysis (-10% to -14%) but no changes were observed in the diaphysis. Interestingly, the cortical thickness was only reduced in the diaphysis with hypoactive PKA (-7%). The cortical bone phenotype was more pronounced in females compared with males. Primary osteoclastic cell cultures from the hyperactive mouse model showed a doubling in osteoclast numbers confirming the increased osteoclastogenesis in this mouse model. These results collectively suggest that PKA activity positively regulates osteoclastogenesis. These genetic data, for the first time, corroborate that PKA is a key positive regulator in osteoclastogenesis.

***Disclosures: CAROLE LE HENAFF**, None*

SAT-470

Development and Biophysical Characterization of a Humanized FSH-blocking Monoclonal AntibodyTherapeutic Formulated at an Ultra-high Concentration *Satish Rojekar[1], Anusha Rani Pallapati[1], Judit Gimenez-Roig[2], Damini Sant[3], Sakshi Gera[2], Funda Korkmaz[2], Farhath Sultana[4], Orly Barak[4], Ofer Moldavski[4], Uliana Cheliadinova[4], Anisa Azatovna Gumerova[5], Hasni Suhasha Kannangara[5], Tal Frolinger[5], Ronit Witztum[5], Anne Macdonald[5], Pevnev Georgii[6], Steven Sims[6], John N. Caminis[6], Marcia Meseck[6], Vitaly Ryu[6], Se-Min Kim[6], Daria Lizneva[6], Tony Yuen[7], Mone Zaidi[7]. [1]Icahn School of Medicine at Mount Sinai, United States, [2]Icahn School of Medicine at Mount Sinai , United States, [3]Max Planck Institute for Biology of Ageing, Germany, [4]Icahn School of Medicine at Mount Sinai , United States, [5]Icahn School of Medicine at Mount Sinai , United States, [6]Icahn School of Medicine at Mount Sinai , United States, [7]Icahn School of Medicine at Mount Sinai , United States

Highly concentrated antibody formulations are oftentimes required for subcutaneous, self-administered biologics. Here, we report the development of a unique formulation for our first-in-class FSH-blocking humanized antibody, MS-Hu6, which we propose to move to the clinic for osteoporosis,obesity, and Alzheimer's disease. The studies were carried out using our Good Laboratory Practice (GLP) platform, compliant with the Code of Federal Regulations (Title 21, Part 58). We first used protein thermal shift, size exclusion chromatography, and dynamic light scattering to examine MS-Hu6 concentrations between 1 and 100 mg/mL. We found that thermal, monomeric, and colloidal stability of formulated MS-Hu6 was maintained at a concentration of 100 mg/mL. The addition of the antioxidant L-methionine and chelating agent disodium EDTA improved the formulation's long-term colloidal and thermal stability. Thermal stability was further confirmed by Nano differential scanning calorimetry (DSC). Physiochemical properties of formulated MS-Hu6, including viscosity, turbidity, and clarity, conformed with acceptable industry standards. That the structural integrity of MS-Hu6 informulation was maintained was proven through Circular Dichroism (CD) and Fourier TransformInfrared (FTIR) spectroscopy. Three rapid freeze-thaw cycles at -80°C/25°C or -80°C/37°C further revealed excellent thermal and colloidal stability. Furthermore, formulated MS-Hu6, particularly its Fab domain,displayed thermal and monomeric storage stabilityfor more than 90 days at 4°C and 25°C. Finally, the unfolding temperature (Tm) for formulated MS-Hu6 increased by >4.80°C upon binding to recombinant FSH, indicating highly specific ligand binding. Overall,we document the feasibility of developing a stable,manufacturable and transportable MS-Hu6 formulation at a ultra-high concentration at industry standards.The study should become a resource for developing biologic formulations in academic medical centers.

***Disclosures: Satish Rojekar**, None*

SAT-471

Positive Effects of Cannabidiol on Primary Rat Osteoclasts and Osteoblasts *Krittikan Chanpaisaeng[1], Jirawan Thongbunchoo[2], Narattaphol Charoenphandhu[3]. [1]National Science and Technology Development Agency, , [2]Department of Physiology, Faculty of Science, Mahidol University, Thailand, [3]Center of Calcium and Bone Research (COCAB), Faculty of Science, Mahidol University, Thailand

Cannabidiol (CBD) has received attention because of its potential therapeutic effects including bone health. This study aims to evaluate the effect of CBD on primary osteoclasts (OCs) and osteoblasts (OBs) from Sprague-Dawley rats. At the age of 14 wks old, bone marrow was isolated from femurs and tibiae and cultured in ?-MEM supplemented with 10 ng/mL M-CSF in 96-well plates at 2x104 cells/well to differentiate into OCs. After 24 hrs, the medium was changed to OC differentiation medium containing 10 ng/mL of M-CSF and RANKL. The osteoclast cultures were fixed with 4% paraformaldehyde and stained for tartrate-resistant acid phosphatase (TRAP). OBs were derived from explant cultures of femurs and tibiae in DMEM supplemented with L-ascorbic acid 2-phosphate (AscP). When the cultures reached confluence, cells were passaged and plated in 96-well and 12-well plates at 1x104 and 5x104 cells/well, respectively. Cells in 96-well plates were allowed to settle overnight and CBD at 0, 0.1, 0.5, 1, 5, 10, and 20 ?M was added to the culture. After 48-hr incubation, MTT assay was performed to evaluate cell proliferation. Cells in 12-well plates were cultured to confluence and the medium supplemented with AscP and 2 mM ?-glycerophosphate was added to stimulate osteoblast maturation and mineralization. Aizarin red S staining was used to detect mineralization. Here, we observed that CBD at the concentration of 1, 5, and 10 ?M suppressed osteoclast multinucleation in a dose-dependent manner. Specifically, CBD at 1 ?M significantly reduced the number of multi-nucleated cells (MNCs) when compared to the culture of vehicle control and CBD at 10 ?M almost completely suppressed osteoclast differentiation. For osteoblast culture, CBD at the concentration of 0.1-1 ?M did not impact the growth of pre-OBs whereas higher doses (5, 10 and 20 ?M) increased pre-OB proliferation compared to control. We selected three doses of CBD at 1, 5, and 10 ?M to study osteoblast mineralization. Alrizarin red S staining of cultures in CBD at 1 and 5 ?M showed an increase in mineralization. On the other hand, CBD at 10 ?M seemed to suppress osteoblast mineralization. Our findings demonstrated that CBD at 1 and 5 ?M presented favorable effect towards bone protection whereas CBD at 10 ?M inhibited MNC formation but also reduced OB mineralization. In conclusion, CBD is a potent regulator of osteoclast and osteoblast functions; therefore, could be used to modulate bone turnover towards bone formation.

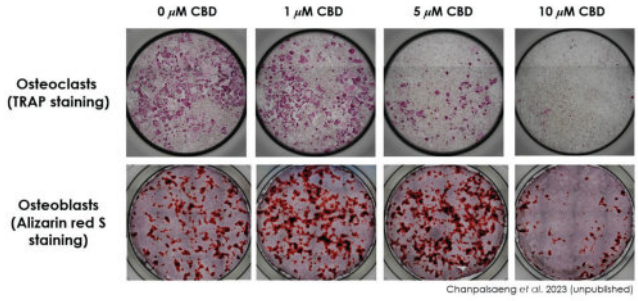

***Disclosures: Krittikan Chanpaisaeng**, None*

SAT-472

Bone-targeted far-red probe for the fluorometric detection of extracellular Cathepsin-K *BEN SWANSON[2], Boya Zhang[2], MARGARET DURDAN[3], Megan Weivoda[4], YUJI MISHINA[2], Colin Greineder[2]. [2]University of Michigan, , [2]University of Michigan, United States, [3], , [4]Mayo Clinic, United States

Cathepsin K (CTSK) is a lysosomal cysteine protease secreted by osteoclasts (OC), which plays a crucial role in ECM proteolysis during bone remodeling. CTSK inhibitors have shown promise to treat osteoporosis, but were halted in human trials due to off-target toxicities. To overcome this, new pharmacologic strategies must be developed and novel research tools are needed to detect changes in CTSK activity at the bone surface. Previous attempts to develop CTSK activity probes lack sensitivity and specificity necessary for high-fidelity detection. We aimed to develop a low molecular weight probe that rapidly circulates and localizes to the bone surface, using a fluorophore-quencher pair to detect extracellular CTSK proteolysis in vitro and in vivo. We synthesized a nine-residue peptide based on the consensus sequence of CTSK, modified with a far-red fluorescent residue adjacent to its C-terminus (Cy5) and broad-spectrum quencher (QSY21) at its N-terminus: QSY21-GHP-GGPQ-K(Cy5)-K(N3) (CTSKr). The C-terminal azidolysine was orthogonally conjugated

to a bisphosphonate dibencocyclooctyne (BP-DBCO) to yield BP-CTSKr. We demonstrated the ability of this BP-CTSKr (10 mM) to detect CTSK protease activity in a fluorometric assay, comparable to a commercially available 7-amino-4-trifluoromethylcoumarin inhibitor screening assay (Abcam). Subsequently, when recombinant CTSK was inhibited by FF-FMK (1 mM), fluorescence signal of BP-CTSKr was abolished. BP-CTSKr efficiently localizes to the surface of hydroxyapatite nanoparticles (HA-NP) in solution. When treated with recombinant CTSK, fluorescent signal from the surface of HA-NP at 670 nm is detected by fluorimeter and confocal at a high quantum yield. Primary mouse OC were differentiated and seeded to bovine bone slabs previously incubated with BP-CTSKr. After 24 hours, 3-D confocal laser microscopy demonstrates extracellular BP-CTSKr fluorescence beneath multinuclear TRAP+ OC, correlating to the resorption pit, exacerbated by LPS treatment. BP-CTSKr was injected systemically in 3-month-old C57BL/6 mice (2 mg/kg IP); no systemic or OC toxicity was observed after 24 hours in vivo. BP-CTSKr fluorescence is detected in frozen lumbar spine and femur sections, localized with TRAP+ OC. These results demonstrate a new approach to detecting extracellular CTSK activity with specificity to the bone microenvironment, an important technology requisite for developing new CTSK-targeted therapeutics.

***Disclosures: BEN SWANSON**, None*

SAT-473

Denosumab Reduces the Number of Circulating Osteoclast Precursor Cells in Postmenopausal Women with Osteoporosis *Jefferson Tsai[2], Kaichi Kaneko[2], Deniece Menez[2], Brian Oh[2], Andrew J. Suh[2], Eugenia Giannopoulou[2], Emily Stein[2], Linda A. Russell[2], Joseph Lane[2], Richard Bockman[3], Kyung-Hyun Park-Min[2]. [2]Hospital for Special Surgery, United States. [2]Hospital for Special Surgery, . [3]Hospital for Special Surgery, Weill Cornell Medical College, United States

Purpose: Osteoporosis is a systemic skeletal disease characterized by low bone mass and increased risk of fracture. Considerable work has been done to improve diagnostic tools to identify low bone mass, but early detection of osteoporosis remains challenging. Therefore, discovering new diagnostic markers that closely correlate with osteoporosis disease activity is imperative.Osteoclasts (OC) are hypothesized to be derived from circulating osteoclast precursor cells (cOCPs) of a myeloid cell origin. We have previously defined a population of cOCPs with high osteoclastogenic potential in postmenopausal women with osteoporosis that shows strong correlations with BMD and CTX, suggesting that the frequency of cOCPs may be indicative of bone quality in these patients. Current strategies for targeting OC in bone diseases such as osteoporosis include denosumab (Dmab), a fully human monoclonal antibody that inhibits RANKL and prevents RANK-mediated OC formation. We hypothesized that Dmab treatment may regulate the frequency of cOCPs. Here, we measured the number of cOCPs in postmenopausal women with osteoporosis on Dmab therapy. Methods: 16 postmenopausal women with osteoporosis on Dmab therapy were recruited for the study. PBMCs were stained with antibodies against different cell surface markers. cOCPs were quantified and analyzed by flow cytometry. CD14+ cells were incubated with macrophage colony stimulating factor and RANKL on a chamber slide and immunocytochemistry staining was performed to analyze RANKL-induced NFATc1 expression. Bone mineral density (BMD) was evaluated using DXA. Results: All 16 participants (mean age+/-SD: 69.3+/-5.3) had osteoporosis prior to beginning Dmab therapy. The duration of therapy was approximately 5 years (mean injection number+/-SD: 10.2+/-5.1). Lumbar spine and total hip T-scores were -1.43+/-1.08 and -2.27+/-0.6, respectively, suggesting that Dmab was effective in increasing BMD. The average number of cOCPs in Dmab patients was diminished (35.9 cOCPs/µL of blood) compared to our cohort of osteoporosis patients without treatment (71.5) and similar to patients with BMD values within normal range (23.1).Conclusions: Dmab treatment lowers the frequency of cOCPs in postmenopausal women with osteoporosis compared to treatment-naïve patients. Our findings indicate that Dmab modulates the frequency of cOCPs and could provide ways in which OC can be therapeutically targeted to prevent pathological bone loss associated with rebound phenomenon.

***Disclosures: Jefferson Tsai**, None*

SAT-474

See Friday Plenary Number FRI-474

SAT-475

Resistance exercise but not aerobic exercise in young males leads to increased serum concentration of ?-aminoisobutyric acid, L-BAIBA *Charalampos Lyssikatos[1], Brandon Yates[1], Ziyue Liu[1], Kamal Awad[2], Andrew Coggan[3], Stuart Warden[4], MARCO BROTTO[5], Lynda Bonewald[6]. [1]Indiana Center for Musculoskeletal Health, United States. [2]The University of Texas at Arlington , United States. [3]Department of Kinesiology, School of Health & Human Sciences, United States. [4]Indiana University School of Health & Human Sciences, United States. [5]University of Texas-Arlington (UTA), United States. [6]Indiana University School of Medicine, United States

BAIBA, a non-proteinogenic aminoacid with two enantiomers, L- and D-, is generated through catabolization of two distinct metabolic pathways from valine and thymine respectively. The enantiomers have been reported to have different or similar actions, depending on assay. We have shown the L-BAIBA is more potent than D-BAIBA in maintaining bone through osteocyte viability and is the form made by contracting murine muscle. In this study, we compared aerobic (endurance) and resistance (anaerobic) exercise in humans for circulating levels of L- and D-BAIBA and related butyric acids. We designed a pilot clinical study in asymptomatic, untrained, young (18-35 years old) adult males. To date four healthy volunteers (LDB1 - 4), age range 22 - 32 years old and BMI: 23.4 - 27.1, have been recruited. The study is taking place at the ICMH Musculoskeletal Function, Imaging and Tissue Resource Core. Three of the four participants completed both the endurance and the resistance exercise, each of 30 min duration but only one did not complete the resistance exercise. Blood samples were collected at baseline, during (15 and 30 min) and after (1, 2, 3 and 24 hrs) exercise. Serum levels of aminobutyric acids were quantitated using LC/MS. Plasma from 30 min was used to determine catecholamines level, an indicator of successful exercise stress response. With endurance exercise, L-BAIBA was detectable only at one time point in one participant (LDB2 - L-BAIBA: 0.085 ??) at 1 hr but was detected in all three participants in the resistance exercise. In two of them (LDB2 and LDB4), there was an increase (L-BAIBA: 0.040 -> 0.045 -> 0.046 for LDB2 and 0.039-> 0.049 -> 0.087 for LDB4) at 1, 2 and 24 hrs after the end of the resistance exercise. We also noticed a similar trend for L-AABA at 3 hrs, after a decrease from baseline. D-BAIBA was detectable after both types of exercise and in two participants (LDB2 and LDB4) was increased at 24 hrs. The ratio of L-BAIBA to D-BAIBA and L-AABA showed similar increases at 1 and 24 hrs after the end of the resistance exercise. This is a small observational pilot study to date with only four participants; however, it was striking that L-BAIBA was mainly observed with resistance and not aerobic exercise. This preliminary data supports the need to perform a larger study with greater power. These results may lend insight to how the different forms of exercise can generate distinct signaling factors correlating with beneficial effects on bone.

***Disclosures: Charalampos Lyssikatos**, None*

SAT-476

Changes in Serum Bone Metabolism Markers Can Predict Improved HR-pQCT Measures during Basic Combat Training - The ARMI Study *Jennifer Coulombe[1], Brittany Bozzini[2], Katelyn Guerriere[3], Stephen Foulis[2], Marinaliz Reynoso[4], Leila Walker[2], Jeffery Staab[2], Mary Bouxsein[5], Julie Hughes[6], Kristin Popp[2]. [1]Center for Advanced Orthopedic Studies, Department of Orthopedic Surgery, Beth Israel Deaconess Medical Center, Harvard Medical School, United States. [2]U.S. Army Research Institute of Environmental Medicine, United States. [3]USARIEM, United States. [4]U.S. Army Research Institute of Environmental Medicine, , United States. [5]Beth Israel Deaconess Medical Center, Harvard Medical School, United States. [6]US Army Research Institute of Environmental Medicine, United States

Stress fractures are a significant burden to the U.S. Army, occurring most commonly during Basic Combat Training (BCT). Bone mineral density (BMD) and bone microarchitecture improve during BCT in many, but not all, trainees. We determined changes in bone metabolism markers (BMM) during BCT and whether those changes predict improvements in bone microarchitecture during BCT.We acquired high-resolution peripheral quantitative computed tomography (HR-pQCT, XTremeCTII, Scanco Medical) scans of the distal tibia (4%) during week 1 (pre-BCT) and week 9 (post-BCT). Trainees provided fasted, rested blood samples pre-BCT, at weeks two, four, six, and eight during BCT, and post-BCT. Procollagen type 1 amino-terminal propeptide (P1NP) was measured by chemiluminescent assays (Immunodiagnostic Systems Limited) and cross-linked collagen telopeptide (CTX) was measured by ELISA (Serum CrossLaps). Bone and BMM data are presented as percent change from pre-BCT levels, with significance evaluated by Wilcoxon signed-rank test. We used sex-stratified multivariate regression models to assess the relationship between changes in HR-pQCT measures and P1NP levels at week four of BCT, adjusting for age, race, BMI, and pre-BCT P1NP levels.Participants included 110 men and 124 women (mean+/-SD; age= 20.7+/-4.0 yrs, BMI= 24.2+/-3.6 kg/m2). In women, P1NP levels were higher than pre-BCT values at every timepoint, with peak levels at week four (+45%, Fig 1A). In men, P1NP levels exceeded pre-BCT only during weeks two and four, with peak levels also at week four (+36%, Fig 1A). P1NP at week four of BCT was associated with increased cortical (Ct.) area (R^2=0.46, $p<0.0001$), Ct. thickness (Th) (R^2=0.42, $p<0.0001$), trabecular (Tb.) bone volume (R^2= 0.23, $p=0.0004$), Tb.BMD (R^2= 0.27, $p<0.0001$), and total (Tt.) BMD (R^2=0.28, $p<0.0001$) in women, and Ct. area (R^2= 0.48, $p<0.0001$), Ct.Th (R^2= 0.43, $p<0.0001$), Tb.BMD (R^2= 0.15, $p=0.001$), and Tt.BMD (R^2= 0.29, $p=0.0002$) in men.These

findings indicate that an increase in P1NP from pre-BCT to week four of BCT is associated with improved bone microarchitecture and density after training. Elevated P1NP without corresponding CTX rise may also suggest bone anabolism via uncoupled formation and resorption.Disclaimer: Supported by U.S. Medical Research and Development Command. The views expressed in this abstract are those of the authors and do not reflect the official policy of the Department of Army, Department of Defense, or the U.S. Government.

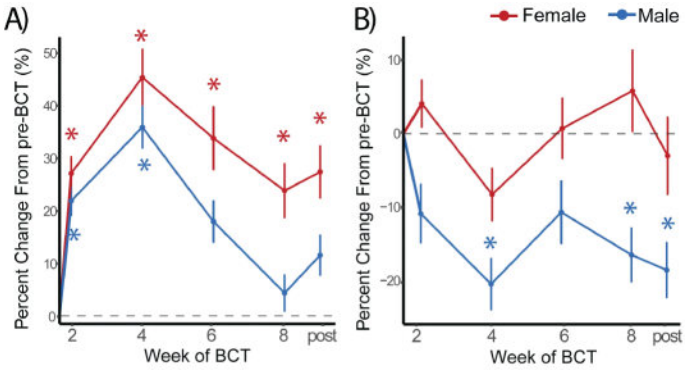

Figure 1: Changes in Serum Bone Turnover Markers during BCT in Men and Women. **A)** P1NP and **B)** CTX. Female and male trainees' P1NP levels peaked at week 4 of BCT (+45.3% and +35.9%, respectively). By contrast, CTX levels in female trainees were never significantly different than pre-BCT levels during BCT but were significantly lower than baseline levels for males during weeks 4 (-20.1%), 8 (-16.1%), and post-BCT follow up (-18.2%). Data are presented as mean and standard error of the mean percent change in P1NP and CTX from pre-BCT levels for female and male trainees. Statistical significance as compared to pre-BCT levels, p-values based on Wilcoxon signed-rank test, * - p<0.01.

***Disclosures: Jennifer Coulombe**, None*

SAT-477

Evaluating a New Physical Activity Metric for Predicting Bone Strength During Growth *Christina Alexander[1], Leigh Gabel[1]. [1]University of Calgary, Canada

Accelerometers are often used to examine relationships between free-living physical activity (PA) and bone health. Free-living PA is usually quantified using minutes spent in different activity intensities (e.g., sedentary, light PA, moderate-to-vigorous PA (MVPA), and VPA). However, new metrics to quantify PA have been proposed, including an intensity gradient (IG) approach that bins the full spectrum of accelerometry data. The IG slope indicates how evenly one's PA is spread across intensities, with the hypothesis that a shallower IG slope (greater time in MVPA and VPA) is beneficial for bone. The purpose of this study is to determine whether the IG metric better predicts bone strength during growth compared with traditional metrics (i.e., MVPA and VPA).In the University of British Columbia's Healthy Bones Study, over 300 healthy children and youth (age range 9-21 years) had their distal tibia scanned using high resolution peripheral quantitative computed tomography (XtremeCT, Scanco Medical). Bone strength (failure load, N) was estimated using finite element analysis. Physical activity was assessed using ActiGraph accelerometers worn on the hip for 7-days. MVPA (min/day) and VPA (min/day) were normalized to accelerometer wear time and IGs were calculated for each participant. Linear regression models examined relationships between PA metrics (MVPA, VPA, and IG) and tibia failure load. Models were adjusted for sex, ethnicity, tibia length, and maturity offset.Average minutes per day of MVPA and VPA were 42 minutes and 15 minutes, respectively, while intensity gradient ranged from -2.16 to -1.26. IG was weakly positively correlated with MVPA and VPA (r = 0.20 and r = 0.39, respectively). MVPA and VPA positively predicted bone strength (p = 0.023 and p= 0.050, respectively). A 1-minute increase in MVPA and VPA was associated with 3.6% and 14.6% greater failure load at the tibia, respectively. IG did not predict bone strength.The novel IG metric encompasses the full spectrum of accelerometry data and provides insight into "how" PA is accumulated. However, for predicting bone strength in youth, IG did not outperform traditional threshold-based approaches that rely on "how much" PA is accumulated. Future work should evaluate alternate IG bin sizes along with metrics that combine PA volumes and patterns.

***Disclosures: Christina Alexander**, None*

SAT-478

Participating in Sports Applying Multidirectional Loading During Youth Reduces Stress Fracture Risk During U.S. Army Basic Combat Training - The ARMI Study *Katelyn Guerriere[1], Ian Hussian[2], Kathryn Taylor[2], Paul Bartlett[2], Leila Walker[2], Nathaniel Smith[2], Kristin Popp[3], Karl Friedl[2], Mary Bouxsein[4], Stefan Pasiakos[2], Susan Proctor[2], Stephen Foulis[2], Julie Hughes[2]. [1]USARIEM, United States. [2]US Army Research Institute of Environmental Medicine, United States. [3]Massachusetts General Hospital, . [4]Beth Israel Deaconess Medical Center, Harvard Medical School, United States

Stress fractures (SF) risk is high during U.S. Army Basic Combat Training (BCT). However, SF risk may be reduced in Soldiers participating in sports applying multidirectional loading (MDS; e.g., soccer, other ball sports) in the two years before military training. History of MDS in youth is also associated with greater bone size, strength, and microarchitecture compared to those participating in sports applying unidirectional loading (UDS; e.g., running) or non-impact loading (NIS; e.g., swimming). Whether participation in MDS at any point during youth reduces SF risk during BCT is unknown. As part of a prospective observational study, participants completed surveys at the beginning of BCT to describe sport participation from kindergarten through young adulthood. Participants were categorized based on the highest level of osteogenic potential reported (MDS > UDS > NIS) or as having no sports participation (NS). Bone density, area, and microarchitecture were assessed using HR-pQCT at the beginning of BCT. ICD-10 medical diagnoses codes were used to identify stress fractures during BCT. Multivariate generalized linear models and least squared means, adjusted for age, height, weight, sex, race, and tobacco use, were used to analyze the relationship between baseline bone parameters and sport category. Multivariate logistic regression models, further adjusted for fracture history, were used to assess the relationship between sport category and SF risk during BCT. Out of 3090 participants (mean+/-SD; age=20.9+/-3.8, 62% male, 42% non-Hispanic white), 2337 were categorized as MDS (76%), 211 as UDS (7%), 30 as NIS (1%), and 508 as NS (16%). SF % was 4.6% in MDS, 8.5% in UDS, 13.3% in NIS, and 8.7% in NS. MDS had greater total area (Tt. Ar), total and trabecular (Tb.) bone mineral density (BMD), Tb. bone volume fraction, Tb. thickness, and cortical thickness than NS (2.07-5.63%; Table). MDS also had greater Tt.Ar., Tt.BMD, and Tb.BMD than UDS (1.68-3.38%; Table). SF risk was 46% lower for MDS (odds ratios(95%CI), 0.54(0.37, 0.78), p=0.001) than NS. SF risk was not different for the other groups compared to NS. These data demonstrate that participating in MDS, but not UDS, during youth improves bone properties and markedly reduces SF risk during BCT. These findings highlight the importance of participating in MDS to prevent bone fragility and reduce SF risk in adulthood.

Bone Outcome	MDS vs UDS	MDS vs NIS	MDS vs NS
Tt.Ar	**1.68 (0.19, 3.20)**	2.87 (-0.93, 6.73)	**2.51 (1.48, 3.56)**
Tt.BMD	**2.24 (0.05, 4.46)**	1.03 (-4.63, 6.77)	**4.38 (2.95, 5.83)**
Tb.BMD	**3.38 (1.05, 5.75)**	2.80 (-3.13, 8.84)	**5.18 (3.68, 6.70)**
Tb.BV/TV	3.17 (-0.31, 6.72)	2.54 (-3.77, 8.96)	**5.07 (3.45, 6.72)**
Tb.Th	0.41 (-5.35, 6.69)	0.41 (-3.70, 4.60)	**2.07 (0.82, 3.34)**
Ct.Th	0.80 (-4.07, 5.82)	-0.34 (-8.71, 8.26)	**5.62 (0.80, 3.17)**

Data are percent differences (upper and lower control limits). Data in bold font indicate significant differences between sport categories. MDS = multidirectional loading sports; UDS = unidirectional loading sports; NIS = non-impact loading sports; NS = no sports participation; Tt.Ar = total area; Tt.BMD = total bone mineral density; Tb.BMD = trabecular bone mineral density; Tb.BV/TV = trabecular bone volume/total volume; Tb.Th = trabecular thickness; Ct.Th = cortical thickness

***Disclosures: Katelyn Guerriere**, None*

SAT-479

Four-year longitudinal assessment of risk factors for bone stress injuries in intercollegiate distance runners *Kenneth Kozloff[1], Melissa Bown[2], Christina Fanning[2], Fiddy Davis[3], Kelly Rogers[4], Ronald Zernicke[1]. [1]University of Michigan, United States. [2]Department of Athletics, University of Michigan, United States. [3]Michigan Performance Research Laboratory, United States. [4]Department of Orthopaedic Surgery, University of Michigan, United States

Bone stress injuries (BSI) are prevalent in sports emphasizing leanness, endurance, and skeletal loading. While individual BSI risk factors have been identified, translating this into actionable models of BSI prevention remains elusive. The Female Athlete Triad Risk Assessment Tool [1] was adapted to identify female [2] and male [3] athletes at high risk for BSI but doesn't account for modifiable factors such as sleep, which has been shown to be associated with BSI in military [4]. Here, we evaluate BSI risk in distance runners using the modified Triad assessment tool and compare risks to those calculated from sleep surveys as an independent predictor of BSI.Male (n=41) and female (n=49) runners from an NCAA D1 Cross Country program were recruited over 4 years. BSI risk scores were evaluated prospectively [2,3] through pre-season surveys and DEXA-derived BMD of the hip and spine. Individual scores on a 0-2 pt scale were summed as follows: Prior BSI (none:0 pt; 1 low risk site:1 pt; >1 high risk site or >2 low risk site:2pt); dietary restriction (none:0pt; some/past DE history:1pt; current DE:2pt); body mass index (BMI>18.5: 0pt; BMI 17.5-18.5: 1pt; BMI-1: 0pt; -1 to -2: 1 pt; <-2: 2 pt). Female surveys included age at menarche (16: 2pt) and cycles over past year (>9 menses: 0pt; 6 to 9:1 pt; <6: 2pt). Sleep was assessed by survey [5] pre-season and after ~8 wks of training. Annual BSI incidence was monitored. Relative risk

(RR) scores for BSI for any year was compared to BSI incidence for subjects scoring 0-1pts on the modified Triad tool and to subjects registering a change of -1 to +1 points on sleep hygiene.A total of 38 (women) and 14 (men) BSI were observed. Of 194 athlete-seasons of data, 160 included complete assessments. Women scoring 6-7 out of 12 max points on the modified Triad tool increased BSI RR 2.1 fold (95% CI 1-4.5). Men scoring 4-5 (out of 8) increased BSI RR 8.2 fold (95% CI 1.4-48). Within-season worsening of sleep hygiene by 4-5 points (17 max) independently increased BSI RR 3.2 fold (95% CI 2.0-5.1) in women, but not men.Predictive tools that incorporate sleep as a modifiable behavior may be combined with other personalized metrics to help identify endurance athletes who are at greatest risk for BSI.Refs: 1.De Souza Br J Sports Med 2014; 2.Tenforde Am J Sports Med 2017; 3.Kraus Br J Sports Med 2019; 4.Firestone Med Sci Sports Exer 2008; 5.Bender Sports Med Open 2018

***Disclosures: Kenneth Kozloff**, None*

SAT-480

Functional Characterization of Novel Lunatic Fringe Variants in Spondylocostal Dysostosis Type-III with Scoliosis *Parker Wengryn[1,] Karina Da Costa Silveira[1,] Connor Oborn[1,] Carrie-Lynn Soltys[1,] Alex Beke[1,] Inara Chacon-Fonseca[2,] Nadirah Damseh[3,] Marco Quesada Rodriguez[4,] Ramsés Badilla Porras[4,] Peter Kannu[1,] [1]University of Alberta, Canada, [2]Lakeridge Health Oshawa, Canada, [3]University of Toronto, Canada, [4]Hospital Nacional de Niños, Costa Rica

Purpose: Rare Mendelian diseases provide a unique opportunity to investigate genetic pathways contributing to normal spinal development and variability in phenotypic presentation. Spondylocostal Dysostosis Type-III (SCD3) is a rare, autosomal recessive disorder characterized by rib fusions, vertebral abnormalities, and varying degrees of scoliosis. SCD3 is caused by variants in the Lunatic Fringe (LFNG) gene encoding a ?-1-3-N-acetylglucosaminyltransferase. This enzyme transfers N-acetylglucosamine to NOTCH1 during somitogenesis to promote normal vertebral formation. We have identified compound heterozygous LFNG variants-of-uncertain-significance (VUS; the genetic variant has an unknown effect on health) in a proband with a SCD phenotype. However, the proband is taller (Height: 10th-25th%), has a longer trunk (Arm span-to-height ratio: 1.07), and more vertebrae (>20) than the six previously reported SCD3 cases. The purpose of our study is to determine whether the c.766G>A (p.G256S) and c.521G>A (p.R174H) LFNG variants lead to diminished N-acetylglucosaminyltransferase activity, protein mis-localization, and/or dysregulated pre-pro-processing. We hope that this will inform the relationship between genotype and phenotype.Methods: HEK293T cells were transiently transfected with 3XFLAG-hLFNG. Fusion protein was immunoprecipitated and assessed with a quantitative glycosyltransferase luciferase assay. NIH3T3 cells were transiently transfected with LFNG-HA, incubated with anti-HA and anti-GM130 antibodies, then assessed for signal colocalization through confocal microscopy. Finally, NIH3T3 cells were transfected with LFNG-HA and whole cell lysate was processed for protein, western blotted, and semi-quantitatively analyzed. Results: The p.G256S and p.R174H variants displayed significantly less enzymatic activity than wildtype. The p.G256S substituion was comparable to negative control whereas p.R174H was significantly more active than p.G256S. Both variants were correctly localized to the Golgi and normally pre-pro-processed.Conclusions: We have discovered the first hypomorphic (p.R174H) and report the fourth functionally null (p.G256S) LFNG variants associated with SCD3. This is the first clinically identified combination of partially active and completely inactive LFNG. This data may suggest that the hypomorphic variant partially rescued the probands height, trunk length, and vertebral number, but not segmentation defects nor scoliosis.

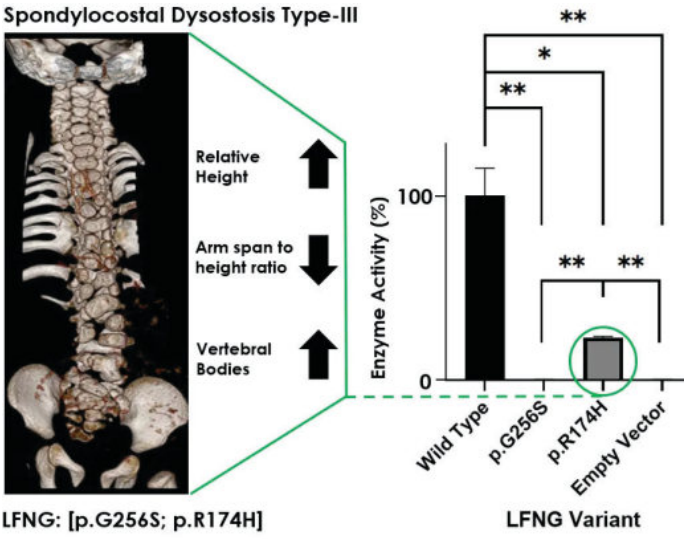

***Disclosures: Parker Wengryn**, None*

SAT-481

The Association Between 24-Hour Activity with Incident Fracture Risk in the Osteoporotic Fractures in Men (MrOS) Study *Lauren S. Roe[1,] Elsa Strotmeyer[2,] Peggy Cawthon[3,] Nancy W. Glynn[4,] Sonia Ancoli-Israel[5,] Kristine Ensrud[6,] Susan Redline[7,] Katie L. Stone[8,] Kelley Pettee Gabriel[9,] Douglas Bauer[10,] Jane A. Cauley[11,] [1], [2]University of Pittsburgh, United States, [3]San Francisco Coordinating Center, United States, [4]University of Pittsburgh School of Public Health, Department of Epidemiology, United States, [5]University of California San Diego, Department of Psychiatry, United States, [6]University of Minnesota and Minneapolis VA Health Care System, United States, [7]Brigham and Women's Hospital, United States, [8]California Pacific Medical Center, Research Institute, United States, [9]The University of Alabama at Birmingham School of Public Health, Department of Epidemiology, United States, [10]University of California, San Francisco, United States, [11]UNIVERSITY OF PITTSBURGH, United States

Lower physical activity (PA) and sleep, and higher sedentary behavior (SB) are individually associated with fractures. Time spent in these behaviors is inherently linked because there is a finite amount of time in a 24-hr period, but previous analyses examining one activity often have omitted information about all other activities. We evaluated the combined role of PA, SB, and sleep on incident fracture risk using compositional data analysis. Men (N=2,910) attending the Year 7 (2007-2009) MrOS visit (mean age 79.0+/-5.1 y) with accelerometry data (SenseWear® Pro3 Armband) were included in this analysis. PA (>1.5 metabolic equivalents of task; METs), SB (<1.5 METS), and sleep at night were measured over an average of 5.1+/-0.3 days. The 24-hr activity compositions were represented as isometric logratios (ILR). These ILRs were used as predictors in Cox proportional hazards regression models to estimate the risk of incident clinical fracture by the proportion of time in one activity relative to all other activities simultaneously. Self-reported fractures were confirmed with radiographic reports. During an average follow-up of 8.7+/-4.4 y, 669 men had any clinical fracture. Mean composition of PA, SB, and sleep was 134 min/day, 896 min/day, and 410 min/day respectively. In minimally adjusted models (age, race, clinic, season of accelerometer wear), more SB at the expense of sleep and PA was associated with greater fracture risk (hazard ratio [HR]: 1.53, 95% confidence interval [CI]: 1.12, 2.07), and more sleep at the expense of PA and SB was associated with lower fracture risk (HR: 0.71, 95% CI: 0.52, 0.97). Further adjustment for height, weight, diabetes history, health status, smoking, number of comorbidities, and number of impaired instrumental activities of daily living did not alter these associations (SB vs. PA/sleep - HR: 1.54, 95% CI: 1.14, 2.08; sleep vs. PA/SB - HR: 0.68, 95% CI: 0.50, 0.92). In contrast, no association between PA vs. sleep/SB existed with fractures in minimally or fully adjusted models. In conclusion, when accounting for the inherent co-dependence of daily activities, men with higher proportions of sleep relative to the proportion of PA and SB had a lower risk of incident fractures, while men with higher proportions of SB relative to the proportion of PA and sleep had an increased risk of fractures. Future studies should evaluate if fracture risk is lowered by increasing PA or sleep at the expense of SB.

***Disclosures: Lauren S. Roe**, None*

SAT-482

The "can do, do do" framework applied to explore physical capacity, physical activity and fall risk factors in FLS patients *MERLE SCHENE[1,] Kenneth Meijer[2,] Donald Cheung[2,] Hanna Willems[3,] Annemariek Driessen[2,] Lisanne Vranken[4,] Joop van den Bergh[4,] Caroline Wyers[4,] [1]Viecuri Medisch Centrum , [2]NUTRIM School of Nutrition and Translational Research in Metabolism, Maastricht University, Netherlands, [3]Amsterdam UMC location University of Amsterdam, Internal Medicine and Geriatrics, Netherlands, [4]Department of Internal Medicine, VieCuri Medical Center, Netherlands

Physical capacity (PC) and physical activity (PA) are two associated, but distinctly separate domains of physical performance. Poor performance in these domains has been associated with an increased fall risk in older persons. Combined, PC and PA can be used to categorize physical performance into four quadrants according to the "can do, do do" framework. This cross-sectional study aims to use this framework to explore physical performance and patient characteristics including fall and fracture risk factors in patients aged >=50 years attending the fracture liaison service (FLS) for fracture risk evaluation. Physical performance of 400 fracture patients was assessed (mean age 64; female 70.8%). PC was measured by 6-minute-walking-test (6MWT) (can't do/can do) and PA by MOX accelerometer (don't do/do do) during 8 days of daily life. Following quadrants were defined based on predefined sex-specific cut-off scores for poor performance: 1."can't do, don't do"; 2."can do, don't do"; 3."can't do, do do"; 4."can do, do do". Correlation and odds ratios (ORs) between PC and PA measures were calculated and patient characteristics including fall and fracture risk factors were compared between groups. Patients performed as follows: 8.3% "can't do, don't do"; 3.0% "can do, don't do"; 19.3% "can't do, do do"; 69.5% "can do, do do". For the "can't do" group the OR for low PA was 9.76 (95%CI: 4.82-19.80), compared to the "can do" group. The "can't do, don't do" was older, had a higher proportions of osteoporosis and prevalent vertebral fractures compared to the "can do, do do" group. Moreover, both the "can't do, don't do" and "can't do, do do" group had lower physical performance on all functional tests, higher proportions of patients with fear of falling, and more patients used a walking aids, compared to the "can do, do do" group. This is the first application of the "can

do, do do" framework to explore fall and fracture risk factors among patients with a recent fracture. Of all FLS patients 20% "can't do", but "do do" while having a high prevalence of fall risk factors compared to patients that "can do, do do", which may indicate a group prone to fall. Subgroup identification following this concept provides additional insight on impaired physical performance of FLS patients and their fall and fracture risk factors and might prove useful for targeted interventions in the future.

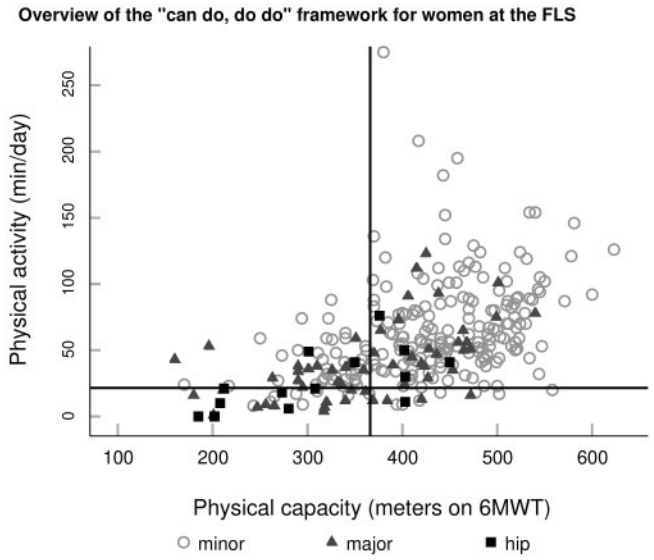

***Disclosures: MERLE SCHENE**, None*

SAT-483

See Friday Plenary Number FRI-483

SAT-484

See Friday Plenary Number FRI-484

SAT-486

Clinical Outcomes and Population Characteristics in Fibrodysplasia Ossificans Progressiva: A Systematic Literature Review *Hind Harrak[1], Amal Souttou[1], Xueqi Qu[2], Caitlin Knox[1]. [1]Regeneron Pharmaceuticals, Inc., United States. [2]Department of Mental Health, Johns Hopkins Bloomberg School of Public Health, United States

Purpose: Despite efforts to better understand fibrodysplasia ossificans progressiva (FOP), a rare autosomal dominant disease characterized by progressive episodic multi-focal heterotopic ossification (HO), population characteristics and natural disease history are ill defined. This systematic literature review (SLR) assessed the current knowledge of FOP, including mortality, comorbidities, recommended management and medication use. HO formation frequency and patterns in the pediatric population were also assessed.Methods: We searched Pubmed, Embase, the Cochrane central register of controlled trials, the Trip database and NICE documents to retrieve relevant studies, restricted to humans but not by language. Studies were kept if they reported at least 1 of the following outcomes: mortality, comorbidity, medication-use pattern, standard of care, or HO in pediatric population. Clinical trials solely aiming to assess treatment of FOP were excluded to avoid potential disease-modifying effects. Two independent reviewers conducted the study selection. Data extraction was conducted by one investigator, and quality controlled by the second reviewer, using the appropriate tools by study design. The SLR was registered on Prospero (CRD42022366914).Results: Thirty-nine studies were selected. Publications were global, covering wide age groups. Study duration varied from 1 day to 33 years and sample size from 3 to 299 patients. Eight studies reported on mortality, and out of 62 reported deaths with recorded cause, 25 were due to cardiovascular or cardiorespiratory failure. Twenty-five publications included information on comorbidities, with eight studies reporting deafness and five studies reporting chronic pain as a comorbidity. The three most affected systems by order of magnitude were cardiovascular, respiratory, and skeletal. Twelve studies provided standard of care recommendations and drug utilization. Eight studies had data on pediatric HO formation.Conclusions: Despite the number of studies included in this SLR, there were important limitations: several studies used the same patient pool, lack of clear definition, outcomes, or follow-up periods. Re-use of the same patient pool meant that duplicate data cannot be ruled out, which inhibited the aggregation of the data or the estimation of background rates. Our SLR highlights the need for detailed information in published studies to allow for critical evaluation and summarization in SLRs, especially in rare diseases.

***Disclosures: Hind Harrak**, Regeneron Pharmaceuticals, Inc., Other Financial or Material Support*

SAT-488

Clinical Features of FGF23-Related Hypophosphatemic Rickets/ Osteomalacia: A Multicenter National Survey in Japan *Makoto Fujiwara[1], Taichi Kitaoka[1], Yasuhisa Ohata[1], Hirofumi Nakayama[2], Yukako Nakano[1], Kenichi Yamamoto[3], Hiroyuki Saitou[1], Chieko Yamada[1], Takeshi Ishimi[1], Ikumi Ueda[1], Tatsuya Nakamichi[1], Rieko Takatani[4], Masanori Minagawa[5], Daisuke Inoue[6], Yasuhiro Takeuchi[7], Seiji Fukumoto[8], Takashi Akamizu[9], Keiichi Ozono[1], Takuo Kubota[1]. [1]Department of Pediatrics, Osaka University Graduate School of Medicine, Japan. [2]The first Department of Oral and Maxillofacial Surgery, Osaka University Graduate School of Dentistry, Japan. [3]Division of Health Sciences, Osaka University Graduate School of Medicine, Japan. [4]Center for Preventive Medical Sciences, Chiba University, Japan. [5]Department of Endocrinology, Chiba Children's Hospital, Japan. [6]Third Department of Medicine, Teikyo University Chiba Medical Center, Japan. [7]Endocrine Center, Toranomon Hospital, Japan. [8]Department of Molecular Endocrinology, Fujii Memorial Institute of Medical Sciences, Institute of Advanced Medical Sciences, Tokushima University, Japan. [9]Department of Internal Medicine, Kuma Hospital, Japan

Background: Fibroblast growth factor 23-related hypophosphatemic rickets/osteomalacia (FGF23-HR/HO) is a rare bone mineralization disorder characterized by high serum FGF23 and hypophosphatemia. X-linked hypophosphatemia (XLH) is the most common heritable cause, while tumor-induced osteomalacia (TIO) is a major acquired one. Due to the rarity of this disease, limited information is available regarding its treatment and prognosis. Objectives: To elucidate the clinical characteristics of XLH and TIO in Japan. Methods: A retrospective questionnaire survey of physicians belonging to the Japanese Society for Bone and Mineral Research was conducted for one year from September 2018 to identify patients diagnosed with FGF23-HR/HO. The clinical information of XLH and TIO patients was analyzed, including anthropometric data, symptoms, and laboratory data. Results: The study analyzed 104 patients (45 males and 59 females), of which 67 had XLH with confirmed PHEX mutations and 37 had TIO. Of the 67 XLH patients, 38 had a family history of the disease. Among the 40 adult patients with XLH (aXLH, age 19-72 years), 31 were diagnosed in childhood, indicating a significantly lower age of onset for XLH compared to TIO (age 32-87 years). aXLH showed significantly lower height standard deviation score (SDS) and weight-SDS, lower serum intact FGF23 (all under 200 pg/mL), and higher serum phosphate levels compared to TIO patients. Pediatric patients with XLH (pXLH, age 1.8-17 years) revealed a significantly higher prevalence of craniosynostosis and foot deformity, while aXLH had a higher prevalence of spinal ligament ossification, enthesopathy, nephrocalcinosis, and periodontitis. In contrast, in TIO, the prevalence of fracture, bone pain, joint pain, and muscle weakness was significantly higher. Regarding treatment, XLH patients received active vitamin D, phosphate, and burosumab in 62%, 47%, and 32% of cases, respectively, while TIO patients received these treatments in 73%, 38%, and 8% of cases, respectively. Tumor resection was performed in 68% of TIO patients. The utilization rate of burosumab and the dosage of alfacalcidol (μg/kg/day) were significantly higher in pXLH, followed by aXLH and TIO patients. Conclusion: aXLH patients exhibit more severe growth disturbance and may require careful prevention and management strategies for the characteristic ectopic calcifications. These findings may be helpful in improving the quality of medical care for this rare disease.

***Disclosures: Makoto Fujiwara**, None*

SAT-490

A qualitative study investigating the experiences of women living with pregnancy and lactation associated osteoporosis in the United Kingdom *Nataliya Gak[1], Ali Abbara[2], Judith Bubbear[3], Alexander Comninos[4], Richard Keen[3]. [1]Department of Rheumatology, Royal National Orthopaedic Hospital NHS Trust, Imperial College London , United Kingdom. [2]Department of Endocrinology, Imperial College London, United Kingdom. [3]Department of Rheumatology, Royal National Orthopaedic Hospital NHS Trust , United Kingdom. [4]Endocrine Bone Unit, Imperial College Healthcare NHS Trust, United Kingdom

Background: Pregnancy and lactation associated osteoporosis (PLO) is a rare and severe form of osteoporosis defined by a reduction in bone mineral density leading to fragility fractures during the last trimester of pregnancy or post-partum when lactating. Despite the severe physical and psychosocial consequences of fracturing around pregnancy, there are currently no data in this regard investigating patients with PLO in the United Kingdom. Objectives: To determine the impact of PLO on physical, emotional, and social wellbeing of women with PLO. Methods: 15 women (age range 32-60 years, mean 40 years) who attended specialist tertiary clinics in the UK, were recruited to take part in semi- structured interviews (duration from diagnosis to interview range 1-32 years, median 3 years). The in-

terviews were video recorded, transcribed verbatim and qualitative data was analysed using emergent coding and thematic analysis.Results: The main themes that emerged were: 1) lack of awareness about PLO in primary and secondary care leading to delays in diagnosis, misdiagnosis and incorrect management; 2) lack of physiotherapy and psychological support specific to PLO needs; 3) acute and chronic back pain impacting on mobility, ability to self-care and care for new-born, resulting in dependence on others (partners, parents, baby-sitters, friends); 4) grieving for the loss of motherhood, self-identity and life normality; 5) anxiety about further possible fractures and future pregnancies; 6) struggling to engaged in social activities important to wellbeing due to mobility issues, loss of self-confidence and emotional distress caused by the diagnosis of PLO.Conclusion: These data demonstrate the physical, and psychosocial impacts of PLO in women in the UK for the first time. They describe a noticeable lack of understanding about PLO and its management in the UK. Better awareness with faster diagnosis and subsequent timely treatment may partially alleviate some of the physical and psychosocial impacts. The themes identified suggest that a multidisciplinary approach with early the involvement of obstetricians, midwives, metabolic bone specialists, spinal surgeons, pain specialists, physiotherapists, and psychologists may better address the needs of women affected by PLO.

***Disclosures: Nataliya Gak**, None*

SAT-491

See Friday Plenary Number FRI-491

SAT-493

Real-World Characteristics and Disease History of Patients With X-Linked Hypophosphatemia Treated with Burosumab: A United States Claims Database Study *KATHRYN DAHIR[1], Heather Heerssen[2], Yang Zhao[2], Angie Dale[2], Ahmed Noman[3], Jeremy Kim[3], Zhiyi Li[2]. [1]Vanderbilt University Medical Center, [2]Kyowa Kirin, Inc., United States, [3]Komodo Health, United States

Purpose: X-linked hypophosphatemia (XLH) is a rare genetic disease characterized by chronic renal phosphate wasting. The clinical presentation typically begins in early childhood and progresses through adulthood. XLH is thus associated with lifetime accumulation of clinical morbidities. In 2018, burosumab became the first United States (US) Food and Drug Administration-approved therapy for treating the underlying pathophysiology of XLH. This study examined patient characteristics and disease history - including XLH-related morbidities, treatments, and procedures - among real-world patients with XLH initiating burosumab in the US.Methods: This retrospective cohort study used Komodo Health's Healthcare Map™, a real-world de-identified patient-level claims database. Included patients had >=1 claim for familial hypophosphatemia between 01/01/2015 and 06/30/2022 and >=1 claim for burosumab between 04/01/2018 and 06/30/2022 (index date was the date of first burosumab claim). The study period was the period prior to the index date and ranged from 1-7 years. Patient characteristics were measured at index while disease history was measured over the study period and stratified by age; all variables were evaluated descriptively. Results: Overall, 1,358 patients were included (mean age 23.5 +/- 19.1 years, 62% female, 41% from the southern US). Approximately half (53%) of XLH patients were <18 years of age at initiation of burosumab. Prior to receiving this treatment, patients had high levels of XLH-related morbidities, many of which appeared early and increased with age group (Figure). Most patients had received some form of conventional therapy for XLH during the study period, including high-dose calcitriol (66% of patients aged <18 years and 56% of patients >=18 years) and/or phosphate supplements (42% of patients aged <18 years and 44% of patients >=18 years), prior to burosumab. Opioid use was prevalent among XLH patients prior to burosumab treatment, and this increased with age (24% of patients aged <18 years and 51% of patients >=18 years). Physical therapy use was observed across all age groups (18% of patients aged <18 years and 40% of patients >=18 years).Conclusions: At the time of initiation of burosumab, approximately half of patients with XLH were <18 years of age and had already experienced a heavy and progressive disease burden. The prevalence of XLH-related morbidities increased with age.Sponsorship: Kyowa Kirin, Inc.

Figure. XLH-related morbidities experienced by patients with XLH prior to burosumab treatment

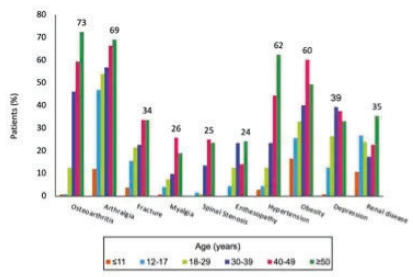

***Disclosures: KATHRYN DAHIR**, Ultragenyx, Kyowa Kirin, Alexion, AM Pharma, Consultant, Ultragenyx, Kyowa Kirin, Alexion-Astra Zeneca, Regeneron, Grant/Research Support*

SAT-495

See Friday Plenary Number FRI-495

SAT-496

Association between work productivity and characteristics of adults with X-linked hypophosphatemia: an analysis of the XLH Disease Monitoring Program *Aliya Khan[1], Ben Johnson[2], Annabel Nixon[3], Jen Liu[3], Zhiyi Li[4], Alison Skrinar[5], Christy Yang[5], Angela Williams[2]. [1]McMaster University, Canada, [2]Kyowa Kirin International, United Kingdom, [3]Chilli Consultancy, United Kingdom, [4]Kyowa Kirin North America, United States, [5]Ultragenyx Pharmaceutical Inc, United States

Objective: X-linked hypophosphatemia (XLH) is a rare, progressive, phosphate wasting disorder that causes substantial musculoskeletal morbidities and functional impairment. The XLH Disease Monitoring Program (XLH-DMP; NCT03651505) is a prospective, 10-year, longitudinal, observational study of adults and children with XLH on or off any treatment. Our study examined the relationship between characteristics of adults with XLH and their work productivity, to understand the broader impact of the disease.Methods: Subjects in the XLH-DMP aged >=18 to <65 years at enrolment were included in the analysis, but those enrolled after 31 December 2019 were excluded to avoid confounding effects of the COVID-19 pandemic on work productivity. Using data collected at enrolment, relationships between work productivity and demographics, medical history, Western Ontario McMaster Universities Osteoarthritis Index (WOMAC®) scores, Patient-Reported Outcomes Measurement Information System (PROMIS) physical function score and the Timed Up and Go (TUG) assessment were evaluated using univariate analysis (ANOVA, chi-squared) to guide the selection of variables for multivariate analyses (multinomial logistic regression). Results: The analysis included 281 adults (75.4% female), with a mean (SD) age of 39.9 (12.3) years; 80.8% were from the USA, 8.5% from Brazil, 7.1% from Canada, and 3.6% from Chile; 53.4% were employed full-time, 15.3% employed part-time and 31.3% not employed. Subjects had undergone a mean (SD) of 3.9 (4.7) surgeries and had mean WOMAC scores of 32.5 (22.5) for pain, 43.3 (24.8) for stiffness and 29.1 (22.8) for physical function, and a mean PROMIS physical function T-score of 41.6 (8.8). Multivariate analysis identified number of surgeries and PROMIS physical function score as significantly associated with work status: subjects with fewer surgeries (odds ratio [OR] 0.88; 95% confidence intervals [CI] 0.82-0.95; p<0.01) and those with better PROMIS physical function scores (OR 1.09; 95% CI 1.02-1.16; p<0.01) were more likely to be in full-time employment compared with being unemployed.Conclusion: Full-time employment levels are low in adults of working age with XLH, suggesting that the disease has a substantial impact on work productivity. Patients' physical function and history of surgery are likely to influence work productivity.

***Disclosures: Aliya Khan**, Kyowa Kirin International, Consultant*

SAT-499

Eagle syndrome: [18F]NaF PET/CT and in-depth tissue analysis *Ruben de Ruiter[1], Sanne Treurniet[1], Björn Busse[5], Jan Jaap Hendrickx[3], Berend Teunissen[4], Adriaan Lammertsma[4], Marelise Eekhoff[1], Felix Schmidt[5]. [1]Department of Endocrinology and Metabolism, Amsterdam University Medical Centers, Vrije Universiteit, Amsterdam Movement Sciences, Netherlands, [5]Department of Osteology and Biomechanics, University Medical Center Hamburg-Eppendorf, Germany, [3]Department of Otolaryngology, Head and Neck Surgery, Amsterdam University Medical Centers, Vrije Universiteit, Netherlands, [4]Department of Radiology and Nuclear Medicine, Amsterdam University Medical Centers, Vrije Universiteit, Netherlands, [5]Department of Osteology and Biomechanics, University Medical Center Hamburg-Eppendorf, Netherlands

Purpose: Eagle syndrome is a rare medical condition, characterized by elongation and calcification of the styloid process. Various theories have been proposed towards the etiology of this styloid calcification, varying from congenital elongation of the styloid process to metaplastic changes following a traumatic stimulus. To elucidate the pathophysiology of Eagle syndrome we performed [18F]NaF PET/CTs in 6 patients presenting with Eagle syndrome followed by detailed bone quality analysis after surgery.Methods: Six patients (age: 36 - 57 years old, men/women: 3/3) were included presenting with Eagle syndrome. Pre-operatively a [18F]NaF PET/CT was performed to evaluate active areas of bone formation, in particular in the stylohyoid region. The styloid process was surgically removed and further analyzed by micro-CT (?CT), quantitative backscattered electron imaging (qBEI) and histopathology including bone histomorphometry.Results: Four out of the six patients showed increased [18F]NaF uptake on the PET/CT scan at the base of the elongated styloid process. Histopathology of the biopsies revealed both cortical and trabecular bone tissue with bone marrow tissue present. Osteoid appeared at the tip in three out of six specimens, indicating the occurrence of longitudinal growth. Three specimens exhibited signs of past fractures (2/6 callus formation and 1/6 pseudoarthrosis). Volumteric tissue mineral density (vTMD) in the styloid processes was compatible with the mineralization of cranial, cortical bone as a control. Following ?CT analysis, qBEI measurements (CaMean, CaPeak, CaLow, CaHigh, StdDev) showed a large mineralization variability in the Eagle sample set significantly different from cortical controls.Discussion: Morphological analysis of the removed calcified tissue obtained from Eagle syndrome patients, revealed cortical and trabecular bone

with cartilage tissue. Growth of the styloid process appeared to be taking place at the tip. The variation in 18F-uptake uptake on the PET/CT may indicate that growth of the styloid process is not occurring at a fixed rate or is a relatively slow process. Elongation of the styloid process may be a result of mechanical forces produced by the stylohyoid ligament, which can also vary over time. Intense uptake on the PET/CT may be the result of a recent fracture as the styloid process appears to heal "normally" with callus formation.

***Disclosures: Ruben de Ruiter**, None*

SAT-500

Cosmic: An open-label, randomized, active-controlled, phase 3 study of setrusumab compared with bisphosphonates in pediatric subjects with osteogenesis imperfecta *Thomas Carpenter[1], MICHAEL BOBER[2], Gary Gottesman[3], Oliver Semler[4], Temis Maria Felix[5], Leanne Ward[6], Hui Wang[7], Heather Byers[9], Stanley Krolczyk[9]. [1]Yale University School of Medicine, United States. [2]Nemours Children's Hospital, Delaware, . [3]Washington University School of Medicine in St. Louis, United States. [4]University Hospital, University of Cologne, Germany. [5]Medical Genetics Service of Hospital de Clínicas de Porto Alegre, Brazil. [6]Children s Hospital of Eastern Ontario, Canada. [7]Ultragenyx Pharmaceutical Inc., United States. [9]Ultragenyx, United States. [9]Ultragenyx,

Setrusumab is a recombinant, fully human monoclonal antibody that selectively binds to and inhibits sclerostin, thereby increasing anabolic bone activity and decreasing bone resorption; setrusumab is in development for the treatment of osteogenesis imperfecta (OI). A Phase 2b study in adults with OI showed increases in bone formation, bone density and bone strength with setrusumab across OI Types I, III, and IV (ASTEROID; NCT03118570) and a pivotal Phase 2/3 study is ongoing to determine the effects of setrusumab on dose, efficacy and safety in pediatric and young adults with OI (Orbit; NCT05125809).This abstract describes the study design of Cosmic, an open-label, randomized, active-controlled, Phase 3 study of setrusumab compared with bisphosphonates in pediatric subjects 2 to <7 years of age with OI Types I, III or IV (NCT05768854). The primary objective is to evaluate the effect of setrusumab vs intravenous bisphosphonates (IV-BP) therapy on reduction in fracture rate, including morphometric vertebral fractures. Participants will receive either setrusumab or IV-BP for up to 24 months during an active-control period. All participants will then enter an extension period for a minimum of 12 months, with those initially assigned to IV-BP transitioning to setrusumab, if desired.The primary endpoint is the annualized rate of all radiographically-confirmed fractures, including morphometric vertebral fractures. Secondary endpoints include the annualized rate of radiographically-confirmed fractures, excluding morphometric vertebral fractures; change from baseline in POSNA-PODCI Sports/Physical Functioning and Pain/Comfort Subscale Scores; serum setrusumab concentration; and the subject incidence of TEAEs, SAEs, and AEs of special interest.Key inclusion criteria include a clinical diagnosis of OI Types I, III, or IV; a history of >=1 fracture in the past 12 months, >=2 fractures in the past 24 months, or >=1 femur, tibia, or humerus fracture in the past 24 months; and prior or current IV-BP. Exclusion criteria includes a history of skeletal malignancies, bone metastases or neural foraminal stenosis; clinical manifestations of Chiari malformation or basilar invagination; current uncontrolled concomitant diseases that may impact bone metabolism; any skeletal condition (other than OI) leading to bone deformity and/or increased risk of fractures; and cardiovascular disease.The Cosmic study is being initiated in the second quarter of 2023.

***Disclosures: Thomas Carpenter**, Ultragenyx, Inozyme, Kyowa Kirin, Consultant, Ultragenyx, Grant/Research Support*

SAT-502

See Friday Plenary Number FRI-502

SAT-503

A PTH Receptor Inverse Agonist (PTH-IA) in Patients with Jansen's Metaphyseal Chondrodysplasia: Rationale and Design for a Phase 1/2 Clinical Trial *Smita Jha[2], Anisha Ninan[2], Rachel Gafni[4], Kelly Roszko[4], Carlos Ferreira[4], Richa Lomash[5], Rodica Stan[5], Elizabeth Ottinger[5], Thomas Gardella[6], Lee Weinstein[2], Harald Jueppner[6], Michael Collins[7]. [2]NIDDK, . [2]NIDDK, United States. [4]National Institutes of Health, United States. [4]National Institutes of Health, . [5]NCATS, United States. [6]Massachusetts General Hospital, United States. [7]NIDCR, United States

Jansen's Metaphyseal Chondrodysplasia (JMC) is a rare disease with ~30 patients currently identified worldwide. JMC is caused by germline, heterozygous gain-of-function pathogenic variants of the parathyroid hormone 1 receptor (PTH1R), the receptor for PTH and PTHrP that lead to its constitutive activation. Phenotypic features of JMC are heterogenous and include short-stature, scoliosis, fractures, bone pain, mineral-ion abnormalities (typically hypercalcemia and hypercalciuria despite low PTH), hypertension, nephrocalcinosis and chronic kidney diseases. There are currently no approved therapies for JMC. We previously demonstrated that PTH-IA, an inverse agonist at PTHR1 suppresses Jansen's PTH1R variant signaling in vitro and in vivo. We propose to evaluate the safety and efficacy of PTH-IA in a Phase 1/2 open-label, first-in-human, dose-escalating, safety and efficacy study. PTH-IA will be administered twice daily subcutaneously. Phase 1 will enroll at least one adult with JMC; Phase 2 will enroll up to five patients?3 years of age. Each phase is divided into three periods: baseline, dose-finding, and treatment (Figure 1). At baseline, patients will undergo blood and urine tests, imaging studies including 18F-NaF PET/CT, and biopsy of dysplastic bone tissue. During dose finding, the dose of PTH-IA will be escalated, and blood and urine sampled serially (for tests including calcium, phosphorus, PTH, PK, bone turnover markers and 1,25(OH)2 vitamin D). The optimal dose will be the minimum dose at which the mean of the two highest PTH values increases to 30-40 pg/mL (in patients with a baseline PTH ?20 pg/mL) in the absence of dose-limiting toxicity. In patients with a baseline PTH >20 pg/mL, the optimal dose will be the dose at which the mean of two highest PTH increases to 55-65 pg/mL. Patients will remain on their optimal dose for the duration of the treatment period (total drug exposure <=28 days) and obtain a second 18F-NaF PET/CT at end of the period. The primary and secondary endpoints of the study are: i) dose limiting toxicities and incidence, severity, seriousness, and causality of all treatment-emergent adverse events ii) pharmacokinetics iii) absolute levels and percentage change from baseline in serum PTH and fractional excretion of calcium iv) optimal dose range of PTH-IA v) change in overall and sentinel skeletal lesion metabolic activity and density on 18F-NaF PET/CT and vi) change in bone turnover markers. We anticipate that the results will inform our understanding of mineral-ion homeostasis and clarify the therapeutic potential of PTH-IA.

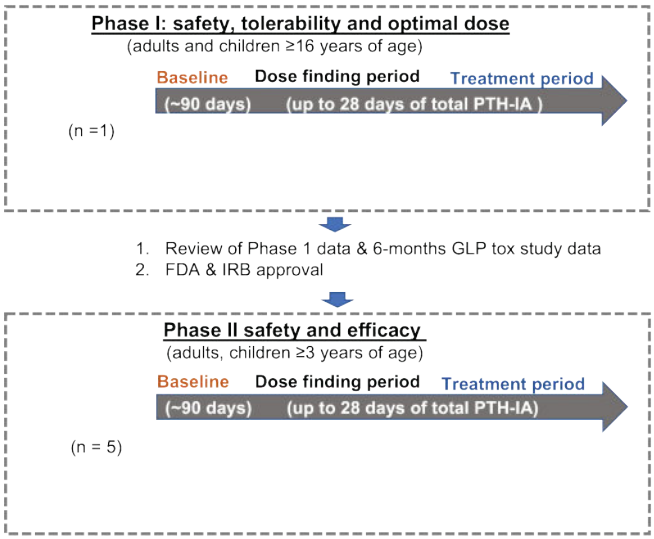

***Disclosures: Smita Jha**, None*

SAT-505

See Friday Plenary Number FRI-505

SAT-506

CALIBRATE: A Phase 3, Randomized, Open-Label Study Evaluating the Efficacy and Safety of Encaleret (CLTX-305) Compared to Standard of Care in Participants with Autosomal Dominant Hypocalcemia Type 1 [NCT05680818] *Michael Mannstadt[1], Lars Rejnmark[2], MARIA LUISA BRANDI[3], Keiichi Ozono[4], Peter Tebben[5], Arun Mathew[6], Mary Scott Roberts[7], Scott Adler[7], Rachel Gafni[8]. [1]Massachusetts General Hospital Harvard Medical School, United States. [2]Aarhus University Hospital, Denmark. [3]FONDAZIONE FIRMO, Italy. [4]Osaka University Graduate School of Medicine, Japan. [5]Mayo Clinic, United States. [6]BridgeBio Pharma, . [7]Calcilytix, United States. [8]National Institutes of Health, United States

Autosomal dominant hypocalcemia type 1 (ADH1), caused by pathogenic gain-of-function calcium-sensing receptor gene (CASR) variants, is characterized by low parathyroid hormone (PTH) levels, hypocalcemia, hypercalciuria, hyperphosphatemia and hypomagnesemia. Current standard-of-care (SoC) (calcium and active vitamin D)?worsens hypercalciuria, which may result in renal complications.Encaleret is an oral calcilytic that functions as a negative allosteric modulator of the calcium-sensing receptor and is under investigation as a potential treatment for ADH1. A phase 2b study [NCT04581629] in 13 adults with ADH1 showed that encaleret led to sustained normalization in mean blood levels of intact PTH, albumin-corrected calcium (cCa), phosphorus, magnesium and 24-hr urine calcium (UCa) excretion over 24 weeks compared with baseline. Encaleret was well-tolerated with no serious adverse events reported.CALIBRATE is a global phase 3 study designed to evaluate the efficacy and safety of encaleret compared to SoC in approximately 60 participants with ADH1. Eligible participants >=16 years-old with ADH1 will enter a

screening period with a SoC optimization and maintenance period (Period 1 [P1]) prior to randomization. Participants will then be randomized 2:1 (encaleret:SoC) into a 20-week dose titration period (Period 2). Doses of encaleret or SoC will be titrated to achieve target cCa concentrations while minimizing UCa excretion. Participants will then enter a 4-week maintenance period (Period 3 [P3]) where doses of encaleret or SoC are intended to be fixed. The primary efficacy endpoint is a composite endpoint: a) cCa within 8.3-10.7 mg/dL AND b) 24-hr UCa within reference range (men: < 300 mg/day; women: < 250 mg/day). Participants who meet both criteria will be considered responders. The primary analysis will be a within-patient comparison of the proportion of responders at the completion of P3 (encaleret) with the proportion of responders at the end of P1 (SoC). Key secondary endpoints include between-treatment arm comparisons as well as the evaluation of mineral homeostasis parameters, renal health, bone health, and patient-reported outcomes. Following completion of P3, eligible participants will have the option to enter a long-term extension (LTE) period with continued access to encaleret.CALIBRATE is recruiting study participants in 12 countries: USA, Canada, Brazil, Netherlands, Belgium, Denmark, France, Italy, Czech Republic, Taiwan, Australia, and Japan.

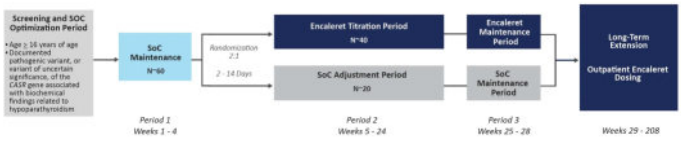

***Disclosures: Michael Mannstadt**, Amolyt, Consultant, Takeda, Consultant, Calcilytix, Grant/Research Support, Takeda, Grant/Research Support, Calcilytix, Consultant*

SAT-508

See Friday Plenary Number FRI-508

SAT-509

Health Assessments of Normotopic Bone in Individuals with Fibrodysplasia Ossificans Progressiva *Robert J. Pignolo[1], Mona Al Mukaddam[2], Geneviève Baujat[3], Angela M. Cheung[4], Carmen De Cunto[5], Edward Hsiao[6], Richard Keen[7], Rose Marino[8], Andrew Strahs[8], Frederick S. Kaplan[2]. [1]Mayo Clinic, United States. [2]University of Pennsylvania, United States. [3]Université Paris Cité, France. [4]University of Toronto, Canada. [5]Hospital Italiano de Buenos Aires, Argentina. [6]University of California San Francisco, United States. [7]Royal National Orthopaedic Hospital, United Kingdom. [8]Ipsen, United States

Purpose: Fibrodysplasia ossificans progressiva (FOP) is an ultra-rare, genetic disorder characterized by cumulative and irreversible heterotopic ossification (HO) in soft and connective tissues. HO progressively restricts movement, leading to cumulative disability and a shortened life expectancy in individuals with FOP. While FOP has been shown to impact bone health, limited studies have investigated normotopic bone health parameters. Here, bone mineral content (BMC), bone mineral density (BMD), and bone strength of the normotopic skeleton were evaluated in individuals with FOP enrolled in a non-interventional natural history study (NHS; NCT02322255). Methods: Individuals with FOP aged <=65 years, with a confirmed ACVR1R206H mutation, were enrolled (N=114) in the NHS. During the study, low-dose whole-body computed tomography (WBCT; excluding head) was performed to assess HO. The accuracy of routine bone assessments using standard techniques in individuals with FOP is limited due to excess bone formation and ankyloses throughout the skeleton. Therefore, WBCT scans obtained at Baseline were evaluated post hoc using a novel computational method, biomechanical computed tomography (BCT; VirtuOst® software), to calculate BMC, BMD, and bone strength at the spine (L1, L2, or adjacent vertebrae) in individuals with FOP aged <18 and >=18 years. BMD z-scores were calculated where normative data were available. Results: BMC, BMD, and bone strength at Baseline are presented (Table). Mean (standard deviation) BMD z-score for individuals aged >=18 years was ?3.0 (1.55; n=33) at Baseline, suggesting that BMD may be lower in adults with FOP compared with unaffected individuals. Normative BMD data were not available for individuals aged <18 years. Conclusion: This is the first time that BCT has been used to evaluate BMC, BMD, and bone strength from WBCT scans in individuals with FOP. BCT could increase our understanding of bone health in individuals with FOP; however, further studies are required to understand the reproducibility of these measurements and their clinical significance for fracture risk and other comorbidities.

Table: Mean (SD) computationally estimated BMC, BMD, and bone strength at Baseline.

	<18 years (n=61)	≥18 years (n=40)
Vertebral body BMC (g)	3.8 (1.96)	5.3 (1.51)
Mid-vertebral BMD (mg/cm^3)	112.1 (31.13)	91.2 (39.11)
Vertebral strength (N)	4,276.1 (1,508.69)	4,872.4 (1,591.22)

BMC: bone mineral content; BMD: bone mineral density; SD: standard deviation.

***Disclosures: Robert J. Pignolo**, Regeneron (Research Investigator), Grant/Research Support, Clementia/Ipsen (Research Investigator), Grant/Research Support, Immediate Past President of the International Clinical Council on FOP, Other Financial or Material Support, Incyte (Research Investigator), Grant/Research Support*

SAT-511

See Friday Plenary Number FRI-511

SAT-512

Real-world utilization of burosumab in patients with tumor-induced osteomalacia: data from a French national registry *JULIEN PACCOU[1], Guillaume Couture[2], Pascale Guillot[3], Nadia Mehsen-Cetre[4], Caroline Morizot[5]. [1]Lille University Hospital, France. [2]Rheumatology Department, CHU de Toulouse, France. [3]Rheumatology Department, CHU de Nantes, France. [4]Rheumatology Department, CHU de Bordeaux, France. [5]Rheumatology Department, CHU de Nancy, France

Tumor-induced osteomalacia (TIO) is a rare paraneoplastic syndrome due to a phosphaturic tumor, which overproduces Fibroblast Growth Factor 23 (FGF-23), causing hyperphosphaturia, hypophosphatemia, low 1,25(OH)2D and osteomalacia. Surgical complete resection is the recommended treatment choice and the standard of care but some tumors cannot be found and others cannot be removed resulting in a persistence or recurrence of the disease. In those difficult situations, burosumab, a fully human monoclonal antibody targeted against FGF-23, is a treatment option. An early access to burosumab, has been set up for TIO patients in France since July 2022. Before that, Kyowa Kirin France had provided access to burosumab at no cost on compassionate grounds for a few number of patients. We retrospectively evaluated patients with definite diagnosis of TIO referred to tertiary Rheumatology Centers between July 2022 and March 2023, investigating clinical and biochemical characteristics before burosumab initiation as well as disease outcome following 2 months of treatment. We included 6 patients: 4 (66.7%) were females, mean age (+/- standard deviation) was 54 +/- 8 years, and mean weight was 74.7 +/- 23.3 kg. Tumor localizations: lower limbs (n=1), lower limbs and chest (n=2), head and neck (n=1), spinal canal (n=1), no localization (n=1). Among these 6 patients, 3 were already under burosumab before July 2022 due to compassionate use. Biochemical data were: serum phosphorus 0.7 +/- 0.3 mmol/L (Reference Range: 0.8-1.5), PTH 65.6 +/- 48.0 ng/mL (RR: 12-50), intact FGF-23, 279.3 +/- 114.4 pg/mL (RR: 25-45). On a scale of 1-100, mean pain was 43 +/- 32 before burosumab initiation (starting dosage 0.5 +/- 0.3 mg/kg rounded to the nearest 10 mg every 4 weeks (20 to 70 mg/4w)). Evaluation of 5 patients was available after 2 months of treatment. Mean pain was 38 +/- 22, mean phosphorus 0.9 +/- 0.4 mmol/L, and burosumab dosage 0.6 +/- 0.3 mg/kg every 4 weeks (30 to 70 mg/4w)). Burosumab was generally well tolerated. Those preliminary findings following burosumab early access for TIO patients in France support benefits in terms of efficacy, safety and ease of treatment. For patients not eligible or refractory to surgery, burosumab appears to be a promising option.

***Disclosures: JULIEN PACCOU**, None*

SAT-514

See Friday Plenary Number FRI-514

SAT-515

Real-life Experience of Burosumab in Two Adult Sisters with X-linked Hypophosphatemia (XLH) from Argentina *Laura Maria Schiro[1], Evangelina Giacoia[1]. [1]Hospital Nacional Prof A Posadas, Argentina

The aim of this presentation is to show the clinical, biochemical and quality of life evolution of two sisters with XLH, under treatment with burosumab.Since the approval of fibroblast growth factor 23 (FGF-23) monoclonal antibody, burosumab, as a treatment for XLH, there are few real-life reported cases of adult patients on the drug. These two sisters were diagnosed in adulthood, having gone through multiple surgical interventions, with erroneous diagnoses. In this way they accumulated sequelae of the disease.At first consultation in 2015, VS, 55 years old, height 4'00", weight 132,3 Lb, SJ, 60 years old, height 4'39",weight 119 Lb. Both suffer from musculoskeletal pain and stiffness, short stature, bowed lower limbs, fractures and pseudofractures due to osteomalacia, and enthesopathy. The variant ChrX:22,196,490 CAG>C was identified in heterozygosity. Since diagnosis, they were replaced with conventional treatment, but they had never achieved proper phosphorus levels, remaining between 1,8 and 2,1 mg/dl (RR2,5-4,5), and showed no clinical or radiographic improvement, leading to lack of compliance. Until the possibility of treatment with burosumab arose, which was initiated in April 2021, at a dose of 50 mg every 4 weeks. After two years of treatment, the phosphorus reached an average between 2.7 and 3.2 mg/dl, in addition to a clear radiological improvement, since it prevented the development of osteomalacia and pseudofractures, prevented the appearance of dental complications and improved the consolidation of previous fractures. The assessment of quality of life using the WOMAC scale was not able to show significant changes in these patients. Depression, which often accompanies chronic diseases, can significantly impact the individual's perception of their quality of life, making it challenging to evaluate the overall effectiveness of the treatment. Regarding the adverse effects, one of the sisters presented vertigo that disappeared after a few weeks.In conclusion, this real life experience highlights the promising efficacy and safety of this new therapy in adult patients with XLH. It is important to highlight that the normal values of phosphatemia were maintained throughout the treatment. Assessing quality of life in individuals with XLH requires a comprehensive approach that includes patient-reported outcomes, biochemistry, clinical evaluations, and monitoring of both physical and mental health parameters.

***Disclosures: Laura Maria Schiro**, None*

SAT-516

Novel Clinical and Molecular Evidence in CYP26B1-Related Disorder *Karina da Costa Silveira[1], Inara Chacon Fonseca[2], Connor Oborn[1], Parker Wengryn[1], Alexander Beke[1], Carrie-Lynn Soltys[1], Oswaldo Artigalas[3], Eric Campos[4], Denise Cavalcanti[5], Peter Kannu[1]. [1]Department of Medical Genetics, University of Alberta, Canada. [2]Clinical Genetics, Durham Region Cancer Centre, Lakeridge Health Oshawa, Canada. [3]Clinical Genetics Unit, Children's Hospital, Grupo Hospitalar Conceicao, Brazil. [4]Genetics & Genome Biology Program, The Hospital for Sick Children, University of Toronto, Canada. [5]Skeletal Dysplasia Group, University of Campinas, Brazil

Introduction: CYP26B1, a P450 cytochrome family member, metabolizes retinoic acid (RA) in the developing embryo to control RA levels. So far, a few individuals with CYP26B1 variants featuring mild to lethal phenotypes have been reported. Here we report two families with CYP26B1-related disorder and describe the functional study of novel pathogenic variants in CYP26B1.Methods: Research-based exome sequencing was performed in family 1 and phenotype-driven Sanger sequencing in family 2. A minigene assay assessed splicing defects. Using a CYP26B1 expression vector (construct), luciferase (DLR) assay analyzed the enzymatic activity of mutant constructs after adding exogenous RA; immunofluorescence (IF) determined if mutant constructs were localized in the endoplasmic reticulum (ER).Results: Siblings from family 1 (11yo and 15yo) present a mild skeletal phenotype including brachycephaly without craniosynostosis, distinctive facial features, arachnodactyly, reduced radioulnar joint movement, conductive hearing loss, and a learning disability. CYP26B1 compound heterozygous variants were identified: p.Pro118Leu; p.Arg234Gln. The stillborn fetus from family 2 presents a lethal phenotype with spina bifida occulta, hydrocephalus, poor skeletal mineralization, joint synostosis, limb defects, and a homozygous point variant in CYP26B1. Minigene assay analysis shows this variant creates an in-frame deletion by introducing a new splice site which excludes part of exon 5 (p.Val361_Asp382del).DLR reveals that the p.Val361_Asp382del variant results in a significantly reduced ability to metabolize exogenous RA (˜3.5 fold decrease compared to the wild-type). The two other variants cause a partial loss of activity with a 1.7 (p.Pro118Leu) and 2.3 (p.Arg234Gln) fold decrease. IF suggests that the CYP26B1 mutant constructs are still localized in the ER.Conclusions: We report here two additional families with pathogenic variants in CYP26B1 including the very first description of a splicing variant causing a lethal phenotype. The splicing variant in family 2 led to a partial deletion of the protein drastically affecting function (but not protein folding) and creating the most severe phenotype reported. The phenotype in family 1 was much milder than what has been previously reported. Our report adds to the genotypic and phenotypic spectrum seen in CYP26B1-related skeletal dysplasia. A complete review of the CYP26B1 mutation phenotype is described in Fig 1.

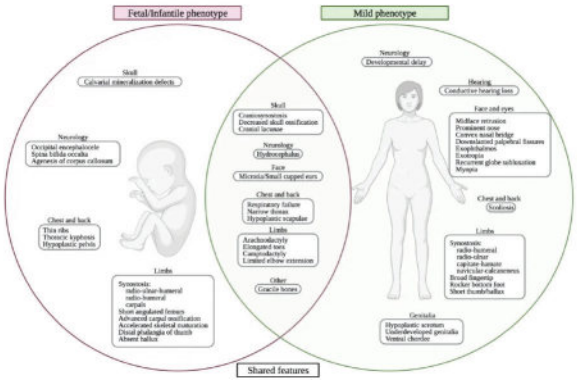

***Disclosures: Karina da Costa Silveira**, None*

SAT-517

Follow-up STOPFOP: A Phase II Clinical Trial to Prevent Heterotopic Ossification in FOP Using Saracatinib (AZD0530) *Vincent Verheij[1], Bernard Smilde[1], Richard Keen[2], Clemens Stockklausner[3], Vijay Zala[4], Alex Bullock[5], Ruben De Ruiter[6], Natasja van Schoor[7], Paul Yu[8], Elisabeth Eekhoff[9]. [1]Department of Internal Medicine, Amsterdam University Medical Center, Amsterdam, The Netherlands, Netherlands. [2]Royal National Orthopaedic Hospital, United Kingdom. [3]Department of Paediatrics, Klinikum Garmisch-Partenkirchen, Garmisch Partenkirchen, Germany, Germany. [4]Research and development, AstraZeneca, Boston, United States of America, United States. [5]Nuffield Department of Medicine, University of Oxford, Oxford, United Kingdom, United Kingdom. [6]AmsterdamUMC, Netherlands. [7]Department of Epidemiology and Biostatistics, Amsterdam University Medical Center, Amsterdam, The Netherlands, Netherlands. [8]Department of Medicine, Brigham and Women's Hospital, Boston, United States of America, United States. [9]Amsterdam UMC, location VU University Medical Center, Amsterdam, The Netherlands, Netherlands

Background: Fibrodysplasia Ossificans Progressiva (FOP) is an autosomal dominant, invalidating disorder marked by severe heterotopic ossifications (HO), severe ankylosis and early death. There are currently no approved treatments in the world except Canada. AZD0530 (saracatinib) was identified by our team as a potent inhibitor of the ALK2-kinase which, through a R206H mutation, causes this rare bone disease. AZD0530 was effective in FOP mouse models. The purpose of this study is to investigate the repositioning of AZD0530, originally designed for ovarian cancer treatment, to treat patients with FOP. This study is funded by the Innovative Medicines Initiative and supported by IFOPA.Methods: The Saracatinib Trial to Prevent FOP (STOPFOP) is a phase 2a, multicentre, 6-month double blind randomized controlled trial of AZD0530 versus placebo, followed by a 12 month trial comparing open-label extended AZD0530 treatment with control data from a previous trial. Due to COVID the study is delayed, but presently we are including 16 otherwise healthy FOP patients, aged 18-65 years, with the classic FOP mutation (R206H). Endpoints are objective change in heterotopic bone volume measured by low-dose whole-body computer tomography, [18F] NaF PET activity and patient reported outcome measures such as the FOP-IADL questionnaire.Discussion: Drug repositioning - using existing, previously researched but unapproved drugs for the treatment of a different disease - is especially useful in rare diseases with limited study populations. It represents an ideal solution for limiting risks in early clinical studies. Using existing pre-clinical and clinical knowledge may also allow more affordable pricing once an indication is approved. With positive study outcome, AZD0530 may provide a rapidly translatable therapy for FOP due to the availability of extensive safety data from over 600 patients in more than 28 registered clinical trials using AZD0530. At the time of writing, 5 patients have already completed the study and all of them elected to continue the medication in an extended study phase, waiting for more results to be analysed once the study is complete.

***Disclosures: Vincent Verheij**, None*

SAT-518

Patients with Fibrodysplasia Ossificans Progressiva show abnormalities in their Gut Microbiome *Ariane Zamarioli[1], Tania Moody[2], Camille Fang[2], Andres Betancourt-Torres[3], Sarah Takimoto[2], Svetlana Lyalina[4], Kelly Wentworth[2], Kristie Yu[5], Vivian Lu[6], Hayley Wallace[2], Samuel Kou[2], Katherine Pollard[4], Edward Hsiao[7]. [1]Department of Orthopaedics and Anesthesiology, Ribeirão Preto Medical School, University of São Paulo, Brazil and Division of Endocrinology and Metabolism, Department of Medicine, University of California, San Francisco, CA 94143, Brazil. [2]Division of Endocrinology and Metabolism, the Institute for Human Genetics, The Ely and Edith Broad Institute for Regeneration Medicine, and the Department of Medicine, University of California, San Francisco, CA 94143, United States. [3]Oral and Craniofacial Sciences Graduate Program, School of Dentistry, University of California, San Francisco, CA 94143, United States. [4]Gladstone Institutes, San Francisco, CA 94158, USA, Department of Epidemiology & Biostatistics, University of California, San Francisco, CA 94158, USA, and Chan Zuckerberg Biohub, San Francisco, CA 94158, USA, United States. [5]Division of Endocrinology and Metabolism, Institute for Human Genetics, Ely and Edith Broad Institute for Regeneration Medicine, Department of Medicine, University of California, San Francisco and California Institute of Technology, Pasadena, CA 91125, United States. [6]Central Michigan University College of Medicine, Mount Pleasant, MI 48859, United States. [7]Division of Endocrinology and Metabolism, the Institute for Human Genetics, The Ely and Edith Broad Institute for Regeneration Medicine, the Department of Medicine, and School of Dentistry, University of California, San Francisco, CA 94143, United States

Background: BMP signaling is critical for normal gut development and function. Fibrodysplasia ossificans progressiva (FOP) is a severe genetic condition that leads to inflammatory flare-ups and heterotopic ossification. 95-98% of patients with FOP show a highly recurrent ACVR1R206H mutation, resulting in increased BMP signaling and abnormal response to Activin A. Patients exhibit a surprising spectrum of bone formation and functional loss, suggesting environmental variables may contribute to phenotypic variability. Patients also report multiple gastrointestinal (GI) symptoms like food selectivity, intermittent bloating, and nausea/vomiting. We previously showed that patients with FOP have significant increases in their clinical and molecular inflammatory responses. We hypothesize that patients with FOP may have microbiota-related inflammatory drivers that contribute to their disease progression.Objective: We assess baseline GI symptoms, and characterize and quantify the gut microbiome in FOP patients vs. siblings living in the same household.Methods: Seven patients with FOP and seven siblings were enrolled and completed surveys on their food preferences, eating habits, and GI symptoms. Shotgun metagenomic sequencing was performed on all stool samples at enrollment (baseline, n=7 pairs) and at one-year follow-up (n=6 pairs).Results: Patients with FOP had significantly more emesis (p=0.01) and were more likely to avoid food requiring chewing (p=0.02). Microbiome analysis at baseline revealed that patients with FOP had significantly lower microbial diversity at the phylum level in community composition (p=0.04) and richness (p=0.03). We detected a higher abundance of Firmicutes and lower abundance of Bacteroidetes (p=0.026) in patients with FOP. Notably, a higher Firmicutes:Bacteroidetes ratio is reportedly related to gut dysbiosis. FOP patients also exhibited a higher abundance of Candidatus Saccharibacteria (p=0.07), which has been associated with inflammatory mucosal diseases, such as inflammatory bowel disease. Conclusion: Patients with FOP show GI symptoms related to their FOP disease manifestations of spinal/esophageal curvatures and jaw ankylosis. Gut microbiomes in patients with FOP showed differences in bacterial composition. Further evaluation is needed to identify if these changes in the microbiome are associated with FOP flare activity or inflammatory status, and if manipulating the microbiome impacts the disease course of patients with FOP.

***Disclosures: Ariane Zamarioli**, None*

SAT-519

Clinical and treatment characteristics of pediatric and adult patients with familial hypophosphatemia compared with demographically matched controls *Zhiyi Li[1], Elizabeth H. Marchlewicz[2], Danae Black[2], Hana Schwartz[2], Yang Zhao[3], Erik Imel[4], Nicole Princic[2]. [1]Kyowa Kirin, United States. [2]Merative, United States. [3], United States. [4]Indiana University School of Medicine, United States

Purpose: Familial hypophosphatemia (FH) is characterized by renal phosphate wasting, rickets, osteomalacia and other musculoskeletal consequences. Understanding of disease progression by age of patients with FH is limited. This study examined the clinical and treatment characteristics of patients with FH across age groups, compared to demographically matched non-FH control patients.Methods: Patients from Merative® MarketScan® Commercial and Medicare claims databases with >1 diagnosis code for FH (ICD10=E83.31) between 1/1/2018-12/31/2021 were included if they had 12 months of continuous enrollment pre- and post-index. Patients treated with burosumab during the study period were excluded. The index date was defined as the date of first FH diagnosis code. FH patients were demographically matched 1:3 to non-FH control patients from MarketScan databases based on age, sex, geographic region, payer, and index year and were stratified by age (0-11, 12-17, 18-29, 30-39, 40-49, 50-64, 65+ years). Clinical and treatment characteristics were assessed in the 12-month follow-up period.Results: Matched FH patients (n=570) and controls (n=1,710) were 57.0% female and had a mean age of 47 years; pediatric patients comprised 10.4% of included FH cases. The most common clinical characteristics associated with FH differed by age: for ages 0-11 years, delayed growth/walking (26.7% FH vs. 0.0% controls), lower limb deformity (26.7% vs. 0.0%), and rickets (20.0% vs. 0.0%); for ages 30-39 years, arthralgia (22.9% vs. 5.7%), kidney disease (21.4% vs. 0.5%) and fractures (11.4% vs. 0.5%); and for ages 65+ years, kidney disease (57.1% vs. 9.5%), osteoarthritis (39.0% vs. 15.2%), and arthralgia (36.4% vs. 16.0%) (all P<0.001). Charlson Comorbidity Index was significantly higher among FH patients and increased with age (0-11 years: 1.1 vs. 0.1; 65+ years: 4.0 vs. 0.6, both P<0.001). Calcitriol (16.7% vs. 1.5%) and oral phosphate supplements (97.9% vs. 0.0%) were prescribed to more FH patients than controls (both P<0.001). Laboratory tests (71.9% vs. 11.6%), physical therapy (31.8% vs. 8.9%), and use of a wheelchair or other walking assistance device (9.3% vs. 0.9%) were more common among FH patients than controls (all P<0.001).Conclusions: Among FH patients, compared to non-FH control patients, the clinical characteristics of the disease are more frequent even among children and young adults and increase with age, suggesting a progressive accumulative disease.

***Disclosures: Zhiyi Li**, Kyowa Kirin, Major Stock Shareholder*

SAT-520

ENPP1 enzyme replacement therapy improves brain calcification but does not rescue skeletal phenotype in a mouse model for craniometaphyseal dysplasia *Ernst Reichenberger[1], Kevin O'Brien[5], Ayano Hatori[1], Thomas Carpenter[3], Koen van de Wetering[4], Lisa Flaman[5], Jennifer Howe[5], Daniel Ortiz[5], Yves Sabbagh[5], I-Ping Chen[1]. [1]University of Connecticut Health, United States. [5]Inozyme Pharma, . [3]Yale University School of Medicine, United States. [4]Thomas Jefferson University, United States. [5]Inozyme Pharma, United States

Craniometaphyseal dysplasia (CMD), a rare genetic bone disorder, is characterized by progressive thickening of craniofacial bones and flared metaphyses of long bones. Patients with CMD often suffer from obstruction of neural foramina and neurological symptoms, such as facial palsy, blindness, deafness, or severe headache. Mutations in ANKH (mouse ortholog ANK), a transporter for small molecules such as citrate and ATP, have been identified for autosomal dominant form of CMD. Knock-in (KI) mice carrying an ANKF377del mutation (AnkKI/KI) replicate many features of human CMD. Mutant ANK protein is rapidly degraded and pyrophosphate (PPi) levels in plasma and bone are significantly reduced in AnkKI/KI mice. PPi is a potent inhibitor of mineralization. To examine the extent to which restoration of circulating PPi levels can prevent the development of a CMD-like phenotype, we treated AnkKI/KI mice with the human recombinant ENPP1-Fc protein IMA2a. ENPP1 is an enzyme that hydrolyzes ATP into AMP and PPi. Male and female Ank+/+ and AnkKI/KI mice (n>=6 per group) were subcutaneously injected with IMA2a (5 mg/kg) or vehicle once a week for 13 weeks, starting at the age of 1 week. PPi and ENPP1 activity levels in plasma were determined at the end point. ENPP1 activity was significantly increased in AnkKI/KI mice injected with IMA2a (Vehicle / IMA2a: 28.15+/-1.65 / 482.7+/-331.2 mOD/minute; p<0.01), which resulted in the successful restoration of plasma PPi levels (Ank+/+ / AnkKI/KI vehicle treatment / AnkKI/KI IMA2a: 0.94+/-0.5 / 0.43+/-0.2 / 1.29+/-0.8 ?M; p<0.01). We examined the skeletal phenotype by Faxitron and ?CT. IMA2a treatment of AnkKI/KI mice did not significantly correct CMD features in femurs, mandibles, and skulls, including the abnormal shape of femurs, increased cortical porosity, hyperostotic mandibles, or narrowed foramina magnum. Calcified nodules were noted in the brain stem of AnkKI/KI mice by ?CT. Interestingly, treatment of AnkKI/KI mice with IMA2a significantly reduced the volume of calcified nodules found in the brain. Brain calcification has not been reported in CMD patients and the extent to which it can induce neurological dysfunction in CMD mice or patients remains unknown. Our data demonstrate that IMA2a is sufficient to restore plasma PPi levels and reduce brain stem calcification but does not rescue the skeletal abnormalities in AnkKI/KI mice in this treatment regimen.

***Disclosures: Ernst Reichenberger**, None*

SAT-521

See Friday Plenary Number FRI-521

SAT-523

See Friday Plenary Number FRI-523

SAT-524

Prrx1Cre-Alplfl/- (PAKO) Mice, a Model to Study Adult HPP Metabolic Phenotypes *VICTORIA DEMAMBRO[1], Jennifer Daruszka[1], Samantha Costa[2], Jose Luis Millan[3], Michael Whyte[4], Anyonya Guntur[1], Dr. Clifford ROsen[5]. [1]MaineHealth Institute for Research, United States. [2]MaineHealth Institute for Research , United States. [3]Sanford Burnham Prebys, United States. [4]Shriners Hospital for Children, United States. [5]Maine Medical Center, United States

Hypophosphatasia (HPP) is caused by loss-of-function mutations in the tissue-nonspecific alkaline phosphatase (TNAP) gene (ALPL) resulting in rickets, bone fragility, muscle weakness and lean body mass when severe in children. Adult HPP has broad expressitivity ranging from simple dental abnormalities to fractures, osteomalacia, chronic muscle weakness/pain as well as chronic fatigue with an estimated carrier prevalence of 1/300. We have reported on the role of TNAP in adipogenesis and mitochondrial function utilizing an Alplko model. Alpl-/- pups exhibited decreased fat mass, adipogenesis, lipid accumulation and mitochondrial function. However, Alpl-/- pups die by postnatal D21 preventing study of these changes into adulthood. We next reported on Prrx1Cre-Alplflfl (Crefl/fl) strain as a model of adult HPP. Prrx1 is highly expressed in the limb bud mesenchyme thus targeting long bones, muscle and the inguinal fat depot (IWAT). Crefl/fl mice exhibited classic bone HPP phenotypes, a 50% reduction in serum TNAP, reduced BMAT and lean mass. Differentiated Crefl/fl BMSCs exhibited no mineralization as well as reduced adipogenesis and mitochondrial function in vitro. However, no significant differences were noted in Crefl/fl IWAT weights, adipocyte size and in vitro adipogenesis despite a 70% decrease in Alpl expression vs. controls. We then hypothesized that TNAP endogenous levels may be affecting the adipogenic phenotype as Prrx1 is highly expressed in IWAT. To test this premise and reduce TNAP levels further we created a Prrx1Cre-Alplflfl X Alpl+/- (PAKO) strain by introducing a null allele into the PrrxCre-Alplflfl colony. Here we report that Crefl/- mice have a 75% reduction in serum TNAP vs. +/f controls coupled with reduced IWAT weight, adipocyte size and BMAT. Interestingly, Crefl/- mice had significantly reduced energy expenditure (EE) vs. controls coupled with reduced running wheel activity and speed. No significant differences were noted in resting EE. However, EE during periods of increased activity was significantly reduced. ANCOVA analysis revealed no significant covariance between body composition, wheel activity or speed with the reduced EE observed in the Crefl/- mice. We surmise that the reduced wheel activity and speed maybe indicative of muscle wasting and fatigue phenotypes. Our data suggest that the PAKO mice are a good model for adult HPP allowing the study of adipogenesis, chronic muscle wasting and fatigue phenotypes with age.

***Disclosures: VICTORIA DEMAMBRO**, None*

SAT-525

See Friday Plenary Number FRI-525

SAT-526

Role of fibroblast activation protein in fibrous dysplasia *Luis Fernandez De Castro Diaz[1], Zachary Michel[2], Layne Raborn[2], Alison Boyce[3]. [1]NIDCR, United States. [2]NIDCR (NIH), United States. [3]National Institutes of Health, United States

Fibrous dysplasia (FD) is a mosaic skeletal disorder arising from de novo activating GNAS mutations during embryogenesis, resulting in expansile fibro-osseous lesions and leading to fractures, pain, and disability. FD tissue is characterized by the replacement of normal bone and marrow by fibrous tissue containing varying amounts of curvilinear trabeculae of poorly mineralized hypercellular woven bone.Fibroblast activation protein (FAP) is a membrane-bound serine protease originally identified in carcinoma-associated fibroblasts (CAFs) in the stroma of most solid tumors. It is associated with tissue remodeling, and growing evidence suggests it plays a role in fibrotic and inflammatory diseases. FAP inhibition was developed for cancer treatment but has not yielded sufficient therapeutic outcomes. However, since FAP is widely expressed by CAFs, a radiolabeled FAP inhibitor has demonstrated to be an effective pan-tumoral tracer, suggesting its potential application for FD nuclear imaging. Moreover, FAP can be detected in serum, and it correlates with disease burden in several disorders, so it could serve as a biomarker in FD. Lastly, due to the high specificity of FAP proteolytic target peptide sequence, and its expression generally confined to fibrotic lesioned tissue, FAP represents a good target candidate for local pro-drug activation, by which a drug coupled to an inactivating peptide can be locally activated upon FAP-mediated cleavage. FD, as a mosaic disease, could significantly benefit from such therapeutic approach, to avoid off target effects of systemically administered drugs.In this study, we measured the expression of FAP in human and mouse FD BMSCs, as well as in tissue treated or not with anti-RANKL therapy. We also measured FAP concentration in FD patient serum and healthy volunteers. We found that (1) in mouse BMSC cultures, expression of the FD-causing G?sR201C resulted in a 2-fold increase of FAP release to the media; (2) cultured human FD BMSCs overexpress FAP in comparison to WT BMSCs; (3) FAP is increased in FD tissue in comparison to normal bone in mice, and decreases with anti-RANKL in both mice and humans; and (4) plasma levels of circulating FAP in FD patients are higher than in healthy volunteers, and it correlates with disease burden.These data support the potential of FAP as a biomarker and imaging radiotracer in FD and open the notion of this protease as a pro-drug activation target in FD.

***Disclosures: Luis Fernandez De Castro Diaz**, None*

SAT-528

Effects of Voxelotor Analog GBT1118 on Bone in Sickle Cell Disease Mice *Liping Xiao[1], Wei He[1], Marja Marie Hurley[2]. [1]UConn Health, United States. [2]UCONN Health School of Medicine, United States

Voxelotor is a sickle hemoglobin (HbS) polymerization inhibitor and has been approved by the FDA for the treatment of hemolytic anemia in sickle cell disease (SCD). Since bone loss is common in SCD, we assessed the effect of GBT1118, an analog of voxelotor on bone in SCD. Four months old female healthy control (Ctrl) and Townes SCD mice were fed with control chow (Teklad 2020 Diet, Veh) or GBT1118 chow (Teklad 2020 Diet with 4 g/kg GBT1118) for 2 months. Dual-energy X-ray absorptiometry analysis showed no significant effect of GBT1118 on bone mineral density. However, micro computed-tomography (uCT) analysis showed that GBT1118 significantly increased femur metaphyseal trabecular thickness (Tb.Th) and decreased trabecular spacing (Tb.Sp) in SCD mice. GBT1118 enhanced bone volume fraction (BV/TV) and trabecular number (Tb.N) in SCD mice, however these changes were not significant. Mid-diaphyseal uCT showed that the enlarged marrow area (Ma.Ar) in SCD mice was reduced with GBT1118 and the drug reversed the decline caused by SCD in cortical area/total area (Ct.Ar/Tt/Ar). Cortical thickness (Ct.Th) was significantly lower in SCD-Veh group vs. Ctrl-Veh, there was a trend increase with GBT1118 treatment. GBT1118 did not alter Tt.Ar or Ct.Ar in SCD mice. There was no difference in serum calcium, phosphate among groups. GBT1118 did not alter serum parathyroid hormone or 1,25 dihydroxyvitamin D level in SCD mice. Serum bone turnover markers Osteocalcin, P1NP, and CTX-1 were not altered by GBT1118 in SCD mice. Von Kossa staining showed the decreased mineralized trabecular number in SCD mice was rescued by GBT1118 (Fig.1A). Bone histomorphometry (Fig.1B-H) showed that there was a significantly decreased mineral apposition rate (MAR), bone formation rate (BRF) and inter-label thickness (Ir.LTh) in SCD-Veh group vs. Ctrl-Veh, which was rescued with GBT1118. Mineralization surface/bone surface (MS/BS) was lower in SCD-Veh vs. Ctrl-Veh, with no rescue by GBT1118. Osteoclast surface/bone surface (Oc.S/BS) and osteoclast number/bone surface (N.Oc/BS) were significantly higher in SCD-Veh group vs. Ctrl-Veh, which was reduced with GBT1118. qPCR analysis of whole tibia showed that GBT1118 inhibits Sost and Trap mRNA expression in SCD mice. We conclude that these are promising results that GBT1118 might be beneficial in SCD-related bone pathology but treating the mice with higher doses of the drug or for longer periods of time at the current dose may be necessary.

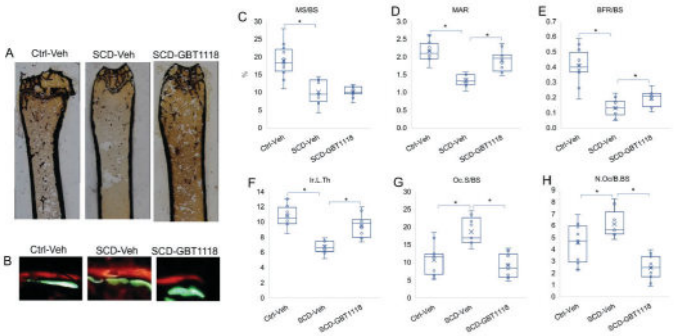

Figure 1. Effect of GBT1118 on bone in SCD mice. (A) von Kossa staining of femur. (B) Calcein and Xylenol Orange double labeling. (C-H) Bone histomorphometry analysis on femur.

***Disclosures: Liping Xiao**, None*

SAT-530

Broad Spectrum Antibiotic Treatment of PDGFR?-cre/ACVR1R206H FOP Mice Improves Survival and Decreases Chronic Heterotopic Ossification *Liam Lam[1], Camille Fang[7], Ariane Zamarioli[3], Aditi Sharma[4], JESSICA PIERCE[5], Michael Hohl[6], Daniel Perrien[6], Edward Hsiao[7]. [1]UCSF, United States. [7]University of California, San Francisco, . [3]Department of Orthopedics and Anesthesiology, Ribeirao Preto Medical School, University of Sao Paulo, Brazil., Brazil. [4]UC San Francisco, . [5]Emory University School of Medicine, United States. [6]Emory University, United States. [7]University of California, San Francisco, United States

Background: Fibrodysplasia ossificans Progressiva (FOP) is a highly penetrant genetic disease that leads to heterotopic ossification (HO) of skeletal muscle due to inflammatory flares caused by a highly recurrent ACVR1R206H mutation that causes Activin A to be misinterpreted as a bone morphogenetic protein (BMP) signal. We previously found that patients with FOP may have alterations in their gut microbiota and that ablation of microbiota reduces injury-induced HO in FOP mice. Pdgfra-cre/Acvr1R206H mice expressing Alk2R206H in fibro-adipoprogenitors spontaneously develop HO resembling that of human patients, leading to reduced muscle function, loss of mobility, and death by 9 weeks old. Here, we tested the ability of broad-spectrum antibiotic ablation of the microbiome to reduce spontaneous, non-injury-induced, HO and improve survival in Pdgfra-cre/Acvr1R206H FOP mice.Methods: At weaning, FOP mice were assigned to ABX or No ABX groups (n=12 each). Mice were given standard drinking water (No ABX) or water containing an established antibiotic cocktail (1.0 g/L Ampicillin, 0.5 g/L Vancomycin, 0.5 g/L Metronidazole,

and 0.5 g/L Neomycin) (ABX) to deplete the microbiota from weaning. Mouse mortality was determined using humane endpoints defined by UCSF-IACUC as >15% weight loss, moribund, or death. HO volume was measured by microCT.Results: Kaplan-Meier curve analysis showed that ABX FOP mice survived longer than No ABX FOP mice (Median odds of survival 54.5 days vs. 41 days, p = 0.048). ABX Wean FOP mice also recovered their body weight, returning to similar levels as WT mice. MicroCT analyses showed a trend toward less HO in ABX Wean mice (45.8% reduction vs. No ABX, p=0.20 by t-test) and a significant 12.7% decrease in tissue mineral density of HO vs. No ABX FOP mice (p=0.11). Conclusion: These results show that ablation of the microbiota with broad spectrum antibiotics started at weaning could improve survival of Pdgfra-cre/Acvr1R206H FOP mice, possibly by decreasing HO and improving body weight. Future investigations are needed to identify the mechanisms by which antibiotic ablation of microbiota mitigates mortality and HO in FOP mice, understand how spontaneous vs. injury-induced HO differ, and elucidate if these effects extend to patients with FOP.

***Disclosures: Liam Lam**, None*

SAT-531

Protein Kinase A: a Promising Therapeutic Target of Fibrous Dysplasia *Zhongyu Liu[1], Ding Bai[1], Xuefeng Zhao[2]. [1]State Key Laboratory of Oral Diseases, National Clinical Research Center for Oral Diseases, Department of Orthodontics and Paediatrics, West China Hospital of Stomatology,Sichuan University, China. [2], China

Fibrous dysplasia (FD) is a skeletal disease caused by postzygotic activating mutations of GNAS. Its symptoms include bone fractures, deformities, and pain. And currently, there is no cure for this disease. The cAMP-dependent protein kinase, also known as protein kinase A (PKA) plays critical roles in metabolism, gene regulation, and disease. However, the role of PKA in FD is unknown. To test our hypothesis that PKA is a therapeutic target for FD, we generated a tetracycline-inducible transgenic mouse model expressing consecutive activating mutation of catalytic subunit alpha of PKA in skeletal stem cell linage (tet-PkacaW197R/Prrx1-Cre). The tet-PkacaW197R/Prrx1-Cre mice developed robust FD-like lesions a few days following administration of doxycycline. Utilizing the PKA inhibitor gene PKI and the FD mouse model (tet-GNASR201C/Linker/Prrx1-Cre) we developed previously, we created a mouse model in which the expression of PKA was effectively suppressed while GNAS-cAMP signaling was elevated (tet-GNASR201C/tet-PKI/Prrx1-Cre). Encouragingly, the tet-GNASR201C/tet-PKI/Prrx1-Cre mice failed to develop FD-like bone lesions, demonstrating that the FD lesion was developed in a PKA-dependent fashion. Furthermore, we found that lesions of FD mice were largely restored following the treatment of small molecular inhibitors of PKA (H89 and rp-cAMPs). Together, these findings suggest that PKA is necessary and sufficient for the initiation and development of FD, making it a promising therapeutic target for FD.

***Disclosures: Zhongyu Liu**, None*

SAT-532

See Friday Plenary Number FRI-532

SAT-533

Generation of a Col1a1 conditional knock-in mouse model for the study of osteogenesis imperfecta *Roy Morello[1], Milena Dimori[1], Charles O'Brien[2]. [1]University of Arkansas for Medical Sciences, United States. [2]Univ of Arkansas for Medical Sciences, United States

Several mouse models are available to study the pathophysiology of osteogenesis imperfecta (OI). Some of these have been genetically modified to introduce a mutation in Col1a1 or Col1a2 to mimic classic dominant OI while others, carrying mutations in other genes, are mimicking rarer, recessive forms of the disease. While these models have been very useful to better understand the disease, they express the underlying mutation in all tissues and thus prevent the study of its potential effects in a tissue-specific manner. To address this important limitation, we designed the first conditional knock-in allele for Col1a1 and generated mice that express the p.Gly1146Arg mutation, known to cause severe OI in human subjects, but only after Cre-specific recombination of the floxed allele. To validate our design we then crossed our Col1a1Gly1146Arg-Floxed/+ mice with the EIIA-Cre mouse strain to verify that offspring with global expression of the mutation exhibit an OI phenotype. Analysis of mice from several litters at 9 weeks of age revealed the presence of runted mice that upon genotyping harbored the recombined allele, Col1a1Gly1146Arg-Floxed/+;EIIA-Cre+. By digital X-ray these mice showed multiple fractures, including bilateral pelvic fractures and severe kypo-scoliosis. Both DEXA and microCT analysis showed severely reduced BMD and BMC, with dramatic reduction of trabecular bone and thinning of cortical bone. Importantly, these mice also showed severe morphological lung defects, confirming our findings in other OI mouse models. In conclusion, we successfully generated a conditional knock-in allele for Col1a1 and verified that its global expression using EIIA-Cre mice causes severe OI. We are breeding these mice with mice expressing Cre in all lung fibroblasts to assess the role of an OI mutation on respiratory function in the context of a healthy skeleton, and with mice expressing Cre in osteocytes to determine whether osteocytes play a significant role in OI disease manifestations compared to osteoblasts. We will also use these mice to study the impact of a severe type I collagen mutation in other tissues as well as during different developmental time points using an inducible Cre.

***Disclosures: Roy Morello**, None*

SAT-534

The Microbiome Contributes to Endochondral Heterotopic Ossification in FOP Mice by Promoting Maturation of Cartilage and Endochondral Bone *JESSICA PIERCE[1], Leslie McCauliff[2], Kela Johnson[2], Michael Hohl[2], Rheinallt Jones[2], Camille Fang[3], Liam Lam[3], ROBERTO PACIFICI[4], Edward Hsiao[5], Daniel Perrien[2]. [1]Emory University School of Medicine, United States. [2]Emory University, United States. [3]University of California San Francisco, United States. [4]EMORY UNIVERSITY, United States. [5]University of California, San Francisco, United States

Endochondral heterotopic ossification (EHO) in Fibrodysplasia Ossificans Progressiva (FOP) is driven by adverse wound healing responses in skeletal muscles, including hyperinflammation, caused by mutations in the Type 1 BMP receptor ACVR1/ALK2. Inflammatory responses to skeletal muscle injury are also modulated by changes in the gut microbiome, and we previously showed that microbiome ablation via an established broad-spectrum antibiotic cocktail (ABX; 1.0 mg/mL ampicillin, 1.0 mg/mL neomycin, 1.0 mg/mL metronidazole, and 0.5 mg/mL vancomycin) significantly reduced injury-induced EHO in tamoxifen-inducible R26creERt2;ALK2R206H-FlEx/w (FOP) mice. This was mediated, in part, by reduced total immune cells and proinflammatory monocytes and macrophages in the injury site, suggesting an indirect contribution of the microbiome to EHO. Here we report the effect of microbiome ablation on the later progression of FOP lesions and muscle repair by analyzing the tissue composition in hindlimb muscles of FOP mice 21 days post-injury (dpi). Twenty-four-day-old FOP mice were given sterile water (CON) or water containing ABX from 10 days before pinch injury of the lower hindlimb muscles until sacrifice at 21 dpi. Ex vivo microCT analysis revealed that median EHO volume in the hindlimbs of ABX-FOP mice (2.44 [1.36,5.65] mm3) was significantly less than in CON-FOP (7.51 [2.59,17.25] mm3, p=0.042 by Mann-Whitney). To further assess soft tissue composition of the FOP lesions, the areas of mature EHO, prehypertrophic and hypertrophic cartilage, fibroproliferative tissue, and regenerating muscle were measured in representative H&E-stained cross-sections of the decalcified hindlimbs. As expected, this confirmed the reduction of mature bone and total lesion size in ABX-FOP mice. The lesions in ABX-FOP mice also contained significantly more cartilage (median=0.18 [0.06,0.37] mm2) compared to CON-FOP mice (0.07 [0.01,0.12] mm2, p=0.049), but significant differences in the relative areas of fibroproliferative tissue and regenerating muscle were not detected. While our previous report demonstrated that microbiome ablation reduced immune cell infiltration at the early stages of FOP lesions, these findings suggest that it may also impair EHO maturation in FOP mice. Future studies are needed to determine whether this is a secondary effect of reduced inflammation in the early lesion or occurs via a direct effect of the microbiome on endochondral bone formation.

***Disclosures: JESSICA PIERCE**, None*

SAT-535

See Friday Plenary Number FRI-535

SAT-536

Electrocardiogram Changes in an Osteogenesis Imperfecta Murine Model (oim) *Krish Sardesai[1], Brittany Lafaver[2], Julian Vallejo[1], Li Lee[3], Lixin Ma[3], Charlotte Phillips[4], Michael Wacker[5]. [1]University of Missouri-Kansas City, School of Medicine, United States. [2]Department of Biochemistry, University of Missouri, United States. [3]Department of Radiology, University of Missouri, United States. [4]University of Missouri-Columbia, United States. [5]University of Missouri-Kansas City School of Medicine, United States

Osteogenesis imperfecta (OI), also known as "brittle bone disease", is a heritable collagenopathy involving the formation of type I collagen, occurring once every 15,000 - 20,000 births. Its pathogenesis is largely due to mutations in COL1A1 and COL1A2 genes. OI is characterized by decreased bone mineral density and increased susceptibility to bone fractures, given that type I collagen is the major structural protein found in bone. Beyond brittle bones, collagen type I contributes to cardiac extracellular matrix and is found in heart valves, interventricular septum, chordae tendineae, and annuli fibrosi; hence, downstream cardiovascular pathologies are a primary cause of mortality in OI, though the specific pathogenesis is largely unstudied. We hypothesize that OI contributes to electrophysiological abnormalities in mice even as young as 4 months concomitant with changes in cardiac structure and function.The osteogenesis imperfecta murine (oim) model replicates OI type III through a homozygous gene mutation of the COL1A2 gene. 4-month old wild-type (WT) and oim (oim/oim) mice underwent conscious electrocardiogram testing (ECG) wherein heart rate variability (HRV), QRS interval, PR interval, ST segment, and corrected QT interval were measured over 20 minutes. Additionally, cardiac function was assessed by in vivo cardiac 7T cine MRI providing parameters such as left ventricular blood volumes and ejection fraction. ECG analysis demonstrated oim mice (combined sexes) exhibit an increase in SD Rate HRV

(18 +/- 4 for WT vs. 25 +/- 6 bpm oim, p<0.05; n=14; female mice alone p=0.058; n=7). Oim mice did not exhibit a significant alteration in conscious heart rate or other ECG parameters. These results are surprising given that oim displayed changes in cardiac structure and function with increased blood volumes in male oim of 21.7% and 60.54%, diastolic and systolic end volumes, respectively with a corresponding decrease in male oim ejection fraction of 16.4% compared to WT littermates (p<0.05; n= 9). It is possible that the high heart rate and variability with conscious mice complicated observing additional differences. While HRV prolongation is normally associated with enhanced vagal tone, studies suggest an increased HRV may also be associated with an increased bone fracture risk, potentially explaining prolongation in oim mice (Stein et al., 2021). These preliminary results suggest understanding changes in ECG may provide additional clinical tools for OI care.

***Disclosures: Krish Sardesai**, None*

SAT-537

A new chemical chaperone rescues cell homeostasis and improves bone collagen content in osteogenesis imperfecta *Nadia Garibaldi[1], Roberta Besio[2], Julen Fernandez[1], Francesca Tonelli[2], Filippo Doria[2], Cecilia Masiero[2], Antonella Forlino[2], Alessandra Carriero[1]. [1]The City College of New York, United States, [2]University of Pavia, Italy

Classical osteogenesis imperfecta (OI) is associated to intracellular collagen accumulations that impairs bone cellular homeostasis and extracellular matrix. We recently focused on the chaperone 4-phenylbutyrate (4-PBA) as a potential OI treatment, but its short half-life and lack of bone specific targeting constitute major limitations. Molecular modeling starting from 4-PBA structure and focused on improving drug stability allowed the identification of a new potentially more stable derivative, MOD-4-PBA. Here, we evaluate MOD-4-PBA efficacy in counteracting OI bone cells stress, and its ability to improve bone matrix properties.To this aim, after its synthesis, we tested MOD-4-PBA efficacy first in vitro in primary osteoblasts (OBs) isolated from the OI murine model Brtl using qPCR-based arrays, western blot, immunofluorescence, thioflavin T labelling of intracellular protein aggregates and protein secretion. We then tested MOD-4-PBA efficacy in improving bone quality in vivo in the Chihuahua zebrafish model of OI, where we evaluated cranial bones mineralization using Alizarin Red in larvae. In adult zebrafish we quantified vertebral length and bone volume using synchrotron microtomography, as well as collagen content, fibers orientation and continuity using second harmonic generation microscopy. MOD-4-PBA administration was well tolerated and non-toxic in Brtl cells. It proved to reduce apoptosis, as confirmed by the low cleaved caspase 3 expression and to modulate the Unfolded Protein Response pathway. The increased expression of the endoplasmic reticulum quality control proteins in treated OBs suggests an attempt of these cells to strongly react to intracellular collagen accumulation. The MOD-4-PBA administration reduced intracellular protein aggregates and increased proteostasis favoring protein secretion (Fig. A). In vivo, in zebrafish larvae, an optimized dose of MOD-4-PBA increased the level of mineralization of cleithrum and branchiostegal ray 3 in both WT and Chihuahua mutants. In adult zebrafish, we observed same vertebral length and bone volume with increased collagen content and fibers continuity even in disoriented fibers (Fig. B). In summary, MOD-4-PBA administration ameliorated cellular homeostasis and proteostasis in OI murine OBs and improved bone collagen content and mineralization in the OI zebrafish Chihuahua, thus paving the way for an innovative approach to complement the current OI therapies.

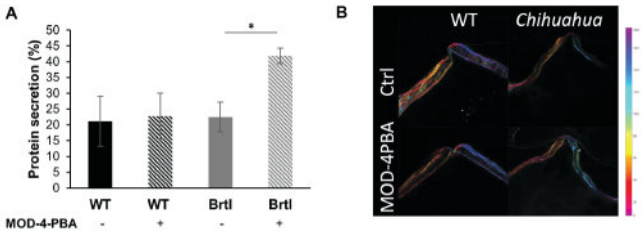

Figure A: Graph representing protein secretion evaluated by radioactively labelling proteins with ^{35}S-L-Methionine and ^{35}S-L-Cysteine in absence or presence of MOD-4-PBA. The experiment was performed in three independent cell preparations. *p<0.05 **B**: Fiber orientation in WT and *Chihuahua* zebrafish vertebral endplates with/out MOD-4-PBA treatment.

***Disclosures: Nadia Garibaldi**, None*

SAT-538

See Friday Plenary Number FRI-538

SAT-539

Potent Parathyroid Hormone 1 Receptor Antagonists Suppress Receptor Activation and Downstream Pathways in Human Primary Osteoblasts *Jonathan Shintaku[1], Elizabeth Rico-Bautista[1], Joe Pontillo[1], Shimiao Wang[1], Anel Castellanos[1], Julie Nguyen[1], Kelsey Retting[1], Beth Fleck[1], Sameer Urgaonkar[1], Stephen F. Betz[1], Stacy Markison[1]. [1]Crinetics Pharmaceuticals, Inc., United States

Parathyroid hormone (PTH) regulates calcium homeostasis by direct and indirect targeting of bone, kidney, and intestine. In bone, PTH stimulates cAMP generation and PKA signaling, which alters expression of genes such as RANKL and OPG. RANKL secretion from osteoblasts activates osteoclasts to promote bone resorption and calcium release from the bone matrix. Primary hyperparathyroidism (PHPT) is diagnosed in about 100,000 people in the United States every year and is characterized by over-secretion of PTH, usually due to parathyroid adenomas or hyperplasia. Approximately 20% of individuals with PHPT are symptomatic, exhibiting skeletal, renal, gastrointestinal, and/or neurological manifestations and increased mortality. Medical intervention seeks to normalize blood calcium levels, increase bone mineral density (BMD) to lower the risk of bone fractures, and reduce the risk of kidney stones. While the first line therapy of partial to total parathyroidectomy is sufficient to treat most individuals, surgery is either declined or insufficient in 10-15% of symptomatic PHPT patients. Alternatives to surgery include calcimimetics, which reduce circulating calcium but have no effect on BMD, or bisphosphonates, which can improve BMD but have no effect on circulating calcium. We hypothesize that targeting PTH action via a PTH1 receptor (PTH1R) antagonist could effectively treat both symptoms of PHPT. Using an iterative medicinal chemistry approach, Crinetics has identified potent non-peptide PTH1R antagonists. In CHO-K1 cells heterologously expressing human PTH1R, compounds demonstrated good potency in functional antagonist assays (IC50<100 nM). Select compounds were then evaluated in normal human primary osteoblasts and human osteosarcoma cells to gauge their therapeutic potential for improving calcium homeostasis and increasing BMD. In both human cellular models, antagonists suppressed PTH-dependent activation of PTH1R in a concentration-dependent manner, with potency comparable to the heterologous system. Antagonist action was also evaluated downstream of PTH1R via expression of functionally relevant genes such RANKL and OPG. The compounds' potent PTH1R antagonist activity in normal human primary osteoblasts strengthens our confidence in their ability to regulate PTH1R activity in patients with PHPT.

***Disclosures: Jonathan Shintaku**, Crinetics Pharmaceuticals, Inc., Grant/Research Support*

SAT-540

See Friday Plenary Number FRI-540

SAT-541

Bone tissue structure and composition of oim middle ear ossicles *MAIALEN UGARTEBURU[1], Luis Cardoso[2], Claus-Peter Richter[3], Alessandra Carriero[2]. [1], [2]The City College of New York, United States, [3]Northwestern University , United States

Hearing loss is a common clinical hallmark of people with Osteogenesis Imperfecta (OI, or brittle bone disease). To date, pathophysiological mechanisms of hearing impairment in OI are uncertain, and structural and compositional properties of the middle ear bones in OI remain poorly studied. In a recent study on the ossicles morphology in the oim mouse model of OI, we found consistent fractures of the incus in the oim middle ear [1]. To explain the mechanism of these fractures, here we investigate the bone tissue structural and compositional properties of the oim middle ear ossicles. We examined bone composition in oim and WT mouse (14 w.o.) ossicles using Raman spectroscopy. On the same bones, we quantified collagen content orientation, continuity, and number of clusters of collagen fibers using second harmonic generation microscopy and a custom-made MATLAB code [2]. On the contralateral ears, we performed synchrotron microtomography to determine ossicular bone tissue porosity at the vascular and cellular level. Bone tissue from the oim ossicles showed no differences in the mineral compositional parameters (mineral-to-matrix ratio, carbonate substitution, and crystallinity) compared to healthy bone. However, they exhibited a decrease in collagen content, as well as in fibers organization and continuity, with an increased number of fibers clusters, and higher lacunar, but not vascular, density volume. These results suggest that potential causes for bone fragility in the oim middle ear bones are to be searched in the collagen organization within the tissue, and in its cellular porosity. These both represent defects within the bone tissue, where a crack can start and easily propagate [3, 4]. Interestingly, structural changes resemble the ones we found in the long bones [3], but not the compositional properties [4], possibly because the middle ear mineralizes during ossification, with no subsequent remodeling. Furthermore, tissue porosity in the ossicles is in contrast with those found in the otic capsule [5], showing that under pathological conditions, different bones of the same hearing system may have different properties according to their physiological function.[1] Ugarteburu, M., et al. ARO 2022[2] Muñoz A., et al. NEBEC 2022[3] Carriero A., et al. Bone 2014[4] Carriero A., et al. JBMR 2014[5] De Paolis, A., et al. JSB 2021

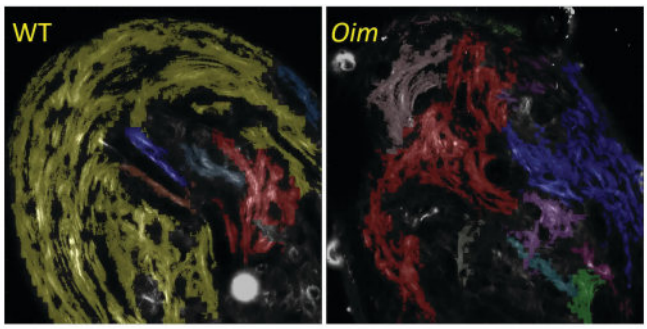

Fig. 1. Clusters of continuous fibers in the bone tissue of WT and *Oim* ossicles.

***Disclosures: MAIALEN UGARTEBURU**, None*

SAT-542

Activating Gcm2 variant enhances tumorigenesis in a cyclin D1-driven mouse model of primary hyperparathyroidism *Jessica Costa-Guda[1], Justin Bellizzi[2], Callie Burke[2], Christina Titarenko[2], Sharon Yaqoob-Krysztofiak[2], Andrew Arnold[3]. [1]University of Connecticut Health Center, United States. [2]UConn Health, United States. [3]University of Connecticut School of Medicine, United States

Germline missense variants in the glial cells missing 2 gene (GCM2) have been associated with familial and sporadic parathyroid tumors, but population-based penetrance is low for most and their potential roles in pathogenesis or clinical management remain unclear. Further, functional evidence has thus far been restricted to demonstrating increased activity in in vitro transcription assays without direct relevance to a parathyroid tumor phenotype, causing difficulty in rigorously classifying the variants e.g. as low-penetrance predisposition alleles, modifiers, pathogenic drivers, variants of uncertain significance (VUS) etc. We therefore evaluated, in a functionally relevant murine system, the ability of one main variant, Gcm2 Y392S (equivalent to human GCM2 Y394S), to accelerate parathyroid tumorigenesis in cooperation with an established parathyroid tumor-driver. Genetically engineered mice harboring Gcm2 Y392S, originally developed at NIDDK on a C57BL/6 background and generously provided by Dr S Agarwal, were crossed with PCD mice, an established model where parathyroid-specific cyclin D1 overexpression (driven by a PTH-CCND1 transgene on an FVB background) causes primary hyperparathyroidism (PHPT). Serum calcium increased over time in both Gcm2Y392S/PCD and PCD mice. By 12 months of age, significantly more Gcm2Y392S/PCD mice had elevated serum calcium compared with PCD mice and by 18 months, serum calcium levels in Gcm2Y392S/PCD mice were significantly higher than in PCD mice. Parathyroid cell proliferation, measured by Ki67 immunostaining, was also significantly higher in Gcm2Y392S/PCD mice than in PCD mice. In contrast, serum calcium levels and parathyroid proliferation in mixed background littermates positive for Gcm2Y392S alone were similar to those of non-transgenic littermates. Thus, in this murine model, Gcm2 Y392S cooperatively enhanced cyclin D1's parathyroid tumorigenic phenotype, but alone was insufficient to cause parathyroid neoplasia or primary hyperparathyroidism. Our observations seem consistent with reports of reduced penetrance for the corresponding human variant GCM2 variant Y394S, further suggesting that Y394S may function more as a modest predisposition allele than as a strongly penetrant germline cause of PHPT. More functional evidence as described here is needed and should also be considered when studying the potential implications or role of germline activating GCM2 variants in genetic counseling and clinical decision-making.

***Disclosures: Jessica Costa-Guda**, None*

SAT-543

Single cell transcriptome analysis of FD/MAS skeletal lesions reveals unique osteoblastic and fibroblastic cell clusters and a gene expression signature that is preserved across multiple cell types *KELLY WENTWORTH[1], Edward Hsiao[2], Fernando Fierro[3], Bryan Le[3], Tania Moody[2]. [1]University of California-San Francisco, Zuckerberg San Francisco General Hospital, United States. [2]University of California, San Francisco, United States. [3]University of California, Davis, United States

Fibrous dysplasia (FD) is a rare skeletal dysplasia characterized by expansile, fibrotic bone lesions that cause significant morbidity. FD exists on a spectrum and can affect one or more bones or occur as part of McCune-Albright Syndrome (MAS), which is defined by polyostotic FD, café-au-lait skin lesions, precocious puberty and various endocrinopathies. FD/MAS is a somatic, mosaic disease caused by a postzygotic activating mutation in GNAS (p.R201H/C), resulting in constitutive Gs-signaling in affected tissues. The precise mechanisms by which this altered signaling causes the FD skeletal phenotype remains unknown, and a more detailed understanding of the cell types present in FD lesions and their transcriptomic profile is needed. Here we report a comprehensive single cell RNA sequencing (scRNAseq) analysis of FD bone lesions (n=4) and compare them to bone from osteoarthritis patients undergoing joint replacement (n=4). Bone fragments obtained from surgical samples were digested and enriched for viable and non-hematopoietic cells. Single cell suspensions were processed for scRNAseq using 10x Chromium technology and sequenced. Following QC and normalization of sample gene expression matrixes, FD and control samples were combined into one dataset for analysis. Integration of the FD and control samples revealed the presence of 3 major cell groups: stromal cells, endothelium, and smooth muscle cells. Each group contained a significant number of genes that were differentially expressed (DE) in FD v. control cells (10638-16384, $p<0.05$), highlighting the significant transcriptomic differences seen in FD cells. Upon subclustering the stromal compartment, 14 cell clusters were identified, including fibroblasts, osteoblasts (OBs), chondrocytes, and skeletal stem/progenitor cells. Intriguingly, FD lesions harbor a unique cluster of OB-like cells that are nearly absent in controls (613 v.10 cells, respectively) and 2 clusters of ECM-producing fibroblasts that are enriched for FD cells (259 v. 14 and 1962 v. 135, respectively). We also identified a significant number of DE genes in FD v. control samples (ranging from 3207-13603 genes per cluster, $p<0.05$), many of which were consistently upregulated in FD across multiple cell types. Altogether, our scRNAseq analysis sheds new light on the altered cellularity and transcriptomic profile of human FD lesions and identifies possible biomarkers and pathways that could be targeted for therapeutic intervention. KW/FF=coauthors

***Disclosures: KELLY WENTWORTH**, None*

SAT-544

See Friday Plenary Number FRI-544

SAT-545

See Friday Plenary Number FRI-545

SAT-546

Progressive Loss of Bone Density in Patients with Esophageal Cancer *Miles Cameron[1], Sarah Judge[1], Andrew Judge[1]. [1]University of Florida, United States

Background: Changes in body composition are common in esophageal cancer (EC). More than 60% of patients, regardless of stage, display signs of cachexia, including weight loss, skeletal muscle atrophy and fat wasting. In the current study, we questioned whether bone density also decreases in patients with EC and associates with oncologic outcomes. Methods: We performed a retrospective review of all patients that received esophagectomy between 2015 and 2020 at University of Florida Health. Patients with pre-existing cardiac disease were excluded. Body composition was measured using PET/CT scans, and patients were classified as having cachexia/myopenia if having an L3 skeletal muscle index below sex- and BMI-dependent cutoffs. A p-value less than 0.05 was considered statistically significant.Results: Bone density was significantly reduced in patients with cachexia relative to those with normal muscle mass (108+/-37.2 HU v. 146+/-55.0 HU, p=0.003). Furthermore, bone density correlated with muscle mass ($p<0.0001$, R=0.5055) and muscle quality/radiodensity (p=0.0002, R=0.4736). Mean rate of bone loss was -12.0+/-27.9 HU/100d between initial and re-staging imaging studies after neoadjuvant therapy. Patients with regional lymph node metastases at surgery (N1-3) had more bone loss than those with N0 disease (-26.6+/-30.8 HU/100d v. -2.71+/-22.1 HU/100d, p=0.03). Similarly, progressive loss of bone was observed in patients with positive lymphovascular (LV) invasion (-41.8+/-32.6 HU/100d v. -3.53+/-20.1 HU/100d, p=0.005) and positive perineural (PN) invasion (-29.8 +/- 32.4 HU/100d v. -3.12 +/- 21.1 HU/100d, p=0.01).Conclusion: Reduced bone mineral density is a key component of cachexia in patients with EC. We demonstrate herein that osteopenia in EC patients associates with several cachexia measures and that progressive loss of bone may predict a worse response to neoadjuvant therapy and a tumor's early metastatic potential. Bone density may serve as a strong predictor of survival and stratification tool for clinical trials. These findings further highlight the need to study mechanisms that lead to bone wasting in tumor bearing hosts.

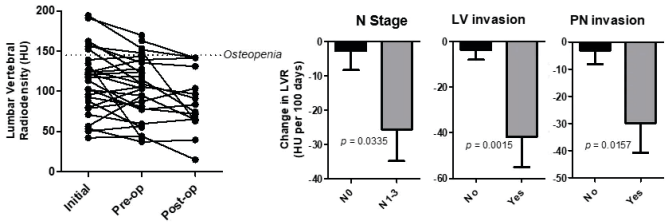

***Disclosures: Miles Cameron**, None*

SAT-547

Higher High-sensitivity Cardiac Troponin I is Associated with Fall and Fracture-Related Hospitalizations in Older Women *Abadi Kahsu Gebre[2], Marc Sim[2], Jack Dalla Via[2], Cassandra Smith[2], Alexander Rodriguez[3], Jonathan Hodgson[2], Catherine Bondonno[2], Wai Lim[4], Elizabeth Byrnes[5], Peter Thompson[4], Richard Prince[6], Joshua Lewis[2]. [2]Edith Cowan University, Australia, [2]Edith Cowan University, , [3]Monash University, , [4]The University of Western Australia, Australia, [5]PathWest Laboratory Medicine, Queen Elizabeth II Medical Centre, Australia, [6]University of Western Australia,

Background: Emerging evidence indicates that individuals with subclinical and clinical cardiovascular disease (CVD) are at increased risk of muscle function decline, falls, and fractures. However, it is unclear if there is an association between high-sensitivity cardiac troponin I (hs-cTnI), a biomarker for myocardial injury, and muscle function decline, injurious fall and fracture-related hospitalizations.Methods: This prospective cohort study included 1179 healthy community-dwelling older women (>=70 years of age) with subclinical plasma levels of hs-cTnI (<15.6 ng/L, in quartiles) measured at baseline (1998). Hand grip strength (HGS) and the timed up-and-go (TUG) test were assessed at baseline. Hip bone mineral density (BMD) was measured by dual-energy X-ray absorptiometry at baseline or year 1 (1999). Data on fall and fracture-related hospitalizations over 14.5 years were obtained from linked health records. Cox proportional hazards regression model was used to determine the association of hs-cTnI (in quartiles) with fall and fracture-related hospitalizations.Results: Compared to women in the lowest quartile of hs-cTnI (Q1), those in the highest quartile (Q4) were older, had higher prevalent chronic diseases, and slower TUG performance (10.3 vs 9.5 seconds, p=0.03). There was no difference in average HGS (Q1 vs Q4;19.9 vs 21.2 kg, p=0.06) or BMD (0.80 vs 0.83 mg/cm2, p=0.58) between the groups. Women in Q4 were more likely to experience injurious falls (43% vs 36%) and fracture-related hospitalizations (30% vs 26%) compared to those in Q1. In a multivariable-adjusted model that accounted for prevalent falls and CVD risk factors, women in Q4 had higher risk of fall-related hospitalization (HR 1.46 95% CI 1.08-1.98) compared to those in Q1. They also had higher risk of fracture-related hospitalization (HR 1.52 95%CI 1.05-2.19), independent of hip BMD.Conclusion: Higher hs-cTnI,a biomarker of myocardial injury, was associated with poorer mobility, and a greater risk of fall and fracture-related hospitalizations in community-dwelling older women.These data indicate the importance of considering cardiac health when assessing musculoskeletal health.

***Disclosures: Abadi Kahsu Gebre**, None*

SAT-548

Association of progression free survival with metabolic activity and radiodensity of the psoas muscle evaluated by preoperative 18F-FDG PET-CT in patients with non-metastatic breast cancer *Yun Kyung Jeon[1], Keunyoung Kim[2]. [1]Pusan National University Hospital, Republic of Korea, [2]Nuclear Medicine, Pusan National University Hospital, Republic of Korea

Background: This study aimed to evaluate the associations of metabolic activity and radiodensity of the psoas muscle measured derived from clinically acquired 18F-fluorodeoxyglucose (F-18 FDG) positron emission tomography/computed tomography (PET/CT) at diagnosis with progression free survival (PFS) in nonmetastatic breast cancer. Methods: This observational study included 249 women from January 2014 and December 2014 in Pusan National University Hospital. All patients undergone surgical resection for stages I-III invasive ductal carcinoma of the breast. Both maximum standardized uptake value (SUVmax) and Hounsfield Unit (HU) of the bilateral psoas muscles were extracted from preoperative performed F-18 FDG PET/CT. We calculated hazard ratios to evaluate the associations between progression free survival with SUVs or HU of psoas muscle using Cox proportional hazard model.Results: Median (range) age of 249 women included in this study was 53 (29-82) years, and median follow-up was 72.5 months (1.9-83.1); 19 patients (7.6%) presented with disease progression. Univariate analyses identified a higher T stage, higher N stage, estrogen receptor negativity, progesterone receptor negativity, human epidermal growth factor receptor 2 positivity, triple-negative breast cancer and higher SUVmax psoas muscle were significantly related to progression free survival (PFS). Lower radiodensity of psoas muscle alone was not significantly related to PFS. Multivariate Cox regression analysis revealed that higher level of N stage (hazard ratio [HR] = 2.240, confidence interval [CI]; 1.349 - 3.716, P = 0.002) and SUVmax (HR = 4.202, CI; 1.488 - 11.863, P = 0.007) as an independent factor for disease progression. Conclusions: Measures of metabolic status of psoas muscle from clinically acquired preoperative F-18 FDG PET/CT scans in nonmetastatic patients provide significant information for PFS.

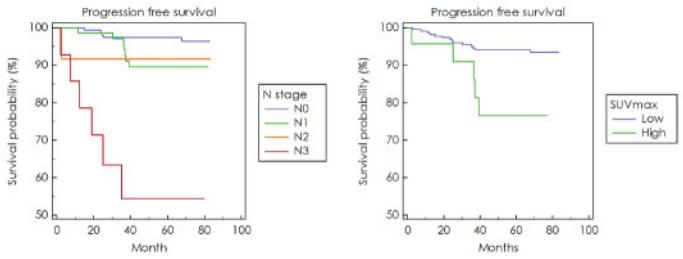

***Disclosures: Yun Kyung Jeon**, None*

SAT-549

Pole Walking Intervention and Fall Risk Factors in Retirement Communities: A Pilot Feasibility Trial *Mohsen Keramati[1], Mahdi Rostami Haji Abadi[1], Saija Kontulainen[1]. [1]College of Kinesiology, University of Saskatchewan, Canada

The effectiveness of exercise interventions in reducing fall and fracture risk in care home residents is unknown. Our purpose was to assess changes in physical function and other fall risk factors, and to explore safety and feasibility of pole walking intervention in retirement care home residents. We recruited 19 residents (mean age 83.8 years; 84% female; 53% with positive fall history) from 4 retirement communities in Saskatoon, Canada to participate in this patient-oriented, multi-site, single-arm pilot feasibility trial. Individually-tailored, supervised group intervention sessions (20-60 min) were offered 3 times/week for 12 weeks at each site. Sessions consisted of posture and balance warm-up, pole walking, strengthening exercises, and stretching. We measured body composition and areal-BMD (DXA), physical function (timed “up & go” [TUG], 6-min walk, 30-s chair stand [30CST], and handgrip strength), health-related quality of life (36-item short-form survey [SF-36]), and fear of falling (falls efficacy scale). We assessed safety by recording adverse events, and feasibility via recruitment, retention and attendance rates, as well as participant-reported intervention acceptability, appropriateness, and feasibility scores. Progression criteria to future RCT were recruitment rate >=1 participant/site/month; retention rate>=80%; mean attendance rate>=70%; mean participant-reported scores >=4.0; and no intervention-related serious adverse event. We assessed changes from baseline to 12-weeks using paired t-tests. Participants improved their mobility (mean change in TUG: -1.5 s; 95% CI: -2.6 to -0.4), lower limb muscle strength (30-CST: 2.5 reps; 1.3 to 3.6), and SF-36 physical functioning score (11.8; 2.9 to 20.7). There were no intervention-related serious adverse events. Recruitment, retention, and mean attendance rates were 2.7 participants/site/month, 84%, and 91%, respectively. Participant-reported acceptability, appropriateness, and feasibility scores were >4.0. In conclusion, pole walking intervention pilot in retirement communities was feasible. Participants improved their physical function over 12 weeks. These findings guide the design of an RCT to examine the efficacy of this intervention in improving fall and fracture risk factors in retirement communities.

***Disclosures: Mohsen Keramati**, None*

SAT-550

Circulating resistin level as a potential biomarker for sarcopenia in older adults *Mi Kyung Kwak[1], Hee-Won Jung[2], Eunju Lee[3], Ji Yeon Baek[4], Il-Young Jang[4], So Jeong Park[5], Jin Young Lee[5], Beom-Jun Kim[3]. [1]Hallym University Dongtan Sacred Heart Hospital, Republic of Korea, [2]Asan Medical Center, , [3]Asan Medical Center, University of Ulsan College of Medicine, Republic of Korea, [4]Division of Geriatrics, Department of Internal Medicine, Asan Medical Center, Republic of Korea, [5]Asan Institute for Life Sciences, Asan Medical Center, Republic of Korea

Background: It is well known that muscles weaken with age, and a situation in which the amount, strength, or performance of muscles is reduced can be referred to as sarcopenia. On the other hand, resistin, which is secreted by adipocytes, myocytes and leukocytes and is known to be pro-inflammatory, is known to directly inhibit myogenesis. However, there are few human studies and only some measurements in a specific group. Therefore, this study investigated the relationship between resistin levels and sarcopenia in older adults.Methods: Blood samples were collected from 247 participants who underwent muscle assessment in a geriatric clinic and resistin levels were measured. Serum resistin levels were measured by enzyme-linked immunosorbent assay (ELISA). Sarcopenia and related parameters were determined using cutoff values for the Asian population.Results: In this study, serum resistin levels were statistically significantly higher in the sarcopenia group than in the non-sarcopenia group (10.65 +/- 5.46 vs. 7.90 +/- 4.22, P<0.001). We observed an association of serum resistin levels with muscle-related parameters, and higher serum resistin levels were significantly associated with lower gait speed (? = -0.205, p=0.001), higher chair-stand time (? = 0.171, p=0.007), and lower Short Physical Performance Battery (? = -0.184, p=0.004). These results were similar in the age- and sex-adjusted model and in the age-, sex-, and BMI-adjusted model. The odds ratio (OR) for sarcopenia increased with each unit increase in serum resistin level, both before and after adjustment (OR=1.10 to 1.13, p=<0.001 to 0.006). In addition, the OR for low muscle mass or strength showed a similar pattern (OR=1.09 to

1.14, p=<0.001 to 0.007). In addition, serum resistin levels were examined by dividing the groups according to sarcopenia status or abnormalities in sarcopenia-related parameters. As a result, resistin levels were statistically significantly higher in cases with sarcopenia, low muscle mass, low muscle strength, and poor physical performance (p=<0.001 to 0.033). Conclusions: Serum resistin levels were associated with sarcopenia or sarcopenia parameters in older adults.

Figure 1. Differences in serum Resistin levels according to sarcopenia status and abnormalities in sarcopenia-related parameters unadjusted (a), adjusted for age and sex (b), adjusted for age, sex, and BMI (c). The estimated means with 95% confidence interval were presented using analysis of covariance. ASM, appendicular skeletal muscle mass; BMI, body mass index; BW, body weight.

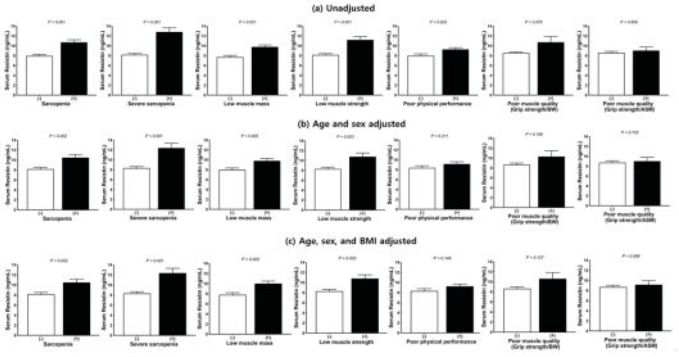

***Disclosures: Mi Kyung Kwak**, None*

SAT-551

Depression is more associated with osteosarcopenia than with other musculoskeletal phenotypes. Data from the SARCOS study *ALBERTO FRISOLI JUNIOR[1], Amanda Kimura[2], Angela Paes[2]. [1]UNIVERSIDADE FEDERAL SAO PAULO, . [2]Universidade Federal Sao Paulo, Brazil

Studies have shown that depression is associated with osteoporosis and sarcopenia. However, the heterogeneity of the latter two conditions and the overlap between them may cause some misinterpretations in the association with depression. To clarify this issue, we assessed the association between depression and osteosarcopenia phenotypes by two different diagnoses of sarcopenia, in older adults. Methods: SARCOS is a prospective cohort study on the association between sarcopenia and osteoporosis and difficult outcomes in older adults with cardiovascular disease. Population: subjects aged > 60 years from the cardiovascular disease outpatient clinic. All patients underwent DXA analysis for appendicular muscle mass, bone mineral density, in addition, handgrip strength and walking speed were measured. Sarcopenia was diagnosed following the EWGSOP II (EW) and SDOC recommendations. Osteoporosis was diagnosed according to the WHO guidelines. Osteosarcopenia was categorized into four phenotypes (osteosarcopenia-OPSAR, sarcopenia-only-SAR, osteoporosis-only-OP, and robust-ROB) for each sarcopenia diagnosis. Depression was considered if the Geriatric Depression Scale was >= 7 points. Regression analyses were adjusted for significant variables for Osteosarcopenia SDOC (Age>80, female sex, previous falls, dementia, diabetes mellitus, previous fracture) and Osteosarcopenia EWGSOPII (female sex, Age>80, Diabetes mellitus, previous fracture, and hospitalizations). Results: In this study, 409 patients were evaluated. The mean age was 77.87(7.6) years, female gender 57.5%(235). Depression occurred in 18.6%(76); osteosarcopenia phenotypes: OPSAR-SDOC:17.8%(73), SAR-SDOC:26.7%(109), OP-SDOC:11.5%(47); p<0.001; and OPSAR-EW:9.5%(39); SAR-EW:8.1%(33); OP-EW:19.8%(81);p=0.337. In patients with depression, 34.2% had OPSAR-SDOC, 28.2% OPSAR-EW; 22% SAR-SDOC, 21.2% SAR-EW; 4.3% OP-SDOC and 19.8% OP-EW. In regression analyses, depression showed odds ratio for OPSAR-SDOC: 3.59 (1.73-7.47; 0.001), SAR-SDOC: 2.05 (1.03-3.96; 0.040); OP-SDOC 0.21 (0.04-0.96;0.045), while for phenotypes with EW, the OR for OPSAR-EW: 2.33 (1.01-5.35; 0.045); SAR-EW: 1.51 (0.59-3.86; 0.382); OP-EW: 1.05 (0.54-2.05;0.862). Conclusions: In our study depression showed greater association with the Osteosarcopenia phenotype than as the other phenotypes, regardless of sarcopenia diagnosis. Implications: These results highlight the importance of differentiating osteosarcopenia phenotypes in clinical practice.

***Disclosures: ALBERTO FRISOLI JUNIOR**, None*

SAT-552

Preliminary Analysis of Weight Loss Associated Musculoskeletal Changes as Assessed by Computed Tomography in the INVEST in Bone Health Trial *Delanie Lynch[5], Allison Avery[2], Caitlyn Dwyer[2], Peggy Cawthon[3], Marjorie Howard[4], Kristen Beavers[2], Ashley Weaver[5]. [5]Wake Forest University School of Medicine , . [2]Wake Forest University, United States. [3]California Pacific Medical Center, United States. [4]Wake Forest University School of Medicine, United States. [5]Wake Forest University School of Medicine , United States

Weight loss improves many obesity-related comorbidities; yet, remains controversial for older adults due to associated musculoskeletal declines and increased fracture risk. Computed tomography (CT) provides accurate, high-resolution measurement of weight loss-associated muscle and bone loss. The purpose of this study is to begin to examine how CT-derived muscle and bone change over 6 months in a geriatric weight loss study.We analyzed a convenience sample of 24 older (68.0+/-4yrs) predominantly white (75.0%) women (66.7%) living with obesity (33.8+/-3kg/m2) and participating in the ongoing INVEST in Bone Health trial (NCT04076618). All participants received caloric restriction targeting 10% weight loss over 6 months (n=24), with some randomized to additional resistance training (n=8) or weighted vest use (n=8). At baseline and 6-months, participants underwent a CT of the trunk and mid-thigh. In each CT, a phantom was imaged to calibrate volumetric bone mineral density (vBMD). Trabecular and cortical vBMD were measured for the total hip and femoral neck. Mid-thigh muscle and intermuscular fat areas were segmented from a single CT slice. Statistical analyses were performed with paired t-tests and partial Pearson's correlations (adjusted for age, sex and weight).Body weight decreased by 11% (-10.3+/-6kg; p<0.01) over 6 months. From baseline, mid-thigh muscle area declined 5% (-6.8+/-6cm2; p<0.01) and intermuscular fat area declined 16% (-1.9+/-3cm2; p=0.01). Trabecular vBMD was not significantly changed (<2% change) for the total hip or femoral neck. Cortical vBMD increased from baseline by 0.6% at the total hip (4.5+/-9mg/cm3; p=0.03) and by 1.9% at the femoral neck (12.9+/-21mg/cm3; p=0.01). Muscle and vBMD changes were not significantly correlated, with the strongest trends between changes in intermuscular fat and hip vBMD (r= -0.34;p=0.14).Significant 6-month weight loss was associated with declines in muscle and intermuscular fat area, while cortical vBMD increased. Only modest correlations were observed between change in muscle and bone outcomes, potentially indicating no causal relationship. However, full interpretation of these results is limited due to the small sample size and lack of analysis by interventional assignment (i.e. resistance training or weighted vest use), which remains blinded at this time. Future work will explore these muscle and bone outcomes longitudinally (i.e. 12-months) in the entire study cohort (n=150).

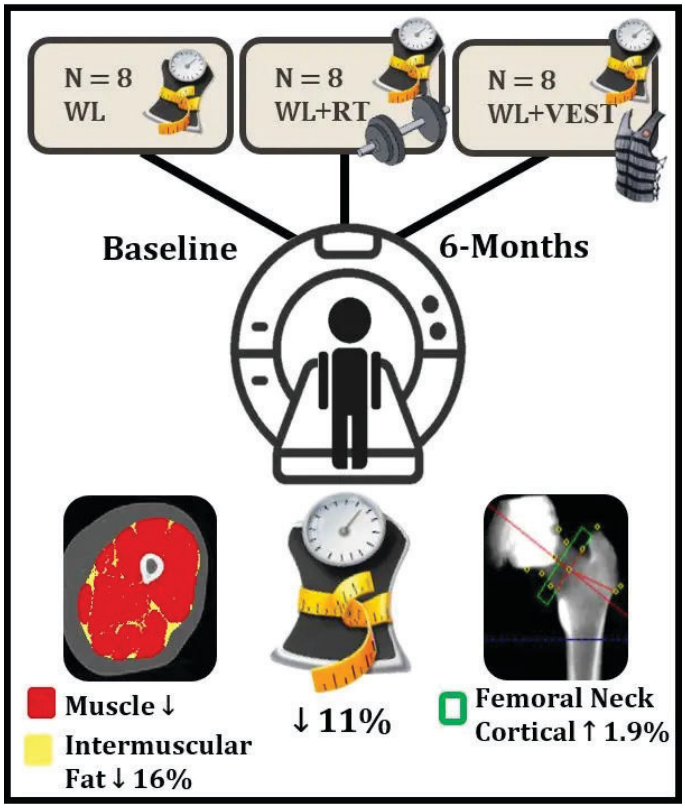

***Disclosures: Delanie Lynch**, None*

SAT-553

ANALGESIC ACTIVITY OF NSAIDs AND PARACETAMOL IN EXPERIMENTAL OSTEOARTHRITIS AND HYPOTHYROIDISM *ROKSOLANA POVOROZNYUK[1], Vladyslav Povoroznyuk[2], Dmytro Nosivets[3], Nataliia Dzerovych[2]. [1], Ukraine. [2]D.F. Chebotarev Institute of Gerontology NAMS of Ukraine, Ukraine. [3]Oles Honchar Dnipro National University, Ukraine

Separate nosological forms of osteoarthritis (OA) and hypothyroidism (HT) differ in their etiology; however, the issue of comorbidity gains the utmost importance for these diseases, which are insufficiently explored in the literature. Analgesics may affect the hormonal activity of the thyroid gland through a direct influence on the synthesis and secretion of hormones or their metabolism, clearance and absorption by tissues. However, an important and unexplored issue is the study of the processes of interaction of analgesics with the hormone

replacement therapy drug L-thyroxine, their ability to affect pain of varying intensity. The aim was to conduct a comparative analysis of the influence of experimental pathologies (OA and HT) on the state of the nociceptive system and the influence of the use of NSAIDs and paracetamol on antinociceptive mechanisms in experimental rats.Materials and Methods. Experimental studies were performed on 240 white mature nonlinear rats of both sexes. Experimental OA was reproduced by a single intra-articular injection of 0.1 ml of Iodoacetic acid solution into the knee joint, which was prepared at the rate of 3 mg of reagent per 50 ?l of sterile saline. Experimental HT was performed by enteral administration of 0.02% carbimazole solution, which was prepared at the rate of 5 mg per 250 ml of saline. The analgesic potential of the studied drugs was evaluated by studying their antinociceptive activity based on the effect on the pain threshold of rats after a single administration of NSAIDs and paracetamol and against the background of a 5-day administration of L-thyroxine using the method of electrical stimulation of the tail root of rats and recording the nociceptive response (vocalization reaction. Conclusions. Hypothyroidism leads to hypoalgesia against the background of OA, which is evidenced by a decrease in the threshold of pain sensitivity by 17% ($p<0.05$) in the comorbid condition versus 24% ($p<0.05$) in OA. Experimental pathological conditions - OA and HT significantly change the antinociceptive activity of drugs. Under the conditions of OA and HT against the background of hormone replacement therapy with L-thyroxine, it was established that these drugs are ranked as follows by the intensity of antinociceptive action: diclofenac sodium (+212%) (p ibuprofen (+144%) (p nimesulide (+134%) (p paracetamol (+116%) (p meloxicam (+104%) (p celecoxib (+93%) ($p<0.001$), which reflects the highest antinociceptive activity of diclofenac sodium.

***Disclosures: ROKSOLANA POVOROZNYUK**, None*

SAT-555

The Relationship between Diet Quality and Sarcopenia: an Analysis of the National Health and Nutrition Examination Survey *Sikarin Upala[1], Moya Alfonso[1], Steven Hecht[1], Darin Ruanpeng[2]. [1]Nova Southeastern University, United States. [2]St Luke's Hospital, United States

Introduction: Sarcopenia is a skeletal muscle disease associated with morbidity and mortality. Factors related to sarcopenia include aging, systemic diseases, physical inactivity, and inadequate energy intake. Limited evidence shows that the levels of sarcopenia symptomology might be better with adherence to healthier diets. However, it is unclear whether the relationship between diet quality and sarcopenia is unique and independent of factors that associate with sarcopenia. This dissertation study aims to determine whether diet quality has a unique relationship with sarcopenia symptomology independent of physical activity and energy intake using publicly available data from the National Health and Nutrition Examination Survey (NHANES) 2011-2012 and 2013-2014. Methods: Eligibility criteria included adult participants aged 18 and older with levels of sarcopenia symptomology (grip strength and appendicular skeletal muscle mass; ASMI) measurement, first 24-hour recall dietary data, physical activity, and energy intake data. Diet quality was assessed using the Healthy Eating Index-2015 (HEI) score. Simple and multiple linear regression analysis was used to determine the relationship between the component of HEI-2015 and levels of sarcopenia symptomology. Energy intake and physical activity were used as covariates. Results: The results from 5,302 participants eligible for this study demonstrated that total HEI-2015 score and scores of the components of HEI-2015 were associated with grip strength and ASMI, but the direction of relationship differs based on the components. Total protein foods had a positive linear relationship with grip strength and ASMI independent of physical activity and total energy intake. The magnitudes of the unique relationship differ based on gender and race and ethnicity. Conclusions: Adequate energy intake and physical activity are essential practice to maintain skeletal muscle strength and skeletal muscle mass. Dietary protein may have a unique beneficial role on these levels of sarcopenia symptomology. Findings from this dissertation study can be applied to practice and further research in the fields of nutrition and sarcopenia.

Table

Multiple Regression Analyses Indicating Unique Relationships Between the Healthy Eating Variables and Sarcopenia Symptomology, While Controlling for Energy Intake and Physical Activity

Variable	ASMI						Grip Strength					
	Estimate	95% CI		*P*	R^2_{Total}	R^2_{Unique}	Estimate	95% CI		*P*	R^2_{Total}	R^2_{Unique}
		LL	*UL*		(%)	(%)		*LL*	*UL*		(%)	(%)
Energy Intake												
Log Total energy intake (kcal)	0.76	0.62	0.90	<.0001	5.8*	4.2	7.14	6.40	7.94	<.0001	14.7*	10.8
Physical Activity												
Log Weekly MET-minutes	0.18	0.13	0.22	<.0001	5.8*	2.3	1.61	1.43	1.79	<.0001	14.7*	5.7
Healthy Eating Variables, Energy Intake, Physical Activity												
Total HEI-2015	-0.01	-0.02	-0.005	0.0003	6.4	0.6	-0.02	-0.04	0.004	0.10	14.7	0
Total Protein Foods	0.12	0.08	0.17	<0.0001	15.1	9.3	0.68	0.42	0.94	<0.0001	15.4	0.7

Note. Estimate = unstandardized regression coefficient; CI = confidence interval; LL = lower limit; UL = upper limit.

R^2_{Total} = Total R^2 of models including Energy Intake, Physical Activity, and each of the diet variables entered as the sole additional predictor in the model. R^2_{Unique} = The unique R^2, for each of the diet variables, calculated as R^2_{Total} – Total R^2 of models including Energy Intake and Physical Activity

* Total R^2 of models including Energy Intake and Physical Activity

***Disclosures: Sikarin Upala**, None*

SAT-556

Lactobacillus Reuteri improved skeletomuscular properties through modulating bile acid profile and vitamin D metabolism in mature male mice *Wen-Xuan Yu[1], Siu-Wai Wan[1], Chun Au-Yeung[1], Yayi Shen[1], Tsz-Hung Kong[1], Liping Zhou[1], Kam-Wah Mok[1], Man-Sau Wong[1]. [1]The Hong Kong Polytechnic University, China

Probiotic supplements have been reported as potential strategies for ameliorating skeletomuscular dysfunction and osteosarcopenia. However, the underlying mechanisms are currently unknown. The present study aimed to compare the effects of probiotics on muscular properties in male mice and explore the role of gut-derived bile acids in modulating vitamin D metabolism and myogenesis.Four-month-old C57BL/6 male mice were randomly assigned to 4 groups and orally administrated with sterile water, 3 x 108 CFU Lactobacillus Reuteri, Bifidobacterium Longum, or Streptococcus Salivarius 3 times per week for 8 weeks. Muscle strength was determined by forelimb and four paws grip strength. Muscular properties were evaluated by measuring muscle mass and fibre cross sectional area of tibialis anterior. Circulating level of 1,25(OH)2D3, the bioactive form of vitamin D, was determined to evaluate its correlation with muscular properties. Serum bile acid profile was determined by targeted metabolomic approach. The effects of selected gut-derived bile acids on myogenesis were further evaluated in mouse myoblast C2C12 cells.The results showed L. Reuteri significantly improved forelimb grip strength ($P<0.05$) and 4 paws grip strength ($P<0.05$) in male mice. S. Salivarius only improved forelimb grip strength ($P<0.05$). Fibre cross sectional area of tibialis anterior was increased by 33.39% ($P<0.01$) in mice treated with L. Reuteri compared to control group. Gastrocnemius and quadriceps mass positively correlated with circulating 1,25(OH)2D3 level ($P<0.05$) which was markedly upregulated in L. Reuteri treated mice ($P<0.01$). There was an evident conversion of primary bile acids into secondary bile acids after administration of probiotics. Relative abundance of secondary bile acids was elevated from 44.95% to 57.82% by L. Reuteri. Among the bile acid profile, deoxycholic acid (DCA) and lithocholic acids (LCA), the typical gut-derived bile acids, were markedly increased in L. Reuteri treated mice. In addition, DCA and LCA further increased myogenesis of C2C12 cells in terms of myoblast number ($P<0.05$) and mean myoblast area ($P<0.05$).In summary, our results indicated that the actions of L. Reuteri in regulating skeletomuscular properties might be associated with bioactivation of vitamin D. As the major gut-derived metabolites, secondary bile acids play an important role in mediating myogenesis. These findings improved our understandings of skeletomuscular-gut axis.

***Disclosures: Wen-Xuan Yu**, None*

SAT-557

See Friday Plenary Number FRI-557

SAT-558

Older Women with Longstanding Type 1 Diabetes Have Lower Femoral Strength and Region-Specific Deficits in Trabecular Bone Mineral Density of the Femoral Neck *Shannon Emerzian[1], David Lee[2], Fjola Johannesdottir[3], I-Hsien Wu[4], John Gauthier[4], Surya Jangolla[4], Marc Gregory Yu[4], Hetal Shah[4], George King[4], Tony Keaveny[5], Klaus Engelke[6], Elaine Yu[7], Mary Bouxsein[8]. [1]Beth Israel Deaconess Medical Center, United States. [2]O.N. Diagnostics, United States. [3]Beth Israel Deaconess Medical Center & Harvard Medical School , [4]Joslin Diabetes Center, United States. [5]University of California, Berkeley, United States. [6]University Hospital Erlangen, Germany. [7]Massachusetts General Hospital, United States. [8]Beth Israel Deaconess Medical Center, Harvard Medical School, United States

Type 1 diabetes (T1D) is associated with an increased risk of hip fracture, but the factors underlying skeletal fragility in older adults with T1D are not well understood. This study assessed regional differences in bone mineral density (BMD) and strength of cadaveric femora from postmenopausal women with longstanding T1D and non-diabetic controls. Whole femora were acquired post-mortem from female Joslin Medalists with T1D >=50yrs (n=11); age and sex-matched non-diabetic control femora were obtained from a tissue bank (n=10). Femora were scanned via axial computed tomography (CT, Siemens). CT scans were analyzed using Medical Image Analysis Framework (MIAF)-Femur, with cortical thickness (Ct.Th) and volumetric BMD (total=Tt; trabecular=Tb) assessed at the total hip (TH) and femoral neck (FN). FN volumes were further divided into quadrants: superior anterior (SA) and posterior (SP) as well as inferior anterior (IA) and posterior (IP). Femoral strength and DXA-equivalent TH and FN areal BMD (aBMD) and T-score were calculated using Biomechanical CT analysis (BCT, O.N. Diagnostics). Individuals were considered high fracture risk if they had either low aBMD (T-score<=-2.5) or fragile bone strength (<=3000N). The ratio of fall force to femoral strength was computed using a soft-tissue attenuated fall force and femoral strength from BCT. Wilcoxon rank sum tests assessed group differences; percent differences are between group medians.The T1D group had an average (mean+/-SD) BMI=25.1+/-3.4kg/m2, HbA1c=8.3+/-0.9%, T1D duration=65+/-5yrs, age at onset=13+/-8yrs, and age at death=78+/-10yrs; age and BMI were not different between groups. 73% of T1D and 40% of controls were considered high risk (p=0.2). TH Tt.BMD and aBMD did not differ between groups. FN aBMD (p=0.07) and Tb.BMD (p=0.06) were lower in T1D (Table). Within the FN, women with T1D had Tb.BMD deficits that were larg-

est in the SP (-35%, p=0.04) and SA (-35%, p=0.10) quadrants. Ct.Th did not differ between groups at any site. Women with T1D also had lower femoral strength (-26%, p=0.03), but similar fall force (p=0.25), resulting in a greater load-to-strength ratio (+28%, p=0.04).These findings reveal deficits in femoral BMD and strength and greater load-to-strength ratio in older women with T1D, indicating increased susceptibility to hip fracture. As hip fractures may initiate in the superior FN, trabecular bone deficits in this region may contribute to the high risk of hip fracture in older adults with T1D.

	Control N = 10[1]	T1D N = 11[1]	p-value[2]
Total Hip			
aBMD (g/cm^2)	0.64 (0.57, 0.79)	0.56 (0.50, 0.67)	0.282
Tt.BMD (mg/cm^3)	210 (189, 255)	184 (171, 214)	0.314
Femoral Neck			
aBMD (g/cm^2)	0.58 (0.54, 0.67)	0.50 (0.44, 0.59)	0.072
Tt.BMD (mg/cm^3)	251 (246, 271)	226 (198, 267)	0.314
Tb.BMD (mg/cm^3)	104 (81, 129)	66 (41, 81)	0.061
Tb.BMD by Quadrant (mg/cm^3)			
Superior-Posterior (SP)	78 (66, 91)	51 (21, 63)	**0.036**
Superior-Anterior (SA)	72 (61, 75)	47 (27, 63)	0.099
Inferior-Anterior (IA)	105 (92, 140)	79 (64, 100)	0.173
Inferior-Posterior (IP)	154 (87, 193)	105 (55, 118)	0.114
BCT Analysis			
Femoral Strength (N)	3,375 (2,662, 4,212)	2,500 (2,125, 3,025)	**0.029**
Attenuated Fall Force (N)	3,960 (3,848, 4,147)	4,109 (3,980, 4,307)	0.245
Load-to-Strength Ratio	1.24 (0.92, 1.49)	1.59 (1.31, 2.04)	**0.036**
High Risk	4 (40%)	8 (73%)	0.198

[1] Median (IQR); n (%); [2] Wilcoxon rank sum test; Fisher's exact test
BMD = Bone Mineral Density; Tt = Total / Integral; Tb = Trabecular; High Risk = high fracture risk by either low aBMD (T-score≤-2.5) or fragile bone strength (≤3000N)

***Disclosures: Shannon Emerzian**, None*

SAT-559

In Patients with Glucocorticoid-Induced Osteonecrosis Severity of Disease Predicts Bone Loss *Olivia Blumberg[1], Alison Heilbronner[2], Alexandra Krez[1], Douglas Mintz[1], Jeri Nieves[3], Donald McMahon[4], Gail Roboz[5], Pinkal Desai[5], Derek Hansen[1], Joseph Lane[1], Richard Bockman[6], Emily Stein[1]. [1]Hospital for Special Surgery, United States. [2], United States. [3]Columbia University and Hospital for Special Surgery, . [4]Columbia University College of Physicians and Surgeons, . [5]Weill Cornell Medical College, United States. [6]Hospital for Special Surgery, Weill Cornell Medical College, United States

Osteonecrosis (ON) and osteoporosis are well-recognized harmful sequelae of glucocorticoid (GC) exposure. However, whether shared factors govern patient susceptibility to both conditions is not well understood. Few studies have investigated the concurrent development of ON and bone loss. This prospective study investigated relationships between patient characteristics, ON severity and progression, and bone loss over 12 months in a cohort with GC-induced ON. We hypothesized that patients with more severe and progressive ON would have greater bone loss by DXA. 28 individuals were enrolled and followed with imaging at baseline, 6 and 12 months including MRI of the bilateral hips, knees and shoulders to diagnose/classify ON and DXA of the spine, hips and forearm. Changes between baseline and 12-month imaging were investigated. Mean age of subjects was 44+/-17 years, 50% women. The most common indications for GC treatment were systemic lupus erythematosus (25%) and acute lymphoblastic leukemia (25%). Mean number of joints with ON at baseline was 4 (range 1 to 6). 23% of joints with ON exhibited collapse. Mean DXA Z-scores at baseline were within the normal range at the spine (0.0), total hip (-0.2), femoral neck (-0.1), 1/3 radius (0.3). Patients with more severe ON at baseline, defined as the number of joints with ON, were younger (r=-0.44, p=0.02) and had higher cumulative oral (r=0.37, p=0.05) and IV GC exposure (r=0.58, p=0.001). Patients with more severe ON at baseline also had more bone loss at the spine (r=-0.57, p=0.002, Figure) and the 1/3 radius (r=-0.37, p=0.05), and tended to have more bone loss at the total hip (r=-0.36, p=0.07) and femoral neck (r=-0.32, p=0.11). Based upon 12-month change in MRI appearance (increased size of lesion, increased edema, joint collapse), ON was classified as progressing in 43% of the cohort. Progression of ON over the course of the study was not significantly related to age, GC exposure or bone loss. No new joints with ON were identified over the 12-month follow-up. In summary, our findings suggest that patients with more severe ON had more ongoing bone loss by DXA on follow-up imaging. Relationships were strongest at the spine, the site known to be most reflective of the harmful skeletal effects of GCs. Future work is needed to investigate the individual and synergistic factors that govern susceptibility to the skeletal effects of GCs and to develop therapeutic approaches to prevent these devastating complications.

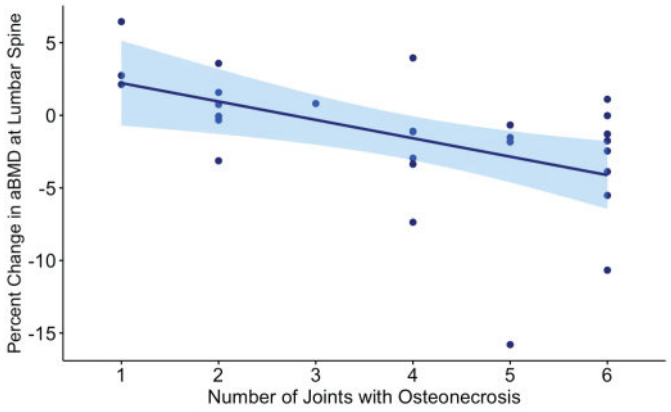

***Disclosures: Olivia Blumberg**, None*

SAT-560

Adolescent girls with type 1 diabetes develop changes in bone prior to evidence of clinical neuropathy *RACHEL USALA[1], IVANA SHEN[2], Mahshid Mohseni[3], Trinity Tedtsen[4], Mary Bouxsein[4], Deborah Mitchell[4], Erica Scheller[5]. [1]Washington University in St. Louis, . [2], . [3]Washington University School of Medicine, United States. [4]Endocrine Unit, Massachusetts General Hospital and Harvard Medical School, United States. [5]Washington University, United States

Neuropathy and skeletal disease are prevalent complications in patients with type 1 diabetes (T1D). However, it remains unknown whether neuropathy directly causes bone disease in patients with T1D or if changes in nerve and bone develop independently. To address this, we conducted a single-centered cross-sectional study. Thirty-three girls aged 12-18 years with and without T1D were enrolled (n=12 control, n=21 T1D). Groups were well matched for age, height, and physical activity. All control and T1D participants had healthy neural exams without clinical neuropathy as assessed by the Michigan Neuropathy Screening Instrument. Participants with T1D had significantly higher Z-scores for weight and BMI. Therefore, bone outcomes were adjusted for BMIz. There were no significant differences in bone mineral density by DXA between control and T1D participants. Differences in bone microarchitectural parameters between groups were observed with high-resolution scans with XtremeCT-II. Among adolescent girls with T1D, there was a decrease in trabecular bone volume fraction at both the distal radius (-5.5%, p=0.095) and the tibia (-7.1%, p=0.017). This was driven predominantly by decreases in trabecular thickness at both sites (-4.2% radius, p=0.007; -5.1% tibia, p=0.034). Cortical parameters including thickness, perimeter, and area remained largely unchanged after adjusting for body size (BMIz) with two exceptions. In the tibia (only), volumetric BMD was increased by 5.8% (p=0.024) and porosity was decreased from 2.1+/-1.6% in the control group to 1.3+/-1.1% with T1D (p=0.012). Predicted failure load trended lower in the T1D tibia relative to control, but was not statistically significant (-9.1%, p=0.242). Biochemically, participants with T1D had lower circulating levels of both CTX (a marker of bone resorption, -34%, p=0.035) and osteocalcin (a marker of bone formation, -25%, p=0.057) compared to controls, identifying a low bone turnover state among young persons with T1D. Our study demonstrates that deficits in trabecular bone microarchitecture, decreased cortical porosity in the tibia, and suppression of bone turnover occur in adolescents with T1D early in the course of disease, prior to the onset of clinical neuropathy. This informs our understanding of the rapid clinical onset and progression of skeletal disease in young girls with T1D and suggests that development of early management strategies for adolescents may help to prevent fracture and related co-morbidities.

***Disclosures: RACHEL USALA**, None*

SAT-561

Glucose dysregulation is associated with lower bone mineral density in adults with cystic fibrosis *Lucia Gonzalez Ramirez[1], Joseph Kindler[2], Elizabeth Ivie[1], Pichatorn Suppakitjanusant[1], William Hunt[1], Vin Tangpricha[1], Tanicia Daley[1], Arlene Stecenko[1], Richard Lewis[2], Thomas Ziegler[1], Jessica Alvarez[1]. [1]Emory University, United States. [2]The University of Georgia, United States

Diabetes and bone disease are common complications of cystic fibrosis (CF). In adults without CF, bone fragility is a concerning complication of diabetes, but the diabetes-bone connection in CF is understudied. This study determined associations between glucose dysregulation and bone mineral density (BMD) in adults with CF. This was a cross-sectional study of 61 adults with CF ages 18-50 years (31% female, 28% Black). Total body BMD was assessed via dual-energy X-ray absorptiometry (DXA), and Z-scores were calculated. During a 2-hour oral glucose tolerance test (OGTT), glucose was assessed at fasting and min 120. OGTT and DXA were performed on the same day. Subjects were classified as having impaired fasting glucose (IFG; fasting glucose >100 mg/dL), impaired glucose tolerance (IGT; 2-hour glucose >140 mg/dL), diabetes (fasting glucose >126 mg/dL or 2-hour

glucose >200 mg/dL), or normal glucose control (fasting glucose <100 mg/dL and 2-hour glucose <140 mg/dL). Linear regression was performed to determine associations between glucose control indices and total body BMD Z-score. Additional analyses included race/ethnicity, sex, age, and body mass index (BMI) as covariates. Twenty-three percent had normal glucose; 34% and 36% had IFG and/or IGT, respectively; and 34% had diabetes. In unadjusted analyses, fasting glucose (p=0.039; Fig 1) but not 2-hour glucose was inversely associated with BMD Z-score. In adjusted analyses, fasting glucose and 2-hour glucose were inversely associated with BMD Z-score (both <0.05). BMD Z-score was significantly lower in those with IFG vs. without IFG (p=0.02; Fig 1), and this difference was maintained after adjusting for covariates (p=0.010). Compared to those with normal glucose control, people with diabetes had lower BMD Z-score (0.74+/-1.42 vs. -0.10+/-1.01), but this difference was not significant (p=0.057). BMD Z-score did not differ between those with both IFG and IGT vs. normal glucose control (p=0.61). In line with studies in non-CF populations, glucose dysregulation is associated with having lower BMD in people with CF. The International Society for Clinical Densitometry recommends assessing hip and spine BMD for clinical evaluations, but unfortunately these measures were not completed for this study. Accordingly, these results highlight the need for additional research focused specifically on diabetes-related bone deficits in people with CF.

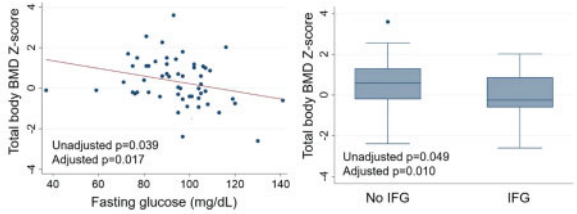

Fig. 1. The inverse association between fasting blood glucose and BMD Z-score (left) and differences in total body BMD Z-score between adults with IFG vs. no IFG (right) in people with CF. Adjusted analyses control for age, sex, race/ethnicity, and BMI. BMD, bone mineral density; IFG, impaired fasting glucose; BMI, body mass index.

***Disclosures: Lucia Gonzalez Ramirez**, None*

SAT-562

Associations of Endothelial Function with Bone Perfusion and Microstructure in Patients with Type 2 Diabetes *Maximilian T. Loeffler[1], Po-hung Wu[2], Amir M. Pirmoazen[3], Gabby B. Joseph[4], Isra Saeed[4], Jing Liu[4], Thomas M. Link[4], Galateia Kazakia[5]. [1]UCSF Radiology and Biomedical Imaging, United States. [2]University of California - San Francisco, . [3]University of Florida Jacksonville, United States. [4]UCSF, United States. [5]University of California, San Francisco, United States

Background: Skeletal fragility is a known complication of type 2 diabetes (T2D). Chronic hyperglycemia promotes endothelial dysfunction, a root cause of micro- and macrovascular complications in T2D. We hypothesize that endothelial dysfunction assessed by pulse amplitude tonometry (PAT) plays a role in the development of diabetic bone disease. The purpose of this study was to investigate the association of PAT with bone perfusion and changes in bone microstructure in T2D patients and non-diabetic controls.Methods: We included 79 participants in this cross-sectional study (39 T2D and 40 age- and sex-matched controls). Inclusion criteria were age 50-70 years, DXA T-score -2.5-0, and no bone disease or use of bone active drugs. HR-pQCT was performed at the distal radius and tibia. Intracortical bone perfusion was assessed using dynamic contrast-enhanced MRI in the distal tibia. Reactive hyperemia index (RHI) was measured by PAT at the index finger. T2D and control participants were compared. Associations between RHI and bone parameters were calculated in linear regression models adjusting for HbA1c.Results: RHI did not significantly differ between T2D participants and controls (p=0.105, Fig. 1). Maximum perfusion slope was 21% higher in T2D (p=0.044). Increasing RHI (=better endothelial function) was significantly associated with longer transition time in the combined group and in T2D participants, but not in controls (Table 1, Fig. 2). RHI was associated with lower Ct.BMD and Ct.Th in the tibia and radius, and with lower Tb.Th and Tb.Sp and higher Tb.N in the tibia in the combined group. Associations were significant for Tb.N and Tb.Sp in T2D participants and for Ct.BMD in controls (Fig. 3). Only in controls, RHI was associated with higher Ct.Po in the tibia and with lower Tb.BMD in the tibia and radius.Conclusion: Better endothelial function was strongly associated with longer transition time in T2D, consistent with neovascularization. This may indicate that those with endothelial dysfunction were unable to mount an adequate response to perfusion demands. Surprisingly, better endothelial function was associated with bone structural decline including decreased cortical BMD and increased porosity in controls. This inverse relationship in the bone-vascular axis could reflect physiologic bone turnover supported by healthy endothelium. A dysregulation of bone remodeling is suggested by the lack of association of RHI with cortical microstructure in T2D.

Table 1: Associations of RHI (marker of endothelial function) with intracortical perfusion in the tibia and bone parameters in the radius and tibia. Beta-values are unstandardized regression coefficients of linear regression models adjusting for HbA1c; AUC= area under the curve, Ct.Po= cortical porosity, Ct.Po.Dm= cortical pore diameter, Ct.BMD= cortical BMD, Ct.Th= cortical thickness, Ct.Ar= cortical area, Tb.BMD= trabecular BMD, Tb.BV/TV= trabecular bone volume, Tb.N= trabecular number, Tb.Th= trabecular thickness, Tb.Sp= trabecular separation

	All		T2D		No T2D	
	Beta	P-value	Beta	P-value	Beta	P-value
Perfusion parameters						
Transition time, s	**9.85**	**0.040**	**19.3**	**0.005**	0.62	0.928
Slope, %/min	-0.01	0.531	-0.04	0.263	0.01	0.592
Max. slope, %/min	-0.01	0.502	-0.02	0.416	0.00	0.808
AUC to peak	0.00	0.570	0.001	0.813	0.003	0.513
Ultra-distal tibia						
Ct.Po, %	0.01	0.097	0.004	0.735	**0.02**	**0.029**
Ct.Po.Dm, µm	-0.004	0.347	-0.004	0.631	-0.003	0.524
Ct.BMD, mg/cm³	**-30.8**	**0.014**	-11.0	0.575	**-42.8**	**0.011**
Ct.Th, mm	**-0.09**	**0.023**	-0.10	0.096	-0.05	0.318
Ct.Ar, mm²	-2.73	0.531	-3.57	0.579	0.79	0.897
Tb.BMD, mg/cm³	-0.61	0.907	-3.12	0.729	**-25.0**	**0.016**
Tb.BV/TV	-0.001	0.887	0.001	0.909	-0.0004	0.956
Tb.N	**0.13**	**0.016**	**0.20**	**0.022**	0.08	0.233
Tb.Th, mm	**-0.01**	**0.014**	**-0.01**	**0.009**	-0.003	0.376
Tb.Sp, mm	**-0.03**	**0.045**	-0.05	0.062	-0.02	0.319
Ultra-distal radius						
Ct.Po, %	0.004	0.288	0.003	0.721	0.01	0.154
Ct.Po.Dm, µm	0.001	0.865	-0.001	0.853	0.003	0.581
Ct.BMD, mg/cm³	**-24.6**	**0.037**	-14.3	0.432	**-34.9**	**0.038**
Ct.Th, mm	**-0.08**	**0.031**	-0.06	0.127	-0.10	0.088
Ct.Ar, mm²	-2.14	0.363	-1.60	0.616	-2.54	0.481
Tb.BMD, mg/cm3	2.64	0.655	-10.5	0.320	**-24.1**	**0.045**
Tb.BV/TV	0.002	0.649	0.004	0.515	0.0002	0.979
Tb.N	0.10	0.078	0.18	0.055	0.05	0.586
Tb.Th, mm	-0.002	0.183	-0.004	0.139	-0.001	0.622
Tb.Sp, mm	-0.01	0.567	-0.02	0.617	-0.01	0.819

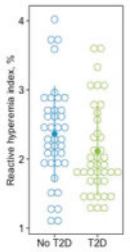

Fig. 1: Dot plot of RHI stratified by T2D status

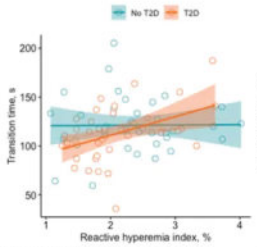

Fig. 2: Scatter plot of intracortical vessel transition time versus RHI stratified by T2D

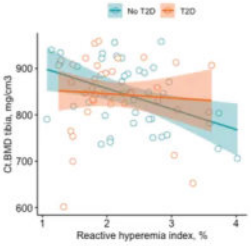

Fig. 3: Scatterplot of cortical BMD versus RHI stratified by T2D

***Disclosures: Maximilian T. Loeffler**, None*

SAT-563

See Friday Plenary Number FRI-563

SAT-564

Low Intensity Vibration and RANKL antibody Reduce Bone Loss after Spinal Cord Injury-induced Immobilization in Rats. *Weiping Qin[1], Yuanzhen Peng[2], Dalton Dietrich[3], Alexander Marcillo[3], Ofelia Furones-Alonso[3], Juliana Sanchez[3], X Guo[4], Helen Bramlett[3]. [1]James J. Peters VA Medical Center/Icahn School of Medicine at Mount Sinai, United States. [2]James J. Peters Veteran Affairs Medical Center, United States. [3]University of Miami, United States. [4]Columbia University, United States

Immobilization-related bone loss occurs in many neurological conditions including stroke, spinal cord injury (SCI), Parkinson's disease, multiple sclerosis, and amyotrophic lateral sclerosis. The rapid and extensive sublesional bone loss after SCI is a difficult medical problem that has been refractory to available interventions except the potent anti-resorptive agent, denosumab (a human monoclonal antibody to RANKL). While promising, this agent has potential to suppress bone formation that might be associated with adverse side effects, highlighting a critical need to develop better treatment options. We previous reported an ability of low-intensity vibration (LIV) to improve selected biomarkers of bone turnover and gene expression and to reduce osteoclastogenesis. In this study, we demonstrate for the first time that a prolonged course of LIV for 8 weeks can protect against loss of bone after SCI in rats. LIV stimulates bone formation and improves osteoblast differentiation potential of bone marrow precursors while inhibiting osteoclast differentiation potential of bone marrow precursors and reducing bone resorption. We further demonstrate a combination of LIV and RANKL antibody reduces SCI-related bone loss more than each intervention alone. Our findings indicate that LIV is efficacious in maintaining sublesional bone mass, suggesting that such physical-based intervention approach would be noninvasive, simple, inexpensive and easy to implement in the treatment of bone loss after SCI. The data that the combination of LIV with RANKL antibody is able to better preserve sublesional bone loss after SCI is also a novel finding, providing a groundwork for the future development of clinical protocols based on activity-based (e.g., LIV) and pharmacological (e.g., RANKL inhibitor) approaches to treat osteoporosis after SCI or other conditions associated with severe immobilization, with a goal to identify more effective and safer therapeutic approaches.

***Disclosures: Weiping Qin**, None*

SAT-565

Bone Structure and Turnover in Postmenopausal Women with Long-Standing Type 1 Diabetes *Viral Shah[1], Shijing Qui[2], Jason Stoneback[3], Lubna Qamar[1], Virginia Ferguson[3], Wendy kohrt[3], Janet Snell-Bergeon[1], Sudhaker Rao[2]. [1]Barbara Davis Center for Diabetes, United States. [2]Henry Ford Hospital, United States. [3]University of Colorado, United States

Purpose: Fracture risk in people with type 1 diabetes (T1D) is increased 2- to 6-fold and may be related to compromised bone quality. We investigated bone histomorphometry in postmenopausal women with T1D and controls without diabetes using a tetracycline double-labeled trans-iliac bone biopsy.Methods: Postmenopausal women with T1D of at least 10 years and women without diabetes were studied to evaluate effects of T1D on bone structural and mechanical properties. After in vivo tetracycline double labeling, participants underwent trans-iliac bone biopsy. An expert (Dr. Qui) who was blinded to study group performed histomorphometry. Static and dynamic histomorphometry measurements were performed and compared between the two groups using Student's -test.Results: The analysis included postmenopausal women with T1D (n=9, mean age 58.4+/-7.1y with 37.9+/-10.9 y of diabetes, and HbA1c 7.1+/-0.4%) and postmenopausal women without diabetes (n=7, mean age 60.9+/-3.3 y and HbA1c 5.4+/-0.2%). There were no significant differences in menopause duration (11.6+/-9.8y vs 8.0+/-5.5 y) or serum PTH (38.6+/-8.1 vs 51.9+/-23.9 pg/mL), CTX 90.4+/-0.2 vs 0.51+/-0.34 ng/mL) or P1NP (64.5+/-26.2 vs 87.3+/-45.3 ng/mL) . Serum 25 (OH) D levels were higher in T1D than controls (53.1+/-20.8 vs 30.9+/-8.2, p<0.05). 75% of T1D participants reported fractures compared to 42.9% in controls. Bone volume, trabecular thickness and cortical thickness were similar between the groups but indices of bone formation and remodeling were non-significantly lower in T1D (Table). Conclusion: Long-standing T1D may affect bone turnover, mainly bone formation, without affecting bone structure. The findings of our study are similar to previous study suggesting T1D is a disease of low bone turnover. Non-significant differences may reflect inadequate statistical power. Further research is needed to understand bone turnover and factors affecting bone turnover in people with T1D.

Table: Differences in bone turnover between postmenopausal women with T1D and without diabetes.

Variables	With T1DM (N=9)	Without T1DM (n=7)	Percent difference (T1D versus controls)#
Bone volume (BV/TV)	17.2±4.6	15.5±2.6	+10%
Trabecular thickness (Tb.Th)	111.4±25.0	103.7±4.9	+7%
Cortical thickness (Ct.Th)	1.60±0.64	1.60±0.39	0%
Osteoid surface (OS/BS)	5.93±3.54	8.44±6.22	-30%
Osteoblast surface (Ob.s/BS)	1.31±0.60	1.94±2.34	-32%
Mineralized surface (MS/BS)	2.71±1.24	4.67±3.56	-42%
Bone formation rate (BFRs)	6.13±2.95	9.66±7.40	-37%
Activation frequency (Ac.f)	0.20±0.08	0.32±0.25	-37%

#Unadjusted, age- and menopausal duration-adjusted differences remained non-significant between groups.

***Disclosures: Viral Shah**, None*

SAT-567

Cortical thickness at the superior aspect of the femoral neck measured by 3D-DXA is impaired in diabetes type 2 patients *Esther Ubago-Guisado[1], Enrique Moratalla-Aranda[2], Sheila González-Salvaterra[3], José J Gil-Cosano[4], Beatriz García-Fontana[5], Cristina García-Fontana[6], Mirella López Picazo[7], Ludovic Humbert[7], Luis Gracia-Marco[8], Manuel Muñoz-Torres[9]. [1]Escuela Andaluza de Salud Pública (EASP), Granada, Spain; Instituto de Investigación Biosanitaria ibs.GRANADA, Granada, Spain; Epidemiology and Control of Chronic Diseases, CIBER of Epidemiology and Public Health (CIBERESP), Madrid, Spain, Spain. [2]Instituto de Investigación Biosanitaria ibs.GRANADA, Granada, Spain; Department of Nuclear Medicine, University Hospital Clínico San Cecilio, Granada, Spain, Spain. [3]Instituto de Investigación Biosanitaria ibs.GRANADA, Granada, Spain; Department of Medicine, University of Granada, Granada, Spain; Fundación para la Investigación Biosanitaria de Andalucía Oriental (FIBAO), Granada, Spain;, Spain. [4]PROFITH "PROmoting FITness and Health through Physical Activity", Research Group, Sport and Health University Research Institute (iMUDS), Departament of Physical Education and Sport, Faculty of Sport Sciences, University of Granada, Granada, Spain, Spain. [5]Instituto de Investigación Biosanitaria ibs.GRANADA, Granada, Spain, Spain. [6]Instituto de Investigacion Biosanitaria ibs.GRANADA, Granada, Spain, , Spain. [7]3D-Shaper Medical, Barcelona, Spain, Spain. [8]Instituto de Investigacion Biosanitaria ibs.GRANADA, Granada, Spain, Spain. [9]Instituto de Investigacion Biosanitaria ibs.GRANADA, Granada, Spain; Department of Medicine, University of Granada, Granada, Spain, Spain

Introduction: Patients with type 2 diabetes (T2DM) have an increased risk of bone fractures compared with non-diabetic controls (doi: 10.3390/jcm11082206). However, areal bone mineral density (aBMD) is increased in these subjects (doi: 10.1001/jama.2011.715) and it could not use as bone fragility predictor. Studies using HR-pQCT techniques has reported an increased cortical porosity in patients with T2DM (doi: 10.1530/EJE-15-0860). However, pQCT images involve a higher radiation and cost than DXA images. 3D-DXA allow cortical and trabecular volumetric parameters assessment from routine DXA. The aim of this study is to evaluate if any 3D-DXA parameter could be used as bone fragility predictor in T2DM.Methods: This case-control study included 91 T2DM patients (40F, 51M) and 135 non-diabetic controls (67F, 68M). 3D-DXA analysis was performed using hip DXA scans and 3D-Shaper software (v2.12, 3D-Shaper Medical, Spain). Differences in aBMD and 3D-DXA parameters between T2DM patients and controls were assessed using Student's t-test.Results: aBMD was significantly higher in the T2DM group compared to controls at total hip (13.2%, p<0.001) and femoral neck (12.0%, p<0.001). 3D-DXA parameters were also higher in the T2DM group compared to controls at total hip (11.2% for integral vBMD, 12.3% for trabecular vBMD, 5.7% for cortical vBMD, 6.3% for cortical thickness and 12.2% for cortical surface BMD, all p<0.001). No differences were found in integral and trabecular vBMD at the neck (p=0.175 and p=0.169, respectively). Cortical thickness at the neck was lower in the T2DM group compared to controls, although the difference was not statistically significant (-2.3%, p=0.174). Cortical thickness at the superior aspect of the neck was lower in the T2DM group compared to controls (-5.9%, p=0.007), as shown by the regions in yellow in the figure.Conclusions: aBMD and 3D-DXA parameters at total hip were higher for T2DM patients than for non-diabetic controls. However, patients with T2DM had significantly lower cortical thickness at the superior aspect of the femoral neck, which could potentially explain the increased risk of femoral neck fractures in this population. Future longitudinal studies are required to confirm this finding.

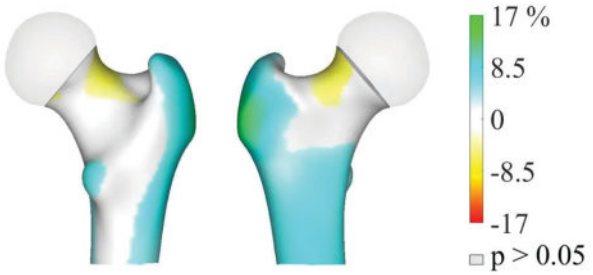

Figure 1: Distribution of the average differences (p<0.05) in cortical thickness between the T2DM group (n=91) and controls (n=135). Regions with non-significant changes (p>0.05) are shown in grey.

***Disclosures: Esther Ubago-Guisado**, None*

SAT-568

See Friday Plenary Number FRI-568

SAT-569

Association of Advanced Glycation End-products with Bone and Muscle Parameters in Obese Individuals With and Without Diabetes *Laurel Walfish[6], Claudie Berger[2], Michelle Wall[3], ANNE-FREDERIQUE TURCOTTE[4], MAHDI HOSSEINITABATABAEI[5], Bettina Willie[6], Fabrice Mac-Way[7], Claudia Gagnon[8], Suzanne Morin[6, 6]McGill University, [2]Research Institute of the McGill University Health Center, Canada, [3]Research Institute of the McGill University Health Centre, Canada, [4], [5]Shriners Hospital for Children, McGill University, [6]McGill University, Canada, [7]L Hotel-Dieu de Quebec, Canada, [8]CHU de Quebec, Universite Laval, Canada

Purpose: Obesity and Type 2 Diabetes Mellitus (T2DM) are associated with poor muscle and bone health. Tissue accumulation of advanced glycation end-products (AGEs) is associated with fractures and decreased muscle strength. We characterized the association between skin AGEs and bone and muscle parameters in adults with obesity, with and without T2DM.Methods: We analyzed baseline data from adults with obesity (body mass index [BMI] >=35kg/m2) participating in a multicenter observational cohort study on the effect of bariatric surgery on bone and muscle health. Skin AGEs, expressed in arbitrary units (AU), were measured by autofluorescence using the AGE Reader (Diagnoptics, UK). We measured total hip trabecular volumetric bone mineral density (vBMD), femoral neck (FN) cross-sectional moment of inertia (CSMI), FN maximal Z-scores and quadriceps muscle cross sectional area (CSA) by quantitative computed tomography, and isokinetic muscle force by dynamometer. Linear regression was used to determine the association between AGEs and the bone and muscle parameters. Covariables included sex, age, T2DM, BMI and percent predicted six-minute walking distance.Results: We included 69 participants (48 females, mean age 45 [SD 10] years) with a mean BMI 42 (SD 4) kg/m2. Twenty-nine (42.0%) participants had a diagnosis of T2DM (mean A1C 7.1 [SD 1.4] %) with a median disease duration of 2 years (interquartile range 1 to 9). Participants with T2DM were significantly older (50 [SD 6] years vs 42 [SD 11] years) and had higher AGEs (2.10 [SD 0.43] AU vs 1.86 [SD 0.47] AU). In the non-adjusted linear regression models (estimates [95% confidence interval]), AGEs were significantly associated with total hip trabecular vBMD (-6.8mg/cm3 [-12.0; -1.7] for each SD AU increase) (Table). When adjusting for T2DM, results remained significant (-5.7mg/cm3 [-11.0; -0.5] for each SD AU increase), but not after adjusting for age. Inclusion of other covariables did not change the estimate. Interactions of sex and T2DM with AGEs were non-significant. There was no association of AGEs with CSMI, maximal Z-scores, CSA or muscle force.Conclusion: Skin AGEs were negatively associated with total hip trabecular vBMD independent of diabetes status in adults with obesity. This association was no longer significant after adjusting for age. There was no association between AGEs and the other measures of bone and muscle parameters, possibly a reflection of our sample size or short duration of diabetes.

Table Unadjusted and adjusted estimates with 95% confidence interval of total hip trabecular vBMD, CSMI, max Z, CSA and Muscle Force for AGEs per 1 SD (0.5 arbitrary units)

Models	Total hip trabecular vBMD (mg/cm^3)	FN CSMI (cm^4)	FN Max Z (cm^3)	Quadriceps CSA (cm^2)	Muscle Force (Newton-Meter)
Unadjusted	**-6.8 (-12.0; -1.7)**	-0.05 (-0.32; 0.21)	-0.045 (-0.150; 0.060)	0.6 (-7.2; 8.4)	-17.8 (-36.9; 1.3)
+ T2DM	**-5.7 (-11.0; -0.5)**	-0.04 (-0.31; 0.24)	-0.031 (-0.139; 0.078)	-0.3 (-8.3; 7.7)	-15.9 (-35.5; 3.6)
+ T2DM + age	-1.7 (-7.6; 4.3)	-0.01 (-0.33; 0.32)	-0.002 (-0.131; 0.127)	0.3 (-9.2; 9.9)	-11.3 (-35.2; 12.6)
+T2DM + age + BMI, sex, %predicted 6 min wd	-1.0 (-7.8; 5.9)	0.01 (-0.26; 0.28)	0.008 (-0.097; 0.113)	1.7 (-5.6; 8.9)	1.9 (-17.5; 21.2)

T2DM: Type 2 diabetes mellitus; BMI: body mass index; % predicted 6 min wd: percentage predicted of 6-minute walk distance; vBMD: volumetric Bone Mineral Density; FN: Femoral Neck; CSMI: cross-sectional moment of inertia; Max Z: maximal Z-scores; CSA: cross-sectional area.

***Disclosures: Laurel Walfish**, None*

SAT-571

Bone Deficits Pertain to the Trabecular Bone in Children with Type 1 Diabetes: Sex and Maturity Matched Case-control Comparison *Yuwen Zheng[1], Munier Nour[2], James (J.D.) Johnston[3], Saija Kontulainen[1], [1]College of Kinesiology, University of Saskatchewan, Canada, [2]College of Medicine, University of Saskatchewan, Canada, [3]College of Engineering, University of Saskatchewan, Canada

Children with type 1 diabetes (T1D) are experiencing a higher risk of fracture, which may be linked to impaired bone development. Our purpose was to assess differences in imaged bone and muscle characteristics between children with T1D and typically developing children (TDC). We matched 56 children with T1D (mean age 11.9yrs, SD 2.1yrs) and 56 TDC (11.5yrs, 1.9yrs) by sex and maturity from 237 participants (6-17yrs, 66 T1D). We imaged the distal radius and tibia with high-resolution peripheral quantitative computed tomography (HR-pQCT) and the radius and tibia shaft bone and muscle with pQCT. We compared limb-specific bone macro- and micro-architecture, density, and estimated strength (stiffness and failure load), along with pQCT-imaged muscle properties (area, density) using MANCOVA. We identified covariates from between-group comparisons (t-tests) of height, body mass, physical activity score, and nutrition (protein, calcium, and vitamin D intakes); only physical activity score differed (14% lower in children with T1D, p=0.003). Bone outcomes differed between the groups (Pillai's trace = 0.736-0.792, p<0.001). Children with T1D had a 5% lower trabecular number and 7% higher separation at the distal radius while cortical and tissue mineral density as well as cortical thickness were 3-18% higher. Children with T1D had 9% lower trabecular thickness at the distal tibia. They also had 4-7% higher cortical density at shaft sites. Muscle density was 3% higher in children with T1D. Findings indicate that children with T1D had deficits in trabecular bone micro-architecture at the distal radius and tibia, while the distal radius cortex had higher density and thickness. Prospective, longitudinal data characterizing bone development in children with T1D vs. TDC, along with endocrine and lifestyle factors contributing to bone development, are warranted to clarify these seemingly contradictory cross-sectional observations.

***Disclosures: Yuwen Zheng**, None*

SAT-573

Growth Hormone Treatment Associated with Increased Vertebral Body Height in Children with Muscular Dystrophy *Malinda Wu[1], Emely Loscalzo[2], Julia See[1], Sonum Bharill[1], Nazanin Yousefzadeh[1], Ethan Gough[1], Janet Crane[1], [1]Johns Hopkins University, United States, [2]Johns Hopkins University ,

Vertebral body reshaping is a phenomenon observed in some children after vertebral fractures (VF). The purpose of this study was to examine if treatment with growth hormone (GH), testosterone (T), and/or zoledronic acid (ZA) impact vertebral body height of children with muscular dystrophy.In this retrospective study, vertebral body heights were measured in patients with Duchenne muscular dystrophy (DMD) and severe Becker MD. All participants were on chronic glucocorticoids and had been referred to endocrinology for concerns of short stature, delayed puberty, and/or osteoporosis. Serial lateral spine X-rays were scored by Genant's grading of VF. Multi-variable linear regression models analyzed change in anterior, middle and posterior vertebral heights while on treatment with GH alone, T alone and ZA with GH and/or T compared to ZA alone.The 27 participants had >400 measures of vertebral height with 34 incident VF noted. Median enrollment age was 13.5 years; median follow-up was 2.3 years. Participants were treated with GH, T and/or ZA according to typical pediatric practice: subnormal growth velocity/short stature, delayed puberty, and clinically significant fractures with low bone density respectively. Most participants were still growing during the study.After adjustment for multiple testing across vertebrae positions, GH was associated with increased vertebral height, reaching statistical significance when used alone of middle height (2.65 mm, P=0.015) or in combination with ZA of posterior height (0.80 mm, P=0.027) relative to ZA alone. In contrast, T alone was associated with decreased vertebral height, reaching statistical significance only of anterior height (-2.70 mm, P=0.032) relative to ZA alone; T with ZA had no specific trend nor statistically significant change relative to ZA alone. Co-variates associated with slight increases in vertebral height included increased age at endocrine referral, follow-up time, and body mass index and decreases in total body less head bone mineral density height-adjusted Z-score. We also observed a previously undescribed phenomenon, where some VF simultaneously both improved and worsened, i.e. changing between wedge or concave VF shapes. This observation was not frequent enough for statistical analysis. Multi-center data, more participants and longer follow-up is needed to explore the association of ZA, GH, and T use on vertebral reshaping.

***Disclosures: Malinda Wu**, None*

SAT-574

See Friday Plenary Number FRI-574

SAT-575

Long-term bone microarchitecture assessment in patients with pregnancy and lactation osteoporosis *maria belen zanchetta[1], lujan lucchini[2], maria florencia scioscia[3, 1]md, Argentina, [2]Universidad del Salvador, Argentina, [3]IDIM, Argentina

Introduction: Previously, we described a severe trabecular bone microarchitecture deterioration in women who suffered vertebral fractures in the last trimester of pregnancy and/or early postpartum (PLO). In this study, our aim was to evaluate long-term changes in bone microarchitecture and bone mineral density (BMD) in this cohort of patients.Materials and methods: Patients with PLO who consulted our institution between 2007 and 2020 were invited to participate. All of them received calcium and vitamin D (VD) supplementation and one received 2 doses of denosumab after the diagnosis. Bone microarchitecture by High-resolution peripheral quantitative computed tomography (HRpQCT) of distal radius (DR) and tibia (DT). Assessments were performed at baseline and then annually.Results: Since 2007, 14 patients consulted for PLO but only 6 were adherent to this long-term follow-up study. Mean age was 28 yo and follow-up time varied from 2 to 14 years. Most patients had no specific risk factors except for one who receive very high glucocorticoid doses for idiopathic

thrombocytopenia during pregnancy and 2 years later was diagnosed with premature ovarian failure. This patient was excluded from the final analysis, as an outlier. Patients had irregular compliance to calcium and vitamin D supplementation. Radius trabecular density after 12-14 months, increased significantly from baseline, mean 4.4 % (range: 0 - 26%). Trabecular thickness increased 20%. Distal tibia trabecular density after 12 -14 months improved significantly (7.1%), and trabecular thickness increased (6-47%). The last assessment (9 to 14 years later) showed a significant improvement in radius Dtrab mean 12% (11 - 26%) and less in tibia (See table 1). Trabecular thickness and number also improved significantly. Dcomp. increased 3.2 % after 12 months at DT and 2.2% at RD during long follow-up. Conclusion: Trabecular bone microarchitecture improved significantly during the first year and continued to improve and maintained after 9 to 14 years. The cortical compartment recovered, to a lesser extent. PLO patients might have impaired cortical bone microarchitecture before pregnancy, probably genetically determined, and that is why there is no significant long-term recovery.Scioscia MF, Vidal M, Sarli M, Guelman R, Danilowicz K, Mana D, Longobardi V, Zanchetta MB. Severe Bone Microarchitecture Impairment in Women With Pregnancy and Lactation-Associated Osteoporosis. J Endocr Soc. 2021 Feb 26;5(5)

DR	Baseline	12-14 m	λ %	Long-term (n:5)	λ Vs basal %
D100	236.7	245.5	3.7	251.9	6.4
Dtrab.	97.1	101.4	4.4	108.6	12
Dcomp.	858.2	856.9	-0.1	876.3	2.1
DT					
D100	235.1	255.1	8.5	252.7	7.4
Dtrab.	117.9	126.3	7.1	125.0	5.9%
Dcomp.	885.9	914.2	3.2	905.6	2.2%

***Disclosures: maria belen zanchetta**, None*

SAT-576

See Friday Plenary Number FRI-576

SAT-578

Altered Bone Mass and Biomarkers in Young Individuals with Long-Duration (10 Years) Type 1 Diabetes *Diana Swolin-Eide[1], Auste Pundziute Lycka[2], Daniel Novak[2], Bjorn Andersson[3], Gun Forsander[2], Per Magnusson[4]. [1]Professor, MD, Sweden. [2]MD, PhD, Sweden. [3]PhD, Sweden. [4]Professor, Sweden

Objective: Diabetes increases worldwide and is the second most common chronic disease during childhood. It is associated with several complications such as increased fracture risk. This study was designed to investigate if individuals with long-duration type 1 diabetes (T1D) have decreased bone mass and how bone biomarkers reflect bone remodeling in relation to healthy matched controls.Methods: Fifty Swedish individuals, age 15.0-17.9 years, with a T1D duration, mean 10.6 +/-2.1 years were included. Their mean HbA1c since their diabetes diagnosis was 57+/-6 mmol/mol. Thus, these individuals had diabetes through the entire puberty and growth spurt. A well-matched control group according to age, gender and geography was recruited. Bone mass was assessed by dual-energy X-ray absorptiometry and peripheral quantitative computed tomography. Clinical follow-up data were retrieved from the NDR-SWEDIABKIDS registry.Results: The groups were well-matched since there were no differences between the groups regarding age, weight, height and BMI. Fourteen individuals (28%) with T1D had sustained 16 fractures, and 18 control subjects (36%) had 19 fractures before study start Total body less head (TBLH) aBMD and TBLH BMC were lower in T1D individuals in comparison with the control group. Lumbar spine L1-L4 BMD and BMC showed no differences between the groups. Trabecular density was reduced in T1D ($p=0.012$) in contrast to cortical density which was unchanged. SSI was unchanged between the groups. PTH, 25(OH) vitamin D, sclerostin, bioactive sclerostin and bone specific ALP were not different between the groups. However, individuals with T1D had reduced CTX levels ($p<0.001$) indicating altered bone resorption.Conclusions: Young individuals with long-duration T1D have altered trabecular bone density and decreased CTX levels already at early ages and before they reach their peak bone mass. Bone health is therefore important to monitor in pediatric diabetes care.

***Disclosures: Diana Swolin-Eide**, None*

LB SAT-580

Semaglutide Does Not Increase Bone Formation In Adults With Increased Fracture Risk *Morten Hansen[2], Eva Wölfel[2], Niklas Jørgensen[3], Richard Eastell[4], Stinus Hansen[5], Morten Frost[2]. [2]Odense University Hospital, . [2]Odense University Hospital, Denmark. [3]Rigshospitalet, Denmark. [4]University of Sheffield, United Kingdom. [5]Hospital of South West Jutland, Denmark

Incretin hormone glucagon-like peptide 1 (GLP-1) receptor agonists (GLP-1Ras) such as liraglutide are commonly used to treat type 2 diabetes (T2D) and obesity. They increase the bone formation marker P-Procollagen type 1 N-terminal propeptide (P-PINP) in obese individuals and preserve bone mass in patients with T2D despite causing weight loss. We tested the effect of semaglutide, a GLP-1Ra, on bone formation in adults with increased fracture risk.In this placebo-controlled, double-blinded clinical trial conducted at two public hospitals in Denmark, adults with a total hip or lumbar spine T-score < -1.0 and/or history of low-energy fracture and without diabetes were randomized (1:1) to receive subcutaneous semaglutide 1.0 mg (or highest tolerated dose) or placebo once weekly for 52 weeks. The primary outcome was the effect of semaglutide compared to placebo on the mean percentage change from baseline to week 52 in P-PINP. Additional outcomes included changes from baseline to week 52 in the bone resorption marker P-Collagen type I cross-linked C-terminal telopeptide (P-CTX), areal bone mineral density (BMD) (by dual-energy X-ray absorptiometry (DXA)), volumetric BMD (vBMD) (by Xtreme computed tomography (CT) II), and bone material strength index (BMSi) at the tibia (by Osteoprobe).Sixty-four individuals (86% female) with a mean age of 63 years (SD 5.5) and BMI ranging from 21 to 39 kg/m2 were enrolled. There were no differences in age, sex, and BMI between groups at baseline. The effects of semaglutide compared to placebo as the differences in mean percentage changes from baseline to week 52 included a nonsignificant 17% increase in P-PINP ($p=0.19$) (Fig. 1). By contrast, P-CTX increased by 54.8% ($p=0.005$). Lumbar spine BMD decreased by 2.1% ($p=0.01$) and total hip BMD decreased by 2.6% ($p=0.001$). Tibial vBMD decreased by 1.5% ($p=0.003$). There were no differences in changes between groups in femoral neck BMD, radial vBMD, or BMSi. With semaglutide, the mean percentage change in body weight was a 9.4% decrease after 52 weeks ($p<0.001$), while there were no change with placebo (Fig. 1). There were no serious adverse events related to semaglutide treatment and no episodes of hypoglycaemia.In conclusions, semaglutide once weekly for 52 weeks was not associated with increased bone formation in adults with increased fracture risk. The bone loss was likely caused by the increase in bone resorption which resulted, in turn, from the loss of body weight.

Figure 1. Mean percentage change from baseline for the bone formation marker P-PINP (broken lines) and body weight (solid lines) for semaglutide (orange) and placebo (purple), respectively

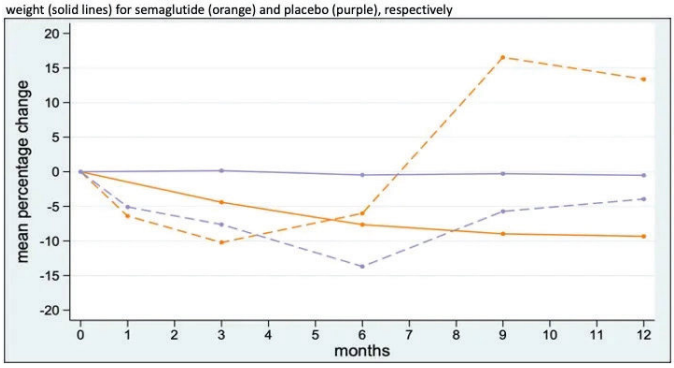

***Disclosures: Morten Hansen**, Novo Nordisk, Other Financial or Material Support, Novo Nordisk Foundation, Grant/Research Support*

LB SAT-581

Vitamin D Supplementation in Primary Hyperparathyroidism: Effects on 1,25(OH)2 Vitamin D and FGF23 levels *Sthefanie Giovana Pallone[1], Monique Nakayama Ohe[1], Livia Marcela dos Santos[1], Isabela Ohki Nacaguma[1], Ilda Sizue Kunii[1], Renata Elen Costa da Silva[1], Sergio Setsuo Maeda[1], Cynthia Maria Alvares Brandao[1], Jose Gilberto Henriques Vieira[1], Marise Lazaretti-Castro[1]. [1]UNIFESP-EPM, Brazil

Background: Primary hyperparathyroidism (PHPT) is a condition characterized by high levels of PTH in the presence of hypercalcemia, and vitamin D deficiency has been associated with more severe presentations. However, Vitamin D supplementation raises safety concerns. Our objective was to understand and monitor specific metabolomic alterations resulting from Vitamin D supplementation in individuals with and without PHPT.Materials and methods: Individuals with and without PHPT received 14,000 IU/week of oral vitamin D3 for 12 weeks. At baseline and endpoint, blood samples were collected to measure 1,25(OH)2vitamin D (1,25(OH)2D), intact FGF23 (FGF23), 25-hydroxyvitamin D (25OHD), PTH, total calcium (tCa) and other biochemical markers. The intact FGF23 was measured using an automated Diasorin LIAISON kit. The 1,25(OH)2D measurement was performed using liquid chromatography and mass spectrometry (LC-MS/MS).Results: 70 subjects with PHPT and

75 healthy individuals (nPHPT) were included at the baseline, and 55 PHPT and 64 nPHPT completed the 12-week protocol. At baseline tCa, PTH, 1,25(OH)2D, and FGF23 concentrations were significantly higher in PHTP, with no difference in 25OHD levels. After the intervention, the 25OHD levels increased significantly in both groups (PHPT: from 22.6.9+/-6.1 to 31.5+/-6.8; nPHPT: from 20.3+/-5.7 to 32.5+/-6.4 ng/mL, p<0.001); the FGF23 levels increased significantly in both groups (PHPT: from 47.9+/-27.1 to 76.3+/-33.3; nPHPT: from 40.5+/-13.9 to 59.8+/-19.8 pg/mL, p<0.001). 1,25(OH)2D levels decreased in both groups (PHPT: from 94.8+/-34.6 to 68.9+/-25.3; nPHPT: from 68.7+/-23.5 to 56.4+/-20.7 pg/mL, p<0.001). No changes in tCa were observed (PHPT: from 11.02+/-0.9 to 11.1+/-0.8; nPHPT: from 9.6+/-0.3 to 9.6+/-0.3 pg/mL, p=0.153), as the same for urinary calcium (p=0.534) and PTH measurements (p=0.516) in both groups. The reduction of 1,25(OH)2D was inversely correlated with the elevation of FGF23 in both groups (r=-0.302, p=0.028).Conclusion: The weekly administration of 14,000IU of Vitamin D3 was safe and the increase in 25OHD after the supplementation did not change the calcium and PTH levels in adults with and without PHPT. Furthermore, a paradoxical decrease in 1,25(OH)2D, associated with an increase in FGF23 levels, was observed in both groups, suggesting a possible mechanism in which FGF23 reduces the production of 1,25(OH)2D, protecting PHPT patients from hypercalcemia in face of vitamin D supplementation.

***Disclosures: Sthefanie Giovana Pallone**, None*

LB SAT-582

Correction of Cross-Sectional Geometry for Porosity Improves Prediction of Human Rib Structural Bending Response *Mary Cole[1], Yun-Seok Kang[1], Amanda Agnew[2]. [1]The Ohio State University, United States. [2]The Ohio State University, United States

Elderly populations are particularly vulnerable to morbidity and mortality following rib fracture. Previous work has shown that rib structural properties are best explained by simplified cross-sectional geometry adjacent to the fracture location, outperforming age, sex, body size, bone mineral density, and simple whole rib geometry. Although cross-sectional geometry treats the rib cortex as a solid object, it contains hundreds of voids representing intracortical pores. The objective of this study was to evaluate whether cross-sectional geometry explains more variance in rib structural properties when calculated on a cortex with pores removed, as opposed to a solid cortex. Mid-level thoracic ribs (n = 191) from an age series (22-108 years, mean = 57.6 +/- 20.2 years) were dynamically loaded to failure in a simplified bending scenario representing a frontal thoracic impact. Structural properties of force, displacement, stiffness, and energy were predicted using cross-sectional geometry calculated from a solid cortex and a porous cortex. Predictors were compared between quantifying all pores, cortical pores only, or trabecularized pores only. Multivariate models included co-variates of age, sex, and section location (anterior or midshaft). Force, stiffness, and yield displacement were best explained by porosity-corrected cortical shape or total area. Peak displacement and energy were more sensitive to age-associated endocortical trabecularization. Compared to the solid cortex, porous cortex cross-sectional geometry explained up to 8.4% more variation in univariate analysis of structural properties and up to 6.1% more variation in multivariate analysis. Except for yield displacement, the strongest multivariate models included porous cortex cross-sectional geometry (45.2-73.3%). The porous cortex also provided a significantly closer multivariate model fit than the solid cortex for yield force, peak displacement, stiffness, and energy, and an equivalent model fit for peak force and yield displacement. Pore morphometry was evaluated as an independent predictor set, including percent porosity, pore density, mean pore area, and pore spatial distribution. With no cross-sectional geometry, pore morphometry still explained moderate variation (37.6-57.4%) in all structural properties except yield displacement. Porosity improves prediction of rib structural properties by accounting for intracortical bone loss, more accurately measuring cortical area and distribution.

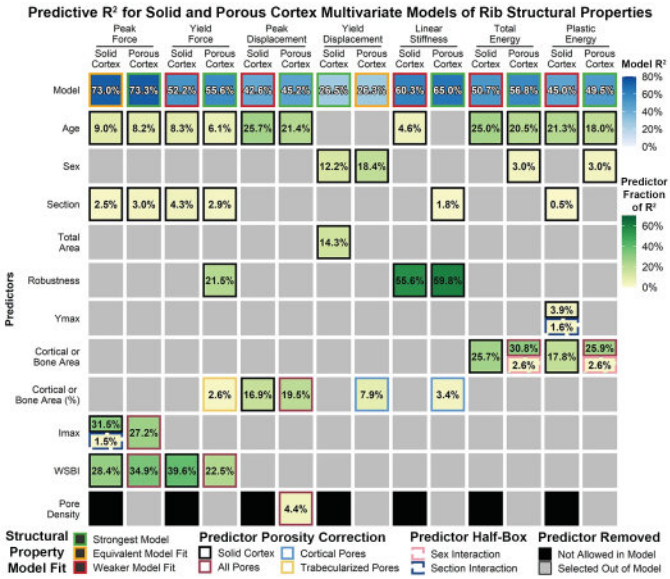

***Disclosures: Mary Cole**, None*

LB SAT-583

Bone size may mediate multiscale relationships with radius cortical porosity in mid-life women *RANDEE HUNTER[1], ERIN BIGELOW[2], Duncan Waanders[3], Todd Bredbenner[4], Karl Jepsen[3], Amanda Agnew[5]. [1]SKELETAL BIOLOGY RESEARCH LABORATORY, United States. [2]UNIVERSITY OF MICHIGAN, United States. [3]University of Michigan, United States. [4]University of Colorado Colorado Springs, United States. [5]The Ohio State University, United States

Growing evidence of the coordinated functional adaptation of bone suggests relationships between multiscale skeletal traits that dictate fracture risk and influence discrepancies in bone strength declines across individuals should be elucidated. The early indicators of subsequent pathological bone loss that likely exist in the radius are not well understood, particularly in mid-life women. Previous work has identified unique relationships between microstructural traits such as porosity and whole-bone geometry in male radii. Thus, the purpose of this study is to investigate the relationship between cortical porosity and whole-bone geometry in the radius of mid-life women representative of ages commensurate with the menopausal transition time period. Left radii of n=20 female post-mortem human subjects (PMHS) aged 40-65 years were imaged on a high-resolution nanoCT system and reconstructed at 8µm to assess multiscale skeletal traits. Cortical porosity was quantified at the 33% site as pore area (Po.Ar), pore number, and cortical pore score (CPS). Correlations were used to investigate the relationships between porosity (Po.Ar/Ct.Ar), pore density (Pore#/Ct.Ar), and CPS with respect to robustness (R; Tt.Ar/length), a measure of whole-bone geometry. There were no significant relationships between any measure of cortical porosity and robustness (p>0.4) for the whole sample; however porosity generally decreased with increasing R, while pore density and CPS increased. When rank-ordering robustness values and separating the sample into “slender” and “robust” radii, contradictory trends emerged between groups for pore density and CPS. Slender radii demonstrated a weak (R=-0.29) decrease in pore density with robustness while robust radii demonstrated a weak increase (R=0.23). A weak positive relationship between CPS and robustness was found for the entire sample (R=0.21) but varied by size category (slender R=0.08; robust R=-0.16). Despite previous evidence that wider male radii have greater CPS, 85% of females in this sample regardless of size category, fell within a CPS range of 11.5-82 mm4 without evidence of increased CPS in robust samples. These results suggest the coordination of multiscale traits may be mediated by bone size in mid-life women but requires a larger sample to investigate these trends. The implications for discrepancies in strength-age trajectories and subsequent fracture risk will be examined using dynamic mechanical testing in future work.

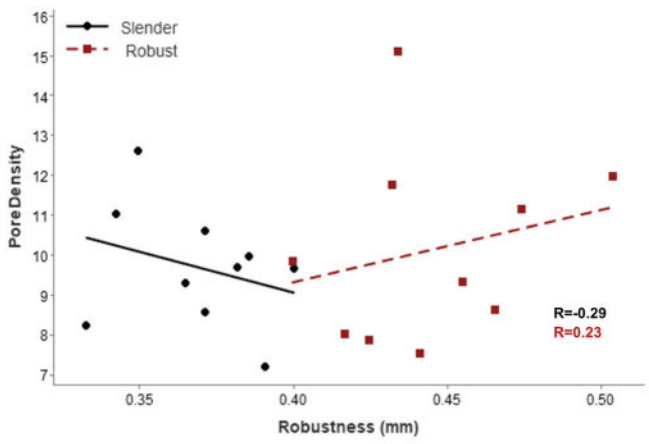

***Disclosures: RANDEE HUNTER**, None*

LB SAT-584

The Use of Clinical Photon Counting CT In Three Dimensional Joint Space Analysis of the Wrist *Jilmen Quintiens[1], Michael Kuczynski[2], Sarah Manske[2], Harry van Lenthe[1], Walter Coudyzer[3], MELISSA BEVERS[4], Joop Van Den Bergh[5]. [1]KU Leuven, Belgium. [2]University of Calgary, Canada. [3]University Hospital Gasthuisberg, Belgium. [4]VieCuri Medical Center, . [5]VieCuri MC Noord-Limburg and Maastricht UMC,

Joint diseases such as osteoarthritis (OA) and rheumatoid arthritis (RA) are typically diagnosed based on radiographs, with a semiquantitative scale based on observed bone erosion and joint space width (JSW) narrowing. This results in floor and ceiling effects, and a significant worsening of condition is required before it can be detected. Moreover, 2D radiographs suffer from overlapping features which confuse the JSW definition. 3D JSW analysis has the potential to improve diagnosis and monitor progression in OA and RA. Previous studies have successfully developed a consensus approach for 3D joint analysis using high-resolution peripheral quantitative computed tomography (HR-pQCT) [1]. Yet, this method is limited by exclusively considering finger joints and by relying on HR-pQCT, a device not easily accessible for clinical applications. This study extends the technique to different articulations of the wrist and performs the analysis with clinical Photon Counting CT (PCCT), which is expected to become widespread in the near future.Five cadaveric wrists were scanned with PCCT (NAEOTOM Alpha, voxel size 0.1 mm) and HR-pQCT (XtremeCT II, voxel size 0.061 mm). Identical full bone masks were delineated on both modalities using image registration. Using the bone masks as input, JS masks were calculated for the scapholunate (SL), capitolunate (CL), radiolunate (RaL), scaphotrapezotrapezoidal (STT) and trapeziometacarpal (TMC) joints. The size of the morphological operations was scaled from PCCT to HR-pQCT by ratio of voxel size, and 3D analysis was performed as described by Stok et al. [1], using the ORMIR_XCT Python package.Using HR-pQCT as the reference value, mean JSW calculations in PCCT showed a RMSE of 0.254 mm. Mean RMSE for minimal JSW was 0.441 mm, a larger relative error (Fig.1).Differences in results between PCCT and HR-pQCT may be partly attributed to pose differences between scanning modalities, which is impossible to correct for. These differences may affect minimal JSW more than mean JSW. For the TMC joint, two specimens showed JS narrowing which decreased minimal JSW values below the voxel size. Moreover, HR-pQCT scans showed stack misalignments in this joint, affecting the JS quantification. In spite of these limitations, these results show that JSW analysis can be extended to different articulating surfaces and imaging modalities with acceptable consistency.[1] Stok et al., Quant Imaging Med Surg 10(2): 314-325, 2020.

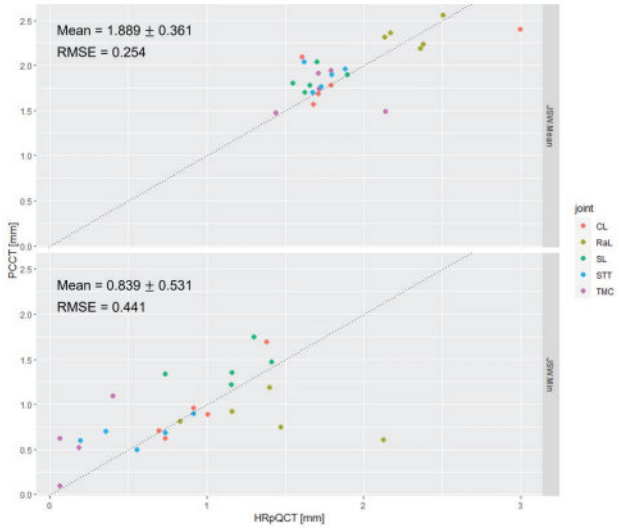

***Disclosures: Jilmen Quintiens**, None*

LB SAT-585

Impact of Ilex paraguariensis Consumption on Rats Offspring Bone Development and Tissue Properties *Natasha Sanz[1], Laureana Villarreal[1], Florencia Buiatti Fagalde[1], Lilian Plotkin[2], Lucas Brun[1]. [1]Bone Biology Laboratory, School of Medicine, National University of Rosario, Argentina. [2]Department of Anatomy, Cell Biology & Physiology, Indiana University School of Medicine, United States

Introduction: Ilex paraguariensis is the herbal species from which Yerba Mate (YM) is derived. It is daily consumed in South American countries as infusions called 'mate' and 'terere', an alternative to tea or coffee. YM leaves contain bioactive compounds like polyphenols and xanthines (mainly caffeine). Previous studies have shown a negative impact of high caffeine consumption on BMD and increased risk of fractures in diets with low calcium intake. On the other hand, we have also observed positive effects of YM compounds on bone cells in vitro, and positive effect of YM infusions on BMD and trabecular bone biomechanical properties in vivo. Therefore, we aimed to evaluate in vivo effects of the YM exposure from embryonic stage up to youth, on bone development and tissue properties of rats. Methods: Ten-week-old Sprague-Dawley rats were divided into 3 groups: Controls consumed water ad libitum; YM group consumed an infusion prepared with 25 g of YM leaves in water at 70°C; YM+ group that consumed a YM infusion prepared with 50 g of YM in water at 90°C. After 30 days old, the rats were euthanized, and their bones were collected. The morphometry measurements were made using Image J 1.40 (NIH, USA) on digitalized radiographs of mandible and tibia bones and on cross sectional photos of femur diaphysis. On mandible, we measure its length (from the most anterior inferior bone point to the condyle), the mandibular area, the height of the jaw and the height of the molars. For femur measurements were total and bone marrow area, cortical thickness, endosteal and periosteal perimeter, internal and external diameter, width and length. For tibia measurements, we recorded the width and length. Three-point bending tests were performed on femurs and mandibles and the following parameters were collected: stiffness, ultimate load, failure load, absorbed energy and cross-sectional moments of inertia (CSMI, only in femur). Radiographs with calcium level patterns were taken, and BMD of tibias were obtained using Image J. All values are reported as mean+/-SD. Statistical tests were conducted using one-way ANOVA or Brown-Forsythe and Welch ANOVA for overall analysis. Only results with significant difference (*) vs control are shown in the Table. Conclusion: Evidence suggests that exposure to YM during the embryonic stage, weaning, and youth can cause changes in bone development and properties. Lower molar width, tibia diaphysis and femur cortical thickness were observed.

	experimental groups					
property	control		YM		YM+	
	mean ± SD	n	mean ± SD	n	mean ± SD	n
Body weight (g)	127.3 ± 12.5	8	121.05 ± 13.6	19	115.6 ± 10.0	10
Femur						
Absorbed Energy (mJ)	23.51 ± 6.48	18	30.36 ± 7.32*	19	27.17 ± 6.18	8
Cortical thickness (mm)	0.41 ± 0.05	18	0.37 ± 0.04*	19	0.43 ± 0.03	10
Mandible						
Ultimate Load (N)	25.04 ± 3.12	13	28.49 ± 3.88*	19	28.74 ± 3.51	9
Stiffness (N/mm)	7.59 ± 0.93	11	8.19 ± 2.32*	18	10.75 ± 2.01*	9
Failure Load (N)	23.80 ± 2.48	12	26.18 ± 2.54	18	26.68 ± 2.99*	9
Molar Width(mm)	5.66 ± 0.22	17	5.54 ± 0.16	19	5.36 ± 0.15*	9
Tibia						
Diaphysis width (mm)	0.206 ± 0.014	16	0.208 ± 0.014	17	0.191 ± 0.007*	10
Epiphysis BMD (mg Ca2+/cm2)	27.67 ± 5.31	16	26.35 ± 7.84	17	22.16 ± 2.89*	10
Diaphysis BMD (mg Ca2+/cm2)	21.00 ± 1.77	14	18.77 ± 3.17	16	15.93 ± 2.78*	10

***Disclosures: Natasha Sanz**, None*

LB SAT-586

High Variabilities in Mouse Femur Strength Due to Specimen Malalignments and Testing Protocols *Ara Nazarian[1], Mason Garcia[2], Maria Buzo Mena[1], Isabella Stewart[1]. [1]Beth Israel Deaconess Medical Center, Harvard Medical School, United States. [2]Boston University, United States

PURPOSE: The 3-point and 4-point bending tests are the most prevalent methods used to determine the mechanical properties of bones in rodents. A study of 100 papers on wild-type mouse femur 3-point and 4-point bending tests reveals considerable variability in the reported mechanical indices. Notably, reported Young's moduli differed by 172% (1.3-17.4 GPa) for 3-point bending and 120% (3.1-12.5) for 4-point bending. We hypothesized that such discrepancies result from variations in testing protocols and specimen malalignment. In this study, we investigate the sensitivity of Young's modulus of rodent femur to the angular orientation of the bone relative to 3- and 4-point bending support and loading pins using finite element analysis (FEA). METHODS: Micro-CT imaging of a 15-week-old wild-type male mouse femur was used to create a 3-dimensional model in Mimics (v21.0; Materialize, Belgium) with appropriate smoothing and thresholding. A hydroxyapatite phantom was used to assign heterogeneous properties to the bone by converting bone attenuation to density, with subsequent density conversion to Young's modulus and a Poisson's ratio of 0.3 [1]. FEA was conducted in Abaqus (Dassault Systèmes, Inc., France). The load and support pins were made in Abaqus with a 2mm diameter and treated as rigid bodies. The support pin span was set at 8 mm, distributed equidistantly from the loading pin, which was placed in the center of the femur for 3-point bending. For 4-point bending, two loading pins were placed 1.3 mm away from the center of the bone, according to the literature. For both 3- and 4-point bending tests, displacement-controlled simulations at 1, 2, 3, and 4 mm of the loading pin(s) were used to determine stress and strain. Simulations were conducted in 5° increments from 0° to +/- 15° from the central axis, with the bones loaded in prone and supine positions, and Young's moduli were calculated from the slopes of the stress-strain curves. RESULT: Our simulations reveal that prone and supine 3-point bending tests with misalignments of up to 15° from the central axis resulted in 8.7% to 132.1% variation in Young's moduli. The 4-point variations were from 3.4% to 33.5% IMPACT: Minor malalignments in bone orientation, an artifact of testing, result in significant variations in 3- and 4-point testing results. Standardizations in testing apparatus and protocols are warranted for more comparable results. REFERENCES: [1] Morgan, E. F., et al. 2003

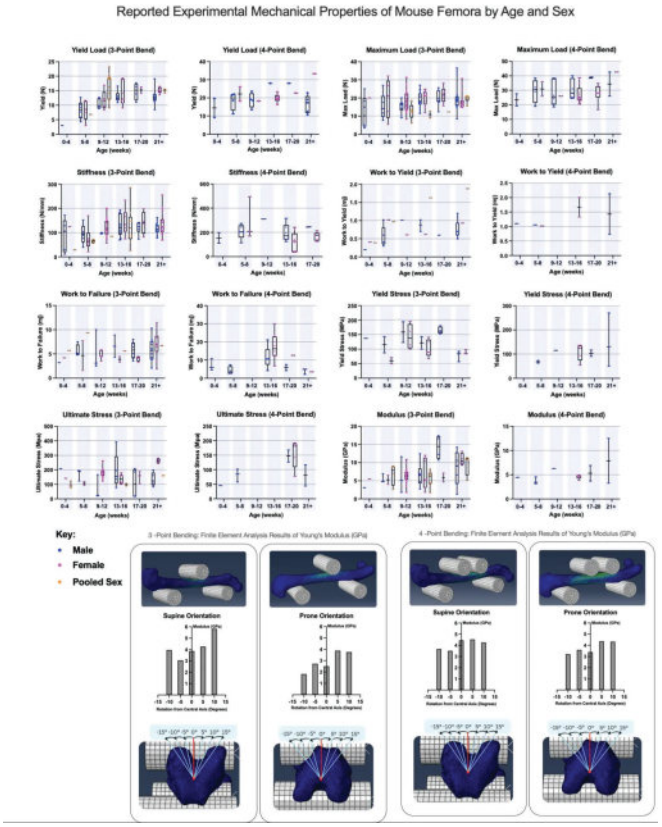

***Disclosures: Ara Nazarian**, None*

LB SAT-587

Transmembrane Protein 53 (TMEM53) Gene Deactivation Underlies Craniotubular Dysplasia (OMIM # 619727) *Michael P. Whyte[1], Robert S. Weinstein[2], Paul H. Phillips[3], Rongsheng Cai[3], G. Bradley Schaefer[3], Michelle A. Hutchinson[3], Gary S. Gottesman[1], William H. McAlister[4], Shenghui Duan[5], Steven Mumm[1]. [1]Shriners Hospitals for Children - St. Louis & Div. Bone & Mineral Diseases, Washington University School of Medicine, United States. [2]Division of Endocrinology, Metabolic Bone Diseases University of Arkansas for Medical Sciences, United States. [3]Arkansas Children's Hospital, United States. [4]Mallinckrodt Institute of Radiology at Children's Hospital, Washington University School of Medicine, United States. [5]Div. Bone & Mineral Diseases, Washington University School of Medicine, United States

Craniotubular dysplasia (OMIM # 619727) denotes the disorder, elegantly reported in 2021 from investigation of four Indian families, caused by a homozygous 4-base exonic insertion or a homozygous small deletion at the exon 2 splice acceptor site within TMEM53. TMEM53 encodes nuclear envelope transmembrane protein 53 involved in BMP-SMAD signaling (*OMIM 619722). We detail the generalized skeletal disorder of a 13-year-old American boy referred in 2018 for progressive vision and hearing loss due to cranial foramina encroachment by bone and associated with compound heterozygosity for a deletion and a missense defect within TMEM53. Steroid therapy for 6 months was ineffective, whereas optic nerve decompressions by curettage of soft overgrown vascular bone improved his vision. Radiographic skeletal survey showed bone tissue accumulation at his skull base, but generalized osteopenia elsewhere. His calvarium and facial bones were widened whereas his optic, auditory, and spinal canals were narrowed. DXA bone density was normal for the whole body assessment, but low in his spine and hip. Biochemical studies of mineral metabolism were unremarkable and bone turnover markers indicated active bone formation. Tetracycline-labeled iliac crest histomorphometry revealed abundant widely spaced "double labels" consistent with twice the expected rate of bone formation. Then, vision loss did not progress during prednisone and zoledronate treatment. Next generation sequencing of a panel of 35 genes underlying high bone turnover or high bone mass was negative. Trio whole genome sequencing subsequently identified in TMEM53: i) a paternally inherited heterozygous 54-base deletion, including the mRNA splice acceptor site for exon 2, and 31 bases of exonic sequence (c. 62-23_92), and ii) a maternally inherited extremely rare, in gnomAD (frequency = 0.000036), heterozygous missense variant (c.650C>T, p.Ser217Leu). In silico missense prediction models, SIFT and Mutation Taster, scored this variant as damaging. Ser217 is highly conserved across species. Thus, bi-allelic deactivation of TMEM53 causes

what is classified as a sclerosing bone disorder, “craniotubular dysplasia.” We find generalized features of poor bone quality and propose “TMEM53-associated skeletal disease”.

***Disclosures: Michael P. Whyte**, None*

LB SAT-588

Muscle-derived FGF21 may negatively regulate bone homeostasis in DMD via promoting bone marrow adiposity *Katsuhiro Murakami[1], Jessica Li[1], Fang Guo[1], Chen Chen[1], Ling Wang[2], Hongshuai Li[1]. [1]University of Iowa, United States, [2]The University of Iowa,

Duchenne Muscular Dystrophy (DMD) is the most common muscular dystrophy seen in children which affects both muscle and bone. Poor bone health is a significant problem for DMD patients which concomitantly contributes to progressively reduced mobility and low quality of life. To date, the pathogenesis of bone abnormalities in DMD is still poorly understood and effective therapies to treat poor bone health in DMD are still lacking. We have previously identified a novel myokine, fibroblast growth factor 21 (FGF21), typically not expressed in skeletal muscle under physiological conditions, is dramatically upregulated in skeletal muscles in DMD mouse models. Systemic neutralization of circulating FGF21 significantly improved bone quality in dystrophic mice. However, how dystrophic muscle-derived FGF21 contributes to the disease progression in DMD, specifically to the poor bone health, has yet to be fully understood. In the current study, we found that rFGF21 treatment significantly increased bone marrow mesenchymal stem cell (BMSCs) adipogenesis and concomintely inhibted osteogenesis; Knockdown of beta-klotho (KLB, an obligate co-receptor of FGF21) using siRNAs blocked the effects of FGF21 on promoting adipogenic differention of BMSCs. Our data demonstrate that FGF21 directly regulats BMSCs differentiation favoring adipogenesis. We further tested in vivo whether elevated FGF21 increases bone marrow adiposity in DMD. We used osmium tetroxide staining with microCT to visualize and quantify bone marrow adipose tissue (BMAT) in tibia of dystrophic mice. Significantly increased bone marrow adiposity was observed in dystrophic mice when compared with WT mice. Excitingly, significantly reduced bone marrow adiposity along with improved bone mass and bone microstructure were observed in muscle conditional FGF21 KO dystrophic mice when compared with their dystrophic loxP controls. Our observations suggest an important role of muscle-derived FGF21 in regulating bone marrow adiposity and affecting bone homeostasis in DMD.

***Disclosures: Katsuhiro Murakami**, None*

LB SAT-589

Bone Loss caused by Adjacent Intervertebral Injury is Blunted by the Ablation of RAGE *Remy Walk[3], KAITLYN BROZ[2], Munish Gupta[3], Simon Tang[4]. [3]Washington University in St. Louis, , [2], , [3]Washington University in St. Louis, United States, [4]Washington University in St Louis, United States

Intervertebral disc (IVD) injury leads to degeneration and inflammation. Needle puncture is a standard animal model to study IVD degeneration. Here, we evaluate the vertebral endplate response. The endplates provide transport to and from the IVD and maintain the structural integrity of the vertebra; the endplates may play a role in IVD degeneration and low back pain. The receptor for advanced glycation end-products (RAGE) is implicated in many inflammatory diseases and has been implicated in skeletal pathology. The objective was to assess vertebral endplate response following IVD injury and the role of RAGE signaling.All procedures were done with WUSM IACUC approval. CC4/5 and CC6/7 IVDs in C57BL/6 mice (n = 10/time point) and RAGE-/- (n = 5/timepoint) were injured with a 30G bilateral puncture confirmed on X-Ray with adjacent IVDs as internal controls. Endplates were imaged on a vivaCT40 at 10µm prior to and following injury. A subset of the IVDs were immediately fixed in 4% PFA and paraffin embedded; 10 µm sections were stained with TRAP activity and Safranin-O/Fast Green. Vertebral endplates were segmented using a custom MATLAB GUI. Weighted averages of the endplates are reported. Paired 2-way ANOVAs were used to determine the effect of injury and time point in Prism 9.4.0.Bone loss was observed at 2 weeks and recovered by 12 weeks following injury in WT while IVD degeneration was sustained throughout. Decreased BV/TV was associated with osteoclast resorption followed by gradual bone formation. Image registration confirmed that the resorption and formation was occurring at the pores within the endplate. Osteoclast activity was correlated with IVD degeneration, suggesting that the degenerative process by the IVD may be driving osteoclast differentiation and subsequent bone resorption. With deletion of RAGE signaling, the endplates are protected from bone loss despite no changes to IVD degeneration.Endplate bone loss, associated with osteoclast resorption, following IVD injury occurs rapidly in the first 2 weeks and returns to baseline by 12 weeks while RAGE deletion prevents bone loss. Osteoclast activity may be a direct response to the inflammatory cascade created by the IVD. Vertebral endplate changes with IVD degeneration may play an important role in the development of low back pain. Future work will investigate whether RAGE inhibition protects the endplate from IVD injury induced changes.

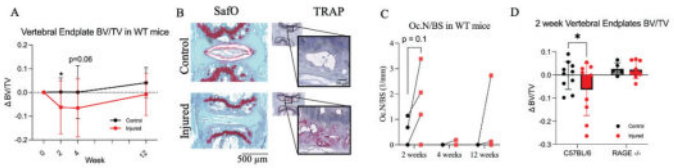

Figure 1: (A) Bone loss in WT vertebral endplates adjacent to an injured IVD was observed at 2 weeks following puncture with BV/TV returning to baseline by 12 weeks. (B) Safranin-O and TRAP stained adjacent sections from 2 weeks following injury demonstrate the correlation between IVD degeneration and osteoclast number. (C) Osteoclast number per bone surface (Oc.N/BS) is increased with injury (p = 0.05). (D) Bone loss is blunted in RAGE -/- mice.

***Disclosures: Remy Walk**, None*

LB SAT-590

Osteocalcin ameliorates cognitive dysfunctions in a mouse model of Alzheimer’s Disease by upregulating glycolysis in neuroglia *Chang Shan[1], Yuying Yang[1], Deng Zhang[1], Shengtian Li[2], Jianmin Liu[1]. [1]Ruijin Hospital, China, [2]Shanghai Jiao Tong University, China

Alzheimer’s disease (AD) is the most prevalent neurodegenerative disorder characterized by the build-up of amyloid ? peptides (A?) and impaired glucose metabolism in the brain. Osteocalcin (OCN), a protein derived from osteoblasts, has been found to influence brain functions, but its impact on AD remains uncertain. This study aimed to investigate the effects of daily intraperitoneal injections of OCN over a 4-week period on anxiety-like behaviors and cognitive impairments in a transgenic AD mouse model (APP/PS1). The results showed that OCN administration led to improvements in various behavioral tests: increased entries into the central area in the open field test, increased time and entries into open arms in the elevated plus maze test, increased time spent in the light chamber in the light-dark transition test, reduced escape latency, and increased preference for the target quadrant in the Morris water maze test. OCN treatment also ameliorated the accumulation of A? in the hippocampus and cortex of AD mice. Additionally, OCN enhanced the neural network function of the brain, particularly by increasing the power of the high gamma band in the medial prefrontal cortex of AD mice. Immunofluorescence analysis revealed that OCN inhibited the proliferation of astrocytes in the hippocampus of AD mice. Furthermore, OCN promoted glycolysis in astrocytes and microglia, as evidenced by increased glucose consumption, lactate production, and extracellular acidification rate. Notably, this effect was diminished when the OCN receptor, Gpr158, was knocked down in astrocytes. These findings highlight OCN as a potential novel therapeutic factor for AD, potentially through reducing A? accumulation and enhancing glycolysis in neuroglia.

***Disclosures: Chang Shan**, None*

LB SAT-591

Fractures and Mortality in Patients with Multiple Myeloma: A Nationwide Korean Case-Control Study *Jeonghoon Ha[1, 1], Republic of Korea

Background: Multiple myeloma (MM), a malignant hematologic disorder, profoundly impacts patients' bone health, heightening their susceptibility to pathologic fractures. These fractures compromise the quality of life and elevate mortality rates. This study examines the relationship between fractures and mortality rates in MM patients, shedding light on the subsequent impact on lifespan. Such an understanding aims to improve therapeutic decision-making, bolster patient outcomes, and potentially increase survival rates in the MM populations. Methods: In this population-based case-control study, data from 14,207 MM patients and age-, sex-, index date-, and comorbidity-matched healthy controls were analyzed in a 1:3 ratio using the Korean National Health Insurance Service database. Differences in mortality due to fractures following an MM diagnosis were compared across fracture sites for up to eight years. Results: Of the 14,207 MM patients, 1,193 (8.4%) experienced vertebral fractures (HR 2.210, 95% CI, 2.017-2.421), 202 (1.4%) had hip fractures (HR 2.502, 95% CI, 2.121-2.952), and 197 (1.4%) suffered upper limb fractures (HR 1.556, 95% CI, 1.343-1.801) during the observation period. The hazard ratios for mortality from any fracture, vertebral fracture, and hip fracture were 1.625 (95% CI, 1.423-1.856). 1.718 (95% CI, 1.481-1.993), and 2.040 (95% CI, 1.483-2.806), respectively (p<0.001 for all). Conclusion: This study establishes a significant correlation between fractures and increased mortality in MM patients. The findings underscore the urgent need for enhanced bone health management in MM patients to mitigate fracture risks and improve survival outcomes, offering critical insights for clinicians to formulate effective, personalized therapeutic strategies for MM patients.

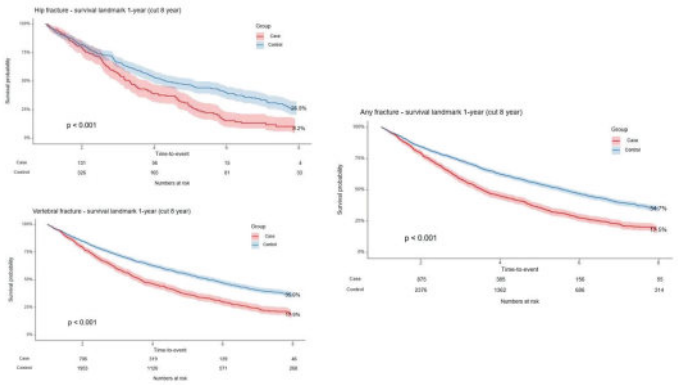

***Disclosures: Jeonghoon Ha**, None*

LB SAT-592

Dementia medications, acetylcholinesterase inhibitors, reduce the risk of all fractures *Charles Inderjeeth[1], Emma Boland[2], Maxine Isbel[2], Diren-Che Inderjeeth[2]. [1]University of Western Australia & North Metropoitan Health Service, [2]SCGH, Australia

Background: Older people are at high risk of osteoporosis and dementia. We reported that in vitro and in vivo mouse models suggest that antidementia medications acetylcholinesterase inhibitors improve bone health through its impact on inhibiting osteoclasts and a potential anabolic effect on osteoblasts (Li, Xu, Inderjeeth et al, Journal Cellular Physiology 2023).Methods: In this aged care, dementia clinic, cohort study we follow-up 744 patients annually for 4 years. The main outcomes assessed were, incidence of new fracture and death. Data was entered into SPSS with analysis of frequency and comparison of groups using Chi-Square Test. Main analysis was demographics at baseline, diagnosis of dementia, prevalence of baseline osteoporosis and fracture, falls risk, dementia medications, osteoporosis medications and follow up incidence of fracture and mortality.Results: There were 744 patients followed up. At baseline fifty-nine percent were female and mean age 81 years (SD6.8). Twenty one percent had prior hip fracture Fifty six percent had dementia and 113 (15.2%) were on dementia medications. During 4 years of annual follow up 137(18%) reported new fractures. Overall mortality rate was 267/744 (36%). Patients with dementia were more likely to die (180/415 vs 87/329; p <0.001) with a trend to more fractures (73/415 vs 64/329; p = 0.078). Patients on dementia medications were less likely to fracture 15/113 vs 122/631 (p = 0.029). Conclusions: Patients with dementia have a higher risk of recurrent fractures and mortality. Treating dementia with Acetyl cholinesterase inhibitors appear to reduce the risk of all fractures. This clinical finding is consistent with our recently published in vitro and in vivo mouse model confirming the benefit of cholinesterase on bone histology, biology and biomarkers.

Risk factor	Fracture (1 year)	Fracture (4 years)	Deceased(1 year)	Deceased(4 year)
Dementia (yes)	26/299	73/415	27/415	180/415
Dementia (no)	17/241	64/329	14/329	87/329
Pearson Chi-Square	0.183	**0.078**	0.181	**<0.001**
Dementia Treatment (yes)	2/78	15/113	3/113	43/113
Dementia Treatment (no)	41/462	122/631	38/631	224/631
Pearson Chi-Square	0.150	**0.029**	0.149	0.602

***Disclosures: Charles Inderjeeth**, None*

LB SAT-593

Weight Loss Exacerbates Bone Loss in Women on Aromatase Inhibitors: A Study of Breast Cancer Survivors *Sandra Naaman, MD, PhD[1], Tamara Vokes, MD[2], John Cursio, PhD[2], Rajesh Jain, MD[2]. [1]Rush University Medical Center, United States, [2]University of Chicago, United States

Background: Breast cancer survivors on aromatase inhibitors (AI) experience abrupt and profound estrogen deprivation. Estrogen loss is associated with overall reductions in lean mass (LM) and redistribution of fat mass (FM), favoring the abdominal region, changes that may contribute to bone loss observed during AI therapy. Since women with breast cancer are frequently counseled to lose weight to reduce breast cancer recurrence risk, we investigated the association of changes in weight, LM, and FM with bone loss in black (B) and white (W) women on AI.Methods: Using a retrospective cohort design, we analyzed B and W females with hormone sensitive breast cancer on AI who completed baseline and follow up BMD's from 1 to 3 years apart. Excluded were patients who did not have both hip and spine BMD available or had metastatic breast cancer or primary hyperparathyroidism. Previously validated equations from our center were used to calculate FM and LM from spine and hip soft tissue measurements. Multivariate linear regression analyses were performed with BMD as the outcome and either weight change or FM and LM change as the predictor(s) in those who gained or lost weight, while controlling for age, race, and height. Results: In 45 subjects who received medications for osteoporosis, there was no significant decrease in BMD during AI therapy. The primary analysis included 153 women (70 B; 83 W) who had not received osteoporosis therapy. Compared to W, B were older (64.8 +/- 10.7 vs. 58.9 +/-9.2, p < 0.001); had higher BMI (30.9 +/- 5.9 kg/m2 vs. 28.2 +/- 6.0 kg/m2, p < 0.01) and higher BMD (lowest T-score -0.8 +/- 1.1 vs. 1.2 +/- 0.9, p<0.01). They also had higher FM (36.7 +/- 10.9 kg vs. 30.9 +/- 11.5 kg, p <0.01) and lower LM (39.8 +/- 5.7 kg vs. 42.0 +/- 5.1 kg, p < 0.02).Among 77 women who lost weight during the study, there was an association between weight loss and decreases in spine BMD (0.003 gm/cm2 decrease per 1 kg loss, figure 1) and total hip (TH) BMD (0.002 g/cm2 decrease per 1 kg loss), regardless of race or BMI. Loss of FM, but not LM, was significantly associated with a decrease in spine BMD (0.005 g/cm2 decrease per 1 kg loss, p=0.01) in these women. There were no significant changes in BMD in those with weight gain.Conclusions: Breast cancer survivors on AI who lost weight experienced greater BMD loss than those who gained weight, irrespective of race or baseline BMI, suggesting a need for close BMD monitoring and consideration for osteoporosis therapy.

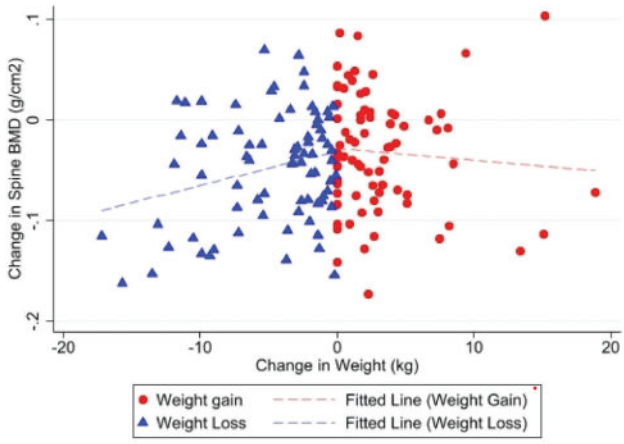

***Disclosures: Sandra Naaman, MD, PhD**, None*

Saturday Orals

LB SAT-594

Effects of Sleeve Gastrectomy on Bone Mass and Microarchitecture Differ By Sex and Menopausal Status *KARIN WU[4], Po-hung Wu[2], Galateia Kazakia[3], Sheena Patel[4], Dennis Black[5], Thomas Lang[3], Tiffany Kim[3], Nicole King[3], Hanling Chang[6], Gaia Linfield[7], Stanley Rogers[3], Jonathan Carter[3], Andrew Posselt[3], Anne Schafer[8], [4], United States, [2]University of California - San Francisco, , [3]University of California, San Francisco, United States, [4], , [5]UC San Francisco, , [6]Liberty University, United States, [7]New York Presbyterian-Weill Cornell Medical Center, United States, [8]University of California, San Francisco and the San Francisco VA Health Care System,

Laparoscopic sleeve gastrectomy (LSG) is a popular and effective treatment for obesity and related comorbidities. However, LSG has been shown to impair intestinal calcium absorption and negatively affect bone metabolism. Studies of skeletal effects have generally examined areal bone mineral density (aBMD) by dual-energy X-ray absorptiometry (DXA), but DXA may be biased in the setting of marked body composition changes and does not provide information about bone microarchitecture. Further, it is not known whether the skeletal impacts differ by sex and menopausal status. In this study, we examined the effect of LSG on aBMD and volumetric BMD (vBMD) and appendicular bone microarchitecture and estimated strength.A prospective cohort of adults (30 premenopausal women, 17 postmenopausal women, 8 men) with severe obesity (BMI 46 +/-7) underwent assessment of skeletal health by DXA, quantitative computed tomography (QCT), high-resolution peripheral QCT (HR-pQCT), and laboratory evaluation preoperatively and 6 and 12 months postoperatively (n=55 preoperatively and n=50 with at least one follow-up scan), although time to last follow-up was longer in some due to the COVID19 pandemic. Log-transformed linear mixed effect models were used to assess how bone parameters change with time after LSG, by sex and menopausal status. The fixed effect of the model was the interaction of time since LSG and sex and menopausal status, and the random effect was the individual participant.Mean 12-month weight loss was 35 kg. Overall median 12-month increase in serum c-telopeptide (CTx) was +87%, and in procollagen-1-N-propeptide (P1NP), +47% (both p<0.001). Predicted total hip aBMD by DXA decreased by 6.8% [95%CI -8.1 to -5.5%] over 12 months. The effect of time on total hip aBMD varied by sex and menopausal status, with a more rapid decline in postmenopausal women (by 7.3% over 12 months, p=0.01; Figure). Predicted spinal vBMD by QCT decreased by 3.4% in postmenopausal women over 12 months (p=0.01), while there was no significant change in spinal aBMD. Radial and tibial vBMD, trabecular bone volume fraction, and estimated strength by HR-pQCT declined, with significant interactions of time on postmenopausal women.In conclusion, axial and appendicular bone mass and microarchitecture decline after LSG, particularly among postmenopausal women. Targeted skeletal health screening and treatment may be warranted in postmenopausal women after LSG.

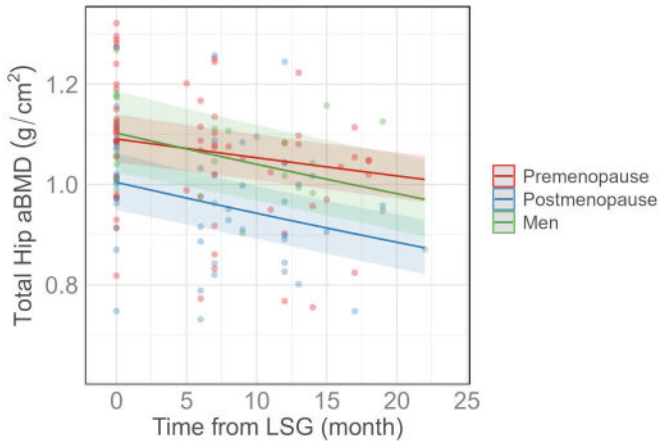

***Disclosures: KARIN WU**, None*

LB SAT-595

Influence of Human Dental Pulp Stem Cells Osteogenic Spheroids Secretome in the Immunomodulatory Potential on Macrophages *Katiucia Paiva[1], Gabriel Albuquerque-Silva[1], Daniel Barrozo-Ferreira[1], Niels Camara[2], [1]ry of Extracellular Matrix Biology and Cellular Interaction, Department of Anatomy, Institute of Biomedical Sciences, University of São Paulo, Brazil, [2]Department of Immunology, Institute of Biomedical Sciences, University of São Paulo, Brazil

In Bone Tissue Engineering, 3D culture models, such as spheroids, has gained more attention for enabling greater cell-cell and cell-extracellular matrix interactions and enhancing regenerative properties of mesenchymal stem cells. Among them, human adult dental pulp stem cells (DPSCs) have attractive properties for bone reconstruction. DPSCs secrete a wide range of biofactors that together are called secretome which can communicate with different cells, including macrophages (M?), being able to polarize them towards the M2/pro-regenerative phenotype that differs from the M1/proinflammatory. It is known that proinflammatory and hypoxic conditions affect the M? polarization. Thus, this project goal was to evaluate the DPSC spheroid secretome influence on M? polarization under an osteogenic, proinflammatory and hypoxic microenvironment. The single 500µm spheroid was formed by 5,5 x 104 DPSCs seeded on u-shape non-adherent 96 wells plates in a basic medium (BM). After spheroid compaction (3-days), differentiation was induced or not by osteogenic medium (OM) for 7 days under hypoxia (2% O2) or normoxia (20% O2). Then, spheroids were incubated or not with TNF-? for 2h and, then, conditioned media (CM) was carried out in an serum-free media for 2 more days. M? derived from THP-1 monocyte lineage were incubated with the spheroids CM for 2 days. M1 and M2 positive controls were induced by LPS and IFN-? or IL-4 and IL-10, respectively. The markers for M1 (IL-6, IL-12, IL-1B, TNF-a, TNFR1B, TIMP-1, CD80, CD96 and CD68) or M2 (IL-10, IL-13, TGF-B, CD200R, MMP-12 and TIMP-2) were evaluated by RT-qPCR analysis. Proinflammatory markers were more upregulated in M1 than M2. Inversely, antiinflammatory markers were upregulated in M2 than M1, except TIMP-2 and IL-10. M? incubated with CM-BM cultivated spheroids expressed more proinflammatory genes than those which was incubated with CM-OM spheroids, excepted TNF-a and IL-12. The same profile was observed for the antiinflammatory genes CD200R, TIMP-2 and MMP-12. M? incubated with CM-OM cultivated spheroids expressed more antiinflammatory genes than proinflammatory ones. Hypoxia microenvironment does not seem to affect the spheroid secretoma. Thus, our data suggest the pro-regenerative immunomodulatory potential of DPSCs spheroids secretome, and OM culture seems to be more important than hypoxia, increasing M2 polarization, even in a pro-inflammatory environment.

***Disclosures: Katiucia Paiva**, None*

LB SAT-596

Bone Marrow Sinusoidal Endothelial Cells Show Fgf23 Upregulation in Murine Beta-Thalassemia and in Response to Direct Administration of Erythropoietin *JACKIE FRETZ[1], Xiuqi Li[1], Larisa Lozovatsky[1], Eileen Chua[1], Karin Finberg[1], [1]Yale School of Medicine, United States

Both iron deficiency and parenteral iron formulations can elevate circulating levels of fibroblast growth factor-23 (FGF23), a hormonal regulator of mineral metabolism classically thought to be produced primarily by osteocytes. Previously, using an Fgf23-eGFP knock-in reporter allele, we identified BM sinusoidal endothelial cells (BM-SEC) as a novel site of Fgf23 upregulation in iron-deficient Tmprss6-/- mice and in mice with phlebotomy-induced anemia. However, the stimuli inducing Fgf23 expression in BM-SEC remain unclear. Here, we used a heterozygous Fgf23-eGFP reporter allele to assess sites of Fgf23 upregulation in the Hbbth3/+ mouse model of non-transfusion dependent ?-thalassemia, which exhibits systemic iron loading and elevated circulating FGF23. Eight-week-old Hbbth3/+ mice showed expected anemia and splenomegaly, which were not altered by the Fgf23-eGFP allele. Anti-GFP immunohistochemistry detected greater Fgf23-eGFP reporter expression in BM-SEC of Hbbth3/+ mice versus Hbb+/+ controls. Fgf23-eGFP expression was also detected in the thymic vasculature but not vasculature of the liver, spleen, or kidney. These thalassemic mice showed a significant induction of circulating intact and c-terminal FGF23 in plasma. Furthermore, introduction of the Fgf23-eGFP allele created a noticeable dosage effect caused by heterozygous Fgf23 disruption. Because we detected both Fgf23 and erythropoietin receptor mRNA in wild-type murine BM-SEC by mining single cell RNA-Seq data from BM stromal populations (PMID: 31130381), and because our anemic mouse models with Fgf23-eGFP reporter expression in BM-SEC all show high serum erythropoietin (EPO), we examined if EPO could induce Fgf23-eGFP reporter expression in BM-SEC of mice with normal iron balance. Fgf23+/eGFP bone marrow plugs, gently flushed from long bones and treated with EPO ex vivo showed significant upregulation of green fluorescence compared to vehicle after 4 and 24 hours of treatment. Additionally, when animals were dosed with EPO for 6 hours, we detected more intense Fgf23 reporter expression in BM-SEC of Fgf23+/eGFP mice treated with EPO compared to saline. This was accompanied by an increase in plasma c-terminal FGF23 expression. Collectively, our studies expand the set of anemic states characterized by Fgf23 upregulation in BM-SEC to include ?-thalassemia and support a model in which EPO acts directly on BM-SEC to upregulate Fgf23 expression.

***Disclosures: JACKIE FRETZ**, None*

LB SAT-597

Addition of ATM Inhibitors to Radium223 Reduces Prostate Cancer Bone Metastases In Vivo *Diane Lefley[1], Callum Jones[1], Sarah Danson[1], Helen Bryant[1], Spencer Collis[1], Janet Brown[1], Penelope Ottewell[1], [1]University of Sheffield, United Kingdom

Rationale/Hypothesis:Bone metastases from prostate cancer are commonly treated with Radium223, and whilst initially effective, patients ultimately experience relapse. Radium223 causes DNA strand breaks within tumour cells that are in close proximity to the bone surface. We hypothesise that relapse is in part due to Radium223 induced activation of DNA damage response pathways, and that inhibition of DNA repair pathways with ATM inhibitors (ATMi) will increase the anti-tumour efficacy of Radium223 in bone.Methods:Male BALB/c nude or C57BL/6 mice received PC3 or RM1 cells, respectively, via intra-cardiac injection. 20mg/kg/day ATMi was administered on day 2, 7 or 10 and Radium223 treatment (50kBq/kg/week or 300kBq/kg/week) commenced 24 hours after first ATMi treatment. Tu-

mour burden was monitored by IVIS and effects on bone and immune cells were monitored by micro-CT, flow cytometry, and heam-analysis.Results:Radium 223 caused an increase in trabecular bone and reduced lymphocytes and monocytes in whole blood, which were not exacerbated with the addition of ATMi. 300kBq/kg Radium223 reduced PC3 tumours in bone by 86% compared with placebo. Addition of either ATMi AZD0156 or AZD1390 to 300KBq Radium223 further reduced bone metastasis by 98.3%. Furthermore, combining AZD1390 with a clinically relevant dose of Radium223 (50mg/kg) synergistically reduced tumour size in bone.Radium223 almost eliminated the growth of RM1 cells in bone when treatment started on day 2 (1.8x106 p/s for placebo vs 3x105 p/s for Radium223) and this effect remained when ATMi was added. Importantly, delaying treatment to mimic the treatment of established tumours (day 7) or large tumours in bone (day 10) resulted in synergistic anti-tumour effects when ATMi was added to Radium223 (tumour burden in bone = 6x104 p/s in placebo vs 1.8x104 p/s; day 10).ConclusionCombining Radium223 with ATMi is more effective at reducing bone metastasis compared with Radium223 alone in vivo.

***Disclosures: Diane Lefley**, None*

LB SAT-598

Oncogenic FLT3 ITD and CD45/PTPRC Control Osteogenesis and Osteoclast Formation *Carolin Lossius[1], Anne Kresinsky[2], Akua Annoh[3], Martina Rauner[4], Lorenz Hofbauer[5], Joerg Mueller[6]. [1]Institute of Molecular Cell Biology, Center for Molecular Biomedicine (CMB), Jena University Hospital, Germany. [2]Research Group Waskow, Leibniz Institute on Aging - Fritz Lipmann Institute, Germany. [3]Division of Nephrology, University Hospital Dresden, Germany. [4]Medical Faculty of the TU Dresden, Germany. [5]TU Dresden University Medical Center, Germany. [6]Institute of Molecular Cell Biology, Center for Molecular Biomedicine (CMB), Jena University Hospital, , Germany

Activating mutations in the receptor tyrosine kinase FLT3 occur in 25 - 30 % of acute myeloid leukemia (AML) patients. In particular, internal tandem duplications (ITD) lead to oncogenic constitutive FLT3 ITD kinase activity with an altered signaling quality promoting leukemic cell transformation. The counteracting role of protein tyrosine phosphatase CD45 on FLT3 activity was demonstrated in vivo using Ptprc-/- mice in a FLT3 ITD knockin background. The inactivation of Ptprc in FLT3ITD/ITD mice resulted insevere hematopoietic phenotypes like leukocytosis, anemia and splenohepatomegaly (Kresinsky et al., Oncogene 2019).Surprisingly, 14-week-old male and female FLT3ITD/ITD Ptprc-/- mice also showed pronounced alterations in bone morphology and microarchitecture. Shortened bones, amorphous epiphyseal plates, high cortical porosity and reduced bone mineral density were observed. Increased trabecular structures were accompanied with severely reduced numbers of osteoclasts (OC), osteoblasts (OB), and virtually absence of adipocytes in the femoral trabecular bones of FLT3ITD/ITD Ptprc-/- mice.Ex vivo differentiation experiments showed reduced capacity in the formation of multinucleated OC of FLT3ITD/ITD Ptprc-/- mice. Their RNAseq data revealed impaired mRNA expression of bone resorption and OC differentiation markers like Oscar, Ocstamp, Dcstamp, Acp5, and Ctsk. Upregulation of proliferation markers and STAT5 target genes indicated pronounced FLT3 ITD signalling activities in the differentiated OC. Thus, oncogenic FLT3 ITD was found to drive proliferation of OC precursor cells, potentially at the expense to produce large, multinucleated OC.In contrast to OC, differentiation and mineralization capacity of FLT3ITD/ITD Ptprc-/- derived OB tended to be reduced compared to control animals. Here, downregulated expression of OB-markers Bmp5, Tgfb1, and Cxcl12 was observed. Further, suppression of adipocyte-related genes like Adipoq and Pparg might explain almost complete absence of adipocyte in situ. Taken together, the observed bone phenotype suggests a previously unnoticed role of FLT3 and CD45 in the formation of the hematopoietic niche and osteogenesis.

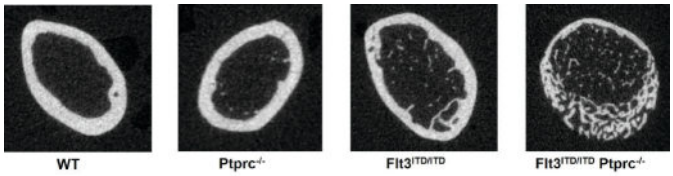

***Disclosures: Carolin Lossius**, None*

LB SAT-599

The Effects of the Nuclear Localization Sequence and C-Terminus of Parathyroid Hormone-Related Protein on the Growth Hormone-IGF-1 Axis *Thomas Rosol[1], Waleed Hashmi[1], Nathan Hoggard[1], Noriko Kantake[1], Megan Turner[1], shiyu yuan[1], Eason Hildreth[2]. [1]Ohio University, United States. [2]The University of Alabama, United States

Osteoarthritis (OA) is a progressive multifactorial joint disease characterized by the degeneration of articular cartilage. Up to now, OA is incurable and treatment options are very limited. Parathyroid hormone-related protein (PTHrP) plays an important role in the regulation of chondrocyte development. In bone, PTHrP acts as a downstream effector, regulating the rate and size of bone formation. PTHrP consists of an N-terminus, a mid-region, a nuclear localization sequence (NLS), and a C-terminus. PTHrP mediates intracrine actions through its NLS which translocates to the nucleus to act as a transcription factor for the regulation of genes involved in growth and metabolism. We intend to explore the cellular and molecular interaction of PTHrP with other factors including signaling molecules such as insulin-like growth factor (IGF-1) whose dysregulation leads to abnormal chondrocyte function and cartilage degeneration in OA. To study the function of NLS and C-terminus of PTHrP in vivo, we generated PTHrP ?/? mice (1-66) that lack the NLS and C-terminus of PTHrP. Pthrp ?/? mice showed stunted growth, altered skeletal development, and most die within 5 days after birth. Previous results show a decrease in IGF-1 levels in these mice, which could lead to defects in cartilage development. Histological analysis by Alcian blue staining and immunofluorescence shows a decrease in the expression of proteoglycans and type II collagen in chondrocytes isolated from Pthrp ?/? mice compared to the control. Overall, the NLS and C-terminus of PTHrP are essential for normal chondrocyte function and may be protective against articular cartilage degeneration.

***Disclosures: Thomas Rosol**, None*

LB SAT-600

A simple and minimal method for differentiation of chondrocytes from human dental pulp stem cells using a thienoindazole derivative small compound TD-198946 *Yuki KANNO[1], Yurika DANTSUJI[1], Monika NAKANO[1], Yuri MATSUI[1], Yoko Kawase-Koga[2]. [1]Department of Oral and Maxillofacial Surgery, Tokyo Women's Medical University, Japan. [2]Tokyo Women's Medical University, Japan

Human dental pulp stem cells (DPSCs) are now considered a type of mesenchymal stem cells and exhibit higher clonogenic and proliferative potential than bone marrow stem cells. Therefore, we hypothesized that human dental pulp stem cells, which have higher proliferative capacity than bone marrow mesenchymal stem cells, could be a new stem cell source for three-dimensional cartilage regeneration. Several studies have shown that a thienoindazole derivative small compound TD-198946 (TD) induces chondrogenic differentiation of mesenchymal cells. In our previous studies, we investigated whether chondrogenic differentiation could be enhanced by the use of TD in the currently known chondrogenic differentiation induction medium. the optimal concentration of TD was 10-7 M. Our previous chondrogenic medium is costly and complicated because it contains seven additives, including two growth factors. Therefore, we hypothesized that the benefits of TD could be maximized by simplifying the medium more. The aim of this study is to establish a highly efficient and low-cost method to induce DPSCs into chondrocytes as a cell source.DPSCs were obtained from dental pulp of premolars or third molars from 24 to 45-year-old patients and cultured in normal medium (NM, control) and chondrogenic medium with/without TD (C, C+TD) for 14-28 days. All procedures of the present experiments were approved by the ethics committee of the Tokyo Women's Medical University (ethics permission #2021-0039). Previous chondrogenic mediums were expensive and complex. Therefore, with reference to other reports, we decided to use a simple medium. This new chondrogenic differentiation medium consists ?-MEM with 5% FBS, 10 ng/mL transforming growth factor (TGF)-?1, 100 nmol/L dexamethasone, 6.25 ?g/mL insulin, 50 nmol/L ascorbic acid-2-phosphate, 110 mg/L pyruvate sodium.Real-Time Quantitative Reverse Transcription PCR (RT-qPCR) results showed that chondrogenic medium supplemented with TD (10-7M) most effectively increased gene expression levels of col2a1and aggrecan, that are chondrogenic differentiation markers. However, expression of sox-9 was not stable.The present results suggested that TD-induced DPSCs are a useful cell source for cartilage regenerative medicine. Furthermore, our new method successfully induced chondrocyte differentiation without the conventionally used bFGF. However, the results for sox-9 varied from cell line to cell line, suggesting that further studies, such as protein-level analysis, are needed.

***Disclosures: Yuki KANNO**, None*

LB SAT-601

TNXB regulates cartilage homeostasis in hemophilic arthropathy through AKT-mediated apoptosis *Qinghe Zeng[1], Jiali Chen[1], Xu Wang[1], Rui Xu[2], Weidong Wang[3], Yuliang Huang[3], Qi Sun[4], Wenhua Yuan[1], Pinger Wang[1], Shuaijie Lv[5], Peijian Tong[5], Hongting Jin[1]. [1]Institute of Orthopaedics and Traumatology, the First Affiliated Hospital of Zhejiang Chinese Medical University, Hangzhou, China, China. [2]Department of Orthopedics, Affiliated Hospital of Jiangxi University of Traditional Chinese Medicine, Nanchang, China., China. [3]Department of Osteology, The Second Affiliated Hospital of Zhejiang Chinese Medical University, Hangzhou, China, China. [4]Department of Orthopaedic Surgery, Fuyang Orthopaedics and Traumatology Affiliated Hospital of Zhejiang Chinese Medical University, Hangzhou, Zhejiang, China, China. [5]Department of Orthopaedic Surgery, the First Affiliated Hospital of Zhejiang Chinese Medical University, Hangzhou, Zhejiang, China, China

Recurrent joint bleeding in hemophilia patients frequently results in hemophilic arthropathy (HA). Drastic degradation of articular cartilage is major characteristic of HA, but its pathological mechanisms has not yet been clarified. DNA methylation is sensitive to environmental factors and likely involved in cartilage damage after hemophilic joint bleeding. Our genome-wide methylation analysis identidied 700 differentially methylated regions (DMRs) associated with HA. The DMR genes (DMGs) were significantly enriched

in extracellular matrix organization. Among these DMGs, Tenascin XB (TNXB) expression was down-regulated in human HA cartilages and in FVIII-KO mouse cartilages following joint bleeding. Further, TNXB knockdown enhanced catabolism and suppressed anabolism in primary chondrocytes. Importantly, the loss of TNXB in FVIII-KO mouse provides a disease-promoting role in HA by augmenting cartilage matrix degeneration and osteoporosis of subchondral bone. In addition, TNXB knockdown promote the chondrocyte apoptosis and inhibited the phosphorylation of Akt. However, AKT agonist dramatically suppressed Extracellular matrix (ECM) catabolism and apoptosis in TNXB-KO chondrocytes.In summary, our study demonstrated that TNXB is a central mediator of cartilage matrix degradation following joint bleeding, which functions by regulating the activation of AKT. These mechanistic insights allow targeted development of potentially new strategies for cartilage protection in HA.

***Disclosures: Qinghe Zeng**, None*

LB SAT-602

Quantitative evaluation of osseous healing using bone mineral density in sagittal split ramus osteotomy. *Hayato Hamada[1,] Kotaro Kaneko[1,] Naoki Ikehata[1,] Yasuyuki Fujii[1,] On Hasegawa[1,] Daichi Chikazu[1,] [1]Tokyo Medical University , Japan

Introduction: Orthognathic surgery, such as Sagittal Split Ramus Osteotomy (SSRO), performed on patients with Ian deformities, is widely employed surgical procedure worldwide. SSRO allows for broad contact area between the divided bone segments, resulting in high postoperative stability and making it an applicability as an osteotomy technique. However, there have been no previous reports conducting a quantitative assessment of the osteogenic healing of the divide bone segments at the surgical site. Therefore, this study presents a quantitativ evaluation using bone mineral density to assess the osteogenic healing between bone segments after SSRO surgery.Materials and methods: The subjects were cases diagnosed with jaw deformities and underwent bilateral SSRO at the department of oral and maxillofacial surgery and orthodontics, Tokyo Medical University Hospital, between December 2021 and July 2022. The Obwegeser-Dal Pont technique was used for the surgical procedur, and bone fixation was performed titanium miniplate. Intermaxillary fixation was not applied postoperatively. Quantitative CT imaging was performed on the subjects at 1month preoperatively, 3 months, 6 months and 1 year postoperatively for evaluatio. Image analysis was conducted using SYNAPSE Vincent Ver.6.7.0003 (Fuji film Medical, Tokyo). Results: The subjects comprised 5 cases involving 10 sides (1 male, 4 females). The age at the time of surgery ranged from 21 to 36 years, with an average age of 26.8 years. Preoperative diagnosis included mandiblar prognathism in 4 cases and facial asymmetry in 1 case. The average BMD was as follows: Preoperatively; 561.4mg/cm3, 3 months postoperatively; 492.8mg/cm3, 6 months post operatively; 473.3mg/cm3, 1 year postoperatively; 476.9mg/cm3.Conclusion: The BMD between the divided bone segments after SSRO showed a decrease up to 6 months post operatively. However,there was no significant difference between the BMD at 6 months and 1 year postoperativly. The findings suggest that the osteogenic healing between the bone segments at 6 months and 1 yea postoperatively is nearly equivalen, indicating a stable bone healing process over time.

***Disclosures: Hayato Hamada**, None*

LB SAT-603

Anabolic Therapy for Treatment of Recurrent Fractures in a Young Patient with Rett Syndrome *Gina Woods[1,] Soumya Kurnool[2,] [1]University of California, San Diego, United States, [2]Endocrinology Fellow, United States

Background: Rett syndrome (RTT) is a rare neurodevelopmental disorder in women that is associated with osteopenia and a 4-fold higher risk of fractures.Patient Case: A 27-year-old ambulatory woman with RTT, osteoporosis, and catamenial seizure disorder presents with recurrent fractures after multiple falls. Initially, she received depot medroxyprogesterone acetate (DMPA) to control menstrual cycle-related seizures which was discontinued after navicular and clavicular fractures from falls. The patient then received two annual doses of zoledronic acid but developed multiple foot fractures after another fall. Subsequently, she was treated with abaloparatide for two years, during which she experienced no further fractures despite additional falls.A repeat DXA after 2 years of abaloparatide showed Z-scores of -2.1 (lumbar spine), -2.7 (R femoral neck), and -2.8 (L femoral neck). There was a statistically significant increase in BMD after anabolic therapy, with a 6.9% increase in the lumbar spine and 8% and 12.5% increases in the left and right femoral neck, respectively. As the patient's Z-scores remained low for her age, abaloparatide treatment was continued for another year.Conclusion: This case highlights the vulnerability of young women with RTT to early and severe osteoporosis. In a case report of 20 patients, DXA scans showed lower BMD in RTT patients compared to age-matched peers, potentially due to reduced bone formation. Ambulatory disability was also associated with a significant decrease in BMD in a 10-year longitudinal study. In this patient's case, her use of carbamazepine and previous treatment with DMPA were additional risk factors for osteopenia, as DMPA reduces ovulation and estrogen levels, resulting in lower BMD. The 2016 Clinical Guidelines for Management of Bone Health in RTT advise against using DMPA for hormonal intervention and recommend bisphosphonates for osteoporosis treatment but make no mention of anabolic agents. A case report of an 18-year-old nonambulatory patient with RTT on carbamazepine showed significant improvement in BMD and no further fractures after 8 months of teriparatide and 3 annual doses of neridronate. Therefore, in young RTT patients with osteoporosis, it is important to address risk factors such as nutritional deficiencies, monitor anticonvulsant use, avoid DMPA, and consider treatment with anabolic agents.

***Disclosures: Gina Woods**, None*

LB SAT-604

A giant parathyroid lesion with innumerable lytic lesions *Muhammad Faiz Muhamad[1,] Anne Mc Gowan[1,] [1]Tallaght University Hospital, Ireland

42 year old South-East Asian woman admitted with persistent vomiting on the background of 6 months history of lethargy, generalised aches and visibly large right sided neck mass. She is a non smoker with medical history of hypertension and hyperlipidaemia.Laboratory results revealed severe hypercalcaemia of 3.16mmol/L, phosphate of 0.91mmol/L, alkaline phosphate of 1338mmol/L and PTH of 1926pg/ml. The Vitamin D level was 31nmol/L, and urine calcium/creatinine ratio was elevated at 1.76mmol/mmol. The clinical diagnosis was made at this stage - severe primary hyperparathyroidism with raised suspicion of parathyroid carcinoma based on the presence of large neck mass and exceedingly high level of PTH(30 times upper limit).The Technetium-99 Sestamibi scan coupled with SPECT/CT neck confirmed the initial finding on the ultrasound of neck as it revealed intense uptake in the right neck mass which representing a giant parathyroid lesion. Osseous abnormalities were seen on the bone windows, concerning for skeletal changes of hyperparathyroidism. The whole nuclear body scan showed uniformly increased uptake affecting the entire skeleton, characterised as a superscan as there was diminished uptake by the kidneys. The SPECT-CT scan of pelvis confirmed the presence of innumerable lytic lesions consistent with Osteitis Fibrosa Cystica.The initial management included rigorous IV fluid, followed by IV bisphosphonates. A 44.9 grams measuring 6cm right parathyroid lesion was resected. Her postoperative course was complicated by development of hungry bone syndrome with prolonged HDU stay.The histology analysis reported a well circumscribed encapsulated lesion with no lymphovascular or perineural invasion or necrosis, suggestive of parathyroid adenoma. The genetic analysis for familial hyperparathyroidism including AIP, CASR, MEN1, CDKN1B and CDC73, was negative to identify a pathogenic variant.Additional results include elevated CTX-1, osteocalcin, P1NP and HCG. The elevation of HCG has been analysed as potential biomarker for parathyroid carcinoma in small studies .This case illustrates a severe skeletal manifestation of hyperparathyroidism caused by a large autonomous parathyroid lesion with underlying chronic vitamin D deficiency. WHO in the year of 2022 listed atypical parathyroid tumour as the third classification, to reflect its unknown potential of malignancy. This lady is under close observation due to concern of possible recurrence.

***Disclosures: Muhammad Faiz Muhamad**, None*

LB SAT-605

Recombinant human monoclonal antibody for fibroblast growth factor 23 (Burosumab, Crysvita®) treatment for FGF23-related hypophoshatemia in an adult patient with severe fibrous dysplasia in McCune-Albright syndrome. *Maria Stelmachowska-Bana?[1,] Karolina Cylke-Falkowska[2,] Wojciech Zgliczy?ski[1,] Waldemar Misiorowski[1,] [1]Department of Endocrinology, Centre of Postgraduate Medical Education, Poland, [2]I Department of Internal Medicine, Biela?ski Hospital, Poland

Background: McCune Albright syndrome (MAS) is a rare mosaic genetic disorder affecting 1/100 000 to 1/1000 000 of the population. It arises from a somatic gain-of-function mutation in GNAS gene. The clinical picture is complex and includes fibrous dysplasia (FD), café-au-lait spots, precocious puberty and other hyperactive endocrinopathies. The degree of FGF23 overproduction is correlated with FD severity, and frank hypophosphatemia occurs only in patients with extensive skeletal involvement, resulting in frequent fractures, pain, increased propensity for deformities, and muscle weakness. Burosumab is a monoclonal antibody that targets FGF23, indicated for the treatment of hypophosphatemic rickets caused by overproduction of FGF23 (XLH, TIO). To date, there is no evidence on the effectiveness and safety of burosumab treatment in adults with FD/MAS.Case presentation: A 27-year-old male with MAS was under the care of the Endocrinology Department for persistent hypophosphatemia despite treatment with oral phosphate supplements and alfacalcidol. MAS was diagnosed at the age of 6 years and his medical history included precocious puberty, multiple fractures, skeletal deformities, muscle weakness and exacerbated skeletal pain due to severe FD. The patient was diagnosed with GH excess at the age of 22 years and has been treated with pasireotide 40 mg every 4 weeks i.m. with normalization of IGF-1 level for age and sex. Because of persistent hypophosphatemia (serum phosphate 0.38 mmol/L) resulting from FGF23 excess (serum FGF23 495kRU/L), bone pain and frequent fractures, the treatment with burosumab has been attempted (1 mg/kg body weight s.c. every 4 weeks). Over the 6-month course of treatment, the patient reported improved general well-being, reduced bone pain and increased muscle strength. Normalization of serum phosphate, PTH and a significant reduction in alkaline phosphatase levels were achieved (serum phosphate 0.83mmol/L, alkaline phosphatase 618.8 IU/l, PTH 51.6 pmol/L). No adverse effects of the short-term therapy were observed.Conclusions: This is the first reported case of burosumab treatment in an adult patient with FGF23-related hypophosphatemia in MAS. In our case, positive effects of the therapy were observed, both in terms of the patient's reported well-being and in terms of calcium-phosphate balance and bone markers. However, a longer follow-up in a larger group of adult patients with MAS seems necessary.

***Disclosures: Maria Stelmachowska-Bana?**, None*

LB SAT-606

Platelet-Rich Fibrin Accelerates Osteogenic differentiation of Human Dental Pulp Stem Cells *Yoko Kawase-Koga[1], Ayano Hatori[2], Eva Dohle[3], Yasuyuki Fujii[4], Yuki Kanno[1], Sarah AI-Maawi[3], Robert Sader[3], Daichi Chikazu[4], Shahram Ghanaati[3]. [1]Division of Maxillofacial Surgery and Stomatology, Department of Oral and Maxillofacial Surgery, Tokyo Women's Medical University , Japan. [2]Department of Oral Health and Diagnostic Sciences, School of Dental Medicine University of Connecticut Health, United States. [3]FORM, Frankfurt Oral Regenerative Medicine, Clinic for Maxillofacial and Plastic Surgery, Goethe University, Germany. [4]Department of Oral and Maxillofacial Surgery, Tokyo Medical University, Japan

[Background] Human dental pulp stem cells (hDPSCs) have demonstrated higher clonogenic and proliferative potentials than bone marrow stem cells and can be easily obtained from extracted teeth in minimally invasive surgeries without any ethical issues. Generally, the conventional culture methods for hDPSCs have used high concentrations (10-20%) serum, such as fetal bovine serum (FBS), to maintain cell viability. However, the use of animal components that are at risk of transmitting pathogens and immune responses to recipients must be considered for the clinical application of stem cell-based therapy. Platelet-rich fibrin (PRF) is a blood concentrate system derived from human peripheral blood obtained through centrifugation without the addition of anticoagulants or external chemicals. PRF performs biological processing of acellular biomaterials with autologous cells and growth factors by combining them with biomaterials to enhance and accelerate the regeneration process within the graft bed. The aim of this study was to evaluate the effectiveness of the PRF-conditioned medium (PRF-CM) compared to FBS general medium in promoting hDPSC proliferation and differentiation. [Methods & Results] Venous blood samples were obtained from 3 healthy donors and immediately centrifuged at medium speed 1200 rpm for 8 minutes. The obtained PRF was cultured for 2 weeks to prepare RPF-CM. hDPSCs were obtained from dental pulp of third molars from 26-31 years old patients and cultured with 15%PRF-CM or 15% FBS in general culture condition and in osteogenic condition. The cell proliferation assay indicated PRF-CM group exhibit lower cell numbers and proliferation rates compared to FBS group. Interestingly, Alizarin Red staining and von Kossa staining in PRF-CM group showed significantly higher calcification than the FBS group by quantification analysis. RT-PCR showed significantly higher expression levels of ALP, osteocalcin, type I collagen alpha 1, and RUNX2 in the PRF-CM group. [Conclusion] This study introduces the novel application of PRF-CM in enhancing the differentiation of hDPSCs, providing an alternative to FBS culture medium, and addressing concerns associated with the use of animal components in clinical settings.

***Disclosures: Yoko Kawase-Koga**, None*

LB SAT-607

The Therapeutic Effect of AAV9-lncR-APDC in Mitigating Periodontitis-Induced Bone Loss *Zoe (Xiaofang) Zhu[1], Jake Chen[1]. [1]Tufts University, United States

Periodontitis, a chronic inflammatory disease that is highly prevalent, triggers an excessive host immune response, leading to alveolar bone resorption and subsequent tooth loss. Our prior research demonstrated that the long noncoding RNA APDC (lncR-APDC) influences bone remodeling by enhancing osteogenesis and inhibiting osteoclastogenesis. The current study explores the role of lncR-APDC in periodontitis progression and therapy. Our experiment with a periodontitis (EP) animal model exhibited exacerbated bone loss and disrupted pro-inflammatory cytokine regulation in lncR-APDC knockout (KO) mice. Single-cell RNA sequencing of EP gingival tissue revealed changes in the proportion and function of epithelial cells and immune cells, including T and B cells, macrophages, and neutrophils due to LncR-APDC silencing. We discovered a new epithelial cell subset (Krt8+, Krt18+, Krt5-, Krt14-) in the lncR-APDC-KO group, which interacts with immune cells through multiple ligand-receptor pairs. Interestingly, the cell-cell communication between macrophages and other cell types, such as neutrophil, T cells and fibroblasts, were extremely active through Trem1/Pglyrp1/Il1 ? axis. The gene Tff2, which was significantly elevated in lncR-APDC KO bone and gingival tissues, has a predicted direct binding site on LncR-APDC. Furthermore, intra-gingival administration of AAV9-lncR-APDC demonstrated remarkable therapeutic effects on periodontitis by alleviating bone mass and inflammation. In conclusion, our results suggest that LncR-APDC plays a pivotal role in the epigenetic control of periodontitis pathogenesis and holds therapeutic potential for periodontitis.

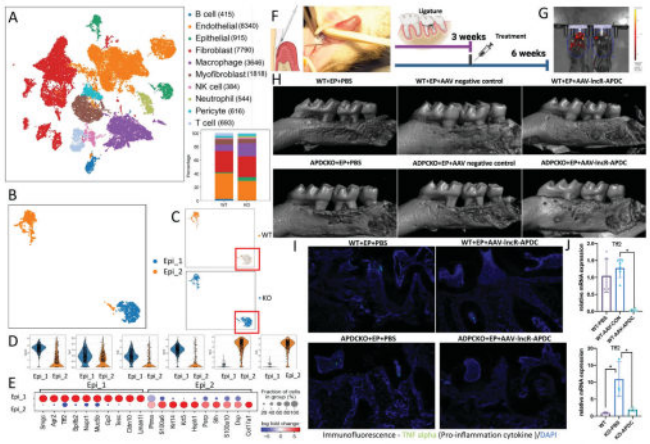

Figure A) the UMAP representation of the 25,161 cells, colored by cell type annotation and the bar plots indicating the percentage of each cell type. B) the subclusters of epithelial cells. C) epithelial cells divided by WT and KO. D) the markers of epithelium. E) DEGs of Epi_1 and Epi_2. F) the AAV-lncR-APDC administration through microinjection on gingival. G) the IVIS imaging of expression of RFP in AAV and PBS group. H) the AAV9-CAG-APDC attenuates the periodontal bone. I) the expression of pro-inflammation cytokine, TNFα. J) the mRNA expression of Tff2 after AAV-APDC treatment in WT group. g) The mRNA expression of Tff2 after AAV-APDC treatment in KO group. * $p < 0.05$.

***Disclosures: Zoe (Xiaofang) Zhu**, None*

LB SAT-608

Roles of osteoblast dopamine D2 receptor in type 1 diabetes-induced bone loss *YASER PEYMANFAR[1], Philip Trackman[2]. [1]Forsyth Institute/ Harvard School of Dental Medicine , United States. [2]The Forsyth Institute , United States

Poor bone health in diabetic patients increases the risk of bone fractures, loss of mobility and can be life threatening. Bone mineral density (BMD) in diabetic patients only partially determines bone strength while there is increasing evidence that the structural integrity of the organic phase of bone made up primarily of type 1 collagen is also important. Extracellular lysyl oxidase (LOX) catalyzes the oxidative deamination of hydroxylysine and lysine residues in collagen, and required for the formation of biosynthetic crosslinks and subsequent stability of functional collagen that ultimately increases bone strength. Lysyl oxidase-dependent cross-linking of bone collagen is deficient in type 1 diabetes, while regulation of lysyl oxidases in diabetes is under-studied. Previously, we have reported that downregulation of bone LOX occurs in type 1 diabetes and is associated with trabecular bone loss and poor collagen structure. Importantly, we have determined that gut-derived peripheral circulating dopamine in diabetic mice is abnormally elevated and is associated with LOX downregulation which in turn adversely affects collagen structure and bone strength. We have seen that blocking of dopamine D2 receptor (D2R) activity pharmacologically with the highly selective antagonist Amisulpride in type 1 diabetic mice rescued trabecular bone loss and partially rescued LOX expression levels in osteoblasts in type 1 diabetic mice.Since the systemic administration of Amisulpride may trigger secondary effects on metabolism and bone turnover, we generated a novel osteoblast-specific dopamine receptor 2 (D2R) knockout mouse using Col1-2.3-cre+/- and D2rfl/fl and control mice in the C57BL6/J background. Type 1 diabetes was induced by streptozotocin following standard protocols. Diabetes was confirmed by measuring blood glucose (glucose>300 mg/dl). Our hypothesis is that bones in osteoblast-specific conditional D2r knockout mice will be resistant to diabetes-induced pathology. Surprisingly but interestingly, our results exhibited a high degree of apparent embryonic lethality in homozygous KO mice. However, micro-CT data indicate that osteoblast heterozygous D2r knockout female mice exhibited femurs rescued from diabetic bone deficiency (n=8), and the same response observed in fewer male mice as well. We are investigating both the apparent embryonic lethality and mechanisms by which D2r regulates bone homeostasis.

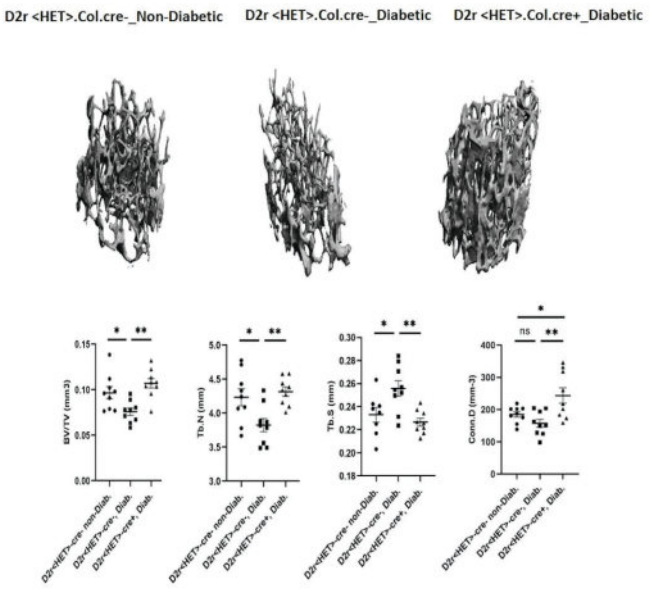

***Disclosures: YASER PEYMANFAR**, None*

LB SAT-609

Effects of Systemically Administered Mes-1022, a Bone-Targeted EP4 Agonist, in Rats with a Critical-Size Femoral Segmental Defect *Jack Chapman[1,] Catherine Julien[1,] Mayumi Umebayashi[1,] Taylor deVet[1,] Michal Kulasek[1,] Aijing Shen[1,] Frank Rauch[2,] Bettina Willie[3.] [1]Co-Author, Canada[.] [2]Shriners Hospital for Children, Montreal, Canada[.] [3]McGill University, Canada

Introduction: Up to 5% of long bone fractures exhibit delayed healing or non-union. Mes-1022, a novel anabolic prodrug, has been shown to promote bone healing when applied locally, but it is unclear whether systemic administration enhances healing. We aimed to evaluate the effect of systemically-administered Mes-1022 on critical-sized bone defect healing and mass and microstructure of the intact contralateral femur.Methods: Ten-week-old female Sprague-Dawley rats (8/group) had a 5 mm osteotomy of the left femoral mid-shaft, stabilized by a unilateral external fixator (Fig 1J,K). Rats received weekly subcutaneous injections of Mes-1022 at 5 mg/kg (high dose), 1.7 mg/kg (low dose), or Vehicle (PBS + 25 nM EDTA). Serum markers and open field activity including rearing were measured pre-osteotomy and throughout study. Rats were sacrificed after 12 weeks and osteotomized and unoperated femora were imaged via micro-CT. Dissected intact femora underwent destructive three-point bending. Data were analyzed by ANOVA followed by post-hoc Tukey testing, with significance at $p < 0.05$.Results: Full bony bridging only occurred in 1 rat, which was treated with high dose Mes-1022 (Fig. 1A-C). At the osteotomy, high dose rats had higher tissue mineral density (TMD) of newly formed lower mineralized bone versus vehicle rats. For unoperated femurs, increased cortical area and max moment of inertia, as well as decreased TMD and medullary area were evident at the mid-diaphysis (Fig. 1G-I) of high dose versus low dose animals. Vehicle and low dose groups had lower porosity when compared to the high dose group. At the distal metaphysis (Fig 1D-F), high dose rats had higher trabecular number and thickness versus low dose rats. There was no difference in mechanical properties between groups. High dose treated rats had a higher rearing count at week 9 compared to low dose rats. P1NP was higher with high dose versus vehicle and low dose at week 1, and with high dose versus vehicle at week 6. TRAcP-5b was lower with high dose versus vehicle at week 10. Serum ALP did not differ between groups.Conclusion: High dose treatment with Mes-1022 enhanced cortical and trabecular microstructural parameters in the contralateral femur diaphysis by stimulating endocortical bone formation and initiating new trabeculae and (re)modeling of existing trabeculae. Histological analysis of callus tissue composition within the osteotomized femur is ongoing to determine if healing was enhanced.

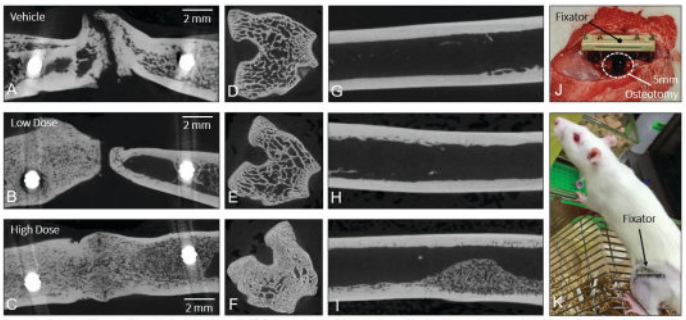

Reconstructed microCT scans of the mid-diaphysis of operated (left) femurs in rats with most advanced healing from each group: vehicle (A), low dose (B), and high dose (C). Representative reconstructed microCT scans of metaphysis of intact (right) femurs for vehicle (D), low dose (E), and high dose (F) rats. Representative reconstructed microCT scans of diaphysis of intact (right) femora for vehicle (G), low dose (H), and high dose (I) rats. Higher-mineralized tissue (> 614 mg HA/cm³), termed quiescent bone, was distinguished from newly formed lower-mineralized tissue (287 - 614 mg HA/cm³) termed non-quiescent bone. External fixator on rat day 6 post-surgery (K), and immediately post implantation during surgery (J). Four titanium pins are threaded through a unilateral bar and then drilled into the femur. The 5 mm osteotomy is created with a gigli wire saw and saw guide.

***Disclosures: Jack Chapman**, None*

LB SAT-610

Sclerostin but not Dickkopf-related protein 1 predicts bone mass and markers of bone turnover in older adults *MARILENA CHRISTODOULOU[1,] Terry Aspray[2,] Isabelle Piec[3,] WILLIAM FRASER[4,] Inez Schoenmakers[5.] [1]University of East Anglia, [2]Translational and Clinical Research Institute, United Kingdom[.] [3]BioAnalytical Facility, University of East Anglia, United Kingdom[.] [4]UNIVERSITY OF EAST ANGLIA, United Kingdom[.] [5]UEA, United Kingdom

Sclerostin (SOST) and Dickkopf-related protein 1 (DKK1) are antagonists of Wnt signalling and inhibit osteoblast activity and indirectly stimulate osteoclast activity. SOST and DKK1 antibody therapy leads to increases in bone mass and bone formation. However, reported associations between plasma SOST and DKK1 concentrations and measures of bone mass and turnover are conflicting.This study in healthy older men and women (n=379; median[IQR] 74.1 [71.5-77.0]y) investigated associations between plasma SOST and DKK1 and (a) BMD and BMC at the hip and femoral neck, (b) markers of bone turnover and Wnt signalling (C-terminal telopeptide (CTX), Procollagen 1 N-terminal Propeptide (P1NP), bone alkaline phosphatase (BAP), osteoprotegerin (OPG) and soluble receptor activator of nuclear factor ?-B ligand (sRANKL) and (c) hormonal regulators (parathyroid hormone (PTH), 1,25-dihydroxyvitamin D (1,25(OH)2D), 25 hydroxy vitamin D (25(OH) D), intact and c-terminal Fibroblast Growth Factor 23 (iFGF23, cFGF23) and KLOTHO). Associations were analysed by univariate (model 1) and multivariate linear regression with adjustment for height, weight and age (model 2) or renal function (CKD-EPI eGFR; model 3).Plasma SOST was significantly, positively associated with BMD and BMC at both sites (all $P<0.001$) and negatively with CTX, P1NP and BAP (all $P<0.01$). Associations of SOST with DKK1, OPG and RANKL were non-significant. SOST was negatively associated with 1,25(OH)2D ($P=0.002$) and positively with cFGF23 and iFGF23 ($P<0.001$ and 0.025). Associations with PTH, 25(OH)D and KLOTHO were non-significant. Multivariate model 2 provided similar results. Adjustment for eGFR attenuated associations with 1,25(OH)2D ($p=0.06$) and iFGF23 ($p=0.07$).Plasma DKK1 was negatively associated only with cFGF23 in univariate and both multivariate models.In conclusion, plasma SOST but not DKK1 was positively associated with bone mass and negatively with markers of both bone formation and resorption, suggestive of a lower rate of bone remodelling. This was independent of body size and renal function.

***Disclosures: MARILENA CHRISTODOULOU**, None*

LB SAT-611

Physiologic Load Induced Strain of 3D Printed Truss Element Amplifies Osteogenic Response of Human Mesenchymal Stem Cells Compared To Static Surface Feature Influence *Ali Kiapour[1,] Se-Hwan Lee[2,] Brendan Stoeckl[2,] Lewis Harrison[3,] Jessee Hunt[4,] Robert Mauck[2,] Su-Jin Heo[2.] [1]Department of Neurosurgery, Massachusetts General Hospital Harvard Medical School, United States[.] [2]University of Pennsylvania, United States[.] [3]4WEB Medical Inc., United States[.] [4]4WEB MEDICAL Inc., United States

INTRODUCTION:Proprietary build themes have been developed to create a hierarchical surface roughness on a Ti truss-based implant using Electron Beam Melting (EBM) technology. This study evaluated how surface features influence MSC morphology, adhesion, clustering, and osteogenic differentiation. We also assessed the amplification effect of dynamic physiologic load-induced strain of a truss element on the osteogenic response of human MSCs beyond the baseline differentiation initiated by static surface technology. METHODS:Three different hierarchical surface roughnesses were fabricated using EBM:1) Smooth Titanium (Smooth), and two proprietary 3D-printed (P3D) titanium surfaces, which consist of a hierarchical surface roughness that spans from the macro to nano-scale having lesser 2) P3D1 or greater 3) P3D2 surface roughness. Human bone marrow-derived MSCs (hMSCs) were obtained, and passage two cells (5×10e5 cells) were seeded onto P3D2 surfaces (10mm×60 mm). A custom bioreactor system was designed to apply 3-point bending

to hMSC-seeded P3D2 surfaces [35µm of cyclic deformation, 1Hz, one time (DL×1), twice (DL×2), or 3 times (DL×3) in daily 3-hour cyclic loading increments on day 1, 2, and 3; Fig.1C] in basal cell growth media]. The Live/Dead assay and RT-PCR were performed after the first dynamic loading.RESULTS:3D scan images (Fig.1A) showed non-uniform 3D peaks and valleys on the P3D1 and P3D2. The areal method analysis showed that P3D1, and P3D2 had similar surface roughness, and the height distribution of P3D2 was sharper compared to P3D1. Live (green)/Dead (red) staining confirmed high cell viability on the P3D2 surface with the application of cyclic tensile strain (Fig.1D). Dynamic loading enhanced all osteogenic gene expression compared to static culture conditions (Fig.1E). BMP2 expression was considerably higher than the static baseline, with a significant increase between DLx1 and DLx2, while ALP, Runx2 and OPN showed amplified expression on DLx1 and leveled off after DL×2. Compared to the static control, OCN expression was higher with each loading event (Fig.1E).CONCLUSION:The hMSCs seeded on the rough Ti surfaces and exposed to dynamic loading experienced amplification in the osteogenic expression (above that seen with surface-feature driven differentiation), indicating synergistic effects of the material microenvironment on differentiation and the macro environment through strain distribution enabled by the truss design.

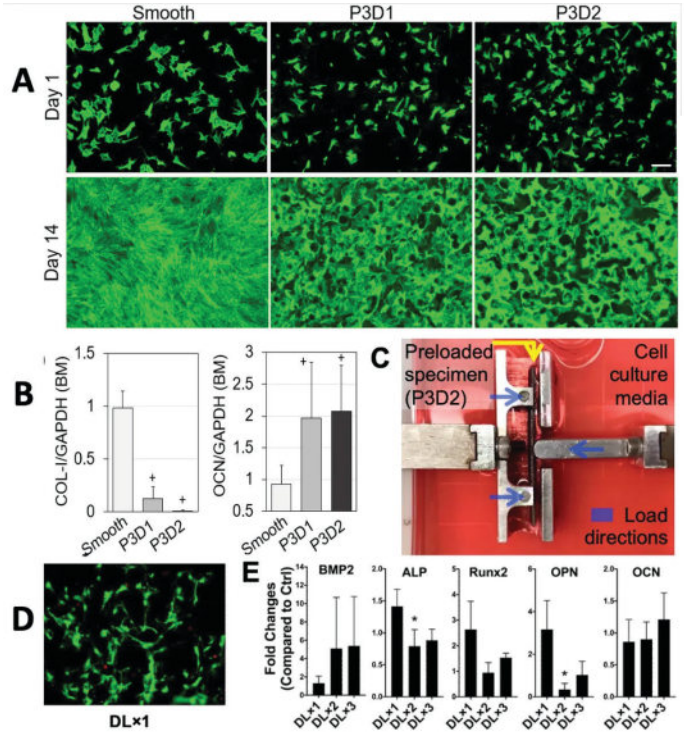

Figure 1: (A) Cell morphology at days 1 and 14. (B) Gene expression in basal media comparing smooth vs. rough titanium surfaces, (C) Image of bioreactor, (D) Live (green)/Dead (red) stain images (5X, after DL×1), (E) Gene expression: BMP2, ALP, Runx2, Osteopontin (OPN), or Osteocalcin (OCN) (n=3, *: p<0.05 vs. DL×1).

***Disclosures: Ali Kiapour**, None*

LB SAT-612

Effect of implant surface roughness and porosity on osteoblastic genes expression in Bone marrow Mesenchymal stem cells *Ali Kiapour[1], Xin Xiaonan[2], Elie Massaad[3], John Shin[3], David Rowe[4]. [1]Massachusetts General Hospital, Harvard Medical School, [2]Department of Reconstructive Sciences, University of Connecticut, United States, [3]Department of Neurosurgery, Massachusetts General Hospital, Harvard Medical School, United States, [4]University of Connecticut Health Center, United States

INTRODUCTION: Hierarchal surface roughness of the 3D printed orthopedic implants can lead to better osteointegration rates compared to conventional PEEK or machined (smooth surface) titanium implants. We compared P3D (Rough Ti),SmTi (Smooth Ti),and PEEK surfaces for bone differentiation through assessing osteogenesis rate and magnitude, including a bone formation regulator and early/late bone differentiation markers.METHODS: BSP-GFP/DMP-RFP transgenic mouse bone marrow stem cells were used to monitor bone mineralization with fluorescently-tagged genes. The BSP and DMP proteins, located in bone tissue and involved in mineralization, were evaluated for gene activation in newly formed osteoblasts and mineral-embedded osteocytes (figure-1a). Low-density, first-passaged cells from the primary bone marrow stromal culture (BMSCs) were seeded at 10e6 cells/mL onto three replicate plates: P3D, SmTi or PEEK. From days 7 through 22, cell constructs were placed under osteogenic conditions. The plates were harvested on days 3,7,14, and 22 and evaluated for fluorescence and RNA expression. Cell entry into osteogenesis was determined by fluorescence intensity at day 22.RESULTS: Significantly greater percentage of BMSC-derived progenitor cells were osteogenic on the P3D Ti surface at day 22 (Figure-1b, p<0.05) as compared to SmTi and PEEK. On each surface, almost all osteogenic markers increased over time with maximum osteogenic gene expression occurring at day 14 (Figure-1c). BMSC-derived progenitor cells cultured on P3D resulted in noticeably (P<0.005) greater increases in the late osteogenic markers Bglap and Phex (indicative of osteocyte formation) by more than 1,000- and 100-fold, respectively, at day 14. At day 22, stem cells cultured on P3D showed significant increases (P<0.005) in early osteogenic markers Alp and Col1A1, by over 15- and 35-fold respectively.DISCUSSION: 3D-printed rough Ti surface enabled a greater proportion of stem cells to enter the osteogenic lineage relative to PEEK and SmTi surfaces. Stem cells on the P3D surface resulted in greater gene expression master regulators of bone differentiation, early bone markers, and markers associated with bony mineralization. Faster and more robust late-stage osteogenic differentiation was demonstrated (>100-fold) increase in osteocalcin and Phex for P3D relative to PEEK and SmTi. These attributes may facilitate a more rapid and stable fixation of the bone-implant interface post surgical intervention.

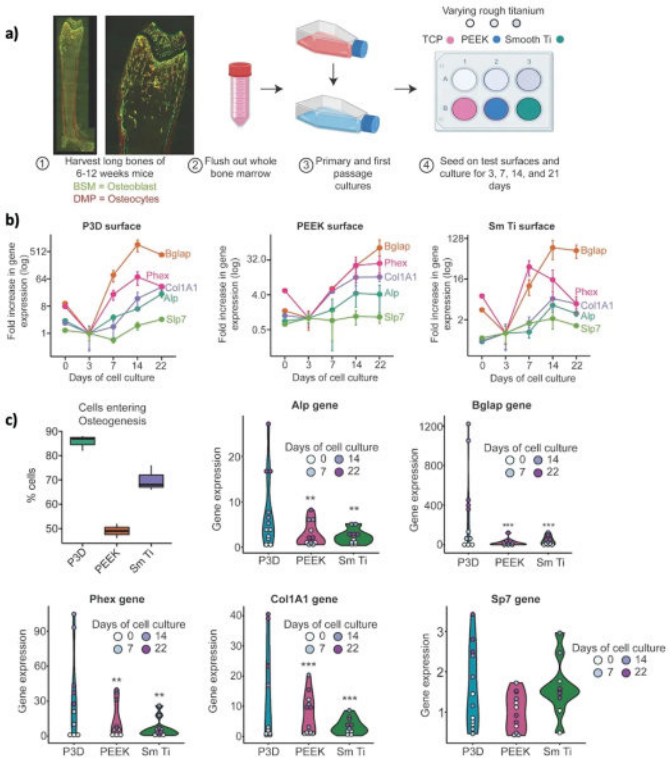

Figure 1. a) Experimental setup b)Osteogenic gene expression over time (day 3, 7, 14 and 22) for the BMSCs cultured on (left) P3D, (middle) PEEK and (right) smooth titanium.
c) Comparison P3D for markers of osteogenic expression versus PEEK and SmTi at each time point of the growth curve.

***Disclosures: Ali Kiapour**, None*

LB SAT-613

Severe Prolonged Hypocalcemia due to Sensipar in a Patient after Monoglandular Parathyroidectomy *Tanya Aggarwal[1], Evgenia Korytnaya[2], Young Min Cho[3]. [1]Northeast Georgia Medical Center, United States, [2]Peach State Endocrinology, United States, [3]Donald & Barbara Zucker School of Medicine, United States

BackgroundCinacalcet is a calcimimetic that is used for treatment of hypercalcemia in patients with primary hyperparathyroidism (PHPT) who are unable to undergo parathyroidectomy. It is sometimes used as a bridge to parathyroidectomy when patients with PHPT present with severe hypercalcemia and surgical treatment is delayed.Case presentationA 78-year-old Caucasian man with hypertension, stage IIIa chronic kidney disease presented from the nursing home (NH) with weakness, and confusion and was found to have a calcium (Ca) level of 15.7 mg/dl, serum creatinine (sCr) of 2.3 mg/dL, PTH of 295.2 pg/ml, phosphorus 1.8 mg/dl. He was treated with intravenous (IV) fluids, subcutaneous calcitonin, and pamidronate IV. Ca and sCr improved to 11.8 mg/dl and 0.95 mg/dl respectively. After discharge, Ca levels increased to 13 mg/dl and he was started on Cinacalcet. ?Computerized tomography of the parathyroid glands showed a solitary right lower pole parathyroid adenoma and parathyroid surgery was planned. Doses of Cinacalcet were gradually titrated over 11 months preceding surgery up to 90 mg three times a day with Ca in the 10-11's

mg/dl range. Monoglandular parathyroidectomy was performed. The patient was readmitted 11 days post-op with Ca 4.7 mg/dl, magnesium 1.2 mg/dl, phosphorus 5.6 mg/dl, vitamin D25OH 113 ng/ml, PTH 16.8 pg/ml, sCr 1.37 mg/dL. A review of the medication list from his NH confirmed the administration of cinacalcet. The patient was started on IV calcium infusion, oral calcium carbonate and calcitriol requiring over 13 grams of elemental calcium per day for two days before his Ca finally improved to 7.7 mg/dl. ?Hypomagnesemia was corrected. Since the patient was on pantoprazole he was switched to calcium citrate (2520 mg of elemental calcium per day) in addition to calcitriol 1 mcg twice a day. Three weeks later hypocalcemia resolved, and he was taken off all supplements.Conclusion:There are currently no guidelines addressing the use of calcimimetics in the preoperative period in patients with PHPT. We describe a case of severe prolonged hypocalcemia due to Cinacalcet in a patient with PHPT who underwent monoglandular parathyroidectomy. There is a need for consensus recommendations addressing the optimal timing for discontinuation of calcimimetics prior to parathyroidectomy. Effective communication between providers involved in the care of such patients is needed to avoid complications

***Disclosures: Tanya Aggarwal**, None*

LB SAT-615

Novel Human Osteoblast Effector Gene EPDR1 Demonstrates Differing Outcomes after Knock-down or Knock-out in Murine In vitro Osteoblastogenesis and During Murine Bone Modeling *Yadav Wagley[1], Parker K. Acevedo[1], Karen Kessell[1], Robert W Goulet[1], Conor S. Locke[1], Tristan Maerz[1], Kenneth M. Kozloff[1], James A Pippin[2], Alessandra Chesi[2], Andrew D. Wells[2], Struan Grant[3], Kurt Hankenson[1]. [1]University of Michigan, United States; [2]Center for Spatial and Functional Genomics, United States; [3]Children s Hospital of Philadelphia / University of Pennsylvania, United States

EPDR1 is a recently characterized human osteoblast effector gene previously identified by intersecting BMD GWAS data with functional genomics in differentiating human mesenchymal stem cells (MSC). Loss of EPDR1 function biases hMSC towards adipogenic differentiation via metabolic and immunologic reprogramming. However, the role of EPDR1 in murine cells and bone development is not known. We generated Epdr1fl/fl mice to investigate its role in osteoblastic and adipogenic differentiation of mouse MSC (mMSC) and to dissect the effect of global loss of EPDR1 function during bone development using whole body knock-out EIIA-Cre mediated genetic recombination. Adenovirus mediated recombination of Epdr1fl/fl mMSC led to a decrease in alkaline phosphatase expression and mineralization similar to our published results with hMSC. The Epdr1 recombined cells showed a general reduction in Runx2, Alpl, Sp7, Ibsp, and Bglap expression suggesting a requirement of EPDR1 function for osteoblastogenesis. However, unlike results observed in hMSC upon EPDR1 silencing, mMSC adipogenesis decreased with Epdr1 recombination and was accompanied by a modest reduction in Pparg gene expression. Next, we crossed the Epdr1fl/fl mice with EIIA-Cre to generate global Epdr1 knock-out mice. These mice appeared normal at birth and showed no developmental abnormalities. Intriguingly, the overall body weight of Epdr1 knockout male mice showed a reduction at 6 months of age that could be associated with reduction in the amount of body fat depots. At the cellular level, mMSC harvested from 1-month old Epdr1-/- showed a minor reduction in mineralization capability, but these differences were not observed with cells harvested from 3- and 6-months old mice. Correspondingly, bone parameters of the 6 months old Epdr1fl/fl and Epdr1-/- mice using microCT imaging of the femurs showed no major genotype differences. Gene expression analysis using the tibial diaphysis and metaphysis from the same mice groups did not establish genotype or sex-specific reduction on bone metabolism. We are currently processing microCT images from the 1-and 3-month-old femur samples, but do not anticipate significant changes. Collectively, these results indicate a compensatory mechanism could exist upon global Epdr1 knock-out in the murine model, and warrants future investigations using conditional loss of Epdr1 function to understand osteoblast and adipocyte cell lineage specific roles in vivo.

***Disclosures: Yadav Wagley**, None*

LB SAT-616

Rapamycin Prevents Senescence and Functional Decline of High-Density Placental Mesenchymal Stem Cells *Kristin Delgado[1], Aaron Sheppard[1]. [1]LSU Health Science Shreveport School of Medicine, United States

Our group has shown that high-density mesenchymal stromal cell (MSC) sheet implantation improves bone healing in a critical-sized bone defect model; however, these cells exhibit increased aging and cellular senescence in prolonged sheet culture, diminishing their therapeutic potential. Promisingly, rapamycin has emerged as a potential agent to rejuvenate aged MSCs. This study aimed to confirm rapamycin's ability to prevent senescence and isolate specific pathways/genes responsible. Human pMSCs were seeded at high density (65,000 cell/cm²) and treated with either rapamycin (10 nM) or control vehicle (DMSO) for up to 7 days. Senescence and autophagy were assessed by senescence-associated ?-galactosidase (SA ?-Gal) staining and DAPI nuclear staining, respectively. Additionally, cell culture media was extracted at different time points to assess senescence-associated cytokines IL-6 and IL-8 via ELISA. Finally, total RNA was extracted for differential gene analysis via GeneChip Clariom A Human Arrays. Rapamycin significantly decreased SA ?-Gal staining at all time points, with 67.7% and 72.9% less area when compared to control at day 4 and 7, respectively. Senescent-associated cytokine IL-6 levels were significantly reduced when compared to control, with 614.3 pg/ml and 286.6 pg/ml decreased at day 2 an 4 of treatment, respectively. Interestingly, IL-8 expression had increased significantly at all time points, with a 979.9 pg/ml difference at day 4 of treatment compared to vehicle. Autophagy-associated vacuoles-stained area had a 3.94-fold increase at day 4 of treatment compared to vehicle. Microarray gene analysis identified a total of 429 genes with a 2-fold or greater change in expression following treatment. FoxO, cellular senescence, and cell cycle pathways are some of many effected with significantly altered expression of FBXO32, PSAT1, CXCL8, and MYC, acting as potential players in rapamycin's anti-aging effects. Rapamycin has proven effective in prolonging pMSC lifespan. Numerous pathways identified in this study may explain rapamycin's anti-aging functionality and lead to the creation of therapeutics specifically targeting relevant genes. The presence of enhanced IL-8 may prove beneficial in stem cell wound healing application. These findings prove rapamycin is a candidate for improving stem cell preparation and support previous studies indicating IL-8 may enhance stem cell viability, results useful in advancing stem cell therapy for bone remodeling.

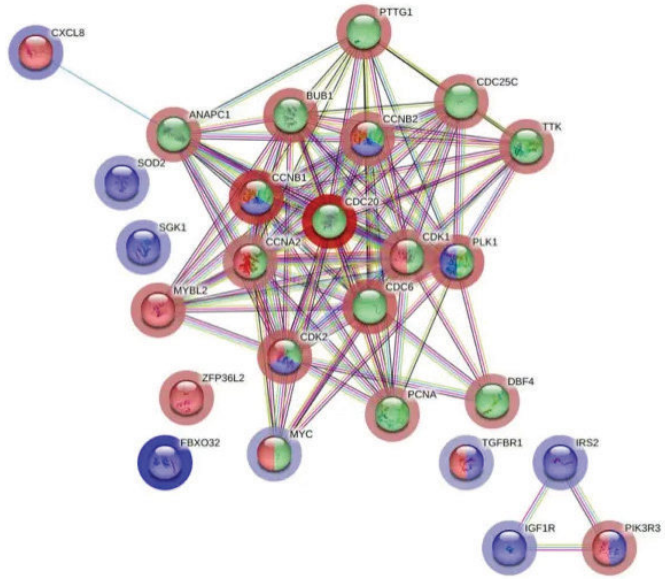

***Disclosures: Kristin Delgado**, None*

LB SAT-617

Investigating The Cell Population That Produces BMP2 In The Periosteum. *David Maridas[1], Laura Gamer[1], Emily Moore[1], Vicki Rosen[1]. [1]Harvard School of Dental Medicine, United States

Our lab previously reported that deletion of BMP2 in Prx1-expressing skeletal progenitors (Bmp2;Prx1 cKO mice) results in longitudinal and appositional growth deficiency of bones in the appendicular skeleton. Additionally, Bmp2;Prx1 cKO mice have fragile long bones that spontaneously fracture and do not heal, reinforcing the central role that BMP2 signaling plays in periosteal function. However, Prx1-Cre targets a wide range of skeletal progenitors, making it unclear if a specific cell population is responsible for producing BMP2. To begin to investigate this question, we used the recently described Ctsk-Cre strain to delete BMP2 in a specific osteogenic subpopulation of cells in the periosteum (Bmp2;Ctsk cKO mice). In contrast to Bmp2;Prx1cKO mice, Bmp2;Ctsk cKO mice did not exhibit alterations in longitudinal or appositional growth at 4 and 12 weeks of age. Concordantly, no spontaneous fractures were detected at 12 weeks of age in Bmp2;Ctsk cKO mice. We then performed femur fractures at 12 weeks of age in Bmp2;Prx1 cKO and Bmp2;Ctsk cKO mice. At 5 days post-fracture, periosteum expansion, callus formation, and chondrogenesis occur similarly in controls and Bmp2;Ctsk cKO mice but are absent in Bmp2;Prx1 cKO mice. Together, our data indicate that Ctsk-Cre driven deletion of BMP2 does not recapitulate the Prx1-Cre phenotype and therefore Ctsk-expressing cells are not a critical source of BMP2 in the periosteum. We were also curious about whether Prx1-Cre deletion of BMP2 results in the loss of the cell population that normally produces BMP2 in the periosteum. To investigate this possibility, we crossed mice carrying the Bmp2-LacZ knock-in (loss of function allele) with the Bmp2;Prx1 cKO mice. In this mouse model (Bmp2;Prx1/LacZ cKO), BMP2 is deleted from the long bones because the LacZ knock-in gene is nonfunctional. However, cells that would otherwise produce BMP2 will be LacZ positive. We found that Bmp2;Prx1/LacZ cKO mice recapitulated the longitudinal and appositional growth phenotype of the Bmp2;Prx1 cKO mice. When fractured, the periosteum of the Bmp2;Prx1/LacZ cKO mice did not expand and callus formation did not occur, yet we detected LacZ staining in cells located at the fracture site, indicating that the cell population responsible for producing Bmp2 during fracture is still present in the adult periosteum even with deletion of Bmp2 with Prx1-Cre. In summary, our data suggest that a subpopulation of periosteal cells that are

Prx1-positive but Ctsk-negative produce BMP2 in the periosteum. Additionally, these cells survive but are dysfunctional in the absence of BMP2.

***Disclosures: David Maridas**, None*

LB SAT-618

Integrated microRNA-mRNA analyses of the osteogenic induction of a helioxanthin derivative in human dental pulp stem cells *Yasuyuki Fujii[1,] Sakura Minami[2,] Ayano Hatori[2,] Yoko Kawase-Koga[3,] Toru Ogasawara[4,] Hayato Hamada[2,] Yuki Kanno[2,] Daichi Chikazu[2,] [1]Tokyo medical university, Japan, [2]Tokyo Medical University, Japan, [3]Tokyo Women's Medical University, Japan, [4]The University of Tokyo, Japan

Dental pulp stem cells (DPSCs) have high proliferative and multilineage differentiation potential in mesenchymal stem cells. Many studies have reported that DPSCs have osteogenic differentiation ability and that small chemical compounds induce osteogenesis of DPSCs. We previously reported that the helioxanthin derivative 4-(4-methoxyphenyl) pyrido[40,30:4,5]thieno[2,3-b]pyridine-2-carboxamide (TH), an osteogenic small molecule, induced the osteogenic differentiation of DPSCs. However, this osteogenesis mechanism of TH in DPSCs are still unknown. The purpose of this study was to identify functional exosomal microRNAs (miRNAs) and the key genes involved in the TH-induced osteogenesis of DPSCs.DPSCs were obtained from dental pulp of the wisdom teeth of three healthy patients and cultured with or without TH (approval No. T2020-0343 by the Institutional Ethics Committee of the Faculty of Medicine, Tokyo Medical University, Japan; approved on January 5, 2021). miRNAs were extracted from DPSCs-derived exosomes. These gene expression patterns were compared using RNA-Seq and miRNA-Seq. To investigate the specific miRNA/mRNA interacting network, these data were analyzed and the functional analyses were generated through the use of Ingenuity Pathway Analysis (IPA, QIAGEN Inc.).Alkaline phosphatase (ALP) staining showed that TH enhanced ALP activity in DPSCs at 7 days. RT-PCR analyses showed that TH-induced DPSCs had significantly higher expression levels of ALP and type 1 collagen alpha 1 in day 7. RNA-Seq and miRNA-Seq showed 869 differentially expressed genes (DEGs) and 18 miRNA-DEGs. Integrated miRNA-mRNA analyses showed these miRNAs have the targeting information of 277 mRNAs in DEGs. Among them, 24 target genes known to be involved in the differentiation of bone cells and 17 target genes known to be involved in the differentiation of osteoblasts were identified. The upstream regulator analysis predicted WNT3a may be responsible for gene expression changes in DPSCs after TH stimulation.The exosomal miRNA regulatory networks might play vital roles in TH-induced osteogenic differentiation of DPSCs. These results provide support for further investigations into the mechanism of osteogenesis in DPSCs.

***Disclosures: Yasuyuki Fujii**, None*

LB SAT-619

Deletion of Ror2 in skeletal muscle promotes intramuscular adipogenesis during aging *Martina Pauk[1,] Hiroaki Saito[1,] Eric Hesse[1,] Hanna Taipaleenmäki[1,] [1]1 Institute of Musculoskeletal Medicine, University Hospital, LMU Munich, Munich, Germany; 2 Musculoskeletal University Center Munich, University Hospital, LMU Munich, Munich, Germany, Germany

Decline in skeletal muscle function during aging involves the accumulation of fatty and fibrotic tissue within muscles. Recently, a specific group of stromal cells called fibro-adipogenic progenitors (FAPs) has been identified as the cellular source of fat and fibrous deposits in muscles. However, the mechanisms behind the differentiation of FAPs into adipocytes or fibroblasts are not well understood. To investigate this question, we isolated FAPs from mouse muscles and induced their differentiation into adipogenic and fibroblast lineages. During this process, an increased presence of the non-canonical Wnt receptor Ror-family receptor tyrosine kinases 2 (Ror2) was observed, suggesting a potential role for Ror2 in the differentiation of adipocytes and fibroblasts. Indeed, inhibition of Ror2 using siRNA, enhanced adipocyte differentiation of FAPs, as indicated by increased Oil Red O staining and the expression of adipogenic markers such as Ppar?, Adiponectin, Perilipin, and Fabp4. On the other hand, absence of Ror2 reduced the differentiation of FAPs into fibroblasts, as demonstrated by decreased collagen production and deposition. To further investigate the impact of Ror2 on the age-related decline of muscle function in vivo, we generated mice with a specific deletion of Ror2 in their skeletal muscles using the Cre-recombinase under the control of the 1.5 kb fragment of the mouse myogenin promoter and the 1 kb mouse Mef2c enhancer element (Myo-Cre+). Muscle-specific deletion of Ror2 in aged female mice (40-55 weeks old) did not affect body weight, muscle weight, or myofiber size. However, it significantly decreased the function of the soleus muscle in Myo-Cre+;Ror2fl/fl mice compared to control, as evidenced by reduced ex vivo muscle contractility and endurance. Histological analysis revealed the infiltration of inflammatory mononuclear cells and necrotic fibers in the muscles of Myo-Cre+;Ror2fl/fl mice, along with increased fatty deposits detected by Oil Red O staining. In summary, our study uncovers the role of Ror2 in regulating FAP differentiation in vitro, while its deletion in muscle leads to increased intramuscular adipogenesis during aging, potentially contributing to reduced muscle function. These findings provide new insights into the function of FAPs and non-canonical Wnt signaling, thereby improving the understanding of age-related decline in muscle function.

***Disclosures: Martina Pauk**, None*

LB SAT-620

VITamin D and OmegA-3 TriaL (VITAL): Genetics, Vitamin D Biomarkers, and Fractures *Meryl LeBoff[1,] Sharon Chou[1,] Dana Ratnarajah[1,] Nancy Cook[1,] Franco Giulianini[1,] Julie Buring[1,] JoAnn Manson[1,] Daniel Chasman[1,] [1]Brigham and Women's Hospital , United States

Supplemental vitamin D is commonly used in the general population to improve bone health. We recently reported that supplemental vitamin D3 (2000 IU/d) vs. placebo did not reduce total, nonvertebral, and hip fractures in 25,871 generally healthy U.S. men (aged >=50) and women (aged >=55) enrolled in the VITamin D and OmegA-3 TriaL (VITAL). The objective of this study was to evaluate modification of randomized vitamin D supplementation by genetic variation in vitamin D metabolism, absorption, and receptor function for 1) changes in vitamin D biomarkers (total 25OHD, PTH and calcium) and 2) incident fractures in a case-cohort. Genotyping using the Global Screening Array was performed by Erasmus Medical Center Rotterdam (Netherlands), with imputation to the TOPMed reference panel. Candidate single nucleotide polymorphisms (SNPs) were selected from vitamin D-related pathways (CYP27A1 [2 SNPs], GC/DBP, CD36, NPC1L1, CYP2R1, FGF23, VDR [2 SNPs], CYP27B1 [2 SNPs], SCARB1, and CYP24A1). Total 25OHD, PTH, and calcium blood levels were measured at baseline and two years of follow-up. Incident fractures in VITAL were reported on annual questionnaires and adjudicated by medical record review. The sample for this study was restricted to individuals of European ancestry (verified by genetics) and comprised of nested incident cases of fractures (N= 834) and an age/sex-matched subcohort (N= 847) selected at random from ~72% of VITAL participants who consented to genetic analysis. This case/subcohort was 68% female with mean (+/-SD) age of 70.4+/-6.8 years and BMI of 26.8+/-5.1 kg/m2. We tested for significant interaction between an additive encoding of genetic variants and randomized vitamin D vs. placebo allocation in association with 2-year changes in blood levels of total 25OHD (N=440), PTH (N=442), and calcium (N=336) and incident fractures. There were no interactions between candidate variants and randomized vitamin D vs. placebo allocation for these circulating measures of vitamin D supplementation or for incident fractures in models adjusted for age, sex, and BMI (Table 1). In VITAL, genetic differences in vitamin D-related pathways did not 1) predict biochemical response to vitamin D supplementation or 2) reveal any genetic profiles that may confer a benefit of vitamin D supplementation on fracture risk. Future VITAL studies will focus on an expanded set of pharmacogenetic hypotheses involving effects of supplemental vitamin D on bone and musculoskeletal outcomes.

Table 1. Fracture SNP Associations adjusted for age, sex, and BMI

Gene	SNP.rs	b	Hazard Ratio	Standard Error	p for interaction
CYP27A1	rs1996992	0.20	1.22	0.07	0.56
CYP27A1	rs13020432	0.08	1.08	0.04	0.48
GC/DBP	rs3755967	-0.23	0.80	0.04	0.50
CD36	rs1049673	0.04	1.04	0.05	0.71
NPC1L1	rs2073547	-0.15	0.86	0.04	0.45
CYP2R1	rs12794714	-0.20	0.82	0.04	0.34
FGF23	rs7955866	0.29	1.33	0.05	0.85
VDR	rs117913411	0.13	1.14	0.08	0.77
VDR	rs117843845	1.10	2.99	0.08	0.08
CYP27B1	rs703842	-0.05	0.95	0.04	0.72
CYP27B1	rs749972457	0.04	1.04	0.04	0.51
SCARB1	rs7485656	-0.11	0.90	0.05	0.73
CYP24A1	rs2762943	-0.05	0.95	0.07	0.57

***Disclosures: Meryl LeBoff**, NIH: 5R01AR059775-09 , Grant/Research Support, Amgen, Major Stock Shareholder, Johnson & Johnson , Major Stock Shareholder, NIH: 5R01AR070854-05 , Grant/Research Support, NIH: 5R01AG071611-03 , Grant/Research Support*

LB SAT-621

Sex differences in the relationship between body fat, vitamin D status and biomarkers of bone and fat metabolism in adult men and women. *Marina Bonanno[1,] Gretel Pellegrini[1,] graciela brito[1,] beatriz oliveri[1,] Susana Noemi Zeni[1,] [1]INIGEM, Argentina

Evidence from diverse studies suggests that obesity is associated with low vitamin D (VD) status evaluated by the levels of 25 hydroxyVD (25HOD). Fat sequestration of VD in fat mass has been pointed out as a plausible explanation for this low levels of circulating VD. Although obesity can be assessed by body mass index (BMI), body fat content appears to provide a clearer picture of health. Our objective was to evaluate according to ranges of obesity the correlation between circulating 25HOD levels, total osteocalcin (OCN), undercarboxilated OCN (ucOCN) and the development of insulin resistance in obese adult women and men. As OCN is involved in glucose homeostasis and to avoid the close relation between obesity and impaired glucose homeostasis we only included in the study, non-diabetic subjects of both genders with normal levels of glycemia and HbA1c, presenting overweight (OW) and obesity (O). Participants aged 40 to 79 years (50 men and 143 women; 96 post and 47 premenopausal) were grouped according to sex and age (40-59 and >60 years). After body composition was recorded by bioimpedance, they were classified according to body fat percentage (%BF) (30-39 or >40). Glucose , triglycerides, HDL cholesterol and waist cir-

cumference (WC) were measured by habitual methods and insuline, leptin, 25HOD and total osteocalcin (OCN) by ELISA. BMI and Insulin resistance was also calculated. Some results (mean +/- SD) are shown as <40 or 40 to 60 years in the following order: men OW and O, women OW BMI (kg/m2): 29.1+/-0.3.a 37.5+/-7.5b 28.9+/-1.49a 37.2+/-7.31b 29.2+/-0.6a 37.3+/-4.9b 28.0+/-1.7a 34.2+/-4.5b% BF: 35.6+/-5.2a 42.5+/-5.4b 35.4+/-1.7a 49.0+/-8.2b 35.5+/-6.2a 45.8+/-4.7b 39.4+/-1.9a 49.1+/-6.9bCC (cm): 105.1+/-1.5a 120.0+/-17.2b 93.6+/-8.1a 108.8+/-15.1a 103.5+/-0.7a 120.1+/-6.7b 9.7+/-9.2a 105.7+/-9.5aGlu (mg/dL): 97.7+/-22.7 99.9+/-17.4 91.1+/-11.8 96.4+/-18.3 95.5+/-30.4a 104.9+/-12.2b 98.2+/-7.2a 97.2+/-10.8aLeptina (ng/ml): 2.4+/-1.9a 15.9+/-15.2c 11.1+/-5.7b 28.3+/-15.7d 2.72+/-3.1a 13.1+/-6.7c 9.6+/-6.0b 21.1+/-13.2dVitamina D (ng/ml): 24.9+/-6.8b 17.4+/-7.4a 20.8+/-6.8b 18.4+/-6.3a 25.0+/-8.5b 17.2+/-4.7a 25.9+/-9.8b 20.0+/-7.5aOCN (ng/mL): 31.1+/-0.5.c 18.6+/-12.6a 32.7+/-10.2c 26.1+/-12.7b 30.4+/-0.2c 30.9+/-13.8c 30.6+/-15.8c 25.6+/-15.9aDifferent letters indicate a p<0.05. 25HOD correlated with %BF but not with BMI Conclusion: The results suggest that the associations of body fat and 25(OH)D was sex-specific, with greater clarity when %BF was used instead of BMI to classify obesity.

***Disclosures: Marina Bonanno**, None*

LB SAT-623

Effects of IL-17 Blockade on Skeletal Microarchitecture in Patients with Axial Spondyloarthritis: An HR-pQCT Study *Insa Mannstadt[1], Donald McMahon[2], Douglas N Mintz[1], Weija Yuan[1], Linda Russell[1], Emma Billings[3], Susan M Goodman[1], Dalit Ashany[1], Emily Stein[1]. [1]Hospital for Special Surgery, United States. [2]Columbia University College of Physicians and Surgeons, . [3]Hospital for Special Surgery ,

Axial spondyloarthritis (AxSpA), a chronic inflammatory rheumatic disease, causes abnormal bone growth at the spine and paradoxically has been linked to osteoporosis and fragility fractures. While tumor necrosis factor alpha inhibitors have been shown to improve skeletal health in patients with AxSpA, the effect of newer medications that block interleukin-17 (IL-17) on bone metabolism remains unclear. This prospective study investigated the impact of IL-17 blockade on bone density (BMD) and microarchitecture in AxSpA. We hypothesized that treatment initiation would be associated with improved BMD and microarchitecture. Skeletal assessments included areal BMD (aBMD) and trabecular bone score (TBS) by DXA, volumetric BMD (vBMD) and microarchitecture by high-resolution peripheral QCT (HRpQCT2) at baseline and 12-months. DXA and HRpQCT measurements from patients were compared to those of age and sex-matched individuals in reference cohorts. Changes in imaging parameters were compared using Wilcoxon and paired t-tests, and predictors of change in HRpQCT were analyzed using multivariate linear regression. Of the 22 AxSpA participants, 55% were female (33% postmenopausal), mean age was 40 years, and mean BMI 30 kg/m2. Half (55%) were HLAB27 positive, mean symptom duration was 10 years, and C-reactive protein (CRP) was elevated in 32% of participants. At baseline, mean DXA and HRpQCT Z-scores were within one standard deviation of the healthy reference population. At 12-months, >80% of participants reported 100% medication adherence. Standardized assessments of disease activity improved, with a decrease in Bath Ankylosing Spondylitis Disease Activity (BASDAI -33%, p<0.01) and Metrology Index (BASMI -22%, p=0.01; Table) There was no significant change in aBMD or TBS. By HRpQCT at the radius, declines were observed in total vBMD (-2%, p=0.04) and trabecular vBMD (-2%, p=0.04). Radial trabecular separation tended to increase (4%, p=0.06). Elevated CRP tended to be associated with the decline in total vBMD (R=0.55, p=0.09). In summary, participants with AxSpA who began IL-17 blockade experienced significant improvements in clinical symptoms but had no change or small declines in BMD and microarchitecture. As our study was not controlled, we lack data regarding whether treatment may have attenuated larger declines associated with disease progression. Larger, controlled studies are needed to further investigate the long-term skeletal effects of IL-17 blockade.

Table: 12-Month Changes in Disease Characteristics and Skeletal Indices After Initiation of IL-17 Blockade

	Baseline	12-months	% change	p-value
Axial Spondylarthritis disease metrics, mean (SD)				
mSASSS	42 (21)	41 (22)	3.2 (21.6)	0.62
BASDAI	**4.8 (2.0)**	**3.2 (2.4)**	**-33.3 (45.8)**	**0.003**
BASMI	**2.62 (1.5)**	**2.1 (1.6)**	**-24.4 (41.9)**	**0.01**
RADIUS HR-pQCT, mean (SD)				
Total vBMD	**313.6 (64.2)**	**301.2 (59.5)**	-2.4 (4.9)	**0.04**
Cortical vBMD	905.5 (72.5)	894.9 (69.4)	-0.6 (1.9)	0.17
Trabecular vBMD	**147.5 (28.4)**	**144.8 (27.0)**	-2.1 (4.5)	**0.04**
Cortical thickness	1.0 (0.21)	1.0 (0.22)	0.57 (7.9)	0.74
Trabecular number	1.5 (0.23)	1.4 (0.22)	-2.2 (6.5)	0.15
Trabecular separation	0.68 (0.13)	0.66 (0.12)	-3.03 (5.1)	0.60
Trabecular thickness	0.22 (0.01)	0.22 (0.01)	0.3 (4.0)	0.73

*Abbreviations: mSASSS (modified Stoke Ankylosing Spondylitis Spinal Score), BASDAI (Bath Ankylosing Spondylitis Disease Activity Index), BASFI (Bath Ankylosing Spondylitis Disease Activity Index), BASMI (Bath Ankylosing Spondylitis Metrology Index), vBMD (volumetric bone mineral density). Bold values indicate p<0.05).

***Disclosures: Insa Mannstadt**, None*

LB SAT-624

Protein phosphatase PPM1A maintains bone homeostasis via regulating TGF-?/Smad2 signaling in osteoblast *Qinwen Ge[1], Kai-ao Zou[1], Ping-er Wang[1], Luwei Xiao[1], Di Chen[2], Xia Lin[3], Peijian Tong[1], Hongting Jin[1]. [1]Institute of Orthopaedics and Traumatology, The First Affiliated Hospital of Zhejiang Chinese Medical University, China. [2]Shenzhen Institutes of Advanced Technology, Chinese Academy of Sciences, China. [3]Zhejiang University, China

Protein phosphatase magnesium-dependent 1A (PPM1A) is a member of the metal-dependent phosphatases family while its role in maintaining bone homeostasis and the precise mechanism by which PPM1A regulates osteogenesis is still largely not elucidated. To explore the role of PPM1A in bone homeostasis in vivo, we generated global Ppm1a knockout (KO) mice. The ?-CT analysis showed that PPM1A deficiency dramatically decreased trabecular bone mass at distal femur metaphysis and lumbar vertebra, but did not alter cortical bone morphology. Compared to wild-type mice, KO mice had lower osteocalcin and ALP expression and unchanged expression of osteoclastic marker cathepsin K. Also, double calcein labelling assay and von Kossa staining revealed Ppm1a ablation reduced trabecular bone mineral apposition. Moreover, KO mice displayed a diminished bone regeneration ability after femoral bone marrow ablation. In vitro, we found an increased Ppm1a mRNA expression during osteogenesis. Conversely, primary osteoblast isolated from KO mice exhibited an impaired osteogenesis as supported by the decreased mRNA expressions of osteogenic genes and reduced ALP staining and ARS staining intensity. Mechanistically, we noted that Ppm1a deficiency reduced the dephosphorylation of Smad2, causing excessive TGF-? signaling, and co-immunoprecipitation assay confirmed the interaction between PPM1A and p-Smad2 in osteoblast. Importantly, Ppm1a?/? osteoblast treated with SD-208, a selective inhibitor for TGF-?/Smad2 signaling activation, showed a restored bone formation phenotype as determined by the increased mRNA expression of osteogenic gene and ALP staining. Similarly, SD-208 treatment in vivo largely rescued the osteogenesis defects and impaired bone regeneration in KO mice, suggesting PPM1A promoted bone formation and bone regeneration mainly by regulating TGF-?/Smad2 signaling. Additionally, we identified that Miltefosine (MF), an FDA approved anti-leishmanial drug, which has been recently reported as a PPM1A activator for Alzheimer's disease, could facilitates osteogenesis in vitro and enhance bone regeneration in vivo while Ppm1a deletion completely blocked this bone anabolic action. Simultaneously, we demonstrated that MF administration strikingly alleviated bone loss in ovariectomy-induced mice. Taken together, this study revealed that PPM1A promoted osteoblastic bone formation via regulating TGF-?/Smad2 signaling and highlighted the potential of MF for osteoporosis treatment.

***Disclosures: Qinwen Ge**, None*

LB SAT-625

Regulation of differential expression and spatial distribution of the endosomal proteins in osteoblasts *Waddell Holmes[1], Marcus Winogradzki[1], Shreya Patel[1], Ahmad Othman[2], Niyati Patel[1], Ryan Ross[1], Jitesh Pratap[1]. [1]Rush University Medical Center, United States. [2]Northwestern University, United States

Recent transcriptomics and proteomics studies with differentiating osteoblasts (OB) revealed endosomal proteins as the most prominent upregulated cluster. The endosomal pathway regulates the fate of the internalized molecules to the plasma membrane, trans-Golgi network, or the lysosome. Endosomes also serve as a platform to control the growth factor signaling output. However, the regulation of expression and subcellular distribution of endosomes during osteoblast differentiation are currently unknown. Here, we utilized multiple OB models to examine the levels and subcellular distribution of the endosomal pathway-related genes via qRT-PCR, western blotting, and confocal microscopy. We found upregulation of mRNA and protein levels of Syntaxin 6 (STX6) and Rab5 in differentiating mouse IDG-SW3 osteoblasts. We found significant upregulation of mRNA levels of early endosomal antigen-1 (EEA1) and Rab7 while protein levels remain unchanged.?Next, to understand the regulation of expression levels and subcellular distribution, we examined the role of Runx2, a master regulator of osteoblast differentiation. We utilized WT and Runx2 knockout (KO) calvarial osteoblasts and found a significant reduction in EEA1 and increased levels of Caveolin-1 and Rab11 in Runx2 KO cells. The distribution and trafficking of endosomes depends on the stability of microtubules (MTs), therefore, we treated OB with MT-targeting agents and found that stabilizing MTs via docetaxel treatment increases the endosomal protein levels. Interestingly, MT depolymerization via vinblastine or nocodazole resulted in the aggregation of EEA1 puncta in Runx2 KO cells without changing the protein levels. Stabilization of MTs via tubacin treatment also yielded endosomal aggregation. These results indicate that changes in the MT dynamics and Runx2 levels can differentially regulate endosomal distribution. Data analysis of Runx2 ChIP-seq studies revealed Runx2 recruitment on STX6 promoter, suggesting a novel Runx2 target gene. Finally, to determine the effect of nutritional stress on endosomal proteins, we examined the serum- and glucose- starved OB and found reduced levels of Rab5 and Rab7.? Taken together, our studies identified the key changes in the endosomal landscape during osteoblast differentiation. Our findings suggest a novel regulation of OB differentiation via endosomal pathway proteins.

***Disclosures: Waddell Holmes**, None*

LB SAT-626

Foci-Xpress: Automated and fast nuclear foci counting tool *Woo-Jin Kim[1], Ki-Tae Kim[1], Hyun-Jung Kim[1], Hye-Rim Shin[1], Heein Yoon[1], Seung Gwa Park[1], Min-Sang Park[1], Hyun-Mo Ryoo[1], Jae-I Moon[1]. [1]Seoul National University, Republic of Korea

Quantification of DNA damage-induced foci can be used to determine DNA damage caused by oxidative stress, radiation, or aging. ?H2AX, a form of phosphorylated histone H2AX induced by DNA double-strand breaks, is one of the most sensitive markers of DNA damage. Counting foci is tedious and time-consuming for researchers. We developed open-source software that automatically counts the number of foci from the indicated image files. We compared the ?H2AX foci counting efficiency, velocity, accuracy, and convenience of the Foci Xpress with those of other conventional methods in an oxidative DNA-induced model. We can adjust the brightness of ?H2AX foci to designate a threshold of foci and assign damaged cells that have 10 or more foci over the threshold in the nucleus. The Foci-Xpress method was much faster than other conventional methods. The accuracy was similar to that of conventional methods. The biggest strength of Foci-Xpress was automation, which freed researchers from analysing equipment while counting. The greater the number of images to be counted, the greater the number of advantages. In addition, automation completely ruled out biases caused by researchers, such as individual or daily variations. Thus, Foci-Xpress is a convincing, convenient, and easily accessible focus-counting tool for cell biologists.

***Disclosures: Woo-Jin Kim**, None*

LB SAT-627

Deciphering the osteoclast regulatory microenvironment *MASAYUKI TSUKASAKI[1], Minglu Yan[2], Kazuo Okamoto[3], Hiroshi Takayanagi[4]. [1]The University of Tokyo, Japan. [2]Department of Immunology, Graduate School of Medicine and Faculty of Medicine, The University of Tokyo, Japan. [3]Department of Osteoimmunology, Graduate School of Medicine and Faculty of Medicine, The University of Tokyo, Japan. [4]The University of Tokyo, Graduate School of Medicine and Faculty of Medicine, Japan

Osteogenic cells play a central role in osteoclast regulation by producing RANKL and OPG. However, the precise molecular mechanisms underlying RANKL/OPG expression have not been fully understood. We explored the epigenomic landscape of osteogenic cells and identified a hitherto undescribed enhancer region in the TNFSF11 gene locus. Transcription factors involved in cell death and senescence act on this enhancer region, and genetic deletion of the enhancer leads to a high bone mass phenotype with decreased osteoclastogenesis. To characterize the OPG-producing osteogenic cells, we analyzed sc-RNAseq data and identified an extracellular matrix factor (EMF) as a marker for OPG-expressing cells. EMF-Cre mediated deletion of OPG resulted in severe osteopenia whereas RANKL-floxed EMF-Cre mice exhibit normal bone volume. Thus, OPG and RANKL are produced by distinct osteogenic subtypes, highlighting the functional diversity of osteogenic cells and the molecular mechanism of osteoclast regulation

***Disclosures: MASAYUKI TSUKASAKI**, None*

LB SAT-628

Senescence osteoclast precursors induce SASP through cGAS-STING *Hirokazu Hattori[1], Kazuki Takaoka[1], Tomoki Kakimoto[2], Sachiko Nosaka[1], Ayaka Hatanaka[1], Masayuki Oshitani[1], Miho Ueta[1], Kazuma Noguchi[1], Hiromitsu Kishimoto[1]. [1]Department of Oral and Maxillofacial Surgery, School of Medicine, Hyogo Medical University, Japan. [2]Department of Oral and Maxillofacial Surgery, School of Medicine, Hyogo Medical University , Japan

Senescence is an unexplained life phenomenon. In recent years, it has become clear that senescent cells do not simply stop cell growth but secrete various proteins such as inflammatory cytokines and chemokines. This secretory phenomenon is called senescence-associated secretory phenotype (SASP). Cyclic GMP-AMP synthase-stimulator of interferon genes (cGAS-STING) pathway, known as an innate immune pathway against DNA during viral infection, has been shown to induce SASP. We hypothesized that SASP factors released by osteoclast precursors (OCPs) undergoing cellular senescence with aging may affect the bone microenvironment. The purpose of this study is to elucidate the differentiation of senescent OCPs and the effects on SASP.RAW264.7 cells were used as OCPs and were cultured to passage (P)5, P10 and P20. To assess replicative senescence, the protein expressions of p53 and p-H2A.X, SA-?-gal, and telomere length were evaluated. To evaluate the ability to differentiate into osteoclasts, the expressions of TRAP and RANK and NFATc1 were evaluated. The concentration of SASP factors (IL-6, TNF-?, NO) in the culture supernatant were measured by ELISA. We extracted exosomes from the culture supernatant. The number of exosome particles was measured by ELISA and the expression of SASP factors (TGF-?1, HIF-1?, iNOS) in exosomes by western blotting, and the expression of miRNAs in exosomes were evaluated. To evaluate SASP induction pathway, the expressions of cGAS-STING pathway were assessed by western blot and ELSIA.P20 showed replicative senescence, and significantly decreased ability to differentiate into osteoclasts compared to P5 and P10. The protein expression levels of RANK and NFATc1 in cells treated with RANKL at P20 were decreased compared with those at P5 and P10. The concentration of SASP factors in the culture supernatant at P20 were significantly increased compared with those at P5 and P10. The number of exosomes at P20 was increased compared with that at P5 and P10. The protein expression level of iNOS in exosomes at P20 was increased compared with that at P5 and P10. The expression of cGAS-STING pathway was significantly elevated at P20.In conclusion, cellular senescence reduces RANKL-induced osteoclastic differentiation of RAW264.7 cells by inhibiting RANK expression. Senescent RAW264.7 cells increase production of SASP factors via cGAS-STING pathway and then release iNOS in exosomes..

***Disclosures: Hirokazu Hattori**, None*

LB SAT-629

The anti-osteoclastic effects of the novel geranylgeranyl diphosphate synthase inhibitor RAM2061 *Molly Muehlebach[1], Sarah Holstein[1], Yashpal Chonker[1], DJ Murry[1]. [1]University of Nebraska Medical Center, United States

Myeloma bone disease affects nearly 90% of myeloma patients, significantly impacting patient morbidity and quality of life. Current treatments include bisphosphonate therapy or monoclonal antibody denosumab, but while both treatments have been found to prevent further skeletal related events, they can be associated with adverse events such as kidney damage and osteonecrosis of the jaw. Our lab has developed a novel bisphosphonate, RAM2061, which inhibits the enzyme geranylgeranyl diphosphate synthase (GGDPS) and has been shown to have anti-myeloma effects in vitro and in vivo. In myeloma cells, we have found RAM2061 depletes intracellular levels of isoprenoid donor geranylgeranyl pyrophosphate (GGPP) necessary for the post-translational modification (geranylgeranylation) of Rab proteins. By inhibiting Rab geranylgeranylation in these cells, Rab-mediated intracellular trafficking is disrupted, inducing ER stress and subsequent apoptosis. Understanding that osteoclasts rely heavily on secretory pathways for bone resorption, we were interested in investigating whether RAM2061 could impair osteoclast activity in the same manner. We hypothesized that RAM2061 will disrupt Rab and Rho protein geranylgeranylation, disrupting intracellular trafficking and cytoskeletal rearrangement necessary for osteoclast function. In RAW264.7 pre-osteoclast cells we demonstrated that RAM2061 induces ER stress and the unfolded protein response pathway (UPR)-mediated apoptosis in a concentration-dependent manner. In mature osteoclasts, we found RAM2061 disrupts osteoclast differentiation by significantly downregulating expression of osteoclast-specific genes and inhibiting tartrate resistant acid phosphatase-positive osteoclast formation. Furthermore, we found RAM2061 inhibits osteoclast resorption at concentrations as low as 200 nM. Upon further investigation, we determined RAM2061 to disrupt Rho protein geranylgeranylation, inhibiting Rho signaling and cytoskeletal rearrangement essential for osteoclast differentiation and function. Therefore, these studies reveal that RAM2061 may represent a novel therapy for treatment of myeloma bone disease and potentially other osteoresorptive diseases.

***Disclosures: Molly Muehlebach**, None*

LB SAT-630

Atenolol reduces human osteoclast resorption, but not differentiation in vitro *Tyler Roy[1], Rebecca Peters[4], David Monroe[3], Aaron Brown[4], Sundeep Khosla[5], Christine Lary[6], Katherine Motyl[7]. [1], [4]MaineHealth Institute for Research, [3]Mayo Foundation, United States. [4]MaineHealth Institute for Research, United States. [5]Mayo Clinic College of Medicine, United States. [6]Northeastern University, [7]MaineHealth, United States

?-adrenergic receptor antagonists (a.k.a. ?-blockers) are associated with increased bone mineral density and reduced fracture risk. In addition to osteoblast-mediated suppression of RANKL, we have shown that ?-blockers also directly suppress primary mouse osteoclastogenesis. While mouse models are convenient for studying osteoclast (OCL) function, primary human OCLs are needed to increase clinical relevance of our findings. Here, we report our protocol for culturing functional OCLs from human peripheral blood mononuclear cells (HPBMCs) isolated from patient-derived blood samples. Specifically, we are using this protocol in an ongoing ancillary study to the Atenolol for the Prevention of Osteoporosis (APO) clinical trial (NCT04905277) to test the effectiveness of atenolol, a ?-blocker on primary osteoclasts derived from women aged 50 to 75. To limit estrogen receptor activity and promote osteoclast differentiation, HPBMCs are cultured in an osteoclastogenic media composed of phenol red-free ?-MEM, charcoal-stripped FBS, M-CSF, and RANKL. OCLs are cultured on plastic and bone slices for 14 days with either vehicle (H2O) or atenolol (15 ?M) throughout osteoclast differentiation. To assess osteoclast number and size, mature osteoclasts cultured on plastic and bone slices are fixed on day 14 and stained for tartrate-resistant acid phosphatase (TRAP). Osteoclasts are imaged and analyzed for number and total TRAP positive area using a semi-automated method we developed using ImageJ. Additionally, media is collected from bone slices on day 14 to quantify levels of carboxy-terminal collagen crosslinks (CTX-1) as a measure of bone resorption. While preliminary data shows atenolol does not affect the number of OCLs or total area covered on bone slices (n=18 participants, with at least 5 replicates each), CTX-1 levels are significantly reduced (59%, p=0.0063, n=8) with 15 µM atenolol treatment throughout all of differentiation. In summary, atenolol treated osteoclasts are less efficient at resorbing bone, which complements the known effect of atenolol to suppress RANKL expression in osteoblasts. While these findings support atenolol as a therapy to prevent osteoporosis, ongoing studies will be necessary to

determine how atenolol influences bone density in vivo and investigate additional molecular and genetic mechanisms of bone loss prevention.

***Disclosures: Tyler Roy**, None*

LB SAT-631

YAP and TAZ regulate adult bone formation and osteocytic bone remodeling

*YASAMAN MOHARRER[5], Ghazal Vahidi[2], DANIEL HORAN[3], TALA AZAR[4], Annemarie Lang[5], Alexander Robling[3], Xiaowei Liu[6], Chelsea Heveran[7], Joel Boerckel[6]. [5]University of Pennsylvania , [2]Montana state university , [3]Indiana University, United States, [4], [5]University of Pennsylvania , United States, [6]University of Pennsylvania, United States, [7]Montana state university, United States

Physical activity induces skeletal adaptation. However, the mechanotransductive mechanisms are unclear. Previously, using genetic methods, we found that the mechanosensitive transcriptional regulators, YAP and TAZ, regulate bone growth and osteocyte network formation. Here, we use global inhibition approaches to test the roles of YAP/TAZ in adult bone growth and osteocyte peri-lacunar remodeling.We injected 8-week-old male C57Bl/6J mice with DMSO or verteporfin (VP) for 2 weeks. VP inhibits YAP/TAZ-TEAD interaction. We evaluated bone formation by Calcein and Alizarin labeling, injected 7 days apart, and quantified the extent of mineralized bone surface (MS/BS), mineral apposition rate (MAR), and bone formation rate (BFR) in coronal and transverse tibial sections. Using a confocal microscope, we identified fluorochrome-labeled osteocytes lacuna, quantified the fluorescence intensity, and measured the lacunae mineral extent. By immunofluorescent staining on coronal sections, we checked if YAP/TAZ inhibition impacts other cell types. We quantified fracture toughness from the maximum and the yield load (KIc-max, KIc-initiation) by 3-point bending of notched femurs.YAP/TAZ inhibition significantly reduced periosteal and trabecular bone MS/BS, but modestly elevated endosteal MS/BS, though this difference was not statistically significant (Fig. 1 A and Fig. 1B). Reduced MS/BS values, without altered MAR indicate that YAP/TAZ inhibition reduced osteoblast recruitment without altering mineral deposition rate. Endomucin immunostaining showed a significant effect of VP treatment on bone marrow vascular morphology, area, and the number of endomucin+ blood vessels (Fig. 1C), highlighting the global nature of YAP/TAZ inhibition, and may explain the contrasts between endosteal and periosteal bone formation responses to YAP/TAZ inhibition. By fluorochrome labeling of osteocyte lacunae, we found that YAP/TAZ inhibition significantly reduced the intensity of the calcein-labeled lacuna, particularly in the anterior tibia, which experiences maximal tensile strains (Fig. 1D), indicating a possible interaction between YAP/TAZ signaling and strain on osteocyte peri-lacunar mineralization. While Kc-max and Kc-initiation values were similar between groups, VP-treated femurs exhibited greater heterogeneity.These findings implicate YAP/TAZ signaling in bone formation and peri-lacunar mineral dynamics, dependent on local activity-associated mechanical cues.

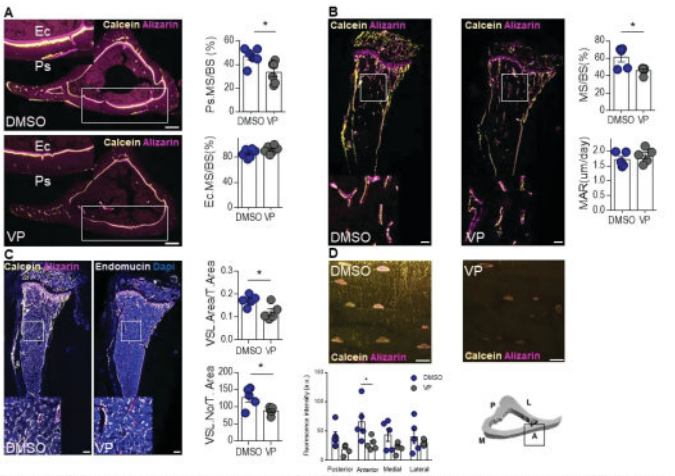

Fig. 1. A. YAP/TAZ inhibition reduces periosteal mineralization. **B.** YAP/TAZ inhibition reduces cancellous mineralization. **C.** YAP/TAZ inhibition reduces vessels area and number in the marrow region. Scale bars=200 μm, Ec=Endosteum, Ps=Periosteum, VSL=Vessel. **D.** YAP/TAZ inhibition reduces osteocytes mineral deposition in the anterior region. Scale bar=5 μm, A=Anterior, M=Medial, P=Posterior, L=Lateral

***Disclosures: YASAMAN MOHARRER**, None*

LB SAT-632

A Prototype High-Resolution Peripheral Quantitative CT Scanner With Photon Counting Detectors For Bone Loss Assessment In Osteoporosis

*Laura Cerbone[1], Russo Paolo[2], Antonio Sarno[2], Luigi Cimmino[2], Giovanni Mettivier[2]. [1]Scuola Superiore Meridionale - University of Naples Federico II, [2]INFN Naples, Italy

Background: While dual-energy X-ray absorptiometry bone represents a fundamental tool for osteoporosis diagnosis, a new technique is available for bone's low-dose imaging, i.e., high-resolution peripheral quantitative CT (HR-pQCT), providing quantitative imaging of the 3D structure of trabecular bone (e.g., in the distal tibia and radius), with an isotropic spatial resolution of 60 μm. We present the design of a new compact HR-pQCT prototype scanner (T4-QCT) for tibia and radius, based on a photon-counting energy-selective detector. T4-QCT scans could also be adopted for CT imaging of metacarpophalangeal finger joints, aiming to improve the characterization of soft and hard tissues.Material and methods: At variance with energy integrating detectors adopted in commercially available HR-pQCT scanners, T4-QCT employs hybrid pixel detectors consisting of a CdTe semiconductor pixel sensor and a Timepix4 readout circuit (448 × 512 square pixels of 55 μm), and a microfocus X-ray tube. Timepix4 spectral imaging performance allows measurement of the x-ray energy deposited in the detector by each interacting photon with a resolution of about 1 keV; this allows the discrimination of bone from soft tissues based on their energy-dependent attenuation, without the need for dual-energy scans. The proposed device will employ 3 Timepix4 CdTe (1-mm thick) pixel detectors in a row, in an offset-detector CT acquisition geometry, with a field of view of 10 cm diameter at the isocenter. This device will be compact and light, with a diameter of 70 cm and a weight below 50 kg.Results: The high granularity of the sensor can lead to an isotropic spatial resolution below 40 μm. CT scans using photon counting detectors effectively increase the image SNR and reduce the radiation dose to the patient. However, this spectral CT scanner's most relevant capability will be separating tissues that exhibit slight differences in densities and Zeff by taking advantage of the different dependence of attenuation coefficients from energy. In addition, the compactness of this scanner with respect to commercially available ones will allow for examining bedridden patients, which might be the case for those suffering from osteoporosis, bone fragility and fractures, and for scanning finger joints for signs of bone disease.Conclusions: T4-QCT is proposed as a new photon-counting scanner for spectral CT osteoporosis and rheumatoid arthritis diagnostic assessment in radius and tibia bone imaging scans.

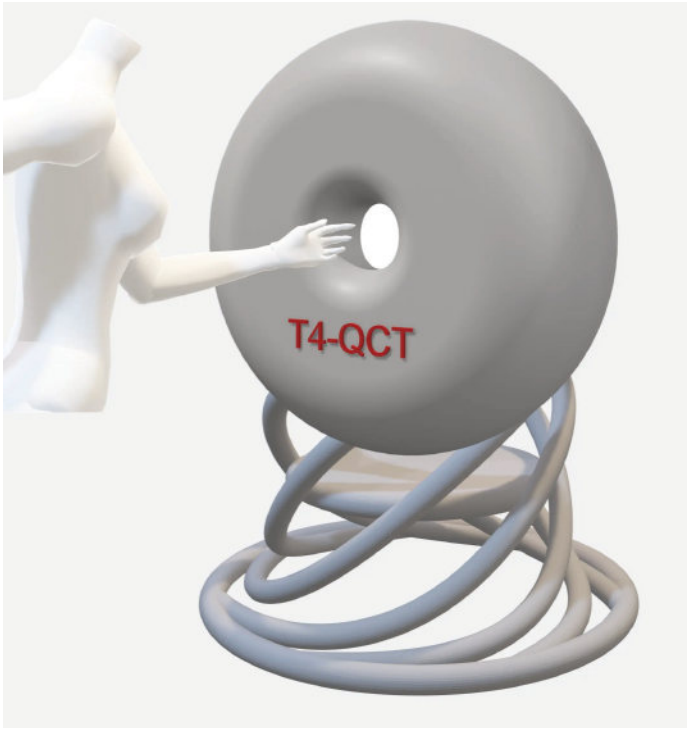

***Disclosures: Laura Cerbone**, None*

LB SAT-633

Improved Fracture Discrimination in Patients With Systemic Lupus Erythematosus using DXA-derived 3D measurements of the Hip

*Edgar Wiebe[1], Elisa Celine Schilling[1], Dörte Huscher[2], Andriko Palmowski[1], Zhivana Boyadzhieva[1], Sandra Hermann[1], Tobias Alexander[1], Falk Hiepe[1], Burkhard Muche[1], Frank Buttgereit[3]. [1]Charité Universitätsmedizin, Dept. Rheumatology, Germany, [2]Charité Universitätsmedizin; Institute for Biometry and Clinical Epidemiology, Germany, [3]Charité Universitätsmedizin, Germany

Background:Patients with systemic lupus erythematosus (SLE) face an increased risk of osteoporosis and fragility fractures (FFx) which may not be adequately captured by areal bone mineral density (aBMD) measurement. Dual energy X-ray absorptiometry (DXA)-derived three-dimensional (3D) analysis has emerged as a promising method for evaluating femur bone structure, showing good correlation with quantitative computed tomography, which has demonstrated good predictive capabilities for fracture risk in postmenopausal non-SLE women.Objectives:We aimed to analyze the discriminative ability of DXA-derived 3D parameters of the femur compared to BMD and trabecular bone score (TBS) for pre-ex-

istent FFx in this SLE cohort.Methods:The prospective observational cohort study Rh-GIOP investigates bone health in patients >=18 years with inflammatory rheumatic diseases and current or prior GC treatment. This cross-sectional analysis assessed baseline visits of all SLE patients meeting the EULAR/ACR 2019 SLE classification criteria. DXA-derived 3D measurements of both femora were obtained using the software 3D-Shaper (v2.12, 3D-Shaper Medical, Barcelona, Spain). Logistic regression analysis was used to develop discrimination models incorporating DXA-based T-Scores, TBS, and 3D-Shaper to detect prevalent FFx, vertebral fractures (VFx), and non-vertebral fractures (NVFx). Area under the curve (AUC) values with 95% confidence intervals were calculated.Results:Baseline data from 110 SLE patients (92% female) were analyzed. The prevalence of FFx was 29%, with 10% having a VFx history. DXA-based T-Scores reached AUC values of 0.61 (0.49; 0.73), 0.47 (0.30; 0.64), and 0.61 (0.48; 0.74) for prevalent FFx, VFx, and NVFx, respectively. In comparison, 3D-Shaper showed better discrimination especially for VFx, with AUC values of 0.66 (0.54; 0.77), 0.77 (0.67; 0.87), and 0.64 (0.52; 0.76). A combined model of 3D-Shaper with DXA and TBS only slightly improved discrimination for FFx (0.67 (0.56; 0.78)) and VFx (0.78 (0.65; 0.91)), but not for NVFx: (0.63 (0.51; 0.75)). TBS alone or in combination with DXA did not enhance the discrimination model.Conclusion:In SLE patients, DXA-derived 3D parameters provide better discrimination of pre-existent fractures than DXA or TBS alone, particularly for VFx. Future longitudinal analyses will show whether these 3D-Shaper parameters can improve fracture prediction in clinical practice.

***Disclosures: Edgar Wiebe**, Novartis, Speakers' Bureau, Novartis, Consultant*

LB SAT-634

Comparative Short Term Recover And Functional Outcome Between Isolated Hip Fracture And Hip Fracture Coexisting With Osteoporotic Vertebral Compression Fracture *Ong-art Phruetthiphat[1], Wasin Kanokwongnuwat[2], Yodhathai Satravaha[3], Chaisiri Chaichankul[2], Pawin Gajaseni[2], Thawee Songpatanasilp[2]. [1]Phramongkutklao Hospital, Thailand. [2]Phramongkutklao hospital, Thailand. [3]Orthodontic department, Mahidol university, Thailand

Background: Fragility hip fractures are also correlated with high mortality, loss in disability-adjusted life year, and financial burden on the healthcare system. The 2 out of 3 osteoporotic vertebral compression fracture (OVCF) is asymptomatic and is common seen in the elderly population. However, current study has not identified the association of hip fracture and OVCF including the recovery and functional outcome. The purpose of this study was to identify a comparison of short-term recovery and functional outcome between Isolated hip fracture and hip fracture coexisting with osteoporotic vertebral compression fracture. Method: A prospective study was performed between 2019 and 2020. The inclusion criteria were those patients with femoral neck fractures or intertrochanteric fractures over 60 years old underwent bipolar hemiarthroplasty or Proximal Femoral Nail Anti-rotation (PFNA), respectively. 81 Patients were classified into 2 groups: Isolated hip fracture (Isolated group) (30.9%), and combined hip fracture and OVCF (Combined group)(69.1%). The severity of OVCF was evaluated by Genant classification. Time Up and Go Test (TUG) was evaluated at 2 weeks, and 6 weeks. In addition, the functional outcome assessed by Harris Hip Score (HHS) was performed at 6 months, and one year. The association of the severity of OVCF, TUG, and HHS were also evaluated.Result: There was no difference in age, gender, comorbidity, ASA class, CCI, and the percentage of intertrochanteric fractures and femoral neck fractures in both groups, as well as the operative parameters. Hip BMD and spine T-score BMD in the combined group was significantly lower than the Isolated group (p = 0.03 and p = 0.033, respectively). The length of hospital (p = 0.022) was significantly shorter, and the 6 weeks TUG (p = 0.042) was significantly lower in the isolated group compared to the combined group. Moreover, the 6 months HHS, and one year HHS in the isolated group was significantly higher than the combined group (p = 0.007 and p =0.005, respectively). In term of severity of OVCF (Grade 1-2 vs grade 0 and grade 3 vs grade 0), the higher grade was significantly lower 6 months HHS (p = 0.014 and p = 0.012, respectively).ConclusionsThe elderly hip fracture combined with OVCF had significantly longer hospital stay, longer time to recover, and worse functional outcome than the isolated group. The severity of OVCF was significantly associated with the worse outcome. This combined group needs more attention during the rehabilitation program.

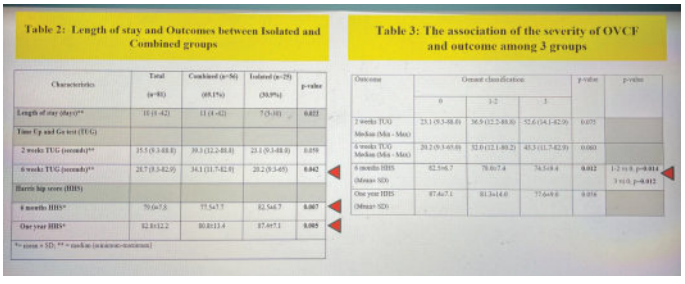

***Disclosures: Ong-art Phruetthiphat**, None*

LB SAT-635

Longitudinal Changes of Cortical and Trabecular Bone Characteristics Associated with Declines in Failure Load in Older Men *John Schousboe[1], Lisa Langsetmo[2], Sheena Patel[3], Andrew Burghardt[4], Peggy Cawthon[5], Mary Bouxsein[6], Nicole Sekel[7], Kristine Ensrud[8]. [1]Park Nicollet Clinic HealthPartners Institute University of Minnesota, [2]University of Minnesota, United States, [3], [4]University of California, San Francisco, United States. [5]California Pacific Medical Center, United States. [6]Beth Israel Deaconess Medical Center, Harvard Medical School, United States. [7]University of Pittsburgh, United States. [8]University of Minnesota and Minneapolis VA Health Care System, United States

Background: Trabecular and cortical bone microstructure are key determinants of fracture resistance. However, the changes in bone microarchitectural parameters that contribute to declines in failure load at older ages are uncertain. Our objective was to estimate the associations of changes in cortical and trabecular bone parameters with changes in failure load of the distal radius and tibia in older men.Methods: 150 men mean (SD) age 83.0 (3.1) years attending the 4th examination at the Pittsburgh and Palo Alto sites of the Osteoporosis Fractures in Men (MrOS) study had high resolution quantitative peripheral computed tomography (HR-pQCT) scans of the distal radius and distal tibia, and had these repeated at the 5th visit a mean (SD) 6.9 (0.6) years later. We used 3D registration to align the baseline and follow-up scans. Cortical parameters were volumetric BMD (Ct.BMD) and thickness (Ct.Th), porosity (Ct.Po), and area (Ct.Ar). Trabecular parameters were vBMD (Tb.BMD), number (Tb.N), and separation (Tb.Sp). Failure load was calculated using finite element analysis and annual changes in failure load, cortical, and trabecular parameters were calculated. We used linear regression to estimate the association of failure load change and each bone parameter change separately, adjusted for age and study site. All parameters with a univariate association with failure load change at p-value <0.10 were included multivariable regression models.Results: After adjustment for age and center, greater losses in Ct.BMD and Tb.BMD were each associated with greater loss of failure load at both skeletal sites. Surprisingly, a decrease in Ct.Po was associated with greater loss of failure load at both skeletal sites (Table). In multivariable analyses, decreases in Ct.BMD, Tb.BMD, and Ct.Po were associated with greater loss of failure load, after consideration of age, center and each other. Effect size was strongest for Ct.BMD. Changes of Ct.Th, Ct.Ar, Tb.N, and Tb.Sp, were not associated with failure load change at either skeletal site.Conclusion: Longitudinal declines in failure load at both the distal tibia and radius in older men are driven especially by declines in Ct.BMD and to a lesser degree by declines in Tb.BMD. We also saw a paradoxical association of changes of Ct.Po with changes of failure load, in the opposite direction of what we hypothesized. Further research is needed to better understand these associations.

Table: Multivariable-Adjusted Associations[a] of Cortical and Trabecular Bone Parameter Changes with Magnitude of Failure Load Loss

Bone Parameter	Effect Size[b] (95% C.I.)	
	Distal Tibia	Distal Radius
Cortical BMD	0.64 (0.54, 0.74)	0.54 (0.42, 0.66)
Cortical Porosity	-0.20 (-0.29, -0.11)	-0.23 (-0.35, -0.12)
Trabecular BMD	0.23 (0.14, 0.33)	0.24 (0.10, 0.38)
R-squared[c]	0.70	0.58

[a]Adjusted for study site
[b]Standard deviations increase of failure load loss per standard deviation increase of bone parameter change
[c]Proportion of failure load change explained by model parameters

***Disclosures: John Schousboe**, None*

LB SAT-636

Assessment of bone health through a photoacoustic quantitative ultrasound (PAQUS) apparatus: a preliminary phantom and clinical study *Zhanpeng Xu[1], Duane Kaufman[2], Rich Hogle[2], Dave Nelson[2], Conor Locke[1], Dara Geva[1], DeAndre Jamison[1], Xueding Wang[1], Rich Morris[2], Kenneth Kozloff[1]. [1]University of Michigan, United States. [2]IF, LLC, United States

Osteoporosis is a significant degenerative disease characterized by loss of bone density and strength, resulting in greater susceptibility to fracture. Development of technologies that enhance early detection of osteoporosis-related changes in bone may help provide timely intervention, reducing fractures and improving overall quality of life. Clinical diagnosis relies on evaluation of bone mineral density (BMD) by DEXA, which provides an incomplete measure of fracture risk. Photoacoustic (PA) imaging is an emerging technology that combines the advantages of high optical contrast and deep ultrasound penetration for non-invasive and non-ionizing quantitative measurement. Spectral information derived from PA reflects a combination of bone microstructure, BMD, and chemical composition that may be useful for evaluating changes in bone health associated with disease or treatment.In the work, a novel photoacoustic quantitative ultrasound (PAQUS) apparatus was developed

for in vivo assessment of the calcaneus. Using 3D printing with dental crown resin, we first made lattice-shaped cubic phantoms of varying density by holding trabecular number constant and varying trabecular thickness (0.630, 0.597, 0.548 mm), resulting in bone volume fractions (BVF) of 0.295, 0.274 and 0.245. Phantoms were then infiltrated with a marrow-mimicking substitute. PA spectra were collected (690-950 nm) and normalized to 800 nm. PA absorbance at 740 nm (hemoglobin) and 930 nm (lipid) were significantly different ($p<0.05$) across phantoms. Next, we created two anatomic phantoms based on a human calcaneus nano-CT volumetric image, and artificially eroded the trabecular structure on one to reduce BVF by 32.5%, mimicking osteoporosis-mediated bone loss. Phantoms were imaged repeatedly and also significantly differed at 740 and 930 nm ($p<0.01$). Lastly, in vivo bilateral PA imaging was conducted at the calcaneus on 32 female Caucasian subjects (20-74 yrs). A significant difference ($p<0.05$) in PA absorption was observed at 740 nm between younger (50 yrs) subjects. Together, results from this preliminary phantom and clinical study demonstrate initial feasibility of PAQUS in assessing human bone mass in a non-ionizing, non-invasive and cost-effective way. Using our multi-spectral approach, PAQUS may provide novel data that may reflect metabolic and compositional changes associated with osteoporosis or response to treatment earlier than conventional measures of BMD alone.

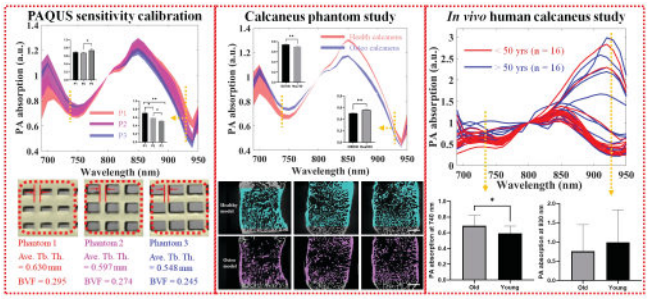

Figure 1. PAQUS sensitivity calibration: Cubic lattice phantoms with different trabecular thicknesses (bone volume fractions), 3D printed from dental resin and infiltrated with marrow substitute, were assessed by PAQUS. PA absorption spectra are plotted as ranges of "mean ± s.d." and differentiated at 740 and 930 nm by unpaired t test. Calcaneus phantom study: Anatomic calcaneal 3D printed phantoms were similarly evaluated, and significant differences of PA spectra were found at 740 and 930 nm. *In vivo* human calcaneus study: *In vivo* assessment of human calcaneus showed distinct age-associated differences at 740 nm. Error bars represent standard error of mean (SEM). *p < 0.05, **p<0.01.

***Disclosures: Zhanpeng Xu**, None*

LB SAT-637

Cold is Associated with Lower Bone Strength in the Midshaft Femur of Medieval Humans *Miranda Cosman[1], Maureen Devlin[1]. [1]University of Michigan, United States

Chronic cold stress decreases bone mass through sympathetic nervous system (SNS) activation in animal models, and is a potential risk factor for bone loss in humans. To test the effects of chronic cold exposure on the skeleton, in this study we used an archaeological sample of Medieval humans from different latitudes as a natural experiment. We studied adults of European genetic ancestry from two sites: Haffjarðarey, Iceland (mean high 45.3°F/low 36.3°F), interred from 1200-1563 CE, and Mistihalj, Bosnia and Herzegovina (mean high 65.8°F/low 52.3°F), interred from 1300-1500 CE, housed at the Peabody Museum at Harvard University. We hypothesized that bone mass would be lower at Haffjarðarey (cold) vs. Mistihalj (warm). Femoral midshaft cortical bone cross-sectional geometry was obtained via computed tomography (45-64 µm). Scans were reconstructed and segmented in Dragonfly (Object Research Systems), then measured using the BoneJ plugin (Domander et al., 2021) in Fiji (2.14.0). We assessed cortical bone area (BA, mm2), cortical thickness (Ct.Th, mm), maximum and minimum area moments of inertia (Imax and Imin, mm4), and the polar moment of inertia (J, mm4). Results indicate that bone strength was higher at the warmer Mistihalj than at the colder Haffjarðarey. In females, BA (+13%, $p<0.07$), Imax (+27%, $p=0.027$) and J (+23%, $p=.047$) were higher at Mistihalj; body mass (estimated by femoral head diameter), Ct.Th, and Imin did not differ between sites. In males, BA (+22%, $p=.001$), Imax (+34%, $p=0.004$) and J (+26%, $p=.014$), and estimated body mass (+10%, $p=0.041$) were higher at Mistihalj; Ct.Th and Imin did not differ between sites. After adjustment for body mass, significance remained for BA ($p=0.028$) and trended for Imax ($p=0.063$). We also observed significant cortical porosity, indicative of bone turnover, in ~75% of femora from Haffjarðarey vs. ~50% of femora from Mistihalj. These results indicate bone mass was lower in Europeans in Iceland compared to counterparts in Bosnia and Herzegovina, and supports the hypothesis that chronic cold is deleterious to bone mass. Ongoing analyses include trabecular bone microarchitecture.

***Disclosures: Miranda Cosman**, None*

LB SAT-638

Results of the Initial Fracture Liaison Service Implementation During the First Year of the Pandemic in a New Public Health System: The Experience of a Third-Level Hospital in Mexico *SALVADOR-ISRAEL MACIAS-HERNANDEZ[1], JANETE-SARAHI DIAZ-GONZALEZ[2], ANDREA OLASCOAGA-GOMEZ DE LEON[3], ROBERTO CORONADO-ZARCO[4], TANIA-INES NAVA-BRINGAS[3]. [1]Orthopedic Rehabilitation Departament, Instituto Nacional de Rehabilitación Luis Guillermo Ibarra Ibarra, Mexico City, Mexico, Mexico. [2]Orthopedic Rehabilitation Departament, Instituto Nacional de Rehabilitación Luis Guillermo Ibarra Ibarra, Mexico City, Mexico., Mexico. [3]Spine Rehabilitation and Osteoporosis Clinic, Instituto Nacional de Rehabilitacion"Luis Guillermo Ibarra Ibarra", Mexico City, Mexico. , Mexico. [4]Deputy Director of Rehabilitation Medicine, Instituto Nacional de Rehabilitacion "Luis Guillermo Ibarra Ibarra", Mexico City, Mexico, Mexico

Introduction: Fracture Liaison Services (FLS) have been shown to be effective in preventing secondary fragility fractures. A previous study by the same group identified a significant gap in the diagnosis and treatment of osteoporosis in patients with fragility fractures. In early 2020, an FLS program was initiated at our hospital. However, its implementation was interrupted by unexpected events, including the COVID-19 pandemic and a new healthcare system in the country. Nevertheless, the program was implemented.Objective: The objective of this study was to examine how the frequency of diagnosis and treatment of osteoporosis changed after the setting of an FLS unit during the first year of its establishment.Materials and Methods: This was a descriptive study conducted by retrospective analysis of one year after the implementation of an FLS. Ethical Considerations: This project is part of the "Impact of a Secondary Prevention Unit for Osteoporosis Fracture Prevention in a Third-Level Institution in Mexico City" project funded by the National Research Council of Mexico through the Health Research Fund, number A3-S-47397. This study was registered as Protocol No. 28/19/AC. The study included patients aged 50 years and above diagnosed with acute low-energy (fragility) fractures of the hip, distal radius, and proximal humerus.Results: A total of 368 patients were included in the study, with a mean age of 78.35 +/- 11.58 years. Of the total, 271 (73.6%) had hip fractures, 66 (17.9%) had distal radius fractures, and 29 (7.9%) had proximal humerus fractures. Of these, only 26 (7.1%) had a previous diagnosis of osteoporosis. During hospitalization, 147 patients (39.9%) were diagnosed with osteoporosis. Of these, 274 (74.5%) received some form of pharmacologic treatment. Supplementation with calcium and vitamin D was indicated in 96 patients (26.1%), while non-pharmacological management, including a calcium-rich diet, exercise, and fall prevention, was indicated in 95 patients (25.8%). At one-year follow-up, 88 (23.9%) of those diagnosed and treated in the hospital were on pharmacologic therapy, 128 (34.8%) were on supplementation, and 131 (35.7%) were on non-pharmacologic therapy.Conclusions: This study shows that despite adverse contexts, the implementation of an FLS significantly increased the proportion of patients diagnosed and treated for osteoporosis after a fragility fracture.Conflict of interest. None.

***Disclosures: SALVADOR-ISRAEL MACIAS-HERNANDEZ**, None*

LB SAT-639

The Association of Bone Mineral Density (BMD) with incident Major Osteoporotic and Hip Fractures Varies by Body Mass Index (BMI) *John Schousboe[1], Neil Binkley[2], William Leslie[3]. [1]Park Nicollet Clinic HealthPartners Institute University of Minnesota, . [2]University of Wisconsin, Madison, United States. [3]University of Manitoba, Canada

Background: Increased BMI and abdominal fat mass increase the precision error of bone densitometry measurement, and may adversely affect its accuracy as well. Our aim was to estimate if the association of femoral neck, total hip, and/or lumbar spine BMD is modified by BMI. We hypothesized that the association of BMD with incident major osteoporotic and hip fractures is weaker among very obese compared to individuals with normal BMI. Methods: Our study population was 82,431 individuals (mean [SD] age 64.8 [11.0] years, 90% female) who had a fan-beam DXA-BMD test in the province of Manitoba between 1998 and 2018. BMI and other predictors were assessed on the date of the BMD test and incident fractures ascertained through linked health claims over a mean (SD) follow-up of 8.5 (5.2) years. Proportional hazards models were used estimate the associations of femoral neck, total hip, and lumbar spine BMD with incident major osteoporotic and hip fractures, adjusted for age and sex and then additionally for FRAX risk factors, use osteoporosis therapy during any part of the follow-up period, tissue fat and soft tissue thickness (at the BMD skeletal site). Statistical differences in strength of association of BMD with incident fractures between BMI categories were tested (p-interaction, T-score*BMI category).Results: The associations of femoral neck and total hip BMD with incident fractures were as strong for those with high or very high BMI as for those with normal BMI (table), but were weaker for underweight individuals (BMI < 18.5 kg/m2) (Table). The associations of lumbar spine BMD with incident fractures did not vary by BMI.Conclusion: BMD is as strong a predictor of major osteoporotic fractures and hip fractures in even very obese individuals compared to those with normal BMI. However, femoral neck and total hip BMD are weaker predictors of these fractures in underweight individuals. Further research is needed to delineate the mechanisms and reasons for these weaker associations.HIPC File Number: 2016/2017-29?

Table: Associations of Bone Mineral Density with Incident Fractures by BMI Category

Incident Fracture	BMI Category	Femoral Neck HR* (95% C.I.)		Total Hip HR* (95% C.I.)		Lumbar Spine HR* (95% C.I.)	
		Model 1†	Model 2‡	Model 1†	Model 2‡	Model 1†	Model 2‡
Major Osteoporotic	<18.5 kg/m² (n=1612)	1.41 (1.10-1.67)	1.29 (1.08-1.54)	1.42 (1.25, 2.62)	1.30 (1.13, 1.50)	1.24 (1.11, 1.38)	1.24 (1.09, 1.41)
	18.5-24.9 kg/m² (n=28987)	1.66 (1.58, 1.74)	1.56 (1.49, 1.64)	1.59 (1.53, 1.64)	1.52 (1.46, 1.58)	1.29 (1.25, 1.33)	1.26 (1.22, 1.30)
	25-29.9 kg/m² (n=28853)	1.71 (1.63, 1.79)	1.62 (1.54, 1.71)	1.61 (1.54, 1.67)	1.54 (1.48, 1.61)	1.29 (1.25, 1.33)	1.26 (1.21, 1.30)
	30-34.9 kg/m² (n=14885)	1.73 (1.62, 1.85)	1.56 (1.46, 1.68)	1.63 (1.55, 1.73)	1.52 (1.43, 1.62)	1.33 (1.27, 1.39)	1.27 (1.21, 1.33)
	35-39.9 kg/m² (n=5415)	1.60 (1.42, 1.85)	1.53 (1.35, 1.74)	1.55 (1.40, 1.71)	1.53 (1.37, 1.70)	1.32 (1.22, 1.44)	1.31 (1.19, 1.43)
	≥40 kg/m² (n=2679)	1.68 (1.39, 2.02	1.49 (1.23, 1.8)	1.65 (1.41, 1.92)	1.48 (1.26, 1.75)	1.34 (1.18, 1.52)	1.26 (1.11, 1.44)
	P-value for difference^	0.002	0.013	0.004	0.02	0.35	0.58
Hip	<18.5 kg/m² (n=1612)	1.53 (1.20, 1.96)	1.46 (1.12, 1.90)	1.51 (1.26, 1.81)	1.40 (1.15, 1.70)	1.19 (1.01, 1.39)	1.20 (1.01, 1.44)
	18.5-24.9 kg/m² (n=28987)	1.99 (1.84, 2.15)	1.89 (1.74, 2.06)	1.84 (1.74, 1.96)	1.78 (1.67, 1.90)	1.16 (1.11, 1.22)	1.14 (1.08, 1.20)
	25-29.9 kg/m² (n=28853)	2.05 (1.88, 2.24)	2.07 (1.88, 2.28)	1.88 (1.75, 2.01)	1.92 (1.70, 2.16)	1.16 (1.10, 1.22)	1.14 (1.08, 1.21)
	30-34.9 kg/m² (n=14885)	2.35 (2.04, 2.71)	2.14 (1.85, 2.49)	2.01 (1.81, 2.24)	1.92 (1.70, 2.16)	1.22 (1.12, 1.33)	1.14 (1.04, 1.25)
	35-39.9 kg/m² (n=5415)	1.95 (1.48, 2.57)	1.96 (1.47, 2.63)	1.82 (1.46, 2.26)	1.87 (1.48, 2.37)	1.20 (0.99, 1.44)	1.23 (1.10, 1.52)
	≥40 kg/m² (n=2679)	2.52 (1.52, 4.20)	2.51 (1.42, 4.42)	2.64 (1.70, 4.11)	2.77 (1.67, 4.49)	1.44 (1.03, 2.01)	1.33 (0.94, 1.87)
	P-value for difference^	<0.001	0.001	<0.001	0.001	0.43	0.86

*per one T-Score decrease
†adjusted for age and sex
‡adjusted for age, sex, FRAX risk factors, osteoporosis drug therapy, diagnosis of diabetes mellitus, skeletal site percent fat, and skeletal site tissue thickness
^p-value HR for <18.5 BMI category being different than HR for 18.5-24.9 kg/m²

***Disclosures: John Schousboe**, None*

LB SAT-640

Frailty is a Predictor of Incident Osteoporotic Fractures in Veterans with Rheumatoid Arthritis *Katherine Wysham[1], Hannah Brubeck[2], Aaron Baraff[2], Punyasha Roul[3], Namrata Singh[4], James Andrews[4], Grant Cannon[5], Gary Kunkel[5], Ted Mikuls[6], Bryant England[6], Dolores Shoback[7], Patricia Katz[8], Jose Garcia[9], Ariela Orkaby[10], Joshua Baker[11]. [1]University of Washington/VA Puget Sound, [2]VA Puget Sound Health Care System, United States. [3]University of Nebraska Medical Center, United States. [4]University of Washington, United States. [5]VA Salt Lake City & University of Utah, United States. [6]VA Nebraska-Western Iowa Health Care System & University of Nebraska Medical Center, United States. [7]San Francisco VA Medical Center & University of California San Francisco, United States. [8]University of California, San Francisco, United States. [9]VA Puget Sound Health Care System & University of Washington & VA Geriatric Research Education and Clinical Center, United States. [10]New England GRECC, VA Boston Healthcare System & Brigham & Women's Hospital, Harvard Medical Center , United States. [11]University of Pennsylvania & Corporal Michael J. Crescenz VA Medical Center, United States

Purpose: Frailty occurs prematurely in rheumatoid arthritis (RA). In this study we evaluated whether frailty predicted incident osteoporotic fractures in Veterans with RA using an externally validated frailty index.Methods: Data were from the Veterans Affairs Rheumatoid Arthritis (VARA) Registry 1/2003-12/2021. Baseline frailty was calculated using the VA Frailty Index (VAFI)1, which is based on diagnostic and CPT codes categorized into 31 deficits including morbidity, function, mood, cognition and geriatric syndromes. Osteoporotic fractures were identified by diagnostic and procedure codes and validated by chart review. High-trauma, periprosthetic and pathologic fractures related to cancer were excluded. Multivariable Cox regression was used to evaluate the relationship between baseline frailty and incident osteoporotic fracture, adjusting for baseline age, sex, race, smoking status, antibody status and prior osteoporotic fracture; and time-varying body mass index, disease activity, prednisone use and RA medication use. The same model was used to evaluate the relationship between baseline frailty and the risk of specific fracture type (extremity, rib, spine, hip and pelvis).Results: Veterans (N=2,930) had a mean age of 64+/-11 years. Cohort characteristics are detailed in Table 1. There were higher rates of baseline frailty in the fracture group (25% vs 17% mild frailty, 10% vs 7% moderate frailty, and 5% vs 2% severe frailty). Over the 21,800 person-years of observation, 240 incident osteoporotic fractures occurred (79 extremity, 58 rib, 47 spine, 43 hip and 13 pelvis). In the multivariable Cox model, prefrail, mild, moderate and severe frailty each had significantly increased risk of incident osteoporotic fracture compared to those who were robust (aHR [95%CI]:1.44 [1.02-2.05], 2.32 [1.56-3.45], 3.30 [2.00-5.46] and 4.92 [2.48-9.80]; all p<0.05, respectively). The relationship between baseline frailty level and incident fracture did not differ significantly by fracture type.Conclusions: Baseline frailty is associated with incident osteoporotic fractures in Veterans with RA in a dose-dependent fashion. We did not find significant differences in the relationship between baseline frailty and risk of fracture by fracture type. Frailty measurement in RA using the VAFI, a validated, automated tool, may prove to be useful in identifying Veterans at high risk for osteoporosis and fractures.1Orkaby AR et al. J Gerontol A Biol Sci Med Sci. 2019

Table 1. Baseline demographics, clinical characteristics and results from multivariable Cox model evaluating the relationship of baseline frailty on incident osteoporotic fracture.

	No Fracture N=2673 (92%)	Fracture N=240 (8%)	Multivariable Model aHRs (95%CI)
Age (mean)	64.3 ± 11.1	64.5 ± 9.9	n/a
Age category			
<55	469 (18%)	41 (17%)	ref
55-64	891 (33%)	93 (39%)	1.24 (0.83-1.85)
65-74	894 (34%)	66 (28%)	1.23 (0.77-1.94)
75+	418 (16%)	40 (17%)	1.62 (0.96-2.74)
Female Sex	305 (11%)	45 (19%)	2.24 (1.54-3.25)§
Black Race	448 (17%)	25 (10%)	0.46 (0.30-0.71)§
BMI†			
<18.5	24 (1%)	2 (1%)	0.49 (0.15-1.55)
18.5-24.9	643 (24%)	64 (27%)	ref
25.0-29.9	979 (37%)	94 (39%)	0.65 (0.48-0.89)§
30.0-34.9	624 (23%)	46 (19%)	0.47 (0.32-0.71)§
35.0-39.9	226 (9%)	21 (9%)	0.60 (0.36-0.98)§
≥40	105 (4%)	12 (5%)	0.70 (0.38-1.29)
Anti-CCP Positivity*			
Positive	1730 (78%)	175 (76%)	1.00 (0.73-1.36)
Negative	497 (22%)	56 (24%)	ref
Smoking			
Never	558 (21%)	58 (24%)	ref
Former	1406 (53%)	114 (48%)	0.83 (0.59-1.17)
Current	645 (24%)	66 (28%)	1.08 (0.74-1.60)
Prior Fracture	747 (28%)	83 (35%)	1.39 (1.05-1.84)§
DAS28ESR† (mean)	3.8 ± 1.6	4.0 ± 1.5	1.16 (1.06-1.28)§
Prednisone use†	892 (33%)	92 (38%)	1.51 (1.14-2.00)§
csDMARD use†	2056 (77%)	183 (76%)	0.83 (0.63-1.11)
bDMARD use†	763 (29%)	65 (27%)	0.92 (0.69-1.22)
Frailty Category			
Robust	824 (31%)	59 (25%)	ref
Pre-Frail	1025 (38%)	86 (36%)	1.44 (1.02-2.05)§
Mild Frailty	461 (17%)	59 (25%)	2.32 (1.56-3.45)§
Moderate Frailty	177 (7%)	25 (10%)	3.30 (2.00-5.46)§
Severe Frailty	64 (2%)	11 (5%)	4.92 (2.49-9.80)§

-BMI: body mass index, CCP: cyclic citrullinated peptide, DAS28ESR: disease activity score 28 with ESR, csDMARD: conventional synthetic disease modifying antirheumatic drug, bDMARD: biologic disease modifying antirheumatic drug, aHR: adjusted hazard ratio.
-n/a: not included in multivariable model, ref: reference category
*Anti-CCP percentage based on total of those without missing data. Missing N=455 (16%).
§- p<0.05
†- time varying covariate in multivariable model

***Disclosures: Katherine Wysham**, None*

LB SAT-641

Does long-term antiresorptive administration lead to atypical fractures at other skeletal sites excluded from the ASBMR atypical femur fracture (AFF) case definition? A systematic review *Lucy Collins[1], Alec Ronan[1], Peter Ebeling[2], Vivian Grill[3], Hanh Nguyen[4]. [1]Department of Endocrinology and Diabetes, Western Health, Victoria, Australia, Australia. [2]Department of Medicine, School of Clinical Sciences, Monash University, Victoria, Australia; Department of Endocrinology, Monash Health, Victoria, Australia, Australia. [3]Department of Endocrinology and Diabetes, Western Health, Victoria, Australia; Department of Medicine, The University of Melbourne, Victoria, Australia, Australia. [4]Department of Endocrinology and Diabetes, Western Health, Victoria, Australia; Department of Medicine, School of Clinical Sciences, Monash University, Victoria, Australia, Australia

BackgroundOsteoporosis affects > 1.3 million Australians. Bisphosphonates and denosumab are approved treatments for osteoporosis with the rare complications of jaw osteonecrosis and AFFs. Cases of AFFs were first reported in 2005, highlighting a state of significantly suppressed bone turnover on biopsy (1). In 2010 and 2013, an American Society of Bone and Mineral Research (ASBMR) Task Force proposed a case definition for these atypical fractures affecting the femoral diaphysis (2, 3). Subsequently, reports of similar atypical fractures at other skeletal sites have been published.AimWe aimed to systemically identify cases of atypical fractures, excluded from the ASBMR AFF case definition in patients receiving anti-resorptive medication (duration > 3 years).MethodA structured search of electronic databases, including PubMed, Medline, Embase, Cochrane and Web of Science and hand-searching of conference abstracts/reference lists was completed. All full-text articles written in English describing atypical fractures were screened for: 1) cases of atypical fractures, excluded from the ASBMR AFF case definition in patients (aged > 18 years) receiving long-term antiresorptive medication, 2) cases published 2005 - 2023.Results7954 citations were identified. 65 articles fulfilled the inclusion criteria. Fractures were more common in females (112/120, 93%). Most frequent fracture sites included the ulna (n=32), tibia (n=12), pelvis (n=10), vertebral pedicle (n=8), sacrum (n=6) and femoral neck (n=5). One atypical fracture was reported in a monogenetic bone disorder (hypophosphatasia). Fractures were commonly atraumatic, with prodromal pain and typically transverse, non-comminuted with evidence of cortical thickening and sclerosis. Non-union was more frequent following conservative management. In most cases, anti-resorptive medication was ceased (41/47, 87%). ConclusionAtypical fractures at sites other than the femoral diaphysis in patients receiving long-term anti-resorptive treatment are important to recognise and may provide insights into the pathogenesis of AFF. A review of the current AFF case definition could be undertaken to include other skeletal sites.

References

1. Odvina CV, Zerwekh JE, Rao DS, et al. Severely suppressed bone turnover: a potential complication of alendronate therapy. J Clin Endocrinol Metab. 2005;90(3):1294-301.
2. Shane E, Burr D, Abrahamsen B, et al. Atypical subtrochanteric and diaphyseal femoral fractures: second report of a task force of the American Society for Bone and Mineral Research. J Bone Miner Res. 2014;29(1):1-23.
3. Shane E, Burr D, Ebeling PR, et al. Atypical subtrochanteric and diaphyseal femoral fractures: report of a task force of the American Society for Bone and Mineral Research. J Bone Miner Res. 2010;25(11):2267-94.

***Disclosures: Lucy Collins**, None*

LB SAT-642

Pharmacologic inhibition of HIF2 prevents trabecular bone loss in ovariectomized mice *Giulia Lanzolla[1], Elena Sabini[1], Mohd Parvez Khan[1], Brittany Laslow[1], Dian Wang[1], Xiaowey Sherry Liu[1], Ernestina Schipani[2]. [1]Department of Orthopaedic Surgery, University of Pennsylvania, Perelman School of Medicine, Philadelphia, 19104, PA, USA, United States. [2]University of Pennsylvania,

Cells of the osteoblast lineage are exposed to a gradient of oxigenation in the adult bone marrow. The transcription factors Hypoxia Inducible Factor 1 (HIF-1) and HIF-2 are key mediators of the cellular response to hypoxia. Loss of HIF2 in the osteoblast lineage promotes bone formation and augments bone mass. Therefore, HIF2 could represent a novel therapeutical target for the treatment of low bone. The study was aimed at evaluating whether the pharmacologic inhibition of HIF2 prevents bone loss in ovariectomized mice. Eight-week-old female mice (FVB/N) were ovariectomized or sham-operated. Next, mice were randomized to be treated with either PT2399 (50 mg/kg), a selective inhibitor of HIF2, or with vehicle by oral gavage, twice daily for 5 weeks. As expected, a significant increase in body weight and a decrease in uterus weight were observed 6 weeks upon ovariectomy. The trabecular bone compartment in both vertebral bodies and distal metaphysis of femurs was analyzed by micro-CT and histomorphometry. Micro-CT analysis showed a significant decrease in bone volume/tissue volume ratio (BV/TV), trabecular number (Tb.N), trabecular thickness (Tb.Th), and bone mineral density (BMD) in OVX mice treated with vehicle compared to sham-operated, whereas trabecular spacing (Tb.Sp) was increased. More importantly, no difference was detectable in any of the parameters listed above between OVX mice treated with PT2399 and sham-operated treated with vehicle. Histomorphometry confirmed micro-CT data. Furthermore, number of osteoblasts over bone surface (Ob.N/BS) was significantly lower in vehicle-treated OVX mice compared to sham-operated. This decrease was prevented by PT2399 administration. Although osteoclast number over BS (Oc.N/BS) did not differ between the four groups, the BS/BV ratio, which is an index of resorptive activity, was significantly higher in OVX mice treated with vehicle compared to sham-operated. PT2399 treatment again normalized this parameter in OVX mice. Taken together, PT2399 fully prevented trabecular bone loss due to ovariectomy in mice, thus representing a new potential anabolic agent to be tested for treating postmenopausal osteoporosis. Modest anemia occurred in mice treated with PT2399, likely due to reduction of renal EPO, which is a direct downstream target of HIF2. Further studies are needed to target PT2399 specifically to bone to prevent anemia and clarify the mechanisms by which PT2399 prevents bone loss.

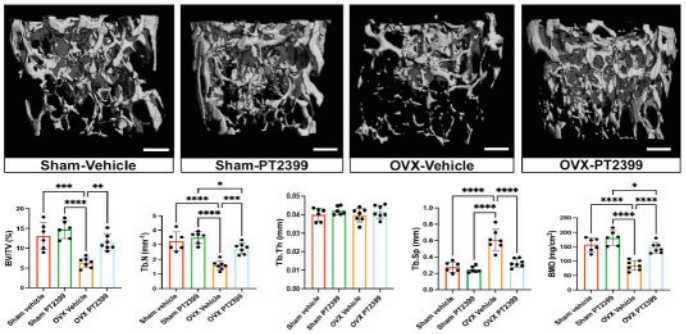

***Disclosures: Giulia Lanzolla**, None*

LB SAT-643

Bisphosphonate Use and Mortality in Olmsted County, MN, USA: A Population-Based Analysis *Richard Lindsey[2], Alanna Chamberlain[2], Elizabeth Atkinson[2], Jad Sfeir[2], Sundeep Khosla[3]. [2]Mayo Clinic, . [2]Mayo Clinic, United States. [3]Mayo Clinic College of Medicine, United States

Bisphosphonates are the most common drugs used to decrease fracture risk in patients with osteoporosis. There has been considerable interest regarding whether bisphosphonates as a class, and zoledronic acid (ZA) in particular, may have broader non-skeletal beneficial effects. Several clinical studies have suggested associations with reduced incidence of cancer, cardiovascular disease, and all-cause mortality. Thus, to address this issue, this study used population-based data from the Rochester Epidemiology Project (REP). The REP allows access to medical records of a wide selection of community members in Olmsted County (Minnesota, USA) to allow population-based analysis of health data in this community over time. We included participants who were at least 50 years of age and were prescribed a bisphosphonate between 2005 and 2021. Individuals who had prior osteoporosis therapy or history of cancer were excluded. We used Cox models adjusting for age, sex, and Elixhauser score to compare mortality of those who used bisphosphonates to propensity score-matched referents. A total of 3,825 patients prescribed bisphosphonates were identified (mean age 70.5 [SD 10.4] years, 85.4% female, 88.9% Caucasian). Alendronate was the primary bisphosphonate used, accounting for 86% of prescriptions, followed by risedronate (7.3%) and ZA (3.6%). Other bisphosphonates included etidronate, ibandronate, and pamidronate. Overall, no significant difference in mortality was observed between those on bisphosphonates and referents (see Table 1). This lack of an effect was consistent when analyzing only those who used alendronate or ZA, although the number of ZA users in this cohort was small (n = 139 out of 3,825). The only statistically significant effect on mortality was observed among males who used ZA (hazard ratio 2.80 [95% CI 1.17-6.69]). The lack of an association between bisphosphonate use and mortality is consistent with some previous data. However, several other observational studies similar in design to this study have suggested a mortality benefit to bisphosphonate use. Furthermore, there is a growing body of mechanistic animal data suggesting ZA may have anti-aging effects, in part by targeting senescent cells. Thus, observational studies may not be able to fully address this question, and randomized clinical trials are likely needed to determine whether bisphosphonate use provides a clinically meaningful mortality benefit.

Table 1

Bisphosphonate	Hazard Ratio All (95% CI)	Hazard Ratio Male (95% CI)	Hazard Ratio Female (95% CI)
All	1.07 (0.98–1.18)	1.20 (0.98–1.48)	1.04 (0.94–1.16)
Alendronate	1.03 (0.93–1.14)	1.06 (0.85–1.34)	1.02 (0.91–1.14)
Zoledronic Acid	1.83 (1.11–3.00)	**2.80 (1.17–6.69)***	1.48 (0.80–2.75)

Risk of all-cause mortality in bisphosphonate users compared to propensity score-matched referents. Adjusted for age, sex, and Elixhauser score.
*$P < 0.05$

***Disclosures: Richard Lindsey**, None*

LB SAT-644

2023 Clinical Practice Guideline Update for Management of Osteoporosis and Fracture Prevention in Canada *Suzanne Morin[1], Sidney Feldman[2], Larry Funnell[3], Lora Giangregorio[4], Sandra Kim[5], Heather McDonald-Blumer[2], Rowena Ridout[6], Nancy Santesso[7], Wendy Ward[8]. [1]McGill University, Canada. [2]University of Toronto, Canada. [3]Patient Partner, Canada. [4]University of Waterloo, Canada. [5]University of Toronto, Women's College Hospital, Canada. [6]Toronto Western Hospital, Canada. [7]McMaster university, Canada. [8]Brock University, Canada

PurposeOver 2 million Canadians live with osteoporosis, a disease that increases the risk for fractures. Fractures result in excess morbidity and mortality, decreased quality of life and loss of autonomy. This Canadian guideline update, to be published on October 10th 2023 in the Canadian Medical Association Journal, is intended to assist healthcare professionals in the delivery of care to optimize skeletal health and prevent fractures in postmenopausal females and in males 50 years of age and older.MethodsWe followed the Grading of Recommendations Assessment, Development and Evaluation (GRADE) Framework and quality assurance as per AGREE II quality and reporting standards. Primary care physicians and patient partners were represented at all levels and throughout the entire process to ensure relevance to target users. The process for managing conflicts of interest was developed prior to and continued throughout the guideline development, informed by the Guideline International Network principles. We considered benefits and harms, patient values and preferences, resources, equity, acceptability and feasibility when developing recommendations; the strength of each recommendation was assigned according to the GRADE Framework. RecommendationsThe 25 recommendations and 10 good practice statements are grouped under the sections of exercise, nutrition, fracture risk assessment and treatment initiation, pharmacologic interventions, duration and sequence of therapy, and monitoring. The management of osteoporosis should be guided by the patient's risk of fracture based on clinical assessment and using a validated fracture risk assessment tool. Exercise, nutrition and pharmacotherapy are key elements of the management strategy for fracture prevention, and should be individualized.InterpretationThis guideline aims to empower healthcare professionals and patients to have meaningful discussions on the importance of skeletal health and

fracture risk across older adulthood. Identification and appropriate management of Canadians with skeletal fragility can reduce fractures, and preserve mobility, autonomy and quality of life in this population.

***Disclosures: Suzanne Morin**, None*

LB SAT-645

Longitudinal Tracking of Patient-Level Indicators Characterizing Osteoporosis Care after Fragility Fracture in U.S. Medicare Fee-for-Service Beneficiaries (2017-2019) Confirms the Osteoporosis Treatment Gap and Provides Insights for Needed Improvement *Jennifer Todd[1], Adrienne Lovink[2], Barton Jones[4], Benjamin Lewing[4], Scott Robinson[4], Cesar Libanati[5]. [1]UCB Pharma, United States. [2]Trinity Life Sciences, United States. [4]Inovalon, United States. [4]Inovalon, United Kingdom. [5]UCB Biopharma srl,

Purpose:Despite increased secondary fracture prevention efforts, most patients experiencing a fragility fracture do not receive treatment (Tx) for underlying osteoporosis (OP). This study aimed to characterize the state of post-fracture care (PFC) in the U.S. by longitudinally tracking a comprehensive set of patient-level metrics inclusive of Tx.Methods:Patients >50 years with a fragility fracture claim from 2017-2019 were identified in Medicare Fee-for-Service (FFS) claims data. Qualifying fractures were identified using ICD-10 codes aligned to comprehensive inclusion/exclusion criteria. Prior non-symptomatic vertebral and traumatic fractures, and fractures associated with cancer or Paget's disease, were excluded. Patients were required to have continuous health plan enrollment with either medical or medical+pharmacy (Rx) coverage during a 6-month lookback period and >=12 months after index fracture (IF). The medical+Rx population was used to calculate Tx metrics due to a lack of Rx data in the medical only group.Results:We identified 1,941,902 patients who experienced a fragility fracture; 71.5% were female. Only 5.8% of all patients and 6.7% of women received a DXA within 3 months of IF. OP was diagnosed based on presence of a diagnosis code in <4% of patients in each group. ~30% of patients in each group experienced a subsequent fracture within 2 years of IF. For the continuous medical+Rx population, Tx initiation within a year was 12.1%: 0.5% received an osteoanabolic (OA), 11.7% received an antiresorptive (AR) and 0.1% received both. Only 3.4% received an OA first; 96.6% received an AR first. Tx initiation rates were slightly higher for women (14.9%); other Tx patterns were similar. Tx persistence at 1 year among those initiating Tx was ~31% in both groups (Table).Conclusion:This analysis confirms the majority of Medicare FFS patients who experienced fragility fractures did not receive Tx to prevent additional fractures. Additionally, it underscores the opportunities to intensify focus on strategies that address pressing gaps in care for these patients: First, investing in PFC by increasing programs and patient reach while ensuring appropriate coding of OP. Second, ensuring care provided to patients aligns to evidenced-based guidelines (risk stratification, choice of OP therapy). Last, implementing simple, effective strategies to improve adherence to interventions with the highest probability to prevent additional fractures.

Table: Selected population characteristics and study results in patients who experienced osteoporosis-related fractures in Medicare FFS (2017–2019)

	All Patients *n = 1,941,902 (100.00%)*		Female Patients *n = 1,388,835 (71.52%)*	
Information on Index Fracture Population (2017-2019) - Total Population (n,%)				
Age (n,%)	1,941,902	100.00%	1,388,835	100.00%
50-64	187,388	9.65%	109,512	7.89%
65-74	669,439	34.47%	459,028	33.05%
75-84	607,580	31.29%	440,079	31.69%
85+	477,495	24.59%	380,216	27.38%
Fracture Types (n,%)	1,941,902	100.00%	1,388,835	100.00%
Spine	393,319	20.25%	275,897	19.87%
Hip	283,354	14.59%	208,411	15.01%
Wrist	212,137	10.92%	196,856	14.17%
Humerus	234,447	12.07%	168,102	12.10%
Other	818,645	42.16%	539,569	38.85%
Study Results - Total Population (n,%)				
DXA[a]				
DXA within 3 months of index fracture (IF)	113,294	5.83%	93,603	6.74%
DXA within 12 months of IF	289,949	14.93%	253,234	18.23%
Coded Diagnosis of Osteoporosis (OP)[b]				
Presence of OP diagnosis code within 6 months of IF	48,705	2.51%	40,564	2.92%
Presence of OP diagnosis code within 12 months of IF	62,896	3.24%	52,662	3.79%
Subsequent Fractures[c]				
Subsequent fracture within 1 year of IF	376,535	19.39%	288,648	20.78%
Subsequent fracture within 2 years of IF	466,207	28.23%	360,190	30.24%
Study Results - Population with Continuous Health Plan Enrollment for Medical+Rx (n, %)				
	All Patients *n = 1,372,110 (100.00%)*		**Female Patients** *n = 1,006,434 (73.35%)*	
Treatment (Tx) Initiation[d]				
Any Tx within 12 months of IF	165,411	12.06%	149,627	14.87%
Both OA and AR Tx within 12 months of IF	1,333	0.10%	1,225	0.12%
Any osteoanabolic (OA) Tx within 12 months of IF	6,453	0.47%	5,796	0.58%
Any antiresorptive (AR) Tx within 12 months of IF	160,291	11.68%	145,056	14.41%
Osteoanabolic first (of those initiating Tx within 12 months of IF)	5,669	3.43%	5,073	3.39%
Antiresorptive first (of those initiating Tx within 12 months of IF)	159,742	96.57%	144,554	96.61%
Treatment (Tx) Persistence[e]				
Persistence on Tx ≥ 12 months (of those initiating Tx)	51,571	31.18%	47,546	31.78%

[a]Patients receiving DXA after index fragility fracture within specified time. [b]Determined by presence of an ICD-10-CM diagnosis of OP on at least 1 inpatient or 2 outpatient claims during follow-up period. Date of first OP code used to determine time to diagnosis. [c]All fracture types reported due to complexity associated with applying detailed inclusion and exclusion criteria at this stage. For 2-year metric, the population with continuous enrollment for medical was used (1,651,459 total and 1,191,104 for women). [d]Patients counted as treated only in the presence of at least 1 script/administration of OP treatment during the 12 months after IF. Categorized into the following Tx types: OA or AR. [e]Stability on therapy defined based on HCP-administered doses and/or doses supplied per pharmacy transactions (excluding abandonment). Differential dosing based on dosing schedule for each drug considered. Medication possession ratio (MPR) = totally day supply (based on any defined pharmacological treatment) divided by time under evaluation (12 months). MPR ≥ 0.80 considered persistent. DXA: dual energy x-ray absorptiometry; ICD-10-CM: ICD-10 Clinical Modification; OP: osteoporosis; IF: index fracture; Tx: treatment; OA: osteoanabolic; AR: antiresorptive; HCP: healthcare professional; MPR: medication possession ratio.

***Disclosures: Jennifer Todd**, UCB Pharma, Other Financial or Material Support*

LB SAT-646

Therapeutic Potential of IL-3 in Ovariectomy-Induced Osteoporosis *Shubhanath Behera[1], Juilee Karhade[1], Garima Pandey[2], Arpita Prasad[1], Adrita Guha[1], Krishna Ezhuthachan[1], Mohan R Wani[1]. [1]National Centre for Cell Science, India. [2]National Centre for Cell Science, Pune, India

IL-3, a cytokine produced by activated T lymphocytes is known to promote the proliferation, differentiation, and survival of hematopoietic stem cells. We have previously reported that IL-3 exhibits both anti-osteoclastic and pro-osteoblastic activity in vitro. We have also shown that IL-3 prevents osteoporotic bone loss in vivo in mice when injected at osteopenic stage. However, the therapeutic potential of IL-3 is not yet delineated. In the current study, we evaluated the therapeutic potential of IL-3 in fully developed osteoporosis in C57BL/6J female mice. IL-3 was administered after 30 days of ovariectomy for the duration of 30 days. At day 60, all mice were euthanized, and bone samples were collected for RNA isolation and μ-CT scanning to assess the alterations in the skeletal structure. We observed that IL-3 significantly improved various skeletal parameters, including femur trabecular BMD; and BV/TV, Tb.Sp., Tb.N., SMI and Conn.Dn. etc. Three-dimensional images of femur trabecular bone showed reversal of bone loss (Figure 1). Moreover, IL-3 showed considerable enhancements in tibial trabecular BV/TV, Tb.N., and Conn.Dn., and displayed improvements in Tb.Sp. and BMD in the tibial trabecular bone region. Considering that bone formation is of paramount importance in the therapeutic context, we examined various signaling molecules associated with osteoblast differentiation and mineralization. Analysis of femur and tibia bones from the IL-3 treated mice revealed an upregulation in the mRNA expression of RUNX2, osterix, osteopontin, osteocalcin, alkaline phosphatase, and collagenase type I. Importantly, in IL-3 knockout mice, we found a significant reduction in bone volume, trabecular BMD, and several other structural skeletal parameters in both male and female mice compared to the wildtype mice. These results indicates the crucial role of IL-3 in maintaining bone homeostasis. Taken together, our results strongly suggest that IL-3 holds a promise as a potential therapeutic agent for treating osteoporosis and maintaining bone health.

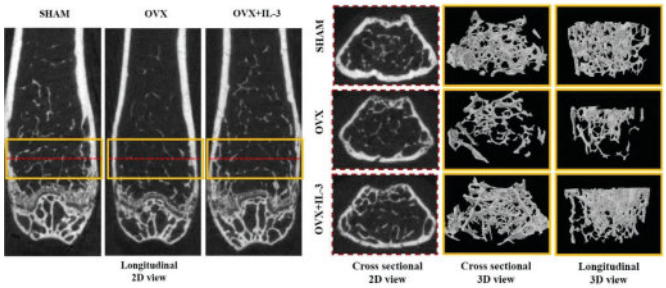

***Disclosures: Shubhanath Behera**, None*

LB SAT-647

Efficacy of Palovarotene for the Reduction of New Heterotopic Ossification in Patients with Fibrodysplasia Ossificans Progressiva: Sensitivity Analyses from the Phase III MOVE Trial *Geneviève Baujat[1], Edward C. Hsiao[2], Robert J. Pignolo[3], Mona Al Mukaddam[4], Staffan Berglund[5], Angela Cheung[6], Carmen De Cunto[7], Patricia Delai[8], Peter Kannu[9], Richard Keen[10], Edna E. Mancilla[11], Rose Marino[12], Andrew Strahs[12], Frederick S. Kaplan[4]. [1]Département de Génétique, Hôpital Universitaire Necker-Enfants Malades, Institut Imagine, Université Paris Cité, France. [2]University of California San Francisco, United States. [3]Department of Medicine, Mayo Clinic, United States. [4]Departments of Orthopaedic Surgery and Medicine, Center for Research in FOP and Related Disorders, Perelman School of Medicine, University of Pennsylvania, United States. [5]Department of Clinical Sciences, Pediatrics, Umeå University, Sweden. [6]University Health Network-University of Toronto, Canada. [7]Pediatric Rheumatology Section, Department of Pediatrics, Hospital Italiano de Buenos Aires, Argentina. [8]Centro de Pesquisa Clinica, Hospital Israelita Albert Einstein, Brazil. [9]Hospital for Sick Children, Canada. [10]Royal National Orthopaedic Hospital, United Kingdom. [11]Children's Hospital of Philadelphia, Perelman School of Medicine, University of Pennsylvania, United States. [12]Ipsen, United States

Purpose: Fibrodysplasia ossificans progressiva (FOP) is an ultra-rare, severely disabling genetic disorder characterized by progressive heterotopic ossification (HO). The phase III MOVE trial (NCT03312634) evaluated the efficacy and safety of the selective retinoic acid receptor-? agonist, palovarotene, in reducing new HO in FOP.1 Using a weighted linear mixed effects (wLME) model, post hoc 18-month interim analyses of MOVE showed that palovarotene reduced annualized new HO volume by 54% compared with patients untreated beyond standard of care from an FOP natural history study (NHS; NCT02322255).1 Palovarotene was generally well tolerated and adverse events were consistent with other systemic retinoids; however, there was a high risk of premature physeal closure in pediatric patients.1 Here, sensitivity analyses are presented to assess the robustness of the 18-month efficacy results previously reported from MOVE. Methods: Mean annualized HO volume assessed by low-dose whole-body computed tomography (WBCT) was compared for palovarotene-treated (MOVE) and untreated (NHS) patients. Sensitivity analyses performed on the wLME model were: inclusion of additional covariates and propensity score quartile as a covariate, extreme annualized new HO volumes of >100.0×103 mm3 set to 100.0×103 mm3, analysis of patients who transitioned from the NHS to MOVE, and propensity score matching and weighting analyses to adjust for baseline differences. A prespecified analysis was also conducted using Generalized Estimating Equations (GEE) modelling without weights. Results: Sensitivity analyses of the wLME model are presented (Table); results showed consistent reductions in annualized new HO volume with palovarotene treatment. Similarly, GEE modelling without weights showed that fitted mean annualized new HO volume was nominally significantly lower, by 54%, in palovarotene-treated (9.4×103 mm3) compared with untreated patients (20.3×103 mm3; nominal p=0.0106). Conclusion: With palovarotene treatment, post hoc sensitivity analyses of MOVE consistently demonstrated reductions in annualized new HO volume. The analyses support previous post hoc findings on the use of palovarotene for reducing new HO, however, the risk-benefit profile of palovarotene treatment should be reviewed on an individual basis. References 1. Pignolo RJ. J Bone Miner Res 2023;38:381-394; 2. Al Mukaddam M. Value in Health 2023;26(6):S20

Table: wLME sensitivity analyses for reductions in annualized new HO volume in palovarotene-treated (MOVE) compared with untreated (NHS) patients.

	% reduction in annualized new HO volume (palovarotene versus untreated)	Nominal p value	Palovarotene (MOVE)	Untreated (NHS)
MOVE IA3 analysis				
wLME analysis[a,1]	53.8	0.0392[f]	N=97	N=101
MOVE IA3 sensitivity analyses				
Analysis with additional covariates[b]	56.2	0.0314[f]	N=97	N=97
Analysis with propensity score quartile as a covariate[c]	56.7	0.0264[f]	N=97	N=97
Analysis with extreme HO volumes >100.0×10^3 mm^3 set to 100.0×10^3 mm^3	51.0	0.0103[f]	N=97	N=101
Analysis of patients who transitioned from the NHS to MOVE[d,1]	51.6	0.0634	N=39	N=39
Propensity score matched analysis[e,2]	76.9	<0.05[f]	N=39	N=39
Propensity score weighted analysis[e,2]	67.2	<0.05[f]	N=58	N=61

[a]Included baseline HO volume divided by baseline age as a covariate. [b]Included baseline HO volume divided by baseline age, baseline age, sex, baseline months since last flare-up, baseline CAJIS, and treatment as covariates. [c]Included propensity score quartile as the only covariate. [d]Included 39 patients who transitioned from the NHS to MOVE. [e]Excluded patients who transitioned from the NHS to MOVE; propensity scores were estimated via a multivariable logistic regression based on baseline age, sex, age-adjusted baseline HO, baseline CAJIS, and time since last flare-up. [f]Statistically significant reduction in mean annualized new HO volume with palovarotene treatment. CAJIS: Cumulative Analogue Joint Involvement Scale; HO: heterotopic ossification; IA3: interim analysis three; NHS: natural history study; wLME: weighted linear mixed effects.

***Disclosures: Geneviève Baujat**, FOP European Consortium (voluntary), Other Financial or Material Support, Alexion (Research Investigator), Grant/Research Support, Clementia/Ipsen (Research Investigator), Grant/Research Support, Clementia/Ipsen (Advisory Board), Other Financial or Material Support, IFOPA Registry Medical Advisory Board, Other Financial or Material Support, Biomarin (Research Investigator), Grant/Research Support, Incyte (Research Investigator), Grant/Research Support, Member of the International Clinical Council on FOP, Other Financial or Material Support, Clementia/Ipsen (Speaker), Speakers' Bureau*

LB SAT-648

Burden of Fractures for Individuals Living with Osteogenesis Imperfecta: Integrating Real-world Claims Data in the United States and Caregiver Panel Interviews *Heather Byers[3], Erru Yang[3], Jenny McCue[3], Yun Guo[2], Stanley Krolczyk[3]. [3]Ultragenyx, United States. [2]Tianjin Happy Life Technology Co., Ltd, China. [3]Ultragenyx,

Purpose: Osteogenesis imperfecta (OI) is a genetic disease characterized by bone fragility and recurrent fractures, characteristically of the long bones, vertebra, and ribs. However, fracture data by body site are limited. This study aims to quantitively and qualitatively better understand fracture burden among individuals with OI.Methods: For quantitative assessment, the IQVIA PharMetrics® Plus commercial database was searched between January 2017-February 2020 for individuals in 3 cohorts: 1) confirmed OI (>=2 ICD-10-CM Diagnosis Codes Q78.0 thirty days apart), 2) X-linked hypophosphatemia (XLH, ICD-10-CM E83.31), and 3) the general population without OI or XLH. All selected individuals required >=12 months of continuous enrollment. Fractures were identified via ICD-10 diagnosis codes and reported by body sites and age groups. For qualitative assessment, insights were gathered from 23 caregivers of individuals with OI through interviews (n=13) and virtual listening sessions (n=10).Results: Diagnosed fractures at any site occurred in 50% (967/1,949), 15% (817/5,281), and 6% (165,367/3,000,631) of individuals with OI, XLH and the general population, respectively. Age of greatest fracture incidence was 65 years for comparators (XLH: 27%, general: 11%). Among individuals with OI, the most common fracture sites were tibia/fibula (17%), radius/ulna (15%), and vertebrae (13%). Finger and toe fractures occurred in 7% and 8% of individuals with OI, respectively, versus <1% of comparators, and were highest in children aged 5-12 (13%-21%). Interviewed caregivers reported finger and toe fractures occur frequently and are commonly self-splinted at home without seeking medical care. Caregivers also stated that children often delay reporting fractures or pain to avoid missing out on activities.Conclusions: Individuals living with OI, especially children, have a high fracture burden that significantly impacts quality of life. Long bone fractures, including long bones of fingers and toes, occur notably more frequently in OI, even compared to patients with other metabolic bone diseases. Despite this significantly higher incidence of finger and toe fractures seen in subjects with OI, caregivers report they are often underreported within the medical record and contribute to high disease burden.

***Disclosures: Heather Byers**, Ultragenyx Pharmaceutical Inc. , Other Financial or Material Support*

LB SAT-649

Long-Term Impact of Palovarotene Treatment on Heterotopic Ossification in Patients with Fibrodysplasia Ossificans Progressiva: Data from the Phase III MOVE Trial *Angela M. Cheung[1], Edward C. Hsiao[2], Robert J. Pignolo[3], Mona Al Mukaddam[4], Geneviève Baujat[5], Staffan Berglund[6], Carmen De Cunto[7], Patricia Delai[8], Peter Kannu[9], Richard Keen[10], Edna E. Mancilla[11], Rose Marino[12], Andrew Strahs[12], Frederick S. Kaplan[4]. [1]Department of Medicine and Joint Department of Medical Imaging, University Health Network, University of Toronto, Canada. [2]University of California San Francisco, United States. [3]Department of Medicine, Mayo Clinic, United States. [4]Departments of Orthopaedic Surgery and Medicine, Center for Research in FOP and Related Disorders, Perelman School of Medicine, University of Pennsylvania, United States. [5]Département de Génétique, Hôpital Universitaire Necker-Enfants Malades, Institut Imagine, Université Paris Cité, France. [6]Department of Clinical Sciences, Pediatrics, Umeå University, Sweden. [7]Pediatric Rheumatology Section, Department of Pediatrics, Hospital Italiano de Buenos Aires, Argentina. [8]Centro de Pesquisa Clinica, Hospital Israelita Albert Einstein, Brazil. [9]Hospital for Sick Children, Canada. [10]Royal National Orthopaedic Hospital, United Kingdom. [11]Children's Hospital of Philadelphia, Perelman School of Medicine, University of Pennsylvania, United States. [12]Ipsen, United States

Purpose: Fibrodysplasia ossificans progressiva (FOP) is an ultra-rare genetic disorder characterized by progressive heterotopic ossification (HO). The phase III MOVE trial (NCT03312634) evaluated palovarotene, a selective retinoic acid receptor-? agonist, in FOP. Post hoc 18-month interim analyses showed palovarotene reduced new HO compared with patients untreated beyond standard of care from an FOP natural history study (NHS; NCT02322255).1 Palovarotene was generally well tolerated with adverse events consistent with other systemic retinoids, but there was a high risk of premature physeal closure in pediatric patients.1 Here, long-term (48 month) efficacy of palovarotene in patients who paused and restarted or stopped treatment in MOVE, due to a partial clinical hold in patients <14 years or dosing interruptions in patients >=14 years, was evaluated. Methods: Mean annualized HO volume changes assessed by low-dose whole-body computed tomography (WBCT) were evaluated to trial completion. Analyses were performed for the MOVE intent-to-treat (ITT) period for: (i) all patients regardless of treatment status (compared with untreated patients from an FOP NHS), (ii) patients who paused and restarted treatment with data in pre-pause, interruption, and post-restart periods (>=2 WBCT scans post-restart), and (iii) patients who paused and stopped treatment. Results: In the ITT period, patients received palovarotene for a mean (standard deviation) of 25.4 (12.5) months and were off treatment for 13.1 (9.3) months. For all patients and for patients who paused and restarted treatment in the ITT period, HO volumes were lower when patients received palovarotene (Table). When patients paused and stopped treatment (n=16), mean annualized new HO volume was 84.9% lower when patients received palovarotene (2.3×103 mm3; mean follow-up: 12.6 months) compared with when they did not (15.6×103 mm3; mean follow-up: 15.7 months). When patients stopped treatment, annualized new HO did not exceed that in untreated patients from the NHS, suggesting no treatment rebound or withdrawal effect. Conclusion: Long-term data from MOVE consistently showed lower annualized new HO volume when patients were treated with palovarotene versus when they were not. The results support previous post hoc findings on the use of palovarotene for reducing new HO. However, the risk-benefit profile of palovarotene should be reviewed on an individual basis. Reference 1. Pignolo RJ. J Bone Miner Res 2023;38:381-394

Table: Analyses of annualized new HO volume from baseline to last visit in the ITT period for all patients and for patients who paused and restarted treatment with data in each period.

MOVE ITT period, all patients[a]			
Treatment (study)	Palovarotene (MOVE) N=97		Untreated (NHS) N=101
Annualized new HO volume (×10³ mm³), wLME LSmean (SEM)	11.2 (3.3)		20.9 (3.7)
wLME reduction in new HO, %	46.4		
wLME estimate (95% CI) (×10³ mm³), p value	-9.7 (-19.8, 0.4), p=0.0585		
MOVE ITT period, only patients with data in all periods[a]			
Time period	Pre-pause N=17	Interruption N=17	Post-restart[b] N=17
Mean duration (months)	20.9	6.8	22.1
Annualized new HO volume (×10³ mm³), mean (SEM)	5.0 (3.5)	29.8 (12.9)	7.7 (5.0)

[a]Baseline total HO, baseline age, sex, baseline months since last flare-up, and baseline CAJIS were included as covariates. [b]Fewer patients paused and restarted palovarotene treatment due to missed WBCT scans and enrolment loss. CAJIS: cumulative analogue joint involvement scale; CI: confidence interval; HO: heterotopic ossification; ITT: intent-to-treat; LSmean: least squares mean; NHS: natural history study; SEM: standard error of the mean; WBCT: whole-body computed tomography; wLME: weighted linear mixed-effect.

***Disclosures: Angela M. Cheung**, Clementia/Ipsen (Research Investigator), Grant/Research Support, Incyte (Research Investigator), Grant/Research Support, Regeneron (Research Investigator), Grant/Research Support, Ipsen, Consultant*

LB SAT-650

Evaluating Setrusumab for the Treatment of Osteogenesis Imperfecta: Phase 2 Data from the Phase 2/3 ORBIT Study *E. Michael Lewiecki[1], Thomas Carpenter[2], Maegen Wallace[3], Peter Smith[4], Erik Imel[5], Hui Wang[6], Heather Byers[8], Stanley Krolczyk[8], Gary Gottesman[9]. [1]University of New Mexico Health Sciences Center, United States. [2]Yale University School of Medicine, United States. [3]University of Nebraska Medical Center, . [4]Shriner's Hospitals for Children, United States. [5]Indiana University School of Medicine, United States. [6]Ultragenyx Pharmaceutical Inc., United States. [8]Ultragenyx, United States. [8]Ultragenyx, . [9]Washington University School of Medicine in St. Louis, United States

Osteogenesis imperfecta (OI) is a rare genetic disorder characterized by bone fragility and low bone mass with no universally-accepted treatment. Setrusumab is a fully-human anti-sclerostin monoclonal antibody that improved bone mineral density (BMD), bone strength, and bone turnover markers in adults with OI (ASTEROID study). The safety and efficacy of setrusumab are further explored in pediatric and young adult cohorts in the Phase 2/3 ORBIT study (NCT05125809).The Phase 2 portion aims to select a setrusumab dosing strategy for patients with OI based on PK/PD, safety, and lumbar spine dual-energy x-ray absorptiometry (DXA) BMD. Subjects with OI Types I, III, or IV, ages 5 to <26 years, were randomized 1:1 to receive 20 or 40 mg/kg setrusumab intravenously monthly. Up to six-month trial data are presented.Twenty-four subjects (50% female, 75% <18 years of age) with OI Type I (n=17/24, 71%) or III/IV (n=7/24, 29%) were enrolled and randomized to receive 20 mg/kg (n=14/24) or 40 mg/kg (n=10/24) setrusumab.Subjects in the 20 mg/kg setrusumab group had a mean (SD) baseline-corrected area under the effect curve (AUEC) for serum P1NP of 4152.7 µg/L*day (4406.5) over the first month of treatment, compared with 5256.4 µg/L*day (5521.3) in the 40 mg/kg group.Mean (SD) change from baseline in lumbar spine BMD in the 20 mg/kg group was 10.5% (6.3%) and 10.2% (3.1%) at M3 and M6, respectively, compared with 10.1% (8.0%) and 21.6% (24.8%) in the 40 mg/kg group (all p<0.05 vs baseline). Mean (SD) baseline BMD Z-score in the 20 mg/kg group of 2.1 (2.8) improved by 0.7 (0.4) at M3 and 0.8 (0.3) at M6, while the 40 mg/kg group improved from 1.1 (1.1) at baseline by 0.6 (0.6) and 1.1 (1.6) at M3 and M6, respectively.Fractures occurred on study and were seen in both groups; additional analyses will investigate incidence over time.Setrusumab treatment in the pediatric cohort resulted in no unexpected adverse events and no significant differences in efficacy across dosing groups or age ranges. Treatment-related adverse events included infusion-related reaction (6/24, 25.0%), and infusion site pain, bone pain, upper respiratory tract infection, and headache (each 1/24, 4.2%).In the Phase 2 portion of ORBIT, significant increases from baseline were observed in P1NP after 1 month of setrusumab treatment, corresponding to BMD improvements at M3 and M6 at both 20 and 40 mg/kg doses. No marked differences in P1NP or BMD were apparent between dosage groups by 6 months.

***Disclosures: E. Michael Lewiecki**, Radius, Consultant, Amgen, Grant/Research Support, Kyowa Kirin, Speakers' Bureau, Radius, Grant/Research Support, Amgen, Consultant, Ultragenyx Pharmaceutical Inc., Grant/Research Support, Amgen, Speakers' Bureau*

LB SAT-651

Influence of Coagulation Factors on Bone Health: Repercussions in Hemophilia Patients *Sara Terreri[1], Giulia Battafarano[2], Stefano Lancellotti[3], Monica Sacco[3], Michela Rossi[2], Jacopo Di Gregorio[2], Laura Di Giuseppe[4], Matteo D'Agostini[8], Ottavia Porzio[5], Leonardo Di Gennaro[3], Maira Tardugno[3], Simone Pelle[6], Salvatore Minisola[4], Renato Maria Toniolo[7], Matteo Luciani[0], Raimondo De Cristofaro[3], Andrea Del Fattore[2]. [1]1Bone Physiopathology Research Unit, Translational Pediatrics e Clinical Genetics Research Division, Bambino Gesù Children's Hospital, IRCCS, Rome, Italy, Italy. [2]Bone Physiopathology Research Unit, Translational Pediatrics e Clinical Genetics Research Division, Bambino Gesù Children's Hospital, IRCCS, Rome, Italy, Italy. [3]Center for Hemorrhagic and Thrombotic Diseases, Foundation University Hospital "A. Gemelli" IRCCS, Catholic University of the Sacred Heart, Rome, Italy, Italy. [4]Department of Clinical, Internal, Anesthesiological and Cardiovascular Sciences, Sapienza University of Rome, Italy, Italy. [8]Clinical Laboratory Unit, Bambino Gesù Children's Hospital, IRCCS, Rome, Italy, Italy. [5]Clinical Laboratory Unit, Bambino Gesù Children's Hospital, IRCCS, Rome, Italy, Italy. [6]"Polo Sanitario San Feliciano - Villa Aurora" Clinic, Rome, Italy, Italy. [7]Department of Orthopaedics and Traumatology, Bambino Gesù Children's Hospital, IRCCS, Rome, Italy, Italy. [0]Pediatric Hematology/Oncology Department, Bambino Gesù Children's Hospital, IRCCS, Rome, Italy, Italy

Background: Hemophilia is a rare inherited X-linked disorder caused by a deficiency of certain blood clotting proteins such as Factor VIII. There are two forms of hemophilia: the more common hemophilia A, which results from a deficiency of coagulation factor VIII, and the less frequent hemophilia B, caused by a deficiency of coagulation factor IX. Coagulation factor deficiency causes both spontaneous and post-traumatic bleeding events. Hemophilia is associated with reduced bone mass and mineral density (BMD) both in adults and children mainly related to impaired mobility and vitamin D deficiency. Due to the rarity of the disease and the heterogeneity among the studies, pathogenesis of bone loss is still under investigation.Objectives: To dissect the mechanism of bone loss in Hemophilia A, we studied the effects on coagulation factors on bone cells and we characterized the osteoclastogenic potential of osteoclast precursors of patients.Patients/Methods: We treated Healthy Donors PBMC (HD-PBMC) and osteoblasts with FVIII, von Willerbrand Factor (VWF), FVIII/VWF, FXa and Thrombin. Osteoclastogenesis and FACS analyses of osteoclast precursors isolated from patients were performed; Alkaline Phosphatase (ALP) staining revealed the effects of coagulation factors on osteoblasts.Results and Conclusions: We showed a significant reduction of mature osteoclasts after treatment of HD-PBMC with FVIII, von Willerbrand Factor (VWF), FVIII/VWF, FXa and thrombin.Interestingly, PBMC isolated from hemophilic patients showed increased osteoclastogenic potential due to alteration of osteoclast precursor population. Moreover, transcriptional analysis revealed increased RANK, TRAF6 (TNF receptor-associated factor 6), CTSK (Cathepsin K) and TCIRG1 (T Cell Immune Regulator 1) genes expression in adult patient's osteoclasts compared to controls. FVIII and VWF treatments led also to a statistically significant reduction of ALP positivity in control osteoblasts. All these data suggest that bone loss observed in patients could be related to altered bone remodelling due to a direct effect of coagulation factors on bone cells. These results may have important implications in the clinical management of hemophilic patients to prevent bleeding as well as preserve the bone health.

***Disclosures: Sara Terreri**, None*

LB SAT-652

Bone Mineralization in 8 adults with Osteogenesis Imperfecta: a bone biopsy study *Delphine Farlay[1], Guilllaume Chevrel[2], Pascale Chavassieux[3], Roland Chapurlat[4]. [1]INSERM, UMR1033; Universite De Lyon, France. [2]Univ. Lyon, INSERM, UMR 1033, F-69008 Lyon, France. [3]INSERM UMR1033, Universite De Lyon, France. [4]INSERM UMR 1033, France

Osteogenesis imperfecta (OI) is an inherited disorder characterized by bone brittleness associated with low bone mass. In adult patients with OI, the incidence of fractures that decreases after puberty remains low until menopause in women and the age of 70 in men. Alendronate is a potent bisphosphonate able to increase BMD of the spine and hip and decrease by ?50% the incidence of vertebral fractures in postmenopausal women with osteoporosis (PMOP). In a clinical trial (ALOIA) that included 64 patients1 receiving either placebo (PBO; calcium + vitamin D) or 10 mg/day of alendronate (ALN) for 3 years, BMD at hip and spine was significantly increased, but no difference in the fracture incidence rate was observed between the 2 groups. The aim of this analysis was to determine the degree of mineralization (DMB) of bone in 8 adults (7 men, 1 woman) with Type I OI (quantitative mutations) from ALOIA study (PBO: n:5, aged 43+14 yrs; ALN: n:3, aged 44+4 yrs) who underwent transiliac bone biopsies after 3 yrs of treatment. Bone histomorphometry was performed and was available in 5 patients. DMB and heterogeneity index (HI) of mineralization were measured by X-ray microradiography. Cortical (Ct) and cancellous (Cn) bone were analyzed. Owing to the small number of samples, no statistical analysis was performed and the data were only descriptive. DMB was elevated in PBO and ALN patients in both Ct (PBO: 1.171+0.032; ALN:1.184+0.043 g/cm3), and Cn (PBO: 1.076+0.035; ALN: 1.092+0.065 g/cm3) bone. HI was low in PBO and ALN patients in both Ct (PBO: 0.108+ 0.013; ALN: 0.110+0.028 g/cm3) and Cn (PBO: 0.159+ 0.035; ALN: 0.125+0.035 g/cm3) bone. By comparison, in PMOP women treated for 8 years with BPs2, DMB was 1.053+0.027 in Ct and 1.014+0.026 g/cm3 in Cn bone, and HI was 0.143+0.022 in Ct and 0.153+0.024 g/cm3 in Cn bone. Histomorphometric analysis showed a great variability of bone turnover among these OI patients, with a trend towards an increase in MAR (0.97+ 0.11 µm/d in PBO, n=3; 0.93 µm/d, n=1 in ALN) compared to normal population (0.59+0.09)3. In conclusion, compared to long-term treated bisphosphonate patients, OI is characterized by a high DMB and a low HI, that may be associated with increased bone brittleness in OI patients. No difference in DMB or HI between ALN and PBO groups was observed, likely due to the small sample size. 1 Chevrel et al. J Bone Miner Res, 21, 2006 2 Farlay et al. J Bone Miner Res, 36, 2021 3 Vedi et al. Metab Bone Dis Rel Res, 5, 1983

***Disclosures: Delphine Farlay**, None*

LB SAT-653

Altered Collagen Secretion and Organization Contributes to the Bone Fragility in a Copb2+/- Mouse Model *Ronit Marom[1], AVA BERRIER[2], Megan Washington[3], I-Wen Song[3], Vittoria Rossi[3], Yuqing Chen[3], Xiaohui Li[3], Brian C. Dawson[3], Joseph M. Sliepka[4], D. Nicole Meyers[5], Cole Kuzawa[5], Lindsay C. Burrage[3], Catherine Ambrose[5], Brendan Lee[3]. [1]BAYLOR COLLEGE OF MEDICINE, United States. [2], . [3]Baylor College of Medicine, United States. [4]University of Washington, United States. [5]University of Texas Health Science Center at Houston, United States

Pathogenic variants in genes encoding subunits of coat protein complexes (coatomers), Golgi proteins, and motor proteins within the secretory pathway are associated with diverse phenotypes, including low bone mineral density and bone fragility, due to a defect in the sorting and transport of proteins between subcellular organelles. We had previously reported heterozygous, loss-of-function variants in COPB2, encoding a subunit of the coatomer complex I (COPI), in individuals presenting with a clinical spectrum of osteopenia, recurrent fractures, and intellectual and developmental disabilities.To better understand how COPB2 haploinsufficiency affects skeletal development, a phenotypic analysis was performed in Copb2+/- mice. Analysis of bone mass using micro-CT imaging showed a 15-20% reduction in spine bone volume/total volume (BV/TV) in 2-month-old Copb2+/- mice, compared to control wild-type littermates. Additionally, in females, the spinal trabecular number, trabecular thickness, and femur cortical thickness were significantly reduced. Polarized light microscopy imaging of Copb2+/- mouse vertebrae stained with picrosirius red showed disorganization of the collagenous matrix, as evidenced by increased yellow-green birefringence. Altered distribution of collagen fibers can affect the mechanical properties of bone and further the underlying collagen trafficking and synthetic defect. Consistent with this, the biomechanical testing of Copb2+/- mice femurs by 3-point bending demonstrated decreased ultimate load and stiffness, indicating reduced bone strength. To correlate these findings with delayed trafficking in vitro, collagen secretion was studied using pulse-chase assay in siRNA-treated cells. An 80% reduction in Copb2 expression was associated with a dramatic decrease in labeled procollagen secretion to the media.In conclusion, our data suggest that altered secretion and distribution of collagen likely contributes to the osteoporosis and bone fragility in patients with COPB2 haploinsufficiency. Understanding the mechanism of COPB2-related disorder will provide insights about procollagen secretion in bone cells, and about the role of intracellular protein trafficking in skeletal homeostasis.

***Disclosures: Ronit Marom**, None*

LB SAT-654

AAV-mediated gene editing of type 1 collagen mutation for Osteogenesis Imperfecta *Yeon-Suk Yang[1], Tadatoshi Sato[1], Sachin Chaugule[1], Zhihao Chen[1], Agustina Rodriguez[1], Hong Ma[1], Jun Xie[1], Guangping Gao[1], Jae-Hyuck Shim[1]. [1]UMass Chan Medical School, United States

Background:Osteogenesis Imperfecta (OI) is the most common rare skeletal disease characterized by bone fragility. The incidence is approximately 1 in 25,000-50,000 in the US. Up to 85% of OI patients have autosomal dominant mutations in either the COL1A1 or COL1A2 gene. The treatments of OI are improving bone strength, reducing fracture risk and pain, and preventing long-term complications. However, treatment options show limited success because they cannot alter the causes of collagen mutations or effectively deliver the drugs to the bone tissue.Methods/results:To develop novel therapeutics to correct collagen mutations in OI, we recently developed a bone-tropic AAV capsid by grafting bone-homing peptides ((AspSerSer)6, DSS) to the VP2 capsid protein (rAAV9.DSS) and confirmed that rAAV9.DSS was highly effective for the transduction of bone-forming osteoblasts (OB) in vitro and in vivo. We also used OIM mice harboring the deletion of a single-nucleotide (G) at 3983 in the Col1a2 gene as a mouse model of the dominant form of human OI (type 3). As a result, OIM mice displayed smaller body sizes, multiple non-union bone fractures, and pelvic bone deformity. µCT analysis demonstrated a significant decrease in trabecular bone mass in the long bones of these mice. CRISPR-Cas9 is one of the most powerful gene editing tools for skeletal rare diseases. We examined CRISPR-Cas9-mediated editing efficiency of the Col1a2 gene in immortalized OIM OB line. The gene-editing efficiency in these cells was substantially increased when CRISPR/Cas9 was coupled with a donor AAV vector containing a promoterless partial mouse Col1a2 complementary DNA sequence (GeneRide designed the optimized Condons for avoiding OIM mutation gRNA targeting, Figure 1) confirmed by NGS (next generation sequencing) analysis. This approach effectively reversed

the dysregulation of osteogenic differentiation by a Col1a2 mutation in vitro. Furthermore, systemic administration of dual AAV vectors lowered bone matrix turnover rates by reducing osteoblast and osteoclast development while improving the cellular network of mechano-sensing osteocytes embedded in the bone matrix. This strategy significantly improved bone architecture/mass/mineralization, skeletal deformities, grip strength, and spontaneous fractures.Conclusion:Taken together, these findings demonstrate that AAV-mediated gene editing effectively corrects a collagen mutation in OI osteoblasts and reverses skeletal phenotypes in OIM mice.

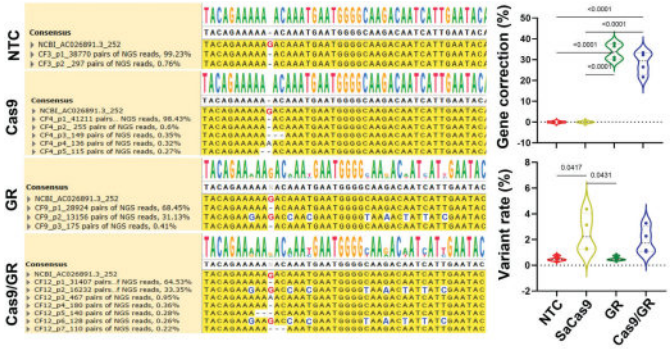

Figure 1. AAV-mediated Col1α2 gene correction in OIM osteoblasts. Immortalized OIM$^{m/m}$ osteoblasts were treated with AAV vectors, and two days later, genomic DNA was extracted and subjected to NGS analysis (n = 4). GR or Cas9/GR restored the missing "G" (red) in the Col1α2 gene, while eight nucleotides (blue) were adapted from GR. Percentage of sequence reads of Col1α2 gene correction (top right) or variants (bottom right) are displayed.

***Disclosures: Yeon-Suk Yang**, None*

LB SAT-655

Challenges of musculoskeletal multimorbidities in sub-Saharan Africa: findings from the Fractures-E3 and MUFASSA studies *Kate Ward[1,] Lisa Micklesfield[2,] Lucy Gates[3,] Tedios Manyanga[4,] Momodou Jallow[5,] Bilkish Cassim[6,] Yoliswa Madela[7,] Anya Burton[8,] Hannah Wilson[9,] Rashida Ferrand[10,] Celia Gregson[11,] [1]MRC Lifecourse Epidemiology Centre, University of Southampton, United Kingdom, [2]SAMRC/Wits Developmental Pathways for Health Research Unit, School of Clinical Medicine, Faculty of Health Sciences, University of the Witwatersrand, South Africa, [3]MRC LIfecourse Epidemiology Centre, University of Southampton, United Kingdom, [4]The Health Research Unit Zimbabwe, , Zimbabwe, [5]MRC Unit The Gambia at LSHTM, Gambia, [6]Department of Geriatrics School of Clinical Medicine, University of Kwa-Zulu Natal , South Africa, [7]Department of Geriatrics School of Clinical Medicine, University of Kwa-Zulu Natal, South Africa, [8]6 Musculoskeletal Research Unit, Bristol Medical School, University of Bristol, United Kingdom, [9]Musculoskeletal Research Unit, Bristol Medical School, University of Bristol, United Kingdom, [10]The Health Research Unit Zimbabwe, LSHTM, Zimbabwe, [11]University of Bristol, United Kingdom

Age-related diseases of bone (osteoporosis) and of muscle (sarcopenia) impact functional ability, through falls and fragility fractures. Currently, there are few data across sub-Saharan Africa quantifying prevalence of musculoskeletal disorders in ageing populations; such data are necessary to plan future healthcare services. The objective is to determine sarcopenia and fall prevalence in women and men in South Africa (SA), The Gambia (Gam) and Zimbabwe (Zim), compare by sex and explore factors associated with outcomes. By household sampling, a community-based sex- and age-stratified sample of urban-dwelling men and women aged 40 years and older were recruited1. Participants had hand grip strength, gait speed, sit-to-stand time and balance measured as part of the Short Physical Performance Battery (SPPB) and self-reported falls in the last year were recorded. Sarcopenia was defined as gait speed <1.0metres/second and grip strength <35.5kg in men and <20kg in women2. Differences between groups were tested using T-tests, Mann-Whitney-U and Chi-squared tests.Sarcopenia was more prevalent in men than women (Table 1). Low gait speed was seen in >75% men and >85% women in all countries, with low grip strength much less prevalent with men ranging from 22-34% and women 4.7-12.2% (sex-differences p<0.001). Those with sarcopenia were older (especially in Zim) with lower BMI. Overall, >=1 fall was reported by 155/885 (18%) in Zim, 174/673 (28.5%) in Gam, & 131/816 (17%) in SA; sarcopenia was associated with falling in Zim only (p=0.05), potentially a function of sample size and age of cohort; only 23.9% of fallers were classified as sarcopenic.Sarcopenia prevalence was low in women which contrasts with other populations. In men prevalence was higher than in the US & Europe1. Self-reported fall prevalence across men and women were similar to elsewhere. There is a need to validate context-specific thresholds for poor functional ability and sarcopenia. The Fractures-E31 and MUFASSA studies are generating important evidence needed to inform future health planning for older people, particularly regarding challenges to functional ability, and healthy ageing.References: 1 Burton A, Drew S, Cassim B et al. Wellcome Open Res 2023, 8:261 (https://doi.org/10.12688/wellcomeopenres.19391.1)2 Westbury et al. J Cachex Sarc Musc 2023 https://doi.org/10.1002/jcsm.13160

	The Gambia (n=698)		Zimbabwe (n=885)		South Africa (n=825)	
	Sarcopenia (n= 77)	No sarcopenia (n= 621)	Sarcopenia (n= 117)	No sarcopenia (n= 768)	Sarcopenia (n= 153)	No sarcopenia (n= 672)
Men (%)	22.0	78	20.7	79.3	28.4	71.6
Women (%)	4.8	95.2	5.7	94.3	9.9	90.1
Age (yrs)*	70 [62 – 77]	56 [49 – 70]	78 [70 – 85]	56 [48 – 67]	65 [56 – 74]	56 [48 – 64]
BMI (kg/m^2)	23.1 (4.2)	27.0 (5.9)	23.5 (4.6)	26.4 (6.4)	27.1 (7.8)	31.0 (9.3)
>1 fall/year (%)	25.9	25.3	23.9	16.5	19.7	15.2
Grip strength (kg)^	26.0 (7.4)	35.5 (9.5)	25.6 (7.1)	40.8 (10.8)	24.7 (7.2)	35.1 (9.5)
Gait speed (m/s)^	0.6 (0.2)	0.7 (0.2)	0.6 (0.2)	0.8 (0.2)	0.7 (0.2)	0.8 (0.3)
Sit-to-stand time (sec)^	19.7 (4.8)	17.6 (5.0)	19.8 (6.8)	16.2 (5.2)	14.5 (8.8)	13.2 (9.7)
SPPB score*	7 [5 – 8]	8 [7 – 9]	7 [5 – 8]	9 [8 – 10]	8 [6 – 11]	10.5 [8 – 12]

***Disclosures: Kate Ward**, None*

LB SAT-656

A Skeletal Muscle-specific Aptamer Facilitates Muscle-targeted Drug Delivery In Vivo *Zongkang Zhang[2,] Shanshan Yao[2,] Hewen Jiang[2,] Huan Xiao[2,] Baoting Zhang[2,] [2]The Chinese University of Hong Kong, , [2]The Chinese University of Hong Kong, Hong Kong

The skeletal muscular disorders, such as sarcopenia and Duchenne muscular dystrophy, are related to serious health consequences. However, one major bottleneck of current pharmacological therapies for skeletal muscle disorders is lack of muscle cell selectivity, leading to low efficacy and off-target side effects when administered systemically. Nucleic acid aptamers are promising escort molecules for drug delivery systems. Utilizing cell-based systematic evolution of ligands by exponential enrichment (cell-SELEX) technology, we identified one aptamer SkMApt1 showed higher affinity and selectivity to skeletal muscle than scramble aptamer both in vitro and in vivo. We previously reported microRNA-487b (miR-487b) is an anabolic suppressor in skeletal muscle during sarcopenia development. To further evaluate the efficacy of SkMApt1-facilitated skeletal muscle-targeted drug delivery, we prepared SkMApt1-functionalized lipid nanoparticles (LNPs) encapsulating antagomiR-487b (Apt1-LNPs-antimiR). The fluorescence labeled antimiR distribution in different tissues were evaluated by ex vivo florescence imaging in mice. The fluorescence signal intensity of Apt1-LNPs-antimiR in skeletal muscle was significantly higher, whereas the fluorescence signal intensities in liver and kidney were significantly lower when compared to scramble aptamer control. Moreover, eight periodic intravenous administrations (once per week) of Apt1-LNPs-antimiR promoted the muscle mass, muscle fiber CSA and muscle strength of muscle-specific miR-487b knockin mice. Apt1-LNPs-antimiR treatment inhibited miR-487b level and elevated Wnt5a protein level in skeletal muscle of muscle-specific miR-487b knockin mice, while blank or scramble aptamer conjugated LNPs-antimiR treatment failed to achieve the above results. Taken together, the above findings suggested that SkMApt1 could be a potential skeletal muscle-targeted moiety to facilitate muscle-targeted drug delivery. Acknowledgments: This study was supported by the Hong Kong General Research Fund (14103420, 14109721, 14103121), and Hong Kong CUHK Direct Grant (4054714).

***Disclosures: Zongkang Zhang**, None*

LB SAT-657

A Randomized Controlled Trial to Investigate the Effect of Luseogliflozin on Bone Microarchitecture in Elderly Patients with Type 2 Diabetes Using High-Resolution Peripheral Quantitative Computed Tomography (HR-pQCT) *Riyoko Shigeno[1,] Ichiro Horie[1,] Norio Abiru[1,] Ryuji Niimi[2,] Ko Chiba[2,] Makoto Osaki[3,] Atsushi Kawakami[1,] [1]Department of Endocrinology and Metabolism, Nagasaki University Hospital, Japan, [2]Nagasaki University Graduate School of Biomedical Sciences, Japan, [3]Nagasaki University, Japan

Aim: Patients with type 2 diabetes (T2D) have an increased risk of bone fractures despite having increased bone mineral density (BMD). In the CANVAS program, an SGLT2 inhibitor canagliflozin was related to an increased fracture risk as early as 12 weeks after initiating the drug in patients with T2D, but other SGLT2 inhibitors did not affect the fracture risk in clinical trials. It remains unclear whether SGLT2 inhibitors lead deterioration of bone quality. We prospectively studied the effect of an SGLT2 inhibitor luseogliflozin on bone microarchitecture and strength in patients with T2D using HR-pQCT.Methods: This is a randomized, open-label, active-controlled trial for elderly (>=60 years) Japanese patients with T2D. We enrolled patients uncontrolled with HbA1c levels of 7.0-8.9 % by the treatment with diet alone or with mono- or combination therapy with metformin (<=?1000?mg/day), ?-glucosidase inhibitor and dipeptidyl peptidase-4 inhibitor. Patients were randomized to either the luseogliflozin (Lusefi) group (added luseogliflozin 2.5 mg) or the control (CTRL)

group (added metformin 500 mg) and have treated for 48 weeks. Bone microarchitecture was evaluated using HR-pQCT (Xtreme CT II, Scanco Medical, Switzerland) in addition to BMD by dual-energy X-ray absorptiometry (DXA) before and 48 weeks after treatment. The primary outcome was 48-weeks change in the predictive bone strength (failure load, kN) determined HR-pQCT in Lusefi group compared to CTRL group using a linear regression model.Result: Of the 22 patients (Female,32%), 20 patients (9 in Lusefi, 11 in CTRL groups) completed the study. There were no significant differences in the changes in BMD measured by DXA before and after treatment in the two groups. As the primary outcome determined by HR-pQCT, the 48-weeks changes in the estimated failure load showed no significant decrease in Lusefi group compared to CTRL group using a linear regression model.Result: Of the 22 patients (Female,32%), 20 patients (9 in Lusefi, 11 in CTRL groups) completed the study. There were no significant differences in the changes in BMD measured by DXA before and after treatment in the two groups. As the primary outcome determined by HR-pQCT, the 48-weeks changes in the estimated failure load showed no significant decrease in Lusefi group compared to CTRL group (?, 35; 95%CI, -215 to 284 at radius, and ?, -147; 95%CI, -330 to 36 at tibia). In the secondary outcomes, cortical porosity (%) in radius tended to decrease after treatment in Lusefi group compared to CTRL group (?, -0.061; 95%CI, -0.12 to 0.0027; p=0.059). The changes in the other HR-pQCT parameters from baseline to 48 weeks showed no significant differences between the two groups.Conclusion: We observed no negative effect of luseogliflozin treatment on bone microarchitecture and bone strength evaluated by HR-pQCT compared to metformin treatment in short standing investigation.

***Disclosures: Riyoko Shigeno**, None*

LB SAT-658

HR-pQCT and Risk Factors in Type 1 Diabetes *Naina Sinha Gregory[1], Andrew J. Burghardt[2], Jye-Yu C. Backlund[3], Mishaela R. Rubin[4], Ionut Bebu[3], Barbara H. Braffett[3], David J. Kenny[3], Thomas M. Link[2], Galateia J. Kazakia[2], Annette Barnie[5], John M. Lachin[3], Rose Gubitosi-Klug[6], Ian H. de Boer[7], Ann V. Schwartz[2]. [1]Weill Cornell Medicine, [2]University of California San Francisco, United States, [3]The George Washington University, United States, [4]Columbia University, United States, [5]University of Toronto, Canada, [6]Case Western Reserve University, United States, [7]University of Washington, United States

Type 1 diabetes is associated with a nearly five-fold greater risk of hip fracture that is not accounted for by the modest decrease in BMD. This discrepancy points to other factors that impact bone strength including bone geometry and microarchitecture. We set out to determine whether type 1 diabetes and its complications are associated with bone geometry, microarchitecture, and strength. This was a cross-sectional study embedded in a long-term observational study. High-resolution peripheral quantitative computed tomography (HR-pQCT) scans of the distal radius and distal and diaphyseal tibia were performed in a subset of 183 participants from the Diabetes Control and Complications Trial/Epidemiology of Diabetes Interventions and Complications (DCCT/EDIC), a long-term follow-up of participants with type 1 diabetes and 94 controls without diabetes. HbA1c, advanced glycation end products (AGEs), and diabetes-related complications were assessed in EDIC participants with >30 years of follow-up. Compared to controls (60 +/- 8 years old and 65% female) , EDIC participants (60 +/- 7 years old, duration of type 1 diabetes 38 +/- 5 years, and 51% female) had lower total bone mineral density (BMD) at the distal radius (-7.9%, 95%CI:(-15.2%,-0.6%), p=0.030) and distal tibia (-11.3%, 95%CI:(-18.5%,-4.2%), p=0.001); larger total cross-sectional area at all sites (distal radius +4.7%, 95%CI:(+0.5%,+8.8%), p=0.030; distal tibia +5.9%, 95%CI:(+2.1%,+9.8%), p=0.003; diaphyseal tibia +3.4%, 95%CI (+0.8%,+6.1%), p=0.011); and poorer radius trabecular and cortical microarchitecture. Estimated failure load was similar between two groups. Among the EDIC cohort, higher HbA1c and AGE and macroalbuminuria were associated with lower total BMD. Macroalbuminuria was associated with larger cross-sectional area and lower cortical thickness at the distal radius. Higher HbA1c and AGE, lower glomerular filtration rate, peripheral neuropathy and retinopathy were associated with deficits in trabecular microarchitecture. These results revealed that type 1 diabetes is associated with lower BMD, larger bone area and poorer trabecular microarchitecture. In those with type 1 diabetes, suboptimal glycemic control, AGE accumulation and microvascular complications, particularly reduced renal function, are associated with deficits in bone microarchitecture and lower BMD.

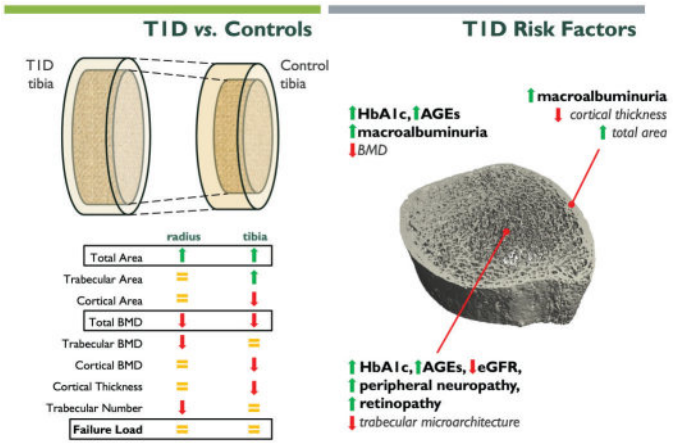

***Disclosures: Naina Sinha Gregory**, None*

LB SAT-659

The importance of kynurenine monooxygenase, KMO in regulation of kynurenine-induced bone loss with age *Dmitry Kondrikov[1], Galina Kondrikova[2], Xing-ming Shi[3], Mark Hamrick[4], Carlos Isales[5], Sadanand Fulzele[6], Meghan McGee-Lawrence[4], William Hill[7]. [1]Department of Pathology and Laboratory Medicine, Medical University of South Carolina, United States, [2]Department of Pathology and Laboratory Medicine, Medical University of South Carolina, United States, [3]Neuroscience and Regenerative Medicine, Augusta University, United States, [4]Cellular Biology and Anatomy, Medical College of Georgia, Augusta University, United States, [5]Augusta University, United States, [6]Division of Endocrinology, Diabetes and Metabolism, Medical College of Georgia, Augusta University, United States, [7]Medical University of South Carolina, United States

Kynurenine pathway metabolites are emerging as important factors in the pathophysiology of aging-related bone loss. Our group has previously shown that the essential amino acid tryptophan is metabolized by IDO-1 in the periphery to generate kynurenine (KYN), and that KYN can act though the aryl hydrocarbon (AhR) receptor signaling pathway to inhibit osteogenesis in bone marrow MSCs via epigenetic regulation of osteogenic genes, while also upregulating osteoclastogenic transcription factors and genes driving osteoclast activity. Further, we recently showed that KYN, acting via KLF6 through the AhR non-canonical XRE pathway, induces senescence and suppresses autophagy in human BMSCs. Also, we demonstrated that KYN pathway metabolites downstream from KYN, 3-hydroxykynurenine (3-HK) and quinolinic acid (QA) act via the AhR signaling pathway also inhibit autophagy, induce Senescence Associated Secretory Phenotype (SASP) molecular expression, and drive senescence in murine and human bone marrow MSCs, similar to KYN.Here, we demonstrate that kynurenine monooxygenase (KMO) plays an important role in kynurenine-induced bone loss. Inhibition of KMO pharmacologically, or by siRNA, prevents KYN-induced senescence, and restores autophagic flux in murine and human BMSCs. KMO inhibition suppresses osteoclast differentiation of human CD14-positive bone marrow and peripheral blood derived macrophages. At the same time, inhibition of KMO promotes osteogenic differentiation of human BMSCs rescuing KYN-induced suppression of osteogenesis. KMO protein levels are higher in osteoblasts and osteocytes in the femurs of aged mice compared to young mice, as well as in mice treated with KYN. KMO gene expression is also elevated with age or KYN treatment in human BMSCs. This suggests KMO levels are potentially increased in response to aging-related factors, including increases in its substrate KYN, thus elevating sub-KMO metabolite levels and possible canonical and non-canonical AhR XRE signaling and gene expression. This makes KMO an attractive target for more precise control of kynurenine pathway effects. Blocking KYN downstream metabolite formation, rather than KYN itself by inhibiting KMO, presents a novel therapeutic target linked to the regulation of kynurenine pathway metabolites and their signaling. As such, inhibiting KMO may allow rescue of bone homeostasis and reduction of bone loss in aged patients.

***Disclosures: Dmitry Kondrikov**, None*

LB SAT-660

Efficacy of Moderate-Dose Denosumab in Fibrous Dysplasia: Secondary Results from a Phase 2 Clinical Trial *VIVIAN SZYMCZUK, National Institutes of Health ; Ramzy Ahmed, Eastern Virginia Medical School, United States; Ibrahim Elbashir, National Institute of Dental and Craniofacial Research, National Institutes of Health, United States; Alison Boyce, National Institutes of Health

Kynurenine pathway metabolites are emerging as important factors in the pathophysiology of aging-related bone loss. Our group has previously shown that the essential amino acid tryptophan is metabolized by IDO-1 in the periphery to generate kynurenine (KYN), and that KYN can act though the aryl hydrocarbon (AhR) receptor signaling pathway to inhibit osteogenesis in bone marrow MSCs via epigenetic regulation of osteogenic genes, while also upregulating osteoclastogenic transcription factors and genes driving osteoclast activity. Further, we recently showed that KYN, acting via KLF6 through the AhR non-canonical XRE pathway, induces senescence and suppresses autophagy in human BMSCs. Also, we demonstrated that KYN pathway metabolites downstream from KYN, 3-hydroxykynurenine (3-HK) and quinolinic acid (QA) act via the AhR signaling pathway also inhibit autophagy, induce Senescence Associated Secretory Phenotype (SASP) molecular expression, and drive senescence in murine and human bone marrow MSCs, similar to KYN.Here, we demonstrate that kynurenine monooxygenase (KMO) plays an important role in kynurenine-induced bone loss. Inhibition of KMO pharmacologically, or by siRNA, prevents KYN-induced senescence, and restores autophagic flux in murine and human BMSCs. KMO inhibition suppresses osteoclast differentiation of human CD14-positive bone marrow and peripheral blood derived macrophages. At the same time, inhibition of KMO promotes osteogenic differentiation of human BMSCs rescuing KYN-induced suppression of osteogenesis. KMO protein levels are higher in osteoblasts and osteocytes in the femurs of aged mice compared to young mice, as well as in mice treated with KYN. KMO gene expression is also elevated with age or KYN treatment in human BMSCs. This suggests KMO levels are potentially increased in response to aging-related factors, including increases in its substrate KYN, thus elevating sub-KMO metabolite levels and possible canonical and non-canonical AhR XRE signaling and gene expression. This makes KMO an attractive target for more precise control of kynurenine pathway effects. Blocking KYN downstream metabolite formation, rather than KYN itself by inhibiting KMO, presents a novel therapeutic target linked to the regulation of kynurenine pathway metabolites and their signaling. As such, inhibiting KMO may allow rescue of bone homeostasis and reduction of bone loss in aged patients.

1041

Identification of one-carbon metabolism and methionine as regulator of bone loss during fasting *Tânia Amorim[1], William Dion[2], Trishya Pagadala[2], Natalie L David[3], Naveen VG Kumar[2], Tristan Pesaresi[2], Nandini K Doshi[2], Rosemary Andrews[2], Andrey Parkhitko[2], Matthew L Steinhauser[4], Pouneh Fazeli[5]. [1]University of Pittsburgh, , [2]Aging Institute, University of Pittsburgh School of Medicine, Pittsburgh, PA, United States, [3]Neuroendocrinology Unit, Division of Endocrinology and Metabolism, University of Pittsburgh School of Medicine, Pittsburgh, PA 2 Aging Institute, University of Pittsburgh School of Medicine, Pittsburgh, PA, United States, [4]1 Aging Institute, University of Pittsburgh School of Medicine, Pittsburgh, PA 2 Center for Human Integrative Physiology, University of Pittsburgh School of Medicine, Pittsburgh, PA, United States, [5]University of Pittsburgh School of Medicine, United States

In non-human models, fasting has beneficial effects on longevity; however, a potential negative effect of fasting is bone loss. Our aim was to test the effect of a prolonged fast on bone microarchitecture and identify novel metabolic regulators of bone turnover. Bone microarchitecture (HR-pQCT) and bone turnover markers (ELISA) were measured during a 10-day, 0-calorie fast in healthy humans [N=12, median age: 29.3yrs (21.8-48.3), 8 premenopausal females]. After fasting, radial Tb.N and BV/TV significantly decreased (-9.2%+7.9 (mean+SD) and -0.7%+0.7, respectively, $p<0.05$ for both), whereas Tb.Th and Tb.Sp increased (10.3%+8.7 and 11.0%+9.4, respectively, $p<0.05$ for both). After 5 days of fasting, P1NP decreased by 55%, $p<0.05$. Using previously published metabolomics data from this study, one-carbon metabolism was identified as one of the most enriched fasting-dependent pathways. This provided rationale for a new hypothesis - one or more one carbon metabolites regulate bone turnover. We systematically manipulated levels of one-carbon metabolites in cultured osteoblasts and methionine was the only candidate to consistently impact metrics of osteoblast function. Gene transcripts related to bone formation (P1NP, ALPL) and osteoblast function (OCN, OPG, ATF4, RUNX2) were significantly attenuated by excess methionine (100 and 500 µmol; ~2-fold reduction, $p<0.05$), an effect also observed at the protein level (RUNX2 and ATF4 immunoblotting). Given the known link between methionine and histone methylation, we tested if manipulating methionine modulates histone methylation. H3K9me and H3K27me histone marks were augmented in osteoblasts cultured in excess methionine. Consistent with western blot assays, we observed a trend towards increased H3K9me and H3K27me3 at ATF4 and RUNX2 promoters in osteoblasts with methionine excess ($p=0.14$). We then conducted a 5-day murine study with 3 groups: vehicle; methionine excess (60mg/day); and 24h fast. Transcripts for Igf1 and Ocn were decreased in femurs of mice treated with excess methionine vs. controls ($p<0.05$), a pattern seen in fasted mice also. Transcription of Mat1A ($p<0.001$) and Bhmt ($p<0.01$) was also increased in the liver of fasted vs. non-fasted mice, supporting the hypothesis that the methionine pathway is upregulated with fasting. In conclusion, a 10-day fast in humans leads to remodeling of bone microarchitecture. Elevations in circulating methionine with fasting may contribute to fasting-associated bone loss.

***Disclosures: Tânia Amorim**, None*

1042

Enhanced lipolysis in osteoblast progenitor cells protects from high fat diet-induced bone dysfunction *Ananya Nandy[1], Elizabeth Rendina-Ruedy[2]. [1]Vanderbilt University Medical Centre, , [2]Vanderbilt University Medical Center, United States

Skeletal homeostasis is maintained by a balance between two highly energy consuming processes, bone formation and resorption. As such, formation of new bone is associated with maturation of stromal cells to matrix and mineral secreting osteoblasts, requiring robust amount of cellular energy or adenosine triphosphate (ATP). Therefore, alterations in systemic metabolism can likely directly influence osteoblast function. In this regard, Type 2 diabetes mellitus (T2DM) is a common metabolic disorder that is associated with increased risk of fracture. In other tissues, impaired lipid metabolism is a key feature of T2DM-related pathologies. Therefore, we tested the hypothesis that the reduced bone formation described in diet-induced obese models of T2DM are a function of disrupted lipid metabolism in osteoblasts. Our data confirm that mice fed a high fat diet display reduced bone microarchitecture along with lower bone formation rates. Interestingly, osteoblast isolated and cultured ex vivo from high-fat diet fed mice contain a higher number of lipid droplets along with reduced bioenergetic profile compared to osteoblasts harvested from mice fed a control diet. Further supporting this observation, bone tibia cortex, devoid of marrow elements, had higher lipid content in the form of triacylglycerol (TAGs) in mice fed a high fat diet compared to control-fed mice. As a further proof of principle, we generated a novel murine model to conditionally delete Plin2 in osteoblast-progenitor cells using Prrx1-Cre, Prrx1-Cre.Plin2 mice along with their littermate, wildtype controls. Disruption of Plin2 has previously been reported to enhance lipolysis, and in this capacity, has been demonstrated to protect other tissues from high-fat diet induced lipid dysfunction. Our data demonstrate the Prrx1-Cre. Plin 2 mice are protected from diet-induced obesity related bone impairments as trabecular microarchitecture are similar to that of wildtype controls, along with comparable bone formation rates. In conclusion, our study shows high fat diet leads to perturbation of lipid metabolism in bone causing decreased bone formation which can be reversed by increasing lipolysis in osteoblasts possibly by increasing utilization of fatty acids by these cells.

***Disclosures: Ananya Nandy**, None*

1043

Stimulation of mitochondria dysfunction in the osteoblast lineage recapitulates part of the effects of aging: evidence from single-cell RNA-seq *Md Mohsin Ali[1], Aaron Warren[1], Ha-Neui Kim[2], Intawat Nookaew[3], Charles O'Brien[4], Maria Jose Almeida[5]. [1]The university of Arkansas for Medical Sciences , United States, [2]Univ. Arkansas for Medical Sciences, Central Arkansas VA Healthcare System, United States, [3]University of Arkansas for Medical Sciences, United States, [4]Univ of Arkansas for Medical Sciences, United States, [5]Central Arkansas VA Healthcare System, Univ of Arkansas for Medical Sciences, United States

Mitochondria dysfunction causes DNA damage, senescence, and loss of proteostasis due, at least in part, to increased production of reactive oxygen species (ROS). All these effects are critical hallmarks of aging, can be interrelated, and have been shown to contribute to skeletal aging. Here, we examined whether mitochondria dysfunction in cells of the osteoblast lineage in vivo is sufficient to promote some of the hallmarks of aging, such as senescence. To this end, we generated mice lacking superoxide dismutase 2 (SOD2) - a critical mitochondrial ROS detoxifying enzyme - in the osteoblast lineage targeted by Osx1-Cre. Specifically, we crossed SOD2-flox and Osx1-Cre mice to generate SOD2?Osx1 and Osx1-Cre control mice. Cultures of bone marrow-derived osteoblastic cells from SOD2?Osx1 mice had lower SOD2 mRNA, increased mitochondrial ROS, and impaired mitochondrial respiration. Osteoblast differentiation markers and mineralization were decreased in cells from SOD2?Osx1 mice. Femoral and vertebral bone mass in female and male SOD2?Osx1 were lower than Osx1-Cre littermates at 3 and 6 months of age. Endosteal mesenchymal cells from long bones were analyzed using single-cell RNA-seq and compared with similar cells obtained from young (6 mo) and old (24 mo) wild-type mice. An initial UMAP plot and cluster analysis, after harmonization of cells from mice of the two experiments, revealed 9 clusters based on expression of cluster-specific markers, including osteocytes, osteoblasts, pre-osteoblasts, osteo-CAR, osteo-X, adipo-CAR, chondrocytes, fibro-1, and fibro-2. Both aging and SOD2 deletion led to a decrease in the proportion of osteoblasts. Overall, the differentially regulated genes with SOD2 deletion and aging exhibited significant overlap, with about 560 genes being commonly up- or down-regulated. Gene Ontology enrichment analysis of differentially expressed genes in osteoblasts revealed that processes related to translation, ribosomes, and ribonucleoproteins were increased with both aging and SOD2 deletion. Senescence, inflammation, and apoptosis processes were increased in osteoblasts with aging but not with SOD2 deletion. On the other hand, processes related to collagen fibril organization and extracellular matrix decreased with age and SOD2 deletion in osteoblasts. These results suggest that mitochondria dysfunction contributes to the decreased osteoblast number and function seen in aged mice, likely via mechanisms independent of cellular senescence.

***Disclosures: Md Mohsin Ali**, None*

1044

N7-methylguanosine tRNA modification regulates bone development by controlling amino acid metabolism *Qiwen Li[1], Quan Yuan[2]. [1]State Key Laboratory of Oral Diseases, National Clinical Research Centre for Oral Diseases, West China Hospital of Stomatology, Sichuan University, China, [2]Sichuan University, China

Organ development requires the optimal translation of mRNA to protein that supports stage-specific function. Transfer RNAs (tRNAs) play an essential role in this process. Dysregulation of tRNA was reported in patients with primordial dwarfism, but the underlying mechanism remains unexplored. Here we demonstrate that METTL1/WDR4 complex-mediated N7-methylguanosine (m7G) tRNA modification regulates skeletal development by controlling amino acid metabolism. Deleting m7G catalytic enzyme Mettl1 using Prx1-Cre severely impairs longitudinal bone growth, manifested as reduced proliferation and maturation of chondrocyte, and retarded bone formation and bone mass accrual. Tamoxifen-induced deletion of Mettl1 in chondrocytes using Acan-CreERT2 greatly impairs endochondral bone formation as well. Furthermore, missense mutation of Wdr4 (p.Arg215Leu) reduces METTL1 levels and the bone growth of Wdr4-R215L/R215L mice is greatly inhibited, phenocopying the primordial dwarfism observed in patients. Mechanistically, m7G tRNA reduction and cleavage sequencing (TRAC-seq) reveals that Mettl1 knockout erases m7G modification and reduces abundance of m7G-modified tRNAs, which alters mRNA translation by two approaches. On one hand, Mettl1 knockout evokes translational stress that relays to GCN2, which stalls general translation initiation by phosphorylating eIF2?. Promoting translation initiation by deleting Gcn2, however, aggravates bone defects of Mettl1-deficient mice, indicating a translational protective response to tRNA dysregulation. On the other hand, Mettl1 knockout selectively upregulates translation of mRNAs related to cellular metabolism, in an m7G tRNAs-decoded codon-dependent manner. Mettl1-deficient cells exhibit active cellular respiration despite of incompetent proliferation and chondral-osteo commitment. Ribosome profiling reveals upregulated translation of branched-chain amino acid transaminase 1 (BCAT1), which catalyzes branched-chain amino acid (BCAA) catabolism to support cellular respiration. However, intracellular ?-ketoglutarate (?KG) levels are restricted as BCAT1 transfers ?-amino group from BCAA to ?KG to form glutamate. Supplementation of ?KG ameliorates the skeletal abnormality of Mettl1-deficient mice. Overall, our study unveils a critical role of m7G tRNA modification in bone development by regulat-

ing cellular metabolism, and reveals that stalling of translation initiation as a quality control mechanism in response to tRNA dysregulation.

***Disclosures: Qiwen Li**, None*

1045

Osteocyte Connexin Hemichannels and Associated PGE2 Release Regulate Adipogenesis and Body Metabolism *FRANCISCA ACOSTA[4], JINGRUO ZHANG[2], Linda Mota[3], Xuewei Wang[2], Elizabeth Hernandez[3], Manuel Riquelme[4], Eric Brey[3], Jean Jiang[5]. [4]UT Health San Antonio, , [2], , [3]The University of Texas at San Antonio, United States. [4]UT Health San Antonio, United States. [5]University of Texas Health Science Center at San Antonio, United States

Obesity leads to a marked decrease in bone quality & increased fragility, & a reduced quality of life. Bone, & most distinctively osteocytes (Ocy, >90% of bone cells), through involvement in biomechanical, inflammatory, & metabolic signaling, provide a strong deduction for the cross-organ regulation of adipose tissue (AT). Recent work has begun to progress on the intricate link between the release of osteokines, obesity, & metabolic homeostasis. Connexin 43 (Cx43) hemichannels (HCs) are transmembrane proteins richly expressed in Ocy that facilitate extracellular communication. Our lab previously found that Ocy Cx43 HCs are mechanosensitive & exchange multiple small molecules, such as prostaglandin E2 (PGE2), a pleiotropic regulator of bone quality & metabolism. Like during obesity, the loss of Ocy Cx43 HCs compromises bone & biomechanical properties. Here, in vivo studies using transgenic mice models with overexpression of Cx43 dominant negative mutants in Ocy: R76W (inhibited gap junctions, enhanced HCs) & ?130-136 (inhibited HCs & gap junctions), or a monoclonal Cx43(M2) antibody that specifically opens Cx43 HCs, high-fat (+/- 60%) diet, we found that impaired HCs (?130-136) increases harmful AT formation, while enhanced HC activity (R76W/M2) decreases it, ultimately improving whole-body energy expenditure & enhancing systemic metabolic function, all of which is likely inextricably linked to Cx43 HC-mediated PGE2 levels. Specifically, ?130-136 mice showed an ~2.5-fold increase in bone marrow (BM) AT (H&E) & a significant increase in global % Fat (DEXA, H&E, AT weights). Enhancement of HCs (R76W/M2) significantly increased BM & serum PGE2 levels, alongside an enrichment in mice activity, food intake, calorie burnout (Indirect calorimetry), & hindered a rise in glucose, triglycerides, AT hypertrophy/whitening, & liver AT. In vitro, work to further corroborate Cx43 HC-PGE2 mediated AT regulation showed that conditioned media (CM) collected from fluid flow-stimulated Ocy hindered BM & AT-derived stem cell adipogenic differentiation, & this inhibition was ablated with CM from Ocy treated with a HC-blocking antibody. Moreover, the direct addition of PGE2 into culture conditions led to similar inhibition of adipogenesis. These results underline the role of Ocy Cx43 HCs, as key bone & systematic metabolic regulators, possibly mediated through the release of PGE2, & present Ocy Cx43 HCs as potential therapeutic targets for obesity & related metabolic conditions.

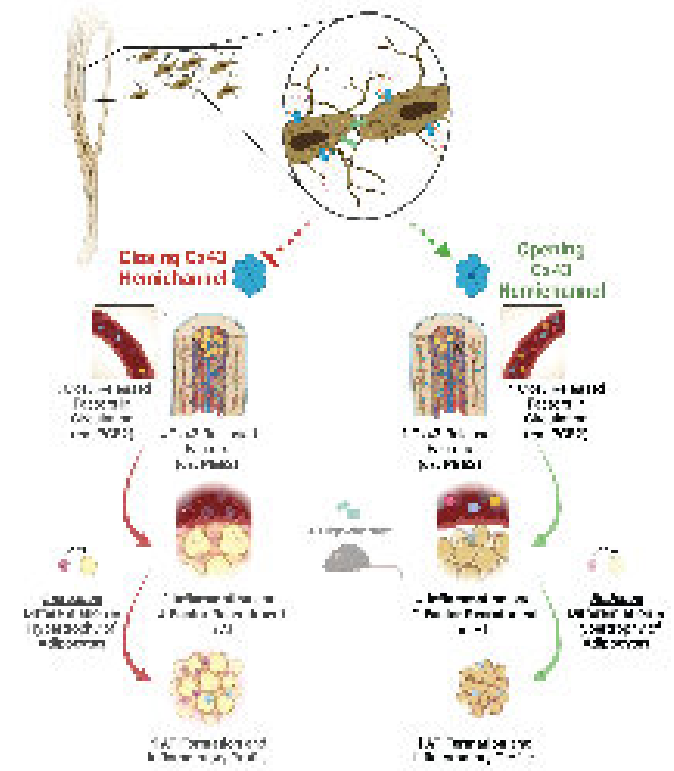

***Disclosures: FRANCISCA ACOSTA**, None*

1046

Synthetic BMP-2 Analog for Specific Targeting of the Skeletal Stem Cell Niche *Eri Takematsu[1], Liming Zhao[2], Charles Chan[2, 1], United States. [2]Stanford University, United States

Age-related skeletal failures, such as osteoarthritis (OA), causes significant morbidity and affect 350 million people worldwide. Diseased and damaged cartilage regenerate poorly, and current standard care for OA focuses on pain medication, physical therapy or invasive joint replacement procedures. We recently showed that a combination of BMP-2 and VEGF inhibition activated skeletal stem cells (SSCs) and induced full thickness cartilage regeneration in critical sized defects in mice and human xenografts (Murphy et al. Nature Medicine 2020). However, the clinical use of BMP-2 is still problematic due to potential off target effects including stimulation of inflammatory cell types such as monocytes and macrophages. This highlights the necessity for more precise targeting strategies that specifically address SSCs and their lineage cells, while avoiding the activation of immunogenic cells, ultimately optimizing their regenerative potential.To address this need, we are developing the synthetic BMP-2s that primarily activate skeletal lineage cells while avoiding activation of immune cells and allowing for tuning in levels of BMP receptor (BMPR) activation. We use machine learning based algorithm's including Alpha-Fold and Rosetta to identify areas of BMP2/receptor engagement and design high affinity nanobodies to specific epitopes that engages with BMPR (Fig.1). We then developed a fusion construct composed of bispecific nanobodies (NBs) that constrain BMPR to be in active configuration thus enabling downstream signaling (Fig.2a). The linker between NB1 and NB2 is cleavable by an enzyme often secreted by monocytes or macrophages, allowing the synthetic BMP-2s to be inactivated near immune cells (Fig.2b). We measured the functional activities of the synthetic BMP-2s using Smad-dependent (p-smad1/5) and independent (p-p38) activities, showing the proof of concept (Fig.2c,d). The synthetic BMP-2s can also tune its activity based on the linker distance, offering a solution to the problem of ectopic bone formation. After selecting the best linker distance and NB combination, the activity of synthetic BMP-2 was verified with in vitro osteogenesis, chondrogenesis and in vivo subcutaneous implantation model.To summarize, we created activity-controllable BMP-2s that have the potential to serve as a next-generation therapy for regenerative medicine, particularly in the context of the diverse genetic and functional makeup of cells in the skeletal stem cell niche.

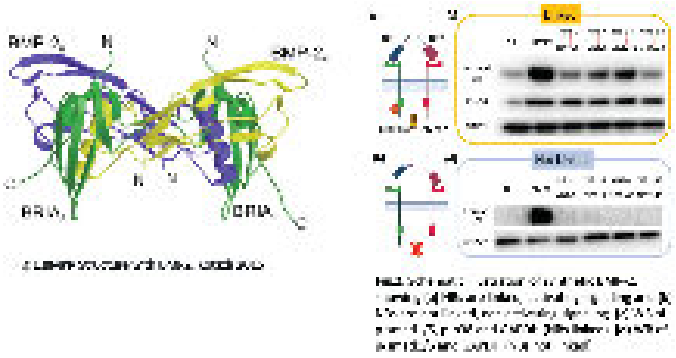

***Disclosures: Eri Takematsu**, None*

1047

SIK2/SIK3 inhibitor increases cortical bone mass in a mouse model of CKD-MBD *Sung-Hee Yoon[1], Han Xie[4], Michael Bruce[4], Daniel Brooks[4], Michael Mannstadt[3], Marc Wein[4]. [1]Massachusetts General Hospital - Harvard Medical School, [4]Massachusetts General Hospital, United States. [3]Massachusetts General Hospital Harvard Medical School, United States. [4]Massachusetts General Hospital,

Chronic Kidney Disease (CKD) is defined as a decrease in renal function with low glomerular filtration rate, albuminuria, and/or structural abnormalities in kidney. Compromised renal function results in inadequate filtration of waste products and minerals and is associated with bone and mineral disease (CKD-MBD). Salt-Inducible Kinases (SIKs) were identified in bone and kidney as key downstream mediators of PTH receptor signaling. SIK inhibition by cAMP/PKA signaling upon PTH receptor activation in kidney leads to increased Cyp27b1 expression and thus 1,25-vitamin-D production. Similarly in bone, SIK inhibition increases Rankl and decreases Sost expression, thus stimulating bone remodeling and net gains in bone mass. These PTH-like effects of SIK inhibitors may be desirable in CKD-MBD with renal osteodystrophy and low 1,25-vitamin-D levels. Thus, we hypothesized that targeting SIKs, downstream of PTH receptor, would improve mineral metabolism and skeletal outcomes in CKD-MBD. To test this, we examined the effects of SIK inhibitor (SK-124) in 0.2% adenine diet induced CKD model in 8-week old CD1 female mice. After 6 weeks of adenine diet-induced CKD, vehicle-treated mice showed expected changes including hyperphosphatemia, increased BUN, hyperparathyroidism, increased CTx bone resorption marker, and decreased trabecular thickness, cortical bone area and thickness, and compromised apparent material properties in femurs. In contrast, daily SK-124 treatment (40mg/kg) in the presence of adenine diet significantly alleviated hyperphosphatemia and hyperparathyroidism, and increased only the bone formation marker P1NP without changing CTx levels. This net bone formation stimulated by SK-124 led to complete rescue of CKD-associated bone changes including improved trabecular thickness and cortical bone area, in addition to significant improvements in structural and apparent material properties. Surprisingly, SK-124 treatment also improved renal function as assessed by serum BUN and creatinine measurements and urinary protein levels in this CKD model. Thus, direct SIK2/SIK3 inhibition may represent a promising new strategy to improve skeletal health for patients with CKD-MBD.

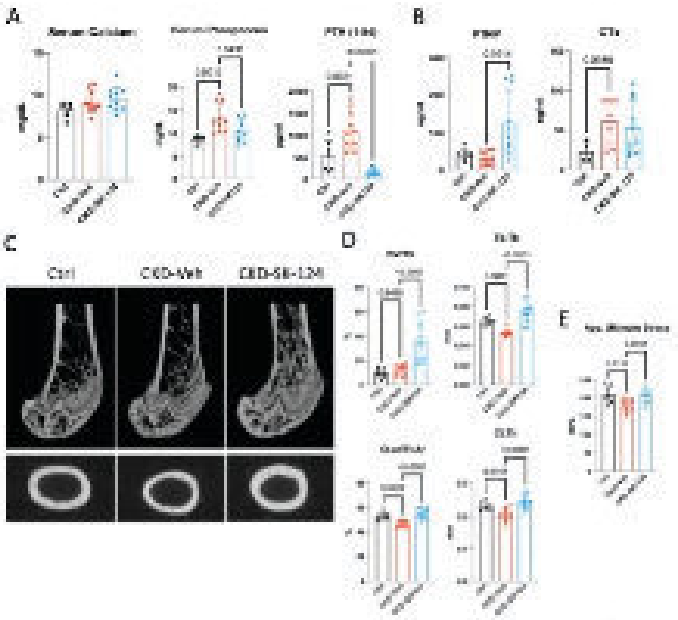

(A) Calcium, phosphorus, and PTH levels and (B) bone turnover markers, P1NP and CTx, measured in serum collected at the time of sacrifice. (C-D) Representative microCT images and analysis in trabecular and cortical bone of femur. (E) Apparent ultimate stress obtained from 3-point bending test in femur.

***Disclosures: Sung-Hee Yoon**, None*

1048

Antisense Oligonucleotides Targeting Notch3 Ameliorate Cortical Bone Osteopenia *Ernesto Canalis[1], Magda Mocarska[1], Lauren Schilling[1], Paymaan Jafar-nejad[2], Michele Carrer[2]. [1]UConn Health, United States. [2]Ionis Pharmaceuticals, Inc., United States

Notch receptors are determinants of cell fate and function and play an important role in the regulation of bone development and skeletal remodeling. Lateral Meningocele Syndrome (LMS) is a monogenic disorder associated with NOTCH3 pathogenic variants that result in the stabilization of NOTCH3 and a gain-of-function. LMS presents with neurological developmental abnormalities and bone loss. We created a mouse model (Notch3em1Ecan) harboring a 6691TAATGA mutation in the Notch3 locus recreating the genetic perturbance observed in LMS. Heterozygous Notch3em1Ecan mice exhibit cancellous and cortical bone osteopenia. We explored whether murine Notch3 antisense oligonucleotides (ASO) targeting either Notch3 or the Notch36691-TAATGA mutation downregulate Notch3 or Notch3 mutant transcripts and ameliorate the osteopenia of Notch3em1Ecan mice. ASOs targeting Notch3 decreased the expression of Notch3 wild type and Notch36691-TAATGA mutant mRNA whereas Notch3 mutant ASOs decreased the mutant transcript fairly selectively and neither ASO caused toxicity in cells from Notch3em1Ecan mice. The effect was specific to Notch3 since ASOs did not downregulate Notch1, Notch2 or Notch4. In vivo, the subcutaneous administration of Notch3 ASO at 50 mg/Kg decreased skeletal Notch3 mRNA by 50 - 60% and the administration of Notch3 mutant ASO decreased Notch36691-TAATGA specifically by ~50%. Microcomputed tomography demonstrated that the administration of either Notch3 or Notch3 mutant ASOs ameliorated the cortical bone osteopenia of Notch3em1Ecan mice, decreasing femoral cortical porosity and increasing cortical thickness and bone volume significantly. Notch3 mutant specific ASOs increased p-moment of inertia ($p < 0.07$) indicating a decrease in skeletal fragility in Notch3em1Ecan mice. The in vivo administration of Notch3 or Notch3 mutant ASOs resulted in no apparent toxicity, but did not ameliorate the cancellous bone osteopenia of Notch3em1Ecan mice. We believe that the beneficial effect of the ASO was limited to cortical bone because Notch3 is preferentially expressed by osteocytes and these cells prevail in the cortical bone compartment. In conclusion, Notch3 and Notch3 mutant specific ASOs downregulate Notch3 or Notch3 mutant expression in skeletal cells and their systemic administration ameliorates cortical bone osteopenia in Notch3em1Ecan mice and decrease skeletal fragility. ASOs may become useful strategies in the management of monogenic disorders of the skeleton.

***Disclosures: Ernesto Canalis**, None*

1049

Development of allele-specific antisense oligonucleotide therapy for fibrodysplasia ossificans progressiva *Rika Maruyama[1], Saeed Anwar[2], Quynh Nguyen[2], Rohini Roy Roshmi[2], Daniel Graf[3], Toshifumi Yokota[2, 1], [2]Department of Medical Genetics, University of Alberta, Canada, [3]Department of Dentistry & Dental Hygiene, University of Alberta, Canada

Fibrodysplasia ossificans progressiva (FOP) is a rare autosomal dominant disorder characterized by episodic heterotopic ossification (HO). It affects approximately 1 in 2 million people worldwide and has no racial, ethnic, or gender preference. More than 95% of cases are caused by a recurrent mutation (c.617G>A; R206H) of activin A receptor, type I (ACVR1)/activin receptor-like kinase-2 (ALK2), a bone morphogenetic protein type I receptor. This mutation is dominant and results in an amino acid change (R206H) within the glycine serine domain of ACVR1. The exact mechanism of FOP remains controversial, but this mutation renders ACVR1 hyperactive and responsive to activin A, triggering HO.Until recently, there were no treatment options for FOP. However, a new drug called palovarotene was approved for the treatment of FOP in Canada in 2022. Although palovarotene has shown promising results in preventing HO, a major drawback is its inability to differentiate between wild-type ACVR1 and ACVR1R206H, which could be potentially harmful to patients. In fact, it is not recommended for use in children.A promising therapeutic strategy for FOP is to reduce the activity of mutant ACVR1 in an allele-specific manner. To this end, we have designed gapmers that selectively knock down ACVR1R206H mRNA. Gapmers are short DNA oligonucleotides with chemical modifications at both ends that can degrade mRNA and selectively silence specific genes. We demonstrated that these gapmers efficiently knocked down ACVR1R206H expression at the RNA level, while ACVR1WT was largely unaffected in human FOP fibroblasts. In addition, the gapmers were able to reduce the amount of ACVR1R206H protein more efficiently than the wild type and suppress osteogenic differentiation induced by activin A. Furthermore, a single systemic injection of the gapmers significantly reduced ACVR1R206H expression in vivo and prevented HO in an FOP mouse model.In conclusion, our results suggest that gapmers targeting ACVR1R206H are promising drug candidates for FOP. These gapmers are considered safe and can be administered systemically via subcutaneous or intravenous injections, which is particularly advantageous for FOP patients because viral vector-mediated gene therapy can induce immune responses and inflammation leading to increased HO. This novel strategy may pave the way for antisense-mediated therapy of other autosomal dominant disorders.

***Disclosures: Rika Maruyama**, OligomicsTx, Major Stock Shareholder*

1050

Cystatin M/E ameliorates bone resorption in both multiple myeloma and sex steroid deficient models through increasing intracellular estrogen concentrations *Perry Caviness[3], Dongzheng Gai[2], Hongwei Xu[2], Oxana Lazarenko[3], Michael Blackburn[3], Jin-Ran Chen[4], Fenghuang Zhan[2, 3]Arkansas Children's Nutrition Center, [2]Myeloma Center, University of Arkansas for Medical Science, United States, [3]Arkansas Children's Nutrition Center, United States, [4]Arkansas Children s Nutrition Center / UAMS, United States

In multiple myeloma (MM), increased osteoclast differentiation leads to formation of osteolytic lesions, leading to severe complications for the majority of MM patients. Currently, bisphosphonates, such as zoledronic acid (ZA), are used to ameliorate increased bone resorption but, due to potential side effects as well as their inability to repair existing osteolytic lesions novel anti-bone resorption agents are required. It was previously shown that in MM patients the absence of osteolytic lesions was strongly associated with an increase in the expression of cystatin M/E (CST6), a cysteine protease inhibitor. In this study, both MM and ovariectomy induced osteoporosis (OVX) mouse models were used to compare the effects of recombinant mouse CST6 to ZA on ameliorating bone loss. For both models, µCT showed that both CST6 and ZA had similar effects on improving percent bone volume (BV/TV %) (MM: 2.64 +/- 0.52, MM + CST6: 3.57 +/- 0.14, MM + ZA: 3.88 +/- 0.53) (Sham: 3.09 +/- 0.60, OVX: 2.33 +/- 0.44, OVX-CST6: 3.23 +/- 0.50, OVX-ZA: 3.85 +/- 0.23). Single cell RNA sequencing showed that treatment with either CST6 or ZA altered the bone marrow cell type ratio in MM mouse models. Both CST6 and ZA inhibited differentiation of non-adherent bone marrow cells into mature osteoclast. However, ZA had a negative impact on the viability of non-osteoclast cells. In breast cancer, loss of CST6 is associated with loss of estrogen receptor ? (ER?), limiting the downstream effects of estrogen. Based on this we propose that CST6 works to improve MM or OVX bone loss models by increasing the expression of estrogen receptors as well as intracellular estrogen concentration in pre-osteoclasts, inhibiting their maturation. For Raw 264.7 cells (+/- RANKL) mRNA levels for ER? and ER? were significantly increased following 200 ng/ml CST6 treatment. In addition to this, intracellular total estrogen concentration was also significantly increased in Raw 264.7 cells following CST6 treatment (Control: 765 +/- 233 pg/ml, 200 ng/ml CST6: 1176 +/- 152 pg/ml) (RANKL; Control: 1366 +/- 44 pg/ml, 200 ng/ml CST6: 1448 +/- 22 pg/ml). Further research is needed to determine the mechanism explaining this increase in intracellular estrogens. Supported by National Cancer Institute (R01 CA236814), U.S. Department of Defense (CA180190) as well as funding from the the Myeloma Crowd Research Initiative Award and the Riney Family Multiple Myeloma Research Program Fund awarded to FZ.

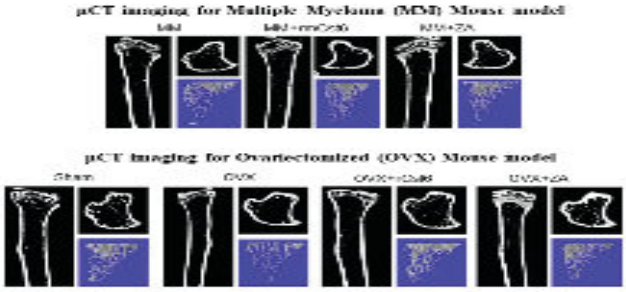

***Disclosures: Perry Caviness**, None*

1051

Long-term OPG:Fc Treatment with Discontinuation Lead to Elevated Microporosities in a Mouse Model Simulating Denosumab Treatment *Johannes Krug[1], Haniyeh Hemmatian[2], Albert Kim[3], Jad Zamerli[3], Annegreet Vlug[4], Katharina Jähn-Rickert[5], Bjoern Busse[5], Michelle McDonald[3], [1]University Medical Center Hamburg-Eppendorf, GER, Germany, [2]University of Melbourne, Department of Medicine-Austin Health, Australia, [3]Garvan Institute of Medical Research, Bone Microenvironment Group, Australia, [4]LUMC, [5]University Medical Center Hamburg-Eppendorf, Germany

Following therapy discontinuation, denosumab-treated osteoporosis patients experience a rebound bone loss with an increase in vertebral fragility fractures. While high-resolution imaging techniques have recently highlighted the importance of bone microporosity as a quantifiable marker of bone mechanical integrity, the structural basis of rebound bone loss associated fragility fractures following denosumab discontinuation remains poorly understood.This study aimed to evaluate bone microporosities, including the osteocyte lacunar and cortical canal networks, in a mouse model of denosumab treatment discontinuation using microcomputed tomography at a nominal resolution of 0.7 µm. Microporosities were quantified in the proximal tibia of mice receiving treatment with an osteoprotegerin Fc (OPG:Fc, 10mg/kg 3 times a week, n=6) or vehicle (n=6) for i) 2 weeks (2+0 weeks), ii) 2 weeks and 12 weeks discontinuation (2+12 weeks), or iii) 8 weeks and 15 week discontinuation (8+15 weeks).In the cancellous bone, lacunar volume was not significantly larger with 2 weeks of treatment either with or without discontinuation, but following 8 weeks of treatment and then discontinuation mean lacunar volume was increased by 13.5% (p=0.002) compared to vehicle. Both discontinuation groups also presented with elevated osteocyte densities (trend in 2+12 weeks: p=0.0529; 8+15 weeks: p=0.008), a finding that was not evident in the 2+0 weeks group. In the cortex, cortical thickness was elevated in the 2+0 week treatment group (p=0.006), while a thinner cortex was evident in both discontinuation groups (2+12 weeks: p=0.024; 8+15 weeks: p=0.005). The cortical bone lacunar characteristics were not altered in any group. The cortical canal volume and number were unchanged with both 2+0 and 2+12 weeks treatment groups, however after 8 weeks of treatment with discontinuation (8+15 weeks) canal volume and number were increased (p=0.006 and p<0.001).In conclusion, in a mouse model, 8 weeks of OPG:Fc treatment with 15 weeks of discontinuation led to elevated trabecular lacunar porosity and cortical canal porosity, outcomes which were not seen following 2 weeks of treatment with or without discontinuation. Therefore, this study shows that bone tissue microporosities compromising mechanical integrity might play a role in the pathogenesis of rebound bone loss and vertebral fractures following denosumab discontinuation, primarily after longer term treatment.

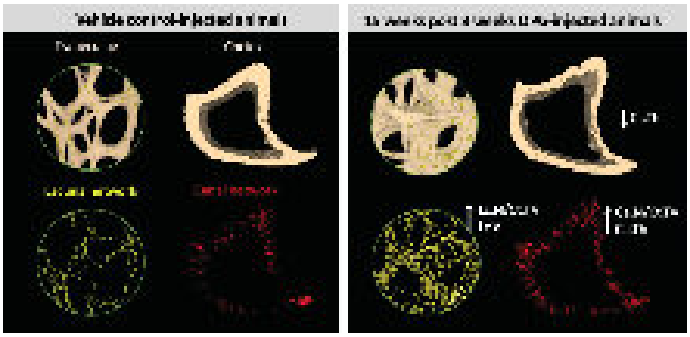

***Disclosures: Johannes Krug**, None*

1052

Interrogating Osteoclast Biology by Live Cell Imaging Reveals Novel Insight into their Cellular and Resorption Dynamics and Real-Time Effects of OPG-Fc and RANKL *Sarah Dallas[1], Kun Wang[1], Charles O'Brien[2], Anthony Meljanac[1], Roya Sabzian[1], Eleanor Ray[1], Vedvignesh Gorjala[1], Yixia Xie[1], Lynda Bonewald[3], David Moore[1]. [1]University of Missouri - Kansas City, United States; [2]Univ of Arkansas for Medical Sciences, United States; [3]Indiana University School of Medicine, United States

Although much progress has been made in defining molecular pathways critical for osteoclast (OCL) function and identifying molecular targets for anti-resorptive therapies, interrogating OCL biology by live cell imaging can reveal novel insights into their function. Transgenic mice with OCL expression of tdTomato (LysM-Cre/tdTom), osteocyte expression of GFP (Dmp1-mGFP) or with GFP-tagged type I collagen (Col-GFP) were crossed in 2-color combinations and confocal or widefield live cell imaging was done in calvarial explants to define OCL dynamic & resorptive behavior in bone and real-time responses to RANKL & OPG-Fc, a RANKL inhibitor. Long term (up to 3d) imaging in LysM-Cre/tdTom/Col-GFP calvaria revealed complex OCL dynamics including fission, fusion, recycling/cytoplasmic exchange, amoeboid-like streaming and extension/retraction of cell processes. Our image resolution allows visualization of OCL sealed zones, revealing that a single OCL can have one or multiple (>=3) sealed zones resorbing simultaneously. In bone tissue, the % of OCL cell-cell encounters resulting in fusion was 6.0% +/- 3.7. In contrast, OCL cultured on plastic had a 10-fold higher % fusion of 67.0% +/- 20.6. OPG-Fc (500ng/ml) caused a rapid change within ~1h to an intricately branched OCL morphology with loss of sealed zones. OPG-Fc increased the complexity of OCL dynamics, with a ~3-fold increase in fissions/OCL/10h (0.32 +/-0.14 vs. 0.12 +/-0.05, p=0.008) and fusions/OCL/10h (0.25 +/-0.10 vs. 0.08 +/-0.07 p= 0.008), while downregulating expression of OCL marker genes, TRAP, DC-STAMP, Atp6v0d2, CTSK, & NFATc1. Computational analysis of motion trajectories showed that OPG-Fc treated OCL had similar velocities as controls. However, OCL in control bones had open, directional trajectories compared to OPG-Fc treated OCL which had compacted trajectories indicating OCL moving in circles. Automated quantitation of real-time GFP-collagen resorption showed arrest of resorption with OPG-Fc. Subsequent treatment with RANKL (200ng/ml) induced fusion, re-formation of sealed zones and re-activation of GFP-collagen resorption. In control bones with already active OCL, RANKL did not induce much fusion, but induced a compacted cell morphology, with intensified actin rings & resorption activity, suggesting direct effects on mature OCL. These results show that mature OCL respond dynamically and reversibly to changes in RANKL signaling and highlight the importance of observing OCL in their natural bone environment.

***Disclosures: Sarah Dallas**, None*

1053

RANKL and OPG mRNA are produced by separate cell populations in murine and human bone *Cecile Bustamante-Gomez[1], Humberto Reyes-Pardo[1], Melda Onal[1], Michela Palmieri[1], Lowry Barnes[1], Jeffrey Stambough[1], Jinhu Xiong[1], Elena Ambrogini[1], Charles O'Brien[1]. [1]University of Arkansas for Medical Sciences, United States

The RANKL/OPG axis controls the location and magnitude of osteoclast formation during skeletal development, growth, and homeostasis. Gene inactivation studies in mice have revealed that different cell types are important sources of either RANKL or OPG for the control of physiologic and pathologic bone resorption. However, due to uncertainties regarding the cell types targeted by various Cre driver strains, the precise identity of the cells providing the RANKL and OPG in bone microenvironments remains unclear. To help clarify this question, we used RNAScope in situ hybridization to detect RANKL and OPG mRNA in murine and human bone sections. Consistent with previous genetic studies, RANKL mRNA was easily detected in bone marrow cells with a morphology consistent with Cxcl12-abundant-reticular (CAR) cells and in a subpopulation of osteocytes. OPG mRNA was easily detected in osteocytes, but only in a small subpopulation of osteoblasts. These findings were similar in murine and human bone sections. Because previous studies have shown that PTH stimulates RANKL and suppresses OPG mRNA abundance in vitro and in vivo, we examined the impact of a single injection of PTH on the expression of these factors in murine bone. Bones were collected and analyzed by RNAScope 1, 6, 12, and 24 hours after injection. One hour after PTH injection, RANKL mRNA signal was strongly increased in CAR-like cells near the bone surface but the levels in osteocytes were not changed. At later timepoints, RANKL mRNA in all cell types was similar to uninjected mice. OPG mRNA levels in osteocytes were potently suppressed one hour after PTH injection but returned to normal by 6 hours. These results suggest that PTH induction of bone resorption is accomplished by stimulating RANKL production by CAR cells and inhibiting OPG production by osteocytes, at least in the short-term. We also detected RANKL mRNA in hypertrophic chondrocytes and OPG mRNA in growth plate chondrocytes and articular chondrocytes. The juxtaposition of OPG and RANKL expression in growth plate chondrocytes suggests that OPG production by pre-hypertrophic chondrocytes acts as a barrier to prevent osteoclastic resorption of the growth plate. Penetration of the growth plate in OPG null mice is consistent with this idea. Moreover, the abundant expression of OPG by articular chondrocytes in humans and mice suggests an important role for this factor in the protection of this tissue from degradation by osteoclasts.

***Disclosures: Cecile Bustamante-Gomez**, None*

1054

RANKL from bone marrow adipogenic lineage precursors is required for bone resorption and pathological bone loss in adult mice *Jiawei Lu[1], Qi He[1], Corben Braun[1], Ken Chen[1], Michael Duffy[1], Jun Li[1], Hanli Guo[1], Jiankang Fang[1], Yilu Zhou[1], Qiushi Liang[1], Yu Lieh Lin[1], Ling Qin[2]. [1]University of pennsylvania, United States; [2]University of Pennsylvania, United States

Bone resorption by osteoclasts is a critical step in bone remodeling. It is well known that osteogenic cells support osteoclastogenesis via synthesizing RANKL. Previous work identified a novel bone marrow mesenchymal subpopulation, marrow adipogenic lineage precursors (MALPs), as a major source for RANKL. Mice with RANKL deficiency in MALPs using Adipoq-Cre had a drastic increase in trabecular bone mass (BV/TV) at 1 and 3 months of age. Using a Tomato (Td) reporter to label MALPs, we found that MALPs first appear inside the bone marrow at birth (P1). To exclude developmental defects and to investigate the role of MALPs-derived RANKL in adult bone, we generated inducible RANKL iCKO mice using Adipoq-CreER. These mice grew normally with no phenotypes. We subjected female iCKO and WT siblings to Tamoxifen (Tam) injections at 3 months of age followed by sham or ovariectomy (ovx) surgery (n=4-8 mice/genotype/surgery). Tam effectively reduced bone marrow RNAKL mRNA by 66% 1 month later. Six weeks post-surgery, we observed striking 3.2- and 1.5-fold increases in femoral and vertebral trabecular BV/TV, respectively, in iCKO mice compared to WT mice. While WT mice developed pathological trabecular bone loss at both sites (femur: 60.7%; vertebra: 25.3%) after ovx, iCKO mice maintained most of their trabecular bone, leading to 5.7- and 1.5-fold more bone than WT ovx mice at these sites. Cortical bone was not affected by either ovx or RANKL knockdown. TRAP staining of femoral sections revealed that compared to WT mice, iCKO mice display 36.8% and 28.4% reduction in osteoclast surface (Oc.S/BS) after sham and ovx surgery, respectively. Ovx increased bone marrow adipocytes by 2.7-fold in WT mice. Interestingly, iCKO mice showed a similar increase of bone marrow adiposity despite strong bone gain, suggesting that high bone mass and high adiposity could co-exist under certain conditions. To study the role of MALP-derived RANKL after bone loss has initiated, we subjected WT and iCKO mice at 3 months of age to sham or ovx mice first and then treated them with Tam 3 weeks later (n=4-6 mice/genotype/surgery). At 6 weeks post-surgery (3 weeks after Tam), we observed a similar high bone mass phenotype in iCKO mice with either sham or ovx, indicating that MALPs-derived RANKL could be targeted for postmenopausal osteoporosis treatment. In summary, our studies demonstrate that MALPs produce RANKL to control adult bone remodeling and postmenopausal bone loss.

***Disclosures: Jiawei Lu**, None*

1055

RANKL signaling drives skeletal muscle into the oxidative profile *Paulo Henrique Cavalcanti de Araujo[1], Maria Eduarda Ramos Cezine[1], Mariana Kiomy Osako[1]. [1]Ribeirao Preto Medical School, University of Sao Paulo, Brazil

The skeletal muscle is vital for energetic homeostasis. A reduced mitochondrial reticulum and oxidative phosphorylation activity in this muscle is seen in metabolic diseases such as obesity and type II diabetes. The receptor activator of NF-?B ligand (RANKL) stimulation induces mitochondrial biogenesis and increases the oxidative capacity in osteoclasts and adipocytes. RANKL may bind to the membrane bound receptor activator of NF-kB (RANK) or to osteoprotegerin (OPG), a decoy receptor that inhibits RANK-RANKL activation. RANK is highly expressed in skeletal muscle, however, the contribution of RANKL to healthy skeletal muscle fiber remains elusive. Here we show that RANKL stimulation in C2C12-derived myotubes induced activation of mitochondrial biogenesis pathways as detected by RNA-seq and western blot. It also expanded the mitochondrial reticulum, as evaluated by mitotracker staining and mitochondrial DNA quantification, and boosted the spare respiratory capacity. The soleus from OPG-/- and OPG+/- mice showed higher respiratory rates compared to C57BL6/J wild type (WT) mice, which correlates with higher serum RANKL levels. RANKL infusion using a mini-osmotic pump in WT mice increased the number of mitochondria and oxidative fibers (type 2A) and boosted the respiratory rate. We also observed an increase in succinate dehydrogenase (SDH) activity in skeletal muscle, in trained, high fat diet-fed WT mice. We found that RANKL increases mitochondrial biogenesis, induces an oxidative profile in skeletal muscle and may protect against obesity-induced metabolism impairment. Our findings reveal a new contribution of RANKL as an osteokine-like protein that impacts muscle fiber metabolism.

***Disclosures: Paulo Henrique Cavalcanti de Araujo**, None*

1056

Efficacy of Osteoporosis Drug Treatment for Reducing Risk of Hip Fracture is the Same in Women and Men *Tony Keaveny[1], David Lee[2], Eric Orwoll[3], Sundeep Khosla[4], Michael McClung[5], Ethel Siris[6], Mary Bouxsein[7], Annette Adams[8], David Kopperdahl[2]. [1]University of California, Berkeley, United States, [2]O.N. Diagnostics LLC, United States, [3]Oregon Health & Science University, United States, [4]Mayo Clinic College of Medicine, United States, [5]Oregon Osteoporosis Center, , [6]Columbia University College of Physicians and Surgeons, United States, [7]Beth Israel Deaconess Medical Center, Harvard Medical School, United States, [8]Kaiser Permanente Southern California, United States

Purpose: The US Preventive Services Task Force does not recommend diagnostic screening of osteoporosis for men due in part to insufficient evidence that osteoporosis drug treatment prevents hip fractures in men. As a result, many high-risk men go untested and untreated for osteoporosis. Addressing that evidence gap, we compared the real-world reduction in risk of hip fracture associated with standard-of-care osteoporosis drug treatment in women versus men.Methods: This was an observational case-cohort study drawing from 341,364 patients age >= 65 in the Kaiser Permanente Southern California healthcare system who had a hip-containing CT scan between 1/1/2005 and 6/30/2018 as part of their care. Cases were selected as all those with a hip fracture after the CT scan; an equal number of sub-cohort patients was randomly selected (sex- and facility-matched) without regard to fracture status. Using data from half the sample, we analyzed fracture risk at 2, 5, and 10 years follow-up after the CT scan; cases were those who fractured their hip during follow-up; controls reached follow-up without fracture. DXA-equivalent bone mineral density (BMD, lowest hip T-score) and femoral strength were measured from the existing CT scans using VirtuOst, and clinical data were obtained from the medical records. Sex-specific multivariate nominal logistic regression was used to obtain an odds ratio associated with osteoporosis drug treatment during follow-up (positive if >= 90 days of any treatment during follow-up). Either BMD or bone strength was included in the statistical model, plus most major risk factors at the time of the CT scan (age, BMI, smoking, alcohol, rheumatoid arthritis, diabetes, glucocorticoid use, secondary osteoporosis, previous major fracture).Results: Complete data were available for 5,144 patients. The odds ratio (for hip fracture) associated with osteoporosis drug treatment versus no treatment varied from 0.30 to 0.46 over the 2- 5- and 10-year follow-ups and was not significantly different between women and men (Table). Showing robustness, the odds ratio was similar regardless of whether BMD or bone strength was used in the statistical model. The 60% risk reduction for women at 2-year follow-up is consistent with results from randomized controlled trials, validating our approach for assessing relative efficacy between the sexes.Conclusion: In this large real-world clinical setting, standard-of-care osteoporosis drug treatment reduced the risk of hip fracture equally in women and men.

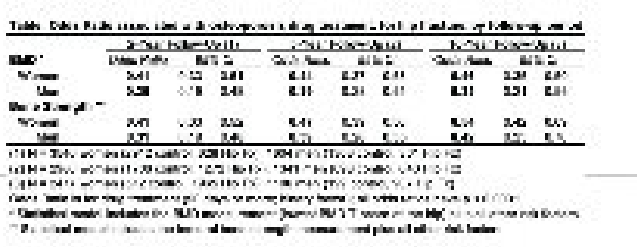

***Disclosures: Tony Keaveny**, O.N. Diagnostics LLC, Major Stock Shareholder*

1057

The association between treatment-related differences in total hip bone mineral density change and fracture risk reduction for BMD measurement intervals of 12, 18 and 24 months: the FINH-ASBMR SABRE Project *Tatiane Vilaca[2], Marian Schini[2], Eric Vittinghoff[3], Li-Yung Lui[4], Susan Ewing[3], Douglas Bauer[5], Mary Bouxsein[6], Richard Eastell[2], Dennis Black[7]. [2]University of Sheffield, United Kingdom, [2]University of Sheffield, , [3]Department of Epidemiology & Biostatistics, University of California, United States, [4]CALIFORNIA PACIFIC MEDICAL CENTER, United States, [5]University of California, San Francisco, United States, [6]Beth Israel Deaconess Medical Center, Harvard Medical School, United States, [7]UC San Francisco,

We have shown a strong association between treatment-related differences in 24 month total hip BMD (THBMD) change and fracture risk reduction. However, the relationships between shorter treatment-related changes in BMD and fracture risk reduction are unknown. In this analysis, we examined whether shorter intervals of BMD measurement were also associated with fracture reductions.We used individual patient data from 22 randomised, placebo-controlled, double-blind trials of antiosteoporosis medications [10 bisphosphonates, 1 odanacatib, 2 hormone therapy, 3 parathyroid hormone receptor agonists, 1 denosumab, and 4 selective estrogen receptor modulator, 1 romosozumab]. For each trial, we calculated the active-placebo difference in mean percent change in THBMD at 12, 18 and 24 months. We also estimated the treatment-related fracture reductions for each trial for the entire follow-up period, using logistic regression for morphometric vertebral fractures and Cox regression for all clinical, non-vertebral, hip and "all" (combination of non-vertebral and clinical or morphometric vertebral) fractures. We performed linear meta-regression to estimate the study-level association (r2 and 95% confidence interval) between treatment-related differences in THBMD changes for each BMD measurement interval and fracture risk reduction. The meta-regression revealed significant associations ($p<0.05$) between treatment-related changes in THBMD at 12, 18, and 24 months and reductions in vertebral, hip, non-vertebral, all and all clinical fractures (table). These findings confirm that treatment related THBMD changes at 12 and 18 months, as well as 24 months are associated with fracture risk reductions in vertebral, hip, non-vertebral, all and all clinical fractures across randomised trials of antiosteoporosis therapies. For all fracture sites, the r2 were very similar at 18 and 24 months.These results support that 12-, 18- or 24-month BMD measurement intervals could be considered for a future trial using BMD as a surrogate endpoint to assess fracture efficacy. However, longer BMD measurement intervals provide more robust association with fracture reduction.

Table Results from meta-regression of between-group (active-placebo) difference in mean percent change in total hip bone mineral density with fracture risk reduction at 12-, 18-, and 24-month

	r^2		
	BMD measurement interval		
Fracture outcome	12 m	18 m	24 m
Vertebral	0.59***	0.69***	0.73***
Hip	0.27*	0.39*	0.41*
Non-vertebral	0.27*	0.49**	0.53**
All	0.44**	0.63***	0.66***
All clinical	0.46***	0.64***	0.71***

BMD bone mineral density; m months. *p<0.05 **p<0.01; ***p<0.001

***Disclosures: Tatiane Vilaca**, None*

1058

Imminent fall risk after fracture *Merle Schene[1], Caroline Wyers[1], Annemariek Driessen[1], Patrick Souverein[2], Marle Gemmeke[2], Joop van den Bergh[1], Hanna Willems[3]. [1]Department of Internal Medicine, VieCuri Medical Center, Netherlands, [2]Division of Pharmacoepidemiology and Clinical Pharmacology, Utrecht Institute for Pharmaceutical Sciences (UIPS), Faculty of Science, Utrecht University, Netherlands, [3]Amsterdam UMC location University of Amsterdam, Internal Medicine and Geriatrics, Netherlands

A high imminent risk of subsequent fracture in the first 2 years after a fracture is well established and subjects with a recent fracture have a high fall risk. We hypothesize that, like subsequent fracture risk, fall risk is also highest immediately after a fracture. This retrospective matched cohort study aims to assess if fall risk is time-dependent in subjects with a recent fracture, compared to fracture-free controls. We used primary care electronic health records from the UK Clinical Practice Research Datalink (CPRD) GOLD. Subjects aged >=50 years with an incident fracture between 1993-2015 were identified and matched one-to-one to fracture-free controls by age, sex and GP-practice. One-year incidence rates (IRs)/1000 person years of first falls and fractures were compared between groups using incidence rate ratios (IRRs). The cumulative incidence and relative risk (RR) of first falls was calculated every 6 months of follow-up, with mortality as competing risk. Analyses were stratified by age, sex and index fracture. In total, 312,230 subjects with an index fracture and 312,230 controls were included (71% women, aged 70+/-12 years, follow-up 6 [3-10] years). The one-year IR for first falls was higher in the fracture cohort compared to the control cohort: in women with a non-major osteoporotic fracture (non-MOF) the IRR was 1.9 (95% confidence interval [CI] 1.8-2.0), and with MOF 1.8 (95% CI 1.7-1.8). In men with non-MOF the IRR was 2.5 (95% CI 2.3-2.7) and with MOF 2.6 (95%CI 2.4-2.8). Similarly, one-year IR of fracture was higher in the fracture cohort: women non-MOF IRR=7.4 (95% CI 6.6-8.3) and MOF IRR=7.0 (95% CI 6.3-7.9) and men: non-MOF 10.2 (95% CI 7.9-13.1), MOF 11.8 (95% CI 8.9-15.5). Correspondingly, the RR of falls was highest in the first few years after fracture compared to controls and declined over time; in the first year women had a 2.2-fold and men a 3.1-fold higher risk, in the second year a 1.5-fold and 2.0-fold risk. Imminent fall risk was present for all ages and index fractures. Similar RR patterns over time were confirmed for imminent fracture and mortality risk. This study demonstrates an imminent fall risk in the first 2 years after fracture, with mortality as competing risk. Corresponding time-dependent risk patterns were confirmed for subsequent fractures and mortality. This

emphasizes the need for combined fall and fracture risk assessment and prevention strategies in adults over 50 years with a recent fracture.

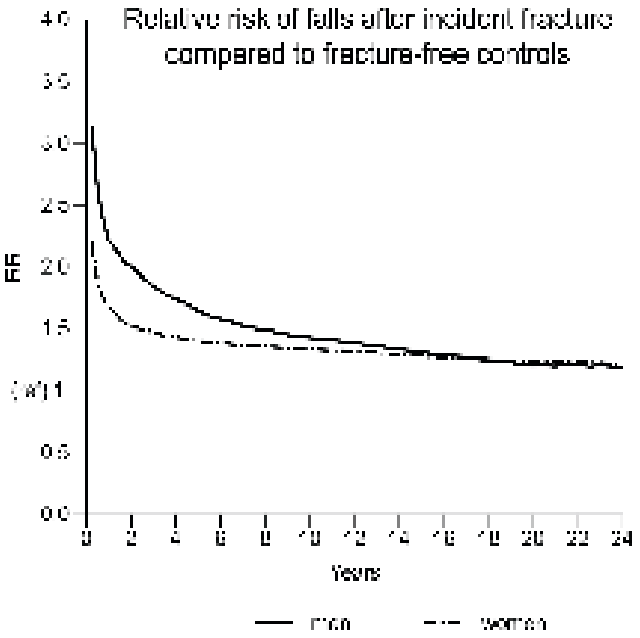

***Disclosures: Merle Schene**, None*

1059

Associations between use of anti-resorptive agents for patients with osteoporosis and all-cause mortality risk: a nationwide population-based study *Kyoung Jin Kim[1], Gi Hwan Bae[2], Seong Hee Ahn[3], So Young Park[4], Ha-Young Kim[5], Kyoung Min Kim[6]. [1]Korea University College of Medicine, Republic of Korea. [2]Gachon University College of Medicine, Republic of Korea. [3]Inha University School of Medicine, Republic of Korea. [4]Kyung Hee University School of Medicine, Republic of Korea. [5]University of Ulsan College of Medicine, Republic of Korea. [6]Yonsei University College of Medicine, Republic of Korea

Although the association between osteoporosis-related fractures and mortality is well-established, it remains uncertain whether osteoporosis drug treatments reduce the risk of mortality. Therefore, we investigated to determine the association between anti-resorptive agents and mortality risk in postmenopausal women with osteoporosis. A total of 117,871 women who diagnosed as osteoporosis by dual-energy X-ray absorptiometry screening were included from the National Screening Program for Transitional Ages health examination from 2008 to 2017. Among them, 11,337 patients who had taken anti-resorptive agents (AR), either bisphosphonate or selective estrogen receptor modulator (SERM), for at least 1 year (AR user group) were matched at a 1:1 ratio to those who had never taken osteoporotic agents (non-user group) by using propensity scores. We estimated the risk of all-cause mortality using multivariable Cox proportional hazard regression models. The mean age of women was 66 years and mean body mass index was 23.2 +/-3.0 kg/m2. In the AR user group, 73.8% was prescribed with bisphosphonates, whereas 26.2% was treated with SERMs. During a median follow-up period of 1.6 years, a total of 121 deaths occurred in the AR user group, and 201 deaths occurred in the non-user group. The mortality rate was 1.99 deaths per 1000 person-years in AR users and 3.36 deaths in non-users, which corresponded to a 45% lower mortality rate in AR users (HR, 0.55; 95% CI, 0.44-0.69). Furthermore, the longer the individuals took AR, the lower the risk of all-cause mortality compared to the control group [HR = 0.55 in 12-24 months, HR = 0.55 in 24-36 months, and HR = 0.50 in >=36 months, p-for trend <0.01]. The mortality risk related to cardiovascular disease (CVD) was lower in the AR group compared to the non-user group (HR = 0.72; 95% CI: 0.64-0.81); however, the interpretation should be approached with caution due to the limited number of events. In the subgroup analysis, the use of AR-related to reduced mortality was more prominent in the calcium or vitamin D replete group compared to the non-replete groups (p for trend <0.001 for both). Taking AR agents contributed to lowering risk of all-cause mortality among postmenopausal women with osteoporosis. Our findings provided real-world evidence regarding the necessity of management of osteoporosis with anti-osteoporotic agents in postmenopausal women.

Figure 1. Cumulative incidence curve of mortality in the AR users (n=11337) with the non-users (n=11337). Hazard ratio (HR) with 95% confidence interval (CI) is shown.

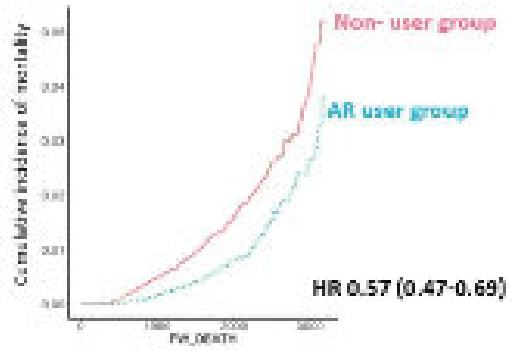

***Disclosures: Kyoung Jin Kim**, None*

1060

Kidney Stone Disease and Risk of Osteoporotic Fractures among U.S. Medicare Beneficiaries *Naim Maalouf[1], Mary Oerline[2], Ryan Hsi[3], Sara Best[4], Joseph Crivelli[5], John Hollingsworth[6], Vahakn Shahinian[2]. [1]University of Texas Southwestern Medical Center, United States. [2]University of Michigan, United States. [3]Vanderbilt University, United States. [4]University of Wisconsin, United States. [5]University of Alabama, United States. [6]NorthShore University HealthSystem, United States

Background: Several observational studies suggest that the presence of kidney stone disease (KSD) may put an individual at higher risk of osteoporotic fracture (OF). Whether this risk varies by fracture site, is influenced by patient age, or differs between men and women remains controversial.Methods: We investigated the association between KSD and OF using U.S. Medicare data from a 20% random sample of beneficiaries. We identified individuals age>=65 years with >=2 physician-coded diagnoses of KSD within a year or >=1 surgical procedure code for KSD between 2011 and 2015. Each patient with KSD was matched with 3 control beneficiaries without KSD based on age, gender, and race. Patients with a diagnosis of OF, primary hyperparathyroidism, or parathyroidectomy in the year preceding or the year following the index KSD event were excluded from KSD patients and controls. The incidence of arm, vertebral, and hip fractures was determined based on claims data over a median of 5.0 years of follow-up from the index KSD date. Cox regression was used to estimate the hazard ratio (HR) for fractures after adjusting for risk factors for osteoporosis.Results: In total, 140,053 KSD cases and 420,091 controls were included in this analysis. Mean age at index stone date was 75.1+/-6.8 years, 38.4% of patients were female, and 95.6% were non-Black. Over the study period, 15,335 OF occurred in KSD patients and 25,391 OF in controls [unadjusted HR: 1.62 (95% CI: 1.59-1.65)]. After adjusting for multiple risk factors/comorbidities (including age, gender, race, osteoporosis diagnosis, obesity, hypertension, CKD, GI disease or bowel resection), the adjusted HR for OF was 1.22 (95% CI: 1.19-1.24). The multivariable adjusted HR (95% CI) for OF in KSD patients vs controls decreased significantly with older age [1.26 (1.22-1.30) for age 65-74, 1.20 (1.16-1.24) for age 75-84, and 1.16 (1.11-1.22) for age >=85 (p for interaction<0.01)], and was significantly higher in women [1.36 (1.32-1.41)] than men [1.11 (1.08-1.14)] (p for interaction <0.01). KSD patients had a significantly higher multivariable adjusted HR for arm [1.31 (1.25-1.37)], vertebral [1.24 (1.20-1.27)], and hip [1.18 (1.14-1.22)] fracture.Conclusions: In this large study of older Medicare beneficiaries, KSD was associated with a higher incidence of arm, vertebral, and hip fractures. The underlying mechanism(s) require further investigation, but these results need to be considered in counseling patients with KSD.

***Disclosures: Naim Maalouf**, None*

1061

Rethinking Fragility Fracture Age Cut-offs: Fractures Beget Fractures Regardless of the Age at Which They Occur *Carrie Ye[1], Suzanne Morin[2], Lisa Lix[3], Eugene McCloskey[4], Helena Johansson[4], Nicholas Harvey[5], JOHN KANIS[6], William Leslie[3]. [1]University of Alberta, Canada. [2]McGill University, Canada. [3]University of Manitoba, Canada. [4]University of Sheffield, United Kingdom. [5]University of Southampton, . [6]UNIVERSITY OF SHEFFIELD, United Kingdom

Fragility fractures are sometimes restricted to those occurring over a certain age (for example, 40 to 50 years), whereas FRAX considers a previous fracture in adult life regardless of age. Although the incidence of fractures increases with age, there is no evidence that fractures occurring in early adulthood are less predictive of future fractures.AIM: To determine whether the age at which a prior fracture occurs modifies its effect on future fracture risk. METHODS: Subjects from the Manitoba BMD Registry with a first DXA between 1996 and 2018 were linked to provincial administrative health data from 1981 onwards to ascertain

all diagnosed fractures occurring before and after the first DXA. Individuals with fractures prior to their first DXA were stratified by the age at first fracture (10-year intervals from age 20-29 to >80 years). Cox regression models estimated hazard ratios (HR) for any incident fracture, osteoporotic fracture, major osteoporotic fracture (MOF) and hip fracture, by age interval at first adult fracture. Models were adjusted for age, sex, body mass index, parental hip fracture, smoker, prolonged glucocorticoid use, rheumatoid arthritis, secondary osteoporosis, high alcohol use, anti-osteoporosis treatment and femoral neck T-score ascertained at the time of first DXA. Linear trend in age effect was tested in the same models.RESULTS: The cohort included 88,696 individuals, 90.3% women, mean age 64.6 years, and mean femoral neck T-score -1.4. Almost one-quarter (21,105, 23.8%) had suffered a prior fracture with a mean age of 57.7 years (range 20.0-102.4 years) at time of first prior fracture. During mean 9.0 years follow-up there were incident fractures in 13,239 (14.6%), including 12,245 (14.0%) osteoporotic fractures, 9440 (10.6%) MOFs and 3068 (3.5%) hip fractures. The adjusted HR for all incident fractures, osteoporotic fractures, MOF and hip fractures were significant in all age groups of first prior fracture and ranged from 1.46 to 2.18 for MOF, and 1.33 to 3.43 for hip fracture (Table). There was no effect modification by age of prior fracture (p-trend >0.1). Sensitivity analyses examining age at last prior fracture, in those with a single prior fracture or those with multiple prior fractures showed similar results.CONCLUSION: Fractures in adulthood predict future fractures regardless of the age at which they occur. Thus, fractures in early adulthood should not be excluded when assessing an individual's ongoing fracture risk.

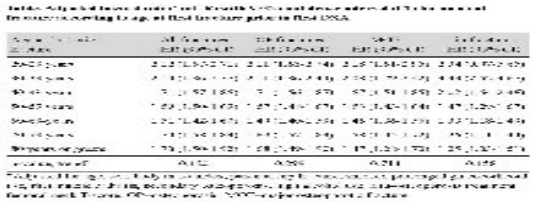

***Disclosures: Carrie Ye**, None*

1062

Effect of BMI-Discordant Abdominal Tissue Thickness on Fracture Probability: The Manitoba BMD Registry *William Leslie[1], Neil Binkley[2], John Schousboe[3], Eugene McCloskey[4], Helena Johansson[5], Nicholas Harvey[6], JOHN KANIS[7]. [1]University of Manitoba, Canada. [2]University of Wisconsin, Madison, United States. [3]Park Nicollet Clinic HealthPartners Institute University of Minnesota, . [4]University of Sheffield, United Kingdom. [5]University of Sheffield Medical School, United Kingdom. [6]University of Southampton, . [7]UNIVERSITY OF SHEFFIELD, United Kingdom

FRAX® considers body mass index (BMI) as a primary input. BMI may not reflect individual variation in body composition and distribution including central obesity.AIM: To examine the effect of BMI-discordant abdominal thickness on FRAX-derived fracture probability for major osteoporotic fracture (MOF) and hip fracture.METHODS: We identified individuals aged 40 years and older at the time of baseline DXA with FRAX assessment in the Manitoba BMD Program. We defined abdominal thickness index (ATI) as the difference between abdominal thickness measured by spine DXA and thickness predicted by BMI using sex-stratified regression. ATI was categorized from lowest (+2 cm) with referent close to zero (-1 to +1 cm). Incident fractures were assessed from linked population-based health data. Hazard ratios (HR) for fracture were estimated from Cox regression adjusted for FRAX probability including competing mortality. Calibration plots compared observed versus predicted 10-year probability according to ATI category.RESULTS: The study contained 73,105 individuals, mean age 64.2 years. During mean 8.7 years observation, 7047 (9.6%) individuals sustained one or more incident MOF, including 2157 (3.0%) hip fractures. Adjusted for FRAX probability, increasing ATI was associated with incident MOF and hip fracture (p-trend <0.001). For the highest ATI category, MOF risk was increased (HR 1.23, 95% CI 1.12-1.35). Similar findings were noted for hip fracture probability (HR 1.28, 95% CI 1.09-1.51). There was significant age-interaction with much larger effects prior to age 65 years (HR 1.44, 95% CI 1.23-1.69 for MOF; 2.29, 95% CI 1.65-3.18 for hip fracture). In contrast, for the subset of individuals with diabetes there was also increased risk for those in the lowest ATI category (HR 1.73, 95% CI 1.12-2.65 for MOF, 2.81, 95% CI 1.59-4.97 for hip fracture). Calibration plots across ATI categories demonstrated deviation from the line of identity in women (calibration slope 2.26 for MOF, 2.83 for hip fracture). An effect of ATI was not seen in men, but this was inconclusive as the sex-interaction terms did not show significant effect modification.CONCLUSION: Greater BMI-discordant abdominal thickness predicted higher risk for fracture when adjusted for FRAX probability, greater in women and younger individuals, with a bimodal effect in diabetes. These data support the need to investigate abdominal thickness as a novel fracture risk factor.

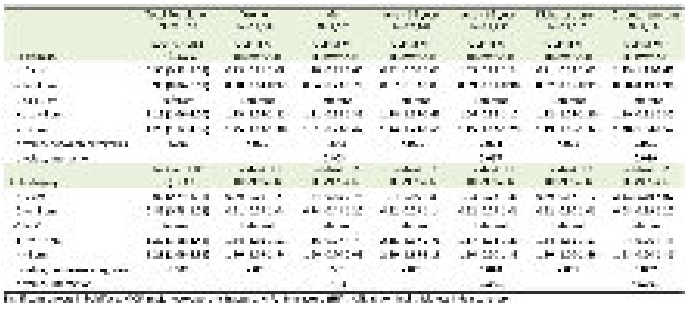

***Disclosures: William Leslie**, None*

1063

A Meta-Analysis of Previous Falls and Subsequent Fracture Risk *Liesbeth Vandenput[1], Helena Johansson[2], Eugene V McCloskey[3], Enwu Liu[1], Marian Schini[4], Nicholas C Harvey[5], Mattias Lorentzon[2], William D Leslie[6], John A Kanis[7], the FRAX Meta-analysis Cohort Group[8]. [1]Mary MacKillop Institute for Health Research, Australian Catholic University, Australia. [2]Mary MacKillop Institute for Health Research, Australian Catholic University and Sahlgrenska Osteoporosis Centre, Department of Internal Medicine and Clinical Nutrition, Institute of Medicine, Sahlgrenska Academy, University of Gothenburg, Australia. [3]Centre for Metabolic Bone Diseases, University of Sheffield and MRC and Arthritis Research UK Centre for Integrated Research in Musculoskeletal Ageing, Mellanby Centre for Musculoskeletal Research, University of Sheffield, United Kingdom. [4]MRC and Arthritis Research UK Centre for Integrated Research in Musculoskeletal Ageing, Mellanby Centre for Musculoskeletal Research, University of Sheffield, United Kingdom. [5]MRC Lifecourse Epidemiology Centre, University of Southampton and NIHR Southampton Biomedical Research Centre, University of Southampton and University Hospital Southampton NHS Foundation Trust, United Kingdom. [6]Department of Medicine, University of Manitoba, Canada. [7]Mary MacKillop Institute for Health Research, Australian Catholic University and Centre for Metabolic Bone Diseases, University of Sheffield, Australia. [8]., Australia

Previous falls are a well-documented risk factor for subsequent fracture but have not yet been incorporated into the FRAX® algorithm.We investigated the association between previous falls and subsequent fracture risk and its relation to sex, age, duration of follow-up, and bone mineral density (BMD) in an international meta-analysis. The resource comprised 891,324 men and women (66.4% female) from 45 prospective cohorts. Previous falls were uniformly defined as any fall occurring during the previous year in 42 cohorts; the remaining three cohorts had a different question construct. During a follow-up of 9,090,849 person-years, 79,953 fractures occurred; 42,805 were hip fractures. Femoral neck BMD was measured in 115,724 individuals. The predictive value of previous falls for incident fracture risk (any fracture, osteoporotic fracture, major osteoporotic fracture, and hip fracture) was investigated using an extension of the Poisson regression model in each cohort and each sex followed by random-effects meta-analyses of the weighted beta coefficients. A previous fall was associated with a significantly increased risk of any fracture both in men (hazard ratio [HR] 1.47, 95% confidence interval [CI] 1.28-1.70) and women (HR 1.39, 95% CI 1.31-1.49) after adjustment for age and duration of follow-up. The HRs were of similar magnitude for osteoporotic, major osteoporotic fracture, and hip fracture. The predictive value was higher in men than women (e.g., for major osteoporotic fracture, HR 1.48 (95% CI 1.23-1.79) in men vs. HR 1.27 (95% CI 1.15-1.40) in women, p for interaction = 0.012) and the HRs associated with previous falls decreased with age in women and with duration of follow-up in men and women for most fracture outcomes. The risk relationship did not materially change when BMD was added to the models and for most fracture outcomes, there was no evidence of an interaction between falls and BMD. Subsequent risk for a major osteoporotic fracture increased 13% and 17% with each additional previous fall in women and men, respectively.In conclusion, a previous self-reported fall confers an increased risk of fracture which seems largely independent of BMD. Previous falls should be considered as an additional risk factor in future iterations of FRAX to improve fracture prediction.

***Disclosures: Liesbeth Vandenput**, None*

1064

Fracture prediction in patients receiving maintenance dialysis: a simple tool *Andrea Cowan[1], Stephanie Dixon[2], Yuguang Kang[2], Nivethika Jeyakumar[3], Amit Garg[1], Kristin Clemens[4]. [1]Division of Nephrology, Department of Medicine, Western University, Canada. [2]ICES, Canada. [3]Lawson Health Research Institute, Canada. [4]Division of Endocrinology and Metabolism, St Joseph's Hospital, Canada

Purpose: Patients receiving maintenance dialysis are at a 5-fold risk of fracture compared to those with normal renal function, with associated poor outcomes. The Fracture Risk Assessment Tool (FRAX) is validated and commonly used in the general population, but lacks information on its performance in those receiving dialysis. Additionally, FRAX does not account for kidney disease specific risk factors including hyperparathyroidism. The 10-year risk predicted by FRAX may also be less meaningful to those receiving dialysis, where the 5-year survival rate is 53%. We sought to create an easy-to-use, short-term fracture risk prediction tool for both clinical and research applications. Methods: Using linked healthcare databases, we conducted a population-based cohort study of adults aged 40-90 years receiving maintenance dialysis with an available parathyroid hormone (PTH) value in Ontario, Canada between January 1, 2010 and September 30, 2017. Patients were followed for 3 years or until death, fracture, or emigration from the province. We developed a prediction model using routinely collected data including patient demographics, comorbidities and laboratory values using Fine and Gray's subdistribution hazards model to account for the competing risk of death. Models were compared using measures of discrimination, calibration and model fit. Models were internally validated using cross-validation. Results: We identified 11,599 individuals receiving dialysis with an average age of 66; 39% were female and 12% had a previous fracture. 839 fractures were observed within 3 years, 44% of which were in the first year, with hip fracture being the most common (299/839). The final fracture prediction model included age, sex, previous fracture, current steroid use, proton pump inhibitor use, calcitriol use, length of time receiving dialysis, and the concentrations of PTH and serum albumin. The c-statistics (equivalent to the area under the receiver operating curve) for 1-year and 3- year fracture prediction were 0.80 and 0.72 respectively indicating good discrimination. Discussion: Our easily implementable fracture risk score in patients receiving maintenance hemodialysis performs well 1 year and 3 -years without requiring bone density measurement or any extra testing or medical visits. Our short-term risk prediction tool will be helpful in identifying those at highest risk of fracture who would benefit from intervention, or inclusion in future clinical trials.

***Disclosures: Andrea Cowan**, None*

1065

Active Learning for the Efficient Annotation of Unlabeled Lateral Spine Images Acquired at Baseline from the Canadian Longitudinal Study on Aging *Barret Monchka[1], John Schousboe[2], J Michael Davidson[1], Douglas Kimelman[1], Didier Hans[3], Olivier Lamy[4], Parminder Raina[5], William Leslie[1]. [1]University of Manitoba, Canada. [2]Park Nicollet Clinic HealthPartners Institute University of Minnesota, . [3]Lausanne University Hospital & University of Lausanne, Switzerland. [4]University Hospital, Switzerland. [5]McMaster University, Canada

BACKGROUND: The Canadian Longitudinal Study on Aging (CLSA) acquired 28,657 vertebral fracture assessment (VFA) images during baseline data collection (2011-2015), but the VFAs had not been previously reviewed by medical experts for presence of vertebral fractures (VFs). Convolutional neural networks (CNNs) are deep learning models that can be used within an active learning (AL) framework to identify the most likely positive cases for expert review.AIM: To use an AL approach to efficiently annotate CLSA baseline VFAs with VF status for use in future research.METHODS: CLSA baseline VFAs were randomly divided into two sets: 60% for initial model development, and 40% for model evaluation and refinement. Six iterations of AL selective sampling were used to annotate 3,032 VFAs from the development set and incrementally improve CNN classification performance. Two ensemble models were constructed using the maximum and mean predicted probabilities of VF from separately trained CNNs. In a seventh AL iteration, the mean ensemble was used to select all VFAs from the 40% sample with predicted probability of VF >= 0.1 (n=725), which were annotated and used to estimate model performance. In the final AL iteration, all previously unlabeled VFAs with predicted probability of VF >= 0.1 (n=249) were annotated and used for model training. Improved ensembles were constructed by re-training on all annotated CLSA VFAs (n=3,891) and subsequently used to estimate the probability of VF for the remaining unlabeled images. VFAs were adjudicated and graded by three expert readers using the modified algorithm-based qualitative (mABQ) method. RESULTS: Through AL selective sampling, 4,006 VFAs were selected for expert review: 115 were excluded due to unevaluable levels or VF uncertainty, and 789 VFs were identified for an estimated prevalence of 2.8% (Grade 2-3 prevalence: 1.7%). CNN performance was assessed after six iterations of AL in 710 patients with VF present in 281 (39.6%). The mean ensemble model achieved high overall balanced accuracy (84.4%) against CLSA VFAs, including when stratified by age (range 81.2% to 88.3%) and sex (males 82.5%, females 85.9%) (Table).CONCLUSIONS: AL is an efficient technique to annotate medical images acquired in longitudinal studies and estimate prevalence from unlabeled data. Researchers using our predictions can select classification cut-offs based on their research objectives in order to prioritize case certainty versus case sensitivity.

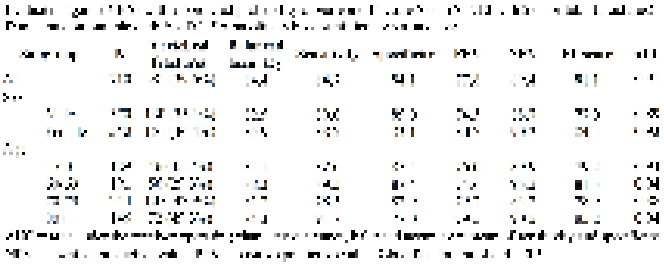

***Disclosures: Barret Monchka**, None*

1066

A Polygenic Risk Score Linked to Fracture Reduction in Adults is Associated with Fracture Reduction in a Multi-Ancestry Sample of Children *Jonathan Mitchell[1], Jonathan Bradfield[2], Shana McCormack[2], Alessandra Chesi[3], Heidi Kalkwarf[4], Dana Duren[5], John Shepherd[6], Kurt Hankenson[7], Andrea Kelly[2], Hakon Hakonarson[2], Struan Grant[8], Babette Zemel[9]. [1]Children's Hospital of Philadelphia, United States. [2]CHOP, United States. [3]Penn, United States. [4]Cincinnati Children's Hospital Medical Center, United States. [5]University of Missouri, United States. [6]University of Hawaii, United States. [7]University of Michigan, United States. [8]Children s Hospital of Philadelphia / University of Pennsylvania, United States. [9]Children s Hospital of Philadelphia, United States

A polygenic risk score, "genetic quantitative ultrasound speed of sound (gSOS)", has been developed using data from adults of European ancestry and is associated with reduced odds of fracture in adults. We aimed to determine if gSOS was associated with the likelihood of having a fracture in a multi-ancestry sample of children.Data from the Children's Hospital of Philadelphia's Center for Applied Genomics were analyzed (N=10,301). Fracture data at the following sites were extracted from electronic health records (EHR): femur, humerus, metacarpal, metatarsal, neck of femur, patella, pelvis, radius/ulna, ribs, scaphoid, tarsal, tibia/fibula and tibia. A total of 21,716 genetic variants were used to calculate gSOS for each participant. Logistic regression models tested for associations between gSOS and the following fracture related outcomes: binary fracture (none or >=1) and fracture location (none, upper limb only, lower limb only, or upper & lower limb). All analyses were adjusted for ancestry and sex differences were assessed using interactions between gSOS and sex (male or female).The sample was comprised of 9,242 (89.7%) children with no history of fracture in their EHR. Of the children with a record of fracture: 581 (5.6%) had 1 recorded fracture, 344 (3.3%) had 2 recorded fractures and 134 (1.3%) had >=3 recorded fractures. Further, 609 (5.9%) had >=1 recorded upper limb fracture, 357 (53.5%) had >=1 recorded lower limb fracture, and 93 (0.9%) had >=1 recorded upper and lower limb fracture. A 1 standard deviation increase in gSOS was associated with reduced odds of having a record of any fracture (OR=0.88, 95% CI: 0.82, 0.94). When considering fracture location, a 1 standard deviation increase in gSOS was associated with reduced odds of having a recorded of upper limb fracture (OR=0.83, 95% CI: 0.75, 0.91). These associations were consistent for both male and female sex.Consistent with the adult literature, and our prior report of gSOS being associated with higher bone mineral density in childhood, a higher gSOS score was associated with reduced odds of having a recorded fracture in childhood. It is therefore likely that having a higher gSOS is a strong genetic marker for enhanced bone accretion in early life that offsets risk for fracture across the lifespan.

***Disclosures: Jonathan Mitchell**, None*

1067

Total Body Bone Mineral Content Trajectories from 8 to 40 years of age: A SITAR Nonlinear Growth Model. *Adam Baxter-Jones[1], Ahmed Elhakeem[2], Stefan Jackowski[3], Erin Barbour-Tuck[1], Marta Erlandson[1]. [1]University of Saskatchewan, Canada. [2]University of Bristol, United Kingdom. [3]Chilrden's Hospital of Eastern Ontario Research Institute, Canada

Introduction: Appropriately modelling repeated measures in cohort studies can improve the understanding of the nonlinear development of Bone Mineral Content across the life-course. Growth-related processes of interest include mean trajectories over time, rates of growth at different ages, timings of peak growth, and variability by sex. One innovative modelling approach is to fit Super Imposition by Translation and Rotation (SITAR) models. SITAR is based on the shape invariant model, which assumes that the study population has a common characteristic curve (fitted as fixed-effects), which by shifting and scaling (by subject-specific random-effects) can be made to fit the form of any individual curve. The aim of this study was to develop velocity curves of BMC development for individuals from 8 to 40. Methods: Data is taken from the Saskatchewan Pediatric Bone Mineral Accrual study (PBMAS). PBMAS is a long running cohort study initiated in 1991 which recruited 251 children aged 8-15 years. Participants underwent up to fifteen annual DXA scans (Hologic QDR-2000, array mode) between 1991 and 2017. 112 males and 127 females in PBMAS with >=1 BMC measure were included in this analysis. SITAR models were fitted with

manually selected knots with number and position informed by the cohort-specific model. All analyses were performed in R version 4.0.2 (R Project for Statistical Computing) and RStudio integrated development environment version 1.3.1 (RStudio Team). Results: Models showed increases in BMC through early life with rapid increases, and emerging sex differences, in adolescence. Age at peak BMC accrual in girls was 12.0 +/- 0.9 yrs with a peak accrual of 260.9 +/- 124.9 (g/yrs), compared to boys whose values were 13.7 +/- 0.9 yrs, peak accrual of 337.6 +/- 71.6 (g/yrs). BMC plateaued in emerging adulthood and started decreasing in the fourth decade of life. Discussion: These models graphically illustrate the nonlinear development of BMC across the life-course and show sex differences in both velocities and distance trajectories. They show peak accrual in adolescence, plateauing in emerging adulthood and the start of bone loss between 30 and 40 years of age. The models described in this paper can be extended to explore associations of early life exposures with trajectories, and associations of trajectories with associated future outcomes. Funding: Canadian Institute of Health Research, Canadian Foundation for Innovation, and Saskatchewan Health Research Foundation.

***Disclosures: Adam Baxter-Jones**, None*

1068

Reliable Quantification of Bone Microstructure from HR-pQCT During Growth Requires Density-Independent Segmentation *Andrew Burghardt[1,] Kyla Kent[2,] Jin Long[3,] Ariana Strickland[3,] Tandy Aye[3,] Mary Leonard[4.] [1]University of California, San Francisco, United States, [2]STANFORD MEDICINE, United States, [3]Stanford University School of Medicine, United States, [4]Stanford School of Medicine, United States

Second generation HR-pQCT uses BMD-based thresholds to segment mineralized bone from soft tissues. This approach does not account for variability in tissue density, which is particularly high during periods of rapid growth in children and adolescents. A density-independent fine structure segmentation method based on the Laplace-Hamming (LH) edge-enhancement operator, significantly improves the accuracy of both trabecular and cortical bone structure measures in adults1. Our goal was to document qualitative improvements in segmentation fidelity in pediatric HR-pQCT scans and compare the impact of segmentation differences on age-related trajectories of structure.Two alternative fine structure segmentation functions were applied within the standard second-generation HR-pQCT image analysis pipeline: (a) the standard BMD-threshold binarization scheme; (b) a fixed-threshold binarization of the edge-weighted, intensity-normalized LH filtered image. Each segmentation approach was used to quantify cortical and trabecular structure in distal tibia HR-pQCT scans acquired at 4.0% proximal to the growth plate in a normative pediatric cohort (n=214; age=5-20). Absolute differences between segmentation methods were calculated for each structure outcome by sex and tanner stage.Qualitatively, BMD-threshold binarizations failed to identify significant amounts of cortical porosity, while also not capturing thin trabecular connections, especially in the central medullary space (Fig. 1). The discrepancy for cortical porosity peaked peri-pubertally in girls (p<0.05), while the difference in trabecular BV/TV decreased with growth for both sexes, with the LH method yielding greater BV pre-pubertally, and lesser BV post-pubertally (p<0.0001). LH detected more trabeculae that were increasingly thinner in boys, compared to BMD-based segmentations (p < 0.01).The standard BMD-based threshold systematically underestimates the quantification of cortical porosity in second-generation HR-pQCT of pediatric subjects. This error is most profound during puberty. Additionally, central medullary trabeculae are often lost by the BMD-based segmentation but rescued by the LH approach. Therefore, fine structure segmentation methods that are independent of BMD are essential to accurately capture age-wise trajectories in bone micro-structure during growth.1. Sadoughi S, et al. A Laplace-Hamming Binarization Approach for Second-Generation HR-pQCT Rescues Fine Feature Segmentation. JBMR 2023

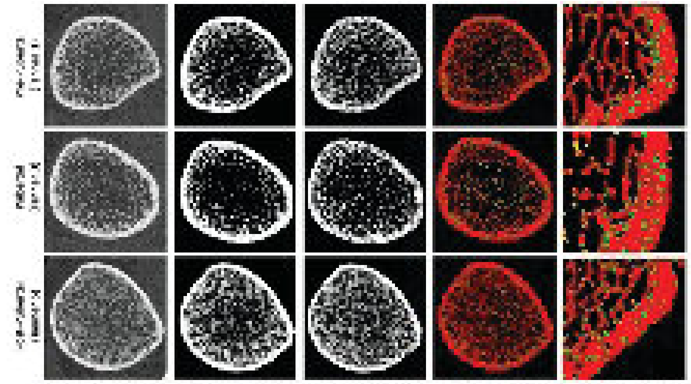

Fig. 1 Representative distal tibia HR-pQCT slices from pre- (top), peri- (center) and pubertal (lower) participants, illustrating fine-structure segmentations using the standard BMD threshold binarization (second column) or Laplace-Hamming binarization (third column), and difference image (last two columns; red = missing; green = overestimated by BMD-based binarization; yellow = rescued by LH-based binarization).

***Disclosures: Andrew Burghardt**, None*

1069

A young-child formula with the synbiotic l reuteri and galacto-oligosaccharides increases bone strength in toddlers: a 6-month randomized Controlled Trial *Nicolas Bonnet[1,] Maria Rosario Capeding[2,] Marc Garcia Garcera[3,] Laura-Florina Kratinger[4,] Jowena Lebumfacil[5,] Lhodie Phee[2,] Ivana Jankovic[6,] Yipu Chen[6,] Delphine Egli[6,] Marie-Noëlle Horcajada[3.] [1]Nestlé research, Switzerland, [2]Clinical Research Unit, Asian Foundation for Tropical Medicine, Inc. (AFTMI), Muntinlupa City, Philippines, Philippines, [3]Nestlé Institute of Health Sciences/ Nestlé Research, Lausanne, Switzerland, Switzerland, [4]Clinical Research Unit, Nestlé Research, Lausanne, Switzerland, Switzerland, [5]Wyeth Nutrition, Makati City, Philippines, Philippines, [6]Nestlé Product Technology Center - Nutrition, Société des Produits Nestlé S.A., Vevey, Switzerland, Switzerland

Toddlerhood is a critical period for bone mass acquisition. This study evaluated the impact of consuming a young child formula containing a synbiotic composed of Limosilactobacillus (L., previously Lactobacillus) reuteri + galacto-oligosaccharides (GOS) on bone quality in healthy young children.In this randomized, double-blind controlled clinical trial performed in the Philippines, children aged 2-3 years received for 6 months a young child formula containing L. reuteri DSM 17938 (at concentration that guarantees 10exp8 cfu/day) + GOS (4g/L) (Experimental Young Child Formula with synbiotic, EYCF, n=91) or a minimally fortified powdered milk mimicking local traditional milks (control milk, CM, n=91). Children were advised to consume 2 servings/day. The tibia quality was assessed at baseline and after 3- and 6-months measuring speed of sound by ultrasound. A linear mixed model with repeated measurements was applied with fixed effects for treatment group, gender, visit, visit x treatment interaction, and baseline values for speed of sound, vitamin D levels in blood and body mass index. Blood bone turnover markers (CTX and P1NP) as well as microbiome composition and function were performed at all timepoints, respectively by ELISA and shotgun metagenomics.Mean age at baseline was 29.6 +/- 3.6 months and 53% were female. The primary outcome, tibia speed of sound measured at 6 months was significantly higher in EYCF compared to CM. The estimated average difference was 58.91 [95% CI = (21.34, 96.48) m/s], p=0.002, in the full analysis set, supported by estimated effect on the per protocol population (p=0.005). A positive effect was already observed after 3 months of intervention 53.00 [95% CI = (7.05, 98.95) m/s] p=0.024. Bone turnover index (CTX/P1NP) was 25% higher in EYCF vs CM [95% CI = (1, 49) %], p=0.041. Microbiome beta diversity analyses based on principal coordinate analysis could differentiate the EYCF samples from CM (p<0.001). L. reuteri abundancy was 15-fold higher in EYCF vs CM (p<0.0001) and a prevalence increase of 7-fold (p<0.0004).Consumption of a young child formula containing the synbiotic L. reuteri + GOS promotes bone strength improving bone quality by increased bone turnover, and induces microbiome changes supporting bone quality improvement in healthy young children.

***Disclosures: Nicolas Bonnet**, Société des Produits Nestlé S.A, Major Stock Shareholder*

1070

Fracture risk, bone mineral density and bone biochemistry: a phase 3, double-blind, placebo-controlled randomized trial of vitamin D supplementation in schoolchildren *Davaasambuu Ganmaa[1], Uyanga Buyanjargal[2], Polyna Khudyakov[3], Adrian Martineau[4]. [1]Channing Division Network of Medicine, Brigham and Women Hospital, Harvard Medical School and Harvard T.H. Chan School of Public Health, Boston, USA, United States. [2]Mongolian Health Initiative, Mongolia. [3]Sage Therapeutics, United States. [4]Blizard Institute, Barts and The London School of Medicine and Dentistry, Queen Mary University of London, United Kingdom

Background:There are numerous observational studies reporting associations between vitamin D deficiency and increased risk of fracture and low bone mineral density (BMD) in children. We previously reported a very high prevalence of vitamin D deficiency in Mongolian schoolchildren living in Ulaanbaatar, the coldest capital in the world. We conducted a phase 3 randomized controlled trial to determine whether a 3-year course of oral vitamin D supplementation influences BMD or fracture risk in this population.ObjectiveTo determine the effects of vitamin D supplementation at a dose of 14,000 IU per week in all participants: (i) fracture incidence (n=8,851), and in a sub-set of participants: (ii) calcaneal bone mineral density (n=1,465) and (iii) serum concentrations of 25-hydroxyvitamin D (25[OH]D) (all participants), parathyroid hormone (PTH), calcium, total alkaline phosphatase (ALP) and bone-specific alkaline phosphatase (BSAP) (n=100 of BMD sub-study) at baseline and 3-year follow-up.MethodsA phase 3 randomized, double-blind, placebo-controlled trial in which 8,851 children were given 14,000 IU/week vitamin D3 supplement or placebo for 3 years. Analyses were conducted for all efficacy outcomes to determine whether the effect of the intervention varied according to baseline 25(OH)D D levels (<10 vs. >=10 ng/mL), calcium intake (<500 vs. >=500 mg/day), and baseline calcaneal BMD z-scores (<-2.00 vs. >=-2.00).ResultsAt baseline 95.6% of participants had vitamin D deficiency (25[OH] D <20 ng/mL) with mean serum 25(OH)D concentration 11.9 ng/mL. The intervention was effective in correcting vitamin D deficiency: end-trial 25(OH)D levels were >=20 ng/mL in 89.8% of participants randomized to vitamin D vs. 5.6% of those randomized to placebo (P<0.001), and this was associated with suppression of PTH concentrations (mean difference -13.6 pmol/L, 95% CI -23.5 to -3.7). However, there was no difference in the proportion of participants randomized to vitamin D vs. placebo reporting at least one fracture (268/4176 [6.4%] vs. 253/4172 [6.1%], respectively; adjusted risk ratio 1.10, 95% CI 0.93 to 1.29, P=0.27) or in mean calcaneal BMD z-score (adjusted mean difference between arms -0.06, 95% CI -0.18 to 0.07, P=0.36).Effects of the intervention on serum BSAP concentrations were modified by baseline 25(OH)D concentration (P for interaction = 0.04) but effects on fracture risk and calcaneal BMD were not (P values for interaction >=0.67).ConclusionsIn a population of children with low baseline vitamin D status, this RCT found that 14,000 IU weekly vitamin D3 supplementation was effective in rendering adequate vitamin D status and suppressing PTH concentrations but it did not affect risk of fracture or calcaneal BMD.

***Disclosures: Davaasambuu Ganmaa**, None*

1071

Bone-Derived PDGF-BB Drives Brain Vascular Calcification During Aging *Jiekang wang[1], Ching-lien Fang[2], Mei Wan[2], Surendra Kumar[4], ke shen[2], huixin hao[2], kangping song[2], Xu Cao[4]. [1]johns hopkins university, . [2]Orthopedic Surgery, United States. [4]Johns Hopkins University, . [4]Johns Hopkins University, United States

Vascular calcification and osteoporosis often coexist in the aging population. While the pathogenesis of large vessel calcifications has been intensively studied, little is known on the mechanisms of microvascular calcification in brain. In fact, brain calcification is a prevalent age-related pathology, affecting over 20% of the elderly population and frequently co-occurring with neuroinflammatory conditions. The present study aims to define the role of bone-derived cues in the pathogenesis of brain microvascular calcification.Using various approaches, including whole-brain micro-CT scanning, susceptibility-weighted imaging (SWI)-based MRI screening, and histological/immunofluorescence analyses, we consistently detected a high incidence of brain calcification nodules in 18- to 24-month-old mice, ranging from 71.4% to 80.9%. The calcification nodules primarily occur in the thalamus regions in aged mice but not in young mice. We recently reported that with aging, preosteoclasts in bone produce higher levels of platelet-derived growth factor-BB (PDGF-BB), which can then enter the bloodstream and cross the blood-brain barrier to regulate brain cell activity. We examined whether bone-derived PDGF-BB is also involved in the development of brain calcification using conditional Pdgfb transgenic (PdgfbcTG) and knockout (PdgfbcKO) mouse models. Young PdgfbcTG mice, in which Pdgfb is overexpressed in preosteoclasts, have much higher serum level of PDGF-BB and recapitulate the thalamic calcification phenotype in aged mice. Conversely, old PdgfbcKO mice, in which Pdgfb is deleted selectively in preosteoclasts, have diminished thalamic calcification. To further explore the molecular mechanisms underlying PDGF-BB-induced brain vessel calcification, we developed an ex-vivo cerebrovascular culture system, in which we treated the isolated brain micro-vessels with recombinant PDGF-BB. PDGF-BB directly promoted microvascular calcification. Osteogenic gene array and scRNA-Seq analyses revealed that PDGF-BB upregulates multiple osteogenic differentiation genes and a phosphate transporter Slc20a1 in cerebral micro-vessels. We also found that PDGF-BB activates ERK signaling and its downstream transcription factor RUNX2, which binds to the promoter regions of Slc20a1 for gene transcription. Our results provide new evidence for the bone-vascular interrelationship and uncover ERK-RUNX2-Slc20a1 signaling as important mediators for PDGF-BB-induced micro-vessel calcification.

***Disclosures: Jiekang wang**, None*

1072

Gut-bone axis: X/A-like cells may mediate the effects on skeletal homeostasis *Caroline de Carvalho Picoli[1], Jeyrie Ramos Aponte[1], Clifford J. Rosen[1], Ziru Li[1]. [1]MaineHealth Research Institute, United States

Background- Bariatric surgery is the most effective treatment for severe obesity and type 2 diabetes. However, this procedure causes various side effects, such as bone loss and increased fracture risks. While changes in gut hormones and microbiota were considered as potential mechanisms, the contribution of the major surgical site (the stomach) has been largely overlooked. X/A-like cells account for ~20% of the endocrine cell in the stomach and produce ghrelin. Vertical sleeve gastrectomy (VSG), the most popular bariatric surgical procedure, reduces ghrelin in humans and rodents. We are sought to understand the roles of X/A-like cells in VSG-caused bone loss. Methods- Firstly, we employed a hand-sewing VSG mouse model. C57BL/6J male mice were fed a HFD for 8 weeks and then underwent VSG. A subgroup of mice received ghrelin supplementation. Secondly, we utilized an inducible X/A-like cell-depletion mouse model. We bred ghrelin (Ghrl)-Cre mice with diphtheria toxin receptor (DTR) mice, which allowed for specific deletion of X/A-like cells following DT injections. Changes in fat mass, glucose and bone were evaluated 4 weeks after VSG or DT treatment. Results- VSG resulted in a significant reduction in fat mass and improvement in glucose metabolism, but it also caused trabecular and cortical bone loss. Interestingly, the supplementation of exogenous ghrelin did not impact these effects, suggesting that ghrelin may not be the critical endocrine factor mediating the effects of VSG on metabolic benefits and skeletal complications. Furthermore, we observed a substantial loss of X/A-like cells following VSG. To further validate the importance of X/A-like cells in the whole-body and bone metabolism, we employed Ghrl-DTR mice treated with DT, resulting in approximately 93% reduction in X/A-like cell numbers. This reduction was associated with a significant improvement in glucose metabolism but also caused trabecular bone loss. The similarity of the effects seen in X/A-like cell depletion with those observed in VSG suggests that these cells may mediate the effects of VSG on glucose and bone metabolism. Conclusions- Our VSG mouse model replicated the metabolic benefits and skeletal complications observed in clinical patients. Ghrelin was not found to be a significant contributor to VSG-induced glucose improvement and skeletal complications. Our findings highlight the significant role of X/A-like cells in skeletal homeostasis through the secretion of unknown factors.

***Disclosures: Caroline de Carvalho Picoli**, None*

1073

Eldecalcitol Prevents Muscle Loss and Osteoporosis in Disuse Muscle Atrophy via NF-?B Signaling in Mice *Haichao Zhang[1], Zheng Ke[2], Shuangshuang Dong[2], Yanping Du[1], Wenjing Tang[1], Minmin Chen[1], Weijia Yu[1], Qun Cheng[1]. [1]Department of Osteoporosis and Bone Disease, Huadong Hospital Affiliated of Fudan University, Research Section of Geriatric Metabolic Bone Disease, Shanghai Geriatric Institute, Shanghai, 201100, PR China , China. [2]Medical Division, Chugai Pharma China Co., Ltd., Shanghai, 200021, PR China, China

IntroductionWe investigated the effect of eldecalcitol (ELD) on disuse muscle atrophy and its molecular mechanisms.MethodTail suspension (TS) was used to mimic disuse muscle atrophy in 6 weeks old C57BL/6J male mice which were randomly assigned to control, TS, and TS-ELD-treated groups (3.5/5 ng) and were injected intraperitoneally twice a week for 3 weeks. Grip strength and gastrocnemius (GAS), tibialis anterior (TA), and soleus (SOL) muscle weights were determined. Oxidative stress was evaluated by malondialdehyde, superoxide dismutase, glutathione peroxidase, and catalase. Bone microarchitecture was analyzed using microcomputed tomography. Effect of ELD on MHC and Atrogin-1 and MuRF-1 of C2C12 myoblasts was assessed by immunofluorescence. ELD influence on NF-?B signaling pathway and vitamin D receptor (VDR) was assessed via immunofluorescence, (co)-immunoprecipitation, and VDR knockdown studies.ResultsELD increased grip strength (P<0.01) and restored TS-induced muscle loss in GAS, TA, and SOL (P<0.05 to P<0.001). Bone mineral density (BMD) and bone architecture was improved in the ELD group by reducing bone loss. Cortical and trabecular BMD of the distal femur were significantly decreased by 12.37% and 28.51%, respectively, which reversed upon ELD administration. Decreased bone surface/total tissue volume (BS/TV) (62.56%), trabecular number (Tb.N) (65.92%), trabecular thickness (Tb.Th) (26.11%) in the TS group as compared to control group (P<0.001). However, their levels were partly restored by 78.22%, 85.68%, and 19.04%, respectively, in the ELD low-dose group (3.5 ng/week). Antioxidant defense system of GAS muscle and serum was altered in the TS group as indicated by the lower levels of SOD, GSH-Px, and CAT in serum (39.04%, 40.53%, and 41.93%, respectively) and in GAS muscle (51.38%, 42.48%, and 50.31%, respectively). In differentiated C2C12 myotubes, the addition of TNF-? elevated the levels of Atrogin-1 and MuRF-1 and decreased the levels of MHC compared with the control cells. ELD inhibited TNF-?-induced myotube atrophy in a concentration-dependent manner. ELD (10 nM) significantly inhibited the expression of MuRF-1 by 38.79% (P<0.001) and Atrogin-1 by 41.52% (P<0.01), increased the diameter of

myotubes (P<0.05), and inhibited the expression of P65 and P52 components of NF-?B and P65 nuclear location, thereby inhibiting NF-?B signaling.ConclusionsELD was beneficial against disuse-induced muscle atrophy via NF-?B inhibition.

***Disclosures: Haichao Zhang**, None*

1074

FGF23 Neutralizing Antibody Ameliorates Abnormal Renal Phosphate Handing in Sickle Cell Disease Mice *Liping Xiao[1], Kai Clarke[1], Marja Marie Hurley[2]. [1]UConn Health, United States. [2]UCONN Health School of Medicine, United States

The mechanisms responsible for the abnormal serum phosphate level in patients with sickle cell disease (SCD) and preserved glomerular filtration rate are not fully understood. Fibroblast growth factor 23 (FGF23), a bone-derived phosphaturic hormone is up regulated by iron deficiency, hypoxia, and high erythropoietin (EPO), which are seen in SCD. In this study, we assessed the involvement of FGF23 signaling pathway in the impaired renal phosphorus handling in kidneys of SCD mice. Six months old healthy control (Ctrl) and Townes SCD mice were subcutaneously injected with control IgG or rat monoclonal anti-FGF23 neutralizing antibody (FGF23Ab, kindly provided by Amgen) at 10mg/kg body weight. Then the mice were housed in metabolic cages. Twenty-four hours later the mice were euthanized for sample collection. Serum biochemistry revealed no differences in creatinine between Ctrl versus SCD mice. Serum intact FGF23 level was higher in SCD-IgG compared with Ctrl-IgG in female, FGF23Ab significantly decreased serum intact FGF23 level in both male and female (Fig. 1A). Although there was no difference in serum Pi between Ctrl-IgG and SCD-IgG urine phosphate/creatinine (Pi/Cr) was significantly higher in SCD-IgG group compared with Ctrl-IgG in both male and female, which was rescued by FGF23Ab treatment (Fig.1B). Analysis of kidneys by Western blot showed that pFGFR1 was significantly higher in SCD-IgG compared with Ctrl-IgG male, which was rescued with FGF23Ab treatment. pFGFR2 and pFGFR4 were significantly higher in SCD-IgG compared with Ctrl-IgG in both male and female, FGF23Ab treatment did not alter pFGFR2 and pFGFR4 expression level. There was no difference in pFGFR3 expression between Ctrl-IgG and SCD-IgG, FGF23Ab treatment significantly decreased pFGFR3 level in SCD kidney. Immunohistochemistry (IHC) staining showed that there was increased phospho p44/42 MAPK (Erk1/2) (pERK), phospho Janus Activating Kinase 3 (pJAK3), and phospho serum glucocorticoid-inducible kinase 1 (pSGK1) in SCD-IgG kidney compared with Ctrl-IgG, which were partially rescued with FGF23Ab treatment (Fig.1C). A significant reduction in the phosphate transporter sodium-phosphate cotransporter NaPi-2a (Npt2a) protein was observed in SCD-IgG kidneys, which was increased by FGF23Ab treatment (Fig.1D). We conclude that FGF23/FGFR1 promotes phosphate wasting in SCD by downregulating expression of the NPT2a via modulation of ERK1/2, JAK3, and SGK1 signaling.

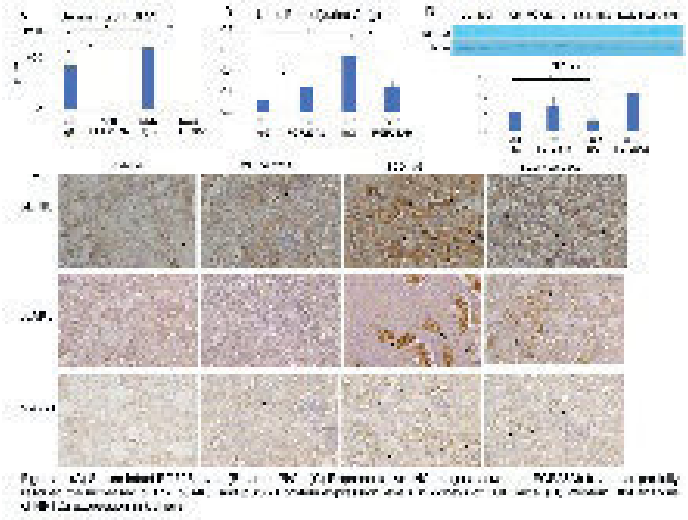

***Disclosures: Liping Xiao**, None*

1075

Implicating peripheral neural mediated MAPK signaling in obesity induced alterations in bone mass *Masnsen Cherief[2], Mario Gomez-Salazar[2], Minjung Kang[2], Mingxin Xu[2], Sowmya Ramesh[2], QIZHI QIN[2], Mary Archer[2], SEUNGYONG LEE[3], Thomas Clemens[4], Ahmet Hoke[2], Aaron James[2]. [2]Johns Hopkins University, United States. [2]Johns Hopkins University, . [3]Midwestern University, Republic of Korea. [4]University of Maryland, Baltimore, United States

Introduction: Recent research suggested that high fat diet (HFD)-associated polyneuropathy may contribute to low bone mass. Here, we show that bone loss induced by HFD was concomitant with a blunted periosteal innervation. Transcriptomic analysis showed a reduced proliferation and differentiation potency in HFD periosteal mesenchymal progenitor cells (pMSCs), associated with reductions in MAPK signaling. Finally, we queried if neural conditioned media (CM) could rescue the proliferation and differentiation abilities of HFD pMSCs. Methods: JHU ACUC approved our experiments. HFD or normal diet (ND) was instituted from 4 to 16 weeks of mice age. µCT was used to quantify cortical and trabecular bone parameters. Skeletal innervation was assessed by the neuronal markers TUBB3. For scRNA-Seq, femur periosteum was digested and sorted to exclude erythrocytes. For pMSCs proliferation and differentiation assays, cells were seeded for further analysis. Results: We demonstrated that HFD led to expected trabecular and cortical bone structural deficits (Fig. 1A-D). In addition, HFD led to a pronounced reduction in skeletal nerve density within the femoral periosteum (Fig. 1E-F). This is the first report of a skeletal neuropathy in any experimental model of diabetes. Next, pMSCs cells were subclustered into MSC progenitors, Pre-osteoblasts, and Osteoblasts (Fig. 2A). Transcriptomics revealed a reduction in 'proliferation' indices, MAPK, WNT and TGFb signaling activity among pMSCs of HFD mice (Fig. 2B). Finaly, HFD reduced proliferation and osteogenic differentiation potential of pMSCs, corroborating our transcriptional data. Next, we exposed pMSCs to dorsal root ganglia (DRG) CM and assessed their response to neural-derived paracrine factors (Fig. 3). DRG CM significantly enhanced the differentiation and proliferation of ND mice pMSCs. Remarkably, DRG CM rescued the proliferaton and osteogenic differentiation potential of HFD pMSCs (Fig. 3A-B). This highlights the potential relationships between skeletal polyneuropathy and defective skeletal progenitor cell function. Conclusion: Metabolic skeletal polyneuropathy is associated with bone architectural deficits and reduced proliferation and osteogenic differentiation in pMSCs, suggesting a direct impact of diabetic neuropathy on bone health. Exposure to physiological neural input has the potential to restore bone health in obesity related bone disease.

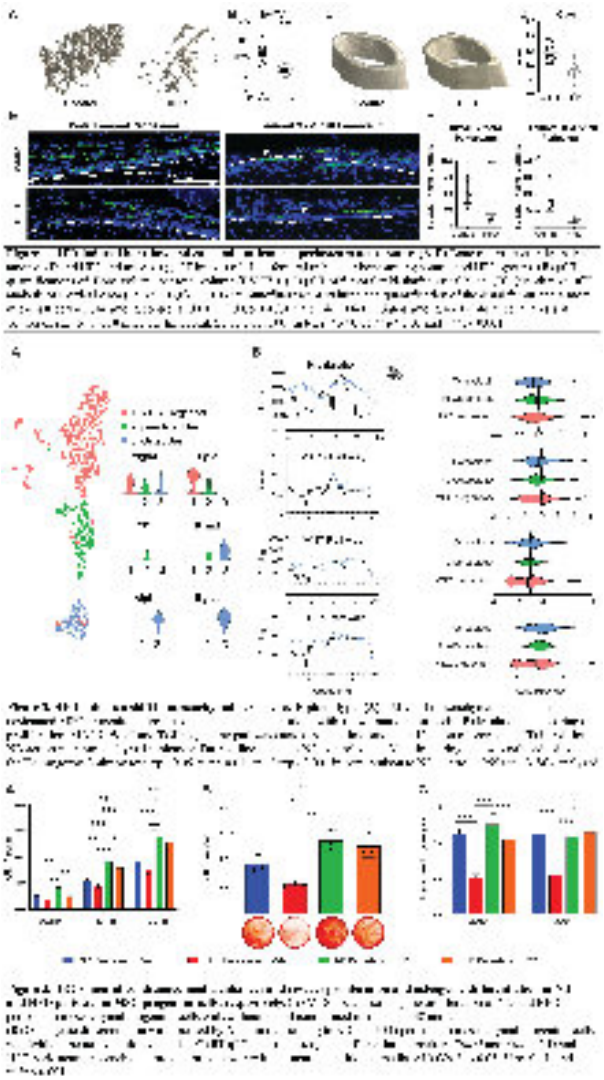

***Disclosures: Masnsen Cherief**, None*

1076

Variants associated with adolescent idiopathic scoliosis perturb an estrogen-sensitive Pax1-Col11a1-Mmp3 signaling axis *Carol Wise[1], Hao Yu[2], Anas Khanshour[2], Aki Ushiki[3], Nao Otomo[4], Yoshinao Koike[4], Elisabet Einarsdottir[5], Yanhui Fan[6], Lilian Antunes[7], Yared Kidane[2], Reuel Cornelia[2], Rory Sheng[3], Yichi Zhang[3], Jimin Pei[8], Nick Grishin[8], Bret Evers[8], Jason Pui Yin Cheung[6], John Herring[2], Chikashi Terao[4], You-Qiang Song[6], Christina Gurnett[7], Paul Gerdhem[9], Shiro Ikegawa[10], Jonathan Rios[2], Nadav Ahituv[3]. [1]Texas Scottish Rite Hospital, United States. [2]Scottish Rite for Children, United States. [3]UCSF, United States. [4]RIKEN Center for Integrative Medicine, Japan. [5]SciLifeLab Sweden, Sweden. [6]Hong Kong University, China. [7]Washington University in St. Louis, United States. [8]UT Southwestern, United States. [9]Uppsala University, Sweden. [10]RIKEN, Center for Integrative Medical Science, Japan

Adolescent idiopathic scoliosis (AIS) is a common and progressive spinal deformity that exhibits striking sexual dimorphism, with girls at more than five-fold greater risk of severe disease compared to boys. Despite its medical significance, insights into the pathogenesis of AIS are just emerging. By genome-wide association and functional studies we previously defined a female-specific AIS risk locus in an enhancer near the PAX1 gene. Here, we sought to define the roles of PAX1 and newly-identified AIS-associated genes in the mechanism of AIS. In a discovery and follow-up meta-analysis association study of nonsynonymous variants within extracellular matrix (ECM) genes (total N=103,757 individuals), we identified significant associations with a variant in COL11A1 (rs3753841; p.(Pro1335Leu); P=7.07e-11, OR=1.118). Using CRISPR mutagenesis we generated Pax1 knockout mice (Pax1-/-), which were viable and displayed a kinked tail phenotype. By RT-PCR in tails of E12.5 Pax1-/- mice, we found reduced expression of AIS-associated genes including Col11a1. Immunofluorescence microscopy in postnatal spines detected overlapping staining of Pax1 and Col11a1 at the cartilaginous endplate-osseous junction encompassing the vertebral growth plate, with reduced expression of Col11a1 in Pax1-/- spines compared to wildtype. To study the role of Col11a1 in growth plate cells (GPCs), primary rib cartilage from Col11a1fl/fl mice was cultured in the presence or absence of Cre-expressing adenovirus. By RT-PCR in these cells, we observed significant upregulation (P<.05) of Mmp3, encoding the matrix metalloproteinase 3 “stromolysin” enzyme that is known to be regulated by Col11a1 in solid tumors. Conversely, endogenous Mmp3 expression was significantly downregulated after lentiviral overexpression of the human COL11A1WT, but not COL11A1P1335L, in Cre-expressing Col11a1fl/fl SV40-immortalized GPCs. These results support negative regulation of Mmp3 expression by Col11a1 that is abrogated by the AIS-associated COL11A1P1335L variant in GPCs. Col11a1 is regulated by estrogen receptor beta (ESR2) in ovarian cells. siRNA-mediated Esr2 knockdown in mouse GPCs significantly increased Col11a1 expression, and significantly decreased Mmp3 expression, as did tamoxifen treatment of these cells. These studies support a new model wherein genetic variation and estrogen signaling increase susceptibility to spinal deformity during adolescent growth via a Pax1-Col11a1-Mmp3 signaling axis.

***Disclosures: Carol Wise**, None*

1077

TYRA-300 Demonstrates Significant Increases in Growth and Bone Length in a Mouse Model of FGFR3-Related Skeletal Dysplasia *Laurence Legeai-Mallet[1], Matthias Guillo[1], Nabil Kaci[1], Jacqueline H. Starrett[2], Ronald V. Swanson[2]. [1]Université de Paris Cité, Imagine Institute, Laboratory of Molecular and Physiopathological Bases of Osteochondrodysplasia. INSERM UMR1163, France. [2]Tyra Biosciences, United States

Achondroplasia (ACH) is the most common human skeletal dysplasia affecting ~1 in 25,000 births. Infants with ACH have an increased risk for death related to critical foramen magnum stenosis leading to cervicomedullary compression. A specific mutation in FGFR3, G380R, causes over 99% of achondroplasia. FGFR3 is expressed in growth plate chondrocytes where it functions to slow endochondral bone formation. The G380R mutation, as well as other activating mutations, results in increased FGFR3 activity, which suppresses chondrogenesis in the growth plate, disturbing long bone elongation. Vosoritide, a C-naturetic peptide analogue, acting exclusively on the MAP kinase pathway, was recently approved as a daily injection to increase annual growth velocity in children with open growth plates. While an important breakthrough, long-term effects on ACH-associated comorbidities are not yet known. TYRA-300 is an oral, highly selective FGFR3 inhibitor currently undergoing a Phase 1/2 clinical trial, SURF301 (Study in Untreated and Resistant FGFR3+ Advanced Solid Tumors). To explore the effectiveness of TYRA-300 in FGFR3-related skeletal dysplasias, TYRA-300 was evaluated in an FGFR3Y367C/+ transgenic mouse model. TYRA-300 administered daily at a 1.2 mg/kg dose for 15 days in the FGFR3Y367C/+ mouse model significantly increased body length in mice by 17.6% compared to the vehicle (Figure 1, p<0.0001) and increased the length of the femur (+24.4%), tibia (+38.3%) and L4-L6 (+23.9%) in mice (p<0.0001). Growth in the skull resulting in elongation (+11.0%) and improvement in the size and shape of the foramen magnum were also observed. Histological staining of the femurs revealed restoration of the hypertrophic zone and secondary ossification center within the epiphysis after TYRA-300 treatment. Collagen X staining also indicated that TYRA-300 improved the structure of the trabecular bone and increased chondrocyte differentiation. These data indicate that inhibiting FGFR3 directly leads to highly increased bone length, as well as foramen magnum diameter, in this preclinical model.

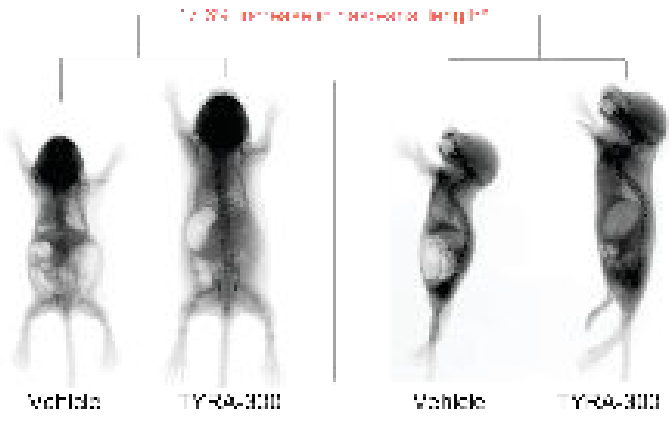

Figure 1. Representative whole body X-ray of vehicle treated heterozygous [illegible] mouse on the left and TYRA-300 treated heterozygous [illegible] mouse on the right. Treatment consisted of daily oral gavage injection of TYRA-300 at 1.2 mg/kg for 15 days starting at day 1 after birth. [illegible] p<0.0001

***Disclosures: Laurence Legeai-Mallet**, Tyra Biosciences, Grant/Research Support*

1078

Conditional Deletion of Runx2 in Cranial Base Chondrocytes Causes Midfacial Hypoplasia *Noriaki Ono[1], RENNY FRANCESCHI[4], Wanida Ono[1], Ariel Arbiv[5], Annabelle Zhou[5], LENA BATOON[4], Ashley Dixon[5], José Brenes[5], SHAWN HALLETT[5]. [1]University of Texas Health Science Center at Houston School of Dentistry, United States. [4]University of Michigan, United States. [5]University of Michigan School of Dentistry, United States. [4]University of Michigan, . [5]University of Michigan School of Dentistry,

The cranial base growth center synchondroses regulate anteroposterior craniofacial growth. Like the long bone growth plate, the synchondrosis is comprised of distinct layers of chondrocytes, but is organized in an opposite-facing mirror-like fashion, facilitating bidirectional cranial base growth. In humans and mice, overactivation of fibroblast growth factor receptor 3 (FGFR3) signaling causes achondroplasia associated with premature fusion of the synchondrosis, while RUNX2 haploinsufficiency causes cleidocranial dysplasia (CCD) with midfacial hypoplasia. Runx2 regulates Fgfr3 expression in vitro; however, signaling mechanisms regulating chondrocytes in the synchondrosis are not well understood. We hypothesize that Runx2 is regulated by FGFR3 signaling and maintains chondrocyte activities in the synchondrosis. To address this, we used a tamoxifen-inducible Fgfr3-creER line and Runx2-floxed alleles to ablate Runx2 in Fgfr3+ chondrocytes. Control, Runx2cHet (Fgfr3-creER; Runx2fl/+) and Runx2cKO (Fgfr3-creER; Runx2fl/fl) mice carrying R26R-tdTomato and Col1a1-GFP reporters were pulsed with tamoxifen at P3 and chased to sequential timepoints. Morphometric analyses of the skull were completed by 3D microCT analyses. EdU labeling and TUNEL assays were conducted to evaluate cell proliferation and apoptosis, respectively. Sections were stained with Safranin-O and TRAP to visualize cartilage matrix and osteoclasts, respectively. Runx2cKO mice showed anteroposteriorly shortened skulls accompanied by synchondroses lacking distinctive chondrocyte layers that prematurely ossified associated with tdTomatoneg/Col1a1-GFP+ osteoblasts in the center of the synchondrosis. Chondrocyte proliferation and apoptosis were both decreased, while TRAP+ osteoclasts were increased, in Runx2cKO synchondroses. Expression of ColX and Fgfr3 were upregulated in Runx2cKO synchondrosis, demonstrating that Runx2 may be a negative regulator of chondrocyte hypertrophy and FGFR3 in the synchondrosis. Therefore, deletion of Runx2 may result in overactivation of Fgfr3 and its subsequent downstream signaling, leading to accelerated chondrocyte hypertrophy, reduced proliferation and precocious ossification of the synchondroses. Our study is the first to demonstrate a possible FGFR3-RUNX2 axis in regulating synchondrosis chondrocytes, and may catalyze the identification of new therapeutic targets to treat midfacial skeletal malformations in humans.

***Disclosures: Noriaki Ono**, None*

1079

The Role of Salt Inducible Kinases in Alveolar Bone Development *Nicha Tokavanich[1], Katelyn Strauss[5], Christian Castro[5], Marc Foretz[3], Wanida Ono[4], Marc Wein[5]. [1]Massachusetts General Hospital, Harvard School of Dental Medicine, United States. [5]Massachusetts General Hospital, United States. [3]University of Paris, Institut Cochin, France. [4]University of Texas Health Science Center at Houston School of Dentistry, United States. [5]Massachusetts General Hospital,

BackgroundAlveolar bone is a specialized part of the jawbones that supports and anchors teeth. It is formed from neural crest mesenchymal cells and regulated by various signaling pathways, including the parathyroid hormone-related protein (PTHrP) pathway. Salt-inducible kinases (SIKs) are key intracellular regulators of PTH/PTHrP signaling in long bones. However, the role of these kinases in jawbone remains unknown.MethodsMice lacking SIK2 and SIK3 were generated using tamoxifen-inducible Ubq-creERt2.Animals were divided into two groups: Sik2f/f ; Sik3f/f (Control) and Ubq-creERt2 ; Sik2f/ f ; Sik3f/f (dKO). Tamoxifen was injected to all mice at P3. Mandibles were collected at P8, P11, P14, P21 and P28. Histology of hemisected mandibles was observed at all time points. Immunohistochemistry, histomorphometry, and micro-CT images at P28 were rendered and analyzed.ResultsSIK2/SIK3 deletion globally at P3 led to small and misshaped mandible without significant difference in tooth eruption. Interestingly, combined ablation of SIK2/SIK3 led to a near complete absence of alveolar bone. Tartrate-resistant acid phosphatase (TRAP) staining revealed fewer osteoclasts in dKO alveolar bone compared to control, and less Calcein labeling was found in dKO mandibles in regions of absent alveolar (inter-radicular and inter-septal) bone. In addition, cells in these regions of dKO mandibles show increased Alkaline Phosphatase and reduced Osteocalcin expression, suggesting arrested osteoblast maturation. Micro CT images showed thicker, but smaller mandibles with increased cortical bone porosity and punched-out lesions surrounding molars.ConclusionConditionally ablated SIK2/SIK3 mandible at P3 causes malformed mandibles with a near complete absence of alveolar bone. Fewer osteoclasts and decreased Calcein labeling suggest that the lack of bone is due to disrupted bone formation. Increased number of immature osteoblasts was seen with decreased mature osteoblasts indicating that the lack of SIK2/SIK3 ablation disrupts the terminal maturation of osteoblasts that produce alveolar bone. Taken together, these data, which contrast with what has been observed to date regarding the role of these kinases in the appendicular skeleton, suggest that SIKs play important roles in osteoblast maturation and differentiation in the alveolar bone.

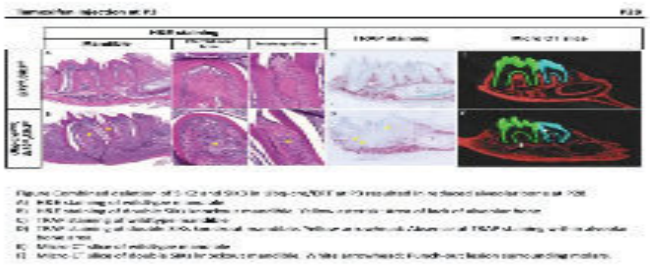

***Disclosures: Nicha Tokavanich**, None*

1080

Nfil3, A Novel PTH Target Involved in Bone development *Omar Al Rifai[1], Rene St-Arnaud[1]. [1]Shriners Hospitals for Children - Canada/ Department of Human Genetics, McGill University - Canada, Canada

Parathyroid hormone (PTH) intermittent administration at low dose promotes bone formation within its osteoanabolic window. It is commonly used for the treatment of osteoporosis; however, its downstream signaling pathway is not fully understood. In our laboratory, we characterized the transcriptional corregulator NACA (alpha chain of the nascent polypeptide-associated complex) as an essential component of the PTH signal transduction cascade that is necessary for its osteoanabolic function, in part by regulating the Bglap and Lrp6 promoters (MCB, 2005; BBA, 2018; IJMS, 2022). ChIP-Seq analysis against NACA identified the Nuclear factor interleukin-3-regulated (Nfil3) as a NACA target induced following PTH treatment depending on NACA availability (Bone, 2020). NFIL3, also known as E4BP4, is a basic domain leucine zipper transcription factor initially characterized as a repressor of gene transcription (MCB, 1992). Little is known about NFIL3's function in bone cells and its role in bone development and PTH signaling was never addressed in vivo. Using molecular biology tools and an animal model, we investigated NFIL3's requirement for bone development ex vivo and in vivo. Our data show that NFIL3 acts as an activator of gene transcription in osteoblasts. ChIP-Seq and RNA-Seq analysis shows that NFIL3 binds to the proximal promoter of osteoblasts differentiation markers such as Alpl, Col1a1, Bglap, Sp7 and Runx2. Nfil3 inactivation in primary osteoblasts decreases the expression of these targets, resulting in decreased mineralization. To assess the function of NFIL3 in vivo, we generated a mouse strain deficient for Nfil3 in osteoblasts and osteocytes (hOC-Cre;Nfil3fl/fl) by breeding Nfil3fl/fl mice with hOC-Cre mice, which express the Cre driver under the control of the human osteocalcin promoter. These mice exhibit a normal trabecular bone phenotype but a reduced cortical bone volume, area, diameter, and thickness as assessed by microcomputed topography. Consistently, three point bending tests and gene expression analysis show a reduction in biomechanical properties of long bones and a decrease in expression of osteoblastic and osteocytic differentiation markers in Nfil3 deficient mice.Our data describe for the first time a role for NFIL3 in bone development in vivo. It demonstrates NFIL3 as a PTH downstream target acting as an activator of gene expression in osteoblasts, supporting a potential role of NFIL3 in PTH signaling in vivo.

***Disclosures: Omar Al Rifai**, None*

SUN-001

Automated immunohistochemistry for TRAcP facilitates osteoclast detection and counting for bone histomorphometry: A validation study *Marie-Josée Bégin[1], Natalie Dion[2], Louis-Georges Ste-Marie[1]. [1]Division of Endocrinology, Department of Medicine, Centre hospitalier de l'Université de Montréal, Université de Montréal, Canada. [2]Department of Pathology, Centre hospitalier de l'Université de Montréal, Université de Montréal, Canada

Histomorphometric analysis of undecalcified bone specimens is the gold standard for diagnosis of complex bone disorders. This analysis requires the measurement of many variables, including osteoclasts (Oc) count per bone perimeter (N.Oc/B.Pm). Oc are identified by their morphology and multinuclearity on Goldner's trichrome stained (GTS) sections. To facilitate Oc count, histological sections are stained by an enzymatic histochemical reaction (EHR) of Tartrate Resistant Acid Phosphatase (TRAcP), an Oc biomarker. This technique has certain limitations including the possible alteration of enzymatic activity by bone tissue preparation with ethanol fixation and methyl methacrylate embedding (EFMMAE). In pathology laboratories, biomarkers such as TRAcP are routinely detected by automated immunohistochemistry technique (AIHC) performed on sections of formalin-fixed and paraffin-embedded (FFPE) of decalcified bone biopsies. We aim to validate the use TRAcP detection by AIHC on sections of undecalcified bone tissue EFMMAE in order to improve Oc identification and counting. To this end, transiliac bone biopsies from 20 adult patients (68.7 +/- 8.7 yo) affected by various metabolic bone diseases were studied. AIHC was performed with a Ventana BenchMark ULTRA system (Roche-Diagnosis) using mouse monoclonal antibody for TRAcP (clone 9C5) on deplastified sections with a protocol usually used for FFPE tissue. Osteoclastic detection by AIHC was confirmed by GTS on consecutive sections (Figure 1), as well as with EHR TRAcP and with AIHC Cathepsin K. The AIHC TRAcP showed a strong positive correlation with N.Oc/B.Pm measurements on GTS (r=0.90), as well as with bone formation rate per bone surface (BFR/BS) (r=0.84). Interestingly, there was a significantly greater detection of Oc with AIHC than with GTS (p<0.001). Furthermore, the difference in Oc counts between the two methods was significantly higher in high turnover states compared to low turnover (p=0.021). Taken together, this study validates the use of AIHC TRAcP on undecalcified bone tissue EFMMAE as an effective technique for Oc detection and outperformed Oc count by standard GTS method, especially in the high turnover states. AIHC should be considered as an alternative and easier method to EHR TRAcP. To our knowledge, this is the first time that AIHC has been successfully performed on undecalcified bone tissue EFMMAE, paving the way for the detection of other cellular biomarkers for clinical purposes.

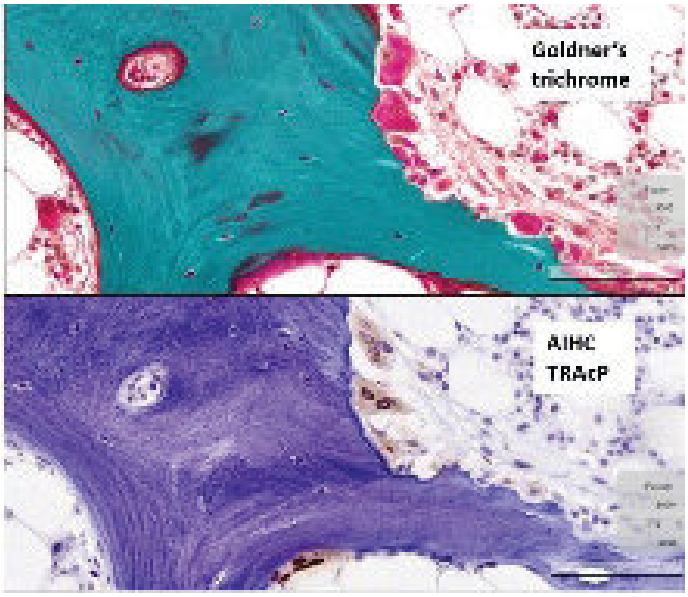

***Disclosures: Marie-Josée Bégin**, None*

SUN-002

Does Bisphosphonate therapy in osteoporosis impact the ability to diagnose primary hyperparathyroidism? *Madhumathi Rao[1], Lawrence Butros[2], Jonathan Webb[3], Hafsa Nebbache[4], Dana Richards[4], Hartmut Malluche[5]. [1]University of Kentucky, . [2]University of Kentucky Internal Medicine, United States. [3]University of Kentucky - Division of Nephrology, . [4]University of Kentucky Pathology and Laboratory Medicine, United States. [5]University of Kentucky Medical Center, United States

Introduction:Primary hyperparathyroidism (PHPT) is now a largely asymptomatic disease, often found incidentally during workup for end organ damage such as osteoporosis (OP). Patients may also be normocalcemic, with only intermittent serum calcium elevation, and remain undiagnosed unless parathyroid hormone (PTH) is checked and found elevated or non-suppressed. Bisphosphonate (BP) therapy is first line for post-menopausal osteoporosis (PMO) and is also recommended in PHPT, as an approach to stabilize bone mineral density (BMD) and offset bone loss.Clinical Cases:We describe the clinical course of three female patients (age 71-80 yrs) with PMO referred to the UK Bone Clinic for worsening BMD despite extended treatment with a bisphosphonate (4-16 yrs). Detailed workup for causes of declining bone density (table 1) showed elevated serum calcium with non-suppressed or elevated PTH, with vitamin D replete status. Bone turnover markers were not elevated, prompting performance of undecalcified bone biopsy with double tetracycline labeling for a better characterization of bone turnover. Paradoxically the biopsy showed evidence of low bone turnover, with resorptive changes and frequent dysmorphic osteoclasts. Further workup with neck ultrasound and sestamibi scans supported parathyroid adenoma. All underwent surgical intervention with subtotal parathyroidectomy, histology showed hypercellular parathyroid. Clinical Lesson:The three patients in this report all had initial diagnosis of PMO and were started on BP therapy. Years later, referral for declining bone density triggered further workup, revealing underlying PHPT but with the phenotype radically altered by BP. We posit that while anti-resorptive therapy addresses bone loss, it could potentially mask a diagnosis of PHPT. Given the population overlap of PHPT and PMO, we propose that diligent efforts should be made to evaluate patients for PHPT prior to treatment with BP, with frequent review subsequently. Of note we also stress the importance of recognizing a non-suppressed PTH in patients with elevated calcium level as an important indicator of PHPT.

	Patient A	Patient B	Patient C
Risk Factors for OP	Glucocorticoids use, Smoking	Early surgical menopause, Family history	Early menopause, Weight loss
Lab Evaluation			
Serum Creatinine (0.6 - 1.10 mg/dL)	1.35	0.66	1.24
Serum Calcium (8.6 - 10.2 mg/dL)	11.1	10.5	10.6
Serum Albumin (3.5 - 4.5 mg/dL)	2.8	2.6	3.5
PTH (12-72 pg/ml)	70	71	54
Vitamin D 25-OH (20.0 - 80.0 ng/mL)	62.6	44.4	43
DEXA Lowest T-scores			
Lumbar Spine	-1.5	-3	-2.2
(Left) Undecalcified bone biopsy (Von Kossa-Goldner trichrome, 20x) showing trabecular bone with osteoid plus osteoclast resorption pits adherent to surface mineralization matrix		(Right) Fluorescent microscopy (20x) of trabecular bone showing isolated single label consistent with low turnover	

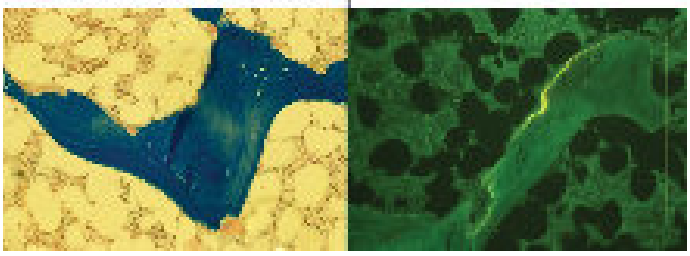

***Disclosures: Madhumathi Rao**, None*

SUN-003

What are we measuring with the 18F-NaF PET/CT in bone diseases? A systematic review of the validation of quantitative 18F-fluoride PET/CT uptake parameters in bone disease *Ruben de Ruiter[1], Jolien Zwama[1], Pieter Raijmakers[2], Maqsood Yaqub[2], Marelise Eekhoff[1]. [1]Department of Endocrinology and Metabolism, Amsterdam University Medical Centers (UMC), Vrije Universiteit, Amsterdam Movement Sciences, Netherlands. [2]Department of Radiology and Nuclear Medicine, Amsterdam University Medical Centers (UMC), Vrije Universiteit, Netherlands

Purpose: The 18F-NaF PET/CT has become an increasingly important tool in clinical practice towards understanding and evaluating diseases and conditions in which bone metabolism is disrupted. Nonlinear regression (NLR) analysis with a two tissue compartment model to determine uptake (Ki) of 18F-fluoride with full dynamic analysis is considered the gold standard for quantification of 18F-fluoride uptake. However, full dynamic analysis is often impractical in a clinical setting, leading to the de development of more simplified semi-quantitative parameters.Methods: We performed a literature search (in PubMed, Embase and Web of Science), including studies using the 18F-NaF PET/CT to measure disease activity in bone-related disorders. Our goal was to first explore if the reported uptake values were validated against full dynamic analysis. Secondly, to investigate if the chosen uptake parameter correlated with a disease specific outcome or marker, validating its use as a clinical outcome or disease marker.Results: Our initial search included 1627 articles leading to 53 studies spanning 27 different bone related conditions in which the 18F-NaF PET/CT was used to quantify 18F-uptake. These were subcategorized into metabolic bone diseases (12 articles), surgery (21 articles), arthritic conditions (16 articles) or other (4 articles). In 7 bone related disorders, dynamic analysis was performed and compared to the thereafter used simplified uptake parameter. The simplified uptake parameters showed a large heterogeneity. SUVmean and SUVmax were most frequently used, though normalization of these values varied greatly between the studies. In some disorders, multiple studies were performed evaluating 18F-uptake as a marker of bone metabolism, however in those cases, the used 18F-uptake was often different for each separate study, making comparison in 18F-uptake reflecting bone turnover as an outcome measure between studies not possible.Conclusions: Should we want to use the 18F-NaF PET/CT to evaluate disease activity or treatment response in various bone related disorders, it is essential to standardize our approach. Ideally the most suitable parameter is determined through dynamic analysis, followed by comparison to simplified uptake parameters and to standardized disease specific biomarkers or outcome of interest.

***Disclosures: Ruben de Ruiter**, None*

SUN-004

Understanding the pathophysilogical link between Alzheimer's disease and osteoporosis. *Sarika Gupta[1]. [1]National Institute Of Immunology, India

Patients with Alzheimer's disease usually have low bone mineral density (BMD) and are more prone to Bone fractures than healthy individual. However, the mechanism behind the accelerated bone loss in AD pateints is unknown. We wanted to understand how the 3XFAD mouse model of familial Alzheimer's disease (FAD) affects age-dependent alteration in bone parameters. According to earlier research, women are more likely than men to experience osteoporosis and AD. In our research, we found that both male and female FAD mice had degeneration in bone micro architecture, with females exhibiting a greater degree of deterioration than males. With age, these alterations in bone micro architecture are seemed to become more pronounced. The mechanical properties of bone, such as bone strength, stiffness, and energy stored in bone, are substantially impaired in FAD mice. Furthermore, in both AD and the presence of the neurotoxic peptide A?42, bone marrow stem cell (BMSC) differentiation to osteoclast was considerably increased, but differentiation to osteoblast was severely impaired. Also, serological studies showed a rise in pro-inflammatory cytokines such as TNF alpha, IL17, and IL18 in AD mice. Increased levels of proinflamatory cytokines have been proven to stimulate osteoclastogenesis. These findings lead us to the conclusion that bone tissue in AD mice begins to deteriorate at a young age, even before AD pathology is evident.

***Disclosures: Sarika Gupta**, None*

SUN-005

Effectiveness of Asfotase Alfa for Treatment of Adults With Hypophosphatasia: Results from a Global Registry *Priya S. Kishnani[1], Gabriel Ángel Martos-Moreno[2], Agnès Linglart[3], Anna Petryk[4], Andrew Messali[4], Shona Fang[4], Cheryl Rockman-Greenberg[5], Keiichi Ozono[6], Wolfgang Högler[7], Lothar Seefried[8], Kathryn M. Dahir[9]. [1]Duke University Medical Center, United States. [2]Hospital Infantil Universitario Niño Jesús, IIS La Princesa, Universidad Autónoma de Madrid, CIBERobn, ISCIII, Spain. [3]Paris-Saclay University, AP-HP and INSERM, France. [4]Alexion, AstraZeneca Rare Disease, United States. [5]University of Manitoba, Canada. [6]Osaka University, Japan. [7]Johannes Kepler University Linz, Austria. [8]University of Würzburg, Germany. [9]Vanderbilt University Medical Center, United States

Objectives: To assess asfotase alfa's effectiveness on mobility, functional status, quality of life (QOL), and pain in adults with hypophosphatasia (HPP).Methods: Patients enrolled in the Global HPP Registry (NCT02306720; EUPAS13514) who had an alkaline phosphatase below the LLN for age and sex and/or a documented ALPL gene variant, initiated asfotase alfa at age >=18 years, and been treated for >=6 months at last follow-up were included. Outcomes were evaluated as mean change from mean baseline (BL) value through 36 months; assessments were not performed at all timepoints for all patients.Results: Among included patients (N=190), median age at treatment start was 45.5 years; 91.1% were characterized as having pediatric-onset HPP. 6MWT distance walked was 404 m (n=31) at BL and improved over time vs BL (change: 93 m at 12 months [95%CI: 47, 138; n=18], 62 m at 24 months [95%CI: 0, 124; n=15], and 45 m at 36 months [95%CI: ?83, 172; n=7]). The SF36v2 Physical Component Summary score was 35.7 (n=48) at BL and improved over time (change: 4.68 at 6 months [95%CI: 0.16, 9.21; n=34], 4.61 at 12 months [95%CI: 1.02, 8.19; n=28], 4.94 at 24 months [95%CI: ?2.23, 12.11; n=22], and 5.13 at 36 months [95%CI: ?0.96, 11.21; n=21]). SF36v2 Mental Component Summary score improvements were not statistically significant at all timepoints. Health Assessment Questionnaire-Disability Index scores were generally unchanged over time. Self-reported Brief Pain Inventory Short Form scores improved at all timepoints from a BL of 4.86 (change: ?0.72 at 6 months [95%CI: ?1.23, ?0.21; n=38], ?1.07 at 12 months [95%CI: ?1.62, ?0.52; n=31], ?1.13 at 24 months [95%CI: ?1.76, ?0.51; n=26], and ?0.97 at 36 months [95%CI: ?1.70, ?0.24; n=23]). The most common AEs were injection site reactions and injection-associated reactions, occurring in 29 (13.4%) and 13 (6.0%) patients, respectively. Eleven serious AEs related to asfotase alfa were reported in 7 patients.Conclusion: Adults with HPP who received asfotase alfa for >=6 months experienced improvements in mobility, physical function, QOL, and pain, which were maintained over 3 years of follow-up.

***Disclosures: Priya S. Kishnani**, Alexion, AstraZeneca Rare Disease, Grant/Research Support, Alexion, AstraZeneca Rare Disease, Consultant, Alexion, AstraZeneca Rare Disease, Other Financial or Material Support*

SUN-007

Coexisting Primary Hyperparathyroidism and Sarcoidosis in a Patient with Recurrent Hypercalcemia *Yasaman Motlaghzadeh[1], Marina Basina[2], Deborah Sellmeyer[3]. [1]Stanford University School of Medicine, . [2]Stanford University School of Medicine , United States. [3]Stanford University, School of Medicine, United States

Background: Primary hyperparathyroidism (PHPT) is the most common cause of hypercalcemia in ambulatory patients. Hypercalcemia associated with elevated levels of 1,25-dihydroxyvitamin D occurs in 10-20% of patients with sarcoidosis. However, the consecutive occurrence of these conditions is rare. We present a patient with PHPT who experienced recurrent hypercalcemia after parathyroidectomy and was subsequently diagnosed with sarcoidosis. Clinical Case: A 69-year-old woman with a history of osteoporosis presented in 2019 with hypercalcemia. Between February 2019 and March 2021 serum calcium ranged from 10.5 to 11.2 mg/dL (ref range: 8.5-10.5 mg/dL), phosphorus ranged from 3.0 to 3.4 mg/dL (ref range: 2.5-4.5 mg/dL), parathyroid hormone (PTH) ranged from 89 to 150 pg/mL (ref range: 15-65 pg/mL), glomerular filtration rate ranged from 54 to 67 mL/min (ref range: >60 mL/min), 25-hydroxy vitamin D level was 24 ng/mL (ref range: 30-100 ng/mL), and calcium: creatinine clearance ratio of 0.015. In March 2021, Sestamibi scan showed a left upper parathyroid adenoma. Following the removal of the adenoma in June 2021, her serum PTH and calcium concentrations declined from 150 to 41 pg/mL and from 11.2 to 9.8 mg/dL, respectively, one-week post-surgery. Pathology report showed hypercellular parathyroid tissue without atypia consistent with parathyroid adenoma. In March 2022, she returned to the clinic with a serum calcium level of 12 mg/dL. Further workup showed a suppressed PTH level of 8 pg/mL (ref range: 10-65 pg/mL) and an elevated 1,25-dihydroxyvitamin D level of 80 pg/mL (ref range: 18-78 pg/mL). The patient underwent a chest CT scan, which showed enlarged mediastinal lymph nodes, followed by endobronchial ultrasound-guided fine-needle aspiration. Pathology showed lymphocytes and collections of histiocytes with features of granuloma; acid-fast and fungal stains were negative. Further testing revealed an elevated angiotensin-converting enzyme level of 65 U/L (ref range: 8-52 U/L), supporting the diagnosis of sarcoidosis. The patient was started on prednisone 20 mg daily and her calcium level normalized within 2 weeks. Conclusion: This case highlights the importance of a thorough evaluation during recurrent hypercalcemia even in patients who previously have been found to have PHPT. While rare, PTH mediated and PTH independent hypercalcemia can occur in the same patient and a complete evaluation is essential to avoid misdiagnosis and unnecessary procedures.

***Disclosures: Yasaman Motlaghzadeh**, None*

SUN-008

Bone Disorganization: A Novel Biomarker Unrelated to Bone Density and Structure that May Hold the Key to The Diagnosis of Atypical, Unusual, or Stress Fractures *Roger Zebaze[1], Cat Shore-lorenti[2], Cherie Chiang[3], Kevin Djopseu[4], Tessa Makebeh[4], Simon Zhang[2], Fran Milat[5], Peter Ebeling[6]. [1]Monash University, . [2]Department of Medicine, School of Clinical Sciences, Monash University, Australia. [3]Department of Endocrinology, Austin Health, Australia. [4]Zeze co, Cameroon. [5]Hudson Institute of Medical Research, Australia. [6]School of Clinical Sciences, Monash University, Australia

Purpose- The cause of many fragility fractures remains a mystery as they are unexplained by reduced bone mineral density (BMD) or degraded microarchitecture. To address this enigma, we recently proposed that fragility in these patients is due to the incorrect arrangement of an otherwise sufficient or even high amount of normal bone tissue (disorganization). Incorrectly positioned (disorganized) components by abnormally transferring loads cause damage; triggering inflammation, and a vicious cascade of events leading to abnormalities and fractures. We further developed and validated a tool to quantify this novel biomarker (disorganization). Here, we test the hypothesis that measures of disorganization are unrelated to bone density or decay, YET associated with Atypical Femoral Fractures (AFFs), Paget Disease of Bone (PDB), and Hypophosphatasia (HPP) (all diseases in which bone is fragility unexplained by BMD or structural decay).Methods-We studied 45 women (10 AFFs and 35 fracture-free peers) mean (SEM) age 68.1(1.83)yrs. In addition, we studied patients withPDBs (2) and HPPs (2). Curves displaying the extent disorganization along the femoral shaft (ALIGNOGRAM) were produced and metrics of disorganization were quantified as previously reported (Zebaze et al, JBMRPlus 2023). Correlations between disorganization metrics, bone structure, and density were assessed.Results-In normal subjects, ALIGNOGRAMs were relatively flat and regular with low Disorganization values (DVs); no abrupt peaks. In all patients with AFFs, PDBs, and HPPs ALIGNOGRAMs were irregular, chaotic with higher DVs and spike-shape peaks corresponding to the most disorganized part of bones (Fig 1). The mean DV (MDV) distinguished AFFs from controls [36.3 (IQR 23.9-60.8) vs 3,139 (IQR 1212-14788)]; p<0.0001. However, DVs along the femur were unrelated to mass or structure. The MDV was not correlated with lateral and medial cortical thicknesses, or periosteal diameter (All R2<0.001; NS). The MDV was also unrelated to density (R2=0.0002; p=0.17).Conclusion-Disorganization is a novel mechanism and a biomarker of bone fragility completely unrelated to bone mass and microarchitecture. This novel biomarker, readily quantifiable from standard X-rays, may hold the key to the cause of fractures that occur in individuals without reduced bone density or structural decay such as AFFs, HPP, or PDB. Larger studies are now needed in larger populations with different bone diseases to confirm our findings.

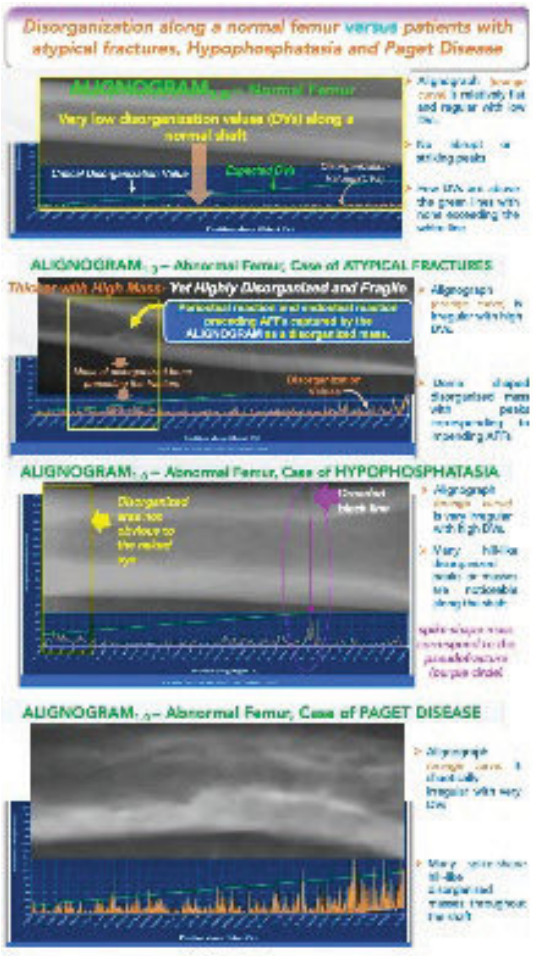

***Disclosures: Roger Zebaze**, None*

SUN-010

Measuring FGF23 in patients treated with Burosumab *Isabelle Piec[1], Allison Chipchase[2], Emma Miler[3], Hari Ramachandran[1], Emma Webb[3], WILLIAM FRASER[4]. [1]University of East Anglia, United Kingdom. [2], . [3]Norfolk and Norwich University Hospitals, United Kingdom. [4]UNIVERSITY OF EAST ANGLIA, United Kingdom

X-linked hypophosphatemia (XLH) is a hereditary, progressive, and lifelong condition that affects both children and adults with an incidence of 1/20,000. The disease is characterised by elevated circulating fibroblast growth factor 23 (FGF23). High FGF23 induces hypophosphatemia, reduced 1,25 Dihydroxyvitamin D concentration and defective bone mineralisation (osteomalacia/rickets). Treatment with burosumab, a fully human IgG1 monoclonal antibody that binds intact FGF23 (iFGF23) decreases rickets severity, prevents enthesiopathy, improves growth, increases serum phosphate and 1,25(OH)2D as well as the ratio of tubular maximum reabsorption rate of phosphate to glomerular filtration rate (TmP/GFR). However, symptoms in some patients are not fully resolved suggesting some free iFGF23 may remain circulating and acting in these patients while concomitantly paediatricians are keen to measure FGF23 to avoid overtreatment with associated potential calcification risk. Measuring FGF23 in patients treated with burosumab is problematic as we and others have observed interference (false positive) of the therapeutic antibody in multiple assays (Immutopics c-terminal FGF23 [cFGF23], MedFrontiers and Immutopics iFGF23) while being seemingly low/normal in the DiaSorin iFGF23 (false negative). We immunoprecipitated burosumab using magnetic A/G beads from samples obtained from treated patients. Cleanliness of the supernatant was checked by western blot and FGF23 was then measured in the supernatant using Immutopics cFGF23. This ELISA measures both intact and cFGF23. We also analysed for the presence of cFGF23 alone by western blot using anti-cFGF23 (186-206) antibody (Quidel). We were only able to detect intact FGF23 by these methods suggesting that either there is no free cFGF23 present or the technique is not sensitive enough to detect the circulating concentration of cFGF23 fragment in patients treated with burosumab. The presence of sufficient circulating intact FGF23 and absence of cFGF23 in patients treated with burosumab could explain the persistence of some symptoms of XLH. In future we may be able to correlate outcome with circulating concentrations of free iFGF23. The changes in efficacy of burosumab in older children and adolescents may partly reflect a requirement for an increased dose of burosumab to fully capture iFGF23.

***Disclosures: Isabelle Piec**, None*

SUN-013

Evaluation of Bone Mineral Density and Microarchitecture using Trabecular Bone Score in Adults with X-Linked Hypophosphatemic Rickets *Luciana Valadares[1], Larissa Moreira[2], Bernardo Cunha[3], Bruno Ferreira[4]. [1]SARAH Network of Rehabilitation Hospitals, . [2] SARAH Network of Rehabilitation Hospitals, Brazil. [3]Universidade do Planalto Central Apparecido dosSantos (UNICEPLAC), Brazil. [4]Centro Universitário Serra dos Órgãos, Brazil

Introduction: X-linked hypophosphatemia (XLH), caused by inactivating mutations in the phosphate regulating endopeptidase homolog X-linked (PHEX) gene, represents the main cause of hereditary hypophosphatemic rickets. Elevated bone mineral density (BMD) of the lumbar spine (LS) has been detected in patients with XLH using dual-energy X-ray absorptiometry (DXA), even in the absence of enthesopathies and/or extraskeletal calcification. Trabecular bone score (TBS) can be used to indirectly assess the bone microarchitecture using DXA images of the LS. However, its utility in patients with XLH is still undefined. Objectives: To evaluate the BMD and microarchitecture in adults with XLH using TBS and to analyze the correlation of the clinical and biochemical parameters with BMD and TBS. Methods: This cross-sectional study included adult patients (aged >18 years) from a single tertiary center in Brazil with XLH confirmed by the occurrence of PHEX mutations. Information pertaining to clinical, biochemical, and densitometric parameters of the patients was retrieved from their medical records. The BMD of three skeletal sites (LS, femoral neck, and total hip) was measured using DXA. TBS was obtained from LS DXA images using the TBS iNsight software. Results: The study group consisted of 16 adults with XLH (15 women and 1 man) with a mean age and height of 30.9 years (+/-12.5) and 143.1 cm (+/-11.7), respectively. Seven patients had an LS BMD Z-score > 2, whereas only 1 had an LS Z-score < -2. The BMD Z-score of LS was significantly higher (median 1.8, range -2.1 to 5.9) than that of the total hip (median 0.2, range -2.1 to 1.3) ($p = 0.028$) and femoral neck (0.6, range -2.0 to 0.6) ($p = 0.023$). There was no correlation between the LS BMD and age ($r = 0.407$, $p = 0.118$), height ($r = 0.186$, $p = 0.491$), body mass index (BMI) ($r = 0.278$, $p = 0.297$), or the biochemical parameters analyzed. The mean TBS was 1.637 (+/-0.12), and no patient showed compromised bone microarchitecture (TBS < 1.350); TBS did not correlate with any of the clinical, densitometric, or biochemical parameters evaluated. Conclusion: We found that adults with XLH had increased BMD in LS when compared with that in total hip and femoral neck, suggesting that the effect of the disease on the axial skeleton differs from that on the appendicular skeleton. No bone microarchitectural compromise was detected using TBS, and the value of using TBS in patients with XLH remains unclear.

***Disclosures: Luciana Valadares**, None*

SUN-014

Temporal Trend of Mortality in Paget's Disease Over 20 years in Quebec, Canada *Laetitia Michou[1], Philippe Gamache[2], Isaora Zefania Dialahy[2], Jason R Guertin[3], Jean-Eric Tarride[4], Jacques P Brown[5], Sonia Jean[2]. [1]Universite Laval, Canada. [2]Institut national de santé publique, Canada. [3]Department of preventive and social medicine and CHU de Québec-Université Laval research centre, Canada. [4]Department of Health Research Methods, Evidence and Impact, Faculty of Health Sciences, Canada. [5]CHU de Québec-Université Laval research centre and Department of Medicine, Université Laval, Canada

Purpose - Paget's disease of bone (PDB) is a chronic focal late-onset metabolic bone disorder. A decline of prevalence, incidence and severity of PDB has been reported in several countries. Although our team has reported a stable prevalence of PDB in Quebec (Canada), the incidence was found to decrease over time. This study aimed at determining the evolution of the mortality in patients with PDB in the province of Quebec by analyzing the medico-administrative data of the Regie de l'assurance maladie du Québec (RAMQ) and to compare it with the general population aged >= 55.Methods - For each fiscal year, the adjusted rate of all-causes mortality in individuals aged >= 55 with PDB and the general population, was determined using the RAMQ data from 2000/2001 to 2020/2021 (population size 2,913,820 in 2019/2020). The case definition relied on one hospitalization or two claims from physicians with the diagnosis code of PDB (CIM-9: 731.x except 731.2, CIM-10: M88). The adjusted rate of mortality was determined in men and women, and by age categories (55-64 years, 65-74 years, 75-84 years and >= 85 years) for each year from 2000/2001 to 2020/2021. The standardized mortality rates ratios and 95% confidence interval were calculated. The percentage of death for each main cause of death was described.Results - The adjusted rate of all-cause mortality in individuals with PDB aged >= 55 varied from 47.1/1000 in 2000-2001 to 54.1/1000 in 2020-2021 (Fig. 1). In the general population, the adjusted mortality rate varied from 27.6/1000 in 2000-2001 to 22.3/1000 in 2020-2021. The absolute number of deaths in individuals with PDB aged >= 55 varied from 410 in 2000-2001 to 655 in 2019-2020. The increase in adjusted rate of mortality in PDB was observed in both men and women. The highest increase in standardized mortality rates ratios in individuals with PDB was observed in the age category of 55-64 years, from 1.90 (0.84-4.30) in 2000-2001 to 11.3 (7.48-16.9) in 2019-2020, followed by the age category of 65-74 years. The most frequent causes of death in individuals with PDB were cardiovascular diseases (27%), cancer (24%) and respiratory

diseases (8%), versus 22%, 31% and 8% in the general population, respectively.Conclusions - We observed an apparent increase in adjusted rate of mortality in individuals with PDB. This increase may be explained by an aging effect of the cohort with PDB in relation with an accelerated decline of incidence of PDB during the past six years.

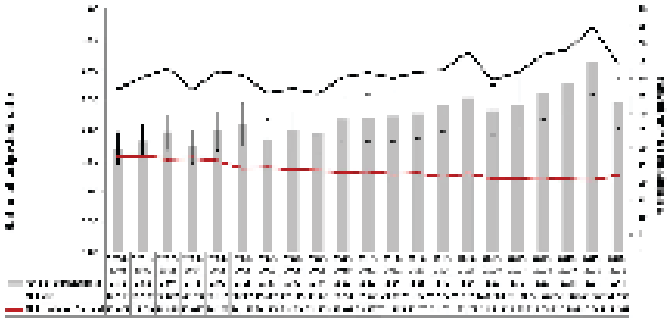

***Disclosures: Laetitia Michou**, None*

SUN-015

Association of parathyroid hormone and hyperparathyroidism on thromboembolic events: a systematic review and meta-analysis *Ernest Zhi Tay[2], Clarise Lam[2], Alexander Rodriguez[2]. [2]Monash University, Australia, [2]Monash University,

Introduction: Parathyroid hormone (PTH) regulates calcium homeostasis. Calcium plays an important role in the coagulation cascade. Calcium supplementation has been shown to transiently increase thrombotic potential. However, there is limited evidence on the role of PTH in thromboembolism. We hypothesised that hyperparathyroidism (HPT) would be associated with thromboembolic events. We also hypothesised that PTH would be associated with thromboembolic events.Method: EMBASE, MEDLINE and ClinicalTrails.gov were searched from inception to 4/8/22 for studies investigating HPT and PTH on acute myocardial infarction (aMI) and stroke. Two independent reviewers screened and extracted data and assessed bias. Random effects models were fitted for meta-analysis and tau2 was reported to investigate effect variance.Results: 3061 records were identified of which 67 articles met our inclusion criteria and 13 studies had outcome data for aMI and stroke enabling meta-analysis. Studies were of low-moderate quality. Study population ranged from 218 to 180,114. Two studies specifically enrolled patients with HPT. Studies applied a threshold of 65pg/mL to determine 'high' PTH. Meta-analysis of five studies comparing high vs. low (<=65pg/mL) PTH showed high PTH was associated with a non-significant increased risk of aMI (RR=1.35 [0.80 to 2.28], tau2 =0.313, n=189,479) but there was an approximate 37% increased risk of stroke (RR=1.37 [1.20 to 1.56], tau2 =0.000, n=291,335). A meta-analysis of four studies examining per 10pg/mL increase in PTH showed that there was an increased risk of aMI (RR=1.36 [1.00 to 1.85, tau2 =0.052, n=3430). When excluding patients with HPT, higher PTH was associated with non-significant increased risk of aMI (RR= [0.99 to 2.52], tau2 =0.198, n=188,274) and stroke [RR=1.33 [0.93 to 1.91], tau2 =0.063, n=3962). In cross-sectional analyses, there was a greater serum level of PTH in patients with an aMI compared to those without (SMD=0.35 [0.25 to 0.44], tau2 =0.031, n=8178, five studies). Interpretation: We showed that (i) HPT was associated with an increased risk of stroke and (ii) PTH levels are higher in individuals with acute MI but this was not associated with MI risk. These data indicate that optimisation of cardiovascular risk should be considered by clinicians treating patients found to have elevated PTH levels. There is scant data for these outcomes in patients with HPT warranting further investigation.

***Disclosures: Ernest Zhi Tay**, None*

SUN-016

COX2-independent Effects of the NSAID Naproxen on Bone *Alexandra Ciuciu[1], Ryan Tomlinson[2]. [1]Thomas Jefferson University , , [2]Thomas Jefferson University, United States

Non-steroidal anti-inflammatory drugs (NSAIDs) inhibit the cyclooxygenase (COX) enzymes COX1 and COX2 that produce prostaglandins driving pain and inflammation. We reported that adult female C57BL/6J mice treated with naproxen for 15 days had significantly decreased bone toughness, reduced strain adaptive bone remodeling, and diminished woven bone formation during stress fracture repair. We also found that naproxen decreased osteocyte dendrite number and the number of MMP13+ osteocytes as compared to vehicle in male mice. Since these effects on bone toughness and healing were not observed in mice treated with the COX2-specific inhibitor, celecoxib, we hypothesized that the effects of naproxen on osteocytes and bone toughness were COX2-independent. To test this hypothesis, naproxen sodium (10.9 mg/kg) or vehicle (ddH2O) was administered to adult (15-18 weeks old) Ptgs2-Y385F and wild-type (WT) mice for 15 days. Mice received six bouts of axial forelimb compression using a 2 Hz rest-inserted sinusoidal waveform of 3 N for 100 cycles. Calcein and alizarin red were injected on day 5 and 12 respectively; drinking water was refreshed every 2-3 days. Right femurs were stored in PBS-soaked gauze at -20ºC before analysis. Both forelimbs were harvested, fixed, embedded in PMMA, sectioned using a low-speed saw, and imaged using confocal microscopy. First, we observed that naproxen significantly decreased trabecular bone volume fraction in Ptgs2-Y385F male mice (-21.5%, p=0.0055) as compared to vehicle treated mice; this effect was not significant in WT male mice or in female mice of either genotype. Next, we found that naproxen significantly decreased bone toughness by three-point bending across all genotypes and sexes (male: p=0.0004; female: p=0.0279; by two-way ANOVA). Surprisingly, naproxen also significantly decreased whole bone bending (section modulus vs. bending moment) intercepts in WT mice (male: p=0.0204; female: p=0.0399) but not Ptgs2-Y385F mice. Finally, we observed that naproxen treatment significantly diminished relative periosteal bone formation rate per bone surface in male Ptgs2-Y385F and WT mice (-28% in Ptgs2-Y385F; -58% in WT; p=0.047 by two-way ANOVA) by dynamic histomorphometry. These results demonstrate COX2-independent effects of naproxen on bone toughness. On-going studies will identify these COX2-independent mechanisms to improve therapeutic options for relief of musculoskeletal pain without impairing bone mechanical properties.

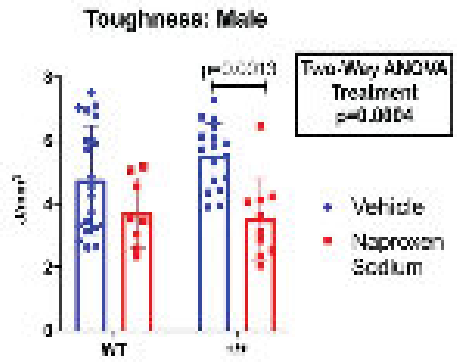

Figure 1: Average bone toughness as determined by standard 3-point bending for vehicle and naproxen sodium treated wild-type (WT) and Ptgs2-Y385F (+/+) mice. (n=8-20 per genotype)

***Disclosures: Alexandra Ciuciu**, None*

SUN-017

Mechanisms of Bone Fragility with Skeletal Growth in Osteogenesis Imperfecta *Anxhela Docaj[2], Asier Muñoz[2], Alessandra Carriero[2]. [2]The City College of New York, , [2]The City College of New York, United States

In classical osteogenesis imperfecta (OI or brittle bone disease) mutations in the genes encoding collagen type I alter collagen structure resulting in bone fragility [1]. We showed that bone fracture resistance is low in the homozygote oim mouse model of OI [1], already at a very young age, with bones getting tougher as the mouse grows and matures [2]. The mechanisms by which OI bone resists fracture varies with skeletal growth. Crack path examination showed for the first time the presence of crack deflections, splitting, and bridging in young (4 w.o.) oim bones, but not in more mature (14 w.o.) ones [2]. These are toughening mechanisms usually observed in healthy bone. Young oim mouse bone showed low resistance to fracture even before the crack forms but not while it grows, while mature oim mouse bone exhibited low toughness during crack grow but not at crack initiation. To determine the mechanisms of bone fragility in oim bones at these stages of skeletal growth, and explain the observed differences in fracture toughness, we here examine changes in the oim bone tissue structure and composition at different ages. We assessed oim bone intracortical porosity with synchrotron microtomography, quantified collagen composition, fibers orientation and organization in oim bones using second harmonic generation microscopy, and determined bone tissue composition, and the presence of advanced glycation end products (AGEs) using Raman spectroscopy and molecular fluorescence. Compared to mature oim bone, young oim bone tissue exhibit high lacunar porosity density, low collagen content, disorganized mineralized fibers with low carbonate substitution and mineral crystallinity, and high CML/CH2-wag and florescent AGEs. These parameters describe a poorly organized bone tissue in young oim mice that can explain their lower fracture resistance compared to mature bone. Cracks favorably initiate in presence of defects, such as lacunae porosity, and in tissue with low plasticity due to poor collagen and mineral properties and interaction. Furthermore, the

increased number of AGEs per collagen content, together with the reduced collagen content, further underlines the controversial role that non-enzymatic crosslinks could possibly have in oim bones. This study suggests that treatments for OI bone fragility should differ in young and mature populations, targeting two different mechanisms of bone fragility.1. A. Carriero, et al., JBMR. 29:6, 20142. A. Docaj, et al., ASBMR, 2020

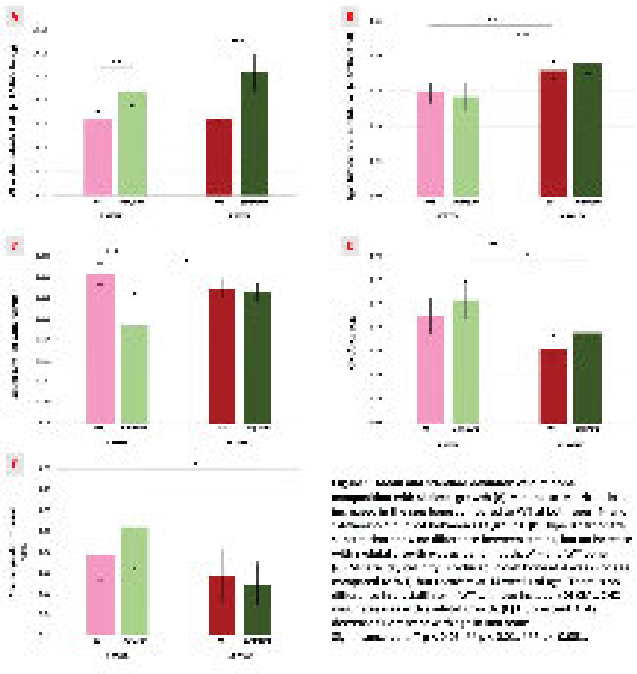

***Disclosures: Anxhela Docaj**, None*

SUN-018

Total Body Irradiation Results in Deficits in Vertebral Bone Structure and Mechanical Properties in Male Rhesus Macaques *Shannon Emerzian[1], Isabel Barnet[2], Trinity Tedtsen[3], Daniel Brooks[4], Sun Park[5], Joseph Moore[5], John Olson[5], Mary Bouxsein[6], J. Mark Cline[5], Jeffrey Willey[5]. [1]Beth Israel Deaconess Medical Center, United States; [2]Harvard Medical School, ; [3]Massachusetts General Hospital, United States; [4]BIDMC/MGH, ; [5]Wake Forest University School of Medicine, United States; [6]Beth Israel Deaconess Medical Center, Harvard Medical School, United States

Patients undergoing high-dose radiation therapy (RT) for cancer treatment have an elevated fracture risk, particularly in healthy bones that absorb dose. However, the effects of low-dose total body irradiation (TBI) on skeletally-mature bone are unclear; determining these responses can help develop countermeasures for adult survivors of radiologic events (e.g, “dirty bomb”). This study quantified aging and late effects of TBI on bone microstructure in rhesus macaque (Macaca mulatta) non-human primates (NHPs).Femora and lumbar vertebrae (LV) were obtained post-mortem from 3 groups of skeletally-mature male NHPs: TBI (n=7 femora; n=5 LV, 18.9+/-2.5yrs of age), age-matched non-irradiated (NR) Controls (n=6 femora; n=4 LV, 18.7+/-2.0yrs), and NR Young NHPs (n=6 femora; n=6 LV, 9.1+/-0.1yrs). TBI received an acute dose of 6.0-6.75Gy. Tissues were harvested ~10yrs after TBI. High-resolution computed tomography (CT, Scanco) scans were used to assess trabecular (Tb) microarchitecture of LV and distal femur; cortical (Ct) bone was assessed at femoral mid-diaphysis. Micro-finite element analysis (µFE) of LV was computed using CT scans. Urinary N-terminal telopeptide crosslinks (NTX) were quantified via ELISA at sacrifice. One-way ANOVA and Tukey post-hoc tests assessed group effects. Data are presented as mean+/-SD; percent differences are calculated between group means.Body mass varied by group, with Young NHPs (18.1+/-3.3kg) larger than TBI (13.9+/-2.7kg, p=0.01) and Controls (14.4+/-4.1kg, p=0.04). TBI resulted in LV Tb deficits: lower bone mineral density (BMD, -20%, p=0.04) and bone volume fraction (BV/TV, -27%, p=0.03) vs Controls (Fig A). LV Tb BMD and BV/TV were similarly lower in TBI vs Young NHPs (-20%, p=0.07; -26%, p=0.04, respectively). µFE stiffness, ultimate force, and apparent modulus were lower in TBI vs Controls (-34%, p=0.11; -30%, p=0.15; -33%, p=0.11) and Young (-37%, p=0.04; -34%, p=0.05; -56%, p=0.048, Fig B). No differences between Control and Young NHPs were detected in LV microarchitecture or µFE measures. By contrast, at the femur, Controls had reduced Tb BMD (-28%, p=0.058) and BV/TV (-32%, p=0.04) vs Young NHPs (Fig C). Yet, TBI had no measurable effect on distal femur Tb bone, Ct bone area (Fig D) and NTX levels vs Young and Control.In the axial skeleton of NHPs, TBI diminished Tb bone microstructure and strength, suggesting TBI exposure could elevate vertebral fracture risk in adult survivors after intentional or accidental radiologic events.

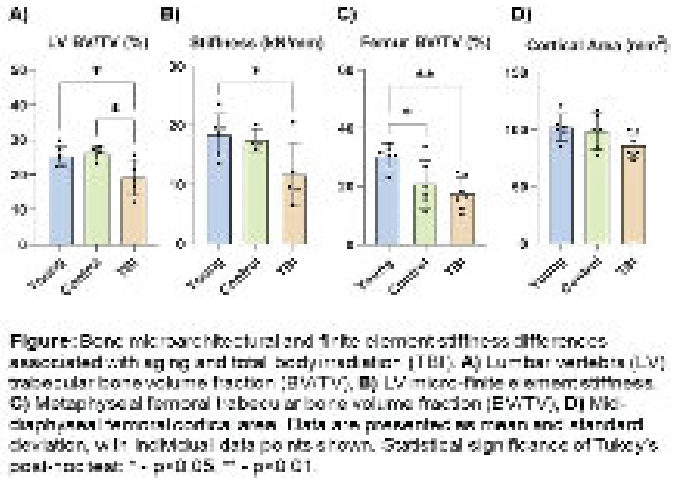

Figure: Bone microarchitectural and finite element stiffness differences associated with aging and total body irradiation (TBI). A) Lumbar vertebra (LV) trabecular bone volume fraction (BV/TV), B) LV micro-finite element stiffness, C) Metaphyseal femoral trabecular bone volume fraction (BV/TV), D) Mid-diaphyseal femoral cortical area. Data are presented as mean and standard deviation, with individual data points shown. Statistical significance of Tukey's post-hoc test: * - p<0.05, ** - p<0.01.

***Disclosures: Shannon Emerzian**, None*

SUN-019

Risk of Vertebral Endplate Failure During Vertebral Fracture *ELISE MORGAN[2], Neilesh Frings[2]. [2]Boston University, United States; [2]Boston University,

Vertebral fracture (VF) is the most common type of osteoporotic fracture1. The vertebral endplate region comprises the cartilage endplate, vertebral endplate (VEP), and underlying subchondral trabecular bone (STB). The endplate region plays a critical role in spinal loading and is frequently involved in VF. Although fracture of the VEP does not always occur during VF2,3, VEP fracture is associated with a higher risk of future disc degeneration and worsening of the VF over time3,4. The conditions responsible for VEP failure are unclear; their identification can aid in evaluating risk of, and prognosis following, VF5. This study used high-resolution micro-finite element (µFE) models to evaluate relative risk of failure in the VEP, STB, and other portions of the vertebral body at the point of onset of VF, and whether the relative risk of VEP failure is associated with VEP and STB microstructure. Models were built from micro-CT scans (0.074mm resolution) of L1 vertebrae (n=21) previously scanned and mechanically tested2. Superior and inferior boundaries of the models were prescribed sample-specific experimentally matched displacements corresponding to the yield point of the compression test. Volumes of interest (VOIs) were defined on coronal image slices and mapped to the model: VEP, STB, and remaining portion of the vertebra, defined as the mid-vertebral body (MVB). Tissue yield was defined by principal strain thresholds reported for trabecular tissue. High strains in the vertebrae were frequently observed in the superior endplate and cortical shell (Figure). The proportion of elements that yielded varied among vertebrae, ranging from 8% to 0.01% of elements, and was not different among VOIs. When normalized to the sample-specific amount of yield, however, the VEP exhibited greater risk of failure than the STB and MVB. These results indicated that at the onset of VF, tissue-level yield typically occurs in the VEP, and to a lesser extent, the rest of the vertebral body. VOI yield fractions did not correlate to average measures of microstructure in the VOIs, suggesting that other factors are responsible for which regions fail first. Overall, these findings emphasize the importance of the VEP in VF pathogenesis. References: [1] Cooper, C., et al., Am J Epi 1993. [2] Hussein, A.I., et al., J Biomech Eng 2018. [3] Holmes, A.D., et al., Spine 1993. [4] Holm, S., et al., Clin Spine Surg 2004. [5] Khosla, S., et al., JBMR 2017.

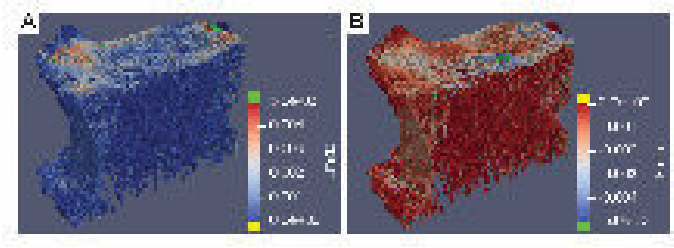

***Disclosures: ELISE MORGAN**, None*

Sunday Orals

SUN-020

Effect of Red Rooibos Consumption on Bone Mineral and Structure in Rats Post-Lactation *Matthew K. Goncharow[1], Jenalyn L. Yumol[1], Michael D. McAlpine[1], Wendy E. Ward [1]. [1]Brock University, Canada

In rats, pregnancy and lactation challenges the maternal skeleton to support skeletal growth of offspring. We previously showed that red rooibos tea (RR) fed pre-pregnancy through to 4 months post-lactation supported a partial recovery in trabecular bone mineral density (BMD) and structure in tibia. The study objective was to determine if RR intake results in similar femur and lumbar vertebrae (L4) BMD and bone structure 4 months post-lactation compared to rats that did not experience pregnancy. Female Sprague-Dawley rats were randomly assigned to one of three groups: 1) no pregnancy+water (GROWTH CON; n=14); 2) pregnancy and lactation+water (PREG CON; n=12); and 3) pregnancy and lactation+water with RR (~2.6 g of red rooibos/kg body weight/day) (PREG TEA; n=14). RR intervention began pre-pregnancy (age 6 weeks) through to 4 months post-lactation (endpoint). Ex vivo measurement of whole femur and L4 area, bone mineral content (BMC) and BMD was conducted using dual X-ray absorptiometry (Scintica InSiGHT) and trabecular (femur neck, L4 body) and cortical bone structure (midpoint of the femur, L4 body) was quantified using micro computed tomography (Skyscan 1176). At femur neck, there were no differences in trabecular bone structure outcomes including bone volume fraction (BV/TV), trabecular number (Tb.N), trabecular thickness (Tb.Th), and trabecular separation (Tb.Sp) among groups. In contrast, cortical bone structure at femur midpoint was different among groups: GROWTH CON had higher cortical area fraction (Ct.Ar/Tt.Ar) and cortical thickness (Ct.Th) than both PREG CON and PREG TEA ($p<0.05$). Similarly, whole femur area and BMD of GROWTH CON were higher than both groups that experienced pregnancy though BMC was higher in the GROWTH CON group compared to PREG CON but not PREG TEA ($p<0.05$). For L4, GROWTH CON group was higher ($p<0.05$) for BV/TV, Tb.N and Ct.Th and lower for Tb.Sp compared to both pregnancy groups though PREG TEA had higher BV/TV, Tb.N and lower Tb.Sp than the PREG CON and suggests a benefit to L4 structure ($p<0.05$). Tb.Th was higher ($p<0.05$) in the GROWTH CON versus PREG CON group while PREG TEA did not differ from either group. BMC and BMD of whole L4 were higher ($p<0.05$) in GROWTH CON group compared to both pregnancy groups while area did not differ among groups. Overall, RR tea supported L4 structure following pregnancy and lactation but did not result in similar outcomes at the femur or L4 compared to the non-pregnant control.

***Disclosures: Matthew K. Goncharow**, None*

SUN-021

Spatio-temporal and 3D imaging analysis of the initial stages of bone marrow formation *Emilio Hara[1], Tsz Long Chu[2], Andrei Chagin[2]. [1]Okayama University, Japan. [2]Karolinska Institutet, Sweden

The cell-cell and cell-matrix interactions are determinant factors in the formation and maintenance of the bone and bone marrow. In an attempt to understand these interactions, it is first necessary to identify the types of cells involved in these processes. For this purpose, we herein performed a spatiotemporal analysis of the first steps of bone formation during the secondary ossification center (SOC). Mouse femur epiphyses were collected at different developmental stages, and the ultrastructure of initially formed minerals was analyzed by scanning electron microscope (SEM), and scanning transmission electron microscope with energy-dispersive x-ray spectroscopy (STEM-EDS). For analysis of cellular components and distribution, we performed immunostaining, OMIC analysis, and tissue-clearing-based 3-dimensional imaging. This approach revealed complex architectures of apatite crystals during the cartilage-to-bone and bone-to-bone marrow transitions. Furthermore, several types of cells related to cartilage matrix degradation/turnover, and newly formed bone and bone marrow were identified and spatially characterized in tissue-cleared 3D images. These results provide important insights into mechanisms underlying the initial steps of osteogenesis within the SOC. Future studies are necessary to clarify their specific roles, and their interactions during these stages.

***Disclosures: Emilio Hara**, None*

SUN-022

Finite Element Analysis of Regenerated Digit Bone *Kevin Hoffseth[1], Mimi Sammarco[2]. [1]Louisiana State University, United States. [2]Tulane University, United States

Purpose: Improving our understanding of how bone regeneration affects structure and mechanical performance at organ and microstructural levels is critical given the vital role of bone in human health. For this purpose, the mouse P3 digit regeneration process has been valuable in studying fundamental mechanisms underlying bone regeneration and healing and their connections to aging. This work details leveraging of µCT to finite element (FE) pipeline for improved analysis of regenerated bone structural quality and mechanical response, specifically the development of a FE-based approach to analyze the mouse P3 digit bone.Methods: Three-dimensional reconstruction of the digit bone is performed using new open-source image processing tools to convert CT images into a three-dimensional, volumetric model [1]. Calibrated µCT scan values and densiometric relationships are used to calculate spatially distinct Young's modulus values in the digit bone [2]. Custom programming scripts process the critical differences in regenerated bone morphology and assign spatially distinct Young's modulus values and create high resolution three-dimensional, volumetric finite element meshes, using 8 node hexahedral elements, implemented as linear elastic and isotropic, and solved in ABAQUS software. The proximal joint end was constrained from displacement and rotation, and distal tip subjected to vertical load for stress analysis, approximating a cantilever beam.Results: Initial results capture the difference in structure and response between uninjured and regenerated bone and effect of structure on potential damage initiation, in particular stress concentrations. Stress analysis results for a representative example of a regenerated digit bone may be seen in Figure 1.Conclusions: Morphologically accurate three-dimensional FE models of regenerated and uninjured mouse P3 digit bone built from µCT data demonstrate the ability to comparatively predict mechanical quality and identify possible sites of failure through stress concentrations. The expected outcome of this ongoing work project is further advancement of our ability to evaluate and predict the structure and mechanical response of regenerated bone, and enable more powerful evaluation of regeneration treatments.References:Hoffseth KF, et al., Bone. 2021;144:115776.Hoffseth KF, et al., J Biomech. 2022;143:111271.

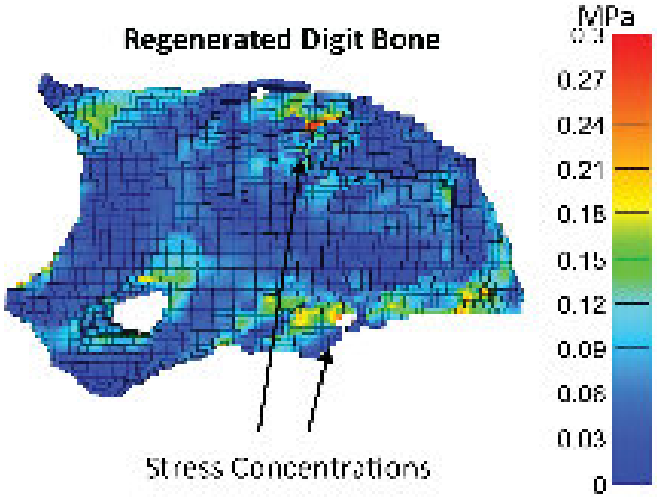

***Disclosures: Kevin Hoffseth**, None*

SUN-023

The contribution of bone structure to sex-specific associations between femoral neck bone mineral density and strength *Karl Jepsen[1], ERIN BIGELOW[2], Robert Goulet[3], Bonnie Nolan[1], Michael Casden[1], Kathryn Kennedy[1], Samatha Hertz[1], Chandan Kadur[1], Gregory Clines[1], Aleda Leis[1], Carrie Karvonen-Gutierrez[4], Todd Bredbenner[5]. [1]University of Michigan, United States. [2]UNIVERSITY OF MICHIGAN, United States. [3]Michigan Medicine, University of Michigan, United States. [4], United States. [5]University of Colorado Colorado Springs, United States

Hip bone mineral density (BMD) is widely used to identify women and men with increased risk of fracturing. Low femoral neck (FN) BMD is an indicator of low strength, but this association has an unresolved sex-specific difference with men showing stronger proximal femurs for a given BMD compared to women. We used validated pseudoDXA images generated from high resolution nanoComputed Tomography (nanoCT) volumes to test how associations among bone structure, BMD, and strength vary by sex. Cadaveric proximal femurs from White female (n=51; 24-89+ years) and male (n=44; 18-89 years) donors were imaged and loaded in a sideways fall configuration to assess strength. Validated neural networks segmented bone from background and cortical from trabecular regions. A validated protocol for generating pseudoDXA images from the nanoCT images was used to generate pseudoDXA BMD, BMC, and area.Strength correlated significantly with BMD for females ($R2=0.61$, $p<0.001$) and males ($R2=0.44$, $p<0.001$) (Fig 1A). The y-intercept differed between sexes ($p<0.001$, ANCOVA); male proximal femurs were 1,059 N stronger than females for a given BMD. In contrast, strength correlated with BMC for females ($R2=0.57$, $p<0.001$) and males ($R2=0.49$, $p<0.001$), but with no difference in the slope ($p=0.69$) or y-intercept ($p=0.08$). Testing bone size-based normalizations found that normalizing BMC by femoral neck width, average total cross-sectional area, and total volume all showed significantly different y-intercepts ($p<0.001$, ANCOVA) suggesting bone-size normalizations led to the sex-difference in the BMD-strength association. We conducted linear regressions across the range of external bone sizes to test if the bone structures giving rise to BMC differ by sex (Fig 1B). A regression of % cortical bone against BMC showed that variation in BMC reflects different proportions of cortical and trabecular bone for men and women. For women, lower values of BMC reflect greater changes in cortical bone and a 50:50 mix of cortical and trabecular bone. For men, the associations were reversed such that lower values of BMC reflected greater changes in trabecular bone than in cortical bone. Thus, the proximal femurs of women are not smaller versions of male proximal femurs but are constructed

in fundamentally different manners. Given the reliance on BMD, it is critical to resolve discrepancies in the associations among BMD, strength, and underlying bone structures so fracture risk prediction is unbiased.

Figure 1

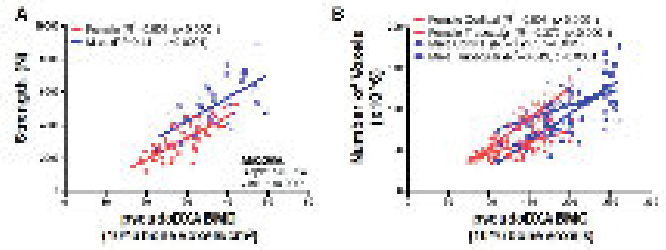

***Disclosures: Karl Jepsen**, None*

SUN-024

MRI-Based Finite Element Modeling of The Proximal Femur Discriminates Between Patients with and without Hip Fractures *Nada Kamona[1], Brandon Jones[1], Emily Tu[2], Iman Fathali[2], Gregory Chang[3], Chamith Rajapakse[4]. [1]Department of Radiology, Department of Bioengineering, University of Pennsylvania, United States. [2]Department of Radiology, University of Pennsylvania, United States. [3]Department of Radiology, New York University, United States. [4]Department of Radiology, Department of Orthopaedic Surgery, University of Pennsylvania, United States

Purpose: Deterioration of trabecular connectivity and thinning of cortical bone are important determinants of bone health because bone microarchitecture contributes substantially to bone fragility.1 Using finite-element analysis (FEA) applied to magnetic resonance (MR) images, we can directly simulate patient-specific bone biomechanics in vivo by reconstructing the 3D morphology of bone. Our goal was to assess bone strength of hip fracture patients using high-resolution MR images of the proximal femur.Methods: Subjects with (n=13) and without (n=13) hip fractures were recruited: 18 females, age 56+/-11.9 yo, BMI 22.7+/-4.0 kg/m2. Fracture and non-fracture groups were matched based on age, height, and weight. Subjects were imaged at the proximal femur with 3T MRI using a spoiled gradient echo sequence, with in-plane resolution of 234x234 ?m and a slice thickness of 1.5 mm2,3. Proximal femur images were manually segmented, and voxel values were inverted and scaled to create bone volume fraction maps, such that bone marrow and bone had values of 0% and 100%, respectively. A custom FEA model was used to simulate patient-specific sideways-fall configuration to mimic the most common direction of hip fracture injuries4. Linear and nonlinear FEA were utilized to estimate whole-bone stiffness (kN/mm) and failure load (kN/mm), respectively4,5. DXA-derived T scores of the total hip and spine were measured for all subjects. Differences between fracture and non-fracture patients were assessed using parametric two-sided t test or nonparametric Wilcoxon signed rank test. Results: An example high-resolution MR image for a fracture patient and the matched control is shown in Figure 1A. Patients with fractures had significantly lower estimated stiffness (P=0.002) and failure load (P=0.007) when compared to matched controls (Figure 1B). On the contrary, total hip T score was not different between fracture and non-fracture groups (P=0.243), while spine T score was erroneously higher in the fracture group (P=0.045). Estimated stiffness and failure load were highly correlated (R2=0.917, P<0.0001, Figure 1C). Neither total hip nor spine T scores were correlated with estimated mechanical properties. Conclusions: FEA applied to high-resolution MR images of the proximal femur can estimate bone mechanical competence, discriminating between hip fracture patients and non-fracture subjects. Bone strength may provide additional information of bone health that is not captured by DXA alone.

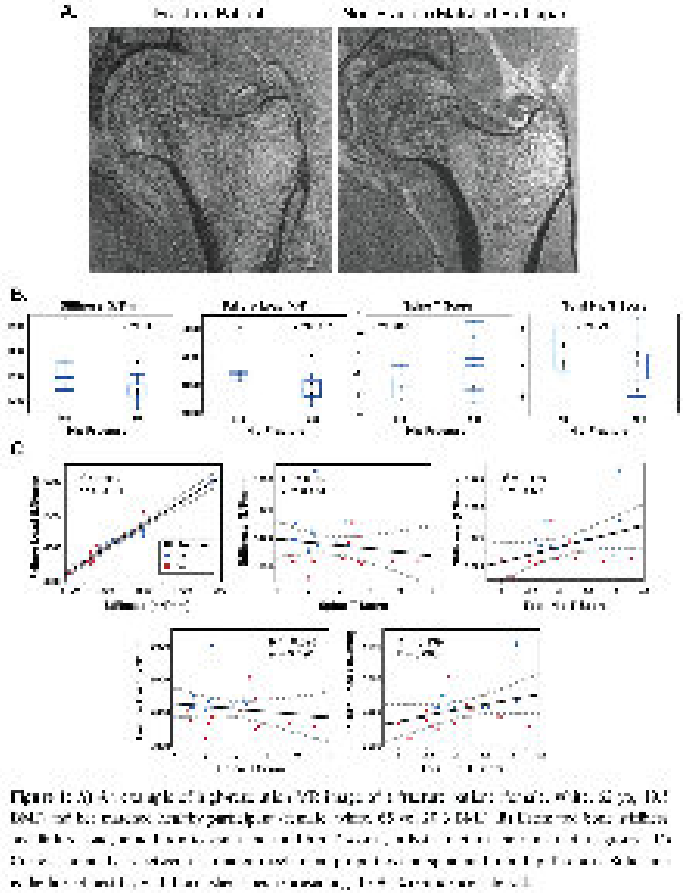

***Disclosures: Nada Kamona**, None*

SUN-025

Trabecular but Not Cortical Bone Responded Similarly to Voluntary Wheel Running in Ovariectomized Mice at Different Skeletal Sites *Dawson B. Kays[1], Jenalyn L. Yumol[1], Ahmad Mohammad[1], Jacob Sweezey-Munroe[1], Rebecca E.K. MacPherson[1], Wendy E. Ward[1]. [1]Brock University , Canada

Mechanical loading is a known stimulus of bone tissue in rodent models but whether long bones respond similarly to exercise is unclear. Knowing this will help inform which long bone should be studied in response to an exercise intervention. The study objective determined if femur and tibia respond similarly to voluntary wheel running (VWR) after ovariectomy (OVX). 24-week-old C57BL6/J mice underwent sham surgery (SHAM; n=20) or OVX (n=20). After 4 weeks, mice were assigned to SHAM (n=10), SHAM+VWR (n=10), OVX (n=10), or OVX+VWR (n=10) for 8 weeks (endpoint). SHAM ran a longer distance compared to OVX (total distance 65+/-9 km versus 29+/-37 km, p<0.05). At endpoint, distal and midpoint regions of femur and at proximal and midpoint regions of tibia were measured using micro computed tomography (SkyScan 1176). Bone mineral density (BMD) of whole femur and tibia were measured using dual energy X-ray absorptiometry (Scintica InSiGHT). As expected, there was a main effect of OVX: distal femur had lower cortical area fraction (Ct.Ar/Tt.Ar) and cortical thickness (Ct.Th), as well as higher trabecular separation (Tb.Sp); femur and tibia midpoint had lower Ct.Ar/Tt.Ar and Ct.Th; and proximal tibia had lower Ct.Ar/Tt.Ar, Ct.Th, bone volume fraction (BV/TV), trabecular number (Tb.N), trabecular thickness (Tb.Th) and higher Tb.Sp compared to SHAM (p<0.05). Whole femur but not tibia BMD was lower (p<0.05) with OVX versus SHAM. To assess whether femurs and tibias responded similarly to VWR, trabecular structure at distal femur and proximal tibia were compared. Also, cortical structure was assessed at these sites, and at femur and tibia midpoint. There was a main effect of VWR at both the distal femur and proximal tibia with higher BV/TV and Tb.N and lower Tb.Sp (p<0.05). There was an interaction (p<0.05) for VWR and estrogen status for Ct.Ar/Tt.Ar and Ct.Th at proximal tibia but not at distal femur. Regardless of VWR, OVX had lower (p<0.05) Ct.Ar/Tt.Ar and Ct.Th compared to SHAM. However, VWR resulted in higher (p<0.05) Ct.Ar/Tt.Ar and Ct.Th in SHAM groups only. At femur but not tibia midpoint, there was a main effect of VWR (higher Ct.Ar/Tt.Ar and Ct.Th, p<0.05). In conclusion, trabecular but not cortical bone responded similarly to exercise when comparing femurs and tibias. These findings support studying multiple skeletal sites to assess the effect of VWR. Findings also suggest that minimal VWR is needed to support bone health following ovariectomy.

***Disclosures: Dawson B. Kays**, None*

SUN-027

Changes in the Microstructural and Mechanical Properties in theMedial Condyle of Human Distal Femur in Advanced Osteoarthritis *Kwangkyoun Kim[1.] [1]Konyang university, college of medicine, Republic of Korea

Objectives: The purpose of this study is to analyze and compare the micro-structural and mechanical properties of subchondral trabecular bone of non-osteoarthritic and osteoarthritic distal femur using micro-images based on finite element analysis.Materials and Methods: Twenty distal femurs were harvested from 10 cadavers. The subchondral trabeculae were obtained from the middle of the articular surface of the medial femoral condyle of distal femurs. A total of 20 specimens were scanned using the micro-CT system. Micro-CT images were converted to micro-finite element model using the mesh technique, and micro-finite element analysis was then performed for assessment of the mechanical properties. Results: According to the results, trabecular bone of osteoarthritic distal femur showed a decrease in trabecular thickness, bone volume fraction, structure model index, and yield stress and an increase in trabecular separation and structure model index.Conclusions: Results of bone morphometry index and strength showed greater deterioration of microstructure and decreased mechanical strength in subchondral trabeculae of the osteoarthritic group.

***Disclosures: Kwangkyoun Kim**, None*

SUN-028

Bone Stress Injury Associates with Increased Cortical Porosity at a Common Fracture Site *Lysanne Michels[1.] Jacob Trend[1.] Theo Hornsey[1.] Philipp Schneider[1.] Andrew Pitsillides[2.] Julie Greeves[3.] Thomas O'Leary[3.] Claire Clarkin[1.] [1]University of Southampton, United Kingdom [2]Royal Veterinary College, United Kingdom [3]Army Health and Performance Research, United Kingdom

IntroductionWomen experience more bone stress injuries (BSIs) in the military than men [1-2], often located along the posterior-medial aspect [3], of which the pathogenesis remains poorly understood. Cortical porosity includes vascular canals and is a critical predictor of bone strength [4]; we therefore aimed to analyse whether differences in the cortical vascular canals associate with bone stress injuries.MethodsHR-pQCT scans (61 ?m) were taken at the tibial diaphysis, a common BSI site, of injured women (n = 5) and sex- and age-matched non-injured controls (n = 6) at the start of the 44-week Officer Commissioning Course in Sandhurst, UK. The volume and diameter of cortical vascular canals were extracted from anterior, medial, lateral, and posterior regions in ImageJ as these are exposed to different strains [3, 5]. In ORS Dragonfly, Distance Mapping was used to divide canals into endosteal (0-40% from the endosteal surface), embedded (41-60%), and periosteal (61-100%) as these are exposed to different blood flows [6].ResultsNo differences between injured and non-injured women were observed when canals or regions were pooled. However, upon regionalisation injured women exhibited larger periosteal canals (61-80% from the endosteal surface) in the posterior (0.338 +/- 0.462 mm3) compared to medial (0.054 +/- 0.040 mm3) and lateral (0.019 +/- 0.014 mm3) regions. These were also wider in the posterior (0.186 +/- 0.048 mm) than lateral region (0.136 +/- 0.010 mm). In contrast, controls exhibited no spatial variation in canal size (fig. 1). As such, posterior periosteal canals were larger in injured than non-injured women (0.048 +/- 0.051 mm3; p = 0.042). DiscussionIncreased canal size in the posterior region could contribute to BSIs originating here, with higher cortical porosity reducing bone strength thus elevating fracture risk [4-5]. These pre-injury differences may point towards a different distribution of or sensitivity to strain linking to fatigue damage [4-5], and can be utilised to identify individuals at risk of bone stress injury thereby allowing for the development of targeted preventions.References[1] Wentz et al. 2011. DOI: 10.7205/milmed-d-10-00322.[2] O'Leary et al. 2020. DOI: 10.1136/jramc-2019-001347.[3] O'Leary et al. 2021. DOI: 10.1007/s11914-021-00671-1. [4] Cooper et al. 2016. DOI: 10.1007/s11914-016-0319-y.[5] Bell et al. 1999. DOI: 10.1016/s8756-3282(98)00143-4.[6] Skedros et al. 1994. DOI: 10.1002/ar.1092390407.

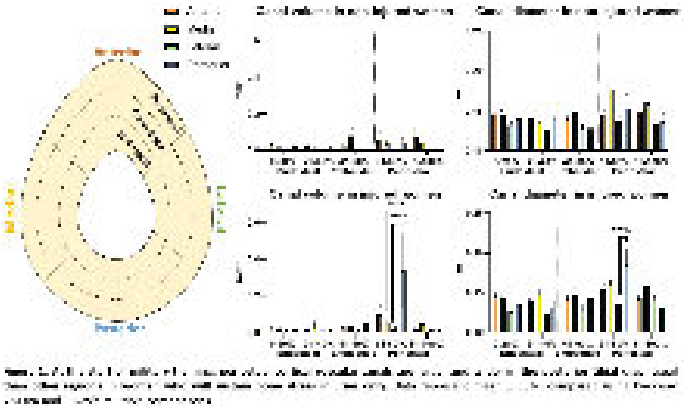

***Disclosures: Lysanne Michels**, None*

SUN-029

Automating quantitative analysis of peri-articular bone microarchitecture in HR-pQCT knee images using deep learning and atlas-based segmentation *Nathan Neeteson[2.] Steven Boyd[2.] [2]University of Calgary, [2]University of Calgary, Canada

High-resolution peripheral quantitative computed tomography (HR-pQCT) is an in-vivo imaging tool allowing direct quantification of bone microarchitecture. However, peri-articular analysis of HR-pQCT knee images requires accurate semantic segmentations of the subchondral bone plate and trabecular bone and the articular contact surface regions of interest (ROIs) on the tibia and femur. Here, we propose a fully automated solution using deep learning for bone segmentation and atlas-based segmentation for contact surface ROI definition.Bone segmentations are generated by a neural network (UNETR) that was pre-trained on 2601 manually segmented HR-pQCT radius and tibia images and retrained on 38 expert-segmented HR-pQCT knee images. Segmentation model performance is evaluated based on the Dice similarity coefficient (DSC) of the ground truth and predicted subchondral bone plate segmentations, calculated using five-fold cross-validation. Articular contact surface ROIs are generated using atlas-based segmentation. A femur or tibia image is downsampled and smoothed then deformably registered to a fixed reference image using a multiscale diffeomorphic Demon's algorithm. The ROI mask is then deformably transformed from the fixed reference to define the contact surface ROIs in the moving image. ROI definition performance is evaluated based on DSC between ground truth and registered ROI masks. The final peri-articular ROIs can then be computed via the intersection of the contact surface ROIs with the bone segmentation, and these ROIs can be used for regional microarchitectural analysis.The bone segmentation model achieves a mean validation set DSC of 0.94 for subchondral bone plate, indicating excellent agreement between the predicted and ground truth bone segmentations. Sample ground truth and predicted segmentations are shown in figure 1. The deformable registration procedure produces registered articular contact surface ROIs with an average DSC of 0.85 (min: 0.75, max: 0.91). Generation of an average atlas from the reference images is ongoing, as is the development of a pipeline for combining the contact surface ROIs and bone segmentations to complete automation of microarchitectural analysis.This work demonstrates that bone segmentation and contact surface ROI definition can both be accurately automated, using deep learning and atlas-based segmentation, respectively. This will allow full automation of peri-articular analysis of knee HR-pQCT images.

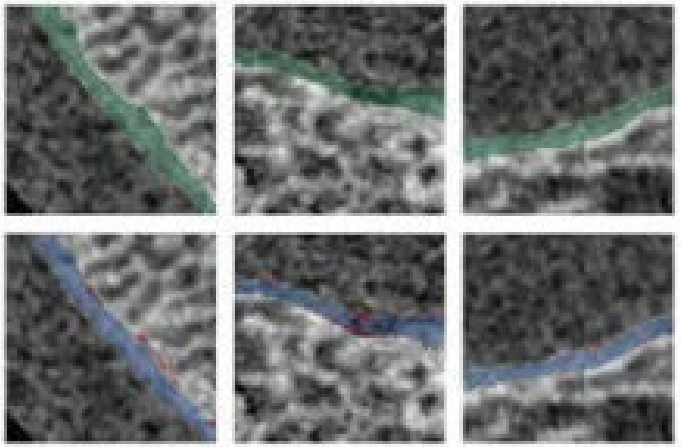

***Disclosures: Nathan Neeteson**, None*

SUN-030

Chromosomal sex (XX vs XY) contributes to bone and muscle mass independently of the gonadal sex (ovaries vs testis) in the 4 core genotype mouse model. *Lilian Plotkin[1.] Matthew Arnett[2.] Dyann Segvich[3.] Padmini Deosthale[1.] Chiebuka Okpara[4.] JULIAN BALANTA-MELO[5.] FABRIZIO PIN[6.] Joseph Wallace[7.] [1]Indiana University School of Medicine, United States [2]I, United States [3]Indiana University-Purdue University Indianapolis, United States [4]Lehigh University, United States [5]Universidad del Valle, Colombia [6], United States [7]Indiana University Purdue University Indianapolis (IUPUI), United States

Vertebrate sexual dimorphism is ascribed to the presence of testis or ovaries, and, hence, to gonad-specific hormone production. Sex differences also stem from the presence of sex chromosomes (XX or XY). To tease out the contribution of chromosome (CS) from gonad (GS) sex, the Sry gene that dictates testis formation was either deleted in XY mice, resulting in XYF mice with ovaries or overexpressed in XX mice, resulting in XXM mice with testis. These mice, together with XY males (M) and XX females (F) form the 4core genotype (FCG) model. It has been shown that levels of estrogen in XXF/XYF and androgen in XXM/XYM are similar. We now show that the musculoskeletal phenotype of 2 and 4 month (m) FCG mice depends on both GS and CS. Mice were scanned for DXA, blood/tissues were

collected, and bones were tested by µCT and 3-point bending. GS/CS effects were assessed by 2-way ANOVA (Tukey post-hoc test). GS influenced body weight (BW), and total/femur/spine BMD at 2m, and BW and total/femur BMD at 4m, all lower in gonadal females (Table1). A GS-CS interaction was found in 2m mouse spine BMD, which was lower in XYF than XYM, but similar in XXF and XXM mice. At 4m, XY mice show lower BW and BMD at the 3 sites than XX mice, whereas % lean mass was higher in XYM and XYF than the respective XX mice, and % fat mass was lower in XYM vs XXM, indicating CS effects (Table2). Skeletal muscle weights were lower in gonadal females (XXF/XYF) than in males (XXM/XYM) at 2m (Table3) whereas soleus muscle weight was higher in XYM than in XXM mice and no different in females. Fewer differences were found at 4m, with a CS-dependent effect in QC weight (higher in XXM than in XYM). µCT showed GS and CS contribution to structural parameters and TMD in femur mid-diaphysis -lower in XYF vs XXF, no different in males- whereas only GS affected marrow cavity and total tissue area and MOI at 4m (Table4). Bone mechanical properties were overall lower in gonadal females (Table5). CS only affected ultimate force - lower in XYF vs XXF, no different in males. GS affected all distal femur trabecular structural parameters, which were lower in gonadal females, but only partially L5 vertebrae (Table4). L5 tissue mineral density TMD depended on CS and was higher only in XXF vs XYF. Finally, GS and CS also affected serum chemokine levels, which might explain changes in bone and muscle cell function (Table6). Thus, while GS has a major role, CS is a so far unrecognized contributor to bone/muscle mass and bone strength.

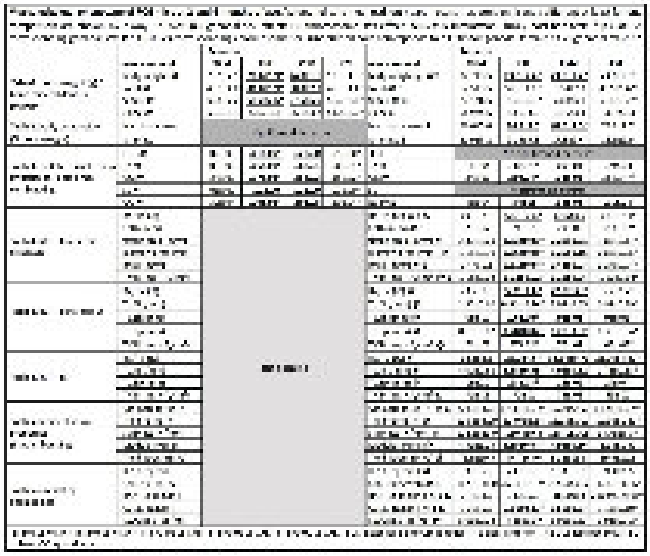

***Disclosures: Lilian Plotkin**, None*

SUN-031

Quantification of the Photon Counting CT Reproducibility And Its Implication For Detecting Bone Remodeling *Jilmen Quintiens[1,] Harry van Lenthe[2,] Walter Coudyzer[3.] [1]Department of Mechanical Engineering, KU Leuven, Belgium. [2]KU Leuven, Belgium. [3]University Hospital Gasthuisberg, Belgium

For the quantification of localized bone strength and bone changes, volumetric methods such as quantitative CT are to be preferred over conventional techniques such as DXA. This due to DXA being a two-dimensional technique, which is dependent on body frame [1]. However, the low resolution of conventional clinical CT limits direct implementation in health care. Photon Counting CT (PCCT) shows potential to overcome this limitation thanks to its higher resolution and better image contrast. The aim of this study was to quantify the reproducibility of PCCT and determine the least-detectable change in volumetric bone density.Using PCCT (NAEOTOM Alpha, Siemens Healthineers), eighth cadaveric wrists were scanned twice with repositioning. For each wrist, the eight carpal bones were delineated. Images were registered onto each other and the difference image was calculated by voxel-wise subtraction. In parallel, a phantom was scanned and a linear relation was fitted, expressing volumetric bone density as a function of Hounsfield Unit (HU). Bone remodeling was defined as all voxels in the difference image that surpassed a predefined threshold and that were part of a cluster of at least 5 voxels.Averaged over all samples, estimated mean intensity difference is 1.75 HU, and estimated standard deviation 142 HU. For a threshold of 250 mgHA/cm³, the total amount of falsely detected remodeling amounts to 0.31% (formation 0.14% +- 0.17%; resorption 0.17% +- 0.39%; Fig.1). This is an acceptable error, hence differences above this threshold are likely to be physiological in nature.Our results compare well to HRpQCT. In a similar ex vivo study with HRpQCT, Christen et al. [2] reported 0.4% remodeling for a threshold of 225 mgHA/cm³. Using the same threshold in an in vivo analysis, remodeling increased to > 5%, due to motion artifacts. For in vivo analyses we hypothesize that PCCT may outperform HRpQCT because of the shorter acquisition time which limits these artifacts.In conclusion, PCCT shows an excellent reproducibility when quantifying volumetric bone density and results are comparable to HRpQCT. This study considers bone remodeling based on image intensity only; however, also voxel size plays an important role, which could favor HRpQCT. In future studies we will 1) repeat the analysis with in vivo measurements and 2) use PCCT for a follow-up study in patients.[1] Alawi et al., Cureus 13(2): e13261, 2021.[2] Christen et al., PLoS One 13: e0191369, 2018.

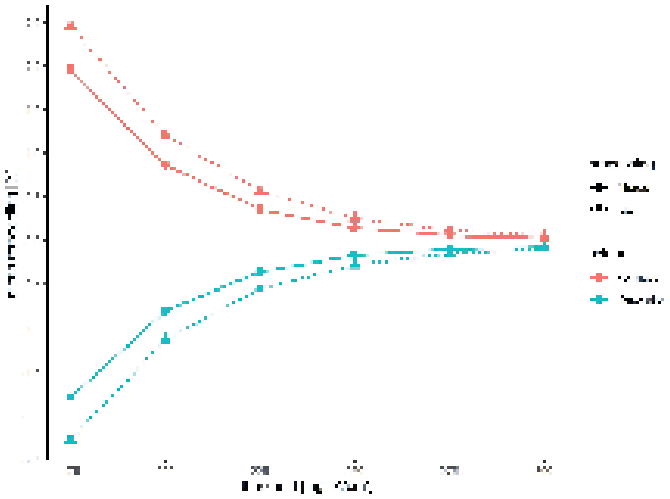

***Disclosures: Jilmen Quintiens**, None*

SUN-032

Type 2 Diabetes Affects Advanced Glycation End-Products and Indentation Properties in Human Bone *Taraneh Rezaee[1,] Rachana Vaidya[2,] Leland O. Barret[3,] Zackery Joseph Silva[3,] Christian Leonarde Ray[4,] Brooke Lynn DeSimone[4,] Lamya Karim[5.] [1]1.Department of Bioengineering, University of Massachusetts Dartmouth 2. Department of Biomedical Engineering, City College of New York of the City University of New York, United States. [2]washington university in st louis , . [3]1. Department of Bioengineering, University of Massachusetts Dartmouth, United States. [4]1Department of Bioengineering, University of Massachusetts Dartmouth, United States. [5]University of Massachusetts Dartmouth, United States

Type 2 diabetic (T2D) patients have 3 times higher fracture risk than non-diabetics [1] despite having normal or high bone mineral density, and this risk may be due to having poor bone quality. Bone quality can be impacted by the accumulation of collagen crosslinks known as advanced glycation end-products (AGEs) that form from non-enzymatic glycation [2]. Our goal was to investigate how tissue-level mechanical behavior of human cortical beams are impacted by altered AGEs in T2D. We hypothesized that T2D bone will have more AGEs and weakened indentation properties compared to non-diabetic bone.We obtained 120 transverse and longitudinal cortical beams from 4 human cadaveric donors (young T2D, young non-diabetic, old T2D, old non-diabetic). Cyclic reference point indentation (cRPI) tests were conducted on all samples using a Biodent system at 6 N, 2 Hz, for 20 cycles. Five indentations were made on the periosteal surface at the proximal end of each beam (~1 mm intervals). Total fluorescent AGEs were measured by a fluorometric assay in all beams and the AGE pentosidine was measured by high performance liquid chromatography in a subset of longitudinal beams (n=48).Young T2D bone had higher AGEs than young non-diabetic in longitudinal beams, with a similar trend in transverse beams. Pentosidine was higher in T2D young vs non-diabetic young beams. These trends were not seen in old donors. cRPI-assessed ID, TID and Avg ED were higher in young T2D vs young non-diabetic bone within longitudinal beams, but there were no differences in the older groups (Table 1). ID, TID, IDI, and Avg ED were higher while Avg US and Avg LS were lower in young T2D bone vs young non-diabetic bone within transverse beams (Table 1). Among older transverse beams, CID was lower in diabetic vs non-diabetic, but no other variables were significantly different. T2D bone had more glycation content than non-diabetic bone as predicted, but this was only observed in young donors. It is possible that T2D has a greater impact in young bone but not in old bone where donors may have faced other more severe health issues such as osteoporosis that have a greater impact on bone health than T2D. Correspondingly, young T2D bone experienced deeper indentation distances than non-diabetic bone as well as reduced stiffness. These results show that young T2D bone with higher AGEs had poor tissue-level mechanical properties.References: [1] Skelly AH, Nursing Clinics, 2006; [2] Tang, et al., Bone, 2007

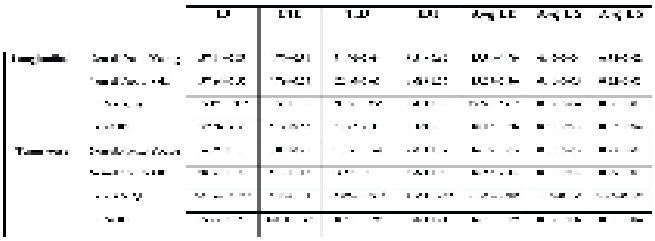

***Disclosures: Taraneh Rezaee**, None*

SUN-033

Developing a "virtual bone biopsy" technique for determining total bone turnover in patients with chronic kidney disease *Saghi Sadoughi[1], Lauren Go[1], Gabby Ramil[1], Aditya Subramanian[1], Po-hung Wu[2], Isra Saeed[1], Joachim H. Ix[3], Galateia Kazakia[1]. [1]University of California, San Francisco, United States, [2]University of California - San Francisco, , [3]University of California, San Diego, United States

Time-lapse HR-pQCT employs sequential scans over time to identify areas and rates of bone formation and resorption. This technique may be well suited to non-invasively measure bone turnover in patients with chronic kidney disease (CKD), who suffer from two extreme subtypes of bone disease: high and low turnover. Because blood biomarkers of bone turnover are unreliable in patients with CKD, the gold standard measure of bone turnover remains iliac crest biopsy. This procedure is invasive, expensive, and available at limited medical centers. Thus, non-invasive "virtual bone biopsy" that can reliably estimate bone turnover in patients with CKD and be measured repeatedly has the potential to revolutionize CKD bone care. The goal of this study was to develop a "virtual bone biopsy" to determine bone turnover in patients with CKD, and to evaluate the technique's sensitivity to measuring turnover over different time periods.Nine individuals with CKD on dialysis (4 women, 5 men; 59 +/- 18 years) were recruited. HR-pQCT scans were acquired on XtremeCT II at the radius and tibia. Patients were scanned at BL (n=9), 2-month FU (n=7), and 4-month FU (n=3). Of the 38 total scans, 5 radius scans were eliminated from analysis due to motion. BL and FU sets were registered using 3D registration and a voxel-wise density difference map was created. A two-step filter approach was then applied to reduce artifacts. Outcome metrics Bone Formation Fraction (BFF) and Bone Resorption Fraction (BRF) were calculated by dividing the number of formation or resorption voxels by BL total bone voxels. Total Bone Turnover (TBT) was calculated as the sum of BFF and BRF (Fig1A-B). Precision metrics were calculated using scan-rescan data in 20 healthy volunteers (9 women, 11 men; 53 +/- 18 years). Two-month TBT (mean +/- SD) was 16.5 +/- 5.9% and 9.9 +/- 4.3% at the radius and tibia, respectively. Four-month TBT was 30.3% (single set) and 17.7+/-3.9% at the radius and tibia, respectively. The 4-month TBT values were 2 to 3 times greater than the LSC at the radius and tibia of 12.1% and 8.2%, respectively, found in our precision study (Fig1C-D).We found that although mean TBT at 2-month FU was greater than LSC at both radius and tibia, not all individual patients had TBT greater than LSC. At 4-month FU, TBT in all patients was greater than LSC, demonstrating adequate sensitivity to detect changes over a 4-month period in patients with CKD. These promising results will be validated against surgical biopsy.

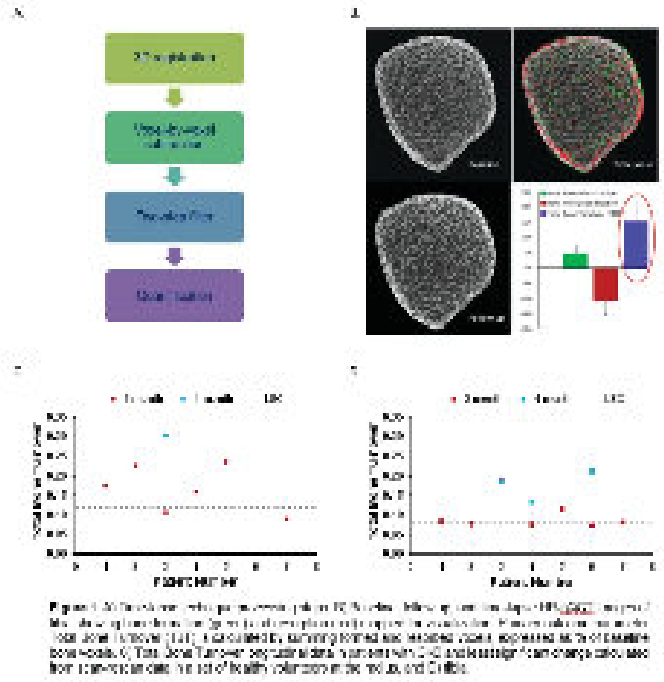

***Disclosures: Saghi Sadoughi**, None*

SUN-034

MRI-Based Finite Element Modeling Approach to Quantify the Relationship between Femoral Geometry and Atypical Femoral Fracture *Ashkan Sedigh[1], Brandon Jones[2], Nada Kamona[2], Christiana Cottrell[2], Rasleen Grewal[2], David Baretto[2], Achala Kankanamge[2], Jianna Kim[2], Elaine Li[2], Kevin Li[1], Makayla Clark[2], Ganen Chinniah[2], Caroline Paik[2], Reva Bhatt[2], Ryan Shams[2], Maegan Sojan[2], Chamith Rajapakse[2], Ani Ural[1]. [1]Villanova University, United States, [2]University of Pennsylvania, United States

Atypical femoral fracture (AFF) that occurs at the subtrochanteric or midshaft region of the femur has been associated with long-term bisphosphonate use. The current clinical population-based studies have not been able to explain the underlying mechanisms of AFF. Moreover, femoral geometrical properties that increase AFF risk have not been conclusively identified. Thus, this study aims to develop a novel MRI-based finite element (FE) modeling approach to identify the relationship between femoral geometry and AFF.Five female human cadaveric femurs were scanned via magnetic resonance imaging (MRI) at an isotropic resolution of 341 ?m. The images were segmented and processed using Simpleware ScanIP to generate FE meshes (~700k elements). The meshes were imported into the FE analysis software, Abaqus, and were subjected to stance loading (Fig. 1A). The fracture process was modeled by the cohesive extended finite element method (XFEM). Homogeneous material properties were assigned to the models based on the literature. The load-displacement data were extracted to assess the influence of femur geometrical properties (neck shaft angle, neck variation angle, neck length, femur neck thickness, and midshaft diameter) on femoral mechanical properties.The simulation results showed that the stiffness, peak load, and displacement at the peak load corresponding to crack formation at the AFF site correlate with the shaft diameter (R=0.79, 0.69, -0.95, respectively) (Fig. 1B). No statistically significant relationships were observed between stiffness, peak load, displacement at the peak load, and other geometrical parameters.This study established a modeling approach incorporating MRI and fracture mechanics-based FE modeling for evaluating the influence of femoral geometrical properties on the mechanical response at the AFF site. The variation in mechanical properties with femoral geometry incorporating the same material properties indicates the significant contribution of femur geometry to the fracture resistance at AFF sites. The modeling process developed here can be adapted to incorporate additional MRI-based geometrical measurements, such as bowing angle, and parameters, such as bone volume fraction, cortical porosity, and collagen fraction. As a result, MRI-based FE models provide a promising new approach for the noninvasive assessment of the femur's geometrical and material properties and identify the multifactorial determinants of AFF.

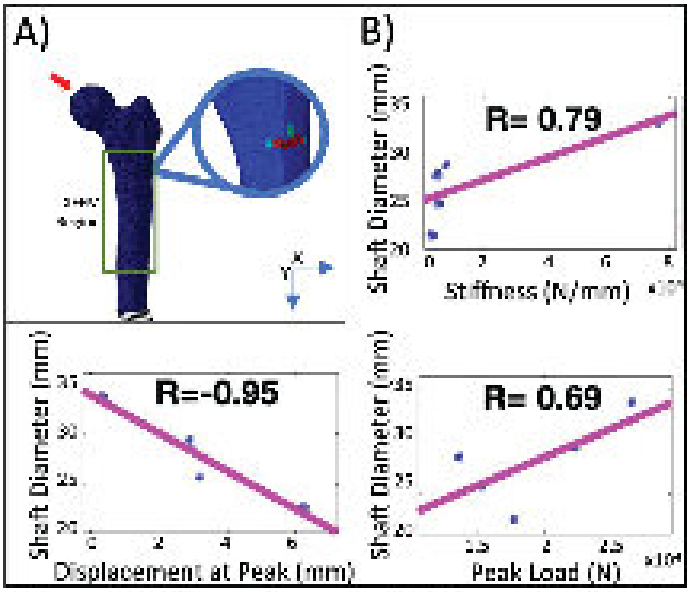

Figure 1. A) Femur FE model with the applied load (red arrow) and crack initiation at the AP1 site. B) Variation of mechanical properties of femur with shaft diameter showing Pearson correlation coefficients.

***Disclosures: Ashkan Sedigh**, None*

SUN-035

Investigation of human cortical bone quality in osteoporosis with and without type 2 diabetes *Praveer Sihota[1], Saroj Kumar[2], Piyush Uniyal[2], Ram Naresh Yadav[2], Vandana Dhiman[3], Ruban Dhaliwal[4], Deepak Neradi[3], Shailesh Karn[3], Sidhartha Sharma[3], Sameer Aggarwal[3], Vijay G Goni[3], Vishwajeet Mehandia[2], Deepak Vashishth[5], Bjoern Busse[1], Sanjay Kumar Bhadada[6], Navin Kumar[2]. [1]University Medical Center Hamburg-Eppendorf, Germany [2]IIT Ropar, India. [3]PGIMER Chandigarh, India. [4]State University of New York Upstate Medical University, . [5]Rensselaer Polytechnic Institute, United States. [6]PGIMER, chandigarh, India, India

Purpose: Individuals with type 2 diabetes mellitus (T2D) are at a higher risk of hip fractures, even with normal to high bone mineral density (BMD). To better understand the factors contributing to this increased risk, we investigated the role of multi-scale cortical bone quality parameters in hip fragility fractures in individuals with T2D. Although T2D is known to cause alterations in cortical bone quality, the specific factors underlying the increased fracture risk remain unclear. Thus, our research aimed to determine if cortical porosity, material properties, or glycation content are independently associated with increased susceptibility to hip fractures in T2D.Method: This cross-sectional observational study investigated the multi-scale bone quality parameters in individuals with type 2 diabetes (T2D) and non-diabetic individuals who underwent hip replacement surgery for their first fragility hip fracture, all recruited from Northern India. We collected inferomedial femoral neck bone tissue specimens and measured cortical porosity using high-resolution micro CT, biomechanical properties using uniaxial compression and nanoindentation, local bone composition with FTIR, gravimetric mineral: matrix ratio, and bone glycation using the fAGE assay. Results: In the study, there was no significant difference in areal BMD between the T2D and non-diabetic groups, but cortical porosity was higher in the T2D group. Biomechanical properties, including ultimate strength, ultimate strain, post-yield strain, toughness, and post-yield energy, were significantly lower in the T2D group. Nanoindentation properties were not different between the groups. The T2D group had a lower gravimetric mineral: matrix ratio, higher FTIR parameters related to glycation content, and higher levels of fAGEs. ANCOVA analysis suggested that the increased cortical porosity explained the decreased ultimate stress observed in the T2D group. Moreover, the higher glycation content in the bone matrix was negatively associated with the nanoindentation-derived E/H ratio, indicating that the bone from T2D patients had reduced plastic deformation.Conclusions: The findings suggest that the increased cortical porosity in T2D individuals may lead to reduced bone strength, while the presence of elevated levels of fAGEs in the bone matrix may contribute to decreased bone deformation and energy absorption, making the bone more brittle and prone to fracture.

Parameters	Non diabetic group (n=35)	Diabetic group (n=31)	p value
Gender (female) n,%	21,60	5,16	
Age (years)	[illegible]	[illegible]	[illegible]
Pre operative HbA1c (%)	[illegible]	[illegible]	<0.001
Femoral neck			
BMD (g/cm²)	[illegible]	[illegible]	[illegible]
FN T score	[illegible]	[illegible]	[illegible]
Cortical porosity (%)	7.9 ± 3.3	14.8 ± 3.3	0.036
Glycation in bone matrix			
FAGE (pg quinine sulfate/µg protein)	[illegible]	[illegible]	[illegible]

Abbreviations: BMD, bone mineral density; FN, femoral neck; fAGE, fluorescent advanced glycation end products

***Disclosures: Praveer Sihota**, None*

SUN-036

3D Cortical Bone Mineral Density Distribution is influenced by genetics and gene-by-diet interactions in mice. *Semahat Serra Ucer Ozgurel[1], Joseph Sheeran[2], Corinne Metzger[4], Matthew Allen[4], James Fleet[1]. [1]University of Texas at Austin, United States. [2]California Institute of Technology, United States. [4]Indiana University School of Medicine, . [4]Indiana University School of Medicine, United States

The heterogeneity and degree of bone mineralization impact the material properties of bone. Tissue-level heterogeneity can be assessed with a bone mineral density distribution (BMDD) determined from 2D-histological sections of bone biopsies using backscatter electron microscopy. Recently, several groups have explored the use of BMDD from 3D-micro-computed tomography (?CT) scans. We further evaluated the ?CT-based BMDD of cortical bone in preclinical mouse models with genetic modifications or treatments that affect bone. In Vitamin D Receptor KO mice, BMDD was shifted to lower density depicted by lower mean degree of mineralization of bone (MDMB), and a lower distribution variance (?2) (n=5-12/genotype) due to the disruption of calcium metabolism. Intermittent PTH (1-34) treatment (100 ng/g/day, 4-wks, n=6-7) also shifted the BMDD to lower a MDMB but with no changes in ?2, indicating that the new bone formed had not yet fully mineralized. MDMB was also lower in 86-wk vs 24-wk old mice, reflecting an imbalance in bone remodeling towards more resorption. In addition, mice with adenine-induced chronic kidney disease (CKD) had decreased MDMB with lower ?2 compared to controls, in agreement with impaired mineralization and longer mineralization lag time observed in CKD patients. We next assessed whether BMDD parameters correlated with material properties parameters from Reference Point Indentation (RPI). In a genetically diverse panel of 11 inbred strains (12 wk old males), we found significant correlations between RPI and BMDD variables, e.g., MDMB and unloading slope, an indicator of material stiffness (r= 0.57, p<.0001, n=162). MDMB from aging/CKD mice also correlated with stiffness from 4-point bending analysis (r=0.63, p<.001, n=25). BMDD parameters (including MDMB and ?2) were significantly different across the panel of 11 inbred strains (n=13-16/strain, see figure), indicating a significant impact of genetics on BMDD. In inbred strains fed 0.25% or 0.5% Ca diets from weaning (n=5-8/line/diet), the BMDD of some, but not all lines were modified by diet, indicating the existence of gene-by-diet (GxD) interactions. Our results show that the 3D ?CT-based BMDD is a useful tool that reflects the material properties of bone and that it can be used to evaluate the impact treatments and genetics on bone. The genetic and GxD effects we saw on BMDD lay the groundwork for a discovery-focused initiative to identify novel genes controlling bone mineralization.

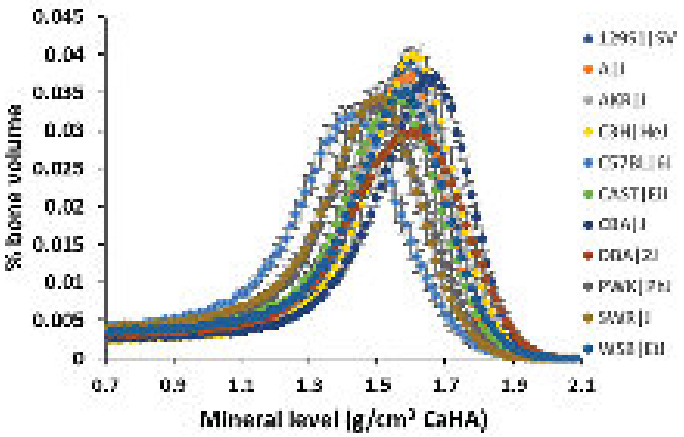

***Disclosures: Semahat Serra Ucer Ozgurel**, None*

SUN-037

Impact Microindentation Measures of Bone Quality is Strongly Correlated with Whole Bone Strength at the Hip, Wrist and Lumbar Spine. *Rachana Vaidya[1], Simon Tang[2], Babak Jahani[3], James Jin[4]. [1]University of Massachusetts Dartmouth, , [2]Washington University in St Louis, United States, [3]Washington University in St.Louis, United States, [4]Washington University in St.Louis , United States

Introduction: Post-menopausal women experience a significant incidence of hip, wrist, and spine fractures, with two-thirds of all fractures occurring in women without osteoporosis, as determined by DXA. While BMD is used to diagnose osteoporosis and predict fracture risk, it does not consider variations in bone composition and structure that affect bone strength. Impact microindentation (IMI) assesses bone quality at the tissue level and provides information beyond BMD. Our objective is to investigate the relationship between IMI, BMD, and bone strength in a cadaver study to better understand the factors contributing to bone strength and improve fracture risk prediction.Methods: We harvested femurs, radii, L4 vertebrae, and tibiae from human cadavers (mean age of 71+/-13 years). DXA measured BMD at different skeletal sites. IMI was performed at the FDA-approved tibia mid-diaphysis site and reported as a Bone score. We mechanically tested bones to calculate fracture force (N) as a measurement of bone strength. We evaluated tissue-level mechanical properties using 3-point bending tests and performed IMI measurements on regions outside the mid-span to reduce bone heterogeneity effects. We investigated the relationships between bone strength, BMD, and bone scores using Pearson's correlation and multivariate regression. Results: Our findings suggest that measuring bone quality using indentation at the tibia is predictive of bone strength at other skeletal sites. Tibia bone score shows higher correlation to bone strength than BMD at the femur (Fig1A) and radius (Fig2A). Adding the tibia bone score measurement to BMD, increases the correlation to bone strength by 20% at the femur (Fig1B) and 10% at the radius (Fig2B). At the spine, tibia bone scores show a strong correlation to bone strength, but not lumbar BMD, and combining the two does not significantly improve the correlation to bone strength(Fig1.3A,B). The beam bone scores were strongly correlated with key measures of material behavior, such as toughness and ultimate stress (Fig1.4). Our results suggest that incorporating measures of bone quality with impact microindentation can improve fracture risk evaluation, particularly in high-risk fracture sites. Significance: IMI provides additional information on bone quality and identifies individuals at increased risk of fractures, allowing for earlier interventions to prevent fractures.

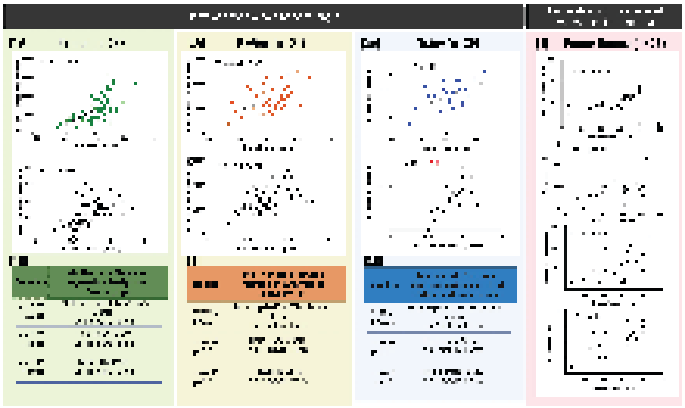

***Disclosures: Rachana Vaidya**, None*

SUN-038

Joint alignment angles and joint space width measured by EOS imaging for patients with an acute anterior cruciate ligament injury in the knee *Isabella Vandergaag[2], Richard Walker[2], Steven Boyd[2]. [2]University of Calgary, , [2]University of Calgary, Canada

The anterior cruciate ligament (ACL) is one of the most frequently injured ligaments among young, athletic individuals1. Many of these patients show early stages of osteoarthrosis (OA) at the 10-year mark following their injury2. Previous research suggests that anatomical factors, such as joint space width (JSW) and quadriceps angle (Q-angle), contribute to both ACL tear incidence and reoccurring injury. These anatomical factors may also contribute to worsening pain, motor functioning, and mental distress for patients during and post recovery3,4. However, there is limited investigation between these anatomical factors and effect on quality of life (QoL) outcomes during the immediate time following injury. Understanding the link between geometric factors and QoL could help develop interventions to prevent worsened clinical outcomes. The long-term purpose of this study is to identify whether JSW and Q-angle can predict the rate of QoL change following ACL injury in a longitudinal study, therefore we aim to determine the use of EOS imaging for measurement of these parameters.Our two cohorts included (1) uninjured individuals (N=30, 50% female) for reproducibility and repeatability of measurements of Q-angle and JSW, and (2) individuals who sustained an acute rupture of the ACL <6 weeks before imaging (N=41, 75% female). Q-angle and JSW was assessed for both populations with manual measurements, X-ray, and EOS Imaging. Wilcox statistical tests and Dunn tests compared the Q-angle and JSW between the two modalities and interrelationships were further explored by linear regression.The accuracy of Q-angle measurement from EOS imaging was confirmed in comparison to manual assessment in the uninjured cohort. Females had significantly higher Q-angle measured by both modalities. JSW assessed by EOS followed the same trends as measured by X-ray, although there was a bias for higher JSW by EOS. Furthermore, the EOS standing position, which is performed with the left leg unloaded, resulted in a significantly higher JSW measurement for uninjured participants in the left leg (Figure 1).We have established reproducibility of our measures of JSW and Q-angle and future work will establish the relationship of baseline anatomical factors to change in QoL measures to better understand their role in acute ACL injury.References1. Hughes G, et al. Sports Med. 2006, 36(5): 411-4282. Lohmander L, et al. Arthritis Rheum. 2004, 50(10): 3145-31523. Dai B, et al. Am J Sports Med. 2012, 40(12): 2756-27634. Palmieri-Smith R, et al. Clin Sports Med. 2008, 27(3): 405-424

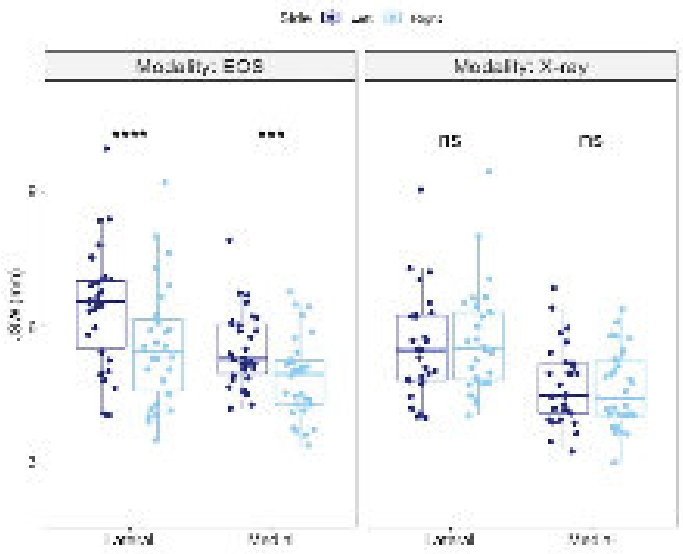

***Disclosures: Isabella Vandergaag**, None*

SUN-039

Comparing Atypical Femoral Fractures with and without bisphosphonate treatment. A case series on patient and fracture characteristics and histological findings. *Georg Zdolsek[1], Hans Peter Bögl[2], Anna Fahlgren[3], Jörg Schilcher[4]. [1]Department of Orthopedic Surgery and Department of Biomedical and Clinical Sciences, Faculty of Health Science, Linköping University, Linköping, Sweden , Sweden, [2]Department of Orthopedic Surgery, Gävle Hospital, Gävle and Department of Biomedical and Clinical Sciences, Linköping University, Linköping, Sweden, Sweden, [3]Department of Biomedical and Clinical Sciences, Division of Cell Biology, Linköping Universi-ty, Linköping, Sweden, Sweden, [4]Department of Orthopedic Surgery and Department of Biomedical and Clinical Sciences, Faculty of Health Science, Linköping University, Linköping, Sweden and Wallenberg Centre for Molecular Medicine, Linköping University, Linköping, Sweden , Sweden

Introduction: Atypical femur fractures (AFF) are insufficiency fractures with a strong association to antiresorptive treatment (ART). Little is known about patients with AFF who are ART naive. We have investigated clinical background, radiological appearance, and histological findings at the fracture site in patients with and without ART to provide insights into the underlying fracture pathophysiology.Method: Between 2008-2021, 19 patients (>50 yrs), with surgically treated incomplete AFF underwent surgical resection of the stress fracture lesion during nailing. Of the 19 patients, 9 (5 women) had no reported exposure to ART (-ART group, mean age 69.6 years, SD 12.4 years) and 10 (9 women, mean age 77.4 years, SD 10.5) had ART treatment (+ART group) on average 6.7 years, (SD 5.1 years). Hematoxylin and eosin staining was performed in all cases to allow basic histological assessment and histomorphometric analyses.Results: The common etiology for AFF in the +ART group was long-term bisphosphonate treatment. There were different etiologies in the -ART group (Paget's disease of bone N=1, adynamic bone disease N=1, hypophosphatasia N=1, coxa vara N=1, extensive lateral bow N=1, heavy loading N=1, unspecified N=3). Fractures in the mid-shaft region, were more frequent in the +ART group (N=9) compared to -ART (N=6) and multiple cortical lesions were more common in the -ART group (N=4) compared to +ART (N=2). The bone volume fraction (BV/TV) was lower in the -ART group, mean 72.0% (SD 7.6) compared to the +ART group, mean 81.3% (SD 5.4), mean difference -9.3% (95% CI -15.6% to -2.9%). There was no difference in specific surface of bone (BS/TV), percentage of alive osteocytes, mean width of fracture gap or bone surface per bone volume

(BS/BV).After surgical fixation all but two patients where the osteosynthesis was removed healed uneventfully. One patient with Paget's disease of bone had avascular necrosis of the femoral head after treatment for infection.Discussion and conclusions: Most patients without ART had an underlying bone metabolic disease which most likely caused the insufficiency fracture. These findings are supported by differences in radiological and histological findings. For a successful orthopedic treatment of AFF-patients with and without ART, a high level of suspicion for underlying bone metabolic pathologies or biomechanical variations is necessary.

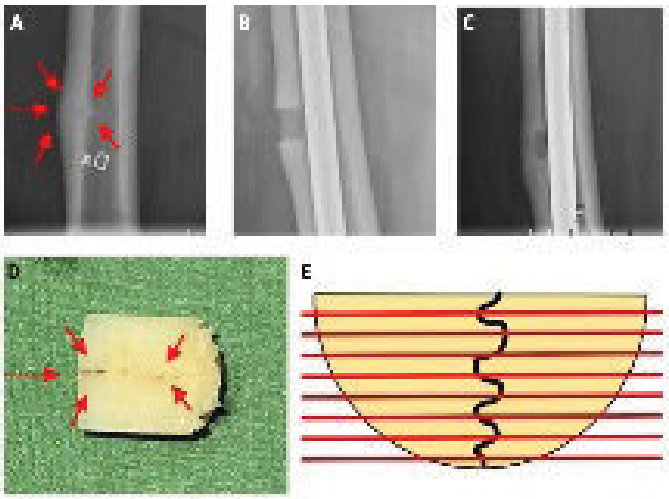

Biopsy preparation: A. Incomplete AFF, B. Cylindrical cortical defect after drill biopsy, C. Healed cortical defect after drill biopsy, D. Cylindrical biopsies cut in half, E. Plane of sectioning of the half cylinder

***Disclosures: Georg Zdolsek**, None*

SUN-040

Fracture Healing Leads to Localized Structural Bone Loss Quantified using Void Space Analysis *Danielle Whittier[1], Matthias Walle[2], Charles Ledoux[3], Penny Atkins[1], Caitlyn Collins[4], Julia Holtmann[5], Matthias Zumstein[6], Patrik Christen[7], Kurt Lippuner[8], Ralph Müller[3]. [1]Institute for Biomechanics, ETH Zurich; Department of Osteoporosis, University Hospital of Bern, Switzerland, [2]ETH Zurich, , [3]Institute for Biomechanics, ETH Zurich, Switzerland, [4]Virginia Tech, United States, [5]Department of Orthopaedic Surgery and Traumatology, University Hospital of Bern, Switzerland, [6]Department of Orthopaedic Surgery and Traumatology, University Hospital of Bern; Sonnenhof Orthopaedics, Bern, Switzerland, Switzerland, [7]Institute for Information Systems, FHNW, Switzerland, [8]Department of Osteoporosis, University Hospital of Bern, Switzerland

High-resolution peripheral quantitative computed tomography (HR-pQCT) has shown rapid changes in bone mineral density (BMD), morphology, and biomechanical properties at the distal radius during fracture healing. However, patient outcomes in terms of BMD are highly variable, suggesting that changes in bone microarchitecture may also play a role in patient-specific recovery and long-term bone strength. This study uses void space analysis to identify regions of adverse localized structural bone loss during fracture healing.Twenty-six patients (21 female, 5 male; aged 18-79 years) with conservatively-treated distal radius fractures were scanned using HR-pQCT (XtremeCT II, 61 µm) at 6 timepoints post-fracture (weeks 1, 3, 5, 12, 26, and 52). The common scan region across timepoints was determine using 3D rigid registration, and total BMD (TtBMD), bone volume fraction (BVTV), and void space volume faction (VSTV) were quantified at the first and last available timepoint for each participant. The cumulative formation of VSTV across sequential timepoints (termed void space expansion) was also quantified to capture structural voids that developed during fracture healing as opposed to those that arose due the fracture incident. Changes in BMD, BVTV, and VSTV between the first and last visit were compared using paired t-tests or Wilcoxon test, depending on data distribution.The median time of the first and last post-fracture visits were 1.1 weeks (IQR = 0.9-1.1) and 52.3 weeks (42.9-54.1), respectively. During this interval, VSTV increased five-fold in size from 1.0% (0.6-9.0%) to 5.5% (2.5-12.4%) (Figure 1A, p=0.01). Void space expansion occurred more rapidly in the first 26 weeks of fracture healing (Figure 1B) and did not necessarily occur in the immediate fracture region, but rather the surrounding area (Figure 1C). In contrast, TtBMD and BVTV did not significantly differ between the first and last study visits, where TtBMD was 283 +/- 55 mg HA/cm3 and 269 +/- 62 mg HA/cm3 (p=0.16) at the first and last visit, and BVTV was 42 +/- 2% and 41 +/- 2% (p=0.48) at the first and last visit, respectively.This study suggests that there may be adverse changes in bone microarchitecture during fracture healing, despite the potential preservation of overall TtBMD and BVTV in the fracture and surrounding region. The formation of void spaces may have long-term implications on patient bone strength and could provide insight into who is at risk of re-fracture.

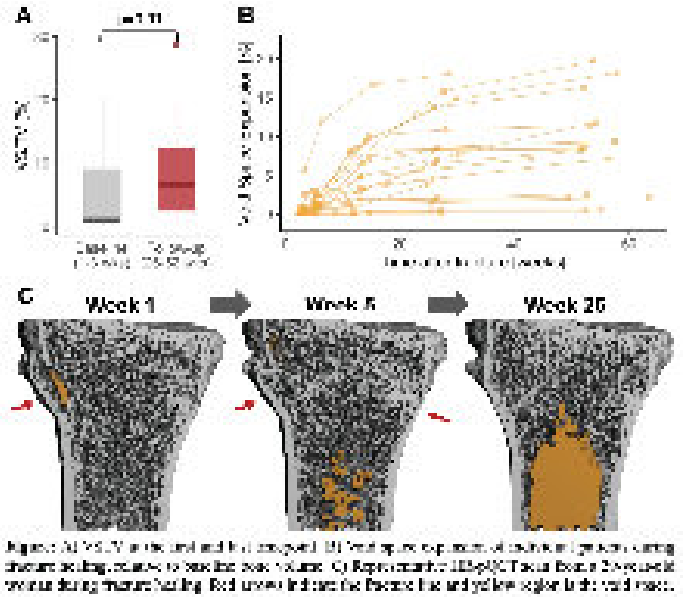

***Disclosures: Danielle Whittier**, None*

SUN-041

Nanoscale Material Properties of Bone Tissue Near Lacunae in Type-1 Diabetics *Maxwyll McConnell[1], Wen Qian[1], Joseph Turner[1], Eleftherios Paschalis[2], Sue Bare[3], Laura Graeff-Armas[4], Joan Lappe[3], Robert Recker[3], Mohammed Akhter[5]. [1]University of Nebraska Lincoln, United States, [2]Ludwig Boltzmann Institute for Osteology, Austria, [3]Creighton University, United States, [4]University of Nebraska Medical Center , United States, [5]Creighton University Osteoporosis Research Center, United States

The risk of skeletal fracture in Type-1 diabetes (T1DM) is much higher than in non-diabetics; however, the data comparing bone tissue's material properties are scarce. We hypothesized that bone quality (structural and material properties) in T1DM patients is compromised. Bone mineral density (BMD) does not explain the elevated fracture-risk in T1DM, and thus, studies characterizing intrinsic material properties in bone tissue are needed. This study quantified the intrinsic material properties of bone tissue at the peri-lacunar space (Figure-1).Using quasi-static nanoindentation, we quantified local/intrinsic material properties of reduced modulus (GPa) and hardness (GPa) in lacunae-near and lacunae-far regions in trabecular bone of the iliac crest bone biopsies from postmenopausal women diagnosed with T1DM (N = 8, T1DM Cases; duration of disease > 10 years), and age- and BMD-matched postmenopausal women controls (N = 4, Control). The lacunae-near region is defined as within 5 micrometers of a lacunae, and the lacunae-far region is from 15-25 micrometers (Figure-2. Indentations were made with a Berkovich tip & target force of 6,000 µN (micronewtons) at a constant loading rate of 400 µN/s (micronewtons per second). For each lacuna, 4 near and 4 far indentations were completed, providing 8 hardness and reduced modulus values. An average of 3 lacunae were analyzed one for each bone sample, with a total of 12 samples analyzed.Results: In trabecular bone tissue near peri-lacunar space, no significant difference between lacunae-near and lacunae-far hardness or reduced modulus within each group (Case, Control) was observed. Thus, the data (near and far) were combined within each group (Case, Control) and analyzed. The combined lacunae (Table-1) show significant difference ($P < 0.05$) in hardness and modulus between the Cases and Controls, both higher in Control (Table-1) compared to Cases (T1DM).These preliminary findings of increased modulus and hardness (peri-lacunar space) in T1DM samples are different from what was previously found at cement lines in the same biopsies and suggest that the lacunar-based mineral accumulation (based on diffusion) mechanism is different than the one governing either interstitial or cement lines. Moreover, they suggest potential canalicular network density differences between Cases and Controls. Additional work is needed to verify the mechanisms governing, and the properties of the bone tissue in the peri-lacunar bone tissue.

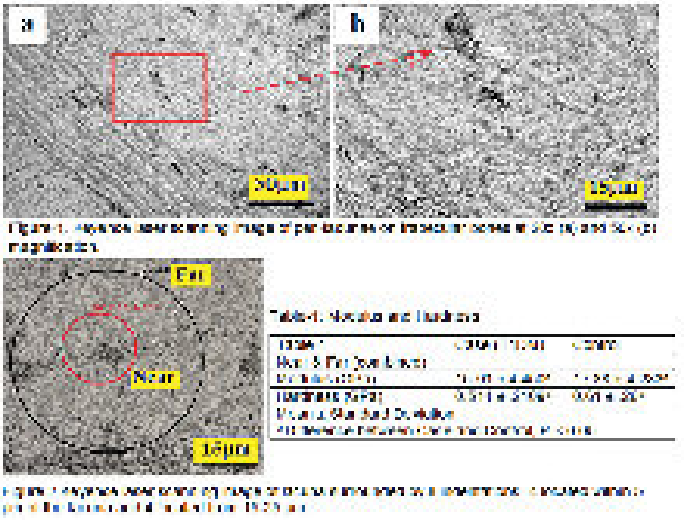

***Disclosures: Maxwyll McConnell**, None*

SUN-042

Improving the rigor of fully convolutional neural networks trained to segment cortical from trabecular bone in high resolution computed tomography images *ERIN BIGELOW[1], Robert Goulet[2], Bonnie Brooker-Nolan[3], Kathryn Kennedy[4], Chandan Kadur[3], James Bird[3], Samantha Hertz[3], Emily Wittrup[3], Kayvan Najarian[3], Todd Bredbenner[5], Karl Jepsen[3]. [1]UNIVERSITY OF MICHIGAN, United States, [2]Michigan Medicine, University of Michigan, United States, [3]University of Michigan, United States, [4]Marquette University, United States, [5]University of Colorado Colorado Springs, United States

Segmenting cortical from trabecular bone is a critical step in the rigorous morphological analysis of computed tomography images. As manual segmentation is impractical for high resolution nano/micro-computed tomography volumes of human femoral necks, a fully convolutional neural network (FCNN) was created using Dragonfly software (Object Research Systems, Inc; Montreal, CA) to reduce personnel time and improve segmentation objectivity. The initial cortical boundary was defined based on work by others that considered mineralized tissue with low porosity as cortical bone. This decision resulted in a 'low porosity-preserving' FCNN, allowing the cortex to thin as resorption-based pores accumulated. This FCNN followed strict and consistent boundary protocols. Ground truth images were created by three trained researchers identifying cortical bone for each slice, and including any voxel selected by at least two researchers. This FCNN utilized 149 slices for training, 17 for validation, and 20 for testing from 20 femoral neck volumes; the patch size was 144 and batch size was 16. The DICE coefficient for this FCNN was 0.98. Despite the high DICE coefficient, we created a quality improvement process to systematically fix errantly segmented voxels. This process resulted in additional slices of ground-truth quality images, which were used to update the FCNN. The updated FCNN used 321 slices from 51 femoral neck volumes, split 70/20/10% for training, validation, and test sets with a patch size of 192 and batch size of 64. The slices were rotated in three directions and added so the network was trained with key features in different orientations. The DICE coefficient was 0.97.To confirm the updated FCNN could be used without substantive error corrections, a study was conducted using 11 femoral neck volumes, comparing morphological parameters following an in-depth quality check to a quality check that removed false positive voxels only. The outcomes showed strong correlations for BV/TV ($R2=0.9915$, $p<0.0001$), Ct.Ar. ($R2=0.9741$, $p<0.0001$), and Tt.Ar. ($R2=0.9959$, $p<0.0001$), confirming the FCNN with minimal error corrections estimated morphological parameters accurately. Thus, we show that a FCNN can be trained to accurately segment cortical from trabecular bone in high-resolution images, saving countless hours in labor and simultaneously improving rigor. The updated FCNN is available for public use.

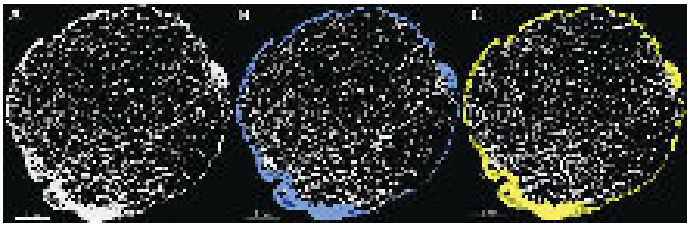

***Disclosures: ERIN BIGELOW**, None*

SUN-044

Mechanical Loading & Withdrawal Relative to Menarche: An Exploratory Application of SITAR Grouping Functions to Radius Adaptations during Human Growth *Jodi Dowthwaite[1], Laure Spake[2], Tim Cole[3], Tamara Scerpella[4]. [1]SUNY Upstate Medical University; Binghamton University, United States, [2]Binghamton University, United States, [3]University College London, United Kingdom, [4]University of Wisconsin, United States

Purpose: Mechanical loading may be osteogenic during growth, but adaptations vary by hormonal milieu. Few human studies have tracked loading and withdrawal relative to menarche to assess estrogen-loading interactions. We evaluated an extreme model of mechanical loading using SITAR group functions to compare growth curves in ex-gymnasts (EX: quit pre-menarche) and gymnasts (GYM: quit post-menarche) vs. the non-gymnast standard (NON), centered by individual ages at menarche. Peak growth velocity (PkV) and magnitude (SIZE) patterns were hypothesized as: 1) NON= late/low PkV, low SIZE; 2) EX= early/high PkV, medium SIZE; 3) GYM= early/high PkV, high SIZE.Methods: From 1997-2023, annual DXA scans yielded 1/3 & ultradistal (UD) radius bone mass, projected area, and areal bone mineral density [BMC (g), AREA (cm2), BMD (g/cm2)]. Age was centered by individual ages at menarche, recentered by grand mean age at menarche (13.2y), and LN-transformed for menarche-centered modeling. For each outcome, we used SuperImposition, Translation And Rotation (SITAR package: R) to model & compare growth curve parameters for EX & GYM vs. the NON standard. Loading was assessed via significant EX & GYM group regression terms for SITAR parameters [SIZE, TIMING, INTENSITY; alpha <=0.05].Results: Longitudinal data for 124 girls were restricted to age 8-<21y in the three groups [NON=61, EX=16, GYM=47]. EX/GYM TIMING showed early PkV for all UD outcomes and 1/3BMC, plus GYM 1/3AREA ($p<=0.05$). For both sites, GYM INTENSITY was higher for AREA & BMC (trend high BMD: $p<=0.20$). In contrast, EX UDBMD INTENSITY was lower (trend low UDBMC & 1/3BMD: $p<=0.14$). GYM SIZE was highest across all outcomes, while EX retained UDBMD SIZE benefits ($p<=0.05$) (EX trend high 1/3AREA, 1/3BMD: $p<=0.17$).Conclusion: Hypotheses were broadly supported, with loading through menarche conferring GYM advantages in bone geometry, mass, and density as SIZE (all), TIMING (all but 1/3BMD), and INTENSITY (all but BMD, both sites). EX & NON patterns suggest pre-menarcheal loading spurs earlier TIMING of radius PkV, while NON TIMING relies on an estrogen boost circum-menarche. In EX, pre-menarcheal loading withdrawal blunted PkV INTENSITY and tempered SIZE benefits, but small sample and heterogeneous loading challenged clarity of EX pattern definition. Furthermore, data were modeled as raw DXA output; thus, radius SIZE comparisons do not account for individual height or weight differences (GYM-EX-NON).

***Disclosures: Jodi Dowthwaite**, None*

SUN-045

Robotic Walking on Bone and Muscle Health in Children with Cerebral Palsy: A Case Study *Erin Hodgosn[1], Leigh Gabel[2], Elizabeth Condliffe[2]. [1]Univeristy of Calgary, Canada, [2]University of Calgary, Canada

Cerebral Palsy (CP) is the most prevalent childhood motor disability affecting ~2-3/1000 children. Weight-bearing physical activity is essential for developing a strong skeleton however, ~1/3 children with CP cannot walk independently, compromising bone health. As such, research into novel robotic trainers provides a promising opportunity for children with mobility impairments. Robotic gait trainers offer partial weight-bearing and independence while providing support and stability. Therefore, the aim of this study is to assess whether the Trexo robotic gait trainer provides sufficient loading to improve muscle and bone health in children with CP.Participants who are unable to walk in community settings are asked to train >=30 mins/day >=5 days/week walking in the Trexo. Bone and muscle health are measured through peripheral quantitative computed tomography (pQCT) prior to and following 3 months of training at the 3%, 38%, and 66% measurements of the participant's tibia. To differentiate between longitudinal growth and intervention effects, bone mineral density (BMD) and content (BMC) are expressed as age-specific z-scores based on normative pQCT data from a healthy population.To date, one 5-year-old male participant has completed baseline and follow-up scans. Trabecular BMD and total BMC at the 3% site were significantly lower compared with reference data in children without CP (-5.9 and -7.1 standard deviations below the mean, respectively). BMD increased by 9.3% (10.3 mg/cm3) at the 3% site with z-score improving to -5.4 at follow-up. BMC increased by 8.4% (4.1 mg/mm) over the trial period with an increase in z-score to -6.7 at follow up. We were unable to analyse the 38% and 66% slices due to significant motion artifact, which is a challenge studying this population. An improvement in BMD and BMC z-scores over 3-months at the distal tibia is encouraging; however, a greater sample size is needed to confirm if it is due to robotic gait training.Preliminary findings suggest the Trexo trainer may be a promising therapeutic device for improving bone health in populations with mobility challenges.

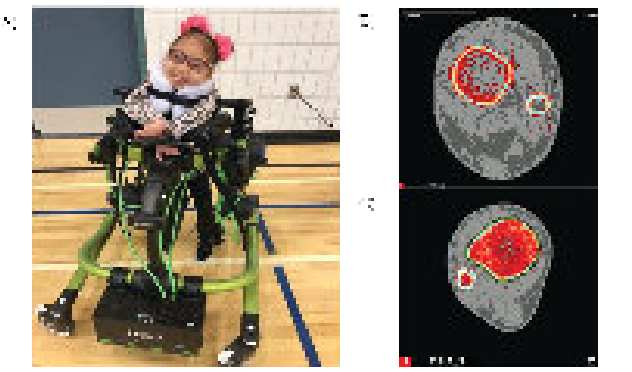

***Disclosures: Erin Hodgosn**, None*

SUN-046

Relative growth rates for height among children and adolescents living with HIV on antiretroviral therapy *Tafadzwa Madanhire[1], Victoria Simms[1], Nyasha Dzavakwa[1], Cynthia Mukwasi-Kahari[1], Rashida Ferrand[1], Nuredin Mohammed[2], Amy MacDougall[2], Kate Ward[3], Celia Gregson[4]. [1]Biomedical Research and Training Institute, Zimbabwe. [2]London School f Hygiene and Tropical Medicine, United Kingdom. [3]MRC Lifecourse Epidemiology Centre, University of Southampton, United Kingdom. [4]University of Bristol, United Kingdom

Purpose: Perinatally acquired HIV is a treatable chronic condition such that through antiretroviral therapy (ART), children with HIV (CWH) are now surviving to adulthood. However, CWH often exhibit impaired growth. We aimed to identify the height growth patterns among CWH and determine age at peak height velocity (PHV).Methods: This is a secondary analysis of data collected prospectively in the ongoing VITALITY randomised controlled trial in Zimbabwe and Zambia. The trial has recruited 840 CWH (11-19 years) established on ART for at least 6 months, to determine whether vitamin-D3/calcium supplementation improves bone mass and strength with follow up to 96 weeks. Height is measured at 12 week intervals with currently (31 March 2023) 135 participants having completed 96 weeks of follow up. Weight and height for age were calculated using 1990 UK reference values, with Z-score<=-2 classifying those underweight and stunted. Analysis of height trajectories was performed using the Superimposition by translation and rotation (SITAR) adjusting for size, pubertal timing and growth rate and fitting the mean and velocity curves by sex.Results: We recruited 447(53.2%) females and 393(46.8%) males and followed them up for 1.37(IQR:1.15-1.1.61) years; at baseline median(IQR) age was 15(13-17) years and 30.0%(n=252) were stunted. CHW were taking ART for median(IQR) 9.8(6.3-12.3) years of their lives and 81.9%(n=688) were on an ART regimen containing tenofovir disoproxil fumarate. Lifetime fracture prevalence was 5.9%(n=50). At baseline (n=840), mean(SD) height for age was -1.70(1.06) and -1.22(1.05) for males and females respectively. Over 48 weeks (n=780), median(IQR) height gains were 3.3(1.1-5.9)cm and 1.2(0.3-3.5)cm for males and females separately. Age at PHV was 15.0 years (PHV:8.2cm/year) and 13.2 years (PHV:5.6cm/year) for males and females respectively.Conclusions: There is a high prevalence of stunting among CWH in Zimbabwe. Both males and females showed delayed PHV compared to regional estimates (females:11.8, males:14.4 years), raising concerns for persistent height deficits in adulthood known to impact human capital and function in later life.

***Disclosures: Tafadzwa Madanhire**, None*

SUN-047

Bone Density in Children with Avoidant/Restrictive Food Intake Disorder - Preliminary Results from an Ongoing Cross-Sectional Study *Eugene Rodrick[1], Kaitlin Proctor[2], Staci Belcher[1], Janasha Goffigan-Holmes[2], Wang Shin Lei[1], William Sharp[2], Joseph Kindler[1]. [1]Nutritional Sciences, University of Georgia, United States. [2]Emory University School of Medicine and Children's Healthcare of Atlanta, United States

Avoidant/restrictive food intake disorder (ARFID) was added to the DSM-5 to characterize patients with severe food avoidance/restriction in the absence of fear of weight gain or body dysmorphia. A robust body of evidence indicates that eating disorders, namely anorexia nervosa, are associated with severe bone deficits, but few studies have evaluated effects of ARFID on bone health. We are currently conducting a cross-sectional pilot/feasibility study in children with ARFID to characterize effects on bone outcomes. Here, we report preliminary results from 7 children (4 males) who have completed study visits. Total body (TB; less head), lumbar spine, hip, and 1/3 radius bone mineral density (BMD) and bone mineral content (BMC) were assessed via dual-energy X-ray absorptiometry (DXA). Z-scores were computed using published pediatric growth charts, which were then adjusted for height-for-age Z-score (HAZ). DXA Z-scores were compared to an expected mean of 0 using one-sample t-tests. The study sample was approximately 9.2+/-4.4 years of age and had an average BMI and height Z-score of 0.57+/-0.70 and -1.2+/-1.4, respectively. TB BMC (-0.97+/-0.74), TB BMD (-0.87+/-0.76), and femoral neck (FN) BMD (-1.18+/-0.69) Z-scores were significantly lower than 0 (all P<0.05; Figure 1). Based on a standard normal distribution, it would be expected that ~16% of children from a healthy population would have a Z-score <-1.0, but in this sample of children with ARFID, about 50% (n=3/6), 33% (n=2/6), and 60% (n=3/5) of subjects had a Z-score <-1.0 for TB BMC, TB BMD, and FN BMD, respectively. HAZ-adjusted bone Z-scores did not differ from 0. Pearson's correlations revealed significant positive associations between BMI Z-score and TB BMC (r=0.85), lumbar spine BMC (r=0.81), and HAZ-adjusted lumbar spine BMC (r=0.87) Z-scores (all P<0.05). In summary, these preliminary results indicate that shorter stature and associated bone deficits may be present in children with highly restricted food intake characteristic of ARFID. We aim to enroll an additional 13 children with ARFID to achieve our intended sample size for this ongoing study, which also includes the use of high-resolution peripheral quantitative computed tomography. Ultimately, results from this study will help inform larger prospective studies to more clearly define effects of ARFID on peak bone strength and inform clinical screening guidelines and interventions.

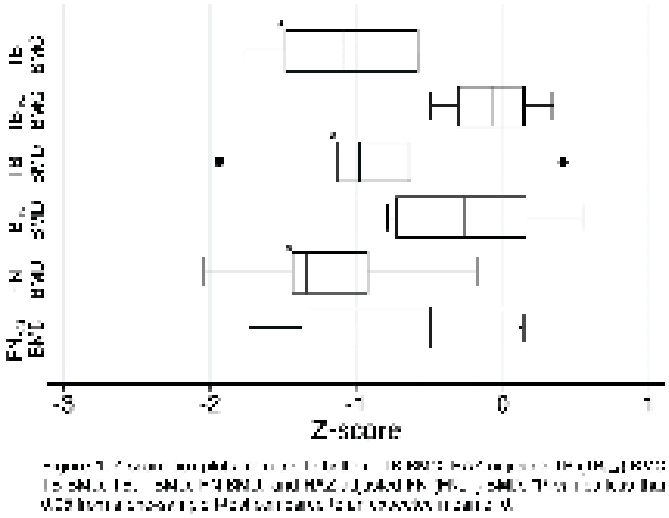

***Disclosures: Eugene Rodrick**, None*

SUN-048

Total Calcium Intake is Associated with Trabecular Bone Density in Adolescent Girls with Type 1 Diabetes *Rylee Saunders[1], Kathleen Kilroe[1], Taisha Joseph[1], Signe Caksa[1], Mary Bouxsein[2], Madhusmita Misra[3], Deborah Mitchell[4]. [1]Endocrine Unit, Massachusetts General Hospital, United States. [2]Beth Israel Deaconess Medical Center, Harvard Medical School, United States. [3]Neuroendocrine Unit, Massachusetts General Hospital, United States. [4]Pediatric Endocrine Unit, Massachusetts General Hospital, United States

Aim: Type 1 diabetes (T1D) confers an increased risk of fracture, lower bone mineral density (BMD), and altered microarchitecture early in the course of disease. Adequate calcium (Ca) intake promotes bone mineralization, thereby increasing BMD. The goal of this analysis was to assess the associations of total daily Ca intake with bone outcomes and compare these associations between T1D and control youth.Methods: This was a cross-sectional analysis of girls ages 10-16 years with (n=62) and without (n=60) T1D. We measured Ca intake with a validated food frequency questionnaire. BMD, microarchitecture, and strength estimates were evaluated with dual energy x-ray absorptiometry and high-resolution peripheral quantitative computed tomography.Results: T1D and control participants had similar age and height, but BMI z-score was higher in T1D (p=0.003). Total daily Ca intake did not differ between groups (950 +/- 488 in T1D vs. 862 +/- 461 mg/day in controls, p=0.306). Serum 25OHD was lower in T1D (26.3 +/- 7.6 vs. 32.6 +/- 9.0 ng/mL, p=<0.001) and PTH was higher in T1D (38.9 +/- 11 vs. 33.4 +/- 9.7 pg/mL, p=0.004). Trabecular volumetric BMD and thickness at the tibia were lower in T1D (p=0.013, p=0.030). Ca intake correlated with trabecular BMD at the radius and tibia among T1D participants (?=0.27, p=0.047, and ?=0.28, p=0.027, ?=0.28 respectively) but not among controls (pinteraction=0.009 at the radius, pinteraction=0.010 at the tibia). Similarly, Ca intake was associated with estimated failure load at the tibia in T1D but not control participants (p=0.038, ?=0.18; pinteraction=0.051). We observed the expected negative association of Ca intake with parathyroid hormone in control (p=0.022, ?=-0.29), but not in T1D participants (pinteraction=0.022). Average glycemia as measured by hemoglobin A1c did not influence the relationship of Ca and PTH among participants with T1D (pinteraction=0.138). Fasting urinary Ca excretion was lower in T1D compared to control participants (p=0.043); we do not have measures of urinary Ca in the fed state.Conclusions: Patients with T1D may be particularly vulnerable to

dietary Ca insufficiency. We hypothesize that the lack of PTH suppression with increasing Ca intake is due to excess urinary losses in the fed state, driving a higher Ca requirement in T1D. Ca intake may be a modifiable risk factor for low BMD among youth with T1D. Ongoing studies will further clarify the role of Ca balance on bone density and accrual in youth with T1D.

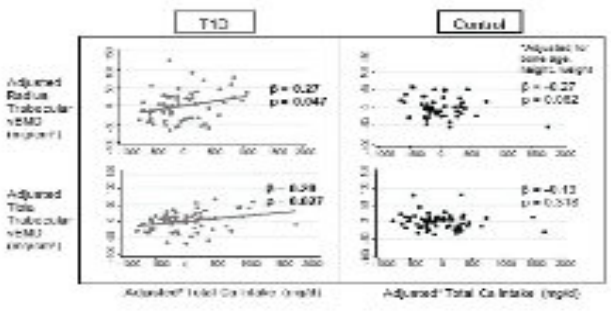

***Disclosures: Rylee Saunders**, None*

SUN-049

Duchenne Muscular Dystrophy and Risk of Fracture *kelly Fuentes[1], Rubén Abdala[1], María José Columbres[2], Bellén Della Pía[2], Stefanía Rapelius[2], Patricia Rearte[2], Oscar Brunetto[2]. [1]Instituto de Diagnóstico e Investigaciones metabólicas , Argentina, [2]División Endocrinología, Hospital Pedro de Elizalde , Argentina

DMD is a rare genetic disease characterized by progressive muscular dystrophy . A high risk of fractures was reported in a patient with DMD which could be due to inmobilization, the pathophysiology of the disease , treatment with glucorticoids (GCs) and increased BMI . Knowledge of the risk factors for the disease contributes to creating preventive strategies that reduce co-morbidities and improve the quality of life in these patients.Objetive: To assess the incidence of first fractures and factors contributing to risk of first fracture in children with DMDMaterials and methodsA retrospective analysis of a cohort of patients with Duchenne Muscular was carried out A total of 27 children under 18 years of age with clinical and molecular diagnosis of DMD were enrolled. The study was approved by the ethics committee and all procedures were performed following the Declaration of Helsinki. The study began in 2010, a total of 27 children were referred to our endocrinology service for their evaluation. Anthropometric variables were evaluated at the start of the study and during follow-up. In addition, annual spine radiographs were performed. Data on long bone (LBF) and vertebral fractures (VF) were recorded. Questionnaires about calcium intake and mobility were also administered. The variables are summarized in mean (SD), median (IQR) and percentage according to their nature.Results: The age of DMD diagnosis was 6.52+/-2.83y and the follow-up time was 7.77 (+/-4.57y).Age of starting GCs was 8.12+/-2.45y and average daily was 0.6+/-0.12 mg/k/d. 7 children with new fractures (VF or LBF) were observed during this period, median time 5.07 (RIQ 3-6.66y) .Cumulative incidences was 0.26 or 26%. Children with fractures presented a delay in the age of diagnosis (8 vs 5.5 y) and increased BMI (p=0.01). No differences were observed in biochemical markers, vitamin D, time and dose of corticosteroids between fractured and non-fractured.Conclusion: We observed a high incidence of fractures in this population, which highlights the importance of a multidisciplinary approach and the creation of strategies to reduce modifiable risk factors to improve the quality of life of these children.

***Disclosures: kelly Fuentes**, None*

SUN-052

Prunes: The Bone Building, Barrier Enhancing, Gut Microbiota Altering Super Prebiotic *NICK CHARGO[2], Kavisha Patel[2], Leon Regnery[2], Narayanan Parameswaran[2], Robert Quinn[2], Laura McCabe[2]. [2]Michigan State University, , [2]Michigan State University, United States

Osteoporosis affects 50% of women in the US. Drug therapies are effective but haven't eliminated this silent disease. Women of all ages are searching for natural treatment options to improve bone health that are convenient, cost effective, and side effect free. Our lab and others have established the gut microbiota and intestinal barrier as key regulators of bone health. Promoting gut health with probiotics or intestinal barrier enhancers effectively prevents several etiologies of bone loss. Prebiotics/fiber increase beneficial gut bacteria and improve overall gut health. Prunes, a common natural fruit and prebiotic, have emerged as an effective way to prevent primary osteoporosis and alter gut microbiota composition, though mechanisms aren't fully understood.Can prunes further benefit the skeletal health of healthy adult female mice? We hypothesized that a prune diet would alter gut microbial composition, improve intestinal barrier function and increase bone volume. To test this, 16-week-old female C57BL/6J mice (n=10/group) were fed control or 25% prune (w/w) AIN-93M diets. At 5d, 10d, 4wks, 8wks, and 16wks sterile blood, bones, and colonic feces were collected. Remarkably, after only 5d on the prune diet, distal femur trabecular bone showed a significant 30% increase in BV/TV% assessed by micro-computed tomography (C: 16.62, P: 21.66, p=0.0026). Strikingly, bone volume continued to increase in the healthy female mice to >300% by 16wks (p<0.0001). Gut responses to the prune diet were also immediate. Colonic microbiota composition (16S rRNA gene sequencing) was significantly altered at early time points, based on PERMANOVA testing of beta-diversity matrices (Pseudo-F=19.647, p=0.001), and changes were maintained at later timepoints. Most importantly, intestinal barrier leakage, determined by serum endotoxin levels, was significantly reduced by 50% (p<0.0001) in the prune diet group after 5d and this benefit was maintained or further improved at later timepoints. The relationship between barrier leaks and low bone density was significant (r=-0.5598, p=0.0103), and the benefit of the prune diet on barrier function was associated with further increases in bone volume. We believe this to be the first study to show that prunes rapidly improve intestinal barrier function and correspondingly increase bone volume in healthy adult female mice. Analyses are currently underway to better understand the osteogenic mechanisms of this delicious snack!

***Disclosures: NICK CHARGO**, None*

SUN-054

Osteoarthritis-Associated Acceleration of Cognitive Dysfunction in a Mouse Model of Alzheimer's Disease *Wei Yao[1], Barton Wise[2], Ming Fan[2], Jill Silverman[2], Michael Pride[2], Yu-Yang Lin[2], Gabriela Loots[3], Blaine Christiansen[2]. [1]University of California, Davis Medical Center, United States, [2]University of California Davis Health, United States, [3]University of California, Davis, United States

Alzheimer's Disease (AD) and osteoarthritis (OA) are two of the most common health conditions affecting the elderly. Several recent studies have described an association between OA and AD, suggesting that prevalent OA increases the likelihood of AD. In this study, we investigated the association between OA and the onset of cognitive dysfunction in a mouse model of AD. APP/PS1 double transgenic mice express a chimeric mouse/human amyloid precursor protein (APP) and a mutant presenilin 1 (PS1), two mutations associated with early-onset cognitive decline and amyloid plaque formation. ?-Amyloid (A?) deposits in the brains of these mice are present by 7 months of age, while cognitive deficits are observable by 9 months. We hypothesized that OA-associated inflammation would be associated with worse early onset cognitive decline in APP/PS1 mice. We subjected 7-month-old male and female APP/PS1-Tg mice and wild type (WT) littermate controls to tibial compression-induced ACL rupture and evaluated their behavior and cognitive function 6 weeks post injury. Knees were assessed with microCT and whole-joint histology to quantify OA, osteophyte formation, and synovitis. A?, Tau, and pTau levels in the brain and knees were measured with ELISA and Western blot. Neurobehavioral tests included open field, novel object recognition, spontaneous alteration, and Morris water maze. We found that ACL injury induced similar OA severity in both WT and APP/PS1 mice, though female APP/PS1-OA mice had greater osteophyte formation than WT-OA mice. In APP/PS1-OA mice, A? in the brain was significantly greater than in the APP/PS1-Sham mice, and A? was increased in femoral subchondral bone and articular cartilage. Cognitive declines were primarily observed in female APP/PS1 mice. In the open field test, female APP/PS1 mice exhibited decreased exploratory behavior compared to WT mice, but no significant differences were observed between OA and Sham mice. For the novel object recognition test, female APP/PS1-OA mice did not have a significant preference for the novel object as would be expected. Significant differences between WT and APP/PS1 mice were also observed during the acquisition phase and the testing phase of the Morris Water Maze test, though no significant differences were observed between Sham and OA mice. These results provide insights about the pathoetiology of both AD and OA and suggest possible common mechanisms connecting OA-associated inflammation to cognitive function.

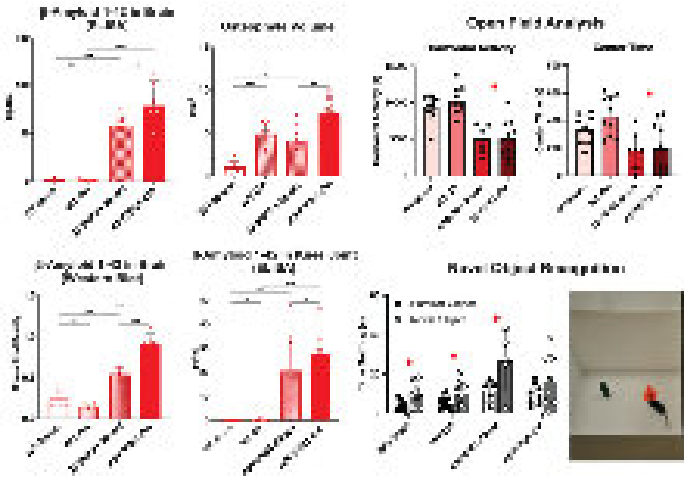

***Disclosures: Wei Yao**, None*

SUN-056

Fibroblast Growth Factor 23 and Physiological Responses to Phosphorus Intake in Pigs *Mariola Grez-Capdeville[1], Brittney P. Kokinos[1], Laura A. Amundson[1], Thomas D. Crenshaw[1]. [1]University of Wisconsin-Madison, United States

Fibroblast growth factor 23 (FGF23), is a bone-derived, protein hormone involved in the regulation of P homeostasis and vitamin D metabolism. FGF23 binds renal FGFR1c/?Klotho receptor complex to induce urinary P excretion and regulate the synthesis of active vitamin D. Biological roles of FGF23 were initially established in studies of humans with disorders of P metabolism and murine models. Pigs offer a large animal model for translational research on bone and mineral metabolism. This study aimed to validate the physiological roles of FGF23 on P metabolism in pigs. Dietary P was altered to assess the time course for synthesis and secretion of FGF23. Growing pigs (n=32) were fed a low P diet (LP, 0.34% P) for 4 days, fasted overnight, and then fed an excessive P diet (HP, 2.50% P) for 5 days. Blood and urine samples were collected throughout the experiment to determine concentrations of P. Pigs were euthanized (n=8/time) at day 4 of LP intake for assessments of baseline (0hr), and at 12, 36, and 108hr after consuming HP. Femur and kidney tissues were collected for assessment of P metabolism based on genes (RT-qPCR) and proteins (Western blot) of interest. Plasma P rapidly increased from approximately 5 to 18 mg/dl within 12hr of consuming HP followed by an increase in urinary P excretion. At maximal urinary P excretion (108hr), plasma P concentrations had recovered to normal physiological concentrations. Sodium-phosphate cotransporter (SLC34A1) protein decreased in pigs fed HP, confirming renal adaptations to P intake. Bone FGF23 mRNA expression was upregulated 20-fold after 12hr of HP relative to LP and reached a 150-fold increase by 108hr. The renal mRNA expression of FGFR1c increased slightly (1.5-fold) at 36hr of consuming HP. The ?Klotho mRNA was not affected by dietary P concentration. However, ?Klotho protein increased in response to HP. Changes in dietary P concentrations affected renal mRNA expression of vitamin D metabolizing enzymes by downregulating 1?-hydroxylase (CYP27B1) and upregulating 24-hydroxylase (CYP24A1) at 108hr. However, in bone, expression of CYP27B1 was not affected and CYP24A1 mRNA was downregulated in HP pigs. We conclude that dietary P induced FGF23 synthesis and that observed responses in pigs are consistent with phosphaturic effects of FGF23 in kidneys to maintain P homeostasis previously described for human and mice. Analyses to measure circulating concentrations of FGF23, PTH, and vitamin D metabolites are in progress.

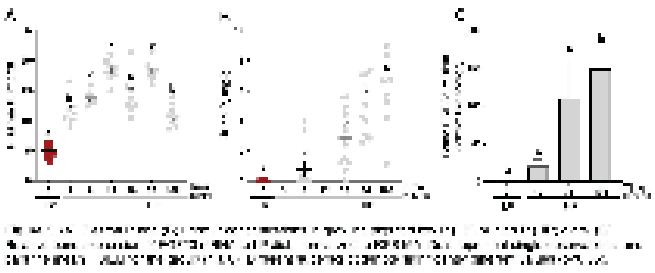

***Disclosures: Mariola Grez-Capdeville**, None*

SUN-057

Membrane Estrogen Receptor-? Signaling in POMC Neurons is Crucial for Normal Bone Metabolism in Female Mice *Yiwen Jiang[1], Karin Horkeby[1], Jianyao Wu[1], Karin Nilsson[2], PETRA HENNING[3], Sofia Movérare-Skrtic[4], Claes Ohlsson[5], Marie Lagerquist[4]. [1]Sahlgrenska Osteoporosis Centre, Centre for Bone and Arthritis Research at Institute of Medicine, Sahlgrenska Academy at University of Gothenburg, Sweden, Sweden. [2], Sweden. [3]UNIVERSITY OF GOTHENBURG, Sweden. [4]Medicine, Sweden. [5]Center for Bone and Arthritis Research at the Sahlgrenska Academy, Sweden

Estrogen receptor-? (ER?) signaling in the central nervous system is involved in the regulation of bone metabolism1,2. We have previously shown that deletion of ER?, specifically in proopiomelanocortin (POMC) neurons, increases bone mass and mechanical strength3. We and others have also revealed that membrane-initiated estrogen receptor-? (mER?) signaling plays an important role in regulating estrogenic effects in bone. However, it remains unknown whether mER? signaling in POMC neurons is involved in mediating estrogenic effects in bone.For this purpose, we have generated a novel ER?-C451Aflox/flox mouse model (C451Af/f) in which the C451A mutation disables the membrane localization of ER?. C451Af/f mice were mated with POMC-Cre mice to breed POMC-C451A mice, lacking mER? signaling in POMC-expressing neurons, and homozygous C451Af/f littermate controls.Phenotyping at 16 weeks of age showed multiple changes between POMC-C451A mice (n=8) and C451Af/f littermate controls (n=9). Areal bone mineral density (BMD), measured by DEXA, was significantly increased in POMC-C451A mice (total body, +5%, p<0.001; lumbar spine, +16%, p<0.001). Cortical thickness and trabecular BMD, measured by pQCT, were increased in long bones (cortical thickness: femur, +13%, p<0.001, tibia, +13%, p<0.001; trabecular BMD: femur, +32%, p<0.05, tibia, +29%, p<0.001). In addition, cortical bone in vertebrae L5 and bone volume fraction (BV/TV), measured by ?CT, were also increased in POMC-C451A mice compared with controls (BV/TV: +37%, p<0.001; cortical thickness: +18%, p<0.01). Uterus weight was unaffected in POMC-C451A mice, suggesting normal sex steroid feedback regulation.In conclusion, our study emphasizes the inhibitory effect of neuronal ER? signaling on bone mass, in contrast to the stimulatory bone effects by peripheral ER? signaling. This demonstrates that mER? signaling in POMC neurons plays an important role in this negative regulation of bone mass.Reference1. Herber CB, et al. Nat Commun, 2019.2. Ohlsson C, et al. Proc Natl Acad Sci U S A, 2012.3. Farman HH, et al. Endocrinology, 2016.

***Disclosures: Yiwen Jiang**, None*

SUN-059

Differential substrate utilization in isolated mitochondria from skeletal muscle of BNIP3 null mice *Rea Victoria P. Anunciado-Koza[1], Victoria Van Berlo[1], Li Tian[1], Calvin Vary[1], Carlos Gartner[1], Robert Koza[1], Anyonya Guntur[2]. [1]CMM, United States. [2]MaineHealth Institute for Research , United States

BNIP3 (Bcl2/adenovirus E1B 19 kDa like interacting protein3), a mitophagy receptor, is an important regulator of cellular function in response to stress. In muscle cells and myotubes, BNIP3 regulates mitophagy and is necessary for maintaining mitochondrial health. To characterize the role of this protein in regulating mitochondrial bioenergetics in the skeletal muscle, we isolated mitochondria from quadriceps femoris of male and female wildtype and Bnip3 KO mice. Next, we utilized a novel Percoll gradient mitochondrial isolation process that yields purified, ATP generation coupled mitochondria, which could be evaluated with the Agilent Seahorse XFe96 analyzer, and subsequently by SWATH liquid chromatography mass spectrometry, to determine mitochondrial respiration and mitochondrial protein expression, respectively. Mitochondrial coupling and electron flow assays using the XFe96 analyzer showed mitochondria derived from BNIP3 null muscle had similar responses to various substrate combinations, except for palmitate, where the mitochondria isolated from male BNIP3-null mice displayed a decrease in oxygen consumption rate. Furthermore, BNIP3 null mitochondria from both male and female mice showed higher activity of electron transport chain Complexes I, II and IV. SWATH proteomics identified a mitochondrial protein expression signature (~450 mitochondrial associated proteins quantified) that were significantly different in the absence of BNIP3 (fold change, Welch's t-Test; P<0.05). We validated selected proteins via western blotting. These data suggest dysregulation of mitochondrial metabolism as a potential mechanistic explanation for some of the metabolic phenotypes seen in the absence of BNIP3 in mice.

***Disclosures: Rea Victoria P. Anunciado-Koza**, None*

SUN-061

Deletion of Fra1 in osteoblasts by Runx2-Cre causes a reduced adipose tissue mass *Julia Luther[1], Mona Neven[1], Olga Winter[1], Lana Rosenthal[1], Michael Amling[1], Jean-Pierre David[1], Thorsten Schinke[1]. [1]Institute for Osteology and Biomechanics (IOBM), University Medical Center Hamburg-Eppendorf, Hamburg, Germany, Germany

The activator protein-1 (AP-1) transcription factor family member Fra1 has been described to cause increased bone mass and decreased adipose tissue mass when ubiquitously overexpressed in mice. Epiblast-specific deletion of Fra1 by More-Cre, conversely, caused

osteopenia due to a decreased bone formation rate. In vitro experiments with primary calvarial osteoblasts showed a reduced mineralizing activity. Osteoclast number and activity was not affected in vivo, however, osteoclasts showed a differentiation defect in vitro.To analyse the cell autonomous phenotype in vivo, we generated mice with an osteoclast- or an osteoblast-specific deletion of Fra1 (Fosl1) using LysM-Cre and Runx2-Cre, respectively. Deletion of Fra1 specifically in osteoclasts did not lead to a change in trabecular bone mass in 12-week- or in 1-year-old LysM-Cre;Fra1fl/fl mice compared to control animals (14.23+/-3.49% (control) versus 12.85+/-2.733% (LysM-Cre;Fra1fl/fl) at the age of 1 year). In addition, osteoclast number per bone perimeter was not affected in young mice (N.Oc/B.Pm: 4,307+/-1,86mm-1 (control) versus 4,928+/-1,42mm-1 (LysM-Cre;Fra1fl/fl)), confirming that Fra1 is not necessary for osteoclast differentiation in vivo. When deleting Fra1 in osteoblasts no significant change in bone mass was observed in 12-week as well as 1-year-old Runx2-Cre;Fra1fl/fl compared to control mice (15.53+/-2.243% (control) versus 13.36+/-0.7766% (Runx2-Cre;Fra1fl/fl) at the age of 1 year). Furthermore, the number of osteoblasts was unchanged in 12-week-old mice (N.Ob/B.Pm: 32,24+/-6,54mm-1 (control) versus 39,38+/-9,66mm-1 (Runx2-Cre;Fra1fl/fl)). However, we could observe a significantly reduced adipose tissue mass accrual in mice with an osteoblast-specific deletion of Fra1, accompanied by a lack of increase in adipocyte cell diameter in 1-year-old Runx2-Cre;Fra1fl/fl mice. Thus, Fra1 expression in Runx2-Cre positive pre-osteoblasts regulates adipose tissue metabolism. In contrast, the bone-anabolic function might be driven by Fra1 expression in early mesenchymal osteoblast progenitors rather than in committed pre-osteoblasts.

***Disclosures: Julia Luther**, None*

SUN-063

Evidence of age-relate bone alterations in a mouse model of Alzheimer's disease *Surendra Kumar[1,] Mei Wan[1,] Ching-Lien Fang[1,] Jiekang Wang[1,] Xu Cao[2,] Janet Crane[2,] Shadpour Demehri[3,] Richard Skolasky[3,] [1]Department of Orthopedic Surgery, Center for Musculoskeletal Research, Johns Hopkins University School of Medicine, Baltimore, Maryland 21205, USA., United States, [2]Johns Hopkins University, United States, [3]Center for Musculoskeletal Research, United States

Osteoporosis and dementia, two common degenerative diseases in the elderly population, often occur simultaneously. Reduced bone mineral density and osteoporosis occur at a much greater rate in patients with Alzheimer's disease (AD), often emerging in the disease before the appearance of significant cognitive decline. Although it is known that the brain regulates bone homeostasis and regeneration, there is limited research investigating bone alterations and how the changes in relation to brain degeneration in mouse models of AD. In this study, we conducted a systemic characterization on the bone phenotype in parallel of brain changes in APPswe/PS1dE9 (APP-PS1) transgenic mice, a well-established mouse model of AD Alzheimer's disease. We found that 9-month-old APP-PS1 mice developed brain degeneration, neuroinflammation, and cognitive impairment, as evidenced by accumulated A? plaque, increased numbers of activated microglia and astrocytes, neuron loss, and declined cognitive functions. Micro-CT analysis of tibial bone samples from 9 month-old APP-PS1 mice and age-matched wild-type littermates (WT) revealed a low-bone-mass phenotype in APP-PS1 mice, characterized by significantly lower bone volume/tissue volume (BV/TV), trabecular thickness (Tb.Th), trabecular number trabecular number (Tb. N), and an increase in trabecular separation (Tb.Sp) relative to wild-type littermates (WT). Cortical bone volume and cortical thickness of tibia were not significantly different in APP-PS1 mice compared to WT mice. Histomorphometry analysis showed a lower osteoblast cell numbers per bone surface (N. Ob/BS) and an increase in osteoclast number per bone surface (N. Oc/BS) in APP-PS1 mice compared to the control group. Moreover, we found a markedly increased bone-marrow adipose tissue in APP-PS1 mice vs. WT mice, as evidenced by higher adipose tissue volume per total volume (%AV/TV) detected by ?CT scan of the osmium tetroxide-stained bone tissue. Consistently, there is increased perilipin+ adipocytes in the bone marrow of APP-PS1 mice vs. WT mice as detected by immunofluorescence staining of tibia bone tissue sections. Together, these findings demonstrate that AD mice have significant bone microarchitectural and cellular changes, which recapitulate age-related bone phenotype. The finding also illuminates a need to define a mechanistic relationship between bone loss and brain deficits in early AD.

***Disclosures: Surendra Kumar**, None*

SUN-064

TERT and STAT5 initiate the osteogenic differentiation of cells in calcific aortic valve disease *Cynthia St. Hilaire[1,] [1]University of Pittsburgh, United States

Calcific aortic valve disease (CAVD) is the pathological remodeling of the aortic valve leaflets which leads to heart failure and high stroke risk. While several mechanisms are known to drive cardiovascular calcification, the initial steps orchestrating the osteogenic reprogramming of cells are not fully understood. Previous studies have shown that over expression of telomerase reverse transcriptase (TERT) primes mesenchymal stem cells to differentiate into osteoblasts. While TERT is best known as the enzymatic cofactor to the telomerase complex that caps telomeres at the end of chromosomes, non-canonical transcriptionally regulatory functions of TERT have been identified. We investigated whether TERT contributes to osteogenic reprogramming of valve interstitial cells. Immunofluorescent imaging revealed that TERT protein was highly expressed in calcified valve leaflets. These phenotypic features were retained in primary valve interstitial cells (VICs) isolated and cultured from diseased tissues. In vitro disease modeling found that TERT levels were increased with osteogenic or inflammatory stimuli, and genetic deletion or reduction of TERT prevented calcification of VICs. Similar results were seen in coronary artery smooth muscle cells (CASMCs) and mesenchymal stem cells (MSCs). In silico analysis of the Runt-Related Transcription Factor 2 (RUNX2) gene promoter identified several putative binding sites for the transcription factor STAT5. Immunofluorescent staining, immunoprecipitation, and proximity ligation assays show that TERT and STAT5 protein colocalize in cells under osteogenic treatment. STAT5 binding to the RUNX2 gene promoter was confirmed with chromatin immunoprecipitation and Cut&Run sequencing. TERT and STAT5 were also found to co-localized in calcified valve tissues. Genetic depletion of TERT or STAT5, as well as pharmacological inhibitors specific for STAT5 prevented calcification of VICs, CASMCs, and MSCs in vitro. Cells from Tert+/+ and Tert-/- mice were used to validate human findings. Together, these data show that TERT in conjunction with STAT5 initiate the osteogenic transition of cardiovascular cells and identify a novel therapeutic target to abate vascular calcification.

***Disclosures: Cynthia St. Hilaire**, None*

SUN-065

Dose Response Effects of Leptin on Polyethylene Particle-Induced Calvarial Osteolysis and Systemic Bone Loss in Leptin-Deficient ob/ob Mice *Russell T. Turner[1,] Kenneth Philbrick[1,] Adam Branscum[1,] Urszula Iwaniec[1,] [1]Oregon State University, United States

Particles generated from wear of prosthesis joint-bearing surfaces (often polyethylene) induce inflammation-mediated periprosthetic bone resorption (osteolysis), a risk factor for implant failure. Additionally, circulating wear particles may induce systemic bone loss. While obesity is a risk factor for implant failure, morbidly obese leptin-deficient ob/ob mice are resistant to osteolysis induced by polyethylene particles placed over their calvaria. Leptin increased osteolysis in ob/ob mice suggesting that the adipokine, an important immune modulator produced by adipocytes in proportion to fat stores, may contribute to implant failure. To investigate this possibility, we performed two dose response studies. In the first study, we administered leptin via s.c. implanted osmotic pumps to 6-week-old female ob/ob mice for 2 weeks at 12, 120 or 400 ng/hr (n=8/group). Compared to untreated ob/ob mice (n=8), changes in cancellous bone volume/tissue volume (BV/TV) were not observed for distal femur metaphysis or 5th lumbar vertebra (LV5). Compared to wild type (WT) mice (n=8), serum leptin was normal in ob/ob mice treated with 120 ng/hr leptin and ~2-fold higher in mice treated with 400 ng/hr. In the second study, polyethylene particles were implanted over calvaria of ob/ob mice. The treatment groups (n=7-10/group) consisted of no treatment, particles, and particles + leptin (12, 120 or 400 ng/hr). Osteolytic bone pitting was not observed in control mice but was present in particle-treated mice. Compared to particle-treated mice, bone pitting was higher in calvaria of mice administered leptin at 120 ng/hr but no further increase was observed at 400 ng/hr. BV/TV was higher in distal femur metaphysis and LV5 in untreated mice when compared to particle-treated mice. In contrast, BV/TV was lower in distal femur metaphysis and LV5 in mice infused with 400 ng/hr leptin but unchanged at lower dose rates. In summary, leptin had no effect on BV/TV in ob/ob mice evaluated 2 weeks following initiation of leptin treatment. Calvarial osteolysis and systemic bone loss were observed in ob/ob mice following particle challenge. Increasing serum leptin to WT levels resulted in an increase in calvarial osteolysis and hyperleptinemia resulted in an increase in systemic bone loss. Taken together, these findings suggest that leptin, while not required for polyethylene particle-induced osteolysis and systemic bone loss, may contribute to implant failure in obese subjects.

***Disclosures: Russell T. Turner**, None*

SUN-067

IL-34 mediated osteolysis exacerbates pathogenic features of Alzheimer's disease *Anny Ho[4,] CHIAKI YAMADA[2,] Bidii Ngala[3,] Amilia Nusbaum[3,] Carolina Duarte[4,] Juliet Akkaoui[5,] Christopher Michael Garcia[6,] William Kochen[4,] Alexandru Movila[3,] [4]Nova Southeastern University, United States, [2], , [3]Indiana University School of Dentistry, United States, [4]Nova Southeastern University, , [5]Florida International University, United States, [6]Indiana University School of Medicine, United States

Alzheimer's disease (AD) is characterized by progressive neurodegeneration and a gradual decline in memory and cognitive functions. The hallmark features of AD are associated with elevated accumulation of aggravated amyloid beta (A?) peptides, hyperphosphorylated Tau (p-Tau), and neuroinflammation. Emerging evidence indicated that inflammatory osteolysis exacerbates AD neurodegeneration and neuroinflammation via unknown molecular mechanisms. Signaling through the colony-stimulating factor-1 receptor (CSF-1r) is critical for maintaining the physiological and pathological signaling of blood myeloid cells and microglia. CSF-1r is activated by macrophage colony-stimulating factor-1 (M-CSF) and interleukin-34 (IL-34). While the impact of M-CSF in bone physiology and pathology is well addressed, it remains controversial whether IL-34-mediated bone osteolysis promotes AD neuroinflammation and neurodegeneration. Surprisingly, we observed that IL-34 plays a critical role in inflammatory osteolysis in wild-type mice. To evaluate the effects of IL-34 on AD cognitive behavioral phenotype and neuroinflammation, female and male triple transgenic 3x-Tg AD mice and corresponding control were randomly divided into two experimental groups (10 mice/sex/group). Mice were subcutaneously injected with 100 µl of

mouse recombinant IL-34 protein solution in PBS or PBS alone over the calvaria bone every other day for 42 days. In addition, we compared the effects of IL-34 and M-CSF on macrophages, microglia, and RANKL-mediated osteoclastogensis in relation to AD pathology. This study demonstrated that local calvaria injection of recombinant IL-34 protein dramatically elevated AD-like memory loss, pathogenic amyloidogenesis, p-Tau, and neuroinflammation-associated RAGE expression in female 3x-Tg mice. Furthermore, IL-34 promoted calvaria inflammatory osteolysis compared to the sham control injected group of female and male mice. Our data also indicated that IL-34-microglia and bone-marrow-derived macrophages isolated from 3x-Tg mice released significantly higher amounts of pro-inflammatory cytokines, TNF-?, IL-1?, and IL-6, compared to M-CSF-proliferated cells in vitro. In addition, IL-34 elevates RANKL-primed osteoclastogenesis in the presence of key AD-associated A?40 and A?42 peptides. Therefore, our data indicated that a novel therapeutic regimen targeting IL-34 could suppress neuroinflammation, neurodegeneration, and elevated bone loss observed in patients with AD.

***Disclosures: Anny Ho**, None*

SUN-068

Angiotensin-(1-7) attenuated LPS-induced osteoclastogenesis and bone resorption via inhibiting the activation of MAPK pathway in macrophages
*Jiayi Ren[1], Hideki Kitaura[1], Takahiro Noguchi[1], Fumitoshi Ohori[1], Aseel Marahleh[3], Jinghan Ma[1], Kayoko Kanou[1], Mariko Miura[1], Kohei Narita[1], Itaru Mizoguchi[1], Aseel Marahleh[0]. [1]Division of Orthodontics and Dentofacial Orthopedics, Tohoku University Graduate School of Dentistry, Japan. [3]Tohoku University, Japan. [0]Frontier Research Institute for Interdisciplinary Sciences, Tohoku University, Japan

Renin-angiotensin-aldosterone system plays a crucial role in regulation of blood pressure and fluid homeostasis. It is reported to be involved in mediating bone-related inflammatory diseases such as osteoporosis. Angiotensin-(1-7), as a well-studied component of RAS recently, is a product of Angiotensin I and II (Ang I, II) cleaved by Angiotensin-converting enzyme 2 (ACE2), binds to Mas receptor (MasR) to counteract inflammatory effects produced by Ang II. However, it remains unclear whether Ang-(1-7) reduces bone resorption by inhibiting osteoclastogenesis. Therefore, the objective is to elucidate the effects of Ang-(1-7) on inflammation-induced osteoclastogenesis. In vivo, mice were supracalvarial injected with Ang-(1-7) or LPS +/- Ang-(1-7) subcutaneously. Micro-CT, tartrate-resistant acid phosphatase (TRAP)-stain and real-time PCR were applied to compare bone resorption and osteoclast formation. In-vitro, RANKL/TNF-? +/- Ang-(1-7) were added to cultures of bone marrow-derived macrophages (BMDM) and osteoclast formation was measured via TRAP staining. The effects of Ang-(1-7) on LPS-induced osteoblasts RANKL expression and peritoneal macrophages TNF-?, IL-6 expression were also investigated. Signaling fluctuation in mitogen-activated protein kinase (MAPK) pathway was studied using Western blot. Consequently, in vivo, Ang-(1-7) attenuated TNF-?, TRAP and Cathepsin K expression from calvaria, and decreased osteoclast number along with bone resorption at the suture mesenchyme. In vitro, Ang-(1-7) tended to reduce LPS-stimulated macrophages TNF-? and IL-6 expression. Additionally, Ang-(1-7) did not inhibit osteoclastogenesis induced by RANKL/TNF-? nor reduce osteoblasts RANKL expression. Ang-(1-7) attenuated the phosphorylation of P38, ERK1/2 in MAPK pathway in LPS activated macrophages. The results suggested a further study in cell-cluster of which affected by Ang-(1-7) during inflammation related bone diseases.

***Disclosures: Jiayi Ren**, None*

SUN-069

Impact of sex hormone deficiency in mice expressing the Alzheimer´s disease-associated risk-factor TREM2 R47H variant in a sex and genotype dependent manner
*JULIAN BALANTA-MELO[1], Padmini Deosthale[2], Rachel Kohler[3], ALYSON ESSEX[4], Chiebuka Okpara[5], Matthew Arnett[2], Madison Gerbig[2], Joseph Wallace[6], Lilian Plotkin[2]. [1]Universidad del Valle, Colombia. [2]Indiana University School of Medicine, United States. [3]Biomedical Engineering, IUPUI, United States. [4]Indiana University , . [5]Lehigh University, United States. [6]Indiana University Purdue University Indianapolis (IUPUI), United States

Expression of the R47H variant of the Triggering Receptor Expressed on Myeloid Cells 2 (TREM2), a risk factor for Alzheimer´s disease in humans and leads to lower bone mass and strength in female but not male 13-month (mo) mice, compared to wild type (WT) littermates. To assess if, as with aging, gonadectomy (GNX) leads to sex-specific musculoskeletal effects, gonad removal or SHAM surgery were performed in 4mo TREM2R47H/+ mice and WT littermates (N=10-12/group). Body weight (BW), BMD and body composition (DXA) were assessed at baseline (0), 3 and 6 weeks (w) post-surgery, and plasma P1NP and CTX at 3 and 6w. After euthanasia at 6w, hindlimb muscles were weighted and femora were tested by µCT, histomorphometry and 3-point bending test. Sexes were analyzed separately by 2-Way ANOVA followed by post hoc multiple comparisons (see Table). At 6w, GNX led to lower BW in males, higher lean mass in females, and higher fat mass in both sexes, independent of the genotype. Also, GNX reduced spine/femur BMD in SHAM R47H males at 3w and total/spine/femur BMD at 6w for all sex/genotypes, compared to baseline. When compared to SHAM mice, GNX led to lower Quadriceps weight in WT males and Quadriceps and Tibialis anterior (TA) in R47H males, whereas it did not change muscle weight in WT females but led to higher TA and Gastrocnemius weight in R47H female mice. Microstructural analysis of femur showed that GNX resulted in lower BA/TA (cortical mid-diaphysis) and Tb.Th (distal) in WT and R47H males, respectively. Moreover, sex hormone deficiency led to lower Ct.Th, BV/TV and Tb.N, and higher Tb.Sp, in WT/R47H males and WT females, but not R47H females. Interestingly, GNX resulted in higher marrow cavity area only in R47H females. Bone formation parameters from femoral mid-diaphysis showed that WT/R47H males and WT females that underwent GNX exhibited lower periosteal MAR and BFR/BS, with no changes in endocortical bone formation or osteoclast-related parameters. At 6w compared to 3w, circulating resorption/formation markers were higher in SHAM/GNX WT males (CTX-I) and SHAM WT females (P1NP) and lower (CTX-I, P1NP) in GNX WT females. GNX also led to sex-dimorphic effects on femur biomechanical properties, with worsening effects in R47H mice and improved parameters in mutant females (Table 1). Thus, R47H TREM2 variant expression is a risk factor that worsens sex hormone deficiency impact in the musculoskeletal system in males, whereas it has a protective role in female mice.

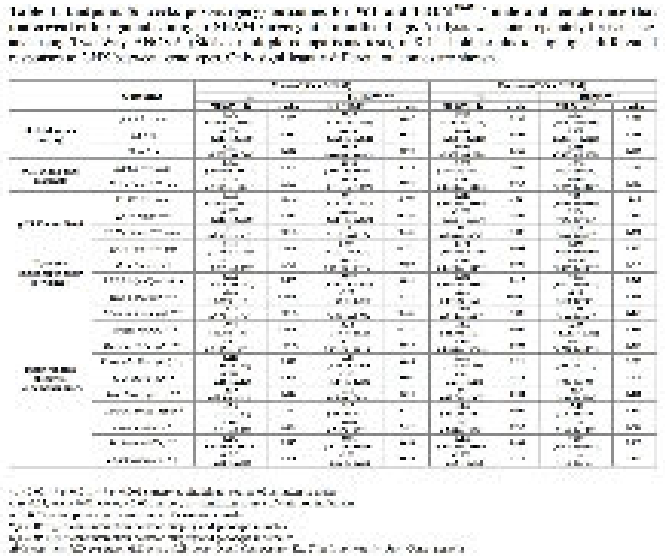

***Disclosures: JULIAN BALANTA-MELO**, None*

SUN-071

Difference between TBS and HR-pQCT in a group of patients with acromegaly
*Mariana Soledad Gonzalez Pernas[1], Fernando Jerkovich[1], Gloria Tubert[2], Debora Katz[3], Dolores Clifton Goldney[1], Patricia Slavinsky[3], Karina Danilowicz[4], Vanesa Longobardi[1], Mariela Sesta[1], Maria Belen Zanchetta[1]. [1]IDIM, Argentina. [2]Hospital Gral de Agudos “Dr. Fernandez”, Argentina. [3]FLENI, Argentina. [4]Hospital de Clinica ‘Jose de San Martin”, Argentina

Introduction: Clinical guidelines suggest performing spinal RX and DXA in acromegalic patients due to the high prevalence of vertebral fractures (VFx) in this population. Trabecular and cortical bone microarchitecture deterioration could better explain the occurrence of these fractures. A prospective study was designed to describe bone and muscular quality in a group of patients with acromegaly. The aim of this cross-sectional analysis was described baseline characteristics of the first female patients included.Methods: Clinical features, BMD and TBS measured by DXA (spine and hip), bone microarchitecture by HR-pQCT) and spine RX or VFA were assessed. The results of HR-pQCT were compared with a control population. A normal IGF-1 value without treatment was defined as remission, controlled disease with normal IGF-1 value under treatment and active disease with elevated values of IGF-1.Results: The first 22 women were included for this analysis; median age was 57 (23-84) yo. Only 4 patients were pre-menopausal. Regarding acromegaly status, 5 were in remission, 13 with controlled disease and 4 actives. None of the patients reported a history of vertebral fracture, 4 VFx were diagnosed in 2 patients. Mean DXA values were within the normal range as follow: LS 1.230+/-0.197g/cm2, TS 0.3+/-1.6, ZS 1+/-1.8; FN 0.942+/-0.157g/cm2, TS -0.7+/-1.2, ZS 0.4+/-1.2. One patient had osteoporosis and 5 patients with osteopenia. Mean TBS value was 1.398+/-0.113 within the normal range. Only 4 patients reported values below the normal range, but very close to the limit of normality (0.8 ULN). Significant trabecular parameters deterioration was found in most patients: total BMD was higher than expected, at the expense of increased cortical density that masks the decrease in trabecular volume and bone density, mainly due to a decrease in trabecular thickness (Table 1). The patients with VFx showed normal TBS values (1.365; 1.491) and abnormal values of trabecular parameters (Radius Tb.BMD: 79, 111; Tb.BV/TV: 6.6, 9.3 - Tibia Tb.BMD: 99,89; Tb.BV/TV: 8.3, 7.4) in HR-pQCT analysis.Conclusions: In this preliminary report, although BMD and TBS values by DXA were within the normal range, trabecular bone microarchitecture was much more severe than expected. A significant trabecular bone compromise with indemnity of cortical compartment was found both in radius and tibia. Specifically

in patients with VFx, TBS measured by DXA did not identify trabecular involvement and was evidenced by HR-pQCT.

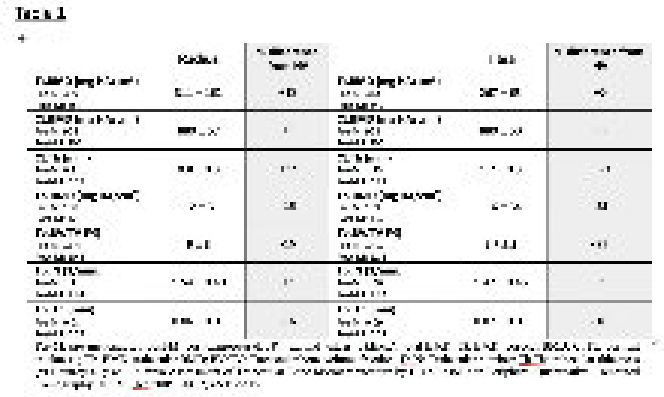

***Disclosures: Mariana Soledad Gonzalez Pernas**, None*

SUN-072

Effects of antiemetic dexamethasone therapy on bone health in cancer patients receiving systemic chemotherapy *A Ram Hong[1.] [1]Chonnam National University Medical School, Republic of Korea

Objective: Chemotherapy-related nausea and vomiting is a critical issue in cancer patients. Dexamethasone plays an important role in mitigating chemotherapy-induced emesis because of its proven benefit in clinical trials, widespread availability in oral form, and low cost. Here, we aimed to investigate the effect of dexamethasone therapy as an antiemetic agent on bone health in patients with solid cancer undergoing systemic chemotherapy. Methods: This study included postmenopausal women and men aged 70 years or older with solid cancer who had been receiving systemic chemotherapy for at least 6 months at Chonnam National University Hwasun Hospital, which included dexamethasone at a dose of 8 mg or more every cycle as an antiemetic agent. Patients receiving anti-osteoporosis treatments, newly diagnosed osteoporosis at baseline, and a history of corticosteroid use within 6 months were excluded. Bone mineral density (BMD) of the lumbar spine (L1-4), femoral neck, and total hip was measured using dual-energy X-ray absorptiometry at baseline and 6 months after chemotherapy. Results: A total of 106 patients from May 2022 through Mar 2023 were included in the analysis. The mean age of the patients was 69.6 +/- 9.5 years, and men comprised 63.2% of the patient population. At baseline, 42.5% had normal BMD and 57.5% had osteopenia according to WHO criteria. Only 1 patient had a history of fragility fracture, and none of them had radiological vertebral fracture at baseline. Twenty-seven of 106 patients were included in the 6-month longitudinal analysis. Of those, 40.7% received calcium and vitamin D supplements during chemotherapy. The mean total dose of dexamethasone was 93.6 +/- 21.1 mg. At 6 months, femoral neck and total hip BMD significantly decreased from baseline with least significant mean changes of -0.026 and -0.044, respectively (P=0.002 and P=0.014, respectively). Lumbar spine BMD did not differ between baseline and 6 months after chemotherapy (least significant mean change of -0.017, P=0.069). Conclusion: Antiemetic dexamethasone therapy, indicative of cyclic glucocorticoid administration, resulted in significant bone loss during 6 months of chemotherapy in patients with solid cancers, especially in regions rich in cortical bone.

***Disclosures: A Ram Hong**, None*

SUN-073

High-Resolution Peripheral Quantitative Computed Tomography (HR-pQCT) as a new Method for Human Osteoarcheology *Peter Herbert Kann[1.] Tanja Pommerening[1.] Rainer Brömer[1.] Christopher John[1.] Peyman Hadji[1.] [1]Evolutionary Osteology Working Group, Philipp's University Marburg, Germany, Germany

In (pre)historic human bones, analysis of bone density and microstructure may be useful for anthropological research to assess skeletal health as well as physical fitness and handedness. Physical strain between arms and legs can be compared. HR-pQCT may provide information on such parameters, but has not been used in (pre)historic bones without soft tissue and bone marrow yet.Three macroscopically intact skeletons of young persons who died 100-125 years ago at an age of approximately 20 years could be identified in the medical-historical-anatomical collection in Marburg/Germany. Distal radii and titiae were measured using HR-pQCCT (XtremeCT, Scanco Medical) and analyzed with the standard evaluation script (software) used for patients in clinical routine. We analyzed (1) the quality of the pseudo-3D images of the bones in comparison to two healthy living persons of the same age group and (2) proved for which quantitative parameters plausible results could be calculated. [Ethical votum: EK_MR_17_03_23_kann].(1) The quality of the pseudo-3D images was completely comparable between the historical bones and those of young living persons. (2) Calculation of trabecular number, cortical thickness and cortical bone density revealed plausible results comparable to young living persons (77.5 + 26.9 % vs. 84.4 + 28.3 % of sex-related mean for persons 20 - 29 years old; n.s. [pooled data]). Calculation of trabecular bone volume / tissue volume and trabecular thickness, however, revealed unplausible results (-29.1 + 24.1 % vs. 104.9 + 11.7 %, p < 0.001).In conclusion, HR-pQCT generates pseudo-3D images of historical bones in good quality. Calculation of trabecular number, cortical thickness and cortical bone density reveals plausible results, whereas this is not the case for trabecular bone volume / tissue volume and trabecular thickness. This can be explained by the calculation's method of these bone parameters (Boutroy et al., J. Clin Endocrinol Metab 2005), which is affected by the absence of soft tissue and bone marrow.

***Disclosures: Peter Herbert Kann**, None*

SUN-074

Bariatric Surgery is Associated with Increased Fracture Risk Among Veterans *Eileen H. Koh[1.] Tiffany Y. Kim[2.] Hui Shen[2.] Mary A. Whooley[2.] Matthew L. Maciejewski[3.] Theodore S. Z. Berkowitz[4.] Valerie Smith[3.] Lygia Stewart[2.] Anne L. Schafer[2.] [1]University of California, San Francisco, United States. [2]University of California, San Francisco and San Francisco Veterans Affairs Health Care System, United States. [3]Durham Veterans Affairs Health Services Research and Development and Duke University, United States. [4]Durham Veterans Affairs Health Services Research and Development, United States

Despite its metabolic and mortality benefits, bariatric surgery has negative skeletal effects. The Roux-en-Y gastric bypass (RYGB) procedure is associated with increased fracture risk in the general bariatric surgery population, who are predominantly premenopausal women. It is unclear whether postoperative fracture risk is increased in men, and whether patients with obesity who undergo sleeve gastrectomy (SG), now the most commonly performed procedure, are more likely to fracture than nonsurgical patients. We compared fracture risk among US Veterans who underwent bariatric surgery from 2000-2020 at a Veterans Affairs (VA) facility or paid for by VA and matched Veterans with obesity who did not have surgery. Surgical patients were matched 1:3 to nonsurgical patients by age, sex, year, and pre-op BMI. We used ICD codes to capture incident fracture from VA electronic health records, VA purchased care claims, and Medicare claims. Cox proportional hazards models were used to determine the relationship between bariatric surgery and subsequent fracture risk. Our surgical cohort, comprised of 8357 patients [3182 RYGB, 4168 SG, 291 adjustable gastric banding (AGB)], was 70% men with mean age 52+/-10 years and BMI 45+/-7 kg/m2. Compared to 25,057 matched Veterans who did not have surgery, surgical patients had higher baseline rates of obesity-related comorbidities including diabetes (48% vs 36%). During an average 7 years follow-up, surgical patients had higher rates of incident fracture (25.1 vs 13.9 per 1000 person-years). Bariatric surgery was associated with a 67% increased risk of incident fracture (HR 1.67, 95% CI 1.56-1.79, p<0.001) after adjustment for race/ethnicity, geographic location, and comorbidities. Bariatric surgery was also associated with incident hip fracture (HR 2.42, 95% CI 1.97-2.96, p <0.001), spine fracture (HR 1.81, 95% CI 1.60-2.05, p<0.001), and radius fracture (HR 2.36, 95% CI 2.03-2.75, p< 0.001). Compared to matched controls, RYGB was associated with increased risk of fracture (HR 1.91, 95% CI 1.73-2.11, p<0.001), as was SG (HR 1.48, 95% CI 1.31-1.67, p<0.001), but there was no difference in fracture rates between RYGB and SG (p=0.18). There was no evidence for an association between AGB and fracture risk (HR 0.97, 95% CI 0.68-1.40, p=0.88). Our findings show that RYGB and SG are associated with increased risk of fracture in this Veteran population of predominantly older men, including at major osteoporotic fracture sites.

***Disclosures: Eileen H. Koh**, None*

SUN-076

Evaluation of the Mandibular Condylar Bone Microarchitecture in People Living with HIV (PLWH) *Michael Levit[1.] Sunil Wadhwa[1.] Michael Yin[2.] Satoko Matsumura[1.] Shin Jung Hsieh[1.] Karolina Kister[1.] Cleber Silva[1.] Jayesh Shah[3.] Anyelina Cantos[3.] Bruno Bohn[4.] Ryan Demmer[4.] [1]Columbia University College of Dental Medicine, United States. [2]Columbia University, United States. [3]Columbia University College of Physicians and Surgeons, United States. [4]University of Minnesota, School of Public Health, United States

Objectives: People living with HIV (PLWH) have been shown to have lower bone density at the spine, hip and radius. However, whether a similar bone phenotype is seen in craniofacial bones is not known. The goal of this study was to evaluate the bone microarchitecture of the mandibular condyle in PLWH.Methods: We recruited 212 participants, which included 88 (22 men, 66 women) HIV-negative participants and 124 (35 men, 89 women) PLWH on combination antiretroviral therapy with virological suppression from a single academic center. Each participant filled out a validated Temporomandibular Disorder (TMD) pain screening questionnaire and had Cone beam computed tomography (CBCT) of their mandibular condyles. Qualitative radiographic evidence of Temporomandibular Joint Disorders-Osteoarthritis (TMJD-OA) assessment and quantitative microarchitecture analysis of their mandibular condylar bones were conducted with CT Analyzer, Bruker Corp. See attached figure for representative trabecular and cortical isolation.Results: There was no statistically significant difference in either self-reported TMD (PLWH: 7.1% vs HIV negative: 11.8% p=0.27) or in radiographic evidence of TMJD-OA (PLWH: 7.8% vs. HIV-negative: 4.2% p=0.585). Linear regression analysis revealed that positive HIV status remained

significantly associated with increased trabecular thickness (0.611 +/- 0.041 vs 0.582 +/- 0.061;p=0.0001), decreased cortical porosity (5.008% +/- 4.214 vs 8.846% +/- 7.082; p<0.0001) and increased cortical bone volume fraction (0.95 +/- 0.042 vs 0.912 +/- 0.071; p<0.0001) after adjusting for race, diabetes, sex and age.Conclusion: Unlike in long bones, PLWH have increased mandibular condylar trabecular bone thickness and cortical bone volume fraction compared to HIV-negative controls.

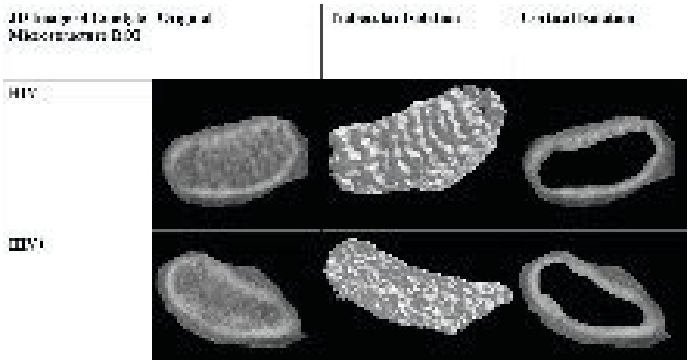

***Disclosures: Michael Levit**, None*

SUN-078

Uncovering the Association of Environmental Stressors on Bone Health in Indigenous Guatemalan Children: Exploring the Interplay between Bone Quality, Body Composition, Nutrition, Maternal Health, and Household Characteristics *Michele Monroy-Valle[1], Hassan Vatanparast[2], Ginny Lane[3]. [1]University of Saskatchewan, , [2]Professor. College of Pharmacy and Nutrition/ School of Public Health. University of Saskatchewan, Canada, [3]Assistant Professor. School of Family and Consumer Sciences. University of Idaho, United States

The environment, diet, and maternal health play a fundamental role in bone elongation during childhood. Economic, societal, community, and emotional elements can cause biosocial stress, which reduces bone development. We explored the association between bone quality, body composition, nutrition, maternal health, and household characteristics among 133 Mayan Indigenous children aged 2 to 5 years old residing in Chichicastenango, Guatemala. We cross-sectionally measured bone quality (Speed of Sound m/s) on the left distal radius and midshaft tibia using Quantitative Ultrasound. We measured body composition by bioimpedance with four electrodes. We gathered data on household factors, such as overcrowding, access to drinking water and sanitation, as well as data on mother and child health. We descriptively analyzed the data and performed statistical modelling. We found that 53.0% (n=70) of children had short stature and potential stunting syndrome [49.2% (n=30) of females and 56% (n=40) of boys]. Stunted children were 2.8 (95% CI 1.3, 6) times more likely to have poor bone quality. More than half of the children (61.4%) lived in rural regions, with 33% lacking access to drinking water and sanitary facilities. Children who lived in a home without water or sanitary facilities were 3.1 (95% CI 1.3, 7.0) times more likely to have low bone quality. Almost three-quarters of the stunted children (70%, n=49) had a short mother. Non-stunted children with taller mothers (height over 145 cm) had higher bone quality than stunted offspring. Mother's height was linked with boys', but not girls', bone quality. However maternal body fat mass was linked with higher bone quality among all children, especially girls. Stunted children, whose mothers' fat mass was low, and lived in a food insecure household had the lowest bone quality. Our findings suggest an intergenerational effect on bone quality in the offspring of malnourished mothers. Furthermore, lack of access to drinking water and sanitation, as well as poor living conditions such as overcrowding, limit access to nutritious meals and a low-inflammatory environment that support healthy growth and development. Low maternal fat mass, stunting, and being food-insecure all increase the likelihood of children having poor-quality bones.

***Disclosures: Michele Monroy-Valle**, None*

SUN-079

Baseline Associations of Age and BMI with Compartmental, Volumetric Bone Mineral Density Tomography in Older Adults Living with Obesity in the INVEST in Bone Health Trial *Delanie Lynch[2], Marjorie Howard[2], Daniel Beavers[3], Erica Lawrence[4], Joshua Stapleton[5], Ashley Weaver[6], Kristen Beavers[3]. [2]Wake Forest University School of Medicine , , [2]Wake Forest University School of Medicine , United States, [3]Wake Forest University, United States, [4]California Pacific Medical Center, United States, [5], , [6]Wake Forest University School of Medicine, United States

Over 50% of older adults (>50 yrs) have low bone mineral density (BMD) and more than 30% are currently living with obesity, with rates rising. Low BMD and obesity both negatively impact overall health and quality of life in the aging population. This study used quantitative computed tomography (QCT) to measure compartmental, volumetric BMD (vBMD) in older adults living with obesity enrolled in a weight loss (WL) trial to explore baseline associations between regional vBMD and age or BMI.The ongoing INVEST in Bone Health trial (NCT04076618) has enrolled 150 older adults (66+/-5 yrs; 69% white; 25% male) living with obesity (34+/-3 kg/m2) to determine effects of a WL intervention with or without weighted vest use or resistance training on bone health. The trial completed enrollment in March 2023 and QCT scans of the hips and lumbar spine were acquired for all participants at baseline. Using a calibration phantom, trabecular and cortical vBMD of the total hip (TH) and femoral neck (FN) and trabecular vBMD of the spine (average of L1-L4) were generated. Analyses were performed using simple linear regression models for the spine and mixed models for the hip, to account for left and right sides. Models explored associations of age and vBMD (adjusted for sex and BMI), and BMI and vBMD (adjusted for sex and age). Pearson's partial correlation was used to analyze relationships between hip and spine vBMD (adjusted for age, sex, and BMI).Greater age (+1 yr) was associated with higher cortical and trabecular vBMD at the hip and spine, but only TH cortical vBMD was significant (+0.9 mg/cm3; p<0.01). Greater BMI (+1 kg/m2) was associated with lower cortical and increased trabecular vBMD for the hip, with strongest associations observed at the FN (cortical: -2.2 mg/cm3; p<0.01; trabecular: +0.9 mg/cm3; p=0.04). Trabecular vBMD of the spine was highly correlated with trabecular vBMD for TH (r=0.76; p<0.01) and FN (r=0.64; p<0.01; see Figure).Unexpectedly, vBMD was positively associated with age, but only significant for TH cortical, which may be due to our relatively active cohort. Consistent with prior studies, BMI was positively associated with trabecular vBMD, likely due to loading from excess adiposity. Regional vBMD measures were highly correlated with each other indicating uniformity across common fracture sites. As the INVEST in Bone Health trial completes follow-up, these outcomes will be explored longitudinally with respect to WL and interventional assignment.

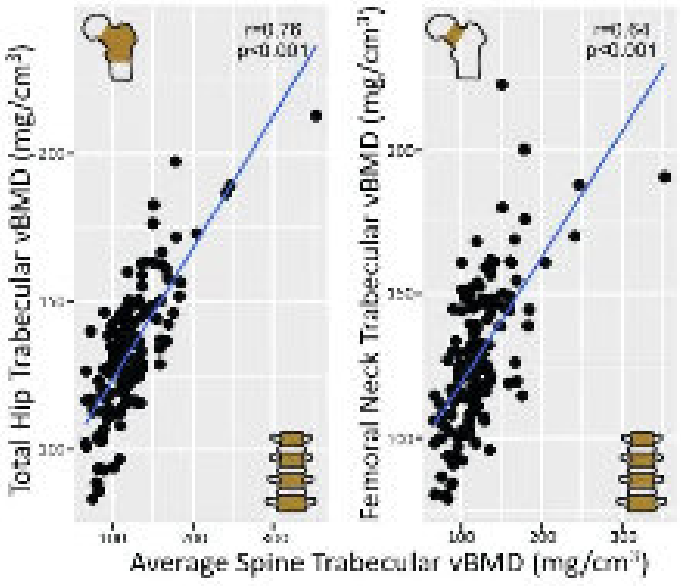

***Disclosures: Delanie Lynch**, None*

SUN-080

Comparative effects of antihypertensive medications on fracture risk in elderly patients with hypertension *Seung Shin Park[3], Hanna Jang[2], Sung Hye Kong[3], Hyunmook Jeong[3], Siyeon Yi[3], Seung Hun Lee[4], Jeonghoon Ha[5], Kwangsoo Kim[3], Jung Hee Kim[3], SANG WAN KIM[6], Chan Soo Shin[7]. [3]Seoul National University Hospital, Korea, Democratic People's Republic of, [2]Seoul National University Bundang Hospital, Korea, Democratic People's Republic of, [3]Seoul National University Hospital, Republic of Korea, [4]Asan Medical Center, Korea, Democratic People's Republic of, [5], Republic of Korea, [6]Seoul National University College of Medicine, Boramae Medical Center, Republic of Korea, [7]Seoul National University College of Medicine, Republic of Korea

Background:Hypertension and osteoporosis commonly coexist in the elderly, and some antihypertensive medications have been reported to potentially lower the risk of fractures. However, there is limited data comparing the effects of different antihypertensive agents and their combinations on fracture risk. We aimed to investigate the individual and combined effects of antihypertensive drugs on fracture risk in this study.Methods:A total of 28,247 patients who received antihypertensive medications for at least one year between 2008 and 2012 at Seoul National University Hospital were retrospectively reviewed using common data model. Patients were categorized into groups based on their antihypertensive medication use: antiotensin receptor blocker (ARB), calcium channel blocker (CCB), beta blocker (BB), ARB with CCB, ARB with BB, ARB with thiazide, CCB with BB, and ARB with BB

and thiazide, for the purpose of analysis. Fracture risks, defined as major osteoporotic fractures (MOFs), vertebral fractures (VFs), and hip fractures (HFs), were analyzed using the Cox proportional hazard model with adjustments made for age, sex, body mass index, previous history of fractures, secondary osteoporosis-related conditions, diabetes mellitus, drug use, and the use of osteoporosis medications.Results:The number of patients using ARB, CCB, BB, ARB with CCB, ARB with BB, ARB with thiazide, CCB with BB, and ARB with BB and thiazide were 5,515, 7,514, 4,940, 5,022, 1,055, 1,965, 1,874, and 362, respectively. Among the total patient population, females accounted for 50.6%, and the average age and BMI were 65.8 years and 24.5 kg/m2, respectively. Compared to the CCB group, the BB group showed a significantly increased risk of osteoporotic fractures (MOFs) and vertebral fractures (VFs) (Hazard ratio (HR) 1.24, 95% confidence interval (CI) [1.01, 1.52] for MOFs; HR 1.40, 95% CI [1.08, 1.91] for VFs). In contrast to the BB group, the ARB with BB group and ARB with BB and thiazide groups demonstrated decreased HRs for VFs of 0.51 and 0.29, respectively (95% CI [0.28, 0.94] and [0.09, 0.93]). No significant differences in fracture risk were observed between the ARB monotherapy group and the ARB with BB, ARB with CCB, or ARB with thiazide groups (HR 1.07, 1.03, and 0.87 respectively). Conclusion:In hypertensive patients with concomitant osteoporosis, prioritizing the use of ARB and thiazide over BB when selecting medications may help reduce the risk of fractures.

***Disclosures: Seung Shin Park**, None*

SUN-081

Hypothalamic-Pituitary-Ovarian Axis Suppression Among Women During U.S. Army Basic Combat Training *Kristin Popp[1], Brittany Bozzini[2], Marinaliz Reynoso[2], Katelyn Guerriere[2], Jennifer Coulombe[3], Nicholas Zurinaga[2], Stephen Foulis[2], Katherine Kuhn[4], Mary Bouxsein[5], Nanette Santoro[4], Julie Hughes[6]. [1]Massachusetts General Hospital, , [2]USARIEM, United States, [3]Center for Advanced Orthopedic Studies, Department of Orthopedic Surgery, Beth Israel Deaconess Medical Center, Harvard Medical School, United States, [4]University of Colorado, United States, [5]Beth Israel Deaconess Medical Center, Harvard Medical School, United States, [6]US Army Research Institute of Environmental Medicine, United States

Hypothalamic-pituitary-ovarian axis suppression can lead to poor bone health and increased risk of bone stress injury. Female trainees overwhelmingly (86%) report menstrual cycle changes during 8-10 weeks of U.S. Army Basic Combat Training (BCT). Whether reported menstrual cycles changes reflect hypothalamic-pituitary-ovarian (HPO) axis suppression during BCT is unknown.Female trainees (n=48) who were not using hormonal contraceptives, provided fasted, rested daily first void urine and weekly blood samples and questionnaires during BCT. Luteinizing hormone (LH), follicle stimulating hormone (FSH), and metabolites of estradiol (E1c) and progesterone (Pdg) were measured by chemiluminescent assays (Siemens Centaur XP) and adjusted for urinary creatinine (cr). We used Mann Whitney U tests to compare maximum values of LH, FSH, E1c, and Pdg between women who had evidence of luteal activity (ELA) or no ELA (NELA) during BCT.Trainees were young (21.1+/-4.9yrs), normal weight (23.7+/-2.9kg/m2) women. Most trainees (75%) reported regular menstrual cycles before starting BCT. During BCT, 36 (77%) trainees reported at least one menstrual period, and 41 (87%) reported changes to either menstrual cycle symptoms, length, or frequency. Hormones normalized to a 28 day menstrual cycle are displayed in figure 1. Only seven trainees had menstrual cycles indicating ELA (i.e. presumed ovulation) during BCT, all with shortened luteal phases ranging from 3-10 days in length. Thus, 85% of women showed NELA and 100% of women displayed menstrual cycle dysfunction. Mean peak hormone concentrations were higher in ELA compared to NELA trainees: E1c, ELA 29.6+/-17.9 vs. NELA 16.7+/-7.4 ng/mg cr (p=0.04), Pdg, ELA 2.9+/-1.3 vs. NELA 1.1+/-0.9 µg/mg cr (p=0.0007); and LH, ELA 27.8+/-23.1 vs. NELA 11.6+/-8.5 mIU/mg cr (p=0.01). FSH was not different between ELA 31.0+/-10.6 and NELA 25.9+/-10.3 mIU/mg cr (p=0.2).Our findings reveal that HPO axis suppression with no evidence of luteal activity is very common during BCT and occurs among menstruating women. This suppression is important to consider in efforts to optimize bone health and reduce bone stress injury risk in female trainees.

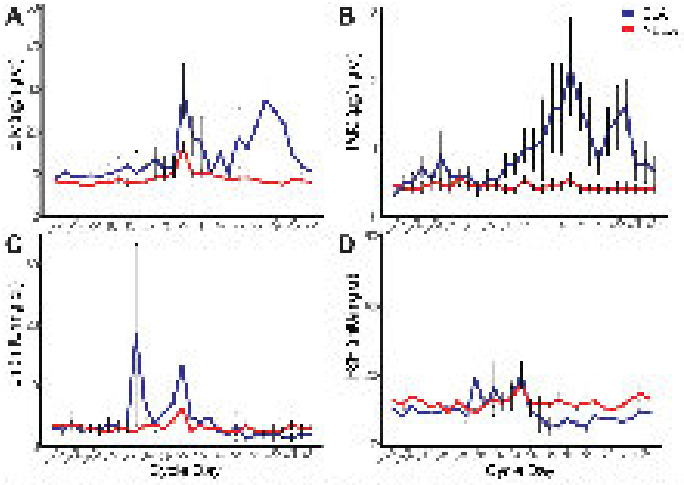

Figure 1.

***Disclosures: Kristin Popp**, None*

SUN-082

Androgen Deprivation Therapy increases the risk of clinical fractures in men with Prostate Cancer *Marsha van Oostwaard[2], Caroline Wyers[2], Yes van de Wouw[2], Marc de Jong[2], maud van Maren[2], Maryska Janssen-Heijnen[3], Joop Van Den Bergh[4]. [2]VieCuri Medical Centre, , [2]VieCuri Medical Centre, Netherlands, [3]Maastricht University, Netherlands, [4]VieCuri MC Noord-Limburg and Maastricht UMC,

Androgen Deprivation Therapy (ADT) is known to increase long-term fracture risk in men with Prostate Cancer (PCa) although the risk of clinical fractures, excluding pathological fractures, is not well known. This study aims to evaluate the risk of clinical and pathological fractures in men with PCa treated with ADT compared to those not treated with ADT. Methods: We conducted a cohort study of men diagnosed with PCa between 2014 and 2019. Data was extracted from electronic health records and fractures were radiographically confirmed. Patients were followed from PCa diagnosis date until death, end of study, or fracture, whichever came first. Follow-up time was divided into 30-day intervals and exposure (current, past or non-ADT use) was determined at each interval based on prescription data. Current ADT use was further stratified by duration of ADT use (0-182 days, 183-730 days, and > 730 days). Cause-specific Cox proportional hazard models were used to estimate the risk of all fractures, the risk of clinical and pathological fractures separately and the risk of mortality with current use of ADT vs. non-ADT use. All analyses were adjusted for age and stage of disease. Results: We included 225 current or past ADT users and 244 non-users, with a mean age of 70.5 (+/-8.3) years. Overall, 30 clinical and 12 pathological fractures during ADT use, and 18 and 0 during non-ADT use were observed, respectively. Current ADT use was associated with an increased risk of all (clinical and pathological) fractures (HR: 5.11; 95%CI: 2.34-11.14) as compared to non-ADT use, while past ADT use was not. Stratification of current ADT use by duration showed an increased risk of all fractures in all ADT duration categories. Current ADT use was not associated with mortality (HR: 1.29; 95%CI: 0.59-2.84) while past use was associated with mortality (HR: 3.59; 95%CI: 1.78-7.24). Associations were similar when only clinical fractures were studied (current ADT use HR: 3.62; 95%CI: 1.57-8.32). The association with pathological fractures could not be studied due to no events during non-ADT use. Conclusion: In addition to the increased risk of pathological fractures, current ADT use was associated with an increased risk of clinical fractures compared to non-ADT use. Therefore, attention is needed for prevention of clinical fractures immediately at the start of ADT.

***Disclosures: Marsha van Oostwaard**, None*

SUN-083

Associations Between the Changes in Gut Microbiota and Bone and Muscle Outcomes After Sleeve Gastrectomy *Angela Yang[1], Julie-Catherine Coll[2], Thibault Varin[3], Serge Simard[3], Suzanne Morin[4], Fabrice Mac-Way[5], André Tchernof[6], Bettina Willie[4], Stéfane Lebel[7], André Marette[3], Claudia Gagnon[8]. [1]Universite Laval, , [2]CHU de Québec Research Centre, Quebec Heart and Lung Institute Research Centre, Canada. [3]Quebec Heart and Lung Institute Research Centre, Canada. [4]McGill University, Canada. [5]CHU de Québec Research Centre, Department of Medicine, Laval University, Canada. [6]Quebec Heart and Lung Institute Research Centre, Department of Medicine, Laval University, Canada. [7]Quebec Heart and Lung Institute Research Centre, Department of Surgery, Laval University, Canada. [8]CHU de Quebec, Universite Laval, Canada

The mechanisms leading to bone and muscle loss after sleeve gastrectomy (SG) remain unclear. We aimed to determine whether changes in the gut microbiota following SG are associated with this bone and muscle loss.This is an exploratory analysis of a multicentre prospective cohort study, in which 70 participants with severe obesity had the following parameters measured before and one year after SG: lumbar spine, total hip, and femoral neck areal bone mineral density (aBMD) and whole-body lean mass by dual-energy X-ray absorptiometry; lumbar spine, total hip, femoral neck, tibia, and radius volumetric BMD (vBMD), bone strength (maximum cross-sectional moment of inertia [CSMI] and maximum section modulus [Z]), and mid-femur muscle cross-sectional area by quantitative computed tomography; serum bone turnover markers (C-terminal crossed-linked telopeptide of type 1 collagen [CTX], procollagen type 1 N-terminal propeptide [P1NP], osteocalcin); lower limb absolute and relative muscle strength by isometric dynamometry. Gut microbiota from stool samples was analyzed by 16S rRNA gene sequencing at baseline and one year after SG. Results are presented as percentage or mean+/-SD. Linear regression analyses adjusted for age and sex were used to assess the associations between microbial, bone, and muscle parameters.A preliminary sample of 19 participants (79.0% women [26.7% postmenopausal], 57.9% with type 2 diabetes, mean age 45.3+/-9.5 years, mean BMI 40.1+/-0.6 kg/m2 at baseline) was analyzed. One year after SG, weight (-26.3+/-6.1%), aBMD (-6.4 to -8.5% depending on skeletal sites), vBMD (-1.0 to -7.4% depending on skeletal sites), whole-body lean mass and mid-femur muscle cross-sectional area as well as lower limb absolute muscle strength all decreased significantly (Table). Bone strength parameters did not change. All serum bone turnover markers increased significantly. Alpha diversity, represented by Shannon (p=0.04) and Simpson (p=0.02) indices, increased significantly while beta microbial diversity did not change (p=0.60).In this preliminary sample, significant associations were identified between bacteria genera and some bone parameters, but not between microbial and muscle parameters. Further analysis of the additional participants is ongoing to confirm that associations observed between gut microbiota composition and bone outcomes after SG persist in the larger cohort.

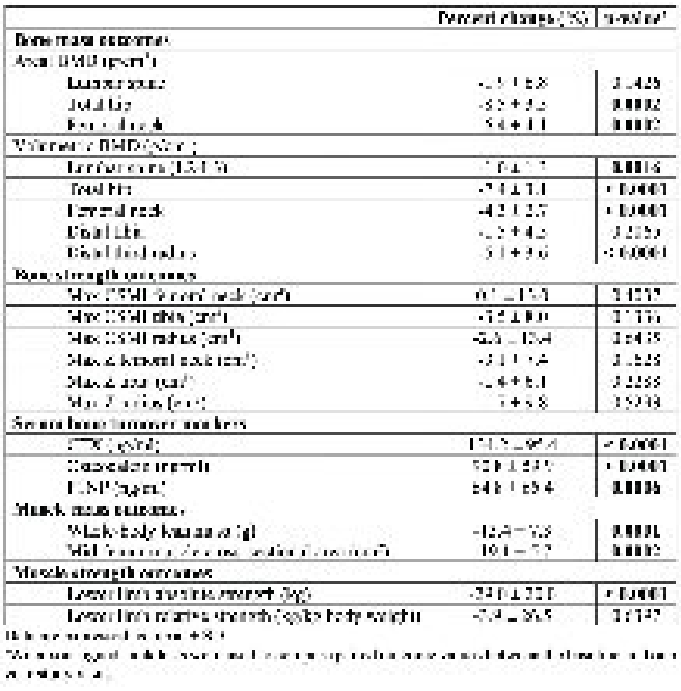

***Disclosures: Angela Yang**, None*

SUN-084

Association of Lower Leg Arterial Calcification with Tibial Bone Microarchitecture and Fracture History in Older Men *BITA ZAHEDI[3], Fjola Johannesdottir[2], Trinity Tedtsen[3], Sheena Patel[4], Peggy Cawthon[5], Andrew Burghardt[6], Kristine Ensrud[7], Charles Ginsberg[8], Nancy Lane[9], Mary Bouxsein[10], Elaine Yu[3]. [3]Massachusetts General Hospital, , [2]Beth Israel Deaconess Medical Center & Harvard Medical School , , [3]Massachusetts General Hospital, United States. [4], , [5]San Francisco Coordinating Center, United States. [6]University of California, San Francisco, United States. [7]University of Minnesota and Minneapolis VA Health Care System, United States. [8]UCSD, , [9]University of California, Davis Medical Center, United States. [10]Beth Israel Deaconess Medical Center, Harvard Medical School, United States

Background: Bone is a highly vascular tissue and it has been postulated that disordered bone blood flow may directly contribute to poor skeletal health. Prior studies have found associations between cardiovascular disease (CVD) and decrease in axial bone mineral density (BMD), although locoregional effects of arterial calcification on bone microarchitecture are not clear. Recently, post-processing analysis of high resolution peripheral quantitative computed tomography (HR-pQCT) has been developed to quantify lower leg arterial calcification (LLAC) with great validity and reliability. The aim of this study is to determine whether LLAC in older community-dwelling men is associated with deficits in volumetric bone mineral density (vBMD) and microarchitecture at the distal tibia. Methods: 1717 men from the Osteoporotic Fractures in Men (MrOS) study completed tibial HR-pQCT with assessment of vBMD, bone microarchitecture, and presence of LLAC. Clinical covariates and medical history were collected, along with spine and hip BMD by DXA and prevalent fracture. Linear and logistic regression were performed with adjustments for age, site, race, body mass index (BMI), self-reported diabetes, cardiovascular disease (CVD), and chronic kidney disease (CKD). Results: Men with LLAC (n=887, 52%) and without LLAC (n=830, 48%) had similar age (84 +/- 4 yrs), BMI (26.8 +/- 3.8 kg/m^2), race (90% White), alcohol use and spine and hip BMD. Men with LLAC were less physically active, more likely to report diabetes and CVD, but less likely to report ever smoking. Furthermore, the LLAC group had slightly lower cortical vBMD (-1.5%) and higher cortical porosity (+5.5%) at the tibia, which persisted after adjustment for covariates (Table 1). Total vBMD and trabecular parameters were largely similar between groups. Men with LLAC were more likely to have prior fracture (OR 1.26, 95%CI 1.03-1.54) even after multivariate adjustment. Conclusion: In this large cohort of older community-dwelling men, we demonstrated a small but significant negative correlation between presence of LLAC and cortical bone microarchitecture at the tibia. LLAC was also associated with prevalent fracture history. Further studies are needed to understand the mechanism underlying the association of vascular calcifications and bone outcomes.

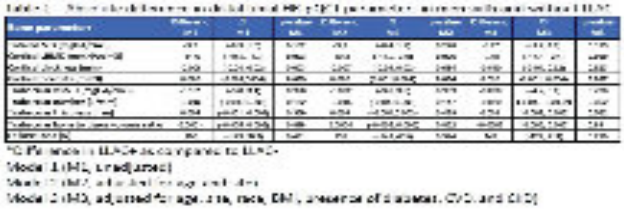

***Disclosures: BITA ZAHEDI**, None*

SUN-085

Treatment With Monthly Romosozumab Injections Increases Areal Bone Mineral Density at the Lumbar Spine and Hip in Women With Chronic Spinal Cord Injury *W. Brent Edwards[1], Laura E. Crack[1], Tudor Muresan[1], Narina Simonian[2], Thomas J. Schnitzer[2]. [1]University of Calgary, Canada. [2]Northwestern University Feinberg School of Medicine, United States

Sublesional bone loss is a known complication of spinal cord injury (SCI) with low bone mineral density (BMD) and increased fracture risk persisting into the chronic phase of injury. While existing literature focuses on pharmaceutical treatment options to prevent bone loss in acute SCI, limited investigations have examined potential therapies to increase BMD in chronic SCI. Romosozumab, a monoclonal antibody that inhibits sclerostin, has illustrated significant bone growth in pre-clinical models and among able-bodied post-menopausal clinical populations. The purpose of this study was to examine the efficacy of romosozumab to increase BMD in women with chronic SCI and an inability to ambulate. Twelve women with a mean (SD) age of 45.4 (9.1) years and injury duration of 15.1 (11.2) years, were administered monthly subcutaneous injections of romosozumab (210 mg) for one year. Areal BMD of the lumbar spine and hip (total hip and femoral neck) were measured at baseline and after 6 and 12 months using dual energy x-ray absorptiometry (DXA). The study is on-going and currently nine of the 12 participants have completed all aforementioned data collection. A preliminary analysis was conducted using longitudinal mixed-effects models to examine

Sunday Orals

the effect of one year of romosozumab treatment on DXA-derived areal BMD measures. Areal BMD at the lumbar spine significantly increased (p<0.001) by an average of 6.1 (3.6)% and 9.3 (3.1)% after 6- and 12-months, respectively (Fig. 1). DXA-derived BMD at the total hip increased (p<0.001) with average gains of 2.2 (2.6)% and 4.1 (3.1)% after 6- and 12-months, respectively. Results were similar when isolating the femoral neck (p=0.014), which increased by an average of 1.8 (6.9)% at 6-months and 4.6 (4.9)% at 12-months. These results are comparable to the treatment efficacy of romosozumab for post-menopausal osteoporosis, which induced an annual increase in areal BMD of approximately 17% at the lumbar spine and 5% at the hip1. These preliminary findings demonstrate that treatment with romosozumab in women with chronic SCI increases areal BMD at the lumbar spine and hip, similar to effects in post-menopausal osteoporosis in able-bodied women. On-going data collection in this clinical trial will lead to further analysis with a larger sample size, and evaluation of bone mineral at the knee and hip using computed tomography.[1] Ishibashi H et al. (2017). Bone. 103:209-215

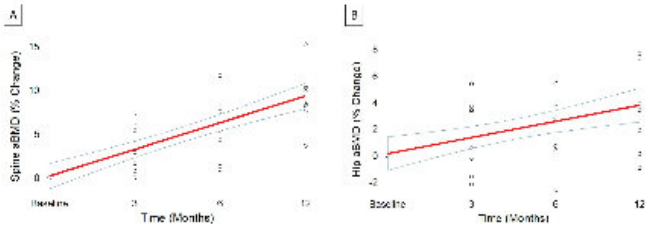

Figure 1. Individual [n=9] and average (95% CI) percentage change in lumbar spine (A) and total hip (B) areal bone mineral density (aBMD) throughout 12 months of treatment with subcutaneous injections of romosozumab (210 mg)

***Disclosures: W. Brent Edwards**, Amgen, Grant/Research Support*

SUN-087

Hip Fractures in Adults with Schizophrenia in Ontario: a Population-based Repeated Cross-sectional Study *Hina Ansari[1], Susan Jaglal[2], Angela M Cheung[3], Paul Kurdyak[4]. [1]Institute of Health Policy, Management and Evaluation, Canada. [2]Toronto Rehabilitation Institute, University Health Network, Canada. [3]Department of Medicine and Joint Department of Medical Imaging, University Health Network, Canada. [4]Centre for Addiction and Mental Health, Canada

Purpose: Individuals with schizophrenia may experience a higher burden of hip fractures. Our study objectives were to describe sociodemographic and clinical characteristics of hip fracture patients with schizophrenia, and quantify their sex-specific annual hip fracture rates relative to the general population.Methods: This repeated population-based, cross-sectional study leveraged multiple individually linked health administrative databases for patients in Ontario, Canada. We included patients aged 40 to 105 years with hip fracture-related hospitalization between April 1, 2009, and March 31, 2019. Schizophrenia diagnosis was ascertained using a validated algorithm. Primary outcome measures were sex-specific age-standardized annual hip fracture rate per 10,000 individuals, and annual percent change in age-standardized rates. Rates were adjusted to the 2011 Ontario population; annual percent change was evaluated using Joinpoint regression.Results: We identified 109,908 index hip fractures with a median[IQR] patient age of 83[75-89] years and 31.4% males. Hip fracture patients with (n=4,251) vs without (n=105,657) schizophrenia were younger at index event [male median[IQR] age: 73[62-83] vs 81[71-87] years (standardized difference, 0.46); female median[IQR] age: 80[71-87] vs 84[77-89] years (standardized difference, 0.32)]. A higher proportion of those with vs without schizophrenia had frailty (54% vs 34%; standardized difference, 0.40), and previous fragility fractures (24% vs 19%; standardized difference, 0.11). The overall age-standardized rate per 10,000 individuals with vs without schizophrenia was 37.5 (95% CI: 36.4-38.6) vs 16.0 (95% CI: 15.9-16.1). Age-standardized rates were threefold higher in men with vs without schizophrenia [31.0 (95% CI: 29.5-32.6) vs 10.1 (95% CI: 9.96-10.2)], and more than twofold higher in women with vs without schizophrenia [43.4 (95% CI: 41.9-44.9) vs 21.4 (95% CI: 21.3-21.6)]. Rates in men with schizophrenia surpassed that of women in the general population. Overall, Joinpoint regression analysis identified a steady annual decrease of 0.7% (95% CI: -1.1% to -0.3%) for both study groups.Conclusions: Findings suggest that individuals with schizophrenia experience an earlier onset and substantially higher burden of hip fractures, with implications for targeted fracture prevention and optimization of bone health management over the course of their psychiatric illness.

***Disclosures: Hina Ansari**, None*

SUN-088

PD-L1 Expressing Myeloid Cells Promote Bone Marrow Immunosuppression and Osteoclastogenesis with Diet-Induced Obesity *Samantha Costa[1], Sergey Ryzhov[2], Moustapha Kassem[3], Dr. Clifford ROsen[4]. [1]MaineHealth Institute for Research , United States. [2]MaineHealth Institute for Research, United States. [3]Odense University Hospital, Denmark. [4]Maine Medical Center, United States

Programmed death ligand 1 (PD-L1) when combined with PD-1 inhibits immune responses and promotes self-tolerance by modulating T-cell function. Previous studies have investigated aberrant PD-L1 expression in tumor-bearing models. Recently, we identified a novel population of PD-L1 expressing myeloid cells within the bone marrow of obese, non-tumor bearing mice. However, the role of PD-1/PD-L1 signaling in osteoclast differentiation resulting in obesity-related bone loss has yet to be explored. We hypothesized obesity-induced bone loss is linked to PD-1/PD-L1 signaling through a pro-osteoclastogenic mechanism. Starting at 8 weeks of age, C57BL/6J mice were fed a high-fat diet (HFD, 60% kcal) or sucrose-matched low-fat diet (LFD, 10% kcal) for 12 weeks. After 12 weeks of HFD-feeding, pre-determined parameters based on body measurements (i.e., body weight >40g and percent body fat >32%) were used to classify obese mice. Compared to LFD-fed mice, obese mice had an increase in MHCIInegPD-L1+ myeloid cells (fully defined as CD11bhighCD11chighMHCIInegF4/80+PD-L1+, p<0.0001). The increase of PD-L1 coupled with the loss of MHCII expression negatively affected T-cell activation and increased immunosuppressive CD39 and CD73 expression (p=0.0019 and p=0.0012). In vitro PD-L1 blockade suppressed osteoclast differentiation (p=0.014), suggesting the PD-1/PD-L1 axis mediates osteoclastogenesis. In addition, PD-1 expressing osteoclast precursors (defined as [B220/CD3/NK1.1]negc-kit+CD115+CD11blowPD-1+) were increased in obese mice compared to LFD-fed mice (1.34-fold higher than LFD, n=10 mice/group, p=0.0042). TRAP staining and histomorphometric analyses revealed obese mice had an increase in osteoclasts (1.82-fold higher than LFD, p=0.0070) and enhanced eroded surface, while no significant changes in osteoblast number and mineralizing surface were observed. As a result, obese mice had decreased femoral (Tb.BV/TV, obese 10.76% vs LFD 12.13%, n=7 mice/group, p=0.020) and tibial (Tb.BV/TV, obese 13.76% vs LFD 20.34%, n=8-10 mice/group, p<0.0001) trabecular bone mass as well as decreased cortical area (Ct.Ar/T.Ar, obese 56.59% vs LFD 58.61%, n=8-10 mice/group, p=0.0245). In summary, obesity creates an immunosuppressive bone marrow microenvironment through increased PD-1 and PD-L1 expression in myeloid and myeloid lineage cells that results in osteoclast-driven bone loss. The impact obesity-induced PD-1/PD-L1 signaling has on osteoclast overactivation remains to be elucidated.

***Disclosures: Samantha Costa**, None*

SUN-091

The Role of Cathelicidin Antimicrobial Peptide in Bone Fracture Repair and Aging *Tuyet Nguyen[1], Tomasa Barrientos de Renshaw[1], Bridgette Furman[1], Puvi Nadesan[1], Vijitha Puviindran[1], Savanna Ma[1], Koji Ishikawa[1], Benjamin Alman[1]. [1]Duke University, United States

The bone repair process becomes less efficient with age resulting in improperly healed fractures, a condition which positively correlates with lower quality of life and higher mortality in geriatric patients. Past murine heterochronic parabiosis experiments have shown that circulatory factors from young mice are able to rejuvenate the fracture repair process in aged animals. Recent studies have specifically identified macrophages as a critical component for this rejuvenated healing phenomenon. Single cell RNA sequencing of bone marrow cells post-injury reveals a unique young macrophage subpopulation. Cathelicidin antimicrobial peptide (Camp) is one of the upregulated genes within this novel young cluster. Previously, Camp has been studied in the context of host response against microbial pathogens and as a therapeutic carcinogenic target, but its role in fracture repair and aging has not been well explored. Through microCT analysis, we have found that the Camp global knockout mouse has poor fracture healing, comparable to older individuals. Additionally, rCAMP administration to primary bone marrow cells from old mice cultured in osteogenic media demonstrates a potential role in promoting osteogenesis. These and future experiments will address the gap in understanding of how macrophage-secreted proteins affect the bone healing process and how this interaction is altered with age.

***Disclosures: Tuyet Nguyen**, None*

SUN-092

Inflammasome activation is an important mechanism in chemotherapy-induced bone loss *Chun Wang[1], Gabriel Mbalaviele[2]. [1]Division of Bone and Mineral Diseases, Washington University School of Medicine, United States. [2]Washington University in St. Louis School of Medicine, United States

Doxorubicin is a widely used chemotherapy drug for the treatment of a variety of tumors including breast cancer. Despite its success in improving survival rates of cancer patients, it causes deleterious side effects, including bone marrow toxicity, neutropenia, irreversible heart muscle damage, osteoporosis, and fracture risk, but the underlying mechanisms remain unknown. We hypothesized that doxorubicin causes DNA damage, which leaks to the cytoplasm, and cell death, which releases DNA to the extracellular environment. We further hypothesized that mislocalized DNA is sensed by inflammasomes, intracellu-

lar protein complexes that propagate inflammation through various mechanisms, including the maturation and secretion of IL-1?. To test these ideas, we used a non-tumor-bearing mouse model, which allowed the assessment of direct tissue off-target effects of this drug in the absence of tumor confounding outcomes. A single injection of 5 mg/kg doxorubicin to wild-type (WT) mice caused NETosis, a form of neutrophil cell death that follows the release to the extracellular space of genomic DNA and granular contents known as neutrophil extracellular traps (NETs). Specifically, doxorubicin administration increased serum levels of NETosis markers such as citrullinated histone 3 and myeloperoxidase. This response correlated with cytopenia, elevated IL-1? serum levels, increased osteoclast number (N.Oc/BS: vehicle = 4.84+/-0.43; doxorubicin = 12.53+/-1.56), and bone loss (BV/TV: vehicle = 29.21+/-3.93%; doxorubicin = 12.29+/-1.82%). Since damaged or mislocalized DNA is mainly detected by inflammasomes assembled by AIM2 or NLRP3 sensors, we determined their role in doxorubicin actions. Consistent with our hypothesis, doxorubicin osteopenic effects were attenuated in animals lacking AIM2 inflammasome or NLRP3 inflammasome, to some extent (BV/TV: WT = 12.29+/-1.82%; Aim2-/- = 23.33+/-4.05%; Nlrp3-/- = 16.68+/-2.05%). Thus, off-target actions of doxorubicin cause inflammasome activation, a response that ultimately, leads to bone loss.

***Disclosures: Chun Wang**, None*

SUN-095

Systemic versus local immune and inflammatory responses to bone fracture *Maryam Rahmati[1], Robert Charles Henry Gresham[2], Kent Leach[3], Mark A Lee[3], Augustine Mark Saiz[3]. [1]Department of Orthopaedic Surgery, UC Davis Health, 4860 Y Street, Suite 3800, Sacramento, CA, 95817, USA , United States, [2]Department of Orthopaedic Surgery, UC Davis Health, 4860 Y Street, Suite 3800, Sacramento, CA, 95817, USA,Department of Biomedical Engineering, University of California, Davis, Davis, CA, 95616, USA , United States, [3]Department of Orthopaedic Surgery, UC Davis Health, 4860 Y Street, Suite 3800, Sacramento, CA, 95817, USA, Department of Biomedical Engineering, University of California, Davis, Davis, CA, 95616, USA , United States

Bone fracture is a major cause of physical disability, quality of life impairment and global socio-economic burden. Providing new treatments to guide bone-healing processes toward regeneration relies on our understanding of the fundamental mechanisms and the key stimulators of fracture healing. There is growing evidence that the homeostasis of the immune system state is crucial for directing bone tissue healing mechanisms. Although some studies have reported that the induced immune responses caused by tissue injury direct wound healing; there is still a knowledge gap in the literature regarding the cellular phenotype of immune responses to the bone fracture at earlier and later time points. Therefore, we aimed to fill this knowledge gap by studying the local versus systemic immune responses to femur fracture at earlier and later time points in mice using flow cytometry. We induced blunt femur fracture in mice using a fracture apparatus and after 0 h, 6 h, 12 h, 24 h, 72 h & 3W collected femur, lung, and bone marrow form the injured and healthy mice. After obtaining a single cell suspension from all tissues, we stained our cells using fluorophore markers for different immune cells and used a BD “Fortessa” 18-color cytometer. We also checked the expression of pro-inflammatory cytokines using a 20-plex inflammatory Luminex panel. Our data demonstrated that after femur fracture there was a higher number of live cells in the injured mice compared to the healthy ones; however, this difference was only significant systemically (in lung and bone marrow), indicating the key role of systemic immune in directing fracture healing. In addition, at the fracture site, the CD 45+ immune cells significantly increased after 6 h of injury and continued to increase throughout the study time. B and T cells, myeloid cells, dendritic cells, and macrophages increased significantly after 72 h. Neutrophils increased significantly after 12 h of injury. Although systemically, B and T cells did not change significantly over time in the injured group compared to the healthy mice, the number of neutrophils increased significantly in the first 12 h systemically and decreased to the healthy level at later time points. These data identified key differences between systemic and local immune responses to bone fracture and addressed the importance of both systems in directing fracture healing.

***Disclosures: Maryam Rahmati**, None*

SUN-097

Dynamic Transcriptional Cell Atlas of Immune Cell Lineage during Alveolar Bone Healing *Weimin Lin[1], Quan Yuan[1]. [1]Sichuan University, China

The bone marrow microenvironment is mainly composed of immune cells and stromal cells that play an important role in bone healing. Although various immune and stromal cell populations have been identified in mouse bone marrow, the dynamics of immune cell populations and how they crosstalk with bone marrow stromal cells during bone healing process still remain unclear.Alveolar bone defect caused by tooth extraction is one of the most common bone injuries in clinical practice. In this study, we used mice alveolar bone defect after molar extraction as a model to explore the dynamic changes of immune cell population during bone healing. Single-cell RNA sequencing was used to identify the immune cell populations in injured bone tissue, including neutrophils, monocyte-macrophages, T cells, B cells, and plasma cells. We observed a rapid increase in T cell population on the 1th day after injury, while their proportions returned to pre-injury levels by the 7th day. Further subcluster analysis revealed that NKT cell cluster accounted for the highest proportion of T cells, and the number of NKT cell subsets also increased on the 1th day after injury. After co-culturing NKT cells with MSCs in vitro, we found that the osteogenic differentiation potential of MSCs was inhibited. After deleting NKT cells by depletion antibody or gene knockout, alveolar bone injury repair process was accelerated. Differential gene analysis indicated that the expression level of Cxcl2 in NKT cells was significantly increased on the 1th day after injury compared with that before injury. Reduction of Cxcl2 by neutralizing antibody or gene knockout could improve the bone healing process. Finally, we designed a porous hydrogel which could release drugs quickly in the early stage and loaded it with NKT cell depletion antibody then applied it locally for alveolar bone repair. Compared with systemic administration, local hydrogel administration could achieve the deletion of NKT cells and accelerate the repair of alveolar bone, while avoiding other potential side effects of systemic administration.In summary, our study revealed a dynamic immune microenvironment during bone injury repair and found that NKT cell populations can impair bone healing by secreting Cxcl2. Deleting NKT cells or reducing the expression level of Cxcl2 can accelerate the repair of bone damage, which reveals the important role of NKT cells in the process of bone repair.

***Disclosures: Weimin Lin**, None*

SUN-098

Eosinophils counteract osteoclast-mediated bone degradation via the secretion of eosinophil peroxidase *Darja Andreev[1], Georg Schett[1], Aline Bozec[1]. [1]Department of Internal Medicine 3 - Rheumatology and Immunology, Friedrich-Alexander-University Erlangen-Nürnberg (FAU) and Universitätsklinikum Erlangen (UKER), Erlangen, Germany. , Germany

A healthy skeleton relies on a balance between bone-forming osteoblasts and bone-resorbing osteoclasts. A shift towards increased osteoclast number and/ or activity can therefore lead to bone loss with increased fracture risk. Hormonal imbalance or an inflammatory environment, as in rheumatoid arthritis (RA), often favors osteoclast differentiation through an overproduction of proinflammatory cytokines and receptor activator of nuclear factor ?B ligand (RANKL) by adaptive immune cells. Far less is known about immune cells and mediators that inhibit osteoclast development. Most consistently, however, Type-2 immunity-related cytokines have been reported to downregulate osteoclasts. Interestingly, these cytokines are highly secreted by eosinophils. Although eosinophils are mainly associated with helminth infection and allergic disease, in recent years several publications shed light on the homeostatic functions of these cells. Hitherto, the impact of eosinophils on bone homeostasis is completely elusive.Herein, we demonstrate that eosinophils, classical innate immune cells, decrease osteoclast differentiation and activity. Mechanistically, eosinophils release eosinophil peroxidase (EPX) that reduces the level of reactive oxygen species (ROS) in osteoclast progenitors, thereby inhibiting RANKL-mediated downstream signaling. Thus, eosinophil deficiency and subsequent EPX loss is associated with increased osteoclast numbers, leading to amplified pathological bone degradation like postmenopausal osteoporosis and arthritis-induced bone depletion. In contrast, hyper-eosinophilia with enhanced EPX protects from osteoporosis and inflammation-mediated bone loss by impairing osteoclast formation. Likewise, therapeutic treatment with EPX during the course of arthritis reduces the number of osteoclasts and as a result mitigates inflammatory bone turnover. This mechanism is also reproducible and highly relevant in human as a high eosinophil number is associated with increased bone mass in healthy subjects and especially in RA patients. Altogether, eosinophils represent a novel link between the innate immune system and bone, resembling an intrinsic immune-mediated brake of excessive osteoclast formation and bone resorption through the secretion of EPX.

***Disclosures: Darja Andreev**, None*

SUN-099

Bioengineered trabecular bone organoid to recapitulate crosstalk between bone and marrow *Yongkuk Park[1], Jungwoo Lee[2]. [1]University of Massachusetts Amherst, , [2]University of Massachusetts-Amherst, United States

Trabecular bone marrow is a multi-functional dynamic tissue that plays a crucial role in maintaining the mechanical structure and mineral homeostasis of the skeleton and supporting continuous blood-forming processes. In vitro recapitulation of trabecular bone marrow function can greatly improve our understanding of the integrated bone and blood and offer therapeutic potential. However, it remains a critical challenge to reproduce hard bone and soft marrow tissue complexity in an integrated platform while maintaining their functional crosstalk for an extended period. Here, we report a modular bioengineered trabecular bone marrow model that effectively represents the complexity of bone and marrow tissues, functioning as an integrated organoid. For the 3D lamellar bone model, we used osteoid-inspired demineralized bone paper (DBP), a 20 um thick section of demineralized bovine bone matrix. The DBP laminated with water-soluble polymer was tailored to be a woven strip. After seeding osteoblasts, a DBP strip was rolled to form a 3D trabecular bone model having a lamellar bone structure with subsurface osteocytes and surface osteoblasts. For the semi-solid marrow model, we utilized a porous hydrogel scaffold mimicking bone marrow sinusoids. We prepared scaffolds having two pore sizes: 500-600 um and 75-100 um. Coating the hydrogel scaffold with type I collagen facilitated bone marrow stromal cell adhesion, while the spherical pore cavities allowed for hematopoietic cell expansion when supplemented with hematopoietic cytokine cocktails. Expanded hematopoietic cells, along with stromal cells, are readily retrieved from larger pores while hematopoietic cells within smaller pores

remain and become the source of replenishment. We then integrated the separately prepared trabecular bone and marrow models, allowing osteogenic cells to provide long-term hematopoietic support in the bone marrow cells. The mobilization and attraction of hematopoietic cells were recapitulated based on osteoblasts' metabolic states. Finally, as a proof-of-concept study, we demonstrated in vitro bone marrow transplantation via a simulating chemotherapy-based preconditioning regime and then introduced new bone marrow cells. Our modular biomaterial strategy offers a promising strategy to recapitulate the complexity and functionality of bone and marrow tissue to study various aspects of osteogenic and hematopoietic cell biology within trabecular bone cavities.

***Disclosures: Yongkuk Park**, None*

SUN-100

Recapitulating acute myeloid leukemia (AML) phenotypes in vitro using a 3D model of the bone marrow microenvironment (BMME) *AZMEER SHARIPOL[1], Maggie Lesch[2], Celia Soto[1], Benjamin Frisch[3]. [1]University of Rochester, [2]University of Rochester Medical Center, United States. [3]University of Rochester School of Medicine and Dentistry, United States

Acute myeloid leukemia (AML) is an aggressive blood cancer characterized by the uncontrolled expansion of dysfunctional myeloid progenitor cells in the bone marrow (BM). AML-driven dysregulation of the BM microenvironment (BMME) leads to loss of normal hematopoiesis and BM failure. With the median diagnosis age of 68 and the growing aging population, AML cases are projected to climb substantially. The standard care for the majority of patients, introduced in the 1970s, results in an abysmal 5-year survival rate of ~30%. The lack of therapeutic advancement is partly due to the challenging task of recapitulating the signaling between AML cells and the BMME components in vitro such as the osteoblastic, mesenchymal stromal (MSC), and endothelial cells, and the matrix. To bridge this gap, our lab aims to develop AML-on-chip models (AML-chip) to study BMME dysregulation in vitro and as a tool to identify new therapeutic targets. Previously, we developed a murine BMME-chip model containing mineralized osteoblastic and flow-induced endothelial components using Emulate Chip-S1™ that can maintain the long-term function of hematopoietic stem and progenitor cells (HSPC) for at least 14 days in vitro (Sharipol et al., 2022). To develop the AML-chip, we cultured AML cells isolated from blast crisis chronic myelogenous leukemia (bcCML) mice in the marrow component of the BMME-chip with MSC, HSPC, and fibrin-hydrogel. At day 14, AML cells were maintained at 29.00+/-2.35% equivalent to disease burden at advanced stages of AML. Flow cytometry showed a 4-fold increase in HSPC in AML-chip, similar to in vivo, which may indicate loss of differentiation. Similar to in vivo experiments, we found that osteoblastic function is lost in AML-chip as shown by reduction of osteocalcin gene expression at day 7 and 14 (41.10+/-13.50% and 16.60+/-5.00% respectively compared to BMME-chip, p=0.04). This finding is reflected in the decrease of mineralization of the osteoblastic cells observed via histochemical imaging. We have previously reported that the chemokine CCL3 is elevated in AML patients as well as murine models, and that elevated CCL3 inhibits osteoblastic function. Strikingly, we found elevated levels of CCL3 in the effluent of AML-chip compared to BMME-chip (918.49+/-192.54 pg/mL and 498.73+/-79.05 pg/mL, p=0.003). Our results indicate that AML-chip can recapitulate the phenotypes reported in vivo, and supports the reliability of our system to recapitulate human AML in future experiments.

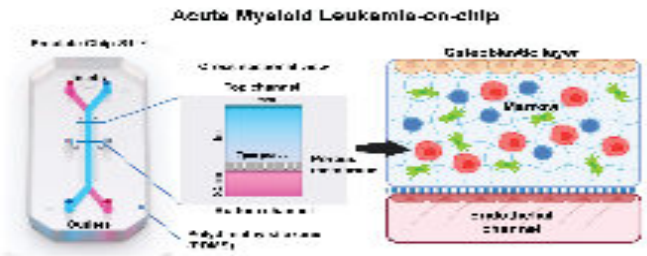

***Disclosures: AZMEER SHARIPOL**, None*

SUN-102

Inhibition of NF-?B Inhibitor Alpha (I?B?) Reduces Type H and L Skeletal Blood Vessels in a Glucocorticoid-Induced Osteotoxic Mouse Model *Sisir Kumar Barik[1], Weixin Zhang[1], Arryn D Otte[1], Janet L Crane[1]. [1]Johns Hopkins University, United States

Osteoporosis and osteonecrosis are well-described adverse effects of chronic glucocorticoid (GC) use; a unifying pathophysiologic change is decreased bone vasculature. Our previous study on young GC-induced osteotoxic (GIO) WT (C57BL/6J) mouse model showed disruption of skeletal angiogenesis through transrepression of nuclear factor kappa B (NF-?B)-mediated preosteoclast (POC) derived platelet-derived growth factor-BB (PDGF-BB) transcription. To further delineate the intracellular signaling mechanism of GC-suppression of angiogenesis, we are disrupting the GC-NF?B-Pdgfb pathway in osteoclasts. We have initially verified the GIO phenotype in GC receptor (GR) floxed (Nr3c1fl/fl) mice intraperitoneally injected with methylprednisolone daily (20 mg/m2/day) or vehicle (veh) for 2, 4, and 6 weeks (n=5-8/group/time point) beginning at postnatal day 14 and further characterized the changes in blood vessels. Micro-CT analysis showed that GIO Nr3c1fl/fl mice have significantly reduced BV/TV at all age groups compared to veh-treated mice. Co-immunostaining at the distal femurs showed reduced CD31hi Emcnhi (Type H vessels) at the metaphyseal region, along with decreased branch points Emcnlow (Type L vessels) in GIO Nr3c1fl/fl mice relative to veh-treated littermates at all age groups. Comprehensive 3D analysis of Type H vessels showed a significant reduction in the vessel diameter, length, area, and volume in GIO Nr3c1fl/fl mice compared to veh-treated mice. Specifically, Type H Vessels were found to be largest in the mid-metaphyseal region and the cortex, with thinner vessels in the angiogenic region towards the growth plate in GIO Nr3c1fl/fl mice. Moreover, thinner vessels were noted at the transition into the diaphysis in GIO Nr3c1fl/fl mice at all the time points. In contrast, veh-treated mice showed a significantly larger volume of Type H vessels identified with CD31hi Emcnhi and time-dependently increased vessel diameter, length, area, and volume nearest to the growth plate, which is the region of angiogenesis. Gene expression analysis on canonical and non-canonical NF-?B pathways from long bones of Nr3c1fl/fl mice showed inhibition of NF-?B inhibitor alpha (I?B?) after 6 weeks, suggesting chronic GC negatively regulates NF-?B signaling. Further experiments disrupting Nr3c1-/- in the osteoclast lineage will help explain the effect of GCs on skeletal angiogenesis and its role in bone formation and development.

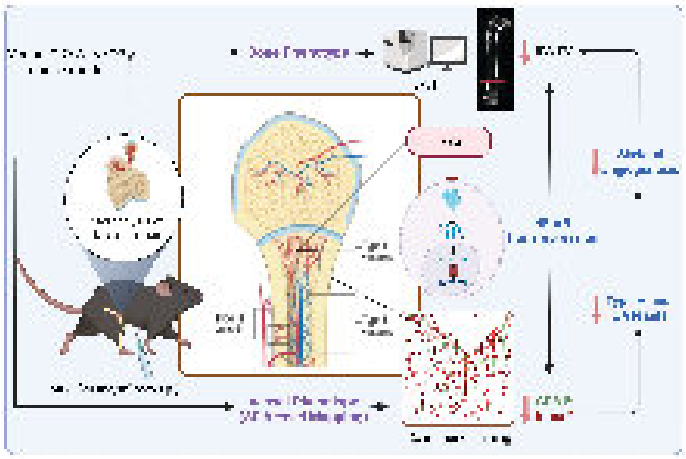

***Disclosures: Sisir Kumar Barik**, None*

SUN-103

The MIP-1?/HMGB1 Signaling Axis Regulates Osteocyte RANKL expression in Multiple Myeloma *ARIC ANLOAGUE[2], MANISH ADHIKARI[2], HAYLEY SABOL[2], Sharmin Khan[3], G. David Roodman[4], Teresita Bellido[5], Jesus Delgado-Calle[6]. [2], [2], United States. [3]University of Arkansas for Medical Sciences, Physiology and Cell Biology, United States. [4]Indiana University, United States. [5]University of Arkansas for Medical Sciences , United States. [6]University of Arkansas for Medical Sciences, United States

Multiple myeloma (MM) is a hematologic cancer characterized by the uncontrolled growth of malignant plasma cells in the bone marrow and devastating bone disease. Bone disease is a hallmark of MM. Reciprocal communication between MM cells and cells of the tumor microenvironment (TME) increases osteoclast differentiation and drives bone destruction, which persists in MM patients even during remission. Current therapies, including bisphosphonates and Denosumab (anti-RANKL antibody), reduce skeletal related events in patients with MM osteolytic disease, but long-term suppression of bone remodeling using these drugs has adverse side effects. Thus, identifying new targets to restore bone resorption to physiological levels is imperative to improve bone health and reduce the potential negative side effects in MM patients. Here we explored the molecular mechanisms regulating RANKL, a pro-osteoclastogenic cytokine essential for osteoclast formation, in the MM TME. Earlier work demonstrated that osteocytes are part of the TME and thus we hypothesize that MM-derived factors stimulate RANKL expression in osteocytes, an abundant cellular source of this cytokine in bone. Treatment of osteocyte-like cells (MLOA5/Y4) with 25% conditioned media (CM) from human JJN3 MM cells or murine 5TGM1 MM cells resulted in a ~2-fold increase in RANKL expression. MIP-1a is produced by MM cells, increases osteoclastogenesis, and it is associated with poor outcomes. Because osteocytes expressed the MIP1? receptors CCR1/3/5, we next investigated whether MM-derived MIP1? regulates RANKL in osteocytes. Recombinant MIP1? increased by ~2-fold RANKL expression in osteocyte-like cells and in ex vivo organ bone organ cultures containing authentic osteocytes. Treatment with a neutralizing anti-MIP1? antibody or siRNA-mediated knockdown

of MIP1? in MM cells fully prevented the RANKL upregulation in osteocytes induced by MM cells. Intriguingly, MIP1? also increased osteocyte production of HMGB1, an alarmin cytokine produced by dying cells capable of enhancing RANKL expression. Thus, we next examined the contribution of HMGB1 to osteocytic RANKL regulation by MM cells. Treatment with a neutralizing anti-HMGB1 antibody or genetic inhibition of HMGB1 in osteocytes prevented osteocyte RANKL upregulation by MM cells. Together, our findings suggest that MM-derived MIP1? stimulates HMGB1 in osteocytes, which in an autocrine manner, regulates RANKL expression. These findings unravel a targetable MIP1?-HMGB1 signaling axis regulating RANKL expression in the MM-TME.

***Disclosures: ARIC ANLOAGUE**, None*

SUN-104

Regulation of Osteoblast Nitric Oxide Generation, Glycolysis, and Metabolic Programming by Prostate Cancer *Katrina Clines[1,] Henry Moon[1,] Gregory Clines[1,] [1]University of Michigan, United States

Osteosclerotic bone metastasis is a dynamic and symbiotic relationship between prostate cancer cells and osteoblasts. How osteoblasts respond during the first encounter, when prostate cancer cells arrive in bone, is uncertain. We hypothesized that an initial step is to recruit local and circulating osteoblasts to the metastatic bone niche. To test the hypothesis, GFP-expressing mouse long-bone primary osteoblast cultures were placed on optically opaque 8 μm pore cell culture inserts with one of the human prostate cancer cell lines ARCaPM, ARCaPE, C4-2B, LNCaP, and 22Rv1 cultured below. Osteoblast migration through the membrane was monitored by fluorescence microscopy in hypoxia. ARCaPM and ARCaPE cells markedly increased migration, while the remaining cell lines repelled osteoblast migration. These data suggested that prostate cancers possess different degrees of osteoblast tropism. We next performed single-cell RNA-seq (scRNA-seq) of osteoblast cultures that migrated through the membrane (Migrat OB) and cultures that migrated in the presence of ARCaPM cells plated below (Migrat OB+PrCa), using the 10X Genomics platform. Significant fold increases in osteoblast gene expression were detected in Nos2 (~1200X), Il13ra2 (~900X), Cxcl5 (~70X), Cxcl3, Cxcl1, Rarb, Mmp13, and Bmp7 in the Migrat OB+PrCa compared to the Migrat OB group. Nos2 encodes inducible nitric oxide synthase (iNOS) that generates nitric oxide (NO). Mouse osteoblasts cultured in ARCaPM-conditioned media (CM) increased osteoblast production of NO (24.6 μM) compared to control media (0.5 μM). NO has numerous biologic actions and was recently reported to increase osteoblast anabolism through the regulation of glycolysis. We next determined the transcriptomic differences in osteoblast glycolytic enzymes and found an increase in Pfkfb3, Pfkp, Aldoa, Tpi1, Gapdh, Pgk1, and Ldha in Migrat OB+PrCa vs. Migrat OB groups. Osteoblasts exposed to ARCaPM CM also significantly increased lactate generation, indicating an increase in glycolysis. An increase in the osteoblast energy supply via glycolysis would be critical for promoting the osteosclerotic response, especially in the hypoxic environment of bone metastasis, thus supplying the cells with substrates for collagen and bone matrix synthesis. We report here how prostate cancer changes osteoblast tropism, secretome, and metabolic programming to support prostate cancer and osteoblast growth.

***Disclosures: Katrina Clines**, None*

SUN-106

Prostate Cancer Bone Metastasis Alters Gut Microbiota Composition by Enhancing Gut Leakiness *Kelly Contino[1,] Jenna Ollodart[1,] Yang Yu[1,] Sidharth Mishra[2,] Laiton Steele[1,] Katherine Cook[3,] Hariom Yadav[2,] Yusuke Shiozawa[1,] [1]Department of Cancer Biology, Wake Forest University Health Sciences, United States, [2]University of South Florida Morsani College of Medicine, United States, [3]Department of Hypertension, Wake Forest University Health Sciences, United States

In a state of dysbiosis, the physical, biochemical, and immune barriers separtating gut bacteria from systemic circulation become compromised. This loss of gut barrier integrity, referred to as “leaky gut”, has been implicated in the pathogenesis of numerous diseases including cancer. The translocation of the gut derivatives as a result of leaky gut has been shown to drive tumorigenesis and cancer progression, including prostate cancer (PCa). Despite this link to tumor formation/progression, the relationship between leaky gut and metastasis, specifically to the bone, remains unexplored. To begin understanding the complex mechanisms between the gut and bone metastasis, the leading cause of death in PCa patients, we intrafemorally inoculated murine PCa cell line RM-1 cells into C57BL/6 mice. Bulk RNA sequencing of intestinal tissue from these mice revealed that markers of intestinal tight junctions (physical barrier) and gut mucosal membranes (biochemical barrier) were downregulated in the intestinal tissue of PCa-bearing mice. This data suggests that bone metastasis alone is capable of inducing leaky gut. To validate these findings, serum ELISAs for LPS binding protein (LBP) and sCD14, well-established markers of leaky gut, were performed. Significantly higher levels of LBP and sCD14 were observed in the serum of PCa-bearing mice, compared to that of sham mice, further supporting the notion that leaky gut occurs as a result of bone metastasis. Then, to examine whether bone metastasis induces changes in gut microbial composition,16s rRNA sequencing of the mouse stool was conducted. Interestingly, elevated levels of Dorea formicigenerans and Ruminococcus gnavus, mucin degrading bacteria known to enhance leaky gut, were found in the stool of PCa-bearing mice. Several butyrate generating bacteria were found to be upregulated in the stool of PCa-bearing mice. Butyrate is a short chain fatty acid known to contribute to bone formation. Clostridum scindens, known to convert glucocorticoids into androgen, was also elevated in the stool of PCa-bearing mice. Conversely, Faecalibaculum rodentium, known to be protective against intestinal tumor growth, was significantly enhanced in the stool of sham mice. Collectively, these results suggest that bone metastasis alters the gut microbiota composition by enhancing gut leakiness. Future studies are clearly warranted to further reveal the mystery of gut-bone metastasis axis.

***Disclosures: Kelly Contino**, None*

SUN-107

Irinotecan’s Effect on Trabecular Long Bone in a Rat Model of Breast Cancer *Bailey Deverell[1,] Kent Algate[1,] Bonnie Williams[1,] Joanne Bowen[1,] Tania Crotti[1,] [1]The University of Adelaide, Australia

Given 90% of people treated for breast cancer with chemotherapy survive five-years post-diagnosis understanding the effects of treatment on bone is essential. Irinotecan, with active metabolite SN-38, is being trialed for breast cancer treatment, yet its effect on bone microarchitecture and turnover is not known. This study aimed to assess irinotecan’s effect on trabecular bone in the femur and tibia of a rat model of breast cancer via micro-CT and histology and on human peripheral blood mononuclear cell (PBMC) viability in culture. Female dark agouti rats were subcutaneously inoculated with breast cancer cells and allocated to vehicle control (n = 8) or irinotecan (175 mg/kg intraperitoneally; n = 8) groups (Ethics: 33965). Rats were euthanised 5 days post-treatment and the femur and tibia were assessed ex vivo via micro-CT for; trabecular thickness (Tb.Th.), trabecular number (Tb.N.), trabecular spacing (Tb.S.), bone volume (BV), and percent bone volume (BV/TV%). Serial sections (5 ?m) of decalcified femur and tibia were stained with tartrate-resistant acid phosphatase (TRAP) and H&E and assessed for multinucleated osteoclast cells on trabecular bone, and adipocytes respectively. TNF? in the rat serum was analysed via ELISA. PBMCs were cultured in vitro with a range of SN-38 concentrations (1 nM - 50 μM) for 48 hours and cell viability assessed via WST-1 assay.Femur and tibia microarchitecture did not significantly differ between groups. Multinucleated TRAP-positive cell number was significantly increased in the tibia of the irinotecan group compared to the vehicle control ($p = 0.033$). Femur and tibia adiposity did not significantly differ between treatment and control groups. TNF? concentration was greater in irinotecan rats (9.145 +/- 1.523) compared to vehicle control (6.300 +/- 1.491), however this was not statistically significant. SN-38 exposure (1 nM - 50 nM) increased cell viability compared to vehicle control in human PBMC culture whilst over 100 nM SN-38 significantly reduced cell viability.Irinotecan increased TRAP+ cells on trabecular bone in the tibia of breast cancer treated rats at five days post treatment. Changes to microarchitecture and adiposity was not evident at this time point. We propose investigating the longer term impacts of irinotecan in the microarchitecture of breast cancer treated rats to align with longer term cancer survivorship.

***Disclosures: Bailey Deverell**, None*

SUN-109

Using Treadmill Exercise and Vibration to Enhance Drug Delivery to Bone Tumors *Michelle Gelbs[1,] Rodrigo Guerra[1,] Eda Biricik[1,] Dillon Murugesan[1,] Vinagolu Rajasekhar[2,] Darren Veach[2,] Pat Zanzonico[2,] Gene DiResta[3,] John Healey[2,] Susannah Fritton[1,] [1]City College of New York, United States, [2]Memorial Sloan Kettering Cancer Center, United States, [3]Microflow Associates, United States

Metastatic bone cancer is frequently treated using systemic administration of chemotherapeutic agents or bone-sustaining medications such as bisphosphonates. Drug delivery to cancerous tumors is affected by vascularity, rate of diffusion of molecules through the tumor, and heightened interstitial fluid pressure. Loading induced bone deformations increase convective transport via interstitial fluid flow in normal bone tissue. We hypothesize that weight-bearing mechanical loading will enhance drug delivery to bone tumors. In this pre-clinical pilot study, two mechanical interventions were analyzed: treadmill walking and standing on a vibrating platform. To model breast cancer bone metastasis, sixteen 12-13-week-old female nude rats were injected in the right proximal tibia with human breast cancer MDA-MB-231 luciferase-expressing cells (1.25-2.5 million cells in 25 μL of serum-free medium) using an IACUC-approved protocol. IVIS bioluminescent imaging was performed on days 0 and 7 post-injection to assess cell viability. After 8-14 days of tumor growth, three radiolabeled tracers/drugs were used to measure the effects of 10-minute mechanical loading protocols on tumor-uptake: 18F-NaF, 89Zr-trastuzumab, and 89Zr-paclitaxel (n=3-5 per group). The tracers were injected via tail vein in awake rats, mimicking clinical drug delivery. In vivo micro-PET/CT imaging was used to assess tracer uptake in the tumor region before and after walking on a treadmill for 10 min at a speed of 5-12 m/min or standing on a vibrating platform (35Hz, 0.3g peak) for 10 min. After sacrifice, right and left tibiae were scanned using high-resolution micro-CT (Skyscan) and then plastic-embedded for histological assessment. The maximum percent of tracer injected dose per unit volume (%ID/mL) was calculated from right (cancer cell-injected) and contralateral left tibial metaphysis volumes of interest. 18F-NaF had the highest %ID/mL within tumor regions, and 18F-NaF uptake was significantly higher in the right, tumor-bearing tibia after treadmill exercise (Fig. 1). Vibration showed an increasing %ID/mL trend in the tumor-bearing tibia. This pilot study demonstrates that exercise and vibration have potential to amplify drug delivery to tumor regions. Utilizing mechanical interventions on tumor bearing limbs represents a potential

clinical intervention that may enhance a drug's uptake and therapeutic effect while potentially decreasing systemic drug dosage and unwanted side effects.

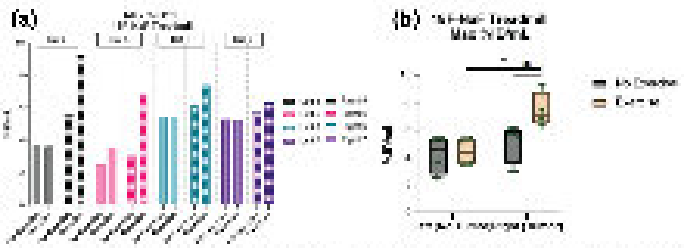

***Disclosures: Michelle Gelbs**, None*

SUN-110

Bone-derived Dickkopf-Related Protein 1 promotes primary breast cancer tumor growth and supports hematopoietic stem and progenitor cells *Emily Eul[1], Biancamaria Ricci[1], Seunghyun Lee[1], Giulia Furesi[1], Roberta Faccio[1]. [1]Washington University in St. Louis , United States

Dickkopf-related protein 1 (Dkk1), a Wnt/?-catenin signaling inhibitor, is produced in the bone, and is best known for suppressing bone formation and increasing bone resorption. Interestingly, Dkk1 is upregulated in cancer patients and correlates with poor prognosis. Recent work has shown that Dkk1 can exert immune suppressive effects by altering the frequency and function of immune cell subsets in various cancer models. However, the role of Dkk1 in breast cancer progression and the mechanisms by which Dkk1 can affect so many immune cell types remain unclear.We found that mice bearing luminal B, ER+ PyMT-B6 tumors exhibit increased Dkk1 expression in the bone and higher systemic serum levels compared to no tumor bearing controls. To assess the role of Dkk1 during breast cancer tumor progression, female C57BL/6 mice were orthotopically injected with PyMT-B6 cells and treated with Dkk1 neutralizing antibody (?Dkk1) or IgG control antibody (10mg/kg every 48 hrs). We observe a striking reduction in tumor growth of ?Dkk1 treated mice, and systemic alterations to immune cell population frequencies. We also find similar results in mice bearing the metastatic basal-like ER- EO771-LMB breast tumors. To study the effects of bone-dervied Dkk1 we utilized osteoblast lineage specific Dkk1 overexpressing mice (2.3kbCol1?1Dkk1Tg) injected with PyMT-B6 cells and observed increases in tumor growth and changes in the immune landscape.To uncover how Dkk1 can modulate a variety of immune cell populations, we investigated the impact of tumor progression and Dkk1 on hematopoietic stem and progenitor cells (HSPCs) in the bone marrow of tumor bearing mice. Based on previous reports indicating that Dkk1 can influence HSPC regeneration and exhaustion, we performed noncompetitive bone marrow transplantation (BMT) assays using Dkk1 overexpressing mice and osteolineage conditional ckO mice, tTA-TetOFFOsx-Cre; Dkk1fl/fl and saw an increase in the engraftment of HSPC populations from over expressing mice. Additionally, we treated mice with PyMT-B6 or EO771-LMB with ?Dkk1 or IgG and discovered that Dkk1 strickingly reduced HSPC frequencies only in the EO771-LMB model, suggesting that Dkk1 may regulate hematopoiesis in a breast cancer subtype dependant manner.Together this data demonstrates that Dkk1 expression is upregulated in the bones and supports breast cancer tumor growth and hematopoiesis, overall, highlighting the existence of a bone-tumor crosstalk to promote tumor progression.

***Disclosures: Emily Eul**, None*

SUN-111

Assessing Targetability and Optimizing Safety of The Acidic Peptide Conjugates Against Bone Cancers *Losha Jung[1], Philip Low[1]. [1]Purdue University, United States

Bone metastasis is very common in breast and prostate cancer patients, but despite the high incidence, five-year survival rates for both are only 20 to 30 percent. Therefore, there is an urgent need to develop a novel therapy to improve the poor prognosis.Many literatures have reported that negatively charged acidic peptides can recognize positively charged calcium heads of hydroxyapatites exposed in damaged bones and thus have utilized these peptides to deliver small molecules. Previously we have confirmed acidic peptide's ability to concentrate fluorescent or radio-imaging agents selectively to prostate and breast cancer-induced bone lesions. Here we have further assessed and optimized the targetability and safety profile of our acidic peptide to determine its usage as a therapeutic agent against bone cancers.First, we performed a biodistribution study by injecting 177Lu-bound chelator-acidic peptide conjugate into tibial tumor-bearing mice and quantifying radioactivity of each organ at different timepoints. Heart, lung, liver, spleen, muscle, blood, and bone marrow all had low radiation exposure (less than 0.2% average injected dose/g). Kidney uptake was initially high (13.2% avg ID/g), but most were excreted by 72 hours (1.28% avg ID/g). Maximum tumor-bearing bone uptake was observed at 1 hour (1.57% avg ID/g), and similar amount was detected 7 days post-injection (1.55% avg ID/g). To further improve the tumor-to-kidney ratio, we then modified our acidic peptide conjugate by incorporating a renal peptidase cleavable sequence as a linker. From left to right, Figure shows kidneys and tumor bearing bones harvested 24 and 48 hours after an injection of the acidic peptide-fluorescent dye conjugate without and with the linker, respectively. Similar fluorescence intensities were measured at the diseased tibias in both groups of mice at all time points, suggesting that the linker does not impair bone lesion uptake or retention. Furthermore, the incorporation of the linker resulted in 1.5 and 3 times lesser kidney uptake at 24 and 48 hour timepoints, respectively. No other offsite localization was observed. Ultimately, the overall tumor-to-kidney ratio has significantly improved. Rapid renal clearance, specific tumor-induced bone lesion uptake, and prolonged bone retention all collectively support that our compound has potential to be a safe and effective vessel to deliver therapeutic warheads to bone cancers.

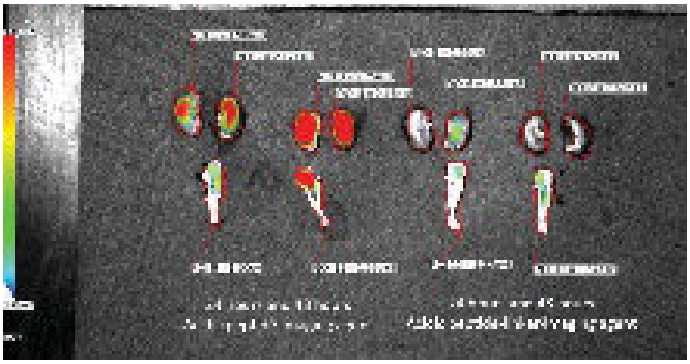

***Disclosures: Losha Jung**, None*

SUN-113

PTHrP intracrine signaling domains oppositely regulate primary breast cancer progression through tumor suppressors LIFR and p27 *JEREMY KANE[1], Courtney Edwards[2], Michael Phan[3], Carolina Vogel[4], Jonathan Lowery[4], Rachelle Johnson[5]. [1], United States. [2]Vanderbilt University , . [3]Vanderbilt University, United States. [4]Marian University, United States. [5]Vanderbilt University Medical Center, United States

Parathyroid Hormone Related Protein (PTHrP) is produced by bone and breast cancer cells to regulate bone homeostasis and mammary development. These actions are elicited through its biological domains which mediate receptor binding and cellular localization and are prone to proteolytic cleavage. In metastatic breast cancer, PTHrP paracrine signaling through the PTH receptor (PTHR1) in osteoblasts promotes tumor induced osteolysis, but breast cancer cells exclusively rely on PTHrP actions inside the cell (i.e., intracrine signaling) to alter tumor suppressor genes. However, the role for PTHrP in breast cancer remains unclear, since clinical and pre-clinical studies have identified both pro-tumorigenic and tumor-suppressive roles for PTHrP. We therefore hypothesized that the PTHrP biological domains have opposing functions in breast cancer progression. To test this, we generated MCF7 cell lines that overexpress full-length PTHrP or truncated forms of PTHrP that lack the nuclear localization sequence (NLS) or the NLS and C-terminus. Following inoculation into the mammary fat pad of 6-week old female athymic nude mice (n=7-10), tumor cells expressing PTHrP that lacks the NLS grew faster and formed larger tumors (>3-fold, $p<0.05$), while tumor cells expressing PTHrP that lacks the NLS and C-terminal region grew slower and formed smaller tumors (65% decrease, $p<0.05$) compared to control MCF7 cells, suggesting the PTHrP NLS functions as a tumor suppressor, while the C-terminus is oncogenic. Immunofluorescence of PTHrP mutant cells revealed that deletion of the PTHrP NLS did not preclude PTHrP from nuclear entry, suggesting that truncated PTHrP peptides that lack the NLS may still enter the nucleus to regulate tumor suppressor genes in breast cancer. Indeed, in vivo staining of DNLS tumors confirmed downregulation of LIFR and p27 (87% decrease, $p=0.0008$). We next conducted in silico analyses to determine which regions contribute to nuclear PTHrP intracrine signaling. DP-bind predicted high DNA binding affinity (9/12 residues) in a "gap" region between the PTHrP NLS and C-terminus enriched with lysine and arginine, which AlphaFold predicted as an ?-helix structure when the NLS is removed. This suggests the gap region facilitates DNA binding in the absence of the PTHrP NLS. These results indicate that individual biological domains of PTHrP may take on novel functions in breast cancer that differentially modulate tumor suppressors, contributing to tumor progression.

***Disclosures: JEREMY KANE**, None*

SUN-114

Breast cancer bone metastasis is mediated by the PTHrP NLS and C-terminal domain in a TGF-?/SNAI2/ZEB1 cascade *DEJA GRANT[1], Julia Ahn[2], Courtney Edwards[3], Jasmine Johnson[4], T. John Martin[5], Rachelle Johnson[4]. [1], United States. [2]Vanderbilt University, United States. [3]Vanderbilt University , . [4]Vanderbilt University Medical Center, United States. [5]St. Vincent s Institute of Medical Research, Australia

Breast cancer cells frequently metastasize to bone, where they may proliferate or enter a dormant state. Parathyroid hormone-related protein (PTHrP) expressed by breast cancer cells promotes tumor outgrowth in bone by increasing bone resorption and stimulating tumor cell exit from dormancy. PTHrP has multiple biological domains that determine its autocrine, paracrine, and intracrine functions, but the role of the PTHrP nuclear localization signal (NLS) and C-terminus is not well understood. To assess the role of PTHrP biological domains in breast cancer bone colonization, we stably expressed full-length secreted PTHrP, PTHrP with deletion of the NLS, or PTHrP with deletion of the NLS and C-terminus in human MCF7 breast cancer cells, which normally lay dormant in bone. MCF7 cells expressing these proteins were termed FLSEC, DNLS, and DNLS+CTERM mutant cell lines, respectively, and inoculated into athymic nude mice by intracardiac injection to facilitate bone colonization (n=8-10/group). Osteolytic lesion area and number, assessed by radiography, and tumor burden in the bone marrow quantified by flow cytometry, were significantly higher in mice inoculated with DNLS (5.9-fold, $p<0.05$) and DNLS+CTERM (4.19-fold, p77% decrease, $p<0.0023$), while ZEB1 was significantly upregulated in DNLS+CTERM cells (2.19-fold, $p<0.05$), compared to MSCV controls. Crosstalk within the TGF-?/Slug/ZEB-1 pathway is exceedingly complex, with bi-directional regulation, depending on the cell type and context. It is also well established that TGF-? positively regulates PTHrP; however, our data suggest that downregulation of Slug may be important for breast tumor progression in bone downstream of PTHrP, and this pathway may or may not converge on ZEB1. Taken together, our data indicate that PTHrP-mediated breast cancer-induced osteolysis involves the NLS and C-terminal domains signaling through EMT-associated pathways.

***Disclosures: DEJA GRANT**, None*

SUN-116

Spatial Cellular Analyses Reveal Changes In Senescent Burden During Multiple Myeloma Tumorigenesis *Marta Diaz-delCastillo[1], Fatima Mustapha[1], Gabriel Alvares Borges[7], Angelo J Guilatco[7], Bilal El Masari[3], Maja Hinge[4], Michael T Gundesen[5], Charlotte G Nyvold[6], Thomas Lund[5], Matthew Drake[7], Megan Weivoda[7], Thomas L Andersen[8]. [1]Molecular Bone Histology lab; Department of Forensic Medicine, University of Aarhus & DanSIC, Denmark. [7]Department of Endocrinology, Diabetes, Metabolism, and Nutrition; Mayo Clinic, United States. [3]Molecular Bone Histology lab; Research Unit of Pathology, Department of Clinical Research University of Southern Denmark, Department of Pathology, Odense University Hospital, & DanSIC, Denmark. [4]Division of Hematology, Department of Internal Medicine, Vejle Hospital, Denmark. [5]Department of Clinical Research, University of Southern Denmark & Department of Hematology, Odense University Hospital, Denmark. [6]Hematology-Pathology Research Laboratory, Research Unit for Haematology & Research Unit for Pathology, University of Southern Denmark & Odense University Hospital, Denmark. [7]Department of Endocrinology, Diabetes, Metabolism, and Nutrition; Mayo Clinic, Denmark. [8]Molecular Bone Histology lab; Department of Forensic Medicine, University of Aarhus; Research Unit of Pathology, Department of Clinical Research, University of Southern Denmark & DanSIC, Denmark

Multiple myeloma (MM) is an incurable clonal plasma cell (PC) cancer that progresses from monoclonal gammopathy of undetermined significance (MGUS). As the premalignant MGUS PCs share many genomic events and chromosomal aberrations with MM cells, the mechanisms of tumorigenesis remain unclear. Recent evidence suggest that cellular senescence in pretumor PCs and/or their bone marrow microenvironment (BMME) may play a role in MM development. Here, we investigate the burden of senescent PC/MM and their BMME in bone biopsies from patients with stable MGUS (no progression > 10 years; n=20), progressing MGUS (progression < 10 years; n=30) and newly diagnosed MM (NDMM). Sections were immunostained for PC marker CD138 and senescent markers LaminB1 and high motility box group-1 (HMGB1), and digitally analyzed with the HALO imaging software. Cells were classified as “senescent” if they displayed double negative staining for LaminB1 and HMGB1 and as “non-senescent” if they were double positive. Biopsies from progressing MGUS and NDMM patients displayed a significantly higher tumor burden than stable MGUS. Moreover, the non-senescent MM cell density was higher in NDMM than in stable MGUS, reflective of the proliferative disease stage. Stable MGUS biopsies showed a significant increase in senescent PCs per total CD138+ cells than progressing MGUS, revealing the accumulation of non-replicative MM precursors in stable premalignant stages. Interestingly, tumor burden was inversely correlated with accumulation of senescent BMME in stable MGUS patients, suggesting a microenvironmental role in tumorigenesis suppression. Next, we characterized the spatial cellular organization within 25-µm radius of senescent and non-senescent CD138+ PC/MM cells. In biopsies from NDMM patients, but not MGUS, we observed increased CD138+ MM cells neighboring senescent CD138+ cells compared to non-senescent CD138+ cells. As the BMME composition was unaffected, the clonal clustering around senescent PC/MM cells seems to be a cell type-specific feature of overt MM. Furthermore, in all disease stages the majority of senescent CD138+ cells cluster around non-senescent PC/MM, while a higher percentage of senescent BMME cells neighbor the senescent CD138+ cells. Overall, our data suggest that PCs may escape senescence and become replicative during MM tumorigenesis. Further studies aim to elucidate the impact of BMME senescence on MM development, which could be extrapolated to other cancer types.

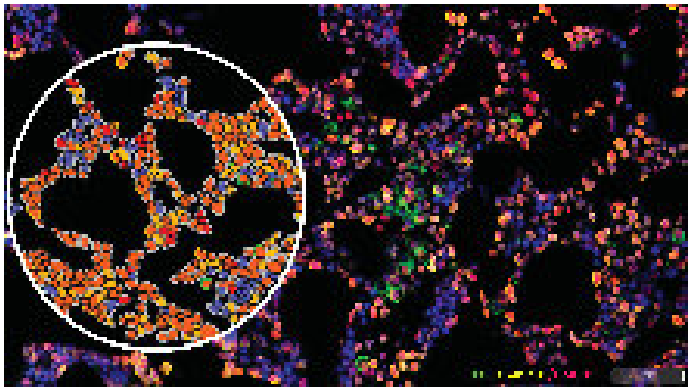

***Disclosures: Marta Diaz-delCastillo**, None*

SUN-117

Detecting Novel Subtypes of Osteosarcoma Using Bayesian Unsupervised Clustering *Sergio Llaneza-Lago[1], WILLIAM FRASER[2], Darrell Green[1]. [1]University of East Anglia, United Kingdom. [2]UNIVERSITY OF EAST ANGLIA, United Kingdom

Osteosarcoma (OS) is a rare and aggressive bone cancer that primarily affects children and young adults. OS has a poor prognosis due to the difficulty in eliminating all tumour cells using currently available treatments, leading to relapse and metastasis. Accurate classification of osteosarcoma into subtypes is essential to optimize treatment pathways and develop targeted drugs. The heterogeneity of OS patients poses a significant challenge to traditional classification methods. One better-suited approach is the Bayesian soft clustering method termed latent process decomposition (LPD). LPD has recently identified a clinically useful aggressive subtype of prostate cancer.The objective of this study is to apply LPD to RNA-seq data from OS patients to detect novel stratifications and characterise them by studying differentially expressed genes and clinical associations.Total RNA expression data plus clinical information of OS patients were downloaded from five publicly available cohorts in the GEO database. Non-biotechnical batch effect was corrected with the R package ComBat. Cohorts were merged and LPD was performed to detect stratifications. OS patients were distributed into groups according to their most representative stratification. Differential expression (DE) analysis was performed using the R package DESeq2 to characterise the identified stratifications. KEGG pathway and GO enrichment analyses were conducted using the R package ClusterProfiler on DE genes. Clinical associations were analysed by assessing relationships between the stratifications and age, gender, survival time, survival status and metastatic occurrence.LPD detected five distinct OS subtypes to which DE genes were identified. These were characterised as a typical cancer-progression subtype, a primary cilium promoter subtype, an indolent subtype associated with muscle development, a bone mineralisation-enriched subtype and a low-prognosis subtype with downregulation of muscle development. Our data highlight the importance of LPD for the in-depth examination of OS subtypes. Further validation and study of these subtypes in other sample cohorts is still required.This preliminary data provides comprehensive insights into the complex genomic processes occurring in OS and a better understanding of its subtypes. This approach will contribute to improving patient care and trial outcomes through better prognosis stratification and facilitate the development of new treatment strategies.

***Disclosures: Sergio Llaneza-Lago**, None*

SUN-118

Investigating the Role of Gli2-mediated Transcription in Paclitaxel-Resistant Bone-Metastatic Breast Cancer *JADE MILLER[1], Julie Rhoades (Sterling)[2, 1], . [2]Vanderbilt University Medical Center, United States

Bone-metastatic breast cancer dysregulates bone homeostasis in part through the secretion of parathyroid hormone-related protein (PTHrP) in a process known as the ‘Vicious Cycle’ of tumor-induced bone disease. The transcription factor Gli2 (Glioma-associated oncogene 2) is a well-established mediator of PTHrP expression and is significantly overexpressed by bone-metastatic tumors in comparison to the primary site through alternative TGF-? signaling in the bone microenvironment.Emerging literature has suggested that Gli2-mediated transcription may also drive multidrug resistance (MDR). MDR most often occurs through overexpression of transmembrane drug efflux transporters, which prevent

chemotherapies from reaching therapeutic concentrations within malignant cells. Gli2 has been implicated as a transcriptional regulator of drug efflux transporters such as p-Glycoprotein (P-gp), breast cancer resistance protein (BCRP), and multidrug resistance protein 1 (MRP1) in various cancers including ovarian, prostate, gastric, and melanoma. Thus, we hypothesized that Gli2 activation also confers a chemoresistant phenotype in bone-metastatic breast cancer through transcriptional upregulation of drug efflux transporters.In our studies, we observed tolerance to paclitaxel (PTX) in bone metastatic clones of MDA-MB-231 and 4T1 cell lines in comparison to parental cell lines. We will use genetic knockdown to inhibit Gli2 and re-sensitize bone-metastatic clones to PTX through reduced expression of drug transporters. Conversely, we will overexpress Gli2 in parental (and PTX sensitive) cell lines to confer a PTX-resistant phenotype. Using these modified cells, we will measure changes in gene and protein expression of the drug transporters to establish the mechanisms of Gli2 modulation of MDR genes in bone metastatic breast cancer.Understanding this mechanism will establish an alternative target for modulating MDR genes. This would be an important step, since decades of clinical trials using efflux transporter-targeted therapeutics have failed due to negative patient outcomes caused by the nearly ubiquitous expression of membrane transporter proteins. Thus, identifying Gli2 as a potential therapeutic target for MDR in bone-metastatic breast cancer could lead to a more effective and less toxic therapy.

***Disclosures: JADE MILLER**, None*

SUN-120

Targeting S1PR1 and p62-mediated signaling as a therapeutic approach to multiple myeloma bone disease *Daniela N. Petrusca[1], Silvia Marino[2], Attaya Suvannasankha[1], Judith Anderson[1], Evgeny Berdyshev[3], Kelvin P. Lee[1], G. David Roodman[1], Deborah L. Galson[4]. [1]Department of Medicine, Hematology/Oncology Division, Indiana University School of Medicine, United States. [2]Department of Physiology and Cell Biology, University of Arkansas for Medical Sciences, United States. [3]Department of Medicine, National Jewish Health, United States. [4]Department of Medicine, Division of Hematology/Oncology, UPMC Hillman Cancer Center, McGowan Institute for Regenerative Medicine, University of Pittsburgh, United States

Multiple myeloma (MM) is an incurable plasma cell malignancy that causes osteolytic bone lesions in most patients. Thus, novel treatments which effectively target both the MM cells and the bone microenvironment are needed. We previously reported that MM-induced upregulation of GFI1 in bone marrow stromal cells (BMSC) causes prolonged suppression of osteoblast (OB) differentiation. In addition, we described the pivotal role of GFI1 in MM proliferation via intracellular S1P-dependent increased c-Myc stability and enhanced extracellular release of S1P for a pro-survival autocrine and paracrine feedback loop through S1PR1. We employed XRK3F2, a p62-ZZ domain competitive inhibitor that can decrease GFI1 expression in both MM cells and in MM-educated BMSC in vitro, in combination with Ozanimod (Oza), a selective S1PR1 functional antagonist. We found S1P levels significantly elevated in the BM plasma of MM patients when compared to healthy donors. Also, S1PR1 and p62 are highly expressed in MM primary cells when compared with healthy donors and negatively correlate with overall survival of MM patients. Microenvironmental soluble factors (IL6, S1P, TNF?, hypoxia) and the direct co-culture of MM cells with BMSC cells, significantly increase S1PR1 transcription as well as GFI1 (mRNA and protein expression) levels in both cell types. We found that XRK3F2 significantly downregulated both p62 and GFI1 levels in MM cells even in the presence of IL-6, and Oza significantly decreased S1PR1 levels even in the MM cells overexpressing GFI1. Each drug alone significantly reduced viability in MM cells and their combination further enhanced the pro-death effect. Either drug alone significantly decreased GFI1 and P-cMyc protein levels in MM cells as well as c-Myc chromatin bound levels. These effects were further accentuated by the drugs in combination. We found that XRK3F2 and OZA, alone and in combination, improve differentiation of pre-OB. Moreover, either drug alone significantly rescued TNF? suppression of OB differentiation, and their combination completely restored it as measured by Col1a1 levels. Oza treatment of MM downregulated IL6 and RANKL levels even in MM cells overexpressing GFI1. IL6 and RANKL increase MM viability and osteoclast recruitment and activation, respectively. These data support the idea that p62 and S1PR1 might be effective targets in MM treatment and the potential of using the Oza-XRK3F2 combination as a novel therapeutic approach for treating MMBD.

***Disclosures: Daniela N. Petrusca**, None*

SUN-121

Myeloid Hif1? stimulates the formation of osteoblastic lesions when apoptosis is induced in a model of prostate cancer bone metastasis. *Hernan Roca[3], Maria Molina Sanchez[3], VERONICA MENDOZA REINOSO[2], LENA BATOON[3], Gustavo V. de Oliveira Fernandes[3], Carlos Pirela[3], AMY KOH[4], John Rubin[3], Laurie McCauley[5]. [3]University of Michigan, United States. [2], United States. [3]University of Michigan, . [4]U OF MICHIGAN, United States. [5]University of Michigan School of Dentistry, United States

Prostate cancer (PCa) preferentially metastasizes to bone, a site rich in myeloid cells and where interaction between cancer and bone cells leads to bone remodeling dysregulation. The result is mixed pathological bone destruction and formation. In human PCa, the formation of osteoblastic bone lesions predominates, resulting in bone pain and is associated with poor prognosis. Cancer growth in bone promotes a hypoxic environment with increased frequency of apoptosis. The clearance of dying cells (efferocytosis) in bone is performed by professional phagocytes, mainly macrophages (M?s). Hypoxia activates the transcription factor Hif1?, which in M?s, even under normal oxygen concentrations, becomes stabilized and activated by efferocytosis of cancer cells. Here we used PCa cells with inducible Caspase-9 mediated apoptosis in a syngeneic mouse model of bone tumor growth to analyze the effect of myeloid Hif1? inactivation when apoptosis is induced in skeletal tumors. LysM-Cre+/- mice were crossed with Hif1?-floxed mice to obtain the Hif1? mutant in myeloid lineage (Hif1?mut), rendering Hif1? inactive in these cells. PCa cells were inoculated via intratibial injection in wild-type (WT (Hif1?flox)) or Hif1?mut mice. Apoptosis was induced at d3 and d5 post-cancer inoculation via intraperitoneal injection of the dimerizer AP20187. Tibiae were collected at d6. Medullary bone volume was significantly higher in tumor-injected tibiae relative to non-injected contralateral bone, demonstrating the predominance of osteoblastic lesions ($p<0.0001$). Histological H&E showed no significant differences in tumor area relative to the total bone marrow area when comparing WT vs. Hif1?mut groups. However, μCT analyses demonstrated a reduced medullary bone volume ($p<0.01$) and fractional bone volume (BV/TV, $p<0.05$) in Hif1?mut vs. WT tibiae-bearing tumors. The analysis of trabecular thickness mimicked the differences in BV/TV ($p<0.05$), while no difference was found in trabecular number between the groups. Immunofluorescence revealed reduced F4/80+ M?s in the tumors ($p<0.05$) of Hif1?mut vs. WT, but no differences in cells lining newly formed bone surfaces within the tumors (F4/80+, CD68+ (phagocytic), TRAP+ (osteoclasts) or OSX+ cells). Altogether, these findings uncover a previously unknown role of myeloid Hif1? in the development of tumor-mediated osteoblastic lesions where cancer cell apoptosis likely accelerates macrophage infiltration/differentiation to promote bone formation.

***Disclosures: Hernan Roca**, None*

SUN-122

Stimulation of Osteoclasts by Extracellular Vesicles without RANKL Released from Adult T-Cell Leukemia *Nitin Pokhrel[1], Amanda Panfil[2], Haniya Habib[1], Sham Seeniraj[1], Ancy Joseph[3], Daniel Rauch[3], Robert Sprung[4], Petra Gilmore[4], Qiang Zhang[4], Reid Townsend[4], Yu Lianbo[5], Ayse Selen Yimaz[6], Rajeev Aurora[7], William Park[7], Lee Ratner[3], Katherine Weilbaecher[8], Deborah Veis[9]. [1]Division of Bone & Mineral Diseases, Musculoskeletal Research Center, Washington University School of Medicine, United States. [2]Veterinary Biosciences, The Ohio State University, United States. [3]Division Molecular Oncology, Washington University School of Medicine, United States. [4]Division of Endocrinology, Washington University School of Medicine, United States. [5]College of Public Health, The Ohio State University, Columbus, Ohio, USA; 6 Department of Biomedical Informatics, Bioinformatics Shared Resource, Comprehensive Cancer Center, The Ohio State University, United States. [6]Department of Biomedical Informatics, Bioinformatics Shared Resource, Comprehensive Cancer Center, The Ohio State University, United States. [7]Department of Molecular Microbiology and Immunology, School Of Medicine, Saint Louis University, United States. [8]Washington University School of Medicine, United States. [9]Washington University in St. Louis School of Medicine, United States

Adult T cell Leukemia (ATL), caused by chronic infection of human CD4+ T cells with HTLV-1, is associated with hypercalcemia and osteolytic lesions. To study the direct effect of HTLV-1-infected T cells (HTLV/T) on osteoclasts (OC), we generated a panel of clonal HTLV/T (n=9 from 2 donors) and ATL patient cell lines (ATL/P) (n=3). Supernatants (sup) from HTLV/T and ATL/P were added to murine and human OC precursors cultured in suboptimal osteoclastogenic conditions. HTLV/T sup variably stimulated OC differentiation (4 high, 1 medium, 4 low), but showed identical effects on murine and human cultures. ATL/P sup all stimulated OC generation. Expression of RANKL and OPG mRNAs by HTLV/T and ATL/P was variable, but we found no correlation between OC effects and either RANKL levels or RANKL/OPG ratio, suggesting an alternative mechanism. Concordantly, we previously showed that osteolysis in a humanized mouse model of HTLV-1 infection was only partially blocked by anti-RANKL antibodies. HTLV/T and ATL/P produce small extracellular vesicles (sEV), known to facilitate HTLV-1 infection. We hypothesized that these sEV also mediate bone loss by targeting OC. We isolated sEV from both HTLV/T and ATL/P, and found they carried most of the activity of sup. In contrast, sEV from uninfected activated T cells had little effect. Pre-treatment of HTLV/T by exosome inhibitor GW4869 blunted the OC stimulatory activity of sup. We further characterized the sEV, finding no viral particles using transmission EM. LC-MS/MS of HTLV/T sEV (n=7) showed no RANKL, but ~18% of sEV proteins correlated with strength of osteoclastogenic effect; gene ontogeny analysis of this group showed increased representation of proteins involved in bone resorption such as cytoskeletal proteins and GTPases. MicroRNA profiling of HTLV/T sEV with high osteoclastogenic activity revealed top microRNAs (mir 21, mir 155, mir 92a1) with previously noted effects on OC. To determine if in vitro findings correlate with true osteolysis, HTLV/T lines (2 high and one low effect) were injected into tibias of immunodeficient NCG mice, and trabecular bone mass was followed by vivaCT. HTLV/T with high in vitro activity caused profound bone loss by 4-8 weeks regardless of RANKL expression ($p<0.01$), while bone injected with the low effect line was not significantly different from uninjected controls.

Our study suggests that sEV, which lack RANKL, directly stimulate OC, likely mediated by multiple components of their cargo.

***Disclosures: Nitin Pokhrel**, None*

SUN-124

PPP1R3C regulates enchondroma formation and mediates cholesterol activity in IDH mutant cartilage tumors *Makoto Nakagawa[1], Nicholas Guardino[1], Eijiro Shimada[1], Vijitha Puviindran[1], Emily Peairs[1], Koji Ishikawa[1], Puviindran Nadesan[1], Banjamin A. Alman[1]. [1]Duke University, United States

Enchondroma (ECA) and chondrosarcoma (CSA) are common cartilage neoplasms that are either benign or malignant, respectively, and frequently associated with mutations in isocitrate dehydrogenase (IDH)1 or IDH2. Although the role of IDH mutations in metabolic reprogramming has been studied, their impact on chondrocytes and CSA is still unclear. Our previous work has shown that IDH mutated chondrocytes and CSA have higher glycogen levels and enhanced glycolysis, suggesting that IDH mutation effectively utilizes glycogen as an energy source. Protein Phosphatase 1 Regulatory Subunit 3 (PPP1R3C), which activates glycogen synthesis, is highly expressed in chondrocytes and CSA expressing a mutant IDH. Here, we investigated the role of PPP1R3C on cartilage differentiation and cell viability in growth plate chondrocytes and CSA, respectively. Deletion of PPP1R3C (Col2a1Cre; Idh1LSL/WT; Ppp1r3cfl/fl) rescued the phenotype of embryos with mutant IDH1 (Col2a1Cre; Idh1LSL/WT) that displays increased Col X-positive length of growth plate chondrocytes at E18.5, a major cause of ECA formation (Figure). Moreover, glycogen levels and cell viability of CSA cells were dramatically increased by PPP1R3C overexpression and significantly decreased by PPP1R3C knockout, respectively. These results indicate that PPP1R3C enhances glycogen synthesis and is responsible for cartilage differentiation and cell viability. We also identified putative binding sites for sterol regulatory element binding protein 2 (SREBP2) on the PPP1R3C promoter sequence. SREBP2 is upregulated by IDH mutation, and the overexpression of SREBP2 in CSA cells increased PPP1R3C expression. Furthermore, ChIP-qPCR revealed that SREBP2 was more strongly recruited to the promoter regions of PPP1R3C under SREBP2 overexpression, indicating that PPP1R3C is directly regulated by SREBP2. Finally, deletion of SCAP (Col2a1Cre; Scapfl/fl), which regulates SREBP2 activity, resulted in disrupted structure in proliferating and hypertrophic chondrocytes at E17.5, whereas overexpression of PPP1R3C (Col2a1Cre; Scapfl/fl; Ppp1r3cOE) partially rescued the phenotype. Taken together, our study sheds light on the mechanisms underlying the role of PPP1R3C in IDH mutated chondrocytes and CSA and highlights PPP1R3C as a potential therapeutic target for the treatment of these neoplasms. We also provide evidence for direct crosstalk between glycogen and cholesterol biosynthesis in growth plate chondrocytes, both upregulated by IDH mutation.

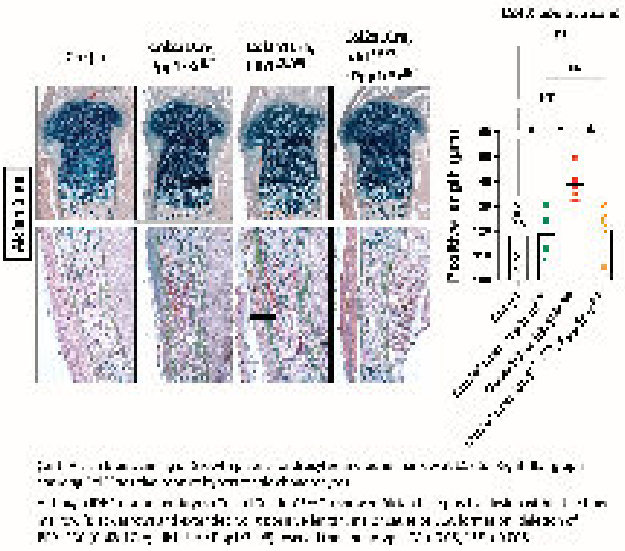

***Disclosures: Makoto Nakagawa**, None*

SUN-125

Effect of acridine orange and zoledronic acid on renal cell carcinoma local bone metastasis model *Keita Oya[1], Hiroyuki Tsuchie[1], Hiroyuki Nagasawa[1], Michio Hongo[1], Yuji Kasukawa[1], Daisuke Kudo[1], Ryo Shoji[2], Fumihito Kasama[3], Kento Okamoto[1], Tsuyoshi Kawaragi[1], Manabu Watanabe[1], Kenta Tominaga[1], Naohisa Miyakoshi[1]. [1]Department of Orthopedic Surgery, Akita University Graduate School of Medicine, Japan. [2]Department of Orthopedic Surgery, Akita Kousei Medical Center, Japan. [3]Department of Orthopedic Surgery, Yuri Kumiai General Hospital, Japan

Purpose:Renal cell carcinoma is one of the carcinomas that can cause bone metastasis, and approximately 30% of patients have bone metastasis at the time of diagnosis. Therefore, renal cell carcinoma is relatively prone to clinical problems due to skeletal related events. Acridine orange (AO) is an acoustic-, light-, and radiation-sensitive substance with a specific affinity for cancer cells and is known to promote apoptosis of cancer cells upon external stimulation. We previously demonstrated that AO inhibited cancer cell growth and zoledronic acid (ZA) prevented bone destruction in a mouse model of breast cancer bone metastasis. This study aimed to investigate the effects of ZA and AO using a mouse model of local bone metastasis of renal cell cancer.Method:Renca, a cell line of renal cell carcinoma derived from BALB/c mice was suspended in 10 ?l of phosphate-buffered saline and injected into the femur of 6-week-old BALB/c mice. ZA was injected subcutaneously every week, starting at 2 weeks after injection of Renca, when the tumor cells in the bone had grown sufficiently. Similarly, AO was injected into the tail vein 2 weeks after the injection of Renca and irradiated with 5 Gy of radiation 2 h later. The mice were divided into Control, ZA, AO, and ZA+AO groups (n=20 per group) based on these interventions, and further subdivided into sacrifice groups (n=10 per group) after 3 and 5 weeks of Renca injection. On the day of sacrifice, ?CT was taken to examine the extent of periosteal reaction (abnormal bone formation rate) due to bone metastasis along the total length of the femur.Results:The ZA, AO, and ZA+AO groups had significantly lower abnormal bone formation rates than the Control group at both 3 and 5 weeks after Renca injection ($p<0.05$). However, there were no significant differences with respect to the ZA, AO, and ZA+AO groups.Conclusion:ZA and AO may inhibit the growth of renal cell cancer bone metastases.

***Disclosures: Keita Oya**, None*

SUN-126

Elevated Parathyroid Hormone during follow-up is associated with inferior event-free survival after lymphatic childhood malignancy in a single center retrospective analysis *Corinna Grasemann[1], Jakob Höppner[2], Stephan Tippelt[3], Maximilian Grasemann[3], Desiree Grabow[4], Gunnar Cario[5], Martin Zimmermann[6], Dirk Reinhardt[3], Michael M Schündeln[3]. [1]University Hospital of Pediatrics and Adolescent Medicine, Division for Rare Diseases, St. Josef-Hospital, Ruhr-University Bochum, Germany. [2]Endocrine Unit, Department of Medicine, Massachusetts General Hospital and Harvard Medical School, United States. [3]Division of Pediatric Hematology and Oncology, Department of Pediatrics III, University Hospital Essen, University of Duisburg-Essen, Germany. [4]German Childhood Cancer Register, University of Mainz, Children's Hospital, Germany. [5]Pediatric Hematology/Oncology, University Hospital Schleswig-Holstein, Campus Kiel, Kiel, Germany., Germany. [6]Hannover Medical School, Department of Pediatric Hematology and Oncology, Hannover, Germany

Introduction: Vitamin D status is investigated as a modifier for the risk and course of multiple malignant diseases. Findings point towards a detrimental role of low vitamin D levels for event free and overall survival (EFS/OS). A vitamin D deficiency is often associated with low calcium stores, which may lead to secondary hyperparathyroidism. We hypothesized that hyperparathyroidism may influence EFS/OS in childhood malignancies.Methods: Real world data from 1547 cases (873 male) of childhood malignancies (397 lymphatic) from a single center tertiary university hospital were anonymized and analyzed. Laboratory data sets with relevance to calcium homeostasis including plasma parathyroid hormone (PTH) and serum 25-OH-vitamin D (25OHD) from 01/2000 - 7/2021 were obtained and filtered for the highest PTH and lowest 25OHD of each patient during the entire observation period. Data on relapse, secondary malignancies and mortality were obtained via chart review; from the German Childhood Cancer registry (Kinderkrebsregister) and from the ALL-BFM study group. Data were stratified for the presence/non-presence of hyperparathyroidism (PTH > 65 pg/ml) and the presence/non-presence of a vitamin D deficiency (25OHD <30 nmol/L). EFS/OS of the entire cohort and six disease specific groups was analyzed. Results:In lymphatic malignancies hyperparathyroidism was associated with inferior EFS (Hazard Ratio (HR) 2.25 [1.38 - 3.66]), but not with inferior OS (HR 1.85 [0.71 - 4.80]) and deficient vitamin D levels did not associate with inferior EFS/OS.In the entire cohort and for the other diagnostic strata neither hyperparathyroidism nor vitamin deficiency during follow-up was associated with inferior EFS/OS.Conclusion: In childhood lymphatic malignancies, hyperparathyroidism at any time during follow-up is associated with inferior EFS and may mediate the discussed effects of low vitamin D. Further prospective and mechanistic studies on this subject are urgently needed.

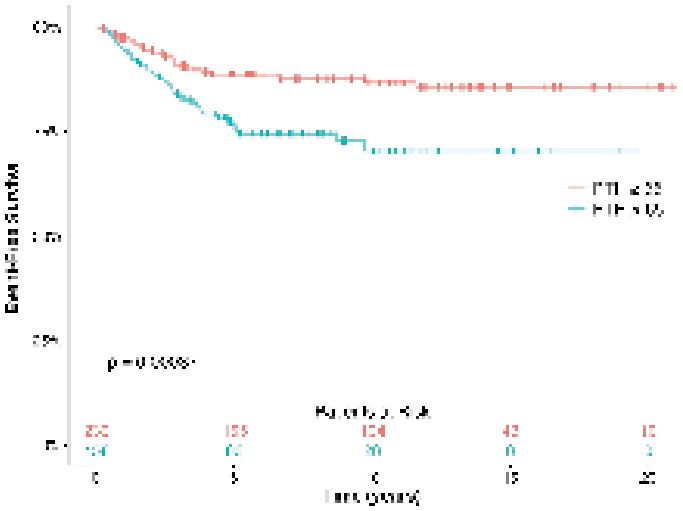

***Disclosures: Corinna Grasemann**, None*

SUN-127

Osteocytes Induce Drug Resistance via the NOTCH3-CXCL12 Signaling Axis in Multiple Myeloma *Hayley Sabol[1,] Cody Ashby[1,] Manish Adhikari[1,] Japneet Kaur[1,] Aric Anloague[1,] Sharmin Khan[1,] Samrat Roy Chodhury[1,] Michela Palmieri[1,] Lawry Barnes[1,] Elena Ambrogini[1,] Carolina Schinke[1,] Intawat Nookaew[1,] Jesus Delgado-Calle[1,] [1]University of Arkansas for Medical Sciences, United States

Multiple myeloma (MM) remains incurable due to disease relapse and drug resistance. Notch signals between MM cells and cells of the tumor niche (TME) confer drug resistance, but the cellular/molecular mechanisms are not entirely known. Using in silico analysis of clinical and transcriptomic public and internal databases, we found that 1) NOTCH3 is up-regulated in MM cells from newly diagnosed MM patients (NDMM) vs. healthy donors, 2) increases in relapsed/refractory MM (RRMM) vs. NDMM patients, and 3) NDMM patients with high NOTCH3 expression have worse responses to Bortezomib (BOR)-based therapies. Because NOTCH3 mRNA levels did not correlate with somatic mutations in NOTCH3, we tested if NOTCH3 is regulated by TME cells and its role in responses to chemotherapy. Osteocytes (Ots), recently defined as key cells in the TME, increased NOTCH3 in MM cells and protected them from apoptosis induced by BOR or VRd (BOR+Lenalidomide+Dexamethasone) in vitro. This protection was lost by NOTCH3 knockdown (NOTCH3KD) and enhanced by NOTCH3 activation (NOTCH3OE) in MM cells. Next, we compared BOR (0.1 mg/kg, 5x/wk) responses in control (C) vs NOTCH3OE MM cells in vivo. All untreated mice bearing C or NOTCH3OE cells died at 4 wks. In mice injected with C MM cells, BOR reduced tumors by 65%, improved survival (7/10 alive), and had 38% more bone mass, 25% more P1NP, and 29% less CTX than untreated mice. In contrast, in NOTCH3OE-bearing mice, BOR only reduced tumors by 23% and did not improve survival (1/10 alive), bone mass, or serum markers, supporting NOTCH3 confers BOR resistance. We then compared the MM cell transcriptome of NDMM patients with high vs. low NOTCH3 expression to find the mechanism for BOR resistance. We found that high NOTCH3 NDMM and RRMM patients had enrichment in chemokine and cell adhesion pathways and CXCL12 upregulation. Ots upregulated CXCL12 and activated the CXCR4/ERK pathway in MM cells in vitro. These effects were blunted in NOTCH3KD and enhanced in NOTCH3OE MM cells. Genetic inhibition of CXCL12 in NOTCH3OE cells prevented Ot's protection and restored BOR/VRd sensitivity, supporting CXCL12 works in an autocrine fashion. Lastly, Plerixafor, a CXCR4/CXCL12 inhibitor, restored NOTCH3OE MM cells sensitivity to BOR/VRd in vitro and in human bones bearing NOTCH3OE tumors cultured ex vivo. Our clinical and experimental data show Ots transmit drug resistance signals and unravel a novel targetable NOTCH3-CXCL12 pro-survival signaling axis in the MM TME.

***Disclosures: Hayley Sabol**, None*

SUN-128

N-cadherin in Osteolineage Cells Restrains a Tgf-?1-driven Vicious Cycle to Reduce Tumor Growth *Toshifumi Sugatani[1,] Roberto Civitelli[1,] [1]Washington University in St. Louis School of Medicine, United States

Tumor growth and metastases are dependent on interactions between the tumor cells and tumor microenvironment (TME) cells. Expression of N-cadherin (Ncad), a calcium-dependent cell-cell adhesion molecule, in transformed cells is the hallmark of epithelial-to-mesenchymal transition, which favors tumor growth and metastasis. While research has focused on Ncad in tumor cells, lesser attention has been given to how Ncad in TME cells may contribute to the interaction between the tumor and the tissue in which it grows. It has been reported that Ncad in cancer associated fibroblasts is pro-tumorigenic. However, we found that Ncad in osteogenic cells present in the TME of breast cancer is anti-tumorigenic. In previous unpublished studies we also found that Tgf-?1, a well-established pro-tumorigenic factor, is upregulated in Cdh2 KO MC3T3-E1 cells (Cdh2KO OB), generated by CRISPR-Cas9 gene editing. Specifically, we found that under Tgf-?1 stimulation, PI3K/Akt/?-catenin signaling and Sp1 and Lef1 mRNA expression are elevated in Cdh2KO OB cells. In turn, binding activity of Sp1 and Lef1 transcription factors to the Tgf-?1 promoter is increased in Cdh2KO OB cells relative to wild type (WT) OB cells. To validate the biologic relevance of these in vitro findings, we generated Tgfbr1 (Tgf-? receptor 1) KO (Tgfbr1KO) tumor cells, also using CRISPR-Cas9, and co-injected them with either Cdh2KO or WT OB cells into the mammary fat pads of C57BL/6J female mice. Injections of WT or Tgfbr1KO tumor cells were also performed as control. After 7, 9, 11, 13, and 15 days inoculation, tumors were measured in size, and after 15 days inoculation, tumors were removed and weighed. Co-injection of WT OB cells greatly enhanced tumor growth, and the effect was enhanced by co-injection of NcadKO OB cells by day 15, corroborating the notion that Ncad in OB cells is anti-tumorigenic. In addition, either WT or Chd2KO OB cells failed to induce tumor growth when co-injected with Tgfbr1KO tumor cell, indicating that Tgf-?1 drives a pro-tumorigenic, feed-forward mechanism via osteogenic cells in vivo. Thus, we propose that Ncad in TME cells with osteogenic signature restrains breast tumor growth by exerting a "breaking" effect on a Tgf-?1-driven vicious cycle.

***Disclosures: Toshifumi Sugatani**, None*

SUN-129

How the administration timing of zoledronic acid affects metastatic bone tumors *manabu watanabe[1,] hiroyuki tuchie[1,] hiroyuki nagasawa[1,] michio hongo[1,] yuji kasukawa[1,] daisuke kudo[1,] fumihito kasama[1,] Keita Oya[1,] takashi kawaragi[1,] Naohisa Miyakoshi[1,] [1]Akita University Graduate School of Medicine, Japan

Introduction:Breast cancer is one of the most common cancers in women; and it presents with various symptoms. In particular, those associated with bone metastasis are known to cause severe pain, and are often accompanied by fractures, which impact negatively on daily life. Bisphosphonate preparations, known as therapeutic agents for osteoporosis, are also used to treat bone metastasis. Zoledronic acid (ZA) is understood to suppress the progression of bone metastases and to relieve pain; however, it is uncertain as to whether the timing of the administration is associated with differences in outcomes. In this study, we administered ZA to breast cancer model mice with bone metastasis, at different points in time, to examine whether the timing of the administration caused differences in the effect. Method:E0771 cells were adjusted to a concentration of 1.0×105/10 µl with PBS and injected into the femurs of C57BL/6N mice. Given that tumor cells in the bone proliferate sufficiently two weeks after tumor administration, 100 ?g/kg of ZA was administered one week before tumor administration, at the same time as tumor administration, and one week after tumor administration. In addition, a group which did not receive ZA was included. Two weeks after tumor administration, the mice were sacrificed and evaluated. Body weight and tumor volume, before tumor administration and at the time of sacrifice, were compared between the groups.Results:Engraftment of tumor tissue was confirmed in all the femurs. There was no significant difference in body weight between the groups at the time of the tumor administration and at the time of sacrifice. In addition, there was no significant difference in tumor volume between the groups.Conclusion:Based on the finding at the time of sacrifice, which was two weeks after tumor administration, the timing of the administration of ZA did not affect the anti-tumor effect of the drug. Moving forward, we believe that it is necessary to confirm the differences in the long- term course and to further evaluate the consequent bone tissue.

***Disclosures: manabu watanabe**, None*

SUN-130

Microtubule Dynamics in Bone Metastasis of Breast Cancer *Shreya Patel[1,] Marcus Winogradzki[1,] Jitesh Pratap[1,] Waddell Holmes[1,] Ahmad Othman[2,] Alan Blank[1,] Niyati Patel[1,] Ryan Ross[1,] [1]Rush University Medical Center, United States, [2]Northwestern University, United States

Bone metastasis (BM) remains a major cause of morbidity in advanced cancer patients. Median survival rates of the two most common BM cancers, breast and prostate, range from 19-25 months and 12-53 months, respectively. Treatment strategies usually rely on surgical resection of tumors, combined with radio- and/or chemotherapies like paclitaxel, which target microtubules (MT). The efficacy of these approaches is diminished by tumor recurrence and drug resistance. Growing evidence points to dysregulated expression of tubulin isotypes as a major driver of chemoresistance. MTs are composed of heterodimers of ?- and ?-tubulins. Tubulin ?3 has been most studied for its resistance to taxanes and vinca alkaloids, with high expression correlating to poor patient outcomes. Tubulin isotypes are distinguished by their c-terminal domain and a variety of post-translational modifications (e.g., acetylation) that facilitate specific protein interaction. Currently, little is known about how microtubules change during bone metastasis. Here, we set out to profile these changes by assessing differences using RNA-Seq data, mass spectrometry, xenograft models, and breast cancer patient samples. RNA-Seq analysis between a set of bone metastatic and a set of non-metastatic breast cancer cell lines (n=10) revealed differential expression of tubulin ? isotypes with increased expression for tubulin ?2a, ?2b, and ?6. Protein levels of tubulin ?2 were higher in the aggressive MDA-MB-231 compared to MCF7 breast cancer cells. Immunohistochemis-

try of BM tumors shows increased ?3 and acetylated ?-tubulin (Ac-?-Tub) staining compared to matched primary tumors. Ac-?-Tub promotes microtubule stability and supports vesicular trafficking. Together these findings suggest specific microtubular changes during cancer cell adaptation to the bone. We and others have reported that Runx2 promotes bone metastasis. Inhibiting Runx2 in MDA-MB-231 leads to decreased Ac-?-Tub as well as tubulin ?2. Mass spectrometry and immunoprecipitations suggest that Runx2 regulates the interaction of MT-associated proteins and HDAC6 with ?-tubulin, preventing its deacetylase activity. Loss of Runx2 sensitized these bone metastatic cells to docetaxel and vinblastine treatment, as well as reduced secretion of IL-6. In summary, our results suggest specific changes in microtubule cytoskeleton during BM, as well as novel therapeutic targets that may lead to more effective chemotherapeutics to inhibit tumor growth in bone.

***Disclosures: Shreya Patel**, None*

SUN-131

Osteoblasts are a source of bone metastases-associated fibroblasts (BMAFs) *Jennifer Zarrer[1], Marie-Therese Haider[2], Nicole Ridlmaier[2], Rafael Preuer[2], Daniel J. Smit[3], Hiroaki Saito[1], Eric Hesse[1], Hanna Taipaleenmäki[1]. [1]Institute of Musculoskeletal Medicine, University Hospital, LMU Munich, Munich, Germany, Germany. [2]Molecular Skeletal Biology Laboratory, Department of Trauma, Hand and Reconstructive Surgery, University Medical Center Hamburg-Eppendorf, Hamburg, Germany, Germany. [3]Institute of Biochemistry and Signal Transduction, University Medical Center Hamburg-Eppendorf, Hamburg, Germany, Germany

In breast cancer bone metastases the abundance of adjacent osteoblasts (OBs) is diminished. To determine the fate of OBs, we combined a lineage-tracing model (Osx-creERt+;Ai9) with intracardiac injection of 4T1 breast cancer cells and performed single cell RNA sequencing (scRNAseq) of tdTomato-positive (tdTom+) OBs in metastases-bearing and healthy control animals. Bioinformatic analysis revealed a distinct cluster of tdTom+ OBs in metastases-bearing mice that express genes related to tumor microenvironment, fibrosis and cancer-associated fibroblast (CAF) proliferation (e.g. Cxcl12, Tnc, Mmps, Pdgfr-?, Pdgfr-?). CAFs reside inside tumors providing a micro-milieu that supports tumor growth. However, little is known about metastasis-associated fibroblasts (MAFs), in particular in bone metastases. Based on our findings, we hypothesized that OBs might abandon the bone surface and become MAFs. Supporting our hypothesis, histological analysis demonstrated elongated tdTom+ OBs within metastases, which we termed bone metastases-associated fibroblasts (BMAFs), while only a few OBs were present on nearby bone surfaces. Consistently, MC3T3-E1- and primary OBs acquired a spindle shape morphology upon stimulation with medium conditioned by 4T1 or MDA-MB-231 breast cancer cells (CCM), which also increased OB migration and OB-induced collagen remodeling. Furthermore, in an ex vivo co-culture model, OBs in the vicinity of cancer cells became elongated and migrated in-between tumor cells. Immunoblot, qRT-PCR, scRNAseq and histological analyses revealed a reduction of OB markers (Runx2, Osx) and an increase of BMAF-associated genes (e.g. Pdgfr-?, Pdgfr-?) in CCM-stimulated OBs and cancer-associated tdTom+ OBs. To elucidate the mechanisms transitioning OBs to BMAFs, we performed RNA sequencing and identified an activated IL-17A signaling pathway in CCM-stimulated OBs compared to controls, which was confirmed by immunoblot and qRT-PCR analyses of downstream targets (C/ebp, Ccl2). Furthermore, recombinant IL-17A promoted OB migration and acquisition of a BMAF phenotype while inhibition of IL-17A signaling using an anti-IL-17 antibody restored the CCM-induced morphological changes and OB migration. In vivo, anti-IL-17A reduced the number and growth of bone metastases determined by bioluminescence imaging and histology. Together, these results demonstrate that OBs give rise to BMAFs at least in part through IL-17A, which might contribute to metastatic growth.

***Disclosures: Jennifer Zarrer**, None*

SUN-132

Investigating Novel RNA Transcripts in Primary Bone Cancer-derived Circulating Tumour Cells *Emma Bull[2], Sergio Llaneza-Lago[2], WILLIAM FRASER[3], Darrell Green[2]. [2]University of East Anglia, . [2]University of East Anglia, United Kingdom. [3]UNIVERSITY OF EAST ANGLIA, United Kingdom

Primary bone cancers (PBCs) are a heterogeneous group of cancers. PBCs primarily arise in children and adolescents. The five-year survival rate for localised disease is ~50% but ~20% for metastatic disease. Standard of care and survival rates have not improved since the 1960s. Better understanding of PBC biology leading to more effective and less toxic treatments is urgently required. Metastasis is the leading cause of bone cancer-related death, but metastatic samples are difficult to obtain because surgery is scantly used at late-stage disease. We recently developed protocols to isolate circulating tumour cells (CTCs) from PBC patient blood to investigate the “seeds” of metastasis at single cell resolution. We identified novel RNA transcripts in CTCs that were not observed in normal or tumour tissue. This data suggests that (i) some novel RNAs are unique to metastasis and/or (ii) pro-metastatic cancer cells are capable of producing their own disease-promoting gene networks. This project aims to validate and characterise the mechanism of action of these novel RNAs. Whole blood samples (7.5mL) were obtained from ten patients with osteosarcoma or Ewing sarcoma. The ClearCell FX (Biolidics) was used to isolate live and viable CTCs. Single CTCs were then manually picked from the output using brightfield microscopy and pipetting. The SMART-Seq® mRNA Single Cell LP kit was used to generate libraries for single cell RNA-seq (scRNA-seq). scRNA-seq revealed 347 significantly differentially expressed genes between CTCs and control cell lines. A completely uncharacterised 2498 base pair transcript that we term LNC441 was expressed in CTCs but not observed in controls. Early bioinformatics analysis suggest that this transcript is a long non-coding RNA housing multiple new and unknown microRNA hairpins. Characterising LNC441 will reveal previously unknown networks promoting PBC metastasis. Our study may identify new therapeutic targets for reducing or halting PBC dissemination.

***Disclosures: Emma Bull**, None*

SUN-133

DDRGK1 regulates proteostasis by modulating the ribosomal protein RPL26 during chondrocyte differentiation in spondyloepimetaphyseal dysplasia *Yangjin Bae[2], Monika Weisz-Hubshman[2], Carolina Leynes[2], Sung Yun Jung[2], Brendan Lee[2]. [2]Baylor College of Medicine, United States. [2]Baylor College of Medicine,

DDRGK1 is a substrate of the ufmylation process, a post-translational modification mediated UFM1.It is required for subsequent ufmylation of other substrates by forming complex with ULF1 (E3 ligase). The physiological importance of DDRGK1 was elucidated by the finding of mutations in Shohat-type Spondyloepimetaphyseal dysplasia (SEMD). Moreover, other genes in this pathway have since been associated with this spectrum of skeletal dysplasias. We previously showed that osteochondroprogenitor-specific (Prx1-Cre; Ddrgk1f/f) and mature chondrocyte- specific (Agn1-CreERT2; Ddrgk1f/f) knockout mouse models recapitulated the SEMD phenotype. In brief, Prx1-Cre; Ddrgk1f/f mice showed severe chondrodysplasia including progressive shortening of the limbs with an abnormal growth plate and a delayed epiphyseal ossification. In Agn1-CreERT2; Ddrgk1f/f mice, we consistently found disorganized growth plate and reduced level of proteoglycan in growth plate and articular cartilage. These in vivo results highlight the essential role of UFM1 modification in cartilage development and homeostasis. Hence, to uncover the potential cartilage-specific complexes and novel substrates of the ufmylation, we have generated ATDC5 (murine chondrocyte cell line) stably expressing the components of the ufmylation machinery, i.e., UFC1-FLAG; UFL1-MYC; HA-HIS-UFM1 via doxcyclin induction and performed IP-MS assay. Based on GO analysis, we found proteins enriched in protein ufmylation (as internal control), ER stress, protein translation pathways and ribosome. Among these, ribosomal protein RPL26 was previously reported as the substrate of UFM1 modification and also the cause of with a human ribosomopathy. Similar to the function of Ddrgk1 in proteostasis, we found that total protein synthesis was reduced by SUnSET assay (Surface Sensing of Translation) when Rpl26 was knockdown in ATDC5, with associated impairment of ATDC5 chondrocyte differentiation. We also found that Sox9 protein level was decreased similarly when Ddrgk1 was knockdown in ATDC5. These data suggest that ufmylation may be a critical post-translational modification for cartilage homeostasis by modulating the protein stability/function of subset of ribosomal proteins such as RPL26. Furthermore, this mechanism underscore the evidence of tissue-specific ribosomal function as a pathological cause of human chondrodysplasia.

***Disclosures: Yangjin Bae**, None*

SUN-134

Loss of function variant in histone reader SPIN4 causes a new X-linked overgrowth syndrome *Julian Lui[1], Jacob Wagner[1], Elaine Zhou[1], Kevin Barnes[1], Lijin Dong[2], Youn Hee Jee[1], Jeffrey Baron[1]. [1]Section on Growth and Development, NICHD, United States. [2]National Eye Institute (NEI), United States

Overgrowth syndromes can be caused by pathogenic genetic variants in epigenetic writers, such as DNA and histone methyltransferases. However, no overgrowth disorder has previously been ascribed to variants in a gene that acts primarily as an epigenetic reader. Here, we studied a male individual with generalized overgrowth of prenatal onset. Exome sequencing identified a hemizygous frameshift variant in Spindlin 4 (SPIN4), with X-linked inheritance. We found evidence that SPIN4 binds specific histone modifications, promotes canonical WNT signaling, and inhibits cell proliferation in vitro and that the identified frameshift variant had lost all of these functions. Ablation of Spin4 in mice recapitulated the human phenotype with generalized overgrowth, including increased longitudinal bone growth. Growth plate analysis revealed increased cell proliferation in the proliferative zone and an increased number of progenitor chondrocytes in the resting zone. We also found evidence that loss of Spin4 in mice led to decreased canonical Wnt signaling in growth plate chondrocytes, potentially contributing to increased pool of progenitor cells in the resting zone.Taken together, our findings provide strong evidence that SPIN4 is an epigenetic reader that negatively regulates mammalian body growth, and that loss of SPIN4 causes an overgrowth syndrome in humans, expanding our knowledge of the epigenetic regulation of human growth.

***Disclosures: Julian Lui**, None*

SUN-136

Piezo1 activation accelerates endochondral osteogenesis-mediated fracture healing and the targeted intervention effect of resveratrol *Donghao Gan[1], Wenjing Zhang[2], Qingyun Jia[3], Guozhi Xiao[1]. [1]Southern University of Science and Technology of China, China. [2]Shenzhen Institute of Advanced Technology, China. [3]Linyi People's Hospital, China

Background Fracture is one of the most common injuries in humans, and despite advances in surgical treatment, approximately 5-10% of patients will progress to delayed union or nonunion. Therefore, it is urgent to explore therpeutic targets for promoting fracture healing and shorten the healing time.Objectives To investigate the effects of Piezo1 activation on bone fracture healing and to explore Piezo1-targeting fracture healing treatment.Methods The expression levels of Piezo1 were determined in human and mice fresh callus tissue. Mice with genetic Piezo1 deletion in chondrocytes or local injection of the Piezo1 activator Yoda1 were utilized to determine the effects on fracture healing. In an effort to define Piezo1-targeting drugs for potential fracture treatment, via virtual docking technology in the constructed compound library, we found that Resveratrol (RSV) may be a PIEZO1-targeting drug. Then, we developed an injectable RSV loaded hydrogel platform as a high payload and sustainable release for fracture treatment.Results Piezo1 expression was elevated in callus tissue chondrocytes in human and bone fracture mouse model. Piezo1 deletion in chondrocytes largely delays fracture healing and callus mineralization. In contrast, local injection of Yoda1 markedly accelerated fracture healing in bone fracture mice. PIEZO1 activation increases, while PIEZO1 siRNA knockdown decreases, expression of osteogenic markers such as RUNX2, Col1a1 and Osterix in primary human articular chondrocytes (HACs) induced by osteogenesis and fluid shear stress stimuli. Interestingly, we found that Yoda1 reduced, while Piezo1 deletion increased, the expression of Runx2-degraded E3 ligase smurf1 in HACs, inhibits ubiquitin-proteasome degradation of Runx2, and promotes Runx2 transcription and osteogenic phenotype. virtual docking simulation revealed Piezo1 molecule with strong binding ability to RSV. Results from primary HACs showed that RSV activates the PIEZO1-mediated calcium flux. Results from in vitro experiments confirmed that RSV decreased the Runx2 degradation and reversed by Piezo1 deletion in HACs. Hydrogel conjugated with RSV were stable and nontoxic, with long time slow release, high cartilage uptake, and penetration capabilities, and is used for in vivo research. When compared with control mice, the RSV-treated mice displayed marked accelerated fracture healing, and upregulated osteogenic genes. Importantly, RSV-induced increases in the bone trabeculae formation, callus mineralization and fracture gap union were dramatically delayed or completely abolished by Piezo1 deletion.Conclusions We establish a critical role of Piezo1 in promoting bone fracture healing and define RSV, Piezo1-targeted compound, as a potential bone fracture treatment.

***Disclosures: Donghao Gan**, None*

SUN-138

SDHA inhibition is involved in Lin28a osteoarthritic chondrocyte reprogramming *ZOHRA BOUCHEMLA[1], Inès Slitine[2], Valentin Duong[2], Fawaz Alzaid[3], Lucie Orliaguet[3], Augustin Latourte[4], Pascal Richette[4], Hang-Korng EA[4], MARTINE COHEN-SOLAL[5], Eric Hay[6]. [1], France. [2]U1132 Inserm, France. [3]Cordeliers Research Center, INSERM, France. [4]U1132 Inserm and Lariboisière APHP hospital, France. [5]Inserm U1132 Bioscar and université Paris-Cité, France. [6]INSERM u1132, France

We have previously shown that Lin28a induces cartilage regeneration during osteoarthritis by inhibiting Let7. Loss of hypoxia is associated with OA progression, inducing energetical metabolism dysfunction. We focused here on the effect of Lin28a on this process and how energetical metabolism is involved in cartilage reprogramming.We performed RNAseq, RT-qPCR, WB, and immunofluorescent staining on murine primary chondrocytes overexpressing or not Lin28a in control or osteoarthritic (Wnt3a) conditions. For ex vivo analysis we used mouse femoral heads and human cartilage explants. Osteoarthritis was induced in WT or TgLin28aflox/flox/Col2CreERt2 by meniscectomy or aging. Knee joints were used for qPCR and histological analysis.In vitro RNAseq analysis showed that Wnt3a induces an increase in oxidative stress associated genes and mitochondrial impairment. Seahorse assay demonstrated a dramatic decrease of the spare respiratory capacity, indicating mitochondrial failure induced by Wnt3a treatment. On the other hand, reduced mitochondrial respiration and increased glycolysis were found with Lin28a overexpression (RNAseq and Seahorse). RNAseq indicates that the mitochondrial enzyme SDHA is oppositely regulated by Wnt3a and Lin28a. In vitro, Wnt3a increases SDHA gene and protein expression whereas Lin28a reduces it. This result was confirmed ex vivo on mouse femoral head explants. In OA mice (meniscectomized or aged), we observe an increase of SDHA expression whereas it is dramatically decreased in TgLin28a mice. This result was confirmed in human OA cartilage samples. To investigate the role of SDHA in chondrocyte protective effect, we used Aptenin5, an SDHA inhibitor. Aptenin5 inhibits the increased expression of mmp13 and adamts5 induced by Wnt3a. This effect was also found in human explants cultured with Wnt3a and Aptenin5. Because SDHA is involved in the conversion of succinate to fumarate, we hypothesized that the accumulation of succinate is responsible for the protective effect on chondrocytes. To demonstrate this, we treated murine chondrocytes and explants with Wnt3a with and without succinate. We found that succinate blocks the pro-catabolic and anti-anabolic effects of Wnt3a.Alltogether, these data indicate that energetic metabolism reprogrammed by Lin28a overexpression participates in cartilage protection during OA through SDHA inhibition. These results suggest that chondrocyte energy metabolism could be a new insight on OA therapeutics.

***Disclosures: ZOHRA BOUCHEMLA**, None*

SUN-140

IL-36Ra modulates IL-1?-induced inflammasome activation in chondrocytes *Sai Rama Krishna Meka[2], Michael Klüppel[2], Pranav Mishra[3], Huseyin Ozkan[2], Esin Ozkan[2], Alfonso Torquati[2], Anna Spagnoli[2]. [2]Rush University Medical Center, . [2]Rush University Medical Center, United States. [3]Rush University,

Background: IL-36 receptor antagonist (IL-36Ra) is emerging as a bone fide anti-inflammatory mediator in injury/damage response, including in osteoarthritisI. IL-36Ra belongs to the IL-36 cytokine family and has been postulated to function as a negative regulator of the IL-36 pro-inflammatory signaling pathway by inhibiting the dimerization of IL-36R and therefore the binding of the other ligands. However, there is emerging evidence that IL-36Ra mediates anti-inflammatory effects independently from IL-36R through interactions with the receptor complex SIGIRR/TIR8II. We hypothesize that IL-36Ra alters inflammatory responses in primary chondrocytes by modulating the gene expression of the IL-1?-induced inflammasome.Methods: Growth Plate Chondrocytes (GPCs) and immature Articular Chondrocytes (iMACs) isolated from P7 mice were treated every other day for a week with IL-36Ra (100 ng/ml) alone; with IL-1? (1 ng/ml) or IL-36? (100 ng/ml) alone and in combination with IL-36Ra (100 ng/ml). Collected mRNAs were subjected to q-RTPCR analysis. Data are expressed as mean + SD, significance was set at $p<0.05$.Results: IL-1? treatment triggered expression of inflammatory response genes such as Mmp13, Nfkbiz (I?B?), Nlrp3 and Irak in both GPCs and iMACs. Interestingly, the inflammatory response observed was several folds higher in iMACs than in GPCs. IL-36Ra exerted a significant reduction in IL-1?-mediated inflammatory gene expression. In particular, IL-36Ra blunted the IL-1? effects on Mmp13, Nfkbiz, Nlrp3 and Irak in GPCs, and on MMP13 and Nfkbiz in iMAC's (Fig 1). Notably, IL-36Ra and IL-36? alone or in combination had not effects, thus highlighting a role for IL-36Ra in response to specific pro-inflammatory environments independently of IL-36? signaling.Conclusion: Our data demonstrate that in chondrocytes, IL-36Ra impairs the IL-1?-induced expression of inflammasome genes. The results suggest that IL-36Ra might have anti-inflammatory effects that are independent of IL-36? signaling. References: I.Li T, Chubinskaya S, Esposito A, Jin X, Tagliafierro L, Loeser R, Hakimiyan AA, Longobardi L, Ozkan H, Spagnoli A. Science Translational Medicine 2019; 11II. Costelloe C, Watson M, Murphy A, McQuillan K, Loscher C, Amstrong M, Garlanda C, Mantovani A, O'Neil L, Mills K, Lynch M. J. Neurochem 2008;15

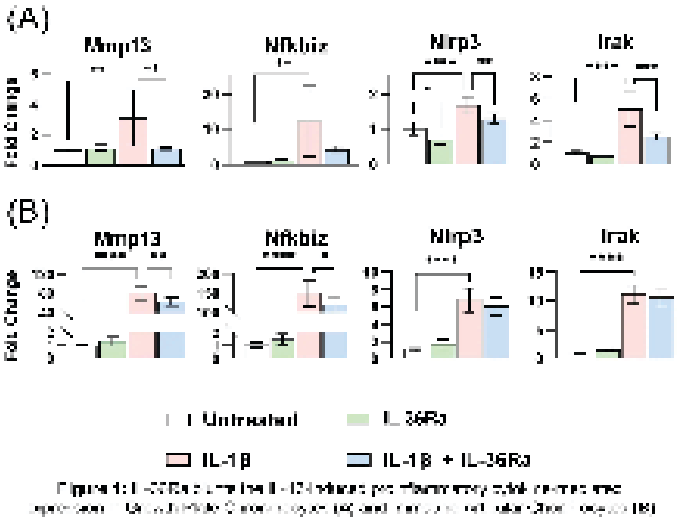

***Disclosures: Sai Rama Krishna Meka**, None*

SUN-141

Transcriptomic Analysis of Growth Plate Chondrocytes in G610C Osteogenesis Imperfecta Mice *JOE KODAMA[1], Kevin Wilkinson[2], Masahiro Iwamoto[3], Motomi Enomoto-Iwamoto[4], Sergey Leikin[5], Satoru Otsuru[2]. [1]University of Maryland, Baltimore, United States. [2]University of Maryland, United States. [3]University of Maryland School of Medicine, United States. [4], United States. [5]Eunice Kennedy Shriver National Institute of Child Health and Human Development, National Institutes of Health, United States

In addition to bone fragility, short stature is a major symptom in patients with Osteogenesis Imperfecta (OI). Currently, there is no effective treatment to enhance longitudinal bone

growth, mainly due to the unknown pathogenesis of growth deficiency in OI. Therefore, there is an unmet need to identify the mechanisms to develop novel therapies for growth deficiency in OI. Previously, we reported that the growth plates of G610C OI mice have abnormalities such as reduced proliferation, suppressed maturation, and reduced cell turnover. Additionally, dilation of the endoplasmic reticulum (ER) in hypertrophic chondrocytes (HCs) was prominent in G610C mice, suggesting that G610C HCs are exposed to cell stress. Treatment with 4-phenylbutyric acid (4PBA; a chemical chaperone) successfully reduced ER size and enhanced bone growth, supporting that cell stress in HCs plays an important role in the pathogenesis of growth retardation in OI. In this study, to further understand the dysfunction of HCs in the growth plate of 4-week-old G610C and WT mice, we performed single-cell RNA sequencing (scRNAseq) on freshly isolated growth plate chondrocytes and spatial resolution RNA sequencing (srRNAseq) in the growth plate using Visium from 10X Genomics. Transcriptomic analysis of both scRNAseq and srRNAseq revealed the upregulation of genes related to cell stress in HCs from G610C mice compared to those from WT mice. This upregulation was rescued by 4PBA treatment. The Ingenuity Pathway Analysis of the differentially expressed genes in HCs identified upregulation of the unfolded protein response and ER stress pathways in G610C HCs. Interestingly, G610C HCs significantly reduced the expression of Vegfa, which is known to be required to induce blood vessel invasion at the chondro-osseous junction. Visualization of blood vessels by intravenous injection of fluorescein-conjugated dextran in 4-week-old mice revealed that blood vessel formation in the trabecular area was significantly suppressed in G610C mice (Figure). Considering the coupling of angiogenesis and osteogenesis, our findings suggest that HC dysfunction induced by cell stress not only contributes to growth deficiency but also partially contributes to the reduced trabecular bone by suppressing blood vessel formation in G610C mice.

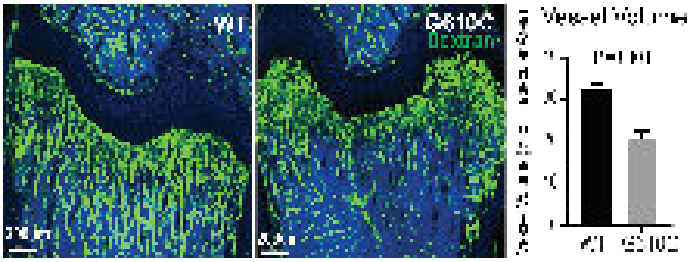

***Disclosures: JOE KODAMA**, None*

SUN-142

Chondroprotection in murine posttraumatic osteoarthritis: Increasing evidence supporting efficacy of abaloparatide *Samantha H Landgrave[1], Toru Ishii[1], Dana Godfrey[1], Terrin Geohring[1], Honey Hendesi[1], David Villani[1], SRIVIDHYA IYER[2], Karin Payne[1], Michael David[1], Douglas Adams[3], Lacey Favazzo[1], Beate Lanske[4], Michael Zuscik[3]. [1]University of Colorado Anschutz Medical Campus, United States. [2] Univ of Colorado, Anschutz Medical Campus, United States. [3]University of Colorado, United States. [4]Radius Health, Inc, United States

Osteoarthritis (OA) is a painful and debilitating disease involving the degeneration of diarthrodial joints, with the hallmark feature being cartilage loss. Currently, treatment options involve only symptom palliation; the absence of a disease-modifying OA treatment is a critical unmet need. Our prior work explored the activation of the parathyroid hormone receptor type I (PTH1R), which is expressed by articular chondrocytes in OA. We have shown that activation of this receptor by the FDA-approved osteoporosis drug Forteo (teriparatide) prevents chondrocyte hypertrophy and apoptosis while stimulating production of cartilage matrix and supporting a chondroprotective effect in a mouse model of posttraumatic OA (PTOA). Recently, the FDA has approved another PTH1R agonist, Tymlos (Abaloparatide), and we hypothesize that this PTH1R agonist could also be an effective chondroprotective drug in PTOA. To address this hypothesis, we examined the effects of abaloparatide (Abl) on knee cartilage and PTOA progression in mice. Using the widely employed destabilization of the medial meniscus (DMM) surgical approach, we induced knee PTOA in 16-week-old C57BL/6 mice. Beginning at 2 weeks after DMM, 40 µg/kg/day of Abl or saline was injected subcutaneously daily for a total of 6 weeks. Tissues were harvested at 8 weeks after DMM surgery. OARSI scores revealed that Abl provided a whole joint tissue protection that approaches statistical significance (Fig 1A). Closer investigation of tibial cartilage structure revealed significant preservation of the uncalcified cartilage in Abl treated mice (Fig. 1B) as shown by Safranin O/Fast Green stains (Fig. 1C). Bulk RNA sequencing of the whole joint was also performed to identify impacts of Abl on gene expression in joint tissues. The volcano plot displays 160 significant differently expressed genes in the abalo DMM compared to saline DMM knees (Fig. 1D). KEGG analysis showed positive activation of Cell Cycle in Abl-treated mice relative to saline controls, and a select group of other differentially expressed genes are presented that suggest a chondroprotective effect (Fig. 1E). These finding provide the first evidence indicating the efficacy of Abl in providing chondroprotection in murine PTOA. Follow-on studies to more deeply analyze the molecular, cellular, and systemic changes induced by Abl treatment will provide a comprehensive view of its potential disease modifying capability in PTOA.

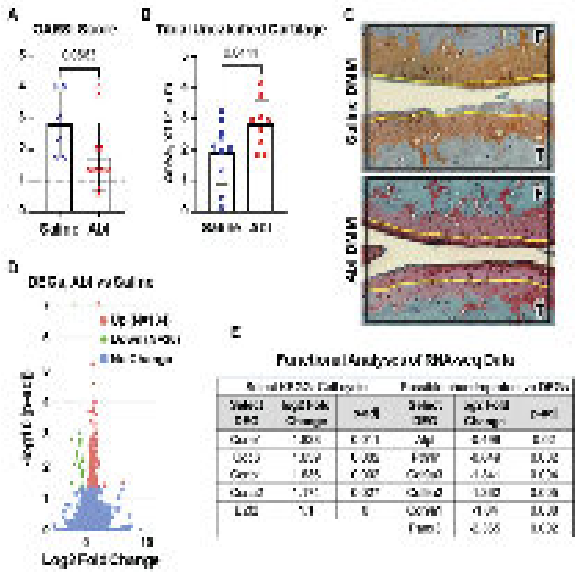

***Disclosures: Samantha H Landgrave**, None*

SUN-143

Hedgehog activation promotes osteogenic cell fates of growth plate resting zone chondrocytes *Shion Orikasa[1], Noriaki Ono[1]. [1]University of Texas Health Science Center at Houston School of Dentistry, United States

The resting zone of the postnatal growth plate is organized by slow-cycling chondrocytes expressing parathyroid hormone-related protein (PTHrP), which include a subgroup of skeletal stem cells that contribute to the formation of columnar chondrocytes. The PTHrP-Indian hedgehog (Ihh) feedback regulation is essential for sustaining growth plate activities; however, molecular mechanisms regulating cell fates of PTHrP+ resting chondrocytes and their eventual transformation into osteoblasts remain largely undefined. In this study, we hypothesized that Hedgehog signaling facilitates osteogenic cell fates of PTHrP+ resting chondrocytes through multiple mechanisms. We utilized a tamoxifen-inducible PTHrP-creER line that can exclusively mark PTHrP+ chondrocytes in the resting zone of the postnatal growth plate without marking any other cell types in long bones. To specifically activate Hedgehog signaling in PTHrP+ resting chondrocytes and visualize the fate of their descendants within growth plate and bone marrow, we also used Patched-1 (Ptch1 encodes a Hedgehog receptor which inhibits its downstream Smoothened signaling) floxed and R26R-tdTomato reporter alleles. All mice received a single dose of tamoxifen at postnatal day (P) 6 and were chased for up to 3 months. Histological and three-dimensional micro-computed tomography (3D micro-CT) analyses were performed at P14, 21, 28, 36, 42, 56, 70, 96. Hedgehog-activated PTHrP+ chondrocytes formed large concentric clonally expanded cell populations within the resting zone ('patched roses') at P21 and generated significantly wider columns of chondrocytes, resulting in hyperplasia of the growth plate at P36. Interestingly, Hedgehog-activated PTHrP+ cell descendants migrated away from the growth plate and eventually transformed into trabecular osteoblasts in the diaphyseal marrow space, leading to increased trabecular bone mass in the diaphysis at P96. Therefore, Hedgehog activation drives resting zone chondrocytes into transit-amplifying states as proliferating chondrocytes and eventually converts these cells into osteoblasts, unraveling a novel Hedgehog-mediated mechanism that facilitates osteogenic cell fates of PTHrP+ skeletal stem cells. These findings provide a solid foundation to understand how therapeutic intervention to the Hedgehog signaling pathway may impact a group of stem cell populations residing in the resting zone of the growth plate of growing individuals and subsequently affect bone formation.

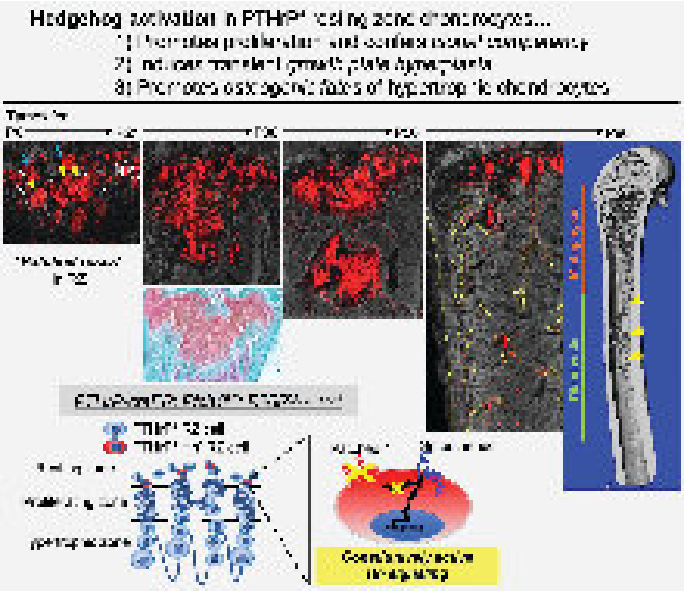

***Disclosures: Shion Orikasa**, None*

SUN-144

Cbf? inhibits osteoarthritis progression through regulating Runx1 stability

*Xian Jin[1], Xiangguo Che[1], Na-Rae Park[1], Dong-Kyo Lee[1], Poo-Reum Choi[1], Ying Cui[1], Hee-June Kim[2], Hee-Soo Kyung[2], Hyun-Ju Kim[1], Jane B. Lian[3], Janet L. Stein[3], Gary S. Stein[3], Je-Yong Choi[1]. [1]Department of Biochemistry and Cell Biology, Cell and Matrix Research Institute, Korea Mouse Pheno-typing Center, KNU Convergence Educational Program of Biomedical Sciences for Creative Future Talents, School of Medicine, Kyungpook National University, Republic of Korea. [2]Department of Orthopedic Surgery, School of Medicine, Kyungpook National University, Kyungpook National University Hospital, Republic of Korea. [3]Department of Biochemistry and University of Vermont Cancer Center, University of Vermont College of Medicine, United States

Abstract: TGF-? signaling is a vital regulator for maintaining articular cartilage homeostasis. Runx transcription factors, downstream targets of TGF-? signaling, have been studied in the context of osteoarthritis (OA). Although Runx partner core binding factor ? (Cbf?) is known to play a pivotal role in chondrocyte and osteoblast differentiation, the role of Cbf? in maintaining articular cartilage integrity remains obscure. This study investigated Cbf? as a novel anabolic modulator of TGF-? signaling and determined its role in articular cartilage homeostasis. Cbf? significantly decreased in aged mouse articular cartilage and human OA cartilage. Articular chondrocyte-specific Cbfb-deficient mice (Cbfb?ac/?ac) exhibited early cartilage degeneration at 20 weeks of age and developed OA at 12 months. Cbfb?ac/?ac mice showed enhanced OA progression under the surgically induced OA model in mice. Mechanistically, forced expression of Cbf? rescued Type II collagen (Col2?1) and Runx1 expression in Cbf?-deficient chondrocytes. TGF-?1-mediated Col2?1 expression failed despite the p-Smad3 activation under TGF-?1 treatment in Cbf?-deficient chondrocytes. Cbf? protected Runx1 from proteasomal degradation through Cbf?/Runx1 complex formation. These results indicate that Cbf? is a novel anabolic regulator for cartilage homeostasis, suggesting that Cbf? could protect OA development by maintaining the integrity of the TGF-? signaling pathway in articular cartilage.

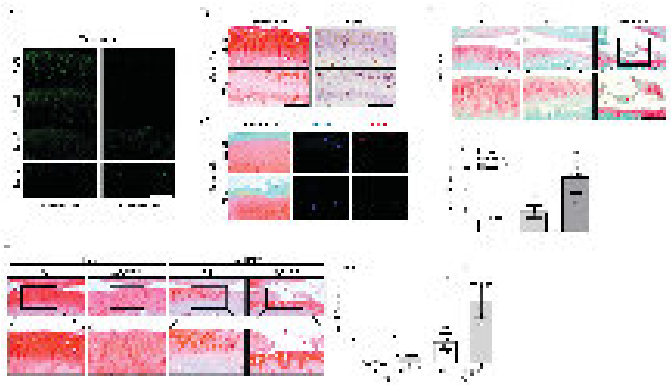

***Disclosures: Xian Jin**, None*

SUN-145

Severe Hypocalcemia Following Lutetium Lu-177 Vipivotide Tetraxetan: How Does It happen?

*Subarna Dhital[1]. [1]University of Wisconsin-Madison, United States

Introduction: Lutetium Lu-177 Vipivotide Tetraxetan (177Lu-Vipivotide Tet) is a radioligand agent approved for use in adults with prostate-specific membrane-positive metastatic castration-resistant prostate cancer previously treated with androgen receptor pathway inhibition and taxane-based chemotherapy (1). Hypocalcemia has been reported in patients receiving 177Lu-Vipivotide Tet but the responsible mechanism is not well characterized. Clinical Case: A 57-year-old man with metastatic castration-resistant prostate cancer presented with hypocalcemia. His treatment history included leuprolide, docetaxel, abiraterone with prednisone, olaparib and cabazitaxel. He also had prolonged treatment with monthly zoledronate for 4.5 years. Because of disease progression, he was started on treatment with 177Lu-Vipivotide Tet.He presented with acute hypocalcemia shortly following the first dose of 177Lu-Vipivotide Tet. At presentation, his corrected serum calcium was 5.7 mg/dL. For the degree of hypocalcemia, he was rather minimally symptomatic with mild acral paresthesia and masseter muscle spasm. Chvostek's and Trousseau's signs were negative on the physical exam. ECG did not show any QT-interval prolongation.His parathyroid hormone level was robustly elevated at 363 pg/mL (23-97). Concomitant 25(OH) Vitamin D level was 26 ng/mL. Serum creatinine was 0.52 mg/dL. Phosphate was 4.5 mg/dL (2.3-4.7). Recent imaging with PET-CT had shown diffuse, markedly avid sclerotic lesions throughout the visualized skeleton. Pelvic, retroperitoneal, and chest areas showed lymphadenopathy.Another notable lab change was the evidence of tumor response reflected by decreasing serum prostate specific antigen concentration (Figure 1). Additionally, total alkaline phosphatase titers had increased markedly, indicative of an increase in bone formation activity.He was treated with intravenous calcium, oral calcium carbonate and citrate, cholecalciferol, and oral calcitriol. Serum calcium levels gradually normalized. Treatment with 177Lu-Vipivotide Tet was resumed 3 months from the last dose. The magnitude of drop in serum calcium was rather low with subsequent dosages.Clinical Lessons:1. Severe hypocalcemia is a risk in patients receiving 177Lu-Vipivotide Tet.2. Low skeletal calcium reserves from androgen deprivation therapy may be a compounding risk factor.3. The background of anti-resorptive therapy common in this patient population could worsen hypocalcemia by limiting calcium mobilization from the uninvolved bone.4. Supplementing calcium and active vitamin D appears to be a reasonable approach for treating hypocalcemia.5. The risk of hypocalcemia appears to be lower with subsequent doses.References: (1) Sartor O et al. Lutetium-177-PSMA-617 for Metastatic Castration-Resistant Prostate Cancer. N Engl J Med. 2021 Sep 16;385(12):1091-1103

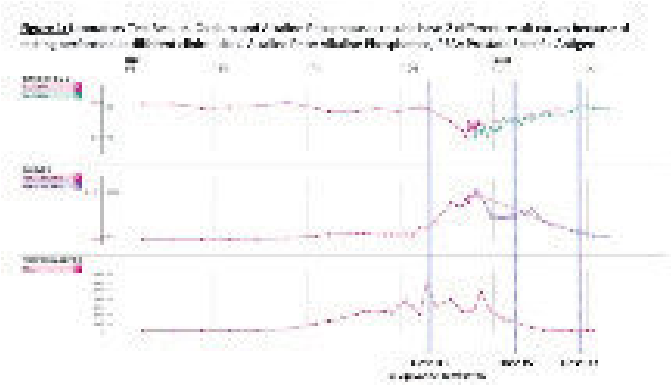

***Disclosures: Subarna Dhital**, None*

SUN-146

Progressive metaphyseal deformities and sclerosis in 11 year fraternal twins with Osteosclerotic metaphyseal dysplasia (OSMD) and Hypophosphatasia (HPP) *Nancy Dunbar[1], Eric Rush[2], Carley Vuillerman[3]. [1]Connecticut Childrens, United States. [2]Childrens Mercy, United States. [3]Boston Childrens Hospital, United States

Osteosclerotic metaphyseal dysplasia (OSMD) is a rare autosomal recessive condition characterized by a distinctive pattern of bony sclerosis limited to metaphyses and undertubulation in the metaphyses and metadiaphyses regions. It is believed to be due to reduced bone resorption by osteoclasts. It is due to biallelic pathogenic variants in the Leucine-rich repeat kinase 1 (LRRK1) gene. There are few cases in the literature and findings are heterogeneous. We report 11 year-old twin sisters with chronic musculoskeletal pain, early tooth loss, frequent fractures and easy fatigability. At age 2 years, they had already lost multiple teeth and sclerotic bones were noted on lower extremity imaging with increased bone mineral density on DXA. Genetic studies for osteopetrosis including CLCN-7, PLEKHM1 and LRP5 were normal. At age 5 years, WES revealed actionable heterozygous variants in the ALPL and TSC2 genes. Treatment for HPP with asfotase alfa was undertaken but discontinued after 9 weeks due to concern for worsening tibial sclerosis.Since the ALPL mutation did not clearly explain the sclerotic bone changes, the WES was re-analyzed at age 8 and results showed that the twins were compound heterozygotes for two mutations in the LRRK1 gene (partial gene deletion and c.5870+1G>C). By age 10, the girls had increasing sclerosis of individual long bones including humeri, femora and tibias with palpable areas of prominence in the metadiaphyseal region that corresponded to areas of bone that are sclerotic and undertubulated. They have experienced symptomatic and asymptomatic fractures in both upper and lower extremities. A bone biopsy with tetracycling labeling will be performed later this month during a planned intramedullary rod surgery. Otherwise, treatment has been supportive including physical therapy and pain control.This report provides additional phenotypic information about LRRK1 mutations and OSMD. It also underscores the importance of revisiting WES results in cases that remain ambiguous to avoid ineffective or deleterious treatments. Further reports documenting the natural history and progression of disease in OSMD are needed as well as basic research into the functional role of LRRK1 in osteoclastic function.

***Disclosures: Nancy Dunbar**, None*

SUN-147

Identification of Novel Somatic Pathogenic Menin 1 Mutations without Germline Origin in an Atypical Parathyroid Tumor *An Nguyen[1], Dolores Shoback[2], Roubin Wu[3], Quan-Yang Duh[4], Janet Chiang[1]. [1]UCSF Endocrinology, United States. [2]UCSF Endocrinology, SFVA Medical Center, United States. [3]UCSF Pathology, United States. [4]UCSF Endocrine Surgery, SFVA Medical Center, United States

Atypical parathyroid tumors (APTs) are rare lesions and can have worrisome features even without invasion or metastases like PT cancer. The loss of parafibromin staining in these tumors suggests a germline or somatic mutation that produces either hyperparathyroidism (HPT)-jaw tumor or familial HPT syndromes. However, parafibromin expression does not exclude a possible mutation.A 69-year-old woman with end-stage renal disease received a living donor kidney transplant after being on peritoneal dialysis for 16 months. While on dialysis and cinacalcet 120mg daily, serum Ca was ~9.0 mg/dL (normal, 8.6-10.4), and PTH values were 1100-1500 pg/mL (normal, 16 -77). One-month post-transplant, PTH remained elevated to 600 pg/mL, serum Ca to 11.8 mg/dL. Neck ultrasound identified a 1.9 x 1.8 x 2.2 cm left posterior hypoechoic candidate lesion with heterogeneity and irregular borders which was co-localizied on Sestamibi scan. PTH level in the washings of the fine needle aspiration of this lesion was >2500 ng/L. At left neck exploration, a large superior parathyroid gland was found to be embedded in the thyroid, requiring lobectomy with parathyroidectomy. Histology revealed a markedlyn enlarged glandtumor with 95% cellularity, without significant mitotic activity, necrosis or infiltration into surrounding tissue. There was retention of nuclear parafibromin staining, consistent with APT. Postoperatively, PTH decreased to 140 pg/mL (serum Ca 9.7 mg/dL) off cinacalcet. The patient denied any family history of MEN. Molecular testing of the tumor revealed pathogenic missense Menin 1 mutation MEN1 p.P320L (40% allele frequency) and pathogenic frameshift MEN1 p.V80W (38% allele frequency) - the latter being a novel mutation. Germline genetic testing was negative for both variants.For molecular testing for somatic mutations, the general cutoff of at least 50% allele frequency strongly supports a germline origin. The MEN1 p.P320L missense mutation is known to result in reduced protein stability leading to rapid degradation and is a germline mutation in hereditary MEN1 and a somatic mutation in sporadic endocrine tumors. The p.V80W mutation in MEN1 is novel and predicted to be pathogenic, given its truncating effect potentially early in protein translation. Overall, this case unites several concepts of recognition, diagnosis, and treatment, as well as application of molecular and genetic testing to identify somatic and germline mutations in APT and in endocrine tumors.

***Disclosures: An Nguyen**, None*

SUN-148

Primary Hyperparathyroidism Presenting with Acute Gout in a Pregnant Female *Keun Young Kim[1], Safiya Elahi[1], sanford Baim[1]. [1]Rush University Medical Center, United States

Introduction: Primary hyperparathyroidism (PHPT) is characterized by elevated serum calcium and elevated or inappropriately normal parathyroid hormone (PTH). Incidence of PHPT in pregnant females is very rare (1%). Musculoskeletal complaints due to pseudogout or gout may be associated with PHPT but are rarely initial presenting symptoms. To our knowledge, there are no reported cases of PHPT presenting as polyarticular gout during pregnancy. We present a rare case of acute gout in a pregnant female that was diagnosed and successfully treated.Case:A 29-year-old pregnant female (17 weeks gestational age) presented with left hand pain, painful lower extremity swelling, and inability to ambulate. Lab results disclosed a calcium of 11.9 mg/dL (9.1-11.2 mg/dL), ionized calcium 1.44 mmol/L (0.95-1.32mmol/L) and inappropriately normal PTH of 61.9 pg/mL (8.0-85.0 pg/mL). C-reactive protein and erythrocyte sedimentation rate were notably elevated. Physical exam revealed pain on motion and palpation, soft tissue swelling and warmth of the left second and third metacarpals, left knee, and both ankle joints. Neck ultrasound showed a right-sided lesion inferior to the thyroid. Left knee arthrocentesis revealed negative birefringent needle-shaped crystals on polarized light microscopy, confirming the diagnosis of gout. The patient underwent resection of the right inferior parathyroid gland; histology confirmed a parathyroid adenoma. Serum calcium levels normalized post-operatively and all joint symptoms resolved on prednisone.Discussion:PHPT in pregnant women is rare and can be complicated by several normal physiologic changes that occur during pregnancy. These include hemodilution, a lower proportion of bound calcium due to reduced albumin levels, and inhibition of PTH-mediated bone resorption by estrogen. Given these multiple effects on serum calcium levels, mild hypercalcemia due to PHPT may go unnoticed during pregnancy with untreated PHPT increasing maternal and neonatal morbidity and mortality.Polyarticular gout is a highly unusual presentation of PHPT. Recognition of both conditions, timely diagnostic studies, and interdisciplinary management were necessary to allow our patient to undergo a successful parathyroidectomy during her second trimester. This case highlights the necessity of monitoring serum calcium, maintaining high suspicion of PHPT when the former is elevated in pregnant patients, and being aware of unusual presentations of PHPT.

***Disclosures: Keun Young Kim**, None*

SUN-149

A stunning case of symptomatic hypocalcemia in a normocalcemic patient *Niloofar Mirsaidi[1], Avani Sinha[1]. [1]Northwell Health - North Shore/LIJ, United States

Introduction: Hypoparathyroidism is a common complication of thyroidectomy and may occur as a result of parathyroid dysfunction from parathyroid injury, disruption in parathyroid blood supply or inadvertent parathyroidectomy. Also known as parathyroid "stunning", transient hypoparathyroidism can result in subsequent hypocalcemia, hypomagnesemia and hyperphosphatemia due to disruption of PTH release and/or production. We discuss a case of hypocalcemia despite normal serum calcium levels in a woman who underwent thyroidectomy and parathyroidectomy with parathyroid reimplantation. Clinical case: A 46-year-old female with PMH of Hashimoto's thyroiditis, thyroid papillary microcarcinoma s/p total thyroidectomy and parathyroidectomy with parathyroid reimplantation, and GERD (on PPI) presented to the ED on POD #3 with worsening bilateral extremity and periorbital numbness suggestive of post-operative hypocalcemia. In the ED, vital signs were normal. Physical exam was notable for decreased tactile sensation in all extremities and positive Chvostek sign bilaterally. Labs showed serum calcium level of 8.5 mg/dL (8.5-10.1 mg/dL), ionized calcium 1.04 mmol/L (1.15-1.33 mmol/dL), intact PTH 4 pg/dL (15-65 pg/dL), and magnesium 1.8 mg/dL (1.6-2.6 mg/dL). Vitamin D levels were normal and phosphorus was elevated. ECG was unremarkable. On arrival to the ED, she was given calcium and calcitriol at doses 25% and 100% greater than her home doses, respectively, and magnesium supplementation was started to keep magnesium > 2.0 mg/dL. Her ionized calcium transiently improved but decreased again to 1.09 mmol/L, yet she reported improved symptoms. After discharge, outpatient labs showed normalization of calcium, PTH, magnesium and phosphorus with associated symptomatic improvement, and supplement doses were decreased accordingly. Conclusions: Parathyroid gland manipulation may cause transient hypoparathyroidism, yet signs and symptoms of hypocalcemia would not be expected with normal serum calcium and mildly decreased ionized calcium. Our patient's presentation was likely due to her body reacclimating to new "normal" levels of PTH and calcium. Higher doses of calcium and calcitriol supplementation may thus be needed postoperatively in certain cases. Magnesium supplementation may further assist in PTH modulation. Furthermore, in patients chronically using PPIs, intestinal calcium absorption may be decreased warranting medication reevaluation at the time of surgery.

***Disclosures: Niloofar Mirsaidi**, None*

SUN-150

Bone microarchitecture and disorganized bone tissue in a young woman with pycnodysostosis and an atypical femur fracture: A case report *Cat Shore-Lorenti[4], Heshan Witanachchi[4], Colin Chen[4], Simon Zhang[4], Hanh Nguyen[2], Christian Girgis[3], Roger Zebaze[4], Peter Ebeling[5]. [4]Monash University, Australia. [2], Australia. [3]Westmead Hospital , . [4]Monash University, . [5]School of Clinical Sciences, Monash University, Australia

Abstract: Pycnodystosis (PYCD) is a rare autosomal recessive lysosomal storage disorder, involving a loss of function mutation of the gene encoding cathepsin K (CTSK). The loss of function of this osteoclastic lysosomal protease reduces bone resorption, increases bone mineral density (BMD), but impairs the structure and material properties of bone. This case report demonstrates that bone fragility in a young woman with PYCD, presenting with an atypical femur fracture (AFF), was not explained by changes in bone density but by microarchitectural defects, disorganized bone and microcracks.Clinical Case: A 24-year-old woman with PYCD presented with an AFF in 2020 following a long history of prior minimal trauma fractures (MTF). PYCD was diagnosed in childhood and as an adult this patient displayed several signs and symptoms, including, but not limited to: short stature; dystrophic nails; short fingers; prominent forehead; prognathism, and; a significant history of 10 peripheral MTFs. Her first MTF occurred at 6-years-of-age. No other medical conditions or significant family history were identified. Her parents were consanguineous.At the time of the AFF, the patient was treatment naïve. Three years prior she gave birth via Caesarean-section and was able to breastfeed her baby for 12 months. Following the AFF, her vitamin D was slightly reduced (45 nmol/L), while P1NP and CTX were high, at 124 ug/L and 518 ng/L, respectively. Other pathology results were unremarkable.In the year following the AFF, BMD was high at the spine (T-score = +3.3), total hip (+5.4); and femoral neck (+6.7). High-resolution peripheral quantitative computed tomography (HR-pQCT) of the distal tibia detected unexpected cortical lucencies and sclerotic lesions in the trabecular compartment of the distal tibia (Fig1). Both total and trabecular volumetric BMD (vBMD) were high and trabecular numbers were increased in both the distal radius and tibia. Disorganization analysis using a novel software showed chaotically disorganized femoral shaft with spike shape masses at locations corresponding to a pseudofracture and sclerotic lesions.Clinical Conclusion: These imaging techniques detected disorganized bone and microarchitectural defects in a treatment naïve patient with PYCD and an AFF. The suppression of bone resorption in PYCD allows the accumulation of microdamage and disorganized bone that produces bone fragility. Antiresorptive therapy should be avoided.

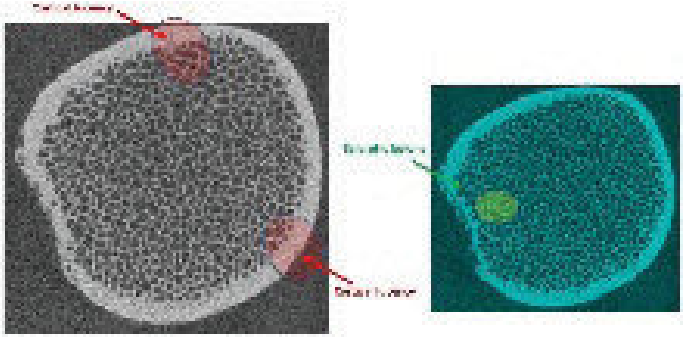

***Disclosures: Cat Shore-Lorenti**, None*

SUN-151

Autosomal Dominant Osteopetrosis, Chiari Malformation and Recurrent Nephrolithiasis: A Rare Association *Joseph Arguinchona[2], Samir Ahmed[2], Krupa Doshi[2]. [2]Mayo Clinic Arizona, United States. [2]Mayo Clinic Arizona,

Background: Osteopetrosis (OP) is a rare, heritable metabolic bone disorder characterized by dense but brittle bone. Rarely, OP is associated with Chiari malformation, described in a handful of case reports. Renal manifestations of osteoporosis are not well documented, with rare case reports of nephrolithiasis. Here we present a patient with a Chiari malformation and recurrent nephrolithiasis who was subsequently diagnosed with autosomal dominant OP.Case Report: A 44-yo white male presented with a DXA scan showing lumbar spine, and left femur neck T-scores of 9.6 and 7.6 respectively. His past history was significant for development of a slipped capital-femoral epiphysis in the right hip at age 13y, requiring pinning. After insidiously presenting with upper back and nuchal pain since late childhood, he was diagnosed with Chiari malformation at age 30y. Surgical correction resulted in complete resolution of pain. In his mid-30's, he developed recurrent nephrolithiasis. He underwent right total hip replacement of previously pinned hip at age 40y. Operative repair was challenging as his bone was very hard and resistant to drilling, and he developed right foot drop postoperatively. He underwent left hip replacement due to severe osteoarthritis at age 43y. Other comorbidities include left tinnitus and progressive hearing loss, hepatic steatosis, hepatomegaly at age 32y, and type 2 diabetes diagnosed at age 41y. He had no known family history of sclerosing bone disease with limited contact with the paternal side of his family. Laboratory findings were unremarkable except for vitamin-D deficiency (Table 1). Stone analysis revealed mixed uric acid and calcium oxalate stones (80%/20%). MRI brain (w/wo contrast) showed diffuse, symmetric thickening of the calvarium. A skeletal survey demonstrated diffusely thickened cortices involving the calvarium, ribs, radius/ulna, and femora supporting a diagnosis of OP. Genetic testing showed a pathogenic variant in the LRP5 gene confirming a diagnosis of autosomal dominant OP.Learning points: OP is a rare sclerosing bone disorder. This case highlights its broad clinical spectrum which includes Chiari malformation and recurrent nephrolithiasis. In addition, expansion of bone into marrow cavities and cranial foramina may result in extramedullary hematopoiesis leading to hepatomegaly and deafness respectively, as experienced by our patient.

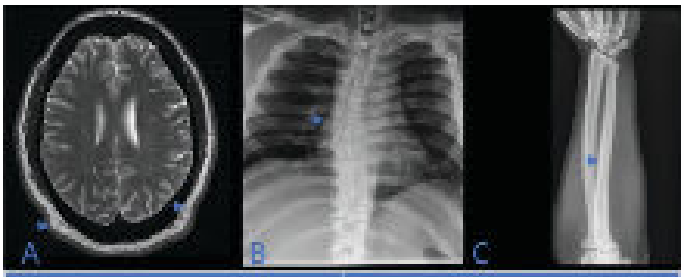

D	Results
Sodium (135 - 145 mmol/L)	137
Chloride (98 - 107 mmol/L)	101
Potassium (3.6 - 5.2 mmol/L)	4.7
Bicarbonate (22 - 29 mmol/L)	24
Calcium (8.6 - 10.0 mg/dL)	9.7
Ionized Calcium (4.50 - 5.30 mg/dL)	4.7
Phosphorous (2.5 - 4.5 mg/dL)	3.8
Creatinine (0.44 - 1.03 mg/dL)	1.01
Parathyroid Hormone (15 - 65 pg/mL)	47.0
Bone Alkaline Phosphatase (0 - 20 mcg/L)	14
Beta-CrossLaps (223-830 pg/mL)	263
Vitamin D 25-OH (30 - 50 ng/mL)	24

[A] Diffusely thickened calvarium with low signal intensity as seen on MR T2 weighted images. [B] Noted deformity/curvature of thoracic spine on plain films. [C] Diffusely thickened cortex seen in radius/ulna plain films. [D] Laboratory studies on evaluation

***Disclosures: Joseph Arguinchona**, None*

SUN-152

Evidence of Reduced Dentin Sialophophoprotein Expression and Impaired Cell Process Formation in Odontoblasts in Patients with Hypophosphatasia *Akira Nozoe[1], Kazuaki Miyagawa[1], Chiho Nakano[1], Shinji Takeyari[2], Makoto Fujiwara[4], Yasuhisa Ohata[4], Keiichi Ozono[2], Takuo Kubota[2], Susumu Tanaka[1]. [1]First Department of Oral and Maxillofacial Surgery, Osaka University Graduate School of Dentistry, Japan. [2]Osaka University Graduate School of Medicine, Japan. [4]Osaka University, . [4]Osaka University, Japan

Background: Hypophosphatasia (HPP) is a genetic disorder characterized by the premature loss of deciduous teeth due to defects in cementum formation. In addition, insufficient calcification of mantle dentin, which is essential for cementum formation, is also observed. But the underlying pathology remains unclear. Our objective of this study is to elucidate the underlying pathogenesis of dental defect in patients with HPP.Methods: We utilized induced pluripotent stem cells (iPSCs) from healthy individuals to generate odontoblast-like cells (ODs) via neural crest cells and mesenchymal stem cells (MSCs). We then examined various parameters, including odontoblastic differentiation markers and protein expressions, morphology, and calcification function using RT-qPCR, western blotting, immunostaining, and alizarin red staining. As a control group, we also induced osteoblast-like cells (OBs) from the same healthy MSCs. In addition, we created an HPP-iPSC from a patient with perinatal severe-type HPP (c.1559delT/c.1559delT: Perinatal), genetically rescued Perinatal-iPSCs by repairing both alleles using the CRISPR-Cas9 system (WT/WT: resHPP), and an odonto-type HPP model (WT/c.550C>T: odonto) from the resHPP-iPSCs using prime editing. We then assessed their isogenic odontogenesis.Results: In WT-ODs, we observed significant increase in DSPP and NES protein expressions, compared to MSCs. The expression of RUNX2 protein increased in the early differentiation stages and then decreased in the late differentiation stages. Additionally, calcification and ALP activity increased over time. We

also noted significant increase in MAPT and NEFL gene expressions, in WT-ODs compared to WT-OBs. Moreover, WT-ODs displayed a polarized nucleus and elongated cell process in one direction, Compared to Perinatal-ODs and Odonto-ODs, resHPP-ODs showed significant increase in ALP activity, DSPP protein expression, and mineralization during odontogenesis. Notably, RUNX2 protein expression was sustained until the late differentiation stage in Perinatal-ODs. The length of cell processes in Perinatal-ODs and Odonto-ODs were shorter than that in resHPP-ODs.Conclusion: We successfully established ODs differentiated from iPSCs. Our findings suggested that reduced DSPP expression, decreased ability to form cell process and lower calcification ability may be involved in the underlying pathogenesis of dental defect in HPP.

***Disclosures: Akira Nozoe**, None*

SUN-153

Comparison of Cd11b+ cells of the mandibular and femoral bone marrow at single-cell resolution *Rachel Phillips[1], Elizabeth Bradley[1], Kim Mansky[2], Amy Tasca[1]. [1]University of Minnesota , United States, [2]University of Minnesota, United States

Osteoclast activity within craniofacial bones orchestrates critical processes such as tooth eruption and skull modeling. Recent lineage tracing experiments in mice demonstrate that proper tooth eruption and skull generation requires embryonic but not adult myeloid cells. These data suggest that cellular ontogeny imparts fundamental differences between adult bone marrow-derived as compared to embryonic-derived tissue resident osteoclast progenitor cell populations; however, we lack essential knowledge about the osteoclast progenitors found in the marrow of craniofacial bones. Moreover, we completely lack transcriptomic data describing craniofacial-derived osteoclast progenitors. This knowledge gap impairs our understanding and treatment of pathological conditions including osteonecrosis of the jaw, primary or metastasized facial bone malignancies and osteomyelitis. Our lab has demonstrated that mandible-derived osteoclast precursors proliferate less, have increased osteoclast size and upregulation of osteoclast genes including Nfatc1, Dc-stamp, Ctsk, and Rank compared to osteoclasts derived from the femur bone marrow. To develop a better understanding of the transcriptome differences between mandible- and femur-derived osteoclast precursors, we performed scRNA sequencing of CD11b+ cells from mandible and femur bone marrow. CD11b+ cells were isolated from the femur and mandible derived bone marrow of 2-month-old male C57Bl/6 mice using Cd11b+ isolation microbeads. Six samples (3 femoral and 3 mandibular) were submitted for single-cell RNA sequencing. Six single cell captures targeting 10,000 cells each were performed by ST G chip for 3' gene expression. Using two-dimensional t-SNE representations of the expression levels of each of the samples, unique cell populations and differentially expressed genes were identified. Femur gene expression levels were used as the baseline for analysis. Differentially expressed genes pathways included up-regulation of TNF-?, AGE-RAGE and FOXO signaling pathways. While genes involved in cell adhesion, Fc gamma R mediated phagocytosis and autophagy pathways were down regulated in mandible derived cells. Currently expression of genes within these pathways are being verified by qRT-PCR. Together this data suggests that mandible derived osteoclast precursors have a unique gene signature compared to femur derived osteoclast precursors.

***Disclosures: Rachel Phillips**, None*

SUN-154

Age-dependent bone formation capacity in the mouse ligature-induced periodontitis model *Mizuho Kittaka[1], TETSUYA YOSHIMOTO[2], Marcus Levitan[1], Roy Choi[3], Anne Gingery[4], Alexander Robling[1], Yasuyoshi Ueki[5]. [1]Indiana University, United States, [2]University of Missouri-Kansas City School of Dentistry, United States, [3]Indiana University School of Medicine, United States, [4]Mayo Clinic, United States, [5]Indiana University School of Dentistry, United States

Periodontitis is an inflammatory disease of the periodontal tissue caused by bacteria. It is well known that susceptibility to alveolar bone loss in periodontitis increases with age. However, the mechanism by which aging exacerbates alveolar bone loss remains unknown. To investigate this age-dependent mechanism of alveolar bone loss, we applied the ligature-induced periodontitis (LIP) model to young (2.5 months old) and mature (8 to 12 months old) mice. Alveolar bone volume (BV) was assessed by microCT at 5 and 14 days after ligature placement. The magnitude of alveolar bone loss compared to the unligated side was comparable between young and mature mice. Surprisingly, the reduction of BV at day 5 was fully recovered by day 14 in young mice. However, no such recovery was observed in mature mice. Dynamic histomorphometry of alveolar bone between days 6 and 10 showed that ligature placement promoted bone formation in both young and mature mice. However, mineral apposition rate (MAR) and bone formation rate (BFR) were lower in mature mice than in young mice. In contrast, the level of osteoclast induction at day 5 was comparable between young and mature mice. These results suggest that impaired bone formation capacity of osteoblasts is a cause of the lack of BV recovery in mature mice, resulting in sustained bone loss. Next, we hypothesized that decreased osteoblast function in mature mice may be due to a pre-existing condition that increases the accumulation of senescent cells in periodontal tissues. qPCR analysis of periodontal tissues revealed that mature mice expressed senescence marker genes (Cdkn2a and Bcl2) and senescence-associated secretory phenotype (SASP) genes (Il17a, Cxcl1, Tnf, and Il1b) at higher levels than young mice, indicating that the accumulation of senescent cells is increased in periodontal tissues of mature mice. Thus, we found that aging affects the bone formation capacity of osteoblasts during LIP and that there is a concomitant accumulation of senescent cells in periodontal tissues. These data suggest that decreased bone formation capacity with age may contribute to increased susceptibility to alveolar bone loss in periodontitis. Furthermore, since pro-inflammatory SASP molecules are known to inhibit osteoblast differentiation and function, depletion of senescent cells by senolytic drugs may be a therapeutic approach to protect against alveolar bone loss in periodontitis, especially in an aging population.

***Disclosures: Mizuho Kittaka**, None*

SUN-156

Development of Cu application using dual-energy computed tomography for detecting medication-related osteonecrosis of the jaw *Satomi Arimoto[1], Akishige Hokugo[1], Kazuki Shigenaga[2], Masahiro Kubo[2], Taro Inagaki[1], Takumi Sato[2], Yujiro Hiraoka[2], Daisuke Takeda[2], Takumi Hasegawa[2], Kiyosumi Kagawa[3], Masaya Akashi[2]. [1]University of California, United States, [2]Kobe University Graduate School of Medicine , Japan, [3]Center for Radiology and Radiation Oncology, Kobe University Hospital, Japan

Introduction: The present study developed an application using dual-energy computed tomography (DECT) focused on Cu for detecting medication-related osteonecrosis of the jaw (MRONJ). Materials and Methods: First, we performed two types of phantom studies using a Cu wire syringe and pig mandible with Cu wire to detect Cu on DECT. Second, DECT examinations of 44 patients with MRONJ were performed to compare lesion and normal bone sites using single-energy CT, DECT, and DECT-Cu applications. Quantitative analyses of the virtual non-calcium CT (VNCa CT) and CT values were performed, and a cut-off value was calculated using receiver operating characteristic analysis. Third, we compared the Cu content in the MRONJ and normal bone groups using inductively coupled plasma atomic emission spectroscopy (ICP-AES). Results: The material-specific differences in attenuation between the two different energies enabled the accurate separation of Cu from Ca in phantom studies. The sensitivity and specificity for single-energy CT, DECT, and DECT-Cu applications were 97.7% and 13.6%, 75% and 81.8%, 81.8%, and 95.5%, respectively. Thus, VNCa CT values obtained on DECT-Cu application images showed the highest area under the curve value and maximal diagnostic efficacy in differentiating lesion sites from normal bone sites. On ICP-AES analyses, the Cu content was significantly higher in the MRONJ group than in the normal bone group. Conclusion: DECT-Cu application demonstrated better diagnostic performance in detecting MRONJ compared with single-energy CT or DECT.

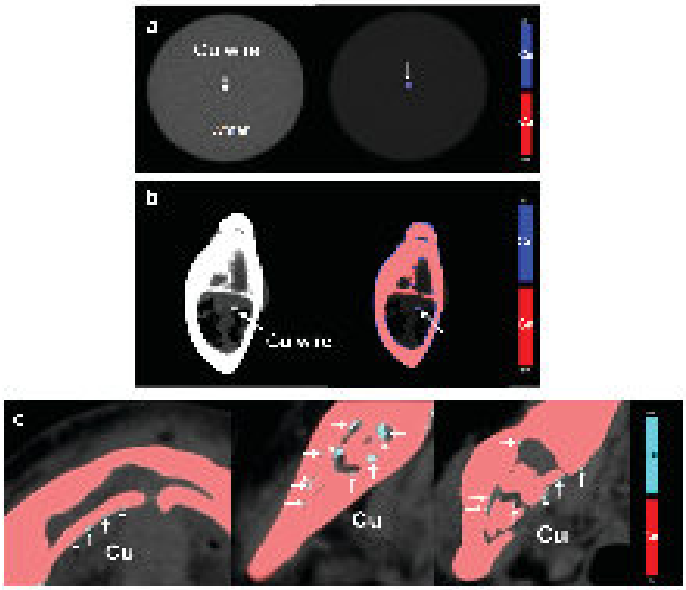

***Disclosures: Satomi Arimoto**, None*

Sunday Orals

SUN-157

Long-Duration Type 1 Diabetes Reduces Resistance to Damage Accumulation in Femoral Cortical Bone in Older Adults *Shannon Emerzian[1], Jarred Chow[1], Ramina Behzad[2], Daniel Brooks[3], I-Hsien Wu[4], John Gauthier[4], Surya Jangolla[4], Marc Gregory Yu[5], Hetal Shah[5], George King[5], Fjola Johannesdottir[6], Lamya Karim[2], Elaine Yu[7], Mary Bouxsein[8]. [1]Beth Israel Deaconess Medical Center, United States. [2]University of Massachusetts Dartmouth, United States. [3]BIDMC/MGH, . [4]Joslin Diabetes Center, United States. [5]Joslin Diabetes Center, Harvard Medical School, United States. [6]Beth Israel Deaconess Medical Center & Harvard Medical School , . [7]Massachusetts General Hospital, United States. [8]Beth Israel Deaconess Medical Center, Harvard Medical School, United States

While type 1 diabetes (T1D) is associated with an increased risk for hip fracture compared to non-diabetics, the factors contributing to skeletal fragility in T1D are not well understood. Previously we demonstrated a reduction in the post-yield properties of cortical bone, suggesting T1D may alter collagen and reduce the ability of cortical bone to resist damage accumulation. To test this hypothesis, cyclic cortical bone material properties and collagen crosslinks were assessed in the excised femora of older adults with T1D and non-diabetic controls.Whole femora were acquired post-mortem from Joslin Medalists, a cohort of individuals with T1D >= 50 years (n=20); non-diabetic control femora of similar age and sex were obtained from a tissue bank (n=14). Impact microindentation (Osteoprobe, Active Life Scientific) was performed on the anterior diaphysis to quantify the Bone Material Strength index (BMSi). Cortical beams (2x2x40mm) were extracted from the midshaft for damage accumulation testing. Fluorescent advanced glycation end products (fAGEs) were quantified by a fluorometric assay and the crosslink pentosidine (PEN) was quantified by HPLC. For damage accumulation testing, beams were cyclically loaded in 4 point bending with incrementally greater displacements (i.e., damage cycles; from 75% to 200% yield displacement in 25% increments). Following each damage cycle, tangent stiffness and percent stiffness degradation relative to baseline were calculated. Mann-Whitney U tests assessed group differences.The T1D group included 11 women and 9 men with an average (mean+/-SD) HbA1c=7.7+/-1.1%, T1D duration=67.5+/-6.0 years, age at onset=12.8+/-7.9 years, and age at death=80.3+/-8.2 years (range 68-92). The control group was 8 women and 6 men; age (p=0.58) and sex (p=0.90) did not differ between groups. BMSi and fAGEs did not differ between groups. PEN was greater by 17% in T1D (p=0.04). At 200% yield displacement, stiffness degradation from baseline was greater in T1D (14%) versus control (10%, p=0.06; Figure). Although no specimens failed in the control group, 25% of T1D specimens failed at or before 200% yield displacement (Figure). Stiffness degradation was not associated with fAGE (r2=0.001, p=0.87) or PEN content (r2=0.001, p=0.92).Long-duration T1D altered the ability of cortical bone to resist damage accumulation induced by cyclic loading. Further investigation is necessary to determine the cause of reduced resistance to damage accumulation in T1D.

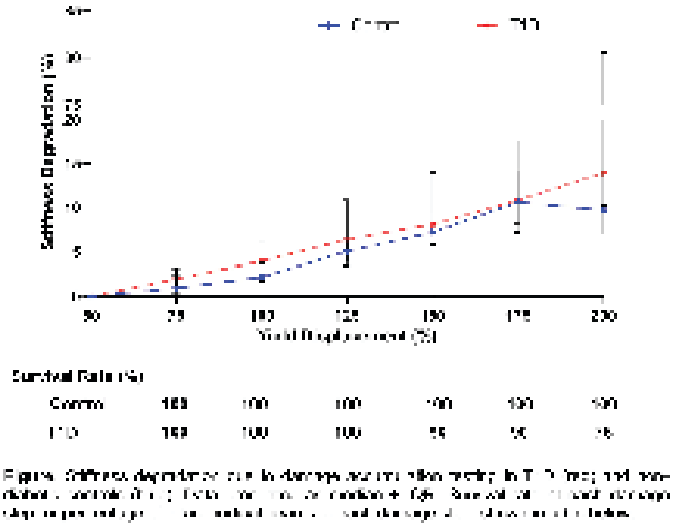

***Disclosures: Shannon Emerzian**, None*

SUN-158

The NAD salvage pathway in osteoblast lineage cells is indispensable for skeletal homeostasis *Olivia Reyes-Castro[1], Aaron Warren[1], Ha-Neui Kim[2], Maria Jose Almeida[3]. [1]University of Arkansas for Medical Sciences, United States. [2]Univ. Arkansas for Medical Sciences, Central Arkansas VA Healthcare System, United States. [3]Central Arkansas VA Healthcare System, Univ of Arkansas for Medical Sciences, United States

Nicotinamide adenine dinucleotide (NAD+) - a critical cofactor for cellular energy metabolism and numerous cellular processes, including cell division, DNA damage repair, and mitochondrial function - can be synthesized via several pathways. NAD+ levels and the expression of nicotinamide phosphoribosyltranferase (Nampt), the rate limit enzyme of the NAD+ salvage pathway, are lower in osteoblastic cells from old when compared to young mice. Moreover, administration of NAD+ precursors to aging mice attenuates the loss of bone mass and the involution of many other tissues. To examine the role of Nampt in osteoblastic cells and whether a decline in Nampt could contribute to skeletal aging, we initially generated mice lacking Nampt in Prx1-cre targeted cells. However these mice exhibited severe developmental phenotypes due to effects in chondrocytes, which precluded the examination of effect of Nampt on bone formation. In the work reported herein, we crossed Nampt-flox and Osx1-Cre mice to generate Nampt?Osx1 and Osx1-cre control mice. Nampt?Osx1 mice were born at the expected Mendelian ratio and were grossly undistinguishable from Osx1-Cre control littermates at birth. Evaluations of body weight, as well as spine and femur DXA BMD at 4 weeks of age revealed no differences between Nampt?Osx1 female or male mice when compared to the respective littermate controls. In contrast, femoral BMD in male and female Nampt?Osx1 mice was decreased at 12 weeks of age compared with Osx1-cre mice. Cultures of bone marrow derived osteoblastic cells from Nampt?Osx1 mice had lower NAD+ levels and exhibited decreased mineralization, as determined by Alizarin Red staining. Micro-CT analysis of femur from male and female Nampt?Osx1 revealed a decrease in cortical thickness due to a decrease in periosteal circumference. No changes were detected at the endosteal circumference. Trabecular bone volume at the distal femur and vertebrae (L5) was also lower in male Nampt?Osx1. These changes were due to a decrease in both trabecular number and thickness. No differences in trabecular bone were found in female. These results indicate that in osteoblast lineage cells Nampt contributes to bone homeostasis. Together with the earlier findings in Nampt?Prx1 mice, these results highlight that the dependency of osteoblast on Nampt is of much lower magnitude than that of chondrocytes.

***Disclosures: Olivia Reyes-Castro**, None*

SUN-160

Tanycytic Thyroid-stimulating Hormone Receptor Activation Increases Blood-hypothalamus Barrier Permeability and Induces Appetite in Female Mice *Hasni Kannangara[1], Jocoll Burgess[1], Sari Miyashita[2], Anisa Gumerova[3], Funda Korkmaz[3], Ronit Witztum[2], Steven Sims[1], Uliana Cheliadinova[1], Georgii Pevnev[1], Ofer Moldavski[3], Tal Frolinger[3], Tony Yuen[4], Ki Goosens[4], Vitaly Ryu[5], Mone Zaidi[6]. [1]Associate Researcher-MSH/QHC/ELM, United States. [2]Postdoctoral Fellow-MSH, United States. [3]Instructor-MSH/QHC/ELM, United States. [4]Associate Professor-MSH/QHC/SSVS/ELM, United States. [5]Assistant Professor-MSH/MSQ/QHC/SSVS/ELM, United States. [6]Professor-MSH/QHC/ELM, United States

In addition to its well-known action to trigger thyroid hormone production, thyroid-stimulating hormone (TSH) is released in the brain, and its receptor (TSHR) has been found in brain sites, including the tanycytes of the third ventricle, that regulate ingestive behavior and convey metabolic information across the blood-hypothalamus barrier (BHB). Our recent work highlights largely undiscovered role for TSHRs in the tanycytes. Here, we tested the hypothesis that tanycytic TSHR activation triggers rapid remodeling of BHB vascular permeability inducing appetite. We compared hypothalamic vascular permeability of food deprived (FD) and ad libitum fed (AL) Tshr+/- and their wild type (WT) counterparts exploiting transmission electron microscopy studies and immunofluorescence for constitutive tight junction protein Claudin-1 and homodimer glycoprotein MECA-32, primarily expressed in tanycytes and endothelial cells, respectively. Fasting significantly increased the organization of tanycytic honeycomb pattern of Claudin-1 and fenestral MECA-32-associated diaphragms in the median eminence and arcuate nucleus implying decreased BHB vascular permeability in Tshr+/- mice. Transmission electron microscopy confirmed immunofluorescence results. In a separate gain-of-function experiment, TSHR activation by the small molecule MS438 increased BHB vascular permeability as evidenced by decreased Claudin-1 and MECA-32 immunostaining. Tanycytic TSHR activation significantly increased both food foraging and intake as during one-hour refeeding after FD. Surprisingly, refeeding restored neuronal activation marker c-Fos expression in the paraventricular nucleus of the hypothalamus, parabrachial nucleus and nucleus of the solitary tract, though failed to do so in the paraventricular nucleus and nucleus of the solitary tract of MS438-injected mice. Collectively, these data infer that modulation of tanycytic TSHRs plays an important role in BHB plasticity in relation with ingestive behavior.

***Disclosures: Hasni Kannangara**, None*

SUN-161

Org43553, the First Low-Molecular-Weight Agonist of the Human Luteinizing Hormone Receptor, Reduces Body Fat. *Daria Lizneva[2], Anisa Gumerova[2], Kseniia Ievleva[2], Orly Barak[2], Funda Korkmaz[2], Judit Gimenez Roig[2], Tal Frolinger[2], Georgii Pevnev[2], Farhath Sultana[2], Darya Vasilyeva[2], Anne Macdonald[2], Natan Kramskiy[2], Soleil Wizman[2], Michelle Orloff[2], Anusha Rani Pallapati[2], Satish Rojekar[2], Vitaly Ryu[2], Ofer Moldavski[2], Tony Yuen[2], Mone Zaidi[3]. [2]Icahn School of Medicine at Mount Sinai, United States. [2]Icahn School of Medicine at Mount Sinai, . [3]Mount Sinai Medical Center, United States

We provide compelling evidence that LH is a pro-lean hormone, and that ORG43553, the first low-molecular-weight agonist of the luteinizing hormone receptor (LHCGR) induces leanness and promotes energy expenditure in mice. We detected Lhcgr transcripts in white adipose tissue (WAT) depots in male and female C57BL/6 mice (qPCR, IHC, RNAscope, Sanger sequencing), but not in Lhcgr-/- mice. Intraperitoneal AlexaFluor-488-labeled hCG bound to gonadal and subcutaneous fat pads in wild type mice, but not in Lhcgr-/- mice. Following i.v. 89Zr-LH injection, radioactivity was detected in mesenteric, inguinal and gonadal WAT. LH, hCG and ORG43553 rapidly induced ERK1/2 phosphorylation in differentiated 3T3.L1 cells. Female and male Lhcgr+/- mice on normal chow and high-fat diet, respectively, became obese, importantly, without changes in sex steroids. The gene-dosage effect of Lhcgr depletion suggests a dominant physiologic action of LH on body composition. 14-week-old male C57BL/6 mice were fed on high-fat diet and injected, i.p., with LH, hCG or vehicle, twice-a-week, for 6 weeks. Both LH and hCG markedly reduced body fat accrual (qNMR) but triggered a rise in serum testosterone. The hCG-induced lean phenotype persisted despite androgen receptor blockade by flutamide-confirming that the pro-lean actions of LH and hCG were largely independent of testosterone. Furthermore that LH failed to inhibit fat accrual in Lhcgr-/- mice testified to its action via the LHCGR. Injection of ORG43553 into male C57BL/6 mice for 9 weeks caused a significant reduction in fat mass (qNMR), with reduced WAT weight in fat depots. Remarkably, serum testosterone remained unchanged confirming that the anti-adiposity effect of ORG43553 was independent of testosterone. To study the mechanism of LHCGR activation on body fat, 3T3.L1 adipocytes were treated with hCG or ORG43553 for 12 hours. This resulted in reduced oil droplet accumulation. 3T3-L1-derived organoids treated with LH, hCG or ORG43553 also displayed a substantial reduction in the differentiated layer compared to vehicle-treated organoids. To study whether, in addition to reducing adipocyte differentiation, LHCGR agonism also enhanced thermogenesis, 3T3-L1 adipocytes were pretreated with ORG43553 for 1 hour before measuring oxygen consumption rate (OCR) on a Seahorse Xf96 Analyzer. ORG43553 increased OCR at baseline and upon oligomycin exposure, indicating mitochondria proton leak (thermogenesis). To confirm increased energy expenditure in vivo, mice were injected, s.c., with ORG43553 or vehicle. Oxygen consumption (VO2) and energy expenditure (EE) increased acutely in ORG43553-treated mice, with no change in locomotor activity. The findings suggest that ORG43553, which has been tested in humans for infertility, can potentially become a candidate drug for obesity.

***Disclosures: Daria Lizneva**, None*

SUN-162

High Fat Diet-induced Bone Loss is Mediated via RANKL-induced Activation of IL1? and TNF? Signaling in Male Mice. *Aruljothi Muralidharan[1], GUSTAVO GOMEZ[2], Chandrasekhar Kesavan[3], Sheila Pourteymoor[4], Destiney Larkin[4], Franklin V Sechriest[4], Subburaman Mohan[3]. [1]LLVARE, United States. [2], . [3]Jerry L. Pettis Memorial VA Medical Center, United States. [4]VA Loma Linda Healthcare System, United States

Obesity and its metabolic complication of type 2 diabetes are recognized as risk factors for bone fragility and osteoporotic fractures. Our research previously demonstrated that high-fat diet (HFD)-induced obesity in adult mice reduced trabecular bone mineral density (BMD) and increased marrow adipose tissue (MAT) only in male mice. To understand this gender-specific effect of a HFD on MAT and BMD phenotypes, we focused on RANKL signaling since its activation is central to obesity-associated metabolic disorders and negatively regulated by estrogen. In this study, we tested the hypothesis that the activation of RANKL signaling causes HFD-induced bone loss. HFD was associated with a 2.9-fold increase in expression of Tnfsf11 (which encodes RANKL) (P<0.01), in the bones of male mice only. Since bone marrow stromal stem cells (BMSC) are common precursors for osteoblastic and adipocytic lineages, we evaluated the expression of Tnfsf11 and Tnfrsf11b during differentiation in vitro. After treatment of BMSCs with osteogenic media, Tnfsf11 expression was decreased by 40% and 90% (P<0.01) on days 3 and 7, respectively, while Tnfrsf11b expression was unchanged. By contrast, adipogenic media treatment of BMSCs increased Tnfsf11 expression 2.8-fold (P<0.01) and decreased Tnfrsf11b expression by 90% (P<0.001) on day 1. RANKL/OPG ratio remained elevated throughout adipocyte differentiation. RANKL treatment suppressed differentiation of BMSCs towards osteoblasts as revealed by markedly decreased expression of Osx, Runx2, Dlx3, Dlx5, and Bsp by 34%-66% (P<0.01) as early as 6 hrs and remained suppressed during the 72 hrs of treatment. By contrast, expression levels of Il-1? and Tnf? were increased by 99-fold and 65-fold, respectively, at 6 h after RANKL treatment in osteogenic media, while expression levels of Mcp1 and Il-11 were unaffected. We next used neutralizing antibodies to IL-1? and/or TNF? to determine the role of these cytokines as effectors of RANKL on osteoblast differentiation. Pretreatment of BMSCs with neutralizing antibodies against TNF?, but not IL-1?, blocked the RANKL suppressive effects on Osx and Runx2 expression. Conclusions: 1) HFD contributes to bone loss by increasing bone resorption, as demonstrated previously, and by suppressing bone formation via RANKL-mediated activation of IL-1? and TNF? signaling, as shown here. 2) Future confirmation of this finding in humans could lead to the development of therapies to alleviate HFD-induced bone loss.

***Disclosures: Aruljothi Muralidharan**, None*

SUN-164

Prediabetes is associated with lower trabecular bone score (TBS): Comparison of TBS according to the prediabetes phenotype *Yong Jun Choi[1], Kyounghwa Ha[1], Dae Jung Kim[1], Yoon-Sok Chung[1]. [1]Ajou University School of Medicine, Republic of Korea

Objective: Diabetes mellitus (DM) is known to be associated with a lower trabecular bone score (TBS) and an increased risk of fracture. However, little is known regarding whether it is associated with poor bone results in pre-diabetic individuals. Despite the fact that both IFG and IGT are characterized by insulin resistance and ?-cell dysfunction, the metabolic abnormalities are quite distinct between the two disorders. Impaired fasting glucose (IFG) was marked by dysfunctional insulin secretion and decreased hepatic insulin sensitivity. In contrast, impaired glucose tolerance (IGT) was related with decreased whole-body insulin sensitivity, followed by a decline in ?-cell function. We examined if TBS differed depending on the prediabetes phenotype. Methods: This was a cross-sectional analysis of baseline data collected from 30- to 64-year-old participants in the Study of the Cardiovascular and Metabolic Diseases Etiology Research Center (CMERC) Cohort Study. A whole-body dual-energy X-ray absorptiometry (DXA) scan and an oral glucose tolerance test were performed. Excluding those with diabetes, liver cirrhosis, chronic kidney disease, or cancer, as well as those on osteoporosis drugs, steroids, or thyroid hormones, or who had ever received hormone replacement treatment, we enrolled 3,276 individuals. Subjects were classified as having normal glucose tolerance (NGT), isolated IFG, isolated IGT, or combined IFG and IGT (IFG+IGT). Statistical analyses were conducted by dividing into three groups (male, premenopausal women and postmenopausal women). Results: Males with isolated IGT exhibited a lower TBS after adjusting for age, weight, vitamin D, Hba1c, cigarette smoking, and alcohol intake (1.466 vs. 1.494, P=0.040). However, statistical significance disappeared when visceral fat was additionally adjusted for. In premenopausal women, patients with isolated IFG had a lower TBS than those with NGT (1.493 vs. 1.513, P=0.044), and statistical significance was preserved even after visceral fat was further adjusted. There were no significant differences in TBS among groups of postmenopausal women. Conclusion: Similar to diabetics, prediabetics have decreased TBS levels compared to NGT people. However, there were gender disparities in the association between TBS and prediabetes. Insulin resistance with visceral fat may have a greater impact on TBS in men, but disruption in insulin secretion may have a greater impact on TBS in premenopausal women.

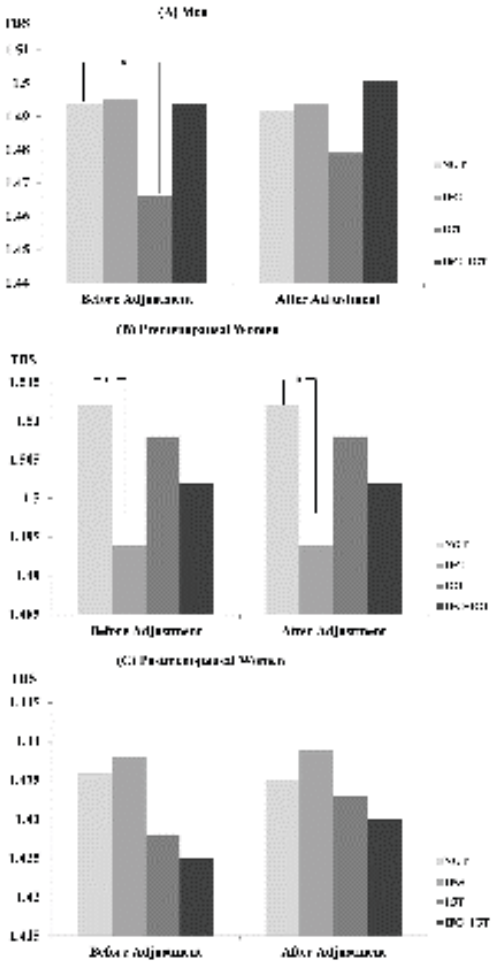

***Disclosures: Yong Jun Choi**, None*

SUN-165

Yiqi Huayu Formula up-regulates type H vessel formation and promotes fracture healing in ovariectomized mice *Kanghui Sun[1], Xiaohui Hu[1], Liqiang Guo[1], Ziyu Huang[1], Yongjian Zhao[1], Dongfeng Zhao[1], Yongjun Wang[1], Bing Shu[2]. [1]Longhua Hospital, Shanghai University of TCM, China, [2], China

Objective: to observe the regulatory effect of Yiqi Huayu Recipe, the basic Chinese compound formula commonly used for bone repair, on H type vessels formation during fracture healing in ovariectomized mice. Methods: 3-month-old C57BL/6 female mice were randomly divided into sham group, model group, and Yiqi Huayu group. The mice in the model group and the Yiqi Huayu group underwent bilateral ovariectomy. Eight weeks after the surgery, all the mice underwent transverse fractures of the left tibias. On the same day after the fracture, the mice were given Yiqi Huayu Formula or physiological saline for gastric perfusion once a day. Results: Micro-CT and histological staining results showed that on the 28th day after fracture, the callus in the sham group and the Yiqi Huayu group basically completed remodeling, while the callus in the model group was still in the shaping stage. The maximum loading force of the healing tibias in the Yiqi Huayu group was significantly higher than that in the model group. The results of flow cytometry and immunofluorescence staining showed that on the 3rd day after fracture, the proportion of type H vascular endothelial cells in the total endothelial cells in the fracture area of the sham group began to increase until the peak was reached on the 7th day. The proportion in the model group increased on the 5th day after fracture, and the proportion of cells at each time point was significantly lower than that of the sham group. The proportion in the Yiqi Huayu group began to increase on the 3rd day after fracture, earlier than that in the model group. Compared with the model group, the Yiqi Huayu Formula significantly increased the production of type H vascular endothelial cells on the 3rd and 5th days after fracture. Conclusion: Yiqi Huayu Formula can improve the formation of type H blood vessels in early stage of fracture healing in ovariectomized mice, which may be partial mechanism of promoting fracture healing in ovariectomized mice.

***Disclosures: Kanghui Sun**, None*

SUN-166

Polycaprolactone and Hydroxyapatite Bioprinting without Using Solvents *Trenton Campos[3], Andy Liu[3], Dean Wertz[3], Carlos Mendez Cruz[3], Chet Friday[3], Michael Hast[3], Rashad Madi[3], Chamith Rajapakse[3]. [3]University of Pennsylvania, United States, [3]University of Pennsylvania, Puerto Rico, [3]University of Pennsylvania,

Introduction: Our goal was to develop a bioink using Polycaprolactone (PCL) and Hydroxyapatite (HA) without using harmful solvents for 3D bioprinting bone grafts. Current methods are cytotoxic and expensive as they dissolve the PCL and HA using solvents such as chloroform to make the bioink sufficiently uniform and viscous for extrusion printing. Methods: Molecular weight 45,000 g PCL pellets and 10 ? m HA powder were used. Dry PCL:HA mixtures were created using varying weight ratios of PCL to HA ranging from 90:10 to 65:35. Compositions were varied at 5% increments. Prior to printing, each mixture was melted in the extruder nozzle and mixed thoroughly to ensure proper dispersion of the HA. The pneumatic extruder nozzle was then placed into the bioprinter. For each composition, four sets of cuboids were printed with varied infill distances (3 and 5 mm) and geometries (grid and triangle) (Figure 1). For each set, two 10 x 10 x 5 mm3 cuboids were printed. Print speed, pressure (PSI), print surface, and layer height were held constant. The increased concentrations of HA resulted in increased bioink viscosity and the temperature was increased to standardize viscosity. After printing, the scaffolds were tested for stiffness (in N/mm2) using a universal test frame. Results: Compositions of PCL:HA were uniformly printed up to ratios of 65:35. There was no decrease in cuboid quality as the HA concentration was increased; however, a small reduction in thickness was noted, likely due to the increased viscosity of the prints. Compression testing showed that print compositions of 75:25 had the greatest stiffness, with a mean maximal load of 2470 N/mm2. Due to a small sample size, further testing is necessary. ANOVA testing showed that there were no statistically significant differences between the stiffness of different infill geometries and lengths (Figure 1). Discussion: Melting dry mixtures of PCL with subsequent HA mixing is a better alternative than the utilization of chloroform to dissolve the PCL. Higher compositions of HA can be obtained and the method is much safer, cost-effective, and less time-consuming. Furthermore, remelting the PCl allows printing to be quickly resumed in contrast to having to redissolve the PCL in chloroform with the alternative method. Further research is needed to investigate the osteogenic and mechanical properties of the newly created PCL:HA prints and determine the optimal concentration for different orthopaedic applications.

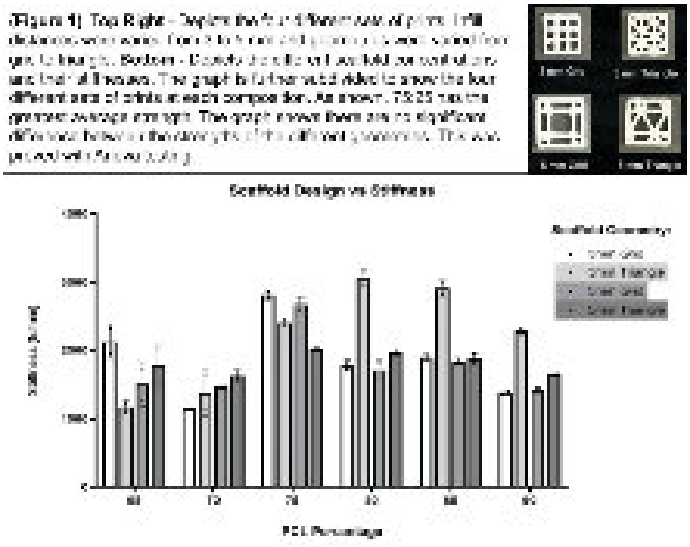

***Disclosures: Trenton Campos**, None*

SUN-168

Two-Pronged Mediation of Adrenal Steroidogenesis by Oxytocin *Uliana Cheliadinova[2], Georgii Pevnev[2], Vitaly Ryu[2], Tal Frolinger[2], Steven Sims[2], Ofer Moldavski[2], Funda Korkmaz[2], Orly Barak[2], Judit Gimenez Roig[2], Farhath Sultana[2], Natan Kramskiy[2], Soleil Wizman[2], Michelle Orloff[2], Tony Yuen[2], Daria Lizneva[2], Mone Zaidi[3], Anisa Gumerova[2]. [2]Icahn School of Medicine at Mount Sinai, United States, [2]Icahn School of Medicine at Mount Sinai, , [3]Mount Sinai Medical Center, United States

Stress-stimulated glucocorticoid release affects diverse biological processes, including pregnancy and childbirth. The controversy surrounding effects of OXT on stress prompted us to investigate its actions on adrenal cortical function in mice. RNAscope and immunohistochemistry provided unequivocal evidence for abundant OXT receptor (OXTR) expression in the adrenal cortex, predominantly in zona fasciculata and zona reticularis. Female mice displayed higher adrenal cortical Oxtr expression, more than a range of other tissues under

study. Oxtr expression was also detected in the adenohypophysis solely in female mice, while both male and female mice expressed Oxtr in the pars intermedia of the hypophysis. Aging impressively attenuated Oxtr expression in female mice in both the adrenal gland and adenohypophysis. For loss-of-function studies, we generated tissue-specific Star-CreERT2/Oxtrfl/fl mice in which the Oxtr was deleted from steroidogenic tissues, namely adrenals and ovaries. Deletion was confirmed by RNAscope and immunohistochemistry. We found no difference in serum corticosterone between tamoxifen-induced and uninduced mice; however, the elevation of serum corticosterone upon ACTH stimulation or after four weeks of stress was attenuated in tamoxifen-induced mice. Bulk RNAseq of adrenals from tamoxifen-induced mice revealed the downregulation of key steroidogenic genes, namely Cyp17a1, Hsd3b3, Hsd17b2, Cyp3a41b, and Serpina6 (a corticosteroid-binding globulin). In gain-of-function studies, a single OXT injection led to a rise of serum ACTH in tamoxifen-induced mice, which was greater in magnitude than uninduced controls. However, after five days of OXT injections, corticosterone levels became elevated, whereas ACTH levels declined to baseline. This suggests that OXT acts directly on OXTRs on corticotropes to initiate a stress-like response, with a negative feedback loop that inhibits further ACTH secretion. Of note is that male mice did not display any difference between tamoxifen-induced and uninduced groups, consistent with their low hypophyseal Oxtr expression. In all, we describe a novel gender-specific two-pronged circuit through which OXT may precisely regulates the production of corticosterone from the adrenal cortex. In the first arm, OXT directly stimulates ACTH secretion through adenohypophysis OXTRs. In the second arm, OXT prevents excessive stress-induced adrenal stimulation by downregulating steroidogenic genes. Our discovery lays the foundation for the emergence of new physiology that may relate to a fundamental role for oxytocin in the stress response during procreation, notably, when levels are elevated during pregnancy and lactation.

***Disclosures: Uliana Cheliadinova**, None*

SUN-169

Maternal But Not Offspring Ablation of Cyp27b1 Impairs Neonatal Growth and Skeletal Development in Mice *Sarah A. Hartery[1,] Beth J. Kirby[1,] Emma C. Walker[2,] Alexandre S. Maekawa[1,] David Bennin[1,] René St-Arnaud[3,] Natalie Sims[4,] Christopher S. Kovacs[1.] [1]Memorial University of Newfoundland, Canada. [2]St. Vincent's Institute of Medical Research and University of Melbourne, Australia. [3]McGill University and Shriners Hospital for Children-Canada, Canada. [4]St. Vincent's Institute of Medical Research and University of Melbourne , Australia

Ablation of Cyp27b1 eliminates calcitriol but does not disturb fetal mineral homeostasis or skeletal development. However, independent of fetal genotypes, maternal loss of Cyp27b1 causes higher fetal serum calcium, lower FGF23, lower renal excretion of calcium and phosphorus, and higher 25OHD and its metabolites, compared to fetuses of WT dams. Since milk from Cyp27b1 null dams has 30% less calcium than WT, we hypothesized that maternal loss of Cyp27b1 would continue to impair offspring skeletal development after birth.Cyp27b1 null and sister WT dams were kept on a calcium-, phosphate-, and lactose-enriched diet and mated to bear only Cyp27b1+/- pups. 48 hours after birth, all pups were cross-fostered to dams that delivered concurrently. Neonatal groups included pups of WT dams fostered by null (WT?null), null fostered by WT (null?WT), and two controls (WT?WT and null?null). Dams and pups were harvested on day 21. Neonatal BMC was measured by PIXImus DXA. Hindlimbs were analyzed by microCT. Neonatal bodies were reduced to ash; mineral content was determined by atomic absorption spectroscopy. Hormones and serum and urine minerals were measured. Maternal behavior was monitored by video surveillance. Milk was collected at day 10 to analyze nutritional content.In comparing all pups nursed by null to all pups nursed by WT, pups nursed by nulls had ~20% lower weight (7.56+/-2.1[SD] vs 9.52+/-1.8 g), BMC (0.15+/-0.04vs 0.19+/-0.04 g), and ash weight (0.26+/-0.07 vs 0.31+/-0.05 g) (all p<0.001). Ash calcium did not differ (30.0+/-2.3 vs 29.1+/-1.1 mg/g, p=NS). Adjustment for body weight accounted for the lower BMC and ash weight. Serum calcium, phosphorus, calcitriol, PTH, FGF23, IGF-I, and urine calcium, phosphorus, and magnesium, did not differ across the four groups. MicroCT showed neonates nursed by null dams had lower cortical thickness, mean polar moment of inertia, cortical area, trabecular bone volume and number (all p<0.01), but femur length was unaffected. No differences were seen in dam behaviors; milk collection and analysis is in progress.In summary, pups nursed by Cyp27b1 nulls, regardless of birth mother, had lower body weight, BMC, ash weight, and impaired bone microstructure, but no changes in systemic mineral homeostasis or total skeletal mineral content, as compared to pups nursed by WT.In conclusion, maternal loss of calcitriol impairs postnatal cortical bone growth and development of the trabecular network, independent of offspring genotype.

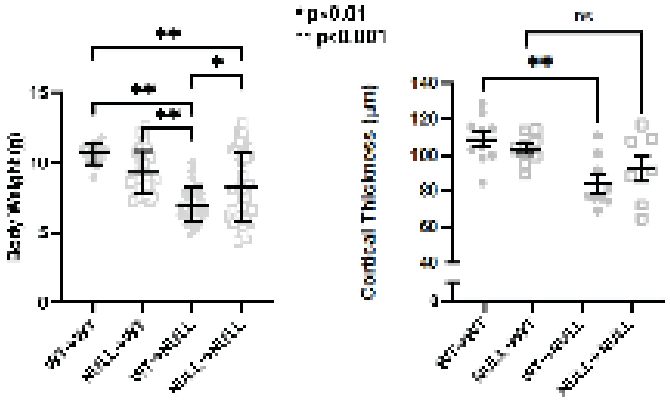

***Disclosures: Sarah A. Hartery**, None*

SUN-171

A long non-coding RNA as a direct vitamin D target transcribed from the anti-sense strand of the human HSD17B2 locus. *Yoshiaki Kanemoto[1,] Akira Hayakawa[2,] Takahiro Sawada[1,] Jinichi Mori[3,] Tomohiro Kurokawa[3,] Shigeaki Kato[1.] [1]Iryo Sosei University, Japan. [2]Research Institute of Innovative Medicine, Japan. [3]Fukushima Medical University, Japan

The known target mRNA genes of VDR are unlikely to account for all of the wide variety of VD actions, and non-coding RNAs(ncRNAs) appear to facilitate physiological and pathological VD actions. However coding regions for ncRNAs are in general not conserved among species. Given the fact that VD analogues are beneficial for bone health, we used in silico and transcriptomic approaches in human cell lines to search for human non-coding RNAs transcriptionally regulated by VD directly, and showed that VD-inducible enhancer RNAs supporting ligand-induced transcription of a VD target mRNA gene in keratinocyte cell line (HaCaT) (Kanemoto et al., JNSV, 67:424-, 2021).In this study, four long non-coding RNAs (lncRNAs), but no microRNAs, were found as VD direct targets by transcriptomic approaches using the VDR KO HaCaT cells, Consensus VDRE -related elements in the promoters of all of the four lncRNA coding regions are present, with documented VDR associations with these regions in ChIP atlas data base. One of these lncRNAs (designated as AS-HSD17B2) is transcribed from the anti-sense strand of the HSD17B2 locus, and the VDR-associated element in the AS-HSD17B2 promoter served as an efficient VDRE in a reporter assay. VD-regulated expression of HSD17B2 was seen also in LNCaP cells. Thus, AS-HSD17B2 represents a direct lncRNA target of VD (Kanemoto et al., Biosci. Res., 42:BSR20220321, 2022), suggesting that cell-type specific non-coding RNAs mediate tissue specific actions of VD. Thus, AS-HSD17B2 is a VDR target lncRNA, that is supposed to mediate VD action in human keratinocytes and prostate cancer. As chromatin environment facilitating production of ncRNAs is distinct among cell types, currently we are assessing if AS-HSD17B2 as well as the other three lncRNAs express osteosarcoma cell lines (U2OS and SaOS2). Transcriptome approach used in our report has also applied to identify VD/VDR target ncRNAs specifically expressed in osteosarcoma cells.

***Disclosures: Yoshiaki Kanemoto**, Tokiwa foundation, Grant/Research Support*

SUN-172

Comparative Analysis of PTH (1-34), PTHrP (1-36), and Abaloparatide Effects on Murine Osteoblast Transcriptome *ZHIMING HE[4,] Michael Mosca[2,] Florante Ricarte[3,] CAROLE LE HENAFF[4,] Nicola Partridge[5.] [4]New York University, . [2]NYU Langone Medical Center, . [3]Department of Molecular Pathobilogy, New York University college of Dentistry, United States. [4]New York University, United States. [5]New York University College of Dentistry, United States

Teriparatide (PTH (1-34)) and its analogs, PTHrP (1-36) and abaloparatide (ABL) have been used for the treatment of osteoporosis, but their efficacy over long-term use is significantly limited. Our laboratory has shown that PTH (1-34), PTHrP (1-36), and ABL exert time and dose-dependent differential responses in osteoblasts, leading us to hypothesize that they may also differentially modulate the osteoblast transcriptome. Here, we treated mouse calvarial osteoblasts with 1 nM of the 3 peptides for 4 h and analyzed the resulting RNA-Seq data. Gene-set enrichment analysis revealed that PTH (1-34) regulated 367 genes, including 194 unique genes; PTHrP (1-36) regulated 117 genes, including 15 unique genes; and ABL regulated 179 genes, including 20 unique genes. There were 74 genes shared exclusively between PTH (1-34) and ABL, 16 genes shared exclusively between PTH (1-34) and PTHrP (1-36), and 83 genes shared among all 3 peptides. The significant differences in the expression of various genes from the 3 peptides indicate gene ontology specific differences, including differences in Wnt signaling, cAMP-mediated signaling, bone mineralization, morphogenesis of a branching structure in biological processes; cytokine receptor/binding activity,

ligand-activated transcription factor activity, cAMP phosphodiesterase activity in molecular functions. The 3 peptides increased Vdr, Cited1 and Pde10a mRNAs in a differential fashion similar to Rankl expression. These findings were confirmed via qRT-PCR with additional cultured samples. mRNA abundance of other genes of interest based on gene/pathway analyses, including Wnt4, Wnt7, Wnt11, Pde10a, Sfrp4, Dkk1, Kcnk10, Hdac4, Epha3, Tcf7, Crem, Fzd5, Pp2r2a, and Dvl3 were also examined; some genes were stimulated similarly by all 3 peptides; others were not. Finally, experiments with siRNA knockdowns of SIK1/2/3 and CRTC1/2/3 in PTH (1-34) treated cells showed that some of these genes are regulated by SIKs and CRTCs (Vdr, Wnt4), while others are not. Although many studies have examined PTH signaling in the osteoblast/osteocyte, ours is the first to examine the global effects of these peptides on the osteoblast transcriptome. Further delineation of which signaling events are attributable to PTH (1-34), PTHrP (1-36) and ABL exclusively and which are shared among all 3 will help improve our understanding of the effects these peptides have on the osteoblast and lead to the refinement of PTH-derived treatments for osteoporosis.

***Disclosures: ZHIMING HE**, None*

SUN-173

Cell surface pathways of PTH and PTH1 receptor *Jonathan Pacheco[1], Karina Pena[1], Sofya Savransky[1], Gerald hammond[1], John Janetzko[2], Jean-Pierre Vilardaga[1]. [1]University of Pittsburgh, United States. [2]Stanford University, United States

The formation of PTH-receptor-arrestin is an important function of the cell membrane to transmit hormone actions. However, the paths and plasma membrane mechanism used by PTH, its receptor and ?-arrestins (?arr) to assemble the ternary signaling complex are not known. We are tackling this fundamental mechanism by using single-molecule and biochemical analyses. Here, fluorescent moieties were attached in the PTH type 1 receptor (PTH1R), PTH, ?arr, and clathrin. By recording dual-color single-molecule imaging at the plasma membrane of live cells, we found that PTH1R exhibits a near-Brownian diffusion, whereas the hormone is randomly confined at the cell surface. The PTH-PTH1R-?arr complex assembles through three sequential steps: 1) receptor collisions with the stationary ligand confined in pre-existing clathrin clusters, 2) phosphoinositide (PIP3) dependent recruitment and conformational change of ?arr molecules in clathrin clusters, and 3) ?arr collision with the ligand-bound receptor. These results provide insight into the cell surface pathway by which a PTH1R-arr complex is assembled and unveil a novel role of PIP3 in regulating PTH1R signaling. They also indicate that the central tenet that formation of cell surface ligand-receptor-arrestin complexes originates exclusively from direct interactions of ligand and ?arr with receptors must be revised.

***Disclosures: Jonathan Pacheco**, None*

SUN-175

Absent LH Signaling Rescues the Anxiety Phenotype in Aging Female Mice *Steven Sims[1], Orly Barak[1], Vitaly Ryu[1], Sari Miyashita[1], Hasni Kannangara[1], Funda Korkmaz[1], Soleil Wizman[1], Anne Macdonald[1], Anisa Gumerova[1], Ki Goosens[1], Mone Zaidi[1], Tony Yuen[1], Daria Lizneva[1], Tal Frolinger[1]. [1]Icahn School of Medicine at Mount Sinai, United States

Clinical studies and experimental data together support a role for pituitary gonadotropins, including luteinizing hormone (LH), otherwise considered solely as a fertility hormones, in age-related cognitive decline. Furthermore, rising levels of LH in post-menopausal women have been implicated in the high prevalence of mood disorders. This study was designed to examine the effect of deficient LH signaling, using the global Lhcgr-/- mouse, on both cognitive and emotional behavior in 12-month-old mice. For this, we established and validated a battery of five tests, including Dark-Light Box (DLB), Y-Maze Spontaneous Alternation, Novel Object Recognition (NOR) and contextual and cued Fear Conditioning (FCT) tests. We found that 12-month-old female mice display a prominent anxiety phenotype on DLB and FCT. This phenotype was not seen in female Lhcgr-/- mice, indicating full phenotypic rescue. Furthermore, there was no effect of depleting LHCGRs on recognition memory or working spatial memory on NOR and Y-maze testing, respectively, in 12-month-old mice, notwithstanding the absence of a basal phenotype in wild type littermates. The latter data do not exclude an effect of LH on cognition documented in previous studies. Finally, male mice and 3-month-old male and female mice did not consistently display deficits on any test. The data collectively document, for the first time, that loss of LH signaling reverses age-related emotional disturbances, a prelude to future targeted therapies that block LH action.

***Disclosures: Steven Sims**, None*

SUN-176

EXT608 for the Treatment of Hypoparathyroidism: Phase 1 Trial Design and Results *Laura Hales PhD[1], Kate Didio MBA[1], Leon Shi PhD[2], Daniel Hall PhD[1], Poul Strange MD PhD[2], Daniel Dickerson MD PhD FAAFP[3], Tarik Soliman PhD[1]. [1]Extend Biosciences, United States. [2]IMD, United States. [3]ICON plc, United States

Extend Biosciences is developing EXT608, a long-acting parathyroid hormone (PTH 1-34)-based therapy designed to replace the physiological effects of PTH with significantly less frequent dosing and improved bioavailability. EXT608 was developed using the company's D-VITylation® platform, which harnesses the biology of vitamin D and the reversible binding properties of the serum-circulating vitamin D binding protein. By utilizing this natural pathway, D-VITylation prevents a vitamin D-conjugated therapeutic from renal clearance, thereby significantly extending its half-life. Bioactivity is not compromised and as such, EXT608 is fully active as-is at the PTH receptor.A double-blind, randomized, placebo-controlled Phase 1 trial involving 24 healthy participants (3:1 active:placebo) across 6 cohorts was conducted with EXT608. The primary endpoint was to characterize the safety and tolerability profile of escalating dose levels of EXT608 when administered to healthy adult subjects as a single injection by 1) observing the incidence, nature, and severity of adverse events (AEs) and withdrawals due to treatment emergent AEs, 2) noting the frequency and severity of post-dose change from baseline in hematology, serum chemistries, urinalysis, electrocardiogram, vital signs, and physical examination findings, and 3) determining the percentage of subjects with injection or infusion site reactions. Secondary endpoints included 1) determining plasma pharmacokinetic parameters, and 2) assessing the pharmacodynamic profile by measuring post-dose change from baseline in serum chemistries and urinalysis. The results show that EXT608 was safe and well tolerated, with no serious adverse events reported. It also shows a dose dependent increase in serum calcium. A prolonged suppression of endogenous parathyroid hormone was also observed, as anticipated. The pharmacokinetic analysis suggests that EXT608 can be effective when dosed once-weekly. The data provide a strong rationale to proceed to the next stage of clinical development and also offer valuable guidance for selecting a starting dose in the Phase 2 trial.

***Disclosures: Laura Hales PhD**, Extend Biosciences, Major Stock Shareholder*

SUN-177

Eldecalcitol Inhibits Bone Turnover And Increases Bone Mass Via Acting On BMSCs *An Xiong[1], Yingying Gu[1], Haibo Li[1], Miaoying Lin[1], Ran Zhang[2], Daniel. D Bikle[3], Zhongjian Xie[1]. [1]National Clinical Research Center for Metabolic Diseases, Hunan Provincial Key Laboratory of Metabolic Bone Diseases, and Department of Metabolism and Endocrinology, The Second Xiangya Hospital of Central South University, China. [2]Department of Medical Laboratory, Hunan Normal University School of Medicine, China. [3] Veterans Affairs Medical Center, University of California San Francisco, United States

Aims: Eldecalcitol (ELD) is one of the active vitamin D analogues that has been shown to inhibit bone turnover and increase bone mass, but the underlying mechanism is unclear. Bone marrow mesenchymal stem cells (BMSCs) are the progenitor cells of osteoblasts, and we hypothesized that ELD increases bone mass by acting on BMSCs. To test the hypothesis, we investigated the effect of ELD on bone mass and osteogenic differentiation of BMSCs in the vitamin D receptor (VDR) conditional knockout mice (cKO).Methods: VDR cKO mice were generated by breeding floxed-VDR mice and PRX1-Cre mice. Floxed-VDR mice were used as a control. Both control and cKO mice were treated with ELD at a dose of 50 ng/kg or vehicle for 4 weeks. Micro-CT was performed to examine the bone mass and bone microstructure morphometrics of femur. Calcein double-labeling, ALP, and TRAP staining were used to examine the bone mineral apposition rate (MAR), the number of osteoblasts, and osteoclasts, respectively. Primary BMSCs were isolated from 8 week-old wild-type mice and cultured in osteogenic medium. Cells were treated with ELD at concentrations of 10-10, 10-9, or 10-8 M for 7 days. The expression of RANK in BMSCs was reduced by siRNA and cells were then treated with 10-9 M ELD for 72 hours. The mRNA and protein expression levels of RANK, RANKL and osteogenic differentiation markers including ALP and RUNX2 were examined by quantitative PCR and western blotting.Results: Micro-CT showed that control mice treated with ELD displayed increases in bone mass, bone volume percentage, and bone trabecular number and decreases in bone trabecular separation compared to vehicle group; Calcein double-labeling, ALP, and TRAP staining showed that control mice treated with ELD displayed reduced MAR, number of positive osteoblasts and osteoclasts compared to the vehicle group. The effects from above were blocked by BMSC conditional knockout of VDR. ELD inhibited expressions of differentiation markers including ALP and RUNX2 and RANKL and promoted RANK expression in a dose-dependent manner in BMSCs. The inhibitory effect of ELD on the expression of ALP, RUNX2 and RANKL was blocked by down-regulation of RANK in BMSCs.Conclusion: ELD inhibits bone turnover and increases bone mass via acting on VDR of BMSCs. ELD suppresses osteogenic differentiation and RANKL expression possibly via promoting RANK expression in BMSCs.

***Disclosures: An Xiong**, Chugai Pharma China Co., Ltd., Grant/Research Support*

SUN-178

Very low dose ACTH treatment increases bone formation in rabbits in vivo and stimulates bone formation gene expression in human osteoblast cultures in vitro *Irina Tourkova[1], Quitterie Larrouture[2], Harry Blair[1]. [1]Pittsburgh VA Medical Center and University of Pittsburgh, United States. [2]University of Pittsburgh, United States

We show that very low dose (0.6 ?g/kg rabbit mass) ACTH daily treatment for five weeks increases bone formation in rabbits. We evaluated adrenocorticotropic hormone (ACTH), cortisol, glucose, and vascular endothelial growth factor (VEGF) in rabbit blood serum as a function of ACTH dose as a single subcutaneous injection. We found that injecting 0.6 ?g per kg rabbit mass did not measurably increase ACTH over no added ACTH in serum in an ELISA over several hours, and had essentially no effect on cortisol (Figure, left panel) or glucose. Actual added serum ACTH is estimated as 1 to 10 pM but is too low to be measured by available rabbit assays (serum half life of ACTH is ~20 minutes). Following this, we evaluated the effect on bone formation after five weeks of treatment with 0.6 ?g/kg rabbit mass ACTH daily by micro-computed tomography (microCT) analysis and fluorescent tetracycline double labeling with one week interval. We revealed that 0.6 µg/kg/day of ACTH treatment increases trabecular bone structure (percent bone volume, bone surface density, and trabecular sickness) in the femoral head on micro-computed tomography images and significantly increased labeling of bone formation with tetracycline estimated by quantification of labeled area, p = 0.0056, n = 3 (Figure, right panel). In vitro, ACTH in as low concentrations as low as 10-12 M increased expression of Collagen type 1 and RunX2 in human osteoblasts differentiating for three weeks on polyethylene terephthalate (PET) membrane inserts with 0.4 micron perforations, which optimizes mineral transport into the matrix and acid transport. VEGF mRNA and the VEGFA receptor FLT-1 and FLK-1 mRNAs were also upregulated at 1 pM ACTH. In related work, mRNA expression of mitochondrial complex 1 (NDUFA5, NDUFS2, NDUFB1, NDUFB6) members, playing key role in energy production, were upregulated by 10-12 M ACTH treatment. An ELISA for complex 1 activity showed similar effects, with maximum activity at 10-9 M but 70% of maximal activity at 10-12 M ACTH.Collectively, our results indicate that very low dose ACTH treatment increases bone formation in vivo and in vitro, and upregulates energy production in human osteoblasts.

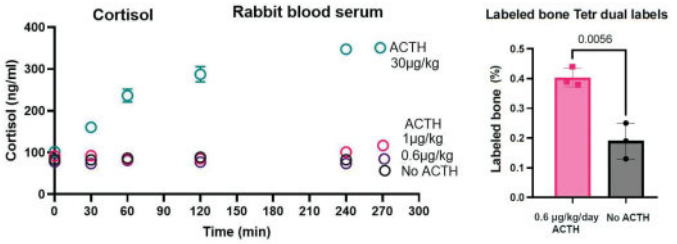

***Disclosures: Irina Tourkova**, None*

SUN-179

Bone Mineral Density in Low Dose vs. Very Low-Dose Estrogen OC users *Taylor Demasi[1], Jordan Beall[1], Michelle Tsang[1], Kristine Giltvedt[1], Mark Kern[2], Shirin Hooshmand[1]. [1]San Diego State University, United States. [2],

Oral contraceptives (OCs) may negatively impact bone health in young females by suppressing the amount of endogenous estrogen in the body. OCs with very low estrogen doses (<=20 mcg EE) may produce more negative consequences than those of low estrogen doses (>20 mcg EE.) The purpose of this study was to compare bone mineral density (BMD) in different doses of OCs.Fifty-six women, aged 18-25 y, who were either using very low (n=22) or low-dose (n=34) OCs were assessed. Participants were required to have taken their OC for at least one year before joining the study. Anthropometrics, physical activity, reproductive health, and habitual calcium and vitamin D intake were evaluated. DXA scans were performed for total body, right and left femur, AP spine, and non-dominant arm.The groups did not differ significantly for height, weight, BMI, age at menarche, average number of days between menstruation, age at first OC use, duration of OC use in years, or calcium and vitamin D intake. Very low dose users were significantly older (+1 yr; p=0.016) and consumed alcohol for a longer duration (+1.2 yr; p=0.021). No differences for BMD were detected for any of the measured bone sites regardless of controlling for age and duration of alcohol use. Although other studies have demonstrated that individuals on very low-dose OCs may have lower BMD compared to low-dose users, these results of this small sample do not agree.

***Disclosures: Taylor Demasi**, None*

SUN-180

A DNA Tetrahedron-based Stem Cell Enrichment Technology in Osteoarthritis Targeted Therapeutic Research *xingyu Chen[1], Taoran Tian[2], wumeng Yin[3], Yunfeng Lin[2]. [1]State Key Laboratory of Oral Diseases, West China Hospital of Stomatology, Sichuan University, , China. [2]Sichuan University, China. [3]State Key Laboratory of Oral Diseases, West China Hospital of Stomatology, Sichuan University, , China

Stem cell therapy is a promising strategy for OA treatment, but reliable sources of stem cells still need to be discovered. In previous studies, we found that the DNA tetrahedron (TDN) exhibits precise editability and a predictable structure. The tetrahedral structure of TDN provides a topological basis for chemical modification, which can be used to combine with stem cell targeting aptamers to construct a stem cell enrichment system for OA treatment. In this study, TDN was initially created and then modified with 1-3 DNA aptamers targeting stem cells, extending from 1-3 vertices (denoted as T1, T2, and T3). The gel electrophoresis results showed that the T1, T2, and T3 synthesis yields were over 80%. Subsequently, the synthesized DNA materials were incubated with positive and negative cells. It was found that the T3 structure had the highest binding efficiency to the membrane of positive BMSC cells, significantly higher than that of randomly arranged monovalent adapters. Following that, biotin was added to the fourth vertex of the T3 structure to achieve effective magnetic separation. Alternatively, thiols were added to the fourth vertex of the T3 structure to covalently connect the inflammatory protein targeting adapter (DTA64) to hyaluronic acid (HA), and the in vitro cell recruitment impact of DTA64-HA-T3 was validated using transwell assays. Finally, a rat OA ACLT model was created, and tissue sections obtained one week later revealed co-localization of the T3 structure and the DTA64 inflammatory protein adaptor, supporting the HA-T3 structure's in vivo targeting site retention. In the future, MSC-specific CD29 and CD44 labeling will be used to confirm the successful stem cell recruitment to the inflamed location in the rat joint cavity. Additionally, micro-CT imaging will assess the degree of joint regeneration and repair. These findings suggest that the TDN framework's topological structure can effectively manage the number and spatial distance of the targeting DNA sequences connected to it, considerably boosting targeting efficiency and specificity. Moreover, the DTA64-HA-T3 stem cell enrichment method shows strong inflammatory targeting in the rat OA joint cavity and good specificity for collecting stem cells in vitro. These findings offer a novel therapeutic option for clinical osteoarthritis and contribute to a significant advancement in treating rat OA.

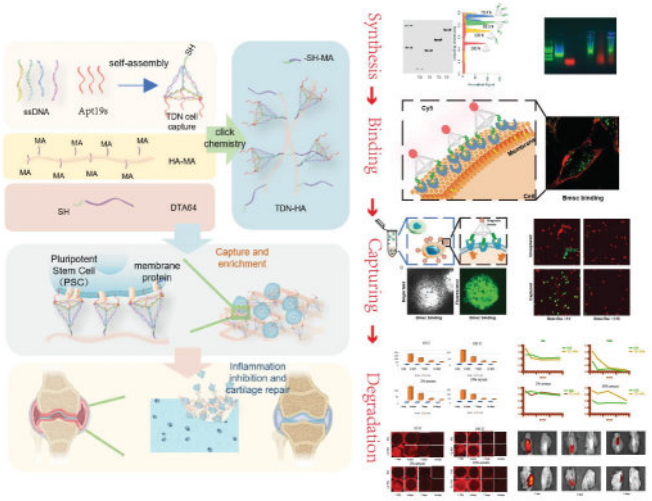

***Disclosures: xingyu Chen**, None*

SUN-181

Targeting Synovial Connexin Hemichannels Ameliorates Osteoarthritis Progression *Rui Hua[1], Yi Tian[1], Manuel A. Riquelme[1], Xuewei Wang[1], Liang Ma[1], Sumin Gu[1], Jean X. Jiang[1]. [1]UT Health San Antonio, United States

Osteoarthritis (OA) is a degenerative joint disease characterized by progressive articular cartilage deterioration, subchondral bone sclerosis, and synovial inflammation. The gap junction protein connexin 43 (Cx43), a key regulator of musculoskeletal homeostasis, is overexpressed in cartilage and synovium of OA patients. However, the contributions of Cx43 to OA pathogenesis remains largely elusive. Cx43 forms hemichannels (HCs) and mediate the release of small molecules (< 1.2 KDa), such as ATP and PGE2, into the extracellular environment. To determine whether deletion of Cx43 in joint tissue could ameliorate OA symptoms, we adopted adeno-associated virus (AAV) mediated Cre expression in Cx43 fl/fl mice using a destabilization of the medial meniscus (DMM) surgery induced OA model. Intra-articular injection of AAV-Cre decreased Cx43 level, with a higher efficiency in the synovium (p=0.001) than in the cartilage (p=0.065). MicroCT analysis showed reductions in subchondral BV/TV, Tb.Th, and BMD with AAV-Cre mediated Cx43 deletion. Moreover,

reduced Cx43 expression mitigated OA-related pain behaviors evaluated by von Frey and open-field tests. To further investigate the role of Cx43 HCs in OA progression, a monoclonal Cx43(M1) antibody that specifically blocks Cx43 HCs was developed. In vivo Evens blue dye uptake assay showed that DMM increased HCs opening by 2 folds, which was inhibited by the antibody. Impeded Cx43 HCs by the antibody improved cartilage structure as quantified by OARSI score, decreased degree of synovitis, along with reduction of MMP13 and Collagen X levels. Subchondral sclerosis and OA pain symptoms were also alleviated in the Cx43 antibody treated group. Remarkably, in vivo distribution of this antibody is predominantly in synovium, including macrophages and fibroblasts, with sustained presence for over 2 weeks. In addition, OA induced increase of M1 macrophages, as indicated by the iNOS/CD68 double positive cells, was attenuated after antibody treatment. In vitro study using mouse macrophages or human synovial fibroblasts demonstrated the inhibition of LPS or IL1?-induced HCs opening and inflammatory genes expression (COX2, ADAMTS 4/5, and MMP3/13) by Cx43 HC-blocking antibody. In summary, our results highlight the crucial role of Cx43 and HCs in regulating pro-inflammatory mediators under OA conditions. Targeting synovial Cx43 HCs, thus, is a potential therapeutic strategy to mitigate the inflammatory environment during OA progression.

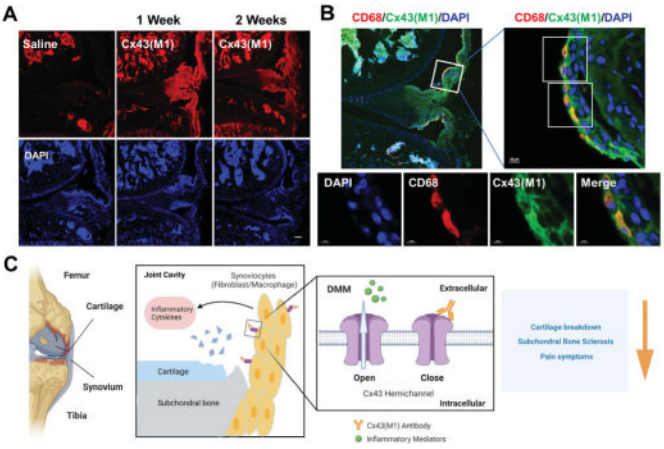

Targeting synovial connexin 43 hemichannel as a potential therapeutic target of OA

(A) *In vivo* distribution of Cx43(M1) antibody shows accumulation primarily in the synovium with sustained presence for over 2 weeks. **(B)** Colocalization of Cx43(M1) antibody with macrophage marker CD68. **(C)** Schematic illustration showing the administration of Cx43(M1) antibody blocks hemichannel opening and release of inflammatory cytokines, thus improving joint structure, subchondral bone sclerosis and pain symptoms.

***Disclosures: Rui Hua**, None*

SUN-182

Therapeutic effect according to the dose of 17?-estradiol in the knee and temporomandibular joints of ovariectomized rats *Hoon Joo YANG[1], Ji Hye OH[2], Jiwon DO[1]. [1]Department of Oral and Maxillofacial Surgery, School of Dentistry, Seoul National University, Seoul, Korea, Republic of Korea. [2]Dental Research Institute, Seoul National University, Seoul, Korea, Republic of Korea

Osteoarthritis (OA) is a degenerative joint disease that mainly affects middle-aged and elderly people. However, progressive condylar resorption (PCR) similar to temporomandibular joint (TMJ) OA has been reported to occur mainly in young women in their teens and twenties. And the patients with PCR have been reported to have low serum 17?-estradiol (E2) levels, even though they are not menopausal. Deterioration of bone cell function and osteoporotic changes due to a decrease in E2 levels may occur systemically, but OA was not observed in the knee joint (KJ) of PCR patients. The purpose of this study was to compare the changes in TMJ with the changes in KJ according to E2 concentration and to evaluate the applicability of estrogen therapy for PCR treatment. In female Sprague-Dawley rats, ovariectomy (OVX) was performed to induce estrogen deficiency, and E2 of 0, 10, 50, and 100 ?g / 100g doses was administered intraperitoneally daily for 4 weeks after 8 weeks of OVX. Bony changes and cartilage inflammation in the TMJ and KJ were evaluated using micro-CT, real-time PCR, histochemical staining, and immunohistochemical staining. OVX induced osteoporotic changes in the TMJ condyle, which were most evident in the posterior area. On the other hand, in the KJ, osteoporotic changes were found in the tibial neck, but no significant changes were shown in the tibial condyle. BMD and BV of the TMJ condyle and tibial neck were significantly increased by all doses of E2, and it was confirmed that 100 ?g / 100g of E2 caused more osteosclerotic changes than in the sham group. The tibial condyle showed no changes with E2 supplementation. In TMJ cartilage, inflammatory changes were observed to increase when 50 and 100 ?g / 100g of E2 were applied, but in KJ cartilage, no significant inflammatory changes were observed in OVX and E2 supplemented groups. Therefore, the study suggests that low dose (10 ?g / 100g) of E2 may have a therapeutic effect on the osteoporotic changes of TMJ, with minimal harmful effects such as inflammation and side effects on other joints. This finding may be useful in developing optimal treatment concentrations of E2 for TMJOA caused by estrogen deficiency in young female patients.

***Disclosures: Hoon Joo YANG**, None*

SUN-184

High Repetition Low Force Task Performance Causes Entheseal Damage and Palmar Muscle Fibrosis in Older Rats with Work-Related Overuse Injuries *Parth R Patel[1], Alex Lambi[2], Steven Popoff[3], Mary Barbe[4]. [1]Center for Translational Medicine, Lewis Katz School of Medicine of Temple University, United States. [2]University of New Mexico, . [3]Lewis Katz School of Medicine at Temple University, United States. [4]Temple University School of Medicine, United States

To better understand the progression of overuse injury, it is crucial to study morphological changes occurring at the tissue level that correlate with functional changes. Using an established rat model of work-related overuse injury, we have shown greater grip strength declines in mature (14-18 mo) rats than young adult rats (3-9 mo) performing the same moderate task, declines that correlated with forearm muscle inflammatory cytokine levels. We sought here to determine if forepaw musculoskeletal changes were also contributors. Experiments were approved by the Institutional Animal Care and Use Committee. Following a 4-week training period, mature female rats went on to perform a high repetition (4 reaches/min), low force (0.29N) task for 9-12wks, 2hrs/day, 3days/wk (HRLF; n=14). Results were compared to age-matched resting Controls (n=11) and animals that trained and then rested for 12wks (Tr+Rest; n=10). We analyzed histologic data from forepaw muscles (thenar, hypothenar, and deep intrinsic) and wrist/forepaw entheses. Muscle fibrosis (percent muscle area with collagen) in combined forepaw muscles was significantly increased in HRLF rats, compared to Tr+Rest and Control rats ($p<0.05$). Forepaw entheses were graded binarily with 1 indicating present each for five domains: attachment site holes, cartilage islands, tidemark fissuring, void space, and vascular invasion. HRLF rats showed significant entheseal changes indicative of damage in the summed average of the five domains, compared to Tr+Rest and Control rats ($p<0.05$ each). Individual domain analysis revealed more attachment site holes and tidemark changes in HRLF forepaw entheses. Using percent change in grip strength from naive to post-task, we performed a Spearman's correlation analysis between percent muscle collagen and change in grip strength and found a moderate inverse relationship ($r=-0.52$, $p<0.05$). We have previously shown that mature rats performing HRLF tasks also develop osteopenia in distal forelimb bones. We extend those results to report here the presence of forepaw histopathology: forepaw muscle fibrosis and entheseal damage following prolonged work-related overuse in very mature rats. The increased muscle collagen content correlated with declines in grip strength. These findings contribute to the understanding of local effects of repetitive overuse injuries in upper extremity tissues and have significant clinical relevance as human females report more work-related overuse.

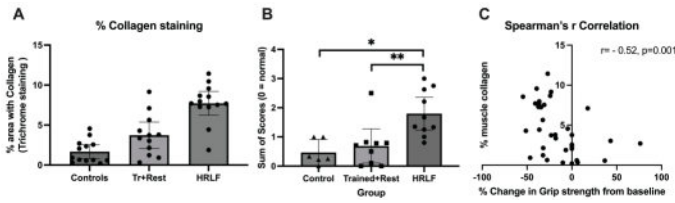

***Disclosures: Parth R Patel**, None*

SUN-185

Sex differences in knee joint pain in relation to joint pathology *Tyler Vesey[1], Peter Caradonna[1], Nic Sian[1], Madison Mueth[1], Victoria Eaton[1], Kathleen Becker[1], Tamara King[1]. [1]University of New England, United States

Osteoarthritis (OA) pain is heterogeneous and mechanisms underlying different OA pain phenotypes are not understood. Many patients report pain during joint use that dissipates with joint rest, defined as mid-stage OA pain. Some patients report development of persistent ongoing pain that is resistant to recommended treatment, defined herein as advanced OA pain. We examined the hypotheses that mid-stage and advanced OA pain have different levels of joint pathology and pathological sprouting of sensory fibers.Male and female C57bl/6 mice received knee joint injections (10 ?l) of different concentrations of monosodium iodoacetate (MIA) to induce mid-stage or advanced OA pain phenotypes. Knee joint pain was assessed 14 days post-injection using analysis of shifts in weight away from the MIA treated knee joint to determine weight bearing associated pain. Conditioned place preference to pain relief was used to determine development of persistent pain characteristic of advanced OA pain in patients. Mid-stage OA pain was defined as weight asymmetry in the absence of persistent pain, advanced OA pain was defined as weight asymmetry and persistent knee joint pain. Following behavioral analysis (D15), knee joint tissue was collected and processed for histology to assess cartilage loss and joint pathology (toluidine blue, H&E) and alterations in innervation of the tibialis anterior muscle using the pan-neuronal marker beta tubulin 3 (BT3). All behavioral testing and image analyses were performed by an experimenter blinded to the treatment and sex of the joint images.Females developed advanced OA pain phenotype at a 5-fold lower dose compared to males. Analysis of joint pathology demonstrates that males and females both demonstrate concentration dependent signs of knee joint OA including cartilage loss, synovitis, and bone remodeling. However, females developed advanced OA pain with less joint pathology compared to males. Analysis of fiber density using BT3 revealed concentration dependent changes in joint innervation corresponding to changes in pain phenotype in males. Studies are ongoing to examine

whether females with advanced OA pain show increased joint innervation with less joint damage compared to males.

***Disclosures: Tyler Vesey**, None*

SUN-186

Phlpp1 and Articular Cartilage Tissue Quality in Osteoarthritis *KATHERINE ARNOLD[1], SAMANTHA WEAVER[3], Jennifer Westendorf[3], Elizabeth Zars[4], Daniel Tschumperlin[5]. [1], , [3]Mayo Clinic, United States, [3]Mayo Clinic, , [4]Department of Orthopedic Surgery, Mayo Clinic, United States, [5]Department of Physiology and Biomedical Engineering, Mayo Clinic, United States

Osteoarthritis (OA) is a chronic and common disease affecting 1 in 4 adults. OA is characterized by articular cartilage deterioration, osteophytes, and other joint changes. Deficient mechanical and structural qualities (e.g., stiffness) are detected in cartilage weeks before histologic signs of OA are apparent in animal models of post-traumatic OA. Atomic Force Microscopy (AFM) micro-indentation is frequently used to measure the stiffness (via the elastic modulus E) of articular cartilage with high spatial resolution and force sensitivity. Phlpp1 is a protein phosphatase that slows chondrocyte proliferation and regeneration, and its genetic deletion in mice results in thicker articular cartilage and higher chondrocyte density. We previously showed that Phlpp1 deletion can protect from injury-induced cartilage degradation; however, we do not know if Phlpp1 deletion affects the mechanical properties of cartilage after injury. As cartilage is a primarily structural tissue, maintenance of the structural integrity is essential for function. Baseline experiments showed no difference in the elastic modulus of healthy adult articular cartilage either with sex or genotype in wildtype (WT) and Phlpp1-/- mice. Next, we examined cartilage tissue quality in WT and Phlpp1-/- mice at 2, 6, and 12 weeks post-DMM (destabilization of the medial meniscus) surgery, which induces post-traumatic OA. Male WT mice showed decreased activity at 12 weeks post-injury, and more histological signs of cartilage damage. Phlpp1-/- mice did not exhibit changes in behavior or cartilage damage. With AFM, we detected significant decreases in elastic modulus of medial condylar cartilage at 6 weeks, local to the injury in WT but not Phlpp1-/- mice. By 12 weeks, cartilage modulus had decreased from 2MPa to ~1MPa on both medial and lateral sides in WT mice. The Phlpp1-/- mice showed only a 25% decrease in modulus at 12 weeks post-DMM. Similar results were seen in female mice, with WT mice showing significant decreases in elastic modulus at 12 weeks post-DMM compared to Phlpp1-/- mice. Histologic scores of the female tibiae were less severe than the males, with no significant changes in score at any timepoint. This study illustrates the differences between DMM on male and female mice, specifically related to the mechanical changes that take place with PTOA and validates Phlpp1 inhibition as a potential therapeutic strategy for articular cartilage preservation after injury.

***Disclosures: KATHERINE ARNOLD**, None*

SUN-187

Differential osseous gene expression in swim-trained anosteocytic and osteocytic teleost fish *JOSEPHINE T. TAUER[1], Tobias Thiele[2], Catherine Julien[3], Lior Ofer[4], Paul Zaslansky[5], Ron Shahar[4], Bettina Willie[6]. [1]Shriners Hospital, Canada, [2]Julius Wolff Institute, Charité - Universitätsmedizin Berlin, Germany, [3]Shriners Hospital for Children-Canada, Montreal; Faculty of Dental Medicine and Oral Health Sciences, McGill University, Canada, [4]Koret School of Veterinary Medicine, The Robert H. Smith Faculty of Agriculture, Food and Environmental Sciences, The Hebrew University of Jerusalem, Israel, [5]Department of Operative and Preventive Dentistry, Charité - Universitätsmedizin Berlin, Germany, [6]McGill University, Canada

Introduction: Osteocytes are considered mechanosensory bone cells that regulate bone (re)modeling in response to mechanical stimuli. Surprisingly, evolutionarily advanced fish lack osteocytes but still exhibit bone formation in response to loading. While there is knowledge of the molecular mechanisms controlling mammalian mechanoadaptation, fish data is lacking. Thus, we aimed to identify molecular mechanisms in anosteocytic bones (ricefish; RF) and osteocytic bones (zebrafish; ZF) after loading.Methods: Fish were trained by swimming for 5 minutes against a current and sacrificed after 1-, 8-, or 24 hours (h). Vertebrae were analyzed using RNA sequencing and compared to non-trained controls (n=6 fish/genotype).Results: At each time point, 26,099 and 21,129 gene reads for ZF and RF have been identified, respectively. After filtering non-skeletal genes (Ayturk et al. JBMR, 2013:28), 14, 54, and 977 differentially expressed genes (DEGs) have been identified in ZF, and 353, 284, and 763 DEGs in RF at 1h, 8h, and 24h, respectively. Enrichment analysis showed in ZF that upregulated DEGs were related to protein translation at 1h, and to DNA transcription and cell cycle processes at 24h, while downregulated DEGs were linked to muscle function, circadian rhythm, and metabolic processes at 24h. In RF, upregulated DEGs were associated with ion channel activity related to metabolic processes in muscle at 8 and 24h, while downregulated DEGs were related to cytoskeletal organization at 8h. Osteoblast differentiation associated enriched DEGs were identified in ZF at 8 and 24 h, but not in RF. Applying a customized ‘osseous analysis panel’ identified 87 ‘osseous DEGs’ (oDEGs) in ZF and 71 in RF, primarily upregulated in ZF and downregulated in RF. Only one upregulated oDEG was identified in RF, myocilin, a regulator of osteoblast differentiation, at 1h and 24h post-training.Conclusion: Zebrafish benefited from numerous osteocytes for bone formation in response to mechanical stimuli, while ricefish exhibited delayed skeletal modeling after swim training. It’s speculated that in anosteocytic bone, non-osteocytic cells, such as bone lining osteoblasts, chondrocytes, and chordoblasts, sense and respond to mechanical load differently over time (Ofer et al. PLoS Biol, 2019:17). Our findings challenge the current paradigm of osteocytes as the exclusive regulators of bone remodeling and suggest the existence of multivariate feedback networks involved in bone remodeling.

***Disclosures: JOSEPHINE T. TAUER**, None*

SUN-189

Cortical Bone Responds to a Single Mechanical Loading Bout in Mice Administered a Bioenergetic Drug *Omar Dervisevic[1], Justin Samuel[2], J Fritton[3]. [1]Department of Biomedical Engineering, City College of New York, United States, [2]CUNY School of Medicine, City College of New York, United States, [3]CCNY, United States

Locally enhancing bone’s response to load-bearing exercise would benefit prevention of osteoporosis. The mechanical threshold for initiating a local response requires large impact loads. Potentially lowering the threshold is our aim by administering the bioenergetic drug, fructose 1,6 bisphosphate (FBP) immediately prior to application of the non-invasive, well-controlled, mouse tibia, cyclic compression model. In an IACUC approved study, 12-wk-old B6 female mice were administered either 12.5% FBP or vehicle control via i.p. injection (pH buffered, sterile saline). 30 minutes later in vivo mechanical loading of the left (L) tibia was completed in 5 minutes (4 Hz, 1200 cycles) under isoflurane anesthesia via ElectroForce LM1. Load groups included, 2N, 6N and 10N (n=10/group). The right (R) tibia serves as paired, intra-animal control for comparison. Double labels (calcein and xylenol orange) were i.p. injected after loading and 3 d before sacrifice that was 10 d post loading bout. Tibias were then scanned by ?CT (Skyscan 1272, 10?m) for structural analyses. Alignment by registration of each scanned tibia with contralateral (Bruker), followed by comparison by % length (Matlab) in all groups revealed relative differences, [L-R]/R at $p<0.05$. In the proximal tibial area that normally responds with formation at 10N (25% of length), greater (8%) cross-sectional max moments of inertia (MOI) were found in loaded limbs from both FBP and vehicle-control, i.e., greater cortical bone geometry to resist bending. In contrast, only the FBP-treated group demonstrated such greater (7%) MOI after the single bout of 6N loading, suggesting a reduced mechanical threshold for response at the time of loading. No significant MOI differences due to 2N loading were found in either FBP or vehicle-control. Other studies in mice suggest bioenergetic drugs that, like FBP, inhibit glycolysis, may also enhance mechanosensitivity. While bioenergetics hold promise in combination with mechanical loading, separating direct effects on the in vivo target-cell population, osteocytes, from indirect effects secondary to increased energy availability is a limitation of studies that utilize multiple drug treatments over weeks. There are also limitations to this current study. However, the pursuit of such a strategy (bioenergetic drug administration only at the time of a single mechanical loading bout) holds the potential to demonstrate mechanism(s).

***Disclosures: Omar Dervisevic**, None*

SUN-190

An in vitro Orbital Flow Model to Study Mechanical Loading Effects on Osteoblasts *Chandrasekhar Kesavan[1], Subburaman Mohan[1]. [1]Jerry L. Pettis Memorial VA Medical Center, United States

Mechanical loading is an important physiological regulator of bone-forming osteoblast function. The fluid flow induced by mechanical loading in vivo is dynamic and oscillatory. Several models have been developed to mimic the in vivo oscillatory flow in cultured osteoblasts, including the commonly employed fluid flow chamber and oscillatory flow apparatus, which requires a complex setup. Since the flow induced by an orbital shaker is also known to produce shear stress and oscillatory flow, we evaluated the utility of this model for studies on mechanical loading effects in osteoblasts. We isolated osteoblasts from adult (12-16-week-old) C57BL/6J mice and plated 10,000 cells on the peripheral edge of the 6-well plate where the flow effect is expected to be high. The plates were subjected to flow at 0.7-, 1.4-, and 3.3-frequency (Hz)/sec for 30- and 50-minutes, respectively, using the orbital shaker in serum-free differentiation medium. The shear stress produced by 0.7-, 1.4- and 3.3-Hz on cells were 1.1-, 3.3-, and 37- dynes/cm2, respectively, as calculated using the formula ?max=??p(2?f)3. The ALP activity measured 72 hours after orbital flow showed a significant increase at 0.7 & 1.4 but not at 3.3 Hz compared to static controls. In addition to ALP activity, we also found significantly increased (25%) osteoblast proliferation at 0.7Hz compared to static controls. Furthermore, expression levels of bone formation markers, Osf2, Hif1a, Vegf, and Cox2, were significantly increased (1.5 to 3-fold, $p<0.05$) in cells subjected to 0.7 Hz flow compared to non-loaded cells. We also evaluated the effect of orbital flow on key signaling pathways (mTOR, JNK, WNT) known to mediate mechanical loading effects on osteoblasts. We found that blocking mTOR and WNT signaling with inhibitors significantly reduced (20-30%) orbital flow-induced ALP activity compared to cells treated with vehicle. By contrast, JNK signal inhibition did not significantly affect flow-induced osteoblast differentiation. In conclusion, our findings demonstrate that the orbital shaker model is an excellent inexpensive model to study mechanical loading effects on osteoblasts in vitro.

***Disclosures: Chandrasekhar Kesavan**, None*

SUN-191

Mechanical Memory Effected Chondrogenesis of Mesenchymal Stem Cells by Using Microgroove-Patterned Hydrogel *Siying Wu[1], Yang Liu[1], Ziyan Wang[1], Hongzhi Liu[1], Chao Liu[1]. [1]Southern University of Science and Technology, China

Purpose: Mechanical stimulation is a critical factor in cartilage regeneration, as it directly activates mechano-sensing molecules and influences stem cell migration and differentiation. Recent studies have also shown that mechanical memory and dosing can impact stem cell fate, with cells retaining a "memory" of their past physical environments. Based on this understanding, we hypothesize that pre-culturing mesenchymal stem cells (MSCs) on microgroove patterned hydrogels with varying widths could generate different elastic moduli and preserve the resulting mechanical memory in the cells, ultimately affecting chondrogenesis.Method: We obtained MSCs from C57BL/6 mice and expanded them in culture dishes for two passages (P0-P1). Subsequently, in passages 2 and 3, the cells were cultured on gelatin hydrogels with flattening and microgroove patterns of varying widths (20-200 um) to achieve pre-mechanical dosing. We then examined the cell mechanics by performing the immune staining of vinculin, phalloidin, and YAP. To study the chondrogenic ability of pre-mechanically dosed MSCs, we carried out staining, western blotting, and qPCR in vitro. Additionally, we validated the chondrogenic repair ability of those MSCs in an articular cartilage full-thickness defect mouse model in vivo (Figure 1a).Result: The microgroove patterned gel substrate has been shown to guide MSC alignment and promote significant cell elongation, resulting in a higher elastic modulus compared to a flat substrate (as depicted in Figure 1b, c). Further investigation will be conducted on the cell mechanics, chondrogenic ability, and the mechanism of pre-mechanically dosed MSCs.Conclusion: This study aims to uncover the underlying mechanism of mechanical memory in MSCs and its impact on chondrogenesis, potentially providing valuable insights into the plasticity of stem cells during development.

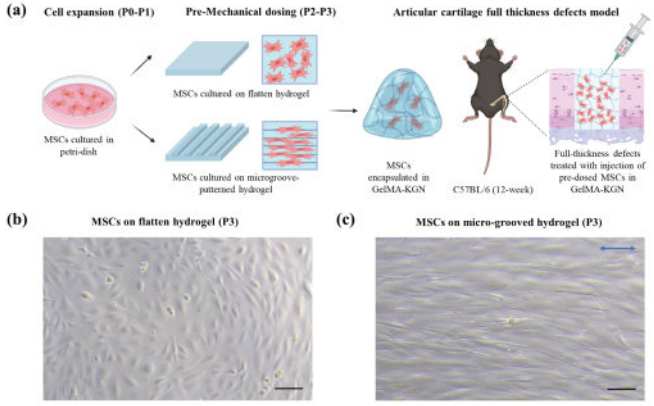

Figure 1. (a) Experimental design: MSCs were expanded from P0 to P1 on a culture dish, pre-mechanically dosed with flatten or microgroove-patterned hydrogel substrates, and then their chondrogenic repair ability was evaluated in a mouse model of articular cartilage full thickness defect. MSCs were cultured on (b) flatten, and (c) microgroove-patterned hydrogel with a width of 20 μm. The blue double-headed arrow indicates the direction of the grooves. Scale bar = 100 μm.

***Disclosures: Siying Wu**, None*

SUN-192

Engineered Bone Analog Models Designed for Testing on the International Space Station *MAXIMILIEN DELEON[1], Sean Howard[2], Omor Khan[2], Anamaria Zavala[2], Angela Kubik[3], Chess Necessary[4], Kendall Nelson[4], Sam Perry[4], Isabel Moore[4], Zach Jacobs[4], Paul Gamble[4], Aykut Satici[2], Mary Farach-Carson[5], Elizabeth Blaber[3], Gunes Uzer[2], Danielle Wu[6]. [1], [2]Boise State University, United States. [3]Rensselaer Polytechnic Institute, United States. [4]Space Tango, United States. [5]University of Texas Health Science Center at Houston, School of Dentistry, United States. [6]University of Texas Health Science Center, United States

Purpose: Bone homeostasis is influenced by mechanical forces that alter anabolic responses and bone quantity/quality. Astronauts lose bone during prolonged spaceflight. To investigate Low Intensity Vibration (LIV) as an effective countermeasure to bone loss in microgravity, we developed 3D Bone Marrow Analogs (BMAs) to be maintained in hardware aboard the International Space Station (ISS). We engineered a perfusable 'Cube Well' system containing 16 BMAs housed within a CubeLab™ containing fluidic and electromechanical systems. We expect LIV to increase anabolic activity of Bone Marrow Stromal Cells (BMSCs) in BMAs to be tested in ground controls and on the ISS.Methods: The CubeLab™ will support automated media changes and preservation steps of BMAs on the ISS [4 Cube Wells/CubeLab™; 2 CubeLabs™: +LIV and -LIV] and matched ground controls. Osteogenic factors are delivered with StemBeads® for controlled release. BMAs consist of hydrogel-encapsulated BMSCs and 3D printed resin scaffolds mimicking trabecular lattices of young (25% BV/TV) or old (15% BV/TV) bone [bone volume/total volume]. To perform experiments within the volume and power limitations on the ISS, CubeLab™ performance is rigorously tested before launch. Studies include testing diffusion rates in and out of the BMAs to assess media change frequency, determining optimal time for solution changes for fixation to assess protein and RNA levels as an index of anabolic activity, assessing extent of mineralization, and verifying full-system integration and automation of fluidic and LIV systems.Results: The Cube Wells satisfied some/most mission success criteria in pre-launch testing. A subpopulation of BMSCs in BMAs attached to the lattice and produced matrix; others remained in a bulk hydrogel. Media changes every 2 days maintain cellularity. Small solutes in BMA exchanged by diffusion by 60 mins. An observed increase in cellularity and collagen production in 25% (young) but not 13% (old) BMAs comparing LIV treated and static groups may be due to the proximity of BMSCs to scaffold surfaces and variable strains. Exposure to LIV (1g, 100 Hz) increased collagen production. Mineralization is being assessed after the addition of osteogenic factors via StemBeads®.Conclusions: BMAs in the Cube Well/CubeLab™ system provide a valuable platform for testing use of LIV as an effective countermeasure to prevent/slow bone loss during microgravity/space flight.

***Disclosures: MAXIMILIEN DELEON**, None*

SUN-193

Osteocytic Connexin 43 Deficiency Attenuates HLS-Induced Epiphyseal Bone Loss in Female, but not Male, C57Bl/6J Mice *Gabriel Hoppock[1], Evan Buettmann[2], Jolene Windle[2], Henry Donahue[2. 1]. [2]Virginia Commonwealth University, United States

Preceding research has shown that gap junction communication and mechanical stimulation, or lack thereof, influence bone development and remodeling, however, the mechanisms by which this occurs remain unclear. Our lab and others have shown deficiency of connexin 43 (Cx43), bone's predominant gap junction protein, in early osteoblasts/osteocytes protects against unloading-induced bone loss in mice.1,2 It is unclear, however, if this protection is due to Cx43 deficiency in osteoblasts or osteocytes, the latter being the most abundant and primary mechanosensory bone cell. To address this, we used a Cx43-deficient mouse targeting later osteoblasts/osteocytes to test the hypothesis that osteocyte-specific Cx43 deficiency protects against hindlimb suspension (HLS)-induced bone loss.All animal procedures were approved by the VCU IACUC. At 6 months of age, male and female osteocyte-specific Cx43 deficient mice (Cx43?OCY) and their wildtype littermates (WT) with C57Bl/6J backgrounds underwent HLS or normal ambulation (control) for 21 days (n=8-11 per group). MicroCT scans were taken on days 1 and 22 and images the left femur was analyzed. Separate 2-way ANOVAs with Bonferroni's post-hoc tests were used to assess female and male mice for significant effects of genotype and HLS ($p<0.05$).At baseline Cx43?OCY mice had decreased diaphyseal cortical bone compared to WT (Figure 1A). In the epiphysis and metaphysis, male mice showed an increase in bone volume due to Cx43 deficiency, but female mice did not. The basal differences between WT and Cx43?OCY mice show osteocytic Cx43 plays a sexually dimorphic role in postnatal bone volume. After 21 days of HLS, significant effects of HLS were found in all female and male epiphyseal and metaphyseal changes as well as in Ct.Ar/T.Ar (Figure 1B). Interestingly, osteocyte-specific Cx43 deficiency protected against HLS-induced decreases in epiphyseal BV/TV in female but not male mice. Cx43 deficiency did not affect HLS-induced decreases in metaphyseal or cortical bone in either male or female mice. These results suggest osteocytic Cx43 deficiency causes increased trabecular and decreased cortical bone basally. The data also show osteocytic Cx43 deficiency protects against HLS-induced epiphyseal bone loss in female mice whereas early osteoblast Cx43 deficiency likely also protects against metaphyseal bone loss, as shown previously by our lab.21. Grimston et al. J Bone Miner Res. 2011. 2. Lloyd et al. J Bone Miner Res 2012.

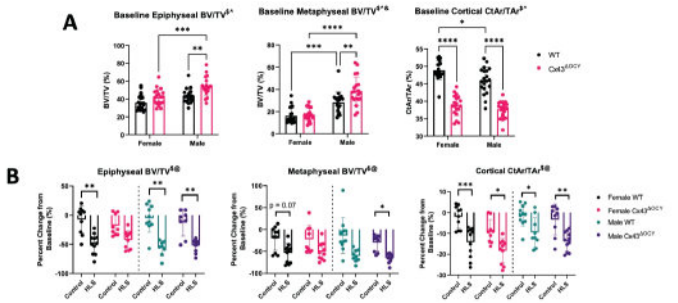

Figure 1. A. Osteocyte specific Cx43 deficiency led to increased trabecular bone but decreased cortical bone fraction. Baseline microCT data for WT and Cx43^{iOCY} female and male mice analyzed by 2-way ANOVA for effects of sex and genotype. $ Significant main effect of sex. ^ Significant main effect of genotype. & Significant main interaction of sex and genotype. **B. Cx43 deficiency protects against HLS-induced epiphyseal bone loss in female, but not male, mice.** Percent change from baseline after 21 days of HLS. Females and males analyzed by separate 2-way ANOVAs for effects of HLS and genotype. $ Significant main effect of HLS in females. @ Significant main effect of HLS in males. * p < 0.05; * p < 0.005; * p < 0.0005; **** p < 0.0001 by Bonferroni post-hoc.

***Disclosures: Gabriel Hoppock**, None*

SUN-194

Renal Osteodystrophy Precision Medicine Project *Valentin David[1], Hartmut Malluche[2], Isidro Salusky[3], Thomas Nickolas[4]. [1]Northwestern University, Feinberg School of Medicine, United States, [2]University of Kentucky Medical Center, United States, [3]University of California, Los Angeles School of Medicine, United States, [4]Columbia University, United States

Renal osteodystrophy (ROD) is a complex disorder of bone metabolism that affects virtually all patients with chronic kidney disease (CKD). ROD is associated with adverse clinical outcomes including bone loss, mineralization and turnover abnormalities, skeletal deformities, fractures, cardiovascular events, and death. Despite current therapies, fracture incidence is 2- to 100-fold higher in adults with compared to those without CKD. Limited knowledge of ROD pathogenesis impedes development of therapeutics aimed at reducing morbidity and mortality of CKD patients.Bone-tissue based information obtained from patients with ROD that includes altered epigenome and transcriptome as a function of disease progression is missing and highly contributes to this critical knowledge gap. We aim to obtain robust and necessary preliminary data assessing the variability and demonstrating the rigor and reliability of single nuclei sequencing in bone by simultaneous profiling of the transcriptome (using 3' gene expression) and epigenome (using ATACseq) to deepen our understanding of how genes are expressed and regulated across different cells and kidney disease stages. Our long-term goal is to create the fundamental infrastructure to facilitate high-impact novel hypothesis-driven clinical and translational research in ROD by building a large-scale data and tissue biorepository integrating clinical, bone quality, transcriptomic and epigenomic data along with stored urine, blood, and bone samples.We have started the collection of bone biopsies from adults with CKD 3-5D and a reference population of kidney-healthy adults with age-related osteoporosis. Our studies will determine the changes in osseous transcriptome and epigenome of patients with ROD vs osteoporosis at the cellular level using single nuclei RNA and ATAC sequencing. Finally, based on these results we will develop a user pipeline with an interactive open access web-based interface.This resource will provide the underpinnings for future research endeavors leading to the elucidation of the pathogenesis of ROD across the spectrum of CKD including dialysis. These results will contribute to our efforts to redefine our understanding of ROD pathogenesis and pathophysiology and the development of disease targeted prevention strategies.

***Disclosures: Valentin David**, None*

SUN-195

miR335-5p and its potential target SERPINB1 as a regulator of bone metabolism in postmenopausal osteoporosis (PMO) *Simran kaur[1], Vandana Dhiman[2], Nainesh Joshi[3], Raman Kumar[4], Mani sangar[5], Ravi Pratap Barnwal[6], Gurpal Singh[7], Sudhaker Dhanwada Rao[8], Sanjay Kumar Bhadada[9]. [1]Phd Student, Department of Endocrinology Post Graduate Institute of Medical Education and Research, , India, [2]Senior Demonstrator, Department of Endocrinology Post Graduate Institute of Medical Education and Research, , India, [3]Research Assistant , India, [4]Department of Endocrinology Post Graduate Institute of Medical Education and Research, , India, [5]Phd Student, Department of Endocrinology Post Graduate Institute of Medical Education and Research, , India, [6]UGC Assistant Professor Department of Biophysics, PU, Chandigarh, India, [7]UGC Assistant Professor University Institute of Pharmaceutical Sciences, PU Chd, India, [8]HENRY FORD HEALTH SYSTEM , United States, [9]PGIMER, chandigarh, India, India

Background:Osteoporosis is a common condition in postmenopausal women, which increases the risk offractures and morbidity. Previous studies have shown that osteoporosis results from anunbalanced pattern of bone remodeling, with higher bone resorption than the formation.Osteoporosis affects approximately 200 million people worldwide. In India, there are around50 million individuals with osteoporosis or low bone mass. Approximately 40% of post-menopausal women and 20% of men suffer fractures each year. In post-menopausal women,osteoporosis is related to increased age and decreased levels of estrogen. Several studies haveshown that microRNAs contribute to the pathogenesis of post menopausal osteoporosis viadysregulated bone homeostasis. In this study, the expression of miR335-5p was investigated inpostmenopausal osteoporosis (PMO) and its potential role in regulating bone metabolism.Aim:To investigate the expression of miR335-5p in PMO and its potential role in regulating bone metabolism.Materials and Methods:Serum samples were collected from postmenopausal women with osteoporosis (n=50) and healthy controls (n=30), and miR335-5p expression was measured using real-time PCR. In silico analysis was performed to identify potential target genes of miR335-5p, using several databases such as miRwalk, Target Scan, miRDB, and miRpath.Results:The results showed that miR335-5p was significantly upregulated in the serum samples of postmenopausal women with osteoporosis compared to controls. Further in silico analysis identified SERPINB1 as a direct target of miR335-5p. SERPINB1 protein is a known inhibitor of neutrophil-derived proteinases, which protects tissues from damage at inflammatory sites. SERPINB1 has also been shown to inhibit osteoclast formation, which may contribute to its protective effect on bone metabolism. Other important genes involved in bone metabolism i.e., RUNX2, SOX4, and MAPK1 are also targets of miR335-5p. The protein tissue atlas showed that SERPINB1 is highly expressed in bone marrow, which supports its potential role in regulating bone metabolism and the pathogenesis of osteoporosis.Conclusion:Targeting miR335-5p and increasing the expression of SERPINB1 protein may be a promising approach to treat PMO. This could be achieved by suppressing osteoclast formation, which may protect tissues from damage at inflammatory sites and thus reduce the risk of fractures and morbidity. Further studies are required to validate these findings and explore the dual-potential therapeutic implications of targeting miR335-5p and SERPINB1 in osteoporosis.

Title: miR335-5p and its potential target SERPINB1 as a regulator of bone metabolism in postmenopausal osteoporosis (PMO)

Authors: **Simran Kaur**, Vandana Dhiman, Nainesh Joshi, Raman Kumar, Mani, Ravi Pratap Barnwal, Gurpal Singh, Sudhaker Rao, Sanjay Kumar Bhadada*

Background:

Osteoporosis is a common condition in postmenopausal women, which increases the risk of fractures and morbidity. Previous studies have shown that osteoporosis results from an unbalanced pattern of bone remodeling, with higher bone resorption than the formation. Osteoporosis affects approximately 200 million people worldwide. In India, there are around 50 million individuals with osteoporosis or low bone mass. Approximately 40% of post-menopausal women and 20% of men suffer fractures each year. In postmenopausal women, osteoporosis is related to increased age and decreased levels of estrogen. Several studies have shown that microRNAs contribute to the pathogenesis of post-menopausal osteoporosis via dysregulated bone homeostasis. In this study, the expression of miR335-5p was investigated in postmenopausal osteoporosis (PMO) and its potential role in regulating bone metabolism.

Aim:

To investigate the expression of miR335-5p in PMO and its potential role in regulating bone metabolism.

Materials and Methods:

Serum samples were collected from postmenopausal women with osteoporosis (n=50) and healthy controls (n=30), and miR335-5p expression was measured using real-time PCR. In silico analysis was performed to identify potential target genes of miR335-5p, using several databases such as miRwalk, Target Scan, miRDB, and miRpath.

Results:

The results showed that miR335-5p was significantly upregulated in the serum samples of postmenopausal women with osteoporosis compared to controls. Further in silico analysis identified SERPINB1 as a direct target of miR335-5p. SERPINB1 protein is a known inhibitor of neutrophil-derived proteinases, which protects tissues from damage at inflammatory sites. SERPINB1 has also been shown to inhibit osteoclast formation, which may contribute to its protective effect on bone metabolism. Other important genes involved in bone metabolism i.e., RUNX2, SOX4, and MAPK1 are also targets of miR335-5p. The protein tissue atlas showed that SERPINB1 is highly expressed in bone marrow, which supports its potential role in regulating bone metabolism and the pathogenesis of osteoporosis.

Conclusion:

Targeting miR335-5p and increasing the expression of SERPINB1 protein may be a promising approach to treat PMO. This could be achieved by suppressing osteoclast formation, which may protect tissues from damage at inflammatory sites and thus reduce the risk of fractures and morbidity. Further studies are required to validate these findings and explore the dual-potential therapeutic implications of targeting miR335-5p and SERPINB1 in osteoporosis.

***Disclosures: Simran kaur**, None*

SUN-196

The Dp1Yey Down Syndrome Mouse Model Exhibits Deficits in Microarchitecture and Strength of the Femur and Lumbar Vertebrae *Joshua Lamantia[1], Kourtney Sloan[2], Randall Roper[3]. [1]Indiana University-Purdue University-Indianapolis, United States, [2], , [3]Indiana University-Purdue University Indianapolis, United States

Down syndrome (DS) is a genetic disorder that affects about 1 in 800 live births, resulting from the triplication of human chromosome 21 (Hsa21). People with DS have distinctive craniofacial features, cognitive deficiencies, and skeletal deficits which can lead to increased risk of fractures, particularly in the femoral neck and lumbar spine. While previous research has studied femoral bone deficits in DS mouse models, little is known about the vertebrae, which are also affected in humans with DS. Understanding when and what kind of skeletal deficits occur is crucial for identifying potential treatments. We used the Dp1Yey DS mouse model, which has all genes triplicated on mouse chromosome 16 that are orthologous to Hsa21. This model accounts for roughly 63% of the genes triplicated in Hsa21 and displays long bone deficits in male but not female mice at 12 weeks based on previous studies. Using micro-computed tomography and 3-point bending, the trabecular and cortical regions of the femur and the 4th lumbar (L4) vertebra in male and female Dp1Yey mice and wildtype controls were quantified at 6 weeks of age. Male Dp1Yey mice exhibited deficits in trabecular and cortical regions of the femur, while female Dp1Yey mice solely presented cortical deficits. Both male and female Dp1Yey mice suffered from significantly lower bone mineral density (BMD) in the L4 vertebra and deficits in trabecular thickness and bone volume fraction (BV/TV). Skeletal abnormalities have been reported in Ts65Dn and Dp1Tyb DS mouse models which show similar but not identical findings. Ts65Dn mice exhibit trabecular and cortical deficits at both 6 and 16 weeks of age in both males and females. In Dp1Tyb mice, trabecular deficits were seen only in males at both 6 and 16 weeks while female Dp1Tyb as compared to control mice did not show any significant trabecular deficits. Cortical deficits, however, were seen in both males and females at these ages. Dp1Tyb and Dp1Yey are thought to be genetically similar, and while the overall conclusions of these mouse models

are consistent, there are small differences in the data that may be attributed to environmental and procedural differences. Our findings suggest that skeletal deficits associated with DS occur early in development, are sex-dependent, and that early treatment may be necessary to improve associated deficits in DS.

***Disclosures: Joshua Lamantia**, None*

SUN-197

A Blueprint to Archive µCT and Bone Histomorphometry Data *Peter Maye[1], Dong-Guk Shin[2], Thomas Andersen[3], Je-Yong Choi[4], David Rowe[5]. [1]UCONN Health, United States. [2]University of Connecticut, United States. [3]University of Southern Denmark, Denmark. [4]School of Medicine, Kyungpook National University, Republic of Korea. [5]University of Connecticut Health Center, United States

The mechanistic regulation of the skeletal system is extremely complex involving a multitude of local and systemic processes that far surpasses what any one individual can conceive. Rapid developments in machine learning approaches bring new possibilities to integrate accumulated knowledge that will advance research and therapeutic development. However, few databases exist that are exclusively dedicated to documenting the skeletal function of genes that would enable machine-learning approaches.The skeletal phenotyping of rodent animal models via µCT and bone histomorphometry analysis yields significant insight into how bone tissue is regulated. However, no central resource exists for storing and accessing datasets generated by skeletal phenotyping. The archiving of bone histomorphometry datasets contributed by generations of investigators over time will undoubtedly become a highly valued resource for a broad user base and will empower systems biology approaches to solve complex mechanisms of skeletal regulation that previously were not possible.Here we detail our resource development plan to build a biomedical data repository to archive and share bone histomorphometry data. This plan has three major objectives: 1) Develop a data ingestion method that is comprehensive in regard to experimental manipulation (genetic, treatment, or combination) for rodent animal models and includes the associated experimental metadata. Maintains high data quality standards by requiring peer-review publication of work and for unpublished studies provides a path to publication in a special issue associated with the repository hosted by the journal Bone. 2) Develop a database system that is scalable and designed for enhanced accessibility and query processing with the proper privacy, backup, and security measures in place. 3) Develop a web portal that exemplifies FAIR principles and includes efforts to harmonize data for interstudy comparisons.This resource will be further supported by an external advisory committee that will establish policies of data governance and the use of scientific emissaries based in North America, Europe, and Asia that will establish a global network of working groups that will be involved in the preliminary testing of applications at progressive stages of development prior to launch. We welcome interested investigators to attend our poster session or contact us (https://bonebase.lab.uconn.edu/contact_us/) to become part of a working group.

***Disclosures: Peter Maye**, None*

SUN-198

The Ts66Yah mouse model displays cortical skeletal deficits associated with Down syndrome *Kourtney Sloan[1], Laurent Meijer[2], Joseph Wallace[3], Yann Herault[4], Randall Roper[5]. [1]Department of Biology, Indiana University-Purdue University, United States. [2]Perha Pharmaceuticals, France. [3]Indiana University Purdue University Indianapolis (IUPUI), United States. [4]Department of Translational Medicine and Neurogenetics, Université de Strasbourg, Centre National de la Recherche Scientifique, Institut National de la Santé et de la Recherche Médicale, Institut de Génétique et de Biologie Moléculaire et Cellulaire, France. [5]Indiana University-Purdue University Indianapolis, United States

Down syndrome (DS) is a genetic condition that alters bone development and maintenance. Many mouse models of DS have been developed but not all have had the appendicular skeleton characterized. The Ts66Yah mouse model has been developed to contain ~50% of human chromosome 21 (Hsa21) orthologous genes on a freely segregating third chromosome, without triplicating the ~35 protein-coding, non-orthologous genes found in Ts65Dn mice, heretofore the most analyzed DS mouse model. Structural properties of male and female 6-, 9-, and 16-week-old Ts66Yah femurs were analyzed using micro-computed tomography (µCT) to understand phenotypes between bone accrual and peak bone mass. Trabecular measurements revealed no genotypic effects compared to wildtype mice at 6 or 16 weeks, but there was a genotypic effect (P=0.048) in trabecular thickness (-5.6% of wildtype) at 9 weeks. There were cortical deficits, including total cross-sectional area (Tt.Ar,-9%), marrow area (Ma.Ar,-12%), periosteal perimeter (Ps.Pm,-4%), and endocortical perimeter (Ec.Pm,-6%), that showed genotypic effects at 6 weeks (P=0.005). At 9 weeks, Ma.Ar (-18.4%) and Ec.Pm (-8%) showed genotypic effects (P<=0.006). Additionally, cortical area fraction (BA/TA) had a genotypic effect (P<0.006) but was increased by 9%. At 16 weeks, there was interactions of genotype and sex (P<=0.02) where only male Ts66Yah mice as compared to wildtype mice showed deficits in Tt.Ar (-18%), Ma.Ar (-29%), Ps.Pm (-7.5%), and Ec.Pm (-16%) in posthoc analyses. Previous studies in Ts65Dn mice showed trabecular deficits in both sexes at 6 weeks and in male mice at 16 weeks, in addition to cortical deficits. These data suggest that trabecular deficits in Ts65Dn mice may be driven by non-orthologous trisomic genes. A potential drawback of the Ts66Yah model may be the lack of trabecular deficits at 6 and 16 weeks and cortical effects in female mice at 16 weeks. However, these results may indicate Hsa21 orthologous genes in Ts66Yah only impact cortical bone, and more trisomic genes are necessary to cause DS-related trabecular deficits. We are also investigating the effect of Dyrk1a, a trisomic gene in Ts65Dn, Ts66Yah, and humans with DS, by breeding Ts66Yah mice with Dyrk1a heterozygous mutant (Dyrk1a+/-) mice to normalize Dyrk1a copy number and treating Ts66Yah mice with a DYRK1A inhibitor and analyzing the resultant femurs. These results and further analyses will help understand the gene-phenotype relationship in DS skeletal deficits.

***Disclosures: Kourtney Sloan**, None*

SUN-199

Comprehensive Characterization of the Ovariectomized Sheep Model of Postmenopausal Osteoporosis *Katie Bisazza[1], Brad Nelson[1], Katie Sikes[1], Jeremiah Easley[1]. [1]Colorado State University, United States

Ovariectomized (OVX) sheep are commonly used for osteoporosis research because they are comparable to humans in bone size and microarchitecture. However, the cellular pathways involved in bone turnover in ovine models of osteoporosis have not been fully elucidated. The objectives of our study were to comprehensively characterize the bone density, protein, and cellular changes in a long-term OVX-corticosteroid combination ovine model, as well as evaluate any clinical and systemic effects. Sixteen skeletally mature ewes were enrolled in the study (CSU IACUC #2060). Ten animals underwent OVX surgery and were administered a high-dosage regimen of corticosteroids. Six animals were used as healthy age-matched controls. In-life imaging and iliac crest bone biopsy collections were performed at baseline (prior to OVX), 3, 6, 9, and 12-months. Parametric data were assessed for statistical differences using a two-way ANOVA and an alpha value of 0.05 or less considered significant. The lumbar spine and tibia were scanned using dual-energy x-ray absorptiometry (DXA) to monitor bone mineral density (BMD). Lumbar spine and tibia BMD of OVX sheep was significantly lower than control animal BMD at 3 and 6-months, while lumbar spine BMD was also significantly lower than controls at 9 and 12-months (Fig. 1A-B). Blood collection and body weights were performed monthly to assess systemic health. Biopsies of the iliac crest were collected at each time point for micro-computed tomography (microCT) analysis to compare bone microarchitecture. Bone volume fraction (BV/TV) of OVX sheep was significantly lower than controls at 3 and 9-months (Fig. 1C). Trabecular number (Tb.N) was also decreased at 6-months (Fig. 1D). Samples were then processed for decalcified histology and stained for histomorphometry analysis. Small bone biopsies were flash frozen for LC/MS untargeted proteomic analysis to evaluate protein production and/or degradation in the bone. Proteomic and histomorphometry data processing is currently ongoing. Large animal preclinical models offer researchers the ability to compare bone changes in the same animals over time, allowing for a more comprehensive insight into the progression of postmenopausal and age-related bone loss. Understanding the cellular pathways involved in osteoporosis disease progression in the sheep model could aid in future cellular therapy research and lead to novel pathway targets for disease treatment in humans.

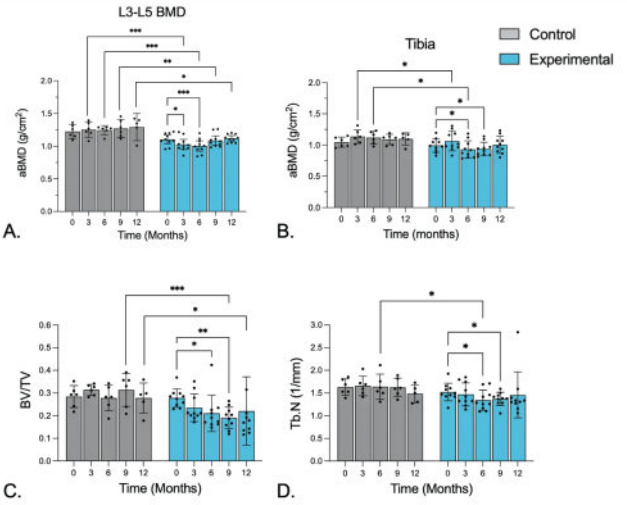

Figure 1. Comparison of bone parameters between OVX (osteoporotic) sheep and age-matched control sheep. *A)* Bone mineral density of the lumbar spine L3-L5 and *B)* the tibia using DXA imaging. *C)* MicroCT bone volume fraction and *D)* trabecular number of iliac crest biopsies. (*) indicates significance of p<0.05.

***Disclosures: Katie Bisazza**, None*

SUN-200

Gene expression profiles in fibroblast growth factor 23 (FGF23)-producing tumors provide new insights on diagnostics and therapeutic intervention.
*Sofya Gronskaia[1], Ruslan Devitiarov[2], Sergey Popov[1], Svetlana Rodionova[3], Yuriy Buklemishev[3], Liudmila Rozhinskaya[1], Oleg Gusev[2], Zhanna Belaya[1]. [1]Endocrinology Research Centre, Russian Federation. [2]Regulatory Genomics Research Center, Kazan Federal University, Russian Federation. [3]National Medical Research Center of Traumatology and Orthopedics named after. N.N. Priorov, Russian Federation

Background: Fibroblast growth factor 23 (FGF23)-producing tumors are histologically known as phosphaturic mesenchymal tumors (PMT). A PMT causes an oncogenic osteomalacia (OOM), which is associated with multiple fractures, severe pain, and muscle weakness.Aim: To analyze gene expression profiles of PMT versus control tissue.Methods: PMT and surrounding control tissue samples were obtained during tumor resection in 5 patients (Age 62 [45; 65], iFGF23 (ELISA Kit Biomedica BI-20700 -113 [50; 203] pg/ml (ref. range 14.8 [3.8;25.0]pg/ml), serum phosphorus 0.51 [0.4; 0.53]mM/L (ref. range 0.74-1.52 mM/l)). Based on histological verification we obtained 4 PMT samples (2 -mandibular bones, 1 - femur bone, 1 - metatarsal bone) and performed bulk RNA sequencing. We used Gene Ontology (GO) and the Kyoto Encyclopaedia of Genes and Genomes (KEGG). Results: A total of 976 genes were differently expressed between PMT and control samples. The four PMT samples were homogeneous according to their gene expression profiles. The genes most up-regulated (n=10) in PMT were LOC105377323/FGF1/MB/SPRY2/LOC105378029/DMP1/FGF23/BMP7/PHEX/LOC124903699. The genes most negatively regulated in PMT were LOC102724638/LOC124901874/LOC124901875/IGLL5/IGKC/IGLC1/LOC105377460/LOC105376032/IGK/IGHG1 (FDR < 0.05). We found that PMT overexpressed genes that are typical for osteoblast activity and differentiation including the most known OPG, RANKL (KEGG: p-value 0.03). We also found increased expression of the Wnt signaling antagonists SOST, DKK1 (KEGG: p-value 0.02). In PMT we found upregulated genes that are typical for secretory active osteocytes surrounded by high phosphate(FGF23/DMP1/ENPP1/PHEX/GALNT3/FAM20C/AKNA/DSPP/MEPE/EN1). Genes and pathways related to mineral ion transport were also up-regulated: Phospholipase D signaling pathway (KEGG p-value 0.003); signaling receptor binding (GO p-value < 0.001); solute: sodium symporter activity (GO p-value 0.004); calcium ion binding (GO < 0.001) and PiT1 (SLC20A1), which encodes the inorganic phosphate transporter. We found that PMT highly expressed osteopontin, CENPK and genes involved in PI3K/AKT (KEGG: p-value 0.006); ERK1/2 pathways (KEGG p-value 0.02) that are associated with castrate-resistant prostate cancer. The most up-regulated pathways in PMT were ECM-receptor interaction and gastric cancer related genes. We identified human membrane protein genes that were highly expressed in the PMT compared to control tissue PHEX/SYT12/PCDH7/RAMP1/CD44/NRG3/ILDR2/ECEL1/CHST3/ LRFN4/PCDH9, FGFR1/EVA1A/AREG/PTGIS/VSIG2/ENPP1/NRCAM/WSCD2.Conclusion: PMT expresses gene that are typical for secretory active osteoblast cells, including RANKL/OPG, phosphaturic genes, and wnt signaling antagonists. Newly identified gene expression profiles may expand our knowledge on diagnostics and therapeutic intervention in PMT.

***Disclosures: Sofya Gronskaia**, None*

SUN-201

Phosphate Signaling Is Mediated via Parathyroid Hormone Receptor 1-PLC-PKC Pathway in Committed Osteogenic Cells
*Nadine Robert[1], Sandeep Chaudhary[2], Mairobys Socorro[1], Sana Khalid[1], Catherine Roberts[1], Juan Taboas[1], Dobrawa Napierala[1]. [1]University of Pittsburgh, United States. [2]Institute of Oral Health Research, University of Alabama at Birmingham, United States

Phosphate (Pi) is a main component of hydroxyapatite crystals that form the skeletal tissues. Pi also acts as a signaling molecule to regulate mineralization. Previous studies demonstrated the involvement of Na+/Pi cotransporters, FGFR1 and Erk1/2 kinase in Pi signaling. However, the molecular mechanisms of Pi sensing and cellular mediators of Erk1/2 activation in response to Pi have not been elucidated. Our goal is to decipher Pi signaling in cells producing bone (osteoblasts) and dentin (odontoblasts). Hence, we selected two committed osteogenic cell lines, the 17IIA11 odontoblast and MLO-A5 osteoblast/pre-osteocytes, which rapidly undergo mineralization in standard osteogenic conditions. From two independent lines of experiments, we observed the 17IIA11 cells failed to respond to Pi, as evaluated by Erk1/2 activation, when the parathyroid hormone receptor 1 (Pth1r) expression is downregulated. Therefore, we hypothesized that Pth1r is required for Pi signaling in committed osteogenic cells. To test this hypothesis, we used shRNA technologies to generate Pth1r-deficient 17IIA11 and MLOA5 stable cell lines. Unlike WT and shScr controls, Pth1r-deficient cells failed to activate Erk1/2 in response to stimulation with Pi nor mineralized under osteogenic conditions. As Pth1r can modulate various signaling cascades, including protein kinase A (PKA)-cAMP and phospholipase C (PLC)-protein kinase C (PKC), we analyzed which signaling axis downstream of Pth1r transmits the response to Pi in the presence and absence of specific pharmacological inhibitors. PKA inhibition with H-89 did not prevent Erk1/2 phosphorylation (pErk1/2) whereas inhibition of phospholipase C (PLC) with D609 attenuated that response. In addition, we observed a dose-dependent decrease of pErk1/2 levels in comparison to untreated controls when PKCs were inhibited by pan-classical PKC inhibitor Bisindolylmaleimide I (GF109203X). To identify which PKC isoform is involved in Pi signaling, we utilized two selective PKC inhibitors Sotrastaurin (inhibits classical PKCs- PKC? and PKC?, but not PKC?) and Staurosporine (inhibits PKC? and PKC?, but not PKC?). We observed a dose-dependent decrease in Erk1/2 activity only with Staurosporin, while Sotrastaurin had no effect on pErk1/2. Our in vitro studies in committed osteogenic cells propose the Pth1r as a candidate receptor/sensor of Pi, that mediates Pi signaling through PLC-PKC? axis.

***Disclosures: Nadine Robert**, None*

SUN-202

A High-Resolution Investigation Into the Impact of Phosphate Homeostasis Dysregulation on Carbon Metabolism in Osteoblasts
*JIE REN GERALD HAR[1], Dylan P. Kuennen[1], Maciek R. Antoniewicz[2], Lauren E. Surface[1]. [1]University of Michigan School of Dentistry, United States. [2]University of Michigan, United States

Background: Chronic kidney disease mineral and bone disorder (CKD-MBD) leads to skeletal fragility, which diminishes the quality of life of patients with CKD. Yet, the molecular mechanisms that mediate the impact of CKD-MBD on bone strength and metabolism are not well-understood. Against this backdrop, we investigate how CKD-induced hyperphosphatemia - a well-characterized indicator of disease progression - influences carbon metabolism in osteogenic cells. Using MC3T3-E1 cells as a model for osteoblasts, we analyzed the impact of hyperphosphatemia on metabolic fluxes over the course of osteoblast differentiation.Method: Hyperphosphatemic conditions were simulated by exposing differentiated and undifferentiated MC3T3-E1 cells to culture media supplemented with 10 mM sodium phosphate (Pi). A GC-MS-based method was employed for the quantification of concentration of metabolites in the culture media at multiple time points over 24 hours. Metabolic fluxes were then calculated from the change in concentration of metabolites in the culture medium normalized to time interval and cell count (Fig. A).Results: We observed that high Pi stimulates an increase in metabolite consumption or production. Subjecting MC3T3-E1 cells to high Pi led to an increase in glycolysis throughout the course of differentiation. Exemplifying this: the presence of high Pi increased lactate production rates by 48% at Day 0 of differentiation, and 75% at Day 21 of differentiation compared to the respective sodium sulfate control. High Pi also increased the flux of TCA cycle-related metabolites - at Day 21 of differentiation, cells cultured in high Pi exhibited a 76% increase in Gln consumption and 77% increase in Cit production against the negative control.We also compared changes in metabolic fluxes over the course of differentiation. Comparing cells at Day 21 against Day 0 of differentiation, we observed that the Gln uptake per cell decreased by 90% while Glu and Asp uptake per cell increased significantly by 235% and 96% respectively over the course of differentiation. In ongoing work, we are employing 13C-metabolic flux analysis to decipher how Pi affects intracellular metabolic fluxes during osteoblast differentiation.In summary, we have established an in vitro workflow to study the local impact of hyperphosphatemia on osteogenic cells. Our findings presented here provide motivation to investigate the consequences of CKD and hyperphosphatemia on bone metabolism in vivo.

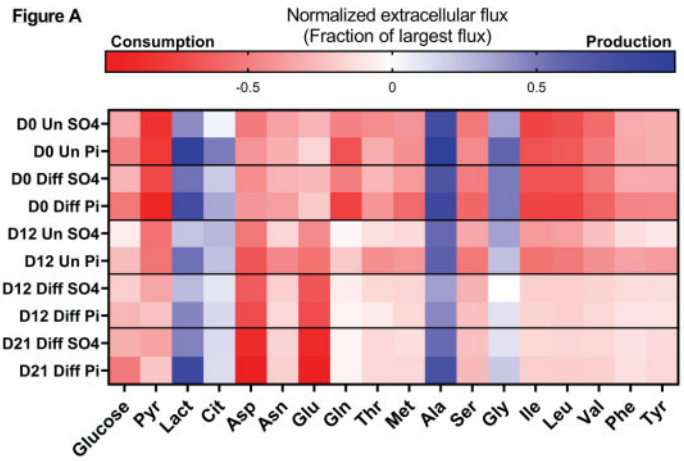

***Disclosures: JIE REN GERALD HAR**, None*

SUN-203

A pilot studies the Relationship between Nucleolin and Copine7-mediated Autophagy
*Joo-Cheol Park[1], Min-Soo Kang[1]. [1]Seoul national university, Republic of Korea

Purpose : we aimed to investigate the relationship between nucleolin and copine7-mediated autophagy in different cell types.Method : To confirm the expression of nucleolin in several cells, we confirmed the expression of nucleolins in normal cells that were treated with noting. And we verified that autophagy was also caused by copine7 in other cells expecting hDPC. Subsequently, nucleolin siRNA and selcopintide were treated and changes were observed in cells with and without autophagy.Results : Expression of nucleolin was confirmed in human dental pulp cells(hDPCs), human periodontal ligament cells(hPDLs),

human gingival fibroblasts(hGF), and SH-SY5Y cells, a neuroblastoma cell line. As a result, nucleolin was expressed in the nucleus of all cells.Conclusions : Nucleolin has been expressed in all cells, especially in the nucleus.

***Disclosures: Joo-Cheol Park**, None*

SUN-204

Genome-wide Analyses Reveal TGF? Signaling as a Regulator of Osteogenic Phosphate Sensing *Dylan Kuennen[1], Long Tran[2], Michael Mannstadt[3], Lauren Surface[2]. [1]University of Michigan, United States. [2]University of Michigan School of Dentistry, United States. [3]Massachusetts General Hospital Harvard Medical School, United States

Organismal phosphate (Pi) is an essential regulator of many cellular processes necessary for healthy tissue and organismal function. The skeleton is a key regulatory site in the control of organismal Pi homeostasis. However, the mechanisms of the Pi-sensing circuitry in osteogenic cells are poorly understood. Using in vitro approaches, our goal is to elucidate how the factors responsible for serum Pi sensing in osteogenic cells enable the endocrine Pi response to inform future therapeutics.To understand the transcriptional response in osteogenic cells during exposure to Pi, we performed an RNA-seq time course on MC3T3-E1, a pre-osteoblast cell line, and OCY454, an osteocytic cell line. We observed differential expression of gene categories related to bone mineralization as well as TGF?, MAPK, and EGF signaling. Based on these findings, we developed two flow cytometry-based readouts of the response to increased extracellular Pi; a Dmp1-2A-mCherry fluorescent reporter and a cell surface antigen stained with an antibody (SEMA7A). Using flow cytometry, we confirmed that inhibiting FGFR1 and ERK signaling blocks these responses to Pi. To identify factors that mediate Pi sensing, we combined our reporters with genome-wide CRISPRi screens and identified ~38 hits common to screens in both reporters. To prioritize physiologically relevant pathways, we intersected these hits with loci associated with circulating Pi and FGF23 levels by GWAS, and identified TGFB2 as a hit that is also top genetic polymorphism associated circulating FGF23 levels, supporting a potential physiological role for TGF? signaling in controlling the endocrine Pi response.We find that TGF-?2 co-treated with Pi enhances the response of osteogenic cells both increasing early Erk phosphorylation and the response of our reporters after 24 hours. We observe that TGF? signaling affects calcium (Ca2+) flux, leading to an increase in extracellular Ca2+, and that an inhibitor of store-operated calcium entry (SOCE) blocks the effect of TGF-?2 suggesting that SOCE mediates this response. Ca2+ may boost the response of osteogenic cells to Pi, likely through calciprotein particle (CPP) formation. We hypothesize that TGF-?2 increases the available extracellular Ca2+ to form CPP with Pi, thereby boosting the Pi response. These results may provide critical insights into Pi homeostasis, particularly in the setting of chronic kidney disease in which both circulating TGF? and FGF23 levels are increased.

***Disclosures: Dylan Kuennen**, None*

SUN-205

Crispant screening in zebrafish as a promising approach for rapid functional screening of osteoporosis candidate genes and known genes for Osteogenesis Imperfecta. *Sophie Debaenst[1], Hanna De Saffel[1], Jan Willem Bek[1], Adelbert De Clercq[1], Tamara Jarayseh[1], Lauren Sahd[1], Andy Willaert[1], Paul Coucke[1]. [1]Ghent University , Belgium

Genome-wide association studies have improved our understanding of the genetic architecture of common complex diseases such as osteoporosis. Nevertheless, to attribute functional skeletal contributions of candidate genes to osteoporosis-related traits and to identify underlying pathogenic mechanisms in other skeletal diseases, such as Osteogenesis Imperfecta, there is a need for efficient and cost-effective in vivo functional testing. To get a quick insight into these pathogenic mechanisms, we aimed to develop a rapid and cost-effective approach for in vivo functional validation of candidate genes through CRISPR-based reverse genetic screens in the zebrafish model system. We used the so-called crispant screening approach, based on CRISPR/Cas9 technology, in order to phenotype directly in FO mosaic founder zebrafish. Compared to a stable knockout model, crispants reduce model generation time, enabling the validation of a large set of genes in a short period of time. Recently, we delivered proof-of-concept for this screening tool by reporting phenotypic and molecular similarities between a stable KO mutant and a crispant for LRP5. In this study, we selected a panel of 6 OI genes (creb3l1, ifitm5, mbtps2, sec24d, serpinf1 and sparc) and 4 Osteoporosis genes (aldh7a1, daam2, esr1 and sost) and micro-injected CRISPR/Cas9 components (gRNA/Cas9) targeting the gene of interest, in one-cell stage zebrafish embryos with an osteoblast-specific Tg(osx:Kaede) transgenic background. NGS amplicon sequencing of pools of injected embryos revealed out-of-frame efficiencies higher than 70%, indicating a high fraction of knock-out alleles for the 10 genes and thus resembling a stable knock-out model. Phenotypic analysis was performed at 7, 14 and 90 days after fertilization, though fluorescence microscopy (osteoblasts), alizarin red bone staining and micro-CT analysis for quantitative analysis of the skeleton. Molecular analysis was performed at 7 dpf through qPCR. Preliminar results are promising, showing skeletal abnormalities, such as fusions, callus formation in the vertebral arches and ectopic mineralization at 90 dpf. Taken together, we showed that crispant screening in zebrafish is a promising approach for rapid functional screening. Moreover, the crispants have the potential to provide new insights into the role of these genes in skeletal biology and can be used as a tool for osteogenic compound screening.

***Disclosures: Sophie Debaenst**, None*

SUN-207

Aging-related declines in skeletal muscle grip strength are prevented via daily oral treatment with an Aryl hydrocarbon receptor (AhR) antagonist, BAY2416964 *KANGLUN YU[3], Meghan McGee-Lawrence[2], DIMA ALHAMAD[3], HUSAM BENSRETI[3], Anik Tuladhar[5], Caihong Dai[5], Joseph Shaver[5], Kehong Ding[5], Rafal Pacholczyk[5], Sadanand Fulzele[5], Carlos Isales[5], Mark Hamrick[5], William Hill[6, 3], . [2]Medical College of Georgia, Augusta University, United States. [3], United States. [5]Augusta University, . [5]Augusta University, United States. [6]Medical University of South Carolina, United States

The Aryl hydrocarbon receptor (AhR) is a cytosolic transcription factor whose activation can be beneficial or harmful; while AhR signaling is important for the detoxification of certain ligands, prolonged or chronic AhR activation may have negative effects on musculoskeletal function. As endogenous AhR ligands like kynurenine increase with age, we tested whether inhibition of AhR would confer a protective effect on the musculoskeletal system during aging.Female C57BL/6 mice were obtained from the NIA rodent colony and treated with vehicle (VEH; Ethanol 10/Solutol 40/Water 50) or BAY2416964 (BAY; 30 mg/kg, Targetmol T10270) via daily oral gavage 5 d/wk for 8 wks (n=8-10 per group). Skeletal muscle endurance and strength were assessed at 0, 4, and 8 wks of treatment via hang-time tests and grip strength meter (Bioseb BIO-GS3). DXA was performed at the same time points to assess body composition and bone density. Skeletal muscles (TA, EDL, Soleus, Quads) and long bones were collected at sacrifice. Muscle fiber size was measured from H&E-stained TA sections. The left tibia and femur from each mouse were used for static and dynamic histomorphometry and microCT analyses. Serum P1NP (bone formation; IDS #AC-33F13) and TRAcP5b (bone resorption; IDS #SB-TR103) were quantified via ELISA, and inflammatory cytokines were measured using a Legendplex panel (Mouse Inflammation 13-Plex). Body weights were stable over the 8-week study in both groups. VEH-treated animals demonstrated a significant age-related decline in forelimb grip strength during the study, but this decline was prevented by BAY (p-treatment <0.0001) by the 8th week, BAY-treated mice had significantly (p=0.0002) greater grip strength than VEH-treated mice. Muscle endurance (hang time), mass, and fiber sizes were unaffected; measurements of mitochondrial function and NMJ morphology are ongoing. Bone endpoints were generally unaffected in the current study, with microCT measures of bone mass and serum and histology-based metrics of bone remodeling largely comparable between VEH- and BAY-treated mice. The minimal impact on bone may have been, in part, due to low bone mass in the aged female mice at the onset of treatment. Together these data suggest that inhibiting AhR via BAY2416964 may prevent age-related declines in skeletal muscle function; future studies will incorporate earlier onset of treatment to determine if benefits observed in muscle function can be conveyed to the bone.

***Disclosures: KANGLUN YU**, None*

SUN-208

Active mTOR is required for de novo bone formation in the regenerating mouse digit tip *Dominik Hanetseder[1], Barbara Schaedl[1], Larry Suva[2], Dana Gaddy[3], Ken Muneoka[4], Lindsay Dawson[5], Regina Brunauer[1]. [1]LBG Ludwig Boltzmann Institute for Traumatology, Austria. [2]Texas A&M University, College of Veterinary Medicine and Biomedical Sciences, United States. [3]College of Veterinary Medicine, Texas A&M University, United States. [4]Texas A&M University, . [5]Texas A&M University College of Veterinary Medicine, United States

Maintaining reparative regeneration and resilience after trauma with age is vital to extending the healthy years of life (healthspan); yet, feasible models to routinely assess resilience are lacking. Mouse digit tip regeneration is one of the few mammalian examples of epimorphic regeneration, the structural regeneration of multiple tissues that is most prominently known for salamander limb regeneration. Mouse digit tip regeneration is induced by a simple amputation surgery, proceeds through a catabolic phase, which is dominated by osteoclast-driven bone resorption, and an anabolic phase, which is dominated by osteoblast-driven bone formation. These regeneration phases are associated with distinct cellular events, are separated and possibly controlled by epidermal wound closure, can be traced in vivo, and exhibit a clearly delayed phenotype with aging. Thus, mouse digit tip regeneration can serve as a feasible model to investigate the role of geroprotector targets in bone regeneration. A central regulator of healthspan is the mTOR (mechanistic Target of Rapamycin) kinase pathway. Rapamycin, the namesake and inhibitor of mTOR, extends healthspan under homeostatic conditions, but whether there is a benefit to regeneration after injury is unknown. In this study, we treated aged (12 month old) CD1 / ICR females with a lifespan-extending regimen of rapamycin (8 mg/kg i.p. every second day) or vehicle, amputated the distal digit tips and tracked the regeneration response for up to 28 days, when regeneration is completed in young mice. We found that rapamycin does not affect the rate of bone degradation, but extends the duration of the catabolic phase, and almost completely inhibits bone formation during the anabolic phase. This inhibition of osteoblast activity is either indirect through an inhibition of epidermal wound closure, or direct through inhibition

of osteoprogenitor proliferation or differentiation. To conclude, our data suggest that geroprotectors that extend healthspan under homeostatic conditions do not necessarily improve reparative regeneration, but that they can in fact even be detrimental to healing after injury.

***Disclosures: Dominik Hanetseder**, None*

SUN-209

Mitochondrial Genetics as a Determinant of Bone Phenotype and Aging

*Sarah Catheline[1], Aric Huber[1], Sarah Murphy[1], Roman Eliseev[1]. [1]University of Rochester, United States

Osteoporosis is the most common bone disease in the world with estimated 200 million cases globally. While aging and sex steroid levels have been considered primary risk factors for osteoporosis, mitochondrial genetics and function are also increasingly recognized as determinants of bone health and aging. Recent studies show that mitochondrial genome variants (haplogroups) in different human populations have developed out of a need to modify mitochondrial coupling efficiency to generate heat based on geographical location. In humans, bone phenotype correlates to mitochondrial haplogroup type, i.e. more efficient and less thermogenic mitochondria correlate with stronger bones. Thus, we hypothesize that mitochondrial DNA (mtDNA) haplogroup and oxidative phosphorylation efficiency are determinants of bone phenotype and aging. To test this, we used two strains of mice, C57BL/6 and C3H, known to have different mtDNA haplogroups and bone phenotype. C57BL/6 mice have less efficient mitochondria than C3H mice. We also used mitochondrial-nuclear exchange (MNX) mice that feature mtDNA from either C57BL/6 or C3H mice inserted into an enucleated embryo from the opposing strain to produce C3H MNX mice or C57 MNX mice. Interestingly, micro CT reveals that despite having more efficient C3H mitochondria, C57 MNX mice show no obvious improvement over WT C57BL/6 mice in measured bone parameters at 3 or 13 months of age. In contrast, female C3H MNX mice that have less efficient C57 mitochondria show a reduction in both trabecular BV/TV and cortical thickness relative to controls at 13 months. This bone loss in the 13-month-old C3H MNX female femurs corresponded to a reduction in energy to yield during biomechanical testing. In vitro, bone marrow stromal, a.k.a. mesenchymal stem, cells (BMSCs) isolated from C57 MNX mice showed greater osteogenic potential at day 0 of culture as illustrated by enhanced alkaline phosphatase staining and increased Sparc and Ibsp expression. These results indicate that initially, C57 MNX BMSCs are more biased towards adopting an osteogenic fate than WT C57BL/6 BMSCs due to their more efficient mitochondria; however, this is no longer the case at days 7 or 14 of osteoinduction. In summary, our data suggest that there is likely sexual dimorphism in the effect of mtDNA haplotype on bone phenotype, and inserting mitochondria from C57BL/6 mice into C3H mice was successful in reducing bone volume in female mice.

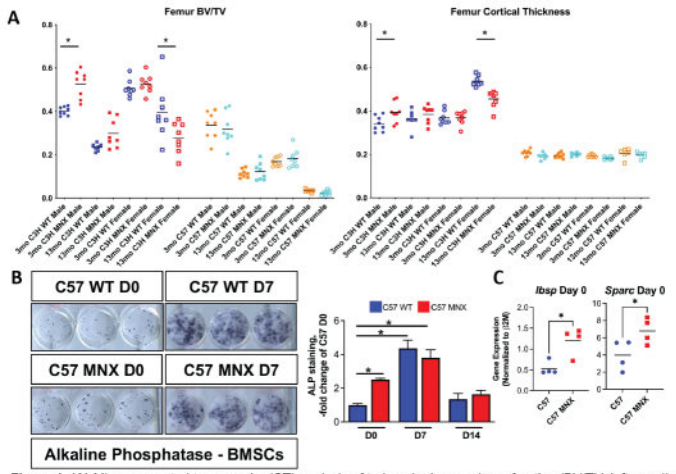

Figure 1. (A) Micro computed tomography (CT) analysis of trabecular bone volume fraction (BV/TV, left panel) and cortical thickness (right panel) from the femurs of C3H WT and C3H MNX (blue and red dots, respectively) and C57 WT and C57 MNX (orange and cyan dots) male and female mice at age 3 and 13 months (N = 8, unpaired t-tests, * indicates $p < 0.05$). **(B)** Images of bone marrow stromal cell (BMSC) isolated from C57 WT and C57 MNX and stained with alkaline phosphatase at day 0 or 7 of culture that is quantified in the graph at the right (N = 6, One way ANOVA, * indicates $p < 0.05$). (C) Quantitative RT-PCR from day 0 BMSC cultures for *Ibsp* and *Sparc* (N = 4, unpaired t-test, * indicates $p < 0.05$).

***Disclosures: Sarah Catheline**, None*

SUN-210

Dissecting the Diversity of Senescence in the Aged Murine Skeleton Reveals Necessity of BCL-2 Expression to Define Age-Related Senescent Cells

*Madison Doolittle[2], Dominik Saul[2], Jennifer Rowsey[2], Stephanie Vos[2], Kevin Pavelko[2], Joshua Farr[2], David Monroe[3], Sundeep Khosla[4]. [2]Mayo Clinic, United States. [2]Mayo Clinic, . [3]Mayo Foundation, United States. [4]Mayo Clinic College of Medicine, United States

Cellular senescence, a hallmark of aging, contributes to age-related bone loss, yet the cells that become senescent in vivo remain poorly understood. This is due to heterogeneity of both skeletal cell types and senescent cell signatures that present technical challenges in delineating the cell types driving this aging phenotype. To address this, we developed and validated a mass cytometry (CyTOF) panel to define, characterize, and profile skeletal senescence at the single-cell level in mice. We enzymatically digested femurs and tibias from cohorts (n=12-15) of young (6-month) and old (24-month) mice to generate single-cell suspensions, which were then purified for mesenchymal cells (Lin-CD45-) before CyTOF analysis. We found that cells positive for the senescence marker p16 were diverse in their expression of senescence-associated markers, while also containing non-senescent (Ki67+) subpopulations. Within p16+ cells, we found a subset positive for the apoptosis resistance marker BCL-2 that was non-proliferative (Ki67-) (Panel A, B; black arrows) and expressed inflammatory and DNA damage markers at a high level. In addition to CyTOF, we also identified these p16+Ki67-BCL2+ ("p16KB") cells using scRNA-seq (Panel C), which revealed that this was a highly secretory cell population that was enriched in senescence-associated secretory phenotype (SASP) gene expression, applied with the SenMayo geneset (Panel D). Altogether, these p16KB cells fulfilled major criteria for senescence through a multiparametric approach. In our skeletal cell clusters, we found that both p16+ and p16KB cells were upregulated in an osteolineage population defined by high expression of CD24. We found this population to be the predominant cluster that was cleared through p16+ senescent cell clearance in aged INK-ATTAC mice. Additionally, we found that CD24 osteolineage cells were also cleared in the bones of aged wild-type (C57BL/6N) mice treated with the senolytic combination of Dasatinib and Quercetin. Upon isolation, CD24+ mesenchymal cells from the bones of aged mice exhibit drastically reduced colony formation efficiency and spontaneous senescence-associated ?-galactosidase expression, consistent with functional outcomes of senescence. In summary, we identified senescent cells in the bone microenvironment through a multiparametric approach and revealed CD24 as a marker present on senescent osteolineage cells in the murine skeleton that are targeted by senolytic therapy.

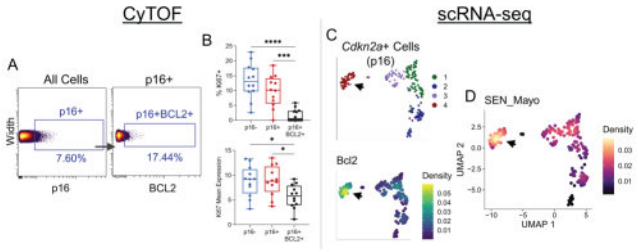

***Disclosures: Madison Doolittle**, None*

SUN-211

Cellular Senescence is a Modifiable Mediator of Skeletal Fragility in Mice with Type 2 Diabetes

*Mitchell Froemming[2], Vojt?ch Pa?ízek[2], MADISON DOOLITTLE[2], Dominik Saul[2], Jennifer Rowsey[2], Stephanie Vos[2], David Monroe[3], Sundeep Khosla[4], Joshua Farr[2]. [2]Mayo Clinic, United States. [2]Mayo Clinic, . [3]Mayo Foundation, United States. [4]Mayo Clinic College of Medicine, United States

Type 2 diabetes (T2D) is a major risk factor for multiple health complications in humans, including poor bone quality and fractures. However, the mechanisms that cause diabetic complications remain unclear. Senescence is a stress-induced growth arrest cell fate that contributes to several pathologies. Characterized by upregulated p16Ink4a expression, apoptosis resistance, telomeric DNA damage (telomere-associated foci [TAF]), and a distinct senescence-associated secretory phenotype (SASP), senescent cells are known to accumulate in various tissues with aging, including bone, where they disrupt tissue function. Despite evidence demonstrating that senescent cells accumulate prematurely in multiple tissues with T2D and promote metabolic dysfunction, the extent to which bone-resident cells in T2D are prone to senescence is incompletely understood. We previously found skeletal fragility, altered bone turnover, and accelerated osteocyte senescence in mice with T2D. Here, we report in T2D mice (relative to age- and sex-matched controls) that osteo- and adipo-progenitors (Lin-/LepR+) from T2D mice expressed significantly higher p16Ink4a mRNA (Panel A) together with several SASP factors. Further, through analysis of various hematopoietic cell populations, we found that p16Ink4a mRNA was significantly higher in B-cells, T-cells and myeloid (Cd14+) cells from T2D mice (Panel A). Using the combination of rt-qPCR, mass cytometry (CyTOF), and complementary imaging techniques, we found that T2D-derived Cd14+ myeloid cells displayed a dramatic SASP (Panel B) and had higher protein levels of p16 and Bcl2 (an anti-apoptotic protein upregulated with senescence) (Panel C). Although these Cd14+ myeloid cells from T2D mice had low and non-significantly different levels of

Sunday Orals

proliferation (assessed by Ki67), interestingly they displayed significantly higher levels of both pATM (a DNA damage marker) and TAFs (Panels C-D). We next removed senescent cells from adult (6-month-old) female and male T2D mice using both genetic (p16-ATTAC) and pharmacological (senolytic) approaches, which after 4 months did not affect trabecular bone, but significantly increased cortical thickness, reduced cortical porosity, and improved femoral strength. These improvements were associated with decreased osteoclasts, increased osteoblasts, and reduced marrow fat. Collectively, our data provide compelling evidence for cellular senescence as a hallmark and modifiable mediator of skeletal fragility in T2D.

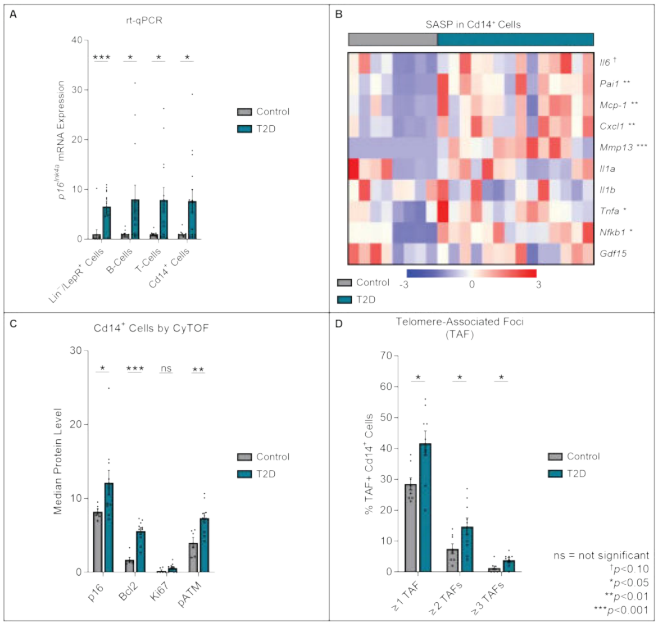

***Disclosures: Mitchell Froemming**, None*

SUN-212

Senescent Cells Evade Macrophage Immune Clearance in Connective Tissue *Zoltan Szilagyi[1], Samantha Przybelski[2], Takako Chikenji[3], Yuki Saito[4], Peter Amadio[2], Tamara Tchkonia[2], James Kirkland[2], Anne Gingery[2]. [1]Indiana University School of Medicine, United States. [2]Mayo Clinic, United States. [3]Hokkaido University, Japan. [4]Sapporo Medical University, Japan

Senescent cell accumulation in musculoskeletal tissues has been increasingly associated with tissue aging and pathology. Connective tissue is important for musculoskeletal structure, protection, and delivery of nutrients to neighboring tissues. Aging connective tissue becomes fibrotic and drives pathologies, limiting activity and range of motion all of which are essential for patient musculoskeletal health and improved health span. We have previously shown that senescent cells accumulate in multiple musculoskeletal connective tissues. Our overarching hypothesis is that senescent cell accumulation contributes to age-related dysfunction of connective tissue by upregulation of immune checkpoint regulators which prevent the clearance of senescent cells. Here we characterized the senescent cell populations in multiple connective tissues from patients and aged animal models. We found that senescent cells from these tissues expressed multiple markers of cellular senescence including p16, p15, p53, and SABG. We also found that immune evasion markers such as CD47, PDL1, and PDL2 were upregulated. Further senescent cells upregulated fibrosis-related genes such as THBS1, which encode thrombospondin 1 protein (TSP1), a CD47 signaling receptor. Using the p16 INK-ATTAC mouse model we found that PD-L1, PD-L2, and CD47 significantly downregulated upon activation of the INK-ATTAC "suicide" transgene which specifically targets senescent cells for removal. We also found that senescence associated secretory factors including TGFß, PAI-1 and interferons type I and type II are expressed in senescent connective tissues and that these factors drive expression of immune evasion markers on senescent cells. When we ablated p16 positive senescent cells using aged mice expressing the INK-ATTAC "suicide" transgene we found that PD-L1, PD-L2, and CD47 were significantly down regulated. Further using a THP-1 macrophage model we assessed the ability of senescent cells to evade macrophage phagocytosis and found that neutralizing antibody to CD47 attenuated immune evasion. In these model systems we found that senescent cells escaped from macrophage phagocytosis and promoted the proliferation of neighboring cells driving tissue dysfunction and pathology. This work indicates that targeting immune evasion as well as the anti-apoptotic pathways in senescent cells may provide a novel therapeutic strategy for removal of senescent cells from aged or diseased musculoskeletal tissues.

***Disclosures: Zoltan Szilagyi**, None*

SUN-214

Osterix-Cre Conditional Indoleamine 2, 3 dioxygenase Knockout Mice were not Protected against Orchiectomy-induced Bone Loss Suggesting that Osteoclasts may be the Main Mediator of IDO1 Effects in Bone *Baolin Kang[1], Wendy Bollag[2], Ke-Hong Ding[1], Debra Irsik[3], Jianrui Xu[1], Meghan McGee-Lawrence[4], Xingming Shi[1], William Hill[5], Sadanand Fulzele[1], Mark Hamrick[1], Carlos Isales[1]. [1]Augusta University, United States. [2]Augusta University and Charles Norwood VAH, United States. [3]Charlie Norwood Augusta VAH, United States. [4]Medical College of Georgia, Augusta University, United States. [5]Medical University of South Carolina, United States

Tryptophan (Trp) is an essential amino acid, and the initial step in its metabolism occurs through the enzymes indoleamine and tryptophan 2,3-dioxygenase (IDO and TDO). We have previously shown that some tryptophan metabolites such as kynurenine (kyn), accumulate with age and contribute to age-induced bone loss, although other downstream tryptophan metabolites have been postulated to have bone-promoting effects. We hypothesized that knocking out IDO1 would be protective against high bone turnover states such as hypogonadism. We had previously reported that a global IDO1 knockout (KO) was protective against trabecular bone loss in orchiectomized (Orx) C57BL/6 mice. To further explore IDO1's role in bone turnover, we used a conditional IDO1 KO mouse (generated by EUCOMM/IMPC) using an osterix-promoter-driven Cre possessing a tet off element, because of concerns of effects of knocking out osterix at an early age on bone development. In an IACUC-approved protocol using male conditional IDO1 KO (cKO) C57BL/6 mice and a sample size of 5 mice/group, we Orx 8-month-old mice and placed them either on a regular or doxycycline-containing diet for eight weeks. At the end of that time mice were sacrificed and bone parameters measured by Digimus and uCT and serum PYD and Trp metabolites determined using ELISA and LC/MS, calibrated using known concentrations of the various metabolites as standards, respectively. There was no significant difference between bone parameters measured: (1)BMD-0.0688+0.0046 vs 0.0647+0.006 (Con vs cKO, gm/cm2; (2)BV/TV-34.6+2.8 vs 33.5+2.7; (3)TbTh-0.166+0.010 vs 0.164+0.013; (4) TbSp-0.470+0.0029 vs 0.471+0.0016; (5)Tb#-2.076+0.088 vs 2.037+0.075. Our results for Trp and its metabolites were only significantly different for xanthurenic acid levels: (1)Trp-7213+/-1318 vs 5954+1270 (nmol/L means+SD, Controls vs cKO for all); (2) kyn-121+/-26 vs 121+/-20; (3) picolinic acid-1656+/-274 vs 1803+/-250m; (4)xanthurenic acid: 19+/-2 vs 14+/-2 (Control vs cKO p<0.02); and (5)quinolinic acid-279+/-25 vs 281+/-93. We also measured PYD levels as an index of bone breakdown and there was no significant difference between the two groups: 3.2+1.4 vs 2.8+1.0 (nmol/L means+SD Control vs cKO, p=0.057). These data suggest that bone osteoprogenitor cell-specific knockout of IDO has little effect on bone; therefore, in the global IDO knockout bone protective effects are likely driven by a bone resorptive role for IDO in osteoclasts during a high bone turnover state such as Orx.

***Disclosures: Baolin Kang**, None*

SUN-215

Detrimental Effects of ?2-Microglobulin on Muscle Metabolism: Evidence from In Vitro, Animal, and Human Research *Beom-Jun Kim[1], So Jeong Park[2], Jin Young Lee[2], Kee ho Song[3]. [1]Division of Endocrinology and Metabolism, Department of Internal Medicine, Asan Medical Center, University of Ulsan College of Medicine, Republic of Korea. [2]Asan Institute for Life Sciences, Asan Medical Center, University of Ulsan College of Medicine, Republic of Korea. [3]Division of Endocrinology and Metabolism, Konkuk University Medical Center, Konkuk University School of Medicine, Republic of Korea

Background: The ?2-Microglobulin (B2M) has been receiving attention as a potential pro-aging factor. Accordingly, it may be involved in muscle metabolism and sarcopenia, a key component of aging phenotypes. To clarify this possibility, we investigated the effects of B2M on in vitro and animal muscle biology and its clinical relevance for sarcopenia parameters in older adults. Methods: In vitro myogenesis was induced in mouse C2C12 myoblasts with 2% horse serum. For in vivo research, C57BL/6 mice aged 3 months were intraperitoneally given 250 ?g of B2M daily, and muscular alterations were assessed one month later. Human blood samples were collected from 158 participants who underwent evaluation of muscle mass and function in an outpatient geriatric clinic of a teaching hospital. Sarcopenia and related parameters were determined using cutoff values for the Asian population. Serum B2M levels were measured using an enzyme-linked immunosorbent assay. Results: Recombinant B2M treatment suppressed myogenesis from mouse C2C12 myoblasts in a dose-dependent manner, and consistently reduced the expression of myogenic differentiation markers. In addition, B2M significantly increased intracellular reactive oxygen species (ROS) levels in myotubes, and treatment with N-acetyl cysteine, a potent biological thiol antioxidant, reversed the decrease of myotube area, myotube area per myotube, nucleus number per myotube, and fusion index by B2M through decreasing oxidative stress. Animal experiments showed that mice with systemic B2M treatment exhibited significantly smaller cross-sectional area of tibialis anterior and soleus muscle, weaker grip strength, shorter grid hanging time, and decreased latency time to fall off the rotating rod, compared to untreated controls. In a clinical study, serum B2M levels were inversely associated with grip strength, usual gait speed and short physical performance battery (SPPB) total score after adjustment for age, sex, and body mass index, whereas sarcopenia phenotype score showed a positive association. Consistently, higher serum B2M levels were associated with higher risk for weak grip strength, slow gait speed, low SPPB total score, and poor physical performance.

Conclusion: These results provide experimental evidence that B2M exerted detrimental effects on muscle metabolism mainly by increasing oxidative stress. Furthermore, we made an effort to translate the results of in vitro and animal research into clinical implication and found that circulating B2M could be one of blood-based biomarkers to predict poor muscle health in older adults.

***Disclosures: Beom-Jun Kim**, None*

SUN-216

APOA1 and APOE proteins related to LXR/RXR pathways as a potential proxy for progression of sarcopenia in community-based prospective cohort

*Sung Hye Kong[2], Seung Shin Park[2], Jung Hee Kim[2], SANG WAN KIM[3], Chan Soo Shin[4], Ok Hee Jeon[5], Do Hyun Han[2]. [2]Seoul National University Hospital, Republic of Korea. [2]Seoul National University Hospital, . [3]Seoul National University College of Medicine, Boramae Medical Center, Republic of Korea. [4]Seoul National University College of Medicine, Republic of Korea. [5]Korea University Colloege of Medicine, Republic of Korea

The study aimed to find protein markers as a proxy for the sarcopenia progression, and markers associated with muscle mass and strength..In this prospective community-based cohort study of the geriatric population aged 70-84 years, muscle mass, function, and performance were measured at the baseline and after 2 years. Among them, 63 participants were nonsarcopenic and the baseline but developed severe sarcopenia after 2 years (non-to-sarcopenic group). As the age, sex, and body mass index (BMI)-matched control, 65 participants who stayed nonsarcopenic both at the baseline and follow-up (stayed robust group) and 43 participants who were severe sarcopenic both at the baseline and follow-up (stayed sarcopenic group) were included. We performed liquid chromatography with tandem mass spectrometry using plasma samples. The definition of sarcopenia was based on the Consensus of Asian Working Groups for Sarcopenia in 2019.In baseline characteristics, the mean age of the patients was 78.5 years and 45% were female. Age, BMI, and underlying diseases were similar among groups, while participants in stayed sarcopenic group were more likely to be men than the other groups. In proteomic analysis, ALDOB, LECT2, USP15, KLKB1, KNG1, APOA1, APOA2, TF, OGN, C4BPB, and AXL proteins were differentially expressed between participants in stayed robust and non-to-sarcopenic groups. CSF1R, KLKB1, PRAP1, ICOSLG, CFD, QSOX1, PODXL, CST3, APOA1, APOE, RBP4, AMBP, SLPI, GAPDH, S100A8, S100A9, C7, IGFBP6, PTGDS, LYZ, B2M, EFEMP1, and MMRN2 proteins were differentially expressed between participants in stayed robust and stayed sarcopenic groups. Interestingly, in pathway analysis of differentially expressed proteins, the LXR-RXR pathway, which represents cholesterol efflux, was one of the most significantly associated pathways between participants in stayed robust and non-to-sarcopenic groups. In association analysis with muscle mass and strength, LXR-RXR pathway was also correlated with both muscle mass and strength, and protein-protein interaction analysis showed key proteins of APOE and APOA1 for muscle mass and strength, respectively. Along with the proteomic analysis, baseline serum HDL levels were significantly different among groups, highest in the stayed robust group, and lowest in the stayed sarcopenic group. Baseline HDL levels were negatively associated with baseline and follow-up appendicular muscle mass in the association analysis.In conclusion, the proteomic analysis showed that 11 and 23 proteins were differentially expressed in participants in non-to-sarcopenic, and stayed sarcopenic groups compared to stayed robust group, respectively. The pathway analysis revealed that LXR-RXR pathway was the key pathway to discriminate stayed sarcopenic and non-to-sarcopenic groups and suggested APOE and APOA1 as key protein markers for muscle mass and strength.

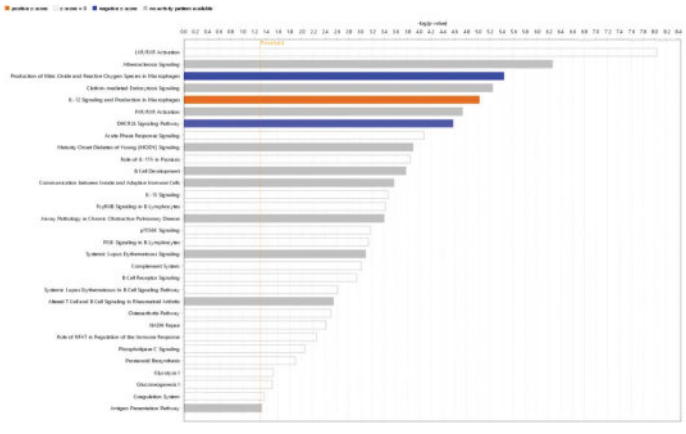

***Disclosures: Sung Hye Kong**, None*

SUN-218

Soft tissue massage alters RANTES and IL-4 cytokine levels in a rat model of induced low back pain

*Carmela Marciano[1], Taylor Hiland[1], Krista Jackson[1], SIERRA STREET[2], Carson Maris[1], Andrew Ehrsam[1], Julia Hum[1], M. Terry Loghmani[3], Tien-Min G Chu[3], Jonathan Lowery[1]. [1]Marian University, United States. [2], . [3]Indiana University, United States

Low back pain (LBP) is a common musculoskeletal complaint that impedes physical function and mobility. Management often involves pain medication such as opioids but there is a need for non-pharmacological and non-invasive interventions. Prior work in human subjects indicates that soft tissue manipulation (STM) such as massage can accelerate return-to-function, improve mental and emotional wellbeing, and reduce the need for opioid medication usage. However, heterogeneity of lifestyles and body conditions, potential co-morbidities, and the inherent mind-body aspect of manual therapies complicate our understanding of the molecular mechanisms underlying these findings. Such a knowledge gap may prevent future therapeutic potential and widespread adoption of this non-invasive approach to pain management and rehabilitation. Thus, in a prior study, we employed a rat model of chronic LBP using Complete Freund's Adjuvant and established a system for delivering instrument-assisted STM (IASTM) wherein force, direction, and duration of therapy were reproducibly applied across conscious subjects. This advancement allowed for demonstrating that IASTM improved gait in rats with chronic LBP and altered plasma levels of several biomarkers such as RANTES. In the present study, we advance this work to evaluate potential changes in soft tissue levels of more than thirty pro- or anti-inflammatory cytokines following IASTM in rats with chronic LBP. Our results indicate that, compared to sham touch, IASTM is associated with reduced soft tissue levels of RANTES and increased soft tissue levels of IL-4, which are pro-inflammatory and anti-inflammatory cytokines, respectively by 120 minutes post-treatment. IASTM was not associated with tissue-level changes in CXCL7, ICAM-1, IL1-ra, IL-6, IP-10/CXCL10, L-selectin, LIX, TNF-?, or VEGF at either thirty or 120 minutes post-treatment. Combined, our findings suggest that IASTM exerts tissue-level effects that are associated with improved clinical outcomes and potentially beneficial changes in pro/anti-inflammatory cytokines in circulation and at the tissue level.

***Disclosures: Carmela Marciano**, None*

SUN-219

Single cell RNAseq analysis reveals that osteoblast biosynthetic activity as well as number decrease with aging

*Intawat Nookaew[1], Aaron Warren[1], Ha-Neui Kim[2], Jinhu Xiong[3], Charles O'Brien[3], Maria Jose Almeida[4]. [1]University of Arkansas for Medical Sciences, United States. [2]Univ. Arkansas for Medical Sciences, Central Arkansas VA Healthcare System, United States. [3]Univ of Arkansas for Medical Sciences, United States. [4]Central Arkansas VA Healthcare System, Univ of Arkansas for Medical Sciences, United States

Bone formation decreases with age both at the periosteum and in endocortical bone but the mechanisms are unclear. Several aging mechanisms have been implicated in the loss of bone mass with aging, including mitochondria dysfunction, loss of proteostasis, and senescence. To examine how transcriptional programs change in a cell-type specific manner with aging, we performed single cell RNA-sequencing (scRNAseq) of mesenchymal cells present at the endosteum and periosteum of mouse bone. To do this, endosteal or periosteal cells were isolated from long bones of 6 and 22 month old female mice expressing tdTomato in cells targeted by an Osx1-Cre transgene. Cells expressing tdTomato were isolated by FACS and subjected to scRNAseq using the 10X Chromium platform. An initial UMAP plot and cluster analysis, after harmonization of cells from mice of the two ages, revealed 9 clusters based on expression of cluster-specific markers, including osteocytes, osteoblasts, pre-osteoblasts, osteo-CAR, osteo-X, adipo-CAR, chondrocytes, fibro-1, and fibro2. In young mice, osteoblasts constituted the majority of the cells at the endosteum while osteo-X cells, characterized by high expression of periostin, were the major cell type at the periosteum. Aging led to a decrease in the osteoblast proportion from 60 to 27% at the endosteum and from 6.8 to 2.4% at the periosteum. Gene Ontology enrichment analysis of differentially expressed genes in osteoblasts of the endosteum revealed that processes related to senescence, inflammation, apoptosis, and translation were increased, while processes related to mitochondria and endoplasmatic reticulum were decreased. In contrast, no changes in these processes were detected in cells from the periosteum. On the other hand, processes related to collagen fibril organization and extracellular matrix, as well as mRNAs encoding collagens and other extracellular matrix proteins, such as Dcn, Lum, and Bglap, decreased with age in osteoblasts, pre-osteoblasts and osteo-CAR cells at both sites. In addition, ribosome and ribonucleoprotein related processes were increased with age in both osteoblast at both sites. Overall, these results suggest that a decrease in osteoblast vigor contributes to the decrease in bone formation that occurs with age at both the periosteum and the endosteum. Moreover, an additional mechanism contributing to reduced bone formation at the endosteum may be increased senescence of osteoblasts and their progenitors.

***Disclosures: Intawat Nookaew**, None*

SUN-220

Deletion of the Mitochondrial Kinase PINK1 Does Not Affect Age-Related Bone Loss *Kimberly Richardson[1], Aaron Warren[1], Maria Jose Almeida[2], Ha-Neui Kim[3]. [1]University of Arkansas for Medical Sciences, United States. [2]Central Arkansas VA Healthcare System, Univ of Arkansas for Medical Sciences, United States. [3]Univ. Arkansas for Medical Sciences, Central Arkansas VA Healthcare System, United States

PINK1 kinase and NAD+-dependent deacetylase SIRT3, localized in mitochondria, play a role in pathological conditions, such as aging, cancer, and Parkinson's disease, most likely by regulating mitophagy. Notably, SIRT3/PINK1-mediated mitophagy does not play a major role under non-stressed conditions. Under stress conditions, however, Sirt3 or Pink1 knockout (KO) mice exhibit overt differences compared to littermate controls. This is in line with evidence that deletion of Sirt3 has no effect on the skeletons of young mice, but Sirt3 KO mice are protected from age-associated bone loss. Nonetheless, the functional significance of SIRT3 deacetylation of PINK1 in the control of mitophagy has not been demonstrated in bone cells. We have investigated here whether PINK1 stimulates osteoclast mitophagy, maintains a functional mitochondrial network, or whether it contributes to age-related bone loss. First, we generated rabbit polyclonal antibodies specific for lysine acetylated PINK1 (K24 and K33). Osteoclasts lacking Sirt3 from aged Sirt3 null or conditional KO mice (under the control of the LysM promoter) exhibited hyperacetylation of PINK1. These results suggest that SIRT3-induced deacetylation of PINK1 might act as a molecular switch to activate mitophagy in osteoclasts during skeletal aging. To address this hypothesis, mice heterozygous for the Pink1 null allele were intercrossed to produce homozygous Pink1 KO mice. Cohorts of Pink1 KO and littermate controls were aged up to 16 months. Pink1 KO mice appeared normal at birth and were indistinguishable from control mice with respect to body weight and femoral length during adulthood. As expected, control mice lost bone mass with age. In contrast to Sirt3 KO mice, however, deletion of Pink1 had no effect on the age-related loss of either cortical or trabecular bone mass of the femur or spine in Pink1 null mice. Likewise, deletion of Pink1 had no effect on RANKL-induced osteoclast formation and the expression of osteoclast markers in cultured bone marrow-derived macrophages. Furthermore, the protein levels of the mitophagy markers Bnip3 and Nix were unaffected by deletion of Pink1 in cultured osteoclasts. These results suggest that PINK1 does not contribute to mitophagic flux in osteoclasts or the development of osteoporosis caused by aging. Based on this evidence, we conclude that PINK1 is dispensable for osteoclast maturation and skeletal involution in mice.

***Disclosures: Kimberly Richardson**, None*

SUN-221

Progranulin inhibits C5a/C5aR1 signaling via direct binding to C5a and its deficiency exaggerates osteoarthritis due to hyper-activation of the complement system *Wenyu Fu[1], Guiwu Huang[1], Chuan-ju Liu[1]. [1]New York University Grossman School of Medicine, United States

The prevalence of osteoarthritis (OA) is increasing globally, with significant economic impacts and negative effects on quality of life. Accumulating evidence demonstrates that complement activation is involved in the pathogenesis of OA, although the molecular events involved remain to be elusive. While previous research has shown that C5 deficiency can attenuate arthritis in mouse OA model, the mechanisms of C5/C5a in OA have not been understood. Our lab has long-standing interest in investigating the role of progranulin (PGRN), a growth factor like molecule, in the pathogenesis of OA. The findings that PGRN bind to cysteine-rich domains (CRDs) of various proteins, together with the fact that complement proteins contain CRDs, suggesting that PGRN may interact with and affect the complement system. We thus conducted solid-phase binding assays to screen the interactions between PGRN and central complement components, including C1-C9, C5a and C3a. Our results showed that PGRN strongly binds to C5 and dose-dependently binds and saturates C5a. Additionally, PGRN/C5a complex formation in mouse sera was confirmed by Co-IP, and PGRN binds to C5a with a high affinity of KD 7.18+/-0.07nM measured by Analytical Surface Plasmon Resonance. Further functional assays demonstrated that PGRN inhibits C5a binding to C5aR1 and effectively blocks C5a binding to cell surfaces, indicating that PGRN acts as a natural antagonist of C5a signaling. PGRN was also found to antagonize C5a's effect on macrophage polarization.ELISA analysis showed a significant increase in C5a levels in the synovial fluid of OA patients than healthy controls, indicating hyperactivation of the complement cascade in OA synovial fluid. PGRN levels were also significantly higher in the synovial fluid of OA patients compared to healthy controls. Furthermore, a positive correlation was found between the levels of PGRN and C5a in OA patients ($r = 0.5475$, $P < 0.0001$). The interaction and interplay of PGRN/C5a were also investigated in vivo using various genetically deficient mice with surgically induced DMM model. The results showed that deletion of C5aR1 partially reversed the exaggerated OA phenotype, including severe cartilage loss and increased OA-associated pain observed in PGRN-/- OA mice. These findings suggest that PGRN interacts with C5a/C5aR1 signaling to regulate macrophage function, and PGRN mitigates OA by suppressing proinflammatory activities of C5a through interrupting C5a/C5aR1 signaling (Fig.1).

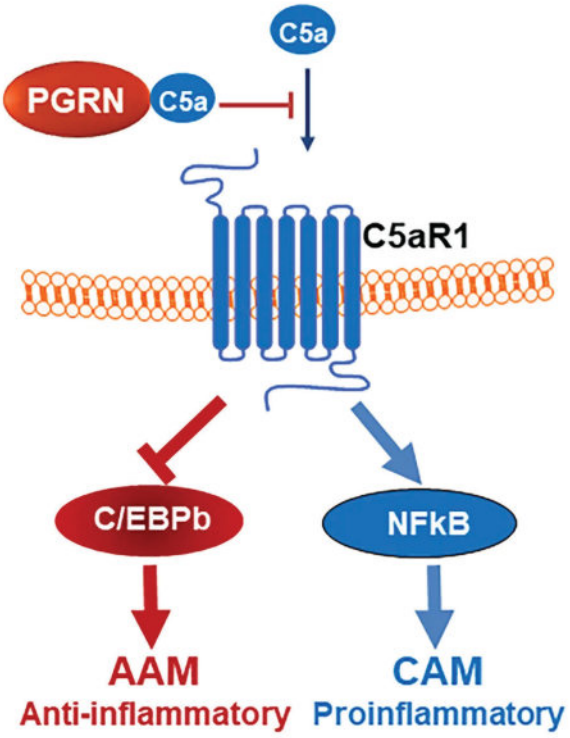

Fig1. A proposed model illustrating the interplays between PGRN and C5a/C5aR1 signaling in regulating macrophage polarization. PGRN directly binds to C5a and inhibits C5a/C5aR1 signaling, and resultant macrophage polarization regulation and OA progression.

***Disclosures: Wenyu Fu**, None*

SUN-222

Rigorous identification of p21+ and p16+ senescent cells by scRNAseq reveals distinct SASP profiles of these cells in bone and across tissues *Dominik Saul[2], MADISON DOOLITTLE[2], David Monroe[3], Sundeep Khosla[4]. [2]Mayo Clinic, . [2]Mayo Clinic, United States. [3]Mayo Foundation, United States. [4]Mayo Clinic College of Medicine, United States

Cellular senescence has been shown to drive multiple age-associated diseases, and clearance of Cdkn2a (p16)+ cells prevents age-related bone loss in mice (Nat Med, 2017). We recently demonstrated the transient appearance of senescent cells during fracture healing and the importance of Cdkn1a (p21), but not Cdkn2a (p16) in this process (eLife, 2021). Specifically, we found that the clearance of Cdkn1a+ cells accelerated the time course of fracture healing. We have also recently demonstrated the importance of Ki67- and Bcl2+ (KB) cells for age-related bone loss (BioRxiv, 2023). Pairing these mechanistic insights with a senescence/SASP gene set that has recently been established by our group (SenMayo, Nat. commun. 2022), we identified Cd45-, KB cells using scRNAdeq data from bone/bone marrow and found them to highly express the canonical markers of senescence, Cdkn2a (p16) and Cdkn1a (p21) (Panel A, B), with only very few cells showing expression of both markers (Panel C). To further characterize these cells, we analyzed the SASP of the selected p21KB vs. p16KB cells. As shown in panel D, this revealed a largely distinct SASP of the 2 populations in bone/bone marrow cells. To expand these findings to other tissues, we next used this approach to identify the p21KB and p16KB cells in scRNAseq data from skeletal muscle, brain, lung and liver. Similar to findings in bone/bone marrow, the p21+ vs the p16+ cells expressed a largely non-overlapping SASP across tissues. Combining the insights from all tissues, Pecam1, Jun and Sema3f stood out from the p21+ cells as consistently expressed SASP markers (Panel E), while Ccl5 dominated within the p16+ senescent cells. Collectively, our findings demonstrate that p21+ or p16+ senescent cells identified in scRNAseq data using rigorous criteria (expression of Cdkn1a and/or Cdkn2a, growth arrest, upregulation of anti-apoptosis genes) express very different SASP profiles not only in the bone microenvironment, but across multiple tissues. Whether these differing SASP profiles account for

varying contributions of p21+ or p16+ senescent cells in modulating tissue repair vs. aging phenotypes is an important question that needs further studies.

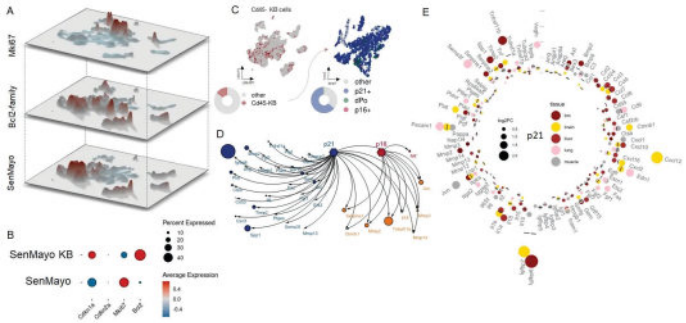

***Disclosures: Dominik Saul**, None*

SUN-223

The Mechanism of the Age-dependent Decline in Bone Formation *Irina Tourkova[1], Quitterie Larrouture[2], Kelichi Onwuka[2], Silvia Liu[3], Jianhua Luo[2], Paul Schlesinger[4], Harry Blair[2]. [1]Pittsburgh VA and University of Pittsburgh , United States, [2]University of Pittsburgh, United States, [3]University of Pittsburgh , United States, [4]Washington University in Saint Louis, United States

We studied the effect of age on proteins critical to bone matrix and mineral transport. Non-quantitative studies reported histological effects, in some cases concluding differences in apoptosis. In contrast, we analyzed quantitative expression of genes and proteins involved in bone formation in aged (18-19 month) and young (3-4 month) C57 black mice. We compared results using cells flushed from femur and tibia in vivo and, for the first time, osteoblasts differentiated from Stromal Stem Cells (SSC) on polyethylene terphthalate (PET) membranes in vitro. Apoptosis did not occur in vitro in bone differentiated from SSC on PET membranes using young or old cells. Age correlated with reduced in mRNAs of mineral transport proteins, alkaline phosphatase (ALP), ankylosis (ANK), and the Cl-/H+ exchanger ClC3. Results were similar in vivo and in vitro. For bone matrix proteins, COL1 and osteocalcin, expression was, as expected, also significantly reduced with age. µCT analysis of lumbar vertebrae showed that trabecular bone of the 18-19 month mice is osteopenic relative to the 3-4 month mice. Additional novel work used gene array analysis to compare osteoblasts differentiated on PET membranes from young and old mice. Results were consistent with known bone formation-related proteins, but we also found additionally major reduction in the pyrophosphatase/phosphodiesterase ENPP2 with age. Since ENPP2 was not previously related to mineral formation, we used silencing ENPP2 with RNAi duplexes to show down-regulation of osteoblast ALP activity and mineralization. In this work, ENPP2 RNAi duplex transfection was documented by fluorescence (Figure, panel A) and real time PCR (Panel B). Decreased osteoblast differentiation was shown by ALP and Alizarin Red (Panel C). Real-time PCR of SSCs differentiated into osteoblasts for 2 weeks confirmed decline in ENPP2 and ALP in transfected cells (Panel D). Further, we analyzed pathways of osteoblast differentiation in vitro on PET membranes. This revealed that cells from older animals had reduced Erk1/2 phosphorylation, decreased SMAD 2 mRNA, consistent with TGF-? pathway regulation, and reduced ?-catenin mRNA and protein consistent with changes in the WNT pathway. Our results suggest that decline in trabecular bone structure reflects, at least in part, reduced osteoblast differentiation and decrease of matrix and mineral transport proteins with age involving multiple signaling pathways.

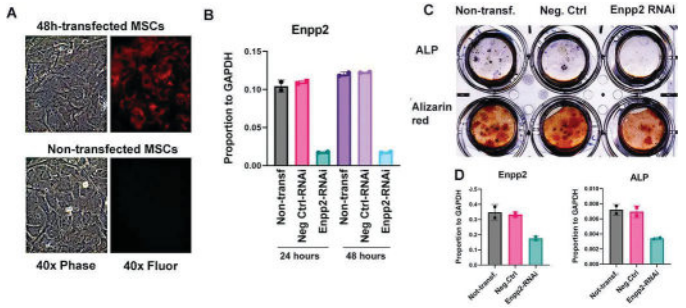

***Disclosures: Irina Tourkova**, None*

SUN-225

Senescence features in pre-malignant plasma cells are associated with stable disease in MGUS and SMM *GABRIEL ALVARES BORGES[1], ANGELO GUILATCO[2], CHRISTINE HACHFELD[3], MING XU[4], FATIMA MUSTAPHA[5], MARTA DIAZ-DELCASTILLO[5], Thomas Andersen[6], TAXIARCHIS KOURELIS[3], TAMAR TCHKONIA[3], JAMES KIRKLAND[3], MATTHEW DRAKE[3], Megan Weivoda[3]. [1], [2]Mayo Clinic/University of Michigan, [3]Mayo Clinic, United States, [4]University of Connecticut, United States, [5]Aarhus University Hospital, Denmark, [6]University of Southern Denmark, Denmark

Multiple myeloma (MM) is a clonal plasma cell (PC) malignancy that progresses from monoclonal gammopathy of undetermined significance (MGUS) and/or smoldering MM (SMM) at rates of 1% and 10% per year, respectively. Despite similar primary genetic abnormalities as MM, MGUS and SMM are non-proliferative, and the mechanisms for disease progression remain unknown. Since oncogenes and DNA damage drive senescence growth arrest, we hypothesized that MGUS and SMM PCs could exhibit senescence features. Differential expression analysis of MGUS and SMM PCs compared to normal (GSE5900) revealed significant increases in the senescence markers CDKN1A and GADD45A. Gene set enrichment analysis showed that MGUS PCs had significant enrichment of senescence phenotyping gene sets that were distinct from aging. We next assessed morphological features of senescence, including the loss of LaminB1 (LoL) and senescence associated distension of satellites (SADS), in MGUS, SMM, and MM PCs, followed by senescence gene expression analysis. PCs from patients with stable MGUS (N=4) exhibited increased number of SADS+ PCs with LoL compared to SMM and MM patient PCs. When SMM PCs were evaluated based on progression (stable vs progressed <=5 years, n=6-8), there remained no differences in SADS or LoL. Despite this, stable SMM patient PCs, but not those from progressors, had increased expression of senescence genes, including CDKN1B, CDKN2A, CDKN2B, TP53, BCL2, and IL1B compared to MGUS PCs. Both stable MGUS and SMM patient PCs showed a significant increase in the expression of the retrotransposable element LINE1, which is increased with senescence, compared to PCs from SMM progressors and MM patients. Overall, our results demonstrate the presence of stage-specific senescence features in PCs from stable MGUS and SMM patients; these senescence features are decreased in PCs from SMM progressors and MM. These findings are consistent with the protective effect of senescence against tumorigenesis. Thus, evaluating PC senescence in MGUS and SMM may have prognostic value to identify patients at risk for progression to MM. Importantly, however, given that stable MGUS patients are at increased risk for osteoporotic fracture and have reduced overall survival due to aging co-morbidities, the senescence-related protection against MM may come at the expense of premature aging. Ongoing studies are evaluating the safety and therapeutic utility of ablating pre-malignant senescent cells in MGUS and SMM.

***Disclosures: GABRIEL ALVARES BORGES**, None*

SUN-226

The Role of cped1 in the Zebrafish Axial and Craniofacial Skeleton *Kurtis Alvarado[2], Ronald Kwon[2], W. Joyce Tang[2], Claire J. Watson[2], David Karasik[3], Donaka Rajashekar[3]. [2]University of Washington, [2]University of Washington, United States, [3]Bar-Ilan University, Israel

Genome wide association studies have identified 7q31.31, also known as the CPED1-WNT16 locus, as a key region harboring genetic variants associated with bone-related traits. These traits include bone mineral density (BMD) in the spine, femoral neck, and skull, as well as facial shape [1,2,3]. It has been speculated that multiple causal genes might underlie genetic effects at the CPED1-WNT16 BMD locus [4]. While knockout studies in mice show Wnt16 is an important regulator of bone structure and strength, little is known about the role of Cped1 in the skeleton. We hypothesized that cped1 contributes to vertebral bone mass and mineralization and craniofacial morphology in adult zebrafish. To test this, we used two mutant lines: cped1w1003 (c.831-844delinsACT), which we have previously described [4], and cped1sa20221 (c.1922 C>A). Both alleles are predicted to lead to a premature stop codon and early truncation of the protein. For analysis, adult 3-month old zebrafish were scanned using microCT, and ImageJ and FishCuT software were utilized to measure vertebral morphology and mineralization. Craniofacial morphology was assessed in SlicerMorph using manual landmarking as we have previously described [5]. RT-PCR revealed a reduction in cped1 transcript levels in cped1sa20221 mutants, supporting cped1 loss of function. Vertebral analysis revealed no significant differences between homozygous mutants and wildtype controls for all traits (Volume, Thickness, Length, and Tissue Mineral Density) and compartments (Neural Arch, Centrum, Haemal Arch) measured for both mutant alleles (w1003: n=8/group; sa20221: n=8/group). Craniofacial analysis revealed cped1w1003 mutants exhibited a significant decrease in skull width (p=0.0206; n=6-7/group); however, no significant difference in this trait was observed for cped1sa20221 mutants (n=7/group). We found little evidence that cped1 contributes to vertebral bone mass and mineralization or craniofacial morphology in adult zebrafish. It is possible zebrafish and mouse orthologs for CPED1 have distinct functions, or that loss of the zebrafish ortholog is compensated for by other genes. Thus, Cped1 knockout studies in mice are needed to better understand the potential for CPED1 to act as a causative gene underlying effects at 7q31.31 on bone-related traits.1. Estrada et al. 2012 Nat Genet; 2. Medina-Gomez et al. 2012 PLoS Genet; 3. Bonfante et al. Sci Adv 2021; 4. Watson et al. 2022 PLoS Genet; 5. Diamond et al. 2023 J Anat

***Disclosures: Kurtis Alvarado**, None*

Sunday Orals

SUN-227

Phenotypic characterization of mice lacking Piezo1 and/or Piezo2 in Col2a1-expressing cells *Laura J Brylka[1], Miriam EA Tschaffon-Müller[2], Simon von Kroge[1], Astrid Schoppa[2], Melanie Haffner-Luntzer[2], Kian M Eghbalian[1], Eva Pawlus[1], Timur A Yorgan[1], Michael Amling[1], Anita Ignatius[2], Thorsten Schinke[1]. [1]University Medical Center Hamburg-Eppendorf, Germany; [2]University Medical Center Ulm, Germany

Piezo proteins function as mechanotransducers in several organ systems including bone. We and others have reported that Piezo1 in osteocytes mediates the bone-anabolic response after mechanical stimulation in vivo. Our analysis of conditional mouse models also indicated that Piezo1 expression in chondrocytes is required for trabecular bone formation below the growth plate. To further analyze the role of Piezo proteins in endochondral ossification, we studied the phenotype of mice lacking Piezo1 and/or Piezo2 in Col2a1-expressing cells.Piezo1Col2a1cre, Piezo2Col2a1cre and Piezo1,2Col2a1cre mice and their Cre-negative littermates were analyzed at different ages using contact radiography, micro-computed tomography (µCT) and bone histomorphometry. While longitudinal bone growth and growth plate thickness were only moderately affected in Piezo1Col2a1cre mice, trabecular bone formation below the growth plate was strongly affected starting from postnatal day 7 (P7, BV/TV in lumbar spine: 9.2 +/- 3.7% vs. 14.0 +/- 2.5% in controls; P14: 5.4 +/- 1.8% vs. 13.2 +/- 2.8% in controls). In addition, Piezo1Col2a1cre mice showed multiple rib bone fractures, most of which occurred in the first week after birth (P7, rib fractures per mouse: 12.9 +/- 3.8). This is possibly explained by a reduced cortical thickness (Ct.Th: 13.5 +/- 1.0 µm vs. 16.1 +/- 1.4 µm in controls) and trabecular bone volume fraction (BV/TV: 9.9 +/- 2.2% vs. 13.8 vs. 3.3%) in ribs of newborn mice, as measured by high-resolution µCT. The skeletal phenotype of Piezo1/2Col2a1cre at P21 was similar to that of Piezo1Col2a1cre mice, while Piezo2Col2a1cre mice had a normal skeletal phenotype.We also performed in vitro transcriptome analyses using ATDC5 and MC3T3-E1 cells to detect novel Piezo1 downstream targets by treating the cells with the Piezo1 agonist Yoda1, or applying mechanical stimulation using laminar fluid flow. We observed the induction of the known target gene Ptgs2, but also other genes such as Ccn2, which is expressed by hypertrophic chondrocytes and essential for endochondral ossification.Our data show that deficiency of Piezo1, but not of Piezo2 strongly affects the formation of trabecular bone below the growth plate, indicating a role for Piezo1 in chondrocyte-to-osteoblast transdifferentiation. It remains to be studied whether Ccn2 or other Yoda1-induced genes are relevant downstream mediators of Piezo1 function in endochondral ossification.

***Disclosures: Laura J Brylka**, None*

SUN-228

Mutations in efemp1 cause changes to bone mass and mineralization in adult zebrafish *Arianna Ericka Gomez[1], Rohda Yase[2], Yi-Hsiang Hsu[3], Ronald Kwon[1]. [1]University of Washington, United States; [2]University of Washington Seattle, ; [3]HSL Institute for Aging Research, Harvard Medical School, United States

EFEMP1 is a member of the fibulin family of extracellular matrix glycoproteins. Several studies have identified EFEMP1 as a biomarker for osteoarthritis and variants in the EFEMP1 gene are linked to connective tissue conditions [1-4]. In mice, Efemp1 is expressed in developing bone and cartilage, and has been found to negatively regulate chondrocyte differentiation in a carcinoma-derived chondrogenic line [5-6]. While multiple studies indicate that Efemp1 is expressed in osteoblasts and their progenitors, animal knockout studies rigorously examining its role in the skeleton are lacking. We hypothesize that efemp1 regulates acquisition of adult bone mass and mineralization in zebrafish. To test this, we used CRISPR0based gene editing to isolate 3 efemp1 mutant lines with deletions in exon 4, and whose alleles are designated as w1014 (8bp deletion), w1016 (13bp deletion), and w1017 (4bp deletion). All three alleles result in premature stop codons predicted to result in nonsense-mediated decay and severe truncation of the protein; therefore, they are predicted to functionally act as null mutants. In preliminary analyses, mutants for all three alleles exhibited similar phenotypic trends and thus we refer to all three mutants as efemp1-/-. MicroCT analysis of 90 day post fertilization (dpf) adult fish revealed that efemp1-/- fish exhibited significantly ($p<0.05$, n= 24 - 30/group) increased centrum volume, tissue mineral density, and thickness, and increased neural arch volume, compared to wildtype controls. Moreover, efemp1-/- mutants exhibited a trend ($p=0.10$) towards having increased standard lengths. efemp1-/- mutants exhibited significant differences in traits following allometric normalization for standard length [7], suggesting that phenotypic differences in efemp1-/- mutants were not solely attributable to differences in developmental progress. Our studies suggest that loss of efemp1 positively influences acquisition of bone mass and mineralization in adult zebrafish. Understanding the role of efemp1 in bone can advance our understanding of genetic influence on skeletal traits and identify a new therapeutic target for osteoporosis.[1] Hasegawa, A. et al. 2017. Arthritis Rheumat.[2] Wu, Q. et al. 2017. Knee.[3] Bizzari, S. et al. 2020. Eur J Med Genet.[4] Driver, S.G.W. et al. 2020. Eur J Hum Genet.[5] Wakabayashi, T. et al. 2010. Biochem Biophys Res Commun.[6] Ehlermann, J. et al. 2003. Gene Expr Patterns.[7] Hur, M. et al. 2018. Zebrafish.

***Disclosures: Arianna Ericka Gomez**, None*

SUN-229

Limb-specific loss-of-function of Prrx1 identifies roles in postnatal skeletal morphogenesis and short-stature signalling pathways *Michael Kluppel[2], Sai Rama Krishna Meka[2], Anna Spagnoli[2], Alessandra Esposito[3], Pranav Mishra[4], Huseyin Ozkan[2], Esin Ozkan[2]. [2]Rush University Medical Center, United States; [2]Rush University Medical Center, ; [3]University of Chicago, ; [4]Rush University,

Background.A global knockout (KO) of the Paired Related Homeobox 1 (Prrx1) gene in mice has previously been shown to lead to perinatal lethality and skeletal abnormalities. In order to prevent the early lethality and assess the roles of Prrx1 in postnatal life, we generated a conditional Prrx1 loss-of-function allele and assessed its effects in postnatal skeletal development and morphogenesis as well as human short-stature signaling pathways.Methods.We generated a mouse strain carrying a floxed Prrx1 allele and crossed these mice with a previously described driver strain in which Cre is expressed under the control of a 2.4kb limb mesenchyme enhancer of Prrx1 (Prrx1-2.4kb enhancer). The skeleton at 4 weeks after birth was assessed using Alcian Blue-Alizarin Red skeletal stains as well as X-Rays and uCT analysis. The role of Prrx1 in regulation of SHOX expression was analyzed by luciferase assays. Data are expressed as mean +/- SD.Results.Prrx1 conditional homozygous mutants survived into adulthood and were fertile. Alcian Blue-Alizarin Red skeletal stains as well as X-Ray and uCT analysis of homozygous Prrx1 mutants showed shortened, thickened, and flattened zeugopod bones in both fore- and hindlimb. The radius also showed significant bowing, and the typical fusion of the distal tibia and fibula observed in wild type mice in the hindlimb was absent in mutants. In addition, the wrist showed morphogenesis defects similar to human Madelung deformity, including altered orientation of specific carpal bones. In the hindlimb, morphogenesis of the calcaneus was altered. Moreover, the skull lacked suture fusion and closure. Quantitative X-Ray analysis demonstrated that forelimb zeugopod length in mutants at 4 weeks of age was reduced to 45.5% +/- 9.6% in males and 43.9% +/- 4.1% in females. Hindlimb tibia length was reduced to 83.3% +/- 7.4% in males and 87.4% +/- 1.1% in females. Since Madelung wrist malformations have been shown to be associated with mutations in enhancers of the short-stature homeobox gene SHOX in humans, we performed preliminary luciferase assays which showed that Prrx1 can positively regulate a transcriptional regulatory element of SHOX mutated in human short-stature patients.Conclusion.Our results demonstrate that Prrx1 plays a critical role in zeugopod bone morphogenesis as well as wrist and ankle formation. Furthermore, our data indicate a mechanistic role for Prrx1 in the regulation of critical regulators of bone formation, including SHOX genes.

***Disclosures: Michael Kluppel**, None*

SUN-231

CRISPR/Cas9 based knockout of sox6 gene severely affects the musculoskeletal health and aging rate in zebrafish *Donaka Rajashekar[1], David Karasik[1], David Karasik[2]. [1]The Azrieli Faculty of Medicine, Bar-Ilan University, Israel; [2]Hebrew SeniorLife, Hinda and Arthur Marcus Institute for Aging Research, Boston, MA, USA., United States

Aging of human musculoskeletal (MSK) traits is linked to many vital functions, disability, frailty, and ultimately survival. Functional integrity of bone and muscle tissues can be achieved via shared molecular signaling pathways. Genetics exert a significant role in losses of both bone and muscle mass and function. Genome wide association studies (GWAS) have discovered multiple candidate genes for age-related MSK traits, including BMD at the lumbar spine and femoral neck. Among them, SOX6 is suggested as one of the strong candidates for its potential association with bone metabolism. Modeling of human disease by knocking-out (KO) sox6 gene in zebrafish (ZF) could aid in discovering potential drug targets or biomarkers for MSK system's aging.KO of sox6 gene in ZF was done by CRISPR/Cas9 technology. In young adult ZF, body weight and length were measured, while swimming performance was determined by 3 min video recordings (n=12 animals per group, KO and wild-type, WT). A cellular senescence (SA-beta-gal) assay was applied at regenerated caudal fins. Expression of selected genes in caudal fins was measured by RT-qPCR. Using micro-CT SKYSCAN 1172 (Bruker), BMD of head bones was measured, and hematoxylin and eosin staining performed for muscle histology (n=8). Deletion of 11 base pairs in sox6 gene had been confirmed by DNA sequencing, and absence of sox6 protein was shown by Western blot. In-crossing of homozygous mutants revealed complications in their reproductive system by producing lower ($p=0.04$) number of eggs than WT. During skeletal growth, sox6-/- (KO) fish had a significant reduction in total body length and weight (both $p<0.0001$) compared to WT siblings. Further, sox6-/- fish had demonstrated slower movement ($p=0.0004$) that resembles of seahorse swimming pattern. Alterations in skeletal muscle fibers morphology were apparent at dorsal and trunk region of sox6-/- adult zebrafish compared to WT siblings. Micro-CT imaging had shown disorganized head bones in sox6-/- (Fig1). A cellular senescence assay had indicated a higher SA-beta-gal; increased expression of cyclin dependent kinase inhibitors (cdkn1a and cdk2ab) in sox6 KO at caudal fins on 4th day of regeneration. This progeric phenotype corresponded to an early death in sox6-/- ZF (max. survival: 7 months and 15 days; log-rank test, $p=0.03$).Knockout of sox6 gene activates premature aging with deterioration of the functional integrity of bone and muscle tissues.

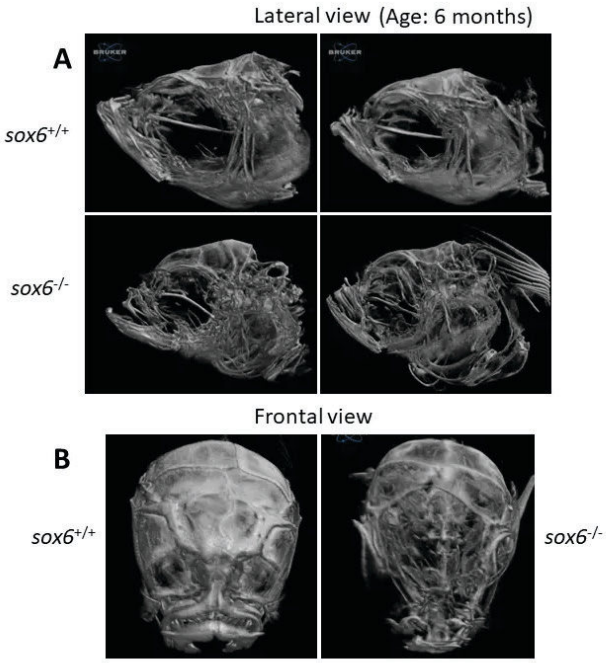

Fig1. micro-CT imaging of zebrafish head bones.

***Disclosures: Donaka Rajashekar**, None*

SUN-232

Translocation Genes tram1 and tram2 Regulate Bone Mass and Mineralization *Kiana Reynolds[4,] Joyce Tang[2,] Anne Onyali[2,] Jyoti Rai[2,] Arianna Gómez[2,] Claire Watson[2,] Yi-Hsiang Hsu[3,] Ronald Kwon[4,] [4]University of Washington, [,2]Department of Orthopaedics and Sports Medicine, University of Washington School of Medicine, Seattle, WA, USA, United States, [3]Institute for Aging Research, Hebrew SeniorLife, United States, [4]University of Washington, United States

Osteoporosis is characterized by decreased bone mineral density (BMD) and increased bone fragility, putting patients at higher risk for fractures. Genome-wide association studies (GWAS) have identified loci harboring genetic variants associated with osteoporosis-related traits. One such locus is the XKR9 locus associated with BMD. The XKR9 locus comprises several genes, and the causal gene at the locus is currently unknown. Here, we examine the skeletal functions of TRAM1, a gene in proximity to XKR9, and TRAM2, a homolog of TRAM1. TRAM1 plays an important role in stabilizing proteins during translocation into the endoplasmic reticulum lumen [1]. Though the function of TRAM2 is not well characterized, it is suggested to play a role in collagen translocation [2]. Currently, no in vivo knockout studies have been published investigating the TRAM genes. We hypothesized that tram1 and tram2 are necessary for adult bone mass and mineralization in zebrafish. To test this, we used CRISPR-based gene editing to isolate tram1w1007 and tram2w1005 zebrafish germline mutants. We also generated tram1w1007;tram2w1005 compound mutants. MicroCT scans were generated at 90 days post fertilization, and ImageJ and FishCuT were used to quantify the impacts on vertebral bone morphology and mineralization. tram1 mutants exhibited significant increases in tissue mineral density (TMD) (centrum TMD, p= 0.0402; haemal arch TMD, p=0.0332; neural arch TMD, p=0.0335; n=13/group) while tram2 mutants showed significant increases in centrum and neural arch volume (centrum volume, p=0.0392; neural arch volume, p=0.0031; n=11/group). Additionally, fish with homozygous mutations in tram1 and heterozygous in tram2 (n=19) showed no significant changes compared to controls (n=5), however tram1;tram2 double mutants exhibited lethality at the larval stage. These findings identify overlapping and distinct roles for tram genes in vivo (Fig. 1). They also provide evidence that variants at XKR9 could act through TRAM1 to influence BMD thereby introducing translocation as an important factor underlying genetic influence on osteoporosis risk.References1. Hegde et al., 2008, J Cell Biol; 2. Stefanovic et al., 2004, Mol Cell Bio.

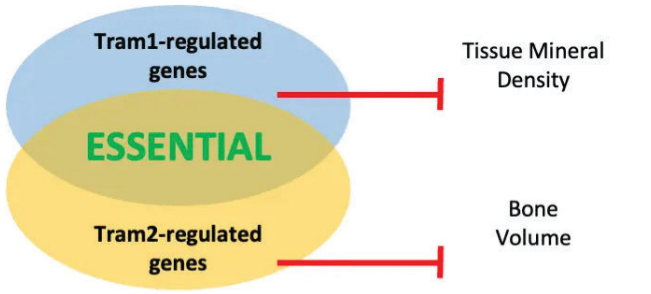

Genotype	Phenotype
tram1$^{w1007/w1007}$	↑ TMD
tram2$^{w1005/w1005}$	↑ centrum/neural arch volume
tram1$^{w1007/w1007}$;*tram2*$^{+/w1005}$	No significant changes
tram1$^{w1007/w1007}$; *tram2*$^{w1005/w1005}$	Lethal at larval stage

Fig. 1 *tram* genes have overlapping and distinct roles *in vivo*.

***Disclosures: Kiana Reynolds**, None*

SUN-233

Investigating the Effects of Antipsychotics on Embryonic Bone Development *Kavindi Weerasinghe[1,] Alister Ward[2,] Clifford Liongue[2,] Jason Hodge[2,] Julie Pasco[2,] Rasika Samarasinghe[2,] Lana Williams[2,] [1]PhD student, Australia, [2]Supervisor, Australia

Antipsychotics are the first line treatment in schizophrenia, a condition involving dysregulation of multiple neurotransmitters including dopamine, serotonin, noradrenaline, histamine and muscarinic pathways. Evidence has shown antipsychotic use decreases bone mineral density and increases fracture risk in adults, with dopamine, serotonin and adrenergic receptors previously been found in bone cells in vitro. Use of antipsychotics during pregnancy, particularly second-generation agents has increased. To date there is no clear evidence of the impact on fetal bone development. Therefore, we aimed to investigate the effects of antipsychotics on embryonic bone formation in-vivo using a zebra fish model. MethodsThe effect of first (chlorpromazine and haloperidol; FGAs), second (olanzapine and quetiapine; SGAs) and third (aripiprazole; TGA) generation antipsychotics on early zebrafish bone development was measured using alizarin red staining. Osteoblasts development marker expression was measured using whole mount in-situ hybridisation method followed by dopamine, serotonin and adrenergic receptor expression profile along with apoptosis studies.ResultsEach antipsychotic dose-dependently inhibited zebrafish bone formation. The FGAs, chlorpromazine and haloperidol, both inhibited bone development at IC50 ~23 ?M and ~3 ?M, respectively. Whereas the SGAs, olanzapine and quetiapine inhibited bone development at IC50 ~73 ?M and ~54 ?M respectively. Aripiprazole, a TGA, inhibited bone development at IC50 ~9 ?M. Expression of osteoblast genes runx2b, col10a and spp1 were reduced with the treatment of 10 µM for FGAs and TGA, where SGAs reduced the bone development with 30 µM demonstrating that these agents are affecting the in-vivo bone development in zebrafish embryos.ConclusionAll tested antipsychotics dose dependently inhibited zebrafish embryos bone development, where FGAs and TGAs were the most potent inhibitors compared to SGAs. This raises further questions regarding the short and long-term effects on bone health of offspring, with future research into dopamine, serotonin and adrenergic signalling pathways to further understand the mechanisms of action.

***Disclosures: Kavindi Weerasinghe**, None*

SUN-234

Elevated PDGFR? Signaling Causes Knee Joint Fusion by Disrupting Synovial Progenitor Differentiation *John Woods[1,] Lorin Olson[1,] [1]Oklahoma Medical Research Foundation, United States

Mouse knee joint development begins at E11.5-E13.5 when a cartilage template is divided in two by the formation of an interzone, an anlage that gives rise to all the structures of a mature joint. Before interzone formation, the cartilage template expresses cartilage genes Sox9 and Col2a1. These genes are downregulated upon interzone formation and replaced by Gdf5, a member of the bone morphogenic protein family. Platelet-derived growth factor receptor-? (PDGFR?) is not expressed in the cartilage template of the limb, but it is expressed in the perichondral mesenchyme and Gdf5+ interzone cells. Based on this expression pattern, we hypothesized that tight regulation of PDGFR? signaling may be crucial for joint development. To investigate this role of PDGFR?, we used gain-of-function (?GOF) and loss-of-function approaches with Prx1-Cre, which is active in the early limb bud mesenchyme. Loss-of-function did not affect joint formation. However, ?GOF mice were born with knee

joints fused by ectopic cartilage and lacking ligaments and menisci. Interzone specification occurred normally in ?GOF mutants up to E13.5, but Gdf5 expression was decreased. Further, there was expansion of Sox9 protein expression into domains that are normally Sox9-negative. These results suggest that elevated PDGFR? signaling interferes with joint progenitor differentiation by redirecting Gdf5+ interzone cells from a synovial connective tissue fate to a Sox9+ chondrogenic fate. Thus, PDGFR? signaling has pro-chondrogenic properties that must be tightly regulated to allow differentiation of ligaments, menisci, and other connective tissue cell types. This property of PDGFR? signaling may be important in other contexts such as de novo cartilage formation in fracture healing.

***Disclosures: John Woods**, None*

SUN-236

Understanding CXXC Finger Protein 1 Action in Osteoblast Differentiation
*Ahmed Al Saedi[1], Katelyn Healey[2], Molly Persky[2], David Maridas[3], Lijie Jiang[2], Vicki Rosen[3], Diana Carlone[4]. [1]Department of Pediatrics, Harvard Medical School and Division of Endocrinology, Boston Children's Hospital, United States. [2]Division of Endocrinology, Boston Children's Hospital, United States. [3]Harvard School of Dental Medicine, United States. [4]Boston Children's Hospital, United States

Skeletal development, remodeling and regeneration are dependent on the activity of mesenchymal progenitor cells (MPCs). Recent data have implicated epigenetics in the regulation of MPC function with links to altered bone formation in both mice and humans. Precisely how epigenetics controls MPC activity and function, including the ability of MPCs to participate in bone formation, remains less clear. Here, we focus on CXXC Finger Protein 1 (CFP1), an epigenetic regulatory factor that mediates transcriptional activation through targeted H3-Lys4 methylation of chromatin. While CFP1 has been identified as a regulator of progenitor cell differentiation in other systems, its role in bone formation remains to be defined. To address this, we deleted Cfp1 in MPCs using Prx1-Cre (cKOPrx1), which resulted in halted chondrocyte differentiation, maturation and primary ossification, implicating this factor as a critical regulator of endochondral ossification. In addition, a decrease in intramembranous ossification within the calvaria was detected in mutant mice consistent with a role for CFP1 as a direct regulator of osteoblast differentiation. To investigate this further, we performed adenoviral deletion of Cfp1 in bone marrow stromal cells (BMSCs) isolated from homozygous floxed-Cfp1 mice. Quantitative RT-PCR (qPCR) analysis revealed a dramatic reduction in the expression of osteoblast markers (Runx2, Osx, Col1a1, Ocn) supporting a role for Cfp1 in bone formation. To further define its role in osteoblast differentiation, we generated Cfp1 knockout MC3T3-E1 cells using CRISPR/Cas9 and mice using Osx1-Cre (cKOOsx1). Studies investigating if changes in osteoblast differentiation occur in the absence of Cfp1 are currently underway. In summary, our recent findings link CFP1 action to both endochondral and intramembranous bone formation.

***Disclosures: Ahmed Al Saedi**, None*

SUN-237

The Role of EGF Containing Fibulin Extracellular Matrix Protein 1 (Efemp1) in Skeletal Development
*Rohda Ahmed Yase[1], Arianna Ericka Gòmez[1], Yi-Hsiang Hsu[2], Ronald Young Kwon[1]. [1]University of Washington Seattle, United States. [2]HSL Institute for Aging Research, Harvard Medical School, United States

EFEMP1 is a member of the fibulin family which encodes an extracellular matrix (ECM) glycoprotein that is expressed in epithelial cells and elastic-fiber-rich tissues. Previous studies in mice show that Efemp1 is expressed in the sclerotome, an embryonic unit that gives rise to bone structures of the axial skeleton. However, the role of EFEMP1 in skeletal development is poorly understood. In this study, we tested the hypothesis that efemp1 is necessary for axial skeletal development in zebrafish. Using CRISPR-based gene editing, we isolated zebrafish germline mutants with an 8 base pair deletion (efemp1w1014), 13 base pair deletion (efemp1w1016), and 21 base pair deletion (efemp1w1015) in exon 4. Whereas efemp1w1014 and efemp1w1016 result in premature stop codons which are predicted to induce loss-of-function in efemp1, efemp1w1015 is an in-frame mutation resulting 7 amino acid deletion. To determine the role of efemp1 in spine development, we analyzed 13 days post-fertilization (dpf) efemp1w1014, efemp1w1015, efemp1w1016 mutants stained with calcein, which binds to actively mineralizing structures. The area of mineralizing vertebrae was measured using FIJI and statistical analyses were performed using Graphpad. We found no significant differences in vertebral mineralized area when comparing homozygous mutants and wildtype controls for efemp1w1014 (n=5-10) and efemp1w1016 (n=7-8). We found a trend (p=0.06) toward decreased vertebral mineralized area for efemp1w1015 mutants (n=4-7). Our results indicate that efemp1 may play a role in spine mineralization. Specifically, whereas mutations predicted to result in loss of Efemp1 (w1014 and w1016) can potentially be compensated for, a mutation predicted to alter Efemp1 protein structure (w1015) appears to result in impaired mineralization. By understanding the role of efemp1 in spine development, we will better understand the role of fibulins in skeletal development and their influence on skeletal traits.

***Disclosures: Rohda Ahmed Yase**, None*

SUN-238

Can early hip fracture surgery improve physical function following fragility fracture in elderly patients with osteoporosis?
*Jun Hwan Choi[1], Soyeon Yoo[2]. [1]Department of Rehabilitation Medicine, Jeju National University Hospital, Republic of Korea. [2]Department of Internal Medicine, Jeju National University Hospital, Republic of Korea

Background and aims: Hip fractures are the most serious osteoporosis-related fracture. Most patients who have had hip fracture surgery do not return to their previous level of function. Although there are studies on the association between early surgery and mortality after hip fracture, there are few studies on the functional prognosis of early surgery. The purpose of this study was to investigate the relations between timing of hip fracture surgery and physical function following fragility fracture in elderly patients. Methods: The patients who underwent hip fracture surgery between January 2019 and December 2022 were retrospectively enrolled through a cohort study. From the cohort data, we only selected patients with a first diagnosis of hip fracture, and excluded patients with acceptable reasons for delay, such as uncorrectable or correctable medical problems and cognitive impairment. Of the 223 patients with fragility hip fracture, 59 patients (12 males, 47 females, mean age 78.6 +/- 11.7) met the study enrollment criteria. Patients were divided into two groups: within 48 hours from arrival at the emergency room to surgery (early surgery group, N=24) or not (delayed surgery group, N=35). All functional outcomes were assessed at the beginning and discharge of in-patient rehabilitation and at 3 months after surgery. The Koval's grade, performance-based physical function (10-meter walk test, timed up and go, Berg balance scale) Results: There was no significant difference between the two groups in the demographic characteristics and type of surgery, and fracture site and side. The mean surgical timing of early surgery group is 35.7 +/- 10.7 hours and delayed surgery group is 85.0 +/- 40.7 hours. The early surgery group had significantly higher level of balance and gait speed at the 3 months after surgery. Conclusions: This study demonstrated that hip fracture surgery within 48 hours of admission is associated with better physical function following fragility hip fracture in elderly patients. Patients who do not require medical stabilization should undergo surgery as soon as possible.

Table. Performance-based physical function at beginning and at discharge after hip fracture surgery

Variables	Early surgery group (n=24)	Delayed surgery group (n=35)	*p*-value
Pre-Koval's grade	1.83 ± 1.27	2.11 ± 1.71	0.497
Koval's grade [1]	6.17 ± 0.38	6.06 ± 0.64	0.455
BBS [1]	27.00 ± 14.30	32.17 ± 12.59	0.148
10MWT (S)[1]	33.21 ± 16.71	32.26 ± 15.42	0.837
TUG (S)[1]	51.44 ± 28.33	43.33 ± 20.37	0.226
Koval's grade [2]	4.91 ± 1.69	4.94 ± 1.59	0.943
BBS [2]	34.08 ± 12.36	36.71 ± 13.12	0.327
10MWT (S)[2]	35.94 ± 31.07	28.08 ± 15.79	0.427
TUG (S)[2]	38.60 ± 29.84	35.26 ± 23.87	0.726
Koval's grade [3]	1.71 ± 1.25	2.86 ± 1.96	0.943
BBS [3]	49.29 ± 10.05	38.07 ± 19.58	0.030*
10MWT (S) [3]	16.78 ± 7.09	26.64 ± 16.21	0.041*
TUG (S) [3]	15.22 ± 7.02	22.23 ± 14.03	0.144

Values represent mean ± standard deviation

Abbreviations: BBS, Berg balance scale; 10MWT, 10 Meter Walk Test; TUG, Timed up and go test

[1]at the beginning of rehabilitation, [2]at the time of discharge after rehabilitation treatment, [3]at the 3 months after surgery

*p<0.05

***Disclosures: Jun Hwan Choi**, None*

SUN-239

Digit Tip Regeneration is Dependent on Mechanical Load and not Innervation
*Connor Dolan[3], Alyssa Falck[3], KIRBY M. SHERMAN[2], Regina Brunauer[3], Dana Gaddy[4], Larry Suva[5], Lindsay Dawson[6], Ken Muneoka[3]. [3]Texas A&M University, . [2]Texas A&M University , . [3]Texas A&M University, United States. [4]College of Veterinary Medicine, Texas A&M University, United States. [5]Texas A&M University, College of Veterinary Medicine and Biomedical Sciences, United States. [6]Texas A&M University College of Veterinary Medicine, United States

The regenerating mouse digit tip and the human fingertip are mammalian models for epimorphic regeneration, and limb denervation in mice inhibits this response. However, limb denervation also causes severe paralysis, impairs appendage use and diminishes mechanical loading of the denervated tissues. Thus, it is unclear whether the regeneration response requires innervation, mechanical load, or both. Herein, we investigated the role of denervation versus mechanical load during mouse digit tip regeneration.To test the specific role of innervation on digit tip regeneration we surgically denervated individual digits to avoid negatively impacting mechanical loading. To test the specific role of mechanical loading, mice were hindlimb unloaded (HU) during regeneration. For both denervation and HU experiments, regeneration was analyzed using in vivo microCT (uCT) to quantify bone volume

and length, and samples were collected throughout for histological and immunohistological quantification of wound closure, blastema formation, osteoclast resorption and proliferation. For all studies, female, 8-week-old CD1 mice were used.Regeneration of sham-operated control digits is completed within 28 days post-amputation (DPA) whereas regeneration of denervated digits is not complete until 42 DPA. The delay in regeneration is not attributed to re-innervation of the digit but is caused by a delayed wound healing response. Treating denervated-digits with Dermabond, a well-established wound dressing, restores wound healing resulting in a restoration of regeneration rate compared to sham-controls digit at 28DPA. Unlike denervation experiments, regeneration was completely inhibited while animals were in HU. At 28DPA, HU-digits were smaller by both bone volume and length, exhibited no histological evidence of blastema formation, had increased osteoclast resorption, and the original amputation wound remained open. Moreover, we also found that removing animals from HU rescues the regeneration response, whereas placing animals in HU during blastema formation attenuates regeneration.Here we show that denervation results in a regeneration response indicating that mouse digit tip regeneration is nerve-independent. In contrast, reducing mechanical loading by hindlimb unloading completely inhibits digit tip regeneration. These studies demonstrate, for the first time, that epimorphic regeneration in mammals requires mechanical load and is independent of innervation.

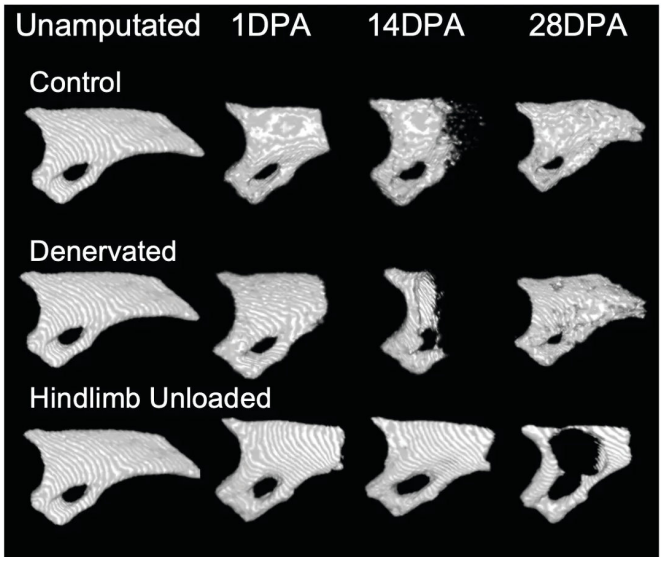

***Disclosures: Connor Dolan**, None*

SUN-240

Development of a novel inorganic polyphosphate-releasing thermoresponsive hydrogel to improve fracture healing outcomes *Rayan BenLetaifa[1,] Deepak Chauhan[2,] Chang-sheng Wang[2,] Hu Zhang[2,] Tarek Klaylat[1,] Derek Rosenzweig[1,] Paul Martinaeu[1,] Xavier Banquy[2,] Rahul Gawri[1.] [1]McGill University, Canada, [2]Universite de Montreal, Canada

INTRODUCTION: Bone fractures are among the most common musculoskeletal injuries. Immune cells play a crucial role in fracture healing, and dysregulation of their function can lead to impaired healing. Inorganic polyphosphates (polyP) have been shown to modulate immune function by closely regulating their functions. At the fracture site, polyPs released by degranulating platelets play a crucial role in initiating coagulation and recruiting immune cells. The objective of the study is to develop a thermosensitive hydrogel with sustained release of polyP to be implanted at the site of fracture to enhance the homing of immune cells.METHODS: Hydrogel formulations and sol-to-gel transition times were tested using several poloxamers, Gellan gum, and poly-N-vinyl-caprolactone (PNVCL). Drug loading of hydrogel formulations was accomplished by mixing dehydrated polymer components with polyP-45-containing distilled water, and supernatant samples were taken at designated time points. Rheological assessments were performed to characterize the viscoelastic properties of the hydrogel. Assays for cell adhesion, cell proliferation, cell survival, and cellular metabolic state to assess the cytocompatibility of the fabricated hydrogel were performed using RBL-2H3 cells, MC3T3 cells, and primary murine BMSCs.RESULTS: The hydrogel formulation consisting of 20% PF-108, 1.5% PNVCL, and 3% Gellan gum (w/v) showed a sol-to-gel transition time of 60 seconds. This formulation was chosen for further analyses and development for its sol-to-gel transition time. polyP release study showed a release concentration of 84.5 μM during the rapid-release phase and maintained a concentration of approximately 37 μM during the extended-release phase. Rheological analyses showed a significantly greater elastic modulus than a viscous modulus. Furthermore, the temperature sweep reveals that the sol-to-gel transition occurs at 35°C. The seeded on the hydrogel showed 92% cell adhesion and 95% cell viability (RBL-2H3, MC3T3, and primary BMSCs).DISCUSSION: This study will generate a novel drug delivery system augmented with a bioactive compound, serving to modulate the body's own immune system to enhance bone healing, improve clinical outcomes, and reduce clinical strain.Finally, after the exhaustion of polyP from the hydrogel, the hydrogel remaining at the site can act as a bio-scaffold, allowing cells to migrate and enhance the development of the fracture callus, thus serving as a dual-purpose bioscaffold.

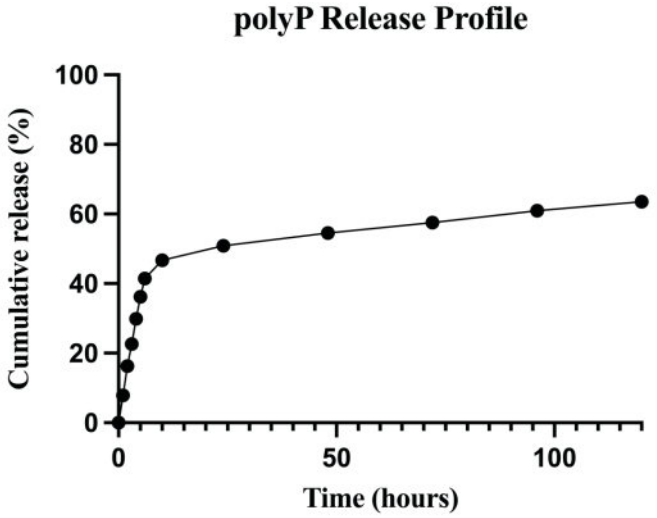

Figure 1: Cumulative release of polyP-45 from hydrogel formulation comprising 20% PF-108 (w/v), 1.5% PNVCL (w/v), 3% Gellan gum. Hydrogel formulation exhibits rapid release during the first 12 hours, releasing approximately 50% of loaded polyP content, and sustained release over the course of 5 days with approximately 65% of polyP being release cumulatively.

***Disclosures: Rayan BenLetaifa**, None*

SUN-241

New possible pharmacotherapy for osteoarthritis: focus on inflammation and cartilage recover *Fabiana Guerra[1,] Seng Manivong[2,] Elie Joe Mikhael[2,] Pierre Sirois[3,] Xavier Banquy[2,] V. Gaëlle Roullin[2,] Patricia Fernandes[1,] Florina Moldovan[2.] [1]Federal University of Rio de Janeiro, Brazil, [2]Universite de Montreal, Canada, [3]Laval University, Canada

Osteoarthritis (OA) is degenerative joint disease characterized by cartilage degradation, joint pain, subchondral bone turnover changes and synovial inflammation, and without curative treatment.1 Our laboratory has previously shown that the synergistic inhibition of endothelin-1 (ETA) and bradykinin (BKB1) receptors, by BQ123 and R954 antagonist peptides respectively, decrease pain and prevent cartilage degradation in an OA rat model.2 The primary objective of this study was to investigate the potential of the concomitant inhibition of the two GPC-receptors (ETA and BKB1) to reduce the inflammatory process in OA; the second objective was to develop nanohydrogel (NG) as a drug-delivery platform for the intra-articular delivery of the two peptides.Methods:Human-derived chondrocytes were treated with BQ123 and/or R954 (25-1000 ?M) to determine cell viability by MTS/LDH assays. The effect on inflammatory protein expression and on catabolic and anabolic markers was assessed by western blotting using specific antibodies of NF?B, COX2, NOS2, COL2A1, SOX9 and MMPs. MMP2 and MMP9 enzymatic activity was also evaluated by zymography. Immunohistochemistry was performed to determine ETA, BKB1, collagen type II and COX2 expression. Cartilage thickness was measured from Safranin-O-stained histology of OA rats knees treated intraarticularly with the ETA/BKB1 antagonists. Additionally, BQ123 and R954 were chemically conjugated to biopolymers to synthesize NG using an ionic gelation process.3Results:Cell viability was not affected by BQ123 or R954. Both activation of the inflammatory proteins NFkB, COX2 and NOS2, and MMPs' catabolic effects were reduced with BQ123/R954 combination after 6 and 24 hours of treatment respectively. In tissue, BQ123/R954 treatment significantly reduced ETA and BKB1 expression, while cartilage thickness was significantly increased in OA rats' knees. NG-BQ123 and NG-R954 were successfully synthesized with a size of ~427 nm and a positive charge of ~41 mV, allowing the rapid internalizing by chondrocytes after 24 hours.Conclusion:We demonstrated that the dual inhibition of ETA and BKB1 reduced both the expression of inflammatory proteins and the activity of cartilage degradation enzymes in vitro, and increased articular cartilage thickness in vivo, thus showing that ETA and BKB1 antagonists could be a promising new treatment for OA. Finally, functionalized peptides NGs for intra-articular treatment were successfully synthesized.

***Disclosures: Fabiana Guerra**, None*

SUN-243

Non-oxidizable fully reduced HMGB1 improves osseointegration in diabetic conditions *Claudia Biguetti[1], Bhuvana Lakkasetter Chandrashekar[2], Peter Elvin[1], Alexandra Arteaga[2], Danieli Rodrigues[2]. [1]University of Texas Rio Grande Valley, United States. [2]University of Texas at Dallas, United States

Diabetes is a metabolic disorder characterized by chronic hyperglycemia and dysregulated inflammatory response, which impairs bone healing and osseointegration of dental implants. The high mobility group box-1 (HMGB1) protein, particularly a non-oxidizable fully reduced isoform of this protein (FR-HMGB1), has been found to enhance SCs proliferation and accelerate bone healing at the injury sites. The present study aimed to assess the potential of FR-HMGB1 to improve osseointegration in both in vitro and in vivo diabetic models. Murine pre-osteoblasts (MC3T3-E1 cells) were treated with 1µg/mL of FR-HMGB1 in a complete culture medium under normal glucose (5.5?mM) or high glucose (30mM) levels. For the in vivo osseointegration model, a titanium screw was inserted in the first upper molar palatine root socket of 12-week-old 129Sv mice. Diabetic (D) mice were produced by administering a high-fat diet for six weeks and two IP injections of streptozotocin (100mg/Kg) one week before implant placement. Control non-diabetic (ND) and D groups were treated with a local injection of 20µL of PBS, while ND- and D-HMGB1 groups were treated with 20µL of FR-HMGB1 (7.5mg/Kg). Five implanted bone samples from each group were harvested at 7 and 21 days post-surgery for histological and microcomputed tomography (MicroCT) analysis (bone to implant contact, BIC %). Our in vitro results demonstrated that the viability of MC3T3-E1 cells was significantly reduced under high glucose levels compared to controls. FR-HMGB1 treatment significantly increased osteoblasts proliferation in normal glucose levels and rescued cell proliferation capacity in diabetic conditions. Clinically, D-Control mice showed inflammation and incomplete epithelization at day 7, while other groups had implants entirely covered by oral mucosa. Histological results demonstrated persistent chronic inflammation in D controls, while D treated with FR-HMGB1 exhibited increased numbers of Runx-2 positive osteoblasts and successful bone formation surrounding implants, comparable to ND control and ND-FR-HMGB1 groups. MicroCT revealed that 80% of both ND control groups and 60% of D mice treated with FR-HMGB1 were successfully osseointegrated (> 60 % BIC %), whereas the average BIC % was significantly reduced in D-Controls. In conclusion, non-oxidizable FR-HMGB1 improved osseointegration in diabetic models, suggesting its potential to be a therapeutic target for implant procedures in diabetic patients.

***Disclosures: Claudia Biguetti**, None*

SUN-244

Nanogels for the drug delivery of antagonist peptides of ETA and BKB1 receptors for OA treatment *Seng Manivong[1], Araceli Garcia Ac[2], Line Séguy[1], Pierre Sirois[3], Xavier Banquy[2], V. Gaëlle Roullin[2], Florina Moldovan[4]. [1]CHU Sainte-Justine, Research Center; Université de Montréal, Faculty of Pharmacy, Canada. [2]Université de Montréal, Faculty of Pharmacy, Canada. [3]Université Laval, Faculty of Medicine , Canada. [4]CHU Sainte-Justine, Research Center; Université de Montréal, Faculty of Dentistry, Canada

IntroductionOsteoarthritis (OA) affects millions of people worldwide with daily physical disability and pain (Glyn-Jones et al., 2015). There is unfortunately no pharmacological cure to date, partly due to the complex and avascular structure of the cartilage representing a major obstacle for drug delivery within the joint (Brown, Kumar and Sharma, 2019). Our laboratory has previously shown that the synergistic inhibition of endothelin-1 (ETA) and bradykinin (BKB1) receptors by two peptides, namely BQ123 and R954 respectively, can decrease pain and also prevent cartilage degradation in an OA rat model (Kaufman et al., 2011). Hence, our goal was to develop a drug delivery system (DDS) for this promising therapy enabling its local and long-term delivery in the cartilage. Biopolymeric nanogels (NG) were selected due to their mimicking extracellular matrix with high-water content, together with their high-loading capacity, and drug-controlled, sustained release to target tissues (Manivong et al., 2023).MethodsFunctionalized chitosan (CH-BQ123 and CH-rhodamine B) / hyaluronic acid (HA-R954) nanogels (NG) were synthesized using an ionic gelation process (Callewaert et al., 2014), resulting in CH-BQ123 NG, HA-R954 NG and fluorescent NG-rhodamine B. Particle sizes (Dh), polydispersity indexes (PdI), and zeta potentials (ZP) were characterized by dynamic and electrophoretic light scattering respectively (DLS and ELS). NG toxicity was determined by MTS/LDH and TUNEL experiments up to 5 days of treatment on human chondrocytes and NG-rhodamine B cell internalization by fluorescence microscopy. Finally, NG efficacy, compared to the free peptides, will be assessed in vitro regarding protein expression of anabolic and catabolic markers, with and without pre-enzymatic digestion of the NG.Results and conclusionCH-BQ123 and HA-R954 NG were obtained with sizes of ~427+/- 58 nm and a positive charge of ~41+/- 6 mV, which will allow the local and persistent deposition of the peptide NG in the negatively charged cartilage. Indeed, NG were rapidly internalized in vitro by chondrocytes without showing any cytotoxicity up to 5 days of treatment. In addition, non-digested NG appears to be able to decrease the catabolic proteins MMP1 and MMP2 expression and to increase aggrecan, the major proteoglycan in articular cartilage, under inflammatory conditions. Overall, CH-BQ123 NG and HA-R954 NG were successfully synthesized and show capacity to deliver peptides to the joint.

***Disclosures: Seng Manivong**, None*

SUN-245

Role of Hypoxia-inducible factor-1? (HIF-1?) in Intramembranous Bone Regeneration *Hoomin Lee[1], Yun Suk Huh[2], Frank Ko[3]. [1]Rush University Medical Center, United States. [2]Inha University, Republic of Korea. [3]Rush University, United States

Intramembranous bone regeneration plays an important role in orthopaedic and dental procedures. Despite the increasing importance of intramembranous bone regeneration, the underlying mechanisms of intramembranous bone regeneration remain unclear. HIF-1? plays a pivotal role in many pathways such as angiogenesis, cell migration and cell differentiation, and is well known to promote bone formation and endochondral bone regeneration through these roles. However, studies to date have yet examine the role of HIF-1? activation or inhibition on intramembranous bone regeneration. We therefore sought to determined the effects of the HIF-1? activation or inhibition on mice that underwent surgical ablation of bone marrow, a well-established intramembranous bone regeneration model. At 4 weeks of age, mice underwent surgery and were administered every 2 days with 30 µg/g of 2-methoxyestradiol (2ME2) or 10 µg/g of dimethyloxaloylglycine (DMOG) to inhibit or activate HIF-1?, respectively. We performed a microcomputed tomography analysis of post-surgery day 7 regenerating bone marrow BV/TV and found that the activation of HIF-1? was not different compared to the control, whereas HIF-1? inhibition by DMOG impaired intramembranous bone regeneration by 25%. These data suggest that HIF-1? is necessary for intramembranous bone regeneration and may improve efficiency of fracture healing or enhance implant fixation.

***Disclosures: Hoomin Lee**, None*

SUN-246

Bioswitchable Delivery of microRNA by DNA origami: Application in Bone Regeneration *songhang li[1], Taoran Tian[2], Yunfeng Lin[2], xiaoxiao cai[1]. [1]State Key Laboratory of Oral Diseases National Clinical Research Center for Oral Diseases, West China Hospital of Stomatology, Sichuan University, China. [2]Sichuan University, China

Background: In recent years, microRNA (miR) therapy has become the main focus of miR research. However, its inherent instability greatly limits its therapeutic applications. In the field of drug delivery, tetrahedral framework nucleic acid (tFNA) constructed using DNA origami as a stable drug delivery system is attracting considerable attention in DNA nanomaterial research because of its good biocompatibility and high cell membrane permeability. Therefore, loading miR on tFNA and transporting them into cells may overcome the limitations of miR instability, thereby expanding the applicability of miRs. However, the loaded miRNA has poor structural stability because it is single-stranded. After entering the cell, the presence of the vector tFNA may affect the efficiency of miRNA due to the lack of detachment mechanism.Aim: This study aims to build a bioswitchable miRNA delivery system based on tFNA with high stability by optimizing the delivery system. And in this study, an RNase H-responsive sequence is applied to connect a sticky-end tFNA (stFNA) and miR-2861, which is a model miR, to target the expression of histone deacetylase 5 (HDAC5) in BMSCs. The resultant bioswitchable nanocomposite (stFNA-miR) enables efficient miR-2861 unloading and deployment after intracellular delivery, thereby inhibiting the expression of HDAC5 and promoting osteogenic differentiation.Methods: Using four specific ssDNA to form stFNA, and assemble it with miR2861 to construct stFNA-miRNA2861; MiR-qPCR were used to verify the opening of the bioswitch. The expression of target protein HDAC5 and osteogenesis-related proteins were observed by western blot and laser confocal microscope; the osteogenic differentiation of BMSCs induced by stFNA-miR2861 was observed by alkaline phosphatase staining and alizarin red staining. Micro-CT was used to analyze the internal structure of bone defects; H&E staining and Masson staining were used to observe the results of repair and collagen formation.Conclusion: Herein, we have confirmed that this delivery system can be successfully assembled. This study verified the effectiveness of the RNase H-activated switch structure in the carrier. In vitro and in vivo experiments verified that the structure of stFNA-miR2861 can promote bone regeneration. In addition, owing to the excellent editability within tFNA, this delivery system can be used as a platform for the delivery of other nucleic acid drugs and nucleic acid-like drugs in the future.

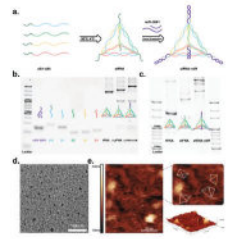

Fig.1Fabrication and characterization of stFNA-miR.

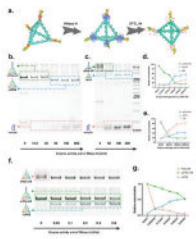

Fig.2 Enzyme cleavage test and the stability of stFNA-miR in an enzymatic environment.

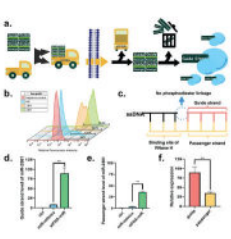

Fig.3 Cellular membrane crossing of the "truck" and screening of the guide strand.

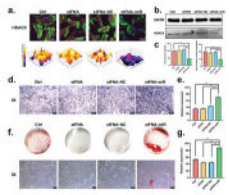

Fig.4 stFNA–miR targeted HDAC5 to promote osteogenic differentiation.

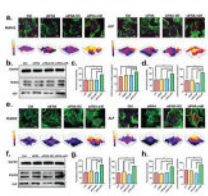

Fig.5 Osteogenesis-related protein expression at five and 14 days.

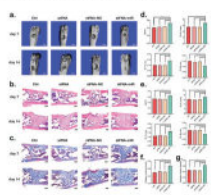

Fig.6 In vivo evaluation of the stFNA–miR at day 7 and day 14.

***Disclosures: songhang li**, None*

SUN-247

Role of Discoidin Domain Receptor 2 in Tooth Socket Healing *RENNY FRANCESCHI[1] Rajay Kamath[1] [1]University of Michigan, United States

Discoidin Domain Receptor 2 (DDR2) is a collagen-activated tyrosine kinase required for skeletal development and regeneration of the calvaria and long bones, however, possible functions in alveloar bone have not been examined. The present study used lineage tracing, as well as global and conditional knockout approaches, to examine functions of Ddr2 in alveolar bone regeneration during tooth socket healing. The following mouse lines were used: DDR2LacZ (where the bacterial LacZ gene is inserted into the Ddr2 locus creating an effective null allele), Ddr2CreERT2; Rosa26GtTdtomato and Gli1CreERT2 Rosa26GtTdtomato for lineage tracing, and the Gli1CreERT2; DDR2fl/fl mice for the selective knockout of Ddr2 in GLI1+ skeletal progenitors. For lineage tracing, 4w old Ddr2CreERT2; Rosa26GtTdtomato and Gli1CreERT2 Rosa26GtTdtomato mice were induced with one dose of tamoxifen and the 1st molars were extracted after 2 or 7 days. In both cases, TdTomato+ cells migrated into the sockets where they co-localized with OSX, a preosteoblast marker. Thus, both DDR2 and GLI1+ cells contribute to socket healing. The considerable overlap observed between DDR2+ and GLI1+ cells suggested that DDR2 largely functioned in GLI1+ cells, which are known to have skeletal progenitor properties. Consistent with localization data, both global Ddr2 (Ddr2LacZ/LacZ) or conditional knockout (Gli1CreERT2; Ddr2fl/fl) mice exhibited reductions in socket healing 1-week post extraction as measured by µCT, but not after 2 or 4 weeks. However, analysis of collagen fibril orientation by picrosirius red staining revealed that collagen fibril orientation was disrupted in tooth sockets at all times examined, suggesting that even though loss of DDR2 only had a transient effect on socket bone fill, it has long-term effects on ECM structure and, potentially, mechanical properties. In summary, this work demonstrates a role for DDR2 in alveolar bone regeneration, a finding that may have therapeutic implications for the treatment of alveolar bone loss asscciated with periodontal disease and other disorders.

***Disclosures: RENNY FRANCESCHI**, None*

SUN-248

Bone-targeted delivery of BMP-2 to promote healing of musculoskeletal injury in a mouse model *Oskar Sundberg[1] Shannon Wu[2] Brendan Shi[2] Varun Sriram[2] Won Kim[3] Dmitriy Sheyn[4] Karen Lyons[2] Weiguang Wang[2] Eldon Hard[1] Matthew Pratt[1] Boris Kashemirov[1] Ichiro Nishimura[5] Thomas Kremen[2] Charles McKenna[1] [1]University of Southern California, United States [2]David Geffen School of Medicine at UCLA, United States [3]University of Ulsan College of Medicine, Republic of Korea [4]Cedars-Sinai Medical Center, United States [5]UCLA School of Dentistry, United States

Musculoskeletal injuries, including rotator cuff tendon tears (RCT), affect millions of individuals annually. Despite surgical treatment, a significant number of RCT repairs fail to heal properly, resulting in suboptimal tissue regeneration. The use of growth factors like bone morphogenic proteins (BMPs) has shown promise in enhancing tendon-bone healing. However, effective delivery strategies remain a challenge. This study describes the design, synthesis and evaluation in a murine model of a bisphosphonate (BP)-based delivery platform for localized targeting and release of a therapeutic BMP cargo.Feasibility was assessed using a previously reported bone imaging-probe (OFS-3) comprised of a bisphosphonate conjugated to a fluorescent dye, linked to an internal quencher via a peptide substrate of Cathepsin K (Ctsk). Male mice underwent Achilles tendon-to-bone repair or sham surgery, followed by local or systemic administration of OFS-3. Imaging was performed at regular intervals up to three weeks post-surgery. Both local and systemic administration of OFS-3 resulted in a localized fluorescent signal at the surgical site, peaking around postoperative day (POD) 7-10. Control groups showed no specific fluorescence, suggesting selective activation at sites where osteoclast Ctsk-activity is associated with bone resorption. Immunohistochemistry staining confirmed the presence of Ctsk-positive cells at early (POD 7) and late (POD 28) time points. Biomechanical testing of repaired hindlimbs receiving OFS-3 injections showed no differences compared to control repaired hindlimbs, indicating that the modified bisphosphonate did not interfere with osteoclast activity and that the delivery platform retained its targeted release function without hindering the healing process.A BP conjugate of BMP2 (BP-BMP2) was then constructed incorporating into the BP-drug linker, the same Ctsk-sensitive peptide sequence used in OFS-3. Evaluation in ATDC5 cells revealed that wt BMP2 and Ctsk-digested BP-BMP2, but not undigested BP-BMP2, stimulate BMP responsive element (BRE) expression in the cells. The results underline the promise of BP-BMP2 as a new approach to improving tendon-bone healing, specifically in the context of RCT repairs.

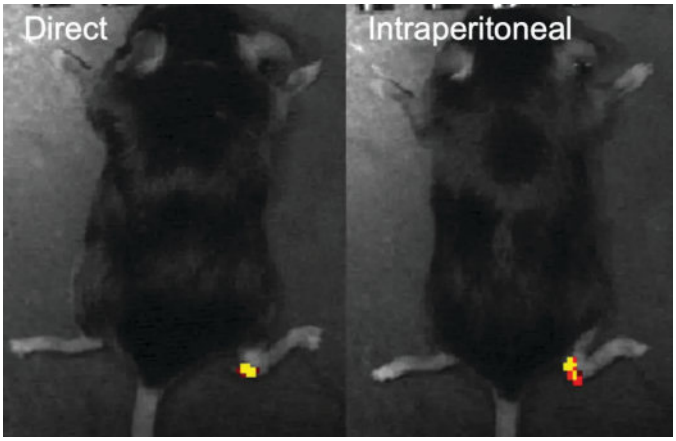

***Disclosures: Oskar Sundberg**, None*

SUN-249

Injectable Phase-Separated Tetra-Armed Polyethylene Glycol Hydrogel Scaffold Allows Sustained Release of Signaling Factors to Enhance the Repair of Cranial Bone Defects *Shant Nepal[1] Jinyan Si[1] Shohei Ishikawa[1] Hiroyuki Okada[1] Shinsuke Ohba[2] Ungil Chung[1] Takamasa Sakai[1] Hironori Hojo[1] [1]The University of Tokyo, Japan [2]Osaka University, Japan

As the global aging population continues to rise, so are the occurrences of bone injuries, including fractures and defects. While most fractures can naturally heal, nonunion fractures and irreversible bone loss require regenerative strategies. One strategy involves the use of biocompatible synthetic hydrogels as scaffolds and drug delivery systems. Previously, we reported the oligo-tetra-armed polyethylene glycol (PEG) hydrogel (oligo gel) to have low swelling, fast and efficient gelation at low polymer content (Hayashi et al., Nat.Biomed. Eng, 2017). We also reported that at low polymer content, tetra-armed PEG gels undergo gel-gel phase separation (GGPS) and provide bio-affinity (Ishikawa et al., arXiv:cond-mat. soft, 2022). Here, we investigated the oligo gel as a scaffold capable of loading and sustained release of signaling factors to enhance bone regeneration using in vitro and in vivo models. First, we assessed GGPS between low content oligo and conventional tetra-PEG gels (tetra gel). As turbidity was reported to be directly correlated with GGPS, we tested and found the oligo gel was significantly more turbid than the tetra gel. Furthermore, when immersed in a solution of hydrophobic microparticles, we observed a significantly higher number of particles adsorbed on the oligo gel than on the tetra gel. We concluded that the greater degree of GGPS occurring in the oligo gel resulted in more hydrophobic regions within its network. Since this may be advantageous when loading signaling factors or proteins, we then characterized the release profiles from the oligo gel and tetra gel using fluorescein-labeled BSA and rhBMP-2. The oligo gel could release both proteins at a slower, sustained rate compared to the tetra gel. This was further confirmed when applied to MC3T3-E1 osteoblast progenitors in vitro. Next, we applied the oligo and tetra gels loaded with rhBMP-2 to a mouse calvarial defect model. After 28 days, micro-CT of treated mice revealed the oligo gel had significantly enhanced bone regeneration, fully covering the defect with new bone, compared to the tetra gel. Immunohistochemistry further revealed the oligo gel-treated new bone had more expression of RUNX2, a master regulator of osteoblasts, suggesting the presence of more osteoblast progenitors compared to the tetra gel-treated new bone. To conclude, we demonstrated that the greater degree of GGPS allowed the oligo gel to sustain rhBMP-2 release and enhance the repair of cranial bone defects.

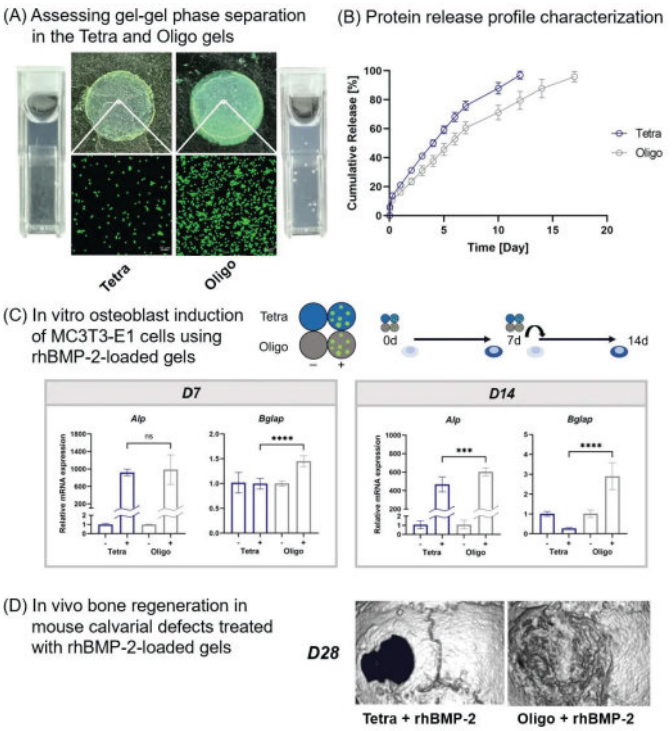

***Disclosures: Shant Nepal**, None*

SUN-251

Changes in skeletal muscle atrophy over time in a rat model of adenine-induced chronic kidney disease *Kento Okamoto[1] Yuji Kasukawa[1] Koji Nozaka[2] Hiroyuki Tsuchie[3] Daisuke Kudo[2] Hayato Kinoshita[2] yuichi Ono[2] Keita Oya[1] SHUN IGARASHI[4] Shuntaro Harata[4] Naohisa Miyakoshi[1] [1]Akita University Graduate School of Medicine, Japan [2]Department of Orthopedic Surgery, Akita University Graduate School of Medicine, Japan [3]Akita university graduate school of medecine, Japan [4], Japan

Purpose:Chronic kidney disease (CKD) causes muscle atrophy through several mechanisms, including the accumulation of uremic substances, insulin resistance, and mitochondrial dysfunction due to impaired renal function. Similarly, muscle atrophy occurs in CKD model rats, but the changes over time are unknown. In the present study, we investigated the changes over time in muscle atrophy, factors related to muscle differentiation and atrophy, and mitochondrial activity in an adenine-induced CKD rat model.Methods:Eight-week-old male Wistar rats were divided into a control group (n=7) with a normal diet for 4 weeks and a CKD group (n=7) with a diet containing 0.75% adenine for 4 weeks. The paraspinal and tibialis anterior muscles were harvested at 12 and 20 weeks of age. Paraspinal muscles were stained for ATPase and the mean cross-sectional areas of type 1 and type 2 muscle fibers were measured. Succinate dehydrogenase (SDH) staining density was measured and mitochondrial activity was assessed. RNA was extracted from the right tibialis anterior muscle, and the expression of PGC-1?, muscle regulatory factors (MyoD, myogenin), and atrogenes (atrogin-1, MuRF-1) were measured by real-time PCR.Results:Type 1 and type 2 muscle cross-sectional areas were significantly decreased in the 12-week CKD group versus the control group ($p<0.05$), while only type 2 muscle cross-sectional area was significantly decreased in the 20-week CKD group ($p<0.05$). SDH staining levels, which reflect mitochondrial activity, were also significantly lower in the 12-week CKD group vs. the control group ($p<0.05$), but there was no significant difference between the two groups at 20 weeks of age. The expression levels of atrogenes (Atrogin-1, MuRF-1) and myogenin were significantly increased ($p<0.05$) and MyoD was decreased ($p<0.05$) in the 12-week CKD group vs. the control group, but there were no significant differences in the expression of muscle regulatory factors or atrogenes at 20 weeks.Conclusion:In the adenine-induced CKD rat model, type 1 and type 2 muscle cross-sectional areas were decreased early after adenine administration, but type 1 muscle cross-sectional area recovered over time. This phenomenon is believed to involve a decrease in mitochondrial activity and an increase in atrogenes.

***Disclosures: Kento Okamoto**, None*

SUN-252

Schwann cells and skeletal stem/progenitor cells in periosteum drive fibrosis and congenital pseudarthrosis of the tibia in NF1 *Simon Perrin[1] Sanela Protic[1] Ingrid Laurendeau[2] Oriane Duchamp de Lageneste[1] Nicolas Panara[2] Cécile-Aurore Wotawa[1] Odile Ruckebusch[3] Marine Luka[4] Cécile Masson[5] Théodora Maillard[6] Stéphanie Pannier[7] Philippe Wicart[7] Smail Hadj-Rabia[8] Katarzyna Radomska[1] Mickael Ménager[4] Dominique Vidaud[6] Piotr Topilko[1] Béatrice Parfait[2] Céline Colnot[1] [1]Univ Paris Est Creteil, INSERM, IMRB, Creteil, France, France [2]INSERM UMR S1016, Institut Cochin, Université de Paris, Paris, France, France [3]Univ Paris Est Creteil, INSERM, IMRB, Plateforme de Cytométrie en flux, Creteil, France., France [4]Paris Cité University, Imagine Institute, Laboratory of Inflammatory Responses and Transcriptomic Networks in Diseases, Atip-Avenir Team, INSERM UMR 1163, Paris, France., France [5]Bioinformatics Core Facility, Institut Imagine-Structure Fe?de?rative de Recherche Necker, INSERM U1163 , France [6]Service de Médecine Génomique des Maladies de Système et d'Organe, Hôpital Cochin, DMU BioPhyGen, Assistance Publique-Hôpitaux de Paris, AP-HP, Centre-Université Paris Cité, F-75014 Paris, France, France [7]Department of Pediatric Orthopedic Surgery and Traumatology, Necker-Enfants Malades Hospital, AP-HP, Paris Cité University, Paris, France, France [8]Department of Dermatology, Reference Center for Rare Skin Diseases (MAGEC), Imagine Institute, Necker-Enfants Malades Hospital, AP-HP, Paris Cité University, Paris, France. , France

The periosteum, the outer layer of bones, is a crucial source of skeletal stem/progenitor cells (SSPCs) for bone healing. The role of periosteum in bone repair disorders is poorly understood but suspected in congenital pseudarthrosis of the tibia (CPT). CPT is a severe pathology marked by tibial bowing leading to spontaneous fractures and fibrous non-union. Half of CPT cases are linked to Neurofibromatosis type 1 (NF1), a genetic disorder caused by mutations in the NF1 gene, encoding the RAS negative regulator neurofibromin. NF1 is characterized by a wide range of symptoms, such as tumors (neurofibromas, NFBs), skin hyperpigmentation and skeletal manifestations, including CPT. While NF1 neurodermatological manifestations are known to arise from NF1 biallelic inactivation in Schwann cells and melanocytes, the cellular origin of CPT remains unknown. Recently, analysis of the Prss56-Nf1 KO mice, revealed that boundary-cap cells, a transient population of neural-crest derivatives, is the population responsible for both neurofibromas and skin hyperpigmentation (Radomska et al.). These results raised the question of a possible common cellular origin of NF1 neurodermatological and skeletal symptoms.In this study, we unraveled the cellular origin and pathogenic mechanisms of CPT through analyses of bone samples from 17 CPT patients and Prss56-Nf1 KO mice. We showed that CPT is associated with NF1 biallelic inactivation in human periosteum. SSPCs in pathological periosteum exhibit NF1 biallelic inactivation and a pro-fibrotic phenotype. We identified an increased proportion of pERK+ Schwann cells (SCs) in pathological periosteum. Overall, analyses of CPT patients revealed SSPCs and SCs as affected cell types in CPT. In parallel, we described the pseudarthrosis phenotype of Prss56-Nf1 KO mice, due to Nf1 loss in boundary cap-derived SSPCs and SCs in periosteum. Single nuclei analyses of the periosteum showed that Nf1 KO SSPCs fail to undergo chondrogenic differentiation leading to fibrogenic differentiation. More strikingly, we identify Nf1 KO SCs as the main driver of fibrotic accumulation in CPT as they acquire a pro-fibrotic function and promote fibrotic fate of wild-type SSPCs via TGF?. We demonstrate that TGF? inhibition prevents pseudarthrosis in Prss56-Nf1 KO mice. These results establish the pro-fibrotic role of boundary cap-derived SCs and SSPCs causing CPT in NF1. This study suggests new therapeutic strategies targeting SC-derived pro-fibrotic factors, including TGF?, for CPT.

***Disclosures: Simon Perrin**, None*

SUN-253

Impaired Fracture Healing in Mice with Targeted Disruption of the Claudin-11 Gene *Charles Rundle[1] Sheila Pourteymoor[1] Subburaman Mohan[1] [1]Jerry L. Pettis Memorial VA Medical Center, United States

The claudin multigene family encodes tetraspan membrane proteins that provide structural and functional components of tight junctions and play important roles in regulating paracellular permeability. However, recent investigations also support a role for the claudins in non-canonical intracellular signaling in bone and in other tissues. In previous studies, we demonstrated that targeted disruption of the Claudin-11 gene in mice significantly reduced the trabecular bone mass by influencing osteoblast-mediated bone formation.To determine whether Claudin-11 functions also mediate bone repair, we examined fracture healing during the endochondral bone formation phase of healing in Claudin-11 knockout and their corresponding wild-type control littermate mice. A standard closed femur fracture was produced in Claudin-11 knockout (n=7) and control (n=7) mice and fracture tissues were examined following four weeks of healing. Both male and female mice were used.Analysis of the fracture callus at four weeks of healing by microCT revealed no significant differences in fracture callus volume between Claudin-11 knockout and control mice. Histology analyses of fracture callus area in trichrome-stained sections, however, revealed that there was a reduced area of woven bone detected when normalized to callus area in Claudin-11 knockout mice compared to control mice (0.19 +/- 0.03 in knockouts vs 0.28 +/- 0.19 in controls, $P < 0.05$). Furthermore, there was a reduction in the number of osteoclasts detected by TRAP

staining in the total callus woven bone (113 +/- 33 in knockouts vs 176 +/- 69 in controls, $P < 0.05$). These observations are consistent with Claudin-11 regulation of both osteoblast and osteoclast development in callus bone formation at this stage of fracture repair. Further time course studies will address the mechanisms for impaired fracture healing in Claudin-11 knockout mice.

***Disclosures: Charles Rundle**, None*

SUN-254

Novel Role of lncRNA H19 in Osteoarthritis Subchondral Bone Remodeling and Treatment *Rongliang WANG[3], Babak Mehrjou[2], Dorsa Dehghan-Baniani[3], Michael Tim yun Ong[3], Hon Fai Chan[3], Gang Li[3], Paul K Chu[4], Wayne Yuk Wai Lee[5]. [3]The Chinese University of Hong Kong, China. [2] City University of Hong Kong, Hong Kong. [3]The Chinese University of Hong Kong, Hong Kong. [4]City University of Hong Kong, Hong Kong. [5]The Chinese University of Hong Kong; CUHK InnoHK Centres, Hong Kong

INTRODUCTION: Emerging evidence suggests that aberrant subchondral bone remodeling upon excessive mechanical loading might play important role in early onset of osteoarthritis (OA). A long non-coding RNA (lncRNA) H19 was reported to be associated with OA progression and regulate mechano-transduction at cellular level, however, its role in OA subchondral bone has not been reported. This study aimed to examine the relationship between H19 and OA subchondral bone remodeling, and to develop a novel strategy for OA treatment via targeting H19. METHODS: Subchondral bone were collected from patients with knee OA undergoing joint replacement surgery. Wild-type C57BL/6 mice and same genetic background transgenic mice with osteocyte-specific deletion of H19 (cKO) mice were used, and OA phenotype was induced by destabilization of the medial meniscus (DMM) surgery. To verify the effect of mechanical stimulation on osteocytes, MLO-Y4 cells were subjected to unidirectional fluid shear stress (FSS) followed by RNA sequencing analysis. We developed a specific gene-delivery system by combining Fe3O4 nanoparticles and metal-organic frameworks (MOFs) to form a magnetic MOFs (MMOFs) for the delivery of anti-H19 antisense oligonucleotides (ASOs) to the target site in the presence of external magnetic field. RESULTS: Human subchondral bones of end-stage OA had higher expression level of H19, which was associated with increased bone mass and more H19 expressing osteocytes. In wild-type mice, DMM surgery led to cartilage damage, subchondral sclerosis, and increased H19 expression in subchondral bone. On the contrary, cKO mice with H19 ablation were much less vulnerable to DMM induced OA phenotypic changes. In MLO-Y4 cells, H19 induced PI3K/AKT/GSK signaling activation and mediated osteocytic mechano-response upon FSS stimulation. Finally, MMOFs were successfully synthesized, and shown as an efficient delivery system with satisfactory distribution to the target site and effectiveness in terms of down-regulating H19 expression, which remarkably alleviated subchondral bone remodeling and OA phenotype. DISCUSSION: Our results provide new evidence that elevated H19 expression in osteocytes could contribute to the aberrant subchondral bone remodeling and subsequently cartilage damage in OA development. H19 appears to be required for osteocytic response to mechanical stimulation, and targeting H19 represents a promising new approach for OA treatment.

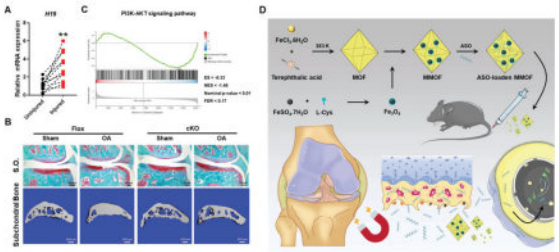

Figure 1. (A) The RNA expression of H19 in human bone samples through qPCR analysis. N=12 for each group. (B) Safranin-O/fast green of knee joint sections and 3D reconstruction of subchondral bone from Flox and cKO mice after DMM surgery. (C) GSEA showing the enrichment of PI3K-AKT signaling pathways in MLO-Y4 cells transfected with control and ASO after FSS stimulation. n = 4 per group. (D) Schematic illustration showed MMOF targeted on H19 inhibition in subchondral bone representing a novel and effective approach for OA treatment. *P < 0.05, **P < 0.01, Results are expressed as mean ± standard deviation (s.d.).

***Disclosures: Rongliang WANG**, None*

SUN-256

Explore the roles of PIEZO1 and YAP in promoting osteogenesis and angiogenesis of 3D-printed vascularized bone organoids under mechanical stimulations *Jia-Fwu Shyu[1], Tzu-Hui Chu[1], Yu-Chih Lo[1], Yi-Ting Lai[1], Yu-Min Tsai[1], Yu-Cheng Kang[1], En-Han Huang[1]. [1]National Defense Medical Center, Taiwan, Province of China

Mechanobiology is an emerging field investigating the translation of physical forces into molecular biological signals. These forces can greatly impact cell behavior, countering or synergizing with other cellular signals from soluble factors. Mechanical forces can stimulate cellular mechanosensors, such as the ion channel PIEZO1 and transcriptional co-activator YAP. These proteins regulate the metabolism of bone cells and remodeling. However, the regulation of PIEZO1 and YAP activity under mechanical stimulation in bone tissue is still unknown. In this proposal, we used compressive and fluidic stimulations to investigate the response of PIEZO1 and YAP in osteoblasts and endothelial cells. Using a 3D bioprinter, polycaprolactone was extruded to simulate the endosteum and trabecular bone. Seeding of osteoprogenitors on PCL was performed to fabricate bone orgaonid. GelMA hydrogels mixed with HUVECs were printed into a hollow tubule vessel structure. The vascularized bone organoid (VBO) was fabricated by insertion of artificial vessel into bone organoid. In the VBO dynamic culture under compression, results from Cell counting kit-8 assay showed viability and proliferation of both osteoblasts and HUVECs for over 28 days. Increased mineralization and bone formation in VBO were observed by Alizarin Red staining and Micro-CT analysis. Western blotting and RT-PCR showed increase expression of PIEZO1 and YAP. Increase immunofluorescence staining for CD31 by confocal microscopy indicated blood vessel formation. In addition, activators (Yoda1) and inhibitors (GsMTx4) of PIEZO1 were used for pharmacological studies of PIEZO1 signaling. It is hoped that these results may provide in-depth insight into mechanotransduction in bone tissue and new methods for treating bone diseases such as osteoporosis and bone fractures.

***Disclosures: Jia-Fwu Shyu**, None*

SUN-257

Neoangiogenesis at chondro-osseous Interfaces in Bone growth and Fracture healing is impaired in absence of Syndecan-1 *Richard Stange[1], Christian Arras[2], Nils Roters[3], Daniel Kronenberg[3], M. Gabriele Bixel[4], Ralf H. Adams[4], Melanie Timmen[3]. [1]University Hospital Muenster, Germany. [2]University Hospital Hamburg, Germany. [3]Institute of Musculoskeletal Medicine (IMM), University Hospital Munster, Germany. [4]Max-Planck-Institute for Molecular Biomedicine , Germany

Background: Neoangiogenesis drives the replacement of mineralized cartilage by trabecular bone during bone growth regulated by molecules like e.g. VEGF, OPG and RANKL. The Heparan sulfate proteoglycan Syndecan-1 (Sdc1) while interacting with VEGF and OPG, plays a role in the communication of osteoclasts and osteoblasts and in the development of blood vessels. To understand the function of Sdc1 in enchondral ossification we analysed bone structure and vessel development in bone growth and fracture healing in mice deficient in Sdc1.Methods: Femora of C57BL/6 WT (n=11) and Sdc1-/- (n=13) mice (male/female) were used for native bone analysis at 4 month age. Female mice (WT n=6-14, Sdc1-/- n=6-8, per time point) underwent midshaft femur fracture stabilized using an intramedullary nail and healed for up to 28 days. Bone structure was analysed using microCT scans with a resolution of 9µm. Fracture callus composition was quantified after Alcian Blue staining as callus area, fibrous tissue, cartilage and trabecular bone in 5µm thick slices. Vascularisation was visualised using an anti-Endomucin antibody in 80µm thick cryosections. Bone marrow isolates (WT/Sdc1-/-) were used to generate endothelial progenitor cells by sequential cultivation on fibronectin. Microvessel development was analysed 4h after plating on matrigel.Results: Bone structure in 4 month old male Sdc1 deficient mice was significantly reduced compare to age matched male WT, whereas female mice of both genotypes did not differ. Sdc1 deficient mice showed a significant less number of vessel buds at the chondro-osseous border at the growth plate at the age of 4 month compared to WT mice in male and female mice. During fracture healing, callus development was delayed with regard to cartilage area at day 7 and trabecular bone area at day 14. A decreased number of vessel buds invading at the borderline of cartilage to bone in the callus were counted in Sdc1 deficient callus tissue. Quantification of microvessel outgrowth of endothelial cells from bone marrow in matrigel revealed a decreased amount of sprouting, but increased length of microvessels of Sdc1-/- cells compared to WT.Conclusion: Syndecan-1 has a significant impact on neoangiogenesis at the chondro-osseous border of the native bone as well as during bone healing in the callus area. This emphasises the importance to further characterise the mechanism, how Syndecan-1 regulates the process of endothelial invasion during enchondral ossification.

***Disclosures: Richard Stange**, None*

SUN-258

Scaffold-based Approach to Regenerating the Cranial Suture Stem Cell Niche through Pore Design *BEN SWANSON[3], Lindsey Douglas[4], Seth Woodbury[4], Maiko Omi[3], Hwa Kyung Nam[4], Peter Ma[4], Nan Hatch[4], YUJI MISHINA[4, 3], . [4]University of Michigan, United States. [3], United States. [4]University of Michigan,

Craniosynostosis is a debilitating disease characterized by premature fusion of cranial bones, caused by depletion of the suture mesenchyme. Previously we reported that scaffold pore size controls differentiation and loss of stemness through YAP/TAZ modulation. Here, we developed a multicompartment scaffold that recapitulates the suture stem cell (SC) niche within engineered bone. We aimed to test the hypothesis that a triphasic scaffold with distinct regions of sufficiently small (S, SC-maintaining) pores sandwiched by large pores (L, favors differentiation), can maintain an SC niche in the bone microenvironment.Nanofibrous, macroporous scaffolds are fabricated from poly (L-lactic acid) by a sugar-sphere method. In a subcutaneous implantation model, CD31 IHC demonstrates the triphasic scaffold's ability to control vascularization, and picrosirus red analysis demonstrates control of ECM composition, regionally. These phenotype differences are more dramatic in center-seeded scaffolds compared to uniformly seeded. In vitro gene expression of primary BMSCs for SC markers indicates that center-seeded triphasic scaffolds have more remarkable maintenance of stemness in the S region versus uniform seeding, suggesting migration from the center to L-pores. We then co-seeded fluorescently labeled naïve and BMP-treated MSCs to either

the center or uniformly and monitored their migration over time to determine that differentiating, but not naïve, MSCs selectively migrate from the S-pores to the L-pores as soon as 48 hours, maintained up to 2 weeks. To further probe this phenomenon and the fate of SCs in the triphasic scaffold, we transplanted primary BMSCs isolated from tamoxifen-induced HoxA11Cre;TdTomato;Col1eGFP mice, seeded to the center region of triphasic scaffolds or monophasic large pore scaffolds, to a parietal bone defect and sacrificed at 2, 4, and 8 weeks. uCT demonstrates the triphasic scaffold's ability to resist bone formation in the center region compared to a large pore scaffold. Confocal microscopy traces the fate of red HoxA11+ SCs and their evolution of Col1eGFP signal. The exact mechanism of migration is still under investigation. Our evidence suggests that a triphasic tissue engineering scaffold can maintain a skeletal SC niche by differential modulation of cell fate. A tissue engineering approach is promising to reestablish the suture SC population to improve the efficacy of surgical craniectomies and re-establish skull growth.

***Disclosures: BEN SWANSON**, None*

SUN-259

Rapid Bone Regeneration via Mesenchymal Stem Cell Recruiting by Framework DNA Nanodevice *Taoran Tian[1], Xingyu Chen[1], Songhang Li[1], Yunfeng Lin[1]. [1]Sichuan University, China

On-site recruiting of endogenous stem cells is promising for eliminating insufficient sources and ethical/regulatory considerations. However, the scant of cell-recruiting devices with high specificity hampers the development of this strategy. Tetrahedral framework DNA nanostructure (tFNA) has been verified to be a potent tool for biomedical purposed-functionalization. To acquire an MSC-targeted binding, we modified the tFNA structure with mesenchymal stem cell (MSC) targeted aptamer Apt19S. The MSC binding tFNA nanodevice was then loaded onto the hyaluronic acid (HA) hydrogel to achieve on-site stem cell recruiting and rapid bone regeneration in craniofacial bone defects. The tFNA was first fabricated via a one-pot approach by annealing four single-strand DNA (ssDNA). Successful fabrication of the tFNA was verified by cryo-EM, DLS, and gel electrophoresis. One to three Apt19S were loaded onto the apexes of the tFNA (denoted as T1, T2, and T3 according to the number of Apt19S attached) to titrate the nanodevice with the best MSC binding affinity. Flow cytometry and laser confocal microscopy indicated that T3 acquired the maximum cell labeling efficiency. Hence, the T3 structure was selected as the MSC capture nanodevice. Further, the remaining apex of tFNA was modified with a thiol group, which could conjugate with the maleimide group on the modified HA strand. The nanodevice-loaded HA hydrogel was then denoted as HA-T3. Rat-derived MSC was cultured and applied to verify the MSC recruiting ability of the HA-T3 hydrogel by a transwell cell culture. With HA-T3 located at the lower chamber of the transwell dish, MSC in the upper chamber migrated and located more onto the siling of the bottom side. Once the MSC recruiting was established in vitro, we set two craniofacial bone defects to verify the efficiency of HA-T3 regarding bone regeneration. Rat skull defect and rat molar tooth extraction socket were created and filled with HA-T3 hydrogel. Animals were sacrificed after 8 weeks of healing. MSC-specialized BRDU staining verified the potent stem cell recruiting in the HA-T3-filled defects, and the enhanced bone regeneration was revealed via micro-CT evaluations. In conclusion, our research established a promising and novel MSC recruiting-facilitated bone regeneration approach. The tFNA-based nanodevice was proven to be a potent tool for the on-site recruiting of endogenous MSC. Further applications could be extended based on our current procedure.

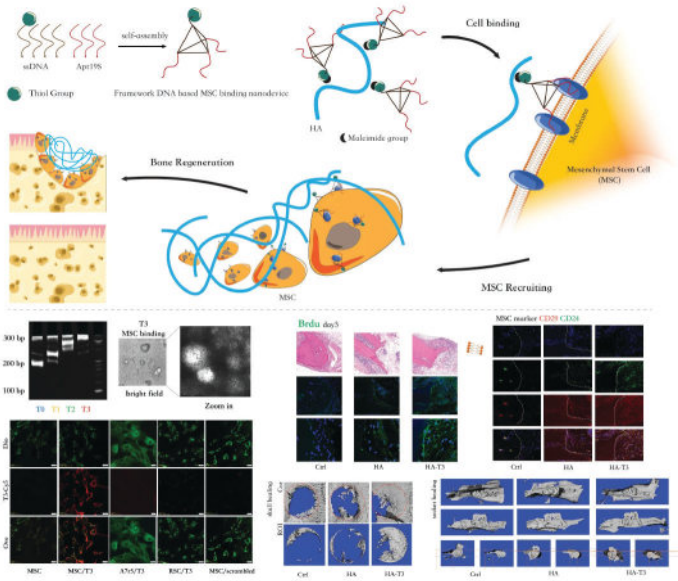

***Disclosures: Taoran Tian**, None*

SUN-260

Title: Mesenchymal cell derived VEGFC promotes lymphangiogenesis and aberrant repair following musculoskeletal injury *Neda Vishlaghi[1], Lei Guo[2], Danielle Griswold-Wheeler[3], Yuxiao Sun[4], Janna Crossley[5], Alec Bancroft[6], Sowmya Ramesh[1], Lin Xu[7], Aaron James[7], Robert Tower[7], Michael Dellinger[7], Benjamin Levi[7]. [1]postdoc, United States. [2]COMPUTATIONAL BIOLOGIST I, United States. [3]research tech I, United States. [4]Research scientist, United States. [5]Research Assistant II, United States. [6]Research Tech II, United States. [7]Professor, United States

Heterotopic ossification (HO) is the abnormal growth of bone that forms in non-skeletal tissues following musculoskeletal trauma. While the role of blood revascularization after a musculoskeletal injury has been well characterized, much less is known about the role of lymphatic vasculature in musculoskeletal tissues during homeostasis and after injury. The lymphatic vasculature is essential in transporting fluids, extravasated leukocytes, and antigen-presenting cells in normal and injured tissues. Here, we combine human HO samples with a mouse model of HO-forming tendon injury to determine the functional role of lymphatic vessels in regulating musculoskeletal injury and repair. Prox1eGFP reporter mice showed expansion of lymphatic vessels in human and mouse tissue following injury, driven by elevated levels of active VEGF-C (Vascular endothelial growth factor C) (4.93+/-0.81 vs. 1.76+/-0.13 in uninjured controls, $p<0.001$). Expansion of lymphatic vessels post-injury was also validated by LYVE1 and PDPN immunostaining. Single-cell transcriptomic analyses identified mesenchymal progenitor cells (MPCs) as one of the major sources of Vegfc, and enzymes known to activate Vegfc post-injury. Lineage-tracing of Vegfc-expressing cells with a novel Vegfcwt/CreERT2;R26wt/mTmG system identified a population of MPCs that underwent a significant expansion after injury and directly contributed to the formation of aberrant HO. Our data confirmed that Vegfc lineage cells were also positive for chondrocyte and osteoblast markers 7- and 21-days post-injury. Conditional ablation of Vegfc within MPCs leads to a significant decrease in lymphatic vessel density (17.89+/-4.76 mm2vs. 7.45+/-2.74 mm2in controls, $p<0.001$) and significantly decreases HO formation (2.06 +/- 0.85 mm3 vs. 3.32 +/- 0.66 mm3 in controls, $p<0.05$). Altogether, these data suggest that soft tissue trauma increases VEGF-C expression, particularly within injured tissue MPCs, contributing to this abnormal cell fate decision of MPCs and lymphatic vessel invasion. VEGF-C signaling inhibition at the time of injury may have therapeutic use in soft tissue trauma as a negative regulator of aberrant MPC differentiation and HO.

***Disclosures: Neda Vishlaghi**, None*

SUN-263

Scaffold With High Curvature Pores Promotes Segmental Bone Defect Repair by Regulating Skeletal Stem Cells *Liu Yang[1], Lin Minmin[1], Pan Yonghao[1], Liu Hongzhi[1], Chao Liu[1]. [1]Southern University of Science and Technology, China

Mechanotransduction of skeletal stem cells (SSCs) plays a crucial role in mediating angiogenesis-osteogenesis coupling in bone repair. However, approaches to regulate SSCs' mechanotransduction for the repair of large bone defects have been lacking. Our previous study identified that pores with high curvature could enhance the proliferation, migration, and osteogenic differentiation of osteoprogenitor cells. In this study, we aimed to investigate whether mechanobiological optimization of pore curvature in 3D scaffolds could regulate SSCs and improve bone regeneration in vivo. All animal procedures were approved by the Southern University of Science and Technology Animal Care and Use Committee. Experiments were performed on 16-week-old female C57BL6 mice (N=27) and Prx1-Cre; tdTomato mice (N=9). Two types of scaffold designs were used: octet truss and Kelvin cell. Subcutaneous implantation was performed to test biological compatibility. Scaffolds were implanted into 2 mm unilateral femoral segmental defects with external fixation. Defects without scaffold were used as controls. At 2, 4, and 8 weeks after surgery, femurs were imaged by micro-computed tomography (?-CT), SSCs and angiogenesis-osteogenesis coupling markers were measured by immunofluorescence staining, collagen fibers were imaged with second harmonic generation (SHG). We fabricated mechanobiological optimized scaffolds (Figure 1A). Octet truss had higher crack resistance and mechanical strength (Figure 1B). After 2 weeks of subcutaneous implantation, octet truss scaffold had the highest Osterix (OSX) and type H vessel volume. Octet truss also had a higher number of perivascular osteoblasts (OSX+) in proximity to type H vessels at the corner of the scaffold (Figure 1C). After 2 weeks in a segmental defect, octet truss group had more paired-related homeobox protein 1 (Prrx1) +, leptin Receptor (LepR)+, and Gli1+ cells within the defects (Figure 1D). Furthermore, the orientation of collagen fibers was aligned with the scaffold surface. Together, high pore curvature alone such as those in acute angles could increase the number of SSCs and promote segmental bone defect repair.

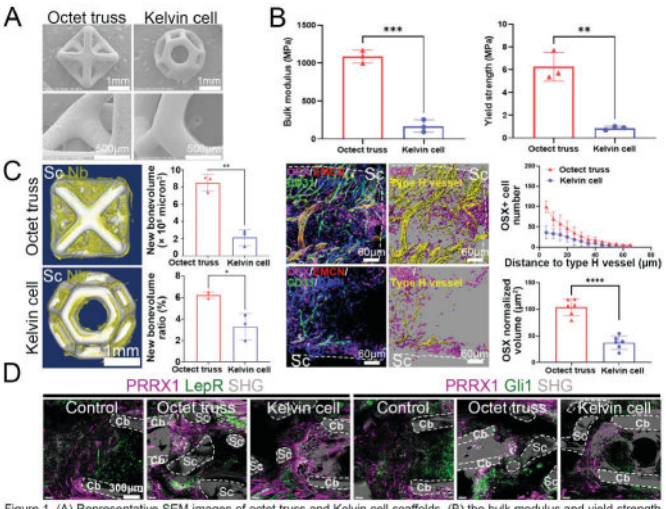

Figure 1. (A) Representative SEM images of octet truss and Kelvin cell scaffolds. (B) the bulk modulus and yield strength of octet truss and Kelvin cell scaffolds. (C) representative images and quantification results of μ-CT 2 weeks after subcutaneous implantation (scale bar = 60 μm), representative maximum intensity projections, 3D surface images and quantification results of OSX, EMCN, CD31 and DAPI immunofluorescence microscopy (scale bar = 60 μm) 2 weeks after subcutaneous implantation. (D) the immunofluorescence images of PRRX1, LepR, Gli1, and SHG in the segmental defects 2 weeks after implantation in femoral segmental defects. n = 3, *p < 0.05, **p < 0.01, ***p < 0.001, ****p < 0.0001. Sc: scaffold, Nb: new bone, Cb: cortical bone.

***Disclosures: Liu Yang**, None*

SUN-264

Nerve Growth Factor Receptor Limits Inflammation to Promote Remodeling and Repair of Osteoarthritic Joints *Lan Zhao[1], Yumei Lai[1], Jian Huang[1]. [1]Rush University Medical Center, United States

Osteoarthritis (OA) is a painful joint disease affecting more than 500 million people around the world. OA is currently incurable, and management of OA focuses on pain relief. Monoclonal antibodies against nerve growth factor (NGF), which had hold promise as a new class of analgesics to treat OA pain, were discontinued for their clinical development, due to joint safety events like rapid progressive osteoarthritis (RPOA) characterized as accelerated bone destruction in osteoarthritic joints. The mechanisms underlying this observation are elusive, and a possible explanation could be that inhibition of NGF signaling negatively regulates joint remodeling and stabilization during OA. However, it is largely unknown whether NGF signaling has a role in non-neuronal skeletal cells and joint pathophysiology. Here we report that nerve growth factor receptor (NGFR) has significant expressions in skeletal cells including chondrocytes and osteoblasts and plays an essential role in enhancing bony changes to stabilize osteoarthritic joints. Both NGF and NGFR were upregulated in both human and murine joints with OA. We generated NgfrAcan-CreER mice, and surgically induced OA. As skeletal progenitor cells (SPC) express Aggrecan, NGFR deficiency in multi-type joint skeletal cells (also the descendent cells of SPC), was continuously induced through weekly injection of tamoxifen during the course of OA progression. We found that NGFR loss-of-function in SPC and descendent osteochondral cells markedly reduced osteophyte growth by 36% and subchondral sclerosis by 21%, which are thought to be a spontaneous reaction of the diseased joints to repair and stabilize themselves during OA. Moreover, NGFR deficiency downregulated BMP-SMAD1 signaling in cultured skeletal cells and in joint tissues, and enhanced the production of RANKL and thus increased the ratio of RANKL/OPG, which promoted osteoclastogenesis and enhanced bone resorption, in the context of osteoarthritic conditions. Further, we found that NGFR loss-of-function exacerbated NF-?B activation induced by inflammatory cytokines like TNF-?, which may underlie weakened BMP-SMAD1 signaling and upregulated RANKL expression. Importantly, NGFR is also negatively associated with NF-?B activation in human OA cartilage. Together, our data suggested that NGFR plays an essential role in non-neuronal joint cells to restrict NF-?B signaling and thus to promote bony remodeling and stabilization of osteoarthritic joints.

***Disclosures: Lan Zhao**, None*

SUN-265

Notch Jagged1 Coating Enhances 3D-Printed Bone Scaffold Vascularization and Callus Formation *Qinqin Xu[1], Solitro Giovanni[1], Shane Barton[1], yufeng dong[2]. [1]LSU Health-Shreveport, United States. [2]Louisana State University,

Rapid angiogenesis and local vascular penetration are essential to deliver cells and growth factors that promote bone callus formation in large bone defect repair surgery. Although multiple cell signaling pathways are involved in regulation of vessel formation, increasing evidence shows that Jagged1 (JAG1)-mediated Notch signaling plays a crucial role in angiogenesis during development. However, it is unknown whether JAG1-mediated Notch activation could be used to enhance vascularization and bone formation during large bone defect repair. Therefore, in this study, 3D-printed biodegradable Polycaprolactone (PCL) scaffolds with similar biomechanical properties to real bone were coated with JAG1 protein or lgG (a control protein) and seeded with angiogenic endothelial stem cells (ESCs). Cell cultures were used to observe the JAG1-induced ESC vessel tube formation. Tetramethylbenzidine (TMB) assay was performed to monitor the controlled release of JAG1 from PCL scaffolds. Finally, a mouse bone defect model was used to test the in vivo repair ability of JAG1 and ESCs loaded scaffolds. Our results demonstrated that ESCs exposed to JAG1 in cultures resulted in a measurable increase of capillary tube formation with thicker tubes and more connections. TMB assay showed the JAG1 protein cross-linked on the surface of PCL scaffold could hold on to and slowly release JAG1 protein over 11 days and possibly even weeks. Histological assessment of transplanted PCL scaffolds showed bone callus formation surrounding the JAG1-coated scaffolds in the bone defect mouse model was significantly increased when compared to lgG- coated scaffolds at 8 weeks after surgery (Figure 1). More importantly, an enhanced expression of angiogenic markers vWF (Brown) and CD31(Green) was observed in the callus adjunct to JAG1-coated scaffolds at 2 weeks after surgery (Figure 1), suggesting that JAG1 induced rapid ESC angiogenic differentiation and local vascularization in these mice. Taken together, our results support the idea that JAG1 protein-coated PCL scaffold could be used as a novel bone substitute for rapid bone defect repair by enhancing ESC angiogenic differentiation/vascularization and subsequent bone callus formation.

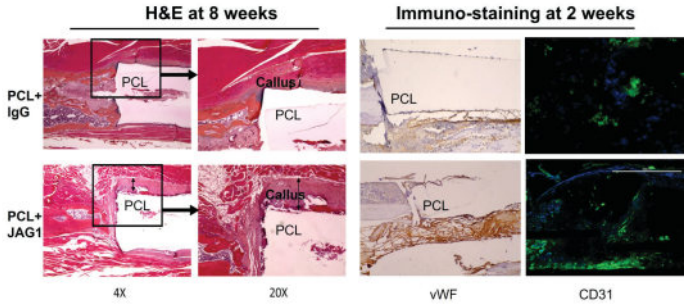

***Disclosures: Qinqin Xu**, None*

SUN-266

The critical role of gender and age in craniofacial bone healing: a microscopic and biochemical study utilizing 129Sv mice *Hagner Andrade[1], Nataira Momesso[2], Gustavo Simionato[2], Mariza Matsumoto[2], Claudia Biguetti[1]. [1]School of Podiatric Medicine, University of Texas Rio Grande Valley, United States. [2]School of Dentistry, São Paulo State University (UNESP), Brazil

Aging may contribute to slower bone healing in craniofacial bones, but there have been insufficient experimental studies that consider this phenomenon in conjunction with biological sex. The objective of this study was to analyze the effect of aging and biological sex on craniofacial bone features in 129Sv mice, as well as their impact on dental socket healing after tooth extraction. A total of 52 129Sv mice were utilized, with 28 being young (3-4 months) and 24 being aged (17-18 months), equally distributed by biological sex. After an upper right incisor extraction, mouse specimens were collected at 7, 14, and 21 days post-surgery for microtomographic (microCT) and comprehensive histological and immunohistochemical analysis. Mandible, skull bones, and maxillae at 21 days were analyzed by microCT, while blood plasma samples were collected to detect key bone turnover markers (P1NP and CTX-1) using enzyme-linked immunosorbent (ELISA) assay. Aged females depicted a significantly decreased fraction of bone mineralized content (BV/TV, %) in alveolar sockets in comparison to young females and aged males at day 7, and aged males at day 14 post tooth extraction. The mandible relative cortical area of aged females was also significantly decreased in comparison with young females. Histological evaluation by hematoxylin and eosin staining and Goldner trichrome revealed that all alveolar sockets healed at 21 days with inflammation resolution and deposition of new bone. In the histomorphometric analysis, B.Ar/T.Ar was significantly lower in aged females in comparison to young females at 14d, and in comparison to aged males at 21 days. Immunohistochemistry for TRAP revealed increased area density for osteoclasts in alveolar sockets of aged females (6.80+/-1.757) when compared to aged males (0.75+/-0.85) or young females (1.56+/-1.96) at 21 days. While a significant increase in CTX-1 levels was detected in the blood plasma of aged females when compared to young females, P1NP levels did not significantly change between young and older females. No significant changes were observed for males. In conclusion, this study demonstrated that age and gender can significantly affect craniofacial bones, especially the maxilla and mandible in females. Considering the altered bone resorption parameters and delayed alveolar bone healing in older female mice, careful deliberation is necessary during the development of pre-clinical models for craniofacial research.

***Disclosures: Hagner Andrade**, None*

SUN-267

Loss of Prdm16 in LepRCre-expressing cells and their descendants does not alter radiation-induced marrow adiposity *Kiana Gunn[1], Wendi Guo[1], Kassandra Spiller[1], Cahil Potnis[1], Colleen Wu[1]. [1]Department of Duke Orthopaedic Surgery, United States

Radiotherapy is received by over 50% of cancer patients as a curative or combinatorial treatment modality. However, an adverse outcome of radiotherapy is the structural weakening of nearby bone, which can lead to bone-related complications like radiation-induced fractures that negatively impact the quality of life of long-term survivors of disease. Radiotherapy induces dramatic changes within cells residing in the bone microenvironment including depleting osteoblasts and expanding marrow adipocytes. Drugs that target the bone remodeling unit are minimally effective in preventing fracture risk for this patient population; therefore, we seek to investigate the mechanisms driving radiation-induced marrow adipocyte expansion.The molecular mechanisms regulating marrow adiposity are poorly understood. Interestingly, gene expression studies show that marrow adipocytes express brown/beige adipocyte-specific markers such as Prdm16. Notably, Prdm16 is required for not only the development and function of brown/beige adipocytes, but also for the regulation of skeletal stem cell proliferation and differentiation. For these reasons, we sought to elucidate the contribution of Prdm16 within skeletal progenitor cells during radiation-induced marrow adipocyte expansion.For this purpose, we utilized the LepRCre driver, as LepRCre-expressing cells label a population of post-natal skeletal progenitor cells found in the bone marrow stroma. Indeed, consistent with previous studies, confocal analysis of LepRCre;Rosa26tdTomato/+ reporter mice revealed marrow adipocytes labeled by tdTomato. Next, we generated LepRCre(-) control and LepRCre;Prdm16fl/fl mutant mice and exposed both cohorts to 4Gy total body irradiation (TBI). qPCR analysis of bone marrow stromal cells revealed diminished Prdm16 mRNA levels in mutant mice when compared to controls demonstrating efficient Cre-mediated recombination, thus validating our murine model. MicroCT and histological analysis of long bones revealed that loss of Prdm16 in LepRCre-expressing cells and their descendants did not attenuate radiation-induced marrow adiposity. In summary, we have shown that loss of Prdm16 in LepRCre-expressing cells and their descendants does not influence adipose volume post-irradiation. This data expands our knowledge of the underlying cellular and molecular mechanisms of radiation-induced marrow adiposity.

***Disclosures: Kiana Gunn**, None*

SUN-268

The Role of Clec3b+ Muscle Cells in Fracture Healing and Heterotopic Ossification *JACOB MOORE[1], EZGI AYDIN[2], Ugur Ayturk[2, 1], . [2]Hospital for Special Surgery, United States

Loss of Clec3b expression results in impaired healing of bone, connective tissue and skin injuries. We previously generated a Clec3b.creERT2 knock-in allele and found that Clec3b+ cells are located in muscle, outer periosteum and connective tissues, and are completely absent in the marrow, endosteum or growth plate. Further, Clec3b+ cells are osteogenically inactive during skeletal development and remodeling, but can contribute to the healing of drill hole injury or BMP2-driven heterotopic ossification (HO).Our goal with the current study was to determine the specific cell types Clec3b+ cells can convert to in trauma situations, and whether these changes are physiologically significant. We induced stabilized long bone fractures in Clec3b.creERT2; Ai14.R26.tdTomato; Bglap.eGFP mice. Using scRNA-seq, flow cytometry and fluorescent histology, we confirmed that Clec3b-lineage cells become fibroblasts, chondrocytes, osteoblasts, osteocytes, and bone marrow stromal cells in the fracture callus. To determine whether these Clec3b-lineage cells arise from the muscle or periosteum, we performed periosteum removal and bone graft transplantation experiments. All results indicated that muscle-resident Clec3b+ cells are the predominant contributors to bone healing. To test the significance of these contributions, we ablated Clec3b+ cells in Clec3b.creERT2; R26.DTA mice during fracture healing. MicroCT analysis showed that Clec3b+ cell-depleted fracture calluses had less bone volume (BV) than same-sex, littermate controls ($p < 0.05$).To determine whether Clec3b+ cells also play a significant role in HO, we activated the Acvr1.Q207D mutation in Clec3b+ cells (which results in BMP-gain-of-function) and confirmed muscle mineralization with microCT. To test loss of function, we depleted Clec3b+ cells with the DTA allele after inducing HO by intramuscular BMP2-injection. Surprisingly, Clec3b+ cell depletion (confirmed by histology) did not reduce but instead increase ectopic bone volume (both TV and BV, $p < 0.05$). These data suggest that Clec3b+ cell apoptosis during HO stimulates bone formation by cells that do not undergo Cre-recombination, either due to inefficient Cre-activation or lack of Clec3b-expression.Overall, our data show that Clec3b+ interstitial muscle cells play significant roles in regenerative and pathologic bone formation processes. Studying the mechanisms regulating Clec3b+ cells can lead to new strategies to promote fracture healing and prevent HO.

***Disclosures: JACOB MOORE**, None*

SUN-270

Identification of LRP1+ human periosteal skeletal stem cells with distinct osteochondrogenic potentials *YOUNGJAE JEONG[1], Lorenzo Deveza[2], LAURA ORTINAU[3], John Dawson[2], Dongsu Park[2, 1], . [2]Baylor College of Medicine, United States. [3]University of Missouri-Columbia,

Human skeletal stem cells (SSCs) are essential for lifelong bone maintenance and repair, and their multipotent differentiation capability to bone, adipocyte, cartilage, and marrow stromal cells makes promising therapeutic options for degenerative bone disorder and bone defects. However, due to heterogeneity and lack of selective markers, it is challenging to identify and isolate rare SSCs. In particularly, the molecular characteristics, function, and regulation of human periosteal SSCs in bone regeneration and repair is not clearly elucidated. Here, using single cell sequencing of human periosteal tissues, we found that the human periosteum contains multiple progenitor clusters and two SSC clusters (PTHRP+ and PTHRP-) expressing known SSC markers, PDPN and CD13. In particular, human periosteal SSCs, but not bone marrow SSCs, have selective expression of a new marker, LRP1 with high expression of Wnt, Notch, and BMP pathway genes. Further, single cell, immunostaining, and FACS analyses of mouse periosteum revealed that Prx1+ mouse P-SSCs also selectively express LRP1. When cultured at single cell level, LRP1+ human P-SSCs are highly clonogenic and long-term repopulating cells with osteochondrogenic but little adipogenic differentiation abilities. Notably, these human P-SSCs reside in perivascular location of human periosteum and repopulate in vivo upon transplantation into immunocompromised mouse calvaria injury. Taken together, our study demonstrates that adult human periosteum contains unique osteochondrogenic stem and progenitor cell subsets and LRP1 is a unique novel marker for endogenous human and mouse P-SSC subsets.

***Disclosures: YOUNGJAE JEONG**, None*

SUN-272

Ctdnep1 deletion in the Cathepsin K-expressing progenitor in the tendons and periosteum causes osteochondroma *Takuto Konno[1], Chisato Sampei[2], YASUHIRO ARASAKI[2], Takashi Nakamura[3], Shigeaki Kato[4], Ryuichi Nishinakamura[5], Yoshinori Asou[6], Yoichi Ezura[7], Tadayoshi Hayata[8]. [1]Tokyo University of Science, Japan. [2], Japan. [3]Department of Biochemistry, Tokyo Dental College, Japan. [4]Iryo Sosei University, Japan. [5]Department of Kidney Development, Institute of Molecular Embryology and Genetics, Kumamoto University, Japan. [6]Tokyo Medical and Dental University, Japan. [7]Tokyo Medical and Dental University, Medical Research Insititute, Japan. [8]Graduate School of Pharmaceutical Sciences and Faculty of Pharmaceutical Science, Tokyo University of Science, Japan

Osteochondroma and fibrodysplasia ossificans progressiva with heterotopic bone and cartilage formation significantly reduce patients' quality of life due to pain and decreased range of motion in the lesion. Recently, cells labeled with Cathepsin K-Cre have been reported to exhibit stemness and ectopic ossification potential in the tendons and periosteum. However, it is not well understood how the ectopic ossification potential of Cathepsin K-Cre-positive cells is suppressed in vivo to maintain tendon and periosteal homeostasis. The CTD nuclear membrane phosphatase Ctdnep1 is a negative regulator of TGF-?/BMP signaling and plays an essential role in endochondral ossification and ovary and kidney homeostasis in mice. Somatic mutations in CTDNEP1 in humans also cause hyperphosphorylation of MYC and genomic instability, leading to medulloblastoma. However, the roles of Ctdnep1 in osteochondroma remain elusive. Here we show that Ctdnep1 suppresses excessive cell proliferation and heterotopic ossification in Cathepsin K-Cre-positive cells in the tendon and periosteum. Deletion of the Ctdnep1 gene in cells positive for Cathepsin K-Cre causes osteochondroma around joints of the ankles and wrists but not those of the knees and elbows. Cathepsin K-Cre; Ctdnep1 (flox/flox) mice showed a marked gait disturbance with a shorter body length and contractures of the wrist and ankle joints. Skeletal preparation showed cartilage masses around the wrist and ankle joints. Micro CT analysis revealed ectopic ossification with low bone mineral density. Histological analysis revealed bone marrow formation in the lesions, suggesting that ectopic endochondral ossification occurred. Gene expression analysis showed that the expression of marker genes for cartilage, tendon, and osteoclasts was significantly elevated in lesions. Furthermore, cell lineage analysis combining fluorescent reporter mice with the CUBIC tissue clearing technique revealed that osteochondromas originated from Cathepsin K-Cre-positive cells, which were positive for phosphorylated Smad2 and Sox9, suggesting that Cathepsin K-Cre-positive progenitor cells transdifferentiated into chondrocytes. Our results demonstrate that Ctdnep1 is a suppressor of transdifferentiation-mediated tumor development in Cathepsin K-Cre-positive progenitor cells in the tendon and periosteum.

***Disclosures: Takuto Konno**, None*

SUN-273

Periosteal CD51+ progenitor cells contribute to local healing *YE CAO[1], IVO KALAJZIC[2], Brya Matthews[3, 1], New Zealand, [2]University of Connecticut Health Center, United States, [3]University of Auckland, New Zealand

The periosteum is a major source of cells that contributes to fracture healing. However, complexity of the fracture model includes response of bone marrow derived skeletal stem/progenitor cells (SSPCs). In this study, we evaluated the response of periosteum and defined populations of periosteal injury-responsive SSPCs using a periosteum-specific scratch injury.Following injury, periosteal progenitors expanded by day 3 and formed fibrocartilage by day 7. Fibrocartilage was gradually replaced by new bone formation with marrow infiltration from day 14 to day 21. Bone and periosteum were remodeled, and healing was complete by day 28.We used multicolor spectral flow cytometry combined with ?SMACreER/tdTom/Col2.3GFP, a lineage tracing model of skeletal progenitors (?SMA+) and osteoblasts (Col2.3+). Within total periosteal CD45- cells, enrichment of ?SMA and CD90 cells was detected on day 3 (10.4% and 27.9%) and day 7 (28.0% and 36.0%) after injury compared with uninjured (3.4% and 17.9%). Markers of progenitors Sca1+CD51+, Sca1-CD51+ were expanded by 7 days after injury.Histologically, most periosteal Sca1 cells were located on the outer periosteum layer. They showed minimal expansion with injury. CD51 and CD90 cells were more abundant in the inner layer and expanded immediately with injury. In contrast with flow result, Sca1+CD51+ cells were rare in the periosteum in situ. Some CD51+ cells were Col2.3+ on day 14 following injury, indicating the contribution of CD51+ cells to osteoblasts.Periosteal Sca1+CD51+ cells were multipotent, and Sca1-CD51+ cells were committed osteoprogenitors in vitro. We further examined the in vivo lineage potential of Sca1-CD51+ and, Sca1+CD51+ cells by subcutaneous transplant. In contrast to the in vitro results, Sca1-CD51+ cells exhibited greater engraftment and more osteoblast formation than the other populations tested.Stimulation of Notch signalling enhances bone healing. Using ?SMACreNICD mice, which have increased Notch signalling in ?SMA+ cells, we found the frequency of CD51+ was tripled in NICD+ mice compared to controls, indicating that CD51+ cells may improve healing at early stages.In conclusion, periosteal Sca1-CD51+ and CD90+ cells are multipotent progenitors that respond rapidly to local injury in vivo. Enhanced bone healing is correlated with the rapid expansion of CD51+ osteoprogenitors.

***Disclosures: YE CAO**, None*

SUN-274

The role of BMP2 in periosteal cell behavior and appositional bone growth *Emily Moore[1], David Maridas[1], Laura Gamer[1], Gavin Chen[1], Ana Garcia Castineiras[1], Kathryn Burton[1], Vicki Rosen[1]. [1]Harvard School of Dental Medicine, United States

The periosteum contains stem/progenitor cells capable of differentiating into cells that contribute to bone growth and repair. Bone morphogenetic protein (BMP) signaling is central to the activation and differentiation of periosteal cells. Mice lacking periosteal BMP2 (Bmp2fl/fl;Prx1Cre) have significantly thinner bones as early as 2 weeks of age and are unable to initiate fracture repair. Here, we investigate the unique phenotype resulting from removal of BMP2 in periosteal lineage cells. Bulk RNAseq analysis of periosteum verified that osteogenesis and BMP signaling were downregulated in Bmp2fl/fl;Prx1Cre mice at birth, consistent with reduced periosteal activity. To further interrogate periosteal BMP signaling in appositional growth, we designed an ex vivo growth model. Briefly, femurs from P7 littermates were exposed to oscillatory fluid flow (FF) using a custom femur holder and platform rocker for 5 consecutive days. Bmp2fl/fl femurs were slightly longer compared to Bmp2fl/fl;Prx1Cre femurs under static conditions and FF did not influence length. Femurs from control mice widened significantly and BMP signaling was upregulated when FF was applied, but this behavior was lost in Bmp2fl/fl;Prx1Cre explants. Histological analysis revealed the cambium layer of the periosteum expanded, bone formation was enhanced, and BMP signaling was upregulated in the mid-diaphysis with FF in controls. The periosteal surface was comparatively inactive in Bmp2fl/fl;Prx1Cre femurs. To further investigate the role of BMP signaling in periosteal cell behavior, we generated a periosteum-derived cell line that expresses established periosteal markers, engages in BMP signaling, and differentiates into chondrocytes and osteoblasts. When treated with BMP2, these cells demonstrate accelerated osteogenic differentiation. We also confirmed these cells are mechanoresponsive using a custom chamber apparatus to apply FF. BMP signaling was not upregulated in response to FF, but Smad1 levels and Bmp2 mRNA expression significantly increased. We speculate that, in response to FF, periosteal cells are priming for BMP signaling to facilitate osteogenic differentiation. This work is the first to suggest a role for BMP signaling in periosteal cell mechanotransduction and we speculate that BMP2 is important for this process. Collectively, we anticipate that our bulk dataset and novel experimental tools will greatly advance our understanding of periosteal activity and subsequent bone formation.

***Disclosures: Emily Moore**, None*

SUN-277

AdipoQ lineage bone marrow progenitors are the major cellular source of M-CSF for bone marrow macrophage development, osteoclastogenesis and bone metabolism *Yongli Qin[1], Kazuki Inoue[1], Yuhan Xia[1], Jie Han[2], Ruoxi Yuan[3], Jun Sun[4], Ren Xu[2], Jean X. Jiang[5], Matthew B. Greenblatt[1], Baohong Zhao[1]. [1]Weill Cornell Medical College and Hospital for special surgery, United States, [2]The first Affiliated Hospital of Xiamen University, China, [3]Hospital for special surgery, United States, [4]Weill Cornell Medical College , United States, [5]University of Texas Health Science Center, United States

M-CSF, encoded by Csf1, is a critical growth factor for myeloid lineage cells, including monocytes, macrophages, and osteoclasts. Tissue-resident macrophages in most organs rely on local M-CSF. However, it is unclear what specific cells in the bone marrow produce M-CSF to maintain myeloid homeostasis. We performed an integrative scRNAseq analysis based on five published bone marrow scRNAseq datasets and human bone marrow scRNA-seq datasets. Although the current paradigm indicates osteoblasts as the main cellular source of M-CSF in bone marrow, we surprisingly found that the osteoblasts do not express Csf1 in vivo. In contrast, we identified that Adipoq-lineage (Adipoq+) bone marrow progenitor cells possess the predominant and highest Csf1 expression level in bone marrow. The Adipoq-lineage progenitors with high CSF1 expression also exist in human bone marrow. We further generated Csf1 conditional knock out (cKO) mice, in which Csf1 is specifically deleted in Adipoq+ cells by crossing Csf1flox/flox mice with Adipoq-cre mice (hereafter referred to as Csf1?Adipoq). Csf1 deficiency in Adipoq+ cells lead to a drastic decrease in bone marrow macrophages and a severe osteopetrotic phenotype in mice with significantly reduced osteoclast numbers and enhanced bone mass. Without exogenous M-CSF, RANKL is able to induce osteoclastogenesis in bone marrow harvested from the control mice, but not from Csf1?Adipoq bone marrow. These results further support an essential role for M-CSF secreted from Adipoq+ bone marrow cells in osteoclastogenesis in vivo. Interestingly, Csf1 is undetectable in other Adipoq highly expressed cells, including peripheral mature adipocytes or mature bone marrow adipocytes. Tissue macrophages in other organs appear normal in Csf1?Adipoq mice. Furthermore, the lack of the Adipoq+ cell-produced M-CSF prevented the estrogen-deficiency induced excessive osteoclast formation and osteoporosis, indicating a potential novel therapeutic strategy for postmenopausal bone loss by targeting M-CSF produced by Adipoq+ cells. Collectively, our data reveal a specifically high Csf1 expression feature of the Adipoq+ bone marrow progenitor cells. These cells constitute approximately only 0.05% of bone marrow cells, but are the major cellular source of M-CSF in bone marrow. These findings challenge the current paradigm and have profound implications for our understanding of bone marrow macrophage development, osteoclastogenesis, bone homeostasis, and pathological bone loss.

***Disclosures: Yongli Qin**, None*

SUN-278

EPDR1 Governs Metabolic and Immunologic Re-programming of Human Mesenchymal Stem Cells During Osteoblast Differentiation *Yadav Wagley[2], Tristan Maerz[2], James A. Pippin[3], Matthew C. Pahl[3], Alessandra Chesi[4], Andrew D. Wells[4], Struan Grant[5], Kurt Hankenson[2]. [2]University of Michigan, , [2]University of Michigan, United States, [3]Center for Spatial and Functional Genomics, United States, [4]Department of Pathology and Laboratory Medicine, United States, [5]Children s Hospital of Philadelphia / University of Pennsylvania, United States

EPDR1 is a novel human osteoblast regulatory gene previously identified by intersecting BMD GWAS datasets with promoter-focused Capture-C and ATAC-seq generated in differentiating human osteoblasts. Recently, we showed that the open chromatin region harboring the BMD variants rs1524068, rs6975644 and rs940347 functions as an osteoblast specific EPDR1 enhancer in hFOB1.19 cells. However, the precise molecular processes controlled by EPDR1 is unknown. Herein, we knocked-down EPDR1 expression in three unique bone-marrow derived human mesenchymal stem cell donor lines (hMSC) using small interfering RNA and evaluated the global transcriptomic changes with or without BMP2 stimulation using osteopermissive media. Globally, 3,861 genes were differentially regulated (1,888 upregulated and 1,973 downregulated) by BMP in non-targeted cells, whereas 2,744 genes were differentially regulated (1,528 upregulated and 1,216 downregulated) in EPDR1 silenced cells. As expected, genes associated with osteoblast differentiation, BMP signaling pathway, Notch signaling pathway and tissue morphogenesis were expressed in non-targeted cells; however, none of these biological processes achieved significance in EPDR1 silenced cells, suggesting major pathway perturbations. To understand these changes, we performed a donor-specific comparison with EPDR1-silenced cells. Of the ~2,300 genes differentially regulated, we observed an upregulation of genes related to inflammatory response, cytokine-mediated signaling pathway, and regulation of T cell activity, while genes related to cell division were decreased. Additionally, we observed differentially expressed genes enriched for pathways involved in regulation of fatty acid metabolic process, regulation of bone resorption, arachidonic acid metabolic process, negative regulation of collagen biosynthetic process and positive regulation of tumor necrosis factor, interferon-gamma, and interleukin-8 production upon BMP2 stimulation. The crystal-structure of EPDR1 protein suggests human EPDR1 folds into a dimer using a monomeric subunit consisting of a deep hydrophobic pocket to bind to hydrophobic fatty acids and function as a lipoprotein carrier. Since EPDR1 is a secreted protein, an immune-reactive profile driven by loss of EPDR1 could be metabolically mediated via disturbances in cellular lipoprotein and fatty acid trafficking. We

conclude that EPDR1 could play an important role in pathophysiological bone turnover later in life and therefore warrants further investigation.

***Disclosures: Yadav Wagley**, None*

SUN-279

In Vivo Tracking of Human Fetal Skeletal Stem Cell Lineage Dynamics at the Single Cell Level *Thomas Ambrosi[1], Rahul Sinha[2], Charles Chan[2]. [1]UC Davis, United States. [2]Stanford University, United States

With the increasing socioeconomic impact of skeletal disorders and the absence of reliable treatments, innovative approaches are required to prevent bone loss and restore skeletal tissues. Skeletal stem cells (SSCs) show great potential as a new therapeutic option; however, progress has been hindered by a lack of understanding regarding the identity and function of these cells in humans. Here, we utilized a combination of prospective flow cytometric isolation and SmartSeq2 single cell RNA-sequencing (scRNAseq) to interrogate the diversity of over 4,000 human SSCs from ten distinct skeletal sites at 20 weeks gestational age. In vivo tracing of lentivirally barcoded fetal human SSCs was combined with scRNA-seq readouts to assess unique clonal dynamics of human growth plate and periosteal SSCs. RNAscope was employed to map SSC subsets in situ. A xenograft model of fetal skeletal elements together with scRNAseq was used to further deconstruct the human SSC lineage tree in fetal long bones. Transcriptomic analysis of single fetal SSCs from distinct skeletal sites revealed diversity of SSCs tied to specialized features correlating with anatomical localization. Intriguingly, gene expression in specific types of SSCs residing in different bone regions was linked to skeletal phenotypes caused by genetic mutations. For example, XYLT1, a gene that if mutated leads to dwarfism, was highly expressed in growth plate SSCs but not cranial, periosteal, pelvic or vertebra SSCs, while SEC24D, a gene associated with craniosynostosis, was highly expressed in suture SSCs. Overall, we identified two major types of SSCs - an osteochondral SSC and a stromal SSC. We also found that growth plate and periosteal SSCs of long bones, representing examples of the two specialized SSC subtypes, presented with distinct clonal dynamics thereby differentially contributing to skeletal development. Functional and bioinformatic approaches highlighted that neither of the two SSC types were dispensable and that they tightly interacted to facilitate proper bone growth and maintenance. Lastly, index-sort analysis of prospectively isolated SSC lineage subsets was able to reconstruct stem cell dynamics and identify additional new subsets of specified, more committed skeletal lineage cell populations. In summary, our research provides novel insights into human skeletal stem cell biology and offers experimental vantage points to study skeletal development and disease at an unprecedented resolution.

***Disclosures: Thomas Ambrosi**, None*

SUN-280

Tryptophan metabolites 3-hydroxy-Kynurenine (3HK) and 3-Hydroxyanthranilic acid (3HAA) induce apoptosis and impede osteogenic differentiation of mesenchymal stem cells *Dima Alhamad[1], Shabiha Sultana[2], Ashley Ellingwood[3], Kyle Burkhart[3], Husam Bensreti[2], Wendy Bollag[4], Sadanand Fulzele[5], Carlos Isales[6], William Hill[7], Mark Hamrick[5], Meghan McGee-Lawrence[8]. [1]1Department of Cellular Biology and Anatomy, Medical College of Georgia at Augusta University, Augusta, GA, 2Graduate School, Augusta University Augusta GA, United States. [2]Department of Cellular Biology and Anatomy, Medical College of Georgia at Augusta University, Augusta, GA. Graduate School, Augusta University Augusta GA, United States. [3]Medical College of Georgia at Augusta University GA, United States. [4]Medical College of Georgia at Augusta University GA. Charlie Norwood VA Medical Center, Augusta, GA, United States. [5]Department of Cellular Biology and Anatomy, Medical College of Georgia at Augusta University, Augusta, GA. Medical College of Georgia at Augusta University GA, United States. [6]Medical College of Georgia at Augusta University GA. Department of Neuroscience & Regenerative Medicine, Medical College of Georgia at Augusta University, Augusta, GA, United States. [7]Charlie Norwood VA Medical Center, Augusta, GA. Department of Pathology, Medical University of South Carolina, Charleston, SC, United States. [8]Medical College of Georgia, Augusta University, United States

Mesenchymal stem cell (MSC) differentiation into osteoblasts is regulated through precise molecular mechanisms that are well positioned to impact bone phenotypes. With aging, both the number of MSCs and their differentiation potential into osteoblasts declines. Concurrently, inflammaging-driven mechanisms increase metabolism of tryptophan into kynurenine (Kyn), which we have previously shown is detrimental to osteoblastic bone formation both in vitro and in vivo. The aryl hydrocarbon receptor (AhR) is best known as a receptor for environmental toxicants, acting as a transcription factor which drives expression of metabolic enzymes such as cytochrome P450 family 1 subfamily A member 1 (CYP1A1). AhR has been reported to be activated by Kyn, but the extent to which other tryptophan metabolites further downstream in the Kyn pathway activate AhR signaling has not yet been tested.We obtained a luciferase reporter vector incorporating the canonical AhR response element (5'-GCGTG-3') and investigated activation of canonical AhR signaling by various tryptophan metabolites in the Kyn pathway. Of the nine compounds tested, only tryptophan, Kyn, and 3-hydroxy-Kyn (3HK) dose-dependently activated AhR transcriptional activity in C2C12 and ST2 mesenchymal cells, with 3HK being the most potent activator. Results were verified by qPCR for CYP1A1, and a time-course study revealed that CYP1A1 expression peaked after 3 hours of Kyn treatment. The metabolism of tryptophan to Kyn, and Kyn to 3HK was inhibited using pharmacological inhibitors of Indoleamine 2,3-dioxygenase (IDO) and Kyn-3-monooxygenase enzymes (KMO) enzymes. These experiments suggested that metabolites downstream of Kyn could mediate negative effects on MSCs. In fact, MTT and TUNEL assays demonstrated significant cell death following treatment of MSCs with 3HK and 3-Hydroxyanthranilic acid (3HAA). Interestingly, cell death was rescued upon scavenging reactive oxygen species with N-acetyl cysteine, suggesting that the mechanism of cell death was attributable to increased oxidative stress. With regards to bone formation activity, the differentiation of MSCs into matrix-producing osteoblasts was blunted upon the introduction of Kyn, 3HK and 3HAA into the osteogenic differentiation media. Together, these results suggest that several intermediate metabolites in the tryptophan-Kyn pathway impede the differentiation of MSCs into osteoblasts through inducing reactive oxygen species leading to apoptosis.

***Disclosures: Dima Alhamad**, None*

SUN-281

Effect of Abaloparatide and Teriparatide on Ctsk+ Periosteal Stem Cells and Cortical Responses *Dhairya Raval[1], Ruiying Chen[1], Dorothy Hu[1], Shawn Berry[1], Lama Alabdulaaly[1], Beate Lanske[2], Roland Baron[3], Francesca Gori[1]. [1]Harvard School of Dental Medicine, United States. [2]Radius Health, Inc., United States. [3]Harvard Medical School and School of Dental Medicine, United States

The periosteum contains a niche of stem cells and progenitors, which contributes to cortical expansion during growth, homeostasis and repair in adults, and responds to anabolic drugs. PTH(1-34) (Teriparatide, TPTD) and the PTHrP analog (Abaloparatide, ABL) are FDA-approved anabolic therapies for osteoporosis. Pre-clinical and clinical studies suggest however, that their influence on the periosteal surface somehow differ, with ABL exerting stronger effects than TPTD. Here we investigated whether ABL and TPTD regulate differentially the periosteal stem cell niche, focusing in particular on periosteal Ctsk+ cells, which include stem cells (PSCs) and non-stem progenitors (PP1 and PP2) and play an important role in periosteal biology. To this aim, 6 weeks old CtskCre;mTmG female mice, in which Ctsk+ cells are GFP+, were treated with vehicle, TPTD or ABL (40ug/kg/day, 5d/week) for 4 weeks. Ctsk+ PSCs, PP1 and PP2 cells were isolated and analyzed by flow cytometry. ABL increased significantly the % of the Ctsk+ PSC population (p=0.015), while TPTD did not significantly affect this stem cell population. While PP1 and PP2 cells were not significantly affected by either treatment, both treatments significantly favor their differentiation into osteo-chondro lineage cells (Lin-THY1.2+6C3-GFP+CD105+) (p=0.01). These data suggest that ABL leads to an accumulation of Ctsk+ PSCs and favor their differentiation, while TPTD favors Ctsk+ periosteal cell differentiation into the osteo-chondro-lineage, w/o affecting the PSC population. Dynamic histomorphometry analysis of cortical bone indicates that both treatments lead to a significant increase in periosteal MS/BS and periosteal BFR/BS. Confirming an increase in periosteal bone apposition, cortical TV and BV/TV, measured by mCT analysis, were significantly increased by both treatments, while cortical thickness was significantly increased only by ABL. Our data raise the possibility that Ctsk+ periosteal cells respond to both TPTD and ABL and that, at the dose of 40 ug/kg/day, ABL, but not TPTD treatment significantly increase the % of Ctsk+ periosteal stem cells. Further understanding of the effects of anabolic agents on periosteal stem cells may have clinical implications for fracture repair and the treatment of diseases associated with bone fragility.

***Disclosures: Dhairya Raval**, None*

SUN-282

Mitochondrial Metabolism Determines Mesenchymal Stem Cell Fate *CHEN YU[3], RUBENS SAUTCHUK JR[2], Roman Eliseev[3]. [3]University of Rochester, , [2], , [3]University of Rochester, United States

Aging-related changes in bone marrow stromal (a.k.a. mesenchymal stem) cells (BMSCs) shift cell fate away from osteogenesis and towards adipogenesis. The mechanism(s) underlying such changes are not completely understood. Mitochondria are important cell organelles that not only produce energy but also determine cell behavior by regulating metabolism, signaling, calcium homeostasis, apoptosis, and other cellular processes. We have previously shown that mitochondrial activation is important during osteogenesis of BMSCs. In aged bone tissue, we observed pathological opening of the mitochondrial permeability transition pore (mPTP) which leads to mitochondrial dysfunction, oxidative phosphorylation uncoupling, and cell death. Cyclophilin D (CypD) is a mitochondrial protein that facilitates opening of the mPTP. We found that CypD is downregulated during osteogenesis of BMSCs leading to lower mPTP activity and, thus, protecting mitochondria from dysfunction. On the other hand, we observed that during adipogenesis, BMSC alternative fate, cells significantly upregulate glycolysis and increase CypD expression and mPTP activity. Confocal imaging shows that mitochondrial morphology remains rounded and fragmented during this process (Figure). CypD gene, Ppif, promoter analysis reveals multiple binding sites for adipogenic C/EBP and inflammatory NF-?B transcription factors. Luciferase assay and ChIP-PCR analysis confirm C/EBP? as a transcriptional activator of CypD. NF-?B p65 translocates to the nucleus during adipogenesis and shows synergistic effect with C/EBP? in inducing Ppif expression, suggesting a potential link between 'inflammaging' and altered BMSC fate. In vitro CypD overexpression enhances, whereas CypD knockdown impairs adipogenesis.

Pharmacological inhibition of CypD by NIM811 also impairs adipogenesis in vitro. Prx-1Cre-mediated deletion of CypD in Ppiff/f mice decreases bone marrow fat in 13-month-old mice. Currently we are pursuing the effect of Prx1Cre-mediated CypD overexpression in mice. In summary, BMSCs maintain or upregulate CypD expression during adipogenesis leading to increased mPTP activity, activated glycolysis and low mitochondrial function, thus establishing a metabolic profile that appears to be favorable for adipogenic lineage. The overall goal of this study is to define the potential role of CypD/mPTP during BMSC adipogenesis, facilitating the understanding of stem cell fate determination and molecular mechanism of age-related bone loss.

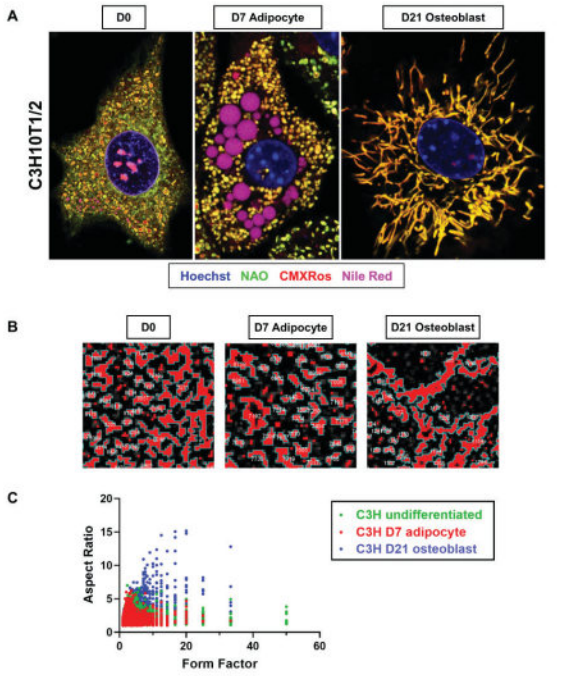

Figure. Mitochondrial network during osteogenesis and adipogenesis in C3H10T1/2.
A) Representative images of mitochondrial morphology in C3H/10T1/2 cells. Cells were cultured in adipogenic media for 7 days or osteogenic media for 21 days. After staining, images were taken by confocal microscopy at 63x magnification. B) Representative images of mitochondrial morphology analysis in C3H10T1/2. Analysis was performed with CMXRos staining using ImageJ. C) Quantification of mitochondrial morphology. For each group, three cells were randomly selected for analysis.

***Disclosures: CHEN YU**, None*

SUN-283

Effect of vitamin D on biochemical markers of bone turnover in people with prediabetes *Lisa Ceglia[1], Saul Malozowski[2], Richard Pratley[3], Irwin Brodsky[4], Erin Leblanc[5], Edith Angellotti[6], Jason Nelson[6], Ellen Vickery[6], Anastassios Pittas[6]. [1]Tufts Medical Center Tufts University, United States. [2]NIH, United States. [3]Advent Health, United States. [4]Maine Health, United States. [5]Kaiser Permanente, United States. [6]Tufts Medical Center, United States

Background: People with glucose intolerance have altered bone turnover, including diminished postprandial suppression of bone resorption. Whether vitamin D can impact bone turnover markers in people with prediabetes has not been studied.Objectives: To determine the effects of vitamin D3 4000 IU/d on 12-month changes in fasting and post-oral glucose tolerance test (OGTT) serum C-telopeptide (CTX) levels, fasting serum procollagen 1 intact N-terminal propeptide (P1NP) and osteocalcin (OC) levels, and fasting serum intact parathyroid hormone (PTH) levels in adults with prediabetes.Research design and methods: This is a post-hoc analysis in a subset of the vitamin D (n=274) and placebo (n=287) groups of the vitamin D and type 2 diabetes (D2d) study - a trial conducted to evaluate whether vitamin D3 lowers risk of diabetes in people with prediabetes. Participants were included in the analysis if they had a baseline and 12-month 75-gram OGTT begun before 9am (to avoid diurnal variation effects on bone turnover) and did not have either a fracture or exposure to osteoporosis drug therapy. Serum was collected at 0', 30', and 120' after the glucose load. Results: At baseline, 41% were women, mean+/-SD age was 59+/-9 y, hemoglobin A1c was 5.9+/-0.2%, and serum 25-hydroxyvitamin D (25OHD) was 28.0+/-9.5 ng/mL. Baseline characteristics of the two groups did not differ. Serum 25OHD increased by a mean 24.3 ng/mL [95%CI 23.1,25.5] with vitamin D vs. 0.2 ng/mL [-1.0,1.4] with placebo at 12 months. PTH levels decreased in response to vitamin D (-3.9 pg/mL [-5.4,-2.5] with vitamin D vs. 0.7 pg/mL [-0.7,2.1] with placebo). CTX rose over 12 mo in both groups, but with >90% power to detect a 15% group difference, we found no statistically significant differences in % change in fasting CTX (6.3% [0.2,12.3] with vitamin D vs. 6.6% [0.6,12.6] with placebo) or in the area under the CTX curve post-OGTT (CTXAUC) (24.2% [-13.6,61.9] with vitamin D vs. 31.2% [-6.4,68.7] with placebo), with or without adjustment for age, gender, race, and baseline calcium intake, 25OHD, and CTX. A subgroup analysis of those aged >=60 y also showed no significant differences between groups. Twelve-month changes in serum P1NP and OC did not differ significantly by group.Conclusion: In a relatively healthy population of people with prediabetes, 4,000 IU/d of vitamin D3 raised 25OHD and lowered PTH levels but had no significant effect on circulating bone turnover markers.

***Disclosures: Lisa Ceglia**, None*

SUN-284

Protein Intake by Source and Longitudinal Measures of Bone Strength at the Distal Radius and Tibia *Lisa Langsetmo[1], Sameneh Farsijani[2], Nicole M Sekel[2], Aarohee P Fulay[2], Jane A. Cauley[3], Kristine Ensrud[4], John Schousboe[5], Andrew Burghardt[6], James M Shikany[7]. [1]Minneapolis VA Medical Center, United States. [2]University of Pittsburgh, United States. [3]UNIVERSITY OF PITTSBURGH, United States. [4]University of Minnesota and Minneapolis VA Health Care System, United States. [5]Park Nicollet Clinic HealthPartners Institute University of Minnesota, . [6]University of California, San Francisco, United States. [7]University of Alabama at Birmingham, United States

We have shown in cross-sectional analysis that dietary protein intake (by source) among older men is associated with high resolution peripheral quantitative computed tomography (HR-pQCT) parameters. It is unclear whether these associations persist over time. Our aim was to assess whether the dietary intake of protein (by source) is related to both baseline and follow-up measures of estimated failure load, as assessed by HR-pQCT, among Osteoporotic Fractures in Men (MrOS) study participants. Men were included who had food frequency questionnaire total energy intake (TEI) between 500 and 5000 kcal/d at visit 4 (2014 -16) and repeat distal radius or tibia HR-pQCT scans at visit 4 and visit 5 an average of 5.9 years later (2019 -22). Two-dimensional registration was used to ensure common region of interest. We used mixed effect regression models to determine the association between protein intake (expressed as % of TEI) and failure load at baseline and follow-up, with both exposure and outcome modeled as continuous variables. Models were adjusted for age, race/ethnicity, visit, center, TEI, education, limb length, smoking, alcohol intake, physical activity level, corticosteroid use, supplement use (calcium and vitamin D), and osteoporosis medications. The study sample included 166 eligible men with mean (SD) age 83.2 (3.2) y, mean TEI of 1505 kcal/d (16.3% protein), and mean (SD) failure load of 6690 (1809) kN at visit 4. In fully adjusted models, non-dairy animal protein and plant protein were not associated with failure load of the distal radius or tibia. There was a consistent positive association between dairy protein and longitudinal HR-pQCT measures of failure load, which was statistically significant for both skeletal sites. While there was no statistically significant association of dietary protein by source with longitudinal change in failure load, there was also no evidence of attenuation of the cross-sectional association over time. In conclusion, higher dairy protein intake was associated with failure load consistent with previous findings and this association persisted among survivors almost 6 years after initial assessment of protein intake.

	Failure Load (kN)	
	Distal Radius	Distal Tibia
Dairy Protein	591 (135, 1047)	997 (25, 1968)
Non-Dairy Animal Protein	83 (-226, 392)	-112 (-758, 535)
Plant Protein	-8 (-526, 511)	122 (-988, 1232)

Adjusted for age, race/ethnicity, center, visit, education, limb length, smoking, alcohol intake, physical activity level, corticosteroid use, supplement use (calcium and vitamin D), and osteoporosis medications.

Beta-coefficient is increase in failure load per SD=3.0% of total protein intake.

***Disclosures: Lisa Langsetmo**, None*

SUN-285

Increased conversion of 25(OH)D to 1,25(OH)2D: A critical requirement for the maintenance of optimal status of active vitamin D metabolite in the context of vitamin D deficiency *Sudhaker Rao[1], Shijing Qiu[1]. [1]Henry Ford Hospital, United States

The active vitamin D metabolite, 1?,25-dihydroxyvitamin D (1,25(OH)2D), is converted from its substrate, 25-hydroxyvitamin D (25(OH)D). This process implicates a positive correlation existing between 25(OH)D and 1,25(OH)2D levels. However, it has been found that many healthy individuals suffering from 25(OH)D deficiency have optimal 1,25(OH)2D levels. The underlying mechanism(s) is not clearly understood.In the current study we examined serum levels of 25-(OH)D, 1,25-(OH)2D, serum corrected calcium (CCa), Creatinine (Cr), and parathyroid hormone (PTH) in 46 heathy women aged 21-73 years. The conversion rate of 25(OH)D to 1,25-(OH)2D was calculated by the ratio of the two metabolites (1,25(OH)2D/25(OH)D). To reveal the percent conversion rate (%), we transformed the unit of measurement for 1,25(OH)2D from pg to ng. The differences in 25(OH)D, 1,25-(OH)2D and 1,25(OH)2D/25(OH)D were compared between subjects with and without vitamin D deficiency (25(OH)D <20 ng/mL) using student t test. In addition, the relationships of CCa, Cr and PTH with 25(OH)D, 1,25-(OH)2D and 1,25(OH)2D/25(OH)D were analyzed using Spearman's correlation coefficient.Among the 46 white women, 28 (61%) with 25(OH)D deficiency (<30 ng/mL). The distribution of dot plots in figure 1 indicated that 1,25(OH)2D/25(OH)D decreased with increasing 25(OH)D levels. Table 1 showed that BMI, 1,25(OH)2D/25(OH)D and PTH were significantly higher in subjects

with 25(OH)D deficiency than in those with 25(OH)D sufficiency. However, there were no significant differences in 1,25(OH)2D, CCa and Cr between the 2 groups. Both BMI and PTH were significantly negatively associated with 25(OH)D levels but positively associated with 1,25(OH)2D/25(OH)D ratio.The results indicated that 1,25(OH)2D level was not significantly decreased in healthy subjects with vitamin D (25(OH)D) deficiency. However, the conversion rate of 25(OH)D to 1,25(OH)2D is likely to increase with decreasing 25(OH) D levels. The potential mechanism is that the lower 25(OH)D levels stimulate PTH secretion, which promotes the conversion of 25(OH)D to 1,25(OH)2D. Since 1,25(OH)2D is the hormonally active vitamin D metabolite, its optimal levels may play a crucial role in the maintenance of mineral homeostasis and skeletal health, even in the context of vitamin D deficiency. Alternatively, the product inhibition of conversion may promote higher conversion rate in the presence of vitamin D deficiency.

Tabble 1. Comparison of age, BMI and biochemical variables between white women with deficient and optimal vitamin D levels

Group	25(OH)D (<30 ng) (n = 28)	25(OH)D (≥30 ng) (n = 18)	p
Age (years)	54.9 (14.1)	54.8 (14.1)	0.787
BMI	27.9 (5.73)	24.7 (3.71)	0.022
$1,25(OH)_2D$ (pg/mL)	34.0 (12.8)	31.4 (8.88	0.424
$1,25(OH)_2D/25(OH)D$ (%)	0.164 (0.072)	0.091 (0.030)	<0.001
Corrected Calcium (mg/dL)	9.44 (0.434)	9.36 (0.524)	0.549
Creatitine (mg/dL)	1.07 (0.186)	1.08 (0.165)	0.822
PTH (pg/mL)	34.8 (10.1)	27.6 (5.90)	0.004

Fig 1.Conversion rate of 25(OH)D to 1,25(OH)2D in white women with deficient and optimal vitamin D levels

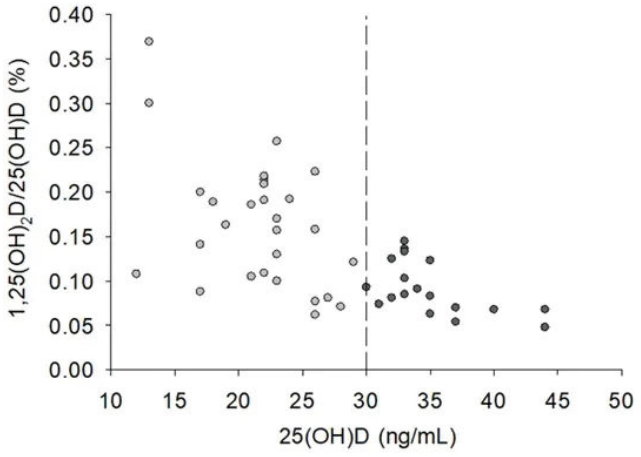

***Disclosures: Sudhaker Rao**, None*

SUN-286

Effect of GIP and GLP-1 infusion on bone resorption in adults with glucose intolerant, pancreatic insufficient cystic fibrosis *Wang Shin Lei[1], XianYan Chen[1], Lingyu Zhao[1], Bradley Phillips[1], Michael Rickels[2], Andrea Kelly[3], Joseph Kindler[4]. [1]University of Georgia, United States. [2]University of Pennsylvania Perelman School of Medicine, United States. [3]The Children's Hospital of Philadelphia, United States. [4]The University of Georgia, United States

Diabetes and bone disease are common complications of cystic fibrosis (CF) in which they primarily occur alongside exocrine pancreatic insufficiency (PI). Gut-derived "incretin" hormones, gastric inhibitory polypeptide (GIP) and glucagon-like peptide 1 (GLP-1), augment postprandial insulin secretion. In CF, PI dampens incretin response and loss of the insulinotropic effect of GIP was recently identified. Since GIP decreases bone resorption, we aimed to determine if GIP-mediated suppression of bone resorption is preserved in individuals with PI-CF. We performed a secondary analysis of specimens from a double-blinded randomized placebo-controlled crossover trial in adults ages 18-40 years (n=22) with PI-CF that determined effects of intravenous infusion of incretins on pancreatic ?-cell response. Subjects were assigned to receive either GIP (4 pmol/kg/min) or GLP-1 (1.5 pmol/kg/min) infusion, along with a placebo infusion completed on a separate day. Three healthy adults without CF also completed testing during GIP and placebo infusions. Serum C-terminal telopeptide (CTX), a biomarker of bone resorption, was assessed before (mins -5 to 0) and during (mins 30 to 80) infusion. CTX incremental area under the curve (iAUC) during infusions was calculated. Effects of incretin infusion on CTX were tested using two-way repeated measures ANOVA with random effects for subject and subject by treatment interaction. CTX decreased significantly under the GIP vs saline condition in PI-CF (time by treatment interaction p<0.01; Fig. 1A). Although the time by treatment interaction was not significant in the three healthy adults (p=0.23), CTX decreased significantly during GIP infusion (p=0.03) but not saline infusion (p=0.50). In PI-CF, CTX-iAUC during GIP infusion was significantly negatively correlated with BMI (r=-0.69, p<0.05) and forced vital capacity (r=-0.64, p<0.05), and marginally negatively correlated with age (r=0.48, p=0.16) and forced expiratory volume (r=-0.58, p=0.08). GLP-1 did not affect CTX (Fig. 1B). These results suggest that the bone anti-resorptive effect of GIP is preserved in PI-CF. We were not powered to test differences between adults with PI-CF and controls, but our results indicate that the effect of GIP infusion on bone resorption might be moderated by nutrition status, pulmonary function, and age. Since the incretin response is perturbed in PI-CF, involvement of the "gut-bone axis" in CF-related bone disease requires further attention.

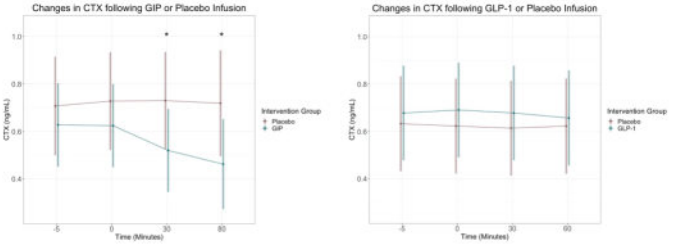

Fig. 1. CTX response to GIP (left) and GLP-1 (right) infusion in adults with PI-CF. Blue circles/bars represent the GIP/GLP-1 infusion and red circles/bars represent placebo (saline) infusion. Data are presented as means and 95% confidence intervals. *Corresponding timepoint during GIP/GLP-1 infusion differs significantly from min -5. CTX, carboxy-terminal collagen crosslinks; GIP, glucose-dependent insulinotropic polypeptide; GLP-1, glucagon-like peptide 1.

***Disclosures: Wang Shin Lei**, None*

SUN-288

Daily Prune Intake, Bone Turnover Markers, and Bone Balance Are Associated with Changes in Bone Mineral Density in Postmenopausal Women: The Prune Study *Ana Carla C Salamunes[1], Janhavi Damani[1], Nancy I Williams[1], Connie M Weaver[2], Connie J Rogers[3], Cindy H Nakatsu[4], Mary Jane De Souza[1]. [1]Pennsylvania State University, United States. [2]San Diego State University, United States. [3]University of Georgia, United States. [4]Purdue University, United States

Background: The Prune Study (NCT02822378) is a 12-month randomized controlled trial (RCT) that investigated the effects of daily prune intake on bone health outcomes in postmenopausal women. We have previously reported that the daily intake of 50g of prunes preserved hip bone mineral density (BMD) (AJCN, 2022). In this analysis of the Prune Study, we aimed to determine (1) if changes in BMD were associated with changes in bone turnover markers (BTM), and (2) if bone balance (BB), calculated using algorithms (Bieglmayer et al., EJCI, 2009), was predictive of changes in BMD. Methods: Postmenopausal women were randomized into three study groups (SG): control group (n=78), 50g/day prune intake (n=79), and 100g/day prune intake (n=78). Dual-Energy X-Ray Absorptiometry scans assessed total body, total hip, femoral neck, and lumbar spine BMD. Fasted blood samples were obtained to assess serum levels of procollagen-1 intact N-terminal propeptide (P1NP) and C-terminal telopeptide (CTX). Changes in BMD and BTM are expressed as percent change from baseline to 12 months (%chg) in completers only (control group n=70, 50g n=67, 100g n=46). Median serum P1NP and CTX from healthy postmenopausal women (BMD T-scores >-1.0 at baseline) were used as the healthy reference values for the estimation of multiple of medians of bone formation (MOMf) and resorption (MOMr), calculated individually. BB was calculated as the ratio MOMf/MOMr at baseline and after 12 months. Subjects whose ratio was >=1 were categorized as in positive BB, <1 categorized as in negative BB. General linear models were fitted to predict %chg BMD, with SG and BB category as fixed factors, and P1NP and CTX as covariates. Results: %chg total hip BMD was higher (p=0.027) in the 50g group compared to the control group. %chg total body BMD was higher (p=0.040), in the positive BB group at 12 months, compared to the negative BB group with no SG effects. SG (p=0.018), BB category at 12 months (p=0.002), and %chg P1NP (p=0.009) were significant predictors of %chg in hip BMD (R2=0.12), with negative effects of control group and negative BB. %chg CTX was a significant predictor of %chg in lumbar spine BMD (p=0.038), but no SG or BB category effects were observed. No effects of intervention group, BB category, or BTM were observed for %chg in femoral neck BMD. Conclusion: BB and %chg P1NP, along with prune intake, have significant effects on %chg hip BMD. BB is a useful indicator of 12-month %chg in hip BMD.

***Disclosures: Ana Carla C Salamunes**, None*

SUN-289

Centers for Medicare & Medicaid Services of USA issues reminders to use 25-OH Testing Wisely. *Ravinder Singh[1]. [1]Professor, United States

We will use 25-OH vitamin D Testing as a case example and educate the attendees about the impact of the changes in reimbursement on practice. The clinical use of the ordering of Vitamin D testing has become very controversial. It has been used as a general screening tool to use this test in only very serious diseases. CMS now restricts its use for only rare disease situations; The measurement of 25(OH) Vitamin D levels will only be considered medically reasonable and necessary for patients with any of the following conditions: Chronic kidney disease stage III or greater. Hypercalcemia, Hypocalcemia, Hyperparathyroidism, Hypoparathyroidism, Osteomalacia, Osteoporosis, Osteopenia, Rickets, Vitamin D deficiency to monitor the efficacy of replacement therapy, Malabsorption states, Cirrhosis (biliary, hepatic), Tuberculosis, Histoplasmosis, Coccidioidomycosis, Berylliosis, Follicular lymphoma, Immunodeficiency with predominantly antibody defects, Sarcoidosis, Hyperalimentation, Cystic fibrosis, Inflammatory Bowel Disease (Crohn's, Ulcerative Colitis), Radiation enteritis, Liver cirrhosis, Psoriasis, Systemic Lupus Erythematosus, Myositis , Obesity, Bariatric surgery, Long-term use of medications known to lower vitamin D levels. To receive payment documentation of this diagnosis is an essential requirement. 1,25 dihydroxy vitamin D has also been misordered and will not be anymore reimbursed by the CMS.

***Disclosures: Ravinder Singh**, None*

SUN-290

Vitamin D Metabolites are Associated with Overuse Musculoskeletal and Bone Stress Injury in Young Adults *Alexander Carswell[1], Thomas O'Leary[2], Paul Swinton[3], Sarah Jackson[2], Jonathan Tang[1], Samuel Oliver[4], Rachel Izard[5], Neil Walsh[6], William Fraser[1], Julie Greeves[2]. [1]University of East Anglia, United Kingdom. [2]Army Health and Performance Research, United Kingdom. [3]Robert Gordon University, United Kingdom. [4]Bangor University, United Kingdom. [5]Defence Science and Technology, United Kingdom. [6]Liverpool John Moores University, United Kingdom

The relationship between vitamin D metabolites and overuse injury is unclear. In a prospective cohort study, we investigated the association between vitamin D metabolites and incidence of lower body (pelvis and lower limb) overuse musculoskeletal and bone stress injury in young adults undergoing 12 weeks of initial military training during all seasons. In 1637 male and 530 female recruits (age, 22.6 +/- 7.5 years; BMI, 24.0 +/- 2.6 kg·m-2; 94.3% white ethnicity), we measured serum 25-hydroxyvitamin D (25(OH)D) and 24,25-dihydroxyvitamin D (24,25(OH)2D) by high-performance liquid chromatography tandem mass spectrometry, and 1,25-dihydroxyvitamin D (1,25(OH)2D) by immunoassay during week 1 of training. We used logistic regression to examine whether vitamin D metabolites were associated with overuse injury, including analysis of whether the relationship between 25(OH)D and 1,25(OH)2D:24,25(OH)2D ratio (with participants categorised into clusters) was associated with overuse injury. During training, 21.0% sustained >=1 overuse musculoskeletal injury, and 5.6% sustained >=1 bone stress injury. After controlling for sex, BMI, 2.4 km run time, smoking, bone injury history, and Army training course (Officer, standard, or Infantry), lower body overuse musculoskeletal injury incidence was higher for participants within the second lowest versus highest quartile of 24,25(OH)2D (OR: 1.62 [95%CI 1.13-2.32; P = 0.009]; 3.2-5.1 versus 7.7-29.6 nmol·L-1) and lowest versus highest cluster of 25(OH)D and 1,25(OH)2D:24,25(OH)2D (OR: 6.30 [95%CI 1.89-21.2; P = 0.003]; 6.9-38.5 nmol·L-1 and 125-307 versus 107.2-222.5 nmol·L-1 and 6-32). Lower body bone stress injury incidence was higher for participants within the lowest versus highest quartile of 24,25(OH)2D (OR: 4.02 [95%CI 1.82-8.87; P < 0.001]; 0.4-3.1 versus 7.7-29.6 nmol·L-1) and lowest versus highest cluster of 25(OH)D and 1,25(OH)2D:24,25(OH)2D (OR: 22.08 [95%CI 3.26-149.4; P = 0.001]), after controlling for the same covariates. Greater conversion of 25(OH)D to 24,25(OH)2D, relative to 1,25(OH)2D (i.e., low 1,25(OH)2D:24,25(OH)2D), and higher serum 24,25(OH)2D were associated with a lower incidence of lower body overuse musculoskeletal and bone stress injury. Serum 24,25(OH)2D may have a role in preventing overuse injury in young adults undertaking arduous physical training. Whether supplementation with vitamin D or its metabolites can decrease 1,25(OH)2D:24,25(OH)2D, and reduce the incidence of overuse injury is unknown.

***Disclosures: Alexander Carswell**, None*

SUN-292

Virtual Spatial Representation of scRNAseq Data Obtained from Human Articular Cartilage *David Rowe[1], Heather Swahn[2], Martin Lotz[3], Dong-Gulk Shin[4]. [1]University of Connecticut Health, United States. [2]Scripps Research, United States. [3]Scripps Institute, United States. [4]University of Connecticut, United States

Imaging the proliferation and maturation of different cell lineages within skeletal models of tissue formation and regeneration play an important role in understanding the cell and molecular mechanisms that control these biological processes. EdU and histone-marking strategies have provided valuable insights, but these technologies have limitations for in vivo marking and lineage tracing. The AurkbCreER mouse was originally developed by the D. Li laboratory (PMID: 32929201) for soft tissue imaging. We obtained this tamoxifen-activated mitosis reporter of the aurora kinase B (Aurkb) gene to evaluate its utility for models important to the skeletal biologist. Three different applications were evaluated. (1) Growth plate: Weaning mice were injected with tamoxifen a at 3-4 weeks of age and followed from 1 to 24 days while receiving a injection of calcein 1 day prior to sacrifice. This protocol labeled very few cells in the resting zone but did label occasion cells in the proliferative zone and many cells in the metaphyseal zone. No activity was observed in the articular cartilage nor in osteocytes under these labeling conditions. Concurrent stains for TRAP and AP distinguished the labeled cells as osteoclasts or osteoblasts. (2) Transplantation: BMSC progenitor cells were implanted in a calvarial defect model, and the recipient mice injected with tamoxifen 1 day after implantation. The implants were harvested at 7, 14 and 21 days post implant while receiving an injection of calcein 1 day prior to sacrifice. Imaging the implanted bone nodule that developed within the defect space clearly distinguished host and donor osteoblastic cells. (3) Cell culture: Mature transgenic mice were injected with tamoxifen 1 day prior to harvesting the bone marrow for osteoblast nodule and osteoclast culture. Time lapse video were recorded to capture the early formation of each cell type, while the transgene expression in a terminal osteoclast culture augmented the clarity of the cell border of the mature osteoclast. Although further characterization of this imaging model will be required, we envision that the reporter line will be valuable when combined with spatial techniques (CODEX and MERFISH) for identifying the precise cell identity of the cell expressing the progeny cell of a in both tissue section and primary cell culture systems.

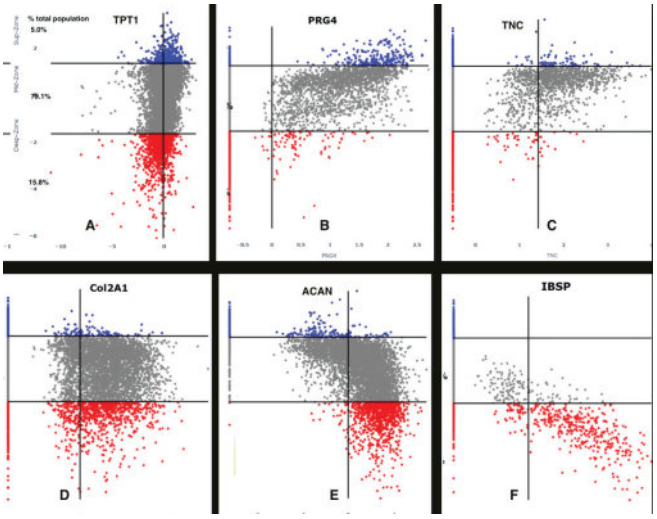

***Disclosures: David Rowe**, None*

SUN-294

Rare Coding Variant in SERT is Associated with Improved Bone Mass in Mice and Humans *Emily Larson[1], Hillary Larson[1], Eric Orwoll[2], Robert Klein[1]. [1]Veterans Affairs Portland Health Care System, United States. [2]Oregon Health & Science University, United States

Common susceptibility loci thus far identified by genome-wide association studies (GWAS) account for a small proportion of the estimated genetic heritability of bone mineral density (BMD). One explanation for the missing heritability is the existence of less common variants with larger biological effects that are poorly detected by GWAS. We hypothesized that genes contributing to biological pathways that regulate BMD could be identified by studying subjects at the phenotypic extremes for BMD. Subjects from the Osteoporotic Fractures in Men Study (MrOS) with the lowest total hip BMD (N =?98) and highest BMD (N =?110) were selected for exome sequencing. We observed an amino-terminal-localized Gly56Ala substitution (rs6355) in the serotonin transporter (SERT or SLC6A4) with a minor allele frequency 4-fold higher in the high BMD pool (4.1%) compared to the low BMD pool (1%). In the entire MrOS European-American population (n=5,008) associations between rs6355 and total hip BMD (maf 1.8%; ? = 0.31; p = 5x10-5) and femoral neck BMD (maf 1.8%, ?= 0.29; p = 1x10-4) were again confirmed. Inspection of the GEFOS Femoral Neck BMD 2012 Data Release provided concordant support for this variant (maf 2.4%; ? = 0.06; p = 0.014). To further explore this novel association, we examined SERT Ala56 mouse knock-in mice (provided by R. Blakely, Florida Atlantic University). Compared to wild-type Gly56Gly littermates, male SERT Ala56Ala knock-in mice demonstrated increased whole body (3.3%; p < 0.01) and femoral (3.3%; p < 0.01) BMD and greater resistance to 3-point bending (12%; p < 0.001). In contrast, no genotype-dependent effect on any skeletal parameter was observed in female SERT Ala56Ala knock-in mice. The rs6355 variant has been demonstrated to exhibit tonic elevation of serotonin (5-HT) transport activity in transfected cells and human lymphoblasts in vitro and when examined in a SERT Ala56 knock-in mouse model leads to an increased 5-HT clearance rate in vivo, along with altered sensitivity to SERT regulatory signaling pathways. The mechanisms whereby this variant results in the acquisition and/or maintenance of increased bone mass are unclear, but our results in both

mice and humans suggest that serotonin signaling is involved in skeletal physiology and manipulating this pathway is a potential target for the treatment of osteoporosis.

***Disclosures: Emily Larson**, None*

SUN-295

A comprehensive single cell transcriptomic atlas of adult human bone marrow *Michael Duffy[3], Shovik Bandyopadhyay[2], Kyung Jin Ahn[2], Kai Tan[2], Ling Qin[3]. [3]University of Pennsylvania, . [2]Children's Hospital of Philadelphia, United States. [3]University of Pennsylvania, United States

Bone marrow (BM) is primarily made of mesenchymal and hematopoietic lineage cells to provide mechanical support and produce blood. While mouse BM has been characterized at the single cell level, the rareness of mesenchymal cells in human BM aspirate has led to a lack of heterogeneity in scRNA-seq datasets and hindered human studies. Here, we developed a robust protocol to enzymatically isolate cells from fresh femoral head BM acquired after total hip arthroplasty. We separately enriched non-hematopoietic (CD45 depletion) and hematopoietic progenitor (CD34 selection) cells and then mixed them with RBC-depleted BM cells at 10:3:3 ratio for scRNA-seq using 10x genomics. From 12 samples (age 52-74, median 65+/-8), we profiled 53,417 hematopoietic and 29,325 non-hematopoietic cells at 3117 genes/cell and identified 35 cell clusters (Fig 1) of hematopoietic (25), mesenchymal (7), endothelial (2), and smooth muscle cells (1). Further analyzing 6 groups of mesenchymal cells, Fibro-mesenchymal stromal cells (MSCs), Osteofibro-MSCs, Osteo-MSCs, Osteoblasts, Adipo-MSCs, and THY1+ MSCs, with distinct markers, only Fibro-MSCs, marked by HAS1, DPT, and PDPN, expressed canonical mesenchymal stem markers and were identified as the most primitive population by CytoTRACE. Contributing a variable proportion of mesenchymal cells (52% +/- 31%, mean +/- SD), THY1+ and Adipo-MSCs highly expressed adipogenic markers. However, THY1+ MSCs had a unique expression profile including THY1 and LBP, and a high CytoTRACE score. We designed a flow panel to sort Fibro-, Thy1+-, Osteo-, and Adipo-MSCs. Fibro-MSCs showed the highest CFU-F forming ability and maintained the highest proliferative status over the long term culture, followed by THY1-MSCs, while Osteo- and Adipo-MSCs grew poorly. Fibro-MSCs also differentiated into osteogenic and adiopogenic cells efficiently in culture, confirming their stem and progenitor properties. CellChat analysis revealed that Adipo- and Thy1+-MSCs produce the highest amount of CXCL12 and KITL to regulate HSPCs and specifically express IL7 to regluate lymphopoiesis. Csf1, a major melopoiesis cytokine, was expressed in Adipo-MSCs, and Notch ligands, which are also important for lymphopoiesis, were mainly produced by arteriol endothelial cells. Together, our work presents a first comphrehensive cellular atlas of adult human bone marrow, identifies a new primitive MSC population, and reveals the importance of adipoprecursors in supporting hematopoeitic function.

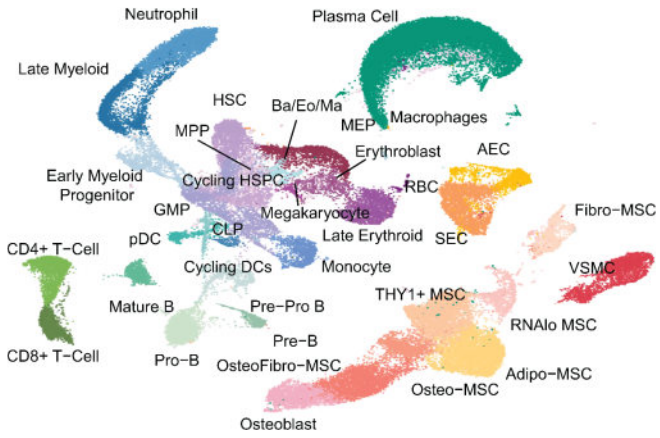

***Disclosures: Michael Duffy**, None*

SUN-297

Genetic Variants Associated with Lower Sclerostin Expression are Strongly Associated with Bone Physiology but not with Cardiovascular Events *James Staley[3], Gill Holdsworth[3], Jen Timoshanko[3], Alison Wolfreys[3], Cesar Libanati[3], Martin Armstrong[3]. [3]UCB Pharma, United Kingdom. [3]UCB Pharma, United States. [3]UCB Pharma, Belgium

Inhibition of sclerostin has been shown to increase bone formation and decrease bone resorption. Romosozumab (Romo), a sclerostin inhibitor, significantly increased bone mineral density and reduced fractures in postmenopausal osteoporosis (FRAME1 & ARCH2 trials). An increase in cardiovascular (CV) serious adverse events has been observed in Romo-treated patients compared to alendronate (ARCH).Genetic approaches such as phenome wide association studies and Mendelian Randomisation allow naturally occurring common genetic variation within a population to be used as a surrogate for the action of a drug, providing supporting data to predict both efficacy and on-target safety profiles. To explore the observations relating to Romo use, researchers have investigated genetic variants associated with lifelong reduced sclerostin expression and their associations with phenotypes, including those related to bone physiology and CV events and risk factors, in large-scale population datasets.In all analyses across research groups, genetically predicted lower sclerostin expression had strong positive effects on bone physiology, including lower lifetime risk of fractures and osteoporosis. There were, however, discrepancies in the results relating to CV events and risk factors between research groups. In our analyses3, we confirmed that variants associated with lower sclerostin expression were associated with phenotypes related to bone physiology but found no association with any phenotypes relating to CV events and risk factors. Other researchers have, however, published evidence linking genetically lower sclerostin expression with increased risk for some CV events, utilising similar data and statistical approaches.We reviewed the evidence and found that inappropriate adjustment for correlation between variants in some analyses (this issue was also raised by Holm et al.4) has led to inflated results of increased CV risk that have been overinterpreted. We also updated our genetic analyses using the latest data, including recently released sclerostin expression and CV event datasets, and the results broadly align with those we found previously. On balance, as a body of work, these investigations provide compelling evidence that genetically lower sclerostin expression is strongly associated with bone physiology, but not CV events.1Cosman NEJM 2016;375:1532-1543; 2Saag NEJM 2017;377:1417-1427; 3Holdsworth JBMR 2021;36:1326-1339; 4Hólm Sci Transl Med 2021;13:eabe8497

***Disclosures: James Staley**, UCB Pharma, Other Financial or Material Support*

SUN-298

Large-Scale Integration of Human Bone Proteomics, Circulating Proteomics and Genetics to Discover Molecular Pathways and Risk Factors of Osteoporotic Fractures *Yi-Hsiang Hsu[1], Sjur Reppe[2], Fangtang Yu[3], Xue Zeng[4], Ming-Ju Tsai[3], Ronald Kwon[5], Kaare Gautvik[2]. [1]HSL Institute for Aging Research, Harvard Medical School, United States. [2]Oslo Univ. Hosp., Oslo, Norway, Norway. [3]HSL Marcus Institute for Aging Research , United States. [4]Amgen, United States. [5]University of Washington, United States

Despite significant progress being made in mapping the basic blueprints (DNA variants) of human diseases, we have yet to comprehensively decipher the myriad end products (proteins) contributing towards these diseases. Thus, proteomics is an emerging tool and a deeper view of proteome alterations in bone tissues from fractures will advance our understanding of molecular pathways and enhance new drug target discovery. In addition, identifying circulating protein biomarkers allows us to identify high risk subjects of fractures. Two proteomics studies were conducted. (1) Bone proteomics was measured by mass spectrometry on human hip bone biopsies from 180 hospitalized adults due to hip replacement surgeries. The whole genome seq was done and DXA FNBMD was measured at non-fracture hip. (2) Serum (circulating) proteomics was measured by OLINK immunoassays in 48,000 UK Biobank subjects. Incident osteoporotic fractures were assessed via eHR. Among them, 237 had osteoporotic fractures and 5,217 had DXA BMD. In both studies, differential protein expression analyses were performed w/wo adjusting for BMD to identify proteins contributing to fractures independently from BMD. Mendelian randomization (MR) analyses were performed to inference causally relations. We observed 6,154 proteins from hip bone biopsies. 198 (88 higher and 110 lower expressed) proteins significantly differentially expressed ($p < 1.7x10-5$) in fracture subjects comparing to controls. These proteins are enriched in terpenoids biosynthesis, ECM-receptors, cytokine-ligand-receptor interactions and TGF-beta, NFKB, PPAR signaling pathways. For example, SOST, VKDPs and EFEMP1 are associated with increased fracture risks. COL6A1, osteoadherin and osteopontin are associated with decreased risks. MR analyses adjusted for BMD identified proteins (e.g. CA2, EIF3I, EFEMP1) associated with fractures independently from BMD. For circulating proteomics, 2,941 proteins were measured. 81 (69 higher and 12 lower expressed) proteins significantly associated with incident osteoporotic fracture (e.g. SOST, GDF15, IL6). In conclusion, we identified novel proteins causally associated with osteoporotic fracture from hip bone biopsies. Not all the fracture-associated proteins observed in bone biopsies could be observed in circulating (plasma); thus, our finding provided tissue-specific molecular insights underlying osteoporotic fractures. We also identified novel circulating proteins predicating risks of incident fractures.

***Disclosures: Yi-Hsiang Hsu**, None*

SUN-299

Exploration of Deep Learning for Automated Segmentation of the Trabecular Compartment of the Mouse Vertebral Body in Micro-Computed Tomography Images *Michael David[1], Veronica Butler[2], Douglas Adams[2]. [1]University of CO Anschutz, United States. [2]University of Colorado, United States

Automated micro-computed tomography (microCT) image segmentation of the trabecular compartment within the rodent vertebral body has been difficult to achieve. Despite a relatively high degree of success in automating this segmentation in long bones, the complexity in spinal anatomy and variation across rodent strains and between vertebral levels has slowed similar approaches for the spine. In this study, we developed a deep learning (DL) model with a U-Net framework to explore the utility of DL-based automation of this segmentation task. To maximize variation in vertebral anatomy for the DL model training

and eventual utility, we used 4th lumbar vertebra microCT images acquired from Diversity Outbred (DO) mice and the 8 founder inbred strains comprising the DO, as well as a subset of these mice following PTH treatment (N = 36, male & female). Following routine microCT scanning (70 kVp, 200 µA, 2000 projections,10 µm discretization), the transverse plane's desired trabecular compartment mask was selected via manual contouring. Each paired serial 2D mask and raw image (~170/vertebra) was imported into Python for DL model development. We used standard protocols for model development, including data scaling (min-max), 22/6/8 train/validate/test splitting, data augmentation (rotation and Gaussian blur), and evaluation metrics (dice score; 0 is poor segmentation, and 1 is perfect). Bone volume fraction and slice-by-slice Tb.Th and Tb.Ar were quantified using BoneJ (ImageJ). On the test set, our DL model accurately segmented the trabecular mask (dice score = 0.92), with resulting bone morphometry metrics being highly correlated (r >= 0.8) between DL and manual segmentation (Fig. 1A). Evaluating the model's performance slice-by-slice highlights the DL model's consistent ability to produce accurate segmentation (dice scores = ~0.88 - 0.95), while also revealing segmentation errors that may occur across a spectrum of anatomical variation (Fig. 1B and 1C). Qualitatively, the errors arise in regions with sparse trabecular architecture and within the posterior region when it resembles vertebral body anatomy (Fig. 1C), which might be eliminated by omitting this anatomical region from the DL model. DL model accuracy may also be improved by developing strain-specific models and increasing the training sample size. Ultimately, our DL model is a first step towards implementing automated high-throughput segmentation of the trabecular compartment of any mouse vertebral body.

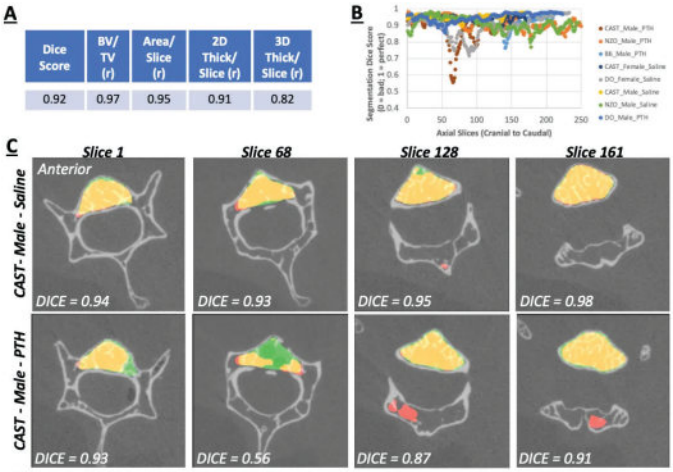

Figure 1. (A) DL model performs well on the test set (dice score ~1) with a high correlation coefficient (r) for bone morphometry between DL and manual segmentation. (B) Volume distribution of dice scores. (C) Slice-by-slice visualization from cranial (leftmost) to caudal (rightmost) of the averaged best (top row) and worst (bottom row) segmented vertebra; manual = green; DL = red; and union = yellow.

***Disclosures: Michael David**, None*

SUN-300

Pharmacogenetic and microRNA mechanisms of beta blocker treatment response in bone *Christine Lary[2], Griffin Scott[2], Hongyu Chen[2], Archana Nagarajan[3], Elizabeth Atkinson[4], David Monroe[5], Aaron Brown[6], Katherine Motyl[7], Sundeep Khosla[8], [2]Northeastern University, , [2]Northeastern University, United States, [3]Tufts University School of Biomedical Sciences, , [4]Mayo Clinic, United States, [5]Mayo Foundation, United States, [6]MaineHealth Institute for Research, United States, [7]MaineHealth, United States, [8]Mayo Clinic College of Medicine, United States

Atenolol, a beta-1 selective beta blocker (BB), is being evaluated to prevent postmenopausal bone loss in the randomized clinical trial, "Atenolol for the Prevention of Osteoporosis". Atenolol inhibits norepinephrine binding of the beta-1 and beta-2 adrenergic receptors (b1-AR and b2-AR) on osteoblasts and osteoclasts (Figure A). Previous pharmacogenetic effects have been found in b1-AR (ADRB1) and in HDAC4, a histone deacetylase that stabilizes ATF4-mediated upregulation of TNFSF11 (RANK Ligand) in osteoblasts. We have also shown that miR-19a-3p, which is associated with BB treatment response for hypertension, and which targets both b1-AR and HDAC4, is positively associated with BB use, bone mineral density (BMD), and reduced fracture risk. However, these associations have not been studied longitudinally with BB treatment. We analyzed pharmacogenetic data using variants from ADRB1, ADRB2, and HDAC4 in a pilot clinical trial performed at the Mayo Clinic in 155 postmenopausal women randomized to placebo, propranolol (40 mg or 80 mg), atenolol (50 mg), or nebivolol (5 mg) daily for 20 weeks. We also collected miRNA-seq data at baseline and endpoint from 24 participants, 9 each from the atenolol group with high response (HR) or low response (LR) based on changes in C-terminal telopeptide (CTX), and 6 from the placebo group. We modeled the change in BMD at the femoral neck (FN), lumbar spine (LS), or ultradistal radius (UDR) or in serum CTX as a function of baseline values, SNP dosage, treatment group, and their interaction. Longitudinal miRNA-seq data was analyzed using negative binomial regression with generalized linear mixed models. An increase in UDR BMD for the propranolol 80 mg group was found compared to placebo for each additional copy of the ADRB1 rs1801252 G allele (Figure B), and an increase in LS BMD and decrease in CTX was found for the atenolol group for each additional copy of the HDAC4 rs11124190 G allele (LS BMD in Figure C). miR-19a-3p was associated with a significant increase in the low responder group over time compared with placebo (OR = 2.8, p= 0.028) and with a trend towards significance in the combined atenolol groups (OR = 2.2, p=0.06, Figure D). Taken together these results are consistent with a mechanism in which genetic variation or miR-19a-3p-induced suppression of b1-AR and HDAC4 is associated with improved treatment response. These results will be validated in an ongoing ancillary study for the APO clinical trial.

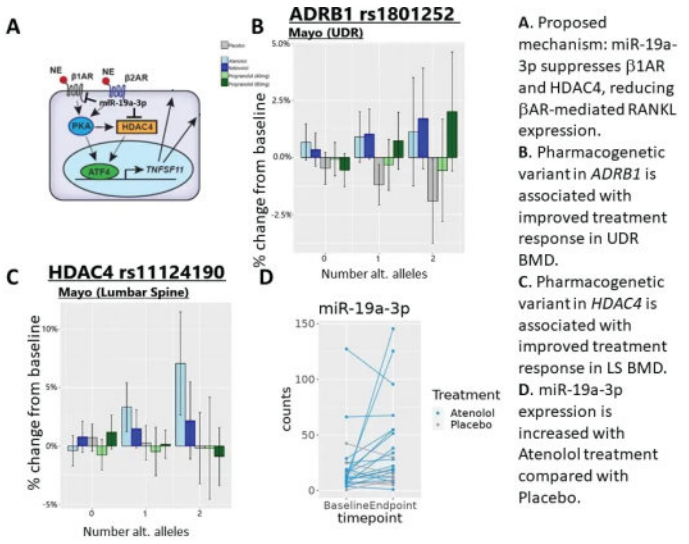

A. Proposed mechanism: miR-19a-3p suppresses β1AR and HDAC4, reducing βAR-mediated RANKL expression.
B. Pharmacogenetic variant in *ADRB1* is associated with improved treatment response in UDR BMD.
C. Pharmacogenetic variant in *HDAC4* is associated with improved treatment response in LS BMD.
D. miR-19a-3p expression is increased with Atenolol treatment compared with Placebo.

***Disclosures: Christine Lary**, None*

SUN-301

Novel Genes and Transcription Factors Related to Skeletal Abnormalities in Down Syndrome *JARED THOMAS[1], Randall Roper[2], [1], [2]Indiana University-Purdue University Indianapolis, United States

Triplication of human chromosome 21 (Hsa21) results in Down syndrome (DS) and dysregulates neurological, cardiovascular, and skeletal development. Increased gene dosage may alter expression of both two- and three-copy genes leading to DS phenotypes. All individuals with DS present with low BMD and have an increased risk for early-onset osteoporosis and fragility fractures. Genetic determinants related to skeletal abnormalities in DS remain poorly understood. Ts65Dn DS model mice are trisomic for ~100 Hsa21 orthologous genes on mouse chromosome 16 (Mmu16) and ~35 Mmu17 non-Hsa21 orthologous genes, and recapitulate skeletal deficiencies observed in humans with DS. At six weeks both male and female Ts65Dn mice showed significantly reduced BMD and impaired trabecular and cortical architecture. Osteocytes regulate bone homeostasis and may contribute to skeletal abnormalities seen in DS. We hypothesized that trisomy alters gene expression genome wide in Ts65Dn mice in the developing skeleton affecting osteoblasts and osteocytes. To test this hypothesis, we performed RNA-Seq on femoral diaphyseal bone from six-week male and female euploid and Ts65Dn mice. Female trisomic compared to euploid mice had 1598 differentially expressed genes (DEGs) (upregulated = 672; downregulated = 926); male trisomic compared to euploid mice had 95 DEGs (upregulated = 93 and downregulated = 2). Female mice showed genome-wide altered expression, in contrast to male mice with the majority of DEGs located on Mmu16 (61%) and Mmu17 (17%). Female trisomic DEGs were identified in pathways related to cell cycle control, mismatch repair and cell cycle checkpoint control. Male trisomic DEGs included those in interferon and PI3K/Akt signaling; both play critical roles in skeletal development and bone formation. Both male and female mice had increased expression of Madcam1 (unknown bone function) and Stfa1 (role in osteogenic differentiation) that may be novel genes related to DS skeletal abnormalities. DEGs found in Ts65Dn mice may derail bone remodeling by impacting bone formation resulting in decreased BMD and weaker bones. Female as compared to male Ts65Dn mice at six-weeks of age display less severe skeletal deficits possibly due to upregulated DEGs that positively affect bone formation. This work identified new candidate genes and pathways involved in altered skeletal development that may provide new potential therapeutic targets for sex-specific treatments for individuals with DS.

***Disclosures: JARED THOMAS**, None*

SUN-302

Augmentation of BMP signaling leads to ectopic cartilages through changes in chromatin structures *YUJI MISHINA[1,] Hiroki Ueharu[1.] [1]University of Michigan,

Dysregulation of proliferation, migration, and differentiation of cranial neural crest cells (NCCs) develop craniofacial anomalies. We have reported that enhanced BMP signaling in NCCs (caAcvr1; P0-Cre mice, mutant mice hereafter) developed ectopic cartilages in the midfacial region at embryonic day 14.5 (E14.5). Pharmacologic rescue experiments using an inhibitor for BMP signaling revealed that a time window for suppression of ectopic cartilage formation is at E11.5, which is a stage before the initiation of the ectopic cartilage formation. We hypothesize that augmentation of BMP signaling directs the multipotency of cranial NCCs towards chondrogenesis. This study aims to reveal the mechanism for cell fate specification of cranial NCCs by BMP signaling. We compared gene expression profiles in cranial NCCs between control and mutant mice at E10.5 by single cell RNA sequence. In the mutant embryos, cranial NCCs formed the ectopic cartilages, but trunk NCCs did not, thus we speculated that genes changed only in cranial NCCs of mutant mice but not in trunk NCCs involve in the formation of ectopic cartilage. Through these 2 way comparisons, we identified 11 genes of which expressions are specifically changed in mutant cranial NCCs. Among these genes, we found that Xist, a main player for X chromosome inactivation, is significantly increased in cranial NCCs of mutant mice. We further observed that cranial NCCs in mutant female embryos have ectopic X chromosome inactivation: one cell has two inactive X chromosomes that are entirely coated with Xist RNA. Surprisingly, ectopic X chromosome inactivation was also found in cranial NCCs of mutant male mice, which should not have X chromosome inactivation. This finding may explain the fact that both male and female mutant mice develop ectopic cartilage in a comparable manner. We demonstrated that silencing of Xist in cranial NCCs decreases chondrogenic differentiation capacity in vitro, and genetic reduction of Xist in mutant mice by deletion of Kdm5C, a known factor positively regulates Xist expression, significantly reduced formation of ectopic cartilages. These results suggested that enhanced BMP signaling develops the ectopic cartilages through induction of ectopic X chromosome inactivation. This is for the first time to demonstrate BMP-Xist axis contributes cell fate specification of cranial NCCs in both sexes.

***Disclosures: YUJI MISHINA**, None*

SUN-303

Does Slc20a2 Deficiency Alter Osteogenic Pathways? *Philip Walczak[1,] Marta Scatena[2,] Cecilia Giachelli[2.] [1]Department of Oral Health Sciences, University of Washington, United States[.] [2]Department of Bioengineering, University of Washington, United States

Background: Slc20a2 encodes the sodium dependent phosphate transporter PiT-2, one of two predominant phosphate transporters in hard tissues. Our lab previously showed that loss of Slc20a2 leads to impaired osteogenesis with shortened bones and decreased bone mineral density concomitant with decreased osteoblast numbers and function. Purpose: We hypothesize that decreased osteoblast numbers and impaired osteogenesis in Slc20a2 -/- mice results from downregulation of key osteogenic signaling pathways. Herein we demonstrate the application of spatial transcriptomic analysis to investigate gene expression in mouse tibias, and its potential alteration by loss of Slc20a2. Methods: C57Bl/6NTac-Slc20a2/Ieg (Slc20a2) mice were used to generate Slc20a2 WT and KO littermates under University of Washington IACUC #201600170. P24 left tibias were collected, formalin fixed, and demineralized. µCT scans of right calcified tibias were obtained to confirm phenotype. Demineralized samples were paraffin embedded and sectioned at 5?m. These slides were used for spatial transcriptomic analysis utilizing the NanoString GeoMX Digital Spatial Profiler (NanoString, Seattle, WA). Regions of interest (ROIs) were selected based on morphology, nuclear staining, and validated using marker genes, specifically proliferative zone, hypertrophic zone, primary spongiosa, and mature cortical bone. Results: µCT scans confirmed decreased bone density, decreased trabecular thickness, and decreased bone volume in P24 Slc20a2 KO compared to WT mice, consistent with previous findings in 10-week-old mice. Spatial transcriptomics allowed interrogation of morphologically distinct ROIs to validate predominant cell types. Genes with consistent differential expression in validated tissues were further investigated. Prickle1, a negative regulator of the canonical Wnt/?-Catenin pathway, was downregulated in Slc20a2 KO compared to WT. Conclusions: P24 Slc20a2 KO mice exhibit impaired osteogenesis compared to their littermates. Spatial transcriptomics enabled in situ whole-transcriptome analysis of Slc20a2 mutant mice to investigate the role of Slc20a2 in osteogenic pathways. Loss of Prickle1 has previously been shown by other groups to lead to shortened appendages and delayed osteoblast differentiation and migration, phenotypic findings observed in Slc20a2 KO mice. These results suggests that Slc20a2 may play a role in Wnt/?-catenin signaling, with deficiencies impairing osteogenesis.

***Disclosures: Philip Walczak**, None*

SUN-304

Osteoporosis-Associated Genes Identified from Transcriptional Profile Reconstruction in Human Peripheral Blood Bulk RNA Sequencing *YUN GONG[2,] XIAO ZHANG[2,] CHUAN QIU[3,] Kuan-Jui Su[2,] Zhe Luo[2,] Qing Tian[2,] Hui Shen[2,] Hong-Wen Deng[2.] [2]Tulane University, United States[,] [2]Tulane University, [,] [3], United States

Bulk RNA sequencing (seq) provides an average gene expression profile for a population of cells. Despite of the cell isolation method has been used (positive or negative), a major limitation of bulk RNA-seq is it fails to identify and characterize cell composition and mask potential cellular heterogeneity in the cell population due to individual complexity of each cell. Therefore, it is essential to determine cell-type specific RNA-seq after cell-type adjustment in bulk RNA-seq data. Here, we performed a comparative analysis between adjusted versus unadjusted cell-type (i.e., classical monocytes) specific bulk RNA-seq data derived from peripheral blood monocytes obtained from 944 independent subjects and investigate their significant gene differences on osteoporosis risk in men. We used Bayesian cell proportion reconstruction inferred using statistical marginalization (BayesPrism) to uncover the cell composition in our bulk RNA-seq data and reconstruct the monocyte-specific transcriptional profile. Next, we will perform the Weighted Gene Co-expression Network Analysis (WGCNA) to identify highly co-expressed clusters of genes associated with bone mineral density (BMD) using unadjusted and adjusted RNA-seq data. Through this comparative analysis, we expect to identify significant and novel BMD-associated genes and networks which could not be identified in the unadjusted bulk RNA-seq.

***Disclosures: YUN GONG**, None*

SUN-305

Identification of genetic risk factors for hip osteoarthritis acting through altered hip shape: findings from a genome-wide association meta-analysis of 43,485 individuals *Benjamin Faber[1,] Monika Frysz[1,] Jiayi Zheng[2,] Huandong Lin[3,] Raja Ebsim[7,] Fiona Saunders[5,] Jenny Gregory[5,] Richard Aspden[5,] Nicholas Harvey[6,] Claudia Lindner[7,] Tim Cootes[7,] Sijia Wang[8,] John Kemp[9,] Jonathan Tobias[1.] [1]University of Bristol, United Kingdom[.] [2]3) CAS Key Laboratory of Computational Biology, Shanghai Institute of Nutrition and Health, University of Chinese Academy of Sciences, Chinese Academy of Sciences, Shanghai, China, China[.] [3]Department of Endocrinology and Metabolism, Zhongshan Hospital, Fudan University, Shanghai, China., China[.] [7]Division of Informatics, Imaging and Data Science, University of Manchester, UK, China[.] [5]Centre for Arthritis and Musculoskeletal Health, University of Aberdeen, UK, United Kingdom[.] [6]University of Southampton, [.] [7]Division of Informatics, Imaging and Data Science, University of Manchester, UK, United Kingdom[.] [8]3) CAS Key Laboratory of Computational Biology, Shanghai Institute of Nutrition and Health, University of Chinese Academy of Sciences, Chinese Academy of Sciences, Shanghai, China., China[.] [9]The University of Queensland, Australia

PurposeHip shape is an important risk factor for hip osteoarthritis (HOA) that is heritable. In this study we aimed to identify new genetic determinants of hip shape, and assess their relationship with HOA.MethodsStatistical hip shape modelling was used to derive 10 orthogonal hip shape modes (HSMs) from DXA images in two cohorts. These include 38,175 UK-Biobank Study participants, as well as 5,310 participants from the Shanghai Changfeng Study. Genome-wide association studies (GWAS) were conducted on the HSMs and resulting summary statistics were meta-analysed using an inverse variance weighted fixed effects method. Statistically independent HSM-associated single nucleotide polymorphisms (SNPs) were identified using GCTA-COJO. HSM-associated SNPs were looked up in a recent GWAS of HOA and pleiotropy was assessed using a Bonferroni corrected p-value threshold of P<1.6x10-4. Statistical fine mapping was used to highlight genes that may be functionally related to hip shape.ResultsAnalysis of the first 10 HSMs identified 308 statistically independent association signals in total (P<5x10-8). These included SNPs that mapped to 8 known HSM-associated loci, as well as a further 261 that mapped to novel loci. SNPs in 17 loci were also associated with HOA. Fine mapping implicated SMAD3 and PLEC as candidate genes that may be involved in the development of hip shape as well as HOA. Rs12901499 intersected SMAD3 and was associated with increased medial femoral head displacement (HSM4: ?=0.05, P=1.7x10-13, Figure 1) and a lower risk of HOA (?=-0.07, P=2.8x10-15). It also colocalized with SMAD3 mRNA expression in cartilage [posterior probability (PP) 98%]. Moreover, rs12541377 intersected PLEC and it was associated with a narrower femoral neck (HSM7: ?=0.05, P=2.55x10-11, Figure 1), and lower HOA risk (?=-0.04, P=2.6x10-6). It also colocalized with PLEC mRNA expression in synovial tissue (PP 96%).ConclusionsWe report the largest hip shape GWAS meta-analysis to date that identifies hundreds of novel loci, many of which are also associated with HOA. Fine mapping highlighted SMAD and PLEC in the development of hip shape and HOA. Both genes warrant further investigation as they could represent potential therapeutic targets for HOA.Figure 1 Legend. Solid Line: +2 Standard Deviations (SD), Dotted Line: -2SD

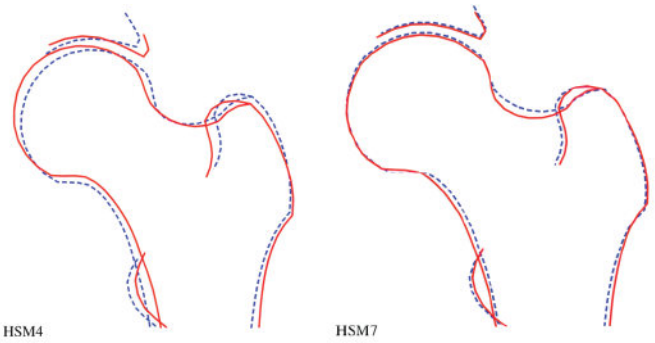

***Disclosures: Benjamin Faber**, None*

SUN-306

Differential transcriptional responses to intracellular infection by S. aureus in osteoclasts and their precursors. *Luke O'Connor[1], Deborah Veis[2,1], [2]Washington University in St. Louis School of Medicine, United States

S. aureus is an opportunistic pathogen that causes 30-50% of all osteomyelitis (OM) cases. During OM, S. aureus survive in colonies, as well as within osteocytes, osteoblasts, and osteoclasts (OCs). We have recently shown that OCs, unlike their bone marrow macrophage (BMM) precursors, allow bacteria to replicate intracellularly and the magnitude of growth increases with OC differentiation . We hypothesized that OC differentiation alters host-pathogen interactions by changing nutrient availability and host defense pathways to favor intracellular S. aureus growth. To test this, we conducted dual RNA-seq to analyze host and S. aureus gene expression at 4 critical infection timepoints: prior to infection, after bacterial internalization (2h), during bacterial metabolic transition (6h), and after bacterial expansion in OCs or killing in BMMs (21h). Bone marrow was cultured from 6-7 week-old male B6/alb mice, and BMMs (MCSF only) or OCs (3 days RANKL) generated prior to infection with USA300 MRSA strain TI3. To ensure data robustness we sequenced 3 batches of pooled samples per cell type, with each pool representing 3 mice and 3 separate infections (total: 18 mice, 10 infections). S. aureus transcripts were aligned to S. aureus USA300_FPR3757 and DESeq2 used to analyze genes differentially expressed by cell type (BMM vs OC) over the time course. In parallel, we used PyModulon to analyze modules of co-regulated genes in bacteria. These analyses show that bacteria in OCs have lower expression of Fur regulated iron scavenging genes as well as genes related to CodY, PerR, PurR, and CymR, which regulate amino acid metabolism. Thus, S. aureus in OCs may be less stressed for iron and amino acids than bacteria in BMMs. Murine host transcripts were aligned to Mm39 and analyzed in DESeq2, followed by supplemental analysis with Gene Ontology (GO) enrichment and using weighted coregulated gene network analysis (WGCNA). GO analysis highlights that OC and BMM responses largely differ in host defense and bacterial response pathways. WGCA of all differentially expressed genes and a subset of genes from the top 10 GO identify Pi3kr1, Id2, and ZO-2 as genes highly interconnected with differential host response and indicate a potential roles for PI3K, TGF-?, and Hippo signaling pathways. Collectively these results suggest OCs have an altered response to infection and provide greater access to nutrients than their BMM precursors, allowing S. aureus expansion in OCs but not BMMs.

***Disclosures: Luke O'Connor**, None*

SUN-307

Subchondral bone migration into trabecular bone in response to direct bone-on-bone contact wear in patients with severe knee osteoarthritis *Meret Keiser[1], Stefan Preiss[2], Stephen J Ferguson[3], Vincent A. Stadelmann[1]. [1]Department of Research and Development, Schulthess Klinik, Switzerland. [2]Department of Knee Surgery, Schulthess Klinik, Switzerland. [3]Institute for Biomechanics, ETHZ, Switzerland

INTRODUCTION: Although it is well established that osteoarthritis (OA) is accompanied by changes in subchondral bone microstructure, such as cortical thickening, little is known about microstructural adaptations at and around full-thickness cartilage defects in severe knee OA. This high-resolution microCT study therefore aimed to describe and quantify subchondral bone changes due to wear under direct bone-on-bone contact in patients with severe OA.METHODS: Ten tibial plateaus showing full-thickness cartilage defects were retrieved from total knee arthroplasty patients. All patients provided signed informed consent. Six 5x5 mm specimens were cut with a diamond saw from the defect, defect-edge, and cartilage region and two from the contralateral side. These were microCT-scanned at a resolution of 3.3 µm. Bone volume fraction (BV/TV) and Tissue Mineral Density (TMD) were analysed layer-by-layer to compute the specimens' density profiles and identify cortical and trabecular bone regions. Bone formation around cortical porosity was derived from the gradient of mineral density around the pores.RESULTS: The subchondral bone plate below full-thickness cartilage defects appears to migrate into trabecular bone through direct thickening and through pockets of bone formation within the trabecular structures. In cases with deep wear grooves, trabecular pores occasionally connect with the joint space before they are completely filled with new bone. The spatial expansion of these effects shows a sharp boundary at the defect-edge, almost immediately disappearing under regions covered with even a minimal layer of cartilage (Fig. 1). Quantitatively, cortical bone was 4-fold thicker below defects than below cartilage. BV/TV and TMD profiles significantly differed between defect, edge, and cartilage specimens, up to 5mm deep. Below defects, cortical porosity and trabecular BV/TV were 85% and 14% higher and TMD 6% lower compared to cartilage specimens. The TMD gradient around pores was greatest in the edge specimens. DISCUSSION & CONCLUSIONS: This is the first study to bring new insights into bone microstructural adaptations below full-thickness cartilage defects in severe knee OA. We observed subchondral plate migration below cartilage defects via trabecular osteogenesis. Our data shows an increased bone formation in defect and edge regions, reflecting the wear of native cortical bone and trabecular corticalisation, causing the cortical layer to migrate down into the trabecular bone.

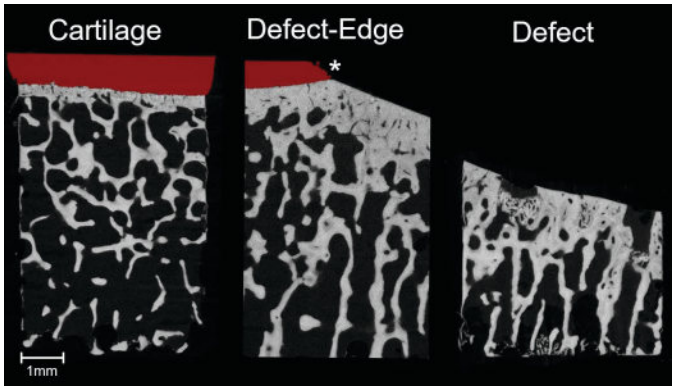

***Disclosures: Meret Keiser**, None*

SUN-308

State-level impact of arthritis pain on patients using a patient-oriented outcomes survey *SIERRA STREET[1], Jonathan Lowery[2,1], [2]Marian University, United States

Arthritis is a group of over 100 joint conditions and diseases that affects more than 54 million adults in the US and places an enormous burden on the US. healthcare system. Despite this, there is a poor understanding of the real-life experiences and daily challenges faced by patients with arthritis. Hence, in collaboration with the Arthritis Foundation, we took a patient-oriented outcomes approach to determine the impact of arthritis on patients through an electronic survey developed with input from patients, healthcare providers, and measurement experts and includes measures from validated questionnaires to allow allowing for comparison to established benchmarks of the general population. Nationwide, the survey has received over 40,000 responses. However, aggregate nature does not allow for examining region-specific differences, which potentially limits the project's ability to influence advocacy efforts at the local, state, healthcare system and/or regional levels. Thus, we initiated a state-focused project to better understand the impact of arthritis on Indiana residents. Among the 515 responses from Indiana, most respondents have osteoarthritis (43%) along with a variety of other forms of arthritis including Rheumatoid Arthritis (32%). Most respondents from Indiana, hereafter referred to as "Hoosiers," are female (79%) and identify as "white" (82. 100% of respondents reported pain in the week prior to taking the survey with an average pain score of 4.92. 29.2% of survey participants indicated a high or moderate pain score, while 58.3% of participants indicated a low pain score.. 62% of Hoosier patients with a higher pain score - i.e., 7 or higher out of 10 -report difficulty with doing all of their regular leisure activities with others compared to 7% of patients with a low pain score of 4 or below. 66% of Hoosier patients report difficulty of all activities with friends that they would like to do compared to 13% of patients with a low pain score. 85% of Hoosier patients with a high pain score report their pain interferes with their day-to-day activities compared to 6.5% of patients with a low pain score. In addition, 75% of Hoosier patients with a high pain score report their pain interferes with their ability to participate in social activities compared to 6% of patients with a low pain score. 50% of patients with a high pain scale reported they felt their choices were respected compared to 82% of patients with a low pain scale. 45% of patients with a high pain scale reported they were able to speak with a professional to get their questions answered compared to the 75% of patients with low pain. Our results indicate that debilitating pain is a major challenge for patients and it is associated with negative impacts on lifestyle and emotional/social health. Future work seek to increase the representation of additional race or ethnics groups, men, and patients with additional forms of arthritis.

***Disclosures: SIERRA STREET**, None*

SUN-309

The Effect of Antiresorptive Agents on Periprosthetic Bone Mineral Density After Non-Cemented Hip Arthroplasty: A Literature Review and Meta-Analysis of Randomized Controlled Trials. *José Francisco Torres-Naranjo[1], Roberto E López Cervantes[2], Roberto Gabriel Gonzalez Mendoza[3], Hugo Gutierrez Hermosillo[4], Darío Esaú Garin Zertuche[5], Luis A Padilla Rojas[6], Pedro Alberto García Hernandéz[7]. [1]Centro de Investigación Ósea, CIO; Asociación Mexicana de Metabolismo Óseo y Mineral , AMMOM, Mexico. [2]CFO, Federación Mexicana de Colegios de Ortopedia y Traumatología, FEMECOT , Mexico. [3]Instituto de Ciencias Aplicadas a la Actividad Física y el Deporte, Centro Universitario de Ciencias de la Salud, Universidad de Guadalajara., Guadalajara, Mexico, Mexico. [4]Asociación Mexicana de Metabolismo Óseo y Mineral, AMMOM, Mexico. [5]Federación Mexicana de Colegios de Ortopedia y Traumatología FEMECOT, Mexico. [6]Federación Mexicana de Colegios de Ortopedia y Traumatología, FEMECOT, Mexico. [7]Facultad de Medicina, UANL, Monterrey, Mexico

Arthroplasty is a common surgical procedure for patients with joint diseases, and its frequency continues to increase. However, its impact on peri-prosthetic bone mass and clinical outcomes is poorly understood. Additionally, the efficacy of osteoporosis medications in managing peri-prosthetic bone loss is uncertain.PurposeThis study aimed to evaluate the effect of antiresorptive agents on periprosthetic bone mineral density after non-cemented hip arthroplasty.MethodsWe conducted a comprehensive search of databases such as "PubMed," "Scopus," "Web of Science," and "ScienceDirect" in August 2022. An additional search was conducted to detect possible related studies not found in the classic search using review and meta-analysis. We included studies that had at least two periprosthetic bone mineral density measurements. When authors did not report numeric bone mineral density, data were iterated from graphs. The primary outcome of interest was the periprosthetic bone mineral density change over time. Given the lack of control or description of various factors in most studies, a random-effects meta-analysis was performed using the "DerSimonian and Laird" approach.ResultsWe conducted a random-effects meta-analysis of 29 studies comprising 1182 adult patients. Six hundred fourteen of whom underwent elective total non-cemented hip arthroplasty surgery and received antiresorptive treatment after the procedure, and 568 controls. Our meta-analysis showed that after hip arthroplasty, there is a significant decrease in bone mineral density (BMD) in the periprosthetic bone. Antiresorptive treatments consistently preserve periprosthetic bone mineral density in Gruen Zone 1 during the 24 months after surgery. In Zone 7, we observed a similar effect only during the first 18 months after surgery. Although not the study's primary objective, we also observed this effect is maintained for up to 60 months.During the literature review, we noted significant variations in the techniques used to acquire and analyze periprosthetic DXA scans.ConclusionsOur findings suggest that after non-cemented hip arthroplasty, there is a significant decrease in BMD in the periprosthetic bone during the first 24 months after surgery. However, the use of antiresorptive agents appears to attenuate this loss. It is important to note that several studies lack adequate information about baseline BMD or other critical factors, highlighting the need for further research to fully understand the effects of surgery on bone health.

***Disclosures: José Francisco Torres-Naranjo**, None*

SUN-310

SENP6 mediated desumoylation regulates osteoarthritis development *Tao Yang[1]. [1]Van Andel Institute, United States

SUMOylation is a reversible posttranslational modification that broadly controls protein-protein interaction, stability, and activity, and plays essential roles in regulating genomic stability, epigenetic states, and stress responses. A genome-wide association study (GWAS) published by the arcOGEN Consortium showed a strong association between human osteoarthritis (OA) and the single nucleotide polymorphisms (SNPs) of the small ubiquitin-like modifier (SUMO) specific peptidase 6 (SENP6), which removes SUMO modifications from specific protein targets. A follow-up study further demonstrated that SENP6 expression decreases in OA hip cartilage relative to non-OA controls. These implicate that SENP6-mediated de-SUMOylation is critical for OA development and that altered SENP6 function could be a target of intervention for treatment of human OA. Here, we found that chondrocyte-specific loss of SENP6 promotes articular chondrocyte (AC) senescence and inflammation and accelerates the onset and progression of post-traumatic OA (PTOA) and age-related OA. Furthermore, loss of SENP6 increases AC senescence and contributes to an abnormal stress response, and an altered epigenetic landscape. Finally, mice with chondrocyte-specific gain of SENP6 expression showed delayed onset and progression of PTOA. Our work overall demonstrated that SENP6-mediated de-SUMOylation contributes to articular cartilage homeostasis, and that increasing the expression level or activity of SENP6 may be used therapeutically to slow down/prevent joint degeneration.

***Disclosures: Tao Yang**, None*

SUN-311

Risk Factors for Skeletal Complications Following Spine Fusion Surgery in Postmenopausal Women *Alexander Dash[1], Emma Billings[2], Han Jo Kim[3], Matthew Cunningham[3], Darren Lebl[3], Francis Lovecchio[3], John Carrino[3], Joseph Raphael[3], Katelyn Vlasartis[4], Donald McMahon[5], Emily Stein[3]. [1]Icahn School of Medicine at Mount Sinai, . [2]Hospital for Special Surgery , . [3]Hospital for Special Surgery, United States. [4]Case Western Reserve University, United States. [5]Columbia University College of Physicians and Surgeons,

Spine fusion surgery is one of the most common orthopedic procedures, with close to 500,000 performed annually in the Unites States alone. Early stability of surgical hardware in bone and de novo bone formation are critical for fusion success. Complications occur in up to one-third of cases, and are more common in patients with underlying skeletal deficits. The FUsion and Skeletal Evaluation in patients unDergoing SPINE surgery (FUSED SPINE) ongoing prospective cohort study of adult men and women investigates the relationship between pre-operative bone quality and post-operative outcomes. Here we present data on a sub-group of postmenopausal women, a group that may be at particular risk for skeletal complications due to the effects of aging and estrogen deficiency. We hypothesized that women with abnormalities in volumetric BMD (vBMD) and microarchitecture would have higher rates of post-operative complications. Pre-operative assessments included areal BMD (aBMD) of the spine, hip, and forearm by DXA, cortical and trabecular vBMD and microarchitecture at the radius and tibia by high resolution peripheral quantitative CT (HRpQCT; Xtreme CT2). Cox Proportional Hazard Models that included clinical characteristics (age, BMI, smoking, alcohol, number of vertebrae included in surgery) and HRpQCT measures were utilized to identify the best predictors of post-operative skeletal complications. Among 50 women enrolled (mean age 65), pre-operative aBMD at the spine was normal; fewer than one-third had DXA measurements in the osteoporotic range at any site. Number of vertebrae included in surgery ranged from 2 to 17; 52% of cases included >=6 levels. Median post-operative follow-up was 15 months. Skeletal complications occurred in 46% of women. In Cox models, earlier time to complication was related to greater number of surgical levels (HR 1.19 95% CI 1.06-1.34), lower tibia total area (HR 0.60 95% CI 0.41-0.86) and lower tibial cortical thickness (HR 0.74 95% CI 0.57-0.95; model p <0.01, Figure). In summary, postmenopausal women with smaller bones, thinner cortices and those having procedures involving a greater number of vertebrae were at highest risk for post-operative complications. Our results highlight the risk of skeletal complications among postmenopausal women who undergo complex multi-level procedures, despite normal appearing DXA. They further illustrate the influence of bone size and cortical integrity on post-operative outcomes in this population.

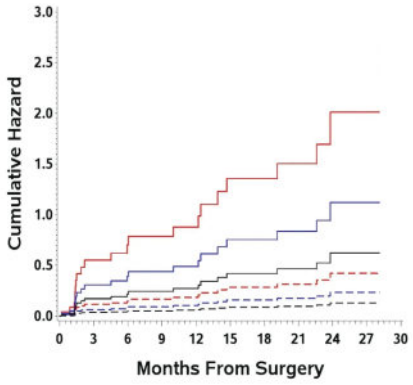

Figure: Lower cortical thickness and greater number of fusion levels associated with increased hazard of post-operative complications. Cumulative hazard shown by tertiles of tibial cortical thickness. Green lines represent lowest tertile (0.6 to <1.2 mm), blue lines represent middle tertile (1.2 to <1.7 mm), red lines represent highest tertile (>=1.7 mm). Dashed lines < 6 surgical levels and solid lines ≥ 6 surgical levels.

***Disclosures: Alexander Dash**, None*

SUN-313

DXA-derived knee shape may provide a useful imaging biomarker for predicting total knee replacement: findings from UK Biobank *Rhona Beynon[1], Fiona Saunders[2], Raja Ebsim[3], Monika Frysz[1], Ben Faber[1], Jenny Gregory[2], Claudia Lindner[3], Richard Aspden[2], Nicholas Harvey[4], Tim Cootes[3], Jon Tobias[1]. [1]University of Bristol, United Kingdom. [2]University of Aberdeen, United Kingdom. [3]University of Manchester, United Kingdom. [4]University of Southampton, United Kingdom

Purpose: Advanced knee osteoarthritis (kOA) is commonly treated with total knee replacement (TKR). We aimed to develop an imaging biomarker for predicting TKR, using knee dual-energy X-ray absorptiometry (DXA) scans obtained from the UK Biobank study. Methods: We used statistical shape modelling (SSM) to generate orthogonal knee shape modes (kSMs) from DXA images of the left knee, excluding osteophytes. A B-score was generated for each individual (n=37,844) by projecting the kSMs along a vector representing the difference between the mean knee joint shape of healthy individuals and those who had undergone TKR. A custom script automatically measured the minimum joint space width (mJSW), which was then binarised for analysis based on whether the medial compartment mJSW fell within the first quartile. For a subset of individuals, osteophytes were manually

graded on a 0-3 scale and an aggregate grade was generated for each knee. Cox proportional hazards models were used to evaluate the relationship between DXA-derived measures and TKR incidence in this sub-sample. We evaluated the predictive ability of DXA-derived variables both independently and in combination with demographic characteristics (age, sex, height, and weight) using Harrell's concordance index (C-index). To assess the accuracy of predicting TKR incidence at five years, we computed the area under the receiver operating characteristic curve (AUC).Results: Full data were available for 6,719 individuals (mean age: 63 years [SD 7.5]; 49% males). B-score, mJSW and osteophyte grade were independently associated with TKR, with hazard ratios (HRs) of 2.63 (2.22,3.11; p<0.001), 2.97 (CI=2.04,4.33; p<0.001), and 8.40 (5.44,12.96; p<0.001), respectively. Corresponding C-statistics were 0.75, 0.63 and 0.75. The model comprising B-score, composite osteophyte grade and demographic variables yielded the best fit and discrimination (C-statistic=0.86). This model showed good discrimination in predicting TKR at 5-years, with an AUC of 0.86, compared to a model with only demographic variables, which had an AUC of 0.73 (Figure 1).Conclusions: An imaging biomarker combining B score (reflecting knee shape) and osteophytes substantially improved prediction of TKR compared with demographic factors alone. These results suggest that DXA-derived imaging biomarkers could prove useful in identifying those at high risk of kOA progression, in whom the focus should be on interventions to slow this process.

Figure 1: Receiver Operating Characteristic (ROC) Curve for Prediction of Knee Replacement at 5 Years (n=6,719).

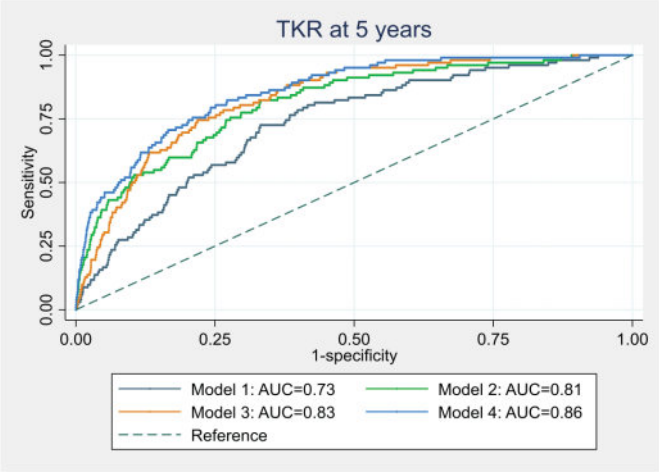

Model 1: age, sex, height, and weight; Model 2: age, sex, height, weight, B-score; Model 3: age, sex, height, weight, composite osteophyte grade; Model 4: age, sex, height, weight, B-score, composite osteophyte grade.

***Disclosures: Rhona Beynon**, None*

SUN-314

Single-cell RNA Sequencing of Human Bone Marrow Mesenchymal Stem Cells Reveals the Cellular Interactions in Osteonecrosis of the Femoral Head *Tian-Ying Li[1], Jia-Qi Wang[1], Xiao-Hua Li[2], Junxiao Yang[3], YUN GONG[5], XIAO ZHANG[5], Hui Shen[5], Li-Jun Tan[2], Hong-Wen Deng[5], Hong-Mei Xiao[1]. [1]Central South University, China. [2]Hunan Normal University, China. [3]Xiangya Hospital, China. [5]Tulane University, United States. [5]Tulane University,

Osteonecrosis of the femoral head (ONFH) and osteoarthritis (OA) are both degenerative chronic diseases that commonly occur on the femoral head of the hip joint. It is known that ONFH and OA have multiple interconnections and can transform into each other, despite their differences in the etiology, symptoms, and pathogenesis. One of the pathogenic factors considered for both diseases is the disrupted osteogenesis process caused by the dysfunction of bone marrow mesenchymal stem cells (BMMSCs), however, the underlying molecular mechanisms still lack consensus. In this study, we collected and enriched BMMSCs with CD271+ magnetic activated cell sorting (MACS) from human bone marrow sampled from patients with ONFH and OA, respectively. The single-cell RNA sequencing (scRNA-seq) was used to generate the transcriptome landscape of cells in bone marrow environments (BMMSCs, macrophages, neutrophils, and endothelial cells, etc.) under both conditions. Next, we further compared these two conditions and analyzed expression differences and cell-cell signaling communication to reveal the participation of different cell types in the pathogenesis of ONFH. Through this study, we expected to provide a new perspective for understanding the pathological changes of degenerative bone diseases and help for the subsequent diagnosis and treatment development.

***Disclosures: Tian-Ying Li**, None*

SUN-315

A Comparison between Osteogenic Capacities of In-Vitro Cell Cultures and Characteristics of Ex-Vivo Bone Fragments Isolated from Human Acetabular Reamings *Christodoulos Constantinou[1], Michael Kain[2], David Freccero[2], Louis Gerstenfeld[3], Paola Divieti Pajevic[4]. [1]Boston University, United States. [2]Boston Medical Center, United States. [3]Boston University School of Medicine, United States. [4]Goldman School of Dental Medicine, Boston University, United States

Osteoporosis (OP) is a bone disease characterized by a decrease in bone mineral density and changes in bone microarchitecture. In the US, OP affects approximately 10 million people, and subsequently increases their risk of bone fracture. Ongoing research targets the prevention and treatment of OP, primarily through clinical trials. Basic science research is utilized less, in part due to costs, as well as the inaccessibility of human specimen procurement. Therefore, devising an accessible and valid model to investigate bone pathologies at the molecular level will enhance the understanding of the connection between cellular pathology and morbidity, and potentially offer insights into osteoporotic risk factors and prevention. In this study, we isolated bone fragments and mesenchymal stem cells (MSCs) from acetabular reamings procured from human elective total hip arthroplasties. We first extracted RNA from the bone fragments and analyzed gene expression using RT-qPCR. We differentiated the isolated MSCs into osteoblasts, and characterized them for their osteogenic properties through biochemical assays and RT-qPCR. We finally compared data between osteoblasts and bone fragments, and further matched them with the respective patients' demographic and clinical information. Initial analysis using data from 6 patients demonstrated that: a) bone fragments expressed osteogenic gene markers significantly more than the corresponding differentiated MSCs, b) cultured osteoblasts produced alkaline phosphatase and hydroxyproline differentially among patients, but at consistent rates within patients, c) biochemical data from osteoblasts followed trends in osteogenic-marker gene expression of respective bone fragments, and d) osteoblasts potentially follow trends in osteogenic capacities to certain demographics and comorbidities, of which race and BMI are of particular interest. The sample size did not allow for correlational analyses in gene expression to validate primary MSCs' ability to maintain a diseased phenotype outside of their in-vivo environment, and further as a model to study molecular factors of osteoporosis. However, our data suggests that determining osteogenic capacities of cultured and differentiated MSCs may offer critical insight into properties of primary cells isolated from patients. Moreover, these cells can potentially be used as a model to investigate molecular-level pathologies of osteoporosis.

***Disclosures: Christodoulos Constantinou**, None*

SUN-316

Wnt10b is required for the bone anabolic effect of a natural antibody that blocks oxidized phospholipids. *Michela Palmieri[1], Intawat Nookaev[2], Maria Jose Almeida[3], Ha-Neui Kim[4], Teenamol E Joseph[1], Stavros Manolagas[3], Charles O'Brien[5], Elena Ambrogini[3]. [1]Division of Endocrinology and Metabolism, Center for Musculoskeletal Disease Research, University of Arkansas for Medical Sciences and the Central Arkansas Veterans Healthcare System, United States. [2]2Department of Biomedical Informatics, University of Arkansas for Medical Sciences, United States. [3]Central Arkansas VA Healthcare System, Univ of Arkansas for Medical Sciences, United States. [4]Univ. Arkansas for Medical Sciences, Central Arkansas VA Healthcare System, United States. [5]Univ of Arkansas for Medical Sciences, United States

Oxidized phospholipids containing phosphatidylcholine (PC-OxPLs), present on oxidized low-density lipoproteins (OxLDL) and apoptotic cells, are pathogenic in many diseases, including osteoporosis, atherosclerosis, and non-alcoholic steatohepatitis. OxPLs decrease Wnt and BMP2 signaling, induce ferroptosis and stimulate pro-inflammatory cytokine production. The natural antibody IgM E06 binds PC-OxPLs and blocks their deleterious effects. Transgenic expression of the antigen-binding domain of E06 (E06-scFv) increases bone mass in 6-month-old mice and attenuates high fat diet- and age-induced bone loss by increasing osteoblast number and function. It was shown earlier that E06-scFv upregulates the expression of Wnt10b and Wnt signaling in vivo, but not other Wnt ligands. We investigated the mechanism(s) mediating the anabolic effect of E06-scFv. Single cell RNA-sequencing (scRNA-seq) of mesenchymal cells, isolated from long bones of 7-month-old female mice, revealed a 3-fold increase in Wnt10b expression (adj-P=3.04E-11) in pre-osteoblasts and osteoblasts obtained from E06-scFv transgenic mice compared to cells from WT mice. Wnt target genes were also upregulated. An integrated analysis of 9 published scRNA-seq datasets from bone resident mesenchymal and hematopoietic cell types revealed that the bulk of Wnt10b in the bone microenvironment originates from cells of the osteoblast lineage. Consistent with this evidence, OxLDL decreased Wnt10b and Wnt target genes in calvaria- and bone marrow-derived osteoblastic cell cultures but had no impact on ferroptosis of osteoblastic cells. Moreover, gene expression markers of ferroptosis, as well as BMP2 signaling pathways, were similar in the mesenchymal cells from E06-scFv and WT mice as determined by scRNA-seq. Expression of inflammatory cytokine genes was also similar in vertebral bone by bulk-RNA-seq, and in myeloid cells by scRNA-seq, of WT and E06-scFv mice. To examine the requirement of Wnt10b in the anabolic activity of E06-scFv, we next determined the effect of Wnt10b deletion on the bone phenotype in WT vs E06-scFv transgenic male mice at 6 months of age. We found that both the increase in BMD by DXA and BV/TV of vertebral and femoral cancellous bone by micro-CT were prevented in E06-scFv

transgenic mice lacking Wnt10b. Collectively, these findings indicate that the bone anabolic effect of E06-scFv is due to increased Wnt10b expression that results from removal of the suppressive effects of PC-OxPL.

***Disclosures: Michela Palmieri**, None*

SUN-317

Inactivation of the Polycomb Repressive Complex 2 in Osteoblasts Increases Trabecular Bone Mass and Results in Mechanically Stronger Bones *Amel Dudakovic[1], Sofia Jerez[1], Christopher Paradise[1], M. Lizeth Galvan[1], Oksana Pichurin[1], Padmini Deosthale[2], Roman Thaler[1], Lilian Plotkin[2], Andre van Wijnen[3]. [1]Mayo Clinic, United States, [2]Indiana University School of Medicine, United States, [3]University of Vermont, United States

Epigenetics, including post-translational modifications of histones, control osteoblast activity and bone formation. The Polycomb Repressive Complex 2 (PRC2) methylates H3 at lysine 27 (H3K27me3), a heterochromatin mark that suppresses gene expression. PRC2 is made of two main structural proteins, Eed and Suz12, and one of two methyltransferases, Ezh1 or Ezh2. We and others showed that Ezh2 inhibition stimulates osteoblast differentiation in vitro and bone formation in vivo. However, Ezh2 loss in osteoblasts (Osx-Cre) is not bone stimulatory in vivo. Thus, the mechanistic understanding of the divergency between Ezh2 inhibition and Ezh2 loss on bone formation remains elusive. These studies build on our findings that Ezh2 is expressed in progenitors while Ezh1 is expressed in committed osteoblasts. We reasoned that loss of the entire PRC2 function will stimulate bone formation. We generated mice in which Ezh1 is depleted globally and Ezh2 is lost in osteoblasts (control = Osx-Cre; Ezh1 KO = Ezh1-/-: Osx-Cre; Ezh2 cKO = Ezh2f/f: Osx-Cre; dKO = Ezh1-/-: Ezh2f/f: Osx-Cre). Ezh1 and Ezh2 dKOs male and female mice exhibited significantly increased trabecular bone (µCT) and bone strength (3-point bending) when compared to controls, Ezh1 KOs, and Ezh2 cKOs (8 weeks). While doxycycline (Cre suppression) prevented this phenotype in dKOs (8 weeks), its removal (8 weeks) to inactivate Ezh2 in osteoblasts (on a Ezh1 null background) lead to a significantly higher trabecular bone mass (14 weeks). We next assessed the effects of targeting PRC2 scaffolding proteins. Eed inhibitors A395 and EED226 enhanced osteogenic differentiation of MC3T3 pre-osteoblasts as assessed by RNA expression (e.g., Bglap and Ibsp) and alizarin red staining (mineral deposition). Similarly, siRNA mediated Eed or Suz12 loss stimulated MC3T3 differentiation. Because Eed can be targeted by small molecules, our initial in vivo studies focused on Eed over Suz12. µCT analysis revealed a significant enhancement of trabecular bone and bio-mechanical bone properties in male and female Eed cKOs (8 weeks). Together, these studies reveal that loss of PRC2 functionality in osteoblasts, through dual Ezh1 and Ezh2 or Eed inactivation, results in high bone mass and mechanically stronger bones. Our findings may enhance the development of novel therapeutic strategies focused on the inactivation of PRC2 to stimulate short-term or sustained bone formation.

***Disclosures: Amel Dudakovic**, None*

SUN-318

Direct Cell Reprogramming to Create Personalized Bone Cell Therapies *Asghar Fallah[1], Peter Kannu[1], Carrie-lynn Soltys[1], Connor Oborn[1], Alex Beke[2], Parker Wengryn[1]. [1]Department of Medical Genetics, University of Alberta, Canada, [2]Department of Medicine, University of Alberta, Canada

Intro: 5-10% of all fractures do not heal causing pain and poor mobility. Currently, there are no treatments for these non-union fractures. Although stem cells are promising, their acquisition is highly invasive. A minimally-invasive alternative utilizes new technology to reprogram patient fibroblasts into a source of therapeutic bone-forming cells-osteoblasts. Therein, we aim to directly reprogram (DR) human fibroblasts into osteoblasts using self-replicating mRNA (srmRNA) for personalized medicine. We hope this will be an effective and safe method to treat fracture non-union clinically.Methods: First, we transduce fibroblasts with an osteoblast-specific reporter system with GFP, enabling the monitoring of differentiation (Fig step1). Next, fibroblast induction into an osteoblastic-state arises through transfection with a custom srmRNA containing OCT4 L-MYC to potentiate multipotency, and RUNX2 and OSX directing cells to an osteoblast fate (Fig step2,3). Adding an interferon blocker (B18R) to media prevents srmRNA degradation and enhances reprogramming. In sum, srmRNA transfection into reporter-integrated fibroblasts, causing reprogramming into osteoblasts; GFP only coexpresses with osteogenic genes, indicating reprogramming. Results: Commercial osteoblasts were transfected with the osteo-specific reporter system, to demonstrate efficacy; GFP expression established significant promoter activity in osteoblasts. RNA gel electrophoresis indicated the successful isolation of srmRNA, based on predicted lengths. Transfection efficiency in fibroblasts was also assessed using various amounts of B18R (200 ng/mL). After 14 days, GFP was expressed in osteo-reporter-transduced cells. After 21 days, alizarin red staining indicated matrix mineralization in reprogrammed fibroblasts (RF), informing osteoblast-like formation. Immunofluorescence analysis of RF showed increased expression of osteoblastic factors, RUNX2 and Osteocalcin. A qPCR analysis of osteoblast marker genes in RF is the next step.Conclusions and future directions: Fibroblasts transfected with osteo-specific srmRNA demonstrated GFP expression and cell matrix mineralization. Suggesting that fibroblasts were successfully reprogrammed to an osteoblast state. We plan to further optimize the process through microRNAs. Single-cell RNA sequencing will also be used for further optimization. We hope that this research lays the groundwork for treatment for non-union fracture.

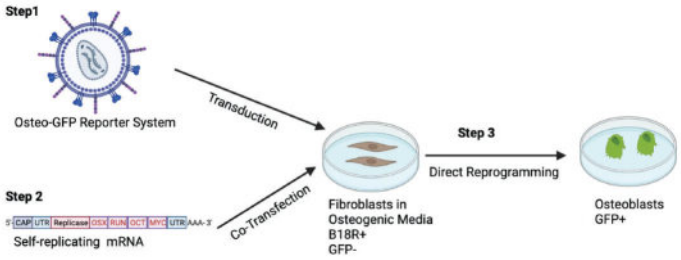

***Disclosures: Asghar Fallah**, None*

SUN-320

C-Jun N-terminal Kinase (JNK) Isoform 2 Augments Human Osteoblast Differentiation by Integrating Bone Morphogenetic Protein Signaling and Canonical Notch Signaling *Yadav Wagley[1], Benjamin Graham[2], Kurt Hankenson[2, 1], [2]University of Michigan, United States

The c-Jun N-terminal kinases (JNK) are evolutionary conserved regulators of proliferation, differentiation, and cell death responses. In vivo studies have shown that Jnk1-/- and Jnk2-/- mice display varying degrees of osteopenia due to impaired bone formation. However, JNK1 and JNK2 isoform specific contribution to human osteoblast differentiation is lesser known. Here, we used small interfering RNA-mediated knockdown of JNK1 and JNK2 in bone-marrow derived human mesenchymal stem cells (hMSC) to evaluate their role in BMP-mediated osteoblast differentiation. Histochemical staining for alkaline phosphatase (ALP) expression and extracellular matrix mineralization using Alizarin red S showed that JNK2 activity is essential for hMSC osteoblastic differentiation, whereas JNK1 activity was dispensable. Gene expression analysis revealed a minimal effect on BMP-dependent RUNX2 and SP7 expression after JNK2 knock-down, but their levels were enhanced in JNK1 silenced cells. Since, BMP signaling requires canonical Notch signaling to promote human osteoblastogenesis, we evaluated JNK-isoform specific effects on Notch signaling components. The expression of Notch ligand JAG1 and downstream Notch target genes HES1 and NOTCH3 was reduced in response to BMP stimulation of JNK2 silenced cells, while the effects were modest after JNK1 knock-down. Consequently, the absolute requirement of JAG1 for BMP-mediated hMSC osteoblastogenesis was established as JAG1 silenced hMSC failed to enhance ALP expression and extracellular matrix mineralization. Finally, we generated JNK2-deficient immortalized hMSC using CRISPR-Cas9 genome editing and subjected these cells to BMP2 stimulation. Corresponding to the results with siRNA, JNK2 knock-out cells failed to produce extracellular matrix mineralization in response to BMP2. Collectively, these results establish a regulatory role of JNK2 in human osteoblast differentiation and suggest that it functions by integrating canonical BMP/SMAD signaling and Notch signaling in human cells.

***Disclosures: Yadav Wagley**, None*

SUN-321

Low, but not High Fluid Shear Stress Affects Matrix Extracellular Phosphoglycoprotein Expression Mainly via Integrin ? Subunits in Preosteoblasts *Jianfeng Jin[1], Hadi Seddiqi[1], Jenneke Klein Nulend[2]. [1]Department of Oral Cell Biology, Academic Centre for Dentistry Amsterdam (ACTA), University of Amsterdam and Vrije Universiteit Amsterdam, Amsterdam Movement Sciences, Netherlands, [2]ACTA-University of Amsterdam and Vrije Universiteit Amsterdam, Netherlands

Introduction: Matrix extracellular phosphoglycoprotein (Mepe) is a member of the extracellular matrix short integrin-binding ligand interacting glycoprotein family of proteins. It plays important multifunctional roles in cell signaling, bone mineralization, and phosphate homeostasis. Mepe expression in bone cells changes in response to pulsating fluid shear stress (PFSS), which is transmitted into cells through integrin-based adhesion sites, i.e., ? and ? subunits. Whether PFSS magnitude controls Mepe expression via modulation of integrin ? and/or ? subunits expression in preosteoblasts is unknown. Therefore, we aimed to test whether low and/or high PFSS affects Mepe expression via modulation of integrin ? and/or ? subunit expression.Methods: MC3T3-E1 preosteoblasts were treated +/- 1h PFSS (0.4 Pa (low-PFSS) or 0.7 Pa (high-PFSS); 1 Hz). Before and after PFSS, cell morphology was observed by light microscopy. Integrin structure was visualized by laser scanning confocal microscopy, and integrin number, area, and fluorescence intensity were quantified by ImageJ. Expression of osteogenic and integrin ? and ? subunit-related genes was assessed by RT-PCR.Results: Preosteoblast morphology, and Runx2, Ki67, Bmp2, Fgf2, Cox2, Dmp1, and Sost gene expression were not affected by low or high-PFSS. Interestingly Mepe gene expression was decreased (0.3-fold) by low, but not high-PFSS. Integrin fluorescence intensity increased (1.1-fold), but integrin area decreased (0.7-0.8-fold) by low and high-PFSS (Fig. 1). Expression of integrin ? subunits 3 and 5-1 was not affected, but integrin ? subunit 5-2 was increased by low (8.0-fold) and high-PFSS (7.3-fold). Expression of integrin ? subunit 1 was increased (2.8-fold) by low-PFSS only, as was expression of integrin ? subunit 1 (2.1-fold) and subunit 3 (5.2-fold). Expression of integrin ? subunit 5 was increased (3.4-

fold) by low/high-PFSS, subunit 5-13 by low (10.8-fold) and high-PFSS (5.2-fold), and subunit 5-123 by low (4.6-fold) and high-PFSS (5.3-fold). Integrin ? subunit 5-12 expression was undetectable.Conclusions: Mepe expression in preosteoblasts was strongly modulated by low, but not high-PFSS. Integrin ? subunit structure and expression were altered by low and high-PFSS, while integrin ? subunit structure and expression were more altered by low-PFSS. This suggests that Mepe-induced changes in preosteoblast mechanosensitivity may drive signaling pathways of bone cell function mainly via integrin ? subunits.

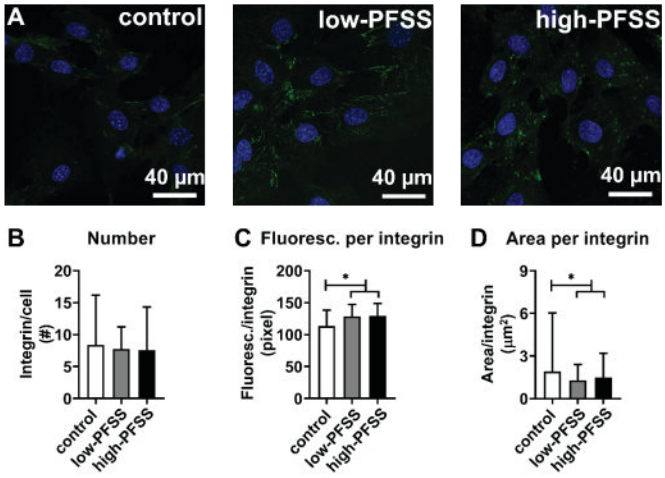

***Disclosures: Jianfeng Jin**, None*

SUN-322

ClC-3 and ClC-5 are essential to drive normal bone mineralization. *Quitterie Larrouture[2], Irina Tourkova[2], Deborah Nelson[3], Paul Schlesinger[4], Harry Blair[2]. [2]University of Pittsburgh, , [2]University of Pittsburgh, United States, [3]University of Chicago, United States, [4]Washington University , United States

Osteoblasts form an epithelial-like layer that separates the extracellular fluid (ECF) that contains the essential components to bone formation from the bone matrix. The production of hydroxyapatite in bone matrix produces a massive number of protons and their removal is essential to avoid stopping the mineralization process. Previously we established that Na/H exchangers 1 and 6 are highly expressed at secretory osteoblast basolateral surfaces and neutralize massive acid loads. We hypothesized that high-capacity proton transport from matrix into osteoblast cytosol must exist to support acid transcytosis for mineral deposition. Gene screening of cultured mineralizing osteoblasts showed dramatic expression of chloride-proton antiporters ClC3 and ClC5. Localization of ClC3 and ClC5 proteins at the apical secretory surface facing the bone matrix was confirmed by antibody labeling, at the EM level, of plasma membrane ClC3, and ClC5, in ClC3 knockout mice (Figure). To study the importance of ClC3 and ClC5 in bone mineralization in vivo and in vitro we used ClC-5 KO mice as well as ClC-3 KO mice. The whole exome sequencing confirmed the deletion of the whole exon 7 in ClC-3 KO mice and the deletion of part of the exon 6 in ClC-5 KO mice. No additional deletions were detected. The ClC-3 KO mice sowed a mildly disordered mineralization (microCT) and serum level of ALP and TRAP compared to WT. Surprisingly, at 3-5 months, body weights of ClC-5 KO females were significantly higher than control mice and 3D morphometry of the lumbar vertebrae showed a significant increase in bone surface/volume ratio in CLC-5 KO mice compared to control. Mass spectrometry-based proteomics confirmed that both KO mice have the presence of modified dysfunctional protein not seen in WT mice). In CLC-3 KO mice the normal CLC-5 protein was increased confirming what we showed previously that cultured ClC-3 KO osteoblasts have an increase in ClC-5 protein expression. After isolation from the bone marrow, CLC-3 KO and CLC-5 KO stromal stem cells were differentiated on PET membrane showing a lower alkaline phosphatase activity, a weak staining with Von Kossa as well as a decrease in collagen production, suggesting a decreased bone turnover. We conclude that regulated acid export, mediated by chloride-proton exchange, is essential to drive normal bone mineralization, and that CLC transporters also regulate fine patterning of bone.Figure: Transmission electron microscopy of mouse vertebrae showing the presence of CLC-5 (immunogold labeling, 12nm) at the apical secretory surface (red arrows) of an osteoblast facing the bone matrix (blue stars).

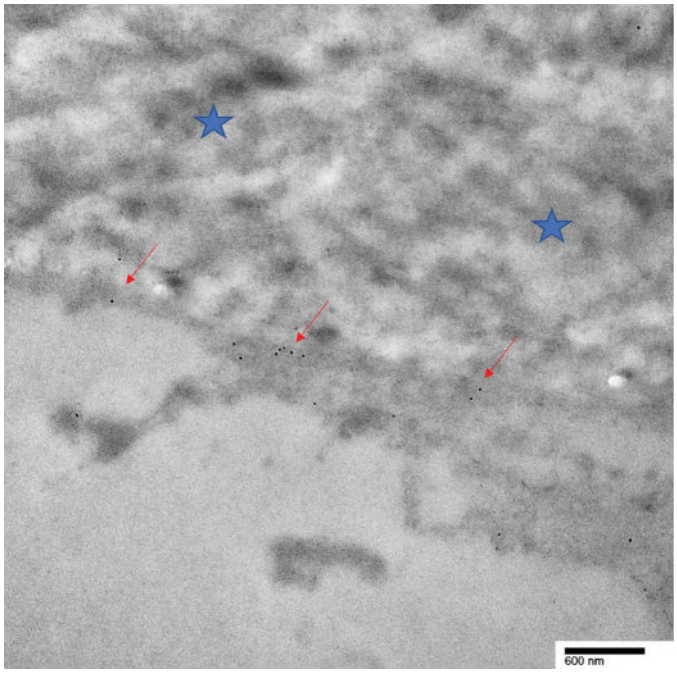

***Disclosures: Quitterie Larrouture**, None*

SUN-323

Muramyl dipeptide enhances bone formation in ovariectomized mice through WNT signaling *Ok-Jin Park[1], Yeongkag Kwon[1], Jiseon Kim[1], Chaeyeon Park[1], Cheol-Heui Yun[1], Seung Hyun Han[1]. [1]Seoul National University, Republic of Korea

Wnt and Nod2 signaling pathways positively regulate bone formation. Here, we investigated whether muramyl dipeptide (MDP), a representative Nod2 ligand, could alleviate post-menopausal osteoporosis through Wnt signaling regulation with an ovariectomy (OVX)-induced mouse osteoporosis model. MDP-administered OVX mice exhibited higher bone volume and mineral density than the control. MDP increased P1NP in the serum and the expression of pGSK3? and ?-catenin in the bone of MDP-administered OVX mice. MDP increased the expression and transcriptional activity of ?-catenin but inhibited the proteasomal degradation of ?-catenin via down-regulating its ubiquitination by GSK3? inactivation in osteoblasts. The induction of pAKT, pGSK3?, and ?-catenin by MDP was not observed in Wnt signaling inhibitor-pretreated osteoblasts or Nod2-deficient osteoblasts. MDP-administered OVX mice exhibited fewer osteoclasts than OVX mice with a decrease in the RANKL/OPG ratio. Conclusively, MDP alleviates estrogen deficiency-induced osteoporosis through canonical Wnt signaling and could be an effective therapeutic against postmenopausal bone loss.

***Disclosures: Ok-Jin Park**, None*

SUN-325

Non-thermal atmospheric plasma induces osteogenic activity in osteoblasts through WNT signaling Pathway *Ashish Ranjan Sharma[1], Supriya Jagga[2], Yeon-Hee Lee[3], Sang-Soo Lee[4]. [1]Hallym University, Republic of Korea, [2]Harvard University, United States, [3]Hallym university , Republic of Korea, [4]Hallym university, Republic of Korea

Non-thermal plasma (NTP: an ionized gas) is being employed for the biological and medical treatment of living tissues. Plasma is composed of free charges (electrons, ions), and free radicals, generating a transient electric field. Reactive oxygen and nitrogen species (ROS and RNS) produced by NTP are thought to be the primary factors that interact with the proteins to exert their biological effects. NTP has been reported as a potent stimulator for various biological activities, like anticancer, sterilization, promoting wound healing, etc. Recent studies have shown a positive effect of NTP on osteogenic induction in stem cells and bone regeneration. However, a clear insight into the mechanism of action of NTP on the osteoblasts is still warranted. Two types of (dielectric barrier discharge (DBD) or Jet) NTPs were treated to serum-free cell culture media with various time intervals (5, 10, 20 min) to generate various plasma-media interfaces for ion exchange. Ionized media showed no mitogenic or cytotoxic effects on murine preosteoblast cells, MC3T3 E-1. Among various NTP ionized mediums, Jet NTP medium (JNTPM, 10 min) showed induction of ALP activity of preosteoblasts after 48 h of treatment. A dose-dependent (% of JNTPM to complete medium) treatment of JNTPM to MC3T3 E-1 cells demonstrated an increased ALP activity from 25%

to 100% of media treatment. Since 25% of JNTPM was enough to induce maximum ALP activity in preosteoblasts, 25% of JNTPM was used for further experiments. Apart from ALP activity, JNTPM enhanced the mRNA expressions of osteogenic markers of osteoblasts like Osterix, Runx-2, bone sialoprotein, Collagen 1, and osteopontin. Moreover, the 7 d JNTPM-treated MC3T3 E-1 cells showed increased collagen synthesis and mineralization. Treatment of JNTPM to MC3T3 E-1 cells transfected with Axin-2 reporter construct showed time-dependent increased reporter activity, implying activation of the Wnt signaling pathway. The increased stabilization of ?-catenin and phosphorylation of GSK3-? further corroborated the activation of Wnt signaling. An N-acetyl-l-cysteine (NAC) treatment suppressed the Axin-2 reporter activity and stabilization of ?-catenin in JNTPM-treated MC3T3 E-1 cells, suggesting a role of ROS in the induction of Wnt signaling and thus osteogenic activity in preosteoblasts. Thus, further studies are required to delineate the cross-talk between ROS and Wnt signaling to understand the osteogenic stimulatory properties of JNTP.

***Disclosures: Ashish Ranjan Sharma**, None*

SUN-326

Mitochondrial dysfunction and integrated stress response in G610C mouse osteoblasts *Elena Makareeva[1], Megan Sousa[1], Laura Gorrell[1], Shakib Omari[1], Satoru Otsuru[2], Sergey Leikin[1]. [1]National Institutes of Health, United States, [2]University of Maryland, United States

Osteoblast cell stress caused by the misfolding of procollagen has been shown to be an important factor in bone pathology resulting from Gly substitutions in osteogenesis imperfecta (OI). Our previously published studies of G610C mice with a Gly610Cys substitution in the triple helical region of the ?2(I) chain of type I collagen revealed increased EIF2? phosphorylation and ensuing integrated stress response (ISR) in osteoblasts without upstream unfolded protein response (UPR). Instead, upregulated expression of Hspa9 and Atf5 encoding mitochondrial paralogues of BIP and ATF4 suggested mitochondrial involvement in the ISR activation, probably via disruption of ER-mitochondria contacts. In the present study, we tested this hypothesis in primary osteoblast cultures by investigating which of the four EIF2? kinases activate the ISR and by imaging mitochondrial dynamics, ATP, and reactive oxygen species (ROS). We observed altered mitochondrial fission, increased ROS production in differentiating osteoblasts, reduced ATP synthesis in mature cells, and EIF2? phosphorylation by GCN2 rather than PERK in response to the G610C mutation. Taken together with our published studies of G610C procollagen trafficking in osteoblasts, these observations suggest the following ISR activation mechanism. Like all secretory proteins, the procollagen precursor of collagen is folded in the ER and exported through ER exit sites (ERESs). Its triple helix misfolding, however, is detected at ERESs rather than in the ER lumen. Blockage and depletion of functional ERESs due to the retention of misfolded procollagen by ERESs disrupts the exit of all secretory proteins and causes their accumulation in the ER. The resulting ER dilation disrupts ER-mitochondria contacts, leading to mitochondrial dysfunction and activation of the mitochondrial, not ER, arm of the ISR, in which EIF2? is phosphorylated by GCN2 rather than PERK. This novel pathway of ISR activation by secretory protein misfolding in the ER may present new opportunities for therapeutic targeting of osteoblast malfunction in classical OI.

***Disclosures: Elena Makareeva**, None*

SUN-327

Orphan GPCR, Gprc5a, is a novel parathyroid hormone-inducible gene and negatively regulates osteoblast proliferation and differentiation in osteoblast-like MC3T3-E1 cells. *Chisato Sampei[1], Kosuke Kato[1], YASUHIRO ARASAKI[2], Yuta Kimura[1], Takuto Konno[1], Kanon Otsuka[1], Masaki Noda[3], Yoichi Ezura[4], Yukihiro Kohara[1], Tadayoshi Hayata[5]. [1]Tokyo University of Science, Japan, [2], Japan, [3]Tokyo Medical and Dental University, Japan, [4]Tokyo Medical and Dental University, Medical Research Insititute, Japan, [5]Graduate School of Pharmaceutical Sciences and Faculty of Pharmaceutical Science, Tokyo University of Science, Japan

Teriparatide is a peptide derived from a parathyroid hormone (PTH) and is an osteoporosis therapeutic drug with potent bone formation-promoting activity. However, its pharmacological actions are not fully understood. To better understand the mechanism of action of teriparatide and identify novel druggable genes that act downstream of PTH signaling, we conducted a screening of teriparatide target genes in mouse osteoblast-like MC3T3-E1 cells. Here we show that Gprc5a, an orphan G protein-coupled receptor is a novel teriparatide-inducible gene and negatively regulates osteoblast proliferation and differentiation. Gprc5a expression was induced by teriparatide in MC3T3-E1 cells, rat osteosarcoma ROS17/2.8 cells, and rat femur. Induction of Gprc5a expression by teriparatide occurred in the absence of protein synthesis and was mediated via the cAMP pathway, suggesting that Gprc5a is a direct target of PTH signaling. Interestingly, Gprc5a expression was induced synergistically by co-treatment with teriparatide and 1?, 25-Dihydroxyvitamin D3 (calcitriol), or retinoic acid in MC3T3-E1. Reporter analysis of a 1 kb fragment of human GPRC5A promoter revealed that the promoter fragment showed responsiveness to teriparatide via the cAMP response element, suggesting that GPRC5A is also a PTH-inducible gene in humans. Gprc5a knockdown promoted cell viability and proliferation, as demonstrated by MTT and BrdU assays. Gprc5a expression was reduced during osteoblast differentiation. Lentivirus-mediated overexpression of Gprc5a suppressed osteoblast differentiation, as indicated by gene expression analysis and mineralization assay. Mechanistic studies showed that Gprc5a interacted with BMPR1A and suppressed BMP signaling induced by BMP-2 and constitutively active BMP receptors, ALK2 (ACVR1) Q207D and ALK3 (BMPR1A) Q233D. Thus, our results suggest that Gprc5a is a novel gene induced by teriparatide that acts in an inhibitory manner on both cell proliferation and osteoblast differentiation and is a candidate for drug targets for osteoporosis.

***Disclosures: Chisato Sampei**, None*

SUN-329

Role of the N-glycosylation Sites for Enzymatic Activity of Tissue-Nonspecific Alkaline Phosphatase and Presence of Bone-Specific Isoforms *Diana Atanasova[1], Lavanya Moparthi[2], Stefan Koch[2], Marwa Abdul Hamid[1], Eva Landberg[1], Sonoko Narisawa[3], José Luis Millán[3], Per Magnusson[1]. [1]Department of Clinical Chemistry, and Department of Biomedical and Clinical Sciences, Linköping University, Sweden, [2]Wallenberg Centre for Molecular Medicine, and Department of Biomedical and Clinical Sciences, Linköping University, Sweden, [3]Sanford Children's Health Research Center, Sanford Burnham Prebys Medical Discovery Institute, United States

Tissue-nonspecific alkaline phosphatase (TNALP) expressed by osteoblasts is known as bone-specific alkaline phosphatase (BALP). BALP is a membrane-bound glycoprotein that facilitates bone mineralization by hydrolysis of the mineralization inhibitor pyrophosphate and of ATP to provide inorganic phosphate, thus controlling the PPi/Pi ratio to enable hydroxyapatite formation. To date, four BALP isoforms can be quantified in serum by HPLC based on different N-linked glycosylation properties. Commercial immunoassays are currently available for the measurement of BALP which reflects bone formation. However, these assays cannot distinguish the individual BALP isoforms. A novel approach to detect the individual BALP isoforms could be to target specific glycoprotein motifs. We have previously demonstrated that all five sites of BALP located at N140, N230, N271, N303 and N430 are glycosylated. In this study, we aimed to study how the five N-glycosylation sites affect the BALP isoform profile with Western blot, enzymatic activity and HPLC after site-directed mutagenesis. The five asparagine (N)-glycan sites were substituted with glutamine (Q) or aspartic acid (D) in the following mutations: N140Q, N230Q, N271Q, N303Q and N430D. Both single and multiple mutations were generated in a human TNALP-expressing plasmid and expressed in Alpl-/- mouse calvarial osteoblasts. Herein, we found that mutating a single N-glycan site did not influence the expression, activity or isoform profile of the expressed BALP in comparison with WT. However, the double substitution of N230Q/N271Q led to decreased protein expression and 9% residual enzymatic activity of WT. N271Q/N303Q and N303Q/N430Q had 57% and 79% residual activity, respectively. N140Q/N230Q, N230Q/N430D and N271Q/N430D slightly changed the activity. The BALP isoform analysis by HPLC of both single and double mutations showed similar BALP isoform patterns as WT. However, a shift in retention time was observed in the double mutations. In conclusion, the presence of BALP isoforms is not dependent on a single N-glycan site. The N-glycan sites N230 and N271 are pivotal for normal activity of BALP. Low BALP protein amounts were found when three N-glycan sites were mutated, which suggests that these N-glycan sites are needed for stable protein expression. Additional studies are needed to understand the structural and functional differences of N-linked glycosylation among the BALP isoforms.

***Disclosures: Diana Atanasova**, None*

SUN-330

Targeted Expression of Claudin (Cldn)-11 in Osteoblasts Increases Trabecular Bone Mass by Stimulating Bone Formation and Reducing Marrow Adiposity in Mice *Weirong Xing[1], Sheila Pourteymoor[2], William Tambunan[2], Subburaman Mohan[3]. [1]Musculoskeletal Disease Center, Jerry L. Pettis Memorial Veteran s Admin., United States, [2]VA Loma Linda Healthcare System, United States, [3]Jerry L. Pettis Memorial VA Medical Center, United States

The claudin (CLDN) family comprises 24 members of 20-34 kDa tetraspan transmembrane proteins of tight junctions. In addition to their established canonical role as barriers controlling the flow of molecules in the intercellular space between cells, a distinct non-canonical role for CLDNs is now emerging in which they serve as mediators of cell signaling. In previous studies, we showed that mice with global deletion of Cldn-11 gene exhibited reduced trabecular bone mass. However, the impact of Cldn11 expression osteoblast lineage cells in vivo remains undefined. Here, we generated osteoblast-specific transgenic lines expressing Cldn11 transgene driven by the ColCAT2.3 promoter and characterized their skeletal phenotype. Micro-CT analysis of distal femoral metaphysis showed that trabecular bone mass was increased by 50% and 38% (both $P<0.01$, n=8-10 per gender), respectively, in the transgenic male and female mice compared to littermate control mice that was caused by a significant increase in trabecular number and reduction in trabecular separation. Trabecular bone mass was also increased by 43% ($P<0.01$) in the proximal tibial metaphysis of transgenic mice of both genders. Histology and serum biomarker studies revealed that increased bone formation, and not reduced bone resorption, is the cause for increased trabecular bone mass in the Cldn11 Tg mice. Accordingly, expression levels of bone formation (Alp, Bsp) but not bone resorption (Ctsk) markers were increased in the bones of Cldn11 transgenic mice. Since bone marrow stromal cells are common precursors for osteoblasts

and adipocytes and marrow adipose tissue (MAT) is known to correlate with trabecular bone mass inversely, we measured MAT by micro-CT of osmium tetroxide labeled bones. MAT was reduced by 86% (P<0.05) in the proximal tibia of transgenic male mice compared to control mice. Accordingly, the expression levels of the adipogenic markers (adiponectin and Asc1) and regulators of MAT (adipsin and leptin), were significantly reduced by 45-53% (P<0.05) in the bones of transgenic male mice. Our data are consistent with the possibility that CLDN11 exerts anabolic effects in osteoblasts by promoting the differentiation of mesenchymal stem cells towards osteoblasts at the expense of adipocytes.

***Disclosures: Weirong Xing**, None*

SUN-331

Functional Validation of Dock9 as a Potential Regulator of Bone Mass with In Vitro and In Vivo Models *Gregory Ottenberg[1], Megan Kraus[1], Dana Godfrey[1], Larry Messner[2], Charles Farber[2], Cheryl Ackert-Bicknell[1]. [1]University of Colorado, United States. [2]University of Virginia, United States

We previously identified osteoblast gene expression gene network modules enriched for genes identified by human genome wide association studies (GWASs) as being associated with bone mineral density (BMD). One module core gene was Dock9, a cell signaling gene that acts on G proteins. Data from International Mouse Phenotyping Consortium suggested that loss of this gene impacted BMD, but this result required validation. We used CRISPR-Cas9 to generate Dock9-/- mutant mice and body composition was measured via DXA in 12-week-old mice. In Dock9 -/- mice, there was an increase in BMD in both males (Dock9-/- = 79.7?3.3 mg/cm2 vs Dock9+/+ = 69.7?3.8 mg/cm2, p = 0.08) and females (Dock9-/-=77.4?2.8 mg/cm2 vs Dock9+/+= 59.4?2.1 mg/cm2, p<0.001), with no increase in bone area (female p = 0.32, male p = 0.95). Female, but not male mice showed an increase in lean mass (Female Dock9-/- = 17.5?0.6g vs Dock9+/+ = 14.8?1.4g, p = 0.011, Male p=0.44), but no difference in fat mass (not shown). Calvarial derived osteoblasts were isolated from neonates and mineralization was monitored in a time course manner using the calcium binding IRDye 800CW BoneTag (Licor). We saw delayed mineralization in Dock9-/- osteoblasts vs Dock9+/+ cells but no change in the rate of mineralization. This resulted in an overall reduction in mineralization (Fig 1 A). To confirm this effect, murine MC3T3-E1 pre-osteoblast cells were treated with siRNAs targeted to Dock9. Western Blots confirmed that DOCK9 was knocked down by Dock9 siRNAs compared to scrambled siRNA controls (Fig 1B). We again observed delayed mineralization, but no change in the rate (Fig 1 C&D.) This resulted in less mineralization in the Dock9 deficient cells as validated by Alizarin Red at the end of the experiment. Quantitative PCR revealed a transient effect on Dock9, Sp7, and Runx2 expression in the siRNA treated cells. Available RNAseq data shows that Dock9 is not expressed in osteoclasts but is expressed highly in osteoblasts and osteocytes. Collectively, our data cannot explain the increased BMD in the absence of Dock9, but do show a primary impact on osteoblast function. This confirms why Dock9 featured prominently in our network analysis and substantiates this gene is a candidate for the BMD GWAS locus. Future studies will investigate if there is in an increase in osteoblast number in vivo increasing overall mineralization, or a suppression of resorption via crosstalk that could explain this increase in BMD.

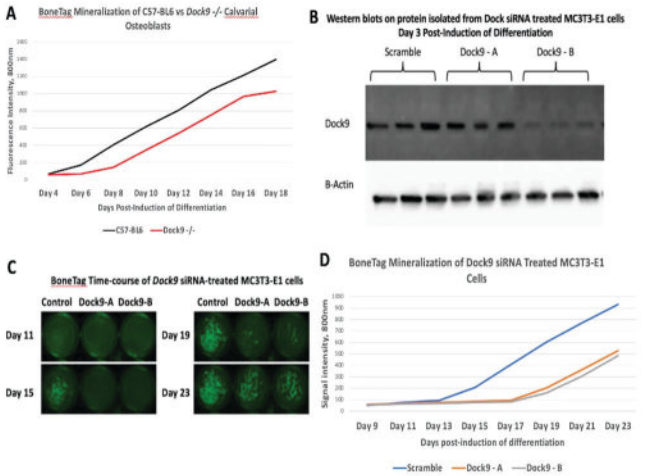

Figure 1: A) Mineralization assay showing delay of onset of mineralization in *Dock9-/-* calverial osteoblasts. B) Western Blot results showing decrease of *Dock9* expression after siRNA treatment. C) BoneTag images of MC3T3-E1 cells after *Dock9* siRNA treatment. D) Mineralization assay showing delay of onset of mineralization in MC3T3-E1 cells after *Dock9* siRNA treatment.

***Disclosures: Gregory Ottenberg**, None*

SUN-334

Azilsartan Inhibits Inflammation-Triggered Bone Resorption and Osteoclastogenesis in vivo via Suppression of TNF-? Expression in Macrophages *ZIQIU FAN[1], Hideki Kitaura[4], Jiayi REN[3], Fumitoshi Ohori[1], Takahiro Noguchi[1], Aseel Marahleh[4], Jinghan Ma[4], Kayoko Kanou[1], Mariko Miura[1], KOHEI NARITA[1], Itaru Mizoguchi[1]. [1]Tohoku University Graduate School of Dentistry, Japan. [4]Tohoku University, Japan. [3]Graduate School of Dentistry, Tohoku University, . [4]Tohoku University,

Introduction: Hypertension is a major risk factor for cardiovascular disease (CVD) and is associated with increased bone loss due to excessive activity of the local renin-angiotensin system (RAS). Angiotensinogen/Angiotensin (ANG) II/Angiotensin II type 1 receptor (AT1R) axis is considered as the core axis regulating RAS activity. Azilsartan is an FDA-approved selective AT1R antagonist that is used to treat hypertension. This study aimed to determine whether azilsartan affects formation of osteoclast, resorption of bone, and the expression of cytokines linked with osteoclastogenesis during lipopolysaccharide (LPS)-triggered inflammation in vivo. Methods: Following a 5-day supracalvarial injection of LPS with or without azilsartan, the proportion of bone resorption and number of osteoclasts were counted. In vitro, the effect of azilsartan on RANKL-or TNF-?-triggered osteoclastogenesis was investigated. Also, whether azilsartan restrains LPS-triggered TNF-? mRNA expression in macrophages and RANKL mRNA expression in osteoblasts were assessed. Results: Azilsartan-treated calvariae exhibited significantly lower bone resorption and osteoclastogenesis than those treated with LPS alone. In vivo, LPS with azilsartan administration resulted in lower levels of receptor activator of NF-?B ligand (RANKL) and tumor necrosis factor-alpha (TNF-?) mRNA expression than LPS administration alone. Nevertheless, azilsartan did not show inhibitory effect on RANKL- and TNF-?-triggered osteoclastogenesis in vitro. Compared to macrophages treated with LPS, TNF-? mRNA levels were lower in macrophages treated by LPS with azilsartan. In contrast, RANKL mRNA expression levels in osteoblasts were the same in cells co-treated with azilsartan and LPS and those exposed to LPS only. Conclusion: These findings imply that azilsartan prevents LPS-triggered TNF-? production in macrophages, which in turn prevents LPS-triggered osteoclast formation and bone resorption in vivo.

***Disclosures: ZIQIU FAN**, None*

SUN-336

Identification of glutamine metabolism as a metabolic vulnerability in osteoclasts *GUOLI HU[1], Yilin Yu[3], Robert Tower[3], Guo-fang Zhang[4], Courtney Karner[3]. [1]UT Southwestern Medical Center, . [3]University of Texas Southwestern Medical Center, United States. [3]University of Texas Southwestern Medical Center, . [4]Duke University, United States

Osteoclasts are bone resorbing cells that are essential to maintain skeletal integrity and function. Excessive osteoclast activity causes both age-related and pathological bone loss associated with several diseases including osteoporosis. While many of the growth factors and molecular signals that govern osteoclastogenesis are well studied, a large gap in our knowledge exists about the role and regulation of cellular metabolism during osteoclastogenesis. Advances in our understanding of differentiation associated metabolic changes will aid in identifying metabolic vulnerabilities that can be exploited therapeutically to reduce bone resorption and pathological bone loss. Here, we used a multifaceted approach to define the metabolomic signature of osteoclasts. When compared to bone marrow monocyte and macrophage cultures, mature osteoclasts (mOC) have significantly increased abundance of amino acids and purine and pyrimidine nucleotides. Osteoclasts must increase the consumption and metabolism of glutamine which provides carbon and nitrogen for amino acid and nucleotide biosynthesis. Importantly, inhibiting glutamine metabolism in mOC resulted in a complete loss of the metabolomic signature and prevented osteoclast differentiation in vitro. Deletion of a floxed Gls allele (Glsfl) in myeloid progenitor cells using LysmCre resulted in significantly higher bone mass at 4- and 6-months of age in male and female mice. The LysmCre;Glsfl/fl bone phenotypes were attributed to a reduction in osteoclast numbers and bone resorption with no change osteoblast parameters. Conversely, expressing a doxycycline inducible Gls allele (tetoGls) using LysmCre (LysmCre;R26rtTA;tetoGls) increased osteoclastogenesis, enhanced bone resorption and rapidly reduced bone mass. Highlighting the therapeutic implications of these findings, genetically inhibiting glutamine metabolism prevented ovariectomy induced bone loss in mice. Collectively, our data provide genetic evidence that glutamine metabolism is essential to regulate osteoclast metabolism, osteoclastogenesis and bone resorption in mice. Moreover, our study demonstrates osteoclasts are reliant on glutamine metabolism like cancer cells. Targeting glutamine dependency using Telaglenastat is being developed as a potential cancer treatment. Our findings indicate it may be possible to repurpose this strategy to prevent excessive bone resorption.

***Disclosures: GUOLI HU**, None*

SUN-337

IGFBP regulates osteoclast differentiation. *Yusaku Hamada[1], Takashi Izawa[2], Yuri Yoshikawa[1], Gohji Kozaki[1], Hiroshi Kamioka[3]. [1]Department of Orthodontics, Graduate School of Medicine, Dentistry and Pharmaceutical Sciences, Okayama University, Japan. [2]Okayama University Grad Sch, Japan. [3]Okayama University Graduate School of Medicine, Dentistry, and Pharmaceutical Sc, Japan

Global deletion of the Igfbp gene results in the suppression of bone turnover. To investigate the role of insulin-like growth factor binding protein (IGFBP) in regulating osteoclast differentiation, we cultured Igfbp?/? bone marrow macrophages (BMMs) and found a reduction in the number of osteoclasts and impaired resorption. To determine the molecular domains of IGFBP that were required for this effect to be manifest, Igfbp?/? BMMs were transfected with constructs which the IGF-binding domains or the thyroglobulin type-1 domain of IGFBP were deleted. We found that both domains were necessary for osteoclastogenesis because expression of the deletion forms of either domain failed to support the formation of functionally mature osteoclasts. Next, to examine whether IGFBP overexpression enhances RANKL-induced osteoclastogenesis, we retrovirally transduced IGFBP into WT BMMs and stimulated with RANKL. Upon RANKL treatment, BMMs transduced with IGFBP-WT vector underwent osteoclastic differentiation more readily and increased bone resorption activity when compared with the BMMs transduced with empty vector. Furthermore, recombinant IGFBP enhance the RANKL-induced osteoclastogenesis in a dose dependent manner. Finally, to discern the mechanism by which IGFBP regulates osteoclast formation, phosphorylation of Akt respond to IGF-I were analyzed. We concluded that IGFBP is an important regulator of osteoclastogenesis and both the IGF-binding domain and the thyroglobulin type-1 domain of IGFBP are essential for the formation of fully differentiated and functional osteoclasts.

***Disclosures: Yusaku Hamada**, None*

SUN-338

A Novel Fluorogenic Probe for Intravital Microscopic Imaging of Enzymatically Active Cathepsin K in Functional Osteoclasts *Eun Jung Lee[1], Seyoung Koo[2], Da Hyeon Yoon[1], Jong Seung Kim[2], SERK IN PARK[1]. [1]Korea University College of Medicine, Republic of Korea. [2]Department of Chemistry, Korea University, Republic of Korea

Cathepsin K (CTSK) is a lysosomal cysteine protease that is essential to the osteolytic activity of functional osteoclasts. Several fluorescence-based probes for CTSK have been developed for preclinical studies on osteoclast inhibitors but the sensitivity and signal intensity are insufficient for real-time live imaging in mice. To overcome this limitation, we synthesized a novel fluorescence resonance energy transfer (FRET)-based fluorogenic CTSK probe and tested its efficacy in vitro using a confocal microscope and in vivo using an intravital microscope. A peptide substrate specific to CTSK was conjugated with a TAMRA fluorophore and a BHQ-2 quencher. Upon addition of a nano-molar range of recombinant CTSK, the TAMRA fluorophore was cleaved from the quencher, resulting in a strong fluorescence signal, which was fully suppressed by odanacatib, a CTSK inhibitor. Notably, our probe exhibited over 60-fold higher sensitivity than previously reported probes. For in vitro imaging, osteoclasts were formed by treating murine bone marrow monocytes with RANKL and M-CSF on collagen-coated plates or dentin discs, followed by fixation, permeabilization and staining with the probe, phalloidin and DAPI. Confocal microscopy demonstrated the subcellular localization of CTSK in osteoclasts (Figure Panel A). A strong fluorescence signal was localized in the ruffled border, indicating that the probe is sensitive and specific to functional CTSK in bone-resorbing osteoclasts. For intravital imaging, we used three different mouse models: an ovariectomy-induced osteoporosis model, a RANKL injection bone loss model, and a bone metastasis model using intra-tibial injection of breast tumor cells. The CTSK probe was administered by tail-vein injection (50?mol), and live real-time images were captured in the proximal tibia with a small skin incision under anesthesia. No significant toxicities were noted in multiple injection groups of mice. Two-photon intravital microscopy showed clear real-time images of osteoclasts on the endosteal surface or trabecular bone of live animals (Figure Panel B). The fluorescence signal was not detectable in negative control mice, and the signal was significantly reduced in mice treated with zoledronic acid or odanacatib. In conclusion, we developed a novel probe for sensitive and specific visualization of functional CTSK in real-time live mice that can be useful in bone biology research and in the development of therapeutics for CTSK or osteoclasts.

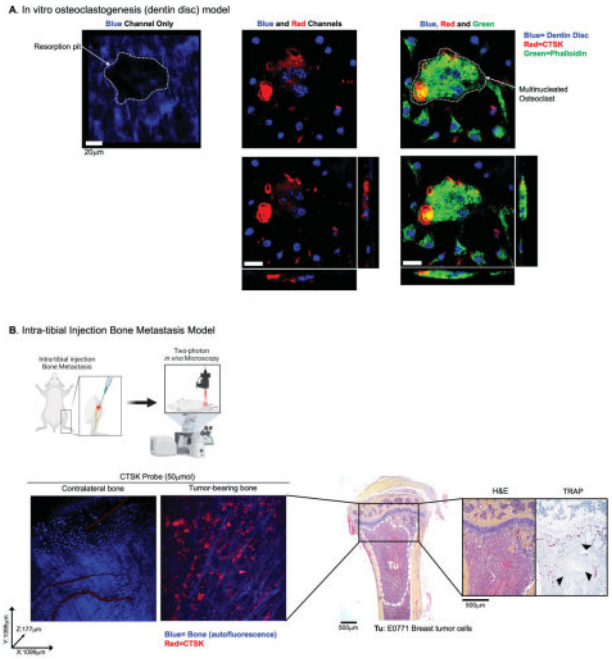

***Disclosures: Eun Jung Lee**, None*

SUN-340

Even in the absence of RANKL and serum, human bone resorbing osteoclasts in vitro are more active when female donors are 60 to 80 years compared to 25-30 years of age *Neha Sharma[1], Jacob B. Olesen[2], Pernille Hermann[3], Julie Therese Skaugen[4], Line Strand Andersen[4], Torben Barington[4], Megan Weivoda[5], Kent Soee[1]. [1]Clinical Cell Biology, Dept. of Pathology, OUH/SDU; Dept. of Clinical Research, SDU; Dept. of Molecular Medicine, SDU, Denmark. [2]Clinical Cell Biology, Dept. of Pathology, OUH/SDU, Denmark. [3]Dept. of Endocrinology, OUH, Odense, DK, Denmark. [4]Dept. of Immunology, OUH, Denmark. [5]Dept. of Hematology, Mayo Clinic, United States

Previously, we reported that the bone resorptive activity of human osteoclasts (OCs) increases with age of the donor, especially caused by OCs making trenches. We are interested in investigating whether the age of the donor has such a strong impact on bone resorbing OCs in vitro that it would still be observed in the absence of fetal bovine serum (FBS) and RANKL.12 female donors were recruited, CD14+ monocytes from their blood were differentiated into OCs using 25 ng/ml M-CSF & RANKL and 10% FBS over 9 days in vitro. OCs were detached, split in two and reseeded at a density of 50,000 cells per bovine bone slice and cultured either 1) with 25 ng/ml M-CSF & RANKL and 10% FBS or 2) with only 25 ng/ml M-CSF. After 72h, conditioned media was collected for TRAcP-activity measurement. Bone resorption was visualized using toluidine blue and bone erosion was quantified using a light microscope, a 100-point grid, and were categorized into pits and trenches. Bone resorption was analyzed in a blinded manner.Group 1 (G1, 25-35 years) and Group 2 (G2, 60-80 years). Osteoclastic bone resorption conducted in the presence of FBS and RANKL clearly showed that OCs from G2 (n=7) were more active than those from G1 (n=5) - and especially made more trenches: 1) eroded surface(ES)/bone surface(BS), G1 3.7% vs G2 6.4%, p=0.005; 2) trench surface(TS)/BS, G1 1.1% vs G2 3.2%, p=0.001); 3) pit surface(PS)/BS, G1 1.5% vs G2 3.0%, p=ns; 4) TS/ES, G1 38.1% vs G2 58.1%, p=0.001. TRAcP activity was 6.4 times higher in G2 compared to G1 (p=0.0002). Osteoclastic bone resorption conducted in the absence of FBS and RANKL gave very similar results showing that OCs from G2 (n=7) were more active than from G1 (n=4): 1) ES/BS, G1 0.7% vs G2 2.2%, p=0.005; 2) TS/BS, G1 0.3% vs G2 0.8%, p=0.005; 3) PS/BS, G1 0.3% vs G2 1.2%, p=0.005; 4) TS/ES, G1 44.2% vs G2 57.8%, p=ns). TRAcP activity was 6.5 times higher in G2 compared to G1 (p=0.03).In conclusion, we replicate our previous findings that increasing age results in more aggressive bone resorbing OCs in vitro and that this is primarily mediated through trench making OCs, in the presence of RANKL and FBS. In their absence, bone resorption is highest in G2, but this seems to be caused both by OCs making pits and trenches. This is an ongoing study and more donors need to be recruited in order to make firm conclusions, but it is clear that increasing age of donor enhances osteoclastic bone resorption in vitro, even in the absence of RANKL and FBS.

***Disclosures: Neha Sharma**, None*

SUN-342

Pim1 contributes to maintenance of bone homeostasis via regulation of osteoclast function *Soo Young Lee[1], Ryeojin Ko[1], Jeongin Seo[1]. [1]Ewha Womans University, Republic of Korea

ObjectiveThe proviral integration site for Moloney murine leukemia virus 1 (Pim1) protein is a highly conserved serine/threonine kinase that is involved in a variety of cellular processes including cell survival, proliferation, and apoptosis. In addition, Pim1 has been shown to regulate the differentiation of osteoclasts. Mature osteoclasts absorb bone matrix by forming an actin ring between themselves and the bone surface. However, the role of Pim1 in the bone-resorbing function of osteoclasts is largely unknown.MethodsIn this study, we generated Pim1-/- mice to investigate the role of Pim1 in the regulation of bone metabolism. We conducted immunofluorescence staining of actin and acetylated tubulin in osteoclast on dentin slices and coverslips in wild-type and Pim1-/- mice. To identify whether Pim1 deletion affects bone growth in vivo, we examined the microstructure of the distal femur from 8 weeks old male mice wild-type and Pim1-/- mice using micro-computed tomography (micro-CT) analysis.ResultsWe demonstrated that Pim1 deletion does not affect the differentiation of osteoclasts. However, a significant reduction in resorption area was observed in Pim1-/- mice. In addition, Pim1-deficient osteoclasts were unable to form normal actin rings, and the acetylation pattern of microtubules was abnormal. Furthermore, an increase in distal femoral bone mass was observed in Pim1-/- mice compared to wild-type mice.Conclusions-These results indicate that Pim1 plays an important role in the bone-resorbing function of osteoclasts. Therefore, the control of osteoclast activity via targeting Pim-1 will provide a novel therapeutic option for the treatment of bone diseases.

***Disclosures: Soo Young Lee**, None*

SUN-343

Orthosilicic Acid Inhibits Human Osteoclast Differentiation and Bone Resorption *Catarina Magnusson[1], Maria Ranjö[2]. [1]Institute of Odontology, Sahlgrenska Academy, University of Gothenburg, Sweden. [2]Institute of Odontology, Sahlgrenska Academy, University of Gothenburg / Department of Odontology, Umeå University, Sweden

Silicon (Si) is a mineral found in our diet and is also present in some bone substitute materials used in the treatment of craniofacial and dentoalveolar bone defects. The bioavailable form of Si and hence, the form with biological relevance, is orthosilicic acid [Si(OH)4]. In vitro studies investigating the effect of Si on osteoblast-like cells have shown osteogenic properties with increased differentiation and function. We have demonstrated that Si inhibits osteoclast differentiation in mouse cells either co-culture from bone marrow (Mladenovic Z et al., Acta Biomater. 2014) or in a monocyte/macrophage cell line (Magnusson C et al., J Biomed Mater Res A. 2021). The present study aimed to further investigate the direct effects of Si on osteoclast differentiation, gene expressions, and bone resorption in human osteoclast precursors.Human CD14+ monocytes were isolated from buffy coat and cultured with M-CSF (25 ng/ml) and RANKL (2 or 25 ng/ml) in medium without or with Si (50 ?g/ml; constituting 75% OSA). The effects of Si on osteoclast differentiation were evaluated by TRAP-staining and the expression of DC-STAMP, cathepsin K, TRAP, and calcitonin receptor by RT-qPCR. The effect of Si on the gene expression of aquaporin9, a potential Si transporter, was also analysed. Bone resorption was determined by the number of resorption pits formed when the cells were cultured on bone slices, and the amount of type I collagen fragments released in the cell culture medium.Silicon inhibited the number of TRAP+ multinucleated cells and significantly inhibited the expression of osteoclast related genes, but increased the expression of aquaporin9. Furthermore, Si significantly inhibited the number of resorption pits and the amount of collagen fragments in the culture medium when cells were cultured on bone slices.In conclusion, our results indicates that orthosilicic acid inhibits osteoclast differentiation and bone resorption in RANKL-stimulated primary human monocytes and that aquaporin9 may facilitate the transmembrane transport of Si.

***Disclosures: Catarina Magnusson**, None*

SUN-344

Transcriptional Reprograming during Human Osteoclastogenesis Identifies Targets for Predicting and Modulating Osteoclast Differentiation and Activity *Morten S. Hansen[1], Kaja Madsen[2], Maria Price[3], Kent Søe[1], Caroline M. Gorvin[3], Morten Frost[1], Alexander Rauch[2]. [1]Odense University Hospital, Denmark. [2]University of Southern Denmark, Denmark. [3]University of Birmingham, United Kingdom

Background: Increased osteoclastogenesis and osteoclast activity are important causes of postmenopausal osteoporosis. Understanding the transcriptional reprogramming during osteoclastogenesis has the power to identify targets for novel anti-osteoporotic drugs.Purpose: Define gene expression dynamics during human osteoclast differentiation for the alignment with bone mineral density related expression and GWAS data, the construction of transcriptional networks and the identification of G-protein-coupled receptors and surface molecules that allow interference with osteoclast activity and the prediction of subject-specific resorptive potential.Methods: Human osteoclasts were differentiated (t=10 days) in vitro from CD14+-monocytes from eight female donors aged 18-49 years. RNA-sequencing was performed at four time points (day 0 prior to and 2-, 5-, and 9-days post-differentiation). GPCRs were targeted with agonist and/or antagonists and FACS based surface molecule expression was determined in relation to bone resorbing activity.Results: We identified 8446 differentially expressed genes with high reproducibility across donors that were grouped into eight temporal patterns which based on network analysis are linked by mutual and temporal dependencies. These patterns were enriched for distinct molecular functions, metabolic pathways, and genes that are flanked by bone mineral density associated SNPs. Compared to normal, osteoporotic bones exemplified gene signatures of mature osteoclasts and absence of precursor related genes. Using pharmacological interference with differentially expressed GPCRs, we found activation of somatostatin receptor 2 (SSTR2) to decrease osteoclast resorption, activation of free fatty acid receptor 4 (FFAR4/GPR120) to decrease both osteoclast numbers and activity, and activation of complement C5a receptor 1 (C5AR1) to increase osteoclast numbers. FACS analysis affirms expression of oxidised LDL receptor 1 (LOX1) and activated CDC42 kinase 1 (ACK1) on precursors to be correlating with activity of the mature cells. Conclusions: We provide a consecutive map of the transcriptional reprogramming during human osteoclastogenesis that highlights the strong implication of osteoclast genes in the aetiology and genetics of human bone loss. Targeting stage specifically expressed GPCRs as well as the quantifying resorption-associated surface molecules highlights the identification of targets and monitors for anti-resorptive treatment options.

***Disclosures: Morten S. Hansen**, None*

SUN-345

Critical role of osteoclast-derived EVs in medication-related osteonecrosis of the jaws (MRONJ) *Sakura Minami[1], Yasuyuki Fujii[1], Ayano Hatori[1], Yusuke Yoshioka[2], Takahiro Ochiya[2], Daichi Chikazu[1]. [1]Department of Oral and Maxillofacial Surgery, Tokyo Medical University, Japan. [2]Department of Molecular and Cellular Medicine, Tokyo Medical University, Japan

Medication-related osteonecrosis of the jaws (MRONJ) is an intractable form of osteonecrosis of the jaw that rarely occurs in patients with malignancies and osteoporosis who are using bone resorption inhibitors such as bisphosphonates (BPs). MRONJ is mainly triggered by surgical invasion such as tooth extraction. However, the detailed mechanism of MRONJ pathogenesis is unknown. Extracellular vesicles (EVs) encode many signaling molecules such as mRNAs, miRNAs, and proteins, and have attracted attention as intercellular communication tools. It has also recently been shown that EVs are also involved in communication between osteoclasts and osteoblasts. The aim of this study is to elucidate the pathomechanism of MRONJ by studying the role of osteoclast-derived EVs . Mouse bone marrow cells were treated with M-CSF and RANKL to induce osteoclastogenesis. Zoledronic acid (ZA) were added to the culture medium to reproduce the MRONJ environment in vitro. EVs were isolated from the culture supernatant by ultracentrifugation and miRNA were extracted from the osteoclast-derived EVs. TRAP staining of the osteoclasts with ZA showed lower osteoclastgenesis. In addition, Phalloidin/Actin staining also showed that ZA significantly decreased osteoclast activity. miRNA Seq analysis identified 11 upregulated and 5 downregulated differentially expressed genes (DEGs) in miRNA of the EVs derived from osteoclasts with ZA. The expression of these DEGs was confirmed by qPCR and miR-146a-5p, and miR-322-3p were upregulated by ZA. An mRNA-seq analysis of the osteoclasts was conducted to identify mRNA target and clarify the molecular and functional mechanism of miRNA of the EVs. Our data demonstrated that BPs attenuate osteoclastgenesis simultaneously changing the characteristics of the osteoclast-derived EVs. We suggest that intercellular communication by the osteoclast-derived EVs may play important roles in the pathogenesis of MRONJ.

***Disclosures: Sakura Minami**, None*

SUN-346

The endosomal RANKL-LGR4 signaling during osteoclast differentiation *Wonbong Lim[1], Beomchang Kim[1], Young Jong Ko[1], Yuria Jang[1]. [1]Department of Premedical Science, College of Medicine, Chosun University, Republic of Korea

LGR4 (Leucine-rich repeat-containing G-protein coupled receptor 4, also known as GPR48) is a membrane receptor and known as a negative regulator of RANK signaling cascade during osteoclast differentiation. Although cell signaling and endocytic membrane trafficking from membrane receptor have traditionally been viewed as distinct processes, it is now recognized that these processes are intimately and bidirectionally linked. In this study, we investigated the difference between membrane-bound LGR4 signaling and internalized LGR4, and whether the LGR4 signaling cascade gives RANKL signal in internalized endosomes as an potential regulator during RANKL-induced osteoclastogenesis. Herein, we showed that LGR4 is endocytosed to endosome after binding to RANKL in osteoclast precursor cells RAW 264.7s. The internalized LGR4 activates LGR4-RANKL signaling in the early endosome. When RANKL is bound to LGR4, it is endocytosed and located in the Rab5 positive ealry endosome. In LGR4-down regulated RAW 264.7 cells, it was analyzed that the early endosome signal increased and the inhibitory phosphorylation of GSK-3beta decreased. Raw 264.7 cells treated with Dynasore (Dynamin inhibitor) confirmed the same reduction in inhibitory P-GSK3B as LGR4 CKO(Conditional Knock-out) cells. With similar results, it was confirmed that the reduced inhibitory P-GSK3B was recovered when DRG2 KO mice were treated with Dynasore, which is similar to the results of DRG2 WT mice. As a result of confirming NFATC1 nuclear translocation by RANKL treatment in LGR4 CKO Raw 264.7 cells and DRG2 KO mouse, nuclear translocation of NFATC1 increased in both groups. In addition, decreased bone density and increaesd TRAP activity in DRG2

KO mice which is known to be increased the early endosome duration were investigated. Taken together, our result showed that the internalized LGR4 could be a potential regulator for the modulation of osteoclast differentiation via RANKL-LGR4 signaling in endosomes.

***Disclosures: Wonbong Lim**, None*

SUN-348

Pharmacological inhibition of protein S-palmitoylation suppresses osteoclastogenesis and ameliorates ovariectomy-induced bone loss *Jianquan Chen[1], Linghui Ma[2], Liwei Zhang[2], Zirui Liao[2], Chunmei Xiu[2]. [1]Hangzhou City University, China. [2]Soochow University, China

Excessive osteoclast formation disrupts bone homeostasis, thereby significantly contributing to pathological bone loss associated with a variety of diseases. Protein S-palmitoylation is a reversible post-translational lipid modification catalyzed by ZDHHC family of palmitoyl acyltransferases, which plays an important role in various physiological and pathological processes. However, its role in osteoclastogenesis remains unexplored. Here, we identified palmitoylation as a novel and critical regulator of osteoclast differentiation. We found that many proteins were palmitoylated in differentiating osteoclasts, whereas pharmacological inhibition of palmitoylation impeded RANKL-induced osteoclastogenesis in vitro, and to a lesser extent, osteoblast formation from MC3T3-E1 cells. Mechanistically, we showed that 2-BP treatment inhibited osteoclastogenesis partly by downregulating the expression of c-Fos and NFATc1 without overtly affecting RANKL-induced activation of osteoclastogenic AKT, MAPK, and NF-?B pathways. Furthermore, we demonstrated that administration of 2-BP protected mice from ovariectomy-induced osteoporosis and bone resorption. Taken together, our study has revealed protein palmitoylation as a key mechanism regulating osteoclast differentiation, thus providing a potential therapeutic target for treating osteolytic bone diseases.

***Disclosures: Jianquan Chen**, None*

SUN-349

Heparan sulfate selectively inhibits the collagenase activity of Cathepsin K *Xiaoxiao Zhang[1], Yin Luo[1], huanmeng Hao[1], Guowei Su[2], Juno Krahn[3], Miaomiao Li[1], Jian Liu[4], Lars Pedersen[3], Ding Xu[1]. [1]University at Buffalo, United States. [2]Glycan Therapeutics LLC, United States. [3]NIEHS, United States. [4]University of North Carolina, Chapel Hill, United States

Cathepsin K (CtsK) is a cysteine protease with potent collagenase activity. CtsK is highly expressed by bone resorbing osteoclasts and plays an essential role in bone remodeling. Although CtsK is known to bind heparan sulfate (HS) with low nanomolar affinity, it remains unknown how HS might regulate the biological functions of CtsK. Here we report that HS can selectively inhibit the collagenase activity of CtsK without inhibiting its peptidase activity. The inhibitory potency of HS directly correlates with the sulfation levels of HS. By X-ray crystallization study of the CtsK-HS complex we discovered that HS could induce CtsK to form a highly stable tetramer. In this structure the complex adopts a 1:4 (HS:CtsK) stoichiometry, and HS is sandwiched at the tetramer interface, holding two CtsK dimers together. If appears that formation of such an oligomeric complex is the key for inhibiting the collagenase activity of CtsK. Based on the crystal structure, we identified eight basic residues that play essential roles in mediating HS-binding. Mutating three key HS-binding residues together was able to greatly diminish CtsK-HS interaction. Interestingly, the HS-binding deficient CtsK mutant retained its full collagenase and peptidase activity, but its collagenase activity could no longer be inhibited by HS. Combined, our findings suggest that HS, which is present both in bone matrix and on osteoclasts surface, likely functions as a natural regulator of the collagenase activity of CtsK. In addition, due to the selective nature of the inhibition, HS-like molecules can be explored as a novel strategy to inhibits the collagenase activity of CtsK in diseases that involve exaggerated bone resorption.

***Disclosures: Xiaoxiao Zhang**, None*

SUN-350

Interventional and integrative subcellular sequencing (i2scseq) clarifies the multi differentiation stages embedded inside mature osteoclast *Hiroyuki Okada[1], Yuta Terui[2], Yasunori Omata[3], Masahide Seki[4], Shoichiro Tani[5], Junya Miyahara[6], Kenta Makabe[6], Asuka Terashima[7], Sanshiro Kanazawa[8], Masahiro Hosonuma[9], Shoko Onodera[10], Fumiko Yano[11], Hiroyuki Kajiya[12], Taku Saito[6], Yutaka Suzuki[4], Koji Okabe[12], Roland Baron[13], Sakae Tanaka[6], Ung-il Chung[14], Hironori Hojo[14]. [1]Center for Disease Biology and Integrative Medicine, Graduate school of Medicine, the University of Tokyo; Department of Orthopaedic Surgery, the University of Tokyo; Department of Oral Medicine, Infection, and Immunity, Harvard School of Dental Medicine, Japan. [2]Department of Single Cell Solution, Product Strategy Department, Marketing Center, Life Business HQ, Yokogawa Electric Corporation, Japan. [3]Department of Orthopaedic Surgery, the University of Tokyo; Bone and Cartilage Regenerative Medicine, the University of Tokyo Hospital, Japan. [4]Department of Computational Biology and Medical Sciences, Graduate School of Frontier Sciences, the University of Tokyo, Japan. [5]Center for Disease Biology and Integrative Medicine, Graduate school of Medicine, the University of Tokyo, Japan. [6]Department of Orthopaedic Surgery, the University of Tokyo, Japan. [7]Bone and Cartilage Regenerative Medicine, the University of Tokyo Hospital, Japan. [8]Department of Oral and Maxillofacial Surgery, Graduate School of Medicine, the University of Tokyo, Japan. [9]Department of Clinical Immuno Oncology, Clinical Research Institute for Clinical Pharmacology and Therapeutics, Showa University; Showa University Pharmacological Research Center, Japan. [10]Department of Biochemistry, Tokyo Dental College, Japan. [11]Department of Biochemistry, Showa University School of Dentistry, Japan. [12]Department of Physiological Science and Molecular Biology, Fukuoka Dental College, Japan. [13]Department of Oral Medicine, Infection, and Immunity, Harvard School of Dental Medicine, United States. [14]Center for Disease Biology and Integrative Medicine, Graduate school of Medicine, the University of Tokyo; Department of Bioengineering, Graduate School of Engineering, the University of Tokyo, Japan

The transcriptome at single-cell resolution clarifies the diversity of cell populations. Single-cell RNA-seq (scRNA-seq) has already been adopted for giant cells such as osteoclasts (OCs) (Omata, Okada, JBMR plus 2022). Although large OCs could not pass through a fluid-based cell dissociation device because of their diameter, acid-producing mature OCs were captured using conventional scRNA-seq.At ASBMR 2022, we presented intra-single cell sequencing (iSCseq) (Okada, bioRxiv 2022). iSCseq is a combinatorial method of high-resolution confocal imaging, picking of intracellular components, including a single nucleus, using the Single CellomeTM System SS2000 (Yokogawa, Japan), and next-generation sequencing at high resolution for mRNA. Our previous results showed that individual nuclei within the same cell are heterogeneous in terms of gene expression.The next version of iSCseq called i2scseq (interventional and integrative subcellular sequencing) can also collect cytoplasm in a small ordinary cell with a 3um probe and capture the living subcellular transcriptome. The average number of genes per cell detected by a 10um probe is much higher, and one by a 3um is equivalent to traditional fluid-based sequencing.i2scseq was used for the in vitro lineage of cells differentiating into OCs. i2scseq clarified that some small cells, which were not morphologically regarded as OCs, were classified into the final cluster of lineages, and vice versa, that giant OC contain immature nuclei in terms of gene expression. With integrative analysis of i2scseq and fluid-based sequencing datasets using a deep machine learning method, large OCs have embedded components at many stages of differentiation.i2scseq clarified the subcellular heterogeneity of mature OCs at a higher resolution than previous iSCseq. We partially solved the question of why conventional scRNA-seq has captured so-called mature OCs. i2scseq is expected to be a core method in cell biology.

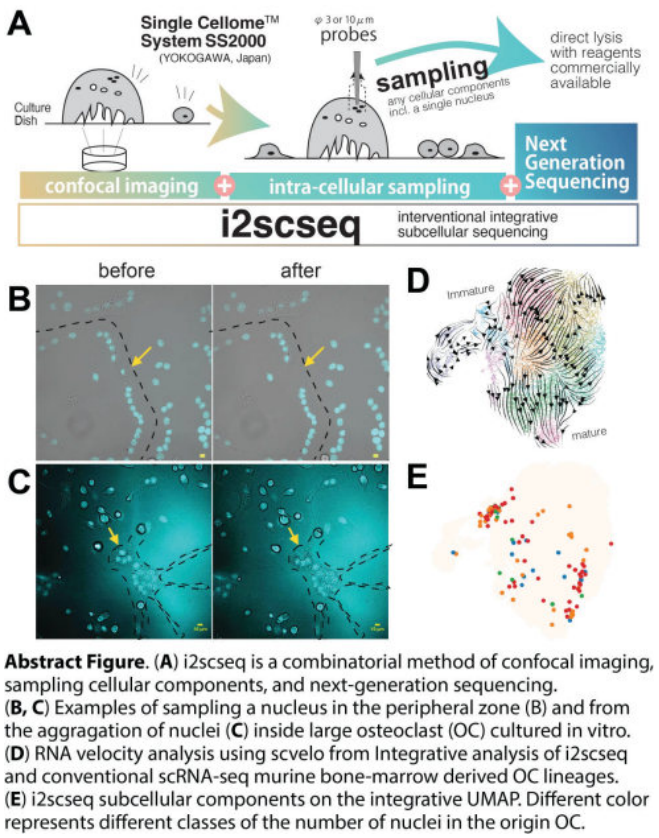

Abstract Figure. (**A**) i2scseq is a combinatorial method of confocal imaging, sampling cellular components, and next-generation sequencing. (**B, C**) Examples of sampling a nucleus in the peripheral zone (B) and from the aggregation of nuclei (**C**) inside large osteoclast (OC) cultured in vitro. (**D**) RNA velocity analysis using scvelo from Integrative analysis of i2scseq and conventional scRNA-seq murine bone-marrow derived OC lineages. (**E**) i2scseq subcellular components on the integrative UMAP. Different color represents different classes of the number of nuclei in the origin OC.

***Disclosures: Hiroyuki Okada**, None*

SUN-351

Role of ATP and ADP in osteoclast mechanotransduction *Svetlana Komarova[1,] Chrisanne Dsouza[1,] [1]McGill University, Canada

Introduction: Physical activity is essential for skeletal health. Upon mechanical loading, ATP and ADP are released from stimulated bone cells and act on purinergic P2 receptors of neighbouring cells. Osteocytes and osteoblasts play important roles in bone response to mechanical loading and have been shown to participate in ATP and ADP-mediated signaling. However, the role of osteoclasts in this process is less understood. The goal of this study was to investigate the role of ATP and ADP in the mechanotransduction of osteoclasts.Methods: Single osteoclasts in primary cultures from 10-12-week-old mice were mechanically stimulated by a gentle touch with a micropipette. Changes in cytosolic free calcium [Ca2+]i were analyzed in fura-2 loaded osteoclasts. Treatment with phosphoenolpyruvate and pyruvate kinase converted all ADP in solution to ATP, and treatment with hexokinase converted all ATP to ADP.Results: Mechanical stimulation with a micropipette resulted in an increase in [Ca2+]i in the primary (stimulated) and the secondary (non-stimulated) neighbouring cells. When cultures were treated with suramin, a broad P2 receptor blocker, primary responders had significantly higher [Ca2+]i amplitude and area under the curve, and secondary responders tended to have a higher area under the curve. In cultures treated with A-804598, a specific inhibitor of P2X7 that is not inhibited by suramin, primary responders tended to have lower calcium response parameters, while secondary responses were abolished. Concentration dependences of osteoclast calcium responses to ATP and ADP demonstrated that more osteoclasts responded with an increase in ATP or ADP concentration. In addition, osteoclasts treated with increasing ADP concentrations demonstrated lower percentage of oscillators and increased amplitude of calcium response. Next, we performed osteoclast mechanical stimulation in the presence of phosphoenolpyruvate and pyruvate kinase, which converted all the mechanotransductive signal to ATP or hexokinase, which converted the signal to ADP. Osteoclasts with mild membrane injury (assessed by the fura-2 loss) demonstrated similar calcium responses in ATP and ADP-rich environments. However, when the mechanotransductive signal to severe osteoclast injury was converted to ADP, the fraction of secondary responders and their [Ca2+]i amplitude were higher.Conclusions: ATP and to a higher degree ADP play important roles in osteoclasts-mediated mechanotransduction.

***Disclosures: Svetlana Komarova**, None*

SUN-352

La, a repurposed RNA-binding protein, regulates osteoclast multinucleation and function. *Jarred M. Whitlock[1,] Evgenia Leikina[1,] Kamran Melikov[1,] Luis Fernandez De Castro Diaz[2,] Sandy Mattijssen[1,] Richard Maraia[1,] Michael Collins[2,] Leonid Chernomordik[1,] [1]NICHD, United States, [2]NIDCR, United States

Multinucleated osteoclasts, essential for skeletal remodeling in health and disease, are formed by the fusion of osteoclast precursors, where each fusion event raises their bone-resorbing activity. Here we show that the nuclear RNA chaperone, La protein has an additional function as an osteoclast fusion regulator. Monocyte-to-osteoclast differentiation starts with a drastic decrease in La levels. As fusion begins, La reappears as a low molecular weight species at the osteoclast surface, where it promotes fusion. La's role in promoting osteoclast fusion is independent of canonical La-RNA interactions and involves direct interactions between La and Annexin A5, which anchors La to transiently exposed phosphatidylserine at the surface of fusing osteoclasts. Disappearance of cell-surface La, and the return of full length La to the nuclei of mature, multinucleated osteoclasts, acts as an off switch of their fusion activity. Targeting surface La in a novel explant model of fibrous dysplasia inhibits excessive osteoclast formation characteristic of this disease, highlighting La's potential as a therapeutic target.

***Disclosures: Jarred M. Whitlock**, None*

SUN-353

The PDE4 inhibitors Roflumilast and Rolipram Rescue ADO2 Osteoclast Resorption Dysfunction *Jung Hong[1,] Angela Bruzzaniti[1,] Rita O'Riley[2,] Dena Acton[2,] Imranul Alam[2,] Michael Econs[2,] [1]Indiana University School of Dentistry, United States, [2]Indiana University School of Medicine, United States

Autosomal Dominant Osteopetrosis type II (ADO2) is a rare bone disease of impaired osteoclastic bone resorption caused by heterozygous missense mutations in the chloride channel 7 (CLCN7). Previous reports have shown that ADO2 knock-in mouse models containing the CLCN7 mutation exhibit elevated bone mass. A CLCN7 mutation is thought to affect not only Clcn7 chloride exchange activity but also affect endosomal-lysosomal trafficking which is critical for formation of the resorption lacunae of active osteoclasts. It is well known that adenylate cyclase is critical for lysosomal acidification in osteoclasts and other cells. Adenylate cyclase catalyze the formation of cyclic adenosine monophosphate (cAMP), an important small second messenger that activates key cellular target proteins. Intracellular cAMP concentration is tightly regulated at the level of its synthesis by adenylate cyclase and hydrolysis by specific phosphodiesterase (PDEs). We investigated the cellular mechanism involved in ADO2 OC dysfunction and found that both immature and mature ADO2 osteoclasts exhibit reduced cAMP levels, compared to wild-type OCs, implicating the signaling pathways that regulate cAMP synthesis or hydrolysis. QPCR analysis revealed higher expression levels of the three PDE4 subtypes (4a, 4b, 4d) in ADO2 osteoclasts compared in WT. Next, we examined the effects of two cAMP specific PDE4 inhibitors, roflumilast and rolipram, on ADO2 osteoclast formation and resorption activity in vitro. Non adherent bone marrow macrophages from ADO2 and WT mice were cultured with RANKL and MCSF in the presence of roflumilast or rolipram (0-250 nM). Roflumilast and rolipram increased osteoclast formation in a dose-dependent manner in both ADO2 and WT osteoclasts. Importantly, the PDE4 inhibitors also displayed a concentration-dependent increase in osteoclast resorption activity which was greater in ADO2 osteoclasts than WT osteoclasts. The key findings from our studies demonstrate that ADO2 mice exhibit reduced cAMP levels and that PDE4 inhibition by rolipram and roflumilast rescue ADO2 osteoclast activity dysfunction in vitro. Further understanding of this mechanism will potentially lead to the development of new approaches for the treatment of clinically affected ADO2 patients.

***Disclosures: Jung Hong**, None*

SUN-354

Proton-Activated Chloride Channel Enhances Endplate Porous Osteoclast Resorption to Induce Spinal Pain *Weixin Zhang[1,] Peng Xue[2,] Shenyu Wang[2,] Jiachen Chu[2,] Janet Crane[2,] Mei Wan[2,] Zhaozhu Qiu[2,] Xu Cao[2,] [1]Johns Hopkins university, , [2]Johns Hopkins University, United States

Proton-activated chloride (PAC) channel is responsive to pathological acidic pH in ischemic brain injury in mice and acid-induced neuronal cell death as a completely new ion channel family. Our PAC structure study revealed that the protein exists in two states: namely, a high-pH resting closed state and a low-pH proton-bound non-conducting state. PAC channel undergoes striking conformational changes when the pH drops from 8 to 4, leading to an opening of the channel and the conduction of anions across cellular membranes, thereby inducing diseases associated with tissue acidosis (acid-induced cell death). Skeletal pain in bone disorders is often associated with aberrant osteoclast-mediated resorption due to very low pH environments. But the role of PAC in pathological osteoclast resorption and spinal pain is still unexplored. Chronic low back pain (LBP) can severely affect daily physical activity and is one of the leading risk factors for the development of immobility and frailty. Aberrant osteoclast-mediated resorption during spinal degeneration leads to the development of a porous endplate that in turn allows for the sensory innervation of the spinal unit, leading to LBP. But the mechanism by which aberrant osteoclast activity occurs during spinal degeneration is unclear. Here, we report that the expression of proton-activated

chloride channel (PAC) is induced specifically in the apical membrane of osteoclasts in the porous endplates via a RANKL-NFATc1 signaling pathway. Extracellular acidosis evokes the ICl, H current in the cell membrane of osteoclasts by activating the PAC-encoded Cl? channel. Thus, a combination of an acidic environment of porous endplates and elevated PAC expression results in enhanced osteoclast fusion and resorption that, in turn, provokes LBP. Further, we find that genetic knockout of PAC significantly reduces endplate porosity and spinal pain in a mouse model of spine degeneration, but it does not affect bone development or homeostasis of bone mass in adult mice. Aberrant osteoclast-mediated resorption is found in most skeletal disorders, including osteoarthritis, ankylosing spondylitis, rheumatoid arthritis, heterotopic ossification, enthesopathy, and Paget disease, in addition to spine degeneration. Thus, elevated PAC expression and PAC activity could be a common mechanism for various bone pathologies and thus a potential therapeutic target.

***Disclosures: Weixin Zhang**, None*

SUN-355

Single Cell Transcriptomic Analysis of Adult Murine Long Bone Reveals a Novel Epcam+ Osteocyte-like Subpopulation *Cesar Morfin[3], Gabriela Loots[2], Aimy Sebastian[3], Nicholas Hum[4], Stephen Wilson[3], Deepa Murugesh[3]. [3]Lawrence Livermore National Laboratory, [2]University of California, Davis, United States, [3]Lawrence Livermore National Laboratory, United States, [4]Lawerence Livermore National Laboratory, United States

The skeleton mediates several diverse functions; in addition to providing mobility, structural and mechanical support it also is a reservoir for blood cell production, mineral storage, and endocrine regulation. While osteoblasts (OB) and osteoclasts are two major cell types that drive remodeling, osteocytes (OCY) make up 95% of all cells in the mineralized bone and are considered the 'master orchestrator'. Current experimental approaches to isolate primary bone cell populations have been hampered by an inability to identify, isolate and study specific subpopulations of bone cells due to the heterogeneity of populations of the MSC lineage. Currently, the differentiation trajectory of bone cells is not clear and is further complicated by the transdifferentiation and plasticity now recognized to occur between cell types of the osteogenic lineage. Single cell RNA (scRNA-seq) technologies can help better define the underlying osteogenic lineages by highlighting specific subpopulations. Previously, Yoshioka et al found several osteoblast subpopulations that were isolated from newborn mouse calvaria which were representative of different maturational stages. In the current study, we isolated primary bone cell populations for scRNA-seq from unlabeled and fluorescently labeled cells (Dmp1-Cre; Ai9 and Bglap-Cre; Ai9) mice to further understand the unique transcriptional signatures, developmental trajectories, and potential novel functions bone cells captured from murine long bones may have. Based on transcriptional signatures, most bone cell populations were captured that include mesenchymal/fibroblast progenitors (MP/FP), osteoprogenitors (OP), pre-osteoblasts (pOB), osteoblasts (OB), osteo-chondro progenitors (OCP), chondrocytes (CH), OCYs, and OB/OCYs. The isolation methods also captured adipo-progenitor populations that also expressed various Wnt, and Bmp1 regulators as well as pro-bone cytokines. Focusing on Sost and Dmp1-expressing OCY subpopulations, we found a population with robust expression of several genes including Epcam, Ndrg1, Prr15, Ramp1 and Pdgfa that have not been previously described in osteocytes. Immunohistochemistry of Epcam in long bones highlighted a population embedded in bone beneath the articular cartilage that is strongly expressing this protein. Further study of these Epcam+ bone cells could provide insights into a previously undescribed OCY-like subpopulation that could be mediating a novel function. Such knowledge could lead towards identifying additional bone cell subpopulations involved in modulating bone metabolism that may open new opportunity for promoting bone formation.Work was conducted under the auspices of the USDOE by LLNL (DE-AC52-07NA27344).

***Disclosures: Cesar Morfin**, None*

SUN-356

Identification of RNA localization elements controlling mRNA transcript enrichment in osteocyte dendrites *Courtney Mazur[1], Christian Castro Andrade[2], Parthena Kotsalidis[2], J. Matthew Taliaferro[3], Marc Wein[1]. [1]Massachusetts General Hospital, [2]MASSACHUSETTS GENERAL HOSPITAL, United States, [3]University of Colorado School of Medicine, United States

Subcellular compartments like neuronal dendrites and fibroblast protrusions contain local transcriptomes that contribute to morphology and function. Trafficking of mRNA within cells is controlled by RNA binding proteins that recognize localization sequences in mRNA, often found in the 3' untranslated region (3'UTR). Our subcellular transcriptomic analysis identified 420 mRNA transcripts enriched in dendrites of osteocyte-like Ocy454 cells compared to cell bodies (log2FC>=1, padj<0.01). These transcripts largely encode for ribosomal proteins, electron transport chain, and cytoskeletal proteins. To learn how osteocytes traffic these specific mRNAs to dendrites, we tested the hypothesis that osteocyte dendrite-enriched transcripts contain localization sequences in their 3'UTRs. We used a heterologous reporter system in which the 3'UTR of one dendrite-enriched mRNA was cloned downstream of the Firefly luciferase (FLuc) coding sequence. Untagged Renilla luciferase (RLuc) served as a control. Ocy454 cells stably expressing one 3'UTR reporter were grown on transwell membranes with 1 ?m pores to facilitate fractionation of dendrites from cell bodies. Relative expression of FLuc mRNA to RLuc mRNA was measured by RT-qPCR in dendrites and cell bodies. For Palld, Fgd3, and 9 of 13 other dendrite-enriched transcripts tested, the 3'UTR was sufficient to promote dendrite localization of FLuc, whereas the 3'UTR of cell body-enriched Pth1r mRNA did not cause dendrite localization. We then cloned 500-1000 nucleotide (nt)-long fragments of the Palld and Fgd3 3'UTRs into our reporter (full lengths 1919 and 2230 nt, respectively). In each case, one fragment caused maximal dendrite localization, indicating that the localization sequence is contained within that region of the 3'UTR. To precisely identify localization sequences, we are performing a massively parallel reporter assay with 260 nt-long sequences tiled at 4 nt intervals across these 11 dendrite-targeting 3'UTRs. To learn why osteocytes localize certain transcripts to dendrites, we investigated the role of Palld on osteocyte morphology. CRISPR-mediated Palld knockout in Ocy454 cells causes a 5-fold reduction in dendrite length and a 2-fold reduction in branching ($p<0.01$). Together our data suggests that dendrite-localized mRNA contributes to osteocyte morphology and is often trafficked via sequences in the 3'UTR. This molecular regulatory mechanism may be a future therapeutic target for osteocyte and bone disorders.

***Disclosures: Courtney Mazur**, None*

SUN-358

Effect of DAMPs Released from Osteocyte Necroptosis on Osteoclastogenesis *Fumitoshi Ohori[1], Hideki Kitaura[2], Takahiro Noguchi[1], Aseel Marahleh[2], Jinghan Ma[1], Kayoko Kanou[1], Mariko Miura[1], Jiayi Ren[1], KOHEI NARITA[1], Itaru Mizoguchi[1]. [1]Tohoku University Graduate School of Dentistry, Japan, [2]Tohoku University, Japan

Necroptosis is a form of regulated cell death that can be triggered by tumor necrosis factor-? (TNF-?) and is related to the activation of receptor-interacting protein 3 (RIP3) and mixed lineage kinase domain-like protein (MLKL). Necroptosis ruptures the plasma membrane leading to the release of damage-associated molecular patterns (DAMPs). During orthodontic tooth movement (OTM), TNF-? expression and osteocyte death have been demonstrated on the compression side. Additionally, osteocytes have been shown to induce osteoclast formation; however, there has been no report regarding the role of osteocyte necroptosis in osteoclastogenesis during OTM. The purpose of this study is to investigate the effect of osteocyte necroptosis on osteoclastogenesis during OTM. As an OTM model, a Ni-Ti closed-coil spring was attached to move the first molar to the mesial direction in eight-week-old male C57BL/6J mice. Histological sections were stained for tartrate-resistant acid phosphatase (TRAP), and osteoclast numbers were determined. To investigate osteocyte necroptosis in OTM, Hematoxylin and Eosin (H&E) staining and immunofluorescence staining were performed. On day 6 of OTM, a large number of osteoclasts appeared on the compression side. H&E staining revealed that necrotic osteocytes also increased on day 6. Furthermore, RIP3 was detected in osteocytes on day 6 with immunofluorescence staining. To obtain high-purity primary osteocytes, Topaz-positive osteocytes were isolated by fluorescence-activated cell sorting (FACS) from Dmp1-Topaz mice whose osteocytes express the green fluorescent protein. Necroptosis was induced by stimulating primary osteocytes with TNF-?, SM-164, and zVAD (TSZ). Necroptosis of osteocytes were detected by immunofluorescence staining. To assess the effect of DAMPs on osteoclastogenesis, bone marrow macrophages derived from bone marrow cells of TNF receptors deficient mice were treated with RANKL and conditioned medium from osteocyte necroptosis. RIP3 and MLKL activation in primary osteocytes was observed 4 and 6 hours after TSZ stimulation, respectively. Although the conditioned medium from viable osteocytes did not affect osteoclastogenesis, the conditioned medium from necroptotic osteocytes significantly enhanced osteoclastogenesis. In conclusion, these results suggest that osteoclastogenesis on the compression side during OTM is enhanced by DAMPs released from osteocytes necroptosis.

***Disclosures: Fumitoshi Ohori**, None*

SUN-359

Live Cell, Confocal and Tissue Clearing/3D Imaging in Mice Expressing a Membrane-GFP targeted to Osteocytes, Odontoblasts and Cementocytes *Yixia Xie[1], David Moore[1], Eleanor Ray[1], Lisa Le[1], Sarah Dallas[1]. [1]University of Missouri - Kansas City, United States

High resolution 3D imaging of cells in hard tissues is challenging due to the light scattering properties of mineralized matrix. Resolving fine detail of osteocyte, cementocyte & odontoblast dendritic processes requires cell-specific staining methods targeting the membrane or specific substructures in the dendrites. Using transgenic mice expressing a membrane-bound GFP driven by the 10kb Dmp1 promoter (Dmp1-mGFP mice) or mice co-expressing Dmp1-mGFP & a LysM-Cre/tdTomato reporter to target osteoclasts, we have used 3D confocal imaging & tissue clearing/3D imaging to define tissue localization of the mGFP reporter and fine cellular detail of osteocytes, odontoblasts & cementocytes in the lower jaw. Samples were counterstained with alexa555-phalloidin to visualize F-actin and DAPI to label nuclei. Dmp1-mGFP mice were also used for confocal live cell imaging to examine osteocyte embedding dynamics. 3D confocal imaging on 50?m cryosections in 7d mandibles showed Dmp1-mGFP expression in osteocytes, odontoblasts, pulpal cells adjacent to odontoblasts and a subset of mature osteoblasts. Membrane-targeting of GFP enabled resolution of branching & fine detail of odontoblast processes (Fig.1) and osteocyte dendrites. Dmp1-mGFP was also expressed in cementocytes in 2mo mice. Dmp1-mGFP also labeled 80-500nm extracellular vesicle-like particles, at the dentin-enamel junction adjacent to odontoblast processes (Fig 1, arrows) and throughout the mineralized bone & cementum matrix, which likely represent matrix vesicles that initiate mineralization. PEGASOS

clearing enabled deep tissue imaging and lightsheet imaging enabled 3D reconstruction of Dmp1-mGFP & LysM-Cre/td tomato expression in the intact mandible and virtual sectioning in any plane. This also revealed Dmp1-GFP expression in a subset of cells in blood vessels supplying the cervical loop region of the incisor. Long term live cell imaging of osteocyte embedding in calvarial explant cultures revealed Dmp1-mGFP first switching on in post mitotic polygonal cells that extended and retracted dendrites during embedding/positioning. Live imaging of osteoclasts & osteocytes revealed that the majority (95%) of osteocytes die during the process of bone resorption. We conclude that the Dmp1-mGFP mouse is a valuable tool for studying differentiation of mineralizing cell types and imaging their fine structure and is compatible with high resolution confocal imaging, tissue clearing/3D lightsheet imaging & live cell imaging.

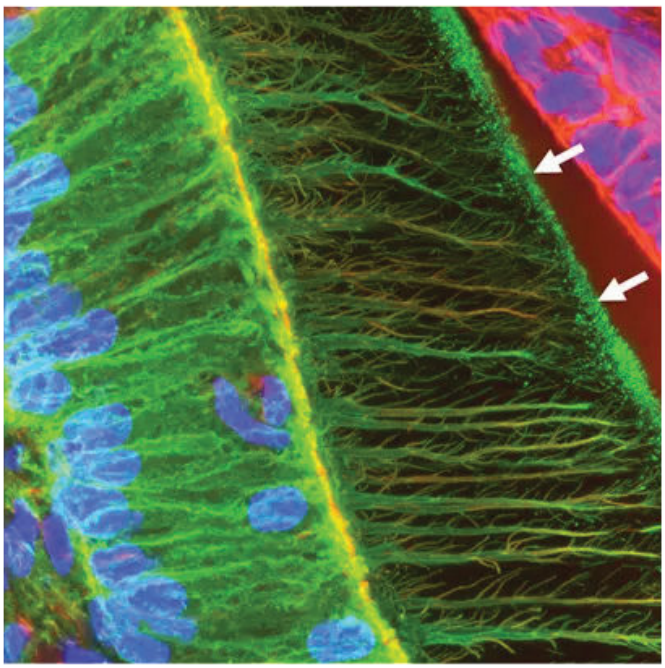

Fig. 1: Dmp1-mGFP expression in odontoblasts showing fine detail of odontoblast processes and GFP positive vesicles close to the dentin- enamel junction (arrows). (green – Dmp1-mGFP, blue = nuclei; red = F-actin)

***Disclosures: Yixia Xie**, None*

SUN-361

Regulation of Lipid Droplet Formation in Osteocytes Under Physiological and Pathological Conditions *MATHILDE PALMIER[1], Yukiko Kitase[2], Lynda Bonewald[3], Matt Prideaux[4]. [1]Inserm, France. [2]Indiana University, School of Medicine, United States. [3]Indiana University School of Medicine, United States. [4]Indiana University, United States

Osteocytes are key regulators of bone formation and resorption. We previously found that fatty acids (FAs) are an important source of energy for osteocyte metabolism through ?-oxidation, but this process is impaired in aged bone. Osteocytes accumulate FAs in the form of lipid droplets (LDs) under pathological conditions such as alcohol or steroid excess. However, questions remain whether osteocytes form LDs under physiological conditions and whether excessive LD accumulation occurs with aging and associated co-morbidities such as obesity and a sedentary lifestyle.To address this, we are investigating LD formation under both physiological and pathological conditions. For physiological in vitro experiments, MLO-Y4 and IDG-SW3 cell lines were treated with BSA-complexed oleic acid (OA) for 24 hrs with the addition of L-carnitine to promote ?-oxidation. 100-250 ?M OA significantly increased expression of the key ?-oxidation regulator Cpt1a and LD-droplet associated gene Plin2 in MLO-Y4 and IDG-SW3 cells. Sost mRNA expression was significantly decreased by OA treatment in IDG-SW3 cells, but there was no change in Tnfsf11/Tnfrsf11b (Rankl/Opg) in either MLO-Y4 or IDG-SW3 cells. This suggests a potential beneficial effect of OA and LDs in young, healthy osteocytes through increased ?-oxidation.To understand the role of LDs in pathological conditions, MLO-Y4 cells were cultured with 100 ?M OA and the CPT1 inhibitor etomoxir to block ?-oxidation. This significantly increased LD accumulation and Plin2 mRNA expression compared to control MLO-Y4 cells, suggesting that impaired ?-oxidation leads to lipid dysregulation in osteocytes. Seahorse ATP rate assay also showed that IDG-SW3 osteocyte energy metabolism was primarily oxidative and that blocking ?-oxidation decreased both mitochondrial and overall ATP production rates. To examine LDs in osteocytes in vivo, obese 18 month female C57Bl/6 mice were fed a high fat diet (HFD) for 5 months. LDs were detected in sections of femoral osteocytes (Figure 1), suggesting a potential link between dietary fat intake, aging, and osteocyte lipid accumulation.Ongoing studies will determine whether exercise of HFD-fed mice reduces LD burden through mechanical strain induced ?-oxidation in osteocytes and if excess LD accumulation in aged osteocytes is a driver of impaired bone health in aging.

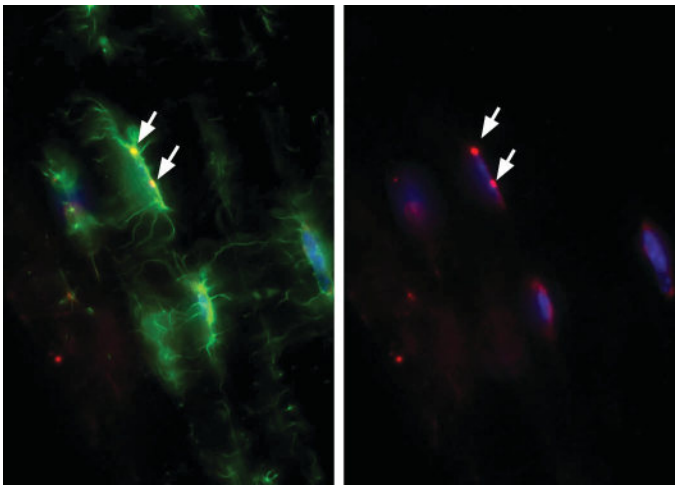

***Disclosures: MATHILDE PALMIER**, None*

SUN-362

Bone formation by osteoid-osteocytes and osteocytes in C57Bl/6 mice *Sarah Ford[1], Svetlana Komarova[2], Katharina Jähn-Rickert[3], Kerstin Tiedemann[2], Elizabeth Zimmermann[2, 1], . [2]McGill University, Canada. [3]University Medical Center Hamburg-Eppendorf, Germany

Purpose: Bone formation is described as occurring on bone surfaces by osteoblasts. However, as bone forming osteoblasts become entrapped in the bone matrix, these so-called osteoid-osteocytes may continue to produce bone matrix while differentiating into osteocytes [1]. Mature osteocytes deeply embedded in the bone have also been observed to remodel their surrounding bone matrix in lactation and hibernation: a process termed perilacunar remodeling [2]. The contribution of osteocyte-driven bone remodeling in the regulation of healthy bone tissue is currently unknown.Methods: Skeletally mature female C57Bl/6 mice received two calcein injections. MMA-embedded undecalcified L3-L5 vertebrae sections were prepared. A region of interest (ROI) of trabecular bone was identified and the bone area of the ROI was measured on brightfield images. Osteocyte lacunae with calcein labels were identified on z-stacks imaged with confocal microscopy. Lacunae were classified (Fig. 1) as osteoid-osteocytes (in or adjacent to the line of osteoblast bone formation) or mature osteocytes (> 3 µm from osteoblast bone formation labels). Bone formation rate (BFR) due to osteoblast activity on bone surfaces followed ASBMR guidelines. BFR of mature osteocytes was measured as follows:BFRosteocyte=(L.Th)/(Ir.L.t) ((sLSocy)/(Ocy.S)) L.Th is label thickness, Ir.L.t is time between calcein injections, and sLSocy is lacunar label length. Ocy.S is total osteocyte surface calculated as the product of lacunar density, bone area and average lacunar perimeter.Results: Active bone formation was observed in 206 +/- 64 lacunae/mm2. Around 80-90% of labeled lacunae were associated with bone forming osteoid-osteocytes (173 +/- 50 lacunae/mm2) and 16% mature osteocytes (33 +/- 6 lacunae/mm2). The osteoblast BFR was 3.17 µm/day and the osteocyte BFR was 0.078 nm/day (not including osteoid osteocytes).Conclusion: Here, we observed that a majority of bone formation at lacunae occurs at osteoid-osteocytes, which should be distinguished from mature osteocytes. BFR due to osteocyte activity may seem small, but perilacunar remodeling is an emerging phenomenon for which the implications on bone quality and bone fragility are not fully understood.References:1. C Palumbo, et al. Cells Tissues Organs. 137:350-358, 1990.2. KJähn-Rickert & EA Zimmermann, Curr. Osteoporos. Rep. 19:391-402, 2021.

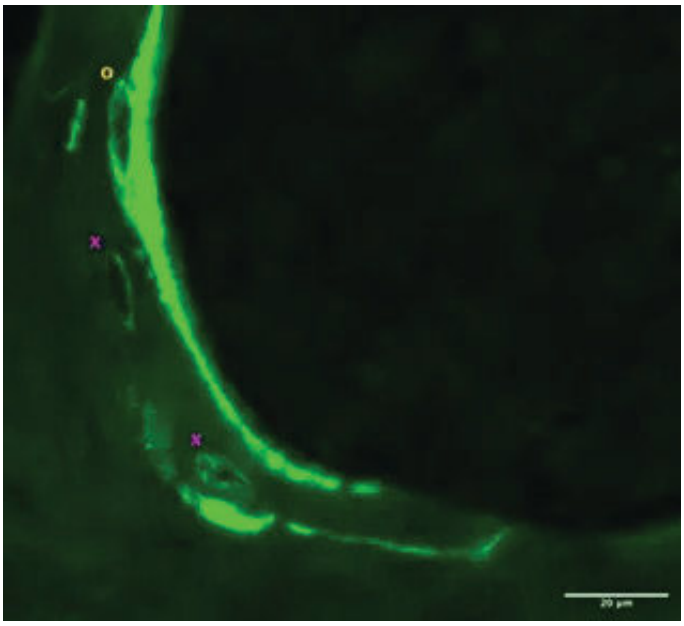

***Disclosures: Sarah Ford**, None*

SUN-364

Is osteocyte function impaired in Jansen disease? *Renata C Pereira[1], Thomas J Gardella[2], Barbara Gales[3], Monica Reyes[4], Harald Juppner[2], Isidro Salusky[5]. [1]Pediatric Nephrology, UCLA, Geffen School of Medicine, United States. [2]Endocrine Unit and Pediatric Nephrology Unit, Massachusetts General Hospital and Harvard Medical School, , United States. [3]Pediatric Nephrology, UCLA, Geffen School of Medicine, , United States. [4]Endocrine Unit, Massachusetts Hospital and harvard Medical School, United States. [5]University of California, Los Angeles School of Medicine, United States

Jansen metaphyseal chondrodysplasia (JMC) is an ultra-rare autosomal dominant disease caused by heterozygous, activating PTH/PTHrP receptor (PTH1R) mutations. Patients display short stature, long bone bowing, craniofacial abnormalities, and growth plate abnormalities that resemble severe rachitic changes. They also exhibit hypercalcemia and hypercalciuria leading to nephrocalcinosis and risk of impaired renal function. Five different PTH1R mutations affecting one of three different amino acids (H223R, T410P/R, and I458K/R) are known to cause JMC. The mutant PTH1R in the growth plates is predicted to slow rates of chondrocyte maturation and hence lead to reduced chondrocyte hypertrophy and reduced formation of primary spongiosa and bone tissue. However, there is currently little known about how the mutant receptors impact processes of bone formation and bone turnover, particularly in young JMC patients. In the current study, we assessed histologically the bone phenotype in two brothers (6 and 8 years old) with JMC (H223R mutation). Serum and urine markers of bone and mineral ion metabolism were also evaluated in both pts:1,25D: 82, 70 pg/ml; PTH: <2.5 pg/ml for both; ALP: 632, 564 IU/L; FGF23: 110, 98 RU/ml; Ca: 10.6, 10.5 mg/dL; P: 3.2, 3.5 mg/dL. Urine NTX: 1757, 1212 (167-578 nM BCE/mM Creatinine). Histomorphometric analyses of dual tetracycline labels in iliac crest biopsies revealed, as compared to age-matched controls, decreased trabecular bone formation, increased mineralization lag time and delayed?? osteoid maturation; reduced connectivity between trabecular plates; decreased cortical thickness consistent with lower turnover osteopenia, and persistent cartilaginous remnants. Bone marrow fibrosis was also detected close to endocortical areas. Immunohistochemical analyses revealed increased osteocytic bone staining for both FGF23 and DMP1 without co-localization and decreased staining for sclerostin. Staining for PTH1R was increased in trabecular bone close to lining cells or cell surface progenitors. Photon silver staining demonstrated osteocyte perilacunar/canalicular abnormalities, including decreased numbers and lengths of dendrites, and osteoid halos, and large lacunae; these findings are similar to those seen with PHEX and SP7 mutations (Fig.1). These intriguing observations suggest that activating PTH1R mutations impair not only maturation of growth plate chondrocytes, the activity of osteoblasts and osteoclasts, but also of osteocyte biology.

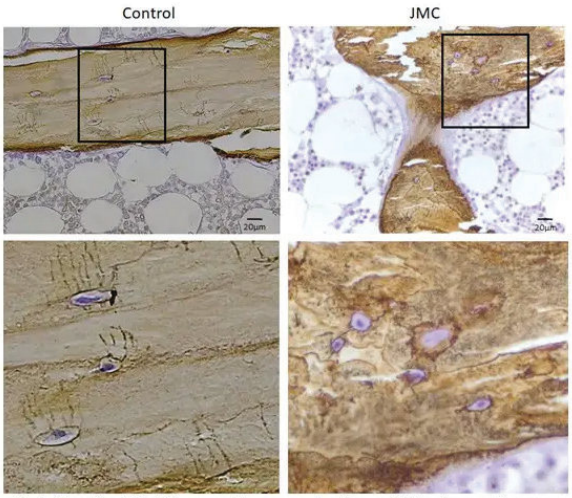

Fig.1: Non-decalcified iliac crest biopsy samples from a JMC patient and an age-matched control were photon silver-stained to assess osteocyte morphology.

***Disclosures: Renata C Pereira**, None*

SUN-365

Investigating Osteocyte Morphology in Crtap -/- Mouse Model of Recessive Osteogenesis Imperfecta *Carolina Leynes[1], Ellen Busschers[1], Mary Adeyeye[1], Iwen Song[1], Yangjin Bae[1], Brendan Lee[1]. [1]Baylor College of Medicine, United States

Osteogenesis Imperfecta (OI) is characterized by short stature and brittle bones. OI type VII has been associated with the loss of CRTAP (Cartilage-associated protein) which is responsible for post-translational modifications of type I collagen via 3-hydroxylation of Pro986 of chain alpha1(I) and Pro707 of chain alpha2(I). Currently, Crtap-/- mice are used as a model for recessive OI as mice present with a decrease in body size, osteo-chondrodysplasia, kyphosis, and severe osteopenia. Furthermore, our lab and others have shown Crtap-/- mice have upregulated transforming growth factor-? (TGF-?) resulting in decreased bone volume to total bone volume (BV/TV), maximum load, and ultimate strength. In addition, an increase in osteoclast, osteoblast, and osteocyte was observed in Crtap-/- mice. Previous studies in children with OI type I and V have also shown an increase in osteocyte number in cortical and trabecular bone compared to age match controls. Given osteocytes' mechanosensory and bone regulatory role via sclerostin and RANKL secretion, we studied morphological changes in osteocytes of Crtap-/- mice. In this study, we collected femurs from Crtap-/- and WT mice of 4 months of age (n=6) and performed phalloidin staining on 30 ?m sections. Using Imaris analysis software, we processed the images and analyzed osteocyte dendrite length, branch depth, branch level, and area. Our analysis showed an increase osteocyte number, consistent with our and others' previous report, and a decrease in dendrite branch length, depth, level, and area in Crtap-/- mice compared to WT control mice. Our data suggest Crtap-/- mice have decrease osteocyte branching complexity which might be correlated to the decrease in bone mass, maximum load, and ultimate strength previously published by our group. Future studies will further determine the changes in dendrite network after 1D11, an anti-TGF-? treatment, in Crtap-/- mice and investigate the underlying molecular changes in osteocytes of OI models such as Crtap-/- mice and additional OI mouse models.

***Disclosures: Carolina Leynes**, None*

SUN-366

Exposure to disuse sensitizes osteocytes to the formation of plasma membrane disruptions (PMD) upon reloading *Anik Tuladhar[1], Wesley McGee[1], Luke Horne[1], Joseph Shaver[1], Mark W. Hamrick[1], Meghan McGee-Lawrence[2]. [1]Augusta University, United States. [2]Medical College of Georgia, Augusta University, United States

Disuse (such as during spaceflight) leads to loss of bone mass and strength. Astronauts can lose approximately 1% to 1.5% of their bone mineral density per month while in space, making it crucial to develop better strategies to maintain bone health during and after spaceflight when returning to gravitational forces. Recently, we and others have reported that osteocytes develop transient, survivable plasma membrane disruptions (PMD) during application of high-impact mechanical loading that allows them to sense and respond to this loading via initiation of mechanotransduction cascades. In the current study, we hypothesized that osteocyte PMD formation may play a role in the sensation and response to normal gravitational loads. To test this, we employed a rotary cell culture system (RCCS) to simulate a microgravity environment and tested whether osteocytes subjected to microgravity demonstrate altered PMD formation upon reloading. Differentiated OCY454 osteocyte-like

cells were grown in 3D collagen coated scaffolds (Alvetex) for 7 days followed by culture in the RCCS system for 3 days. Gene expression analyses (RT qPCR) revealed that 3 days of disuse via RCCS culture up-regulated mRNA expression of Sost by 30 fold as compared to static controls, validating previously reported effects of disuse from RCCS in this cell line. A subset of cell-seeded scaffolds were subjected to reloading via turbulent fluid shear stress (TFSS) (n=5 biological replicates) in the presence of fluorescent dextran (10 kDa) in the culture media which acts as a PMD tracer. Reloading following culture in microgravity conditions induced the formation of significantly more PMD (+17%) as compared the abundance of PMD formed from TFSS in static controls, suggesting that the cells exposed to microgravity became sensitized to PMD formation upon high-impact reloading. In ongoing studies, we are investigating whether exposure to disuse conditions alters PMD-induced mechanotransduction, PMD repair processes, or mechanisms of post-wounding cell survival downstream of the PMD event.

***Disclosures: Anik Tuladhar**, None*

SUN-368

Irisin modulates murine osteocytic osteolysis in a sex and age-specific manner *Anika Shimonty[1], Fabrizio Pin[1], Matt Prideaux[1], Gang Peng[1], Lynda Bonewald[1]. [1]Indiana University School of Medicine, United States

Irisin, a hormone generated by the proteolytic cleavage of Fibronectin type III Domain Containing protein 5 (FNDC5) has been described to have beneficial effects on the brain and fat, but effects on bone are contradictory [1], as some studies have found positive effects but our studies have shown that irisin deletion protects against bone loss due to ovariectomy [3]. Recently we have shown that irisin deletion also protects against bone loss with lactation and a low calcium (Ca) diet in females but exacerbates male mice bone loss due to a low Ca diet. To determine if irisin plays a role in bone loss with aging, 5 and 20-month (mo)-old mice were compared. No differences were observed between WT and FNDC5 global KO female mice (BV/TV; 57.5% WT:58.5% KO), however, male KO mice, 5 and 20 mo, had higher BV/TV (60.8% KO:57.6% WT) but less biomechanical strength compared to WT males (ultimate force; 18.5N KO:22.1N WT, stiffness;78.6Nmm KO:94.3Nmm WT). With a low Ca diet, both 5 and 18 mo female KO were partially protected against bone loss and weakness: (BV/TV;43.2% KO:40.4% WT), ultimate force (17.8N KO:15.7N WT) and stiffness (59.8Nmm KO:43.4 Nmm WT). In contrast, both 5 and 18-mo male KO mice lost more bone and had lower bone volume (BV/TV; 48.6% KO:55.4% WT) on a low Ca diet and lower ultimate force (14.9N KO:18.4N WT). To begin to identify responsible molecular mechanisms, RNAseq was performed on osteocyte-enriched bone from 5 mo old animals as two major functions of the osteocyte are to remove their perilacunar matrix to provide calcium and to produce RANKL to activate osteoclasts. Sex differences showed that the female WT osteocyte transcriptome had higher expression of genes responsible for osteocytic osteolysis including Acp5, Ocstamp, Dcstamp, Ctsk, Tnfsf11, and Mmp13 compared to WT males. This difference was not evident in KO females compared to KO males. On a low Ca diet, KO females had lower expression of osteocytic osteolysis genes such as Tnsfs11 and Ocstamp compared to WT females. Analysis of the osteocyte transcriptome is ongoing. In summary, in young females irisin aids or primes the osteocyte to release Ca under Ca-demanding conditions to possibly aid in offspring survival, however in the aging female, this effect of irisin on osteocyte function becomes detrimental with sex hormone and/or Ca deficiency. In contrast, irisin appears beneficial for males at any age, but especially with aging.1.Maak et al, Endocr Rev, 20212. Kim et al, Cell, 2018

***Disclosures: Anika Shimonty**, None*

SUN-369

Vitamin D Receptor Agonist Eldecalcitol Prevents Aging Postmenopausal Osteoporosis by Inhibiting Ferroptosis and Apoptosis of Senescent Osteocytes *Yan Zhang[1], Zheng Ke[2], Shuang-shuang Dong[2], Chun-zhu Gong[1]. [1]Shenzhen Pingle Orthopaedic Hospital, China. [2]Chugai Pharma China Co., Ltd, China

Active vitamin D analog eldecalcitol is clinically applied in treatment of postmenopausal osteoporosis. This study aims to determine the role of eldecalcitol in protection of osteocytes from senescence and the underlying mechanism. The MLO-Y4 osteocytes were exposed to D-gal, one classical inducer of senescence. The ovariectomized (OVX) mice with D-gal treatment were intraperitoneally injected with eldecalcitol. Eldecalcitol reversed senescent phenotypes of MLO-Y4 cells by improving cell morphology and density, decreasing accumulation of ?-gal-positive cells, and down-regulating expression of P16, P21, and P53. Treatments with Z-VAD-FMK or ferrostatin-1 could recover viability of D-gal-treated MLO-Y4 cells. Flow cytometry showed the reduction in percentage of apoptotic cells after eldecalcitol treatment, which enhanced the expression ratio of Bcl-2/Bax. Eldecalcitol reduced cellular ROS and MDA productions, elevated JC-1 aggregates, and up-regulated expression of Nrf2 and GPX4. Eldecalcitol exhibited osteopreserve effects without changes in serum levels of calcium and phosphorus of aging OVX mice. The confocal imaging displayed that eldecalcitol improved osteocytic network organization. The analysis by transmission electron microscopy showed that the ablation of vitamin D receptor led to a reduction in amounts of osteocytes and dendrites in cortical bone. Eldecalcitol decreased senescent osteocytes in tibial diaphysis by SADS assay, attenuated mRNA expression of SASP factors and down-regulated protein expression of senescence-related factors and caspase-3 in osteocytes-enriched bone tissue fraction. The treatment of aging OVX mice with eldecalcitol restored levels of ferroptotic biomarkers in osteocytic fraction. Furthermore, it reduced 4-HNE expression, stimulated Nrf2-positive staining, and promoted nuclear translocation of Nrf2 in osteocytes. The present study revealed the ameliorative effects of vitamin D analog eldecalcitol on apoptosis and ferroptosis of senescent osteocytes, potentially contributing to its protection against aging postmenopausal osteoporosis.

***Disclosures: Yan Zhang**, None*

SUN-371

F-Actin Bundles and Cross-linkers in Osteocyte Dendrites *Rosa Guerra[1], Megan Coffin[1], Shannon Modla[1], Velia Fowler[1], Liyun Wang[1]. [1]University of Delaware, United States

Introduction: Osteocytes are the master orchestrators of bone remodeling, and their extensive dendrite network enables them to sense the external mechanical signals and communication with other cells.1,2 With aging, the dendrites deteriorate with bone quality declined.3 Similar to epithelial microvilli and inner ear stereocilia4, osteocyte dendrites are thought to contain rigid tightly packed cross-linked F-actin bundles as in previous mechanosensing models.5 However, the dendrite cytoskeleton details have not been revealed experimentally due to their entombment in a mineralized bone matrix and the high resolution needed to resolve the F-actin fibers (5-7 nm diameter). The goal of this study is to optimize protocols for high-resolution STED imaging and transmission electron microscopy (TEM) of the dendrite cytoskeleton of cultured osteocytes.Methods: MLO-Y4 cells were seeded at a density of 4,000 cells/cm2 onto collagen-coated coverglass and cultured in alpha-MEM with 2.5% fetal bovine serum and 2.5% calf serum for 2-4 days. The F-actin cytoskeleton and selected cross-linkers were stained with SiR-Actin (in live cells), phalloidin and fimbrin and actinin antibodies (in 4% paraformaldehyde fixed cells), followed with STED (pixel ~16.5 nm) and confocal imaging (pixel ~100-200 nm). Additional TEM images (pixel ~0.55 nm) were also taken of cells on coverslips, fixed with 1% osmium tetroxide and 1% glutaraldehyde with an overnight 0.5% uranyl acetate staining and embedding in resin.Results/Conclusions: In cultured osteocytes, there were a few long cellular protrusions containing linear or curved F-actin fibers in a semi-parallel fashion. These fibers were neither located at the center (under confocal) nor formed compact bundles (observed under STED and TEM). Under STED (Fig. 1), fimbrin and actinin were found along the F-actin fibers and they were not fully co-localized with F-actin fibers in the dendrites as suggested in a previous study.6 Overall, the F-actin cytoskeleton of 2D cultured osteocytes is arranged differently than the previous linear actin core model. To understand osteocyte dendrites in vivo, better models are needed.References: (1) Schaffler, Calcif Tissue Int, 2014 (2) Bonewald, JBMR, 2011 (3) Tiede-Lewis, AGING, 2017 (4) Pelaseyed, J Cell Sci, 2018 (5) Wang, PNAS, 2007 (6) Murshid, J Bone Miner Metab, 2007

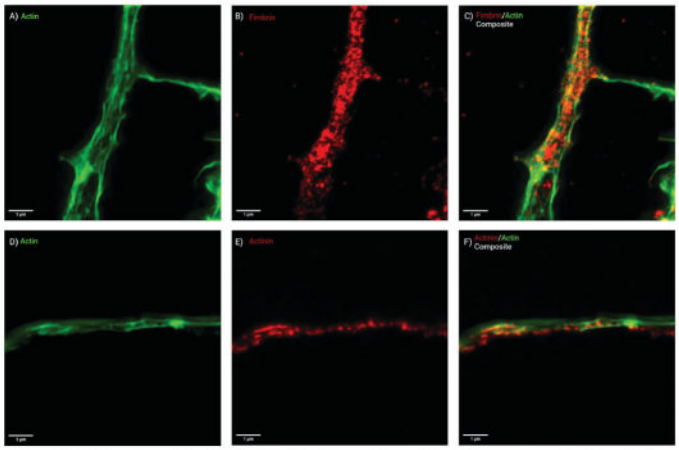

Figure 1) STED imaging of the distribution of fimbrin, actinin, and F-actin in osteocyte dendrites. (A-C): Fimbrin (red) and F-actin (green) staining in branched dendrites. (D-E): Actinin (red) and F-actin (green) staining on a thin dendrite. Scale bar = 1 µm.

***Disclosures: Rosa Guerra**, None*

SUN-372

Sex Differences in in vivo Osteocyte Ca2+ Signaling and Gap Junction Inhibition *JAMES BOORMAN-PADGETT[1], Randy Valcourt[2], Bridget Saw[3], Jelena Basta-Pljakic[2], Mia Thi[4], David Spray[3], Mitchell Schaffler[5, 1], United States. [2]City College of New York, United States. [3]Albert Einstein College of Medicine, United States. [4]ALBERT EINSTEIN COLLEGE OF MEDICINE, United States. [5]The City College of New York, United States

INTRODUCTION: Osteocytes (Ot) in vivo exhibit a highly coordinated Ca2+ signaling response to mechanical loading, in which number of responding Ot increases in proportion to increasing applied strain [1,2]. Earlier studies established this signaling pattern in female mice. Whether Ot in males respond similarly to loading is unknown. Here, we compared

Ot Ca2+ signaling responses to loading in male vs female mice and further tested whether signaling in both sexes responded similarly to gap junction inhibition.METHODS: Osteocyte Ca2+ signaling responses to mechanical loading were examined in tamoxifen inducible GCaMP6f Ca2+ indicator mice (4 mo, n=22F/30M). Studies used urethane anesthesia, which unlike isoflurane does not interfere with gap junctions [3]. This allowed us to test gap junction function using the inhibitor carbenoxolone (CBX). 3rd metatarsals (MT3s) were cyclically loaded to test strains of 250-3000 ??; 2-photon microscopy was used to image Ca2+ fluorescence in diaphyseal Ot during loading [1,2]. CBX was given after the first (baseline) loading bout and 20 minutes were allowed for diffusion into the bone; loading and imaging studies were then repeated. Cumulative in vivo fluorescent signal intensity as a function of time was calculated for each osteocyte in the region of interest (>1000 cells/group). Ot Cx43 gene and protein expression were determined.RESULTS: Ot in male mice showed ~40% greater cumulative fluorescent signal intensity with loading than Ot in female mice [Fig 1A] and occurred at all strain levels. Blocking gap junctions slightly reduced cumulative signal intensity in males. In contrast, blocking gap junctions in females dramatically attenuated Ca2+ signal intensity. Cx43 mRNA and protein levels were significantly higher in male than female Ot [Fig 1B, 1C - mRNA: 1.4-fold; Protein: ~2.5-fold].DISCUSSION: Our studies reveal unexpected differences in loading-induced osteocyte Ca2+ signaling in male and female mice. The reasons underlying this sex difference in Ot response to loading remain obscure, but may include sex hormones effects and/or intrinsic biological differences between males and female cells [4,5]. Indeed, the more profound Ot response to gap junction inhibition in female mice may reflect such a biological difference, as female Ot express comparatively less Cx43 at both gene and protein levels.REFERENCES:1)Lewis+ PNAS 2017 2)Lewis+ JoVE 2023 3)Burt+ Cir Res 1989 4)Lewis+ Bone 2021 5)McNamara+ Curr Ost Rep 2021

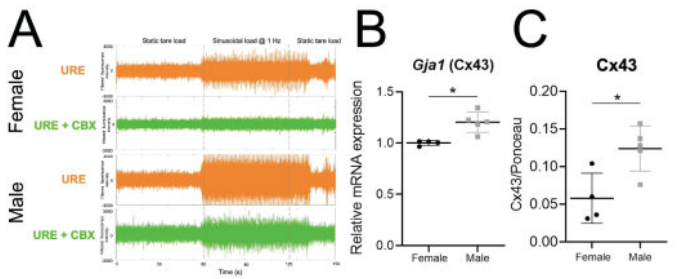

Figure: (A) Overlaid fluorescence intensity traces from ~1000 osteocytes during mechanical loading protocol at 2000 με. (B) Gene expression of *Gja1* in bones of female and male mice (C) Protein expression of Cx43 in bones of female and male mice

***Disclosures: JAMES BOORMAN-PADGETT**, None*

SUN-373

Disparate impact of osteocyte oxygen-sensing mechanisms on bone quality

*Kristina Wells[1], Sarah Mendoza[4], Alice Wong[1], Deepa Murugesh[3], Gabriela Loots[4], Clare Yellowley[5], Damian Genetos[6]. [1]UC Davis, United States. [4]University of California, Davis, . [3]Lawrence Lvermore National Lab, United States. [4]University of California, Davis, United States. [5]University of California School of Veterinary Medicine, United States. [6]University of California Davis, United States

Bone strength involves bone quantity and quality, with bone quantity receiving greater engagement and investigation than bone quality. Ideal osteoanabolic therapies will involve both the quantity and the quality of bone matrix. We have recently demonstrated that constitutive osteocytic oxygen sensing (degradation resistant HIF2a, HIF2cDR) or a regulatory protein upstream of oxygen sensing (Vhl cKO) produce unique high bone mass phenotypes. While both disruptions increase cortical and trabecular bone, HIF2cDR does not phenocopy Vhl KO either in quantity of bone produced or apparent bone organization. Understanding overlapping and unique contributions to bone quality in Vhl cKO vs. HIF2cDR will identify ideal targets for osteoanabolic therapies. We developed mice with osteocyte-enriched (10kb-Dmp1-cre) deletion of Vhl, Hif1a, or Hif2a or degradation-resistant HIF1A or HIF2A and established distinct impact of these deletions on bone strength, which was increased in Vhl cKO and reduced in HIF2cDR mice compared to wild-type controls. We next used ?CT to evaluate total mineral density distribution of knockout and transgenic femora. Both Vhl cKO and HIF2cDR mice had reduced mid-cortical peak mineral and mean mineral density, indicating impaired tissue material properties despite distinct impact on bone strength. Collagen alignment, analyzed by second-harmonic generation, was altered in each genotype relative to wild-type controls. Finally, we sought a potential mechanism for the differences in bone quality. SPARC - a matrix mineralization protein involved in collagen fibrillogenesis- is regulated by both hypoxia and Vhl in myriad cell types; absence of SPARC causes osteopenia and impairs both the organic and mineral content of bone. IHC staining revealed higher Sparc levels in both HIF2acDR and Vhl cKO compared to wild-type bones, with greater staining in Vhl cKO compared to Hif2cDR. In summary, manipulating oxygen-sensing pathways in osteocytes elicits high bone mass phenotypes with diverse outcomes on bone quality.DKM and GGL conducted work under the auspices of the USDOE by LLNL (DE-AC52-07NA27344)

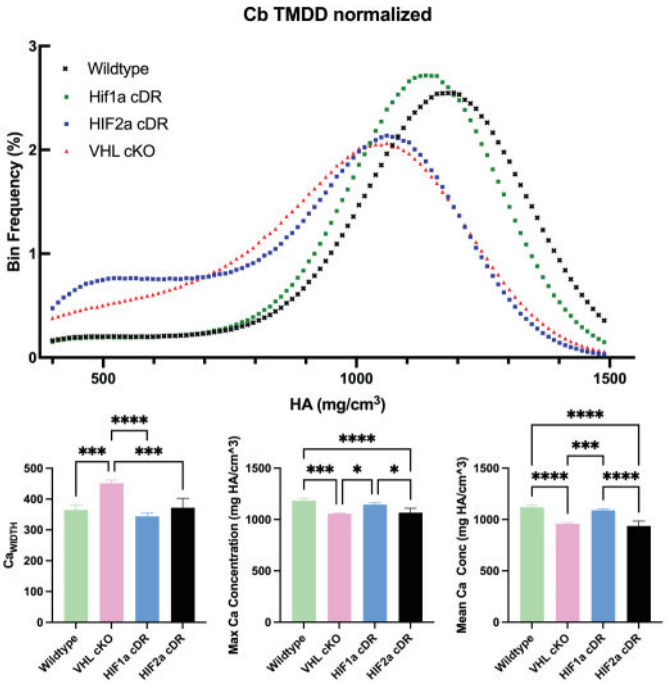

***Disclosures: Kristina Wells**, None*

SUN-374

Assessing Fracture Probability in Patients with Different Types of Fractures Using a Pretrained Artificial Neural Network Model Trained with Demographic, Anthropometric, and Densitometric (DXA) Characteristics

*Carlos Cure Cure[1], Sergio Luscher[2], Jose Ferretti[3], Gustavo Roberto Cointry[3], Ricardo Francisco Capozza[2]. [1]Biomelab Research Center , Colombia. [2]Center for P-Ca Metabolism Studies (CEMFoC), Natl Univ of Rosario and Arg NRC (CONICET), Argentina. [3]National University of Rosario,

Bone mineral density (BMD) by DXA is the reference for defining an individual's skeletal health status. We developed and validated an artificial neural network (ANN) model to evaluate this subject by demographic, anthropometric, and densitometric values and the corresponding fractured or non-fractured status into the ANN. After training, we can establish the probability of belonging to the fractured or non-fractured group.The study sample is 478 post-menopausal women (mean age 62.5 +/- 8.6 years) randomly selected from a sample of 1960 women divided into two equal groups of fractured (n: 239) and non-fractured (n: 239). Among the fractured women, only those previously regarded as osteoporotic and with low-trauma fractures were included. The sample was subdivided into 334 participants in the training set, 72 participants in the validation set, and the remaining 72 participants in the testing set, the latter consisting of women with fractures in various locations, namely: fx-humerus, fx-wrist, fx-spine, fx-hip, and fx-other-regions. The ANN input variables included age, weight, height, body mass index (BMI), lean mass (LM) of upper and lower extremities, trunk, and total body, and bone mineral content (BMC) of upper and lower extremities, trunk, and total body. The ANN outcome variable was dichotomous, established at 0 for non-fractured and 1 for fractured. The ANN was built with the training and validation data and tested with the testing set, the outcome variable of which was unknown to the network. The ANN performance was evaluated by simultaneous discrimination and calibration. After the training processes, the best final ANN was a multilayer perceptron network that determined 12 input variables (age, weight, height, BMI, LMs, and BMCs) as significant features. The ANN discriminant power for the test set was excellent (area under the ROC Analysis curve = 0.81 +/- 0.03).The test set of fractured women was evaluated by the neural network, and then the means and variances of the probabilities obtained in the different groups of fractured women were calculated. The probabilities obtained and the significance of the difference calculated compared to the group of women fractured in other regions were: fx-hip= 0.80 $p < 0.01$; fx-spine= 0.60 $p < 0.05$; fx-wrist= 0.65 $p < 0.05$; fx-humerus= 0.70 $p < 0.01$. We conclude that the trained neural network model can provide fracture probability values consistent with the osteoporotic or non-osteoporotic characteristic of the fracture site.

***Disclosures: Carlos Cure Cure**, None*

SUN-375

Assessment of osteoporosis and vertebral fracture risk by opportunistic bone mineral density (BMD) measurement on Choline PET/CT in patients with prostate cancer (Horm-Os Project) *Astrid Dauchez[1], Olivier Fogel[1], Charles Dariane[2], Jacques Fechtenbaum[1], Sylvain Bodard[3], Sylvain Guinebert[3], François Allioux[4], Marc-Olivier Timsit[2], Christian Roux[1], Fabien Hyafil[4], Karine Briot[1]. [1]Cochin Hospital, Rheumatology, France. [2]European Hospital Georges Pompidou, Urology, France. [3]Necker Hospital, Radiology, France. [4]European Hospital Georges Pompidou, Nuclear medecine, France

Androgen deprivation therapy (ADT) is central in the management of prostate cancer (PCa) but is associated with osteoporosis and fracture. DXA is recommended when starting ADT. Opportunistic measurement of bone mineral density (BMD) on CT has been proposed to improve osteoporosis screening. Choline PET/CT (chPET/CT) is frequently used to search for metastasis or relapse of PCa.The objectives were to demonstrate the feasibility of using chPET/CT in comparison to CT for opportunistic screening of osteoporosis and to describe pet/ct-derived BMD and prevalence of osteoporotic vertebral fracture in patients with PCa.We searched for PCa patients with chPET/CT from our tertiary center, then identified those with a CT within 6 months before or after the PET/CT for comparison. BMD estimation was performed on a 200mm² trabecular bone area on L1 vertebrae in axial section. Demographic and treatment information were collected. Spearman coefficient and t-test were used for continuous variables and chi square test for dichotomous variables.We identified 93 patients including 29 with a CT within 6 months. The mean age was 74 y-o, mean BMI was 27 kg/m², 12 patients had fractures, 20 had metastasis, 39 were already on ADT with a mean duration of 21.4 months. We compared chPET/CT and CT BMD values on the 29 patients who had both, the mean BMD were similar, 125 +/- 51 and 128 +/- 42 HU respectively and correlated well (k=0.7; p<0.001). The mean chPET/CT BMD of all patients was 125 HU +/- 51. Increasing age was significantly correlated with decreased BMD (k=-0.3; p<0.001). There was no correlation between BMI and BMD (k=0.02; p=0.87). The mean BMD in patients on ADT was 114 HU +/- 56, compared 127 HU +/- 42 in others (p=0.17), there was a trend toward a negative correlation between BMD and ADT duration (k=-0.3; p=0.1). We found a significant decreased BMD for patients with fracture (87 +/- 43 vs 131 +/- 49; p<0.01). A cut-off of 100 HU has been suggested to define risk for bone complications. The 23 patients with BMD<100 HU were more likely to have fracture compared to others (30% vs 7% of fracture; p<0.01).We demonstrated the feasibility of using chPET/CT for opportunistic screening for osteoporosis in PCa. Bone disease was frequent, 13% patients had fractures, 25% had BMD<100 HU. Pet/ct-BMD seemed useful for screening patients at risk of fracture. A prospective study will validate the interest of this approach and its impact on the management of osteoporosis in PCa patients.

***Disclosures: Astrid Dauchez**, None*

SUN-376

The key importance of vertebral fractures rather than forearm fractures in the identification of high fracture risk of in younger postmenopausal women *Klaus Engelke[1], Claus-C Glueer[2], Frederike Thomasius[3], Bernd Schweikert[4], Jost von Petersdorff[5], Peyman Hadji[3], Alireza Moayyeri[6], Cesar Libanati[7]. [1]University Hospital Erlangen, Germany. [2]Christian Albrechts Universitaet zu Kiel, Germany. [3]Frankfurter Hormon- und Osteoporosezentrum, Germany. [4]Icon, Germany. [5]Algonaut GmbH, Germany. [6]UCB, United Kingdom. [7]UCB Biopharma srl,

Background: To identify patients at high(est) fracture risk, prior fracture history is key, particularly of fractures that are strong predictors of future fracture. Especially in younger postmenopausal women, forearm fractures (FF) are recognized as sentinel fracture. But vertebral fractures (VF) are stronger risk factors for subsequent VF and hip fractures (HF). Unfortunately, VF are often unrecognized, which may substantially contribute to the gap in osteoporosis care at younger age and the early stoppage of the fracture cascade. Aims: (1) To prove larger predictive power of VF compared to FF, hypothesizing that this advantage is even larger at younger age. (2) To identify a range of risk factors that facilitate identification of patients with high likelihood of prevalent vertebral fractures. Methods: We used a large representative German insurance database (DB), (a) to calculate absolute 1 and 3-year VF and HF risk after an index VF or FF, (b) to determine out of 32 cRF previously identified by a literature review of 2267 peer-reviewed publications those that best predicted VF fracture. Predictive power of cRFs was examined using age-adjusted sex-specific Cox proportional hazard models including interactions between the selected predictor and age. Calculations were performed separately for age ranges of 50-70 and 70-90 years. Results: The DB included 214,453 women aged 50-70 and 154,221 aged 70-90. VF were better index fractures than FF to predict subsequent VF (table). At younger age, the predictive power was 5-10 fold stronger for VF compared to FF for prediction of VF. At young age VF were also stronger predictors for HF with comparable strength of VF and FF for prediction of HF at older age. We identified 11 cRF with HR>3.0 and another 10 cRF with HR>2.0 associated with VF in the last 4 years. Discussion: Diagnosis of VF is important for fracture risk determination especially at younger age. Risk factor gradients of VF decline with age but are higher compared to forearm fractures. As hip fractures are rare at younger age, VF rather than FF, need more attention to overcome the in osteoporosis care gap in younger age groups. The large number of 20 cRF with strong association with prevalent VF indicates realistic potential to develop better strategies, e.g. using advanced diagnostic procedures such as VFA. This will substantially improve the identification of high-risk patients to help reduce costly fractures later in life and improve patients' lives.

predictor	Age adjusted HR for incident VF				Age adjusted HR for incident HF			
age range	50-70		70-90		50-70		70-90	
years after index fx	1	3	1	3	1	3	1	3
VF	63.5	18.0	8.9	5.3	7.6	3.2	1.6	1.9
FF	3.6	2.8	1.8	1.7	4.5	2.4	1.9	1.8

cRF with HR≥3.0: Morbus Alzheimer, Morbus Parkinson, falls, immobility, hip fx, hypernatremia, MGUS, oral glucocorticoids (high dose), peripheral arterial disease, schizophrenia, transplantations,
additional cRF with HR≥2.0: anticoagulants, COPD, pulmonary hypertension, atrial fibrillation, Cushing syndrome, growth hormone deficiency, heart failure, stroke, opioids, oral glucocorticoids (low/medium dose)

***Disclosures: Klaus Engelke**, Clario, Inc, Grant/Research Support*

SUN-377

Variance in Bone Strength is conferred by Diversity of its Structure *Ali Ghasem-Zadeh[7], Haniyeh Hemmatian[2], Olga Panagiotopoulou[3], Phil Salmon[4], Rita Hardiman[2], Narelle McGregor[5], Natalie Sims[6], ego seeman[7]. [7]Austin Health, University of Melbourne, Australia. [2]The University of Melbourne, Australia. [3]Monash University, Australia. [4]Bruker-MicroCT, Belgium. [5]St. Vincent's Institute of Medical Research , Australia. [6]St. Vincent's Institute of Medical Research, Australia. [7]Austin Health, University of Melbourne,

Introduction Resistance to fracture is achieved by adding bone to, and removing bone from, its periosteal and three components of its endosteal surface. These events modify the spatial distribution and mineral content of the bone volume without necessarily alerting its mass. In tubular bones, similar amounts of bone are used to assemble large differences in the size, shape, and microarchitecture of adjacent cross sections along the length of bone 1,2. We hypothesized that i) in vitro, differences in size, shape, and architecture of adjacent cross-sections along the whole length of a bone are assembled using differences in void volume, not bone volume, ii) likewise, in vivo, regional differences in bone morphology are largely achieved by differences in void volume, not bone volume.Methods We quantified macro-structure of the cross-sections of 5 radii and 5 femora using CT-Scan (300 microns) and micro-structure of the cross-sections of the distal and proximal metaphyseal-diaphyseal regions (1/3 of bone length) of 18 radii and 5 femora using HR-pQCT (82 micron). Distal radius and tibia of 94 women (age:57+/- 6.3 yrs.) scanned by HR-pQCT. Finite element analysis was used to estimate bone strength.Results Bone mass was constant along the diaphysis of radii, the femoral neck and along the distal third of the femur (Fig). Along the metaphysis, the constant mass was fashioned with a large void volume and high surface area/matrix volume (trabecular bone) while at the mid-diaphysis the same mass was fashioned with a small intracortical and medullary void volume and low surface area/matrix volume (cortical bone). Preliminary FEA showed a reduction in strains in areas with increased cortical thickness and the moment of inertia. In-vivo results revealed that larger bones are assembled with relatively less cortical mass, which is characterized by higher cortical porosity and lower matrix mineral density.Conclusion Larger bones are not assembled using more mass, they are assembled using more void - mass is minimized to facilitate mobility. Moreover, maintaining optimal strains is achieved by diversity in structure more than mass.References:1. Ghasem-Zadeh A, et al. Bone. 2017 Aug; 101:206-213. PMID: 28502884 2. Zebaze RM, et al. J Bone Miner Res. 2007 Jul;1055-61. PMID: 17501625.

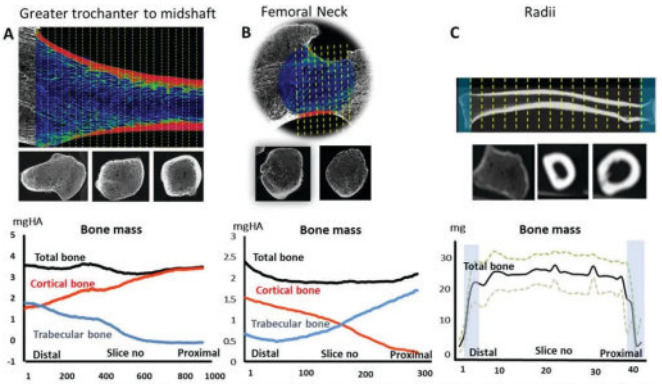

Fig. Coronal section and axial images of cross sections along the greater trochanter to midshaft (**A**), femoral neck (**B**), and radius (**C**). Trabecular and cortical bone fashioned within different pattern and with same amount of bone volume in each cross-section. Metaphysis is large, with mainly void volume, and the smaller diaphysis is exclusively cortical bone with a small medullary void volume.

***Disclosures: Ali Ghasem-Zadeh**, None*

Sunday Orals

SUN-378

Physical Function Tests for the Prediction of Fracture Risk in Older Women

*Giulia Gregori[1], Lisa Johansson[2], Kristian Axelsson[3], Henrik Litsne[1], Mattias Lorentzon[4]. [1]Sahlgrenska Osteoporosis Centre, Institute of Medicine, University of Gothenburg, Gothenburg, Sweden, Sweden. [2]Institute of medicine, . [3]Institute of Medicine, Sahlgrenska Academy, Gothenburg University, . [4]Sahlgrenska Academy, University of Gothenburg, Sweden

Background: Physical function is an important risk factor for fracture. Previous studies have found that physical tests including the one leg standing (OLS) time and timed up and go test (TUG) predict fracture risk. The aim of this study was to determine which physical function test is the most optimal predictor of fracture risk when adjusting for clinical risk factors (CRFs), used in the fracture risk assessment tool (FRAX), and bone mineral density (BMD).Methods: In total, 2,321 Swedish women 77.7?1.6 years old (mean?SD) from the SUPERB study were included in this analysis. Five different physical function tests were conducted at baseline: hand grip strength, OLS, TUG, gait speed, and chair stand test. Incident fractures were identified using by X-ray or review of medical records and subsequently categorized as major osteoporotic fractures (MOF; hip, spine, proximal humerus, and forearm), hip fractures, and any fractures. Multivariate Cox regression (hazard ratios [HR] and 95% confidence intervals [CI]) analyses were performed to investigate the association between all physical function tests (included in the same model) and incident fracture, with age, body mass index (BMI), FRAX CRFs and femoral neck (FN) BMD used as covariates. Results: During a median (IQR) follow-up time of 7.5 (2.9) years (IQR), there were 579 (24.9%) MOF, 163 (7%) hip fractures and 779 (33.6%) any fractures. After adjusting for age, BMI, CRFs included in FRAX, and additionally for BMD, OLS was the only physical function test consistently associated with increased risk of all fracture outcomes (Table). Gait speed was only associated with the risk of hip fracture regardless of adjustment, and chair stand test with MOF and any fracture only in fully adjusted models (Table).Conclusions: Among the five physical function tests, this study demonstrates that OLS time is the strongest predictor of MOF, hip fracture, and any fracture in older women, indicating that this test should therefore be considered as an additional assessment tool for improving fracture prediction in older women.

Table. Association between physical function tests and fracture risk in older women.

	Grip Strength (N)	One Leg Standing (s)	Time Up and Go (s)	Gait Speed (m/s)	Chair Stand (n/s)
	HR (95% CI)	HR (95% CI)	HR (95% CI)	HR (95% CI)	HR (95% CI)
Major osteoporotic fracture					
Model 1	1.01 (0.93 to 1.11)	**1.14 (1.04 to 1.26)**	0.94 (0.84 to 1.05)	**1.12 (1.00 to 1.26)**	1.08 (0.98 to 1.20)
Model 2	0.99 (0.91 to 1.09)	**1.12 (1.02 to 1.24)**	0.96 (0.87 to 1.08)	1.11 (0.99 to 1.24)	**1.11 (1.01 to 1.22)**
Hip fracture					
Model 1	1.03 (0.87 to 1.22)	**1.32 (1.10 to 1.60)**	1.03 (0.84 to 1.26)	**1.34 (1.09 to 1.66)**	1.14 (0.95 to 1.36)
Model 2	0.99 (0.83 to 1.17)	**1.30 (1.06 to 1.55)**	1.08 (0.88 to 1.31)	**1.29 (1.05 to 1.60)**	1.19 (0.99 to 1.43)
Any fracture					
Model 1	1.01 (0.94 to 1.09)	**1.13 (1.04 to 1.22)**	0.94 (0.85 to 1.04)	1.09 (0.99 to 1.21)	1.07 (0.98 to 1.17)
Model 2	0.99 (0.92 to 1.07)	**1.11 (1.02 to 1.20)**	0.97 (0.88 to 1.06)	1.09 (0.98 to 1.20)	**1.10 (1.01 to 1.20)**

Associations were studied using Cox proportional hazard models. Hazard ratios (HR) per SD are shown with 95% Confidence Intervals. Significant HRs are shown in bold. All physical function test variables were included simultaneously. Model 1: adjusted for age, BMI, CRFs included in FRAX (previous fracture, family history of hip fracture, current smoking, rheumatoid arthritis, oral glucocorticoid use, alcohol consumption, secondary osteoporosis). Model 2: model 1 + Femoral Neck BMD.

***Disclosures: Giulia Gregori**, None*

SUN-379

Assessment of Trabecular Bone Score using updated TBSTT on top of bone mineral density, body composition and bone turnover markers in Anorexia Nervosa - The AN-BO Study

*Judith Haschka[1], Martina Behanova[1], Didier Hans[2], Annina Arens[1], Christian Muschitz[3], Larisa Dzirlo[4], Julia Binder[5], Jochen Zwerina[1], Heinrich Resch[6], Roland Kocijan[1]. [1]Ludwig Boltzmann Institute of Osteology at Hanusch Hospital of OEGK and AUVA Trauma Center Meidling, 1st Medical Department Hanusch Hospital, Vienna, Austria. [2]Centre des Maladies Osseuses-Département de l'Appareil Locomoteur, Hôpital Orthopédique, Lausanne, Switzerland. [3]St. Vincent Hospital, Medical Department II, Vienna, Austria. [4]St. Vincent Hospital, Medical Department III, Vienna, Austria. [5]Department of Obstetrics and Gynecology, Medical University of Vienna, Vienna, Austria. [6]Karl Landsteiner Institute for Gastroenterology and Rheumatology at Rheuma-Zentrum Wien Oberlaa and St. Vincent Hospital, Medical Department II, Vienna, Austria

BackgroundAnorexia Nervosa (AN) is a well-known risk factor for secondary osteoporosis. Despite low bone mineral density (BMD), reduced trabecular bone score (TBS) in AN has been reported previously. Presence of soft tissue leads to alterations in X-ray absorption, may underestimate TBS values and is especially of interest when comparing patient populations with different body compositions. The updated TBS software (TBS iNsight®v4.0) provides a new algorithm accounting for soft tissue thickness (TBSTT) instead of body mass index (BMI, TBSBMI).Purpose & MethodsThe aim of the study was to assess TBS using both TBS algorithms (TBSTT and TBSBMI) in adult females with AN compared to controls (CTRL). Further, BMD (lumbar spine LS; total hip; femoral neck; body composition: lean body mass LBM; fat mass FM; bone mineral content, BMC; GE Lunar iDXATM) as well as 25(OH)vitamin D, bone turnover markers (BTM; CTX, P1NP) and serum sclerostin levels were assessed. Differences between groups were evaluated by independent-samples T-test or Mann-Whitney U test. Results are presented as mean+/-SD or median(IQR), depending on normality distribution.Results60 female patients with AN (N=34) and CTRL (N=26) of comparable age (22.8 (7.1) vs. 25.0 (4.0) years, p=0.145) but different BMI (14.7 (1.6) vs. 22.4 (4.0), p<0.001) were analyzed. TBSTT (1.319+/-0.09 vs.1.502+/-0.07, p<0.001) and TBSBMI (1.317+/-0.10 vs.1.548+/-0.09, p<0.001) were significantly lower in AN patients. Soft tissue thickness was lower in AN (cm, 13.8+/-1.0 vs.18.6+/-2.1, p<0.001). BMD at all sites of AN patients were reduced (p<0.001 for all), being lowest at LS (0.973+/-0.149 vs. 1.289+/-0.146). TBSTT and TBSBMI correlated with BMD at all sites (p<0.001). BMC, LBM and FM were decreased in AN (p<0.001). AN patients had lower 25(OH)vitamin D (ng/ml; 26.7+/-11.0 vs. 32.9+/-9.5, p=0.028) and P1NP (36.9 (42.5) vs. 47.4 (31.9), p=0.05), but higher CTX (0.73 (0.5) vs. 0.37 (0.3), p=0.001) and sclerostin (12.6 (10.0) vs.8.7(6.9), p=0.003). Duration of amenorrhea was negatively correlated with TBSBMI (?=-0.36, p=0.05) and BMD of LS (?=-0.64, p<0.001).ConclusionAdult AN patients have lower TBSTT and TBSBMI despite reduced BMD at all sites. BTM indicate an uncoupling of bone turnover in AN patients.Differences in soft tissue thickness were displayed by the new algorithm. Although, the impact in these cohorts of under- and normal-weight controls was low, greater differences may arise if body composition varies despite comparable BMI.

***Disclosures: Judith Haschka**, None*

SUN-380

Microstructural Imaging of Bone by Photon-Counting Detector Computed Tomography

*Andrew Burghardt[1], Aida Korajac[2], Andreas Strassl[2], Saghi Sadoughi[3], Galateia Kazakia[1], Janina Patsch[2]. [1]University of California, San Francisco, United States. [2]Medical University of Vienna, Austria. [3]UCSF,

The quantification of bone quality by high-resolution peripheral quantitative computed tomography (HR-pQCT) improves fracture risk prediction1, however few systems are available worldwide, they are exclusively approved for research purposes, and the technology is limited to imaging the peripheral skeleton. In the last year clinical CT systems with photon counting detectors (PCD-CT) - a generational advance in imaging performance - have been introduced2. The goal of this study was to evaluate the accuracy of PCD-CT for bone structure quantification.Cadaveric phantoms comprised of 20 1-cm metaphyseal sections of distal radius and tibia bone3 were imaged by µCT (24.5µm), 1st- and 2nd-generation HR-pQCT (82µm, 61µm), and PCD-CT (Naeotom Alpha, Siemens Healthineers). PCD-CT scans were acquired at 120kVp in Ultra-High Resolution (UHR) mode (200mAs, 16.1mGy). A 15mm FOV was reconstructed across 1024x1024 matrix using the Br92 kernel (146µm pixel size, 150µm slice thickness). Spatial resolution (10% MTF) and noise performance (SNR) were measured in idealized density and wire phantoms. Standard density, geometry, and structure measures were quantified from the cadaveric phantom images and evaluated for accuracy by linear regression and Bland-Altman analysis.Scan time for each bone section was <10s for PCD-CT, compared to 3.2 and 2.0 minutes for 1st and 2nd-gen HR-pQCT. Qualitatively, PCD-CT provides an exquisite depiction of cortical and trabecular microstructural features (Fig. 1, top). PCD-CT noise performance (SNR=20.5) was superior to 1st- and 2nd-gen HR-pQCT (SNR=15.4 and 7.1). The spatial resolution of PCD-CT (10% MTF = 132 µm) was comparable to 1st-gen HR-pQCT (10% MTF = 138 µm), and inferior to 2nd-gen HR-pQCT (10% MTF = 95 µm). Accuracy of PCD-CT was high (R2>0.9) for BV/TV and Tb.N, and comparable to HR-pQCT (Fig.1, bottom).Photo-counting detector CT provides significant advantages for measuring human bone structure in vivo, including superior noise performance and scan time, while spatial resolution is comparable to 1st-gen HR-pQCT and accuracy was comparable to 2nd-gen HR-pQCT. Given the potential for wide availability and existing regulatory approval, PCD-CT represents an exciting opportunity to translate quantitative microstructural skeletal imaging to a clinical platform.1 Langsetmo L, et al., doi: 10.1002/jbmr.34332 Hsieh SS, et al., doi: 10.1109/trpms.2020.30202123 Burghardt AJ, et al., doi: 10.1002/jbmr.1795

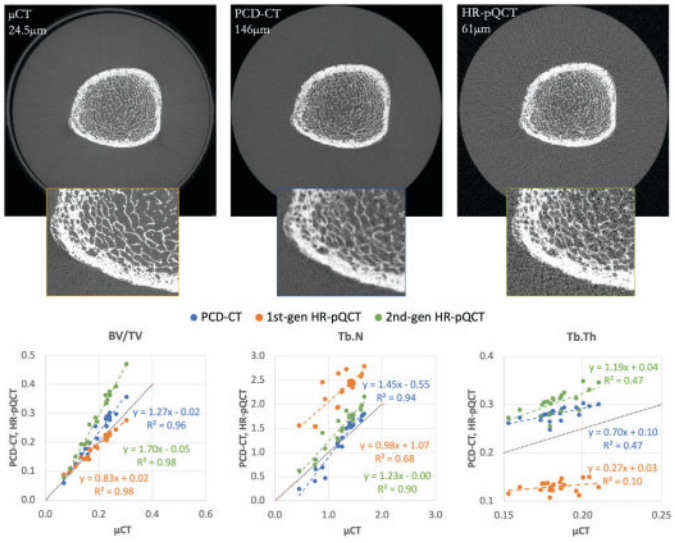

***Disclosures: Andrew Burghardt**, Siemens Healthineers, Other Financial or Material Support*

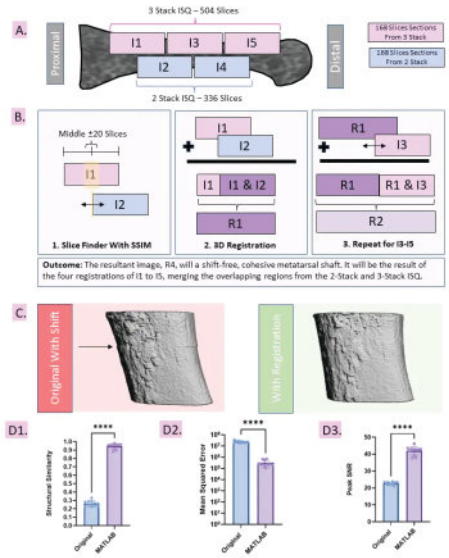

Figure 1 – (A) The 3-Stack and 2-Stack HR-pQCT ISQ files were divided into 168 slice subregions. These subregions were labeled accordingly. (B) These subregions were pulled into the custom MATLAB code for registration into a single, cohesive scan. A "slice finder", governed by the structural similarity index function, selected identical slices from the adjacent subregions. As shown in this first box, the first slice of I2 was compared to 40 different slices in I1 with this "slice finder" until an identical image was identified. Next, I1 and I2 were registered starting at the matching slice. This created R1, or the first registered subregion. Following this, the cycle was repeated, but using R1 and I3. This process was continued for four registrations, until (C) a complete, cohesive image was reconstructed. (D1) Structural similarity index and (D3) peak signal to noise ratio were significantly increased ($p<0.0001$) and the mean square error (D2) was significantly decreased ($p<0.0001$).

***Disclosures: Andrea Jacobson**, None*

SUN-381

Custom MATLAB Registration Script for Stack Shift Correction of Multistack HR-pQCT Scans of the Metatarsals *Andrea Jacobson[1], Austin Sventeckis[2], Michael Kuczynski[3], Sarah Manske[4], Stuart Warden[5], RACHEL SUROWIEC[6]. [1]Department of Biomedical Engineering, Indiana University Purdue University Indianapolis, United States. [2]Department of Physical Therapy, Indiana University Purdue University Indianapolis, United States. [3]McCaig Institute for Bone and Joint Health, Department of Radiology, Cumming School of Medicine, University of Calgary, Canada. [4]University of Calgary, Canada. [5]Indiana University School of Health & Human Sciences, United States. [6]Indiana University Purdue University,

The metatarsals are commonly injured in athletes and military recruits as well as in some disease states (e.g. Charcot neuropathy). High resolution peripheral quantitative computed tomography (HRpQCT) is a novel tool for measuring bone parameters in vivo. Scan stacks are limited to 168 slices (10.2mm), and each new stack creates a "stack shift" which could alter evaluation outcomes. Metatarsal pathologies may extend beyond the 10.2mm single stack length, necessitating a protocol for correcting stack shifts. This work aimed to create a stack shift correction to enable accurate assessment of multistack metatarsal HRpQCT scans.A convenience sample of two participants had two HRpQCT scans (Scanco XtremeCTII) taken of the metatarsal forefoot region: one 2-stack scan (336 slices) and one 3-stack (504 slices) centered at the midshaft of the 2nd metatarsal (voxel 60.7 µm). The stacks were positioned to overlap at points of stack shift, which would occur at slices 168 and 336 in the 3-stack scan (Fig.A). The first, second, and third metatarsals were cropped from each data set to test the reconstruction of 6 unique bones. The stacks were divided into 168 slice subregions (Fig. A) and imported to MATLAB for image registration. To register these images, the custom code had two main functions. First, as shown in Figure B, the "slice finder" used structural similarity index (SSIM) to find the most similar slices between neighboring subregions. Next, four 3D registrations were performed until all neighboring subregions were combined into one cohesive image, as shown in Figure C. The two slices adjacent to each stack shift (slices 168-169 and 336-337) were compared before and after the registration (n=12) using three metrics: SSIM, mean squared error (MSE), and peak signal to noise ratio (PSNR). Paired one-tailed t-tests were run to evaluate each metric's before and after registration results.The SSIM value was significantly larger ($p<0.0001$) post-registration and close to a value of 1 (0.95+/-0.03) compared to prior to the registration (0.26+/-0.03) (Fig. D1). The MSE was significantly lower post-registration ($p<0.0001$) (Fig. D2). Additionally, the PSNR value was significantly larger ($p<0.0001$) post-registration (Fig. D3).The custom MATLAB registration script significantly improved the stack shift in both regions of the metatarsal scan. With these promising results, next steps are to perform microarchitectural and mineral density analyses on resultant, registered images.

SUN-382

Cortical thickness as measured by 3D-DXA is associated with prior fracture in Blacks but not Whites when controlling for age and areal BMD T-score *Rajesh Jain[1], Mirella López Picazo[2], Ludovic Humbert[2], Tamara Vokes[1]. [1]University of Chicago, United States. [2]3D-Shaper Medical, Spain

Introduction: Black patients are known to have greater areal BMD (aBMD) than White patients. Some studies suggest aBMD may not be as predictive of fracture in Black patients, and Black patients are known to fracture at about 50% the rate at a given aBMD. Some of these differences appear to relate to differences in bone structure. New software can provide quantitative CT-like 3D models based on 2D hip DXA images, allowing for analysis of cortical and trabecular volumetric parameters from routine DXA. We sought to determine whether there were differences between Black and White patients in 3D-DXA parameters and/or their association with fragility.Methods: This is a secondary analysis of patients previously recruited as part of their clinical care at an osteoporosis center in Chicago, IL. Patients with active cancer were excluded. All patients had undergone a fracture questionnaire, a DXA scan, and vertebral fracture assessment (VFA). 3D-SHAPER software (v2.12, 3D-Shaper Medical, Spain) was retrospectively run on hip DXA scans. 95% patients had DXA of both femurs, and the worst parameter was used in analysis. We analyzed either vertebral fracture on VFA or history of fracture after the age of 50 as an outcome of bone fragility. We compared 3D-DXA parameters by race using t-tests, and we used logistic regression to analyze the association between fractures and 3D-DXA parameters.Results: There were 368 Black and 407 White women with Blacks being older but with greater aBMD (Table 1). Cortical surface BMD and total hip volumetric BMD (vBMD) measurements were strongly correlated with total hip aBMD (correlation coefficient p= 0.90-0.97, $p<0.001$ for all), while cortical thickness of the femoral neck less so ($p=0.43$, $p<0.001$).Most 3D-DXA parameters were superior in Blacks vs. Whites (Table 1). When adjusting for age only, total hip trabecular, cortical, and integral vBMD were associated with fracture in Whites, but not Blacks (per SD worsening: OR 1.7-2.2, $p<0.001$ vs. OR 1.1-1.2, p=NS, respectively). When also adjusting for lowest T-score, trabecular vBMD of the total hip was the strongest 3D-DXA predictor of prior fracture in Whites, but in Blacks we found that cortical thickness of the femoral neck was the strongest predictor.Conclusion: 3D-DXA software demonstrates superior bone structure in Black patients, and cortical thickness of the femoral neck may be an important parameter to uniquely predict fracture in Black patients.

	3D-DXA Parameters		Associations with Fracture[1]	
	Black (368)	White (407)	Black (368) OR per SD worsening	White (407) OR per SD worsening
Age	69.4 ± 11.0	63.8 ± 11.1	-	-
Lowest T-score	-2.0 ± 1.2	-2.4 ± 1.0	-	-
Fracture history	23.4%	27.5%	-	-
Integral vBMD (TH), mg/cm³	288.3 ± 61.1	269.5 ± 51.0	0.6 (0.4-1.0, p=0.06)	1.6 (0.9-2.8, p=0.08)
Trabecular vBMD (TH), mg/cm³	141.2 ± 43.1	127.2 ± 37.3	0.7 (0.5-1.1, p=0.13)	**1.8 (1.1-3.0, p=0.02)**
Cortical vBMD (TH), mg/cm³	768.3 ± 92.2	754.1 ± 79.6	**0.6 (0.4-0.9, p=0.02)**	1.2 (0.8-1.8, p=0.49)
Cortical Surface BMD (TH), mg/cm²	144.4 ± 27.0	137.3 ± 21.7	0.7 (0.4-1.1, p=0.14)	1.2 (0.7-2.0, p=0.57)
Cortical thickness (TH), mm	1.84 ± 0.16	1.79 ± 0.13	1.2 (0.9 – 1.8, p=0.21)	0.9 (0.6 – 1.4, p=0.79)
Cortical thickness (FN), mm	1.60 ± 0.18	1.51 ± 0.14	**1.5 (1.1 – 2.0, p=0.009)**	0.8 (0.6-1.1, p=0.24)
Cortical thickness (lateral FN), mm	1.01 ± 0.12	0.97 ± 0.10	**1.5 (1.2-1.9, p=0.002)**	0.9 (0.7-1.2, p=0.44)
Cortical thickness (medial FN), mm	2.72 ± 0.34	2.53 ± 0.26	1.3 (1.0 – 1.7, p=0.08)	0.8 (0.6 – 1.1, p=0.15)

[1]Controlled for Age and lowest areal BMD T-score
TH: total hip; FN: femoral neck, SD: standard deviation, OR: odds ratio
Bold 3D-DXA parameters are significantly different across race; bold odds ratio are statistically significant.

***Disclosures: Rajesh Jain**, None*

SUN-383

Portable USB-powered Radiation-free Bone Mineral Density Measurement at the 1/3 Radius *Jonathan Kaufman[1], Gangming Luo[1]. [1]CyberLogic, Inc., United States

The goals of this study were to determine the ability of a new clinical ultrasound device (UltraScan 650, CyberLogic, Inc., NY, USA, Fig. 1) to estimate bone mineral density (BMD) at the 1/3 radius.The UltraScan 650 is a portable USB-powered tabletop sonometer, and performs evaluation of the BMD with a 10 second radiation-free test. The device measures the radius in thru-transmission, and computes the BMD in grams per square centimeter, as would be measured by DXA. A clinical IRB-approved study was carried out in which 77 adults (age range 21-83, 75% female) were measured at the 1/3 radius using the UltraScan 650 and DXA (Hologic QDR 4500). BMD ranged from 0.45 - 0.92 g/cm2). A linear regression showed that BMD obtained with the UltraScan 650 and the BMD obtained with DXA had a linear (Pearson) correlation of 0.93 (P<0.001). The data presented demonstrate that the UltraScan 650 is an excellent proxy for BMD as would be measured by DXA at the 1/3 radius. Indeed, we found that forearm ultrasound measurements yield results that are very closely associated with those from DXA. These clinical results are also consistent with previously reported simulated and in vitro studies, and the present clinical data provides strong support for the proposed methods in ultrasonically estimating BMD. A new device, the UltraScan 650, has been shown to have the potential to enlarge the scope of ultrasound bone assessment in particular and of bone screening in general.The portability and simplicity in use of the radiation-free ultrasound scanner, combined with its high degree of accuracy and precision in estimating radial BMD, provides a basis by which to expand ultrasonic assessment to the primary and community care settings. This will in turn provide an opportunity to reduce the incidence of osteoporotic fractures through early and timely therapeutic interventions.

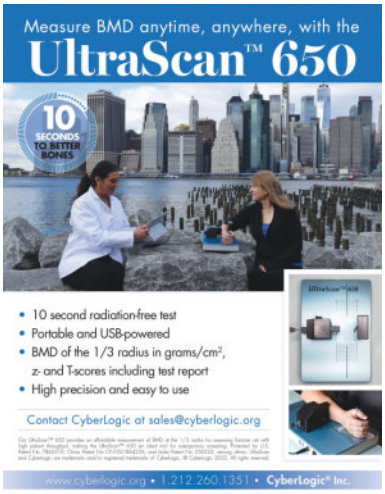

***Disclosures: Jonathan Kaufman**, CyberLogic, Inc., Major Stock Shareholder*

SUN-384

Prediction of progressive collapse in osteoporotic vertebral fractures using conventional statistics and machine learning *Jin Hwan Kim[1], Sung Tan Cho[2], Soonchul Lee[3], Hyun Il Lee[4]. [1]Inje University, Ilsanpaik Hospital, Republic of Korea. [2]INJE University ILSANPAIK Hospital, Republic of Korea. [3]Department of Orthopaedic Surgery, CHA University School of Medicine, Republic of Korea. [4]Department of Orthopedic Surgery, Ilsan Paik Hospital, Inje University, Republic of Korea

Background: Few studies have investigated the risk factors of progressive osteoporotic vertebral fracture (OVF). Furthermore, machine learning has not been applied in this aspect. The purpose of this study is to determine prognostic factors for the progression of OVF following conservative treatment.Methods: The study involved the progression of collapse (PC) and non-PC groups based on the compression rate (15%). Clinical data, fracture site, OVF shape, Cobb's angle, and anterior wedge angle of the fractured vertebra were evaluated. The presence of intravertebral cleft and the type of bone marrow signal change were analyzed using magnetic resonance imaging. Multivariate logistic regression analysis was performed to identify prognostic factors. In machine learning methods, decision tree (DT) and random forest (RF) models were used.Results: There were no significant differences in clinical data between the groups. The proportion of fracture shape (p<0.001) and bone marrow signal change (p=0.01) were significantly different between the groups. Moderate wedge shape was most observed in the non-PC group (31.7%), whereas the normative shape was most observed in the PC group (54.7%). The Cobb's angle and anterior wedge angle at diagnosis of OVFs were higher in the non-PC group (13.2+/-10.9; p=0.001, 14.3+/-6.6; p<0.001) than in the PC group (10.3+/-11.8, 10.4+/-5.5). The bone marrow signal change at the superior aspect of the vertebra was more frequently found in the PC group (42.5%) than in the non-PC group (34.9%). Feature importance using machine learning revealed that vertebral shape at initial diagnosis was the main factor of progression of vertebral collapse. Furthermore, the RF model was better at predicting progression (AUC=0.727, multivariate logistic regression=0.724, DT=0.688).Conclusion: The initial shape of the vertebra and bone edema pattern on MRI are useful prognostic predictors for the progression of collapse in OVFs.

***Disclosures: Jin Hwan Kim**, None*

SUN-385

Opportunistic Vertebral Fracture Detection from Computed Tomography Studies by Artificial Intelligence - preliminary results *Daniel Arian Kraus[5], Shahin Zandieh[2], Judith Haschka[3], Heinz Redl[4], Jochen Zwerina[5], Roland Kocijan[5]. [5]Ludwig Boltzmann Institute of Osteology, Austria. [2]Department for Radiology and Nuclear Medicine at Hanusch hospital of OEGK, Austria. [3]Ludwig Boltzmann Institute for Osteology, Hanusch Hospital Vienna, . [4]Ludwig Boltzmann Institute of Traumatology, Austria. [5]Ludwig Boltzmann Institute of Osteology,

IntroductionVertebral fractures belong to the most common osteoporotic fractures, although not always clinically evident. Nevertheless, vertebral fractures increase the risk of further osteoporotic fractures and require assessment and treatment in most cases. The aim of this preliminary analysis was to identify higher grade vertebral fractures by the prototype of a deep learning artificial intelligence software in a high-risk collective of patients with pulmonary diseases.MethodsThe artificial intelligence Flamingo (ImageBiopsy Lab®) detects vertebral fractures from thoracic and abdominal computed tomography (CT) studies. It can be applied to already existing CT scans and predicts a class probability for every voxel using a 3-dimensional convolutional neural network. This retrospective analysis comprised 30 patients with thoracic and/or abdominal CT studies from the pulmonary outpatient clinics of Hanusch hospital Vienna. In total, 458 vertebral bodies from T1-L4 were analyzed. CT studies were screened for fractures by a trained radiologist and classified according to the Genant classification. In the next step, the same CT studies were reviewed by Flamingo for vertebral fractures and classified into no fracture (Genant 0/1), moderate fracture (Genant 2) and severe fracture (Genant 3). Sensitivity and specificity were tested.ResultsDatasets of 29 subjects (mean age 76 +/- 9.9, 51.7 % male) were available. In total, 19 higher-graded vertebral fractures in 9 subjects were identified by the radiologist. Flamingo correctly identified 76 % of subjects (22 out of 29) with fractures (Genant 2/3) and without (Genant 0/1) compared to the radiologist. Furthermore, 69 % of subjects (20 out of 29) were correctly classified in no fracture (Genant 0/1), Genant 2 or Genant 3 fracture compared to the radiologist. Moreover, in 14 % of subjects (4 out of 29) at least 1 fracture (Genant 2/3) was identified correctly, whereas the remaining subjects (10.3 %, 3 out of 29) were assessed incorrectly. Overall, Flamingo reported a sensitivity of 89.5 % and specificity of 98.0 % for identification of higher-grade vertebral fractures (Genant 2/3).ConclusionThe artificial intelligence Flamingo revealed promising preliminary results in opportunistic fracture detection of higher-grade vertebral fractures (Genant 2/3) from existing CT scans. The application of artificial intelligence could reduce the gap of undiagnosed and untreated vertebral fractures and thus osteoporosis.

***Disclosures: Daniel Arian Kraus**, None*

SUN-386

Osteosarcopenia Presents a Risk for Self-Reported Incident Falls, Fractures, Frailty, Life Satisfaction and Activities of Daily Living in Community-Dwelling Older Adults: Results From the Canadian Longitudinal Study on Aging (CLSA) *Ahreum Lee[1], Caitlin McArthur[2], George Ioannidis[1], Gustavo Duque[3], Jonathan D Adachi[1], Lauren E Griffith[1], Lehana Thabane[1], Alexandra Papaioannou[1]. [1]McMaster University, Department of Health Research Methods, Evidence, and Impact, Canada. [2]Dalhousie University, School of Physiotherapy, Canada. [3]Dr. Joseph Kaufmann Chair in Geriatric Medicine, Department of Medicine, McGill University, Canada

Background/Purpose: To investigate whether older adults with osteosarcopenia have a higher risk of experiencing falls, fractures, frailty, decline in life satisfaction, limitations in activities of daily living (ADL), and reduced physical function compared to those without osteopenia/osteoporosis and sarcopenia.Methods: This study included Caucasian participants aged 65 years or older who completed physical measurements at baseline and a 3-year follow-up within the Canadian Longitudinal Study on Aging (CLSA) 2015 comprehensive baseline interview. Osteopenia/osteoporosis was defined as a BMD T-score -1 standard deviation (SD) by the World Health Organization definition, and sarcopenia was defined by the Sarcopenia Definition Outcomes Consortium, which involves low grip strength and/or low gait speed. Osteosarcopenia was defined as the coexistence of osteopenia/osteoporosis and sarcopenia. This study assessed any self-reported incident falls and fractures occurring within the 12 months prior to the 3-year follow-up, as well as frailty (measured through the Rockwood Frailty Index), life satisfaction (measured through the Satisfaction With Life Scale, SWLS), ADL (measured through the Older American Resources and Services Modules), and physical function (measured through timed up and go, chair rise, and standing balance tests). We conducted multivariable logistic and linear regressions, with subgroup analyses conducted by sex. Odds ratio (OR), coefficient (?) and 95% confidence intervals (CI) are reported.Results: This study included a total of 8,888 participants with a mean (SD) age of 72.7 (5.6) years, of which 49.1% were females. At baseline, 30.1% of participants had neither osteopenia/osteoporosis nor sarcopenia, 18.4% had sarcopenia only, 29.2% had osteopenia/osteoporosis only, and 22.3% had osteosarcopenia. The results showed that males with osteosarcopenia had a higher risk of experiencing incident falls and fractures compared to males without osteopenia/osteoporosis or sarcopenia, with an adjusted odds ratio of 1.90 (95% CI: 1.15, 3.14) and 2.60 (95% CI: 1.14, 5.91), respectively. In addition, participants with osteosarcopenia had worse ADLs and a decrease in their SWLS than those without, with an estimated ? 0.110 (95% CI: 0.029, 0.192) and -0.660 (95% CI: -1.133, -0.187), respectively.Discussion/Conclusions: Osteosarcopenia presents a greater risk for self-reported incident falls and fractures among males, as well as poorer life satisfaction and ADL for females and all participants.

***Disclosures: Ahreum Lee**, None*

SUN-388

Parental History of Hip Fracture and Future Fracture Risk: an International Meta-analysis to Inform Updates of FRAX *Eugene McCloskey[5], Helena Johansson[2], Nicholas Harvey[3], Enwu Liu[4], Marian Schini[5], Liesbeth Vandenput[4], Mattias Lorentzon[6], William Leslie[7], John Kanis[4], and the FRAX Meta-analysis Cohort Group [8]. [5]University of Sheffield, United Kingdom. [2]University of Gothenburg, Sweden. [3]University of Southampton, . [4]Australian Catholic University, Australia. [5]University of Sheffield, . [6]Sahlgrenska Academy, University of Gothenburg, Sweden. [7]University of Manitoba, Canada. [8], United Kingdom

We have undertaken a meta-analysis of international prospective cohorts to quantify the relationship between a parental history of hip fracture history and future fracture incidence. We additionally explored the predictive value of this risk factor when adjusted for age, sex, time since baseline and femoral neck bone mineral density (BMD).The analysis dataset comprised 281893 men and women from 40 cohorts in 28 countries followed for a total of 2.42 million person-years. We investigated the relationship between parental hip fracture history and the risk of any clinical fracture, any osteoporotic fracture, major osteoporotic fracture (MOF) and hip fracture alone using an extended Poisson model in each cohort. Covariates examined were age, sex, BMD and duration of follow up. The results of the different studies were merged by using the weighted ?-coefficients.After adjustment for age and time since baseline, a parental history of hip fracture was associated with higher risk of incident fracture across all of the fracture outcome categories in both men and women. For example, the hazard ratio [HR (95% CI)] for MOF was 1.21 (1.13-1.29) in women and 1.18 (1.05-1.33) in men, with no difference between the sexes. The association appeared stronger for the prediction of incident hip fractures alone (1.40, 1.26-1.56 and 1.37, 1.05-1.80 in women and men respectively). Associations were similar in the subset of cohorts in which BMD was measured and the relationship was largely unchanged when BMD was included in the analysis. Furthermore, the magnitude of associations did not vary by age and/or follow-up time. In this large international cohort meta-analysis, parental history of hip fracture increased the risk of future fracture, especially hip fracture. The association appears independent of sex, age and femoral neck BMD. We conclude that parental history of hip fracture should continue to play a role as an important, easily captured, fracture risk factor in future iterations of tools such as FRAX.

***Disclosures: Eugene McCloskey**, Osteoporosis Research Ltd, Other Financial or Material Support*

SUN-389

Defining Imminent Risk Using FRAX Multipliers for Patients with Recent Fragility Fractures *Prism Schneider[2], Kaja Matovinovic[2]. [2]University of Calgary, Canada. [2]University of Calgary,

Purpose: The Fracture Risk Assessment Tool (FRAX) estimates a 10-year probability of major osteoporotic fracture (MOF) using clinical risk factors, including prior fracture history as a binary variable. However, prior fractures affect future risk differently depending on recency and site, with MOF risk being highest in the first two years following an index fracture (imminent risk). Therefore, the FRAX tool may underestimate true risk, resulting in missed opportunities for osteoporosis management. To address this, multipliers based on age, sex, and fracture type have been proposed to adjust FRAX scores. Modified FRAX scores may more accurately predict MOF risk in patients with recent fragility fractures, allowing earlier identification of those eligible for pharmacologic intervention. Methods: Standard and modified FRAX scores were calculated for patients with non-hip MOFs. Patients 50 years or older with distal radius or humerus fractures were included. Patients under 50 years and hip fractures were excluded. Age- and sex-based FRAX multipliers for acute distal radius and proximal humerus fractures were used to adjust FRAX scores (McCloskey et al. 2021). Low, intermediate, and high-risk of MOF was defined as less than 10%, 10-20%, and greater than 20%, respectively. Paired sample t-tests were used to compare FRAX score pre- and post-modifier. Results: A total of 142 patients, with a mean age of 65 years were included. Most patients were female (90.1%), with 75.4% sustaining distal radius fractures and 24.6% sustaining proximal humerus fractures. In the distal radius group, average MOF risk pre- and post-multiplier was 17.2 and 21.0, respectively ($p<0.05$). Seventeen percent of patients in the distal radius group moved from intermediate to high-risk after multiplier adjustment. Average FRAX scores pre- and post-adjustment in the proximal humerus group were 16.1 and 23.0, respectively ($p<0.01$), with 28.6% moving from intermediate to high-risk. Conclusion: This study demonstrates the clinically significant impact of modified FRAX scores in patients with recent fragility fractures. Seventeen percent of the distal radius group and 28% of the humerus group moved from intermediate to high MOF risk post-multiplier. Consequently, patients previously ineligible for pharmacologic management, now met criteria. Multiplier-adjusted FRAX scores may more accurately identify patients with imminent fracture risk, facilitating earlier risk reduction interventions.

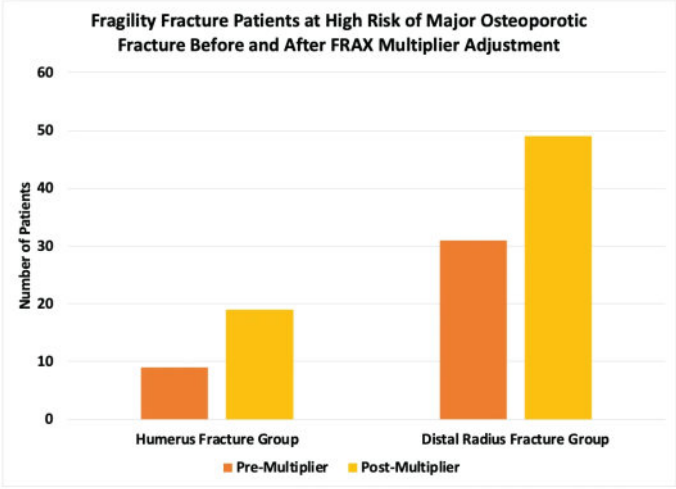

***Disclosures: Prism Schneider**, None*

SUN-391

Adjusting for Level-specific Trabecular Bone Score (TBS) Differences Reduces FRAX®-based Treatment Reclassification in Patients with Vertebral Exclusions Due to Structural Artifact: The Manitoba BMD Registry *William Leslie[1], Heenam Goel[2], Neil Binkley[3], Eugene McCloskey[4], Didier Hans[5]. [1]University of Manitoba, Canada. [2]CentraCare, St. Cloud, United States. [3]University of Wisconsin, Madison, United States. [4]University of Sheffield, United Kingdom. [5]Lausanne University Hospital & University of Lausanne, Switzerland

L1-L4 trabecular bone score (TBS) is a FRAX®-independent risk factor for fracture. Lumbar vertebrae affected by structural artifact are usually excluded from BMD measurement; how such exclusions affect TBS is uncertain. Since TBS values increase from cranial

to caudal, excluding lower vertebral levels reduces TBS and conversely increases TBS when upper lumbar vertebral levels are excluded. This can affect FRAX-based treatment when close to an intervention threshold.AIM: To examine the effect of adjusting for level-specific TBS differences in individuals with vertebral exclusions due to structural artifact on TBS-adjusted FRAX-based treatment recommendations.METHODS: We identified 71,209 individuals (mean age 64 years, 89.8% female) undergoing baseline TBS and FRAX calculations through the Manitoba Bone Density Program, where structural artifact resulting in vertebral exclusions was carefully ascertained. We compared FRAX-based treatment recommendations from the American Association of Clinical Endocrinologists (AACE) for TBSL1-L4 and from the non-excluded vertebral levels before and after adjusting TBS for mean level-specific differences.RESULTS: We computed mean differences between TBSL1-L4 and individual lumbar vertebrae in the 46,781 individuals without vertebral exclusions: L1 (+0.096), L2 (+0.008), L3 (-0.058) and L4 (-0.046). In the 24,428 individuals with vertebral exclusions, adjusting TBS using these level-specific factors gave excellent agreement with TBSL1-L4 (mean difference -0.001). Among those with baseline MOF risk >15%, TBS vertebral exclusions reclassified FRAX-based treatment in 10.6% of individuals compared with TBSL1-L4, whereas this was reduced to 7.2% after adjusting for level-specific differences (Figure). In 11,131 patients where L1-L2 was used for BMD reporting (the most common exclusion pattern with the largest TBS effect), treatment reclassification was reduced from 13.9% to 2.4%, respectively. Among individuals with baseline hip fracture risk >2%, TBS vertebral exclusions reclassified 7.1% compared with TBSL1-L4, but only 4.5% after adjusting for level-specific differences. When L1-L2 was used for BMD reporting, treatment reclassification from hip fracture risk was reduced from 9.2% to 5.2%.CONCLUSION: TBS and FRAX-based treatment recommendations are affected by vertebral level exclusions for structural artifact. Adjusting for level-specific differences in TBS reduces reclassification in FRAX-based treatment recommendations.

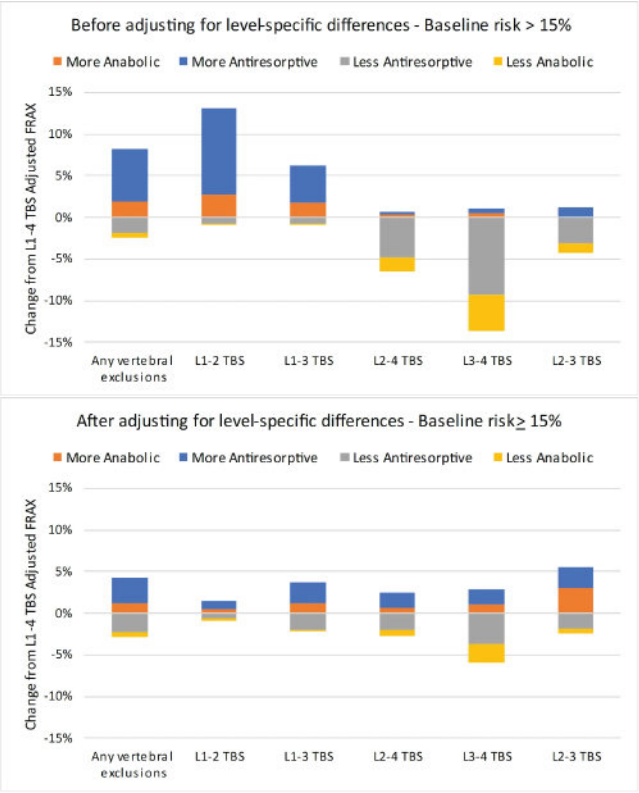

***Disclosures: William Leslie**, None*

SUN-392

BONEcheck: a digital tool for personalized fracture risk assessment *Dinh Tan Nguyen[1], Thao P. Ho-Le[2], Liem Pham[3], Vinh P. Ho-Van[4], TIen Dat Hoang[4], Thach Tran[5], Tuan Nguyen[6]. [1]University of Technology Sydney, . [2]School of Biomedical Engineering, University of Technology, Sydney, Australia., Australia. [3]Saigon Precision Medicine Research Center, Saigon, Vietnam, Viet Nam. [4]Faculty of Engineering and Information Technology, Hatinh University, Hatinh, Vietnam, Viet Nam. [5]Garvan Institute of Medical Research, Australia. [6]University of Technology Sydney , Australia

Background and Aim: Osteoporotic fracture is a significant public health burden associated with increased mortality risk and substantial healthcare costs. Accurate and early identification of high-risk individuals and mitigation of their risks is a core part of the treatment and prevention of fractures. We aimed to introduce a digital tool called 'BONEcheck' for personalized bone health assessment. Methods: The development of BONEcheck primarily utilized data from the prospective population-based Dubbo Osteoporosis Epidemiology Study and the Danish Nationwide Registry. BONEcheck has 3 modules: input data, risk estimates, and risk context. Input variables include age, gender, prior fracture, fall incidence, bone mineral density (BMD), comorbidities, and genetic variants associated with BMD. By utilizing published methodologies, BONEcheck generates output related to the likelihood of fracture and its associated outcomes. The vocabulary utilized to convey risk estimation and management is tailored to individuals with a reading proficiency at level 8 or above. Results: The tool is designed for men and women aged 50 years and older who either have or have not sustained a fracture. Based on the input variables, BONEcheck estimates the probability of any fragility and hip fracture within 5 years, skeletal age, subsequent fracture, genetic risk score, and recommended interval for repeating BMD. The probability of fracture is shown in both numeric and human icon array formats. The risk is also presented in the context of treatment and management options based on Australian guidelines. Skeletal age was estimated as the sum of chronological age and years of life lost due to a fracture or exposure to risk factors that elevate mortality risk. In its entirety, BONEcheck is a system of algorithms translated into a single platform for personalized osteoporosis and fracture risk assessment. Conclusions: BONEcheck is a new system of algorithms that aims to offer not only fracture risk probability but also contextualize the efficacy of anti-fracture measures concerning the survival benefits. The tool can enable doctors and patients to engage in well-informed discussions and make decisions based on the patient's risk profile. Public access to BONEcheck is available via website https://bonecheck.org and in Apple Store (iOS) and Google Play (Android).

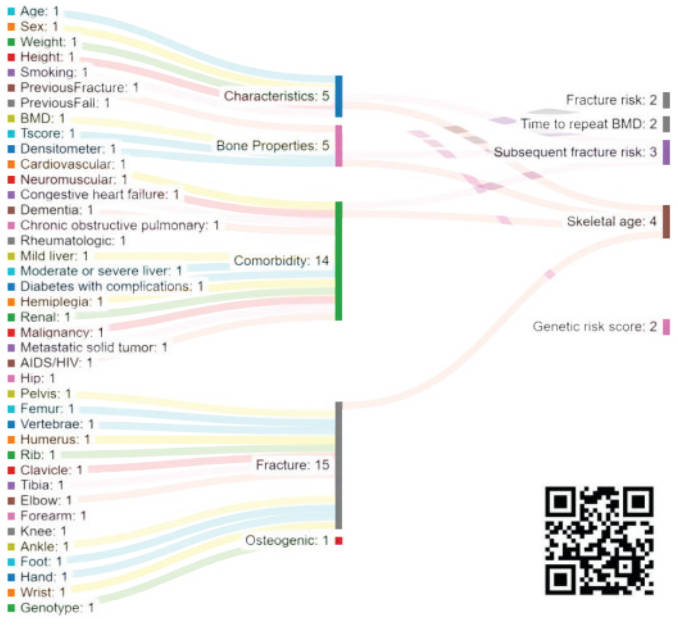

***Disclosures: Dinh Tan Nguyen**, None*

SUN-393

Nine-year survival after intertrochanteric fracture in elderly with chronic kidney disease *Ong-art Phruetthiphat[1], Attaporn Lawanprasert[2], Yodhathai Satravaha[3], Thawee Songpatanasilp[1], Chatlert Pongchaiyakul[4]. [1]Phramongkutklao Hospital , Thailand. [2]Chulabhorn hospital, Thailand. [3]Department of Orthodontics, Faculty of Dentistry, Mahidol University, Thailand. [4]Faculty of Medicine, Khon Kaen University, Thailand

BackgroundOsteoporotic hip fracture is becoming the world's major health issue as the majority of population ages [1,2]. Previous literatures demonstrated that older age, male gender, co-morbidities such as liver diseases, chronic kidney disease, heart pathology and Charlson index more than 2 were associated with increased mortality [3-7]. However, lack of data demonstrated the long-term survivors of elderly hip fracture combining with CKD. The primary outcome of this study was to identify long-term survivors of hip fracture in each stage of CKD. Secondary outcome was to demonstrate the risk factors associated with the survivors after hip fracture combined with CKD.Study Design & MethodsAfter IRB Approval, 443 intertrochanteric fractures over 60 years were recruited in this study. Patients' demography,comorbidity and mortalitywere collected.The study categorized patients into non-CKD (chronic kidney disease) and CKD groups. The former group (Stage 1; n = 39) was defined as those patients with a glomerular filtration rate (GFR) of at least 90 mL per minute (ml/min), while the other group was GFR less than 90 ml/min (n = 404). Furthermore, dividing into five subgroups by CKD groups (Stage 2, 3a, 3b, 4, and 5). The overall survivors from 1 year to 9 years were identified after PFNA fixation for intertrochanteric fractures as shown in table 1 and figure 1. We further compared the short to long term survival time in-

cluding the median survival time of hip fracture patients over 60 years in each stage of CKD as demonstrated in table 2 and figure 2. In addition, the regression analysis was performed to identify the association of risk factors and one year mortality as illustrated in table 3.ResultsThe survival rate after surgery was 89.6% at 1 year, 74.1% at 3 years, 59.9% at 5 years, and 37.8% at 9 years. Although CKD was not significantly increased the mortality (p=0.072), the Kaplan-Meier curve was significantly different (p <0.001) in each CKD stage especially in CKD 5 (Figure 1). In addition, the incidence rate of mortality was highest in CKD 5 (17.4%) and the median survival time in CKD 5 was 3.3 years. Multivariate regression analysis identified that heart disease, operative time more than 60 minutes, pulmonary embolism, poor to fair functional outcome (HHS) were significantly increased mortality.ConclusionsCKD stage 5 is associated with the highest mortality rate during short term period and the shortest median time of survival in mid to long-term period. In addition, heart disease, longer operative time, pulmonary embolism, and poor to fair HHS were associated with increased mortality. This vulnerable group required intensive care in all follow up periods

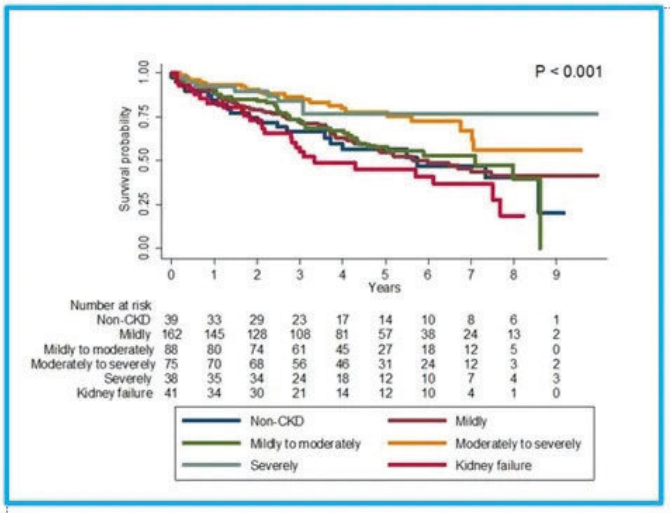

Figure 2 The comparison the survivors among each stage of CKD after hip fracture from 1 to 9 years

***Disclosures: Ong-art Phruetthiphat**, None*

SUN-394

Dentists' Perspective on Osteoporosis Therapy: A Pilot Survey Study
*Sudhaker Rao[1], Vivek Bhan[2], Rebecca Simon[3]. [1]Henry Ford Hospital, United States. [2]Michigan State University, United States. [3]Henry Ford Health System, United States

Osteoporotic fractures are a major public health problem worldwide. Effective therapies have been available since 1995 with bisphosphonates (BPs) as the most commonly used first line drugs. However, long term BP related rare osteonecrosis of the jaw (ONJ), which may occur after dental procedures or in some cases spontaneously, has become a major barrier in initiating or interruption in therapy. The estimated incidence rate of ONJ is quite low; <0.01%in patients taking oral and 1-10% taking IV BPs. Although the risk of ONJ is low, many dentists require "clearance" for invasive dental procedures and often request "drug holiday" to avoid ONJ. There are no recommendations for such practices by the American Dental Association. In this pilot study we aimed to determine the dentist's perception and practice pattern to mitigate ONJ.After approval from Institutional Review Board, we e-mailed an online 7-point survey questionnaire to licensed dental practitioners who are members of the Michigan Dental Society (MDA) to ascertain the range of approaches dentists would take to treat patients who were using OP medications. Only registered members of the MDA were surveyed to ensure the integrity of the data being collected. A second reminder email was sent 4 weeks and the survey was closed 2 months after the initial mailing.Of the total 4808 members emailed, 30 dentists completed the survey. Respondents were 50% female and 20 worked in suburban area, 6 in urban, and 4 in rural area. 57% of the dentists have been practicing for >20y, 9 for 5-20y, and 4 for <5y. When asked about interruption of OP medications for low-risk dental procedures such as cavities; 73% never stopped therapy, 13% stopped in certain scenarios, and 13% reported stopping after discussion with patient's provider. When asked about interruption of OP medications for high-risk dental procedures (tooth extractions), 83% would interrupt therapy, 20% would interrupt in certain scenarios, 3% would always interrupt therapy, and 60% would interrupt therapy after discussion with patient's provider.Despite the rarity of ONJ and no specific guidelines from the ADA, this small pilot survey on practice patterns of dentists in Michigan is a barrier to an effective therapy to reduce the burden of a major public health problem. The responses indicate an urgent need for education of our dentist colleagues on the rationale and validity of interrupting OP therapy.

***Disclosures: Sudhaker Rao**, None*

SUN-395

Automated Deep Learning-based CT-Scout View Assessment of Prevalent Vertebral Fractures
*Eren Bora Yilmaz[1], Till Yannik Fricke[2], Claus-C Glueer[3], Carsten Meyer[2]. [1]Christian-Albrechts-Universität Kiel , . [2]Ostfalia University of Applied Sciences, Germany. [3]Christian Albrechts Universitaet zu Kiel, Germany

Automated detection and grading of vertebral fracture status on computed tomography (CT) scout scans using artificial intelligence (AI) may be useful for both diagnosis and opportunistic prognostic evaluation of fracture risk (no added radiation dose). 2D localizer images (scout scans) taken as part of a CT protocol to select the scan range usually cover a larger area of the spine than the final 3D CT volume and thus may provide more comprehensive information on prevalent vertebral fractures, a key risk factor for future fracture. Aim: To develop and test an AI tool for classification and grading of fractures on CT scout scans. Method: "fNet" is a deep CNN that was previously applied to 3D CT volumes (Yilmaz et al., 2023) and was modified to work with 2D scout scans. It was used to classify the fracture status of individual vertebrae based on 2D image patches centered on vertebral bodies (47 × 47 mm at 1 mm/px) that were extracted using ground truth vertebral body center coordinates. The model was trained on scout scans from the Diagnostik Bilanz dataset (147 scout scans from 7 centers, 1798 vertebrae, 127 fractured, 101 with fracture grade>=2, 32 with grade 3). Ground truth (vertebral body center coordinates and per-vertebra fracture status) for T4-L4 was previously annotated by a trained radiologist using slices of 3D CT volumes. Experiments were conducted in a 4-fold cross-validation setting also used to compute mean confidence intervals (noted +/- in the following). Results: For classifying osteoporotic fractures (positive class; Genant SQ grades 1 - 3) versus normal vertebrae (negative class; Genant SQ grade 0 and deformities), the model achieved 90.6%+/-1.5% ROC-AUC. At a classification threshold of ?=0.05 the sensitivity was 81%+/-4%, the specificity 86%+/-1.3%. When regarding Genant SQ grades 2 and 3 as positive class, ROC-AUC, sensitivity and specificity (?=0.05) were 91.5%+/-0.8%, 85%+/-2% and 85%+/-1.0%, respectively. Finally, with only SQ grade 3 as positive class, we obtained 95.9% 0.8%, 87%+/-7% and 90.6%+/-0.8%, respectively. Discussion: In previous experiments on 3D CT volumes instead of scout scans we reported AUC=98.4%+/-0.4%for the classification of "0-1 vs 2-3". 2D vs 3D differences and image quality of the scout scans could be reasons for lower AUC. Conclusion: To our knowledge this is the first automatic vertebral fracture assessment method on CT scout scans. We demonstrated robust classification performance across three fracture classification tasks.

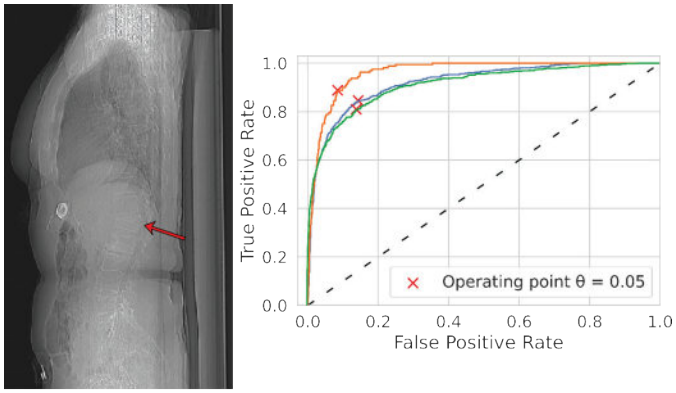

Figure: Vertebral fracture detection on CT scout scans. Left: Arrow indicates indicates Genant SQ grade 3 fracture fracture that was correctly detected by the model. Right: ROC-Curves for binary classifications of fracture grades "0 vs 1-3" (green line), "0-1 vs 2-3" (blue line), and "0-2 vs 3" (orange).

***Disclosures: Eren Bora Yilmaz**, None*

SUN-396

Empowering Egyptian Postmenopausal Women: A Novel Decision Tree-Based Osteoporosis Screening Tool with High Sensitivity and Predictive Value
*Abdulhafez Selim[1], Marina Dangelo[1], Sahar Ghoname[2], Paula Karabelas[3]. [1]PCOM, United States. [2]Ain Shams University School of Medicine, Egypt. [3]Independent Investigator, United States

Osteoporosis remains a significant public health concern in Egypt, particularly among postmenopausal women, necessitating the development of new, effective screening tools for prompt diagnosis. This study constructs and validates an osteoporosis screening tool based on a decision tree (DT) model. Four DT algorithms, namely, classification and regression tree; chi-squared automatic interaction detection (CHAID); quick, unbiased, efficient statistical tree; and C4.5, were applied to 395 patients, of whom 286 were abnormal and

109 normal. The investigation revealed that the DT algorithms have insignificantly different performances concerning accuracy, sensitivity, specificity, and area under the curve. Each algorithm possesses its unique performance. The Decision Tree for Postmenopausal Osteoporosis Screening (DTPOS) tool was developed from the best performance of CHAID's algorithms. The age of 58 years and a BMI cutoff of 22.1 were the crucial predictors of our tool. DTPOS provides a sensitivity of 91.3% and a positive predictive value of 81.8%, which may be used to identify subjects at risk of osteopenia and osteoporosis in community-based screening since it is simple to administer.

***Disclosures: Abdulhafez Selim**, None*

SUN-397

Establishing Japanese Osteoporosis Equivalent Vertebral Strength using Biomechanical CT (E-JOS Vertebral Study) *Junta Mawatari[1], Taro Mawatari[1], David Lee[2], Shoji Baba[1], Satoshi Hagio[1], Koichiro Kawano[1], Reima Sueda[1], Satoru Harada[1], Yasuharu Nakashima[3], Tony Keaveny[2]. [1]KKR Hamanomachi Hospital, Japan. [2]O.N. Diagnostics, LLC, United States. [3]Kyushu University, Japan

Purpose: The purpose of this study was to establish osteoporosis equivalent vertebral bone strength using biomechanical CT in a Japanese cohort and to investigate the differences in bone strength between Japanese and American women. Methods: A total of 120 female patients aged 55-90 years who underwent CT scans including the lumbar spine and bone mineral density within 3 months before and after the CT scan were randomly selected up to 20 patients in each 5-year age group. The study was single-center, retrospective in design, and used anonymized CT data analyzed with biomechanical CT. Results and Discussion: This cohort does not deviate significantly from the Japanese standard in terms of bone mineral density. The correlation between vertebral strength and bone density by DXA in women was strong (R2 = 0.81). However, most of the DXA examinations were taken at L2-L4 and did not include L1, which was judged to be unsuitable for determining the vertebral strength reference value in this study from the viewpoint of consistency with past data and the influence of posterior vertebral elements and degeneration. Therefore, the osteoporosis equivalent vertebral strength and osteopenia equivalent vertebral strength of Japanese patients were calculated from the volumetric density of L1 on CT images. The strength thresholds for Japanese women were 4,000N and 5,500N for osteoporosis-equivalent and osteopenia-equivalent vertebral strength, respectively. These values were 500N lower than the reported values for American women. In addition, the decrease in vertebral strength was greater than the rate of decrease over time in bone mineral density in the spine, femoral neck, and total hip. Conclusion: This study established osteoporosis equivalent vertebral strength using biomechanical CT in a Japanese cohort. The results showed lower values of osteoporosis equivalent vertebral bone strength in Japanese women compared to American women, highlighting the need for tailor-made medical care that comprehensively takes height, weight, and bone strength into account. The study suggests that a separate standard for osteoporosis diagnosis and treatment should be established for Japanese women based on their unique physical characteristics.

***Disclosures: Junta Mawatari**, None*

SUN-398

Associations Between Weight, Bone Mineral Density And Bone Marrow Adipose Tissue In Older Women and Men With Obesity *Joshua Stapleton[1], Katelyn Greene[2], Delanie Lynch[2], Denise Houston[3], Ashley Weaver[4]. [1], [2]Wake Forest School of Medicine, [3]Wake Forest University School of Medicine, Department of Gerontology & Geriatric Medicine, United States. [4]Wake Forest University, United States

Bone mineral density (BMD) and bone marrow adipose tissue (BMAT) are common metrics for the assessment of bone health and fracture risk in older adults and could be associated with changes in weight. This study measured volumetric BMD (vBMD) and BMAT from dual energy computed tomography (DECT) of older adults with obesity undergoing an active weight loss intervention to investigate baseline and 6-month change associations between weight, vBMD and BMAT.DECT scans were collected at baseline (n=186) and 6-month follow-up (n=163) in older adults (mean+/-SD: age 71.6+/-4 yrs; BMI 34.3+/-4.2 kg/m2, 65% women, 74% white) participating in the UPLIFT trial (NCT03074643; NCT03819478), a 6-month caloric restriction and aerobic exercise intervention targeting ~10% weight loss. Participants received DECT scans (140 and 80 kvp) of the lumbar spine using a Mindways Model 3 calibration phantom as the standard reference for vBMD and BMAT quantification. Scans of the L2 vertebra were analyzed using QCTPro™ software (Fig 1A,B) to calculate vBMD and BMAT fraction at baseline and 6 months. vBMD was calculated from the 140 kvp CT, while BMAT was calculated using DECT and material projection of known yellow and red marrow references. Unadjusted Pearson correlation was used for regression of outcome by sex.At baseline, BMAT (mean+/-SD: 40+/-28%) was negatively associated with weight in men (R= -0.4, p<0.01) and women (R= -0.41, p<0.01; Fig 1C); however, vBMD (105+/-43 mg/cm3) was not in men (R=0.16, p=0.29) or women (R=0.18, p=0.09). Over 6 months, body weight decreased by 8% (7.9+/-5.2 kg, p<0.01), which was negatively associated with vBMD change in women (R= -0.22, p=0.04;), but not vBMD change in men (R= -0.19, p=0.22; Fig 1D), or BMAT change in men (R=0.05,p=0.72) or women (R=0.01, p=0.92). At baseline, vBMD was negatively associated with BMAT in women (R= -0.31, p<0.01) and men (R= -0.35, p=0.02). At 6 months, changes in vBMD and BMAT were negatively associated in women (R= -0.27, p=0.01), and men (R= -0.28, p=0.06; Fig 1E).This study used DECT scans to explore cross-sectional and longitudinal associations between lumbar vBMD and marrow adiposity with obesity and weight loss. Baseline weight likely plays a significant role in BMAT fraction in the spine. Spine BMD loss was associated with marrow adiposity gains in older adults with obesity undergoing weight loss over 6 months. Results suggest a dynamic relationship between BMD and BMAT in the context of obesity and weight loss.

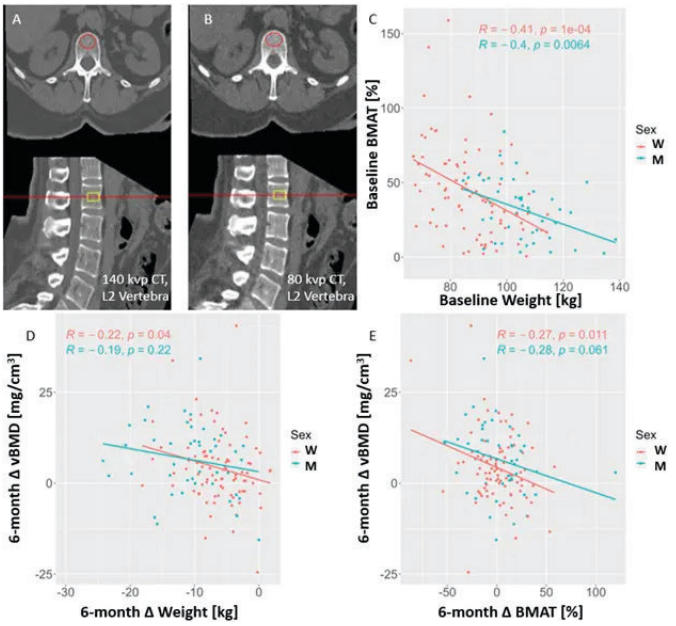

***Disclosures: Joshua Stapleton**, None*

SUN-400

Body composition by DXA in the prediction of 10-years incident fragility fractures: The OsteoLaus Cohort *Colin Vendrami[1], Enisa Shevroja[1], Elena Gonzalez Rodriguez[1], Guillaume Gatineau[1], Didier Hans[1], Olivier Lamy[2]. [1]Center of Bone Diseases, Rheumatology Unit, Bone and Joint Department, CHUV, Lausanne, Switzerland, Switzerland. [2]Internal Medicine Unit, Internal Medicine Department, CHUV, Lausanne, Switzerland, Switzerland

Background: Half of fragility fractures occurs in patients with normal bone density or medium/low estimated risk. The ability of body composition parameters to predict incident fragility fractures (IFF) remains unclear.Objectives: To analyze the association of body composition parameters by Dual-X-Ray Absorptiometry (DXA) and IFF (hip, humerus, forearm or radiologic vertebral low trauma fractures) over 10 years (y).Methods: Postmenopausal women from the OsteoLaus cohort were followed each 2.5y for 10y. We included those with body composition assessment by DXA (Hologic Discovery A) at baseline (n=1025) and the IFF for each follow-up separately. Patient's DXA values mean's differences between the IFF versus no IFF groups were compared using t-test and boxplots. The DXA parameters with significant difference between the two groups were further tested in univariate (M0) and multiple logistic regression model (M1-3) with stepwise adjustment for known covariables: age (M1), weight, height (M2), and femoral neck BMD T-Score (M3).Results: After excluding for previous glucocorticoid therapy, 995 participants remain at baseline (mean+/-standard deviation: age 62.7+/-7.6y, BMI 25.6+/-4.5kg/m2 and femoral neck T-Score -1.05+/-1.03). After 2.5y, 5y, 7.5y and 10y, 29/882 (3.2%), 82/799 (9.3%), 118/715 (14.2%) and 97/570 (14.5%) participants had one or more IFF/no IFF. Participants with IFF at 7.5y had higher (p<0.05) subtotal fat (+1660gr.), percent fat (PFAT, +1.3%), android fat (+186.3gr.), visceral fat (VFAT, +71.1gr.), and lower subtotal bone mineral density (BMD, -0.02gr/cm2). Total or appendicular lean mass did not differ between the IFF and no IFF group. Most of these results were not significant using a more conservative p-value<0.002 second to Bonferroni adjustment. In the logistic regressions, VFAT and subtotal PFAT were positively associated with IFF at 5y (M0) and VFAT at 7.5y (M0). Total BMC was negatively associated with IFF after 5y (M0,M2,M3), 7.5y (M1,M3) and 10y (M0-M2). Total BMD was negatively associated with IFF after 2.5y (M0), 5y (M0-M2), 7.5y (M0-M3) and 10y (M0-M2).Conclusions: As expected, DXA body composition parameters are not independent predictors of IFF. However, some bone and fat parameters could be involved in the fracture risk. Since IFF are complex and multifactorial event, further investigations considering time-to-event using cox regressions and a competing risk analysis are planned.

***Disclosures: Colin Vendrami**, None*

SUN-401

Are you a 'Crunchie™' or a 'Malteser™'? The Importance of the Use of Vernacular Language & Visual Messaging in Communication with Patients who have Osteoporosis. *Eamonn Brankin[1]. [1]NHS Lanarkshire / University of Glasgow / Glasgow Caledonian University/University of Strathclyde, United Kingdom

Are you a 'Crunchie™' or a 'Malteser™'? - The Importance of the Use of Vernacular Language and Visual Messaging in Communication to Patients with Osteoporosis.A perennial problem for all clinicians is in the accurate communication of clinical issues and descriptions of disease to patients. In describing osteoporosis and the reasons for fragility fracture risk, the challenge is in using language and visual imaging relevant to the patient to help him/her better understand the nature of osteoporosis and why this places the individual at increased risk of fragility fracture. In the UK, well known brands of chocolate sweet include the 'Crunchie™' chocolate bar and 'Maltesers™' chocolate sweets. In general patients understand the nature of these common chocolate / honeycomb sweets and how, in the former, the 'scaffolding' structure of the honeycomb is more robust and stronger, whereas, in the latter, the internal scaffolding structure is much less robust, with less inherent structural strength and so more likely to compression/damage. Over an approximate 12 month period, these descriptors were used to help explain the nature of osteoporosis and subsequent fragility fracture risk in 68 consecutive new patients at the osteoporosis clinic. In every case patients reported that they understood the analogy and felt that these descriptors were a significant help to them in understanding their disease, the reasons why they are now at risk of further fragilty fracture and why taking medication for this condition makes sense. Working with the Royal Osteoporosis Society, regular talks are given to patient groups by our osteoporosis service's clinicians and the most common memorable take home message patients report back is that he/she is now a 'Malteser'! Numerous studies have shown in the past that improved patient understanding of their disease results in better adherance to medication and improved outcomes. By using local language and the analogy of well known chocolate branding, patients' understanding of their disease is improved, which results in improved drug concordance, patient behaviour, clinical management and ultimately patient wellbeing and outcomes.

***Disclosures: Eamonn Brankin**, None*

SUN-402

Estimating 'Skeletal Age' by Bone Loss in Elderly Men and Women *Ngoc Huynh[1], Krisel De Dios[1], Thach Tran[1], Tuan Nguyen[2]. [1]University of Technology Sydney, Australia. [2]University of Technology Sydney , Australia

Background and Aim: Skeletal Age is defined as the age of the skeleton as a result of a fracture or exposure to risk factors that elevate the risk of fracture. Higher rates of bone loss are associated with an elevated risk of both fracture and mortality. In this study, we aimed to assess the impact of bone loss on bone fragility by estimating skeletal age using bone loss in elderly men and women. Methods: We analyzed the data from the Study of Osteoporosis Fracture (SOF) and Osteoporotic Fractures in Men (MrOS) that included 9704 women and 5994 men aged 64 years and above. Bone mineral density (BMD) at the femoral neck was measured at baseline and subsequent visits. Mortality was ascertained from death certificates and hospital records. We limited the analysis to those with at least 3 BMD measurements (3848 women and 2925 men). The linear regression model was used to estimate the rate of change in BMD for each individual. The multivariable Cox's proportional hazard model was used to quantify the contribution of the rate of BMD change to mortality, adjusted for age, body mass index, smoking status, alcohol consumption, dietary calcium intake, estrogen and bisphosphonate treatment. The magnitude of the association between bone loss and mortality was then transformed into the number of years of life lost using Gompertz's law of mortality and the US life table. Skeletal age is then determined by the sum of chronological age and years of life lost. Results: In women, the average rate of change in femoral neck bone mineral density (BMD) was found to be -0.61 +/- 1.2% [mean+/-SD] per year, while in men, it was -0.16 +/- 0.9% per year. Throughout the study, 1942 women and 1949 men died. For women, each standard deviation [SD] increase in femoral neck BMD loss was linked to a 1.2-fold (95%CI, 1.1-1.3) increase in total mortality, while for men, the increase was 1.4-fold (95%CI, 1.35-1.5) after adjusting for age, baseline FNBMD, BMI, smoking and drinking status. Additionally, each SD increase in bone loss was associated with a loss of 1.9 years and 3.5 years of life in women and men, respectively. For the same rate of bone loss, men experienced a more substantial loss of years of life than women. Moreover, a 60-year-old woman with a femoral neck BMD loss of more than 2% is estimated to have a skeletal age of 63.5 years. Conclusion: In elderly men and women, excess bone loss is associated with an increased loss of years of life and accelerated bone fragility.

***Disclosures: Ngoc Huynh**, None*

SUN-403

Second hand smoking is associated with elevated risk of fracture in community dwelling, non-smoking adults *Sung Joon Cho[1], Junyeong Ahn[1], Chul Sik Kim[2], Yumie Rhee[1], Namki Hong[1]. [1]Department of Internal Medicine, Severance Hospital, Endocrine Research Institute, Yonsei University College of Medicine, Republic of Korea. [2]Division of Endocrinology, Department of Internal Medicine, Yongin Severance Hospital, Yonsei University College of Medicine, Republic of Korea

Active smoking is widely known as an independent risk factor of various diseases. Yet, the risk of fracture in non-smokers exposed to second hand smoking is not well understood. A total of 5,089 non-smokers aged 40 to 69, who participated in the Korean Genome and Epidemiology Study (KOGES; study no. 4851-302) from 2001 to 2018, were analyzed. The participants were classified into two groups; currently exposed to second hand smoking and unexposed, with further categorization of second hand smoking exposures into three groups on the tertiles of the exposure time per week. Newly-developed fracture outcome was defined by sites based on self-reported questionnaire; overall, vertebral, hip, non-vertebral, and non-vertebral non-hip. The mean age of participants was 52 years (52.6% women). Incidence rate in second hand smoking exposed group was higher than those without exposure (incidence rate ratio 1.16, age-adjusted log rank p=0.001). Exposure to second hand smoking was associated with higher risk of fracture at overall sites (hazard ratio [HR] 1.35, p=0.004) after adjustment for age, sex, BMI, which remained robust after further adjustment for education, bone density of midshaft tibia, muscle mass, and c-reactive protein level (HR 1.28, p=0.022). Individuals at highest exposure time tertile had highest risk of fracture (HR 1.36, p=0.010) than lowest exposure tertile (HR 1.12, p=0.528) compared to non-exposed as referent, suggesting potential dose-response relationship. When fracture outcome was grouped by sites, second hand smoking showed association with elevated risk of non-vertebral (HR 1.41, p=0.003) or non-vertebral non-hip (HR 1.40, p=0.005) fractures, whereas the association was attenuated with vertebral fracture (HR 1.02, p=0.942). Second hand smoking was an independent risk factor for fracture (HR 1.28, p=0.017) after adjustment for FRAX major osteoporotic fracture probabilities. In summary, second hand smoking was associated with elevated risk of fracture in non-smoking adults, independent of clinical predictors.

***Disclosures: Sung Joon Cho**, None*

SUN-405

Areal BMD at Baseline Predicts HR-pQCT Parameters 14 Years Later: Findings from the Osteoporotic Fractures in Men (MrOS) Study. *Lauren Carlson[1], Eric Orwoll[2], Andrew Burghardt[3], Peggy Cawthon[4], Kristine Ensrud[5], Lisa Langsetmo[6], Mary Bouxsein[7], Jane A. Cauley[8]. [1]University of Pittsburgh, United States. [2]Oregon Health & Science University, United States. [3]University of California, San Francisco, United States. [4]San Francisco Coordinating Center, United States. [5]University of Minnesota and Minneapolis VA Health Care System, United States. [6]Minneapolis VA Medical Center, United States. [7]Beth Israel Deaconess Medical Center, Harvard Medical School, United States. [8]UNIVERSITY OF PITTSBURGH, United States

Areal bone mineral density (aBMD) measured via DXA is an integrated measure of both trabecular and cortical BMD. High- resolution peripheral quantitative computed tomography (HR-pQCT), allows for a non-invasive assessment of cortical and trabecular volumetric bone mineral density (vBMD) and estimated strength by failure load. A small (n=78) cross-sectional study examined the correlation between total hip aBMD and HR-pQCT vBMD parameters taken at the same time. At the cortical bone, the resulting correlations were 0.12 and 0.24 at the radius and tibia, respectively. At the trabecular bone, the resulting correlations were 0.43 and 0.63 at the radius and tibia, respectively. The correlation between DXA total hip and failure load measured by HR-pQCT were 0.59 and 0.71 at the radius and tibia, respectively. The objective of the current study was to examine if total hip aBMD at baseline was associated with these same HR-pQCT parameters measured an average of 14 years later.A total of 2,424 community-dwelling older men aged 65 years and older at baseline participated. Hip aBMD was measured at baseline and HR-pQCT parameters, 14 years later. Total hip aBMD measurements were significantly associated with all HR-pQCT measures taken 14 years later. HR-pQCT measurements of trabecular bone were more strongly associated with aBMD (Table 1). Unadjusted Pearson correlations between total hip aBMD and trabecular vBMD at the distal radius and distal tibia were 0.51 and 0.54 ($p<0.05$), respectively. Unadjusted Pearson correlations between total hip aBMD and cortical vBMD at the distal radius and distal tibia were 0.17 and 0.22 ($p<0.05$), respectively. Total hip aBMD was also strongly associated with failure load at the distal radius and distal tibia. Unadjusted Pearson correlations were 0.52 and 0.60 ($p<0.05$). Models adjusted for age, comorbidities, race, site, quality of life, and walk speed showed total hip aBMD as a significant predictor of HR-pQCT measurements taken 14 years later.In conclusion, aBMD measurements from DXA were significantly associated with HR-pQCT measurements taken 14 years later. Trabecular vBMD and failure load measurements were more highly correlated with aBMD than cortical vBMD.

Table 1. Total Hip DXA as a Predictor of HR-pQCT Parameters

HR-pQCT Variable	Unadjusted Pearson Coefficient	Unadjusted p-value	Adjusted R-squared*	Adjusted P-value*
Distal Radius Cortical	0.17	<0.001	0.11	<0.001
Distal Tibia Cortical	0.22	<0.001	0.14	<0.001
Distal Radius Trabecular	0.51	<0.001	0.28	<0.001
Distal Tibia Trabecular	0.54	<0.001	0.34	<0.001
Distal Radius Failure Load	0.52	<0.001	0.30	<0.001
Distal Tibia Failure Load	0.60	<0.001	0.15	<0.001

*Adjusted for age, comorbidities, race, site, quality of life, and walk speed

***Disclosures: Lauren Carlson**, None*

SUN-404

Effect of Race/Ethnicity on United States FRAX Calculations and Treatment Qualification: A Registry-Based Study *William Leslie[1,] [1]University of Manitoba, Canada

Since 2008 the United States has had four race/ethnic FRAX® calculators: White ("Caucasian"), Black, Asian, and Hispanic. The ASBMR Task Force on "Clinical Algorithms for Fracture Risk" has been examining the implications of retaining race/ethnicity in the US FRAX calculators.AIM: To compare treatment qualification based upon existing US FRAX race/ethnicity calculators and a hypothetical US population-based FRAX calculator. METHODS: The study sample consisted of all DXA assessments in Manitoba women aged 50 years or older from 1996-2018, with at least one year of prior coverage to assess FRAX inputs. Race/ethnicity was self-identified (119,243 White, 485 Black, 2,816 Asian, insufficient Hispanic for analysis). We computed FRAX scores according to each US calculator and the proportion exceeding intervention cutoffs (>20% for major osteoporotic fracture, MOF; >3% hip for fracture, and combined with prior fracture and T-score criteria as per the Bone Health and Osteoporosis Foundation, BHOF). We then estimated these measures for a hypothetical population-based FRAX calculator derived as the weighted mean for the US population based upon current US Census Bureau statistics.RESULTS: With identical inputs, the highest FRAX measurements were seen with the White FRAX calculator, lowest measurements with the Black calculator, with intermediate measurements for the Asian and Hispanic calculators. The percentage of women with FRAX scores exceeding the hip fracture treatment threshold was 32.0% for White, 1.9% for Black and 19.7% for Asian women; the MOF treatment threshold was exceeded for 14.9% of White, 0.0% of Black, and 3.5% of Asian women. Disparities in treatment qualification were reduced when additional BHOF criteria including DXA T-score were considered. When fracture risk was recalculated for non-White women using the White FRAX calculator, mean values for Asian women slightly exceeded those for White women but for Black women remained substantially below those for White women. When using a single population-based FRAX calculator for non-White women the mean probability of fracture and treatment qualification increased across the age range, and for Asian women slightly exceeded that for White women.CONCLUSION: Use of a single population-based FRAX calculator, rather than existing US race/ethnic FRAX calculators, will reduce differences in treatment qualification and may ultimately enhance equity and access to osteoporosis treatment.

Proportion of women with high fracture risk according to self-reported race/ethnicity using race/ethnicity-concordant FRAX calculator and population-based FRAX calculator.

WHITE WOMEN	WHITE FRAX MOF ≥ 20%	WHITE FRAX HIP ≥ 3%	WHITE FRAX BHOF GUIDELINES	POP-BASED FRAX MOF ≥ 20%	POP-BASED FRAX HIP ≥ 3%	POP-BASED FRAX BHOF GUIDELINES
50-59 years	2.8%	5.2%	20.3%	1.4%	3.6%	19.5%
60-69 years	9.2%	16.9%	33.0%	5.4%	13.1%	31.0%
70-79 years	23.1%	55.4%	61.4%	16.5%	49.4%	57.2%
80+ years	41.7%	87.1%	87.5%	29.1%	81.7%	83.1%
All ages	14.9%	32.0%	43.4%	10.0%	28.0%	40.9%
BLACK WOMEN	**BLACK FRAX MOF ≥ 20%**	**BLACK FRAX HIP ≥ 3%**	**BLACK FRAX BHOF GUIDELINES**	**POP-BASED FRAX MOF ≥ 20%**	**POP-BASED FRAX HIP ≥ 3%**	**POP-BASED FRAX BHOF GUIDELINES**
50-59 years	0.0%	0.0%	13.1%	0.8%	0.8%	13.1%
60-69 years	0.0%	0.0%	19.3%	1.0%	4.0%	21.8%
70-79 years	0.0%	3.0%	15.0%	1.5%	15.8%	21.1%
80+ years	0.0%	17.9%	50.0%	7.1%	71.4%	75.0%
All ages	0.0%	1.9%	18.4%	1.4%	10.3%	22.5%
ASIAN WOMEN	**ASIAN FRAX MOF ≥ 20%**	**ASIAN FRAX HIP ≥ 3%**	**ASIAN FRAX BHOF GUIDELINES**	**POP-BASED FRAX MOF ≥ 20%**	**POP-BASED FRAX HIP ≥ 3%**	**POP-BASED FRAX BHOF GUIDELINES**
50-59 years	0.8%	2.5%	26.3%	1.5%	5.1%	26.3%
60-69 years	1.3%	10.9%	42.1%	6.4%	21.8%	43.7%
70-79 years	7.4%	42.4%	58.3%	19.0%	59.8%	68.5%
80+ years	18.2%	82.5%	84.4%	39.6%	94.8%	94.8%
All ages	3.5%	19.7%	43.6%	9.7%	29.8%	47.2%

MOF, Major osteoporotic fracture. BHOF, Bone Health and Osteoporosis Foundation.

***Disclosures: William Leslie**, None*

SUN-407

Trajectories of Areal Bone Mineral Density Significantly Differ by Patterning of Femoral Neck Area and Bone Mineral Content Across the Menopausal Transition *Aleda Leis[1,] Karl Jepsen[1,] Kerry Richards-McCullough[2,] Tom Richards[2,] ERIN BIGELOW[3,] Robert Goulet[4,] Carrie Karvonen-Gutierrez[5,] [1]University of Michigan, United States, [2]University of Michigan , United States, [3]UNIVERSITY OF MICHIGAN, United States, [4]Michigan Medicine, University of Michigan, United States, [5], United States

Clinical use of areal bone mineral density (aBMD) to identify individuals at risk of fracturing assumes that aBMD change reflects bone mineral content (BMC) change. However, differences in the rate and magnitude of BMC and bone area changes over time may affect the reliability of aBMD. Understanding how different trajectories of BMC and area affect aBMD is thus central to improving our use of DXA measures to monitor bone health. This study examined the differential impact of BMC and area trajectories across the menopausal transition (MT) on aBMD. The Michigan Bone Health and Metabolism Study (MBHMS) is a longitudinal study of women; participants aged 24-50 were recruited in 1992 and followed near-annually through 2010. Femoral neck bone data were assessed using DXA. The sample included 138 women with an observed non-surgical final menstrual period (FMP); a DXA scan 10 years prior to FMP; and at least one post-FMP DXA. Group-based growth trajectory modeling was used to determine trajectory groups of area and BMC. Smoothed loess curves were constructed to examine trajectories of aBMD within each area (lowest, middle, highest) and BMC (slowest decline, moderate decline, and fastest decline) trajectory combination. Cross-tabulations of area and BMC trajectory group showed very few individuals in both the BMC fastest decline trajectory group and the area lowest trajectory group, and in the BMC slowest decline trajectory group and area highest trajectory group. The most common combinations were lowest area/slowest decline BMC (23.2%) and middle area/moderate decline BMC (21.0%). Those in the highest area/fastest decline BMC trajectory groups had the largest decline in aBMD from first to last study visit (mean 13.3% decrease, SD 8.7%; Fig. 1), while those in the highest area trajectory and the slowest BMC decline trajectory had the least decline in aBMD (mean 2.2% decrease, SD 5.9%). Understanding bone health with aging using trajectories of BMC and area change represents a novel approach to examining the significant heterogeneity across the MT, a critical life stage for musculoskeletal health. Notably, our analysis showed women who started at higher aBMD with significant BMC loss may not have been identified earlier as high risk though they show the greatest loss pattern. This information may be highly informative in identifying women at greatest risk for low aBMD and future risk for fracture.

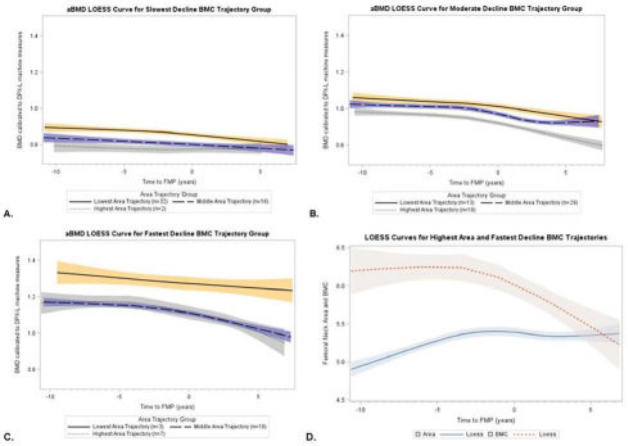

Figure 1. Loess curves for (A) aBMD by area trajectory group for those in the slowest decline BMC trajectory group, (B) aBMD by area trajectory group for those in the moderate decline BMC trajectory group, (C) aBMD by area trajectory group for those in the fastest decline BMC trajectory group, and (D) femoral neck area and BMC for those in the highest area and fastest decline BMC cross-tab trajectory group.

***Disclosures: Aleda Leis**, None*

SUN-408

Rate of bone loss is associated with fracture risk: The Study of Osteoporotic Fractures *Krisel De Dios[1,] Ngoc Huynh[2,] Thach Tran[3,] Tuan Nguyen[4,] [1]University of Technology Sydney, , [2], , [3]Garvan Institute of Medical Research, Australia, [4]University of Technology Sydney , Australia

ObjectiveAlthough the link between low bone mineral density and fracture is well established, the association between aged-related bone loss and fracture remains controversial. In this study, we aimed at testing the hypothesis that excessive bone loss is associated with increased fracture risk in elderly women.MethodsThis study involved 5581 women who were a part of the Study of Osteoporotic Fractures (SOF) and had undergone a minimum of three bone mineral density (BMD) assessments. BMD at the femoral neck was measured using DXA (Hologic QDR 1000) between 1992 and 2008. The rate of BMD change was determined by utilizing a linear mixed-effects regression model. The incidence of fragility fractures (after 3 BMD measurements) was ascertained by reviewing hospital discharge records

or physician reports. Cox's proportional hazards model was utilized to assess the association between bone loss and fracture risk, while also accounting for pre-defined covariates such as BMD, age, BMI, smoking, drinking, physical activity, prior and family history of fractures. ResultsDuring the median follow-up of 13 years (IQR: 9-17), there were 1470 incident fractures, yielding fracture incidences of 25 per 1000 person-years (95% CI: 23-26). We found 679 women with a hip fracture rate of 8 per 1000 person-years (95% CI: 7-9). Bone loss was significantly associated with an increased risk of any fragility fracture (adjusted hazard ratio: 1.18; 95% CI: 1.07-1.30) and hip fracture (1.30; 95% CI: 1.13-1.50). Importantly, those with an excess annual bone loss (e.g., at least 2% per year) were associated with a 2-fold (95% CI: 1.01-4.0) increase in the risk of hip fracture.ConclusionThese data support the hypothesis that bone loss at the femoral neck is a risk factor for fracture, independent of age and baseline BMD. This suggests that repeated measurements of BMD can be useful in identifying individuals who are at high risk of fracture.

***Disclosures: Krisel De Dios**, None*

SUN-409

Association between a Social Determinants of Health Index and Bone Mineral Density and Odds of Osteoporosis among Puerto Rican Adults

*Liam Fouhy[1], Xiyuan Zhang[1], Kelsey Mangano[2], Bess Dawson-Hughes[3], Katherine Tucker[1], Sabrina Noel[1]. [1]University of Massachusetts Lowell, United States. [2]University of Massachusetts, Lowell, United States. [3]Tufts University, United States

Social determinants of health are known to play a key role in development of chronic conditions, however, to our knowledge, few studies have examined these factors in relation to bone health. Puerto Rican adults are at increased risk for osteoporosis, which has only recently been appreciated. Thus, it is imperative to understand whether social determinants contribute to bone health inequities in this population. This study aimed to examine the relationship between social determinants, based on a derived index, and bone mineral density (BMD), at hip and spine sites, and osteoporosis among Puerto Rican adults from the Boston Puerto Rican Osteoporosis Study. In the BPROS, there were valid data on bone mineral density (BMD) for 955 participants, using dual-energy x-ray absorptiometry (DXA). Osteoporosis at the femoral neck and/or lumbar spine was defined as T-score <= 2.5 SD below peak bone mass. Questionnaires assessing sociodemographic, perceived stress, health and health behaviors and food insecurity were administered by trained interviewers. A social determinant index was calculated by summing the values of 0 or 1 for each of the following variables: educational attainment (<8 grade), income to poverty ratio (<130% of the year specific index), marital status (married vs. not), housing stability (owned home vs. rented), perceived stress, and food security (food insecure vs. secure). A total possible score ranged from 0-7 points. General linear regression models were used for BMD outcomes and logistic regression for odds of osteoporosis. Models were adjusted for 1: age, BMI, height, and sex/estrogen status; model 2: also, for alcohol use, and smoking status; model 3: also, for serum vitamin D status. Higher social determinant scores were inversely associated with BMD at the femoral neck (?: -0.007, P=0.03), trochanter (?: -0.006, P=0.05), total hip (?: -0.008, P=0.01), and lumbar spine (?: -0.011, P=0.01). A poorer social determinant score (higher score) was associated with increased odds of osteoporosis (OR: 1.93, 95% CI: 1.13, 3.28). These results provide valuable data to inform future interventions to address bone health inequities among Puerto Rican adults living on the US mainland.

Table 1. Associations between a social deprivation index and bone mineral density at hip and spine sites (n=792)

Femoral Neck	β±SE	Lower CI	Upper CI	P-value
Model 1	-0.007 ± 0.003	-0.013	-0.005	0.03
Model 2	-0.007 ± 0.003	-0.013	-0.002	0.04
Model 3	-0.007 ± 0.003	-0.013	-0.0007	0.03
Trochanter				
Model 1	-0.007 ± 0.003	-0.013	-0.001	0.02
Model 2	-0.006 ± 0.003	-0.012	-0.0003	0.06
Model 3	-0.006 ± 0.003	-0.012	-0.00007	0.05
Total Hip				
Model 1	-0.009 ± 0.003	-0.016	-0.003	0.007
Model 2	-0.008 ± 0.003	-0.015	-0.001	0.02
Model 3	-0.008 ± 0.003	-0.015	-0.002	0.01
Lumbar Spine				
Model 1	-0.011 ± 0.004	-0.019	-0.002	0.01
Model 2	-0.011 ± 0.004	-0.019	-0.002	0.01
Model 3	-0.011 ± 0.004	-0.019	-0.002	0.01

Table 2. Associations between a social deprivation index and odds of osteoporosis in Puerto Rican Older adults (n=894)

Osteoporosis	OR	Lower CI	Upper CI	P-value
Model 1	1.75	1.08	2.85	0.02
Model 2	1.76	1.06	2.93	0.03
Model 3	1.92	1.13	3.27	0.02

***Disclosures: Liam Fouhy**, None*

SUN-410

Associations of Cardiorespiratory Fitness with HR-pQCT Bone Parameters in Older Adults: The Study of Muscle, Mobility and Aging (SOMMA)

*Nina Heilmann[2], Kerri Freeland[2], Reagan Moffit[2], Nancy Glynn[2], Lauren S. Roe[3], Tong Yu[2], Nicole Sekel[2], Kristen Koltun[2], Katelyn Guerriere[4], Julie Hughes[4], Bradley Nindl[2], Ashley Weaver[5], Paolo Caserotti[6], Peggy Cawthon[7], Anne Newman[2], Jane A. Cauley[8], Elsa Strotmeyer[2]. [2]University of Pittsburgh, . [2]University of Pittsburgh, United States. [3], . [4]US Army Research Institute of Environmental Medicine, United States. [5]Wake Forest University, United States. [6]Department of Sports Science and Clinical Biomechanics and the Center for Active and Healthy Ageing, Denmark. [7]San Francisco Coordinating Center, United States. [8]UNIVERSITY OF PITTSBURGH, United States

Cardiorespiratory fitness and bone mass and strength decline with age, yet few studies have assessed the relationship of cardiorespiratory fitness with bone health in older adults. Physical activity (PA) is related to cardiorespiratory fitness and is recommended for preventing bone loss and osteoporosis. Whether cardiorespiratory fitness is associated with bone health independent of PA is unknown. The Study of Muscle, Mobility and Aging (SOMMA) included baseline assessments of VO2peak from treadmill cardiopulmonary exercise testing using the modified Balke protocol. We investigated associations of absolute VO2peak (mL/min) with bone mineral density (BMD) from dual-energy X-ray absorptiometry (DXA) and bone microarchitecture and strength from high-resolution peripheral quantitative computed tomography (HR-pQCT) collected in the SOMMA Bone Ancillary Study at the year 1 visit. In 124 men (age 76.2+/-4.3 years, 93% White) and 189 women (age 76.2+/-4.2 years, 87% White), relative VO2peak (mL/kg/min) was higher in men (23.8+/-5.5) vs. women (19.6+/-4.6; p<0.001). Bone outcomes differed between men and women (p<0.001) so analyses were stratified with sex-specific z-scores used in linear regression. Models (Table 1) were adjusted for age (years), race (White/non-White), weight (kg), >=1 alcoholic drink/week (y/n), total activity counts from valid wrist-worn accelerometry (>=3 days with >=10 h wear), comorbidity count (0-7), and limb length. In men, higher VO2peak was associated with higher tibial (standardized[std] ?=0.26, p<0.05) and radial (std ?=0.30, p<0.05) failure load, but not with DXA or other HR-pQCT parameters. Higher VO2peak was associated with higher radial trabecular (Tb) BMD (std ?=0.26, p<0.05) and cortical (Ct) area (std ?=0.25, p0.05) after adjusting for total activity. Associations were consistent when adjusting for moderate-to-vigorous PA instead of total activity counts. No significant associations were found between VO2peak and bone outcomes in women. Positive associations of VO2peak with failure load found in older men suggest cardiorespiratory fitness is associated with bone outcomes in a sex-specific manner. Future studies need to explore reasons for sex differences of VO2peak and bone outcomes.

Table 1. Adjusted linear regression std β coefficients of VO_2peak associations with DXA and HR-pQCT outcomes

	VO_2peak (mL/min)	
	Women mean 1350±257	**Men** mean 1966±429
Distal tibial HR-pQCT	*n=170*	*n=111*
Est. Failure load, N	0.05	**0.26***
Ct.BMD, mg/cm^3	0.12	0.11
Tb.BMD, mg/cm^3	-0.05	0.14
Ct.Ar, mm^2	0.08	0.14
Tb.Ar, mm^2	0.10	0.09
Distal radial HR-pQCT	*n=153*	*n=105*
Est. Failure load, N	0.07	**0.30***
Ct.BMD, mg/cm^3	0.13	0.18
Tb.BMD, mg/cm^3	-0.03	0.15
Ct.Ar, mm^2	0.08	0.22
Tb.Ar, mm^2	0.001	0.07
DXA parameters	*n=163*	*n=112*
Total hip BMD, mg/cm^2	-0.02	0.09
FN BMD, mg/cm^2	-0.08	0.04

***P<0.05**; Models adjusted for age (years), race (White/non-White), weight (kg), ≥1 drink/week (y/n), total activity counts (ActiGraph), comorbidity count (0-7), and tibia/ulna length. Abbreviations: cortical BMD (Ct.BMD), Ct. area (Ct.Ar), FN (femoral neck), trabecular BMD (Tb.BMD), Tb. area (Tb.Ar)

***Disclosures: Nina Heilmann**, None*

Sunday Orals

SUN-412

Trends in Hip Fracture Rates in Elderly Male Veterans *Amna N. Khan[1], Nabeel Khan[2], Robert B. Jones[3], Robert Adler[4], Yu Xiao Yang[2]. [1]University of Pennsylvania and Corporal Michael J Crescenz VAMC, United States. [2]Corporal Michael J Crescenz VAMC and University of Pennsylvania, United States. [3]Division of Endocrinology, University of Pennsylvania and Corporal Michael J Crescenz VAMC, United States. [4]McGuire VA Medical Center, United States

BACKGROUNDHip fractures account for about 17% of osteoporotic fractures and have the highest one-year mortality, approximately 20-30%. Half of those who survive one year post-hip fracture require assistance with ambulation and a quarter require long-term care. Hip fracture care accounts for 72% of all fracture-related medical expenses. Recent studies in Medicare health plan enrollees report that hip fracture rates may no longer be declining in women 65 years of age or older, raising concern for a widening care gap. Osteoporotic fracture has been less studied in older men, who have a poorer prognosis after hip fracture. We assessed the recent trends of hip fracture incidence in a nation-wide male veteran population older than 50 years of age.METHODSUsing data from the US Veterans Affairs Informatics and Computing Infrastructure (VINCI) 2002-2019, we calculated the annual age-standardized hip fracture incidence (standardized to the age distribution of eligible population in 2019) and analyzed the incidence trends (i.e., annual percent change [APC]) using joint point regression. As secondary objectives, we determined the annual proportion of hip fracture patients who received a) dual energy X-ray absorptiometry (DXA) before and/or after the fracture and/or b) osteoporosis medication after the hip fracture over the study period. RESULTSIn this retrospective cohort analysis of US male veterans age 50years and older, we observed a sharp but statistically non-significant decline of -8.41% APC in age-standardized hip fracture incidence between 2002-2006. However, this was followed by a statistically significant steady increase of 1.81% APC in age-standardized hip fracture incidence between 2006 and 2019.Additionally, fewer than 6% of men underwent a DXA scan one to two years after a hip fracture. Fewer than 0.5% received osteoporosis medications within 3 years prior and/or one to two years after a hip fracture during this study period.CONCLUSIONSDespite well described methods to reduce hip fractures and associated morbidity and mortality, hip fracture incidence is not decreasing in older male veterans. Our study highlights the need to pay more attention to the risk of fracture in aging men.

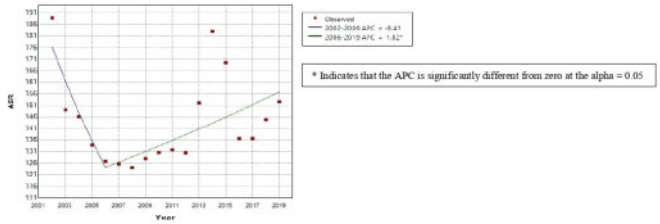

Age standardized rate of fractures per 100,000 veterans between 2002-2019. Annual Percent Change (APC) was calculated for each segment.

***Disclosures: Amna N. Khan**, None*

SUN-414

Post-Operative Outcomes among Women with Postmenopausal Osteoporosis who underwent Elective Spine Surgery: A Retrospective Cohort Study *Junjie Ma[1], Tzu-Chieh Lin[1], Tingting Gong[2], Hsu-Chih Chien[1], Brett Freedman[3], Alan Daniels[4], Kyle Mitsunaga[5], Sigurd Berven[6], John Dimar[7], Zachariah Pinter[3], Mary Oates[1], Xiaodong Li[1], Jiannong Liu[8]. [1]Amgen Inc., United States. [2]Chronic Disease Research Group, United States. [3]Department of Orthopedic Surgery, Mayo Clinic, United States. [4]Department of Orthopedic Surgery, Warren Alpert Medical School of Brown University, United States. [5]Queens Medical Center, United States. [6]Department of Neurosurgery and Orthopaedic Surgery, University of California, United States. [7]Norton Leatherman Spine Center, University of Louisville Department of Orthopedic Surgery, United States. [8]Hennepin Healthcare Research Institute, United States

BackgroundOsteoporosis (OP) is a common condition among postmenopausal women, and it may increase risk of poorer health outcomes after spine surgery. The purpose of this study is to investigate the association between history of OP and post-operative outcomes among a cohort of postmenopausal women who underwent elective spine surgery.MethodsA retrospective cohort study was conducted using the U.S. Medicare data (20% sample). Postmenopausal women who underwent elective spine surgery between January 1, 2013 and December 31, 2017 were included. History of OP was defined as having OP diagnosis, fracture diagnosis, or OP medication use before the elective spine surgery. Baseline characteristics and health outcomes during the hospitalization for the primary surgery and within 90 days and 2 years after discharge were described for patients with and without history of OP. Multivariable Cox models were used to evaluate the association between history of OP and the risk of revision surgery, fracture at any site, and death.ResultsThe study included 14,225 patients. Among them, 6,524 (45.9%) had history of OP. Patients with history of OP were older (75.3 years +/- 6.7 vs. 72.5 years +/- 5.1) and had more comorbidities (CCI: 1.4 +/- 1.7 vs. 1.1+/- 1.5) compared to those without history of OP. Among 6,524 patients with OP, 36.5% (N = 2,380) were treated with OP medication after surgery. Patients with history of OP had a higher percent of fractures and deaths during hospitalization (fractures: 2.1% vs. 1.6%; deaths: 0.35% vs. 0.14%) and within 90 days after discharge (fractures: 2.4% vs. 0.9%; death: 1.8% vs. 0.7%). A higher event rate of revision surgery, fractures, and deaths were observed within 2 years after discharge in patients with history of OP compared with those without OP. After adjusting for age, race, baseline comorbidities, and baseline medication use, Cox models showed a statistically significant association between history of OP and the risk of fractures (HR: 2.52, 95% CI: 2.21, 2.86) and death (HR: 1.54, 95% CI: 1.30, 1.83), and a marginal association between history of OP and revision surgery (HR: 1.19, 95% CI: 1.00, 1.41) after discharge.ConclusionAmong postmenopausal women who undergo elective spine surgery, a history of osteoporosis is associated with a significantly higher risk of fractures at any site and death after discharge. These findings highlight the importance of screening and appropriately treating patients for OP prior to spine surgery.

Figure 1. Post-surgery outcomes during hospitalization, and within 90 days and 2 years after discharge

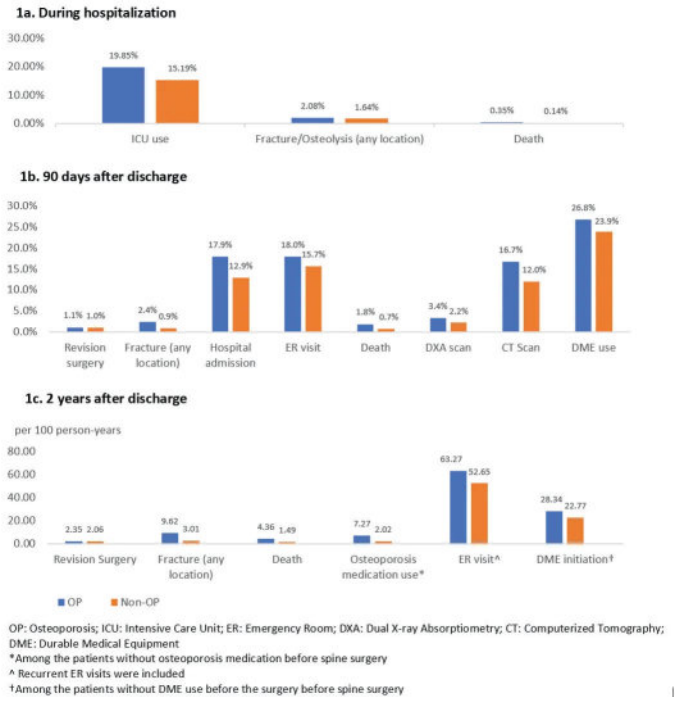

OP: Osteoporosis; ICU: Intensive Care Unit; ER: Emergency Room; DXA: Dual X-ray Absorptiometry; CT: Computerized Tomography; DME: Durable Medical Equipment
*Among the patients without osteoporosis medication before spine surgery
^ Recurrent ER visits were included
†Among the patients without DME use before the surgery before spine surgery

***Disclosures: Junjie Ma**, Amgen, Other Financial or Material Support*

SUN-415

Functional outcome, mortality, and risk factors in centenarian patients with hip fractures *HO YEON CHUNG[1], Byung-Woong Jang[2], Ha-Young Kim[3], Yong-Chan Ha[4]. [1]Department of Endocrinology and Metabolism, Kyung Hee University Hospital at Gangdong, Kyung Hee University College of Medicine, Republic of Korea. [2]Department of Orthopaedic Surgery, Soonchunghyang University Hospital Seoul, Republic of Korea. [3]Department of Internal Medicine, Gangneung Asan Hospital, University of Ulsan College of Medicine, Republic of Korea. [4]Department of Orthopaedic Surgery, Seoul Bumin Hospital, Republic of Korea

Introduction: Increasing longevity has caused the very old population to become the fastest-growing segment. The number of centenarians (over 100 years old) is increasing rapidly. Fractures in the elderly lead to excessive medical costs and decreased quality of life with socioeconomic burdens. However, little research has thoroughly examined the functional outcomes and mortality of hip fractures in centenarians. The purpose of this study was to 1) investigate the characteristics of hip fractures, mortality, and functional outcomes and 2) assess the risk factors for mortality in centenarians.Materials & Methods: This is a retrospective observational study. Sixty-eight centenarian hip fracture patients were admitted to the 10 institutions from February 2004 to December 2019. Fifty-six patients with 1-year follow-up were finally included. The following data were obtained: sex, age, body mass index (BMI), Charlson comorbidity index (CCI) value on the operation day, Koval's classification for ambulatory ability, type of fracture, the time interval from trauma to surgery, American Society of Anesthesiologists (ASA) grade, surgery-related complications, and duration of hospital stay. Postoperative Koval's classification (at 1-year after surgery), and information about death were also collected. Multivariate analysis was performed to analyze the risk factors affecting mortality one year after surgery.Results: Mortality rates were 26.8% at six months and 39.3% at one year. The 90-day mortality was 19.6%, and one of them (2.1%) died in the hospital. The 1-year mortality rates for the community ambulatory and non-community ambulatory groups were 29 and 52%, respectively. Only nine (16.1%)

were able to walk outdoors one year after surgery. The remaining 47 patients (83.9%) had to stay indoors after surgery. Multivariate analysis demonstrated that the pre-injury ambulatory level (adjusted hazard ratio (HR) = 2.884; p = 0.084) was associated with the risk of mortality.Conclusions: We report a 1-year mortality rate of 39.3% in centenarian patients with hip fractures. The risk factor for mortality was pre-injury ambulatory status. This could be an important consideration in the planning of treatments for centenarian hip fracture patients.

***Disclosures: HO YEON CHUNG**, None*

SUN-416

A Comparative Analysis Of Opportunistically Identified Vertebral Fractures Using CT Scans Across 4 NHS Organisations. Do Patients Survive Long Enough To Potentially Benefit From Fracture Prevention Interventions: The ADOPT study *Jack Boylan[1], Jane Turton[1], Daniel Chappell[2], Viki Sanders[2], Janine Connor[3], Rebecca Barbary[4], Elizabeth Gadd[5], Deborah Wellburn[6], Rachel Eckert[7], Alexandra Guy[6], Bilal Khan[6], Yuriy Arlachov[4], Madeline Sampson[6], Mark Baxter[6], Madhavi Vindlacheruvu[2], Elizabeth Curtis[8], Michael Stone[1], Sahota Opinder[9], Kenneth Poole[10], Muhammad Javaid[11]. [1]Bone Research Unit, Cardiff and Vale UHB, United Kingdom. [2]Cambridge University Hospitals NHS Foundation Trust, United Kingdom. [3]Bradford Teaching Hospitals NHS Foundation Trust, United Kingdom. [4]Nottingham University Hospitals NHS Trust, United Kingdom. [5]University Hospital Llandough, United Kingdom. [6]University Hospitals Southampton NHS Foundation Trust, United Kingdom. [7]University of Oxford , United Kingdom. [8]University of Southampton, UK, United Kingdom. [9]University of Nottingham , United Kingdom. [10]University of Cambridge, United Kingdom. [11]University of Oxford, United Kingdom

BACKGROUND: Vertebral fractures increase morbidity, mortality and fracture risk. Despite effective interventions, up to 70% remain undiagnosed. One recommendation for improving identification is re-reading existing CT scans that include the spine. However, these patients often have significant comorbidities. It is not clear how many patients survive long enough to potentially benefit from fracture prevention interventions.Objective: To describe survivorship of patients with vertebral fractures identified by opportunistic re-reading of existing CT scans.METHODS: Consecutive CT scans of adults aged 50 and over from 2017 that included an image of the thoracic or lumbar spine were re-read by clinicians with experience in identifying vertebral fractures using the grade 2/3 semi-quantitative Genant score in Cambridge, Cardiff, Nottingham and Southampton. Date of death was extracted from the hospital record system up to 5 years after the index CT scan. Log-rank tests were used to test for survival differences.RESULTS: 2084 consecutive scans were re-read. 50.5% were women, mean age 71.3 years. The commonest scan types were “CT Abdomen / Pelvis with contrast” (n=576) and “CT Thorax (n=356). CTPA accounted for 138 scans. 282 (13.5%) patients had a moderate or severe fracture, of whom 156 (55.3%) had died by 60 months. 28.4% had died by 12 months and 37.2% had died by 24 months. Survival was significantly shorter in those with index CTPA scans (Figure).DISCUSSION: In this audit population, most patients with vertebral fractures diagnosed using their 2017 CT scans survived more than two years. The opportunistically identified vertebral fracture population should benefit from secondary fracture prevention.

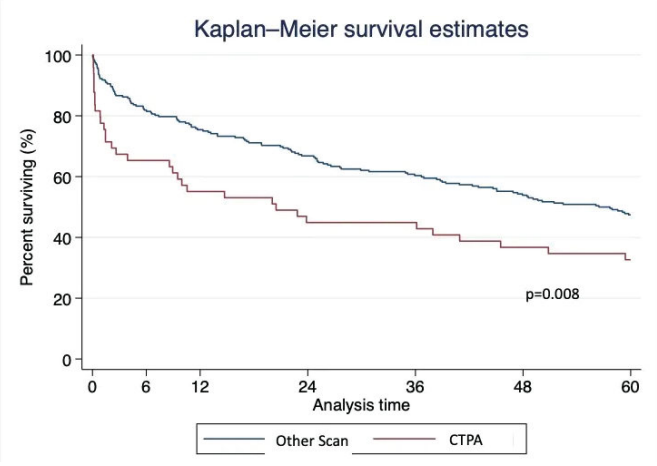

***Disclosures: Jack Boylan**, None*

SUN-417

Sensitivity Of Modelled Fracture Liaison Service Impact To Subsequent Fracture Risk Uncertainty *Rafael Pinedo-Villanueva[1], Thierry Thomas[2], Bernard Cortet[3], JULIEN PACCOU[4], Christian Roux[5], Muhammad Javaid[1]. [1]University of Oxford, United Kingdom. [2]Hopital Nord - CHU de St-Etienne, France. [3]Service de Rhumatologie, France. [4]Lille University Hospital, France. [5], France

Purpose: Previous models of FLS impact have often used data from other countries where recent national epidemiological data are missing. We want to highlight the importance of accurate national subsequent fracture risks when estimating the benefits, resource use and budget impact of Fracture Liaison Service (FLS) implementation.Methods: A microsimulation model was run to estimate the expected impact of FLS implementation in France. It was populated by 500+ inputs characterising current practice and FLS operation in the country, and run using (1) a lower set of 10-year subsequent fracture risks obtained from stratifying and extrapolating 3-year data from the FRACTOS Study in France, and (2) a set of 10-year observed risks from Denmark which were 2.5 to 4.4 times higher (e.g. risk of spine fracture after hip fracture for women = 1.4% vs. 4.7%). Patient benefit was measured in subsequent fractures avoided and quality of life gained; resource use in hospital bed days, surgeries, clinic consultations, temporary rehabilitation days, and patient-years of institutional social care; and budget impact in health and social care costs. The model was run for the yearly 396,700 patients aged 50 years or older who have a fragility fracture in France and produced results for the first 5 years of FLS implementation. Results using each set of risks were compared to measure the sensitivity of modelled FLS impact to the different levels of fracture risk.Results: All FLS patient benefit, resource use savings, and cost savings were 3 to 4 times higher when the simulation was run using the higher risks from Demark compared to the lower estimated rates from France (see Table 1). For example, fractures avoided over 5 years were estimated at 8,972 under the higher risk set instead of 2,783 under lower risk set, and quality-adjusted life years (QALY) gain at 7,173 compared to 2,066, respectively. Savings were also 3 to 4-times higher under the higher risk set, however new investment for the expected FLS operation was only 10% higher (€307.2 vs €269.8 million) leading to a much more favourable cost-effectiveness ratio under the higher risk set (€36,196 vs. €124,366 / QALY).Conclusions: Models simulating the impact of FLS are highly sensitive to subsequent fracture risks, hence estimates informing policy implementation must use accurate national values that lead to more precise estimates of patient benefit, resource use, budget impact, and cost-effectiveness.

Table 1 - Expected FLS patient benefit and budget impact under two levels of 5-year subsequent fracture rates

	Lower rates	Higher rates	Ratio
Patient benefit			
Fractures avoided	2,783	8,972	3.2
QALYs gained	2,066	7,173	3.5
Resource use (avoided)			
Hospital bed days	16,310	51,696	3.2
Surgical procedures	1,880	5,965	3.2
Clinic consultations	8,671	27,365	3.2
Temporary rehabilitation days	11,920	38,443	3.2
Institutional social care (patient-years)	129	563	4.4
Cost savings			
Healthcare (€)	9,439,408	29,868,719	3.2
Social care (€)	4,682,505	19,015,394	4.1
FLS new investment			
Extra staff, DXA, lab, drug costs (€)	269,760,926	307,196,986	1.1
Cost-effectiveness			
Incremental cost-effectiveness ratio	€124,366/QALY	€36,196/QALY	3.4

***Disclosures: Rafael Pinedo-Villanueva**, None*

SUN-418

Fall Injury Associations with Fall-Risk Increasing Drugs (FRID) Use in Older Black and White Men and Women: the Health, Aging and Body Composition Study *Jimmie Roberts[1], Kerri Freeland[2], Lingshu Xue[2], Kristine Ruppert[2], Jeanine Buchanich[2], Jennifer Pruskowski[2], Jane A. Cauley[3], Elsa Strotmeyer[2]. [1]University of Pittsburgh Graduate School of Public Health, . [2]University of Pittsburgh, United States. [3]UNIVERSITY OF PITTSBURGH, United States

Medications that increase fall risk, defined as fall-risk increasing drugs (FRIDs), are more often prescribed now than 20 years ago, with increases mainly due to antihypertensive, antidepressant, and anticonvulsant use. The association of FRIDs and falls has been examined in older adults, but fall injury risk is largely unknown. We hypothesized that FRID use would be associated with higher fall injury risk in 1,205 community-dwelling older Black and White adults with medication and fall data in the Health, Aging, and Body Composition Study (Health ABC; 2007-2008 clinic visit with 2 years of follow-up; 84+/-3 years; 54%

women; 35% Black). Medications used in past 30 days were brought to the visit. The Stopping Elderly Accidents, Deaths & Injuries (STEADI-Rx) definition of FRIDs included any use (yes, N=1052/no, N=153) of FRIDs in the past month: antidepressants, antipsychotics, anticonvulsants, opioids, benzodiazepines, sedative hypnotics, antihistamines, muscle relaxants, and antihypertensives. Fall injuries were self-reported every 6 months for 2 years. Those with >=1 FRID were more likely to be married, have a prior year hospital stay, lower physical activity (walking/stair climbing), higher BMI, physiologic hypertension, >=1 mg/L Cystatin-C, diabetes, higher Center for Epidemiologic Studies Depression scores, and more non-FRID medications use (all p<0.05). Of participants, 81% were taking antihypertensives (Table 1), with lower use of all other FRIDs. In chi-square analysis of FRIDs by fall injury, antidepressant (16.3% vs. 9.2%), antihistamine (5.6% vs. 2.9%), and muscle relaxant use (82.5% vs. 80.6%), respectively (all p<0.05), were higher in those with fall injury vs. no injury. FRID use (yes/no) was entered in multivariable Generalized Estimating Equations (GEE) models for repeated fall injuries over time. Adjusting for demographics, lifestyle/behavioral factors, comorbidities, and non-FRID medication count, STEADI-Rx FRID use was not associated with fall injury (AOR=0.92, 95%CI: 0.56-1.48). Results were similar for count of FRIDs and fall injuries (AOR=1.02, 95%CI: 0.93-1.12). In similarly adjusted sensitivity analysis, antihypertensive use entered separately (yes, N=976/no, N=229; AOR=1.07, 95%CI: 0.71-1.61) had no association with fall injuries, though other FRID use (yes, N = 458/no, N=747) had borderline increased fall injury risk (AOR=1.31; 95%CI: 0.98-1.75; p=0.07). Including antihypertensive use with other FRID use may impact fall injury risk.

Table 1. FRID Class Prevalence (%): Overall, for 1 FRID Medication Only, and Stratified by Fall Injury (yes/no)

Medication Classes	Overall (N=1205)	Use of 1 FRID medication only* (N=643)	Fall Injury Occurrence		
			Yes (N=252)	No (N=953)	P-value
Antidepressants, %	10.7	1.1	16.3	9.2	**0.001**
Antipsychotics, %	0.7	0	0.8	0.6	0.68
Anticonvulsants, %	6.9	0.3	7.9	6.6	0.46
Opioids, %	15.6	1.3	17.9	15.3	0.33
Benzodiazepines, %	8.5	0.6	9.5	8.2	0.50
Sedative hypnotics, %	2.2	0.2	1.6	2.4	0.63
Antihistamines, %	3.5	0	5.6	2.9	**0.04**
Muscle Relaxants, %	9.4	0.5	14.3	8.1	**0.003**
Antihypertensives, %	81.0	49.3	82.5	80.6	0.48
*Percent's shown as a proportion of overall use.					

***Disclosures: Jimmie Roberts**, None*

SUN-420

Validation of the Swiss FRAX model for fracture risk assessment using 10-years fracture data from the OsteoLaus Study *Enisa Shevroja[1], Vendrami Colin[3], Elena Gonzalez Rodriguez[3], Guillaume Gatineau[4], Olivier Lamy[5], Didier Hans[4]. [1]Lausanne University Hospital, Switzerland, [3]CHUV, , [3]CHUV, Switzerland. [4]Lausanne University Hospital & University of Lausanne, Switzerland. [5]University Hospital, Switzerland

Background : FRAX provides the fragility fracture risk in the next 10 years. FRAX score threshold is currently recognized as reimbursement criteria for dual X-ray absorptiometry (DXA) acquisiton and certain osteoporosis treatments in Switzerland. Further, Swiss national guidelines recommend its use in treatment decision-making. Objectives : To investigate the FRAX performance at predicting the occurrence of incident major osteoporotic fractures (MOF) during 10 years of follow-up. Methods : 944 Swiss postmenopausal women (mean age 62.7+/-7.6y) from the OsteoLaus cohort were included in this analyses. The participants had FRAX assessed at baseline, had undergone a DXA and had incident and prevalent MOF data at baseline and 4 follow-up visits every 2.5 years, with a total follow-up period of 10 years. T-tests were used to study the difference of FRAX adjusted for clinical risk factors (CRF) and of FRAX adjusted for bone mineral density (BMD) and trabecular bone score (TBS) between fractured and non-fractured groups. FRAX sensitivity and specificity were assessed for cutoffs of 10%, 20%, and moderate and high risk age-adjusted cutoffs as recommended by the Swiss national guidelines. Results : The 10y MOF incidence in the low risk group (FRAXTBS<10%) was 10%, moderate risk (10%<FRAXTBS<20%) was 25% and high risk (FRAXTBS>20%) was 48%; and for FRAXCRF the 10y MOF incidence was 11.7%, 23% and 29%, respectively. Both FRAXCRF and FRAXTBS were significantly higher in the fractured group. The sensitivity of FRAXTBS cutoff 10% was 66%, specificity was 42%; the sensitivity of FRAXCRF cutoff 20% was 20%, specificity 7.5%. The sensitivity and specificity of the FRAXTBS age-dependent cutoff was 18% and 7%, respectively. Conclusions : The fully adjusted FRAX model, comprising adjustment for CRF, BMD and TBS performs better in fracture prediction than the only CRF adjusted model. The age-dependent FRAX cutoffs used currently in Switzerland show a low sensitivity and specificity in the 10 years fracture prediction in the OsteoLaus cohort. Further analysis will study more FRAX performance parameters; and take into account time dependent fracture occurrence and the possible effect of antiosteoporotic treatment use in FRAX performance.

***Disclosures: Enisa Shevroja**, None*

SUN-421

Associations of Metabolic Syndrome (MetS) with Fall Rates and Fall Injuries: Results from the Objective Physical Activity and Cardiovascular Health in Older Women (OPACH) *Chen Hu[1], Kerri Freeland[1], Michael LaMonte[2], Marcia Stefanick[3], Kristine Ensrud[4], Jane Cauley[1], Andrea LaCroix[5], Elsa Strotmeyer[1]. [1]University of Pittsburgh, United States. [2]University of Buffalo, United States. [3]Stanford University, United States. [4]University of Minnesota Twin Cities, United States. [5]University of California San Diego, United States

MetS is an increasingly prevalent disorder that consists of a cluster of metabolic conditions. Previous studies found individual MetS components were associated with falls and fall injuries in older adults, though the association of MetS, as a constellation, with these outcomes is unknown. We aimed to evaluate whether MetS was associated with higher fall rates and fall injury risk among older women in a community-based cohort in the OPACH, an ancillary study of the Women's Health Initiative (WHI). Participants were 5,548 women (mean 79.0+/-6.7 years; 63.4% White; 30.8% obese) who had a blood draw and physical measurements during 2012-2013, and >1 month of fall calendars over a 13-month follow-up. MetS (Y/N) was defined as having?>=3 of 5 criteria per NCP/ATP-III guidelines: waist circumference?>88 cm, fasting glucose >=100 mg/dL or hypoglycemic medication use, systolic BP?>=130 or diastolic BP?>=85 mmHg, high-density cholesterol?<50 mg/dL, and triglycerides >=150 mg/dL. Falls and fall injuries were ascertained by monthly fall calendars and telephone interviews. Poisson regression examined MetS associations with fall rates. Weighted logistic regression was used for MetS associations with fall injuries (Y/N), while accounting for sampling strategies for interviews. MetS (N=1,125) was present in 20.3% the cohort and 43.6% (N=2,417) reported >=1 fall. Fall injuries were reported in 35.6% (508/1,428) over mean 11.9+/-2.3 mo. of follow-up. In unadjusted models, MetS was associated with 17% higher fall rates (RR=1.17, 95%CI=1.10-1.24) and 17% higher odds of fall injuries (OR=1.17, 95% CI=1.02-1.34). After adjusting for age, race (White/Black/other), ethnicity (Hispanic/non) and obesity (BMI>=30) the association persisted between MetS and fall rates (RR=1.12, 95%CI=1.04-1.20), but the association between MetS and fall injuries was attenuated to null (OR=1.08, 95%CI=0.93-1.24). In addition to MetS, obesity was an independent risk factor of higher fall rates (RR=1.16, 95%CI=1.08-1.25). Age-stratified adjusted analyses found MetS associated with higher fall injuries (OR=1.18, 95%CI=1.00-1.39) in women aged 65-85 years (N=1,159), but a non-significant inverse association (OR=0.83, 95%CI=0.57-1.10) in women aged >85 years (N=269). MetS was associated with higher fall rates in women >=65 years and injurious falls in women <85 years. Further studies should evaluate potential mechanisms of individual MetS components and how comorbidities may contribute to these associations.

***Disclosures: Chen Hu**, None*

SUN-422

Skeletal Age for mapping the impact of fracture on mortality using clinical data *Thach Tran[1], Dinh Tan Nguyen[2], Lisa Langsetmo[3], Nancy Lane[4], Tuan Nguyen[5]. [1]Garvan Institute of Medical Research, Australia. [2]University of Technology Sydney, . [3]Minneapolis VA Medical Center, United States. [4]University of California, Davis Medical Center, United States. [5]University of Technology Sydney , Australia

Fragility fracture is associated with an increased risk of mortality, though mortality is not part of patient-doctor risk communication. We used the Danish nationwide registry-based data to propose a new metric called "Skeletal Age" to convey the combined risk of fracture and fracture-related mortality for an individual. This study sought to estimate Skeletal Age for specific fracture sites using self-reported and clinically measured data.Skeletal Age is conceptually defined as the age of an individual's skeleton resulting from a fragility fracture. Thus, for an individual with a fracture associated with increased mortality risk, the skeletal age would be expected to be higher than the individual's chronological age. Skeletal Age is estimated as the sum of chronological age and the number of years of life lost (YLL) associated with each fracture site for an individual with specific risk profiles. Cox's proportional hazards model was employed to determine the hazard of mortality associated with a specific fracture for a given risk profile including age, BMD, BMI, lifestyle factors, and the presence of comorbidities, and the hazard was then transformed into YLL using the Gompertz law of mortality.The study involved 5994 community-dwelling elderly men in the Osteoporotic Fractures in Men Study (MrOS) with an average age of 73.6 (+/- 5.9) years. During a median follow-up of 13.9 years (IQR: 8.5, 17.5), 1085 men had sustained a fragility fracture followed by 694 deaths (~11.8 deaths/100 person-years). Hip, other proximal, and lower leg fractures were associated with a significantly increased risk of death. On average, a fragility fracture was associated with 1 to 9 years of life lost, with the loss being greater in younger patients with a hip, femur, or pelvis fracture. A 60-year man with a hip fracture is estimated to have a Skeletal Age of 68.1 (95% CI: 66.9, 69.2); whereas the estimated skeletal age for a 70-year man with a hip fracture is 76.3 (75.4, 77.1). Skeletal Age was also estimated for each age and specific fracture associated with increased mortality risk (Figure).Our results reemphasize that most fractures are associated with increased mortality risk and hence reduced life expectancy. The findings were consistent in both registry-based and clinical data. The proposed Skeletal Age supplements the traditional relative risk as a metric for conveying the mortality consequence of fracture, making the doctor-patient risk communication more intuitive.

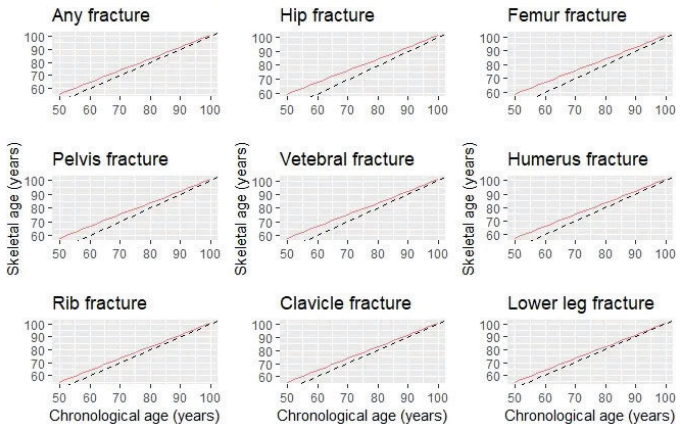

***Disclosures: Thach Tran**, None*

SUN-424

Volumetric BMD, Failure Load, and Other HR-pQCT Measurements Are Associated with Clinical and Hip Fracture Risks: Follow-up 6.2 Years *Tong Yu[1], Elsa Strotmeyer[1], Andrew Burghardt[2], Kristine Ensrud[3], Lisa Langsetmo[4], Eric Orwoll[5], Peggy Cawthon[6], Mary Bouxsein[7], Jane Cauley[1]. [1]University of Pittsburgh, United States. [2]University of California San Francisco, United States. [3]University of Minnesota, Minneapolis VA Health Care System, United States. [4]University of Minnesota, United States. [5]Oregon Health and Science University, United States. [6]University of California San Francisco, California Pacific Medical Center, Research Institute, United States. [7]Harvard medical school, United States

Current fracture prediction relies on clinical risk factors combined with areal bone mineral density (aBMD) measurements. However, deficits in bone microstructure, measured by high resolution peripheral quantitative computed tomography (HR-pQCT), may also contribute to age-related increases in fracture risk. Previous studies have shown associations between HR-pQCT parameters and clinical fracture, but most studies did not examine hip fracture, the most devastating consequence of osteoporosis, specifically.The analytic sample included 1794 men (median 84 years) with HR-pQCT and DXA scans at Year 14 visit of MrOS. The outcomes were incident clinical fractures and hip fractures. Failure load was estimated using finite element analysis. We used Cox models with standardized HR-pQCT parameters as predictors of fracture risk, adjusting for clinical sites, limb length and total hip aBMD with clinical risk factors (CRFs) for fractures or FRAX 10-year probability of osteoporotic fractures with FN aBMD. We compared incidence rates of clinical fracture across quartiles of failure load and presence of low femoral neck (FN) aBMD by T score (<=-1) vs normal.Over 6.2 years of follow-up, 318 men had at least one incident clinical fracture, including 74 hip fractures (23%). One standard deviation (SD) decrement of total volumetric (v) BMD at distal radius was significantly associated with increased risk of clinical fracture (HR=1.44, 95%CI 1.23-1.68) and hip fracture (HR=1.84, 95%CI 1.32-2.57) after adjusting for total hip aBMD and CRFs. (Table). Results were in the same direction for failure load (HR=1.48 for clinical fracture, HR=1.69 for hip fracture). On the contrary, one SD lower of total area at distal radius was significantly associated with reduced risk of hip fracture (HR=0.55) but not clinical fractures. Adjusting for FRAX with FN aBMD instead of total hip BMD and CRFs further strengthen the associations. Associations with parameters at distal tibia are weaker than those at distal radius. Higher quartiles of distal tibia failure load and vBMD were associated with a decreasing fracture incidence rate in both normal and low FN aBMD groups.In community-dwelling older men, lower failure load and total vBMD are robust predictors for risks of clinical fractures and hip fractures. Lower total area was associated with reduced hip fracture risk. HR-pQCT parameters provide fracture prediction independent of existing fracture risk assessment tools.

Table. Estimated hazard ratios (per decrement SD) and 95% confidence intervals (CI) of volumetric BMD, total bone area and failure load for clinical fractures and hip fractures.

	Model 1[1] (Total hip aBMD + CRFs)		Model 2[2] (FRAX with FN aBMD)	
Clinical Fracture				
Distal radius	N = 1651; Fx = 286		N = 1656; Fx = 287	
Total vBMD[3]	**1.44**	**1.23 - 1.68**	**1.68**	**1.46 - 1.93**
Total area	0.90	0.79 - 1.02	0.90	0.79 - 1.02
Failure load	**1.48**	**1.26 - 1.73**	**1.69**	**1.47 - 1.95**
Distal tibia	N = 1672; Fx = 299		N = 1677; Fx = 300	
Total vBMD	**1.45**	**1.23 - 1.70**	**1.65**	**1.44 - 1.89**
Total area	0.93	0.81 - 1.07	0.93	0.81 - 1.06
Failure load	**1.51**	**1.28 - 1.79**	**1.69**	**1.47 - 1.93**
Hip Fracture				
Distal radius	N = 1651; hip = 64		N = 1656; hip = 64	
Total vBMD	**1.84**	**1.32 - 2.57**	**2.73**	**2.01 - 3.70**
Total area	**0.55**	**0.43 - 0.70**	**0.56**	**0.44 - 0.72**
Failure load	**1.69**	**1.19 - 2.40**	**2.54**	**1.85 - 3.49**
Distal tibia	N = 1672; hip = 71		N = 1677; hip = 71	
Total vBMD	**1.40**	**1.00 - 1.95**	**2.22**	**1.67 - 2.94**
Total area	**0.71**	**0.55 - 0.94**	**0.70**	**0.53 - 0.91**
Failure load	**1.25**	0.89 - 1.74	**2.04**	**1.54 - 2.69**

[1] Model 1 adjusted for clinical sites, ulnar/tibia length, total hip aBMD and clinical risk factors (CRFs) including age, race, fall history and prevalent fracture after age 50.
[2] Model 2 adjusted for clinical sites, ulnar/tibia length, FRAX 10-year probability of osteoporotic fracture risk with FN aBMD (age, race, clinical risk factors for fractures implicitly included).
3 Hazard ratios for total vBMD, total area and failure load were estimated in separated models, and not mutually adjusted for each other.

***Disclosures: Tong Yu**, None*

SUN-425

Association of Serum Pentosidine with Fracture in Women from the Canadian Multicentre Osteoporosis Study *Lindsie Blencowe[1], Andrea Bozovic[2], Vathany Kulasingam[2], George Tomlinson[2], Evelyn Wong[2], Claudie Berger[3], Jerilynn Prior[6], Robert Josse[5], Brian Lentle[6], Alexandra Papaioannou[7], Suzanne Morin[8], William Leslie[9], Stephanie Kaiser[10], Christopher Kovacs[11], DAVID GOLTZMAN[8], Jonathan Adachi[12], Angela Cheung[13]. [1]University of Toronto, University Health Network, . [2]University Health Network, Canada. [3]Research Institute of the McGill University Health Center, Canada. [6]University of British Columbia, Canada. [5]St. Michael s Hospital, University of Toronto, Canada. [6]University of British Columbia, . [7]McMaster University , Canada. [8]McGill University, Canada. [9]University of Manitoba, Canada. [10]Dalhousie University, Canada. [11]Memorial University of Newfoundland, Canada. [12]St. Joseph s Hospital/McMaster University, Canada. [13]University Health Network-University of Toronto, Canada

Purpose: The glycation of bone collagen results in compounds known as advanced glycation end-products (AGEs). The accumulation of AGEs in bone has been associated with increased fracture risk. Pentosidine (PEN) is a cross-link AGE found in bone. Serum PEN has been shown to correlate with the PEN content of bone and may be a useful biomarker. Serum PEN was assessed in women participating in the Canadian Multicentre Osteoporosis Study (CaMos) to explore its association with fracture.Methods: Total serum PEN was assessed using liquid-chromatography tandem mass spectrometry in stored serum samples from 1200 women (aged 41-72 years), at year 10 in CaMos. The association between serum PEN and All Fractures (any site), Major Osteoporotic Fracture (MOF), Fragility Fracture (FF, defined as low trauma, nonvertebral fractures, excluding the head, hand and foot), Hip Fracture (HF) and Vertebral Fracture (VF, Genant Grade >1) was explored using multivariable logistic regression. We adjusted for age or estimated glomerular filtration rate (eGFR), as age and eGFR are the most significant predictors of serum PEN. Given the limited number of fractures in the cohort, we could only adjust for one covariate at a time. Serum PEN quartiles were used in the analyses to allow for non-linear associations with fracture. Our analyses explored timepoints at years 1-10 and 11-15 for All Fractures, MOF, FF, and HF and at years 10 and 16 for VF.Results: Serum PEN ranged from 0.31 to 41.0 nmol/g albumin (median 0.92 nmol/g). From years 1-10 and years 11-15 there were 250 and 176 total fractures, 87 and 55 MOF, 149 and 102 FF, 11 and 18 HF, respectively. For years 10 and 16, there were 77 and 16 VF, respectively. After Age adjustment, serum PEN was associated with FF (years 11-15) (OR: 2.12, 95% CI: 1.11-4.02), but was not associated with any other fracture outcomes or timepoints. After eGFR adjustment, the 3rd quartile serum PEN level was significantly associated with MOF and FF (years 1-10 and years 11-15) (ORs: 2.27-2.93, 95% CIs: 1.18-6.89) and was associated VF at year 10 (OR: 2.14, 95% CI: 1.03-4.48) but was not associated with All Fractures. There were too few HFs (all time points) and VFs (year 16) to be able to interpret and draw conclusions from the results.Conclusions: Our results suggest that there may be an association between serum PEN levels and fracture, particularly fragility fracture. Further exploration into the utility of serum PEN as a fracture biomarker is warranted.

***Disclosures: Lindsie Blencowe**, None*

SUN-426

Hip fracture rate and osteoporosis treatment in long-term care: Ontario Osteoporosis Strategy *Hajar AbuAlrob[1], Susan Jaglal[2], Crystal MacKay[3], Cathy Cameron[2], Yinan Li[4], Haley Golding[4], Lesley Plumptree[4], Ravi Jain[5], George Ioannidis[1], Loretta Hillier[6], Alexandra Papaioannou[1]. [1]McMaster University, Canada. [2]University of Toronto, Canada. [3]Westpark Hospital, Canada. [4]Institute for Clinical Evaluative Sciences, Canada. [5]Osteoporosis Canada , Canada. [6]Ontario Osteoporosis Strategy, Canada

Aim: This population-based study reports trends in hip fracture rates and osteoporosis treatment according to fracture risk level in long-term care (LTC) adults >=65 years from 2014/15-2018/19.Methods: Osteoporotic fracture were identified using Public Health Agency of Canada algorithm and ICD-10 codes. Health administrative data was linked using unique, encoded identifiers and analyzed at ICES. Fracture risk was determined using the Fracture Risk Scale (FRS). FRS predicts hip fracture over a 1-year period using data readily available in RAI MDS 2.0 and LTC-specific risk factors and consists of 8 risk levels (1 lowest risk, 8 highest risk).Results: There has been a 41.2% increase in the age standardized rate of hip fracture in LTC (from 223.6 per 10,000 in 2014/15 to 315.7 per 10,000 in 2018/19). The rate increased for both women (+47.0%) and men (+56.5%), adults 66-79 years (+63.8%) and 80+ years (+28.5%), and across setting (+85.6% in rural +44.7% in urban). From 2014/15 to 2018/19 the proportion of LTC residents 66+ not investigated or treated within 6 months after discharge from a hip fracture decreased from 83% to 73%. The overall rate of osteoporosis treatment among LTC residents at high-risk of fracture (Fracture Risk Scale score 4+) increased by 8.7% (23.3% in 2014/15 to 25.4% in 2018/19). Among LTC residents at high fracture risk (FRS 4+), treatment rate was higher for females than males (31.2% for women vs 11.6% for men 2018/19), adults 80+ years compared to 66-79 (19.3% for 66-79 age group, 26.3% for 80+ 2018/19), and large LTC facility size compared to small and medium (11.5% for small, 22.1% for medium, 26.2% for large, in 2018/19). Conclusion: The hip fracture rate in LTC in Ontario, Canada has increased over time, and is higher for women and seniors 80+ years. Treatment rate for LTC residents at high risk for fracture has increased over time, and treatment rate varies across age groups and LTC facility size. Residents in LTC are at very high risk for fracture and need individualized treatment. Care needs to be patient centred and individualized based on goals of care and life expectancy. Fracture Risk Scale score should be used to identify those at high risk for fracture in LTC.

***Disclosures: Hajar AbuAlrob**, None*

SUN-427

Abaloparatide Increases Distal Femur BMD Post Total Knee Arthroplasty *Neil Binkley[1], DIANE KRUEGER[2], Gretta Borchardt[3], Brian Nickel[3], Paul Anderson[3]. [1]University of Wisconsin, Madison, United States. [2]UNIVERSITY OF WISCONSIN, United States. [3]University of Wisconsin, United States

Purpose: Osteoporosis is common in total joint replacement patients and increases risk for adverse outcomes including revision surgery and periprosthetic fracture. Existing data indicates total knee arthroplasty (TKA) leads to rapid distal femur bone loss. We hypothesized that Abaloparatide (ABL) would mitigate this loss. The purpose of this preliminary analysis is to evaluate the effect of ABL begun ~3 months prior to TKA on distal femur BMD.Methods: Female and male TKA candidates age >= 55 years were enrolled in this open-label 18-month study. Those with clinical osteoporosis, defined as T-score <= -2.5, or < -1.0 with prior low-trauma fracture, received subcutaneous ABL up to 80 mcg daily. Subjects with osteopenia but without fracture comprised the an untreated control (CON) group. BMD was measured at the lumbar spine, total hip, 0.3 radius and distal femur at screening (~3 months pre-TKA), 1 week pre-op, 6 and 15-months post-op. Distal femur BMD was measured at regions of interest (ROIs) placed at 15% and 25% of femur length. Groups were compared at baseline by t-test. For this preliminary analysis in study completers (n = 10 ABL/17 CON) BMD change at all measured sites was assess by ANOVA.Results: To this point, 27 of the planned 29 ABL subjects and all 29 controls have been recruited. Mean (SD) age and BMI did not differ between ABL and CON groups; 70.6 (7.4) vs. 68.5 (7.0) years and 31.9 (6.5) vs. 30 (4.6) kg/m2 respectively. ABL group screening BMD was lower (p <= 0.05) at all measured sites. ABL was administered for mean (SD) 89 (67) days prior to TKA. At the 15% distal femur ROI, BMD percentage change from screening was higher than control (p < 0.05) at pre-op, 6 and 15 months by 1.6%, 5.5% and 8.6% respectively. Similarly, at the 25% ROI BMD change was greater (p < 0.05) at 6 (3.6%) and 15 months (5.2%; Table). At 15 mo, spine and total hip BMD change from baseline was greater (p < 0.001) in the ABL group (9.9% and 6.3% respectively).Conclusion: In this preliminary analysis, ABL increased distal femur BMD following TKA. This increase was demonstrable with ~3 months of treatment.

	Control			Abaloparatide			Difference: ABL - Control		
Timepoint	Pre-op	6 mo	15 mo	Pre-op	6 mo	15 mo	Pre-op	6 mo	15 mo
L-spine	0.4 (1.6)	1.2 (2.9)	3.0 (4.9)	2.5 (2.4)	7.1 (4.3)	12.9 (5.5)	**2.1***	**5.9§**	**9.9§**
Total Hip	0.2 (0.9)	-0.9 (2.3)	-1.1 (2.8)	2.1 (2.1)	3.3 (5.1)	5.2 (3.8)	**1.9†**	**4.2§**	**6.3§**
1/3 Rad	-0.9 (3.5)	-1.1 (3.4)	-1.2 (3.2)	0.9 (2.5)	-0.8 (2.8)	-3.1 (3.3)	1.8	0.3	**-1.9***
15% Distal Femur	-0.9 (1.1)	1.2 (5.9)	-3.1 (5.8)	0.7 (2.3)	6.7 (5.5)	5.5 (5.3)	**1.6***	**5.5†**	**8.6§**
25% Distal Femur	-0.1 (1.7)	-1.9 (5.2)	-3.5 (4.9)	-0.3 (2.0)	1.7 (4.1)	1.7 (3.1)	-0.2	**3.6***	**5.2†**

Notes: Mean (SD) % BMD change from baseline; different ABL and CON: * = p < 0.05; † = p < 0.01; § = p < 0.001

***Disclosures: Neil Binkley**, None*

SUN-428

Most patients on denosumab with hypocalcemia continued treatment without further hypocalcemia on follow-up *Cherie Chiang[1], Nadia Pocci[1], Jasmine Seah[1], Sharjeel Ahmad[1], Peter Mount[1]. [1]Austin Health, Australia

Impaired renal function is a known risk factor for hypocalcemia in de novo denosumab use, however the prevalence of hypocalcemia in established denosumab users with declining eGFR is unknown. We conducted a retrospective longitudinal cohort study to assess the incidence and risk factors of hypocalcemia in patients on long-term established or de novo denosumab treatment stratified by severity of kidney disease. 312 patients prescribed denosumab at Austin Health from 2016-2020 who had follow-up pathology were included. The breakdown of CKD stages at baseline was CKD 2 = 70%, CKD 3a = 20%, CKD 3b = 9%, CKD 4 = 1%, at most recent follow-up was: CKD 2 = 65%, CKD 3a = 19%, CKD 3b = 10%, CKD 4 = 6%. Hypocalcemia (any low total or corrected or ionised Ca) was found in 26% (total calcium = 2.0 +/- 0.17, corrected calcium 2.2 =+/- 0.16, iCa = 1.06 +/- 0.08 mmol/L). Compared to the normocalcemic cohort, the hypocalcemic cohort had a higher CKD stage at baseline (p = 0.015), lower eGFR (p < 0.001), lower albumin (p < 0.001), lower corrected calcium (p 1 year), hypocalcemia was present in 27% (72/263), neither recent eGFR or change in eGFR was associated with hypocalcemia. Of the 81 hypocalcemic subjects, 2 patients had hypocalcemic symptoms requiring admission, 57 continued denosumab (13/57 had eGFR < 45) and 3 patients had recurrent low corrected calcium. Of the 32 subjects with baseline eGFR < 45, 13 ceased denosumab (6 deceased, 1 declining eGFR, 3 clinician's choice, 3 no information). Of the 19 who continued denosumab (follow-up 3.3 +/- 2.4 years, recent mean eGFR 37 +/- 10), only one patient had an asymptomatic low corrected Ca of 2.0 and albumin of 23 g/L on recent pathology. In conclusion, hypocalcemia was common in de novo or established denosumab use, mostly driven by low albumin. Hospital presentations due to symptomatic hypocalcemia were rare. Hypocalcemia was not associated with magnitude of eGFR decline, most hypocalcemic patients continued denosumab without further episodes.

***Disclosures: Cherie Chiang**, Amgen, Grant/Research Support*

SUN-430

Effects of Abaloparatide on Cortical and Trabecular Compartments by 3D-DXA in Men with Osteoporosis *Ruban Dhaliwal[1], John Boxberger[2], Yamei Wang[3], Bruce Mitlak[2], Ludovic Humbert[4], Neil Binkley[5]. [1]State University of New York Upstate Medical University, . [2]Radius Health, United States. [3]Radius Health, Inc., United States. [4]3D-Shaper Medical, Spain. [5]University of Wisconsin, Madison, United States

Abaloparatide (ABL) increases bone mineral density (BMD) in men with osteoporosis. In the Abaloparatide for the Treatment of Men with Osteoporosis (ATOM) trial, DXA-measured BMD change with ABL 80 ?g/day was greater than placebo (PBO) at the lumbar spine, total hip, and femoral neck. The purpose of this study was to evaluate the effects of ABL on cortical and trabecular compartments of the proximal femur in men with osteoporosis using 3D-DXA modeling. Blinded hip DXA images from all randomized patients in the ATOM trial (n=149 ABL; n=79 PBO) were retrospectively analyzed using 3D-DXA 3D-Shaper software (v2.12.0, 3D-Shaper Medical) to evaluate changes from baseline at months 6 and 12 at the total hip. Comparisons from baseline were made using paired t tests. Between-group comparisons were made for percent change from baseline data based on a mixed-effect repeated-measure model with treatment, visit, treatment-by-visit interaction and DXA scanner as fixed effects. Other covariates include body mass index (BMI), age, and value at baseline. At 12 months, significant within group increases from baseline (P<0.0001) in integral volumetric BMD (vBMD) (3.7%), trabecular vBMD (7.0%), cortical thickness (1.1%), and cortical surface BMD (sBMD; 1.7%) were observed with ABL. Mean percent change from baseline was greater for ABL compared to PBO (P<0.01) for all 4 variables (integral vBMD, trabecular vBMD, cortical thickness, cortical sBMD) at 12 months (Figure).

Greater increases (P<0.0001) were also observed at 6 months between ABL and placebo for integral vBMD (2.5% vs 0.04%) and trabecular vBMD (5.7% vs ?0.2%). In conclusion, in men with osteoporosis in ATOM, 12 months of treatment with ABL improved cortical and trabecular 3D-DXA parameters at the total hip, consistent with the results in postmenopausal women in the ACTIVE study.

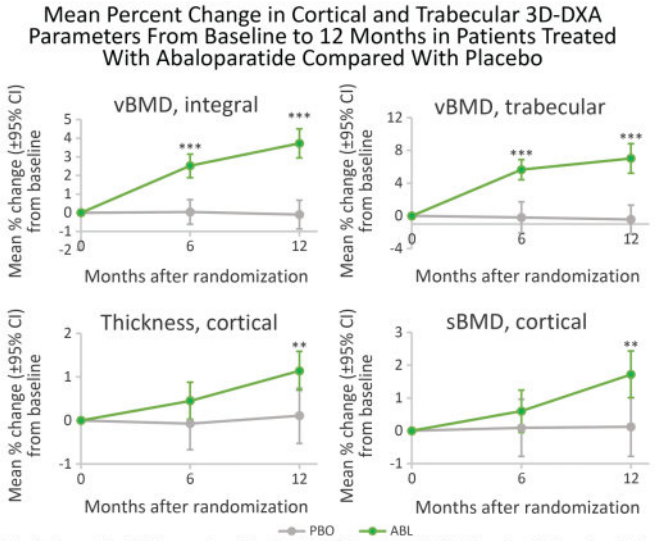

ABL, abaloparatide; BMD, bone mineral density; CI, confidence interval; PBO, placebo; sBMD, surface BMD; vBMD, volumetric BMD.
** P<0.01; *** P<0.0001

***Disclosures: Ruban Dhaliwal**, Amgen, Consultant, Alexion, Consultant, Takeda, Grant/Research Support, Radius Health, Inc, Grant/Research Support, Alexion, Grant/Research Support, Ultragenyx, Consultant, Radius Health, Inc, Consultant, Shire, Grant/Research Support, Ascendis, Consultant*

SUN-431

Impact of Bisphosphonate Use Following Hip Fracture: A Decade-Long Follow-Up of a Cohort Within a Private Healthcare System *Betiana Perez[1], Maria Eugenia Vera[1], Luisa Carmen Plantalech[1], Maria Diehl[1]. [1]Hospital Italiano de Buenos Aires, Argentina

Bisphosphonate use after hip fracture is useful for secondary prevention and may reduce post-fracture morbidity and mortality. Aims To evaluate the long-term impact of bisphosphonate use after hip fracture in mortality and morbidity. Methods Retrospective cohort study of patients >=50 years from a closed health system hospitalized for a fragility hip fracture between July 2005 and December 2010. Deaths and readmissions were analyzed. Kaplan Meier survival analysis and Cox regressions were performed. Sensitivity analysis with propensity score matching (PSM), considering age, sex, previous fracture and comorbidities was employed to adjust for prescription bias. Results We included 965 patients. The median age was 82.4 years (IQR 77.8-86.6), and 80.7% were female. Secondary prevention with bisphosphonates was administered to 39% of cases within the year after hip fracture. Mortality in the first year was 14.9% and at 10 years 73.2%. Median survival was 5.6 years. The median survival of patients with hip fracture treated with bisphosphonates was 8.33 years, and for those not treated it was 4.06 years (p<0.0001), and remained significantly different after PSM (p= 0.022). Median survival free of readmissions was 2.93 years; 4.02 years for treated with bisphosphonates, and 2.09 years for not treated (p<0.0001), and also remained different after PSM (p= 0.045). Multivariate Cox regression showed that secondary prevention with bisphosphonates remains an independent predictor of survival and survival free of readmissions, even after adjusting for significant covariates (table 1). Conclusions Bisphosphonates positively impacted survival and readmissions in our study after adjusting by demographic variables, comorbidities. However, we could not assess other relevant covariates such as educational level and social support.

	Mortality	Readmissions
Age (each year)	1.08(1.07-1.09) [a]	1.04 (1.03-1.05) [a]
Male sex	1.22(1.01-1.48) [b]	1.12 (0.92-1.37)
Intracapsular fracture	1.46(1.22-1.74) [a]	1.32 (1.10-1.59) [c]
Charlson Index (each point)	1.14(1.08-1.20) [a]	1.17 (1.11-1.23) [a]
Dementia	1.74(1.46-2.07) [a]	1.23 (1.03-1.48) [d]
Congestive heart failure	1.68(1.30-2.17) [a]	1.99 (1.50-2.65) [a]
Secondary prevention with bisphoshonate	0.68 (0.58-0.80) [a]	0.72 (0.61-0.86) [a]

a. p<0.0001 b. p=0.043 c. p=0.003 d. p=0.026

***Disclosures: Betiana Perez**, None*

SUN-432

A Randomized, Double-blind, Phase III Study to Compare SB16 (Proposed Denosumab Biosimilar) to Reference Denosumab in Patients with Postmenopausal Osteoporosis *Richard Eastell[1], Bente Langdahl[2], Yoon-Sok Chung[3], Rafal Plebanski[4], Edward Czerwinski[5], Eva Dokoupilova[6], Jerzy Supronik[7], Jan Rosa[8], Anna Rowi?ska-Osuch[9], Ki Hyun Baek[10], Audrone Urboniene[11], SoHui Ahn[12], Young Hee Rho[12], Jisuk Ban[12]. [1]University of Sheffield, United Kingdom. [2]Aarhus University Hospital, Denmark. [3]Ajou University Hospital, Republic of Korea. [4]Klinika Zdrowej Kosci, Poland. [5]Krakowskie Centrum Medyczne sp z oo, Poland. [6]MEDICAL PLUS sro; Masaryk University, Czech Republic. [7]OsteoMedic sc A Racewicz J Supronik, Poland. [8]Affidea Praha sro, Czech Republic. [9]ETG Warszawa, Poland. [10]Yeouido St Mary's Hospital, Republic of Korea. [11]JSC Saules seimos medicinos centras, Lithuania. [12]Samsung Bioepis, Republic of Korea

Introduction: SB16 is a human monoclonal antibody to the receptor activator of nuclear factor ?? ligand that has been developed as a proposed biosimilar to reference denosumab (brand name: Prolia, DEN hereafter).Objective: This Phase III study was a randomized double-blind study to compare efficacy, safety, pharmacokinetics (PK), pharmacodynamics (PD) and immunogenicity of SB16 with DEN in postmenopausal osteoporosis (PMO) patients (NCT04664959). Results up to Month 12 are presented here.Methods: PMO patients were randomized in a 1:1 ratio to receive either 60 mg of SB16 or DEN subcutaneously at Month 0, Month 6, and Month 12. At Month 12, patients in DEN were re-randomized in a 1:1 ratio to switch to SB16 or maintain DEN. The primary endpoint was percent (%) change from baseline in lumbar spine bone mineral density (BMD) at Month 12. Equivalence between SB16 and DEN was declared if the 95% confidence interval (CI) of least squares means (LSMeans) difference of % change in lumbar spine BMD at Month 12 was within the pre-defined equivalence margin. Other secondary efficacy, PD (serum C-telopeptide of type I collagen [CTX] and procollagen type I N-terminal propeptide [P1NP]), PK and safety endpoints were also measured.Results: Among 457 patients, 225 patients were randomized to SB16 and 232 patients to DEN. Baseline characteristics were comparable between SB16 and DEN. The mean % change from baseline in lumbar spine BMD at Month 12 was 5.6% and 5.3% in SB16 and DEN, respectively (Figure 1), and the difference in LSMeans was 0.39, 95% CI [?0.36, 1.13] for the per-protocol set, and 0.33, 90% CI [?0.25, 0.91] for the full analysis set, both within the pre-defined equivalence margin. The mean % change from baseline in total hip BMD at Month 12 was 3.5% and 3.2% in SB16 and DEN, respectively. The mean % change from baseline in femoral neck BMD at Month 12 was 2.8% and 2.3% in SB16 and DEN, respectively. The incidence and distribution of adverse events were comparable between SB16 and DEN up to Month 12. Serum CTX, P1NP and denosumab concentrations were comparable between SB16 and DEN up to Month 12. The median % change from baseline in serum CTX concentration over time was a decrease of at least 50% at all time points. Only 3 subjects (1 in SB16 and 2 in DEN) had non-neutralizing anti-drug antibodies.Conclusion: This study demonstrated biosimilarity of SB16 to DEN through equivalent efficacy and comparable PD, PK, immunogenicity and safety up to Month 12.

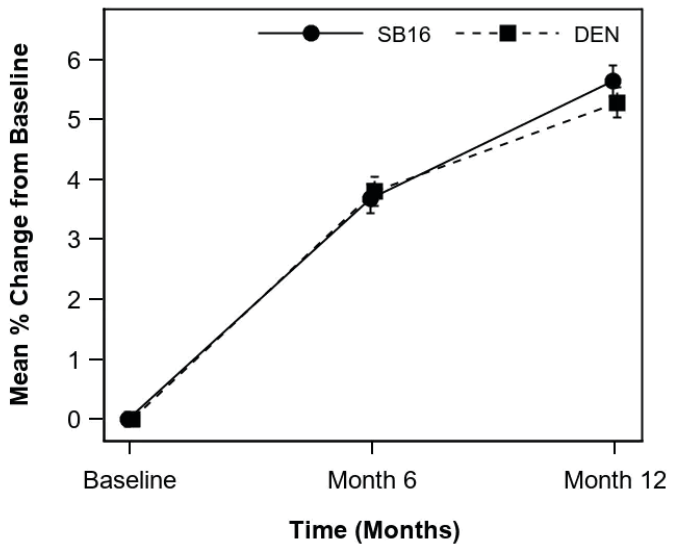

***Disclosures: Richard Eastell**, Takeda, Consultant, UCB, Speakers' Bureau, Biocon, Consultant, Pharmacosmos, Grant/Research Support, UCB, Consultant, Sandoz, Consultant, Alexion, Grant/Research Support, Immunodiagnostic Systems, Consultant, Haoma Medica, Consultant, Samsung Bioepis, Consultant, CL Bio, Consultant, Amgen, Speakers' Bureau, Roche, Grant/Research Support, Alexion, Speakers' Bureau*

SUN-433

A Real-World Review of the Use of Romosozumab for Fracture Risk Reduction and Bone Optimization in an Orthopaedic-Based Fracture Liaison Service *Michael Gardner[1], Andrea Fox[1]. [1]Stanford University School of Medicine, United States

The novel bone-forming medication, romosozumab, was approved by the FDA in 2019 for use in postmenopausal females with a high risk of fracture. There is limited data on real-world experience with romosozumab in the US. This retrospective review describes the experience of 131 postmenopausal women at high risk of fracture who completed one year of romosozumab therapy between 2019-2022 in the setting of an orthopedic Fracture Liaison Service (FLS) clinic. Women were referred to the FLS for very recent fracture (n=84, 64.1%), bone optimization prior to elective surgery (n=35 patients, 25.7%), and high risk of fracture risk identified via DXA BMD or FRAX assessments (n=12 patients, 9.2%). Patients ranged in age from 51-93 with a mean age of 73 years. Forty-one patients (31.3%) were treatment naïve, while 90 (68.7%) had used a variety of antiresorptive (n=53, 55.7%) or anabolic (n=9, 0.1%) agents in the past. Reasons for selecting romosozumab as the treatment agent of choice included patient preference (32.8%), contraindications to PTH analogs (32.8%), current hypercalcemia or history of hyperparathyroidism (19.1%), aversion to daily injections (11.5%), cost as a hindrance to PTH analogs (10.7%), prior PTH intolerance (7.6%), and provider preference (4.6%). BMD increased at all measured sites over 12 months of therapy with romosozumab. Mean spine T-score improved from -1.99 to -1.14 with mean right hip increasing from -2.28 to -1.86. Few fractures on therapy were observed (n=9) during the treatment course. Of the 35 patients treated for bone optimization prior to surgical intervention, 18 patients (85.7%) met expected outcomes per surgical follow-up notes, 14 surgeries were still pending and 3 (14.3%) of patients had a documented interoperative or postoperative complication related to bone. Overall, treatment with romosozumab was well tolerated. The most commonly reported side effects were myalgias (9 patients, 6.9%) , injection site reactions (8 patients, 6.1%) , and headaches (3 patients, 2.3%) . Romosozumab was found to be an effective option for osteoporosis treatment in postmenopausal women at high fracture risk and those referred for surgical bone health optimization in an orthopedic-based FLS.

***Disclosures: Michael Gardner**, None*

SUN-435

Effect of risedronate on bone loss after hematopoietic stems cell transplantation: A Prospective, Double-blinded, Randomized Controlled Trial *Jeonghoon Ha[1], Jinyoung Kim[1], Chaiho Jeong[1], Jeongmin Lee[1], Yeeje Lim[2], Ki-Hyun Baek[1]. [1]The Catholic University of Korea, Republic of Korea. [2]Seoul National University Bundang Hospital, Republic of Korea

Background Bone marrow transplantation (BMT) is an effective treatment for hematological diseases; however, it often leads to bone loss, the complex causes of which are not fully understood. Although bisphosphonates are recommended for these patients, there is limited evidence, particularly regarding risedronate. This study aims to evaluate risedronate as a potential solution for preventing bone loss in bone marrow transplant recipients. Methods We conducted a prospective, double-blinded, randomized controlled trial with 50 allogeneic BMT patients to assess the efficacy and safety of risedronate in preventing post-transplant bone loss. Participants were randomized into treatment (35 mg risedronate weekly) (n=26) or placebo groups (n=24), with both receiving calcium and vitamin D supplements. Intention-to-treat and per-protocol analyses were conducted. The primary endpoint was the change in bone mineral density (BMD) at the lumbar spine and femoral neck, measured at baseline, 24, and 48 weeks using dual-energy X-ray absorptiometry. Secondary endpoints included changes in serum calcium, phosphorus, 25-hydroxyvitamin D, osteocalcin, and carboxy-terminal cross-linked telopeptide of type I collagen (1CTP) levels. Results There were no statistically significant differences in age, gender, underlying hematologic conditions, bone turnover markers, and BMD between the two groups. At week 48, lumbar BMD decreased from baseline in both groups, with a 1.5% decrease in the risedronate group and a 6.5% decrease in the placebo group. For femoral neck BMD, there was an 8.7% decrease from baseline to week 48 in the risedronate group, compared to a 12.1% decrease in the placebo group. Total hip BMD decreased by 7.7% at 48 weeks in the risedronate group, in contrast to an 11.2% decrease in the placebo group. For 1CTP, levels rose rapidly in the placebo group 8 weeks after transplantation and then declined. In the risedronate group, levels rose slowly until week 24 and then declined. Overall, 1CTP levels were more suppressed in the risedronate group throughout the study. Conclusion Administering risedronate at a dose of 35 mg weekly for 48 weeks following allogeneic hematopoietic stem cell transplantation did not entirely prevent post-transplant bone loss. However, it reduce bone loss without serious side effects when compared to the placebo group.

***Disclosures: Jeonghoon Ha**, None*

SUN-436

Trends in osteoporosis drug initiation and use among community dwelling older adults *Kaleen Hayes[1], Sulbh Aggarwal[2], Suzanne Cadarette[2]. [1]Brown University, . [2]University of Toronto, Canada

Background: Many different therapy options exist for the treatment and prevention of osteoporosis. Introduction of new therapeutic options, updates to practice guidelines, media coverage of adverse drug events, and healthcare policy changes have likely affected the use of osteoporosis medications over time.Objective: To estimate the number of older adults with use of osteoporosis drugs and describe trends over time in Ontario, Canada, 1996-2022.Methods: The Ontario Drug Benefit (ODB) program covers prescription drugs listed on the formulary for all residents aged 65 years or older. We leveraged pharmacy claims (ODB) data to identify all community-dwelling older adults (aged 66 or more years) with dispensed prescriptions for oral bisphosphonates (alendronate, etidronate, risedronate), intravenous bisphosphonate (zoledronic acid), denosumab, teriparatide, nasal calcitonin, or raloxifene (females only) between May 27, 1996 (date of earliest claim) and December 31, 2022. The number of patients with initial use (no prior exposure history) and any use of each medication was plotted by calendar year, and patient age was summarized using descriptive statistics.Results: In total, we identified 712,036 unique community-dwelling older adults with use of an eligible osteoporosis medication during the study period (mean age=75.6 [standard deviation=7.2] years). Risedronate was the most common osteoporosis medication used, with 460,647 unique users, followed by alendronate (n=310,482), etidronate (n=303,620), denosumab (n=193,104), and raloxifene (n=22,205). Teriparatide (n=233) and calcitonin (n=1,669) were the least commonly used osteoporosis medications, likely due to ODB formulary restrictions for these medications and calcitonin's removal from the Canadian market in 2013. Large shifts were observed in the total number of users of any osteoporosis medication annually, from n=28,403 in 1997 to a peak of n=240,640 in 2009, then to n=200,912 in 2022. Shifts were especially large for denosumab (from n=12,580 in 2012 to a peak of n=114,778 in 2022) and etidronate (from a peak of n=126,478 in 2002 to virtually no users beyond 2017).Conclusion: We observed major fluctuations in the number of users of osteoporosis medications over time that likely reflect changes in policy, public perception, and clinical practice. Consideration must be given to the absolute number of users of each medication as well as time-trends when designing pharmacoepidemiologic studies of drug safety and effectiveness in this population.

***Disclosures: Kaleen Hayes**, None*

SUN-438

Effect of combination therapy of eldecalcitol and risedronate on aromatase inhibitor induced bone loss in postmenopausal women with early-stage breast cancer: an open-label randomized trial *Yasuo Imanishi[1], Takumi Imai[2], Hisako Fujii[3], Rei Aida[2], Yuki Nagata[4], Tetsuo Shoji[4], Shinichiro Kashiwagi[5], Tsutomu Takashima[5], Masanori Emoto[1]. [1]Department of Metabolism, Endocrinology, and Molecular Medicine, Osaka Metropolitan University Graduate School of Medicine, Japan. [2]Department of Medical Statistics, Osaka Metropolitan University Graduate School of Medicine, Japan. [3]Department of Health and Medical Innovation, Osaka Metropolitan University Graduate School of Medicine, Japan. [4]Department of Vascular Medicine, Osaka Metropolitan University Graduate School of Medicine, Japan. [5]Department of Breast Surgical Oncology, Osaka Metropolitan University Graduate School of Medicine, Japan

As aromatase inhibitors (AIs) induces bone loss and increases fracture risk in women with hormone-positive, early-stage breast cancer (EBC), antiresorptive bone agents are

recommended to the patients with risk of fragility fractures. We aimed to compare the bone quantity and quality of the combination therapy of eldecalcitol and risedronate with risedronate alone in an open-label randomized control trial for 24 months. Postmenopausal women with hormone receptor-positive EBC (TNM stage 0-3A) treated with risedronate more than 12 months, and with T< -1.0 bone mineral density (BMD) at lumber spine (LS), femoral neck (FN), or total hip (TH), or fragility fractures on LS were randomly assigned to combination therapy or risedronate monotherapy. The primary outcome of this study is group difference in the change of LS BMD at 24 months, and BMD at FN and TH, and trabecular bone score (TBS) were also assessed for 24 months. A total of 200 patients were enrolled to the study between October 2012 to December 2019. Excluding the patients with no follow-up BMD data, 98 patients in each group were selected as a full analysis set. The increase in LS, FN and TH BMD at 24 months was larger in combination therapy group compared to monotherapy group, with a group difference (combination therapy minus monotherapy) estimate of 0.020 g/cm2 (95% confidence interval (CI) 0.010 to 0.029 g/cm2, p<0.001) for LS, 0.013 g/cm2 (95% CI 0.005 to 0.021 g/cm2, p=0.001) for FN, 0.017 g/cm2 (95% CI 0.008 to 0.025 g/cm2, p<0.001) for TH. However, no group difference was detected in the change in TBS at 24 months (estimate 0.008, 95% CI -0.006 to 0.021, p=0.266). Patients with osteopenic to osteoporotic status after risedronate treatment may be added on eldecalcitol in order to avoid bone loss induced by AIs.

***Disclosures: Yasuo Imanishi**, Chugai Pharmaceutical, Grant/Research Support*

SUN-439

Prognostic effect of Vitamin B12 and D levels on post hip fracture recovery *Angela G Juby[1], Christopher MJ Davis[2], Paula M Zubick[3], Mary Dunwald[3], Sebastian Lackey[4], Hoa Kong[4]. [1]University of Alberta, Faculty of Medicine and Dentistry, Canada. [2]University of Alberta, Faculty of Kinesiology, Canada. [3]University of Alberta Hospital Fracture Liaison Service, Canada. [4]Alberta Bone & Joint Health Institute, Canada

PurposeEpidemiological studies on the impact on bone of Vitamin B12 deficiency vary, but generally suggest that the lower the B12 level the higher the homocysteine level, and the higher the fracture risk. Yet other studies only showed an increased fracture risk with low plasma folate levels, but not plasma B12. Mouse studies also suggest low B12 may affect fracture healing. There are no reported studies evaluating the potential effects of B12 levels on post hip fracture recovery. This study was done to assess the prognostic effect of Vitamin B12 status on hip fracture outcomes. The hypothesis was that Vitamin B12 levels would be negatively associated with length of stay in post hip fracture patients.MethodsRetrospective analysis of hip fracture patients enrolled in a Fracture Liaison Service (FLS) in Alberta, Canada. Vitamin D and B12 levels measured on admission. Fracture outcomes were assessed by length of acute care stay (LOS-A), length of total hospitalisation (acute and rehabilitation) (LOS-T), and discharge location (compared to baseline). B12 and D levels were evaluated as both continuous and categorical variables (low <400pmol/L, sufficient >=400pmol/L; low < 80nmol/L, sufficient >=80nmol/L, respectively). Outcomes were corrected for patients' age and sex.ResultsData obtained from 456 patients seen between January 2017 and October 2019 (pre COVID-19). Age averaged 80.6 years (51-100), median 83yr, and included 354 females (77.6%). Low B12 was identified in 57.3% females, 57.8% males. Low D occurred in 55.9%. LOS assessments excluded those who died (10 patients, all in acute stage). Average LOS-A was 11.9 (2.2-119.3) days and LOS-T was 34.3 (2.6-445.9) days. LOS-A and LOS-T were significantly positively associated with age (p<.001) but not B12 or D categories. There was no interaction between age, gender, and B12 or D levels. LOS-A was weakly positively associated with absolute B12 levels (p=0.03) but not D levels (p=0.7). LOS-T showed no such association. LOS-T was correlated with LOS-A (p<.001).ConclusionsBoth absolute B12 and D levels, and categorical B12 and D status did not appear to be associated with acute or total hospital length of stay in this post hip fracture cohort. Longer length of stay was associated with increased age.

***Disclosures: Angela G Juby**, None*

SUN-440

Antiresorptive Therapy to Reduce Fracture Risk and Effects on Dental Implant Outcomes in Patients with Osteoporosis: A Systematic Review and Consensus Statement *Aliya A. Khan[1], Dalal S. Ali[1], Reza Mirza[2], Archibald Morrison[3], Salvatore Ruggiero[4], Gordon Guyatt[2], Sotirios Tetradis[5]. [1]Division of Endocrinology and Metabolism, McMaster University, Canada. [2]Department of Health Research Methods, Evidence, and Impact at McMaster University, Canada. [3]Citadel Oral and Maxillofacial Surgery, Canada. [4]NYCOMS, United States. [5]University of California, Los Angeles, United States

Background: Placement of a dental implant in a patient on antiresorptive therapy has been hypothesized to increase the risk of Medication-Related Osteonecrosis of the Jaw (MRONJ) and/or impact implant survival. In patients with osteoporosis, the risk of MRONJ with antiresorptive therapy is only marginally higher than observed in the general population1. Due to the invasive nature of implant placement and the increased risk of MRONJ seen in patients undergoing an oral procedure or event2, the International ONJ Taskforce further evaluated this issue.Methods: A systematic review of the literature was conducted and evaluated the outcomes of implant placement in individuals with osteoporosis or osteopenia receiving antiresorptive therapy. The risk of implant failure was evaluated in comparison to age matched individuals not on antiresorptive therapy.Results: Seven studies reported comparative risk estimates of dental implant failure with and without antiresorptive therapy for osteoporosis or osteopenia. A random-effects meta-analysis revealed a non-significant increased risk with antiresorptive agents with wide confidence intervals (RR 1.56, 0.43 - 5.70). The data were reviewed by the International Taskforce, and consensus was achieved on the graded recommendation3,4.Conclusion: In patients with osteoporosis on antiresorptive therapy, the Taskforce suggests that antiresorptive therapy does not need to be stopped prior to proceeding with dental implant (weak recommendation, very low-quality evidence). Current evidence does not suggest an association between antiresorptive therapy and implant failure. There is no evidence that cessation of bisphosphonate or denosumab therapy improves implant survival or reduces the development of MRONJ. Cessation of denosumab is not advised as it has been associated with rebound bone loss and an increased risk of multiple vertebral fractures. This presentation will provide the recommendations of the International Taskforce and also provide details regarding possible pathogenesis and differences in healing following dental extraction in comparison to implant placementReferences: 1.Khan, et al., Diagnosis and Management of ONJ: A Systematic Review and International Consensus. JBMR, 2015. 30(1): p. 3-23. 2.Watts, et al., Invasive Oral Procedures and Events in Postmenopausal Women With Osteoporosis Treated With Denosumab for Up to 10 Years. JCEM, 2019. 104(6): p. 2443-2452. 3.Mirza et al OI (submitted) 4. Tetradis et al OI (submitted)

***Disclosures: Aliya A. Khan**, Alexion, Amgen, Ascendis, Chugai, Radius, Takeda, Grant/Research Support*

SUN-441

Is it necessary to repeat BMD for patients receiving denosumab? Baseline results from a Quality Improvement initiative *Tayyab Khan[1], Mohammed AlAgha[2], Jenny Thain[2], Kristin Clemens[3]. [1]Department of Medicine, Western University, Canada. [2]Western University, Canada. [3]Division of Endocrinology and Metabolism, Western University, Canada

The utility of repeating Bone Mineral Densitometry (BMD) to monitor patients' response to anti-osteoporosis therapy has been questioned as a vanishingly small number of patients taking antiresorptive therapies (ie. bisphosphonates or denosumab) have convincing evidence of bone loss. This could be particularly the case for denosumab, which is the most potent among anti-resorptive therapies. In this quality improvement project, we aimed to reduce the proportion of patients who receive BMD testing every 2 years or less while on denosumab. As the first step in this process, we assessed the proportion of participants who had convincing evidence of bone loss defined as loss of BMD at the same site on repeat measurements, or loss of BMD at multiple sites on one measurement, and those who required a change in therapy. We then implemented our test of change (a policy to promote repeating BMD at >2year intervals in patients receiving denosumab) and measured outcome, process and balance measures. We included postmenopausal women being treated with denosumab at our institution who had at least two repeat BMD measurements following a baseline study. Prior to the implementation of our intervention, 20 consecutive patients with a mean age of 64.9 + 6.7 years had received denosumab for 7.1 + 3.4 years. Baseline BMD T scores were -2.6+1.2 at the lumbar spine (LS) and -2.4 + 0.5 at the femoral neck (FN). The average interval between baseline and first repeat, and between first and second repeat BMD was 23.0 + 11.7 months and 28.0 + 17.9 months, respectively. Only one of twenty patients (5%) experienced significant loss of LS BMD which stabilized on repeat measurement. No patient experienced a decrease in FN BMD from baseline to the first repeat BMD, while only one of 19 (5.2%) experienced loss in BMD at this site between first and second repeat measurement. No patient experienced loss of BMD at both sites between the baseline and final measurements. Four patients experienced fractures while on denosumab, but none of them were candidates for more potent therapies due to concerns regarding cost or contraindications. Our initiative suggests that among postmenopausal women treated with denosumab at the Osteoporosis and Bone Disease Program in London, Ontario, no patient demonstrated convincing loss of BMD at repeat measurements. We will investigate the utility and safety of reducing BMD testing in patients taking denosumab at our centre.

***Disclosures: Tayyab Khan**, Amgen, Speakers' Bureau*

SUN-443

Cardiovascular Risk and Fracture Risk Among Women Initiating Treatment with Romosozumab or Denosumab *Ye Liu[1], Tarun Arora[2], Jingyi Zhang[1], S. Bobo Tanner[3], Jeffrey Curtis[1]. [1]University of Alabama at Birmingham, United States. [2]Foundation for Advancing Science, Technology Education and Research, United States. [3]Vanderbilt University Medical Center, United States

Background: Romosozumab (romo) and denosumab (dmab) are recommended for postmenopausal women with osteoporosis (OP) at high risk of fracture. The U.S. prescribing information includes a boxed warning that romo should not be initiated in patients with prior myocardial infarction or stroke in the prior year. For all other patients without recent MI or stroke, the warning recommends to consider whether the benefits of romo outweigh its risks. This study evaluated CV and fracture risks among patients who initiated romo referent to dmab users.Methods: We used Medicare data from 1/1/2017 to 9/30/2021 to identify women age >=55 newly initiating romo or dmab after 4/1/2019. Claims data was linked to electronic medical record (EMR) data from multiple PCORNet Clinical Research Networks. Comorbidities and medical history were identified from claims while biometric data and lipid test results were obtained from the EMR. The ACC/AHA pooled cohort risk equation was used

to calculate the 10-year CV risk. The FRAX algorithm was used to calculate 10-year risk of hip and major fracture (clinical spine, forearm, hip, or shoulder). We set the 75 percentile of each risk score as the cut-off for high CV and fracture risk. A scatter plot with 95% prediction ellipse was used to illustrate the relationship between CV risk versus the risk of fractures (Figure 1) at a patient level and to compare the cohort of romo vs. dmab patients. Multivariable logistic regression was used to evaluate the relationship between high CV or fracture risk and medication initiation.Results: A total of 197,515 new users of romo (n=14,596) or dmab (n=182,919) were eligible for analysis and 1072 were linked to PCORNet data. Figure 1 showed romo users had lower CV risk but comparable or higher risk for hip or major fracture compared with dmab users. Romo was more likely to be prescribed to patients with higher fracture risk but lower CV risk, compared with dmab. The odds ratios (95% CI) for initiating romo vs. dmab for high CV risk, hip fracture risk, and major fracture risk were 0.46 (0.26, 0.80), 0.97 (0.47, 2.01), and 1.83 (0.89, 3.75), respectively.Conclusion: In this cohort of older women with claims data linked to EHR data, patients with high CV risk were less likely to be given romo compared with dmab. These data suggest that the boxed warning regarding CV risk for romo appropriately influences clinical decision making of physicians when prescribing anabolic medications for osteoporosis patients.

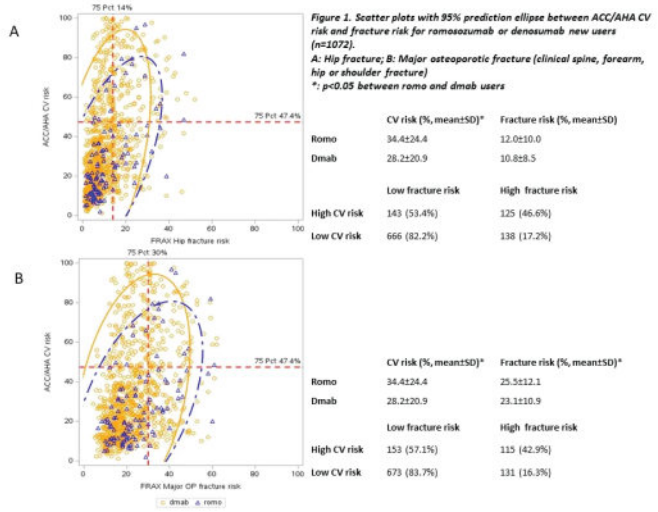

Figure 1. Scatter plots with 95% prediction ellipse between ACC/AHA CV risk and fracture risk for romosozumab or denosumab new users (n=1072).
A: Hip fracture; B: Major osteoporotic fracture (clinical spine, forearm, hip or shoulder fracture)
**: p<0.05 between romo and dmab users*

	CV risk (%, mean±SD)*	Fracture risk (%, mean±SD)
Romo	34.4±24.4	12.0±10.0
Dmab	28.2±20.9	10.8±8.5
	Low fracture risk	High fracture risk
High CV risk	143 (53.4%)	125 (46.6%)
Low CV risk	666 (82.2%)	138 (17.2%)

	CV risk (%, mean±SD)*	Fracture risk (%, mean±SD)*
Romo	34.4±24.4	25.5±12.1
Dmab	28.2±20.9	23.1±10.9
	Low fracture risk	High fracture risk
High CV risk	153 (57.1%)	115 (42.9%)
Low CV risk	673 (83.7%)	131 (16.3%)

***Disclosures: Ye Liu**, None*

SUN-444

Femur Geometrical Phenotypes in Atypical Femoral Fractures *Rashad Madi[2,] Julio Ojea Quintana[2,] Christiana Cottrel[2,] Rasleen Grewal[2,] Ani Ural[3,] Bruce J. Kneeland[2,] Gregory Chang[4,] Chamith S. Rajapakse[2,] [2]University of Pennsylvania, [,2]University of Pennsylvania, United States[,3]Villanova University, United States[,4]New York University, United States

Osteoporosis is a bone disorder characterized by the deterioration of bone microarchitecture, leading to fragility fractures in older individuals (1). Bisphosphonates are commonly employed as a first-line treatment for osteoporosis due to their ability to inhibit osteoclast function by binding to the bone's mineral matrix (2). Despite their effectiveness, long-term use has been associated with potential side effects, including atypical femoral fractures (AFF) (3). Our study investigates the demographic and radiological factors influencing AFF pathogenesis to improve prevention, diagnosis, and treatment strategies.Methods: We conducted a retrospective analysis of 65 patients who experienced AFFs after being treated with bisphosphonates for 3-15 years. The sample population consisted of 62 females and 3 males with an average age of 70.9 +/- 8.8 years. We utilized Sectra MSK (Version 24.2.6.5829, Linkoping, Sweden) to measure the following parameters on hip X-rays: 1) the distance from the lesser trochanter to the fracture, 2) medial and lateral cortical thicknesses, 3) femoral offset and 4) femoral neck angle (Figure 1).Results: The average distance from the lesser trochanter to the AFF was 59.1 mm (IQR: 32.3-96.9). The medial cortex width measured 7.3 mm (IQR: 6.5-8.4), while the lateral cortex width was 10.9 mm +/-2.5. Additionally, patients exhibited a femoral offset of 43.9 mm +/-7.1 and a femoral neck angle of 128.7° +/-4.8.Discussion: The etiology of AFFs is still not well understood. Several studies have identified potential geometrical features of the femur that may contribute to AFF formation in certain patients and at particular lateral subtrochanteric locations. Factors such as a decreased femoral shaft neck angle and increased femoral offset have been associated with heightened stress on the lateral subtrochanteric area, potentially explaining why fractures occur there (4). Recent advances in imaging analyses, such as CT and MRI finite element analyses, will facilitate further examination of the influence of geometrical, compositional, and biomechanical factors on AFFs. By integrating these findings with demographic and risk factor data, clinicians may be better equipped to predict which patients are at a high risk of developing AFFs before initiating bisphosphonate therapy. This information could help us consider alternative osteoporosis treatments or the implementation of more frequent bisphosphonate-free holidays for high-risk patients.

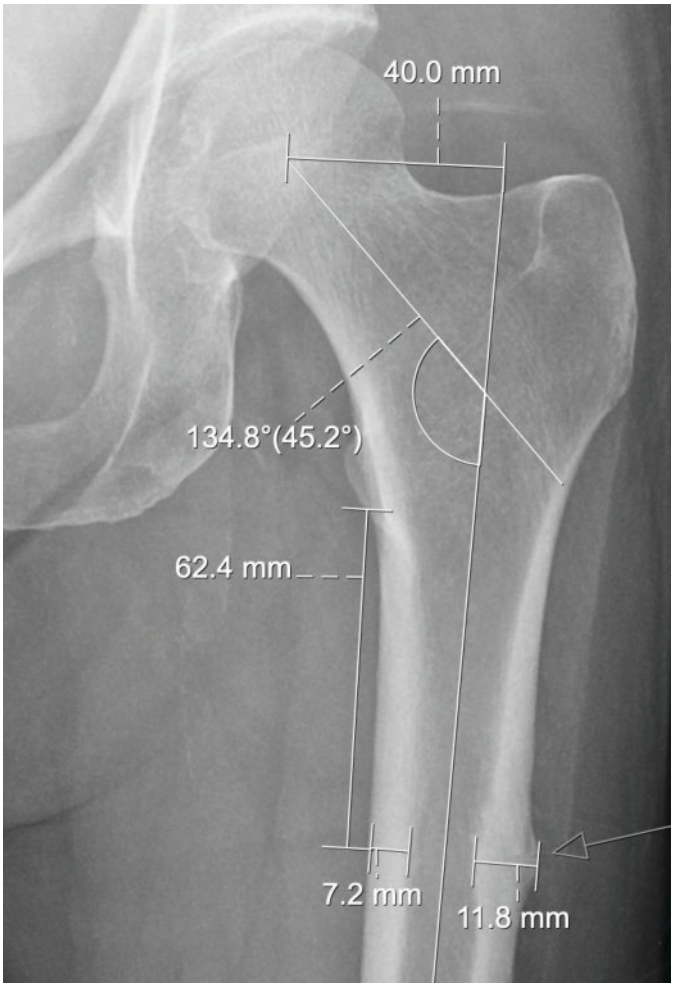

***Disclosures: Rashad Madi**, None*

SUN-445

Effectiveness of zoledronic acid treatment within 14 days of hip fracture surgery. *Betiana Perez[1,] Ariela Kitaigrodsky[1,] Natalia Aliquo Maciel[1,] Ullman Tamara[1,] Lucia Coli[1,] Rodrigo Greco[1,] Ivan Huespe[1,] Mirena Buttazzoni[1,] Maria Diehl[1,] [1]Hospital Italiano de Buenos Aires, Argentina

Treatment with zoledronic acid (ZA) within 90 days after surgical repair of a hip fracture reduces the occurrence of clinical fractures and mortality. However, there is limited available data regarding the effectiveness of using ZA within the first two weeks. As lockdown limited follow-up during Covid-19 pandemic, ZA began to be indicated during hospitalization with calcium and vitamin D supplementation in our institution. AimTo evaluate the effectiveness of administering ZA within 14 days after surgical resolution of a hip fracture.MethodsRetrospective cohort study of patients >=65 years from a closed health system hospitalized in a tertiary care hospital for a fragility hip fracture between 04/2018 and 04/2022, comparing patients who received ZA within 14 days after surgery (Early-ZA) with those treated between days 15 and 90 after surgery (Later-ZA). The main outcome was the combined event of death or refracture. Analysis was made with chi2 or Fisher for qualitative variables and Wilcoxon for quantitative variables. We performed Kaplan-Meier survival analysis and Cox regressions. We adjusted the regression analysis considering age, Charlson Index and length of the initial hospital stay as potential confounders.ResultsOut of 848 patients, 220 received ZA within 90 days: 163 (74%) within 14 days following hip fracture surgery (Early-ZA) and 57 (26%) between days 15 and 90 (Later-ZA). Median age Early-ZA 88 (IQR 81-92) and Later-ZA 85 (IQR 80-88) p=0.054; 14% male without differences between groups (15.3% vs 10.5%, p=0.36). Median Charlson Comorbidity Index was significantly higher in patients receiving Early-ZA (median 5 IQR 4-5; vs Later-ZA 0 IQR 0-1; p<0.0001). Median hospitalization for hip fracture was 7 days (IQR 5-9) for both groups (p=0.76). During a median follow-up of 502 days, 38 patients died (17.3%); 27 had new fractures (12.3%). Regarding the combined outcome (death or refracture) we did not observe significant differences (Figure), with a crude HR of 1.314 (95%CI 0.74-2.35), and an adjusted HR of 1.011 (95%CI 0.46-2.22). ConclusionsZA administration during in-hospital stay enhances access to secondary fracture prevention. We did not observe differences in the combined outcome of refracture or

mortality between Early-ZA and Later-ZA after hip fracture in this preliminary study. After adjusting for confounding variables, HR changed substantially, suggesting a higher burden of comorbidities in patients treated in the first two weeks.

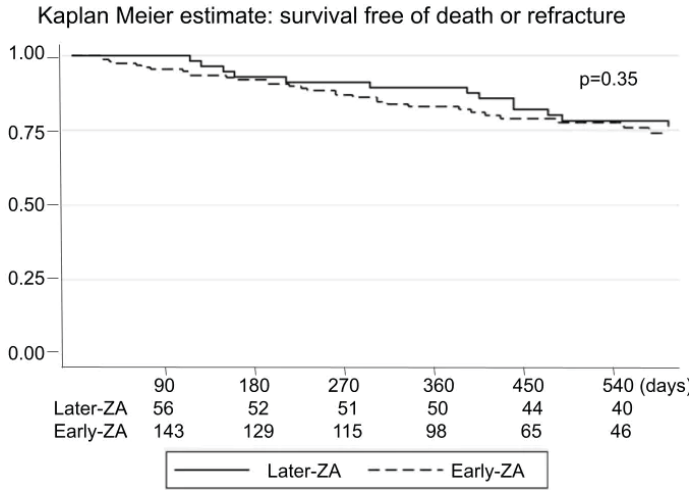

***Disclosures: Betiana Perez**, None*

SUN-446

Baseline FRAX Score and Effectiveness of Romosozumab in Patients with Osteoporosis at a High Risk of Fracture in Japan: A Multicenter Retrospective Study *Akimitsu Miyauchi[1,] Etsuro Hamaya[2,] Junichiro Shimauchi[2,] Cae Tolman[3.] [1]Miyauchi Medical Center, Japan. [2]Amgen K.K., Japan. [3]Amgen Asia, China

Background: FRAX® has been incorporated into the initiation criteria for pharmacological treatment in the Japanese guidelines for prevention and treatment of osteoporosis (OP) (Orimo H, 2012). Efficacy of romosozumab on clinical, osteoporotic and major osteoporotic fractures was significantly greater in patients at high baseline FRAX probability compared with placebo in the FRAME study (McCloskey EV, 2021). Previously, we conducted a chart review of patients with OP at a high risk of fracture who received romosozumab for 12 months and then transitioned to another OP therapy for >=6 months to better understand the therapeutic profile of romosozumab in a real-world setting in Japan (Miyauchi A, 2021). In this analysis of the real-world study, we aim to explore the relationship between baseline fracture probability as measured by FRAX and the effectiveness of romosozumab based on absolute and percentage change in bone mineral density (BMD) from baseline. Methods: In this observational, multicenter, retrospective medical chart review, data were collected from 19 sites across Japan during the baseline period (12 months before romosozumab initiation [ie, index date]), the romosozumab treatment period (12 months), and a follow-up of >=18 months after the index date. Baseline FRAX scores were calculated with actual femoral neck BMD (g/cm2) or T-score. This analysis will include data collected from treatment-naïve patients during the baseline and the 12-month romosozumab treatment period.Results: Of the 462 treatment-naïve patients included in the chart review, baseline FRAX score was available for 217 patients (mean [SD]: 27.0 [10.68]) and baseline lumbar spine T-score was available for 346 patients (mean [SD]: -2.58 [1.31]). Final results will be reported on the day of presentation.Conclusion: Results of this study may provide insights into the clinical management of Japanese patients at higher baseline fracture risk receiving romosozumab treatment.

***Disclosures: Akimitsu Miyauchi**, None*

SUN-447

Parathyroid hormone levels following denosumab therapy vs. zoledronic acid therapy for osteoporosis *Pnina ROTMAN PIKIELNY[1.] [1]MEIR MEDICAL CENTER, ENDOCRINE INSTITUTE, Israel

Background:Denosumab (DMAb) and zoledronic acid (ZA) are potent, anti-resorptive agents used to treat patients with osteoporosis. It has been suggested that they increase parathyroid hormone (PTH) levels in response to their antiresorptive effect, and that PTH elevation might be responsible for DMAb modeling actions on bone. The timeline and magnitude of PTH elevation post-DMAb and ZA has not been characterized in a large patient population.Objective:To characterize PTH levels post-DMAb injection vs. baseline and vs. ZA infusion.Material and Methods:Female osteoporotic patients, >=50 years, treated with DMAb or ZA, 2008-2020 were included if PTH was 2mg/dl, vitamin D <50nmol/l or hyperparathyroidism. Post-injection PTH levels were linked time-wise to previous injections. Results: A total of 35,375 women, >=50 years received DMAb or ZA for the first time in 2008-2020; 26,341 met the exclusion criteria. Of the remaining women, 5,640 received a first DMAb injection and 3,394 ZA. The DMAb group was older (73.2 vs. 69.8 years), was treated more frequently with osteoporosis medications before the injection (56.5% vs. 50.3%) and more had sustained a fracture (15.8% vs. 13.9%) compared to the ZA group. Vitamin D level was 80.9+/-21.9 nmol/l. Repeat PTH was available for 2,206 DMAb patients and 1,444 ZA. Among 772 PTH measurements in the first month post-DMAb, it was >1.5ULN in 156 (20.1%) and >2.5ULN in 74 (5.1%), whereas among 807 PTH measurements 5-months post-injection, it was >1.5ULN in 112 (13.9%) and >2.5ULN in 9 (1.1%). One-month post-ZA, PTH was >1.5ULN in 35/169 (20.7%) and >2.5ULN in 11 (6.5%), and decreased to >1.5ULN in 23/213 (10.7%) and to >2.5ULN in 2/213 (0.9%), 5 months after injection.DiscussionThis is the first study to examine PTH levels in a large population receiving DMAb or ZA injections, with precisely-timed PTH measurements post-injection. PTH levels increased by >1.5ULN in 20% of osteoporotic patients who received DMAb or ZA, while it increased to >2.5ULN in ~5% post-injection. PTH levels declined gradually after treatment in both groups. It seems that PTH elevation is related to the antiresorptive effects of the drugs and is not a disease phenomenon. It is suggested to avoid checking PTH in the first few months post-DMAb and ZA therapy.

***Disclosures: Pnina ROTMAN PIKIELNY**, None*

SUN-448

A Single Dose of Zoledronic Acid after Stopping Denosumab in Early Hormone-receptor-positive Breast Cancer Patients: a Randomized Controlled Trial *Georg Pfeiler[1,] Christian F. Singer[1,] Dominik Hlauschek[2,] Diether Manfreda[3,] Ferdinand Haslbauer[4,] Paul Sevelda[5,] Kristin Koeck[6,] Karl Tamussino[7,] Arno C. Reichenauer[8,] Florian Fitzal[9,] Dietmar Heck[10,] Richard Greil[11,] Anita Jallitsch-Halper[2,] Christian Fesl[2,] Michael Gnant[12.] [1]Department of Gynecology and Gynecological Oncology and Comprehensive Cancer Center, Medical University of Vienna, Vienna, Austria, Austria. [2]ABCSG, Austrian Breast and Colorectal Cancer Study Group, Vienna, Austria, Austria. [3]Doctor's office Manfreda, Klagenfurt, Austria, Austria. [4]Department of Internal Medicine, Salzkammergutklinikum Hospital Vöcklabruck, Vöcklabruck, Austria, Austria. [5]Department of Gynecology, Karl Landsteiner Institute for Gynecologic Oncology and Senology, Hospital Hietzing, Vienna, Austria, Austria. [6]Department of Gynecology and Obstetrics, Hospital Klagenfurt, Klagenfurt, Austria, Austria. [7]Department of Gynecology and Obstetrics, Medical University of Graz, Graz, Austria, Austria. [8]Department of Surgery, Hospital BHB St. Veit, St. Veit/Glan, Austria, Austria. [9]Department of General Surgery and Breast Health Center of the Comprehensive Cancer Center, Medical University of Vienna, Austria, Austria. [10]Department of Hematology and Oncology, Ordensklinikum Linz - Barmherzige Schwestern, Linz, Austria, Austria. [11]Department of Internal Medicine III with Haematology, Medical Oncology, Haemostaseology, Infectiology and Rheumatology, Oncologic Center, Paracelsus Medical University Salzburg, Salzburg, Austria, Austria. [12]Medical University of Vienna, Comprehensive Cancer Center, Vienna, Austria; ABCSG, Austrian Breast and Colorectal Cancer Study Group, Vienna, Austria, Austria

Background: The placebo controlled randomized phase III ABCSG-18 trial demonstrated that denosumab significantly reduced clinical fractures in postmenopausal patients with breast cancer. Concern exists about a potential rebound effect after treatment discontinuation with denosumab. In line with this, an earlier analysis of ABCSG-18 showed an increased risk for vertebral and multiple vertebral fractures after stopping denosumab. We have therefore conducted a randomized sub-study investigating the use of a single dose of zoledronic acid (ZA) at the end of denosumab therapy. Here we present the first data on bone turnover markers (BTM).Patients And Methods: Patients of the ABCSG-18 trial who had completed denosumab treatment were randomized to a single dose of ZA 5mg i.v. versus nil(=SOC). ZA was administered 8 months+/-4 weeks after the last dose of denosumab (day 1 of this sub-study). DXA scans, lateral spine X-rays and BTM (CTX and osteocalcin) were assessed at baseline and at 6, 12 and 18 months thereafter. New fractures were assessed throughout. The percent change from baseline was derived and compared between arms with stratified Wilcoxon rank sum tests.Results: 50 patients with a median age of 71 years were randomized into this prospective sub-study. 24 received ZA, and 26 did not. Patient groups were well balanced with respect to baseline bone health factors. All patients of the ZA arm and 25 of the SOC arm received 7 doses of denosumab in the ABCSG-18 trial. At baseline, mean CTX was 0.57 ng/ml in both arms, mean osteocalcin was 19.5 ng/ml in the ZA arm and 18.8.ng/ml in the SoC arm. Percentage change of CTX differed significantly between the two arms with a median decrease of CTX after 6 months (-50.0%) and 12 months (-49.5%) in the ZA arm, and a median decrease after 6 months (-7.0%) and after 12 months (-6.5%) in the SOC arm. Accordingly, osteocalcin decreased by a median 17.0% after 6 months and 13.9% after 12months in the ZA arm, but increased by 110.8% after 6 months and by 29.4% after 12 months in the SOC arm. No significant difference of the BTM could be seen after 18 months. Importantly, the observed increase of BTM in the SOC arm was driven by a few patients with major changes - up to 778.6% for CTX and up to 679.6% for osteocalcin.Conclusion: These first data of the randomized sub-study of the ABCSG-18 trial demonstrate that a single

dose of ZA prevents a high bone turnover state that occurs in some patients of the SOC arm after stopping denosumab.

***Disclosures: Georg Pfeiler**, Pfizer, Roche, AstraZeneca, Seagen, MSD, Gilead, Accord Healthcare, Daiichi, Novartis, Lilly, Speakers' Bureau, Pfizer, Roche, Seagen, Novartis, AstraZeneca, Daiichi, MSD, Lilly, Gilead, Consultant, Pfizer, Accord Healthcare, Roche, AstraZeneca, MSD, Grant/Research Support*

SUN-449

Introduction of a Standardized Hip Fracture Order Set Improves Osteoporosis Medication Initiation and Persistence: A Population-Based Before-After Analysis *Gabriel Larose[1], Saeed Al-Azazi[1], Lisa Lix[1], Eric Bohm[1], William Leslie[1]. [1]University of Manitoba, Canada

Background: Osteoporosis-related fractures pose a great burden for society, with a high risk of subsequent fractures after a first fragility fracture. Introducing standardized care can improve the rate of initiation of osteoporosis treatment. This project evaluated osteoporosis medication initiation, persistence and fracture prevention after hip fracture.Methods: Within the Canadian health system, our region introduced a hip fracture order set (OS) that included recommendations for the initiation of osteoporosis medication for secondary prevention beginning in one of the hospitals in 2015 (Group 1). A control group (Group 2) had delayed introduction of the same OS in other hospitals (after 2017). A retrospective cohort study was conducted using linked administrative health data. All women and men 50+ years with surgical treatment for a low-energy hip fracture between 2010 and 2019 were included. Individuals were followed until 2021 for evaluation of osteoporosis medication initiation, medication persistence at 1 year and secondary fractures. Group comparisons used chi-square tests. Logistic regression models tested the impact of patient factors on initiation and persistence of osteoporosis medication.Results: Group 1 (early OS) included 813 patients and Group 2 (delayed OS) included 2150 patients. No significant differences in demographics, socioeconomic status or comorbidities were observed. A significant increase in osteoporosis medication initiation by 30 days post-fracture was seen with OS introduction (Figure 1). Group 1 treatment initiation was 9.7% in the year before and 47.8% in the year after OS introduction (P<0.001). This increase was sustained in later years and contrasted with Group 2 where no comparable change was seen. Similar improvements were seen in medication initiation by 90 days, 180 days and 365 days post-fracture. Persistence on osteoporosis medication at 1 year was also increased (Group 1 year before OS: 16.8%; year after OS: 35.0%, p<0.001). Logistic regression showed a significant impact of sex, diagnosis of osteoporosis, and OS utilization on medication initiation and persistence at 1 year. No difference in secondary fragility fractures was observed (Group 1: 19.8%; Group 2: 18.8% p=0.38).Conclusion: Introduction of the hip fracture OS significantly increased osteoporosis medication initiation and persistence at one-year post-fracture. However, there were no significant differences in secondary fractures.

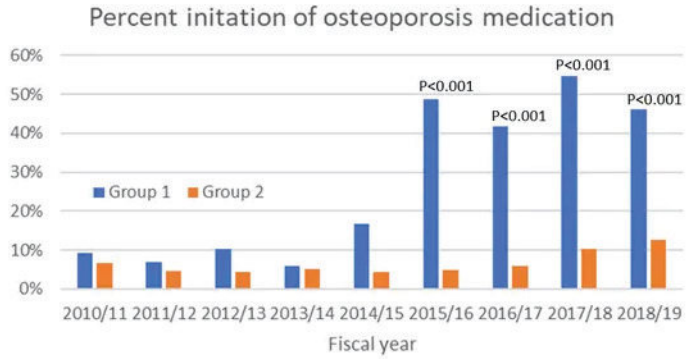

***Disclosures: Gabriel Larose**, None*

SUN-450

Evaluation and treatment of Osteoporosis after hospitalization with hip fractures: how effective are we *Catherine Anastasopoulou[1], Sri Ram Teja Sathi[2], Corina Nava Suarez[2], Sana Ahsun[2], Abhiram Javvaji[2], Michael Ngu[3]. [1]Sidney Kimmel Medical College at Jefferson University, United States. [2]Einstein Endocrinology, United States. [3]Einstein Medical Center, United States

Background: Hip fractures substantially increase the risk of major morbidity and death in older patients. Osteoporosis is a major risk factor for hip fracture. Patients with hip fractures have an increased risk for recurrent fractures following the first one [1] and low bone mineral density appears to be an additional and independent indicator for future fracture risk [2]. It is, therefore, important to assess bone mineral density to evaluate and properly treat osteoporosis after a hip fracture to decrease the risk for recurrent fractures [3,4].Purpose: The purpose of our study was to identify how effective we are in evaluating and treating osteoporosis in patients who have sustained a hip fracture.Methods: A total of 260 patients with a fragility hip fracture (low-trauma) occurring between 2015 and 2019 were identified from medical records at a large tertiary care hospital in USA. Data was collected about demographics, recurrent fractures, DXA scans, 25 hydroxy vitamin D levels, and type of treatment offered.Results: Out of 260 patients, 172 (66.1%) were female and 88 (33.9%) were male with a median age 79 [35-105]. Demographics showed 121 of total 260 (50.3%) were African American, 95 (36.5%) Caucasian, 14 (5.3%) Asian, and 21 (8.0%) other. 19 of the total 260 (7.3%) had a DXA scan done, and 20 (7.6%) received osteoporosis treatment after hip fracture. Of the 20 patients treated, 16 received bisphosphonate (one patient got IV medication and 15 oral therapy), 2 denosumab, 1 estrogen, and 1 teriparatide. 20 patients (7.6%) had a subsequent fracture. 25 hydroxy vitamin D level was checked in 101 (38.8%), vitamin D was supplemented in 91 (35%) and calcium supplements were initiated in 40 (15.3%) patients.Conclusion: In the post-operative follow up for fragility hip fracture, osteoporosis is still underrecognized and undertreated. In our study, fragility hip fractures, which already indicate significant osteoporosis complication, did not prompt physicians into further action. This calls for initiatives to increase awareness for better recognition and treatment of osteoporosis and further studies could help identify barriers to promote interventions.

***Disclosures: Catherine Anastasopoulou**, None*

SUN-451

The efficacy of sequential therapy with romosozumab followed by denosumab compared to denosumab alone in hemodialysis patients *Yuichiro Tamagawa[1], Hitoshi Tanigawa[2]. [1]Japan Community Health care Organization Shiga hospital, Japan. [2]Center for Regenerative Medicine and Skeletal Development, Uconn Health, United States

Hemodialysis patients have a high rate of osteoporosis and are a high-risk group for fractures. However, some osteoporosis drugs are contraindicated to severe renal failure patients, and treatment strategies for patients with severe osteoporosis aren't well established. Romosozumab is a monoclonal anti-sclerostin antibody that has the dual effect of increasing bone formation and suppressing bone resorption, reducing the risk of fracture within 12 months. This study aimed to compare the effects of one year of romosozumab followed by one year of denosumab (group R) to two years of denosumab (group D) on bone mineral density (BMD) and bone metabolism markers in hemodialysis patients with severe osteoporosis. This study was a single-center, retrospective study. 19 patients were in group R and 23 in group D, they are all hemodialysis patients. All patients were given these treatments as their first treatment for osteoporosis. Both groups showed significant increase in BMD(T-score) at the lumbar spine and femoral neck after 6 months treatment (group D: +0.32; group R: +0.70), with group R showing a significant increase compared to group D in BMD at the lumbar spine (p=0.0024). The bone metabolism marker P1NP increased significantly in group R at 6 months (+57.4%, p=0.002 vs baseline), and decreased significantly at 12 months (-17.4%, p=0.001 vs baseline). Adverse events were few and none were fatal, including cardiovascular events. P1NP level of group D showed a consistent decrease from baseline. The bone resorption marker TRACP-5b also showed a significant decrease compared to baseline after 6 months in both groups (group D: -42.9%; group R: -17.4%), with group D showing a consistently greater decrease in all the periods. No obvious fractures were not observed. These results suggest that romosozumab treatment followed by denosumab may be a potentially good strategy for hemodialysis patients with severe osteoporosis.

***Disclosures: Yuichiro Tamagawa**, None*

SUN-452

Cost-Effectiveness of Four Treatment Approaches for Osteoporotic US Women and Men With a Recent Hip Fracture *Mickael Hiligsmann[1], Yamei Wang[2], LENY PEARMAN[4], John Caminis[4], Stuart Silverman[5], Andrea Singer[6], Jean-Yves Reginster[7]. [1]Maastricht University, Netherlands. [2]Radius Health, Inc., United States. [4]Radius Health, . [4]Radius Health, United States. [5]Cedars-Sinai/UCLA, United States. [6]MedStar Georgetown University Hospital, United States. [7]University of Liège, Belgium

Hip fracture is the most severe osteoporotic-related event, with dramatic consequences to the patients' quality and quantity of life. Furthermore, hip fractures substantially increase the risk of a subsequent fracture, especially in the near term. Common treatment approaches for these patients at very high fracture risk include sequential treatment with an anabolic agent (either abaloparatide [ABL] or unbranded teriparatide [TPTD]) followed by an antiresorptive agent (eg, alendronate [ALN]), or monotherapy with ALN. Many patients at very high fracture risk do not receive osteoporosis medication; unfortunately, "no treatment" must therefore be included as a comparator. Few economic evaluations have assessed the cost-effectiveness of these four treatment approaches, and in particular in patients with a recent hip fracture. Using a microsimulation-based Markov model previously validated, lifetime healthcare costs (in 2022 dollars) and quality-adjusted life years (QALYs) were estimated for the four treatment approaches: sequential ABL/ALN, sequential unbranded TPTD/ALN, ALN monotherapy, and no treatment. Analyses were conducted in US women and men aged 50-90 years who had a recent hip fracture and bone mineral density T-score <=?2.5. In both sexes and over the full age range, no treatment was dominated (ie, it incurred higher costs for lower QALYs) by ALN monotherapy, and sequential unbranded TPTD/ALN was dominated by sequential ABL/ALN. Between the two remaining approaches, sequential ABL/ALN was cost-effective compared to ALN monotherapy in men aged >=50 years and in women aged >=55 years at the US threshold for cost-effectiveness, estimated at $150,000

per QALY gained. Results were robust over various sensitivity analyses. By example, probabilistic sensitivity analyses revealed that sequential ABL/ALN was cost-effective in at least 90% of the simulations in both US men and women aged 70 years. In conclusion, this study suggests that sequential ABL/ALN is the most cost-effective intervention among the four treatment approaches in both US men (aged >=50 years) and women (aged >=55 years) with osteoporosis and a recent hip fracture. Treating patients with recent hip fractures by sequential ABL/ALN could lead to cost-effective use of healthcare resources.

***Disclosures: Mickael Hiligsmann**, ViiV, Grant/Research Support, Amgen, Grant/Research Support, Mylan Pharmaceuticals, Other Financial or Material Support, UCB, Consultant, Radius Health, Inc., Grant/Research Support*

SUN-453

Pharmacokinetic Equivalence of CT-P41 to Reference Prolia: A Randomized Phase I Study in Healthy Male Subjects *Anhye Kim[1], Janghee Hong[2], Wonsuk Shin[1], Hyounggyoon Yoo[1], Jin-Gyu Jung[2], Jean-Yves Reginster[3], Sunghyun Kim[4], Yunju Bae[4], Jeehye Suh[4], Sera Kim[4], Eunkyung Lee[4], Stuart Silverman[5]. [1]Department of Clinical Pharmacology and Therapeutics, CHA Bundang Medical Center, CHA University School of Medicine, Republic of Korea. [2]Chungnam National University, Republic of Korea. [3]Division of Public Health, Epidemiology and Health Economics, University of Liège, Belgium. [4]Celltrion, Inc., Republic of Korea. [5]Cedars-Sinai/UCLA, United States

Purpose: CT-P41 is a human monoclonal antibody developed as a biosimilar to the reference product, Prolia. This study aimed to demonstrate pharmacokinetic (PK) equivalence of the proposed biosimilar, CT-P41 to US-licensed Prolia in healthy male subjects.Methods: In this double-blind, parallel-group, phase I trial, healthy male subjects were randomized (1:1) to receive a single 60 mg subcutaneous injection of CT-P41 or US-licensed Prolia and followed up until Day 253. The primary endpoints for PK equivalence were area under the concentration-time curve from time zero to infinity (AUC0-inf), AUC from time zero to the last quantifiable concentration (AUC0-last) and maximum serum concentration (Cmax). PK equivalence was concluded if 90% CIs for geometric least-square means (GLSMs) ratios were within the equivalence margin of 80-125%, using ANCOVA. Additional PK, pharmacodynamics (PD) measured with bone turnover marker (serum type 1 C-telopeptides [s-CTX]), safety, and immunogenicity were evaluated as secondary objectives.Results: Of the 154 randomized subjects aged from 28 to 55, 151 subjects (CT-P41:74; US-licensed Prolia: 77) received the study drug. The 90% CIs of GLSMs ratios for all primary endpoints were within the prespecified equivalence margin (AUC0-inf: 100.39-114.65; AUC0-last: 99.92-114.28; Cmax: 95.20-107.34). Secondary PK parameters and mean serum concentrations were comparable between the treatment groups. As serum concentrations of CT-P41 and US-licensed Prolia increased, serum level of s-CTX was decreased by 87% from baseline (Figure 1). Median % change from baseline of s-CTX was comparable between the treatment groups and trended toward back to baseline.Overall, 55 (74.3%) and 59 (76.6%) subjects reported >=1 treatment-emergent adverse event (TEAE) in the CT-P41 and US-licensed Prolia treatment groups, respectively. The most frequently reported TEAE was blood calcium decreased (CT-P41: 37.8%; US-licensed Prolia: 45.5%), and all were Grade 1 or 2 in intensity. No treatment-emergent serious adverse event was reported. The immunogenicity profiles were comparable between the treatment groups.Conclusions: In conclusion, PK equivalence for single-dose administration of CT-P41 and US-licensed Prolia was demonstrated in healthy male subjects. Mean serum concentrations, secondary PK parameters, PD, and safety profiles, including immunogenicity, were comparable between the treatment groups and no new safety signals with CT-P41 were identified.

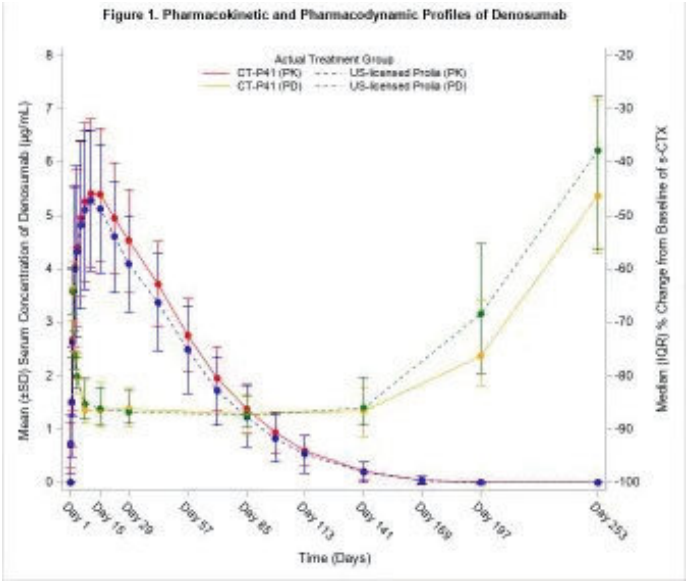

***Disclosures: Anhye Kim**, Celltrion, Inc., Grant/Research Support*

SUN-454

Allograft vs Cement Void Filler and Postoperative Metabolic Drug Therapy: Impact on Pain, Function, and Height Restoration in the 1-Year Period After Kyphoplasty for Vertebral Compression Fractures *Moshe Schneiderman[1], Jeri Nieves[2], Edward Yoon[3], Joseph Lane[3]. [1]Hospital for Special Surgery; SUNY Downstate College of Medicine, United States. [2]Columbia University and Hospital for Special Surgery, . [3]Hospital for Special Surgery, United States

PURPOSE: Osteoporotic VFs are a serious public-health issue. Both the actual treatment of the fracture and the metabolic drug therapy may influence patient outcomes. Although cement kyphoplasty is a valuable tool in the treatment of VFs, the use of cement comes with risks, including potential embolization to the lungs or heart. To lessen these risks, we switched to performing kyphoplasty using structural allograft beads of bone, which are too large to enter the venous system. We tested the allograph vs cement for functional efficacy and analyzed the impact of metabolic drug therapy on pain, function, and height restoration in the year following kyphoplasty.METHOD: We performed a retrospective study of patients who underwent kyphoplasty between January 2018 and April 2023 for osteoporotic VFs and were treated by the same surgeon at the same institution in a large urban area. Patients with at least one MRI/CT or PROMIS-29 completed within the 1-year postoperative period were included. A total of 100 patients met these criteria. Vertebral height restoration was measured by comparing pre- and post-operative MRI/CT. Postoperative PROMIS-29 NRS Pain and Physical Function scores were recorded. A linear mixed-effects model for repeated measures was used to analyze the data. Independent variables included allograft vs cement and duration of postoperative osteoporosis drug therapy. Gender, smoking status, weekly alcohol consumption, and time since surgery were included as covariates.RESULTS: Allograft was associated with less postoperative pain (p=.03) and greater physical function (p=.009) than cement kyphoplasty during the 1-yr postoperative period. For anterior height, there was a dose-response relationship between postoperative time on teriparatide (p=.02), or on denosumab (p=.03), and increased height retention over the 1-yr period. For medial height, allograft was associated with significantly greater height retention than cement (p<.001) over the 1-yr period. Abaloparatide also showed a dose-dependent effect on height retention: Longer time on the drug was associated with greater medial (p=.03) and posterior (p=.001) height retention.CONCLUSIONS: Allograft kyphoplasty is associated with significantly less pain, greater physical function, and greater medial height restoration. There was no difference in anterior or posterior height restoration between allograft and cement. Metabolic drug therapy after kyphoplasty improves retention of vertebral height.

***Disclosures: Moshe Schneiderman**, None*

SUN-456

Effect of geographic region on zoledronic acid-related fracture risk reduction in postmenopausal osteoporosis *Austin Thompson[1], Elaine Yu[2], Annette Adams[3], Mary Bouxsein[4], Richard Eastell[5], Dennis Black[6]. [1]University of California, San Francisco, , [2]Massachusetts General Hospital, United States, [3]Kaiser Permanente Southern California, United States, [4]Beth Israel Deaconess Medical Center, Harvard Medical School, United States, [5]University of Sheffield, United Kingdom, [6]UC San Francisco,

Geographic differences in osteoporosis prevalence exist. Bisphosphonates (BP) are commonly used to treat osteoporosis, yet some evidence suggests the bioavailability or effectiveness of BPs may vary by geographic regions. Additionally, important differences in BP treatment and incidence of hip and atypical femoral fractures by race have been documented. We sought to evaluate whether the fracture reduction effects of zoledronic acid (ZOL) is greater in Asian regions compared to non-Asian regions.This secondary analysis of the Health Outcomes and Reduced Incidence with Zoledronic Acid Once Yearly (HORIZON) Pivotal Fracture Trial included postmenopausal women with osteoporosis and/or vertebral fractures who were randomly allocated to receive ZOL or placebo. Radiographs were used to assess morphometric vertebral fractures at baseline and at 12, 24, and 36 months, and clinical fractures were ascertained and adjudicated at each interview and clinic visit. Each participating clinical site was categorized as an Asian or non-Asian regional site. Estimated associations between ZOL treatment and fracture outcomes (morphometric vertebral, hip, non-vertebral, any clinical, and clinical vertebral fractures) were quantified as risk ratios (RR) or hazard ratios (HR) with 95% confidence intervals (CI) using a log-binomial regression and proportional hazard models, respectively. Effect modification by geographic region was evaluated using an interaction term for treatment and geographic region in each model. Among 7,765 post-menopausal women (1,090 from Asian regions), baseline characteristics were similar between treatment and placebo groups; although, women from Asian regions were more likely to be younger, have lower BMI, have lower BMD, and have baseline vertebral fracture. Those treated with ZOL were less likely to have morphometric vertebral fractures compared to women on placebo (RR 0.32, CI 0.26-0.39). This association differed by geographic region (RR 0.20, CI 0.11-0.34 in Asian regions; RR 0.35, CI 0.29-0.44 in non-Asian regions, p = 0.048) (Figure). In general, the other fracture outcomes followed a similar trend, although not statistically significant.These results suggest morphometric vertebral fracture risk reduction with ZOL treatment may vary by geographic region (Asian vs. non-Asian), though substantial risk reductions existed in each region. Future research should substantiate these findings with bone markers.

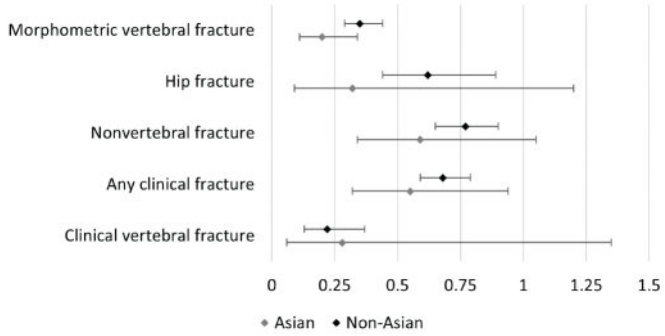

***Disclosures: Austin Thompson**, None*

SUN-457

Comparative Microarchitecture Changes of Alendronate or Raloxifene after Denosumab (CARD HR-pQCT) *Joy Tsai[1], Mackenzie Jordan[2], Savannah Ryan[2], Benjamin Leder[3]. [1]MASSACHUSETTS GENERAL HOSPITAL, United States, [2]Massachusetts General Hospital, United States, [3]Massachusetts General Hospital Harvard Medical School, United States

Background: When denosumab is discontinued, antiresorptive therapy is necessary to mitigate high bone turnover bone density losses. In the CARD study, we demonstrated that after 12-month of denosumab, 12-months of alendronate was better able to maintain bone mineral density gains versus 12-months of raloxifene (manuscript in press). In this exploratory analysis, we wished to evaluate the comparative changes in peripheral compartmental volumetric bone mineral density and microarchitecture among those receiving alendronate and raloxifene.Methods: Postmenopausal women (60-81yo) at high fracture risk received denosumab 60-mg SC every 6 months for 12-months followed by 12-months of alendronate 70 mg weekly (N=26) or raloxifene 60 mg daily (N=22). Total, trabecular, and cortical density (Tot.vBMD, Tb.vBMD, Ct.vBMD) and cortical porosity (Ct.Po) were measured by high-resolution peripheral quantitative CT (HR-pQCT) of the distal tibia and radius.Results: As shown in the figure below, after 12-months of denosumab treatment, Tot. vBMD and Ct.vBMD at the tibia increased significantly. These increases were maintained during months 12-24 in both those randomized to alendronate or to raloxifene, with no significant between-group differences. Tb.vBMD at the tibia did not significantly change after 12-months of denosumab but then trended toward an increase between months 12-24 in both the alendronate and raloxifene groups with no significant between group differences. At the radius, similar changes in Tot.vBMD, Ct.vBMD, Tb.vBMD were observed. Ct.Po remained stable over the entire study period at the radius and tibia in both treatment groups.Conclusions: 12-months of denosumab modestly improved compartmental bone density without significantly changing cortical porosity at both the distal tibia and distal radius. These vBMD changes were maintained by both 12-months of alendronate or raloxifene. In conjunction with the previously presented aBMD by DXA results, these results support the consideration of raloxifene after short term denosumab as alternate therapy for those who cannot or do not wish to take bisphosphonates.

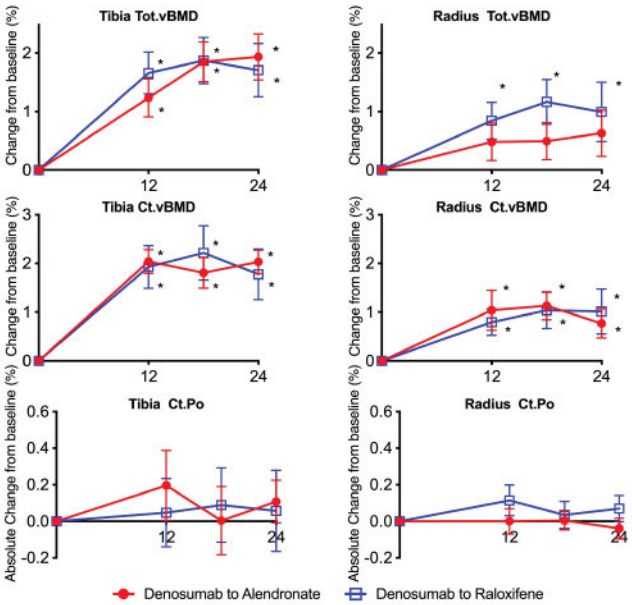

Figure. Mean % change (SEM) in bone density. *P<0.05 within group change from month 0.

***Disclosures: Joy Tsai**, Amgen, Other Financial or Material Support*

SUN-458

The long-term effect of omeprazole on BMD in patients treated with calcicum, vitamin D and antiresorptive drugs *Vaclav Vyskocil[1], Radka Stepanova[2], Marie Simeckova[2]. [1]Charles University Hospital, Czech Republic. [2]ANOVA, Czech Republic

The authors analyzed a group of 399 patients treated with omeprazole for more than 2 years to determine the negative impact on BMD in patients treated with calcium, vitamin D, and antiresorptive drugs. The control group consisted of 340 patients selected to match the demographics of the study group. The primary endpoints were changes in BMD in the spine and hip, incidence of fractures, and their number in selected locations - hip, spine, upper limbs, lower limbs except for the hip, and other locations.The effect of the dose and duration of omeprazole treatment and of BMI on changes in spine and hip (active group) was tested. Additionally, the effect of vitamin D level was examined, the threshold was set to 50 nmol/L and 75 nmol/L. Majority of the treated patients had BMI higher than 25 (81.1%), respectively higher than 30 (44.5%), vitamin D values higher than 50 nmol/L was in 81.7% of patients. The mean age was 72.5 (+/-4.32) years. The most frequently used dose of omeprazole was 40 mg in 44.1% and 20 mg in 40.6% patients. The average duration of treatment was 6.4 (+/-3.23) years. The t-test for indepentend groups, linear models and Poisson regression were used for statistical testing.Results:No statistically significant difference was found in the spine and left hip BMD between groups. The effect of omeprazole dose and duration of treatment examined by a linear model was not statistically significant on both variables. The effect of BMI on BMD % change in the spine or hip was not statistically significant, both in the group with a threshold of 25kg/m2 and 30kg/m2. No statistically significant effect of vitamin D treatment was found on BMD changes in the hip or spine in both subgroups (thresholds of 50 nmol/l and 75 nmol/l). Similarly, the dose or duration of omeprazole treatment did not affect the number of fractures . Regarding the interaction of dose and duration of omeprazole treatment and the occurrence of fractures for the above-mentioned 5 locations, statistical significance was not found.The effect of dose or duration of omeprazole treatment on BMD or fracture occurrence was not proven considering vitamin D levels and BMI. Additional analysis of extended sample as well as update of clinical data needs to be performed.

***Disclosures: Vaclav Vyskocil**, None*

SUN-459

Clinical and Radiological Characteristics of Southeast Asian Women with Atypical Femoral Fracture Compared with Age Matched Controls with Similar Bisphosphonate Exposure *Kuan Swen Choo[1], Le Roy Chong[1], Jemima Koh[1], Li Hnn Goh[1], Thomas FJ King[1], Linsey Utami Gani[1]. [1]Changi General Hospital, Singapore, Singapore

Bisphosphonate (BP) remains the 1st line of osteoporosis treatment in most patients due to its effectiveness in reducing osteoporotic fractures. Asians have upto 6 times higher risk of developing atypical femoral fracture(AFF) compared to Caucasians, with those from Southeast Asia displaying the highest incidence. In this study, we aim to characterize the clinical risk factors and femoral geometries in Singaporean women with AFF compared with age matched controls with similar BP exposure. We hope to elucidate predisposing risk factors for AFF in patients on BP.Methods: A case control study was conducted on female subjects admitted to Changi General Hospital, Singapore, with AFF from 2009 to 2022. 35 subjects were matched to 35 controls in terms of age. AFF was ascertained by the ASBMR 2014 criteria. Demographic data, clinical and medication history, and bone mineral density were extracted from the hospital electronic database. Femoral geometry parameters obtained from full-length lower limb radiographs were analysed for lateral bowing angle, femorotibial angle, femoral neck-head offset ratio, femoral neck-shaft angle, hip axis length, femoral offset, lever-arm ratio, line bisecting long axis of femur and pelvic center, and femoral shaft lateral cortical thickness index. 2 groups comparison were tested based on the nature and distribution of the outcomes.Results: The 2 groups of AFF and controls were well matched in their demographics and clinical characteristics (Table1). 26 out of the 70 subjects had previous osteoporotic fracture. Mean duration of BP use was similar in both groups [77.3 versus 73.4months for AFF and controls (p-value 0.608)]. Pre-BP treatment BMD in the AFF group were significantly higher at femoral neck. BMD at the time of AFF were also higher compared to controls at the time of recruitment. There were no significant differences in the femoral geometry parameters, except femoral head-neck offset ratio was statistically smaller in AFF group [0.671 versus 0.695, p-value 0.018], but the small ratio difference was unlikely of clinical significance.Conclusion: In a well-matched group of women with similar BP exposure, there were no significant differences in clinical characteristic and femoral geometry that suggest higher risk for AFF formation. We observed higher BMD at pre-BP treatment and time of fracture for patients with AFF. Further studies are needed to elucidate predisposing factors for AFF development in this high-risk group.

Table 1: Comparison of demographics, clinical variables, bone mineral density (BMD) and femoral geometries between the AFF and control groups.

	Overall (*n*= 70) *n* (%)	AFF (*n*= 35) *n* (%)	Control (*n*= 35) *n* (%)	*p* value
(a) Demographics and Clinical Variables				
Age (years), mean (SD)	74.6	74.5 (9.99)	74.7 (9.81)	0.914
BMI (kg/m^2), median (IQR)	22.6 (20.9, 26.9)	24.4 (21.8, 27.2)	22.1 (20.0, 26.3)	0.087
Race				0.308
Chinese	61 (87)	29 (83)	32 (91)	
Malay	6 (9)	4 (11)	2 (6)	
Indian	2 (3)	2 (6)	0 (0)	
Others	1 (1)	0 (0)	1 (3)	
Smokers	0 (0)	0 (0)	0 (0)	1
Charlson comorbidity score, median (IQR)	4.0 (3.0, 5.0)	4.0 (3.5, 5.0)	4.0 (3.0, 5.0)	0.181
Diabetes mellitus	16 (23)	9 (26)	7 (20)	0.776
Glucocorticoid (>3months in the last 1 year)	4 (6)	1 (3)	3 (9)	0.614
Proton pump inhibitor (>6 months in the last 1 year)	12 (17)	4 (11)	8 (23)	0.342
History of osteoporotic fracture	26 (37)	14 (40)	12 (34)	0.805
History of AFF	5 (7)	5 (14)	0 (0)	0.167
25OHD (µg/L), median (IQR)	28.6 (25.9, 34.2)	27.5 (25.1, 30.8)	31.7 (28.0, 36.1)	0.021
Osteoporosis treatment				
Bisphosphonate	67 (96)	32 (91)	35 (100)	0.239
Denosumab	26 (37)	9 (26)	17 (49)	0.083
Raloxifene (SERM)	2 (3)	1 (3)	1 (3)	1
Strontium	10 (14)	6 (17)	4 (11)	0.734
Duration of bisphosphonate (months), mean (SD)	75.2 (29.3)	77.3 (35.4)	73.4 (23.1)	0.608
(b) Bone mineral Density (BMD)				
Pre-BP treatment				
T-score femoral neck, mean (SD)	-2.19 (0.99)	-1.80 (1.04)	-2.50 (0.85)	0.009
T-score total hip, mean (SD)	-2.33 (1.05)	-1.97 (1.28)	-2.55 (0.83)	0.084
T-score lumbar spine, mean (SD)	-1.99 (1.12)	-1.91 (1.33)	-2.05 (0.93)	0.882
At time of AFF/ recruitment of control				
T-score femoral neck, mean (SD)				
T-score total hip, mean (SD)	-2.12 (1.01)	-1.59 (1.10)	-2.48 (0.79)	0.002
T-score lumbar spine, mean (SD)	-2.01 (1.11)	-1.51 (1.21)	-2.34 (0.92)	0.010
	-1.41 (1.41)	-1.02 (1.50)	-1.80 (1.20)	0.034
(C) Femoral geometry parameters				
Lateral bowing angle (varus -, valgus +), mean (SD)	-3.87 (5.21)	-4.65 (5.15)	-3.12 (5.24)	0.236
Femorotibial angle, mean (SD)	179 (7.44)	179 (8.84)	179 (5.96)	0.426
Femoral head-neck offset ratio, mean (SD)	0.683 (0.042)	0.671 (0.041)	0.695 (0.039)	0.018
Femoral neck-shaft angle, mean (SD)	129 (6.78)	128 (7.32)	130 (6.12)	0.366
Hip axis length (cm), mean (SD)	10.5 (0.62)	10.5 (0.63)	10.5 (0.63)	0.974
Femoral offset (cm), mean (SD)	11.7 (14.1)	9.98 (6.88)	13.3 (18.6)	0.581
Lever arm ratio, mean (SD)	0.705 (0.047)	0.693 (0.053)	0.715 (0.038)	0.174
Line bisecting the long axis of femur & pelvic center, mean (SD)	12.5 (1.20)	12.8 (1.41)	12.2 (0.907)	0.145
Femoral-shaft lateral cortical thickness index, mean (SD)	0.265 (0.054)	0.280 (0.059)	0.249 (0.043)	0.017

***Disclosures: Kuan Swen Choo**, None*

SUN-460

Impact of Multidisciplinary Fracture Liaison Service in Post-fracture Care in Acute Hospital *Yasumasa Yoshino[1], Yohei Asada[1], Hidemi Muramatsu[2], Takahiro Toda[3], Takao Tobe[3], Shiho Asai[4], Masahiro Hidaka[5], Mitsuhiro Morita[6], Nobuyuki Fujita[6], Atsushi Suzuki[1]. [1]Department of Endocrinology, Diabetes and Metabolism, Fujita Health University, Japan. [2]Nursing Department, Fujita Health University Hospital, Japan. [3]Department of Pharmacy, Fujita Health University Hospital, Japan. [4]Food and Nutrition Service Department, Fujita Health University Hospital, Japan. [5]Department of Rehabilitation, Fujita Health University Hospital, Japan. [6]Department of Orthopedic Surgery, Fujita Health University, Japan

?Purpose? Fracture Liaison Service (FLS) is nowadays well accepted as effective coordinator-based system to prevent secondary fracture. Japan Osteoporosis Society offered multidisciplinary approach with a framework named as Osteoporosis Liaison Service (OLS)-7 (Suzuki A: Endocr J in press) in order to provide coordinated care for patients with osteoporosis. In this study, we aimed to explore the efficacy of multidisciplinary team care for post-fracture patients in acute care hospital.?Methods?The patients with primary osteoporosis (n=75, M/F=19/56, age 79.8 +/- 8.6 years old), who admitted to our hospital due to hip fracture or new clinical vertebral fracture, were recruited from 2018 to 2020. At enrollment, risk assessment as well as guidance of nutrition, medication and exercise were provided according to the OLS-7. On discharge, anti-osteoporotic medications were initiated. The questionnaires to each patient were conducted at 6, 12, 24, and 36 months after fracture.?Results? The study subjects included 65 hip fractures and 10 clinical vertebral fractures. OLS-7 includes 7 elements: (1) Fracture risk assessment, (2) Prevalent fracture and other causes of secondary osteoporosis, (3) Nutrition, (4) Fall risk and exercise, (5) Medication review and guidance, (6) QOL and ADL, (7) Database. Multidisciplinary team was in charge of assessment and guidance on post-fracture patients with OLS-7 framework. Medications for secondary fracture prevention was initiated in all patients. The breakdown was 41 bisphosphonates, 27 denosumab, 3 teriparatide, 1 romosozumab and 3 alfacalcidol alone. A total of 35 patients discontinued the medication at 36 months (11 died, 2 poor general condition, 10 refused to continue, 10 were unreachable, and 2 developed other skeletal dysplasia). Of the 40 patients confirmed alive at 36 months, 38 continued the medication, and 2 discontinued. Secondary fractures were observed in 12 cases in 10 patients.?Conclusion?Medication adherence was 95.0 % in surviving patients with a continuous approach, though it stayed at 50.7 % of the patients at enrollment.

***Disclosures: Yasumasa Yoshino**, None*

SUN-461

Co-morbidity in Patients with Fragility Fracture and Impact on Osteoporosis Treatment Choices *Amina Anwar[1], Lucas Steele[1], Aamir Kadri[2], Madhumathi Rao[2]. [1]University of Kentucky College of Medicine, United States. [2]University of Kentucky,

Introduction Among patients who sustain a fragility fracture, <20% receive treatment for osteoporosis. The 2020 AACE guidelines characterized these patients as very high risk for re-fracture and recommended osteo-anabolics as first line for secondary fracture prevention. However, patients with fragility fractures have a high burden of co-morbidities that can significantly impact choice of osteoporosis therapy. We undertook a study of patients who sustained a fragility fracture to characterize their co-morbidity and evaluate the impact on subsequent therapy choices in the context of AACE guidelines and FDA label indications. Methods Retrospective chart review of patients with fragility fracture treated at a single institution from 2021-2022, and obtained data regarding demographics, co-morbidities, osteoporosis risk factors, lab values, clinical outcomes, and post-fracture treatment. We characterized the distribution of comorbidity and estimated the proportion of patients who post-fracture care. In addition, we approximated the proportion of patients where co-morbid conditions could preclude the use of osteo-anabolic agents. Proportions compared using Chi-square analysis and means using the independent sample t-test with significance at p=0.05. Results 197 patients with mean age 78 years (SD=9.6 years), gender distribution 76.1% female (n=150). Major comorbidities included diabetes (32%), coronary artery disease (CAD) (28.4%), COPD (23.4%), dementia (21.8%), chronic kidney disease (CKD) stage 3 or worse (19.8%), chronic malnutrition (48.7%); 64% used ambulatory or assistive devices pre-fracture. There was a significantly higher prevalence of comorbidities in men - CKD stage 3 or worse (p=0.049), diabetes (p=0.012), CAD (p=0.001). Mortality was 10.7% (n=21), re-hospitalization 13.7%, and 23.4% (n=46) followed up for care. We projected use of osteo-anabolic agents was not feasible in 23.4% of male patients and 32.7% of female patients based on comorbidity. Conclusion Patients with fragility fracture carry a significant disease burden that appears more pronounced in men. Almost a third of female patients, and a quarter of male patients were ineligible for first-line anabolic treatment based on co-morbid conditions, hence detailed clinical workup should inform decision-making for osteoporosis treatment. In addition, there are clearly significant barriers to post-fracture osteoporosis treatment that need to be overcome so as to close the treatment gap.

***Disclosures: Amina Anwar**, None*

SUN-462

KY-265, a Novel Benzofuran Derivative, has Osteogenic Effects on Femur Cortical but not Trabecular Bone in Ovariectomized Female Rats *Megumi Yamamoto[1], Masafumi Ando[1], Yuma Ito[1], Masaki Fukui[1], Kazuya Otake[1], Yoshimichi Shoji[1], Eiichi Hinoi[2], Hiroaki Shirahase[1], Tatsuya Kitao[1]. [1]Kyoto Pharmaceutical Industries, Ltd., Japan. [2]Gifu Pharmaceutical University, Japan

Osteoporosis develops due to an imbalance between bone formation via osteoblasts and bone resorption via osteoclasts, and is treated with parenteral and oral resorption inhibitors and parenteral osteogenic drugs. A number of small osteogenic molecules have been reported, which have not been successfully developed. In the present study, we synthesized a novel benzofuran derivative, 3-{4-[2-(2-ethoxyethoxy)ethoxy]phenyl}benzofuran-5-carboxamide (KY-265), and examined its effects on osteoblast differentiation and experimental osteoporosis.Mouse-derived mesenchymal stem cells (ST2) and rat bone marrow mesenchymal stem cells (MSCs) were cultured for 4 days with or without KY-265, and alkaline phosphatase (ALP) activities were determined. Female rats were ovariectomized and orally administered KY-265 at 3 or 10 mg/kg/day for 8 weeks. The femur was scanned using in vivo micro-computed tomography (micro-CT) before OVX and after repeated administrations. Plasma bone-type ALP activity was determined and the isolated femurs were scanned using dual-energy X-ray absorptiometry (DEXA).In ST2 cells and MSCs, KY-265 enhanced ALP activities at 10-7 - 10-5 M, indicating the promoting effects on osteoblast differentiation. In female rats, ovariectomy markedly reduced the uterine weight but had little effect on plasma bone-type ALP activity. In DEXA scanning, ovariectomy reduced areal bone mineral density (aBMD) in distal but not diaphyseal femurs. KY-265 significantly increased distal femur aBMD in ovariectomized (OVX) rats. Micro-CT after administration demonstrated that OVX significantly reduced femur metaphysis trabecular and cortical bone volumes, but not diaphysis cortical bone volume. KY-265 did not affect the reduced metaphysis trabecular bone volume or micro-architectural parameters in OVX rats. On the other hand, KY-265 significantly increased metaphysis cortical bone volume. Changes in micro-CT parameters over the experimental period further suggested that KY-265 promoted cortical but not trabecular bone growth, resulting in an increased cortical bone strength index.The present findings showed that KY-265 has osteogenic effects on cortical bone but not trabecular bone, possibly via promoting osteoblast differentiation, being a potential candidate for bone fracture and osteoporosis therapies.

***Disclosures: Megumi Yamamoto**, None*

SUN-463

From Sea to Bone: Marine Sulfated Polysaccharides as Dual Regulators in Bone Remodeling *Jessica S. Landeros-Juárez[1], Enrique Hernández-Garibay[2], Rodrigo Beas-Luna[3], Pierrick Fournier[1], Patricia Juárez[1]. [1]Ensenada Center for Scientific Research and Higher Education, Mexico. [2]Centro Regional de Investigación Pesquera de Ensenada, Mexico. [3]Faculty of Marine Sciences, Autonomous University of Baja California, Mexico

Bones are active living tissue in constant turnover. An imbalance in bone remodeling could lead to bone diseases such as osteoporosis. Nowadays, some therapeutants protect bones from disease or delay the outcome of such pathologies. However, long-term consumption causes adverse side effects. In this work, we characterized the anabolic and antiresorptive effect of a sulfated polysaccharide isolated from three species of brown macroalgae. Chemical characterization of sulfated polysaccharides extracted by acid hydrolysis confirmed that they were mainly composed of fucose (14.5-31.5%), organic sulfates (26.5-41.5%), and uronic acids (42-44%). In mineralization assays on mouse bone marrow cells (BMCs) or preosteoblasts MC3T3-E1, measured with alizarin red staining, the sulfated polysaccharides showed an increase in mineralization as compared to controls after 21 days of culture. In contrast, in osteoclastogenesis assays, sulfated polysaccharides significantly decreased osteoclast formation induced by the cytokines RANKL and M-CSF in a dose-dependent manner. In gene expression studies of osteoprotegerin (OPG) and RANKL, we found a downregulation in the expression of RANKL gene but not OPG. This change in the gene expression ratio RANKL/OPG suggests that sulfated polysaccharides could modulate the bone remodeling process by inhibiting the RANKL signaling pathway.Finally, the effect of sulfated polysaccharides on bone remodeling was evaluated ex vivo using bone calvaria from 4-6-day-old Balb/c mice. After 7 days of culture, the histomorphometric analysis showed that new bone area and the number of osteoblasts increased significantly (i. e. 30-60% and 22-31%, respectively. One-way ANOVA, Bonferroni's Post-test, P>0.05) compared to control-treated calvaria. We demonstrated that sulfated polysaccharides have a dual effect on the bone remodeling process by promoting mineralization and inhibiting osteoclast formation in a dose-dependent manner in vitro. These novel findings suggest that sulfated polysaccharides are anabolic molecules with biomedical potential for treating bone-related diseases.

***Disclosures: Jessica S. Landeros-Juárez**, None*

SUN-464

From bench to bedside: Transcriptome profiling in a medaka fish osteoporosis model identifies CXCL9 as a blood marker that predicts the risk for osteoporotic hip fractures in men *Christoph Winkler[1], Quang Tien Phan[1], Kevin Yiqiang Chua[1], Aizhen Yin[1], Woon-Puay Koh[1], [1]National University of Singapore, Singapore

Bone homeostasis requires reciprocal communication between bone-forming osteoblasts and bone resorbing osteoclasts to maintain bone health. Communication failures result in bone diseases, such as osteoporosis, where uncontrolled osteoclast activity results in excessive bone resorption and bone fractures. To identify novel signalling factors implicated in osteoblast-osteoclast communication, our lab had earlier conducted transcriptome profiling of bone cells in a medaka fish osteoporosis model, which allows high-resolution live imaging of dynamic bone cell behaviour in intact specimen. In this model, transgenic induction of the osteoclast inducer Rankl resulted in excessive osteoclast formation and osteoporotic bone lesions. We showed that under Rankl+ conditions, osteoblasts strongly upregulated expression of the chemokine Cxcl9l. This chemokine in turn led to osteoclast recruitment and differentiation at bone matrix and excessive bone resorption. Mutations in cxcl9l and its cognate receptor cxcr3.2, or treatment with chemical Cxcr3.2 antagonists prevented excessive osteoclast formation and protected medaka bone form osteoporotic lesions. To validate a possible association of the CXCL9 ortholog and osteoporosis or fracture risk in humans, we conducted a matched case-control study nested in the prospective, population-based Singapore Chinese Health Study. This study included 55 men and 119 women who had experienced a hip fracture with an average of 6.3 years after their blood was collected. Participants were matched individually to controls who did not develop hip fractures. We found significantly higher levels of CXCL9 in pre-fracture blood samples of men with subsequent hip fractures compared with their non-fracture controls. Surprisingly, no such differences were seen in women. This suggests that elevated CXCL9 levels affect older men and women differently, possibly due to changes in sex hormone levels during aging. These findings open the possibility that early interventions targeting CXCL9-CXCR3 signalling could be beneficial in preventing hip fractures in older men. This work is funded by a grant from the Singapore Ministry of Education (MOE-T2EP30221-0008).

***Disclosures: Christoph Winkler**, None*

SUN-466

Spatial and time-dependent inhibition of human osteoclastic bone resorption with cathepsin K inhibitors. A time-lapse study *PREETY PANWAR[1], Jacob Olesen[2], Galia Blum[3], Jean-Marie Delaisse[4], Kent Soe[5], Dieter Bromme[1], [1]University of British Columbia, Canada, [2]University of Southern Denmark, Denmark, [3]The Hebrew University, Israel, [4]Odense University Hospital, KI, University of Southern Denmark, Denmark, [5]Odense University Hospital, University of Southern Denmark, Denmark

Therapeutic approaches that regulate bone resorption by inhibiting cathepsin K (CatK), an essential collagenase in osteoclasts (OCs), have gained attention in past decades. Bone resorption requires a directed OC movement over the bone surface. Using live cell imaging, we monitored the movement and bone resorptive activity of human OCs for 72h and analyzed any change in the resorptive behaviour during dose dependent inhibition of CatK by an ectosteric (T06) and active site-directed inhibitor, odanacatib (ODN). These experiments were performed using 3-5 different human donors and the number of OCs analyzed in each experiment was between 55 and 150. CatK inhibition of OCs by both inhibitors caused drastic changes in resorption speed (Control (147.2 ?m2/h), T06 (500 nM; 42.9 ?m2/h) and ODN (15 nM; 40.3 ?m2/h); $P < 0.0001$). The majority of these CatK-inhibited OCs showed frequent stops (Control; 10% and T06 (1µM; 95%) and ODN (50 nM; 95%); P 80% of the monitoring time. Surprisingly, we also observed frequent fusions of OCs during ongoing bone resorption in control and CatK-inhibited OCs, which both increased their resorption speed up to 10-20%. Fifty percent inhibition of CatK activity displayed a 2-fold increase in OC-fusion ($P < 0.0001$) during ongoing bone resorption, possibly in an attempt to compensate for the CatK-inhibition. Nevertheless, more fusion could not counterweigh the overall loss of resorption speed in the presence of inhibitors. Finally, we were also able to detect the localization of active CatK in bone resorbing OCs by using an activity-based protease inhibitor and confirmed the ectosteric inhibition by T06. In conclusion, with these data we are able to show, using live cell imaging, how OCs respond to CatK-inhibition with respect to movement, bone resorption, and that they seemingly attempt to compensate for inhibition by reactivating fusion.

***Disclosures: PREETY PANWAR**, None*

SUN-467

The beneficial effect of a probiotic mix on bone and lean mass is dependent on the diet in mice. *Klara Sjogren[1], Lina Lawenius[1], Yiwen Jiang[1], Karin Horkeby[1], Jianyao Wu[1], Karin Nilsson[2], Sofia Movérare-Skrtic[3], PETRA HENNING[4], Claes Ohlsson[5], [1]Sahlgrenska Osteoporosis Centre, Sweden, [2], Sweden, [3]Medicine, Sweden, [4]UNIVERSITY OF GOTHENBURG, Sweden, [5]Center for Bone and Arthritis Research at the Sahlgrenska Academy, Sweden

We have previously demonstrated that a probiotic mixture of Lacticaseibacillus paracasei DSM13434, Lactiplantibacillus plantarum DSM 15312 and DSM 15313 (L. Mix) prevents bone loss in ovariectomized (ovx) female mice and postmenopausal women1,2. It is unknown if the beneficial effects of probiotics are modified by the diet. The purpose of the present study is to test if the effects of L. Mix on bone mass is modified by the fat content in the diet.Ten-week-old mice were subjected to either sham or ovx surgery and treated with L. Mix at a concentration of 109 colony forming units/mL or vehicle in the drinking water for 12 weeks. We fed the mice a high fat diet (HFD) with 60% kcal from fat (D12492, Research Diets) or a control low fat diet (LFD) with 10% kcal from fat (D12450J). At the end of the experiment, mice were analysed by dual-energy X-ray absorptiometry (DXA) and dissected bones by peripheral quantitative CT (pQCT).As expected, mice on a HFD had increased body weight and fat % measured by DXA compared to mice on a LFD. L. Mix treatment resulted in higher total body BMD ($p = 0.012$ for the overall treatment effect) and protected mice from loss of BMD after ovx in mice on a LFD but not in mice on HFD (Figure 1). In addition, L. Mix increased total body lean mass in mice on LFD ($p= 0.035$ for the overall treatment effect) but not in mice on HFD. More detailed analysis of the long bones by pQCT showed that L. Mix increased the cortical thickness both in the tibia ($p=0.026$) and femur ($p=0.053$) in mice on LFD but not in mice on HFD.In conclusion, data indicates that the beneficial effect of a probiotic mix on bone and lean mass is dependent on the diet. The LFD may promote the production of some necessary metabolite or cause changes in gut microbiota composition and nutrient absorption. These findings indicate that a combination of certain probiotic bacteria and a healthy diet is beneficial for the musculoskeletal health. Ohlsson, C., et al. PloS one 9 (2014)Jansson, P.A., et al. The Lancet Rheumatology 1 (2019)

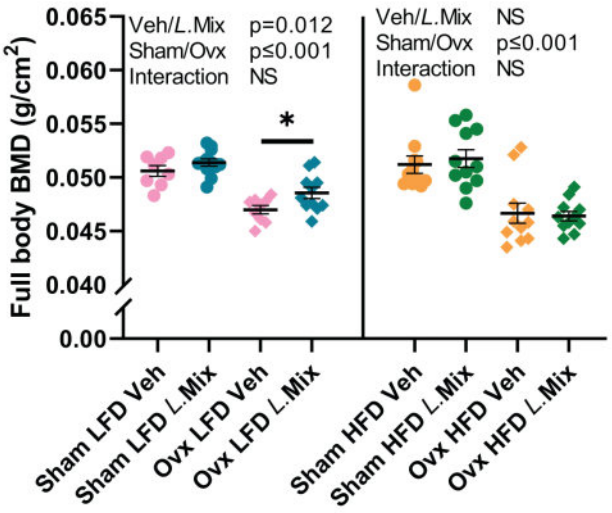

***Disclosures: Klara Sjogren**, Probi AB, Grant/Research Support*

SUN-468

Sclerostin Loop3-LRP4 Interaction Required by Sclerostin for Antagonizing Wnt Signaling and Osteogenic Potential in Osteoblasts *Luyao Wang[1], Xiaohui Tao[1], Hewen Jiang[2], Ning Zhang[2], Dijie Li[1], Jin Liu[1], Yuanyuan Yu[1], Yihao Zhang[1], Aiping Lyu[1], Baoting Zhang[2], Ge Zhang[1], [1]Law Sau Fai Institute for Advancing Translational Medicine in Bone and Joint Diseases (TMBJ), School of Chinese Medicine, Hong Kong Baptist University, Hong Kong, [2]The Chinese University of Hong Kong, Hong Kong

Sclerostin becomes a novel bone anabolic target. Sclerostin loop2 was reported to bind to YWTD repeats within LRP5/6 of osteoblasts, thereby antagonizing bone anabolic Wnt/?-catenin signaling pathway. Humanized sclerostin antibody which targeted sclerostin loop2 promoted bone formation, whereas imposed sever cardiovascular events in clinical trials. In our published work, sclerostin loop3 was notably found to contribute to the antagonistic effect of sclerostin on bone formation, while the cardiovascular protective effect of sclerostin was independent of loop3. Targeting sclerostin loop3 by our screened sclerostin loop3-specific aptamer promoted bone formation in SOSTki mice, ovariectomized osteoporotic rats and Col1a2+/G610C mice, without increasing cardiovascular risk. The sclerostin loop3 aptamer for osteogenesis imperfecta was granted Orphan Drug Designation by US-FDA (DRU-2019-6966). However, how sclerostin loop3 participates in the antagonistic ef-

fect of sclerostin on bone formation remains unclear. In our pull-down and biolayer interferometry (BLI) studies, sclerostin loop3 was found to bind to LRP4 in osteoblasts (Fig.1a-b). It was reported that osteoblastic LRP4 could facilitate the binding of sclerostin to LRP6 for antagonizing bone formation. After identification of the interaction residues, LRP4m (LRP4-Y200A, G201A, L214A, D215A, I216A, Y217A, H218A, C219A) was designed to genetically block sclerostin loop3-LRP4 interaction in vitro. The antagonistic effect of sclerostin on Wnt signaling and osteogenic potential in osteoblasts were inhibited upon LRP4m, while no changes in Wnt signaling and osteogenic potential were found in the absence of sclerostin before and after expression of LRP4m (Fig.1c-d). Based on the interaction, a peptide tool LRP4-Pep was designed to pharmacologically block sclerostin loop3-LRP4 interaction. The antagonistic effects of sclerostin on Wnt signaling and osteogenic potential in osteoblasts were inhibited after pretreatment of the exogenous LRP4-Pep (Fig.1e-f). Sclerostin loop3-LRP4 interaction was required by sclerostin for antagonizing Wnt signaling pathway and osteogenic potential in osteoblasts in vitro.

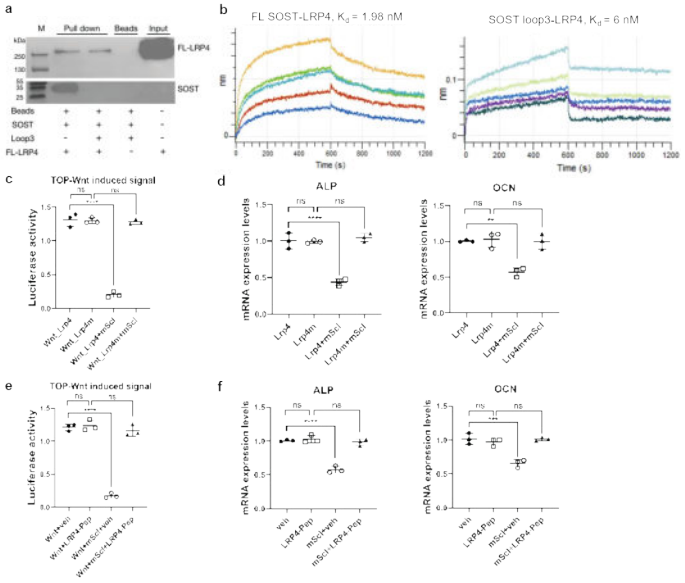

***Disclosures: Luyao Wang**, None*

SUN-469

Post-prandial timing of PTH treatment alters the osteoanabolic effect in mice *Santosh Thapa[1], Elizabeth Rendina-Ruedy[2]. [1], . [2]Vanderbilt University Medical Center, United States

Osteoporosis and osteopenia are late-onset diseases affecting a staggering 54 million people in the U.S. While anabolic agents that increase bone formation, such as intermittent parathyroid hormone (iPTH), have aided in the management of osteoporosis, patients still experience adverse side-effects. Therefore, continued development of refined therapeutic options is necessary. Our lab and others have recently demonstrated that PTH's osteoanabolic effect relies on exogenous substrates, including fatty acids, to support the energy requirements of bone formation by the osteoblast. As such, we aimed to test the hypothesis that the osteoanabolic actions of iPTH can be enhanced by synchronizing PTH treatment with exogenous substrate availability. The study included 12-week-old male and female C57BL/6NJ mice. A subset of mice experienced standard light/ dark cycle conditions (light 7am-7pm; dark 7pm-7am), while the other subset was acclimated to a reverse light/dark cycle (light 7pm-7am; dark 7am-7pm) regimen. Mice were further divided to receive a subcutaneous injection of PTH (100 µg/kg bodyweight) or vehicle control (Veh) 5 days/ week for 4 weeks. Importantly, treatment injections occurred ~4 hours into the active dark cycle to allow for food ingestion and postprandial substrates circulation. Male mice receiving PTH during their dark cycle demonstrated an increase in BMD as early as 2 weeks following treatment, which was maintained at 4 weeks as well. The increase in BMD was only documented in female mice after 4 weeks of receiving PTH treatment during the dark cycle. There was no detectable difference in bone turnover markers, serum CTx and PINP was elevated in mice receiving PTH, regardless of timing. (C-terminal telopeptide of type I collagen) and PINP (Procollagen type I N-propeptide), in male mice following 2 weeks of treatment in either light/dark cycle. Female mice displayed differences in serum CTx and PINP as early as 2 weeks. By 4 weeks, serum PINP remained elevated in female mice during both light/dark cycle groups. These data are compelling and provide strong evidence that the timing of iPTH treatment can significantly alter the osteoanabolic activity. Ongoing analyses are currently underway to assess bone microarchitecture, histology, and gene expression. Data from this study is expected to enhance clinical applicability and efficacy of the treatment of osteoporosis.

***Disclosures: Santosh Thapa**, None*

SUN-470

Affinity-targeting of Anti-sclerostin Antibody to the Bone Surface Significantly Increases Therapeutic Efficacy in an Ovariectomy Mouse Model of Osteoporosis *Boya Zhang[2], BEN SWANSON[2], Margaret Durden[3], Megan Weivoda[3], YUJI MISHINA[2], Colin Greineder[2]. [2]University of Michigan, United States. [2]University of Michigan, . [3]Mayo Clinic, United States

Background: We previously demonstrated targeting of globular proteins to the bone surface by site-specific modification with bisphosphonate or deca-aspartate affinity ligands. Bone accumulation of targeted proteins was further enhanced by extending circulation time via Fc-mediated recycling. Proteins anchored to the bone surface were shown to retain activity for at least 24 hours. Here, we extend this work by evaluating the impact of affinity targeting on bone accumulation and retention of anti-sclerostin antibody and determining if improved pharmacokinetics enhance therapeutic effects in a murine osteoporosis model. Methods: Deca-aspartate ligands were fused to the C-termini of murine specific anti-sclerostin antibody (Anti-SOST-D10) and non-therapeutic control IgG (IgG-D10). Blood, organ, and bone pharmacokinetics were determined in 14-week-old female C57BL/6J mice via quantitative radiotracing. Age-matched female mice were subjected to bilateral ovariectomy and treated weekly with i.v. administration of 5 mg/kg anti-SOST-D10, untargeted anti-SOST antibody, IgG-D10, or vehicle. Treatment outcomes were assessed by micro-computed tomography (uCT) phenotype analysis.Results: At 24 hours post-injection, both anti-SOST-D10 and IgG-D10 demonstrated markedly increased biodistribution to bone as compared to untargeted anti-SOST. Furthermore, bone levels of anti-SOST-D10 continued to increase out to 7 days, while anti-SOST decreased steadily to nearly undetectable levels (Figure 1A). In ovariectomized mice, weekly injection of anti-SOST-D10 produced significant increases in BV/TV, as compared to anti-SOST, IgG-D10, and vehicle controls (0.111+/-0.008 vs. 0.074+/-0.006 vs. 0.049+/-0.005 vs. 0.041+/-0.011 for femur, $p < 0.001$, and 0.256+/-0.019 vs. 0.217+/-0.019 vs. 0.170+/-0.017 vs. 0.172+/-0.014 for L4 vertebrae, $p < 0.001$) (Figure 1B). Other indices demonstrated a similar pattern between groups, with significantly increased connective tissue density ($p<0.001$) and decreased SMI in anti-SOST-D10 treated animals ($p<0.001$).Conclusions: Affinity-targeting of anti-sclerostin antibody increased bone accumulation and retention and enhanced therapeutic effects in ovariectomized mice. These results suggest that bone targeting may enable lower doses and longer dosing intervals of anti-sclerostin antibody therapy without reduction in therapeutic efficacy. Future studies will be needed to determine the translational potential of this strategy and its impact on off-target toxicities.

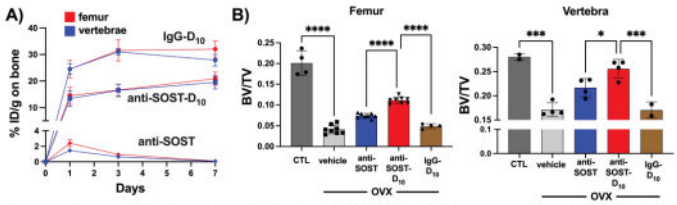

Figure 1: A: Bone PK of IgG-D_{10}, anti-SOST-D_{10}, anti-SOST. n=4 for each time point, data presented as mean±SD. **B: Bone volume fraction (BV/TV) of femur (left panel) and vertebrae (right panel).** n=4 for CTL and OVX+IgG-D10, n=8 for all other groups, data presented as mean±SD. *$p < 0.05$, ***$p < 0.001$, ****$p < 0.0001$.

***Disclosures: Boya Zhang**, None*

SUN-471

PTH Stabilizes YAP1 in Bone Marrow Stromal Cells through Src-dependent YAP-Tyrosine 428 Phosphorylation to Affect Osteoblast and Adipocyte Differentiation *Sara Monaci[1], Mengrui Wu[2], Roland Baron[3], Dr. Clifford ROsen[4], Francesca Gori[5]. [1]Harvard, United States. [2]Zhejiang University, China. [3]Harvard Medical School and School of Dental Medicine, United States. [4]Maine Medical Center, United States. [5]Harvard School of Dental Medicine, United States

PTH affects mesenchymal cells and cells of the osteoblast (OB) lineage, including osteocytes. Yes-associated protein 1 (YAP) is, together with TAZ, a key transcription factor for the Hippo pathway. YAP can be phosphorylated at various serine residues following its interaction with LATS1/2. This alters YAP cytoplasmic stability through ubiquitination and prevents its translocation to the nucleus to activate the transcription of target genes. Here, we show that in the marrow stromal cell line W20 and in Ocy454 cells, PTH stabilizes YAP, leads to its nuclear translocation, and promotes target gene expression. This effect is mediated through a decrease of YAP interaction with LATS1/2, preventing YAP ubiquitination. Examination of the YAP LATS1/2-binding site residues revealed 2 novel consensus sequences for tyrosine (Y) phosphorylation: Y375 and Y428. To determine Y375 or Y428's role in YAP function and in its stabilization by PTH, we mutated each of these two Y to prevent phosphorylation (Y375F and Y428F). Y428F favored YAP interaction with LATS1/2, leading to major YAP instability. This led to a significant decrease in YAP target genes expression and OB as well as adipocyte (AD) differentiation. We developed an antibody specific for phosphorylated YAP Y428 and showed that PTH induced Y428 phosphorylation. Preventing Y428 phosphorylation (Y428F) increased LATS1/2 binding and serine phosphorylation upon PTH stimulation, decreasing YAP stability and transcriptional activity. PTH-induced Y428 phosphorylation required Src tyrosine kinase activity which, when blocked by dasatinib, prevented PTH effects on YAP stability and on OB and AD differentiation, similar to

Y428F mutation. In contrast, mimicking Y428 phosphorylation (Y428D) restored YAP stability and mimicked the effects of PTH, showing the specificity of the Y428 phosphorylation event. Interestingly, preventing the phosphorylation of Y375 (Y375F) had opposite effects on the responses to PTH. Similar observations on the effects of PTH on YAP stability were made in the Ocy454 osteocyte cell line. These results demonstrate that 1/ PTH stabilizes YAP and allows its translocation into the nucleus by regulating the interaction of YAP with LATS1/2 via Src activation and tyrosine phosphorylation of Y428; 2/ These events regulate the OB and AD differentiation of marrow stromal cells in vitro. Thus, phosphorylation of YAP at specific tyrosine residues is critical for PTH-induced marrow stromal cell differentiation.

***Disclosures: Sara Monaci**, None*

SUN-472

11?-Hydroxysteroid Dehydrogenase Type 1 protects against Ovariectomy-induced Osteoporosis by inhibiting Osteoclast Activation *Hao Chen[1], Hanwen Li[2]. [1]Institute of Translational Medicine, The Affiliated Hospital of Yangzhou University, China. [2]The First Affiliated Hospital of Soochow University, China

Objectives: Osteoporosis is a worldwide problem in postmenopausal women and the elderly. 11?-Hydroxysteroid dehydrogenase type 1 (11?-HSD1) is a bi-directional enzyme that primarily activates glucocorticoids (GCs) in vivo, which is a considerable potential target as a treatment for osteoporosis. Previous studies have demonstrated its effect on osteoblasts, while our study aims to demonstrate its role in osteoclastogenesis.Methods: In vivo, we performed ovariectomy-induced osteoporosis (OVX) with 11?-HSD1 global knock-out (KO) mice and the wild type (WT) mice to see the bone phenotypes and osteoclasts number. Furthermore, we generated osteoclastic-specific knockout of 11?-HSD1 mice (Ctsk-cre::11?-HSD1fl/fl) and performed OVX surgery with these mice. Micro-CT analysis, H&E, immunofluorescence staining and qPCR were performed to evaluate the bone phynotypes and osteoclastogenesis. In vitro, bone marrow mesenchymal stem cell (BMSC) and bone marrow-derived macrophages (BMM) of the KO and WT mice were extracted to test their osteogenic and osteoclastogenic abilities. Finally, we conducted the high-throughput sequencing to find out the related genes or signaling pathways to explain how 11?-HSD1 influence osteoclast activation. Results: We found that KO mice were resistant to osteoclast activation and the loss of bone trabeculae. The similar effect was observed in osteoclastic specific knock out of 11?-HSD1 mice. In vitro, we observed the osteoclastogenic ability of the BMM from the KO mice were significantly attenuated. Similarly, BVT-2733, a classic inhibitor of 11?-HSD1, also suppressed the osteoclastogenesis without affecting osteogenic effect. Finally, with high-throughput sequencing, we found that the Hippo signaling was enriched in the 11?-HSD1 induced osteoclastogenic process. Then, the YAP1 activator and inhibitor was used to confirm this, and the results demonstrated that the Hippo signaling was the key as the bridge.Conclusions: Our study revealed that, in the process of osteoporosis, 11?-HSD1 expression in osteoclasts is abnormally increased, which activates osteoclastogenesis and promotes osteoporosis. Hence, 11?-HSD1 might become a new target for treating osteoporosis by cutting off the activation of osteoclastogenesis.

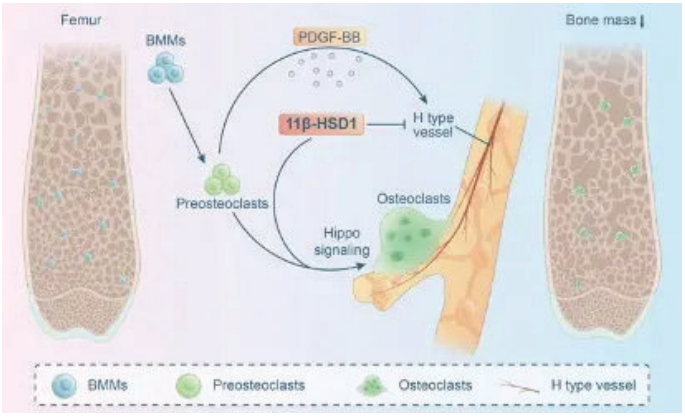

***Disclosures: Hao Chen**, None*

SUN-473

A Longitudinal Study of Bone Strength Development at the Radius and Tibia from Childhood into Adolescence in Children Exposed to Recreational Gymnastics *Marta Erlandson[1], Brendan Ernst[2], Matthew Chapelski[2], Stefan Jackowksi[3], Adam Baxter-Jones[1]. [1]University of Saskatchewan, Canada. [2]University of Saskatchewan , Canada. [3]CHEO Research Institute , Canada

Bone development in childhood and adolescence is important because the bone that is accrued during the early years can have a profound impact on bone health throughout the lifespan. Bone responds to mechanical loading such as that from physical activity (PA). We have previously shown that exposure to recreational gymnastics in early life (4 to 6 years of age) provides skeletal benefits at the distal radius at 7 to 12 years of age; with no differences observed at the radial shaft or tibia. The purpose of this follow-up study was to identify if the positive effects of recreational gymnasts' bone development in childhood (7 to 12 years of age) were maintained into adolescence (11-16 years of age). Methods: In 2006 recreational gymnasts and non-gymnasts, between the ages of 4 and 6 years, were recruited into the Saskatchewan's Young Recreational Gymnast Study (YRGS); a mixed longitudinal study. One hundred and twenty-six children underwent repeated anthropometry, physical activity and dietary assessments, and peripheral Quantitative Computer Tomography (pQCT) scans (distal and shaft sites of the radius and tibia). At the last measurement occasion (2016) children were aged between 11 and 16 years. Multilevel modeling was used to assess the effect of gymnastics exposure on area, density, content, and estimated strength controlling for confounders of growth, maturation, PA, and diet. Results: Gymnastics exposure was a significant independent predictor at the distal radius (4%) on total area (25.43 +/- 6.95mm2), total content (9.58 +/- 2.42mg/mm), total density (14.19 +/- 6.46mg/cm3), trabecular density (13.07 +/- 6.21mg/cm3), and estimated strength (3.17 +/- 1.07mg2/mm4) with a confidence interval of 95% (p0.05). Discussion: Gymnastics exposure during childhood (4 to 6 years of age) significantly predicted improvements at the distal radius during adolescence (11 to 16 years of age). The positive effects of recreational gymnastics at the wrist observed in childhood are seen to be maintained in adolescence when the effects of growth are controlled. The results provided further evidence that exposure to childhood recreational gymnastics exposure is advantageous to bone development at the wrist in adolescence. Funding: Canadian Institute of Health Research, Canadian Foundation for Innovation, and Saskatchewan Health Research Foundation.

***Disclosures: Marta Erlandson**, None*

SUN-475

Non-Steroidal Anti-inflammatory Drugs are Associated with Increased Risk of Stress Fractures during U.S. Basic Combat Training *Julie Hughes[1], Jeffery Staab[1], Kristin Popp[2], Ian Hussian[1], Leila Walker[1], Ronald Matheny[3], Karl Friedl[1], Stefan Pasiakos[1], Susan Proctor[1], Mary Bouxsein[4], Stephen Foulis[1], Kathryn Taylor[1], Katelyn Guerriere[1]. [1]Military Performance Division, US Army Research Institute of Environmental Medicine, United States. [2]Massachusetts General Hospital, . [3]Military Operational Medicine Research Program, United States. [4]Beth Israel Deaconess Medical Center, Harvard Medical School, United States

Non-steroidal anti-inflammatory drugs (NSAIDs) are prescribed to 80% of soldiers and have been shown to blunt adaptive bone formation from physical activity which may predispose to stress fracture during physically rigorous military training. In a retrospective analysis of trainees undergoing U.S. Army Basic Combat Training (BCT), stress fracture risk was five-fold higher in those prescribed NSAIDs compared to those who were not. These results have not been confirmed in a prospective study of BCT. Whether the frequency of NSAID use modulates their association with stress fracture risk has not been studied. Trainees volunteered for a prospective observational study of injury risk factors during BCT and completed weekly surveys during BCT describing NSAID use. ICD-10 codes were used to identify stress fractures during BCT. Multivariate logistic regressions, adjusted for age, sex, race/ethnicity, BMI, and the number of weekly surveys collected, were used to assess the relationship between NSAID use and stress fracture risk during BCT. NSAID use during BCT was evaluated in three ways: ever used (yes/no), average number of days used per week (continuous), total weeks used during BCT (continuous). To account for reverse causation, NSAIDs exposure was lagged by excluding NSAID use two weeks before stress fractures were diagnosed. Of 2,482 participants (mean+/-SD; age=20.7+/-3.7, BMI= 24.7+/-3.5), 62% were male, 44% were Non-Hispanic White, and 24% were Non-Hispanic Black. We identified 49 trainees with at least one diagnosed stress fracture during BCT (16 men, 33 women). Stress fracture risk was greater for NSAID users compared to nonusers (odds ratios(95%CI)); 4.9(2.2,10.9). In men, stress fracture risk was 3.6-fold (2.3,5.5) greater for every 1-day increase in the average number of days NSAIDS were used per week and 2.1-fold (1.5,3.0) greater for each additional week NSAIDs were used. There were no significant relationships between the frequency of NSAID use and stress fractures in women. Stress fracture risk during BCT was nearly 5-fold greater in trainees using NSAIDs than those who were not. In men, stress fracture risk increased progressively when the frequency of NSAIDs use also increased. These results corroborate previous results and provide further evidence to recommend conservative approaches to NSAID prescriptions during BCT.

***Disclosures: Julie Hughes**, None*

SUN-476

Is There a Causal Relationship Between Physical Activity and Bone Microarchitecture? A Study of Adult Female Twin Pairs *Frida Nissen[1], Vivenne F C Esser[2], Minh Bui[3], Shuai Li[3], John Hopper[3], Ashild Bjornerem[4], Ann Kristin Hansen[5]. [1], . [2]BHlthMedSc(Hons), Australia. [3]PhD, Australia. [4]UiT The Arctic University of Norway, Norway. [5]MD PhD, Norway

The reasons for the association between physical activity (PA) and bone microarchitecture traits are unclear. We examined whether these associations were consistent with causation and/or with shared familial factors using a cross-sectional study of 47 dizygotic and 93 monozygotic female twin pairs aged 31-77 years. Images of the nondominant dis-

tal tibia were obtained using high-resolution-peripheral quantitative computed tomography. The bone microarchitecture was assessed using StrAx1.0 software. Based on a self-completed questionnaire, a PA index was calculated as a weighted sum of weekly hours of light (walking, light gardening), moderate (social tennis, golf, hiking), and vigorous activity (competitive active sports) = light + 2*moderate + 3*vigorous. We applied Inference about Causation through Examination of FAmiliaL CONfounding (ICE FALCON) to test whether cross-pair cross-trait associations changed after adjustment for within-individual associations. Within-individuals distal tibia cortical cross-sectional area (CSA) and cortical thickness were positively associated with PA (regression coefficients (?) = 0.20 and 0.22) while porosity of the inner transitional zone was negatively associated with PA (? = -0.17), all p < 0.05. Trabecular vBMD and trabecular thickness were positively associated with PA (? = 0.13 and 0.14), and medullary CSA was negatively associated with PA (? = -0.22), all p <= 0.01. Cross-pair cross-trait associations of cortical thickness, cortical CSA and medullary CSA with PA attenuated after adjustment for the within-individual association (p = 0.048, p = 0.062 and p = 0.028 for changes). In conclusion, increasing PA was associated with thicker cortices, larger cortical area, lower porosity of the inner transitional zone, thicker trabeculae, and smaller medullary cavities. The attenuation of cross-pair cross-trait associations after accounting for the within-individual associations were consistent with PA having a causal effect on the improved cortical and trabecular microarchitecture of adult females, in addition to shared familial factors.

***Disclosures: Frida Nissen**, None*

SUN-477

The Influence of Eight Months of Ballistic and Conventional Resistance Exercise Training on Bone Mineral Content in Postmenopausal Women: The REPROOF Study *Ogulcan Caliskan[1], Elisa Marques[1], Jonathan Folland[1], Katherine Brooke-Wavell[1]. [1]Loughborough University, United Kingdom

High load, progressive resistance training is recommended for osteoporosis prevention and management, but the effectiveness of lower load, higher velocity exercise on BMD is unclear. Fast ballistic resistance exercise involves moving as explosively as possible with a light/moderate load, attempting to launch the load, if possible, to maximise rate of force development. The aim was to investigate the influence of ballistic and conventional resistance training, relative to control, on BMC and BMD in postmenopausal women.The Resistance Exercise Programme on Risk of Osteoporosis and Osteoarthritis in Females (REPROOF) study was an eight-month randomised controlled trial. Participants were healthy women aged 50-75 years, >4 years postmenopause and without osteoporosis or other conditions/medications affecting bone. They were randomly allocated to ballistic resistance training (BRT), conventional resistance training (CRT) or control (CON) groups. Both RT groups attended similar twice-weekly training sessions, including warm-up and resistance exercises (hack squat and unilateral calf raise). The heaviest weight that could be lifted for one repetition maximum (1RM) was determined monthly and used to progressively increase the load. This ranged up to 50%1RM in BRT and the maximum load that could be lifted 8 times in CRT. Both hips and lumbar spine were measured by dual X-ray absorptiometry(GE iDXA). Mean femoral neck, total hip and lumbar spine BMC and BMD were the main and secondary outcomes, respectively. Comparisons between groups were made using linear regression models adjusting for baseline values.111 of 133 screened women were randomised (38 BRT, 39 CRT and 32 CON) of whom 82 (28 BRT, 29 CRT and 25 CON; 63.1+/-3.7 years; 24.5+/-3.5 kgm-2; femoral neck T-score -1.0 and lumbar spine T-score -0.8) completed the study and were included in the analysis. Mean adherence was 98.3%in BRT and 98.0% in CRT. BRT improved total hip BMC by mean (95%CI) 0.33 (0.07, 0.59) g (p=0.01) and BMD by 0.008 (0.001, 0.014) g cm-2 (p=0.02) relative to CON (Figure1). There were no other statistically significant differences between groups.Ballistic resistance training increased total hip BMC and BMD, whilst conventional resistance training did not. This contrasts with previous findings that high load resistance training is necessary for skeletal adaptation. Ballistic resistance exercise was feasible in healthy postmenopausal women and may have a role in osteoporosis prevention.

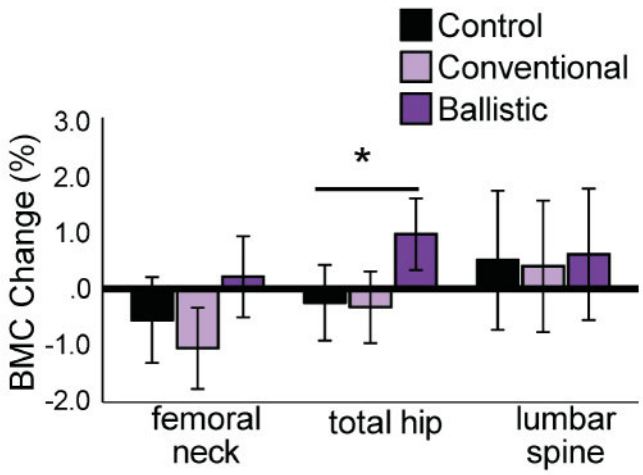

Figure 1: Mean (95% CI) BMC Change
*ballistic significantly different from control

***Disclosures: Ogulcan Caliskan**, None*

SUN-478

Applying novel analytic methods to 24-hour physical activity and sleep behaviors to determine associations with HR-pQCT parameters at the distal limbs in older adults: The Study of Muscle, Mobility and Aging (SOMMA). *Lauren S. Roe[1], Tong Yu[6], Nina Heilmann[6], Nicole M. Sekel[3], Kristen Koltun[6], Julie Hughes[4], Katelyn I. Guerriere[5], Kerri Freeland[6], Peggy Cawthon[7], Nancy W. Glynn[8], Kelley Pettee Gabriel[9], Bradley Nindl[3], Paolo Caserotti[10], Elsa Strotmeyer[6], Jane A. Cauley[11]. [1], [6]University of Pittsburgh, [3]2Neuromuscular Research Laboratory/Warrior Human Performance Research Center, Department of Sports Medicine and Nutrition, University of Pittsburgh, United States. [4]US Army Research Institute of Environmental Medicine, United States. [5]U.S. Army Research Institute of Environmental Medicine, Military Performance Division, United States. [6]University of Pittsburgh, United States. [7]San Francisco Coordinating Center, United States. [8]University of Pittsburgh School of Public Health, Department of Epidemiology, United States. [9]Department of Epidemiology, The University of Alabama at Birmingham, United States. [10]Department of Sports Science and Clinical Biomechanics and the Center for Active and Healthy Ageing, University of Southern Denmark, Denmark. [11]UNIVERSITY OF PITTSBURGH, United States

Optimal time in moderate to vigorous intensity activity (MVPA), light intensity activity (LPA), and sleep are critical for bone health in older adults but are often considered separately. Given the finite 24-hrs in a day, MVPA, LPA, sedentary behaviors (SB), and sleep are inherently co-dependent. We examined associations between the composition of accelerometer-derived MVPA [>3940 vector magnitude counts (vcm)/min], LPA (2860-3940 vcm/min), SB (<2860 vcm/min), and sleep with High-Resolution peripheral Quantitative Computed Tomography (HR-pQCT) measures. This study included community-dwelling older men (n=105) and women [n=167; mean age: 76.2+/-4.52 yrs (same for men and women)] enrolled in the Study of Muscle, Mobility and Aging (SOMMA) Bone Ancillary Study. Participants wore an ActiGraph GT9X on their nondominant wrist for five 24-hr periods after the SOMMA baseline visit. At the 12-mo visit, distal radius (DR) and tibia (DT) estimated failure load, total volumetric bone mineral density (vBMD), and cortical and trabecular vBMD, bone area, and thickness were obtained from HR-pQCT. Compositional data analysis methods were applied to estimate associations between 24-hr movement profile (distribution of MVPA, LPA, SB, and sleep) with sex-specific standardized HR-pQCT parameters in linear regression models for men and women separately. Isotemporal compositional substitution methods were applied to estimate hypothetical changes in predicted continuous HR-pQCT measures (not standardized) if 30 minutes of MVPA displaced 30 minutes of SB. Mean composition of MVPA, LPA, SB, and sleep for men was 159, 95, 755, and 431 min/day, and for women was 206, 104, 687, and 442 min/day. In minimally adjusted models (age and race), the 24-hr movement profile was associated only with DR cortical area (Ct.Ar) in men (p=0.047), and DR trabecular thickness (Tb.Th) in women (p=0.01). Subsequent adjustment for ulna length, body mass index, and smoking status did not change results (p-values: for Ct.Ar=0.046, for Tb.Th=0.006). Theoretically displacing 30 min of SB for 30 min of MVPA increased the predicted Ct.Ar for men by 0.56 mm2 (mean: 74.48 vs. 75.04 mm2) and Tb.Th for women by 0.002 mm2 (mean: 0.23 vs. 0.24 mm2). Replacing SB with MVPA was related to improved Ct.Ar and Tb.Th at the non-weightbearing DR, a robust predictor of clinical and

major osteoporotic fractures, but no association were found between 24-hr activity composition with HR-pQCT measures at the weightbearing DT.

***Disclosures: Lauren S. Roe**, None*

SUN-479

The Effect of 9 Months Whole Body Vibration, With or Without Osteogenic Exercise, on Indices of Bone Strength and Fracture Risk: the VIBMOR Trial *Belinda Beck[1], clinton rubin[2], Mark Forwood[1], Amy Harding[1], Luke Buizen[3]. [1]Griffith University, Australia. [2]State University of New York at Stony Brook, United States. [3]University of New South Wales, Australia

PurposeThe purpose of the VIBMOR randomised controlled trial was to determine the efficacy of low-intensity whole-body vibration (LIV), bone-targeted, high-intensity resistance and impact training (HiRIT), or the combination of LIV and HiRIT, on risk factors for hip fracture in postmenopausal (PM) women with osteopenia and osteoporosis.MethodsPostmenopausal women with low aBMD at the hip or spine, with or without a history of fragility fracture and on or off antiresorptive osteoporosis medications (OP meds), were recruited. Exclusions included: cognitive impairment, uncontrolled cardiovascular disease, anabolic bone medications, regular HiRIT or LIV in preceding 12 mths, malignancy, current or recent chemotherapy, conditions and medications adversely influencing bone health, recent fragility fracture, and unable to undertake 9 mths 2/wk supervised exercise training. Participants were randomly allocated to 9 mths of either LIV, HiRIT, LIV+HiRIT, or control (low-intensity home exercise) followed by 12 mths detraining. Allocation was block-randomized, stratified by use of OP meds. Testing occurred at baseline (T0), 9 mths (T1) and 21 mths (T2). The primary outcome was total hip aBMD (DXA, Norland Elite). Secondary outcomes included anthropometrics, aBMD at the spine, femoral neck, trochanter and whole body, 3D hip and pQCT indices of bone strength, lean and fat mass, functional performance, posture, muscle strength and power, balance, falls, and intervention compliance. Exploratory outcomes included bone turnover markers, pelvic floor health, quality of life, physical activity enjoyment, adverse events, and fracture. An economic evaluation was conducted. ResultsData collection was finalised Dec 2022 and data entry/cleaning was completed April 2023. Total study n was 252 (Con 62, LIV 64, HiRIT 61, LIV+HIRIT 65). Mean age was 68.7 +/- 7.0 yrs, height 160.4 +/- 11.9 cm, weight 64.1 +/- 11.9 kg and LS BMD T-score -1.2 +/- 1.0. Compliance with each intervention was CON 80.5 +/- 29.9%, LIV 85.1 +/- 21.3% and HiRIT 78.9 +/- 12.1%. Our submission is an 'initiated trial abstract' per the Abstract guidelines. Full data analysis is underway and results will be available by the ASBMR Annual Meeting.ConclusionsThe VIBMOR trial is the first to compare the effect of LIV alone or in combination with HiRIT on risk factors for hip fracture in PM women with low bone mass. Findings are highly relevant to those with low bone mass who are unwilling to take or adversely affected by OP meds.

***Disclosures: Belinda Beck**, The Bone Clinic PTY LTD, Major Stock Shareholder*

SUN-480

Clinical Outcome Assessment Instruments for Neurofibromatosis Type 1 (NF1)-Related Skeletal Manifestations: A Targeted Literature Review *Ayo Adeyemi[1], Maria Marfa[2], Inga Gru?[3], Gail Doughton[4], Damien Simoneau[5]. [1]Alexion, AstraZeneca Rare Disease, Boston, MA, USA, United States. [2]Alexion, AstraZeneca Rare Disease, Barcelona, Spain, Spain. [3]IQVIA, New York, NY, USA, United States. [4]Alexion, AstraZeneca Rare Disease, Cambridge, UK, United Kingdom. [5]Alexion, AstraZeneca Rare Disease, Zurich, Switzerland, Switzerland

Purpose: People with NF1 can experience skeletal manifestations (SM), e.g. scoliosis; however, no approved pharmacotherapies for SM are currently available. To inform future clinical study design, identification of fit-for-purpose clinical outcome assessments (COA) is needed. Here, we aimed to develop a conceptual model to assess signs, symptoms and impacts of NF1-related SM. Then, the landscape of COAs used for NF1-related SM was reviewed to identify potential fit-for-purpose tools in this population.Methods: Information from a targeted literature review was used to create a preliminary conceptual model of the patient experience and identify relevant instruments for measuring these concepts. Information on content validity and psychometric criteria were included. Four sources were queried: published literature (PubMed, Cochrane Library and Embase), clinical trials, PROQOLID™, and PROLABELS™. Searches included disease and outcome-related terms and were limited to human studies in English with available abstracts, published <=10 years prior.Results: The conceptual model identified scoliosis as a core sign/symptom of NF1-related SM, with impacts on emotional, physical, social and general wellbeing. Across the 4 sources, 156 unique COAs relevant to NF1 were identified, of which 5 were related to SM: Scoliosis Research Society (SRS) Patient Questionnaire (v7 and 22), Early Onset Scoliosis 24-item Questionnaire (EOSQ24), Neck Disability Index (NDI), and Japanese Orthopedic Association (JOA) Scoring System. SRS instruments were the most relevant tools available to measure symptoms and impacts specific to scoliosis. Although the EOSQ24 focuses on measuring impacts, it does not cover signs/symptoms specific to SM. The NDI and JOA partially cover symptomatic cord compression/myelomalacia and cervical compression myelopathy, respectively. Other NF1-related and general quality of life tools were identified to better support concepts in the conceptual model: INF1-QOL and PedsQL NF1, and PedsQL core module. The content validity and psychometric properties of the tools were mostly seen as low as it relates to SM in patients with NF1.Conclusions: The signs, symptoms, and impacts of SM are varied and not covered comprehensively by any single instrument. The use of a combination of instruments, including generic tools maybe considered to capture the several domains of patient quality of life impacted by NF1-related SM.

***Disclosures: Ayo Adeyemi**, Alexion, AstraZeneca Rare Disease, Major Stock Shareholder, Alexion, AstraZeneca Rare Disease, Other Financial or Material Support*

SUN-481

Changes in Volumetric Bone Mineral Density and Microarchitecture in Adults With X-linked Hypophosphatemic Rickets: a Longitudinal Case Control Study *Thomas Funck-Brentano[1], Arnaud Vanjak[2], Agnes Ostertag[3], Corinne Collet[2], Bert Rietbergen[4], MARTINE COHEN-SOLAL[5]. [1]Univserité de Paris, France. [2]Université Paris Cité INSERM U1132 Bioscar, France. [3]INSERM U1132 Biscar, France. [4]Eindhoven University of Technology, Netherlands. [5]Inserm U1132 Bioscar and université Paris-Cité, France

X-Linked Hypophosphatemia (XLH) is the most common type of inherited rickets. Although the clinical features of this rare disease are well characterized, bone mineralization, microstructure and biomechanical changes over time are poorly known. Our aim was to analyze changes in bone properties assessed by High Resolution peripheral Quantitative Computed Tomography (HRpQCT) in the appendicular skeleton of adults with XLH. At baseline, each XLH patient (N= 14 adults; 9 females; age 50 +/- 15 years) was matched by sex, age and body mass index to a minimum of two healthy controls (N= 34). Patients and their matched controls were assessed by DXA and HRpQCT at baseline. Each continuous variable was compared between XLH patients and their matched controls using a paired T-test with multiple controls, according to the method described by Ury et al. Nine XLH patients were then followed for a median duration of 4 years with a new HRpQCT evaluation. For HR-pQCT, we evaluated 12 parameters at the tibia and the radius. After Bonferroni correction for multiple testing, a P value < 4.2x10-3 was considered significant. All participants gave their written consent to participate to the study and ethical approval was obtained by the local ethical committee.HRpQCT demonstrated that total volumetric BMD was decreased at the radius (mean difference -87.85 mgHA/cm3 +/- 22.24, P=0.001). Cortical thickness was decreased (-165.27 µm +/- 48.42, P=0.002) was with a preserved Cortical area in relation to an increased total area due to metaphyseal enlargement. A trend in trabecular bone volume fraction was also observed lower with fewer trabecular number (-0.60/mm² +/- 0.10, P<0.001). However, bone strength evaluated by micro-finite element analyzes revealed unaffected bone stiffness and maximum failure load. Similar trends were observed at the tibia. At follow-up cortical vBMD had further decreased at the tibia (-33.44 mgHA/cm3 +/- 25.65, P=0.004) as well as total vBMD (P nominal =0.02). Analysis of bone microarchitecture revealed a decreased cortical area and increased trabecular area suggesting of cortical trabecularisation over time. However, no significant change was observed at the radius.In adult XLH patients, bone mineral density and microarchitecture is impaired at the appendicular skeleton. With time, alterations of mineralization and microarchitecture worsen. The impact of secondary hyperparathyroidism on these changes could not be analyzed in this pilot study. The respective impact of conventional or targeted therapies for XLH should be further assessed in the future.

***Disclosures: Thomas Funck-Brentano**, None*

SUN-482

New Heterotopic Ossification Lesions in Patients with Fibrodysplasia Ossificans Progressiva Measured by PET/CT vs CT Only *Dinko Gonzalez Trotter[1], Jennifer McGinniss[1], Aris Economides[1], Kusha Mohammadi[1], Andrew Rankin[1], Bret Musser[1], Scott Mellis[1], Eduardo Forleo-Neto[1], Gary Herman[1]. [1]Regeneron Pharmaceuticals, Inc., United States

Purpose: Fibrodysplasia ossificans progressiva (FOP) is an ultra-rare disorder caused by mutations in the activin-A receptor type 1 (ACVR1) gene that render it responsive to activin-A. FOP is characterized by the deposition of bone in soft tissues known as heterotopic ossification (HO) and episodic painful flare-ups. Garetosmab, a fully human monoclonal antibody against activin-A, is being investigated for the prevention of new HO lesions in patients with FOP.Methods: This post hoc analysis compared the change from baseline in the number and volume of new HO lesions identified by 18F-labeled sodium fluoride (a bone-seeking tracer that measures bone deposition and turnover) positron emission tomography (PET) and X-ray computed tomography (CT) imaging (measures bone volume). Baseline and 28-week PET/CT and CT-only scans acquired during the initial double-blind, placebo-controlled period of the LUMINA-1 (NCT03188666) phase 2 study were independently read by two sets of blinded readers and an adjudicator for the presence and volume of new lesions. Number and volume of new lesions were compared between the two imaging modalities.Results: The number of patients with new lesions as detected by PET/CT and CT only was 14/44 (31.8%) and 12/44 (27.3%), respectively. The mean number (standard deviation) of new lesions per patient by PET/CT through Week 28 was 0.68 (1.57) vs 0.86 (1.95) detected by CT only. In patients with new lesions, the mean number of new lesions per patient was 2.14 (2.18) vs 3.17 (2.62) as detected by PET/CT vs CT only, respectively. The mean volume (cm3) of new lesions through Week 28 per patient detected by PET/CT was 6.05 (14.88) vs 5.94 (21.13) by CT only. In the subset of patients with new lesions, the mean volume of new lesions per patient detected by PET/CT was 19.02 (21.60) vs 21.79 (36.98)

by CT only. Moderate agreement between PET/CT and CT only detection was observed when identifying patients with new lesions, with a kappa coefficient of 0.46 (standard error: 0.146; 95% confidence interval: 0.17-0.74). Placebo vs garetosmab groups, respectively, showed aggregate new lesion number/volume (cm3) of 27/245.3 vs 3/21.3 by PET/CT, and 37/261.8 vs 1/0.1 by CT only.Conclusions: CT only imaging showed similar performance to PET/CT in the detection and characterization of new HO lesions and provides a viable option for the assessment of therapies that may inhibit the formation of new HO lesions in patients with FOP.

***Disclosures: Dinko Gonzalez Trotter**, Regeneron Pharmaceuticals, Inc., Major Stock Shareholder, Regeneron Pharmaceuticals, Inc., Other Financial or Material Support*

SUN-485

Bone microarchitecture and strength in Osteogenesis Imperfecta using HR-pQCT: comparison with normative data taking into account limb length and deviating axial scan angles *MELISSA BEVERS[1], Bert Rietbergen[2], Arjan Harsevoort[3], Koert Gooijer[3], Hans Feenstra[3], Guus Janus[3], Caroline Wyers[4], Joop Van Den Bergh[5]. [1]VieCuri Medical Center, , [2]Eindhoven University of Technology, Netherlands. [3]Expert Center for adults with Osteogenesis Imperfecta Isala Hospital, Netherlands. [4]VieCuri Medical Centre, Netherlands. [5]VieCuri MC Noord-Limburg and Maastricht UMC,

Purpose: Patients with osteogenesis imperfecta (OI) have increased bone fragility and fracture risk. High-resolution peripheral quantitative CT (HR-pQCT) has been used to study bone microarchitecture in OI as compared to non-OI groups, but short stature and bone deformities in OI may cause deviations in scanned region and limit comparison. The aim of this study was to assess bone microarchitecture and strength in adults with OI as compared to normative data using HR-pQCT with a limb-length dependent scan protocol and by taking into account deviating scanned regions. Methods: Limb-length dependent HR-pQCT scans of the distal radius and tibia were obtained from 118 adults with OI (41.8 [IQR: 25.1] year old). To evaluate potential deviations in the scanned region, the axial scan angle was computed using a new algorithm that quantifies the angle between the areal center of the bone on the first and last slice of a scan. The angle was compared to that of limb-length dependent HR-pQCT scans of 13 healthy young women. It was considered to be deviated when being outside the fence of 1.5xIQR from Q1 and Q3 in those women. Bone microarchitecture and strength were quantified and compared to normative data from literature (Warden et al. Osteoporos Int 2021). Results: 102 radius and 105 tibia scans could be analyzed, of which the axial scan angle was found to be deviating in 11 (radius; 10.8%) and 14 (tibia; 13.3%). In the radius scans without deviating angle, total BMD was low (Z-score: -1.0+/-1.8) as were trabecular BMD (Z-score: -1.6+/-1.3) and number (Z-score: -2.5+/-1.4) and total bone stiffness (Z-score: -1.4+/-1.5). Trabecular separation was high (Z-score: -2.7 [2.7]). Trabecular thickness and cortical BMD and microarchitecture were normal. Larger deviations were seen at the tibia. In the scans with a deviating axial angle, deviations from the normative data were smaller or similar (cortical bone) but more often larger (total and trabecular bone) than in the scans without deviating angle, most pronounced at the tibia (Fig.1). Conclusion: Bone microarchitecture and strength in OI are impaired, in particular at the trabecular compartment. It likely contributes to the increased fracture risk in OI and may provide valuable insights to improve treatments of reduced bone quality. Scans with a deviating scanned region, likely due to bone deformities and scan positioning limitations in OI, should be excluded in HR-pQCT studies on OI, especially when comparing study groups.

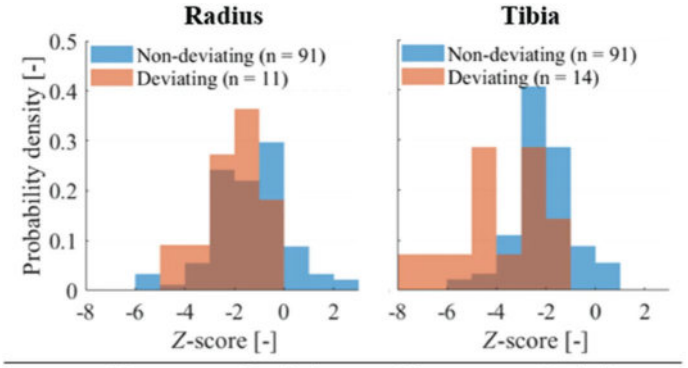

	Non-deviating	Deviating	Non-deviating	Deviating
Z<-1	51 (56%)	9 (82%)	78 (86%)	14 (100%)
Z<-4	4 (4%)	1 (9%)	5 (5%)	7 (50%)

Fig.1: Z-scores for bone stiffness at the distal radius (left) and tibia (right) from scans with and without deviating axial angle.

***Disclosures: MELISSA BEVERS**, None*

SUN-486

New Insights into the Skeletal Consequences of Trisomy 21 from the Plasma Metabolome and Lipidome of Patients *COLE DAHLSTROM[1], ALYSSA FALCK[2], KIRBY M. SHERMAN[3], Matthew Galbraith[4], Joaquin Espinosa[4], Dana Gaddy[5], Larry Suva[6]. [1]Texas A&M University, , [2], United States. [3]Texas A&M University , , [4]Colorado University- Anschutz, United States. [5]College of Veterinary Medicine, Texas A&M University, United States. [6]Texas A&M University, College of Veterinary Medicine and Biomedical Sciences, United States

Bone turnover is a complex and coordinated activity that results from two processes: bone resorption and new bone formation. CTX-I and P1NP are biochemical markers of bone resorption and formation that we measured in a series of bisphosphonate-naïve individuals diagnosed with trisomy 21 (Ts21) (20 female; 20 male, n=40) and control age-matched patients (20 female; 20 male, n=40). Ts21 females had significantly increased CTX-I (p=0.0442); however, once corrected for vitamin D and thyroid hormone status, no significant differences were observed. However, age stratification of patients revealed a significant and sustained decline in both CTX-1 and P1NP in female Ts21 patients between ages 20 and 40 (p=0.02) that was not observed in control. No significant correlations were observed in males with Ts21, indicative of sexual dimorphism in bone turnover markers in Ts21 patients. We next performed a detailed metabolomic analysis of plasma from these patients using Vanquish UHPLC coupled online to a Q Exactive high resolution mass spectrometer. Profiles were analyzed using Maven in conjunction with the KEGG database and the metabolomic profiles correlated with measured CTX-1 and P1NP levels. Several fatty acid (FA) metabolites (e.g. palmitic acid, acylcarnitine) had strong positive correlations with P1NP in control patients (p=0.0225 & p=0.001 respectively) but were not correlated in Ts21, suggesting that Ts21 osteoblasts may have alterations in their energy utilization of FAs. Similarly, aspartate and glutamine, which are both required for mitochondrial energy production, were diminished in plasma from patients with Ts21 compared to control, supporting the conclusion of mitochondrial dysregulation in Ts21. Furthermore, metabolites that impact bone cell function such as tauroursodeoxycholic acid and picolinic acid (both known to be bone anabolic) were positively correlated with P1NP levels in control but not Ts21 (p=0.0008 & p=0.0045 respectively), further implicating systemic diminution of osteoblast activity in Ts21 patients. Collectively, these studies provide new insight into the circulating metabolome of Ts21 patients and suggest that both osteoclast (CTX-I) and osteoblast (P1NP) activity may be compromised when disconnected from bone-promoting circulating metabolites. As Ts21 patients age, the continued miscommunication between the metabolome and bone cell function is likely contributing to the increased fracture risk that we and others have reported.

***Disclosures: COLE DAHLSTROM**, None*

SUN-487

A Prospective Study to Evaluate Patient-Reported Quality of Life Before and After Asfotase Alfa Treatment in Adults with Pediatric-Onset Hypophosphatasia *Kathryn Dahir[1], Steven Ing[2], Chad Deal[3], Andrew Messali[4], Toby Bates[4], Eric T. Rush[5]. [1]Vanderbilt University Medical Center, United States. [2]The Ohio State University Wexner Medical Center, United States. [3]Cleveland Clinic Foundation, United States. [4]Alexion, AstraZeneca Rare Disease, United States. [5]Children's Mercy Kansas City; University of Missouri - Kansas City School of Medicine, United States

Purpose: To evaluate the impact of asfotase alfa on patient-reported outcomes (PROs) in adults with pediatric onset hypophosphatasia (HPP).Methods: A longitudinal telephone-based survey was administered to adults with pediatric-onset HPP at baseline (prior to asfotase alfa initiation) and follow-up (3 [3M], 6 [6M], and 12 months [12M] post-initiation). Demographics and PROs (Patient Health Questionnaire-9 [PHQ-9], Patient-Reported Outcomes Measurement Information System [PROMIS-29], Routine Assessment of Patient Index Data 3 [RAPID3], and Work Productivity and Activity Impairment-Specific Health Problem [WPAI-SHP]) were assessed (Figure). McNemar's or Cochran-Mantel-Haenszel tests or paired t-tests were performed, as appropriate.Results: Among 50 enrolled patients, 29 were evaluable at 12M. Mean age at baseline was 46 (+/-15.4) years; 80% were female and 94% were White. At 12M, a statistically significant improvements from baseline were observed for PHQ-9 total score (10.6 baseline vs 4.2 12M, P<0.0001), PROMIS-29 domain scores (physical functioning: 38.0 vs 46.5, P<0.0001; anxiety: 57.5 vs 47.9, P<0.0001; depression: 52.6 vs 47.4, P=0.003; fatigue: 63.3 vs 51.3, P<0.0001; sleep disturbance: 58.8 vs 51.6, P=0.0008; social roles and activities: 42.6 vs 50.7, P=0.0001; pain interference: 63.8 vs 54.9, P<0.0001), and RAPID3 domain scores (functional status: 2.7 vs 1.1, P<0.0001; pain tolerance: 6.0 vs 3.2, P<0.0001; global health estimate: 5.1 vs 2.7, P<0.0001). WPAI-SHP domains showed significant improvement at 12M in presenteeism (39.6% vs 14.0%, P<0.0001), activity impairment (64% vs 30.0%, P<0.0001), and work productivity loss (41.9% vs 20.0%, P=0.012); however, the significant improvement seen at 6M in absenteeism (4.7% vs 0%, P=0.025) was not maintained at 12M (vs 8.0%, P=0.65). By 12M, the use of analgesic medications decreased from baseline (20%, n=10 vs 10.3%, n=3).Conclusion: Treatment with asfotase alfa improved anxiety, depression, physical functioning, fatigue, sleep, pain, and improved work and social relationships. These results illustrate the potential utility of adapting existing PRO instruments validated in diseases phenotypically similar to HPP.

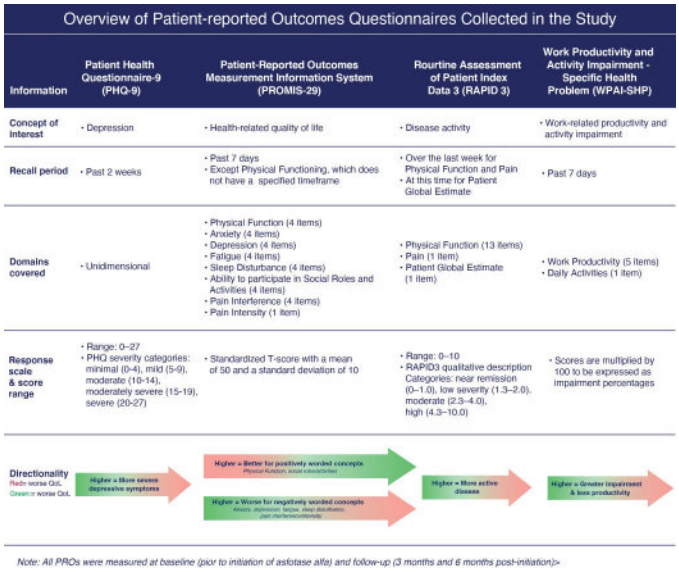

***Disclosures: Kathryn Dahir**, Alexion, AstraZeneca Rare Disease, Consultant, Alexion, AstraZeneca Rare Disease, Grant/Research Support*

SUN-488

A 14-day repeated oral administration of meclizine in child patients with achondroplasia to evaluate safety and pharmacokinetics *Masaki Matsushita[1], Kenichi Mishima[1], Yasunari Kamiya[1], Kenta Sawamura[1], Hiroshi Kitoh[2], Shiro Imagama[1]. [1]Nagoya University Graduate School of Medicine, Japan. [2]Aichi Children's Health and Medical Center, Japan

Achondroplasia (ACH) is a skeletal dysplasia characterized by shorten-limbed short stature. We employed a drug repositioning strategy and found meclizine, which has been used as an anti-motion sickness for more than 50 years, inhibited the fibroblast growth factor receptor 3 (FGFR3) signalings. Meclizine also revealed enhancing bone growth in a mouse model of ACH, and the plasma concentration of meclizine was lower than that for anti-motion sickness. A previous single-dose study of meclizine 25 and 50 mg for child patients with ACH showed no serious adverse events. According to the instruction of Pharmaceuticals and Medical Devices Agency, we performed additional pre-clinical studies using rats and dogs, including 2-week-repeated dose toxicity studies, toxicokinetic and pharmacokinetics (PK) studies, genotoxicity studies, safety pharmacology, pharmacodynamic studies, and juvenile animal toxicity studies. Thus, we conducted current study to evaluate the safety and PK for child patients with ACH after a 14-day-repeated dose of meclizine. Current study enrolled twelve patients with ACH, aged 5-10 years. Patients were randomly divided into meclizine 12.5 mg/day group (n = 6) and 25 mg/day group (n = 6), and they took meclizine after meals for 14 days. The adverse events (AEs) and PK were assessed. The patients were subjected to blood sampling immediately before drug dosing and at 1, 2, 3, 4, and 6 h after dosing on Days 1 and 14, and 10 and 24 h on Day 14 for PK evaluation. No patients experienced serious AEs in either group. The average maximum drug concentration (Cmax), peak drug concentration (Tmax), area under the curve (AUC0-24h), and terminal elimination half-life (t1/2) on Day 14 of meclizine 12.5 and 25 mg were 167 and 266 ng/mL, 3.7 and 2.8 h, 1170 and 1780 ng·h/mL, and 7.4 and 7.9 h, respectively. Cmax and AUC were increased in a dose-dependent manner. AUC0-6h on Day 14 was 1.5 times that on Day 1. The AUC0-24h on Day 14 revealed negatively correlation with patient weight. As proposing regimen of meclizine 12.5 and 25 mg in patients weighting <20 kg and >=20 kg, respectively, the coefficient of variation value for AUC0-24h was reduced from 54 to 21%. Compartment models demonstrated that the plasma concentration of meclizine achieved at steady state on Day 14. Meclizine 12.5 or 25 mg/day depending on the patients' weight is recommended for long-term administration of phase 2 clinical trial in child patients with ACH.

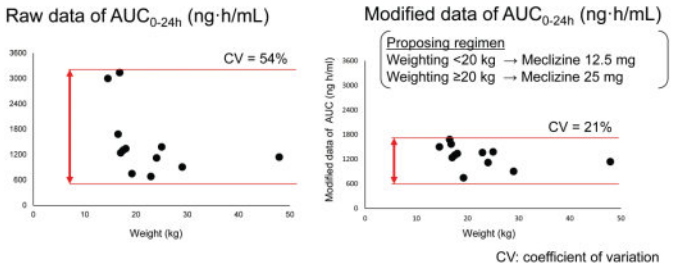

***Disclosures: Masaki Matsushita**, Japan Agency for Medical Research and Development, Grant/Research Support*

SUN-489

A Multicenter Study Evaluating Hypertension in Children with X-Linked Hypophosphatemia *Irene Chen[5], Anna Ryabets-Lienhard[2], Sreya Molakalapalli[3], Jennifer Ringrose[5], Leanne Ward[4], Robert T Alexander[5], Chelsey Grimbly[5]. [5]University of Alberta, Canada. [2]Children's Hospital Los Angeles, . [3]Children's Hospital of Los Angeles, United States. [4]Children s Hospital of Eastern Ontario, Canada. [5]University of Alberta,

X-linked Hypophosphatemia (XLH) is associated with elevated fibroblast growth factor 23 (FGF23) resulting in renal phosphate wasting and decreased 1,25 dihydroxyvitamin D. It is a multi-system disease with significant co-morbidities. Current treatment options include conventional therapy (phosphate and 1,25 dihydroxy vitamin D) or burosumab (anti-FGF23 therapy). High rates of hypertension (HTN) have been reported in adults, but it is unclear if HTN develops in childhood. We present data on HTN in pediatric XLH.Methods: We evaluated medical records of children (<18 years of age) with XLH followed at two tertiary care centers, the Stollery Children's Hospital (Edmonton, Canada), and the Children's Hospital of Los Angeles (Los Angeles, United States) from 2014-2022. Patients were included if they had three or more blood pressure (BP) recordings. Clinical data was collected including laboratory and treatment data and renal ultrasound results. HTN was defined as systolic or diastolic BP (SBP, DBP) greater than the 95th percentile for age, sex and height on three or more occasions, as per the Fourth Report on the Diagnosis, Evaluation, and Treatment of High Blood Pressure in Children and Adolescents. Descriptive analyses were performed. Results: Our cohort included 56 children (35 female, 63%) with XLH. HTN was found in 19 children (34% of the cohort, n=10 female), diagnosed at a mean age of 7.9 years (SD 4.2). SBP was higher than DBP with a SBP percentile average of 76 and DBP percentile average of 58 ($p<0.01$). 14 children had isolated systolic HTN, 4 had a combination of diastolic and systolic HTN, and 1 child had isolated diastolic HTN. HTN was not associated with body mass index, serum parathyroid hormone levels, nephrocalcinosis, or average weight-based phosphate or 1,25 dihydroxyvitamin D treatment over the study period. Furthermore, BP percentiles did not change with initiation of Burosumab therapy.Conclusion: Children with XLH demonstrate a high prevalence of hypertension as a third of our cohort met criteria for HTN. It is unclear why children with XLH develop HTN. FGF23 has been associated with vascular morbidity and elevated FGF23 drives the pathology in XLH. We did not see that anti-FGF23 treatment (Burosumab) lowered BP percentiles, but this could be confounded by a small sample size and the limited duration of follow up. HTN is an important comorbidity in XLH, and further studies are needed to identify risk factors.

***Disclosures: Irene Chen**, None*

SUN-490

microRNA Signature in Adult Patients with Hypophosphatasia *Roland Kocijan[1], Zora Messner[2], Benjamin Hadzimuratovic[3], Julia Feurstein[3], Jochen Zwerina[3], Andreas Diendorfer[4], Matthias Hackl[4], Heinrich Resch[2], Judith Haschka[5]. [1]Ludwig Boltzmann Institute of Osteology, . [2]St. Vincent Hospital Vienna, 2nd Medical Department, Vienna, Austria, Austria. [3]Ludwig Boltzmann Institute of Osteology at Hanusch Hospital of OEGK and AUVA Trauma Centre Meidling, 1st Medical Department Hanusch Hospital, Vienna, Austria, Austria. [4]TAmiRNA GmbH, Vienna, Austria, Austria. [5]Ludwig Boltzmann Institute for Osteology, Hanusch Hospital Vienna,

Background&Purpose Hypophosphatasia (HPP) is a rare genetic disorder, characterized by hypomineralization, recurrent fractures, musculoskeletal pain and extra-skeletal manifestations. The serological hallmark is low TNSALP (tissue non-specific alkaline phosphatase) activity and accumulation of natural substrates, such as PLP (Pyridoxalphosphate). Data on microRNAs (miRNAs) are lacking. Methods Circulating miRNAs, PLP and established bone turnover markers were analyzed in a cohort of adult HPP patients and healthy age- and sex-matched controls (CTRLs) in a cross-sectional design. Next-generation sequencing (NGS) of serum samples was performed and validation of selected miRNAs is ongoing using Reverse-transcriptase-quantitative PCR (RT-qPCR; TAmiRNA). Results Serum of 22 adult HPP patients and 23 CTRLs (47.9+/-14.2 vs.45.9+/-8.8 years, p=0.980) were analyzed. Alkaline phosphatase levels (ALPL) were significantly lower in HPP than

CTRLs (U/L;23+/-11 vs. 54+/-28, <0.0001). PLP-levels were above the reference range in 55% of patients (µg/L;36.3+/-98.2). 91% of patients reported musculoskeletal pain, 14 patients had history of fractures and 1 patient reported poor fracture healing. No patient had a history of seizures, diffuse neurological symptoms (e.g.headache) were reported of 41% of patients. In total, 84 miRNAs were differentially regulated in HPP vs. CTRLs (44 up- and 40 down-regulated, p-adj0.7, LOG FC 0.8/-0.8, p-adj.<0.05; e.g. miR-1-3p muscle, miR-107 brain, miR-26b-5p osteogenesis). Conclusion Adult HPP patients show a distinctive miRNA-signature compared to healthy population and an association to clinical manifestations. Differently regulated miRNAs display not only an affection of the musculoskeletal system including osteogenic differentiation/proliferation and muscle strength/dystrophy, but also display extra-skeletal manifestations in adult HPP.

***Disclosures: Roland Kocijan**, ALEXION, Grant/Research Support, ALEXION, Speakers' Bureau*

SUN-492

A Phase 1, Open-label, Dose-escalating Study to Evaluate the Safety, Tolerability, Pharmacokinetics, and Pharmacodynamics of ALXN1850 in Adults With Hypophosphatasia *KATHRYN DAHIR[1], Derek Dunn[2], Jawad Hasan[2], Amy Shannon[2], Wei-Jian Pan[2]. [1]Vanderbilt University Medical Center, [2]Alexion, AstraZeneca Rare Disease, United States

Hypophosphatasia (HPP) is a rare, inherited disorder associated with recurrent fractures/pseudofractures, orthopedic/dental burden, pain, mobility impairments, and diminished quality of life. ALXN1850 is an investigational enzyme replacement therapy being developed for the treatment of HPP.1-3 The primary objective of this study was to assess the safety and tolerability of ALXN1850 administered by IV weekly as 1 dose and SC for 3 weeks. Secondary objectives included pharmacokinetics (PK) of 1 IV and 3 SC doses, absolute bioavailability of SC, pharmacodynamic (PD) effects of 1 IV and 3 SC doses, and immunogenicity potential of ALXN1850. Of the 23 adult patients with HPP who signed informed consent, 15 were dosed, and each cohort of 5 received ALXN1850 (15, 45, or 90 mg) as 1 IV dose weekly and SC for 3 weeks; 3 patients missed doses due to COVID-19 but did not discontinue the study. Following IV and SC doses, peak and total exposure of ALXN1850 increased dose dependently (15-90 mg). Effective t1/2 was estimated at 3-6 days depending on dose. Mean bioavailability of SC doses was ~43% (range: 6%-75%). ALXN1850 achieved maximal lowering (nadir) of plasma inorganic pyrophosphate (PPi) in 7 days; ~40% post-dose PPi concentrations were below the limit of quantification (0.75µM). Mean PPi concentration was reduced for 3-4 weeks post-dose. There was no apparent impact of immunogenicity on ALXN1850 PK/PD. ALXN1850 has acceptable safety, tolerability, and PK profiles, demonstrating a sustained reduction in PPi concentrations in patients with HPP. These results will inform the selection of an appropriate therapeutic dose in future studies.References:1. Baumgartner-Sigl S et al. Bone. 2007;40(6):1655-1661.2. Whyte MP et al. J Clin Invest. 1985;76(2):752-756.3. Whyte MP. Academic Press. 2012:771-794.Acknowledgments: The authors would like to thank the patients, their families, and the investigators of the trial (NCT04980248), and Loredana Cuccia (Medical Lead/Medical Monitor, Alexion, AstraZeneca Rare Disease) for their commitment to this research. Medical writing and editorial support were provided by Danielle Dalechek, MSc, of Oxford PharmaGenesis Inc., Newtown, PA, USA, and were funded by Alexion, AstraZeneca Rare Disease, Boston, MA, USA.

Safety Overview Table

Safety finding, n (%)	Description (N = 15) of 4 weeks treatment with ALXN1850
Any TEAE	12 (80.0%); 46 events
Related TEAE	10 (66.7%); 29 events
Injection site reactions (ISRs)	8 (53.3%); 10 out of 41 (24.4%) SC injections led to an ISR event* • Four patients with 1 ISR (erythema) • One patient with 1 ISR (soreness, swelling, and redness) • One patient with 1 ISR (erythema and bruising) • One patient with 3 ISRs, 1 per each SC administration (erythema and pruritus; erythema and ecchymosis; erythema) • One patient with 1 ISR (bruise) Four patients had 1 ISR each of erythema, not reported as TEAEs but included in this ISR total. One patient experienced induration following the IV dose, which is not included in this ISR total
Injection associated reactions • **Systemic reactions**	1 (6.7%) Headache (grade 1), considered related to study drug,*** occurred following the start of the IV dose and resolved the same day following medical intervention.
TESAE	1 (6.7%) Atrial fibrillation (grade 3) considered not drug related***
TEAE/TESAE leading to study drug withdrawal	0
Immunogenicity (ADA+)**	4 (26.7%) Only 1 (6.7%) was treatment emergent; ADAs persisted to the end of the study. Per protocol, patient was offered follow-up via the HPP registry. No patients tested NAb+

*Most cases of erythema resolved in less than 2 hours following the SC dose. There was no pattern observed in the timing of SC administration (ie, first, second, or third dose) and the occurrence of erythema.
**Assays for measuring anti-ALXN1850 antibodies and neutralizing antibodies (NAbs) were fully validated for precision, specificity, selectivity, sensitivity, robustness, and drug tolerance following the current 2019 FDA guidance on ADA method validation.
***By the investigator.
ADA, antidrug antibody; AE, adverse event; HPP, hypophosphatasia; IV, intravenous; NAb, neutralizing antibody; SC, subcutaneous; TEAE, treatment-emergent adverse event; TESAE, treatment-emergent serious adverse event.

***Disclosures: KATHRYN DAHIR**, Alexion, AstraZeneca Rare Disease, Consultant*

SUN-493

Utilization of EMR Filters to Identify Potential Cases of Occult Hypophosphatasia in a Single Health System *Camille Moeckel[1], Joshua Chen[1], Zara Karuman[1], Masayo Mesler[1], Edward Fox[1]. [1]Department of Orthopaedics and Rehabilitation, Penn State Milton S. Hershey Medical Center, United States

Occult hypophosphatasia (HPP) is a rare metabolic bone disorder caused by mutations in the ALPL gene; it is characterized by a wide variety of clinical symptoms including a persistently low tissue-non-specific alkaline phosphate (ALP). ALP is important for mineralization of the bones and teeth. Therefore, HPP can have serious consequences if left undiagnosed. Identifying patients with HPP can be challenging because a low ALP is uncommonly encountered in clinical practice and HPP has a nonspecific clinical presentation in milder forms. Electronic medical record (EMR) systems have become an integral part of patient care, and there is growing interest in their potential to improve disease surveillance and early diagnosis. The purpose of this study is to investigate the use of EMR filters in the identification of potential cases of occult HPP in a large, rural health system. After IRB approval, our Information Technology department utilized filters to identify adult patients (>18) who had visited the health system from 2014 to 2018 and had two consecutively low ALP levels (serum alkaline phosphatase <=30 IU/L). Patient charts that met the search criteria were then reviewed by the research team to confirm the potential diagnosis and collect data on their clinical characteristics. Exclusion criteria for patients included the presence of diseases and treatments known to decrease ALP levels, such as active cancer, multiple myeloma, overt hypothyroidism, malnutrition, pernicious or profound anemia, multiorgan/hepatic failure, bisphosphonate therapy, chronic glucocorticoids, and ongoing chemotherapy. Of the 733,860 unique patients seen between 2014 and 2018, 273 patients were identified with two consecutively low ALP levels. Among these patients, 28 were identified after chart review as potentially having occult HPP. Common symptoms reported included musculoskeletal pain, recurrent fractures, myalgia, chondrocalcinosis, and dental problems, such as periodontal disease. In conclusion, the utilization of EMR filters to identify potential cases of occult HPP has shown to be an effective approach; by leveraging the power of EMRs, healthcare providers can quickly identify patients at risk for HPP and initiate appropriate interventions. Going forward, the next step would be to contact the identified patients for further evaluation and management. By taking a proactive automated approach to screening and diagnosis, outcomes can potentially be improved for patients with HPP.

***Disclosures: Camille Moeckel**, None*

SUN-494

Prevalence of ENPP1 variants among patients with ossification of the posterior longitudinal ligament *Hajime Kato[1], Shivani Srivastava[2], Paul Stabach[3], Soichiro Kimura[4], Takashi Sunouchi[4], Yoshitomo Hoshino[4], Naoko Hidaka[4], Minae Koga[4], DEMETRIOS BRADDOCK[5], Nobuaki Ito[6,1], [2]Department of Pathology, Yale University, United States. [3]Department of Pathology, Yale Universty, United States. [4]Division of Nephrology and Endocrinology, The University of Tokyo Hospital, Japan. [5]YALE UNIVERSITY, United States. [6]The University of Tokyo Hospital, Japan

Background: Ossification of the posterior longitudinal ligament (OPLL) is a multifactorial disease that is caused by genetic and environmental factors. On the other hand, some hereditary FGF23-related hypophosphatemic rickets/osteomalacia (heterozygous PHEX mutation, homozygous ENPP1 mutation, homozygous DMP1 mutation) are known to develop OPLL. We, therefore, hypothesized that mild or undiagnosed cases of these diseases are included in the patients diagnosed with OPLL.Methods: We prospectively evaluated the frequency of cases with low-frequency variants (allele frequency in gnomAD: <0.5%) in the exonic regions of PHEX, ENPP1, and DMP1 genes in patients who underwent surgery for OPLL at our hospital. Clinical and biochemical data (i.e. calcium, phosphate, FGF23) of were collected. Plasma inorganic pyrophosphate (PPi) levels, which ENPP1 produces by hydrolyzing ATP, were also measured to evaluate the effect of the detected variants on ENPP1 catalytic activity.Results: The total of 50 patients with OPLL were included in this study (median age, 68 years [range, 37-86 years]; 14 women [28%]). All OPLL patients underwent genetic testing, and four types of heterozygous rare ENPP1 variants (c.802T>C [p.Y268H], c.1352A>C [p.Y451C], c.2089G>A [p.V697M], c.2335A>C [p.T779P]) were found in seven patients (14%). Clinical and biochemical data analysis showed that FGF23 levels of the OPLL patients with ENPP1 variants (median: 46 pg/mL [range: 36-102 pg/mL]) were higher than those of OPLL patients without ENPP1 variants (median: 36 pg/mL [range: 14-86 pg/mL]) (p=0.01). All of seven OPLL patients with heterozygous ENPP1 variants presented low plasma PPi levels (median: 1.8µM [range: 1.0-1.9 ?M], reference value 2-5 ?M). In vitro kinetic assays showed p.Y268H, p.Y451C, p.V697M and p.T779P variants possessed a catalytic velocity of 5%, 30%, 30%, and 1%, respectively, compared with that of wild-type ENPP1.Conclusion: This study revealed that patients with heterozygous ENPP1 variants were included in patients with OPLL and the prevalence of ENPP1 variant in this cohort was 14%. The establishment of the appropriate diagnostic criteria to select cases with pathogenic ENPP1 variants would be warranted.

***Disclosures: Hajime Kato**, None*

SUN-496

A patient-centred and multi-stakeholder co-designed, mixed methods, observational, prospective study protocol: Example of the adolescent experience of treatment for X-linked hypophosphatemia (XLH) *Vrinda Saraff[1], Pedro Arango-Sancho[2], Justine Bacchetta[3], Annemieke M. Boot[4], Christine P. Burren[5], Amish Chinoy[6], Poonam Dharmaraj[7], Juan David González-Rodríguez[8], Iva Gueorguieva[9], Wesley Hayes[10], Agnès Linglart[11], Maria Amelia Gómez Llorente[12], Héctor Ríos[13], Dirk Schnabel[14], Pol Harvengt[15], Karen M.A. Bailey[16], Fiona Glen[16], Paul Joos-Vandewalle[17], Angela J. Rylands[18], Angela Williams[18], Elin Haf Davies[19]. [1]Department of Paediatric Endocrinology and Diabetes, Birmingham Women's and Children's Hospital NHS Trust, United Kingdom. [2]Department of Pediatric Nephrology, Hospital Sant Joan de Deu, Spain. [3]Centre Hospitalier Universitaire (CHU) de Lyon, Hôpital Femme-Mère-Enfant, France. [4]University Medical Center Groningen, Department of Pediatric Endocrinology, University of Groningen, Netherlands. [5]Bristol Royal Hospital for Children, United Kingdom. [6]Department of Paediatric Endocrinology, Royal Manchester Children's Hospital, United Kingdom. [7]Department of Paediatric Endocrinology, Alder Hey Children's NHS Foundation Trust, United Kingdom. [8]Department of Pediatric Nephrology, Santa Lucia General University Hospital, Spain. [9]Centre Hospitalier Universitaire (CHU) de Lille, France. [10]Department of Nephrology, Great Ormond Street Hospital, United Kingdom. [11]Assistance Publique Hôpitaux de Paris, Université Paris Saclay, Bicêtre Paris-Saclay Hospital, France. [12]Department of Pediatric Nephrology, Virgen de las Nieves Universitary Hospital, Spain. [13]Department of Pediatric Nephrology, Vall d´Hebron Universitary Hospital, Vall d´Hebron Institut de Recerca, Spain. [14]Department of Pediatric Endocrinology and Diabetes, Charité Universitätsmedizin Berlin, Germany. [15]XLH Belgium (Belgium X-Linked Hypophosphatemic Rickets [XLH] Patient Association), Belgium. [16]Open Health, United Kingdom. [17]Global Medical Affairs, Kyowa Kirin International, United Kingdom. [18]Medical Affairs, Kyowa Kirin International, United Kingdom. [19]Aparito, United Kingdom

BackgroundXLH is a rare, genetic, life-long disease caused by PHEX pathogenic variants. It is associated with progressive accumulation of musculoskeletal features and symptoms that evolve across the patient's lifetime if untreated. Although the disease is well characterised in children and adults, there are limited data describing the health outcomes and experiences of adolescents, particularly at end of skeletal growth (EOSG), a crucial phase during transition to adulthood.To explore these unmet needs, a collaborative, patient-centric, mixed-methods protocol was developed to assess functionality and health-related QoL (HRQoL) in adolescents with XLH at EOSG, including caregiver perspectives.MethodsMy XLH (NCT05181839) is a 12-month, multicentre, non-interventional, observational, prospective study using a mixed-methods approach. Research questions and methodology were designed collaboratively by patient-centred outcome research specialists, adolescents with XLH, caregivers, expert European physicians, and specialist technology providers.Descriptive analyses of quantitative and qualitative data will assess the experiences of adolescents and caregivers in the pre-index (before EOSG) and post-index (after EOSG) periods. Targets of 30 adolescents and 15 caregivers were considered sufficient to reflect diversity of opinions and experiences.The study setting is specialist centres in Europe that treat adolescents with XLH with burosumab.The target population is adolescents aged 12-17 years with genetically confirmed XLH treated with burosumab for >=12 months and confirmed as approaching EOSG. Patients non-adherent to treatment, or scheduled for orthopaedic surgery during the study will be excluded.Data will be collected for 4 weeks before and 26 weeks after EOSG. Analyses will be conducted to describe characteristics, symptoms, activities, and experiences of adolescents during treatment pre- and post-EOSG (with comparisons over time between patients continuing and discontinuing treatment post-index). Caregivers will be interviewed about their experiences and support needs of adolescents.ResultsRecruitment began on 24 November 2021. As of 18 April 2023, 24 patients have been enrolled. Enrolment is due to be completed by end of December 2023. Data analysis is planned to commence in 2024. ConclusionOur multistakeholder, mixed-methods research design in a rare disease offers an inclusive approach to better understand patient and caregiver experience.

***Disclosures: Vrinda Saraff**, Kyowa Kirin, Consultant*

SUN-497

Evidence Based Guidelines On Diagnosis, Management and Monitoring of X-Linked Hypophosphatemia (XLH) in The Pediatric and Adult Population 2023 *Aliya A. Khan[1], Dalal Ali[2], MARIA LUISA BRANDI[3], Eric Rush[4], Gordon Guyatt[1], Natasha Appelman-Dijkstra[5], Catherine Chaussain[6], Suzanne Jan De Beur[7], Thomas Carpenter[8]. [1]McMaster University, Canada. [2], . [3]FONDAZIONE FIRMO, Italy. [4]Children's Mercy Kansas City, United States. [5]Leiden Center for Bone Quality, Netherlands. [6]Université Paris Cité and APHP, France. [7]Johns Hopkins University, United States. [8]Yale University School of Medicine, United States

Background: Over the past 5 years, there have been rapid advances in our understanding of the multisystem manifestations of XLH and the development of new treatment paradigms. To offer guidance to clinicians and to promote evidence-based care, an International Working Group (IWG) of 52 experts in guideline development methodology and XLH in the pediatric and adult population has convened to develop new evidence-based guidelines on the evaluation, management, and monitoring of XLH.Methods: Four systematic reviews and meta-analyses were completed using the GRADE methodology addressing the management of XLH in relation to patient important outcomes and surrogate outcomes. In addition to the systematic reviews, expert clinical practices were captured with a comprehensive, 280 item questionnaire developed by the panel and administered to 44 experts treating patients with XLH. Data derived from the questionnaire were captured in expert-opinion based narrative reviews that address: 1) diagnosis of XLH including the role of genetic testing, 2) dental complications, 3) indications for treatment, 3) selection of treatment, 4) disease and treatment monitoring, 5) pregnancy and lactation in XLH, 5) agenda for future research.The new international guidelines on XLH will be reviewed by stakeholders including professional medical societies and patient advocacy organizations interested in endorsing these guidelines.Conclusions: These new guidelines will be presented for the first time internationally at the upcoming meeting of the ASBMR in October 2023.International Working Group Members:Aliya A. Khan (Chair), Dalal S. Ali, Maria L. Brandi, Eric Rush, Hajar Abualarob, Hatim Alalwani, Abdulrahman Alamri, Rana Aldabbagh, R.Todd Alexander, Farah Alsarraf, Natasha Appelman-Dijkstra, Signe Sparre Beck-Nielsen, Martin Biosse Duplan,Tom Carpenter, Catherine Chaussain, Martine Cohen-Solal, Rachel K. Crowley, Karel Dandurand, Guido Filler, Lisa Friedlander, Seiji Fukumoto, Claudia Gagnon, Paul Goodyer, Corinne Grassmann, Chelsey Grimbly, Gordon Guyatt, Dieter Haffner, Erik A. Imel, Suzanne M. Jan de Beur, Kassim Javaid, Sarah Khan, Aneal Khan, Anna Lehman, Willem F. Lems, E. Michael Lewiecki, Agnès Linglart, Outimaija Makitie, Karen McAssey, Ciara McDonnell, Reza D. Mirza, Emmett Morgante, Archibald Morrison, Anthony Portale, Frank Rauch, Lars Rejnmark, Yumie Rhee, Salvatore Ruggiero, Heide Siggelkow, Sotirios Tetradis, Laura Tosi, Pablo Florenzano Valdes, Leanne M. Ward

***Disclosures: Aliya A. Khan**, Amgen, Amolyt and Takeda, Consultant, Alexion, Amgen, Ascendis, Chugai, Radius, Takeda, Grant/Research Support*

SUN-499

Investigating PTH-Independent CaSR Inhibition on Renal Calcium handling: Rationale and Design for a Phase 2 Clinical Trial (NCT05735015) *Iris Hartley[2], Rachel Gafni[2], Kelly Roszko[2], Karen Pozo[2], Kimberly Ampuero[2], Ananth Sridhar[3], Arun Mathew[3], Mary Scott Roberts[3], Scott Adler[3], Edward Nemeth[4], Michael Collins[2]. [2]National Institutes of Health, United States. [2]National Institutes of Health, , [3]Calcilytix Therapeutics, Inc., United States. [4]MetisMedica, Canada

Parathyroid hormone (PTH) and the Calcium-sensing receptor (CaSR) are the primary regulators of blood and urinary calcium levels. The relative and/or hierarchical contributions of PTH and the CaSR in regulating renal calcium handling, an important physiologic focus of their action, are not well understood, largely due to their intertwined physiology. CaSR activation and inhibition directly impact PTH secretion, thus confounding the ability to isolate their independent effects on calcium regulation. We propose that studying patients with absent or insufficient circulating PTH, as is seen in postsurgical hypoparathyroidism (PSH), with the oral negative allosteric CaSR modulator encaleret will reveal PTH-independent CaSR effects on calcium handling. We further hypothesize that encaleret will sufficiently lower urine calcium and increase blood calcium levels to serve as a primary or adjuvant oral treatment option for patients with PSH. To test these hypotheses, we have designed an open-label, phase 2, proof-of-principle study using encaleret to evaluate PTH-independent effects of CaSR modulation on renal calcium handling in PSH. The study will enroll up to 10 patients with PSH >1 year since surgery (permanent PSH) and up to 5 patients with PSH <1 year since surgery. Calcitriol will be discontinued, calcium supplementation continued and adjusted, and encaleret 162 mg administered every 12 hours for 5 inpatient days. Patients will undergo serial sampling of markers of mineral metabolism and 24-hour urine assessments. This dose, the highest studied to date, was selected to avoid missing a drug effect due to inadequate dosing. Participants with <1 year of PSH will be studied to assess the ability of high dose encaleret to identify PTH reserve in early PSH. The primary and secondary endpoints are: 1) change in fractional excretion of calcium and 2) the proportion of patients who achieve a concomitant normal fasting albumin-corrected blood calcium level and normal 24-hour urinary calcium excretion. Exploratory endpoints include pharmacokinetics, changes in albumin-corrected and ionized blood calcium, intact PTH, cyclic AMP excretion, 1,25-(OH)2 Vitamin D, C-telopeptide, procollagen type 1 N-propeptide, and urinary supersaturation analyses. We anticipate that the results will inform our understanding of renal mineral physiology and clarify the potential of encaleret as a treatment option for patients with PSH.

***Disclosures: Iris Hartley**, Calcilytix Therapeutics, Inc., Grant/Research Support*

SUN-500

Age at diagnosis of XLH amongst children with and without a family history: Findings from the International XLH Registry *Suma Uday[1], Kerry Sandilands[2], Angela Williams[2], M. Zulf Mughal[3]. [1]Birmingham Women's and Children's Hospital & Institute of Metabolism and Systems Research, University of Birmingham, United Kingdom. [2]Kyowa Kirin International, United Kingdom. [3]Department of Paediatric Endocrinology & Metabolic Bone Disease, Royal Manchester Children's Hospital & The Faculty of Biology, Medicine & Health, University of Manchester, United Kingdom

Background: X-linked hypophosphatemia (XLH) is a rare, progressive, genetic phosphate wasting disorder leading to rickets, lower limb deformities as well as short and disproportionate stature. The condition is inherited in the majority, however spontaneous mutations are reported in ?30% of cases. Its rarity, coupled with its diverse clinical manifestations, may lead to delayed diagnosis and subsequently delayed treatment initiation. The objective of this analysis is to investigate if there is a delay in diagnosis for children without a family history (FH) compared to those with a FH.Methods: The International XLH Registry (NCT03193476) is a multicentre, prospective, non-interventional study initiated in 2017, aiming to recruit 1,200 people with XLH, collecting data prospectively for a period of 10 years. All participants of all ages with a confirmed diagnosis of XLH, regardless of their treatment and management, are included in the Registry.Results: At the database lock for the first analysis (29 March 2021), 579 participants had entered the registry before 30 November 2020, of which 360 were children. Date of diagnosis and data for FH were available for 195 of the 360 children. Of 195 children, 121 (62%) reported FH of XLH, defined as having a biological parent(s) affected, whereas 74 (38%) had no FH of XLH. Of those with a FH, the biological mother was affected in 77%, biological father affected in 22%, and both affected in 1% of cases. Children aged <18 years with no FH were significantly older at time of diagnosis (3.96 years) compared to those with a FH (1.47 years), p<0.001. Males (n=74) and females (n=121) did not differ in terms of age at diagnosis.Conclusions: All XLH patients without a FH of XLH were diagnosed significantly later than patients with a FH. Younger patients with a FH appear to be diagnosed more quickly than older patients, suggesting increased disease awareness.

Age Group Years	FAMILY HISTORY OF XLH		NO FAMILY HISTORY OF XLH		P-value
	n	Age at XLH Diagnosis (years), Mean (SE)	n	Age at XLH Diagnosis (years), Mean (SE)	
<5	28	0.43 (0.06)	4	0.97 (0.15)	p=0.07
5 < 12*	58	1.43 (0.25)	38	4.31 (0.34)	p<0.001
12 < 18*	35	2.36 (0.51)	32	3.92 (0.51)	p=0.002

***Disclosures: Suma Uday**, Kyowa Kirin International, Grant/Research Support*

SUN-501

Efficacy of growth hormone therapy on height in children with achondroplasia *Takuo Kubota[1], Hirofumi Nakayama[2], Takeshi Ishimi[3], Chieko Yamada[3], Yukako Nakano[3], Ikumi Ueda[3], Tatsuya Nakamichi[3], Hiroyuki Saitou[3], Kenichi Yamamoto[4], Makoto Fujiwara[6], Yasuhisa Ohata[6], Taichi Kitaoka[1], Keiichi Ozono[1]. [1]Osaka University Graduate School of Medicine, Japan. [2]Department of Pediatrics, Graduate School of Medicine, The first Department of Oral and Maxillofacial Surgery, Graduate School of Dentistry, Osaka University , Japan. [3]Department of Pediatrics, Osaka University Graduate School of Medicine, Japan. [4]Department of Pediatrics, Division of Health Sciences, Osaka University Graduate School of Medicine, Japan. [6]Osaka University, . [6]Osaka University, Japan

Background: Achondroplasia (ACH) is a skeletal disorder with marked short stature and short limbs. The mean adult height has been reported to be 130.4 cm in males and 124.0 cm in females, respectively, in Japan, resulting in difficulties of daily life. Growth hormone (GH) therapy is available in children with ACH in Japan, although evidence on the efficacy of GH therapy on height growth is limited. Aim: To elucidate the efficacy of GH therapy on height growth in children with ACH. Methods: Children with ACH who visited our department from January 2011 to December 2022 and received GH therapy were included in this study. Height data between a year before and 5 years after the initiation of GH therapy were collected annually. Height SD values for healthy and ACH children and annual growth velocity (AGV) were evaluated. No further data were included after discontinuation of the therapy. A height increase due to lower limb lengthening was subtracted from the height measured. Results: Forty?one children (25 males) with ACH were included in the study. The median age was 4.00 years (range: 3.04 to 8.50) at the beginning of GH therapy. Height SD at that time was ?4.95 +/- 0.75 (mean +/- SD) for healthy children and ?0.24 +/- 0.71 for children with ACH. AGV was 4.45 +/- 1.62 cm. Regarding the efficacy of the therapy, the mean height SD of ?4.28, ?4.01, ?3.69, ?3.83, and ?3.84 for healthy children significantly increased 1 to 5 years after GH therapy, respectively, compared to that at the therapy initiation. In addition, the mean height SD of 0.25, 0.51, 0.95, 1.03 and 1.18 for children with ACH significantly increased in 1 to 5 years after GH therapy, respectively. AGV was 7.40, 5.76, 5.66, 4.84 and 4.77 cm 1 to 5 years after GH therapy, respectively, and significantly higher 1 to 3 years after GH therapy compared to that at the therapy initiation. Four and one patients underwent adenotonsillectomy and lower limb lengthening, respectively, after GH therapy initiation. GH therapy in 3 patients was changed to C-type natriuretic peptide analogue treatment. Except for the medical treatment change, no discontinuation of GH therapy occurred. Discussion: Height SD for both healthy and ACH children, and annual growth velocity were improved at least 1 to 3 years during GH therapy in this study, which shows the efficacy of GH therapy on height in children with ACH. Adult height needs to be evaluated in many patients with ACH after GH therapy.

***Disclosures: Takuo Kubota**, BioMarin Pharmaceutical Japana, Speakers' Bureau, Eli Lilly Japan, Grant/Research Support, Novo Nordisk Pharma, Speakers' Bureau*

SUN-503

Pharmacokinetics and Pharmacodynamics of Garetosmab in Patients with Fibrodysplasia Ossificans Progressiva *Yuhuan Wang[1], Jenny-Hoa Nguyen[1], Ruben De Ruiter[2], Jeanne Mendell[1], Dushyanth Srinivasan[1], John Davis[1], Elisabeth Eekhoff[3]. [1]Regeneron Pharmaceuticals, Inc., United States. [2], Netherlands. [3]Amsterdam UMC, location VU University Medical Center, Amsterdam, The Netherlands, Netherlands

Purpose: Fibrodysplasia ossificans progressiva (FOP) is a rare disorder caused by mutations in the bone-morphogenetic protein (BMP) type-1 activin-A receptor, characterized by episodes of soft tissue swellings, flare-ups, and progressive heterotopic ossification (HO) in skeletal muscles throughout the body. Garetosmab is an investigational fully human monoclonal antibody against activin-A that prevents formation of new HO. We report pharmacokinetic (PK) and immunogenicity data of garetosmab from the LUMINA-1 study.Methods: LUMINA-1 (NCT03188666) was a phase 2, randomized, double-blind, placebo-controlled study evaluating the safety and efficacy of garetosmab (10 mg/kg every 4 weeks intravenous) in adults with FOP over 28 weeks, followed by a 28-week open-label treatment period and a subsequent open-label extension. The PK, immunogenicity, concentrations of BMP9, and comparative exposure-response (E-R) analyses for efficacy and safety were performed with trough concentrations of functional garetosmab in serum (Ctrough) as exposure variables. Results: PK data were analyzed in 44 patients who received garetosmab. Plots of Ctrough over time showed that steady-state PK was reached 12-16 weeks after the first dose of garetosmab. After reaching steady state, Ctrough averaged (SD) 105 (30.8) mg/L. There was no meaningful difference in the PK profiles between patients who did and did not experience epistaxis. Immunogenicity assessments showed anti-garetosmab antibody formation with a persistently low titer in one patient (1/43; 2.3%), with no apparent impact on garetosmab PK or clinical effects. Median concentrations of BMP9 were approximately 40 pg/mL at baseline. Levels did not show treatment-related changes over time nor were differences seen between patients who did and did not experience epistaxis. The comparative E-R analyses demonstrated no association between Ctrough and efficacy (number of new HO lesions versus baseline) or safety (incidence or severity of treatment emergent adverse events of special interest, eg epistaxis or death).Conclusions: PK steady state was reached within ~12 weeks of starting garetosmab and no association was observed between higher serum exposures to functional garetosmab and the likelihood of experiencing adverse events. Incidence of anti-garetosmab antibodies was low and concentrations of BMP9 in serum had no apparent association with epistaxis. Garetosmab is being further evaluated in the phase 3 OPTIMA trial (NCT05394116).

***Disclosures: Yuhuan Wang**, Regeneron Pharmaceuticals, Inc., Other Financial or Material Support, Regeneron Pharmaceuticals, Inc., Major Stock Shareholder*

SUN-504

A Phase 1/2, Open-Label, Multiple Ascending Dose Clinical Study to Evaluate the Safety, Tolerability, Pharmacokinetics, and Pharmacodynamics of INZ-701 in Adults with ENPP1 Deficiency *Yves Sabbagh[1], Robert Wermers[2], Rainard Fuhr[3], Dirk Schnabel[4], Terra Arnason[5], Alix Besancon[6], Borut Cizman[1], Deborah Wenkert[7], Kurt Gunter[1]. [1]Inozyme Pharma, United States. [2]Mayo Clinic, United States. [3]Parexel International GmbH, Early Phase Clinical Unit Berlin, Germany. [4]Charitè, Universitätsmedizin Center for Chronic Sick Children, Pediatric Endocrinology, Germany. [5]University of Saskatchewan, Division of Endocrinology, Canada. [6]Hôpital Universitaire Necker Enfants Malades, Endocrino-diabetologie pediatrique , France. [7]Wenkert and Young, LLC, United States

Background: ENPP1 Deficiency is a rare disorder due to inactivating mutations in the ENPP1 gene. It is characterized by low levels of inorganic pyrophosphate (PPi), a critical regulator of mineralization; subsequent pathologic soft tissue calcification results in ~50% infant mortality and life-long musculoskeletal and cardiovascular morbidities. No targeted therapy exists for this disease. INZ-701 is a recombinant ENPP1-Fc investigational product which has demonstrated efficacy in preclinical models of ENPP1 Deficiency.Purpose: To determine the safety, tolerability, immunogenicity, pharmacokinetics and pharmacodynamics of INZ-701 following subcutaneous administration in adults with ENPP1 Deficiency. Methods: Phase 1/2, multicenter, open-label, multiple ascending dose study including three cohorts of three adults each, with genetic confirmation and PPi <1300 nM (NCT04686175). Participants were dosed at Day 1, then twice weekly from Day 8 to the end of the study.

Results: In all 3 dosing cohorts as of January 10, 2023, INZ-701 was well-tolerated with no related serious or severe adverse events. Low titers of non-neutralizing anti-drug antibodies (<160) were observed in 7/9 patients. Rapid increase in mean PPi from baseline of 426+/-407 nM of was noted in all patients, reaching the healthy volunteer range within 6 hours of the first dose. Mean PPi across the 0.2, 0.6, and 1.8 mg/kg dosing groups from day 32 through last data cut was 1299+/-490 nM, 1472+/-516 nM, and 1462+/-233 nM, respectively. Six of eight evaluable participants showed improvements in overall health on the Global Impression of Change (GIC) scale, as reported by both participants and clinicians. Long half-life of approximately 126 hours and drug accumulation as shown by a greater than dose proportional exposure suggests the potential for once weekly dosing. All participants enrolled in the phase 2 portion of the study.Conclusions: INZ-701 demonstrated a rapid and sustained increase in PPi levels in all participants, was well tolerated, and exhibited a favorable safety profile with a potential for once weekly dosing. Improvements in GIC score were observed in 6/8 patients and this ongoing study will elucidate the impact of INZ-701 on additional clinical and functional endpoints.

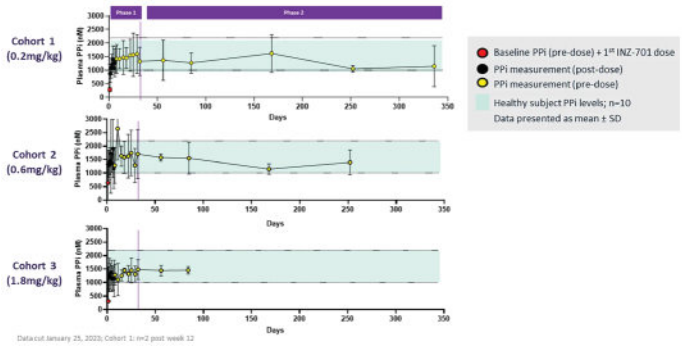

***Disclosures: Yves Sabbagh**, Inozyme Pharma, Other Financial or Material Support*

SUN-506

Medical care use among patients with monogenic osteoporosis due to rare variants in LRP5, PLS3, or WNT1 *Sara Verdonk[1], Silvia Storoni[1], Lidiia Zhytnik[2], Wenchao Zhong[2], Gerard Pals[3], Barend van Royen[4], Mariet Elting[3], Alessandra Maugeri[3], Elisabeth Eekhoff[5], Dimitra Micha[6]. [1]Amsterdam UMC location Vrije Universiteit Amsterdam, Department of Internal Medicine Section Endocrinology, Rare Bone Disease Center Amsterdam, Amsterdam Movement Sciences, Netherlands. [2]Amsterdam UMC location Vrije Universiteit Amsterdam, Department of Human Genetics, Rare Bone Disease Center Amsterdam, Amsterdam Movement Sciences, Netherlands. [3]Amsterdam UMC location Vrije Universiteit Amsterdam, Department of Human Genetics, Netherlands. [4]Amsterdam UMC location University of Amsterdam and location Vrije Universiteit Amsterdam, Department of Orthopedic Surgery and Sports Medicine, Netherlands. [5]Amsterdam UMC, location VU University Medical Center, Amsterdam, The Netherlands, Netherlands. [6]Amsterdam UMC locateon Vrije Universiteit Amsterdam, Department of Human Genetics, Rare Bone Disease Center Amsterdam, Amsterdam Movement Sciences, Netherlands

PurposePathogenic variants in the LRP5, PLS3, or WNT1 genes can significantly affect bone mineral density, causing monogenic osteoporosis. Much remains to be discovered about the phenotype and medical care needs of these patients. The purpose of this study was to examine the use of medical care among Dutch individuals identified between 2014 and 2021 with a pathogenic or suspicious rare variant in LRP5, PLS3, or WNT1. In addition, the aim was to compare their medical care utilization to both the overall Dutch population and the Dutch Osteogenesis Imperfecta (OI) population.MethodsThe Amsterdam UMC Genome Database was used to match 93 patients with the Statistics Netherlands (CBS) cohort. Patients were categorized based on their harbored variants: LRP5, PLS3, or WNT1. Hospital admissions, outpatient visits, medication data, and diagnosis treatment combinations (DTCs) were compared between the variant groups and, when possible, to the total population and OI population.ResultsCompared to the total population, patients with an LRP5, PLS3, or WNT1 variant had 1.61 times more hospital admissions, 2.0 times more opened DTCs, and a greater proportion using medication. Compared to OI patients, they had 0.61 times fewer admissions.ConclusionDutch patients with an LRP5, PLS3, or WNT1 variant appear to require on average more medical care than the total population. As expected, they made higher use of care at the surgical and orthopedic departments. Additionally, they used more care at the audiological centers and the otorhinolaryngology (ENT) department, suggesting a higher risk of hearing-related problems.

Table 1. Admission incidence rate comparing the number of hospitalizations of Dutch patients with a pathogenic or a rare suspicious variant in *LRP5*, *PLS3* or *WNT1* to the total population between 2013 and 2019.

Mean yearly admission incidence rate on average per person	0-24 y	24-44 y	45-64 y	≥65 y	Total
LRP5, *PLS3*, or *WNT1* cohort	0.48	0.13	0.31	0.53	0.31
Total Dutch population	0.10	0.12	0.20	0.44	0.20
Incidence rate ratios:	4.69	1.04	1.58	1.22	1.61

Admissions include both day-case and inpatient admissions.

***Disclosures: Sara Verdonk**, None*

SUN-507

Development of an 18F-NaF PET/CT-Based Tool for Quantification and Characterization of Soft Tissue Calcification in Hyperphosphatemic Familial Tumoral Calcinosis (HFTC) *Aaron Sheppard[1], Faraz Farhadi[2], IRIS HARTLEY[3], Rachel Gafni[7], Michael Collins[5], Babak Saboury[6], Kelly Roszko[7]. [1]NIH, United States. [2]Geisel School of Medicine, Dartmouth, United States. [3]NIDCR/NIH, . [7]National Institutes of Health, United States. [5]NIDCR, NIH, United States. [6]Clinical Center, Department of Radiology and Imaging Sciences, NIH, United States. [7]National Institutes of Health,

Hyperphosphatemic familial tumoral calcinosis (HFTC) is a rare disorder which results from a deficiency of FGF23 signaling. Biochemical abnormalities include hyperphosphatemia and an elevated calcium x phosphate product, which likely drives the development of disabling soft tissue calcification. The study of HFTC and its response to treatment suffers from the lack of a quantitative technique to measure disease burden and activity. To address this, we developed 18F-NaF PET/CT and CT only imaging and analysis techniques to characterize and quantify calcifications in the NIH HFTC cohort. 11 patients with HFTC underwent either CT or 18F-NaF PET/CT imaging and the PET and CT voxel-level data were exported to and analyzed with MIM and MATLAB software. Analyses included CT-based bone data - volume and density (Hounsfield Units, HU), and PET-based mineral metabolic activity (Standardized Uptake Value, SUV).82% of patients had ectopic calcifications. The most frequently occurring and largest lesions were at the hips (n=9) and shoulders (n=5), 546.5 +/- 573.5 cm3 and 388.8 +/- 535.1 cm3 respectively. Large variations in total lesion volume and individual lesion volume over the cohort illustrated the great degree of heterogeneity in HFTC. Calcifications were also identified in the sclera of the eye, the colonic mucosa, the brain parenchyma and meninges/dura, and the para-vertebral region of the neck. In one patient who had four CT scans, we found that surgical intervention or repeated trauma increased the rate of growth of the lesions. Another patient had two 18F-NaF PET/CT scans, and voxel-by-voxel analysis found that the lesion increased in volume and density while decreasing in metabolic activity. These data demonstrate the utility of 18F-NaF PET/CT in identifying and quantifying the presence and mineral metabolic activity of calcific lesions and illustrate that CT and PET data provide complementary information that may inform the underlying pathomechanisms of calcification in HFTC. This technique will be useful in quantifying response to treatment in HFTC and likely applicable to other diseases of ectopic calcification.

***Disclosures: Aaron Sheppard**, Ultragenyx, Grant/Research Support*

SUN-509

Bronchial Obstruction in Osteogenesis Imperfecta can be detected by the Forced Oscillation Technique (FOT) *SILVIA STORONI[1], SARA VERDONK[2], Dimitra Micha[1], Patrick M.C. Jak[1], Marianna Bugiani[1], Elisabeth Eekhoff[3], Joost G. Van den Aardweg[1]. [1]Amsterdam UMC, Netherlands. [2]VUmc, Netherlands. [3]Amsterdam UMC, location VU University Medical Center, Amsterdam, The Netherlands, Netherlands

ABSTRACT Introduction Respiratory complications are a primary cause of death in individuals with Osteogenesis Imperfecta (OI), occurring three times more frequently than in the general population. However, current pulmonary function tests such as spirometry and body plethysmography are sometimes difficult to perform by OI patients, while reference values are not always applicable. The Forced Oscillation Technique (FOT) requires no effort from the patient and is a more patient-friendly method for detecting respiratory abnormalities. Objective This study investigates the potential value of FOT in the evaluation of respiratory function and the clinical management in OI patients. Methods Spirometry, body plethysmography and FOT (Modified Master Screen IOS) were performed in twelve OI patients, including two with OI type IV, two with OI type III, and eight with OI type I. Each patient underwent four FOT measurements, two before and two after the administration of salbutamol. Results FOT provided sufficient data to identify obstructive and possibly also restrictive pulmonary patterns. The resistance at 8 Hz decreased after administration of salbutamol, indicating that FOT is able to measure (sensitively) bronchial obstruction and its relief by therapy ($P < 0.05$). There appears to be a correlation between the relative change in forced expiratory volume in 1 second (FEV1) and the relative change in respiratory resistance at 8 Hz after salbutamol ($r^2=0.15$). Conclusions Bronchial obstruction can be detected by FOT in patients with OI during quiet breathing, making it an easily executable alternative to other lung function measurements. It also has the potential to provide information on expiratory flow limitation, restriction and reduced lung compliance.

***Disclosures: SILVIA STORONI**, None*

SUN-510

18F-NaF PET/CT is a Sensitive Tool for Detection of Prevalence and Activity of Enthesopathies in X-linked Hypophosphatemia *Aaron Sheppard[1], Babak Saboury[2], Juan Carlos Quintana[3], Oscar Contreras[3], Macarena Jimenez[4], Danisa Ivanovic-Zuvic[5], Annette Madison[5], Michael Collins[1], Pablo Florenzano[5]. [1]National Institutes of Health, National Institutes of Dental and Craniofacial Research, United States. [2]National Institutes of Health, Department of Radiology and Imaging Sciences, United States. [3]Pontificia Universidad Catolica de Chile, Radiology Department, Chile. [4]Pontificia Universidad Catolica de Chile, Endocrinology Department, Chile. [5]Pontificia Universidad Catolica de Chile, Endocrinology D, Chile

X-linked hypophosphatemia (XLH) is a rare metabolic bone disorder characterized by increased FGF23 production, which leads to chronic hypophosphatemia. Clinically, it presents with impaired skeletal mineralization and abnormal soft-tissue calcifications, including enthesopathies (Ens), leading to pain and diminished quality of life (QoL). To date, the natural history of Ens in XLH has been ill defined, due to the lack of a sensitive quantitative tool for its characterization and follow-up. Adult patients with genetically confirmed XLH were included. Clinical evaluations included severity surveys to assess QoL (SF23V), pain (BPI) and functionality (WOMAC/6MWT). 18F-NaF PET/CT scans, which can detect both the presence and metabolic activity of Ens, were acquired for all patient, and a comprehensive review of each patient's scan was performed. A subset of 14 common tendon/ligament insertion sites were chosen for further analysis, characterizing each site as CT-positive only (CT+) (macro-En) or PET-positive/CT-negative (PET+/CT-) (micro-En). Associations of macro- and micro-Ens with relevant clinical variables were performed, including linear regressions and Pearson's correlations. 20 patients were included, 70% women. Mean age at study was 35 years (21-62), with a mean age at diagnosis of 10 years (0.3-32). 18F-NaF PET was able to detect developing Ens in many locations before detection by CT (14.6% of all Ens). Notably, the number of PET+/CT- Ens was negatively correlated with age (r=-0.634, p=0.0027). The number of CT+ Ens had an insignificant positive correlation with age (r=+0.29, p=0.200). In addition, 18F-NaF PET offered synergistic information to CT, allowing the differentiation between metabolically active (PET+) vs stable (CT+/PET-) Ens. To illustrate, only 25% of macro-Ens at the ischial tuberosity were 18F-NaF avid, while 95.7% at the Achilles tendon were 18F-NaF avid. This, the first study to describe the use of 18F-NaF PET in characterizing Ens in XLH, demonstrated the ability of this modality to detect early En development at many sites. The fact that the number of detectable micro-Ens (PET+/CT-) was negatively correlated with age, suggests a progression pattern from a metabolically active early-lesion to a more structurally detectable, inactive lesion. 18F-NaF PET/CT is a promising tool that opens a window to better understand the natural history of the disease and may be used to assess the response of early Ens to therapeutic interventions.

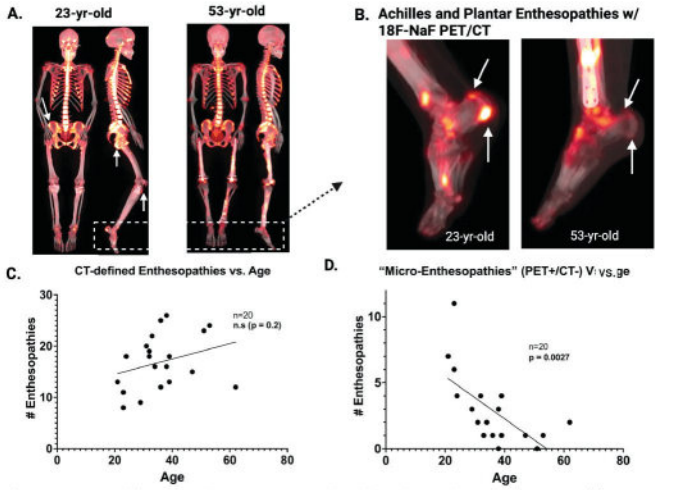

[18]F-NaF PET/CT differentiates between active and stable enthesopathies (Ens) in XLH. *(A) maximum intensity projection (MIP) of [18]F-NaF PET scan overlayed on CT MIP for a 23-yr-old patient and a 53-yr-old. (B) A focused look at the heel of the same 23- and 53-yr-old patients. Increased [18]F-NaF PET signal is greatest at the Achilles and plantar ligament in the younger patient, illustrating how this modality may detect the actively forming Ens earlier in life. (C) The number of CT+ Ens was insignificantly positively correlated with age, whereas (D) the number of PET+/CT- Ens was negatively correlated with age*

Disclosures: Aaron Sheppard*, Ultragenyx, Grant/Research Support*

SUN-512

3D-DXA reveals dramatic effects of burosumab on trabecular and cortical envelopes in symptomatic adults with X-linked Hypophosphatemia. *Rucha Patki[1], Karl Insogna[2], Thomas Carpenter[2], Keerti Murari[3], Stephen Parziale[4], Yanhong Deng[4], Ludovic Humbert[5], Mirella Lopez Picazo[5]. [1]Yale School of Medicine, United States. [2]Yale University School of Medicine, United States. [3]Optum Medical, Carmel/Brewster Campus, United States. [4]Yale School of Public Health, Yale Center for Analytical Sciences, United States. [5]3D-Shaper Medical, Spain

Burosumab heals fractures and improves osteomalacia in symptomatic adults with XLH but its effect on bone mineral density has not been well characterized. A study using quantitative backscattered electron imaging and FTIC of iliac crest bone biopsies, reported complex changes in cortical and trabecular bone mineralization following a year of burosumab treatment (doi: 10.1002/jbmr.4641).To quantify the effect of burosumab on trabecular and cortical bone density in the hip, a weight-bearing skeletal site prone to fracture in XLH, hip DXA scans and 3D-Shaper software (v2.12.1,3D-Shaper Medical, Spain) were used to analyze scans from 20 subjects who participated in the Phase 3 burosumab trial. DXA scans were obtained prior to and 6, 12 and 18-24 months after beginning treatment with 1mg/kg of drug every 4 weeks. The Month 6 BMD data were considered baseline for subjects receiving placebo for the first 6 months of the trial. Data were analyzed using a repeated-measures multivariate model that included age, gender, height, weight and time-point as covariates. Areal BMD at the total hip (TH) and femoral neck (FN) showed highly significant increases compared to baseline at every time point. For the TH, increases between 6 and 12 mo., 6 and 18-24 mo. and 12 and 18-24 mo. were highly significant. At the FN, increases between 6 and 12 mo. and 6 and 18-24 mo. were significant. The trabecular volumetric BMD (vBMD) at TH showed a progressive, highly significant and dramatic 13.6% increase over the study course. The trabecular vBMD at the FN also showed a significant 14.1% increase. At both skeletal sites, the interval increases from baseline in trabecular vBMD were also highly significant.Cortical surface BMD which incorporates cortical density and thickness, increased significantly between 6 and 12 mo. (p=0.03) and between 6 and 18-24 mo. (p= 0.01) for the FN. There was also a significant increase in the FN cross-sectional moment of inertia (CSMI), a predictor of strength, at 12 (p<0.05) and 24 (P<0.002) mo. compared to baseline (Figure1).We conclude that burosumab dramatically increases trabecular bone density in the TH and FN as well as the amount of FN cortical bone and increases FN CSMI. Since fractures in XLH often occur in cortically-enriched, weight-bearing lower extremity bones, including the FN, these changes may help explain the drug's efficacy in healing all fractures including FN and suggests that it may reduce the risk for future hip fractures.

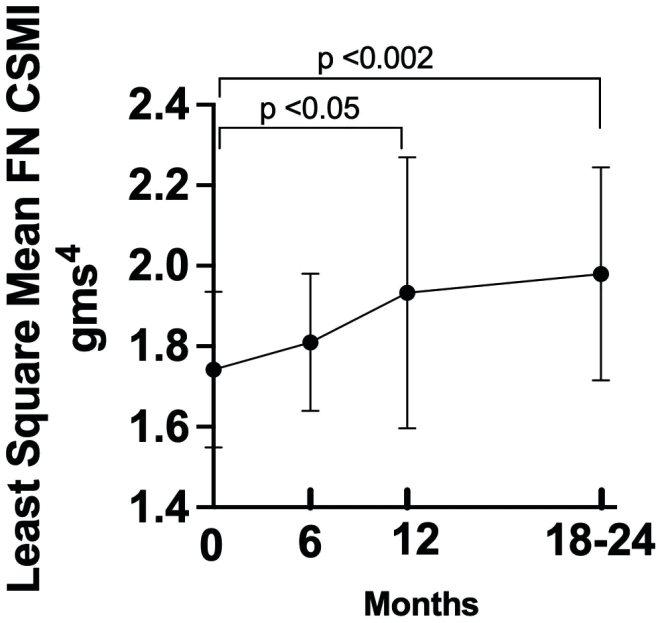

Disclosures: Rucha Patki*, None*

SUN-513

Assessment of Serum Alkaline Phosphatase, Serum Phosphate, Rickets Severity Score, Spinal Stenosis, Nephrocalcinosis, and Renal Function with Burosumab or Conventional Therapy Among Patients with X-linked Hypophosphatemia (XLH): Results from a Multinational, Long-term, Prospective Outcomes Disease Monitoring Program (DMP) *Leanne Ward[1], KATHRYN DAHIR[7], Hamilton Cassinelli[3], Pablo Florenzano[4], Erik Imel[5], Aliya Khan[6], Jill Simmons[7], Suzanne Jan De Beur[8], Carolina Moreira[9], Anna Ryabets-Lienhard[10], Zhiyi Li[11], Zunqiu Chen[12], ANTONIO NINO[13], Thomas Carpenter[14]. [1]Children s Hospital of Eastern Ontario, Canada. [7]Vanderbilt University Medical Center, . [3]CEDIE, Centro de Investigaciones Endocrinologicas Dr Cesar Bergada, Division de Endocrinologia, Hospital de Niños Ricardo Gutierrez, Argentina. [4]Pontificia Universidad Catolica de Chile, Chile. [5]Indiana University School of Medicine, United States. [6]McMaster University, Canada. [7]Vanderbilt University Medical Center, United States. [8]Johns Hopkins University, United States. [9]Endocrine Division (SEMPR), Department of Internal Medicine, Federal University of Parana, Brazil. [10]Children's Hospital Los Angeles , . [11]Kyowa Kirin, Inc., United States. [12]Ultragenyx Pharmaceutical Inc., United States. [13]Ultragenyx, United States. [14]Yale University School of Medicine, United States

Purpose: To provide an update from the XLH DMP, which is an ongoing, non-interventional, prospective study with a 10-year planned duration, that characterizes disease progression and long-term effectiveness and safety of burosumab and other treatments (NCT03651505).Methods: Children (peds; <18 years) and adults (>=18 years) at DMP enrollment (Month 0; M0) were grouped according to burosumab treatment: Group 1 (Gr1) began burosumab in a prior clinical trial and have the longest exposure among the study population; Group 2 (Gr2) began commercial burosumab prior to/during the DMP; Group 3 (Gr3) had no burosumab exposure, but most received conventional therapy (CT; eg, oral phosphate and active vitamin D). Results from patients (pts) who completed Year 3 (Y3) at data cutoff are reported.Results: As of February 2023, 347 peds and 461 adults were enrolled in the DMP; mean (SD) age at M0 was 9.0 (4.8) years and 39.0 (14.7) years, respectively. Mean duration of burosumab exposure was similar between peds (133.1 [65.5] weeks) and adults (135.0 [72.0] weeks). At Y3, mean serum alkaline phosphatase was lower in peds receiving burosumab vs CT (Gr1: 287.3 [151.6] U/L; Gr2: 277.0 [142.4] U/L; Gr3: 474.5 [170.2] U/L). Additionally, mean serum phosphate levels were higher in peds receiving burosumab vs CT (Fig 1A). Mean serum phosphate levels were also higher in Gr1 and Gr2 adults vs Gr 3 adults (Fig 1B). Rickets severity scores (RSS) in Gr1 peds remained low at Y3 (-0.1 change from M0) and improved in Gr2 peds (-0.7 change from M0); no Gr3 pts had completed RSS at Y3. At M0, 75 (16%) adults across all 3 groups reported an existing diagnosis of spinal stenosis (SS) or spinal cord (SC) compression, including 36 pts (37%) in Gr1, 28 pts (14%) in Gr2, and 11 pts (7%) in Gr3. The majority of pts who had a previous diagnosis of SS or SC compression did not report worsening of their condition and did not undergo a related surgery at Y3. Comparing M0 to Y3, 4 pts (2 each from Gr2 and Gr3) had renal ultrasound score increases of >=2 and 1 pt from Gr2 showed improvement with score decreases of >=2; no Gr1 pts had score increases >=2. Burosumab was not associated with declines in renal function (as assessed by eGFR), urinary protein/creatinine ratio, or any new safety concerns in peds or adults.Conclusions: Long-term exposure to burosumab for up to 3 years in the DMP was consistent with its previously reported benefits vs CT and positively affected markers of disease activity.

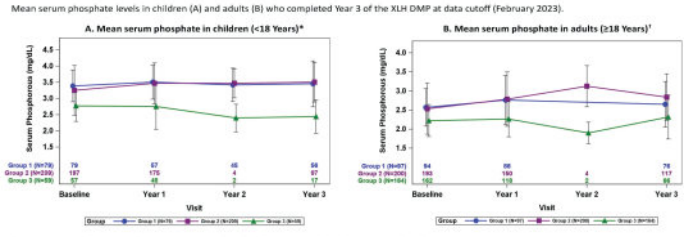

***Disclosures: Leanne Ward**, Ultragenyx Pharmaceutical Inc., Grant/Research Support, Ultragenyx Pharmaceutical Inc. , Consultant*

SUN-515

A Systematic Literature Review of the Impact and Measurement of Mobility Impairment in Rare Bone Diseases *Inês Alves[1], Gabor Barton[2], Edward Hsiao[3], Luca Sangiorgi[4], Jaymin Upadhyay[5], Ingunn Westerheim[6], Alexander Artyomenko[7], Kim Croskery[7]. [1]Associação Nacional de Displasias Ósseas (ANDO), Portugal. [2]Liverpool John Moores University, United Kingdom. [3]University of California San Francisco, United States. [4]IRCCS Istituto Ortopedico Rizzoli, Italy. [5]Harvard Medical School, United States. [6]Osteogenesis Imperfecta Federation Europe (OIFE), Belgium. [7]Ipsen, United Kingdom

Purpose: Rare bone diseases (RBDs) are a group of over 700 genetic disorders involving the skeletal system. While existing research characterizes the impact of mobility impairments in few specific RBDs, there is a lack of evidence on impacts on activities of daily living (ADLs) and quality of life (QoL) across RBDs. Furthermore, tools capable of measuring RBD-related mobility in real-world settings need to be identified. This systematic literature review aimed to investigate: 1) the impact of mobility impairment on ADLs and QoL in individuals with RBDs, and 2) the adequacy of tools for measuring mobility in RBDs. Methods: Searches of MEDLINE/Embase, Google, and conference proceedings were performed. Studies published between 2011-2022, in people with the 461 RBDs listed in the 2019 Nosology and Classification of Genetic Skeletal Disorders, were included. Non-English language studies, animal/cell studies, narrative reviews, and editorial letters were excluded. Risk of bias was minimized by two independent reviewers assessing each full-text article for inclusion. Data from included studies were extracted into a pre-specified extraction grid. Results: Of 4,587 studies identified, 113 met the inclusion criteria, in which only 39 different RBDs were investigated (population sizes: 1-959 individuals). Mobility impairments were described for 58 cohorts of individuals with RBDs; most common issues were with joint function and gait. In the cohorts of individuals identified under objective 1 (N=58), mobility impairment was associated with a negative impact on ADLs (n=47; most commonly walking [27/47; 57.4%]) and QoL (n=36; most related to pain [29/36; 80.6%]). Overall, 61 mobility tools were identified, including 34 functional assessments, 22 questionnaires, and 5 technologies/applications. Only 9 tools were evaluated as valid, reliable, or responsive in an RBD population, and therefore considered adequate (Table). Few digital tools were identified, with no assessment of their adequacy or use in a remote setting. Conclusion: Many tools used to measure mobility in RBDs were identified, reflecting a lack of consensus on the most appropriate tools. No adequate tools capable of capturing multiple factors impacting individuals' daily lives in a remote setting were identified. Development of adaptable tools, or exploring novel uses of existing tools, would facilitate data collection in the real world, better characterizing the impacts of mobility impairments across RBDs.

Table: Mobility tools deemed adequate for the assessment of mobility in RBDs

Mobility tool	RBDs assessed
Brief Pain Inventory Short Form (BPI-SF)	Hypophosphatasia (HPP) Morquio A syndrome **X-linked hypophosphatemia (XLH)**
Functional independence measure (FIM)	Achondroplasia **Mucopolysaccharidoses (MPS)**
FOP-Physical Function Questionnaire (FOP-PFQ)	**Fibrodysplasia ossificans progressiva (FOP)**
International Classification of Functioning, Disability and Health (ICF) self-report questionnaire	**Skeletal dysplasias**
Patient-Reported Mobility Assessment (PRMA)	**Fibrodysplasia ossificans progressiva (FOP)**
Patient Reported Outcome Measure Information System (PROMIS)	**Osteogenesis imperfecta (OI)** Proteus syndrome **X-linked hypophosphatemia (XLH)**
Western Ontario and McMaster Universities Osteoarthritis Index (WOMAC)	Nail patella syndrome (NPS) **X-linked hypophosphatemia (XLH)**
Modified Performance-Oriented Mobility Assessment-Gait (mPOMA-G)	**Hypophosphatasia (HPP)**
Pediatric Gait, Arms, Legs, and Spine (pGALS) examination	**Mucopolysaccharidoses (MPS)**

Bold indicates tools reported to be valid, responsive, or reliable, and therefore deemed adequate for mobility measurement in the assessed RBD.

***Disclosures: Inês Alves**, None*

SUN-516

Identification of progenitor cells that contribute to heterotopic ossification in normal and inflammatory environment *Qian Cong[1], Yingzi Yang[2]. [1]Harvard University, Harvard School of Dental Medicine, Armenia. [2]Harvard University, United States

Heterotopic ossification (HO) is a debilitating condition characterized by the pathologic formation of ectopic bone that occurs as a common complication after injury or as a manifestation of particular genetic disorders. The identity of progenitor cells that contribute to GNAS mutation induced heterotopic ossification relevant to progressive osseous hetero-

plasia (POH) is unknown, which limits the effective treatment or prevention of ectopic bone formation and expansion. Based on our single-cell RNA sequencing analysis from a well-established POH mouse model, we found that PDGF signaling was much increased in ectopic cell population. Utilizing an inducible lineage-tracing mouse (Gnasf/f; Pdgfr?-CreERT2; Rosa26LSL-TdTomato), we found that Pdgfr?+ progenitor cells were induced to become osteoblasts in POH. Moreover, local induction with Tamoxifen tibia subcutaneous injection cause dramatic HO compared to systemic Tamoxifen injection, suggesting that Pdgfr?+ cells is the major cell population in HO formation which will be promoted by an inflammatory microenvironment. Importantly, pharmacological inhibition of Pdgfr? abolished HO without affecting normal bone homeostasis, providing a previously unrecognized therapeutic rationale to prevent HO. Since we found that the ectopic bone invaded into deep muscular region 3 months post Ad-Cre injection in POH mouse models, we tested the hypothesis that the muscle satellite cells and committed muscle cells could also be reprogrammed to form ectopic bone. Consequently, Gnas mutant mature myotube cells cannot reprogram to ectopic bone. Skeletal muscle precursors and muscle satellite cells in vivo contributed minimally to heterotopic ossification, and this contribution was not increased by cardiotoxin injection, which induces muscle regeneration and mobilizes muscle stem cells. Taken together, Pdgfr?-expressing progenitor cells respond to an inflammatory trigger, differentiate into osteoblast, contribute to heterotopic bone formation and expansion in animal models of POH. The understanding of the cellular basis of heterotopic ossification aids in the development of targeted, cell-specific therapies for the treatment and prevention of heterotopic ossification.

***Disclosures: Qian Cong**, None*

SUN-517

Inhibition of ACVR1 with a Neutralizing Antibody Significantly Inhibits Recurrence of Trauma-induced Heterotopic Ossification Following Resection in a Burn and Tenotomy Mouse Model *Nanditha Das[1], Johanna Jimenez[1], Andrew Murphy[2], Aris Economides[1], Sarah Hatsell[1], Kalyan Nannuru[1]. [1]Regeneron Pharmaceuticals Inc, United States. [2]Regeneron Pharmceuticals Inc., United States

Heterotopic ossification (HO) can occur in an acquired form due to severe trauma, or in the rare genetic diseases such as Fibrodysplasia Ossificans Progressiva (FOP). Both forms of HO arise from the endochondral ossification process, resulting in ectopic bone formation in soft tissues, including muscles and tendons, hence the molecular mechanisms that drive these processes are postulated to be similar. FOP mutations in ACVR1 impart neofunction to the receptor by gaining responsiveness to Activin A, and inhibition of Activin A with a neutralizing antibody completely abrogates HO in mouse FOP models and human FOP patients. However, we have shown previously that blocking Activin A did not alter either the incidence or severity of trauma HO, suggesting that Activin A induced signaling does not drive HO development in trauma HO patients who have WT ACVR11. On the other hand, we and others2 have previously shown that inhibiting BMP signaling using an ALK3-Fc ligand trap or small molecule inhibitors can reduce ectopic bone formation in mouse models of trauma and burn-induced HO. We further showed that inhibiting BMP signaling by blocking ACVR1 prophylactically using an ACVR1 neutralizing antibody significantly reduced the formation and progression of trauma-induced HO in a burn/tenotomy mouse model.Trauma HO patients sometimes undergo resection surgery to remove HO, so establishing efficacy of ACVR1 blockade against recurrent HO following surgical resection is necessary. Hence, we tested whether our neutralizing ACVR1 antibody prevents HO recurrence post-resection. After inducing the models using the Achilles tenotomy and burn injury, mice were allowed to develop HO for 6 - 7 weeks, after which they underwent HO resection and ACVR1 antibody treatment at 25 mg/kg once weekly was initiated. The mice were treated for 12 weeks post-resection. We observed a significant inhibition in HO recurrence and its progression post-resection surgery in the ACVR1 antibody treated mice compared to isotype control treated group. These data, together with our previous data, suggest that ACVR1 signaling plays a major role in the development and recurrence of trauma-induced HO and blocking it offers an effective therapeutic option.References:1. Activin A does not drive post-traumatic heterotopic ossification, Bone. 138:115473, 20202. Strategic Targeting of Multiple BMP Receptors Prevents Trauma-Induced Heterotopic Ossification, Mol. Ther. 25:8, 2017.

***Disclosures: Nanditha Das**, Regeneron Pharmaceuticals Inc., Other Financial or Material Support*

SUN-518

Sexually Dimorphic Low Bone Mass in Down Syndrome Mice is Associated with Decreased Testis Weight but not Compromised Reproductive Hormone Levels *ALYSSA FALCK[1], KIRBY M. SHERMAN[2], Dana Gaddy[3], Sophia Schutmaat[1], Abigail Leon[1], Larry Suva[4]. [1]Texas A&M University, United States. [2]Texas A&M University , . [3]College of Veterinary Medicine, Texas A&M University, United States. [4]Texas A&M University, College of Veterinary Medicine and Biomedical Sciences, United States

Down syndrome (DS), the result of trisomy at human chromosome 21 (Ts21), manifests in a variety of clinical, behavioral, and physical abnormalities. People with Ts21 have low bone mass and increased fracture risk, associated with decreased bone formation. Interestingly, these skeletal complications are more prevalent in Ts21 men, despite low-normal hormone levels in the HPG axis including testosterone. We previously demonstrated low bone mass in male DS mice of both TS65 and DP16 strains is a result of low bone accrual, however the female TS65 bone phenotype is unknown. Given the well-established importance of sex steroids for normal bone accrual in both humans and mice, we hypothesized that the low bone accrual in Ts65 and DP16 DS mouse models might be associated with deficiencies across the reproductive axis. Therefore, 3-month-old male and female DP16 and Ts65 DS mice were assessed for whole body BMD by DEXA, tibial bone volume by microCT, and reproductive function by serum reproductive hormone levels and gonadal and accessory sex gland tissue wet weights. Whole body BMD measurements confirmed low bone mass in male Ts65 and DP16 mice; however, no bone phenotype was evident in TS65 DS females. Despite normal reproductive hormone levels, male DS mice had significantly decreased testis, but not seminal vesicle, weights compared to WT. Female DS Ts65 and DP16 mice did not show significant differences in ovarian or uterine weights compared to WT. These murine data are entirely consistent with previous human data demonstrating that testosterone, FSH and LH levels in Ts21 men are all in the low normal range, providing evidence that the hypothalamic-pituitary-gonadal axis is intact. Collectively, these data demonstrate for the first time that the low bone mass phenotype of male DS mice is independent of reproductive hormone levels and that female Ts65 DS do not have low bone mass at 3 months of age. Thus, the sexual dimorphism evident in the human Ts21 bone phenotype is replicated in DP16 and Ts65 DS mice. These data further validate the utility of multiple DS mouse lines to accurately reflect the human Ts21 phenotype and provide novel insight into the cellular and molecular mechanisms of low bone formation in DS. Importantly, it provides further evidence that low bone mass of Ts21 patients and DS mice is not simply the result of low sex steroid levels, as previously speculated in the field.

***Disclosures: ALYSSA FALCK**, None*

SUN-519

role of calcium related signalling in osteoblasts: what we learned From Osteogenesis Imperfecta *Roberta Besio[1], Barbara M Contento[1], Nadia Garibaldi[1], Marta Filibian[1], Stephan Sonntag[2], Doron Shmerling[3], Francesca Tonelli[1], Marco Biggiogera[1], Marisa Brini[4], Andrea Salmaso[4], Milena Jovanovic[5], Joan Marini[5], Antonio Rossi[1], Antonella Forlino[1]. [1]University of Pavia, Italy. [2]LIMES-Institute, University of Bonn, Germany. [3]PolyGene AG, Switzerland. [4]University of Padova, Italy. [5]National Institute of Child Health and Human Development, United States

Osteogenesis imperfecta (OI) is a group of inherited brittle bone diseases associated to skeletal deformities and bone fragility and mainly due to defects in collagen type I. Both altered bone matrix and impaired osteoblast homeostasis have been described in OI. Even if the molecular basis of the disease has been deeply investigated, is still largely poorly defined. The characterization of the rarest recessive OI forms has been and will be extremely relevant to further elucidate the disease pathophysiology. Mutations in TMEM38B, encoding the TRIC-B potassium channel necessary for intracellular Ca2+ homeostasis, cause the autosomal recessive OI type XIV characterized by defects in osteoblast (OB) differentiation and activity. To understand the molecular mechanisms underlying OB impairment in OI type XIV, a Tmem38b osteoblast specific conditional knock-out mouse (Runx2Cre;Tmem38bfl/fl, cKO) was generated and used to investigate pathways relevant for OB differentiation. Among these, the SMAD pathway, acting downstream the TGF-? and the Ca2+-dependent CaMKII, was evaluated.At the cellular level, the Ca2+ imbalance caused delayed osteoblast differentiation and decreased collagen synthesis associated with reduced collagen incorporation in the extracellular matrix and poor mineralization. The osteoblast malfunction was proved to be associated to the impaired SMAD signalling detected in mutant mice, and validated in OI patient osteoblasts. The reduced SMAD phosphorylation and nuclear translocation were mainly caused by alteration in Ca2+ calmodulin kinase II (CaMKII)-mediated signalling and to a less extend by a lower TGF-? reservoir. Indeed, TGF-? treatment only partially rescued SMAD signalling, osteoblast differentiation and matrix mineralization, underlying the relevance of CaMKII-SMAD axes on osteoblast function. In conclusion, our study established the TRIC-B role in osteoblasts and strengthen the contribution of the CaMKII-SMAD signalling in bone.

***Disclosures: Roberta Besio**, None*

SUN-520

Skeletal phenotype in mice with a homozygous truncating PTH1R mutation resembles skeletal abnormalities in Eiken Syndrome *Jakob Höppner[1], Thomas Gardella[2], Monica Reyes[3], PATRICK HANNA[4], Harald Jueppner[2], Ignacio Portales Castillo[4]. [1]Endocrine Unit, Massachusetts General Hospital and Harvard Medical School, United States. [2]Massachusetts General Hospital, United States. [3]Massachusetts General Hospital , United States. [4],

Eiken syndrome is an ultra-rare disease characterized by delayed bone ossification that is caused by homozygous mutations in the parathyroid hormone/parathyroid hormone-related protein receptor (PTH1R). One of these mutants, R485X-PTH1R, lacks most of the receptor C-terminal tail, and in vitro exhibits impaired interaction with ?-arrestins, which are necessary for normal PTH1R desensitization. In transfected HEK293 cells, R485X-PTH1R exhibits increased basal cAMP signaling as well as enhanced PTHrP-stimulated cAMP formation responses. To investigate how this PTH1R mutant impacts endochondral bone formation in-vivo, we used iGONAD (improved genome editing via oviductal nucleic acids

delivery) to generate R485X "humanized" hPTHR1 mice, which express the human PTH1R under the control of the endogenous mouse promoter. The resulting R485X-hPTHR1 knock-in mice were viable in both heterozygous and homozygous states and were analyzed at different ages along with age-matched controls. Homozygous R485X-PTH1R mice had short tails, but otherwise appeared normal. Heterozygous mice were indistinguishable from WT littermates. Whole mount skeletons of homozygous mice exhibited reduced mineralization of the long bones and carpals on postnatal days 1-6. Histology of H&E-stained tibial sections revealed expanded zones of proliferative and hypertrophic chondrocytes in the growth plate. Analysis of explant cultures of metatarsals obtained at postnatal day 1, 4 and 10 confirmed a major delay in mineralization of bones from homozygous mutant vs. WT mice. Beyond day 21, metatarsal mineralization and growth plate histology appeared similar in mutant and WT mice; however, the mutant tarsal bones and vertebrae appeared shorter and misshapen. Homozygous R485X mice exhibited normocalcemia but serum PTH levels tended to be elevated suggesting moderate PTH-resistance. These homozygous R485X-hPTH1R mutant mice thus recapitulate the main features of patients with Eiken Syndrome (delayed ossification). Further, the results support an important role for the PTH1R C-tail and its interaction with ?-arrestins which may have a previously unrecognized role in regulating PTH1R signaling during endochondral bone formation.

***Disclosures: Jakob Höppner**, None*

SUN-522

Genetic Modulation of Hedgehog Signaling Influences Exostoses Elongation, Orientation, and Proliferation in a Mouse Model of Hereditary Multiple Exostoses (HME) *Sarah Catheline[1], Christina Mundy[2], Maurizio Pacifici[3]. [1]University of Rochester, United States. [2]Children's Hospital of Philadelphia, United States. [3]The Children's Hospital of Philadelphia, United States

Hereditary Multiple Exostoses (HME) is a congenital pediatric disorder in which cartilaginous tumors called osteochondromas or exostoses develop perpendicular to growth plates of skeletal elements. Most HME patients have a mutation in?EXT1?or?EXT2 causing heparan sulfate (HS) deficiency. Normally, HS-rich proteoglycans (HSPGs) restrict growth factor availability, and the HS deficiency in HME growth plates could result in freely available growth factors, inducing exostosis formation. However, it is unknown why the exostoses grow orthogonally to the growth plate main axis. The Indian hedgehog (IHH)/PTHrP signaling axis is critical for growth plate zonal organization, and hedgehog proteins bind HSPGs. Thus, HS deficiency in HME could allow the proteins to escape the growth plate and trigger a neo IHH-PTHrP axis within perichondrium, causing orthogonal exostosis formation. To test this novel thesis, we used AggrecanCreERT2? mice to drive?Ext1?deletion in chondrocytes and perichondrium in 5 week-old mice. To ask whether hedgehog signaling is necessary and sufficient for exostosis formation, we combined this model with: (a) conditional deletion of hedgehog receptor?Smo?resulting in Hedgehog loss of function (LOF); or (b) conditional deletion of?Ptch1, a negative regulator of signaling, resulting in gain of function (GOF). Acan-Cre+/-ERT2; Ext1f/f;?Smof/f?mice displayed delayed exostosis formation 10 days after tamoxifen relative to Acan-Cre+/-ERT2; Ext1f/f?(Ext1 mutant) mice, significantly decreasing exostosis number and size 4 weeks post tamoxifen. In contrast,?Acan-Cre+/-ERT2; Ext1f/f; Ptch1f/+?mice showed greater number of exostoses at 10 days relative to Ext1?mutant mice, resulting in significantly longer, wider and more numerous exostoses by 4 weeks. Notably, Ext1 mutants showed enriched cell proliferation marked by Ki67 in perichondrium at the site of new exostoses, while LOF mice lacked proliferating perichondrial cells and GOF mice showed the greatest number of Ki67-positive cells, suggestive that hedgehog helps initiate perichondrial proliferation. ?-catenin expression throughout the exostoses, and Pthrp-LacZ specifically present at their leading edge, both increased in Ext1 mutant mice and were further increased in GOF mice, suggesting that crosstalk between these pathways is important in exostosis formation. Our current data implicate IHH/PTHrP signaling as a critical regulator of osteochondroma formation and orthogonal growth.

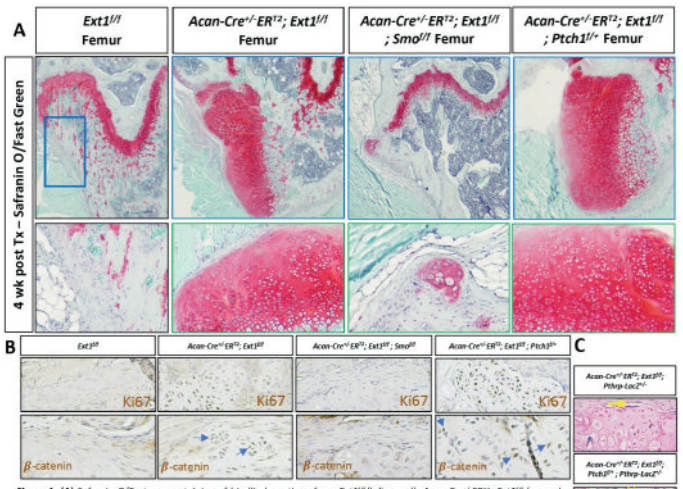

Figure 1. (A) Safranin O/Fast green staining of hindlimb sections from *Ext1$^{f/f}$* (left panel), *Acan-Cre$^{+/-}$ER^{T2}; Ext1$^{f/f}$* (second from left), *Acan-Cre$^{+/-}$ER^{T2}; Ext1$^{f/f}$; Smo$^{f/f}$* mice (third from left) and *Acan-Cre$^{+/-}$ER^{T2}; Ext1$^{f/f}$; Ptch1$^{f/+}$* mice (right panel) at 9 weeks of age, 4 weeks post tamoxifen (tx) (a single tx injection, 75μg/g body weight). Blue box indicates zoomed area in bottom panels. **(B)** Ki67 IHC (top panels) and β-catenin IHC (bottom panels) from the same genotypes as in **(A)** at 6.5 weeks of age, 10 days post tx induction; blue arrows indicate β-catenin+ cells. **(C)** β-gal/Nuclear fast red staining of hindlimb sections from *Acan-Cre$^{+/-}$ER^{T2}; Ext1$^{f/f}$; Pthrp-Lacz$^{+/-}$* or *Acan-Cre$^{+/-}$ER^{T2}; Ext1$^{f/f}$; Ptch1$^{f/+}$; Pthrp-Lacz$^{+/-}$* mice 2 weeks post tx. Yellow arrows indicate *Pthrp+* cells.

***Disclosures: Sarah Catheline**, None*

SUN-524

KMT9? maintains bone homeostasis via JAK1-STAT3-mediated osteogenesis *Shuang Jiang[1], Quan Yuan[1], Mingyue Lyu[1]. [1]Sichuan University, China

Maintenance of bone homeostasis depends on coordinated bone formation by osteoblasts and bone resorption by osteoclasts. Disruption in this tightly-regulated process results in skeletal disorders, such as osteoporosis or osteopetrosis. Autosomal recessive osteopetrosis (ARO) is a lethal genetic disease, characterized by increased bone mineral content and density. However, the mechanism underlying ARO is still unclear and the treatment strategy is limited. Lysine methyltransferase 9 (KMT9) is newly identified as a histone methyltransferase that writes the monomethylated mark on lysine 12 of histone H4. Here we raise the possibility that KMT9?-mediated JAK1-STAT3 signaling pathway is highly relevant in the onset of ARO.First, we generated a mouse model with Kmt9? specific knockout in mesenchymal stem cells by crossing Kmt9?fl/fl mice with Prx1-Cre mice. It was first noted that Kmt9?-knockout mice exhibited stunted growth of limbs, especially the femurs, compared to their littermates. To further identify the extent of the skeletal defects, we analyzed the femurs of Kmt9?-knockout mice using a micro-CT scanner. Notably, micro-CT analysis revealed that the femurs of Kmt9?-knockout mice were shorter, deformed, and exhibited increased cortical mineral density and cortical thickness. This finding was reproduced via histomorphometry, which showed massively increased amounts of trabecular bone and reduced bone marrow space in the mutant mice. Interestingly, we also observed an increase of growth plate thickness in the absence of KMT9?.Considering the mutant mice resemble the major symptoms of the human disease, we extracted information from public sequencing data in bone tissue of patients with autosomal dominant osteopetrosis. A significant enrichment of JAK-STAT signaling pathway in bone of patients was then noticed. To uncover the mechanism driving skeletal disorder in low-level KMT9? setting, we silenced KMT9? in mesenchymal stem cells using siRNA and traced the cellular responses. As expected, we found a surge of expression in JAK1-STAT3 pathway with KMT9? deficiency. We therefore proposed a possibility that the hyperactive bone formation in Kmt9?-knockout mice may directly or indirectly come from JAK1 and STAT3 actions.Taken together, these data demonstrates that KMT9? is vital for skeletal development and bone homeostasis through JAK1-STAT3-mediated osteogenesis and suggest it be a potential target for ARO diagnosis and management.

***Disclosures: Shuang Jiang**, None*

SUN-526

PDGFR?-STAT5 Signaling Hijacks Growth Hormone Pathway to Promote Skeletal Gigantism *Hae Ryong Kwon[1], Lorin Olson[1]. [1]Oklahoma Medical Research Foundation, United States

Autosomal dominant platelet-derived growth factor receptor beta (PDGFR?) gain-of-function mutations cause skeletal gigantism in mice and humans with the rare genetic disease Kosaki overgrowth syndrome. However, the cellular basis and molecular mechanisms of these disorders are still being discovered. We previously showed that mice with a gain-of-function PDGFR? D849V point mutation on a Stat1-deficient background develop skeletal overgrowth. Skeletal stem cells (SSCs) isolated from these mice exhibit increased colony formation, suggesting overactive stem and progenitor cells as a cellular origin of overgrowth. Single-cell RNA transcriptomics with SSCs-derived colonies revealed in-

creased expression and phosphorylation of signal transducer and activator of transcription 5 (STAT5) and overexpression of the STAT5 target gene, insulin-like growth factor 1 (IGF1). We hypothesized that PDGFR? causes skeletal overgrowth by activating local STAT5-IGF1 signaling in the skeletal lineage. To investigate the significance of STAT5 and IGF1 in the overgrowth phenotype, we conditionally deleted Stat5, Igf1, or IGF1 receptor Igf1r, from the axial skeleton of PDGFR?D849VStat1-/- mice. For conditional gene deletion, we utilized Prx1-Cre which targets mesenchymal cells in the early limb bud including bone, cartilage, muscle connective tissue and dermal fibroblasts, but not skeletal muscle. Longitudinal and appositional skeletal overgrowth of PDGFR?D849VStat1-/- mice was normalized by deletion of Stat5, Igf1, or Igf1r, suggesting the importance of STAT5 and IGF1 signaling. With lineage tracing and immunostaining, we found that PDGFR? is expressed around the growth plate, suggesting paracrine actions of IGF1 leading to enhanced growth. We propose that by directly phosphorylating STAT5 in Prx1-lineage skeletal cells, PDGFR?D849V hijacks the growth hormone (GH) signaling pathway to promote skeletal overgrowth. Our work establishes the cellular basis of skeletal growth disorders caused by PDGFR? mutations and gives new insight into a role of STAT5 in skeletal development and genetic disease.

***Disclosures: Hae Ryong Kwon**, None*

SUN-527

Osteopathy in Gorham-Stout Disease Animal Model *ERNESTO SOLORZANO[1], Gabrielle Robinson[5], Hope Ball[5], Adam Sanchez[3], Alexander Powell[3], Michael Kelly[4], Fayez Safadi[5], [1], United States, [5]Northeast Ohio Medical University, , [3]NEOMED, United States, [4]Cleveland Clinic Foundation, United States, [5]Northeast Ohio Medical University, United States

Gorham-Stout Disease (GSD) is a rare condition associated with aggressive lymphatic invasion into bone leading to massive bone loss. To date, the mechanism of bone loss identified in GSD remains to be elucidated. Most recently, a lymphatic-specific KRAS somatic activating mutation was identified in GSD patients. A mouse model recapitulating this mutation in Prox1 expressing lymphatic cells showed detrimental lymphatic valve formation. To better understand the abnormal bone loss present in GSD patients, we generated a tamoxifen-induced lymphatic endothelial cell KRAS somatic activating mutation in mice and characterized the skeletal phenotype. These mutant animals exhibited decreased body weight compared to wild-type littermates. In addition, we observed extensive lymphatic fluid accumulation in the thoracic cavity in comparison to wild-type littermates. Soft tissue immunohistochemical analysis of LYVE-1 (lymphatic endothelial cell marker) revealed lymphatic vessel invasion into the kidneys. Subsequently, bone mineral density, content, and area were all found to be decreased in KRAS mutants compared to wild-type mice. These results were also observed in KRAS mutant spine, femur, and tibia compared to wild-type controls. In addition, a decrease in total fat and lean muscle mass was also observed. Further, we next assessed bone mRNA expression and found a decrease in Runx2 and Collagen type I in mutant mice. However, the expression of osteoclast-related markers (TRAP, DC-Stamp, and Cathepsin-K) was increased in mutants compared to wild-type animals. When assessing bone marrow-derived macrophages, we found a decrease in cell proliferation associated with decreased total osteoclast count in mutant compared to wild-type. Interestingly, TRAP activity per osteoclast was increased in mutant compared to wild-type. Our findings show how a lymphatic-specific KRAS mutation leads to a decrease in bone mass in vivo and induces cell-autonomous changes in osteoclast differentiation ex vivo. For this reason, we predict mutant lymphatic tissue actively secretes bone-regulating factors capable of modulating bone homeostasis. In conclusion, our studies are the first to describe abnormal bone phenotypes found in KRAS mutant mice. Future studies aimed to identify lymphatic secreted factors responsible for bone loss and changes in osteoclast homeostasis observed in the GSD mouse model.

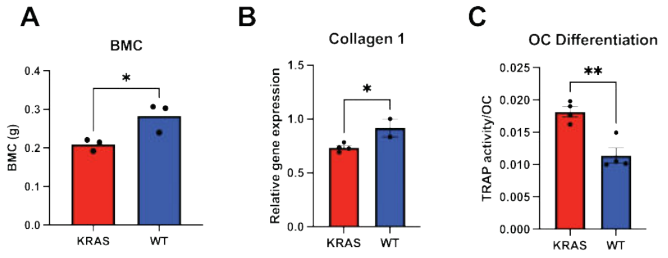

Figure 1. Osteopathic changes found in GSD animal model. Lymphatic specific KRAS activating mutation led to a decrease in bone mineral content (BMC) on mutant animals (KRAS) when compared to wild-type (WT) (**A**). Bone mRNA expression of collagen 1 was decreased in KRAS when compared to WT (**B**). Osteoclast (OC) TRAP activity per cell was higher in KRAS animals when compared to WT (**C**).

***Disclosures: ERNESTO SOLORZANO**, None*

SUN-528

Unraveling Immune Alterations in the Pathogenesis of Pachydermoperiostosis through a Cross-Omic Analysis Informed by Heterotopic Ossification *jinsen lu[1], [1]Botnar Research Institute, United Kingdom

Pachydermoperiostosis (PDP) is a rare genetic osteo-related disorder with enigmatic etiology. Prior research has associated immune dysregulation with aberrant bone remodeling and cutaneous thickening. Building upon these findings, this study endeavors to examine immune alterations to further elucidate the pathophysiological processes of PDP.Comprehensive imaging and blood tests were performed on a PDP patient, his asymptomatic brother, and healthy controls. Single-cell sequencing of PBMCs revealed immune cell shifts in the PDP patient, including decreased NK cells, CD4 T helper cells, CD8 T cells, and increased B cells. A CTX-injured BMP4 transgenic mouse model was applied as PDP model to complement the human study. Lesion tissues were collected at different time points, and bulk RNA sequencing, histology, and micro-CT were conducted to trace tissue morphogenesis on mice models. Time-course clustering and WGCNA identified six functional clusters related to abnormal tissue morphogenesis in mice models. In the human study, top genes were mapped to identified murine clusters and validated via RT-PCR. NK cells displayed upregulated CPQ, COL6A2, and NSG1 (related to tissue morphogenesis) and altered immune response via upregulated THEMIS2 and downregulated AOAH. CD8 T cells showed upregulated CD300A and downregulated COTL1, influencing their activation and function, while downregulated SKAP2 and S100A9 affected their migration. CD4 T helper cells exhibited upregulated S100A4 and downregulated TMEM263, impacting their activation and communication, as well as altered chemotaxis due to downregulated MTURN and S100A8. B cells demonstrated upregulated CSTB and FCGR2B affecting their activation, migration, and antibody production, while downregulated S100A9, TLE4, HMGB2, PLPP5, and CXCR4 potentially contributed to PDP pathogenesis through regulating cell migration, cell cycle and inflammatory response.In conclusion, this study unveils novel insights into PDP pathogenesis, emphasizing the significance of immune cell population dynamics, altered gene expression, and mechanistic understanding, providing a foundation for future research and potential targeted therapies for PDP.

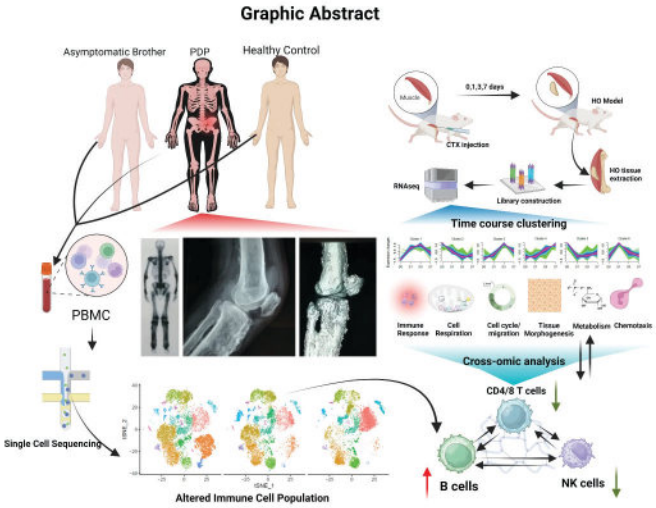

***Disclosures: jinsen lu**, None*

SUN-529

Distinct molecular mechanisms of bone and lung pathologies in a G610C Mouse Model of OI *ELENA MAKAREEVA[1], Megan Sousa[1], Muthulakshmi Sellamani[1], Edward L. Mertz[1], Satoru Otsuru[2], Sergey Leikin[3], [1]NIH, United States, [2]University of Maryland, United States, [3]National Institutes of Health, United States

Lung function in osteogenesis imperfecta (OI) is affected by both chest deformities and intrinsic lung tissue pathology. Alveolar disruption has been reported in mouse models and bronchial wall thickening in humans. The present study aims to provide mechanistic insights into the causes of the lung-intrinsic pathology in a G610C mouse model of moderate OI, which carries the same mutation in type I collagen alpha2(I) chain as in Old Order Amish patients. We previously demonstrated that bone pathology in G610C mice is largely caused by osteoblast and hypertrophic chondrocyte malfunction because of misfolded procollagen accumulation in the ER and consecutive cellular stress, specifically integrated stress response (ISR). Surprisingly, we found that lung pathology in G610C mice is more severe than bone pathology, homozygous (Hom) G610C neonates die at birth from lung failure caused by poorly developed saccular structures and massive parenchymal bleeding. In Hom E18.5 embryos, bone pathology was comparable to severely affected yet surviving Het animals while the lung pathology was more dramatic. In lung fibroblasts, unlike osteoblasts, we observed no ER disruption in electron microscopy (EM) and no ISR marker gene

upregulation in single cell (scRNASeq) or spatially resolved (srRNASeq) RNASeq. Instead, EM, histology, immunofluorescence, scRNASeq, srRNASeq, and in situ mRNA hybridization revealed deficient extracellular matrix (ECM) deposition, myofibroblast deficiency, and disorganization of lung epithelial cells, which filled the developing lung saccules instead of lining them. Altered gene expression by myofibroblasts and epithelial cells suggested abnormal cell interactions with the deficient ECM. In Het embryos, the lung pathology was less severe, but in 3- and 5-week-old Het mice we observed alveolar disruption, reduced alveolar surface/volume ratio, and increased respiratory frequency and volume/minute at rest (potentially compensating for the alveolar surface loss). In addition, many 3- and 5-week-old Het mice had lesions with inflammatory cell infiltration and various degrees of fibrosis, probably resulting from weak ECM being prone to injury. In 10-week-old Het mice, the alveolar disruption, lesions, and respiratory abnormalities were less pronounced, likely because of continuous lung remodeling in mice. These observations suggest that disruption of rapidly forming ECM and cell-ECM interactions by secreted mutant collagen molecules in embryos and young animals is the primary cause of the lung-intrinsic pathology in G610C mice, which is distinct from bone pathology.

***Disclosures: ELENA MAKAREEVA**, None*

SUN-530

Complex Abnormalities in Osteoblasts/Osteocytes of X-Linked Hypophosphatemia: Analysis of PHEX-Knockout Human iPS Cells Generated by CRISPR/Cas9 Genome Editing *Toshimi Michigami[1], Tatsuro Nakanishi[2], Miwa Yamazaki[2], Kanako Tachikawa[2], Ayu Ueta[2], Masanobu Kawai[2], Keiichi Ozono[3]. [1]Osaka Women's and Children's Hospital, Japan. [2]Osaka Women's and Children's Hospital, Japan. [3]Osaka University Graduate School of Medicine, Japan

X-linked hypophosphatemia (XLH) is caused by inactivating variants of the PHEX gene, which is highly expressed in mature osteoblasts and osteocytes. Although overproduction of FGF23 is responsible for hypophosphatemia and impaired vitamin D metabolism, pathogenesis of XLH is still not fully understood. Studies using Phex-deficient Hyp mice have suggested complex defects in osteoblasts and osteocytes: however, it is unclear whether the findings in Hyp mice are indeed shared by human XLH, partly due to the difficulty in obtaining sufficient numbers of osteoblasts/osteocytes from patients. Therefore, we herein generated PHEX-knockout (KO) human induced pluripotent stem (iPS) cells in order to use as a cell model for XLH. By applying CRISPR/Cas9-mediated gene ablation to an iPS clone derived from a healthy male, we obtained PHEX-KO iPS cells with a deletion extending from exon 1 to exon 3 and a frameshift. The parental iPS cells isogenic except for the PHEX gene were used as a control in the study. There was no obvious difference in cell viability/cytotoxicity between the PHEX-KO and isogenic control iPS cells. We then induced these iPS cells to differentiate into osteoblast-lineage by culturing in the presence of beta-glycerophosphate and ascorbic acid up to 49 days. The expression of PHEX was markedly increased by time in the isogenic control iPS cells, while the PHEX-KO cells completely lacked the functional PHEX transcripts. The expression of RUNX2, the master transcription factor of osteoblast differentiation, peaked on Day 28 in both the PHEX-KO and isogenic control iPS cells. We confirmed the increased production of FGF23 in the osteoblast-lineage cells differentiated from PHEX-KO iPS cells. Interestingly, in vitro mineralization was accelerated in the PHEX-KO iPS cells, which reminded us of ectopic calcification such as ossification of posterior longitudinal ligament (OPLL) often observed in adult patients with XLH. Extracellular levels of pyrophosphate, an inhibitor of mineralization, and adenosine triphosphate (ATP) in the conditioned media were elevated in the osteoblast-lineage cells derived from PHEX-KO iPS cells compared to those from isogenic control iPS cells, and this appeared to be associated with the reduced alkaline phosphatase activity. In addition, PHEX-KO iPS cells showed increased expression of multiple molecules such as DMP1, osteopontin, RUNX2, and FGF receptor 1, which was similar to the observations in the osteoblasts/osteocytes of Hyp mice. The expression of EGR1, a target of FGFR signaling, was also increased in the PHEX-KO iPS cells, suggesting an enhanced activation of FGFR signaling. The expression of KLOTHO was very low in the osteoblast-lineage cells from both iPS cells. Taken together, these results suggest that complex intrinsic abnormalities of osteoblasts/osteocytes may underlie the pathogenesis of XLH.

***Disclosures: Toshimi Michigami**, None*

SUN-531

SP7/Osterix Neomorphic Mutation S309W-Zebrafish Model Recapitulates Human High Bone Turnover Disease *Diane Sepich[1], Gary S. Gottesman[4], William H. McAlister[3], Michael P. Whyte[4], Lilianna Solnica-Krezel[1], Steven Mumm[4]. [1]Department of Developmental Biology, Washington University School of Medicine, United States. [4]Division of Bone and Mineral Diseases, Washington University School of Medicine, United States. [3]Mallinckrodt Institute of Radiology, Washington University School of Medicine, United States. [4]Division of Bone and Mineral Diseases, Washington University School of Medicine,

SP7 encodes the osteoblast-specific transcription factor osterix, which is critical for osteoblast development and function. In 2020, we reported (Whyte et al. Bone 137:115364) a de novo SP7 missense mutation (c.926C>G, p.S309W) in a young woman with high bone turnover resembling juvenile Paget's disease (JPD). JPD features rapid bone remodeling throughout the skeleton, presents in infancy or early childhood with fractures and deformity, is characterized by elevated serum alkaline phosphatase (ALP), and is usually caused by recessive mutations in TNFRSF11B encoding osteoprotegerin (OPG). She began fracturing her lower extremity long bones during infancy, then developed skull deformity and hearing loss. At age 15, radiographs revealed generalized osteosclerosis, hyperostosis, scoliosis, and craniofacial/dental defects, and DXA showed elevated bone mineral density (Z-score +5.1 at lumbar spine and T-score +3.3 at wrist). Bone turnover markers (serum ALP and urine hydroxyproline) were elevated. Iliac crest biopsy was consistent with rapid skeletal remodeling. She responded to alendronate therapy. Sanger sequencing of the OPG gene was negative, whereas whole exome sequencing identified the SP7 variant S309W. Independent publication of a second patient with the identical mutation and similar clinical characteristics supports the SP7 neomorphic variant as causal. Herein, we created a zebrafish model of our patient's allele using CRISPR/cas9, called sp7stl838. The homozygous mutants and heterozygous siblings exhibit frequent scoliosis of caudal vertebra. Initial micro computed tomography analysis of homozygous mutant and WT sib showed altered vertebral morphology, teeth not mounted in bone, and fractures in the caudal (tail) fin. Additionally, the mutant fish have altered growth of the premaxilla, maxilla, and dentary and other bones in the head. Cranial sutures between the frontal plates of the neurocranium ridge-up rather than overlap as in WT. The mid-region of the face centered on the nose, appears to have reduced bone density, while scales (which are dermal bone) have increased bone density. Histologic staining for bone and cartilage shows early excessive mineralization due to overactive sp7 (see figure). Thus, the zebrafish sp7 allele recapitulates some of our patient's JPD, with additional features. Our findings confirm c.926C>G, p.S309W as the causal mutation for Type 4 JPD and provide a good model for further study of this SP7 neomorphic mutation.

***Disclosures: Diane Sepich**, None*

SUN-533

Altered Desensitization of PTHrP Signaling as a Mechanism for Delayed Ossification in Eiken Syndrome *Ignacio Portales Castillo[1], Jakob Hoeppner[2], Thomas Dean[2], Brendan Creemer[3], Ross Cheloha[3], Sofya Savransky[4], Jean-Pierre Vilardaga[5], Roberto Civitelli[6], Harald Jueppner[2], Thomas Gardella[2]. [1]Washington University St. Louis, . [2]Massachusetts General Hospital, United States. [3]Chemical Biology in Signaling Section, Laboratory of Bioorganic Chemistry, National Institutes of Diabetes and Digestive and Kidney Diseases, United States. [4]Department of Pharmacology and Chemical Biology, School of Medicine, University of Pittsburgh, United States. [5]University of Pittsburgh, School of Medicine, United States. [6]Washington University in St. Louis School of Medicine, United States

Eiken syndrome is a rare disease characterized by delayed bone mineralization that is caused by homozygous mutations in the parathyroid hormone/PTH-related protein receptor (PTH1R). In some cases, hypocalcemia with elevated serum PTH also occurs. These clinical features seem consistent with a gain-of-function (G-O-F) effect of the mutation, given that the PTH1R acts during endochondral bone formation in response to PTHrP to delay growth plate chondrocyte differentiation and prevent premature ossification, and throughout life in response to PTH to maintain calcium homeostasis. The mechanisms, however, by which the PTH1R mutations of Eiken syndrome result in altered bone development and mineral ion physiology are unknown. The main signaling pathway activated by the PTH1R in response to either endogenous ligand is cAMP, which is normally regulated at least in part by interaction with ?arrestins. Here, we present results of our assays in vitro of three reported PTH1R mutations (R485X, E35K and Y134S) of Eiken syndrome which support a G-O-F effect of the mutations on cAMP signaling and suggest a plausible mechanism to explain the delayed bone mineralization phenotype. In HEK293 cells, and compared to PTH1R-WT, PTH1R-R485X, which has a truncated C-terminal tail and hence lacks important sites of ?arrestin interaction, exhibited elevated basal and prolonged PTHrP-induced cAMP signaling responses. The E35K and Y134S mutants, which are altered in the receptor's extracellular N-terminal domain at or near key sites of ligand contact, exhibited little or no change in

initial rates of PTHrP-induced cAMP signaling, but signaling after washout of unbound PTHrP was reduced, leading to a blunted desensitization response to PTHrP re-exposure. Each mutant was defective for recruiting ?arrestin2 to endosomes, but the defect for E35K and Y134S was specific for stimulation with PTHrP, not PTH; defects which parallel the impaired termination of initial PTHrP-induced cAMP signaling (R485X) and the impaired desensitization to PTHrP re-exposure (E35K, Y134S). The combined results suggest that a G-O-F effect of the studied mutations on either the constitutive or PTHrP-stimulated cAMP signaling by the PTH1R due in part to a weakened interaction with ?arrestin2 is a plausible mechanism underlying the delayed ossification seen in these Eiken syndrome patients.

***Disclosures: Ignacio Portales Castillo**, None*

SUN-534

The dynamics of P3 bone regeneration are compromised in Ts65 male Down syndrome mice *KIRBY M. SHERMAN[1,] CATRINA SILVEIRA[1,] Abigail Leon[3,] Hannah M. Smith[3,] Mingquan Yan[3,] Ken Muneoka[3,] Dana Gaddy[4,] Larry Suva[5,] Lindsay Dawson[6,] [1]Texas A&M University , [3]Texas A&M University, United States, [3]Texas A&M University, [4]College of Veterinary Medicine, Texas A&M University, United States, [5]Texas A&M University, College of Veterinary Medicine and Biomedical Sciences, United States, [6]Texas A&M University College of Veterinary Medicine, United States

Down Syndrome (DS), trisomy of human chromosome 21 (Ts21) is associated with mammalian embryologic and postnatal abnormalities. Ts21 individuals typically exhibit hallmark skeletal defects such as low bone mineral density (BMD) that predisposes this vulnerable group to skeletal injuries. Using multiple DS mouse lines that parallel the low BMD observed in Ts21 patients, Dp16(16)1Yey (Dp16) and Ts65Dn, transformative progress has been made in determining how low BMD in DS translates to skeletal repair. We demonstrated that fracture healing is severely impaired in Dp16 mice, with a nearly 100% occurrence of fracture non-union, characterized by failure of the cartilaginous callus to bridge the fracture gap. Underscoring the clinical relevance of our observations using murine DS lines, a fracture non-union was recently reported in a Ts21 patient. Here, to investigate intramembranous bone regeneration in DS, Ts65Dn male mice and WT controls were subjected to distal amputation of the digit tip (P3) and assessed via longitudinal ?CT and histological analysis. In this model, targeted osteoclast and osteoblast activities are spatially and temporally separated in vivo over the course of intramembranous bone regeneration. To fine-tune the analysis of P3 regeneration in the DS setting, we deployed our in-vivo ?CT staging system that distinguishes the 5 stages of the regeneration response based on osteoclast- and osteoblast-mediated anatomical changes.After P3 amputation, Ts65Dn males (n=8) show significantly delayed bone resorption and attenuated P3 bone regeneration compared to WT males (n=16; P<=0.0001). Intriguingly, ?CT staging revealed that osteoclast recruitment and the initiation of osteoclastic resorption (stage 2) was temporally indistinguishable between DS and WT mice, yet osteoclast resorption (stage 3) is prolonged in DS mice. Histological and ?CT analysis revealed that DS mice progress to stage 5 (initiation of bone regeneration) slower than WT mice, consistent with defects in osteoblast recruitment and/or activity. The osteoblast defect does not resolve, and Ts65Dn mice never achieve WT bone regeneration volume, even 2 months post amputation.Collectively, these data demonstrate that both intramembranous bone regeneration and endochondral fracture healing are severely impacted in DS mice. Future studies to identify the cellular and molecular deficits inherent in DS bone repair are critical to enable bone repair treatment options in people with Ts21.

***Disclosures: KIRBY M. SHERMAN**, None*

SUN-536

Respiratory Distress in Hypophosphatasia: The Case for Defects in Lung and Diaphragm in HPP Sheep *CLAIRE STENHOUSE[2,] JOSHUA BERTELS[2,] ALYSSA FALCK[3,] Lauren White[2,] Yava Jones-Hall[2,] Larry Suva[4,] Dana Gaddy[5,] [2]Texas A&M University, United States, [2]Texas A&M University, [3], United States, [4]Texas A&M University, College of Veterinary Medicine and Biomedical Sciences, United States, [5]College of Veterinary Medicine, Texas A&M University, United States

Hypophosphatasia (HPP) is an inherited disorder of mineral metabolism in individuals with loss of function mutations in the tissue-nonspecific alkaline phosphatase gene (ALPL). Patients with severe HPP have low serum ALPL enzymatic activity, musculoskeletal defects, and respiratory complications. We created a sheep model of HPP that recapitulates the human HPP phenotype. Interestingly, neonatal HPP lambs commonly have respiratory complications at birth and an increased incidence of developing pneumonia compared to wildtype (WT) control lambs. Prophylactic antibiotic administration to 1-day old lambs increased survival rates of HPP sheep to >1 year of age without evidence of respiratory symptoms (wheezing, labored breathing, nasal discharge). To better characterize the respiratory phenotype of HPP sheep, WT and homozygous HPP sheep were sacrificed at 1 year of age, and lung pathology, diaphragm function and rib mineralization assessed. Lung histology demonstrated pathologies consistent with pleural fibrosis, emphysema, and congestion in HPP sheep despite no respiratory symptoms at the time of sacrifice. Interestingly, rib mineralization in HPP sheep was indistinguishable from WT as measured by DEXA and microCT. However, isolated diaphragm muscle fibers from both genotypes demonstrated increased stiffness in 1-year old HPP sheep compared to WT, suggesting that compromises in diaphragm function also contribute to respiratory complications in HPP. To determine if the observed postnatal respiratory deficiencies were also apparent during development, lungs and rib mineralization were assessed in WT and HPP fetuses on gestational Day 100 (GD100). Like 1 year old HPP sheep, significant lung pathology was present on GD100, and fetal rib mineralization was not different between genotypes. These data provide the first direct evidence that the postnatal HPP lung phenotype is programmed during fetal development. Collectively, these data in HPP sheep demonstrate that the postnatal HPP respiratory phenotype has origins during fetal development and suggest that respiratory distress syndrome in human HPP is not solely the result of impaired rib mineralization and may also involve defects in both lung and diaphragm development and function. The observed abnormalities in multiple tissues that contribute to asymptomatic respiratory deficiencies in HPP suggest the potential need for monitoring or managing underlying respiratory deficiencies in mild to moderate HPP patients.

***Disclosures: CLAIRE STENHOUSE**, None*

SUN-537

Prkar1a deletion in osteoblasts causes severe bone pathology with change in gene expression leading to impairment of osteoblast differentiation and increased osteoclast activity. *CAROLE LE HENAFF[2,] ZHIMING HE[2,] Brandon Finnie[2,] Joshua Johnson[2,] Maria Pacheco[2,] Yasaman Nahaei[2,] Juhee Jeong[2,] Henry Kronenberg[3,] Lawrence S Kirschner[4,] Nicola Partridge[5,] [2]New York University, United States, [2]New York University, [3]Massachusetts General Hospital, United States, [4]Department of Cancer Biology and Genetics, Division of Endocrinology, Diabetes, and Metabolism, Department of Internal Medicine, The Ohio State University, United States, [5]New York University College of Dentistry, United States

PTH (1-34) was the first osteoanabolic hormone for treating osteoporosis. PTH acts through PTHR1 and Protein Kinase A (PKA) activation to regulate osteoblastic gene expression. However, hyperactive PTHR1 and its downstream signaling pathway (Gs?) are involved in several bone diseases including hyperparathyroidism, Jansen's metaphyseal chondrodysplasia and Fibrous Dysplasia-McCune-Albright Syndrome. Hyperactive PKA due to a mutation in PKA regulatory subunit 1A (Prkar1a) is found in Carney disease and has been linked to benign tumor formation while its impact on bone formation or remodeling remains unknown. Our study aimed to elucidate the effects of increased PKA activity and better understand the actions of PTH in bones. One-month-old C57Bl/6J male and female col1CREERT/Prkar1afl/fl mice or Prkar1afl/fl mice received tamoxifen weekly for 3 weeks to delete Prkar1a in osteoblasts and increase PKA activity. In both sexes, Prkar1aob-/- mice demonstrated bone pathologies in their skulls, femurs and vertebrae and tumors in their tails. MicroCT showed cortical bone breakdown with apparent trabecular bone in the cortical area in femurs, vertebrae, tails and skulls. RNA-Seq was conducted with femoral trabecular bone. The data showed a complete change in gene expression and an impairment of osteoblast differentiation with a defect in ossification. This was confirmed by qPCR analyses. In both sexes, cortical and trabecular bone RNAs showed a large increase in Bsp mRNA levels (3-6 fold) with a sharp decrease in Bglap (0.2-0.4 fold) showing a change in osteoblast differentiation. The RNAseq and qPCR confirmed the high bone turnover in Prkar1aob-/- mice with a 2-3 fold upregulation of Rankl. These paralleled the huge increase in osteoblast activity shown by serum-P1NP levels (6.5-13 fold), only single fluorescent labeling and a substantial increase in osteoclast activity shown by CTX levels (4.4-12 fold) and TRAP staining (increased osteoclast number and size). Furthermore, PTH-responsive-genes were significantly changed: Sost expression was decreased to 0.1-0.2 fold, and Mmp13 was increased by at least 3 fold. It was evident that there was a profound modification of gene expression of chemokines and Wnt members together with enhanced osteoclastogenesis. High PKA activity in osteoblasts appears to be involved with high bone turnover and pathological events mimicking diseases from a hyperactive PTHR1/PKA pathway.

***Disclosures: CAROLE LE HENAFF**, None*

SUN-539

PDGFR? Signaling in Osteoprogenitors Contributes to the Pathogenesis of Fibrous Dysplasia *Cyril Thouverey[1,] Alessandro Corsi[2,] Mara Riminucci[3,] [1]University Hospital of Geneva, Switzerland, [2]Sapienza University, Italy, [3]University La Sapienza, Italy

Fibrous Dysplasia (FD) is a rare bone disorder caused by somatic gain-of-function mutations of the GNAS gene, which encodes Gs? protein. FD bone lesions are characterized by the replacement of normal bone and marrow by a fibro-osseous tissue containing proliferating fibroblast-like osteoprogenitors (OPs) and elevated number of osteoclasts. Platelet-derived growth factor B (PDGFB) and PDGF receptor type ? (PDGFRB) are overexpressed in human FD bone lesions. To determine whether PDGF/PDGFR? signaling contributes to FD pathogenesis, we generated a mouse model of FD that lacks PDGFR? in leptin receptor-positive (LEPR+) OPs (GnasR201C;Lepr-Cre;Pdgfrbf/f) and compared its phenotype with that of Lepr-Cre and GnasR201C;Lepr-Cre mice at 5 months of age. Bone phenotypes were analyzed by micro-CT, 3-point bending test, histomorphometry and gene expression analyses. Bone lesions of GnasR201C;Lepr-Cre mice exhibited increases in Pdgfb (+65%, p=0.06) and Pdgfrb (+139%, p=0.06) expressions in comparison to healthy bone tissue of Lepr-Cre littermates. GnasR201C mice showed increased cortical bone vol-

ume (+39%, p=0.028) with elevated number of osteolytic cavities (x14.3 per total volume, p=0.0001), decreased cortical volumetric bone mineral density (vBMD; -2%, p=0.04), and altered bone mechanical properties (plastic energy: -55%, p=0.005) at femoral midshaft lesions. Deletion of PDGFR? in LEPR+ cells in GnasR201C mice decreased number of osteolytic cavities (-62% vs GnasR201C;Lepr-Cre, p=0.002), augmented cortical vBMD (+1.2% vs GnasR201C;Lepr-Cre, p=0.04) and restored bone mechanical properties (plastic energy: +107% vs GnasR201C;Lepr-Cre, p=0.02). Those beneficial effects were associated with reduced osteoclast number (-44% vs GnasR201C;Lepr-Cre, p=0.0001), osteoid surfaces (-63% vs GnasR201C;Lepr-Cre, p=0.002) and fibrotic bone marrow volume (-66% vs GnasR201C;Lepr-Cre, p=0.02). Consistent with these findings, bone lesions of GnasR201C;Lepr-Cre;Pdgfrbf/f mice displayed reduced expressions of Rankl (-55%, p=0.02), Csf1 (-74%, p=0.003), fibronectin (-61%, p=0.06) and Timp1 (-77%, p=0.007) in comparison to those of GnasR201C;Lepr-Cre mice. In conclusion, our results indicate that PDGFR? signaling in OPs contributes to the pathogenesis of FD.

***Disclosures: Cyril Thouverey**, None*

SUN-541

Bone Marrow Adiposity May Be a Key Player in Cystic Fibrosis related Bone Disease *Claire Dumortier[1], Johan Sergheraert[1], Mezhoura Ouhamou[1], Olivier Piot[2], Emilie Buache[2], Nicolas Goffin[2], Christophe Chauveau[3], Sophie Gangloff[1], Denise Al Alam[4], Frédéric Velard[1]. [1]URCA, EA 4691 BIOS, France. [2]URCA, EA 7506 BioSpeCT, France. [3]ULCO, ULR 4490 MabLab, France. [4]The Lundquist Institute, Torrance, Harbor-UCLA Medical Center, United States

Purpose: Cystic Fibrosis related Bone Disease (CFBD) affects 50% of cystic fibrosis (CF) adult patients. Osteoblasts obtained from CF patients' induced pluripotent stem cells (iPSCs) evidenced delayed maturation phenotype as already observed on primary mature cells (Velard, 2014; Delion, 2016). They have also shown an higher level of PPARG (the adipocyte transcription factor) than healthy donors-derived control line. A relationship exists between low bone density and increased medullar adiposity in several pathologies (Verma, 2002; Piccinin, 2014, Schafer, 2015; Bredella, 2009). So, we hypothesised that adipocyte differentiation would be triggered in cells bearing mutation in CFTR gene, which causes CF. Up to date, medullar adiposity has never been investigated in CFBD.Methods: Bone marrow mesenchymal stem cells (MSC) from non CF patients have been differentiated into adipocytes during 21 days with or without Inh172, a CFTR pharmacological inhibitor. Oil Red'O, Bodipy®, Perilipin, FABP4 (adipocytes specific proteins) and PPARG stainings were performed. RAMAN microspectroscopy was used to assess lipid content. MicroCT analysis of 10 weeks-old F508del CFTR mice was performed to determine bone marrow adiposity. Results: Lipid vesicles were 50% bigger when CFTR inhibitor was adding in the medium (n=6 donors, p<0.05). However, no change in PLIN1, FABP4 and PPARG genes or protein expression, or adiponectin and leptin secretion were highlighted. Lipid droplets spontaneous generation was evidenced by RAMAN, Oil Red O and BODIPY stainings, in MSC cultured in presence of Inh172 and without any differentiation triggering factors. This reflects the spontaneous adipocyte commitment of MSC associated with impaired CFTR function. In addition, we evidenced increased bone marrow adiposity in mice bearing F508del CFTR mutation compared to wildtype littermates.Conclusion: These data are the first proof of concept that CFTR loss of function influences size and content of mature adipocytes lipid vesicles, as well as MSC commitment towards adipocyte lineage. More, increased bone marrow adiposity observed in CF mice tibia enforced the idea of a defective lipid metabolism in CF context, sustained by recent studies that have highlighted the major role of lipid deregulations on CFTR function (Aureli, 2016. Loberto, 2020). The hypothesis of increased medullar adiposity in CF patients is a promising axis to better understand and cure CFBD.

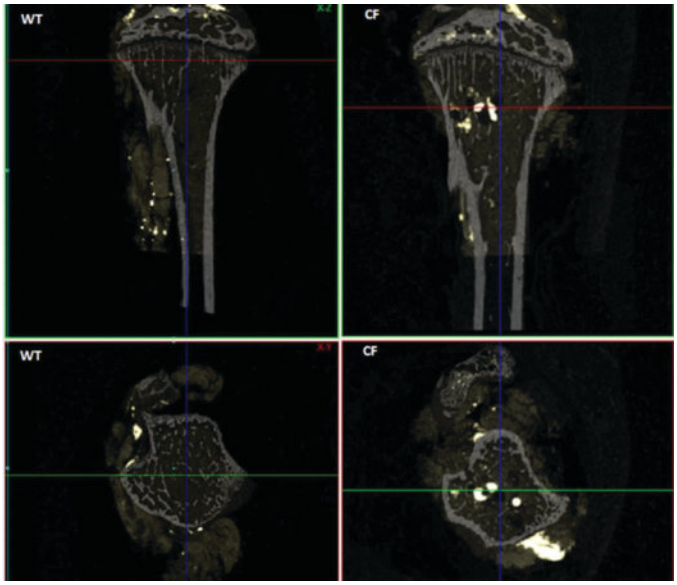

***Disclosures: Claire Dumortier**, None*

SUN-542

GNAS AS2 DMR Methylation Depends on STX16/NESP55 ICRs and Has Diagnostic Potential in AD-PHP1B *YORIHIRO IWASAKI[1], Monica Reyes[2], Harald Jueppner[3], Murat Bastepe[4]. [1], . [2]Massachusetts General Hospital , United States. [3]Massachusetts General Hospital, United States. [4]Massachusetts General Hospital, Harvard Medical School, United States

BACKGROUND: Gs? is a signaling protein essential for the actions of numerous hormones. It is encoded by GNAS, an imprinted locus giving rise to Gs? mRNA and alternatively spliced transcripts from additional first exons within differentially methylated regions (DMRs), including NESP55, antisense (AS), XL, and A/B. Parent-specific methylation of these GNAS DMRs is crucial for Gs? expression and the pathogenesis of diseases caused by GNAS mutations. Perturbed GNAS methylation, especially A/B hypomethylation, leads to pseudohypoparathyroidism type 1B (PHP1B). We recently generated human embryonic stem cell (hESC) models of autosomal dominant PHP1B (AD-PHP1B) by deleting either of the two GNAS imprinting control regions (ICRs), namely del-STX16 and del-NESP55. These models revealed that interaction between the two GNAS ICRs is critical for regulating A/B methylation in the zygote/early embryo. Recently, a new DMR located between AS and XL (AS2) was shown to be hypomethylated in some PHP1B variants.METHODS: We analyzed AS2 methylation levels in wild-type (WT), del-STX16/del-NESP55 hESCs using MSRE-qPCR. We also analyzed GNAS methylation by MS-MLPA in several AD-PHP1B patients with either a STX16 deletion, a GNAS-STX16 duplication upstream of AS2, or a retrotransposon insertion downstream of AS2.RESULTS: In WT hESCs, the AS2 DMR had lower methylation levels than other GNAS DMRs (~3.5 vs. ~50%). Maternal deletion of STX16- or NESP55-ICRs resulted in further hypomethylation at AS2 DMR (3.6 vs. 0.03%, p<0.0001 for del-STX16; 3.5 vs. 0.6%, p=0.0015 for del-NESP55). In contrast, methylation levels at AS and XL were not significantly reduced. AS2 was hypomethylated in AD-PHP1B patients with a STX16 deletion (n=7) or a GNAS-STX16 duplication (22.2+/-4.7% and 18.1%, respectively), but it was normal (53.7+/-1.5%) in seven patients from one family with a retrotransposon insertion. DISCUSSION: Based on our findings, the AS2 DMR, unlike AS and XL DMRs, is critically regulated by GNAS ICRs in the zygote/early embryo, similar to A/B DMR. In addition, the extent of GNAS methylation abnormalities, including AS2 hypomethylation, depends on the locations of genomic aberrations that presumably disrupt nascent NESP55 transcripts. Thus, analysis of AS2 DMR can help determine where a disease-causing AD-PHP1B mutation is located within GNAS/STX16.

***Disclosures: YORIHIRO IWASAKI**, None*

SUN-543

Human Femur Erlenmeyer Flask Deformities Result from Disrupted Metaphyseal Bone Modeling with Mutations in ANKH, COL10A1, FLNA, LRRK1, MMP9, MMP13, PLEKHM1, PTH1R, SFRP4 and SNX10 *Robert Brommage[1]. [1]BoneGenomivs, United States

Metaphyseal dysplasias involve defects in metaphyseal bone development, usually with normal stature and minimal growth plate disturbances. These genetic disorders include craniometaphyseal dysplasia (ANKH, mouse Ank), Schmid metaphyseal chondrodysplasia (COL10A1), frontometaphyseal dysplasia (FLNA), Gaucher's disease (GBA), osteosclerot-

ic metaphyseal dysplasia (LRRK1), metaphyseal anadysplasia (MMP9 and MMP13), Jansen metaphyseal chondrodysplasia (PTH1R), Pyle's disease (SFRP4), and osteopetroses resulting from PLEKHM1 and SNX10 mutations. Disruptions of the homologous mouse genes result in similar metaphyseal abnormalities.Metaphyseal bone modeling during growth involves 1) endocortical bone formation, 2) periosteal bone resorption, 3) consolidation of existing peripheral trabeculae into cortical bone and 4) removal of central trabeculae from marrow regions. The Erlenmeyer flask deformity (see attachment) results from disruption of these processes.During linear growth periosteal osteoclasts below the growth plate resorb bone to decrease bone width. Osteoblasts simultaneously add bone to endocortical surfaces, which includes incorporation of existing trabeculae (compactation). Small islands of calcified cartilage remain within this cortical bone. Calcified cartilage below the growth plate is transformed to mineralized bone trabeculae, which are then resorbed several centimeters from the growth plate. A full understanding of the normal spatial and temporal coordination of these complex processes must include the actions of each of these known metaphyseal dysplasia genes.Developmental metaphyseal dysplasias occur when these processes are compromised. Radiologic Erlenmeyer flask deformities (EFD) with thin cortices result from failure of periosteal osteoclasts to resorb bone and concurrent lack of bone formation by endocortical osteoblasts. Metaphyseal trabeculae within the marrow cavity are not properly removed.A literature survey of 55 publications (92 subjects) describing skeletal phenotypes in Pyle's disease subjects found EFD (all publications), genu valgum (36), thin cortices (28), S-shaped tibia (23), fragility fractures (19), and dysplasias in skulls, clavicles, ribs, and digits (all > 20).Mouse mutants provide good models for these human dysplasias. Mouse gene knockouts of Lrrk1 and Sfrp4 were observed (in the author's laboratory) to have relevant bone abnormalities prior to the identification of human LRRK1 and SFRP4 mutations.

Human Erlenmeyer Flask Deformity

Osteopetrosis and Erlenmeyer-Flask Deformity. Heczey A, Louis C. N Engl J Med. 2015; 373:e12.

Pyle disease (metaphyseal dysplasia) presenting in two adult sisters. Soares DX, Almeida AM, Barreto AR, Alencar E Silva IJ, de Castro JD, Magalhães Pinto FJ, Dias DA, Aguiar LB. Radiol Case Rep. 2016; 11:405-410.

***Disclosures: Robert Brommage**, None*

SUN-546

Circulating 25(OH)D >= 50 ng/mL is Not Associated With Increased Falls

*Neil Binkley[1], Gretta Borchardt[2], Joan Lappe[3], Chris Sempos[4]. [1]University of Wisconsin, Madison, United States. [2]University of Wisconsin, United States. [3]Creighton University, United States. [4]Vitamin D Standardization Program, United States

Purpose: Falls are a common cause of unintentional injury including fracture in older adults. High circulating 25(OH)D has been reported to increase falls risk; thus, recent osteoporosis Guidelines recommend 25(OH)D not exceed 50 ng/mL. The purpose of this secondary analysis of a 4-year randomized trial of vitamin D supplementation in postmenopausal women was to evaluate the association of retrospectively standardized 25(OH)D concentration with falls.Methods: This study recruited 2,303 healthy postmenopausal women age 55+ in rural Nebraska. Excluding missing data (n=194) 2,109 were followed for 4 years. The treatment group received vitamin D3 2000 IU/daily. Circulating 25(OH)D was measured at baseline and annually initially using the Diasorin Liaison; subsequently, retrospectively standardized 25(OH)D (s25D) results were obtained using stored sera analyzed by HPLC following the Vitamin D Standardization Program protocol. Falls were captured by diary. Incidence for >=1 fall and >= 2 falls was assessed by study year and correlated with 4 levels of s25D (<= 20 ng/mL, 20-29 ng/mL, 30-49 ng/mL and >= 50 ng/mL) at start of each year. Subsequently association between s25D and falls was evaluated using multivariable logistic regression.Results: Mean baseline age was 65 (range 55-91) years. Mean (SD) s25D at baseline was 32.6 ng/mL (8.3) with no difference between treatment and placebo groups. s25D remained stable in the placebo group and increased to 41.3 ng/mL at year 1 in the treatment group then remained stable. Falls incidence rate did not differ by treatment group. At each individual year 1-4 and over the entire study duration the incidence rate for one or more falls varied from 19.3-36.4% and for 2 or more falls from 4.5-14.6%. Over all 4 years of follow-up there was a statistically significant association between s25D and falls incidence (both >=1 fall and 2 or more falls per year). This significant association appears to have been driven by lower falls rates in the < 20 ng/mL group. In the multivariate analysis, no consistent effect of s25D group on falls was observed.Conclusion: In this cohort of postmenopausal women, higher s25D concentration was not associated with greater falls risk.

Table: Crude falls incidence by standardized 25(OH)D group

	Study year				
s25D	1	2	3	4	All Years*
One or more falls/year [≥ 1 falls/year]					
< 20	19.3 (23/119)	20.9 (14/67)	24.7 (18/73)	19.7 (14/71)	*20.9 (69/330)
20-30	25.4 (171/674)	27.6 (141/511)	25.2 (121/480)	29.5 (122/413)	26.7 (555/2078)
30-50	27.6 (348/1261)	27.7 (337/1217)	29.1 (338/1164)	29.0 (333/1150)	28.3 (1356/4792)
≥ 50	36.4 (20/55)	25.5 (50/196)	27.7 (59/213)	26.3 (60/228)	27.3 (189/692)
Two or more falls/year [≥ 2 falls/year]					
< 20	5.9 (7/119)	4.5 (3/67)	6.9 (5/73)	7.0 (5/71)	*6.1 (20/330)
20-30	9.9 (67/674)	10.6 (54/511)	8.5 (41/480)	12.4 (51/413)	10.3 (213/2078)
30-50	9.5 (120/1261)	8.6 (105/1217)	10.6 (123/1164)	9.7 (111/1150)	9.6 (459/4792)
≥ 50	14.6 (8/55)	10.2 (20/196)	12.7 (27/213)	11.4 (193/1862)	11.7 (81/692)

Note: Data presented as percent (# who fell/# in s25D group); * = p < 0.05

***Disclosures: Neil Binkley**, None*

SUN-547

Sarcopenia definitions And their Association with Non-fracture injurious Falls in older Swedish women From the SUPERB study

*Anoohya Gandham[1], GIULIA GREGORI[2], Lisa Johansson[3], Helena Johansson[4], Nicholas Harvey[5], Liesbeth Vandenput[6], Eugene McCloskey[9], JOHN KANIS[8], Marian Schini[9], Henrik Litsne[4], Kristian Axelsson[10], Mattias Lorentzon[11]. [1]Mary MacKillop Institute for Health Research, Australian Catholic University, Victoria, Australia, Australia. [2]University of Gothenburg, . [3]Institute of medicine, . [4]Sahlgrenska Osteoporosis Centre, Institute of Medicine, University of Gothenburg, Sweden, Sweden. [5]University of Southampton, . [6]Australian Catholic University, Australia. [9]University of Sheffield, United Kingdom. [8]UNIVERSITY OF SHEFFIELD, United Kingdom. [9]University of Sheffield, . [10]Institute of Medicine, Sahlgrenska Academy, Gothenburg University, . [11]Sahlgrenska Academy, University of Gothenburg, Sweden

Purpose: To investigate the prevalence and predictive value of three commonly used sarcopenia definitions for the risk of injurious falls in a population of older Swedish women, when adjusted for fracture risk assessment (FRAX)-based risk factors and previous falls. Methods: Of 3,028 older women aged 75 to 80 years included in the Swedish SUPERB-cohort, 2,883 had complete data on the used sarcopenia definitions and were used in all further analyses. Sarcopenia was defined based on the Sarcopenia Definitions and Outcomes Consortium (SDOC) (low handgrip strength and gait speed), revised European Working Group on Sarcopenia in Older People (EWGSOP2) and Asian Working Group for Sarcopenia (AWGS) (low appendicular lean mass index (ALMI; appendicular lean mass (kg)/height (m2)) and hand grip strength (kg))) definitions. ALMI was obtained from dual-energy X-ray absorptiometry (Hologic Discovery A). Self-reported questionnaires captured the occurrence of falls in the past 12 months and FRAX-based clinical risk factors. Incident injurious falls, without concurrent fracture, were identified using national registers and ICD-10 codes (W00-W19 code and a S00-T14 diagnosis, but not a simultaneous fracture code). Cox regression (hazard ratios (HR) and 95% confidence intervals (CI)) analyses were performed without adjustment and after adjustment for age, FRAX variables and previous falls. Results: Sarcopenia prevalence was 4% (n=129) defined by SDOC, 12% (n=360) according to EWGSOP2 and 10% (n=296) for AWGS. During a median (IQR) follow-up time of 6.6 (5.7-7.3) years there were 491 injurious falls without fracture. Sarcopenia according to EWGSOP2 and AWGS was not associated with an increased risk of injurious falls in any model, regardless of adjustment (p >0.05). Individuals with sarcopenia defined by SDOC had a more than 2-fold increase in the risk of injurious falls compared with women without sarcopenia (HR: 2.27; CI:1.64-3.15). Adjusting this model for clinical risk factors used in FRAX and previous falls resulted in a slightly attenuated association between SDOC prevalence and injurious falls (HR:1.85; CI:1.32-2.60). Conclusion: These findings suggest that sarcopenia definitions confined to muscle function and strength such as SDOC, rather than including DXA-based ALMI (EWGSOP2 and AWGS), lowers the prevalence but improves prediction of injurious falls in this population of Swedish older women.

***Disclosures: Anoohya Gandham**, None*

SUN-548

Cross-calibration of body composition between Hologic and Inbody 970 *Ha Young Kim[1], Deog-Yoon Kim[2], Yong-Chan Ha[3], Hyoung-Moo Park[4], Dong-Won Byun[5], Young-Kyun Lee[6]. [1]Gangneung Asan Hospital, University of Ulsan College of Medicine, , Republic of Korea. [2]Kyung Hee University Hospital, Republic of Korea. [3]Seoul Bumin Hospital, Republic of Korea. [4]Grace Hospital, Republic of Korea. [5]Soon Chun Hyang University Hospital, Republic of Korea. [6]Seoul National University Bundang Hospital, Republic of Korea

Background: The aim of this study was to investigate the correlation body composition measured by the Hologic Discovery QDR W and the Inbody 970 and to calculate the conversion rate between the two devices. Methods: The 120 subjects were men and women in aged 20-79 years old. All participants were scanned twice on both the Hologic Discovery QDR W (Hologic, Bedford, MA) DEXA system and the Inbody 970 (Biospace Co., Seoul, Korea) using the manufacturers' standard scanning and positioning protocols. Results: In the correlation coefficient for muscle mass between the two devices, all regions showed a very high correlation of 0.9 or more. The values were 0.96 (0.95 - 0.98) for the right arm, 0.96 (0.94 - 0.97) for the left arm, 0.96 (0.95 - 0.97) for the right leg, and 0.97 (0.95 - 0.98) for the left leg. body composition analysis of two machines by gender was compared. In the CCC for muscle mass between the two devices in woman, all regions showed moderate or strongly correlation. Body composition analysis of two machines according to age of each sex was compared. The CCC values of total muscle mass in female were 0.69 (0.46 - 0.83) in age 18 - 34, 0.66 (0.5 - 0.77) in age 35 - 64 and 0.36 (0.11 - 0.56) in age over 65. Conclusion: This prospective comparision study between DXA and BIA demonstrated that BIA is an good laternative device for measuring muscle mass and diagnosing sarcopenia. However, relatively lower correlation in gender and age differences between two device should be considered.

***Disclosures: Ha Young Kim**, None*

SUN-550

Correlation between serum immunoglobulin E levels and skeletal muscle mass in Korean adults: a cross-sectional study *Hyeonmok Kim[1]. [1]Seoul medical center, Republic of Korea

Despite evidence from experimental and field studies suggesting the detrimental effects of serum immunoglobulin E (IgE) on muscle metabolism, there are limited clinical studies in terms of circulating IgE with sarcopenia-related phenotypes. Thus, this study investigated the correlation between serum IgE levels and indices of muscle mass and risk of sarcopenia. This is a population based cross-sectional study from the Fifth Korea National Health and Nutrition Examination Surveys (KNHANES V), which includes participants a total of 2,241 (1,115 men and 1,126 women). Total lean mass (TLM) and appendicular skeletal muscle mass (ASM) was measured by dual energy X-ray absorptiometry.The findings demonstrates that before and after adjustment for confounding variables, higher IgE levels were significantly associated with lower ASM/Weight in men (r=-0.064, P=0.034) and with lower TLM and ASM/Weight in women (r=-0.069, P=0.035 and r=-0.089, P=0.006, respectively). When participants were divided into two groups according to sarcopenia status calculated by ASM/Weight, participants with sarcopenia demonstrated 88.4% and 121.8% higher serum IgE levels than those without sarcopenia (P<0.001 and P<0.001, respectively). The risk of sarcopenia of men and women were 3.41 fold and 5.69 fold (95% confidence interval=1.45-8.01 and 1.49-21.82 respectively) higher in subjects with in the highest serum IgE quartile than in those in the lowest quartile after adjustment for potential confounders.These findings suggests that increased serum IgE levels could be an independent risk factor for the development of low muscle mass, especially skeletal muscle mass.

***Disclosures: Hyeonmok Kim**, None*

SUN-551

Jump power assessment using computer vision-based deep learning motion analysis to detect possible sarcopenia *Sang Wouk Cho[1], Eun-young Park[2], Na-rae Park[2], Sookyeong Han[3], Yumie Rhee[4], Namki Hong[5]. [1]Department of Integrative Medicine, Yonsei University College of Medicine, Republic of Korea. [2]Department of Internal Medicine, Endocrine Research Institute, Severance Hospital, Yonsei University College of Medicine, Seoul, Korea , Republic of Korea. [3]Department of Internal Medicine, Endocrine Research Institute, Severance Hospital, Yonsei University College of Medicine, Seoul, Korea, Republic of Korea. [4]Yonsei University College of Medicine, Republic of Korea. [5]Division of Endocrinology, Republic of Korea

Peak countermovement jump power measured using ground force plate is associated with impaired physical function and higher risk of fracture in older adults. However, ground force plate is available at research setting, limiting the clinical applicability. We developed a video-based pose landmark regression model to estimate the peak jump power and tested clinical utility for sarcopenia screening.Participants who visited Osteoporosis Clinic, Severance Hospital, Korea were prospectively enrolled after obtaining written consent between March and August 2022. Individuals were instructed to perform three jump attempts under video recording, followed by grip strength (GS) and 5-time chair rise test (CRT). After detecting anatomical landmarks using Mediapipe for each frame of jump motion videos, an open-source deep learning pose estimation model, velocity, acceleration, force, and power were estimated. LightGBM-based model was built to predict jump power from motion data in 80% train set. In 20% hold-out set, clinical utility of predicted jump power was tested against detecting possible sarcopenia by Asian Working Group for Sarcopenia 2019 definition (low GS or low CRT performance).A total of 661 jump motion data from 221 patients (mean age 62 years; 78% women; possible sarcopenia 45%) were analyzed. In test set, average difference between predicted and actual jump power was 0.27 W/kg (95% limit of agreement -4.9 to +5.5 W/kg; concordance correlation coeffficient 0.93). Lower predicted jump power was associated with elevated odds of possible sarcopenia (adjusted odds ratio 1.27, 95% CI 1.02 to 1.58, p=0.029) after adjustment for age, sex, and body mass index. Motion data-based predicted jump power showed better discriminatory ability compared to age (AUROC 0.71 vs. 0.63, p=0.021), with comparable discriminatory performance to actual jump power (0.71 vs. 0.74, p=0.096).Computer vision -based prediction of jump power using motion video data can be useful to detect possible sarcopenia.

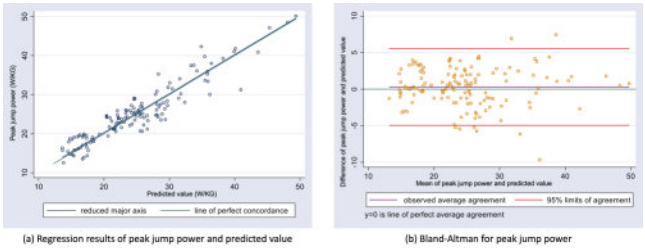

(a) Regression results of peak jump power and predicted value (b) Bland-Altman for peak jump power

***Disclosures: Sang Wouk Cho**, None*

SUN-552

Vertebral Bone Marrow Fat Is Associated With Sarcopenia In Korean Older Adults *Seunghyun Lee[1], Jhii-Hyun Ahn[2], Namki Hong[3], Jae Seung Chang[4], Kyu-Sang Park[5], Moon Young Kim[6], Jung Soo Lim[7]. [1]Wonju Severance Christian Hospital, Yonsei University Wonju College of Medicine, Wonju, Korea, . [2]Department of Radiology, Wonju Severance Christian Hospital, Yonsei University Wonju College of Medicine, Wonju, Korea, Republic of Korea. [3]Division of Endocrinology, Republic of Korea. [4]Department of Sports Science, Hannam University, Daejeon, Korea, Republic of Korea. [5]Department of Physiology, Wonju Severance Christian Hospital, Yonsei University Wonju College of Medicine, Wonju, Korea, Republic of Korea. [6]Department of Internal Medicine, Wonju Severance Christian Hospital, Yonsei University Wonju College of Medicine, Wonju, Korea, Republic of Korea. [7]Yonsei University Wonju College of Medicine, Republic of Korea

Mesenchymal stem cells (MSCs) are precursors of adipocytes, osteoblasts, and myocytes. Recent studies suggested that vertebral bone marrow fat (vBMF) can be a diagnostic marker for osteoporosis, and it is explained by the competition of osteoblastogenesis and adipogenesis when MSCs are differentiated. However, the association between vBMF and sarcopenia or myokines remains unclear.Among 1,894 participants of a population-based cohort study between May 2018 and August 2019, a total of 310 subjects (114 men, 196 women) were enrolled. Those with alcoholism, a history of steroid use, liver diseases other than fatty liver, malignancy, high body mass index (BMI) (>= 35 kg/m2), high fasting blood glucose (>= 200 mg/dL), L-spine compression, metal artifact, and missing data were excluded. Bone mineral density and muscle mass (MM) were assessed by dual-energy X-ray absorptiometry. vBMF (%) was defined as the average of L1-3 proton density fat fraction using quantitative MRI. The presence of low MM, low muscle function (MF), and sarcopenia were defined based on the Asian Working Group Society 2019 guideline. Moreover, serum concentrations of myokines such as myostatin and decorin (DCN) were quantified by using commercially available ELISA kits according to the manufacturer's instructions. The median age was 66 [61-72] years, and BMI was 25.3 [23.4-27.5] kg/m2. Approximately 44%, 48%, and 23% of the subjects had low MM, low MF, and sarcopenia, respectively. Those with sarcopenia had higher vBMF than normal subjects (59.8 [56.0-62.4] vs. 55.0 [46.8-59.2], p<0.001). Higher vBMF had a higher prevalence of low MM, low MF, and sarcopenia according to unadjusted logistic regression analysis (all, p<0.05). However, there was an association between vBMF and low MM or sarcopenia after adjusting for covariates (adjusted OR 1.78 [1.10-2.89], p=0.020; adjusted OR 1.45 [1.01-2.08], p=0.044, respectively). For myokines, partial correlation analysis revealed a significant correlation between vBMF and DCN after adjusting for age group, sex, and BMI (r=0.200, p<0.001).Intriguingly, our findings suggest a link between vBMF and sarcopenia or DCN levels in Korean older individuals. Further research is needed to understand better how vBMF interacts with sarcopenia and myokines.

***Disclosures: Seunghyun Lee**, None*

Sunday Orals

SUN-553

Physical Function Assessment in Older Adults- Self-Report May Not Reflect Actual Physical Performance *Jeri Nieves[1], Donald McMahon[4], Heather Berman[3], Peter Prescott[3], Felicia Cosman[4], Joseph Lane[3]. [1]Columbia University and Hospital for Special Surgery, , [4]Columbia University College of Physicians and Surgeons, , [3]Hospital for Special Surgery, United States, [4]Columbia University College of Physicians and Surgeons, United States

Introduction: Functional ability is a marker of successful treatment after fracture. Poor physical function is associated with high risk of another fracture. The methodology to assess functional ability varies greatly, from self-reported measures to physical performance tests; the gold standard is likely the Short Physical Performance Battery (SPPB). The aim of this study was to see if self-reported measures, using 3 separate scales, are a good proxy for tested performance. Methods: Subjects included patients enrolled in pelvic fracture healing study (n=64; SF-36 used) and patients recruited from our osteoporosis clinic into the Fragile Bone Registry (FBR; n=188; PROMIS-29 used). In-person testing of physical performance included SPPB-which combines 4-meter walk speed, time for 5 chair stands and ability to maintain balance in 3 positions) and Timed Up and Go (TUG- the time to stand, walk 3 meters, turn, and walk 3 meters back). Self-reported measures of physical performance: SF-36 physical function, PROMIS-29, and Lower Extremity Activity Scale Score (LEASS) were completed under supervision by a research assistant. Self reported measures and TUG were compared to SPPB. Results: In the FBR, of participants whose physical performance by SPPB scored in the lowest quintile, 27% were in the highest quartile for PROMIS ($p<0.001$ fisher's exact test) and the kappa (level of agreement) was 0.7. Similar findings were found for the LEASS. For subjects who tested in the highest quartile of TUG, 22% were in the lowest quartile by PROMIS ($p<0.001$ Fishers' Exact Test, Kappa = 0.72). From regression analysis, PROMIS explained 32% and LEASS explained 11% of the variance in SPPB. The other performance test, TUG, explained 48% of the variance in SPPB. PROMIS was able to explain 29% and LEASS explained 12% of the variance in TUG. In pelvic fracture patients we were able to assess the relationship between changes in SPPB, TUG and SF-36 over 8 weeks. The correlation between the % differences in SPPB and SF-36 over 8 weeks was $r=0.44$ ($p=0.002$). Change in SF-36 explained 19% of the change in SPPB (Shrout-Fleiss ICCR = 0.55). The ICCR between changes in SPPB and TUG was 0.49, but TUG change only explained 13% of SPPB change. Conclusion: SPPB is likely more responsive to change in physical performance than TUG. Self-reported assessments of lower extremity physical function may not be reflective of tested physical performance in either cross-sectional or longitudinal evaluations.

***Disclosures: Jeri Nieves**, None*

SUN-555

Mapping the context of sedentary behaviour (MAPS-B) in older adults who are frail: A feasibility study *Isabel Rodrigues[1], Rachel Swance[1], Suleman Tariq[1], Alexa Kouroukis[1], Jonathan Adachi[2], Steven Bray[1], Qiyin Fang[1], George Ioannidis[3], Dylan Kobsar[1], Carolyn Leckie[1], Alexander Rabinovich[1], Rong Zheng[1], Alexandra Papaioannou[1]. [1]McMaster University , Canada, [2]St. Joseph s Hospital/ McMaster University, Canada, [3]McMaster University, Canada

Older adults who are frail are likely to be sedentary. Individuals with frailty are also at higher risk of falls and fractures. Prolonged sedentary time can decrease muscle and bone strength. Prior interventions to reduce sedentary time in older adults have not been successful as there is little research about the context of sedentary behaviour. We determined the feasibility to measure context (posture, location, purpose, social environment) of sedentary behaviour among older adults who are frail. We defined "feasibility process" using recruitment (20 participants within two-months), retention (85%), and refusal (20%) rates and "feasibility resource" if the measures capture context and are all participants willing to use the measures. We conducted a mixed-methods longitudinal study. Context was assessed using activPAL4TM placed on the anterior mid-thigh to assess posture (e.g., sitting), a McMaster engineering indoor positioning system (IPS) to assess functional location in the home (e.g., kitchen), and the Activities Collected over Time over 24-hours [ACT24] diary to understand purpose and social environment. We chose three measures as one measure alone does not capture all domains of context. We assessed feasibility in winter and spring over 1 weekend and 2 weekdays. We approached ~80 individuals through physicians' offices, community posters, and newspaper/radio advertisements, and 58 expressed interest in the study. Of the 58 individuals, 37 (28 female, Morley frail score>2) declined to enroll citing medical mistrust or worsening medical health (64% refusal). We enrolled 21 participants (13 female, 19 Caucasian) within two months; mean age 72.3+/-5.8 years. Eighteen participants were frail and 3 prefrail and all participants had probable sarcopenia using the Fit-Frailty App; ~30% had osteoporosis or a prior fragility fracture. After the initial study visit, one participant withdrew citing medical mistrust with the devices and another withdrew after the winter period citing worsening health (95% retention). All participants were willing to use activPAL4TM and 12 completed ACT24 while eight preferred a hard-copy diary. The diaries were not completed with detail making it challenging to precisely time synchronize the diary to the other measures. Six participants used the IPS, although they cited difficulties utilizing the system. The other 15 participants were not comfortable setting up the IPS. We met our criteria for recruitment and retention but experienced high refusal rates. Linking data between measures was complicated due to timeframe misalignment. The diaries did not accurately capture purpose. Participants found it challenging to configure the IPS.

***Disclosures: Isabel Rodrigues**, None*

SUN-556

Opportunistic Computed Tomography Analysis Reveals Severe Muscle Degeneration in Critical Care Patients *Ainsley C.J. Smith[1], Kirsten N. Bott[2], Brandon M. Hisey[3], Chel H. Lee[4], Kevin J. Solverson[3], Christopher Grant[5], Steven K. Boyd[2], Christopher J. Doig[3], Sarah L. Manske[2]. [1]Department of Radiology, Cumming School of Medicine, University of Calgary; McCaig Institute for Bone and Joint Health, University of Calgary; Department of Biomedical Engineering, University of Calgary, Canada, [2]Department of Radiology, Cumming School of Medicine, University of Calgary; McCaig Institute for Bone and Joint Health, University of Calgary, Canada, [3]Department of Critical Care, Cumming School of Medicine, University of Calgary, Canada, [4]Department of Critical Care, Cumming School of Medicine, University of Calgary; Department of Mathematics and Statistics, University of Calgary , Canada, [5]Department of Critical Care, Cumming School of Medicine, University of Calgary; Department of Clinical Neurosciences, University of Calgary, Canada

Purpose: Muscle loss is a common complication of critical illness that can lead to long-term physical impairment and poor quality of life. However, it is unclear who is most susceptible to critical illness induced muscle loss. Computed tomography (CT) images are acquired at several time points during a patient's intensive care unit (ICU) stay. These CT images can be repurposed to evaluate muscle cross-sectional area (CSA), a measure of muscle loss, across different patient populations. The objectives of this study were to: 1) measure changes in muscle CSA over the course of critical illness using clinically acquired CT images and 2) determine risk factors associated with critical illness induced muscle loss.Methods: We retrospectively acquired abdominal CT scans of ICU trauma and sepsis patients. Patients were included if they had a CT scan within 48 hours of ICU admission (baseline) and a second CT scan taken >14 days later, prior to discharge (follow-up). We assessed mean psoas muscle CSA (cm2) by segmenting the psoas muscle at L3 using an automated segmentation algorithm with manual correction. We acquired patient demographic and illness-related information using electronic medical records.Results: Critical care patients (n = 43) had a median time between scans of 19 [IQR: 15, 25] days. Patients had a median psoas CSA of 14.10 [IQR: 9.79, 19.91] cm2 at baseline and a median psoas CSA of 10.76 [IQR: 8.46, 14.70] cm2 at follow-up ($p < 0.001$). Univariate regression revealed that muscle CSA loss was greater in trauma patients than sepsis patients ($p < 0.01$). Univariate regression indicated a trend towards greater muscle CSA loss in younger patients ($p = 0.05$) and in males compared to females ($p = 0.07$). Multivariate regression suggested that illness type (trauma or sepsis) had a greater impact on muscle loss than sex or age. Univariate regression found that patients with greater illness severity, assessed with APACHE-IV scores, trended towards greater percent change in muscle per day in the ICU ($p = 0.06$).Conclusion: Critical care patients experienced a mean 24% decline in psoas muscle CSA over the course of their ICU stay. Our results indicate that patients with more muscle at ICU admission, typically young males with traumatic injuries, may experience a greater absolute muscle loss. Future research should focus on establishing muscle CSA thresholds to determine who is at risk of severe weakness and may benefit most from preventative interventions.

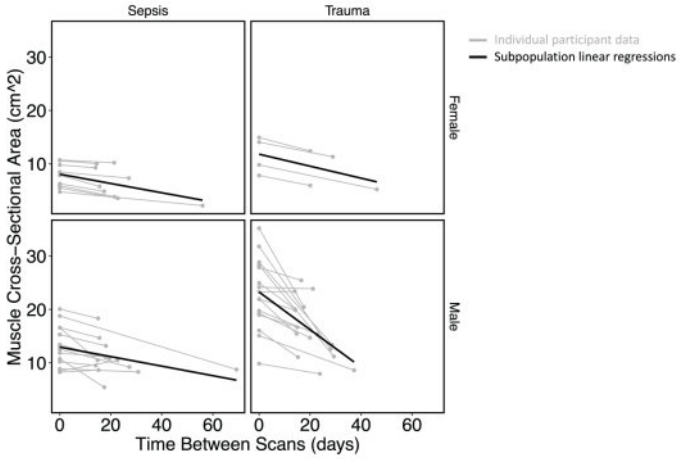

***Disclosures: Ainsley C.J. Smith**, None*

SUN-558

Validation of a Fall Rate Prediction Model for Community-Dwelling Older Adults: A Meta-Analysis with three Cohorts *Christina Wapp[1], Anne-Gabrielle Mittaz Hager[2], Toni Rikkonen[3], Roger Hilfiker[2], Emmanuel Biver[4], Heikki Kröger[5], Serge Ferrari[4], Marcel Zwahlen[6], Philippe Zysset[1]. [1]ARTORG Center for Biomedical Engineering Research, University of Bern, Switzerland. [2]HES-SO Valais-Wallis, School of Health Sciences, Physiotherapy, Switzerland. [3]Kuopio Musculoskeletal Research Unit (KMRU), University of Eastern Finland, Finland. [4]Division of Bone Diseases, Department of Medicine, Geneva University Hospitals and Faculty of Medicine, University of Geneva, Switzerland. [5]Orthopaedics and Traumatology, Department of Orthopaedics, Traumatology and Hand Surgery, Kuopio University Hospital, Finland. [6]Institute for Social and Preventive Medicine, University of Bern, Switzerland

Background: Since most of the fragility fractures in older adults are caused by falls, the risk of fracturing increases together with the number of falls. Accordingly, the prediction of an expected fall number potentially helps to identify individuals at risk of fragility fractures. So far, only a few studies have analysed the risk of falling with rate ratios that enable the calculation of an expected fall rate. This analysis aimed to meta-analyse three previously developed fall rate prediction models that included the history of falls as the main predictor. Methods: The three cohorts GERICO [1], Swiss CHEF Trial [2] and Kuopio Fall Prevention Study [3] were used for a two-stage meta-analysis. Separate fall rate prediction models have been developed previously. All three models included the number of falls during 12 months prior to the baseline as a predictor, which was treated as a factor with 0, 1, 2, 3, 4 or >= 5 falls. In the first stage, negative binomial regression models for every cohort were fit. In the second stage, the resulting coefficient estimates were used to derive overall coefficients with a random effect meta-analysis. Additionally, external model validation was performed by applying the three data sets to the models derived in the first stage, as well as the newly derived model in the second stage.Results: In total, 1855 community-dwelling older adults were included in the analysis (226 male, 1629 female; mean age 74 years). 1810 prior falls and 1565 incident falls were reported. The coefficients for the prior fall number were consistent among the three studies (Figure 1). Higgin's I2 was used as a measure for heterogeneity, ranging from 0 to 55.39%. The overall coefficient estimates derived from the meta-analysis indicated that the expected fall rate increases with the increasing number of previous falls. External model validation revealed that the prediction errors for the three data sets were independent of the model it was applied to (e.g., GERICO dataset applied to 1) GERICO model: 0.82; 2) SCT model: 0.82; KFPS model: 0.81; overall model: 0.81).Conclusion: This analysis introduces a meta-analysed and externally validated fall rate prediction model for community-dwelling older adults. Thereby, the prior number of falls was shown to be a robust predictor for future falls among different cohorts.[1] Biver et al., RevMedSuisse, 2015. [2] Mittaz et al., BMC Geriatrics, 2019. [3] Vilpunaho et al., BMJ Open, 2019.

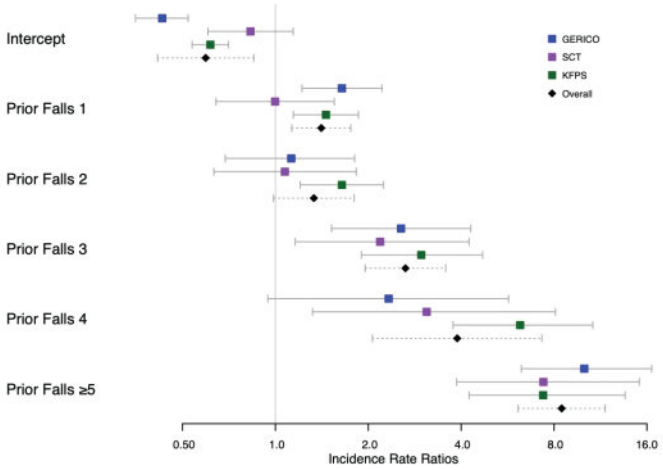

Figure 1. Incidence rate ratios with 95% confidence intervals for the first and second-stage models. Legend: GERICO = Geneva Retirees Cohort, SCT = Swiss CHEF Trial, KFPS = Kuopio Fall Prevention Study.

***Disclosures: Christina Wapp**, None*

SUN-559

Global Balance Of The Spine, An Independent Contributor To Physical Impairments And Predictor Of Incident Falls In Older Adults: The SAFE 3-Year Longitudinal Cohort Study *Hars Melany[1], Antonio Faundez[2], Marie-Josée Begin[3], Maiwenn Terrien Ferey[1], Jacques Fechtenbaum[4], Karine Briot[4], Christian Roux[4], Francois Herrmann[5], Serge Ferrari[1], Stephane Genevay[6], Sana Boudabbous[7], Andrea Trombetti[8]. [1]Division of Bone Diseases, Geneva University Hospitals and Faculty of Medicine, Switzerland. [2]Division of Orthopaedics and Trauma Surgery, Geneva University Hospitals and Faculty of Medicine & La Tour Hospital, Switzerland. [3]Division of Bone Diseases, Geneva University Hospitals and Faculty of Medicine & Division of Endocrinology, Department of Medicine, Centre Hospitalier Université Montréal, Switzerland. [4]Department of Rheumatology, Cochin Hospital, Assistance Publique-Hôpitaux de Paris, France. [5]Division of Geriatrics, Geneva University Hospitals and Faculty of Medicine, Switzerland. [6]Division of Rheumatology, Geneva University Hospitals and Faculty of Medicine, Switzerland. [7]Division of Radiology, Geneva University Hospitals and Faculty of Medicine, Switzerland. [8]Division of Bone Diseases, Geneva University Hospitals and Faculty of Medicine & Division of Geriatrics, Geneva University Hospitals and Faculty of Medicine , Switzerland

BackgroundFalls remain the leading cause of fractures in older adults and may result from several intrinsic and extrinsic risk factors. Among them, the role of the global balance of the spine (since recently easily evaluated with the advent of EOS® technology) has never been fully established. In the SAFE cohort, we aimed to determine the association between global balance of the spine, physical function and falls in community-dwelling older adults. MethodsSAFE is an ongoing prospective 3-year longitudinal cohort study conducted in Geneva (Switzerland) among community-dwelling adults aged >=65 years without history of instrumented spinal surgery. All subjects undergo at baseline and 3-year a comprehensive assessment battery including: full skeleton 2D/3D radiographs in the standing position by EOS® low-dose biplane X-ray imaging system, DXA imaging, and physical function tests. Prospective falls and fractures are also collected over the 3-year. Spino-pelvic parameters measured include, among others, the spino-sacral angle (SSA) and the C7-central sacral line (C7-CSL) distance for sagittal and coronal balance, respectively.ResultsAmong the 110 subjects (mean age, 75 years; 76% female) included in the final cross-sectional analysis, 40 (36%) reported one or more falls in the past 12 months, 19 (17%) had a Short Physical Performance Battery (SPPB) score <=9 and 8 (7%) were sarcopenic. Global sagittal balance was independently associated with physical performances after controlling for potential confounders (adjusted regression coefficient SPPB/SSA= 0.04, 95%CI [0.01-0.08]; p=0.024). Global coronal balance was independently associated with both 1-year retrospective falls (OR C7-CSL/faller=1.59, 95%CI [1.10-2.30]; p=0.015) and 3-year incident falls (n=66 first subjects in the longitudinal analysis; OR C7-CSL/faller=2.23, 95%CI [1.23-4.03]; p=0.008 and IRR C7-CSL/number of falls=1.55, 95%CI [1.21-1.98]; p=0.001), after controlling for potential confounders including age, sex, comorbidities, vertebral fractures and physical performances by SPPB score.ConclusionsOur results suggest that global sagittal balance of the spine is an independent contributor to physical impairments, while global coronal balance is an independent predictor of incident falls in older adults. Further ongoing longitudinal analysis will fully reveal whether global balance of the spine relates to fractures and the role of compensating mechanisms.

***Disclosures: Hars Melany**, None*

SUN-560

Association of circulating sclerostin level with frailty in Korean older adults *Seong Hee Ahn[1], Hee-Won Jung[2], Eunju Lee[2], Ji Yeon Baek[2], Il-Young Jang[2], So Jeong Park[3], Jin Young Lee[3], Eunah Choi[3], Yun Sun Lee[3], Beom-Jun Kim[4], Seongbin Hong[1]. [1]Department of Endocrinology and Metabolism, Inha University Hospital, Inha University School of Medicine, Republic of Korea. [2]Division of Geriatrics, Department of Internal Medicine, Asan Medical Center, University of Ulsan College of Medicine, Republic of Korea. [3]Asan Institute for Life Sciences, Asan Medical Center, Republic of Korea. [4]Department of Endocrinology and Metabolism, Asan Medical Center, University of Ulsan College of Medicine, Republic of Korea

Background: Sclerostin has recently been recognized not only as an osteokine, but also as a myokine that plays an essential role in bone and muscle crosstalk. Although both osteoporosis and sarcopenia are closely related to aging, the relationship between circulating sclerostin and frailty reflecting on biological age has never been investigated. Therefore, we evaluated the association of serum sclerostin levels with frailty and its related parameters in a cohort of ambulatory, community-dwelling Korean older adults.Methods: Blood samples were collected from 247 participants who underwent a comprehensive geriatric assessment, and serum sclerostin level was measured using an enzyme-linked immunosorbent assay. Phenotypic frailty and deficit accumulation frailty index were assessed using widely validated approaches, proposed by Fried and Rockwood groups, respectively.Results: After adjusting for sex, age, and body mass index, the frail participants presented 35.5% and 33.3% higher serum sclerostin levels than those with robustness and prefrailty, respectively (both P < 0.001). Consistently, circulating sclerostin level was positively related to frailty index (? =

0.205, P = 0.001), and the odds ratio (OR) per standard deviation increment of serum sclerostin level for phenotypic frailty was 1.87 (P = 0.003). Furthermore, compared with those in the lowest serum sclerostin quartile, the participants with the highest quartile had 38.5% higher frailty index (P = 0.026) and 9.91-fold higher risk for phenotypic frailty (P = 0.039). Conclusions: These data provide clinical evidence that circulating sclerostin level might be a potential biomarker for assessing the risk of frailty in humans.

***Disclosures: Seong Hee Ahn**, None*

SUN-561

Successful Pancreas-Kidney Transplantation Recipients Need Better Care for Osteoporosis *Yohei Asada[1], Yasumasa Yoshino[1], Hiroaki Sumioki[1], Yuka Nakajima[1], Sayumi Kanie[1], Izumi Hiratsuka[1], Megumi Shibata[1], Takeshi Takayanagi[1], Yusuke Seino[1], Atsushi Suzuki[1]. [1]Fujita Health University, Japan

Purpose:Simultaneous pancreas-kidney transplantation (SPK) could eliminate both insulin injections and maintenance dialysis and also improve life expectancy in type 1 diabetes (T1DM) patients with kidney failure. Recent advances in immunosuppressive therapy have improved the engraftment rate for pancreas transplantation (PTx). At the same time, long-term immunosuppressive medications could cause a decrease of bone mineral density (BMD), leading to an increased risk of fracture. The aim of this study is to evaluate the bone turn over and bone mass in successful post-PTx recipients.Methods: T1DM patients (n=34, M/F=11/23, age 46.7 +/-8.7 years old) who underwent PTx from 2013 to 2021 were enrolled in this study. The breakdown was 28 SPK and 6 PTx after kidney transplantation (PTA). All patients were received prednisolone (4.9 +/- 0.5 mg/day) throughout the observation period. Lumbar spine (LS) and femoral neck (FN) BMD was examined at baseline, 1 and 2 years after PTx as well as bone turnover markers. Total FN 2D-DXA images were analyzed using 3D-SHAPERTM Software. There were 15 patients with anti-osteoporotic treatment; 9 with denosumab (Dmab group) and 7 with active vitamin D alone (Vit D group), whereas 18 patients were observed without treatment (Control group).Results: All patients had become insulin-free and free from hemodialysis. Their serum creatinine and creatinine clearance remained stable during study period. At the baseline, the average LS and FN BMD T-scores were -1.35 +/-0.97 and -2.04 +/-0.76, respectively, and 12 patients were categorized as osteoporosis. After 2 years, the percent change from baseline in LS BMD was -3.1%($p<0.05$) in control group, +0.6% in Dmab group, and +0.5% in Vit D group. Trabecular bone score was not significantly changed in all groups. FN areal BMD (aBMD), trabecular volumetric BMD (vBMD), cortical surface BMD (sBMD), cortical thickness (Cth) decreased in control group (-5.9%, -9.7%, -4.6%, -3.9%). In Dmab and Vit D groups, aBMD, vBMD, sBMD and Cth were not changed. There was a significant decrease in serum BAP and TRACP-5b in the Dmab group at 1year after PTx and serum BAP decreased in Vit D group.Conclusion: Bone structure would deteriorate after PTx without treatment, and the recipients should be monitored for bone health regularly, and if necessary, receive appropriate interventions.

***Disclosures: Yohei Asada**, None*

SUN-562

Bone remodelling and responsiveness to mechanical stimuli in type 1 diabetes mellitus: the role of neuropathy *Matthias Walle[1], Ankita Duseja[2], Danielle Whittier[3], Tatiane Vilaca[4], Margaret Paggiosi[5], Richard Eastell[4], Ralph Müller[3], Caitlyn Collins[3]. [1]ETH Zurich, . [2]Department of Oncology and Metabolism, University of Sheffield, Sheffield, United Kingdom. [3]Institute for Biomechanics, ETH Zurich, Zurich, Switzerland, Switzerland. [4]University of Sheffield, United Kingdom. [5]Department of Oncology and Metabolism, University of Sheffield, Sheffield, UK, United Kingdom

Type 1 diabetes mellitus (T1DM) has been linked to increased osteocyte apoptosis, local accumulation of mineralised lacunar spaces and microdamage suggesting an impairment of the mechanoregulation network in affected individuals. Diabetic neuropathy might exacerbate this dysfunction through direct effects on bone turnover, and indirect effects on balance, muscle strength, and gait. However, the in vivo effects of impaired bone mechanoregulation on bone remodelling in humans remain underexplored. Based on previous ex vivo studies we hypothesised that individuals with T1DM would demonstrate impaired bone turnover and mechanoregulation.We assessed consenting participants with T1DM without (n=6) and with distal symmetric sensorimotor polyneuropathy (T1DM+, n=14) and controls (n=9) at baseline and 4-year follow-up. We tested nerve conduction in participants with T1DM using DPNCheck (Neurometrix). We used longitudinal high-resolution peripheral quantitative computed tomography (XtremeCT, Scanco Medical AG, 82 ?m) at the standard distal sites to assess bone turnover. We used 3D rigid image registration to identify local trabecular bone formation (Tb.F) and resorption (Tb.R) sites and quantified mechanical stimuli at these sites using micro-finite element analysis (Fig 1A-C). We calculated odds ratios to determine the likelihood of bone formation (ORF) and resorption (ORR) with increasing/decreasing strain in percent as markers for mechanoregulation.At the distal radius, Tb.F was 26% reduced in T1DM (p=0.56) and 56% in T1DM+ ($p<0.05$, Fig. 1D) compared to controls. Tb.F correlated positively with nerve conduction amplitude ($r=0.74$, $p<0.05$, Fig. 1E) in participants with T1DM and negatively with glycated haemoglobin (HbA1c) ($r=-0.45$, $p<0.05$). Additionally, ORF was 30% reduced in T1DM compared to controls, regardless of neuropathy status (p0.65).Our findings represent in vivo evidence suggesting that bone formation in individuals with T1DM is in a state of low responsiveness to mechanical stimuli, resulting in impaired bone formation rates; these relate to the degree of neuropathy and level of diabetes control. Adverse effects were more severe at the radius than the tibia, possibly resulting from differences in site-specific mechanical loading. These findings could have implications for understanding the alterations in bone quality in T1DM.

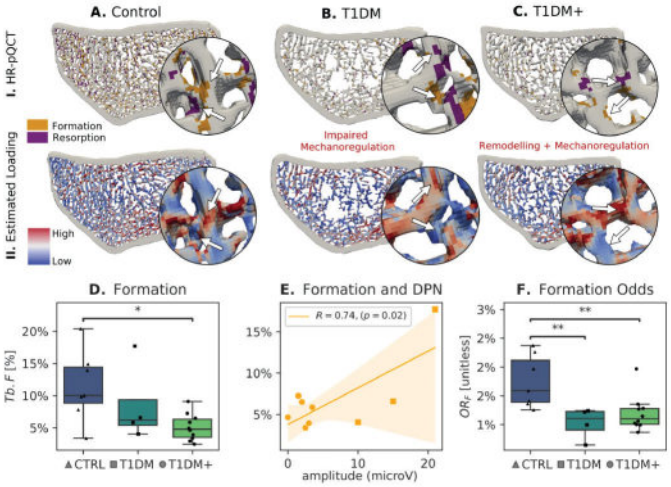

Fig. 1: (I) Distal radius cross-sections (10 slices) showing bone formation and resorption in (A) controls, (B) T1DM, and (C) T1DM+ participants. (II) Local mechanical loading estimates. (D) Bone formation and (E) correlation with P1NP. (F) Mechanoregulation of bone formation sites (* p<0.05, ** p<0.01).

***Disclosures: Matthias Walle**, None*

SUN-564

Effect of microvascular disease on bone blood flow regulation in older adults with Type 1 Diabetes: preliminary findings *ADINA DRAGHICI[1], Elaine Yu[2], Mary Bouxsein[3], J. Andrew Taylor[4, 1], United States. [2]Massachusetts General Hospital, United States. [3]Beth Israel Deaconess Medical Center, Harvard Medical School, United States. [4]Physical Medicine and Rehabilitation, Harvard Medical School, Schoen Adams Research Institute at Spaulding Rehabilitation , United States

Skeletal fragility is an important complication of Type 1 Diabetes (T1D), particularly among older adults. Microvascular disease (MVD), one of the most serious consequences of diabetes, has been linked to worse bone health in T1D, suggesting a potential direct pathophysiologic link between vascular disease and bone deficits. However, altered vascular control in bone remains unexamined. These preliminary data derive from our investigation of a key vascular mechanism for blood flow regulation in bone - myogenic vasoconstriction. Our recent data in young healthy adults has shown for the first time that myogenic vasoconstriction is an active regulator of blood flow in bone, but this mechanism has yet to be explored in T1D.In older adults with T1D (N=10, 63+/-2yrs), we characterized myogenic vasoconstriction in the tibia via custom-made near infrared spectroscopy (total hemoglobin, tHb) and in the whole leg (reflective primarily of muscle) via Doppler ultrasound. Results were compared to data in young healthy adults (N=13, 26+/-4 yrs). We employed leg dependency (lowering the leg below heart level) to increase arterial transmural pressure and engage myogenic vasoconstriction. Responses were assessed during 5min supine, 5min seated with legs extended (Level 1), and 5min seated with 90deg knee flexion (Level 2). In those with T1D, increased perfusion pressure at both levels (?23+/-2 and ?33+/-1mmHg; $p<0.01$) was accompanied by proportional declines in whole leg blood flow (?-6.14+/-2.24 and ?-10.4+/-1.90cm/s; $p<0.01$), indicating myogenic vasoconstriction of a similar magnitude in young adults. Tibial tHb decreased proportionally as well (?-3.40+/-2.79 and ?-6.14+/-2.24?M; $p<0.05$), indicating vasoconstriction in the tibial vasculature; however, this response was up to 5X greater than in young adults. Interestingly, those with T1D and MVD (N=5) had a strong tendency for greater tibial vasoconstriction at both levels compared to those with no MVD (N=5) (Level 1: ?-7.02+/-2.83 vs 0.23+/-4.71?M, p=0.1; Level 2: ?-10.6+/-2.46 vs -3.66+/-3.66?M; p=0.08) despite similar vasoconstriction in the whole leg. There were no age differences between T1D groups. Hence, older adults with T1D have compromised bone blood flow that appears to be worse in those with MVD. These preliminary results represent the first direct assessment of bone blood flow in older adults with T1D providing a strong foundation for the potential mechanistic link between MVD and diabetes-induced bone loss.

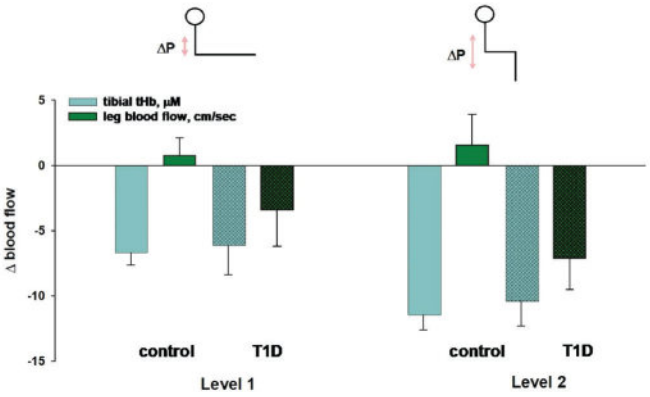

***Disclosures: ADINA DRAGHICI**, None*

SUN-565

Validation of Maturity Prediction for Children and Adolescents with Type 1 Diabetes *Zahra Ghafouri[1], James (J.D.) Johnston[2], Munier Nour[3], Saija Kontulainen[1]. [1]College of Kinesiology, University of Saskatchewan, Saskatoon, SK, Canada, Canada. [2]College of Engineering, University of Saskatchewan, Saskatoon, SK, Canada, Canada. [3]College of Medicine, University of Saskatchewan, Saskatoon, SK, Canada , Canada

Introduction: At the same chronological age, the range in somatic maturity can be large, particularly around the adolescent growth spurt. Thus, validated estimates of somatic maturity are essential in clinical research when assessing skeletal growth and development. Predictive equations, based on predicting years from peak height velocity (i.e., maturity offset, MO) have been validated for typically developing children and adolescents. The predictive accuracy of these equations has not been assessed in children and adolescents with type 1 diabetes (T1D). Validation is needed, as sex-specific impairments in growth velocity during the pubertal growth spurt have been reported in adolescents with T1D, which may affect predictive accuracy. The objective of this study is to assess agreement and differences between predicted and observed MO in female and male children and adolescents with T1D. Methods: We obtained prospective measures of height from health records of participants in the Bone Strength Development Study in Children with T1D (BSDS). We applied the Preece-Baines Model and defined age at peak height velocity (APHV) for 22 participants (12 females and 10 males). We calculated observed MO by subtracting age at each measurement from APHV for male (Nobservations = 109, age 6-18 years) and female (Nobservations = 144, age 3-17 years) participants. We used Moore et al. maturity prediction equations to predict MO at each measurement time. We used sex-specific linear regression models to report model-fit (R2) for the agreement and paired t-tests to report mean differences (?) with 95% confidence intervals, between observed and predicted MO. Significance was set to p <0.05.Results: Predicted MO explained 86% and 87% of the variance in the observed MO in male and female participants, respectively. Predicted and observed MO means did not differ significantly in male (? 0.18, 95% CI -0.02 to 0.38) nor female (? 0.09, 95% CI -0.06 to 0.25) participants.Conclusion: The maturity prediction equation estimated MO within 2 months from the observed offset in both female and male children with T1D. These findings warrant cross-validation in a larger sample of children with T1D. Nevertheless, initial findings suggest that the commonly used Moore et al. equation may offer a reliable and practical solution to estimate biological maturity in studies assessing growth and development in children and adolescents with T1D.

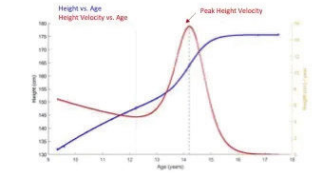

Fig 1. Example of Preece-Baines model to estimate age at peak height velocity (APHV) for a male participant

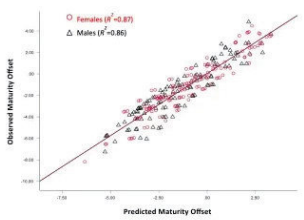

Fig 2. Scatter-dot graph of regression line between predicted and observed maturity offset (MO) in children and adolescents with T1D

***Disclosures: Zahra Ghafouri**, None*

SUN-566

Chronic kidney disease is associated with lower cortical measures at proximal femur as assessed by 3D-DXA *M. Kužma[1], Z. Kužmová[1], L. Humbert[2], M. Lopez Picazo[2], J. Falat[1], J. Smaha[0], P. Jackuliak[1], Z. Killinger[0], J. Payer[1]. [1]5th department of Internal Medicine, Comenius University Faculty of Medicine, University Hospital , Bratislava, Slovakia, Slovakia. [2]3D-Shaper Medical, Barcelona, Spain, Spain. [0]5th department of Internal Medicine, Comenius University Faculty of Medicine, University Hospital , Bratislava, Slovakia, Slovakia

Introduction: Patients with chronic kidney disease (CKD) has 2-14 fold increase in fracture risk, especially in later stages of the CKD. The gold standard for the diagnosis of osteoporosis represents DXA, but its use is limited due to lack of possibility to measure trabecular and cortical characteristics and interference of aortic calcifications with BMD. Specific information about bone microstructure and turnover could be obtained by bone biopsy, but this is limited due to invasiveness.Aim: To compare several non-invasive DXA-derived methods used for assessment trabecular and cortical parameters, such a s trabecular bone score (TBS), 3D-Shaper and hip structure analysis (HSA) in subjects across all CKD stages.Patients and methods: In total, 89 CKD (38 females / 51 males; mean age 69,5 years) subjects were included in the analysis. According to glomerular filtration rate (GFR) there were 12; 23; 10; 14; 14 and 16 subjects in stage G1, G2, G3a, G3b, G4 and G5, respectively. BMD at lumbar spine (LS) and proximal femur (hip and neck) was analyzed by Hologic Horizon device. LS TBS was analyzed by TBS Insight software. Proximal femur parameters such as cortical and trabecular volumetric (v) BMD, cortical thickness (CTh) and surface (s) BMD and HSA parameters such as buckling ratio (BR), cross-sectional area (CSA) and section modulus (Z) were analyzed by 3D-Shaper-research v. 2.12.1. In all subjects bone turnover markers such as CTx, P1NP and Osteocalcin was measured.Results: Cross-sectional comparison between each CKD stage showed gradually decreasing LS BMD, cortical vBMD (neck and TH), TH Cth and neck BR starting from G3b, G4 and G5 stages; but not in earlier stages of CKD (G1-G3a). Comparison of means between earlier stages (G1-G3a) versus later stages (G3b-G5) of CKD showed significant differences in CTx (386 vs. 1053 ng/l); TH aBMD (0,991 vs 0,859 g/cm2), cortical vBMD at TH (831 vs 795 mg/cm3) and neck (837 vs.788 mg/cm3), TH cortical sBMD (170 mg/cm2) and TH Cth (2,03 vs 1,92 mm) (all p<0.05). Among all subjects, strong positive associations between GFR and cortical parameters (neck/TH vBMD and TH Cth) were observed (p<0.01).Conclusion: This study showed that later stages of CKD (G3b - G5) CKD have lower cortical bone parameters, such as vBMD, sBMD and CTh, as assessed by 3D Shaper. In addition, most of the cortical parameters are associated with GFR, showing direct relationship of kidney function and bone. These results agree with the previous findings provided by bone histomorphometry. As such, it is likely that 3D Shaper as non-invasive DXA derived method can be of use in assessment of fracture risk in CKD subjects especially in later stages of the disease. However, further prospective studies with greater amount of subjects and fracture data are needed.

***Disclosures: M. Kužma**, None*

SUN-567

Role of Selcopintide in Alleviating the Progression of Diabetic Periodontitis *Jihyun Hong[1], Joo-Cheol Park[1]. [1]Seoul National University, Republic of Korea

Diabetes mellitus (DM) is a systemic metabolic disorder characterized by hyperglycemia which can lead to various complications, including periodontitis. Periodontitis is a chronic inflammatory disease that affects the supporting tissues of the teeth, including the periodontal ligament (PDL), cementum, alveolar bone, and gingiva. Hyperglycemia can lead to oxidative stress and inflammation, which can exacerbate periodontitis by affecting the host response to bacterial pathogens. Mitochondria are the primary source of ROS, and their dysfunction can contribute to the development and progression of diabetic periodontitis. Therefore, regulating mitochondrial function and suppressing the production of pro-inflammatory cytokines are important to alleviate the progression of diabetic periodontitis. Copines are a family of ubiquitous Ca2+ -dependent, phospholipid-binding proteins. Our previous studies have demonstrated that Selcopintide (SCPT), CPNE7-derived peptide, can promote the regeneration of the PDL and enhance the attachment activity of human periodontal ligament cells (hPDLCs). Furthermore, CPNE7 has been shown to be involved in DNA damage repair by removing ROS on human dental pulp cells. It suggests that CPNE7 may be a potential therapeutic target for the treatment of diabetic periodontitis. Therefore, this study aimed to explore the effect and mechanism of SCPT on the expression of inflammatory cytokines and oxidative stress in the development of diabetes mellitus-periodontitis, as well as potential therapeutic strategies. In vitro, hPDLCs were stimulated by high glucose (35mM) and LPS to reflect the high glucose status and the infection of periodontitis causative bacteria. mRNA expressions of inflammatory cytokines were quantified, and reactive oxygen species was measured. The protein expression level of mitochondrial function-related markers in the cells were also detected by Western blot. Our study demonstrates that the expression of inflammatory cytokines increased when the cells were stimulated by both high glucose and LPS compared to when they were stimulated by only control or LPS. However, when treated with SCPT, this effect was alleviated. Reactive oxygen species of the cells with treated both of high glucose and LPS was also reduced after treating SCPT with the upregulation of mitochondrial functions. In conclusion, SCPT can alleviate the progression of diabetic periodontitis by regulating oxidative stress and its anti-inflammatory effects.

***Disclosures: Jihyun Hong**, None*

SUN-569

Evaluation of PTH-Ca Axis in Normocalcemic Primary Hyperparathyroidism
*Reiko Inoue[1], Fukuo Kosokabe[1], Kota Ishizawa[1], Yoshiyuki Ban[1], Daisuke Inoue[1]
[1]Teikyo University Chiba Medical Center, Japan

Background & Aim: Normocalcemic primary hyperparathyroidism (NPHPT) is defined by normal serum calcium (Ca) and elevated PTH. Although vitamin D repletion is recommended upon diagnosis, differentiation between NPHPT and secondary hyperparathyroidism (SHPT) due to vitamin D deficiency is often difficult. And we do not know what proportion of subjects with normal Ca and high PTH are indeed diagnosed NPHPT in the real-world setting. The aim of the present study was to evaluate PTH-Ca axis and to explore clinical indicators differentiating between NPHPT and SHPT in possible PHPT cases with high intact PTH levels.Subject & Method: We screened 1,101 patients given ICD 10 codes of hyperparathyroidism at our hospital from January 2012 to September 2022 for possible NPHPT, excluding those under the age of 20, those with chronic kidney disease (eGFR<30), and those with other apparent hypercalcemic conditions (N=704). We further excluded 11 cases diagnosed and treated for PHPT at other hospitals. Of the remaining 386 cases, we identified 215 subjects with intact PTH levels above 50 pg/ml for further analysis.Result: Of the 215 cases analyzed, 70 had PHPT with apparent hypercalcemia, and the remaining 145 were suspected to have NPHPT or SHPT. Of these, 17 cases were subsequently diagnosed with PHPT, including 10 MIBI-positive cases and 7 cases developing overt hypercalcemia after vitamin D supplementation. Among the remaining 128 cases, 74 had their 25(OH)D levels measured: among them 19 had probable NPHPT based on 25(OH)D >20 ng/ml (with or without vitamin D supplementation) and intact PTH >65 pg/ml, 34 had possible NPHPT based on intact PTH levels of 50-65 pg/ml, and 21 had vitamin D-deficient SHPT whose PTH normalized after vitamin D supplementation. In the probable NPHPT group (N=19), the pre-supplementation levels of Ca, PTH and 25(OH)D were 9.5+/-0.5 mg/dl, 85.8+/-31.6 pg/ml, and 21.5+/-7.2 ng/ml, respectively. There was no difference in bone parameters including BMD and TBS between the NPHPT and SHPT groups, but the product of intact PTH and Ca values was significantly higher than SHPT in the NPHPT group.Conclusion: 25(OH)D >20 ng/ml and intact PTH >65 pg/ml may be indicative of NPHPT. Further observation of the natural course and reassessment after achieving complete sufficiency with 25(OH)D >30 ng/ml will be necessary.

***Disclosures: Reiko Inoue**, None*

SUN-570

Association of Sodium-Glucose Cotransporter 2 Inhibitor Use With Risk of Osteoporotic Fracture Among Older Women: A Nationwide, Population-Based Cohort Study
*Seunghyun Lee[1], Min Heui Yu[2], Namki Hong[3], KYOUNG JIN KIM[4], Hae Kyung Kim[5], Yumie Rhee[6], Minyoung Lee[5], Kyoung Min Kim[7]
[1]Wonju Severance Christian Hospital, Yonsei University Wonju College of Medicine, Wonju, Korea, [2]SENTINEL team, Division of Endocrinology, Department of Internal Medicine, Yonsei University College of Medicine, Seoul, Korea, Republic of Korea, [3]Division of Endocrinology, Republic of Korea, [4]Korea University College of Medicine, Republic of Korea, [5]Institute of Endocrine Research, Department of Internal Medicine, Yonsei University College of Medicine, Seoul, Korea, Republic of Korea, [6]Yonsei University College of Medicine, Republic of Korea, [7]Yongin Severance Hospital, Yonsei University College of Medicine, Republic of Korea

Sodium-glucose cotransporter-2 inhibitor (SGLT2i) is a widely recommended anti-diabetic medication (ADM) due to its cardioprotective and renoprotective benefits. However, the effects of SGLT2i on fracture risk have been debated. The Canagliflozin Cardiovascular Assessment Study showed that SGLT2i increased hip fracture risk during the mean 6-year follow-up period. However, in most other large randomized controlled trials of SGLT2i, SGLT2i use was not associated with increased fracture risk. Although the fracture risk associated with SGTL2i use is controversial, there are concerns regarding fracture risk due to the increased risk of falls caused by volume depletion or disturbance of calcium phosphate balance. Therefore, in the present study, the association between SGLT2i use and fracture risk in elderly women (>= 65 years of age) who were newly prescribed ADMs was investigated using a national cohort database.?We used the data for this population-based cohort study obtained from the National Health Insurance Service of Korea between January 1, 2013, and December 31, 2020. Women older than 65 years old diagnosed with type 2 diabetes mellitus who were newly prescribed ADMs other than glucagon-like peptide-1 receptor agonists and thiazolidinedione and who had available comprehensive health check-up data were included.A total of 1,333 SGLT2i users was analyzed and compared with covariate (e.g., body mass index (BMI), age-matched non-SGLT2i users at a 1:2 ratio (n = 2,626). After propensity score matching, mean age (70.3 years vs. 70.3 years, p = 0.830), BMI (27.4 kg/m2 vs. 27.4 kg/m2, p = 0.924), number of oral ADMs (1.4 vs. 1.3, p = 0.092), and other covariates were well-balanced between SGLT2i users and non-SGLT2i users. During the follow-up period, SGLT2i use was associated with a significantly increased risk of vertebral fracture compared with non-SGLT2i use (incidence rate 19.2 vs. 13.8 per 1,000 person-years; hazard ratio 1.40, 95% confidence interval 1.00-1.96, p = 0.049). Regarding the risk of other types of fracture, any fractures, hip fractures, and non-hip or non-vertebral fractures, significant differences were not observed between SGLT2i users and non-SGLT2i users.In conclusion, SGLT2i use showed a 40% higher risk of vertebral fracture than non-SGLT2i use in elderly women. Although further validation is required, SGLT2i should be cautiously prescribed in older women due to the potential association with fracture risk in this vulnerable population.

***Disclosures: Seunghyun Lee**, None*

SUN-571

Hypothyroidism and Future Fracture Risk Prediction From a Prospective Outpatient Fracture Liaison Service
*Brittany Carde[1], Leah Kennedy[1], Sarah Hamilton[1], Stephanie Yee[1], Kim Rondeau[1], Jacques van der Merwe[1], Emma Billington[1], Prism Schneider[1]
[1]University of Calgary, Canada

Background: There are conflicting reports in the literature regarding the relationship between hypothyroidism and fragility fracture (FF) risk. Some reports suggest a significantly prolonged bone remodeling cycle in patients with hypothyroidism and increased bone mass. These result in increased bone stiffness, thus equating to increased FF risk. This study aimed to compare FF risk between those with and those without a pre-existing diagnosis of hypothyroidism at the time of initial FF presentation.Methods: In August 2020, we introduced a 3i OFLS at a single Level 1 trauma centre. Active case finding was used to identify patients over the age of 50 with a new FF to their wrist, shoulder, or pelvis. Following informed consent, enrolled patients met with the OFLS nurse at their initial fracture assessment and underwent a complete bone health history, including hypothyroidism assessment. Thyroid-stimulating hormone levels, future fracture risk using the Fracture Risk Assessment Tool (FRAX), and bone mineral density (BMD) were captured. T-tests and Chi square analyses were used to compare age, sex, and FF type between those with and without hypothyroidism and a Wilcoxon rank sum test was used to compare FRAX with and without BMD between these two groups.Results: Within the first 12-months, 128 patients with a new FF were enrolled, with 26 (25.5%) having a pre-injury diagnosis of hypothyroidism. There was no difference in the mean age between groups (mean age= 68 [+/- 8] years for those with hypothyroidism and 65 [+/- 11] years without; p =0.11), but there were significantly more females in the hypothyroidism group (100% vs. 84%; p=0.04). The majority of participants had suffered a distal radius fracture (58% in the hypothyroidism group and 60% in those without hypothyroidism). When factoring in BMD, significantly higher FRAX scores were observed in the hypothyroidism group (mean FRAX=19 [+/- 9]) compared to those without hypothyroidism (mean FRAX=16 [+/- 10]; p=0.04). However, when excluding BMD in FRAX calculations, there was no difference between the groups.Conclusions: The results of this study support the discordance in the literature around use of BMD in fracture risk prediction in patients with pre-fragility fracture diagnosis and treatment. Interpretation of fracture risk in the setting of hypothyroidism warrants further investigation for accurate prediction of future fracture risk and decision-making around indications for initiation of osteoporosis pharmacotherapy.

***Disclosures: Brittany Carde**, None*

SUN-572

The Association between Intrahepatic Lipid Content and Bone Microarchitecture and Strength (Assessed by HR-pQCT): The Maastricht Study.
*VEERLE VAN HULTEN[1], Johanna Driessen[2], Marleen van Greevenbroek[3], Carla van der Kallen[3], Annemarie Koster[4], Martijn Brouwers[3], Eline Kooi[5], Pieter Dagnelie[6], Coen Stehouwer[3], Joop Van Den Bergh[7]
[1]Maastricht University, [2], Netherlands, [3]Department of Internal Medicine, MUMC+, Netherlands, [4]Department of Social Medicine, Maastricht University, Netherlands, [5]Department of Radiology, MUMC+, Netherlands, [6]School for Cardiovascular Diseases, Maastricht Universiity, Netherlands, [7]VieCuri MC Noord-Limburg and Maastricht UMC,

Background: It is known that type 2 diabetes (T2D) is associated with a number of comorbidities, such as an increased fracture risk, possibly due to impaired bone quality. T2D has also been associated with non-alcoholic fatty liver disease (NAFLD) characterized by a high intrahepatic lipid (IHL) content. In turn, NAFLD has been shown to be a risk factor for osteoporotic fractures.Purpose: To determine the association of IHL content with parameters of bone microarchitecture and strength assessed by high-resolution peripheral quantitative computed tomography (HR-pQCT).Methods: This study includes cross-sectional data from 2104 participants of the Maastricht Study who underwent a HR-pQCT scan (first generation) at the distal radius. MRI was performed to determine IHL content, expressed as the percentage of hepatic triglyceride content in the total liver volume. Multiple linear regression models were used to investigate the association of IHL content with HR-pQCT parameters of bone microarchitecture and strength. Analyses were stratified by sex due to inherent differences in bone metabolism, and were adjusted for glucose metabolism status, age, comorbidities, medication and lifestyle factors.Preliminary Results: We included 1057 men and 1047 women. Male participants were on average 60 (+/-8.7) years old, and female participants were on average 58 (+/-8.8) years old. After adjustment, IHL content was positively associated with total bone mineral density (BMD) and cortical BMD in the distal radius in men and women, and with trabecular BMD, cortical area, stiffness, and failure load in women (Table 1). When BMI was added to the linear regression model, all significant associations between IHL content and HR-pQCT parameters were strongly attenuated and not statistically significant.Conclusion: These findings suggest that bone quality may not be impaired in individuals with an increased IHL content, and that bone strength may even be greater in women with NAFLD. However, it is possible that this finding is at least partially

due to the association of BMI with IHL content and with bone density, stiffness and failure load, since no statistically significant associations between IHL content and HR-pQCT parameters remained when BMI was added to the linear regression model.

Table 1: The association between IHL content and bone architecture and bone strength in the distal radius (assessed by HRpQCT)

	IHL content	
	Men (ß (95% CI)) †	Women (ß (95% CI)) †
Tt.BMD (mg HA/cm³)	0.76 (0.13; 1.39) * ⇑	0.90 (0.23; 1.57) * ⇑
Ct.BMD (mg HA/cm³)	0.70 (0.05; 1.35) * ⇑	1.05 (0.29; 1.81) * ⇑
Tb.BMD (mg HA/cm³)	0.17 (-0.2; 0.55)	0.52 (0.12; 0.91) * ⇑
Tt.Ar (mm²)	-0.58 (-1.30; 0.14)	0.08 (-0.42; 0.59)
Ct.Ar (mm²)	0.18 (0.00; 0.36)	0.20 (0.08; 0.32) * ⇑
Tb.Ar (mm²)	-0.70 (-1.42; 0.03)	-0.06 (-0.57; 0.45)
Ct.Th (mm)	0.00 (0.00; 0.01)	0.00 (0.00; 0.01)
Tb.N (mm⁻¹)	0.00 (0.00; 0.01)	0.00 (0.00; 0.01)
Tb.Sp (mm)	0.00 (0.00; 0.00)	0.00 (0.00; 0.00)
Log Ct.Po (%)	0.00 (-0.01; 0.00)	0.00 (-0.01; 0.00)
Stiffness (kN/mm)	-0.10 (-0.15; 0.34)	0.28 (0.12; 0.43) * ⇑
Failure load (kN)	4.94 (-6.45; 16.33)	12.51 (5.19; 19.83) * ⇑

** Denotes statistically significant finding*
† Adjusted for age, educational level, time gap (time in months between baseline visit and HR-pQCT scan), alcohol use, smoking behavior, medication affecting bone metabolism, estimated glomerular filtration rate, moderate-to-vigorous physical activity and history of cardiovascular disease.
CI, confidence interval; Ct.Ar, cortical area; Ct.BMD, cortical density; Ct.Po, cortical porosity; Ct.Th, cortical thickness; HbA1c, glycated hemoglobin; IHL, intrahepatic lipid; NGM, normal glucose metabolism; Tb.Ar, trabecular area; Tb.BMD, trabecular density; Tb.N, trabecular number; Tb.Sp, trabecular separation; Tt.Ar, total area; Tt.BMD, total density.

***Disclosures: VEERLE VAN HULTEN**, None*

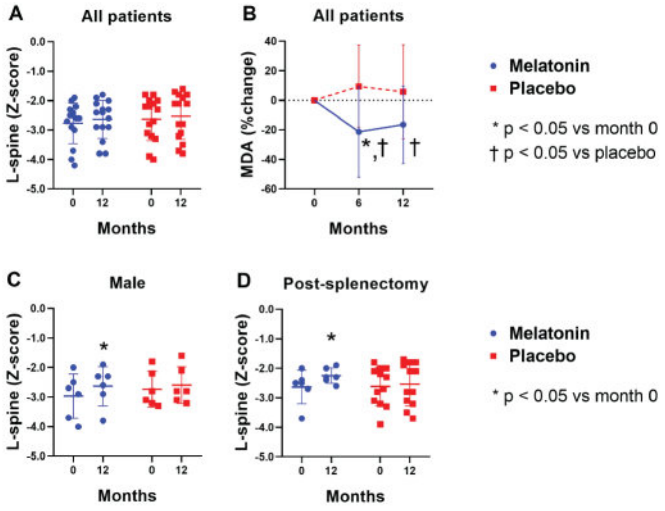

***Disclosures: Pokpong Piriyakhuntorn**, None*

SUN-573

Effects of Melatonin Supplement on Bone Mineral Density in Thalassemia Patients with Iron Overload and Low Bone Mineral Density: A Randomized Controlled Study *Pokpong Piriyakhuntorn[1], Adisak Tantiworawit[1], Mattabhorn Phimphilai[2], Tawika Kaewchur[3], Piangrawee Niprapan[1], Nattayaporn Apaijai[4], Krekwit Shinlapawittayatorn[4], Nipon Chattipakorn[4], Siriporn C. Chattipakorn[4]. [1]Division of Hematology, Department of Internal Medicine, Faculty of Medicine, Chiang Mai University, Thailand. [2]Division of Endocrinology, Department of Internal Medicine, Faculty of Medicine, Chiang Mai University, Thailand. [3]Division of Nuclear Medicine, Department of Radiology, Faculty of Medicine, Chiang Mai University, Thailand. [4]Cardiac Electrophysiology Research and Training Center, Faculty of Medicine, Chiang Mai University, Thailand

Background: Low bone mineral density (BMD) is commonly found in thalassemia patients, leading to increased incidence of bone fracture. It is known that iron-overloaded condition in thalassemia patients increased circulating oxidative stress, which resulted in decreased BMD. Melatonin is a powerful antioxidant. It improves bone quality in postmenopausal osteopenia. However, the effect of melatonin on bone in thalassemia patients with iron-overloaded and low BMD conditions has not been investigated.Aim: To investigate the effect of melatonin supplementation on bone health in thalassemia with iron- overloaded and low BMD conditions.Methods: We conducted a randomized controlled study at CMU Outpatient Hematology Clinic. Thalassemia patients who had a Z-score of BMD at L-spine, femoral neck, or total hip of less than -2.0, indicating low BMD, and serum ferritin level of more than 500 ?g/L, characterized as iron overload, were recruited in the study. 30 patients were allocated to orally receive either melatonin 20 mg/day or placebo at bedtime for 12 months. BMD in each patient was re-evaluated at 12 months. Bone turnover markers (BTM), malondialdehyde (MDA as an oxidative stress marker), and back pain score were assessed at baseline, 6, and 12 months. The outcome was the alterations of BMD at various sites as well as changes in serum BTM, MDA, and back pain score.Results: Thirty patients were enrolled in the study. Twelve patients were male. The mean age was 31.1+/-5.7 years old. Twenty-eight patients were identified as beta-thalassemia, and 25 were patients with transfusion dependence. At 12 months after interventions, we found that patients in both groups had no significant change in BMD at L-spine, femoral neck, or total hip, when compared to their baseline (Figure 1A). No significant change of serum CTX, P1NP, or SOST in both groups were found at 6-, 12-months. There was a significant reduction of serum MDA between groups at 6 and 12 months (Figure 1B). Back pain was significantly reduced at 12 months in only melatonin group. Melatonin significantly improved BMD at L-spine in males (Figure 1C) and patients with splenectomy (Figure 1D).Conclusion: Melatonin 20 mg/day for 12 months did not improve BMD in iron-overloaded thalassemia with low BMD. However, melatonin significantly reduced circulating oxidative stress and back pain score in those patients. Surprisingly, we observed the improvement of BMD at L-spine in male and post-splenectomy subgroups.

SUN-575

Areal bone mineral density, trabecular bone score and 3D-DXA analysis of proximal femur in psoriatic disease *Eric Toussirot[1], Renaud Winzenrieth[2], Francois Aubin[3], daniel wendling[3], Charline Vauchy[4], Maxime Desmarets[4]. [1]INSERM CIC_1431, France. [2]GALGO, Spain. [3]CHU, France. [4]INSERM CIC, France

Objectives: To evaluate bone mineral density (BMD) and bone quality, with assessment of the cortical and trabecular compartments, in patients with psoriasis (PsO) alone or with psoriatic arthritis (PsA).Methods: Patients with PsA and patients with PsO alone were evaluated and compared to control subjects matched for age, sex and body mass index category. Areal BMD (aBMD) was determined for the lumbar spine, femoral neck, total hip and total body using dual-energy X-ray absorptiometry (DXA). Bone quality was evaluated by using trabecular bone score (TBS) at the lumbar spine, and by 3D DXA-based analysis (3D Shaper) for the proximal femur.Results: 196 subjects including 52 patients with PsA and 52 patients with PsO and their respective paired controls were analyzed. Patients with PsA had comparable aBMD, TBS and 3D DXA analysis parameters compared to their paired controls. After adjustment for confounders, patients with PsO alone were characterized by a higher aBMD at the left femur and higher cortical 3D DXA derived parameters (total hip cortical surface BMD and total hip cortical thickness) than their paired controls (Figure 1). TBS was decreased in PsO compared to their controls.Conclusion: Patients with PsA had normal bone mass and bone quality parameters. Patients with PsO were characterized by higher femoral neck bone density by DXA and cortical parameters by 3D DXA-based analysis, supporting no increased risk for hip fracture. Conversely, bone texture by TBS assessment was decreased in patients with PsO, which may be associated with impaired vertebral bone resistance.Figure 1: 3D spatial distribution of differences in the cortical bone between the patients with psoriasis (PsO) (left femur N = 52, right femur N= 52) and their paired controls. Increases in cortical sBMD, vBMD and thickness are presented in blue-green color while decreases are presented in yellow-red color. Results are given for the right and left hips. Each figure shows the anterior and posterior view of the proximal femur. Results illustrate differences in percentage between PsO and controls. DXA-based 3D parameters were higher in patients with PsO, especially for the left femur. Differences were significant for cortical parameters.

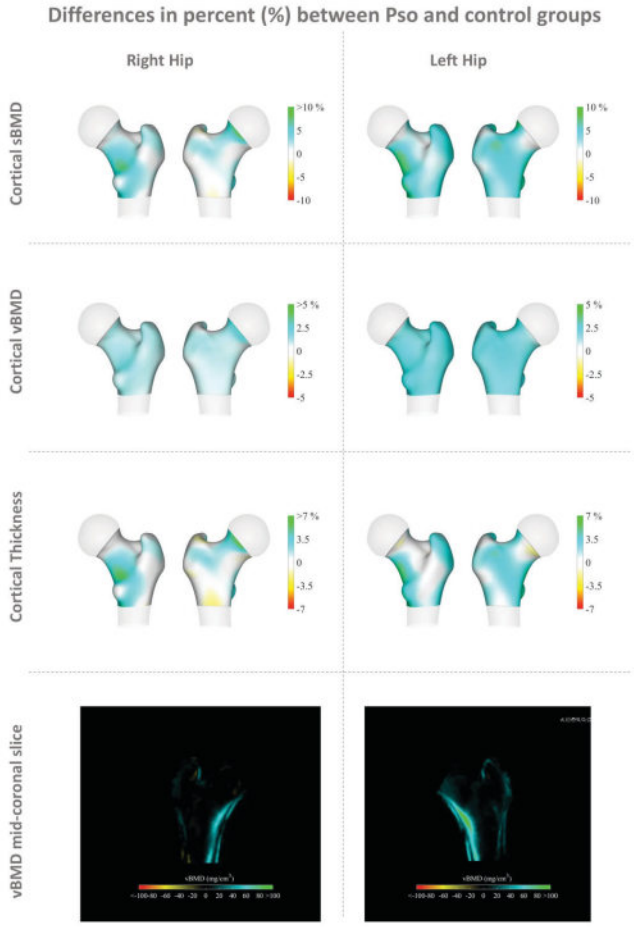

***Disclosures: Eric Toussirot**, None*

SUN-577

Type 2 Diabetes is Associated with Better Bone Microarchitecture, higher BMD, but Impaired Physical Function and Increased Risk of Incident Fracture in Older Swedish Women from the SUPERB study. *Lisa Johansson[1], Kristian Axelsson[2], Mattias Lorentzon[3], Henrik Litsne[4], Michail Zoulakis[5]. [1]Institute of medicine, , [2]Institute of Medicine, Sahlgrenska Academy, Gothenburg University, , [3]Sahlgrenska Academy, University of Gothenburg, Sweden, [4]Sahlgrenska Osteoporosis Centre,University of Gothenburg, , Sweden, [5]Sahlgrenska Osteoporosis Centre, Institute of Medicine,University of Gothenburg, Sweden

Several studies have shown that type 2 diabetes mellitus (T2DM) is associated with incident fracture, but it is not clear if the risk increase is due to impaired bone microarchitecture, low bone material strength index (BMSi) or poor physical function. The aim of this study was to determine if T2DM is associated with bone microarchitecture, BMSi, physical function, and risk of incident fracture in older Swedish women.In total, 3028 Swedish women, 75-80 years old were included in the prospective SUPERB study. At baseline, information on clinical risk factors (CRFs) was collected using questionnaires. Bone mineral density (BMD) was measured with dual-energy X-ray absorptiometry, bone microarchitecture with HR-pQCT (XtremeCT), and BMSi obtained using the Osteoprobe device (n=630). Physical function was assessed using timed up and go (TUG), one leg standing (OLS), grip strength, chair stand test and by measurements of gait speed. Data on incident fractures were retrieved from a regional x-ray archive.At baseline, the 294 women with T2DM were compared to women (n=2714) without diabetes. Women with T2DM had higher BMD at all sites (total hip 4.7%, femoral neck (FN) 3.9% and lumbar spine L1-L4 5.4%, all p<0.01) than women without. At the ultradistal tibia, T2DM women had a greater cortical area (7.3%, p<0.01) and density (1.2%, p=0.03), as well as higher trabecular bone volume fraction (8.6%, p<0.01). There was no difference in BMSi between groups (n=630; T2DM 77.8+/-8.1 vs. controls 78.1+/-7.3, p=0.81). Women with T2DM performed significantly worse on all physical function tests than their non-diabetic controls. For example, grips strength was 10.1% lower, gait speed 10.2% slower, and TUG time 13.1% (p<0.001 for all comparisons) slower in women with T2DM than in those without.During 7.3 (4.4, 8,4) years (median (IQR) of follow-up there were 1071 incident any fractures, 797 major osteoporotic fractures (MOF), and 232 hip fractures. In adjusted (for age, BMI, FRAX CRFs and FN BMD) Cox regression models T2DM was associated with an increased risk of any fracture (HR 95% CI 1.26 [1.04-1.53], but the associations with MOF (HR 1.16 [0.92-1.46]) or hip fracture (HR 1.31 [0.85-2.00]) did not reach statistical significance.In conclusion, older women with T2DM have considerably better bone microarchitecture, and no different BMSi, but substantially poorer physical function than nondiabetic women, which could be the principal reason for the increased fracture risk observed in T2DM women.

***Disclosures: Lisa Johansson**, None*

SUN-578

People Living with HIV Show High Bone Marrow Adiposity and Low Volumetric Bone Mineral Density at the Femoral Neck using Data-Driven Spatial Image Analysis Techniques *Julio Carballido-Gamio[1], Magdalena Posadzy[2], Po-Hung Wu[2], Katie Kenny[3], Isra Saeed[2], Thomas Link[2], Phyllis Tien[4], Roland Krug[2], Galateia Kazakia[2]. [1]University of Colorado Anschutz Medical Campus, United States, [2]University of California, San Francisco, United States, [3]University of California, Berkeley, United States, [4]University of California, San Francisco & Department of Veterans Affairs Medical Center, United States

People living with HIV (PLWH) have increased risk for osteoporosis and fractures. However, the pathophysiology of this comorbidity is not fully understood. Low areal and volumetric bone mineral density (aBMD and vBMD), poor bone microarchitecture, high bone marrow adiposity (BMA), and correlations of BMA with vBMD and bone microarchitecture have been reported in PLWH at the proximal femur. However, the spatial localization of these phenomena is largely unknown. The purpose of this work was to investigate if there are regions in the proximal femur manifesting stronger associations of BMA with vBMD - indicative of high bone deterioration - using data-driven image analysis techniques. Fifty-one PLWH and 51 age-matched seronegative controls (SNC) were recruited for this study. Using quantitative computed tomography (QCT) and magnetic resonance imaging (MRI), vBMD and BMA maps of the non-dominant proximal femur were generated. Using a framework like voxel-based morphometry (VBM), image registration was used to spatially normalized all parametric maps to a common template, enabling voxel-wise Spearman partial correlations of BMA with vBMD for each group. Partial correlations were adjusted for age, body-mass-index (BMI), sex, and bone shape (90% variance) and yielded maps of correlations and P-values for each group. P-value maps were corrected for multiple testing using false discovery rate (FDR).The FDR-corrected Spearman partial correlation maps of BMA with vBMD are shown in Figures 1 A-D where voxels with no significant correlations were rendered transparent. As expected, BMA and vBMD were negatively correlated in both groups. However, these correlations had distinct patterns between groups with stronger associations in the femoral head in SNC, and in the femoral neck in PLWH. These findings reflect the observed low vBMD and high BMA in the femoral neck of PLWH shown in Figures 1 E-F. However, maps in Figure 1 also show high BMA in the superior aspect of the femoral head in PLWH that is not accompanied by low vBMD at the same region.Using data-driven image analysis techniques we showed that in PLWH there is a synergistic phenomenon of high BMA and low vBMD in the femoral neck, probably predisposing them to an increased risk of fracture. Another important observation was the independent increase in BMA - with respect to vBMD - observed at the femoral head in PLWH suggesting that BMA might provide independent information from vBMD in assessments of bone fragility.

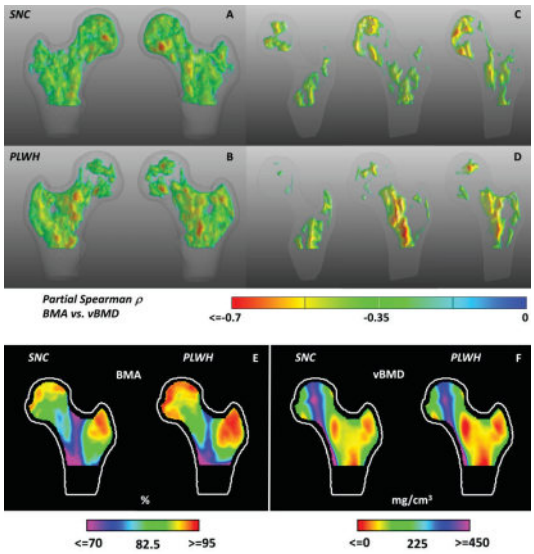

Figure 1. A-B Anterior and posterior views of three-dimensional renderings of FDR-corrected Spearman partial correlation maps of BMA with vBMD. **C-D** Posterior, central, and anterior cross-sections of A-B maps. **E-F** Central cross-sections of mean BMA and vBMD maps. Non-significant correlations in A-D were rendered transparent. The cortical bone was excluded from all analyses.

***Disclosures: Julio Carballido-Gamio**, None*

SUN-579

Correlates of MiR-144-3p With Bone Remodeling in Obese Patients With T1DM: Role of Aging And Thyroid Function *SOUAD DAAMOUCH[2], DAVID CARRO VAZQUEZ[2], Matthias Blüher[3], Lorenz Hofbauer[4], Matthias Hackl[5], Martina Rauner[6, 2], [, 2], Austria. [3]Department of Medicine and Clinic of Endocrinology and Nephrology, Germany. [4]TU Dresden University Medical Center, Germany. [5]TAMIRNA, Austria. [6]Medical Faculty of the TU Dresden, Germany

The incidence of type 1 diabetes mellitus (T1DM) is increasing worldwide. Studies have now revealed that obesity is present more often in these patients than previously thought. Furthermore, patients with T1DM are vulnerable to bone loss, however, the underlying causes are not fully understood. Previous studies have reported miR-144-3p to be upregulated in type 2 diabetes mellitus (T2DM) and to impair bone remodelling. Here, we hypothesized that miR-144-3p could play a role in diabetic bone disease associated with T1DM. We collected human serum samples (n=60 in total) from female and male patients with T1DM and non-diabetic individuals with an average age of 51 years. This cohort had an average BMI of 45 kg/m², reflecting severe obesity. Controls were matched according to age, sex, and BMI. Bone turnover markers including OCN and CTX were assessed using ELISA, and we collected clinical parameters such as HbA1c, cortisol, triglyceride, cholesterol, and thyroid-stimulating hormone (TSH) levels. miR-144-3p in the serum was measured by qPCR. As expected, a significant negative correlation was observed between HbA1c level and OCN in patients with T1DM ($r = 0.19$, $p=0.02$) compared to non-diabetic subjects. This difference was also observed in women only, who showed additional differences in CTX ($r = 0.36$, $p = 0,02$; $r = 0.38$, $p<0.02$), while men did not display any differences in bone turnover markers. Unexpectedly, circulating miR-144-3p was significantly downregulated (-37%, $p<0.05$) in patients with T1DM compared to healthy subjects. However, no significant associations were found for HbA1c, OCN, or CTX with miR-144-3p. Although no correlation with bone turnover markers was noted, a significant negative correlation between miR-144-3p and aging was observed in T1D men compared to healthy individuals ($r = 0.36$, $p<0.02$). This observation was associated with a low TSH level ($r = 0.85$, $p<0.003$), highlighting a potential thyroid disorder, which is a common secondary complication in T1DM patients. Additionally, TSH was also negatively correlated with aging in T1D patients compared to control subjects ($r = 0.90$, $p<0.0003$). Hence, this study identified miR-144-3p as a potential target for investigating the mechanisms underlying altered bone remodelling in T1DM, aging, and thyroid disorders. Further investigations are needed to validate miR-144-3p as a biomarker and to evaluate its role in bone remodelling.

***Disclosures: SOUAD DAAMOUCH**, None*

LB SUN-580

Prediction of change in bone mineral density in patients with primary hyperparathyroidism after parathyroidectomy by using flotillin-1 extracellular vesicle-microRNAs *Seunghyun Lee[1], Sunyoung Park[2], Namki Hong[3], Yongnyun Kim[4], Jongju Jeong[5], Hogyeong Gwak[2], Hyo-Il Jung[2], Yumie Rhee[6]. [1]Wonju Severance Christian Hospital, Yonsei University Wonju College of Medicine, Wonju, Korea, [, 2]Department of Mechanical Engineering, Yonsei University, Republic of Korea. [3]Division of Endocrinology, Republic of Korea. [4]Yonsei University Health System, Republic of Korea. [5]Department of Surgery, Thyroid Cancer Clinic, Severance Hospital, Yonsei University College of Medicine, Republic of Korea. [6]Yonsei University College of Medicine, Republic of Korea

Primary hyperparathyroidism (PHPT) is characterized by hypercalcemia, increased parathyroid hormone (PTH) secretion, and higher fracture risk due to bone loss. While surgery can cure PHPT, only 30% of cases show improved bone mineral density (BMD) after surgery. Prior research has suggested potential BMD changes markers, such as PTH, and procollagen type 1 N-terminal propeptide (P1NP), but their validity is disputed. Accordingly, our team proposed circulating free miR-122-5p and miR-375 as predictive markers. However, due to increased stability of miRNAs in extracellular vesicle (EV), we propose an ExoBONE assay for a complementary assay of prediction of BMD using EV miRNAs, providing a more accurate marker..We consecutively enrolled patients who underwent parathyroidectomy for PHPT at Severance Hospital between July 2017 and June 2021, excluding those without a one-year post-surgery BMD, recent users of bone metabolism affecting medications, or those with insufficient specimens: 28 patients were included (specific EV group). Twelve healthy volunteers (control group) also participated. Osteoblast-derived EVs were isolated using microbeads coated with flotillin-1(FLOT-1) antibody. Sixteen miRNAs, which are related to osteoporotic fracture, were profiled from FLOT-1 EVs. 'BMD improvement' was defined by least significant change values, which were 3.32% for the lumbar spine, 5.82% for the femur neck, and 4.71% for the total hip.The specific EV group had a mean age of 54.1, with the control group at 29.3, and both were mostly women. Notable differences were seen in miRNA levels of miR-19b-3p, miR-21-5p, miR-93-5p, miR-124-3p, miR-148-3p, and miR-375 for FLOT-1 EV before and after surgery. Among them, preoperative miR-148-3p and miR-375 showed significant association with femur neck BMD improvement, even after adjusting for age, sex, PTH, and P1NP (miR-148-3p, odds ratio 0.67 [0.50-0.90], p=0.007; miR-375, odds ratio 1.00 [1.00-1.00], p=0.001). Due to the minimal odds ratio observed in miR-375, miR-148-3p was considered a better predictive marker.In conclusion, our study proposes miR-148-3p from FLOT-EVs as a marker to validate BMD improvement after surgery in patients with PHPT. ExoBONE assay could significantly enhance BMD monitoring, improve the identification of patients at higher risk of persistent bone loss post-surgery, and provide a potential tool for better understanding bone metabolism regulation.

***Disclosures: Seunghyun Lee**, None*

LB SUN-581

Clustering HR-pQCT Parameters Reveals Three Clusters with Unique Density, Morphology, Microarchitecture & Mechanics in Older Men and Women: the Study of Muscle, Mobility and Aging (SOMMA) *Morgan Bolger[2], Kerri Freeland[2], Megan Marron[2], Nina Heilmann[2], Tong Yu[2], Lauren Roe[2], Nicole Sekel[2], Kristen Koltun[2], Katelyn Guerriere[3], Julie Hughes[4], Bradley Nindl[2], Ashley Weaver[5], Paolo Caserotti[6], Peggy Cawthon[7], Anne Newman[2], Jane A. Cauley[8], Elsa Strotmeyer[2]. [2]University of Pittsburgh, United States. [2]University of Pittsburgh, [, 3]USARIEM, United States. [4]US Army Research Institute of Environmental Medicine, United States. [5]Wake Forest University School of Medicine, United States. [6]University of Southern Denmark, Denmark. [7]California Pacific Medical Center, United States. [8]UNIVERSITY OF PITTSBURGH, United States

Age-related changes to bone density, morphology, and microarchitecture do not occur uniformly across the population and the common phenotypes beyond BMD are not well defined. We hypothesized that unsupervised clustering of high-resolution peripheral quantitative computed tomography (HR-pQCT) measures at the distal tibia (DT) and radius (DR) separately, would reveal unique skeletal phenotypes in the Study of Muscle, Mobility and Aging (SOMMA; year 1 visit), a cohort of community-dwelling older women and men (60% women; 87% white). HR-pQCT parameters at the DT (N=321; 76.3+/-4.7 years) and DR (N= 295; 76.1+/-4.5 years) were within-sex standardized as z-scores, then used to form clusters: density (Tt.BMD, Ct.BMD, Tb.BMD), geometry (Tt.Ar, Ct.Ar, Tb.Ar, Ct.Th), microarchitecture (Tb.Th, Tb.N, Tb.Sp), and bone length (Le). Fuzzy c-means clustering found 3 clusters, then discretized by the highest membership coefficient. DT cluster 1 (Figure 1; DTC1, n=121) had the highest Tt.BMD, Tb.BMD, Ct.Ar, Ct.Th, and Tb.Th. DT cluster 2 (DTC2, n=86) had the highest Tb.Sp and lowest Tb.BMD and Tb.N. DT cluster 3 (DTC3, n=114) had the highest Tt.Ar, Tb.Ar, and Le and lowest Tt.BMD, Ct.BMD, Ct.Ar, Ct.Th (all $p<0.05$). For DR, (DRC1, N=98; DRC2, N=103; DRC3, N=94) the same associations were seen for Tt.BMD, Tt.Ar, Ct.Ar, Tb.Ar, Ct.Th, and Le. The external bone size (Tt.Ar/Le) was higher in DTC3 (2.23+/-0.37) vs. DTC1 (1.95+/-0.30) and DTC2 (1.97+/-0.35). The estimated failure load (FL) was higher in DTC1 (11.1+/-3.1 kN) vs. DTC2 (9.1+/-2.7 kN) and DTC3 (8.9+/-3.0 kN, $p<0.05$ for all) with no difference in DTC2 vs. DTC3 ($p=0.58$). The cortical load fraction (Ct.LF) was highest in DTC2 (47+/-10%), followed by DTC1 (41+/-9%), and lowest in DTC3 (33+/-9%; all $p<0.05$), meaning DTC2 relied relatively more on the cortical and DTC3 on trabecular bone to achieve similar FL. For femoral neck (FN) DXA, FN BMD was lower in DTC2 (0.82+/-0.12 g/cm2) and DTC3 (0.84+/-0.12 g/cm2) vs. DTC1 (0.93+/-0.16 g/cm2), driven by higher FN area in DTC3 vs. DTC1 (5.41+/-0.54 vs. 5.18+/-0.54 cm2) and lower BMC in DTC2 vs. DTC1 (4.32+/-0.84 vs. 4.84+/-1.12 g). Similar associations in external bone size, FL, Ct.LF and FN measures were found for DR clusters. In summary, for both DT and DR sites, clusters with high-Tt.BMD, Ct.Ar, (C1), medium-Tt.BMD, Ct.Ar (C2), and low-Tt.BMD, Ct.Ar with high-Le and Tb.Ar (C3) were captured. Whether unique skeletal phenotypes differ in risk factors, muscle function, and fracture incidence need to be studied.

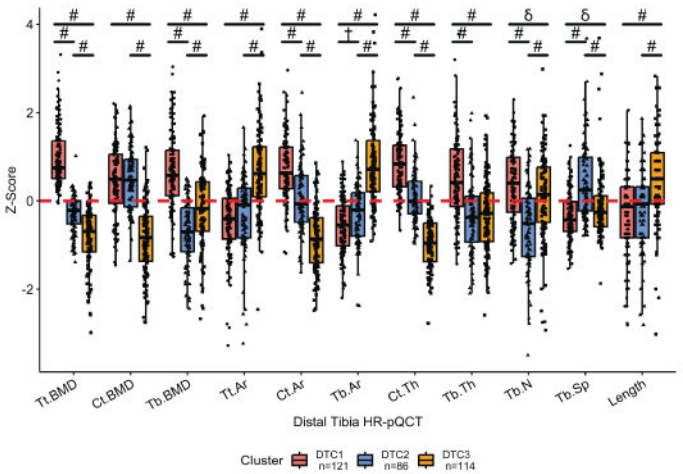

Figure 1: Box plots of standardized z-scores of HR-pQCT parameters for the distal tibia used to derive cluster assignments. Between groups pairwise Student's t-test or Wilcoxon test δ p<0.05, † p<0.01, ‡ p<0.001, # p<0.0001. *Abbreviations*: distal tibia cluster 1 (DTC1), distal tibia cluster 2 (DTC2), distal tibia cluster 3 (DTC3), total bone mineral density (Tt.BMD), cortical BMD (Ct.BMD), trabecular BMD (Tb.BMD), total area (Tt.Ar), cortical area (Ct.Ar), trabecular area (Tb.Ar), cortical thickness (Ct.Th), trabecular thickness (Tb.Th), trabecular number (Tb.N), trabecular spacing (Tb.Sp), and tibia length (Le).

***Disclosures: Morgan Bolger**, None*

LB SUN-582

Trabecular Bone Texture from Clinical MRI Scans Reflects Biomechanical Properties of Bone *Alexander Dash[1], Ryan Breighner[2], Fernando Quevedo Gonzalez[4], Matthew Koff[4], Olivia Blumberg[4], Alison Heilbronner[5], Emma Billings[6], Matthew Cunningham[4], Han Jo Kim[4], Jeri Nieves[7], Emily Stein[4]. [1]Icahn School of Medicine at Mount Sinai, , [2]Hospital for Special Surgery/Weill Cornell Medicine, United States, [4]Hospital for Special Surgery, United States, [4]Hospital for Special Surgery, , [5], United States, [6]Hospital for Special Surgery , , [7]Columbia University and Hospital for Special Surgery,

There is a need for opportunistic screening methods to improve identification of individuals poor bone quality. Our group has recently published a method for evaluation of bone quality based upon clinical MRI scans. Greater heterogeneity (irregularity) of trabecular bone texture was associated with worse bone quality-postmenopausal women with fragility fractures had greater texture heterogeneity compared to age-matched controls and individuals with greater texture heterogeneity had lower volumetric BMD and more abnormal microarchitecture by high-resolution peripheral QCT. The present study investigated relationships between MRI-based texture and biomechanical properties of bone using CT-based finite element analysis (FEA). We hypothesized that individuals with greater texture heterogeneity would have lower stiffness and compressive strength. Forty-three individuals included in this prospective study had vertebral imaging at L1-2. Trabecular bone texture was calculated from T1-weighted MRIs. A gray level co-occurrence matrix characterized the distribution and spatial organization of voxelar signal intensities to derive the following texture features: contrast (variability), entropy (disorder), angular second moment (ASM; uniformity), and inverse difference moment (IDM; local homogeneity). Texture features were calculated in five directions relative to the image plane. Analyses were performed utilizing the average of all offsets and individually in the vertical (cranio-caudal) direction to correspond with the direction of vertebral loading in FEA. Whole bone stiffness and compressive strength were calculated from phantom calibrated lumbar QCT (Abaqus and Matlab). Spearman rank correlation was used. Mean age of subjects was 61+/-10 years, 56% were female, 83% non-Hispanic White. Patients with lower whole bone stiffness had greater texture heterogeneity, specifically, higher contrast (r=-0.38, p<0.05) and entropy (r=-0.36, p<0.01) and lower IDM (r=0.39, p<0.01) and ASM (r=0.36, p<0.05, Figure). Lower compressive strength was similarly associated with greater texture heterogeneity. Relationships were comparable using the average value of texture features in all directions and the vertical direction individually. In summary, trabecular bone texture was directly related to biomechanical properties of vertebral bone. These results provide further evidence that MRI-based texture analysis may be a useful tool for identification of patients with skeletal fragility.

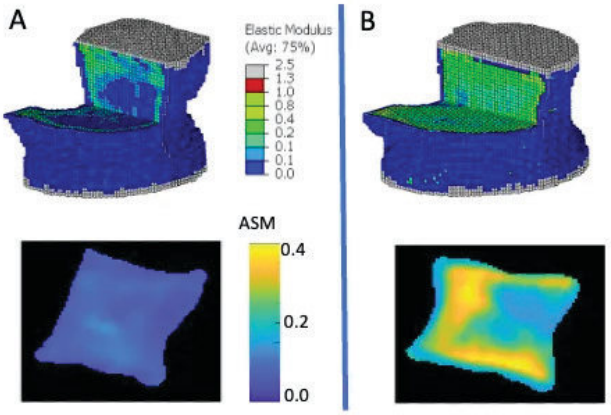

Figure: Representative vertebral images from L1 of 2 individuals using CT-based finite element analysis (FEA, above) and MRI-based texture mapping (below). Panel A is from an individual with low stiffness by FEA and low uniformity (angular second moment, ASM) by MRI. Panel B is from an individual with high stiffness by FEA and high ASM.

***Disclosures: Alexander Dash**, None*

LB SUN-583

Factors involved in the development of cortical porosity: a cross-sectional study in healthy subjects using HR-pQCT *Jin Ikenaga[1], Ko Chiba[1], Narihiro Okazaki[2], Kazuteru Shiraishi[3], Makoto Osaki[3]. [1]Nagasaki University Graduate School of Biomedical Sciences, Japan, [2]Nagasaki University Hospital, Japan, [3]Nagasaki University, Japan

Purpose: The purpose of this study is to investigate factors involved in the development of cortical porosity using data from a cohort study assessed by high-resolution peripheral quantitative computed tomography (HR-pQCT).Methods: The subjects were 520 healthy individuals (260 men, 260 women, 20-97 years old, all Japanese) of the cohort study (J-CaraT study: Japanese study of bone microarchitecture and mineral density in a normative cohort measured by HR-pQCT).Background information (age, height, weight, etc.), areal bone mineral density (BMD) of the lumbar spine and proximal femur by dual-energy x-ray absorptiometry (DXA), calcaneus speed of sound (SOS) by quantitative ultrasound (QUS), blood tests (WBC, RBC, Hb, Plt, Ca, P, ALP, TP, Alb, BUN, Cre, eGFR, Na, K, Cl, AST, ALT, GTP, UA, CRP, TC, TG, HbA1c, intact PTH, TRACP-5b, total P1NP, Pentosidine, 25-OH Vitamin D) was assessed.HR-pQCT imaging of the distal radius and tibia was performed (XtremeCT II, SCANCO Medical AG, Brüttisellen, Switzerland) and volumetric BMD (total BMD, cortical BMD, trabecular BMD), cortical bone microarchitecture (cortical porosity: Ct.Po, cortical thickness, etc.), and trabecular bone microarchitecture (BV/TV, trabecular thickness, trabecular number, trabecular separation, etc.) were measured. Correlations between Ct.Po and other parameters were analyzed using Pearson's correlation coefficients and partial correlation coefficients corrected for age, height and weight.Results: Ct.Po was positively correlated with age in both men and women (men: radius r=0.58, tibia r=0.41, women : radius r=0.55, tibia r=0.64, p<0.01). Ct.Po did not correlate with any measurements of DXA or blood tests. Ct.Po was negatively correlated with Ct.BMD (men: radius r=-0.45, tibia r=-0.79, women : tibia r=-0.54, p<0.01). Ct.Po was positively correlated with Tb.BMD (men: radius r=0.29, tibia r=0.35, women: radius r=0.29, tibia r=0.38, p<0.01). Ct.Po was positively correlated with Tb.Meta.BMD (men: radius r=0.37, tibia r=0.38, women: radius r=0.35, tibia r=0.42, p<0.01).Conclusion: Cortical porosity increased with age, especially after age 50 in women. None of the parameters in DXA and blood tests could be predictive markers of cortical porosity.Trabecular BMD was positively correlated with cortical porosity, and higher trabecular BMD was associated with higher cortical porosity. Its pathogenesis is unknown and further investigation is required.

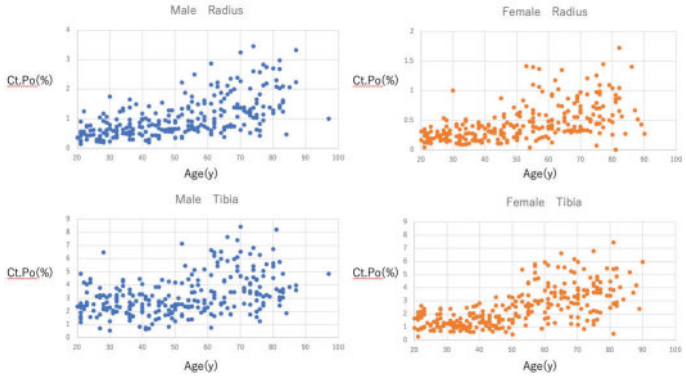

***Disclosures: Jin Ikenaga**, None*

LB SUN-584

Mitochondria dysfunction in osteoblast lineage cells does not impact the bone adaptive response to mechanical loading *Ana Resende-Coelho[1], Mohsin Ali[2], Aaron Warren[1], Stuart Berryhill[3], Jeff Thostenson[4], Jinhu Xiong[5], Maria Almeida[1]. [1]Division of Endocrinology and Metabolism, University of Arkansas for Medical Sciences, Little Rock, USA, United States. [2]University of Arkansas for Medical Sciences , United States. [3]Bone Biomechanics, Histology and Imaging Core (BHIC), University of Arkansas for Medical Sciences, Little Rock, AR, USA, United States. [4]Department of Biostatistics, University of Arkansas for Medical Sciences, Little Rock, AR, USA, United States. [5]Department of Orthopedic Surgery, University of Arkansas for Medical Sciences, Little Rock, USA, United States

Mechanical loading, such as induced by exercise, is efficient in increasing bone formation and bone mass. The bone response to mechanical loads is less effective with aging, but the mechanisms responsible remains unknown. The number of osteoblasts and bone mass decreases in old mice due to several mechanisms of aging that are common to many organs, including mitochondria dysfunction and the production of reactive oxygen species (ROS). Superoxide anions produced during oxidative phosphorylation are promptly converted into hydrogen peroxide by superoxide dismutase 2 (SOD2) within the mitochondria. Mice with deletion of SOD2 in osteoblast lineage cells (SOD2?Osx1) have decreased bone mass. Here, we tested whether an increase in ROS and mitochondrial dysfunction in osteoblast lineage cells contribute to the decreased bone adaptive response to mechanical loading. To this end, we performed axial tibial loading in SOD2?Osx1 mice and Osx1-cre littermates controls. A reduction in SOD2 mRNA and an increase in mitoROS in bone marrow-derived osteoblastic cells from SOD2?Osx1 mice were confirmed by qPCR and MitoSOX Red staining, respectively. An 8.5N axial load was applied to the left tibia of 10-month-old female SOD2?Osx1 (n=8) and control mice (n=8) to achieve +1200 μ? peak strain at the tibial midshaft, for five consecutive days per week for 2 weeks. The load was applied in 1200 cycles with 4 Hz triangle waveform and 0.1 s rest time between each cycle. The right leg served as a non-loaded control. After sacrifice, cortical thickness was assessed by μCT at tibial midshaft and at 5 mm proximal from the tibiofibular junction. Model-estimated pairwise analysis revealed that the main effect of loading was significant (Midshaft: p=0.003, Proximal: p=0.0004). The Tukey-adjusted p-values of the 4 pairwise differences of genotype/loading combinations revealed significant differences in Osx1-cre unloaded vs. loaded for Midshaft (p=0.045) and Proximal (p=0.016) and SOD2?Osx1 unloaded vs. loaded only for Proximal (p=0.036). The interaction contrast comparing the loading differences between the genotypes revealed that the response to loading was not affected by genotype. Our results indicate that impaired mitochondrial function in osteoblast lineage cells has no major impact on the response to mechanical loading in bone, suggesting that an increase in ROS does not interfere with the response to loading with aging.

***Disclosures: Ana Resende-Coelho**, None*

LB SUN-585

Bioprinting of a 3D Heterocellular Human Organoid for Reproducing Physiological Bone Remodeling *Chris Steffi[1], Anke de Leeuw[1], Gian Nutal Schädli[1], Xiao-Hua Qin[1], Matthias Rüger[1], Ralph Mueller[2]. [1]ETH Zürich, Switzerland. [2]ETH Zurich, Switzerland

Bone remodeling, orchestrated by osteoclasts and osteoblasts, plays a pivotal role in maintaining skeletal integrity. However, current 3D bioprinting approaches often overlook key cell types involved in bone remodeling, such as monocytes, macrophages, and osteoclasts. To address this research gap, we aimed to develop an advanced bone remodeling model by incorporating these crucial cell types and exploring their interactions in an in vitro setting.In our study, bone organoids were 3D bioprinted using alginate, gelatin, graphene oxide bioinks. By encapsulating human mesenchymal stem cells (hMSCs) or primary osteoblasts within the bioink, we mimicked the initial steps of bone development. Furthermore, to induce maturation of the hMSCs into osteoblasts, we subjected the organoids to cyclic mechanical compression, effectively stimulating cell-matrix production. Over a 4-week culture period, the hMSCs or osteoblasts successfully differentiated and mineralized the extracellular matrix. Building upon this foundation published previously, we then reseeded monocytes, osteoblasts or both into the mineralized organoids using a fibrin-based bioink. The fibrin-based bioink not only facilitated the adhesion of cells to the mineral surface but also supported their subsequent differentiation.To assess the functionality of our organoid, we cultivated it with receptor activator of nuclear factor kappa-? ligand and macrophage colony-stimulating factor, pivotal factors known to drive osteoclast differentiation and activation. The non-destructive evaluation of mineral maturation was achieved through time-lapsed micro-CT scans, which provided valuable insights into the dynamic changes occurring within the organoid. Our findings revealed a significant reduction in tissue mineral density and bone volume upon the inclusion of osteoclast precursors. These results underscored the active participation of osteoclasts in the bone remodeling process. Histology analysis confirmed the presence of multinuclear tartrate-resistant acid phosphatase-positive osteoclasts, responsible for bone resorption, as well as alkaline phosphatase-positive osteoblasts, actively engaged in mineral deposition. Multinucleated cells are shown in Fig 1. By incorporating multiple cell types and studying their interactions non -invasively, our 3D bone organoid provides a novel and sophisticated platform for investigating the intricate mechanisms underlying bone remodeling.

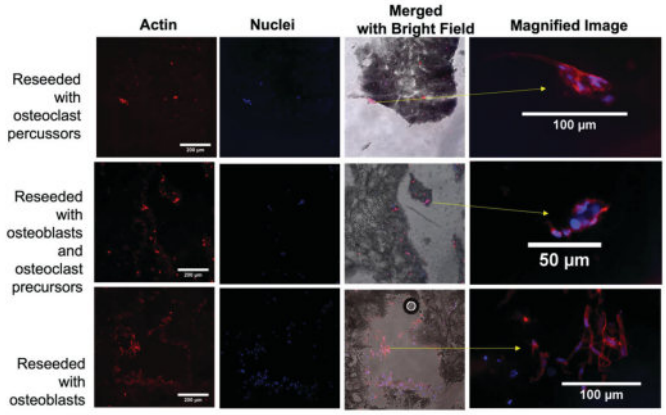

Figure 1: Confocal microscopy images of cryosections of the organoids. The actin was stained with phalloidin, and nuclei were stained with NucBlue Fixed Cell Reagent (DAPI). Osteoblast-encapsulated organoids were cultured for four weeks and were subdivided into three experimental groups. Group 1 was reseeded with osteoclast precursors, group 2 was reseeded with osteoblasts and osteoclast precursors, and Group 3 was reseeded with osteoblasts (n=3).

***Disclosures: Chris Steffi**, None*

LB SUN-586

Effects of In Utero and Lactational Exposure to Dolutegravir-Based cART In Sprague Dawley Rats *Abhayavarshini Sridhar[1], Ryan Ross[2], Jean Harry[3], Helen Cunny[3]. [1]Rush University, United States. [2]Rush University Medical Center, United States. [3]NIH/NIEHS, United States

Introduction: Combination antiretroviral therapy (cART) has dramatically reduced the risk of Mother-to-Child HIV Transmission during pregnancy and breastfeeding. Despite its positive effects, cART increases the risk for osteoporosis in adults and may inhibit bone development in children, which increases the risk of late-life osteoporosis. Recently, the World Health Organization (WHO) has recommended dolutegravir (DTG) as the preferred treatment for pregnant women. However, the effects of early exposure to maternal DTG-based cART on bone are unclear. In the current study, we evaluated the effects of perinatal exposure to DTG/ABC (Abacavir)/3TC (lamivudine) in uninfected Sprague Dawley (SD) rats to understand its effects on bone independent of HIV.Methods: Female SD rats were bred between 10-13 weeks of age. Pregnant rats were treated with DTG/ABC/3TC or vehicle via oral gavage starting at gestational day 6. Maternal treatment continued throughout gestation and lactation. Upon weaning, the offspring received a cART-free rodent diet. On postnatal day 573 (~18 months), offspring were sacrificed. Femoral length was measured using digital hand-held calipers. Micro-computed tomography was used to evaluate trabecular bone architecture in the distal femoral metaphysis. Results were evaluated using a two-way ANOVA. To date, 10 cART and 15 vehicle treated samples have been evaluated.Results: Trabecular bone volume fraction (BV/TV) was significantly affected by treatment, with a significant 29% and non-significant 27% reduction in BV/TV of cART treated female and male rats compared to vehicle treated controls, respectively (Fig 1). cART treatment also affected trabecular number and spacing, with an overall decrease in trabecular number and increase in trabecular spacing. Femoral length was also affected by cART, with a significant increase in length in cART treated males, but not in females.Conclusion: Our prelim-

inary data suggests that exposure to DTG-based cART during early skeletal development has long-lasting negative effects on trabecular bone mass and potentially influences bone growth. Importantly, impaired bone mass accrual can increase the risk for osteoporosis later in life, and therefore children born to HIV infected mothers may be at an increased risk for osteoporosis even if uninfected themselves. Future work is aimed at assessing bone strength, matrix composition, and cellular dynamics.

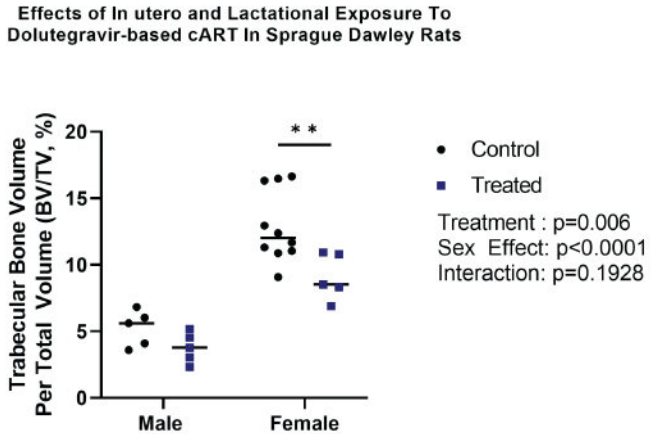

***Disclosures: Abhayavarshini Sridhar**, None*

LB SUN-587

Prediction of curve progression and progression to surgical threshold in adolescent idiopathic scoliosis with bone microarchitecture phenotyping by an unsupervised machine learning protocol - a 6-year longitudinal study till skeletal maturity and beyond *Guangpu Yang[3], Adam Yiu Chung Lau[2], Alec Lik Hang Hung[2], Tsz Ping Lam[3], Jack Chun Yiu Cheng[3], Wayne Lee[3], Anubrat Kumar[2], Raymond Chung Wai Wan[2]. [3]The Chinese University of Hong Kong, China. [2]Prince of Wales Hospital, China. [3]The Chinese University of Hong Kong, Hong Kong

IntroductionAdolescent Idiopathic Scoliosis (AIS) is a 3D spine deformity that may cause serious health problems. Early prediction of curve progression in AIS is essential in guiding timely interventions, and bone qualities have been shown to be an important prognostic factor in AIS. High resolution peripheral quantitative computed tomography (HRpQCT) provides low-radiation and 3D evaluation of bone microarchitecture but generates a long list of quantitative parameters hindering easy interpretation.ObjectiveOur study aims to (a) utilize unsupervised machine learning to identify hidden bone microarchitecture phenotype clusters amongst HRpQCT parameters in AIS, (b) investigate the clusters' association with risk of progression to surgical threshold in AIS, and (c) validate their association to curve progression in a separate cohort of AIS patients.MethodsA total of 207 AIS girls were staged for skeletal maturity using the validated Thumb Ossification Composite Index (TOCI) and they were all at peripubertal peak height velocity. Patients were followed up longitudinally for 6 years in the primary cohort (N=101) and for 3 years in the validation cohort (N=106). Bone qualities were evaluated by HRpQCT and three bone microarchitecture phenotype clusters were identified by Fuzzy C-Means.ResultsIn the primary cohort, patients with Phenotype-1 had normal bone characteristics. Phenotype-2 was characterized by significantly lower periosteal perimeter and trabecular area, while Phenotype-3 had significantly lower cortical density and thickness and compromised trabecular microarchitecture (Fig 1A-1C). Upon the 6-year follow-up, these bone characteristics were persistent till skeletal maturity (Fig 1D-1F), and Phenotype-3 was associated with curve progression to surgical threshold (OR=4.88, P=0.029). In the validation cohort, Phenotype-2 (adjusted OR=5.02, P=0.027) and Phenotype-3 (adjusted OR=4.22, P=0.039) were associated with curve progression >= 6°during the 3-year follow-up.ConclusionThis 6-year longitudinal study revealed that bone microarchitecture phenotype clustered by unsupervised machine learning was persistent throughout the rapid peripubertal growth period till skeletal maturity with validated success in the prediction of curve progression and progression to surgical threshold in early presenting AIS girls. With further expanded trials, these findings have important implications in guiding the clinical management of early AIS.

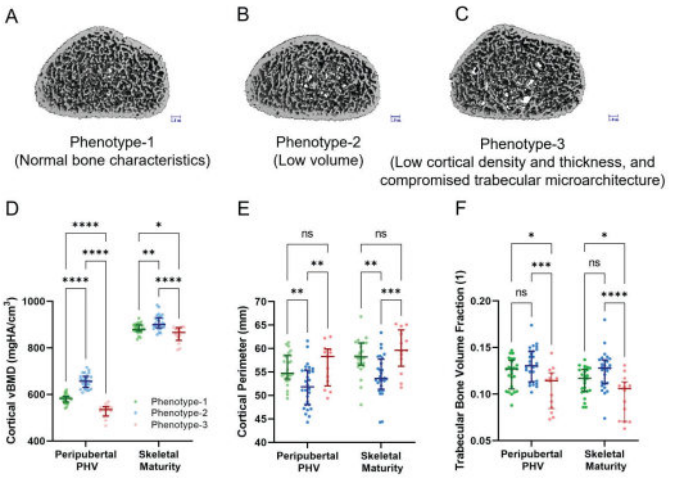

***Disclosures: Guangpu Yang**, None*

LB SUN-588

TATR: Modeling a Target And Timed Release strategy for TrkB agonist drug delivery to cochlear bone *Oskar Sundberg[1], Judith Kempfle[2], Boris Kashemirov[1], David Jung[3], Charles McKenna[1]. [1]University of Southern California, United States. [2]Department of Otolaryngology, Eaton-Peabody Laboratory, Massachusetts Eye and Ear Infirmary; Department of Otolaryngology, UMass Memorial Medical Center, UMass Chan Medical School, United States. [3]Department of Otolaryngology, Massachusetts Eye and Ear Infirmary, Harvard Medical School, United States

Sensorineural hearing loss (SNHL) related to aging is associated with loss of inner ear sensory hair cells (HCs), cochlear spiral ganglion neurons (SGNs), and ribbon synapses between HCs and SGNs, stimulating intense interest in therapies to restore synaptic function. Selective and potent agonists of tropomyosin receptor kinase B (TrkB) are known that can promote regeneration of SGN neurites, however local delivery of drugs to the inner ear remains a challenge due to several factors, including clearance by inner ear fluid.Bisphosphonates strongly complex calcium ions in hydroxyapatite matrices, enabling them to tightly bind to bone. This property offers the potential for bone-specific drug delivery, which has been demonstrated to provide more effective concentrations of antibiotics to infected bone tissue by attachment of the drug cargo to a bisphosphonate via a pH-sensitive linker that cleaves in situ ('target and release', TAR). Bisphosphonate-conjugated fluorescent imaging probes triggered by cathepsin K secretion at bone resorption sites have also been recently implemented.Cochlear bone is an intriguing depot target for bisphosphonates but an instigating drug release mechanism other than bone resorption is indicated to access SGNs, e.g. by adjusting the rate of drug release at physiological pH inherently, via synthetically accessible structural changes in the linker moiety ('target and timed release', TATR) (Fig. 1A). To this end, we have synthesized a small library of bisphosphonate-equipped TATR model conjugates incorporating tunable self-immolating linkers pioneered by Santi et al. and incorporating a quinine-standardized chromophore (7-AMC) as the drug cargo to facilitate determination of release kinetics. The conjugates were designed to exhibit half-lives ranging from 36 h to 450 h, with the drug release timing dependent on synthetic adjustment of the cleavable linker structure. Release kinetics were determined experimentally at pH 7.4 and the time-dependent concentrations for single compartment cochlear dilution were simulated using FluidSIM4 for bolus drug, the parent conjugate and released drug (61 uM at t = 0). As shown in Fig. 1B, under the selected conditions, the TATR-generated free drug concentration could be maintained within an arbitrary therapeutic dose range of 5 - 0.5 uM well over tenfold longer than the bolus drug concentration, demonstrating the potential of this new approach to drug delivery in the cochlea.

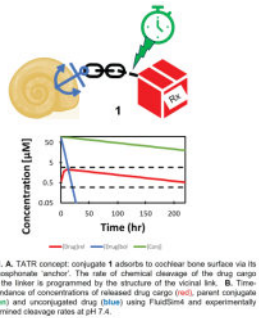

Fig 1. A. TATR concept: conjugate **1** adsorbs to cochlear bone surface via its bisphosphonate 'anchor'. The rate of chemical cleavage of the drug cargo from the linker is programmed by the structure of the vicinal link. **B.** Time-dependance of concentrations of released drug cargo (red), parent conjugate (green) and unconjugated drug (blue) using FluidSim4 and experimentally determined cleavage rates at pH 7.4.

***Disclosures: Oskar Sundberg**, None*

LB SUN-589

Undercarboxylated Osteocalcin Predicts Fat Accumulation in cART Initiating People Living with HIV *Niyati Patel[1], Bryan Dulion[1], Itzel Lazcano[1], Ryan Ross[1]. [1]Rush University Medical Center, United States

The initiation of antiretrovirals (ARVs) is associated with rapid changes in bone and fat mass, which may be related phenomenon. We've reported that bone-derived undercarboxylated osteocalcin (ucOCN) is associated with fat accumulation in women living with HIV and in a mixed gender cohort of people initiating ARVs. The extent of bone and fat change and the amount of ucOCN released with ARV initiation is dependent on ART regimen. We leveraged data and serum from the AIDs clinical trial group (ACTG) to determine whether the association between ucOCN and body fat change is ARV-specific.Data and samples were obtained from a randomized clinical trial of treatment-naïve HIV-infected patients assigned to either - raltegravir (RAL), atazanavir/ritonavir (ATV/r), or darunavir/ritonavir (DRV/r), each in combination with TDF/FTC. Serum was collected at baseline (pretreatment) and 48 weeks post ARV initiation. Circulating ucOCN was measured using ELISA (Biolegend). Total body and trunk fat was assessed using dual energy x-ray absorptiometry (DXA) at baseline and 96-weeks post initiation. The change in ucOCN and fat parameters were evaluated according to treatment using a repeated measures two-way ANOVA. The association between the 48-week change in ucOCN and the 96-week change in fat parameters was evaluated using linear regression after adjusting for the baseline fat parameter. Regression analyses were run with the entire cohort and then separately by treatment.ucOCN, total body fat, and trunk fat increased over time, but there were no treatment effects. In the total cohort, change in unOCN was positively associated with total fat gain (?=0.15, p =0.046). The association between ucOCN and trunk fat was similar, but not significant (?=0.08, p =0.061). When run separately, there were no associations between ucOCN and fat in the RAL or ATV/r groups. There were, however, significant associations between the change in ucOCN and total body (?=0.35, p=0.014) and trunk fat gain (?=0.20, p=0.017) in the DRV/r group.These findings provide further confirmation of a bone-fat hormonal connection in people living with HIV and for the first time, suggest that the relationship between these two organ systems may be ARV specific. Ultimately, identifying the mechanisms associated with ARV associated complications can help to improve the quality of life of HIV infected patients.

***Disclosures: Niyati Patel**, None*

LB SUN-590

Bidirectional Regulation of PTH and Bone Mass by Subfornical Organ *Lu Zhang[1], Nian Liu[1], Jie Shao[1], Dashuang Gao[1], Yunhui Liu[1], Yingzi Zhao[1], Chuanliang Han[1], Di Chen[1], Liping Wang[1], William Weijia Lu[1], Fan Yang[1]. [1]Shenzhen Institute of Advanced Technology Chinese Academy of Sciences, China

The central nervous system modulates the body homeostasis including bone metabolism and hormone secretion. Our recent studies found that the central nervous system modulates bone metabolism through parathyroid hormone (PTH). In mammals, PTH is secreted through the parathyroid glands and modulates bone turnover and calcium homeostasis, however mechanism underlying central neural regulation of PTH in mammals remains unknown. In our study, we identified the subfornical organ (SFO) and the paraventricular nucleus (PVN) as two important brain nuclei that responded to serum PTH and calcium changes. Using chemogenetics, we found that serum PTH was suppressed by stimulation of GABAergic neurons in SFO followed by a decrease in trabecular bone mass. Conversely, stimulation of glutamatergic neurons in SFO promoted serum PTH and bone mass. The paraventricular nucleus (PVN) is downstream of the SFO, and chemogenetic activation of glutamatergic neurons in PVN induced an increase in serum PTH and bone mass. In summary, our study demonstrates for the first time that distinct neuronal subtypes in the SFO are responsible for bidirectional regulation of serum PTH and bone metabolism, which is mediated through the PVN and the peripheral nervous system. These findings reveal important central neural nodes and will advance our understanding of the central neural regulation of PTH at the molecular, cellular and circuit level.

***Disclosures: Lu Zhang**, None*

LB SUN-591

Hearing Loss and Risk of Osteoporotic Fracture: Population-Based Cohort Study from the United Kingdom *Yana Vinogradova[1], Nadeem Qureshi[1], Seyed Alireza Hashmeinsab[2], Daniel Prieto Alhambra[2], Laura Canals Ruiz[5], Michaela Ratzinger[5], Adrian Salas[5], Sara Khalid[2]. [1]Faculty of Medicine & Health Sciences, University of Nottingham , United Kingdom. [2]Nuffield Department of Orthopaedics, Rheumatology and Musculoskeletal Sciences, Oxford University, United Kingdom. [5]Amgen, . [5]Amgen, Austria. [5]Amgen, Argentina

BACKGROUND: Hearing loss and osteoporosis (OP) incidence both increase with age. While data suggest increased risk of hearing loss with low bone mineral density (BMD), the association between hearing loss and OP fracture is not well understood.AIMS: We assessed the association between hearing loss and major OP fracture (MOP; clinical spine, wrist/forearm, shoulder/proximal humerus and hip).METHODS: Using READ and ICD-10 diagnosis codes, we identified individuals aged >=60 years in the UK Clinical Practice Research Datalink (CPRD) GOLD database, diagnosed with hearing loss (HL; index event) from 1January2001 to 16December2021, in CPRD for >= 1 year before index event, with no history of secondary OP causes. Individuals were followed from index date to 1) MOP, or 2) death, migration/transfer out, practice last collection date, end of study or follow-up (1 year) and matched with up to 5 individuals without HL by birth and index year, sex, general practice. Incidence rates and Cox proportional Hazard Ratios (HL vs no HL; stratified by low/high fracture risk [prior fracture, OP diagnosis and/or treatment]; adjusted for ethnicity and other confounders) were calculated for MOP and hip fracture outcome. Multivariate logistic regression was used to assess risk factors for MOP and hip fracture in the HL cohort.RESULTS: 237,297 and 829,431 individuals with and without HL were included, respectively; median [IQR] age, 74 [67-81] and 72 [66-79] years, respectively; men, 52% and 53%; women, 48% and 47%. The HL cohort had longer follow-up and greater frailty (severe electronic frailty index, 5.9% vs 2.7%). After adjustment, the HL loss cohort had increased 1-year risk of MOP and hip fracture (Table). Significant risk factors for 1-year MOP and hip fracture (both) included older age, fracture history, falls, OP diagnosis, chronic obstructive pulmonary disorder, cardiovascular disease and comorbidities; additional risk factors for 1-year MOP included severe frailty and heavy alcohol use; additional risk factors for 1-year hip fracture included moderate smoking and rheumatoid arthritis.CONCLUSION: We observed a 10% higher risk of MOP and an 8% higher risk of hip fracture in individuals with hearing loss versus those without hearing loss and identified several risk factors. Our data suggest individuals with hearing loss should be considered for BMD or fracture risk assessment. Our data require external validation.

Table. Fracture incidence in individuals with and without HL – data from UK CPRD GOLD

Fracture risk	Hearing loss (N=237,297)			No Hearing loss (N=829,431)		
	Low	High	Overall	Low	High	Overall
Follow-up, median (IQR), years	4.4(2.1,7.7)	3.4(1.5,6.4)	4.2 (1.9, 7.4)	3.6(1.6,6.6)	2.8(1.2,5.5)	3.4 (1.4, 6.4)
Major Osteoporotic Fracture (MOP)						
Incidence rate (95% CI) per 1,000 person-years	16.08 (15.83, 16.34)	36.66 (35.90, 37.44)	20.11 (19.86, 20.36)	13.17 (13.04, 13.30)	32.92 (32.47, 33.37)	16.58 (16.44, 16.7)
Adjusted HR (95% CI)	1.10 (1.08, 1.12)					
Hip fracture						
Incidence (95% CI) per 1,000 person-years	4.36(4.23, 4.49)	9.28(8.9, 9.68)	5.32 (5.19, 5.45)	3.68(3.61, 3.75)	8.69(8.46,8.96)	4.54 (4.47, 4.61)
Adjusted HR (95% CI)	1.08 (1.05, 1.11)					

CI, Confidence Interval, HR, Hazard Ratio (matched by age and sex, stratified by low/high fx risk (diagnosis of OP, use of OP medications, previous OP fx) adjusted for lifestyle factors, morbidities and medications); IQR, inter quartile range.

Figure. Risk factors for 1-year fracture risk in individuals with hearing loss (Odds Ratios and 95% CIs)

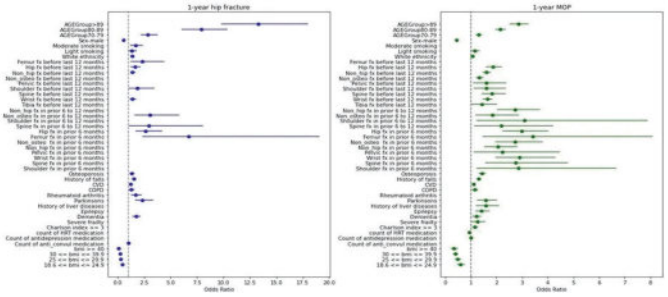

***Disclosures: Yana Vinogradova**, None*

LB SUN-592

Skeletal effects of hypoparathyroidism (HypoPT); data from the Canadian National Hypoparathyroidism Registry (CNHR) *Aliya Khan[1], Salma Hussein[1], Habiba Afifi[2], Hajar AbuAlrob[2], Dalal Ali[1], Ragad Abu Fardeh[2], Abdulrahman Almoulia[2], Ayman Azharruddin[2], David Bole[2], Manoela Braga[1], Prakash Chandra[3], Alice Cheng[4], Rapheal Cheung[5], James Edward Massey Young[1], Naqiah Firdous[2], Hetal Juta[2], Sarah Khan[2], Tayyab Khan[5], Jouma Malhem[2], Hadia Malik[2], Shehryar Mehmood[2], Adam Millar[4], Emmett Morgante[2], Faizan Naveed[2], Humaira Niazi[2], Terri Paul[5], Ally Prebtani[1], Zubin Punthakee[1], Joseph Shaban[5], Reema Shah[1], Muhammed Shrayyef[4], Cherry Tagra[2], Susan Teschke[1], Ibrahim Treki[6], Rida Tauqir[2], Stan Van Uum[5], Robert Wilson[5], Michel Ovize[7]. [1]McMaster University, Canada. [2]Bone Research and Education Centre, Canada. [3]LMC, Canada. [4]University of Toronto, Canada. [5]Western University, Canada. [6]Windsor Regional Hospital, Canada. [7]Amolyt, Canada

Introduction: the CNHR registry was established in 2014 with the objectives of identifying the etiology, presentation, natural history and current treatment of hypoPT(1)Methods: 105 patients with hypoPT were included in this prospective study. Patients completed baseline assessments including 3 site bone mineral density (BMD), trabecular bone score (TBS), fracture risk assessments, and bone biomarkers. Baseline data is presented.Results:A total of 105 participants were enrolled, mean age was 51.9 years(Y) (SD=16.4), mean age of disease onset was 39.7 Y (SD=17.3), mean duration of disease 11.3 Y (SD=8.6), mean BMI kg/m2 was 28.9(SD=7.8), 17% (n=18) were male,(M) 83% (n=87) were female(F) of whom 54% (n=47/87) were premenopausal and 46% (40/87) were postmenopausal females (PMF). 71% (75/105) had postsurgical hypoPT. 29% (n=30/105) had non-surgical hypoPT. The mean total Hip BMD gm/cm2 (n=88) was 1.04(SD=0.20), L1-L4 BMD gm/cm2 (n=86) was 1.20(SD=0.22), FN BMD gm/cm2 was 0.98(SD=0.19), 1/3 radius BMD gm/cm2 (n=81) was 0.83 (SD=0.13), TBS score (n=69) 1.33(SD=0.14). 11% (12/105) had an osteoporotic T-score (T score<=-2.5) at any site, 25% (10/40) of the PMF had an osteoporotic T score at any site and 5% (2/47) of pre-menopausal F had an osteoporotic T score at any site. 14%

(12/87) of F had an osteoporotic T score at any site and 0% of M had an osteoporotic T score at any site. A total of 14% (15/105) had a prior fragility fracture, 30% (12/40) of PMF had a fragility fracture and 2% (1/47) of premenopausal F had a fragility fracture. 15% (13/87) of F had a fragility fracture and 11% (2/18) of M had a fragility fracture. 16% (17/105) of the total sample had an osteoporotic T-score at any site OR a prior fragility fracture, 35% (14/40) of PMF, 2% (1/47) of premenopausal F, 17% (n=15/87) of F and 11% of M(1/18) had an osteoporotic T-score at any site OR fragility fracture. 11% (2/18) M had osteopenia and 57% (23/40) PMF had osteopenia. The mean age at first fragility fracture was 63.1 years (SD=12.4). 23% (3/13) had a hip fracture, 23% (3/13) had a spine fracture, 8% (1/13) had a wrist fracture, 8% (1/13) had a humerus fracture, and 15% (2/13) had a rib fracture. Conclusion:The effects of hypoPT on bone strength are not fully understood at this time. (2) We observed a significant prevalence of osteopenia (57.5%) and osteoporosis in PMF who had co-existing hypoPT in whom 35% had osteoporosis by BMD criteria or a prior fragility fracture.

***Disclosures: Aliya Khan**, Amolyt, Grant/Research Support, Alexion, Grant/Research Support, Takeda, Grant/Research Support, Ascendis, Grant/Research Support*

LB SUN-593

Fracture risk among stroke survivors according to post-stroke disability and stroke type *Dagyeong Lee[1], Dong Wook Shin[1], In Young Cho[1]. [1]Department of Family Medicine/Supportive Care Center, Samsung Medical Center, Sungkyunkwan University School of Medicine, Republic of Korea

Background: Stroke survivors face physical and cognitive challenges, including impaired coordination and balance, which can lead to an increased dependency and a higher risk of falls. We aimed to investigate the impact of post-stroke disability status and stroke type on the risk of fracture of various site compared to the matched comparison group. Method: This retrospective cohort study used data from Korean National Health Insurance System (KNHIS) database (2010-2018) and included a total of 223,358 stroke patients and a 1:1 matched comparison group. Stroke survivors were grouped based on the severity of their post-stroke disability and stroke type (hemorrhagic vs. ischemic). The primary outcome was the incidence of newly diagnosed fracture. Cox proportional hazard regression analyses were used to calculate the hazard ratios (HR) of fractures after adjusting for potential confounders.Results: Stroke survivors had an increased risk of overall fractures compared to a matched comparison group (adjusted hazard ratio [aHR] 1.40, 95% confidence interval [CI] 1.37-1.43). This relative risk was particularly higher for hip fractures (aHR 2.42, 95% CI 2.30-2.55) compared to vertebral fractures (aHR 1.29, 95% CI 1.25-1.34) or other fractures (aHR 1.19, 95% CI 1.15-1.23). The risk of hip fractures was highest among stroke survivors with severe post-stroke disability (aHR 4.82, 95% CI 4.28-5.42), while the risk of vertebral or other fractures was highest among those with mild post-stroke disability. There was no significant difference in fracture risk between hemorrhagic and ischemic stroke survivors when stratified by disability status.Conclusion: Our findings showed an increased risk of subsequent fractures among stroke survivors, particularly those with post-stroke disability and for the hip fracture. Bone health assessment and treatment are warranted as an essential part of stroke management.

***Disclosures: Dagyeong Lee**, None*

LB SUN-594

Peripheral quantitative ultrasound measured bone mineral density is associated with age and menopause in midlife women with and without HIV *Ryan Ross[1], Niyati Patel[1], Elizabeth Daubert[2], Kathleen Weber[2]. [1]Rush University Medical Center, United States. [2]Hektoen Institute of Medicine, United States

An estimated 75% of people with osteoporosis are undiagnosed. Women with HIV (WWH) and socio-demographically similar women without HIV (WWoH) have a greater osteoporosis risk than the general population due to life circumstances including poor nutrition, low physical activity, high prevalence of smoking, alcohol, and substance abuse, co-morbidities, and use of high-risk medications. Therefore, effective point-of-care osteoporosis screening is critical to identify and treat osteoporosis early and reduce the burden of osteoporotic fractures.MACS/WIHS Combined Cohort Study (MWCCS) participants from the Chicago Cook County Clinical Research Site had bone mineral density (BMDUS Index) assessed at the non-dominant distal radius using an Ultrascan650 (CyberLogic) quantitative ultrasound (QUS) instrument. Clinical, socio-demographic and lifestyle factors were collected concurrently. Menopause status was dichotomized as pre vs. postmenopausal based on participant self-report of menstrual bleeding and final menstrual period >12 months. Differences in BMD and menopausal and HIV status were compared using t-tests. Pearson correlation was used to assess the association between continuous BMD and age. Linear regression was used to test the association of BMD with menopausal status, HIV serostatus, and age. All analyses were performed using SAS software.108 (69% WWH; 31% WWoH) had a valid BMDUS Index. Mean age was 55+/-8 years, 83% were menopausal, 80% were Black, 50% were current and 31% former cigarette smokers, and 11% were former injection drug users. Mean BMD was 0.59+/-0.09 g/cm2. 32 participants (30%) were osteoporotic, 42 (39%) osteopenic, and 34 (31%) were normal. Age was negatively associated with BMD (?=-0.035, p=0.011). Postmenopausal women had significantly lower BMD (0.64 vs. 0.58, p=0.013) and there was no significant effect of HIV. In multivariate models including both age and menopause, age was the primary driver of low BMD.We investigated the feasibility of using an FDA cleared portable, rapid, QUS-based instrument in a cohort of women at high risk. Consistent with DXA, BMDUS Index was lower in postmenopausal and older women. Age was a more significant predictor of BMD than menopausal status, which could be due to the relatively small number of premenopausal women (n=18/17%). The Ultrascan650 can be an effective, rapid point-of-care screening method for identifying women at risk for low bone mass with little participant burden or cost.

***Disclosures: Ryan Ross**, None*

LB SUN-595

Distinct defects in early innate and late adaptive immune responses typify impaired fracture healing in diet-induced obesity *Reyad Elbarbary[1], Deepak Kumar Khajuria[2], Irene Rider[3], Fadia Kamal[4], Christopher Norbury[3]. [1]The Pennsylvania State University , United States. [2]Pennsylvania State University, College of Medicine, United States. [3]Department of Microbiology and Immunology, The Pennsylvania State University College of Medicine, United States. [4]Penn State College of Medicine, United States

Most of bone fractures heal through three main phases: inflammatory, repair, and remodeling. Around 10% of fracture patients suffer from impaired healing that requires surgical intervention, a huge burden on the healthcare system. The rate of impaired healing increases with metabolic diseases such as obesity-associated hyperglycemia/type 2 diabetes (T2D), an increasing concern given the growing incidence of obesity/T2D. Immune cells play pivotal roles in fracture healing, and obesity/T2D is associated with defective immune-cell functions. However, there is a gap in knowledge regarding the stoichiometry of immune cells that populate the callus and how that population changes during different phases of healing. Here, we used flow cytometry, global RNA-seq, single-cell RNA-seq, immunofluorescence staining, and qPCR to characterize the repertoire of immune cells in the fracture callus and to identify populations specifically enriched in the fracture callus relative to the unfractured bone or bone marrow. Our analyses identified two waves of immune-cell infiltration into the callus: the first wave occurs during the early inflammatory phase, while the second takes place during the late repair/early remodeling phase. Innate immune cells were activated during the early inflammatory phase, but in later phases they returned to homeostatic numbers and activation levels. Of the innate immune cells, distinct subsets of activated dendritic cells were particularly enriched in the inflammatory healing hematoma. In contrast to innate cells, B and T cells were enriched and activated in the callus primarily during the late repair phase. The Diet-Induced Obesity (DIO) mouse, an established model of obesity-associated hyperglycemia and insulin resistance, suffers from multiple healing defects. Our data show that DIO mice exhibit dysregulated innate immune responses during the inflammatory phase, and clear defects in all lymphocyte compartments during the late repair phase, which was accompanied by substantially reduced bone formation. Further investigation of the adaptive immune cells identified specific enrichment of antigen experienced (CD44+) memory CD4+ T (TCD4+) cells in the callus of wild-type (WT) mice, which consisted primarily of effector memory (CD62L-, TEM) cells. DIO mice showed blunted TCD4+ response, and specific depletion of the TCD4+ cells in WT mice recapitulated the DIO healing phenotype and resulted in 50% reduction in bone formation. Our data characterized immune populations that are enriched/activated in the callus during two distinct phases of fracture healing. The data also identified, for the first time, defects in the healing-associated immune response in DIO mice, particularly the adaptive immune system, which will facilitate future development of immunomodulatory therapeutics for impaired fracture healing in obesity/T2D patients.

***Disclosures: Reyad Elbarbary**, None*

LB SUN-596

Role of Interleukin-4 in Osteogenic Differentiation of Dental Mesenchymal Cell *Hyewon Kim[1], Kyoung-Hwa Kim[2], Shin-Young Park[1]. [1]Department of Dental Science and Dental Research Institute, School of Dentistry, Seoul National University, Seoul, Korea, Republic of Korea. [2]Department of Periodontology, Dental Research Institute, School of Dentistry, Seoul National University, Seoul, Korea, Republic of Korea

Local cytokine networks, which have not yet been fully understood, control bone remodeling. Interleukin-4 (IL-4) is a pleiotropic cytokine that plays a major role in the modulation of T helper cells and mediates the regeneration of multiple tissues. This study aimed to create cells that stably express IL-4 using recombinant adeno-associated virus (AAV) and investigate its osteogenic differentiation capacity. The cDNAs of human IL-4 were cloned into AAV vectors of serotype 1, 2, 5, and 6. Rat dental pulp stem cells (rDPSCs) and human dental pulp stem cells (hDPSCs) were used. Gene transfer efficacy and the location of AAVs in cells after transduction were examined using AAV-ZsGreen1 vector. After the transduction, supernatants were collected at days 1, 3, 7, and 14. Supernatants IL-4 levels were assessed by using ELISA. Osteogenic differentiation was carried out with the IL-4 transduced cells, and their capacity was investigated by ALP staining, ARS staining, qPCR, and western blotting. AAV2-ZsGreen1 showed the highest level of gene transfer in all cell types of this study. The expression of IL-4 in rDPSC and hDPSC was high in the order of AAV2, AAV1, AAV6, and AAV5 groups. Expression of osteogenic differentiation markers, Runx2, Collagen 1, and ALP, was highest in the AAV2-IL-4 group, and ALP and ARS staining were also the darkest in the AAV2-IL-4 group. The osteogenic differentiation potential was shown to be the best in the AAV2 group. In addition, IL-4-transduced dental pulp stem cells

differentiated into osteogenic lineage via the extracellular signal-regulated kinase (ERK) signaling pathway. As a result, AAV vectors of serotype 2 showed the highest transduction efficiency in dental mesenchymal cells and the highest osteogenic differentiation potential. ERK signaling pathway play important roles in the regulation of IL-4-induced osteogenic differentiation. This study demonstrated that IL-4-transduced dental mesenchymal cells can be used in the clinical applications.

***Disclosures: Hyewon Kim**, None*

LB SUN-597

N?-(1-Carboxymethyl)-L-lysine drives cell metastasis and cancer stemness in osteosarcoma through RAGE-mediated NF-?B signaling *Ting-Yu Chang[1], Rong-Sen Yang[2], Shing-Hwa Liu[1]. [1]National Taiwan University, Taiwan, Province of China. [2]National Taiwan University Hospital, Taiwan, Province of China

N?-(1-Carboxymethyl)-L-lysine (CML), an advanced glycation end product (AGE), is believed to play a role in cancer progression. Recent studies have shown that CML promotes cancer cell growth and metastasis, however, the underlying mechanism remains unclear. Here, we found that CML and receptor of AGE (RAGE) were highly expressed in human osteosarcoma tissues with advanced stage using IHC staining (Figure 1A). The subcutaneous tumor growth and tumor weight were not affected under CML accumulation in mice induced with streptozotocin (STZ) in vivo (Figure 1B, C; n = 7/group). However, the number of nodules was significantly increased in STZ-treated mice compared to control mice in a tail-vein injection model of metastasis (Figure 1D; n = 6/group; p < 0.05). CML (25 and 50 ?M) treatment induced migration and invasion abilities (Figure 1E; n >= 3), as well as epithelial-mesenchymal transition (EMT) process in MG63 and U2OS cells. Additionally, treatment with CML in osteosarcoma cells increased the formation of tumor spheres and expression of cancer stem cell markers (Figure 1F, G; n >= 3). Pretreatment with a RAGE neutralizing antibody (5, 10 ?g/mL) blocked CML-induced cell migration/invasion, tumor sphere formation and cancer stem cell markers expression (Figure 1H-J; n >= 3). Furthermore, the activation of NF-?B was inhibited after administration of RAGE antibody (Figure 1K; n >= 3), indicating that CML promotes osteosarcoma cell migration, invasion, and stemness through the RAGE-mediated NF-?B pathway. Our study suggested that CML plays a significant role in promoting stemness and metastasis of osteosarcoma. These findings shed light on a potential link between CML/RAGE and osteosarcoma progression.

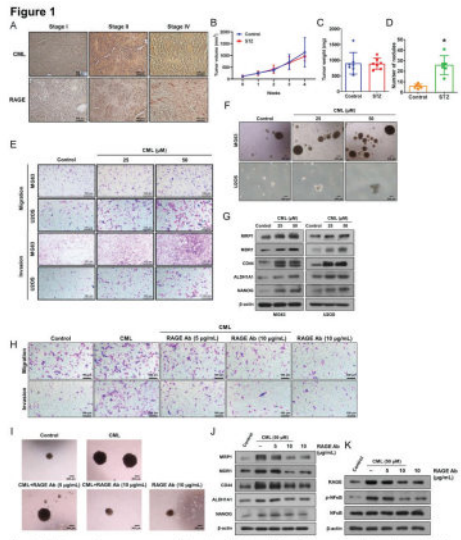

Figure 1. CML increases the cancer stemness and migration and invasion abilities of osteosarcoma cells by activating the RAGE-NF-κB signaling pathway. **(A)** CML and RAGE IHC staining in human osteosarcoma tissue microarray (n = 40) with different stages were shown. Scale bar, 100 μm. **(B, C)** MG63 cells were injected subcutaneously into the dorsal flanks of mice with or without prior treatment with STZ (n = 7 per group). The tumor growth was measured weekly, and the tumor weight was recorded after euthanizing. **(D)** MG63 cells were intravenously injected in mice with or without pretreatment with STZ. The metastatic tumor nodules in the lungs were examined and quantified. n = 6 per group. *, $P < 0.05$. **(E)** The images of migration/invasion were shown with CML (25 and 50 μM) treatment in MG63 and U2OS cells. Scale bar, 100 μm. **(F)** Self-renewal activity was determined by using the sphere formation assay in the presence or absence of CML treatment. **(G)** The protein expression of cancer stemness markers were determined in the indicated cells. **(H – J)** Blocking of RAGE using anti-RAGE antibody attenuates the CML-induced migration/invasion abilities and sphere formation. **(K)** The protein expression level of RAGE, p-NF-κB and NF-κB were examined with pretreatment with anti-RAGE antibody for 2 h in the presence or absence of CML (50 μM) treatment.

***Disclosures: Ting-Yu Chang**, None*

LB SUN-598

Phosphorylation of RXR ? at serine 265 is critical for the development of lung metastasis in the PYmT mouse model of breast cancer progression. *Jiarong Li[1], Richard Kremer[1]. [1]Research Institute of the McGill University Health Centre, Canada

Retinoid X receptor alpha(RXR ?) belongs to the nuclear receptor superfamily and acts as a transcription factor. RXR? forms heterodimers with other nuclear receptors, including the vitamin D receptor(VDR), the retinoic acid receptor (RAR), the PPAR gamma receptor and the thyroid hormone receptor (TR), to modulate gene transcription. Furthermore, RXR? can interact with other nuclear receptors, such as estrogen receptor (ER) and progesterone receptor (PR), to modulate the transcriptional activity of target genes involved in breast cancer progression. We previously showed that phosphorylation of serine 260 in the human RXR? leads to conformational changes and is critical for RXR? heterodimerization, translocation to the nucleus and transcriptional activity in a keratinocyte model of tumour progression(JCI1999;103(12):1729;JBC2008 ;283(8):4943JBC 2017 Jan 27;292(4):1490) .Here, we aimed to further investigate the significance of this critical amino acid phosphorylation site in vivo in a mouse model of breast tumor progression, the PYmT model. For this purpose, we used CRISPR/Cas-9 mediated genome engineering to create a FVB/Nj PYmT mouse model with serine(S)265alanine(A) point mutation in the mouse RXR? locus(the mouse amino acid equivalent of serine 260 in the human RXR ?) to prevent serine 265 phosphorylation. Cas9 mRNA and gRNA were generated by in vitro transcription and the point mutation S265A(TCA>GCA) donor oligo were co-injected into fertilized eggs for Knockin (KI) mouse production. At sacrifice the average tumor number/animal was 9.7 +/-0.2 (N=28) vs 9.67 +/-0.25 (N=24 P= 0.88) and and total tumour volume 6.85+/-0.33 cm3 vs 7.0 +/-0.23 cm3 (P=0.7) in control animals vs KI animals (). By Kaplan Meier analysis, average survival was 95 +/-1.2 days in control animals vs 92.6 +/-2.4 days in KI animals(P=0.3). In contrast, metastatic spread to lungs assessed by H & E staining at sacrifice showed that the number of metastatic lesions in KI animals more than doubled compared to controls(20 +/- 4.4 vs 8.6+/-2.2 ,P=0.028) .Signalling pathways linked to tumor progression and metastatic spread were then analyzed by real time PCR and immunofluorescence(IF) staining of breast tumors .A significant increase of AKT1 expression (2.78 fold change (FC), P= 0.012), estrogen receptor alpha (ER?)expression, (FC=8.6 ,P<0.001), CXCR4/SDF1 pathway expression(CXCR4 FC of 4.6 ,P<0.001 and SDF1 FC of 5.5, P<0.001), CD31(FC=3.7, P<0.001) as well as EMT markers mRNA expression(CDH1 FC=2.86, P=0.023, Vimentin FC=3.26 P<0.001, Zeb2 FC= 4.4 P<0.001 and snail FC= 4.2 P<0.001) were significantly increased in KI tumors compared to controls . IF staining confirmed these results.In summary, our results demonstrate that phosphorylation of the mouse RXR ? at serine 265 is critical for breast cancer metastatic spread independently of tumor growth. The underlying mechanism appears to involve ER expression, CXCR4/SDF1 and EMT.

***Disclosures: Jiarong Li**, None*

LB SUN-599

Low Intensity Vibration Alters Small-Chain Fatty Acid Metabolism in a Murine Model of Complete Estrogen Deprivation *Gabriel Pagnotti[1], Monte Willis[2], Trupti Trivedi[3], Sutha K John[4], Laura E. Wright[4], Yun She[4], Sreemala Murthy[4], William Thompson[4], clinton rubin[5], Khalid S. Mohammad[2], Theresa Guise[6]. [1]UT - MD Anderson Cancer Center, . [2]Indiana University School of Medicine, United States. [3]MD Anderson Cancer Center, University of Texas, United States. [4]Indiana University, United States. [5]State University of New York at Stony Brook, United States. [6]MD Anderson Cancer Center, United States

Aromatase inhibitors are highly effective to treat post-menopausal, breast cancer patients by suppressing estrogen (E2) synthesis. However, many adverse effects, such as bone loss, musculoskeletal pain and increased fat deposition, limit compliance. Mechanical stimuli, like those produced from exercise and physical activity, have known benefit for bone and muscle anabolism; yet practical considerations can limit patients' ability to perform the high energy loading exerted on weak skeletal tissue. This can result in fat accumulation and weakness. Low intensity vibration (LIV), a physiologically low-magnitude mechanical signal, has preserved bone in cancer models and suppressed adiposity in ovariectomized mice and diet-induced obesity. We hypothesized that LIV would deter excess fat while suppressing the production of harmful fatty-acid byproducts and improve musculoskeletal endpoints in E2-deprived mice. C57Bl/6 female mice (n=10/group) ovariectomized at 8w of age and given daily aromatase inhibitor letrozole were treated with LIV or mock-LIV (CTL) for 4w prior to and 24w post-surgery 1x/d, 5d/w for 24w. Body composition derived from DXA scans quantified lean and fat tissue indicating a 41% (p<0.001) slowing of fat gain with LIV treatment. In addition, LIV significantly increased lean mass (p<0.02) over the 28w-treatment period. Free-fatty acids were analyzed in serum using serum metabolomics analysis. Short-chain acylcarnitines (C2-C7), fatty acid metabolites implicated in insulin resistance and metabolic disease at abnormal concentrations, were increased after 24w of E2-deprivation compared to baseline. However, LIV-mice also had lower levels of C2-C7 compared to CTL-mice. Further, medium-chain (C8-C14) acylcarnitines increased (p<0.001) after 28w of E2-deprivation but did not lower in LIV-mice compared to CTL-mice. Marginal glucose intolerance, shown by a greater area under the curve (p=0.05), was observed in LIV-mice compared to CTLmice. In summary, acetylcarnitine (C2) and hexanoylcarnitine (C7) were identified as two novel biomarkers that, in addition to medium-chain species, increased with E2-deprivation-associated musculoskeletal defects, but which only C2 and C7 decreased with LIV. These data suggest that the impact of E2-deprivation on musculoskeletal tissue supports production of potentially harmful fatty-acids in cancer patients while also supporting the role of mechanical signals in protecting lean tissue mass while limiting the accrual of fat.

***Disclosures: Gabriel Pagnotti**, None*

LB SUN-600

Analysis of cartilage in Sox9 SUMOylation deficient mice *Megumi Iimori[1], Shizuka Yamamiya[1], Masafumi Inui[1]. [1]Laboratory of Animal Regeneration, Department of Life Sciences, School of Agriculture, Meiji University, Japan

Sox9 is a transcription factor essential for vertebrate chondrocyte differentiation. While Sox9 is known to be negatively regulated by SUMOylation in cultured cells, its in vivo role remains unclear. To address this, we generated mutant mice with a Sox9K396R mutation, where the SUMOylation target residue (lysine 396) is mutated to arginine. In these mice, the endochondral ossification process was delayed, and Sox9 target gene were upregulated in chondrocyte, indicating that Sox9 is also negatively regulated by SUMOylation in vivo. Next, we investigated the effect of this mutation on long bone development and homeostasis. Firstly, immunofluorescence analysis of embryonic long bones showed that the Col2a1-expressing chondrocyte region and the Col10a1-expressing hypertrophic chondrocyte region were wider in Sox9K396R mice compared to wild-type mice, suggesting a delay in the chondrocyte hypertrophy process. Secondly, the growth plate thickness of adult long bones were greater in 8-week-old Sox9K396R mice than in wild-type mice. However, this difference became smaller in 12 months of age, indicating a delayed growth plate closure in Sox9K396R mice. Furthermore, we investigated whether suppression of SUMOylation affects age-related degeneration of knee articular cartilage in Sox9K396R mice. We found that articular cartilage thickness was reduced in 8-week-old, 12-month-old, and 16-month-old medial femoral condyles in Sox9K396R mice compared to wild-type mice, suggesting an influence on articular cartilage thickness. At 8 weeks old, there was no difference in Safranin O staining while some wild-type articular cartilage showed reduced staining at 12 months old, whereas no reduction was observed in Sox9K396R mice. At 16 months old, Safranin O staining was reduced in both wild-type and Sox9 mutant mice. These results suggest that age-related cartilage degeneration may be partially suppressed in Sox9K396R mice by enhanced Sox9 function. In conclusion, this study demonstrates that Sox9 SUMOylation negatively regulates Sox9 function during both development and adult stages, which in turn may affect skeletal morphogenesis and cartilage homeostasis.

***Disclosures: Megumi Iimori**, None*

LB SUN-601

Bmp7 Controls Molecular And Mechanical Properties Of Articular Cartilage *Haiming Lin[1], Daniel Young[2], Lindsey Westover[3], Adetola Adesida[4], Antoine Dufour[2], Daniel Graf[1]. [1]School of Dentistry, University of Alberta, Canada. [2]University of Calgary, Canada. [3]Faculty of Engineering, University of Alberta, Canada. [4]Department of Surgery, University of Alberta, Canada

Introduction: Osteoarthritis (OA), the most common form of arthritis, is associated with cartilage degeneration. Bone morphogenetic protein 7 (Bmp7) levels are reduced in end stage human OA cartilage. Its deletion in mouse limbs leads to synovium inflammation and articular cartilage changes by 8 weeks, however, the joint appears histologically normal at 4 weeks. We recently discovered that loss of BMP7 in the nasal septum changes molecular properties of chondrocytes, predisposing to subsequent septum deviation and expression of molecular markers associated with OA. Here we tested if deletion of Bmp7 in limbs similarly leads to changes in chondrocyte properties that might be associated with subsequent cartilage degradation.Methods: To delete Bmp7 in the limbs, we created BMP7fl/fl:Prrx-Cre (mutant) mice. Knee cartilage from 4-/8-week-old mutant and control mice were collected and sent for quantitative shotgun proteomics. 8-week-old femur condyles were tested by a mechanical tester to measure stiffness. 8-week-old mice were run on a treadmill for 6 weeks. Knee joints were collected, processed histology and immunofluorescence.Results: Quantitative shotgun proteomics on control and mutant knee epiphyses followed pathway identification by using STRING shows that both femur and tibia cartilage showed significant molecular differences at 4 weeks. Amongst them were changes to extracellular matrix, protein translation, energy metabolism, and mechanotransduction. Differential expression of Col1, Fibrillin 1, Cox5a, ATP13A1, KIAA1199, RPL38, PDLIM7 were validated by immunofluorescence at both 4 and 8 weeks. Mutant cartilage was stiffer than control. After treadmill running, joints of mutants but not controls showed scattered hypertrophic chondrocytes and increased expression of ColX and MMP13.Conclusion: Our study establishes that loss of Bmp7 is associated with early molecular changes in chondrocytes before any histological changes to cartilage appearance are apparent. While mutant cartilage showed altered stiffness, OA-like changes became only apparent following strenuous exercise. BMP7 appears to maintain hyaline cartilage properties at an early stage and shows a protective effect from developing OA.

***Disclosures: Haiming Lin**, None*

LB SUN-602

Protein phosphatase SCP4 regulates cartilage development and endochondral osteogenesis via FoxO3a dephosphorylation *Kaiao Zou[1], Pinger Wang[2], Zhen Zou[2], Wenhua Yuan[2], Jiali Chen[2], Jianbo Xu[1], Hongfeng Ruan[1], Jianying Feng[3], Xia Lin[4], Hongting Jin[5]. [1]Institute of Orthopaedics and Traumatology, The First Affiliated Hospital of Zhejiang Chinese Medical University (Zhejiang Provincial Hospital of Chinese Medicine), Hangzhou, China. , China. [2]Institute of Orthopaedics and Traumatology, The First Affiliated Hospital of Zhejiang Chinese Medical University (Zhejiang Provincial Hospital of Chinese Medicine), Hangzhou, China., China. [3]School of Stomatology, Zhejiang Chinese Medical University, Hangzhou, China., China. [4]Michael E. DeBakey Department of Surgery, Baylor College of Medicine, Houston, Texas, USA., China. [5]Institute of Orthopaedics and Traumatology, The First Affiliated Hospital of Zhejiang Chinese Medical University, Hangzhou, China., China

Background: This study investigated the function of protein phosphatase SCP4 in cartilage development and endochondral osteogenesis. Methods: SCP4 knockout mice (SCP4-/-) and chondrocyte progenitor-specific knockout mice (SCP4Col2ER) were constructed and assessed for differences in bone formation using whole skeleton staining. ABH/OG staining was used to compare chondrocyte differentiation and cartilage development. Relevant pathways were analyzed using RNA-sequence and GO enrichment, further validated by immunohistochemical staining, Co-IP, and Western Blot.Results: SCP4-/- mice have a much smaller embryonic size than their littermates, this phenotype was even more pronounced in SCP4Col2ER mice. The number of chondrocytes in the growth plate was significantly reduced, the cells were irregularly arranged, increased in size, and accompanied by an increased number of vacuolated cells when compared with littermate controls. Signaling pathways and GO terms suggested that SCP4 may have contributed to this phenotype by regulating apoptosis in chondrocytes. Tunel-positive cells were increased dramatically in the growth plates of SCP4Col2ER mice, and the key pro-apoptotic proteins Caspase3/8/9 were remarkably up-regulated. The nuclear transcription factor FoxO3a has been reported to be a substrate for SCP4 dephosphorylation as well as a regulator of apoptosis. The expression of pFoxO3a was significantly upregulated in chondrocytes of SCP4Col2ER mice growth plate. In vitro, pFoxO3a and Caspase3/8/9 expression was enhanced in primary chondrocytes knocked down for SCP4. Furthermore, Co-IP and Western Blot demonstrated the dephosphorylation of FoxO3a by SCP4 in chondrocytes. Conclusions: Our results demonstrated that SCP4 has an important protective role during chondrogenesis and endochondral ossification, mediated through FoxO3a, resulting in normal skeletal formation during the embryonic period.

***Disclosures: Kaiao Zou**, None*

LB SUN-603

A novel mutation in the cysteine rich extracellular domain of the CaSR causing Familial Hypocalciuric Hypercalcemia *Naim Maalouf[1], Sarah Haroon[2]. [1]University of Texas Southwestern Medical Center, Dallas, United States. [2]UTSW, Department of Endocrinology and Mineral Metabolism, United States

A 46 yo male of Taiwanese origin was referred for evaluation and management of hypercalcemia. Hypercalcemia was first noted at age 41 years with initial labs demonstrating serum calcium of 12.0 mg/dL and a PTH reportedly in the normal range. Prior to referral to our clinic, he underwent parathyroidectomy on 2 separate occasions. Initial pre-operative localization studies were inconclusive, and he underwent neck exploration with excision of an enlarged right superior parathyroid gland. Following his first neck surgery, his serum calcium remained elevated. He underwent selective venous sampling of neck veins and a chest CT followed by excision of thymic tissue which was thought to contain parathyroid tissue on frozen section. The permanent section, however, revealed no evidence of parathyroid tissue. Due to persistent hypercalcemia he was referred to our clinic. He denied a history of kidney stones but did endorse polyuria, polydipsia, thirst and fatigue. He had a now 2-year-old son who was noted to be hypercalcemic without a concomitant PTH level during a hospital admission for diarrhea at the age of 8 months. No other family members had known hypercalcemia. He had normal cognition and his physical exam was unremarkable. Labs demonstrated a high Ca of 10.6-11.2 mg/dL, low phosphorus of 2.2 mg/dL and PTH of 34 pg/mL. His GFR was >60 mL/min. Magnesium was 1.8 and 2.6 mEq/L on different occasions (normal range 1.4-1.8 mEq/L). 24 hour urine calcium values were 143 and 198 mg/day with a Ca/Cr clearance ratio of 0.009 and 0.012, respectively. DXA showed T scores of -1.7 at lumbar spine, -1.3 at L hip, and +0.1 at the 1/3 radius. Due to findings of hypercalcemia, non-suppressed serum PTH, and relative hypocalciuria, familial hypocalciuric hypercalcemia (FHH) was suspected. He was referred for genetic testing which revealed a heterozygous variant c.1661T>A in exon 5 of the CASR gene, resulting in amino acid change 554 from isoleucine to asparagine (p.I554N). This novel base change was felt to represent a pathologic missense mutation in the CASR even though it has not been previously described, as substitutions at the adjacent amino acids (553 and 555) have been reported in association with FHH. The mutation is located in the cysteine-rich extracellular domain of the calcium sensing receptor.

***Disclosures: Naim Maalouf**, None*

LB SUN-604

Romosozumab Therapy in Adult Monogenetic Osteoporosis *Rodrigo Montero-Lopez[1], Alexandra Blaschitz[1], Katharina Tischlinger[1], Markus Klinger[2], Daniel Cejka[3], Wolfgang Högler[1]. [1]Department of Paediatrics and Adolescent Medicine, Johannes Kepler University Linz, Linz, Austria, Austria. [2]Institute of Nuclear Medicine, Kepler University Hospital, Linz, Austria, Austria. [3]Dept. of Internal Medicine III, Nephrology, Transplantation Medicine, Rheumatology, Geriatrics, Ordensklinikum Linz-Elisabethinen, Linz, Austria., Austria

BACKGROUND: Romosozumab (ROMO) is a monoclonal antibody targeting sclerostin, an inhibitor of the Wnt/ß-catenin pathway. Clinical trials show benefits for postmenopausal women or men over 50 years with osteoporosis. However, there have been no studies assessing the effect of ROMO on monogenetic osteoporosis. Here we describe the impact of ROMO in adult patients with WNT1 and COL1A1 mutations.METHODS: We conducted an analysis of two patients with monogenetic osteoporosis treated with ROMO (210mg s.c.), along with oral colecalciferol and calcium supplementation. Densitometry (Hologic Horizon; lumbar spine, femoral neck) and HRpQCT (Scanco XtremeCT-II; tibia 22.0mm, tibia 30%) were conducted before and after 12 months of treatment. HRpQCT results were compared with those of healthy controls (unpublished data).CASE 1: A 40-year-old Caucasian man presented with a history of long-bone fractures from moderate trauma since early childhood and multiple vertebral fractures. Whole Exome Sequencing identified a novel, heterozygous variant in WNT1 (c.761C>A). DXA-measured bone mineral density (BMD) was significantly reduced (LS-BMD T-score -6.8, FN-BMD T-score -4.1). Tibial trabecular volumetric BMD was very low (Tb.vBMD Z-score -4.1) with a cortical vBMD within normal range (Ct.vBMD Z-score +1.0). After one year of ROMO, aBMD had substantially increased (LS-BMD +41%, FN-BMD +24%). Volumetric BMD increased in trabecular compartment (Tb.vBMD +7.5%, Ct.vBMD -0.2%). No fractures or cardiovascular events were reported.CASE 2: A 50-year-old Caucasian woman was diagnosed in infancy with osteogenesis imperfecta type I with multiple long-bone and vertebral fractures. NGS Panel showed a novel heterozygous variant in COL1A1 (c.2334dup). Prior to starting ROMO she had reduced BMD (LS-BMD T-score -2.2, FN-BMD T-score -2.4). Tibial Tb.vBMD was low (Z-score -4.3), Ct.vBMD was within normal range (Z-score +0.0). After 12 months of ROMO, aBMD increased by 6-9% (LS-BMD T-score -1.5, FN-BMD T-score -2.0). Tb.vBMD increased substantially (+78.7%, Z-score -3.6) and Ct.vBMD decreased slightly by -3.1% (Z-score -0.4). Two radius fractures occurred 1 and 6 months after starting ROMO and no cardiovascular events were reported.DISCUSSION: ROMO treatment for 12 months substantially improved aBMD and vBMD, most notably in trabecular bone. Larger cohorts are required to confirm if ROMO may be an effective therapeutic option for monogenetic osteoporosis caused by WNT1 and COL1A1 mutations.

***Disclosures: Rodrigo Montero-Lopez**, None*

LB SUN-605

Multiple Vertebral Fractures (VFs) as the presenting manifestation of Amyloidosis and response to bisphosphonate (BP) therapy with long-term follow-up *Vijayalakshmi Donthireddy[1], Abeselom Geletu[1], Sudhaker Rao[2], David Willens[1]. [1]Henry Ford Health, United States. [2]Henry Ford Hospital, United States

Spontaneous VFs are a rare clinical presentation of amyloidosis, which commonly affects kidney, heart, liver, and bone marrow. Only 16 cases have been reported. Although BPs have been used in a few patients, long-term outcome with such therapy is unknown. We present a 52y old white woman who was otherwise healthy till April 2016 spontaneously developed upper and lower back pain. Imaging studies confirmed multiple VFs T3, T7, and T12 and underwent vertebroplasty. This was soon followed by additional VFs of L1 and L2 and had vertebroplasty again. Extensive evaluation including kidney biopsy confirmed primary amyloidosis. She received stem-cell transplant in 2017 with stable course since. Spine BMD T-score prior to VFs was -2.7 and femoral neck BMD was -1.5. Serum levels of Ca (total and ionized), PTH, 25OHD and 1,25-D were all normal. Weekly alendronate was started soon after the initial VFs in early 2017 until 2021, then switched to zoledronic acid (received 2 courses in 2021 and 2022) with 40-50% decline in CTX and osteocalcin in response to BP therapy. No new VFs or other fractures occurred since 2016 except the cascading VFx related to previous vertebroplasty. Her amyloidosis is now in remission.Serial CT scans before and after sustaining VFs and the most recent are shown in Figure. L1 and L2 VFs occurred soon after vertebroplasty of T12. Also, other thoracic VFs occurred after T3 and T7 vertebroplasty a few months later, a cascading VF phenomenon well described in patients with osteoporosis. But no new VFs or other fractures since July 2021.To the best our knowledge this is the longest BP treated patient with amyloidosis and VFs with no progression of VFs or other fractures. It is unclear if VFs were due to amyloid deposits within the vertebrae compromising bone quality or due to usual OP, although multiple VFs at this young age is very unusual. Also, it is unclear if the lack of progression of VFs or other fractures an expected response to BP therapy or remission of amyloidosis with stem cell transplantation. For now, we plan to continue BP therapy with close monitoring to avoid AFF. We contemplated anabolic therapy, but reluctant to consider because of potential for malignancy. Suggestions and experiences are welcome!

***Disclosures: Vijayalakshmi Donthireddy**, None*

LB SUN-606

Infigratinib Reduces Premature Bone Fusion at Sutures in a Mouse Model of Craniosynostosis *Greg Holmes[1], Susan M. Motch Perrine[2], Abdul Rashid Abdulai[1], Yuhan Hsi[2], Cecil S. Qiu[3], Morgan L. Paull[3], Bhavik P. Shah[3], Joan T. Richtsmeier[2], Ethylin Wang Jabs[1]. [1]Department of Genetics and Genomic Sciences, Icahn School of Medicine at Mount Sinai, United States. [2]Department of Anthropology, Pennsylvania State University, United States. [3]QED Therapeutics, Inc, United States

Purpose: Fibroblast growth factor (FGF) signaling is a key regulator of skeletal development. Gain-of-function receptor mutations of FGFR1, FGFR2, and FGFR3 result in a variety of craniosynostosis (CS) syndromes, in which suture fusion prevents normal skull development and leads to increased intracranial pressure, adversely affecting neurological development. Pharmacological antagonism of the FGFR signaling pathway is an attractive avenue for ameliorating the effects of activating FGFR mutations. Infigratinib is a selective FGFR1-3 tyrosine kinase inhibitor, and therefore may be an effective therapeutic agent for the amelioration of premature suture closure and other sequelae of FGFR activation. Infigratinib treatment improves long bone growth in mouse models of achondroplasia and of hypochondroplasia, and it is being evaluated in clinical trials for children with achondroplasia. To determine the efficacy of infigratinib in reducing the severity of suture fusion we used the Crouzon syndrome mouse model (Fgfr2cC342Y/+) that has progressive postnatal coronal suture fusion. Methods: Unaffected wildtype (WT) mice were treated with vehicle and Fgfr2cC342Y/+ littermates were treated with either vehicle, 0.5 mg/kg, or 2.0 mg/kg infigratinib by daily subcutaneous injection between postnatal days (P) 2 and 15 (n=10 per treatment group). After sacrifice on P16, skulls were scanned by microcomputed tomography (microCT). Scans were acquired using the 300 kv tube of a GE v|tome|x L300 nano/microCT scanner alongside a hydroxyapatite (HA) phantom with known densities. Results: MicroCT revealed a wide array of changes in the degree of suture fusion and skull shape in this model. The degree of suture fusion in Fgfr2cC342Y/+ mice treated with 2.0 mg/kg infigratinib was equivalent to that of WT littermates for the coronal, maxillary-palatine, and lateral occipital-squamous sutures as well as the presphenoid-sphenoid synchondrosis. Morphological analysis of the cranial vault and the mandible revealed that shape was most similar between specimens treated with 2.0 mg/kg infigratinib and WT littermates. Conclusions: Treatment with 2.0 mg/kg infigratinib reduced premature bone suture fusion in a mouse model of craniosynostosis, suggesting the potential to ameliorate intramembranous bone phenotypes in conditions like craniosynostosis.

***Disclosures: Greg Holmes**, QED Therapeutics, Inc, Grant/Research Support*

LB SUN-607

Sclerostin Antibody induces changes in Osteogenesis Imperfecta craniofacial bone *Hsiao Sung[1], Braden Terner[1], Hane Eun[1], Esmeralda Blaney Davidson[2], Kenneth Kozloff[1]. [1]University of Michigan, United States. [2]Radboud umc, Netherlands

Osteogenesis Imperfecta (OI) is characterized by low bone density and high bone fragility. Craniofacial and dentoalveolar abnormalities are present in all OI types. Currently, antiresorptive bisphosphonates are widely used to reduce bone fragility in OI. However, there are limitations to its use, such as the potential for osteonecrosis of the jaw, leading to the exploration of alternative anabolic approaches to the disease. Multiple studies have shown that the sclerostin antibody (SclAb) increases long bone mass and strength in OI models. However, little is known about its effect on craniofacial bone and teeth and whether

there is any variation in its effectiveness on endochondral and intramembranous-originated bone.3-week-old WT and Brtl/+ OI mice received subcutaneous SclAb (SclAb VI, Amgen, and UCB) treatment or vehicle injection (PBS) at 25 mg/kg, 2X/week, for five weeks. Skulls were scanned using high-resolution MicroCT (Skyscan 1176, Kontich, Belgium). Dragonfly 2.0 (ORS, Denver, USA) was used to delineate regions of interest and to perform measurements of the maxilla, mandible, temporomandibular joint (TMJ), and teeth. Statistical analysis was performed with two-way ANOVA, $p<0.05$ was considered significant. SclAb significantly increases the bone volume fraction in both WT (maxilla-79%, mandible-89.5%) and Brtl/+ (maxilla-67.8%, mandible-75.4%) (fig.1). These results are consistent with previous long bone and alveolar bone defect regeneration studies. SclAb also increases the bone thickness of TMJ articular tubercle and mandibular condyle neck in WT and Brtl/+ (0.35mm, 0.27mm versus control WT 0.34mm and control Brtl/+ 0.24mm) (fig.2). An increased TMJ thickness was previously observed in sost-/- mice. Brtl/+ mice have increased alveolar bone loss with a high presence of osteoclastic activity compared with treated Brtl/+. SclAb increases the dentin/tooth ratio (Fig.3), suggesting potential SclAb effects on odontoblasts. We did not observe any cementosis as reported in sost-/- mice. Importantly, SclAb impacts bone thickness but has minimal effects on the maxilla, mandible, and TMJ lengths, consistent with our previously reported cranial findings.In conclusion, SclAb increases craniofacial bone mass across multiple bone types in an OI mouse model, including dentin and condylar neck thickness. These SclAb-induced effects have potential clinical applications for jawbone and tooth regeneration for OI and other craniofacial bone disease patients.

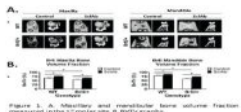

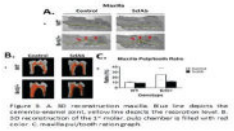

***Disclosures: Hsiao Sung**, None*

LB SUN-608

Unique chemical probes to assess Ghrelin proteolysis in plasma of men and women with obesity *Daniel Castrogiovanni[1], Tyler Lalonde[2], Leonard G. Luyt[3], Jean-Alain Fehrentz[4], Maria F Andreoli[5], Mario Perello[1], Nicolas De Francesco[1]. [1]IMBICE, UNLP, CONICET, CIC-PBA, Argentina. [2]Scintica Instrumentation Inc. , Canada. [3]University of Western Ontario , Canada. [4]IBMM, France. [5]IDIP and CONICET, Argentina

Since plasma ghrelin can undergo des-acylation and proteolysis, the aim of this work was to investigate the extent to which enhancement of these reactions is associated with the decrease of ghrelin in plasma after food intake or in individuals with obesity. Unique analogs of natural ghrelin were developed to monitor changes in plasma ghrelin levels. Levels of ghrelin, desacyl-ghrelin (DAG), glucose, insulin, ghrelin des-acylation, and ghrelin proteolysis were assessed in plasma before and after a test meal in 40 people (n=21 males) with normal weight (NW, n=20) or overweight/obesity (OW/OB, n=20). Preprandial ghrelin and DAG levels were lower, whereas preprandial ghrelin proteolysis was approximately 4.6-fold higher in the plasma of males that were OW/OB. Ghrelin proteolysis in males positively correlated with glycemia. Ghrelin and DAG levels were also lower in females with NW or OW/OB. Ghrelin and DAG levels decreased postprandially in males and females, independently of BMI, and ghrelin proteolysis increased postprandially approximately 2 folds only in individuals with NW. Ghrelin des-acylation remained unaffected by BMI or feeding status in both sexes. This current study highlights that ghrelin proteolysis increases in males with obesity as well as after a meal in lean individuals. Therefore ghrelin proteolysis may be an important checkpoint and, consequently, a putative pharmacological target to control circulating ghrelin levels in humans.

***Disclosures: Daniel Castrogiovanni**, None*

LB SUN-609

Effect of vitamin D supplementation on fracture healing: a randomized controlled trial in a paediatric population with hypovitaminosis D *Michael Bullen[1], Christine Rodda[2], Peter Pivonka[3]. [1]University of Melbourne, Western Health, Australia. [2]University of Melbourne, Australia. [3]Queensland University of Technology, Australia

Objective: The primary objective of this study was to assess the effect of vitamin D supplementation on fracture healing in a vitamin D deficient paediatric population.Methods: We performed a double blind, randomized placebo-controlled trial in participants aged 8 - 18 years who had sustained an acute distal radius fracture managed with cast immobilisation. Participants with a serum vitamin D level of 12.5 - 50 ng/mL were randomly allocated to a single oral dose of 150,000 international units of cholecalciferol or placebo. Follow-up was performed at two, six and twelve weeks post-injury. The primary outcome was peripheral quantitative computed tomography (pQCT) derived measures of fracture healing at six weeks post-injury. Secondary endpoints comprised clinical and plain radiograph fracture healing assessment, changes in bone mineral density (BMD) and cross-sectional area (CSA) in the uninjured limb, and dietary calcium intake.Results: A total of 28 participants (median age 12 y; 79 % male) were randomized, with complete primary outcome data for 23 (82 %). There was no difference in fracture callus trabecular density (coefficient 13.95; 95% confidence interval [CI], -23.45 to 51.35; p=0.44), cortical density (coefficient 0.96; 95% CI, 0.83 to 1.11; p=0.55), trabecular area (coefficient -24.5; 95% CI -59.2 to 10.11; p=0.15) or cortical area (coefficient 0.88; 95% CI 0.58 to 1.33; p=0.53) between the two groups. The strength-strain index was higher in the placebo group compared to the vitamin D group (coefficient 64; 95% CI 9.05 to 118.94; p=0.025). There was no difference in clinical or plain radiograph assessments of fracture healing, nor BMD & CSA of the uninjured limb, and dietary calcium intake between the two groups.Conclusions: Vitamin D3 supplementation did not improve fracture healing in a vitamin D deficient paediatric population, as measured by pQCT.

***Disclosures: Michael Bullen**, None*

LB SUN-610

Osteocalcin Improves Glucose Tolerance, Insulin Sensitivity and Secretion *Terry Dowd[1], Noorulain Paracha[1], Evan Kello[1], Paul Mastrokostas[1], Devorah Segall[1], Lawrence Mitelberg ?[1], Naif Hassan[1], Yosef Gedailovich[1], Alexis Rizzo[1]. [1]Brooklyn College, United States

Osteocalcin deficient mice (Ocn-/-), on a mixed 129/BL6J background, were reported to show glucose intolerance, reduced insulin sensitivity and insulin secretion at 1-6 mos of age. In contrast, two studies in Ocn-/- mice on different backgrounds (C3H/BL6 (5-6 mos.) and C57BL/6N (5 and 9 mos.)) found no effect on glucose metabolism. To determine the role of Ocn in glucose metabolism we conducted glucose tolerance tests (GTT), insulin tolerance tests (ITT) and glucose stimulated insulin secretion (GSIS) on 9.5 month-old male Ocn-/- and Ocn+/+ mice on a pure C57BL/6J background and fed a normal chow diet. Mice were fasted for 5 hours during the day with access to water for GTT and ITT. The GTT and ITT were separately conducted by an intraperitoneal injection of either glucose for GTT (2 g/kg BW) or insulin (0.5 U/kg BW) for ITT and measurement of blood glucose at 0, 15, 30, 60, 90 and 120 minutes post injection via a tail nick and glucometer. Blood glucose values vs. time were plotted as mean +/- SEM. Two-way repeated measure ANOVAs were used to assess significance for all tests. The GTT results for 20 male Ocn+/+ and Ocn-/- mice gave a significant main effect of osteocalcin ($p< 0.01$) with significantly ($p <= 0.05$) greater blood glucose for Ocn-/- at most time points. Insulin sensitivity (ITT) results for 19 Ocn+/+ and 28 Ocn-/- also showed a significant main effect of osteocalcin ($p <= 0.05$) with significantly increased blood glucose at several time points for Ocn-/- indicating insulin insensitivity. Insulin secretion (GSIS) was conducted after an overnight fast (12 hours) and an intraperitoneal injection of glucose (3 g/kg BW). Blood insulin concentrations were measured at time 0, 3, 8, 17 and 28 minutes post glucose injection using an insulin elisa assay. A significant main effect of osteocalcin ($p <= 0.05$) was shown with insulin significantly reduced in Ocn-/- at several time points. Our results confirm the role of Ocn in glucose metabolism and insulin sensitivity and demonstrate a role in insulin secretion in older male mice on a C57BL/6J background. The results may differ from previous reports due to differences in background, age, or experimental procedures which led to the discrepancies. Our data indicates a delayed onset of the effect of Ocn on glucose metabolism occurring at 9.-10 months in male C57BL/6J mice and highlights the importance of background on phenotype. These results may be relevant to the elderly since osteocalcin is reduced with age.

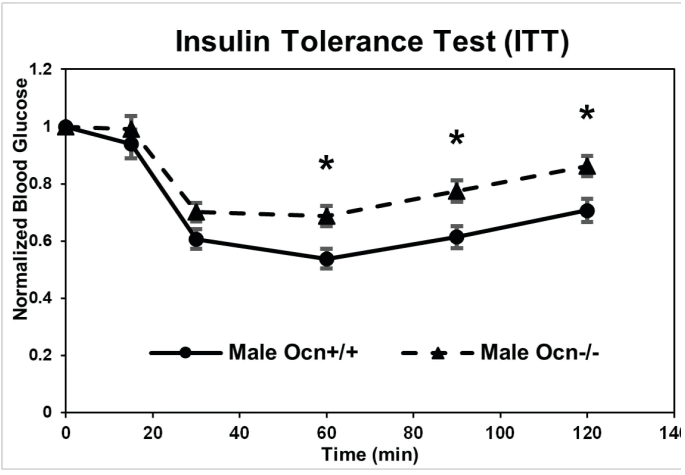

***Disclosures: Terry Dowd**, None*

LB SUN-611

AAV2-FGF18 Gene Therapy Protects Cartilage and Subchondral Bone in a Mechanically Induced Model of Osteoarthritis *Alex Goraltchouk[1], Judith Hollander[2], Jingshu Liu[3], Ellyn Xu[3], Frank Luppino[2], Li Zeng[3], Alexey Seregin[1]. [1]Remedium Bio, Inc., United States. [2]Remedium Bio, Inc, United States. [3]Department of Immunology, Tufts University, United States

Osteoarthritis (OA) is a debilitating degenerative pathology of cartilagenous joints affecting over half a billion people. Prevalence rates continue to grow, driven mainly by aging global population and increasing rates of obesity. To date, only the chondroanabolic treatment regimen of a series of intra-articular injections of Fibroblast Growth Factor 18 (FGF18) has demonstrated clinically meaningful efficacy in placebo-controlled human trials. We induced OA in adult male Sprague-Dawley rats using destabilization of the medial meniscus (DMM). Treatment included rhFGF18 (positive control), PBS (negative control), and 3 dose levels of AAV2-FGF18. Durability, redosability, and biodistribution were measured by quantifying nLuc bioluminescence. Transcriptomic analysis was performed by RNA-seq on primary human chondrocytes in culture and rat knee joints. Morphological analysis was performed on whole knee joints stained with Safranin O/Fast Green and anti-PRG antibody. Dose-dependent reductions in cartilage defect width and depth were observed following AAV2-FGF18 treatment. Defect width was reduced by up to 76% and cartilage thickness in the thinnest zone was increased by up to 106% relative to control. PBS-treated joints exhibited severe cartilage erosion, bone void formation, subchondral bone remodeling, and cases of near-complete subchondral bone collapse. In contrast, AAV2-FGF18-treated joints appeared significantly more anatomically normal, with only marginal cartilage erosion and regional glycosaminoglycan loss. While effective at reducing cartilage lesions, treatment with repeated rhFGF18 injections increased joint swelling and decreased PRG4 expression. In contrast to in vitro RNA-seq analysis, which showed a high degree of concordance between rhFGF18- and AAV2-FGF18-treated chondrocytes, in vivo transcriptomic analysis revealed few gene expression changes following protein treatment, suggesting transiency of effect. Conversely, gene therapy exhibited a high degree of localization and durability (>12 months) in both healthy and OA joints, upregulating several chondroanabolic genes while downregulating OA and fibrocartilage associated transcripts.Intra-articular FGF18 gene therapy treatment for OA can provide benefits to both subchondral bone and cartilage, with a high degree of durability and localization. In contrast to rhFGF18 protein injections, the gene therapy is not limited by pharmacokinetics and possesses superior safety and efficacy.

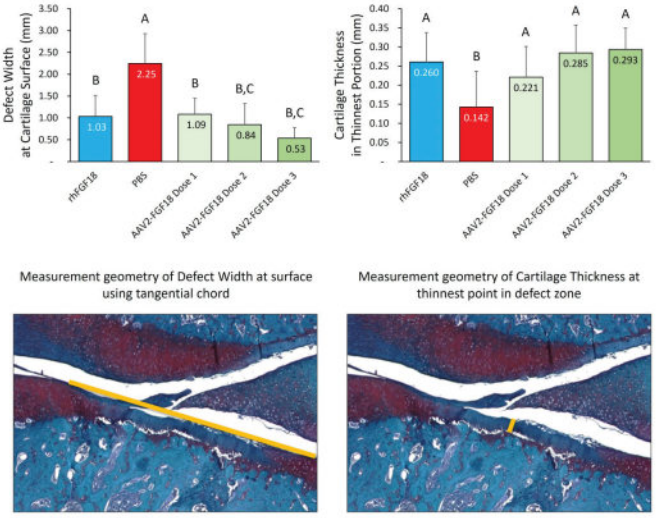

***Disclosures: Alex Goraltchouk**, Remedium Bio, Inc., Major Stock Shareholder*

LB SUN-612

Hierarchical surface roughness using a 3D-printed interbody implant promotes optimal bone formation and integration on Fluorescence image cytometry *Ali Kiapour[1], Xiaonan Xin[2], Elie Massaad[3], John Shin[3], David Rowe[4]. [1]Massachusetts General Hospital, Harvard Medical School, . [2]Department of Reconstructive Sciences, University of Connecticut, United States. [3]Department of Neurosurgery, Massachusetts General Hospital, Harvard Medical School, United States. [4]University of Connecticut Health Center, United States

INTRODUCTION: Novel 3D-printed titanium implantable devices with the surface roughness which is the by-product of the printing process can yield to better tissue-implant interaction and fusion as opposed to conventional PEEK or smooth titanium implants. This study aimed at comparing 3D-printed Ti (P3D) with smooth Ti (SmTi) and PEEK surfaces for their bone differentiation capability by utilizing transgenic bone marrow stem cells that fluoresce when osteogenesis is initiated. Also, gene expression was evaluated longitudinally with a comprehensive panel of bone-related genes that include a master transcriptional regulator of bone formation, and early-and late-stage markers for bone differentiation. METHODS: We evaluated mesenchymal stem cells obtained from the bone marrow of a transgenic mouse in which the expression of two genes critical for the proper mineralization of bone could be monitored fluorescently (Fig-1a). The P3D surface with hierarchical surface roughness (Fig-1b) was produced Electron-Beam Melting (EBM) 3D-Printing process. The surface characterization was done scanning electron microscopy. The SmTi and PEEK discs with matching sizes were also obtained. All samples were cleaned and sterilized before seeding.RESULTS: Significantly greater percentage of BMSC-derived progenitor cells were osteogenic on the P3D Ti surface at day 22 (Fig-1c, $p<0.05$) as compared to smooth Ti & PEEK. Approximately 86% of the stem cells were osteogenic on the P3D surface compared to less than 49% and 70% on the PEEK and SmTi surfaces, respectively. The magnitude of gene expression was substantially higher for most markers on the P3D surface (greatest at day 14) vs. PEEK or SmTi.DISCUSSION: The P3D-printed surface tested in the current study enabled a more rapid and robust bone formation. The P3D rough Ti surface enabled a significantly greater proportion of the BMSC-derived progenitor cells (vs. PEEK and SmTi) to enter the osteogenic lineage and resulted in significantly greater gene expression for a broad spectrum of bone-related molecules that includes a master regulator of bone differentiation, early bone markers and late bone markers associated with bony mineralization and osteocyte formation. Accelerated osteogenic differentiation indicative of osteocyte formation was observed at an early timepoint the P3D surface relative to the smooth surfaces as indicated by large and significant increases in the late bone markers of Blap and Phex.

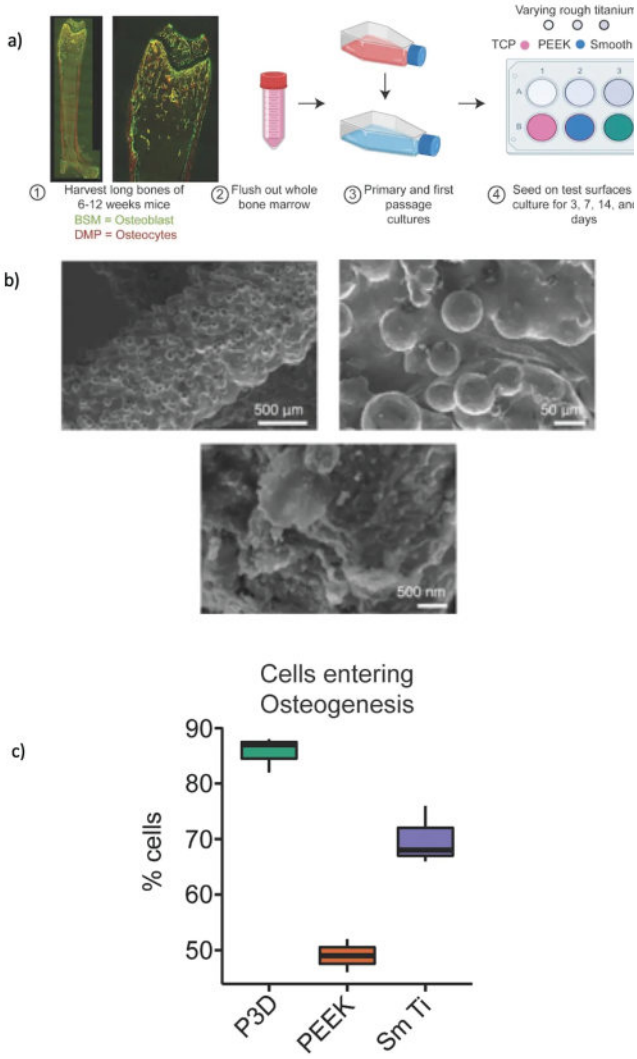

Figure 1: a) Experiment setup. b) Scanning Electron Microscopy of the P3D. c) Percentage of cells that entered osteogenesis at day 22.
surface at three different magnifications shows hierarchical surface roughness spanning from the macro to nanometer scale. A. 500 micrometer scale (macro). B. 50 micrometer scale. C 500 nanometer scale (nanometer scale).

***Disclosures: Ali Kiapour**, None*

LB SUN-613

Bibliometric analysis highlights lesser-studied pathways in bone remodeling
*Emily Davis[1], Jacob Snyder[1], Elicza Day[1], Gabriella Battiston[1], SIERRA STREET[2], Kyung Kang[1], Julia Hum[1], Jonathan Lowery[1]. [1]Marian University, United States, [2],

Osteoporosis (ie, low bone mass) is a common medical condition that places individuals at elevated risk of fracture and greater likelihood of disability, loss of independence, and death. Both anti-resorptive and anabolic medications are available and are generally successful at stabilizing and/or promoting gains in bone mass. However, each current medication has significant drawbacks which present considerable challenges for the long-term management of this chronic condition. Unfortunately, there are relatively few new candidate therapies in the drug development pipeline, which presents an urgent need to identify new treatment targets for increasing bone mass. However, a report from 2018 identified a striking lack of heterogeneity among molecular pathways studied in the bone remodeling field, with just three pathways (Wnt, Mitogen-activated protein (MAP) kinase, and the Transforming Growth Factor (TGF)-beta superfamily) accounting for more than 50% of publications and 46% of NIH-funded grants between 2008-2017. Further, adding Parathyroid Hormone (PTH), this list of four pathways accounts for nearly 55% of United States National Institutes of Health (NIH) grants funded during that period. In this study, we update the prior analysis to the time period of 2018-2022 to a) examine the heterogeneity of molecular pathways studied in the bone remodeling field in that time and b) determine if functional evidence exists for lesser-known pathways which might hold therapeutic potential. We used a combination of search terms in the PubMed and NIH RePORTER databases to detail the relative popularity of more than 144 pathways, with the RANK Ligand (RANKL) pathway having the greatest frequency of publications and grants (32.5% and 16.1%, respectively) from 2018-2022. For publications, RANKL is followed by TGF-beta superfamily (26.6%), MAP kinase (22.2%), Fos/Jun (22%), and Wnt (21.2%). Given that many of these publications overlap, we combined search terms to find that just these top five pathways account for 75.3% of publications in the bone remodeling field from 2018-2022. The popularity of just these top five pathways (by publication) in NIH-funded grants exceeds 48% of all grants awarded in the bone remodeling field from 2018-2022. Adding PTH to this list accounts for greater than 52% of NIH-funded bone remodeling grants in 2018-2022. This current lack of diversity in research may restrict discovery of novel therapeutic approaches. Our study highlights several pathways for which functional evidence supports a role in the regulation of osteoblasts and/or osteoclasts in vivo. Future work is required to determine therapeutic potential for these pathways intersect and we call for an expansion into lesser-studied pathways in order to broaden the collective focus of the field.

***Disclosures: Emily Davis**, None*

LB SUN-614

Synergistic effects of lysophosphatidic acid (LPA) and 1,25-dihydroxy vitamin D in osteocytes to promote the skeletal synthesis of fibroblast growth factor-23 (FGF23)
*Birol Ay[1], Sajin Marcus Cyr[2], YORIHIRO IWASAKI[3], Stefan Offermanns[4], Petra Simic[2], Murat Bastepe[5]. [1]Massachusetts General Hospital/Harvard Medical School, United States, [2]Endocrine Unit, Department of Medicine, Massachusetts General Hospital and Harvard Medical School, United States, [3]Massachusetts General Hospital, , [4]Department of Pharmacology, Max Planck Institute for Heart and Lung Research, Germany, [5]Massachusetts General Hospital, Harvard Medical School, United States

The synthesis of the bone-derived phosphaturic hormone fibroblast growth factor 23 (FGF23) is stimulated by lysophosphatidic acid (LPA) in response to kidney injury. Previous studies suggest that skeletal FGF23 production increases upon activating the heterotrimeric G?q/11 signaling pathway. Since LPA acts via multiple G proteins, including G?q/11, we hereby investigated the role of G?q/11 signaling in LPA-induced FGF23 synthesis. We also explored the cellular pathways downstream of LPA, using mice with conditional ablation of G?q and G?11 in osteocytes (G?q/11Dmp1KO). We also used osteocyte-like OCY454 cells, in which LPA was shown to stimulate FGF23 synthesis when administered with 1,25-dihydroxy vitamin D (1,25D). Serum total and intact FGF23 levels were mildly elevated in 2-month-old G?q/11Dmp1KO mice compared to control littermates (1.3-fold and 1.2-fold, respectively) at baseline. The levels rose in both controls (1.4-fold, p=0.0004 and 1.4-fold, p=0.0004, respectively) and G?q/11Dmp1KO littermates (1.5-fold, p=0.0001 and 1.5-fold, p=0.0001, respectively) 24 hours after intraperitoneal LPA (50 mg/kg) injection. In OCY454 cells, LPA/1,25D treatment led to a significant increase (5-fold, p=0.007) in FGF23 mRNA levels at 24 hours, but G?q/11 inhibitor YM254890 could not blunt this elevation. Whole transcriptome analysis identified a greater number of differentially expressed genes (DEG) after a 2 or 8 hour-treatment with LPA and 1,25D together (1157 and 657 DEGs) than LPA (306 and 475 DEGs) or 1,25D alone (12 and 140 DEGs), suggesting synergism between LPA and 1,25D. Several DEGs were unique or dramatically more expressed in the LPA/1,25D treatment group compared to the individual treatments, including MAPK signaling targets Dusp5 and Dusp6. Several cellular pathways unique to the combined LPA/1,25D treatment were also identified, including MAPK and NF-KB signaling. Accordingly, LPA/1,25D treatment led to ERK1/2 phosphorylation in OCY545 cells, and the LPA/1,25D-induced FGF23 synthesis was blocked by MEK1 inhibitor U0126. Our results indicate that LPA and 1,25D synergize in osteocytes to stimulate FGF23 production. The pathways mediating the effect of LPA/1,25D on FGF23 synthesis include MAPK and NF-KB signaling. These findings increase our knowledge of the mechanisms governing FGF23 synthesis and can lead to the discovery of new drug targets for treating FGF23-related disorders.

***Disclosures: Birol Ay**, None*

LB SUN-615

Overexpression of Nuclear Factor I-C (NFI-C) causes skeletal and growth defects in mouse.
*Dong-seol Lee[1], Joo-Cheol Park[2]. [1]School of Dentistry, Seoul National University, Republic of Korea, [2]Seoul National University, Republic of Korea

Nuclear factor I-C (NFI-C) transcription factors are crucial regulators of various organ development and stem cell biology. Among their family, Nfic knockout mice show malformation in all mineralized tissues, but it remains unclear which stage of development Nfic is involved. We previously reported that Nfic induces the differentiation of ameloblast, odontoblast, and osteoblast. However, the question remains whether Nfic participates in skeletal development. Here, we demonstrate that NFI-C gain of function confirmed NFI-C did not cause abnormalities in skeletal formation during the fetal period but caused abnormalities in skeletal formation after birth. This study aimed to investigate the effect of the NFI-C gene, one of the factors regulating cartilage and bone development, on skeletal dysplasia during development. First, we constructed NFI-C-overexpressing transgenic mice using the prix1 promoter. It was observed that the mice overexpressed with the NFI-C gene at 5 days and 6 weeks were smaller than normal mice. In addition, the NFIC overexpressing mice showed short fingers or toes, especially the fourth and fifth fingers were short or underdeveloped, like Feingold's syndrome. It was also confirmed that mesenchymal-specific overexpression of NFI-C caused problems in limb development and calvarial bone formation, but ossification of the femur increased compared to wild-type mice. In addition, We investigated whether the expression levels of markers of bone and cartilage were altered in the Nfic-overexpressing mice at P1. The gene expression of Mycn-1, Sox6, TGF-?1, Fgf1, Fgf2, and FGFR2 was decreased in Nfic-overexpressing mice, whereas the expression of Sox9, Sox5, mir19 and mir92 was not altered. Therefore, it is thought that if the expression of the NFI-C gene can be appropriately controlled, it could be helpful to regenerate bone and cartilage damaged by various causes, including skeletal genetic diseases and osteoporosis. This work was supported by Basic Science Research Program through the Ministry of Education of the Republic of Korea and National Research Foundation (Grant No. No. NRF-2021R1A2C1095165).

***Disclosures: Dong-seol Lee**, None*

LB SUN-616

A mechanosensor protein, Filamin A, mediated embryonic palate fusion through ?-catenin/Smad2: A bioinformatics-oriented study
*Ziyi Wang[1], Satoru Hayano[2], Yao Weng[3], Xindi Mu[3], Mitsuaki Ono[3], Toshi Oohashi[3], Hiroshi Kamioka[4]. [1]Okayama university, Japan, [2]Department of Orthodontics, Okayama University Hospital, Japan, [3]Department of Molecular Biology and Biochemistry, Okayama University Graduate School of Medicine, Dentistry and Pharmaceutical Sciences, Japan, [4]Okayama University Graduate School of Medicine, Dentistry, and Pharmaceutical Sc, Japan

This study aimed to elucidate the key mechanisms and genes associated with cleft palate through a comprehensive bioinformatics analysis. By re-analyzing bulk RNA-seq data (GSE45568 and GSE185279) and conducting literature mining, we identified Filamin A (Flna) as a pivotal gene and Epithelial-Mesenchymal Transition (EMT) as a significant biological event in cleft palate development. Immunofluorescence analysis of in vivo embryonic palates revealed increased Flna expression in medial edge epithelial (MEE) cells and EMT cells within the epithelial triangle. In ex vivo cultured palates, various experimental interventions such as mechanical stimuli, a TGF-? inhibitor, and a RhoA inhibitor resulted in significant alterations in Flna expression. Flna, as a mechanosensor, is increased in response to mechanical stimuli on the ex vivo cultured embryonic palate. Through re-analysis of single-cell RNA-seq data (GSE155928), we newly identified an EMT cell cluster and observed a significant correlation between the expression of Flna and Ctnnb1. In the ex vivo cultured embryonic palate, the knock-down of Flna disrupted the palate fusion. Knockdown of Flna in both ex vivo cultured palates and HaCaT cells led to substantial changes in Ctnnb1/Smad2 expression. Additionally, our study consistently observed a correlation between Flna expression and MEE cell morphology in both in vivo and ex vivo cultured palates across all experimental conditions. These findings suggested that Flna may play a critical role in palate fusion by connecting mechanotransduction and the Wnt/TGF-?/Smad signaling pathways.

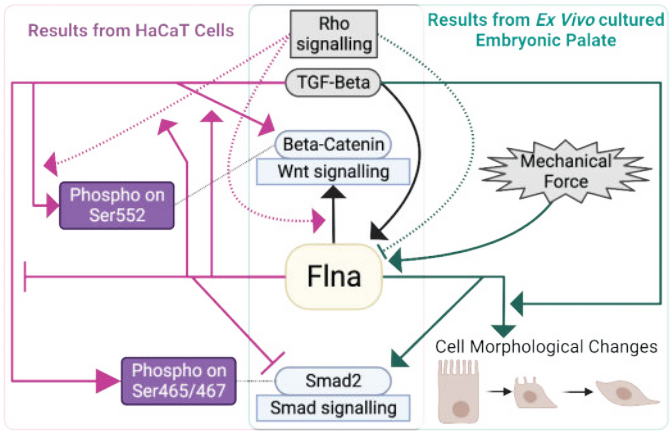

***Disclosures: Ziyi Wang**, None*

LB SUN-617

Collagen XII regulates cell migration required for regeneration and repair after Achilles tendon injury. *Yayoi Izu[1], kei Fujihara[1], Taiju Yoneda[1]. [1]Okayama University of Science, Japan

Achilles tendon injuries are common in athletes and the elderly. Because regeneration and repair of tendon is difficult due to poor vascularization and highly organized structure, resulting in clinical problems of re-tears and dysfunction after surgical reconstruction. Tendon regeneration and repair requires migration of tendon stem/ progenitor cells (TSPCs) at the site of injury. We previously demonstrated that collagen XII provides physical binding between adjacent tenocytes, thereby regulating tendon development and maintenance (Izu et al. Matrix Biol. 95:52-67. 2021). Here, we elucidate the role of collagen XII during tendon repair and regeneration by using Col12a1 null mice. Neonatal and adult mice are used as regeneration and repair models, respectively. The gait and the angle of plantar to floor analysis revealed that these were restored in wild-type mice by 2 weeks after injury, whereas Col12a1 deficient mice did not recover even 4 weeks after injury in regeneration model. Similarly, wild type repair model also showed not fully but functionally recover by 4 weeks after injury, whereas no recovery symptoms were observed in Col12a1 deficient mice. Histological analysis demonstrated an inflammatory response 3 days after injury in both genotype in regeneration model. By 2 weeks after injury, fiber like structure was found at the transection sites in wild type but not in Col12a1 deficient mice. To elucidate the cell migration ability of Col12a1 deficient cells, a wound healing assay was performed using primary tenocytes derived from neonatal FDL tendons. The results showed that the number of migratory cells were reduced in Col12a1 deficient compared to the wild type. Interestingly, the wild type tenocytes migrated toward the wounded sites, whereas Col12a1 deficient tenocytes migrated in disorganized fashion and lost directionality. Furthermore, the response to chemotaxis was analyzed by a transwell assay using TGF-b1, no genotype specific difference was observed. Collectively, our results suggest that collagen XII is involved in regulatory mechanisms of migration in TSPCs, tenocytes, and scar-forming fibroblasts in regeneration and repair. The function of collagen XII in cell-cell binding via matrix bridge formation suggests that this may be a novel mechanism for cell migration and/or guidance in tissue development and regeneration.

***Disclosures: Yayoi Izu**, None*

LB SUN-618

Unraveling the Cellular Activators of Osteoclastic Bone Resorption - The Key Role of Bone Surface Osteoprogenitors *Bilal M. El-Masri[1], Christina M. Andreasen[1], Xenia G. Borggaard[1], Viktoria B. Kofod[1], Malene H. Nielsen[1], Kaja S. Laursen[2], Jesper S. Thomsen[3], Anne Marie Brüel[3], Mads S. Sørensen[4], Lars J. Hansen[4], Michelle Macdonald[5], Julia F. Charles[6], Jean-Marie Delaisse[1], Thomas L. Andersen[1]. [1]Dept. of Clinical Research, University of Southern Denmark, Denmark, [2]Dept. of Forensic Medicine, Aarhus University, Denmark, [3]Dept. of Biomedicine, Aarhus University, Denmark, [4]Dept. of Otorhinolaryngology - Head and Neck Surgery and Audiology, Rigshospitalet, Denmark, [5]Healthy Ageing Theme, Garvan Institute of Medical Research, Australia, [6]Dept. of Orthopaedic Surgery, Brigham and Women's Hospital, Harvard Medical School, United States

The activation of osteoclastic bone resorption and its cellular orchestrators remain poorly characterized. We utilized highly sensitive in situ hybridization on human bone samples and rodent models as a direct approach to identify spatially the key cells that orchestrate the activation of osteoclastic bone resorption through the RANKL/OPG-pathway across skeletal sites, and during anti-RANKL treatment.The study demonstrates that RANKL is expressed mainly by bone surface osteoprogenitors (bone lining cells, reversal cells or canopy cells) and much less by osteocytes proximate to osteoclasts in human (3% vs 30%), rat, and mouse bone. Conversely OPG is expressed mainly by osteocytes and less by bone surface osteoprogenitors. The RANKL+ bone surface osteoprogenitor populations which proximate to osteoclasts also express MMP13, RUNX2, and DMP1 in humans and mice, and CD56, CD271 and PTHR1 in humans.As these osteoprogenitors, not osteocytes, are the most abundant Rankl+ Dmp1+ population in mice, we selectively knocked out Rankl in Dmp1+ cells using Dmp1-cre;Rankl-fl/fl mice. We validated that Cre was expressed by bone surface cells in these mice. μCT analysis of the distal femoral metaphysis revealed a significantly higher trabecular bone volume in 15-week-old male and female Cre+ compared to Cre- mice. RNA-based histomorphometry revealed a significant reduction in Col1a1high osteoblast surfaces in Cre+ compared to Cre- mice but surprisingly no change in Acp5+ osteoclast surfaces.In 7-week-old healthy female mice treated with OPG:Fc for 2 weeks, Rankl+ bone surface cells remained abundant, even though no Acp5+ osteoclasts were present. Interestingly, both the bone surface cells and osteocytes had a significantly increased Rankl/Opg expression ratio in OPG:Fc treated mice compared to vehicle, which may explain the rebound following anti-RANKL treatment discontinuation. On the other hand, at skeletal sites with an extremely high endogenous expression of Opg by fibrocytes, like the temporal bone of the inner ear of rats, we observed nearly no Rankl+ bone surface cells or osteocytes. This supports the concept of local regulation of RANKL expression by bone surface cells.Collectively, this study supports the concept that bone surface osteoprogenitors activate bone-resorbing osteoclasts through RANKL signaling in response to local (osteocytic) and systemic (e.g. PTH) signals and that they contribute to the rebound following anti-RANKL treatment discontinuation.

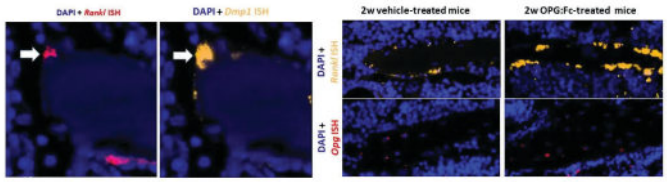

***Disclosures: Bilal M. El-Masri**, None*

LB SUN-619

Identification of metaphyseal Nestin-GFPbright stromal cells as a skeletal stem cell subpopulation in growing trabecular bone *Shinichirou Ito[1], Toshihide Mizoguchi[1], Masataka Kasahara[2]. [1]Tokyo Dental College, Japan, [2]Tokyo Dental College, Department of Pharmacology, Japan

‹Objective›Two distinct types of Nestin (Nes)-GFP+ stromal cells in the bone marrow (BM) can be detected based on their GFP expression levels (Nature 502(7473):637, 2013). Nes-GFPdim cells are observed throughout BM and overlap with leptin receptor (LepR)+ skeletal stem cells (SSCs). In contrast, Nes-GFPbright cells localize to peri-arterial niches and the metaphysis, and arterial Nes-GFPbright cells are considered a hematopoietic stem cell niche. However, the skeletal role of the metaphyseal Nes-GFPbright (hereafter Met-Nes-GFPbright) cell population remains elusive. Herein, using a Cre/LoxP-based strategy, we assessed the fate of Met-Nes-GFPbright cells during bone growth.‹Methods and Results›To examine the relationship between Met-Nes-GFPbright cells and LepR+ SSCs, we analyzed bone tissue of LepR-creER;Rosa26-loxP-stop-loxP-tdTomato(R26-Tom);Nes-GFP mice labeled on postnatal day 14 (P14). After 48-h labeling, some LepR-creER-labeled cells were observed to overlap with Met-Nes-GFPbright cells, indicating that Met-Nes-GFPbright cells are a subpopulation of LepR+ SSCs. As induced Cre expression in Nes-creER mice was detectable only in Met-Nes-GFPbright cells, and not in Nes-GFPdim cells, this mouse line was applied for lineage-tracing analysis of Nes-creER/Tom cells labeled on P1. Significant increases in the absolute number of Nes-creER/Tom cells was observed by P9; however, most were lost by P57. We further examined the appearance of Nes-creER/Tom cells according to the growth stage of bone tissues, and found that the absolute number of these cells increased up to P14 labeling, and became almost undetectable at P56 labeling. To examine the role of Nes-creER/Tom cells, these cells were depleted using Nes-creER;R26-Tom;R26-diphteria toxin A (DTA) mice during bone growth (P6 to P12) and analyzed on P14. Micro-CT showed that the trabecular bone volume was significantly decreased by cell depletion. These results prompted us to investigate the potential of Nes-creER/Tom cells to differentiate into osteoblasts using Nes-creER;R26-Tom;type I collagen (Col1)(2.3 kb)-GFP mice. Lineage-tracing analysis revealed that Nes-creER/Tom cells labeled on P14 significantly contributed to Col1 (2.3 kb)-GFP+ mature osteoblasts after a 1-week chase.‹Conclusion›Based on the findings, Met-Nes-GFPbright cells are a subpopulation of skeletal stem cells that transiently contribute to trabecular bone growth via osteoblastic differentiation.

***Disclosures: Shinichirou Ito**, None*

LB SUN-620

The Interrelationship of Supplemental Vitamin D and Vitamin K Status on Incident Fractures: Results from the VITamin D and OmegA-3 TriaL (VITAL) *Sharon Chou[1], Sarah Booth[2], Dana Ratnarajah[1], Nancy Cook[1], Gregory Kotler[1], Xueyan Fu[2], Julie Buring[1], JoAnn Manson[1], Meryl LeBoff[1]. [1]Brigham and Women's Hospital , United States. [2]Tufts University, United States

Vitamin D and vitamin K are both involved in bone metabolism. We recently reported in the VITamin D and OmegA-3 TriaL (VITAL) that daily supplemental vitamin D (2000 IU/d) vs. placebo did not reduce fracture risk in 25,871 U.S. men (aged >=50) and women (aged >=55) enrolled from 50 states.1 While vitamin D stimulates transcription and translation of osteocalcin (OC) and matrix Gla protein (MGP), vitamin K is needed to carboxylate and activate these proteins. Older adults have low vitamin K intakes, and it has been proposed that vitamin D effectiveness on bone health is attenuated by low vitamin K status. Currently, there are limited data on the interaction of vitamin D and vitamin K statuses and effects of supplemental vitamin D on fracture risk. In this VITAL ancillary study, we tested in a case-cohort sample of 1,162 participants with fractures and an age-sex-matched subcohort size of 2,652, whether baseline low vitamin K status modifies the effects of supplemental vitamin D on incident total, non-vertebral, and hip fractures. The mean (+/-SD) age of participants was 68.3+/-7.2 years and the mean BMI was 27.3+/-5.3 kg/m2. 60.6% of the case-cohort participants were female and 81.2% were Non-Hispanic White. Fractures were reported on annual questionnaires and adjudicated through medical record review. To assess vitamin K function, percent undercarboxylated osteocalcin (%ucOC) and dephosphorylated undercarboxylated MGP ([dp]ucMGP) were measured in fasting baseline blood samples. High levels of %ucOC and (dp)ucMGP indicate low vitamin K status. %ucOC was calculated from measures of ucOC and total OC. The ucOC, total OC and (dp)ucMGP, were measured by sandwich ELISAs (IDS-iSYS Multi-Discipline Automated System). The effects of supplemental vitamin D on total, nonvertebral, and hip fractures were not modified by baseline levels (above or below the median) of %ucOC and (dp)ucMGP (Table 1; hip fractures not shown due to low power). In the largest randomized controlled trial of supplemental vitamin D vs. placebo on fractures, low vitamin K status does not explain the lack of effect of vitamin D supplementation on fracture prevention. Ongoing analyses are examining whether low baseline vitamin K status in combination with low baseline vitamin D levels are associated with increased incident total, non-vertebral, and hip fractures in VITAL.1. LeBoff MS, et al. NEJM 2022

Table 1. Effects of vitamin D supplementation vs. placebo on fractures, stratified by vitamin K status

		Total Fractures						Nonvertebral Fractures					
Subgroup		Vitamin D		Placebo				Vitamin D		Placebo			
Parameter	Strata	N tot.	N event	N tot.	N event	HR (95% CI)	p for interaction	N tot.	N event	N tot.	N event	HR (95% CI)	p for interaction
[dp]ucMGP	<median	954	344	963	357	0.90 (0.74-1.10)	0.356	954	315	963	341	0.86 (0.71-1.05)	0.211
	>median	832	225	840	231	1.03 (0.82-1.31)		832	217	840	220	1.04 (0.82-1.32)	
%ucOC	<median	833	250	893	288	0.91 (0.73-1.13)	0.366	833	231	893	276	0.88 (0.70-1.10)	0.301
	>median	896	295	857	270	1.05 (0.85-1.30)		896	278	857	256	1.04 (0.83-1.29)	

***Disclosures: Sharon Chou**, None*

LB SUN-621

Correlation between 25OHD and age, body weight, BMI and season of the year in supplemented and not supplemented women *Jose L Mansur[1], María J Castro[2]. [1]Center of Endoc and Osteoporosis La Plata Argentina, Argentina. [2]Dept FisicoMatem, Fac Farmacia y Bioq, Univ Buenos Aires, Argentina

The 25OHD value of the population depends on several factors.Our objective was to analyze 25OHD levels in women and the relation between 25OHD with age, BMI, weight and season.Patients and methods: retrospective study of 25OHD in 730 women (528 without supplementation (not suppl) and 202 with supplementation (suppl) of 100.000 IU/month for more than 3 months). Data are shown as media +/- standard deviation, Spearman Rank Correation coefficient, Student Test, ANOVA with post hoc Tuket test, Test chi PearsonResultsNot suppl: Age: 52.8+/-14.6. BMI: 26.6+/-6.0 Weight: 68.6+/-16.1; 25OHD: 21.7+/-8.4Suppl Age: 63.4+/-11.3 BMI: 25.7+/-5.3 Weight:63.7+/-13.5; 25OHD: 44.5+/-10Suppl women were older (p<0,0001), and have less BMI (p=0.0113) and weight (p<0.0001)1. Age and 25OHNot Suppl: 65: 20.98+/-9.0Suppl 65: 45.6+/-11.7Younger women have less 25OHD in suppl.2. 25OHD and BMINot Suppl: 30: 18.2+/-7.5Suppl 30: 40.8+/-9.8Obese women have less 25OHD (not suppl and suppl)3. 25OHD in each season:Not Suppl: Winter: 18.1+/-6; Spring: 21.6+/-8; Summer: 26.6+/-9; Fall 24.1+/-9Suppl Winter: 43.9+/-10; Spring: 44.7+/-9; Summer: 49.1+/-11; Fall 43.2+/-13In not suppl winter is less than the other seasons, and spring is less than summer (Anova p<0.001). In suppl no diference.4. Association between 25OHD and BMI and WeightNot Suppl: BMI: p<0.0001 # Weight: p<0.0001 #Suppl: BMI: p=0.0135 # Weight: p<0.0001 #5. Association between 25OHD and BMI and Weight in each season:In not supplemented women 25OHD is associated with BMI and weight in Winter, Spring and Summer. In supplemented women 25OHD is associated with BMI and weight only in Winter.Discussion: We found that BMI and body weight have negative correlation with 25OHD in suppl and not suppl women. It is possible that body weight correlates better than BMI because the amount of body fat would be more important than BMI. In summer values are higher but with a mean lower than 30 ng/mL. Obese women have less 25OHD. The combination of obesity and winter has more risk of lower 25OHD. Younger women has less 25OHD in suppl women.We think that seems necessary detailing always the season of the year and whether it is obese or non-obese people in all the studies about 25OHD.

***Disclosures: Jose L Mansur**, None*

LB SUN-622

Comparative miRNA Profiling Reveals Differential Expression Patterns between SWR/J and TallyHo/JngJ Mouse Models *DAVID CARRO VAZQUEZ[1], Lejla Emini[2], Martina Rauner[3], Johannes Grillari[4], Lorenz Hofbauer[5], Matthias Hackl[6]. [1], Austria. [2]bone lab dresden, Germany. [3]Medical Faculty of the TU Dresden, Germany. [4]Ludwig Boltzmann Institute for Experimental and Clinical Traumatology, Austria. [5]TU Dresden University Medical Center, Germany. [6]TAMIRNA, Austria

Type 2 diabetes mellitus (T2DM) increases the susceptibility to bone fragility. We hypothesize that microRNAs could be involved in the underlying mechanism and be used as biomarkers for diagnosis of diabetic bone disease. To test this hypothesis, we aimed to detect dysregulated miRNAs using the polygenic murine model TallyHo/JngJ (TH), that recapitulates adolescent-onset T2DM in humans, as well as the recommended control SWR/J and a strain-matched non-diabetic control (TH-ND). RNA isolation and small RNA next generation sequencing (NGS) were performed for untargeted genome-wide miRNA analysis in serum, bone marrow and femora bone samples from all three groups. Metabolic and bone phenotype parameters were also determined in all animals. Significantly (Benjamini-Hochberg adjusted p<0.2) regulated miRNAs were further analyzed with miRnet 2.0 for miRNA~mRNA target network construction and with the FANTOM5 browser for their cell-type enrichment to identify putative donor cells. TH and TH-ND mice showed no differential bone phenotype and miRNA regulation. When comparing TH-ND with SWR/J mice, mmu-miR-351-5p and mmu-miR-322-3p appeared to be upregulated while mmu-miR-449a-5p and mmu-miR-6240 were downregulated in both bone marrow and serum. mmu-miR-6240 was downregulated while mmu-miR-1a-3p was upregulated in both femur tissue and serum. mmu-miR-196b-5p was downregulated in femur and upregulated in serum. Finally, mmu-miR-677-3p appeared to be downregulated in both bone marrow and femur. miRnet 2.0 analysis using these miRNAs revealed target genes such as Myc, Bcl2 and Gab1 which play roles in insulin secretion and Wnt, Ca2+ and Hippo signaling. FANTOM5 analysis showed that three of these miRNAs, hsa-miR-424-3p (homolog to mmu-322-3p), hsa-miR-1-3p and hsa-miR-196b-5p are highly expressed in mesenchymal stem cells or their derived cells such as skeletal muscle cells and osteoblasts. In conclusion, our comparative miRNA profiling sheds light on differential expression patterns between SWR/J and both subgroups of TallyHo/JngJ. There is no significant difference between the miRNA expression patterns of TH and TH-ND mice suggesting that the differential miRNA regulation observed in SWR/J mice may be due to its different genetical background. These findings contribute to the growing knowledge of bone complications associated with T2DM and emphasize the need for continued exploration using more representative animal models to advance our comprehension of this disease.

***Disclosures: DAVID CARRO VAZQUEZ**, None*

LB SUN-623

COMPENSATORY GAIT PATTERNS ARE RELATED TO SUBCHONDRAL BONE REMODELING IN RAT OA *Markia Bowe[1], Joshua Yarrow[1], Kyle Allen[1]. [1]University of Florida, United States

Pathologic subchondral bone modeling and/or remodeling are likely connected to abnormal movement patterns in OA. Here, subchondral bone plays an important role in joint function, working together with the articular cartilage to dissipate 30%-40% of the joint loads. Since abnormal loads may accompany changes in movement patterns, it is important to clarify how the relationship between altered movement and subchondral bone pathology is affected during disease progression. However, very few studies evaluate these pathologic subchondral bone changes within the context of mechanics. Furthermore, even fewer studies assess abnormal changes in movement and subchondral bone microstructure over multiple stages of disease progression. In this study, we evaluated the relationship between altered movement patterns and pathologic microstructural changes in subchondral bone in OA. 40 Lewis rats were split into groups of naïve rats and OA rats. OA was induced in one limb using two common models known to progress at different rates. Here, the medial meniscus transection (MMT) and medial collateral ligament transection (MCLT) models were treated as fast-progressing and slow-progressing OA models, respectively. At 2, 4, 8, and 12 weeks after OA induction, animals underwent gait testing and in vivo MicroCT imaging. Both MMT and MCLT rats had similar compensatory gaits, where OA animals spent more time on their operated and contralateral limbs throughout the experiment and had spatially and temporally symmetric gaits. Changes in subchondral bone microarchitecture were also similar across both groups. Cortical and trabecular thickness increased in OA rats, along with trabecular number and bone volume. More severe changes were seen in the subchondral bone of MMT rats, as expected. However, osteophytes only formed in MMT rats, presenting an important difference in pathologic bone structure between MMT and MCLT animals.

***Disclosures: Markia Bowe**, None*

LB SUN-624

Doxorubicin induced senescence in the knee, a new mouse model to study degenerative arthritis *Vidyani Suryadevara[1], Mohammad Hajipour[1], Ariana Martin[2], Frezghi Habte[1], Noeen Malik[1], Edwin Chang[1], Dilyana Mangarova[1], Kerem Nernekli[1], Lucia Baratto[1], Lisa C. Adams[1], Jonathan Cotton[3], Bernd Pichler[3], Nicolas Be?zie?re[3], Heike Daldrup-Link[1]. [1]Stanford University, United States; [2]Meharry Medical College, United States; [3]Werner Siemens Imaging Center, Germany

Purpose: Senescence plays a key role in several mechanisms leading to osteoarthritis (OA), as evidenced by the amelioration of OA progression by senlolytic therapies. We developed a new mouse model to induce senescence using doxorubicin in the knee joints, which was further validated by PET-CT using a novel ?-galactosidase-based radiotracer, [18F]-PyGal.Methods: Senescence was induced by treating 20,000 primary chondrocytes with 400nM doxorubicin for five days, followed by the assessment of cell morphology, ?-galactosidase activity, and secretion of IL-6 and CXCL5. As approved by the animal care committee at Stanford, 12 mice aged 12-months (6 males, 6 females) received an intra-articular injection of 400nM doxorubicin in 50ul of PBS into the left knee. The right knee was injected with 50ul of PBS and served as the control (C). All mice underwent microCT (V=60 kV, I=167?A with rotation steps of 0.4°ß, 20u resolution), followed by intravenous injection of 250uCi [18F]-PyGal and positron emission tomography (PET). After imaging, the mice were sacrificed to collect knees for histological assessment of senescent markers using traditional ICC staining for p-16, p-21, and X-gal markers. Significant differences between the control and senescence groups were compared using t-tests.Results: Chondrocytes treated with doxorubicin had significantly elevated levels of IL6 (C: 18.39+/-5.10 pg/mL; S: 58.85+/-1.43pg/mL, p<0.005), CXCL5 (C: 153.8162+/-38.14pg/mL, S:1163.24+/-169.09pg/mL p<0.005) and beta-gal activity (C: 9.16+/-0.7%, S: 90+/-2%, p<0.0005). Senescent cells exhibited a 2.28-fold higher uptake of [18F]-PyGal than controls (C 1754+/-247.22, S 3704.23+/-570.76, p=0.005). Doxorubicin-treated left knees demonstrated significantly higher expression of p-16, p-21, and ?-gal markers than controls. MicroCT analysis revealed changes in the bone microarchitecture of doxorubicin-treated knees compared with control knees. In 12-month-old mice, significantly higher retention of [18F]-PyGal (0.47+/-0.18 %ID/g, 0.47+/-0.12 %ID/g) radiotracer in senescent knees was seen as compared to control knees (0.22+/-0.03%ID/g, 0.29+/-0.08, p=0.02, p=0.03 female and male respectively).Conclusions: Intra-articular doxorubicin administration as a preclinical model to induced senescence in the knee joints of mice. Senescent cells in doxorubicin-treated joints can be detected with [18F]-PyGal. This new model may be useful for studying the efficacy of senolytic therapy.

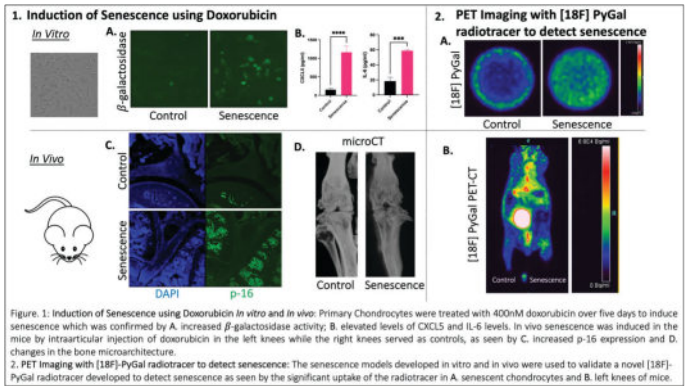

Figure. 1: Induction of Senescence using Doxorubicin *In vitro* and *In vivo*: Primary Chondrocytes were treated with 400nM doxorubicin over five days to induce senescence which was confirmed by A. increased β-galactosidase activity; B. elevated levels of CXCL5 and IL-6 levels. In vivo senescence was induced in the mice by intraarticular injection of doxorubicin in the left knees while the right knees served as controls, as seen by C. increased p-16 expression and D. changes in the bone microarchitecture.
2. PET Imaging with [18F]-PyGal radiotracer to detect senescence: The senescence models developed in vitro and in vivo were used to validate a novel [18F]-PyGal radiotracer developed to detect senescence as seen by the significant uptake of the radiotracer in A. senescent chondrocytes and B. left knees of mice.

***Disclosures: Vidyani Suryadevara**, None*

LB SUN-625

Connecting HIPPO signaling to chromatin action during early osteoblast and adipocyte differentiation *Atenisa Caci[1], Alexander Rauch[1]. [1]1 Department of Clinical Research, University of Southern Denmark, Odense, Denmark; 2 Department of Endocrinology and Metabolism, Odense University Hospital, Odense, Denmark, Denmark

Background: Stromal cells of the bone marrow (BM-MSCs) give rise to osteoblasts, chondrocytes, and adipocytes. A network of about 200 transcription factors (including TEAD1) is pivotal for osteoblast, while efficiently inhibiting fat cell differentiation. YAP/TAZ have been previously recognized as pro-osteogenic and anti-adipogenic regulators, however, not through binding to TEAD1 but RUNX2 and PPAR-?, respectively.Purpose: Identify transcriptional mechanisms of the HIPPO signaling contributing to lineage commitment of BM-MSCs.Methods: TEAD1, RUNX2 and YAP1 binding, enhancer activity and gene expression profiles have been established during early in vitro differentiation of BM-MSCs using ChIP and RNA-seq. Quantification of Hippo signaling through YAP1/TAZ during BM-MSC differentiation using western blot and immunostaining and its impact on differentiation upon pharmacological inhibition or genetic knock down.Results: Genome-wide binding analysis confirmed YAP1 as a transcriptional coactivator in BM-MSC. Gain of YAP1 binding upon osteogenic stimulation was highly predictive for enhancer and gene activation, in contrast loss of YAP1 chromatin association marks enhancers that are deactivated upon adipogenic stimulation. Importantly, YAP1 binding dynamics show much stronger correlation with TEAD1 compared to RUNX2(ROC test pvalue:Ob up<2.2e-16,Ob down= 1.806e-13,Ad up<2.2e-16,Ad down<2.2e-16), indicating an unappreciated role of TEAD1 in BM-MSC differentiation (Figure1A). Immunostaining showed clear lineage selective dynamics in nuclear localization of YAP1(Cohen's estimation: 1dAdvsMsc= -0.1; 1dObvs0hMsc = 1.31(large)) (Figure1B) and reduction in nuclear YAP1 protein levels correlate with reduced genome-wide occupancy of both YAP1 and TEAD1 upon adipogenic stimulation, indicating cofactor-dependent dissociation. Besides controlling HIPPO target genes, YAP1 binding in cells exposed to osteogenic condition was associated with WNT-signaling, while loss of YAP1 binding upon adipogenic stimulation correlates with repression of those genes. Pharmacological inhibition and genetic ablation of YAP1 strongly reduces mineralization, with opposing effects on lipid droplet formation.Conclusion: From our genome wide binding pattern, we suggest TEAD1 as the major sequence specific rheostat of Hippo signaling that is implicated in lineage determination of BM-MSCs.

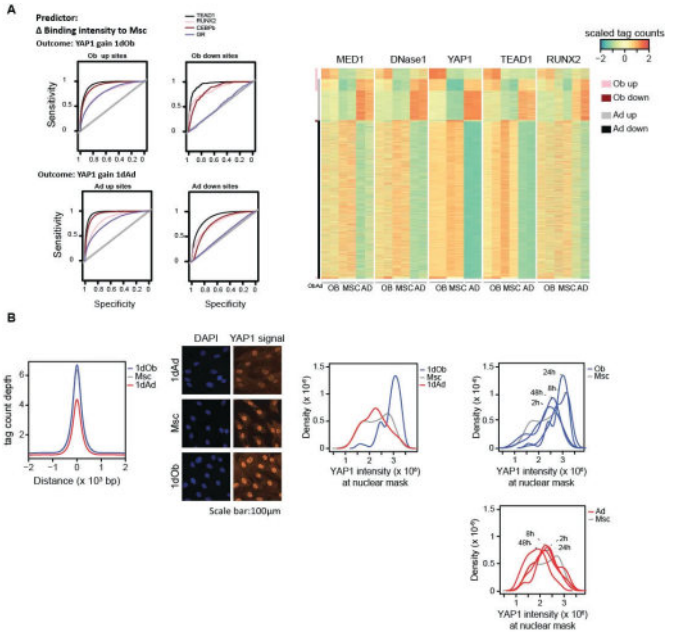

***Disclosures: Atenisa Caci**, None*

LB SUN-626

Inhibition of Dot1L histone methyltransferase activity promotes osteogenic differentiation *Alexander Tress[1], Drew Dauphinee[1], Alayna Grzybowski[1], Marta Stetsiv[1], Archana Sanjay[2], Rosa Guzzo[1]. [1]UConn Health, United States; [2]UCHC, United States

Posttranslational modifications of histones by chromatin modifying enzymes play a key role in determining transcriptional activity, making them attractive targets for skeletal repair and regeneration. Several histone methyltransferases are known to control bone formation. The Disruptor of telomeric-silencing 1-like (Dot1L) is the only known histone methyltransferase that catalyzes the di-methylation of lysine 79 in histone 3 (H3K79me2), a modification associated with gene expression. Our group previously demonstrated that loss of Dot1L expression in Prrx1+ mesenchymal progenitors impaired chondrocyte differentiation and endochondral bone growth in mice; however, the functional contribution of Dot1L to bone cell differentiation remained unexplored. Here, we examined the effects of Dot1L depletion, as well as the direct effects of Dot1L enzymatic inhibition on osteogenic differentiation in mouse mesenchymal stem/stromal cells and MC3T3-E1 osteoblasts. Mesenchymal stem/stromal cells harvested from the bone marrow (BM) of adult Dot1Lfl/flPrrx1Cre mice exhibited significantly higher numbers of colony forming units, with increased proliferative capacity relative to cells from Dot1Lfl/fl mice. Genetic depletion of Dot1L in BM derived mesenchymal stem/stromal cells resulted in increased levels of osteogenic genes (ie. Sp7, Ibsp, Osteocalcin), as well as elevated activity of alkaline phosphatase, and increased matrix mineralization relative to controls. Western blot analyses performed over a time course of osteogenic differentiation in mouse MC3T3-E1 cells showed significant down-regulation of H3K79me2 protein levels as compared to undifferentiated cells. Thus, we evaluated the impact of inactivating Dot1L methyltransferase activity in MC3T3-E1 cells by treating cells with a Dot1L-specific inhibitor under osteogenic conditions. Our results confirmed that inhibitor treatment accelerated osteogenic gene induction, and matrix mineralization in differentiating MC3T3-E1 osteoblasts. Results from the mouse cell line treated with the Dot1L inhibitor paralleled the effects of Dot1L protein loss in mouse primary mesenchymal stem/stromal cells. Taken together, our study indicates that Dot1L-H3K79me2 restricts osteogenic

differentiation, and that temporal inhibition of H3K79me2 may offer a novel approach for stimulating osteoblast differentiation.

***Disclosures: Alexander Tress**, None*

LB SUN-627

Analysis of Runx2 transcriptional regulation by DNA methylation on DMR via Epigenome Editing *Yutaro Kawa[1], Jun Ohgane[2], Masafumi Inui[1]. [1]Laboratory of Animal Regeneration, Department of Life Sciences, School of Agriculture, Meiji University, Japan. [2]Laboratory of Genomic Function Engineering, Department of Life Sciences, School of Agriculture, Meiji University, Japan

Runx2 is a transcription factor essential for bone formation and its haploinsufficiency causes dysplasia of the skull and clavicle in mice and humans (known as cleidocranial dysplasia or CCD). Mutant mice with the Runx2 expression levels at 70% of that of wild type displayed abnormal skeletal development, demonstrating that a quantitatively precise level of Runx2 is essential for normal bone formation. Interestingly, identical twin CCD patients have reported phenotypic differences involving excessive teeth, suggesting that epigenetic mechanisms contribute to the quantitative regulation of Runx2. We hypothesize that transcriptional regulation by DNA methylation is involved in the process. Previous report have indicated the presence of a tissue-specific differentially methylated region (T-DMR) upstream of the transcriptional start site of Runx2-I in several mammals, and the methylation rate of this region inversely correlates with Runx2 expression during osteoblast differentiation. Therefore, in this study, our aim is to elucidate whether changes of DNA methylation level of this Runx2-I T-DMR could affect Runx2 expression using Cas9-based epigenome-editing tools. We designed guide RNAs targeting Runx2-I T-DMR, transfected them along with CRISPRoff-v2.1 into MC3T3-E1 cells, and found that the methylation level in the proximity of the gRNA target sites increased from 0%-10% to 20-30%. Furthermore, we increased the methylation level to 40-60% by optimizing the selection conditions of the transfected cells. Currently, we are examining whether this increase of methylation level could affect Runx2-I expression level as well as osteoblast differentiation process of MC3T3-E1 cells. In addition to the previously reported T-DMR, we are also examining the effect of this epigenome-editing on the activity of known and novel promoter/enhancer regions of Runx2. In this presentation, we will discuss the technical evaluation of epigenome-editing and the methylation variation in Runx2-I T-DMR, as well as its physiological function.

***Disclosures: Yutaro Kawa**, None*

LB SUN-628

Peptidylarginine deiminase 2 plays a key role in osteogenesis by enhancing RUNX2 stability through citrullination *Hye-Rim SHIN[1], Hyun-Jung KIM[1], Heein Yoon[1], Min-Sang Park[1], Byung-Gyu Kim[2], Jae-I Moon[1], Woo-Jin Kim[1], Seung Gwa Park[1], Ki-Tae Kim[1], Ha-Neui Kim[3], Je-Yong Choi[4], Hyun-Mo Ryoo[1]. [1]Department of Molecular Genetics and Dental Pharmacology, School of Dentistry and Dental Research Institute, Seoul National University, Republic of Korea. [2]Center for Genomic Integrity, Institute for Basic Science (IBS), Republic of Korea. [3]University of Arkansas for Medical Sciences, Little Rock, United States. [4]Kyungpook National University, Republic of Korea

Peptidylarginine deiminase (PADI) 2 catalyzes the post-translational conversion of peptidyl-arginine to peptidyl-citrulline in a process called citrullination. However, the precise functions of PADI2 in bone formation and homeostasis remain unknown. In this study, our objective was to elucidate the function and regulatory mechanisms of PADI2 in bone formation employing global and osteoblast-specific Padi2 knockout mice. Our findings demonstrate that Padi2 deficiency leads to the loss of bone mass and results in a cleidocranial dysplasia (CCD) phenotype with delayed calvarial ossification and clavicular hypoplasia, due to impaired osteoblast differentiation. Mechanistically, Padi2 depletion significantly reduces RUNX2 levels, as PADI2-dependent stabilization of RUNX2 protected it from ubiquitin-proteasomal degradation. Furthermore, we discovered that PADI2 binds to RUNX2 and citrullinates it, and identified ten PADI2-induced citrullination sites on RUNX2 through high-resolution LC-MS/MS analysis. Among these ten citrullination sites, the R381 mutation in mouse RUNX2 isoform 1 considerably reduces RUNX2 levels, underscoring the critical role of citrullination at this residue in maintaining RUNX2 protein stability. In conclusion, these results indicate that PADI2 plays a distinct role in bone formation and osteoblast differentiation by safeguarding RUNX2 against proteasomal degradation. In addition, we demonstrate that the loss-of-function of PADI2 is associated with CCD, thereby providing a new target for the treatment of bone diseases.

***Disclosures: Hye-Rim SHIN**, None*

LB SUN-629

Sorting Nexin 10 (SNX10) Limits Osteoclast Size by Arresting Cell Fusion in late Osteoclastogenesis *Maayan Barnea-Zohar[1], Nina Reuven[1], Sabina Winograd-Katz[1], Merle Stein[2], Sarah-Agnes Elkaim[1], Jan Tuckermann[2], Benjamin Geiger[1], Ari Elson[1]. [1]The Weizmann Institute of Science, Israel. [2]University of Ulm, Germany

Multi-nucleated osteoclasts (OCLs) are formed by regulated fusion of monocyte precursor cells that is induced by RANKL. Cell fusion is required for generation of active OCLs, but the extent of fusion is limited and OCL sizes typically fall within a finite and reproducible range. The mechanisms that arrest osteoclastogenic cell fusion and determine maximal OCL size are unknown. We show that the vesicular trafficking protein sorting nexin 10 (SNX10), whose loss induces autosomal recessive osteopetrosis, participates in regulating the maximal size of OCLs. Mice homozygous for the osteopetrosis-inducing R51Q mutation in SNX10 are massively osteopetrotic due to inactivity of their OCLs, which do not form ruffled borders. In culture, RANKL induces monocytes from these mice to fuse uncontrollably to generate OCLs whose sizes are up to 1000-fold larger than those of control OCLs, in the square millimeter range. Dramatically large OCLs are observed also ex vivo, when GFP-labelled OCLs are visualized in femurs and tibias of SNX10 mutant mice using two-photon microscopy combined with second harmonics generation microscopy. R51Q SNX10 OCLs exhibit reduced endocytosis, suggesting that their deregulated fusion is caused by disruption of physiological membrane homeostasis. The R51Q mutation destabilized the SNX10 protein, suggesting that loss of SNX10 deregulates OCL fusion. In agreement, we observed osteopetrosis, OCL inactivity, deregulated OCL fusion, and giant OCLs ex vivo also in SNX10-knockout mice. We conclude that OCL size is limited by an active, genetically-regulated, and OCL-cell autonomous mechanism that arrests cell fusion during osteoclastogenesis. This mechanism requires SNX10 but, surprisingly, this function of SNX10 is non-redundant, as disrupting this single protein deregulates cell fusion and abolishes control of OCL size.

***Disclosures: Maayan Barnea-Zohar**, None*

LB SUN-630

Cholesterol sulfate inhibits osteoclast differentiation and survival by regulating the AMPK-Sirt1-NF-?B pathway *Jin Ha Park[1], Jiae Lee[1], Gong-Rak Lee[1], Hye In Lee[1], Minjeong Kwon[1], Hee Jin Kim[1], Mi-Ock Lee[2], Woojin Jeong[1]. [1]Department of Life Science and the Research Center for Cellular Homeostasis, Ewha Womans University, Republic of Korea. [2]ollege of Pharmacy and Bio-MAX Institute, Research Institute of Pharmaceutical Sciences, Seoul National University, Republic of Korea

Cholesterol sulfate (CS) is an activator of retinoic acid-related orphan receptor ? (ROR?). CS treatment or ROR? overexpression attenuates osteoclastogenesis in a collagen-induced arthritis mouse model. However, the mechanism by which CS and ROR? regulate osteoclast differentiation remains largely unknown. Thus, we aimed to investigate the role of CS and ROR? in osteoclastogenesis and their underlying mechanism. CS inhibited osteoclast differentiation, but ROR? deficiency did not affect osteoclast differentiation and CS-mediated inhibition of osteoclastogenesis. CS enhanced adenosine monophosphate-activated protein kinase (AMPK) phosphorylation and sirtuin1 (Sirt1) activity, leading to nuclear factor-?B (NF-?B) inhibition by decreasing acetylation at Lys310 of p65. The NF-?B inhibition was restored by AMPK inhibitor, but the effects of CS on AMPK and NF-?B were not altered by ROR? deficiency. CS also induced osteoclast apoptosis, which may be due to sustained AMPK activation and consequent NF-?B inhibition, and the effects of CS were significantly reversed by interleukin-1? treatment. Collectively, these results indicate that CS inhibits osteoclast differentiation and survival by suppressing NF-?B via the AMPK-Sirt1 axis in a ROR?-independent manner. Furthermore, CS protects against bone destruction in lipopolysaccharide- and ovariectomy-mediated bone loss mouse models, suggesting that CS is a useful therapeutic candidate for treating inflammation-induced bone diseases and postmenopausal osteoporosis.

***Disclosures: Jin Ha Park**, None*

LB SUN-631

Osteoclast-specific deletion of the beta 1-adrenergic receptor influences bone in mice, but does not rescue isoproterenol-induced bone resorption in vivo *Ryan Neilson[1], Claire Morrow[2], Daniel Brooks[3], Audrie Langlais[4], Karen Houseknecht[5], Christine Lary[6], Katherine Motyl[7]. [1]MHIR, United States. [2]Maine Health Institute for Research, United States. [3]BIDMC/MGH, . [4]MaineHealth Institute for Research, . [5]University of New England, United States. [6]Northeastern University, . [7]MaineHealth, United States

The sympathetic nervous system (SNS) promotes bone loss by suppressing bone formation and increasing RANKL-dependent osteoclast recruitment. Emerging evidence indicates the SNS may also work through beta-adrenergic receptor (?AR) activity directly in osteoclasts to promote bone resorption. Although ?1AR-selective antagonists may be more effective at reducing fracture risk and increasing bone mineral density clinically, no studies have examined the role of ?1AR specifically in bone resorption. To test the hypothesis that

SNS-mediated bone loss may work through ?1AR in osteoclasts, we generated an osteoclast-specific knockout of Adrb1 using the myeloid-lineage specific Lysozyme 2 promoter-driven Cre recombinase (a.k.a. LysM-Cre) model (Adrb1fl/flLyz2Cre/+). Efficiency of deletion was confirmed in primary osteoclasts and whole bone using qPCR. Consistent with our hypothesis, 16-week-old female Adrb1fl/flLyz2Cre/+ (Cre/+) mice had higher trabecular number (p=0.0297, n=10) and lower trabecular separation (p<0.0001, n=10/genotype), suggestive of slower trabecular bone loss as the mice aged from 8 to 16 weeks of age (compared to Adrb1fl/fl littermates). Consistent with this, in vitro bone resorption (CTX-1 levels in media from osteoclasts plated on bone chips) showed a trend towards reduction (by 54% (p=0.139, n=3)) despite a lack of changes in TRAP stain. However, in contrast to our hypothesis, male Adrb1fl/flLyz2Cre/+ mice did not exhibit a trabecular phenotype but had lower cortical area fraction (p=0.0179, n=10) at 8 weeks of age. To test if an osteoclast-specific deletion of Adrb1 would protect against SNS-mediated bone loss, we treated 8-week-old female Adrb1fl/flLyz2Cre/+ mice and Adrb1fl/fl littermates with isoproterenol (6 mg/kg) for 14 days. Both genotypes lost trabecular bone in a comparable manner, indicating that alone, Adrb1 in the osteoclast does not contribute significantly to SNS-induced bone loss. Importantly, ?2AR is more highly expressed in mice and humans, and ongoing studies in the lab are examining the effects of osteoclast specific ?2AR deletion, as well as conditional double knockout, since receptor compensation may occur. In summary, Adrb1 has a role in cortical acquisition in male mice and trabecular bone maintenance in female mice, but further studies are needed to determine the mechanism of bone loss prevention by ?1AR-selective antagonists.

***Disclosures: Ryan Neilson**, None*

LB SUN-632

Effect of change of the extracellular physical environment on differentiation of osteoclast precursors *Miho Ueta[1], Kazuki Takaoka[1], Hirokazu hattori[1], Tomoki Kakimoto[1], Sachiko Nosaka[1], Ayaka Hatanaka[1], Masayuki Oshitani[1], Kazuma Noguchi[1], Hiromitsu Kishimoto[1]. [1]Department of Oral and Maxillofacial Surgery, School of Medicine, Hyogo Medical University, Japan

[Introduction] Osteoclasts (OCs) are differentiated from monocyte/macrophage-lineage hematopoietic precursor cells which are termed OC precursors (OCPs) in the bone microenvironment. OCPs are drawn from the bloodstream to bone by various factors released at sites undergoing resorption in the bone microenvironment, and subsequently differentiate into OCs following stimulation with the RANK ligand (RANKL). The purpose of this study is to investigate the effect of change of the extracellular physical environment as from blood to bone on the differentiation of OCPs in the bone microenvironment. [Materials and Methods] RAW264.7 cells were used as osteoclast precursors, and cultured on either plastic cell culture dishes (solid condition as bone) or ultra-low attachment surface dishes (fluid condition as blood). We performed cell proliferation assay. After addition of RANKL, we counted the total numbers of cells with large multinucleated OC-like cells, and determined TRAP staining by TRAP solution kit (Oriental Yeast Co., Ltd., Japan). To perform immunohistochemistry, cells were collected using iPGell (GenoStaff, Japan), and stained with NFATc1. RANK, NFATc1, c-Fos and mTOR were detected by Western blot analysis. [Results] The cell proliferation of RAW264.7 cells increased under fluid condition compared with under solid condition. mTOR protein expression level under fluid condition were higher than under solid condition. On day 7, RANKL induced the formation of large multinucleated OC-like cells under solid condition, but failed to differentiate into OC-like cells under fluid condition. TRAP staining cells were significantly decreased under fluid condition, compared with under solid condition. Similarly, NFATc1 positive cells were lower under fluid condition compared with under solid condition by immunohistochemistry. RANK, c-Fos and NFATc1 protein expression levels under fluid condition were lower than under solid condition. [Conclusions] These results of this study indicate that the change of the extracellular physical environment (from fluid condition as blood to solid condition as bone) of OCPs may induce be one of the factors regulating that OCPs differentiate into OCs via up-regulated RANK.

***Disclosures: Miho Ueta**, None*

LB SUN-633

Osteocyte single-cell ATAC sequencing shows genomic accessibility variations in mice with chronic kidney disease (CKD) *Mohammad Niroobakhsh[1], Xierzhatijiang Sulaiman[1], RAFIOU AGORO[1], Yamil Marambio[1], Dan Eaton[2], Magdalena Preciado López[2], Jun Wan[1], Kenneth White[1]. [1]Indiana University School of Medicine, United States. [2]Calico Life Sciences , United States

BackgroundOsteocyte malfunction is linked to common bone diseases such as aging, osteoporosis, and CKD, however it has been difficult to isolate cell-specific changes in vivo in models of these diseases. At the individual cellular level, understanding osteocyte genomic accessibility reprogramming is critical for identifying the contribution of osteocytes to the metabolic bone disease associated with CKD.MethodMale wild-type mice were placed on an adenine-containing or control diet (0.2%, n=5) for 4 weeks. Femurs, tibia, and humeri were collected and bone cells isolated using sequential digests of collagenase and EDTA. Following subtraction of marrow cells, sequencing libraries were prepared using the 10X Genomics protocol and single-cell ATAC sequencing (scATACseq) was carried out. Data processing and analysis included integration, filtering, dimension reduction, and differentially accessible region (DAR) analysis for enriched chromatin motifs. Osteocytes and osteoblasts were identified with chromatin accessibility encompassing their marker genes Dmp1, Phex, and Col1a1.ResultsTwenty-three distinct bone cell population clusters were identified by scATACseq, in which one cluster was identified as an osteocyte/osteoblast cluster which was 3% (147/4920) of the cells from the control group and 2% (165/8408) from the mice with CKD. In osteocyte/osteoblasts, based upon pathway analysis Dtwd1, Col12a1, and genes related to DNA metabolism, chromatin organization, and skeletal morphogenesis were significantly more open at promoter region peaks in CKD than controls. The up-regulated DARs were enriched with binding motifs for transcription factors Atf3, FosL2, and c-Jun. Pcdh17, Hpn, and genes related to cadherin binding and vasculogenesis were significantly more closed in CKD than in controls. The downregulated DARs in CKD osteocytes were enriched with motifs for SOX gene family members, suggesting unique cell- and disease-specific transcriptional regulation.ConclusionA novel workflow was developed to understand osteocyte genetic reprogramming profiles at the single-cell level. Genes involved in DNA metabolism, chromatin organization, and skeletal morphogenesis were found to be significantly more open in CKD osteocyte/osteoblasts whereas cadherin binding and vasculogenesis were significantly more closed. Thus CKD causes dynamic shifts in chromosomal accessibility which may help to predict skeletal outcomes and provide new therapeutic targets.

***Disclosures: Mohammad Niroobakhsh**, None*

LB SUN-634

Motion artifact masquerading as femur fracture on DEXA: A case report *Maria Fariduddin[1], Subhash Kukreja[2], Michele Obeid[1], Kristen DeCarlo[3]. [1]University of Illinois at Chicago, United States. [2]University of Illinois, United States. [3]University of Illinois ,

A 41 y/o female with spastic quadriplegic cerebral palsy underwent a DEXA scan for osteoporosis screening. Femur image was read as atypical femur fracture based on transverse appearance on DEXA images. Further history revealed that the patient has no known diagnosis of osteoporosis, never been on bisphosphonates and is not on glucocorticoids. She is bed bound and non-weight bearing with no hip pain or history of hip trauma. Given the DEXA findings, bilateral hip X-rays were obtained which did not show any evidence of fracture. Atypical femur fractures (AFF) are defined as stress fractures occurring along the lateral shaft of the femur with minimal or no trauma. The major features which suggest this diagnosis include involvement of the subtrochanteric region and femoral shaft, transverse or short oblique orientation, medial spike in complete fractures, absence of comminution and no or minimal trauma. All the major features need to be present for a fracture to be designated as atypical. Minor features are cortical thickening and localized periosteal or endosteal thickening often referred to as “beaking” seen on imaging, presence of pain, bilateral occurrence, use of bisphosphonates or other antiresorptive agents, glucocorticoids or proton pump inhibitors. The DEXA in this case included all major features without any minor features. On close examination, a blurring of the upper femur was seen, suggesting that there may have been motion artifacts during the scan. The findings on the DEXA scan were determined to be secondary to rotation of the femur at the diaphysis giving an appearance of a femur shaft fracture caused by movement during the scan. This highlights the limitations of DEXA scan and how motion artifacts can lead to a false appearance of fracture which in turn can lead to unnecessary tests and patient anxiety. This emphasizes the importance of educating patients about lying still during the DEXA scan akin to CT imaging. However, this is challenging for patients with mental and physical impairments and raises the need to create a process of communication to the interpreting physician when there is excessive movement during the study in an effort to improve the accuracy of DEXA scan interpretation. This case illustrates that for the diagnosis of AFF, clinicians should carefully examine for typical findings of AFF and in the absence of these findings, should consider the possibility that the apparent fracture may reflect a motion artifact.

***Disclosures: Maria Fariduddin**, None*

LB SUN-635

DXA-derived 3D Parameters of the Hip Discriminate Fragility Fractures in Patients with Axial Spondyloarthritis *Edgar Wiebe[1], Elisa Celine Schilling[2], Dörte Huscher[3], Andriko Palmowski[2], Zhivana Boyadzhieva[2], Sandra Hermann[2], Frank Buttgereit[2], Burkhard Muche[2]. [1]Charité Universitätsmedizin, Dept. Rheumatology , Germany. [2]Charité Universitätsmedizin, Dept. Rheumatology, Germany. [3]Charité Universitätsmedizin; Institute for Biometry and Clinical Epidemiology, Germany

Background: Axial Spondyloarthritis (axSpA) is related to osteoporosis and fragility fracture risk possibly not reflected by measurement of areal bone mineral density (aBMD) alone. DXA-derived three-dimensional (3D) analysis has emerged as a promising method for evaluating bone structural properties of the femur, showing good correlation with quantitative computed tomography, which has demonstrated good predictive capabilities for vertebral fractures in axSpA patients.Objective: Our objective was to investigate the discriminative performance of DXA-derived 3D parameters of the femur in comparison to aBMD and trabecular bone score (TBS) for pre-existent fragility fractures (FFx).Methods: This cross-sectional analysis is part of the Rh-GIOP prospective observational cohort study focusing on bone health in inflammatory rheumatic diseases. We analyzed baseline visits of axSpA patients fulfilling the ASAS 2009 classification criteria. Using 3D-Shaper software (v2.12, 3D-Shaper Medical, Barcelona, Spain), we derived various parameters (integral, trabecular and cortical volumetric BMD, cortical thickness and cortical surface BMD) from hip DXA scans. Logistic regression analysis was used to develop discrimination models incorporating DXA-based T-Scores, TBS, and 3D-Shaper parameters to detect pre-existent FFx in total, vertebral fractures (VFx), and non-vertebral fractures (NVFx). Area under the curve (AUC) with 95% confidence intervals were calculated.Results: 80 axSpA patients (64% male) were analyzed. The prevalence of FFx was 34%, with 15% having a history of VFx. DXA-T-Scores showed AUC values of 0.62 (0.48; 0.75), 0.54 (0.39; 0.70), and 0.64 (0.50; 0.78) for any FFx, VFx, and NVFx, respectively. DXA-derived 3D parameters exhibited better discrimination for fragility fractures, with AUC values of 0.75 (0.64; 0.86), 0.81 (0.69; 0.94), and 0.72 (0.59; 0.85). Incorporating these parameters in a logistic regression model with DXA and TBS further improved discriminative performance (any FFx: AUC 0.78 (0.67; 0.89), VFx: AUC 0.86 (0.74; 0.98), NVFx: AUC 0.75 (0.63; 0.88)). TBS alone or in combination with DXA did not enhance the discrimination of the model.Conclusion: Our results suggest that DXA-derived 3D hip parameters offer superior discrimination of pre-existent FFx compared to DXA or TBS alone in axSpA. Future longitudinal analysis will determine whether DXA-derived 3D measurements of the femur can improve fracture prediction in clinical practice.

***Disclosures: Edgar Wiebe**, Novartis, Consultant*

LB SUN-636

Levels of Serum and Urine N-terminal Telopeptides of Type I Collagen (NTx) Correlate in Patients with Osteopenia *Dania Salih Bacha[1], Lea El-Hage[1], Kelly Brake[1], James Bena[2], Jessica Colon-Franco[3], Kevin M. Pantalone[1], Leila Zeinab Khan[1]. [1]Endocrinology and Metabolism Institute, Cleveland Clinic Foundation, Cleveland, Ohio, United States. [2]Lerner Research Institute, Cleveland Clinic Foundation, Cleveland, Ohio, United States. [3]Pathology Institute, Cleveland Clinic Foundation, Cleveland, Ohio, United States

Purpose: Bone turnover markers (BTMs) are biomarkers released during bone remodeling. They have high utility in assessing responsiveness and adherence to osteoporosis treatment. One marker of bone resorption is N-terminal telopeptide of type I collagen (NTx) which is released from osteoclasts and can be measured in either serum or urine. Compared to serum NTx, urine NTx is impacted by both the circadian rhythm and the day-to-day variability in creatinine excretion, and it has to be collected from the second void of the day. This can be cumbersome for patients and clinicians. The primary purpose of this study is to measure the correlation between serum and urine NTx in patients with osteopenia not previously receiving anabolic or antiresorptive treatment for bone health.Methods: In this prospective, 6-month cohort study, 40 participants who met the study eligibility criteria and were diagnosed with osteopenia on Dual X-ray Absorptiometry (DXA) scan, were enrolled at Cleveland Clinic Foundation (CCF). Patient demographics and clinical characteristics were summarized. Participants were monitored with blood and urine testing at the time of enrollment and throughout the duration of the study. Lab tests were obtained exclusively at CCF laboratories. The urine samples were collected from the second void of the day and at the same time the blood samples were drawn. Spearman's correlation evaluated the association between urine and serum NTX levels. Graphically, the linear best fit model is shown.Results: The mean age of the cohort was 66.7 +/- 6.3 years, 95% were female, and 90% were Caucasian. All participants had an eGFR of at least 60 mL/min. The median (IQR) serum and urine NTx levels were 17.0 nmol bone collagen equivalents (BCE) [13.7, 20.6] (reference range: 6.2 - 19.0 nmol BCE), and 64.7 nmol BCE/nmol creatinine [42.5, 90.9] (reference range: 5.0 - 65.0 nmol BCE/nmol creatinine), respectively. A moderate correlation was observed between the urine and serum NTx levels (r value= 0.52, P-value<0.001, Fig.1). Conclusion: A moderate correlation between urine and serum NTx levels was observed. Since serum NTx has a smaller biological intrasubject variability, and is easier to obtain, compared to urine NTx, clinicians may consider using it interchangeably with urine NTx.

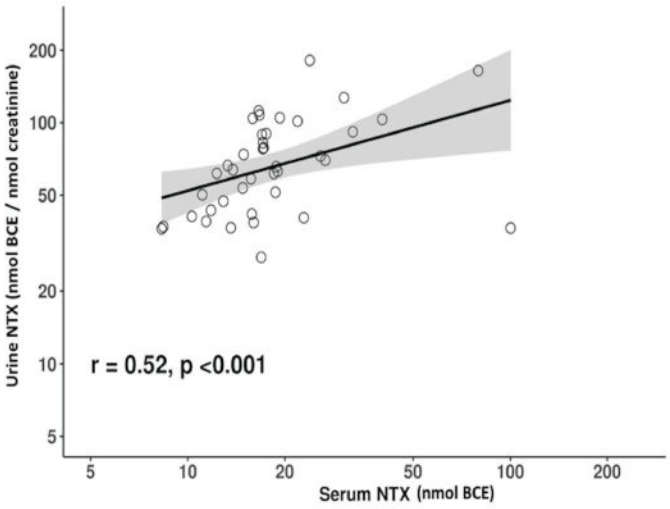

***Disclosures: Dania Salih Bacha**, None*

LB SUN-637

The validation of osteoporosis self-assessment tool for Asians using fracture probability according to BMI and age in Korean postmenopausal women : Ajou Bone Love Data *Bom-Taeck Kim[1], Junghwa Shin[2], Kwangyoon Kim[1], Sangmi Lee[3], Hanna Kim[4], Okyu Noh[5], Yoon-Sok Jung[6], Yong Jun Choi[6]. [1]Department of Family Practice & Community Health, Ajou University School of Medicine, Republic of Korea. [2]Department of Family Medicine, Korea University School of Medicine, Republic of Korea. [3]Pyeongtaeck Saint Mary's Hospital, Republic of Korea. [4]B&Viit Eye Center, Republic of Korea. [5]Department of Radiation Oncology, Ajou University School of Medicine, Republic of Korea. [6]Department of Endocrinology and Metabolism, Ajou University School of Medicine, Republic of Korea

Fracture probability in postmenopausal women depends on factors such as bone mineral density (BMD), body mass index (BMI), and age. The association of these factors with frac-

tures has been reported; however, the association of fracture probability with BMI and age was not assessed concurrently. Therefore, we investigated fracture risk according to different BMI and age groups in postmenopausal women. Medical records of 22,142 women aged >=50 years who underwent BMD measurement between January 2006 and December 2014 at Ajou university hospital were checked for exclusion criteria that are known to interfere with normal bone metabolism, such as thyroid illness, rheumatoid arthritis, and prescription of hormone replacement treatment. Overall, 6,503 women with baseline BMD were included, and their fracture records after BMD measurements were identified. They were categorized into seven age groups of 5-year interval (50-54, 55-59, 60-64, 65-69, 70-74, 75-79, and >= 80 years) and five BMI groups according to the Korean Society for the Study of Obesity Guideline: underweight (BMI < 18.5), normal (18.5 <= BMI < 23), overweight (23 <= BMI < 25), Obese I (25 <= BMI < 30), and Obese II&III (BMI >= 30). Women in each age and BMI group were investigated for T-score distribution and fracture incidence. The distribution of BMD for normal, osteopenia, and osteoporosis was 28.4%, 45.5%, and 26.1%, respectively. Osteoporosis prevalence was 53%, 27.7%, 24.7%, 23.5%, and 20.2% for underweight, normal, overweight, obese I, and obese II & III, respectively. Fracture rates were 10.3%, 6.3%, 7.2%, 8.4%, and 7.4% for underweight, normal, overweight, obese I, and obese II & III, respectively. Regardless of BMI, osteoporosis increased significantly with advancing age; however, fracture risk significantly increased only in women aged >=70 years (Table 1). Fracture risk did not follow the trend of osteoporosis when age and BMI were considered together. Underweight women were at increased risk of fracture from age 65 years. However, belonging to BMI groups other than underweight did not significantly increase fracture risk in older women, irrespective of BMD.

Table 1. Fracture rate (%) in BMI and age groups

	Underweight	Normal	Overweight	Obese I	Obese II&III	Total
50–54	2.7	3.7	5.7	5.0	2.9	4.4
55–59	13.6	6.2	6.0	8.3	4.9	6.8
60–64	15.4	5.3	9.9	8.7	9.3	8.0
65–69	3.2	8.1	6.1	8.0	10.8	7.5
70–74	57.1	15.1	11.6	18.5	10.0	15.8
75–79	23.1	19.0	7.6	8.0	12.0	12.3
≥ 80s	15.4	8.3	17.1	6.0	0.0	10.1
Total	10.3	6.3	7.2	8.4	7.4	7.3

***Disclosures: Bom-Taeck Kim**, None*

LB SUN-638

Skeletal HR-pQCT Phenotypic Cluster Associations with Lower Leg Power in Older Men and Women: the Study of Muscle, Mobility and Aging (SOMMA) *Morgan Bolger[1], Kerri Freeland[3], Megan Marron[3], Nina Heilmann[3], Tong Yu[3], Lauren Roe[3], Nicole Sekel[3], Kristen Koltun[3], Katelyn Guerriere[4], Julie Hughes[5], Bradley Nindl[3], Ashley Weaver[6], Paolo Caserotti[7], Peggy Cawthon[8], Anne Newman[3], Jane A. Cauley[9], Elsa Strotmeyer[3, 1], [3]University of Pittsburgh, United States, [3]University of Pittsburgh, , [4]USARIEM, United States, [5]US Army Research Institute of Environmental Medicine, United States, [6]Wake Forest University School of Medicine, United States, [7]University of Southern Denmark, Denmark, [8]California Pacific Medical Center, United States, [9]UNIVERSITY OF PITTSBURGH, United States

The association between bone and muscle with age may be driven by mechanical loading and muscle-bone interactions. Skeletal phenotypic clusters were identified based on high-resolution peripheral quantitative computed tomography (HR-pQCT) scans of the distal tibia (DT) and distal radius (DR) of older men and women in the Study of Muscle, Mobility and Aging (SOMMA) at year 1. We hypothesized that the phenotypic clusters would differentially associate with muscle function measures including stair climb ascend power (Watts=W; best of 3 laps), single leg press peak power (W; 40-70% 1-RM) and strength (1-RM, kg), and maximum grip strength (kg). Fuzzy c-means clustering found 3 clusters using within-sex standardized z-scores for the HR-pQCT measures at separate sites, DT (N = 321; 76.3+/-4.7 years; 61% women; 87% white) and DR (N = 295; 76.1+/-4.5 years; 61% women; 87% white). For both sites, cluster 1 (C1) was high-total BMD (Tt.BMD), cortical area (Ct.Ar); cluster 2 (C2) was medium-Tt.BMD, Ct.Ar; and cluster 3 (C3) was low-Tt.BMD, Ct.Ar with higher trabecular area. No sex or race differences were found by cluster though men and women were analyzed separately in multivariate linear regression for muscle function. For women DTC3 was slightly older vs. DTC2, and DTC3 was taller with lower BMI vs. DTC2 & DTC1. For men, DTC3 was taller vs. DTC2 & DTC1, and weighed less vs. DTC2. For women, stair climb power was lower in DTC3 vs. DTC1. For men, DTC3 had lower leg power and leg strength vs. DTC1 (all p<0.05). At the DR site, no significant differences in any muscle function measure were observed between clusters for women or men. In linear regression models (Table 1, ref. C1) for women, DTC3 was associated with lower stair climb power, though not significant after adjusting for age, race, weight and height, and significantly associated (p<0.05) with lower leg press power after covariate adjustment. For men, DTC3 was associated with lower stair climb and leg press power and leg strength after covariate adjustment. No significant relationship was found between clusters and muscle function at the DR. These associations support the concept of bone phenotypic-specific associations with muscle function (power in women; power and strength in men) at the load-bearing DT site but not at the non-load bearing DR, highlighting relative the importance of mechanical loading to muscle-bone interactions.

Table 1. Standardized β regression coefficients of the distal tibia (DT) and distal radius (DR) categorical clusters (referenced vs. cluster 1; women DTC1=72; men DTC1=49; women DRC1=58; men DRC1=40) as predictors of sex-specific muscle function z-score (per SD for all) outcomes: stair climb power (Watts=W), leg press power (W), leg strength (kg), and grip strength (kg).

			Distal Tibia				Distal Radius			
	Women	Men	Women		Men		Women		Men	
	Mean ± SD		C2	C3	C2	C3	C2	C3	C2	C3
n			54	69	32	45	69	51	34	43
Power										
Stair climb power (W)	147.8±37.6	185.0±41.0	-0.21	-0.19	-0.19	**-0.44***	-0.12	-0.19	-0.20	-0.32
Leg power (W)	284.7±84.4	480.5±144.2	-0.04	**-0.41***	-0.31	**-0.54***	-0.01	-0.12	-0.03	-0.34
Strength										
Leg strength (kg)	141.2±40.5	204.8±53.7	0.07	-0.28	-0.28	-0.32	-0.20	-0.08	-0.05	-0.05
Grip strength (kg)	23.5±5.4	36.5±8.0	0.18	-0.09	-0.10	-0.11	-0.01	0.04	0.16	0.12

***p≤0.05;** All models adjusted for age (years), race (White/non-White), height (m), weight (kg), and stair climb power is additionally adjusted for moderate-to-vigorous activity time (min), drinker (≥1/week), smoking (y/n).

***Disclosures: Morgan Bolger**, None*

LB SUN-639

Global Prevalence of Osteoporosis in Rheumatoid Arthritis: Systematic Review and Meta-analysis *Khalid Almutairi[1], Johannes Nossent[1], David Preen[1], Helen Keen[1], Charles Inderjeeth[2], [1]The University of Western Australia, Australia, [2]University of Western Australia & North Metropoitan Health Service,

Background: Rheumatoid Arthritis (RA) patients have a higher risk of developing osteoporosis, which increases morbidity, mortality rates, and healthcare costs [1]. However, there is limited data on the prevalence of osteoporosis and associated risk factors in RA. Objective: Estimate the global prevalence of osteoporosis in RA patients, identify associated risk factors, and determine high-risk RA patients who require preventive osteoporosis treatment.Methods: We searched several databases (MEDLINE, Scopus, ProQuest Central, Web of Science, EMBASE, CINAHL, and Google Scholar) to estimate the global prevalence of osteoporosis in RA populations. We also evaluated the influence of geographical location, prevalence methods, and diagnostic criteria on prevalence estimates from 1980 to 2023.Results: We included 29 studies involving 31,473 RA patients with osteoporosis out of 130,989 RA populations. The global prevalence of osteoporosis in RA was estimated at 21.5% (95% confidence interval (CI) 16.5-27.0), with a prediction interval of 1.4% - 56.1% (Figure 1). The point-prevalence of osteoporosis was 19.2% (95% CI 13.3-25.8), while the period-prevalence was 27.1% (95% CI 18.9-36.3). The highest pooled prevalence of osteoporosis was observed in Asia (30.0%; 95% CI 22.1-38.6), while Europe (13.4%; 95% CI 8.9-18.7) and North America (13.3%; 95% CI 11.0-15.9) had lower estimates. Factors influencing osteoporosis prevalence included continents, prevalence methods, and diagnostic osteoporosis criteria. The World Health Organization (WHO) osteoporosis criteria exhibited greater consistency in prevalence estimates in RA populations, regardless of demographic characteristics.Conclusion: The estimated global point- and period-prevalence of osteoporosis in RA were 19.2% and 27.1%, respectively. Higher prevalence rates observed in Asia may be influenced by restricted healthcare access or variations in risk environments, highlighting the significance of the WHO criteria in predicting and guiding preventive treatment. Reference:1. Hauser B, Riches PL, Wilson JF, Horne AE, Ralston SH. Prevalence and clinical prediction of osteoporosis in a contemporary cohort of patients with rheumatoid arthritis. Rheumatology 2014;53(10):1759-66.

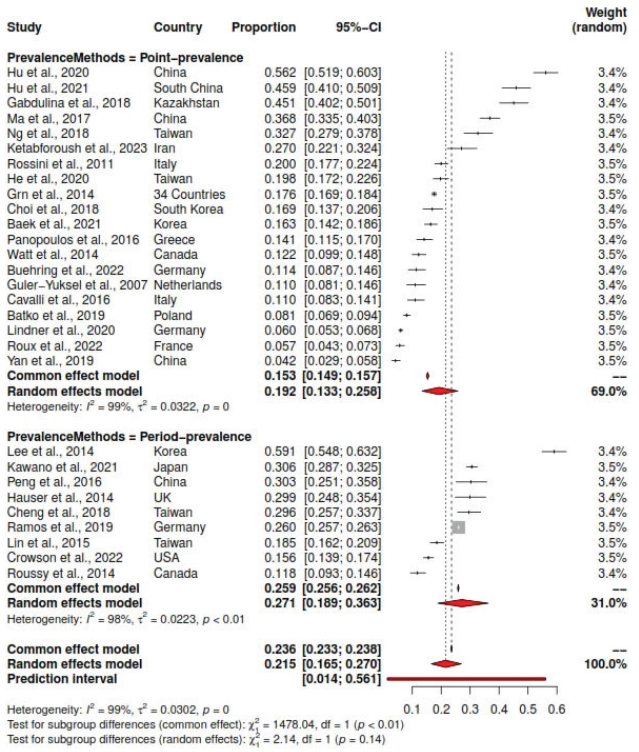

Figure 1: Global point- and period- prevalence of osteoporosis in Rheumatoid Arthritis populations and prediction interval between 1980- 2023.

***Disclosures: Khalid Almutairi**, None*

LB SUN-640

Is poor glycemic control a risk factor for the development of Osteoporosis in Type 2 Diabetes Mellitus?: A Cross-Sectional Study *Jessica Margaux Mercado[1], Katrina Marie Mendoza[1], Jayrick Aguirre[1], Maria Jocelyn Isidro[1], Monica Therese Cating-Cabral[1]. [1]Makati Medical Center, Philippines

This study aimed to determine the relationship between poor glycemic control and the risk of osteoporosis in patients with Type 2 Diabetes Mellitus (T2DM) in a private tertiary hospital in the Philippines. The charts of 171 T2DM patients who underwent bone densitometry (BMD) were reviewed and the risk of osteoporosis was determined with the exposure of interest being poor glycemic control. Statistical analysis was performed via Wilcoxon-Mann-Whitney Test, Chi-square Test or Fischer's Exact Test, Simple logistic regression, Multiple logistic regression, and Stepwise Regression. From a study population of 171, 48 (28.07%) had osteoporosis. Poor glycemic control was not a risk factor in the development of Osteoporosis in patients with T2DM (OR 1.18, 95% CI 0.56-2.51). However it was seen that T2DM patients with older age had 1.08x odds of having osteoporosis (5% CI 1.01-1.16), and T2DM patients who have hypertension have 2.37x increased risk of developing osteoporosis (95% CI 1.05-5.36). Biguanide use among T2DM patients reduces risk of osteoporosis by 60% (95% CI 0.17-0.9). In conclusion, glycemic control did not present any association with the risk of developing Osteoporosis in Filipino patients with Type 2 Diabetes Mellitus. However, other coexisting factors such as increased age, presence of Hypertension and Biguanide use could be considered as independent risk factors for the development of Osteoporosis.

***Disclosures: Jessica Margaux Mercado**, None*

LB SUN-641

Lean Mass and Fat Mass Phenotypes in Association with Bone Mineral Density in Middle Aged Asian Chinese Women *Mya-Thway Tint[1], Li Ting Ang[2], Mabel Shu Fung Kouk[2], Melvin Khee Shing Leow[2], Seng Bin Ang[3], Kok Hian Tan[3], Shiao Yng Chan[4], Peter D Gluckman[5], Yap-Seng Chong[6], Keith M Godfrey[7], Nicholas Harvey[8], Cuilin Zhang[4], Johan G Eriksson[2]. [1]Agency for Science, Technology and Research, Singapore, [2]Singapore Institute for Clinical Sciences, A*STAR, Singapore, [3]KK Women's and Children's Hospital, Singapore, [4]Department of Obstetrics and Gynaecology, National University of Singapore, Singapore, [5]University of Auckland, New Zealand, [6]Yong Loo Lin School of Medicine, National University of Singapore, Singapore, [7]MRC Lifecourse Epidemiology Unit, University of Southampton, United Kingdom, [8]University of Southampton,

BackgroundUntil recently, bone health research primarily focuses on osteoporosis and consequent fractures in older age. Women have lower bone mineral density (BMD) than men, hence they have higher incidence of osteoporotic fractures. Studies are sparse in younger populations, in whom early interventions optimizing bone health might be most beneficial. Lean mass (LM) and adiposity defined by higher BMI are known to be positively associated with BMD. To understand their differential contributions to bone health, this study examined the associations of LM, fat mass (FM), and LM-FM phenotypes with BMD in middle aged Asian Chinese women.MethodsA total of 272 Chinese women from the Growing Up in Singapore Towards healthy Outcomes (GUSTO) cohort underwent dual energy X-ray absorptiometry for measurements of LM, FM, and BMD at the femoral neck(FN), lumbar spine(LS) and total body(TB). Handgrip strength was also measured. Using multivariable linear regression analyses, we studied the associations between LM, FM and four LM-FM phenotypes based on dichotomized high vs. low LM and FM, and BMD. The cut-off for FM was 35%, the threshold proposed for prediction of metabolic syndrome among Chinese women, and for LM was appendicular LM index (ASMI), 5.4kg/m2 based on Asian Working Group for Sarcopenia guidelines.ResultsMean(SD) of age of women was 44(4) years. Percentages of women with osteopenia based on T-scores of BMD-FN, BMDLS, and BMDTB were 22.8%, 9.9% and 11.8%, respectively. 72.3% of women had FM>35%. LM was significantly and positively associated with BMD at all sites even after the adjustment for FM and age. FM by contrast was inversely associated with BMDTB. 18.6% of women had low LM and lower handgrip strength <18 kg-force, and 12.1% had low LM- high FM. Compared to women with high LM-low FM, women with low LM-low FM and low LM-high FM had lower BMD in all sites, while women with high LM-high FM had higher BMD possibly attributed to higher ASMI (Table1). Dose-response in these relationships was observed.ConclusionLM, but not FM, was significantly and positively associated with BMD in middle aged Asian Chinese women. Such findings highlight the need for earlier intervention well before osteoporosis develops. Women with low LM-high FM may be at heightened risk for sarcopenic adiposity later in life with consequent osteoporosis and metabolic diseases. Preserving or accruing LM while reducing adiposity is important for women's health over life span.

Table 1 Associations between body composition phenotypes, bone mineral density and hand-grip strength

Body composition phenotypes	Metabolic phenotypes	N (%)	B (95%CI)	P
T-scores of total body BMD				
Lean mass (kg)		272	0.12(0.09, 0.15)	**0.000***
Fat mass (kg)		272	-0.04(-0.06, -0.02)	**0.000***
High lean-lower adiposity	Healthy body composition	56 (20.6%)	Reference	
Low lean-higher adiposity	Sarcopenic adiposity	33 (12.1%)	-0.97 (-1.41, -0.52)	**0.000**
Low lean-lower adiposity	Sarcopenia	18 (6.6%)	-0.68 (-1.23, -0.12)	**0.017**
High lean-higher adiposity	High adiposity	165 (60.7%)	-0.22 (-0.53,0.10)	0.177
T-scores of lumbar spine BMD				
Lean mass (kg)		272	0.10(0.07, 0.13)	**0.000***
Fat mass (kg)		272	0.00(-0.03, 0.02)	0.646*
High lean-lower adiposity	Healthy body composition	56 (20.6%)	Reference	
Low lean-higher adiposity	Sarcopenic adiposity	33 (12.1%)	-0.72 (-1.14, -0.30)	**0.001**
Low lean-lower adiposity	Sarcopenia	18 (6.6%)	-0.89 (-1.40, -0.37)	**0.001**
High lean-higher adiposity	High adiposity	165 (60.7%)	0.09 (-0.20,0.39)	0.529
T-scores of femoral neck BMD				
Lean mass (kg)		272	0.07(0.04, 0.09)	**0.000***
Fat mass (kg)		272	0.02(0.00, 0.04)	0.084*
High lean-lower adiposity	Healthy body composition	56 (20.6%)	Reference	
Low lean-higher adiposity	Sarcopenic adiposity	33 (12.1%)	-0.63 (-1.00, -0.25)	**0.001**
Low lean-lower adiposity	Sarcopenia	18 (6.6%)	-0.60 (-1.07, -0.14)	**0.011**
High lean-higher adiposity	High adiposity	165 (60.7%)	0.20 (-0.06,0.47)	0.130
Hand grip strength				
High lean-lower adiposity	Healthy body composition	56 (20.6%)	Reference	
Low lean-higher adiposity	Sarcopenic adiposity	33 (12.1%)	-27.12 (-52.79, -1.44)	**0.039**
Low lean-lower adiposity	Sarcopenia	18 (6.6%)	-9.97 (-41.83, 21.89)	0.538
High lean-higher adiposity	High adiposity	165 (60.7%)	-8.97 (-27.34, 9.40)	0.337

* Models adjusted for fat mass and age. * Models adjusted for lean mass and age. The rest of the models adjusted for age.
Fat mass was dichotomized as higher and lower adiposity based on cut off % fat mass associated with metabolic syndrome in large population of Chinese. Lean mass was dichotomized as higher and lower lean mass based on Asia Working Group for Sarcopenia (AWGS) guidelines, i.e., 5.4kg/m^2 for women.

***Disclosures: Mya-Thway Tint**, None*

LB SUN-642

Denosumab improves bone mineral density and microarchitecture in patients with rheumatoid arthritis: randomized controlled trial by HR-pQCT *Ko Chiba[1], Naoki Iwamoto[2], Kounosuke Watanabe[2], Kazuteru Shiraishi[2], Atsushi Kawakami[2], Makoto Osaki[2]. [1]Nagasaki University Graduate School of Biomedical Sciences, Japan. [2]Nagasaki University, Japan

Introduction: This pre-specified exploratory analysis investigated the effect of denosumab on bone mineral density (BMD) and bone microarchitecture in patients with rheumatoid arthritis (RA) treated with conventional synthetic disease-modifying anti-rheumatic drugs (csDMARDs).Materials and Methods: In this open-label, parallel-group study, patients were randomly assigned (1:1) to continuous treatment with csDMARDs plus denosumab or continuous treatment with csDMARD therapy alone for 12 months. BMD and bone microarchitecture were measured by dual-energy X-ray absorptiometry (DXA) and high-resolution peripheral quantitative computed tomography (HR-pQCT) (UMIN000030575 and jRCTs071180018).Results: Of 46 patients enrolled in the primary study, 43 were included in the full analysis set. The mean age was 65.3 years, 88.4% were female, and 60.5% had osteoporosis. Areal BMD of the lumbar spine increased from baseline to 6 and 12 months in both groups, but the increase was higher in the csDMARDs plus denosumab group. Areal BMD of the total hip and femoral neck increased from baseline to 6 and 12 months only in the csDMARDs plus denosumab group. Cortical volumetric BMD and cortical thickness of the distal tibia increased in the csDMARDs plus denosumab group at 6 and 12 months but decreased in the csDMARD therapy alone group. Trabecular bone parameters of the distal tibia improved only in the csDMARDs plus denosumab group at 12 months.Conclusion: Denosumab may be recommended for patients with RA treated with csDMARDs to increase BMD and improve bone microarchitecture.

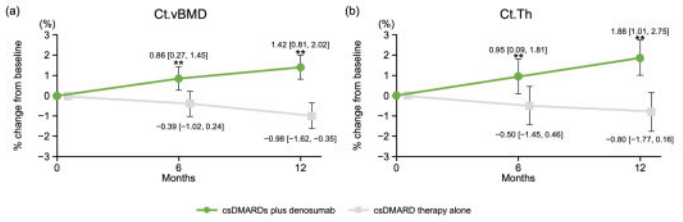

***Disclosures: Ko Chiba**, Daiichi Sankyo Company, Limited, Grant/Research Support*

LB SUN-643

Differences in long term bisphosphonate treatment between older adults in the United States and Canada *Kaleen Hayes[3], Sulbh Aggarwal[2], Michael Adegboye[3], Andrew Zullo[3], Sarah Berry[4], Arman Oganisian[3], Angela Cheung[5], Suzanne Cadarette[2]. [3]Brown University, . [2]University of Toronto, Canada. [3]Brown University, United States. [4]Hebrew SeniorLife/Beth Israel Deaconess Medical Center, United States. [5]University Health Network-University of Toronto, Canada

Background: Oral bisphosphonates (BP; alendronate, risedronate, ibandronate) are first-line therapy for osteoporosis (OP) in the US and Canada. Clinical guidelines recommend long-term treatment (>=3 years) with BP therapy to reduce fracture risk. Prior studies suggest that adherence to BPs is higher in Canada than in the US, yet there has been no direct comparison of long-term therapy between the two countries.Objectives: To describe and compare long-term BP use between the US and Canada.Methods: We leveraged claims data from: 1) a 20% random sample of Medicare Fee-for-Service beneficiaries (US cohort) and 2) universal healthcare administrative data from Ontario, Canada (ON cohort). In each cohort, we identified community-dwelling residents aged >=66 years newly initiating alendronate, risedronate, or ibandronate between 01/2008 and 12/2016. We excluded those with exposure to a non-OP-dosed BP or other OP medication in the 365 days prior to first oral BP use. We followed patients until 12/2019 to identify the proportion with >=3 years of BP use (proportion of days covered >=80%, using 3-year rolling windows) and Kaplan-Meier (KM) estimates for long-term use by the end of follow-up, censoring on death, insurance disenrollment, or end of data.Results: The US cohort comprised 518,781 individuals initiating oral BPs (88% female, mean age 78 [standard deviation (SD) 7.6] years, 76% alendronate; 5.4% with a prior major osteoporotic fracture [3.0% hip fracture]) and the ON cohort comprised 279,448 individuals initiating oral BPs (77% female, 37% alendronate, mean age 76 [SD 7.2] years), 8.9% with a prior fracture [3.6% hip fracture]). The prevalence of long-term BP therapy was lower in the US cohort (crude proportion: 17% [n= 86,379], KM estimate: 25%) vs. the ON cohort (crude proportion: 42% [n=116,907], KM estimate: 52%). Around 17% vs. 8% in the US and ON cohorts had only one oral BP prescription, respectively. The median length of long-term BP therapy was 4.0 (interquartile range [IQR] 2.3) years in the US cohort and 5.3 (IQR: 3.7) years in the ON cohort. Of those without long-term BP therapy, 6% in the US cohort vs. 17% in the ON cohort switched to another OP medication. Conclusions: The proportion of older adults with long-term BP therapy in ON is double that of US Medicare beneficiaries, but was low in both populations. Future research should explore the impact of lower BP exposure on fracture risk and identify strategies to promote long-term therapy.

***Disclosures: Kaleen Hayes**, None*

LB SUN-644

Title: unexpected bone loss and new vertebral fractures after 1 year romosozumab. Teaching point: what are the most likely reasons for an unfavorable treatment response? *willem lems[1]. [1]amsterdamumc.nl, Netherlands

IntroductionRomosozumab is a new anabolic drug, in the FRAME and ARCH study, a large increase in BMD of spine and hips was found, and a reduction in fractures But what to do and how to interprete an unfavorable treatment response?Clinical CaseA 83-year old women presented after a fracture of the distal radius. Her medical history revealed chronic back pain and a family history of a hip fracture, no other risk facors for osteoporosis.At physical examnination her height was 159 cm (prior 168 cm), weight 55 kg. DXA/VFA showed osteoporosis of the lumbar spine and hips (T-scores -3.2 and -3.1 respectively) and vertebral fractures (T 12 Genant Grade 3, L1 Genant Grade 1). Blood tests, including bone markers, showed no evidence of secondary osteoporosis, and she was treated with romosozumab for one year. After 1 year, new vertebral fractures were detected (T 8 Genant Grade2, T 9 Genant Grade 3, L4 Genant Grade 1) and an increased collapse of L1 (now Grade 2). Moreover, we found a BMD loss of the hips of 7.6% and a mild increase of the BMD of the spine of 2.5%. Why did this patient show an unexpected and unfavorable response to romosozumab?1) Non adherence to therapy. However, our patient confirms that she has used all her medication, and we observed the classical pattern of changes in bone markers, with an early (transient) rise in P1NP and a mild decrease over time in CTX.2) A new comorbidity during the one year treatment with romosozumab, However, nor medical history nor physical eaxmination nor the lab tests (including PTH, paraproteins) revealed a new cause of secondary osteoporosis.3) Pretreament with antiresorptive drugs (which may lead to a blunted response). However, she was not pretreated with an antiresorptive drug.Clinical LessonAn unexpected and unfavorable treatment response may occur during romosozumab, in our patient probably a (bad) chance finding. Since the number of patients treated with romosozuamb is probably rising, it is important for clinicians to check in patients with an unfavorable response for nonadherence, new comorbidities and for pretreatment with antiresorptives as a possible explanation.

TITLE

Introduction:
Romosozumab is a new anabolic drug, in the FRAME and in the ARCH study, a large mean increase in BMD of the spine and of the hip and a reduction in incidence of vertebral fractures, compared to placebo and alendronate, was found. But what to do and how to interprete an unfavorable response?
Clinical case
An 83-year-old woman presented 3 months after a fracture of the distal radius.. History revealed chronic back pain. She reported a family history with a hip fracture, but no other risk factors for osteoporosis. At physical examination her height was 159 cm (prior 168 cm), weight 55 kg (body mass index 21.8 kg/m2). DXA/VFA showed eoporosis of the lumbar spine and total hip (T-scores respectively -3,2 and -3,1) and vertebral fractures (Th12 Genant Grade 3, L1 Genant Grade 1).Blood tests , including bone makers, showed no underlying cause of secondary osteoporosis, and she was treated with romosozumab for one year.
After 1 year treatment, new vertebral fractures were detected (Th8 Genant Grade 2, Th9 Genant grade 3, L4 Genant grade 1), increased collapse of fracture L1 (now Genant Grade 2) and a stable fracture of Th12 (Genant Grade 3), Moreover, we found a decrease in BMD of the hips of 7.6% and a mild increase of the BMD of the spine of 2.5%.

Why did this patient show the unexpected and unfavorable response to romosozumab?
1)Non adherence to therapy. However, our patient confirms that she has used all her medication, and we observed the classical the pattern of changes in bone markers, with an early rise after 2 months in P1NP and a decrease over time in CTX.
2)A new comorbidity during the one-year treatment with romosozumab. However, nor history nor physical examination (no loss of height) nor the repeated laboratory tests (including PTH, paraproteins) revealed a new cause of secondary osteoporosis.
3) Pretreatment with anti-resorptive osteoporotic drugs. However, this patient was not pre-treated with any antiresorptive drug.
Clinical Lesson
An unfavorable treatment response may occur during romosozumab, in our patient probably a (bad) chance finding. Since the number of patients treated with romosozumab is rising, it is important for clinicians to check for nonadherence, new comorbidities and for pretreatment with antiresorptives as a possible explanation.

***Disclosures: willem lems**, None*

Sunday Orals

LB SUN-645

RANKL inhibition creates a pro-osteoclastic environment, leading to an overshoot in serum TRAP and accelerated bone resorption following treatment withdrawal *Albert Kim[1], Ariel Castro-Martinez[2], Victoria Taylor[2], Suraj Dhakal[2], James Smith[2], Jacqueline Center[3], Christian Girgis[4], Peter Croucher[3], Michelle McDonald[5, 1], [2]Skeletal Diseases Program, Garvan Institute of Medical Research, Australia, [3]Garvan Institute of Medical Research, Australia, [4]Westmead Hospital , , [5]Skeletal Diseases Program, Garvan Institute of Medical Research, The University of Sydney, Australia

Cessation of denosumab (dmab) leads to a rapid loss in bone mineral density (BMD) due to accelerated bone resorption by osteoclasts. Optimal timing and approaches of sequential therapy have not yet been defined. This is likely due to a lack of understanding of the cellular mechanisms at play, and optimal serum turnover marker assessment. We sought to examine temporal changes in RANKL signalling and serum TRAP5b compared to typical bone turnover markers CTX and P1NP, to define alternative tools to guide sequential treatment. We also aimed to determine the role of osteoclast precursors in this bone loss.Seven-week-old female C57BL/6 mice were treated with 2-weeks of saline or thrice-weekly OPG:Fc (10mg/kg) to inhibit RANKL then withdrawn from therapy (OPG-W)). Longitudinal BMD and serum was measured throughout the study. Mice were harvested at weeks 2, 8, 11 and 13 to allow a large serum collection for concurrent measures of RANKL, TRAP5b, P1NP and CTX respectively and at week 8 bone samples assessed for RANKL mRNA. At week 6 bone marrow samples were analysed for osteoclast precursors defined as NK1.1- Ter119- CD3-Ly6G-, B220-, CD11blo, CD117int, CD115+.Following OPG:Fc withdrawal, BMD was increased 24% at week 8 in OPG-W mice ($p<0.01$), declining at week 10 and normalised to vehicle levels by week 13. Serum TRAP, CTX and P1NP were all suppressed in OPG-W treated mice to week 8 ($p<0.001$). An overshoot in serum TRAP occurred in OPG-W treated mice at week 11 ($p=0.01$), whereas serum P1NP and CTX remained equivalent to vehicle. By week 13, serum TRAP, P1NP and CTX were all significantly higher in OPG-W treated mice ($p<0.01$). Serum RANKL levels were elevated with OPG:Fc at week 2 ($p<0.001$), peaking 13 fold higher at week 8 ($p<0.0001$), returning to control levels by week 11. Bone surface RANKL mRNA was significantly elevated above vehicle at week 8 ($p<0.01$), prior to the overshoot in serum TRAP levels. At week 6, osteoclast precursors were elevated in bone marrow in OPG-W treated mice ($p<0.05$).We show that rebound decline in BMD has already occurred by the time bone turnover markers used in clinical practice (P1NP and CTX) rise above vehicle levels. A significant overshoot in serum TRAP occurs earlier and prior to bone loss and may better inform sequential therapy following dmab discontinuation. Prior to the rise in serum TRAP, RANKL levels are elevated in bone and serum, providing a pro-osteoclastogenic signal for accumulated osteoclast precursors..

***Disclosures: Albert Kim**, None*

LB SUN-646

First Oral hPTH(1-34) Tablet Treatment for Osteoporosis Demonstrates Rapid Pharmacodynamic Effect on Plasma Levels of Endogenous PTH(1-84) *Arthur C. Santora[2], Gregory Burshtein[2], Constantin Itin[2], Hillel Galitzer[2], Anke Hoppe[2], Chana Sternberg[3], Miranda Toledano[2], Yoseph Caraco[4, 2]Entera Bio, United States, [2]Entera Bio, Israel, [3]CSC Ltd, Israel, [4]Hadassah Medical Center, Israel

Introduction: Entera is developing EB613 [hPTH(1-34) tablets, EBP05] as the first oral anabolic therapy for the treatment of osteoporosis. In a 6-month, 161-patient, placebo-controlled Phase 2 study, EB613 produced rapid dose-proportional increases in biochemical markers of bone formation, reductions in markers of bone resorption, and increased lumbar spine, total hip, and femoral neck Bone Mineral Density (BMD) in postmenopausal women with low BMD or osteoporosis.A Phase 1 study comparing EB613, subcutaneous (SC) injection hPTH(1-34) 20 ?g (Forteo®) and a new generation of Entera's oral peptide delivery platform is ongoing. One of the objectives of this study is to rapidly evaluate the pharmacodynamic (PD) effects of our oral hPTH(1-34) tablets. An increase in plasma ionized calcium should result in decreased secretion and plasma concentrations of endogenous PTH(1-84). Thus, a reduction in plasma PTH(1-84) should provide an early PD marker indicating systemic exposure and pharmacologic activity with our oral hPTH(1-34) tablets.Methods: This Phase 1 open label, exploratory, cross-over study evaluating PK, PD and safety in healthy male volunteers is being conducted at Hadassah Medical Center, Israel. In the first phase of the study, EB613 (1.5 mg and 2.5 mg) tablets and SC injection Forteo® were administered in a randomized order to 15 subjects. Endogenous PTH(1-84) was measured with a intact PTH immunoassay as an early PD marker of the pharmacologic effect of the treatments.Results: Mean plasma PTH(1-84) levels following a single administration of both oral EB613 doses and Forteo® rapidly decreased in all subjects. EB613 showed comparable maximal decreases in levels of PTH(1-84) as Forteo®. Treatments were well tolerated, with safety consistent with previous studies.Conclusion: EB613 oral tablets rapidly decreased plasma concentrations of PTH(1-84) after a single dose. The early results available from this ongoing study indicate that plasma PTH(1-84) may serve as an early PD marker indicating systemic exposure and pharmacologic activity with our orally administered hPTH(1-34) tablets.

***Disclosures: Arthur C. Santora**, Entera Bio, Other Financial or Material Support*

LB SUN-647

The Impact of Stopping Oral Bisphosphonates on Plasma Advanced Glycation End Products *Tatiane Vilaca[1], Fatma Gossiel[2], Casper Schalkwijk[3], Richard Eastell[1, 1]University of Sheffield, United Kingdom, [2]The University of Sheffield, United Kingdom, [3]Maastricht University Medical Center, Netherlands

Atypical femur fractures (AFFs) have been associated with the long-term use of bisphosphonates (BP), but the risk of these fractures decreases within the first year of stopping the treatment. The mechanism for this increased risk of AFF is unknown. Advanced glycation end products (AGEs) are the result of non-enzymatic reactions between sugars and macromolecules. The accumulation of AGEs compromises the bone matrix quality and affects bone material properties. Animal models have shown that high doses of bisphosphonates (BP) promote bone accumulation of AGEs; however, the effect of therapeutic doses of BP on circulating AGEs in humans is not known. We investigated the effects of the use and withdrawal of licenced doses of oral BP on serum levels of AGEs. We hypothesise that bisphosphonates would lead to an increase in serum levels of AGEs and that levels would decrease after stopping BP.We used ultra-performance liquid chromatography with tandem mass spectrometry to measure N?-carboxy-methyl-lysine (CML) and N?-carboxy-ethyl-lysine (CEL), and Methylglyoxal-derived hydroimidazolone (MG-H1), and high-performance liquid chromatography with fluorescent detection to measure pentosidine. We used automated immunoassays to measure the C-telopeptide of type I collagen (CTX) and intact pro-collagen I N-propeptide (PINP). We used samples from 48 postmenopausal women from the TRIO/TRIO offset study, who received oral BPs (alendronate 70mg weekly or risedronate 35 mg weekly or ibandronate 150 mg monthly) for 96 weeks and were followed for 96 weeks after stopping therapy. We measured AGEs and bone turnover markers at baseline, after 48 and 96 weeks of BP therapy, and after 48 and 96 weeks of BP discontinuation. We log transformed variables that were non-normally distributed and used mixed effect analysis to compare the several timepoints.The use of BPs did not affect levels of AGEs ($p>0.05$); however, after discontinuation, there was a decrease in CML (mean 9.3% p 0.05). In contrast, BP use led to a decrease in both CTX and PINP, followed by an increase after BP discontinuation without reaching baseline levels.Levels of AGES decreased after stopping BPs. This decrease was associated with an increase in bone turnover markers and could account for reducing the risk of AFF when stopping BP therapy.

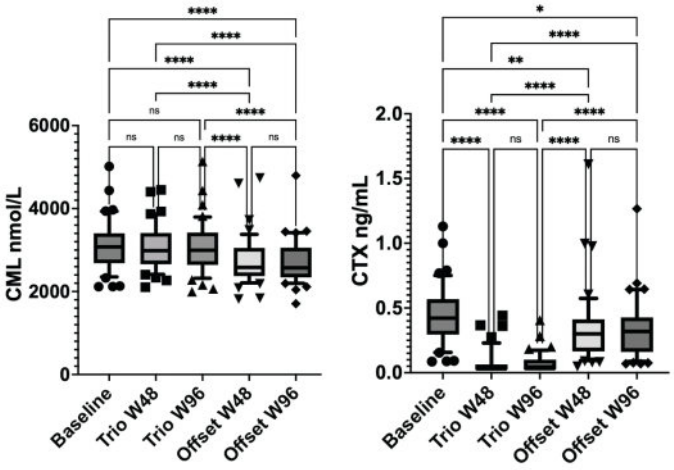

***Disclosures: Tatiane Vilaca**, Pharmacosmos, Grant/Research Support, Alexion, Grant/Research Support, Pharmacosmos, Consultant*

LB SUN-648

KTA inhibits RANKL-induced Osteoclast Differentiation and Attenuates Lipopolysaccharide-induced Bone Loss in Mice *Saroj Kumar Shrestha[1], Se woong Kim[1], Yunjo Soh[1, 1]Jeonbuk National University, Republic of Korea

IntroductionInhibitors of osteoclast differentiation have been used to treat bone diseases. The current study aimed to demonstrate that kalkitoxin thiol amide (KTA), a marine product isolated from the marine cyanobacterium Moorena producens, could be a novel therapeutic for osteoclast-related diseases.Material and MethodsEffects of KTA on osteoclast differentiation were studied in TRAP+ multinucleated cells using M-CSF/RANKL-stimulating bone marrow cells. F-actin ring formation, pit formation assay, RT-PCR, western blot and ?CT were carried out to examine the effect of KTA on bone loss.ResultsKTA suppressed RANKL-mediated osteoclast differentiation and bone resorption activity in vitro and attenuated osteoclast-specific marker gene expression, including dendrocyte-expressed seven-transmembrane proteins (DC-STAMP), tartrate-resistant acid phosphatase, matrix metallopeptidase 2, and matrix metallopeptidase-9. Likewise, molecular analyses showed that KTA attenuated RANKL-mediated MAPK signaling pathways by inhibiting the phosphorylation of ERK1/2 and p38. KTA also suppressed MMP-2, MMP-9, cathepsin K, and c-fos protein expression. Furthermore, KTA inhibited LPS-induced osteolytic bone loss,

BMD (bone-marrow density), trabecular number (Tb. N), trabecular separation (Tb.S), bone volume/trabecular volume (BV/TV), and eroded surface/bone surface (ES/BS) ratios. KTA suppressed RANKL-induced osteoclastogenesis dose-dependently by reducing cathepsin K, ERK1/2, and p38 MAPK signaling pathways in vitro, thus preventing LPS-induced bone loss in vivo.ConclusionKTA significantly suppresses bone loss in-vitro and in-vivo, suggesting that KTA could effectively treat osteoclast-related bone diseases such as osteoporosis.

***Disclosures: Saroj Kumar Shrestha**, None*

LB SUN-649

Evaluation of the bone mineral density and trabecular bone score in adults with X-linked hypophosphatemic rickets *Alberth Burnier[1], Macarena Jimenez[1], Danisa Ivanovic-Zuvic[2], Annette Madison[1], Pablo Florenzano[1]. [1]Endocrinology Department, School of Medicine. Pontificia Universidad Católica de Chile., Chile. [2]Endocrinology Section, Hospital del Salvador. Santiago, Chile. , Chile

X-linked hypophosphatemia (XLH), the most common cause of hereditary hypophosphatemia, manifests as rickets in children and osteomalacia in adults. Reports of bone mineral density (BMD) in this population have been discordant, with a trend toward higher BMD in the lumbar spine. There is limited data on trabecular bone score (TBS), whole body and forearm BMD measurements in these patients. Aim: To describe BMD and TBS inpatients with XLH, and to determine its association with clinical and biochemical phenotype. Method: Adult subjects with PHEX-confirmed XLH were included. All patients underwent lumbar spine, femoral neck, whole body and forearm GE/Lunar DEXA scans. Z-scores were defined compared to NHANES database. Clinical and biochemical data were obtained to determine its association with BMD. Results: Twenty-five adults were included, 18 (72%) women, median age of 35y (21-66). All patients were hypophosphatemic, 64% had elevated alkaline phosphatase and 52% had secondary hyperparathyroidism. Mean BMD at lumbar spine and the whole body was 1.405 gr/cm2 (Z-score: 2.1) and 1.190 gr/cm2 (Z-score: 1.1), respectively, both significantly higher than normal range ($p<0.05$). Mean BMD at the radius 33% was 0.596 gr/cm2 (Z-score: -1.7) , and 0.362 gr/cm2 (Z score: -0,5) at the ultra-distal radius, both significantly lower than the norm-based population ($p<0.05$). Mean TBS was 1.519 with a mean Z-score of 1.43, significantly higher than the normal population ($p<0.05$). Mean BMD at the femoral neck was 0.888 gr/cm2 (Z-score: -0.7). The rate of exposure to conventional treatment was negatively correlated with the whole body BMD ($p=0.009$, $r=-0.6$) and lumbar spine BMD ($p=0.02$, $r=-0.53$). Other clinical and biochemical parameters, such as alkaline phosphatase, PTH, vitamin D or FGF23 did not significantly correlate with BMD at any sites. Conclusions: Our population presents with higher lumbar spine BMD, whole body BMD and TBS compared to reference data, and lower BMD at the 33% and ultra-distal radius. Exposure to treatment is associated to lower BMD in the whole body and lumbar spine BMD. These findings suggest that the increased BMD at the spine could not only be explained by paraspinal calcifications, and that appropriate conventional treatment could have an impact on the high spine BMD phenotype of subjects with XLH.

***Disclosures: Alberth Burnier**, None*

LB SUN-650

Effect of Burosumab on Growth Trends in Patients with X-Linked Hypophosphatemia *Thomas Carpenter[1], Leanne Ward[2], Suzanne Jan De Beur[3], Hamilton Cassinelli[4], Erik Imel[5], Jill Simmons[6], Anna Ryabets-Lienhard[7], Jerry Li[8], Eric Chen[9], Antonio Ramirez[9]. [1]Yale University School of Medicine, United States. [2]Children s Hospital of Eastern Ontario, Canada. [3]Johns Hopkins University, United States. [4]CEDIE, Centros de Investigaciones Endocrinologicas Dr Cesar Bergada, Division de Endocrinologia, Hospital de Niños Ricardo Gutierrez, Argentina. [5]Indiana University School of Medicine, United States. [6]Vanderbilt University Medical Center, United States. [7]Children's Hospital Los Angeles , . [8]Kyowa Kirin, . [9]Ultragenyx Pharmaceutical Inc., United States

X-linked hypophosphatemia (XLH) is a rare, musculoskeletal disorder due to PHEX pathogenic variants characterized by rickets/osteomalacia leading to bone pain, skeletal deformities, and short stature. This initial analysis explores growth patterns in patients treated with burosumab from the XLH Disease Monitoring Program (DMP; NCT03651505) supplemented with data from prior XLH studies via DataLink, a compilation of clinical trial data.To assess the impact of XLH on age-dependent growth velocity, we explored records of patients (regardless of burosumab treatment) aged <25 years at entry into the DMP or other XLH studies with Center for Disease Control (CDC) reference values. We then examined height Z-score by age in the study population regardless of burosumab status. To assess the impact of burosumab, changes in height Z-score from first burosumab dose or observation (burosumab-naïve) were examined separately by duration of treatment or observation. Records represent study visits by treatment status; patients may have multiple records by age. Data are presented based on availability of endpoints for each record.As of June 2023, data were available from 592 patients aged <25 years at study entry. Mean CDC reference growth velocity peaked at age 13 years in males and 11 in females. In patients with XLH (burosumab-naïve and treated combined), mean growth velocity peaked at age 15 years in males and 12 in females, remaining above CDC values through age 18 when growth stopped in both cohorts.At the last record of each patient (burosumab-naïve and burosumab-treated combined), a downward trend in absolute height Z-score was seen from age 1 (n=17 records; mean (SD) -1.0 [1.7]) to age 8 years (n=44 records; mean [SD] -1.7 [1.4]). After age 8, mean height Z-scores stabilized (range of means [SD] -1.6 [1.1] to -2.1 [1.2]) through age 18.Height Z score changes from baseline in treated and burosumab-naïve patients age <8 were compared by duration of treatment/observation at each record date (Figure 1). Over the first 3 years, height Z-score decreased in burosumab-naïve patients and remained constant in treated patients ($p<0.001$).XLH is associated with growth delays, with the greatest delays in the first 8 years of life. Available study data in a limited population suggest burosumab treatment in this period may mitigate early negative impacts of XLH on growth velocity. Future analyses will explore its effect on final height.

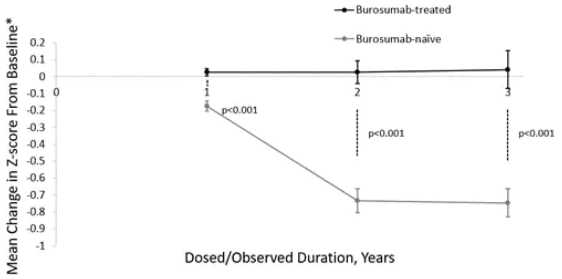

n, records =			
Burosumab Treated	474	100	58
Burosumab-naïve	876	369	297

*Baseline defined as time of first observation or burosumab treatment

***Disclosures: Thomas Carpenter**, Ultragenyx Pharmaceutical Inc., Grant/Research Support, Kyowa Kirin, Consultant, Ultragenyx Pharmaceutical Inc., Consultant*

LB SUN-651

(Towards Establishing Clinically Useful Treatment Guidelines for ERT in HPP Patients) Understanding the Impact of Discontinuing Enzyme Replacement Therapy in Adult Patients with Hypophosphatasia *Kathryn Dahir[1], Scout Dahir[2], Margo Black[1], Emery Mason Campbell[1], Cheryl Rockman-Greenberg[3]. [1]Vanderbilt University Medical Center, United States. [2]Vanderbilt University, United States. [3]Max Rady College of Medicine, Rady Faculty of Health Sciences, University of Manitoba, Canada

Hypophosphatasia (HPP) is a rare, genetic disorder caused by loss-of-function mutations in the ALPL gene. Disease presentation is variable, including skeletal, non-skeletal rheumatologic and neurological manifestations. HPP has no cure, but the advent of enzyme replacement therapy (ERT) has resulted in sustained improvement of disease burden. However, in the real-world, clinical practice setting, some patients discontinue ERT therapy due to perceived lack-of-benefit, side effects or restricted access. To anticipate and improve management of patients who discontinue ERT, comprehensive treatment guidelines are required that better identify these subgroups. The data regarding discontinuation of ERT in adults is limited to a published case series of 6 highly affected Canadian patients who lost access to ERT. Reasons for discontinuation of ERT in less affected individuals are unknown. The current study was based on the hypothesis that, in contrast to the Canadian cohort, cohorts at the Nashville site who discontinued asfotase alfa ERT (StrensiqTM) manifest different disease burden and characteristics. To test this hypothesis, the clinical characteristics of 39 HPP patients were recorded prior to treatment and the patients then longitudinally followed in an ongoing study: 10.3% (n=4) electively stopped ERT due to perceived lack of efficacy, 28.2% (n=11) stopped ERT due to adverse events (hypersensitivity or injection side reactions), 5.1% (n=2) lost access to ERT, and 56.4% (n=22) continued ERT. Patients who electively stopped ERT were all female, had lower body mass index, and started ERT later in life compared to patients continuing ERT. Further, these 4 patients who electively stopped ERT experienced at baseline fewer musculoskeletal complications, including osteoarthritis (-69.4%), joint stiffness (-45.0%), fractures (-33.6%), and increased mobility (+16.6%) when compared to 2 patients stopping ERT due to adverse events. In contrast, fatigue and neurological complications of headaches and abnormal balance were the predominant disease features of those 4 patients who electively stopped ERT. All patients with adverse events or restricted ERT access suffered from high disease burden, thus making it important to devise sustainable treatment guidelines and access for these patients. These observations show that discrete disease burden may inform on ERT adherence and may aid in the development of effective, safe, and individualized ERT guidelines.

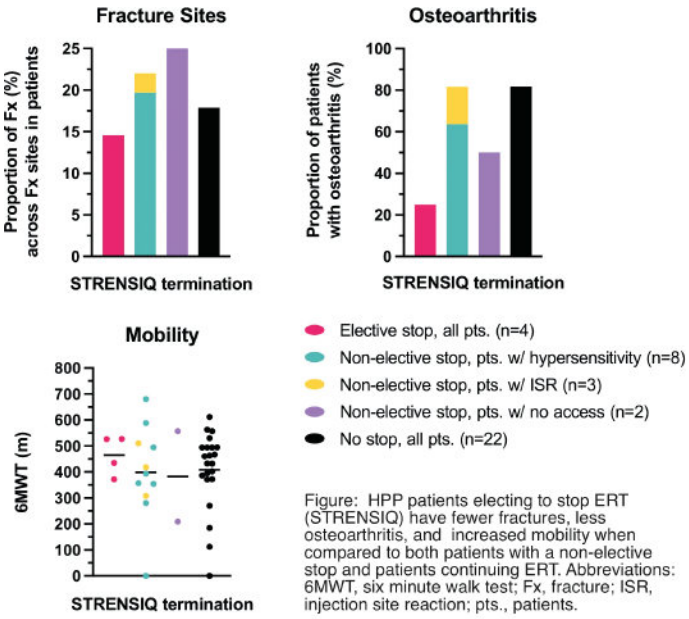

Figure: HPP patients electing to stop ERT (STRENSIQ) have fewer fractures, less osteoarthritis, and increased mobility when compared to both patients with a non-elective stop and patients continuing ERT. Abbreviations: 6MWT, six minute walk test; Fx, fracture; ISR, injection site reaction; pts., patients.

***Disclosures: Kathryn Dahir**, None*

LB SUN-652

Eneboparatide, A Novel Investigational PTH1R Agonist, Maintains Calcium Homeostasis Without Deleterious Effects on Bone *Mark Sumeray[2], Michel Ovize[2], Soraya Allas[2], Guillaume Ravel[2], Myriam Aouadi[2], Michael Culler[2]. [2]Amolyt Pharma, France. [2]Amolyt Pharma, United States

Eneboparatide (EBO) is a novel PTH type 1 receptor (PTH1R) agonist with a short half-life and high affinity for the R0 receptor conformation. This profile is expected to result in maintenance of serum calcium (sCa) in chronic hypoparathyroidism (cHP) by recycling Ca from the glomerular filtrate and enhanced intestinal Ca absorption while avoiding the net bone resorptive effects of continuous PTH1R exposure. To explore this, data were examined from studies in non-human primates (NHP), healthy human volunteers (HV) and patients with cHP. NHP received daily sc EBO injections for 39 weeks at doses within and above the anticipated human therapeutic dose range. In HV, EBO was administered up to 80 µg/day for 2 weeks. In a phase 2 study cHP patients received sc EBO administration for 3 months starting at 10 or 20 ?g/day. sCa, 1,25 dihydroxy vitamin D (1,25 OH Vit D), bone biomarkers, and 24h urinary Ca (uCa) were measured in HV and patients. Bone mineral density (BMD) was measured in cHP patients by dual-energy X-ray absorptiometry. In NHP, BMD was measured by quantitative computed tomography, and bone histology was evaluated. In NHP, BMD, bone structure and turnover markers remained unchanged over 39 weeks. In HV there were no changes in bone biomarkers. In cHP patients, EBO had no significant effect on BMD and induced a modest, balanced increase in bone biomarkers (CTX and P1NP), consistent with resumption of physiologic bone turnover. Bone biomarkers and sCa levels were not correlated. In HV there was no increase in uCa despite marked elevation of sCa at higher doses of EBO. In cHP patients with hypercalciuria at baseline, uCa excretion was correlated with sCa levels. EBO treatment normalized uCa which was no longer correlated with sCa levels. Despite withdrawal of active Vit D supplements, EBO treatment maintained stable, normal levels of 1,25 OH Vit D. The collective data from NHP, HV and cHP patients indicate that EBO does not induce net bone loss. Further, treatment of HV with EBO maintains renal capacity to reabsorb Ca as sCa increases, while in cHP patients, EBO restores normal renal Ca reabsorption. EBO stimulated renal conversion of 25-0H to 1,25-0H Vit D allows continued intestinal Ca absorption despite the removal of supplements. These data suggest that restoration of Ca homeostasis with EBO in cHP is likely due to a sustained effect on renal Ca reabsorption and intestinal Ca uptake without deleterious effects on bone.

***Disclosures: Mark Sumeray**, Amolyt Pharma, Other Financial or Material Support*

LB SUN-653

Injury-induced and Spontaneous Heterotopic Ossification in a New Acvr1 R206H Mouse Model for FOP *Salin A. Chakkalakal[1], Douglas W. Roberts[1], Jeffrey Xi[1], Maurizio Pacifici[2], Eileen M. Shore[1]. [1]Perelman School of Medicine, University of Pennsylvania , United States. [2]The Children's Hospital of Philadelphia, United States

Fibrodysplasia ossificans progressiva (FOP) is a rare disorder of heterotopic endochondral ossification (HO). In FOP, HO occurs in the absence or in response to tissue injury. Most patients with FOP share a heterozygous single nucleotide substitution (c.617G>A; R206H) in ACVR1 that encodes the bone morphogenetic protein type I receptor ALK2. A conditional Acvr1R206H/+ knock-in mouse (Acvr1[R206H]FlEx/+) was previously created to investigate disease pathogenesis. Once induced, the Acvr1R206H-expressing mice formed HO in response to injury. However the engineered allele in this model is null for Acvr1 prior to Cre-recombination, a possible complication. We developed an alternative knock-in mouse (Acvr1ARC-R206H/+) in which the engineered allele expresses wild-type R206 Acvr1 prior to Cre recombination and R206H following Cre. Here, we characterize the HO phenotype of this new model. Using our established approach for injury-induced HO, Acvr1R206H expression was activated globally via rt-tetO-Cre and leg skeletal muscle was then injured by cardiotoxin (ctx). Progression to HO was examined by histology and HO volume quantified by microCT over 2 weeks post-injury. Previously defined histologic stages of HO progression and altered muscle repair were identified, but with more robust chondrogenesis (5 dpi) and an apparent slower transition from cartilage to bone. We used the same rt-tetO-Cre system to examine 'spontaneous' HO progression in the absence of ctx injury. We found that HO developed more slowly than in response to ctx tissue injury. Little HO was detected by microCT at 3 weeks, but consistently formed by 4 weeks. Upon specific expression of Acvr1R206H in skeletal mesenchymal progenitor cells (Acvr1ARC-R206H/+;Prrx1-Cre), no extra bone was detected during embryogenesis; however at birth, development effects were indicated by reduced body length, malformed limbs with webbed digits, fused joints, and spine and skull malformations. Within 2 weeks after birth, spontaneous HO occurred that was more robust and rapidly progressive than that induced by global Cre induction, supporting the importance of cell interactions to regulate cell fate. Overall, our new FOP mouse shows more robust phenotypes than a previously described model. It is the first model for global induction of spontaneous (non-injury-induced) HO, providing a novel, patient-relevant system to investigate the initiation, progression, and cell mechanisms that regulate heterotopic ossification.

***Disclosures: Salin A. Chakkalakal**, None*

LB SUN-654

A Cell Culture Model Suggests a Key Function for Paracrine Signaling in the Development of Bone Fibrous Dysplasia *Amin Cressman[1], David Morales[1], Zhenyang Zhang[1], Fernando Fierro[1], Rakel Runarsdottir[1]. [1]Stem Cell Program, University of California Davis, United States

Fibrous Dysplasia/McCune Albright Syndrome (FD/MAS) is a rare disease caused by gain-of-function mutations in the gene coding for Gsalpha protein. We modelled the disease in a dish by modifying human bone marrow derived multipotent stromal cells (MSCs) to over-express either wild type Gsa or mutant Gsa (R201C and R201H). As additional control, MSCs were transduced with a lentivirus without over-expression of Gsa. MSCs expressing mutant Gsa (R201C or R201H), but not wild-type Gsa, show significantly higher levels of cAMP, impaired cell motility, and marked morphological changes that resemble excess RhoA signaling. Mutant Gsa also significantly inhibits osteogenic differentiation, measured by alkaline phosphatase activity at day 10 and mineralization (Alizarin Red S staining) at day 21. Interestingly, MSCs expressing mutant Gsa show decreased cell proliferation, but co-cultures with unmodified MSCs show increased cell growth as compared to controls. Even more, treatment of unmodified MSCs with supernatants derived from modified cells suggests that MSCs expressing mutant Gsa release signals that induce cell proliferation. Finally, we show that these supernatants induce activation of the canonical Wnt pathway on unmodified cells. A proteomic analysis of these supernatants lists a number of potential candidates driving this paracrine signaling. Our findings shed new light on the mechanism by which mutant Gsa may cause FD/MAS phenotype and offers a new platform to test potential therapeutic interventions.

***Disclosures: Amin Cressman**, None*

LB SUN-655

Sexual Dimorphism in Treatment Effect of Anti-Siglec 15 in Adult Mice with Moderate-to-Severe Osteogenesis Imperfecta *Ketsia Seide[1], Holly LoTurco[1], Erin Carter[1], Nancy Pleshko[2], Priyanka Kothari[3], Sol Langermann[3], Shanmugam Selvam[3], Cathleen Raggio[4]. [1]Hospital for Special Surgery, United States. [2]Temple University, United States. [3]Nextcure, Inc., United States. [4]HSS, United States

Purpose: Osteogenesis imperfecta (OI) is a heterogeneous type 1 collagenopathy characterized by bone fragility. Gaps persist for effective pharmacological treatment in adult patients. We previously demonstrated that a monoclonal antibody targeting the sialic acid-binding immunoglobulin-like lectin 15 (Siglec 15) immunoreceptor [1], NP159 (NextCure), improves bone quality and decreases fractures in female oim mice. We have now extended the study to evaluate efficacy in male oim mice. Methods: In this portion of the study, eighty male mice (20 wildtype (WT) saline, 20 WT NP159, 20 oim/oim saline, and 20 oim/oim NP159) were treated from age 14 -26 weeks with either NP159 (10mg/kg weekly x1 month then biweekly) or weekly saline. Faxitrons at 14 and 26 weeks were taken to evaluate fracture incidence and healing. Tibias and femurs were analyzed post-sacrifice for femoral length, microcomputed tomography (micro-CT) , biomechanical testing and Fourier Transform Infrared Spectroscopy (FTIR). These results were compared to a previous study completed with female mice.Results: With treatment, 90% of male oim/oim NP159 vs. 85% of female oim/oim NP159 seen earlier, had no new fractures. Micro-CT showed decreased trabecular separation with NP159 treatment in both oim/oim males and females (p=0.05). Cortical porosity was normal in the male mice treated with NP159, in contrast with females

who showed increased porosity. There were no changes in the bone mineral density for male or female mice. NP159 increased stiffness of the bones in both sexes. FTIR in females showed a normalization of mineral:matrix ratio, increased acid phosphate and decreased collagen maturity. In contrast, the males showed no similar changes. Conclusion: Overall the results show promising trends for the use of NP159 treatment for OI. Fracture incidence was reduced. Sexual dimorphism was seen with treatment and is consistent with dimorphism both in humans and previously reported treated mice models. The observed cortical and trabecular bone changes support the premise that NP159 works as both an antiresorptive and a bone formation agent, and seems to be favorable for bone strength in both sexes as indicated by the increased stiffness shown on biomechanical testing. References 1. Sato, D., Takahata, M., … Iwasaki, N. Bone 2018; 116, 172-180. We thank NextCure for their ongoing support of this project (CLR).

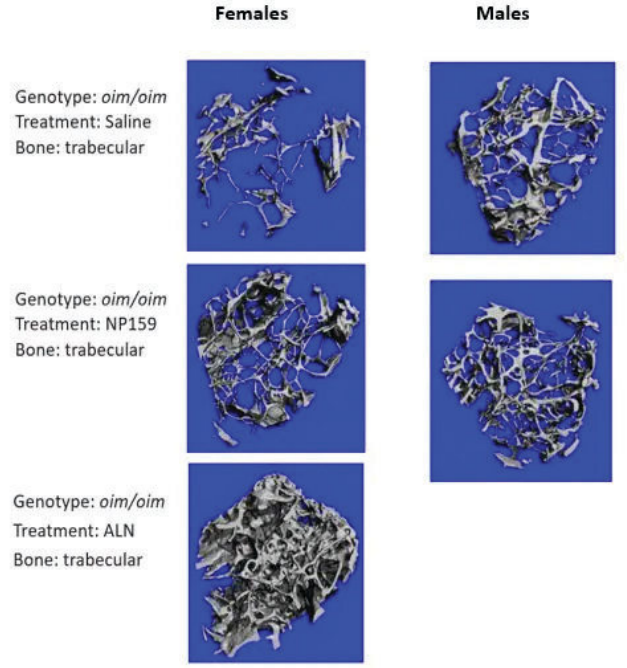

Micro-CT 3D images of *oim/oim* trabecular bone

***Disclosures: Ketsia Seide**, None*

LB SUN-656

Forearm Muscle Strength Assessment by Means REMS Technology *Paola Pisani[1], Fiorella Anna Lombardi[1], Chiara Stomaci[1], Fabiola Rosa Contaldo[2], Maurizio Muratore[3], Tommaso De Marco[4], Luigi Antelmi[4], Sergio Casciaro[1]. [1]Istituto di Fisiologia Clinica, Consiglio Nazionale delle Ricerche, Lecce, Italia, Italy. [2]Università del Salento, Dipartimento di Ingegneria dell'Innovazione, Lecce, Italia, Italy. [3]Vito Fazzi Hospital, ASL-LE, Lecce, Italy, Italy. [4]R&D Department, Echolight S.p.a., Lecce, Italy, Italy

Muscle Diseases, also known as myopathies, are a group of disorders that affect the human muscle system and their main manifestation is skeletal muscle weakness, reduced muscle function, and sometimes muscle wasting. Sarcopenia represents a main contributor to the burden of musculo-skeletal conditions. It is a medical term used to describe the loss of skeletal muscle mass, strength, and function. The literature shows that muscle and bone are physiologically related, and therefore sarcopenia and osteoporosis coexis, in fact, it is estimated that over 30% of fractured individuals are also affected by sarcopenia. Therefore, the aim of this study is to assess the level of forearm muscle strength by means of a Radiofrequency Echographic Multi Spectrometry (REMS)-based algorithm.For the evaluation of the forearm musculature, when the patients was in supine position with the elbow joint fully extended, an ultrasound scans of the dominant forearm by using a 40-mm linear probe (EchoStation device made by Echolight S.p.a., Italy) was performed in the transverse projection considering ulna and radius as reference anatomical sites. In addition, to estimate the MVC (maximum voluntary contraction) of the dominant arm for each subject, a hand dynamometer grip was used and only the maximum obtained value was included in the subsequent analyses.In this study, 30 healthy subjects were enrolled, with a mean age of 40 years and BMI in the range of 18.5-29.1 kg/m2. The automatic REMS-based algorithm used to investigate lumbar and femoral sites, was optimised in order to extend its use for muscle assessment. An automatic identification and analysis of the region of interest (ROI) of the forearm muscles allows to predict MVC value. An accurate data analysis showed a high correlation between the value of MVC and the corresponding value predicted by the algorithm (MVCREMS) with a Pearson's coefficient of 0.94 (p-value < 0.001).The obtained data demonstrate that REMS technology can estimate the muscle strenght of the dominant forearm. Therefore, REMS lets have innovative possibilities for the assessment of both muscle and bone, enabling an overall estimation of musculo-skeletal pathology by improving prevention and diagnosis.

***Disclosures: Paola Pisani**, None*

LB SUN-657

A pilot study of low-intensity vibration training to reduce symptoms and improve gait and stability in cancer survivors with chemotherapy-induced peripheral neuropathy (NCT04170075) *Kerri Winters-Stone[1], Kendra Braun[1], Becky Chan[1], Stephanie Krasnow[1], Sydnee Stoyles[1], Nathan Dieckmann[1], Eric Roeland[1], Clinton Rubin[2]. [1]Oregon Health & Science University, United States. [2]Stony Brook University, United States

Background: Chemotherapy-induced peripheral neuropathy (CIPN) is a debilitating and dose-limiting side effect of systemic cancer therapy. CIPN can persist after treatment ends and is associated with functional impairments, abnormal gait patterns, postural instability, and injurious falls. Low-intensity vibration (LIV) may reduce symptoms of CIPN and improve gait and stability, but it has never been tested.Methods: We conducted a pilot randomized controlled trial comparing LIV to usual care (UC) on symptoms and mobility in cancer survivors with persistent CIPN (n=40). Participants completed chemotherapy for early-stage adult-onset cancer within the previous 5 years and self-reported the presence of any CIPN. Participants assigned to LIV were asked to complete 2 x 10-minute LIV sessions daily for 12 weeks using a vibration platform (Marodyne LiV®; dose: 30 Hz, 0.4g). While standing on the LIV platform, participants were encouraged to slowly sway in a clockwise fashion . Outcomes included self-reported CIPN using the FACT/GOG-NTX, assessing the presence and severity of CIPN. Postural sway was measured using an instrumented (iSWAY, Mobility Lab, Clario, Inc) 30-second quiet stance test. Gait was measured using a 7-foot instrumented timed-up-and-go test (iTUG). Given our small sample size for this pilot, we report effect sizes using Cohen's d. Analyses were repeated, limiting the LIV group to those with compliance rates above 50%.Results: Overall, 38 participants provided pre- and post-data for analysis (age: 60.1 + 9.4 years; 22.6 + 17.6 months past chemotherapy completion). One statistical outlier was removed from the outcome analysis (n=20 in LIV and n=17 in UC). On average, LIV participants completed 82% of prescribed sessions with 1 moderate adverse event (foot discomfort). There was a small positive effect size of LIV vs UC for CIPN symptoms (Cohen's d = 0.4), which increased to moderate when removing non-compliant participants (Cohen's d = 0.6). There were moderate to large effect sizes favoring LIV vs UC for TUG time (Cohen's d = 0.6), step number (Cohen's d = 0.6), centroidal sway frequency (Cohen's d = 0.8), and sway velocity (Cohen's d = 0.5). Effect sizes improved slightly when removing non-compliant participants.Conclusions: LIV shows promise for CIPN symptom relief and improving stability and gait in cancer survivors with persistent symptoms. A larger, fully powered controlled trial that includes falls as an outcome is warranted.

***Disclosures: Kerri Winters-Stone**, None*

LB SUN-658

Glucocorticoids Inhibit Longitudinal Advance of Cortical Bone Basic Multicellular Units in the Rabbit *Lindsay Loundagin[1], Kim Harrison[1], Beverly Hiebert[2], Arash Panahifar[3], Ning Zhu[3], Terra Arnason[4], Kurtis Swekla[5], Peter Pivonka[6], David Cooper[1]. [1]Department of Anatomy, Physiology and Pharmacology, College of Medicine, University of Saskatchewan, Saskatoon, Canada, Canada. [2]Max Rady College of Medicine, University of Manitoba, Winnipeg, Canada, Canada. [3]BioMedical Imaging and Therapy Beamline, Canadian Light Source, Saskatoon, Canada, Canada. [4]Medicine Department of Endocrinology, Faculty of Medicine & Dentistry, University of Alberta, Edmonton, Canada, Canada. [5]Animal Care and Research Support Office, Office of the Vice President of Research, University of Saskatchewan, Saskatoon, Canada, Canada. [6]School of Mechanical, Medical, and Process Engineering, Queensland University of Technology, Brisbane, Australia, Australia

Cortical bone remodeling is performed by basic multicellular units (BMUs), which couple resorption and formation to replace discrete packets of bone. This coupling is the foundation of classic histomorphometric evaluation of BMU dynamics. For example, the rate at which formation longitudinally advances may be directly evaluated with sequential fluorochrome labels and has been used to indirectly infer the rate of resorption (i.e., longitudinal erosion rate; LER), assuming synchronized and equal advance of resorption and formation fronts. In the case of glucocorticoid-induced osteoporosis, bone formation is greatly reduced and BMUs have been described as uncoupled, with formation being absent or delayed, such that inferring LER is not feasible. To address this knowledge gap and test the hypothesis that glucocorticoids alter LER we used an in vivo imaging protocol to track individual remodeling events and determine the LER of cortical BMUs in rabbits treated by ovariohysterectomy (OVH), glucocorticoids (GC), a combination thereof (OVH+GC) and SHAM controls (n=5 per group). Ten weeks post OVH or sham surgery, and two weeks after the initiation of dosing (daily subcutaneous injections 1ml of saline or 1.5mg/kg/day of methylprednisolone sodium succinate), the right tibiae were scanned in vivo using in-line phase contrast micro-CT (voxel size=13?m) at the Canadian Light Source synchrotron.

Following two additional weeks of dosing, the rabbits were euthanized and ex vivo images were collected using desktop micro-CT (voxel size=5?m). The datasets were co-registered in 3D and LER was calculated as the distance traversed by BMU cutting-cones in the 14-day interval between scans. The median LERs of OVH and SHAM rabbits were similar at 41.28 and 40.06µm/day [1] (p=0.307), respectively. BMUs in the GC and OVH+GC group were largely arrested, indicated by a median LER of 2.89 and 3.10µm/day, respectively, both of which were significantly slower than LER in OVH and SHAM (p<0.001). Despite the lack of longitudinal advance, radial resorption of the remodeling space was evident in many of the GC and OVH+GC BMUs (Fig. 1). It is known that GCs disrupt BMU coupling, primarily impacting osteoblasts; however, our results provide a novel 4D perspective that suggests, in addition to impaired formation, GC treatment can also lead to the creation of remodeling spaces that fail to progress longitudinally.[1] Previously reported by Harrison et al. JBMR. 2022 Nov; 37(11): 2244-2258.

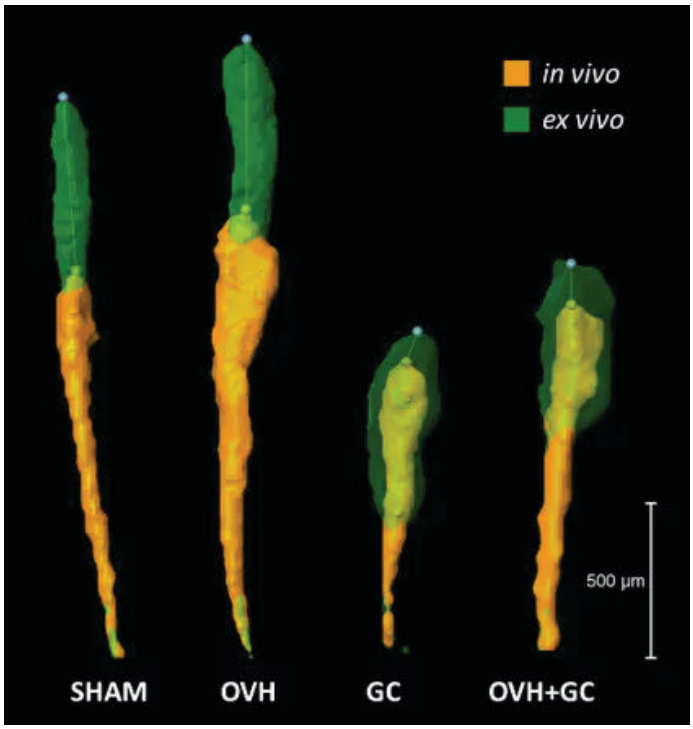

***Disclosures: Lindsay Loundagin**, None*

LB SUN-659

The enzyme 11?-hydroxysteroid-dehydrogenase influences bone metabolism and bone mineral density through local inactivation of prednisolone *Martina Blaschke[1], Ina Dressel[1], Regine Köpp[2], Gabriele Armbrecht[3], Stephan Sehmisch[4], Mlladen Tzvektov[5], Frank Streit[6], Holger M. Reichardt[7], Claus-C Glueer[8], Heide Siggelkow[2]. [1]Clinic of Gastroenterology, Gastrointestinal Oncology and Endocrinology, Germany. [2]Clinic of Gastroenterology, Gastrointestinal Oncology and Endocrinology, University Medical Center, Germany. [3]Center for Muscle and Bone Research, Charité; 12203 Berlin, Germany. [4]Clinic for Trauma Surgery, Orthopedics and Reconstructive Surgery, University Medical Center, Germany. [5]Department of General Pharmacology, University Medicine Greifswald, Germany. [6]Department of Clinical Chemistry, University Medical Center, Germany. [7]Institute for Cellular and Molecular Immunology, University Medical Center, Germany. [8]Christian Albrechts Universitaet zu Kiel, Germany

Glucocorticoids (GC) are inactivated in the kidneys by 11?-hydroxysteroid dehydrogenase type 2 (11?-HSD2) and reactivated at sites of inflammation by 11?-hydroxysteroid dehydrogenase type 1 (11?-HSD1). We investigated the role of 11?-HSD1 in the activation and inactivation of glucocorticoids by analyzing effects in bone in vitro and in vivo.Two different human osteoblast-like cell models were stimulated with prednisone, or prednisolone with or without inhibition of 11?-HSD1 activity. Subsequently, GC metabolites were analyzed in combination with adipogenic and osteogenic differentiation. The in-vivo study included 216 patients treated with prednisolone or methylprednisolone for different inflammatory diseases. Bone mineral density (BMD), fractures, and history of falls were investigated in combination with genotyping for single nucleotide polymorphisms of HSD11B1 as parameter of 11?-HSD1 activity.In our study, the conversion of prednisone to prednisolone and vice versa in human models of mesenchymal stem cells is catalyzed by 11?-HSD1. This mechanism affects cell differentiation. In patients treated with prednisolone for inflammatory diseases, the oxidative capacity of the enzyme is the main factor influencing BMD.Further investigations of patients and the development of pharmaceuticals influencing 11?-HSD1 enzyme function should therefore also focus on its oxidative capacity.

***Disclosures: Martina Blaschke**, None*

LB SUN-660

Impact of HIV on tibial bone density, geometry, and strength in midlife Zimbabwean Women and association between pQCT outcomes and fracture *Micheal O'Breasail[1], Cynthia Mukwasi-Kahari[4], Tafadzwa Madanhire[4], Victoria Simms[4], Lisa Micklesfield[3], Rashida Ferrand[4], Celia Gregson[5], Kate Ward[6]. [1]Monash University, Australia. [4]The Health Research Unit (THRU) Zimbabwe, Biomedical Research and Training Institute, Harare, Zimbabwe ; LSHTM, Zimbabwe. [3]SAMRC/Wits Developmental Pathways for Health Research Unit, School of Clinical Medicine, Faculty of Health Sciences, University of the Witwatersrand, South Africa. [4]The Health Research Unit (THRU) Zimbabwe, Biomedical Research and Training Institute, Harare, Zimbabwe ; LSHTM, United Kingdom. [5]University of Bristol, United Kingdom. [6]MRC Lifecourse Epidemiology Centre, University of Southampton, United Kingdom

Background: HIV and its treatment are associated with deficits in bone and an increased risk of fracture; however, limited data are available from sub-Saharan African women during midlife, and importantly during the menopause transition. We used peripheral QCT to measure tibial bone density, geometry, and strength in pre- peri-, and postmenopausal Zimbabwean women living with (WLWH) and without HIV (WLWOH). and determined whether pQCT measures were associated with self-reported fractures.Methods: Tibia pQCT scans were obtained from 384 women aged 40-61 years (n=191[49%] +Ve). pQCT outcomes were: 4% total area (Tot.A4, mm2), trabecular volumetric bone mineral density (Trab.vBMD, mg/cm3), and compressive bone strength (BSIc, g2/cm4); 38% cortical vBMD (Ct.vBMD, mg/cm3), total area (Tot.A38, mm2), and Stress-Strain Index (SSI, mm3). Height (m) weight (kg) and menopause status based on last menstrual period were recorded (pre=regular period; peri= irregular period/ ammenhorea <= 12 months; post > 12months after last period). Linear regression investigated differences adjusting for age, menopause stage, and height, and then additionally for weight. In all women, odds ratios were calculated to test whether pQCT measures were associated with self-reported 1) any fracture; 2) major osteoporotic fracture.Results: Women were of mean(SD) age 49.6(5.8) years and BMI 29.0(6.1) kg/m2. Weight and BMI were lower in WLWH (both p<0.001), with no differences in age or height. All unadjusted pQCT outcomes except Tot.A4 were lower in WLWH (all p<0.05, Figure 1). These relationships were robust to adjustment for age, menopause stage, and height (all p<0.001) apart from Tot.A38. Further adjustment for weight attenuated only the between-group difference in SSI. BSIc and SSI were associated with lower odds of previous major osteoporotic fracture (OR[95%CI]: BSIc, (0.46 [0.26;0.79]); SSI, 0.53 [0.29;0.93]). Conclusion(s): In perimenopausal Zimbabwean women, HIV impacts both tibial trabecular and cortical bone density. These relationships were robust to adjustment for age, menopause status and height, though the addition of weight to the models reduced the effect size. In the whole group, pQCT outcomes were associated with self-reported MOF. Further investigation will explore in greater detail how body composition and its determinants may explain the observed HIV-related differences and fracture risk.

Table 1. Linear regression to determine the extent of between-group differences between perimenopausal Zimbabwean women aged 40-61 years

N=384	Unadjusted model		Adjusted for age, menopause, and height		Adjusted for age, menopause, height, and weight	
Tibia 4%	MD [95% CI]	p-value	MD [95% CI]	p-value	MD [95% CI]	p-value
Trabecular vBMD (mg/cm^3)	-16.1 [-23.4; -8.8]	**<0.001**	-16.1 [-23.3; -8.8]	**<0.001**	-8.10 [-15.10; -1.08]	**0.024**
Total CSA (mm^2)	-9.36 [-33.90; 15.20]	0.454	2.04 [-19.80; 23.90]	0.854	8.29 [-14.40; 31.00]	0.474
BSIc (g^2/cm^4)	-0.139 [-0.182; -0.097]	**<0.001**	-0.131 [-0.171; -0.091]	**<0.001**	-0.0637 [-0.0985; -0.0289]	**0.001**
Tibia 38%	MD [95% CI]	p-value	MD [95% CI]	p-value	MD [95% CI]	p-value
Cortical vBMD (mg/cm^3)	-13.0 [-20.3; -5.8]	**<0.001**	-11.1 [-17.2; -5.0]	**<0.001**	-12.3 [-18.7; -6.0]	**0.001**
Total CSA (mm^2)	-12.4 [-22.8; -2.0]	**0.020**	-6.76 [-15.60; 2.13]	0.136	2.46 [-6.26; 11.20]	0.579
SSI (mm^3)	-120 [-180; -60]	**<0.001**	-83.3 [-134.0; -32.6]	**0.001**	-27.5 [-76.8; 21.8]	0.273

MD = mean difference; CI = confidence interval. Women without HIV as the reference group, such that negative values mean those with HIV have lower values.

***Disclosures: Micheal O'Breasail**, None*

1081

ER? signaling in resident synovial macrophages promotes inflammatory arthritis via the activation of cellular metabolism *Yuuki Imai[1], Noritaka Saeki[2]. [1]Ehime University Prote-Science Center, Japan. [2]Ehime university, Japan

Rheumatoid arthritis is an autoimmune disease that exhibits sex differences in prevalence and pathogeneses. It has been suggested that female sex hormones are related to such sex differences, however molecular mechanisms of sex hormones and these receptors remain unclear in rheumatoid arthritis. Especially, the functions of sex hormone receptors in macrophages are largely unknown.We found the levels of ER? mRNA was the highest among examined sex hormone receptors (ER?, ER?, Gpr30, PR, AR) in synovial macrophages derived from serum-transfer arthritis (STA) by RT-qPCR. Thus, myeloid-specific ER? knockout mice (cKO, LysMCre; ER?flox/flox) and littermate control mice (Ctrl, ER?-flox/flox and LysMCre; ER?flox/+) were established and induced experimental arthritis. Development of STA pathogenesis was significantly inhibited in female cKO compared to Ctrl, but not in male. Flow cytometry analysis showed that the proportions of blood-monocyte subpopulations were almost comparable between Ctrl and cKO, and parabiosis with Ctrl and cKO indicates similar STA pathogenesis, suggesting that ER? signaling in resident synovial macrophages promotes inflammatory arthritis. scRNA-seq analysis using synovial cells obtained from STA on day 3 showed increased cell number of resident synovial macrophage clusters (Lyve1+ cluster and Cx3cr1+ cluster) in cKO compared to Ctrl. Gene ontology analysis against highly expressed genes in Ctrl than cKO showed significant enrichment in the biological process termed “metabolic process” in both Lyve1+ and Cx3cr1+ clusters and in the pathway termed “positive regulation of cell death” in Lyve1+ cluster. To understand cellular metabolism dependent on ER? signaling in macrophages, extracellular acidification rate (ECAR) and oxygen consumption rate (OCAR) were analyzed by flux analyzer using bone marrow macrophages derived from Ctrl and cKO. ECAR and OCAR were significantly reduced in cKO-derived macrophages under M1 and M2 conditions, respectively.Collectively, these data suggested that ER? signaling promotes arthritis pathogenesis via the activation of cellular metabolism in resident synovial macrophages.

***Disclosures: Yuuki Imai**, None*

1082

Itaconate-producing neutrophils regulate local and systemic inflammation following trauma *Robert Tower[2], Janna Crossley[2], Sonya Ostashevskaya-Gohstand[2], Stefano Comazzetto[2], Jessica Hook[2], Lei Guo[2], Neda Vishlaghi[2], Conan Juan[2], Lin Xu[2], Alexander Horswill[3], Gerta Hoxhaj[2], Jessica Moreland[2], Benjamin Levi[4]. [2]University of Texas Southwestern Medical Center, . [2]University of Texas Southwestern Medical Center, United States. [3]University of Colorado, United States. [4]UT Southwestern Medical Center, United States

A fundamental question following injury or infection relates to the ability of the immune response to both initiate and halt the inflammatory process. Due to the evolving role of cellular metabolism in regulating cell fate, function, and inflammation, tendon from control mice or mice subjected to a dorsal burn and full transection of the Achille’s tendon (known to promote the formation of heterotopic ossification [HO]), were evaluated by metabolic profiling to determine its impact on healing outcomes. In addition to bioenergetic changes associated with injury, we observed a significant increase in the immunomodulatory metabolite itaconate following injury (120+/-43-fold increase relative to uninjured tendon, $p<0.001$). In the context of infection and injury, macrophages have previously been shown to produce itaconate to facilitate their conversion from a more pro- to anti-inflammatory state. Single-cell RNA sequencing and subsequent molecular and metabolomic validation identified a highly mature neutrophil subtype, not macrophages, as the primary producers of itaconate following trauma (2.47+/-0.32-fold increase in itaconate in neutrophils relative to macrophages, $p<0.05$). This neutrophil-mediated itaconate production was similarly found in response to TNF? or a simulated bacterial infection in both mouse and human neutrophils, suggesting a conserved response to various forms of inflammation. These mature itaconate-producing neutrophils are highly inflammatory, producing cytokines that promote local HO formation (e.g. Il1b, Tnf) before cycling back to the bone marrow. In the bone marrow, treatment with itaconate was shown to alter hematopoiesis, skewing progenitor cells towards the granulocyte monocyte lineages (132+/-46%, $p<0.01$) and away from the megakaryocyte erythrocyte lineages (-72+/-11%, $p<0.01$), thereby regulating systemic inflammation. Therapeutically, exogenous itaconate was found to reduce injury site inflammation, promoting tenogenic differentiation and impairing aberrant vascularization with disease, ameliorating effects on HO (2.0+/-0.6mm3 vs 3.1+/-1.4 mm3 total HO in control, $p<0.05$). These results demonstrate a therapeutic potential for exogenous itaconate to mitigate HO and present an intriguing role for cycling neutrophils as a sensor of inflammation induced by injury, potentially regulating immune cell production in the bone marrow, through delivery of endogenously produced itaconate.

***Disclosures: Robert Tower**, None*

1083

Inflammation Activates Wnt Canonical Signaling and Induces New Bone Formation Through Toll-Like Receptor 2 *Petra Henning[1], Ali Kassem[2], Anna Westerlund[1], Lei Li[1], Pernilla Lundberg[2], Cecilia Engdahl[1], Vikte Lionikaite[1], Pernilla Wikström[2], Catharina Lindholm[1], Pedro P. C. de Souza[3], Sofia Movérare-Skrtic[1], Ulf H. Lerner[1]. [1]Sahlgrenska Academy at University of Gothenburg, Sweden. [2]University of Umeå, Sweden. [3]Federal University of Goias, Brazil

It is well established that inflammatory processes in the vicinity of bone often induce osteoclast formation and bone resorption. Effects on bone formation by inflammatory processes are, however, much less studied. The present study assessed the effect on bone formation by locally induced inflammation. The Toll-like 2 receptor (TLR 2) agonists Pam2 (synthetic ligand) and LPS from Porphyromonas gingivalis were injected once subcutaneously above skull bones of 5-weeks-old mice. Five days after injection, the calvarial bones were dissected and analyzed by ?CT, static and dynamic histomorphometry, immunohistochemistry (IHC), gene expression, and in situ analyses. Both agonists induced new bone formation primarily at endocranial surfaces. Bone formation at pericranial and intracranial surfaces was also observed. New bone formation could be observed in close vicinity to osteoclasts, but excessive new bone was mainly observed at a distance from osteoclasts and bone resorption cavities. Inflammation increased endocranial bone formation rate due to increased mineralizing surfaces. The injection resulted in progressively increased calvarial thickness during the subsequent 23 days. Treatment with antibodies neutralizing RANKL robustly decreased osteoclast numbers and inflammation-induced bone loss as expected but did not affect the increase of bone formation. Similar observations were made with zoledronic acid. In areas close to new bone formation, there was an abundance of proliferating cells as assessed by Ki67 labeling. TLR 2 activation increased mRNA expression of genes encoding bone matrix proteins (Col1a1, Bglap), Alpl and the osteoblastic transcription factors Runx2 and Sp7, as assessed by qPCR. These observations were confirmed by RNAScope demonstrating the presence of cells expressing Runx2 mRNA. IHC showed robust Runx2 and alkaline phosphatase protein expression in osteoblasts in areas with new bone formation. qPCR analysis showed that TLR 2 activation increased the mRNA expression of Lrp5, Lrp6 and Wnt7b and decreased the expression of Sost and Dkk1. RNAScope demonstrated expression of Wnt7b mRNA in areas with new bone formation. In conclusion, these data suggest that inflammation, not only stimulates osteoclastogenesis, but also locally activates new bone formation through canonical WNT signaling. Importantly, this process is independent of bone resorption and, therefore, should be regarded as inflammation-induced bone modeling.

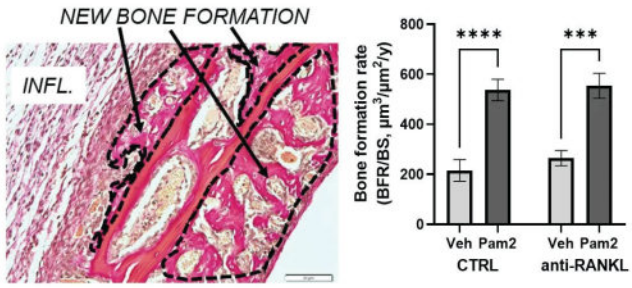

Fig. Inflammation induced bone modelling. Histology showing new bone formation (arrows) in inflammation model. Quantification of bone formation rate induced by Pam2 in the absence and presence of anti-RANKL

***Disclosures: Petra Henning**, None*

1084

Temporal osteoclast ablation reduces adaptive immune reactivity in the bone marrow microenvironment *MARGARET DURDAN[1], Anders Narum[3], ANGELO GUILATCO[1], Christine Hachfeld[3], GABRIEL ALVARES BORGES[3], David Monroe[4], Sundeep Khosla[5], Megan Weivoda[3]. [1]Mayo Clinic/University of Michigan, . [3]Mayo Clinic, . [3]Mayo Clinic, United States. [4]Mayo Foundation, United States. [5]Mayo Clinic College of Medicine, United States

Osteoclasts (OCs) are myeloid derived, bone resorbing cells. More recently, OCs have also been reported to have immune functions, including regulation of T cell responses in vitro. However, our understanding of the role for OCs in T cell regulation in vivo is limited. Our in vitro studies revealed that polarization of OCs on bone restricts OC antigen uptake and presentation. Thus, we hypothesize that bone-resorbing OCs in vivo may indirectly impact T cell activation through the release of resorption-derived products. To test this, we evaluated the impact of temporal OC ablation on bone marrow T cells in male and female adult mice. Tamoxifen (TAM)-inducible Cathepsin K CreERT2 mice (CtskCreERT2) were crossed with mice transgenic for conditional Diphtheria Toxin Fragment A (DTA). 4 months old male and female CtskCreERT2-DTA and DTA littermates were treated with 10mg/kg TAM daily for five days (induction) followed by once weekly (maintenance) for

one month (n=5-7). Prior analysis of this regimen revealed the Cre-reporter expression was restricted to OCs on the bone surface; there was no evidence of Cre activity in osteocytes, periosteum, or bone marrow. TRAP staining of vertebral cryosections confirmed significant reduction in OCs in TAM-treated CtskCreERT2-DTA mice compared to DTA littermates. Consistent with this, vertebral BV/TV, Tb.Th, Tb.N were significantly increased, along with a significant decrease in SMI. Flow cytometry analysis of bone marrow immune cells revealed that OC ablation decreased Natural Killer T cells (NKT) populations ($p<0.05$) in male and female CtskCreERT2-DTA mice, along with nearly significant decrease in Th17 cells ($p=0.06$). Single cell RNA sequencing (scRNA seq) of a subset of female mice (n=3) confirmed decreased NKT and NK cells in CtskCreERT2-DTA compared to TAM treated DTA littermates, as well as decreased effector cytotoxic CD8 T cell and increased naïve CD8 T cells; a trend for increased Treg populations in CtskCreERT2-DTA female mice was also noted. There were no significant changes to macrophage, monocyte, or dendritic cell populations, but decreased mature B and plasma cells. Altogether these results show that temporal OC ablation induces an immune tolerance phenotype, suggesting that OC or OC resorption may help to maintain immune reactivity in the bone marrow niche. These findings raise important questions regarding the impact of anti-resorptive therapies on the efficacy of immune therapies in cancer bone disease.

***Disclosures: MARGARET DURDAN**, None*

1085

Critical environmental control of B cell lymphopoiesis in the bone marrow through VEGF and PDGF signaling in skeletal stem/progenitor cells *Seppe Melis[1,] Marion Mesnieres[1,] Dana Trompet[1,] Laura Tack[1,] Roger Valle-Tenney[1,] Christa Maes[1,] [1]KU Leuven, Belgium

The bone marrow (BM) microenvironment plays vital roles in hematopoiesis, supporting hematopoietic stem cells (HSCs) and their lineage differentiation. However, the cellular-molecular control of B cell development in the BM remains incompletely understood. Analyzing hypoxia signaling in osteolineage cells, we found that Osx-Cre-mediated conditional knockout (cKO) of von Hippel-Lindau (Vhl), a negative regulator of hypoxia-inducible factor (HIF), led to a marked high bone mass and BM hypervascularization. Here, we investigated the impact on hematopoiesis. Flowcytometry revealed that Vhl cKO mice showed drastically impaired B lymphopoiesis, with >2-fold reduced circulating and BM-resident B cells, from juvenile ages onward. The deficit was due to a specific differentiation block at the transition from pre-pro- to pro-B cells in the BM. To elucidate the mechanism by which activated HIF signaling in bone cells led to a block in B cell development, we next tested the impact of Osx-Cre-driven conditional transgenic (cTg) over-expression of VEGF, the major angiogenic downstream target of HIF. VEGF cTg mice, like Vhl cKO mice, exhibited increased trabecular bone and vascularization, and drastically reduced B cells. The impact was B cell-specific, as the frequency of HSCs, myeloid progenitors and other blood cells was unaltered. Known niche-derived B lymphopoiesis regulators (IL-7, Cxcl12, SCF, Flt3l) were expressed normally. However, data from immunofluorescence, 3D deep-tissue imaging, qPCR and flowcytometry, altogether implicated increased platelet-derived growth factor receptor (PDGFR) signaling in the phenotype. VEGF cTg mice had more metaphyseal (H-type) blood vessels, associated with a dramatic expansion and altered distribution of reticular and perivascular skeletal stem/progenitor cells (SSPCs) marked by PDGFR?, PDGFR? and LepR. Strikingly, the metaphyseal and endosteal bone areas where the expanded PDGFR?+ cells localized, specifically corresponded to the regions of B220+ B cell depletion in VEGF mutants. Finally, evidencing its mechanistic involvement, we found that deletion of PDGFR? in Osx+ cells prevented the SSPC expansion in VEGF cTg mice, normalized bone mass, and rescued B lymphopoiesis.This work thus uncovers a critical environmental control of B lymphopoiesis in the hypoxia-sensitive BM, through VEGF and PDGFR? signaling in SSPCs determining the architecture, cellular composition and functionality of the B cell-supportive stromal-vascular niche.

***Disclosures: Seppe Melis**, None*

1086

Addressing the Gap: Does US FRAX Adequately Account for Racial and Genetic Differences in Postmenopausal Women's Fracture Risk? *Qing Wu[1,] Jongyun Jung[2,] [1]The Ohio State University College of Medicine, United States, [2]The Ohio State University, United States

The current US Fracture Risk Assessment Tool (FRAX) presents unresolved concerns regarding the adjustment of racial and ethnic factors, leading to potential healthcare disparities in fracture risk assessment among US postmenopausal women. Our study investigates the influence of race and genetics on fracture prediction performance, aiming to identify opportunities for enhancing the precision of FRAX. Using genomic and phenotypic data from the Women's Health Initiative (WHI) study, we calculated a Genome-Wide Polygenic Risk Score (GPS) employing the LDPred algorithm with 103,155 genetic variants. We categorized GPS into High (top 25%), Medium (25% to 75%), and Low (bottom 25%) groups. We estimated fracture probability with FRAX integrated with bone mineral density (BMD) in the WHI study (N=1522), focusing on major osteoporotic fractures (MOF) and hip fractures as primary outcomes. We derived the observed 10-year fracture probability for MOF using the cumulative incidence function while accounting for competing mortality risk. We computed the FRAX score with BMD for the 10-year probability of MOF and hip fracture. We applied a multivariable Cox proportional hazard model adjusted for baseline FRAX probability to assess the hazard ratio for GPS and race concerning survival time to the first fracture or death. Our findings reveal that FRAX with BMD significantly underestimates MOF risk in minority women, including African American, Hispanic, and other ethnic groups. Multivariate analysis shows that African American and Hispanic women have a 64% and 48% lower hazard than Caucasian women after adjusting the FRAX score. Moreover, the 10-year probability of MOF, adjusted for the FRAX score, is 47% and 62% higher in the median and high GPS groups, respectively, compared to the low GPS groups. These results remain consistent in sensitivity analyses using hip fracture outcomes and additional adjustments for FRAX probability and other factors. We conclude that the current US FRAX with BMD inadequately adjusts for race/ethnic differences. Incorporating accurate racial adjustments and genetic differences could significantly improve FRAX performance in fracture risk assessment.

Table 1. Adjusted Hazard Ratios (HR) and 95% Confidence Intervals (CI) for Fracture Incidence by Race and GPS Group: Multivariate Cox Proportional Hazard Model Analysis in WHI Data with BMD and Genetic Information (N=1,522)

	Major Osteoporotic Fracture	Hip Fracture
	HR (95% CI)	HR (95% CI)
Adjusted for FRAX probability		
Not-Hispanic White	1 (Reference)	1 (Reference)
Black or African-American	0.36 (0.21-0.56)	0.31 (0.16-0.45)
Hispanic/Latino	0.52 (0.40-0.68)	0.43 (0.22-0.59)
Others*	0.27 (0.18-0.45)	0.20 (0.11-0.32)
Adjusted for FRAX probability		
Low GPS (<25%)	1 (Reference)	1 (Reference)
Medium GPS (25% - 75%)	1.47 (1.24-1.61)	1.52 (1.35-1.72)
High GPS (>75%)	1.62 (1.38-1.82)	1.75 (1.41-1.93)
Adjusted for FRAX probability and GPS		
Not-Hispanic White	1 (Reference)	1 (Reference)
Black or African-American	0.33 (0.19-0.53)	0.30 (0.15-0.39)
Hispanic/Latino	0.49 (0.39-0.66)	0.39 (0.18-0.57)
Others*	0.25 (0.16-0.44)	0.21 (0.16-0.33)
Adjusted for FRAX probability and Race		
Low GPS (<25%)	1 (Reference)	1 (Reference)
Medium GPS (25%- 75%)	1.35 (1.18-1.51)	1.39 (1.21-1.58)
High GPS (> 75%)	1.52 (1.24-1.73)	1.59 (1.32-1.75)

*Others include American Indian or Alaskan Native and Asian or Pacific Islander participants.

***Disclosures: Qing Wu**, None*

1087

Associations of Race, Skin Pigmentation, and Genetic Similarity with Bone Mineral Density in Adolescents *Catherine Gordon[1,] Abby Fleisch[2,] Marie-France Hivert[3,] Lisa Rokoff[2,] Sheryl Rifas-Shiman[3,] Emily Oken[3,] [1]Department of Pediatrics, Baylor College of Medicine, United States, [2]Center for Interdisciplinary Population & Health Research, MaineHealth Institute for Research, United States, [3]Department of Population Medicine, Harvard Medical School, United States

Background: Use of race and ethnicity in clinical decision-making has come under scrutiny, including in the evaluation of bone mineral density (BMD) by dual-energy x-ray absorptiometry (DXA). Rates of osteoporosis and fracture appear to be lower in Black adolescents and adults.Purpose: To evaluate the associations of reported race, skin pigmentation, and genetic similarity with BMD in a cohort of adolescents.Methods: We conducted a cross-sectional analysis of 509 adolescents (mean age 17.5y, range 16-20y) in the Boston-area Project Viva cohort. Exposures were maternal report of adolescent race and ethnicity, self-report of skin pigmentation, and principal components (PC) derived from genome-wide genotyping arrays. The outcome was BMD Z-score (BMDz) standardized for age, sex, and height. We conducted linear regression analyses with the three exposures individually and in combination.Results: Participants were 65% non-Hispanic White (NHW) and 14% non-Hispanic Black (NHB). They identified varying skin pigmentation across 6 categories ranging from "extremely fair" (8%) to "dark brown" (3%), which did not track exactly with reported race. BMDz was higher in those who identified as NHB vs. NHW (?: 0.96, 95% CI: 0.66, 1.26) and those reporting darker skin pigmentation (e.g., 1.22, 95% CI: 0.57, 1.87 for dark brown vs. fair). Darker skin pigmentation remained associated with higher BMDz within strata of NHB and NHW. The first PC derived from genome-wide genotyping arrays (PC1) captures the variance across the most diverse genetic architecture in a population; NHB participants had a higher value of PC1. PC1 strongly predicted BMDz (9.80, 95%CI: 6.50, 13.10), even after including self-reported race (9.37, 95% CI: 1.24, 17.50) or skin pigmentation (10.19, 95% CI: 4.77, 15.61); whereas both race (0.05, 95% CI: -0.82, 0.92 for NHB vs. NHW) and skin pigmentation (0.16, 95% CI: -0.78, 1.10 for dark brown vs. fair) no longer predicted BMDz after adjustment for genetic similarity.Conclusions: Although genetic similarity reflected in the first PC of genome-wide genotyping arrays strongly predicted BMD, this information is not generally available in clinical settings. Further, whether the relationship between BMD and fracture risk differs by race, skin pigmentation, or genetic similarity, independent of other risk factors, is uncertain. We recommend re-evaluation of adolescent BMD reference data to exclude consideration of race.

***Disclosures: Catherine Gordon**, None*

1088

Multiscale Analysis Identifies Cell Types and Genes Associated with Bone Mineral Density *Ryan C Chai[1], Mischa Lundberg[2], Monika Frysz[3], J H Duncan Bassett[4], Graham R Williams[4], Peter I Croucher[1], John P Kemp[5]. [1]Bone Biology, Garvan Institute of Medical Research, Australia. [2]The University of Queensland Diamantina Institute, The University of Queensland, Australia. [3]University of Bristol, Musculoskeletal Research Unit, Bristol Medical School, United Kingdom. [4]Molecular Endocrinology Laboratory, Department of Medicine, Imperial College London, United Kingdom. [5]Mater Research Institute-University of Queensland, Translational Research Institute, Australia

Background: Bone mineral density (BMD) is a major determinant of bone strength and fracture risk. Genome-wide association studies (GWAS) have identified many variants associated with BMD; however, the underlying cell types and genes remain unclear. Identifying the cellular mechanisms of these genetic determinants is crucial for understanding the pathogenesis of skeletal diseases and developing new therapeutics. We hypothesised that a multiscale approach of integrating GWAS, single cell RNA sequencing (scRNA-seq) data and knockout mouse models would identify cell types and genes associated with BMD. Methods: scRNA-seq was used to define the transcriptome of cells isolated from mouse femurs. Hypergeometric tests were used to identify cell types enriched for genes involved in monogenetic skeletal disorders. MAGMA gene-set analysis was used in conjunction with GWAS of 448,010 participants in the UK-Biobank Study to identify cell types that are enriched for BMD-associated genes. Disease- and BMD-associated genes were validated using skeletal phenotyping data from the mouse genome informatic (MGI) database and in-depth functional analysis of the skeleton in 1000 unselected single gene deletions in mice. Results: scRNA-seq analysis of 133,942 cells identified 34 cell types, including multiple clusters of myeloid, lymphoid, osteoblastic, chondrocytic and vascular cells, each with distinct transcriptional profiles. Osteoblasts and osteoclasts were enriched for genes that cause monogenetic low and high bone mass skeletal disorders respectively. Osteoblasts, chondrocytes, endothelial cells and vascular smooth muscle cells were enriched for BMD-associated genes. Cell type-specific BMD-associated genes were more likely to result in abnormal BMD when deleted in mice. In-depth skeletal phenotyping validated the critical functions of 15 BMD-associated genes, including the novel endothelial cell-specific gene SLC9A3R2, which when deleted in mice resulted in reduced trabecular bone mass.Conclusions: Our multiscale approach identifies cell types, including bone resident cells and vascular cells, in which genetic determinants of BMD may function to influence pathogenesis of monogenetic and polygenetic skeletal disorders with abnormal BMD. This provides a resource to prioritise genes to accelerate development of patient-centred therapeutics for skeletal diseases.

***Disclosures: Ryan C Chai**, None*

1089

Femoral Neck Width Genetic Risk Score Is A Novel Independent Risk Factor For Hip Fractures *Jonathan H Tobias[1], Maria Nethander[2], Benjamin F Faber[1], Sophie Heppenstall[1], Raja Ebsim[3], Timothy Cootes[3], Claudia Lidner[3], Fiona R Saunders[4], Jenny S Gregory[4], Richard M Aspden[4], Nick C Harvey[5], John Kemp[6], Monika Frysz[7], Claes Ohlsson[8]. [1]Musculoskeletal Research Unit, University of Bristol, United Kingdom. [2]Sahlgrenska Osteoporosis Centre, Centre for Bone and Arthritis Research, Institute of Medicine, Sahlgrenska Academy at University of Gothenburg, Sweden. [3]Division of Informatics, Imaging and Data Sciences, The University of Manchester, United Kingdom. [4]Centre for Arthritis and Musculoskeletal Health, University of Aberdeen, UK, United Kingdom. [5]Medical Research Council Lifecourse Epidemiology Centre, University of Southampton, , United Kingdom. [6]The University of Queensland, Australia. [7]University of Bristol, United Kingdom. [8]Center for Bone and Arthritis Research at the Sahlgrenska Academy, Sweden

Purpose: We investigated whether femoral neck width (FNW) is related to hip fracture independently of femoral neck bone mineral density (FN-BMD) using a genetic approach. Methods: FNW was derived from points automatically placed along the outline of the proximal femur in left hip DXA scans from 38,150 individuals (mean age 63.8 years, 48.0% males) in UK Biobank (UKB). Subsequent GWAS identified 71 independent genome-wide significant FNW SNPs. FNW and FN-BMD SNPs were used to generate genetic risk scores (GRSs), which were examined in relation to incident hip fracture in UKB (excluding the FNW GWAS population; n=338742, 3222 cases) using a Cox proportional hazards model, with sex and baseline age as covariates. Participants were subsequently classified according to binarized FNW and FN-BMD GRS scores, using a 10% cut-off for high/low risk. Results: MAGMA analyses identified different gene sets between FNW GWAS (cartilage differentiation, hedgehog, skeletal development) and FN-BMD GWAS (runx1/Wnt signalling), demonstrating distinct underlying biology of these traits. In multivariable Mendelian Randomisation (MVMR), greater genetically determined FNW increased risk of all hip fractures (OR 1.53; 95% CI 1.29-1.82 per SD increase in FNW) and femoral neck fractures (OR 1.58;1.30-1.92), but not trochanteric or forearm fractures. Greater genetically determined FN-BMD decreased fracture risk at all four sites. FN-BMD GRS was associated with reduced risk of incident hip fractures (HR 0.83;0.80-0.86), and FNW GRS with increased risk of hip fractures (HR 1.08;1.05-1.12) and femoral neck fractures (HR 1.10;1.06-1.15). Individuals with genetically determined low FN-BMD had a more pronounced increased risk from genetically determined high FNW (p=0.04 for FN-BMD GRS x FNW GRS interaction for hip fracture prediction). Using the 10% cut-off for high/low risk, subjects in the high-risk GRS group for both FNW GRS and FN-BMD GRS had a more than two-fold increased risk of hip fractures compared with those in the low-risk group for both binarized GRSs.Conclusions: The underlying biology regulating FNW and FN-BMD differs. DXA-derived FNW is causally related to hip fractures independently of FN-BMD and adds information beyond FN-BMD for hip fracture prediction. FNW derived from DXA analyses or a FNW GRS may contribute clinically useful information beyond FN-BMD for hip fracture prediction.

***Disclosures: Jonathan H Tobias**, None*

1090

Associations Between Gut Microbiota Composition and Incident Fractures in the FINRISK Cohort *LOUISE GRAHNEMO[1], Oleg Kambur[2], Teemu Niiranen[3], Rob Knight[4], Veikko Salomaa[2], Aki S. Havulinna[5], Claes Ohlsson[6]. [1]University of Gothenburg, Sweden. [2]Finnish Institute for Health and Welfare, Helsinki, Finland, Finland. [3]Finnish Institute for Health and Welfare, Helsinki, Finland; Department of Internal Medicine, University of Turku, Turku, Finland; Division of Medicine, Turku University Hospital, Turku, Finland, Finland. [4]University of California San Diego, La Jolla, California, USA, United States. [5]Finnish Institute for Health and Welfare, Helsinki, Finland; Institute for Molecular Medicine Finland (FIMM), HiLIFE, University of Helsinki, Helsinki, Finland, Finland. [6]Center for Bone and Arthritis Research at the Sahlgrenska Academy, Sweden

The gut microbiota (GM) can regulate bone mass in mice and humans, but there is no study on the association between GM composition and incident fractures. A previous human study determining the association between GM composition and bone mineral density indicated that large sample sizes (n>6000) are required to account for the multiple testing when evaluating the high number of taxa present at genus/species levels.The present study mainly aimed to determine whether the overall GM composition - reflected by the alpha diversity (Shannon diversity), beta diversity, and relative abundances of the 10 most abundant phyla (average relative abundance >= 0.0094%) - is associated with incident fractures in the large FINRISK cohort (n=7043, 1092 incident fracture cases, median follow-up time 18 years) with GM composition quantified using shallow shotgun metagenome sequencing. Associations were tested using Cox regression models adjusted for age, sex, prevalent fractures, medications, and recent antibiotic use.We observed that higher alpha diversity was associated with decreased fracture risk (hazard ratio [HR] 0.92 per standard deviation increase in Shannon diversity, 95% confidence interval 0.87-0.96, P=0.006). For beta diversity, the first principal component was associated with decreased fracture risk (Aitchison distance, HR 0.90, 0.85-0.96, P=0.0007). We next determined the associations between the 10 most abundant phyla and fracture risk. Following Bonferroni correction ($p<0.05/10=5.0\times10-3$ required), Proteobacteria was associated with increased fracture risk (HR 1.14; 1.07-1.20, $P=1.0\times10-5$), while Tenericutes was associated with decreased fracture risk (HR 0.90; 0.85-0.96, $P=5.4\times10-4$). The strengths of these associations were mainly unchanged after further adjustments for diet.Explorative sex-stratified analyses showed that Shannon alpha diversity associated with fractures in women (HR 0.88; 0.82-0.95) but not in men (HR 0.99; 0.90-1.08). Further explorative analyses demonstrated that Proteobacteria was associated with increased (HR 1.13, 1.04-1.23) and Tenericutes with decreased (HR 0.90, 0.82-0.99) risk of major osteoporotic fractures (hip, humerus, forearm, and vertebral fractures, n=458) with similar effect sizes as observed for fractures at any bone site.In conclusion, the overall GM composition is associated with incident fractures in the large FINRISK cohort. Further studies are warranted to determine the underlying mechanism.

***Disclosures: LOUISE GRAHNEMO**, None*

1091

A novel periosteal cell type, identified by single cell RNA sequencing, senses mechanical loading and in response to it differentiates into osteoblasts *XUEHUA LI[1], Intawat Nookaew[2], Jinhu Xiong[3, 1], United States. [2]University of Arkansas for Medical Sciences, United States. [3]Univ of Arkansas for Medical Sciences, United States

Mechanical loading stimulates periosteal bone formation and osteocytes are considered to be the major cells sensing and transducing mechanical signals in bone. However, a complete understanding of the identity of mechanosensitive cells in periosteum is lacking. To determine which cell types are responding to mechanical stimulation in periosteum, we isolated periosteal cells from loaded tibia at different time points and performed 10X-based single cell RNA sequencing (scRNA-seq). The left tibiae of 7-month-old female C57BL/6J mice were loaded with 9N at 1 bout per day for 1, 2, and 5 days. Periosteal cells were then isolated 12 hours after loading for 12-hour time point and 24 hours after the last set of loading for the 2- and 5-day time points. scRNA-seq identified 8 clusters: Fibro-1, Fibro-2, Osteo-X, Osteoblasts, Chondrocytes, Articular Chondrocytes, Tenocytes, and a new cluster we refer to as Fibro-L. Comparing clusters between the control and 12-hour groups, we found that the number of Fibro-L is greatly increased within 12 hours after loading. The dramatic change of the cell number in this cluster within 12 hours cannot be explained by cell proliferation but the change in gene expression profile induced by mechanical loading. Differential gene expression analysis of this cluster showed increased expression of Ptgs2,

Lif, and Il-6 which are classic early response genes to mechanical loading. To confirm the increased expression of these genes in periosteum, we localized their mRNA using RNAscope based in-situ hybridization. Tibiae collected 4 hours after loading were used for RNAscope. Consistent with scRNA-seq analysis, we found increased Ptgs2, Lif, and Il-6 expression in osteocytes as well as cells at the periosteal surface, suggesting that periosteal cells are also capable of sensing mechanical stimulation. Differential gene expression analysis of this cluster at later time points showed that proliferation related genes such as Ki67 and Top2a were significantly elevated. In addition, RNAscope showed a dramatic increase of Top2a expression in the tibial periosteum 5 days after loading, demonstrating increased cell proliferation in periosteal cells. More importantly, cells in the Fibro-L cluster became Sp7 and Spp1 positive at day 5 consistent with their differentiation towards osteoblasts. Taken together, our results provide evidence that a subset of periosteal cells may directly sense mechanical loads and differentiate into osteoblasts.

***Disclosures: XUEHUA LI**, None*

1092

RESPONSE OF BONE TO MECHANICAL LOADING IS HERITABLE AND CORRELATES WITH OSTEOCYTE LACUNAR MORPHOLOGY IN MICE *Nicole Migotsky[2], John Shuster[2], Surabhi Kumar[2], Charles Farber[3], Matthew Silva[4]. [2]Washington University in St Louis, . [2]Washington University in St Louis, United States. [3]University of Virginia, United States. [4]Washington University in St. Louis School of Medicine, United States

Mechanical loading is a potent anabolic and anti-catabolic stimulus for bone. Many bone traits are heritable, but little is known about the influence of genetics on the response of bone to increased mechanical loading. In this study we utilized two murine models of genetic diversity, the diversity outbred (DO) population and the eight inbred founder strains (Founders) that were crossbred to create the DO. We hypothesized that loading-induced bone formation varies with mouse genetic background and sex, is moderately heritable, and correlates with osteocyte lacunar morphology. The right tibia of 220 skeletally mature (5 mo-old) mice, including females and males, were loaded in axial compression to a peak tensile strain of 1500 µ?. The diaphyseal cortical responses to loading were assessed using classic dynamic histomorphometry and time-lapse µCT (comparing pre- and post-loading scans). Because osteocytes are thought to regulate the mechanoresponsiveness of bone, loading responses were correlated to lacunar morphology determined in a separate cohort of mice. Loading increased bone formation in a strain/sex dependent manner, with the inbred strain 129S1 having the largest response to loading on both periosteal and endocortical surfaces (ANOVA). Inbred strain A/J did not have a measurable response on either bone surface. Additionally, loading reduced bone resorption in a strain/sex dependent manner. For every measurement of periosteal bone formation, the outbred population (DO) had a higher increase due to loading than the inbred population (Founders). While sex differences were found in some inbred strains, there was no main sex effect when looking at all inbred or all outbred mice as a population. Broad-sense heritability (H2) was calculated for each bone formation outcome in the Founders. All periosteal formation outcomes have heritability over ~80%. Lacunar volume fraction positively correlated with increased loading response, while lacunar aspect ratio negatively correlated with increased loading response. Overall, bone responses to mechanical loading vary with genetic background and are moderately to highly heritable. Additionally, the volume fraction and elongation of osteocyte lacunae are significantly correlated with loading response indicating a relationship between osteocyte morphology and mechanosensitivity. This work supports further use of these genetically diverse mouse models to investigate how genetics regulates bone mechanoresponsiveness.

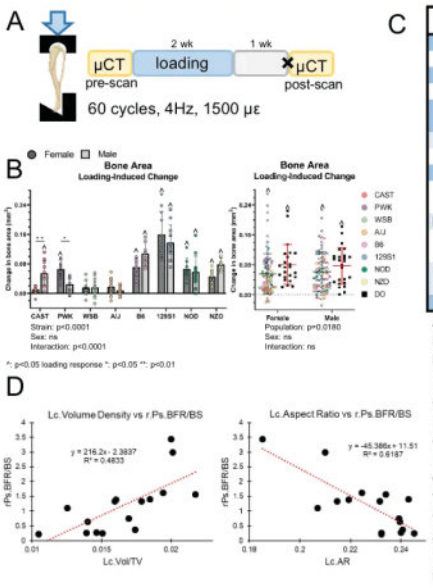

C

Trait	Heritability (H^2)
Ec.BFR/BS	0.970
Ct.Ar	0.953
Ps.MAR	0.950
Ct.Th	0.946
Ps.BFR/BS	0.943
Ec.MAR	0.936
Ec.Form/BV	0.921
pMOI	0.893
Ps.MS/BS	0.870
Ct.Ar/Tt.Ar	0.860
Tt.Ar	0.850
Ps.Formed/BV	0.792
Ma.Ar	0.546
TMD	0.459
Ec.Resorb/BV	0.436
Ps.Resorb/BV	0.355
Ec.MS/BS	0.317

A) Timeline of loading to induce bone formation. Mice were loaded for 2 weeks to 1500 µε. µCT was taken before loading and 1 week after the last bout. B) Loading-induced change in bone area in the Founders (left) and DO (right) as a representative outcome. C) Heritability values for all loading outcomes. D) Correlations of Lc.Vol/TV (left) and Lc.Aspect Ratio (right) to BFR. More elongated lacunae respond more to loading.

***Disclosures: Nicole Migotsky**, None*

1093

Regulation of Intracellular cAMP Levels in Osteocytes by Mechano-sensitive Focal Adhesion Kinase *Garyfallia Papaioannou[1], Tadatoshi Sato[2], Parthena Kotsalidis[1], Katelyn Strauss[1], Thomas Dean[1], Matthew Stokes[3], Thomas Gardella[1], Marc Wein[1]. [1]Massachusetts General Hospital, Harvard Medical School, United States. [2]Massachusetts General Hospital, Harvard Medical School and UMass Medical School , United States. [3]Cell Signaling Technology, United States

Introduction Osteocytes are the primary mechano-sensors in bone. Mechanical loading is sensed across their dendritic projections leading to transient reductions in tyrosine kinase focal adhesion kinase (FAK) activity. Previous studies suggested that FAK controls sclerostin expression in osteocytes, and pharmacologic FAK inhibition increases bone formation. However, our understanding of the signaling pathways downstream of FAK in osteocytes is incomplete. This study aims to identify novel bone anabolic pathways controlled by FAK. Methods/Results We performed tyrosine-focused phospho-proteomic profiling via tandem mass spectrometry in osteocyte-like Ocy454 cells to identify FAK substrates. We analyzed the tyrosine phospho-proteome of cells lacking FAK (via CRISPR ??) or treated with pharmacologic FAK inhibitors vs controls. Surprisingly, Gs?, PTH1R, and phosphodiesterase 8A (PDE8A), all proteins associated with cAMP signaling, were found as potential FAK targets based on their reduced tyrosine phosphorylation in both FAK KO or FAK inhibitor treated cells. A Glosensor system was used to measure cAMP levels in HEK293 cells. FAK pharmacologic inhibition or gene deletion increased basal and ligand-stimulated (ligands: isoproterenol, PGE2, PTH) cAMP levels. In Ocy454 cells, both phosphorylated protein kinase A substrate levels and cAMP target genes (Rankl, Wnt4) were increased by FAK inhibitors +/- PTH treatment. Mutating FAK phospho-acceptor sites in Gs? and PTH1R had no effect on PTH or FAK inhibitor stimulated cAMP levels. In addition, FAK inhibitor augmented cAMP levels even in the presence of forskolin that activates adenyl-cyclase downstream of Gs?. Therefore, PDE8A is a possible target and PDE8A inhibition (via PF04957325) in Ocy454 cells led to molecular changes (increased cAMP, PKA activity, cAMP target genes) similar to FAK inhibition. In vitro kinase assay showed that PDE8A is directly phosphorylated by FAK. Initial experiments measuring PKA activity in bones of mice after acute treatment with the FAK inhibitor VS6063 (60mg/kg) and/or PTH (5nmol/Kg) suggest that the effect of FAK inhibition on cAMP signaling also operates in vivo. Conclusion FAK inhibition acts synergistically with signals that activate adenyl-cyclase to increase intracellular cAMP. Mechanically-regulated FAK can modulate intracellular cAMP levels via effects on PDE8A. These data suggest a novel mechanism of crosstalk between mechanical and cAMP-linked hormonal signaling in osteocytes.

***Disclosures: Garyfallia Papaioannou**, None*

1094

Piezo1 Regulates cGMP/PKG Signaling in Osteocyte Mechanotransduction *Yizhong Hu[1], Xinchen Wu[1], Fuhua Wang[1], Yingzi Yang[2]. [1]Harvard School of Dental Medicine, United States. [2]Harvard University, United States

Mechanical stimuli and osteocyte mechanotransduction are critical for maintenance of healthy adult bone. Following mechanical stimulation, increased [Ca2+]in initiates downstream signaling activities modulating bone anabolic responses. Enhanced cGMP/PKG signaling resulting from increased [Ca2+]in promotes osteoblast and osteocyte differentiation.

Recent works from our lab and others have demonstrated that the force-gated calcium ion channel Piezo1 at the cell membrane is required for load-induced bone adaptation. RNA-seq analysis of Piezo1-deficient mouse bones further demonstrated reduced cGMP/PKG signaling. We therefore hypothesize that Piezo1 regulates early mechanotransduction events through the cGMP/PKG pathway.To test this hypothesis, we generated a Piezo1-/- OCY454 osteocyte cell line using CRISPR-Cas9 (Fig. 1A). After 21-day differentiation, Piezo1-/- OCY454 expressed lower levels of osteocyte genes (DMP1, SOST, PHEX, TNFSF11) but higher levels of osteoblast genes (SP7, RUNX2, BGLAP) than WT OCY454, suggesting that Piezo1 deficiency impedes osteocyte differentiation. Furthermore, bulk RNA seq analysis of the differentiated Piezo1-/- and WT OCY454 revealed downregulation of hippo signaling and upregulation of Wnt signaling.In WT OCY454, stimulation by fluid shear stress and Yoda1 treatment, a Piezo1 activator, induced PKG activation measured by increased VASP Ser239 phosphorylation. These effects were abolished in Piezo1-/- OCY454, suggesting that mechanically stimulated Ca2+-dependent PKG activation acts through Piezo1(Fig. 1B). Furthermore, mRNA and protein levels of PKG1 and PKG2 decreased significantly in Piezo1-/- OCY454. Pharmacological activation of YAP, a downstream effector of Piezo1, increased prkg1/2 mRNA and PKG1/2 protein levels, suggesting that Piezo1 may transcriptionally modulate PKG signaling via YAP. Using primary BMSCs isolated from Piezo1f/f mouse, deletion of Piezo1 by Ad-Cre infection reduced osteogenic differentiation measured by ALP staining, consistent with published studies (Fig. 1C). Importantly, PKG activation by 8-pCPT-cGMP treatment rescued osteogenic differentiation defects in Ad-Cre-infected Piezo1f/f BMSCs measured by the number of ALP-positive CFUs. Taken together, these results indicate that Piezo1 regulates cGMP/PKG signaling in osteogenic differentiation and mechanotransduction.

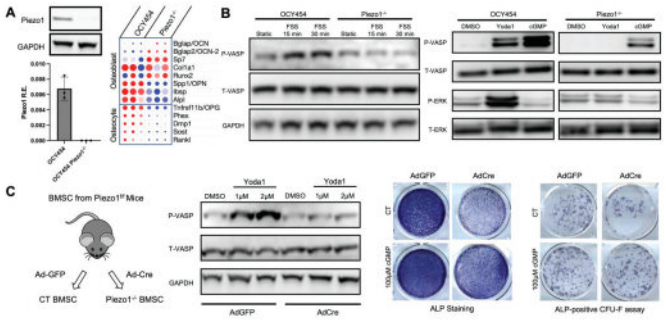

***Disclosures: Yizhong Hu**, None*

1095

Effects combining mechanical loading with sclerostin antibody, parathyroid hormone, or bisphosphonate treatment on mechanoregulation in trabecular bone in mice *Julia K. Griesbach[1], Friederike A. Schulte[1], Claudia Weigt[1], Marcella von Saglis-Soglio[1], Floor M. Lambers[1], Peter J. Richards[2], Michaela Kneissel[2], Gisela Kuhn[1], Ralph Mueller[3]. [1]ETH Zürich, Switzerland, [2]Musculoskeletal Disease Area, Novartis Institutes for Biomedical Research, Switzerland, [3]ETH Zurich, Switzerland

Osteoporosis is a prevalent disease leading to low bone mass and increased bone fragility often treated with medications such as parathyroid hormone (PTH), sclerostin antibodies (SclAB), or bisphosphonates (BIS). Further, mechanical loading can cause an anabolic bone response. We investigated how the combination of mechanical loading and three pharmacological treatments affects bone mechanoregulation.In vivo micro-computed tomography scans were obtained from the 6th caudal vertebra of ovariectomized (OVX) C57BL/6JRcc mice, treated with mechanical loading only at 0N and 8N (n=27/27) and/or with PTH (n=9/9), SclAB (n=10/10) or BIS (n=9/10), respectively. Formation, quiescent and resorption volumes were identified by registering the scans of week 20 and 22. Strain energy density (SED) was estimated using micro-finite element analysis at week 20. Conditional probabilities associating volumetric remodeling events with SED levels were calculated and parametrized. Area under the curve (AUC) for the receiver operating characteristic and the correct classification rate (CCR) of remodeling probabilities were compared to OVX 0N using unpaired Student's t-test with Bonferroni correction.Concurrent loading improved trabecular bone volume fraction (OVX: 0.0% to 14.5%; PTH: 37.5% to 66.3%, SclAB: 21.1% to 50.2%; BIS: 14.6% to 27.0%; p<0.05). All groups exhibited mechanoregulation, where bone was more likely to be formed in areas with high SED and resorbed in areas with low SED (Fig. 1A,B). While SclAB increased mechanoregulation in formation with and without loading, PTH only had this effect when combined with loading (Fig. 1C). Mechanoregulation of resorption was not significantly affected by PTH or SclAB (Fig. 1 D). BIS decreased mechanoregulation of resorption and formation compared to OVX 0N (Fig. 1C,D). Overall, mechanoregulation of the remodeling process increased when combining PTH or SclAB with mechanical loading and decreased when using BIS without loading (Fig. 1E).Combining mechanical loading and pharmacological treatments affects the mechanoregulatory response in bone. The combination of PTH or SclAB with mechanical loading will target the remodeling response more to the mechanical demands, while BIS treatment will cause a more untargeted response. These insights shed new light on the mechanisms of combined mechano-pharmacological treatments and might help clinicians make more informed treatment plans including physical therapy as an additional option.

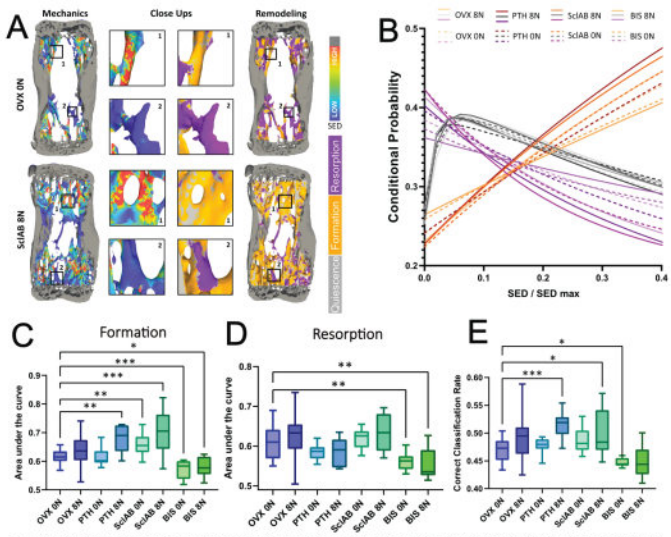

Fig. 1: A) Qualitative comparison mechanical environment and bone remodelling for OVX 0N and SclAB 8N; B) Conditional probabilities for formation (orange), quiescent (grey) and resorption (purple); Area under the curve of the receiver operating characteristic for C) formation and D) resorption; E) correct classification rate *: p<0.05; **:p<0.01; ***:p<0.001

***Disclosures: Julia K. Griesbach**, None*

1096

Allelic Effects at the Cped1 Locus Interact with Parathyroid Hormone to Impact Bone Strength in Mice *Yingping Wang[1], Dana Godfrey[1], Robert Maynard[2], Nicole Szeto[1], Veronica Butler[1], Michael David[1], Gregory Ottenberg[1], Douglas Adams[1], Cheryl Ackert-Bicknell[1]. [1]University of Colorado, United States, [2]University of North Carolina, United States

Teriparatide is a recombinant peptide consisting of the first 34 amino acids of Parathyroid Hormone (PTH) and is an anabolic drug for treating osteoporosis. Available data suggests that not all patients respond to Teriparatide, and that response may be genetic. We conducted a Genome-wide Gene-Environment Association study (GWEAS) using Diversity Outbred (DO) mice, with intermittent PTH as the environmental variable. We treated 1173 mice with either PTH (40 ?g/kg/day) or saline for 4 weeks, starting at 12 weeks of age (equal male:female and PTH:saline). Mice were genotyped using the GigaMUGA array. Femur strength was measured in 3-point flexure. Genetic loci were mapped by fitting mixed-effects linear models at each marker and regressing the phenotype on the haplotype probabilities. In model 1, PTH treatment was an additive covariate and in model 2 PTH treatment was an interactive covariate with genotype. In model 1 we identified a quantitative trait locus (QTL) with a peak LOD at 22.31 Mbp (LOD = 8.23, CI = 21.38 to 22.35 Mbp), but in Model 2 the LOD dropped to 4.71, suggesting that this locus interacted with PTH to impact strength. This locus encompassed 6 genes: Kcnd2, Tspan12, Ing3, Cped1, Wnt16 and Fam3c, and is concordant with the human CPED1/WNT16 locus for BMD and fracture. We looked for cis-expression QTL (eQTL) to see if local genetic effects impacted femoral gene expression at this locus, as mapped in a discrete set of PTH naïve 188 female DO mice. No cis eQTL were found for Kcnd2 or Wnt16. For Ing3 and Fam3c, cis eQTL were found but the allele effects did not match those of our strength QTL, eliminating these 4 genes. A strong cis eQTL was found for Tspan12 (LOD 11.90) and the allele effects partially match our strength QTL. No primary eQTL was found for Cped1, but we have shown previously that Cped1 is highly alternatively spliced. When conditioning on the long transcript for Cped1 in a mediation analysis, we found an eQTL for Gm26719 (LOD = 20.79), which is likely a mis-annotated transcript for Cped1. Using mice homozygous for a CRISPR-induced mutation of Cped1, we measured a significant reduction in femoral strength for male Cped1mut femurs (16.7 +/- 1.7 N) relative to Cped1+/+ (18.2 +/- 2.5 N). Future studies will determine how these mice respond to PTH. We cannot rule out Tspan12 as contributory to the primary QTL, but the available data strongly support Cped1 as causative, and that this genetic locus interacts with PTH to impact bone strength.

***Disclosures: Yingping Wang**, None*

1097

ROI-based Spatial Transcriptomics as a Novel Approach to Reveal the Mechanism of Quiescent Bone Lining Cells Reactivation *Ahyoun Choi[1], Ji Yeon Lee[2], Sung Hye Kong[2], Chan Soo Shin[2], Sunghoon Kwon[3], Sang Wan Kim[2]. [1]Interdisciplinary Program in Bioengineering, Seoul National University, Republic of Korea. [2]Department of Internal Medicine, Seoul National University College of Medicine, Republic of Korea. [3]Department of Electrical and Computer Engineering, Seoul National University, Republic of Korea

Anabolic agents such as parathyroid hormone (PTH) and anti-sclerostin antibody (Scl-Ab) are highly effective in treating severe osteoporosis by increasing bone mass and restoring bone microstructures. One of the mechanisms by which these agents work is the modeling-based bone formation by reactivating quiescent bone lining cells (BLCs). Given that BLCs make up 80% of the trabecular bone surface, reactivating these cells has emerged as a promising target for osteoporosis treatment due to their potential contribution to bone formation. However, the underlying mechanisms are not fully understood.To investigate the molecular mechanisms underlying the reactivation of BLCs, we utilized a Dmp1-CreERT2:mTmG or Osteocalcin-CreERT2:mTmG mouse model to create four groups: active osteoblasts (Obs), inactive Obs (presumably BLCs), and reactivated Obs with PTH or Scl-Ab. This lineage tracing mouse model rendered target Obs to express green fluorescent proteins (GFP), which allowed us to specifically isolate region-of-interests (ROIs) containing them from mouse calvaria sections using our in-house spatially resolved laser activated cell sorter (SLACS). We performed ROI-based spatial transcriptomics on each group, generating transcriptome data from 100 ROIs in 48 male mice, with 6 mice in each group.Our analysis revealed the reactivated Obs exhibited features consistent with the response of anabolic agents, including increased expression of Col1a1 and Bglap genes and upregulation of canonical Wnt signaling. Notably, the Scl-Ab-treated group showed similar expression patterns to the active group in the Dmp1-CreERT2 mouse model, while the PTH-treated group had the distinct expression profile. Furthermore, differential gene expression analysis revealed upregulation of Kras gene in both the active and Scl-Ab-treated groups, compared to the inactive group. Gene set enrichment analysis showed downregulation of transforming growth factor-beta (TGF-?) signaling in the Scl-Ab-treated group, along with differential expression of Dcn, Apc, and Mmp13 genes. Our findings suggest that Kras and TGF-? signaling could be involved in the interconversion between mature osteoblasts and BLCs.In summary, spatial transcriptomics combined with lineage tracing mouse models sheds light on the genetic characteristics of BLCs and reactivated osteoblasts. Further functional studies are required to elucidate the possible role of Kras or TGF-? signaling in BLC reactivation.

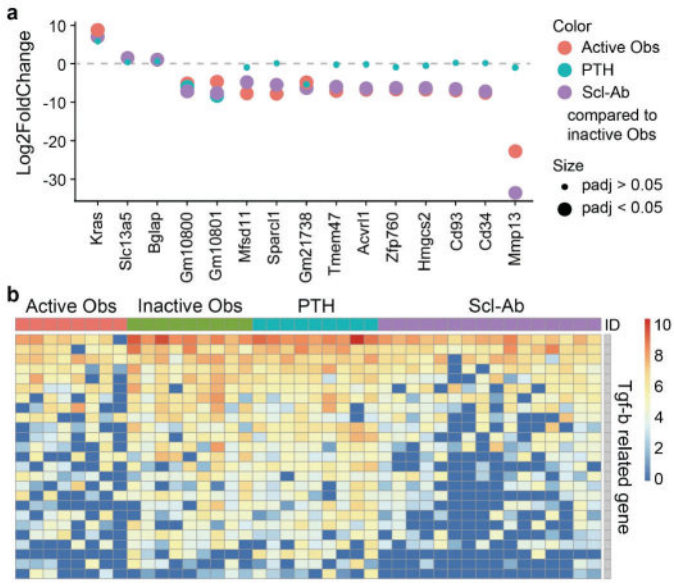

***Disclosures: Ahyoun Choi**, None*

1098

Integrated Transcriptomic and Proteomic Profiling of Responses to Clinical and Novel Bisphosphonates Reveal Extraskeletal Effects and Protection Against Senescence *Jinsen Lu[8], Srinivasa Rao Rao[8], Haoqun Zhan[8], Helen Knowles[8], Eleanor Platt[2], Lucy Frost[2], Tiffany Allen[2], Gayle Marshall[2], Killian Huber[8], Ludwig Bauer[8], Benedikt Kessler[8], Anne Horne[3], Ian Reid[3], Chas Bountra[8], F Hal Ebetino[4], Shuting Sun[4], Emilio Roldan[5], James L Kirkland[6], Sundeep Khosla[7], R Graham Russell[8], James Edwards[8]. [8]University of Oxford, United Kingdom. [2]Medicines Discovery Catapult, United Kingdom. [3]University of Auckland, New Zealand. [4]BioVinc, United States. [5]Qualix, Spain. [6]Mayo Clinic, United States. [7]Mayo Clinic College of Medicine, United States. [8]University of Oxford,

Although bisphosphonates (BPs) are well established for treating bone disorders, many clinical and other studies suggest BPs also have beneficial extra-skeletal effects on cardiovascular disease, respiratory infections, some cancers, neurodegeneration and mortality. However, the mechanisms by which BPs induce such effects are unclear. Using multi-cell screening and studies of BP-treated aged mice and human patients, combined with genomic, transcriptomic, and proteomic analysis, we explored the hypothesis that BPs exert direct effects outside the skeleton to impact multiple aspects of aging.In multiple cell types, established and novel BPs (incl ZOL, ALN, OX14) increased cell growth at low doses (live cell imaging analysis, 1nM-0.1uM, up to 36%, p<0.01). Using fluoro-tagged BPs (ROX-RIS, FAM-ZOL, 0.1uM) to study whether BPs gain access to non-skeletal cells, we showed internalization and co-localization with lysosomal and endosomal organelles (kidney, liver, epithelia, cardiovascular, lung, prostate cells) in vitro. In vivo spatial transcriptomic analysis revealed differentially expressed genes/pathways in multiple organs of aged (24mth) ZOL-treated (125ug/kg) animals vs. untreated, including senescence markers SESN3, CLEC2J and ASB9 (p<0.05) with a shift in cellular composition toward those of young (12wk) untreated mice. Similarly, a 5000-plex plasma proteome analysis from osteopenic patients before/after ZOL treatment (36mth) showed significant alterations in ~400 proteins including GTPase regulators, and markers of senescence, autophagy and inflammatory responses. Following this, a mass spectrometry-based cellular thermal shift assay confirmed multiple ZOL-protein interactions (TP-MAP analysis). Reassuringly FPPS was the most BP-bound protein, but we found many similarly stabilized proteins previously unassociated with BP action such as PHB2, FOSL1, CLTB (p80 genes including those linked to cell cycle regulation, and senescence (e.g. CCDC68, CDC14B, IGFBP5, PRKACB, p<0.001). Functional cellular analyses confirmed pre-treatment of cells with BPs protected against the onset of DNA damage-induced senescence (SA-?-gal, ?-H2AX, x2 fold, p<0.01). These multi-omic analyses reveal both novel BP-binding proteins and unidentified transcriptomic/proteomic alterations in non-skeletal cells via which BPs might protect against human aging-linked disorders.

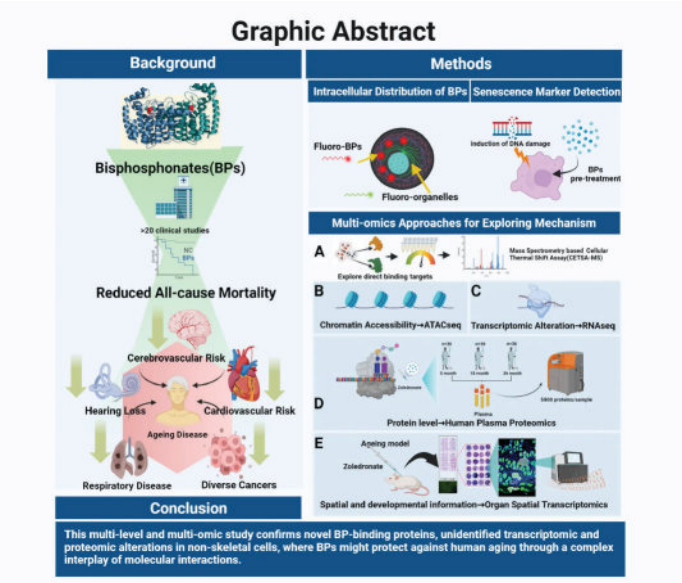

***Disclosures: Jinsen Lu**, None*

1099

Mouse model of uncoupled bone remodeling upon discontinuation of anti-RANKL antibody therapy

*Koji Ishikawa[1], Soji Tani[1], Nobuhiro Sakai[2], Yoshifumi Kudo[1], Hideyo Horiuchi[3], Hiromi Kimura-Suda[4], Masamichi Takami[5], Mayumi Tsuji[6], Katsunori Inagaki[1], Yuji Kiuchi[7], Takako Negishi-Koga[8]. [1]Department of Orthopaedic Surgery, School of Medicine, Showa University, Japan. [2]Department of Dental Education, School of Dentistry, Showa University, Japan. [3]Department of Applied Chemistry and Bioscience, Faculty of Science and Technology, Chitose Institute of Science and Technology, Japan. [4]Graduate School of Science and Engineering, Chitose Institute of Science and Technology, Japan. [5]Department of Pharmacology, School of Dentistry, Showa University, Japan. [6]Pharmacological Research Center, Showa University, Japan. [7]Department of Pharmacology, School of Medicine, Showa University, Japan. [8]Department of Medicine for Orthopaedics and Motor Organ, Juntendo University , Japan

The discontinuation of denosumab (anti-RANKL antibody) therapy may lead to an increased risk of multiple vertebral fractures in various pathological conditions. However, the pathophysiology underlying this risk is largely unknown.Eight patients who underwent discontinuation after multiple injections of denosumab had higher levels of TRAP-5b, the so-called “overshoot” phenomenon, compared to their pre-treatment levels. The rate of decrease in bone mineral density (BMD) during the withdrawal period was higher than in age-matched non-treated patients, suggesting a decrease in BMD independent of age-related physiological bone metabolism.To know the pathology of bone loss after discontinuation, we analyzed mice injected with anti-RANKL antibody. Overshoot and significant bone loss were observed in mice receiving continuous anti-RANKL antibody administration after treatment cessation, resembling the original pathology (Figure A and B). Bone mass rapidly decreased during overshoot (in vivo CT), and the ratio of mineral contents in the bone matrix was also reduced (FTIR). This deterioration of bone structure and quality resulted in bone fragility (three-point bending test). Furthermore, in mice long out of overshoot, bone resorption recovered, but osteoblast numbers and bone formation remained markedly reduced, even at the late phase (16 weeks after discontinuation). In the bone marrow, the number of Sca-1- and PDGFR?-expressing osteoblast progenitors (P?S cells) and ALP-positive early osteoblasts was greatly reduced (Figure C). These results suggested that sustained inhibition of osteoblastic lineage cells resulted in long-lasting bone loss.To explore the mechanism of overshoot of bone resorption, osteoclastic lineage cells were examined. Just before the overshoot, bone marrow cells contained a higher number of osteoclast precursor cells (c-Fms +cells), which formed TRAP+ mature osteoclasts more effectively than the control. RANKL levels were also elevated in mice injected with anti-RANKL antibody during overshoot. We found that these mice had higher amounts of RANKL-enriched extracellular vesicles (EVs) in sera, and that purified EVs stimulated osteoclastogenesis (Figure D). Thus, the accelerated bone resorption due to the accumulation of RANKL-bearing EVs and the long-term suppression of bone formation uncoupled from bone resorption leads to the severe bone loss that is characteristic of denosumab treatment discontinuation.

Figure

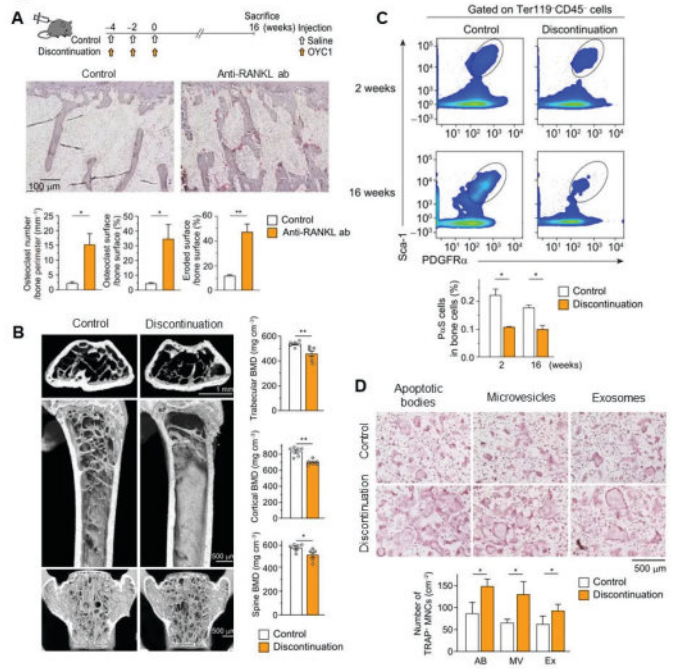

A. Schematic of the experimental setting for the mouse model of anti-RANKL discontinuation (Upper). Bone histomorphometric analysis in the proximal tibia of control (n = 3) and discontinuation mice (n = 3) 8 weeks after the last injection (Middle: TRAP staining).
B. Representative μCT images of the distal femur and spine of control (n = 8) and discontinuation mice (n = 8) 16 weeks after the last injection (Upper, axial view of metaphyseal region; middle, longitudinal view of femurs; lower, coronal view of spine).
C. The percentage of osteoblastic progenitors characterized by surface expression of PDGFRα and Sca-1 positive cells (PαS cells) in the femur of control (n = 4) and discontinuation mice (n = 4).
D. Effect of extracellular vesicles isolated from control and discontinuation mice serum during the overshoot period on the osteoclastogenesis of normal bone marrow monocyte/macrophage lineage cells. Representative images and the number of TRAP⁺ multi nucleated cells are shown (n = 4/groups).

***Disclosures: Koji Ishikawa**, None*

1100

Osteocyte RANKL is Critical for the Development of Cortical Porosity and High Bone Turnover in an Animal Model of Chronic Kidney Disease

*Corinne Metzger[3], Mizuho Kittaka[2], Alec Laplant[3], Yasuyoshi Ueki[2], Matthew Allen[3]. [3]Indiana University School of Medicine, . [2]Indiana University School of Dentistry, United States. [3]Indiana University School of Medicine, United States

Skeletal fragility and high fracture rates are common in chronic kidney disease (CKD). They contribute to reduced quality of life and increased mortality. A key component of bone loss in CKD with secondary hyperparathyroidism is cortical bone deterioration through both cortical thinning and the development of cortical porosity. Cortical porosity development progresses rapidly in both human CKD patients and animal models demonstrating it is a phenotype not directly tied to basal levels of intracortical remodeling (which is lacking in most rodents). We hypothesize that receptor activator of nuclear factor-?B ligand (RANKL), specifically from osteocytes, drives high bone resorption within cortical bone leading to the development of cortical porosity. To explore this hypothesis, we utilized male and female Dmp1-cre RANKL fl/fl mice after 10 weeks of adenine-induced CKD (Ad-CKD; 0.2% dietary adenine). All Ad-CKD mice regardless of sex or genotype had elevated blood urea nitrogen indicating reduced renal function and high parathyroid hormone (PTH). Micro-computed tomography of the distal femur revealed ~30% lower cortical thickness between wild-type Ad-CKD and wild-type control (CON) in both sexes. Cortical porosity was present in both sexes of wild-type Ad-CKD mice (average of 9.7% in male, 6.1% in females). Trabecular osteoclast-covered surfaces of the distal femur were ~3-fold higher in wild-type Ad-CKD mice compared to matched CON with corresponding higher bone formation rate. Ad-CKD mice lacking osteocyte RANKL had no statistical differences in cortical thickness or cortical porosity compared to sex- and genotype-matched CON groups with 3-6% differences in cortical thickness and cortical porosity values at or under ~2%. Additionally, Ad-CKD mice lacking osteocyte RANKL had no statistical differences in osteoclast-covered trabecular surfaces compared to matched CON groups. Likewise, there were no statistical increases in bone formation rate due to CKD in the transgenic Ad-CKD groups compared to matched controls. Overall, these data demonstrate that osteocyte RANKL is critical for the development of cortical porosity, cortical thinning, and high bone turnover seen in CKD with high PTH. Additionally, these data show that osteocyte RANKL is a key link between high circulating PTH and CKD-induced bone alterations. Anti-RANKL ligand

Monday Orals

therapy in CKD is potentially an attractive mechanism to prevent cortical bone deterioration and protect skeletal integrity.

***Disclosures: Corinne Metzger**, None*

Networking Reception

1101

Induction of Osteocalcin+ Osteoblast Apoptosis Stimulates Paradoxical Bone Formation Via Osteoprogenitor Recruitment *LENA BATOON[4], AMY KOH[2], Laurie McCauley[3], Hernan Roca[4]. [4]University of Michigan, [2]U OF MICHIGAN, United States. [3]University of Michigan School of Dentistry, United States. [4]University of Michigan, United States

Billions of cells in the body undergo apoptosis daily - a crucial process for tissue homeostasis and organ development. In bone, osteoblasts routinely undergo apoptosis yet the relevance of this process remains underexplored. We generated a murine model with conditional expression of inducible caspase-9 (iCasp9) activated in the presence of Cre. Caspase-9 is an apoptosis-initiating enzyme and iCasp9 activity can be induced via a dimerizer (AP). To generate mice with inducible osteocalcin(OCN)+ osteoblast apoptosis, iCasp9 mice were crossed with OCNcre. OCNcre-iCasp9 mice at 3 weeks were injected intraperitoneally with AP or vehicle. Immunofluorescence of the vertebrae confirmed an increase in cleaved caspase-3+ apoptotic cells at 9h ($p<0.05$) and reduction in OCN+ osteoblasts at 24h ($p<0.01$) post AP injection, validating the model. Long-term AP treatment for 5 weeks induced a paradoxical increase in vertebral bone volume fraction ($p=0.0001$) irrespective of gender. Dynamic histomorphometry with calcein and xylenol orange injected at 7 and 2 days pre-harvest revealed that AP treatment enhanced bone formation rate ($p<0.05$) and mineral apposition rate ($p<0.05$). There was no change in TRAP+ osteoclasts or serum N-terminal telopeptide of type I collagen, indicating that the bone accrual was not due to changes in bone resorption. Increase in fractional bone volume did not translate in improved mechanical strength examined via compression testing likely due to disruption of the lacunocanalicular network. Long-term AP treatment increased empty osteocyte lacunae along with reduced canaliculi number and length. The number of sclerostin-expressing osteocytes was unaltered. To further understand the cellular mechanism, we stained for the pre-osteoblast growth factor amphiregulin (AREG) and osteoprogenitor markers osterix (OSX) and alpha-smooth muscle actin (?SMA). Induction of OCN+ cell apoptosis was associated with elevated AREG expression ($p<0.05$) and OSX+ cells in the bone marrow ($p<0.05$). ?SMA+ cells directly associated with bone surfaces were also increased ($p<0.01$). Interestingly, a similar long-term AP treatment regimen in OSXcre-iCasp9 mice did not trigger the bone increase observed with OCNcre-iCasp9 mice. Collectively, this work establishes the importance of osteoblast apoptosis in promoting osteoprogenitor recruitment and bone accrual. Importantly, it exposes the potential of targeting this mechanism to promote bone formation in the clinical setting.

***Disclosures: LENA BATOON**, None*

1102

Stat3 Persistent Activation in Osteoblasts Leads to High Bone Mass in Mice *Mariana Moraes de Lima Perini[1], Elizabeth Scott[2], Olivia Reul[2], Hong Du[3], Cong Yan[3], Jiliang Li[1]. [1]Department of Biology, Indiana University Purdue University Indianapolis, United States. [2]Department of Biomedical Engineering, Indiana University Purdue University Indianapolis, IN 46202, United States. [3]Department of Pathology and Laboratory of Medicine, Indiana University School of Medicine, IN 46202, United States

Signal Transducer and Activator of Transcription 3 (Stat3) plays an important role in bone formation and maintenance. Our previous studies have shown that osteoblast-specific deletion of Stat3 decreased bone mineral density (BMD) and strength. While overexpression of Stat3 in osteoblasts may increase osteogenic potential, overexpression of Stat3 in many other cell-types is associated with a wide range of cancers including prostate, breast cancer, etc. Stat3 overexpression is found throughout the tumor ecosystem in these cancers, in tumor cells, immune cells, and cancer-associated fibroblasts. To assess the consequences of Stat3 persistent activation in osteoblasts, we bred Osterix-tTA,tetO-EGFP/cre mice with CCSP-rtTA/(tetO)7-Stat3C bitransgenic mice to generate a doxycycline-controlled Osterix-tTA,tetO-EGFP/cre and Stat3c binary transgenic mouse model that over-expresses Stat3C (the constitutively active form of Stat3) selectively in osteoblasts lineage (OB-Stat3C mice). At 20 weeks of age, both male and female OB-Stat3C mice showed a significant increase in BMD and bone mineral content (BMC) compared to their littermate controls. Micro-CT analysis of the distal femur showed a significant increase in trabecular bone volume (520%; 882%), BV/TV (245%; 485.9%), trabecular number (174.5%; 257%), and trabecular thickness (26.7; 69.6%) for both male and female OB-Stat3C mice, respectively, when compared to their respective controls. Both histological images and micro-CT 3D reconstruction images (Figure 1) showed an excessive growth of trabecular bone not only in the distal part of the femur, but through the entirety of the femurs in both male and female OB-Stat3C mice. Bending tests of the femurs of male OB-Stat3C mice showed a significant increase of 119.77% in failure force while their females counterparts showed a significant increase of 55.22% compared to their respective controls. Furthermore, we did not observe any primary bone tumors even in 18-month-old mice. More importantly, we observed astonishing amounts of newly formed lamellar bone in the bone marrow of those mice, suggesting that Stat3 in osteoblasts and osteocytes not only stimulate lamellar bone formation but also does not induce tumor growth.

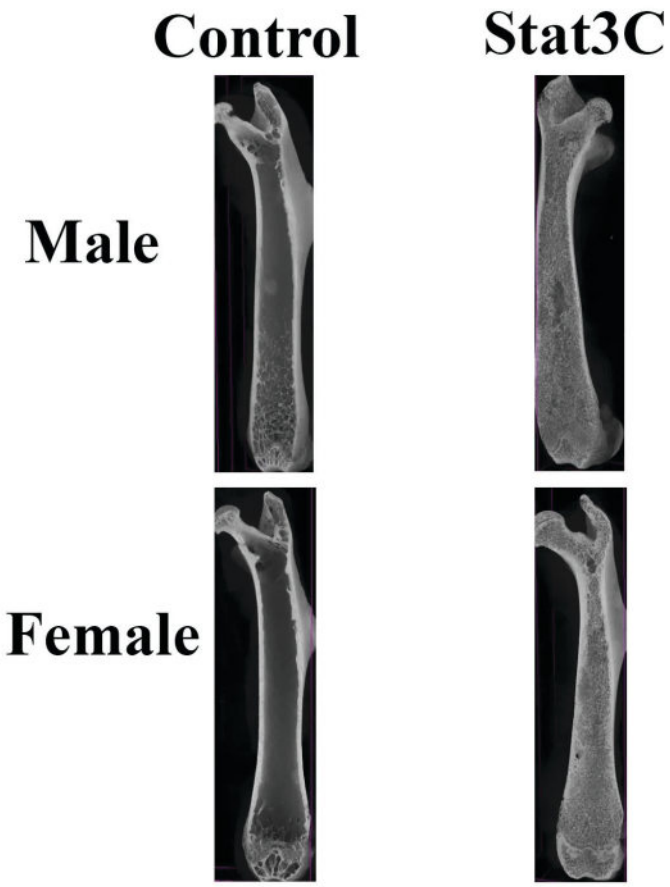

***Disclosures: Mariana Moraes de Lima Perini**, None*

1103

miR-219a-5p Improves Bone Mass in Mice and is Enriched in Osteoblast-derived Extracellular Vesicles *David Monroe[1], JAPNEET KAUR[2], Naureen Javeed[3], Madhusudhan Bobbili[4], Johannes Grillari[4], Joshua Farr[3], Jennifer Rowsey[3], Stephanie Vos[3], Ming Ruan[3], Sundeep Khosla[5]. [1]Mayo Foundation, United States. [2]University of Arkansas for Medical Sciences, [3]Mayo Clinic, United States. [4]Ludwig Boltzmann Institute for Traumatology, Austria. [5]Mayo Clinic College of Medicine, United States

We previously demonstrated that miR-219a-5p plays an osteo-anabolic role in cultured osteoblastic cells based on increased miR-219a expression during differentiation, enhancement of osteogenic marker expression with miR-219a mimics, and suppression of osteoblastic differentiation with a miR-219a antagonist. To test these effects in vivo, we developed a novel mouse model to express miR-219a under the control of a Cre-inducible system ("miR-219a-FLIP"). In the unrecombined state, the ubiquitous CAGGS promoter drives expression of EGFP, followed by an mCherry cassette with the miR-219a-5p sequence embedded in its 3' UTR in the reverse orientation (Fig 1A). Following Cre expression, a two-step recombination process results in loss of EGFP and expression of mCherry and miR-219a (Fig. 1B). We used the Actb-Cre to express miR-219a in all tissues and analyzed the bone phenotype at 4 months of age. We found significant ($p<0.05$) increases in BV/TV (+23%) and Tb.Th (+8%), with a trend for increased Tb.N. (+12%), in female mice at the spine. At the femur, significant increases in BV/TV (+46%) and Ct.Th (+7%) were observed, with a trend for increased Ct.Th (+4%). Similar trends were found in male mice. Osteoclast number was 2.9-fold decreased with no change in osteoblast number or activity, suggesting an anti-resorptive phenotype. We also found that miR-219a was present in EVs isolated from mouse calvarial osteoblasts. To validate this finding in vivo, we developed another novel mouse model where we could tag EVs from a select cell- or tissue-type using Cre mouse models. Using a similar design as in the miR-219a-FLIP model, we developed the "CAGS-SNORKEL" model where the SNORKEL protein (encoding a fusion of the EV-associated CD81 tetraspanin with various epitope tags) is expressed upon exposure to Cre. This model was crossed with either Prx1-Cre (early osteoblast progenitors) or Osteocalcin-Cre (late osteoblast/osteocyte), SNORKEL+ EVs isolated from bone marrow plasma using a magnetic bead protocol, and miRNA-seq performed. We found that miR-219a was enriched in osteoblast-derived EVs,

suggesting that miR-219a may perform its bone anabolic function, in part, through EV-mediated mechanisms. Cell culture studies further demonstrated that miR-219a increased Wnt activity through targeting of the Wnt inhibitor, Gsk3?. In summary, our data demonstrate that miR-219a is bone anabolic in vivo and may stimulate Wnt activity in bone using EV-mediated mechanisms.

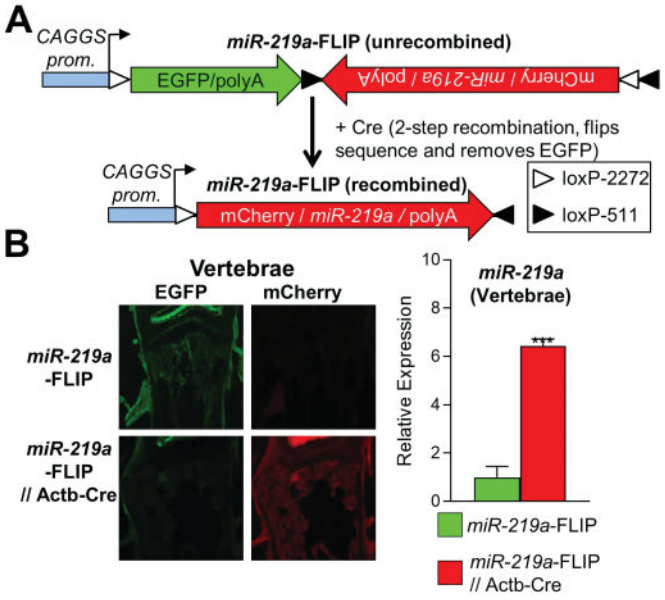

***Disclosures: David Monroe**, None*

1104

Dual inhibition of sclerostin and Notum induces synergistic osteoanabolic action in mice *Roy Byung-Jun Choi[1], Alexander Robling[1], Jung Min Hong[2]. [1]Indiana University School of Medicine, United States. [2]Indiana University School of Dentistry, United States

The Wnt pathway has been an obvious target for designing skeletal therapies, mainly based on the Wnt inhibitor sclerostin. The sclerostin-neutralizing agent romosozumab was recently approved to treat patients at increased fracture risk. However, significant adverse events were found in clinical trials, prompting the FDA to assign a 'black-box warning' to patients at higher risk for cardiovascular complications. Thus, reducing the dose of sclerostin antibody while maintaining the anabolic potential of the drug will likely provide a safer and more cost-effective strategy to harness Wnt for fracture prevention. Previously, we reported that simultaneous pharmacological or genetic inhibition of the Wnt antagonists sclerostin and Dkk1 could be optimized to create potentiated effects in the cancellous bone compartment. This highly efficacious approach allowed significantly reduced drug dose yet maintained full (or improved) anabolic potential. We looked for other candidates that might be co-inhibited along with sclerostin to potentiate effects in the cortex. To start, we used genetic clues for molecules that preferentially affect the cortical compartment. Another Wnt inhibitor that has major effects on cortical but not cancellous bone is Notum, a secreted deacylase that removes palmitoylated modifications from Wnt ligands, thereby neutralizing Wnt's ability to interact with Fzd-Lrp5/6. Previously, we found Notum deletion mice had an additive effect on cortical bone formation in the absence of sclerostin. We looked at Notum as target to inhibit, alongside sclerostin, to improve cortical bone specifically. We generated double knockout mice in both Sost and Notum (Sost-/-;Notum-/-) and compared them to single knockouts and WT controls. Further, we performed analogous experiments with pharmacologic inhibitors, rather than genomic mutations. i.e., co-treatment of WT mice with sclerostin antibody and a small molecule inhibitor of Notum (LX-5061). Each experiment included evaluation by DXA-derived radiography, μCT, biomechanical testing and bone dynamic histomorphometry to assess the distal and midshaft femur, and lumbar vertebrae. Inhibition/deletion of Notum alone had mild cortical effects while co-suppressing/deleting sclerostin and Notum significantly improved bone mass and strength. Pharmacologic studies largely supported the genetic studies, suggesting that co-inhibiting sclerostin and Notum might be viable for treating low bone-mass disease in aged patients.

***Disclosures: Roy Byung-Jun Choi**, None*

1105

PTH regulates osteogenesis and suppresses adipogenesis through Zfp 467 in a feed-forward, PTH1R-cyclic AMP-dependent manner *Hanghang Liu[1], Phuong T. Le[1], Akane Wada[2], Isabella Le[1], Andrew Lee[1], Jun Zhou[2], Francesca Gori[2], Roland Baron[2], Clifford J. Rosen[1]. [1]MaineHealth Institute for Research, United States. [2]Harvard School of Dental Medicine, United States

Conditional deletion of the PTH1R in mesenchymal progenitors reduces osteoblast differentiation, enhances marrow adipogenesis and increases zinc finger protein 467 (Zfp467) expression. In contrast, genetic loss of Zfp467 increased Pth1r expression and shifts mesenchymal progenitor cell fate towards osteogenesis and higher bone mass. In this study, we hypothesized PTH1R and ZFP467 could constitute a feedback loop that facilitates PTH-induced osteogenesis and that conditional deletion of Zfp467 in osteogenic precursors would lead to high bone mass in mice. Similar to global Zfp467-/- mice that have significantly higher bone formation and bone volume assessed by ?CT and histomorphometry analysis, Prrx1Cre; Zfp467fl/fl but not AdipoqCre; Zfp467fl/fl mice exhibit high bone mass and greater osteogenic differentiation similar to the Zfp467-/- mice. qPCR results revealed that PTH suppressed Zfp467 expression primarily via the cyclic AMP/PKA pathway. Not surprisingly, PKA activation inhibited the expression of Zfp467 and gene silencing of Pth1r caused an increase in Zfp467 mRNA transcription. Dual fluorescence reporter assays and confocal immunofluorescence demonstrated that genetic deletion of Zfp467 resulted in higher nuclear translocation of NF?B1 that binds to the P2 promoter of the Pth1r and increased its transcription. As expected, NF?B1 was found heterodimerize with RelB to transactivate the transcription of Pth1r, higher protein level of NIK and activated non-canonical NF?B pathway was also observed in Zfp467 deficient osteoblasts. In addition, Zfp467-/- cells had enhanced production of cyclic AMP and increased glycolysis in response to exogenous PTH. And the osteogenic response to PTH was also enhanced in Zfp467-/- calvarial osteoblasts, and the pro-osteogenic effect of Zfp467 deletion was blocked by gene silencing of Pth1r or a PKA inhibitor. In conclusion, our findings suggest that loss or PTH1R-mediated repression of Zfp467 results in a pathway that increases Pth1r transcription via NF?B1 and thus cellular responsiveness to PTH/PTHrP, ultimately leading to enhanced bone formation.

***Disclosures: Hanghang Liu**, None*

1106

Spatial transcriptomic analysis of a pre-clinical model of Nf1-deficient fractures pseudarthrosis *Jonathan Rios[1], Yared Kidane[1], Conan Juan[2], Carol Wise[3], Robert Tower[4]. [1]Scottish Rite for Children, United States. [2]UTSouthwestern Medical Center, United States. [3]Texas Scottish Rite Hospital, United States. [4]University of Texas Southwestern Medical Center,

Patients with Neurofibromatosis type 1 (NF1) may develop fracture pseudarthroses characterized by a persistent fibrotic, hypomineralized callus with a high re-fracture risk. Prior pre-clinical studies demonstrated impaired osteogenic potential of cultured periosteal and bone marrow progenitor cells in vitro. Delayed fracture healing phenocopying patient pseudarthrosis has been demonstrated in Postn-cre;Nf1flox/- (herein Nf1Postn) mice; however, molecular analyses of such delayed fracture healing is lacking.Spatial transcriptomics provides unprecedented resolution of cell type-specific gene expression profiling within the context of normal and diseased tissues. Here, we performed spatial transcriptomic analyses of fracture calluses from Nf1Postn and control mice. Spatial transcriptomic analysis was performed on control and Nf1Postn calluses 10 days after distal tibia osteotomy fracture using the 10X Genomics mouse FFPE Visium protocol.Spatial transcriptomic analysis detected a median 2,168 and 2,203 expressed genes per spot under tissue, with an average 4,315 and 4,631 unique molecular identifiers (UMI) per spot from 61,642 and 85,469 mean reads per spot, respectively. Graph-based clustering analysis detected eight tissue/cell types mapping to the fracture calluses, each with associated expression biomarkers that informed their predicted identities. Gene set enrichment analysis (GSEA) demonstrated significantly increased expression of pathways involved in cartilage development and chondrocyte differentiation (Cartilage), collagen deposition in the extracellular matrix (Ossifying perichondrium), and bone remodeling and biomineralization (Woven bone) within spatial clusters. Additionally, expression of genes representative of different morphogenetic pathways, such as BMP, TGF-?, and WNT, were spatially restricted within the fracture callus. Finally, GSEA analysis demonstrated reduced expression of pathways required for proper skeletal development and fracture healing, including BMP signaling, chondrogenesis, cartilage development, extracellular matrix, and bone remodeling pathways, in the Nf1Postn fracture compared to control. This study is the first to apply unbiased spatial transcriptomic analysis to resolve molecular gradients within a fracture callus and to spatially resolve molecular dysregulation leading to delayed fracture healing in a pre-clinical disease model.

***Disclosures: Jonathan Rios**, None*

1107

Microbiome-Induced Intestinal Th17 Cells and Musculoskeletal ?? T Cells Improve Fracture Healing *Hamid Y Dar[1], Daniel Perrian[1], Subhashis Pal[1], Andreea Stoica[1], Sasidhar Uppuganti[2], Jeffry S Nyman[2], Rheinallt M Jones[1], M. Neale Weitzmann[1], Roberto Pacifici[1]. [1]Emory University, United States. [2]Vanderbilt University Medical Center, United States

IL-17 is a driver of the inflammatory phase of fracture repair. This cytokine is produced in the callus by ?? T cells and Th17 cells. However, the origin of the ?? T cells and Th17 cells involved in fracture repair, the mechanism by which they are home to the callus, and their contribution to fracture healing are unknown. Using a model of murine femoral fracture that heals by endochondral ossification, we found that femoral fractures were followed within 2- days by an expansion of callus ?? T cells. Their activation and release of IL-17 caused systemic inflammation and increased gut permeability. Demonstrating the relevance of ?? T cells, fractures did not increase gut permeability and fracture repair was delayed in TCRd-/- mice, a strain lacking ?? T cells. When the gut microbiota contained the Th17 cell-inducing taxa segmented filamentous bacteria (SFB), increased gut permeability led to the expansion of intestinal Th17 cells, higher callus levels of IL-17 with a peak at day 3- after fracture, and faster fracture repair. Studies using Kaede mice, a strain expressing a photo-convertible fluorescent protein that allows direct tracking of intestinal lymphocytes, demonstrated that fractures increased by ~ 3 folds the migration of intestinal Th17 cells to the callus with a peak at day 3. These studies also showed the existence of a small pool of microbiome-induced intestinal ?? T cells that migrate to the callus. IV injection of eGFP+ Th17 cells confirmed that fractures increased the tropism of Th17 cells toward the callus. Mechanistically, fractures increased the S1P-receptor-1 (S1PR1) mediated migration of Th17 cells from the intestine to the bloodstream. In addition, fractures increased the homing of circulating Th17 cells to the callus by upregulating the expression by callus stromal cells of CCL20, a ligand for the chemokine receptor CCR6 expressed by Th17 cells. Attesting to the relevance of these mechanisms, the fracture-induced increase in callus IL-17 levels was prevented, and fracture repair was impaired, by the deletion of ?? T cells, depletion of the microbiome by antibiotics, and lack of SFB in the gut microbiome. These findings demonstrated the relevance of the gut microbiome, ?? T cells, and Th17 cell trafficking for fracture repair. Modifications of microbiome composition via Th17 cell-inducing bacteriotherapy and avoidance of broad-spectrum antibiotics may represent novel therapeutic strategies to improve fracture healing.

Microbiome-Induced Intestinal Th17 Cells and Musculoskeletal γδ T Cells Improve Fracture Healing

Hamid Y. Dar[1,2], Daniel S. Perrien[1,2], Subhashis Pal[1,2], Andreea Stoica[1,2], Sasidhar Uppuganti[3], Jeffry S. Nyman[3,4], Rheinallt M. Jones[2,5], M. Neale Weitzmann[1,2,6], and Roberto Pacifici[1,2,7]

[1]Division of Endocrinology, Metabolism and Lipids, Department of Medicine, and [2]Emory Microbiome Research Center, Emory University, Atlanta, Georgia, USA. [3]Department of Orthopedic Surgery, Vanderbilt University Medical Center, Nashville, TN 37232, USA. [4]Department of Veterans Affairs, Tennessee Valley Healthcare System, Nashville, TN, USA. [5]Division of Pediatric Gastroenterology, Hepatology, and Nutrition, Department of Pediatrics, Emory University, Atlanta, Georgia, USA. [6]Atlanta VA Health Care System, Department of Veterans Affairs, Decatur, Georgia, USA. [7]Immunology and Molecular Pathogenesis Program, Emory University, Atlanta, GA.

IL-17 is a driver of the inflammatory phase of fracture repair. This cytokine is produced in the callus by γδ T cells and Th17 cells. However, the origin of the γδ T cells and Th17 cells involved in fracture repair, the mechanism by which they are home to the callus, and their contribution to fracture healing are unknown. Using a model of murine femoral fracture that heals by endochondral ossification, we found that femoral fractures were followed within 2- days by an expansion of callus γδ T cells. Their activation and release of IL-17 caused systemic inflammation and increased gut permeability. Demonstrating the relevance of γδ T cells, fractures did not increase gut permeability and fracture repair was delayed in TCRd-/- mice, a strain lacking γδ T cells. When the gut microbiota contained the Th17 cell-inducing taxa segmented filamentous bacteria (SFB), increased gut permeability led to the expansion of intestinal Th17 cells, higher callus levels of IL-17 with a peak at day 3- after fracture, and faster fracture repair. Studies using Kaede mice, a strain expressing a photo-convertible fluorescent protein that allows direct tracking of intestinal lymphocytes, demonstrated that fractures increased by ~ 3 folds the migration of intestinal Th17 cells to the callus with a peak at day 3. These studies also showed the existence of a small pool of microbiome-induced intestinal γδ T cells that migrate to the callus. IV injection of eGFP+ Th17 cells confirmed that fractures increased the tropism of Th17 cells toward the callus. Mechanistically, fractures increased the S1P-receptor-1 (S1PR1) mediated migration of Th17 cells from the intestine to the bloodstream. In addition, fractures increased the homing of circulating Th17 cells to the callus by upregulating the expression by callus stromal cells of CCL20, a ligand for the chemokine receptor CCR6 expressed by Th17 cells. Attesting to the relevance of these mechanisms, the fracture-induced increase in callus IL-17 levels was prevented, and fracture repair was impaired, by the deletion of γδ T cells, depletion of the microbiome by antibiotics, and lack of SFB in the gut microbiome. These findings demonstrated the relevance of the gut microbiome, γδ T cells, and Th17 cell trafficking for fracture repair. Modifications of microbiome composition via Th17 cell-inducing bacteriotherapy and avoidance of broad-spectrum antibiotics may represent novel therapeutic strategies to improve fracture healing.

***Disclosures: Hamid Y Dar**, None*

1108

Dysregulation of the Unfolded Protein Response Outputs by Diet-Induced Obesity may Impede Fracture Repair. *Lakshmi Kolora[1], Sara Higsley[1], Dana Godfrey[1], Kartik Shankar[2], Douglas Adams[3], SRIVIDHYA IYER[4]. [1]Department of Orthopedics, University of Colorado Anschutz Medical Campus, United States. [2]Department of Pediatrics, University of Colorado, Anschutz Medical Campus, United States. [3]University of Colorado, United States. [4] Univ of Colorado, Anschutz Medical Campus, United States

Obesity increases skeletal fragility and hinders fracture repair in humans and rodent models, but its biological basis is unknown. Endoplasmic reticulum (ER) stress, due to protein processing deficits, mediates development of obesity-related comorbidities including diabetes, but its contribution in the context of bone repair remains unaddressed. The Unfolded Protein Response (UPR) engages transcriptional (IRE1/XBP1s and ATF6) and translational (PERK) outputs that aid protein folding and transiently repress protein synthesis, respectively, to relieve ER stress. To comprehensively assess the UPR during fracture repair in obese backgrounds, 17-week-old diet-induced obese (DIO) and DIO control mice (Jax Labs) were administered tibial fracture by osteotomy. DIO mice exhibited lower callus bone volume (~32 %), strength (~35 %), and stiffness (~33%) at 28 days post-fracture (dpf). DIO suppressed expression of osteogenic (RunX2, Sp7, Col1a1) genes and augmented adiposity (Fabp4, Ppar?) in cultures of 10dpf callus. Notably, obesity also inhibited the expression of several IRE1/XBP1s targets in callus cultures, concomitant with apoptosis. The ATF6 protein levels were, however, unaffected. Furthermore, callus culture lysates obtained from DIO mice exhibited elevated PERK activity, as evidenced by increase in phosphorylation of PERK and its downstream target eIF2?. The expression of Gadd34 (a phosphatase that reverses p-eIF2? phosphorylation) was suppressed, substantiating a protracted PERK-induced translational arrest. In line with these findings, single-cell profiling of 10 dpf callus revealed ~3-fold increase in bipotential Cxcl12-abundant reticular (CAR) cells with obesity. However, CAR cell-dependent endothelial, B-cell and neutrophil niches were decreased, but adipocytes were increased ~10-fold in the obese callus. Per gene ontology analyses, DIO was associated with suppression of protein synthesis processes and upregulation of inflammatory genes in CAR cells. Further confirming a role for aberrant UPR in skeletal repair deficits, the ER stress attenuator TUDCA mitigated the HFD-induced low callus bone volume, and rescued the osteo to adipocytic skewing of the callus transcriptome. Our findings demonstrate that obesity dysregulates PERK and IRE1/XBP1s outputs during osteogenic fracture repair, a phase reliant on protein synthesis and processing, and underscores the potential of modifying the UPR to improve fracture repair in obese diabetic populations.

***Disclosures: Lakshmi Kolora**, None*

1109

YAP regulates periosteal progenitor cell proliferation through both cell intrinsic and extrinsic co-transcriptional programs *MADHURA NIJSURE[2], Annemarie Lang[2], Elizabeth Seidl[2], Christopher Panebianco[2], Miriam Baitner[2], Gabrielle Tanner[2], Dakota Jones[2], Annapurna Pranatharthi-Haran[2], Greg Szeto[3], Nathaniel Dyment[2], Joel Boerckel[2]. [2]University of Pennsylvania, . [2]University of Pennsylvania, United States. [3]Seagen Inc, United States

Bone fracture repair activates the transcriptional regulator, YAP, in periosteal cells and initiates periosteal cell proliferation. Deletion of YAP, and its paralog TAZ, from Osterix-expressing cells impairs periosteal cell proliferation and periosteal expansion1. The transcriptional mechanisms by which YAP drives periosteal expansion are unclear. YAP does not directly bind to DNA but forms a complex with other transcription factors to regulate transcriptional activity. It is therefore important to identify both YAP transcriptional programs and the associated transcription factor partners.To this end, we used a gain-of-function model to induce expression of constitutively active YAP (YAPS127A) upon treatment with doxycycline. We isolated periosteal cells from 4-day old fracture calluses and treated them with 1?M doxycycline in vitro. We performed orthogonal Bulk mRNA sequencing (RNA-seq) and Assayed for Transposase Accessible Chromatin with sequencing (ATAC-seq) to quantify YAP-induced messenger RNAs and YAP-regulated chromatin accessibility, respectively. This analysis identified YAP target genes and putative transcription factor binding partners in periosteal cells.Gene set variation analysis revealed 236 gene sets most relevant to progenitor pool expansion during fracture repair (Fig 1A). YAPS127A activation significantly enriched gene sets involving cell cycle progression and Smad2/3 signaling and suppressed gene sets marking caspase pathways involved in apoptosis. Specifically, YAPS127A upregulated both cell intrinsic factors, such as Cdk6, and cell extrinsic or secreted factors, such as Bmp4 and Cyr61. Analysis of DNA motifs present in differentially accessible chromatin revealed enrichment of chromatin loci containing the consensus binding motifs of the TEAD and Smad2/3 transcription factors (Fig 1B). YAPS127A activation elevated canonical YAP-TEAD complex target genes and enriched Smad2/3-target gene sets, supporting roles for both TEAD and Smad2/3 as putative transcriptional co-effectors of YAP in periosteal osteoblast precursors. We further validated YAP-TEAD binding in periosteal cells by immunoprecipitating YAP and probing for TEAD (Fig 1C).Finally, to define the impact of YAP/TAZ signaling on cell proliferation in vivo, we deleted YAP/TAZ from Osterix expressing cells in mice. There was a significant decrease in proliferation and cell numbers of both Osterix-targeted cells and non-targeted cells, confirming that YAP/TAZ signaling functionally regulates periosteal progenitor proliferation through both cell intrinsic and extrinsic mechanisms (Fig 1D).Together, these data reveal that YAP and TAZ regulate proliferation-associated gene

expression partially through TEAD and promote functional periosteal expansion for fracture repair.References:1. Kegelman+, JBMR 2020

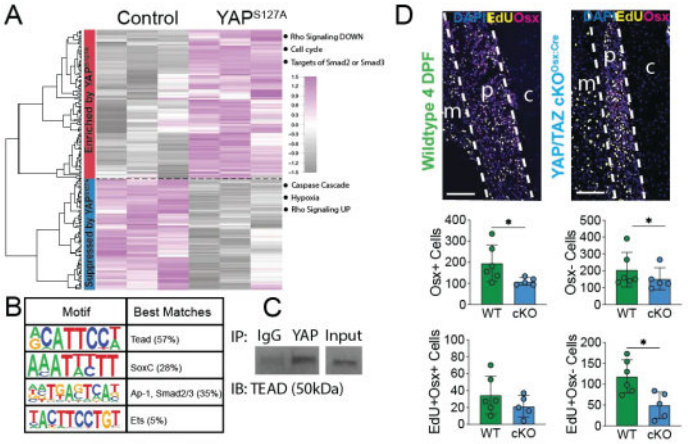

Figure 1. A. Gene Set Variation Analysis revealed 236 differentially regulated gene sets after YAP^{S127A} expression. **B.** TEAD Binding motifs were 57% enriched in open chromatin in YAP^{S127A} expressing cells. **C**. TEAD co-immunoprecipitates with YAP in periosteal cells. **D**. Immunofluorescence staining in callus-adjacent periosteum 4 days post fracture. p = periosteum, c = cortical bone, m = muscle; Scale Bar = 100 μM.

***Disclosures: MADHURA NIJSURE**, None*

1110

Neutrophil-derived TGF?1 causes age-related osteoporosis and delays fracture healing *Han Jiao[1], Jinxiao Fan[1], Shida He[1], Brendan Boyce[2], Jinbo Li[1]. [1]Hebei Medical University, China; [2]University of Rochester Medical Center, United States

During aging, enhanced myeloid lineage commitment promotes neutrophil generation, but neutrophil effects on bone homeostasis remain poorly understood. We generated Ly6G-CreERRosaDTA (Ly6G-DTA) mice in which tamoxifen induced diptheria toxin expression in neutrophils (Ly6G+) and caused specific ablation of >99% neutrophils in BM. Of note, femoral trabecular bone mass, thickness, number and mineral density in adult (8-mon-old) Ly6G-DTA mice were significantly higher than in WT littermates (BV/TV: 44.8+/-3.2% vs 22.1+/-2.0% in WT mice; p<0.001), associated with markedly increased bone formation and bone resorption, but cortical thickness was normal. Transplant of Ly6G-DTA mouse BM cells into 2-mon-old immunodeficient NSG mice caused a significant increase in trabecular bone mass and mineral density, suggesting that Ly6G+ neutrophils negatively regulate bone mass. TGF?1+CCR5+ neutrophil numbers increase in BM during aging and cause bone loss. Single-cell RNA-Seq data revealed that TGF?1+ neutrophils are a terminally differentiated subset in which pro-osteoclast differentiation signaling was highly activated and associated with high Il-1? and Dap12 transcription. To further determine the role of neutrophil-derived TGF?1 on bone aging, we next generated Ly6GCreERTGF?1fl/fl (TGF?1-cKO) mice and found that inducible deletion of Tgf?1 from Ly6G+ neutrophils caused significant decrease in TGF?1 protein levels in BM and impairment of neutrophil NET formation and phagocytosis. In addition, TGF?1-cKO mice have higher trabecular bone mass (BV/TV: 45.2+/-6.2% vs 22.1+/-2.0% in WT mice; p<0.001) and mineral density (BMD: 1.07+/-0.19 vs 0.40+/-0.07 g/cm3 in WT mice; p<0.001) than WT littermates, associated with markedly increased bone formation and resorption, similar to Ly6G-DTA mice. RNASeq analysis of tibial fracture callus of 4- (young) and 20-mon-old (aged) mice revealed that neutrophil chemotaxis and TGF? signaling pathways were more highly activated in aged callus. Notably, callus and woven bone volume were higher in Ly6G-DTA and TGF?1-cKO mice than WT littermates at 2-, 3- and 4-week post fracture (Woven bone: 5.2+/-1.9 mm3 in DTA, 5.3+/-1.6 mm3 in TGF?1-cKO vs 2.3+/-0.4 mm3 in WT mice; p<0.01), associated with increased bone formation and decreased callus fibrosis. These findings define novel roles of neutrophils and neutrophil-derived TGF?1 in bone homeostasis and fracture repair; blockade of neutrophils or TGF?1 might prevent age-related osteoporosis and enhance fracture repair.

***Disclosures: Han Jiao**, None*

1111

First Results of the Global ALPL Gene Variant Classification Project *Mariam R Farman[1], Catherine Rehder[2], Theodora Malli[3], Cheryl Rockman-Greenberg[4], Kathryn Dahir[5], Gabriel Ángel Martos-Moreno[6], Agnès Linglart[7], Keiichi Ozono[8], Lothar Seefried[9], Guillermo del Angel[10], Florian Högler[1], Francesca Barbazza[1], Lisa K John[1], Sewmi M. A. Delana Mudiyanselage[1], Erica Burner Nading[2], Erin Huggins[2], Eric T Rush[11], Ahmed El-Gazzar[1], Priya S Kishnani[12], Gerald Webersinke[3], Wolfgang Högler[1]. [1]Department of Paediatrics and Adolescent Medicine, Johannes Kepler University Linz, Austria; [2]Duke University Medical Center, Division of Medical Genetics, Dept of Pediatrics, United States; [3]Laboratory for Molecular Genetic Diagnostics, Ordensklinikum Linz, Austria; [4]Department of Pediatrics and Child Health Rady Faculty of Health Sciences, University of Manitoba, Canada; [5]Vanderbilt University Medical Center, Program for Metabolic Bone Disorders, United States; [6]Departments of Pediatrics & Pediatric Endocrinology, Hospital Infantil Universitario Niño Jesús, IIS La Princesa, Madrid, Spain. Department of Pediatrics, Universidad Autónoma de Madrid, Spain; [7]8 AP-HP, Paris Saclay University, INSERM, Bicêtre Paris Saclay hospital, France; [8]9 Department of Pediatrics, Osaka University Graduate School of Medicine, Japan; [9]Julius-Maximilian University, Germany; [10]Alexion, AstraZeneca Rare Disease, United States; [11]Division of Clinical Genetics, Children's Mercy Hospital Kansas City, United States; [12]Duke University Medical Center, Division of Medical Genetics, Department of Pediatrics, United States

ObjectivesHypophosphatasia (HPP) is an inherited multisystem disorder predominantly affecting the mineralization of bones and teeth. HPP is caused by pathogenic variants in ALPL, which encodes tissue non-specific alkaline phosphatase. A major challenge in diagnosing HPP is interpreting variants in ALPL classified as variants of uncertain significance (VUS) according to ACMG/AMP criteria, creating uncertainty in patients and treating physicians resulting in diagnostic delays. The ALPL gene variant classification project was established to reclassify VUS and to continuously assess and update genetic, phenotypic, and functional variant information in the ALPL gene variant database (https://alplmutation-database.jku.at/), an open-access archive for interpretations of the clinical significance of variants reported in ALPL. We aim to report the first results of newly classified variants in this project.MethodsAn international, multidisciplinary consortium of HPP experts has been established to reclassify the submitted VUS using a multi-step process adhering to the ACMG/AMP variant classification guidelines. These steps include a clinical phenotype assessment, deep literature review including artificial intelligence technology, molecular genetic assessment, and in-vitro functional testing (episomal pcDNA3 vectors used in a co-transfection model to express a variant in renal MDCK-II cells to measure ALP residual activity and assess dominant negative effect).ResultsCurrently, the ALPL database has 429 variants and 594 genotypes. The number of VUS reclassified or classified by the ALPL gene consortium since its inception in Feb 2021 is 58, as shown in the table below.VariantsNumber of VariantsReclassified to date58-Reclassified with functional testing-Reclassified from literature2813New submissions classified20Out of the 58 classified or reclassified variants, 4 were pathogenic, 29 likely pathogenic, 2 were likely benign, 1 benign, and 21 remained VUS. 84 new genotypes and 57 new phenotypes were added to the variants in the ALPL database.Through studying the submitted and reported phenotypes, we discovered distinct new phenotypes - asymptomatic heterozygote individuals featuring the typical biochemical signature of HPP (c.1225C>T, c.466C>T, c818C>T, c.244G>A, c.244G>C, c.906C>A, c.83A>G and c.299C>T) and heterozygote individuals with massive ectopic calcification (c.1559del and c.1250A>G).ConclusionThis classification project and the ALPL gene variant database serve the global medical community and widen the genotypic and phenotypic HPP spectrum by classifying ALPL variants based on ACMG/AMP criteria, thus facilitating improved genetic counselling and medical decision-making for affected patients and families and as a repository for clinicians and scientists to query a variant and view evidence of its pathogenicity.

***Disclosures: Mariam R Farman**, None*

1112

Development of bone targeted anti-TGF? antibody for the treatment of osteogenesis imperfecta *I-Wen Song[1], Dianne Nguyen[1], Alyssa Tran[1], Ben Greene[2], James Cao[2], Xiaoyou Ying[2], Anna Park[2], Elizabeth Masterjohn[2], Denise Honey[2], Shiguang Liu[2], Sandesh Nagamani[1], Brendan Lee[1]. [1]Baylor College of Medicine, United States; [2]Sanofi, United States

Osteogenesis imperfecta (OI) is a genetic skeletal disorder for which, currently, there are no FDA-approved therapies. We, and others, have previously shown that excessive TGF? signaling is a key pathogenic driver in OI and that inhibition of TGF? could be a potential mechanism-specific approach for treatment. In a phase 1 study with fresolimumab, an anti-TGF? antibody, we found that individuals with moderate OI, i.e., OI type IV had increase in lumbar spine areal bone mineral density whereas individuals with the more severe forms, i.e., OI types III and VIII did not. This suggested a dose-specific effect based on disease severity that correlates with treatment studies in preclinical models of OI of varying severity. Here, we report on the pharmacodynamics and pharmacokinetics of fresolimumab and preliminary results in generating a bone-targeted anti-TGF? antibody to improve efficacy and safety. We found that peak plasma levels of fresolimumab were higher in individuals with

OI who received 4 mg/kg dose compared to 1 mg/kg. The plasma levels dropped to 84% of the peak level by day 15 and returned to baseline by day 90. Overall, an anabolic window, i.e., lower CTX and higher P1NP levels as compared to baseline values, were observed in 4 out of 8 participants. In the 4 mg/kg cohort, suppression in bone turnover marker osteocalcin was observed at day 30 and 180 together with an anabolic window. This alluded to the possible need for a higher anti-TGF? concentration in OI bone. Therefore, we generated a bone-targeted anti-TGF? antibody, 1D11-D10. After a single dose administration in WT mice, 1D11-D10 showed increased distribution to bone (lumbar and femur) and reduced concentrations in plasma, kidney and heart as compared to untargeted 1D11. Moreover, 1D11-D10 has a longer half-life of 76 days in bone compared to 16.3 days for 1D11 (t1/2 ratio=4.7). Importantly, at 0.3, 1, and 5 mg/kg 3 times/week dosing of Col1a2G610C/+ OI mice, 1D11-D10 showed comparable effect on bone mass at 1mg/kg and a trend towards higher efficacy at 5mg/kg comparing to untargeted 1D11. These data supported the effective bone targeting and a potential increased efficacy and safety profile for 1D11-D10. As bone targeted anti- TGF? therapy may offer wider therapeutic index, this may be important for clinical translation in OI and other skeletal diseases with TGF? dysregulation.

***Disclosures: I-Wen Song**, None*

1113

Standard bone microarchitecture assessment using HR-pQCT in adults with Osteogenesis Imperfecta: does it tell the whole story? *MELISSA BEVERS[1], Arjan Harsevoort[2], Koert Gooijer[2], Caroline Wyers[3], Hans Feenstra[2], Bert Rietbergen[4], Joop Van Den Bergh[5], Guus Janus[2]. [1]VieCuri Medical Center, [2]Expert Center for adults with Osteogenesis Imperfecta Isala Hospital, Netherlands, [3]VieCuri Medical Centre, Netherlands, [4]Eindhoven University of Technology, Netherlands, [5]VieCuri MC Noord-Limburg and Maastricht UMC,

Purpose: Osteogenesis imperfecta (OI) is a heterogenous disorder associated with bone fragility. In an ongoing study, we observed inhomogeneities in the trabecular compartment on high-resolution peripheral quantitative CT (HR-pQCT) scans, which potentially influence standard HR-pQCT analyses. The aim of this study was to assess bone microarchitecture in adults with OI using HR-pQCT and to evaluate whether inhomogeneities in the microarchitecture are captured by or influence standard HR-pQCT parameters. Methods: Limb-length dependent HR-pQCT scans of the distal radius and tibia were obtained from 118 adults with OI (41.8 [interquartile range (IQR): 25.1] year old). Cortical and trabecular microarchitecture were quantified using standard HR-pQCT analyses and compared to normative data from literature (Warden et al. Osteoporos Int 2021). Scans were also visually evaluated. Results: 91 radius and 91 tibia scans were analyzed after exclusion of scans with insufficient quality or deviating axial scan angles. At the radius, trabecular number (Tb.N) was low (Z-score: -2.5+/-1.4), and trabecular separation (Tb.Sp) was high (Z-score: -2.7 [2.7]). Trabecular thickness (Tb.Th), cortical thickness (Ct.Th), and cortical porosity (Ct.Po) deviated less from the normative data. 12% and 31% of the patients had a Z-score <-4 for Tb.N and Tb.Sp, respectively, and 0-3% had a Z-score 4 for Tb.Th, Ct.Th, and Ct.Po. The deviations from normative data were larger at the tibia. Void volumes of variable size were seen in the trabecular compartment, more often at the tibia and with corresponding highly negative Z-scores for Tb.N and Tb.Sp (Fig.1a). Local sclerotic spots and thickened trabeculae were also observed, mainly at the tibia and together or not with an increased Tb.Th (Fig.1b). A high Tb.Th was also seen in the absence of these thickened bone spots. In the cortex, locally increased porosity and reduced mineralization density were seen, mainly near the periosteum and not always fully captured by the standard HR-pQCT analyses (Fig.1c). Conclusion: The cortical and trabecular bone in adults with OI show local inhomogeneities. Standard HR-pQCT analyses do not give a complete impression of bone microarchitecture in OI and should be extended to better capture local inhomogeneities, e.g. by detection and evaluation of void volumes and local sclerotic regions in the trabecular bone and by evaluation of cortical and trabecular bone at a broader range of mineralization densities.

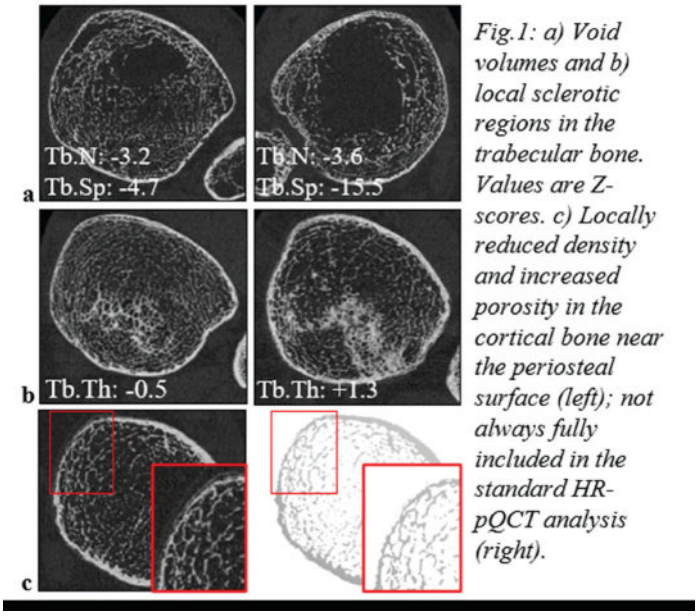

Fig.1: a) Void volumes and b) local sclerotic regions in the trabecular bone. Values are Z-scores. c) Locally reduced density and increased porosity in the cortical bone near the periosteal surface (left); not always fully included in the standard HR-pQCT analysis (right).

***Disclosures: MELISSA BEVERS**, None*

1114

Improved Skeletal Dynamics in Adults Treated With Palopegteriparatide for Hypoparathyroidism: 52-Week Analysis of Phase 3 PaTHway Trial *Aliya A Khan[1], Mishaela R. Rubin[2], Dolores M. Shoback[3], Peter Schwarz[4], Lynn Kohlmeier[5], Andrea Palermo[6], Bart L. Clarke[7], Erik Eriksen[8], Elena Tsourdi[9], Filomena Cetani[10], Rajesh Jain[11], Carol Zhao[12], Bryant Lai[12], Jenny Ukena[12], Christopher T. Sibley[12], Michael Ominsky[12], Aimee D. Shu[12], Lars Rejnmark[13]. [1]McMaster University, Canada, [2]Columbia University, United States, [3]UCSF/VA Medical Center, United States, [4]Rigshospitalet, Denmark, [5]Endocrinology and Spokane Osteoporosis, United States, [6]Unit of Metabolic Bone and Thyroid Disorders, Fondazione Policlinico Campus Bio-medico and Unit of Endocrinology and Diabetes, Campus Bio-medico University, Italy, [7]Mayo Clinic E18-A, United States, [8]Oslo University Hospital, Norway, [9]Technische Universität Dresden Medical Center, Germany, [10]University Hospital of Pisa, Endocrine Unit, Italy, [11]University of Chicago, United States, [12]Ascendis Pharma Inc, United States, [13]Aarhus University Hospital, Denmark

Purpose: Evaluate the temporal changes in and relationship between skeletal endpoints in response to palopegteriparatide (TransCon PTH), a prodrug with sustained release of PTH(1-34), in individuals with chronic hypoparathyroidism. Methods: PaTHway is a phase 3 trial of TransCon PTH with a randomized, placebo-controlled 26-week blinded period and 156-week open-label extension. Serum bone turnover markers (BTM) of bone formation (procollagen type 1 N-terminal propeptide [P1NP]) and bone resorption (C-telopeptide [CTx]) were assessed at baseline and weeks 12, 26, 38, and 52. Bone mineral density (BMD) was assessed by DXA at the lumbar spine, total hip, and distal 1/3 radius at baseline, weeks 26 and 52. Skeletal endpoints are reported herein for participants randomized to TransCon PTH with week 52 data (n=59). Results: At baseline, participants in the TransCon PTH group had a mean (SD) age of 49 (13) years; 75% were female, 41% of whom were postmenopausal. Through week 52, 81% (48/59) maintained normal serum calcium (8.3-10.6 mg/dL) and independence from conventional therapy (<=600 mg/day of elemental calcium and no active vitamin D). TransCon PTH treatment initially increased CTx and P1NP; responses peaked by week 12 and 26, respectively, and then declined through week 52 (Fig). From weeks 26 to 52, BTM decreased most in those with the highest values at week 26. Mean baseline BMD was high, as expected in hypoparathyroidism. With exposure to TransCon PTH over 52 weeks, mean BMD Z-scores and T-scores declined from above 0 toward age- and/or sex-matched norms at the lumbar spine and total hip, with a smaller magnitude of change from week 26 to 52 (Fig). Changes in BMD at the spine and hip were consistent across age, sex, and postmenopausal status, and at week 26 were inversely correlated with changes in P1NP and CTx at week 12 (R: -0.23 to -0.48). Conclusions: TransCon PTH treatment resulted in mobilization of calcium from the low bone turnover state in adults with hypoparathyroidism. Increases in BTM were correlated with declines from disease-elevated BMD at baseline. After week 26, BTM normalized toward sex and menopausal status appropriate levels and corresponded to lesser declines in BMD through week 52, similar to the results through week 110 in the Phase 2 PaTH Forward trial. These 52-week results reflect temporal changes trending toward a new skeletal steady state closer to age-appropriate norms with continued use of TransCon PTH in hypoparathyroidism.

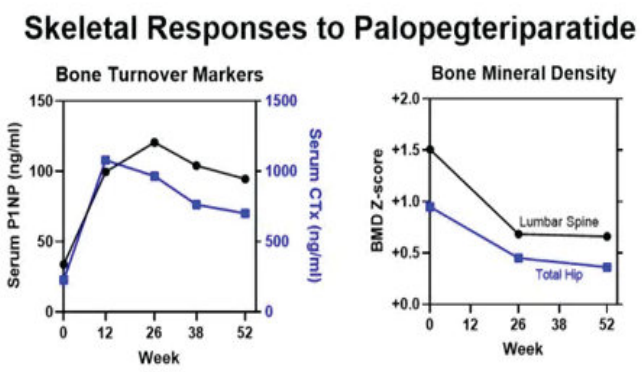

***Disclosures: Aliya A Khan**, Amolyt, Ascendis, Chugai, Radius, Takeda, Ultragenyx, Grant/Research Support, Amgen, Speakers' Bureau, Amgen, Alexion, Amolyt, Ascendis, Ultragenyx Speakers' Bureau: Amgen, Consultant, Amgen, Alexion, Ascendis, Takeda, Utragenyx, Other Financial or Material Support, Amgen, Alexion, Ascendis, Takeda, Ultragenyx, Other Financial or Material Support*

1115

Newly Diagnosed Hyperparathyroidism After 3 Years Of Burosumab In Children Affected With X-Linked Hypophosphatemia *Volha ZHUKOUSKAYA[1], Alexandra ERTL[2], Jugurtha BERKENOU[2], Christelle AUDRAIN[2], Claire BARDET[3], Catherine CHAUSSAIN[3], Anya ROTHENBUHLER[2], Agnès LINGLART[2]. [1]Université Paris Cité, Laboratory Orofacial Pathologies, Imaging and Biotherapies URP2496 and FHU-DDS-Net, Dental School, and Plateforme d'Imagerie du Vivant (PIV), Montrouge; APHP Hôpital Cochin, Paris, France. [2]AP-HP, Endocrinology and diabetes for children, Reference center for rare diseases of the Calcium and Phosphate Metabolism, DMU SEA, OSCAR filière, EndoRare and BOND ERN, Bicêtre Paris Saclay Hospital, France. [3]Université Paris Cité, Laboratory Orofacial Pathologies, Imaging and Biotherapies URP2496 and FHU-DDS-Net, Dental School, and Plateforme d'Imagerie du Vivant (PIV), Montrouge, France

Background/aim: Hyperparathyroidism (HPHT) is a common feature in patients with X-linked hypophosphatemia (XLH) especially when treated with vitamin D analogues and phosphate supplements. Although the exact mechanism is not clear, it is assumed that phosphate supplements taken chronically stimulate parathyroid hormone (PTH) secretion. We prospectively assessed the effect of a novel pathogenetic treatment anti-FGF23 (burosumab) on PTH levels in children with XLH.Patients and methods: 37 XLH-children (23 girls / 14 boys; 8.8+/-3.2 years) were switched from conventional therapy to burosumab and completed at least three years of burosumab therapy. Subjects with secondary HPTH at baseline were excluded from analysis. The biochemical parameters of calcium-phosphate metabolism were measured at baseline (M0) and then every 6 months under burosumab (M6 up to M36). According to our national guidelines, the target serum phosphate upon burosumab was >1.2 mmol/l (>3.7 mg/dl). Results: After three years of treatment with burosumab, there was a global increase of PTH levels from 39.1+/-18.2 (M0) to 54.8+/-27.6 ng/l (M36) (18.5-88 ng/l) (p=0.001). Four subjects of 37 (10.8 %) developed secondary HPTH with mean+/-SD PTH levels equal to 110+/-17.9 ng/l. The subjects who developed HPTH tended to be older (10.0+/-1.2 vs 8.7+/-3.4 yrs, p=0.43, respectively) and had significantly higher PTH levels at baseline (62.8+/-22.5 vs 36.3+/-15.7 ng/l, p=0.004, respectively), in comparison to those without HPTH. Subjects with HPTH tended to have higher levels of serum phosphate at M36 (1.33 vs 1.19 mmol/l, p=0.11, respectively) and higher delta of phosphate increase from M0 to M36 (94% vs 63%, p=0.051, respectively), in comparison to those without HPTH. None of the children developed tertiary hyperparathyroidism. Conclusion:This is the first study describing the effect of anti-FGF23 treatment on PTH secretion in children with XLH. Although the benefit on phosphate homeostasis and bone mineralization has been fully demonstrated, we suggest that prolonged anti-FGF23 treatment may stimulate PTH secretion thus leading to development of hyperparathyroidism after three years of treatment. Nonetheless, longer follow-up study is needed to better understand and describe this phenomenon.

***Disclosures: Volha ZHUKOUSKAYA**, None*

1116

The serine synthesis pathway drives osteoclast differentiation through epigenetic regulation of NFATc1 expression *Steve Stegen[1], Karen Moermans[1], Ingrid Stockmans[1], Bernard Thienpont[2], Geert Carmeliet[1]. [1]Clinical and Experimental Endocrinology, KU Leuven, Belgium. [2]Laboratory for Functional Epigenetics, KU Leuven, Belgium

Mature osteoclasts display a specific metabolic profile, characterized by mitochondrial respiration to accommodate the bioenergetic demands of bone resorption, next to glycolysis that likely contributes to local acidification for dissolving bone mineral. However, whether metabolic adaptations are drivers of osteoclast differentiation or rather a consequence of an altered cellular state is poorly understood.Here, using mass spectrometry-based metabolomics and in vivo models, we identify the serine synthesis pathway (SSP) as a critical regulator of osteoclast differentiation. During early osteoclastogenesis, prior to NFATc1 induction, RANKL transiently activates the SSP, evidenced by enhanced 13C-glucose incorporation in serine and glycine, and increased expression of SSP enzymes. In contrast, mature osteoclasts relied more on serine and glycine uptake. The transient stimulation of the SSP is physiologically important, as deletion of the rate-limiting enzyme phosphoglycerate dehydrogenase (PHGDH) in osteoclast precursors (Lysozyme M-Cre) resulted in a high-bone-mass phenotype, caused by decreased bone resorption with no effect on bone formation. At the cellular level, the SSP is essential to initiate osteoclast differentiation, evidenced by a decrease in TRAP-positive osteoclasts and osteoclast-related gene expression in PHGDH-null cells, whereas proliferation or cell survival was not affected. As a mechanism, we found that the SSP-enzyme phosphoserine aminotransaminase 1 generates ?-ketoglutarate (?KG), which in turn stimulates ?KG-dependent demethylases that remove the repressive histone mark H3K27me3 at the Nfatc1 transcription start site and thereby activate gene expression. In vitro supplementation of cell-permeable ?KG fully rescued the differentiation defect in PHGDH-null osteoclasts by restoring H3K27Me3 levels and osteoclast-related gene expression. Finally, our findings also hold translational potential, since administration of the PHGDH inhibitor NCT-503 fully prevented bone loss in ovariectomized mice by reducing bone resorption, while bone formation was maintained.Together, this study reveals a RANKL-induced metabolic-epigenetic coupling mechanism in osteoclasts whereby SSP-dependent ?KG synthesis is linked to histone demethylation and Nfatc1 transcription (Fig 1). Moreover, PHGDH inhibition prevents estrogen deficiency-induced bone loss, suggesting that modulation of the SSP might be an appealing strategy to treat osteoporosis.

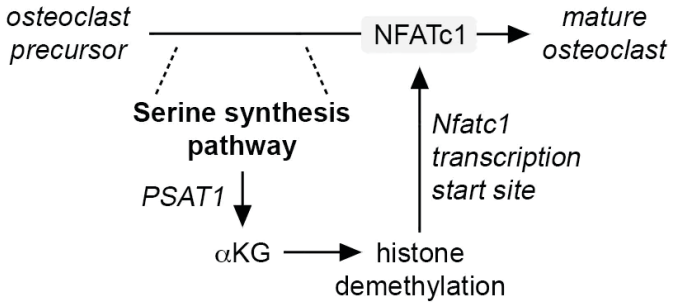

***Disclosures: Steve Stegen**, None*

1117

Bap1 Promotes Osteoclast Function By Metabolic Reprogramming *nidhi rohatgi[1], Wei Zou[2], Steven Teitelbaum[2]. [1]Washington University in St. Louis, United States. [2]Washington University in St. Louis School of Medicine, United States

Treatment of osteoporosis most commonly diminishes osteoclast number which suppresses bone formation thus compromising fracture prevention. Bone formation is not suppressed, however, when bone degradation is reduced by retarding osteoclast functional resorptive capacity, rather than differentiation. We find deletion of deubiquitinase, BRCA1-associated protein 1 (Bap1), in myeloid cells (Bap1?LysM), arrests osteoclast function but not formation. Bap1?LysM osteoclasts fail to organize their cytoskeleton which is essential for bone degradation. Consequently, bone mass increases in the mutant mice. The deubiquitinase activity of Bap1 modifies osteoclast function by metabolic reprogramming. Bap1 deficient osteoclast lineage cells upregulate the cystine transporter, Slc7a11, by enhanced H2Aub occupancy of its promoter. SLC7A11 controls cellular ROS levels and redirects the mitochondrial metabolites away from the TCA cycle, both of which are necessary for osteoclast function. Thus in osteoclasts, Bap1 appears to regulate the epigenetic-metabolic axis and is a potential target to reduce bone degradation while maintaining osteogenesis in osteoporotic patients.

***Disclosures: nidhi rohatgi**, None*

1118

Osteoclast Diversity Highlighted by Transcriptomic and Metabolic Analyses in vitro and in vivo *Julia Halper[1], Maria-Bernadette Madel[1], Valeriia Rezapova[1], Adrien Mahler[1], Konstantin Zaitsev[2], Maria Firulyova[2], Alexandre Gallerand[1], Rafael Argüello[3], Abdelilah Wakkach[1], Didier Pisani[1], Matthieu Rouleau[1], Stoyan Ivanov[1], Claudine Blin-Wakkach[1]. [1]Université Côte d'Azur, Laboratory of Molecular Physio-Medicine- CNRS- UMR7370, France. [2]ITMO University, Computer Technologies Department, Russian Federation. [3]Aix Marseille Univ-CNRS- INSERM, CIML, France

Osteoclasts (OCL) are myeloid cells with various origins, leading to phenotypic diversity. Previously, we showed that monocytes and dendritic cells give rise to two distinct populations of OCLs (MN- and DC-OCLs). Here, we explore OCL heterogeneity at the single cell level and characterize metabolic and functional traits, confirming heterogeneity of mature OCLs.Combination of bulk RNAseq of MN- and DC-OCLs with single-cell RNAseq on mature OCLs from bone marrow (BM-OCLs) revealed metabolic differences. Energetic properties of the subpopulations were defined by SCENITH (Argüello, 2020). Glycolytic and oxidative metabolism, bone resorptive and immune function were analysed in vitro. Metabolic analysis was performed on OCLs extracted ex vivo from Sham and osteoporotic mice (OVX).Transcriptomics identified different OCL clusters and markers, namely CD200 (adj.pVal=1.37*e-05) and CD16/32 (adj.pVal=0.00159) for steady-state and inflammatory OCLs, respectively; in line, MN-OCLs highly expressed CD200 (pVal<0.001) while DC-OCLs were predominantly CD16/32+ (pVal<0.0001) by FACS. Metabolic analysis of CD200+ OCLs revealed an important dependence on both glucose and mitochondrial metabolism, as MN-OCLs. No significant differences were observed in mitochondrial mass, ROS, resorption and antigen presentation capacity between these OCLs. In strong contrast, the CD16/32+ population, as DC-OCLs, displayed a shift from mitochondrial to glycolytic capacity (pVal<0.0001); reduced oxidative metabolism was accompanied by low mitochondrial mass (pVal<0.001) that produced less ROS (pVal<0.001), but increased lactate production through anaerobic glycolysis (pVal<0.01). Their resorption capacity was diminished (pVal<0.001) while antigen presentation was strikingly increased (pVal<0.0001).Importantly, OCLs isolated ex vivo from OVX mice had lower CD200+ but higher CD16/32+ percentage compared to Sham (pVal<0.05). As expected, these ex vivo OVX-OCLs displayed higher glucose dependence (pVal<0.05) than Sham-OCLs, but also a tendency towards increased mitochondrial dependence. Whether energetic demands are divergent for in vitro and ex vivo OCLs is currently under investigation.Here, we reveal the existence of 2 OCL subpopulations that clearly differ in metabolic, resorptive and immune properties, with varying proportions in OVX versus Sham. These findings support the prospect of targeting pathological OCL subsets to improve therapeutic approaches against pathologic bone loss.

***Disclosures: Julia Halper**, None*

1119

Attenuation of NAD+ Metabolism in Osteoclasts Contributes to the Bone Protective Effects of Estrogens *ADRIANA CARVALHO[1], Kimberly Richardson[2], Aaron Warren[2], Maria Jose Almeida[3], Ha-Neui Kim[4, 1], . [2]University of Arkansas for Medical Sciences, United States. [3]Central Arkansas VA Healthcare System, Univ of Arkansas for Medical Sciences, United States. [4]Univ. Arkansas for Medical Sciences, Central Arkansas VA Healthcare System, United States

Mitochondria are a central node of the effects of RANKL on osteoclast formation and bone resorption. NADH oxidation to NAD+ is critical for Complex I activity and the generation of ATP by the electron transport chain. NAD+, in turn, promotes multiple redox reactions and the activity of NAD+-dependent enzymes such as Sirt3. Estrogens attenuate early stimulatory effects of RANKL on Complex I and mitochondria activity of osteoclast precursors. However, how these early effects of estrogens impact osteoclastogenesis remains unclear. Here, we examined the contribution NAD+ metabolism to the anti-osteoclastogenic effects of estrogen. Addition of RANKL to bone marrow-derived macrophages (BMMs) caused an increase in mitochondrial respiration, NAD+ levels, and NAD+/NADH ratio; and 17?-estradiol (E2) prevented all these effects. We next decreased NAD+ levels using FK866, a specific inhibitor of Nampt - the critical enzyme in the NAD salvage pathway. FK866 reduced NAD+ levels, NAD+/NADH ratio, ATP levels, mitochondria respiration, RANKL-induced osteoclast formation, and promoted apoptosis in osteoclast progenitors. While the effects of FK866 were stronger than the ones caused by E2, these findings support the idea that changes in NAD+ mediate the effects of estrogens. To determine the significance of these results to bone in vivo, we next used mice with decreased levels of NAD+ in the macrophage lineage. Specifically, we generated mice lacking one Nampt allele in LysM-cre targeted cells (Nampt?LysM). BMMs from these mice exhibited lower Nampt expression and NAD+ levels. Nampt?LysM mice and Nampt-flox littermate controls were sham-operated or ovariectomized (OVX) at 5 months of age and bone mass was determined 6 weeks later, using DXA BMD and micro-CT. Cortical and trabecular bone of sham-operated Nampt?LysM mice were indistinguishable from control. OVX decreased cortical thickness in the femur and trabecular bone volume in the spine of control mice but these effects were attenuated in the Nampt?LysM mice. Overall these results suggest that an increase in NAD+ levels in osteoclasts contributes to the increase of bone resorption in estrogen deficiency. Along with earlier evidence that the NAD+-dependent mitochondrial deacetylase Sirt3 also contributes to the increase in bone resorption in estrogen deficiency, collectively these findings indicate that inhibition of NAD+ is a functional consequence of suppressive actions of estrogens on osteoclast mitochondria.

***Disclosures: ADRIANA CARVALHO**, None*

1120

Vitamin K-Dependent Carboxylation in Osteoblasts Regulates Osteoclastogenesis through Gas6 *Mathieu Ferron[1], Diep Ngoc Thi Pham[1], Monica Pata[1], B. Ashok Reddy[1], Julie Lacombe[1], Amélie Germain[1], Céline Schott[1]. [1]Institut de recherches cliniques de Montreal, Canada

Interventional and observational studies in humans suggest that vitamin K (VK) plays a role in the regulation of bone remodeling. In cells, VK functions as a co-factor for the ?-carboxylase (GGCX), an enzyme responsible for the conversion of glutamic acid residues (Glu) into ?-carboxyglutamic acid (Gla) residues in specific secreted proteins. This post-translational modification is notably present in osteocalcin, the most abundant non-collagenous protein in bone extracellular matrix (ECM) and an osteoblast-derived hormone affecting glucose metabolism. However, gain- and loss-of-function mouse models of osteocalcin have shown that this protein does not affect bone remodeling and is not required for normal bone ECM mineralization. Therefore, the mechanism and the Gla protein(s) through which VK influences bone density and/or quality remain to be characterized. To address this question, we generated mice lacking ?-carboxylation specifically in osteoblasts by breeding mice harboring a Ggcx floxed allele with the hOC-Cre transgenic line, which express Cre recombinase in osteoblasts. Histological analysis revealed that these Ggcxff;hOC-Cre mice have increased bone mass at 6 months of age. This phenotype appears to be caused by a decrease in the number of multinucleated bone resorbing osteoclasts. In co-cultures experiments, GGCX-deficient osteoblasts were less effective than control osteoblasts at supporting the generation of large osteoclasts. In contrast, osteocalcin-deficient osteoblasts did not display this phenotype, suggesting the involvement of another osteoblast derived Gla protein. Among all known Gla proteins, we found that, beside osteocalcin, Gas6 was the most highly expressed in osteoblasts. In cell culture assays, recombinant ?-carboxylated Gas6 dose-dependently increases the size of osteoclasts and the number of nuclei per osteoclasts in presence of RANKL and M-CSF. Genes involved in osteoclast differentiation were not affected by recombinant Gas6, suggesting that Gas6 might be involved in pre-osteoclast fusion. The Gas6 receptor tyrosine kinases, MerTK and AXL, were expressed in pre-osteoclasts and two different AXL inhibitors completely block osteoclast generation in co-culture assays, indicating that Gas6 signaling through these receptors is required to support pre-osteoclast fusion. This work identifies Gas6 as a novel osteoblast derived Gla protein regulating osteoclast maturation and potentially mediating the effect of VK on bone turnover.

***Disclosures: Mathieu Ferron**, None*

1121

Optimizing spatial transcriptomics in mouse bone from the single gene to the whole transcriptome identifies regional changes in response to applied load *Samia Saleem[1], Erica Scheller[1], ALEC BEEVE[2], Katherine Minielly[1], Lisa Lawson[3], John Shuster[1], David DeBruin[4], Michelle Brennan[5], Matthew Silva[6]. [1]Washington University, United States. [2], . [3]Washington University in St. Louis, . [4]St. Louis University , United States. [5]Saint Louis University , United States. [6]Washington University in St. Louis School of Medicine, United States

Spatial transcriptomics allows for resolution of gene expression in the spatial dimension from the single-gene to the whole transcriptome. However, methods are not well optimized for bone, which limits current applications. To overcome this, we optimized protocols for single gene RNAscope prior to adaptation for whole transcriptome analysis (WTA) using the NanoString GeoMx platform. This workflow was used to analyze gene expression in the periosteum and cortical bone after biomechanical loading of the mouse tibia. Specifically, 5-month old C57Bl/6 mice were loaded unilaterally to -2200 µ? for 5-days and sacrificed 4-hours after the final loading bout. Non-loaded and loaded tibias were harvested and transverse paraffin sections from the mid-diaphysis were prepared for analysis. Spatial capture tools were used to subdivide each section into regions of maximum tensile and compressive strain, resulting in four areas of interest (AOIs) per section (max compressive-bone; max compressive-periosteum; max tensile-bone; max tensile-periosteum). Periosteal and cortical bone AOIs expressed gene profiles in accordance with tissue type, providing evidence of successful AOI selection (ex. Postn, Bglap, Sparc, and Aspn enriched in periosteum; Mepe, Dmp1, and Dkk1 enriched in bone). The resulting spatial transcriptomic datasets were also validated against prior bulk tissue RNAseq. This identified 128 overlapping DEGs between gene sets ($p<0.05$, $Log2FC>|0.5|$) including known responders such as Bglap, Col1a1, Gja1, and Phospho1. Regression analysis of overlapping genes revealed relatively high concordance in fold change between techniques ($r2=0.556$, $p<0.001$). AOI-based subanalysis of the spatial data in bone vs periosteum identified 224 vs 809 significant DEGs with loading, respectively. Gene ontology analysis revealed an upregulation of genes associated with collagen fibril organization and mineralization in bone, while key genes and pathways associated with collagen biosynthesis, vesicle transport, osteoblast differentiation, and angiogenesis were more prominent in the periosteum. Further characterization based on FEA-determined stress maps identified a spectrum of loading-induced gene changes with maximal upregulation of osteoanabolic genes and pathways at sites of maximum compression. Overall, this

novel workflow substantially expands our capabilities for spatial WTA in bone tissues while clarifying the relationship between applied stress and regional skeletal adaptation.

***Disclosures: Samia Saleem**, None*

1122

Obesity impairs revascularization and bone healing in a mouse model of ischemic osteonecrosis *Zhuo Deng[1], Maria Aguirre[1], Harry Kim[1], Yinshi Ren[1]. [1]Scottish Rite Hospital, United States

Osteonecrosis (ON) of the femoral head (ONFH) is the major form of ON and affects patients in their early 30s. With the arising concerns of obesity worldwide, it is found that obesity is highly correlated to the increased incidences of ONFH. However, it is unclear if obesity directly affects the progression and healing of ON. The purpose of this study is to investigate the effects of obesity on bone healing and revascularization in an established mouse model of ischemic ON.A total of 27 mice are randomly assigned into three groups at the young adult age of 3 months: Group 1) Control mice fed with normal diet (ND); Group 2) Obese (Ob) mice fed with high-fat-diet (HFD) containing 60% kcal and Group 3) Weight Loss (WL) mice was initially fed with HFD and then switched to normal diet to reduce body fat. ON was surgically induced on the right distal femoral epiphysis and the left side serves as Sham control. All mice are sacrificed at 4 weeks after the surgery. Micro-CT, IHC and histomorphometry were used to measure bone remodeling and vascularization. Endothelial cell (HUVEC) tube formation assay and qPCR were performed to investigate the effects of LDL on endothelial cells.At 4 weeks after surgery, all mice in the control group had a complete revascularization of ON bone, while the Ob group had a significant reduction in re-vascularized marrow space ($p<0.05$) and endomucin positive vessel areas (50% reduction, $p<0.05$) (Figure 1). Histomorphometry on HE and TRAP staining showed significantly reduced osteoblasts($p<0.01$) and osteoclasts($p<0.01$) in Ob mice compared to control. WL animals show rescued bone remodeling and revascularization. Serum LDL was significantly increased in the Ob group compared to both control and WL groups. Addition of 100 μg/ml oxLDL markedly reduced endothelial cell branching in the tube formation assay with reduced total length ($p<0.05$), number of nodes ($p<0.01$) and branches ($p<0.05$), indicating decreased vascularization. Notch signaling is known to stimulate angiogenesis. Downstream gene analysis revealed that oxLDL decreased Notch4 and DLL1 expression ($p<0.05$), and activation of Notch signaling in HUVEC cells rescued the tube formation defect induced by oxLDL.Our study is the first to investigate the role of obesity in osteonecrosis bone healing. We identified a potential LDL-Notch signaling cascade that blocked angiogenesis in ON, providing novel thoughts for future treatment of ON.

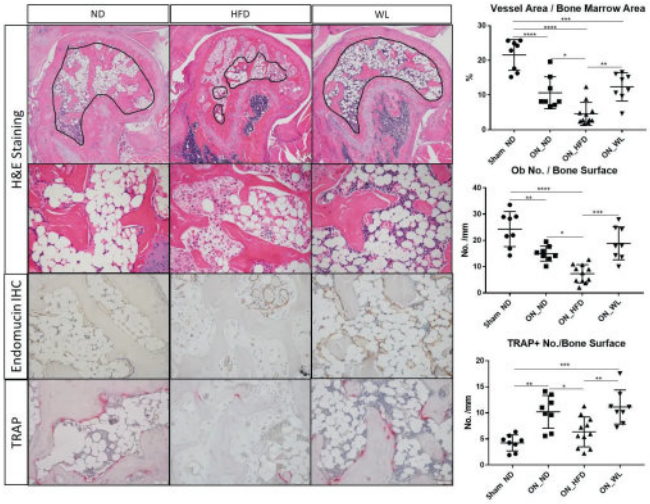

***Disclosures: Zhuo Deng**, None*

1123

CircFam190a: a positive regulator of osteoclast differentiation via acting as a scaffold for HSP90?/AKT1 *Kun Chen[1], Mingyou Xu[1], Zhi Li[1], Xingshi Yuan[1], Xifu Shang[1]. [1]The First Affiliated Hospital of USTC, Division of Life Sciences and Medicine, University of Science and Technology of China, China

The identification of key regulator factors that control osteoclasteogenesis is of vital importance. Accumulating evidence indicates that circular RNAs (circRNAs) are discrete functional entities. However, the complexities of circRNAs expressions as well as the extent of their regulatory functions during osteoclastogenesis are yet to be revealed.Using circular RNA sequencing, we identified 1013 circular RNAs during osteoclastogenesis. Among these, circFam190a, generated from the Fam90a gene, caught our attention [Attachment Figure1]. In mice with ovariectomy surgery, a condition characterized by hyperactive osteoclasts, circFam190a expression was significantly elevated. Similarly, the expression level of circFAM190A in post-menopausal osteoporosis patients was significantly up-regulated. In vitro culture studies demonstrated a significant increase in circFam190a expression during Rankl-induced osteoclastogenesis. These findings indicate a close relationship between circFam190a and osteoclasts, motivating us to further investigate.For in vitro function studies, circFam190a was found to enhance osteoclast formation and function, while its knockdown inhibited osteoclast formation. In vivo, overexpression of cirFam190a induced significant bone loss, whereas knocking down cirFam190a prevented pathological bone loss in an ovariectomized (OVX) mice osteoporosis model [Attachment Figure2]. Mechanistically, our data suggest that cirFam90a enhances the combination of AKT1 and HSP90?, promoting AKT1 stability. Moreover, the use of the AKT signaling inhibitor MK2206 successfully rescued circFam190a's osteoclast hyperactive phenotype in mice.Altogether, our findings highlight that circFam190a, a circular RNA that binds directly to HSP90? and AKT1, is an important positive regulator of osteoclasteogenesis [Attachment Figure3]. Targeting circFam190a could efficiently ameliorate OVX-induced osteoporosis. These findings contribute to our better understanding of the mysterious of circular RNA and bone metabolism, and provide potential therapeutic targets for treating pathological bone loss.

Attachment Figure

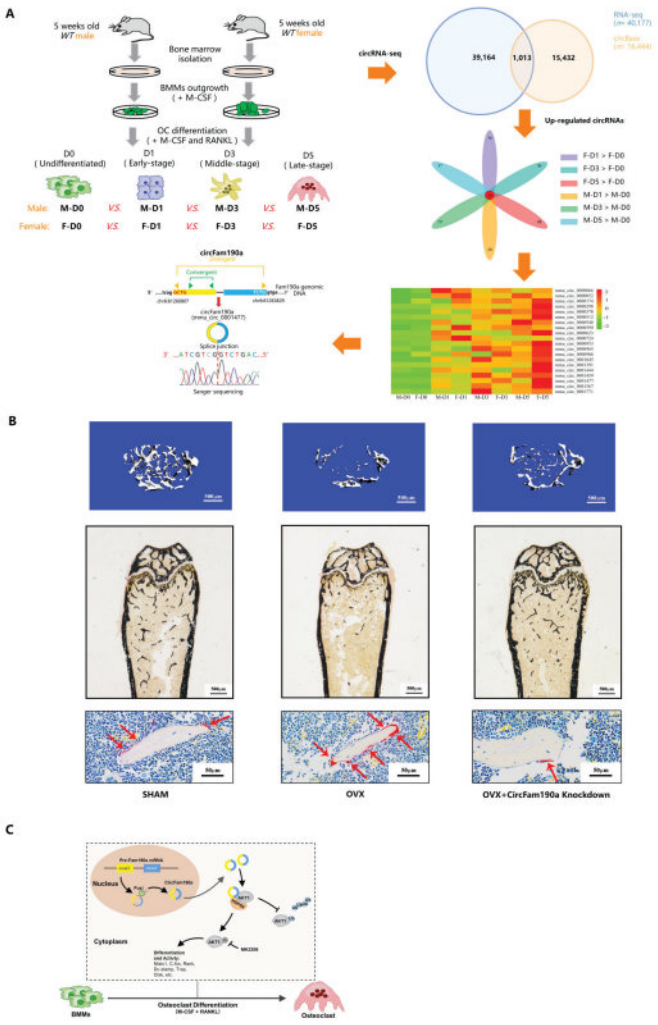

***Disclosures: Kun Chen**, None*

1124

Altered Mitochondrial Protein Acetylation in Osteoclasts May Lead to Skeletal Disintegration in Young Adult Male Mice Exposed to Ionizing Radiation *Gareeballah Balla[1], Kimberly Richardson[2], Qiang Fu[3], Nukhet Aykinburns[2], Ha-Neui Kim[4]. [1]University of Arkansas for Medical Sciences , United States. [2]University of Arkansas for Medical Sciences, United States. [3]Institute of Nuclear Medicine, United States. [4]Univ. Arkansas for Medical Sciences, Central Arkansas VA Healthcare System, United States

The damaging effects of ionizing radiation (IR) on bone mass have been well documented in mice and humans. Biomarker studies conducted in patients indicated that increased bone resorption is a predominant source of bone loss. However, the mechanisms leading to the acute activation of osteoclasts that follows exposure to IR remain unknown. SIRT3, the primary mitochondrial deacetylase, plays a crucial role in maintaining mitochondrial quality control during stressful conditions, such as aging, and oxidative stress, most likely by promoting deacetylation of its target proteins. Here, we examined the contribution of osteoclast mitochondria to the adverse effects of low-dose IR. Cultured bone marrow-derived macrophages were exposed to ?-radiation (2 or 4 Gy), which resulted in an increase in osteoclast size and activity; and this was associated with an increase in mitochondrial respiration and mRNA levels of SIRT3. To determine the significance of these findings to bone in vivo, we next subjected 6-month-old male SIRT3 KO mice and WT littermates to 4 Gy total body irradiation with fractionated exposures for 3 months. Low-dose IR exposures caused a dramatic decrease in trabecular, but not cortical bone mass, in both the femur and the spine of WT mice, as determined by DXA and micro-CT. Notably, the IR-induced bone loss was greatly attenuated in SIRT3 KO mice. Consistent with the high trabecular bone mass, the serum marker of bone resorption, CTX was dramatically lower in irradiated SIRT3 KO mice than in irradiated WT littermate mice. Our proteomic analysis of SIRT3-deficient osteoclasts revealed a dramatic increase in acetylation of ATPIF1 and SOD2, which are essential for mitophagy and mitochondrial ROS, respectively. Knockdown of either ATPIF1 or SOD2 in osteoclast progenitors impaired resorptive activity and suppressed mitophagy, suggesting an important role in osteoclast function and mitochondrial quality control. In addition, Mito-TEMPO, a mitochondrial superoxide scavenger, dose-dependently decreased RANKL-induced osteoclast formation in ex vivo cultures from mice exposed to radiation. These results demonstrate that SIRT3 plays an essential role in excessive bone resorption that occurs with IR exposure by promoting deacetylation in osteoclast mitochondria. Understanding the mechanisms of mitochondrial quality control and protein acetylation in osteoclasts could pave the way for developing novel strategies to counteract radiation-induced bone loss.

***Disclosures: Gareeballah Balla**, None*

1125

TrkA signaling dictates sensory nerve ingrowth and bony bar formation after growth plate injury *Xin Xing[1], Zhao Li[1], Sowmya Ramesh[1], Austin Chen[1], Mary Archer[1], Ziyi Wang[1], Qizhi Qin[1], Neelima Thottappillil[1], JiHye Yea[1], Mingxin Xu[1], Manyu Zhu[1], Thomas Clemens[2], Aaron James[1]. [1]Johns Hopkins University, United States. [2]University of Maryland, Baltimore, United States

Purpose: Injuries to the growth plate often lead to the formation of a bony bar, causing bone growth limitations, limb length discrepancies, and angular deformities in children. However, the mechanisms underlying this undesirable bony repair remain poorly understood. Recent studies have implicated TrkA+ sensory nerves in the regulation of skeletal cells and tissues, suggesting their potential role in the tissue response to growth plate injury. Methods: A drill hole injury was created in the distal epiphysis of 4-week-old male C57BL/6 and nerve growth factor (NGF)-eGFP reporter mice to model bony bar formation in growth plate injury. ?CT analysis, histology, TUBB3, and CD31 immunofluorescent staining were employed to assess bony bar formation, innervation, and angiogenesis at 1 and 6 weeks post-injury. Temporary inhibition of TrkA signaling was achieved in 4-week-old male TrkAF592A mice with 1NMPP1 treatment, and its effects were evaluated by ?CT analysis and immunofluorescent staining (TUBB3, CD31). Conditioned medium from dorsal root ganglia (DRG) was isolated for ex vivo organ culture of the injured growth plate, and EdU incorporation assay and Runx2 immunostaining were performed at 1 week post-culture. Results: ?CT analysis and histological staining revealed longitudinal disruption of the growth plate through the drill hole injury, resulting in a progressive increase in bone tissue formation at the injury site from day 7 to day 42 (Fig A). NGF expression, nerves, and blood vessels were found to be absent in the uninjured growth plate (day 0). Exuberant sprouting of nerves and vasculature into the growth plate injury site was identified at 1 week post-injury, which persisted above baseline at 6 weeks post-injury (Fig A). Inhibition of TrkA signaling significantly reduced bony bar formation at 6 weeks (-17% BV/TV) in the injured growth plate, along with decreased innervation (1.75-fold), and vascularization (2.42-fold) at 1 week post-injury. Ex vivo organ culture experiments demonstrated that conditioned medium from DRG-derived sensory neurons resulted in a 1.82-fold increase in EdU-positive cells and a 4.48-fold increase in Runx2-positive cells in the injured growth plate (Fig C). Conclusions: To our knowledge, this study represents the first investigation into the role of TrkA+ sensory nerves in the growth plate's response to injury. The findings contribute to our understanding of pathologic endochondral ossification and may facilitate the development of future preventative biological treatments.

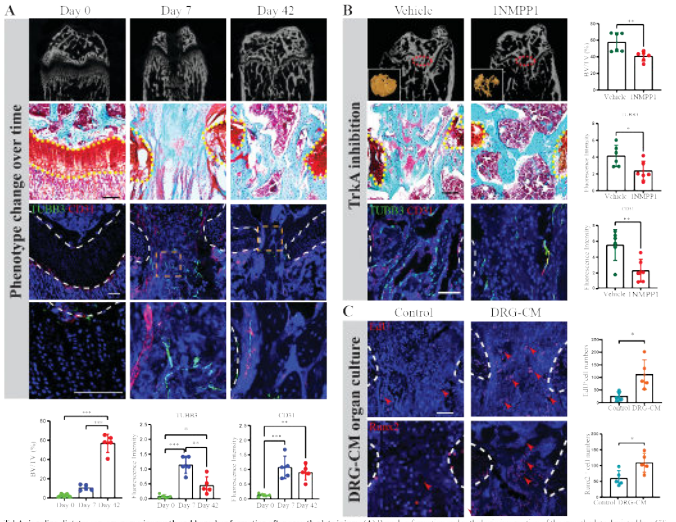

TrkA signaling dictates sensory nerve ingrowth and bony bar formation after growth plate injury. (A) Bony bar formation and pathologic innervation of the growth plate depicted by µCT images, Safranin O/Fast green staining, TUBB3, and CD31 immunofluorescent (IF) staining at day 0, 7, and 42. Quantitative analysis includes BV/TV measured by µCT and semiquantitative analysis of TUBB3 and CD31 expression. N=5 (B) Inhibition of TrkA+ sensory nerves reduce bony bridge formation as observed in µCT images, Safranin O/Fast green staining of the injured growth plate in TrkA^{F592A} mice treated with 1NMPP1 or vehicle control at day 42 after injury. TUBB3 and CD31 IF staining was performed at day 7 after injury. Quantitative analysis includes BV/TV and semiquantitative analysis of TUBB3 and CD31 expression. N=4-6 (C) Dorsal root ganglion-derived conditioned medium (DRG-CM) modulates the metabolism of in vivo cultured injured growth plate, as indicated by EdU incorporation and Runx2 IF staining. N=5. Scale bars: 100 µm. Data presented as mean +/-1 SD. *P<0.05, **P<0.01, and ***P<0.001.

***Disclosures: Xin Xing**, None*

1126

Accelerated Physical Decline after Fracture in Older Men - the Prospective STRAMBO Study *Pawel Szulc[1], Joshua Lewis[2], Roland Chapurlat[3]. [1]INSERM UMR 1033, University of Lyon, Hopital E. Herriot, Pavillon F, France. [2]Edith Cowan University, Australia. [3]INSERM UMR 1033, France

Prospective data on the loss of muscle strength and physical function after a fracture are scarce. Few studies have compared fracture-related loss of muscle strength and physical function with normal ageing-related decline. Our aim was to compare the loss of muscle strength and physical function after an incident fragility fracture to normal ageing-related decline in a prospectively followed cohort of older men.In 823 men aged 60-87 years, grip strength measurements and clinical tests (chair stands, balance) were performed every 4 years for 12 years. Incident vertebral fractures were assessed every 4 years on the lateral spine DXA scans. Self-reported low trauma non-vertebral fractures were confirmed by health professional. In 155 men with incident fracture, we compared the status on the first visit after fracture vs. that on the last visit before the fracture. In men without fracture (controls), we compared the status on the first follow-up (4 years) vs. baseline.After adjustment for confounders, the loss of grip strength was 41% higher (0.28SD, p<0.01) in men with incident fracture vs. controls. Men with fracture were more likely to become unable to stand for 10s with closed eyes (OR=4.80, 95%CI: 1.49-15.42, p<0.01) or to have an incident deterioration on the chair stand test (OR=2.45, 95%CI: 1.49-4.05, p<0.001) vs. controls. The risk of decline on the dynamic balance tests (tandem walk) was higher in men with fracture vs. controls: forwards (OR=2.04, 95%CI: 1.22-3.42, p<0.01), backwards (OR=2.25, 95%CI: 1.31-3.85, p<0.005).The decline after fracture was also greater in anatomical regions remote from the fracture site. Grip strength decreased more (34%, 0.24SD, p<0.05) in men who had no upper limb fracture vs. controls. The risk of decline in the tests of the lower limbs was higher in men who had no lower limb fracture, e.g., chair stands (OR=2.73, p<0.001) or tandem walk backwards (OR= 2.08, p<0.05). Men with incident vertebral fracture had 38% higher loss of grip strength (0.29SD, p<0.05) as well as higher risk of decline on the chair stands (OR=2.42, p<0.01) and on the backward tandem walk (OR=2.53, p<0.01).In older men followed prospectively, fractures were associated with greater loss of muscle strength and higher risk of physical function decline vs. normal ageing. This rapid decline was general and not limited to the fracture site. Thus, rehabilitation programs to prevent this post-fracture functional decline are urgently needed.

***Disclosures: Pawel Szulc**, None*

1127

AI-based Osteoporosis Screening with Chest Radiographs: Correlation Analysis between AI-Score and T-Scores *Mingyu Kim[1], Sung Jin Bae[2], Jung-Min Koh[2], Gaeun Lee[1], Namkug Kim[2], Miso Jang[2]. [1]Promedius Inc., Republic of Korea. [2]Asan Medical Center, Republic of Korea

Osteoporosis is a major public health challenge with significant implications for global health. Given the heightened treatment uptake and compliance rates resulting from raising awareness of osteoporosis, osteoporosis screening emerges as the most effective approach. In this study, we investigated the correlation between T-scores and an AI-score outputs from an AI model for osteoporosis screening with chest radiographs. The AI model was trained using deep learning by matching chest radiographs with DXA-based osteoporosis diagnosis.

The training data were obtained from the Health Screening and Promotion Center in Asan Medical Center, Korea (IRB No 2019-1226). The model achieved AUC of 0.91 and 0.88 for internal and external test set, respectively (Jang et al., J. Bone Miner Res. 2022, 37, 369-377). Using the test set, we evaluated the Spearman correlation coefficient between the AI-score and the T-scores (Femoral neck and Lumbar spine). Our findings revealed correlation coefficients of -0.594 and -0.741 for T-scores from the Femoral neck and Lumbar spine, respectively. AI-score is continuous values between 0 and 1. Negative correlation is due to inverse relation between the T-score and the AI score. Here, only correctly classified by AI model to either of non-osteoporosis or osteoporosis data were used for correlation analysis. Notably, the T-score from the Lumbar spine demonstrated a 24.7% higher correlation than that from the Femoral neck. This implies that the AI model easily learns lumbar spine structure in chest radiograph where femoral neck does not cover. Despite the promising results of our study, several limitations should be acknowledged. The AI model and evaluated data were limited to a specific medical center in Korea, which may introduce variations in correlation tendencies with other populations. In addition, the AI-score distribution in the figure is highly skewed towards 0s and 1s indicating that the need of T-score calibration by training AI model to estimate T-score directly. In conclusion, our study highlights the potential of AI-based screening models to predict T-scores across a continuous range from normal to osteoporosis. This correlation function can be used for monitoring individual patients for appropriate treatment as well as enabling early-stage detection even in the absence of discernible symptoms. Future research should consider broader population samples and further refinement of the AI model to enhance its clinical utility.

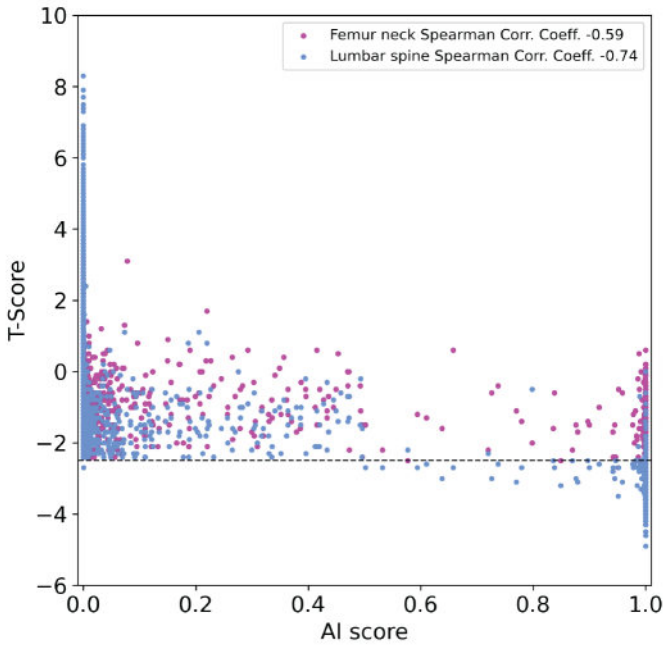

***Disclosures: Mingyu Kim**, None*

1128

Bone-Targeted Pre-Conditioning Prevents Bone and Muscle Injury in Australian Army Recruit Training: The PREFIT Study *Belinda Beck[1], Graeme Jones[2], Stephan Rudzki[3], Mark Barclay[4], Paul Scuffham[1]. [1]Griffith University, Australia. [2]University of Tasmania, Australia. [3]Canberra Sports Medicine, Australia. [4]Kapooka Health Centre, Australia

PurposeBone will adapt to progressive mechanical loading but overly rapid training increments such as occurs in Army recruit training (ART) causes bone stress injuries. We hypothesized that bone-targeted training prior to ART would reduce injuries during ART. Our aims were to determine 1. if bone-targeted preconditioning could reduce musculoskeletal injuries and costs during ART at the Army Recruit Training Centre (Kapooka, NSW, Australia), and 2. factors related to incidence of musculoskeletal injury during ART.MethodsPREFIT was a prospective, voluntary controlled trial of 45mins 5d/wk bone-targeted preconditioning offered to candidates to the Australian Army scheduled to enlist within 5 months. At baseline, enlistment and march out we collected biometrics, health history, medications, heel BUA (QUS, Achilles, GE); muscle strength and power (TTM Muscle Meter; GymAware, respectively); functional reach; #push-ups, #sit-ups, shuttle run performance, vitamin D; prior physical activity (BPAQ); dietary calcium (AusCal) and prior injuries. Preconditioning adherence and musculoskeletal injuries sustained during 12-week ART were monitored. We compared rates and costs of musculoskeletal injury in recruits who did and did not undertake PREFIT training and examined predictors of injury.ResultsWe enrolled 91 candidates into PREFIT training of which 37 entered recruit training (54 decided not to enlist). Only 25 completed sufficient PREFIT training prior to enlisting to qualify as 'pre-trained'. 349 platoon-mates consented to be controls. Mean age was 22+/-5.4yrs. 19% of the PREFIT-group versus 61.2% of non-PREFIT trained recruits sustained an injury. 10.7% of the PREFIT group sustained a musculoskeletal injury versus 37.7 % of the non-PREFIT group. There was insufficient power to examine bone injuries, but for every 1-unit increase in BUA or #push-ups, the odds of a bone injury was 0.97 and 0.96 times lower, respectively (p=0.033; p=0.041). Variables associated with a lower extremity injury and bone injury included height, BUA, leg power, #push-ups, #sit-ups, shuttle run, smoking, and previous medication. Total medical cost was $1308/PREFIT recruit versus $2,241/non-PREFIT recruit, i.e. almost double. No PREFIT recruit was discharged due to injury versus 4 non-PREFIT.ConclusionsA bone-targeted preconditioning program was a simple strategy to reduce musculoskeletal injury and cost to the Army for recruit training. Taller, stronger, fitter recruits are less at risk.

***Disclosures: Belinda Beck**, None*

1129

Improved Real-World Prediction of Hip Fracture Using CT-Based Measurements of Bone, Muscle, and Soft Tissue in Women and Men *Tony Keaveny[1], David Lee[2], Mary Bouxsein[3], Eric Orwoll[4], Sundeep Khosla[5], Michael McClung[6], Ethel Siris[7], David Kopperdahl[2], Annette Adams[8]. [1]University of California, Berkeley, United States. [2]O.N. Diagnostics, United States. [3]Beth Israel Deaconess Medical Center, Harvard Medical School, United States. [4]Oregon Health & Science University, United States. [5]Mayo Clinic College of Medicine, United States. [6]Oregon Osteoporosis Center, . [7]Columbia University College of Physicians and Surgeons, United States. [8]Kaiser Permanente Southern California, United States

Introduction: Reflecting the biomechanics of hip fracture, we hypothesized that combined measurements related to bone strength, postural instability, body size, and soft tissue cushioning can improve clinical prediction of hip fracture compared to standard of care. Specifically, using measurements taken only from a patient's hip-containing CT scan, we developed a method ("Biomechanical CT Plus", BCT+) for identifying patients at high risk of hip fracture and then compared fracture prediction for BCT+ versus BMD and FRAX.Methods: Our case-cohort sample of 11,461 patients was drawn from 271,389 patients age >= 65 who had a hip-containing CT scan (start of observation) during clinical care. Cases were all those with a hip fracture after the CT scan; an equal number of sub-cohort patients was randomly selected (sex- and facility-matched). Using the CT scan, over 50 measurements in the hip region were taken of: 1) strength (by finite element analysis), density (volumetric and areal, including DXA-equivalent hip BMD T-score), and geometry of the bone; 2) muscle morphology; 3) body composition; and 4) soft tissue thickness. Hip fracture status and risk factors for FRAX were taken from electronic records. The BCT+ model was formulated by sex-specific logistic regression (nine variables were chosen) for patients from half the facilities (outcome = hip fracture status at five years). For the other facilities, fracture prediction for the BCT+ model was compared against predictions from hip BMD T-score (lower of femoral neck/total hip) and FRAX 10-year probability of hip fracture (with femoral neck BMD T-score).Results: Overall, there were 4,959 hip fractures at five years. For BCT+, risk of hip fracture increased with higher values of age, bone volume, intra-muscular % fat content, and body-composition total area (women only) and with lower values of femoral strength, ratio of trabecular-to-cortical volumetric BMD, muscle size (area), body-composition % fat content (women only), and posterior fat thickness (women only). Area under the ROC curve was significantly higher (p<0.0001) for BCT+ (0.79, 95% CI: 0.77-0.80) than for BMD (0.72, 0.71-0.74) and FRAX (0.73, 0.72-0.75); these trends persisted by sex (women: 0.79/0.72/0.74, respectively; men: 0.78/0.72/0.73). For all specificity values, sensitivity was highest for BCT+ (Figure).Conclusions: In a real-world clinical setting, prediction of hip fracture was improved by BCT+ compared to current standard of care.

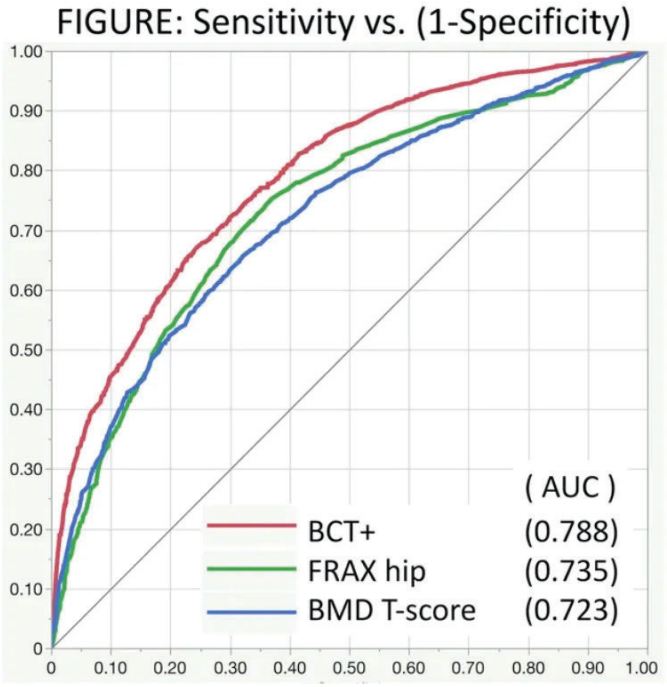

***Disclosures: Tony Keaveny**, O.N. Diagnostics LLC, Major Stock Shareholder*

1130

Fracture following Kidney and Simultaneous Pancreas-Kidney Transplantation is predicted by DXA-derived Bone Mineral Density and Advanced Hip Analysis *Tahira Scott[1], Jasna Aleksova[2], Ryan Gately[1], Harpreet Kaur[3], Carmel Hawley[1], Mirna Vucak-Dzumhur[3], Mina Khair[1], James Elhindi[4], Grahame Elder[5]. [1]Faculty of Medicine, The University of Queensland, Princess Alexandra Hospital, Australia. [2]School of Clinical Sciences, Monash University, Hudson Institute of Medical Research, Australia. [3]Westmead Hospital, Western Sydney Local Health District, Australia. [4]Westmead Hospital, University of Sydney, Australia. [5]Westmead Hospital, Univeristy of Notre Dame,University of Sydney, Garvan Institute of Medical Research, Australia

Patients with kidney failure have accelerated trabecular and cortical deterioration and elevated fracture risk that remains high following kidney transplantation. Contributing factors include chronic kidney disease-mineral and bone disorder and immunosuppressive treatment. BMD is less predictive of fracture in patients with kidney failure. This study aimed to determine if the DXA-derived trabecular bone score (TBS) and advanced hip analysis (AHA) improved BMD-based fracture prediction.Patients from two Australian transplant centres receiving kidney or simultaneous pancreas-kidney (SPK) transplants were included. Baseline information included demographics, medications and lab. data. A DXA scan was performed as soon as practical post-transplant to provide BMD, TBS and AHA parameters; femoral neck, calcar and shaft cortical thickness (CTh), and the femoral neck buckling ratio (BR), an indicator of structural instability defined as radius/CTh. Patients received treatment to reduce post-transplant BMD loss based on a risk algorithm(1). Parameters with skewed distributions were log transformed, and hazard ratios were determined using Kaplan Meier and Cox proportional hazard models with multivariable adjustment.Of 357 kidney and SPK transplant recipients, 289 (83%) received a kidney-only transplant. Mean age was 48+/-13 years, 62% were male, 20% had type 1 diabetes mellitus (T1DM) and median dialysis vintage was 29 months (IQR: 12, 60). There were 81 incident fractures, with median time to fracture or censoring 4.4 years (2.5, 5.5). Incident fracture was predicted by T1DM (p<0.001), former smoking (p=0.017), lower 25OHD (p=0.045), axial BMD (p<0.01), CTh (all sites p<=.01) and the BR (p=0.004; HR 1.83 (1.34, 2.49) for each log-unit increase), but not by the TBS. After multivariate adjustment, T1DM, 25OHD, smoking, prevalent fracture and hip BMD remained significant predictors. Using the BMD-based risk algorithm, inclusion of an interaction parameter for BR above or below the median improved the model fit (HR 2.36 (0.96, 5.80); p=0.06). Fracture risk increased from low-risk and low BR, to low-risk high BR, and high risk (Fig. 1).DXA-derived BMD, AHA cortical parameters and the BR predict incident fracture in kidney and SPK transplant recipients but TBS does not. AHA by DXA is readily available and may improve fracture risk assessment, particularly in kidney and SPK transplant patients whose BMD suggests fracture risk is low.1. Elder G. Transplantation 2023

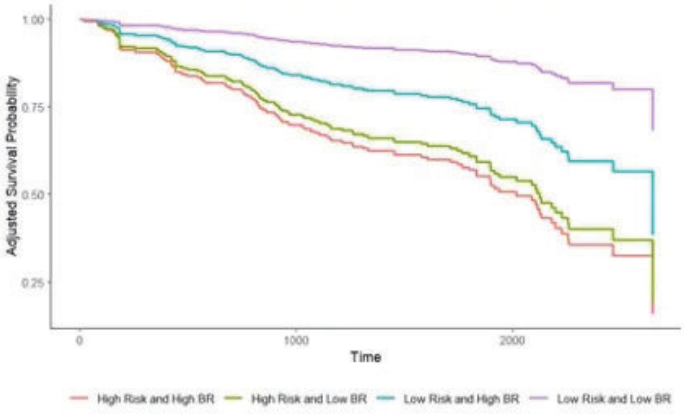

***Disclosures: Tahira Scott**, None*

1131

Exploring a Whole New World of Bone: Osteomorphs and Insights Utilizing an Ovariectomized Cynomolgus Monkey Model *Alana Stahl[1], Alexandra Olsen[2], Andrew Sawatsky[1], Brent Edwards[3], Roman Krawetz[4]. [1]McCaig Institute for Bone and Joint Health, Faculty of Kinesiology, Canada. [2]McCaig Institute for Bone and Joint Health, Department of Biomedical Engineering, Canada. [3]McCaig Institute for Bone and Joint Health, Faculty of Kinesiology, Department of Biomedical Engineering, Canada. [4]McCaig Institute for Bone and Joint Health, Department of Biomedical Engineering, Department of Cell Biology and Anatomy, Cumming School of Medicine, University of Calgary, Canada

Antiresorptive treatments for osteoporosis include denosumab (DMAb) and alendronate (ALN), which inhibit the function and survival of osteoclasts and the action of osteoclasts, respectively. Osteomorphs are osteoclasts that have been recycled via fission into smaller, highly mobile units. These osteomorphs can then fuse together to form new osteoclasts when needed. Though their mechanics remain elusive, osteomorphs play a role in bone resorption and therefore are likely active players in osteoporosis. The purpose of this study was to determine the effects ALN and DMAb have on osteoclast and osteomorph survival in a non-human primate model of osteoporosis.Adult cynomolgus monkeys were ovariectomized and randomly assigned to 12 monthly injections of s.c. vehicle (VEH; n = 6), s.c. DMAb (25 mg/kg, n = 6), or i.v. ALN(50 ?g/kg, n = 6). Other groups received 6 months of VEH followed by 6 months of DMAb (VEH-DMAb; n = 6) or 6 months of ALN followed by 6 months of DMAb (ALN-DMAb; n = 6. After sacrifice, the humeri were fixed, decalcified, then paraffin embedded. Sections were stained with TRAP and CD115 and the slides were fluorescently imaged. Tissue cytometry (TissueQuest) was performed on the images to detect and quantify cells expressing none, either or both marker. The number of cells/mm2 for all cell populations of interest (osteoclasts and osteomorphs) was analyzed.Cells expressing TRAP alone (osteoclasts) and those expressing both CD115 and TRAP (osteomorphs) were detected within all treatment groups (Fig. 1). Animals receiving treatment (ALN or DMAb) had significantly lower TRAP cell counts than the VEH group. There were no differences in the number of osteomorphs (CD115 and TRAP double positive cells) between any treatment groups.DMAB inhibits RANK ligand (RANKL), which in turn prevents osteoclasts from resorbing bone. It has been suggested that blocking RANKL inhibits the fusion of osteomorphs into osteoclasts, causing the accumulation of osteomorphs, which has never been previously observed in a non-human primate. Interestingly, while we observed a decrease of osteoclasts with treatment (as expected), osteomorph numbers were not impacted by ALN or DMAb. This resulted in an increase in the relative abundance of osteomorphs vs. osteoclasts in animals, particularly in the DMAb treatment group. Further research is required to understand the role of osteomorphs and if these cells play a role in rebound resorption after DMAb cessation.

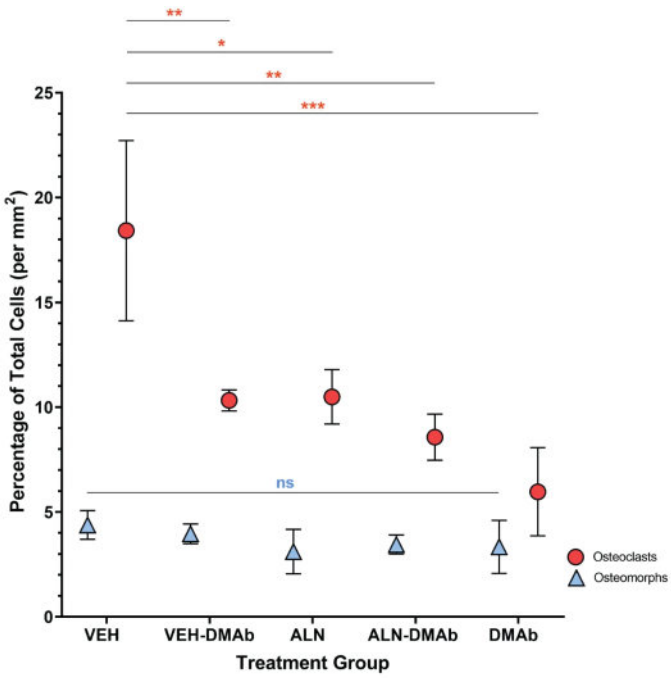

***Disclosures: Alana Stahl**, None*

1132

Delineating the role of Fshr in Bone Remodeling Using Novel Genetic Mouse Models *Mingxin Sun[1], Hongqian Chen[1], Li Xing[1], Libin Chen[1], Dr. Clifford ROsen[2], Mone Zaidi[3], Peng Liu[1]. [1]Laboratory of Bone and Adipose Biology, Shanxi Medical University, Taiyuan, China, China. [2]Maine Medical Center, United States. [3]Mount Sinai Medical Center, United States

FSH, secreted by anterior pituitary gonadotropic cells, has been traditionally held as a hormone that solely regulates reproduction through its G-protein-coupled receptor, the FSHR. However, there is increasing evidence for roles of FSH in the regulation of bone and adipose tissue remodeling, vascular function, lipid homeostasis, and cognition [e.g. Cell, 2006 PMID: 16630814; Nature, 2017, PMID: 28538730; Nature, 2022; PMID: 35236988]. Nevertheless, the extragonadal expression and function of the FSHR has been debated. To address this challenge and to precisely localize Fshr expression, we created a Fshr promoter-driven ZsGreen reporter mouse line. We found strong Fshr expression in the osteoclast, osteoblast, bone lining cells, and osteocytes. To understand the role of the FSHR in bone formation, we further developed floxed Fshr cKO mice, which we bred with a 10 kb Dmp1-CreERT2 line. We used micro-CT and NMR to sequentially assess bone and adipose tissues in mice on normal chow or high fat diet (HFD). Significant increases in bone mass were noted in both male and female tamoxifen (TMX)-induced Fshr cKO mice, on both normal chow and HFD, compared with the respective uninduced controls. In addition, we found an increase of markers of bone turnover, including osteocalcin, PINP and TRACP5b (ELISA). Histomorphometric parameters of bone resorption were also elevated, indicating that both bone formation and bone resorption were increased in Fshr cKO mice. Surprisingly, on quantitative NMR and micro-CT, we also noted a marked reduction of visceral adipose tissue in male Fshr cKO mice, but not in females fed on normal chow. There were no differences in subcutaneous adipose tissue in both sexes. However, when fed on HFD, both males and females showed a significant reduction in visceral and subcutaneous adipose tissue. We also studied the ovariectomized and aged Fshr cKO mice to find increased bone mass in the Fshr cKO, while trabecular bone was lost in the respective uninduced controls. To study the mechanism underpinning the bone conservation in Fshr cKO mice, we performed RNA-seq on femur-derived RNA from Fshr cKO and uninduced control mice on normal chow and HFD. We found that sclerostin (Sost) expression was downregulated by 10-fold in Fshr cKO mice fed on HFD compared with uninduced controls. However, there was an unexplained increase in Sost expression by 2-fold in the Fshr cKO mice fed on normal chow. In addition, we found a 5-fold increase in Lcn2 expression. The results collectively demonstrate that the selective deletion of the Fshr in osteocytes in adult, aging and ovariectomized mice, yields a remarkably robust bone conservation, while also resulting in a lean phenotype, via a yet uncharacterized mechanism.Our results suggest that removing the inhibition of bone formation by the Fsh-Fshr complex could have therapeutic implications.

***Disclosures: Mingxin Sun**, None*

1133

Denosumab inhibits the transition from erosion to formation in cortical remodeling of osteoporotic patients, similar to bisphosphonates *Xenia Borggaard[1], Jean-Paul Roux[2], Jean-Marie Delaisse[3], Shuang Huang[4], Pascale Chavassieux[5], Christina Andreasen[6], Thomas Andersen[7]. [1]Odense University Hospital, Denmark. [2]INSERM, UMR 1033, Universite de Lyon, France. [3]Odense University Hospital, KI, University of Southern Denmark, Denmark. [4]Amgen Inc, United States. [5]INSERM UMR1033, Universite De Lyon, France. [6]ODENSE UNIVERSITY HOSPITAL, Denmark. [7]University of Southern Denmark, Denmark

Osteoporosis is caused by an imbalance between bone resorption and bone formation, causing low bone mass and fragile bones. Denosumab inhibits maturation of osteoclasts thereby increasing BMD and reducing osteoporotic fractures. The increased BMD is presumably caused by closure of remodeling spaces and secondary mineralization. However, many questions concerning its effect on cortical bone remain unanswered. In this study, we use a series of new histomorphometric endpoints to investigate the intracortical and periosteal effect of denosumab treatment within bone biopsies collected during the FREEDOM study.The study included 164 iliac crest bone biopsies from osteoporotic patients treated with denosumab or placebo for 2-3 years. Goldner Trichrome stained sections cut from the biopsies were scanned under polarized light using Olympus VS200 microscope. Cortical area and area/size of intracortical pores were semi-automatically measured using VS200 Desktop 3.2.1 & DNN TruAI software. Each intracortical pore was manually classified according to their remodeling stage (eroded, eroded-formative, formative, or quiescent), and the percentage of eroded and formative periosteal surfaces were measured.In total, 8411 intracortical pores were measured and classified. The analysis revealed a significant reduction in mean pore diameter ($p = 0.002$), but no reduction in mean pore area ($p = 0.15$) or decrease in cortical porosity ($p = 0.077$) in patients treated with denosumab compared to placebo. Despite the reduction in mean pore diameter, the prevalence of eroded pores was not changed ($p = 0.78$) but their contribution to the total pore area increased significantly ($p < 0.001$) in the denosumab-treated patients. In contrast, prevalence, size, and contribution to the total pore area of eroded-formative and formative pores were significantly reduced ($p < 0.001$) in the denosumab-treated patients. On the periosteal surface, denosumab-treatment resulted in a significant reduction of formative surfaces ($p = 0.036$), while the prevalence of eroded surfaces increased significantly ($p = 0.009$) compared to placebo.The cortical histomorphometry demonstrates that denosumab delays the transition from erosion to formation in the remaining intracortical and periosteal remodeling events, likely due to an absence of osteoclasts and their coupling factors. We observed no modeling-based bone formation on the periosteal surfaces, as previously shown in femurs of denosumab-treated monkeys.

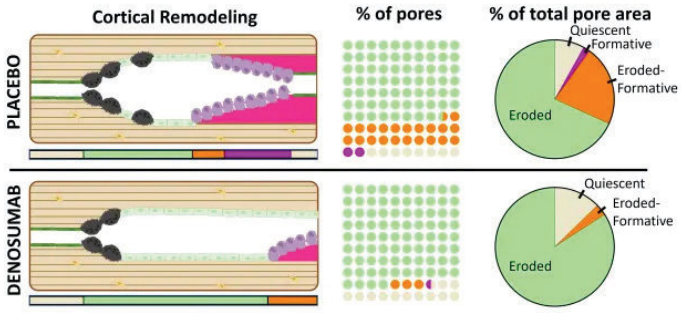

***Disclosures: Xenia Borggaard**, Amgen, Consultant*

1134

Preliminary Data From a First-in-Human, Randomized, Double-blind, Placebo-Controlled, Phase 1 Study of MBX?2109, a Once-Weekly Parathyroid Hormone Replacement Therapy, in Healthy Adults *Mary Jane Geiger[1], Martin Frenzel[2], Richard Bergstrom[3], Patricia Carney[1], Richard DiMarchi[4]. [1]MBX Biosciences, United States. [2]Cytel Inc, United States. [3]B2S Life Sciences, United States. [4]MBX Biosciences and Indiana University, Department of Chemistry, United States

Background: Hypoparathyroidism (hypoPT) is a rare condition characterized by parathyroid hormone (PTH) deficiency resulting in hypocalcemia and hyperphosphatemia. Standard of care with large doses of active vitamin D and calcium fails to adequately and consistently control serum calcium and disease symptoms. MBX 2109 is a novel PTH peptide prodrug being developed as a treatment for hypoPT. The N- and C- termini are respectively extended by 2 and 1 amino acids, with the same fatty acid attached at each end of the prodrug. MBX 2109 chemically converts to active drug by an intramolecular cyclization controlled by temperature and pH. This releases a fatty acylated, N-terminal dipeptide of MBX 2109 and an active drug containing a C-terminal fatty acid with full and selective binding potency for the PTH type 1 receptor. The fatty acids bind plasma proteins and extend circulating residence time of MBX 2109 and active drug. We evaluated the safety, tolerability, pharmacokinetics (PK), and pharmacodynamics (PD) of single and multiple ascending doses

(SAD/MAD) of MBX 2109 in healthy adults.Methods: This was a phase 1, randomized, double-blind, placebo-controlled, SAD/MAD trial (NCT05158335) in 76 healthy adults. SAD/MAD cohorts comprised up to 8 or 10 adults each (6-8 active, 2 placebo) who received subcutaneous doses of 50-600 ?g (SAD, 5 dose levels) or 200-900 ?g (MAD, 4 dose levels, 4 doses once weekly [QW]). Endpoints included plasma concentrations of MBX 2109 and active drug, albumin-adjusted serum calcium, and intact PTH(1-84) levels.Results: After single MBX 2109 doses, MBX 2109 and active drug concentrations increased linearly and dose proportionally (Figure). The geometric mean half-life of MBX 2109 and active drug was ~3.4-4.2 and ~5.5-6.9 days, respectively, across dose groups, supporting QW dosing. MBX 2109 200-900 ?g QW were associated with dose-related increases in mean albumin-adjusted serum calcium and concomitant suppression of mean intact PTH(1-84) levels. MBX 2109 was generally well tolerated (mostly mild treatment-emergent adverse events [AEs]) with no drug-related serious or severe AEs. No doses were associated with dose-limiting toxicity. Injection site reactions were generally mild (primarily erythema).Conclusions: MBX 2109 and active drug PK and PD support QW administration and demonstrate MBX 2109's pharmacologic effect in healthy adults, supporting advancement into phase 2 clinical development.

Figure. Arithmetic Mean Concentration Time Profiles by Dose for the MBX 2109 Prodrug (A) and Active Drug (B) After Single Doses of MBX 2109.

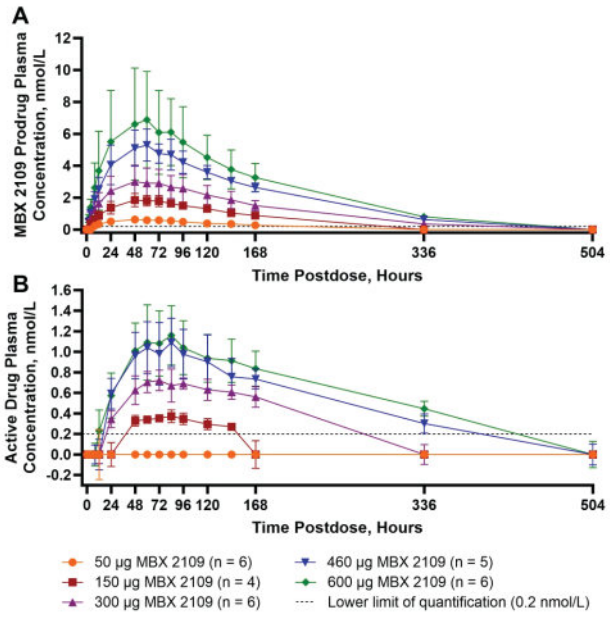

***Disclosures: Mary Jane Geiger**, MBX Biosciences, Other Financial or Material Support*

1135

The Longevity Gene SLC13A5 as a Novel Target For The Prevention of Age-Related Bone Loss *Naomi Dirckx[1], Hannes A. Baukmann[2], Jasmine Wu[1], Andreas L Birkenfeld[3], Marco F Schmidt[2], Dipender Gill[4], Stephen Burgess[5], Grit Zahn[6]. [1]Department of Orthopaedics, University of Maryland School of Medicine, Baltimore, MD 21201, United States. [2]biotx.ai GmbH, Am Mühlenberg 11, 14476 Potsdam, Germany , Germany. [3]Department of Diabetology Endocrinology and Nephrology, Internal Medicine IV, University Hospital Tübingen, Eberhard Karls University Tübingen, 72074 Tübingen, Germany , Germany. [4]Department of Epidemiology and Biostatistics, School of Public Health, Imperial College London, London, UK, United Kingdom. [5]MRC Biostatistics Unit, University of Cambridge. Address: East Forvie Building, Robinson Way, Cambridge, CB2 0SR, UK., United Kingdom. [6]Eternygen GmbH, Westhafenstrasse 1, 13353 Berlin, Germany, Germany

Citrate, a critical TCA cycle intermediate, is present in bone at high concentrations (1-5 wt%) where it is bound to mineral apatite surfaces in a pattern compatible with a structural role. We previously showed that osteoblasts use a specialized metabolic pathway, mediated by the plasma membrane citrate transporter SLC13A5, to regulate uptake, endogenous production and deposition of citrate into bone. Loss of function of this pathway impairs mineralization of bones and teeth in young mice and in children with mutations in SLC13A5 due to increased mineral citrate. Since other studies have suggested that deletion of Slc13a5 in mice mitigates age-related cardiovascular and metabolic pathologies and reducing the expression of the I'm not dead yet (Indy) gene, an orthologue for Slc13a5, increases lifespan in Drosophila melanogaster and C. elegans, we hypothesized that SLC13A5 exerts a unique function in skeletal aging in mice. Furthermore, we translated our findings in humans using a drug target Mendelian Randomization (MR) approach from UK biobank data.We compared young (10 wks) and aged (52 wks) osteoblast-specific Slc13a5 (Slc13a5Oc-cre) mutant mice to littermate Slc13a5fl/fl controls of the respective age. While young female Slc13a5Oc-cre mice exhibited reduced cortical thickness ($p<0.01$) and increased fragility (reduced ultimate moment, $p<0.05$) in 3pt bending tests as we reported earlier, old female Slc13a5Oc-cre mice exhibited a striking reversal of the phenotype marked by a 50% increase in elasticity (Young's modulus, $p<0.05$) without affecting the moment of fracture. Similarly, old male Slc13a5Oc-Cre mice show significant widening of the bone ($p<0.001$) and increased bone strength by 3pt bending (increased ultimate moment, $p<0.05$), while young male mutants were phenotypically normal. In humans, we observed that SNPs associated with reduced function of SLC13A5, indicated by increased plasma citrate levels, were associated with lower risk of osteoporosis in UK Biobank participants (-0.0034 +/-0.0013, $p<0.0097$), while an association between osteoporosis risk and plasma citrate levels in general, was not found (-0.000443 +/-0.0011, $p<0.6877$), indicating that the effect is mediated by SLC13A5. Together, our mechanistic data in mice and MR studies in humans suggest that reducing the function of SLC13A5 in older age has beneficial effects on age related bone loss, which renders pharmacological inhibition of SLC13A5 as a promising approach to treat osteoporosis.

***Disclosures: Naomi Dirckx**, None*

1136

Impaired Fracture Healing in Novel Transchromosomic TcMac21 Down Syndrome Mice *Catrina Silveira[1], KIRBY M. SHERMAN[2], Alyssa Falck[3], Lindsay Dawson[4], Dana Gaddy[5], Larry Suva[6]. [1]Texas A&M University, Departments of Veterinary Physiology & Pharmacology, United States. [2]Texas A&M University , . [3]Texas A&M University, . [4]Texas A&M University College of Veterinary Medicine, United States. [5]College of Veterinary Medicine, Texas A&M University, United States. [6]Texas A&M University, College of Veterinary Medicine and Biomedical Sciences, United States

Down Syndrome (DS) (trisomy of human chromosome 21 (Hsa21) (Ts21)) occurs in approximately one in 800 live births. Low BMD in Ts21 is secondary to low bone mass accrual, which contributes to significantly increased fracture risk and fracture non-union. Recently we demonstrated that long-bone fracture healing is significantly impaired in DP16 DS mice, ultimately resulting in fracture non-union. These results prompted us to investigate long-bone fracture repair using novel human transchromosomic (Tc) mouse models using Tc1 and Tc(HSA21q;MAC)1Yakaz (TcMac21) murine DS models. Tc1 carries 158 of 213 functional Hsa21 protein coding genes but is mosaic (with each individual Tc1 animal unique), whereas TcMac21 contains 93% of Hsa21 protein coding genes, and is not mosaic. Thus, TcMac21 is the most complete genetic DS mouse model to date, yet no detailed skeletal analyses have been reported. Both Tc1 and TcMac21 replicate multiple DS phenotypes including cardiac, craniofacial, and neurocognitive abnormalities. Tc1 DS mice have no basal bone phenotype regardless of age or gender. Like DP16 DS mice, male TcMac21 DS mice have decreased BMD at both 8 weeks and 4 months of age as well as significantly decreased BV/TV, with increased Tb. Sp and decreased Ct. Th compared to WT. Despite the differences in basal bone phenotype, both TcMac21 and Tc1 DS mice exhibit significantly impaired fracture healing. Fractures were induced using the middle phalanx (P2) non-stabilized fracture model. P2 fractures were induced on digits II and IV of the hindfeet of 16-week-old male TcMac21 and Tc1 DS mice. Following fracture, sequential in vivo ?CT was utilized to determine anatomical changes over 42 days post fracture (DPF). Analysis revealed that both male TcMac21 and Tc1 DS mice exhibited lower percent fracture healing (0 of 8; 0% and 1 of 14; 7.1% respectively) at 42 days DPF compared to WT counterparts. Collectively, these data demonstrate that TcMac21 DS mice (like other DS mice) exhibit a low bone mass phenotype and that both TcMac21 and Tc1 DS mice have impaired fracture healing. TcMac21 is a new humanized model of DS, with a freely segregating Hsa21 with which to further study the skeletal complications of DS. Ongoing studies targeting identification of the cellular mechanisms specific to DS bone repair in multiple Tc and other DS mouse strains will be paramount to translate clinically to the management of fracture non-union in Ts21 humans.

***Disclosures: Catrina Silveira**, None*

1137

Correction of Paradoxical Mineralization in murine CKD-MBD with ENPP1 Enzyme Biologics *Hana Kim[1], Tayyaba Ishaq[1], Paul Stabach[1], Thomas Carpenter[2], William O'Neill[3], Demetrios Braddock[1]. [1]Yale University Department of Pathology, United States. [2]Yale University Department of Pediatric Endocrinology, United States. [3]Emory University, Department of Nephrology, United States

Background: Chronic Kidney Disease-Mineral & Bone Disorder (CKD-MBD) is a prevalent mineralization disorder characterized by medial arterial calcifications and decreased bone mass, in which bone mass inversely correlates with vascular calcifications in a 'Paradoxical Mineralization' disorder to underscore the confusing pathogenesis. Plasma levels of pyrophosphate (PPi) are reduced in CKD patients, suggesting a potential role for the enzyme producing PPi, ENPP1, in the pathogenesis of CKD-MBD.Experimental Plan: To induced CKD we placed mice on a high phosphate, high calcium, low magnesium diet (1.2% Ca, 1.8% Pi, 0.04% Mg) and alternated adenine between 0.15% - 0.3% over 33 weeks in a manner similar to previous murine CKD models induce with an alternating adenine diet (Jia et al. BMC Nephrology 2013, 14:116). Once the animals had developed renal failure (BUN>60 mg/dl) we began dosing the mice with weekly doses of either vehicle or soluble

(1118) or bone targeted (2000) ENPP1-Fc, monitoring BUN and plasma PPi concentrations weekly. At 33 weeks the animals were sacrificed and aortic vascular calcifications were chemically quantitated, and subcutaneous calcifications and cardiac calcifications were assessed by weight and micro-CT, respectively. Bone mineralization in the animals was assessed using biomechanical testing of femurs and micro-CT analysis of tibias.Results: The high-adenine, high-phosphate diet induced progressive renal failure in CKD mice, marked by elevated BUN levels and reduction of plasma PPi levels, which inversely correlated with BUN and markedly dropped on the final week for the diseased groups. With respect to the untreated CKD group, both variants of our ENPP1 enzyme significantly reduced aortic calcification, maintaining low levels comparable to the wild-type. Additionally, comparison of bone biomechanical properties showed significant improvement in stiffness and maximum load in both treatment groups. Micro-CT scans of tibial trabecular bone also showed improved trabecular number, thickness and spacing in the biologic-treated mice. Finally, untreated CKD mice demonstrated an inverse correlation between vascular calcification and Trabecular BV/TV, cortical thickness, and maximum load of femurs in biomechanical testing, reproducing the paradoxical mineralization present in human CKD-MBD.Conclusions: Our studies demonstrate that a modified version of the alternating adenine diet reproduces paradoxical mineralization present in humans with CKD-MBD and demonstrates prevention of vascular calcification and amelioration of the bone mineral abnormalities with ENPP1 biologics, suggesting a role for ENPP1 in the pathogenesis of CKD-MBD, and treatment of the mineralization phenotype with recombinant ENPP1-Fc.

***Disclosures: Hana Kim**, None*

1138

Pooled single-cell CRISPRi screen in hFOB1.19 cells identifes effector genes at BMD GWAS loci *Mitchell Conery[1], James Pippin[2], Yadav Wagley[6], Andrew D. Wells[2], Benjamin F. Voight[4], Babette Zemel[5], Kurt Hankenson[6], Alessandra Chesi[4], Struan Grant[7]. [1]University of Pennsylvania/Children's Hospital of Philadelphia, United States, [2]Children's Hospital of Philadelphia, United States, [4]University of Pennsylvania, United States, [5]Childrens Hospital of Philadelphia, United States, [6]University of Michigan, United States,

[7]Children s Hospital of Philadelphia / University of Pennsylvania, United States

Genetic factors strongly influence bone mineral density (BMD) and osteoporosis risk over time. To date, genome-wide association studies (GWAS) have discovered over 1,100 independent BMD signals; however, the causal variant(s) and respective effector gene(s) for the majority of these loci remain unknown. We previously published the results of a 3D genomics-based 'variant-to-gene' mapping method for BMD loci based on ATAC-seq, RNA-seq, and chromatin confrmation capture data from hMSC-derived osteoblasts. We have since applied this approach, which links putative causal variants in open chromatin to candidate effector genes via chromatin interactions with open promoters, to a dataset derived from the human fetal osteoblast 1.19 cell line (hFOB). For validation of both sets of fndings at scale, we conducted a CRISPRi screen in hFOBs differentiated for fve days. To reduce background noise and avoid issues stemming from non-random assortment of guide RNAs, we executed the screening process at a low multiplicity of infection (~1 guide RNA per cell). We targeted 89 GWAS-tagged distal regulatory elements linked to one or more known osteoblast-expressed genes via chromatin interaction and observed effects on gene expression in a 1Mb range via single-cell RNA sequencing (scRNA-seq). Post-screening, we used CellBender to denoise our data and a two-tiered strategy to eliminate cellular debris and doublets. This approach employed the clustering of low-complexity cells and stringent fltering of droplets exhibiting >90,000 unique molecular identifers (UMIs) or >10% mitochondrial reads. We ultimately retained 27,383 high-quality cells that received a single unique guide. Using SCEPTRE and the top 15 expression principal components as covariates, we identifed 22 successful CRISPRi perturbations for 19 of the targeted elements. We observed eight connections implicated via our mapping strategy, for example, CPED1, a locus previously reported by our group, as well as 14 novel implicated genes including two HOXD genes that suggest an important role for developmental patterning in the establishment and maintenance of BMD. These results warrant confrmation of the BMD modulating effects of all 22 genes with siRNA knockdown and paired functional assays. In conclusion, our strategy in the osteoblast-lineage has yielded crucial functional insights for BMD GWAS loci and provides a methodological framework for studying the genomics of other musculoskeletal traits and diseases.

***Disclosures: Mitchell Conery**, None*

1139

Measuring in vivo musculoskeletal metabolism at a single-organelle level *Kai Chen[1], Nathan Pavlos[2], Jiake Xu[2], Matthew Greenblatt[3], Killugudi-Swaminatha Iyer[2], Haibo Jiang[4]. [1]The University of Western Australia, Australia, [2]University of Western Australia, Australia, [3]Weill Cornell Medical College, United States, [4]University of Hong Kong, China

Metabolism refers to a series of chemical reactions that occur within living organisms. Musculosketal system is highly metabolically active and exhibits enormous metabolic heterogeneity, which is challenging to measure. An in vivo investigation of metabolism is critical as it is difficult to recapitulate in vitro, where cells exhibit distinct metabolic behaviors and dependencies. Therefore, the holistic understanding of musculoskeletal biology and diseases requires the in vivo spatial mapping of the chemistry and metabolism across organelles, cells, and matrix. However, this remains unresolved with existing molecular imaging approaches. The mineralized nature of musculoskeletal tissues poses additional challenges to this endeavor.Here, using correlative electron and ion microscopy (CEIM), we have developed an imaging platform specialized for the musculoskeletal system, enabling the in vivo metabolic profiling of cells and matrix down to a single-organelle level. Electron microscopy (EM) provided the ultrastructural details, and the same area, mapped by ion microscopy (IM) using nanoscale secondary ion mass spectrometry (NanoSIMS) intrument, enabled the visualization of chemical elements (e.g., 1H, 12C-, 31P-, 32S-) with a spatial resolution down to approximately 40 nm. Following the oral administration of stable isotope-labelled (i.e., 13C, 15N) amino acids in mice over time periods ranging from minutes to weeks, we spatiotemporally profiled the chemcial elements and metabolic heterogeneity across single cells (e.g., osteoblasts, osteoclasts, chondrocytes, tenocytes, myocytes) and single organelles (e.g., ER, Golgi apparatus, secretory grannules, mitochondria) in vivo. Furthermore, our data also revealed the diverse matrix renewal patterns and aging-related decline throughout the musculoskeletal system. Taken together, our study delivered a landscape of nanoscale metabolim and matrix renewal in the musculoskeletal system in vivo.

***Disclosures: Kai Chen**, None*

1140

A CNP Analog as Adjuvant Treatment for the Growing Osteogenesis Imperfecta Mouse: A Pilot Study *MICHAEL BOBER[1], Ketsia Seide[2], Jack Mulcrone[2], Erin Carter[2], Nancy Pleshko[3], Cathleen Raggio[4]. [1]Nemours Children's Hospital, Delaware, [2]Hospital for Special Surgery, United States, [3]Temple University, United States, [4]HSS, United States

Purpose: Osteogenesis imperfecta (OI) is a heterogenous type 1 collagenopathy characterized by bone fragility. Bisphosphonates decrease fracture incidence and are utilized to manage moderate to severe forms of OI in children. C-type natriuretic peptide (CNP) is produced in the growth plate and positively regulates linear bone growth. This study aims to evaluate if the addition of a CNP Analog (vosoritide) to standard bisphosphonate (alendronate (ALN)) therapy will reduce fracture incidence, improve growth, increase bone mineral density (BMD), and/or improve bone strength in a growing oim/oim mouse model of moderate-to-severe OI.Methods: Starting at 2 weeks of age, growing oim/oim mice (N=17) were divided into 4 groups, saline-treated (controls, N=8), and treated oim/oim mice where all received weekly ALN and one of 3 CNP dosages: 20 ug/kg 5 days/week (20x5) (N=3), 20 ug/kg 3 days/week (20x3) (N=3), or 10 ug/kg 3 days/week (10x3) (N=3). Faxitron images were taken at 2 and 14 weeks (sacrifice) to asssess femoral length, vertebral height, and other bone microstructural parameters by microcomputed tomography analysis. Results: At sacrifice, mice in the 20x5 group had no new fractures, compared to 1 fracture in 1 mouse in both the 20x3 and 10x3 groups. All 3 treatment groups had increased femoral lengths compared to the untreated oim/oim mice (Fig 1); the greatest increase was in the 20x5 group with the 20x3 and 10x3 having similar increases. All treated groups had an increase in vertebral height; both the 20x5 and 10x3 groups had higher vertebral heights than the 20x3 group, but were not different from each other. In comparison to untreated oim/oim mice, all 3 dosage groups had increased cortical bone tissue mineral density (TMD), cortical bone mineral density (BMD), cortical bone thickness, trabecular bone volume fraction (BVF), trabecular BMD, and trabecular bone number. All 3 dosage groups had decreased trabecular bone separation (Fig 2).Conclusion: In this preliminary pilot study, it appears that the adjuvant treatment with a CNP analog results in an overall increase in both femoral and vertebral heights without compromising fracture reduction. In addition, the combination treatment appears to have an additive beneficial effect on both trabecular and cortical bone, the latter of which was not seen with bisphosphonates alone. Continued enrollment will yield the best dosage to maximize the positive bone effects.We thank BioMarin for their grant support.

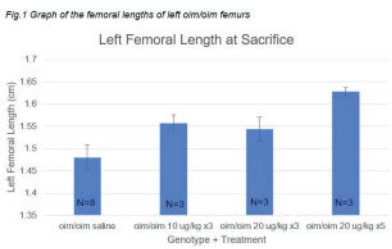

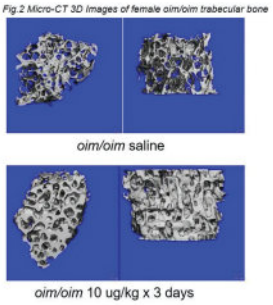

***Disclosures: MICHAEL BOBER**, Biomarin, Consultant*

Monday Orals

Author Index